ISCBFM
International Society for
Cerebral Blood Flow & Metabolism

Barcelona
BRAIN 2011

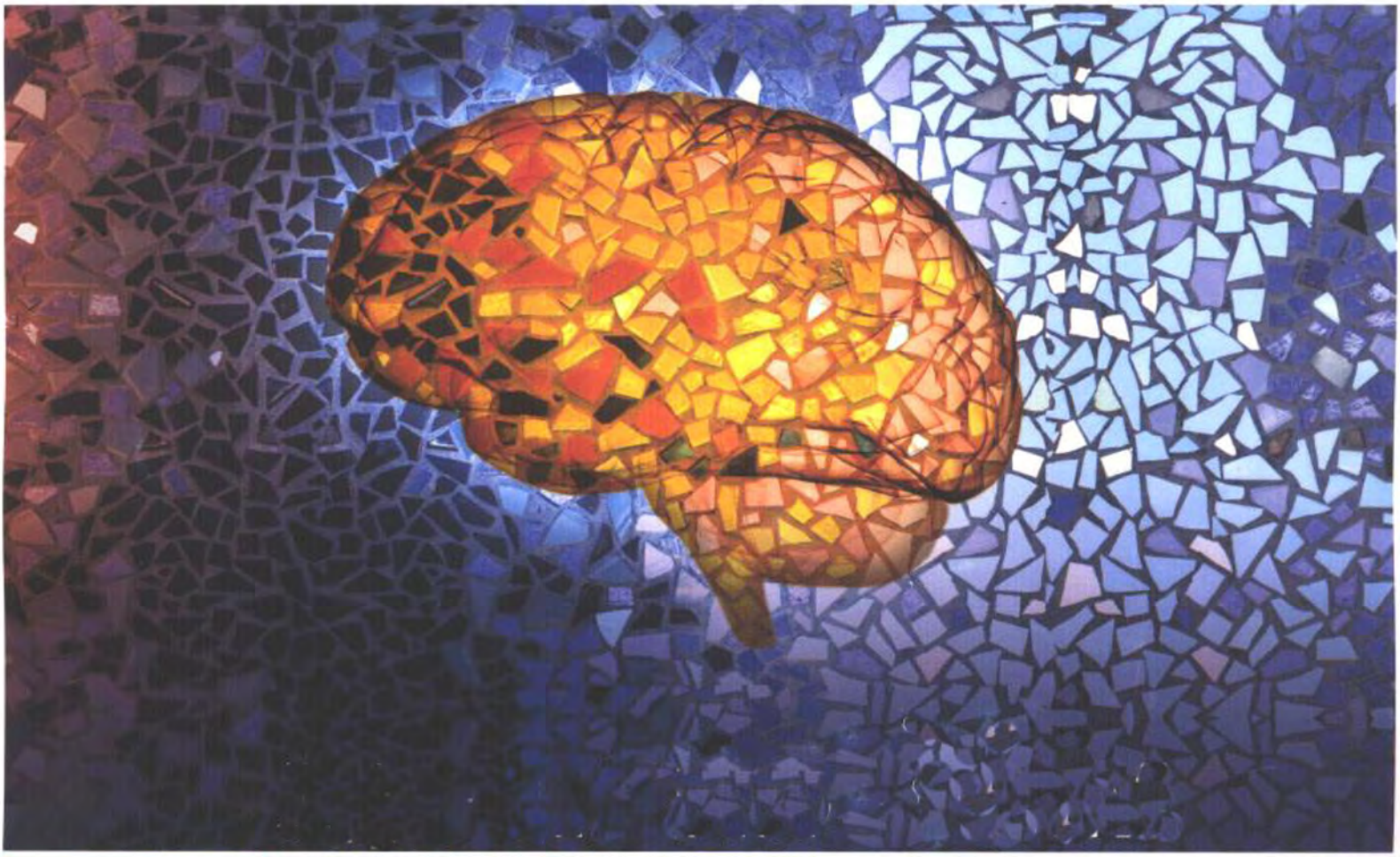

XXVth International Symposium on Cerebral Blood Flow, Metabolism, and Function
&
Xth International Conference on Quantification of Brain Function with PET

Barcelona, Spain, May 25- 28, 2011

The State-of-the-Art in Brain Research

www.kenes.com/brain

4

NEUROPROTECTIVE EFFECT OF MEDICINAL HERBS ON CEREBRAL ISCHEMIA IN MALE WISTAR RATS

S.S. Raza, M.M. Khan, F. Islam

Toxicology, Jamia Hamdard University, New Delhi, India

Objectives: The use of herbs to treat disease is almost universal among non- industrialized societies. The WHO estimates that 80% of the world´s population presently uses herbal medicine for some aspect of primary health care. Herbal medicine is a major component in all traditional medicine systems, and a common element in Unani, Sidha, Ayurvedic and Homeopathic systems in India.

Cerebral Ischemia induces production of oxygen free radicals and other reactive oxygen species (Allen et. al., 2009). These react with and damage a number of cellular and extracellular elements. Free radicals also directly initiate elements of the apoptosis cascade by means of redox signaling . Accumulated evidence suggests that ROS can be scavenged through utilizing natural antioxidant compounds present in foods and medicinal plants. In the present study two herbs were used with an objective:

- To study the neurobehavioural and neurochemical changes associated with cerebral ischemia.
- To study the efficacy of herbal extract for prevention of cerebral ischemia.

Hesperidin a flavonone glycoside (flavonoid) found abundantly in citrus fruits.It acts as an antioxidant and anti-inflammatory agent (Galati et. al., 1994) and Silymarin, the mixture of flavonolignans extracted from blessed milk thistle (*Silybum marianum*) having antioxidant property.

Material and methods: Male Wistar rats were pretreated with oral hesperidin (25 mg/kg) and silymarin (100, 200 and 400 mg/kg 30-min before occlusion) dissolved in normal saline and 5% PEG respectively. The middle cerebral artery of adult male Wistar rats was occluded for 2 hr and reperfused for 22 h as per the published method (Longa et. al., 1989) with some modification (Salim et. al., 2003).

Results: Both were found as a good antioxidant in up-regulating the status of enzymatic and non-enzymatic endogenous antioxidants, lowering the TBAR's level, lowering proinflammatory cytokines level, and recovering results close to baseline with better functional and behavioural outcome.

Conclusion: These results suggest the neuroprotective potential of hesperidin as well as silymarin in cerebral ischemia is mediated through their antioxidant activities.

References:

- Allen, C.L., Bayraktutan, U., 2009. Oxidative stress and its role in the pathogenesis of ischemic stroke. Int. J. Stroke. 4, 461-470.
- Galati, E.M., Monforte, M.T., Kirjavainen, S., Forestieri, A.M., Trovato, A., Tripodo, M. M., 1994. Biological effects of hesperidin, a Citrus flavonoid (Note I): antiinflammatory and analgesic activity. Farmaco. 40, 709-712.
- Longa, E.Z., Weinstein, P.R., Carlson, S., Cummins, R., 1989. Reversible middle cerebral artery occlusion without craniectomy in rats. Stroke. 20, 84-91
- Salim, S., Ahmad, M., Zafar, K.S., Ahmad, A.S., Islam, F., 2003. Protective effect of Nardostachys jatamansi in rat cerebral ischemia, Pharmacol. Biochem. Behav. 74, 481-486.

13

THE BLOOD-BRAIN BARRIER IN ALZHEIMER'S DISEASE

W. Banks

Internal Medicine, VA/ University of Washington, Seattle, WA, USA

About a dozen hypotheses have suggested ways in which blood-brain barrier (BBB) structure or function are altered in Alzheimer's disease (AD). These include disruption or loss of integrity of the BBB, secretion of neurotoxic substances by brain endothelial cells, and altered reabsorption of cerebrospinal fluid. New hypotheses have been put forth as the BBB is understood to be not just a barrier, but a dynamic, regulatory interface controlling the exchange of substances between the CNS and blood. More recently, the neurovascular hypothesis as advanced by Zlokovic et al. states that decreased efflux of amyloid beta protein contributes significantly to the amyloid burden of the brain. Jaeger et al. has shown that knockdown inb mice of the BBB efflux pump protein LRP-1 results in decreased efflux of amyloid beta protein from the brain, increased amyloid beta protein in the brain, and cognitive deficits. Inflammation induced by lipopolysaccharide both inhibits efflux out of brain and increases influx into brain of amyloid beta protein, providing a mechanism by which neuroinflammatory influences at the BBB could result in increased amyloid burden in brain. The BBB plays a crucial role in determining the degree to which potential therapeutics cross the BBB. Efflux transporters such as p-glycoproteins influence the uptake and accumulation by brain of traditional small molecules and antibodies, whereas saturable transporters influence the uptake of antisense oligonucleotides, peptides, and proteins. Ghrelin, leptin, and insulin represent gastrointestinal peptides that readily cross the BBB and have positive effects on cognition in mouse models of Alzheimer's disease. Intranasal delivery has been shown to be effective in bypassing the BBB and delivering insulin and exendin to the CNS in quantities sufficient to affect cognitive processes.

15

CURATIVE EFFECTS OF INTRA-ARTERY THROMBOLYSISOF ACUTE ISCHEMIC STROKE WITHIN 6~9 HOURS INFARCTION OF CAROTID ARTERIAL SYSTEM

Y. Jun, X.J. Tao, Z. Jun

Department of Neurology, Urumqi General Hospital, Lanzhou Command, PLA, Urumqi, China

Objective: To evaluate the curative effects and security of intra-artery thrombolysis for acute infarction of carotid arterial system in 6~9 hours time window.

Methods: Analyzed retrospectively the 27 patients treated with selective intra-arterial thrombolysis using urokinase(500 000 to 1.5 million units) within 6~9 hours after the acute infarction of carotid arterial system. The patients were admitted from Jan 2005 to Jan 2010, including 20 men and 7 wemen, aged from 32 to 79 years old with averge of 60 years. After digital subtraction angiography examination, urokinase were administered locally through microcatheters by micropump at rate of 15,000 unit/min. the total dosage of UK was 500 000 units to 1.5 million units. Angiograms were graded according to the Thrombolysis in Cerebral Infarction (TICI) .

Results: 10 occulisons were found in internal carotid artery, 15 occulisons were found in median cerebral artery, and 2 occulisions were found in anterior cerebral artery. After thrombolysis, 5 cases were totally recanalized (TICI: 3 grade), 15 cases were partially recanalized (TICI: 2 grade), 7cases were not recanslized (TICI: 0~1 grade). The tatal mortality were 14.8 percent, while the ratio of recanalization were 74.1 percent. The mortality of 20 atherthrombosis patients were 0, while the ratio of recanalization were 90%. However, the mortality of cardioembolism patients were 57.1 percent, and the ratio of recanalization were only 28.5%. Compared with prethrombolysis, the Barthel index of atherthrombosis patients increased significantly (35.7±12.9 versus 68.3±23.7, $P< 0.05$), while the mRS decreased obviously (4.0±0.6 versus 2.3±1.1, $P< 0.05$). In comparison with prethrombolysis, no significant changes of the Barthel index(16.4±20.6 versus 22.1±25.3, $P>0.05$) and mRS(4.0±1.4 versus 5.0±1.1, $P>0.05$) were observed in cardioembolism patients.

Conclusion: Intra-arterial thrombolysis is a safe and effective theraputic method for acute ischemic stroke within 6~9 hours atherthrombosis infarction of carotid arterial system.

Key words: Thrombolytic therapy; stroke; time window; internal carotid artery; anterior cerebral artery; middle cerebral artery

17

DELAYED CEREBRAL ISCHEMIA IN ASSOCIATION WITH SPREADING DEPOLARIZATION BUT ABSENT PROXIMAL VASOSPASM AFTER ANEURYSMAL SUBARACHNOID HEMORRHAGE

J. Woitzik[1], J. Dreier[1], N. Hecht[1], I. Fiss[1], N. Sandow[1], S. Major[1], J. Manville[2], P. Schmiedek[2], M. Diepers[2], E. Muench[2], H. Kasuya[3], P. Vajkoczy[1], COSBID Study Group

[1]Charité - Universitätsmedizin Berlin, Berlin, [2]Universitätsmedizin Mannheim, Mannheim, Germany, [3]Tokyo Women's Medical University, Tokyo, Japan

Objektive: It was measured recently that clusters of spreading depolarization (SD) occur time-locked to the development of delayed cerebral ischemia (DCI) after aneurysmal subarachnoid hemorrhage (aSAH). Currently it is assumed that DCI is primarily induced by proximal vasospasm. Surgical placement of nicardipine prolonged-release implants (NPRIs) has been shown to significantly reduce proximal vasospasm and DCI.

Aim: In the present study, we tested in 13 patients with major aSAH whether DCI is associated with SD when proximal vasospam is abolished by NPRIs.

Patients and methods: After clipping of the ruptured aneurysm, 10 nicardipine prolonged release implants were placed next to the proximal intracranial vasculature. SDs were recorded using a subdural 6-contact strip electrode. SD-associated changes of tissue partial pressure of oxygen ($ptiO_2$) and perfusion changes were measured with a Clark type probe and thermal-diffusion regional cerebral blood flow probe. The degree of proximal vasospasm was assessed by digital subtraction angiography. DCI was assessed by repeated neurological examinations and repeated CT and/or MRI scans.

Results: 534 SDs were recorded in 10 of 13 patients (77%). Digital subtraction angiography revealed no vasospasm in 7 of 13 patients (53%) and mild or moderate vasospasm in 3 patients each (23%). Five patients developed DCI. In three of these patients, clusters of SD occurred and serial neuroimaging revealed delayed ischemic stroke although proximal vasospasm was absent. There was no significant correlation between the degree of proximal vasospasm and the occurrence of DCI. In contrast, the number of SDs and the total duration of the electrocorticographic depression period correlated significantly with the occurrence of DCI.

Conclusion: Our findings confirm that DCI is associated with SD and provide evidence that SDs occur abundantly after aSAH even if proximal vasospasm is significantly reduced or abolished. The persistence of SDs may explain, at least partially, why robust reduction of proximal vasospasm has not been sufficient in the clinic to improve outcome.

22

INHIBITION OF VEGF SIGNALING PATHWAY ATTENUATES HEMORRHAGIC TRANSFORMATION AFTER THROMBOLYTIC TREATMENT IN RATS

T. Shimohata[1], M. Kanazawa[1], H. Igarashi[2], T. Takahashi[1], K. Kawamura[1], A. Kakita[3], H. Takahashi[4], T. Nakada[2], M. Nishizawa[1]

[1]Department of Neurology, [2]Department of Center for Integrated Human Brain Science, [3]Department of Pathological Neuroscience Resource Branch for Brain Disease Research, [4]Department of Pathology, Brain Research Institute, Niigata University, Niigata, Japan

Objective: To investigate whether inhibition of vascular endothelial growth factor (VEGF) signaling pathway can attenuate hemorrhagic transformation (HT) after tissue plasminogen activator (tPA) treatment.

Background: The benefits of tPA thrombolysis are heavily dependent on time to treatment, and use of tPA may be associated with HT, especially when tPA is administered beyond the therapeutic time window. An angiogenic factor, VEGF, might be associated with the blood-brain barrier (BBB) disruption after focal cerebral ischemia: however, it remains unknown whether HT after tPA treatment is related to the activation of VEGF signaling pathway in BBB.

Methods: Rats subjected to acute cerebral ischemia by injection of autologous thrombi (Okubo S, et al. 2007) were assigned to a permanent ischemia group and groups treated with tPA (10 mg/kg) at 1 h or 4 h after ischemia. Anti-VEGF neutralizing antibody (RB-222) or control antibody was administered simultaneously with tPA. At 24 h after ischemia, we evaluated the effects of the antibody on the VEGF expression, matrix metalloproteinase-9 (MMP-9) activation, degradation of BBB components (type IV collagen, endothelial barrier antigen), and HT. Outcomes at 24 h after ischemia were scored using the 5-point motor function scale (Anderson M, et al. 1999).

Results: Delayed tPA treatment at 4 h after ischemia promoted expression of VEGF in BBB, MMP-9 activation, degradation of BBB components, and induction of HT. Compared with tPA and control antibody, combination treatment with tPA and the anti-VEGF neutralizing antibody significantly attenuated VEGF expression in BBB, MMP-9 activation, degradation of BBB components, and HT. It also improved motor outcome and mortality at 24 h after ischemia ($P = 0.001$ and $P = 0.007$, respectively).

Conclusions: The therapeutic time window of tPA prolonged by the anti-VEGF neutralizing antibody. Inhibition of VEGF signaling pathway will be a promising therapeutic strategy for attenuating HT after tPA treatment.

27

TRANSLATIONAL REPROGRAMMING TO STRESS RESPONSES AFTER BRAIN ISCHEMIA

D.J. DeGracia

Department of Physiology, Wayne State University, Detroit, MI, USA

2011 is the 40th anniversary of Hossmann and colleague's[1] discovery of protein synthesis inhibition in reperfused neurons. Subsequent work established that protein synthesis remained inhibited, decoupled from energy charge, in neurons destined for delayed neuronal death after both focal and global ischemia. The translation block contributed to delayed neuronal death, at least partly, by preventing translation of pro-survival mRNAs such as c-fos or hsp70.

The Burda et al.[2] demonstration that eukaryotic initiation factor 2 was phosphorylated during early reperfusion opened investigations of ribosome regulation that eventually vindicated Paschen's suggestion[3] that post-ischemic translation arrest was part of the neuronal intracellular stress response. However, the molecular biology of ribosome regulation could not explain the persistent translation arrest.

Seminal work by Hu and colleagues[4] revealed that masses of ubiquinated proteins aggregated in post-ischemic neurons, providing insight into upstream triggers leading to expression of the heat shock response, and to the realization that stress response effectors could succumb to protein aggregation. Hence, the mechanism of co-translational aggregation, where ribosomes and associated cofactors are damaged, was advanced to explain the persistent shut-off of protein synthesis in the selectively vulnerable neurons.

Our lab has continued to investigate the post-ischemic neuronal intracellular stress response. Advances in molecular biology have revealed the complexity of mRNA regulation when cells experience exogenous stressors. Our investigations of mRNA-containing structures in reperfused neurons have shown that ribosome regulation is only the initiating step in the stress response program. We have shown that mRNA transforms into cytosolic structures, mRNA granules, which separate the mRNA from the ribosomes[5]. The mRNA granules persist until the death of selectively vulnerable neurons. The composition of the mRNA granules correlates with whether or not the cell is capable of the selective translation of pro-survival mRNAs such as hsp70. Our current work indicates that the persistent translation arrest is due, at least in part, to a dysfunction in the control and handling of mRNA in selectively vulnerable neurons due to alterations in mRNA binding proteins such as HuR. The dysfunction in mRNA handling appears to occur in parallel to co-translational aggregation. Thus at least two major mechanisms contribute to persistent translation arrest in vulnerable neurons.

Reference:

[1] Kleihues P, Hossmann K (1971) Protein synthesis in the cat brain after prolonged cerebral ischemia. Brain Res 35:409-418.

[2] Burda J, Martin ME, Garcia A, Alcazar A, Fando JL, Salinas M (1994) Phosphorylation of the a subunit of initiation factor 2 correlates with the inhibition of translation following transient cerebral ischemia in the rat. Biochem J 302:335-338.

[3] Paschen W (1996) Disturbances of calcium homeostasis within the endoplasmic reticulum may contribute to the development of ischemic-cell damage. Med Hypotheses 47:283-288.

[4] Hu BR, Martone ME, Jones YZ, Liu CL (2000) Protein aggregation after transient cerebral ischemia. J Neurosci 20:3191-3199.

[5] Jamison JT, Kayali F, Rudolph J, Marshall MK, Kimball SR, DeGracia DJ (2008) Persistent Redistribution of Poly-Adenylated mRNAs Correlates with Translation Arrest and Cell Death Following Global Brain Ischemia and Reperfusion. Neuroscience. 154: 504-520

30

ELECRTOENCEPHELOGRAPHIC (EEG) & MINI MENTAL STATE EXAMINATION (MMSE) FINDINGS AMONG HIV POSITIVE PATIENTS

J.K. Adam[1], C. Kelbe[2], D. Kelbe[2], M. Botha[1], W. Rmaih[1]

[1]Biomedical and Clinical Technology, Durban University of Technology, Durban, [2]Neurology, Bay Hospital, Richards Bay, South Africa

Objective: To study the role of Folstein's Mini Mental State Examination (MMSE) and the Electroencephalogram (EEG) in the clinical evaluation of patients at risk of cognitive impairment in HIV disease.

Methods: 80 HIV-positive patients were categorized into 2 groups according to their current immune status (HIV or AIDS). Group 1 consists of asymptomatic HIV-seropositive individuals (HIV) with CD4 counts above 200 cells/ml^3, and group 2 consists of individuals with Acquired Immunodeficiency Syndrome (AIDS) with CD4 counts below 200 cells/ml^3. 36 were males and 44 were females, ranging between the ages of 18 - 60 years were recruited from The Bay Hospital, Richards Bay, Kwa-Zulu Natal, South Africa. Demographically, 99% of the patients selected were Black and 1% Caucasian. For the detection of cognitive impairment in each patient, MMSE and EEG were performed. The EEG findings were then correlated with results of MMSE, immunosuppression, opportunistic infections, medication (Highly Active Antiretroviral Therapy) and disease classification.

Results: MMSE was significantly associated with the EEG results (P=0.008), immunosuppression (P=0.016), opportunistic infections (P=0.018), and disease classification (P=0.030). EEG did not associate with immunosuppression (P=0.838), opportunistic infections (P=0.074), and disease classification (P=0.259). Neither the MMSE nor the EEG were associated with HAART intake. The mean MMSE score for the AIDS group was 24, marginally less than that of the matched HIV group scoring 27. 21 patients had a score less than 24, indicative of dementia. EEG was abnormal in 16 patients and borderline in 8 cases.

Conclusion: MMSE may be a sensitive test in detecting cognitive impairment and monitoring its course in AIDS/HIV. EEG abnormalities may indicate a risk of HIV cognitive impairment in otherwise stable individuals.

Keywords: EEG, MMSE, HIV, AIDS

31

MAGNETIC RESONANCE PERFUSION IMAGING OF RESTING-STATE CEREBRAL BLOOD FLOW IN PRECLINICAL HUNTINGTON´S DISEASE

R. Wolf[1], G. Grön[2], F. Sambataro[3], N. Vasic[2], N. Osterfeld[4], P. Thomann[5], B. Landwehrmeyer[2], M. Orth[2]

[1]Department of General Psychiatry, University of Heidelberg, Heidelberg, [2]University of Ulm, Ulm, Germany, [3]Italian Institute of Technology, Parma, Italy, [4]Central Institute of Mental Health, Mannheim, [5]University of Heidelberg, Heidelberg, Germany

Introduction: Several functional neuroimaging studies have suggested that task-related brain activation differences in clinically pre-symptomatic carriers of the Huntington's disease (preHD) could serve as biomarkers for future clinical trials. However, little is known about brain perfusion physiology in preHD during the brain's resting-state.

Methods: We assessed differences in baseline regional cerebral blood flow (rCBF) using a novel magnetic resonance imaging (MRI) method based on perfusion images obtained with continuous arterial spin labeling (cASL) in 18 healthy controls and 18 preHD individuals. High-resolution structural MRI data was collected in order to test for early changes of brain volume.

Results: Compared to healthy controls, preHD individuals showed decreased rCBF in regions of the prefrontal cortex (Brodmann areas 5, 9, 9/46 and 10). PreHD individuals near to symptom onset additionally showed decreased rCBF in the left putamen. Increased rCBF in preHD was found in the bilateral precuneus and the right hippocampus. RCBF network analyses revealed an abnormal pattern of spatiotemporal covariance in the left dorsolateral prefrontal cortex in preHD far and near to motor onset. rCBF changes in the medial and lateral prefrontal cortices were associated with measures of cognition. Compared to healthy controls, preHD individuals showed decreased grey matter volume in the medial frontal gyrus (BA 10).

Conclusions: These data suggest early and focal cortical changes of frontostriatal baseline perfusion in preHD independent of early reductions of grey matter volume. This study also demonstrates the feasibility of detecting individually quantifiable rCBF changes in preHD with a robust and stable MRI-technique that would be suitable to longitudinal multi-site application.

37

INTRODUCTION

A. Meisel

Neurology, NeuroCure Clinical Research Center, Charite Universitätsmedizin, Berlin, Germany

Glucose is the main source of energy for the mammalian brain. The main consumers of energy in the brain are neurons. Since neurons are largely intolerant against changes in energy supply, regulation of glucose metabolism is essential for brain function. The rationale for this symposium is to highlight the multifaceted role and regulation of glucose metabolism in the CNS as well as pathophysiological consequences. Mechanisms have evolved to counteract imbalances in metabolic and oxygen supplies. We will focus on several highly relevant mechanisms:

1) regulation of the glucose metabolism and energy homeostasis of the organism by the CNS;

2) regulation of cerebral blood flow by glucose metabolism;

3) intercellular regulation of metabolism and

4) regulation of neuronal cell death by glycolytic enzymes. Insights into mechanisms keeping metabolic homeostasis in the brain might provide new potential therapeutic approaches for treatment of neurodegenerative diseases as well as CNS tumors.

38

CAPILLARY $B_{40\ \&\ 42}$ AMYLOID CORRELATES WITH NFTS, AND LRP POSITIVE CAPILLARIES IN THE CALCARINE CORTEX OF ALZHEIMER BRAINS

B. Jeynes[1], **J. Provias**[2]

[1]Faculty of Applied Health Sciences, Brock University, St. Catharines, [2]HHS Department of Pathology and Molecular Medicine, McMaster University, Hamilton, ON, Canada

Objective: The correlation of parenchymal and vascular amyloid deposition and the pathogenesis of neurofibrillary tangles in Alzheimer's disease remains an area of intense research. This study was undertaken to examine a quantitative relationship between capillary amyloid deposition and the densities of neurofibrillary tangles [NFTs] and lipoprotein receptor-related protein [LRP] positive capillaries within the calcarine cortex of Alzheimer [AD] brains.

Methods: Cortical samples were taken from the calcarine cortex of ten confirmed, using Braak & Braak staging and CERAD level criteria, AD brains. Coronal sections were cut, with multiple contiguous sections for each case, and stained using immunohistochemistry techniques for tau protein, beta- amyloid n-terminus $_{[40\ \&\ 42]}$ and LRP. Segments of cortex were randomly selected in each case and section areas of ten field- diameters, contiguous, full and of comparable cortical widths were observed at 250x magnification. The densities of neurofibrillary tangles [NFTs] and $\beta_{40\ \&\ 42}$ and LRP positive capillaries were recorded. Density data was analyzed using Spearman's non-parametric statistical analysis.

Results: Our results indicate that there is a positive correlation between the density of NFTs and the densities of both $\beta_{40\ \&\ 42}$ positive capillaries in the calcarine cortex of AD brains. In addition, we observed that there were also positive correlations between the densities of $\beta_{40\ \&\ 42}$ and LRP positive capillaries.

Conclusions: Based on these results we infer that there may be a pathogenic association between capillary amyloid burden and the pathogenesis of NFTs. Further we also infer that LRP may facilitate amyloid accumulation within cerebral capillaries.

39

OLIGOVASCULAR SIGNALING IN CNS PHYSIOLOGY AND PATHOLOGY

K. Arai

Radiology and Neurology, Massachusetts General Hospital/Harvard Medical School, Charlestown, MA, USA

Pathophysiologic responses in brain after central nervous system (CNS) diseases are highly complex. Over the past several decades, study of CNS physiology and pathology has focused on intra-neuronal mechanisms. In recent years, however, this neuron-based model has gradually shifted to a more integrated paradigm that highlights cell-cell interactions. In this regard, the concept of the neurovascular unit emphasizes the importance of multiple brain cell types in many CNS diseases. Within this conceptual framework, brain function and dysfunction are manifested at the level of cell-cell signaling between neuronal, glial and vascular elements. In particular, attention has focused on the study of how cerebral blood vessels and brain cells communicate with each other. Traditionally, cerebral endothelial cells have been thought as inert pipes for blood flow to the brain. But, emerging data now suggest that the cerebrovascular system does not merely provide inert plumbing to deliver blood for the brain. Instead, cerebral endothelial cells may comprise a rich source of molecular signaling that contributes to brain homeostasis and function. The most well-documented example of these endothelial-brain interactions comprise the neurovascular niche. It is now accepted that cell-cell signaling between cerebral endothelium and neuronal precursor cells help mediate and sustain pockets of ongoing neurogenesis and angiogenesis in adult brain. Although data are strongest in terms of supporting endothelial-neuronal interactions, it is likely that similar interactions occur in white matter as well. White matter damage is a clinically important part of several CNS diseases such as stroke. However, compared to the mechanisms of neuronal injury in gray matter, white matter pathophysiology remains relatively understudied and poorly understood. This presentation aims at summarizing recent advances in the dissection of cell-cell interactions in white matter. First, the basic steps involved in oligodendrocyte (OLG) maturation will be introduced. OLG is one of the major cell types in the CNS white matter, and OLG differentiation/maturation in adult brain is an important event for white matter maintenance and repair. Next, we will overview the phenomena of white matter damage in CNS diseases especially for stroke. Under ischemic conditions, several deleterious signal cascades are activated and OLGs eventually die. On the other hand, in the penumbra, the number of oligodendrocyte precursor cells (OPCs) may even increase as the brain attempts to repair itself. Finally, we will survey recent data to support the idea that cell-cell trophic coupling in white matter is critical for maintaining white matter homeostasis. We will mainly discuss the interaction between cerebral endothelium and OLG/OPC (i.e. oligovascular signaling). Trophic interactions between vessels and OLG/OPC play critical roles in white matter homeostasis. In turn, cell-cell trophic coupling is disturbed under diseased conditions that incur oxidative stress, and this may contribute to white matter injury. Taken together, a deeper understanding of the mechanisms of oligovascular signaling in normal and pathologic conditions may lead us to new therapeutic targets for stroke and other neurodegenerative diseases.

40

DECOMPRESSIVE CRANIECTOMY AS AN EFFICIENT TREATMENT OPTION FOR TRAUMATIC BRAIN INJURY: OUR EXPERIENCE

G. Bunc[1], J. Ravnik[1], M. Vorsic[1], **T. Velnar**[1,2]

[1]Department of Neurosurgery, University Medical Centre Maribor, Maribor, [2]Department of Neurosurgery, University Medical Centre Ljubljana, Ljubljana, Slovenia

Objectives: In 10% to 15% of patients after severe traumatic brain injury (STBI) the intracranial pressure rises significantly and does not react to conservative treatment or to external ventricular drainage placement. Patients with intracranial pressure (ICP) higher than 20mmHg not responding to intensive care measurements, show higher morbidity and mortality. In such cases, decompressive craniectomy (DC) may be employed for lowering the elevated ICP. Prospective studies lack sufficient data about DC outcome with regard to conservative treatment. The aim of this study was to analyse our experience with DC in treatment of STBI.

Methods: The retrospective study at the University Medical Centre, Maribor, Slovenia was conducted from 2005 to 2008. Patients with STBI were included (Glasgow Coma Scale rated from 3 to 8) in whom DC was performed due to a rise in ICP that was not responsive to conservative measurements. A classical, mostly unilateral DC of 10cm in diameter was performed. After the DC, ICP and CPP were continuously monitored. Success of the treatment was rated by GOSE score (Glasgow Outcome Scale Extended) at patient discharge and during follow-up. All postoperative complications and timing of DC were reviewed. The success of treatment was rated according to patients' age, initial GCS (Glasgow Coma Scale) and the time from injury to DC.

Results: From 2005 to 2008, 118 patients with severe brain injury were treated. DC was employed in 14 patients, 43% of patients died, 14% remained in persistent vegetative state and 7% severely disabled. A favourable treatment outcome was achieved in 36%. Rated by GOSE score (GOSE 1 to 4), poor treatment outcome was observed in 64% (average GOSE 1.4) and favourable in 36% (average GOSE 6.5). Before and after DC, the average ICP has fallen from (46 ± 19)mmHg to (17 ± 11)mmHg, respectively ($p=0.003$). Patients treated by DC later than 24 hours after injury, those with GCS rated from 6 to 8 ($p=0.0038$) and those younger than 50 years, had a better treatment outcome.

Conclusions: To date, no prospective, randomised and controlled studies relating to DC in severe brain injuries were performed. Although a straightforward comparison among them is not possible due to the various parameters they considered, they all demonstrated a successful treatment outcome on patients' survival after DC, ranging from 16% to 69%. The results of our study showed 43% mortality. Among the surviving patients, a favourable outcome was documented in 50% and a poor outcome in the other 50%. Using GOSE, a successful outcome was observed in 36% and a poor outcome in 64%. These results are thus comparable to those reported in other retrospective studies. The disadvantage of our study is that only a small number of patients treated by DC were included. DC effectively reduces the rise in ICP following a severe brain injury. Patients with lower neurological dysfunction and patients younger than 50 years benefit the most.

41

LUMBOPERITONEAL SHUNT MIGRATION: FROM LUMBAR SPINE TO THE AMBIENS CISTERN

G. Bunc[1], J. Ravnik[1], M. Vorsic[1], **T. Velnar**[1,2]

[1]Department of Neurosurgery, University Medical Centre Maribor, Maribor, [2]Department of Neurosurgery, University Medical Centre Ljubljana, Ljubljana, Slovenia

Objectives: Displacement of the distal end of lumboperitoneal shunt from the peritoneal cavity and migration proximally is a rare complication. We report a case of lumboperitoneal shunt failure where migration of the catheter into the ambiens cistern took place.

Methods: A 19-year old patient was admitted due to a severe traumatic brain injury. On admission, he was unconscious. CT scan showed diffuse cerebral oedema with contusional haematomas. One month after the admission, posttraumatic hydrocephalus was diagnosed and LP shunt was inserted in order to avoid the infected wound at the neck region. After initial improvement, the ventricles widened again and neurological recovery deteriorated, requiring VP shunting procedure. In the meantime, the infected wound in the neck was properly healed allowing safe insertion of the VP shunt.

Results: The patient recovered well after the VP shunt insertion. After a few months of rehabilitation he was able to speak and walk by assistance. A slight left sided hemiparesis was present.

Conclusions: LP shunt may be a convenient alternative to VP shunt for treating communicating hydrocephalus. Causes of LP shunt failure include infection, obstruction and displacement with migration of the tube distally or proximally. The patient has had the LP shunt inserted because of the infected wound at the neck region not allowing to safely perform the VP shunt when posttraumatic hydrocephalus was diagnosed. The mechanism for proximal shunt migration may result from rotational and lateral movements of lumbar spine and flexion and extension of the head and neck, causing steady upward migration of the catheter. In our case, loosening of the anchoring sutures and higher intraabdominal and respiratory pressure during the early phase of patient´s recovery from the unconscious state may have influenced the intradural pressure and cerebrospinal fluid flow. Acting as a windlass, they may cause the proximal migration of the LP shunt. We believe the LP shunt must be fixed properly with suture collars to the subcutaneous tissue at three locations: I) where lumbar portion comes out of the thoracolumbar fascia, II) at the centre portion at flank and III) at abdominal incision site. This in particular is necessary for the one-piece LP systems.

45

SUPPRESSION OF NFKB SIGNALING PATHWAY BY EPIGALLOCATECHIN GALLATE ATTENUATES DIABETIC ENCEPHALOPATHY

A. Kuhad, K. Chopra

University Institute of Pharmaceutical Sciences, Panjab University, Chandigarh, India

Objective: Diabetes mellitus produces numerous neurophysiological and structural changes in the brain and it is associated with moderate cognitive deficits. The etiology of diabetes associated cognitive decline is multifactorial and involves insulin receptor down regulation, neuronal apoptosis and glutamatergic neurotransmission. The study was designed to evaluate the impact of epigallocatechin gallate on cognitive function and neuroinflammatory cascade in streptozotocin-induced diabetes.

Research design & method: Streptozotocin-induced diabetic rats were treated with epigallocatechin gallate or with vehicle for 10 weeks. Morris water maze was used for behavioral assessment of memory. Cytoplasmic and nuclear fractions of cerebral cortex and hippocampus were prepared for the quantification of acetylcholinestrease activity, oxidative-nitrosative stress (lipid peroxidation, superoxide dismutase, catalase, non protein thiols, total nitric oxide), tumor necrosis factor-alpha (TNF-α), interleukin-1beta (IL-1β), p56 subunit of NFκβ and caspase-3.

Results: After 10 weeks of steptozotocin injection, the rats produced significant increase in transfer latency which was coupled with enhanced acetylcholinestrease activity, increased oxidative-nitrosative stress, TNF-α, IL-1β, caspase-3 activity in cytoplasmic lysate and active p65 subunit of NFκβ in nuclear lysate of cerebral cortex and hippocampus regions of diabetic rat brain. Interestingly, co-administration of epigallocatechin gallate significantly and dose-dependently prevented behavioral, biochemical and molecular changes associated with diabetes. Moreover, diabetic rats treated with insulin-epigallocatechin gallate combination produced more pronounced effect on molecular parameters as compared to their *per se* groups.

Conclusions: Collectively, the data reveal that activation of NFκβ signaling pathway is associated with diabetes induced cognitive impairment and point towards the therapeutic potential of epigallocatechin gallate in diabetic encephalopathy.

47

BENEFICIAL ACTIVATION OF MICROGLIA BY POST-MECHANICAL INJURY ASTROCYTES IN VITRO ENHANCES THE PRODUCTION AND RELEASE OF BDNF THROUGH P38 MAPK

H. Yang[1], Z. Liang[2], J. Li[1], Q. Yao[1], G. Ju[1], S.-W. You[1], Groups of Neural Regeneration and Neurodengenerative Diseases

[1]The Fourth Military Medical University, Xi'an, China, [2]Emory University, Atlanta, GA, USA

It has long been promulgated that microglial cells serve entirely beneficial versus detrimental dialectic role in central nerve system (CNS). However, the capability of inducing neuroprotection by harboring elevated trophic factors and BDNF in particular following traumatic CNS injury has become a crucial but elusive issue. Also a gap still remains in understanding of the cellular and molecular mechanisms that contribute to the beneficial endogenous neuroprotection. In this study, we demonstrate the possibility that some diffusible factors from post-mechanical injury astrocytes can evoke elevation of BDNF synthesis/release by beneficial activation of microglial cells, and the microglia-derived BDNF can exert a demonstrable biological role in promoting dorsal root ganglion (DRG) neurite outgrowth and intimate contact with microglia. Furthermore, the post-injury astrocytes-evoked synthesis and secretion of BDNF in microglia could be dependent on the activation of p38 MAPK signaling pathway. Inhibition of the p38MAPK by SB203580 could reduce BDNF level, and reversely activation of p38MAPK by anisomycin increased BDNF levels. The above results indicate the neuroprotective potential of microglial source for the increased BDNF levels after activation mainly caused by microenvironmental soluble molecules released from injured astrocytes, and BDNF production and release from microglia is up-regulated through mediation of 38-MAPK-signaling pathway. Therefore, seeking to discover these molecules that contribute importantly to the beneficial activation of microglia might be a novel clinical therapeutic strategy for CNS injury or neurodegenerative disease.

50

PRESURGICAL LOCALIZATION OF EPILEPTIC FOCI IN TEMPORAL LOBE EPILEPSY COMPLICATING WITH DEPRESSIVE DISORDERS AND 3 YEARS FOLLOW-UP

L. Kangyong[1], G. Yihui[2], Z. Jimin[3], X. Heding[4], Z. Ting[1], D. Qiaoying[3], L. Liqin[2], Z. Ling[3], S. Liwei[3], W. Chen[2], S. Bomin[5], S. Xiaojiang[1]

[1]Shanghai JiaoTong University Affiliated Sixth People's Hospital, [2]Fudan University Affiliated Huashan Hospital, [3]Fudan University Affiliated Fifth People's Hospital, [4]Shanghai Mental and Healthy Center, [5]Shanghai JiaoTong University Affiliated Ruijin Hospital, Shanghai, China

Objective: To evaluate the values of video-EEG, MRI and FDG-PET in the localization of epileptic foci in temporal lobe epilepsy complicating with depressive disorders and to discuss the relationship between improvements in depressive disorders and localization of surgery.

Methods: Pre-surgical examinations of video-EEG, MRI and FEG-PET of 60 patients were analyzed. The values of video-EEG, MRI and FDG-PET in the pre-surgical evaluation in temporal lobe epilepsy were compared based on the postsurgical results of seizure control. The parameters mainly including HAMA, HAMD and ADL were observed and analyzed pre-surgery and post-surgery in order to discuss the effects of surgery for depressive disorders.

Results:

1) MRI was able to distinguish normal brain structure from lesions. Patients with hippocampal sclerosis in MRI demonstrated a good seizure control after surgery. The sensitivity of interictal PET was higher than MRI for the localization of temporal lobe epilepsy. Usually the area of hypometabolism in PET was larger than the epileptic foci.

2) To all the patients underwent surgery, HAMD was improved significantly compared to that of pre-surgery（$P< 0.05$). Surprisingly, it is important that HAMD of patients with epileptic foci in left temporal lobe and hippocampus is higher than those with epileptic foci in right temporal lobe and hippocampus（$P< 0.001$).

Conclusions:

1) Combination of video-EEG, PET and MRI improved the accuracy of localization of epileptic foci and reduced the need of intracranial recording.

2) Incision the epileptic foci accurately not only controlled the seizures, but also improved the symptoms of the depressive disorders.

Key words: Temporal lope epilepsy; Epileptic foci; EEG; MRI; FDG-PET

51

THE ROLE AND MECHANISM OF AUTOPHAGY-LYSOSOMAL PATHWAY IN THE BRAIN ISCHEMIC INJURY MODEL OF RATS

L. Kangyong[1], Z. Ting[2], S. Liwei[1], S. Jijun[3], W. Fen[4], Z. Yunjiao[1], L. Qiang[2], Z. Ling[1], S. Xiaojiang[2]

[1]Fudan University Affiliated Fifth People's Hospital, [2]Shanghai JiaoTong University Affiliated Sixth People's Hospital, Shanghai, [3]Soochow University Affiliated Second Hospital, [4]Department of Neurobiology, Soochow University, Suzhou, China

Objective: This study used the rat brain ischemic injury model to investigate whether the autophagy-lysosomal pathway plays a key role after brain ischemic injury(BII) and explore the proboble mechanisim.

Methods: First, building the brain ischemic damage model of rats with thread bolt method. Then Induction of autophagy is manifested by accumulation of autophagosomes (APs), observable under transmission electron microscopy (EM). Two hallmarks of autophagy, i.e., the microtubule-associated protein light chain 3 (LC3)-II and the autophagy-related gene ATG12-ATG5 conjugates, were explored by biochemical and confocal microscopic analyses of brain tissues. Meanwhile, we introduce rapamycin -inducer of autophagy to exert on the model rat to explore the changes of LC3-II and ATG12-ATG5 conjugates.

Results: Under EM, both APs and autolysosomes were markedly accumulated in neurons from 4 h onward after BII. Western blot analysis showed that ATG12-ATG5 conjugate was markedly redistributed during 3 to 14 days in brain tissues after BII. LC3-II conjugate was initially unchanged but was drastically upregulated from 24 h onward in the pre-AP-containing fraction after BII. LC3-II immunostaining was mainly located in living neurons under confocal microscopy. Rapamycin not only improve the ischemic symptoms model rats but also upgrade the level of LC3-II and ATG12-ATG5 conjugates.

Conclusion: These results clearly show that the autophagy-lysosomal pathway is persistently activated after BII. Because the autophagy-lysosomal pathway is the chief machinery for bulk elimination of aberrant cell components, we propose that activation of this pathway serves as a protective mechanism for maintaining cellular homeostasis after BII.

Key words: Brain ischemic injury,autophagy, LC3-II , ATG12-ATG5

52

CEREBRAL TRANSPLANTATION OF VESICULAR MONOAMINE TRANSPORTER-2 TRANSGENE DECORATED CELL IN TREATING MONKEYS WITH PARKINSON'S DISEASE

L. Kangyong[1,2], S. Liwei[2], Z. Ting[1], C. Yanbo[3], W. Fen[4], T. Jin[4], Z. Yunjiao[2], Z. Ling[2], S. Xiaojiang[1]

[1]Shanghai JiaoTong University Affiliated Sixth People's Hospital, [2]Fudan University Affiliated Fifth People's Hospital, Shanghai, [3]Xuzhou Medical College, Xuzhou, [4]Soochow University, Suzhou, China

Background: VMAT2 and DAT have direct impacts on the DA transportion and its adjustment of cytoplasmic concentration, the impaired VMAT2 cannot effectively act its function to limit the endogenous and exogenous toxic damage to the mitochondria, leading to monoaminergic neuron degradation. However, if effective measures to enhance gene expression can be taken, the increase in the expression of exogenous VMAT2 in the substantia nigra dopaminergic neurons can be administered for an effective treatment of PD.

Objective: Evaluation of VMAT2 gene-modified cells for the treatment of Parkinson´s disease, as well as the role of dopamine metabolism.

Methods:

1) To establish unilateral monkey model of PD by injecting MPTP unilaterally into the internal carotid artery. To slowly inject MPTP along with the direction of internal carotid artery blood flow, observe the Parkinson´s disease-like symptoms of monkey and make a video recording after injection for two weeks, and determine the successful model through behaviors and EMG;

2) VMAT2 gene cloning, VMAT2 gene restructuring Plasmid was transfected into monkey skin fibroblasts and engineering cell lines expressing of VMAT2 gene were established through the SV40 virus gene transformation;

3) To implant VMAT2 gene-modified cells into specific target of brain in monkeys with Parkinson´s disease by stereotactic technology, we observed alterations in behavior, histology and the content of dopamine in cerebrospinal fluid; and effects on brain metabolism and cognitive function, immune rejection as well as short-term and long-term therapeutic effects.

Results:

1) Western Blot showed that VMAT2 expression significantly enhance in monkey skin fibroblasts after transgenes;

2) Motor and non-motor symptoms were significantly improved and the content of DA species in cerebrospinal fluid increased in post-transplanted PD monkeys;

3) SPECT results indicated that VMAT2 imaging increased clearly.

Conclusion: All engineered cells with VMAT2 gene expressed human VMAT2 gene in vitro and vivo, meanwhile, engineering cells stocked in the PD monkey brain and played a role in the treatment of Parkinson´s disease by stereotactic technology implanting into specific target of PD monkey brain.

Keywords: PD monkey ,VMAT2, MPTP, DAT, DA

53

3-N-BUTYLPHTHALIDE (NBP) PROTECTS PC12 CELLS AGAINST MPP+-INDUCED CYTOTOXICITY BY UP-REGULATION OF AUTOPHAGY

L. Kangyong[1,2], Z. Ting[1], Z. Ling[2], S. Jijun[3], S. Liwei[2], S. Xiaojiang[1]

[1]Shanghai JiaoTong University Affiliated Sixth People's Hospital, [2]Fudan University Affiliated Fifth People's Hospital, Shanghai, [3]Soochow University Affiliated Second Hospital, Suzhou, China

Background: Autophagy is a key and highly conserved degradation pathway for the turnover of dysfunctional organelles or aggregated proteins in cells. Wasted intracellular macromolecules are delivered to lysosomes, where they are degraded into biologically active monomers such as amino acids that are subsequently recycled to maintain cellular metabolic turnover and homeostasis. Autophagosomes and autolysosomes are induced in acute and chronic neurological disorders including stroke, brain trauma, Parkinson's disease (PD) and other neurodegenerative diseases. The l-isomer of 3-n-butylphthalide (NBP) was extracted as a pure component from seeds of Apium graveolens Linn. Synthesized dl-NBP received approval by the State Food and Drug Administration of China for clinical use in stroke patients in 2002. Previous studies showed that NBP had beneficial effect on stroke through multiple actions.

Objective: The aim of this study was to investigate the neuroprotective effect of 3-n-butylphthalide (NBP) on cell damage caused by MPP+ and explore the probable mechanism.

Methods:

(1) MTT assay was used to measure cell vitality;

(2) LC3-II and α-synuclein expression were detected by Western Blot;

(3) Alterations in position between cytoplasm and nucelus, the expression of LC3-II and α-synuclein and its co-localization were assayed through fluorescence microscopy;

(4) Changes in autophagosome formation, lysosomes, and apoptotic bodies were observed by TEM.

Results: MTT results showed that NBP, to certain extent, to resist cell viability decreased induced by MPP+($P< 0.05$); NBP could increase the expression of LC3-II($P< 0.001$), and reduced α-synuclein ($P< 0.05$); The fluorescent signal for NBP -induced LC3-II up-regulation and the reduced α-synuclein could be seen; Electron microscopy showed increased autophagosome formation induced by NBP.

Conclusion: These results suggest that neurotoxin, MPP+ causes the aggregation of α-synuclein and damages the PC12 cells, and NBP may have a neuroprotective effect for PD cell model induced by MPP+ through enhancing LC3-II expression and up-regulating the level of autophagy to resist the oxidative stress.

Keywords: Parkinson´s disease, α-synuclein, autophagy, NBP

54

PROLONGED DRAINAGE REDUCES THE RECURRENCE OF CHRONIC SUBDURAL HEMATOMA

G.J. Yu, C.Z. Han, M. Zhang, H.T. Zhuang, Y.G. Jiang

Qingdao Haici Hospital, Qingdao, China

Background: Recurrence of chronic subdural hematoma (CSH) is a significant problem in neurosurgical practice. Various risk factors associated with patient's characteristics and the pathogenesis of CSH have been investigated in many studies, but controversial findings are not uncommon. Therefore we made a retrospectively investigation focusing mainly on the factors associated with surgical techniques. in order to find out the factors which may affect the recurrence rate of CSH.

Methods: The medical records of 97 consecutive patients with 121 CSHs, who were treated with burr-hole craniostomy and continuous drainage, were retrospectively reviewed. The relationships between the recurrence rate and some factors associated with surgery, such as location of burr-hole, thickness of residual hematoma, location of drainage catheter, intracapsular air postsurgery, duration of drainage were investigated.

Results: The average recurrence rate was 6.6% in this whole series. For patients with less than three days of drainage, the recurrence rate was16.3%, whereas for those with 3 and more days of drainage, the recurrence rate was only 1.3%. The duration of drainage significantly related to recurrence rate. In addition, a higher recurrence rate seemed to be associated with more intracapsular air postsurgery, but it did not reach statistically significant level in this study. Prolonged duration of drainage did not increase the frequency of infection in this series.

Conclusion: We found in this study that the duration of drainage play an important role in the treatment of CSH and three full days of drainage seems to be necessary, especially for patients of 60 years and over. We presumed that it takes at least 3 days of drainage for outer membrane of CSH to get the restoration of a normal balance between coagulation and fibrinolysis after surgery, which is necessary for termination of the vicious cycle and resolution of the hematoma.

56

F18-FDG PET/CT COULD LOCALIZE HYPERMETABOLIC CERVICAL MUSCLES IN A PATIENT AFFECTED BY IDIOPATHIC CERVICAL DYSTONIA.

B. Paghera, F. Caobelli, F. Motta, R. Giubbini

Nuclear Medicine, University of Brescia, Brescia, Italy

Objectives: Idiopathic cervical dystonia (ICD) is characterized by an abnormal head and neck posture attributable to involuntary tonic or phasic contractions of neck muscles [1]. Electromyography (EMG) is the most widely used method to identify dystonic muscles in ICD; however, not every neck muscle can be explored with a needle electrode and its accurate placement is often difficult in patients with a severe dystonic posture. F18-FDG PET/CT provides both metabolic and anatomic information on hypermetabolic lesions and may be useful to localize dystonic skeletal muscles showing enhanced F18-FDG uptake due to sustained contraction.

Methods: A 51 year-old woman without evidence of an identifiable cause of secondary dystonia was referred to our Nuclear Medicine Department to undergo a brain F18-FDG PET/CT for suspected metabolic alterations in basal ganglia. She suffered rotational torticollis and right laterocollis, not relieved despite conventional muscle relaxant therapy. We performed a brain F18-FDG PET/CT 30 min after intravenous injection of 181 MBq F18-FDG.

Results: Brain uptake was unremarkable, whereas an increased F18-FDG uptake was observed in right trapezius and right longus colli muscle (fig.1). After a neurological clinical re-evaluation, a diagnosis of ICD was made according to international standard criteria [2] and the patient underwent BT therapy on the affected muscles with a clear symptoms regression.

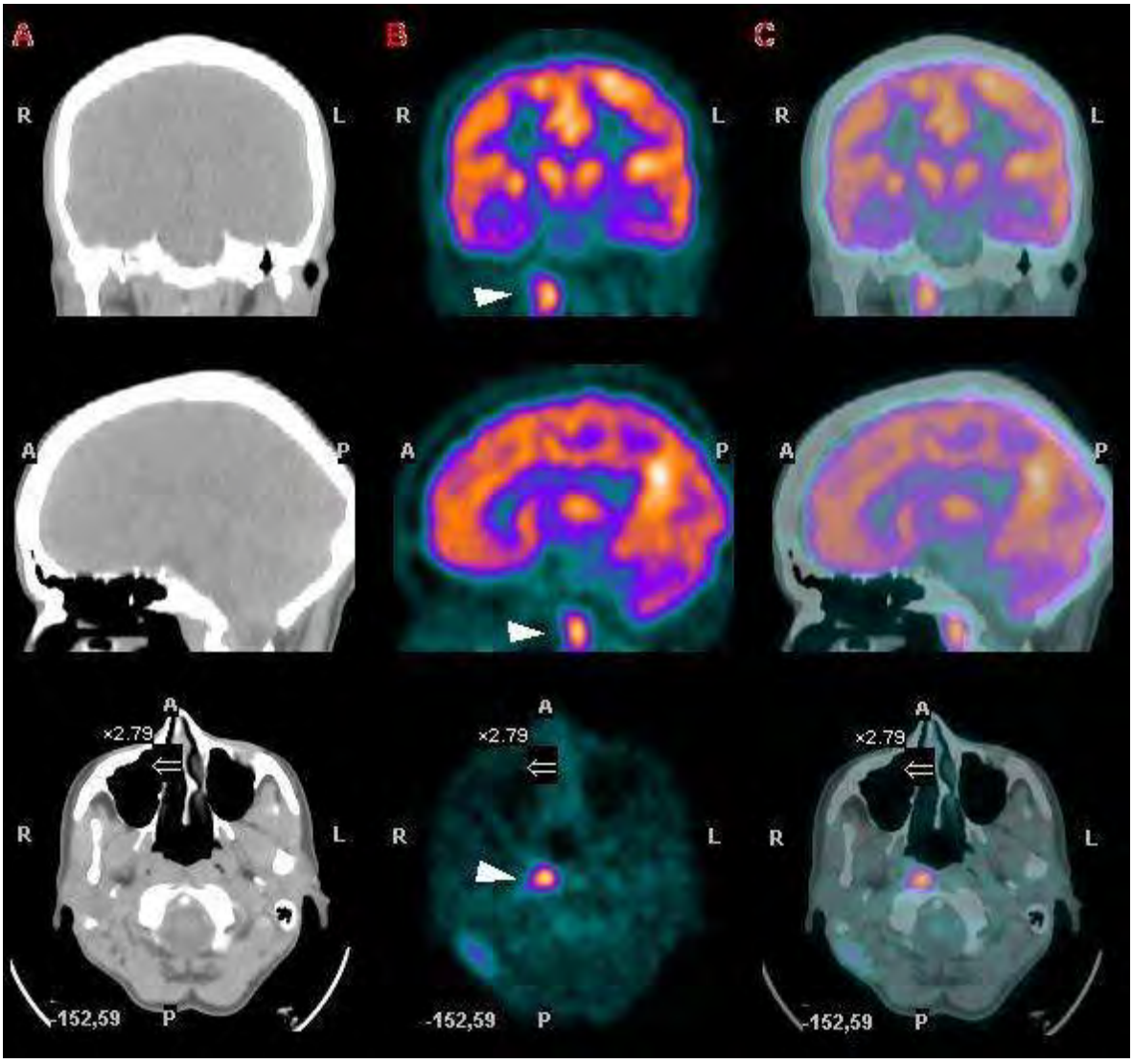

[fig. 1]

Conclusion: Skeletal muscle F18-FDG rest accumulation is relatively low, although even in healthy subjects, variable symmetric uptake may be observed in head and neck muscles because of stress-induced muscle tension [3]. In our case, F18-FDG uptake by cervical muscles was asymmetric and unilateral. Since our patient was not under muscle relaxant medications and she was in a sitting position with her head and neck in the usual abnormal involuntary posture, the observed hypermetabolic character of the cervical muscles can be interpreted as being a result of involuntary active contraction.F18-FDG PET/CT may be a non-invasive alternative to EMG to identify dystonic cervical muscles and this identification could lead to successful clinical results after targeted intramuscular BT treatment [4].

References:

[1] Dauer WT, Burke RE, Greene P, Fahn S. Current concepts on the clinical features, aetiology and management of idiopathic cervical dystonia. Brain. 1998;121:547-60.[2] Albanese A, Barnes MP, Bhatia KP, et al. A systematic review on the diagnosis and treatment of primary (idiopathic) dystonia and dystonia plus syndromes: report of an EFNS/MDS-ES Task Force. Eur J Neurol. 2006;13:433-44.

[3] Cook GJ, Fogelman I, Maisey MN. Normal physiological and benign pathological variants of 18-fluoro-2-deoxyglucose positron-emission tomography scanning: potential for error in interpretation. Semin Nucl Med. 1996;26:308-14

[4] Sung DH, Choi JY, Kim DH, Kim ES, Son YI, Cho YS, Lee SJ, Lee KH, Kim BT. Localization of dystonic muscles with ^{18}F-FDG PET/CT in Idiopathic Cervical Dystonia. J Nucl Med 2007;48:1790-5.

Figure legend

Fig.1: from up to down, coronal, sagittal and transaxial CT images (line A), PET images (line B) and fused PET/CT images (line C). The hypermetabolic longus colli muscle is evidenced by white triangle.

64

THE EFFECT OF INTRAHIPPOCAMPAL INJECTION OF ASCORBIC ASID ON SPATIAL LEARNING AND MEMORY IN ADULT MALE RATS

K. Esmaeilpour Bezenjani[1,2], Y. Masoumi Ardakani[1,2], M. Abbasnejad[2]

[1]Kerman Neuroscience Research Center (KNRC), [2]Department of Biology, Faculty of Sciences, Shahid Bahonar University of Kerman, Kerman, Iran

Introduction: Ascorbic acid (AA) is present in high concentration with heterogeneous distribution in mammalian brain. Previous studies have shown that release of various neurotransmitters such as the glutamate, acetylcholine and dopamine might be involved in the central AA release. On the other hand all of this neurotransmitters and CA1 are involved in learning and memory so; the aim of the present study is to evaluate the effect of intrahippocampal (CA1) administration of ascorbic acid on spatial learning and memory in adult male rats.

Methods: 42 adult male NMRI rats (250-300g) in 6 groups were used in this study including: control group (no injection), sham-operated group received normal saline as vehicle, four groups received different doses of ascorbic acid (6,12,24and48µg/rat). All injections were given in 5 consecutive days, 30 min after each injection, Morris Water Maze, was used as a method to measure learning and memory task, spatial learning and memory parameters were subjected to analysis of variance (ANOVA).

Results: The results indicated intrahippocampal microinjection of AA (12 and 24 µg/rat) significantly enhanced some spatial learning and memory parameters such as, escape latency and path length to reach the hidden platform.

Conclusion: Our findings show that AA into the CA1 have a decreasing effect on spatial learning and memory.

71

MOLECULAR CHAPERONES AND MITOCHONDRIAL FUNCTION AFTER BRAIN ISCHEMIA

R. Giffard, L. Xu, L. Voloboueva, Y.-B. Ouyang

Anesethesia, Stanford University, Stanford, CA, USA

Objectives: Mitochondrial dysfunction contributes to ischemic brain injury both by production of increased free radicals and oxidative stress, especially during reperfusion, and by reducing the availability of ATP for essential cellular functions. Molecular chaperones, members of the heat shock protein 70 family in particular, have been studied by several labs and shown to protect the brain from both focal and global ischemia. We have studied the ability of Hsp70 family members to protect from ischemia both in vitro and in vivo, and have identified several settings in which members of this family can contribute to mitochondrial protection.

Methods: Primary astrocyte and neuronal cultures, neurosphere cell culture, forebrain and focal cerebral ischemic models were used in the experiments. Live fluorescence imaging was used for mitochondrial membrane potential, free radicals and free calcium measurement. Mitochondrial respiration was measured using an oxygen electrode and complex activities were assayed spectrophotometrically. Immunohistochemistry and Immunoblotting were done as routine.

Results: While the best known function of these chaperones is facilitating protein folding and binding unfolded proteins, it has become clear that the cytosolic localized Hsp72 can influence a variety of cell compartments and functions to improve cell survival. In addition to protecting mitochondria by reducing stress in the cytosolic compartment, Hsp72 also has anti-inflammatory effects and reduces oxidative stress. Several pro-inflammatory cytokines are known to inhibit mitochondrial function. Grp75/mortalin is the mitochondrial localized member of the Hsp70 family, and it too can reduce ischemic brain injury and improve mitochondrial function under stress, in vitro and in vivo. These effects include protection from reduced activity, protection of mitochondrial membrane potential and reduced generation of free radicals. We have previously shown that in global ischemia astrocytes in the CA1 region of hippocampus suffer oxidative stress and loss of glutamate transporter 1, which feeds back and contributes to neuronal cell death. Overexpression of either Hsp72 or the mitochondrial antioxidant enzyme SOD2 preserves astrocyte function and neuronal survival. Lastly we investigated the contribution of mitochondrial dysfunction to reduced neurogenesis under stress conditions. We observe that the doublecortin positive young neurons are especially vulnerable to mitochondrial inhibition, and that they can be protected by overexpression of the mitochondrial chaperone Grp75.

Conclusions: Mitochondrial protection due to overexpression of molecular chaperones can contribute to preservation of neurogenesis as well as protection of astrocytes and neurons from ischemic injury.

73

KLEBSIELLA PNEUMONIAE B5055 INDUCED MOUSE MODEL OF SEPSIS ASSOCIATED BRAIN INFLAMMATION IN BALB/C MICE: AN EXPERIMENTAL MODEL

V. Kumar[1], V. Malhotra[2]

[1]Department of Biochemistry, Queen's University, Kingston, ON, Canada, [2]Malhotra Diagnostic Laboratory, Chandigarh, India

Background: Autopsy studies from septic patients reveal various cerebral lesions including ischemia, hemorrhage, microthrombi, microabscesses, multifocal necrotizing leukoencephalopathy and bacterial invasion of nervous system.

Objective: No such animal model of sepsis has been developed which in true sense represents the brain inflammation associated with evolving sepsis. Present study comprises of development of a mouse model of sepsis induced brain inflammation.

Methods: A mouse model of sepsis associated brain inflammation was developed by directly placing a selected dose (10^2 cfu) of *Klebsiella pneumoniae* B5055 entrapped in fibrin-thrombin clot into the peritoneal cavity of mice. Various cytokines (i.e. IL-1α, TNF-α, IL-10) and other inflammatory markers [i.e malondialdehyde (MDA), myeloperoxidase (MPO) and nitric oxide (NO)] in serum and brain were estimated by ELISA, biochemical methods and histopathology.

Results: Establishment of bacterial colonies in brain led to significant ($p< 0.05$) increase in neutrophil infiltration into the brain along with significantly ($p< 0.05$) increased levels of pro-inflammatory cytokines (TNF-α and IL-1α) in comparison to IL-10 levels and other inflammatory mediators like NO, MDA and MPO. Also the animals survived till 5^{th} day of post sepsis development.

Conclusion: This mouse model of sepsis induced brain inflammation may prove helpful to study immunopathogenesis of brain inflammation observed during bacterial sepsis and may also prove helpful to study behavioral changes associated with sepsis.

76

MRI STUDY IN PSYCHOPATH AND NON PSYCHOPATH OFFENDERS

A.A. Calzada Reyes

Cognitive Neuroscience, Cuban Neuroscience Center, Havana, Cuba

Previous studies have suggest that the psychopathy is associated with structural and functional abnormalities in fronto-temporo-limbic regions, but most structural findings have been isolated and not yet replicated, is unclear whether findings are apply only to psychopathic or violent behaviours in general. The current study used IBASPM for segmentation of structural MRI images to compared 44 grey matter volume symmetrical regions of both brain hemispheres and evaluate the CC morphometry in 97 extreme violent offenders, 29 psychopaths and 68 non psychopaths and and 73 healthy non violent men. Both violent groups exhibited decreased total gray matter volume, right inferior orbitofrontal gyrus, right middle cingulate, cuneus, and lingual gyrus bilaterally and increased volume in right rolandic operculum and postcentral areas. Compared to controls the psychopath group displayed reduction in right superior orbitofrontal gyrus, left putamen and increased volume left inferior parietal gyrus. Reduced grey matter volume in non psychopath offenders was detected left middle frontal and middle occipital gyri compared to controls. Not differences between psychopath and non psychopaths group were found. The length of the CC did not differ significantly among the groups studied, while one increase corpus callosal thickness in violent group was found. Analyses of total score PCL-R scale revealed negative associations with brain volumes of key regions implicated in psychopathic behaviour. VBM analysis of gray matter revealed areas of atrophies in the thalamus bilaterally and in the left hippocampus in violent group. These findings provide new evidence for neuroanatomical differences in violent individuals but also suggest that fronto-limbic-striatal system and inferior parietal region morphometric abnormalities may underlie the poor inhibitory control, moral decision-making and reward/punishment deficits associated with psychopathy.

77

EDARAVONE INHIBITS DNA PEROXIDATION AND NEURONAL CELL DEATH IN NEONATAL HYPOXIC-ISCHEMIC ENCEPHALOPATHY MODEL RAT

M. Itoh, Y. Takizawa, Y.I. Goto

National Center of Neurology and Psychiatry, Kodaira, Japan

Objective: Neonatal hypoxic-ischemic encephalopathy (HIE) is the most frequent neurological disease in the perinatal period. The major cause of neonatal HIE is oxidative stress, which induces DNA peroxidation and apoptotic neuronal death.

Methods and results: We examined 8-hydroxy-2'-deoxyguanosine (8-OHdG) expression to evaluate brain damage in neonatal HIE[1] and the therapeutic effect of edaravone, a free radical scavenger[2,3]. Using high-performance liquid chromatography and immunohistochemistry, the 8-OHdG levels of neonatal HIE model Sprague-Dawley rats which were subjected to left common carotid artery ligation and 2-hour hypoxia[4], significantly increased after 24-48 hours of HI insult, but decreased after 72 hours. Moreover, the number of apoptotic cells with terminal deoxynucleotidyl transferase-mediated dUTP nick end labeling and karyorrhexis significantly increased after 24-72 hours of HI insult. In a therapeutic experiment, edaravone was administered intraperitoneally (9 mg/kg) after HI insult every 24 hours. Edaravone reduced both the apoptotic neuronal cell number and 8-OHdG expression after 24-48 hours of HI. From a double immunofluorescent study, DNA peroxidation occurred in apoptotic neuronal cells with 8-OHdG expression.

Conclusion: Edaravone may inhibit the number of apoptotic neuronal cells and 8-OHdG expression within 48 hours after HI insult.

References:

1. Warner DS, et al. Oxidants, antioxidants and the ischemic brain. J Exp Biol 2004; 207: 3221-3231.

2. Uno M, et al. Inhibition of brain damage by edaravone, a free radical scavenger, can be monitored by plasma biomarkers that detect oxidative and astrocyte damage in patients with acute cerebral infarction. Free Radic Biol Med 2005; 39:1109-1116.

3. Noor JI, et al. Edaravone inhibits lipid peroxidation in neonatal hypoxic-ischemic rats: an in vivo microdialysis study. Neurosci Lett 2007; 414: 5-9.

4. Rice JE, et al. The influence of immaturity on hypoxic-ischemic brain damage. Ann Neurol 1981; 9: 131-141.

78

ASSESSMENT OF MILD DEGENERATIVE DEMENTIA WITH [11C]DTBZ AND [11C]PIB POSITRON EMISSION TOMOGRAPHY

R.L. Albin[1,2], J.F. Burke[1], R.A. Koeppe[3], B. Giordani[4], M. Kilbourn[3], S. Gilman[1], K.A. Frey[3]

[1]Neurology, University of Michigan, [2]GRECC, VAAAHS, [3]Radiology, [4]Psychiatry, University of Michigan, Ann Arbor, MI, USA

Objectives: We assessed the relationship between consensus clinical diagnostic classification and neurochemical positron emission tomography (PET) imaging of striatal vesicular monoamine transporters (VMAT2) and cerebrocortical deposition of aβ-amyloid in mild degenerative dementia.

Methods: 76 subjects with mild dementia (MMSE $\geq$ 18) underwent a conventional clinical evaluation followed by [^{11}C]dihydrotetrabenazine (DTBZ) PET imaging of striatal VMAT2 and [^{11}C]Pittsburgh compound-B (PiB) PET imaging of cerebrocortical aβ-amyloid deposition. Clinical and psychometric evaluations were based on the Uniform Data Set (UDS) of the National Alzheimer Coordinating Center (NACC). Clinical classifications were assigned by consensus of an experienced clinician panel using conventional criteria. PET imaging data were not used for clinical classification. Neuroimaging classifications were assigned as Alzheimer disease (AD), Frontotemporal dementia (FTD), or Dementia with Lewy bodies (DLB) on the basis of the combined [^{11}C]DTBZ and [^{11}C]PiB results.

Results: Thirty six subjects were classified clinically as mild AD, 26 as FTD, and 8 as DLB. There were only modest or insignificant differences in demographic, clinical, and psychometric features between the 3 clinically classified subject groups. PET neuroimaging classifications consisted of AD in 46, FTD in 15 and DLB in 15 subjects. There was only moderate agreement between clinical consensus and PET neuroimaging classifications across all dementia subtypes, with discordant classifications in approximately 33% of subjects (Cohen's k = 0.46). Discordant classifications were least frequent in clinical consensus AD (20%), followed by DLB (29%), and were most common in FTD (58%). When subjects were compared by neuroimaging classification, there were only modest or insignificant differences in demographic, clinical, or psychometric features of each group. Similarly, comparison of subjects with discordant clinical-neuroimaging classifications and concordant clinical-neuroimaging failed to reveal any marked differences in demographic, clinical, or psychometric features of groups.

Conclusions: Accurate clinical classification of mild neurodegenerative dementia is challenging. PET can distinguish subgroups corresponding to neurochemically-defined pathologies, and may augment clinical classification. This may be useful in disease-modifying therapeutic trials and other prospective research involving subjects in the early stages of neurodegenerative dementias.

79

TREATMENT OF ISCHEMIC STROKE BY INO IN RODENTS - PROOF OF CONCEPT

N.A. Terpolilli[1,2], S.W. Kim[2], S. Thal[2], N. Plesnila[3]

[1]Neurosurgery, [2]Institute for Surgical Research, Munich University, Munich, Germany, [3]Royal College of Surgeons in Ireland, Dublin, Ireland

Our laboratory demonstrated that inhalation of nitric oxide (NO) dilates cerebral vessels in areas of diminished pO2. We therefore hypothesized that NO supplied by inhalation is released via an oxygen-tension- dependent mechanism preferentially depositing NO in regions of low perfusion. In order to test this hypothesis, cerebral blood flow was lowered to 30% of baseline by carotid banding. Under these conditions, NO release shifts to the arteriolar side and, subsequently, increases blood flow. Following experimental cerebral ischemia iNO selectively dilates arterioles in the ischemic penumbra, thereby increasing collateral blood flow and reducing brain damage after transient and permanent middle cerebral artery occlusion by ~40%. This translated into a significantly better neurological outcome 7 days after experimental ischemic stroke. Cerebral autoregulation, endogenous NO synthase expression, and bleeding time were not affected by long term NO inhalation.

iNO may thus provide a completely novel strategy to improve penumbral blood flow and neuronal survival in stroke or other ischemic conditions.

Since ischemia is one of the major mechanisms leading to secondary brain damage after traumatic brain injury (TBI) we hypothesised that inhaled NO (iNO) also acts within the traumatic penumbra, redistributing the blood flow to areas in need and thereby reducing peri-contusional ischemia and secondary brain damage after TBI. After experimental controlled cortical impact (CCI) trauma iNO singificantly reduced intracranial hypertension while improving cerebral blood flow in mice. Furthermore, lesion volume 24h after CCI was significantly improved by NO inhalation when it was started within one hour after trauma. Analog to the data obtained after ischemic stroke iNO significantly improved functional outcome after traumatic brain injury.

80

FREE RADICAL SCAVENGER EDARAVONE ADMINISTRATION PROTECTS AGAINST TISSUE PLASMINOGEN ACTIVATOR INDUCED OXIDATIVE STRESS AND BLOOD BRAIN BARRIER DAMAGE

V. Lukic-Panin, K. Deguchi, T. Yamashita, J. Shang, X. Zhang, F. Tian, N. Liu, H. Kawai, T. Matsuura, K. Abe

Okayama University, Okayama, Japan

One of the therapeutics for acute cerebral ischemia is tissue plasminogen activator (t-PA). Using t-PA after 3 hour time window increases the chances of hemorrhage, involving multiple mechanisms. In order to show possible mechanisms of t-PA toxicity and the effect of the free radical scavenger edaravone, we administered vehicle, plasmin, and t-PA into intact rat cortex, and edaravone intravenously. Plasmin and t-PA damaged rat brain with the most prominent injury in t-PA group on 4-HNE, HEL, and 8-OHdG immunostainings. Such brain damage was strongly decreased in t-PA plus edaravone group. For the neurovascular unit immunostainings, occludin and collagen IV expression was decreased in single plasmin or t-PA group, which was recovered in t-PA plus edaravone group. In contrast, matrix metalloproteinase-9 intensity was the strongest in t-PA group, less in plasmin, and was the least prominent in t-PA plus edaravone group. *In vitro* data showed a strong damage to tight junctions for occludin and claudin 5 in both administration groups, while there were no changes for endothelial (NAGO) and perivascular (GFAP) stainings. Such damage to tight junctions was recovered in t-PA plus edaravone group with similar recovery in Sodium-Fluorescein permeability assay. Administration of t-PA caused oxidative stress damage to lipids, proteins and DNA, and led to disruption of outer parts of neurovascular unit, greater than the effect in plasmin administration. Additive edaravone ameliorated such an oxidative damage by t-PA with protecting outer layers of blood-brain barrier (*in vivo*) and tight junctions (*in vitro*).

81

THROMBIN TOXICITY CONTRIBUTES TO NEUROVASCULAR DAMAGE DURING ACUTE ISCHEMIA

B. Chen[1,2], Q. Cheng[2], P.D. Lyden[1,2]

[1]Neurology, Cedars-Sinai Medical Center, Los Angeles, [2]Neuroscience, University of California, San Diego, La Jolla, CA, USA

Objectives: Ischemic stroke is caused by sudden loss of blood flow to the brain and results in massive neuronal and vascular injury. The exact mechanism of ischemic cell death is not fully understood. Here we test the hypothesis that thrombin, a blood-derived coagulation factor, might cause blood-brain barrier disruption and the subsequent neuronal death by activating protease activated receptor-1 (PAR-1).

Methods: Ischemic stroke was induced in adult Sprague Dawley rat by occluding the middle cerebral artery for 4 hours followed by a short reperfusion. 2MDa FITC-dextran was injected to label severe vascular disruption. Using the syringe pump, thrombin, thrombin inhibitor, PAR-1 agonist peptide, and/or PAR-1 antagonist, were infused during ischemia. Brain tissues were fixed and sectioned for immunohistochemistry examination.

Results: Intraarterial thrombin infusion caused significant increase in both vascular leakage labeled by FITC-dextran and cell death labeled by TUNEL staining, whereas intravenous infusion of argatroban, a direct thrombin inhibitor, reduced such damage. Immunostaining showed thrombin accumulation in ischemic brain region adjacent to vascular disruption. Double staining of thrombin and cell type specific antibodies revealed significant thrombin association with neurons. Evidence of PAR-1 activation were found in the ischemic region as well. Infusion of PAR-1 agonist peptide TFLLR mimicked the thrombin toxicity on neurovascular unit, and PAR-1 antagonist SCH79797 significantly decreased the number of damaged vessels and neuronal cells.

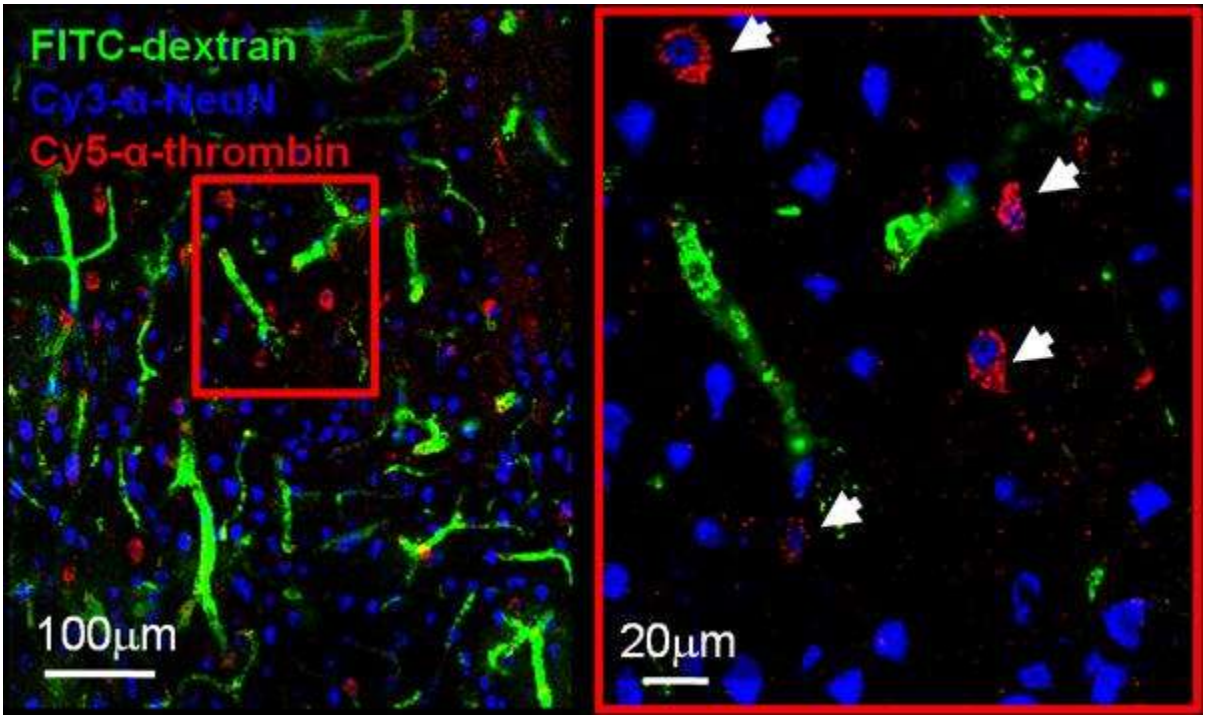

[thrombin associated with neurons in ischemic brain]

Conclusions: Thrombin contributes to ischemic injury during acute stroke by activating cellular receptors in neurovascular unit.

82

USE OF POPULATION-DERIVED INPUT FUNCTIONS AND VENOUS BLOOD SAMPLING FOR L-[1-^{11}C]LEUCINE PET DETERMINATION OF REGIONAL RATES OF CEREBRAL PROTEIN SYNTHESIS

G. Tomasi[1], C.B. Smith[2], K.C. Schmidt[2]

[1]Comprehensive Cancer Imaging Center, Imperial College Faculty of Medicine, Hammersmith Hospital, London, UK, [2]Section on Neuroadaptation and Protein Metabolism, National Institute of Mental Health, Bethesda, MD, USA

Objectives: The L-[1-^{11}C]leucine PET method (1,2) for determination of regional rates of cerebral protein synthesis (rCPS) requires measurement in arterial blood of total C-11 (Cba*), $^{11}CO_2$, plasma [^{11}C]leucine (Cpa*) and plasma leucine (Cpa). As a possible alternative to arterial blood sampling, we investigated the use of population-derived input functions together with a limited number of venous blood samples for estimating rCPS.

Methods: We generated normalized population time-activity curves (TACs), Cpa*_pop and Cba*_pop, from the averages of measured Cpa* and Cba* TACs (normalized by injected dose/body weight) from 12 conscious control subjects. Arterial blood $^{11}CO_2$ was set to zero. We tested population-derived input functions in 6 propofol-anesthetized subjects with fragile X syndrome. In the test subjects, complete arterial blood sampling was carried out. We also drew 3-4 venous samples at 15-30 min intervals and measured total blood C-11 (Cbv*), plasma [^{11}C]leucine (Cpv*), and plasma leucine (Cpv).

We calculated rCPS in 11 regions-of-interest (ROIs) using spectral analysis with iterative filter (SAIF) (3) with the measured individual arterial plasma and whole blood TACs. These rCPS estimates were regarded as the “true” ones and were compared with rCPS values determined with population-derived input functions. We used two approaches:

A: For each test subject, measured venous samples were employed to scale Cpa*_pop by multiplying it by mean [Cpv*(t_i)/Cpa*_pop(t_i)] to obtain individual plasma TACs (Cp*_indiv). Cba*_pop was scaled by mean [Cbv*(t_i)/Cba*_pop(t_i)] to obtain Cb*_indiv.

B: We accounted for lag of venous plasma behind arterial plasma by scaling Cpa*_pop by mean [Cpv*(t_i)/Cpa*_pop(t_i-D)] to obtain Cp*_indiv, where D is the best-fitting arterial-to-venous plasma delay, averaged across the 6 subjects. The same method was employed to derive Cb*_indiv.

The input functions Cp*_indiv and Cb*_indiv obtained with Methods A and B were used with SAIF to estimate kinetic model parameters, and mean [Cpv(t_i)] was used as the unlabeled plasma leucine concentration to determine rCPS.

Results: Method A yielded good rCPS estimates, with mean absolute error of 5.4% and mean bias of +4.5% (Fig 1A). Method B provided better results (Fig 1B) with mean absolute error of 4.6% and negligible bias (-1.3%). In Figure 1A & B, the X-axes represent “true” rCPS values and the Y-axes represent rCPS estimated by means of Methods A and B, respectively. Lines of identity are shown in blue. The difference between arterial and venous plasma leucine concentrations accounts for some of the error. Mean absolute difference between Cpa and Cpv was 1.9%.

Conclusions: These preliminary results suggest that use of population-derived arterial plasma and whole blood TACs along with venous blood samples may provide good estimates of rCPS at the ROI level. They also suggest that rCPS estimates are improved by including correction for arterial-to-venous delay.

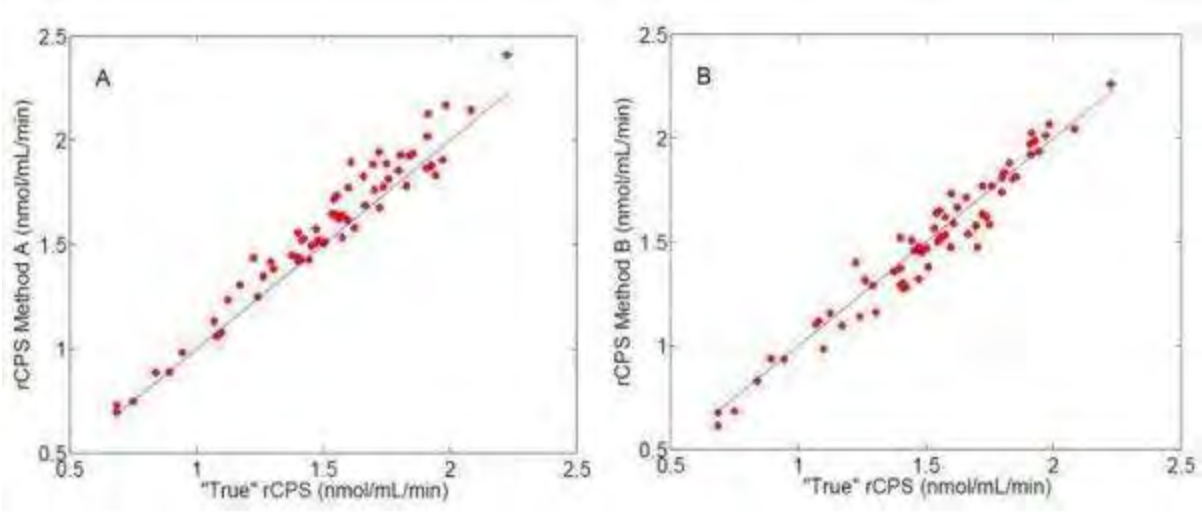

[Figure 1]

References:

(1) Smith et al.,JCBFM 2005;25:629-40.

(2) Schmidt et al.,JCBFM 2005;25:617-28.

(3) Veronese et al.,JCBFM 2010;30:1460-76.

84

ROLES OF THE KEAP1/NRF2 SYSTEM IN THE REGULATION OF PENTOSE-PHOSPHATE PATHWAY ACTIVITY IN ASTROGLIA CULTURED IN HIGH GLUCOSE ENVIRONMENTS

S. Takahashi, Y. Izawa, N. Suzuki

Department of Neurology, Keio University School of Medicine, Tokyo, Japan

Objectives: Cultured astroglia respond to acutely increasing glucose concentrations by enhancing pentose-phosphate pathway (PPP) activity to reduce reactive oxygen species (ROS) toxicity (1). The high-glucose environments associated with diabetes mellitus may have deteriorating effects on brain parenchymal cells (i.e., neurons and astroglia) as well as vascular endothelial cells. PPP is a minor pathway (contributing approximately 2-3%) of glucose metabolism that generates NADPH, which in turn increases the reduced form of glutathione (GSH) to detoxify ROS through the activity of glutathione peroxidase. A rate-limiting enzyme of PPP, G6PDH is regulated by both allosteric and transcriptional mechanisms. The Keap1/Nrf2 system is a master regulator of phase-2 detoxifying enzymes, including G6PDH (2). We investigated the roles of the Keap1/Nrf2 system in the regulation of PPP activity in astroglia cultured in high-glucose environments.

Methods: Cultured astroglial cells were prepared from newborn Sprague-Dawley rats (3). Cells were cultured in DMEM with 10% FBS containing 5 mM glucose for 10 days. Then, the cells were exposed to sulforaphane (10 μM), a Nrf2 activator, thapsigargin (1 μM), an ER stress inducer, or hexosamine (1-10 mM), a precursor of N-acetylglucosamine generated through the hexosamine biosynthetic pathway (HBP), another minor pathway of glucose metabolism. PPP activity was measured using a modification of the method described by Hothersall et al (4). Briefly, cells were incubated with tracer doses of [1-^{14}C]glucose or [6-^{14}C]glucose for 60 min and the difference between $^{14}CO_2$ derived from [1-^{14}C]glucose and [6-^{14}C]glucose was thought to be an indicator of PPP activity. Bip expression, an ER stress indicator, or the translocation of Nrf2 from the cytosol to the nucleus was assessed using immunohistochemistry. The ROS production rates were assessed semiquantitatively using the fluorescent intracellular ROS indicator H_2DCFDA (5).

Results: Fifteen hours of exposure to sulforaphane caused the translocation of Nrf2 from the cytosol to the nucleus without inducing Bip expression. Both thapsigargin and hexosamine induced Bip expression and Nrf2 translocation. All three drugs enhanced the PPP activities by 70-90% and reduced the ROS production rates by 10-30%.

Conclusions: PPP activity in astroglia is regulated by the Nrf2-mediated transcription of G6PDH. High-glucose environments could induce N-acetylglucosamine synthesis through an increased flux into HBS, which induces the abnormal glycosylation of proteins and triggers ER stress. Hexosamine did, indeed, induce ER stress, as evidenced by the enhanced Bip expression in cultured astroglia. Nrf2 reportedly is a direct substrate of PERK, an ER stress transducer protein kinase (6), and the phosphorylation of Nrf2 facilitates its dissociation from the adaptor protein Keap1 and its translocation to the nucleus. Finally, hexosamine induced PPP activation and ROS reduction in a dose-dependent manner. These findings indicate that the Keap1/Nrf2 system plays important roles in the regulation of PPP activity in astroglia, which may exert a protective role against ROS toxicity in high-glucose environments.

References:

1. Izawa et al, Brain09 in Chicago

2. Thimmulappa et al, Cancer Res, 2002

3. Takahashi et al, PNAS, 1995

4. Hothersall et al, Arch Biochem Biophys,1979

5. Izawa et al, Brain Res, 2009

6. Cullinan et al, Mol Cell Biol, 2003

85

PREDICTION OF MOTOR FUNCTION BY DIFFUSION TENSOR TRACTOGRAPHY IN PATIENTS WITH BASAL GANGLION HEMORRHAGE

P. Zheng, J.-S. Zeng, Y.-J. Guo, G.-Y. Li

Neurosurgery, Shanghai Pudong New Area People's Hospital, Shanghai, China

Introduction: Hemorrhagic stroke is one of the leading causes of death and the most common cause of long-term adult disability. An accurate estimation of prognosis is very important for hemorrhagic stroke patients. Impairment of motor function caused by pyramidal tracts injury is common in these patients. Here, we performed a MR diffusion tensor tractography (DTT) to predict the impairment of motor function in patients with basal ganglion hemorrhage and explore its clinical value.

Methods: DTT was performed in 33 patients with basal ganglia hemorrhage within two weeks after onset. To visualize the course of pyramidal tracts and classify patients into four groups according to the fiber ratio of PTs, calculated by dividing the number of the PT number of the affected hemisphere by that of the unaffected hemisphere as follows: type A, the fiber ratio was less than 1/4; type B, less than 1/2; type C, more than 1/2 and type D, more than 3/4. The motricity index of upper extremity (UMI) was used to evaluate the motor function at onset and after six months of onset. UMI scores of different groups were compared among the different groups and a Spearman analysis was performed to correlate the UMI scores with different integrity of pyramidal tracts.

Results: There were no differences in the UMI scores at onset among the four groups ($p>0.05$). The UMI scores obtained at 6 months after onset were significantly unequal and influenced by the DTT type ($p< 0.05$). There was a significant correlation between the integrity of the pyramidal tracts and the UMI scores after 6 month of onset ($r=0.7312$, $p< 0.05$).

Group	Case number	Fiber number in affected hemisphere	Fiber number in unaffected hemisphere	Fiber ratio group	Initial UMI scores	UMI scores 6 months after onset
A	4	41±15	208±21	<1/4	8.61±5.07*	46.38±15.64
B	11	87±14	226±18	<1/2	8.76±4.93*	68.30±10.70#
C	12	124±22	219±29	>1/2	9.70±6.96*	78.81±12.89#
D	6	198±18	232±23	>3/4	10.72±9.89*	84.00±12.02#

[UMI scores distributed among different DTT types]

Conclusion: There was a positive correlation between the integrity grade of pyramidal tracts

and the motor function, showing that the more seriously pyramidal tracts damaged, the worse the motor function was. The DTT findings of pyramidal tract in acute cerebral hemorrhage may valuably predict the motor function outcome.

86

DETERMINATION OF TIME-COURSE CHANGE RATE FOR ARTERIAL XENON USING THE TIME COURSE OF TISSUE XENON CONCENTRATION IN XENON CT

S. Sase[1,2], M. Honda[2], H. Takahashi[3], H. Ikeda[3], M. Kobayashi[3], N. Matsumoto[3], M. Suzuki[3]

[1]R&D, Anzai Medical Co., Ltd., [2]Department of Neurosurgery, Toho University School of Medicine, Tokyo, [3]Department of Internal Medicine, Division of Gastroenterology and Hepatology, St. Marianna University School of Medicine, Kawasaki, Japan

Introduction: In calculating tissue blood flow (TBF), such as cerebral blood flow (CBF), according to the Fick principle, time-course information on arterial tracer concentration is indispensable and has a considerable influence on the accuracy of calculated TBF. In TBF measurement by xenon CT (Xe-CT), non-radioactive xenon gas is administered by inhalation as a tracer, and end-tidal xenon is used as a substitute for arterial xenon. There has been the assumption that the time-course change rate for end-tidal xenon concentration (Ke) and that for arterial xenon concentration (Ka) are substantially equal. Respiratory gas sampling is non-invasive to the patient and Ke can be easily measured by exponential curve fitting to end-tidal xenon concentrations. However, it is pointed out that there would be a large difference between Ke and Ka in many cases. In Xe-CT, accurate Ka determination would be the key to establishing quantitativeness.

Purpose: The goal of this work was to develop a method of determining the Ka value using the time course of tissue xenon concentration in Xe-CT.

Methods: We incorporated Ka into the Kety autoradiographic equation as a parameter to be solved, and developed a method of least squares to obtain the solution for Ka from the time-course changes in xenon concentration in the tissue. We applied this method of least squares to the data from Xe-CT abdominal studies performed on 17 patients; the solution for Ka was found pixel by pixel in the spleen, and its Ka map was created for each patient. Xe-CT cerebral studies were also performed on a healthy man at different ages (28 and 32 years), and Ka and CBF maps were created.

Results: On one hand, we obtained the average value of the Ka map of the spleen as the calculated Ka (Ka_calc) for each patient. On the other hand, we measured Ka (Ka_meas) using the time-course changes in CT enhancement in the abdominal aorta for each patient (Fig. 1).

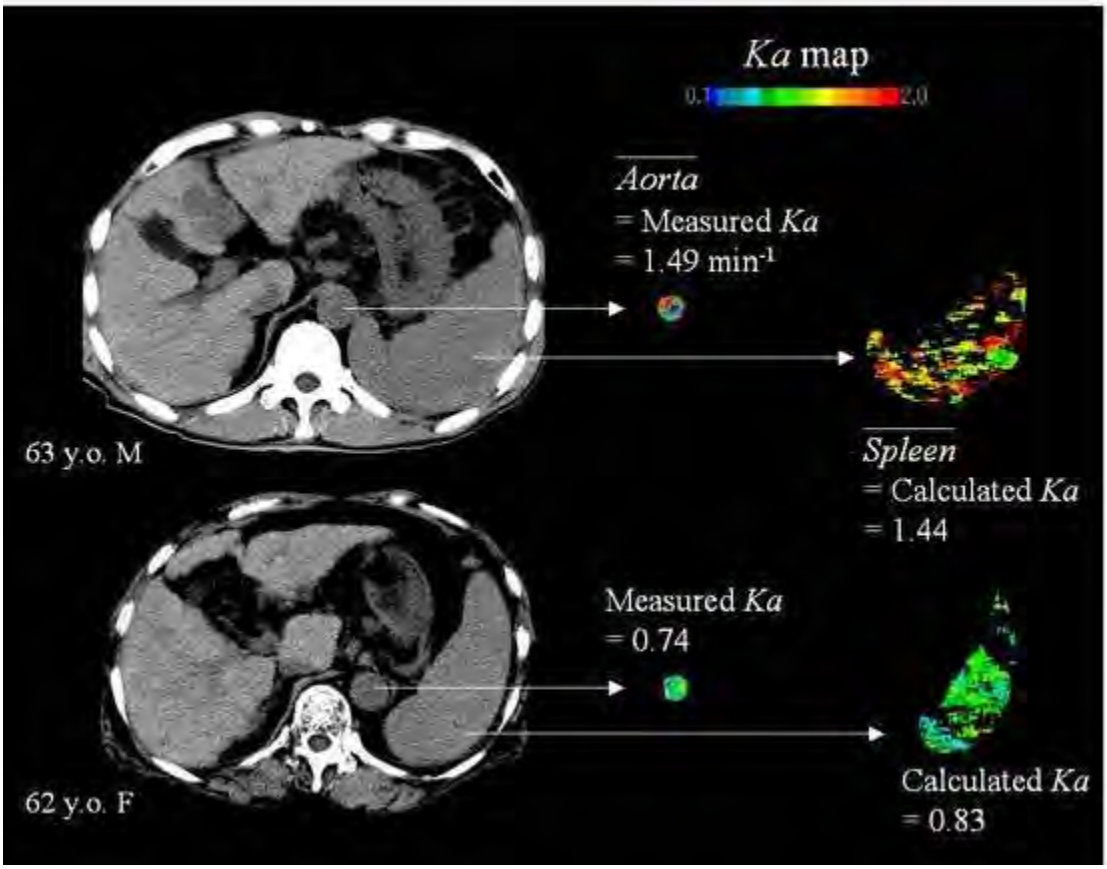

[Fig. 1]

There was a good correlation between Ka_calc and Ka_meas (r = 0.966, *P*< 0.0001), and these two values were close to each other (Ka_calc = 0.935 x Ka_meas + 0.089). This demonstrates that Ka_calc would be close to the true Ka value. In the cerebral studies on the same subject, there was a considerable decrease in the Ka_calc value (1.07 to 0.85 min^{-1}) although CBF values were close, suggesting a reduction in the diffusing capacity of the lung (Fig. 2).

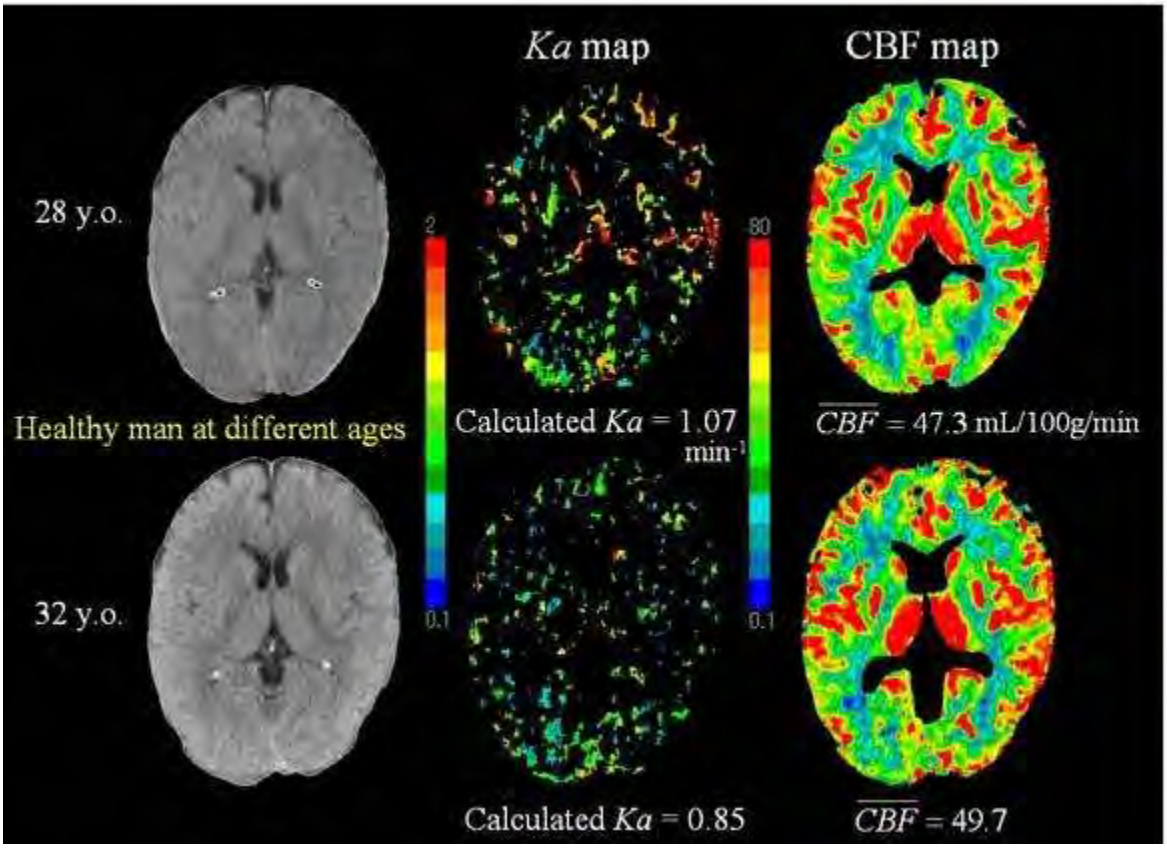

[Fig. 2]

Conclusions: Accuracy of TBF by Xe-CT can be improved with use of the average value of the Ka map of an organ like the spleen or the brain that has a single blood supply (only arterial inflow). Quantitativeness of CBF images by means of the proposed method could not be influenced by the pulmonary functions of the patient because of no use of respiratory xenon data in obtaining Ka, and therefore, the applicability of Xe-CT/CBF would be widened besides its increase in accuracy.

87

EVENT RELATED POTENTIALS (ERP) IN STRESS AND NONSTRESS CONDITIONS BEFORE AND AFTER CHRONIC EXERCISE

Z.G. Özünal[1], S. Sabırlı[2], S. Şen[3], S. Karamürsel[4], B. Ömer[5], S. Yildiz[6], Y. Üresin[3]

[1]Pharmacology, Izzet Baysal Medical Faculty, Bolu, [2]Pharmacology, Harran Medical Faculty, Urfa, [3]Pharmacology, [4]Physiology, [5]Biochemistry, [6]Sports Medicine, Istanbul Faculty of Medicine, Istanbul, Turkey

Introduction: Stress is a common condition for life. Exercise training alters stress response. Event Related Potential (ERP) is a quantitative parameter to evaluate stress response. Salivary cortisol is a noninvasive and valid parameter in clinical stress research. It is interesting to investigate exercise training's effect on stress response with ERP, cortisol and blood pressure.

Objective: In this study our objective is to investigate the chronic exercise's effect on stress response.

Method: Volunteers were included in a chronic exercise program consisted of 60 minute walking three times a week for eight months. Cardiometabolic parameters were measured and ERPs, salivary cortisol levels and blood pressure responses with and without cold stress conditions were recorded before and after exercise intervention. Twenty volunteers aged between 26-56 were included in the study. Cold stress was applied by immersing one hand into 10ºC cold water. Electroencephalographic activity was measured with BrainAmp (Brain Vision, Germany) from 32 recording sites with electrodes referenced to ear lobe . Electrooculographic (EOG) activity was recorded bipolarly with electrodes placed at the outer canthus and below the eye. Artefacts were eliminated by manual method after automatic ocular correction. ERPs were recorded with mismatch negativity and novelty paradigms. In mismatch paradigm, which evaluates preattentive process of cognition, two different auditory stimuli (S1, S2) and in novelty paradigm which evaluates automatic attention switch mechanism, additional novel stimuli were given. ERPs to autitory stimuli were averaged.

Salivary sample was taken with cotton swap and cortisol measured with electrochemiluminescence immunassay method (Elecsys). Blood pressure was checked with validated blood pressure device (Omron). ERP results were evaluated with Greenhouse Geisser test, and cortisol, blood pressure and cardiometabolic test results compared with Wilcoxon test.

Result: In mismatch negativity paradigm peaks were extracted and difference waves were evaluated. The amplitudes and latencies of difference waves were not statistically different. Novelty paradigm compounds standart (S1) and target stimuli (S2) responses were compared in four conditions. There was no statistically significant difference. The novel stimuli (S3) response's p3a component latencies were different between groups. Before exercise, systolic and diastolic blood pressure increased with cold stress ($p< 0.05$), but after exercise, only the increase in sistolic blood pressure was statistically significant. After chronic exercise, systolic blood pressure values were lower ($p< 0.05$) than before chronic exercise levels. Salivary cortisol levels increased with cold stress but did not reach to a significant level.

Conclusion: Our study showed parallel result with a cold pressor test study mentioning no significant effect on mismatch negativity while contradictory results on novelty paradigm. In our study, while cold stress test did not decrease P50 gating, did not increase N100 amplitude, and

did not elicit P3a responses, did alter p3 latency. Chronic exercise changed basal systolic blood pressure levels and reduced diastolic blood pressure response to cold stress.

This work was supported by Scientific Research Projects Coordination Unit of Istanbul University. Project number 3024.

88

RELATIONSHIP BETWEEN AQP4 AND BLOOD-BRAIN BARRIER DAMAGE FOLLOWING INTRACEREBRAL HEMORRHAGE

Y.P. Tang, Q. Dong

Department of Neurology, Huashan Hospital, Fudan University, Shanghai, China

Objective: The purpose of this study was to examine the role of AQP4 on blood-brain barrier damage after ICH by using $AQP4^{-/-}$mice.

Background: Intracerebral hemorrhage (ICH) is associated with high morbidity and mortality. To date, little is known about the role of Aquaporin-4.

Design/methods: ICH was induced by microinjecting 5 μl autologous whole blood into the striatum of mice. We compared neurological deficits, brain edema contents, Evans blue leakage and ultrastructure of brain microvessels. With protein array, we detected expression of cytokines between $AQP4^{+/+}$ and $AQP4^{-/-}$ mice following ICH, and then, expression of cytokines were tested by Elisa. After injection of IL-1ra, TNFbp, LNMMA and PTIO by ventricle, we detected blood-brain barrier damage with Evans blue and electron microscope between $AQP4^{+/+}$ and $AQP4^{-/-}$ mice following ICH. After blocking IL-1βreceptor and TNFα receptor with inhibitor, we detected blood-brain barrier damage of $AQP4^{-/-}$ mice following ICH.

Results: Our experiments showed a significant increase of AQP4 expression following ICH in $AQP4^{+/+}$ mice. AQP4 deletion aggravated neurological deficits, brain edema, Evans blue leakage and microvessel damage. With antibody array and Elisa techonology, our experiments showed a significant increase of IL-1β, IL-6, IL-12, TNFα, and NO after ICH. Eventually, after blocking IL-1βreceptor and TNFα receptor with inhibitor, $AQP4^{-/-}$ mice showed a decrease of Evans blue leakage, which suggests IL-1β and TNFα play an important role on blood-brain barrier damage of $AQP4^{-/-}$ mice after ICH.

Conclusions: These results suggest that AQP4 deletion increases blood-brain barrier damage. Its mechanism is partially ascribed to excessive expression of cytokine. Further studies on the protective role on blood-brain barrier of activated AQP4 expression following ICH may provide useful therapeutic target for ICH-induced brain injury.

Study supported by: This research was supported by two grants of the National Natural Science Foundation of China (30570632) (30700252)

89

RELATIONSHIP BETWEEN AQP4 AND BRAIN EDEMA, CELLS DEATH AND APOPTOSIS FOLLOWING INTRACEREBRAL HEMORRHAGE

Q. Dong, Y. Tang

Department of Neurology, Huashan Hospital, Fudan University, Shanghai, China

Objective: The purpose of this study was to examine the role of AQP4 in edema formation, cells death and apoptosis after ICH by using $AQP4^{-/-}$mice.

Background: Intracerebral hemorrhage (ICH) is associated with high morbidity and mortality. To date, little is known about the role of Aquaporin-4.

Design/methods: ICH was induced by microinjecting 5 μl autologous whole blood into the striatum of mice. We compared neurological deficits, brain edema contents, specific gravity of brain tissue surrounding hematoma, Evans blue leakage and ultrastructure of brain microvessels , cells death and apoptosis rate, expression of caspase3,8,9,Bcl2,IL-1β receptor and TNFα receptor with western blot, cytokine with protein array between $AQP4^{+/+}$ and $AQP4^{-/-}$ mice following ICH. Eventually, death and apoptotic rate were detected after astrocytes cocultured with IL-1β, TNFα, SNP, LPS.

Results: Our experiments showed a significant increase of AQP4 expression following ICH in $AQP4^{+/+}$ mice. AQP4 deletion aggravated neurological deficits, brain edema, Evans blue leakage and microvessel damage. It also reduced the specific gravity of brain tissue surrounding hematoma. Our experiments also showed a significant increase of cells death and apoptosis rate and caspase3,8,9,bax protein expression following ICH in $AQP4^{-/-}$ mice, when compared to $AQP4^{+/+}$ mice following ICH. With antibody array and Elisa techonology, our experiments showed a significant increase of IL-1β, IL-6, IL-12, TNFα, and NO after ICH. AQP4 deletion did not alter expression of IL-1β receptor and TNFα receptor. Eventually, death and apoptotic rate were same between astrocytes from $AQP4^{+/+}$ and astrocytes from $AQP4^{-/-}$ mice after astrocytes cocultured with IL-1β, TNFα, SNP, LPS.

Conclusions: These results suggest that AQP4 deletion increases ICH damage, including edema formation, blood-brain barrier damage, cells death and apoptosis rate. Its mechanism is partially ascribed to excessive expression of cytokine without change of IL-1βreceptor and TNFα receptor.

Study supported by: This research was supported by two grants of the National Natural Science Foundation of China (30570632) (30700252)

90

WIDESPREAD AND PROLONGED INCREASED *(R)*-[^{11}C]PK11195 BINDING AFTER TRAUMATIC BRAIN INJURY

H. Folkersma[1], R. Boellaard[2], M. Yaqub[2], R.W. Kloet[2], A.D. Windhorst[2], A.A. Lammertsma[2], W.P. Vandertop[1], B.N.M. van Berckel[2]

[1]Neurosurgical Center Amsterdam, [2]Nuclear Medicine & PET Research, VU University Medical Center, Amsterdam, The Netherlands

Objective: Traumatic brain injury (TBI) elicits strong inflammatory responses involving activation of resident microglia in brain tissue. Activated microglia can be visualised and quantified using (R)-[^{11}C]PK11195 and PET. The purpose of this study was to measure (R)-[^{11}C]PK11195 binding as an indirect marker of neuronal damage after TBI in humans.

Methods: Dynamic (R)-[^{11}C]PK11195 PET scans were acquired in eight consecutive patients with an initial moderate (GCS 8-13, n=5) or severe (GCS< 8, n=3) Glasgow Coma Scale, six months after TBI. For co-registration purposes, an individual high resolution MRI-scan of the brain was acquired within one week after the PET scan. Seven age- and gender matched healthy controls underwent the same scanning protocol. A modified supervised reference tissue extraction method (SVCA4) combined with a basis function implementation of SRTM was used to derive quantitative (R)-[^{11}C]PK11195 BP_{ND} images. Regional binding potentials (BP_{ND}) were obtained by projecting volumes of interest (VOI) onto parametric (R)-[^{11}C]PK11195 BP_{ND} images. Whole brain BP_{ND} was defined as the volume-weighted average of these regional VOI values. (R)-[^{11}C]PK11195 BP_{ND} was assessed using the simplified reference tissue model.

Results: Whole brain analysis revealed a significantly increased (R)-[^{11}C]PK11195 BP_{ND} in TBI patients (BP_{ND} = 0.22 ± 0.08) six months after head injury, as compared with age-and sex-matched healthy controls (BP_{ND} = 0.12 ± 0.06) (p=0.02). Regional analysis indicated that increased (R)-[^{11}C]PK11195 binding was widespread over the brain.

Interpretation: Prolonged and widespread increased (R)-[^{11}C]PK11195 binding six months after TBI is indicative of diffuse neuronal damage.

91

BLOCKAGE OF P-GLYCOPROTEIN AT THE BLOOD BRAIN BARRIER BY LOW SPECIFIC ACTIVITY ^{11}C-LANIQUIDAR

L. Moerman[1], C. Dumolyn[1], P. Boon[2], F. De Vos[1]

[1]Laboratorium of Radiopharmacy, Ghent University, [2]Laboratory for Clinical and Experimental Neurophysiology, Ghent University Hospital, Ghent, Belgium

Objectives: Variations in P-glycoprotein (P-gp) expression at the blood brain barrier may play a role in several brain disorders. Measurement of P-gp functionality with PET tracers may be an important tool to investigate these diseases. Luurtsema et al. (2009) synthesized ^{11}C-laniquidar, which act as a substrate in performed in vivo studies. They suggested that studies with co-injection of cold laniquidar could be useful. Thereby, we investigated differences in brain uptake of ^{11}C-laniquidar between a low (0.025 mg/kg body weight) and high (60 mg/kg body weight) dose of i.v. administered ^{11}C-laniquidar.

Methods: The synthesis of ^{11}C-laniquidar was slightly modified to Luurtsema et al. (2009). To investigate the influence of the dose of laniquidar on the brain uptake, wild-type mice were injected i.v. with 5.55 MBq ^{11}C-laniquidar at a high or low specific activity (S.A.). Mdr1a(-/-) knock-out mice were incorporated as control animals, and underwent the same procedures. All mice were killed 1, 10 and 30 min post injection (n = 3 at all time points). Brain and blood were isolated, weighted and counted for radioactivity. The results were expressed as % injected dose (ID)/g organ.

Results: The high S.A. ^{11}C-laniquidar formulation averaged around 44 GBq/µmol, representing an administered dose of 0.025 mg/kg body weight, while the low S.A. formulation averaged around 18 MBq/µmol, which represents a therapeutical dose of 60 mg/kg body weight. At all time points, injection of the high S.A. ^{11}C-laniquidar in wild-type mice resulted in a statistical significant lower brain uptake (0.7 ± 0.2 % ID/g at 30 min) compared to the low S.A. formulation (3.1 ± 0.3 % ID/g at 30 min; P = 0.004). The ^{11}C-laniquidar blood concentration at all time points was not significantly different between the high and low S.A. formulation in wild-type mice (P = 0.558). No effect of S.A. on ^{11}C-laniquidar uptake in brain could be demonstrated in P-gp knock-out mice. The brain uptake averaged around 3.3 % ID/g at all time points and was not statistically different from the wild-type mice with the low S.A. formulation.

Conclusions: These results clearly demonstrate the bivalent character of laniquidar, acting as a substrate at low doses (≤ 0.025 mg/kg body weight). At higher doses the administered amount of laniquidar is high enough to block the P-gp transporters facilitating the uptake in the brain to a level comparable to the mdr1a(-/-) knock-out mice.

References: Luurtsema G. et al., Nuclear Medicine and Biology, 36 (2009): 643-649

92

ISCHEMIC MODEL FOR ALZHEIMER'S DEMENTIA

R. Pluta[1], A. Kiryk[2], M. Ulamek[1], M. Jablonski[3], L. Kaczmarek[2]

[1]Laboratory of Ischemic and Neurodegenerative Brain Research, Mossakowski Medical Research Centre, [2]Laboratory of Molecular Neurobiology, Nencki Institute of Experimental Biology, Warsaw, [3]Department of Orthopaedics and Rehabilitation, Lublin Medical University, Lublin, Poland

Objectives: Recent data suggest that neurovascular insufficiency may precede cognitive decline and onset of Alzheimer's disease (AD). Brain ischemia (BI) and impaired beta-amyloid peptide clearance across the ischemic blood-brain barrier (BBB) may contribute to the onset and progression of AD dementia (1). BI negatively affects the synthesis of proteins required for memory and learning, and may eventually lead to amyloid plaques development and to neuritic injury and neuronal death (1). Impaired clearance of beta-amyloid peptide from the brain tissue by the cells of the BBB unit may lead to its accumulation on neurovessels and in brain. The accumulation of beta-amyloid peptide on the brain blood vessels, known as cerebral amyloid angiopathy (CAA), is associated with cognitive decline and is one of the hallmarks of AD pathology. CAA can severely disrupt the integrity of the neurovascular wall resulting in hemorrhages that exacerbates neurodegenerative process and increases inflammatory response. Here, we present the role of BI and molecular mechanisms in ischemic BBB responsible for AD and CAA pathogenesis. First, we study ischemic changes, including vascular degeneration that contributes to different stages of the AD. Next we show the role of the ischemic BBB, a key beta-amyloid peptide transportation system in- and outside brain, whose pathology is observed early in AD. Finally, we present characteristic behavioral changes for AD following BI injury.

Methods: We used 16 females Wistar rats. The animals were divided for two groups. First group with 10-min BI (n=8) (2) and second was used as sham-operated control (n=8). All rats underwent behavioral tests: neurological examination, rotarod, elevated plus maze, open field, novel object recognition and object location memory, T-maze and Morris water maze 1 year after BI. After behavioral examination brains of animals were fixed by perfusion for neuropathological studies.

Results: After BI locomotor hyperactivity positive correlated with increased hippocampus neuronal alterations. Following BI impairment in habituation and reduced anxiety were observed. Ischemic brain injury results in reference and working memory deficits. Moreover, BI injury in experimental animals leads to progression of spatial memory for up to 1 year. Above abnormalities were connected with significant brain atrophy, associated with diffuse neuronal loss in the brain cortex, and in the CA1 sector of the hippocampus.

Conclusions: Taken together supportive evidence from both experimental and clinical studies indicates that the decline in progressive cognitive activities could not be explained only by direct contribution of primary BI injury, but rather by a progressive result of the additive effects of the ischemic lesions, Alzheimer's factors and aging. On the other hand, the abnormal ischemic expression and metabolism of amyloid precursor protein (1) and ischemic injury properly may constitute a *vicious cycle*, which leads to ischemic type neurodegeneration and finally to full cognitive decline of Alzheimer's type. The data presented here support an essential role of BI and ischemic BBB mechanisms in contributing to both, onset and progression of AD.

References:

1. Pluta R. Ischemia-reperfusion pathways in Alzheimer's disease. Nova Science Publishers, New York, 2007.

2. Pluta R et al. Acta Neuropathol 83: 1-11, 1991.

93

NITRIC OXIDE MECHANISM IN THE PROTECTIVE EFFECT OF NARINGIN AGAINST EXPERIMENTAL ANIMAL MODEL OF POST-STROKE DEPRESSION (PSD)

V. Gaur, A. Kumar

Division of Pharmacology, University Institute of Pharmaceutical Sciences, Panjab University, Chandigarh, India

Background and aims: The present study has been designed to explore the nitric oxide mechanism in the protective effect of naringin against I/Rinduced neurobehavioral alterations, oxidative damage and mitochondrial dysfunction in mice.

Methods: Laca mice (25-30 g) were subjected to twice BCCAO occlusion (5 min) at the interval of 10 min, followed by 96 h reperfusion. Naringin (50and 100 mg/kg) was administered for 10 days, starting 7 days before animals were subjected to I/ R injury. On day 10, various neurobehavioralparameters followed by biochemical parameters and mitochondrial enzyme complex activities were assessed.

Results: Ischemia reperfusion injury caused significant (increased immobility period, neurological score and decreased locomotor activity), oxidativedamage (increased lipid peroxidation and nitrite concentration and depleted reduced glutathione, Glutathione-S-transferase, superoxidedismutaseand catalase) and altered mitochondrial enzyme complex activities (complex I to IV) as compared to sham treatment. Naringin (50 and 100 mg/kg)treatment significantly attenuated neurobehavioral alterations, oxidative damage and restored mitochondrial enzyme complex activities ascompared to control (ischemia reperfusion) group. Further, protective effect of naringin (50 mg/kg) was attenuated by L-arginine (100 mg/kg) orsildenafil (5 mg/kg) pretreatment. Further, L-NAME (10 mg/kg) or 7-NI (10 mg/kg) pretreatment with naringin (50 mg/kg) significantly potentiatedtheir protective effect as compared to their treatment alone.

Conclusion: Present study suggests the involvement of nitric oxide mechanism in the protective effect of naringin against post stroke depressioninduced neurobehavioral, biochemical and cellular alterations in mice.

94

FLOW-METABOLISM UNCOUPLING AND EXTENDED LONGEVITY AS OBSERVED IN A TRANSGENIC MICE MODEL

A.-L. Lin[1,2], T. Duong[1], H. Van Remmen[3], A. Richardson[3], P. Fox[1,2]

[1]Research Imaging Institute, [2]Department of Psychiatry, [3]Barshop Institute for Logevity and Aging Studies, University of Texas Health Science Center, San Antonio, TX, USA

Objective: Mitochondrial integrity is generally viewed as being highly associated with lifespan and healthspan. Recent studies, however, indicate that longevity can be increased by *reduced* mitochondrial function. Specifically, increased lifespan is observed in mice with a mitochondrial mutation in an assembly protein (*Surf1*$^{-/-}$) for electron-transport chain complex IV, which results in a reduction in the level of cytochrome c oxidase (1). The flow-metabolism relationship in the mice, however, remains unknown. The purpose of the study is to use the multi-metric neuroimaging methods (e.g. MRI and PET) to determine the basal cerebral blood flow (CBF), cerebral metabolic rate of oxygen ($CMRO_2$) and glucose (CMR_{Glc}), and the flow-metabolism coupling relationship in the *Surf1*$^{-/-}$ mice.

Methods: Wild type (WT) and *Surf1*$^{-/-}$ mice (N =2, respectively) were used for the study. MRI studies were performed at a 11.7T Biospec system. CBF was acquired using MRI arterial spin labeling (ASL) technique (2). $CMRO_2$ was determined by the Fick's principle: $CBFxOEFxCaO_2$, where OEF is the oxygen extraction fraction and CaO_2 is the oxygen content (assuming the same in both types of mice, 15.0 g/dl, (3)). OEF was measured with the Quantitative BOLD technique (4). CMR_{Glc} was determined with the 18F-FDG using PET. 18F-FDG (0.39 MBq/g of body weight) dissolved in saline was injected through the tail vein. The emission data was acquired for 20 min after 40 min of injection.

Data Analysis: ASL and OEF analysis employed codes written in Matlab. FDG images were analyzed to obtain CMR_{Glc} using the mean standardized uptake value (SUVmean) method. Student t test was used to determine the statistical significance of the CBF, $CMRO_2$ and CMR_{Glc} between the WT and the *Surf1*$^{-/-}$ mice.

Results: The quantitative CBF, OEF, $CMRO_2$, and CMR_{Glc} values and their relative changes between the WT and the *Surf1*$^{-/-}$ mice are listed in the Table 1. The basal CBF and CMR_{Glc} of the *Surf1*$^{-/-}$ mice were 18.3% ($P < 0.05$) and 85.2% ($P < 0.001$) higher, respectively, compared to those of the WT. $CMRO_2$ was found lower (4.8%), but not significant ($P > 0.5$).

Conclusions: At normal conditions, the basal CBF, $CMRO_2$ and CMR_{Glc} are tightly coupled (5). In the *Surf1*$^{-/-}$ mice, the flow-metabolism relationship was found deviated (uncoupled). Our data further demonstrated that their metabolic pathway has shifted from oxidative to glycolytic metabolism (with dramatic increases in CMR_{Glc} and CBF, but no significant change in $CMRO_2$). It is thus speculated that the lifespan of the *Surf1*$^{-/-}$ mice is extended due to the metabolic pathway shifting. With the novel mice model and the concurrent MRI-PET measurements, it our goal to further study the impact of mitochondrial function on longevity, cognitive integrity and neurodegenerative disorders.

	CBF (ml/g/min)	OEF	CMRO2	CMRGlc(SUVmean)

			(ml/g/min)	
WT	1.09±0.03	0.38±0.04	0.062±0.012	28.7±5.3
Surf1-/-	1.29±0.04	0.31±0.05	0.059±0.008	53.1±6.1
%change (Surf1-/- vs. WT)	18.3±4.6	-18.4±5.8	-4.8±1.1	85.2 ± 9.1

[Table 1]

References: (1) Dell´agnello, Hum Mol Genet 2007;

(2) Muir, MRM 2008;

(3) Schöler, EJA 2009;

(4) He, MRM 2008;

(5) Raichle, PNAS 2001.

97

COMPARATIVE EFFECTIVENESS OF HEMOSTATIC THERAPY IN EXPERIMENTAL WARFARIN-ASSOCIATED INTRACEREBRAL HEMORRHAGE

S. Illanes[1,2], W. Zhou[1], S. Schwarting[1], S. Heiland[3], R. Veltkamp[1]

[1]Neurology, University of Heidelberg, Heidelberg, Germany, [2]Instituto de Ciencias Clínica Alemana-Universidad del Desarrollo, Santiago, Chile, [3]Neuroradiology, University of Heidelberg, Heidelberg, Germany

Background and purposes: Intracerebral hemorrhage associated with oral anticoagulants has a poor prognosis. Current treatment guidelines are based on case series and plausibility only, and a common consensus on effective hemostatic therapy is missing. We compared the effectiveness of diverse hemostatic approaches in a previous established mouse model of warfarin-associated ICH (W-ICH).

Methods: Male C57BL/6 mice received anticoagulant treatment with warfarin (0.4 mg/Kg for 3 days). ICH was induced by striatal injection of collagenase in mice with an International normalised ratio (INR) between 4-5. 30 min later mice received an intravenous injection of either saline (200µl n=15), prothrombin complex concentrate (PCC, 100U/Kg, n=10), fresh frozen plasma (FFP, 200µl, n=13), recombinant human factor VII activated (FVIIa, 3.5 mg/Kg, n=8 and 10 mg/Kg, n=8) or tranhexamic acid (TA, 400 mg/Kg, n=12). ICH volume was quantified on T2* weighted images after 24 hours.

Results: Mean hematoma volumes were 7.4±1.8 mm³ in the non-warfarin controls and 21.9±5.0 mm³ in the warfarin group receiving saline. PCC (7.5±2.3 mm³) and FFP (8.7±2.1) treatment resulted in significantly smaller hematoma volume compared to saline. FVIIa (10mg/kg: 14.7±3.4; 3.5mg/kg: 15.0±6.8 mm³) and TA (16.2±4.1 mm³) were less effective. Water content in the hemorrhagic hemisphere was similar in all groups except for TA in which it was significantly increased.

Conclusions: PCC and FFP effectively prevent hematoma growth in murine W-ICH whereas factor VIIa was less effective. TA exacerbates perihematoma edema in this mouse W-ICH model.

99

ND-308, A NOVEL COMPOUND, AMELIORATES CEREBRAL INFARCTION IN RATS BY ANTI-INFLAMMATORY ACTION

G.X. Liang

Department of Integrative Medicine, Yuhuangding Hospital, Qingdao University Medical College, Yantai, China

Cerebral ischemia is a prevalent human disorder, and the search for effective remedies continues. Puerarin has been clinically prescribed in China to treat patients with stroke and coronary artery disease since 1998. The present study was conducted to investigate the neuroprotective effects of ND-308 , one of the novel derivatives from puerarin, against focal cerebral ischemic infarct in rats, and to discuss the possible mechanism. A rat models of focal cerebral ischemia-reperfusion injury was established by middle cerebral artery occlusion using modified filament method. The behavioral test was used to measure neurological deficit scores for evaluation of the ischemic damage of brain. The cerebral infarct volume and edema were assessed to evaluate the brain patho-physiological changes. Immunohistochemistry and enzymelinked immunosorbent assay (ELISA) were used to detect the expression of TNF-α, NF-κB and IL-1β proteins, and TUNEL assay was employed to examine the cell apoptosis. The results showed that ND-308 markedly decreased the neurological deficit scores, reduced infarct volume and the edema compared with the model group. Meanwhlie ND-308 significantly reduced the—levels. Taken together, our results indicate that indicate that ND-308 exerts the protective potential against cerebral ischemia injury and its neuroprotective effects may be due to the anti-inflammatory effects.

100

OXYGEN-GLUCOSE DEPRIVATION INDUCES GAP-43 INTERACTION WITH GEPHYRIN TO REGULATE $GABA_A$ RECEPTOR ACTIVITY IN DEVELOPING CORTICAL NEURONS

C.-Y. Wang[1,2], Y.-P. Song[3], Y.-T. Hsu[3], C.-H. Lin[4], Y.-Y. Sun[3], C.-C. Hung[3], C.Y. Hsu[2], **Y.-H. Lee**[1]

[1]Physiology, National Yang-Ming University, Taipei, [2]China Medical University Hospital, Taichung, [3]Medical Sciences, Taipei Medical University, [4]Nursing, Kang-Ning Junior College of Medical Care and Management, Taipei, Taiwan R.O.C.

Introduction: Neonatal hypoxia-ischemia (HI) remains a frequent cause of childhood epilepsy and cerebral palsy. The injury often associated with spreading depression at acute stage and long term effect on the onset of epilepsy. Recent studies reported decrease of $GABA_A$ receptor function in the cerebral cortex of hypoxic neonatal rats, but the underlying mechanism is unknown. During brain injury, activity-dependent plasticity proteins, such as growth-associated protein 43 (GAP43), is highly expressed in the injured neurons to facilitate axonal regeneration. However, whether GAP43 contributes to the synapse development abnormalities during neonatal brain injury remains poorly understood.

Objective: We used proteomic approach to reveal that GAP43 could interact with gephyrin, a scaffold protein for $GABA_A$ receptor trafficking and clustering at postsynaptic density, in developing cortical neurons. Importantly, oxygen-glucose deprivation (OGD), which represents hypoxia-ischemia insult, significantly increased the GAP43-gephyrin interaction. Therefore, the present study aimed to examine the role and mechanism of GAP43-gephyrin interaction in the regulation of $GABA_A$

receptor clustering and activity during OGD insult in developing neurons.

Methods: Primary cultured rat cortical neurons at 4 days-in-vitro were used as the experimental system. The OGD insult, i.e. 2hr hypoxia (1% O_2) in the absence of glucose followed by 22hr normoxia in the presence of glucose, was used as the in vitro model for ischemic brain injury. Ser41Asp (S41D) and Ser41Ala (S41A) GAP-43 mutants which mimicked PKC-phosphorylated and unphosphorylated GAP-43 were established respectively for investigating the causal relationship between GAP43 activity and $GABA_A$ receptor activity. The interactions among GAP43, gephyrin and $GABA_A$ receptor were assessed by immunofluorescent double labeling and co-immunoprecipitation. The surface $GABA_A$ receptor presentation and activity of the developing cortical neurons were measured by biotinylation assay and muscimol-induced intracellular calcium ($[Ca^{2+}]_i$) elevation, respectively.

Results: We found that OGD insult increased the interaction between GAP43 and gephyrin accompanied by the reduction of surface $GABA_AR$ activity. Treatment with PKC inhibitor Ro318220 also had the same effect. Furthermore, S41D-GAP43 mutant interact with gephyrin better than the S41A-GAP43 mutant, and neurons expressing S41D-GAP43 mutant had much higher degree of gephyrin-$GABA_AR\gamma2$ interactions than those expressing S41A-GAP43 mutant. In addition, blockade of calcineurin-mediated dephosphorylation of pS41-GAP43 by FK506 also increased gephyrin-$GABA_AR\gamma2$ interactions, suggesting that PKC-phosphorylated GAP43 facilitates gephyrin-$GABA_AR$ interaction. However, the surface $GABA_AR$ activities in S41D-transfected and FK506-treated neurons were lower than their respective control, suggesting that phosphorylated GAP43 might induce $GABA_AR$ internalization by promoting gephyrin-$GABA_AR$ interaction.

Conclusion: OGD insult in developing cortical neurons impairs $GABA_A$ receptor presentation and activity via induction of GAP43-gephyrin interaction. This study revealed a novel role of GAP43 in the alteration of GABAergic transmission and subsequent neurological deficit during neonatal HI.

(Supported by grants NSC 99-2321-B-010-015, 96-2320-B-010-039-MY3 from National Science Council, and DOH99-TD-B-111-004 from Taiwan Department of Health Clinical Trial and Research Center of Excellence.)

108

MICROGLIAL SENESCENCE AND NEURODEGENERATION: CONNECTING THE DOTS

W.J. Streit

Neuroscience, University of Florida, Gainesville, FL, USA

Microglia are essential for providing neuroprotection in the normal CNS and particularly following acute CNS injury. There is now evidence suggesting that chronic neurodegenerative states may arise in large part because of microglial degeneration and associated loss of microglial neuroprotective function. Although it is clear that a main reason for microglial degeneration is advanced age there may be other factors, including undue oxidative stress, that exacerbate normal microglial senescence, and thus the preservation of microglial cell function may become a target for developing novel neuroprotective strategies. The role of microglia in Alzheimer's disease (AD) pathogenesis remains unknown. Although many studies maintain that chronic microglial activation in the AD brain is detrimental and contributes to neurodegeneration, anti-inflammatory drugs show little promise for AD treatment or prevention. This presentation provides support for a novel theory of microglial involvement in AD, the microglial dysfunction hypothesis, claiming that the neurofibrillary degeneration of AD is the result of declining microglial neuroprotection due to aging-related microglial senescence and degeneration. I will report histopathological findings from humans covering the spectrum from none to severe AD pathology, including patients with Down's syndrome, showing that degenerating neuronal structures positive for tau (neuropil threads, neurofibrillary tangles, neuritic plaques) are invariably colocalized with severely dystrophic (fragmented) rather than with activated microglial cells. Using Braak staging of AD neuropathology, I will demonstrate that microglial dystrophy precedes the development of tau pathology. Amyloid deposits devoid of tau-positive structures are found to be colocalized with non-activated, ramified microglia, suggesting that amyloid-beta protein does not trigger microglial activation. In contrast, microglia associated with amyloid deposits marked by tau pathology (neuritic plaques) are always dystrophic. The histopathological findings to be presented also indicate that when microglial activation does occur in the human brain in the absence of an identifiable acute CNS insult, it is likely to be the result of systemic infectious disease. Overall these observations strongly argue against the belief that neuroinflammatory changes contribute to AD dementia, and they have the potential to change our views on AD pathogenesis and may thus profoundly influence future treatment approaches.

109

BONE MESENCHYMAL STROMAL CELLS ENHANCE SKILLED MOTOR FUNCTION AND INCREASE AXONAL CONNECTIONS AFTER STROKE IN MICE

Y. Li[1], Z. Liu[1], R.L. Zhang[1], L. Zhang[1], Y. Cui[1], X. Sang[1], M. Chopp[1,2]

[1]Neurology, Henry Ford Hospital, Detroit, [2]Physics, Oakland University, Rochester, MI, USA

Objectives: To characterize reorganization of the corticospinal tract (CST) and elucidate the neuroanatomical mechanisms underlying motor functional recovery after treatment of stroke with bone mesenchymal stromal cells (BMSCs), we investigated axonal connections of the CST between the contralesional cerebral cortex and the stroke-impaired side of the spinal cord using adult CST-yellow fluorescent protein (YFP) mice subjected to semi-pyramidotomy.

Methods: Adult male CST-YFP mice, in which the CST was transgenically labeled with YFP, were subjected to right hemispheric pyramidotomy (PT) at the medulla level along with (w) right permanent middle cerebral artery occlusion (MCAo); or PT without (w/o) MCAo (sham) surgery. One day after surgery, the mice were randomly selected to receive 0.4 ml of phosphate-buffered saline (PBS) or $1x10^6$ BMSCs in PBS injected into a tail vein. A Foot-Fault test and a single pellet reaching test were performed before MCAo as a baseline, and 3 days after MCAo and weekly thereafter to monitor skilled motor functional deficit and recovery. To retrogradely label axonal pathways between the impaired left forelimb and the cerebral cortices, 10 µl of trans-synaptic tracer pseudorabies virus (PRV)-614-m red fluorescent protein (RFP) were injected into the left forelimb flexor muscles 4 weeks after stroke (4 days before sacrifice). The brain and cervical cord were processed for vibratome sectioning to detect the YFP labeling in the denervated side of the spinal cord and the RFP labeling in the cortical pyramidal neurons with a confocal imaging system.

Results:

1) Significant functional improvements were evident in mice subjected to PT-w-MCAo and treated with BMSCs (n=9) compared to PBS treated mice (n=9, $p< 0.05$), but not in mice subjected to PT-w/o-MCAo treated with either PBS (n=9) or BMSCs (n=10).

2) Both CST-YFP axonal density in the denervated side of the spinal cord and PRV-RFP labeled pyramidal neurons in the left intact hemispheric cortex were significantly increased in the PT-w-MCAo mice, compared to PT-w/o-MCAo mice ($p< 0.05$).

3) BMSCs significantly enhanced both CST-YFP axonal density in the denervated side of the spinal cord and PRV-RFP labeled pyramidal neurons in the left intact hemispheric cortex in PT-w-MCAo mice ($p< 0.05$), but not in PT-w/o-MCAo mice.

4) The behavioral outcome assessed by both Foot-Fault test and single pellet reaching test were highly correlated, respectively, with the CST-YFP axonal density in the denervated side of the spinal cord and numbers of PRV-RFP labeled pyramidal neurons in the left contralesional cortex (Foot-Fault vs CST-YFP, $r=0.82$, $p< 0.01$; Foot-Fault vs PRV-RFP, $r=0.61$, $p< 0.05$; single pellet reaching vs CST-YFP, $r=0.76$, $p< 0.01$; single pellet reaching vs PRV-RFP, $r=0.60$, $p< 0.05$).

Conclusions: Our data suggest that BMSCs amplify stroke-induced contralesional neuronal remodeling, which contributes to motor recovery after stroke.

110

ENGINEERED NANOPARTICLES FROM METALS AG, CU AN AL (50-60 NM) INDUCE OXIDATIVE STRESS, BBB BREAKDOWN AND BRAIN PATHOLOGY

H.S. Sharma[1], A. Sharma[1], D.F. Muresanu[2]

[1]Surgical Sciences, Uppsala University, Uppsala, Sweden, [2]Neurology, University of Medicine & Pharmacy, Cluj-Napoca, Romania

The possibility that chronic exposure of nanoparticles leads to breakdown of the blood-brain barrier (BBB) and brain pathology by inducing oxidative stress and increased nitric oxide production was examined in a rat model using biochemical and morphological approaches. Separate group of rats (Male Sprague Dawley, body weight 200-250 g, age 18 to 22 weeks old) were treated with Ag, Cu or Al nanoparticles (50 mg/kg, i.p.) once daily for 7 days, whereas, the control group received saline under identical conditions. These rats were tested on the 8th day for sensory and cognitive dysfunction using Rota rod performance, grid walking, inclined plane angle tests and stride length test using standard procedures. After that the BBB permeability was measured using Evans blue albumin and radioiodine tracers in several brain areas. Brain edema formation was examined d by measuring brain water content and oxidative stress parameters e.g., Myeloperoxidase (MP), Malondialdehyde (MD) and glutathione (GT) were measured in various brain regions. Using immunohistological methods, upregulation of neuronal nitric oxide synthase (nNOS) immunoreactivity was examined on paraffin sections under light microscope. In these serial sections, cell changes were seen at light microscopy using Nissl or Haematoxylin and Eosin. Rats treated with Cu and Ag nanoparticles exhibited mild to moderate sensory motor dysfunction as seen by reduction in time for staying on Rota rod (16 rpm, 120 sec to 80 sec), decline in the angle of inclined plane (from 60 to 40°), placement error of forepaws during grid walking (from 0 % to 34%) and increase in stride length between two hind-limbs while walking (from 45 mm to 85 mm). These changes were only mildly affected by Al treatment. We observed as significant increase in MP and MD levels (MP 4±1 U/g to 9±2 U/g, $P < 0.01$; MD 24±4 nM/g to 56±8 nM/g, $P< 0.01$) in the brains of Cu and Ag treated rats, whereas, GH showed a significant decline (from 1.8±0.04μM/g to 0.8±0.04 μM/g, $P< 0.01$) in Cu and Ag treated rats. Changes in Al treatment were not significant in any one of these oxidative stress parameters. A significant increase in brain water and BBB breakdown to Evans blue and radioiodine tracers were observed in Cu and Ag treated but not in Al treated rats. The number of dark and distorted neurons in various brain regions was significantly increased in Cu and Ag treated but not in Al treated rats. A significant increase in the number of nNOS positive neurons was seen in the cortex, hippocampus, cerebellum, thalamus and hypothalamus in these nanoparticles treated rats as compared to normal rats. Interstingly, the occurrence of nNOS positive neurons were seen into areas showing BBB disruptions to Evans blue leakage, Taken together these observations are the first to demonstrate that nanoparticles depending on their tie (Cu and Ag and but not Al) are able to induce severe oxidative stress and nNOS expression leading to BBB disruption and cell injury.

112

ESTIMATED RELATION BETWEEN CEREBRAL BLOOD FLOW AND BACKGROUND ELECTROENCEPHALOGRAM ACTIVITY SIGNALS WITH MISSING SAMPLES IN NEONATES DURING QUIET SLEEP

M.C. Arango Granados[1], D.A. Botero[1], A.F. Catelli Infantosi[2], D.M. Simpson[3]

[1]Neurophysiology, Universidad de la Sabana, Chía, Colombia, [2]Biomedical Ingeneering, Federal University of Rio de Janeiro, Rio de Janeiro, Brazil, [3]Institute of Sound and Vibration Research, University of Southampton, Southampton, UK

Background: There is a relationship between the demand and supply of cerebral blood flow (CBF) during sleep in newborns (NB) [1,2]. There is not much information about the relationship between spontaneous neuronal activity (NA) and CBF [3]. Therefore, a prospective analytical study was designed to relate NA (EEG) with CBF (cerebral Doppler velocimetry) and explain that specific interaction, taking into special account the existence of missing samples in both signals [4,5].

Methods: A set of signals from twenty normal newborns (up to 7 days of birth) was recollected, during quiet sleep (Tracé Alternant -TA- and High Voltage Slow -HVS- patterns). EEG power (pEEG) and frequency parameters within frequency bands of interest (power in delta - *Pdel* - and theta - *Ptet* -, estimated at each second in F4T4 derivation), and the mean velocity from Doppler velocimetry (from the ipsilateral middle cerebral artery) were obtained. To investigate the association between EEG and CBF in time (cross correlation function -CCF-) and frequency domains (magnitude square coherence -MSC-), signal processing techniques with missing samples were developed. To establish the statistical significance level, a computational method based in the Monte Carlo simulation was applied [4,5,6].

Results: In TA, the pEEG median in *Ptet* had the higher CCF values (0.243), at a lag around 6s, while *Pdel* obtained smaller values. In the frequency parameters, there was a higher variability between individuals, with a CCF median very close to 0 (independent from the lag value). The maximum CCF value for the 84.6% of the NB was statistically significant ($p \leq 0.005$). In HVS, the pEEG median in *Ptet* was smaller than in TA, but still the 40% of the NB obtained statistical significance ($p \leq 0.05$). About the frequency parameters, the HVS had a behavior similar to the TA. The *Pdel* values were even smaller than those in TA. About the frequency domain analysis, the median of the spectrum during TA evidenced an energy concentration (EC) of 3600mv^2/Hz around 0.1Hz. Meanwhile, during HVS, the EC at 0.1 Hz fell (1900mv^2/Hz), while other frequencies acquired a greater importance, resulting in a similar EC. To study the coherence between EEG and CBF parameters, the best results obtained from the CCF were used. During TA, the median MSC value was of 0.38 in 0.1Hz. Meanwhile, during HVS, the median MSC value was of 0.15 in 0.1Hz. In addition, the coherence at frequencies < 0.07Hz (very low frequencies -VLF-) grew up to 0.22. In TA, 92.3% of the NB had a statistically significant MSC ($p \leq 0.005$). In HVS, 50% of the NB achieved statistical significance.

Conclusions: The CCF reveals a 6s delay between NA and CBF, meaning that a change in the NA is followed by a change in the CBF. The coherence indicates a significant association between NA in *Ptet* and CBF about 0.1Hz (autonomous nervous system) during TA [7,8,9]. During HVS this association, although present, has fewer cases reaching statistical significance. However, the second peak in the VLF observed probably means an increased influence of other control mechanisms different from the neurogenic regulation.

114

CEREBRAL PERFUSION (HMPAO-SPECT) IN PATIENTS WITH "DEPRESSION WITH COGNITIVE IMPAIRMENT" VERSUS "MILD COGNITIVE IMPAIRMENT" AND "DEMENTIA OF ALZHEIMER´S TYPE"

W. Staffen[1], J. Bergmann[2], U. Schönauer[1], H. Zauner[3], M. Kronbichler[2], S. Golaszewski[1], G. Ladurner[1]

[1]Neurology, Priv. Med. Univ. of Salzburg, Christian Doppler Clinic, [2]Center of Cognitive Research Salzburg, Salzburg, [3]Rehab. Center Großgmain, Großgmain, Austria

Purpose: Comparative evaluation of regional brain perfusion measured by HMPAO-SPECT of patients with mild cognitive impairment (MCI), dementia of Alzheimer's type (DAT) and depressed patients with cognitive impairment (DCI).

Methods: 736 persons were investigated by reasons of suspected cognitive dysfunction. After exclusion of patients with other forms of dementia than DAT or relevant accompanying disorders SPECT-data of 149 MCI, 131 DAT, 127 DCI patients as well as 123 controls without any cognitive impairment were analysed. Relative cerebral blood flow of 34 anatomical regions was assessed with an automated analysis software (BRASS).

Results: Calculation of global forebrain perfusion discriminated demented from not demented patients. Compared to controls DCI patients showed hypoperfusion of thalamus, lentiforme nucleus and medial temporal cortex. MCI patients differed significantly from controls concerning perfusion in both hemispheric temporal, parietal and in the (right hemispheric) posterior part of cingulate gyrus areas. MCI and DCI patients differed in parietal, temporal superior and right hemispheric cingulate gyrus posterior cortices. Global forebrain and regional perfusion was more extensively reduced in DAT and discriminated them from controls, MCI and DCI. Frontal perfusion disturbance was only present in DAT patients.

Conclusion: Automated analysis of HMPAO-SPECT MCI patients showed significant perfusion deficits in regions also involved in DAT, but ROC analysis demonstrated only moderate sensitivity and specificity differentiating DAT from controls and DCI. Frontal hypoperfusion seems to correspond with conversion from MCI to DAT. Finally results of DCI patients raises the question of depression as an early symptom of neurodegeneration again.

115

RESIDENT ENDOTHELIAL CELLS SURROUNDING DAMAGED ARTERIAL ENDOTHELIUM REENDOTHELIALIZE THE LESION WITHOUT ANY INVOLVEMENT OF FOREIGN PROGENITOR CELLS

Y. Itoh[1], H. Toriumi[1], S. Yamada[1], Y. Tomita[1], H. Hoshino[2], N. Suzuki[1]

[1]Neurology, [2]Preventive Medicine for Cerebrovascular Disease, Keio University School of Medicine, Shinjuku, Japan

Objective: Endothelial repair of the cerebral artery after its damage is critical for prevention of thrombosis, maintenance of vascular tone and protection of the brain by blood-brain barrier. In this study, we evaluated endothelial repair processes in denuded pial vessels to clarify mechanisms for reconstructing endothelium.

Methods: Tie2-green fluorescent protein (GFP) transgenic mice were employed for the non-invasive identification of endothelial cells (EC). We confirmed through histochemical analysis that Tie2-GFP positive cells were positive for PECAM and von Willebrand factor and were surrounded with cells positive for α-smooth muscle actin. Closed cranial window (3 mm in diameter, with the center at 2.5 mm lateral and 2.5 mm posterior to bregma) with a metal bar to secure the head to a holder was installed under 1.5% isoflurane anesthesia. Tail vein was catheterized for the drug injection. EC in a 350-μm long segment of the middle cerebral artery were damaged through photochemical reaction of intravenously injected rose bengal (20 mg/g weight) with green laser (diameter 250 μm, wave length at 532 nm, light power 150 μW, duration 150 sec).

Results: The endothelial damage induced platelet thrombosis and the artery was loosely occluded at the end of photochemical reaction. Within 6 hours, the artery was recanalized and ECs were detached from the luminal surface of the injured artery, which was then covered with a platelet carpet. Platelets, in the size of 2 to 4 μm, were morphologically identified by confocal laser microscopy in CAG-EGFP mouse as well as in wild type mouse injected with Rhodamine-6G. All cells except red blood cells and hair are fluorescently visualized in CAG-EGFP mouse.

Within 24 hours, re-covering of denuded artery started at the proximal edge and then at the distal one with tips of resident ECs moving toward the defect (fig1). The repair rate was faster at the proximal edge than at the distal one († $p < 0.05$). Elongation and proliferation of ECs were also observed during endothelial repair (fig2. ** $p < 0.01$, * $p < 0.05$ compared with cell length before the endothelial damage). Reendothelialization with EC proliferation peaked at 2-3 days (fig1. maximum rate at 4 μm/hr at the proximal border, ** $p < 0.01$, * $p < 0.05$ compared with baseline) and ended at 5 days together with normalization of EC length. Growth of EC tips at both edges was completely continual in time and in place, and no islands of newly developed ECs distant from preexisting ECs, suggesting possible involvement of foreign progenitor cells, were confirmed.

Conclusions: Our *in vivo* study demonstrated continual reendothelialization processes, i.e. migration, elongation and proliferation of resident ECs, in the pial artery without any involvement of foreign progenitor cells. Therefore resident EC might be a better target to accelerate endothelial repair process. Meanwhile, prevention of thrombosis, vasospasm and treatment for blood-brain barrier dysfunction should be considered.

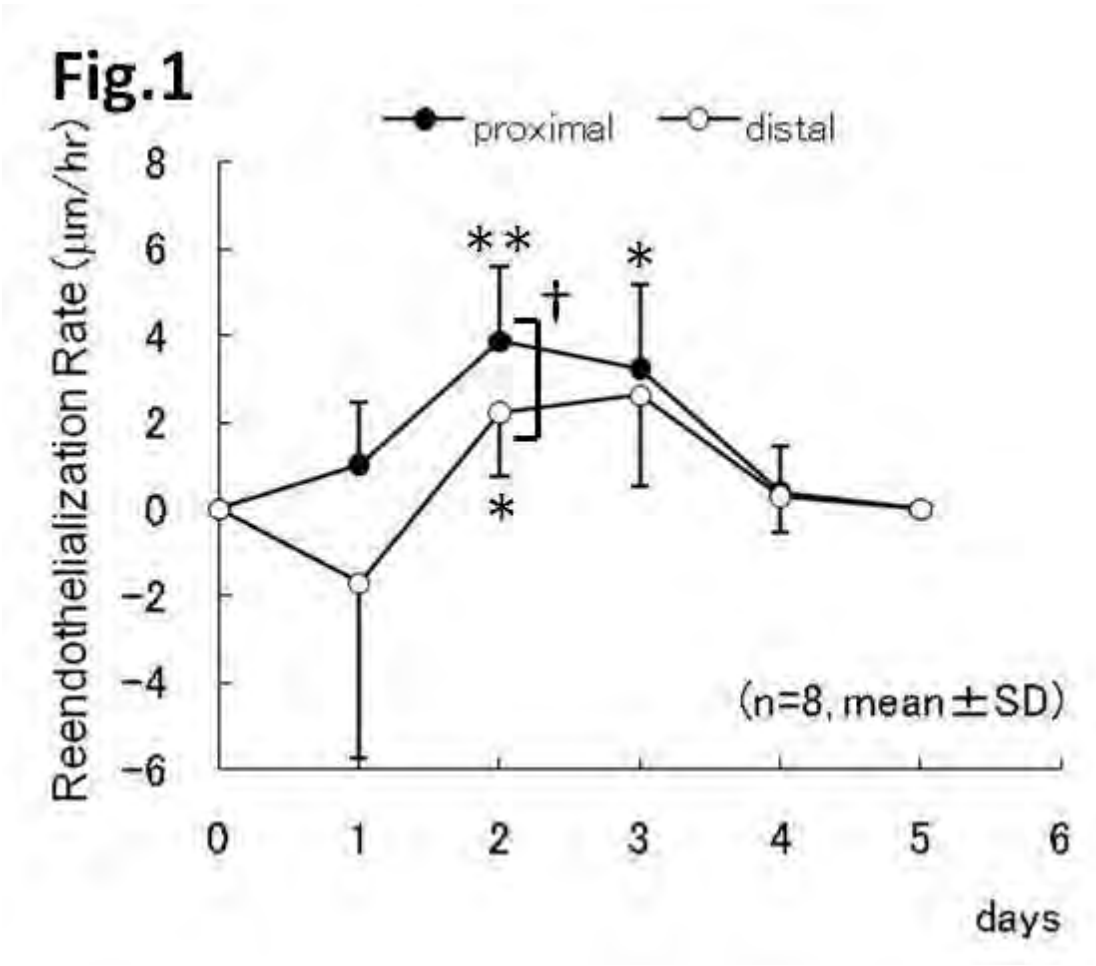
Fig.1
proximal
distal
Reendothelialization Rate (μm/hr)
8
6
4
2
0
−2
−4
−6
**
*
†
*
(n=8, mean±SD)
0
1
2
3
4
5
6
days

[fig1]

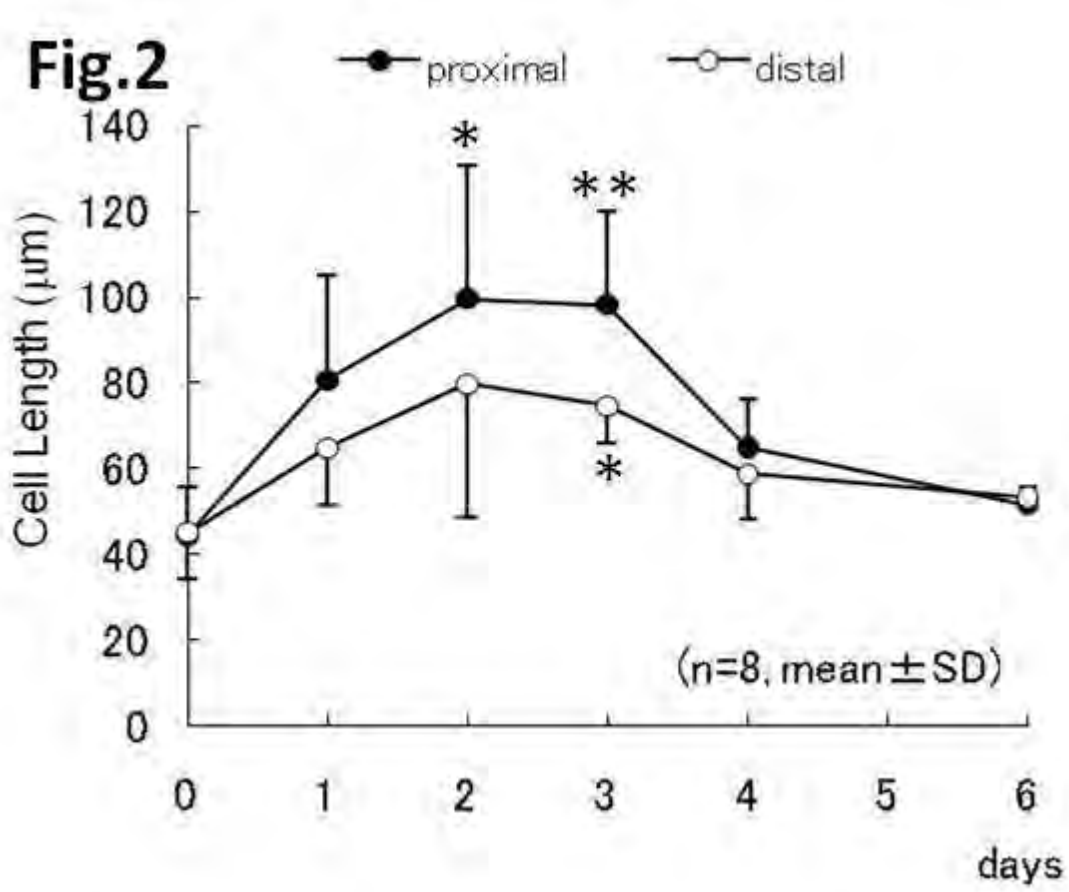
Fig.2
proximal
distal
Cell Length (μm)
140
120
100
80
60
40
20
0
*
**
*
(n=8, mean±SD)
0
1
2
3
4
5
6
days

[fig2]

116

GINSENOSIDE RD FOR ACUTE ISCHEMIC STROKE: LABORATORY AND CLINICAL EVIDENCE

R. Ye[1], Q. Yang[2], Y. Zhang[1], X. Liu[1], J. Yang[3], Y. Yan[4], Y. Song[5], X. Liu[6], H. Ren[7], Y. Wu[8], Z. Li[9], W. Chen[10], Y. Xu[11], J. Xia[12], L. Xiong[2], G. Zhao[1]

[1]Department of Neurology, [2]Department of Anesthesiology, Xijing Hospital, the Fourth Military Medical University, Xi'an, [3]Department of Neurology, Lanzhou Military Command General Hospital, Lanzhou, [4]Department of Neurology, the First Affiliated Hospital of Chongqing University of Medical Sciences, Chongqing, [5]Department of Neurology, the First Hospital of Shaanxi Province, Xi'an, [6]Department of Neurology, Nanjing Military Command General Hospital, Nanjing, [7]Department of Neurology, the First Affiliated Hospital of Kunming Medical College, Kunming, [8]Department of Neurology, the First Affiliated Hospital of Nanchang University, Nanchang, [9]Department of Neurology, School of Medicine, Xi'an Jiaotong University, Xi'an, [10]Department of Neurology, Wuhan General Hospital of Guangzhou Military Command, Wuhan, [11]Department of Neurology, the First Affiliated Hospital of Zhengzhou University, Zhengzhou, [12]Department of Health Statistics, the Fourth Military Medical University, Xi'an, China

Objectives: Ginsenoside Rd (Rd), one of the main active ingredients in *Panax ginseng*, has previously been demonstrated to protect against ischemic insult in vitro and in vivo. Here we sought to systematically define the preclinical characteristics of the neuroprotection afforded by Rd in experimental stroke models, and confirm its efficacy in humans after acute ischemic stroke.

Methods: For experimental investigations, we used permanent and transient middle cerebral artery occlusion (p/tMCAO) to evaluate the effects of Rd. In dose-response study, we compared the efficacy of Rd (0.1-200 mg/Kg) with two other established neuroprotectants: PBN and edaravone. In therapeutic window study, Rd was administered at 0 h, 2 h, 4 h, or 8 h after the reperfusion or the onset of artery occlusion. Infarct volume was measured on post-operative day (POD) 1 and 7, and neurological deficits were assessed up to POD 42 using modified neurological severity scores, modified sticky-tape test, and corner test. Furthermore, we probed whether the protection of Rd is present in females and aged animals. For clinical trial, we conducted a randomized, double-blind, placebo-controlled trial involving 390 patients with acute ischemic stroke in a 3:1 ratio to receive a 14-day intravenous infusion of Rd or placebo within 72 hours after the onset of stroke. The primary end point was the distribution of disability scores on the modified Rankin scale at 90 days. Neurological function score and activities-of-daily-living scale were included as secondary end points.

Results: Rd at the doses of 10-50 mg/Kg significantly reduced the infarct volume and improved the neurological outcome for up to 6 weeks after pMCAO or tMCAO. Subanalysis showed that both cortex and striatum were protected. Comparatively, Rd was significantly more effective than edaravone, and slightly more effective than PBN. Importantly, Rd was effective even when administered up to 4 h after the recirculation of tMCAO or the onset of pMCAO. Furthermore, in female rats or 16-month-old rats, the salutary effects of Rd were still observed and sustained for up to 6 weeks after ischemia. In clinical research, the efficacy analysis was based on 386 patients (Rd group: 290, placebo group: 96). Rd significantly improved the overall distribution of scores on the modified Rankin scale, as compared with the placebo (P = 0.02 by the CMH test; odds ratio: 1.74; 95% CI: 1.08-2.78). There was significant difference between the two groups when we categorized the scores into 0 to 1 versus 2 to 5 (P = 0.01 by the CMH test; odds ratio:

2.32; 95% CI: 1.23-4.38). Besides, Rd improved the National Institutes of Health Stroke Scale ($P < 0.01$ by the analysis of covariance; least squares mean: −0.77; 95% CI: −1.31 to −0.24).

Conclusions: These experimental and clinical results indicate that Rd is a promising neuroprotectant with superior neuroprotective efficacy and wide therapeutic window. Further investigations should be encouraged to confirm whether Rd is beneficial in ischemic stroke.

117

BRAIN EXTRACELLULAR FLUID AND SERUM S-100B LEVELS IN SEVERE TRAUMATIC BRAIN INJURY USING INTRACEREBRAL MICRODIALYSIS

C. Winter

Neurosurgery, Royal Brisbane and Women's Hospital, Brisbane, QLD, Australia

Objectives: To use intracerebral microdialysis to sample the brain extracellular fluid (ECF), enabling us to compare S-100B levels in the brain and intravascular compartments, to comment on ECF and serum S-100B correlation with patient outcome and to suggest a possible relationship with blood brain barrier (BBB) function.

Methods: A prospective study of brain extracellular fluid (ECF) and serum S-100B levels in 12 patients with severe head injury (GCS ≤ 8) was undertaken using intracerebral microdialysis. S-100B levels in both serum and brain ECF dialysate were measured at regular intervals and patient outcomes were assessed at 6 months using the Glasgow Outcome Scale (GOS). The patients were divided into two outcome groups; group A containing 8 survivors with either a good recovery or moderate disability and group B containing 4 patients who died.

Results: Peak serum levels of S-100B were significantly greater in group B (mean 6.03 ng/ml) compared with group A (mean 0.73 ng/ml) (P = 0.009), though 6 of the latter group had values less than the lower limit of detection of the assay. Group A had a mean peak S-100B in the brain extracellular compartment of 186 ng/ml compared to 150 ng/ml in group B. There was no significant difference between the mean peak brain ECF S-100B concentrations between the 2 outcome groups (P = 0.932).

Conclusions: We report that serum S-100B in 12 severely head injured patients was significantly higher in those patients in the poor outcome group, and that there was no significant difference in ECF S-100B between the good outcome and poor outcome groups. These results are consistent with the body of literature which concludes that there exists a strong correlation between elevated serum S-100B and a worse patient outcome following TBI. The brain ECF S-100B levels however suggest that serum S-100B level may not merely be a result of the primary parenchymal damage but may in part reflect blood-brain barrier compromise secondary to the head injury. We suggest that the ratio of brain ECF S-100B to serum S-100B may provide a biochemical measure of BBB function.

References:

1.Blyth BJ, Farhavar A, Gee C, Hawthorn B, He H, Nayak A, Stocklein V, Bazarian JJ. Validation of Serum Markers for Blood-Brain Barrier Disruption in Traumatic Brain Injury. J Neurotrauma. 2009 Sep;26(9):1497-1507

2.Nylen K, Ost M, Csajbok LZ, Nilsson I, Hall C, Blennow K, Nellgard B, Rosengren L. Serum levels of S100B, S100A and S100BB are all related to outcome after severe traumatic brain injury. Acta Neurochir (Wien). 2008 Mar;150(3):221-7, discussion 227

3.Winter CD, Iannotti F, Pringle AK, Trikkas C, Clough GF, Church MK A microdialysis method for the recovery of IL-1beta, IL-6 and nerve growth factor from human brain in vivo. *J Neurosci. Meth.* 2002; 119: 45-50

118

INFLUENCE OF PUMP-FLOW MANAGEMENT DURING SELECTIVE CEREBRAL PERFUSION ON REGIONAL AND GLOBAL CEREBRAL BLOOD FLOW, VASCULAR RESISTANCE AND METABOLIC RATE

P.L. Haldenwang[1], T. Klein[2], O. Liakopoulos[3], M. Zeriouh[3], A. Sterner-Kock[4], H. Christ[5], T. Wahlers[3], J.T. Strauch[1]

[1]Cardiothoracic Surgery, Ruhr University of Bochum, Bochum, [2]University of Cologne, [3]Cardiothoracic Surgery, [4]Experimental Medicine, [5]Institute for Medical Statistics, Informatics and Epidemiology, University of Cologne, Cologne, Germany

Objective: Although hypothermic selective cerebral perfusion (SCP) is widely used for cerebral protection during aortic surgery, little is known about the ideal pump-flow management during this procedure. This study explored cerebral hemodynamics and metabolism at high- vs. low-pump-flow rates.

Methods: 20 pigs (32-38 kg) were cooled on cardiopulmonary bypass (CPB) to 25°C. After 10min of HCA the animals were randomized to 60min of SCP, at two different pump-flow rates : low-flow at 10 ml/kg/min (n=13) vs. high-flow at 20 ml/min (n=7), Fluorescent microspheres were injected at baseline, coolest temperature, respectively at 5,15,25 and 60 min of SCP, to calculate cerebral blood flow (CBF), cerebral vascular resistance (CVR), metabolic rate ($CMRO_2$) sagittal (SSP) and intracranial pressure (ICP) .

Results: Global CBF decreased during cooling to 49% of the baseline value (from 61±13 to 30±17 ml/min/100g). It recovered during the initial 15min of SCP, reaching baseline values in the low-flow perfusion group (65±29 ml/min/100g), with a significant increase (p=0.015) in the high-flow-group (139±41ml/min/100g). After 60 min of SCP the CBF slightly decreased (56±26 ml/min/100g) in the low-flow-group, but showed an dramatic decrease (30±6 ml/min/100g) in the high-flow-group. The pattern of global CBF change as a function of time was seen in all brain areas, with some regional differences: the frontal cortex, the area with the highest regional blood flow (RBF) (70±14 ml/min/100g) offered a mostly stable RBF, with no significant differences between groups after 15min of SCP. During the last 35min of SCP the cortical RBF decreased in both groups, reaching lower levels in the high-flow group (23±8 vs. 47±25 ml/min/100g). The RBF of cerebellum (68±16 ml/min/100g), pons (57±21 ml/min/100g) and hippocampus (42±16 ml/min/100g) remained stable during the first 25 min of low-flow-SCP but increased dramatically during the initial period of high-flow SP to 230%(cerebellum), 500%(pons) respectively 400%(hippocampus). During the last 35min of SCP the RBF decreased in the high-flow-group, reaching only 46%(cerebellum), 87%(pons and hippocampus). CVR increased in all animals during cooling to 25°C: from 1.1±0.4 to 2.2±0.8 mmHg/ml·min·100g. It stayed stable in both groups at 0.6 to 0.9 mmHg/ml·min·100g during the first 25 min of SCP and increased during the last 35 min of SCP to 1.1±0.7 (low-flow) and 2.3±0.7(high-flow). ICP did not change during cooling to 25°C (11±3mmHg). Group differences occurred after starting the SCP: whereas the ICP decreased slowly to 10±2 mmHg at low-flow pressure, it showed a sudden rise to 17±3 mmHg in the high-flow group (p=0.001). SSP changes presented a similar pattern: whereas the low-flow perfusion resulted in a slight SCP decrease, alternating between 7 and 9 mmHg, the high-flow perfusion induced a persistent increase up to 13±3 mmHg (p=0.007). Cooling to 25°C reduced the $CMRO_2$ from 3.5 ±0.7 to 1.0±0.3 ml/min/100g. During SCP it recovered slightly reaching 51% in the low-flow- and 75% in the high-flow group.

Conclusion: High-flow SCP doesn't improve RBF and $CMRO_2$ when compared to low-flow SCP at 25°C: When provided for more than 25 min it increases CVR with following higher ICP and SSP as clinical signs for cerebral edema.

119

THE EFFECTS OF HIGH ALTITUDE AND DEXAMETHASONE ON PLASMA S-100B LEVELS (A MEASURE OF BLOOD-BRAIN BARRIER FUNCTION)

C. Winter[1,2], T. Whyte[1], J. Cardinal[3], R. Kenny[4], S. Rose[5]

[1]Neurosurgery, Royal Brisbane and Women's Hospital, [2]Neurosurgery, University of Queensland, [3]Chemical Pathology, Royal Brisbane and Women's Hospital, Brisbane, QLD, Australia, [4]CAE Solutions, Tokyo, Japan, [5]Centre for Advanced Imaging, University of Queensland, Brisbane, QLD, Australia

Objectives: Acute Mountain Sickness (AMS) or altitude sickness occurs in certain individuals who ascend to high altitude (a hypobaric hypoxic 'stress') and may relate to mild cerebral oedema associated with a disturbed blood-brain barrier (BBB). We aim to evaluate the effect of ascending to high altitude (3700 m) on plasma S-100B levels (a measure of blood-brain barrier function) and seek a correlation with the symptoms of altitude sickness. Dexamethasone is a drug prescribed to treat or prevent the effects of high altitude, and is also known to attenuate BBB dysfunction. We aim to confirm the effects of dexamethasone on both plasma S-100B levels and the symptoms of altitude sickness.

Methods: A prospective study of fourteen healthy subjects who climbed Mt Fuji was undertaken. Serial blood samples were taken at baseline, 1400m, 2590m, 3700m (the summit) and during the descent at 2590m. Further baseline samples were taken over the next two days and the trek was then repeated with samples taken at the same altitudes. Twelve subjects completed both ascents. At the beginning of the second ascent 6 subjects were prescribed a standard course of Dexamethasone used for the prevention and treatment of Acute Mountain Sickness. Each blood sample was centrifuged for 3 minutes at 7,200 rpm (4400 g) using a battery powered portable centrifuge, the plasma pipetted off and placed immediately into dry ice. The volunteers documented Lake Louise Questionnaire assessment of acute mountain sickness at each bleed point.

Results: Baseline plasma S-100B levels taken before the first ascent ranged between 0.08 - 0.53 pg/ml with an average of 0.15 pg/ml for the initial 14 subjects. The range for the peak S-100B values reached during the first ascent was 0.17 - 0.6 pg/ml with the mean average peak value for the first ascent being 0.37 pg/ml. This was an approximate 3 fold rise in the mean average peak plasma S-100B levels compared to baseline. Five of the six subjects who took dexamethasone on the second ascent had a significant reduction in mean average peak value from 0.36 pg/ml during the first ascent to 0.19 pg/ml on the second ascent.

Conclusions: Ascending to 3700m resulted in elevation of plasma S-100B levels suggesting that the hypobaric hypoxic stress resulted in increased 'leakiness' of the BBB. Furthermore, those subjects who were prescribed dexamethasone, a drug known to attenuate BBB dysfunction, showed significantly lower values during the second ascent, further supporting this hypothesis. Plasma S-100B levels did not however correlate with symptoms of altitude sickness, suggesting that although the BBB may become 'leakier' during ascent to high altitude, the development of AMS may relate to other processes or that the BBB dysfunction is one part of a multifactorial aetiology.

References:

1. Blyth BJ, Farhavar A, Gee C, Hawthorn B, He H, Nayak A, Stocklein V, Bazarian JJ.

Validation of Serum Markers for Blood-Brain Barrier Disruption in Traumatic Brain Injury. J Neurotrauma. 2009 Sep;26(9):1497-1507.

120

PROGESTERONE AND ALLOPREGNANOLONE EXACERBATE HYPOXIC-ISCHEMIC BRAIN INJURY IN IMMATURE RATS

M. Tsuji, A. Taguchi, T. Ikeda

Department of Regenerative Medicine and Tissue Engineering, National Cerebral and Cardiovascular Center Research Institute, Suita, Japan

Objectives: Progesterone (PROG) and its metabolite, allopregnanolone (ALLO, 3α-hydroxy-5α-pregnan-20-one, 3α,5α-tetrahydroprogesterone) are neuroactive steroids that are present at high concentrations in the fetal brains of humans and rats. The PROG and ALLO concentrations decrease right after birth. ALLO is a potent positive modulator of γ-aminobutyric acid A ($GABA_A$) receptor function (1). We examined the effect of exogenous administration of these steroids in an immature rat model of hypoxic-ischemic encephalopathy.

Methods: Seven-day-old (experimental paradigm, P7), 14 day-old (P14), and 21 day-old (P21) male and female Wistar rats underwent left carotid artery ligation, followed by 120 min, 80 min, and 50 min of hypoxic (8% oxygen) exposure, respectively. The duration of the hypoxic exposure was optimized to obtain similar degrees of brain injury in each age groups. PROG (10 mg/kg), ALLO (10 mg/kg), or vehicle were administered intraperitoneally, immediately before, and then subcutaneously at 6 h and 24 h after the start of the hypoxic exposure. In a different experimental paradigm, the $GABA_A$ receptor antagonist, Bicuculline (2 mg/kg) was administered intraperitoneally immediately before and subcutaneously, 6 h after each ALLO injection. Seven days after the hypoxic-ischemic insult, the brains were removed and dissected into coronal 2-mm sections. We then measured the area of the contralateral and ipsilateral hemispheres in each brain section. The hemispheric volume for each brain was estimated by summing the hemispheric area of the brain slices and then multiplying by the section interval thickness. We evaluated the neuropathological injury in hematoxylin-eosin-stained sections from four brain regions (cortex, hippocampus, striatum, thalamus) using a semi-quantitative scoring system, as described previously (2).

Results: Treatment with either PROG or ALLO significantly reduced the ipsilateral hemispheric volume after the hypoxic-ischemic insult in P7 ($p < 0.01$) and P14 ($p < 0.05$), but not P21 rats compared with vehicle-treated rats. Both steroid treatments increased (exacerbated) the total neuropathologic injury score in P7 rats, however, only the treatment with PROG showed any statistically significant changes ($p < 0.01$). This detrimental effect was similar in the four brain regions examined. The mortality was significantly higher in the ALLO treated animals ($p < 0.05$). Treatment with lower doses of ALLO (3 mg or 1 mg) was less detrimental. The $GABA_A$ receptor antagonist, Bicuculline partially abolished the exacerbating effect of ALLO.

Conclusions: These findings indicate that both PROG and ALLO exhibit adverse effects in hypoxic-ischemic brain injury in immature rats. Our results in immature rats are in contrast with the results of an adult stroke model that showed neuroprotective effects of the two compounds (3). These contrasting results may be due to developmental changes of $GABA_A$ receptor function. GABA depolarizes immature neurons while hyperpolarizing mature neurons (4). Our studies indicate that $GABA_A$ receptors may be involved in the detrimental effect of ALLO in immature animals.

References:

1. Paul SM, Purdy RH. FASEB J 1992; 6: 2311-22.

2. Tsuji M, et al. Exp Neurol 2004; 189: 58-65.

3. Sayeed I, et al. Ann Emerg Med. 2006; 47: 381-9.

4. Ben-Ari Y, et al. Physiol Rev. 2007; 87: 1215-84.

121

SELECTIVE B_1-ADRENORECEPTOR ANTAGONISTS PROVIDE NEUROPROTECTION AGAINST TRANSIENT FOREBRAIN ISCHEMIA IN RATS

T. Goyagi, T. Nishikawa

Anesthesiology, Akita University Graduate School of Medicine, Akita-City, Japan

Introduction: Selective β_1-adrenoreceptor antagonists provide neuroprotective effects after focal cerebral ischemia in experimental settings[1,2]. Recently, post-treatment but not pre-treatment with β_1-adrenoreceptor antagonists provide neuroprotection after forebrain ishemia[3]. The present study was conducted to evaluate whether selective β_1-antagonists, esmolol and landiolol, would provide brain protection in a dose-response manner following transient forebrain ischemia in rats.

Material and Methods: Adult male S.D. rats were anesthetized with halothane to maintain normocapnia and normoxia. Rats received intravenous infusion of saline 0.5 mL/hr, esmolol 20, 200, 2000 mcg/kg/min, or landiolol 5, 50, 500 mcg/kg/min (n=10 in each group). Infusion was initiated 30 min prior to ischemia and continued for 24 hr. Forebrain ischemia was induced by hemorrhagic hypotension and occlusion of the bilateral carotid arteries, and was confirmed by isoelectric EEG. At the end of 10-min ischemia, rats were reperfused. Neurological examination was done at 1, 4 and 7 days after ischemia. Seven days after ischemia, the brains were stained with hematoxylin and eosin. Intact cells in the CA1 hippocampal region were counted. The data were analyzed using Kruskal-Wallis test and ANOVA. $P < 0.05$ was considered statistically significant.

Results: Neurological deficit scores were lower in the rats treated with esmolol or landiolol at 1 day, 4 days and 7 days after ischemia, compared with saline-treated rats ($P< 0.05$), whereas no difference was found among the different doses of esmolol or landiolol. The number of intact neurons in the CA1 hippocampal region was significantly larger in the rats treated with esmolol or landiolol than saline-treated rats, although there was no difference in the number of intact neurons between esmolol- and landiolol-treated rats.

Conclusion: Administration of selective β_1-adrenoreceptor antagonists improved neurological and histological outcomes following forebrain ischemia in rats, irrespective of their doses.

References

1. Goyagi T, et al. β-Adrenoreceptor antagonists attenuate brain injury following transient focal ischemia in rats. Anesth Analg 103:658-63, 2006.

2. Goyagi T, et al. Post-treatment with selective beta1 adrenoceptor antagonists provides neuroprotection against transient focal ischemia in rats. Brain Res 1343: 213-7, 2010.

3. Iwata M, et. al. Posttreatment but not pretreatment with selective β-adrenoreceptor 1 antagonists provides neuroprotection in the hippocampus in rats subjected to transient forebrain ischemia. Anesth Analg 110:1126-1132, 2010.

122

METASTATIC BRAIN NEOPLASM: PRELIMINARY PERFUSION CT STUDY

C.C.T. Lim[1,2], D.L.H. Cheong[1,3], K. Lim[4], T.S. Koh[5,6]

*[1]Neuroradiology, National Neuroscience Institute, [2]Neurology, Duke NUS Graduate Medical School, Singapore, [3]A*Star-NUS Clinical Imaging Research Center, National University of Singapore, 117456, [4]Radiation Oncology, National University Hospital, Singapore, [5]School of Electrical and Electronic Engineering, Nanyang Technological University, 639798, [6]Department of Oncologic Imaging, National Cancer Center, 169610, Singapore*

Background and aims: Cerebral metastases depend on angioneogenesis to recruit blood supply. Although tumor perfusion may predict control and outcome, to date perfusion changes in response to radiotherapy have not been well studied. We used longitudinal dynamic contrast enhanced reducing temporal resolution CT perfusion (CTP) before and after radiotherapy to study tumor perfusion and permeability in cerebral metastasis.

Patients and methods: Patients with four or fewer cerebral metastases from lung cancer and being treated with palliative whole brain radiotherapy (WBRT) were enrolled after IRB approval. Serial CTP before, 0, 6 and 16 weeks after WBRT were obtained for the largest tumor. CTP were done at a reducing temporal resolution manner where scan duration of 90 s was covered by 30 acquisitions at reducing temporal resolutions of 1, 2, 4 and 8 s for acquisitions 1-10, 11-20, 21-25, and 26-30, respectively. Microcirculation parameters of intracranial tumors including cerebral blood flow (CBF), volume (CBV), vascular mean transit time (MTT) and permeability (PS) were determined using a two-compartment distributed parameter method.

Results: Two woman patients (aged 58 and 46 years) completed enrollment.

Patient 1 only completed first two scans with the largest metastatic tumor diameter showing only slight decrease (from 31 to 29mm) before and after WBRT. Most CTP parameters also had insignificant changes (Fig 1, circles) although PS had the largest increase (from 37.12±49.89 to 42.77±70.77 ml/min/100ml). Four months after diagnosis of brain metastasis, MRI showed stable tumor response.

Patient 2 had two metastatses within the CTP coverage (Fig 2). The largest tumor largest diameter reduced from 27 mm before WBRT to 16 mm 22 weeks after WBRT. All CTP parameters of the two tumors (Fig 1, triangles and squares) decreased from before WBRT to 16 weeks after WBRT (Fig 2 rightmost column). However, PS was very high at 6 weeks after WBRT for the largest tumor (410.71±491.69 ml/min/100ml) and at immediately after WBRT for the smaller tumor (470.20±617.70). 11 months after diagnosis, the largest metastatic tumor progressed (largest diameter 40 mm) and required surgical removal. The other smaller tumors remained in stable response.

Conclusion: The reducing temporal resolution acquisition strategy allows tracking of contrast enhancement for longer time with lesser CT acquisitions thereby may improve quality of CTP parameters such as PS and reduces the radiation dosage. Preliminary results suggest that persistent increased of PS immediately and 6 weeks after radiotherapy may be a marker of late relapse, even though CTP findings 16 weeks after radiotherapy showed normalization.

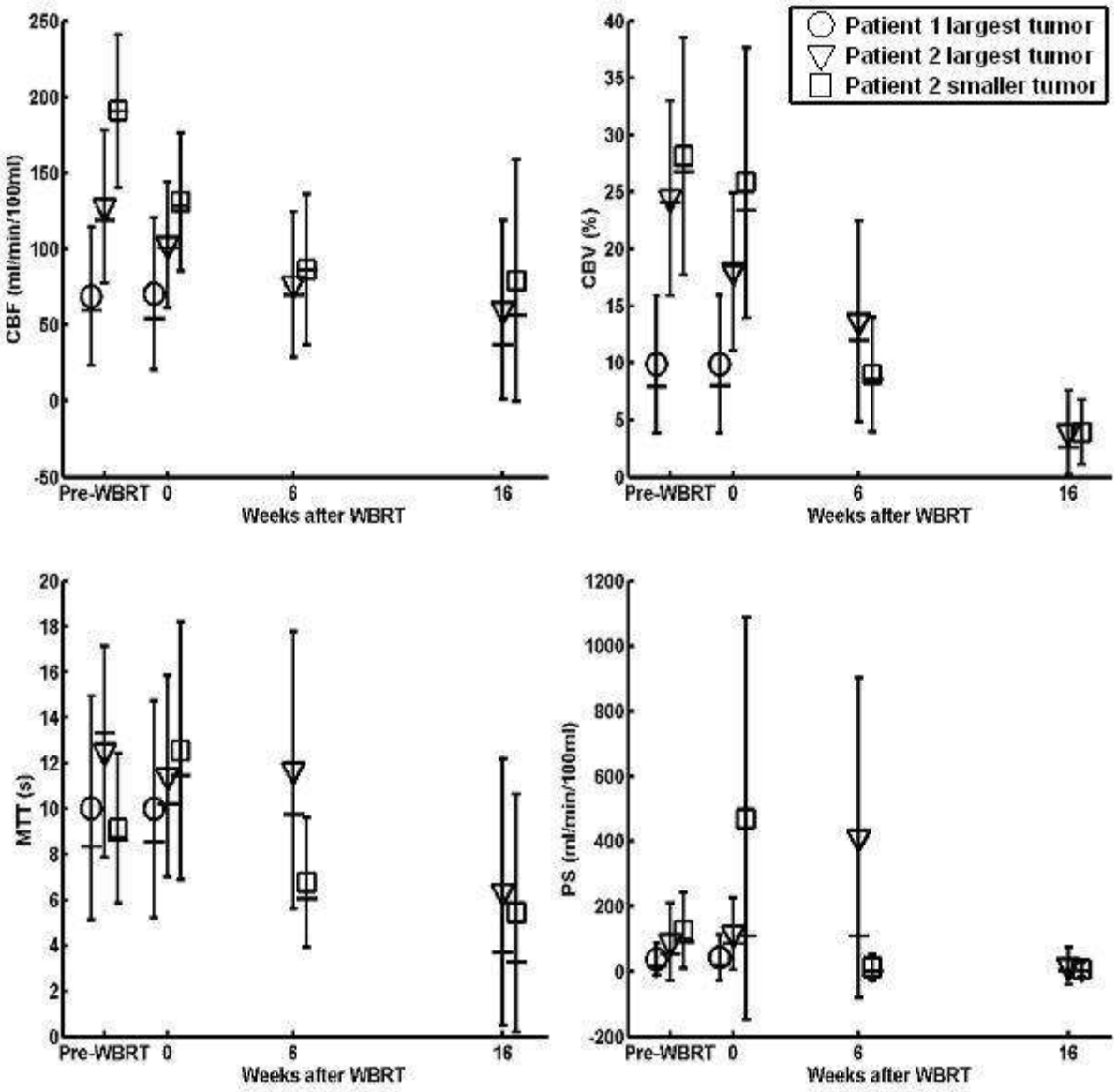

[Fig 1. CTP parameters mean±SD and median (dash)]

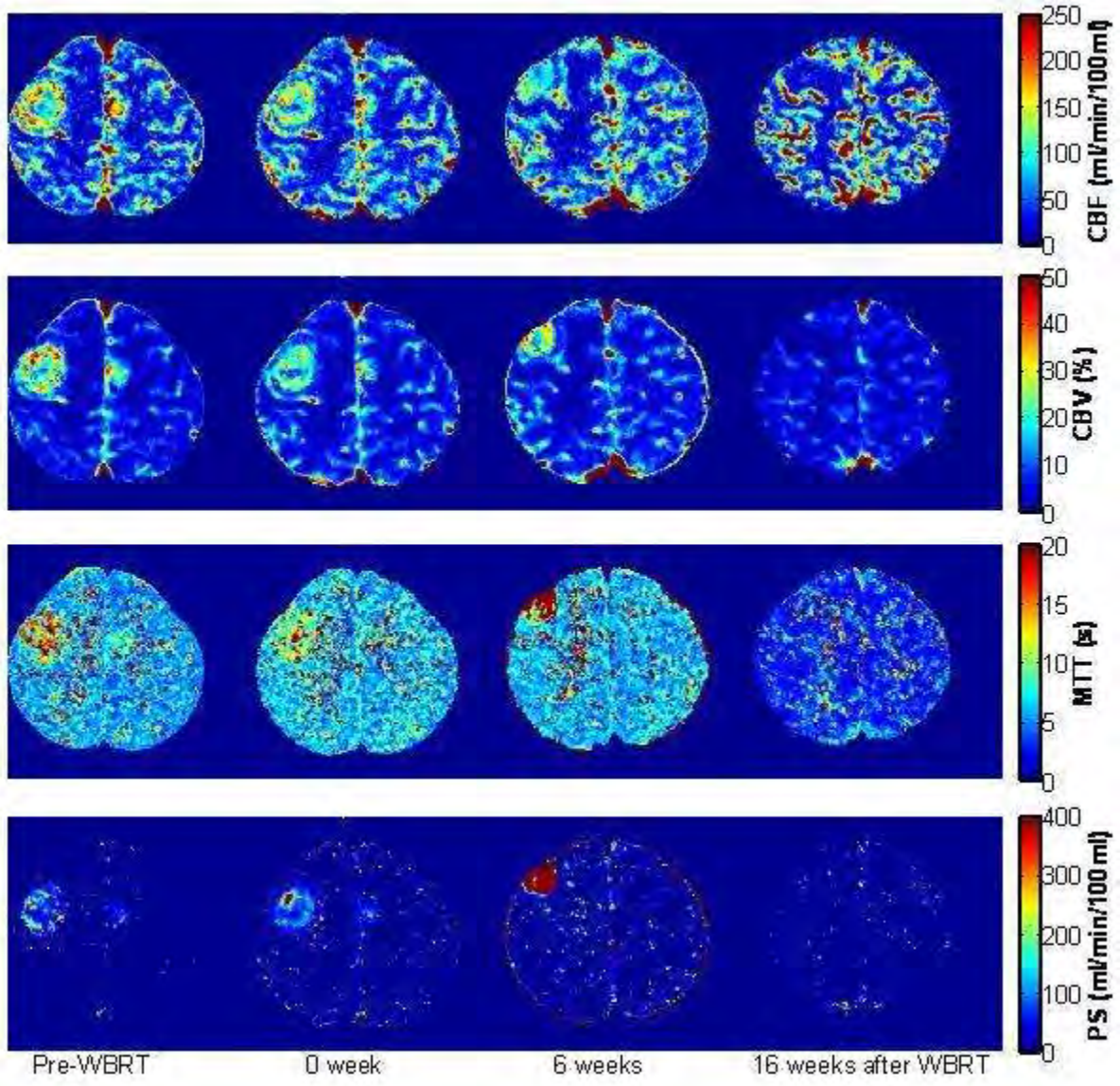

[Fig 2. Patient 2 longitudinal CTP parameter maps]

123

HUMAN CHROMOSOME 21 AND NEUROPATHOGENESIS OF DOWN SYNDROME: ASSOCIATION BETWEEN GENE OVERDOSAGE, BRAIN ABNORMALITIES, AND MENTAL RETARDATION

M. Rachidi, C. Lopes

University of French Polynesia, Punaauia, French Polynesia

Down syndrome (DS), caused by a genomic imbalance of human chromosome 21 (HSA21), is mainly observed as trisomy 21 and is the major genetic cause of mental retardation (MR). MR and associated neurological and behavioural alterations results from dysregulation in critical HSA21 genes and associated molecular pathways. Gene expression, transcriptome, proteome and functional genomics studies, in human, trisomic and transgenic mouse models have shown similar genotype/phenotype correlation and parallel outcomes suggesting that the same evolutionarily conserved genetic programs are perturbed by gene-dosage effects. The expression variations caused by this gene-dosage imbalance may firstly induce brain functional variations at cellular level, as primary phenotypes, and finaly induce neuromorphological alterations and cognitive deficits as secondary phenotypes. The identification of trisomic genes overexpressed in the brain and their function, their developmental regulated expression and their downstream effects, their interaction with other proteins, and their involvement in regulatory and metabolic pathways is giving a clearer view of the origin of the MR in DS. This lead to the identification of potential targets in the altered molecular pathways involved in mental retardation pathogenesis, such as Calcineurin, NFATs and MAPK pathways, that may be potentially corrected, in the perspective of new therapeutic approaches. Treatment of DS mouse models with NMDA receptor or $GABA_A$ antagonists allowed post-drug rescue of cognitive deficits. Besides these new pharmacotherapies, the regulation of gene expression by microRNAs or small interfering RNAs provide exciting possibilities for exogenous correction of the aberrant gene expression in DS and provide potential directions for clinical therapeutics of mental retardation. Herein, we highlight the genetic networks and molecular mechanisms implicated in the pathogenesis of mental retardation in Down syndrome and, thereafter, we outline some of the therapeutic strategies for the treatment of this yet incurable cognitive disorder with hard impact on public health.

125

FUSION OF NEAR-INFRARED AND MAGNETIC RESONANCE SPECTROSCOPY DELIVERS NOVEL MULTIMODAL INVESTIGATION OF NEONATAL HYPOXIC-ISCHAEMIC BRAIN INJURY

I. Tachtsidis[1], A. Bainbridge[2], S. Faulkner[3], S. Mahoney[1], D. Price[2], D. Thomas[4], E. Cady[2], N. Robertson[3], X. Golay[4]

[1]Medical Physics and Bioengineering, University College London, [2]Medical Physics and Bioengineering, University College London Hospitals, [3]Institute for Women's Health, [4]Institute of Neurology, University College London, London, UK

Introduction: Neonatal brain injury after hypoxia-ischaemia (HI) involves a complex cascade of events involving initial necrosis and delayed programmed cell death. Using magnetic resonance spectroscopy (MRS), our piglet model previously defined the biphasic pattern of energy disruption during and after HI[1]. However, the precise relationship between energy failure and cell death remains unclear.

Aim: To combine near-infrared spectroscopy (NIRS) with MRS during and after cerebral HI in the piglet thereby enabling simultaneous measurement of cerebral oxygenation, haemodynamics and energy metabolism.

Methods: Experiments were under UK Home Office guidelines. An anaesthetised and ventilated newborn piglet (aged < 24hr) was positioned in the bore of a 9.4 Tesla Varian spectrometer with a 60mm diameter MRS surface coil and two end-on optodes (~30mm apart, midline equidistant) on the intact scalp.

Whole-brain proton (1H) and phosphorus (31P) MRS were acquired every minute. 1H MRS used PRESS (repetition time (TR) 5sec, echo time 288ms, 12 averages, 2x2x2cm voxel centred entirely within brain); 31P MRS used simple pulse-acquisition (TR 10sec, 12 averages). Spectra were analysed (AMARES; jMRUI software) to give the peak-area ratios Lactate (Lac)/N-acetylaspartate (NAA), NAA/creatine (Cr), phosphocreatine (PCr)/inorganic phosphate (Pi), and nucleotide triphosphate (NTP)/total exchangeable phosphate (epp=PCr+Pi+3NTP).

Broadband light was passed through a 610nm long-pass filter and transmitted to the head via an optic-fibre bundle. Reflected NIRS spectra (650-980nm) were collected via a second optic-fiber bundle onto a spectrograph with a cooled CCD detector. Exposure was typically 1-2sec. Absolute changes in oxyhaemoglobin ($\Delta[HbO_2]$), deoxyhaemoglobin (Δ[HHb]) and cytochrome-c-oxidase redox state (Δ[ox-redCCO]) were measured; concentration changes in total haemoglobin ($\Delta[HbT]=\Delta[HbO_2]+\Delta$[HHb]) and haemoglobin difference ($\Delta[Hbdiff]=\Delta[HbO_2]-\Delta$[HHb]) were then derived. Simultaneous 31P MRS and NIRS were done during brief hypoxia (SaO_2 down to 60%) and 1H MRS and NIRS during HI (~25mins bilateral carotid occlusion and hypoxia).

Results: Brief hypoxia alone resulted in large changes in brain oxygenation and haemodynamics(Fig.1(a)). However,Δ[ox-redCCO], PCr/Pi, and NTP/epp remained in their normal ranges. These results contrast with our recent healthy adult studies were we demonstrated significant linear correlation between estimated cerebral oxygen delivery and Δ[ox-redCCO][2].

HI resulted in a rapid drop in brain oxygenation closely followed by a reduction in Δ[ox-redCCO];

NAA/Cr declined quickly with Lac/NAA increasing shortly afterwards (Fig.1(b)). Upon insult reversal there was a hyperaemic phase followed by slow recovery of brain oxygenation. During recovery there was a period of reduced Δ[ox-redCCO] and increased oxygenation while Lac/NAA began to decline followed by [ox-redCCO] overshoot.

Conclusion: Combining MRS with NIRS data suggest a switching between anaerobic and aerobic metabolism during HI and a hyperoxic phase at the start of reperfusion. Such multimodal imaging may improve understanding of the haemodynamic and metabolic responses of newborn brain during and after HI and the relation between cell death and energetics; and may direct therapies targeting oxidative stress immediately post HI.

References:

[1]Lorek A. et al. Pediatr.Res.,36,699-706(1994).

[2]Tisdall M. et al. JBO,12:2,024002(2007).

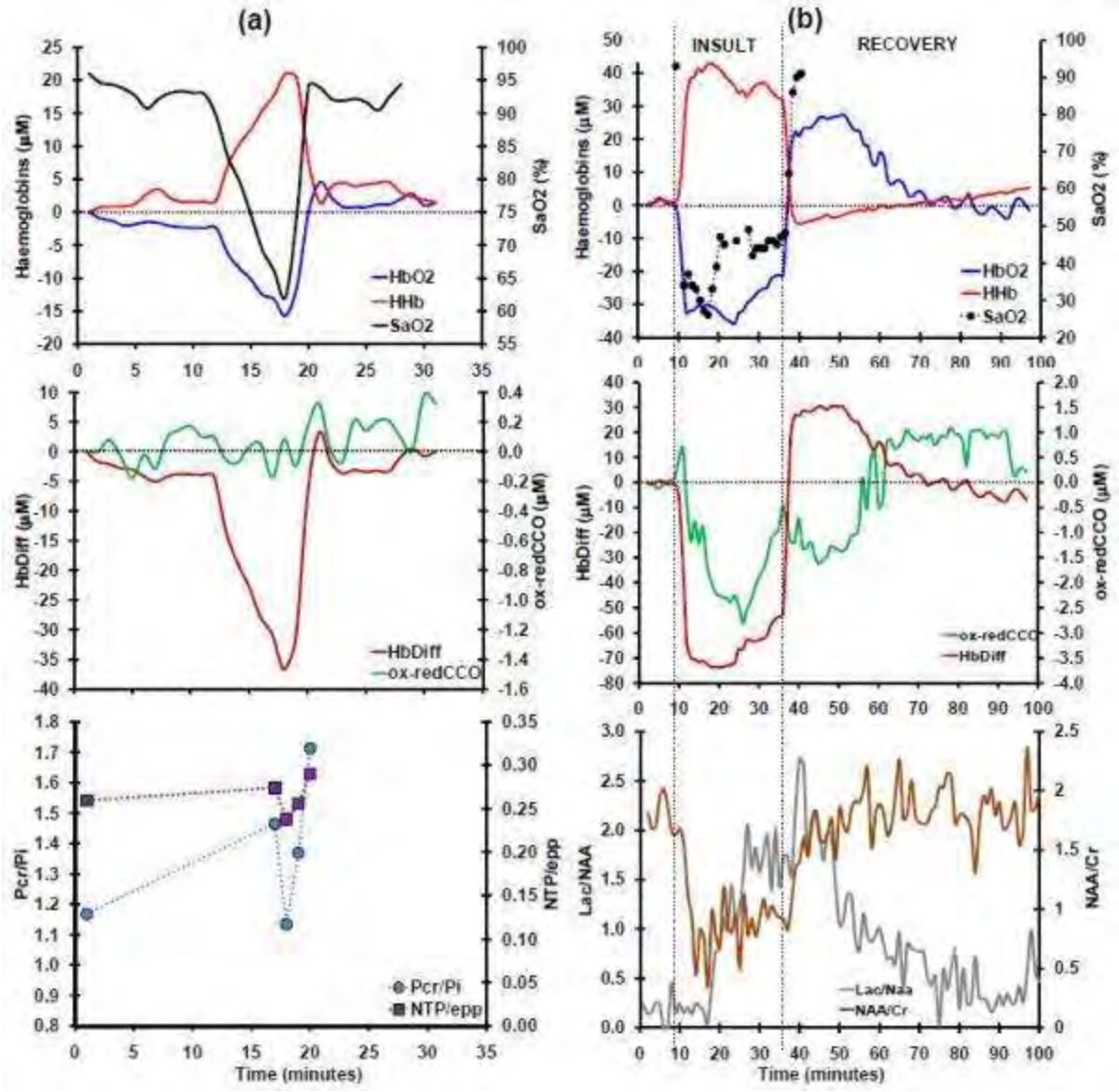

[Figure 1]

(a)31P MRS and NIRS results during the brief hypoxia; (b)1H MRS and NIRS results during the HI.

126

BRADYKININ-ANTAGONIST ABOLISHES THE EFFECT OF ANGIOTENSIN CONVERTING ENZYME INHIBITORS AND ANGIOTENSIN RECEPTOR BLOCKERS ON THE LOWER LIMIT OF CBF AUTOREGULATION

O.B. Paulson[1,2], S.T. Sigurdsson[1,3], A.H. Nielsen[3], S. Strandgaard[3]

[1]Neurobiology Research Unit, N-9201, Copenhagen University Hospital, Rigshospitalet, Copenhagen, [2]Danish Research Center for Magnetic Resonance, Copenhagen University Hospital, Hvidovre, [3]Dept. of Nephrology, Copenhagen University Hospital, Herlev, Denmark

Objectives: Autoregulation denotes the constancy of cerebral blood flow (CBF) within rather wide physiological limits of arterial blood pressure; below a certain limit of blood pressure CBF starts to decline..The lower limit of autoregulation of CBF can be modulated with both angiotensin converting enzyme (ACE) inhibitors and angiotensin receptor blockers (ARB). The bradykinin 2 (B2) receptor antagonist (Hoe 140) abolishes the effect of ACE-inhibition on autoregulation of CBF. The influence of bradykinin antagonism on ARB-induced changes was the subject of this study.

Methods: CBF was measured in Sprague-Dawley rats with laser Doppler technique. The blood pressure was lowered by controlled and stepwise bleeding. Six groups of rats were studied: a control group and five groups given drugs intravenously: an ACE-inhibitor (enalaprilat), an ARB (candesartan), Hoe 140, a combination of enalaprilat and Hoe 140, and a combination of candesartan and Hoe 140.

Results: In the control group the lower limit of CBF autoregulation was 54 ± 9 mmHg (mean ± SD), in the enalaprilat group 46 ± 6, with candesartan it was 39 ± 8, with Hoe 140 53 ± 6, with enalaprilat/Hoe 140 52 ± 6, and with candesartan/Hoe 140 50 ± 7. There was a statistically significant difference between both the enalaprilat group and the candesartan group vs. control. Bradykinin-inhibition with Hoe 140 abolished the effect of enalaprilat and candesartan on autoregulation of CBF.

Conclusion: The bradykinin antagonist abolished not only the effect of the ACE inhibitor but also the effect of the ARB on the lower limit of CBF autoregulation. Thus, bradykinin seems to have an integral role in how the RAS modulates the cerebral circulation.

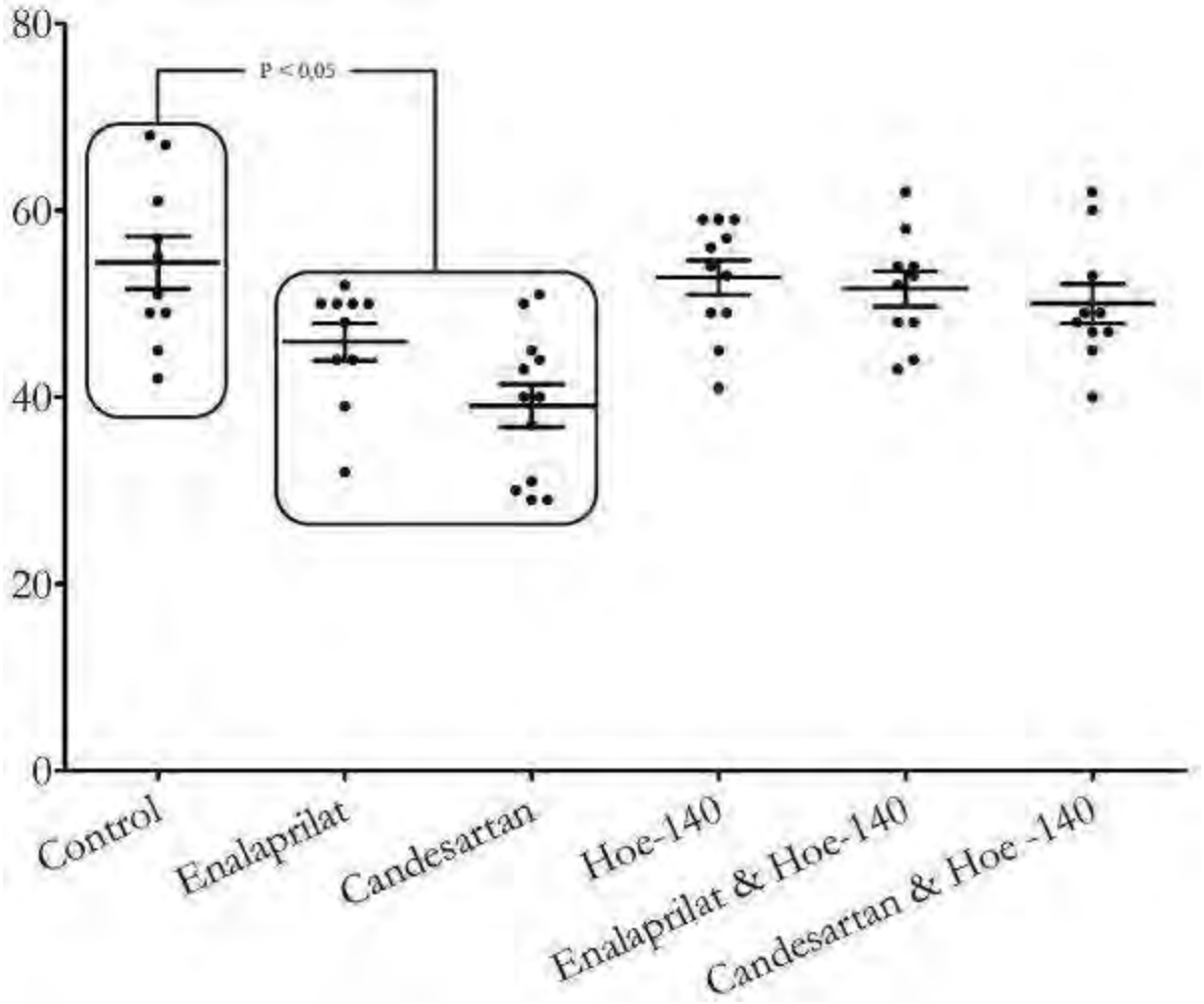

[Figure]

The figure shows a scatter plot of the results and the bars are standard error of means. The reduction of the lower limit of CBF autoregulation following inhibition of angiotensin by ACE-inhibitors or ARB is abolished by the bradykinin receptor blocker.

128

TOF-PET DETECTOR DEVELOPMENT AND IDENTIFICATION OF TINY TUMORS USING BRAIN PHANTOM

N.N. Mondal

Physics Group, Variable Energy Cyclotron Center (VECC), Kolkata, India

It is important to keep on eye on detection efficiency, energy, time and spatial resolutions, resolving power, signal to noise ratio (SNR) and so on, when a TOF-PET detector is developed. This kind of information can be perceived earlier of the proposed detector by the help of Monte Carlo Simulation (MCS) based on GEANT. An extensive MCS studies are performed in order to find detection efficiencies, spatial resolutions and resolving powers of the TOF-PET detector. Cerium activated Lutetium Oxyorthosilicate (Lu_2SiO_5:Ce in short LSO), Barium Fluoride (BaF_2) and BriLanCe 380 (Cerium doped Lanthanum tri-Bromide, in short $LaBr_3$) scintillation crystals are studied in view of their good time and energy resolutions and shorter decay times. The results of MCS show that spatial resolution, detection efficiency and resolving power of LSO are better than those of BaF_2 and $LaBr_3$, although it possesses inferior time and energy resolutions. Instead of the conventional position reconstruction method, position vector (PV) method is utilized in order to produce high-tech images. Validation is a momentous step to ensure that this imaging method fulfills all purposes of motivation will be discussed by reconstructing images of two tiny tumors in a brain phantom. X-ray, CT, MRI, NMR, TOF-PET and PET/CT imaging techniques are available. RPC-PET and GEM-PET are now in R&D stage and their performance will be discussed.

129

IMPACT OF ISCHEMIC PRECONDITIONING ON EXCITATORY POSTSYNAPTIC CURRENT (EPSC) AND AMPA / KAINATE-ACTIVATED CURRENTS IN PRIMARY CORTICAL NEURONS

S. Maysami[1,2], A. Pearson[2], V. Jessick[2], R. Simon[2], Z. Xiong[2], R. Meller[2]

[1]Faculty of Life Sciences, The University of Manchester, Manchester, UK, [2]Dow Neurobiology, Legacy Health Research, Portland, OR, USA

Ischemic preconditioning is described as non-injurious ischemic stimuli that activate different signaling pathways to protect neuronal cells from a subsequent injurious ischemic insult. Rapid ischemic tolerance occurs 30 -60 min following the preconditioning event, and our recent studies suggest a synaptic mechanism may mediate the protection. Here we report our observations on primary cortical neurons from rat (Sprague-Dawley: 14 DIV) subjected to brief oxygen-glucose deprivation (30 min: ischemic preconditioning). Preconditioning significantly reduced the frequency of EPSCs recorded from cortical neurons, when measured approximately 30-45 min after 30min preconditioning (oxygen-glucose deprivation). Ischemic preconditioning reduced AMPA and kainate-activated current amplitude and increased the desensitization time constant of AMPA-activated current. Concentration response demonstrated a shift to the right in both AMPA and kainate current amplitude. Hence, here we demonstrate for the first time that ischemic preconditioning can regulate EPSC and kinetics of AMPA / Kainate activated currents in neurons to potentially minimize the susceptibility of these cells to ischemic-injury.

This work is supported by NIH grant R01 NS059588 to R. Meller.

133

GLIAL GLYCOLYTIC GAPDH ACTIVITY MODULATES THE RESTING CEREBRAL METABOLIC RATE OF GLUCOSE AND CA^{+2}- DEPENDENT EXCITATORY NEUROTRANSMITTER RELEASE

C. Poitry-Yamate[1], M. Cotte[2], A. Giannocelli[3], L. Lecomte[1], B. Lanz[1], M. Jourdain[1], J. Susini[2], G. Margaritondo[1], R. Gruetter[1]

[1]Centre d'Imagerie Biomédicale, Ecole Polytechnique Fédérale de Lausanne, Lausanne, Switzerland, [2]European Synchrotron Radiation Facility, Grenoble, France, [3]ELETTRA Synchrotron Facility, Trieste-Basovizza, Italy

Objective: CMR_{02}/CMR_{glc} human PET studies indicate that the brain uses glycolysis independently, or in combination with oxidative metabolism during evoked functional brain activity (1). We addressed the question whether this occurs during resting functional brain activity to elucidate cellular compartmentation of brain energy metabolism that underlies function. The direct contribution of glycolysis to resting CMR_{glc} was assessed using iodoacetate (IAA), an inhibitor of glycolysis. The thio-ether bond between IAA with the active center of GAPDH enabled identifying the cellular locus of IAA, and assessing the cell-type specific role of GAPDH activity on resting CMRglc and Ca^{+2}-dependent neurotransmitter release.

Methods: Dynamic *in vivo* γ photon-based ^{18}FDG PET and *β* photon-based ^{18}FDG detection were performed in parallel, in the presence and absence of IAA (50-55mg/kg), to determine the time course of DG in rat cerebral tissue and blood. The cellular distribution of endogenous Ca^{+2}, and exogenous IAA and Mn, a calcium analogue, were determined in a CNS model of the dark-adapted retina *ex vivo* using synchrotron based high energy x-ray fluorescence (HEXRF) mapping and spectromicroscopy.

Results: CMR_{glc} was 20.4 ± 0.6 µmol/100g/min, an expected metabolic activity in rodents under isoflurane anesthesia (2). Glycolysis contributed >35% to resting CMRglc as deduced from CMR_{glc} in the presence of IAA. IAA exerted its effect in 3 additional ways: steady-state levels of ^{18}FDG6P were lowered >30%; imaged ^{18}FDG6P across the brain was fairly uniform, yet the regional variance of ^{18}FDG6P within a volume of interest was raised by > 70%, suggesting that IAA --a derivative of acetate, a glial-specific substrate - had a differential effect on the brain's major cell types. HEXRF mapping demonstrated IAA's localization to glia and its absence in excitatory and inhibitory neurons. Synaptosomal calcium/Mn uptake into first -and second-order excitatory retinal neurons was moreover reduced by 75% and >95% by IAA binding to GAPDH.

Conclusion: These results indicate that glycolysis alone can contribute substantially to resting CMR_{glc}, and that the flow of glucose through glycolysis and oxidative metabolism is not necessarily continuous within the same cell. Since GAPDH isoforms are reported to catalyze either glycolytic flux or synaptic vesicular glutamate uptake/vesicle-membrane fusion activity, but not both (3,4), the present study suggests a role for glial glycolytic GAPDH activity in supporting basal CMR_{glc} and Ca^{+2}-dependent excitatory neurotransmitter release. This imposes an obligatory coupling between oxidative CMR_{glc} in neurons and glycolysis in glia.

References:

(1) Fox PT et al., 1988. Science, 241:462-464.

(2) Toyama H et al., 2004. J Nucl Med 45:1398-1405.

(3) Glaser PE et al., 2002. Proc Natl Acad Sci. 99:14104-14109.

(4) Ikemoto A et al., 2003. J Biol Chem 278: 5929-5940.

134

THE SPATIO-TEMPORAL DISTRIBUTION OF SMOOTH MUSCLE ACTIN-POSITIVE CELLS IN A RAT MODEL OF STROKE: THE EXPRESSION OF DEFINITIVE CELL MARKERS

P.J. Wookey[1], V. Sharma[2], T.W. Ling[2], S.S. Rewell[1], D.L. Hare[1], D.W. Howells[3]

[1]Medicine, University of Melbourne, [2]Cardiology, Austin Health, [3]Florey Neurosciences Institute, University of Melbourne, Heidelberg, VIC, Australia

Introduction: In brain, non-neuronal cell types that are activated following ischaemic events are thought to play an important role in the restriction of damage, particularly neuronal death, around and within the infarct. However, the identity of cell types is often complicated by the limited range of specific markers tested and poor resolution of markers in relation to cell structure. Knowledge of these cells might aid in the formulation of strategies to restrict damage and its neurological consequences.

Aims: In the spontaneous hypertensive rat (SHR) model of induced stroke, the spatio-temporal distribution of smooth muscle actin-positive (αSMA+) cells was investigated in the peri-infarct region. Furthermore, additional markers expressed by these cells were investigated to confirm cell identity. Finally, the expression of feline leukaemia virus C receptor 2 (FLVCR2) recently associated with pericytes in the developing brain was also investigated.

Methods: The SHR model of stroke was generated by the temporary occlusion of the middle cerebral artery which resulted in an infarct in the region of the lateral striatum and the cortex of the frontal lobe. Staining of αSMA+ cells for spatio-temporal analysis was performed using a standard immuno-histochemical protocol including an amplification step. A series of coronal paraffin sections was cut through the region of infarct from at least two brains. Every third section was processed and stained using a monoclonal antibody against αSMA. The images were captured at high magnification and analysed using MCID software with settings adjusted such that the brown stain was highlighted. Secondly, frozen sections were also cut in the coronal and sagittal planes, and positive cells that expressed αSMA, NG2, glial acidic fibrillary protein (GFAP) and FLVCR2 analysed using multi-channel immuno-fluorescence and confocal microscopy with Z-plane devolution to confirm coincident expression.

Results: At day 3 (post-ischaemic insult), on the ipsilateral compared to contralateral side, high densities of αSMA+ cells were located principally in three main concentrations. The first (A) being the most dense, was found in the medial corpus callosum, adjacent to the junction between the striatum and lateral ventricle. The second (B, < dense than A) was located further ventral approximately midway through the striatum adjacent to the lateral ventricle, and the third (C, low density), on the lateral border of the striatum, adjacent the dorsal endopiriform nucleus. By day 7, few cells in these regions were αSMA+. Confocal analysis of individual αSMA+ cells demonstrated both GFAP+ (predominant in A) and GFAP- (predominant in B & C) phenotypes corresponding to astroglia and putative pericytes, respectively. In B & C two morphologically distinct populations of pericytes were evident, one integrated in vessel walls and the other loosely associated with micro-vessels. FLVCR2 was expressed by the putative pericytes and a subset of the GFAP+ cells.

Conclusions: Putative pericytes (αSMA+, GFAP-) and astrocytes (αSMA+, GFAP+) were discovered in the peri-infarct region principally located in three defined regions with maximal numbers about day 3 post-ischaemia. This peak coincides with the period of maximal neuronal death in the infarct region and suggests a role for these cells in restricting damage.

135

HIGENAMINE PROTECTS HYPOXIA-INDUCED BRAIN APOPTOSIS BY ACTIVATION OF NRF-2 AND PI3K PATHWAYS AND REDUCES HMGB1 RELEASE

Y.M. Ha[1], M.K. Park[2], H.J. Kim[1], H.G. Seo[1], J.H. Lee[1], **K.C. Chang**[1]

[1]Gyeongsang National University, Jinju, [2]Seoul National University, Seoul, Republic of Korea

Ischemic stroke causes a very extensive health problem throughout the world. Reactive oxygen species (ROS) and inflammation play key roles in ischemic injury in the brain. The purpose of this study was to test our hypothesis that higenamine protects brain cells from ischemic damage, in which heme oxygenase (HO)-1 induction plays a key role. Higenamine increased HO-1 expression in C6 cells in both hypoxia and normoxia, in which the former was much more significant than the latter. Higenamine significantly and concentration-dependently protected the C6 cells against hypoxic injury. The increased cell viability by higenamine in hypoxia was significantly inhibited by ZnPPIX, an inhibitor of HO-1. Phosphoinositol-3-kinase inhibitor, LY 294002 inhibited increasing phosphorylation of Akt and HO-1 induction by higenamine in C6 cells. Higenamine increased Nrf-2 luciferase activity and translocated Nrf-2 to nucleus in C6 cells. Apoptosis induced by glucose/glucose oxidase in C6 cells was prevented by higenamine, which effect was reversed by LY 294002. Administration of higenamine (i.p) significantly reduced brain infarct size, mortality rate, blood MPO activity and tissue expression of HMGB1 in middle cerebral artery occluded rats, which were inhibited by ZnPPIX. Recombinant HMGB1 caused apoptosis in C6 cells by increasing Bax/bcl-2 ratio and cytochrome c release, which was diminished by higenamine. Taken together, it is concluded that higenamine, at least in part, protects brain cells against hypoxic damages by up-regulation of HO-1. Thus, higenamine may be beneficial for the use of ischemic injuries such as stroke.

138

INFLAMMATORY CYTOKINES CAN INCREASE THE PERMEABILITY OF BLOOD-BRAIN BARRIER IN HIGH ALTITUDE CEREBRAL EDEMA

Q.Q. Zhou, Y.J. Luo, P. Guo

Department of High Altitude Disease,College of High Altitude Military Medicine, Third Military Medical University, Chongqing, China

Background: Inflammatory cytokines can increase of permeability of blood-brain barrier (BBB) in the cerebral edema. Whether high altitude hypoxia environment exposure could raise the permeability of blood-brain barrier wasn't clear.

Objective: To explore the relationship between the permeability change of BBB and inflammatory cytokines in rats which were exposed to the different altitudes.

Methods: The rats were directly exposed in the different altitudes and time, the contents of TNFα, ET in brain were measured by radioimmunoassay, the activities of NO, SOD, MDA, GSH AND GSH-PX in the brain were measured by chemical method, the content of VEGF in the brain was detected using ELISA, the permeability of blood-brain barrier was measured by EB transmittance, and the percentage of brain water content by brain wet-dry gravimetric method.

Results: The activities of VEGF, TNFα, ET, NO, SOD, MDA and GSH in the rats' brain were gradually roused with the increase of altitude and exposure time. The most obvious increase of activity was found in high altitude area (5000m)-9d group. Meanwhile, the permeability of BBB to EB and brain water content also elevated accordingly. Histo- and ultramicrostructure detections showed that there were many lanthanum nitrate granules leaking from the cortex vessel of rat brain. Furthermore, the content of brain inflammatory mediators and brain water contents is positively correlated. These suggested that VEGF, TNFα, ET, NO, SOD and MDA played an important role in the increase of the permeability of BBB, which involved in the high altitude cerebral edema.

Conclusion: VEGF, TNFα, ET, NO, SOD and MDA played an important role in the increase of the permeability of BBB during high altitude environment exposure. They were the key factors for the increase of the permeability of BBB, which was directly related to high altitude cerebral edema. This work was supported by the “Eleventh Five-Year Plan” for Sci & tech Research of the Chinese PLA (No.2008Z093), and the National Science and Technology Ministry (No. 2009BAI85B03).

140

INTERVENTION EFFECT OF GINKGO BILOBA EXTRACT ON THE LEAKAGE OF CEREBRAL MICROVASCULAR IN HIGH ALTITUDE HYPOXIA EXPOSURE

Q.Q. Zhou, Y.J. Luo, Y.X. Gong

Department of High Altitude Disease, College of High Altitude Military Medicine, Third Military Medical University, Chongqing, China

Objective: To observe the protective effect of ginkgo biloba extract (GBE) on the blood-brain barrier of rats, and stated its mechanism initially.

Methods: 48 SD rats were randomly divided into 4 groups. The experimental high altitude cerebral edema model in rat was in hypoxic surroundings, through modeling 7000 meters altitude in low-voltage for 3 days. GBE pretreatment group are given GBE at the standard of 60mg/kg/day by the first three days of hypoxia, GBE anaphase treatment group are given GBE by the same dose at the time of 24 hours after hypoxia to the end of decompression hypoxia. To evaluate the influence of GBE on the brain water content by exposing to hypoxia with the method of doing wet ratio; observing the influence of GBE on blood-brain barrier permeability by exposing to hypoxia with the anthanum nitrate tracer method.

Results: The results showed that the brain water content was significantly increased under high altitude exposure, for 80.53 +0.06%, higher than 74.62 +0.05% brain water content of the plain control group. to the animal brain water content of the intervention given GBE intervention group Under altitude exposure was significantly lower than the animals of simple exposed to high altitude, in between the plain control group and the high altitudes control group for 76.35 +0.03%. The brain water content in the GBE early intervention group was lower than GBE late intervention group ($P< 0.01$), showed that GBE early pretreatment can alleviate the cerebral edema induced by hypoxia at some extent is better than the effects of GBE late treatment interventions enter after plateau. Ultrastructure observing of rat brain showed that the cerebral cortex the lanthanum nitrate less leakage, and most of the lanthanum granules concentrated in the cerebral blood vessels in the plain control group. The cerebral cortex visible leakage more the lanthanum nitrate, and dispersed in the brain cortex in the high altitude control group. Lanthanum nitrate leaking out of cerebral cortex in the early GBE intervention group significant lower than the high altitude control group, the grana of lanthanum nitrate was concentration on the surface of endothelial cells. leaking of lanthanum nitrate in cerebral cortex in the later stage GBE intervention group more mult than in the early GBE intervention group, but low significant than the high altitude control group. These result showed that the GBE pre-treatment and post-treatment intervention can protect the blood-brain barrier, abatement the injury of tight junctions between endothelial cells, reduce or prevent the lanthanum nitrate leakage to the brain tissue.

Conclusion: GBE has some protective effect on the increasing of the permeability of the blood-brain barrier when it is exposed to hypoxia.

This work was supported by the “Eleventh Five-Year Plan” for Sci & tech Research of the Chinese PLA (No.2008Z093), and the National Science and Technology Ministry (No. 2009BAI85B03).

141

CEREBRAL BLOOD FLOW MEASUREMENT AND ITS CLINICAL VALUE IN THE POPULATION WHO RAPID ENTRY TO HIGH ALTITUDE REGIONS

Q.Q. Zhou, Y.J. Luo, P. Guo

Department of High Altitude Disease, College of High Altitude Military Medicine, Third Military Medical University, Chongqing, China

Objective: To investigate the relationship of cerebral blood flow with acute high altitude cerebral edema and the clinical value of cerebral blood flow measurement in rapid entry population to the plateau.

Methods: The cerebral blood flow of 496 persons who rapid ascended to high altitude regions was observed in higher altitude regions (>4800m).

Results: The cerebral blood flow of rapid entry population to high altitude was more obviously increased than that of those as the lower altitude region. The cerebral blood flow of acute high altitude response and acute mountain sickness in rapid entry population to high altitude were higher than those of the adaptation population to high altitude. “Mountain sickness prophylactic” was used to prevent acute mountain sickness or to inspire oxygen or carrying oxygen can decreased significant the cerebral blood flow of rapid entry persons to high altitude and acute mountain sickness' patients in rapid entry population to high altitude regions, decreased the morbidity of acute mountain sickness.

Conclusion: Monitoring the cerebral blood flow of rapid entry persons to high altitude, may not only detect the mountain sickness, but also predict susceptive persons with acute mountain sickness. Therefore, the determination of cerebral blood flow may proved an important theoretical basis for forecasting the incidence of acute mountain sickness in rapid enter population to high altitude regions, and early treatment and prevention of acute mountain sickness.

This work was supported by the “Eleventh Five-Year Plan” for Sci & tech Research of the Chinese PLA (No.2008Z093), and the National Science and Technology Ministry (No. 2009BAI85B03).

142

RELATIONSHIP BETWEEN WATER CONTENT OF BRAIN AND CEREBRAL EDEMA OF RATS EXPOSED AT THE DIFFERENT ALTITUDE REGIONS

Q.Q. Zhou, Y.J. Luo, P. Guo

Department of High Altitude Disease, College of High Altitude Military Medicine, Third Military Medical University, Chongqing, China

Objective: To investigate the pathogenesis of acute high altitude cerebral edema, and the relationship between the water content of brain and cerebral edema in rats exposed in different altitude gradient.

Methods: 178 healthy adult kunming rats were randomly divided into seven groups, each 26 rats, they were transported separately to Golmud (2807m), Mt.kunlun (4750m), Lanzhou (1500m) and executed by dislocation of the cervical vertebra at differential time in plateau. The animals of Golmud and Mt.kunlun from Lanzhou transported by car to Golmud city in two days, at Golmud city stay for three days, except that some executed animals, the rest animals were transported to the station of Mt.kunlun from Golmud city in a day. The rest animals were executed within 1, 3, 5, 7, 9 day separately after enter to plateau. The brain and viscera were takan to observe the water content of tissue and their histomorphology. The wet-dry ratio and water content of brain tissue were measured; samples were taken from the brain tissue and other viscera and fixed later for light microscopy and electomicoscopy observation.

Results: After rats rapidly enter higher altitude region from lower altitude region, their wet-dry ratio and water content of brain tissue were obviously increased with altitude increased. At the high altitude regions with prolonged stay, the wet-dry ratio and water content of brain tissue were obviously increased, especially at 7day, after enter into high altitude regions. The value was highest, significantly different compared that at 1, 3, 5 days. Histological examinations showed that neurons swelling and vascular degeneration in intracytoplsmic neurons. The peripheral gap of gliocyte and microvaessels was increases, these changes were marked in the 7 day group.

Conclusion: Rats rapid entry into higher altitude regions from lower altitude regions may result in formation of acute high altitude cerebral edema, which attack within 5-7 days after being entered into high altitude regions from lower altitude region.

This work was supported by the “Eleventh Five-Year Plan” for Sci & tech Research of the Chinese PLA (No.2008Z093), and the National Science and Technology Ministry (No. 2009BAI85B03).

143

ANALYSIS OF THERAPEUTIC EFFECT AND INFLUENCING FACTORS ON HIGH ALTITUDE CEREBRAL EDEMA TREATED ON THE SPOT AT HIGH ALTITUDE REGIONS

Q.Q. Zhou, Y.J. Luo, P. Guo

Department of High Altitude Disease, College of High Altitude Military Medicine, Third Military Medical University, Chongqing, China

Objectives: To investigate the curative effect of treatment on the spot in high altitude regions for high altitude cerebral edema (HACE).

Methods: Hosptalization cases of the past 50 years were studied by retrospoetive survey, according to epidemiological studies and retrospective case series, analyzing on the therapeutic effect of HACE treated at high altitude region on the spots, and the factors of influence therapeutic effect were sought.

Results: Through treatment on the spot for HACE of 328 cases in high altitude regions, 319（97.3%）cases was successfully cured, average hosptalization time was 8.9 days. Analysis of 328 cases showed that the multiple organ dysfunction were, leading factors of influencing therapeutic effect, in which 56 per cent of them were accompanied by high altitude pulmonary edema, 41 per cent of them are accompanied by renal insufficiency, 14 per cent of them are accompanied by cardiac insufficiency, three organ lesion at the same time account for 12.5 per cent. five organ damage involved in 6 patients, four organs involved in 11 patients, three organs involved in 24 cases, respectively, 1.83% of total cases, 3.35%, 7.32%; three organs by A total of 41 cases of loss of cases, accounting for 12.5% of all cases. Multiple deaths associated with MODS, can be seen in patients with high altitude cerebral edema are more or less to the existence of late MODS, particularly heavy and very heavy patients with high altitude cerebral edema, indicating that high altitude cerebral edema complicated by MODS is the effect of local treatment major factor. Therefore, strengthening the HACE complicated by the diagnosis and treatment of MODS, is to improve the success rate of treatment of high altitude cerebral edema, an important guarantee. HACE complicated by multiple organ dysfunction syndrome after clinical treatment should be adhered to: multi-channel oxygen to ensure adequate oxygen inhalation; early mechanical ventilation; early dehydration diuretic to reduce intracranial pressure; early use of mild hypothermia therapy to reduce the oxygen consumption of brain tissue; early treatment of complications, to prevent the occurrence of multiple organ failure.

Conclusion: HACE accompanied by multiple-organ dysfunction syndromes was the primary factors of influencing, strengthen the treatment of high altitude cerebral edema complications is an important measure to improve the cure rate.

This work was supported by the “Eleventh Five-Year Plan” for Sci & tech Research of the Chinese PLA (No.2008Z093), and the National Science and Technology Ministry (No. 2009BAI85B03).

144

EARLY DIAGNOSIS AND CLASSIFICATION TREATMENT OF HIGH ALTITUDE CEREBRAL EDEMA

Q.Q. Zhou, Y.J. Luo, P. Guo

Department of High Altitude Disease, College of High Altitude Military Medicine, Third Military Medical University, Chongqing, China

Background: For a long time on treatment of high altitude cerebral edema only way is to find the patient, and rapidly transported to low altitude region. But the long-distance transportation, transit and other factors not timely treatment, mortality is high.

Objectives: To investigate early diagnosis and classification treatment of high altitude cerebral edema.

Methods: Screening patients suspected of high altitude cerebral edema (HACE), by acute mountain sickness symptoms indexing, observed the early symptoms, signs and laboratory examinations.

Results: Early diagnosis of high altitude cerebral edema have necessary the conditions: ① recently entered the plateau from the plains (above 3000m), or by the plateau into the higher altitudes, severe headache, vomiting (all symptoms of acute mountain sickness scores were>4); live in the highlands by the bed, a small flow of oxygen and no relief after symptomatic treatment. ② Cyanosis, retinal abnormalities: including papilledema, optic disc hyperemia, retinal artery spasm. ③ MRI examination can be found in the brain parenchyma T1wI low signal and high signal on T2WI spots or small sheet changes. ④ Blood examination showed WBC increased. ⑤ Continuous and progressive development of hypoxemia and respiratory alkalosis. ⑥ Abnormal EEG examination revealed mainly slow performance.Principle of classification treatment of High altitude cerebral edema in high altitude regions is: (1) Light cerebral edema: Treatment with bed rest, oral furosemide, prednisone, methyl-testosterone, 1 or 2 times / day, given the appropriate analgesia and sedation.(2)Moderate cerebral edema: Treatment with absolute bed rest, intermittent oxygen inhalation or skin download carrying oxygen, intramuscular injection of furosemide, dexamethasone, anisodamine, promethazine or diphenhydramine, 1-2 times / day, changed to oral administration after stop vomiting. (3)Severe cerebral edema: Treatment with absolute bed rest, continuous oxygen inhalation, if necessary, tracheal intubation or incision pressurized inhalation oxygen. The first intramuscular injection of dexamethasone or diphenhydramine, followed by intravenous infusion of 10% glucose plus dexamethasone, furosemide, and vitamin C, 2-3 times /day, and head cooling, alternate energy medicine or energy mixture. (4) Very severe cerebral edema: Treatment of severe cerebral edema in addition to the treatment principles, mainly handling with complications. Given antibiotics if with infection; Increase the dose of diuretic dehydration with heart failure; pressurized oxygen inhalation, implementation of hibernation therapy, increase the amount of dehydration drugs. The patients may be delivery to low altitude region after condition stable.

Conclusions: Early detection of patients, early diagnosis and treatment in high altitude region by grade, can reduce mortality and improve the cure rate is the key to treatment of high altitude cerebral edema. This work was supported by the “Eleventh Five-Year Plan” for Sci & tech Research of the Chinese PLA (No.2008Z093), and the National Science and Technology Ministry (No. 2009BAI85B03).

145

SIGNALING REGULATING MECHANISMS OF OCCLUDIN IN THE BLOOD-BRAIN BARRIER PERMEABILITY CHANGES

Q.Q. Zhou, Y.J. Luo, P. Guo

Department of High Altitude Disease, College of High Altitude Military Medicine, Third Military Medical University, Chongqing, China

Objectives: To investigate the effects and signaling regulating mechanisms of occludin in Blood-Brain Barrier Permeability.

Methods: Through literature review to explore the signaling regulatory mechanisms of occludin in the blood-brain barrier permeability changes.

Results: As an important transmembrane protein in brain microvascular endothelial cells (BMVECs) tight junction, occludin play a crucial role in regulation of blood-brain barrier (BBB) permeability under physiological, as well as pathological conditions. Abnormal expression of occludin can increase BBB permeability and fluid leakage. We describe several current understanding of signaling mechanisms about occludin in regulating BBB Permeability.

Ⅰ. Under stress condition, ATP-sensitive K^+ channel is blocked by some cytokines, such as INF-γ, leading to expression of occludin decreased and aquaporin-4 increased, causing dysfunction of BBB and the consequent increasing in BBB leakage.

Ⅱ. The expressions of VEGF and its receptors increased under stress condition, occludin rearranged, conformation of ZO-1 and actins changed, linking to the disruption of tight junctions, causing a breakdown in equilibrium of BBB permeability.

Ⅲ. Hypoxia and reoxygenation stress leads to an increased production of reactive oxygen species (ROS), can make changes in localization and structure of occluding, which critically important to function of tight junctions in regulation and maintenance of BBB's permeability and leading to a hyperpermeability.

Ⅳ. Occludin phosphorylation state can affect BBB permeability. Via PI3K/PKB signaling pathways, activation of PI3K by oxidative stress can induce tyrosine phosphorylation and dissociation from actins cytoskeleton of occludin. Via Rho/RhoK signaling pathways, activation of RhoK is involved in phosphorylation of occludin, claudin-5, myosin light chain phosphatase(MLCP) and myosin light chain-2 (MLC2). Via Rho/PKC signaling pathways, activation of PKC can act on occludin, ZO and claudin-5, cause their serine phosphorylation and conformational changement of occludin and actin. An end result of these signaling events is leading to hyperpermeability of BBB.

Conclusion: Under stress conditions, blocked ATP-sensitive K^+ channels, increased ROS , VEGF and its receptor expression, activation of PI3K ,RhoK and PKC, etc, which interact with phosphorylation and redistribution of occludin, claudin and ZOs, can increase BBB permeability.

This work was supported by the “Eleventh Five-Year Plan” for Sci & tech Research of the Chinese PLA (No.2008Z093), and the National Science and Technology Ministry (No. 2009BAI85B03).

146

EPIDEMIOLOGICAL CHARACTERISTICS OF HIGH ALTITUDE CEREBRAL EDEMA COMPLICATED BY MULTIPLE ORGAN DYSFUNCTION SYNDROME IN QINGHAI-TIBETAN PLATEAU

Q.Q. Zhou, Y.J. Luo, F.Y. Liu, S.Z. Li, X.Z. Zhang, W. Gao

Department of High Altitude Disease, College of High Altitude Military Medicine, Third Military Medical University, Chongqing, China

Objectives: To investergate the Characteristics and the incidence of high altitude cerebral edema complicated with Multiple Organ Dysfunction Syndrome on the Qinghai-Tibetan Plateau.

Methods: Retrospectively by way of questionnaire survey for inpatient cases of mountain sickness 11 central hospitals in the Qinghai-Tibet Plateau over the past 50 years, statistical analysis the high altitude cerebral edema complicated by the incidence of MODS, looking for cause and pathogenesis of the MODS.

Results: The epidemiological study covered 4,095 inpatient cases of MODS from Qinghai, Tibetan high altitude areas. Data screening of the 4,095 cases with ASMS was conducted according to scoring criteria for high altitude MODS, and of these, 103 patients had symptoms consistent with the diagnostic criteria, with the detection rate being 2.5%. Of the 103 patients, 14 patients suffered from 3-organ damage, 25 patients from 4-organ damage, 34 cases from 5-organ damage, and 30 cases from 6-organ damage. The damaged organs were lung (100%), cerebrum (100%), blood (90%), heart (80%), kidney (61%), body fluid internal environment (42%), liver (25%), stomach and intestine (27%).Comparison of leukocytes and their classification showed no significant difference in leukocyte count or in leukocyte type between primary HAPE and recurrent HACE. The leukocyte count of the patients with A-MODS was strikingly higher than that of the patients without MODS. Simultaneously, such cytokines as TNF, IL-1, IL-2, IL-6, and IL-8 in patients with AMS were remarkably higher than in healthy controls at high altitude, whereas the IL-4 level in ASMS patients was remarkably lower than in healthy people at high altitude.The above results indicate that the probability of A-MODS is relatively high. Once HACE is complicated by MODS, the patient´s condition would rapidly deteriorate and become more serious. The effect of oxygen therapy was poor, and the response to usual treatment was not significant. If treatment was delayed, the prognosis would be poor and the mortality rate would be high. All the death cases were due to MODS or multiple organ failure. A-MODS not only increased the severity of the patient's condition but was also associated with markers of multi-organ injury. Therefore, it is an important significance to elevate diagnosis rate of A-MODS and to enhance its treatment to increase the cure rate of AMS and reduce its mortality rate that monitoring effectively to early damage condition of organs.

Conclusion: Acute mountain sickness complicated by MODS is the main factor influencing therapeutic efficacy, and timely and effective treatment on the spot at high altitude is important to relieve MODS. This work was supported by the “Eleventh Five-Year Plan” for Sci & tech Research of the Chinese PLA (No.2008Z093), and the National Science and Technology Ministry (No. 2009BAI85B03).

147

PATHOGENESIS OF HYPOXIC MICROVASCULAR CEREBROPATHY AT HIGH ALTITUDE AND RELATIONSHIP IT WITH HIGH ALTITUDE CEREBRAL EDEMA

Q.Q. Zhou, Y.J. Luo, P. Guo, B. Zhou

Department of High Altitude Disease, College of High Altitude Military Medicine, Third Military Medical University, Chongqing, China

Objective: To study the mechanisms of high altitude cerebral edema and the way to rescue it.

Methods: Through the observation of animal experiments and populations rapid entrying to high altitude regions. The pathogenesis of hypoxic microvascular cerebropathy at high altitude regions from the system, organ, cellular and molecular levels was analyzed.

Results:

(1) Brain's blood stream was higher than who lived in lower altitude areas. The brain's blood stream of acute mountain sickness was obviously higher than the native also.

(2) Animal experiments proved that blood vessels of brain were extensive, the mount and density of opened micro-vessels increased, the distance between these vessels shorted, the speed of cerebral blood stream slower and stasis, and leakage and bloody were observed around the microvessels when exposed acutely to lower oxygen concentration.

(3) The scene experiment conducted in high elevation area proved that the ET in brain release increased at early stage and decreased 3 days late after enter the plateau. NO release were increased distinctly from 1st to 10^{th} day, and decreased at 13^{th} day but still higher than that level at 5^{th} day. SOD, GSH and β-endorphin in brain increased and GSH-PX decreased notably as elevation increased and the time prolong. Brain water content and wet-weight of brain increased.

(4)With altitude raising and time prolonging, the activities of TNFa, NO and ET in the brain rose. Their most obvious rise was seen during at 9th day after ascending 5000m.

(5) With altitude going up, the expression of VEGF and VEGF mRNA in the brain of rats rose, and they also rose gradually with time prolonging under high altitude exposure. Their most obvious rise was seen at 9th day after ascending 5000m. At the same time, the EB and water content in the brain of mice showed the same change trends.

(6) The ultrastructures and histology of brain revealed that under hypoxia or plateau condition, the neurons of brain intumescence, rounded, dendrite disappeared, plasma degenerated to vacuoloid, glial cells. The intumescence, the electric dense decreased.

Conclusion: Hypoxia in plateau will increase the permeability of brain vessels and caused energy metabolism obstruction, these factors act together to lead to high altitude cerebral edema happened which is mixed type cerebral edema.

This work was supported by the “Eleventh Five-Year Plan” for Sci & tech Research of the Chinese PLA (No.2008Z093), and the National Science and Technology Ministry (No. 2009BAI85B03).

148

ANALYSIS OF BRAIN AREAS ASSOCIATED WITH THE ATTRACTIVENESS OF POTATO CHIPS BY MEMRI

T. Hoch[1], S. Kreitz[2], M. Pischetsrieder[1], A. Hess[2]

[1]Department of Chemistry and Pharmacy, Food Chemistry, Emil Fischer Center, [2]Department of Experimental and Clinical Pharmacology and Toxicology, Institute for Pharmacology and Toxicology, University of Erlangen-Nuremberg, Erlangen, Germany

Aims: The purpose of the represent study was to identify processes in the brain of rats responsible for food craving. The activity of numerous brain areas were measured to provide a comprehensive and differentiated overview over the processes connected with food craving. Therefore, rats were fed with potato chips as the food of interest. Manganese-enhanced magnetic resonance imaging (MEMRI) [1] was used to quantify the activity of defined brain areas.

Methods: Three groups of male Wistar rats (initial weight 257 ± 21 g) received different foods ad libitum additional to their standard chow pellets: Salted potato chips (N = 16), a mixture of 35 % fat and 65 % carbohydrates (sunflower oil and maltodextrine) as a model for potato chips (N = 16) and powdered standard chow (N = 16), respectively. For familiarisation these test foods were presented ad libitum over a period of 7 days followed by 7 days with standard pellets only. Subsequently, osmotic pumps, filled with a solution of manganese chloride ($MnCl_2$, 200 µL, 1 M) were implanted dorsally, subcutaneously into the rats under isoflurane anesthetisation. Over the period of disposal (7 days, rate: 1 µL/h) and accumulation of $MnCl_2$ in the rat brain, the animals had ad libitum access to their known test food. The activity of the different brain areas were quantified by MEMRI after this period with the following scanner parameters (MDEFT): TR = 4 s, TE = 5.2 ms, TI = 1000 ms, matrix = 256 x 256, FOV = 2.80 cm x 2.80 cm, 2 averages and 64 slices with 0.80 mm thickness. Signal intensities of 166 distinct brain areas were measured by using a digital version of a rat brain atlas [2]. Z-scores for each brain area were calculated for conducting statistical analyses (ANOVA) to discover significant differences ($P < 0.05$) between the three groups. Visualization was performed with Amira®.

Results: Significant differences between brain activities depending on the provided test food were detected by MEMRI. It became evident that the brain activity of the potato chips fed group differed from the activity of the standard chow fed group in brain areas associated with reward or addiction, motion, food intake and alertness or sleep. The brain activities of the rats fed with the mixture of fat and carbohydrates also showed significant differences with regard to the rats fed with powdered standard chow. The number of differences, however, was lower and the differences corresponded only partly to the brain activities of the potato chips fed rats.

Conclusions: It can be concluded that I) intake of snack foods like potato chips induces activity in several specific brain areas not connected to the consumption of standard chow, II) the induction of brain activity is not predominantly caused by additional caloric intake from carbohydrates and lipids III) intake of potato chips affects brain activity in areas related with reward or addiction, motion and activity.

References:

[1] Silva et al. 2004, NMR in Biomedicine, 8, 532-543

[2] Paxinos, Watson 2007, Academic Press

150

BRAIN AROMATASE AND COGNITION: [11C]VOROZOLE PET STUDIES IN HEALTHY HUMAN SUBJECTS

A. Biegon[1], N. Alia-Klein[1], D. Alexoff[1], S.-W. Kim[2], J. Logan[1], D. Pareto[3], F. Telang[1], G.-J. Wang[1], J. Fowler[1]

[1]Medicine, Brookhaven National Lab, Upton, NY, [2]NIAAA, Bethesda, MD, USA, [3]Institut de Recerca Hospital Universitari Vall d'Hebron, Universitat Autònoma de Barcelona, Alta Tecnologia, Barcelona, Spain

Introduction: Aromatase is the final enzyme catalyzing estrogen biosynthesis. Vorozole is a potent and selective aromatase inhibitor, and [11C]vorozole was found to be a useful PET tracer for brain aromatase in rodents and non-human primates. Recent PET studies have revealed that the regional distribution pattern of aromatase in the human brain is unique, with the highest levels found in the thalamus. In contrast, primate and rodent brain studies show low levels in thalamus and high levels in amygdala.

Objective: To gain an insight into the possible functions subserved by estrogen synthesis in the human thalamus and amygdala, we have examined the relationship between aromatase availability in these two regions and neuro-psychological assessment of higher brain function in healthy volunteers.

Methods: Sixteen healthy volunteers (8 men and 8 women) were administered the multidimensional personality questionnaire (MPQ) and the California verbal learning test (CVLT) prior to a PET scan with [11C]vorozole. Blood input data and brain regional time activity curves over a 90 minute acquisition period were collected from each subject and analyzed using the 2 compartment model to obtain the total distribution volume (VT) values, which where then correlated with CVLT performance and traits control/constraint in the whole group as well as in men and women separately.

Results: Verbal learning and memory (CVLT1-5) showed a statistically significant negative correlation with thalamic VT ($R=-0.546$, $p< 0.03$). However, this correlation originated exclusively from the women ($R=-0.73$, $p< 0.04$); with no apparent contribution from the men ($R=-0.13$, $p=0.75$). Conversely, VT in amygdala was significantly and negatively correlated with CVLT performance in men ($R=-0.76$, $p< 0.02$) but not in women ($R=-0.11$, $p=0.78$). A similar double dissociation between regions and genders was found with regard to control/constraint: Trait control was positively and significantly correlated with thalamic aromatase availability in men ($R=0.94$, $p< 0.0005$) but not in women ($R=0.46$, $p=0.25$). Conversely, trait constraint (composite of control and harm avoidance) was positively correlated with VT in amygdala of women ($R=0.87$, $p< 0.005$) but not men ($R=0.19$, $p=0.6$).

Conclusion: These results suggest that estrogen synthesis in the human brain modulates cognitive function in a sex- and region specific manner.

151

COMPUTATIONAL MODELLING OF THE PIGLET BRAIN TO SIMULATE NEAR INFRARED SPECTROSCOPY AND MAGNETIC RESONANCE SPECTROSCOPY DATA COLLECTED DURING PHYSIOLOGIC INSULTS

T. Moroz[1], M. Banaji[2], C.E. Cooper[3], N.J. Robertson[4], I. Tachtsidis[1]

[1]Department of Medical Physics and Bioengineering, University College London, London, [2]Department of Mathematics, University of Portsmouth, Portsmouth, [3]Department of Biological Sciences, University of Essex, Colchester, [4]Institute for Women's Health, University College London, London, UK

Objectives: Piglets are commonly used as models for human neonates[1]. The purpose of this work is to increase understanding of the metabolic and circulatory processes occurring during anoxic, hypoxic and ischaemic insults in piglets. Towards that goal we have developed a computational model to simulate variables measured by near infrared spectroscopy (NIRS) and magnetic resonance spectroscopy (MRS) during these insults.

Methods: The model described here is an extension of the existing BrainSignals model[2]. This is a physiological model of circulation and mitochondrial metabolism. It was developed to model the brain of healthy adults, with an interest in predicting NIRS measured variables, including the concentration changes of oxygenated haemoglobin (HbO_2), deoxygenated haemoglobin (Hb) and cytochrome c oxidase (Cu_A). We altered and enhanced the model to simulate the physiology and metabolism of the anaesthetised piglet brain. The model structure is illustrated in Figure 1a. It now includes the metabolites which are measured by 31-P MRS, namely phosphocreatine (PCr), inorganic phosphate (P_i) and ATP. Their interactions involve a feedback whereby the phosphorylation potential influences the rate of production of ATP. PCr concentration is calculated from the concentrations of ATP and ADP and the pH, assuming that the reaction catalysed by creatine kinase is always effectively at equilibrium.

Results: Figure 1 shows the effect of changing the arterial oxygen concentration on some of the model variables. Figure 1b shows the relationship between the PCr/P_i concentration ratio, and the change in Cu_A oxidation. Cu_A continues to become more reduced after PCr concentration is close to zero. Figure 1c shows the concentrations of ATP and PCr. As seen experimentally[3], the ATP concentration remains constant until the arterial oxygen saturation is low, and the buffering capacities of PCr have been exceeded. The position and shape of this drop would be expected to change if glycolysis were represented in the model. At low oxygen concentrations, glycolysis becomes an important source of ATP production. The graphs shown are for the steady state, but the model is also used to simulate dynamic data. For example, we are comparing its outputs with measurements from a study involving brief anoxias in piglets [3]. The inputs are the blood pressure, arterial oxygen saturation, and pH measured by MRS, taken from the study.

Conclusions: The model is a promising tool to help understand the MRS and NIRS measurements, and further analyse results from piglets during physiologic insults . It will be refined to predict these measurements more accurately. We are currently extending the model to include lactate as measured by proton MRS, and pH. We will also use the model to study hypoxic-ischaemic insults.

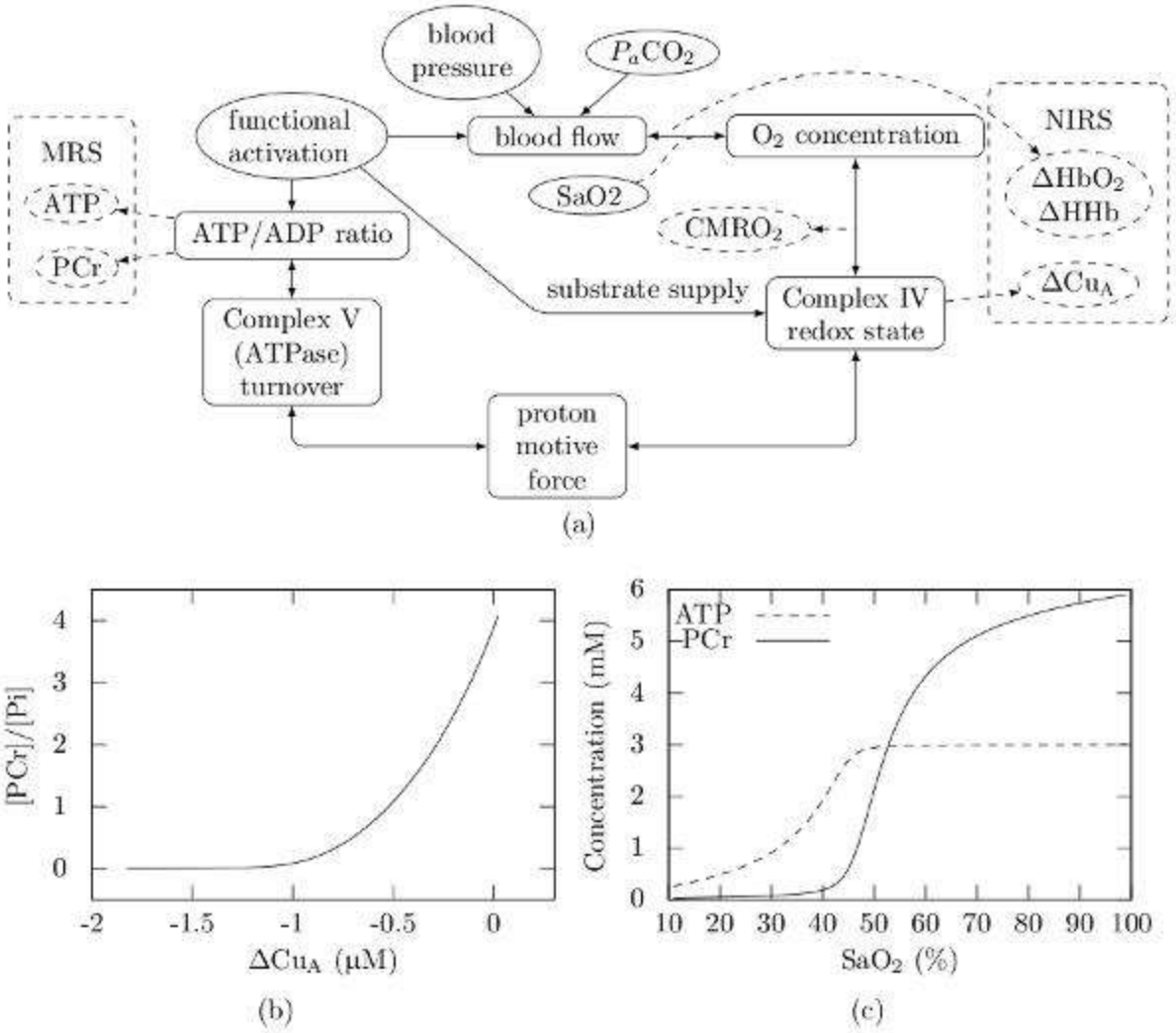

[Figure 1]

a) Model structure. Inputs are shown in solid ovals, and outputs in dashed ovals

b) Modelled [PCr]/[Pi] ratio vs change in Cu_A concentration

c) Modelled ATP and PCr concentration vs arterial oxygen saturation

References:

[1] Cady et al. J Neurochem, 107(4):1027-1035(2008)

[2] Banaji et al. PloS Comput Biol, 4(11):e1000212(2008)

[3] Springett et al. J Cereb Blood Flow Metab 20(2):280-289(2000)

152

REGULATION OF CELL CYCLE AND CELLULAR PROLIFERATION BY ALTERED LIPID METABOLISM IN STROKE

R.M. Adibhatla, J.F. Hatcher, A. Gusain

Neurological Surgery, University of Wiscosnin, Madison, WI, USA

Introduction: Expressions of cell cycle regulating proteins are altered after stroke. Post-mitotic neurons enter an aberrant cell cycle after stroke, resulting in cell death. Cell cycle inhibition has shown dramatic reduction in infarction after stroke. Sphingomyelin (SM) synthase (SMS) transfers the phosphocholine group from phosphatidylcholine (PC) to ceramide to form sphingomyelin and release DAG; and serves as a bridge between glycerophospholipids and sphingolipids. D609 (tricyclodecan-9-yl-xanthogenate), a PC-phospholipase C (PC-PLC) inhibitor also inhibits SMS and increases ceramide. Ceramide can induce cell cycle arrest by up-regulation of Cdk inhibitors p21 and p27 through activation of protein phosphatases 1 and 2A.

Methods: Spontaneously hypertensive rats (SHR) were subjected to 1 hr middle cerebral artery occlusion (tMCAO) and reperfused. D609 (50 mg/kg i.p., saline) was administered at the onset of reperfusion. Infarction volumes were measured using TTC. *In vitro* studies were conducted using primary mouse neuronal and astrocyte cultures, microglia (N9 and BV-2) and macrophage (RAW 264.7) cell lines. Lipid analyses were performed by TLC and GC. Protein expression was performed by immunoblotting and immunocytochemistry. Cell proliferation assays were performed by BrdU incorporation and cell viability was determined by trypan blue exclusion.

Results: D609 reduced the infarct volume after stroke by 35% and 60% at 1 and 3 d reperfusion, respectively. D609 reduced PC-PLC activity and expression, acidic sphingomyelinase expression; phospho- retinoblastoma (Rb); oxidized PC (OxPC, a lipid peroxide) protein-adduct and increased p21 expression over 3 d reperfusion. Primary neuronal cultures subjected to OGD/reoxygenation showed increased expression of Cdk4, evidence of entry into the cell cycle. D609 increased the p27 expression and reduced the neuronal death after OGD/reoxygenation. Microglia and macrophage cell lines and primary astrocyte cultures exposed to D609 exhibited concentration-dependent inhibition of cell proliferation (cell counting, BrdU incorporation) without affecting cell viability. Exposure of BV-2 and N9 microglia cultures to D609 resulted in significantly increased ceramide levels without inducing cell death. Immunocytochemical studies showed increased p21 expression with D609 treatment and significantly arrested cell proliferation, which correlated with the increase in ceramide.

Conclusions: D609 may provide benefit through inhibition of SMS and increased ceramide levels. Others have also shown that D609 inhibited bFGF-stimulated astrocyte proliferation by increasing ceramide through SMS inhibition. Ceramide may induce cell cycle arrest by up-regulating p21 and causing hypo-phosphorylation of Rb protein (through Cdk inhibition and/or increased protein phosphatase activity). Ceramide may have pleiotropic effects: intermediate ceramide levels may cause cell cycle arrest whereas high levels induce apoptosis. Microglia/macrophages are the major source for ROS, pro-inflammatory cytokines as well neurotrophic factors. Reducing microglia/macrophage proliferation by D609 may attenuate the inflammatory response as well as oxidative stress (evidenced by the reduction in OxPC protein adducts with D609 treatment). D609 may at the same time prevent mature neurons from entering the cell cycle/dying. However, it is unclear how D609 affects proliferation of individual neural cells (astrocytes or microglia). D609 may be acting on both PC-PLC as well as SMS.

LMV-601, a pure enantiomeric isomer of D609, a more specific PC-PLC inhibitor, may help resolve these issues.

Support by NIH

154

IS WATER DIFFUSION DECAY IMAGING (DDI) ABLE TO PROBE SYNAPTIC PLASTICITY?

R. Nicolas[1], J. Pariente[1], X. Franceries[1,2], N. Chauveau[1], L. Saint-Aubert[1], F. Aubry[1], H. Gros-Dagnac[1]

[1]INSERM, Imagerie Cérébrale et Handicaps Neurologiques, UMR 825, [2]Université de Toulouse; UPS, INPT; LAPLACE (Laboratoire Plasma et Conversion d'Energie), Toulouse, France

Introduction: Diffusion signal (S/S_0 decay) changes traducting an *ADC* decrease, induced by ischemia [2], ouabaïn [3], NMDA [3], kaïnate [4], osmotic swelling [2], brain activation [10] and Mg2+ and Ca2+ action [2] is correlated to G to F actin conversion [5,6,7,8,9], highly present in dendrites and spines (~20% of total proteins). This fact was supported by the Le Bihan´s seminal paper treating the role of water in cell biology/biophysic [1]. He hypothesized that water interacting with actin cytoskeleton should be the fundamental event determining the water diffusion decay shape (S/S_0=f(*b*, *ADC*)) obtained by increasing b-factor in DWI images. Brain *ADC* maps changes in cerebral activation suggest that this signal could be a marker of immediate synaptic-plasticity activation changes. Diffusion Decay Imaging (DDI) could be a sensitive marker to the loss of dendritic connexions in PreDemential Alzheimer´s Disease (PDAD) and to dendritic reorganization in acute stroke and brain activation.

Patients and methods: S/S_0 signal from DWI images constituting a DDI acquisition were acquired with parameters TR/TE=4168.8/70.4 ms for PDAD patients (8), aged (6) and young (4) control subjects, and a patient 4 days after stroke *(b*=0,10,30,100,200,500,750,1000,1500,2500 s/mm², in bold for stroke acquisition). For both, diffusion time was t_d=26.36ms (Δ=34.8 ms, δ=25.3 ms). Parameters and paradigms for visual stimulation *ADC*-fMRI (3B) aquired simultaneously with BOLD (3A) and for HR-DWI-fMRI (3C) were given in Fig. 3.

Results: The stroke patient exhibit the well-know DDI change in infarcted areas corresponding to *ADC* decrease (Fig. 1). Mean DDI signal of registered, segmented brain areas were analyzed by bilateral t-test (Fig. 2) and statistical significances for a DDI change (corresponding to an *ADC* increase) were seen only in grey matter (GM) for aged vs young and aged vs PDAD patients (Fig. 2).

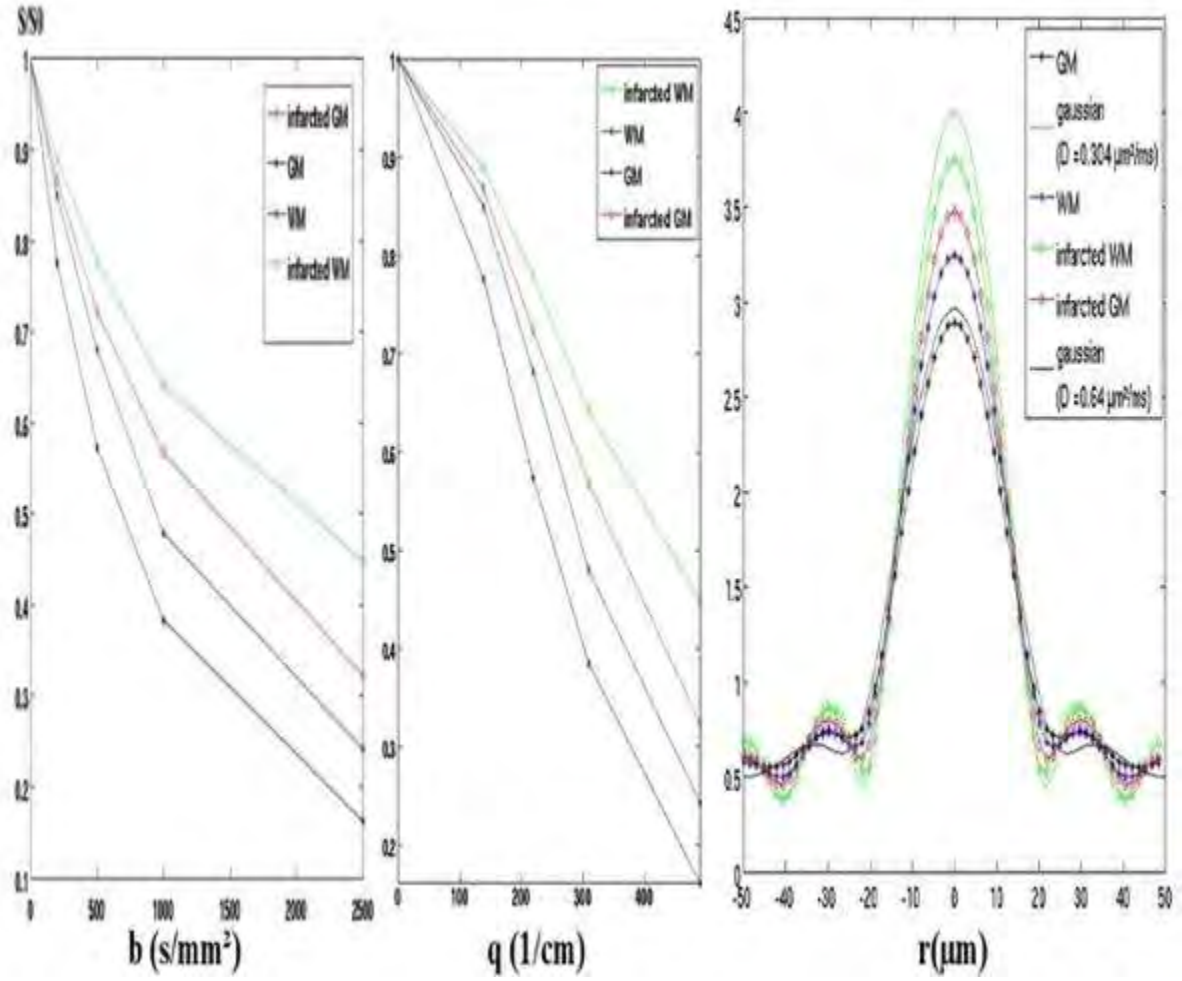

[Fig 1. Signal of healthy and infarcted GM and WM]

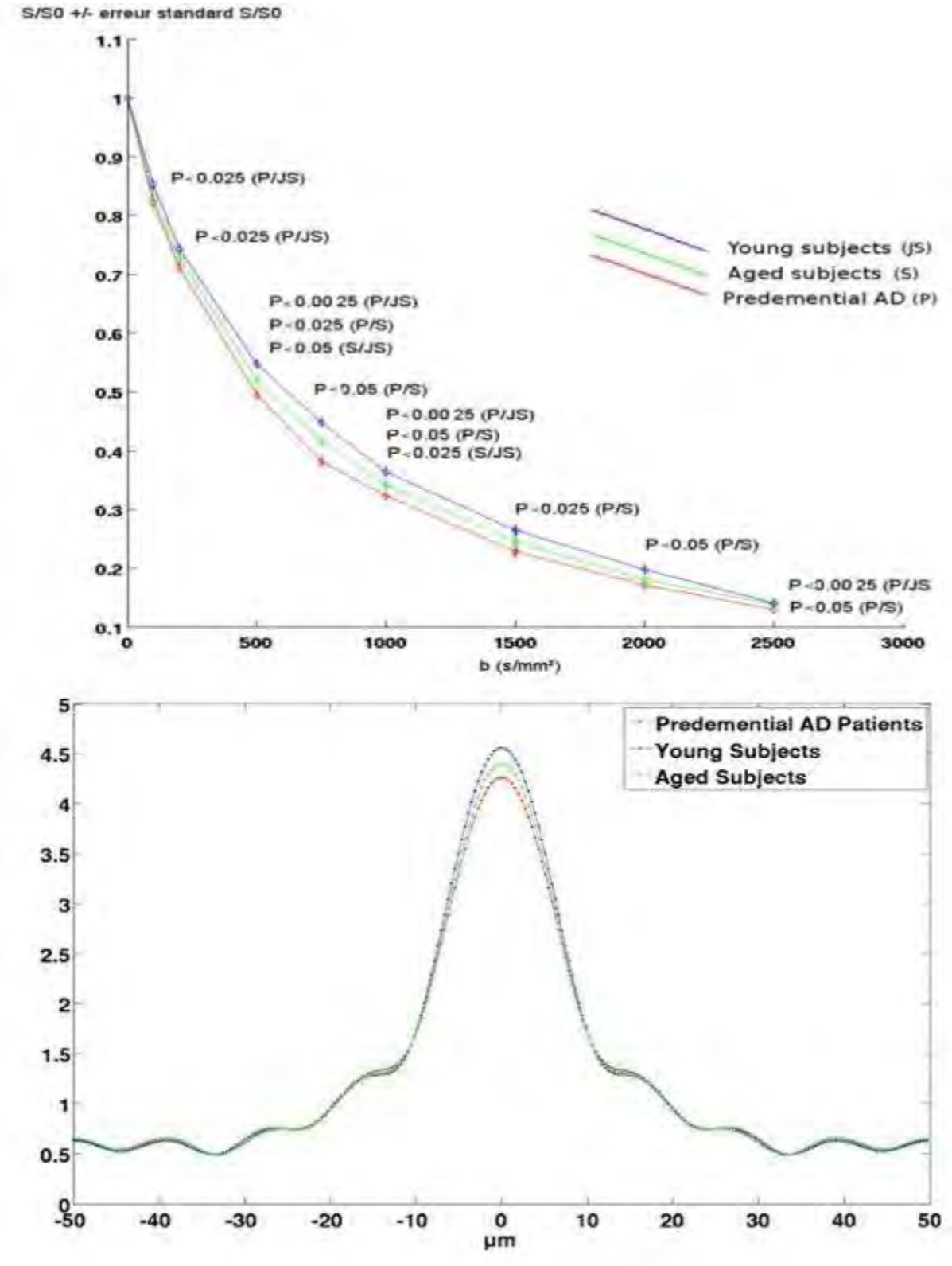

[Fig. 2 DDI and q-space signal for PDAD patients]

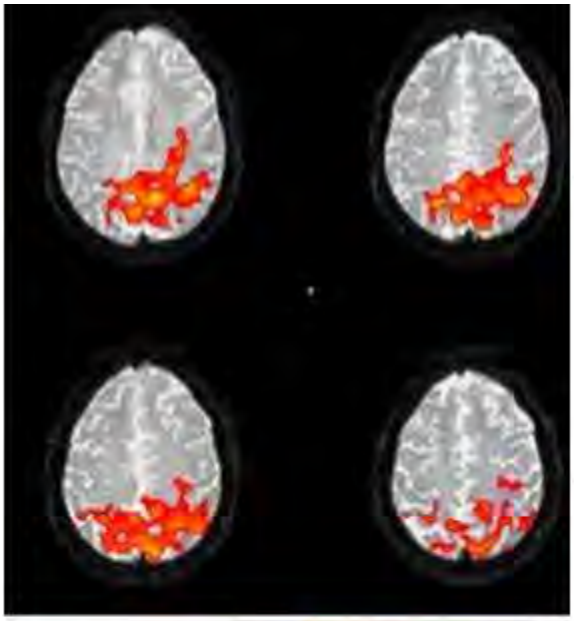

3A (BOLD)

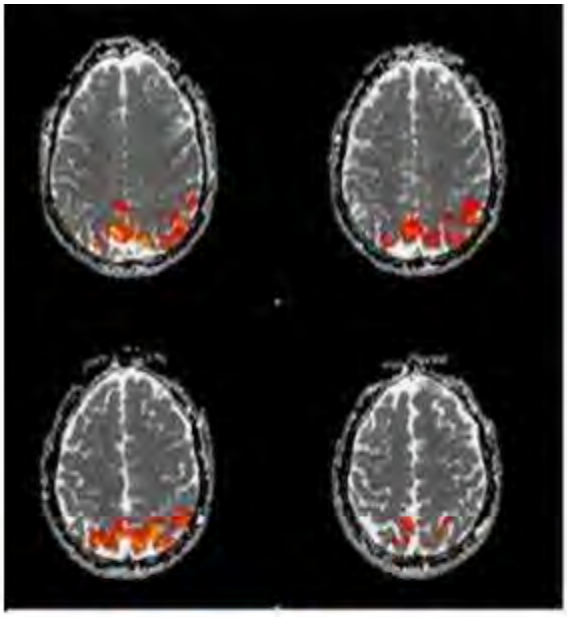

3B (ADC)

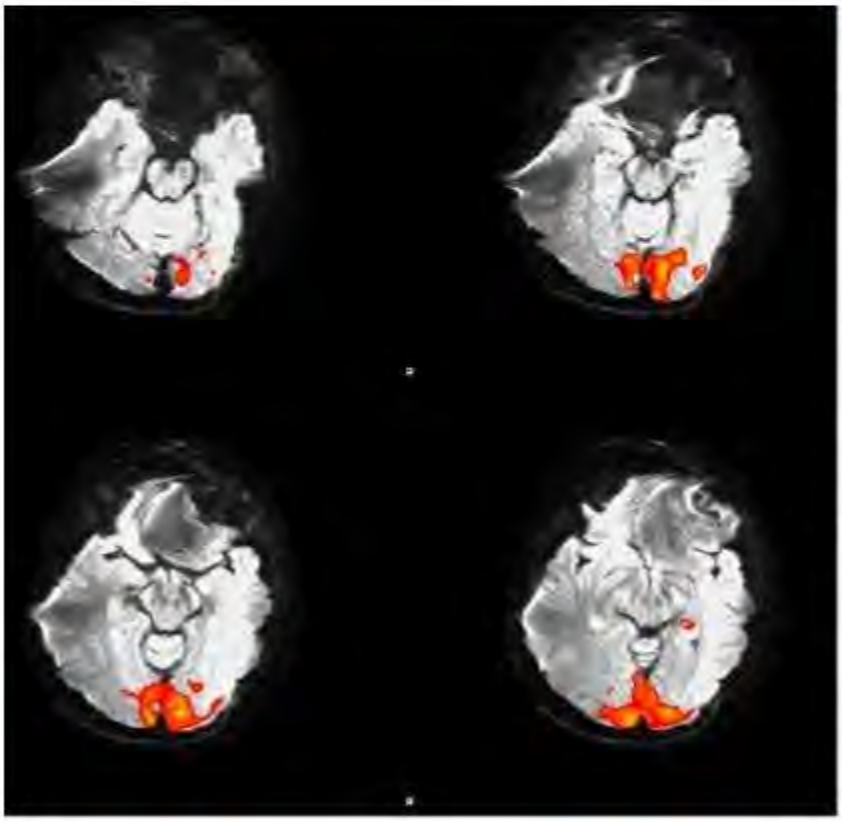

3C (DWI HR (1.2 x 1.2 x1.2 mm)

Experimental Design : Visual checkboard (5 stimulations, 5 resting state) with b=1000 s/mm², FSL P< 0.05, smoothing=8 mm.

3A, 3B : (2x2x4 mm, TR=26 s, 3 averages in 3 directions (FH, AP, RL)

3C : HR-DWI,TE=92 ms, TR=2.41 s, 16 averages in one direction)

[Fig. 3 Brain activation in BOLD, ADC, HR-DWI maps]

Conclusion: *ADC decrease*, as stated may be linked to F-actin increase (stress fibers [5]) in stroke and in brain activation by NMDA-related synaptic actin reorganization [6] . ADC *increase* with age and in PDAD could be caused by decrease of F-actin in synaptic loss before cellular loss. The biologic events underlying these pathologic cases sustain the hypothesis that the cytoskeleton may influence the DDI signal.

Bibliography:

[1] D. Le Bihan, Physics in Medicine and Biology, 52(7), (2007), pp. R57-R90.

[2] J.M. Hakumäki, Journal of Cerebral Blood Flow and Metabolism, 20(2), 2000), pp. 405-411.

[3] W.B. Veldhuis, M. Van der Stelt, Journal of Cerebral Blood Flow and Metabolism,23,(2003),pp. 62-74.

[4] T. Ebisu, W.D. Rooney, S.H. Graham, Magnetic Resonance in Medecine,36(6),1996,pp. 821-828.

[5] S.J. Atkinson, M.A. Hosford,The Journal of Biological Chemistry,279(7-13),(2004),pp.5194-5199.

[6] S. Halpain, A. Hipolito, L. Saffer, The Journal of Neuroscience,18(23),(1998),pp.9835-9844.

[7] L.H. Zeng, L. Xu, N.R. Rensing, P.M. Sinatra, The Journal of Neurosciences,27,(2007),pp. 11604-11613.

[8] J. Moran, M. Sabanero, I. Meza, American Journal of Cell Physiology,271(6),(1996),pp. C1901-C1907.

155

AGE DEPENDENCE OF VMAT2 DENSITY ESTIMATES: COMPARISON OF RACEMIC DTBZ TO (+) DTBZ BINDING AND DEPENDENCE ON PET SCANNER

V. Sossi[1,2], K. Dinelle[2], J. Mckenzie[3], A.J. Stoessl[3]

[1]Physics and Astronomy, [2]UBC PET Imaging, [3]Pacific Parkinson's Research Centre, University of British Columbia, Vancouver, BC, Canada

Background: An accurate determination of tracer binding as a function of age is important for providing insights into the physiology of normal aging, when differentiating disease induced changes from those due to aging and for assessing disease effects in subjects of different age. The vesicular monoamine transporter type 2 tracer ^{11}C-dyhydrotetrabenazine (DTBZ), in its racemic form (±) and active (+) enantiomer, is a good marker for the assessment of the pre-synapatic integrity of the dopaminergic system, since deemed less susceptible to disease and pharmacological regulation than markers estimating dopamine (DA) synthesis or DA transporter. Previous studies presented conflicting reports on the influence of aging on VMAT2 density: a significant age related decline in (±) DTBZ binding (0.77% year) (1) and DTBZ+ (0.5% year) (2), while others reported no significant age effect(3). Here we compare the effect of aging as a function of DTBZ form, scanner characteristics and two different tissue input analysis methods.

Methods: 11 subjects (age 57.9 ±12.2) underwent a DTBZ+ scan on the GE Advance (resolution ~$(8mm)^3$. Five of these subjects also underwent a (±)DTBZ scan on the same scanner, while six subjects underwent a DTBZ+ scan on the Siemens high resolution research tomograph (resolution $(2.5mm)^3$). The scanning protocol and image analysis were identical in all cases. The tissue input Logan and the simplified reference tissue methods (SRTM) were used to yield BP_{ND}.

Results: Consistent with our earlier results(3), no significant age relation was found for the BP_{ND} obtained with (±)DTBZ for either method (p ranging from 0.46 to 0.67). In contrast, the results for the same 5 subjects when scanned with DTBZ+ yielded a highly significant age relation for the caudate with SRTM ($p < 0.01$, decline 0.4%/yr), with corresponding trend when Logan method was used ($p = 0.07$, decline 0.35%yr). In the putamen significance was not reached for this subsample ($p = 0.32$, decline 0.36% and $p = 0.26$, decline 0.35% yr respectively). However, when data from all 11 subjects were included, very significant declines ($p < 0.015$, decline range 0.53% /yr -0.6%/yr) were observed in both the caudate and putamen, consistent between methods. A very similar, significant age related decline was observed for the subset of 6 subjects scanned with DTBZ+ on both scanners, even though the values of the BP_{ND} were on average 55% higher on the HRRT. On average SRTM yielded 5% lower BP_{ND} values.

Conclusion: These results indicate that (+) DTBZ is more sensitive to healthy aging related declines in VMAT2 binding sites compared to (±)DTBZ and provide a partial explanation for the discrepant literature reports. Different age relation parameters must thus be used when age-correcting (±)DTBZ and DTBZ+ derived PET measures. The estimated decline/yr appears independent of scanner and tissue input analysis method. There is therefore no need to perform an age-dependence study for different scanners. Results are currently being confirmed with a larger subject group.

1. Frey et al, 1996 Ann Neurol 40 873-84

2. Bohnen et al, JCBFM 2006 26 1198-1212

3. Troiano et al, Synapse 2010 64(2):146-51

157

GALACTOSYLTRANSFERASE B3GALT2 IS REQUIRED FOR DENDRITE OUTGROWTH OF THE LAYER V PYRAMIDAL NEURONS IN THE MOUSE CEREBRAL CORTEX

J. Bi, M. Hewitt, H. Fang

National Research Council of Canada, Institute for Biological Sciences, Ottawa, ON, Canada

Factors that regulate neurite outgrowth are important in determining the wiring of the central nervous system. Glycosylation is known to play a role in regulation of neurite outgrowth. However, the underlying mechanisms remain unclear. Here we describe that a UDP-Gal:ß GlcNAc ß- 1,3-galactosyltransferase (B3GalT2) is strongly expressed in neurons in the layers V and VI of the cerebral cortex and in the hippocampus during postnatal development of the mouse brain. We also show that cortical layer V pyramidal neurons of B3GalT2 gene knockout mice exhibit reduced apical dendrite length, reduced spine numbers, and aberrant apical dendrite direction. Together, our results demonstrate for the first time that B3GalT2 is an important regulator of neuritogenesis.

160

NON-INVASIVE MONITORING OF ANGIOGENESIS AFTER STROKE WITH MRI

J. Adamczak[1], P. Böhm-Sturm[1], J. Jikeli[1], T. Kallur[1], B. Cohen[2], M. Neeman[2], M. Hoehn[1], T.D. Farr[1]

[1]Max-Planck-Institute for Neurological Research, Köln, Germany, [2]Department of Biological Regulation, The Weizmann Institute of Science, Rehovot, Israel

Background and aims: Angiogenesis in the brain is up-regulated in response to stroke (Slevin, *et al*., 2006. Clin Sci. 111: 171-83) and a few studies have attempted to image this process with magnetic resonance imaging (MRI). For example, using steady-state contrast enhanced MRI (SSCE-MRI), changes in microvessel density following permanent middle cerebral artery occlusion (MCAO) were observed in rats (Lin, *et al*., 2008. JCBFM. 42: 1-11). The primary aim of the present project is to characterize a time course of this response in a transient stroke mouse model. An additional strategy to look at angiogenesis will be to use transgenic mice that over-express a hemagglutinin-epitope (HA) tagged ferritin (Ferr) MRI-reporter in response to activation of the vascular endothelial cadherin (VECad) promoter (Cohen, *et al*., 2007. Nat Med. 13(4): 498-503).

Methods: 13 male adult VECad-HaFerr mice and 17 age-matched wildtype FVB mice received 30min of MCAO using the intraluminal filament technique. MRI was performed 7 days before, and 14 and 21 days after MCAO. The SSCE-MRI protocol included a combination of T_2 and T_2* sequences before and after injection of contrast agent (Sinerem, 30 mg/kg i.v.), as well as a diffusion-weighted MRI scan. Regions of interest (ROIs) were drawn on theT_2 maps (infarct core and peri-infarct zone (PIZ)) and copied into the corresponding relaxivity (R_2) and vessel density (Q) maps (Jensen and Chandra, 2000. MRM. 44: 224-30). Animals were sacrificed at day 21 and brain tissue processed for immunohistochemistry.

Results: Prior to stroke R_2 was significantly higher in the hippocampus, but not in the cortex or striatum, of VECad-HAFerr mice ($t(28)= -2.812$, $p=0.009$). MCAO produced extensive lesions (Fig1A) and final group sizes were (n=5 wildtype, n=2 VECad-HAFerr). There were no significant changes in microvessel density (quantity Q) over time in either region (Fig1A). However, R_2 decreased significantly after stroke in both the infarct core ($F(2,10)= 36.934$, $p< 0.0001$) and PIZ ($F(2,10)= 21.312$, $p< 0.0001$) (Fig1C+D, respectively). Interestingly, R_2 was slightly higher in the PIZ of the VECad-HAFerr mice (Fig1D). Immunohistological analysis showed dilated microvessels in the ischemic hemisphere compared to the contralateral side (Fig1B) but actual microvessel density counts are pending.

Conclusions: SSCE-MRI derived measurements of microvessel density (Q) did not show changes in the infarct core or PIZ after MCAO in mice. This could partially be due to the inherent image noise in the Q maps, particularly since changes in R_2 were observed in the infarct core. It appears that higher R_2 values are present in VECad-HAFerr mice, but more animals are needed to conclude this.

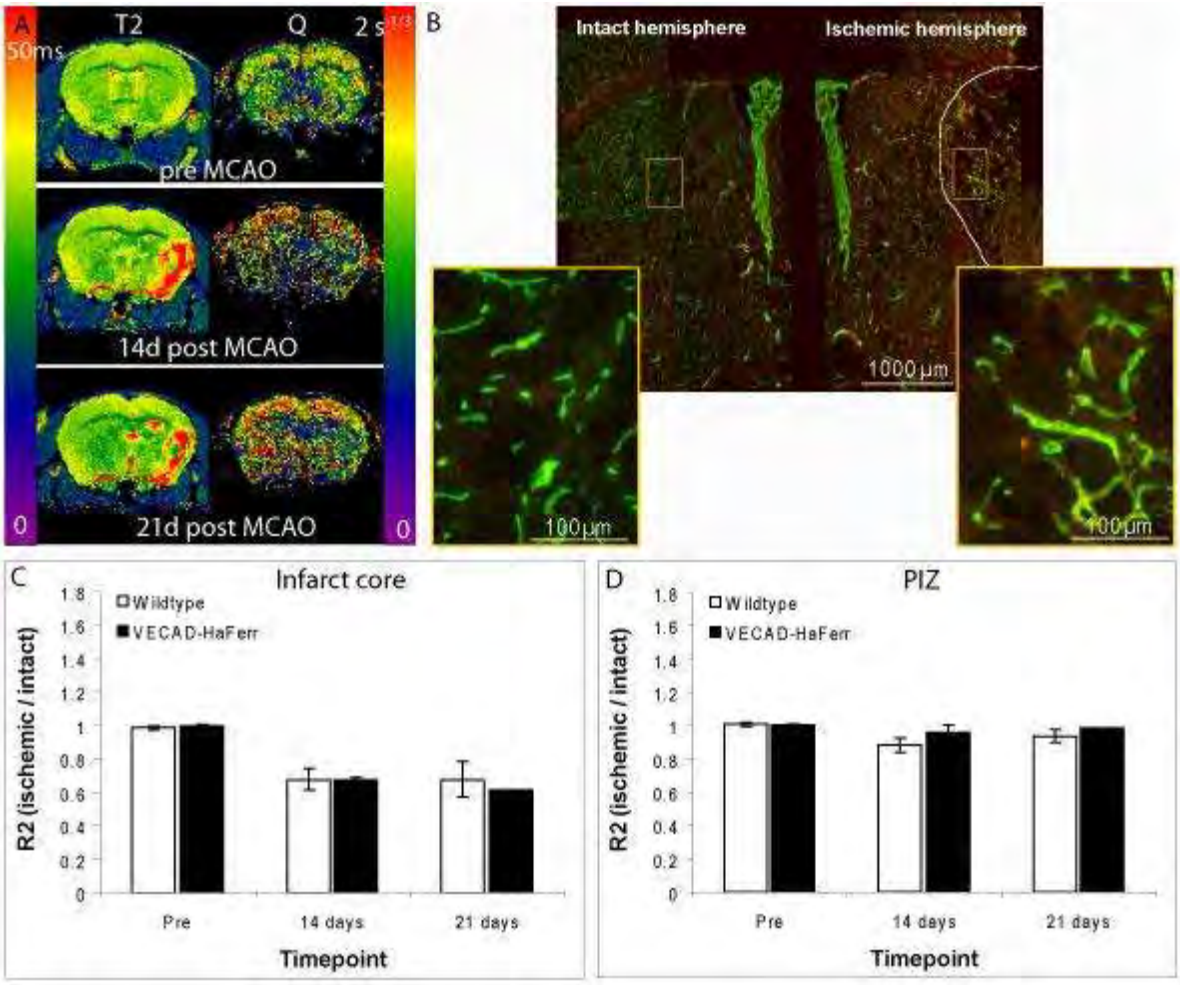

[Figure1]

A: T_2 and corresponding Q maps from a representative wildtype mouse at all measured time points. B: Laminin (green) and GFAP (red) stained tissue sections illustrating the microvessels in the intact and ischemic hemispheres. The white dotted line illustrates the infarct boundary and the boxes are displayed in higher magnification. C+D: Relaxivity values over time, expressed as a ratio of the ischemic to intact hemisphere, in the infarct core (C) and PIZ (D).

161

CEREBRAL BLOOD VOLUME FRACTION MAPPING IN MICE BY RAPID STEADY STATE T_1 MAGNETIC RESONANCE IMAGING

T.-A. Perles-Barbacaru[1], F. Berger[2], H. Lahrech[1]

[1]Functional and Metabolic Neuroimaging, [2]Brain Nanomedicine Group, INSERM U836, Grenoble Institute of Neurosciences, University Joseph Fourier, Grenoble, France

Most quantitative approaches for cerebral blood volume fraction (BVf) mapping by magnetic resonance (MR) imaging require intravenous (i.v.) injections of contrast agents (CA) [1,2], presenting limitations for longitudinal studies in mouse models of brain dysfunction. In this study, we demonstrate that the Rapid-Steady-State-T_1 ($RSST_1$) MR-technique, previously used with i.v. injections [1] in rats, can be used with intraperitoneal (i.p.) injections of Gd-DOTA to safely and reliably acquire serial cerebral BVf maps in mice. To achieve this aim, we compared the BVf after i.v. and i.p. CA injections in the same mouse.

BVf maps were acquired in NMRI mice (n=6) in a 47/40 Bruker Biospec-USR-AV-III scanner using a 3D inversion-recovery prepared MDEFT sequence (TE=1.2 ms, TR_{echo}=6.5 ms, α=10°, matrix 32×32, FOV 15×15 mm^2, 8 coronal slices × 0.7 mm). A dynamic $RSST_1$-scan (TR=750 ms, T_{inv}=303 ms, 6 s/repetition) was acquired over 65 minutes with the i.v. injection (0.7 mmol/kg) administered at 5 minutes and the i.p. injection (6 mmol/kg) administered at 15 minutes into the scan. The BVf maps were obtained according to $S_{norm}(t) = (S_{post}(t) - < S_{pre}>)/S_0$, where $S_{post}(t)$ is the post-contrast, $< S_{pre}>$ the average pre-contrast and S_0 the proton density weighted signal (TR=10 s, T_{inv}=9 s, duration 1 min 20 s). The normalized signal $S_{norm}(t)$ equals the BVf when the CA is confined to the intravascular compartment and when blood $T_1 < T_{inv}/5 \approx$ 60 ms [1]. To confirm this condition, we measured T_1 and T_2 in plasma sampled 30 minutes after i.p. administration of 6 mmol/kg Gd-DOTA (n=4) and used these plasma samples in an *in vitro* BVf experiment with the $RSST_1$-technique as described in [1], expecting BVf=1.

An i.p. dose of 6 mmol/kg Gd-DOTA was safe [3] and yielded plasma T_1 and T_2 of 4.6 ± 0.3 ms and 5.7 ± 0.5 ms, respectively, demonstrating that the intravascular protons relax to thermal equilibrium with little transverse relaxation effects. The average BVf was 1.01 ± 0.01 in the *in vitro* experiment.

In mouse brain and blood vessels, 15 minutes after i.p. administration of 6 mmol/kg Gd-DOTA, a steady state signal was obtained for a duration of ≥ 20 minutes with an amplitude equal to the peak signal amplitude after i.v. injection, corresponding to the thermal equilibrium magnetization of the vascular space and leading to equivalent cerebral BVf measures of 0.023 ± 0.003. However, regions of interest including ventricles exhibit a CA leakage profile, such as typically observed in skin or muscle tissue.

Cerebral BVf mapping in mice is feasible with the $RSST_1$-MR-technique. The time window after i.p. CA injection is ≥ 20 minutes and can be used for acquiring BVf maps with increased spatial resolution or for determining functional changes of the BVf during the time interval. Compared to i.v. injections, i.p. CA administration in mice is less traumatic with practically no risk for emboli or hypervolemia, and can therefore be used repeatedly in longitudinal studies such as for monitoring tumor angiogenesis.

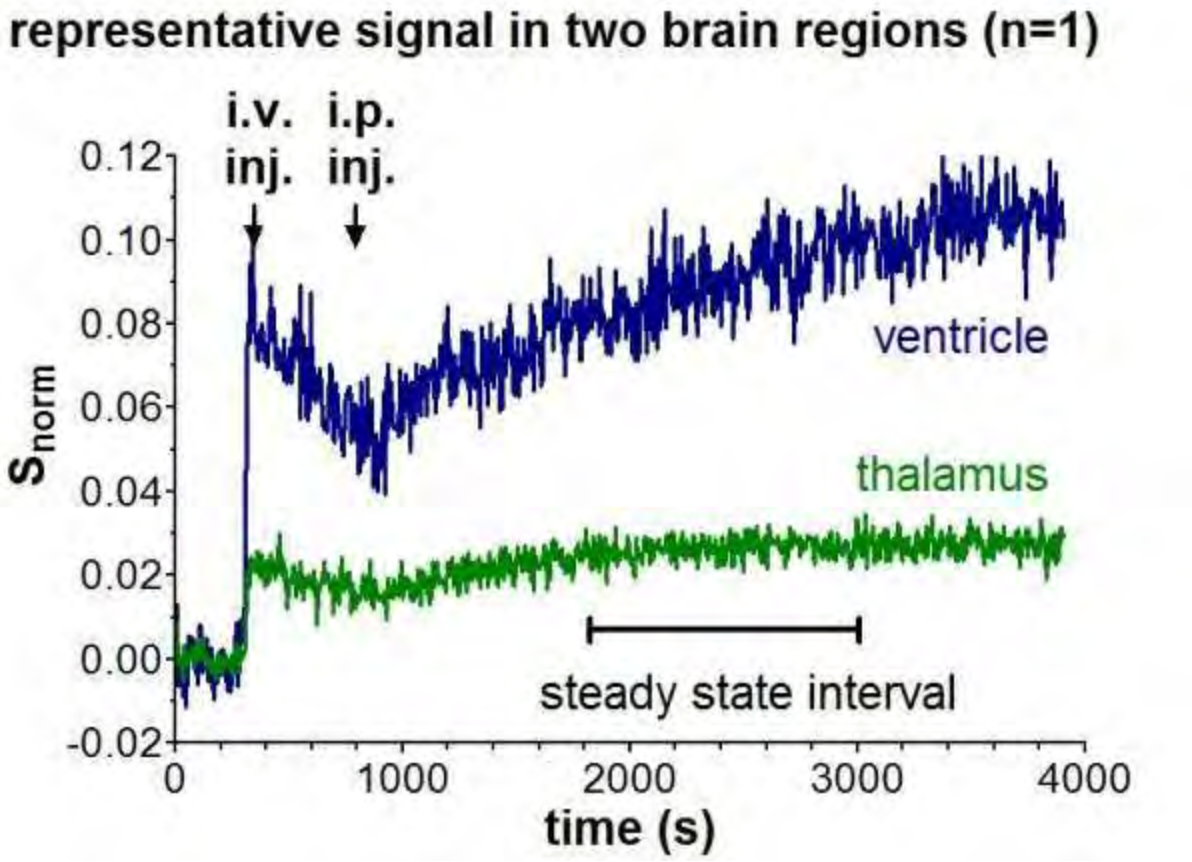

[Graph]

References:

[1] Perles-Barbacaru, JCBFM 2007;

[2] Schwarzbauer, MRM 1993;

[3] Moreno, NMR Biomed 2006

162

APPLICATION OF NETWORK CONCEPTS TO ISCHEMIC BRAIN INJURY

D.J. DeGracia

Department of Physiology, Wayne State University, Detroit, MI, USA

Objectives: The intracellular effects of ischemia on neurons are currently modeled as an "ischemic cascade" in which a linear causal sequence of cellular and molecular events generates cell death. Neuroprotective therapies based on this model have sought to inhibit a "bottle neck" point in this cascade to prevent cell death. However, neuroprotective therapies have encountered a frustrating "translational roadblock" [1]. Thus, much effort to identify and overcome weaknesses in clinical and preclinical stroke research has occurred. One avenue for contributing to this effort is to determine if alternative models can account for the mass of empirical data.

Methods: We apply network dynamical concepts to interpret the empirical data and thereby derive an alternative theoretical understanding of ischemic brain injury [2].

Results: A systems biology approach allows us to view the effects of ischemia on brain cells as generating a complex, intracellular chemical network displaying nonlinear dynamics. The course-grained dynamics of this network are inferred from the fact that there are only two mutually exclusive outcomes for a neuron after ischemia: recovery or death, which occur as a function of the magnitude of the ischemic insult. Any two-state dynamical system is "bistable" and this property sets strict limits on the network behavior: any specific node is constrained to contribute to either recovery or death. Thus all pro-damage and all pro-survival nodes may be aggregated, in a nonlinear fashion, to total damage (D_T) and total induced stress responses (S_T), respectively. Thereby the complex chemical network induced in neurons by ischemia can be effectively reduced to a two-dimensional (2D) circuit representing the bistable competition between D_T and S_T. The resulting 2D post-ischemic state space describes the core system dynamics, serving as a "phase diagram" of all possible chemical networks and their associated post-ischemic cell phenotypes as a function of ischemic intensity. This bistable state space offers the advantage over the "cascade" concept by providing formal definitions of cell death and survival. Cells die when $D_T > S_T$, but survive when $S_T > D_T$. The model implies that targeting individual nodes for therapeutic purposes will be ineffective because of nonlinear interactions in the network. Instead, the model indicates that the appropriate target of neuroprotective therapy is to seek to shift the competition between D_T and S_T in favor of S_T. This gives rise to the counter-intuitive notion that drug efficacy is independent of its binding-target specificity.

Conclusion: Application of network concepts to brain ischemia gives rise to an alternative, bistable network model of ischemic cell injury which is, both in principle and in practice, amenable to empirical verification. This model provides a unified systematic accounting of the response of brain cells to ischemic injury and gives rise to a completely novel concept of neuroprotection.

References:

[1] Endres M, Engelhardt B, Koistinaho et al (2008) Improving outcome after stroke: Overcoming the translational roadblock. Cerebrovasc Dis. 25:268-78

[2] DeGracia DJ (2010) Towards a dynamical network view of brain ischemia and reperfusion: Parts I-IV. *J Exp Stroke Transl Med*. 3: 59-114

163

^{18}F-LABELLED ALKYL-SUBSTITUTED SPIROCYCLIC PIPERIDINES - POTENTIAL RADIOTRACERS FOR PET IMAGING OF Σ_1 RECEPTORS

W. Deuther-Conrad[1], A. Maisonial[1], S. Fischer[1], A. Hiller[1], D. Schepman[2], E. Große Maestrup[2], U. Funke[1], J. Steinbach[3], B. Wünsch[2], P. Brust[1]

[1]Forschungszentrum Dresden-Rossendorf, Institut für Radiopharmazie, Forschungsstelle Leipzig, Leipzig, [2]Universität Münster, Institut für Pharmazeutische und Medizinische Chemie, Münster, [3]Forschungszentrum Dresden-Rossendorf, Institut für Radiopharmazie, Dresden, Germany

Objectives: Neuroprotective effects mediated by signal transduction via the transmembrane σ_1 receptor localised in the endoplasmatic reticulum make this receptor a promising target for novel approaches in the therapy of neurodegenerative diseases. Furthermore, behavioural changes are assumed to be related to alterations in the expression of σ_1 receptors mainly expressed in the striatum. Thus, molecular imaging of σ_1 receptors of the brain may hold potential in diagnostics and drug development, and we have compared in mice radiotracer properties of a series of new ^{18}F-labelled spirocyclic piperidine derivatives with high affinity and selectivity for σ_1 receptors.

Methods: Radiosynthesis of fluoromethyl- ([^{18}F]WMS1850), fluoroethyl- ([^{18}F]fluspidine), fluoropropyl- ([^{18}F]WMS1813), and fluorobutyl-([^{18}F]WMS1847) substituted derivatives was performed by nucleophilic substitution of the corresponding tosylate precursors using K[^{18}F]F-K222-carbonate complex. Organ distribution of radiotracers applied i.v. was determined in female CD-1 mice at 5, 30, 60, and 120 min p.i. Spatial distribution of the radiotracer binding sites in the brain was examined by ex vivo autoradiography at 45 min p.i. Target specificity was investigated in blocking studies with pre-application of 1 mg/kg of the σ_1 receptor ligand haloperidol by assessing the organ distribution of the respective radiotracer at 60 min p.i. The metabolic stability in vivo of each radiotracer was evaluated by radio-TLC and -HPLC analyses of brain, plasma, and urine samples.

Results: The radiotracers were obtained with radiochemical yields of 35-53%, radiochemical purities >98.5%, and specific activities >150 GBq/µmol. All radiotracers readily passed the blood-brain barrier with high brain uptake values at 30 min p.i.: [^{18}F]fluspidine = 4.71 ± 1.39 % ID/g, [^{18}F]WMS1813 = 3.18 ± 0.68 % ID/g, [^{18}F]WMS1850 = 2.65 ± 0.68 %ID/g, and [^{18}F]WMS1847 = 1.78 ± 0.16 %ID/g. High initial radioactivity uptake was also observed in peripheral organs which express σ_1 receptors such as spleen, thymus, kidney, and stomach. In brain as well as in these organs the uptake of radioactivity was significantly reduced in mice pre-treated with haloperidol. Distribution patterns of the radiotracer binding sites in brain were resembling for all four radiotracers with [^{18}F]fluspidine possessing the highest target (facial nucleus)-to-nontarget (olfactory bulb) ratio (4.69 at 45 min p.i.). The metabolic stability in vivo was high for all radiotracers (75% parent radiotracer in plasma at 30 min p.i.), and none of the peripherally detected radiometabolites crossed the blood-brain barrier.

Conclusion: Fluoroalkylated spirocyclic piperidines are high affinity ligands for σ_1 receptors with high brain uptake, specific binding, and good metabolic stability. Within the herein reported series of ^{18}F-labelled derivatives, the in vivo data identify [^{18}F]fluspidine as the most suitable radiotracer for further development in molecular imaging of σ_1 receptors. [^{18}F]fluspidine radiosynthesis is selected for transfer to an automated radiosynthesis module for further preclinical development.

164

DEVELOPMENT OF AQUAPORIN-4 PET IMAGING

T. Nakada[1,2]

[1]Center for Integrated Human Brain Science, Brain Research Institute, University of Niigata, Niigata, Japan, [2]Neurology, University of California, Davis, Martinez, CA, USA

Objective: Aquaporin-4 (AQP-4) is a membrane protein in the aquaporin family of water transporters which is widely expressed in the central nervous system (CNS). Although much remains to be elucidated, evidence continues to accumulate that AQP-4 is actively involved not only in vital physiological brain function such as neural-flow coupling, but also in pathophysiological processes of CNS diseases including brain edema, multiple sclerosis, and Alzheimer's disease. The study was focused on developing selective AQP-4 ligands for clinical positron emission tomography (PET) imaging.

Method: One of the AQP-4 inhibitors previously identified in our laboratory, TGN-020 (2-nicotinamido-1,3,4-thiadiazole), was chosen as base substrate (Figure 1). The synthesis of ^{11}C-TGN-020 was performed using [carboxyl-^{11}C]-nicotinic acid and a TRACERlab FXC (GE Healthcare) automated versatile synthesizer. The target radioligand was synthesized in a suitable amount (300 MBq average) and radiochemical purity (>95%) for further studies in vivo.

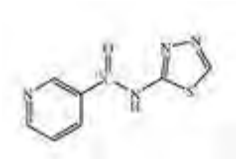

[Figure 1]

Results: TGN-020 PET images of wild type (WT) and AQP-4 null mice (KO), obtained on a GE eXplore VISTA animal PET system, showed distinct differences highly consistent with known distribution of AQP-4 in the brain. Clear differences were observed in the localized contrast due to this ligand in brain and skeletal muscle tissue of WT and KO animals, tissues known to have selective distribution of AQP-4. Less significant differences were found in other tissues not known to have selective AQP-4 distribution. These results are consistent with ligand selectivity for AQP over other proteins, but suggest some degree of non-selectivity for AQP-4 over other AQP isozymes. Nevertheless, TGN-020 appears to be sufficient as ligand for clinical AQP-4 PET development.

Conclusion: The study demonstrated that ^{11}C-TN020 is an appropriate PET ligand for analysis of AQP-4 distribution in human brain clinical PET studies. All necessary toxicology studies have been completed at the point of this abstract submission. Following final approval by the University of Niigata Institutional Review Board (IRB), clinical AQP-4 images of human brain are expected to emerge.

Supported by grants from the Ministry of Education, Culture, Sports, Science, and Technology (Japan) and University of Niigata.

165

NOVEL AND PROMISING RADIOTRACERS FOR PET IMAGING OF THE ENDOCANNABINOID SYSTEM: FATTY ACID AMIDE HYDROLASE (FAAH) INHIBITORS

A.A. Wilson[1], J. Parkes[1], A. Garcia[1], S. Houle[1], J. Tong[2], N. Vasdev[1]

[1]PET Centre, [2]Human Neurochemical Pathology Laboratory, CAMH and University of Toronto, Toronto, ON, Canada

Introduction: Fatty Acid Amide Hydrolase (FAAH) is the enzyme responsible for hydrolysing endocannabinoids such as anandamide. As such it plays a major role in setting the tone of the cannabinoid system in the human brain, regulating anandamide levels, and terminating signaling at cannabinoid receptors. There is substantial evidence that dysfunction of FAAH biochemistry plays a major role in addiction, and in psychiatric and neurological illnesses. Thus the ability to measure the levels of FAAH in the living human brain would be extremely useful, but no human PET or SPECT studies on FAAH have been reported as yet. We have synthesised a series of six novel carbon-11 labeled aryl carbamate inhibitors of FAAH using recently developed [^{11}C]CO_2 fixation chemistry and evaluated them as potential PET radiotracers for FAAH imaging via ex vivo biodistribution studies in rat brain in conjunction with pharmacological challenges.

Methods: [^{11}C]-labelled radiotracers were synthesised by one-pot coupling of alkylamines, [^{11}C]CO_2, and substituted phenols to generate a series of aryl carbamates, radiolabelled in the key carbonyl position. Radiotracers were evaluated ex vivo in rats upon tail-vein injection. Rats were sacrificed at various time points post-injection, and tissue samples were dissected, counted, and weighed. Specific binding to FAAH was investigated by pretreatment of animals with the prototypical FAAH inhibitor URB597 (2 mg/kg IP). For metabolism and mechanism of binding studies, whole brains were excised post-radiotracer injection, homogenised, and extracted exhaustively with 80% aq. acetonitrile to determine the time course and fraction of radioactivity that was irreversibly bound to brain parenchyma.

Results: Radiotracers were synthesised in unoptimised radiochemical yields of 5-10% (uncorrected, based on [^{11}C]CO_2, at EOS) in 25-30 min from EOB with specific activities of 70-150 GBq/μmol. Brain uptake of the six radiotracers varied from moderate (0.7 SUV) to excellent (4.2 SUV) with little washout over time, which is characteristic of irreversible binding. In all cases, highest regional uptake of radioactivity was seen in the cortex, intermediate in the cerebellum, and lowest in the hypothalamus, reflecting the reported distribution of FAAH. Pre-treatment with the well-characterised FAAH inhibitor, URB597, reduced brain uptake of radioactivity for all radiotracers by 65-95% depending upon region. Homogenised brain extractions experiments on selected radiotracers demonstrated unequivocally that they were irreversibly bound to FAAH, consistent with the mechanism of action of this class of compounds as FAAH inhibitors.

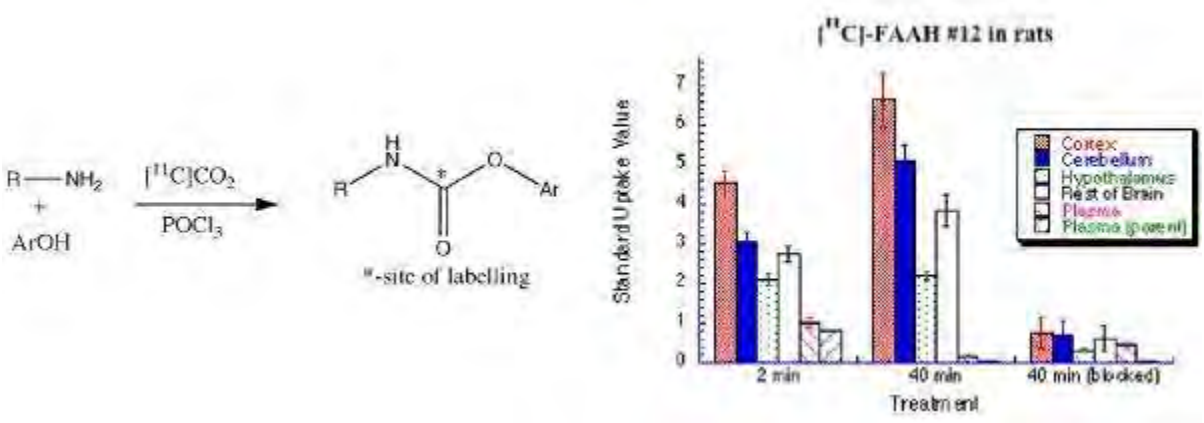

[combi1]

Conclusions: Several [^{11}C]-carbamate radiotracers demonstrate highly favourable properties for PET imaging of FAAH, including excellent brain uptake, appropriate regional heterogeneity, and specificity of binding based on ex vivo biodistribution studies in conscious rat brain. More detailed kinetic analyses of binding are underway to determine the optimal candidate(s) for human PET imaging of FAAH.

166

A CONTROL SYSTEMS VIEW OF THE ASTROCYTE-NEURON LACTATE SHUTTLE HYPOTHESIS

M. Cloutier[1], F.B. Bolger[2], J.P. Lowry[2], P. Wellstead[1]

[1]Hamilton Institute, [2]Department of Chemistry, National University of Ireland, Maynooth, Ireland

The astrocyte-neuron lactate shuttle (ANLS) hypothesis is based upon the proposition that astrocytic lactate can fuel neuronal activity during stimulation. We used a mathematical model of brain energy metabolism, calibrated and validated by *in vivo* measurements of energy substrates, to interpret the ANLS as a control mechanism that enhances the neuronal regulation of ATP concentration during transient energy demands. In rest conditions, results from the model predict that neurons use mainly glucose to sustain their energy requirements. By contrast, during physiological stimuli, the model predicts that neurons dynamically increase their lactate (LAC) usage to produce the additional amount of energy required, resulting in almost perfect regulation of ATP. This perfect adaptation between energy demand and supply is possible because of two major mechanisms: a strong regulation of mitochondrial activity in neurons and a favourable LAC gradient, whereby the additional LAC is supplied through changes in astrocytic metabolism.

The predictions from our model are consistent with *in vitro* and *in vivo* observations reported in the literature for comparable conditions. Also, as a specific test of the role of astrocyctes, model predictions were compared with *in vivo* glucose and LAC data obtained from experiments in which propanolol was used to artificially reduce glycogen breakdown in astrocytes. Both the *in vivo* and *in silico* limiting of glycogen breakdown produced an imbalance in LAC supply that is coherent with the interpretation of ANLS as a dynamic response to neuronal stimulation.

Our mathematical representation of brain energy metabolism also suggests a cybernetic interpretation of the metabolic regulation in terms of the control components that act to reduce ATP variations in neurons (but not in astrocytes). In this control systems view, the internal regulation of neuronal metabolism is equivalent to feedback control and the additional supply of substrate by an external system (i.e. the astrocytes) is a feedforward control mechanism. Given that brain energy metabolism is a process with a very fast turnover rate, the use of a feedforward system to reduce ATP variations in neurons corresponds perfectly with that expected in a well designed control system. A conclusion from this interpretation is that both sides of the ANLS debate have some foundation. Specifically, in the rest state neuronal energy supply is regulated by internal feedback, with astrocytic lactate playing a negligible role. However, during periods of high activity the astrocytic contribution provides the fast transient feedforward supplementation of energy needed to maintain ATP levels.

167

EFFECT OF ANGIOTENSIN II AND XINKANG ON APOPTOSIS, CYTOKINES AND MMPS IN ENDOTHELIAL CELL AND SMC

J. Liang, J. Tan, L. Shao, **X. Liang**

Qingdao University, School of Medicine, Yantai, China

Introduction: Xinkang capsule, a preparation made of several Chinese medicinal herbs, has been successfully used to prevent or treat the cerebrovascular and cardiovascular diseases. The mechanisms of the effects remain uncertain.

Objective: To study the effects of angiotensin II in different concentrations and different action time on apoptosis ratio and the expression of cytokines in vascular endothelial cells , and on MMPs in vascular smooth muscle cells and the influences of Xinkang on it. Methods Flow cytometer was used to measure the apoptosis ratio and the expression of Fas , Bcl-2. RT—PCR , to measure the changes of MMPs. IL-6, IL-10 were evaluated by ELISA means.

Results:

(1) Apoptosis ratio and the expression of Fas, Bcl-2, IL-6 were induced and increased but IL-10, decreased by angiotensin II with the increase of concentrations and action time.

(2) MMPs were also induced and increased by angiotensin II in SMC, especially in high concentrations. And MMP-9 was earlier than MMP-1 and MMP-2.

(3)The effects of angiotensin II were significantly inhibited when cells were pretreated with the Xinkang.

Conclusions: Xinkang capsule may have the inhibition effect against AngII, and also may have the regulative effect on apoptosis ratio and the expression of Fas , Bcl-2, IL-6, IL-10, and MMPs.

169

TRANSFUSION OF ENDOTHELIAL PROGENITOR CELLS PROMOTES ANGIOGENESIS AND REDUCES CEREBRAL ISCHEMIC DAMAGE IN DB/DB DIABETES MICE

J. Chen, S. Chen, C. Zhang, J. Wang, W. Zhang, Y. Chen

Wright State University, Dayton, OH, USA

Introduction: There is accumulating evidence showing that circulating endothelial progenitor cells (EPCs) are reduced and dysfunctional in diabetic patients. EPCs based therapy represent a promising strategy for promoting angiogenesis and tissue repair in diabetes. This study was designed to investigate the effect of EPCs transplantation in promoting angiogenesis and treating ischemic stroke in diabetes.

Methods: Male adult db/db type-2 diabetic mice and the db/+ control mice were divided into four groups (n=5-7/group) for middle cerebral artery occlusion (MCAO) surgery or sham surgery, and EPCs or vehicle transfusion. EPCs were cultured from the bone marrow of db/+ mice and injected ($1x10^5$ cell/100 µl) via tail vein 2 hrs after MCAO. Mice were sacrificed 2 or 7 days after surgery. The levels of circulating EPCs (CD34+KDR+ cells) were determined by flow cytometry. Ischemic volume and cerebral microvascular density were determined histologically on brain sections by Fluoro-J and anti-CD31 antibody staining, respectively, as previous reports.

Results:

1) The db/db mice had a lower level of circulating EPCs (170±19 n/ml and 480±50 n/ml, db/db sham vs db/+ sham, P< 0.01), lower cerebral microvascular density in cortex (338±29 capillaries/mm^2 and 416±32 capillaries/mm^2; db/db sham vs db/+ sham, P< 0.01) and higher infarct volume after MCAO (in day 2: 35.2±1.6% and 23.2±2.0%; db/db MCAO vs. db/+ MCAO, P< 0.01);

2) following MCAO surgery, the levels of circulating EPCs were increased in day 2 in both db/db (306±23 n/ml, vs sham, P< 0.01) and db/+ mice (1720±105 n/ml, vs sham, P< 0.01), and returned to basal level in day 7 (200±21 n/ml in db/db mice, 585±52 n/ml in db/+ mice, vs sham, P>0.05). However, the increase of circulating EPCs in day 2 was less in db/db mice (db/db MCAO vs db/+ MCAO, P< 0.01);

3) EPCs transfusion increased circulating EPCs more in db/+ mice (in day2: 1660±130 n/ml and 8840±189 n/ml; in day 7: 660±30 n/ml and 1840±189 n/ml; db/db vs db/+, P< 0.01);

4) EPCs transfusion increased the microvascular density in peri-infact area in day 7 (328±22 capillaries/mm^2 and 193±18 capillaries/mm^2 in db/db mice, 425±29 capillaries/mm^2 and 288±21 capillaries/mm^2 in db/+ mice, vs vehcile, P< 0.01), but not in day 2 (180±17 capillaries/mm^2 and 165±17 capillaries/mm^2 in db/db mice, 225±19 and 230±20 capillaries/mm^2 in db/+ mice, vs vehicle, P>0.05), and decreased ischemic damage in day 7 in both db/db mice (20.5±2.0% and 30.1±2.5%, vs vehicle, P< 0.01) and db/+ mic (14.5±2.0% and 25.8±2.2%; vs vehicle, P< 0.01).

Conclusion: The data indicate that lower level and/or dysfunction of circulating EPCs might be responsible for the worse outcome in db/db mice exposed to ischemia. EPCs transfusion therapy could be an avenue for treatment of ischemia stroke in diabetes.

171

MOLECULAR MECHANISMS OF BLOOD-BRAIN BARRIER REGULATION DURING HEALTH AND DISEASE

R. Daneman

UCSF, San Francisco, CA, USA

The blood vessels of the central nervous system (CNS) form a barrier that is crucial for proper brain function and to protect the CNS from injury and disease. In patients with multiple sclerosis (MS), there is a breakdown of this blood-brain barrier (BBB) at the site of active lesions, which allows for immune cells and molecules to enter the CNS and attack the myelin causing neural degradation and paralysis. Although the properties of the BBB are manifested in the endothelial cells, transplantation studies have identified that they are induced by interactions with the CNS microenvironment. Determining the mechanisms regulating BBB function may prove vital to develop therapeutics to restore the BBB in MS patients, preventing immune infiltration and demyelination. To understand the cellular and molecular mechanisms that regulate blood-brain barrier formation we have used microarray analysis to compare the gene expression of endothelial cells purified from the CNS with endothelial cells purified from non-neural tissue, and thus have generated a comprehensive resource of transcripts that are enriched in the BBB forming endothelial cells of the brain. Through this comparison we have identified novel tight junction proteins, transporters, metabolic enzymes, signaling components, and unknown transcripts whose expression is enriched in CNS endothelial cells. This analysis has led to the identification that neural stem cell-derived Wnt/beta-catenin signaling is required for CNS angiogenesis, but not angiogenesis in non-neural tissue, and also induces BBB-specific gene expression. Furthermore, we have identified a role for pericytes in regulating the permeability of CNS vessels by inhibiting the expression of molecules that increase vascular permeability. In particular, pericytes limit the expression of leukocyte adhesion molecules in CNS endothelial cells, which limits CNS immune infiltration. This has led to a model for BBB formation in which CNS endothelial cells are induced to express BBB-specific genes during angiogenesis, and then the functional properties of the BBB are regulated by pericytes and astrocytes.

173

SPATIAL COMPARISON OF HIGH-DENSITY DIFFUSE OPTICAL TOMOGRAPHY AND FMRI MAPPING OF THE VISUAL CORTEX

A. Eggebrecht, B. White, S. Ferradal, A. Snyder, J. Culver

Radiology, Washington University School of Medicine, St Louis, MO, USA

Objectives: Near infrared spectroscopy (NIRS) has long promised to extend functional neuroimaging to the bedside. Recent improvements in image quality have been achieved through high-density diffuse optical tomography (HD-DOT) methods with estimates of resolution near 1-1.5 cm (White et al., 2010). However, spatial comparisons have not been made to either the underlying MRI anatomy, or to subject matched fMRI studies. We herein provide an across-subject comparison demonstrating that the imaged HD-DOT exhibit gyral-specificity to the cortical structure. Additionally, cross-modal validation is provided by comparing visual cortical maps obtained via subject-anatomy-registered HD-DOT with those obtained with fMRI.

Methods: A high-density array (24 sources and 28 detectors) is placed over the visual cortex to record activations to visual stimuli (Fig. 1,d). The subject-specific anatomical MR (Fig. 1,a) is segmented (Fig. 1,b) and used to create a head model of optical properties for use with the DOT reconstructions. Activations recorded with DOT (Fig. 1,e) in response to the visual stimuli are directly co-registered to the subject-specific anatomical MRI. The fMRI activation (Fig. 1,g) is smoothed to match the DOT point-spread function of 13 mm. Visual cortex was mapped using standard visual stimuli (Sereno et al., 1994) consisting of phase encoded retinotopic stimuli (Fig. 1,i): 10 Hz reversing flickering checkerboard wedges moving clockwise or counterclockwise and annuli moving in or out of the center of the visual field. Cortical activations for both DOT and fMRI are visualized using the Caret software package (Van Essen et al., 2001).

Results: In response to the rotating wedges, a strong activation is localized within the contralateral visual cortex as measured by both DOT (Fig. 1,e&f) and fMRI (Fig. 1,g&h). Activations from each of the four quadrants (Fig. 1,j) map onto the cortical surface at well defined loci with the positions of all four quadrants in agreement between DOT (Fig. 1,k) and fMRI (Fig. 1,l). Images for the annuli (radial mapping) also show agreement between the two modalities.

Conclusions: Functional neuroimaging with DOT is able to localize and map regions of the visual cortex in good agreement with the current gold standard fMRI. This validates both the HD-DOT data sets and the subject specific head modeling approach presented. As the validity of DOT is further established and demonstrated, we have a stronger foundation for applying DOT to analyzing cortical function in adults and children at the bedside as well as in answering fundamental neuroscience questions for which fMRI is ill suited such as freely behaving or ICU stricken subjects.

References:

Sereno M.I., McDonald C.T., Allman J.M. "Analysis of retinotopic maps in extrastriate cortex," Cerebral Cortex, 4, 601-620, (1994).

Van Essen, D.C., Dickson, J., Harwell, J., Hanlon, D., Anderson, C.H. and Drury, H.A. "An Integrated Software System for Surface-based Analyses of Cerebral Cortex," Journal of American Medical Informatics Association", 8(5): 443-459, (2001).

White B.R. & Culver J.P., “Quantitative evaluation of high-density diffuse optical tomography: in vivo resolution and mapping performance,” J. Biomed Optics, 15, 026006-1--026006--14, (2010).

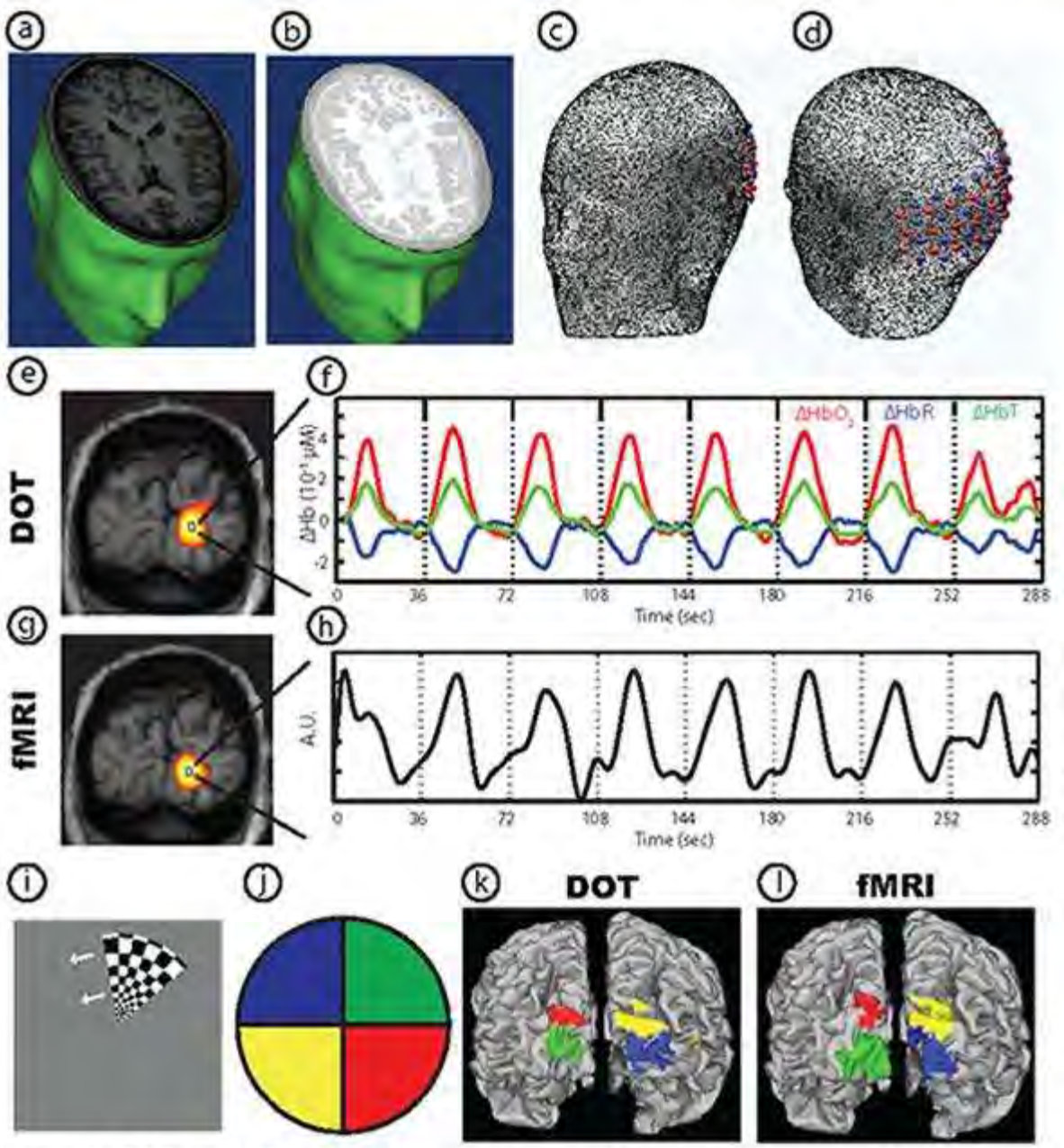

Figure 1: DOT and fMRI of human retinotopy. A T1-weighted anatomical MRI **(a)** is segmented into five tissue types **(b)** to assign the relevant optical properties in a subject-specific MRI-derived head mesh **(c)** which along with optode placements **(d)** provides for an accurate DOT light model. Because the DOT model is created within MRI space, direct voxelwise comparisons are possible between DOT **(e,f)** and fMRI **(g,h)**. Visual cortex was mapped using a standard 10 Hz reversing rotating checkerboard wedge **(i)**. Relative to the stimulus position **(j)**, activations in response to a wedge in the center of the colored quadrant are shown on the cortex as measured via DOT **(k)** and fMRI **(l)**.

[DOT and fMRI of human retinotopy]

174

HISTOLOGICAL EVIDENCE REVEALS MRNA GRANULES ARE CYTOPLASMIC STRUCTURES

J.T. Jamison, J.J. Szymanski, D.J. DeGracia

Physiology, Wayne State University, Detroit, MI, USA

Introduction: The death of selectively vulnerable neurons following global brain ischemia and reperfusion correlates with irreversible translation arrest (TA) [1]. We previously reported that sequestration of poly-adenylated mRNAs away from the small ribosomal subunit in the form of mRNA granules correlated with prolonged TA in reperfused neurons [2]. Although the mRNA granules colocalized with the known mRNA binding proteins eIF4G, PABP and HuR, the nature of the mRNA granules remained unclear. To further discern the nature of mRNA granules formed in post-ischemic neurons we here describe additional colocalization studies with markers of known intracellular structures.

Methods: We performed double labeling with fluorescent in situ hybridization (FISH) for polyA mRNAs and immunofluorescence (IF) for markers detecting endoplasmic reticulum, Golgi apparatus, mitochondria, nucleus, neurofilaments, microtubules, ribosomal subunits, and nuclear transport proteins. Ten minutes of normothermic global brain ischemia was induced in male Long Evans rats using bilateral carotid artery occlusion with hypovolemic hypotension, followed by various durations of reperfusion. Experimental groups (n=5 per group) were: (1) non-ischemic sham operated controls, and 10 min of ischemia followed by: (2) 1hr, (3) 8hr, (4) 16 hr, (5) 36 hr, and (6) 48 hr reperfusion. Brains were perfusion fixed with 4% PFA, 50 micron slices through dorsal hippocampus prepared, and double labeled by FISH/IF for polyA mRNA and the markers listed above. Images acquired under 63X oil immersion were evaluated for colocalization.

Results: mRNA granules did not colocalize with ribosomal subunits, mitochondria, neurofilament or microtubule markers. There was very slight colocalization of mRNA granules with markers of endoplasmic reticulum and the Golgi apparatus. Interestingly, mRNA granules clearly outside of the nuclear boundary showed colocalization with the widely-used neuronal marker NeuN. There were not major changes of these patterns of colocalization as a function of reperfusion duration.

Conclusion: Lack of colocalization of the mRNA granules with markers of major subcellular organelles indicates these are primarily cytoplasmic structures. This information is of technical use for future biochemical characterization of mRNA granules. The cytoplasmic nature of the mRNA granules is consistent with our previously hypothesized assignment of mRNA granules as HuR granules [3]. HuR granules are known to be involved in mRNA regulation under conditions of cellular reprogramming, thereby supporting the notion that mRNA granules are markers of the intracellular stress response induced in neurons by brain ischemia and reperfusion.

Citations:

[1] Hossmann KA. Disturbances of cerebral protein synthesis and ischemic cell death. Prog. Brain Res. 1993; 96:161-177.

[2] Jamison JT, Kayali F, Rudolph J, Marshall M, Kimball SR, DeGracia DJ. Persistent

redistribution of poly-adenylated mRNAs correlates with translation arrest and cell death following global brain ischemia and reperfusion. Neuroscience. 2008;154(2):504-20.

[3] DeGracia DJ, Jamison JT, Szymanski JR, Marshall MK. Translation Arrest and Ribonomics In Post-ischemic Brain: Layers and Layers of Players. J Neurochem. 2008;106(6):2288-301.

175

DIFFERENTIAL INDUCTION OF PYRUVATE DEHYDROGENASE KINASE AND PHOSPHATASE EXPRESSION AFTER TRAUMATIC BRAIN INJURY IN RAT: IMPLICATION FOR GLUCOSE METABOLISM

G. Xing, M. Ren, W. Watson, J.T. O'Neill, A. Verma

Uniformed Services University of the Health Sciences, Bethesda, MD, USA

Background: Dysregulated brain glucose metabolism is a metabolic characteristic in people with traumatic brain injury (TBI). The mechanism is unknown. Pyruvate dehydrogenase (PDH) is the rate-limiting enzyme coupling cytosolic glycolysis to mitochondrial citric acid cycle, and plays a critical role in maintaining homeostasis of brain glucose metabolism. Brain PDH activity is tightly controlled by balanced activities between PDH kinase (PDK1-4) and PDH phosphatase (PDP1-2): phosphorylation of PDHE1α1 subunit (p-PDHE1α1) by PDK inhibits PDH activity whereas dephosphorylation of p-PDHE1α1 restores PDH activity. We hypothesized that the balance between PDK and PDP expression was disrupted following TBI.

Objectives: To determine PDK and PDP isoenzyme mRNA and protein expression and in rat brain at various time after controlled cortical impact (CCI).-induced TBI.

Methods: CCI was induced in young adult male Sprague-Daley rats (170-200g) with a penetration depth of 2.5 mm, at a velocity of 4 m/s. Brain samples were analyzed at 4 hr, 1 d, 3 d and 7 d post TBI with immunohistochemistry, in situ hybridization, RT-PCR and western blot techniques.

Results: PDK (1-4) and PDP (1-2) mRNA were expressed in rat brain with regions-specific patterns. PDK2 and PDP1 appear to be the dominant PDK and PDP isoenzymes in rat brain, respectively. PDK isoenzyme (1-3) mRNA increased significantly whereas PDP1 mRNA decreased significantly in brain at various time post CCI-TBI. Compared to naïve controls, PDK isoenzyme (PDK1-4) protein increased significantly in ipsilateral and contralateral CCI whereas PDP isoenzyme (PDP1-2) protein level decreased significantly in ipsilateral CCI and contralateral CCI at 4h, 24h, 3- and 7-day post-CCI, respectively. The craniotomy (Sham CCI) group showed similar patterns in PDK and PDP proteins as those found in CCI group.

Conclusions: The divergent induction of PDK and PDP expression after TBI could favor increased phosphorylation of PDHE1α1 and thus inhibited PDH activity and glucose utilization in the injured brain. Further study should determine if pharmacological means that can prevent or restore the lost balance between PDK and PDP can improve glucose utilization and functional outcome in TBI.

Funded by GEMI Fund and HJF grant.

176

EDARAVONE IS EFFECTIVE TO AMELIORATE THE SENSORY NEUROLOGIC DEFICIT DEVELOPED IN CHRONIC PHASE OF CEREBRAL INFARCTION IN MICE

T. Matsuyama[1], N. Doe[1], T. Nakagomi[1], A. Nakano-Doi[1], O. Saino[1], M. Takata[1,2], S. Lu[1,3], O. Mimura[2], H. Tachibana[3], A. Taguchi[4]

[1]Institute for Advanced Medical Sciences, [2]Department of Ophthalmology, [3]Department of Internal Medicine, Hyogo College of Medicine, Nishinomiya, [4]Department of Cerebrovascular Disease, National Cardiovascular Research Center, Suita, Japan

Introduction: Edaravone, a potent scavenger of hydroxyl radical, may be a useful neuroprotective agent to treat the stroke patients. Although a number of clinical studies have approved the efficacy of edaravone, whether it might improve long-term neurologic deficit has not been approved even by experimental models, in which ischemia-reperfusion injury was temporally ameliorated by edaravone. In this study, we attempt to evaluate the effect of edaravone-treatment at stroke onset on neurologic deficit of chronic phase by using a recently developed reproducible and simple model of permanent cerebral ischemia in mice (J Clin Invest, 2004).

Materials and methods: Focal cerebral ischemia was produced by occluding the middle cerebral artery (MCA) of adult CB17 mice (Taguchi et al., 2010). Animals were treated with edaravone (n=8; MCA-Eda) or PBS (n=7; MCA-PBS) post-stroke. It was administered intravenously 1 and 3 hours (3mg/kg, each) after MCA occlusion, followed by subcutaneous injection twice per day for 3 days (10 mg/kg, each). On 14 and 28 days post-stroke, animals were tested behaviorally using the open-field task (including light-induced activity) and hot plate test (for sensitivity to pain). Motor deficiencies were scored on a 3-point modified scale. Sensitivity to pain was measured between 50-64℃ at hot plate. After behavioral testing, brains were removed and subjected to immunohistochemistry for MAP2 and ATF3 to examine the neuronal loss and infarct volume.

Results:

1. Locomotion activity on day 14 is significantly lower in post-stroke mice compared with sham-operated mice (n=8), but lightning-induced activity is higher in edaravone-treated group than PBS-treated animals. On day 28, the locomotion activity was not different among the 3 groups.

2. Sensitivity to pain was lower in two post-stroke groups than sham-operated mice on day 14, but was not different between the MCA-Eda and MCA-PBS. However, on day 28 the sensitivity was significantly higher in MCA-Eda than MCA-PBS, though these two groups still showed lower sensitivity than the sham-operated animals.

3. No detectable motor deficits were observed in all mice post-stroke on day 14 and 28.

4. Immunohistchemistry revealed that all mice developed loss of MAP2-staining at ipsilateral ventral posterior thalamic nucleus (VPM and VPL) where stress-induced ATF3-positive cells are expressed. The volume of MAP2-loss and the number of ATF3-cells was not different between the two post-stroke groups. However, the ipsilateral brain volume was significantly larger in MCA-Eda than MCA-PBS group (ipsi/contra volume: 0.72 vs. 0.65, $P < 0.05$).

Discussion: The results clearly demonstrate that treatment with edaravone at stroke onset is

effective for improving sensory neurologic deficit derived from the cortical infarction produced by permanent MCA occlusion. Although edaravone has been reported to ameliorate brain edema and tissue injury, and to delay neuronal death and neurological deficits, most of the reports involved the short-term effect, and using the ischemia-reperfusion model. The present study may support for the first time that radical scavenger is a therapeutic drug which can improve neurologic symptoms caused by cerebral infarction often seen in clinical cases.

177

EVALUATION OF PSF-BASED DYNAMIC ROW-ACTION MAXIMUM LIKELIHOOD ALGORITHM RECONSTRUCTION FOR BRAIN PET

M. Ibaraki[1], K. Matsubara[1], T. Mizuta[2], A. Ohtani[2], K. Tanaka[2], K. Nakamura[1], H. Yamaguchi[1], T. Kinoshita[1]

[1]Akita Research Institute of Brain and Blood Vessels, Akita, [2]Shimadzu Corp., Kyoto, Japan

Objectives: Iterative reconstruction algorithms incorporating a point spreading function (PSF) have been developed for improving the spatial resolution of PET images. The aim of this study was to evaluate a noise property of the PSF-based dynamic row-action maximum likelihood algorithm (Dynamic RAMLA or DRAMA) for actual human PET images. Specifically, by measuring image noises and contrasts of the reconstructed images, we investigated whether the PSF-based DRAMA provided better performance than the conventional DRAMA in terms of the trade-off between image noise and contrast

Methods: Each healthy volunteer received a $H_2{}^{15}O$ PET with 3min scanning (n=2) or a ^{18}F-FDG PET with 60min-uptake, 5min scanning (n=1). A GSO-based 3D PET (Eminence PET/CT, Shimadzu Corp.) was operated with 64-bit list-mode [1]. 3D sinograms acquired were converted to 2D sinograms by a Fourier rebinning algorithm followed by the 2D DRAMA reconstruction, a modified version of RAMLA using a ´subset-dependent´ relaxation parameter for noise suppression [2,3]. The PSF kernel, obtained by measuring a point source, was incorporated in the system matrix of DRAMA by the manufacture. Combinations of various numbers of main-iteration in DRAMA (1 to 10) and various degree of post-reconstruction Gaussian filtering (2 to 7 mm FWHM) were applied to test the trade-off between image noise and contrast. The all images were segmented into gray-matter and white-matter regions, and then the image contrast was defined as an average count ratio of gray-to-white matter. The image variance was estimated by a sinogram bootstrap method on a pixel-by-pixel basis [3,4], and the average image noise in white-matter region was calculated.

Results: Characteristic curves of image noise as a function of image contrast were compared between the PSF-based DRAMA and the conventional DRAMA, as shown in Figure 1 for FDG image. Results for $H_2{}^{15}O$ (n=2) were similar with FDG. The incorporation of PSF shifted the characteristic curve toward higher image contrast. Although the different setting of the relaxation parameter in DRAMA provided slightly different results, the PSF-based DRAMA had better performance in terms of the trade-off between noise and contrast. These results represent that the PSF-based DRAMA provides the images with lower noise than the conventional DRAMA at the condition of similar image contrast, or the images with higher contrast at the condition of similar image noise as shown in Figure 2.

Conclusions: The PSF-based DRAMA is superior to the conventional DRAMA in terms of the trade-off between image noise and contrast.

References:

[1] Ibaraki M, et al. J Nucl Med. 2008;49(1):50-59.

[2] Tanaka E, Kudo H. Phys Med Biol. 2003;48(10):1405-1422.

[3] Ibaraki M, et al. Ann Nucl Med. 2009;23(7):627-638.

[4] Buvat I. Phys Med Biol. 2002;47(10):1761-1775.

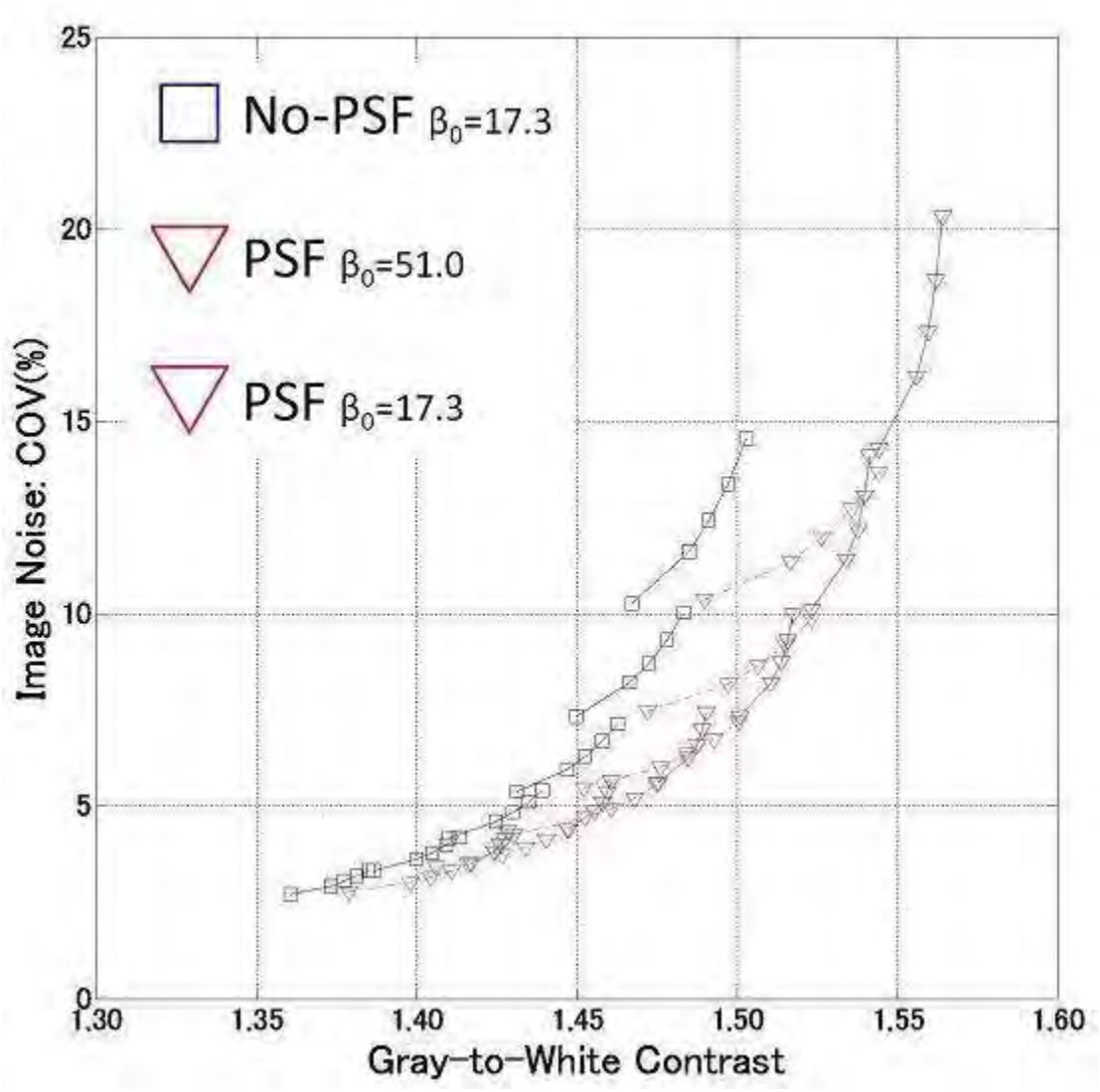

[Figure 1]

Figure 1: Characteristic curves for FDG images: image noise as a function of image contrast for the PSF-based DRAMA (red) and the conventional DRAMA (blue).

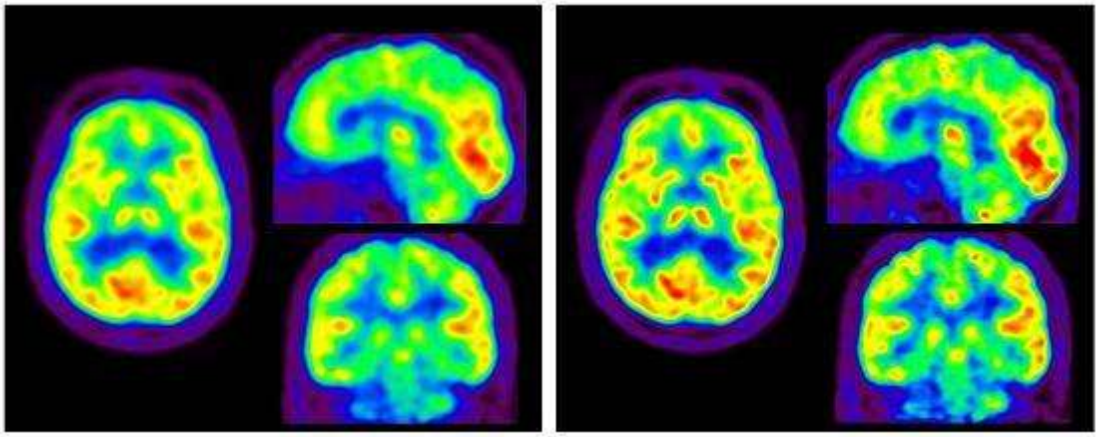

[Figure 2]

Figure 2: FDG images with the conventional DRAMA (left) and the PSF-based DRAMA (right).

179

OMEGA-3 POLYUNSATURATED FATTY ACIDS PROTECT AGAINST ISCHEMIC INJURY *VIA* FORMATION OF PHOSPHATIDYLSERINE AND ACTIVATION OF THE AKT SIGNALING PATHWAY

W. Zhang[1,2], X. Hu[2], M. Chu[1], S. Lu[1], H. Gao[1], F. Zhang[2], G. Cao[1,2], J. Chen[1,2], Y. Gao[1]

[1]Department of Anesthesiology of Huashan Hospital, State Key Laboratory for Medical Neurobiology and Institute of Brain Sciences, Fudan University School of Medicine, Shanghai, China, [2]Department of Neurology, University of Pittsburgh School of Medicine, Pittsburgh, PA, USA

Background: Recent studies have demonstrated that dietary supplementation or pharmacological administration of omega-3 polyunsaturated fatty acids (n-3 PUFA) confers remarkable neuroprotection in models of cerebral ischemia or neonatal hypoxic/ischemic brain injury. While it is likely that n-3 PUFA treatment attenuates ischemic brain injury by directly protecting neurons and by ameliorating cerebral pro-inflammatory reactions, the precise mechanism underlying the neuroprotective effect of n-3 PUFA is poorly understood. The present study was aimed to investigate the role of the Akt pro-survival signaling pathway in mediating neuroprotection conferred by n-3 PUFA in both in vitro and in vivo models of hypoxic/ischemic neuronal injury.

Methods: Dietary supplementation of n-3 PUFA began at day 2 of pregnancy in the dams. Hypoxic/ischemic (H/I) brain injury was induced in 7-day-old newborn rats by means of ipsilateral common carotid artery occlusion followed by hypoxia (8% oxygen for 2.5 hrs). Brains were assessed for cell death and PI3-K/Akt activation at 0-24 hrs after H/I, and for cerebral tissue loss at 7 days after H/I. Neurological performance was analyzed in additional animals using gait testing and righting reflex up to 2 weeks after H/I. Oxygen-glucose deprivation (OGD) was induced in primary cortical-neuron cultures to study the direct neuroprotective effect of n-3 PUFA, where DHA or EPA (0-40 μM) was applied to cultures 24 hr prior to OGD.

Results: Supplementation of n-3 PUFA protected against H/I in neonatal rats, resulting in significantly reduced brain tissue loss and neuronal apoptosis, and improved neurological performance after H/I. Activation of the PI3-K/Akt pathway was diminished in H/I brains, whereas n-3 PUFA treatment promoted this survival pathway. To further support an essential role of PI3-K/Akt in mediating neuroprotection, intracerebral administration of the PI3-K inhibitor LY294002 significantly ablated the neuroprotective effect of n-3 PUFA in H/I animals. In primary neuron cultures, DHA and EPA protected against OGD-induced mitochondrial damage and cell death, which was also dependent on the PI3-K/Akt activity. Mechanistically, DHA or EPA treatment increased the production of phosphatidylserine, the major cell membrane-bound acidic phospholipid, thus facilitating the membrane translocation and subsequent activation of Akt. Inversely, reduction in membrane production of phosphatidylserine by serine depletion in culture medium or shRNA-mediated knockdown of the phosphatidylserine synthetase PSS1 attenuated the promoting effects of DHA and EPA on Akt activation and neuronal survival after OGD.

Conclusions: Supplementation of n-3 PUFA protects against hypoxic/ischemic neuronal injury in neonatal rats and in cultured neurons. The direct neuroprotective effect of n-3 PUFA is mediated, at least in part, by promoting the production of cell membrane phosphatidylserine and facilitating the membrane translocation and activation of Akt.

181

ADIPONECTIN PROVIDE VASCULARPROTECTIVE EFFECTS AGAINST ISCHEMIC DAMAGE IN MOUSE BRAIN

T. Urabe[1], K. Yatomi[2], N. Miyamoto[1], M. Liu[1], H. Oishi[2], H. Arai[2], N. Hattori[1]

[1]Department of Neurology, [2]Department of Neurosurgery, Juntendo University School of Medicine, Tokyo, Japan

Background and aims: The adipocyte-derived bioactive protein, adiponectin, is specifically expressed in adipose tissue. Adiponectin has attracted attention in recent years as a therapeutic target for the metabolic syndrome. Furthermore, recent reports have shown that adiponectin has anti-atherosclerotic, anti-diabetic, and anti-inflammatory properties. Recent clinical studies have suggested that plasma adiponectin plays a role in cerebrovascular disease (CVD). The present study was designed to determine the serial changes in adiponectin expression in the brain and plasma after transient focal cerebral ischemia in mice.

Methods: C57BL/6 mice (n=100) were subjected to 60 min of middle cerebral artery occlusion followed by 1, 3, 6, 12, 24, 48, 72 h and 7 day reperfusion. Mouse plasma adiponectin levels were determined with adiponectin enzyme-linked immunosorbent assay (ELISA) kit. Expression of adiponectin was assessed by immunohistochemistry, western blot analysis, and reverse transcription-polymerase chain reaction (RT-PCR). Antibodies for adiponectin, CD31, endothelial nitric oxide synthase (eNOS), and von Willebrand factor (vWF) were used in the immunohistochemical analysis.

Results: Cerebral ischemia-reperfusion injury resulted in a transient rise in the acute phase and decrease in the late phase, in plasma adiponectin levels ($P < 0.05$). The same insult resulted in upregulation of adiponectin expression, with two peaks at 3 and 24 h after reperfusion ($P < 0.05$). Adiponectin protein was negligible in nonischemic contralateral hemispheres, but relatively high levels of the protein were detected in the ischemic hemisphere. Adiponectin mRNA was detected in epididymal fat but not in nonischemic or ischemic cerebral hemisphere. Immunoreactivity for eNOS was detected in cells stained positive for vWF, an endothelium maker, and eNOS/adiponectin double-positive endothelial cells were detected in the peri-ischemic area. Adiponectin accumulated only in endothelial cells of ischemic brain in response to cerebral ischemia.

Conclusions: We outlined the time course of adiponectin changes in response to transient focal ischemia in mice. Ischemic stroke elicits transient elevation in plasma adiponectin levels during the acute phase, and circulating adiponectin accumulates in damaged vessels during the late phase. Adiponectin protects against the pathologic damage of ischemic stroke. Based on our findings, we propose that time-targeted administration of adiponectin could be therapeutically beneficial in patients with ischemic stroke.

184

BRAIN AND WHOLE-BODY IMAGING IN RHESUS MONKEYS OF ^{11}C-NOP-1A, A PROMISING PET RADIOLIGAND FOR NOCICEPTIN/ORPHANIN FQ PEPTIDE RECEPTORS

Y. Kimura[1,2], M. Fujita[1], J. Hong[1], T.G. Lohith[1], R. Gladding[1], S.S. Zoghbi[1], J.A. Tauscher[3], K.S. Rash[3], Z. Chen[3], C. Pedregal[4], V.N. Barth[3], V.W. Pike[1], R.B. Innis[1]

[1]Molecular Imaging Branch, National Institute of Mental Health, National Institutes of Health, Bethesda, MD, USA, [2]Molecular Imaging Center, National Institute of Radiological Sciences, Chiba, Japan, [3]Eli Lilly & Co., Lilly Research Laboratories, Indianapolis, IN, USA, [4]Lilly S.A., Madrid, Spain

Objectives: The nociceptin/orphanin FQ peptide (NOP) receptor is a G-protein coupled receptor with sequences similar to the classic opioid receptor, and, based on animal studies, NOP may be involved in the pathophysiology of anxiety disorders and substance abuse. We developed a new NOP radioligand that has high affinity (K_i = 0.15 nM) and appropriate lipophilicity (measured logD = 3.41) for PET brain imaging: ^{11}C-NOP-1A, ((S)-3-(2´-fluoro-6´,7´-dihydrospiro[piperidine-4,4´-thieno[3,2-c]pyran]-1-yl)-2-(2-fluorobenzyl)-N-methylpropanamide). The purposes of this study were: 1) to assess the utility of ^{11}C-NOP-1A to quantify NOP receptors in monkey brain; and 2) to estimate the radiation safety profile of this radioligand based on its biodistribution in monkeys.

Methods: A pair of baseline and blocking PET scans were acquired from head to thigh on three rhesus monkeys for ~110 min after injecting ^{11}C-NOP-1A (3 baseline scans: 229 ± 13 MBq, 3 blocking scans: 239 ± 15 MBq, Head and peripheral images were taken at the same scans). In the blocking scans, a nonradioactive receptor antagonist (LSN2558114; 1 mg/kg i.v.) was administered prior to ^{11}C-NOP-1A. In all scans, arterial blood was sampled to measure unmetabolized ^{11}C-NOP-1A and radiometabolites in plasma. In the brain, preset volumes of interest from the monkeys' MRI were transferred to the coregistered PET images. Distribution volume was calculated with a compartment model using brain and arterial plasma data. For the whole body, radiation-absorbed doses were calculated using the Medical Internal Radiation Dose scheme.

Results: After injection of ^{11}C-NOP-1A, uptake of radioactivity in brain was relatively high (peak concentrations of ~5 SUV), peaked early at about ~12 min, and thereafter washed out quickly. Brain time-activity curves were well fit using a one-tissue compartment model (table). Distribution volume (V_T; mL · cm^{-3}) was highest in neocortex (~20) and lowest in hypothalamus and cerebellum (~13). LSN2558114 blocked ~50 - 70% of uptake and reduced V_T in all brain regions to ~7. The whole body scans showed that radioactivity was distributed in brain, organs containing large volumes of blood, and organs involved in metabolism and excretion. The effective dose in human estimated from the baseline scans in monkeys was 5.0 μSv/MBq.

Conclusions: These initial results strongly suggest that ^{11}C-NOP-1A is a useful radioligand to quantify NOP receptors in monkey brain with specific binding of more than 50% of total uptake and that its radiation dose is similar to that of other ^{11}C-labeled ligands for neuroreceptors. Thus, ^{11}C-NOP-1A is a promising candidate to measure NOP receptors in humans.

	VT (ml/cm^3)		

	Baseline	Blocked	Baseline /Blocked	In vitro*
Frontal cortex	18.1	6.6	2.8	+++
Occipital cortex	20.4	6.6	3.1	N/A
Hipothalamus	12.6	7.4	1.7	++
Cerebellum	12.9	6.7	1.9	++
Values are mean from 3 monkeys, * +++, high binding, ++ moderate binding of ^{125}I[Tyr^{14}]N/OFQ in primate CNS from Bridge et al. Neuroscience (2003), N/A: not available				

[Distribution volume of 11C-NOP-1A in monkey brain]

186

AN INVESTIGATION OF THE METABOLISM OF THE RAT BARREL CORTEX DURING SUSTAINED TRIGEMINAL NERVE STIMULATION

N. Just[1], R. Gruetter[1,2]

[1]LIFMET, EPFL and UNIL, Lausanne, [2]Radiology Department, Hopital Universitaire de Genève, Geneva, Switzerland

Introduction: In rodents, prolonged activation of the somatosensory cortex is limited due to anesthesia and habituation. Since Hyder *et al.(1)* showed a one hour BOLD activation of the rat primary somatosensory cortex upon forepaw stimulation and concluded that oxidative glycolysis is the primary source of energy during cortical activation, investigations have been challenging and controversial (2).Trigeminal nerve stimulation (TGN) allows investigating the BOLD fMRI activation of the rat barrel cortex (3). Here, functional proton MRS was conducted during sustained TGN stimulation allowing measurement of metabolic changes during barrel cortex activation.

Materials and methods: Male SD rats (n=15 for fMRI; n=10 for fMRS, 350±40g). Orally intubated; Catheterized for α-chloralose and physiology control (pH ~7.4, pCO2~39-mmHg, MABP ~130mmHg, Temperature =37.5ºC ± 0.5ºC). All the experiments were performed on an actively shielded 9.4T/31cm bore magnet (Magnex, Varian) with a quadrature T/R 17mm surface coil. First and second order shims were adjusted using FASTMAP (4). fMRI was performed as described in (3, 5). fMRS: Localized ^{1}H-MR spectroscopy was performed using SPECIAL(6) in a 2x2x4 mm^3 VOI localized in the activated barrel cortex and after re-adjusting the shims using FASTMAP. Blocks of fids were summed over each 10-minute period per rat and then summed over the 10 animals resulting in a stimulation spectrum and a rest spectrum. Spectra contaminated by extra-cerebral lipid signals were discarded. Metabolite concentrations were calculated using LCmodel (7). Statistics were performed using a paired-test. A pvalue < 0.05 was considered significant.

Results and discussion: Reproducible BOLD fMRI time-courses were obtained in rats upon sustained TGN stimulation. In the activated area in the barrel cortex, shimming resulted in water linewidths of 15-19 Hz. A difference spectrum resulting from the subtraction of stimulated and rest spectra, was obtained. An exponential multiplication corresponding to 0.6Hz line broadening was applied to the stimulation spectrum to match the linewidth of the rest spectrum before subtraction allowing investigation of the BOLD-free difference spectrum. Positive Glu (2.15, 2.4 ppm) and Lac (1.32ppm) peaks were seen as well as negative Gln (2.46ppm) and Asp (2.6 and 2.8ppm). Spectra were averaged across subjects and LCmodel quantification was performed. During stimulation, lactate (Lac:+42%; +0.32±0.01µmol/g) and Glutamate (Glu: +4.2%; 0.45±0.02µmol/g) increased significantly (p< 0.01) whereas Glutamine (Gln: -8%;-0.3±0.01µmol/g) and Aspartate (Asp: -13%;-0.3±0.02µmol/g) showed a tendency to decrease although not significantly. However, Glucose (Glc) levels were unchanged. This result can be attributed to the variability between subjects. Using sustained TGN stimulation, concentration changes of Glu and Asp in the rat barrel cortex were in agreement with concentration changes observed (Glu=+3%; Asp=-15%) during stimulation in the human visual cortex.

Conclusion: Sustained TGN stimulation is possible in the rat barrel cortex to study neurochemical consequences of activation.

References:

1. Hyder F et al. PNAS; 1996; 93:7612-7617.

2. Xu S et al. Neuroimage. 2005;28:401-409.

3. Just N et al. 2010.28:1143-1151.

4. Gruetter et al. MRM. 1993; 29:804.

5. Just N et al. Proc. 18th ISMRM scientific Meeting, Stockholm, Sweden, 1199.

6. Mlynarik V et al. MRM. 2006; 56:965.

7. Provencher SW. MRM. 1993; 30:672.

187

A NON-SELECTIVE CALCIUM CHANNEL BLOCKER, BEPRIDIL, AMELIORATES THALAMIC PATHOLOGY AND IMPROVES FUNCTIONAL RECOVERY IN MCAO RATS

A. Lipsanen[1], T. Sarajärvi[1], P. Mäkinen[1], S. Peräniemi[2], M. Hiltunen[1], J. Jolkkonen[1]

[1]Institute of Clinical Medicine - Neurology, [2]Department of Biosciences, University of Eastern Finland, Kuopio, Finland

Introduction: We have previously shown increased amyloid precursor protein (APP) and β-amyloid (Aβ) and calcium depositions in the ipsilateral thalamus in rodents following focal cerebral ischemia (van Groen et al., 2005, Hiltunen et al., 2009). Interestingly, calcium and Aβ showed an overlapping distribution pattern in the thalamus of rats subjected to middle cerebral artery occlusion (MCAO) (Mäkinen et al., 2008).

Aim: The aim of this study was to investigate whether chronic treatment with bepridil, a non-selective calcium channel blocker, would decrease calcium and amyloid load in the thalamus and whether this is associated to improved behavioral outcome in MCAO rats.

Material and methods: Male Wistar rats (295-344 g) were subjected to sham-operation or transient MCAO (120 min). Bepridil (50 mg/kg, p.o., once a day) was administrated for 27 days starting the administration two days after MCAO (n=5). Sham-operated (n=6) and MCAO control rats (n=7) were treated with the vehicle. Sensimotor impairment was assessed using the cylinder, tapered/ledged beam-walking and limb-placing tests (Figure 1). After the follow-up, animals were sacrificed for qualification of calcium, $A\beta_{40}$ and $A\beta_{42}$ levels.

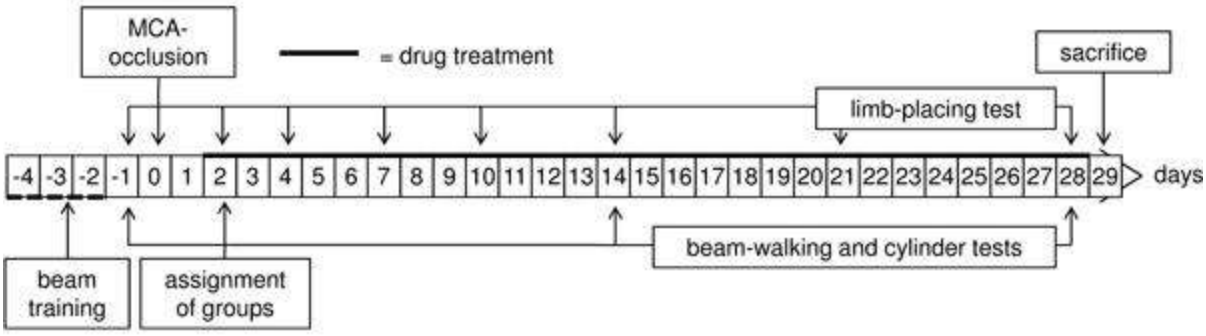

[Figure 1: Study design]

Results: In vehicle treated MCAO rats calcium and amyloid-β -load in the thalamus was significantly higher compared to sham-operated animals. Bepridil decreased calcium ($p< 0.05$), soluble $A\beta_{40}$ ($p< 0.05$) and $A\beta_{42}$ ($p< 0.05$) in the ipsilateral thalamus compared to vehicle treated MCAO rats. Bepridil treatment did also improve spontaneous forelimb use (cylinder test) in MCAO rats ($p=0.05$). Other behavioral tests showed no significant differences between experimental groups.

Conclusions: Chronic bepridil treatment did partially prevent secondary pathology in the

thalamus in MCAO rats and this was reflected to improved behavioural outcome. Prevention of secondary pathology in the thalamus by calcium channel blockers may provide a novel treatment to facilitate functional recovery after stroke.

References: Hiltunen et al. Focal cerebral ischemia in rats alters APP processing of Aβ peptide degrading enzymes in the thalamus. *Neurobiol Dis* 35:103-113, 2009

Mäkinen et al. Coaccumulation of calcium and β-amyloid in the thalamus after transient middle cerebral artery occlusion in rats. *J Cereb Blood Flow Metab* 28:263-268, 2008

van Groen et al. Transformation of diffuse β-amyloid precursor protein and β-amyloid deposits to plaques in the thalamus following transient occlusion of the middle cerebral artery in rats. *Stroke* 36:1551-1556, 2005

188

ANTI-APOPTOTIC MECHANISMS ARE INVOLVED IN SEVOFLURANE PRECONDITIONING AGAINST FOCAL CEREBRAL ISCHEMIA IN RATS

H. Wang[1], S. Lu[1], Q. Yu[1], H. Shi[1], M. Chu[1], H. Gao[1], W. Liang[1], F. Zhang[1,2], J. Chen[1,2], Y. Gao[1]

[1]Department of Anesthesiology of Huashan Hospital, State Key Laboratory of Medical Neurobiology and Institute of Brain Sciences, Fudan University, Shanghai, China, [2]Center of Cerebrovascular Disease Research, University of Pittsburgh School of Medicine, Pittsburgh, PA, USA

Objectives: Neuroprotection conferred by volatile anesthetic preconditioning (APC), such as that by sevoflurane, has been demonstrated in both in vivo and in vitro

models of cerebral ischemia; yet the underlying mechanism is poorly understood. In the present study, we investigated whether sevoflurane APC attenuates the expression of anti-apoptotic and pro-apoptotic members of the Bcl-2 family and/or the activation of the JNK and p53 pro-death signaling cascades in a rat of focal cerebral ischemia and reperfusion.

Methods: Male Sprague-Dawley rats were randomly assigned to sham, vehicle, Sevoflurance APC groups. In the APC group, rats received 1 minimum alveolar concentration (MAC) sevoflurane in air 30 min/day for 4 consecutive days, whereas animals in the vehicle group inhaled ambient air. Animals were subjected to focal ischemia for 60min by filament occlusion of the middle cerebral artery. At 24h after ischemia (n=3 per condition), rats were sacrificed and brains were harvested. Immunofluorescent staining of cleaved caspase-3 was performed with the counterstaining of Hoechst 33258. Other sets of animals were euthanized at 0, 6, 12 and 24 h after reperfusion (n = 4/group/per time point) for assessing the relative levels of cleaved caspase3, Bcl-2, Bcl-xl, Bax, Bid, p-JNK and p53 by Western blots.

Results: In comparison with the vehicle-treated group, sevoflurane APC significantly inhibited the activation of caspase3 ($p< 0.05$) at 6h and 24h after reperfusion, as shown by Western blot analysis. Similarly, the numbers of cleaved caspase3 positive cells in the sevoflurane APC group were robustly decreased in both cortex and striatum of the ipsilateral hemisphere, compared to the vehicle group ($p< 0.01$). Sevoflurane APC also significantly increased the levels of Bcl-2 and Bcl-xl and suppressed the levels of Bax and Bid at 3, 6, and 24h after reperfusion ($p< 0.05$), resulting in a significantly increased ratio of anti-apoptotic proteins over pro-apoptotic proteins. Moreover, sevoflurane APC markedly decreased the levels of p-JNK and p53 in the nuclear fraction at 6 and 24h after reperfusion ($p< 0.05$).

Conclusion: Suppression of apoptotic responses may contribute to the neuroprotection against focal ischemic brain injury conferred by sevoflurane preconditioning.

189

CHANGES IN EXTRACELLULAR POTASSIUM CONCENTRATIONS ($[K]_E$) WITHIN THE PHYSIOLOGICAL RANGE AFFECT EXTRACELLULAR ADENOSINE LEVELS ($[ADO]_E$) AND DYNAMICS IN ASTROCYTIC CULTURES

T. Kulik[1], H.R. Winn[2]

[1]Neurology, University of Rochester Medical Center, Rochester, [2]Neurosurgery, Mount Sinai School of Medicine, New York, NY, USA

Introduction: Ado is an endogenous purine nucleoside, a neuro-modulator, vasoregulator and a retaliatory metabolite. We (1) have shown in astrocytic cultures that $[Ado]_e$ correlate with oxygen tension: during hypoxia, $[Ado]_e$ rises rapidly and reaches a concentration sufficiently high to evoke vasodilatation *in vivo*. Upon re-oxygenation, $[Ado]_e$ swiftly returns to baseline levels. Similar changes in Ado have been observed *in vivo* (2) where blockade of Ado receptors attenuates hypoxic hyperemia (3). In addition, hyperoxia depresses $[Ado]_e$ (1).

In vivo, $[K^+]_e$ is increased with neuronal activation and hypoxia. Increases in physiological $[K+]_e$ attenuate Ado kinase and increase Na/K ATPase activity; both of these mechanisms may therefore affect $[Ado]_e$.

Objective: The present study tested the hypothesis that changes in $[K^+]_e$ within the physiological range influence $[Ado]_e$ in astrocytic cultures. Previous studies (4) of potassium/Ado interactions have utilized pathological concentrations (>30 mM) of $[K^+]_e$.

Methods: Primary cultures were established from the brain of rat pups, purified based on differential adhesion, trypsinized after 11 days in vitro (DIV), attached to microcarrier beads and subsequently grown in spinner flasks. After 23 DIV, O_2 tension in the culture vessel was rapidly changed by flushing the vessel with N_2 or O_2. Utilizing a fluorometric technique, we were able to measure pO_2 in our culture in real-time. ph and $[K^+]_e$ were continuously measured using electrodes. Culture supernatant was sampled, cleaned with SPE, and analyzed with HPLC.

Results: In the presence of augmented potassium concentrations, we measured $[Ado]_e$ in normoxic (pO_2=154 mmHg) and hypoxic (pO_2< =3 mmHg) astrocytes as previously described (1). During normoxia (**Fig. 1**), exogenously elevated potassium levels (5, 10 and 15 mM) increased resting $[Ado]_e$ significantly ($p< 0.05$) at all time periods (60, 300 and 600 s) as compared to baseline potassium levels (3.2 mM).

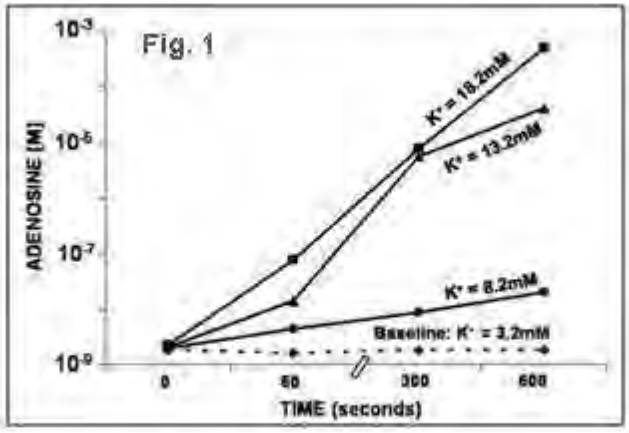

[Fig. 1]

During induced hypoxia, $[K^+]_e$ in our culture remained stable. When we exogenously increased potassium during hypoxia, neither the rate of accumulation nor the steady state $[Ado]_e$ was affected. However, with re-oxygenation (**Fig. 2**), $[K^+]_e$ in a dose dependant fashion retarded clearance of elevated $[Ado]_e$.

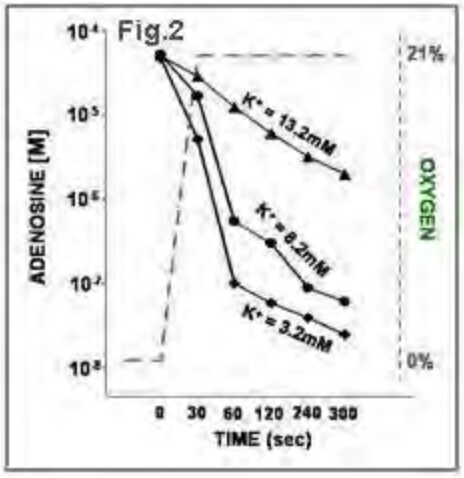

[Fig. 2]

Conclusion: During normoxia and hypoxia, changes in physiological levels of potassium affect $[Ado]_e$: elevated $[K^+]_e$ during normoxia causes resting $[Ado]_e$ to increase, whereas augmented $[K^+]_e$ during re-oxygenation attenuates clearance of $[Ado]_e$. We speculate that this potassium/Ado reciprocal interaction serves as a means of communication between neurons and astrocytes. The mechanism responsible for the increase in $[Ado]_e$ evoked by potassium may be an increase in Na/K ATPase activity and/or an attenuation of Ado kinase activity. Both mechanisms would augment $[Ado]_e$ and could influence CBF.

References:

1. Kulik et al, *Glia* 58:1335-44, 2010;

2. Morii et al, *Am J Physiol (Heart)* 253:H165-75, 1987;

3. Miekisiak et al; *J CBF Metab* 28:1656-64, 2008;

4. Latini and Pedata, *J Neurochem* 79:463-84, 2001.

190

GENDER-DEPENDENT NEURONAL NOS MODULATION MEDIATES PROTECTIVE BLOOD-FLOW REDISTRIBUTION DURING STROKE IN NEONATAL RATS

C. Charriaut-Marlangue[1], S. Renolleau[1], S. Villapol[2], O. Baud[2], P. Bonnin[3]

[1]Hopital Universitaire Robert Debré, [2]INSERM U676, [3]Hopital Lariboisière, INSERM U965, Paris, France

Objective: Research into neonatal ischemic brain damage is impeded by the lack of a complete understanding of the mechanisms. We recently demonstrated that two different intracranial hemodynamic patterns were displayed during neonatal ischemia, characterized by the presence or the absence of an increase in the mBFV of the BT (Abstract A 303-0022-00199 Bonnin et al.). The goal of this study was to explore the role of NO and specific NO synthases as key mediators involved in the cerebral arterial vasodilation underlying collateral recruitment in the P7 rat pup.

Material and methods: Ischemia was performed in Wistar P7 rats of both sexes (Renolleau et al., 1998). Animals were treated with either PBS (n=12), L-NAME (n=11), 7-NI (n=9) or L-NIO (n=18) 1 hour before ischemia. In another set of experiments, animals were subjected to inhaled NO (iNO). Blood flow velocities (BFVs) were measured in basilar trunk upstream the circle of Willis, and in the posterior cerebral arteries downstream before, during ischemia, and after release of CCAs occlusion using an echocardiograph (Vivid 7, GE Medical Systems ultrasound®, Horten, Norway) equipped with a 12-MHz linear transducer (12L) as previously reported. Lesion volumes were evaluated at 48 hours post-injury on cresyl violet-stained sections.

Results: Data indicated that both endogenous (as shown after L-NAME treatment) and exogenous NO (iNO exposure) modify the redistribution of blood flow through the circle of Willis during ischemia and modulate the volume of the ischemic brain lesion. Neuronal NOS (nNOS) mediated collateral recruitment and a significant gender effect for Ser^{847} phosphorylation in L-NIO-treated animals was detected with higher levels in females than in males. Endothelial NOS inhibition was associated with extended nNOS overactivation during ischemia and reperfusion in males, leading to a large lesion size at 48 hours. Finally we demonstrated the harmful effects of high blood flow during ischemia and reperfusion induced by an excess of exogenous NO (iNO exposure).

Conclusions: Intracranial BFV changes are mediated by NO production via neuronal NOS (nNOS), and the modulation of nNOS activity modulation through Ser^{847} phosphorylation is gender-dependent. Inhaled NO increases collateral recruitment and appears to be beneficial when administrated at low doses during ischemia. Together, these findings strongly support the role of NO and nNOS in modulating blood flow and lesion development and extent during ischemia.

- Bonnin P, Renolleau S, Leger PL, Deroide N and Charriaut-Marlangue C. (2011) Abstract A-303-0022-00199 - Brain 2011.

- Renolleau S, Aggoun-Zouaoui D, Ben-Ari Y, Charriaut-Marlangue C. (1998) Stroke 29:1454-1460; discussion 1461.

191

MIGRAINE MUTATIONS INCREASE THE VULNERABILITY OF BRAIN TO ISCHEMIC STROKE

K. Eikermann-Haerter[1], J.H. Lee[1], I. Yuzawa[1], C. Liu[2], Z. Zhou[1], H.K. Shin[1], Y. Zheng[1], T. Kurth[3], C. Waeber[1], M. Ferrari[4], A. van den Maagdenberg[5], M. Moskowitz[1], C. Ayata[1,6]

[1]Radiology, [2]Neuroradiology, Massachusetts General Hospital/Harvard Medical School, Charlestown, MA, USA, [3]Neuroepidemiology, UPMC University Paris, Paris, France, [4]Neurology, [5]Human Genetics, Leiden University Medical Centre, Leiden, The Netherlands, [6]Neurology, Massachusetts General Hospital/Harvard Medical School, Boston, MA, USA

Introduction: Migraine is the most common neurological condition affecting young to middle-age adults. Migraine with aura is associated with increased stroke risk both during and between attacks. The biological basis for this association is unknown. Stroke risk is also increased in familial hemiplegic migraine (FHM), a monogenic migraine subtype with hemiplegic auras in addition to the common aura forms. Mutant mice carrying human missense mutations causing FHM type 1 have been generated.

Background and aims: Glutamatergic mechanisms have been implicated in pathogenesis of FHM and common forms of migraine. Glutamate excitotoxicity also plays a pivotal role in stroke pathogenesis. We hypothesized that genetic mutations conferring migraine susceptibility via glutamatergic mechanisms increase the vulnerability of brain to ischemic stroke as one mechanism to explain the migraine-stroke association.

Material and methods: In transgenic mice, we examined the impact of two allelic FHM type 1 mutations ($Ca_v2.1$ R192Q and S218L) on stroke pathophysiology and outcome using established stroke models, optical and magnetic resonance imaging, and electrophysiological recordings.

Results: Compared to wild-type (WT), both FHM1 mutant mouse strains developed larger infarcts (grey bars) and brain swelling (white bars) after transient filament middle cerebral artery occlusion (fMCAO), with 100% mortality within 24h in the S218L homozygous group. Functional outcomes were worse when assessed in the S218L mutants compared to WT, using a combined death and neurological disability score as a clinically relevant endpoint.

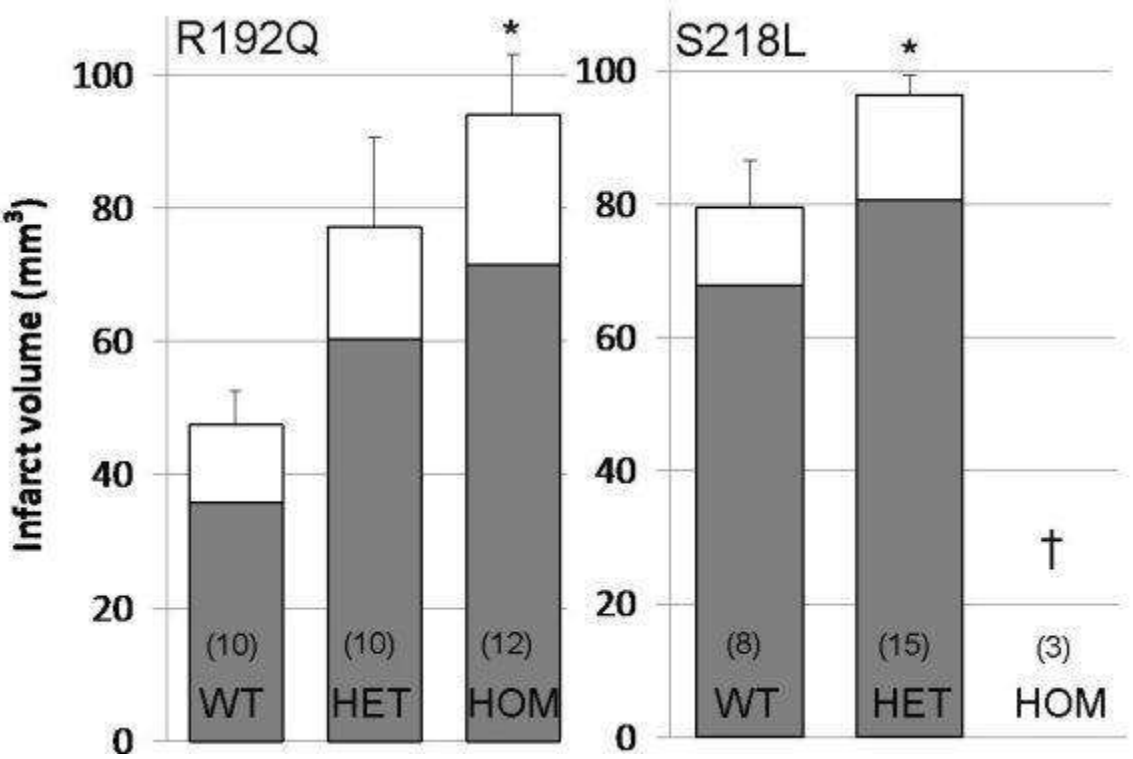

[Enlarged infarcts after 60min fMCAO in FHM mutants]

As underlying mechanisms, we found evidence for an enhanced susceptibility to ischemic depolarizations that are known to promote infarct growth, and to worsen stroke outcome. We identified an earlier onset of anoxic depolarization and more frequent peri-infarct depolarizations in both mutant strains, compared to their WT littermates.

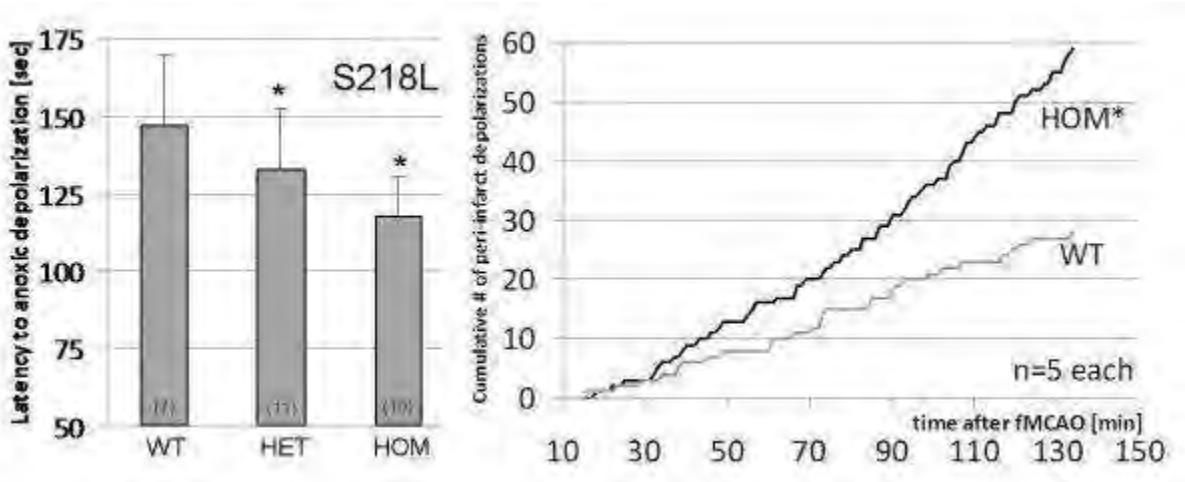

[Enhanced susceptibility to ischemic depolarization]

Increased susceptibility to ischemic depolarizations was associated in mutants with rapid expansion of infarct core on diffusion-weighted MRI, and with larger areas of CBF deficit, assessed using laser speckle flowmetry.

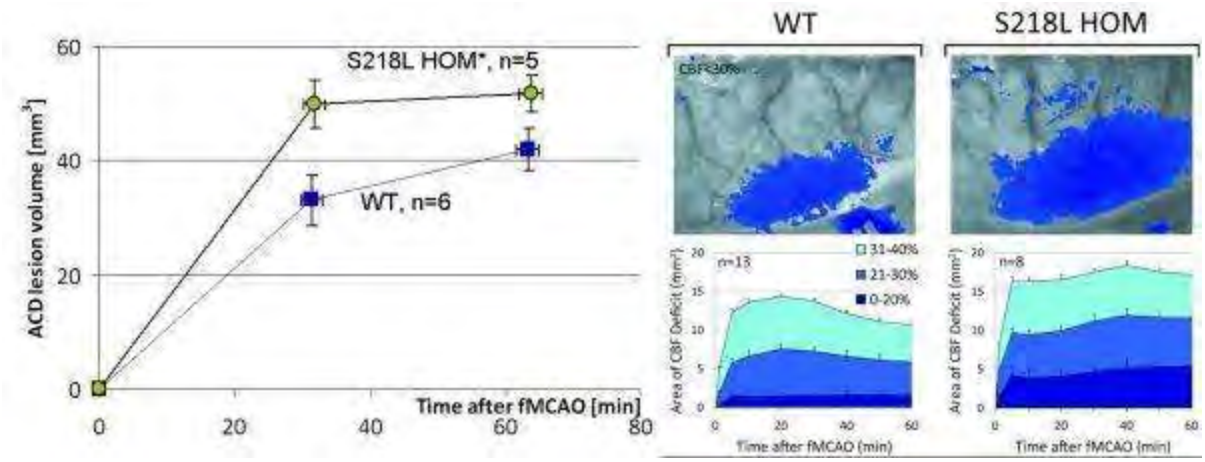

[Rapid growth of infarct core and CBF deficit]

As a result, blood flow required for tissue survival (i.e., viability threshold) was higher in mutants when analyzed by spatially co-registering the laser speckle perfusion map during ischemia with the infarct that developed 48 hours later. Mutant cortex infarcted when blood flow dropped below 42±3% of baseline, whereas in WT, a reduction to 35±2% was necessary to produce an infarct ($p < 0.05$).

Underscoring the importance of parenchymal mechanisms such as neuronal hyperexcitability and ischemic depolarizations, the glutamate (NMDA)-receptor antagonist MK-801 was selectively more efficacious in reducing infarct size in FHM1 mutants than in WT (45% vs 23% infarct reduction, compared to untreated mice of the same genotype), and completely abolished differences in infarct sizes between genotypes.

Conclusion: We present experimental evidence that FHM1 mutations in $Ca_V2.1$ channels render the brain vulnerable to ischemic stroke. Given the overlap between more common forms of migraine and FHM in glutamatergic hyperexcitability, we propose that enhanced susceptibility to ischemic depolarizations may predispose migraineurs to infarction during ischemic events.

192

POTASSIUM- AND EET-MEDIATED FUNCTIONAL HYPEREMIA: A MATHEMATICAL MODEL

H. Farr[1,2], T. David[1]

[1]Centre for Bioengineering, University of Canterbury, [2]Van der Veer Institute for Parkinson's and Brain Research, Christchurch, New Zealand

Introduction: Functional hyperemia is the mechanism by which increased neuronal activity is matched by a rapid and regional increase in blood supply. However, little is known about the pathways that control functional hyperemia, despite its importance for fMRI imaging and in early Alzheimer's Disease pathology. It is known that it is achieved through “neurovascular coupling”, the intercellular communication system between cells comprising the neurovascular unit (neurons, astrocytes and arterioles). The delivery of a request for increased nutrients from neuron to arteriole is facilitated by chemical processes that occur in the astrocyte, a star-shaped glial cell with branches that surround both synapses and arterioles.

Objective: The objective of this study was to create a mathematical model that described potassium- and EET-mediated neurovascular coupling operating in a network of neurovascular units within a vascular tree.

Methods: We have created a model of an entire neurovascular unit including the synaptic cleft, astrocyte, and both active layers of the arteriole (smooth muscle cells (SMCs) and endothelial cells (ECs)) using the work of Filosa and Blanco and Higashimori et al. as a guide. We combine existing SMC, EC, astrocyte and muscle contraction equations and the vascular tree model of David et al. and extend them to produce a more physiologically correct model that takes into account important potassium transport systems (Na-K pump and BK and KIR ion channels).

Results: We provide a model which successfully accounts for many observations seen in experiment. The model is capable of simulating the approximate 15% arteriolar dilation caused by a 60-second neuronal activation. Figure 1 is a summary of the neurovascular response to a 60-second neuronal activation (glutamate-induced increases in astrocytic IP3, calcium and EET, which then effect increases in perivascular potassium (pvK) and arteriolar radius).

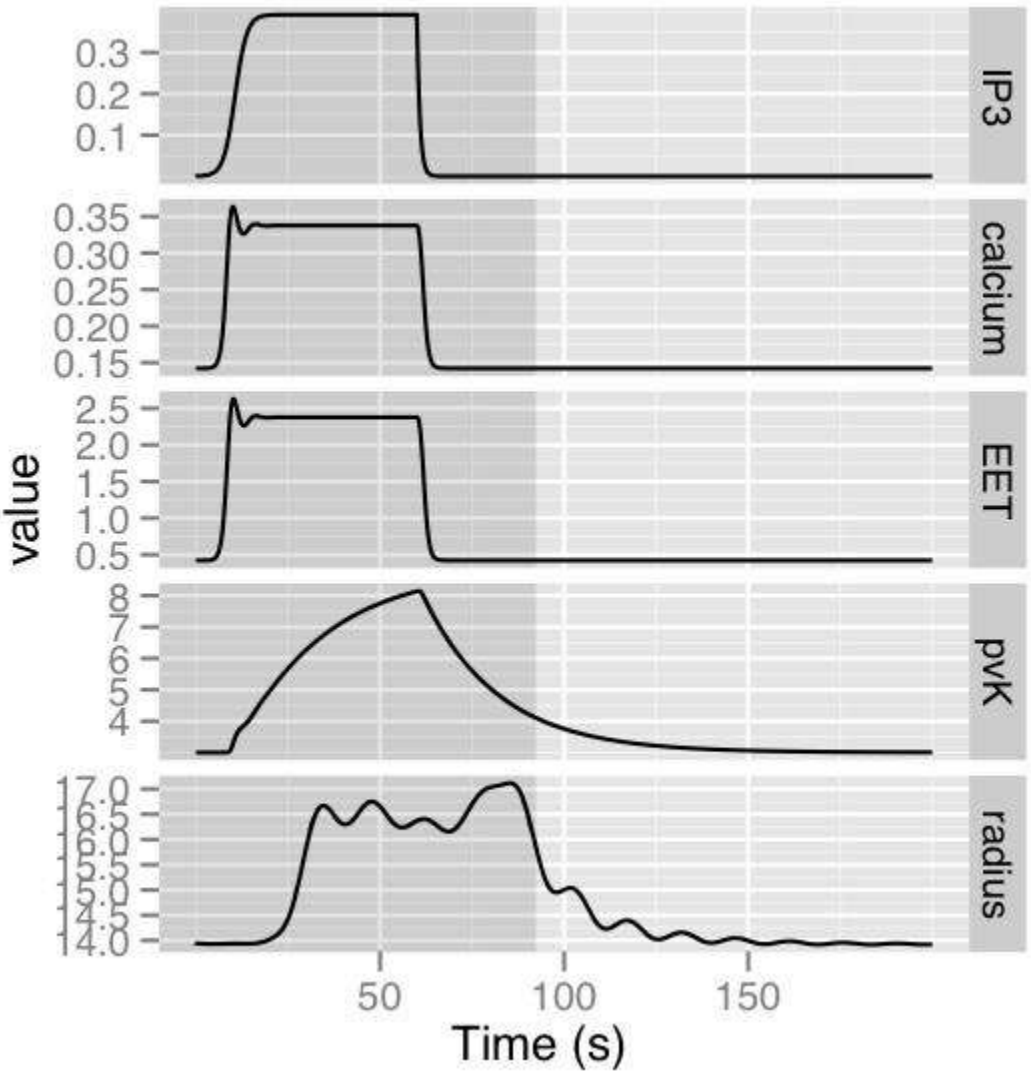

[Figure 1]

Furthermore, the phenomena seen in the work of Girouard et al. can be replicated, whereby a small increase in the calcium concentration at the astrocyte endfoot can cause dilation, whereas a large increase causes vasoconstriction. Extending this model into several neurovascular units operating within a vascular tree allows us to simulate changes in larger tissue areas, and provides us with a physiological replacement for the phenomenological metabolic autoregulation model used in the work of David et al.

Conclusions: These results successfully support the hypothesis of a potassium- and EET-mediated exchange of information between arteriole and astrocyte (as proposed by Filosa and Blanco).

193

TRANSPLANTATION OF ALLOGENEIC BONE MARROW MONONUCLEAR CELLS AMELIORATES BRAIN INJURY FOLLOWING TRANSIENT FOCAL ISCHEMIA IN RATS

F. Kamiya, M. Ueda, C. Nito, N. Kamiya, T. Inaba, S. Suda, Y. Katayama

Divisions of Neurology, Nephrology and Rheumatology, Department of Internal Medicine, Nippon Medical School, Bunkyo-ku, Japan

Objectives: Transplantation of bone marrow cells reportedly exert neuroprotection against cerebral ischemia [1]. We have previously shown the effects of 'autologous' bone marrow mononuclear cells (BMMCs) on brain damage following transient focal ischemia in rats [2]. However, it remains uncertain whether 'allogeneic' BMMC transplantation is also neuroprotective in the rat model. The present study was designed to examine whether brain injury in response to transient focal ischemia can be ameliorated by allogeneic BMMC transplantation in rats.

Methods: Under halothane anesthesia, male Sprague-Dawley rats were subjected to 90 min focal ischemia using intraluminal technique, followed by administration of $1x10^7$ allogeneic BMMCs (allogeneic BMMC group), $1x10^7$ autologous BMMCs (autologous BMMC group) or vehicle (vehicle group) via the femoral vein immediately after reperfusion (n = 8, each). Allogeneic BMMCs were obtained from the femurs of other donor rats, isolated by density gradient centrifusion. Autologous BMMCs were collected from the right femur of each rat, isolated by the same way. Animals were decapitated at 24 hrs after reperfusion to assess infarct volume using 2,3,5-triphenyltetrazolium chloride (TTC) staining method. Statistical significance was set at $p < 0.05$.

Results: The transplanted allogeneic BMMCs as well as the autologous BMMCs significantly decreased infarct volume 24 hrs after reperfusion compared with vehicle. There was no statistical significance in infarct volume between the allogeneic and autologous BMMC groups. No adverse events were observed after the allogeneic BMMC transplantation.

Conclusions: Intravenous administration of either allogeneic or autologous BMMCs showed neuroprotection in rat transient focal ischemic model when administered immediately after reperfusion. The allogeneic BMMCs may provide a potent and safe treatment equal to the autologous BMMCs in this model.

References:

[1] Bliss T, et al. Cell transplantation therapy for stroke. Stroke 2007; 38: 817-826

[2] Kamiya N, et al. Intra-arterial transplantation of bone marrow mononuclear cells immediately after reperfusion decreases brain injury after focal ischemia in rats. Life Sci 2008; 83: 433-437

194

TIME COURSE OF DOPAMINE SYNTHESIS CAPACITY IN STRIATUM BEFORE AND AFTER RISPERIDONE TREATMENT IN SCHIZOPHRENIA: A PET STUDY WITH [^{11}C]DOPA

H. Takano, H. Ito, H. Takahashi, R. Arakawa, T. Suhara

Molecular Imaging Center, National Institute of Radiological Sciences, Chiba, Japan

Background and aim: Antipsychotic efficacy is thought to be mediated mainly through the blockade of postsynaptic dopamine (DA) D_2 receptors. However, studies have also found indications of striatal presynaptic dopaminergic hyperactivity in schizophrenia, and the effect of antipsychotic treatment on DA synthesis capacity remains unclear. The aim of this study was to measure the time course of DA synthesis capacity before and during treatment with risperidone by using positron emission tomography (PET) with [^{11}C]DOPA.

Method: The study included 9 unmedicated patients with schizophrenia (men, 5;women, 4; mean [standard deviation {SD}] age, 33.8 (7.3) years) who were scanned before (baseline), 1 day after, and 1 month after initiating oral risperidone treatment (2-6 mg/day). Dynamic scanning was performed for 64 min with a PET scanner (SIEMENS ECAT HR+). The overall uptake rate constant k_i of [^{11}C]DOPA, which indicates net DA synthesis capacity, was determined for the whole striatum and its functional subdivisions including limbic striatum (LST), associative striatum (AST), and sensorimotor striatum (SMST) [1] by graphical plot analysis with the occipital cortex as reference region [2]. Patients' symptoms were evaluated using the positive and negative symptom scale (PANSS) on the day PET was performed. Significance was set at $P < .05$.

Result: The mean (SD) PANSS scores and k_i values at each time point are shown in Table. Repeated-measures analysis of variance (ANOVA) revealed a significant main effect of time on the PANSS total scores; in contrast, no significant change was observed in k_i values for the whole striatum and the subdivisions at 3 time points. However, a highly significant negative correlation was observed between the change in k_i values at 1 month after risperidone treatment from baseline and the k_i values at baseline in the whole striatum (Pearson's correlation, $r = -0.947$, $P < .001$). Furthermore, the coefficient of variation for k_i values in the whole striatum decreased at 1 month of treatment: 14.7% at baseline, 13.1% at 1 day after treatment, and 5.5% at 1 month after treatment. No significant correlations were observed between k_i change rates and change in symptoms.

	Baseline	After 1 Day	After 1 Month	P
Total PANSS score	85.1 (22.2)	82.3 (21.4)	73.2 (25.4)	0.000
ki values				
Whole striatum	0.0143 (0.0021)	0.0137 (0.0018)	0.0146 (0.0008)	0.670

LST	0.0131 (0.0017)	0.0129 (0.0020)	0.0118 (0.0014)	0.929
AST	0.0139 (0.0024)	0.0132 (0.0022)	0.0146 (0.0009)	0.484
SMST	0.0161 (0.0031)	0.0155 (0.0019)	0.0167 (0.0016)	0.996

[Change in PANSS and striatal DA synthesis capacity]

Conclusion: In this study, k_i values decreased in patients with high baseline k_i, while patients with low baseline k_i values increased, and variations in k_i at baseline tended to converge through 1 month of risperidone treatment. Thus, patients with different baseline values may show different patterns of change in DA synthesis capacity after antipsychotic treatment; risperidone may stabilize presynaptic DA function, especially after 1 month of treatment.

References:

[1] Martinez et al., J Cereb Blood Flow Metab, 23: 285-300, 2003

[2] Ito et al., Nucl Med Commun, 27:723-731, 2006

195

EVALUATION OF THE SUBJECT MOTION IN MEASUREMENTS FOR CBF, OEF AND $CMRO_2$ BY ^{15}O PET

K. Matsubara, M. Ibaraki, K. Nakamura, H. Yamaguchi, K. Kudo, A. Umetsu, F. Kinoshita, T. Kinoshita

Department of Radiology and Nuclear Medicine, Research Institute for Brain and Blood Vessels, Akita, Japan

Objectives: Regional cerebral blood flow (CBF) and oxygen metabolism (OEF, $CMRO_2$) can be measured by positron emission tomography (PET) with ^{15}O-compounds, i.e. $[^{15}O]CO$, $[^{15}O]O_2$ and $[^{15}O]H_2O$. Because of relatively long study period, 60 - 90 min, the subject motion may occur and affect the consistency during the emission scans. We aimed to reveal how often the subject motion occurs in brain ^{15}O PET study and how the motion affects CBF, OEF and $CMRO_2$.

Methods: PET images acquired from the patients with stroke (n = 130) were investigated. ^{15}O PET studies included a transmission scan for attenuation correction and three static emission scans with the inhalation of $[^{15}O]CO$, $[^{15}O]O_2$ and the injection of $[^{15}O]H_2O$ (Figure 1) [1]. The stress tests by CO_2 gas and acetazolamide (ACZ) with $[^{15}O]H_2O$ PET were also performed. The head of subject was fixed by the head fixation instruments during the scans. The emission images were registered as shown in Figure 1, and rigid body transformation matrices for translation (t_x, t_y, t_z) and rotation (r_x, r_y, r_z) between each images were estimated, by the algorithm based on normalized mutual information criterion [2]. All emission images except for $[^{15}O]CO$ image were corrected for the subject motion by the image realignment by estimated transformation matrices to $[^{15}O]H_2O$ (rest) image. $[^{15}O]CO$ image realigned to $[^{15}O]O_2$ image was realigned to $[^{15}O]H_2O$ image additionally. The mismatch between transmission and emission images was corrected by the realignment of transmission image with the assumption of no motion between transmission and $[^{15}O]CO$ scans. All the image registrations were computed by SPM8 software.

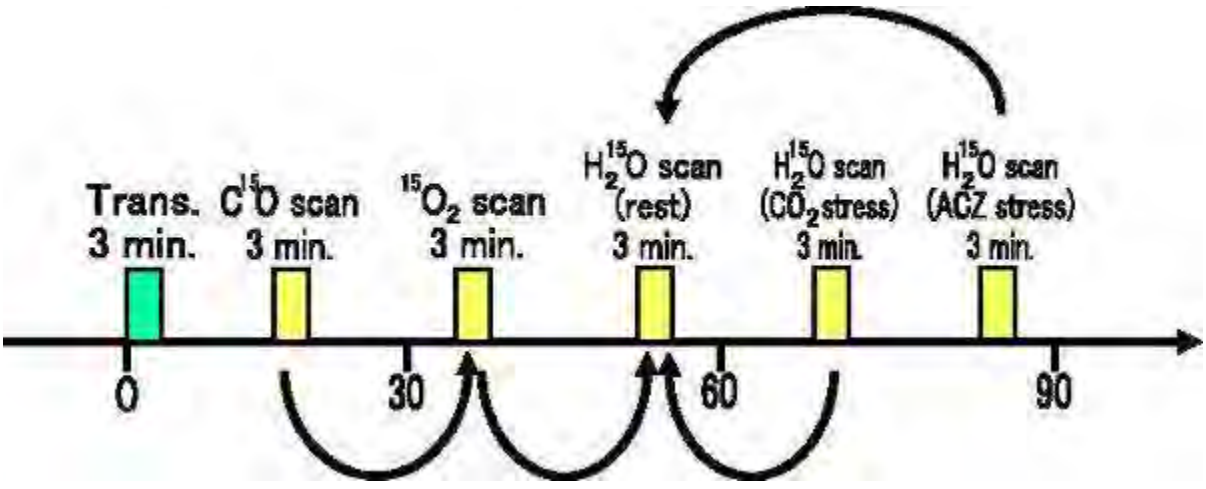

[Figure 1]

Figure 1: Study protocol of ^{15}O PET and direction for image co-registration.

Results: The z direction motion was observed most frequently: [^{15}O]CO to [^{15}O]O_2: 6/130 (4.6 %), [^{15}O]O_2 to [^{15}O]H_2O (rest): 1/130 (0.8 %), [^{15}O]H_2O (CO_2 stress) to [^{15}O]H_2O (rest): 4/130 (3.1 %), [^{15}O]H_2O (ACZ stress) to [^{15}O]H_2O (rest): 8/130 (6.2 %). Few considerable motions in the other directions were estimated. The original and realigned [^{15}O]O_2 images in a case of considerable motion between [^{15}O]O_2 and [^{15}O]H_2O were shown with [^{15}O]H_2O (rest) image in Figure 2. The consistency with [^{15}O]H_2O image was improved by the realignment of [^{15}O]O_2 image apparently. $CMRO_2$ calculated from [^{15}O]CO, [^{15}O]O_2 and [^{15}O]H_2O images was changed between original and motion-corrected images by 4.6 % in cortical region and 58.0 % in white matter. OEF was also affected: 2.6 % in cortical region and 35.4 % in white matter.

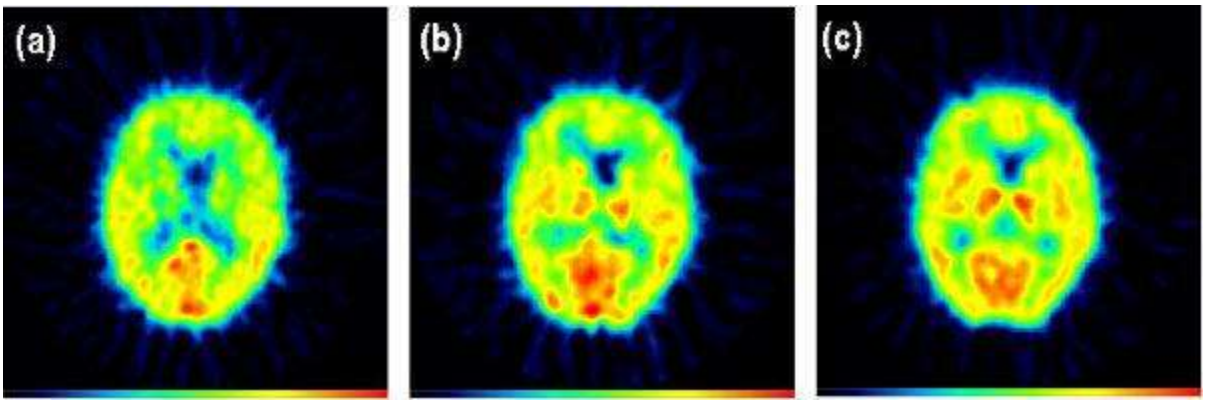

[Figure 2]

Figure 2: (a) Original, (b) realigned [^{15}O]O_2 images, (c) [^{15}O]H_2O (rest) image as a reference. Please note that the slice number is corresponding among the depicted images.

Conclusions: Although the considerable subject motion is less frequently, the motion correction in the case that the subject motion occurs is necessary for the precise estimation of OEF and $CMRO_2$.

References:

[1] Ibaraki, M., et al., 2008, J. Nucl. Med. 49, 50-59

[2] Studholme, C., et al., 1998, Proc. Med. Imaging 3338, 132-143

199

IMPACT OF INTRACRANIAL BLOOD FLOW REDISTRIBUTION ON STROKE SIZE DURING ISCHEMIA-REPERFUSION IN 7-DAY-OLD RATS

P. Bonnin[1,2], S. Renolleau[3,4], P.-L. Leger[4], N. Deroide[2], C. Charriaut-Marlangue[4]

[1]Physiologie Explorations Fonctionnelles Multidisciplinaires, APHP, Hôpital Lariboisière, [2]U965, INSERM, [3]Réanimation, APHP, Hôpital Trousseau, [4]U676, INSERM, Paris, France

Objective: Animal models have been developed to understand the pathophysiological mechanisms underlying ischemic disease and to study neuroprotection. Nevertheless, these models produce heterogeneous lesion volumes including animals without lesion. We hypothesized that the absence of cerebral lesion could be partly explained by the opening of the intracranial arterial collaterality through the circle of Willis and/or through the cortical anastomosis between the vascular beds of the three terminal cerebral arteries (anterior, middle, posterior cerebral arteries).

Material and methods: Ischemia was performed in Wistar P7 rats (Renolleau et al., 1998). Briefly, anesthetized rats were exposed to left middle cerebral artery electocoagulation (MCAo) followed by a 50 minutes occlusion of either the left common carotid artery (first sets of experiments, I/R-1, n=68) or both common carotid arteries (second set of experiments, I/R-2, n=30). Blood flow velocities (BFV) were measured, in the internal carotid arteries and basilar trunk upstream the circle of Willis, and in the posterior cerebral arteries downstream 1) before, 2) during ischemia, and 3) after release of CCA(s) occlusion using an echocardiograph (Vivid 7, GE Medical Systems ultrasound®, Horten, Norway) equipped with a 12-MHz linear transducer (12L) as previously reported (Bonnin et al. 2008). Cortical regional cerebral blood flow (rCBF) was monitored in the MCA territory by laser Doppler flowmetry. Lesion volumes were evaluated at 48 hours post-injury on cresyl violet-stained sections.

Results: At 48 hours after ischemia 41 to 48% (I/R-1 model) and 30% (I/R-2 model) of rats did not present a lesion. Those rats displayed increased mean BFV in both right internal carotid artery and basilar trunk in I/R-1 model, and increased mean BFV in the basilar trunk (BT) in I/R-2 model. In contrast, no significant changes in mean BFV were observed in lesioned rats. Furthermore, mean BFV in the BT was inversely correlated to the size of the lesion (R^2=0.72, $p< 0.0001$) in the I/R-2 model.

Conclusions: Two different intracranial hemodynamic patterns were displayed during ischemia, characterized by the presence or the absence of an increase in the mBFV of the right ICA and BT. The first pattern was correlated with the lack of a lesion and the second with its occurrence. Ultrasound imaging points it out and predicts absence or presence of ischemic lesions. This novel approach should greatly help preclinical studies.

- Bonnin P, Debbabi H, Mariani J, Charriaut-Marlangue C, Renolleau S. (2008a) Ultrasound Med Biol 34:913-922

- Renolleau S, Aggoun-Zouaoui D, Ben-Ari Y, Charriaut-Marlangue C. (1998) Stroke 29:1454-1460; discussion 1461.

201

IMMATURITY OF ENERGY METABOLISM IN NEONATAL BRAIN UNDERLIES ITS RESISTANCE TO HYPOXIA-ISCHEMIA: ^{31}P-MRS AND MITOCHONDRIA RESPIRATION STUDY IN NEWBORN RATS

I. Juranek[1], L. Baciak[1,2], S. Kasparova[2], Z. Sumbalova[3], J. Kucharska[3], T. Liptaj[2]

[1]Department of Biochemical Pharmacology, Institute of Experimental Pharmacology & Toxicology, Slovak Academy of Sciences, [2]Laboratory for in vivo NMR, Faculty of Food and Chemical Technology, Slovak Technical University, [3]Pharmacobiochemical Laboratory, 3rd Department of Internal Medicine, School of Medicine, Comenius University, Bratislava, Slovak Republic

Cerebral hypoxia-ischemia is a major cause of mortality and morbidity of neonates. Based on clinical findings, the brain of newborn infants is generally considered to be quite susceptible to hypoxic-ischemic insult. However, some data from studies using newborn mammals suggest that the neonatal brain may be rather resistant to hypoxia-ischemia. This controversy may result from experimental conditions used in those studies, e.g. from the degree of hypoxia applied, its duration, the postnatal age/maturity of newborns and animal species used. In the present study, we tested our original hypothesis that susceptibility of the neonatal brain to hypoxic-ischemic insult may be related to cerebral energy metabolism maturity; i.e. we supposed that the more mature cerebral energy metabolism, the higher the susceptibility of the neonatal brain to hypoxia-ischemia. We used newborn rats of various age (1, 4, 7 and 10-day old). To record postnatal maturation of energy metabolism in rat brain, we applied non-invasive approach of *in vivo* phosphorus magnetic resonance spectroscopy (^{31}P-MRS) on rat pups. Survival rate of the pups exposed to severe hypoxia (zero-oxygen environment) was inversely related to the maturity degree of their brain energy metabolism. In parallel experiments, activities of respiratory chain complexes were evaluated in isolated brain mitochondria; they increased with increasing postnatal age and surprisingly reached their maxima in different age groups. Mitochondrial content of alpha-tocopherol and coenzyme Q9/Q10 also increased along with the postnatal age of pups. Efficiency of oxidative phosphorylation was found to increase within the first two weeks of pups' life. To follow immediate cerebral energy metabolism alterations due to lack of oxygen in the neonatal brain, naïve pups of all age groups were challenged by 10-min anoxia, and ^{31}P-MRS was applied before, during and after the insult. The decrease of adenosine triphosphate and phosphocreatine and increase of inorganic phosphate reflected well acute brain energy metabolism failure in the pups exposed to anoxic conditions. Pups were left to recover for 15 min under air atmosphere. Both, the acute anoxic energy metabolism failure and short-term postanoxic energy metabolism deficit (at 15 min of brain reoxygenation) were inversely proportional to the maturity degree of brain energy metabolism. In conclusion, our data indicate that the maturation of brain energy metabolism in the neonatal period may be involved in increasing susceptibility of newborns to hypoxic-ischemic insult. In addition, our findings suggest that the inefficiency of neonatal brain energy metabolism, in particular that of cerebral mitochondria oxidative phosphorylation, may strikingly contribute to a relative resistance of neonates to hypoxic-ischemic insult. If this suggestion is confirmed, its significance for neonatology practice should become relevant.

Acknowledgement: The study was partially supported by the Structural Funds of EU (ITMS 26240220040), EU COST Programme (Action CM1001), Slovak State Programme for R&D (2003SP200280203) and Slovak Grant Agency VEGA (2/0083/09, 2/0048/11, 2/0011/11).

202

SEVOFLURANE PRECONDITIONING CONFERRED NEUROPROTECTION VIA ATTENUATING BLOOD-BRAIN-BARRIER DAMAGE AFTER FOCAL CEREBRAL ISCHEMIA IN RATS

Q. Yu[1], S. Lu[1], H. Wang[1], H. Gao[1], Y. Gan[1,2], P. Li[1], M. Chu[1], W. Liang[1], F. Zhang[1,2], J. Chen[1,2], Y. Gao[1]

[1]Department of Anesthesiology of Huashan Hospital, State Key Laboratory of Medical Neurobiology and Institute of Brain Sciences, Fudan University, Shanghai, China, [2]Center of Cerebrovascular Disease Research, University of Pittsburgh, Pittsburgh, PA, USA

Objectives: Preconditioning by inhalational anesthetics protects against ischemic neuronal injury in vivo and in vitro. The underlying mechanism of neuroprotection may involve reduced excitotoxicity, increased expression of antioxidants, and both anti-apoptotic and anti-inflammatory effects. However, the impact of inhalational anesthetics on blood-brain-barrier (BBB) after stroke is unknown. During post-ischemic reperfusion, the upregulation of cell adhesion molecules (CAMs) and matrix metalloproteinases (MMPs) attributes to the adhesion of leukocytes in the inflammatory sites and degradation of neurovascular matrix, respectively. We therefore tested the hypothesis that sevoflurane preconditioning offers neuroprotection by attenuating BBB leakage via suppression of CAMs and MMPs after focal cerebral ischemia.

Methods: Adult male Sprague-Dawley rats were randomly assigned to sham, vehicle or sevoflurane- preconditioning (sevo-pre) groups. The rats were exposed to ambient air (sham and vehicle group) or 1.2% sevoflurane (sevo-pre group) for 30min per day for 4 consecutive days, and then at 24 hours after preconditioning, subjected to middle cerebral artery occlusion (MCAO) for 60 min. Neurological deficits were assessed up to 3 days after ischemia. BBB integrity was assessed by transmission electron microscopy (tEM) and examining the levels of CAMs, MMPs and occludin (a tight-junction protein) 2 days after ischemia. All data are presented as mean±SEM; and statistic analysis was performed using ANOVA and *post hoc* Fisher's PLSD tests, with $P< 0.05$ considered statistically significant.

Results: tEM (n=4/group) showed that the BBB in vehicle group was severely disrupted after ischemia and reperfusion, indicated by the shrinking of blood vessels, swelling of astrocytic perivascular processes, decreased but intact tight-junctions, and disruption of basement membranes. In the sevo-pre group, the endothelial cells were only slightly shrunken, and the tight-junctions and basement membranes were intact. Furthermore, sevoflurane preconditioning markedly alleviated neurological deficits after strokes ($P< 0.05$, n=8/group). Determined by Western blots (n=4/group) and immunofluorescence (n=4/group), ischemia-induced increases in intercellular adhesion molecule-1 (ICAM-1) and vascular cell adhesion molecule-1 (VCAM-1) were attenuated in sevo-pre group (178±56% and 98±23% over sham group, respectively), compared to the vehicle group (582±119%, $P< 0.05$; 758±121%, $P< 0.01$, respectively). Upregulated MMP-9 (1589±254% over sham group) and MMP-2 (920±286% over sham group) after ischemia was also attenuated in sevo-pre group (MMP-9, 116±31%, $P< 0.01$; MMP-2, 153±50%, $P< 0.05$). The results were confirmed by gelatin zymography (n=4/group). Ischemia-induced decreases of occludin (10.1±7.3% over sham group) was also reduced by sevoflurane preconditioning (48.3±11.7%, $P< 0.01$).

Conclusion: Repeated preconditioning with sevoflurane confers potent neuroprotection against ischemic brain injury partially by suppressing ICAM-1- and VCAM-1-mediated leukocytes adhesion and reducing MMPs-mediated degradation of neurovascular tight-junctions, thus

preserving the BBB integrity. Sevoflurane preconditioning may be a potential novel therapy for ischemic brain injury.

205

EFFECT OF DIABETES ON MRNA GRANULE FORMATION AFTER PERMANENT FOCAL BRAIN ISCHEMIA

M.K. Lewis, J.C. Dunbar, D.J. DeGracia

Physiology, Wayne State University School of Medicine, Detroit, MI, USA

Objective: Stroke outcome is worsened in diabetic patients compared to non-diabetics. The underlying etiology of worsened diabetic stroke outcome remains an open question. We previously showed that post-ischemic translation arrest involved, at least in part, sequestration of poly-adenylated mRNAs away from ribosomes in the form of mRNA granules. Here, we investigated the effect of diabetes on mRNA granules after permanent focal cerebral ischemia.

Methods: Diabetes was induced in male Long Evans rats via a single I.P. injection of 55 mg/kg streptozocin. After 7 days, if blood glucose > 300 mg/dL, animals were then subject to normothermic, unilateral focal cerebral ischemia by middle cerebral artery occlusion (MCAO) [1]. Experimental groups were (n=5 animals/group): non-diabetics given MCAO for 2, 4, 6 and 8 hrs of permanent ischemia, and diabetics given MCAO for 30 minutes, 1, 4 and 6 hrs of permanent ischemia. Animals were perfusion-fixed in 4% PFA and 50 micron slices through the entire extent of the striatum were taken for evaluation. To detect mRNA granules, slices were double-labeled for poly-A binding protein via immunofluorescence histochemistry and for poly-adenylated mRNAs via fluorescent in situ hybridization (FISH). The volume of tissue containing mRNA granules was determined by evaluating areas containing mRNA granules in every second slice through the extent of the striatum, followed by 3 dimensional volumetric reconstruction. In addition, polyA FISH was performed with markers of intracellular organelles including endoplasmic reticulum, Golgi and mitochondria.

Results: In the non-diabetic groups, MCAO resulted in ipsilateral necrosis of striatal and cortical territory fed by the MCA, which increased with ischemia duration. In general, cortical areas lateral to and striatal areas medial to core showed evidence of mRNA granulation. At 2 hr MCAO, animals showed only mRNA granules and no core. As ischemia duration increased, areas previously occupied by mRNA granulation became necrotic so that by 8 hr MCAO, most affected tissue was necrotic and little showed evidence of mRNA granules. In terms of the relative proportions of necrotic or mRNA-granule-containing areas, the 1 hr ischemia diabetic animals resembled the 2 hr non-diabetics, and the 4 and 6 hr diabetic MCAO groups resembled the 6 and 8 hr MCAO non-diabetic groups. In all instances, mRNA granules did not colocalize with organelle markers, indicating they are cytoplasmic structures.

Conclusions: Ischemia-induced mRNA granulation and necrosis were more extensive at earlier time-points in the diabetic group compared to the non-diabetics. Under the assumption that the diabetics and non-diabetics received equivalent amounts of ischemia [2] at the fixed MCAO time points, our observations suggest that diabetes predisposes the neurons to increased sensitivity to ischemic damage.

References:

[1] Rizk NN, Rafols JA, Dunbar JC. Cerebral ischemia-induced apoptosis and necrosis in normal and diabetic rats: effects of insulin and C-peptide. Brain Res. 2006;1096:204-12

[2] DeGracia DJ. Towards A Dynamical Network View of Brain Ischemia And Reperfusion. Part I: Background and Preliminaries. J Exp Stroke Transl Med 2010; 3(1): 59-71

206

CHRONIC RESVERATROL TREATMENT RESTORES VASCULAR RESPONSIVENESS OF CEREBRAL ARTERIOLES IN TYPE 1 DIABETIC RATS

D.M. Arrick, H. Sun, **W. Mayhan**

Cell and Integrative Physiology, University of Nebraska Medical Center, Omaha, NE, USA

Introduction: Decreased dilation of cerebral arterioles via an increase in oxidative stress may be a contributing factor in the pathogenesis of diabetes-induced complications that lead to cognitive dysfunction and/or stroke.

Aim: Our goal was to determine whether resveratrol, a polyphenolic compound present in red wine, has a direct protective effect on cerebral arterioles during Type 1 diabetes (T1D).

Materials and methods: We measured responses of cerebral arterioles in untreated and resveratrol-treated (10 mg/kg/day) nondiabetic and diabetic rats to eNOS- and nNOS-dependent agonists, and a NOS-independent agonist. In addition, we harvested brain tissue from nondiabetic and diabetic rats to directly measure the levels of superoxide under basal conditions. Further, we used Western blot analysis to determine the protein expression of eNOS, nNOS, SOD-1 and SOD-2 in isolated cerebral arterioles and/or brain tissue from untreated and resveratrol-treated nondiabetic and diabetic rats.

Results: We found that T1D specifically impaired eNOS- and nNOS-dependent reactivity of cerebral arterioles, but did not alter NOS-independent vasodilation. While resveratrol did not alter responses in nondiabetic rats, resveratrol prevented T1D-induced impairment in eNOS- and nNOS-dependent vasodilation. In addition, superoxide levels were higher in brain tissue from diabetic rats and resveratrol reversed this increase in superoxide. Further, eNOS and nNOS protein were increased in diabetic rats, resveratrol produced a further increased eNOS and nNOS protein in nondiabetic and diabetic rats. SOD-1 and SOD-2 proteins were not altered by diabetes or resveratrol treatment.

Conclusion: Our findings suggest that resveratrol restores vascular function and oxidative stress in T1D. We suggest that our findings may implicate an important therapeutic potential for resveratrol in treating T1D-induced cerebrovascular dysfunction.

207

EXERCISE TRAINING RESTORES NOS-DEPENDENT RESPONSES OF CEREBRAL ARTERIOLES AND IMPROVES ISCHEMIC BRAIN DAMAGE IN DIABETIC RATS

D.M. Arrick, H. Sun, W.G. Mayhan

Cellular & Integrative Physiology, University of Nebraska Medical Center, Omaha, NE, USA

Introduction: Exercise training (ExT) has been shown to play a significant role in the prevention cardiovascular-related diseases. However, the effects of ExT on the brain remain largely unknown.

Aims: Our goals were to examine whether ExT could normalize impaired nitric oxide synthase-dependent (NOS) dilation of cerebral arterioles and to determine the influence of ExT on transient focal ischemia-induced brain damage during type 1 diabetes (T1D).

Materials and methods: We measured the diameter of pial arterioles in sedentary and exercised nondiabetic and diabetic rats in response to eNOS-dependent (ADP), nNOS-dependent (NMDA) and a NOS-independent (nitroglycerin) agonist. Superoxide levels were measured in brain tissue under basal conditions in sedentary and exercised nondiabetic and diabetic rats. In addition, a right middle cerebral artery occlusion (MCAO) was performed and we examined infarct size 24 hr after a 2 hr occlusion.

Results: ADP and NMDA produced dilation of pial arterioles that was similar in sedentary and exercised nondiabetic rats, but produced only minimal vasodilation in sedentary diabetic rats. ExT restored impaired ADP- and NMDA-induced vasodilation in diabetic rats. Nitroglycerin produced similar responses of pial arterioles in sedentary and exercised nondiabetic and diabetic rats. Superoxide levels were similar in sedentary and exercised nondiabetic rats, were increased in sedentary diabetic rats, and were normalized by ExT in diabetic rats. We found that eNOS protein was increased in diabetic rats and further increased by ExT and nNOS protein was not influenced by T1D, but was increased by ExT. Diabetic sedentary rats had a significantly larger infarct volume than that observed in nondiabetic sedentary rats. Diabetic exercised rats had a significantly smaller infarct volume when compared to sedentary nondiabetic and diabetic rats.

Conclusions: We conclude that ExT can alleviate impaired eNOS- and nNOS-dependent responses of pial arterioles during T1D. The normalization of cerebral vasoreactivity may contribute to the decreased ischemic brain damage observed by ExT in T1D.

210

NEUROPROTECTIVE EFFECT OF LOW-DOSE ALCOHOL CONSUMPTION ON TRANSIENT FOCAL CEREBRAL ISCHEMIA

H. Sun[1], W. Xiong[2], D.M. Arrick[1], W.G. Mayhan[1]

[1]Cellular and Integrative Physiology, [2]Surgery-General Surgery, University of Nebraska Medical Center, Omaha, NE, USA

Background and aims: Alcohol is one of the most commonly used chemical substances, and transient focal cerebral ischemia is one of the most common types of stroke. High-dose alcohol consumption has been found to exacerbate cerebral ischemia/reperfusion (I/R) injury. However, the influence of low-dose alcohol consumption on cerebral I/R injury has not been investigated. We recently examined the influence of low-dose alcohol consumption on cerebral I/R injury and determined the role of PPARgamma in reduced cerebral I/R injury during low-dose alcohol consumption.

Methods: C57BL/6J mice were fed liquid diets with or without 1% alcohol for 8 weeks. Transient focal cerebral ischemia was induced by middle cerebral artery occlusion (MCAO) with an intraluminal filament for 1 hour. Cerebral I/R injury was evaluated at 24 hours and 72 hours of reperfusion by 2,3,5-triphenyltetrazolium chloride (TTC) staining and DNA fragmentation assay. In addition, we measured protein expression and DNA-binding activity of PPARgamma in peri-infarct parietal cortex and the effects of PPARgamma agonist, rosiglitazone (20 mg/kg/day in diet for 2 weeks prior to MCAO), and PPARgamma antagonist, GW9662 (3 mg/kg/day in diet for 2 weeks prior to MCAO), on 1-hour MCAO/24-hour reperfusion-induced brain injury.

Results: Compared with nonalcohol-fed mice, total infarct volume was reduced by 46% at 24 hours of reperfusion and 41% at 72 hours of reperfusion in 1% alcohol-fed mice. Consistently, the magnitude of cerebral I/R-induced increase in DNA fragmentation was significantly less in 1% alcohol-fed mice compared to nonalcohol-fed mice. Eight-week 1% alcohol consumption produced an upregulation in PPARgamma expression and activity in parietal cortex. Although PPARgamma expression and activity reduced following cerebral I/R in peri-infarct parietal cortex, they were still significantly greater in 1% alcohol-fed mice compared to nonalcohol-fed mice. In addition, rosiglitazone significantly reduced total infarct volume in nonalcohol-fed but not 1% alcohol-fed mice. In contrast, GW9662 significantly increased total infarct volume in 1% alcohol-fed but not nonalcohol-fed mice.

Conclusions: Our findings suggest that low-dose alcohol consumption protects the brain against I/R injury, and neuroprotective effect of low-dose alcohol consumption may be related to an upregulation of PPARgamma.

213

REAL-TIME INTRAVITAL FLUORESCENCE IMAGING REVEALS THAT HYDROXYL RADICAL PLAYS A CRUCIAL ROLE IN DELAYED NEURONAL DEATH

S. Yamamoto, Y. Wang, T. Sakurai, S. Terakawa

Photon Medical Research Center, Hamamatsu University School of Medicine, Hamamatsu, Japan

Objective: This study was designed to explore the relationship between *in situ* hydroxyl radical (•OH) production and delayed neuronal death induced by transient forebrain ischemia in rats.

Methods: In anesthetized adult SD rats (300 g), hippocampal CA1 neurons were stained with hydroxyphenyl fluorescein (HPF, 1 mM), a •OH indicator, by pressurized bolus injection (Wang et al., 2010). To obtain intravital fluorescence images in the CA1 region, we employed an imaging fiber bundle (1 mm outer diameter) including 20,000 fibers coupled to the multi-pinhole confocal scanner (CSU-21, Yokogawa, Japan) equipped with 10x objective lens. This fiber-coupled confocal microscope (FCM) is capable to observe the confocal images in deep brain regions (Sakurai et al., 2006). 10-min forebrain ischemia was induced by 4-vessel occlusion using a balloon occluder (Wang et al., 2010), and fluorescence intensities of HPF were recorded during ischemia and 180-min reperfusion. •OH scavenger, edaravone (1-phenyl-3-methyl-5-pyrazolone, Mitsubishi Tanabe Pharma, Japan); 0.3, 1, and 3 mg/kg, was intravenously injected before ischemia. Their effects on the •OH production and on the delayed (7 days later) neuronal death were analyzed.

Results: Edaravone dose-dependently increased the number (mean $\pm$ SD/500 μm) of residual CA1 neuron 7 days after transient (10 min) forebrain ischemia (sham = 102 $\pm$ 9, ischemia alone = 19 $\pm$ 10, ischemia with edaravone 0.1 mg = 34 $\pm$ 5, ischemia with edaravone 1 mg = 72 $\pm$ 5.5, ischemia with edaravone 3 mg = 83 $\pm$ 3, n=6/each). During and following ischemia, edaravone (3 mg) did not affect the cerebral blood flow change in CA1 measured by laser-Doppler flowmetry. Transient forebrain ischemia significantly increased the fluorescence intensity of HPF, that is, the •OH production, in CA1 during the early period of reperfusion (reaching the plateau level 60 min after reperfusion). Edaravone dose-dependently suppressed the •OH production following ischemia (mean $\pm$ SD % of basal HPF intensity) measured by FCM (ischemia alone = 163 $\pm$ 6, ischemia with edaravone 0.3 mg = 150 $\pm$ 12, ischemia with edaravone 1 mg = 136 $\pm$ 5, ischemia with edaravone 3 mg = 118 $\pm$ 8, n=4/each). Edaravone (3 mg), at the most effective dosage, did not change the fluorescence intensity of Mito-SOX, a fluorescent superoxide ($\bullet O_2^-$) indicator, measured by FCM.

Conclusions: Edaravone provides the dose-dependent neuroprotection against delayed neuronal death in CA1. The treatment with edaravone produces the dose-dependent reduction of •OH, but not $\bullet O_2^-$, in hippocampus in parallel with the neuroprotective effects. Our results indicate that: 1) •OH, but not $\bullet O_2^-$, plays a crucial role in delayed neuronal death induced by transient forebrain ischemia; and 2) FCM is useful to obtain the fluorescence images in the brain in which two-photon microscopy does not reach.

Supported by the grant from JSPS #16390407 (SY)

References:

1. Wang Y, Yamamoto S, Miyakawa A et al. Intravital oxygen radical imaging in normal and ischemic rat cortex. *Neurosurg* 2010; 67:118-128.

2. Sakurai T, Yamamoto S, Miyakawa A et al. Fiber-coupled confocal microscope for real time imaging of cellular signals in vivo. *Proc of SPIE* 2006; 6088:608803-1-608803-6.

214

FUNCTIONAL AND MORPHOLOGICAL REPAIR OF NEWBORN STRIATAL NEURONS IN ADULT RAT BRAIN AFTER A TRANSIENT MIDDLE CEREBRAL ARTERY OCCLUSION

F.-Y. Sun, X. Sun, Q.-W. Zhang, J.-J. Guo, K.-Y. Li, L.-M. Zhang, Y.-L. Huang

Department of Neurobiology, Medical Center, Fudan University, Shanghai, China

Introduction: Our previous work had demonstrated that newborn striatal neurons induced by ischemic injury coud differentiate into mature neurons and functionally integrate with local neural networks. In this study, we investigate whether newborn striatal neurons could form long projection to the substantia nigra for functional repair of the brain after ischemic injury.

Methods: Cerebral ischemic injury was induced by a transient middle cerebral artery occlusion (MCAO) in adult rats. Retrovirus containing GFP report gene was injected into the lateral ventricle to label newborn cells and a retrograde tracer fluorogold (FG), into the substantia nigra to trace projection neurons from the striatum. Patch-clamp recording and confocal analyses with fresh-prepared striatal slices were used to study functional and morphological behaviors of newborn striatal neurons.

Results: GFP-expressing (GFP^+) cells in the ipsilateral striatum expressed GAD_{67} or ChAT, which are a GABAergic or cholinergic synthetic enzyme, respectively. GFP^+ neurons showed neurite and its branches, formed synapses with preexisting neurons. These newborn striatal neurons possess actively recycled synaptic vesicle and neurotransmitter release capacity. They also could fire action potentials and receive both excitatory and inhibitory synaptic inputs. Thus, ischemia-induced newly formed striatal GABAergic and cholinergic neurons could become functionally integrated into local neural networks.

We further found that NR1 and D_2L, proteins for NMDA and dopamine D_2 receptors respectively, expressed on the membrane of newborn striatal neurons, suggesting that NMDA and dopamine D_2 receptors exists in the newly generated striatal neurons. Moreover, GFP^+ neurons showed positive staining with FG, a retrograde tracer. Thus, these newborn striatal neurons can develop long projection to the substantia nigra and, NMDA and dopamine D_2 receiving glutamate and dopamine inputs, respectively.

Conclusion: Putting together, stroke-induced adult neurogenesis in non-neurogenic regions should be very important endogenous compensatory mechanism in brain repair after stroke attack. The results also provided positive evidences that enhancement of neurogenesis should be beneficial and helpful for brain repair after injury.

Acknowledgement: We thank National Nature Science Foundation of China (81039920) for the financial support.

216

COMBIANTION THERAPY OF GLUCOCORTICOIDS AND PROTEASOME INHIBITORS AS NOVEL TREATMENT OPTION FOR ACUTE ISCHEMIC STROKE

C. Kleinschnitz[1], K. Blecharz[2], T. Kahles[3], T. Schwarz[1], P. Kraft[1], K. Göbel[4], S.G. Meuth[4], M. Burek[2], T. Thum[5], G. Stoll[1], **C. Foerster**[6]

[1]Neurology, [2]Dept. of Anesthesia and Critical Care, Experimental Anesthesia, University Hospital Wuerzburg, Wuerzburg, Germany, [3]Weill Cornell Medical College, New York, NY, USA, [4]Neurology - Inflammatory Disorders of the Nervous System and Neurooncology, University of Münster, Münster, [5]Institute for Molecular and Translational Therapeutic Strategies, OE8886, IFB, Hannover Medical School, Hannover, [6]Experimental Anesthesia, University Hospital Wuerzburg, Wuerzburg, Germany

Objectives: Brain edema caused by disruption of the blood brain barrier is detrimental in ischemic stroke and its treatment options are limited. While glucocorticoids potently stabilize the blood brain barrier and ameliorate tissue edema in neoplastic and inflammatory central nervous system disorders, they are ineffective in patients with acute ischemic stroke. Our study identifies excessive proteasomal glucocorticoid receptor degradation as an important mechanism causing pharmacological insensitivity of brain microvascular endothelial cells to glucocorticoids under hypoxic conditions.

Methods: In vitro and in vivo, restoration of glucocorticoid sensitivity was achieved by inhibition of the proteasomal pathway by Bortezomib accompanied by treatment with a specific glucocorticoid. In mice subjected to transient middle cerebral artery occlusion, this combination therapy moreover significantly reduced brain edema and infarct volumes, while the respective monotherapy was ineffective.

Results: In mice subjected to transient middle cerebral artery occlusion, this combination therapy moreover significantly reduced brain edema and infarct volumes, while the respective monotherapy was ineffective.

Conclusions: This combined approach, application of proteasome inhibitors and a glucocorticoid, might open new avenues for the treatment of brain edema following ischemic stroke.

218

ADMINISTRATION OF ENDOTHELIAL PROGENITOR CELLS OR THEIR SECRETED FACTORS ENHANCES THE NEURO-ANGIOGENIC RESPONSES IN A MICE MODEL OF CEREBRAL ISCHEMIA

A. Morancho[1], A. Rosell[1], M. Navarro-Sobrino[1], E. Martínez-Saez[2], L. García-Bonilla[1], S. García[1], V. Barceló[1], A. Penalba[1], S. Lope-Piedrafita[3], J. Montaner[1]

[1]Laboratorio Investigación Neurovascular, Institut de Recerca Hospital Universitari Vall d'Hebron, Universitat Autònoma de Barcelona, [2]Departamento de Neuropatología, Hospital Universitari Vall d'Hebron, [3]Servei RMN, Universitat Autònoma de Barcelona, Barcelona, Spain

Objectives: Demonstrate that therapies with endothelial progenitor cell (EPCs) and secretion factors enhance the neuro-angiogenesis responses in a model of cerebral ischemia in mice.

Methods: We used a model of permanent cerebral ischemia induced by occlusion of middle cerebral artery. The study by magnetic resonance imaging (MRI), including T2WI, DTI and T2 map sequences, was performed 24h and 2 weeks after the ischemia. The EPCs were maintained in basal medium 24h to obtain conditioned media (CM). After the first MRI, animals were randomized to a group of treatment: vehicle, EPCs or CM. We also performed a sham non-ischemic group. After the second MRI, brains were obtained to determine capillary density (CD31), neuroblasts (DCX), neurons (NeuN) and axonal organization (NF and MAP2).

Results: EPCs secreted angiogenesis-related growth factors (VEGF, FGF, PDGF-BB). MRI study showed that infarct size (T2WI) and severity (ADC, FA, T2map) were similar between groups before treatment. However, after two weeks, the loss of cortical Angiogenesis tissue was smaller in the group of EPCs compared to the vehicle (19% and 24%, p=0.1). In the peri-infarct areas, an increase of the FA was detected, indicating structural changes in neural columns in the EPCs and CM groups ($p< 0.05$), accompanied by an increase of capillaries in both groups ($p< 0.05$) (figure A and B). Finally, more neuroblasts were identified in the subventricular zone and dentate gyrus although the number of mature neurons did not change.

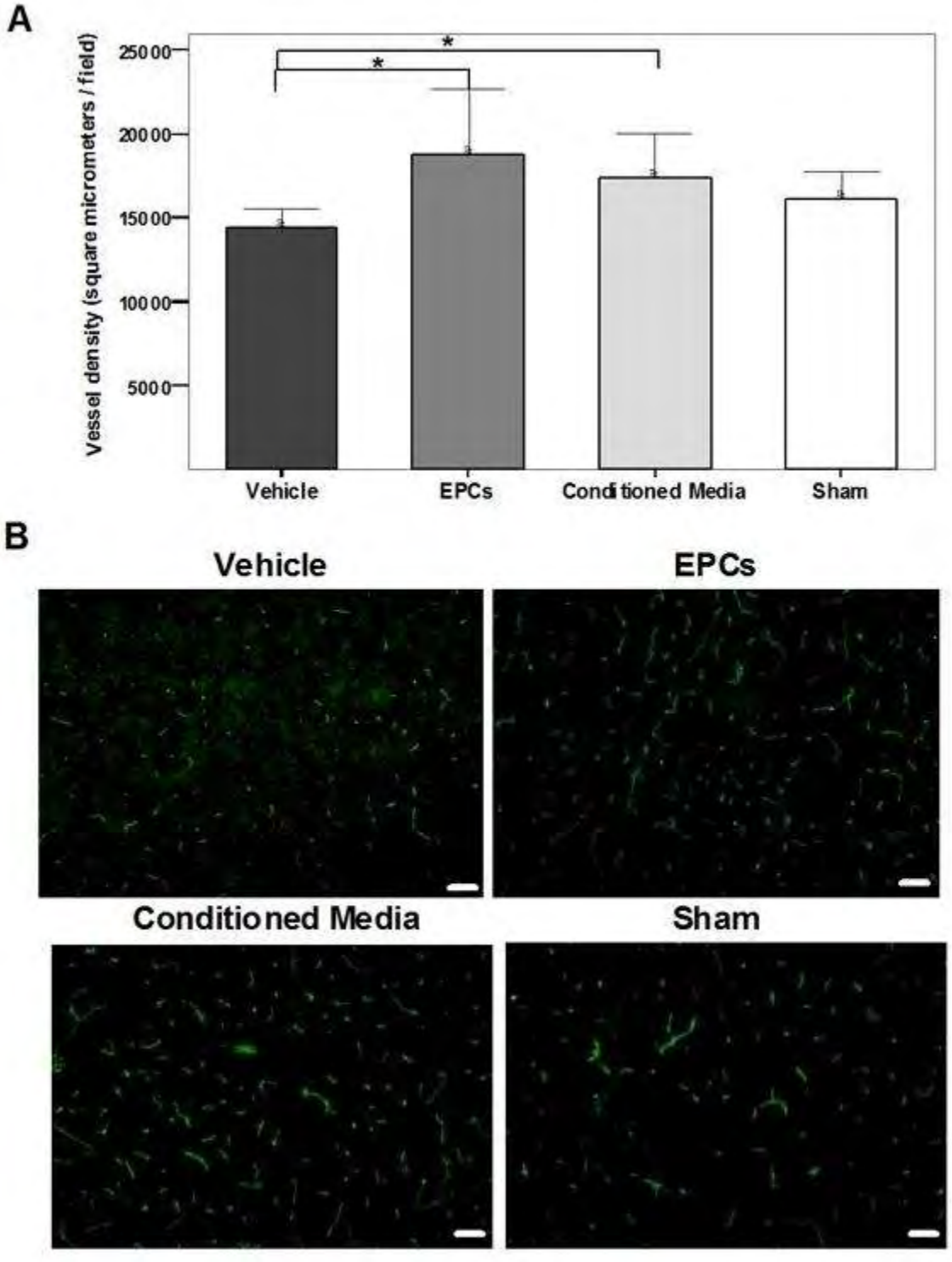

[Angiogenesis]

Conclusions: Treatment with EPCs or their secretion factors improves neuro-angiogenic response after cerebral ischemia in mice.

219

A NEW MOUSE MODEL OF FOCAL TRANSIENT CEREBRAL ISCHEMIA BY DISTAL OCCLUSION OF THE MIDDLE CEREBRAL ARTERY

A. Morancho, A. Rosell, S. García, D. Giralt, V. Barceló, J. Montaner

Laboratorio Investigación Neurovascular, Institut de Recerca Hospital Universitari Vall d'Hebron, Universitat Autònoma de Barcelona, Barcelona, Spain

Objectives: Rodent stroke models provide the experimental backbone for the *in vivo*

determination of the mechanisms of cell death and neurorepair. Of them, transient models of ischemia, where the blood flow is restored after the ischemic insult, are the best models to assure the arrival of specific treatments into the injured area. Our aim was to develop a reproducible model of transient focal cerebral ischemia by distal artery occlusion.

Methods: Adult male Balb/c mice (n=19) were anesthetized and the left middle cerebral artery (MCA) was exposed via the transtemporal approach, involving a small craniotomy. The distal MCA was occluded for 60 min by compressing it with a blunted needle. Cerebral blood flow (CBF) was measured continuously by laser-Doppler flowmetry using a flexible fiberoptic placed directly on the top of the parietal branch of the M1 bifurcation beginning 5 min before MCAO, during the occlusion and 5 min after the occlusion. Occlusion was considered when the CBF decreased by more than 80% of the baseline, and reperfusion when the CBF increased more than 75% of the baseline value. Physiologic parameters were evaluated (n=4) before and after the ischemia period and the ischemic lesion was evaluated at 24h after occlusion by TTC staining and immunolabeling (NeuN and CD31). The corner test was performed to evaluate functional impairment.

Results: A total of 17 animals (88%) completed the surgery achieving the occlusion and reperfusion criteria. There were no differences in the measured physiological parameters (pH, pCO2 and pO2) before and after the ischemia. The infarct volume at 24h was 37.7±12.1 mm^3 representing a 20.7±7% of the ipsilateral hemisphere but there was no significant edema in the ipsilateral hemisphere (0.96±0.04 mm3). Mortality rate was 10.5% during the surgical procedure. The corner test at 4 and 24h after the ischemia represented by the laterality index was 0.4±0.16 at 4h and 0.45±0.19 at 24h showing an impairment of the motor activity and the loss of symmetry (p=0.018 at 4h and p=0.003 at 24h versus pre-surgery values). Immunohistochemistry confirmed a severe ischemic lesion since the number of neurons and vessels was significantly reduced when compared to the contralateral hemisphere (p=0.004 and p=0.05, respectively).

Conclusions: We have set up a highly reproducible and little invasive model of focal transient cerebral ischemia in mice, by distal occlusion of the MCA. After 60 min of ischemia, animals showed reproducible cortical infarcts, impaired functional outcome and tissue damage. This study shows that it could be a good ischemia-reperfusion model to assess cortical localized death, repair and treatment screening.

220

DIHYDROTESTOSTERONE MAY PROMOTE A NEUROPROTECTIVE RESPONSE TO ISOFLURANE PRECONDITIONING IN ISCHEMIC AGED MALE MOUSE BRAIN

W. Zhu[1], N.L. Libal[2], P.D. Hurn[2], S.J. Murphy[2]

[1]Department of Neurology, the Affiliated Nanjing Benq Hospital of Nanjing Medical University, Nanjing, China, [2]Anesthesiology and Perioperative Medicine, Oregon Health and Science University, Portland, OR, USA

Objectives: Isoflurane preconditioning (IsoPC) in experimental stroke is neuroprotective in young male mouse brain, with the neuroprotective benefits of IsoPC being lost in androgen-deficient castrated males and restored in dihydrotestosterone (DHT) treated castrates[1,2]. Because male sex steroid levels are not constant during life and can begin to decline during the middle years of life (andropause), it seems likely that androgen loss during aging might have a similar effect on the aging male brain's response to Iso PC as castration did in the young male brain. We evaluated the ischemic sensitivity of IsoPC aged male brain and the effect of DHT on this ischemic sensitivity.

Methods: Gonadally intact aged C57BL/6 male mice (20 to 22 months old) received either no hormone or a subcutaneous 0.5 mg DHT pellet 7 to 8 days before preconditioning and experimental stroke. Aged males $\pm$ 0.5 mg DHT were preconditioned for 4 h with air (sham preconditioning, Sham PC) or 1.0% IsoPC, and then underwent 2 h of middle cerebral artery occlusion via intraluminal filament 24 h after preconditioning. Laser-Doppler flowmetry (LDF) was used to monitor cortical perfusion. Blood and brains were collected at 22 h reperfusion. Plasma DHT levels were measured in duplicate by radioimmunoassay and hemispheric infarct volumes (% contralateral structure) were determined by digital image analysis of 2 mm thick coronal brain slices stained with 2,3,5-triphenyltetrazolium chloride.

Results: Relative LDF changes were equivalent among groups. IsoPC had no effect on hemispheric infarct volume in aged males (46 $\pm$ 5%, n=11) compared to Sham PC aged males (41 $\pm$ 6%, n=10) but significantly ($p< 0.05$) decreased hemispheric infarct volume in DHT-treated aged male mice (22 $\pm$ 5%, n =3) compared to Sham PC DHT-treated aged males (45 $\pm$ 6%, n=3). Plasma DHT levels were higher in DHT-treated aged males (0.24 $\pm$ 0.09 pg/ml, n=6) compared with aged males (0.13 $\pm$ 0.04 ng/ml, n=20) mice regardless of preconditioning group.

Conclusions: IsoPC neuroprotection observed in young male brain is lost in aged male brain but is restored in the presence of DHT. Our findings suggest that androgen availability during IsoPC may influence experimental stroke outcomes in aged mouse brain. Future studies will need to address the role of androgens as well as determine what mechanisms are involved in IsoPC neuroprotection in aging ischemic male brain. Clinically, our findings suggest that isoflurane anesthesia and androgen availability during “at-risk” cardiovascular surgical procedures may influence perioperative stroke outcomes in aging men.

References:

1. Kitano et al. 2007. J Cereb Blood Flow Metab 27:1377-86

2. Zhu et al. 2010. Neuroscience 169:758-69

221

A NEW APPROACH TO CENTRAL NERVOUS SYSTEM RADIOTRACER DISCOVERY USING HIGH PERFORMANCE LIQUID CHROMATOGRAPHY

A.A.S. Tavares[1], D. Dewar[1], S. Pimlott[2]

[1]Institute of Neuroscience and Psychology, University of Glasgow, [2]West of Scotland Radionuclide Dispensary, University of Glasgow and North Glasgow University Hospital NHS Trust, Glasgow, UK

Objectives: To date, the early stage of central nervous system (CNS) radiotracer discovery has been mainly focused on screening unlabelled compounds according to their partition coefficient (Log P) and their affinity/selectivity values. Both measures are simplistic and do not account for the complex process of brain entry, non-specific binding and kinetics of the compound and there is a need for better selection models at the early stages of radiotracer discovery. This prompted us to examine an alternative *in vitro* high throughput screening approach based on high performance liquid chromatography (HPLC), where we investigated existing radiotracers and compared our HPLC measures with *in vivo* human measures.

Methods: Twelve molecules, which have previously been used as radiotracers in human studies were screened using HPLC and four different measures were determined, according to previously established methodology [1-3]. 1) Log P; 2) permeability (P_m); 3) percentage of plasma protein binding (%PPB); 4) membrane-compound equilibrium constant (K_m). The *in vivo* measures of percentage injected dose (%ID) and BP_{ND} (defined at equilibrium as the ratio of specifically bound to nondisplaceable radiotracer in tissue) were obtained from previously published studies or in house measurements in healthy human volunteers. Relationships between brain entry measurements (Log P, P_m and %PPB) and *in vivo* %ID as well as, membrane-compound interactions (K_m) and specific binding *in vivo* (BP_{ND}) were investigated. Best fitting models and nonlinear regression were used to adjust the values of the variables in the model to find the curve that best predicts Y (%ID or BP_{ND}) from X (Log P, P_m, %PPB or K_m). Log P values obtained using *in silico* packages (ChemDraw 8.0 package and ADME Suite 5.0 package) and flask methods (from literature or measured in house) were compared with Log P values obtained using HPLC.

Results: Log P exhibited the weakest correlation with *in vivo* brain uptake (r^2=0.47). The Log P values determined were highly variable depending on the methodology used. %PPB and P_m showed good correlation (r^2=0.68 and r^2=0.77, respectively) with the %ID and K_m presented the strongest correlation with the *in vivo* measure, BP_{ND} (r^2=0.86). %PPB showed a parabolic relationship with %ID (highest %ID found at %PPB=60%), while P_m and K_m showed a logarithmic and exponentially decreasing relationship with %ID and BP_{ND}, respectively.

Conclusion: The described relationships between high throughput HPLC measures (%PPB, P_m and K_m) and *in vivo* measurements may provide selection criteria, that could be used to target and rank candidates at early stages of CNS radiotracer discovery that are most likely to succeed .

Acknowledgments: The authors thank Dr. Hank Kung, Dr. Franklin Aigbirhio and Dr. Frederic Bois for kindly providing ADAM, PIB and Iomazenil reference compounds, respectively; and Dr. James Patterson for providing *in vivo* data on AMT. Adriana Tavares was funded by Scottish Imaging Network: A Platform for Scientific Excellence (SINAPSE) studentship.

References:

[1] Yang C. et al. Advanced Drug Delivery Reviews 1996; 23:229-56.

[2] Valko K. et al. Journal of Pharmaceutical Sciences 2003; 92(11):2236-48.

[3] Valko K. Journal of Chromatography A 2004; 1037:299-310.

222

A NEW PHASE MASK FOR HIGH RESOLUTION BRAIN VENOGRAPHY

E. Casciaro, R. Franchini, S. Casciaro

Institute of Clinical Physiology, National Research Council, Lecce, Italy

Objectives: Most modern imaging diagnostic techniques, as functional Magnetic Resonance Imaging (fMRI) and High-Resolution BOLD Venography (HRBV), are based on the physical phenomenon so called Blood Oxygen Level Dependent (BOLD) effects which is due to the paramagnetic behaviour of venous blood: fMRI techniques are based on the BOLD contrast to detect neuronal activation sites, and HRBV techniques are able to image small venous vessels up to sub-millimeter dimensions thanks to induced magnetic field distortions, in and around draining vessels, that are responsible of MR signal dropout and phase contrast with surrounding tissues.

A key point to perform effective BOLD venography is the choice of an appropriate phase mask for the image processing, because phase masking represents the data processing step where magnitude and phase information are merged.

In literature, the Conventional phase masks (CM) are based on linear formulas with an exponent be able to determine the shape. These ones do not optimize vessel contrast-to-noise ratio (CNR) for all phase values because they do not take into account the intrinsic image signal-to-noise ratio (SNR).

Our aim was to improve vessel contrast in high resolution brain venography, and we had proposed a novel image processing procedure to obtain HRB venograms based on a new phase mask (NM) filter that maximizes the contrast of venous MR signals.

Methods: The effectiveness of the new algorithm was assessed both on digital phantoms and on acquired MR human brain images, and then compared with venographic results of phase masking methods in recent literature. The digital phantom consisted of a simulated MR dataset with given SNRs, while real human data were collected by scanning healthy volunteers with a 3.0-T MR system and a 3D gradient echo pulse sequence.

Results: With this procedure, vessel contrast is enhanced by reducing vessel signal in relation to its phase values according to a novel analytical function.

The NM was more effective than the CM both on the digital phantoms and on the acquired MR images. A quantitative comparison based on phantom indicates how this phase enhancement can lead to a significant increase in the CNR for all considered phase values as well as for all vessel sizes of clinical interest. Likewise, the in vivo brain venograms reveal a better depiction of the smallest venous vessels and the enhancement of many details undetectable in conventional images (Fig.1).

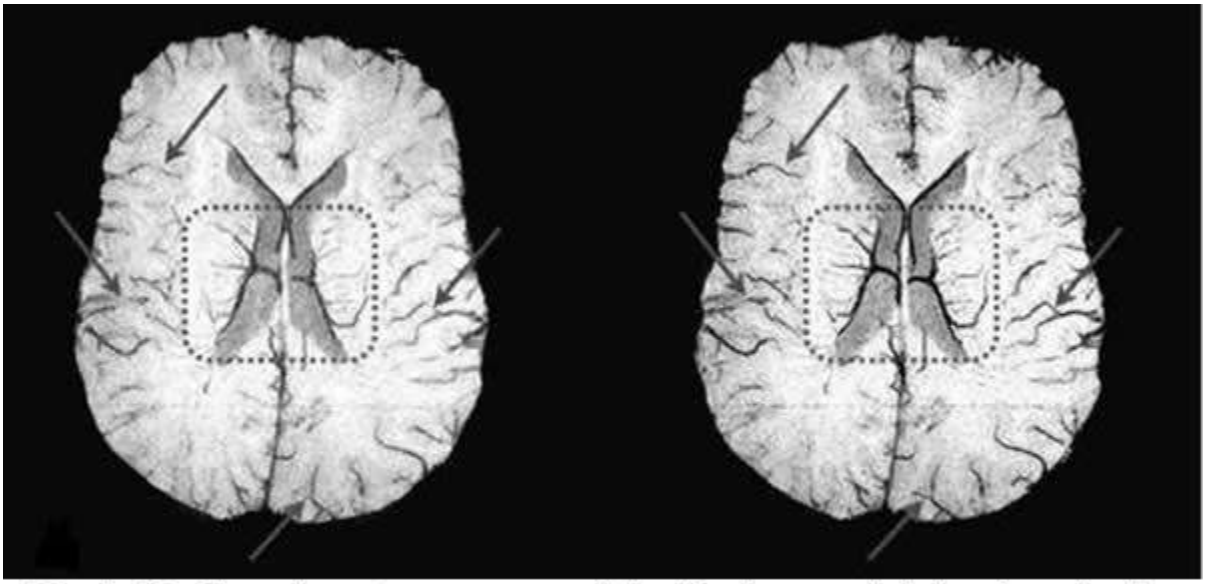

Fig. 1: The figure shows two venograms obtained in the same brain location using the conventional mask (left) and new mask (right). The overall contrast of the veins is higher in the venogram elaborated with the new mask. Arrows highlight improvements.

[The conventional mask and new mask]

Conclusions: The validity of this new method is critically evaluated both with theoretical considerations and experimental data, and the quality of the new venograms is compared with that ones realized as suggested in the current literature. The results demonstrate indubitably the striking advantages of this new technique and give to it scientific fundament as a significant improvement of BOLD venographic technique.

References:

[1] Predicting BOLD signal changes as a function of blood volume fraction and resolution, Y.-C.N Cheng, EM.Haacke, NMR Biomed 14 (2001)468-477

223

INCREASED NEUROREGENERATIVE CAPACITY OF VASCULAR ENDOTHELIAL GROWTH FACTOR OVEREXPRESSING MICE AFTER BRAIN ISCHEMIA

R. Kunze, K. Bieber, H. Marti

Physiology and Pathophysiology, University of Heidelberg, Heidelberg, Germany

Objectives: Vascular endothelial growth factor (VEGF), a key regulator of angiogenesis, exerts also neurotrophic and neuroprotective effects. VEGF is up-regulated during hypoxia and ischemia in the brain and can improve outcome after stroke, when administered exogenously. Neurogenesis occurs in discrete regions of the adult mammalian brain such as the subventricular zone (SVZ), and is stimulated upon brain ischemia. The present study aimed to analyse, whether VEGF overexpression in adult mouse brain affects neurogenesis upon transient brain ischemia.

Methods: Wild-type (WT) mice and mice overexpressing VEGF (V1)[1] were exposed to focal cerebral ischemia for 45 min by using the reversible filament occlusion model. Mice received daily intraperitoneal injections of BrdU up to day 3 after removal of the monofilament. Mice were sacrificed 3, 7, 14 or 21 d after transient middle cerebral artery occlusion (MCAO), brains were removed and cryosections were stained immunohistochemically for BrdU and nestin. SVZ of brains from WT and V1 mice were dissected, adult neural stem cells (NSC) were isolated and cultured as neurospheres *in vitro*. The cellular phenotype was characterised by immunocytochemistry. RT-PCR and ELISA were applied to analyse the expression of mVEGF, mVEGFR-1, mVEGFR-2 and $hVEGF_{165}$ transgene. To study migration, neurospheres were embedded into a 3-dimensional matrix, cultured for up to 24 h and the outgrowth of cells was determined. Neurospheres were exposed to 1 % hypoxia or grown in culture medium deficient in growth factors. The ratio of dead and proliferating cells was quantified by propidium iodide staining and FACS analysis.

Results: As compared to WT mice, in V1 mice the number of BrdU / nestin double-positive cells within the penumbra adjacent to the infarct area was highly increased 3 to 21 d after transient brain ischemia. SVZ-derived adult NSC isolated from V1 and WT mice expressed endogenous VEGF and VEGFR-2, whereas NSC from V1 mice also strongly produced the $hVEGF_{165}$ transgene. Furthermore, VEGF overexpression promoted migration of NSC *in vitro* as well as protected the cells against cell death by hypoxia and growth factor depletion.

Conclusions: Our results indicate that VEGF increases neurogenesis after transient cerebral ischemia probably by enhancing survival and migration of adult NSC.

References: [1]Wang Y, Kilic E, Kilic U, Weber B, Bassetti CL, Marti HH, Hermann DM. 2005. VEGF overexpression induces post-ischaemic neuroprotection, but facilitates haemodynamic steal phenomena. *Brain* 128: 52-63.

224

LOCAL AND REMOTE ACTIVATED MICROGLIA: A LONGITUDINAL DTI-GUIDED PET-STUDY WITH [^{11}C]-PK11195 IN ACUTE SUBCORTICAL STROKE

B. Radlinska[1,2], C. Paquette[2,3], M. Sidel[1,2], J.-P. Soucy[1,4], R. Schirrmacher[1,3], J. Minuk[1,2], A. Thiel[1,2,3]

[1]McGill University, [2]SMBD Jewish General Hospital, [3]Lady Davis Institute for Medical Research, [4]Montreal Neurological Institute, Montreal, QC, Canada

Objectives: Following subcortical ischemic stroke, activated microglia (AMG) can be seen not only in the local surroundings of the infarct itself, but also in remote brain regions with fibre tract connections to the affected area [1,2]. [^{11}C]-PK11195 is a PET ligand that binds to the cholesterol transporter protein (TSPO) which is expressed on the outer mitochondrial membrane of microglia when they become activated during post-stroke neuroinflammation [3], and can thus be used to image AMG *in vivo* after stroke. In this prospective longitudinal study, we investigated the temporal dynamics of AMG locally in the area of the infarct and remotely along the stroke affected fibre tracts. We also related AMG activity to pyramidal tract (PT) damage using diffusion tensor imaging (DTI).

Methods: 18 patients underwent DTI-MRI, [^{11}C]-PK11195-PET and behavioral testing within 2 weeks and 6 months of acute sub-cortical stroke. In 12 subjects the PT was affected by the stroke (PT-group) and in 6 patients it was not (nonPT-group). Standardized volumes-of-interest (VOIs) were placed along the PT at the level of the brainstem, oval centre and the infarct. Tracer uptake ratios (ipsilateral/contralateral) were calculated for each VOI and related to tract damage (measured as fractional anisotropy ratio R_{FA}) and clinical outcome (measured by the Rivermead Motor Function Test RMFT). 6 control subjects underwent the same protocol but only once.

Results: At 2 weeks post-stroke, local AMG activity in the infarct was increased in both patient groups as compared to the control group ($P < 0.01$). Increased uptake ratios were found along the PT at the level of the pons, midbrain and internal capsule only in PT-group patients (Fig.1), whereas no AMG was observed retrograde to the lesion at any time point. This remote anterograde AMG persisted at 6 month follow-up, and was significantly correlated with initial PT damage, as assessed by DTI-MRI in the same tract portion ($r = -0.92$, $P < 0.01$). After controlling for PT damage, initial AMG activity in the brainstem showed a positive correlation with clinical outcome ($p = 0.67$, $P = 0.035$), whereas persisting AMG activity in the infarct tended to be negatively correlated ($p = -0.62$,$P = 0.052$) (Fig.2).

Conclusions: This DTI-guided [^{11}C]-PK11195-PET study in acute sub-cortical stroke demonstrates that local and remote AMG display differential temporal dynamics. Both local and remote AMG is associated with anterograde PT damage as measured by DTI, and both may contribute differently to clinical outcome.

References:

1. Myers R, Manjil LG, Frackowiak RS, Cremer JE. [3H]PK 11195 and the localisation of secondary thalamic lesions following focal ischaemia in rat motor cortex. Neurosci Lett 1991; 133(1):20-24.

2. Radlinska BA, Ghinani SA, Lyon P, Jolly D, Soucy JP, Minuk J et al. Multimodal Microglia Imaging of Fiber Tracts in Acute Subcortical Stroke. Annals of Neurology 2009; 66(6):825-832.

3. Benavides J, Quarteronet D, Imbault F, Malgouris C, Uzan A, Renault C et al. Labelling of "peripheral-type" benzodiazepine binding sites in the rat brain by using [3H]PK 11195, an isoquinoline carboxamide derivative: kinetic studies and autoradiographic localization. J Neurochem 1983; 41(6):1744-1750.

226

GLYBURIDE REDUCES MORTALITY AND IMPROVES NEUROLOGICAL OUTCOME IN RAT EXPERIMENTAL STROKE MODELED ON SEVERE HUMAN STROKE

J.M. Simard, N. Tsymbalyuk, V. Gerzanich

Neurosurgery, University of Maryland School of Medicine, Baltimore, MD, USA

Objective: To study a rat model of stroke that incorporates critical elements encountered in human stroke, including large infarcts predisposing to malignant cerebral edema, 4.5 hours ischemia before reperfusion, use of recombinant tissue plasminogen activator (rtPA), and prolonged delay of supplementary treatment with glyburide, to ameliorate cerebral edema.

Methods: Middle cerebral artery occlusion was produced using a thread occluder (LDF reduction >75%). Reperfusion was obtained 4.5 hours later by removing the thread and infusing IV rtPA (0.9 or 10 mg/kg). We studied 3 groups of rats:

(i) rats with reperfusion alone (vehicle controls; n=10);

(ii) rats with reperfusion supplemented with glyburide at reperfusion (n=7);

(iii) rats with reperfusion at 4.5 hours supplemented with glyburide 10 hours after ischemia (n=6).

Glyburide treatment consisted of a loading dose (10 microg/kg IP) plus start of constant infusion (200 ng/hour subcutaneously). Outcome measures included mortality and neurological assessments using a modified Garcia scoring system (mGS; 0=dead; 15=normal).

Results: In the 3 groups (all with 0.9 mg/kg rtPA), mortality was 60%, 0% and 17%, mean mGS at 24 hours was 2.6±1.1, 9.0±1.0 and 7.8±1.7 ($P< 0.05$), and mean mGS at 48 hours was 2.0±1.0, 11.3±0.6 and 9.3±2.0 ($P< 0.01$), respectively. In separate groups (both with 10 mg/kg rtPA), with reperfusion alone (n=22) vs. reperfusion plus glyburide at reperfusion (n=17), serial measurements for 14 days showed consistently better scores with glyburide, culminating in mean mGS at 14 days of 3.0±1.2 vs. 11.3±1.6, respectively ($P< 0.01$).

Conclusion: Glyburide significantly improves outcome in a rat model that recapitulates critical elements encountered in human stroke.

227

INCREASED ACTIVATION OF ACID-SENSING ION CHANNELS IS ASSOCIATED WITH ISCHEMIC BRAIN INJURY IN DIABETIC CONDITIONS

T. Yang[1], X. Li[1], M. Li[1], K. Inoue[1], D. Branigan[1], X. Chu[1], R. Simon[2], **Z. Xiong**[1,2]

[1]Robert S. Dow Neurobiology Laboratories, Portland, OR, [2]Neurobiology, Morehouse School of Medicine, Atlanta, GA, USA

Animal and human studies have linked diabetes/hyperglycemia in the acute phase of ischemic stroke to worsening of clinical outcome. Although a host of possibilities have been suggested, the cellular and molecular mechanism for this worsening of ischemic injury in the setting of hyperglycemia remains elusive. We hypothesize that increased activation of acid sensing ion channels (ASICs), a novel family of proton-gated cation channels, plays a role in increased ischemic brain injury associated with diabetes/hyperglycemia. Using in vitro and in vivo hyperglycemia/diabetes models, we determined the neuroprotective effect of ASIC blockade in ischemia. The degree of ischemic brain injury and protection by ASIC1a blockade were also compared between diabetic and non-diabetic mice. 24 hours after a 45 min middle cerebral artery occlusion, diabetic mice showed a dramatically increased infarct volume compared to non-diabetic mice. ICV injection of the ASIC1a inhibitor PcTX1 largely reduced the infarct volume, and the relative reduction in the infarct volume by PcTX1 is significantly greater in diabetic mice than in non-diabetic mice. In addition, neurons cultured under hyperglycemic conditions had an increased amplitude and density of acid-activated current. Western blotting demonstrated an increased ASIC1a expression in cortical tissues isolated from diabetic mice or neurons cultured in hyperglycemic conditions. Thus, increased ASIC1a expression and activation play an important role in the increased ischemic brain injury associated with diabetic/hyperglycemic conditions.

228

ULTRASONIC EVALUATION OF CEREBRAL VASOREACTIVITY IN THE BRAIN TISSUE AND THE MAJOR CEREBRAL ARTERIES

T. Shiogai[1], M. Koyama[1], T. Mizuno[2], M. Nakagawa[2], H. Furuhata[3]

[1]Department of Clinical Neurosciences, Kyoto Takeda Hospital, [2]Department of Neurology, Kyoto Prefectural University of Medicine, Kyoto, [3]ME Laboratory, Tokyo Jikei University School of Medicine, Tokyo, Japan

Background: Cerebral vasoreactivity (CVR) has been evaluated not only by conventional transcranial Doppler sonography (TCD) but also using various neuroradiological perfusion imaging. Acetazolamide (ACZ) CVR evaluation has been conducted in risk assessment for cerebral infarction and hemorrhage, clarified pathophysiology, and evaluation of treatments. CVR in the major cerebral arteries has been evaluated using conventional TCD, and this has shown some correlation with cerebral blood flow measurements in the brain tissue from other neuroradiological modalities. Our previous study of ultrasound perfusion imaging showed that power modulation imaging (PMI) utilizing transient response high power images, is superior to conventional second harmonic imaging in evaluation of the contra-lateral cerebral hemisphere. Compared to conventional TCD, transcranial color duplex sonography (TCDS) is able to measure much more accurately on the basis of angle-collected velocities in the intracranial major vessels.

Objectives: To confirm the reliability of CVR analysis in the brain tissue through transcranial PMI, ACZ CVR was evaluated and correlated with CVR in the major cerebral arteries by TCDS.

Methods: Time-averaged maximum velocity (Vmax) in the middle and posterior cerebral arteries (MCA and PCA) was measured by TCDS and after a bolus intravenous Levovist®, transcranial PMI images were obtained via bilateral temporal windows in 11 stroke patients (ages: 40-80 years, mean 67). Peak intensity (PI) and time to PI (TPI) before and after ACZ were measured and CVR calculated on the basis of time-intensity curves in five regions of interest (ROI); bilateral basal ganglia (BG) and thalamus (Th), and contra-lateral temporal lobe (TL). PI and TPI via bilateral temporal windows were correlated in the identical BG and Th ROIs. Correlations between Vmax and PI/TPI in the corresponding vascular territories were evaluated before and after ACZ and in CVR.

Results:

1) Vmax and PI increased while TPI decreased after ACZ.

2) Despite evident depth attenuation in PI, this was not evident in TPI or CVR.

3) PI and TPI on the identical BG and Th ROIs were closely correlated.

4) Vmax in the ipsilateral MCA and PCA closely correlated with PI and TPI in the ipsilateral BG/TL and Th, respectively.

5) Easily disrupted PI/TPI CVR resulted in poor correlations with Vmax CVR.

Conclusions:

1) There are close relationships between velocity changes in the major arteries and brain tissue perfusion in the corresponding vascular territories.

2) There is some possibility of overlooking easily disrupted CVR in the brain tissue utilizing CVR evaluation in the major arteries.

229

A TRIAL OF INTRAVENOUS GRANULOCYTE COLONY-STIMULATING FACTOR FOR ACUTE ISCHEMIC STROKE

S. Takizawa, Y. Moriya, A. Mizuma, Y. Ohnuki, E. Nagata, W. Takahashi, H. Kawada, K. Ando, S. Takagi

Division of Neurology, Department of Internal Medicine, Tokai University School of Medicine, Isehara, Japan

Objectives: Granulocyte colony-stimulating factor (G-CSF: Filgrastim) may be useful for treatment of acute ischemic stroke owing to its anti-inflammatory, anti-apoptotic, and neurogenetic properties. We have already established that administration of hematopoietic cytokines in the subacute phase of cerebral infarction is effective for functional recovery, facilitating proliferation of intrinsic neural stem/progenitor cells and transition of bone marrow-derived neuronal cells [1], and providing a favorable microenvironment for neurogenesis through up-regulation of IL-10 in mice [2]. Here, we examined the safety and tolerability of G-CSF over a broad dose range, and investigated the effectiveness of G-CSF given in the acute (within 24 hours) or subacute (7 days) phase of ischemic stroke.

Methods: In a dose escalation study, three intravenous dose regimens (150, 300 and 450 μg/body/day for 5 consecutive days) of G-CSF were tested in 18 patients in Tokai University Hospital. Administration of G-CSF was skipped when leukocyte count exceeded 40,000/μL. Other routine medications were given to all patients. Main inclusion criteria were 24-hour (n=9) or 7-day (n=9) time window after stroke onset, and infarct localization to the middle cerebral artery territory. We monitored leukocyte count every 6 hours and spleen size by means of an echogram 3 times during treatment. Neurologic functions including NIHSS, mRS and BI, and MRI were examined.

Results: We observed no increase of thromboembolic events and no serious adverse events, including drug-related platelet reduction and splenomegaly. G-CSF (150 and 300 μg/body/day) increased leukocyte count within 40,000/μL, as expected. Although leukocyte count exceeded 40000/μL in the case of G-CSF (450 μg/body/day), it rapidly declined when administrations were skipped. We did not observe significant differences in clinical outcome between acute-phase and subacute-phase G-CSF treatments, but improvement of neurologic function (difference of NIHSS between before and 1 month after treatment) appeared to be better in the case of acute-phase treatment, though the difference was not statistically significant (6.6±3.9 vs. 4.3±4.9; p=0.29).

Conclusions: G-CSF was well-tolerated at 150 and 300 μg/body/day in patients with acute ischemic stroke, with the leukocyte count remaining below 40,000/μL. In contrast to our experimental studies, administration of G-CSF in the acute phase of ischemic stroke resulted in a better (though not significantly so) outcome than subacute-phase treatment. The results indicate that administration of G-CSF in the acute phase may contribute to functional recovery of ischemic human brain. Further study with more patients seems justified.

References:

[1] Kawada H, Takizawa S, Takanashi T, et al. Administration of hematopoietic cytokines in the subacute phase after cerebral infarction is effective for functional recovery facilitating

proliferation of intrinsic neural stem/progenitor cells and transition of bone marrow-derived neuronal cells. *Circulation,* 113: 701-710, 2006.

[2] Morita Y, Takizawa S, kamiguchi H, et al. Administration of hematopoietic cytokines provide a favorable microenvironment for neurogenesis after stroke. *Neurosci Res*, 58: 356-360, 2007.

230

"BRUSH SIGN" ON SUSCEPTIBILITY-WEIGHTED MR IMAGING INDICATES THE SEVERITY OF MOYAMOYA DISEASE

N. Horie[1], M. Morikawa[2], K. Hayashi[1], K. Suyama[1], I. Nagata[1]

[1]Neurosurgery, [2]Radiology, Nagasaki University School of Medicine, Nagasaki, Japan

Introduction: Susceptibility weighted image (SWI) is a high spatial resolution 3D gradient echo MR imaging technique showing magnetic inhomogeneity, and has been applied to various pathologies of the brain. Here, we first evaluate the efficacy of SWI in Moyamoya disease (MMD).

Methods: Thirty three consecutive MMD patients were prospectively analyzed in this study. Routine MR imaging including SWI was performed and increased signal intensity of medullary veins were classified as follows, Stage 1: none, Stage 2: few (moderate) and Stage 3: brush like (severe). The SWI stage was evaluated in correlation with clinical presentations, and cerebral hemodynamics on SPECT.

Results: The patients were 12 male and 21 female, and consist of 4 asymptomatic, 13 TIA, 9 infarct and 7 hemorrhage. There was no difference in age and Suzuki's stage among clinical presentations, although there was a significant difference not in CBF, but in CVR among the groups. On the other hand, SWI stage was significantly higher in TIA group and infarct group than asymptomatic group ($p < 0.01$). Higher SWI stage significantly had lower CBF and CVR in middle cerebral artery area ($p < 0.05$).

Conclusions: Increased signal intensity of medullary veins on SWI named "brush sign" indicates a part of misery perfusion in MMD. Brush sign on SWI could predict the severity of MMD without hemodynamic assessment.

231

ASSESSING CEREBRAL BLOOD FLOW AND OXYGEN SATURATION CHANGES IN EXPERIMENTAL TRAUMATIC BRAIN INJURY BY USING SUSCEPTIBILITY WEIGHTED IMAGING

Z. Kou[1], Y. Shen[1], C. Kreipke[2], T. Petrov[2], J. Hu[1], E.M. Haacke[1]

[1]Radiology, [2]Anatomy and Cell Biology, Wayne State University School of Medicine, Detroit, MI, USA

Introduction: Traumatic brain injury (TBI) has an incidence rate of 1.5 million annually in the United States. Following the primary injury, the secondary effects of head injury often result in the decrease of cerebral blood flow (CBF). CBF and brain tissue oxygenation are proving to be crucial parameters to monitor in intensive care units along with others. However, despite this progress, CBF is still not routinely measured in neurosurgery or neurology. Part of the reason is due to the invasive manner of many of the available techniques or the limited spatial and temporal resolution of regional measurements.

Our objective is to use susceptibility weighted imaging (SWI) as a means to monitor functional blood oxygenation changes and quantify the CBF changes in animals after trauma. In addition, we also used arterial spin labeling (ASL) to measure the CBF changes in arterial perspective.

Material and methods: Six male Sprague-Dawley rats (weighting 350-400g) were inflicted diffuse traumatic brain injury by using Marmarou weight drop model. The rats were scanned over four time points: pre-trauma, 4h, 24h, and 48h post-trauma.

MR imaging protocol included T_2-weighted imaging, T_1-weighted imaging, ASL, and SWI. All of the MRI measurements were performed on a 4.7T horizontal-bore magnetic resonance spectrometer (Bruker AVANCE).

By using flow-compensated SWI phase signal as a measurement of susceptibility caused by brain tissue oxygenation, we further related this signal to venous blood flow changes by assuming the constant cerebral metabolic rate (CMRO2). This change in flow is independent of blood vessel orientation.

Results: Five rats survived after trauma and one died. A blood phase analysis using filtered SWI phase images suggested that the CBF dropped after trauma in five rats by 26% on average and 46% in the worst case, all at 4 hours post trauma. SWI revealed three rats were recovering 48h post trauma and two were deteriorating. ASL showed up to a 28% CBF decrease 4h after trauma in the medial dorsal cortex and the temporal pattern of recovery from trauma after 48h. The data also revealed the physical size differences of venous vessels pre and post trauma. The CBF changes on veins measured by SWI are in good agreement with the CBF changes on arteries measured by ASL.

The temporal CBF changes as seen with the SWI approach showed a similar temporal evolution of trauma as seen in other studies. The relative changes in CBF measured by SWI demonstrated multiple episodes of transient hypoperfusion, which is consistent with the published data on humans in an effort to continuously monitor cerebral oxygenation and CBF in patients with brain trauma.

Conclusions: Compared with the traditional invasive manner of clinical monitoring of cerebral

vascular damage and reductions in blood flow, this method offers a novel, safe, and noninvasive approach to quantify changes in oxygen saturation and cerebral blood flow and to visualize structural changes in blood vasculature after TBI. It could also be used along with ASL in a complementary way to assess the blood flow changes after trauma.

232

NEUROPROTECTIVE EFFECT OF ACUTE ETHANOL ADMINISTRATION IN RAT WITH TRANSIENT CEREBRAL ISCHEMIA

X. Ji[1], Y. Wang[1], F. Wang[1,2], Y. Luo[1], X. Liu[1], F. Ling[1], Y. Ding[1,3]

[1]XuanWu Hospital, Beijing, [2]Ningxia Medical University, Yinchuan, China, [3]School of Medicine, Wayne State University, Detroit, MI, USA

Objective: Numerous studies have shown that mild to moderate alcohol consumption is inversely associated with risk of ischemic stroke, suggesting ethanol may have a neuroprotective effect. We want to test this hypothesis in a rat transient cerebral ischemia model, and further characterize the properties of ethanol as a possible treatment for acute ischemic stroke.

Methods: Sprague-Dawley rats were subjected to 2 hours middle cerebral artery occlusion. Three sets of experiments were conducted (1) to test whether various doses of ethanol (0.5g/kg, 1.0 g/kg, 1.5 g/kg) has neuroprotective effect; (2) to test whether the protective effect of ethanol can be improved by pairing it with hypothermia; and (3) to test whether ethanol affects intracranial hemorrhage after administration of recombinant tissue plasminogen activator (rtPA) or urokinase (UK).

Results: Dose of 1.5g/kg ethanol was effective in reducing infarct volume and behavioral dysfunction after transient middle cerebral artery occlusion. The protective effect of ethanol could be further improved by pairing it with hypothermia, and ethanol did not increase cerebral hemorrhage when given in combination with rtPA or UK.

Conclusions: Our study suggests that a dose of 1.5g/kg ethanol administrated after the onset of reperfusion has neuroprotective effect, can be added to hypothermia therapy, and do not interfere with or complicate rtPA or UK therapy.

233

MODELS OF PERINATAL BRAIN INJURY

H. Hagberg

Institute of Reproductive and Developmental Biology, Imperial College, London, UK

Cerebral palsy (CP) is the commonest cause of severe disability in children (2-3/1000 births) and a major cost to sufferers, their families and society. It costs 1 M$ to treat and care for one patient with CP in the US over the person's lifetime. An improved understanding of the fundamental mechanisms of brain injury is urgently needed in order to find strategies for the next generation of brain protective treatments for term and preterm brain injury. CP results from a number of disparate insults to the developing brain acting alone or in combination, and in at least two of these categories there is reason to believe that significant progress can now be made: hypoxic ischemic encephalopathy (HIE) in term infants and brain injury in preterm infants. There are several animal models of HIE avaiable including the Vannucci model in rodents, hypoxia-ischemia in piglets or fetal sheep that all proved helpful in the development of hypothermic treatment of HIE. The etiology of preterm brain injury - predominantly white matter damage (WMD) - is more complex but ischemia-reperfusion and/or infection-inflammation are believed to be important factors. WMD can be induced by antenatal or postnatal administration of microbes (E. coli or Gardnerella vaginalis), virus (border disease virus) or bacterial products (lipopolysaccharide, LPS). Alternatively, various hypoperfusion paradigms or administration of excitatory amino acid receptor agonists can be used. Irrespective of which insult is utilized, the maturational age of the CNS and choice of species seem critical. Generally, lesions with similarity to human WMD, with respect to distribution and morphological characteristics, are easier to induce in gyrencephalic species (rabbits, dogs, cats and sheep) than in rodents, the rabbit model being the only one resulting in motor deficits with similarities to CP. LPS is the infectious agent most often used to produce WMD in immature dogs, cats, or fetal sheep. The mechanism whereby LPS induces brain injury is not completely understood but involves activation of toll-like receptor 4 on immune cells with initiation of a generalized inflammatory response resulting in systemic hypoglycemia, perturbation of coagulation, cerebral hypoperfusion, and activation of inflammatory cells in the CNS. LPS and umbilical cord occlusion both produce WMD with quite similar distribution in 65% gestational sheep. Furthermore, low doses of LPS that by themselves have no adverse effects in fetuses or immature rats/mice (maturation corresponding to preterm or near term human fetus/neonate), dramatically increase brain injury to a subsequent hypoxic-ischemic challenge, implicating that bacterial products can sensitize the immature CNS.

234

EDARAVONE TREATMENT CONFERS NEUROPROTECTION AGAINST TRAUMATIC BRAIN INJURY IN RATS

G.H. Wang[1,2], Z.L. Jiang[1], T.J. Ren[1], Y.Q. Gao[2], J. Chen[2,3]

[1]Department of Neuropharmacology, Institute of Nautical Medicine, Nantong University, Nantong, [2]State Key Laboratory of Medical Neurobiology, Fudan University, Shanghai, China, [3]Center of Cerebrovascular Disease Research, University of Pittsburgh, Pittsburgh, PA, USA

Objectives: Traumatic brain injury (TBI) is the leading cause of neurological disability in young adults, for which an effective neuroprotective strategy is currently unavailable. TBI is known to cause the initial tissue loss by trauma and, subsequently, a cascade of events such as brain edema, blood-brain barrier (BBB) disruption, apoptosis, and pro-inflammatory reactions that trigger the so-called secondary brain damage and long-term neurological deficits. While the mechanism underlying the secondary brain damage following TBI remains elusive, oxidative stress has been thought to play a central role. Edaravone is a novel synthetic small molecule free-radical scavenger that has shown neuroprotective effect in animal models of cerebral ischemia and currently is being used clinically to treat stroke patients in Asian countries. Edaravone is also effective in scavenging alkoxyl radicals in TBI patients (*J Neurotrauma*. 2006, 23:1591-9). Therefore, in the present study, we have investigated the neuroprotective effect of edaravone in a rat model of TBI.

Methods: TBI was induced in the right cerebral cortex of male adult SD rats (250-280 g body weight) using the Feeney's weight-drop method. Edaravone (0, 0.75, 1.5, or 3 mg/kg) or vehicle was intravenously administrated twice at 2 and 12 hr after TBI. Neurological deficits (sensory-motor dysfunction), brain water content (gravimetric analysis), BBB damage (Evans blue extravasations), and hippocampal CA3 cell death (Nissl staining) were quantitatively assessed 3 days after TBI. Moreover, the effect of edaravone treatment on oxidative stress parameters and pro-inflammatory cytokines was determined using neurochemical assays and ELISA, respectively. All data are presented as mean±SEM; and statistic analyses were performed using Student's *t*-test (for single comparison) or ANOVA and *post hoc* student Newman-Keuls tests (for multiple comparisons), with $P < 0.05$ considered statistically significant.

Results: Compared to vehicle treatment, administration of edaravone significantly reduced neurological deficits (n=10/group), brain water content (n=6/group), BBB damage (n=6/group) and CA3 neuron loss (n=4/group) after TBI in a dose-dependent manner. At the optimally effective dose (1.5 mg/kg), edaravone treatment (n=6/group) also significantly attenuated TBI-induced oxidative stress (decreased formation of nitric oxide and hydroxyl radicals and increased anti-oxidant reserves, compared to vehicle treatment), production of pro-inflammatory cytokines (TNF-α, IL-6 and IL-1β), and caspase-3 activation (the number of cells containing active caspase-3) in the brain.

Conclusions: Our results demonstrate that systemic administration of the synthetic free-radical scavenger edaravone is neuroprotective in the rat model of TBI, resulting in not only reduced brain edema and neuronal degeneration but also improved neurological functions. These results reinforce the importance of oxidative stress in the pathogenesis of secondary neuronal injury following TBI. Since edaravone has been used clinically in treating stroke patients without apparent adverse effects, edaravone may be a novel candidate neuroprotectant for the treatment of clinical TBI.

235

USING DYNAMIC MOLECULAR IMAGING TO STUDY PHASIC RELEASE OF DOPAMINE IN ATTENTION DEFICIT HYPERACTIVITY DISORDER

R.D. Badgaiyan[1,2]

[1]Psychiatry, SUNY at Buffalo, Buffalo, NY, [2]Massachusetts General Hospital/Harvard Medical School, Boston, MA, USA

Objectives: Neurotransmission is dysregulated in most psychiatric conditions. However, because of the lack of a reliable technique to study acute changes in neurotransmission, the nature of dysregulation remains unclear. For example, the status of the dopamine system in attention deficit hyperactive disorder (ADHD) is controversial because indirect measures have reported either hyper or hypoactive system. To resolve the controversy we used a dynamic molecular imaging technique to directly detect, map and measure dopamine released phasically in ADHD patients.

Methods: The study was conducted on healthy control volunteers and ADHD patients. After positioning the volunteers in the PET camera, an intravenous bolus (10-15 mCi) of the dopamine receptor ligand ^{11}C-raclopride was administered at high specific activity. Immediately after the injection, the PET data acquisition and the control condition of a modified Eriksen's flanker task was initiated. The task had a control and a test condition. In both conditions volunteers were shown a series of 7 arrowheads pointing either to the left or right. They were asked to indicate direction of the arrowhead located at the center (target) as quickly and as accurately as possible. In the control condition the target and flanker arrows pointed to the same direction but in the test condition these arrowheads pointed to different directions. Thus, response execution in the test condition required inhibition of responses indicated by a majority of stimuli (flankers). The ligand concentration was dynamically measured in both, control and test conditions using a PET camera. The rate of ligand displacement from receptor sites was then estimated by a newly developed receptor kinetic model (1-6).

Results: The rate of ligand displacement increased significantly ($t>3.0$) in the right caudate in healthy volunteers in the test condition, which required inhibition of unwanted responses (see the figure). In ADHD patients the rate increased in the caudate bilaterally. The ligand binding potential was also lower, indicating increased dopamine release.

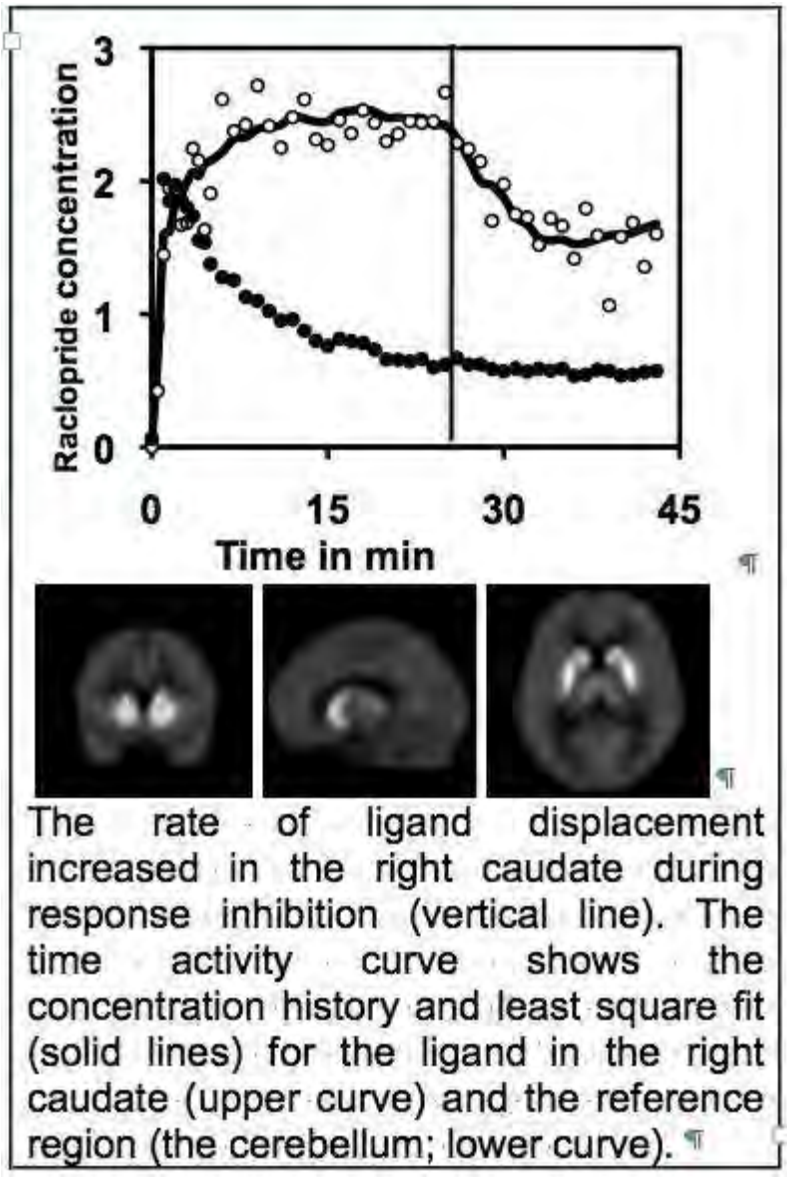

The rate of ligand displacement increased in the right caudate during response inhibition (vertical line). The time activity curve shows the concentration history and least square fit (solid lines) for the ligand in the right caudate (upper curve) and the reference region (the cerebellum; lower curve).

[Phasic Release of Dopamine in Healthy Volunteers]

Conclusions: The results indicate that phasic release of striatal dopamine is significantly increased in ADHD during response inhibition. The study provides the first direct evidence of dysregulated dopamine neurotransmission in ADHD and indicates that the dynamic molecular imaging can be used to study pathophysiology of psychiatric conditions.

References:

1. Badgaiyan RD. Dopamine is released in the striatum during human emotional processing. NeuroReport. 2010;21:1172-6.

2. Badgaiyan RD, Fischman AJ, Alpert NM. Dopamine release during human emotional processing. Neuroimage. 2009;47(4):2041-5.

3. Badgaiyan RD, Fischman AJ, Alpert NM. Explicit Motor Memory Activates the Striatal Dopamine System. NeuroReport. 2008;19(4):409-12.

4. Badgaiyan RD, Fischman AJ, Alpert NM. Striatal dopamine release in sequential learning. NeuroImage. 2007;38(3):549-56.

5. Badgaiyan RD, Fischman AJ, Alpert NM. Striatal dopamine release during unrewarded motor task in human volunteers. Neuroreport. 2003;14(11):1421-4.

6. Alpert NM, Badgaiyan RD, Livini E, Fischman AJ. A novel method for noninvasive detection of neuromodulatory changes in specific neurotransmitter systems. NeuroImage. 2003;19(3):1049-60.

236

PROTECTION OF BLOOD BRAIN BARRIER (BBB) VIA ACTIVATION OF CANNABIONOID RECEPTOR 2 (CB_2) IN BRAIN MICROVASCULAR ENDOTHELIAL CELLS (BMVEC)

Y. Persidsky[1], S. Ramirez[1], J. Hasko[1], M. Zhang[2], H. Dykstra[1], S. Fan[1], R. Tuma[2]

[1]Pathology and Laboratory Medicine, [2]Physiology, Temple University School of Medicine, Philadelphia, PA, USA

Objectives: To prove whether CB_2 activation in BMVEC protects BBB from inflammatory insults.

Methods: We assessed expression of CB_2 in human brain tissues and primary human BMVEC by immunostaining and Western blot. Barrier tightness was evaluated after application of highly selective CB_2 agonists (O-1966 and JHW-155) with or without inflammatory stimuli. To evaluate whether the anti-inflammatory effect of CB_2 activation applies to brain endothelial cells, we profiled the expression of genes commonly involved in the regulation of inflammatory response and autoimmunity. We also investigated whether CB_2 stimulation would diminish leukocyte adhesion *in vivo*. Mice were implanted with cranial windows allowing visualization of leukocytes in brain microvessels.

Results: CB_2 were detected in BMVEC by immunofluorescence and Western blot. Pre-treatment with pro-inflammatory cytokines, TNFα and IL-1β led to 1.8- or 2.5-fold enhancement of CB_2 expression, respectively. Enhanced endothelial CB_2 expression was found brain tissues affected by HIV encephalitis as compared to controls. Next, we tested whether CB_2 activation could increase barrier structural integrity. BMVEC were cultured on gold electrodes of an ECIS apparatus allowing assessment of transendothelial resistance (TEER). Application of CB_2 agonists resulted in dose- and time-dependent augmentation of tightness of BMVEC monolayers (10-15% increase in TEER as compared to controls, $p< 0.001$). To understand the mechanism underlying this effect, we evaluated expression of tight junction proteins in BMVEC treated with CB_2 agonists. Four-hour stimulation of CB_2 with O-1966 and JWH-133 caused 2.2-2.7-fold increase in the amount of occludin and claudin-5 in the membranous fraction of cell lysates. Next, we sought to determine whether a CB_2 agonist could protect BBB integrity after disruption by pro-inflammatory stimuli (like lipopolysaccharide, LPS or CD40 ligand, CD40L). Treatment of BMVEC monolayers with LPS (50 ng/ml) led to a drop of TEER (80% of control) and O-1966 reversed this change ($p< 0.05$). After CD40L application, average TEER measurements showed a fast 5-20% drop in resistance in a dose-dependent manner. CB_2 agonists reversed TEER drop caused by CD40L. 92 genes relevant to inflammatory responses were analyzed in TNFα BMVEC activated in the presence of the CB_2 agonists. The array analyses revealed that 33 gene targets were upregulated more than 2-fold in the TNFα-treated BMVEC when compared to untreated control cells. The addition of either O-1966 or JWH-133 resulted in the suppression of 28 and 32 genes out of the 33 upregulated by TNFα. Next, we investigated whether CB_2 stimulation would diminish leukocyte adhesion *in vivo* using cranial windows. Selective CB_2 agonist was injected simultaneously with LPS (6 mg/kg) and white cell adhesion was monitored at 0, 4 and 24 h by intravital fluorescence microscopy. LPS injection substantially increased leukocyte adhesion by 4 h (~8-fold), the CB_2 agonists significantly attenuated leukocyte adhesion after LPS injection (50% by O-1966, $p< 0.05$). This effect was completely reversed by CB_2 antagonist. The CB_2 agonist prevented enhanced permeability caused by LPS *in vivo.*

Conclusions: CB_2 activation in brain endothelium enhances BBB function under physiologic

conditions and prevents its damage by inflammatory insults *in vitro* and *in vivo* proving novel therapeutic approach.

238

TEMPORAL DYNAMICS OF ENDOGENOUS NEUROGENESIS,ANGIOGENESIS AND OLIGODENDROGENESIS AFTER FOCAL CEREBRAL ISCHEMIC INJURY

M. Chu[1], S.D. Lu[1], Y.L. Guo[1], H. Gao[1], J. Zhang[1], Y. Gan[2], P.Y. Li[1,2], J. Chen[1,2], Y.Q. Gao[1]

[1]State Key Laboratory of Medical Neurobiology and Institute of Brain Sciences, Fudan University, Shanghai, China, [2]Department of Neurology, University of Pittsburgh School of Medicine, Pittsburgh, PA, USA

Background and purpose: Stroke is the leading cause of serious long-term disability in adults in the US. Recent discoveries have demonstrated that ischemic stroke can trigger multiple processes of repair, including neurogenesis, angiogenesis and oligodendrogenesis in adult brain, aiming towards neurovascular remodeling in peri-infarct areas during stroke recovery. The understanding of theses endogenous restorative responses to stroke, however, is very limited. The present study aimed to clarify the temporal dynamics of neurogenesis, neovascularization and white matter injury/repair occurred in a murine cerebral ischemia-reperfusion injury model.

Methods: Transient focal cerebral ischemia was induced in C57/BL6 mice by unilateral middle cerebral artery occlusion (MCAO) for 60 minutes. 5-bromo-2'-deoxyuridine (Brdu) was administered intraperitoneally to lable newly generated cells. Animals were sacrificed on day 1, 3, 7, 14 or 28 of reperfusion (n=5 per group). Immunohistochemistry stainings of BrdU and cell-specific markers were used to determine the presence of neurogenesis (nestin, doublecortin (DCX), Tuj1) and oligodendrogenesis (NG2). Functional vessels were identified by transcardial perfusion of FITC-conjugated tomato lectin, which labels endothelial cells only in perfused vessels. White matter injury was evaluated by immunohistochemistry staining of myelin basic protein (MBP) and neurofilament (NF) 200.

Results: The number of BrdU+/nestin+ cells increased markedly in the ischemic brain up to 7 days after MCAO and decreased thereafter. The number of DCX+ cells in the ischemic hemisphere were increased compared to the contralateral hemisphere since 7 days after ischemia. BrdU+/Tuj1+ cells was observed in the peri-infarct regions since 14 days after ischemia. The post-stroke neovasculation, as measured by total vascular branch points, dramatically decreased in the peri-infarct regions at 1 day after ischemia. Vascular density was then partially recovered in the peri-infarct regions beginning at 3 days and further increased at 7, 14 and 28 days after ischemia. Neovascularization was not observed in the ischemic core area. The post-stroke angiogenesis began to be observed at 3 days and further increased at 14 and 28 days after MCAO. Oligodendrogenesis, quantified as the number of BrdU+/NG2+ cells, significantly increased in the penumbra from day 3 until day 28 after ischemia. NF-200 immunoreactivity was essentially absent in the penumbra at day 1, while the loss of MBP immunoreactivity began at day 3 after ischemia. The loss of NF-200 and MBP continued until 28 days after ischemia, suggesting a persistent white matter injury.

Conclusions: Our study provides a detailed temporal analysis of neurogenesis, angiogenesis and oligodendrogenesis in a rodent stroke model. Neurogenesis and neovascularization were substantially activated early after ischemic stroke and persisted for several weeks. Despite the sustained presence of newborn oligodendrocyte progenitors, white matter injury after ischemic stroke is almost irreversible without any intervention. These findings provide insight into the future development of therapeutic strategies targeting the establishment of integrated neurovascular units in the ischemic brain.

Keywords: Neurogenesis; angiogenesis; white matter injury; cerebral ischemia.

240

DELAYED CEREBRAL POST-ARTERIOLE DILATION IS CONSISTENT WITH OBSERVATIONS AT MULTIPLE SPATIAL AND TEMPORAL SCALES: EVIDENCE FROM MATHEMATICAL MODELLING

M.J.P. Barrett[1], M.H. Tawhai[1], V. Suresh[1,2]

[1]Auckland Bioengineering Institute, [2]Department of Engineering Science, University of Auckland, Auckland, New Zealand

Background and aims: Observations from different neurovascular imaging modalities provide conflicting evidence about the presence and/or extent of volume changes in post-arteriole blood vessels. At the level of individual vessels, two-photon imaging during functional activation shows a rapid increase in arteriolar diameter, but little or no increase in capillaries or venules[1]. In contrast, 'bulk' measurements of flow-volume relationships show large increases in arterial volume[2], and smaller - but still significant - increases in venous volume[3]. Here, we reconcile these competing observations using a dynamic, biophysically based mathematical model of the hemodynamic response.

Methods: We use the widely known Windkessel model that represents blood flow as analogous to electrical current, and networks of blood vessels as analogous to electrical resistances and capacitances. The model also includes a novel description of vascular compliance, viscoelastic effects, and stimulus-driven vasodilation. Experimental observations at progressively more detailed scales are used to constrain and validate the model, following a 'top down' approach. In addition, we test the assumption that post-arteriole vessels do not dilate, and use the model to predict observations at progressively more aggregated scales, following a 'bottom up' approach.

Results: Model predictions of the total, arterial, and venous steady state flow-volume relationships agree well with experimental observations, as do predictions of transient changes in flow and volume during functional activation. The model also predicts rapid arteriole dilation during activation. Interestingly, this is accompanied by slow increases in capillary and venule diameter that - for brief stimulation - are near indistinguishable from baseline noise. When assuming no dilation of capillaries or venules, there are only minor differences between the model predictions at the single vessel scale. However, predictions at more aggregated scales are qualitatively and quantitatively different from experimental observations.

Conclusions: The model presented here is able to reproduce the main features of experimental observations over a range of spatial and temporal scales. These results suggest that arterial dilation represents the majority of regional cerebral blood volume increases during functional activation, especially during brief stimulation. However, passive dilation in capillaries and venules may be increasingly significant during extended stimulation. This is an important consideration when interpreting or comparing results from neurovascular imaging modalities, such as optical methods and magnetic resonance imaging.

References:

1. Hillman *et al. NeuroImage* 2007; 35(1):89-104

2. Ho *et al. J Cereb Blood Flow Metab* 2010; doi:10.1038/jcbfm.2010.126 (in press)

3. Chen and Pike *NeuroImage* 2010; 53(2):383-391

243

DEVELOPMENT OF A NEW METHOD TO REDUCE GLOBAL PHYSIOLOGICAL TRENDS IN FNIRS MEASURES OF BRAIN ACTIVATION

S. Brigadoi[1,2], F. Scarpa[1], S. Cutini[1], P. Scatturin[1], R. Dell'Acqua[1,3], G. Sparacino[2]

[1]Department of Developmental Psychology, [2]Department of Information Engineering, [3]Centre for Cognitive and Brain Sciences, University of Padova, Padova, Italy

Objectives: Functional near-infrared spectroscopy (fNIRS) is a non-invasive optical neuroimaging method used to investigate functional activity of the cerebral cortex evoked by cognitive, visual, auditory and motor tasks, detecting regional changes of oxy- and deoxy-hemoglobin concentration [1]. In order to estimate the stimulus-evoked hemodynamic response (≈0.1 Hz), it is essential to identify and reduce the global physiological noise (Figure1), which is mainly constituted by heart beat (≈1 Hz) respiration (≈0.2 Hz), vasomotor waves (or Mayer´s waves, ≈0.1 Hz), as well as very low frequency oscillations (≈0.04 Hz) [2]. The aim of the present work is to develop a method for the reduction of these global physiological trends.

Methods: The proposed method is based on the use of a “reference signal”, acquired by a detector placed on the scalp at a distance of 1 cm from the source (creating a reference channel), against the 3 cm of standard channels. Since the depth-penetration of the reference channel is limited [2], the signal acquired includes global physiological trends but no stimulus-evoked hemodynamic response (HR). Due to their quasi-periodic nature, physiological trends are modeled, on a trial by trial basis, as a sum of a variable number of sine waves. Model order is chosen through the Akaike´s information criterion according on the number of dominant low frequencies components (< 0.18 Hz) detectable in the spectrum. Amplitude and frequency of the sine waves are found using a least squares fit and a grid search method [3], respectively. This reconstruction of the physiological trends, derived from the reference signal, is then subtracted from the raw channels data. Finally, HRs are estimated with a Bayesian approach presented in [4].

Results: The proposed method has been evaluated on 30 simulated subjects, generated according to real data acquired in [4]. Each HR is estimated from ≈45 trials. The estimation error computed on the HRs estimated using the proposed method is 47% lower than that obtained without the use of the reference channel (7.9% vs 14.8% respectively). An example is reported in Figure1. Furthermore, a two times lower estimation error was obtained on single trial.

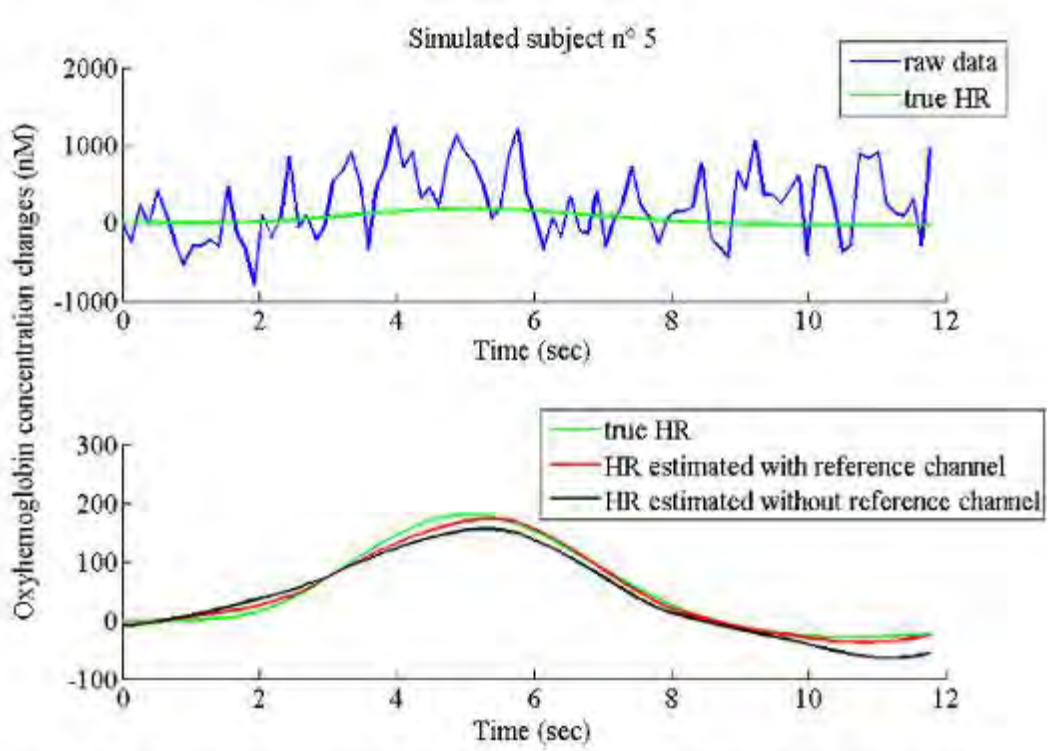

Figure 1: True HR (green) compared with raw data (blue), HR estimated with and without the use of the reference channel (red and black respectively).

[Figure 1]

Conclusions: The proposed method provides a valuable reduction of physiological noise. It allows single-trial analysis, necessary to quantify HR spatio-temporal variability. On simulated data, it provides a remarkable improvement on HR estimation, and its application and evaluation on real data are required.

References:

[1] Obrig, Villringer, “Beyond the Visible - Imaging the Human Brain With Light”. Journal of Cerebral Blood Flow & Metabolism, vol 23, 2003

[2] Zhang, Strangman, Ganis, “Adaptive filtering to reduce global interference in non-invasive NIRS measures of brain activation: How well and when does it work?”. NeuroImage, vol 45, 2009

[3] P. Handel, “Evaluation of a standardized sine wave fit algorithm”, Proc. IEEE NORSIG, 2000

[4] Scarpa, Cutini, Scatturin, Dell'Acqua, Sparacino, “Bayesian filtering of human brain hemodynamic activity elicited by visual short-term maintenance recorded through functional near-infrared spectroscopy (fNIRS)”. Optics Express, vol 18, 2010

244

A NOVEL MODEL OF IN SITU EMBOLIC STROKE IN THE ANAESTHETIZED MONKEY (MACACA MULATTA)

C. Orset, V. Agin, L. Chazalviel, M. Gauberti, A.R. Young, D. Vivien

U.919, INSERM, Caen, France

Introduction: The lack of relevant stroke models in large animals is a limitation for the development of innovative therapeutic/diagnostic approaches. Considered as being the last stage in pre-clinical investigations, non-human primate models of focal cerebral ischaemia are of seminal importance in the translation from the incontrovertible proof of experimental neuroprotection to the suggested therapeutic benefit in the clinical setting.

Objectives: To develop a model of thromboembolic stroke that allows drug-induced reperfusion in anaesthetized monkeys; to follow the ischaemic insult with 3T MRI techniques; to assess their neurological status over a three-month interval.

Material and methods: Anaesthetized (Sevoflurane, 2.5%) and during full physiological and biochemical monitoring, 6 male monkeys underwent enucleation, the right MCA was exposed[1] and purified alpha-thrombin was injected directly (600 µL via a micropipette) into the MCA. The orbit was reconstructed and the monkeys underwent MRI studies (T2, FLAIR, ADC, DWI, PWI and MRA) prior to, and following the acute (2 hr) and chronic stages (24 hr to 3 months) of stroke. Neurological status was assessed longitudinally throughout the study using a modified stroke scale[2].

Results: No mortality or haemorrhagic transformation of the lesion was evidenced. In 4 monkeys, the MRI data showed an hyperintense signal that encompassed the putamen, the caudate nucleus and the internal capsule with sparing of the parasylvian cortex. Only 2 animals had additional cortical involvement that covered the entire MCA territory following injection of thrombin into the M1 segment of the MCA. Sequential MRI allowed one to follow the temporal evolution of these ischaemic regions (Figure 1). The associated major clinical deficits were contralateral motor and sensory dysfunctions, visual-spatial neglect and a decrease in autonomy.

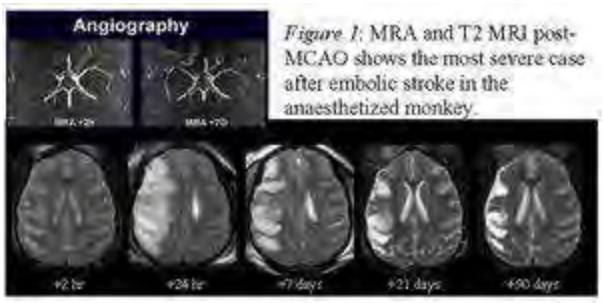

Figure 1: MRA and T2 MRI post-MCAO shows the most severe case after embolic stroke in the anaesthetized monkey.

[Figure 1]

Conclusion: Only 2/6 monkeys had a clot that remained in place for at least 2 h (Figure 1) and whose neurological function was notably altered. We do not consider this model as being

severe enough in which to assess the effects of thrombolysis. It is envisaged that the model can be improved to establish a more severe ischaemic lesion in order to correspond to the clinical situation, even to the extent where mortalities and haemorrhagic transformation of the lesion could, and should, be expected in this type of study.

References:

1. Young et al., J. Cereb. Blood Flow Metabol., 1996;16:1176-1188.

2. Kito et al., J. Neurosci. Methods, 2001;105:45-53.

245

[^{11}C]FLUMAZENIL RELATIVE DELIVERY IMAGES MAY REPLACE [^{18}F]FDG PET IN EPILEPSY SURGERY INVESTIGATIONS

T. Danfors[1,2], E. Kumlien[1], J. Sörensen[2], M. Lubberink[2,3]

[1]Neuroscience/Neurology, [2]PET Centre, [3]Medical Physics, Uppsala University Hospital, Uppsala, Sweden

Introduction: Epilepsy is one of the most prevalent neurological disorders and affects approximately 0.6 % of the population. About 30-40% of patients with focal epilepsy continue to have seizures despite appropriate medical therapy. Surgical treatments should be considered in this important subset of patients.

Before surgery an extensive evaluation with video EEG monitoring, magnetic resonance imaging, and neuropsychological assessment is performed. In many cases, further investigations with subtraction ictal SPECT co-registered to MRI (SISCOM) or positron emission tomography (PET) scans may be needed. Two commonly used PET tracers are [^{18}F]fluorodeoxyglucose ([^{18}F]FDG) and [^{11}C]flumazenil ([^{11}C]FMZ). [^{18}F]FDG provides information of glucose metabolism and [^{11}C]FMZ distribution of GABA-A receptors. In addition dynamic [^{11}C]FMZ scans can give relative cerebral blood flow (CBF), or delivery, (R_1) estimates.

Aims of the study: To assess weather the [^{11}C]FMZ R_1 image can substitute the [^{18}F]FDG scan in pre-surgical epilepsy investigations.

Methods: Seventeen consecutive patients who all had undergone preoperative epilepsy surgery investigation without conclusive results, underwent 40 min dynamic scans after injection of 4 MBq/kg [^{11}C]FMZ and 20 min static scans starting 30 min after injection of 3 MBq/kg [^{18}F]FDG. One patient was excluded due to different scanning days but the rest were scanned during the same day. To our knowledge, no patient had a seizure in-between the scans.

Images were acquired using an ECAT Exact HR+ scanner (Siemens/CTI, Knoxville) and reconstructed using filtered back projection applying all appropriate corrections. Volumes of interest were drawn over pons on a co-registered T2-weighted MRI scan. [^{11}C] FMZ R_1 and binding potential (BP_{ND}) images were constructed using reference parametric mapping (RPM) which is a basis function implementation of the simplified reference tissue model (1), using pons as reference tissue (2). FDG and FMZ images were co-registered using a mutual information algorithm. Volumes of interest were drawn over areas with reduced [^{18}F]FDG uptake, as well as contra-lateral areas, and transferred to [^{11}C]FMZ R_1 images. Correlation and agreement of ratios between pathological and contra-lateral [^{18}F]FDG SUV and [^{11}C]FMZ R_1 images were assessed using linear regression and Bland-Altman analysis.

Results: Ten patients had focal uptake changes in booth FDG- and [^{11}C]FMZ-PET and 6 were considered normal. Figure 1 shows [^{11}C]FMZ BP_{ND} and R_1 as well as [^{18}F]FDG SUV images for a typical patient. Mean pathological to contra-lateral ratios were 0.81 ± 0.11 for [^{18}F]FDG and 0.91 ± 0.07 for [^{11}C]FMZ R_1. Correlation between [^{18}F]FDG and [^{11}C]FMZ R_1 ratios was 0.77 (Pearson), and intra-class correlation coefficient was 0.71. Mean difference between [^{11}C]FMZ R_1 and [^{18}F]FDG SUV ratios was 12% (CI 2-21%).

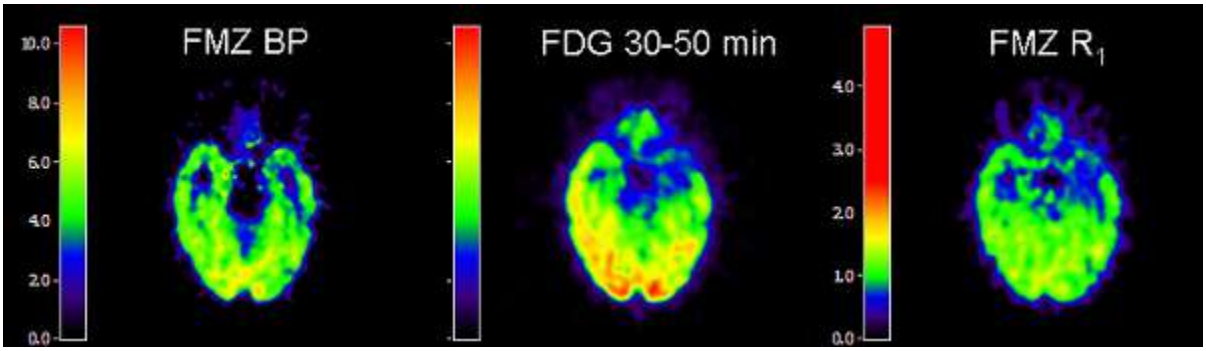

[Figure 1 -. [11C]FMZ BP, [18F]FDG SUV and [11C]FMZ]

In conclusion a positive correlation between [^{18}F]FDG and [^{11}C]FMZ R_1 pathological to contra-lateral ratios was found, with [^{18}F]FDG yielding significantly lower ratios. The present work suggests that [^{11}C]FMZ R_1 images may substitute [^{18}F]FDG imaging in pre-surgical epilepsy investigations.

References:

1. Gunn RN et al (1997) Neuroimage 6:279-287

2. Klumpers UM et al (2008). J Cereb Blood Flow Metab 28:579-587

246

NUCLEOPHILIC ^{18}F-DIRECT LABELING APPROACH AND EVALUATION OF THE 5-HT$_{2A}$ RECEPTOR PET LIGAND [^{18}F]MH.MZ IN DANISH LANDRACE PIGS

M.M. Herth[1], H. Hansen[1], A. Etrrup[1], V. Kramer[2], N. Gillings[1], F. Rösch[2], G.M. Knudsen[1]

[1]Rigshospitalet, Copenhagen, Denmark, [2]Johannes Gutenberg-Universität, Mainz, Germany

Objective: The 5-HT$_{2A}$ receptor is among the most interesting receptors within the serotonergic system because of its implications in physiological processes such as appetite, emotion, depression and Alzheimer's disease [1]. Therefore, in vivo studies of 5-HT$_{2A}$ receptor availability would significantly advance the understanding of the biological principles of the mentioned disorders and contribute to the development of appropriate therapies. Positron emission tomography (PET) is an appropriate tool to measure in vivo directly and non-invasively the pharmacologic parameters of ligand-neuroreceptor interactions. Currently, [^{18}F]altanserin and [^{11}C]MDL100907 are the most frequently used PET tracers to probe for 5-HT$_{2A}$ receptor, however [^{18}F]altanserin gives rise to a lipophilic metabolite which complicates quantification and [^{11}C]MDL100907 has the disadvantage of a short half-life and slow kinetics. [^{18}F]MH.MZ combines the advantages of the two existing PET tracers and previously published data showed promising characteristics as a new and improved 5-HT2A receptor radiotracer [2,3]. The first aim of this study is to evaluate the binding characteristics of [^{18}F]MH.MZ in a non-rodent PET approach using pig as an experimental animal. The second aim is to simplify the described 2-step labelling procedure of [^{18}F]MH.MZ to an ^{18}F-direct labelling approach.

Methods:

a) Chemistry: An aclylated tosyl precursor was synthesized similar to published synthesis of MH.MZ [3]. ^{18}F-direct labeling was optimized regarding temperature, precursor concentration and used solvent systems. Zemplen-deprotection strategy led to the final product (figure 1).

b) Biology: Three female Danish Landrace pigs (~20 kg) were used to study the in vivo brain distribution of the tracer. After intravenous injection of the tracer, the pigs were scanned for 150 min in list-mode in high resolution research tomography (HRRT) scanner. Two scans with ketanserin (5 mg/kg/h bolus infusion and 3 mg/kg/h infusion) blocking after 90 min was obtained. Arterial input measurements and radio-metabolite analysis were done, and regional radioactivity were measured by co-registration to an MRI-based atlas of the pig brain.

Results:

a) Chemistry: Optimization led to a radiochemical yield of about > 30%.The final formulation of the injectable solution including a semi-preparative HPLC took no longer than 100 min and provided ^{18}F-labeled tracer with a purity > 96%. Typical specific activities (A_s) were between 5-10 GBq/µmol. Thereby, amounts of ~ 25 GBq of [^{18}F]fluorine were used as starting radioactivity.

b) Biology: µPET experiments of [^{18}F]MH.MZ showed a accumulation in the frontal cortex areas as expected. No lipohilic metabolite could be detected. However, slow kinetics were determined and a ketanserin challenge during the scan time was not able to displace [^{18}F]MH.MZ from receptors.

Conclusions: [^{18}F]MH.MZ could be obtained as an injectable solution in radiochemical yields of about 40% within a synthesis time of about 100 minutes. PET data suggests that the tracer is

able to visualize the 5-HT_{2A} receptor in the pig brain. But the slow kinetics may complicate the quantification.

References:

[1] Naughton M et al., Hum Psychopharmacol, 2000;15:387-415.

[2] Debus F et al., Nucl Med Biol, 2010;37(4):487-495.

[3] Herth MM et al., Nucl Med Biol, 2009;36:447-454.

247

SMALL DEEP INFARCTS OF THE BRAIN ARE NOT ALL LACUNAR STROKE BY GENE EXPRESSION ANALYSIS

G.C. Jickling[1], B. Stamova[1], B.P. Ander[1], H. Xu[1], X. Zhan[1], Y. Tian[1], D. Liu[1], S.C. Johnston[2], P. Verro[1], F.R. Sharp[1]

[1]Neurology, University of California Davis, Sacramento, [2]Neurology, University of California, San Francisco, CA, USA

Objective: Determine whether gene expression profiles can distinguish lacunar from non-lacunar causes of small deep infarcts (SDI).

Background: SDI including lacunar stroke account for greater than one quarter of all ischemic strokes and are associated with increased risk of cardiovascular disease and dementia. Though lipohylinosis of small penetrating arteries (lacunar stroke) is the most common cause, embolic occlusion of arterial or cardioembolic origin have been described. Determining which SDI are of lacunar, arterial or cardioembolic cause is challenging, but nevertheless important to deliver optimal stroke prevention therapy.

Methods: A total of 184 ischemic strokes and 60 controls were analyzed.

Lacunar stroke was defined as a lacunar syndrome associated with infarction < 15mm of the striatum, internal capsule, corona radiata, thalamus or pons. RNA was isolated from whole blood and processed on Affymetrix U133 plus2 microarrays. Differentially expressed genes between acute lacunar strokes (n=30) and non-lacunar strokes (n=86) were identified using an ANCOVA (FDR$\underline{\geq}$0.05, fold change>|1.5|). A prediction model able to discriminate lacunar from non-lacunar stroke was generated using linear discriminant analysis and evaluated using cross-validation and a second test cohort (n=36). The model was then applied to predict etiology in SDI of unclear cause (size >15mm or SDI with potential embolic source) (n=32).

Results: A 41 gene profile discriminated lacunar from non-lacunar strokes with greater than 90% sensitivity and specificity. Of the 32 SDI of unclear cause, 17 were predicted to be of lacunar etiology and 15 were predicted to be of non-lacunar etiology. Independent predictors of lacunar SDI were non-Caucasian race/ethnicity and absence of ipsilateral arterial disease. The identified profile largely represents immune differences between stroke subtypes.

Conclusions: Gene expression profiles distinguished lacunar from non-lacunar stroke. SDI of unclear cause were predicted to be of lacunar and non-lacunar etiology, suggesting comprehensive workup is required to identify potential cardioembolic and arterial causes. Further study is required to evaluate the gene profile in a second cohort and determine the clinical and treatment implications of SDI predicted to be of non-lacunar etiology.

249

REVERSIBLE AND REGIONALLY SELECTIVE DOWNREGULATION OF BRAIN CANNABINOID CB_1 RECEPTORS IN CHRONIC DAILY CANNABIS SMOKERS

J. Hirvonen[1], R.S. Goodwin[2], C.-T. Li[1], G.E. Terry[1], S.S. Zoghbi[1], C. Morse[1], V.W. Pike[1], N.D. Volkow[2], M.A. Huestis[2], R.B. Innis[1]

[1]Molecular Imaging Branch, National Institute of Mental Health, National Institutes of Health, Bethesda, [2]Chemistry and Drug Metabolism Section, National Institute on Drug Abuse, National Institutes of Health, Baltimore, MD, USA

Background and aims: Cannabis (marijuana, hashish) is the most widely used illicit drug, and chronic cannabis smoking can result in dependence. The effects of the main psychoactive ingredient of cannabis, Δ^9-tetrahydrocannabinol (Δ^9-THC), are mediated via cannabinoid CB_1 receptors in the brain. In rodent brain, cannabinoid CB_1 receptors downregulate after chronic exposure to cannabis but recover during abstinence. To see if such reversible downregulation occurs in humans, we used positron emission tomography (PET) to image brain cannabinoid CB_1 receptors in chronic daily cannabis smokers.

Methods: We admitted male chronic daily cannabis smokers (N=30) to a closed and monitored inpatient research unit for about four weeks. We imaged cannabis smokers with PET and [^{18}F]FMPEP-d_2 at two time points: on the day following admission and after about four weeks of abstinence. Healthy male subjects (N=28) with less than 10 times lifetime cannabis exposure underwent a single PET scan with [^{18}F]FMPEP-d_2. Arterial blood was sampled during PET scans to estimate receptor binding as distribution volume (V_T), which is the ratio at equilibrium of the concentration of radioactivity in brain to that of the parent radioligand in plasma.

Results: At baseline, V_T of [^{18}F]FMPEP-d_2 was about 20% lower in cannabis smokers than in healthy control subjects in cortical, but not in subcortical brain regions or cerebellum. Decrease in V_T correlated with years of cannabis smoking: subjects who had smoked cannabis for a longer period had smaller V_T than subjects who had smoked cannabis for a shorter period. In the cannabis smokers that had the second PET scan after about four weeks of continuously monitored abstinence (N=14 subjects), V_T increased significantly but only in those regions that had showed decreased V_T at baseline. The fraction of free (non-protein bound) radioligand in plasma was not different between groups at baseline, or between the two time points among cannabis smokers.

Conclusions: Chronic daily cannabis smoking is associated with reversible downregulation of cortical cannabinoid CB_1 receptors in human brain. Cannabinoid CB_1 receptor downregulation could be among neuroadaptations that promote cannabis dependence in human brain.

250

NEUROPROTECTION IN ACUTE ISCHEMIC STROKE: SAFETY AND EFFICACY ANALYSIS OF ALIAS (ALBUMIN IN ACUTE STROKE) PART 1 CLINICAL TRIAL

M.D. Ginsberg[1], M.D. Hill[2], R.H. Martin[3], Y.Y. Palesch[3], S.D. Yeatts[3], B.D. Waldman[3], C.S. Moy[4], D. Tamariz[1], K.J. Ryckborst[2], W. Barsan[5]

[1]Neurology (D4-5), Univ. of Miami Miller School of Medicine, Miami, FL, USA, [2]Clinical Neurosciences, Univ. of Calgary, Calgary, AB, Canada, [3]Division of Biostatistics and Epidemiology, Medical University of South Carolina, Charleston, SC, [4]Office of Clinical Research, National Institute of Neurological Disorders and Stroke, Bethesda, MD, [5]Emergency Medicine, University of Michigan, Ann Arbor, MI, USA

Objectives: High-dose 25% albumin (ALB) is highly neuroprotective in rodent stroke models [1]. Following a successful dose-escalation pilot clinical trial [2,3], we designed the ALIAS Multicenter Clinical Trial to assess whether ALB (dose 2 g/kg) would confer neuroprotection in acute ischemic stroke. After 434 subjects were enrolled, the Data and Safety Monitoring Board (DSMB) suspended enrollment due to a safety concern. We conducted extensive unblinded analyses and proposed protocol modifications that permitted the trial to resume (as "ALIAS Part 2"). Here we present the safety data and an efficacy exploration of the Part 1 Trial.

Methods: The Part 1 trial comprised 2 cohorts -- subjects who received thrombolysis and those who did not. Inclusion criteria were: acute ischemic stroke; age ≥18; ability to treat within 5 hours of stroke onset; and baseline NIH Stroke Scale ≥6. Major exclusion criteria included recent or current congestive heart failure, myocardial infarction, or cardiac surgery. Patients were randomized 1:1 to ALB or placebo (saline). The primary outcome was the NIHSS and modified Rankin Scale (mRS) at 90 days.

Results:

Safety analysis: This was performed in 424 subjects who had received ≥20% of study drug (ALB 207, saline 217). The major safety concern was an imbalance in overall deaths by treatment. Deaths in the ALB (9 deaths) and saline groups (9) were similar on days 1-4, while on days 5-30 there were 15 deaths in the ALB group compared to 6 in the saline group. By contrast, death rates beyond 30 days were identical in the two groups (20 each). Large strokes (with or without medical complications) were the predominant cause of death throughout days 1-30 and were more frequent in ALB than in saline subjects, but no single cause completely explained the differential death rates. Further analysis revealed that 90-day deaths were similar in the subgroup with age < 84 *and* with 48-h IV fluids ≤4200 ml *and* out-of-hospital strokes. Thus, these changes were introduced into the Part 2 protocol to enhance safety.

Exploratory efficacy analysis: This was conducted in a "target population" of those Part 1 subjects who would have satisfied the more stringent Part 2 eligibility criteria: i.e., age ≤ 83, normal baseline troponin or CK-MB level, and out-of-hospital stroke. In the N=255 thrombolysed subjects of the target population, a favorable primary outcome (NIHSS 0-1 *and/or* mRS 0-1 at 90 days) was attained in 46.7% of ALB subjects vs. 36.6% of saline subjects, (absolute benefit, 10.1%; risk ratio [RR] 1.30, 95% CI 0.9-1.7); and *dramatic* improvement (defined as 90-day NIHSS 0-1 *or* mRS 0-1 *or* DNIHSS [baseline minus 90d) of ≥10]) was seen 63% of ALB compared to 49% of placebo subjects (RR 1.29, CI 1.08-1.53, p=0.005, adjusted for age and baseline NIHSS).

Conclusions: ALIAS Part 1 led to protocol modifications to improve safety in Part 2 and revealed suggestions of efficacy. The Part 2 Trial has now recruited ~400 subjects.

References:

[1] Belayev L et al. Stroke 2001;32:553-60.

[2] Ginsberg MD etl al. Stroke 2006;37:2100-6.

[3] Palesch YY et al. Stroke 2006;37:2107-14.

252

MAGNETIZATION TRANSFER IMAGING TO DIAGNOSE DEGENERATION OF THE DESCENDING CORTICOSPINAL TRACT FOLLOWING UNILATERAL CEREBRAL HYPOXIA-ISCHEMIA

U.I. Tuor[1,2], M. Qiao[1], C. Smith[2], D. Kirk[2], T. Foniok[1], A. Kirton[3]

[1]National Research Council of Canada, Institute for Biodiagnostics West, [2]Experimental Imaging Centre, [3]Pediatrics and Clinical Neurosciences, University of Calgary, Calgary, AB, Canada

Introduction: Perinatal cerebral hypoxia-ischemia and stroke resulting in focal ischemic lesions are major causes of morbidity and adverse neurodevelopment in children. Subacute magnetic resonance (MRI) imaging of such ischemic infarcts have often observed diffusion and T_2 changes in the descending cortico-spinal tract (DCST) (1,2,3). DCST imaging abnormalities are associated with poor motor outcome in humans and may represent early Wallerian degeneration. Imaging sequences with magnetization transfer (MT) contrast have been reported more sensitive than T_2 for detecting degenerative changes (3,4), and might therefore improve identification of DCST degeneration following perinatal stroke. Clinical applications of such imaging biomarkers include improved prognostication, patient selection for and evaluation of new treatments.

Objective: To determine whether the detection of MRI abnormalities in the DCST with MT imaging is different from that with T_2 imaging in a neonatal rat model of unilateral cerebral hypoxia-ischemia.

Methods: Seven day old Wistar rat pups were subjected to either sham surgery or unilateral cerebral hypoxia-ischemia produced by occlusion of the right common carotid artery under isoflurane anesthesia followed by exposure to 65 minutes of hypoxia (8% O2). At 1 or 7 days following the hypoxia-ischemia, the rats were anesthetized and MRI scans (multiple spin-echo, and MT on/off resonance) were acquired using a 9.4T MRI system (5). Scans were used to determine T2 and MT ratio maps. Values were measured in ipsilateral and contralateral selected regions of interest including the cerebral peduncle of the DCST, the parietal cortex and a non-ischemic control region of pontine nuclei. Ipsilateral-contralateral differences were converted to a % of contraleral for comparison between sequences and to sham controls.

Results: At 1 day post-insult, T_2 was increased and MTR was decreased ipsilateral to the hypoxic-ischemic insult (Fig). Quantitative analysis demonstrated significant ipsilateral vs contralateral differences in parietal cortex and the cerebral peduncle of the DCST but no changes in the pontine nuclei (e.g. Fig). Changes in MT in the cerebral peduncle were less apparent and smaller in magnitude than changes in T_2. At 1 week post-insult, both the T_2 and MT imaging changes had normalized.

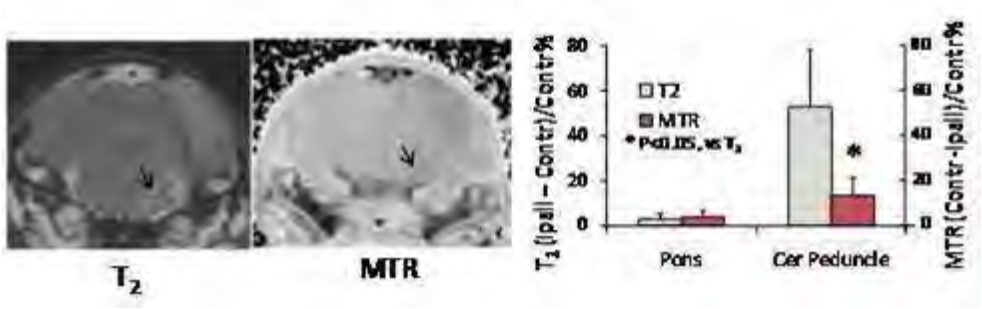

[figure2]

Conclusions: This study provides original results of a direct comparison of acute and subacute T_2 and MTR imaging changes in the DCST following unilateral infarction in neonatal brain. Reductions in MT ratios in the cerebral peduncle are modest compared to those in T_2 images. This indicates no added diagnostic benefit of MT ratio imaging for detection of DCST abnormalities soon after (1 to 7 days) a hypoxic-ischemic infarct.

Supported by the Heart and Stroke Foundation of Alberta.

References:

1. Kirton A, et. al *Stroke*, (2007) 38(3):974-80.

2. Domi T, et al. (2009) *Stroke,* 40:780-7.

3. S. Lama, et al. JCBF Metabol (2009) 29,S526-43 Abs 323

4. Lexa et al, (1993) Ann NY Acad Sci, 679:336-40;

5. Da Rocha et al, (2007) Mov Disord, 22:238-44.

6. Tuor, UI, et al. (2008) J CBF Metab 28: 1613-23.

255

SPHINGOSINE KINASE AND SPHINGOSINE 1-PHOSPHATE PATHWAYS AS NOVEL THERAPEUTICAL STRATEGIES TO MODULATE INFLAMMATION AND MICROGLIA ACTIVATION

R. Kacimi[1,2], M.A. Yenari[1,2], J.S. Karliner[2,3]

[1]Neurology Department, University California San Francisco, [2]San Francisco Veterans Affairs Medical Center, [3]Cardiology Department, University California San Francisco, San Francisco, CA, USA

Sphingolipids have evolved as new signaling regulators of diverse biological processes. Particularly, the sphingolipid metabolites, ceramide and sphingosine-1-phosphate (S1P), have emerged as a new class of potent bioactive molecules, implicated in a variety of cellular processes. It is generally believed that ceramide and sphingosine induce growth arrest and cell death in multiple situations of cellular stress. S1P produced by SPHK isoenzymes, and is up-regulated in cells via activation of G-protein-coupled receptors, growth factor receptors and cytokine receptors and variety of stress insult and disease processes. Conversely, S1P the product of sphingosine phosphorylation, tthrough transactivation of five cognate G protein-coupled receptors namely endothelial cell differentiation gene receptors (EDGs/S1P1-5), promotes proliferation, differentiation, enhances cell survival and inhibits apoptosis in different cellular systems. However, the role of S1P receptor subtypes and sphingosine kinase pathways in brain inflammation and tissue damage are not well defined. We undertook this study to sought to elucidate the role of S1P receptor subtypes and sphinosine kinase (SPHK) in cultured microglia activated by endotoxin.

We found that S1P1 agonists SEW-1 and FTY720 and endogenous ligand S1P had no significant effect on LPS induces NO, nor they affect LPS response when co-cultured with microvascualar endothelial cells (bEND.3). However, preincubation with S1P3 antagonist (CAY10444) prevented dose dependently NO accumulation, while JTE-013, a S1P2-specific antagonist & S1P1 antagonist VPC23019 were less potent on NO accumulation. We initially showed expression of SPHK1/ 2 in BV2 cells by immunofluorescence microscopy using selective antibodies. We further compared the effect of the novel SPHK1 antagonist ((2-(p-Hydrozyanilino)-4(p-chlorophenyl) tiazole, SKI) and the classical dimethyl sphingosine (dimethyl sphingosine, DMS)**.** SKI and DMS both dose dependently blocked LPS induced iNOS and COX2 protein expression and NO generation but SKI effect was more potent (n=8-12 experiments, *P< 0.01). Similarly, SP1R3 blockade with SKI pretreatment was effective in preventing iNOS expression and NO accumulation in BV2 cells after stimulation with a second TLR4 agonist Kdo2-Lipid (ADi[3-deoxy-D-manno-octulosonyl]-lipid A (ammonium salt) (n=3-5 independent experiments, * P< 0.01). Moreover, SKI but not DMS prevented microglia cell death as determined by light microscopy, MTT assay and calcein live cell stain. We also found that SKI preserves microvascular endothelial cells bEND.3 morphology and integrity compared to DMS in single monolayer. Moreover, SKI markedly prevents microglia induced inflammation and endothelial cell injury in a co-culture model.

Our findings indicate that sphingosine phosphorylation promotes immune responses in microglia and its blockade, especially SPHK1 and to lesser extent S1P3 attenuates these responses. This inhibition also led to decrease cell death due to immune cell activation. Our data suggests that targeting aspects of the sphingolipid pathway may be a new strategy to inhibit microglia activation and underlying inflammation induced injury as it occurs in stroke, trauma, and sepsis.

256

QUANTIFICATION OF SIGMA-1 RECEPTORS IN RAT BRAIN USING ^{11}C-SA4503 AND MICROPET

N. Kuzhuppilly Ramakrishnan[1], A. van Waarde[1], A.A. Rybczynska[1], A.K.D. Visser[1], K. Ishiwata[2], C.J. Nyakas[3,4], P.G.M. Luiten[4], R.A.J.O. Dierckx[1]

[1]Nuclear Medicine and Molecular Imaging, University of Groningen, Groningen, The Netherlands, [2]Positron Medical Center, Tokyo Metropolitan Institute of Gerontology, Tokyo, Japan, [3]Semmelweis University, Budapest, Hungary, [4]Molecular Neurobiology, University of Groningen, Haren, The Netherlands

Objectives: The sigma-1 receptor, a unique orphan receptor, is strongly expressed in neurons and glia. Sigma-1 receptors are implicated in cellular differentiation, neuroplasticity, neuroprotection, and cognition [1]. Sigma-1 agonists are potentially useful in the treatment of neurodegenerative diseases, stroke, and depression. PET studies of sigma-1 receptors have been performed in primate brain but not in the aging brain of rodents.

Quantification of sigma-1 receptors in rat brain is of interest for the study of animal models of human disease and for the study of mechanisms of action of sigma-1 ligands. The aim of this study was to quantify sigma-1 receptors in rat brain using the agonist radiotracer ^{11}C-SA4503 and microPET.

Methods: Sigma-1 receptors in young (6 weeks), middle aged (16-18 months) and aged (24 months) Wistar Hannover rats were visualized using ^{11}C-SA4503. A canula placed in a femoral artery was used for blood sampling. The time-dependent uptake of ^{11}C-SA4503 in rat brain was measured using a Siemens/Concorde microPET Focus 220 camera, and various tracer-kinetic models were fitted to this data, using plasma radioactivity as input function. Radioactive metabolites in plasma were quantified using reversed-phase HPLC. A biodistribution study was also performed.

Results: Aged and middle aged rats metabolised ^{11}C-SA4503 to a significantly lesser extent than the young rats. Apparent distribution volume (from Logan plots) calculated with the uncorrected plasma values as input, did not show any significant difference between the young, middle aged and aged rats. However, when the same was calculated using plasma input corrected for metabolites, middle aged and aged rats showed a significant reduction in the apparent distribution volume in the entire brain. In the biodistribution study, the aged animals showed region specific differences in the uptake of ^{11}C-SA4503: cerebral cortex in the aged rats had a significantly higher uptake, cerebellum had a non significant increase and rest of the brain had a non significant decrease. Therefore, the scan data is now being further evaluated to quantify regional distribution volumes of ^{11}C-SA4503.

Conclusions: Results indicate that sigma-1 receptors are quantifiable as the distribution volume of ^{11}C-SA4503 (from a Logan plot) in rats. Further, metabolite correction of the plasma input function has a large impact on the calculated distribution volume; therefore this correction seems essential. Biodistribution studies indicate regional differences in the brain. This method of sigma-1 receptor quantification can now be used, in conjunction with behavioural or lesion methods, to study sigma receptors in animal models of neuropsychiatric disorders and also to evaluate sigma ligands in these animal models.

References:

1. van Waarde A, Ramakrishnan NK, Rybczynska AA et al. The cholinergic system, sigma-1 receptors and cognition. *Behav Brain Res*. 2010.

257

MILD HYPOTHERMIA ATTENUATES INTERCELLULAR ADHESION MOLECULE-1 INDUCTION VIA ACTIVATION OF EXTRACELLULAR SIGNAL REGULATED KINASE-1/2 IN A FOCAL CEREBRAL ISCHEMIA MODEL

H.S. Han

Physiology, Kyungpook National University School of Medicine, Daegu, Republic of Korea

Intercellular adhesion molecule-1 (ICAM-1) in cerebral vascular endothelium induced by ischemic insult triggers leukocyte infiltration and inflammatory reaction. We investigated the mechanism of hypothermic suppression of ICAM-1 in a model of focal cerebral ischemia. Rats underwent 2 hour of middle cerebral artery occlusion and were kept at 37^{o}C or 33^{o}C during occlusion and rewarmed to normal temperature immediately after reperfusion. Under hypothermic condition, robust activation of extracellular signal regulated kinase-1/2 (ERK1/2) was observed in vascular endothelium of ischemic brain. Hypothermic suppression of ICAM-1 was reversed by ERK1/2 inhibitor. Phosphorylation of signal transducer and activator of transcription 3 (STAT3) in ischemic vessel was attenuated by hypothermia. STAT3 inhibitor suppressed ICAM-1 production induced by stroke. ERK1/2 inhibitor enhanced phosphorylation and DNA binding activity of STAT3 in hypothermic condition. In this study, we demonstrated that hypothermic suppression of ICAM-1 induction is mediated by enhanced ERK1/2 activation and subsequent attenuation of STAT3 action.

259

[F-18]WAY DERIVATIVES FOR THE STUDY OF BRAIN 5-HT1A RECEPTORS IN RAT

J.Y. Choi[1,2], C.H. Kim[2], T.J. Jeon[1], B.-S. Kim[3], K.S. Woo[3], G.I. An[3], T.H. Choi[3], Y.H. Ryu[1]

[1]Department of Nuclear Medicine, Yonsei University College of Medicine, Gangnam Severance Hospital, [2]Department of Pharmacology, Yonsei University College of Medicine, [3]Radiopharmaceutical Research, Korea Institute of Radiological & Medical Sciences, Seoul, Republic of Korea

Introduction: The serotonin 1A receptors (5-HT_{1A}) in the central nervous systems are strongly implicated in psychiatric disorders such as depression, schizophrenia and Alzheimer´s disease. Thus, a number of [F-18]WAY derivatives are developed for measuring 5-HT_{1A} receptor densities in the brain. Among these radioligands, [^{18}F]FCWAY, [^{18}F]MPPF, and [^{18}F]MEFWAY have been reported as useful PET agents for imaging 5-HT_{1A} receptors. However, there have been few reports on the comparative study of these radioligands.

Objectives: The purpose of this research is to compare the uptakes of [F-18]WAY derivatives in rat brains and to find optimal candidate for preclinical study.

Method: For in vivo experiment, male Sprague-Dawley rat was anesthetized with 2.0 % isoflurane in oxygen and placed in the gantry with its head centered in the field of view. A catheter was inserted into the tail vein and fluconazole was injected at an infusion rate for 1 h. Radioactivity (13.1-19.6 MBq) was promptly injected over 1 min to the catheter and dynamic PET scans (Siemens, Inveon PET/CT) were performed for 120 min. Control rats were injected with [^{18}F]FCWAY, [^{18}F]MEFWAY or [^{18}F]MPPF alone with no treatment. Regions of interests are hippocampus, frontal cortex, cerebellum and skull. Fluconazole, antifungal drug was tested the ability for defluorination of the radioligands.

Result: PET experiments indicated that authentic [^{18}F]FCWAY revealed extensive skull uptake due to defluorination, while [^{18}F]MPPF showed little defluorination. (skull uptake : [^{18}F]FCWAY > [^{18}F]MEFWAY >>[^{18}F]MPPF). This skull uptake was efficiently reduced by fluconazole. Moreover, [^{18}F]MPPF revealed fast uptake and short lasting time in the brain. This data supported that [^{18}F]MPPF had moderate affinity to 5-HT_{1A} ^{18}F]FCWAY was the highest while radioactivity in receptor-rich regions is two times higher than that of receptor-poor areas.

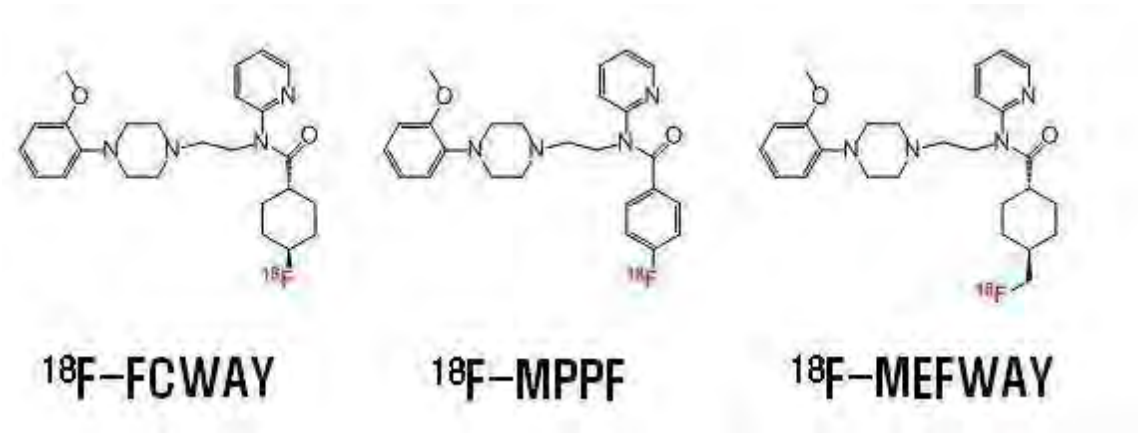

receptor. In fluconazole pretreatment group (60mg/kg intravenously), the brain uptake of [**Conclusion:** We conclude that defluorination of [^{18}F]FCWAY or [^{18}F]MEFWAY in rat brain was almost completely blocked by fluconazole, probably through the inhibition of CYP2E1. In the comparative study of PET images, inhibitor treated [^{18}F]FCWAY was the highest brain uptake. We suggest that fluconazole-treated [^{18}F]FCWAY may serve as an optimal radioligand for investigating 5-HT$_{1A}$ receptors in rat models of neuropsychiatric disorders.

References:

1. Saigal, N. et al. Synthesis and biological evaluation of a novel serotonin 5-HT$_{1A}$ receptor radioligand, ^{18}F-Mefway in rodents and imaging by PET in non-human primate. *J. Nucl. Med.* **2006***, 47*, 1697-1706.

2. Tipre, D. N. et al. PET imaging of brain 5-HT$_{1A}$ receptors in rat in vivo with ^{18}F-FCWAY and improvement by successful inhibition of radioligand defluorination with miconazole. *J. Nucl. Med.* **2006***, 47*, 345-353.

3. Ryu, Y. H. et al. Disulfiram inhibits defluorination of ^{18}F-FCWAY, reduces bone radioactivity, and enhances visualization of radioligand binding to serotonin 5-HT$_{1A}$ receptors in human brain, *J. Nucl. Med.* **2007***, 48*, 1154-1161.

260

ANALYSIS OF HYPERPERFUSION BY POSITRON EMISSION TOMOGRAPHY AFTER SUPERFICIAL TEMPORAL ARTERY-MIDDLE CEREBRAL ARTERY ANASTOMOSIS IN PATIENTS WITH MOYAMOYA DISEASE

Y. Kaku[1], K. Fukuda[1], M. Isozaki[1], N. Nakajima[1], H. Iida[2], K. Iihara[1]

[1]Neurosurgery, [2]National Cerebral and Cardiovascular Center Research Institute, Osaka, Japan

Objectives: Moyamoya disease (MMD), characterized by progressive stenosis/occlusion of the terminal internal cerebral artery and its branches of unknown etiology, may cause ischemic and hemorrhage injuries. Surgical revascularization remains the mainstay treatment. Superficial temporal artery (STA)-middle cerebral artery (MCA) anastomosis is usually indicated for symptomatic patients based on the degree of hemodynamic compromise. Despite the favorable long-term outcome after successful bypass surgery, increasing evidence suggests that in MMD, this surgery may be complicated with temporary neurologic deterioration owing to focal cerebral hyperperfusion at the site of the anastomosis during the acute stage. No previous study, however, analyzed hyperperfusion using positron emission tomography (PET) after STA-MCA anastomosis in patients with MMD.

Methods: We performed positron emission tomography (PET) and fluid-attenuated inversion recovery (FLAIR) magnetic resonance imaging (MRI) before and 2-7 days and 3-4 months after STA-MCA anastomosis on 22 sides of 17 patients with adult MMD. Here, postoperative hyperperfusion was defined as postoperative increase of cerebral blood flow (CBF) greater than normal value +2SD (56.4 ml/100g/min). To compare the PET parameters related to hyperperfusion precisely among the different time points after surgery, reslicing and fusion of the FLAIR MRI and PET images was performed.

Results: Seven patients (8 sides, 36.4 %) had symptomatic cerebral hyperperfusion. The CBF value in patients with postoperative hyperperfusion significantly increased from 37.2±4.4 ml/100g/min on preoperative baseline (n=4) to 80.0±17.5 ml/100g/min (n=6) at the time of hyperperfusion. Preoperative increased cerebral blood volume (CBV) (6.23±2.44 ml/100g) remained higher (6.92±2.12 ml/100g) at hyperperfusion than normal value +2SD (4.31 ml/100g). In contrast to the interval changes of CBF, cerebral metabolic rates of oxygen ($CMRO_2$) slightly, but not significantly, increased from 3.63±0.40 ml/100g/min to 4.73±1.79 ml/100g/min during postoperative hyperperfusion. Interestingly enough, 67% (4/6 cases) remained within the normal range even at its peak of hyperperfusion, whereas the other 2 cases with markedly increased CMRO2 were complicated with postoperative seizure. As a result, OEF significantly decreased from 0.56±0.05 at baseline to 0.41±0.10 at hyperperfusion. During the follow-up period, in the region of postoperative hyperperfusion, CBF and $CMRO_2$ returned to normal level and CBV and OEF improved compared with the preoperative status.

Conclusions: This report illustrates, for the first time, cerebral blood flow and metabolism of hyperperfusion after STA-MCA anastomosis in MMD. As reported in post CEA hyperperfusion, prolonged recovery of high CBV values during acute postoperative periods also may be a key mechanism underlying postoperative hyperperfusion in patients with MMD. However, $CMRO_2$ during postoperative hyperperfusion showed heterogeneous changes depending on the development of seizure. Taken together, the present study clearly demonstrated that postoperative symptomatic hyperperfusion may be characterized by increased CBF caused by persistent loss of vascular autoregulation with normal $CMRO_2$ unless the patients developed

seizure. In patients complicated with postoperative seizure, both CBF and $CMRO_2$ markedly increased.

265

PROLONGED MODERATE HYPOXIA IMPAIRS NEURO-GLIA-VASCULAR COUPLING IN THE SOMATOSENSORY CORTEX ACCOMPANIED BY PARECHYMAL MICROVESSEL DILATION AND ASTROGLIA SWELLING IN MICE

I. Kanno[1], K. Masamoto[2], H. Takuwa[1], H. Kawaguchi[1], Y. Tomita[3], N. Suzuki[3], T. Obata[1]

[1]Biophysics Group, Molecular Imaging Center, National Institute of Radiological Sciences, Chiba, [2]The University of Electro-Communications, [3]Neurology, Keio University School of Medicine, Tokyo, Japan

Objective: To examine the robustness of neuro-glia-vascular coupling under prolonged moderate hypoxia in mice.

Methods: Two groups of mice were selected and a closed cranial window was fixed to the skull above the somatosensory cortex of all animals before experimentation began (Tomita 2005). The groups were kept in either an 8% oxygen (n=6) or 10% oxygen (n=5) chamber for one month. Two of the 8% oxygen mice were kept alive for another three months in room air. Cortical CBF responses to air puffs (10Hz for 20sec) were weekly measured using LDF for all mice under awake state. The bodies of the animals rested on a floating ball, the rotation of which was recorded to determine the locomotion of each mouse (Takuwa 2010). Then, the cranial window was fixed to the stage of a two-photon microscope. 3D images with 0.5 micrometer x-y resolution were acquired at the same parenchymal region after a fluorescent dye (sulforhodamine 101) was intraperioneally administered (Masamoto 2010).

Results: Although the CBF responses of the 10% oxygen mice were approximately constant at 25% over the month, those of the 8% oxygen mice reduced week-by-week from 25% to < 5% at one month. The locomotion of both the 10% and 8% oxygen groups was unchanged throughout the month. The parenchymal microvessels of the 10% oxygen mice had a maximum dilation of 30% at 2~3 weeks, but they constricted again almost to the baseline diameter at one month. The vessels of the 8% oxygen mice dilated rapidly to 30% after the first week, to 40% after the second week and thereafter the dilation was sustained for the rest of the month. The cell body of astroglia in the 8% oxygen mice were observed to gradually swell to 70% of the original size over the month, but the foot process did not lengthen. The two 8% oxygen mice kept alive for another two months in room air demonstrated sustained impairment of CBF response, although the diameter of the microvessels had returned to the baseline level.

Discussion: The present study demonstrated a new model for the impairment of neuro-glia-vascular coupling. Since the locomotion level was unchanged during the experiment period for both the 10% and 8% oxygen groups, it can be concluded that the cortical neuronal activity was normal during course of the experiment. Morphological change to the microvessels is not a plausible explanation for the declined CBF response because impairment was sustained even when the microvessel diameter returned to the baseline level after the animals were breathing room air for more than three months. Therefore, the impairment of neuro-glia-vascular coupling might be caused by disruption to signal transmission between the neuron and the microvessel, e.g. malfunction in the pathways from either neuron to astroglia or from astroglia to the vessels. Further experiments are necessary to clarify these questions.

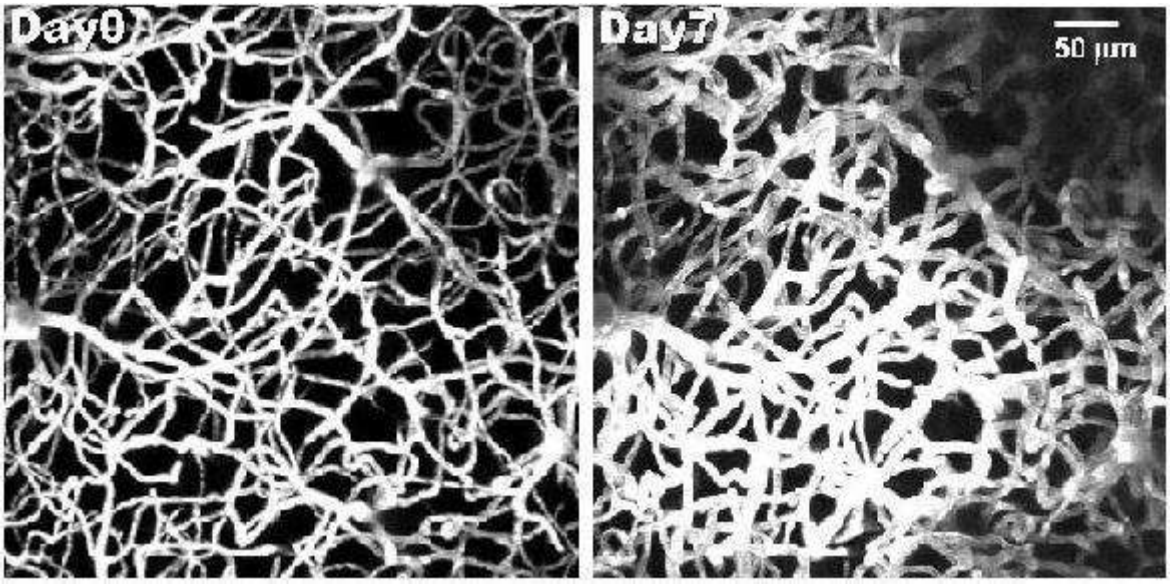

[Fig.2]

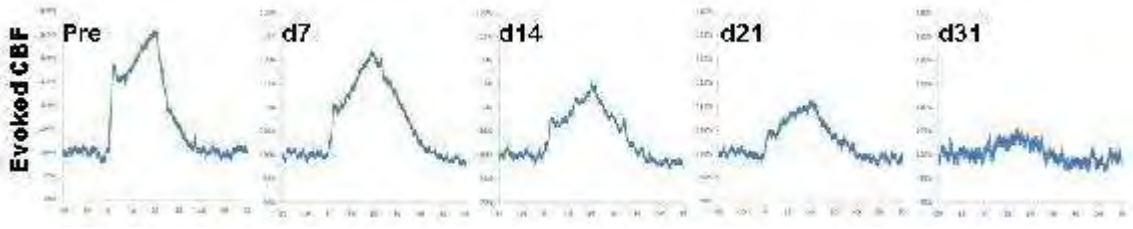

[Fig.1]

Conclusion: Exposure to 8% oxygen for one month impaired the CBF response to somatosensory stimulation in mice. This could be used as a new model to study impairment of neuro-glia-vascular coupling.

266

IS MENTALIZATION THE DOMINANT COMPONENT OF THE CBF RESPONSE TO ACTIVE AND PASSIVE MOTOR PARADIGMS? A FUNCTIONAL TCD STUDY

A.M. Salinet, R.B. Panerai, T.G. Robinson

Cardiovascular Sciences Department, University of Leicester, Leicester, UK

Introduction: Temporal and spatial patterns of cerebral activity in response to cognitive and motor paradigms have been reported [1-3]. To our knowledge this is the first study addressing the contribution of the cognitive component of passive and active motor paradigms in a healthy population aged $\geq$50 years.

Objective: We tested the hypothesis that the response of cerebral blood flow velocity (CBFv) measured using transcranial Doppler (TCD) ultrasonography is similar for passive and active motor and cognitive paradigms.

Methods: In seven right-handed healthy subjects (60.3±8.4 years, 5 male), continuous recordings of arterial blood pressure (ABP, Portapres), bilateral middle cerebral artery CBFv (using TCD), heart rate (3-lead ECG) and end-tidal CO_2 ($ETCO_2$, Capnograph) were obtained at rest and during sequential passive, active and cognitive (participants imagine elbow movement) elbow flexion and extension. Each paradigm was performed twice in random order with the dominant hand.

Results: Figure 1 shows the temporal response of CBFv in the contralateral hemisphere during the performance of the three paradigms. For the cognitive and active paradigms, changes in CBFv had a similar pattern reaching a peak seconds after the beginning the stimulus and decreasing gradually during the activity. However, during passive exercise, CBFv rose steeply immediately after the beginning of the exercise, and was maintained until just after the end of the exercise. In the ipsilateral MCA, the increase in CBFv was greater during the cognitive paradigm than during both the passive and active paradigms. ABP changes were similar during the 3 paradigms, with increases associated with activity and maintained throughout. $ETCO_2$ varied slightly during the intervention, within the limits of normocapnia.

Conclusion: Similar haemodynamic responses were observed for all 3 paradigms, indicating that mentalization is an important contributor, resulting in both contralateral and ipsilateral haemodynamic changes. Further reproducibility studies are needed before this approach can be extended to patients with stroke or other cerebrovascular conditions.

References:

1. Khushu, S., S. S. Kumaran, et al. (2001). "Functional magnetic resonance imaging of the primary motor cortex in humans: response to increased functional demands." Journal of Biosciences 26(2): 205-215.
2. Matteis, M., C. Caltagirone, et al. (2001). "Changes in cerebral blood flow induced by passive and active elbow and hand movements." Journal of Neurology 248(2): 104-108.

3. Moody, M., R. B. Panerai, et al. (2005). "Cerebral and systemic hemodynamic changes during cognitive and motor activation paradigms." American Journal of Physiology-Regulatory Integrative and Comparative Physiology 288(6): R1581-R1588.

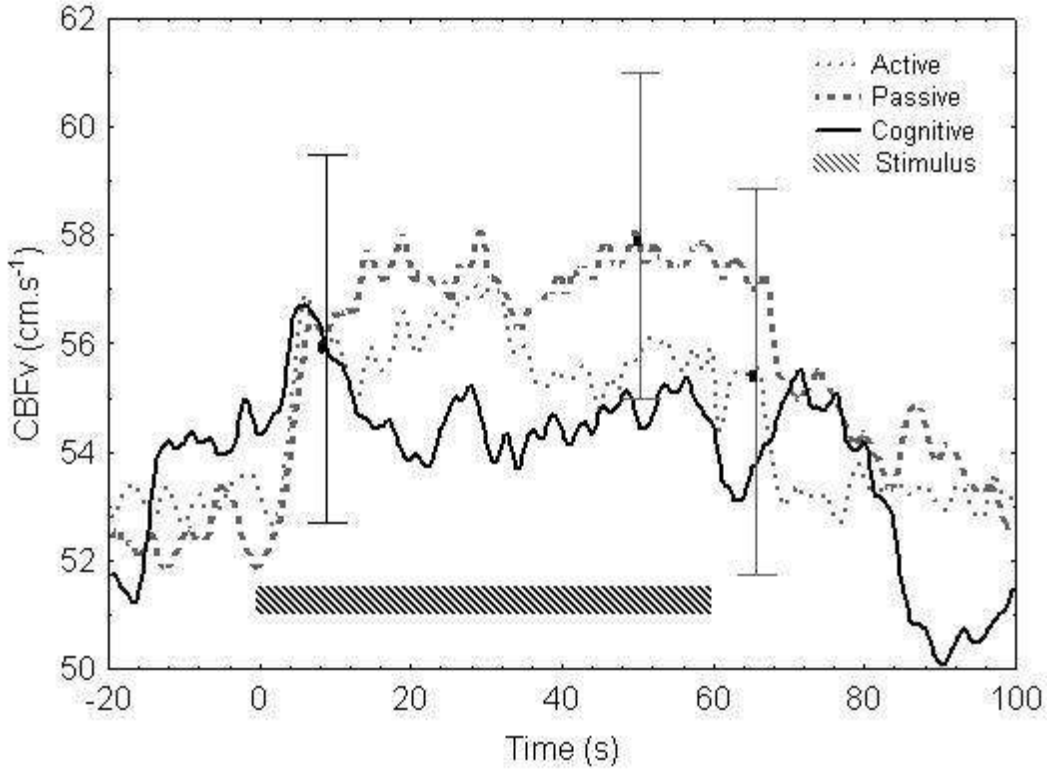

[Temporal response of CBFv]

267

EFFECTS OF PPAR GAMMA AGONIST ON NO PRODUCTION, HYDROXYL RADICAL METABOLISM DURING CEREBRAL ISCHEMIA AND REPERFUSION IN DB/DB MICE

Y. Ito, Y. Asano, M. Yamasato, R. Nishioka, N. Araki

Department of Neurology, School of Medicine, Saitama Medical University, Saitama, Japan

Introduction: Peroxisome proliferator-activated receptor (PPAR gamma) agonist, pioglitazone, protects against cerebral injury by anti-oxidant mechanisms. It is suggested that hyperglycemia during acute cerebral ischemia is associated with poor prognosis. The purpose of this study is to investigate the effects of pioglitazone on NO production, hydroxyl radical metabolism and ischemic change of hippocampal CA1 during cerebral ischemia and reperfusion in *db/db* mice, an animal model of type 2 diabetes.

Methods: (1) *db/db* mice [n=16] were used. Pioglitazone 20 mg/kg/day was given in 8 mice for 4 days (pioglitazone group), and others were used as contol group. Both NO production and hydroxyl radical metabolism were continuously monitored by *in vivo* microdialysis. Microdialysis probes were inserted into the bilateral striatum. The *in vivo* salicylate trapping method was applied for monitoring hydroxyl radical formation via 2,3 dihydroxybenzoic acid (2,3-DHBA), and 2,5 dihydroxybenzoic acid (2,5-DHBA). A Laser Doppler probe was placed the skull surface. Blood pressure, blood gases and temperature were monitored and maintained within normal ranges throughout the procedure. Forebrain cerebral ischemia was produced by occlusion of both common carotid arteries for 10 minutes. Levels of nitric oxide metabolites, nitrite (NO_2^-) and nitrate (NO_3^-), in the dialysate were determined using the Griess reaction. (2) CA1 neurons: Hippocampal CA1 neurons were analyzed into three phases (severe ischemia, moderate ischemia, survive), and the ratio of the number of surviving neurons was calculated (survival rate).

Results: (1) Blood Pressure: pioglitazone group (65.8 ± 12.9 mmHg; mean ± SD) showed significantly lower than that of the control group (104.7 ± 31.7), 30 minutes before ischemia, ischemia and 10-50 minutes after the start of reperfusion ($p< 0.05$). (2) Cerebral Blood Flow (CBF): pioglitazone group (82.4 ± 22.9 %; mean ± SD) showed significantly higher than that of the control group (59.9 ± 11.0), 50, 90-100 minutes after the start of reperfusion ($p< 0.05$). (3) Nitric oxide metabolites: 1) NO_2^- ; There were no significant differences between the groups. 2) NO_3^- ; pioglitazone group (121.7 ± 15.9 %; mean ± SD) showed significantly higher than that of the control group (104.0 ± 10.7), 20-40 minutes after the start of reperfusion ($p< 0.05$). (4) Hydroxyl radical metabolites: 1) 2,3-DHBA; pioglitazone group (98.6 ± 1.45%; mean ± SD) showed significantly lower than that of the control group (106.1 ± 4.3), 20 minutes after the start of reperfusion ($p< 0.05$) (Figure 1). 2) 2,5-DHBA; There were no significant differences between the groups. (5) Survival rate in CA1 area: There were no significant differences between the groups.

Conclusion: These *in vivo* data suggest that pioglitazone influences on the CBF and hydroxyl radical production in *db/db* mice, and may protect against cerebral ischemic injury following ischemia and repurfusion.

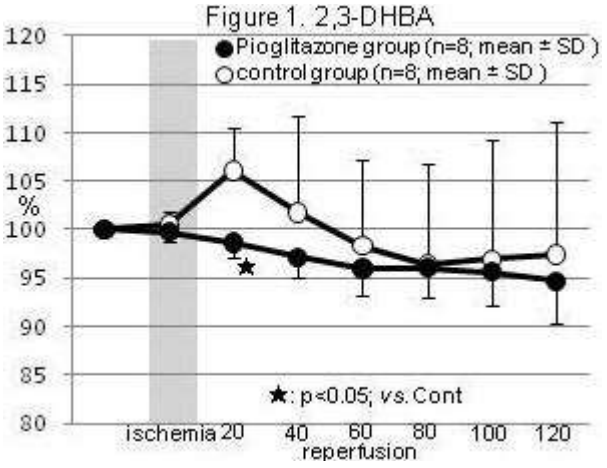
Figure 1. 2,3-DHBA
Pioglitazone group (n=8; mean ± SD)
control group (n=8; mean ± SD)
120
115
110
105
%
100
95
90
85
80
★: p<0.05; vs. Cont
ischemia
20
40
60
80
100
120
reperfusion

[2,3-DHBA]

268

ADMINISTRATION OF HIGH DOSE OF BENDIOCARB ON MEMBRANA PAPYRACEA ON EMBRYONIC DAYS 3 AND 10

J. Danko, E. Petrovova, D. Mazensky, K. Vdoviakova, S. Flesarova

University of Veterinary Medicine and Pharmacy, Kosice, Slovak Republic

The aim of the study was to investigate toxicity of bendiocarb to central nervous system of chick embryo. Bendiocarb (1600 mg/egg) was administered over the embryo through *membrana papyracea* on embryonic day (ED) 3 and 10.

The annual application of the synthetic pesticides to food crops in the European Union exceeds 140,000 tones, an amount that corresponds to 280 grams per EU citizen per year.

Bendiocarb is the most widely used carbamate insecticide used to control disease vectors (mosquitoes, flies, household and agricultural pests). The blockage of acetylcholine esterase caused by bendiocarb persists for approximately 24 hours and subsequently the situation returns to normal after acute exposure because the insecticide does not accumulate in mammalian tissues. The purpose of the present study was to observe the effect on central nervous system (CNS) in the chick embryos applied *in ovo* with high bendiocarb dose (1600 mg/egg).

Fertile white Leghorn chicken eggs (113 eggs) were incubated in a thermostat with forced circulation of air (37.5 ± 0.5 °C and relative humidity of 60 %). The application dose (200 µL - water for injection, acetone, bendiocarb) was applied directly over the embryo on the top of the innner shell membrane, *membrana papyracea.* At the time of sampling (9 ED for application on 3 ED, and 17 ED for application on 10 ED), the embryos were removed from the eggs, weighed, fixed and processed by a standard way for histological examination. The parts of embryos were embedded in paraffin and a microtome was used to cut sections. To observe the microscopical changes in the CNS, part of the sections was stained with haematoxylin-eosin and the remaining sections were stained immunohistochemically for observation of caspase activity. Statistical comparison of differences among groups was performed using GraphPad Prism. Value of $P < 0,05$ was considered significant.

The microscopic findings in the CNS were negative in comparison with the control. Part of the neck was sampled for this examination (including spinal cord cross section) and no histological changes were observed in CNS as far as neurons and intercellular space was concerned.

On 3 ED we observed (in the viewing field of size 887.5µm^3) one cell (0,20 %) with caspase activity in both treated and control embryos. On 10 ED we observed one cell (0.20 %) with caspase activity in comparison with the control which contained five (1 %) nerve cells with caspase activity.

Application of bendiocarb to survived chick embryos produced no macroscopic or microscopic changes in the tissue of the CNS both on 3 ED and 10 ED. The chick embryos showed low caspase activity of nerve cells. The apoptotic cells in the CNS were presented in both treatment and control embryos. It may be related to physiological apoptosis occurring during embryogenesis and physiological elimination of excessive neurons at generation of synapses.

269

BLOOD VOLUME FRACTION MAPPING IN MICE FOR ANGIOGENESIS ASSESSMENT IN A NOVEL HUMAN GLIOBLASTOMA STEM CELL MODEL

T.-A. Perles-Barbacaru[1], F. Tiar[2], L. Pelletier[2], D. Wion[2], F. Berger[2], H. Lahrech[1]

[1]Functional And Metabolic Neuroimaging, [2]Brain Nanomedicine Group, INSERM U836, Grenoble Institute of Neurosciences, University Joseph Fourier, Grenoble, France

The tumor blood volume fraction (BVf), an important parameter related to angiogenesis, can help predict response to antiangiogenic therapies in preclinical and clinical studies. Here, we quantified the BVf in a novel orthotopic glioblastoma mouse model **[1]** using the Rapid-Steady-State-T_1 ($RSST_1$) MRI technique **[2]** with a clinically approved contrast agent.

One to three months after tumor implantation (5×10^5 human glioblastoma stem cells) in the caudate nucleus (Bregma level, 2 mm right, 2.5 mm depth), nude mice (n=6) were imaged in a 47/40 Bruker Biospec USR AV III scanner (FOV=15×15 mm^2, 8 slices of 0.7 mm). Gd-DOTA (6 mmol/kg,12 ml/kg) was administered intraperitoneally 5 minutes after the start of a dynamic $RSST_1$ acquisition (Inversion Recovery prepared Modified-Driven-Equilibrium-Fourier-Transform (MDEFT), $TR/TR_{echo}/T_{inversion}/TE$=750ms/6.5ms/303ms/1.2ms, α=10°, matrix 32×32, duration=6s/repetition) of 60 minutes duration, followed by a T_1-weighted acquisition (Multi-Slice-Multi-Echo, TR/TE=300ms/6.3ms, NA=8, matrix 128×128, duration=5min7s). Prior to Gd-DOTA injection, T_2-weighted (Rapid-Acquisition-Relaxation-Enhanced imaging, $TR/TE_{effective}$=3.5s/33ms, NA=6, matrix 128×128, duration=5min36s), T_1-weighted and proton density weighted MDEFT images $TR/TR_{echo}/T_{inversion}/TE$=10s/6.5ms/9s/1.2ms, duration=1min20s) were acquired. Contrast enhancement was quantified as $(S_{post\_T1w}-S_{pre\_T1w})/S_{pre\_T1w}$, S_{post_T1w} and S_{pre_T1w} being the T_1-weighted (T1w) pre- and post-contrast signal, respectively. The BVf maps were obtained according to $S_{norm}=(S_{post}-S_{pre})/S_0$ **[2]**, where S_{pre} and S_{post} are the average pre- and post-contrast $RSST_1$ signals during the steady state phase, while S_0 is the proton density weighted signal. When the Gd-DOTA is confined to the vascular compartment the normalized signal equals the BVf: S_{norm}=BVf **[2]**.

During the 1st month, tumor growth was not detectable with either MR technique. During the 2nd month, the tumor occurrence was hardly visible on T_2 weighted acquisitions, but contrast enhancement in the order of 50 to 400% could be observed on T_1 weighted acquisitions. The diagram displays typical $S_{norm}(t)$ time courses (n=1). No contrast agent leakage in the tumor region was observed after Gd-DOTA injection (vertical arrow), similar to the $RSST_1$ signal from a major vessel. A typical Gd-DOTA leakage profile as observed in muscle tissue is shown for comparison. Fifteen to 35 minutes after Gd-DOTA injection the signal is in a steady state (horizontal arrow) reflecting the thermodynamic equilibrium signal from the vascular compartment. Under the assumption that Gd-DOTA is confined to the vascular compartment after intraperitoneal injection **[3]**, the BVf in the tumor region is 0.034 ± 0.010 (range 0.020 to 0.043) while it is 0.023 ± 0.004 (range 0.018 to 0.029) contralateral to the tumor. In most mice, clinical signs appeared 3 months after tumor implantation.

This novel glioblastoma model develops slowly and mimics the cellular heterogeneity encountered in clinical tumors. During the 2nd month of tumor development, the tumor vasculature appears impermeable to Gd-DOTA and allows noninvasive acquisition of quantitative micro- and macrovascular BVf maps for angiogenesis assessment using the $RSST_1$ technique. This novel glioblastoma model is useful for the evaluation of new treatment strategies such as antiangiogenic agents.

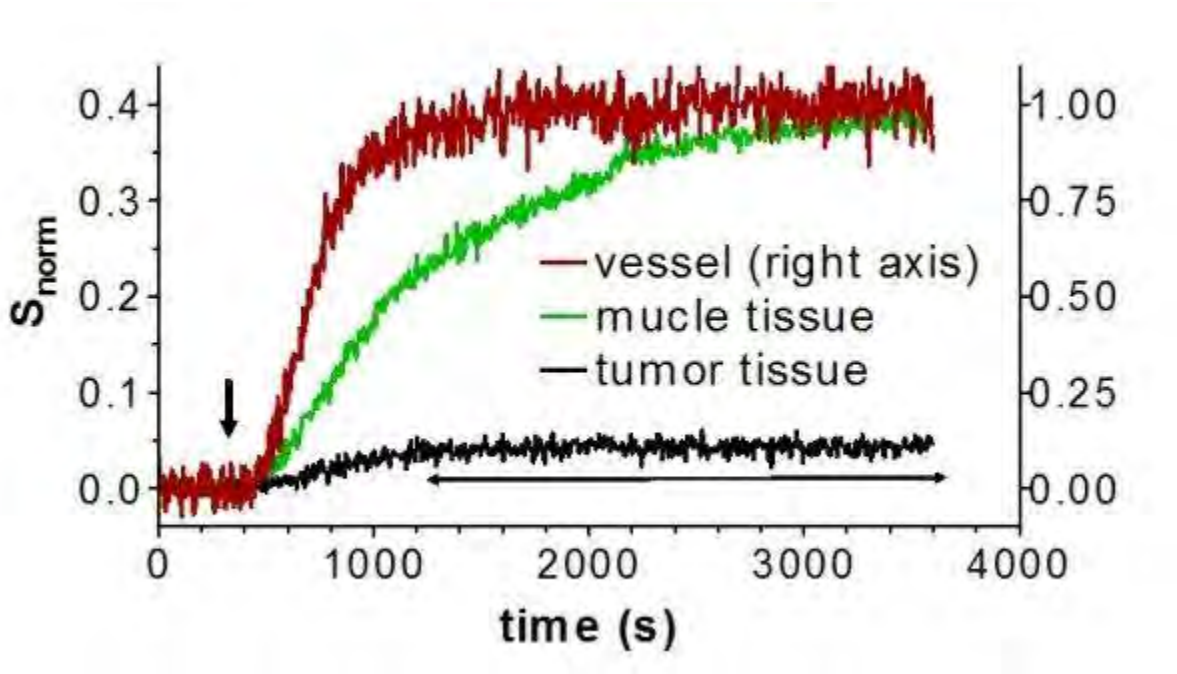

[diagram]

[1] Platet et al, Cancer Lett. 2007;

[2] Perles-Barbacaru and Lahrech, JCBFM 2007;

[3] Moreno, NMR Biomed 2006

270

MINOCYCLINE AMELIORATES BLOOD BRAIN BARRIER PERMEABILITY CHANGES IN THE RAT STREPTOZOTICIN MODEL OF DIABETES

R.D. Egleton[1], A.J. Marcelco[1], N.A. Proper[1], S. Hom[2], C.R. Campos[3], B.T. Hawkins[4]

[1]Pharmacology, Marshall University Medical School, Huntington, WV, [2]Pharmacology, University of Arizona, Tucson, AZ, [3]Laboratory of Toxicology and Pharmacology, National Institute of Environmental Health Sciences, Research Triangle Park, NC, [4]Division of Hematology, University of Washington School of Medicine, Seattle, WA, USA

Objectives: The modulation of cerebrovascular function in diabetes is believed to play a significant role in the development of neurological disease in diabetic patients. Several recent studies have shown that the blood brain barrier (BBB) of diabetic patients is compromised (1). Further studies with the streptozotocin (STZ) rat model of diabetes have shown a significant and prolonged change in functional and molecular properties of the BBB (2, 3). Minocycline, a tetracyclic antibiotic has been shown to be neuroprotective in diseases that have altered BBB function (4). In this study we investigated the effect of minocycline on STZ induced BBB changes in the rat.

Methods: Diabetes was induced via an I.P. injection of 65 mg/kg STZ. At 7 days post injection with STZ, rats were injected twice daily with either 22.5 mg/kg minocycline of sterile saline I.P. At 14 days post STZ injection rats were anesthetized with a ketamine based anesthetic and used for either in situ perfusion with [^{14}C]sucrose or were used for microvessel isolation and subsequent Western blot analysis (detailed methods in reference 2). From the in situ perfusion study, single time point unidirectional uptake coefficients were calculated (K_{in}). Western blot analysis was carried out for tight junction proteins (Claudin-5, ZO-1 and occludin).

Results: As seen previously, STZ diabetes lead to a significant increase in BBB permeability to [^{14}C]sucrose with an increase in K_{in} by approximately 30% ($p < 0.05$). Minocycline therapy prevented this increase from occurring, and in fact decreased BBB permeability to sucrose below control levels in STZ treated rats (~70% of control). This decrease in permeability was also seen in control animals that were given minocycline, indicating that the effect of minocycline was not specific to the STZ treated animals themselves. Subsequent Western blot analysis showed that minocycline did not affect the levels of either ZO-1 or occludin, it did however significantly increase the expression of claudin-5 at the BBB (~60 and 45 % for control and STZ treated animals respectively). Treatment with minocyline did not significantly affect the course of diabetes as measured by glucose, ketones and lipid levels in the rats.

Conclusions: Minocycline, a tetracycline antibiotic with neuroprotective actions, prevents the changes seen in BBB permeability induced by STZ in the rat. These changes may be due to an increased expression seen in Claudin-5, not only in STZ treated rats, but also in the control treated rats. Claudin-5 has previously been reported to be responsible for modulating BBB permeability to low molecular weight markers such as sucrose. The mechanism by which minocycline up-regulates Claudin-5 is as yet unknown, however previous studies indicate that minocycline interacts with multiple signaling pathways involved with CNS inflammation and apoptosis; pathways known to regulate claudin-5 function and expression.

References:

1. Starr, J.M., et al., J Neurol Neurosurg Psychiatry, 2003. 74(1): p. 70-6.

2. Hawkins, B.T., et al., Diabetologia, 2007. 50(1): p. 202-11.

3. Huber, J.D., et al., Am J Physiol Heart Circ Physiol, 2006. 291(6): p. H2660-8.

4. Kim, H.S. and Y.H. Suh, Behav Brain Res, 2009. 196(2): p. 168-79.

271

COMPARISON OF TWO ADMINISTRATION TIMES AND DOSES OF RT-PA ON POST-ISCHEMIC OUTCOMES IN A THROMBO-EMBOLIC MOUSE MODEL OF CEREBRAL ISCHEMIA

M. El Amki[1], **D. Lerouet**[1], B. Coqueran[1], C. Orset[2], D. Vivien[2], M. Plotkine[1], C. Marchand-Leroux[1], I. Margaill[1]

[1]Pharmacologie de la Circulation Cérébrale EA4475, Université Paris Descartes, UFR des Sciences Pharmaceutiques et Biologiques, Paris, [2]INSERM U919, Université de Caen Basse-Normandie, Centre Cyceron, Caen, France

Introduction: Thrombolysis with recombinant tissue plasminogen activator (rt-PA) is the only treatment for ischemic stroke. Nevertheless, its use remains limited due to its short therapeutic time window and the increased risk of post-ischemic hemorrhagic transformation (HT). Since Korninger *et al.* showed that the rat's fibrinolytic system is 10-fold less sensitive to rt-PA than the human one[1], all *in vivo* experimental studies have been using rt-PA at 10 mg/kg in rodents instead of 0.9 mg/kg in human. However, recent data showed that rt-PA at 0.9 mg/kg is almost as beneficial as at 10 mg/kg in a model of cerebral ischemia (CI) in rats[2].

In this context, we compared the effects of “human” and “rodent” doses of rt-PA, given at early or delayed time after stroke.

Methods: Ischemia was induced in anesthetized male Swiss mice (25-32 g) by *in situ* microinjection of purified human thrombin in the left middle cerebral artery[3].

Experiment 1:

Thrombolytic effect of 0.9 or 10 mg/kg rt-PA, administered intravenously (10% bolus plus 90% perfusion) 30 min after ischemia, was evaluated by recording the cerebral blood flow (CBF) for 120 min post-ischemia.

Experiment 2:

Rt-PA (0.9 or 10 mg/kg) or vehicle (saline) was administered 30 min or 4h after ischemia. Sensorimotor functions were evaluated at 24h using a grading scale on 16 points. Mice were then anesthetized, transcardially perfused with saline and their brains were removed and frozen. Cryostat-cut coronal sections were used to quantify (1) hemorrhagic score[4], and (2) cortical lesion and edema after cresyl violet staining.

Results: Ninety minutes after rt-PA administration, CBF was only partially restored in ischemic mice treated with 0.9 mg/kg rt-PA (70% of basal level), while 10 mg/kg rt-PA led to a rapid and total reperfusion as soon as 40 min after injection.

Early administration of 0.9 or 10 mg/kg rt-PA reduced neurological deficit (40% and 50%; $P=0.053$ and $P< 0.01$, respectively), lesion volume (65% and 77%; $P< 0.001$) and brain edema (64% and 76%; $P< 0.001$), but had no effect on post-ischemic HT.

The delayed administration of both rt-PA doses had no more effect on neurological deficit, brain lesion and edema, and worsened HT (x3.1 at 0.9 mg/kg, $P< 0.01$; x4.9 at 10 mg/kg, $P< 0.001$).

Conclusion: Our results show that despite reperfusion differences, low and high doses of rt-PA exert similar beneficial effects when administered early after CI, while a delayed treatment shows no more neuroprotective effects and even increases post-ischemic HT.

1. Korninger *et al.* 1981. *Thromb Haemost*, 46:561.

2. Haelewyn *et al.* 2010. *J Cereb Blood Flow Metab*, 30:900.

3. Orset *et al.* 2007. *Stroke*, 38:2771.

4. Haddad *et al.* 2008. *Eur J Pharmacol*, 588:52.

272

INTRAVENOUS IMMUNOGLOBULIN ALLEVIATES COGNITIVE DEFICITS AFTER GLOBAL CEREBRAL ISCHEMIA IN C57/BL6 MICE AND PROVIDES TIME- AND DOSE-DEPENDENT NEUROPROTECTION

R. Heikkinen[1], T. Malm[1], H. Koivisto[1], M. Takalo[1], A. Muona[2], H. Tanila[1,3], M. Koistinaho[2], J. Koistinaho[1,4,5]

[1]Department of Neurobiology, A.I. Virtanen Institute for Molecular Sciences, Biocenter Kuopio, University of Eastern Finland, [2]Medeia Therapeutics Ltd, [3]Department of Neurology, Kuopio University Hospital, [4]Department of Oncology, [5]School of Pharmacy, University of Eastern Finland, Kuopio, Finland

Objectives: Intravenous immunoglobulin (IVIG) has been traditionally used to treat autoimmune diseases. Recent studies suggest that IVIG is neuroprotective also against acute ischemic attack. Even though IVIG has several potential mechanisms to attenuate the detrimental inflammatory responses caused by neurodegenerative processes, it is not known whether IVIG could provide neuroprotection in global brain ischemia. The aim of this study was to test the neuroprotective potential of IVIG in a mouse model of global ischemia, especially when IVIG is administered after the ischemic insult. In addition, we determined the most effective therapeutic dose and the time window for IVIG treatment after global ischemia.

Methods: Wild-type C57/Bl6 mice underwent bilateral reversible compression of common carotid arteries for 17 minutes. Mice were treated with a single dose of 0.1, 0.5 or 1.0 g/kg immunoglobulin or diluent intravenously, 1, 3 or 6 hours after global ischemia. Minocycline was used as positive control. A neurological test battery for motor functions, anxiety, and spatial learning and memory was performed during post-operative weeks 3 and 4. Histological outcome was analyzed by NeuN-staining.

Results: After global ischemia, spatial learning and neuronal survival at the CA1 of the hippocampus were restored by 1.0 g/kg dose of IVIG given 1 and 3 hours after ischemia but not when administered at 6 hours. IVIG proved to be as protective as minocycline, when measured by spatial learning and histological staining. Treatment with IVIG did not protect from motor deficits but decreased post-ischemic anxiety when administered at 1h time point.

Conclusions: A single dose of 1g/kg IVIG given 1 or 3 hours after ischemia proved to be the most efficient in restoring spatial learning, which correlated well with neuroprotection seen in CA1. Differential effects seen in motor and navigation tasks confirm IVIG as valuable treatment for conditions with hippocampal damage. Further studies will provide the mechanism behind the neuroprotective effect of IVIG in global ischemia.

273

EFFECT OF IL-1 RECEPTOR ANTAGONIST (IL1-RA) ADMINISTERED SUBCUTANEOUSLY AFTER EXPERIMENTAL STROKE (REPERFUSION TIME) IN RATS WITH DIFFERENT STROKE RISK FACTORS

J.M. Pradillo, H. Boutin, C. Drake, A. Denes, B.W. McColl, N.J. Rothwell, S.M. Allan

Neurosciences, Faculty of Life Sciences, University of Manchester, Manchester, UK

Introduction: Stroke is a leading cause of death and disability worldwide. Although several successful treatments have been demonstrated in experimental stroke, there has been a lack of translation to the clinic[(1)]. Most experimental stroke studies do not address key clinical co-morbidities and risk factors, such as atherosclerosis, high blood pressure, chronic and/or acute inflammation due to chronic inflammatory disease, infections and age, which may explain this lack of translation. Inflammation contributes to poor outcome after stroke, and the proinflammatory cytokine interleukin-1 (IL-1) is a key mediator of experimental ischaemic brain injury[(2,3)]. Recently, we have demonstrated that peripheral administration of IL-1 receptor antagonist (IL-1Ra) at the time of middle cerebral artery occlusion (MCAo) is neuroprotective in young and healthy rats[(4)]. In the present study, we tested whether IL-1Ra administered at reperfusion after focal MCAo is also neuroprotective in animals with different risk factors for stroke, as well as effects on the post-stroke systemic inflammatory response.

Methods: 15 months old Corpulent (JCR:LA Cp/Cp, a model of atherosclerosis and obesity) and Lean rats were used. Experimental stroke was induced by transient MCAo (90 min). IL-1ra or placebo was administered subcutaneously (50 mg/kg) at time of reperfusion and 6h after. 24h after MCAo, infarct volume was assessed by MRI (T_2W images). Blood-brain barrier (BBB) disruption was assessed ex vivo by IgG immunostaining. The systemic inflammatory profile was assessed by cytometric bead array (CBA) and different behavioural tests were used to determine functional outcomes.

Results: IL-1ra reduced (by approx 50%) infarct volume in lean and corpulent rats, and also reduced BBB disruption in both groups. IL-1Ra improved behavioural outcome (adhesive removal test) only in lean rats, and no significant effect of treatment on the systemic inflammatory response was observed in either strain of rat. In accordance with previous data[(5)], inflammatory status and BBB disruption were worse in corpulent animals compared to the lean cohort.

Conclusions: IL-1ra is neuroprotective when administered subcutaneously time of reperfusion after cerebral ischaemia in animals with different stroke risk factors.

References:

(1). Dirgnal U. (2006) J Cereb Blood Flow Metab. 26:1465-78;

(2). McColl B.W. et al. (2009) Neuroscience. 158:1.049-1061;

(3) Allan S.M. et al. (2005) Nat Rev Immunol. 5(8):629-40;

(4) Greenhalgh A.D. et al. (2010) Br. J Pharmacol. 160(1):153-9; Drake C. et al. (2010) (unpublished).

This work was supported by MRC and the European Union's 7th Framework Programme (FP7/2008-2013) under grant agreements n° 201024 and n° 202213 (European Stroke Network).

275

SELECTIVE CYCLOOXYGENASE TYPE 1 INHIBITION PROMOTES NEUROLOGICAL RECOVERY IN A MOUSE MODEL OF TRAUMATIC BRAIN INJURY

H. Girgis, B. Palmier, N. Croci, M. Soustrat, M. Plotkine, C. Marchand-Leroux

Laboratoire de Pharmacologie de la Circulation Cérébrale (EA 4475), Université Paris Descartes, Paris, France

Introduction: The role of cyclooxygenase (COX) family of enzymes in traumatic brain injury (TBI) is still controversial. In rat models of TBI, the pharmacological inhibition of the inflammation-induced isoform, the COX-2, was shown to be neuroprotective [1, 2, 3]. However, the genetic disruption of either COX-2 [4, 5] or COX-1 [5], the constitutive isoform, had no effect in mouse models of TBI. Therefore, we investigated the effect of selective and non selective COX inhibitors on deleterious consequences of TBI: the neurological deficit and the cerebral œdema.

Methods: Closed head injury model was realised in anaesthetised Swiss male mice by mechanical percussion using a weight-drop device.

For the time-course studies, COX-2 protein expression was evaluated by Western Blot and brain 6-keto-prostaglandin F1 alpha (6-Keto-$PGF_{1\alpha}$), a major prostacyclin metabolite, was measured by Enzyme immunoassay. A single dose of a preferential COX-2 inhibitor, meloxicam (2 mg/kg) or a selective COX-1 inhibitor, valeroyl salicylate (20 mg/kg), was administered intraperitoneally 10 minutes after TBI. Another group of mice received 3 doses of a non selective COX inhibitor, indomethacin (5 mg/kg) at 10 minutes, 6 and 12 hours after trauma.

Post-traumatic neurological deficit was evaluated by “Exit Circle Test” and “Irwin's Criteria” at 6 and 24 hours. Animals were then sacrificed for the determination of cerebral œdema.

Results: COX-2 expression was significantly increased at 6 and 12h after injury. This was associated with an increased production of 6-Keto-$PGF_{1\alpha}$ which was reduced by all COX inhibitors. While meloxicam had no effect on post-traumatic neurological deficit, both indomethacin and valeroyl salicylate significantly promoted neurological recovery at 6 and 24h after TBI. However, no COX inhibitor had an impact on cerebral œdema.

Conclusion: Our results show that COX-2 is not implicated in post-traumatic consequences. However, in a mouse model of TBI, we demonstrate for the first time that COX-1 inhibition is beneficial for neurological recovery independently of an eventual anti-œdematous effect. Our findings are consistent with recent data [6] suggesting a significant deleterious role of COX-1 in neuroinflammatory brain pathologies.

1) Cernak et al. Exp Brain Res. 2002; 147: 193-199.

2) Gopez et al. Neurosurgery. 2005; 56: 590-604.

3) Hakan et al. Neurol Res. 2010; 32: 629-635.

4) Ahmad et al. J Neurosci Res. 2008; 86: 3605-3612.

5) Kelso et al. BMC Neurosci. 2009; 10: 108.

6) Bosetti & Choi. Cell Cycle. 2010; 9: 2919-2920.

276

BUYANG HUANWU DECOCTION CAN PROMOTE THE PROLIFERATION OF NEURAL PROGENITOR CELL AND NEUROGENESIS INDUCED BY ISCHEMIA STROKE VIA JAK2/STAT3-HES1 CROSSTALK

X. Chen, J. Shen

The University of Hong Kong, the School of Chinese Medicine, Hong Kong, China

Objectives: Buyang Huanwu Decoction (BHD), a classic traditional Chinese medicine (TCM) formula, has been used for recovering neurological dysfunctions and treating post-stroke disability in China for about 200 years. The molecular mechanisms are still unknown. In order to explore the molecular mechanisms of the formula for stroke treatment, we investigated the effects of BHD on modulating cellular growth signals and improving neural stem cells proliferation and differentiation in the experimental rat stroke model by the occlusion of middle cerebral artery (MCAO).

Methods: BHD was orally administrated to the rats for 14and 28 days after MCAO. We detected the proliferation-promoting effects by immunofluorescent staining of thymidine analog 5-bromo-2′-deoxyuridine (BrdU). We also detected the differentiation-promoting effects by immunofluorescence double staining of doublecortin (DCX) and neuron-specific nuclear antigen (NeuN) and astrocyte marker (GFAP). To understand its mechanisms, we investigated the expressions of proteins involved in Jak/stat3 pathway and hes1 which is important signaling molecule to maintain the neural stem cells at the early stage and improve neurogenesis on the later period.

Results: The results showed that the formula stimulated the proliferation of the neural stem cells at dentate gyrus of hippocampus in the ischemic brains. BHD could increase the number of the double staining positive cells. We found the formula remarkably up-regulated the expressions of p-Jak,p-stats3, Cylin D1and hes1 in vitro.

Conclusion: These result indicated that BHD could improve the neural stem cell proliferation and differentiation, and the underlying mechanism were related to activate Jak/p-Stat3 -hes1 crosstalk.

277

MITOCHONDRIAL IMMP21 GENE MUTATION INCREASES ISCHEMIC BRAIN DAMAGE, ENHANCES ROS PRODUCTION, ACTIVATES INTRINSIC CELL DEATH PATHWAYS, AND INHIBITS MITOCHONDRIAL FUNCTION

Y. Ma[1,2], S.L. Mehta[1], B. Lu[3], **P.A. Li**[1]

[1]Pharmaceutical Sciences, BRITE, North Carolina Central University, Durham, NC, USA, [2]Pathology, Ningxia Medical University, Yinchuan, China, [3]Institute for Regenerative Medicine, Wake Froresh University School of Medical, Winston-Salem, NC, USA

Objectives: Mutation of the inner mitochondrial membrane peptidase 2-like (Immp2l) gene affected the signal peptide sequence processing of mitochondrial proteins cytochrome c1 and glycerol phosphate dehydrogenase 2. Mutant Immp2l impairs fertility by enhancing oxidative stress. Although mutation of Immp2l gene is associated with Tourette syndrome, its influence in the central nervous system is unknown. The objectives of this study are to explore the effects of mutant Immp2l on ischemic outcome and to determine the underlying mechanisms responsible for its detrimental effects on brain after stroke.

Methods: Male Immp2l mutant and wild-type mice were subjected to 1 hour focal cerebral ischemia under normoglycemic conditions. Their brains were harvested after 5- and 24-hrs of reperfusion.

Results: The results showed that infarct volume increased from 12% of hemisphere in the wild-type to 30.9% in the mutant mice. In situ detection of superoxide revealed a significant elevation of superoxide production in the mutant mice. Mutation of Immp2l significantly increased the levels of cleaved caspase-3 in the cytosolic and nuclear fractions and apoptosis-inducing factor (AIF) in the nuclear fraction at 5 and/or 24 hrs of recovery. Mitochondrial respiratory rate, oxygen consumption and complex activities were decreased in the mutant mice at 5hrs of recirculation compared to wild-type mice.

Conclusions: Our results suggest that mutation of Immp2l gene increases ischemic brain damage by enhancing superoxide production, causing activation of mitochondria-initiated cell death pathways and damaging mitochondrial functional performance.

References: Lu-B, Poirier C, Gaspar T et al. Biology of Reproduction 2008; 78:601-610.

AcknowledgementsNational Institute of Health (7R01 DK075476) and the Golden Leaf Foundation.

278

DIRECT ARTERIOLAR CONTRIBUTION TO CORTICAL OXYGEN SUPPLY - EVIDENCE FROM THE GEOMETRY OF THE CORTICAL MICROCIRCULATION AND TISSUE METABOLIC STATES

G. Salahura, A. Sun, M. Jepson, **K. Kasischke**

Dept. of Neurology, Center for Neural Development and Disease, University of Rochester Medical Center, Rochester, NY, USA

Many models of neurovascular coupling are based on the notion that cortical oxygen demand is exclusively satisfied by oxygen diffusion from the capillary network. Frequently made assumptions are that the cortical oxygen distribution is relatively uniform and can be approximated by an average brain oxygen tension. However, direct electrode measurements have reported perivascular oxygen gradients at the cortical surface [1] for a long time. Recently, two independent studies using high-resolution optical measurements have confirmed the existence of steep perivascular oxygen gradients in the cortex [2,3] and implied pial and penetrating arterioles as direct, primary oxygen sources in addition to the capillary network. The former study was based on the two-photon lifetime imaging of phosphorescence quenching, the latter on two-photon imaging of cylindrical NADH tissue patches which are congruent with capillary free tissue cylinder surrounding penetrating arterioles. Notably, these capillary free peri-arteriolar tissue spaces also exist in the human cortex and they were described in vascular casts as early as 1930 [4]. Their existence has been confirmed [5] and their pathophysiological relevance can now be recognized in experimental stroke models [6,7]. Here, we follow up on our high-resolution in-vivo microangiographies in the mouse somatosensory cortex [3] and show that brain tissue cylinders surrounding cortical arterioles are generally capillary-depleted and that their radius is a function of the intravascular pO_2. We further find no evidence for anatomical capillary recruitment in the cortex. In summary, our results imply the permanent existence of significant oxygen gradients in the cerebral cortex which is a central element in the understanding of the possible purpose of the hemodynamic response [8].

References:

[1] Vovenko E, Pflügers Arch. 437, 617-23, 1999

[2] Sakadzić S et al, Nat. Methods 7, 755-9, 2010

[3] Kasischke KA et al JCBFM, advance online publication, Sept 22, 2010

[4] Pfeifer RA. Angioarchetiektonik des menschlichen Gehirns, Springer, Berlin, 1930.

[5] Duvernoy HM et al., Brain Research Bulletin 7, 519-79, 1981

[6] Pulsinelli WA & Duffy TE, Science 204,626-8, 1970

[7] Welsh et al., Science 198, 951-3

[8] Buxton F, Front. Neuroenergetics, 2:8, 2010

279

MEASUREMENT OF CEREBRAL GLUCOSE CONSUMPTION USING AN MR-COMPATIBLE APD-BASED HIGH RESOLUTION BRAINPET AND AN IMAGE DERIVED INPUT FUNCTION

H. Herzog[1], H. Hautzel[2], C. Weirich[1], L. Tellmann[1], E. Rota Kops[1], J. Scheins[1], N.J. Shah[1]

[1]Institute of Neuroscience and Medicine - 4, Forschungszentrum Juelich, [2]Department of Nuclear Medicine, University of Duesseldorf, Juelich, Germany

Introduction: Previous studies using the high resolution research tomograph (HRRT) demonstrated the feasibility of obtaining an image-derived input function (IDIF) from regions-of-interest (ROIs) placed over the carotid artery. Since the APD-based BrainPET developed by Siemens and operated within a standard Siemens 3T MAGNETOM Trio MR scanner offers a central resolution of 3mm, we explored the possibility of utilising an IDIF for dynamic FDG-studies acquired with the BrainPET.

Material and methods: We report on studies of the cerebral metabolic rate of glucose consumption (CMRglc) in three patients after intravenous injection of FDG. Starting with the bolus injection BrainPET data were acquired in listmode for 60 min and iteratively reconstructed using OP-OSEM. All corrections necessary for quantitative imaging were performed. The resulting dynamic image files consisted of 23 frames with eight frames per 5 sec after the tracer's entry into the brain and three frames per 10 min at the end. Venous blood samples were withdrawn every 10 minutes from 5 to 55 min to obtain venous plasma samples as well. The average ratio P/V of plasma to venous blood was 1.09. - The eight 5 sec frames were summed and bi-sided isocontour ROIs were defined over the carotid artery so that the corresponding time-activity curve represented the plasma input function after multiplication with P/V (IDIF-A). When the IDIF-As were compared to the venous plasma samples, they were about 40% lower than the plasma sample at 5 min, but reasonably similar at 55 min, that is, a spillover from the FDG accumulated in the brain must be assumed. To assess this spillover a background ROI was placed between the carotid arteries. Next, a correction was performed by fitting a corrected IDIF (= IDIF-B) to the venous blood samples and applying two fitting parameters representing the partial volume effect at the carotid artery and the spillover. At a further step, IDIF-C was created by replacing the data of IDIF-B from 5 to 55 min by the plasma blood samples. Finally, the IDIF-D was obtained by fitting the data of IDIF-C between the blood peak and 5 min to a three-exponential curve. - Parametric images of CMRglc were calculated using the Patlak plot implementation offered in PMOD together with dynamic FDG images and the four different IDIFs. Furthermore, the individual plasma glucose level of each patient was considered. The lumped constant was 0.52.

Results: Using IDIF-A directly derived from ROIs over the carotid arteries, the whole brain CMRglc (n=3) was 36.0 +/- 8.8 µmol/min/100g. The correction procedure to obtain IDIF-B yielded 0.46 +/- 0.02 for the PVE parameter and 0.75 +/- 0.14 for the spillover parameter. With IDIF-B as plasma input the whole brain CMRglc decreased by 21% compared to 16%, if IDIF-C and IDIF-D were used as plasma input.

Conclusion: The preliminary studies reported here show the feasibility of IDIF when using a high resolution MR-compatible BrainPET. The BrainPET allows an efficient sampling of the blood peak passing through the carotid artery by short time frames of a few seconds.

280

IN VIVO EVIDENCE FOR REDUCED STRIATAL VESICULAR MONOMINE TRANSPORTER (VMAT2) EXPRESSION IN COCAINE ABUSERS

B. Lopresti[1], D. Martinez[2], N.S. Mason[1], P. Keating[1], M. Himes[1], J.C. Price[1], C.A. Mathis[1], W.G. Frankle[3], R. Narendran[1]

[1]Radiology, University of Pittsburgh, Pittsburgh, PA, [2]Psychiatry, Columbia University, New York, NY, [3]Psychiatry, University of Pittsburgh, Pittsburgh, PA, USA

Aim: PET studies in cocaine abusers (CA) have shown that lower dopamine (DA) transmission in the striatum following a psychostimulant challenge is associated with higher relapse rates. Post-mortem studies have demonstrated reduced availability of VMAT2 in CA relative to healthy controls (HC). Indeed, lower VMAT2 availability in CA may explain this impairment of DA neurotransmission, as VMAT2 regulates the size of the vesicular DA pool that is available for stimulant-induced release. In this work, we used PET and the VMAT2 radioligand [^{11}C]-(+)-dihydrotetrabenazine (DTBZ) to assess in vivo VMAT2 availability in CA and confirm the post-mortem findings.

Methods: 12 cocaine abusers (CA) and 12 matched HC subjects were recruited (Age: 41±8(HC) vs. 43±8 (CA); Gender: 4F/8M per group; Smoking: 7 smokers/group). All CA were monitored for abstinence for a minimum of two weeks before they underwent scanning. [^{11}C]DTBZ binding potential (BP_{ND}) was measured in the three functional subdivisions of the striatum (limbic (LST), associative (AST), and sensorimotor striatum (SMST), as defined in Martinez 2003) with kinetic analyses based on the arterial input function (20/24 subjects) and the simplified reference tissue method (4/24). Occipital cortex was used as a non-specific reference region.

Results: No significant differences in [^{11}C]DTBZ occipital cortex (OCC) distribution volume V_T were observed between HC and CA groups (HC: 5.3±0.4; CA: 5.6±0.7; n=10/group, p=0.32). A repeated measures ANOVA demonstrated that CA had significantly lower [^{11}C]DTBZ binding in the striatal subdivisions relative to HC (region factor: $p< 0.0001$; group factor: $p< 0.0001$; group-by-region interaction: $p =0.14$). Significant reductions in [^{11}C]DTBZ BP_{ND} in CA were observed in the LST (-10%), AST (-16.3%), and SMST (-13.4%) compared to HC (see table).

Conclusion: The results of this study are consistent with post-mortem reports of lower VMAT2 availability in the striatum of CA subjects. The findings also suggest a compensatory downregulation of vesicular DA storage in response to chronic cocaine abuse and/or a loss of dopamine nerve terminals. Further research is necessary to understand the clinical relevance of this finding and its relation to relapse in abstinent CA subjects.

This work was supported by NIDA, ARRA, and NCRR/CTSA

Region	Controls, n=12	Cocaine Abusers, n=12

LST	2.2±0.3	1.9±0.2
AST	2.3±0.2	2.0±0.2
SMST	3.0±0.2	2.7±0.2

[[C-11]DTBZ BPND Measures]

281

EFFECTS OF MICROCOIL-INDUCED CAROTID STENOSIS ON LOCAL CEREBRAL BLOOD FLOW IN MICE

L. Ferrington[1], C.M. Gliddon[2], J. McCulloch[1], K.J. Horsburgh[1]

[1]University of Edinburgh, Edinburgh, UK, [2]University of Otago, Dunedin, New Zealand

Introduction and objective: Cognitive impairment associated with old-age is widely considered to be a part of normal aging; however these symptoms place an increasing burden upon society, both socially and economically. The mechanisms underlying this cognitive deterioration remain to be fully elucidated, but it is thought that chronic cerebral hypoperfusion may contribute to white matter abnormalities, which in turn may induce cognitive impairment in the elderly. Animal models of chronic cerebral hypoperfusion may be used to examine causative mechanisms linking reductions in blood flow with white matter pathology and subsequent cognitive impairment, and the insights into the processes of cognitive deterioration that may be gained could suggest novel targets for therapeutic intervention.

Aim: The aim of this study was to measure local cerebral blood flow (LCBF) in white and grey matter regions of the mouse brain following microcoil and sham surgery.

Methods: *Animals/Surgery:* Under isoflurane/oxygen anaesthesia, the left and right carotid arteries of 25-30g male C57bl6/ Jax mice (n=55) were wrapped around 0.18mm coils. Sham operated animals were identically prepared without placement of microcoils.

Measurement of Local Cerebral Blood Flow: [^{14}C]-iodoantipyrine autoradiographic imaging was used to measure lCBF in white and grey matter regions of the mouse brain in separate groups of animals 1 day and 30 days after surgery. lCBF was measured in 18 anatomically distinct and functionally diverse brain regions identified with reference to a mouse stereotaxic atlas.

Statistics: data were analysed using 1-way ANOVA with Newman-Keuls post-hoc test for multiple comparisons ($p< 0.05$).

Results: *Comparison between sham and microcoiled animals:* At 1 day post-surgery, there was a significant reduction in lCBF in the prefrontal cortex of the microcoiled group compared to shams, which returned to sham levels at 30 days post-surgery. However, at 30 days there was a significant difference in lCBF between sham and microcoiled animals in temporal cortex which was not present at 1 day. There was no significant difference in lCBF in any other brain region at either time point.

Comparison between microcoiled animals: There was a significant decrease in lCBF in 5 of the 18 brain regions at 1 day compared to 30 days in the microcoiled groups.

Comparison between shams: There was a significant decrease in lCBF in 7 of the 18 brain regions of interest at 1 day compared to the 30 day sham blood flow levels.

Conclusions: This study demonstrates a complex effect upon blood flow following the bilateral wrapping of microcoils around the common carotid artery and its corresponding sham surgery. Although the significant reduction in lCBF in temporal cortex at 30 days in the microcoiled animals compared with sham appears to replicate data generated by laser-Doppler studies, there was no difference in lCBF between sham and microcoiled animals in any other brain

region. Futhermore, there were significant reductions in lCBF at 1 day in some brain regions of both groups when compared to their 30 days counterpart, suggesting that the surgical procedure may in fact alter blood flow, rather than the implantation of microcoils per se.

283

ESTROGEN RECEPTOR BETA-MEDIATED ANTI-INFLAMMATORY EFFECT OF DIHYDROTESTOSTERONE DURING CYTOKINE-INDUCED INFLAMMATION IN HUMAN BRAIN VASCULAR SMOOTH MUSCLE CELLS

K.L. Osterlund[1,2], R.J. Handa[1], R.J. Gonzales[1]

[1]Basic Medical Sciences, University of Arizona, Phoenix, AZ, [2]Biomedical Sciences, Colorado State University, Fort Collins, CO, USA

Introduction: The pathophysiological processes that influence the progression and severity of cardiovascular disease remain an area of investigation. Studies suggest that vascular inflammation plays a key role in the etiology of cardiovascular disease, particularly stroke[1]. Previous studies have demonstrated that gonadal steroids modulate vascular inflammation. Consistent with this, our recent studies show that, in human vascular smooth muscle (VSM) cells, chronic treatment with the potent androgen, dihydrotestosterone (DHT), decreases expression of the pro-inflammatory mediator cyclooxygenase-2 (COX-2) during cytokine-induced inflammation or ischemia. This occurs through an androgen receptor (AR)-independent mechanism[2,3] since it cannot be blocked by co-treatment with the anti-androgen, bicalutamide. Because estradiol has also been shown to reduce vascular inflammation[4], we hypothesized that this was a mechanism for DHT's action. Although DHT cannot be aromatized to estradiol in the same fashion that testosterone can, it can be converted to 5alpha-androstane- 3beta,17beta-diol (3β-diol) which is a selective estrogen receptor (ER) β ligand[5]. Blood vessels express AR[6], ERα[6,7], ERβ[7], and 3beta-hydroxysteroid dehydrogenase[8] (the enzyme that converts DHT to 3β-diol) and the presence of these receptors and enzyme allows for potential androgenic and estrogenic effects which can influence vascular inflammation.

Objective: Determine if DHT decreases cytokine-induced COX-2 expression in brain VSM cells via metabolism to 3β-diol and subsequent activation of ERβ.

Methods: Human brain VSM cells were treated (18h) with vehicle, DHT (10nM) or 3β-diol (10nM) then exposed to the cytokine IL-1β (6h, 5ng/ml) in the continued presence of hormone. In some experiments 1h prior to DHT treatment, one of the following steroid hormone receptor antagonists was added to the treatment media: the AR antagonist bicalutamide (1μM), the non-selective ERα/ERβ antagonist ICI 182,780 (1μM), or the selective ERβ antagonist PHTPP (1μM). All cell treatments were performed in media containing 2% charcoal stripped FBS. Following hormone/drug treatment, whole cell lysate was collected and COX-2 levels were measured via Western blot.

Results: Both DHT and its estrogenic metabolite 3β-diol reduced IL-1β-induced increases in COX-2 expression. The AR antagonist did not block the effect of DHT whereas both the non-selective ER antagonist and the selective ERβ-antagonist inhibited the effect of DHT.

Conclusion: DHT appears to be protective against cerebrovascular inflammation via conversion to 3β-diol and subsequent activation of ERβ.

References: [1] del Zoppo and Mabuchi 2003 *Journal of Cerebral Blood Flow & Metabolism*. [2]Osterlund et al 2010 *AJP Endocrinology & Metabolism*. [3]Osterlund and Gonzales unpublished data. [4]Sunday et al 2006 *AJP Endocrinology & Metabolism*.[5]Handa et al 2008 *Hormones & Behavior*. [6]Gonzales et al 2007 *Journal of Cerebral Blood Flow & Metabolism*. [7]Shih et al 2008 *Journal of Neurosurgery*. [8]Nakamura et al 2005 *Endocrine Journal*.

Support: *AHA KLO, UA Sarver Heart Center Grant KLO*

289

COMPARISON OF HYPERTENSION, HYPERVOLEMIA, AND TRANSFUSION TO AUGMENT CEREBRAL OXYGEN DELIVERY AFTER SUBARACHNOID HEMORRHAGE

R. Dhar[1], M. Scalfani[1], A. Zazulia[1,2], T. Videen[1,2], C. Derdeyn[1,2,3], M. Diringer[1,3]

[1]Neurology, [2]Radiology, [3]Neurological Surgery, Washington University in St. Louis School of Medicine, Saint Louis, MO, USA

Introduction: Critical reductions in cerebral blood flow (CBF) and oxygen delivery (DO_2) underlie the development of delayed cerebral ischemia (DCI) after subarachnoid hemorrhage (SAH). If DO_2 is not promptly restored then irreversible injury (i.e. cerebral infarction) may result. Induced hypertension and hypervolemia, the primary means of treating DCI, aim to raise CBF; transfusion has been proposed as an alternate strategy, primarily to improve DO_2. The relative effects of these interventions on CBF and DO_2 have not been assessed, specifically their ability to restore DO_2 to regions where it is impaired.

Objective: Compare the ability of hypertension, hypervolemia, and transfusion to improve DO_2 and minimize proportion of the brain with impaired oxygen delivery.

Methods: We analyzed data from three prospective studies employing ^{15}O-PET imaging to measure the effects of:

1) a fluid bolus of 15 ml/kg normal saline (n=9);

2) raising mean arterial pressure 25% (n=12);

3) transfusing one unit of red blood cells (n=17), to aneurysmal SAH patients at risk for DCI.

All patients had PET at baseline and then immediately after the intervention to measure CBF and DO_2. We compared change in global DO_2 between groups as well as response in regions with low DO_2

at baseline (defined as < 4.5 ml/100g/min), using repeated measures ANOVA.

Results: The three groups were similar except that the fluid bolus cohort had more patients with symptoms of ischemia and lower baseline CBF. Global DO_2 did not rise significantly after any of the interventions, except when transfusing patients with hemoglobin < 9 g/dl. All three interventions improved CBF and DO_2 to regions with low baseline DO_2, but the rise in DO_2 was greater after transfusion (+23%) vs. hypertension (+14%) vs. hypervolemia (+10%); $p< 0.001$. Transfusion also resulted in a greater reduction in brain regions with low DO_2 (by 47% vs. 7% for fluid bolus and 12% with hypertension) but this difference was not significant.

Conclusions: Induced hypertension, hypervolemia, and transfusion all improve DO_2 to vulnerable brain regoins at risk of ischemia after SAH. However, transfusion may provide the greatest benefit, especially among patients with anemia. The clinical significance of this difference remains to be established.

295

REDUCTION OF THE LONG-TERM CONSEQUENCES OF AXONAL INJURY BY MINOCYCLINE FOLLOWING CLOSED HEAD INJURY IN MICE: POTENTIAL ROLE OF SAPPA

E. Siopi, A.H. Cho, S. Homsi, N. Croci, M. Plotkine, C. Marchand-Leroux, M. Jafarian-Tehrani

EA4475 Pharmacology of Cerebral Circulation, Paris Descartes University-UFR Pharmacy, Paris, France

Introduction: Traumatic axonal injury (TAI) is a detrimental consequence of traumatic brain injury (TBI) that refers to extensive lesions in white matter tracts and for which no treatment is available. It has been recently reported that an endogenous neuroprotector, the soluble form a of the amyloid precursor protein (sAPPa) is able to reduce TAI [1]. However, the emergent post-traumatic neuroinflammatory environment compromises sAPPa production [2] and may promote TAI development and subsequent white matter atrophy. Hence, the aim of this study was to examine the effects of an anti-inflammatory drug, minocycline, on post-TBI sAPPa production as well as on the long-term TAI consequences.

Methods: The mouse model of TBI by mechanical percussion was applied on anesthetized Swiss mice, as previously described [3]. Minocycline was injected (i.p.) at 5 min (90 mg/kg), 3 h and 9 h (45 mg/kg) post-TBI [3]. The ELISA and the cresyl violet staining were used to measure sAPPa production and TAI-induced atrophies, respectively. Immunohistochemistry of GFAP and CD11b was also used to measure gliar scar formation.

Results: A decrease of sAPPa production was observed at 24h post-TBI ($P < 0.001$), that was significantly attenuated by minocycline ($P < 0.01$). A corpus callosum atrophy ($P < 0.05$), striatal atrophy ($P < 0.001$) and ventriculomegaly ($P < 0.01$), accompanied by an increased GFAP and CD11b immunolabeling ($P < 0.01$) were observed at 3 months post-TBI. All the above consequences were significantly reduced by minocycline.

Conclusion: Inhibition of the acute phase of post-TBI neuroinflammation by minocycline is associated with the sparring of sAPPa and the protection of the white matter tracts in the long-term, emphasizing the potential role of minocycline as a promising neuroprotective treatment in TBI [4], and highlighting sAPPa as a therapeutic target.

(1) Thornton et al., Brain Res 2006; 1094:38-49.

(2) Lesné et al., J Neurosci. 2005; 25(41):9367-77

(3) Homsi et al., J Neurotrauma 2010; 27:911-921

(4) www.clinicaltrials.gov clinical trial with minocycline in head injured patients (USA, février 2010)

297

VASCULAR ENDOTHELIAL GROWTH FACTOR REGULATES THE MIGRATION OF OLIGODENDROCYTE PRECURSOR CELLS

K. Hayakawa, L.-D.D. Pham, A.T. Som, B.J. Lee, S. Guo, E.H. Lo, **K. Arai**

Radiology and Neurology, Massachusetts General Hospital/Harvard Medical School, Charlestown, MA, USA

Objectives: Oligodendrocyte precursor cells (OPCs) are widely distributed in adult brain. After brain injury, OPCs may contribute to myelin repair. However, the precise mechanisms remain unknown. In gray matter, vascular endothelial growth factor (VEGF) is an essential mediator for neurogenesis and angiogenesis. We investigated if VEGF might also affect white matter recovery by regulating OPC function.

Methods: The mouse middle cerebral artery occlusion-reperfusion model and the lysophosphatidylcholine-induced focal demyelination model were used to induce white matter injury in vivo. Cultured OPCs were prepared from brain cortex of rat neonates.

Results: In both mouse white matter injury models, the corpus callosum was damaged and OPCs migrated toward the injured area. Immunostaining demonstrated that OPCs expressed VEGF-receptor2/KDR/Flk-1. Cultured OPCs were used to investigate how VEGF may regulate OPC function. VEGF did not promote proliferation or differentiation in OPC cultures, but VEGF significantly promoted OPC migration in a concentration-dependent manner (Figure). In addition, VEGF-treated OPCs showed reorganization of the actin cytoskeleton especially in their processes. VEGF-induced migration and actin reorganization were inhibited by co-treatment with a neutralizing antibody for Flk-1. VEGF also prompted the binding of FAK with paxillin. A FAK inhibitor PF573228 reduced VEGF-induced OPC migration. Finally, we assessed the involvement of reactive oxygen species (ROS) in VEGF-induced OPC migration. VEGF rapidly produced ROS in OPCs, and VEGF-induced OPC migration was increased when antioxidants were deprived from the culture media.

Conclusions: After stroke and brain injury, VEGF may enhance white matter repair by promoting OPC migration. The underlying mechanisms involve the activation of Flk-1 receptors, FAK-mediated cytoskeletal responses, and free radical signaling. These results demonstrate that VEGF not only mediates neurogenesis and angiogenesis in gray matter, but also plays a novel role in OPC homeostasis for white matter maintenance and repair.

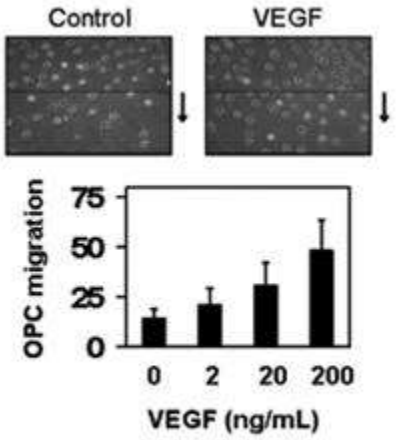

Figure: VEGF promoted OPC migration.

[VEGF and OPC migration]

298

MINOCYCLINE REDUCES THE OLFACTORY BULB LESIONS AND OLFACTORY IMPAIRMENT INDUCED BY TRAUMATIC BRAIN INJURY IN MICE : LONG-TERM STUDY

E. Siopi, S. Calabria, M. Plotkine, C. Marchand-Leroux, M. Jafarian-Tehrani

EA4475 Pharmacology of Cerebral Circulation, Paris Descartes University-UFR Pharmacy, Paris, France

Introduction: Olfactory dysfunction can often arise after traumatic brain injury (TBI) and, while it has a considerable impact on daily life, no neuroprotective treatment is available. Olfactory bulb lesions result from the immediate loss of olfactory neurons, due to the site and severity of the mechanical insult. However, there is increasing awareness that diseases involving persistent neuroinflammation demonstrate marked deterioration of the olfactory bulbs [1]. Since TBI triggers multiple neuroinflammatory cascades that persist up to months or years after TBI, we examined the effects of an acute anti-inflammatory treatment with minocycline on short and long-term post-TBI olfactory behaviour, and on olfactory bulb integrity at 12 weeks post-TBI.

Methods: The mouse model of TBI by mechanical percussion was applied on anesthetized Swiss mice, as previously described [2]. The treatment protocol included three injections of minocycline (i.p.) at 5 min (90 mg/kg), 3 h and 9 h (45 mg/kg) post-TBI [2]. An olfactory behaviour test, based on the innate aversion to an unpleasant odor (acetic acid), was run from 1 up to 12 weeks post-TBI. At 12 weeks post-TBI, the mice were anaesthetized and sacrificed by transcardial perfusion (PFA 4%). Digital images of the whole brains were taken and the surface of ipsilateral and contralateral olfactory bulbs was measured using ImageJ software (NIH).

Results: TBI induced a deficit in olfactory behaviour that was significant from 2 ($P< 0.05$) to at least 12 weeks ($P< 0.001$) post-TBI, reflected by a diminution of the innate aversion to acetic acid. Additionally, a substantial post-TBI olfactory bulb atrophy was observed at 12 weeks post-TBI ($P< 0.001$) that was strongly correlated with the olfactory impairment ($n = 33$; $r = -0.62$; $P=0.001$). The acute post-TBI treatment with minocycline was able to attenuate both the behavioural dysfunction ($P< 0.01$) and the olfactory lesions ($P< 0.01$) in the long-term after TBI.

Conclusion: Inhibition of the acute phase of post-TBI neuroinflammation by minocycline is associated with the sparring of olfactory bulb tissue and a consequent improvement of olfactory behaviour. These results emphasize the potential role of minocycline as a promising neuroprotective agent [3] for the treatment of olfactory lesions and deficits in TBI.

(1) Doty et al., Annu. Rev. Psychol. 2001; 52: 423-452.

(2) Homsi et al., J Neurotrauma 2010; 27: 911-921.

(3) *www.clinicaltrials.gov clinical trial with minocycline in head injured patients (USA, février 2010).*

300

IMAGING DNA AND GENE ACTIVATOR PROTEIN INTERACTION BY MRI IN LIVE BRAINS

P.K. Liu, C.H. Liu, J.Q. Ren, C.-M. Liu

Radiology/A.A. Martinos Center for Biomedical Imaging, Mass General Hospital/Harvard Medical School, Charlestown, MA, USA

Protein-DNA interaction is an important step in epigenetic signal transduction. Short DNA mimicking binding domain of activator protein-1 (AP1) has been used as a decoy to interfere the interaction between AP1 protein and mouse genome, but its intracellular transport mechanism is not clear. Here, we aimed to visualize and investigate intracellular transport of AP1-binding DNA and the effect of such DNA aptamer upon amphetamine (AMPH)-induced hyper-activities. Only double-stranded DNA aptamer with AP1 consensus sequence binds to AP1 protein. To visualize protein-DNA interaction in vivo, we labeled a short AP1-targeting DNA with superparamagnetic iron oxide nanoparticles (SPION-AP1) for magnetic resonance imaging (MRI). We measured changes in R2* value, or the frequency of T2 signal reduction, to represent SPION-AP1 retention. After intracerebroventricular (0.04 mg Fe per kg) or intraperitoneal (4 mg Fe per kg to mice with BBB-bypass) injection to C57black6 mice, we observed SPION-AP1 retention by MRI in normal mice but not in mice with a dominant negative mutation of activator protein-1. Additionally, we demonstrated the utility of SPION-AP1 in an MR imaging platform for in vivo detection of altered protein-DNA interaction associated with psychostimulant exposure in C57black6 mice. We also observed that AP1-binding DNA, at a dose of 100-fold of imaging dose, suppressed amphetamine-induced hyper-activity. When AP1-binding DNA was labeled with gold or SPION and delivered to the brain for intracellular localization in tissue samples under electron microscopy, we observed electron-dense particles in neuronal endosomes and endoplasmic reticulum where gene translation occurs. The data suggest that neural cells retained SPION-AP1 as the result of SPION-AP1 binding to AP1 protein and excluded SPION-AP1 rapidly when mutant AP1 protein is present. Together, we demonstrated transport of intracellular MRI probe for binding to AP1 protein and such binding provides a window for MRI. This technology is based on the capability of normal active brains to rapidly exclude non-targeting (unbound) MR probe and retain targeting (target bound) MR probe thereby provide an extended window for MRI assessment of mRNA level.

302

PHENYLEPHRINE PRESERVES AUTOREGULATION AFTER FEMALE TBI BUT AGGRAVATES DYSREGULATION IN MALES THROUGH K CHANNEL INHIBITION VIA ET-1, ERK, AND O2-

W.M. Armstead[1], J. Riley[1], C. Kreipke[2], M. Vavilala[3]

[1]University of Pennsylvania, Philadelphia, PA, [2]Wayne State University School of Medicine, Detroit, MI, [3]University of Washington School of Medicine, Seattle, WA, USA

Objectives: Traumatic brain injury (TBI) contributes to morbidity in children and boys are disproportionately represented. Hypotension is common and worsens outcome after TBI. ERK mitogen activated protein kinase (MAPK) is upregulated more in males and reduces CBF after fluid percussion brain injury (FPI). Increased cerebral perfusion pressure (CPP) via phenylephrine (Phe) sex dependently improves impairment of cerebral autoregulation after FPI through modulation of ERK MAPK upregulation, which is aggravated in males, but blocked in females. Activation of ATP and Calcium sensitive (Katp and Kca) channels produce cerebrovasodilation and contribute to autoregulation, both impaired after FPI. Endothelin-1 (ET-1) contributes to impaired autoregulation of K channel function via release of superoxide (O2-). This study hypothesized that K channel function impairment and thereby dysregulation after FPI will be prevented by Phe in a sex dependent manner through modulation of ET-1, O2- , and ERK MAPK upregulation.

Methods: Pial artery diameter was determined before and after FPI in untreated, pre- and post-injury (30 min before or 30 min after) Phe, BQ 123, U 0126, and polyethylene glycol superoxide dismutase and catalase (PEGSOD), ET-1, ERK antagonists and free radical scavenger) treated male and female newborn pigs equipped with a closed cranial window. CSF ET-1 and ERK were quantified by ELISA. Data (n=5) were analyzed by repeated measures ANOVA, with significance determined at p less than 0.05.

Results: The Katp channel agonists cromakalim and calcitonin gene related peptide (CGRP) and Kca agonist NS 1619 produced vasodilation which was impaired more in males than females after FPI. Phe pre- and post-treatment prevented reductions in cerebrovasodilation to cromakalim, CGRP, and NS 1619 in females, but further reduced dilation to these K channel agonists in males after FPI. Co-administration of BQ-123, U 0126, or PEGSOD with Phe fully restored dilation to cromakalim, CGRP, and NS 1619 in males after FPI, but had no further effect on K channel agonist mediated dilation after FPI in females. Similar effects were noted for pial artery dilation during hypotension. CSF ET-1 release was greater in males than females after FPI, which was blunted by PHE in females, but aggravated in males. CSF ERK upregulation was blocked by BQ 123 and PEGSOD.

Conclusions: These data indicate that elevation of CPP with Phe sex dependently prevents impairment of cerebral autoregulation during hypotension after FPI through modulation of ET-1 release and subsequent sequential O2- and ERK MAPK upregulation mediated impairment of Katp and Kca induced cerebrovasodilation. These data suggest the role for sex dependent mechanisms in cerebral autoregulation after pediatric TBI.

304

OLIGODENDROCYTES PRODUCE MATRIX METALLOPROTEINASE-9 IN RESPONSE TO INTERLEUKIN-1BETA DURING FOCAL WHITE MATTER INJURY

L.-D.D. Pham, K. Hayakawa, M.-N. Nguyen, A.T. Som, S. Guo, E.H. Lo, **K. Arai**

Radiology and Neurology, Massachusetts General Hospital/Harvard Medical School, Charlestown, MA, USA

Objectives: White matter damage is a clinically important part of stroke. However, compared to the mechanisms of neuronal injury in gray matter, white matter pathophysiology remains relatively understudied and poorly understood. Both interleukin-1beta (IL-1beta) and matrix metalloproteinase-9 (MMP-9) are well known deleterious factors to lead neuronal damage during stroke. Here, we ask whether these mediators may also play a role in oligodendrocyte responses after white matter injury.

Methods: Lysophosphatidylcholine(LPC)-induced focal demyelination model was used to induce white matter injury in vivo. Cultured oligodendrocytes were prepared from brain cortex of rat neonates. Standard molecular techniques were used to assess cell signaling responses.

Results: Stereotaxic injection of LPC into the corpus callosum induced focal demyelination of the damaged white matter tracts. Western blot analysis and immunostaining showed that both IL-1beta and MMP-9 expression were increased in the damaged area. Importantly, some of MMP-9 positive cells were overlapped with olig2 staining, suggesting that oligodendrocytes directly produced MMP-9 in this model of focal white matter damage. Next, we used cultured oligodendrocytes to ask how IL-1beta upregulates MMP-9 in these cells. Our oligodendrocyte cultures expressed the mature oligodendrocyte markers Olig2 and MBP. Gelatin zymography showed that MMP-9 secretion was observed 48 hrs after IL-1beta treatment (Figure). WST and LDH assays confirmed that IL-1beta treatment did not induce oligodendrocyte death. Because a MEK inhibitor U0126 inhibited IL-1beta-induced MMP-9 secretion, MEK/ERK pathway might be involved in this phenomenon.

Conclusions: IL-1beta and MMP-9, well known as deleterious factors in stroke, were upregulated in demyelinated tracts after focal white matter injury in vivo. IL-1beta induced MMP-9 production via MEK/ERK pathway in cultured oligodendrocytes. White matter is susceptible to ischemic stress and white matter damage is a clinically important part of stroke. Damage to oligodenrocytes causes loss of myelin synthesis and interruption of proper axonal function. The current results suggest that blocking the ERK signaling pathway may be a potential therapeutic approach for interrupting the IL-1beta-MMP-9 cascade and rescuing white matter damage after stroke and brain injury.

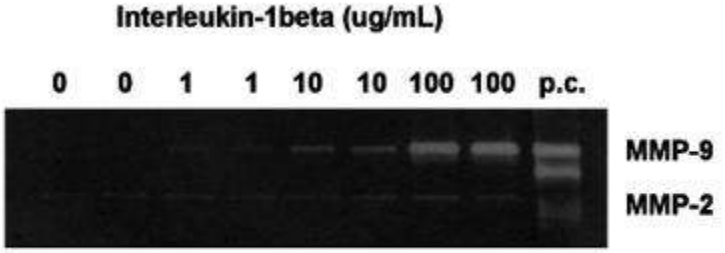

Figure: Gelatin zymography showed that IL-1beta induced MMP-9 secretion in oligodendrocyte cultures.

[IL-1beta and MMP-9]

305

DEEP HYPOTHERMIA ACTIVATES THE SUMO CONJUGATION PATHWAY

W. Paschen, L. Wang, M. Qing, W. Yang, G.B. Mackensen

Department of Anesthesiology, Duke University Medical Center, Durham, NC, USA

Objectives: Various cardiovascular operations involve use of cardiopulmonary bypass (CPB) that requires a period of circulatory arrest. To protect organs from damage induced by ischemia, surgery is usually carried out during deep hypothermia. Recently, we have shown that deep hypothermic cardiopulmonary bypass (DHCPB) activates the small ubiquitin-like modifier (SUMO) conjugation pathway (1), and that SUMO conjugation is also massively activated after cerebral ischemia (2,3). Here we describe in more detail the duration and extent of hypothermia required to activate this process.

Materials: Anesthetized male 12-14 weeks-old rats (n=5/group) were subjected to CPB as decribed before (3). Control animals were kept at 37^{o}C during CPB, while body temperatures of experimental animals was reduced to 30, 24 or 18^{o}C. At the end of the experiments, brains were quickly removed, frozen and dissected into the cortex, striatum, hippocampus and cerebellum. Hypothermia-induced changes in levels of SUMO conjugated proteins were evaluated by Western blotting, using SUMO1 and SUMO2/3 specific antibodies, and image analysis. The high molecular weight area in each lane was cropped and analyzed. Membranes were then stripped and reprobed for beta-actin as loading control. For quantification, levels of SUMO conjugated proteins were related to beta-actin levels. Statistical analysis was performed using ANOVA followed by Fisher´s PLSD test (*, **, ***: $p< 0.05$, $p< 0.01$, $p< 0.001$).

Results: DHCPB induced a significant rise in levels levels of SUMO1 and SUMO2/3 conjugated proteins and decrease in levels of free SUMO1 and SUMO2/3 in all brains regions investigated. Examples of hypothermia-induced changes in levels of SUMO2/3 conjugated proteins in the hippocampus are illustrated in Figures 1 + 2.

Figure 1

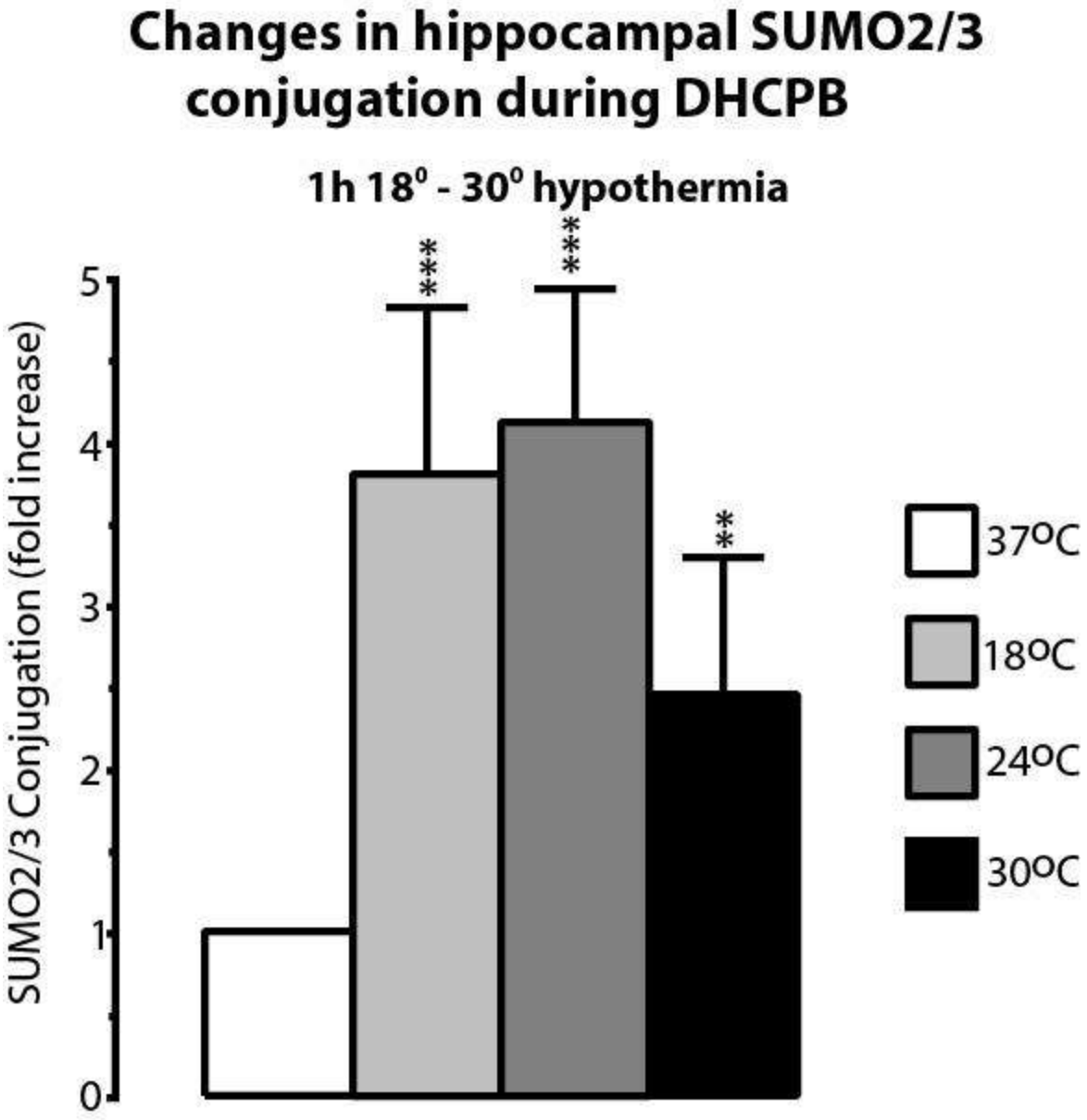

[Figure 1]

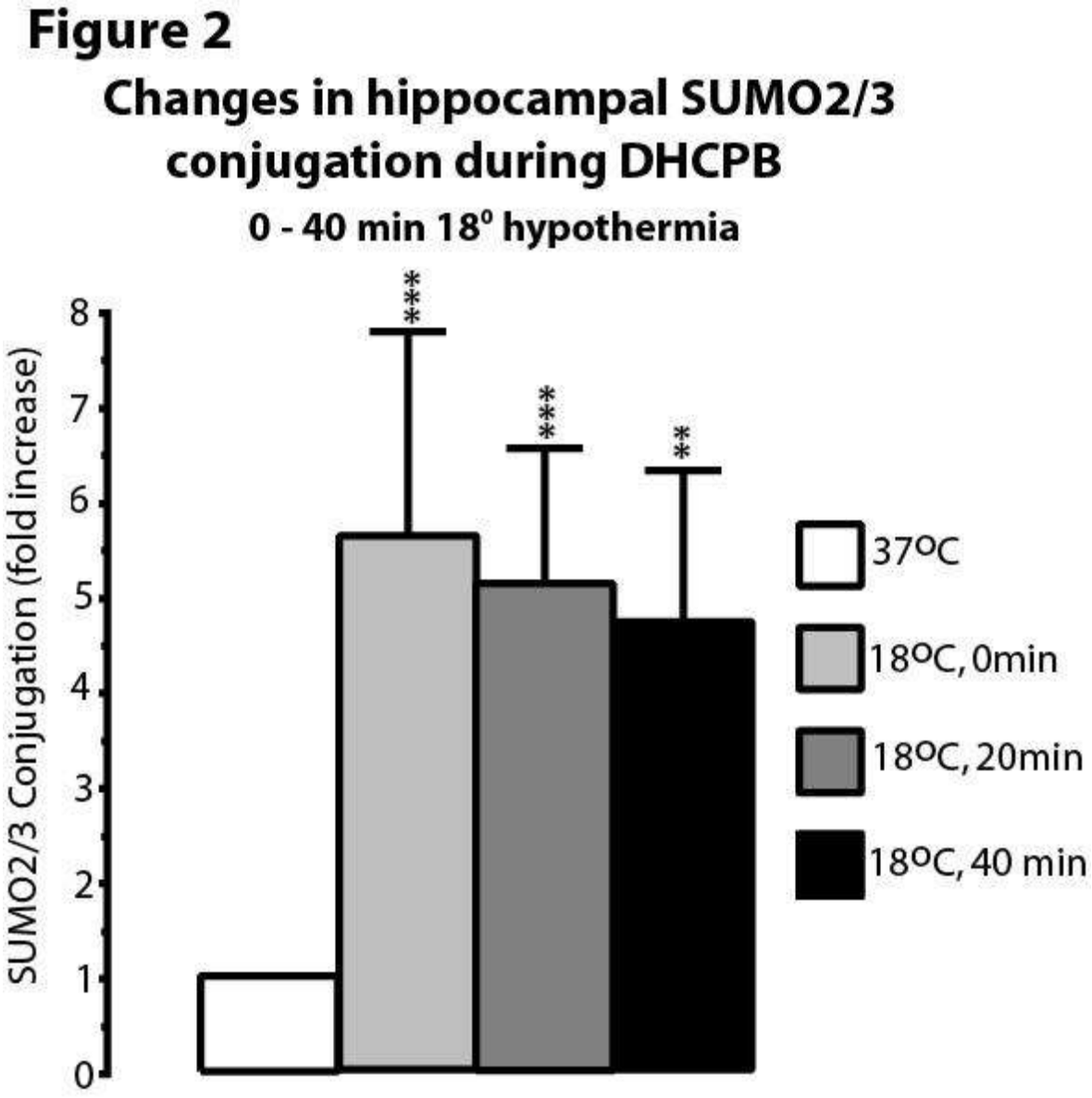

[Figure 2]

In the hippocampus, 1h 18°C and 24°C hypothermia induced an about 4-fold increase in levels of SUMO2/3 conjugated proteins (Figure 1), and this process was already fully activated immediately after the brain temperature had reached 18°C (Figure 2, 0 min). This suggests that hypothermia-induced activation of the SUMO conjugation pathway is a fast stress response.

Conclusion: Many SUMO conjugation proteins are transcription factors or other nuclear proteins involved in gene expression and genome stability. A substantial change in levels of SUMO conjugated proteins can therefore be expected to have a major impact on the fate of cells. We have found that SUMO2/3 conjugation protects neurons from damage induced by ischemia-like conditions (Daetwyler et al., Brain ´11). We therefore conclude that the rise in levels of SUMO conjugated proteins observed during DHCPB may play a major role in the protective effects provided by hypothermia. The SUMO conjugation pathway could become an

exciting new target for therapeutic intervention by providing a means of increasing the resistance of neurons to a transient interruption of blood supply.

References:

1) Yang et al., J Cereb Blood Flow Metabol. 2009; 29:886-890.

2,3) Yang et al., J Cereb Blood Flow Metabol 2008; 28:269-279 + 892-896.

4) Jungwirth et al., J Thorac Cardiovasc Surg 2006; 131:805-812.

306

PROTECTIVE EFFECT OF ETHANOL IN RAT WITH TRANSIENT CEREBRAL ISCHEMIA

X. Ji, **Y. Wang**, F. Wang, Y. Luo, X. Liu, F. Ling, Y. Ding

Cerebral Vascular Disease Institute, XuanWu Hospital, Capital Medical University, Beijing, China

Objective: Numerous studies have shown that mild to moderate alcohol consumption is inversely associated with risk of ischemic stroke, suggesting ethanol may have a neuroprotective effect. We want to test this hypothesis in a rat transient cerebral ischemia model, and further characterize the properties of ethanol as a possible treatment for acute ischemic stroke.

Methods: Sprague-Dawley rats were subjected to 2 hours middle cerebral artery occlusion. Three sets of experiments were conducted (1) to test whether various doses of ethanol (0.5g/kg, 1.0 g/kg, 1.5 g/kg) has neuroprotective effect; (2) to test whether the protective effect of ethanol can be improved by pairing it with hypothermia; and (3) to test whether ethanol affects intracranial hemorrhage after administration of recombinant tissue plasminogen activator (rtPA) or urokinase (UK).

Results: Dose of 1.5g/kg ethanol was effective in reducing infarct volume and behavioral dysfunction after transient middle cerebral artery occlusion. The protective effect of ethanol could be further improved by pairing it with hypothermia, and ethanol did not increase cerebral hemorrhage when given in combination with rtPA or UK.

Conclusions: Our study suggests that a dose of 1.5g/kg ethanol administrated after the onset of reperfusion has neuroprotective effect, can be added to hypothermia therapy, and do not interfere with or complicate rtPA or UK therapy.

308

REACTIVE ASTROCYTES EXPRESS HIGH-MOBILITY GROUP BOX 1 IN WHITE MATTER STROKE

K. Hayakawa, L.-D.D. Pham, **K. Arai**, E.H. Lo

Radiology and Neurology, Massachusetts General Hospital/Harvard Medical School, Charlestown, MA, USA

Objectives: Astrocytes comprise the most numerous non-neuronal cell type in mammalian brain. Within a few hours of virtually any type of brain injury, surviving astrocytes in the affected region become hypertrophic and proliferate, a process termed reactive astrogliosis. It was recently discovered that reactive astrocytes may secrete a nuclear protein called high-mobility group box 1 (HMGB1). HMGB1 is a multifunctional molecule that can also promote neurovascular remodeling and recovery after neuronal injury. Here, we investigated how HMGB1 may be involved in reactive gliosis in white matter.

Methods: Lysophosphatidylcholine(LPC)-induced focal demyelination model was used to induce white matter injury in vivo. Cultured astrocytes were prepared from brain cortex of rat neonates.

Results: Stereotaxic injection of LPC into the corpus callosum induced myelin loss within 2-5 days. Immunostaining with anti-GFAP antibody revealed that reactive gliosis occurred in the injured area by 5 days after LPC injection. Importantly, these GFAP-positive cells expressed HMGB1 (Figure). To further dissect the underlying mechanisms, we next used an interleukin-1beta (IL-1beta)-induced model of reactive astrocytes in culture. Exposure of rat primary astrocytes to IL-1beta for 24 h elicited a dose-dependent HMGB1 response. Immunostaining and western blots of cell lysates showed increased intracellular levels of HMGB1. MAP kinase signaling was involved. Levels of phospho-ERK were increased by IL-1beta, and the MEK/ERK inhibitor U0126 decreased HMGB1 upregulation in the stimulated astrocytes. Since HMGB1 is a nuclear protein, the role of the nuclear protein exporter CRM1 was assessed as a candidate mechanism for linking MAP kinase signaling to HMGB1 release. IL-1beta increased CRM1 expression in concert with a translocation of HMGB1 from nucleus into cytoplasm. Blockade of IL-1b-stimulated HMGB1 release with U0126 was accompanied by a downregulation of CRM1.

Conclusions: Expression of HMGB1 was increased in reactive astrocytes after white matter injury in vivo. Cell culture experiments showed that the ability of reactive astrocytes to upregulate HMGB1 involved inflammatory cytokine signaling and activation of ERK signaling and CRM1 nuclear protein export mechanisms. Traditionally, it was assumed that reactive astrocytes contribute to glial scarring that impedes neuronal remodeling and recovery. Our data here suggest that reactive astrocytes may also contribute to HMGB1-mediated recovery and repair after white matter injury.

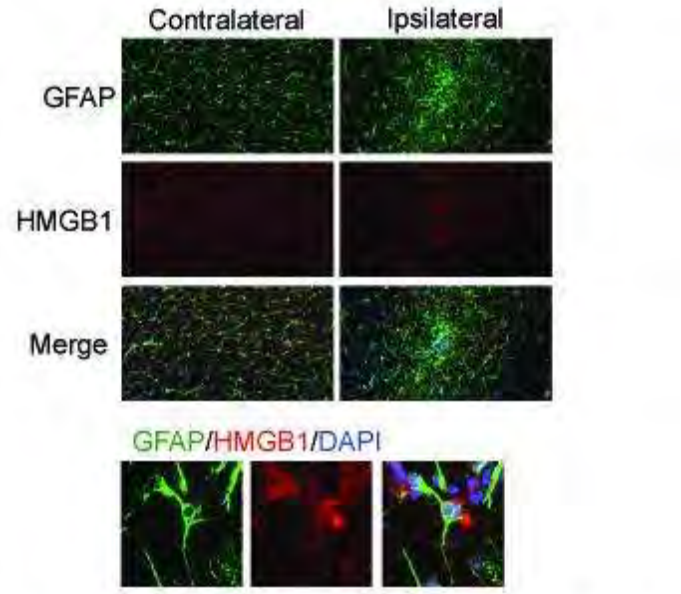

Figure: Reactive gliosis occurred in the injured area by 5 days after LPC injection into the corpus callosum. These GFAP-positive cells expressed HMGB1.

[reactive astrocyte and HMGB1]

309

NEUROVASCULAR COUPLING AT DIFFERENT LEVELS OF CEREBRAL ISCHEMIA IN A RAT MODEL

W.B. Baker[1], Z. Sun[2,3], T. Hiraki[2], M. Reivich[2], A.G. Yodh[1], J.H. Greenberg[2]

[1]Physics and Astronomy, [2]Neurology, University of Pennsylvania, Philadelphia, PA, USA, [3]Neurosurgery, General Hospital of Chinese PLA, Beijing, China

Objectives: In this study, we monitored the cerebral blood flow, oxygenation, metabolic, and electrical functional responses to forepaw stimulation in rats at different levels of cerebral ischemia. We are particularly interested in differences that arise between hemodynamic and electrical responses as the blood flow to the brain is lowered.

Methods: Graded ischemia was induced in 21 Sprague-Dawley rats with unilateral carotid, bi-lateral carotid, and bi-lateral carotid with uni-lateral vertebral artery occlusion. The drops in cerebral blood flow due to these occlusions were heterogeneous across rats, enabling us to observe functional responses at many different flow levels from no ischemia to severe ischemia. In this model, we regard flow as the fundamental variable affecting functional responses. Our functional stimulation protocol consisted of a 3 Hz, 1.5 mA, 4 second duration pulse train sent to the rat's forepaw every 30 seconds. For each condition of each animal, 32 pulse trains were delivered. We measured changes in surface cerebral blood flow and blood oxygenation using the independent imaging techniques of laser speckle flowmetry (LSF) (1) and optical intrinsic spectroscopy (OIS) (2). A compartmental model was employed to calculate changes in cerebral oxygen metabolism ($CMRO_2$) from the measured hemoglobin and flow changes (3). For all of the hemodynamic parameters, we quantified the functional response by taking the peak value reached due to the forepaw stimulation minus the baseline value (average over the 5-second pre-stimulation interval) over a ROI established by a correlation coefficient threshold of 0.8 with the stimulus (4). We also measured the somatosensory evoked potential (SEP) with an electrode placed at the edge of the forepaw activation area. The difference between the first positive and negative peaks in the SEP signal quantifies the strength of the electrical response. To compare across animals, all of the hemodynamic and electric responses for each animal were normalized by the average pre-ischemic response.

Results: Figure 1 shows the mean hemodynamic (i.e., flow, total-hemoglobin (HbT), oxy-hemoglobin (HbO), deoxy-hemoglobin (HbR), and the metabolic rate of oxygen ($CMRO_2$)) and electrical responses of the rats as a function of flow level. Here, the flow levels are discretized into bins of width 10 percentage points of the pre-ischemic level, asterisks indicate statistically significant differences (0.05 Bonferroni level) from the SEP response at the given flow level, and the lines on top of the bars are standard deviations.

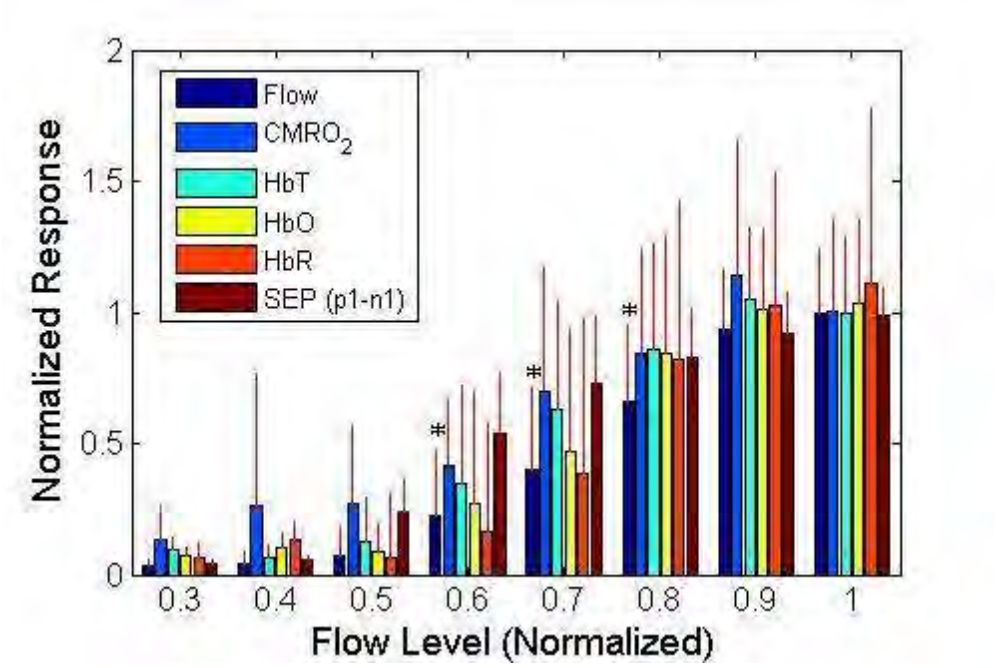

[Figure 1]

Conclusion: We found that the functional flow response to forepaw stimulation in rats decays more rapidly than the electrical response, but the metabolic response does not. In other words, during functional stimulation the brain can sustain neuronal firing and oxygen consumption at more severe ischemic levels than the vasculature's ability to locally increase flow.

References:

1. Briers, J D. 2001, Physiol. Meas., 22, R35-R66.

2. Dunn, A K, et al. 2003, Opt. Lett., 28, 28-30.

3. Dunn, A K, et al. 2005, NeuroImage, 27, 279-290.

4. Durduran, T, et al. 2004, J. Cereb. Blood Flow Metab., 24, 518-525.

311

ATTENUATED PERI-INFARCT DEPOLARIZATION AND IMPROVED CBF FOLLOWING LESION-INDUCED PRECONDITIONING IN THE SPONTANEOUSLY HYPERTENSIVE RAT

L. Zhao, **T. Nowak**

Department of Neurology, University of Tennessee Health Science Center, Memphis, TN, USA

Objectives: Peri-infarct depolarizations (PIDs) contribute to the evolution of ischemic injury in stroke, in part due to an impact on perfusion (Strong et al. 2007). Previous studies of ischemic preconditioning (PC) demonstrated that protection was associated with early improvement in penumbral CBF (Zhao and Nowak 2006), but interpretation was complicated by interacting effects of prior anesthesia. The present studies investigated PIDs and associated perfusion responses in a model of PC induced by cortical freeze lesions that avoided such confounds.

Methods: Male Spontaneously Hypertensive Rats (SHR, 250-300 g) received a preconditioning cortical lesion under isoflurane anesthesia, produced by application of a liquid nitrogen-chilled 2 mm diameter stainless steel rod to the thinned skull overlying middle cerebral artery (MCA) territory (7 mm lateral, 4 mm caudal to bregma, 10 second exposure). Sham animals experienced the same surgery and anesthesia (~20 min duration) without lesioning. The following day rats (n = 9-10/group) were subjected to permanent tandem occlusion of the MCA and ipsilateral common carotid artery (CCA), and edema-corrected infarct volume was assessed at 24 h. In other animals (n = 9/group) the dorsal skull was bilaterally thinned, vessels were occluded, and anesthesia was transitioned to i.v. alpha-chloralose. PID-associated flow transients were monitored by speckle contrast perfusion imaging (FLPI, Moor Instruments, Inc., Wilmington, DE), after which infarct volume was assessed at 4 h.

Results: Preconditioning reduced final infarct volume, without an impact of the sham procedure (116 ± 4, 113 ± 11 and 85 ± 14* cubic mm in Naïve, Sham and PC groups, respectively; mean ± SD, * $P < 0.05$ vs. Naïve and Sham). PID incidence was reduced by preconditioning (17 ± 5, 16 ± 6 and 7 ± 2*), as was acute infarct volume at the end of the imaging procedure (112 ± 14, 118 ± 10 and 93 ± 17* cubic mm). PIDs invariably elicited hyperemic flow responses in adequately perfused cortex, typically associated with transient hypoperfusion more proximal to the ischemic core. In Naïve and Sham animals a small subset of these events produced persistent CBF deficits and expansion of the severely ischemic territory, whereas PC rats more often exhibited gradual CBF recovery.

Conclusions: The brief lesioning procedure permitted study of injury-induced protection without confounding anesthesia effects. Preconditioning robustly reduced 24 h infarct volume and an effect was also detected at 4 h following perfusion imaging. PC rats exhibited both reduced PID incidence and attenuated vasoconstrictive responses to such events, identifying candidate mechanisms underlying preconditioning protection in this model.

References:

Strong AJ, Anderson PJ, Watts HR, Virley DJ, Lloyd A, Irving EA, Nagafuji T, Ninomiya M, Nakamura H, Dunn AK, Graf R. (2007) Peri-infarct depolarizations lead to loss of perfusion in ischaemic gyrencephalic cerebral cortex. *Brain* 130:995-1008

Zhao L, Nowak TS, Jr. (2006) CBF changes associated with focal ischemic preconditioning in the Spontaneously Hypertensive Rat. *J. Cereb. Blood Flow Metab.* 26:1128-1140

313

MULTIMODAL HIGH-FIELD MRI IN ALCOHOL DEPENDENCE REVEALS FUNCTIONALLY SIGNIFICANT DEFICITS IN REGIONAL BRAIN BLOOD FLOW AND WHITE MATTER INTEGRITY

D.J. Meyerhoff[1], T.C. Durazzo[1], A. Mon[1], A. Kuceyeski[2], A. Raj[2]

[1]Radiology and Biomedical Imaging, UCSF/VAMC, San Francisco, CA, [2]Weill Cornell Medical College, New York, NY, USA

We have used multimodal MR to study brain injury and recovery from brain injury in alcohol dependent individuals in treatment. Previous studies have shown that brain injury measured by structural MRI, 1H MR spectroscopic imaging, perfusion and diffusion MRI at 1.5T is widespread and related to cognitive deficiencies and relapse propensity. We also showed that chronic smoking in alcoholics has a compounding effect on brain injury and cognition and that it appears to hamper recovery from brain abnormalities during abstinence from alcohol. Here we report on new multimodal findings and analyses using our 4T MR scanner, focusing on neocortical perfusion with arterial spin labeling and related white matter injury using diffusion tensor imaging data.

Here, we used 4T isotropic volumetric coronal 3D T1w MPR, axial continuous arterial spin labeling (cASL) perfusion with short-TE 2D gradient-echo EPI (2.4x2.4x3.0mm3) and axial whole-brain diffusion weighted imaging using double-refocused SE EPI (2x2x3mm3, 40 contiguous slices, 6 diffusion directions, 0 and 800s/mm2, 4 averages, 2xGRAPPA). FSL's FreeSurfer was used to parcellate the brain into neocortical and subcortical white matter regions. Cerebral blood flow was measured in those regions by coregistering with cASL perfusion maps. DTI data were processed using FSL's Tract Based Spatial Statistics (TBSS) for voxelwise, group-level analysis, FSL's permutation-based program randomise for statistics, and threshold-free cluster enhancement for multiple comparison corrections. Graph theory-based analyses of networks and probabilistic tractography were used to characterize anatomical connections between parcellated cortical regions.

12 alcoholics at entry into treatment had significantly lower blood flow than 9 controls in dorsolateral prefrontal and orbitofrontal cortices, anterior cingulate, insula, nucleus accumbens, hippocampi, amygdala, and anterior corpus callosum and centrum semiovale. Blood flow was 30% lower in cortical and WM regions and by up to 50% lower in subcortical regions. Effect sizes ranged from 1.1 to 1.7 and were not much different in 20 similar alcoholics at 5 weeks of abstinence from alcohol, suggesting little short-term blood flow recovery during sobriety. This new 4T multimodal processing approach is much more sensitive to alcohol effects than our 1.5T lobar perfusion analyses. DTI analyses in 36 alcoholics vs. 12 controls revealed lower fractional anisotropy (FA) ($p < 0.05$, corrected) in the anterior corona radiata, callosal genu, external capsule and inferior fronto-occipital fasciculus. Specific smoking effects were observed in the callosal splenium (not genu) and the anterior limb of the internal capsule ($p< 0.05$, uncorrected). Those alcoholics with lower FA in the fornix, bilateral hippocampal formations (cingulum), and left cerebral peduncle (corticospinal tract) ($p< 0.04$, uncorrected) relapsed within 12 months of baseline studies. In a similar cohort, fiber network eccentricity was significantly smaller, suggesting a smaller number of long-distance connections in alcoholics compared to controls. Further, regions with significantly fewer connections include regions within the dorsolateral prefrontal, orbito frontal, and prefrontal cortices.

These exciting novel observations at 4T expand on our earlier findings of chronic alcohol and

smoking-related abnormalities at 1.5T, highlighting specific injury to functionally significant regions of the brain reward system in anterior and limbic brain regions. Support: AA10788, DA025202, DA024136.

314

EDEMA EFFECT CORRECTION BY IMAGE ANALYSIS TO ESTIMATE INFARCTION VOLUME FOR ANIMAL MACO MODELS

W. Zhao[1], Q. Shen[1], L. Belayev[2], M.D. Ginsberg[3]

[1]Biomedical Engineering, University of Miami, Coral Gables, FL, [2]Neuroscience Center, Louisiana State University School of Medicine, New Orleans, LA, [3]Neurology, University of Miami, Miller School of Medicine, Miami, FL, USA

Introduction: Histopathological analysis has long been regarded as the "gold standard" for the quantitative assessment of tissue injury in animal models. This method typically utilizes perfusion-fixed, paraffin-embedded brain material for the localization and measurement of zones of infarction. A change in infarction volume in response to a treatment or an alteration of experimental physiological conditions constitutes a quantitative, geometric signal of crucial value for comparative analysis.

Objective: Brain swelling (edema) is a common complication of ischemic stroke, such as is produced by experimental middle cerebral artery occlusion (MCAo). Because of this, the infarct volume computed by integration of directly measured infarct areas must be corrected for the effects of brain swelling. The standard correction method, accepted by most laboratories, compares non-infarcted volumes between the ipsilateral hemisphere and the contralateral hemisphere, and regards the volume-difference as the corrected infarct volume. However, the method induces errors when the infarction volume is relatively small and the edema exists in the rest part of the brain. The objective of this study is to create a refined method for edema correction.

Materials and experimental description: Following 2h MCAo by intraluminal suture model, rats of saline- (n=9) and drug- (stilbazulenyl nitrone (STAZN)) (n=10) treated groups were perfusion-fixed under halothane anesthesia following a 3-day survival period. Brain sections of 10μm thickness for each animal were H&E stained and viewed by a Nikon microscope equipped with a Sony 3CCD camera to investigate cellular alterations, and digitized by a Xillix digital camera to form TIFF format files for image processing.

Methods: In order to correct the effects of brain swelling, we designed a software-based semi-automated "de-edema" method. Digitized H&E stained histology sections were input to our Image Processing (IP) software package. The software required user to define the midline of the brain through an interactive user interface. Mirrored by the defined midline, the software mapped the ipsilateral half of the brain section into the contralateral half of the brain section. The mapping used a nonlinear transformation based on the Delaunay triangulation structure, which matched corresponding triangles in two halves of the brain. These triangles were constructed by control points that had the maximum correlation coefficients between two halves of brain section. The algorithm dealt with a global non-linear transformation, which ensured non-infarcted and infarction areas to be proportionally mapped.

Results: We applied the designed method to the above mentioned histological sections. Each brain section was processed, and its ispilateral, contralateral and infarct areas were measured. Integrating the 2D information, we obtained corresponding volumes. Without the de-edema processing, the saline- and STAZN-treated group had 13.1+/-3.3% and 6.2+/-0.2.4% edema effects, respectively. After the de-edema processing, these values became 0.7+/-0.2% and 1.0+/-0.4%, respectively. The results demonstrated a significant de-edema effect ($p < 0.01$).

Conclusion: The non-linear mapping algorithm ensures two halves of the brain sections to be “mirrored” so that the brain swelling can be effectively corrected. This semi-automated procedure does not involve much of operator's time and knowledge of the anatomy. Software-based edema correction is a feasible approach in infarction volume estimation.

316

INTRATHECAL DRUG DELIVERY TO THE HUMAN CENTRAL NERVOUS SYSTEM

Y. Hsu, T.J. Harris, M. Hettiarachchi, A.A. Linninger, Laboratory for Product and Process Design

Bioengineering, University of Illinois at Chicago, Chicago, IL, USA

Treatments of neurological disorders such as Parkinson's and Alzheimer's diseases, or tumors require the efficient delivery of therapeutic agents to specific target areas in the brain. However, most large molecular weight drugs do not cross the blood brain barrier preventing them from reaching affected brain regions. *Intrathecal drug administration* bypasses the blood brain barrier by delivering macromolecules from the spinal canal directly into the brain. This drug infusion modality shows great potential for administering proteins, functionalized nanoparticles, or even inducing gene therapy via viral vectors to the central nervous system.

Prior clinical studies demonstrated that intrathecally delivered drugs such as morphine or Baclofen travel towards the cervical spine much faster than can be explained by pure diffusion. The hypothesis of this presentation is that pulsations of the cerebrospinal fluid are responsible for this remarkable acceleration in drug transport. Our Cine MRI studies on normal and diseased patients show that cerebrospinal fluid pulsations with a stroke volume of 1-4cc per cardiac cycle induce oscillatory convective flow patterns inside the spinal canal. These pulsations cause a drastic increase in transport speed in the laminar cerebrospinal fluid flow in the canal due to micro-mixing.

To investigate the effect of cerebrospinal fluid pulsations on drug transport in the central nervous system, a surrogate model of a human spinal canal was constructed. The distribution of a radionucleotide in the model was quantified by single photon emission computed tomography. The spatiotemporal dispersion of the radionucleotide Technetium-99m under pulsatile flow was compared to a control experiment with stagnant flow field. The quantitative comparison of the dispersion fronts suggests that the cerebrospinal fluid pulsations cause a two to five-fold acceleration of radionucleotide dispersion. We also developed a theoretical model for intrathecal drug distribution based on computational fluid dynamics. Our computer simulations affirm our hypothesis that convection is the main driver for accelerated species transport.

The quantitative understanding of the fundamental transport mechanisms allows the rational design of intrathecal delivery. To demonstrate the novel method of patient-specific therapy design, we reconstructed the cerebrospinal fluid-filled subarachnoid spaces of a specific human central nervous system using advanced image reconstruction techniques. The computer model accounts for the complex geometry of the subarachnoid space, as well as the production, elimination, and pulsations of cerebrospinal fluid. The cerebrospinal fluid flow field and species transport were resolved by solving the momentum and species transport equation. We designed a treatment plan for a spastic patient. Intrathecal Baclofen infusion -an anti-spasticity drug- into the L2 vertebrae was simulated. The infusion parameters such as injection rate and drug concentration were designed to match clinical treatment requirements. The goal of the treatment plan is to maintain therapeutic concentrations of Baclofen at targets sites in the central nervous system and to monitor toxicity. This computational model possesses potential to predict the dispersion of a wide range of therapeutic agents, with user defined infusion parameters. Patient-specific therapy design using advanced medical images and scientific software is expected to enhance the safety and efficiency of intrathecal delivery in clinical applications.

318

RELATIONSHIP BETWEEN PERSONALITY TRAITS AND DOPAMINE D_2 RECEPTOR AVAILABILITY

Y. Eguchi[1,2], H. Takano[1], H. Ito[1], R. Arakawa[1], F. Kodaka[1], H. Takahashi[1,3], H. Matsuda[2], T. Suhara[1]

[1]Molecular Neuroimaging, Molecular Imaging Center, National Institute of Radiological Sciences, Chiba, [2]Nuclear Medicine, Saitama Medical University International Medical Center, Hidaka, [3]Psychiatry, Kyoto University Graduate School of Medicine, Kyoto, Japan

Background and aims: Dopamine plays important roles for various human behaviors. The relationships between dopamine D_2 receptor binding and personality traits in healthy subjects have been investigated using positron emission tomography (PET), but the results have been inconsistent. Although the reasons are not entirely clear, small sample sizes and heterogeneity in subjects, such as age and gender, may be to blame. In this study, we have examined the association between individual personality traits and striatal dopamine D_2 receptor availability using PET with [^{11}C]raclopride, in a relatively uniform and larger study population.

Subjects and methods: Forty-two healthy male volunteers aged 20 to 43 years participated in the study. They showed normal results on T_1-weighted magnetic resonance (MR) imaging (1.5T, Intera, Phillips), and the MR images were used for anatomical reference.

Personality Assessment:

We assessed individual personality traits using the revised NEO personality inventory (NEO PI-R) [1]. This test consists of five dimensional domains (neuroticism, extraversion, openness to experience, agreeableness, and conscientiousness) that correspond to a five-factor model of personality traits, with each domain comprising six personality trait facet scales. The results of NEO PI-R are presented as T scores with a mean of 50 and a standard deviation of 10.

PET Measurement:

Striatal dopamine D_2 receptor binding was measured using PET (Siemens HR+) with [^{11}C]raclopride. Dynamic PET scanning was performed for 60 min in three-dimensional mode. Binding potential (BP_{ND}) was calculated using the simplified reference tissue method with the cerebellum as reference region [2].

Data analysis:

After each image was anatomically standardized to the Montreal Neurologic Institute stereotactic brain, volumes of interest were manually delineated for the striatum, which was divided into three functional subdivisions: limbic striatum (LST), associative striatum (AST), and sensorimotor striatum (SMST) [3]. The relations between striatum [^{11}C]raclopride BP_{ND}s and NEO PI-R T scores were analyzed using partial correlation coefficients adjusted for age.

Results: The NEO PI-R average T score of each of the domains was 53.6, 55.0, 58.3, 47.5, and 46.4, respectively, indicating that the subjects did not seem to have any evident deviation of personality. A significant negative partial correlation was observed between BP_{ND} for dopamine D_2 receptors in the whole striatum, AST, and SMST and the dutifulness facet (conscientiousness domain) when controlled for age (Pearson's correlation, r=-0.39, -0.36, and -

0.41, respectively, $p< 0.05$). There were no significant partial correlations between BP_{ND}s and any of the other personality facet scales.

Discussion and conclusion: The present results suggest that people who are more dutiful, that is, rigid and faithful to their ethical principles, tend to have lower striatal dopamine D_2 receptor binding, whereas those who are less dutiful, namely, more casual, tend to have higher D_2 binding. The human behavior exemplified by dutifulness and rigidness might be partially affected by dopamine D_2 availability in the striatum, especially AST and SMST.

References:

[1] Costa et al., NEO-PI-R professional manual. Psychological Assessment Resources, 1992

[2] Gunn et al., Neuroimage, 6: 279-287, 1997

[3] Martinez et al., J Cereb Blood Flow Metab, 23: 285-300, 2003

321

ENDOTHELIAL PROGENITOR CELL DYSFUNCTION IN CEREBRAL AMYLOID ANGIOPATHY ASSOCIATED STROKE

K. Hayakawa, K. Arai, E.H. Lo

Radiology and Neurology, Massachusetts General Hospital/Harvard Medical School, Charlestown, MA, USA

Objectives: Cerebral amyloid angiopathy (CAA) is associated with hemorrhagic stroke. But how the vascular deposition of beta-amyloid (Aβ) damages vessels is not fully understood. One idea is that vascular integrity requires constant maintenance by endothelial progenitor cells (EPCs). Is it possible that Aβ interferes with EPCs thus making brain vessels more vulnerable? Recent studies suggest that the receptor for advanced glycation endproducts (RAGE) may regulate EPC migration (Chavakis et al 2007). But RAGE is also a receptor for Aβ. Here, we ask whether Aβ1-40 can interfere with RAGE-mediated interactions between EPCs and brain endothelium. If so, this raises the possibility that CAA may impact neurovascular integrity by perturbing EPC-mediated endothelial homeostasis and repair.

Methods: EPCs were obtained from Sprague-Dawley rat spleen. Early EPCs were used for each independent experiment between days 3 and days 5 after seeding. Immunophenotyping of EPCs were performed days 5 using each CD34, CD133 (Prominin-1), Flk-1 (VEGFR2) and von Willebrand Factor (vWF) antibody in immunohistochemistry. Cell adhesion assay was performed after 24 hours incubation with or without IL-1β to assess interactions between EPCs and RBE.4 rat brain endothelial eclls. Ac-LDL labeled EPCs (1×10^4 cells/well) were incubated in RBE.4 monolayer cultured onto collagen I -coated 24 well plates at 37°C. The numbers of adhered cells were quantified by directly counting the number of ac-LDL positive cells.

Results: IL-1β -stimulated EPCs were significantly more adherent to the RBE.4 endothelial monolayer. An integrin mechanism may be involved since IL-1β upregulated β2 integrin levels on EPCs, and CD18, CD11a and CD11b neutralizing antibodies significantly decreased the adherence between stimulated EPCs and the RBE.4 monolayer. Next, we asked which corresponding receptor on endothelial cells was involved. Neutralizing antibodies for RAGE, toll-like receptor (TLR) 2 and TLR4 were co-incubated with RBE.4 for 1 hour before testing. Blockade of RAGE but not TLR2 or TLR4 significantly reduced the adherence between stimulated EPCs and the endothelial monolayer. Exposure of RBE.4 to Aβ1-40 for 24 hours reduced RAGE expression on its membrane. Consequently, Aβ1-40 inhibited the adherence between IL-1β -stimulated EPCs and RBE.4.

Conclusions: Targeted adhesion between EPCs and brain endothelial cells may be mediated by an interaction between endothelial RAGE and β2 integrins on EPCs. Aβ1-40 interfered with this interaction between EPCs and brain endothelium. These initial findings suggest that rescuing cell-cell interactions between circulating EPCs and brain endothelium may be a therapeutic strategy to improve endogenous neurovascular repair after CAA associated stroke.

References:

Chavakis E, Hain A, Vinci M, Carmona G, Bianchi ME, Vajkoczy P, Zeiher AM, Chavakis T, Dimmeler S (2007) High-mobility group box 1 activates integrin-dependent homing of endothelial progenitor cells. Circ Res 100:204-12.

324

EXPRESSION AND LOCALIZATION OF LRRN3 MEMBRANCE PROTEIN IN HUMAN EMBRYO DORSAL ROOT GANGLION

A. Pan, M. Li, H. Huang, H. Wu, Z. Li, X. Yan

Anatomy & Neurobiology, Xiangya School of Medicine, Central South University, Changsha, China

Objectives: To explore the expression and localization of membrance protein LRRN3 of dorsal root ganglion in human embryo at the mRNA and protein levels.

Methods: RT-PCR, Noethern Blotting, Western Blotting, immunocytochemistry staining and Immunofluorescence were used to detect membrance protein LRRN3.

Results: RT-PCR production cDNA of LRRN3 C-terminal domain protein were detected in DRG, and the lenth is about 500 bp; Northern blot analysis showed that mRNA were detected and there were no statistical significance between consecutive conceptus age DRG, the mRNA lenth is about 3.6kb; Western blot analysis showed membrance protein LRRN3 were detected and the relative molecular mass is about 79 kD; immunocytochemistry staining and Immunofluorescence detection showed membrance protein LRRN3 were detected in DRG sensory neurons.

Conclusion: The expression of LRRN3 suggests that LRRN3 is closely associated with embryonic development,morphogenesis and repair following injury.

325

REACTIVE ASTROCYTES CONTRIBUTES TO STROKE RECOVERY: A POTENTIAL ROLE OF HMGB1 IN EPC-MEDIATED NEUROVASCULAR REPAIR

K. Hayakawa, K. Arai, E.H. Lo

Radiology and Neurology, Massachusetts General Hospital/Harvard Medical School, Charlestown, MA, USA

Objectives: Glial scarring is traditionally thought to impede brain plasticity after stroke. However, emerging data now suggest that reactive astrocytes may also contribute to neurovascular remodeling, in part via the release of high-mobility group box1 (HMGB1) (Hayakawa *et al* 2010a; Hayakawa *et al* 2010b). Recent study suggests that HMGB1 may contribute to endothelial progenitor cells (EPCs) homing after tissue injury (Chavakis *et al* 2007). EPCs play an important role for tissue vascularization and endothelium homeostasis in stroke. In this pilot study, we assessed the feasibility of using small interference RNA (siRNA) against HMGB1 in a mouse model of stroke recovery.

Methods: Five days after cerebral ischemia, mice were stereotaxically injected control siRNA or HMGB1 siRNA in intra-cerebro-ventricular (i.c.v.). siRNAs for i.c.v. injection were prepared according to the in vivo siRNA transfection protocol for brain delivery from PolyPlus Transfection. Four μL of the siRNA complexes were i.c.v.-injected as 1μL /min of flow rate of mice under anesthesia. To detect accumulated EPCs in the ischemic brain, Flk1 and CD34 double positive cells were measured in the peri-infarct cortex by using FACS analysis over the course of 14 days after stroke. Behavioral tests were also performed over 14 days post-stroke.

Results: Over the course of 14 days after stroke, GFAP and HMGB1 double positive reactive astrocytes were upregulated in peri-infarct cortex. These double positive cells were coexpressed with chromosome region maintenance 1 (CRM1), which is related with translocation of HMGB1 from nucleus before release. At this time, proliferation markers (phospho-ERK and Ki67) were upregulated in CD31 positive microvessels, and EPCs were also accumulated in the peri-infarct cortex in parallel with a steady improvement in neuroscore and functional outcome of these post-stroke mice. HMGB1-siRNA-treated mice demonstrated a significant decrease in HMGB1-positive reactive astrocytes. Correspondingly, this reduction of astrocyte HMGB1 was associated with a worsening of behavioral recovery. Finally, our pilot data suggest that EPC numbers and vascular density may also be slightly decreased in treated brains.

Conclusions: Astrocytic HMGB1 may contribute to neurovascular repair after brain injury by mediating EPCs migration into the ischemic peripheral region. Augmenting these astrocyte-EPC pathways may offer a novel way to improve stroke recovery.

References:

1. Chavakis E, Hain A, Vinci M, Carmona G, Bianchi ME, Vajkoczy P, Zeiher AM, Chavakis T, Dimmeler S (2007) High-mobility group box 1 activates integrin-dependent homing of endothelial progenitor cells. *Circ Res* 100:204-12.

2. Hayakawa K, Arai K, Lo EH (2010a) Role of ERK map kinase and CRM1 in IL-1beta-stimulated release of HMGB1 from cortical astrocytes. *Glia* 58:1007-15.

3. Hayakawa K, Nakano T, Irie K, Higuchi S, Fujioka M, Orito K, Iwasaki K, Jin G, Lo EH, Mishima K, Fujiwara M (2010b) Inhibition of reactive astrocytes with fluorocitrate retards neurovascular remodeling and recovery after focal cerebral ischemia in mice. *J Cereb Blood Flow Metab* 30:871-82.

326

EFFECTS OF INFRARED LIGHT THERAPY ON ENDOTHELIAL PROGENITOR CELLS IN MOUSE FOCAL CEREBRAL ISCHEMIA

K. Hayakawa, A. Vahabzadeh-Hagh, K. Arai, E.H. Lo

Radiology and Neurology, Massachusetts General Hospital/Harvard Medical School, Charlestown, MA, USA

Objectives: Experimental and clinical studies suggest that near infrared (NIR) light therapy may influence outcomes after stroke. However, the mechanism by which NIR light may induce beneficial effects in the ischemic brain is unclear. Recent data suggest that endothelial progenitor cells (EPCs) play an important role for neurovascular recovery in stroke (Rosell *et al* 2009; Rouhl *et al* 2008). In this study, we assessed the effect of NIR light therapy on EPCs during stroke recovery.

Methods: Beginning at 5 days following cerebral ischemia, mice received NIR light treatments (810 nm, 37 mW/cm^2) to the left parietal region of the head every 4 days, for a total of 3 treatments. To detect accumulated EPCs in the ischemic brain, Flk1 and CD34 double positive cells were measured in the peri-infarct cortex using FACS analysis over the course of 14 days after stroke. Behavioral tests (neuroscore, corner test, and foot-fault test) were also performed over these 14 days. A mouse angiogenesis protein array was used to further examine the effect of light therapy on day 14.

Results: Over the course of 14 days after stroke, Flk1/CD34 double positive EPCs appeared to increase in peri-infarct cortex in parallel with a steady improvement in neuroscore and functional outcome. Exposure to NIR light during stroke recovery augmented the accumulation of EPCs and improved behavioral outcomes in comparison to the control, unexposed group. The angiogenesis protein array demonstrated an upregulation of endostatin, CXCL16, Ang-1, Ang-3, b-FGF-2, MIP-1, and SDF-1 in the light therapy group compared to controls on day 14 after stroke.

Conclusions: Exposure to NIR light during stroke recovery may enhance migration of EPCs into the ischemic peripheral region by upregulating angiogenic factors. NIR light therapy may offer a novel way to promote neurovascular repair in the setting of ischemic brain injury.

References:

Rosell A, Arai K, Lok J, He T, Guo S, Navarro M, Montaner J, Katusic ZS, Lo EH (2009) Interleukin-1beta augments angiogenic responses of murine endothelial progenitor cells in vitro. *J Cereb Blood Flow Metab* 29:933-43.

Rouhl RP, van Oostenbrugge RJ, Damoiseaux J, Tervaert JW, Lodder J (2008) Endothelial progenitor cell research in stroke: a potential shift in pathophysiological and therapeutical concepts. *Stroke* 39:2158-65.

327

THE CNS IMMATURITY PRESERVES BLOOD-BRAIN BARRIER INTEGRITY AFTER NEONATAL STROKE

D. Fernandez-Lopez[1], J. Faustino[1], R. Daneman[2], L. Zhou[3], N. Derugin[4], M. Wenland[5], B.A. Barres[3], Z.S. Vexler[1]

[1]Neurology, University of California, San Francisco, [2]Anatomy, University of California San Francisco, San Francisco, [3]Neurobiology, Stanford University, Palo Alto, [4]Neurosurgery, University of California, San Francisco, [5]Radiology, University of California San Francisco, San Francisco, CA, USA

Objectives: It is increasingly recognized that the immaturity of the CNS at birth affects ischemic injury and recovery. In many brain diseases, including stroke, BBB breakdown is an important contributing factor to injury. We recently showed that paracellular diffusion is better preserved after neonatal than after adult acute stroke. We also showed that in contrast to adult stroke, neutrophil transmigration is minimal in neonatal stroke (*Faustino et al, ISC, 2009*)

We asked if the pattern of expression of the BBB proteins after stroke differs between two ages, contributing to the relative integrity of the barrier after neonatal stroke.

Methods: Postnatal day 7 and adult rats were subjected to a transient 3hr middle cerebral artery occlusion (MCAO). Diffusion-weighted MRI was used to identify injured animals and guide tissue dissection. Albumin extravasation and Gd-enhanced T1W MRI were used to establish BBB permeability 24hr after reperfusion in relation to histological outcome. Endothelial cells were isolated by immunopanning through negative (CD45, PDGFRb) and positive (CD31) selection and endothelial transcriptosome (31,042 total probe sets; the significance thresholds > 2-fold change) was used to determine the effect of age on stroke-induced changes in endothelial gene expression. Expression of the tight junction (TJ) and extracellular matrix proteins was determined by Western blot and immunofluorescence.

Results: In contrast to a 14-fold increase in albumin extravasation into ischemic-reperfused tissue in the adult, only a 2-fold increase was observed in the neonate. BBB permeability to a small molecule, GdDTPA, was low (< 10%) at 24 hours after neonatal stroke based on Gd-enhanced T1W-MRI.

The endothelial transcriptome data sets revealed significant up-regulation of 1241 probes in injured regions in adult and 726 probes in neonates after stroke. The patterns of up-regulated genes were largely non-overlapping (1017 unique probes in adults and 503 probes in neonates). The patterns of down-regulated genes and the signaling pathways involved were vastly different as well between the two ages. Differential changes in the gene expression of claudin-5 and occludin and the basal lamina components laminin and collagen IV were among key differences between the two age groups. Lower gene and protein expression of the basal lamina components laminin and collagen IV in naive adults compared to neonates were also observed.

The patterns of TJ protein expression changes after stroke also differed between neonatal and adult rats. A significant 2-fold increase in claudin-5 expression was observed in injured cortex of neonates whereas expression remained unchanged in adults. Occludin expression tended to increase in neonatal but decreased in adult rats. ZO-1 expression was unaffected in neonatal but was significantly reduced in adult rats.

Summary and conclusions: We demonstrate that fundamental structural and functional aspects of the BBB are better preserved after neonatal than after adult acute stroke. Using highly purified endothelial cells we show the profoundly different gene expression patterns in the immature and adult CNS vasculature after stroke. The better preserved expression of TJ and extracellular matrix components likely contributes to the integrity of the BBB in injured neonates.

Support: AHA 0655236Y (ZV), NS44025 (ZV), NS55915 (ZV),

328

THE SCAVENGER RECEPTOR CD36 MODULATES INJURY AFTER NEONATAL FOCAL STROKE

M.-S. Woo[1], X. Wang[1], J. Faustino[1], N. Derugin[1], M. Wendland[2], P. Zhou[3], C. Ladecola[3], Z. Vexler[1]

[1]Neurology, [2]Radiology, University of California, San Francisco, CA, [3]Neurology and Neuroscience, Weill Cornell Medical College, New York, NY, USA

Objectives: The scavenger receptor CD36 participates in multiple cell-type specific biological functions through its capacity to bind an array of ligands, including anionic phospholipids, collagen, advanced glycosylation end products, TSP-1 and OxLDL, or via cooperation with other receptors. It plays a key role in phagocytosis of apoptotic material and generation of reactive oxygen species. The CD36 contributes to brain damage after transient middle cerebral artery occlusion (MCAO) in the adult. Compared to wild type (wt) mice, injury is smaller in CD36 knockouts (CD36-/-) and lack of CD36 is associated with elimination of oxidative burst in brain macrophages.

We asked if CD36 exacerbates injury after neonatal focal stroke.

Methods: P10 CD36-/- and wt mice (C57BL6) were subjected to a transient 3hr MCAO. Diffusion-weighted MRI was used to identify injured animals to guide tissue dissection and monitor injury progression. Injury volume was determined in Nissl-stained coronal sections 24 hr after MCAO. Iba1+/IB4+/cleaved caspase-3+/DAPI+ immunofluorescence was performed in adjacent coronal sections, Z-stacks of images acquired (25x oil objective), and 3D image analysis performed (Volocity software) to determine macrophage accumulation and phagocytosis of apoptotic neurons. Considering that CD36 may trigger multiple intracellular signaling pathways through the dynamic association of signaling molecules in lipids, including Src family kinases Fyn and Lyn, expression of Fyn, Lyn and the associated downstream signalling molecules p-Pyk, p-p130cas was determined in injured and contralateral brain tissue by Western blot at 24 hr.

Results: MRI-identifiable volumes of injury during MCAO (tissue with reduced ADC values) were similar in CD36-/- and wt groups, 64±12% (n=10) and 60±14% (n=11) of ipsilateral hemisphere, respectively. At 24 hrs, various degree of injury recovery was observed in 55% wt but not in CD36-/- pups. The overall injury volume was significantly higher in CD36-/- than in wt pups, 50±6% Vs. 28±26%, respectively ($p< 0.0028$). The number of cells with cleaved caspase-3 was similar in both groups in both the core and penumbra. The number of and the surface of activated microglial cells/macrophages tended to be lower in injured regions of CD36-/- pups. The protein levels of Fyn and Lyn were significantly reduced in ischemic-reperfused regions in wt compared to CD36-/- mice (35±35% Vs. 75±25% for Fyn, $p=0.028$; and 32±22% Vs. 76±14% for Lyn, $p=0.006$, for wt and CD36-/-, respectively). These changes were associated with a significant decrease in phosphorylation of Pyk2 but not p-p130cas in wt animals but not in CD36-/-.

Summary and conclusions: These data shows that the lack of the scavenger receptor CD36 adversely interferes with the ability of neonatal mice to recover from stroke. The study suggests that injury exacerbation may in part occur through CD36-induced Src kinase-mediated signaling. These data also demonstrate that genetic deletion of the CD36 differentially affects injury after neonatal and adult stroke.

Support: AHA 0655236Y (ZV), NS44025 (ZV), NS55915 (ZV)

329

INDUCTION OF 20-HETE SYNTHASE IN RAT MODEL OF BRAIN ISCHEMIA: A PET STUDY WITH ^{11}C-LABELED SPECIFIC 20-HETE SYNTHASE INHIBITOR

T. Kawasaki[1], T. Marumo[2], T. Mori[1], K. Shirakami[1], Y. Ago[3], H. Hashimoto[3], H. Amada[2], R. Suzuki[2], H. Doi[1], T. Matsuda[3], A. Baba[3], H. Onoe[1]

[1]RIKEN, Center for Molecular Imaging Science, Kobe, [2]Taisho Pharmaceutical Co., Ltd, Saitama, [3]Osaka University, Osaka, Japan

Objectives: 20-Hydroxyeicosatetraenoic acid (20-HETE), an arachidonic acid metabolite, which is produced following cerebral ischemia, has been shown to contribute to the ischemia/reperfusion injury by mediating vasoconstriction and inflammation. Positron emission tomography (PET) imaging of 20-HETE synthase expression or activity might be useful for monitoring of vasoconstrictive and inflammatory processes of patients with brain ischemia. To develop a suitable PET probe for 20-HETE synthase imaging, we recently have synthesized specific 20-HETE synthase inhibitors, ^{11}C-labeled N-(3-methyl-4-morpholin-4-yl) phenyl-N-hydroxyimido formamide (TS-011-Me), ^{11}C-labeled 2-Dimethylaminohexyloxy imidazole (20-HETE1), and have performed PET studies with rat model of brain ischemia.

Methods: Rat model of brain ischemia was made by induction of transient occlusion of the MCA (t-MCAO) by the intraluminal filament method. On days 3-28 after the occurrence of cerebral ischemia, dynamic PET scan was performed for 90 min with a PET scanner for small animals (microPET focus220) under 1.5% isoflurane anesthesia following a bolus injection of ^{11}C-labeled radioligands through the cannula implanted into tail vein. Binding potential (BP) was calculated by the multilinear reference-tissue model 2 (MRTM2) in PMOD software (PMOD Technologies, version 3.0) using cerebellum ROI as the reference region.

Results: In PET study with the normal rats, [^{11}C]TS-011-Me and [^{11}C]20-HETE1 showed a high uptake of radioactivity in the kidney, liver, and other organs in which 20-HETE synthase-was known to be rich. In addition, total uptake of [^{11}C]20-HETE1 in the brain was higher than that of [^{11}C]TS-011-Me. To determine the time course of 20-HETE synthase function over 28 days after the induction of cerebral ischemia in rat brain, we performed PET with [^{11}C]20-HETE1. PET imaging showed a significant increase in [^{11}C]20-HETE1 uptake on the cerebral regions of injured hemisphere compared with those in the contralateral side on days 7 and 10 after the induction of ischemia. In vivo [^{11}C]20-HETE1 binding of the lesioned area was displaced by an excess amounts of 20-HETE1 co-injection (10 mg/kg).

Conclusions: [^{11}C]20-HETE1 provides quantitative information of the time course of 20-HETE synthase function in rat model of brain ischemia. [^{11}C]20-HETE1 might be a useful PET probe to study the changes in 20-HETE synthase function in patients of cerebral ischemia.

330

PIDD AND BACH1 INDUCTION IN MOTOR NEURONS AFTER TRANSIENT SPINAL CORD ISCHEMIA IN RABBITS

M. Sakurai[1], T. Kawamura[2], H. Nishimura[3], H. Suzuki[4], K. Abe[5]

[1]Cardiovascular Surgery, [2]Anethegiology, [3]Virus Research, [4]Pathology, National Hospital Organization Sendai Medical Center, Sendai, [5]Neurology, Okayama University, Okayama, Japan

Objective: The mechanism of spinal cord injury has been thought to be related to the vulnerability of spinal motor neuron cells against ischemia. However, the mechanisms of such vulnerability are not fully understood. Because we previously reported that spinal motor neurons were lost probably by programmed cell death, we investigated a possible mechanism of neuronal death by immunohistochemical analysis for PIDD, p53 and Bach1.

Methods: We used a rabbit spinal cord ischemia model with use of a balloon catheter. The spinal cord was removed at 8 hours, 1, 2, or 7 days after 15 min of transient ischemia, and histological changes were studied with hematoxylin-eosin staining. Western blot analysis for PIDD, p53 and Bach1., temporal profiles of PIDD, p53 and Bach1. immunoreactivity, and double-label fluorescence immunocytochemical studies were performed.

Results: The majority of motor neurons were preserved until 2 days, but were selectively lost at 7 days of reperfusion. Western blot analysis revealed scarce immunoreactivity for PIDD, p53 and Bach1 in the sham-operated spinal cords. However, they became apparent at 8 hours after transient ischemia, which returned to the baseline level at 1 day. Double-label fluorescence immunocytochemical study revealed that both PIDD and p53 and Bach1 and p53 were positive at 8 hours of reperfusion in the same motor neurons, which eventually die.

Conclusion: This study demonstrated that immunoreactivities for both PIDD and a p53 and, Bach1 and p53 were induced in the same motor neuron, which eventually die. The induction of Bach1proteins at the early stage of reperfusion might be one factors responsible for the delay in neuronal death, and the induction of PIDD and p53 may be implicated in the programmed cell death change after transient spinal cord ischemia.

332

VALUE OF MONTREAL COGNITIVE ASSESSMENT IN IDENTIFYING PATIENTS WITH VASCULAR COGNITIVE IMPAIRMENT NO DEMENTIA AFTER CEREBRAL INFARCTION

R. Zhao

The Affiliated Hospital of Medical College, Qingdao University, Qingdao, China

0bjective: To investigate the value of Montreal Cognitive Assessment (MoCA)in identifying patients with vascular cognitive impairment no dementia（VCIND） after cerebral infarction.

Methods: Among the 119 cases of cerebral infarction,71 subjects diagnosed with VCIND and 48 controls without cognitive impairment were assessed by the Mini-Mental State Examination(MMSE) and MoCA.Their demographic data and vascular risk factors were also documented.

Results:

1. No significant differences were found between the two grops on age,gender,education level（P>0.05）.
2. Total scores of MoCA and MMSE in the VCIND group were significantly lower compared with that in control group(P< 0.05).There was high correlation between total scores of MoCA and MMSE by Pearson correlation analysis (r=0.779, P< 0.05).
3. According to the ROC curve analyses,with the best cut-off score of 21,MoCA can provide a sensitivity of 83.1％and a specificity of 72.9% while the best cut-off score of MMSE is 26 with a sensitivity of 69.0% and a specificity of 66.7%.
4. Except language and abstraction, significant differences in other sub-items of MoCA were found between the two groups (P< 0.05).
5. Logistic regression analysis showed that hypertension, diabetes mellitus, smoking and leukoaraiosis had correlation with VCIND (P< 0.05).

Conclusions: MoCA has higher sensitivity and specificity than MMSE in screening VCIND, and the optimal cut-off point of MoCA is 21.Patients with VCIND have extensive cognitive domains impairment. Hypertension, diabetes mellitus, smoking and leukoaraiosis are risk factors of VCIND.

333

VALUE OF THE MONTREAL COGNITIVE ASSESSMENT FOR THE DETECTION OF VASCULAR COGNITIVE IMPAIRMENT IN CEREBRAL SMALL VESSEL DISEASE

R. Zhao

The Affiliated Hospital of Medical College, Qingdao University, Qingdao, China

Objective: To study the validity of Montreal Cognitive Assessment in cognitive impairment caused by cerebral small vessel disease(SVD).

Methods: According to the diagnostic criteria ,103 patients with SVD were divided into two groups, cognitive impairment group(n=62) and the control(n=41). All the patients were assessed with MoCA and MMSE.

Results:

1. No significant differences were found between the two groups on age, gender and education level (P>0.05).
2. The total scores of MoCA and MMSE were (18.08±3.16),（25.53±2.91）respectively in the cognitive impairment group. There was high correlation between the total scores of MoCA and MMSE by using spearman correlation coefficient(r=0.522,P＝0).
3. Total scores of MoCA and MMSE in the cognitive impairment group were significantly lower compared with that in control group. Except attention, significant differences in other sub-items of MoCA were found between the two groups（P< 0.05), however only total score, memory and recall had differences between two groups by MMSE.
4. According to the ROC curve analyses, with the best cut-off score of 22/23, MoCA can provide a sensitivity of 91.9% and a specificity of 95.1%.

Conclusion: MoCA has higher sensitivity and specificity than MMSE in screening cognitive impairment caused by SVD, and the optimal cut-off point of MoCA is 22/23.

335

IMPLICATION OF CREB-BDNF SIGNALING IN NICOTINE-INDUCED NEUROPROTECTION

K. Kitagawa, T. Sasaki, Y. Terasaki, M. Kawamura, S. Okazaki, Y. Sugiyama, N. Oyama, Y. Yagita

Department of Neurology, Osaka University, Suita, Japan

Background and purpose: Nicotine and the stimulation of nicotine acetylcholine receptors (nAChR) in the central nervous system play an important role in neuroprotection. Previous studies showed that the treatment with nicotine increased the level of phosphorylation of the cAMP response element binidng protein (CREB), but it remains unclear whether nicotine treatment could induce CRE-mediated gene expression, especially in the promoter region of brain-derive neurotrophic factor (BDNF) gene. The aim of this study is to clarify the effect of nicotine treatment on CRE activity, CREB-BDNF signaling, and glutamate-induced neurotoxicity. We also examined the effect of alpha-bungarotoxin (α-BTX), blocker for α7 nAChR, on nicotine treatment in cultured neurons.

Methods: Primary neuronal cultures of the rat cortex were prepared from E18-E19 rat embryo. Cells were cultured in himudified atmosphere of 5%CO2 and used after 10 d in vitro. Cells were treated with 1nM to 100 μM nicotine for 6 hours before exposure to glutamate of 100 μM for 15 min. LDH assay was used for cell injury 24 hr after glutamate exposure using Cytotoxity detection kit. α-BTX was added to final concentration of 50 nM before treatment of nictoine at 10 μM. Phosphorylation of CREB (pCREB) was evaluated with immunoblotting with anti-pCREB antibody. The CRE transcriptional activity was quantified by luciferase assay. Cortical neurons were transfected with purified adenovirus, adeno CRE-Luc (firefly) and adeno-TK-Luc (renilla). The relative firefly luciferase-based CRE-reporter activities were standardized to the corresponding Renilla luciferase. About 400 bp BDNF exon IV fragment was cloned into the pGL5 luciferase reporter vector. A BDNF exon IV promoter mutant (mutant-BDNF) was generated in the consensus CRE sequence by exchanging nucleotides using Quickchange Mutagenesis Kit.

Results: Nicotine treatment at 10 μM increased the level of CREB phosphorylation, CRE transcriptional activity and mitigated cell injury after glutamate exposure. However, nicotine at 1 nM to 1 μM did not show significant effect. Nicotine treatment also enhances BDNF exon IV promoter activity, but mutant-bdnf activity was unaffected after nicotine treatment. Treatment with α-BTX inhibited enhancement of CRE activity and BDNF-luc activity by nicotine and diminished the protective effect against glutamate toxicity.

Conclusions: Our result suggests that nicotine treatment in cultured neurons enhanced CRE-BDNF signaling through α7 nAChR activation. Stimulation of α7 nAChR could be a potential target for neuronal protection in stroke and other neurological diseases.

336

IMPAIRED VASCULAR RESPONSES OF INSULIN RESISTANT RATS AFTER MILD SUBARACHNOID HEMORRHAGE

A. Institoris[1,2], J.A. Snipes[2], P.V. Katakam[2], F. Domoki[1], F. Bari[3], D.W. Busija[2]

[1]Department of Physiology, University of Szeged, Szeged, Hungary, [2]Department of Physiology and Pharmacology, Wake Forest University School of Medicine, Winston-Salem, NC, USA, [3]Department of Medical Physics and Medical Informatics, University of Szeged, Szeged, Hungary

Insulin resistance (IR) impairs cerebrovascular responses to several stimuli in Zucker obese (ZO) rats. However, cerebral artery responses after subarachnoid hemorrhage (SAH) have not been described in IR. Hemolysed blood (300µl) or saline was infused (10µl/min) into the cisterna magna of 11-13 week-old Zucker obese (ZO) (n=25) and lean (ZL) rats (n=25). One day later, dilator responses of the basilar artery (BA) and its side branch (BA-Br) to acetylcholine (Ach, 10^{-6} M), cromakalim (10^{-7} M, 10^{-6} M) and sodium nitroprusside (SNP, 10^{-7} M) were recorded with intravital videomicroscopy. The baseline diameter of the BA was increased in the ZO but not the ZL rats 24h after the blood injection. Saline injected ZO animals showed reduced dilation to ACh (BA=7±4% vs. 21±5%; BA-Br=20±5% vs. 37±8%) compared to ZL rats. Blood injection blunted the response to ACh in both the ZO (BA=4±3%; BA-Br=11±3%) and ZL rats (BA=7±2%; BA-Br=16±4%). Cromakalim (10^{-6} M)-induced dilation was significantly reduced both in the blood injected ZO animals compared to the saline control (BA=11±3% vs. 27±5%; BA-Br=23±7% vs. 43±11%), and in the blood injected ZL rats compared to their saline control (BA=24±4% vs. 29±3%; BA-Br=39±3% vs. 58±9%). No difference in SNP reactivity was observed. Western blot analysis of the basilar artery showed a lower baseline level of neuronal nitric oxide synthase (nNOS) expression and an enhanced cyclooxygenase-2 (COX-2) level in the blood injected ZO animals. In summary, cerebrovascular reactivity to both endothelium- and smooth muscle-dependent stimuli is severely compromised by SAH in IR animals.

Supported by the National Institutes of Health Grants HL-030260, HL-065380, HL-077731, and HL-093554, Hungarian Scientific Research Fund (OTKA K81266).

337

QUANTITATIVE ANALYSIS OF DOPAMINE TRANSPORTER BINDING IN HUMAN BRAIN USING POSITRON EMISSION TOMOGRAPHY WITH [^{18}F]FE-PE2I

T. Sasaki[1,2], H. Ito[1], R. Arakawa[1], C. Seki[1], H. Takano[1], F. Kodaka[1], H. Takahashi[1], K. Takahata[1], S. Fujie[1], H. Fukuda[1], T. Nogami[1], M. Suzuki[1], H. Fujiwara[1], Y. Kimura[1], A. Varrone[3], C. Halldin[3], T. Nishikawa[2], T. Suhara[1]

[1]Molecular Imaging Center, National Institute of Radiological Sciences, Chiba, [2]Section of Psychiatry and Behavioral Sciences, Tokyo Medical and Dental University Graduate School, Tokyo, Japan, [3]Department of Clinical Neuroscience, Karolinska Institutet, Stockholm, Sweden

Introduction: Dopamine transporter (DAT) is of major interest in the pathophysiology of several neurological and psychiatric disorders including Parkinson's disease, schizophrenia, attention-deficit/hyperactivity disorder (ADHD) and high-functioning autism. [^{18}F]FE-PE2I was recently developed as a radioligand to measure DAT binding using positron emission tomography (PET). In this study, the kinetics of [^{18}F]FE-PE2I in living human brain were investigated.

Methods: Ten healthy men (20-39 years of age) underwent a 90-min dynamic PET scan after intravenous injection of 166-200 MBq of [^{18}F]FE-PE2I (specific radioactivity: 48-329 GBq/μmol). Arterial input function was determined by frequent arterial blood sampling and HPLC analysis. Using kinetic parameters determined by 2-tissue compartment model analysis, binding potential (BP_{ND}) values were calculated as DVR-1, where DVR was the ratio of total distribution volume (V_T) between the target region and the reference region, cerebellum (Indirect kinetic method). Considering the production of radiometabolite which had been reported to cross the blood-brain barrier and bind to DAT, analyses were done using either the input function calculated from parent radioligand (method 1) or the input function calculated from parent radioligand+radiometabolite (method 2). BP_{ND} values were also quantified by the simplified reference tissue model (SRTM) method.

Results: A rapid brain uptake of [^{18}F]FE-PE2I was observed. The highest regional radioactivity was observed in the striatum during PET scan. In method 1 and 2, regional time-activity curves could be well described by the two-tissue compartment model with four rate constants, K$_1$, k$_2$, k$_3$ and k$_4$. Rate constants and V_T in the putamen by method 1 and 2 are shown in table 1. The K$_1$ value was not different between two methods. The k$_3$, k$_4$, and also k$_3$/k$_4$ values were significantly smaller in method 2 than in method 1. BP_{ND} values by method 1 as well as those by SRTM method are shown in table 2. BP_{ND} values by both methods were in good agreement (r=0.99) (figure 1). In method 2, however, BP_{ND} values were reliably calculable not in all regions, especially in brain regions with relatively low specific binding.

	K1	k2	k3	k4	V_T
parent input (method 1)	0.29 ± 0.05	0.073 ± 0.022	0.133 ± 0.031	0.043 ± 0.007	17.3 ± 4.6

parent + radiometabolite input (method 2)	0.29 ± 0.05	0.065 ± 0.013	0.049± 0.017	0.033 ± 0.009	11.2 ± 2.1

[(Table 1) Rate constants and VT in putamen]

	caudate head	putamen	thalamus	midbrain
parent input (method 1)	4.03 ± 0.94	4.42 ± 0.83	0.19 ± 0.10	0.54 ± 0.13
SRTM method	3.48 ± 0.56	3.91 ± 0.54	0.26 ± 0.07	0.58 ± 0.11

[(Table 2) BPND values]

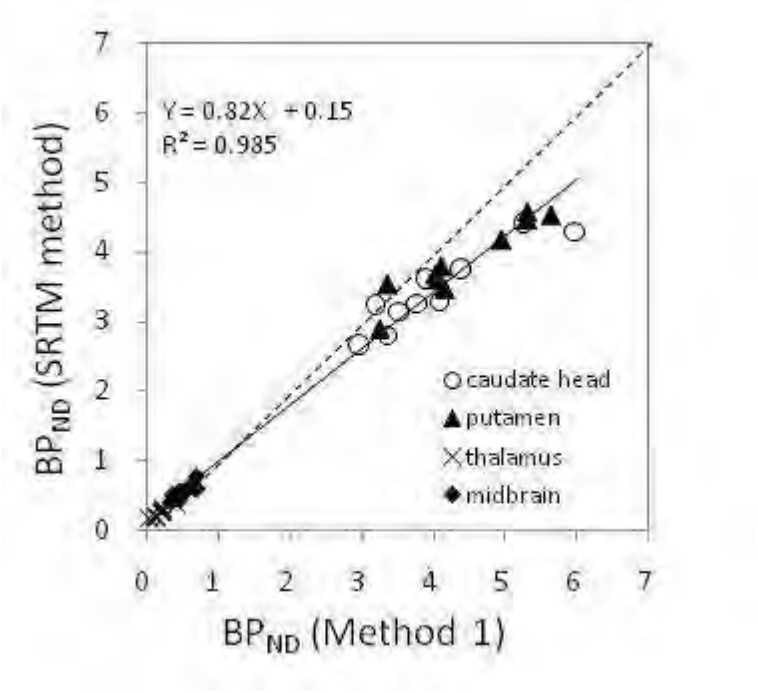

[(Figure 1) BPND values by method 1 and SRTM method]

Conclusions: Regional distributions of [^{18}F]FE-PE2I were in good agreement with regional distributions of DAT in the postmortem human brain measured with [^{18}F]FE-PE2I (1) and in the living human brain measured with [^{11}C]PE2I (2). BP_{ND} values by indirect kinetic method and

SRTM method were in good agreement unless radiometabolite were taken into account, indicating the validity of SRTM method which is one of non-invasive quantification methods.

References:

1. Varrone, A. et al. Synapse. 2009

2. Seki, C. et al. Ann. Nucl. Med. 2010

338

THE ISCHEMIC PENUMBRA: AN EXPERIMENTAL CONCEPT WITH CLINICAL IMPACT

W.-D. Heiss

Max-Planck-Institute for Neurological Research, Cologne, Germany

With the occlusion of a cerebral artery the perfusion of the tissue usually is not completely blocked, but maintained at a severely reduced level for an unpredictable period. As a result function of the tissue is disturbed, but morphology is not damaged immediately. These early experimental findings led to the concept of the "penumbra" suggesting that hypoperfused functionally impaired tissue can survive for some time and even recover, if sufficient reperfusion is re-established within a limited time period, which depends on the level of residual flow. Irreversible tissue damage starts in the area with the lowest residual flow and progresses to the more peripheral areas with less disturbed perfusion. This centrifugal progression of irreversible tissue damage is accompanied by a complex cascade of interconnected electrophysiological, molecular, metabolic and perfusion disturbances. In these processes waves of depolarisations, the peri-infarct spreading depressions, inducing activation of ion pumps and liberation of excitatory transmitters play an important role; the drastically increased metabolic demand in addition to the reduced oxygen supply cause further hypoxia and lactacidosis, which further damage the tissue.

In order to translate these experimental findings into clinical research methods like positron emission tomography (PET) are required which allow non-invasive determination of regional cerebral blood flow, regional metabolic rate of oxygen and regional oxygen extraction fraction. Together these measures can identify the areas which are critically perfused but morphologically intact, i. e. penumbra, and the regions which are irreversibly damaged. In animal experiments the transition of penumbra to infarction could be followed and the effect of reperfusion after ischemia of different severity and duration could be evaluated. Selective PET studies supported the validity of the concept of the penumbra in patients and were also able to demonstrate the efficacy of reperfusion strategies.

The original PET methods for detection of the penumbra require arterial blood sampling and complex logistics and are limited for routine application. Therefore, tracers were developed for non-invasive detection of irreversible tissue damage (flumazenil as a marker of neuronal integrity) and of hypoxic tissue changes (fluoromisonidazole, a tracer for hypoxic cells). But also these methods require complex instrumentation and radioactive tracers.

A widely applicable diagnostic tool for stroke patients is perfusion- / diffusion weighted magnetic resonance imaging (PW-DW-MRI), and the "mismatch" between perfusion and diffusion changes was widely applied as a surrogate marker of the penumbra. However, selection of patients based on these criteria usually did not predict efficacy of treatment. Comparative studies of MRI imaging and PET showed a considerable false-positive rate of irreversible damage indicated by DWI. The PW estimation of blood flow was highly variable when compared to quantitative values from PET studies, and the PW-DW-mismatch significantly overestimated the penumbra as defined by PET. Advanced analytical procedures of MRI data may improve the reliability of these surrogate markers, but they should be validated on quantitative measures. With these improved non-invasive and widely available methods the concept of the penumbra finally will be introduced into clinical practice and will be used widely for therapeutic decisions in stroke patients.

341

THE NMDA-RECEPTOR GLYCINE SITE MEDIATES XENON NEUROPROTECTION AGAINST HYPOXIC/ISCHEMIC INJURY

P. Banks[1,2], N. Franks[1,2], **R. Dickinson**[1,2]

[1]Anaesthetics, Pain Medicine & Intensive Care, [2]Biophysics Section, Imperial College London, London, UK

Goals & Objectives: The inert anaesthetic gas xenon is neuroprotective. We have shown that xenon inhibits NMDA-receptors[1,2] and this is plausible as a mechanism underlying xenon neuroprotection. However, whether NMDA-receptor antagonism actually mediates xenon neuroprotection is not known. We recently showed that xenon inhibits NMDA-receptors by competing with the co-agonist glycine at the glycine-binding site[3]. Here we test the hypothesis that inhibition of the NMDA-receptor at the glycine site underlies xenon neuroprotection against hypoxia/ischemia. If this hypothesis is correct xenon neuroprotection should be attenuated at elevated glycine concentrations.

Methods: We use an *in-vitro* model of hypoxia/ischemia using organotypic hippocampal brain-slices from mice, subjected to oxygen-glucose deprivation (OGD). Neuronal injury is quantified by propidium-iodide (PI) fluorescence.

Results: We show that 50% atm xenon is neuroprotective against hypoxia/ischemia when applied immediately after injury, or after a delay of 3 hours following injury. To validate our method, we show that neuroprotection by gavestinel is abolished when glycine is added, confirming that NMDA-receptor glycine-site antagonism underlies gavestinel neuroprotection. We then show that adding glycine abolishes the neuroprotective effect of xenon, consistent with competitive inhibition at the NMDA-receptor glycine-site mediating xenon neuroprotection.

Discussion & conclusion: We have shown that xenon neuroprotection against hypoxia/ischemia can be reversed by elevating the glycine concentration. This is consistent with competitive inhibition by xenon at the NMDA-receptor glycine-site mediating xenon neuroprotection. Not only does this provide a molecular mechanism (competitive inhibition), but it also, for the first time, clearly identifies the NMDA-receptor as playing a major role in xenon neuroprotection.

1. Franks, N. P., Dickinson, R., de Sousa, S. L. M., Hall, A. C. & Lieb, W. R. *Nature* **396**, 324 (1998).

2. de Sousa, S. L. M., Dickinson, R., Lieb, W. R. & Franks, N. P. *Anesthesiology* **92**, 1055-1066 (2000).

3. Dickinson, R., Peterson, B. K., Banks, P., Simillis, C., Martin, J. C., Valenzuela, C. A., Maze, M. & Franks, N. P.. *Anesthesiology* **107**, 756-67 (2007).

343

EFFECT OF PROPOFOL ON AUTOPHAGY - MEDIATED STRESS RESPONSE IN MOTOR NEURON AFTER TRANSIENT SPINAL CORD ISCHEMIA IN RABBITS

Y. Watanabe[1], M. Sakurai[2], T. Kawamura[1], K. Abe[3]

[1]Anesthesiolosy, [2]Cardiovascular Surgery, National Hospital Organization Sendai Medical Center, Sendai, [3]Neurology, Okayama University, Okayama, Japan

Objective: The mechanism of spinal cord injury has been thought to be related to the vulnerability of spinal motor neuron cells against ischemia. The aim of this study was to investigate whether propofol could protect against ischemic spinal cord damage by suppressing autophagic change.

Methods: We used a rabbit spinal cord ischemia model with use of a balloon catheter. In transient ischemia and treatment with vehicle group and treatment with propofol group, saline or propofol was administered intravenously 10 minutes before the induction of ischemia. Spinal cord was removed at 8 hours, and 1, 2, and 7 days after 15 minutes of transient ischemia. Cell damage was analyzed by counting the number of motor neurons and histological changes. Western blot analysis used for microtubule-associated protein light chain 3(LC3) andγ-aminobutyric-acid type-A (GABAA) -receptor-associated protein (GABARAP), temporal profiles of LC3 and GABARAP immunoreactivity were performed.

Results: In the Group I, about 85% of motor neurons were preserved until 2 days after reperfusion, but were serectively lost at 7 days. In contrast, in the Group P, motor neurons were presereved after 2 days. Western blot analysis and immunoreactivity for LC3 and GABARAP demonstrated that the induction of LC3 and GABARAP were slightly detectable in the sham group samples, which was then strongly enhanced at 8 hours, and was preserved until 2 days after reperfusion in the Group I. In the group P, LC3 and GABARAP were detectable but did not admit enhancement.

Conclusions: Propofol eased the functional deficits and increased the number of motor neuons after ischemia. This study indicates that propofol may protect motor neurons from ischemic injury by suppressing augtophagic change. These results suggest that propofol is a therapeutic agent in the treatment of ischemic spinal cord injury.

344

MAGNETIC RESONANCE IMAGING MEASUREMENT OF CEREBRAL BLOOD FLOW RESPONSE TO THE THIGH CUFF MANOEUVRE

M.A. Horsfield, N.P. Saeed, R.B. Panerai, A.K. Mistri, T.G. Robinson

Cardiovascular Sciences, University of Leicester, Leicester, UK

Introduction: Poor cerebral blood flow autoregulation is implicated in a number of diseases, notably stroke and head injury. We present initial findings from a novel MRI-based method using the thigh-cuff manoeuvre that allows regional assessment of autoregulation. This method has previously been compared to the traditional transcranial Doppler method (*1*).

Subjects and methods: Ten normal subjects were studied. The subjects lay in the MRI scanner and large inflatable cuffs were applied, one to each leg, and inflated to 20 mm Hg above systolic BP. Rapid MRI scanning of the head was performed for 4 minutes using a gradient-echo EPI sequence, with a set of slices covering the head acquired at a rate of one per second. Pressure in the thigh-cuffs was rapidly released at 3 minutes. The procedure was performed three times.

The time-series of images was analysed pixel-by-pixel to evaluate the signal drop and recovery that resulted from the thigh-cuff manoeuvre. First, a 2-D spatial blur was applied (full-width half-maximum [FWHM] 5mm), then any low-frequency (< 0.0125 Hz) signal variation and drift was removed, and signal changes normalised by converting to a percentage change from baseline. A 15-second segment of data after the thigh-cuff release was used to assess both the maximum signal reduction, and the time to return to baseline.

Results: Of the ten subjects, one withdrew because of intolerance to the thigh-cuff pressure, and six of those remaining completed all three repeats with no significant image quality problems due to motion.

In these six subjects, consistent drops in signal intensity were seen in many areas of the brain in all three runs. The coefficient of variation (CoV) in the amplitude of the signal drop over the three runs averaged over all pixels and all subjects was 21%. The largest signal drops, of the order of 6-10%, were seen in the vicinity of large vessels such as the anterior cerebral artery, middle cerebral artery, great central vein and sagittal sinus.

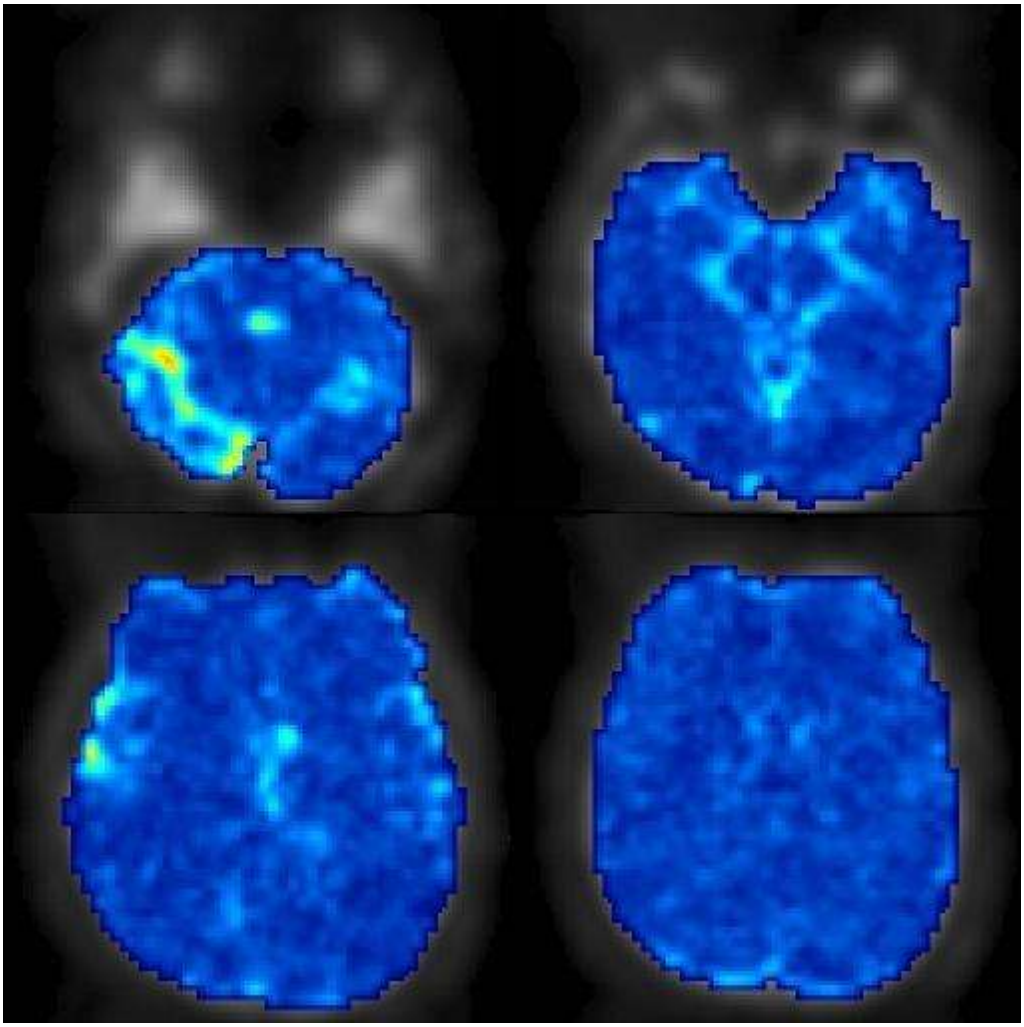

[Figure 1]

Figure 1. Maximum signal drop in four representative slices for one subject.

Due to the greater sensitivity to noise, more spatial blurring was used when evaluating the time to return to baseline (FWHM=20 mm). The time to return to baseline also varied, with those areas showing the largest signal drops taking longer to return to baseline. The mean time to return to baseline averaged over all pixels and all subjects was 6.7 seconds, with a between-runs CoV of 20.1%.

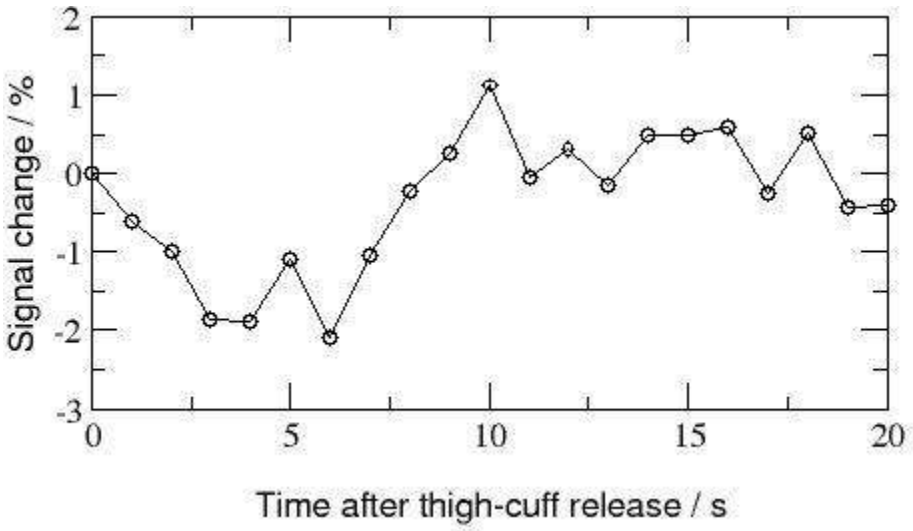

[Figure 2]

Figure 2. Time-course of signal change in a region surrounding the anterior cerebral artery.

Conclusions: We present a novel MRI method for visualising blood flow changes in response to the thigh-cuff manoeuvre. This has potential for mapping autoregulatory response, and the changes that occur in in diseases such as stroke.

1. N.P. Saeed et al. "Measurement of cerebral blood flow responses to the thigh cuff maneuver: a comparison of TCD with a novel MRI method." *JCBFM (in press).*

346

NEAR INFRARED SPECTROSCOPY AS A MEASURE OF VASCULAR REACTIVITY IN BRAIN INJURY.

D.T. Highton[1], A. Ghosh[1], J. Bal[1], I. Tachtisidis[2], C. Kolyva[2], C. Elwell[2], M. Smith[1]

[1]Neurocritical Care, National Hospital for Neurology and Neurosurgery, University College London Hospitals, [2]Department of Medical Physics and Bioengineering, University College London, London, UK

Objectives: Continuous monitoring of cerebral autoregulation (CA) might identify therapeutic windows and novel treatment targets, thus potentially improving outcome in brain injury. However, no widely accepted bedside monitoring modality has emerged. Growing evidence supports a relationship between Near infrared spectroscopy (NIRS) derived indices of vascular reactivity and established indices[1-2]: pressure reactivity index (PRx) and mean velocity index (Mx), calculated from intracranial pressure (ICP) and transcranial Doppler flow velocity respectively. We explore the relationship between these indices in the time and frequency domains to investigate the utility of NIRS as a surrogate of CA.

Methods: 25 ventilated severely brain-injured patients were studied during a period of clinical stability. One hour of multimodal neuro-monitoring data was gathered including ipsilateral ICP, middle cerebral artery flow velocity (FV) and NIRS (NIRO 100, Hamamatsu Photonics). NIRS indices of CA were derived in an identical fashion to Mx and PRx using a moving correlation coefficient of 30 consecutive 10-second time averaged data points of NIRS variables and arterial blood pressure (ABP). Thus multiple indices based on both absolute and relative concentration of haemoglobin species were produced. These were compared with Mx and PRx using correlation and Bland-Altman analysis while the underpinning relationships between ICP, NIRS and FV were investigated using cross-spectral and wavelet based techniques (complex Morlet wavelet, Matlab Mathworks).

Results: Significant correlation and agreement was found between the majority of NIRS variables, Mx and PRx - most notably those derived from the total haemoglobin index (THI) [PRx ($r = 0.72$ $p < 0.001$) Mx ($r = 0.50$ $p < 0.05$), 95% limits of agreement, PRx (-0.45 - 0.34), Mx (-0.60 - 0.63)]. Coherence between THI, ICP and FV revealed bands of high coherence > 0.5 in all traces in frequencies < 0.05Hz (a frequency band commonly associated with autoregulatory mechanisms, ICP slow waves and PRx[3]), but these did not extend over the entire spectrum and varied with time. The wavelet phase coherence between ICP, FV and ABP was closely related to PRx ($r = 0.95$ $p < 0.001$) and Mx ($r = 0.93$ $p < 0.001$) . Using the same method THI/ABP coherence correlated with PRx ($r = 0.64$ $p < 0.001$), Mx ($r = 0.54$ $p < 0.05$) and enabled focused assessment of areas of high ABP power more clearly establishing relationships in individual waveforms. An example of the data generated is shown in figure 1.

Discussion: NIRS derived indices of CA are significantly related to both PRx and Mx but agreement is limited by the complex, non-stationary, non-linear relationship between ICP, FV and NIRS variables. Wavelet based techniques aid the interpretation of such complex time variant signals as they can focus analysis to specific features of interest within the time and frequency domains simultaneously, producing qualitative and quantitative evidence of CA not possible with other methods.

References:

(1) Zweifel. J Neurotrauma 2010; 27(11):1951-1958

(2) Steiner. Neurocritical care 2009;10(1):122-8

(3) Lee. Stroke 2009;40(5):1820-6

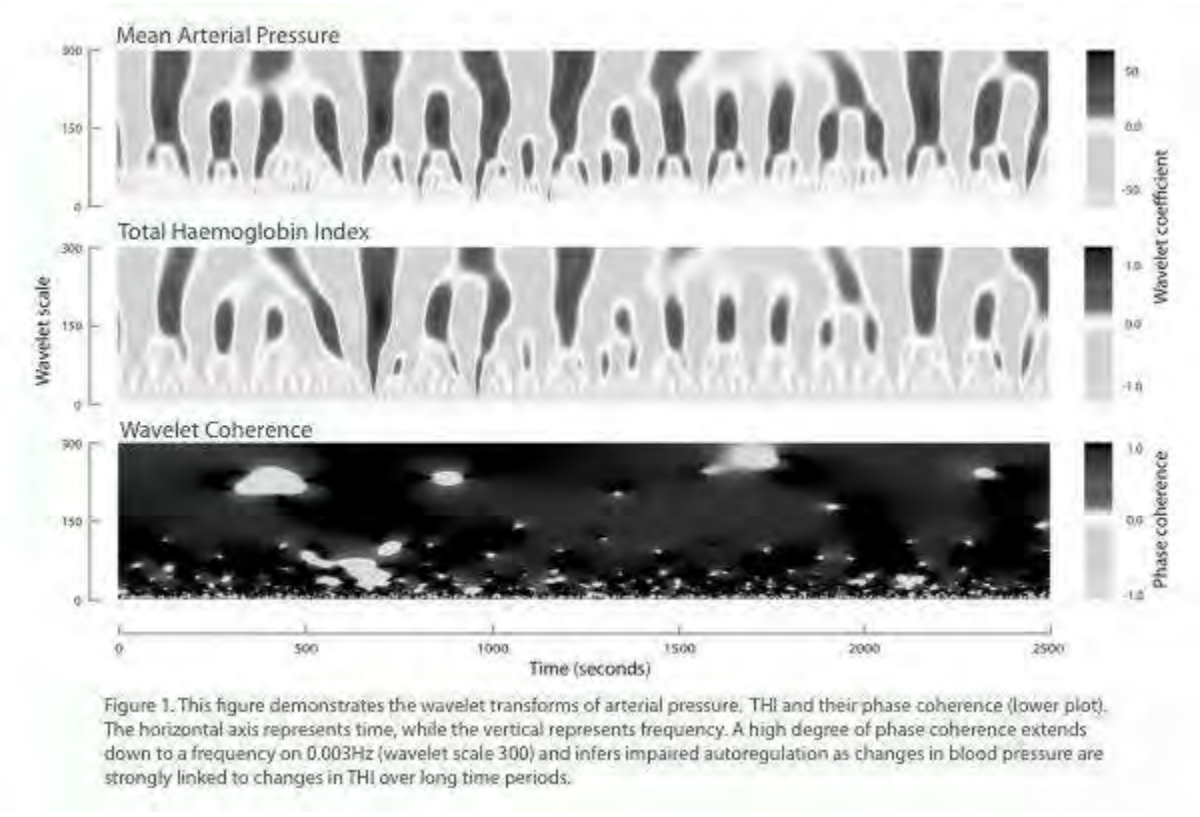

Figure 1. This figure demonstrates the wavelet transforms of arterial pressure, THI and their phase coherence (lower plot). The horizontal axis represents time, while the vertical represents frequency. A high degree of phase coherence extends down to a frequency on 0.003Hz (wavelet scale 300) and infers impaired autoregulation as changes in blood pressure are strongly linked to changes in THI over long time periods.

[Wavelet Transform]

347

FOCAL NEURONAL DAMAGE IN PATIENTS WITH NEUROPSYCHOLOGICAL IMPAIRMENT FOLLOWING DIFFUSE TBI: EVALUATION USING ^{11}C-FLUMAZENIL PET WITH STATISTICAL IMAGE ANALYSIS

N. Kawai, T. Tamiya

Department of Neurological Surgery, Kagawa University Faculty of Medicine, Kita-gun, Japan

Objectives: This study was conducted to identify the regional neuronal damage in patients with neuropsychological impairment following diffuse traumatic brain injury (TBI) compared with normal control subjects. In addition, measures of the neuropsychological tests were correlated with the regional flumazenil (FMZ) binding potential (BP) reduction to clarify the relationship between cognitive impairment and regional neuronal damage.

Methods: We performed ^{11}C-flumazenil positron emission tomography (FMZ-PET) study using 3D stereotactic surface projection (3D-SSP) statistical image analysis in 8 diffuse axonal injury (DAI) patients (mean 29.1 ± 11.1, range 19-46 years). All patients underwent the Wechsler Adult Intellectual Scale, The Third Edition (WAIS-Ш) to assess the general intelligence. Twenty healthy control subjects (mean 24.4 ± 2.8, range 22-30 years) were studied to obtain the normal data base for 3D-SSP.

Results: Group comparison showed a significant regional low FMZ uptake in the bilateral medial frontal gyri, the anterior cingulate gyri, and the thalamus.

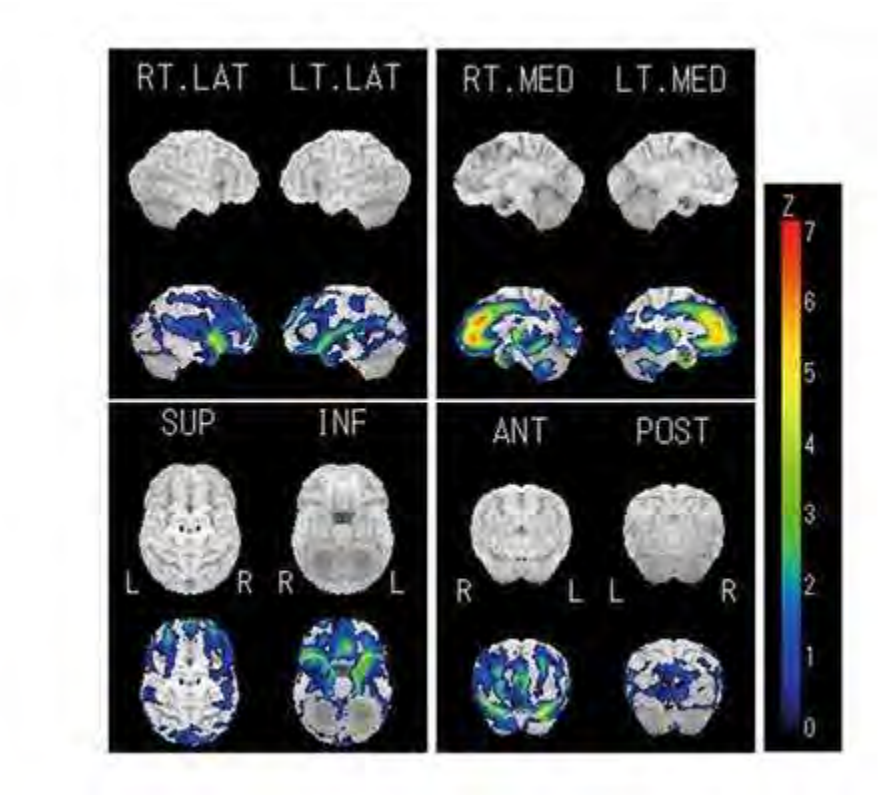

[Fig. 1]

Individual analysis also showed decreased FMZ uptake in these regions; however, the distribution and “extent” of low FMZ uptake were different in each individual case. Full-scale IQ (FIQ) and performance IQ (PIQ) negatively correlate with the degree of FMZ BP reduction in the right thalamus. FIQ, verbal IQ (VIQ) and PIQ also negatively correlate with the FMZ BP reduction in the left medial frontal gyrus.

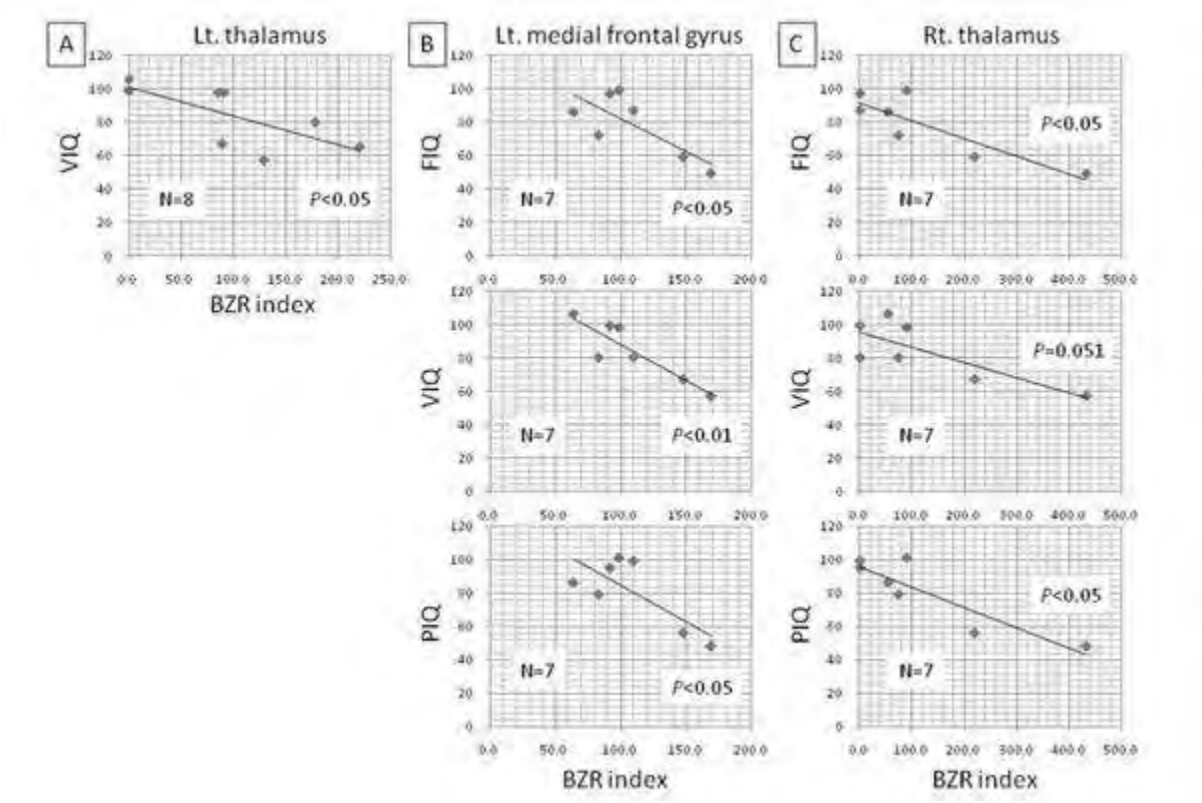

[Fig. 2]

Conclusions: DAI uniformly induces neuronal damage in the medial frontal cortex and the thalamus, which may be related to underlying cognitive impairment in diffuse TBI patients. Future studies to confirm a common area of focal neuronal damage and a direct correlation to the neuropsychological test may validate the use of FMZ-PET for the functional diagnosis of neuropsychological impairment after TBI.

349

SIMPLIFIED KINETIC MODELLING OF THE 5-HT_{2A} TRACER [^{11}C]MDL-100907 IN RATS

A.K.D. Visser, E.F.J. De Vries, A.T.M. Willemsen, A. Van Waarde, R.A.J.O. Dierckx

Nuclear Medicine and Molecular Imaging, University Medical Center Groningen, Groningen, The Netherlands

Objectives: The serotonin 5-HT_{2A} receptor is involved in prefrontal cortex functioning in stress and depression. The use of [^{11}C]MDL-100907 for non-invasive PET imaging of 5-HT_{2A} receptor expression has been fully validated in humans [1]. In rats, however, only brain region-cerebellum tracer accumulation ratios have been applied as a measure of receptor expression [2]. Animal models are of great interest, especially for therapy evaluation. A validated non-invasive method to measure receptor binding potential (BP) is needed to perform longitudinal studies. The question is whether pharmacokinetic modeling using a reference tissue as the input function instead of multiple arterial blood samples is feasible.

Therefore, we calculated BP of [^{11}C]MDL-100907 using a simplified reference tissue model (SRTM) and compared results with distribution volume (DV), calculated from Logan plots.

Materials and methods: Two groups of animals (N= 7/group) were used, whereof two animals were scanned simultaneously for 90 minutes. In one group of animals, unlabeled MDL-100907 (0.2 mg/kg) was injected together with 25 (±11) MBq of [^{11}C]MDL-100907 to block tracer binding. The other group received the same amount of tracer with vehicle. From all animals, 15 arterial blood samples were taken for calculation of the arterial input function and at 6 time points extra blood was taken for metabolite analysis. We used a SRTM to calculate BP with cerebellum as a reference tissue and Logan plots to calculate DV using a metabolite corrected arterial input function. Regions of interest were drawn around various brain areas on an MRI template.

Results: The tracer was highly metabolized in both groups, with on average 23 (±5) and 29 (±5) % parent after 10 min in the control and blocked group, respectively. BP (SRTM) and DV (Logan) showed the same distribution between brain regions: Frontal cortex > striatum > rest cortex > amygdala > hippocampus > brainstem > cerebellum. In all brain regions, blocking of the receptor resulted in significantly lower BP and DV, with exception of the cerebellum. No regional differences in DV were found in the blocked group (fig).

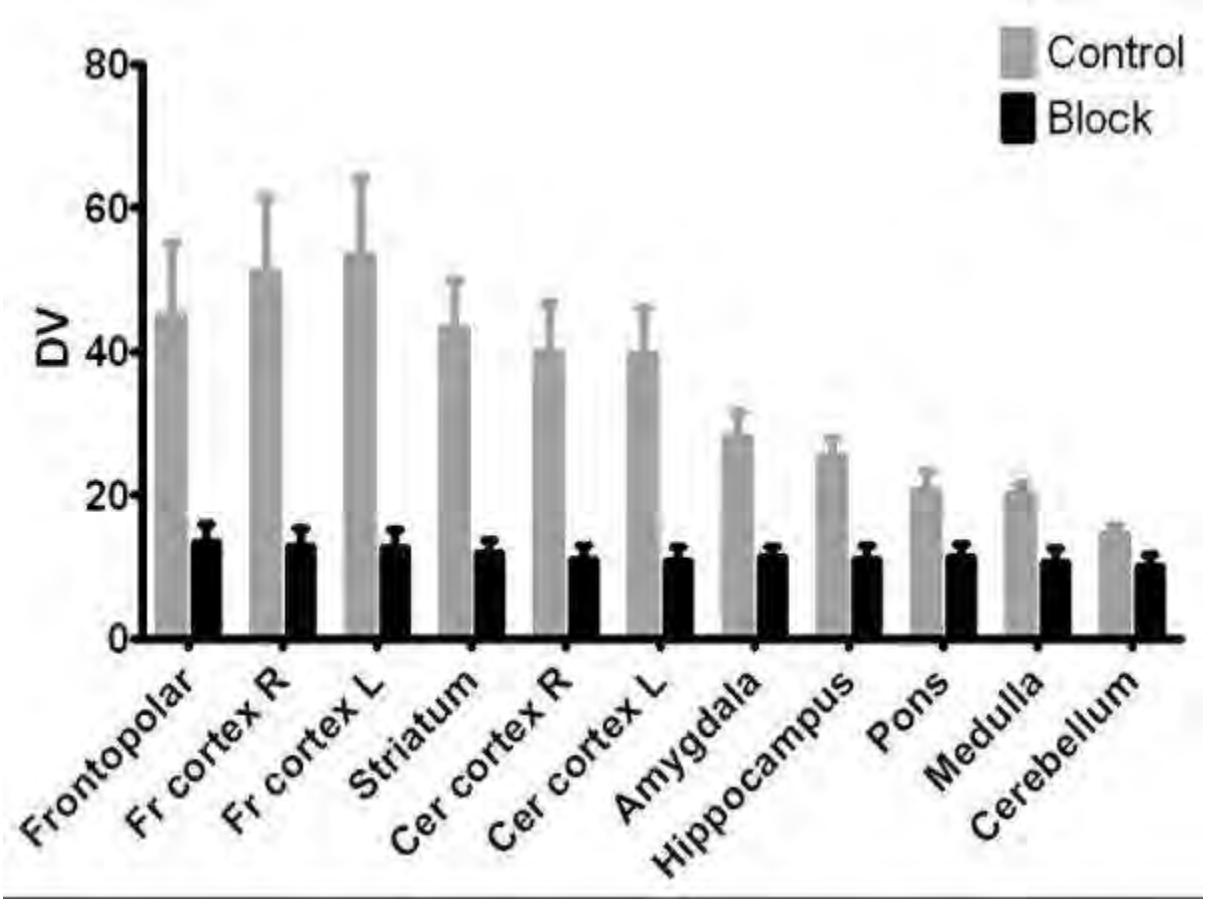

[Distribution Volume control vs block]

Conclusions: As there is no significant difference in DV in cerebellum, between blocked and control animals, receptor mediated tracer uptake in cerebellum seems negligible. Therefore, this region seems a valid reference region. The absence of a significant difference between brain regions in the blocked group indicates similar non-specific binding. Therefore, we conclude that the SRTM seems a valid approach for kinetic modeling of 5-HT_{2A} receptor expression, which can be applied in longitudinal studies in rats.

References:

(1) Meyer et al. *Neuroimage*, 50(3):984-993 (2010)

(2) Hirani et al. *Synapse*, 50(3):251-260 (2003)

350

CLINICAL IMPLICATIONS FOR SOLUBLE FORMS OF RECEPTOR FOR ADVANCED GLYCATION END PRODUCTS (RAGE) IN PATIENTS WITH ACUTE ISCHEMIC STROKE

C. Yokota, M. Fukuda, K. Sato, K. Toyoda, K. Minematsu

Cerebrovascular Medicine, National Cerebral and Cardiovascular Center, Suita, Japan

Background and aims: A secreted isoform of receptor for advanced glycation end products (RAGE), termed soluble RAGE (sRAGE), involves sRAGE and endogenous sRAGE (esRAGE). sRAGE was proteolytically cleaved from the cellular surface by the action of matrix metalloproteinases, and esRAGE was secreted extracellularly. Both isoforms are considered to neutralize the adverse effects of RAGE signaling by acting as a decoy[1,2]. The AGEs-RAGE system was regarded to play a role on development of not only atherosclerosis[3] but also neuronal inflammation[4]. Few studies were addressed the pivotal roles of the AGEs-RAGE system in acute stroke patients. We aimed to examine plasma sRAGE/esRAGE levels associated with clinical features in acute stroke patients.

Methods: We enrolled prospectively 381 patients (male 227, 72 years in average) admitted within 3 days of stroke onset from December 2007 to October 2009. Clinical features on admission including risk factors and stroke severity were assessed and recorded by experienced stroke physicians. Blood samples for measurement of plasma glucose, lipid, and sRAGE levels were obtained within 3 days after the stroke onset. Renal function was assessed using the estimated glomerular filtration rate (eGFR) calculated from the Japanese equations[5]. Patients were divided into three equal categories based on tertiles of the plasma sRAGE/esRAGE levels.

Results: Median values of sRAGE/esRAGE levels were 891/250 pg/ml in brain infarction (n=247), 853/270 pg/ml in transient ischemic attack (n=39), and 728/200 pg/ml in brain hemorrhage (n=95). sRAGE levels correlated significantly with age, smoking habit, atrial fibrillation (AF), body mass index (BMI), eGFR, and NIHSS scores on admission by the simple regression analyses. Among these concomitant risk factors, the lowest tertile of sRAGE was associated with normal eGFR (≥ 90 ml/min/1.73m^2) (OR, 2.81; 95%CI, 1.62-4.87) by the multiple regression analysis. esRAGE had significantly correlations with age, smoking habit, BMI, AF, brain hemorrhage, diastolic blood pressure, HDL cholesterol, and eGFR by the simple regression analyses. By the multiple regression analyses, the lowest tertile of esRAGE was associated positively with smoking habit (1.38; 1.03-1.88), diastolic pressure (1.02;1.001-1.03), eGFR (2.01; 1.17-3.64), and negatively with the frequency of AF (0.43;0.23-.81).

Conclusions: Both plasma sRAGE and esRAGE levels in patients with acute stroke correlated with eGFR. The lower level of plasma esRAGE rather than sRAGE could be a biomarker for hypertensive cerebral angiopathy.

1. Malherbe P, et al. : *Brain Res Mol Brain Res*. 1999;71:159-170.

2. Yonekura H, et al: *Biochem J*. 2003;370:1097-1109.

3. Falcone C, et al.: *Arterioscler Thromb Vasc Biol*. 2005;25:1032-1037.

4. Rong LL, et al: *FASEB J*. 2004;18:1818-1825.

5. Matsuo S, et al: *Am J Kidney Dis*. 2009;53:982-992.

351

ANGIOGENIC FUNCTION OF CCM GENES IN ENDOTHELIAL CELLS DERIVED FROM CEREBRAL CAVERNOUS MALFORMATIONS

Y. Zhu, Q. Wu, J.-F. Xu, I.E. Sandalcioglu, U. Sure

Department of Neurosurgery, University of Duisburg-Essen, Essen, Germany

Objective: Cerebral cavernous malformation (CCM) is one of the most frequent vascular malformations in brain and clinically presents recurrent headaches, seizures, hemorrhagic stroke and/or focal neurologic deficiency. CCMs appear as either sporadic or familial forms (around 20%) and loss-of-function mutations in *CCM1-3* genes are frequently detected in familial CCMs. However, the functions of these genes remain unclear. Indeed, the current *in vitro* studies on these genes were performed mostly in commercial purchased normal endothelial cells and the results appeared discrepancy. The present study aimed to investigate the role and the signaling of *CCM1-3* genes in the key steps of angiogenesis using endothelial cells derived from CCMs (CCM-ECs).

Methods: CCM-ECs were isolate, purified and cultured from the fresh operative specimens of sporadic CCMs. *CCM1-3* were silenced by the specific siRNAs in CCM-ECs and in control cultures (HBMEC and HUVEC). The efficiency of gene silencing was proven by real-time PCR. Cell proliferation and apoptosis, migration and tube formation, the expression of phosphor-p38, phospho-Akt and phosphor-Erk1,2 were analyzed after silencing individual *CCM* genes.

Results: Silencing *CCM1* inhibited endothelial proliferation in an order of HUVEC< HBMEC< CCM-EC, whereas the most significant increase in cell migration was observed in CCM-EC after *CCM1* silencing. *CCM3* deletion significantly promoted proliferation, reduced apoptosis in all three types of endothelium, but accelerated cell migration exclusively in CCM-EC. Interestingly, *CCM2* siRNA influenced neither cell proliferation nor migration. Silencing *CCM3* and, to a lesser extent, *CCM1 and CCM2* stimulated the growth and extension of sprouts selectively in CCM-EC. Loss of *CCM1*, *CCM2* or *CCM3* did not significantly influence the formation of the tube-like structure. However, the maintenance of tube stability was distinctly different in CCM-EC and in HUVEC after silencing *CCM1, CCM2* or *CCM3*. Western blot revealed that knockdown of *CCM2* and *CCM3,* but not *CCM1,* commonly activated p38, Akt and Erk1,2 in CCM-ECs.

Conclusions: The unique response of CCM-ECs to *CCM1-3* siRNA, in comparison to HBMEC and HUVEC, indicates that some of angiogenic functions of CCM genes are context-dependent, and therefore, CCM-EC is particular valuable for further studies on the pathogenesis of CCMs. The activation of p38, Erk1,2 and Akt signal proteins in *CCM2*- or *CCM3*-silenced CCM-ECs suggests a possible involvement of these common pathways in the pathogenesis of CCMs. However, the specific signalling mediating the distinct function of *CCM* genes in the pathogenesis of CCMs needs to be further elucidated.

352

HYPERPERFUSION SYNDROME FOLLOWING SUPERFICIAL-MIDDLE CEREBRAL ARTERY ANASTOMOSIS IN PATIENTS WITH MOYAMOYA DISEASE: EVIDENCE FROM CEREBRAL BLOOD FLOW STUDIES

K. Furuya, A. Ogawa, T. Shinohara, T. Watanabe, S. Takanashi, T. Nakagomi

Neurosurgery, Teikyo University School of Medicine, Tokyo, Japan

Introduction: Cerebral hyperperfusion, a state characterized by a significant increase in cerebral blood flow (CBF) relative to the homologous area of the contralateral hemisphere, may complicate a number of neurological and neurosurgical conditions. Temporary postoperative neurological deterioration associated with hyperperfusion has also been reported after extracranial-intracranial bypasses. Moyamoya disease is characterized by gradual stenosis of the intracranial portion of the internal carotid arteries (ICA). In turn, fine vessels called moyomoya vessels develop and cause ischemic and/or hemorrhagic stroke. Superficial temporal-middle cerebral artery anastomosis (STA-MCA anastomosis) is a standard surgical therapeutic option in patients with moyamoya disease. Most patients undergo improvements in their clinical symptoms immediately after surgery. We experienced three patients with moyamoya disease who suffered from severe neurological deterioration after STA-MCA anastomosis caused by hyperperfusion.

Case report and result: These are 2 males and 1 female patients, ranging in age from 20 to 39 year-old (mean: 32.6). Unilateral moyamoya disease includes 1 patient. Neurological deterioration including aphasia, sensory disturbance, motor weakness and generalized convulsion began from 2 days after surgery and lasted for over 14 days. Preoperative single photon emission computed tomography (SPECT) disclosed reduction of CBF in the resting state. In all patients, the cerebral perfusion reserve estimated by acetazolamide infusion was severely disturbed in the affected lesion. After surgery, SPECT demonstrated focal intense accumulation of the tracer on the side of the surgery**.** Magnetic resonance (MR) imaging did not show any abnormalities except for the postoperative change. MR digital subtraction angiography in 2 patients and three dimensional computed tomographic angiography in 1 patient revealed hyperperfusion on the side of the surgery where the cerebral perfusion reserve was severely disturbed preoperatively. This collective evidence strongly supports the notion that hyperperfusion following STA-MCA anastomosis could occur in the poor perfusion reserve area preoperatively and could cause temporary neurological deterioration.Cerebral ischemia creates a situation in which the resistant vessels dilate maximally in order to increase local CBF. After a long period of dilatation, the vessels might become atonic and lose the capacity for normal autoregulation. Excessive blood flow directed into a poorly autoregulated vascular bed may induce local cerebral edema resulting in transient localized cortical dysfunction. The cases we present herein supports the hypothesis that the neurological deterioration is closely related to increased blood flow and volume in chronically ischemic regions of the brain. In contrast to carotid endarterectomy, STA-MCA anastomosis rarely causes transient hyperperfusion syndrome, probably because the bypass flow through the STA is rather less than the ICA flow. This syndrome after STA-MCA anastomosis is rare, but must be considered in patients manifesting neurological deterioration. The explanation as to why patients with postoperative hyperperfusion in the previously hypoperfused areas experience transient neurological deficits still remains unknown.

Conclusion: Hyperperfusion without already extensive irreversible damage invariably predicted minute (or absent) infarct and excellent spontaneous recovery, so that these patients would not

be rational candidates for stroke treatment. Therefore, we have to keep in mind that hemodilution or induced hypertension therapy might be contraindicated in such patients.

353

ACTIVATION OF THE CANONICAL NOTCH-SIGNALING PATHWAY MEDIATES ISCHEMIC BRAIN INJURY IN MICE

Q. Yang, L. Hou, H. Dong, X. Li, Q. Wang, H. Dong, L. Xiong

Department of Anesthesiology, Xijing Hospital, Fourth Military Medical University, Xi'an, China

Objective: The canonical Notch-signaling pathway (CNSP) is characterized by γ-secretase-dependent release of Notch intracellular domain from cell membrane and subsequent translocation to the nucleus, where it activates a transcriptional program in coupling with the essential transcriptional factor RBP-J[1]. Ablation or attenuation of Notch receptor expression can remarkably impact stroke outcome in rodents[2,3], suggesting that Notch signaling may be an important determinant for ischemic brain injury. However, while the vessel-enriched Notch (Notch-3) functions mainly on cerebrovascular regulation[2], it remains unknown whether the pathogenic participation of Notch in ischemic injury involves a neuronal component. In the present study, using both transgenic and pharmacological approaches, we have demonstrated for the first time that neuronal activation of CNSP is obligatory in promoting neuronal cell death and neurological impairment after transient focal cerebral ischemia (tFCI).

Methods: tFCI was induced for 1 hr in 8-10 weeks old male C57BL/6 mice by filament occlusion of the middle cerebral artery. CNSP was assessed in brain tissues at 0-72 hr after tFCI by quantifying the released Notch intracellular domain (rNICD) and mRNA expression of Notch target genes Hes1 and Hes5 using Western blot analysis and real-time PCR, respectively. To determine the contributing role of Notch signaling in ischemic brain injury, tFCI was induced in forebrain-neuronal-specific Notch-RBP-J conditional knockout (Notch-RBP-J-cko) mice and wild type (WT) littermates, and in mice treated with the γ-secretase/Notch inhibitor DAPT (*s.c.*, 100mg/kg, 2 hrs before tFCI). Neurological performance (Garcia score), infarct volume (TTC staining), and cell death (TUNEL) were examined at 72 hr after tFCI. Statistical analyses were performed using ANOVA and *post hoc* Fisher's PLSD tests, with $P < 0.05$ considered statistically significant.

Results: Compared to sham-operated animals, the levels of rNICD (*$P < 0.05$, n=5/group) and Hes1 and Hes5 mRNA were significantly increased at 2-72 hrs after tFCI. The Notch-RBP-J-cko mice, generated by crossing the RBP-J-floxed mice to CamKIICre mice, were viable and healthy and showed no macroscopic abnormalities by gross observations. However, Notch-RBP-J-cko mice exhibited improved neurological performance and significantly reduced infarct volume (*$P < 0.05$, n=8/group) and neuronal cell death after tFCI compared to WT littermates. Moreover, administration of DAPT, which prevented the generation of rNICD, significantly improved neurological score and reduced infarct volume after tFCI (*$P < 0.05$, n=10/group). None of the above manipulations of Notch in animals resulted in changes in cortical blood flow (laser Doppler flowmetry) or other physiological parameters during tFCI compared to control animals.

Conclusion: The results provide novel evidence suggesting that activation of the neuron-specific γ-secretase/Notch/RBP-J signaling pathway contributes to ischemic brain injury by mediating neuronal cell death. Notch signaling thus may represent a new therapeutic target for the treatment of ischemic stroke.

References:

1. Kopan et al. *Cell* 2009, 137: 216-33.

2. Arboleda-Velasquez et al. *Proc Natl Acad Sci U S A.* 2008, 105:4856-61.

3. Arumugam et al. *Nat Med* 2006, 12: 621-23.

354

PAVLOVIAN FEAR CONDITIONING DETECTS MILD HYPOXIC-ISCHEMIC BRAIN INJURY IN NEONATAL MICE

M. Pekna[1], K. Järlestedt[1], A.L. Atkins[1], H. Hagberg[2,3], C. Mallard[1]

[1]Institute of Neuroscience and Physiology, [2]Department of Obstetrics and Gynecology, University of Gothenburg, Gothenburg, Sweden, [3]Institute of Reproductive and Developmental Biology, Imperial College London, London, UK

Pavlovian fear conditioning assesses learning deficits associated with injury to the hippocampus and amygdala in rodents. The aim of this study was to establish whether Pavlovian fear conditioning could be used to detect memory deficits following mild hypoxic-ischemic (HI) injury in neonatal mice.

Brain injury was induced in mice at postnatal day 9 (P9) by 30-minute HI. At P49 and P50, animals were tested for: 1. Fear conditioning with a shock-paired tone and light; 2. Fear conditioning with a delayed shock-paired tone and 3. Fear conditioning with a shock-paired tone and additional, more salient contextual cues. Outcome was assessed as percent freezing behavior over a 2-minute period.

Both shock-paired tone and light and shock-paired tone with added contextual cues enhanced tone-induced freezing behavior in the control group, but not in the HI group. However, shock-paired tone with added contextual cues also enhanced contextual cue-induced freezing in the control group, which resulted in less tone-enhanced freezing. In trace fear conditioning with a 20-second delay between the tone and the shock, freezing behavior did not differ between control and HI animals. Hippocampal and amygdala volume were smaller in the ischemic hemisphere of the HI mice.

In summary, we have shown that Pavlovian fear conditioning is a sensitive method to detect memory impairments following mild HI injury in neonatal mice. Using both shock-paired tone and light as conditioned stimuli and a short delay between the conditioned stimuli and the shock is the most effective way to detect mild damage to the hippocampus and amygdala.

355

QUANTIFYING BOLUS DISPERSION IN ARTERIAL SPIN LABELLING TO MONITOR HAEMODYNAMICS IN VASCULAR DISEASE

M. Chappell[1,2], B.J. MacIntosh[3], **S.J. Payne**[1]

[1]Institute of Biomedical Engineering, [2]FMRIB Centre, University of Oxford, Oxford, UK, [3]Department of Medical Biophysics, University of Toronto, Toronto, ON, Canada

Objectives: The non-invasive ASL MRI technique is designed to create a well-defined bolus of contrast at the labelling site. By the time the blood water label has reached the brain tissue of interest, however, dispersion will have altered its shape. This has implications for perfusion quantification, but it may also be an indicator of hemodynamic changes in disease or with age [1]. Quantification of dispersion requires the fitting of a model to temporally sampled data. However, a large number of models exist with a variety of physiological reality and complexity. We sought to investigate appropriate models for dispersion quantification in a realistic clinical population.

Methods: Data were acquired from 24 patients with varying degrees of carotid stenosis both pre and post carotid endarterectomy (mean age 70 years). A pulsed ASL preparation and time-resolved angiographic readout were used to acquire 20 inflow phases with a temporal resolution of 78 ms at 3T. Five ASL models were considered

1) No dispersion,

2) Gamma-variate function,

3) convolution with a Gaussian dispersion function [2]

4) as 3 but with modified Gaussian function [3],

5) as 3 but with a gamma function.

Fitting was performed using a probabilistic method that has previously been applied to ASL [4]. Models were assessed based on the 'free-energy' of the model fit, which is an approximation to the Bayesian model evidence: a measure of 'goodness-of-fit' that includes a penalty for model complexity. Three ROIs was placed manually at the inlets to the left and right middle cerebral arteries (MCA-L and -R) and vertebrobasilar artery (VBA) at the level of the Circle of Willis. The mean value of the free energy was calculated in each ROI. The significance of improvement in free energy between models was tested using a one-tailed T-test at $p < 0.05$.

Results: The figure shows the free energy within each ROI across all patients for the models considered, along with bars indicating significant differences. Lower log(free energy) is better and indicates that models based on the convolution with a dispersion function are superior. Mean values of the model parameters consistently indicated a greater degree of dispersion in the VBA than the MCAs. Significant differences in dispersion pre and post surgery were found for models 2, 3 and 5.

Conclusions: Dispersion of an ASL bolus can be quantified in major arteries from time resolved angiographic images. Greatest model fit was achieved where models based on convolution of the ideal bolus with a dispersion function were employed. This has the advantage that effects of

the sequence on the bolus shape can be separated from dispersion. This patient population considered here is likely to exhibit greater dispersion than a younger healthy population.

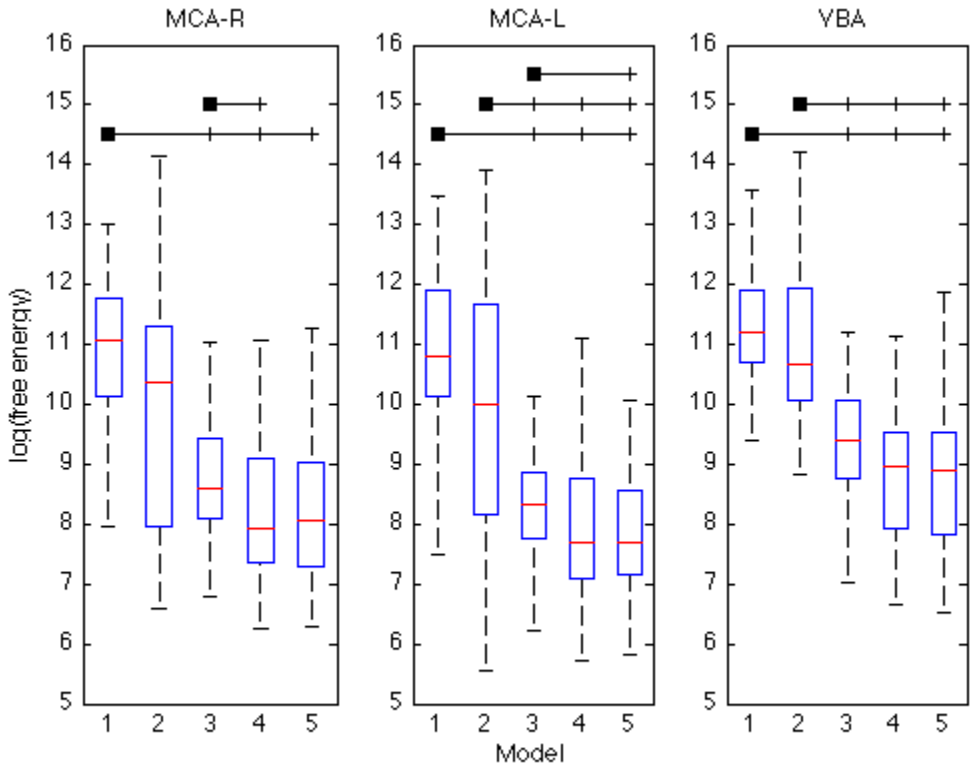

[Figure: Model comparison at artery inlets.]

References:

1. MacIntosh et al., Stroke, in press, 2011.

2. Hrabe and Lewis, J. Magn. Reson. Med. 167:49-55, 2004.

3. Ozyurt et al., Proc. Int. Soc. Magn. Reson. Med., Stockholm, 2010.

4. Chappell et al., IEEE Trans. Sig. Proc. 57:223-236, 2009.

357

CALCULATIONS OF ARTERIAL TRANSIT TIME, TOTAL TRANSIT TIME AND MEAN DISTRIBUTION TIME USING PULSED TIME-RESOLVED ARTERIAL SPIN LABELING MRI

A. Bibic[1], L. Knutsson[1], F. Ståhlberg[1,2], R. Wirestam[1]

[1]Department of Medical Radiation Physics, [2]Department of Diagnostic Radiology, Lund University, Lund, Sweden

Introduction: Arterial spin labeling (ASL) is a non-invasive MRI technique for quantification of blood perfusion. The technique employs the arterial water as an endogenous freely diffusible tracer magnetically labeled by a 180° radiofrequency pulse. The aim of this work was to adapt a previously published quantitative ASL method, based on a macroscopic model (1), to a clinical MRI scanner.

Methods: The ASL data were acquired using a 3T MRI unit (Philips Achieva) in a healthy volunteer using the QUASAR pulse sequence (2). The project was approved by the local ethics committee, and the volunteer gave written informed consent before participation. The imaging parameters were as follows: TR/TE/ΔTI/TI1=4000/23/300/40ms, 64x64 matrix, 7 slices, FOV=240x240mm^2, flip angle 35°, SENSE factor 2.5, 48 averages with V_{enc}=4cm/s and 24 averages without arterial suppression. The difference between non-velocity-encoded and velocity-encoded data, for each sampling point, was used to calculate the arterial input function (AIF), from which the bolus duration was subsequently estimated (Fig. 1a). Using ROI data (cf. Fig. 1b), the total transit time (TTT) and the mean distribution time (MDT) were extracted from the fitting of experimental data to Eq. 1 (1).

The ATT=TTT-MDT is the time it takes for blood plasma to travel from the labeling plane to the beginning of the capillary bed, where MDT (referred to as CTT in ref. (1)) is the time it takes for the intravascular water to distribute from the capillary bed to the parenchyma. Finally, TTT (referred to as MTT in ref. (1)) is the total transit time from the labeling plane to the imaging plane. C_0 represents the input function, τ is the bolus duration and T_1=1.66 s is the longitudinal blood relaxation time (3). The least-squares fitting was performed using a locally developed computer program (IDL 6.3, Research Systems Inc.).

Results: Fig. 1a shows the AIF, and from this curve the bolus duration was estimated to be 900ms. The ROI in Fig. 1b represents the region for which the transit-time parameters were extracted. Fig. 1c shows the least-squares fit of the ASL model to the experimental data. The obtained numerical values of TTT, MDT and ATT were 1.77s, 0.57s and 1.20s, respectively.

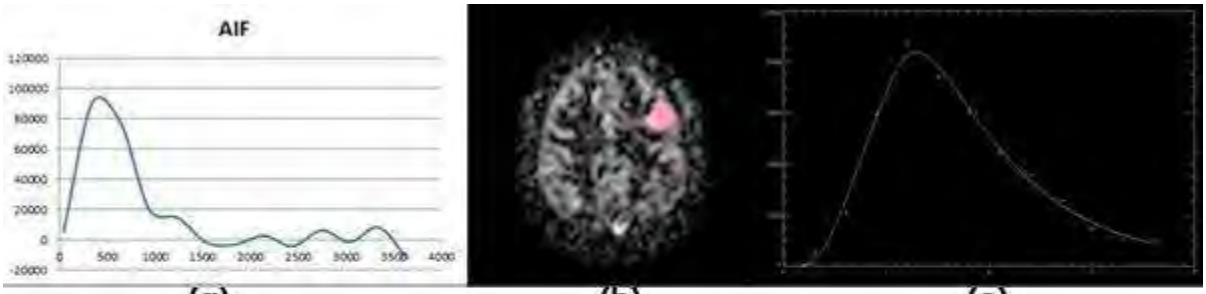

$$c(V,t) = \frac{c_0}{2} exp\left(\frac{TTT}{2MDT}\right)\left(erfc\left(\frac{TTT}{4MDT \cdot t} - \sqrt{\left(\frac{1}{4MDT} + \frac{1}{T_1}\right)t}\right) \times exp\left(-\frac{TTT}{\sqrt{MDT}}\sqrt{\frac{1}{4CTT} + \frac{1}{T_1}}\right)\right)\Bigg|_{t=t-\tau}^{t=t} \quad \text{eq. 1}$$

[Fig1]

Conclusions: The employed model has previously been validated in an animal study using a 7T small-bore animal MR system and a continuous ASL sequence (1). In the present study, we applied the concept to human subjects and employed a 3T clinical MRI scanner and a clinically more appropriate pulsed ASL sequence. The obtained time parameters seem numerically reasonable, and the obtained ATT values were in agreement with previously published results (4). The future goal is to compare these results with other techniques, and to apply the proposed concept to suitable patient groups.

References:

1. Kelly ME et al, Phys. Med. Biol. 54 (2009) 1235-1251.

2. Petersen ET et al, MRM 2006;55:219-32.

3. Lu H et al, MRM 2004;52:679-682.

4. Qiu M et al, MRM 2010;63:374-384.

358

INVESTIGATION OF CEREBRAL AUTOREGULATION IN ACUTE ISCHEMIC STROKE WITH DIFFUSE OPTICS

R.C. Mesquita[1,2], C.G. Favilla[3,4], M.N. Kim[1], M.T. Mullen[3], J.H. Greenberg[3], J.A. Detre[3], S.E. Kasner[3], A.G. Yodh[1]

[1]Department of Physics & Astronomy, University of Pennsylvania, Philadelphia, PA, USA, [2]Institute of Physics 'Gleb Wataghin', University of Campinas, Campinas, Brazil, [3]School of Medicine, University of Pennsylvania, Philadelphia, PA, [4]School of Medicine, University of Florida, Jacksonville, FL, USA

Introduction: A major goal in the care of acute ischemic stroke (AIS) is optimization of cerebral blood flow (CBF) in order to prevent additional damage in the ischemic penumbra. Following AIS, cerebrovascular autoregulatory mechanisms become impaired and CBF becomes dependent on cerebral perfusion pressure. Clinically, there is no bedside perfusion monitor available to optimize CBF in individual patients.

Objective: Current guidelines recommend the empirical use of flat head-of-bed (HOB) to maximize CBF following AIS. Transcranial Doppler ultrasonography (TCD) indicates that flat HOB is associated with increased macrovascular blood velocity. Here, we employed Diffuse Correlation (DCS) and Optical (DOS) Spectroscopies to monitor microvascular perfusion and oxygenation during HOB manipulation in AIS patients. Relative CBF changes (rCBF) obtained from DCS were compared to simultaneous measurements of blood velocity from TCD (vTCD). In addition, auxiliary measurements of heart rate and systolic, diastolic and mean arterial (MAP) blood pressures were used to investigate the relationships between rCBF, vTCD, and systemic variations due to HOB.

Material and methods: Fifteen patients with unilateral middle cerebral artery cortical infarction were enrolled within the first 24-72 hours of onset. Optical probes were combined with a TCD headframe and placed bilaterally on scalp, overlying prefrontal cortex. The source detector separations varied from 0.5-2.5 cm. Diffuse optical, TCD and systemic parameters were measured sequentially at HOB angles of 0^o, 15^o, 30^o, 0^o, -5^o, and 0^o, with a temporal resolution of 2.7s. Changes in the ipsilesional hemisphere were compared to changes in the contralesional hemisphere, and statistical results were derived from averages over a period of 5 minutes at each HOB position.

Results: Both DCS and TCD demonstrated impaired autoregulation in the infarcted region during HOB manipulations. Across the whole population, HOB positioning at 15^o resulted in a 5.5(±3.4)% increase in rCBF ipsilesionally and a flat HOB resulted in 28(±8)% increase, relative to HOB at 30^o. Similarly, flat HOB resulted in a 6.2(±2.2)% increase in vTCD relative to 30^o in the ipsilesional hemisphere on TCD. Changes in the contralesional hemisphere were significantly smaller and within values found for a healthy population (rCBF=17(±5)% and vTCD=3.6(±0.8)% from 30^o to flat HOB, $p< 0.01$). In approximately 20% of the patients, decreasing HOB from 30^o to 0^o did not increase rCBF in the ischemic region. Although TCD blood velocity and rCBF were found to be uncorrelated in the ipsilesional hemisphere ($r=0.08$, $p=0.57$), the correlation between either parameter with MAP was higher (ΔMAP=2.7(±3.1)% at 30^o, $r=-0.77$ and -0.61 for TCD and DCS, respectively, $p< 0.08$), compared to the contralesional side ($r=-0.58$ and -0.38 for TCD and DCS, respectively).

Conclusions: The feasibility of diffuse optics as a bedside monitoring tool for AIS patients has

been previously demonstrated. Our results compare DCS to TCD and systemic changes during HOB manipulation. The large perfusion changes observed in the infarcted hemisphere provide evidence for impaired autoregulation following AIS in most patients. The absence of CBF augmentation in ~20% of patients is not fully understood, but indicates the potential for individualized stroke management based on each patient's unique hemodynamic balance.

359

NEUROPROTECTIVE EFFECTS OF NIGELLA SATIVA OIL ON HALOPERIDOL INDUCED DEFICIT IN RAT MODEL

T. Malik[1,2], S. Hasan[2], S. Pervaz[2], D.J. Haleem[1], T. Fatima[3]

[1]Neurochemistry , Biochemical Neuropharmacology Unit, Biochemistry Department, University of Karachi, [2]Pathology and Microbiology, [3]Biomedical Biological Sciences, Aga Khan University Hospital, Karachi, Pakistan

Introduction: The neuropathological status of Haloperidol (HP) induced Extrapyramidal symptoms (EPS) remains unclear, but several lines of evidence suggest that persistent neuronal alterations in the basal ganglia cause EPS produced by HP provoked oxidative stress.

Objective: The aim of this study was to evaluate the possible protective effects of the antioxidative agent “Nigella sativa (NS)” oil on HP induced neuropathological alterations and related motor symptoms in the rodent striatum (Str).

Material and methods: To achieve these objectives HP was administered alone and with NS oil. EPS was monitored in HP treated groups and the animals treated with NS alone and placebo.

Results: In the HP treated group displayed a high degree of motor impairment ($p < 0.00$) shown on rota rod experiment, vacuous chewing movements ($p < 0.00$) were higher along with grossly disturbed the large fraction of the cytoarchitectonic pattern ($p< 0.05$), histopathology with nerve cell depletion concomitant shrunken cytoplasm, nuclear membrane breakdown and chromatin disorganization. Scarring was also a prominent feature owing profusion of astrogliosis in the dorso and ventro lateral regions of the caudate putamen and in the core of nucleus accumbens. Moderate levels of halo and pyknotic neurons were also observed in HP treated rodents. The morphological HP induced neuronal changes were almost absent in the HP plus NS treated groups ($p < 0.00$). However minor astrogliosis was observed with no obvious indication of cell loss and 82% normal neuronal densities were observed using quantitative, analytic approach in the NS plus HP treated Str.

Conclusion: We conclude that NS therapy has preventive effects on HP induced neuronal degeneration in the Str. We believe that further preclinical research into the utility of NS may indicate its usefulness as a protective agent from irreversible EPS during neuroleptic treatment.

360

D-CYCLOCERINE REDUCES NEUROINFLAMMATION IN A MOUSE MODEL OF CLOSED HEAD INJURY

A. Biegon[1], J. Dhawan[1], M. Nawrocky[1], A. Alexandrovich[2], R. Yaka[2], E. Shohami[2]

[1]Medicine, Brookhaven National Lab, Upton, NY, USA, [2]Pharmacology, Hebrew University, Jerusalem, Israel

Introduction: Neuroinflammation is a prominent feature of traumatic and ischemic brain injuries, and appears to follow a conserved temporal and anatmocial course, with peak levels of activated micrgolia (measured with [3H]PK11195 autoradiography or other methods) peaking 7 days after injury . However, no animal studies examined neuroinflammation at times longer than 7 days postinjury and the effect of NMDA receptor manipulation on long-term neuroinflammation in conjunction with changes in long-term functional outcome.

Objective: Examine the effect of D-cycloserine (DCS) on long-term regional neuroinflammation in mice killed 4 weeks after injury, which showed significant functional imrpovement in vivo.

Methods: Male Sabra mice were subjected to closed head injury consisting of weight drop over the intact skull above the left parietal-motor cortex. Mice were assessed for neurological and cognitive deficits 1 hr after injury and randomized to treatment with a single i.p injection of saline or DCS 10mg/Kg (N=8/treatment) 72 hours later. Neurological and cognitive follow-up continued till day 28, when animals were decapitated and cryostat brain sections processed for quantitative autoradiography with the neuroninflammation marker [3H]PK11195.

Results: We found that CHI -induced neuroinflammation persisted through 28 days post injury and was significantly ameliorated by DCS given 72 hr post injury, a treatment which also improved behavioral and functional endpoints. The long-term effects of the injury as well as the treatment exhibited regional specificity. Thus, the highest values of [3H]PK11195 specific binding were found in the hippocampus and somatosensory cortex in the injured hemisphere of saline-treated mice. DCS treatment reduced the binding in the cortex and hippocampus of the injured hemisphere by 39-44% but had no effect on striatal neuroinflammation. DCS treatment also reduced neuroinflammation in the non-injured hemisphere to values found in intact mice. This effect, too, was seen in hippocampus and cortex but not striatum. The DCS treated animals were previously shown to demonstrate significant improvement in neurological and memory deficits relative to vehicle treated mice when tested in vivo (Adeleye et. al., 2010).

Conclusions: Traumatic brain injury in mice results in bilateral neuroinflammation which persists for more than 4 weeks after injury. A single dose of the NMDA receptor indirect agonist DCS, which was shown to improve sensorymotor and cognitive performance in these mice, also reduced neuroinflammation in the NMDA receptor rich hippocampus and cortex but not in the striatum, were NMDA receptor density is relatively low,

361

PERI-INFARCT DEPOLARIZATIONS (PIDS) IN PERMANENT FOCAL BRAIN ISCHEMIA IN THE RAT CAN BE INITIATED BY AN ADDITIONAL ISCHEMIC INSULT

A. Kharlamov, V.E. Yushmanov, S.C. Jones

Anesthesiology, Allegheny Singer Research Institute, AGH, Pittsburgh, PA, USA

In focal ischemia the peripheral region around the ischemic core undergoes spontaneous repetitive cortical spreading depolarizations known as peri-infarct depolarizations (PIDs) (Hossmann, Cerebrovasc Brain Metab Rev, 1996, 8: 195). PIDs are characterized by transient propagating changes in CBF (Strong et al., Brain, 2007, 130: 995; Luckl et al., J Neurosci Res, 2009, 87: 1219) caused by increased $[K^+]_{ex}$ (Branston et al., J Neurol Sci, 1977, 32: 305; Strong et al., JCBFM, 1983, 3: 86). We hypothesize that after ischemia both spontaneous and hypotension-mediated decreases in CBF initiate PIDs along the periphery of the ischemic region (characterized by low CBF and the depletion of brain tissue $[K^+]$, $[K^+]_{br}$) and that variations in PID speed during propagation are not related to local CBF.

In 13 male Sprague-Dawley rats (0.5-1.5% isoflurane, 70% N_2O balance O_2) focal ischemia was induced by unilateral distal (M2 branches) MCA transection and bilateral CCA occlusion. Mean arterial blood pressure was continuously recorded and stored. Arterial blood gases (p_aCO_2, p_aO_2) and pH were measured. Hypotension (60-70 mmHg) was created by temporary (2-3 min) blood withdrawal from the femoral artery catheter. CBF was constantly monitored by laser speckle flowmetry over a thin cranial bone window before and for 4 h after ischemia every 35s (n=5) or 12 s (n=8). PID velocity and local CBF were determined between each CBF frame. Images of 35 μm brain sections histologically stained for $[K^+]_{br}$ were stacked, aligned with CBF images, and analyzed using ImageJ.

PIDs (n=37) varied in flow level, duration, and direction. Most (91%) PIDs were associated with monophasic hypo-perfusion CBF propagations. Mean PID speed, calculated as the average of each PID segment, was 3.1±0.3 mm/min. The COV of each segmental PID velocity was 34%. The first spontaneous PID occurred at 18.5±5.9 min after ischemia. Average elapsed PID time was 2.4±0.2 min. The direction of the PIDs within bone window varied from unidirectional (n=26, 70%) in different directions to bidirectional (n=11, 30%). The route of PIDs followed the edges of the depressed $[K^+]_{br}$ at 4 h after ischemia. Fifty-seven percent of the PIDs were associated with (and may have resulted from) an additional ischemic insult caused by spontaneous or deliberate hypotension (74±3 mmHg at the beginning of PID vs. 103±2 mmHg pre-PID pressure, Fig. 1). Deliberate hypotension during first hour after ischemia was always accompanied with a PID. No correlations between mean arterial pressure and CBF changes during PIDs or between segmental PID speed and CBF were observed. Hypotension resulted in further CBF decrease in the ischemic core to 85±2% of the pre-hypotension level at the beginning of PID, and even more CBF decrease during the PID (to 69±2%). Substantial variations in PID speed during their propagation occurred. Our data suggest that additional post-ischemic CBF decrease caused by hypotension initiates PIDs and the variations in PID propagation speed are not related to local CBF.

Support: NIH NINDS NS66292 and NS30839.

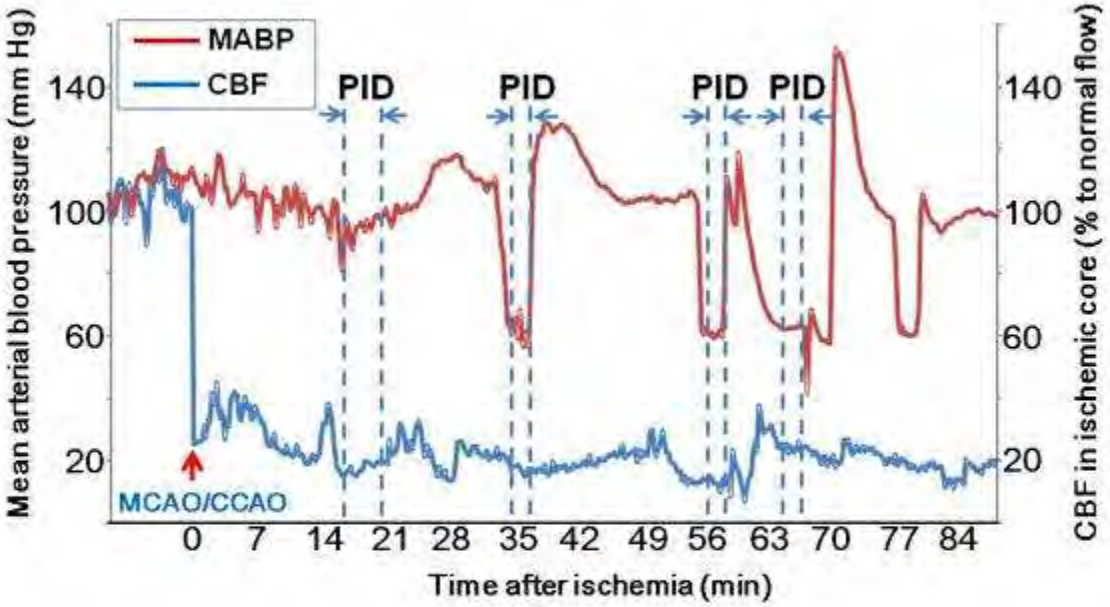
MABP
CBF
PID
PID
PID
PID
140
100
60
20
MCAO/CCAO
0
7
14
21
28
35
42
49
56
63
70
77
84
Time after ischemia (min)
Mean arterial blood pressure (mm Hg)
CBF in ischemic core (% to normal flow)

[Fig 1]

363

FOCAL CEREBRAL ISCHEMIA IN THE TNFA-TRANSGENIC RAT: EFFECT ON A TNF RECEPTOR-MEDIATED ANTI-APOPTOSIS PATHWAY

L.C. Pettigrew[1,2], S.D. Craddock[2]

[1]Medical Research Service, Department of Veterans Affairs Medical Center, [2]Stroke Program, Sanders-Brown Center on Aging, and Department of Neurology, University of Kentucky Medical Center, Lexington, KY, USA

Objectives: Tumor necrosis factor-alpha (TNFα) is an inflammatory mediator that becomes elevated in ischemic brain. Active TNFα will bind to its receptor, TNFR1, to initiate one of two dialectical paths: 1) promotion of apoptosis through activation of caspase 8 or 2) release of a nuclear transcription factor, NFκB, for upregulation of anti-apoptotic factors. Phosphorylation of an inhibitory protein, IκB, is a key step preceding release of NFκB to inhibit apoptosis. We hypothesized that overexpression of the murine TNFα gene will alter regional levels of TNFα protein, TNFR1, or the IκB phosphorylated/total protein (phos/tp) ratio in the brain of a transgenic (TNFα-Tg) rat subjected to focal ischemia.

Methods: TNFα-Tg and wild type (WT) rats (n = 3 - 7 per group and sampling time) underwent middle cerebral artery occlusion (MCAO) for 1 hr. Ischemic core (IC) and penumbral (PN) tissues were sampled after 30 min or 24 hr of reperfusion. TNFα protein and IκB phos/tp ratio were determined by Linco multiplex; TNFR1 expression was quantified by western blot.

Results: The TNFα levels in IC and PN of TNFα-Tg rat brain were unchanged at 30 min but fell below non-ischemic control levels at 24 hr ($p \leq 0.02$; Fisher's test; Table 1). The TNFα levels in IC and PN of WT rats could be measured only at 24 hrs (p=NS compared to non-ischemic WT controls). TNFα levels were significantly higher in IC ($p \leq 0.003$) and PN ($p \leq 0.01$) of the TNFa-Tg rat than in WT animals at both sampling times.

Groups	Control (Mean ± SD)	30 Min (Mean ± SD)	24 Hr (Mean ± SD)
Non-ischemic Tg Control	78.5 ± 31.4	-	-
Tg IC	-	75.3 ± 29.3	46.3 ± 12.4
WT IC	-	0	4.0 ± 6.9
Tg PN	-	75.4 ± 29.4	39.0 ± 7.5
WT PN	-	0	4.6 ± 8.0

[Table 1: TNFa Protein Levels (pg/100 ug protein)]

Non-ischemic TNFα-Tg and WT animals were equivalent in expression of TNFR1. In ischemic TNFα-Tg rats, TNFR1 expression increased in both IC and PN at 30 min ($p \leq 0.004$) and at 24 ($p \leq 0.0001$) hrs in IC. For ischemic WT animals, TNFR1 expression remained unchanged at 30 min but was increased in both IC and PN at 24 hrs ($p \leq 0.006$). In ischemic TNFα-Tg rats, IκB phos/tp ratio peaked at 30 min in PN ($p \leq 0.001$) and remained elevated at 24 hrs in IC ($p \leq 0.03$), compared to ischemic WT controls.

Conclusions: We found that TNFα increased in both IC and PN after MCAO in TNFα-Tg rats and remained several fold higher than in WT rats 24 hrs afterward. TNFR1 expression became elevated in the TNFα-Tg animal during early reperfusion and showed regional heterogeneity not observed in WT rats. Increased IκB phos/tp ratio was observed in penumbral tissue during early reperfusion, perhaps secondary to upregulation of TNFR1. We conclude that cerebral ischemic injury in the TNFa-Tg rat will initiate a TNFR-regulated anti-apoptotic pathway that may limit caspase-mediated apoptosis.

364

MONITORING BRAIN OXYGENATION AND METABOLISM IN THE ADULT DURING FRONTAL LOBE FUNCTIONAL ACTIVATION USING A NOVEL SEVEN WAVELENGTH NEAR-INFRARED SPECTROMETER

T. Zhu, J.F. Ahmed, I. Tachtsidis

Medical Physics and Bioengineering, University College London, London, UK

Introduction: Near-infrared spectroscopy (NIRS) utilises 2-4wavelengths in the near-infrared region to measure the changes in brain tissue oxy- and deoxy-haemoglobin ([HbO_2] [HHb]) and hence monitor the haemodynamic and oxygenation changes following brain functional activation.

Aim: To monitor frontal lobe brain activation using a modified seven wavelengths NIRS system (749,772,777,811,852,910,915nm) that is also capable of measuring the brain tissue redox changes in cytochrome-c-oxidase ([CtOx]) which is an indicator of oxidative metabolism and may also serve as a marker of transient brain activity.

Methods: A study was done in 17 young healthy volunteers (9 Male-8 Female). NIRS measurements were obtained using a modified 7-wavelength NIRO 30(Hamamatsu Photonics KK), while simultaneously monitoring mean blood pressure (MBP), heart rate (Portapres) and scalp blood flow (SF) changes (laser Doppler). The NIRS optodes were placed on top of the Fp1 location with the interoptode spacing of 4cm. Following a 120sec rest period, the volunteers attempted to solve anagrams for 1min followed by 30sec rest. This was repeated 10 times with the total experiment lasting 18.5min.

All activation blocks were averaged to represent the general response of individual subject. The averaged activation block was then divided using 25-second time windows, overlapped by 96 percent to find the maximum mean [HbO_2] changes, minimum mean [HHb] changes and maximum mean [CtOx] changes. The two-sample t-test with 5% significant level ($\rho \leq 0.05$) assessed the significance of these responses.Activation was then defined as a significant increase in [HbO_2] and a significant decrease in [HHb] that occurs in the same time period. After identifying activation we report the significant changes in [CtOx] that occurred in the activation period.

Results: Of the 17 subjects, seven demonstrated activation according to the above criteria. In those seven subjects we found a heterogeneous response in [CtOx], two demonstrating a significant decrease (Group A) and five demonstrating a significant increase (Group B). The Figures (a) and (b) show the results from the two groups with the systemic changes. The mean(±SEM) response in Group A, for [HHb] is -0.01(±0.02)uMolar, [HbO_2] is 0.59(±0.04)uMolar, [CtOx] is -0.021(±0.010)uMolar, MBP is 4(±0.2)mmHg and SF is 2.5(±0.6)%. In Group B, for [HHb] is -0.26(±0.03)uMolar, [HbO_2] is 0.33(±0.03)uMolar, [CtOx] is 0.195(±0.015)uMolar, MBP is 2.3(±0.2)mmHg and SF is 4.4(±0.6)%.

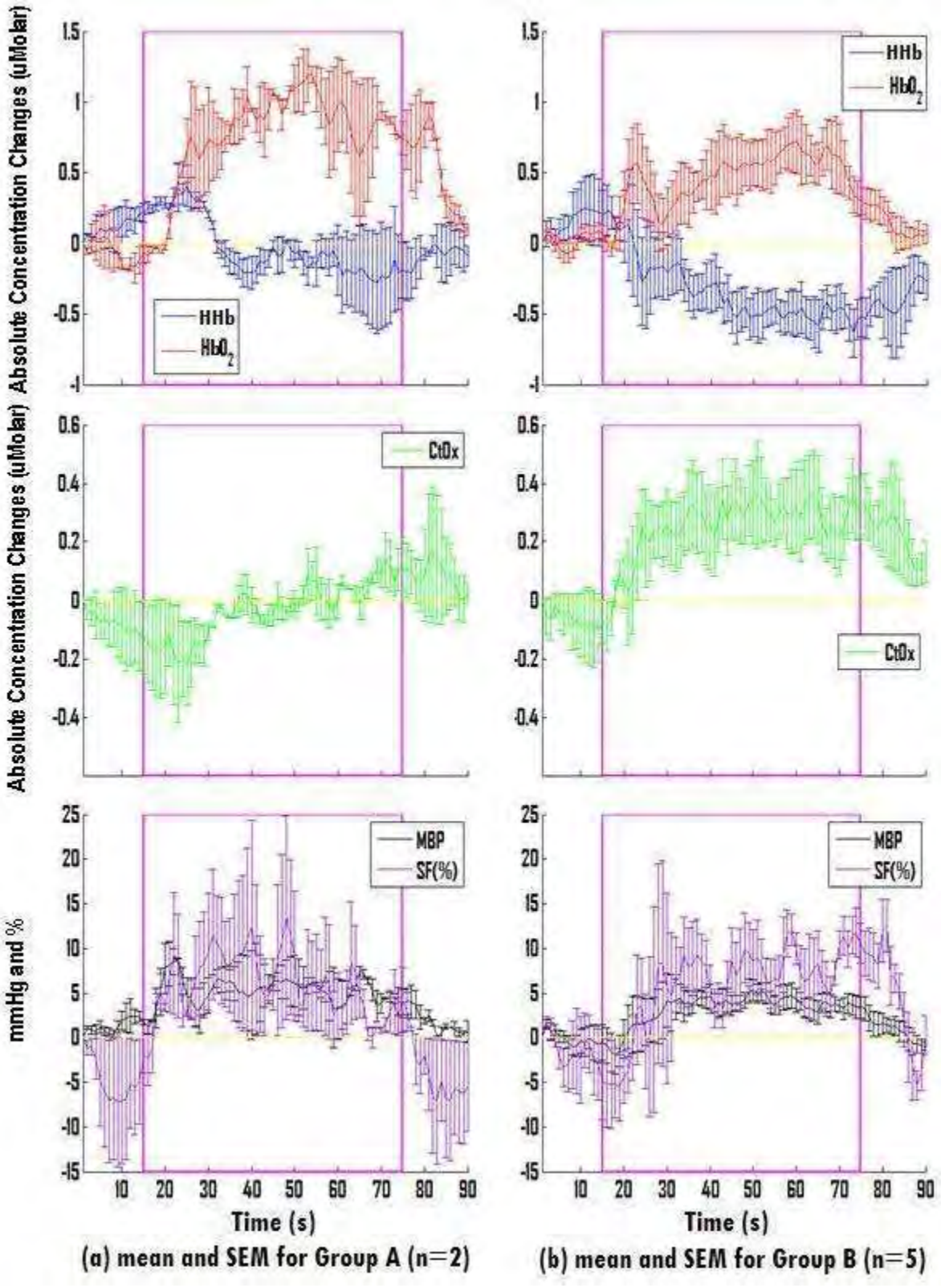

[mean and SEM for Group A & B]

Discussion: Measuring brain haemodynamics, oxygenation and metabolism during frontal lobe activation can offer further insights to brain neuronal activation. In this study, we show haemodynamic changes that were followed by significant changes in [CtOx] during frontal lobe activation. In a study by Heekeren et al. [1], significant increases were observed in [CtOx] following visual stimulation. We observed a significant increase in five subjects but a significant decrease in two. In addition, we found significant systemic changes during the stimulation period as reported previously [2]; and also differences in the magnitude and the timing profile of the haemodynamic response between the two subject groups. Further studies and analysis is underway to investigate the [CtOx] response during frontal lobe functional activation.

References:

[1] Heekeren_H.R_et_al._(1999)_Journal_of_Cerebral_Blood_Flow_and_Metabolism_19:592-603

[2] Tachtsidis_I._et_al._(2009) _Advances_in_Experimental_Medicine_and_Biology_645:307-314

365

INCREASES IN CEREBROVASCULAR IMPEDANCE IN OLDER ADULTS

R. Zhang, Y.S. Zhu, B.Y. Tseng, S. Shibata, B.D. Levine

Institute for Exercise and Environmental Medicine, Texas Health Presbyterian Hospital Dallas and University of Texas Southwestern Medical Center, Dallas, TX, USA

Pulsatile cerebral blood flow (CBF) in response to pulsatile changes in arterial pressure is determined by cerebrovascular impedance. So far, few studies have measured cerebrovascular impedance due to relative inaccessibility of the cerebral circulation and limitation of methods for measuring CBF with high temporal resolution. This study explored a novel method to measure cerebrovascular impedance. Arterial pressure in the common carotid artery (CBP, applanation tonometry), CBF velocity in the middle cerebral artery (CBFV, transcranial Doppler) and end-tidal CO_2 ($ETCO_2$, capnography) were measured simultaneously in 6 healthy young (28 ± 4 yr, 3 women) and 9 elderly subjects (70 ± 6 yr, 7 women). Transfer function method was used to estimate cerebrovascular impedance index between pulsatile changes in CBFV and CBP. Estimation of cerebrovascular impedance revealed frequency dependant characteristics in the frequency range from 0.78 Hz to 10 Hz. Specifically, impedance modulus decreased and phase increased, indicating “high-pass filter” properties of the cerebral vasculature at these time scales. When comparisons were made between the groups, impedance modulus in the elderly increased by 38% in the frequency range of 0.78 - 4 Hz and by 24% in the frequency range of 4 - 6 Hz relative to the young ($p< 0.05$). Moreover, increases in impedance in the elderly were correlated with reductions in CBFV. These findings demonstrate the feasibility of assessing cerebrovascular impedance using the method developed in this study. Furthermore, increases in cerebrovascular impedance in the elderly suggest the presence of cerebral vasoconstriction which may contribute to reduction in brain perfusion.

367

CNS DRUG DELIVERY: MOLECULAR TARGETING AT THE BLOOD-BRAIN BARRIER

T.P. Davis, P.T. Ronaldson

Medical Pharmacology, University of Arizona College of Medicine, Tucson, AZ, USA

The blood-brain barrier (BBB) constitutes a physical and biochemical barrier between the brain and the systemic circulation. This dynamic structure regulates critical processes of nutrient uptake and waste removal, thus enabling the BBB to maintain homeostasis of the brain. However, characteristics of the BBB involved in homeostatic control (i.e., tight junction (TJ) protein complexes, functional expression of membrane drug transporters) are also significant obstacles to effective CNS drug delivery. As paracellular permeability is limited by TJs between adjacent endothelial cells, drug development is often focused on improving affinity for specific uptake transporters while circumventing drug efflux mechanisms. In fact, the utility of endogenous BBB uptake transporters as facilitators of CNS drug delivery has been a subject of considerable controversy. Furthermore, the complexity of CNS drug delivery is underscored by the fact that BBB integrity may be compromised in response to pathophysiological stressors. Recently, our laboratory has shown that pain/inflammation in the periphery can dramatically affect both BBB TJ protein complexes and endogenous drug transport mechanisms. In particular, we observed that paracellular permeability to vascular markers (i.e., sucrose) and therapeutic drugs (i.e., morphine, codeine) were increased in response to peripheral inflammatory pain. These increases in xenobiotic permeability were directly related to discrete changes in constituent proteins of BBB TJ complexes. We also demonstrated that pain/inflammation in the periphery can significantly alter functional expression of CNS drug transporters that are endogenously expressed at the BBB endothelium (i.e., P-glycoprotein (P-gp) and Organic Anion Transporting Polypeptide 1a4 (Oatp1a4)). Although CNS drug efflux, mediated by P-gp, is increased during pain/inflammation, we identified Oatp1a4 as a transporter target that may be exploited to optimize delivery of therapeutic agents to the brain. One critical consideration in these studies was that, prior to our work, underlying biochemical mechanisms responsible for changes in BBB TJ complexes and/or transporters during peripheral inflammatory pain had not been identified. Our data provides evidence for involvement of the transforming growth factor-β (TGF-β) pathway, an intracellular signaling mechanism known to regulate endothelial cell function at the BBB. Of particular interest are processes mediated by activin receptor-like kinase 5 (ALK5), a TGF-β receptor that is involved in regulation of vascular permeability. Pharmacological targeting of ALK5 receptors represents a novel approach for altering BBB physiology (i.e., expression of TJ proteins and endogenous transporter systems such as Oatp1a4) and, ultimately, CNS drug delivery. Overall, results from our studies may profoundly impact drug development and/or design as well as treatment of CNS disease. This teaching session will outline BBB mechanisms that determine CNS drug uptake, present highlights of our recent studies, and demonstrate how these data may translate to optimization of CNS drug delivery to the patient.

Studies described in this teaching session were supported by National Institutes of Health Grants R01-NS39592, R01-NS42652, and R01-11271 to TPD.

368

DOES VELOCITY-SELECTIVE ARTERIAL SPIN LABELING IMPROVE CBF MEASUREMENTS IN PATIENTS WITH CEREBROVASCULAR DISEASE?:A COMPARATIVE STUDY IN MOYAMOYA DISEASE PATIENTS

D. Qiu, M. Straka, R. Bammer, M. Moseley, G. Zaharchuk

Lucas Center for Imaging, Stanford University School of Medicine, Stanford, CA, USA

Introduction: Velocity-selective arterial spin labeling (VSASL) (1) is a recently developed non-invasive MR method for cerebral blood flow (CBF) measurement. It is expected to be insensitive to arterial transit time, which limits the accuracy of standard ASL in pathologies with slow blood flow and/or collateral flow, such as stroke. However, the theoretical advantage of VSASL is yet to be verified with clinical data. In this study, we compared the performance of VSASL and a 3D-FSE pseudocontinuous ASL (pcASL) (2) with long post-label delay (PLD) time, using ASL calibrated bolus perfusion CBF (CAD-CBF) as well as gold-standard xenon CT CBF.

Methods: Fourteen patients with Moyamoya disease are included in this study. The MR sequences were performed at 3T (GE Healthcare MR750), and included 3D SPGR T1-weighted images, 3D-FSE pcASL (voxel size = 4x4x4mm^3, PLD =1s, 1.5s, 2s, 2.5s, and 3s) and VSASL (3.4x3.4x7.7mm^3, PLD=1.6s), and bolus contrast perfusion-weighted imaging (PWI) (EPI, 2.3x2.3x5mm, TR/TE = 1800/40ms). Quantitative CAD-CBF images were calculated as previously described (3), and was used as a reference for the comparison between pcASL (PLD = 3s) and VSASL. Eight of the 14 patients (57%) received xeCT CBF (3). MR and CT images were co-registered and re-sliced to the same space for quantitative analysis. The T1-weighted image was segmented to create gray matter (GM) and white matter (WM) masks. Mean CBF values were measured in the entire imaged brain region and in GM and WM using masks created above.

Results: CBF maps obtained with pcASL showed substantially higher SNR than VSASL, and were relatively free from anatomical artifacts. The expected reduction in arterial transit artifacts with increasing PLD in the pcASL CBF maps was obvious. VSASL typically had lower SNR, and in some cases was able to make better quantitative CBF measurement, but was not immune to arterial transit artifacts as might be expected theoretically. Table 1 shows mean and standard deviation of CBF measurements of the different techniques. VSASL showed higher deviation from CAD-CBF compared to pcASL with 3s PLD. Among the 8 cases with xeCT, VSASL showed comparable accuracy in CBF measurement with pcASL with 3s PLD using xeCT as gold standard.

Region	VSASL	pcASL(PLD=3s)	CAD	VSASL-CAD	pcASL(PLD=3s) - CAD	Xenon CT (n=8)	VSASL-xeCT	pcASL(PLD=3s) - xeCT
CBF in Brain (ml/100g/	39.7(10.7)	36.0 (5.4)	33.6(5.5)	6.2(8.1)	2.4 (4.4)	30.1(4.8)	5.7(10.1)	5.3 (8.4)

min)								
CBF in GM (ml/100g/min)	48.0(13.9)	45.4 (7.9)	39.8(5.9)	39.8(5.9)	5.6 (4.4)	36.3(6.8)	6.2(15.5)	7.1 (11.9)
CBF in WM (ml/100g/min)	30.2(9.3)	27.2 (5.5)	21.3(4.8)	21.3(4.8)	5.8 (7.4)	24.1(5.0)	3.0(7.2)	2.4 (8.0)

[Table 1. shows the mean (SD) of CBF values.]

Discussion: To our knowledge, this is the first report of VSASL in clinical patients with severe prolongations in arterial arrival times. Although VSASL is theoretically advantageous over standard ASL, it is currently limited by SNR and also appears to be prone to erroneous measurement in slow-flow regions. Further development of VSASL techniques may enable more accurate CBF measurements in patients with cerebrovascular disease.

References:

1. Wong et al., MRM 2006.

2. Dai et al., MRM 2008.

3. Zaharchuk et al., MRM 2010.

Acknowledgements: NIH R01-NS066506; Lucas and Oak Foundation; GE Healthcare; and Eric C. Wong for providing the VSASL sequence and post-processing tools.

370

PLATELET ACTIVATING FACTOR ANTAGONISM ELICITS HIGH-GRADE ISCHEMIC NEUROPROTECTION IN FOCAL CEREBRAL ISCHEMIA IN RATS

L. Belayev[1], L. Khoutorova[1], T.N. Eady[1], K.D. Atkins[1], A. Obenaus[2], J. Alvarez-Builla[3], N.G. Bazan[1]

[1]Neuroscience Center of Excellence, Louisiana State University, New Orleans, LA, [2]Non-Invasive Imaging Laboratory, Loma Linda University, Loma Linda, CA, USA, [3]Depto. de Quimíca Organica, Universidad de Alcala, Madrid, Spain

Introduction: Recently, we have demonstrated that signaling mediated by platelet activating factor (PAF) is involved in synaptic plasticity, memory, and neuronal protection. LAU-0901, a novel platelet-activating factor receptor antagonist, was examined in models of focal cerebral ischemia in rats and mice. LAU-0901 improved behavioral deficits and reduced infarct volumes when administered at 2 h after middle cerebral artery occlusion (MCAo) onset. In addition, LAU-0901 conferred enduring neuroprotection in animals allowed to survive for several weeks after stroke. We used magnetic resonance imaging (MRI) in conjunction with behavior and immunohistopathology to expand our understanding of this novel therapeutic approach.

Methods: Male Sprague-Dawley rats (260-349g) were anesthetized with isoflurane/nitrous oxide and mechanically ventilated; rectal and cranial temperatures were regulated at 36-37.5°C. Rats received 2 h MCAo by retrograde insertion of an intraluminal suture. Animals were treated with LAU-0901 (60mg/kg; n=5) or vehicle (45% cyclodextran; IP; n=6) 2 h from MCAo onset. Behavioral function was evaluated at 24 h, 72 h, and 7 days, and a grading scale of 0-12 was employed (0=normal and 12=maximal deficit). Diffusion weighted (DWI) and T2-weighted imaging (T2WI) MRI were carried out on a 4.7T magnet on days 1, 3 and 7 after MCAo. Apparent diffusion coefficient (ADC) and 3D volumetric analysis were conducted. Seven days after MCAo, brains were perfusion-fixed and infarct volume was measured. Immunohistochemistry was conducted on the adjacent sections. The number of GFAP (reactive astrocytes), ED-1 (activated microglia/microphages) and NeuN (neurons) - positive cells were counted in the cortex and striatum at the level of the central lesion.

Results: All animals showed similar values for rectal and cranial temperatures, arterial blood gases, and plasma glucose during and after MCAo. LAU-0901 treatment significantly improved behavioral scores compared to vehicle on day 1, 3 and 7. Total lesion volumes computed from T2WI were significantly reduced by LAU-0901 treatment on day 1 (by 84%), day 3 (by 90%) and day 7 (by 96%), which was consistent with decreased edema formation. In addition, T2WI revealed signficantly decreased cystic lesion development and decreased ventricular enlargement in the LAU-0901 group compared to controls. LAU-0901 increased ADC in the cortex and striatum on day 1. The total infarct, cortical and subcortical volumes were reduced by LAU-0901 compared with vehicle-treated rats by 80%, 100% and 64%, respectively. No cortical infarct was observed in LAU-0901-treated rats. LAU-0901 treatment significantly decreased ED-1 and increased NeuN and GFAP-positive cell count compared to vehicle group.

Conclusions: MRI, behavior and histopathology confirms marked neuroprotective efficacy of LAU-0901, a novel PAF inhibitor, in focal cerebral ischemia and might provide the basis for future therapeutics in patients suffering ischemic stroke.

371

QUANTITATIVE APPLICATION OF HYPR-LR TO DYNAMIC PET DATA FOR IMPROVED GRAPHICAL ANALYSIS

J.M. Floberg[1], J.E. Holden[1], J.P. Weichert[2], L.T. Hall[2], C.A. Mistretta[1], B.T. Christian[1]

[1]Medical Physics, [2]Radiology, University of Wisconsin, Madison, WI, USA

Objective: Local Highly constrained back-PRojection Reconstruction (HYPR-LR) is an image processing tool that uses a temporally summed composite image from a dynamic set of images to improve signal-to-noise ratio (SNR) in individual frames, making it a useful potential tool for dynamic PET data [1]. However, under certain (e.g. nonsparse) conditions, HYPR-LR can distort time series PET data. The aim of this work is to improve the quantitative accuracy of HYPR-LR by using multiple composite images, at the potential cost of some loss of SNR improvement, to improve the kinetic analysis of PET data.

Methods: HYPR-LR was evaluated with simulated and real Pittsburgh Compound B (PIB) data. HYPR-LR processing was performed using multiple composite images formed to reflect the tracer's kinetics. Simulated image data were calculated using the published kinetic rate constants of Price *et al.* and the Zubal phantom, with Poisson noise added to the reprojected sinograms [2],[3]. Parametric images of simulated data were generated with the plasma based Logan graphical method [4]. Percent error from the known parameters was used to evaluate the accuracy of the HYPR-LR estimates. Parametric images of real subject data were generated using the reference region Logan graphical method [5], and evaluated for an improvement in the Logan bias by measuring mean and maximum binding potentials (BP_{ND}) before and after HYPR-LR processing, and the volume of pixels above a 1.1 BP_{ND} threshold.

Results: The noise free simulations show that with our method of forming multiple composites, HYPR-LR introduces relatively minor errors at boundary regions, a maximum of 2% for individual frames and 5.5% for the parametric image. In simulations with added noise, our implementation of HYPR-LR reduces noise in both individual frames and parametric images by approximately 2 fold, and substantially reduces the bias in the BP_{ND} estimates (Figure 1). The real PIB data results are consistent with the simulations. The mean and maximum BP_{ND} in the frontal and parietal cortex increase with HYPR-LR processing, as does the number of voxels exceeding the 1.1 BP_{ND} threshold.

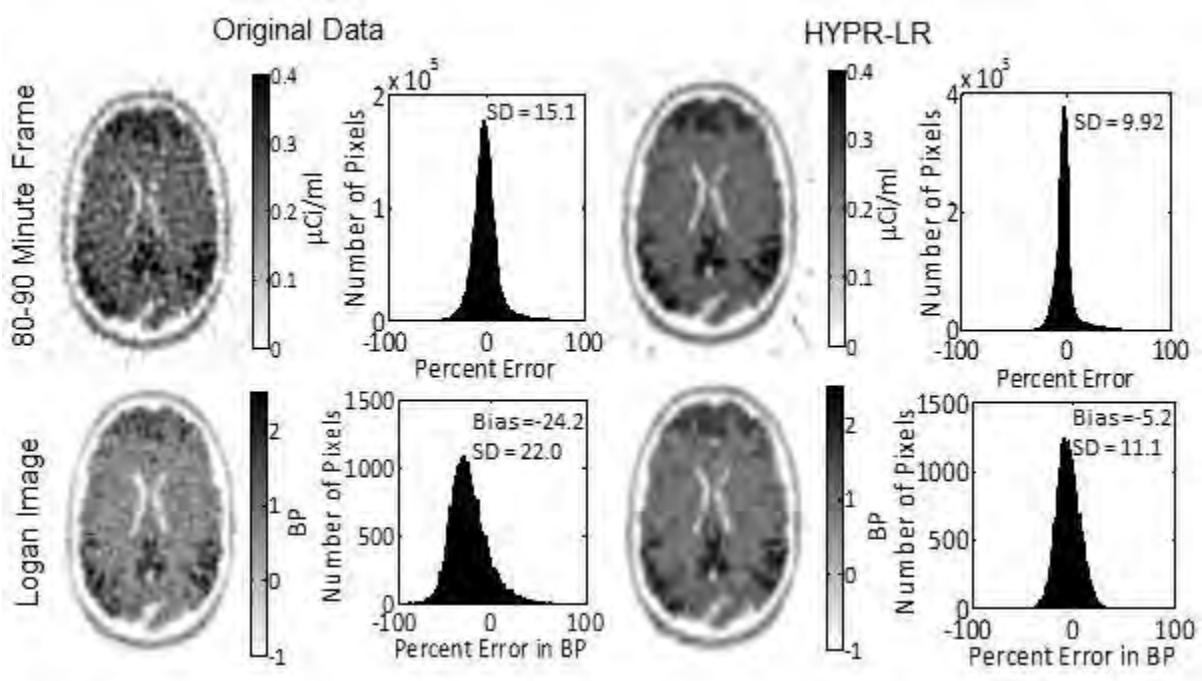

[Figure 1]

Figure 1: HYPR-LR processing with our proposed technique reduces voxel noise in individual frames (top) and reduces bias in BP_{ND} estimation (bottom). The histograms show percent error for nonzero voxels in all frames of the study (top), and percent error in BP_{ND} for voxels falling above 1.1 in the parametric image (bottom).

Conclusions: We have introduced a method for applying HYPR-LR to PET data using multiple composite images based on a radiotracer's time course that provides substantial reductions in image noise and the associated bias when using multiple time graphical methods for BP_{ND} estimation, while introducing minimal errors into the data. These improvements could increase the sensitivity of dynamic studies with radiotracers that suffer from high noise and low uptake.

References:

[1] Christian et al; J Nucl Med 2010; 51;1147-1154.

[2] Price et al; JCBFM 2005; 25:1528-1547.

[3] Zubal et al; Med Phys 1994; 21;299-302.

[4] Logan et al; JCBFM 1990; 10;740-747.

[5] Logan et al; JCBFM 1996; 16;834-840.

374

SEXUALLY DIMORPHIC EXPRESSION OF X-CHROMOSOME GENES IN BLOOD FOLLOWING ISCHEMIC STROKE IN HUMANS

B. Stamova[1], Y. Tian[1], G. Jickling[1], V. Patel[1], H. Xu[1], D. Liu[1], B.P. Ander[1], C. Bushnell[2], X. Zhan[1], R. Turner[1], R. Davis[3], P. Verro[1], W. Pevec[4], N. Hedayati[4], D. Dawson[4], J. Laird[5], J. Khoury[6], E. Jauch[7], A. Pancioli[8], J. Broderick[6], F.R. Sharp[1]

[1]Neurology, UC Davis / MIND Institute, Sacramento, CA, [2]Womens Health Center of Excellence, Wake Forest University Medical Center, Winston-Salem, NC, [3]UC Davis / MIND Institute, [4]Vascular Surgery, [5]Cardiology, UC Davis School of Medicine, Sacramento, CA, [6]Neurology, [7]Emergency Medicine, University of Cincinnati, Cincinnati, OH, [8]Emergency Medicine, University of South Carolina, Charleston, SC, USA

Objectives: Gender differences affect the risk, etiologies, response to treatment and outcome of ischemic stroke (IS). These may relate in part to sexually dimorphic differences in the immune system which we assess in this study by measuring RNA expression of cells in blood. Thus, this study focused on X chromosome-linked genes expressed in women and men following ischemic stroke to identify

(1) genes whose expression pattern indicates significant gender-diagnosis interaction in blood of IS patients at < 3h (pre-treatment), 5h (post-treatment) and 24h (post-treatment) following IS compared to non-stroke controls;

(2) differences in the temporal gene expression between males and females following IS.

Methods: RNA levels in whole blood were measured on Affymetrix U133 Plus2.0 expression arrays from IS patients (n=35 men; n=26 women) at ≤3h, 5h and 24h (183 samples) following the onset of the stroke and compared to healthy controls (n=58) and controls with vascular risk factors (n=51). 888 probe sets (683 genes) on the X-chromosome were analyzed. Analysis involved

(1) ANCOVA to assess the Gender by Diagnosis interaction adjusting for age and gender and

(2) a Mixed Model ANOVA to assess the Gender-by-Time interaction adjusting for batch. Significance was defined as a Benjamini-Hochberg FDR-corrected $p < 0.05$ and a $|FC|>1.2$.

Results: Female-specific expression after stroke was noted for 37, 140 and 61 X chromosome genes at 3, 5 and 24h, respectively, when compared to controls. Similarly, male-specific expression after stroke was noted for 23, 18 and 31 X chromosome genes at 3, 5 and 24h, respectively, when compared to control. The female-specific IS genes were associated with post-translational modification, small molecule biochemistry and cell-cell signaling/ interactions. Male-specific genes were associated with cellular movement and development, immune cell trafficking and cell death. There were many more X chromosome genes regulated in women compared to men following IS.

Conclusions: The changes in expression of these X chromosome genes could be a result of the stroke, could contribute to the stroke injury, and/or might be due to an interaction with the thrombolytic treatment (at 5h and 24h). Identification of the genes that contribute to injury or modulate response to thrombolysis could guide development of gender-specific stroke treatments.

375

THE EFFECTS OF DIESEL EXHAUST PARTICLES ON NEURAL TUBE DEVELOPMENT IN THE EARLY STAGE CHICKEN EMBRYO

H. Şimşek[1], A. Çolak[2], A. Çetinkal[3], S. Kaya[4], H. Kaya[5], A. Haholu[6], M.N. Demircan[2]

[1]Neurosurgery, Çorlu Military Hospital, Tekirdag, [2]Neurosurgery, GATA Haydarpaşa Training Hospital, [3]Neurosurgery, Kasımpaşa Military Hospital, Istanbul, [4]Neurosurgery, GATA Military Medical Faculty, [5]Pulmonology, Bilkent Rehabilitation Center, Ankara, [6]Pathology, GATA Haydarpaşa Training Hospital, Istanbul, Turkey

Particulate matter is an important cause of air pollution and its toxicity on various organs has been reported. Diesel exhaust particles (DEP) constitute a considerably large portion of this potentially toxic particulate matter. Therefore, we established our study to investigate the effects of DEP on neural tissue and neural tube development in early stage chicken embryos. Four study groups and one control group, each of which included 24 objects were designed. Eggs were incubated for 30 hours. Solutions of DEP containing 10, 50, 100, and 200 µg/0,1 ml were prepared with serum saline. In the end of thirty hours, embryos in the control group were administered 0,1 ml of serum saline, the others were administered 0,1 ml of diesel exhaust particle solutions under the embryonic discs. After 72nd hour of the incubation, embryos were excised and their levels of development were evaluated macroscopically. Subsequently, neural tissue and neural tube development were evaluated histopathologically. The difference between the embryos that were defined as *poorly* and *well* developed, was found statistically significant ($p< 0.05$). Neural tube defects were detected in 16 of 104 embryos. Statistically significant association between the administration of DEP and development of neural tube defect was identified ($p=0.037$). Thus, the direct neurotoxic effects of DEP, which the whole population encounters inevitably, have been shown in the early stages of embryonic development. Further studies are needed to identify the effects of these particles in the later stages of embryonic development.

377

AGE-RELATED DECLINE IN LECTIN BINDING IN THE RAT BRAIN FOLLOWING BRAIN PATHOLOGY IN HEAT STRESS

H. Sharma[1], A. Sharma[1], R.J. Castellani[2], M.A. Smith[3]

[1]Surgical Sciences, Uppsala University, Uppsala, Sweden, [2]Pathology, University of Maryland School of Medicine, Baltimore, MD, [3]Pathology, Case Western Reserve University, Cleveland, OH, USA

Role of lectins in neuropathology of hyperthermia caused by heat stress is not well understood. The lectins such as *Ricinus communi* Agglutinin, (ricine, RCA120, RCA-1) and Wheat Germ agglutinin (WGA) are commonly used as specific markers for primary sensory afferents and neuronal membrane proteins, respectively. Since heat stress is a disorder of thermal sensory information processing system of the CNS, selective alteration in neurochemical metabolism, cell membrane permeability, neuronal, and non-neural functions could occur. These changes in hyperthermia could, in turn, influence lectin-binding sites in the brain. Accordingly, structural and functional changes in the brain could be demonstrated at an early stage by examining specific lectin reactivity in heat stress.

The present study was undertaken to examine RCA-1 and WGA immunoreactivity in brain of normal and heat stressed animals in two different age-groups. Wistar male rats (age 10-12 wks; 24-28 wks) were exposed to heat stress in a B.O.D. incubator at 38°C for 4 h. The animals were perfused transcardially under urethane anesthesia (0.8 g/kg, i.p.), with a paraformaldehyde-based fixative in phosphate buffer (pH 7.4, about 100 ml) preceded by a brief saline rinse. The brains were removed, embedded in paraffin, and processed for lectin immunoreactivity using standard protocol. The unstressed animals (n=5) served as controls. Young animals subjected to heat stress exhibited profound brain dysfunction, e.g., breakdown of the blood-brain barrier (BBB) function, consequent development of vasogenic brain edema, and neuronal, glial, and myelin damage. These animals showed virtually a complete absence of RCA binding in cortical astrocytes, as well as in the pons, and medulla. The lectin immunoreactivity in white matter and microvessels was much less intense as compared to the control. The controls exhibited strong binding of these lectins in microvessels and choroid plexus followed by astrocytes of cerebral cortex, pons, medulla, and white matter. The WGA activity was absent in neuronal membranes of hypothalamus, pons, medulla, and was markedly reduced in the cerebral microvessels and in white matter following 4 h heat exposure. In controls, the WGA activity was strongly localized in the cerebral vessels, choroid plexus, and neuronal membranes of pons, medulla and hypothalamus followed by the white matter. On the other hand, only a mild to moderate decrease in these lectin bindings were seen in adult rats after identical heat exposure. Pretreatment with neuroprotective drugs, such as naloxone or indomethacin markedly enhanced the lectin binding intensity in the brains of heat exposed rats. This effect was most pronounced in young rats as compared to adult animals after drug treatment. Taken together these observations are the first to demonstrate that lectin-binding sites are altered in heat stress in an age-related manner. Furthermore, neuroprotective drugs could restore lectin-binding sites in the brain of heat stressed rats. In conclusion, our result shows that lectin-binding sites are important indicators of neural injury or repair mechanisms in the setting of heat stress, and raise important implications for therapeutic intervention in a spectrum of neurologic diseases.

379

ASTROCYTES ARE SUSCEPTIBLE TO HYPERTHERMIA INDUCED BRAIN PATHOLOGY IN NORMAL AND IN CU NANOPARTICLES TREATED RATS - MODULATION BY NEUROCHEMICALS

A. Sharma[1], D. Muresanu[2], H. Pant[3], H.S. Sharma[1]

[1]Surgical Sciences, Uppsala University, Uppsala, Sweden, [2]Neurology, University of Pharmacy & Medicine, Cluj-Napoca, Romania, [3]Laboratory of Neurochemistry, National, Institutes of Neurological Disorders and Stroke, Bethesda, MD, USA

Our earlier study in a rat model of HS exhibited marked increase in BBB permeability to proteins in various brain regions indicating endothelial cell dysfunction. An increased BBB permeability alters the CNS fluid microenvironment and results in brain edema formation and brain pathology. To examine the possibility of glial cell involvement in HS-induced neuropathology we investigated the changes in specific astrocytic marker, the glial fibrillary acidic protein (GFAP) immunoreactivity in the CNS following HS. In addition, influence of copper (Cu) nanoparticles (50-60 nm) and drugs modifying opioid receptors (naloxone) or prostaglandin synthesis (indomethacin) on GFAP activation in HS were also investigated. Male Wistar rats (age 10-12 weeks) either intact or treated with Cu nanoparticles (50 mg/kg, once daily for 7 days) were subjected to HS in a B.O.D. incubator (38° C; rel. humid. 45-50%, wind velocity 28.6 cm/sec) for 4 h. After the end of the experiment, the animals were perfused transcardially under anesthesia (Equithesin 3 ml/kg, i.p.) with a paraformaldehyde-based fixative (about 100 ml, pH 7.4) preceded with a brief 0.9% saline rinse. The GFAP immunoreactivity was developed using standard protocol on 3-µm thick paraffin sections from selected brain areas. Animals kept at room temperature were used as control. The stressed animals showed profound hyperthermia (+3.56±0.23° C), behavioral prostration BBB damage and cell injury. These changes were exacerbated in nanoparticles treated rats after HS. A massive increase in GFAP immunoreactivity was observed in the thalamus, hypothalamus, pons, brain stem, cerebellum, hippocampus, caudate nucleus and cerebral cortex in normal animals subjected to HS. Interestingly, the spinal cord of these animals also showed a massive increase in GFAP immunoreactivity in dorso-lateral gray matter at all levels examined. The GFAP immunoreactivity in control animals showed only mild staining in glia limitans and around the central canal. Nanoparticles treated rats showed an exacerbation of hyperthermia, BBB leakage and GFAP immunoreactivity in the CNS. Activation of astrocytes in the CNS was closely seen in the areas showing BBB disruption and brain pathology in normal or nanoparticles treated rats. This suggests that astrocytes are sensitive indicators of thermal injury. To further understand this point, separate groups of rats were treated with naloxone or indomethacin in separate group of rats (10 mg/kg, i.p. 30 min before HS). These treatments are known to reduce BBB disruptions and brain edema following HS. Examination of GFAP immunoreactivity in these animals after 4h HS revealed marked diminution in astrocytic activation in normal or Cu nanoparticles treated group. These observations are the first to demonstrate that breakdown of the BBB caused by hyperthermia is crucial for GFAP activation. Furthermore activation GFAP is associated with brain pathology. Obviously, leakage of serum elements in the CNS fluid microenvironment due to BBB disruption is instrumental in GFAP activation. Taken together our results strongly indicate that astrocytes appear to play active roles in thermoregulatory changes in the CNS following heat exposure.

380

NEUROPROTECTIVE EFFECTS OF CEREBROLYSIN FOLLOWING NANOPARTICLES INDUCED HSP 72 KD, HO-2, C-FOS EXPRESSIONS AND BRAIN PATHOLOGY IN HEAT STRESS

D.F. Muresanu[1], A. Sharma[2], R. Patnaik[3], H.S. Sharma[2]

[1]Neurology, University of Pharmacy & Medicine, Cluj-Napoca, Romania, [2]Surgical Sciences, Uppsala University, Uppsala, Sweden, [3]Biomedical Engineering, Institute of Technology, Banaras Hindu University, Varanasi, India

The possibility that chronic exposure of nanoparticles will exacerbate stress reaction following hyperthermia and induce brain pathology was examined using upregulation of heat shock protein (HSP 72kD) and hemeoxygenase-2 (HO-2) immunohistochemistry in the rat brain. Engineered nanoparticles from Ag or Cu (≈50-60 nm) were administered (30 mg/kg, i.p.) once daily for 1 week in young male rats and on the 8th day these animals were subjected to 4 h heat stress at 38^{o} C in a BOD incubator. In these animals and stress reaction, blood-brain barrier (BBB) permeability and brain pathology were examined. Subjection of nanoparticles treated rats to heat stress showed exacerbation HSP and HO-2 upregulation as compared to normal rats in several parts of the brain exhibiting leakage of Evans blue albumin or radioiodine tracers. Interestingly, these brain areas also show profound brain edema formation and cellular damage following heat exposure. The enhanced brain pathology after heat stress was most pronounced in Ag treated animals. Pretreatment with Cerebrolysin (5 ml/kg, i.v.) either 30 min before or after heat stress significantly attenuated HSP or HO-2 expression and reduced brain pathology in nanoparticle treated rats. In drug treated animals, BBB disruption, brain edema formation and brain pathology in nanoparticles treated heat stressed animals were also minimized. These results show that chronic nanoparticles treatment exacerbate hyperthermia induced HSP and HO-2 response and enhanced brain pathology. These neuropathological changes were significantly attenuated by Cerebrolysin, a mixture of various neurotrophic factors and peptides. This indicates that Cerebrolysin treatment cold be a promising approach to induce neuroprotection in hyperthermia induced brain pathology caused by nanoparticles intoxication.

384

INDUCED PLURIPOTENT STEM CELLS TRANSPLANTED IN MOUSE ISCHEMIC BRAIN

H. Kawai, T. Yamashita, Y. Ohta, K. Deguchi, S. Deguchi, X. Zhang, Y. Ikeda, T. Matsuura, K. Abe

Department of Neurology Graduate School of Medicine, Dentistry and Pharmaceutical Sciences Okayama University, Okayama, Japan

Stroke is a major neurologic disorder and one of the leading causes of death in human. Induced pluripotent stem (iPS) cells can be produced from basically any part of patients, with high reproduction ability and pluripotency to differentiate into various types of cells, suggesting that iPS cells can provide a hopeful therapy for cell transplantation. However, transplantation of iPS cells into ischemic brain has not been reported. In this study, we showed that the iPS cells fate in a mouse model of transient middle cerebral artery occlusion (MCAO). Undifferentiated iPS cells (5×10^5) were transplanted into ipsilateral striatum and cortex at 24 h after 30 mins of transient MCAO. Behavioral and histologic analyses were performed at 28 day after the cell transplantation. To our surprise, the transplanted iPS cells expanded and formed much larger tumors in mice postischemic brain than in sham-operated brain. The clinical recovery of the MCAO+ iPS group was delayed as compared with the MCAO+PBS (phosphate-buffered saline) group. iPS cells formed tridermal teratoma, but could supply a great number of Dcx-positive neuroblasts in the ischemic lesion. iPS cells have a promising potential to provide neural cells after ischemic brain injury, if tumorigenesis is properly controlled.

385

SYNERGISTIC BENEFIT OF COMBINED AMLODIPINE PLUS ATORVASTATIN ON NEURONAL DAMAGE AFTER STROKE IN ZUCKER METABOLIC RAT

H. Kawai, S. Deguchi, K. Deguchi, T. Yamashita, Y. Ohta, J. Shang, F. Tian, X. Zhang, N. Liu, W. Liu, Y. Ikeda, T. Matsuura, K. Abe

Department of Neurology Graduate School of Medicine, Dentistry and Pharmaceutical Sciences Okayama University, Okayama, Japan

Stroke is a major neurologic disorder and leading cause of death in the world. We compared neuroprotective effects of single or combination therapy of amlodipine (AM) and atorvastatin (AT) in such a metabolic syndorome model Zucker rat after 90 min of transient middle cerebral artery occlusion (tMCAO). The animals were pretreated with vehicle, AM, AT, or the combination of AM plus AT for 28 d, and at 24 h of tMCAO, infarct volume and immunohistochemical analyses were performed. The combination of AM plus AT treatment decreased the infarct volume stronger than each single treatment with AM or AT. The numbers of positive cells of oxidative stress markers such as 8-hydroxy-2'-deoxyguanosin (8-OHdG), 4-hydroxy-2-nonenal (4-HNE), and advanced end glycation products (AGE), and inflammation markers such as tumor necrosis factor alpha (TNF-α) and monocyte chemoattractant protein-1 (MCP-1) decreased dramatically in the combination-treated group compared with single AM or AT treated group. The present study showed that single AM or AT treatment showed neuroprotective effects both with antioxidative and antiinflammatory mechanisms, but combination therapy of AM plus AT presented a further synergistic benefit in acute ischemic neural damages.

387

NEUROPROTECTION INDUCED BY BRDYKININ B2 RECEPTOR ANTAGONIST HOE-140 IN SPINAL CORD INJURY IS MEDIATED THROUGH NITRIC OXIDE-RELATED MECHANISMS

A. Sharma[1], H. Sharma[1], L. Feng[2]

[1]Surgical Sciences, Uppsala University, Uppsala, Sweden, [2]Neurology, Norman Bethune International Peace Hospital Army, Shi Jia Zhuang, China

Role of Bradykinin in spinal cord injury (SCI) induced breakdown of the blood-spinal cord barrier (BSCB) and edema formation is not well known. Previously we showed that bradykinin B2 receptor antagonist (HOE-140, Hoechst, Frankfurt, Germany) in low doses is able to thwart BSCB disruption, edema formation and cell injury in a rat model of SCI. Recent studies suggest that bradykinin may stimulate endothelial nitric oxide synthase (NOS) through B1 receptor mediated events. However, the role of B2 receptors in NOS upregulation is still not known. Thus, in present investigation we wanted to see whether bradykinin B2 receptor is somehow involved in SCI induced neuronal NOS (nNOS) activation.

We used HOE-140, a specific B2 receptor antagonist in lower dose to ascertain the role of bradykinin in spinal cord trauma induced alterations in nNOS expression, BSCB permeability, spinal cord blood flow (SCBF), edema formation and cell changes in our rat model. However, HOE-140 in higher doses may have some B2 receptor agonistic activity as well. SCI was produced in Equithesin anaesthetized animals by making a longitudinal incision into the right dorsal horn at the T10-11 segment. The animals were allowed to survive 5 h after the injury.

A focal trauma to the rat spinal cord significantly increased the BSCB permeability to Evans blue, [131]I-sodium in five spinal cord segments examined, e.g., C4, T5, T9, T10-11 and T12. These spinal cord segments also showed marked upregulation of nNOS activity and exhibited profound reduction in the SCBF (mean -30 %). Measurement of spinal cord water content showed significant increase in all the above spinal cord segments. Profound nerve cell, glial cell and myelin damage were seen in these spinal cord segments that are most pronounced around the vicinity of the lesion site. A close correlation between upregulation of nNOS and cell injury is clearly seen after SCI. Extravasation of lanthanum was largely present within the endothelial cell cytoplasm and also found occasionally in the basal lamina. Pretreatment with lower doses of B2 receptor antagonist HOE-140 (0.1 mg to 1 mg/kg, i.v.) 30 min prior to trauma significantly attenuated spinal cord pathology and upregulation of nNOS expression. The SCBF showed marked improvement in this group. This effect of HOE-140 was also seen when the compound was administered 10 to 15 after SCI, but no neuroprotection is seen when the compound was given 30 min after injury. Interestingly, increasing the dose of HOE-140 from 2 mg to 5 mg/kg, i.v. (either 30 min before or 10 min after injury) did not exhibit any neuroprotection. In fact, there was an exacerbation of tracers extravasation, edema formation, cell injury and nNOS expression.

These observations are the first to suggest that bradykinin B2 receptors play an important role in SCI induced nNOS expression and spinal cord pathology. An early blockade of bradykinin B2 receptors in the spinal cord following trauma is necessary to induce neuroprotection. Furthermore, the neurodescructive effects of bradykinin appears to be mediated through mechanisms involving nitric oxide, not reported earlier.

388

GLUCOCORTICOID-INDUCED TNF RECEPTOR-STIMULATED T CELLS SERVE AS A NEGATIVE REGULATOR FOR CNS REPAIR AFTER CEREBRAL INFARCTION

M. Takata[1,2], T. Nakagomi[1], S. Kashiwamura[1], A. Nakano-Doi[1], O. Saino[1], H. Okamura[1], O. Mimura[2], T. Soma[3], A. Taguchi[4], T. Matsuyama[1]

[1]Laboratory of Neurogenesis and CNS Repair, Institute for Advanced Medical Sciences, [2]Department of Ophthalmology, [3]Department of Hematology, Hyogo College of Medicine, Nishinomiya, [4]Department of Cerebrovascular Disease, National Cardiovascular Research Center, Suita, Japan

Introduction: Accumulating evidences suggest that immune response affects the restoration of the injured CNS. Although $CD4^+$ T cells serve as a negative regulator in post-stroke neurogenesis (Saino et al., J Neurosci Res, 2010), the identity of their subsets remains unclear. Glucocorticoid-induced TNF receptor (GITR), a multifaceted regulator of immunity belonging to the TNF receptor superfamily, is expressed on activated $CD4^+$ T cells.

Herein, we show that GITR triggering suppress the expression of neural stem/progenitor cells which were induced by ischemic stroke (iNSPC: Nakagomi et al, Eur J Neurosci, 2009) using a murine model of cortical infarction.

Materials and methods: Focal cerebral ischemia was produced by occluding the middle cerebral artery(MCA) of adult CB17 mice and SCID mice. This procedure can allow us to make highly reproducible cortical infarction (Taguchi et al., J Exp Stroke Transl Med,2010). Animals were treated intraperitoneally with agonistic GITR antibody (GITR-Ab), Fc fusion protein (GITR-Fc) blocking the GITR-GITRL interaction, or control rat IgG (1 mg/kg of protein/each injection) 3 hours and 3 days post-stroke. The infiltration of T cells to the ischemic area was assessed by immunohistochemistry and by FACS analysis of T cells extracted from post-infarct brain. Post-stroke inflammatory state was analyzed by PCR for IFN-γ, TNF-α, and IL-10. Induction of iNSPCs was assessed by immunohistochemistry and PCR for nestin and Sox2. To investigate whether activated T cells could directly affect on the iNSPC in vivo, T cells obtained from CB-17 mice, which was triggered either by GITR or by control IgG, were transplanted into post-stroke SCID mice. To assess cortical function after these treatments, mice were subjected to behavioral testing using a modification of the open field task on day 30.

Results: Immunohistochemistry for CD3, CD4 and GITR revealed that $CD4^+$T cells started to infiltrate as early as 3 hours after the MCA occlusion, but they were almost negative for GITR. The number of $GITR^+$T cells in the post-ischemic cortex was gradually increased, and on 7 days post-infarction, over 50% of $CD3^+$T cells were GITR-positive. This was confirmed by FACS of extracted T cells from the ischemic region. The ratio of $GITR^+$T cells/$CD4^+$T cells in the splenocytes also significantly increased after stroke. These findings indicate that the $CD4^+GITR^+$T cells were preferentially accumulated at the infarct area. The post-stroke mice treated with GITR-Ab revealed elevated inflammatory responses with enhancing iNSPC-apoptosis. In contrast, administration of GITR-Fc decreased inflammatory responses with inhibiting the iNSPC-apoptosis. Administration of GITR-triggered T cells, but not untriggered T cells, to post-stroke SCID mice reduced post-stroke iNSPC-expression. Mice treated with GITR-Ab or GITR-triggered T cells showed higher locomotion than control, while animals treated with GITR-Fc reduced their hyperactivity to the control level.

Conclusion: These observations indicate that GITR triggering on $CD4^+$T cells following stroke

works as negative regulators for CNS repair via enhancing apoptosis of iNSPCs. These findings also raise the possibility that the blockade of GITR-GITRL interaction can be a novel immune-based therapy in stroke treatment.

390

INFLUENCE OF ANGIOTENSIN-(1-7) ON INOS EXPRESSION AFTER FOCAL CEREBRAL ISCHEMIA-REPERFUSION IN RATS

Y. Zhang, J. Lu

Department of Neurology, Nanjing Brain Hospital / Nanjing Medical University, Nanjing, China

Purpose: To investigate influence of Ang-(1-7) on the inducible nitric oxide synthase (iNOS) activity and gene expression following focal cerebral ischemia/reperfusion in rats.

Methods: Cerebral ischemia/reperfusion injury was induced by intraluminal thread occlusion of middle cerebral artery in the adult male Sprague-Dawley (SD) rats. Ang-(1-7) or artificial cerebrospinal fluid (aCSF) was continuous administrated by implanted Alzet osmotic minipumps into lateral cerebral ventricle after reperfusion. Experimental animals were divided into sham-operated group (sham operation + aCSF), aCSF treatment group (MCAO+aCSF) and Ang-(1-7) treatment groups [MCAO+Ang-(1-7)] at low (1pmol/0.5μl/h), medium (100pmol/0.5μl/h) or high (10nmol/0.5μl/h) dose levels. The activity of iNOS in ischemic tissues were measured by iNOS detection kits. Reverse transcription(RT)-PCR was used to determine messenger RNA (mRNA) of the iNOS in ischemic tissues.

Results: The cerebral ischemic lesion resulted in a significant increase of iNOS expression compared with sham operation group. The high-dose Ang-(1-7) markedly enhanced (iNOS) activity and gene expression compared with aCSF treatment group at 24 hours and 48 hours after reperfusion ($P < 0.01$), whereas medium and low-dose Ang-(1-7) didn´t stimulate iNOS activation ($P > 0.05$).

Conclusions: These findings indicate that Ang-(1-7) overdose(high-dose:10nmol/0.5μl/h) upregulate iNOS expression in ischemic tissues following focal cerebral ischemia/reperfusion in rats, however, no significant changes in iNOS expression were found in medium and low-dose Ang-(1-7) groups after the ischemic insult.

391

EFFECT OF SOLUBLE CILOSTAZOL ON CEREBRAL BLOOD FLOW AFTER ACUTE ISCHEMIC STROKE IN MICE

S. Lu[1,2], T. Nakagomi[1], A. Nakano-Doi[1], M. Takata[1,3], N. Okamoto[3], O. Mimura[3], Y. Ito[4], A. Taguchi[5], H. Tachibana[2], T. Matsuyama[1]

[1]Laboratory of Neurogenesis and CNS Repair, Institute for Advanced Medical Sciences, [2]Department of Internal Medicine, [3]Department of Ophthalmology, Hyogo College of Medicine, Nishinomiya City, [4]Pharmaceutical and Technology Institute, Kinki University, [5]Department of Cerebrovasular Disease, National Cardiovascular Center, Osaka, Japan

Introduction: Cilostazol (CLZ) is an inhibitor of Type III phosphodiesterase that increases intracellular cyclic AMP levels by restraining platelet aggregation. Increasing evidence has shown that CLZ has a significant preventing action of stroke recurrence. However, its efficiency on acute cerebral infarction has not been elucidated. For medication of acute stroke patients, injection may be performed more easily than oral administration. To this purpose, we attempted to enhance solubility by using 2-hydroxypropyl-β-cyclodextrin (HPβCD). In this study, we examined the effect of soluble cilostazol on cerebral blood flow (CBF) and on endothelial proliferation with phospho-eNOS (p-eNOS) expression, after focal cerebral ischemia to evaluate its acute action.

Material and methods: Focal cerebral ischemia was produced by occluding the left middle cerebral artery of adult C.B-17/icr$^{-+/+}$ mice. Animals were administered intraperitoneally with 50μl of fine particle suspensions of 0.5% CLZ in 5% HPβCD (soluble CLZ: ca.0.027%), which were prepared using a Microfluidizer, an impact-type emulsifying comminution device, 30min after stroke. The local CBF was measured in the cerebral cortex by using Laser Speckle Blood Flow Imager (Omegazone laser speckle blood flow imager, Omegawave, Inc, Tokyo, Japan), which can represent local CBF continuously and two-dimensinally, in mice treated with CLZ, vehicle (5% HPβCD) or PBS every 10, 20, 30mins and 1 hour after the injection. To assess the direct effect of CLZ on endothelial cells (EC), we applied CLZ (1ng/ml) to the cultured EC from mice brain (1x10^{4}cells/dish), and determined its proliferative effects by BrdU labeling with observing the change in expression of both eNOS and p-eNOS by Western blot analysis.

Results: The CBF at the ischemic cortex was reduced to less than 50% of control and was not changed after injection of HPβCD or PBS. However, CLZ-treated groups (1 mg/kg) showed a significant increase in the ipsilateral CBF from 20 to 30 min after the injection compared to the other control groups ($p < 0.05$). The CBF was not significantly different among the groups at 1 hour, indicating its temporal effect. When applied the CLZ with 0.1 and 1.0 ng/ml, the number of BrdU-labeled ECs was increased (ca. 1.5 times) dose-dependently compared with the control. However, when applied 2.5 ng/ml its proliferative action turned to reduce and 5 ng/ml of CLZ showed no proliferative effect on ECs. Western blot analysis showed that expression of p-eNOS was selectively increased in the ECs cultured with 1.0 ng/ml of CLZ solution.

Conclusions: These results indicate that cilostazol contributes to improve the microcirculation around the ischemic region (penumbra) through upregulation of endothelial activity in post-stroke brain. Its proliferative action to endothelial cells may also be involved in the beneficial effects. Our study suggests that infusion of cilostazol solution is a therapeutic option in treating acute ischemic stroke patients.

392

VALPROIC ACID PREVENTS HEMIN TOXICITY THROUGH HO-1 DOWNREGULATION BY REGULATING AN UBIQUITIN-PROTEOSOMAL PATHWAY

K.J. Kwon[1], K.S. Cho[1], S.J. Jeon[2], S.-H. Han[1], C.Y. Shin[1]

[1]Department of Neurology, Institute of Biomedical Science and Technology, Center for Geriatric Neuroscience Research, Konkuk University, [2]Department of Pharmacology, Pharmacy and Research Institute of Pharmaceutical Sciences, Seoul National University, Seoul, Republic of Korea

Valproic acid (VPA) is commonly used in the treatment of bipolar disorder and as an anticonvulsant. In the nervous system, it has been reported that VPA increases neuronal growth and synaptogenesis, improves learning and memory, and has neuroprotective effect in acute neuronal injury, such as cerebral ischemia, via activating ERK and GSK-3 pathway. Hemin is released from hemoglobin after CNS hemorrhage and is present at high micromolar concentrations in intracranial hematomas. This highly reactive compound has cytotoxic effects via a variety of oxidative and nonoxidative mechanisms. The Heme oxygenase-1 (HO-1) is an inducible and redox-regulated enzyme and is believed to be a cytoprotective and anti-inflammatory enzyme. The purpose of current investigation was to assess the effect of VPA on hemin toxicity through the expression of HO-1 protein. We investigated the effects of VPA on HO-1 protein in primary cortical neurons, and on hemin-induced cell death *in vivo*. VPA significantly decreased the expression levels of HO-1 protein in concentration-dependent manner in primary cortical neurons. Expression level of HO-1 mRNA was not affected by VPA. VPA did not change the cell viability and the ROS generation in primary cortical neurons. An inhibitor of JNK pathway, SP600125, inhibited VPA mediated changes in HO-1 expression. VPA concentration-dependently increased ERK1/2 and JNK activation in primary cortical neurons. Reduction of HO-1 expression by VPA was prevented by MG132, a reversible proteosome inhibitor, and VPA increased HO-1 ubiquitination. Hemin induced the cell death and this toxicity prevented by VPA. These protective effects mediated by inhibition of the HO-1 protein expression. Based on these findings, our results indicate VPA inhibits the expression of HO-1 protein in rat primary cortical neurons through ubiquitin-proteosomal degradation by JNK pathway, and suggest VPA may provide a therapeutic strategy to attenuate the intracerebral hemorrhagic injury.

393

EFFECTS OF ELECTROACUPUNCTURE ON N-METHYL-D-ASPARTATE RECEPTOR-RELATED SIGNALING PATHWAY IN THE SPINAL CORD OF NORMAL RATS

H.N. Kim, Y.R. Kim, J.Y. Jang, H.K. Shin, **B.T. Choi**

School of Korean Medicine, Pusan National University, Yangsan, Republic of Korea

Objective: This study examined the roles of the N-methyl-D-aspartate receptor (NMDAR) on the modulation of related spinal signaling pathway after electroacupuncture (EA) stimulation in a non-pain rat model.

Methods: Bilateral 2 Hz EA stimulations (1-2-3.0 mA) were needle-delivered in men for 30 min at acupoints corresponding to Zusanli (ST36) and Sanyinjiao (SP6). NMDAR and related signaling were analyzed by behavioral, Western blot and immunohistochemical analysis.

Results: Thermal sensitivity of the hindpaw was strongly inhibited by EA stimulation, but this EA analgesia was reduced by pre-intrathecal injection with the NMDAR antagonist MK801. We examined the phosphorylation of the NMDAR NR2B subunit with related extracellular signal-regulated kinase (ERK), p38, phosphatidylinositol 3-kinase (PI3K) and cAMP response element-binding protein (CREB) in the L4-5 segments of the spinal cord corresponding to hindpaw afferent inputs by Western blot analysis. Phosphorylation of the NR2B subunit of NMDAR, CREB and especially PI3K were significantly induced by EA stimulation. However, these marked phosphorylations were not observed in MK801 pre-treated rats. Because the phosphorylation of PI3K and CREB by NMDAR is closely related with calcium influx, two calcium chelators (Quin2 and TMB8) were injected intrathecally. EA analgesia was reduced by pre-treatment with both calcium chelators, similar to the NMDAR antagonist. Phosphorylation of PI3K and CREB induced by EA was also inhibited by TMB8. Double-labeling staining showed a large proportion of phosphorylated PI3K or CREB and NeuN colocalization in the laminae VI-VI of the dorsal horn.

Conclusion: The calcium influx by NMDAR activation may play an important role in EA analgesia of non-pain animal model by modulating the phosphorylation state of spinal PI3K and CREB.

394

HUD REGULATES THE CPG15 EXPRESSION VIA THE 3'-UTR

X.-H. Chen, Z.-H. Wang, S.-J. Li, Y. Qi, J.-J. Zhao, X.-Y. Liu, Y. Han, P. Xu

State Key Laboratory of Medical Neurobiology, Fudan University, Shanghai, China

Objectives: The candidate plasticity related gene 15 (cpg15) plays important roles in neural development and plasticity. However, the mechanism by which the cpg15 expression is regulated remains largely unclear. The present study is to investigate whether the 3'-untranslated region (UTR) play roles in regulating the expression of the candidate plasticity related gene 15 (cpg15) gene and whether HuD, a neural-specific RNA binding protein, is involved in the regulation.

Methods: The rat cpg15 coding sequence followed with or without its 3'-UTR were inserted downstream the GFP coding sequence in the pEGFP-C2 vectors, and the recombinant vectors were used to express the GFP-cpg15 fusion gene in SH-SY5Y cells. The expression levels of GFP-cpg15 mRNA were detected by real-time RT-PCR, and the GFP-CPG15 fusion proteins were detected by Western blotting using anti-GFP antibodies 48 hours after cell transfection.

Results: The presence of the 3'-UTR significantly decreases the GFP-cpg15 fusion gene expression, and over-expression of HuD increases the GFP-cpg15 expression, which depends on the presence of the 3'-UTR. In addition, deletion of HuD domains RRM1 plus RRM2 or Hinge region plus RRM3 attenuates the function of HuD in enhancing the cpg15 expression.

Conclusions: The 3'-UTR might be a negative cis-element for cpg15 gene expression. HuD could up-regulate the cpg15 expression and this regulation is the 3'-UTR-dependent. The present study gives the first report on the posttranscriptional regulation of cpg15 expression and the important role of HuD in the regulation.

Keywords: cpg15; HuD; regulate; expression; 3'-UTR

395

NEUROPROTECTIVE EFFECTS OF BONE MARROW MESENCHYMAL STEM CELLS OVER-EXPRESSING GDNF ON RATS WITH INTRACEREBRAL HEMORRHAGE AND NEURONS EXPOSED TO HYPOXIA/REOXYGENATION

Y.Q. Lan[1], Y.C. Xian[2], Z. Ling[3], G.X. Qing[2]

[1]Department of Anatomy and Neurobiology, Tongji University School of Medicine, Shanghai, [2]Department of Neurobiology, Luzhou Medical College, [3]Department of Endocrine, Affiliated Hospital of Luzhou Medical College, Luzhou, China

Objective: The present study aims to investigate whether administration of BMSCs over-expressing GDNF provides more efficient neuroprotection for the rats with intracerebral hemorrhage (ICH) and neurons exposed to hypoxia/reoxygenation.

Methods: Primary rat BMSCs were transfected with rat GDNF gene using virus vector (GDNF/BMSCs) and blank virus plasmid (BVP/BMSCs). GDNF mRNA levels in transfected cells were measured by real time RT-PCR, GDNF proteins from supernatant in the cultures were measured by Elisa assay, and GDNF-positive cells were detected by immunocytochemistry. Differentiation of BVP/BMSCs and GDNF/BMSCs in vitro were performed by immunostaining. Primary rat cortical neurons of rats were exposed to hypoxia for 4 h and then reoxygenated with GDNF/BMSCs (GDNF/BMSCs group) or BVP/BMSCs (BMSCs group) treatment for 12 h, 1 d, 2 d, 3 d, 5 d. Hoechst 33258 staining was used to evaluate apoptosis of cells. GDNF/BMSCs, BVP/BMSCs and saline (GDNF/BMSCs, BMSCs and control groups) were injected into right striatum 3 d after rat ICH induced by injecting collagenase. Modified Neurological Severity Scores and H&E staining were performed to evaluate neurological function and lesion volume at 1 and 2 weeks after transplantation. Immunostaining was used to observe differentiation of grafted cells (NF-200 for neurons, GFAP for astrocytes). The GDNF level and apoptosis were evaluated by western blotting and TUNEL, respectively.

Results: Extrinsic GDNF mRNA and protein from GDNF/BMSCs were stably expressed. The number of NF^+ GDNF/BMSCs was significantly increased compared to BMSCs in vitro. In contrast, the number of $GFAP^+$ BMSCs was not significantly different compared to that from GDNF/BMSCs in vitro. GDNF/BMSCs group significantly lowered apoptosis compared to BMSCs group at given time. GDNF/BMSCs group significantly improved functional deficits and reduced lesion volume compared with the BMSCs group. Stable GDNF expression in the GDNF/BMSCs group was detected at given time in the host brain. The NF^+ grafted cells in the GDNF/BMSCs group were more than BMSCs group. GDNF/BMSCs group was significantly decreased apoptotic cells compared with BMSCs group.

Conclusion: These results suggest that GDNF/BMSCs prefer to differentiate into neurons in vitro and in vivo, and provide better neuroprotection for the rats with ICH and neurons exposed to hypoxia/reoxygenation.

396

SUBSTITUTION OF ARTERIAL BLOOD-BASED QUANTIFICATION BY COMBINING IMAGE-DERIVED INPUT FUNCTIONS WITH VENOUS BLOOD DATA IN NEUROIMAGING WITH [CARBONYL-^{11}C]WAY-100635

A. Hahn[1], L. Nics[2], P. Baldinger[1], J. Ungersböck[2], R. Frey[1], W. Birkfellner[3], S. Zgud[1], A. Höflich[1], P. Dolliner[2], W. Wadsak[2], M. Mitterhauser[2], R. Dudczak[2], S. Kasper[1], R. Lanzenberger[1]

[1]Department of Psychiatry and Psychotherapy, [2]Department of Nuclear Medicine, [3]Center for Medical Physics and Biomedical Engineering, Medical University of Vienna, Vienna, Austria

Objectives: Full quantification of neuronal receptors usually requires an arterial input function. Although for the radioligand [*carbonyl*-^{11}C]WAY-100635 non-invasive quantification methods have been established, recent comparisons demonstrate the limited applicability of models based on reference regions [1]. The aim of this study was to substitute arterial blood samples-based quantification. Here, we introduce a novel approach to quantify serotonin-1A (5-HT_{1A}) receptor binding with minimally invasive measures by combining data from image-derived input functions and venous blood samples.

Methods: Eleven [*carbonyl*-^{11}C]WAY-100635 scans of 8 healthy women (mean age±sd=55.1±3.1years) were taken from an ongoing clinical study (GE advance PET scanner, 4.36mm full-width at half-maximum (FWHM), voxel size=3.125x3.125x4.25mm). Arterial blood samples were taken automatically for the first 3 minutes and manual arterial and venous samples were drawn simultaneously at 2, 5, 10, 20, 35 and 50 minutes thereafter. Arterial input functions (AIF) were obtained by correcting for delay, plasma/whole blood ratio and radioactive metabolites in plasma [2] using arterial samples only.

Cerebral blood vessels were defined automatically from the dynamic PET records using linear discriminant analysis [3]. Image-derived input functions (IDIFs) were obtained after partial volume correction in PMOD 3.1. Similar to AIFs, IDIFs were corrected with data (plasma/whole blood ratio,metabolites,delay) from venous blood samples (IDIF+V).

PET scans were normalized to MNI-space with SPM8 and regions of interest were taken from an atlas: frontal, orbitofrontal, parietal, temporal, occipital and cingulate cortices, insula, amygdala-hippocampal complex, midbrain, cerebellar gray (excluding vermis) and white matter. 5-HT_{1A} binding potentials (BP_P) were quantified separately using AIF and IDIF with a 2-tissue compartment model by fixing K1/k2 to that of cerebellar white matter [1,4].

Results: Average variability between arterial and venous blood samples was small for plasma/whole blood ratio (1.4%) and within reported reproducibility values [4] for metabolite fractions (maximum 23% at 5min). Compared to IDIFs, the peaks of AIFs were slightly lower (mean difference Δ=7±19kBq/cm^3,$p>0.05$), but emerged significantly later (Δ=5.1±5.9s,$p< 0.05$) with higher full-width at half-maximum (Δ=15.5±4.1s,$p< 0.001$).

Regression analysis showed excellent agreement of BP_P between AIF and IDIF+V with R^2=0.96 across subjects (Figure 1). Slope and intercept were 1.12 and -0.04, respectively, indicating that BP_P from IDIF+V were 12% higher. This might be attributed to the dispersion of the AIF peak, which is also reflected by the lower estimates of K1 obtained with AIFs (Δ=0.11±0.08ml/cm^{3}min,$p< 0.001$).

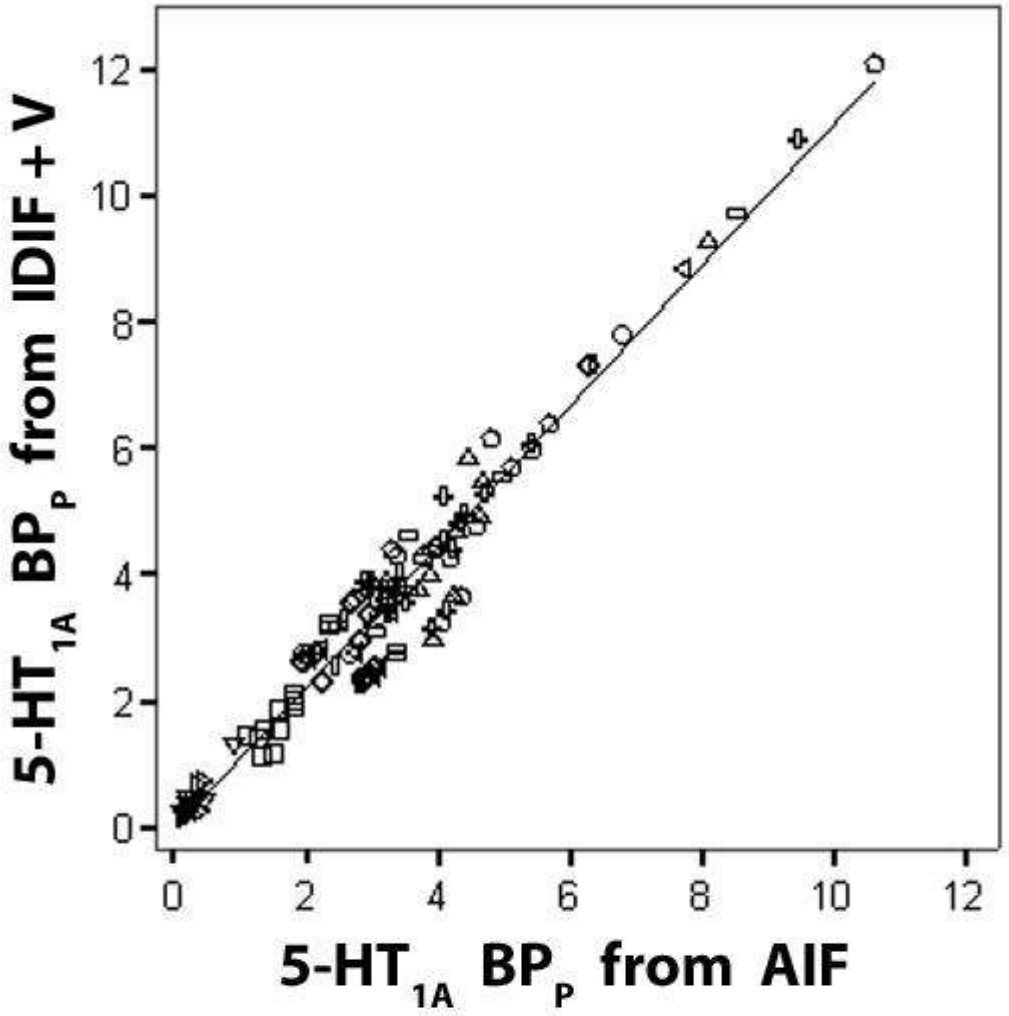

Figure 1: Regression analysis of 5-HT_{1A} binding potentials BP_P obtained from arterial input functions (AIF) and the combination of imaged-derived input functions with venous blood data (IDIF+V).
$R^2 = 0.96$, slope = 1.12, intercept = -0.04. Symbols represent different regions of interest.

[Figure 1]

Conclusions: This study demonstrates the proof-of-principle to substitute arterial cannulation with a combination of IDIFs and venous blood data even for radioligands with fast metabolism. In contrast to previous approaches [5], this method maintains the possibility of full compartmental quantification while reducing patient burden and technical demands.

References: [1] Biol Psychiatry 68(2):170-178;2010.

[2] Eur J Nucl Med Mol Imaging 37(S2):S242;2010.

[3] NeuroImage 52(S1):S155-156;2010.

[4] J Cereb Blood Flow Metab 27(1):185-195;2007.

[5] Eur J Nucl Med Mol Imaging 36(3):463-471;2009.

Disclosure: This research was supported by a grant from the Austrian National Bank (OeNB12809). A. Hahn is recipient of a DOC-fellowship of the Austrian Academy of Sciences at the Department of Psychiatry and Psychotherapy.

398

KINETICS OF CEREBRAL BLOOD FLOW DURING MODERATE INTENSITY STEADY-STATE CYCLE ERGOMETER EXERCISE

M. Hiura[1], N. Kinoshita[1], S. Izumi[1], T. Nariai[2]

[1]Faculty of Sports and Health Studies, Hosei University, [2]Department of Neurosurgery, Tokyo Medical and Dental University, Tokyo, Japan

Introduction: It has been demonstrated that change in cerebral blood flow (CBF) during exercise would be related to that in both cardiac output (CO) and arterial carbon dioxide tension (P_aCO_2). Considering that pulmonary oxygen uptake ($\dot{V}O_2$) is attributable to CO and skeletal muscle metabolism for oxygen, the kinetics of CBF during exercise would be related with that of $\dot{V}O_2$. With respect to neural mechanisms that regulate the circulation during exercise, central command and the exercise pressor reflex arising from skeletal muscles are to be mediating resetting the carotid baroreflex. However, there is paucity of information for CBF response during the on-transit and off-set phase of dynamic exercise.

Aims: The purpose of the present study is to investigate the kinetics of CBF during exercise in association with that of P_aCO_2 and $\dot{V}O_2$ and to examine if CBF would remain stable during steady-state exercise where P_aCO_2 and $\dot{V}O_2$ have plateau phase.

Methods: 7 healthy young males (age, 24.1 ± 3.1 yr; height, 1.71 ± 0.07 m; body mass, 64.7 ± 5.8 kg) performed constant workload of exercise bouts (10 min) by cycle ergometer with moderate intensity corresponding to the level of 10~20 % below lactate threshold (LT). Respiratory gas analysis and the middle cerebral blood flow mean velocity (MCA V_{mean}) were measured simultaneously using the transcranial Doppler method. P_aCO_2 was estimated (eP_aCO_2) using end-tidal pressure of CO_2 and tidal volume. We assumed that MCA V_{mean} could be used as an index of the global CBF.

Results: 1) The kinetics of $\dot{V}O_2$, eP_aCO_2 and MCA V_{mean} at the initial phase of the exercise was expressed by a monoexponential curve fitting model. The response of MCA V_{mea} during the transition from rest to exercise mimicked that of $\dot{V}O_2$ and the time constant (τ) for $\dot{V}O_2$ were related to τ for MCA V_{mean} (R^2 = 0.73). 2) As MCA V_{mean} remained stable during the steady phase of eP_aCO_2, relationship between eP_aCO_2 and MCA V_{mean} were investigated both at onset and off-set of exercise, separately. There was tendency that MCA V_{mean} was correlated well at off-set of exercise rather than at on set; (R^2 = 0.72 ± 0.08 vs. 0.41 ± 0.11, $p < 0.05$).

Discussion: We demonstrate that response of MCA V_{mean} during the transition from rest to exercise mimicked that of $\dot{V}O_2$ and that τ for $\dot{V}O_2$ correlated with that for MCA V_{mea}. As the initial phase of $\dot{V}O_2$ kinetics at the onset of steady-state exercise (the phase II response) is thought to closely represent the kinetics of muscle oxygen consumption, it is likely that the enhanced utilization of oxygen within muscles would be reflected in the corresponding area of brain such as motor cortex and would contribute to the related neuronal activity that affects CBF.

Conclusion: Considering that exercise starts with central command and afferent signals from contracting muscles generate the perception and integration of various sensory input in brain, we speculate that increase in both CO and muscle metabolism would have association with that of CBF.

399

GINKGOLIDE B PREVENTED NEURONAL DAMAGE IN ACUTE CEREBRAL ISCHEMIA BY SUPPRESSING CALCIUM INFLUX

M. Thura[1], K. Hokamura[2], S. Yamamoto[1], H. Koyama[3], M. Suzuki[4], K. Umemura[2]

[1]Photon Medical Center, [2]Department of Pharmacology, Hamamatsu University School of Medicine, Hamamatsu, [3]Regeneration and Advanced Medical Science, Gifu University Graduate School of Medicine, Gifu, [4]Center for Molecular Imaging Science, RIKEN, Kobe, Japan

Introduction: Ginkgolide B (GB) is one of the derivatives of ginkgo biloba extract. It has been reported that GB protects neuronal apoptosis through inhibiting platelet activating factor. However, its effects on focal ischemia and on glutamate excitotoxicity, one of the major mechanisms in acute cerebral ischemia, remain unclear.

Objective: In the present study, we examined whether GB could be neuroprotective against acute cerebral ischemia, and if so, we sought to determine its mechanisms.

Methods:

1) The study in rat focal ischemia model: The effects of GB (0.3, 0.1 and 0.3 mg/kg) on acute cerebral infarction was investigated using middle cerebral artery occlusion (MCAO) in rats induced by photochemically induced thrombosis (Umemura *et al* 1993). 24 hours later, neurological examination was performed, and the infarct volume was measured. Ischemic cerebral blood flow (CBF) was measured by laser-Doppler flowmetry in the frontal cortex.

2) The study using cultured rat cortical neurons: The possible neuroprotective mechanism was explored in primary cortical neurons. The effect of GB (0.2, 0.6, 2 and 6 μM) on the process of neuronal cell death upon glutamate 300 μM exposure was investigated. Cell death was assessed using propidium iodide (PI), a fluorescence marker, and neuronal swelling was observed under a differential interference contrast microscope. Change in intracellular calcium concentration $[Ca^2]_i$ was monitored using fluo-3/AM, a fluorescent Ca^{2+} indicator, under confocal laser microscope (Thura et al 2009).

Results:

1) The study in rat focal ischemia model: Administration of GB immediately after induction of MCAO improved neurological scores significantly after 24 hours and infarct size was reduced by 37.5% in 0.3 mg/kg group. However, GB did not improve the ischemic CBF following MCAO, suggesting the neuroprotective mechanism is independent of improving CBF.

2) The study using cultured rat cortical neurons: Co-administration of GB significantly reduced glutamate-induced neuronal death after 6 hours in a dose-dependent manner. It also suppressed glutamate-induced neuronal swelling. These findings indicated that GB prevented neuronal necrosis upon glutamate exposure. GB reduced glutamate-induced increased in $[Ca^2]_i$ in a dose-dependent manner, while it could not suppress AMPA-induced $[Ca^2]_i$ increase. GB decreased NMDA-induced $[Ca^2]_i$ increase in the neurons recorded in glycine 15 μM containing artificial cerebrospinal fluid (aCSF) but could not do so in the neurons in Mg^{2+} free aCSF.

Conclusions: In the present study, we observed GB is protective against: 1) cerebral infarction

following MCAO; and 2) neuronal necrosis induced by glutamate with suppression of $[Ca^2]_i$ increase independently of AMPA. We also observed 3) GB decreased NMDA-induced $[Ca^2]_i$ increase in the presence of glycine. We conclude that GB plays a protective role in the process of neuronal necrosis by inhibiting the glycine site upon NMDA activation.

References:

(1) Umemura K, Wada K, Nakashima M *et al*, 1993, Evaluation of the combination of a tissue-type plasminogen activator, SUN9216, and a thromboxane A2 receptor antagonist, vapiprost, in a rat middle cerebral artery thrombosis model. Stroke 24, 1077-1082.

(2) Thura M, Hokamura K, Yamamoto S *et al*, 2009, GIF-0173 protects against cerebral infarction through DP1 receptor activation. Experimental Neurology 219, 481-491

400

IMPAIRED CAMP AND RHO GTPASES SIGNALING CONTRIBUTE TO PRION-INDUCED ENDOTHELIAL BARRIER BREAKDOWN IN BLOOD-BRAIN BARRIER

I. Cooper[1], B. Mohar[1], M. Salmona[2], V.I. Teichberg[1]

[1]Neurobiology, Weizmann Institute of Science, Rehovot, Israel, [2]The Mario Negri Institute for Pharmacological Research, Milano, Italy

Prion is the infectious particle responsible for transmissible spongiform encephalopathy, a fatal neurodegenerative disease of humans and animals. Since the disease may be acquired from iatrogenic sources like blood transfusion, we addressed the question whether prions may invade the brain from circulating blood. To this aim, we studied the interactions of the peptide PrP 106-126, which corresponds to the 106-126 amyloidogenic region of the cellular human prion protein, with brain capillary endothelial cells using an in-vitro model of the BBB. PrP 106-126 was found to cross an in-vitro barrier formed by pig brain capillary endothelial cells (PBEC) displaying high transendothelial electrical resistance (TEER). The PrP 106-126 at 100 µM, was toxic to PBEC as shown by assays of LDH release and MTT reduction as well as by direct cell counting. Though the PrP 106-126 caused a cumulative rate of cell death averaging 20% and about 50% reduction of the TEER, the latter remained of substantial amplitudes indicating that the PBEC maintained confluency at the different time points. The decrease of the TEER was accompanied by a 23% increase of the average size of the PBEC along with a disappearance of the tight and adherence junctions claudin-5, occludin and VE-cadherin but not of ZO-1 immunoreactivities from the cell surface. Exploring the effects of the prion protein on the cytoskeleton elements, we observed stress fibers formation in the endothelium cytoplasm. Moreover, we found that cyclic AMP, a known barrier protective compound is reduced while the GTPase RhoA is being activated upon prion peptide exposure. Inhibition of the RhoA signaling pathway reversed the PrP 106-126-induced barrier breakdown. These results are compatible with a mechanism by which PrP 106-126 crosses the endothelial cell barrier by a coordinated cell killing process and re-modeling of the intercellular junctions and cytoskeleton.

403

VOXELBASED PARAMETRIC CORRELATION OF FDG-PET WITH BIOMARKER PROFILE IN PATIENTS WITH EPISODIC MEMORY IMPAIRMENT

M. Gartenschlaeger[1], I. Yakushev[2], H.G. Buchholz[1], A. Fellgiebel[2], M. Schreckenberger[1]

[1]Nuclear Medicine, [2]Psychiatry, University Medical Center, Mainz, Germany

Aim: Beside FDG-PET, several CSF- and hemochemistry biomarkers have been introduced into clinical routine to assist detection of Alzheimer disease (AD) at a pre-dementia state, such as amyloid $\beta_{1\text{-}42}$,(Aβ), tau protein phosphorylated at threonine 181 (p-tau_{181}), total tau (t-tau) in CSF and ApoE-status in peripheral blood. Our interest was to demonstrate in which respect the various laboratory biomarkers correlate with FDG-PET findings.

Material and methods: Retrospective evaluation of 58 patients with episodic memory disturbance, without manifest dementia. All patients had been studied with FDG-PET (150 MBq 18-F-FDG, under standardized resting conditions, Siemens ECAT Exact Scanner, 3d-mode). FDG images were spatially normalized using the preprocessing tools of SPM and a FDG template. The results of

- Neuropsychologial tests
- CSF: Aβ, p-tau_{181}, t-tau
- Peripheral blood: ApoE-status

were correlated voxelwise to PET-data using SPM 5. All statistics were performed with $p< 0.001$ uncorrected and $p< 0.05$ corrected on cluster level using small volume correction.

Results: A positive correlation was found for MMSE and glucose metabolism in the left posterior lateral parietal lobe ($z=4.24$). Negative correlation could be demonstrated for p-tau_{181} ($z=3.61$) and t-tau ($z=4.82$) on one hand and FDG-uptake in the posterior part of the cingulate gyrus.

Conclusion: Among CSF biomarkers, t-tau shows the strongest and p-tau_{181} also demonstrates a significant inverse correlation with FDG-uptake in the posterior part of the cingulate gyrus.

405

PARTIAL VOLUME CORRECTION OF (R)-[^{11}C]VERAPAMIL PET IMAGES USING CHOROID PLEXUS DEFINED ON CONTRAST ENHANCED-MRI

S. Wang[1], M. Feldmann[1,2], R. Hinz[1], M. Koepp[2], A. Jackson[1], M.-C. Asselin[1]

[1]Wolfson Molecular Imaging Centre, The University of Manchester, Manchester, [2]Department of Clinical and Experimental Epilepsy, UCL Institute of Neurology, London, UK

Aims: P-Glycoprotein (P-gp) is an efflux pump that has been hypothesised to play a key role in drug resistance in epilepsy. P-gp function and expression can be imaged in the human brain *in vivo* using PET with (R)-[^{11}C]Verapamil (VPM). The hippocampus is one of the most important epileptogenic regions in temporal lobe epilepsy (TLE) patients, but this region cannot be quantitatively analyzed in VPM-PET images due to the spill-over of radioactivity from the adjacent choroid plexus (CP) (Langer et al, 2007). The aim of this study is to implement and evaluate an MR-based partial volume correction (PVC) method for HRRT PET images using contrast-enhanced MRI (CE-MRI).

Material and methods: A pilot CE-MRI study was conducted in 6 healthy volunteers to determine the reproducibility of the position of the CP. An algorithm was implemented to automatically segment the CP from the pre- and post-contrast MR images. The automatically segmented CP was compared against the CP manually delineated. A group of 7 subjects (1 healthy volunteer and 6 TLE patients) underwent both VPM-PET and CE-MRI scans for subsequent MR-based PVC (Rousset et al, 1998). The segmented CP from CE-MRI was incorporated into a modified probabilistic brain atlas using a multi-atlas propagation approach (Heckemann et al, 2006). A simulation study was performed to assess the effect of misregistration on PVC.

Results: Automatic segmentation and manual delineation of CP resulted in an average overlap (Dice coefficient) of 73% and 75% in the test-retest study, respectively. VPM uptake in the ventricles corresponded to the segmented CP from the CE-MRI after matching the spatial resolution of the two images, as demonstrated in Figure 1. Despite this very good correspondence, MR-based PVC increased VPM uptake in most of the gray matter regions including the hippocampus (Figure 2A), which was expected to decrease. The simulation study revealed that MRI-PET misregistration in the inferior-superior direction as small as 2mm led to overcorrection in the hippocampus (Figure 2B). As an alternative method, the segmented CP blurred to the spatial resolution of PET images was subtracted from the hippocampus. After CP-based erosion VPM uptake in the hippocampus was reduced to reach similar level as other temporal lobe regions not affected by spill-over from CP.

Conclusions: The CP can be reproducibly segmented from CE-MRI and corresponds to the high uptake region in the ventricles of the VPM-PET images. However, the sensitivity of MR-based PVC methods to coregistration errors is exacerbated by the small size of the hippocampus and the high contrast with the CP. The CP-based erosion method can be applied to eliminate spill-over from CP not only to a region but also to parametric maps . Creation of probabilistic map of CP is being investigated to extend the CP-based erosion method for subjects without CE-MRI scans.

References:

Langer et al (2007) Epilepsia 48: 1774-84

Rousset et al (1998) J Nucl Med 39: 904-11

Heckemann et al (2006) NeuroImage 33: 115-26

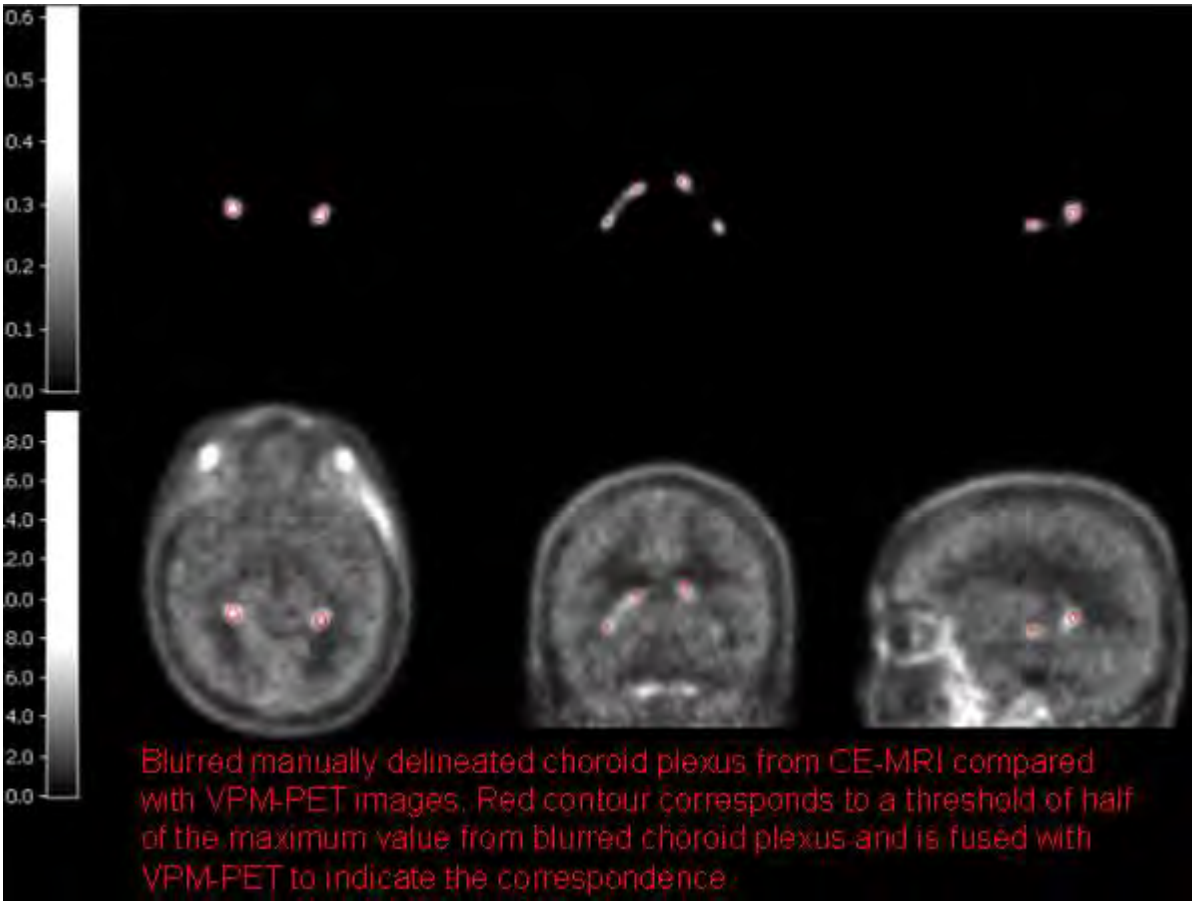

[Figure 1]

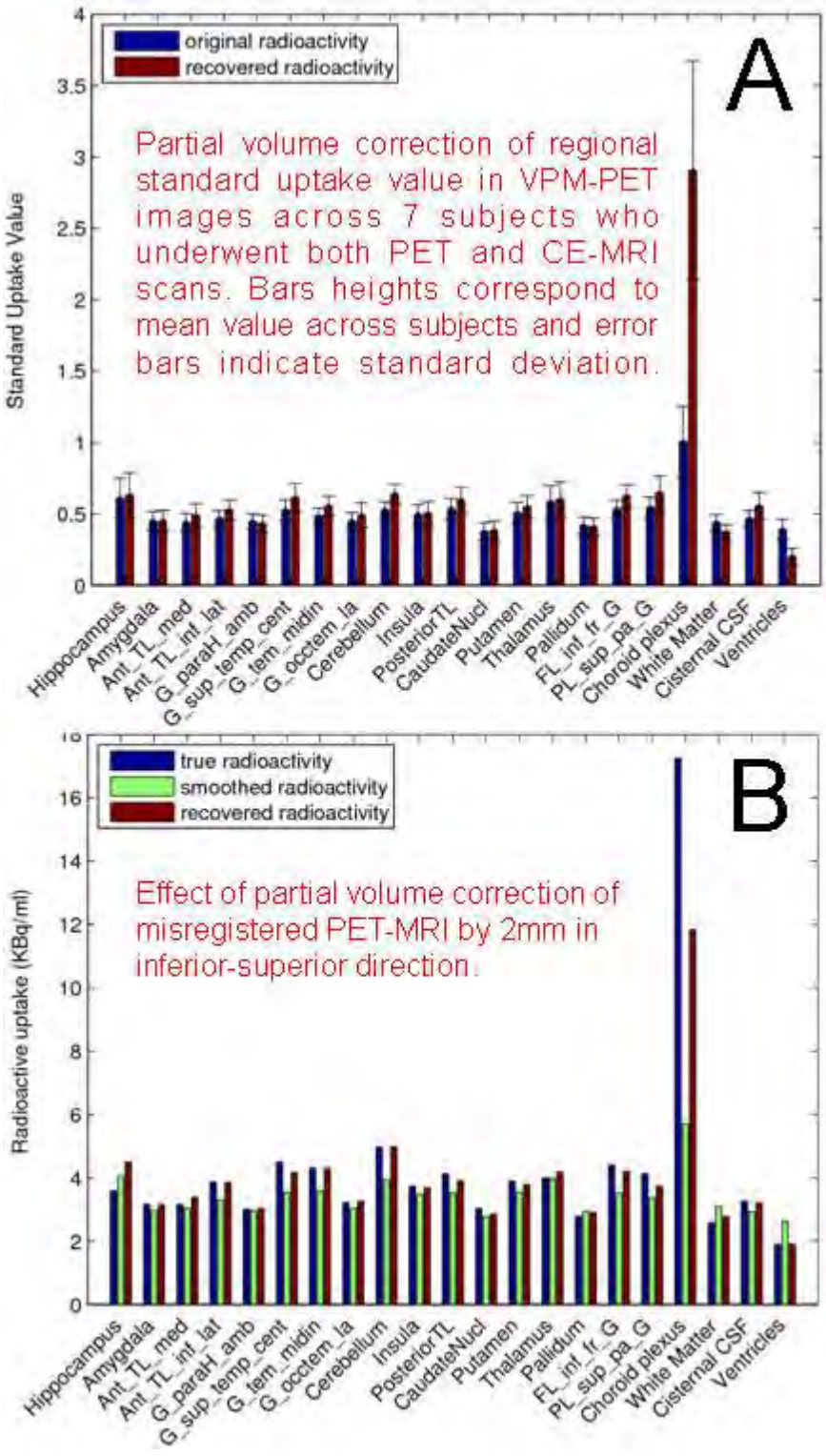
original radioactivity
recovered radioactivity
A
Partial volume correction of regional standard uptake value in VPM-PET images across 7 subjects who underwent both PET and CE-MRI scans. Bars heights correspond to mean value across subjects and error bars indicate standard deviation.
Standard Uptake Value
Hippocampus
Amygdala
Ant_TL_med
Ant_TL_inf_lat
G_paraH_amb
G_sup_temp_cent
G_tem_midin
G_occtem_la
Cerebellum
Insula
PosteriorTL
CaudateNucl
Putamen
Thalamus
Pallidum
FL_inf_fr_G
PL_sup_pa_G
Choroid plexus
White Matter
Cisternal CSF
Ventricles
true radioactivity
smoothed radioactivity
recovered radioactivity
B
Effect of partial volume correction of misregistered PET-MRI by 2mm in inferior-superior direction.
Radioactive uptake (KBq/ml)

[Figure 2]

407

THE ROLE OF ABC TRANSPORTERS IN NEURO-INFLAMMATORY EVENTS AT THE BLOOD-BRAIN BARRIER

G. Kooij[1], M. Mizee[1], J. van Horssen[1], P. van der Valk[2], A. Reijerkerk[1], **H.E. de Vries**[1]

[1]Molecular Cell Biology and Immunology, [2]Pathology, MS Center Amsterdam, VU University Medical Center, Amsterdam, The Netherlands

At the blood-brain barrier (BBB), the ATP binding cassette (ABC) transporters drive cellular exclusion of a variety of compounds, thereby protecting the brain from neurotoxic compounds. Recently it is described that ABC transporters may also be involved in removal of inflammatory agents from immune cells. In a variety of neuroinflammatory disorders including multiple sclerosis (MS), a defective function of the BBB has been described, based on structural differences. However, lowered expression of ABC transporters at the BBB may lead to enhanced exposure of the brain to inflammatory mediators, thereby aggravating the inflammatory process at the vasculature.

We therefore set out to study the regulation of ABC transporters at the BBB in MS using our well-defined post-mortem patient material. Dominant loss of P-glycoprotein (P-gp: ABCB1) was detected in active MS lesions. Moreover, we have identified that the interaction of activated T-cells with brain endothelial cell cultures leads to a reduction of P-gp expression and function through regulation of the NF-kB signalling route (Kooij et al., J Autoimmun 2009). Our data therefore indicate that in MS not only at the structural level of the blood-brain barrier alterations occur but that also the endothelial efflux barrier properties are affected, exposing the brain to higher levels of inflammatory agents.

Strikingly, in MS lesions, reactive astrocytes start to express a number of these ABC transporters including multi-drug resistance protein-1 (MRP-1) and P-gp. Expression was not solely localized in astrocytic endfeet contacting the vasculature but was found distributed along the whole cell body. Importantly, in vitro cultures of primary human astrocytes derived from MS lesions were found to have enhanced function of MRP-1 and P-gp compared to astrocytes isolated from non-neurological controls. In vitro data using human astrocytes further revealed that both efflux pumps are involved in the secretion of monocyte chemoattractive protein 1 (MCP-1 / CCL-2), which was found to act as the leading chemoattractant for monocyte recruitment across the BBB. Blocking the activity of astrocytic ABC transporters reduced cellular migration across the BBB in vitro, emphasizing that ABC transporters are modulators during inflammation at the BBB (Kooij et al., Brain in press). Since the ATP binding cassette (ABC) transporter P-glycoprotein (P-gp: ABCB1) drives cellular exclusion of a variety of compounds, we finally investigated its role as immunomodulator in the animal model for MS experimental allergic encephalomyelitis (EAE). P-gp knockout mice (mdr1a/1b-/-) showed significantly decreased clinical symptoms of EAE (Kooij et al., PlosOne 2009).

Taken together, our work highlights a new immunomodulatory role of P-gp, revealing a possible new target for immunotherapy.

408

CEREBRAL BLOOD FLOW CHANGES IN THE NON-DOMINANT LANGUAGE AREAS AFTER APHASIC STROKE ARE DIRECTLY AFFECTED BY DOMINANT HEMISPHERIC DAMAGE

G. Uruma, W. Kakuda, M. Abo

Department of Rehabilitation Medicine, Jikei University School of Medicine, Tokyo, Japan

Background: It still remains unclear whether there is a significant interaction between regional cerebral blood flow (rCBF) changes in the left language areas and in the right homologus one, and how rCBF changes are influenced by disruption of interhemispheric neural connection with the onset of stroke if there is such an interaction. The objective of this study was to clarify the influence of rCBF changes in language-relevant areas of the dominant hemisphere on rCBF in each region in the non-dominant hemisphere in post-stroke aphasic patients.

Methods: Twenty-seven Japanese aphasic patients (age:45-89, 16 male and 11 female) with left hemispheric cerebrovascular lesions were studied. All patients were right-handed and the time between the onset of the first-ever stroke and 99mTc-ethylcysteinate dimmer single photon emission computed tomography (SPECT) ranged from 11 to 245 days. The type and severity of aphasia was diagnosed by a cognitive rehabilitation specialists and a speech therapist within 2 days prior to SPECT evaluation. Patients with multiple cerebral lesions seen on brain CT and/or MRI were excluded from the study. In each subject, we measured rCBF by means of SPECT. The SPECT images were analyzed by the statistical imaging analysis programs easy Z-score Imaging System (eZIS) and voxel-based stereotactic extraction estimation (vbSEE). Segmented into Brodmann Area (BA) levels, regions of Interest (ROIs) were set in language-relevant areas bilaterally, and changes in the relative rCBF as average negative and positive Z-values were computed fully automatically. To assess the relationship between rCBF changes of each ROIs in the left and right hemispheres, the Spearman ranked correlation analysis and stepwise multiple regression analysis were applied.

Results: In all patients, the negative Z-value was dominantly found in left ROIs, and the positive Z-value was dominantly found in right ones oppositely. Spearman correlation analysis revealed several significant negative relationships between rCBFs in some left ROIs and ones in the right cortex homologous to language areas. A stepwise regression analysis revealed some rCBF of the left ROIs independently and negatively influenced some of the right ones(R^2 = 0.57 to 0.70, $P < 0.00001$), especially, the rCBF decrease in left BA22 significantly influenced the rCBF increase in right BA39, BA40, BA44 and BA45. Globally, a negative and asymmetric influence of rCBF changes in the language-relevant areas of the dominant hemisphere on the right hemisphere was found.

Conclusions: The results suggested that the chronic increase in rCBF in the right language-relevant areas is due at least in part to reduction in the trancallosal inhibitory activity of the language-dominant left hemisphere caused by the stroke lesion itself and indicate the presence of interhemispheric neural connections via the corpus callosum, which can be described as asymmetrical with varying tightness. These findings may offer new perspectives for the development of novel rehabilitation strategies for post-stroke aphasic patients by influencing these neural connections with the application of electrophysiologic intervention as like transclanial magnetic stimulation.

410

DISTRIBUTION OF CALCITONIN GENE-RELATED PEPTIDE (CGRP) AND ITS RECEPTOR COMPONENTS IN HUMAN AND RAT SPINAL TRIGEMINAL NUCLEUS

S. Eftekhari, L. Edvinsson

Department of Clinical Sciences, Division of Experimental Vascular Research, Lund University, Lund, Sweden

Objectives: Calcitonin gene-related peptide (CGRP) has a key role in migraine pathophysiology and is associated with activation of the trigeminovascular system. The trigeminal ganglion, storing CGRP and its receptor components, project peripheral to the intracranial vasculature and central to different regions in the brain stem with Aδ- and C-fibers; this constitutes an essential part of the pain pathways activated in migraine attacks. In patients, a migraine active region in the brainstem has been demonstrated with positron emission tomography (PET). Therefore it is of importance to identify the regions within the brainstem that processes nociceptive information from the trigeminovascular system, such as the spinal trigeminal nucleus (STN).

Methods: The indirect immunofluorescence method was used to study the distribution of CGRP and its receptor components, calcitonin like receptor (CLR) and receptor amplifying peptide 1 (RAMP1), in human STN, and compare with that of rat, using a set of newly characterized antibodies (Eftekhari et al., Neuroscience 2010). Double immunostainings with CGRP and CLR, CLR and RAMP1 were performed. In addition, double immunostaining with CGRP and a marker against myelin (MBP) was performed.

Results: We observed immunoreactivity for CGRP and its receptor components in the STN. The highest density of CGRP immunoreative fibers were found in a network around fiber bundles in the superficial laminae. Besides immunoreactive fibers, CGRP positive neurons were found in the rat brainstem (on the level of the inferior olive and the hypoglossal nucleus). However, no positive neurons were found in the human brainstem. CGRP fibers did not co-localize with the MBP marker, suggesting that the CGRP fibers belong to unmylinated fibers. The CLR and RAMP1 expression were predominately found in fibers in the spinal trigeminal tract region, with some fibers spanning into the superficial laminae. Co-localization between CGRP and its receptor components was rarely noted.

Conclusions: This study demonstrates the expression of CGRP and its receptor components in the STN, and for the first time indicating the possibility of CGRP signaling in the human STN. Our morphological results suggest that STN could be involved in migraine pathophysiology and act as a possible site for the recently developed CGRP receptor antagonists.

References: Eftekhari, S., Salvatore, C.A., Calamari, A., Kane, S.A., Tajti, J., and Edvinsson, L. (2010) Differential Distribution of Calcitonin Gene-Related Peptide and Its Receptor Components in the Human Trigeminal Ganglion. *Neuroscience* 169: 683-696.

411

INFLUENCE OF PET SCAN DURATION ON DIAGNOSTIC ACCURACY OF FLORBETABEN TO IMAGE B-AMYLOID IN ALZHEIMER'S DISEASE (AD)

O. Sabri[1], S. Tiepolt[1], M. Patt[1], S. Hesse[1], H.-J. Gertz[2], C. Reininger[3], H. Barthel[1]

[1]Department of Nuclear Medicine, [2]Department of Psychiatry, University of Leipzig, Leipzig, [3]Bayer Healthcare, Berlin, Germany

Introduction: Florbetaben is a promising ^{18}F-labeled β-amyloid targeting PET tracer currently under global clinical development. In a multicenter Phase 2 trial we verified similar sensitivity and specificity for florbetaben scans across the imaging start time points 45, 90 and 110 min p.i., with highest values attained 90 min p.i.. For PET tracers used in dementia there is the obvious desire to simplify clinical use without loss of accuracy, for instance by reducing scan duration. The effect of scan duration on diagnostic accuracy has not yet been investigated for florbetaben and was, thus, addressed in this single-center evaluation.

Methods: The florbetaben PET scans (300 ± 60 MBq, ECAT EXACT HR+ scanner) obtained from 50 subjects (age 69±8yrs, 22/28 females/males) imaged at our facility as part of a multi-center Phase 2 trial were analyzed: 25 patients with mild to moderate probable AD (NINCDS-ADRDA and DSM IV-TR criteria, MMSE score 18-26, CDR=0.5-2) and 25 healthy volunteers (HVs, MMSE score ≥28, CDR=0). For each subject, scans of 3 different durations (5 min, 10 min, and 20 min) were generated from dynamic datasets starting 90 min p.i.. The images were randomized and each image visually assessed in a consecutive manner by three experts blinded to the subject's identity and group affiliation but not to scan duration. The experts scored the degree of tracer uptake (as a reflection of β-amyloid load) using an established scale, and determined the degree of diagnostic confidence (0 -100%). Furthermore, a 10% re-read was carried out.

Results: For all three scan durations, 20 of the 25 AD patients and 1 of the 25 HVs were scored as positive for β-amyloid ($p < 0.001$). The resulting sensitivity and specificity were 80% and 96% for all scan durations analyzed. Diagnostic confidence across readers was high (20 min: 97±6%, 10 min: 97±6%, 5 min: 95±8%, n.s.). This was accompanied by a high, not significantly different inter-reader agreement rate ($kappa_{20min}$=0.94, $kappa_{10min}$=0.94, $kappa_{5min}$=0.89). Intra-observer agreement rate was highest for the 20 min scan (kappa=1.00) and lower for the 10 min (kappa=0.71) and 5 min (kappa=0.80) scan duration (p=0.002 and 0.003 as tested against 20 min scan duration).

Conclusions: The above results require verification in a multi-center, multi-camera environment, however, they indicate that the visual assessment of florbetaben PET scans enables discrimination between subjects with AD and HVs with high diagnostic confidence, and inter- as well as intra-observer agreement. A reduction of scan duration from 20 min to at least 10 min did not adversely affect the diagnostic performance. Thus, shortening scan duration appears conceivable for future use of florbetaben in a clinical setting in which a quantification of the PET data is not required.

This trial was supported by Bayer Healthcare, Berlin (Germany)

413

EXTENSIVE BRAIN WHITE MATTER INTEGRITY IMPAIRMENT IN PATHOLOGICAL GAMBLING

J. Joutsa[1,2], J. Saunavaara[3], R. Parkkola[2,4], S. Niemelä[5], V. Kaasinen[1,2]

[1]Neurology, [2]Turku PET Centre, University of Turku, [3]Medical Imaging Centre of Southwest Finland, [4]Radiology, [5]Psychiatry, University of Turku, Turku, Finland

Introduction: Pathological gambling is classified as an impulse control disorder in DSM-IV. Several previous MRI studies have shown brain white matter integrity impairment in various substance use disorders, but there are no previous studies in pathological gambling, a form of behavioral addiction.

Objective: To study possible changes in regional brain gray and white matter volumes, and axonal white matter integrity in pathological gamblers compared to healthy controls.

Design: Between-group analyses using statistical parametric mapping and voxel-based morphometry in structural T1-images and tract based spatial statistics for diffusion tensor parameters. Correlation analyses with gambling-related behavioral measurements.

Participants: Twelve clinically diagnosed (DSM-IV) male pathological gamblers and twelve BMI- and age-matched healthy male volunteers.

Main Outcome Measures: Diffusion tensor parameters: fractional anisotropy and mean diffusivity. Regional volumes of structural magnetic resonance imaging.

Results: In pathological gamblers, widespread reductions in white matter integrity (lower fractional anisotropy, higher mean diffusivity) were seen in multiple brain regions including the corpus callosum, the cingulum, the superior longitudinal fascicle, the inferior fronto-occipital fascicle, the anterior limb of internal capsule, the anterior thalamic radiation, the superior coronal radiation, the inferior longitudinal fascicle and the uncinate / inferior fronto-occipital fascicle. There were no regional volumetric differences in gray or white matter between pathological gamblers and controls.

Conclusions: Pathological gambling is associated with extensive impairment of several brain white matter tracts. The diffusion impairment is not explained by substance abuse or other major neurological or psychiatric diseases, but resembles previous findings in individuals with substance addictions.

414

AUTOMATED REGIONAL AND VOXELWISE QUANTIFICATION OF B-AMYLOID BRAIN LOAD AS IMAGED BY FLORBETABEN PET USING THE HERMES BRASS TOOL

H. Barthel[1], D. Butzke[1], M. Diemling[2], M. Senda[3], B. Sattler[1], J. Seibyl[4], H.-J. Gertz[5], M. Pessel[6], C. Reininger[6], O. Sabri[1]

[1]Department of Nuclear Medicine, University of Leipzig, Leipzig, Germany, [2]Hermes Medical Solutions, Stockholm, Sweden, [3]Institute of Biological Research and Innovation, Kobe, Japan, [4]Molecular NeuroImaging, New Haven, CT, USA, [5]Department of Psychiatry, University of Leipzig, Leipzig, [6]Bayer Healthcare, Berlin, Germany

Introduction: Florbetaben is currently under global clinical development to evaluate its efficacy in detecting cerebral β-amyloid deposition in the brain by means of PET. In addition to visual scan interpretation, quantification via standardized uptake value ratios (SUVRs) and “whole brain β-amyloid load” (total brain volume affected by β-amyloid) may be of significant value. Recently, in a pilot trial, we identified the Hermes BRASS module as a potential tool that permits operator-independent determination of both of these quantitative parameters. The aim of this present study was to evaluate the diagnostic performance of this tool when analyzing multi-center florbetaben data.

Methods: Within the Hermes BRASS software, a normal database was generated utilizing the florbetaben PET scans from 93 cognitively normal, PET-negative healthy volunteers (HVs). A total of 27 VOIs were defined within the brain by adapting the AAL template to the data. The, thus, generated normal database was used to analyze 145 florbetaben PET scans obtained from a multi-center Phase 2 trial. This cohort included 77 patients with probable AD (NINCDS-ADRDA and DSM IV-TR criteria, MMSE score 18-26, CDR=0.5-2) and 68 HVs (MMSE score ≥28, CDR=0). The composite SUVR results obtained with BRASS were then compared to those obtained using a modified AAL volume of interest (VOI) based template applied to the PET scans after MRI-based grey matter segmentation (with the subject's own MRI).

Results: Using florbetaben-BRASS, the analysis of all PET datasets was possible without interventions by the operator (mean analysis duration = 41±4 sec). The composite SUVRs in ADs as determined by BRASS correlated significantly with those determined by the reference method ($r=0.80$, $p< 0.001$). The composite SUVRs obtained with the reference method and those obtained by BRASS discriminated equally well between the ADs and the HVs ($p< 0.001$, Cohen's $d = 1.37$ for both approaches). In the ADs and HVs, 3.2±2.7 vs. 0.1±0.4 ($p< 0.001$, Cohen's $d = 1.61$) neocortical regions were defined by BRASS as pathologic (z-score > 2.5). Furthermore, the “whole brain β-amyloid load” as determined by voxelwise analysis within BRASS was 18.6±25.7 vs. 0.8±3.7ml for the ADs and HVs ($p< 0.001$).

Conclusions: In this study, the florbetaben-BRASS software could be validated against the reference method and demonstrated excellent ability in discriminating between ADs and HVs, both on a regional and a voxel-based level. Thus, this software has great potential in supporting the visual interpretation of florbetaben PET image data in a rapid, user friendly and operator-independent manner.

This project was supported by Bayer Healthcare, Berlin (Germany)

416

EXTENDING ADAPTIVE SEQUENTIAL DESIGN (ASD) FOR IMPROVED REAL-TIME TI OPTIMISATION IN ARTERIAL SPIN LABELLING

A.G. Gardener, S. Clare, P. Jezzard

FMRIB, University of Oxford, Oxford, UK

Objectives: Arterial spin labelling (ASL) uses magnetically-labelled blood as an intrinsic contrast agent to investigate cerebral blood flow (*f*). Paired control and labelled images are acquired and the difference (ΔM) gives *f*-dependent signal; imaging at several post-label times (TIs) between labelling and acquisition allows perfusion quantification[1]. Low SNR in ΔM benefits from optimising acquisition strategy. Historically, repeat measures at fixed TIs are performed, using literature values (i.e.: arterial arrival time (δτ) and *f*) generally based on data from healthy adult subjects. This may not be optimal for a specific subject due to age, physiological, or pathological differences. Adaptive Sequential Design (ASD) allows real-time scanner-based optimisation of TIs during scans, based on a direct search algorithm[2].

Methods: ASD runs within the image processing pipeline on the reconstruction computer; online *f* and δτ best-fits for each voxel ΔM time-course are found; distribution of all voxel fits considered; new optimal TI set generated and fed-back to protocol; takes < 1 second. Process is repeated using voxel fits for all data collected to iteratively generate second improved TI set, and so on. Previously, voxels included for fitting were from thresholding ΔM to approximate grey matter, which may fail where ΔM is outside norm. This study uses an independent voxel selection not reliant on perfusion for robust TI optimisation. Using a 3T Siemens Verio system four acquisition schemes were employed for 10 TIs (0.8-1.8s). Evenly distributed sampling (EDS) followed standard fixed multi-TI measurements; ASD1 self-generated a voxel mask from ΔM during image reconstruction; ASD2 used a prior-acquired double inversion recovery[3] (DIR) sequence to generate independent voxel masks. The DIR image used GE-EPI acquisition with grey-matter weighting (64^2 voxels; $3x3x6mm^3$; five slices; TI1/2=3.2/0.5s; TR=20s; TE=18ms) acquired at start and then stored in memory for subsequent ASL scans (QUIPSS2 technique[4], TI1=0.7s post-label; same setup as DIR except TR=3.2s). Eight TI blocks acquired for each scheme taking ~10mins; additionally a co-multiplied scanner-generated mask of PCA territory was acquired with ASD2 (hypothesis - this region would have longer δτ, therefore optimal TIs would fall later). All TIs were recorded and data sets fitted to the Buxton model in Matlab for *f* and δτ.

Results: Figure 1A: ASD1 self-generated mask, DIR GM-image and ASD2 mask; blue box showing PCA territory.

Figure 1B: distribution of mean TIs (four subjects) for four schemes - ASD1 / ASD2 are similar; ASD2-PCA showing longer TIs as expected.

Figure 1C: representative *f* and δτ maps. For EDS/ASD1/ASD2/ASD2-PCA: averaged *f*=53,55,55,62 (±13ml/100g/min) and δτ=431,391,432,492 (±100ms), showing longer δτ for PCA-only region.

Conclusions: Using DIR images to create online tissue masks improves tissue specificity for real-time TI optimisation, independent of ΔM. Simple segmentation can weight optimal TIs for specific brain regions. Future work will integrate more complex segmentations and different

tissue masking and will apply the technique to stroke patients where perfusion can be regionally impaired.

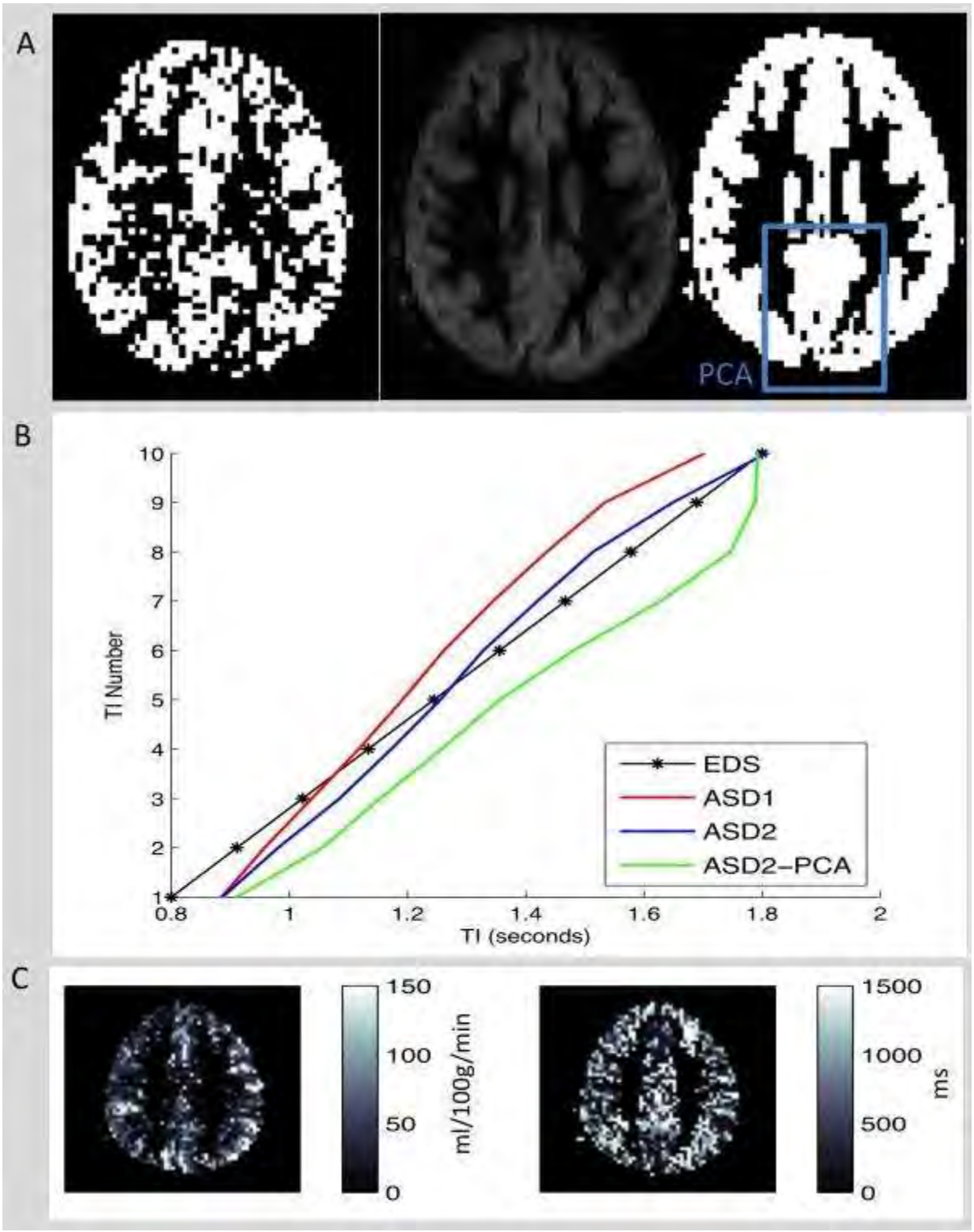

[Figure1]

References:

[1]Buxton, MRM, 1998.

[2]Xie, MRM, 2010.

[3]Redpath, BJR, 1994.

[4]Wong, MRM, 1998.

418

COMPARATIVE OXIDATIVE ENERGY DEMANDS IN CORTEX AND SUBCORTEX BY HIGH FIELD CALIBRATED FMRI

B.G. Sanganahalli[1,2], P. Herman[1,2], D.L. Rothman[1,2,3], H. Blumenfeld[2,4], F. Hyder[1,2,3]

[1]Diagnostic Radiology, [2]Quantitative Neuroscience with Magnetic Resonance in Medicie, [3]Biomedical Engineering, [4]Neurology, Neuroscience, Neurosurgery, Yale University, New Haven, CT, USA

Objectives: Energetic basis of neural activity provides a solid foundation for non-invasive neuroimaging with calibrated fMRI. Our earlier studies with calibrated fMRI have shown that changes in cortical electrical activity correlate well with changes in CMR_{O2} [1-3]. To convert cortical and subcortical BOLD signals into ΔCMR_{O2} by calibrated fMRI, we need reliable measurements of BOLD, CBV, CBF as well as extracellular neural signals (LFP,MUA) measured from both cortical and subcortical regions. Neural activity patterns and microvasculature are known to be different in cortical and subcortical areas [4]. Because oxidative demands in cortex and subcortex are unknown, we evaluated regional energetics with high field calibrated fMRI in rat.

Methods: Animal preparation: Sprague-Dawley male rats were tracheotomized and artificially ventilated ($70\%N_2O,30\%O_2$). During the animal preparation 2% isoflurane was used for induction. Intraperitoneal line was inserted for administration of α-chloralose (46±4 mg/kg/hr) and D-tubocurarine chloride (1 mg/kg/hr). Forepaw stimuli (2mA, 0.3 ms, 3Hz): Stimulation was achieved by insertion of thin needle copper electrodes under the skin of the forepaw. fMRI (n=10): All fMRI data were obtained on a modified 11.7T Varian horizontal-bore spectrometer using a 1H surface coil (Ø = 1.4 cm) [1]. Neural and CBF measurements (n=10): Tiny burr holes above the contralateral somatosensory regions [4.4 mm lateral and 1.0 mm anterior to bregma] and ventral posterior lateral (VPL) thalamic nuclei [3.0 mm lateral and 3.0 mm posterior to bregma] were drilled and tungsten microelectrodes (FHC Inc, Bowdoinham, ME) with fine laser Doppler flow probes (400 μm diameter) were inserted up to layer 4 for $S1_{FL}$ and 5 mm ventral for the thalamic nuclei (VPL) with stereotaxic manipulators (Kopf). Neural data and LDF were processed as described earlier [1]. The LDF data were adjusted to the arterial spin labeling measurements to get the CBF data and CMR_{O2} was calculated using the measured hemodynamic signals as described earlier [1-3].

Results: During somatosensory stimulation we measured BOLD, CBV, and CBF to calculate ΔCMR_{O2} in cortex and subcortex and compared these with neural recordings. While we find that neural-BOLD, neural-CBV, and neural-CBF relationships differ significantly between cortex and subcortex, quite surprisingly we report that ΔCMR_{O2} values are quite similar in these different regions. These regional energetic estimates from calibrated fMRI are in agreement with neural recordings.

Conclusion: These results suggest that neurometabolic couplings are similar in cortex and subcortex, but neurovascular couplings are quite different. Therefore understanding the role of subcortical regions in influencing cortical activation is vital for cortical fMRI data interpretation. The difference in the neurovascular coupling probably originates in the different neural and vascular structure of these two areas [4].

References:

[1] Sanganahalli et al (2009) J neurosci 29: 1707-1718.

[2] Herman et. al (2009) J Neurochem 109: 73-79.

[3] Hyder et al, (2010) Front Neuroenerg 19 : pii 18

[4] Ebner and Armstrong-James (1990) Prog Brain Res 86: 129-141.

Acknowledgements: This work was supported by grants from NIH (R01 MH-067528, P30 NS-52519).

419

PRE-TREATMENT OF FG2216 IS NEUROPROTECTIVE IN MICE FOLLOWING TRANSIENT FOCAL CEREBRAL ISCHAEMIA

R. Chen[1], A. Jani[1], M. Papadakis[1], K. Yeoh[2], S. Nagel[3], C. Schofield[2], A.M. Buchan[1]

[1]Nuffield Department of Medicine, Acute Stroke Programme, University of Oxford, [2]Department of Chemistry, University of Oxford, Oxford, UK, [3]Department of Neurology, University of Heidelberg, Heidelberg, Germany

Objectives: FG-2216 {2-(1-chloro-4-hydroxyisoquinoline-3-carboxamido) acetic acid} is a member of a novel class of small molecules that inhibit hypoxia inducible factors (HIF) - Prolyl Hydroxylases (PHD or EGLN enzymes), which regulate both the stability and activity of HIF. FG-2216 induces erythropoietin expression both *in vitro* and in animals[1], as well as in healthy human subjects (www. Fibrogen.com/programs/fg-2216). The objectives of this study were to determine whether FG2216 when administered systemically confers neuroprotective effects in mice after transient focal cerebral ischaemia.

Methods: Male, 8-12 week old C57/B6 mice received a single dose of FG2216 (20 or 60 mg/kg) or vehicle through a tail vein injection. One day or immediately after the injection, the mice were subjected to 45min of middle cerebral artery occlusion (MCAO) under anesthesia with 1.5 % isoflurane in O_2/N_2O (1:3). At 24h post-ischaemia, behavior was assessed using a neuroscore (0: no deficit - 5: severe deficit)[2]. Thereafter mice were sacrificed and brains were fixed with 4% formaldehyde by cardiac perfusion, and embedded with paraffin. Infarct volumes and HIF1a expression levels were determined using histological and immunohistochemistry techniques.

Results: Mice receiving FG2216 one day before the MCAO had better neuroscores and smaller infarct volumes than mice in the vehicle control group, with only the low-dose (20 mg/kg) comparison reaching statistical significance (Neuroscores: 2.0±0.6 vs 4.5±0.3, p=0.03; Infarct volumes: 27.0±8.1% vs 47.4±5.3%, p=0.04). Mice having high-dose FG2216 showed a trend to have better neuroscores (Neuroscores: 3.3±0.6 vs 4.4±0.5, p=0.28), and smaller infarct volumes (28.3±6.6% vs 49.3±9.5%, p=0.17), compared to the vehicle control mice, however neither of them were significant.

Whereas mice received FG2216 immediately before the MCAO had similar neuroscores and infarct volumes to mice having vehicle in either low or high dosages. Mice having high-dose FG2216 had unexpected significant worse neuroscores (3.0±1.2 vs 4.75±0.5, p=0.03) but similar infarct volumes (48.8±5.5 vs 44.6±8.6, p=0.66) compared to those having low-dose FG2216 immediately before the MCAO.

HIF1a was upregulated not only in the ipsilateral hemisphere but also in the contralateral hemisphere in all the animals 24h after MCAO. Whereas HIF1a stains were more prominent in the ipsilateral hemisphere than in the contralateral hemisphere.

Conclusions: Pre-treatment of FG2216 one day, but not immediately, before cerebral ischaemia is neuroprotective. HIF activation upon ischaemic injury is swift, but the HIF transcription is delayed and limited. Additional therapeutic activation can lead to an earlier and more robust activation of HIF target genes, which confers benefit of the intervention.

References:

1. Hsieh MM, Linde NS, Wynter A, Metzger M, Wong C, Langsetmo I, Lin A, Smith R, Rodgers GP, Donahue RE, Klaus SJ, Tisdale JF. HIF prolyl hydroxylase inhibition results in endogenous erythropoietin induction, erythrocytosis, and modest fetal hemoglobin expression in rhesus macaques. *Blood* 2007; **110** (6): 2140-7.

2. Bederson JB, Pitts LH, Tsuji M, Nishimura MC, Davis RL, Bartkowski H. Rat middle cerebral artery occlusion: evaluation of the model and development of a neurological examination. *Stroke* 1986; **17:** 472-6.

420

CONCURRENT BOLD FMRI AND OPTICAL MEASURES OF SPONTANEOUS FLUCTUATIONS IN CORTICAL HEMODYNAMICS

M. Jones, M. Bruyns-haylett, A. Kennerley, J. Berwick

Department of Psychology, University of Sheffield, Sheffield, UK

Introduction: It has long been known that there are spontaneous low frequency fluctuations in BOLD fMRI signals that occur in the absence of stimuli and now spatial correlations in these low frequency BOLD fMRI spontaneous fluctuations are now used extensively to infer functional connectivity between brain regions. Although great care is taken to remove sources of noise from resting state fMRI data, it would be reassuring to have empirical evidence that spontaneous fluctuations in fMRI signals are related to underlying cerebral hemodynamics and not to non-physiological sources. We have previously developed methods for conducting 2-dimensional optical imaging spectroscopy in a small bore magnet (3T) with a medical endoscope, thus enabling concurrent measurements of sensory evoked cortical hemodynamics and BOLD fMRI in rat.

Aims and objectives: The aims of the present investigation were to (i) Adapt this multi-modal methodology to high field strength (7T) MRI (ii) Ascertain whether it is possible to simultaneously measure spontaneous fluctuations in cerebral hemodynamics with optical and fMRI techniques (iii) Investigate whether spontaneous BOLD fMRI signals and the underlying hemodynamics have similar temporal structure (iv) To investigate whether time series of spontaneous BOLD fMRI signals can be predicted from the underlying hemodynamics

Methods: Hooded Lister rats were anaesthetised with urethane. The skull overlying the whisker barrel somatosensory cortex was thinned to translucency. A plastic chamber was attached to the skull to allow attachment of a surface coil and a medical endoscope. The medical endoscope was use to both illuminate the cortex and relay images of the cortical surface to a high speed CCD camera while the animal was within the bore of the MRI machine. The cortex was illuminated sequentially with four wavelengths of light (495 ± 31 ;587 ± 9 nm;559 ± 16 nm; 575 ± 14 FWHM) with a high speed filter changer synchronised to image capture. The subsequent 'multi-wavelength' optical imaging data were used to estimate changes in total hemoglobin concentration (Hbt), oxyhemoglobin concentration (HbO_2) and deoxyhemoglobin concentration (Hbr) using a modified Beer Lambert Law corrected for the wavelength dependency of the light photon path length by the results of a Monte Carlo simulation (MCS) of light transport through brain tissue. Whisker stimuli were used as functional localisers to enable localisation of whisker barrel somatosensory cortex in both modalities. 'Activation maps' were generated and used to select regions of interest to from which to derive time series. Continuous fMRI and optical data were then collected concurrently in the absence of stimuli or tasks.

Results: Robust measures of spontaneous fluctuations in cortical hemodynamics were evident in both optical and BOLD fMRI measures of cortical hemodynamics. Fluctuations at both 0.1Hz and at slower frequencies were observed in both modalities. Reasonable predictions of BOLD fMRI time series could be derived from the optical hemodynamic data using standard models.

Conclusion: Multi-modal imaging of spontaneous cortical hemodynamics provides powerful confirmation of the hemodynamics origin of spontaneous fMRI signals at different frequencies and will allow greater characterisation of these cerebral hemodynamics fluctuations in health and disease.

421

UNILATERAL TACTILE STIMULI EVOKE CONTRALATERAL CORTICAL BUT BILATERAL THALAMIC ACTIVITY

B.G. Sanganahalli[1,2], P. Herman[1,2], D.L. Rothman[1,2,3], H. Blumenfeld[2,4], F. Hyder[1,2,3]

[1]Diagnostic Radiology, [2]Quantitative Neuroscience with Magnetic Resonance in Medicie, [3]Biomedical Engineering, [4]Neurology, Neuroscience, Neurosurgery, Yale University, New Haven, CT, USA

Objectives: The main tactile somatosensory pathway, the medial lemniscal system of the thalamus has a well defined pathway but it has been mainly studied by cross sectional studies and evoked electrical potentials [1]. Because different peripheral sensory pathways converge onto these subcortical regions, these are important sites for studying the interplay across different sensory modalities [2-6]. The aim here is to describe thalamic and cortical responses to forepaw stimuli in rat brain by high field fMRI and neural recordings [7]. Changes in BOLD and CBV signals were compared with MUA measurements from the same regions.The results demonstrate potential of fMRI at 11.7T to study system wide (cortical and subcortical) integration of sensory inputs [6].

Methods: Animal preparation: Sprague-Dawley male rats were tracheotomized and artificially ventilated (70%N_2O,30%O_2). During the animal preparation 2% isoflurane was used for induction. Intraperitoneal line was inserted for administration of α-chloralose (46±4 mg/kg/hr) and D-tubocurarine chloride (1 mg/kg/hr). Forepaw stimuli (2mA, 0.3 ms, 3Hz): Stimulation was achieved by insertion of thin needle copper electrodes under the skin of the forepaw. fMRI (n=10): All fMRI data were obtained on a modified 11.7T Varian horizontal-bore spectrometer using a ^{1}H surface coil (Ø = 1.4 cm) [7]. Neural measurements (n=5): Tiny burr holes above the contralateral somatosensory regions [4.4 mm lateral and 1.0 mm anterior to bregma] and bilateral ventral posterior lateral (VPL) thalamic nuclei [3.0 mm lateral and 3.0 mm posterior to bregma] were drilled and tungsten microelectrodes (FHC Inc, Bowdoinham, ME) inserted up to layer 4 for $S1_{FL}$ and 5 mm ventral for the thalamic nuclei (VPL) with stereotaxic manipulators (Kopf). Neural (LFP and MUA) data were processed as described earlier [7].

Results: We used 11.7T fMRI of BOLD and CBV and electrophysiology to study thalamocortical activity in anesthetized rats. We observed contralateral cortical but bilateral subcortical activations during unilateral forepaw stimuli with fMRI and these localized activations were confirmed by independent neural recordings. There were no significant differences between the contralateral and the ipsilateral thalamic responses, but the thalamic activations were more pronounced in medial and lateral portions of the laterodorsal thalamic nucleus.

Conclusion: These experiments provide early insights into understudied interactions between cortical and subcortical areas and which should provide a mechanistic basis to understand sensory signaling in the brain. Our results show that there is a strong ipsilateral thalamic activation which is not a part of the medial lemniscal pathway. Future ablation studies will be important in revealing the mechanistic basis of the bilateral thalamic responses. These results have significance in understanding the role of both cortical and subcortical areas during sensory processing [6].

References:

[1] Davidson (1964) J Comp Neurol. 124:377-390.

[2] Grunwerg and Krauthamer (1990) Neurosci Lett 111:23-27.

[3] Alloway et al (2008) J Comp Neurol 510:100-116.

[4] Driver and Noesselt (2008) Neuron 57:11-22.

[5] Cauller et al (1998) J Comp Neurol 390:297-310.

[6] Meredith and Stein (1986) J Neurophysiol 56:640-642.

[7] Sanganahalli et. al (2009) J Neurosci 29:1707-1718.

Acknowledgements: This work was supported by grants from NIH (R01 MH-067528, P30 NS-52519).

422

BLOOD LACTATE ELEVATION ALTERS FMRI AND NEUROPHYSIOLOGICAL RESPONSES DURING ACUTE HYPOGLYCEMIA

B.G. Sanganahalli[1,2], L. Jiang[1], P. Herman[1,3], R.I. Herzog[4], R.S. Sherwin[4], D.L. Rothman[1,3,5], F. Hyder[1,3,5], K.L. Behar[1,3,6]

[1]Diagnostic Radiology, [2]Quantitative Neuroscience with Magnetic Resonance in Medicine, [3]Quantitative Neuroscience with Magnetic Resonance in Medicie, [4]Int Med Endocrinology, [5]Biomedical Engineering, [6]Psychiatry, Yale University, New Haven, CT, USA

Objectives: Hypoglycemia can impair performance during a variety of cognitive tasks in humans [1-4]. Intensive insulin therapy in individuals with type 1 diabetes increases the risk of severe hypoglycemia and potential CNS injury. While glucose is the major fuel of mature brain, blood-borne monocarboxylic acids (MCA; e.g., lactate, ketone bodies) can be utilized as fuels under certain conditions. Blood lactate has been shown to be consumed by the brain during hypoglycemia, although the extent of functional support provided by lactate (and other MCA's) is not clear. MRS studies suggest that blood lactate can support basal energetics, although its capacity to support task-evoked activity is unclear [2,3]. A better understanding of blood MCA utilization by the brain could lead to new treatment strategies for hypoglycemia and other disorders of glucose transport/metabolism. In this study we used fMRI and neurophysiological methods to assess the degree to which lactate can support functional brain activation during limiting hypoglycemia.

Methods: Animal preparation: Sprague-Dawley male rats were tracheotomized and artificially ventilated (70%N_2O,30%O_2). During the animal preparation 2% isoflurane was used for induction. Intraperitoneal line was inserted for administration of α-chloralose (46±4 mg/kg/hr) and D-tubocurarine chloride (1 mg/kg/hr). Forepaw stimuli (2mA,0.3 ms,3Hz): Stimulation was achieved by insertion of thin needle copper electrodes under the skin of the forepaw. fMRI (n=6): All fMRI data were obtained on a modified 11.7T Varian horizontal-bore spectrometer using a ^{1}H surface coil (Ø=1.4 cm) [5]. Neural measurements (n=5): Tiny burr holes above the contralateral somatosensory regions [4.4mm lateral and 1.0mm anterior to bregma] were drilled and tungsten microelectrodes (FHC Inc, Bowdoinham, ME) inserted up to layer 4 for S1FL with stereotaxic manipulators (Kopf). Neural (LFP and MUA) data were processed as described earlier [5]. Hypoglycemia was produced by hyperinsulinemic-glucose clamp resulting in well-controlled stepped reduction in glycemic levels. [2-3].

Results: We found that BOLD signal change in somatosensory cortex ($S1_{FL}$) was suppressed during acute hypoglycemia (~2 mM). Blood lactate elevation (~3 mM) during limiting hypoglcemia led to a transient increase in the response not only at $S1_{FL}$, but dispersed in multiple brain regions. Baseline neurophysiological responses (both LFP and MUA) were suppressed during hypoglycemia and lactate elevation led to significant recovery in these responses, thus confirming changes observed by fMRI.

Conclusion: We conclude that elevation of blood lactate can serve as an alternate fuel during limiting hypoglycemia. Furthermore, blood lactate supports greater delocalization of fMRI activity during limiting hypoglycemia, in contrast to the highly focal activity supported by glucose. Our findings suggest a complex role for lactate in the energetics of neural activation when blood glucose is limiting.

References:

[1]. Jones TW. et al, 1990, Diabetes, 39, 12,1550-5.

[2]. Jiang L.et al, Proc. Intl. Soc. Mag. Reson. Med. 17: 5994. (2009).

[3]. Jiang L. et al, 2009, Diabetes, 58, 1266-74.

[4]. Tyson RL. et al. 2003, Brain Res. 992, 1, 43-52.

[5] Sanganahalli et. al (2009) J Neurosci 29:1707-1718.

Acknowledgements: This work was supported by grants from NIH:NIDDK R01-DK027121 and ARRA supplement, NINDS R01-NS051854 and P30-NS052519 (QNMR Core Center), and JDRF 4-2004-807.

423

UP-REGULATION OF HUMAN CEREBROVASCULAR CONTRACTILE RECEPTORS IS GENDER DEPENDENT

H. Ahnstedt[1], H. Säveland[2], O. Nilsson[2], L. Edvinsson[1]

[1]Experimental Vascular Research, Clinical Sciences, Lund University, [2]Neurosurgery, Lund University Hospital, Lund, Sweden

Objectives: Sexual dimorphism is observed in arterial hypertension and cerebral ischemia. Estrogen has been shown to regulate endothelin and angiotensin receptor expression in spontaneous hypertensive rats. Up-regulation of cerebrovascular contractile receptors that is observed after cerebral ischemia and subarachnoid hemorrhage can be induced by incubation of isolated arteries in serum-free culture medium at 37°C for 48 hrs. In the present study, we investigated if up-regulation of contractile receptors after organ culture is different in human female cerebral arteries than in male arteries.

Methods: Human cerebral arteries, obtained during neurosurgery for treating patients with brain tumor or severe epilepsy, were dissected free from adhering tissue, cut into cylindrical segments and incubated in serum-free culture medium at 37°C for 48 hrs. Incubation of isolated arteries is used as an *in vitro* method to study mechanisms involved in cerebrovascular receptor up-regulation in detail. Contractile responses of 5-hydroxtryptamine type 1B (5-HT_{1B}), angiotensin II type 1 (AT_1) and endothelin type A and B (ET_A and ET_B) receptors were evaluated both in female and male arteries using a sensitive myograph.

Results: In female cerebral arteries, 5-HT_{1B} contraction was similar to that of males. Vascular sensitivity to angiotensin II (Ang II) and endothelin-1 (ET-1) were markedly lower in female cerebral arteries than in males after incubation. A stronger concentration of Ang II was required to produce the equivalent contraction as in male cerebral arteries. No ET_B receptor-mediated contraction was observed in females, while in males contractile responses were observed. As for AT_1 receptor-mediated contraction, a higher concentration of ET-1 was required to elicit the same ET_A receptor-mediated contraction in female arteries as in the respective preparations from males.

Conclusions: There is a sexual dimorphism in vascular responses of AT_1 and ET receptors after incubation of human cerebral arteries. Up-regulation of AT_1 and ET_B receptors is minor in female cerebral arteries compared to in male arteries.

References:

1. Nuedling S et al. **17 Beta-estradiol regulates the expression of endothelin receptor type B in the heart**. *Br J Pharmacol* 2003, **140**(1):195-201.

2. Silva-Antonialli MM et al. **A lower ratio of AT1/AT2 receptors of angiotensin II is found in female than in male spontaneously hypertensive rats**. *Cardiovasc Res* 2004, **62**(3):587-593.

425

GENDER-ASSOCIATED GENE EXPRESSION IN THE BLOOD OF ISCHEMIC STROKE PATIENTS

Y. Tian[1], **B. Stamova**[1], G. Jickling[1], H. Xu[1], D.-Z. Liu[1], B.P. Ander[1], C. Bushnell[2], X. Zhan[1], R. Turner[1], R.R. Davis[3], P. Verro[1], W.C. Pevec[4], N. Hedayati[4], D.L. Dawson[4], J.R. Laird[5], J. Khoury[6], E.C. Jauch[7], A. Pancioli[8], J.P. Broderick[6], F.R. Sharp[1]

[1]Departments of Neurology and the MIND Institute, University of California at Davis, Sacramento, CA, [2]Wake Forest University Medical Center, Winston-Salem, NC, [3]Departments of Pathology and the MIND Institute, [4]Departments of Vascular Surgery, [5]Departments of Cardiology, University of California at Davis, Sacramento, CA, [6]Departments of Neurology, [7]Departments of Emergency Medicine, University of Cincinnati, Cincinnati, OH, [8]Departments of Emergency Medicine, Medical University of South Carolina, Charleston, SC, USA

Background and purpose: Although gender is an important determinant of risk factor profiles, treatment, outcome, and stroke etiology, the basis for this is unknown. We postulated that there are gender specific gene expression changes associated with stroke.

Methods: Blood samples were obtained from 61 acute ischemic stroke patients (35 males and 26 females) at ≤3h, 5h and 24 h following ischemic stroke and from 89 controls (35 males and 54 females) which included healthy and subjects with at least one vascular risk factor. The stroke patients were treated with recombinant tissue plasminogen activator with or without eptifibatide after the 3h blood samples were obtained. RNA was isolated and processed on Affymetrix Human U133 Plus 2.0 Arrays. An ANCOVA were used to identify the gender-associated stroke genes included with the age, gender and batch as co-variates. Genes with a Benjamini-Hochberg false discovery rate (FDR) corrected p≤0.05 and fold change FC $\geq$ |1.5| were considered significant.

Results: There were 571genes whose expression significantly changed between male stroke subjects and male controls, but not in female stroke compared to female controls at ≤3h of stroke onset. Of the 571 genes 91 were over-expressed at all three time points (≤3h, 5h, 24h). There were 684 genes whose expression significantly changed between female stroke subjects and female controls, but not in male stroke subjects compared to male controls at ≤3h of stroke onset. Of the 684 genes 79 were over expressed at all three time points (≤3h, 5h, 24h). Most of the male-specific stroke genes were involved in the cell cycle, integrin-mediated signaling, actin cytoskeleton signaling, cell junction assembly. Most of the female-specific stroke genes were involved in the inflammatory and immune response and response to steroid hormone stimulus - especially for estrogen. Within stroke group analysis revealed that most of the significantly differentially expressed genes between stroke male and female patients were located on the X and Y chromosomes.

Conclusions: Our findings demonstrate that gender has an effect on gene expression in peripheral blood of stroke patients probably representing different gender-related immune responses. Assessing the changes of gene expression in cells in blood may provide unique insights into genders effects on the molecular pathophysiology of stroke.

Keywords: Stroke; Gender; blood; gene expression profiles; Microarray

428

MEASUREMENT OF CEREBRAL PHYSIOLOGY USING QUANTITATIVE MRI

D. Bulte, M. Kelly, J. Xie, P. Jezzard

FMRIB Centre, University of Oxford, Oxford, UK

Objectives: Most functional MRI methods suffer from being non-quantitative. Either it is not a measure of a single physiological parameter or it only produces relative changes in a parameter during the performance of a task or stimulus. Here we present a short, robust paradigm for obtaining whole brain images of resting CBF, CBV, AAT and OEF and estimates by two different methods of the theoretical BOLD maximum. The technique uses a combined hyperoxia and hypercapnia paradigm with a modified CBF measurement sequence.

Methods: 6 healthy volunteers were scanned on a 3 Tesla Siemens Verio with a 32-channel head coil, using a pseudo-Continuous ASL sequence[1] and gradient-echo EPI readout (TR=3.91s, TE=22ms, 6/8 k-space) which had been modified to preserve its BOLD "contamination". Twenty-six axial slices in ascending order (4×4×5.5mm voxels, 0.5mm inter-slice gap) were prescribed. Labelling duration was 1.4s with five different post labelling delay times. The 18-minute paradigm consisted of delivering, via a sealed facemask, 2x2 minute blocks of 4% CO2 in air and 2x3 minute blocks of 50% oxygen, balance nitrogen. Each hypercapnia block was followed by 1 minute of normal air, each hyperoxia block by 2 minutes. BOLD-weighted images were produced by averaging the tag and control images, each image was averaged with both its predecessor and subsequent image to provide equivalent temporal resolution. The BOLD data during the hyperoxia and normal air phases were used to produce resting CBV images using the hyperoxia contrast method[3]. The ASL data from the normal air and hyperoxia periods were used to produce a resting CBF image and an arterial arrival time image, by fitting the data to the ASL kinetic model[4]. The BOLD signal changes and the CBF changes during the hypercapnia periods relative to normal air periods were used to produce an estimate of the theoretical maximum BOLD value *M*[5,6]. The OEF may be calculated using the equation for *M* by Hoge *et al*[6]

$M=TE.A.CBV_0.[dHb]_{V0}^{\beta}$, rearranged as: $OEF = \{[M/(TE.A.CBV_0)]^{(1/\beta)}\}/v_b^{max}$

where: A=1, β=1.3, v_b^{max}=72.3. The value for A is dependent on numerous factors, but is between 0.04 and 4.3 and will tend to be lower at higher fields. A comparison *M*-image was produced from the hyperoxia BOLD data[7].

Results: The figure shows the data from a single slice from one representative subject. Although noisy the values are all within reasonable physiological ranges.

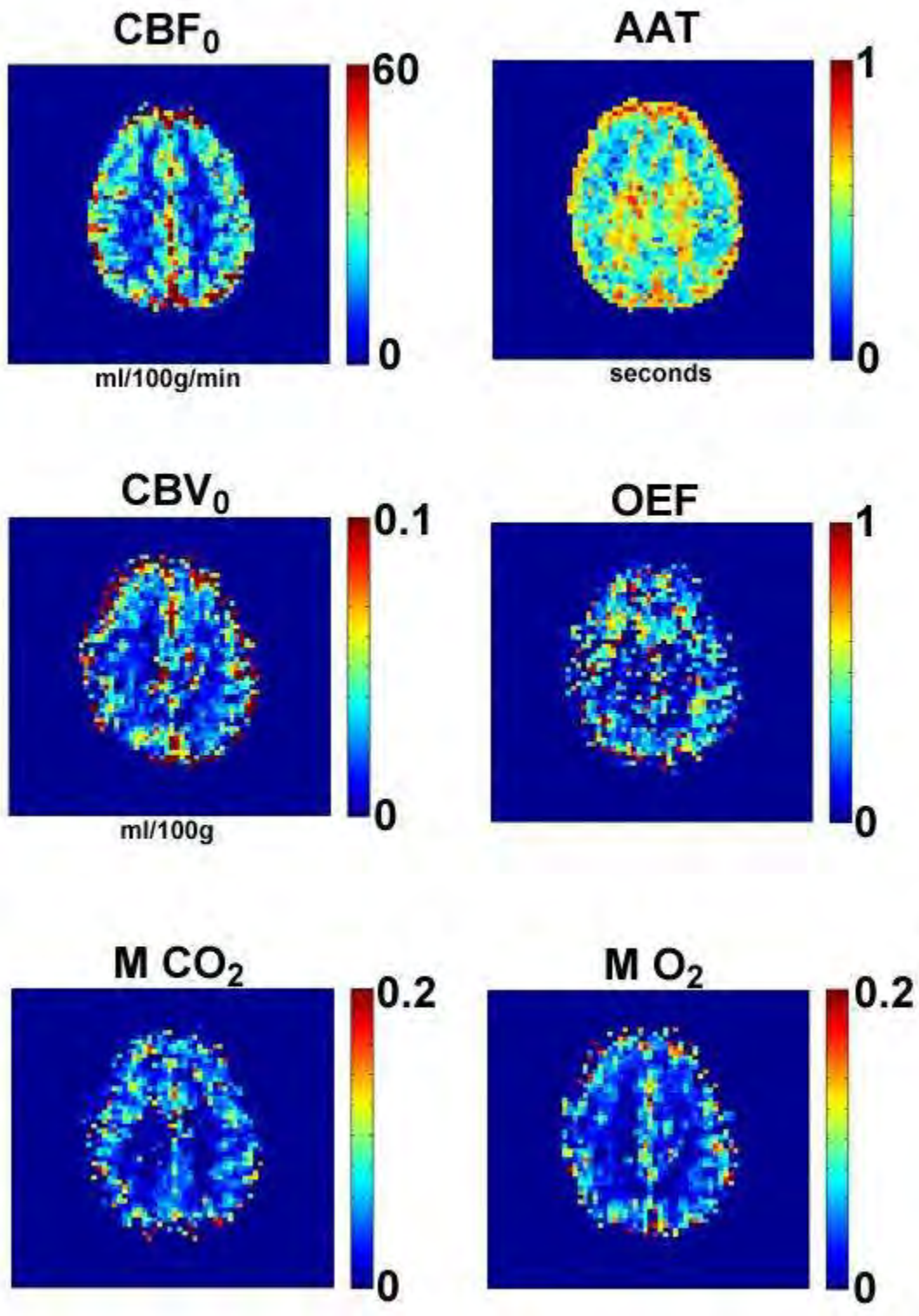
CBF0
60
0
ml/100g/min
AAT
1
0
seconds
CBV0
0.1
0
ml/100g
OEF
1
0
M CO2
0.2
0
M O2
0.2
0

[Figure 1]

Conclusions: The technique introduced here shows promise as a means of producing clinically relevant cerebral metabolic and physiological data from single subjects without contrast agents. This level of diagnostic imaging information was previously only available from Oxygen-15 PET.

References:

1. Dai W*, et al*. Magn Reson Med 2008:(6):1488-1497.

2. Xie J*, et al*. Magn Reson Med 2008:(4):826-834.

3. Bulte DP*, et al*. J Magn Reson Imaging 2007:894-899

4. Buxton RB*, et al*. Magn Reson Med 1998:(3):383-396.

5. Davis TL*, et al*. Proc Natl Acad Sci U S A 1998:(4):1834-1839.

6. Hoge RD*, et al*. Magn Reson Med 1999:(5):849-863.

7. Chiarelli PA*, et al*. Neuroimage 2007:(3):808-820.

429

PLGF KNOCKOUT AFFECTS HYPOXIA-INDUCED BRAIN ANGIOGENESIS AND VESSEL PERMEABILITY

M. Freitas-Andrade[1], C. Charlebois[2], D. Stanimirovic[1,2], M. Moreno[2]

[1]Cellular and Molecular Medicine, Ottawa University, [2]Cerebrovascular Research Group, National Research Council of Canada, Institute for Biological Sciences, Ottawa, ON, Canada

Placental growth factor (PlGF) is a vascular endothelial growth factor (VEGF) homolog known to act synergistically with VEGF in mediating pathological angiogenesis in the peripheral system (1) and to promote vessel stabilization in tumors (2). After focal cerebral ischemia, simultaneous upregulation of VEGF and PlGF has been reported in different cell types in the CNS (3) but the role of PlGF in brain angiogenesis remains elusive.

This study investigates the effect of PlGF knockout in hypoxia-induced brain angiogenesis and blood brain barrier (BBB) permeability.

PlGF wild-type ($PlGF^{+/+}$) and knockout ($PlGF^{-/-}$) mice (1) were subjected to mild hypoxia (10% oxygen) or normoxia for 7, 14 and 21 days. Brain sections from three frontal cortical areas were obtained for immunofluorescent analysis of endothelial cell (CD31), pericyte/smooth muscle cell (NG2, desmin) and BBB (fibrinogen) markers. Images were subjected to microscopy-coupled quantitative analysis. Angiogenesis was investigated, *in vitro,* using brain endothelial cells (BEC) from $PlGF^{+/+}$ and $PlGF^{-/-}$ mice plated on Matrigel™. Cells were exposed to 2-hr, 3-hr or 4-hr hypoxia followed by 16-h reoxygenation and capillary-like-tube (CLT) formation was evaluated (4). Protein expression of VEGF and VEGFR-2 were measured in BEC.

In $PlGF^{+/+}$ animals, a significant ~40% increase in angiogenesis ($CD31^{+}$ cells) was evident after 7 days hypoxia compared to normoxic controls, while in $PlGF^{-/-}$ this effect only occurred after 14 days hypoxia. No differences in pericyte/smooth muscle cell total coverage between the two genotypes were measured. However, after 14 days hypoxia, a significant increase in fibrinogen accumulation and extravasation was measured in $PlGF^{-/-}$ microvessels. A number of these microvessels displayed an abnormally large lumen filled with fibrinogen clots; these vessels were surrounded by reactive astrocytes, lacked pericyte/vascular smooth muscle cell coverage and endothelial VEGF expression, and regressed after 21 days hypoxia.

In vitro studies indicate that, $PlGF^{+/+}$ BEC form CLT networks in Matrigel™ just after 2-hr hypoxia, with the cells continuing elongating and forming complex interconnections over time. In contrast, the angiogenic response of $PlGF^{-/-}$ BEC started only after 3-hr hypoxia, with the cells exhibiting a highly vacuolated cytoplasm and shorter CLT networks, which highly regressed after 4-hr hypoxia. In $PlGF^{-/-}$ hypoxic BEC, VEGF protein levels were significantly increased whereas VEGFR-2 expression was decreased compared to $PlGF^{+/+}$ BEC.

This study shows both *in vitro* and *in vivo* that the lack of PlGF delays brain angiogenesis in response to hypoxia, an effect likely associated to the decrease in VEGFR-2 expression observed in $PlGF^{-/-}$ BEC. The delayed angiogenic response likely promotes hypoxic stress in $PlGF^{-/-}$ mice that leads to fibrinogen accumulation and extravasation. This affects vessel integrity as indicated by the lack of endothelial VEGF expression and pericyte coverage in the $fibrinogen^{+}$ vessels, which results in vessel regression after 21-days hypoxia.

1. Carmeliet, P., *et al*. Nature Medicine **7**, 575-583 (2001)

2. Hedlund, E.M., *et al*. PNAS **106**, 17505-17510 (2009)

3. Beck, H., *et al*. J Neuropath Exp Neurol **61**, 339-350 (2002)

4. Moreno, M. J., *et al.* Glia **53**, 845-857 (2006)

431

CAN CAROTID REVASCULARIZATION FOR STENOSIS IMPROVE BLOOD FLOW AND COGNITIVE FUNCTION?

Z. Ghogawala[1,2], J. Curran[2], M. Westerveld[3], L. Stabile[2], D. Langer[4,5], A. Berenstein[6,7], S. Amin-Hanjani[8]

[1]Yale University, New Haven, [2]Wallace Trials Center, Greenwich Hospital, Greenwich, CT, [3]Florida Hospital, Orlando, FL, [4]Hofstra University School of Medicine, [5]North Shore University Hospital, Manhasset, [6]Albert Einstein College of Medicine, [7]Roosevelt Hospital, New York, NY, [8]University of Illinois at Chicago, Chicago, IL, USA

Objectives: To determine if patients with extracranial carotid stenosis experience improved blood flow and cognitive function following revascularization.

Methods: Patients with significant (>60%) unilateral carotid stenosis were included. Cerebral blood flow values were measured using a commercially available quantitative phase contrast MRA (qMRA) for the ipsilateral and contralateral ICA and MCA vessel flow rates. Patients underwent qMRA pre-operatively and 1 month post-operatively. Flow asymmetry was calculated using a simple ratio, (*ipsi-contra flow/contra flow*) of the vessel flow rates. Pre-operative flow impairment was defined as an ipsilateral flow at least 15% less than contralateral flow and improvement in flow was defined as at least 15% increase in the flow ratio from pre-operative to 1 month post-operative. Only patients with unilateral disease were included. Patients with major stroke were excluded. Patients underwent cognitive testing pre-operatively and 1, 6, and 12 months post-operatively.

Results: A total of 29 patients were enrolled in this pilot study (17 right sided stenosis, 12 left). 25 subjects (86%) completed follow-up at 6 months and/or 1 year. Mean age was 72 years, 59% were male, and 28% were symptomatic at baseline. Pre-operative ICA flow impairment was observed in 62% of patients and MCA flow impairment in 32% of patients. ICA flow improvement was observed in 83% of patients who were previously ICA flow impaired, compared to 45% of the patients who had normal baseline ICA flow (P=0.03). Similarly, 44% of the patients with pre-operative MCA flow impairment demonstrated improvement following carotid revascularization, compared to 26% of patients with normal MCA flow (P=0.3). Following revascularization, patients with baseline flow impairment demonstrated an average of 70% and 40% improvement in flow ratio in the ICA and MCA vessels respectively (Figure 1); this was statistically significant for patients with baseline ICA flow impairment (P< 0.01). Patients who experienced flow improvement following revascularization were more likely to demonstrate clinically significant cognitive improvement at 1 year in both attention (Trail Making A) and executive functioning (Trail Making B). In particular, 100% of patients with improvement in MCA flow demonstrated a clinically significant improvement in executive functioning (Trail Making B) compared to only 39% of patients who did not demonstrate MCA flow improvement (P = 0.01).

Conclusions: Patients with hemodynamically significant >60% ICA carotid stenosis were more likely to experience an improvement in flow following carotid revascularization. In addition, patients with improved cerebral blood flow demonstrated greater cognitive benefit compared to patients that did not experience flow improvement.

References: Ghogawala Z, Westerveld M, Amin-Hanjani S. Cognitive outcomes after carotid revascularization: the role of cerebral emboli and hypoperfusion. Neurosurgery. Feb 2008;62(2):385-95.

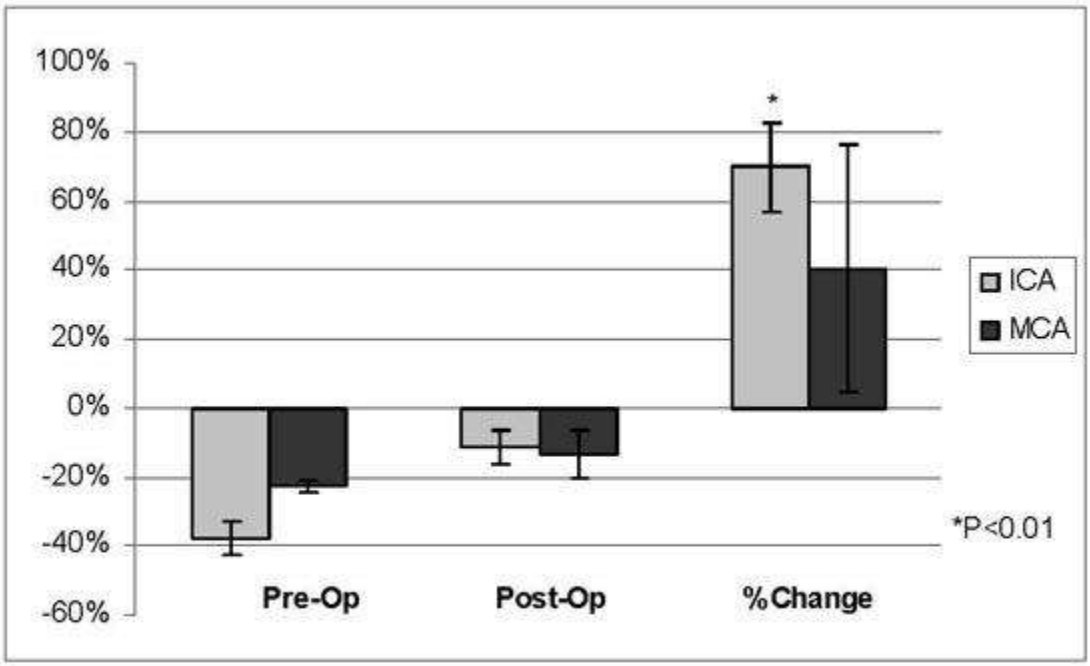

Figure 1. *Change in blood flow among patients with baseline flow impairment.*

[Figure 1]

432

NADPH OXIDASE AND THE PROMOTION OF HYPERGLYCEMIA-INDUCED HEMORRHAGIC TRANSFORMATION IN EXPERIMENTAL STROKE

S.J. Won[1,2], X.N. Tang[1,2], S.W. Suh[1,2], M.A. Yenari[1,2], **R.A. Swanson**[1,2]

[1]Neurology, University of California, San Francisco, [2]Neurology, San Francisco Veterans Affairs Medical Center, San Francisco, CA, USA

Intracerebral hemorrhage is a major factor limiting use of tissue plasminogen activator (tPA) treatment for acute stroke. Clinical studies show that hyperglycemia at the time of tPA infusion increases the risk of symptomatic brain hemorrhage, independent of prior diabetes. We previously showed that glucose, when present at the time of reperfusion could exacerbate ischemic injury, presumably by 'fueling' NADPH oxidase. Here we used an animal model of tPA-induced hemorrhagic transformation to determine if we could recapitulate the clinical observation that hyperglycemia exacerbates this hemorrhage, and whether it could be prevented by a NADPH oxidase inhibiting treatment. Sprague-Dawley rats (n=6-8/ group) were subjected to mechanical occlusion of the left distal middle cerebral artery, plus 90 min of bilateral common carotid artery occlusion. tPA infusion was begun 10 minutes prior to vessel reperfusion, and given at a dose of 10 mg/kg with 10% as an intravenous (IV) bolus and the remainder over 30 min. Hyperglycemia was induced by administering 50% glucose in 3 divided doses 5 min before ischemia onset, 40 min after ischemia onset, and 5 min before reperfusion in order to attain ischemic blood glucose levels 15.0 ± 2.1 mM (hyperglycemia) at the time of reperfusion. Blood glucose levels in normoglycemic animals were measured and maintained at 5.9 ± 1.8 mM. Brains were harvested 1 hour or 3 days later to evaluate the effect of hyperglycemia on oxidative stress, blood-brain barrier breakdown, and hemorrhage volume. Rats that were hyperglycemic at the time of tPA infusion had diffusely increased blood-brain barrier permeability in the post-ischemic territory, and a 3 - 5 fold increase in intracerebral hemorrhage volume ($P < 0.05$). The hyperglycemic rats also had increased superoxide generation in the brain parenchyma and vasculature during reperfusion. The hyperglycemia-induced superoxide production, blood-brain barrier disruption, and hemorrhage were all attenuated by blocking superoxide by NADPH oxidase with apocynin (2.5 mg/kg given IV 10 min prior to reperfusion). These findings establish a cause-effect relationship between hyperglycemia and hemorrhage in the setting of tPA treatment for acute stroke. This effect of hyperglycemia appears to be mediated by superoxide generated by NADPH oxidase. The adjunctive treatment with apocynin might suggest a new therapeutic approach to decrease brain hemorrhage in tPA treated patients.

433

VASCULAR ENDOTHELIAL GROWTH FACTOR (VEGF) SIGNALING AND ITS POTENTIAL ROLE AT THE BLOOD BRAIN BARRIER IN DIABETES

A. Marcelo, R. Egleton

Pharmacology, Physiology, and Toxicology, Marshall University, Huntington, WV, USA

Objectives: Diabetes is a risk factor for stroke and vascular dementias. Clinical studies using gadolinium-DTPA have shown increased permeability of the blood brain barrier in diabetic patients (1). This was also seen in an animal model of diabetes, and the increase in permeability may be associated with the decreased expression of tight junction proteins, particularly occludin and ZO-1 (2). However, the mechanism of the permeability increase has not been elucidated. Other studies at the blood-retinal barrier have observed similar changes in permeability and decreased expression in occludin, and have suggested that vascular endothelial growth factor (VEGF) may play a role (3). VEGF is known to regulate permeability and angiogenesis, and the present study investigates the potential role of VEGF at the blood brain barrier in a streptozocin (STZ) model of diabetes.

Methods: Male Sprague-Dawley rats were injected with either 65 mg/kg STZ or sterile 0.9% saline to induce diabetes. At 14 days post injection, rats were sacrificed and used for real-time PCR analysis or for microvessel isolation. Blood glucose was analyzed, and diabetic rats were grouped based on blood glucose levels as follows: low (< 300 mg/dl), mild (≥300 mg/dl), and high (≥ 400 mg/dl). mRNA and protein expression of VEGF and its receptors, Flt-1and Flk-1, were analyzed.

Results: Real-time PCR analysis showed that there were increased expressions of VEGF and its receptors, Flt-1 and Flk-1 (2-3 fold each) in the microvessels of STZ-treated rats compared to control. Western analysis showed that there was no appreciable change in VEGF in rats with mild glucose, but there was an increase of VEGF in rats with high glucose (~30%) compared to control. There were also glucose-dependent changes in the protein levels of both Flt-1 and Flk-1. No changes in protein levels were seen at low glucose; however both Flt-1 and Flk-1 were slightly elevated in animals with mild glucose levels (15% higher than control). For the animals with high glucose, the levels of both Flt-1 and Flk-1 were reduced compared to control (by 20 and 30%, respectively).

Conclusions: Previously we reported changes in BBB permeability in the STZ model of diabetes. VEGF signaling is an important regulator of angiogenesis and BBB permeability. The present results suggest changes in the brain microvasculature may be due to the interactions of these receptor systems based on the relative diabetic state. The changes in VEGF are dependent on differences in blood glucose; a small glucose elevation increases receptor number, while a larger elevation in glucose concentration decreases receptor numbers. These changes in VEGF signaling may play a role in diabetic-related diseases, and may be an important target for therapeutic intervention.

References:

1. Starr, J., et al. (2003). J Neurol Neurosurg Psychiatry 74: 70-75.

2. Hawkins, B., et al. (2007). Diabetologia 50(1): 202-211.

3. Antonetti, D., et al., (1998). Diabetes 47: 1953-1959.

434

REST AND DNMT3A MODULATE MIR29C MEDIATED BRAIN DAMAGE AFTER FOCAL ISCHEMIA

R. Vemuganti[1,2], G. Pandi[1], V.P. Nakka[1], A. Dharap[1,2]

[1]Neurological Surgery, [2]Neuroscience Training Program, University of Wisconsin, Madison, WI, USA

Transcription factor REST/NRSF controls neural gene expression in neural and non-neural cells. The microRNA mir29c which is expressed at a high level in normal brain has several REST-binding sites in its gene promoter. We observed that REST plasmid dose-dependently prevented mir29c promoter vector expression in vitro. We presently report that transient middle cerebral artery occlusion (MCAO) in adult rats induced REST expression and concurrently repressed mir29c expression. We also observed that knocking-down REST with a siRNA or treatment with a premir29c restored post-ischemic mir29c levels and induced significant neuroprotection. On the other hand, treatment with antagomir29c promoted neuronal death. Bioinformatics analysis showed that the de novo methyltransferase DNMT3a is a strong down-stream target of mir29c and cotransfecting with premir29c prevented the expression of DNMT3a 3'-UTR vector in vitro. Concurrent with mir29c down-regulation, DNMT3a was upregulated following focal ischemia; and treatment with a DNMT3a siRNA decreased ischemic cell death. Thus, following stroke, disruption of the REST-mir29c-DNMT3a pathway mediates brain damage. Funded by a NIH grant NS061071.

435

COMPARISON OF AWAKE AND ANESTHETIZED NON-HUMAN PRIMATE BENZODIAZEPINE BP_{ND} WITH [^{11}C]FLUMAZENIL AND EQUILIBRIUM ANALYSIS

C.M. Sandiego[1], T. Mulnix[1], X. Jin[1], K. Fowles[1], S. Ford[1], J.-D. Gallezot[1], D. Lee[2], D.W. Campbell[2], A. Amanda[2], R.N. Gunn[3], L. Wells[3], E.A. Rabiner[3], S.A. Castner[2], G.V. Williams[2], K. Cosgrove[2], R.E. Carson[1]

[1]Department of Diagnostic Radiology, [2]Department of Psychiatry, Yale University, New Haven, CT, USA, [3]GSK, London, UK

Objectives: Neuroreceptor imaging in the awake non-human primate (NHP) is ideal for improving upon translational research approaches in humans. NHP-PET studies are typically conducted under anesthesia, affecting the interpretability of receptor binding measures. Specifically, anesthetic agents can enhance the affinity of GABA to $GABA_A$ receptors. Isoflurane dose-dependently increased DVR of [^{11}C]flumazenil, a $GABA_A$ benzodiazepine receptor antagonist, compared with the awake condition in humans [1]. The goal of this study is to compare [^{11}C]flumazenil BP_{ND} in anesthetized and awake studies in the NHP. We hypothesized that BP_{ND} would be higher in the anesthetized monkeys. To perform awake NHP studies we used motion-tracking technology to permit NHP imaging without head restraint. Furthermore, scan time was minimized to reduce stress by using bolus/infusion methods, allowing for acquisition only during the equilibrium phase.

Methods: Rhesus monkeys were trained to sit in a custom chair, tilted back 45º while the Focus-220 scanner was tilted forward 45º. The Vicra system was used to track motion, with its tool mounted onto the animal's scalp via skin glue. [^{11}C]Flumazenil was administered as a bolus/infusion (K_{bol}=90 min). Animals were positioned in the scanner ~45 min post-injection, and listmode and motion-tracking data were acquired for 25-35 min. The listmode data were binned into sub-frames based on an intra-frame motion threshold of 2 mm and minimal sub-frame duration of 3 sec [2]. Sub-frames were reconstructed with FBP and resliced to a reference orientation using the motion data. A transmission image from an anesthetized study for the same animal was resliced to the awake reference orientation and used to reconstruct sub-frames with attenuation and scatter correction [3]. Isoflurane anesthetized monkeys were scanned for 90 min with the same bolus/infusion protocol. Unpaired anesthetized (n=20) and awake (n=3) datasets were analyzed by equilibrium analysis. To assess the quality of equilibrium, percent change per min (PCPM) in radioactivity concentration was calculated across animals for ROIs. Mean BP_{ND} images were computed for anesthetized and awake images in NHP template space, using the pons as a reference region where, $BP_{ND}=(C_{ROI}/C_{PONS})-1$.

Results: Mean PCPM were generally positive for anesthetized and negative for awake groups, respectively: frontal(+0.13±0.30,-0.33±0.54), occipital(+0.23±0.13,0.44±0.40)*, temporal(+0.17±0.13,-0.27±0.68), insula(+0.16±0.15,-0.27±0.68)*, and pons(+0.26±0.45,-1.09±-1.12),*p< 0.001. Mean BP_{ND} values between awake and anesthetized conditions showed close agreement when analyzed by regions, BP_{ND}(awake) =1.15BP_{ND}(anesthetized)+0.059, r^2=0.92, or by individual pixels, BP_{ND}(awake)=1.02BP_{ND}(anesthetized)+0.48, r^2=0.74, in average BP_{ND} images (Fig. 1).

Conclusions: In this initial dataset, there was excellent agreement of [^{11}C]flumazenil BP_{ND} values between awake and anesthetized conditions. These data suggest that K_{bol} should be adjusted for awake NHP-PET to avoid potential bias. BP_{ND} was slightly higher for awake

monkeys, in contrast with the human study, perhaps due to differences in equilibrium or stress-induced changes. Results in a larger cohort with an adjusted K_{bol} and cortisol measurements will be necessary to fully characterize anesthesia-induced changes in [^{11}C]flumazenil binding.

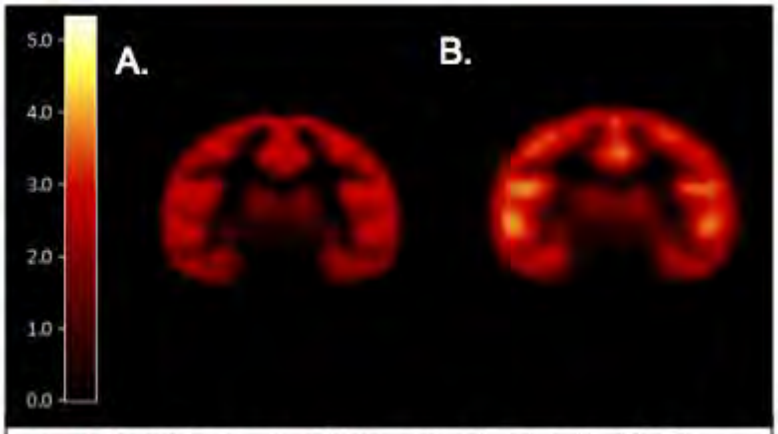

Figure 1 Mean BP_{ND} images of [^{11}C]flumazenil A. Anesthetized NHP image (n=20) B. Awake NHP image (n=3) post smoothed with a 3-mm Gaussian. Images are in NHP template space.

[Mean BPND images of [11C]flumazenil]

References:

[1] Gyulai FE et al., *Anesthesiology*, 2001;95(3):585-93.

[2] Jin X et al., IEEE MIC Conference Record, 2010.

[3] Sandiego CM et al., NRM abstract, 2010.

436

IS [^{11}C]CUMI-101 BINDING TO 5-HT$_{1A}$ RECEPTORS SUSCEPTIBLE TO INTRAVENOUS CITALOPRAM CHALLENGE IN HUMANS?

L.H. Pinborg[1,2,3], L. Feng[1], M. Haahr[1], N. Gillings[4], A. Ettrup[1], H.D. Hansen[1], S. Yndgaard[5], C. Svarer[1], G.M. Knudsen[1,3]

[1]Neurobiology Research Unit, N9201, [2]Epilepsy Clinic, N8501, [3]The Lundbeck Centre for Integrated Molecular Brain Imaging, [4]The PET & Cyclotron Unit, [5]Department of Thoratic Anaesthesiology, Rigshospitalet, Copenhagen University Hospital, Copenhagen, Denmark

Introduction and hypothesis: We previously failed to demonstrate a translation of intravenous citalopram challenge into a change in 5-HT$_{2A}$ binding of [^{18}F]altanserin binding(1). Whether we consider changes in radioligand binding following pharmacological challenges to be the result of simple competition between radioligand and 5-HT or the result of agonist-mediated receptor internalization, the fact that most of the 5-HT$_{2A}$ receptors are located intracellularly and [^{18}F]altanserin is an antagonist radioligand are likely to be the most important explanations. Here we present our preliminary results in three healthy subjects using citalopram challenge and the new 5-HT$_{1A}$ agonist radioligand [^{11}C]CUMI-101. Our hypothesis is that [^{11}C]CUMI-101 binding to 5-HT$_{1A}$ receptors is reduced following acute citalopram challenge.

Methods: [^{11}C]CUMI-101was synthesized as previously described(2). [^{11}C]CUMI-101was injected as a bolus and PET (high-resolution research tomography scanner, Siemens AG) data were subsequently collected for 120 minutes. Arterial blood samples were obtained during PET scanning and metabolite corrected using HPLC as previously described(3). Thirty minutes after ending the first PET experiment one hour of constant Citalopram (H. Lundbeck A/S, 0.15 mg kg^{-1}) infusion started. Thirty minutes after Citalopram infusion started a second [^{11}C]CUMI-101-PET experiment was conducted similar to the first experiment. MRI was conducted on a Siemens Magnetom Trio 3 T MR scanner (Invivo, FL, USA) and co-registred to the PET image. VOIs were automatically delineated on each individual's MRI in a strictly user-independent fashion(4). Kinetic modeling (unconstrained 2-tissue compartment modeling and simplified tissue reference modeling) was done in PMOD (version 3.0).

Results:

		Cerebellum			Thalamus			Prefrontal cortex		
		Subject 1	Subject 2	Subject 3	Subject 1	Subject 2	Subject 3	Subject 1	Subject 2	Subject 3
K_1	Baseline	0.26	0.41	failed	0.34	0.47	failed	0.32	0.43	failed
	Citalopram	0.31	0.59	0.39	0.39	0.58	0.44	0.36	0.49	0.42
	% diff.	**20.4**	**44.7**		**15.9**	**23**		**13.4**	**14**	
V_T	Baseline	3.48	4.01	failed	5.24	6.38	failed	9.14	9.79	failed
	Citalopram	4.5	4.23	4.94	6.69	6.64	6.63	11	9.86	12.73
	% diff.	**29.1**	**5.3**		**27.5**	**4**		**20.4**	**0.7**	
BP_P	Baseline				1.76	2.37	failed	5.65	5.98	failed
	Citalopram				2.19	2.42	1.69	6.5	5.63	7.79
	% diff.				**24.4**	**1.9**		**15**	**-5.8**	
R_1	Baseline				1.3	1.14	1.12	1.24	1.08	1.03
	Citalopram				1.24	1.12	1.09	1.19	1.04	1.1
	% diff.				**-4.5**	**-1.6**	**-2.9**	**-4.4**	**-4**	**7.6**
BP_{ND}	Baseline				0.5	0.51	0.41	1.62	1.31	1.36
	Citalopram				0.46	0.5	0.34	1.35	1.29	1.52
	% diff.				**-9.8**	**-2.6**	**-18.1**	**-16.8**	**-1.7**	**11.1**

[table]

In subject 3 the final analysis of blood data in the baseline situation is to be completed.

Conclusion: Our preliminary results do not imply a decrease in [^{11}C]CUMI-101 binding to 5-HT_{1A} receptors following intravenous citalopram challenge. The literature suggests a decrease in regional cerebral blood flow following intravenous administration of citalopram. Our K_1 and R_1 values do not imply a quantitatively important reduction in tracer delivery following citalopram challenge. Our results do not imply that the use of cerebellum as a reference region is hampered by the increase in extracellular 5-HT following citalopram infusion. Recent unpublished data (Hendry-N et al.) suggest that [^{11}C]CUMI-101 behaves as an antagonist on rodent cortical 5-HT_{1A} receptors. Sensitivity of [^{11}C]CUMI-101to acute pharmacological challenge in monkeys has been demonstrated but at much larger doses of citalopram (2-4 mg kg^{-1})(5). Thus, the challenge paradigm and the radiotracer may not be optimal for measuring acute changes in extracellular 5-HT. Further studies are needed to draw more firm conclusions using this experimental set-up.

References:

(1) Pinborg et al. (2004) *J Cereb Blood Flow Metab* 24:1037-45

(2) Kumar et al. (2007) *Eur J Nucl Med Mol Imaging* 34:1050-60

(3) Gillings-N (2009) *Nucl Med Biol* 36:961-65

(4) Svarer et al. (2005) *Neuroimage* 24:969-79

(5) Milak et al. (2010) *J Cereb Blood Flow Metab*: Epub ahead of print

437

PRECONDITIONING NEURAL STEM CELLS WITH MINOCYCLINE ENHANCES NEUROPROTECTION AFTER ISCHEMIC STROKE IN RATS

H. Sakata[1,2], K. Niizuma[1,2], H. Yoshioka[1], G.S. Kim[1], M. Katsu[1], J.E. Jung[1], P. Narasimhan[1], T. Tominaga[2], P.H. Chan[1]

[1]Neurosurgery, Stanford University School of Medicine, Stanford, CA, USA, [2]Neurosurgery, Tohoku University Graduate School of Medicine, Sendai, Japan

Objectives: The efficacy of grafting neural stem cells (NSCs) is limited because of poor cell survival in ischemic stroke. A hostile host-brain environment is responsible, and is caused in part by the production of reactive oxygen species after ischemic reperfusion injury. Minocycline, a broadly-used antibiotic, has demonstrated neuroprotective properties in a wide range of neurological diseases. Here we assess the hypothesis that preconditioning with minocycline protects grafted cells from ischemic reperfusion injury and enhances their neuroprotective effect in stroke.

Methods: NSCs were harvested from the subventricular zone of GFP transgenic Sprague-Dawley rats (postnatal day 1). The NSCs were pretreated with 0, 1, 3, or 10 μM minocycline for 24 hours. Adult male Sprague-Dawley rats were subjected to 90 minutes of transient middle cerebral artery occlusion. We stereotactically delivered the NSCs to the ischemic penumbra in the cortex 4.5 hours after reperfusion. Neurological recovery was assessed weekly, and the lesion volume and the number of surviving NSCs were measured histologically 4 weeks after grafting. Apoptotic death of the NSCs was analyzed by the TUNEL method, and the concentration of BDNF was quantified by enzyme-linked immunosorbent assay 2 days after grafting. For *in vitro* study, NSCs were subjected to oxygen-glucose deprivation (OGD) and reoxygenation. Cell viability was quantified by LDH assay, WST-1 assay, and TUNEL staining. Early production of superoxide was analyzed using hydroethidine. The effect of minocycline on gene expression was examined by real-time RT-PCR array and assays. Whole cell fractions were obtained from the NSCs and used for Western blot analysis. In a siRNA study, NSCs were pretreated with Nrf2-siRNA or control-siRNA for 48 hours.

Results: The minocycline-pretreated NSC group showed attenuated infarct size and enhanced neurological recovery compared with the non-pretreated NSC group. Survival of the NSCs was significantly higher in the minocycline-pretreated group 28 days after transplantation. LDH assay, WST-1 assay, and TUNEL staining demonstrated that minocycline pretreatment offered cytoprotection against OGD and reoxygenation. In accordance with the *in vitro* study, TUNEL staining showed a 75% decrease in grafted cell death in the minocycline-pretreated NSC group 2 days after transplantation. Ethidium signals in the NSCs remarkably increased after ischemic reperfusion, but this signal increase was reduced in minocycline-preconditioned NSCs both *in vivo* and *in vitro*. Real-time RT-PCR array and Western blot analysis revealed that minocycline preconditioning significantly up-regulated the expression of Nrf2 (2.7-fold), and Nrf2-regulated antioxidant genes, NQO1 (20-fold) and HO-1 (4.0-fold), after OGD and reoxygenation. Pretreatment of cells with Nrf2-siRNA abolished the cytoprotective effects of minocycline under OGD and reoxygenation. Minocycline-pretreated NSCs, which were also treated with Nrf2-siRNA, failed to show neuroprotective effects in the ischemic brain. Minocycline-pretreated NSCs expressed higher levels of trophic factors such as BDNF (2.0-fold), NGF (1.8-fold), GDNF (3.4-fold), and VEGF (2.8-fold) *in vitro*. The level of BDNF was increased by 40% in the ischemic brain grafted with minocycline-pretreated NSCs.

Conclusions: Preconditioning with minocycline reprograms NSCs to tolerate oxidative stress after ischemic reperfusion injury and to express higher levels of trophic factors. Minocycline-pretreated NSCs offer enhanced neuroprotection in stroke compared with non-pretreated NSCs.

438

SPECT BRAIN PERFUSION ABNORMALITIES IN MILD TRAUMATIC BRAIN INJURY: A QUALITATIVE ANALYSIS BY USING EASY Z-SCORE IMAGING SYSTEM, EZIS

T. Nakagomi, K. Furuya, J. Tanaka, S. Takanashi

Department of Neurosurgery, Teikyo University School of Medicine, Tokyo, Japan

Introduction: Mild traumatic brain injury (mTBI) is a common neurologic disorder and frequently associated with neurocognitive dysfunctions. Most patients recover fully from mTBI, but some patients have persistent neurocognitive problems, including problems with cognition, emotion, and behavior. Magnetic resonance (MR) imaging is now routinely used in mTBI patients and proven very useful to delineate organic lesions responsible for cognitive impairments. In some cases, however, no lesion can be detected on serial MR imaging including FLAIR and T2* images as well as T1/T2 images despite its great sensitivity and specificity.

Aim: In this paper, the role of single-photon emission CT (SPECT) study as a complementary technique to MR examination was investigated in diagnosing lesions responsible for neurocognitive dysfunctions in patients with mTBI.

Materials and methods: Seventeen consecutive patients (Four women and 13 men; age range, 20-72 years: median age : 39.4 years) were included in this study. All of the patients suffered from a single episode of mTBI (Glasgow Coma Scale = 13-15, as well as loss of consciousness) due to traffic accident and had computed tomography (CT) scans within 6 hours following injury. They have persisting neurocognitive impairments lasting more than 3 years, which were confirmed by the neuropsychological tests, including Mini-Mental State Examination, Wechsler Memory Scale-R, Wechsler Adult Intelligent Scale-R, Trail Making Test-B (TMT-B), and non paired Miyake Paired Test, and so on. In these patients, Tc99m-ECD SPECT studies were performed, and changes in cerebral blood flow (CBF) was analyzed by using easy Z-score imaging system (eZIS), in addition to serial MR studies including FLAIR and T2* images.

Results: On serial MR images, thirteen patients showed traumatic lesions either in the cerebral cortex, or in the subcortical structures, including the basal ganglia, corpus callosum, and so on. In five patients, ventriculomegaly was detected in the chronic stage. One patient showed subarachnoid hemorrhage (SAH) alone, which was diagnosed by initial CT scans. In three patients, neither CT nor serial MR images detected traumatic lesions. On the other hand, focal areas of hypo-perfusion were detected in all patients on SPECT images using eZIS. The sites of abnormality were in the following order: frintal lobes (82.3%), temporal lobes (58.8%), parietal lobes (35.3%), hippocampus (35.3 %), occipital lobes (29.4%), basal ganglia(23.5%), thalamus (23.5%), cingulate gyri (23.5%), and cerebellum (5.9%). In four patients whose abnormality was not detected by MR images, SPECT studies using eZIS showed hypo-perfusion areas in the cerebral cortex (100%) , in the hippocampus (25%) or in the cingulated gyrus (25%).

Conclusion: MR examination alone cannot fully explain the focal lesions responsible for neurocognitive dysfunction following mTBI. However, addition of SPECT study using eZIS enable us to understand legions where blood flow was decreased, i.e., where neuronal functions conceivably might be reduced. In conclusion, SPECT study using eZIS is very useful as a complementary technique to MR examination in diagnosing lesions responsible for neurocognitive dysfunctions in patients with mTBI.

439

MEASURING BRAIN OXYGENATION AND THE CEREBRAL METABOLIC RATE OF OXYGEN CONSUMPTION IN HUMANS USING A QUANTITATIVE BOLD MRI APPROACH

T. Christen, G. Zaharchuk

Stanford University School of Medicine, Palo Alto, CA, USA

Objectives: We have recently developed an MRI method to measure the level of blood oxygenation (SO2) in the rat brain [1]. The technique is based on extraction of the oxygenation information from T2* measurements using a mathematical model and measurements of T2, B0, and the cerebral blood volume (CBV). The objective of this study was to translate the method for human use. Estimates of MR_SO2 were obtained on healthy volunteers by combining MR relaxometry, Arterial Spin Labeling (ASL) and bolus contrast Perfusion Weighted Imaging (PWI) measurements. By adding information of the cerebral blood flow (CBF), we also derived estimates of the cerebral metabolic rate of oxygen consumption (MR_CMRO2).

Methods: Five normal subjects were scanned at 3T using the following protocol:

- T2* maps and T2 maps were acquired using multiecho echo sequences.

- ASL_CBF maps were acquired using pseudocontinuous labeling [2].

- Hemodynamic maps (CBF, CBV, MTT, and Tmax) were created using Bolus PWI [3] [4] and scaled using the recently described CAD method [5].

- MR_SO2 maps were derived using (1-MR_SO2)=(R2*-R2)/(CBV.g.Dc.Hct.B0). Where Hct=0.42*0.85 is the microvascular hematocrit fraction and $\Delta\chi=0.264*10^{-6}$ is the difference between the magnetic susceptibilities of fully oxygenated and deoxygenated hemoglobin.

- MR_CMRO2 maps were derived using MR_CMRO2=(SaO2-MR_SO2)*CBF*Ca/0.8. Where SaO2 (arterial saturation)=0.98 and Ca=836 mmol of O2 per 100mL of blood.

All acquisitions were coregistered using SPM8. Regions of interest were manually drawn over the entire brain. Voxels with T2>150ms (CSF) and MR_SO2 values < 0 or >100% were considered as out of the range of validity and were excluded.

Results: Parametric maps from one subject are presented in Figure 1. Blood oxygenation in human brain is believed to be homogeneous over the brain. However, the MR-SO2 map shows contrast between white and gray matter. Possible explanations could be the presence of iron or anisotropy of magnetic susceptibility in WM [6]. T2* (53±2 ms) and T2 (69±1 ms) values averaged over the entire brain are consistent with the literature. A mean CAD correction factor of 3.0±1.0 was found in the 5 subjects leading to a scaled CBV of 4.0±0.3% and a CBF of 34±4 mL/100g/min. MR_SO2 (60±1%) and MR_CMRO2 (121±9 mmol/100g/min) values are in line with previously reported oxygenation values. An average of 15% voxels were excluded according to our criteria.

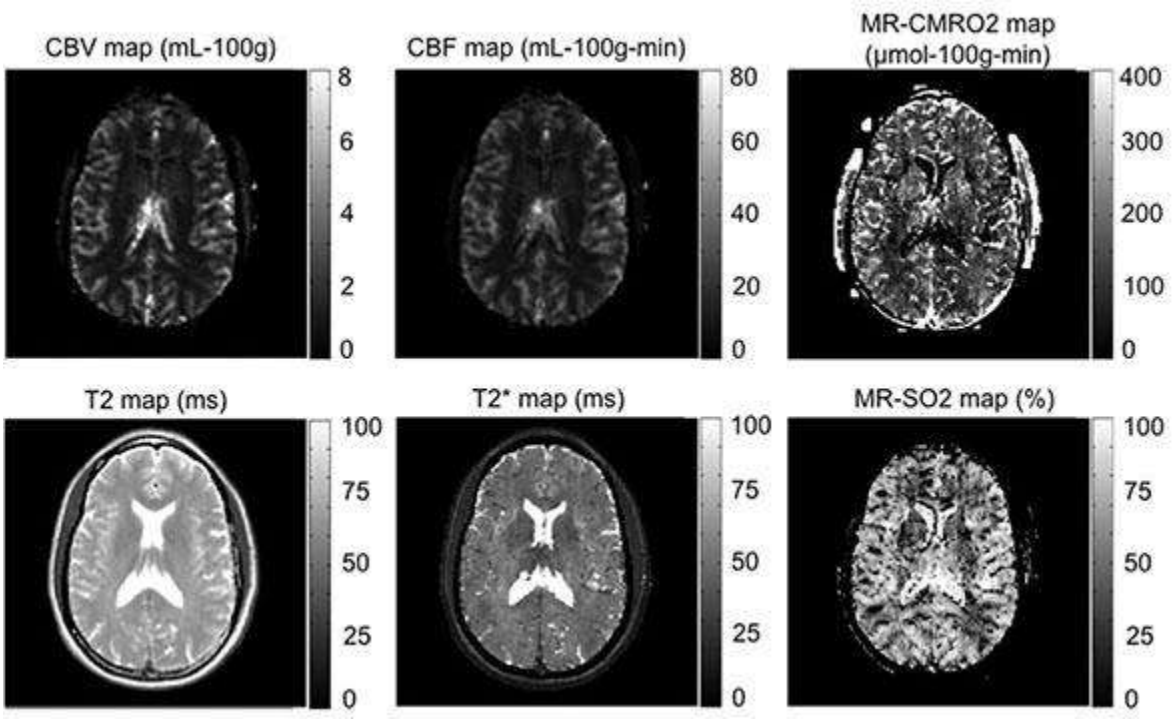

[Maps in one subject.]

Conclusions: This study suggests that MR_SO2 and MR_CMRO2 maps can be obtained in human brain using a quantitative BOLD approach. Although the global values are in agreement with prior reports, further insights are needed to understand the apparent WM/GM contrast in the MR_SO2 maps. Applications to pathologies such as stroke or cancer will also help to elucidate the meaning and utility of such parameters.

References:

[1] T Christen et al, NMR in biomed, 2010.

[2] Dai et al., MRM, 2008.

[3] Newbould et al., MRM 2007.

[4] Straka et al., JMRI 2010.

[5] G Zaharchuk et al, MRM, 2010.

[6] Lee et al, Neuroimage, 2010.

441

A PROGRESSIVE TREATMENT OF ALZHEIMER'S LIKE SYMPTOMS' USING CURCUMIN LOADED SOLID LIPID NANOPARTICLES

V. Kakkar, I.P. Kaur

Department of Pharmaceutics, University Institute of Pharmaceutical Sciences, Panjab University, Chandigarh, India

AD is a progressive neurodegenerative brain disorder that affects major brain areas including the cortex and limbic system, and is characterized by progressive decline in memory with impairment of at least one other cognitive function. AD begins as a deficiency in the production of the neurotransmitter acetylcholine. The National Institute of Health predicts, if the current trend continues, there will be more than 8.5 million AD patients by the year 2030 in USA alone. Aluminium (Al) is the most abundant metal known for its neurotoxicity in humans. It gains easy access to the central nervous system under normal physiological conditions and accumulates in different brain regions. It has been reported to be involved in the etiology of several neurodegenerative diseases. In this study, we have investigated the effects of curcumin loaded solid lipid nanoparticles(C-SLNs) vis-à-vis free curcumin after intake of aluminium chloride (100 mg/(kg day)) for 90 days months in the drinking water. Exploration studies to elaborate upon the behavioral, biochemical and histochemical functions of lateral sections of whole brain were also conducted .

Envisaging the compromised bioavailability of curcumin a potential pluripotent molecule, it was packaged into solid lipid nanoparticles. Our pharmacokinetic studies on LC/MS/MS revealed an increase in 32-155 times bioavailability of the developed formulation as compared to free curcumin at various dose ranges.

Post cognitive losses after aluminium chloride as estimated by Morris water maze were followed by administration with free curcumin (50 mg/kg/day) and various doses of C-SLNs (1, 12.5, 25, 50 mg/kg/day) for a period of 8 weeks. The animals were sacrificed at the end of study and biochemical estimations were done in the brain homogenates. Further the blood of the animals was analysed for the changes in blood lipid profile. Our studies indicate that aluminium intake adversely affect the spatial learning and memory abilities of mice. Aluminium intake also inflicts oxidative stress-related damage to lipids, membrane (LPO), and endogenous antioxidant enzyme activity (SOD, GSH and CATALASE) and acetylcholinestrase. The compromised antioxidant system might be playing a crucial role in the observed Al-induced alterations.

We have observed that per oral administration of C-SLNs at all the doses significantly reversed the memory losses, as was evident from the morris water maze, histopathology and biochemical estimations as compared to free curcumin. In conclusion, the results of the present study implicates that aluminium treatment exerts its neurotoxic effects by altering the overall physiology of brain, and natural polyphenol curcumin in its highly bioavailable form (C-SLNs) is highly effective in treating the induced cognitive losses.

References:

Kaur, I.P., Bhandari, R., Bhandari, S. and Kakkar, V. (2008). “Potential of solid lipid nanoparticles in brain targeting.”J Controlled Release, 108-114.

Vandita Kakkar, Sukhjit Singh , Dinesh Singla , Indu Pal Kaur " Exploring solid lipid

nanoparticles to enhance the oral bioavailability of curcumin". Molecular Nutrition and Food Research 2010 , DOI: 10.1002/mnfr.201000310.

442

TRANSLATIONAL NEUROSCIENCE: FOCUS ON RADIATION DOSIMETRY OF PET TRACERS

S.M. Moerlein[1], R. Laforest[1], T.O. Videen[2], J.A. Antenor-Dorsey[2], J.S. Perlmutter[1,2]

[1]Radiology, [2]Neurology, Washington University School of Medicine, St Louis, MO, USA

Introduction: Development of new PET radiopharmaceuticals for brain imaging requires intensive investigation and validation using preclinical studies in animals. For promising biomarkers that warrant further application in human subjects, it is necessary to verify that the proposed radiotracers are safe for use in clinical studies. An important aspect of this translational process is the estimation of the internal radiation dosimetry of novel PET tracers used for brain imaging.

Objective: To develop systematic methodology for preclinical assessment of the internal radiation dosimetry of potential PET radiopharmaceuticals for brain imaging. Such methodology will streamline the translation of experimental tracers used in preclinical animal research to radiopharmaceuticals for clinical studies in human subjects.

Methods: Whole-body PET imaging of nonhuman primates was used to estimate the human internal dosimetry of a series of positron-emitting PET neuroligands. A CTI/Siemens ECAT 953B scanner was used for repeated sequential images taken from head to pelvis of adult baboons. Imaging began immediately after i.v. injection of tracer, and continued continuously for 2-3 hours. Four different radioligands were studied: the D2 ligands [^{18}F]NMB and [^{11}C]NMB, the D1 ligand [^{11}C]NNC 112 and the DAT ligand [^{11}C]CFT. Four bed positions containing volumes of interest (VOI) representative of all major organs were scanned. The attenuation- and decay-corrected VOI data were used to generate time-activity curves, and organ residence times were calculated by analytical integration of a multi-exponential fit to these curves. Human radiation doses were estimated using OLINDA/EXM 1.0 and the standard human model.

Results: These whole-body PET measurements demonstrated tracer biodistribution patterns that were not unexpected based on what is known of the metabolic pathways and rodent data. Each radioligand that we evaluated had unique radiation dosimetry characteristics, dependent on the particular chemical structure, radionuclide, as well as the molecular location of the radiolabel. The rank order for the dose equivalent was [^{18}F]NMB > [^{11}C]NNC 112 > [^{11}C]NMB > [^{11}C]CFT. For all radiotracers, the critical organ that determines the maximum permissible dose for human studies was not the brain, but rather extracerebral organs. The critical organs for were: [^{18}F]NMB (lower large intestines, 158 μGy/MBq); [^{11}C]NNC 112 (kidneys, 16.7 μGy/MBq); [^{11}C]NMB (heart wall, 10.5 μGy/MBq). The absorbed radiation dose to the brain was much lower for all radioligands, demonstrating that the dose-limiting organ and target organ for imaging were different.

Conclusions: Whole-body PET imaging of primates is a useful technique for estimation of human radiation dosimetry, and is a valuable tool in the translational development of new PET tracers for human use. The radiation dose to critical organs limits the amount of tracer that can be administered to humans for brain imaging. This dosimetry-defined limit may impact the statistical power of human brain imaging studies when compared to preclinical PET experiments using the same tracers in animals.

443

DEVELOPMENT OF A NEW SIMPLIFIED SOFTWARE MODIFYING AUTOMATED ROI ANALYSIS SOFTWARE, 3DSRT FOR EVALUATING HYPERPERFUSION AFTER REVASCULARIZATION SURGERY

K. Fukushima[1], T. Hosoya[2], K. Fukuda[3], Y. Kaku[3], K. Iihara[3]

[1]Radiology, National Cerebral and Cardiovascular Center-Hospital, Suita, [2]FUJI FILM RI Phama. Co. Ltd., Tokyo, [3]Neurosurgery, National Cerebral and Cardiovascular Center-Hospital, Suita, Japan

Objectives: Cerebral hyperperfusion syndrome is a rare but serious complication of carotid revascularization, including carotid endarterectomy (CEA) and carotid stent placement, which can occur in patients with preoperative impairments in cerebral hemodynamics. The Objectives of this study were to develop a new simplified software for evaluating hyperperfusion after revascularization surgery and to evaluate usefulness of it.

Patients and methods: Ten patients with unilateral internal carotid artery (ICA) stenosis (> 70%) undergoing CEA were enrolled in the present study. No patient had stenosis > 50% or occlusion in the cotralateral ICA or middle cerebral artery. Cerebral vascular reserve (CVR) was measured using SPECT and I-123 IMP according to dual table ARG method before CEA. To evaluate hyperperfusion after CEA, brain SPECT was performed using I-123 IMP a day after CEA. To perform an ROI analysis of the brain with improved objectivity and excellent reproducibility, we used automated ROI-based analysis software for the brain, the so-called 3DSRT and modified it for calculating asymmetric index (AI), cerebellar ratio (CR) and relatively increase rate (RIR) for evaluating hyperperfusion after CEA. By using a newly developed software, three slices: periventricular, basal ganglia and cerebellar cortex levels were selected automatically in the transaxial slices of brain SPECT in a default setting. Moreover, we can displace slices up and down and add another slice as needed for selecting most appropriate slices for evaluating hyperperfusion.

Result: By using a newly developed software, we could easily calculate hyperperfusion indices such AI, CR and RIR after CEA with objectivity and excellent reproducibility. These indices were useful for evaluating hyperperfusion after CEA.

Conclusion: We developed a new software modifying 3DSRT for evaluating hyperperfusion after revascularization surgery. Further studies are necessary to clarify general clinical values of hyperperfusion indices such as AI, CR and RIR.

446

PREDICTION OF MALIGNANT BRAIN SWELLING FOLLOWING MCA INFARCTION IN ELDERLY BY EARLY INFARCT VOLUMETRY STANDARDIZED WITH BRAIN VOLUME

E. Kumura[1], Y. Goto[1], A. Nishino[1], K. Taniwaki[1], T. Koyama[1], T. Yuguchi[1], T. Yoshimine[2]

[1]Department of Neurosurgery, Hanwa Memorial Hospital, [2]Department of Neurosurgery, Osaka University Graduate School of Medicine, Osaka, Japan

Objective: Malignant brain swelling (MBS) following MCA territory infarction is a devastated life-threatening condition. As one of quantitative predictors of MBS, the volume of diffusion-weighted high-intensity area (DHV) ≥ 145cm^3 on early MR images is demonstrated (1). This volume threshold, however, might not fit to aged patients with brain atrophy. In the present study, we analyze what percentage of DHV on early MR images occupied within brain volume (BV) provides reliable information for the prediction in aged patients at risk of MBS in acute MCA territory infarction.

Methods: Between June 2007 and September 2010, both MR (DWI, MR angiogram) and CT images were taken in 69 consecutive patients with MCA territory infarction within 48 hours of onset. Of these, 37 patients were older than 75 y.o. (84±6, aged group) and 32 patients were under 75 y.o. (65±10, younger group). On each patient, DHV was measured as voxels sum of high-intensity area on DWI, and BV on CT images was measured as voxels sum of brain tissue. To eliminate effects of brain atrophy, we calculated value of DHV divided by BV (DHV/BV). When patient's neurological state deteriorated progressively due to massive mass effect of infarction, MBS was diagnosed. We compared two groups on scores of Glasgow Coma Scale (GCS) on admission, values of DHV/BV and scores of modified Rankin Scale (mRS) at 3 months after onset.

Results: Scores of GCS on admission in aged group were significant lower than those of younger group (11±3, 13±2, respectively, $p< 0.05$).The BV of aged group was significant smaller than that of younger group (1035±154cm^3, 1131±157cm^3, $p< 0.05$). The BV was correlated negatively to age where BV= 1418.2-4.5x age ($r=-0.33$, $p< 0.01$). Of aged group, 10 patients developed MBS and their DHV/BV values were 20±12%. The rest 27 patients whose DHV/BV values were 4±3%did not develop MBS ($p< 0.01$, ANOVA). Receiver operating characteristic (ROC) analysis revealed DHV/BV>7.8% as a MBS predictor with 90% sensitivity and 85% specificity ($p< 0.01$). In younger group, 4 patients whose DHV/BV values were 14±10 developed MBS, while the rest 28 patients with low DHV/ BV values did not (3±4%, $p< 0.01$). In this group, MBS was predicted with 75% sensitivity and 96% specificity by DHV/BV>11.6% determined with ROC analysis ($p< 0.01$). In both groups, patients with MBS showed definitely worse scores of mRS than those of without MBS (5.5±0.9, 3.2±1.5, $p< 0.01$, ANOVA). As for patients with MBS, however, there was no difference between aged and younger group on mRS scores (5.5±0.7, 5.3±1.5).

Conclusion: In elderly ≥75 y.o., infarct volume exceeding 7.8% of brain volume is a reliable marker to predict malignant brain swelling following acute MCA territory infarction.

Reference: (1) Oppenheim C, et al., Stroke31; 2175-81, 2000.

447

PREVENTION OF ALTEPLASE-INDUCED HEMORRHAGIC INFARCTION BY CILOSTAZOL IN EXPERIMENTAL ISCHEMIA-REPERFUSION MICE

Y. Kasahara[1], T. Matsuyama[2], K. Nagatsuka[1], A. Taguchi[1]

[1]Department of Cerebrovascular Disease, National Cerebral and Cardiovascular Center, Osaka, [2]Institute for Advanced Medical Sciences, Hyogo College of Medicine, Hyogo, Japan

Objectives: The use of antiplatelet agent is recommended for secondary prevention of cerebral infarction. However, most of the antiplatelet agents have the risk to increase bleeding events, including cerebral hemorrhage. Recently, cilostazol was shown to be superior to aspirin for secondary prevention of stroke with fewer hemorrhagic events (1). In this study, we investigated the effects of cilostazol on alteplase-induced cerebral hemorrhage using highly reproducible ischemia-reperfusion model in mice (2).

Methods: CB-17mice were fed a diet with 0.3% w/w of cilostazol, 0.1% w/w of aspirin or a additive-free diet for 7 days before induction of ischemia. Transient ischemia was induced by ligation of left middle cerebral artery for 90 or 180 minutes. Alteplase (10mg/kg) or same volume of saline was administered at 5 minutes before reperfusion. Reperfusion-related hemorrhagic transformation was evaluated at 24 hours after induction of ischemia (N=3 in each group).

Results: All of the mice that received saline before reperfusion, including mice after 90 and 180 minutes ischemia in any diet group, showed no cerebral hemorrhage at 24 hours after stroke. In contrast, all of the mice that received alteplase and fed with aspirin or additive-free diet showed hemorrhagic transformation. However, no mice that received alteplase and fed with cilostazol showed hemorrhagic transformation.

Conclusion: Our results showed that administration of cilostazol reduces the risk of alteplase-induced cerebral hemorrhage. These findings indicated therapeutic time window of thrombolytic therapy by alteplase could be extendible in patients medicated with cilostazol, and antithrombotic treatment could be safely started with cilostazol within 24 hours after injection of alteplase.

References:

1. Shinohara Y et al. Lancet Neurol. 2010

2. Kasahara Y et al. Brain Res. 2010

448

EFFECT OF GRADED OXYGEN CHALLENGE ON VASCULAR AND METABOLIC PARAMETERS

F. Xu, P. Liu, H. Lu

Advanced Imaging Research Center, University of Texas Southwestern Medical Center, Dallas, TX, USA

Objectives: Oxygen (O2) therapy has anecdotally been suggested to improve outcome in patients with neurological disorders including cerebral palsy (1), traumatic brain injury (2), and cerebral ischemia (3). However, much controversy still exists as to the real benefit of such treatment and the associated mechanism (4). The present study will therefore investigate how O2 content change in the arterial blood affects the cerebral metabolism rate of oxygen (CMRO2) in healthy adults.

Methods: Nine young healthy subjects (28±5 yo, 2 F 7 M) were studied. Each subject participated in a 50 min session with a graded O2 challenge in which they breathed four levels of O2 in the following order: 21%O2 for 8min, 14%O2 for 18min, 50%O2 for 15min, and 98%O2 for 12min.

The total arterial oxygen content ($[O2]_a$) was calculated for each O2 level as $[O2]_a=(Y_a x C_h+p_a O2 x C_d)/C_h$, accounting for both the dissolved and hemoglobin-bound oxygen. Y_a (%) is arterial oxygenation measured by PulseOximeter, paO2 (mmHg) is arterial O2 tension measured by oxygen gas sensor from the exhaled air, C_h and C_d are associated with hemoglobin oxygen-carrying capacity and plasma oxygen-dissolving capacity, and were taken from literature (5).

Four global physiologic parameters were determined under each breathing condition, including venous oxygenation (Y_v), oxygen extraction fraction ($OEF=[O2]_a-Y_v$), CBF, and CMRO2 (i.e. OEFxCBF). These measurements would allow a complete characterization of vascular and metabolic responses to graded O2 challenges. Y_v and CBF were measured at the sagittal sinus by MRI techniques (6,7) and CMRO2 was calculated based on the arterial-venous difference (7).

Results: Correlation analysis between arterial oxygen content and each of the physiologic parameters revealed that $[O2]_a$ was positively correlated with Y_v ($P< 0.001$), but negatively correlated with CBF and CMRO2 ($P< 0.001$). That is, hyperoxia increased both arterial and venous oxygenation, but decreased blood flow and brain metabolism. The opposite changes occurred during hypoxia. The OEF was relatively independent of the O2 level ($P=0.64$), suggesting that tissue extracts identical amount of O2 from each unit of blood flow regardless the level of arterial O2 content.

Conclusions: We found that O2 has a suppressive effect on CBF and oxygen metabolism. The reduction of CBF in response to O2 has been reported previously (8). However, to our knowledge, this is the first report of a suppression effect of O2 on brain metabolism. Although this finding appears paradoxical in that brain consumes less oxygen when there is more oxygen available in the blood stream, the observed change is consistent with the principle of a coupling between neural and vascular responses. It is therefore possible that the lower CBF during hyperoxia may be a manifestation of coupling to reduced neural activity.

References:

1) Rosenbaum, J Child Neurol 18 Suppl 1:S89-94 (2003);

2) Gunnarsson and Fehlings, Curr Opin Neurol 16:717-723 (2003);

3) Calvert et al. Brain Res 951:1-8 (2002);

4) Collet et al. Lancet 357:582-586 (2001);

5) Guyton AC Textbook of

Medical Physiology Elsevier: Saunders (2005);

6) Lu and Ge MRM, 60:357 (2008);

7) Xu et al. MRM 62:141 (2009);

8) Sicard and Duong Neuroimage 25:850 (2005).

450

PREDICTION OF MALIGNANT BRAIN SWELLING BY EARLY INFARCT VOLUMETRY STANDARDIZED WITH BRAIN VOLUME IN ACTUE MIDDLE CEREBRAL ARTERY INFARCTION

Y. Goto[1], E. Kumura[1], A. Nishino[1], T. Koyama[1], K. Taniwaki[1], T. Yuguchi[1], T. Yoshimine[2]

[1]Department of Neurosurgery, Hanwa Memorial Hospital, Osaka, [2]Department of Neurosurgery, Osaka University Graduate School of Medicine, Suita city, Japan

Objective: Since malignant brain swelling (MBS) following MCA infarction is mortal, early detection of patients at a risk of MBS is of importance. As one of quantitative predictors of MBS, the volume of high intensity area on diffusion weighted imaging (DHV) larger than 145cm^3 has been reported. (1). The volume threshold, however, may not be simply applicable whose brain already being atrophied.

In the present study, we analyze what percentage of DHV on early MR images occupied within brain volume (BV) provides the most reliable prediction of MBS in acute patients with MCA infarction.

Methods: We analyzed data from 69 consecutive patients (76 y.o., 38-98y.o.) admitted to our hospital from June 2007 to September 2010 for acute ICA or MCA infarction within 48 hours of onset. Both MR images (DWI, MR-angiogram) and conventional CT images (8mm slice thickness) were performed at the time of admission. Using a DICOM image processing software (OsiriX), DHV was measured as a voxel sum of high intensity area on axial MR images. BV on CT images was measured in similar manner. To exclude effects of brain atrophy, we calculated DHV/BV of each patient. When patient's neurological state deteriorated rapidly due to massive mass effect of MCA infarction, MBS was diagnosed. Patients were classified into MBS group and non-MBS group. We compared both groups for potential predictors of MBS, scores of Glasgow Coma Scale (GCS) on admission, DHV values, DHV/BV values and scores of modified Rankin Scale (mRS) at 3 months after onset. To obtain the optimal threshold value of DHV and DHV/BV for predicting MBS, receiver operator characteristic (ROC) analysis was used.

Results: Of 69 patients, 14 patients developed MBS (MBS group, 78±8y.o.) and the rest 55 patients did not (non-MBS group, 74±12y.o.). On admission, MBS group showed lower scores of GCS than that of non-MBS group (10±3, 12±3, respectively, $p< 0.01$). Although BV of two groups was almost equal (MBS 1107±199cm^3, non-MBS 1072±153cm3), there was a close correlation between age and BV($r=-0.33$, $p< 0.01$) indicated as BV= 1418.2-4.5xage. The DHV of MBS group was 188±104cm^3 which was significant larger than that of non-MBS group (40±42cm^3, $p< 0.01$). Similarly, DHV/BV of MBS group was 18.1±11.3% which was significantly higher than that of non-MBS group (8.6±3.6%, $p< 0.01$). Applying ROC analysis revealed that DHV threshold value for MBS prediction was 101cm^3 (sensitivity 86%, specificity 91%) and DHV/BV threshold value was 7.8% (sensitivity 86%, specificity 87%). At 3 months after stroke, patients with MBS showed absolutely worse outcome compared with those without MBS on scores of mRS (5.4±1.0, 3.2±1.5, $p< 0.05$).

Conclusion: Development of MBS is highly predictable regardless of age-related brain atrophy when the rate of diffusion-weighted hyper-intense volume within brain volume exceeds 7.8%.

Reference: (1) Oppenheim C, et al., Stroke31;2175-81, 2000.

451

VALIDATION OF MRI AND ^{18}F-FDG-PET COREGISTRATION IN PATIENTS WITH PRIMARY BRAIN TUMORS

N. Ortega López[1,2], R.G. Mendoza Vasquez[1], G. Adame Ocampo[3], E. Alexanderson Rosas[1], A.A. Cayetano Alcaraz[1], M.A. Celis[4]

[1]Unidad PET-CT Ciclotron, Facultad de Medicina, Universidad Nacional Autonoma de Mexico (UNAM), [2]Unidad PET-CT, Hospital Medica Sur, [3]Unidad PET-Ciclotrón, Facultad de Medicina, Universidad Nacional Autonoma de Mexico (UNAM), [4]Departamento de Radioneurocirugía, Instituto Nacional de Neurología y Neurocirugía "Dr. Manuel Velasco Suárez" (INNN), Mexico City, Mexico

Purpose: To evaluate the role of PET and MRI fused image study in patients with primary brain tumors previously treated, to determine the presence of radionecrosis *vs* residual tumor viability.

Materials and methods: Primary brain tumors were diagnosed by biopse and MR. ^{18}FDG-PET scan and T1 enhanced MRI follow-up studies were performed between 3 and 5 months after treatment. The ^{18}F-FDG uptake was semiquantitavively calculated by a region-of-interest based Tumor hotspot/ normal brain tissue index.

Results: Fifty-seven patients were studied, 37 had high grade gliomas; 9 had Oligoastrocytomas; 5 had Embrionary tumors; 1 had a meningyoma and 1 had an Oliodendroglial tumor. All MR studies showed tumor enhancement, without determine wether if it was radionecrosis or tumor viability. PET/MR fused study diagnosed 21 negative studies (30%) and 36 positive results (70%). Tumor hotspot/ normal brain tissue index correlated well with the visual analysis registered.

Conclusion: Visual analysis in the contrast enhanced MR upperestimates the tumoral area, without defining a possible diagnosis between tumor viability and radionecrosis. Metabolic activity in the ^{18}F-FDG PET study in the enhanced area, determines the presence of residual tumor viability. So, coregistration can be used to obtain a more specific diagnosis optimizing the cinical use.

453

MCA BLOOD FLOW VELOCITY CHANGES IN RESPONSE TO TARGETED CO_2 COMPARISON BETWEEN TRANSCRANIAL DOPPLER ULTRASOUND AND PHASE CONTRAST MRI

J. Leung[1], A. Mohanta[1], A. Behpour[1], N. Sokol[1], **A. Kassner**[1,2]

[1]Diagnostic Imaging, Hospital for Sick Children, [2]Medical Imaging, University of Toronto, Toronto, ON, Canada

Objectives: Measurement of cerebral blood flow (CBF) change in response to a vasoactive stimulus, a parameter known as cerebrovascular reactivity (CVR), is an increasingly relevant tool for the clinical assessment of cerebrovascular disease.[1] Two non-invasive imaging approaches to quantify CBF velocity are transcranial Doppler ultrasonography (TCD) and phase contrast magnetic resonance angiography (PCMRA), yet previous attempts to correlate their readings, with and without a stimulus, have produced inconsistent results.[2] These studies, however, suffer from a lack of control of subject arterial CO_2 and O_2 levels, which directly influence CBF. We therefore propose to apply precise end-tidal PCO_2 ($P_{ET}CO_2$) and PO_2 ($P_{ET}O_2$) targeting to compare blood flow velocities in the middle cerebral artery (MCA) using both TCD and PCMRA.

Methods: Four healthy male volunteers (21-31 years) had their blood flow velocity in their left and right MCA measured during baseline and hypercapnia using TCD and MRI. Reproducible delivery of a CO_2 stimulus was achieved using a computer-controlled gas sequencer (RespirAct™, Thornhill Research Inc., Toronto, Canada).[3] Subject $P_{ET}O_2$ values were clamped at 100mmHg and $P_{ET}CO_2$ levels were either held at 40mmHg (baseline) or 45mmHg (hypercapnia) during imaging. TCD evaluation was conducted with a 2.0MHz ultrasound machine (iU22 xMatrix; Philips Electronics, Best, The Netherlands) by an experienced sonographer (AM). Subjects were exposed to the stimulus while the sonographer determined the time-averaged peak velocity (TAPV) in the MCAs. Using the same stimulus, baseline and hypercapnia PCMRA scans were then performed on a 3.0T MRI scanner (MAGNETOM Tim Trio; Siemens Medical Solutions, Erlangen, Germany) on the MCAs of each subject. The imaging parameters for the PCMRA sequence were: TR/TE=53/5ms, FA=30°, matrix=364×448, voxel size=0.4×0.4×5mm, bandwidth=399Hz/pixel, V_{enc}=100cm/s, time=3.5min. TAPV from the PCMRA data was selected from the voxel in the MCA that exhibited the highest time-averaged velocity. Subject CVR for both modalities was then expressed as a percent change in velocity, divided by the change in $P_{ET}CO_2$. The mean and coefficient of variation (CV) for each group of measurements were calculated and statistical paired t-test analysis was performed between TCD and PCMRA velocities, as well as between the corresponding CVR values.

Results: PCMRA produced markedly lower mean velocities during both baseline and hypercapnia relative to TCD values. TCD velocities also had high CV (35.1% baseline; 30.4% hypercapnia) compared to PCMRA (20.5% baseline; 19.3% hypercapnia), although correlation between modalities was good (r^2=0.47, p=0.06 baseline; r^2=0.64, p=0.02 hypercapnia). For CVR, the CV was much better for PCMRA (29.7%) versus TCD (65.3%), and the correlation between the two was very low (r^2=0.11, p=0.43).

Conclusions: Both TCD and PCMRA were able to measure the same physiological flow parameters in the MCA. TCD provided, on average, higher TAPV measurements but also had higher variation compared to PCMRA. Consequently, PCMRA appears to be more reliable

based on the consistency of the CVR calculations. However, a larger study is required for a more extensive statistical analysis.

References:

1. Mandell DM, et al., Stroke, **39**:2021-8, (2008);

2. Valdueza JM, et al., AJNR, **18**:1929-34, (1997);

3. Slessarev M, et al., J Physiol., **581**:1207-19, (2007)

454

HYPOGLYCEMIA-INDUCED NEURON DEATH IS PREVENTED BY LACTATE ADMINISTRATION

S.W. Suh[1,2], S.J. Won[1], B.H. Yoo[1,3], M.W. Lee[2], B.Y. Choi[2], J.H. Kim[2], M. Sohn[4], B.G. Jang[2]

[1]Neurology, UCSF, VAMC, San Francisco, CA, USA, [2]Physiology, Hallym University, College of Medicine, Chuncheon, [3]Anesthesiology, Inje Paik Hospital, Inje University, School of Medicine, Seoul, [4]Nursing, Inha University, Incheon, Republic of Korea

Introduction: Hypoglycemia-induced brain injury is a serious obstacle to maintain optimal blood glucose level in patients with diabetes. Tight blood glucose control can reduce the risk of diabetic complications, but also increases the unwanted risk of hypoglycemic episodes. It can result from tight control of blood glucose with insulin or other hypoglycemic agents, sulphonylurea (Seltzer, 1989). Studies using animal models have demonstrated that extensive neuronal death occurs after profound and prolonged hypoglycemia as seen in diabetes patients (Auer et al, 1984; Suh et al., 2003, 2004, 2007). However, hypoglycemic neuronal death is not a simple result of glucose deprivation, but is instead the end result of a multi-factorial process involving glutamate receptor stimulation, production of reactive oxygen species, Zn^{2+} release, and activation of poly(ADP-ribose) polymerase-1 (PARP-1) after glucose reperfusion. A key event in this cascade is the activation of PARP-1 (Suh et al., 2003). Activated PARP-1 consumes cytosolic NAD. Since NAD is required for glycolysis, hypoglycemia-induced PARP-1 activation may render cells unable to utilize glucose even when glucose availability is restored. Pyruvate or lactate, however, can be metabolized in the absence of cytosolic NAD. Our previous study demonstrated that pyruvate administration after hypoglycemia significantly reduced neuronal injury and cognitive impairment (Suh et al., 2005).

Objectives: Here we tested whether lactate also could improve outcome in rats subjected to insulin-induced hypoglycemia by terminating hypoglycemia with glucose alone or glucose plus lactate.

Results: Lactate (500 mg/kg, ip) administered without glucose was not sufficient to promote EEG recovery from an isoelectric state during hypoglycemia. Even lactate administration with glucose prolonged EEG recovery after hypoglycemia. However, supplementation of glucose with lactate reduced neuron death approximately 70% in the cerebral cortex, and CA1, subiculum and dentate gyrus of the hippocampus. Hypoglycemia-induced superoxide production and microglia activation in these areas was also substantially reduced by administration of lactate.

Conclusions: These results suggest that lactate may significantly improve outcome after severe hypoglycemia by circumventing a sustained impairment in neuronal glucose utilization resulting from PARP-1 activation. Furthermore, lactate may prevent hypoglycemia-induced neuronal death by intervening in the glucose reperfusion-induced neuron death pathway.

References:

Seltzer HS (1989) Drug-induced hypoglycemia. A review of 1418 cases. Endocrinol Metab Clin North Am 18:163-183

Auer RN, Olsson Y, Siesjö BK (1984) Hypoglycemic brain injury in the rat. Correlation of density of brain damage with the EEG isoelectric time: a quantitative study. Diabetes 33:1090-1098.

Suh SW, Aoyama K, Chen Y, Garnier P, Matsumori Y, Gum E, Liu J, Swanson RA (2003) Hypoglycemic neuronal death and cognitive impairment are prevented by poly(ADP-ribose) polymerase inhibitors administered after hypoglycemia. J Neurosci 23:10681-10690.

Suh SW, Garnier P, Aoyama K, Chen Y, Swanson RA (2004) Zinc release contributes to hypoglycemia-induced neuronal death. Neurobiol Dis 16:538-545.

Suh SW, Aoyama K, Matsumori Y, Liu J, Swanson RA (2005) Pyruvate administered after severe hypoglycemia reduces neuronal death and cognitive impairment. Diabetes 54:1452-1458.

Suh SW, Gum ET, Hamby AM, Chan PH, Swanson RA (2007) Hypoglycemic neuronal death is triggered by glucose reperfusion and activation of neuronal NADPH oxidase. J Clin Invest 117:910-918.

455

2-AMINO-[3-^{11}C]ISOBUTYRIC ACID AS AN IN VIVO IMAGING AGENT FOR THE ASSESSMENT OF BLOOD-BRAIN BARRIER PERMEABILITY

M. Okada[1], T. Kikuchi[1], H. Wakizaka[2], A.B. Tsuji[3], T. Okamura[1], M.-R. Zhang[1], K. Kato[1]

[1]Molecular Probe Group, [2]Biophysics Group, [3]Diagnostic Imaging Group, National Institute of Radiological Sciences, Chiba, Japan

Introduction: The blood-brain barrier (BBB) plays an important role for protecting the central nervous system by limiting the entry of substances from blood. The abnormalities of the BBB function are associated with neurological disorders. 2-Aminoisobutyric acid (AIB) is a neutral amino acid that hardly penetrates BBB in normal condition, and is taken up into brain cells rapidly. These biological characters render the isotopic labeled AIB suitable as a marker for BBB dysfunction. So far *in vitro* and *ex vivo* studies of BBB dysfunction have been carried out using ^{14}C-labelled AIB, however there is no *in vivo* imaging study demonstrated by PET. Although the *in vivo* assessment of BBB dysfunction by PET was straightforward method, difficult synthesis of ^{11}C-labelled AIB hampered the access. In this work, the development of an efficient method for the synthesis of ^{11}C-labeled AIB (2-amino-[3-^{11}C]isobutyric acid: [3-^{11}C]AIB) and the evaluation of its feasibility as an *in vivo* imaging agent for the assessment of the BBB function with small animal PET become a significant research topic.

Methods: The synthesis of [3-^{11}C]AIB chosen in this study involved the base-promoted α-[^{11}C]methylation of iodo[^{11}C]methane and methyl *N*-(diphenylmethylen)-D,L-alaniate, followed by hydrolyses. The chemical form of the radioactive compounds in the plasma and the brain after intravenous injection of [3-^{11}C]AIB to rat was determined with a high performance liquid chromatography in conjunction with a high sensitive positron detector. The small animal PET study was conducted with a typical BBB disruption model rat using lipopolysaccharide. Rats were received a unilateral-intrastriatal injection of lipopolysaccharide for inducing the BBB disruption. To the contralateral region, the same volume of saline was injected as a control. Immediately after the 60 minutes of PET scan, Evans blue was administrated intravenously to the rat for assessment of the BBB permeability with staining.

Results: The treatment of iodo[^{11}C]methane and methyl *N*-(diphenylmethylen)-D,L-alaniate with tetrabutylammonium fluoride (TBAF) in DMSO underwent the α-[^{11}C]methylation with about 80% radiochemical conversion (decay-corrected). Followed by the deprotection by base and acid hydrolyses, 72% of high overall radiochemical conversion was achieved for [3-^{11}C]AIB preparation. The synthesis protocol was a one-pot manner and hydrophilic interaction chromatography mode HPLC provided efficient method for the isolation of [3-^{11}C]AIB. The metabolite of [3-^{11}C]AIB in the rat plasma and brain was not detected up to 60 minutes after administration. The PET study clearly demonstrated that [3-^{11}C]AIB was significantly accumulated in the lesion side compared with the control side. Because the significant Evans blue staining was observed in the lesion side, the high accumulation of [3-^{11}C]AIB was considered to be associated with the enhanced BBB permeability.

Conclusions: Using TBAF as a base for the incorporation of the [^{11}C]methyl-group into sterically hindered alanine analog, we could achieve the efficient and remote-controlled synthesis of [3-^{11}C]AIB without any technical difficulty. The results suggest that [3-^{11}C]AIB is an useful *in vivo* imaging agent for the assessment of BBB permeability with PET. And we are undertaking the further radiopharmaceutical studies of [3-^{11}C]AIB.

456

HIPPOCAMPAL MYO-INOSITOL METABOLISM IS DIFFERENT BETWEEN ALZHEIMER´S DISEASE AND SUBCORTICAL ISCHAEMIC VASCULAR DEMENTIA

A. Shiino[1], T. Watanabe[2], Y. Shirakashi[2], E. Kotani[3], S. Morikawa[1], T. Inubushi[1], I. Akiguchi[2]

[1]Biomedical MR Science Center, Shiga University of Medical Science, Ohtsu, [2]Center of Neurological and Cerebrovascular Diseases, Takeda Hospital, Kyoto, [3]Neurosurgery, Shiga University of Medical Science, Ohtsu, Japan

Objectives: The mechanism of neurodegeneration between Alzheimer's disease (AD) and subcortical ischaemic vascular dementia with Binswanger type (BD) are different, but the two types of dementia shows hippocampal atrophy causing difficulty to discriminate. We assessed metabolites change of the hippocampus of the two diseases using magnetic resonance spectroscopy (MRS).

Methods: Subjects were clinically diagnosed patients of 31 BD and 99 AD. Additionally, 45 healthy elderly subjects were recruited as controls. Two-sample t-test was applied for providing voxel-wise group comparisons of volumes of grey matter (VBM)[1].We measured N-acetylaspartate (NAA), glutamine and glutamate (Glx), and myoinositol (mIns) concentration quantitatively by MRS[2] using 1.5T MR scanner.

Results: As expected, VBM showed higher t-values of medial temporal structures and posterior cingulate and precuneal cortices (PCC) in both the AD and BD groups, which means significant atrophy in those regions. When compared the results with AD, BD showed less atrophy in amygdala, hippocampus, and parahippocampus, and more atrophy in PCCAs expected, decrease in NAA and Glx concentration of the hippocampus was observed both in AD and BD patients corresponded with hippocampal atrophy. However, mIns concentration of the hippocampus was increased in AD and decreased in BD. Half-normal plot analysis indicated that the sum of mIns of the bilateral hippocampi was the most powerful factor for discrimination between AD and BD. The mechanisms of the opposite manner of mIns of the two diseases are unknown, but different glial responses to the different mechanism of the neuronal degeneration of the disease are supposed.

Conclusions: Proton MRS can provide useful information about pathologic aspect of AD and BD. The differences of mIns concentration of the hippocampus would be one of the marker for differentiation between AD and BD pathology.

References:

Ashburner J: A fast diffeomorphic image registration algorithm. *Neuroimage* 2007;38:95-113.

Provencher SW: Estimation of metabolite concentrations from localized in vivo proton NMR spectra. *Magn Reson Med* 1993; 30:672-679.

459

NEUROVASCULAR COUPLING IS IMPAIRED IN CHRONICALLY AGED SPONTANEOUS HYPERTENSIVE RATS

N. Calcinaghi[1], M. Wyss[1,2], R. Jolivet[1], A. Singh[1], A. Buck[2], C. Matter[3], B. Weber[1]

[1]Institute of Pharmacology and Toxicology, University of Zürich, [2]PET Center, Division of Nuclear Medicine, University Hospital Zürich, [3]Institute of Physiology and Cardiovascular Center, Zürich University and University Hospital Zürich, Zürich, Switzerland

Objectives: Normal brain functions depend on the continuous blood-borne supply of oxygen and energy substrates. An increase in neuronal activity exerts spatially and temporally closely orchestrated changes in energy metabolism and cerebral blood flow (CBF). Neurovascular coupling is guaranteed by the neurons, astrocytes and the vasculature that act in concert to maintain a proper cerebral perfusion. A complex cerebral vascular autoregulation maintains CBF during variations in arterial pressure within a certain range (Iadecola and Davisson 2008). Chronic hypertension causes structural and functional alterations in resting CBF and stimulated hyperaemia (Jennings, Muldoon et al. 2005). Our study investigates the age- and hypertension-induced functional changes on neurovascular coupling and the effects of antihypertensive treatment.

Methods: A combination of multi-wavelength spectroscopy and laser speckle imaging was used to spatiotemporally characterize the hemodynamic response in the primary somatosensory cortex upon 4-seconds deflections at 4 Hz of a single vibrissa in the contralateral face of α-chloralose-anesthetized rats. Studies were performed comparing 10, 20 and 40 week old Spontaneous Hypertensive Rats (SHRs) to age matched control Wistar-Kyoto Rats (WKRs).

Arterial blood pressure (BP) was continuously monitored during experiment via a femoral catheter. Additionally, 30 week old SHRs were treated with Losartan, an angiotensin II type 1 receptor antagonist, or Verapamil, a calcium channel blocker, and imaged after 10 weeks of treatment. Drugs were administered in the drinking water.

Results: Mean Arterial BP of WKRs (10 week old 103±13 mmHg, 20 week 96±17, 40 week 104±20; mean±sd, n=7, 13, 14, respectively) were significantly different ($p< 0.05$) from SHRs (10 week old 138±15 mmHg, 20 week 152±12, 40 week 147±18; mean÷sd, n=5, 9, 14, respectively). The hemodynamic responses were similar in 10 week old SHRs compared to age-matched WKRs whereas they showed a trend in reduction in 20 week old SHRs versus WKRs. In contrast, hemodynamic responses were significantly ($p< 0.05$) reduced in 40 week old SHRs versus WKRs. SHRs treated with Losartan or Verapamil indicated a tendency in reversing the hypertension-evoked changes of hemodynamic parameters but not a complete recovery.

Conclusions: In our study with WKRs and SHRs of different ages, only in 40 week old SHRs alterations of the functional hemodynamic response were observed, suggesting delayed effects of chronic hypertension on neurovascular coupling. Treatment with Losartan or Verapamil when SHRs are already 30 week old could not completely reverse the hypertension-induced dysfunction. In conclusion, this work provides new insights about the effects of age and chronic hypertension on alterations of neurovascular coupling.

References:

1. Iadecola, C. and R. L. Davisson (2008). "Hypertension and cerebrovascular dysfunction." Cell Metabolism 7(6): 476-484.
2. Jennings, J. R., M. F. Muldoon, et al. (2005). "Reduced cerebral blood flow response and compensation among patients with untreated hypertension." Neurology 64(8): 1358-1365.

460

CLINICAL TRIAL OF AUTOLOGOUS BONE MARROW MONONUCLEAR CELL TRANSPLANTATION FOR STROKE PATIENTS

A. Taguchi[1], K. Kajimoto[1], H. Moriwaki[1], K. Saito[1], Y. Kasahara[1], K. Miyashita[1], H. Naritomi[2], K. Nagatsuka[1]

[1]National Cerebral and Cardiovascular Center, Suita, [2]Senrichuou Hospital, Toyonaka, Japan

Objectives: We had demonstrated that intravenous transplantation of hematopoietic stem/progenitor cell after stroke enhances functional recovery in experimental model through activation of endogenous neurogenesis[1.2]. Cell based-therapies using autologous bone marrow derived hematopoietic stem/progenitor cells were initiated in patients with limb and myocardial ischemia with promising results[3.4]. Based on these observations, we have started phase 1/2a clinical trial of cell-based therapy for patients with severe cerebral embolism[5].

Methods: Main inclusion criteria are following: patients with cerebral embolism, aged 75 or younger and more than (or equal to) 10 in NIHSS score at day 7 after onset of stroke. On day 7-10 after onset of stroke, patient has 25ml (low dose group, n=6) or 50ml (high dose group, n=6) of bone marrow aspiration. Autologous bone marrow derived mononuclear cells, the rich cell fraction of hematopoietic stem/progenitor cells, are purified by density gradient method and administrated intravenously in the day of cell aspiration. Primary endpoint is the safety and improvement of NIHSS, compared with our historical control.

Results: We have treated 6 patients in low dose group and are now recruiting patients in high dose group. No adverse effects were observed in low dose group and some patients showed significant improvement of regional cerebral blood flow at 6 months after cell transplantation, compared with 1 month. No enrolled patients showed worsening of NIHSS score at 30 days after treatment, compared with before.

Conclusion: Autologous bone marrow mononuclear cells transplantation with 25ml of bone marrow aspiration is likely safe and feasible, even in patients with severe cerebral embolism. We will do statistical analyze after completing 12 patients. When the autologous bone mononuclear cell plantation is shown to be safe in 12 patients and likely to be improve functional recovery in some patients, we will proceed phase 2 clinical trial that includes patients with milder cerebral infarction.

References:

1. Taguchi et al. J Clin Invest. 2004

2. Nakano-Doi et al. Stem Cells 2010

3. Taguchi et al. Eur J Vasc Endovasc Surg. 2003

4. Schächinger V et al. N Engl J Med. 2006

5. ClinicalTrials.gov ID: NCT01028794

461

MONITORING OF CEREBRAL BLOOD FLOW AND OXYGEN METABOLISM IN PATIENTS WITH SUBARACHNOID HEMORRHAGE EMPLOYING A TIME-RESOLVED SPECTROSCOPY

N. Yokose[1], K. Sakatani[2], T. Igarashi[1], T. Hoshino[1], S. Nakamura[1], N. Fujiwara[1], Y. Murata[1], T. Suma[1], T. Hirayama[1], Y. Katayama[1], E. Ohmae[3], T. Suzuki[3], M. Oda[3], Y. Yamashita[3]

[1]Division of Neurosurgery, [2]Division of Optical Brain Engineering, Department of Neurological Surgery, Nihon University School of Medicine, Tokyo, [3]Central Laboratory, Hamamatsu Photonics K.K., Shizuoka, Japan

Background: Arterial vasospasm is the most common cause of delayed ischemic neurological deficits in patients with aneurysmal subarachnoid hemorrhage (SAH). Transcranial Doppler sonography (TCD) has been used to detect vasospasms after SAH, but its sensitivity is not high. In addition, TCD does not provide information about the cerebral circulation and oxygenation in the cortex. Near infrared spectroscopy (NIRS) appears to be an attractive alternative method, since it can measure concentration changes of oxyhemoglobin (Oxy-Hb) and deoxyhemoglobin (Deoxy-Hb) in the cortical vessels. Various studies have shown the usefulness of NIRS for detecting cerebral ischemia during carotid endarterectomy; however, it is difficult to apply NIRS to the diagnosis of vasospasm after SAH, since commercially available NIRS, which employs continuous wave (CW) light, does not provide quantitative values of the baseline Hb concentrations. In contrast to CW-NIRS, time-resolved near infrared spectroscopy (TR-NIRS) permit quantitative measurement of the Hb concentrations. In this study, we examined whether TR-NIRS can detect cerebral ischemia caused by vasospasm in patients with aneurysmal SAH.

Subjects and methods: We investigated eight age-matched controls and 14 aneurysmal SAH patients, including 10 patients with WFNS grade V and four patients with grade II. Employing TRS (TRS-10, Hamamatsu Photonics K.K, Japan), we measured the cortical oxygen saturation ($CoSO_2$) and baseline concentrations of oxygenated Hb Oxy-Hb, Deoxy-Hb and total Hb (=Oxy-Hb+ Deoxy-Hb) in the middle cerebral artery territory. The concentrations of Hb were expressed in μM. In addition, we measured blood flow velocity of the MCA (M1 portion) by TCD (Nicolet Biomedical Inc., USA). Measurements of TRS and TCD were performed repeatedly for 14 days after SAH. Angiography was performed day seven after SAH or when TRS or TCD indicated occurrence of vasospasm.

Results: In six patients, the $CoSO_2$ and hemoglobin concentrations remained stable after SAH; Digital subtraction angiography (DSA) did not reveal vasospasm in these patients. In eight patients, however, $CoSO_2$ and total hemoglobin decreased abruptly between five and nine days after SAH. DSA revealed diffuse vasospasms in six out of eight patients. The reduction of $CoSO_2$ predicted occurrence of vasospasm at a cut of value of 3.9-6.4% with 100% of sensitivity and 85.7% of specificity. TCD failed to detect the vasospasm in four cases, which TR-NIRS could detect. Finally, TR-NIRS performed on day 1 after SAH revealed significantly higher $CoSO_2$ than that of controls ($p=0.048$); but there was no significant difference in total hemoglobin.

Conclusion: TR-NIRS detected vasospasm by evaluating the CBO in the cortex, and may be more sensitive than TCD, which assesses the blood flow velocity in the M1 portion. The cerebral oxygen metabolism in SAH might be reduced by brain damage due to aneurysmal rupture.

462

THE EFFECTS OF AGING ON MONOAMINERGIC TRANSMISSION: [11C]-DASB AND [11]-RACLOPRIDE UPTAKE IN THE AGED RODENT BRAIN

E.A. Hoekzema[1], S. Rojas[2], R. Herance[2], D. Pareto[2,3], S. Abad[4], X. Jiménez[4], F.P. Figueiras[4], F. Popota[4], A. Ruiz[4], È. Torrent[4], N. Flotats[4], F.J. Fernández-Soriano[4], M. Rocha[5], M. Rovira[4], V.M. Víctor[5,6], **J.D. Gispert**[2,3,4]

[1]Dept. de Psiquiatria i Medicina Legal, Universitat Autònoma de Barcelona, [2]Institut d'Alta Tecnologia - PRBB, Barcelona, [3]Centro de Investigación Biomédica en Red en Bioingeniería, Biomateriales y Nanomedicina (CIBER BBN), Zaragoza, [4]CRC Centre d'Imatge Molecular, Barcelona, [5]University Hospital Doctor Peset Foundation and CIBERehd, [6]Department of Physiology, University of Valencia, Valencia, Spain

Introduction: Aging alters the neurotransmission and molecular imaging studies in humans have demonstrated marked changes in the dopaminergic and serotonergic systems. These have been associated to age-dependent deterioration in cognitive and mood functions. Rodent models play an important role in aging research, as they allow more invasive and treatment-based studies and permit the study of normal aging without neurodegenerative pathology as a confounding factor.

Aim: In this study, we aimed to assess the effect of age on the dopaminergic D2-like receptor (D2R) and the serotonergic transporter (5-HTT), using in vivo molecular imaging with the radioactive compounds [^{11}C]-raclopride and [^{11}C]-DASB in old and young rats.

Methods: Two sets of male OFA rats consisting of 6 young adult animals (~2 months old) and 6 aged animals of over 20 months old were scanned after the administration of [^{11}C]-raclopride and [^{11}C]-DASB. Binding potentials were calculated using the Simplified Reference Tissue Model in the striatum, for the [^{11}C]-raclopride scans, and in the frontal cortex and midbrain for the [^{11}C]-DASB ones.

Results: We observed a robust decline in striatal [11C]-raclopride uptake in the aged rats in comparison to the young control group ($p < 0.001$), comprising a 41% decrement in striatal binding potential. In addition, the old rats were characterized by increments in 5-HTT binding, as indicated by increased cerebral [^{11}C]-DASB binding potentials. Visual inspection of the data suggested that the frontal cortex was a site of considerable age-dependent difference. We observed a substantial increment in [^{11}C]-DASB binding potential in the frontal cortex ($p < 0.001$), and a more modest increase in the midbrain ($p = 0.004$).

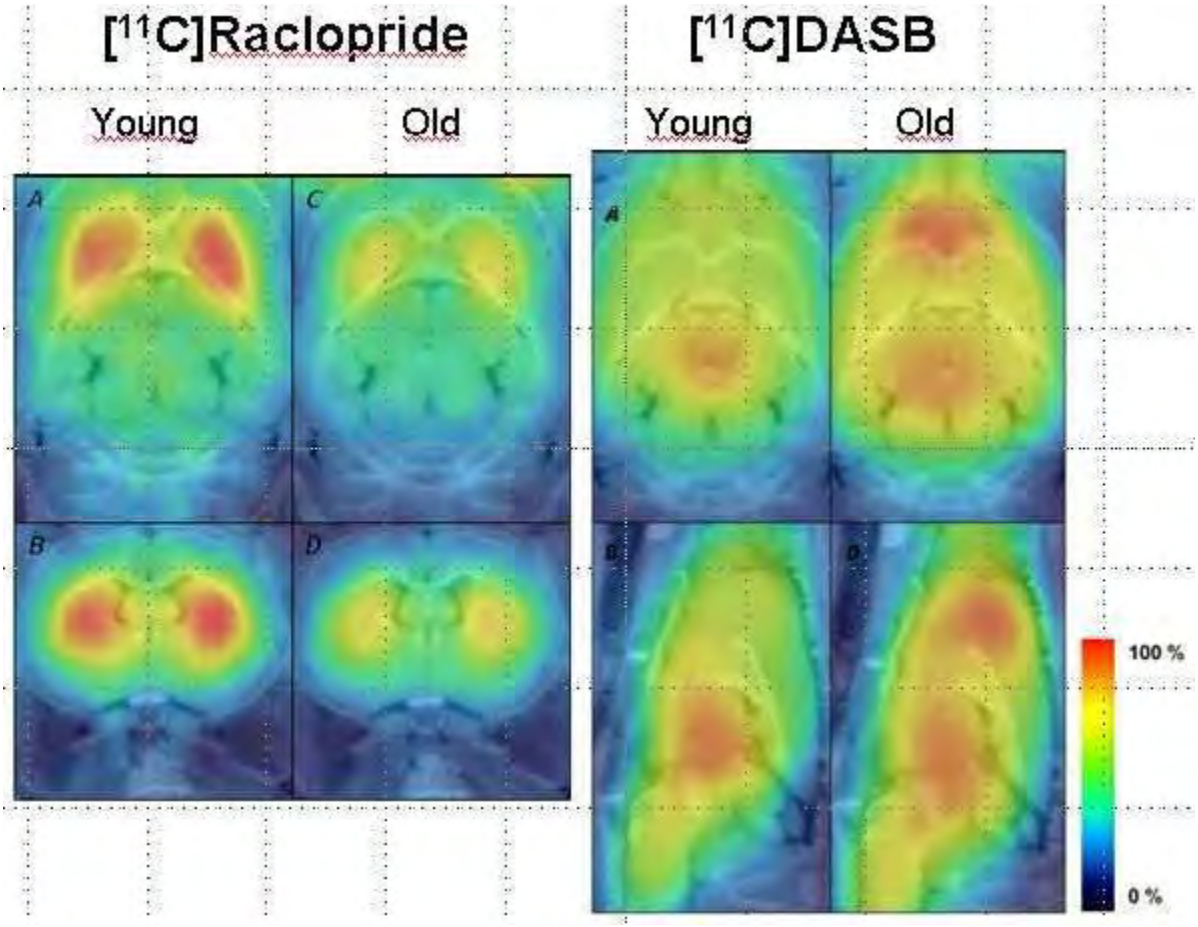

[PET pannel]

Conclusions: Our findings support the existence of age-related alterations in the dopaminergic and serotonergic systems, which can be monitored in vivo with molecular imaging techniques. Studies in humans have consistently reported age-dependent decrements in D2-like receptor availability in agreement with our results. On the other hand, while human imaging studies predominantly report reductions in 5-HTT binding, our in-vivo rat results point to age-related increments in 5-HTT uptake, a finding in line with the majority of the in vitro studies in rodents. Therefore, species differences or other environmental factors may account for the discrepancy between the findings in aged rodents and humans. Despite not being a particular high-density 5-HTT site, the especially strong age-related [11C]-DASB binding increases in the frontal cortex is of great importance due to its prominent role in mood regulation and depression. Considering the increased prevalence of depression and depressive symptoms in the elderly, age-related increases in [^{11}C]-DASB binding may impact the effectiveness of serotonin-specific reuptake inhibitors (SSRIs) in aged patients. Hence, understanding the effects of aging in the serotonergic transporter of the rodent brain may be of great importance for the preclinical development of new drugs for depression and other mood disrders.

463

ACETAZOLAMIDE REACTIVITY AND OXYGEN METABOLISM IN LACUNAR PATIENTS WITH WHITE MATTER LESIONS

T. Nezu[1], C. Yokota[1], K. Fukushima[2], T. Uehara[1], K. Toyoda[1], H. Iida[3], K. Minematsu[1]

[1]Cerebrovascular Medicine, [2]Radiology, National Cerebral and Cardiovascular Center, [3]Bio-Medical Imaging, National Cerebral and Cardiovascular Center Research Institute, Suita Osaka, Japan

Objectives: White matter lesions (WMLs) were the cause of cognitive impairment, dementia, and disability in elderly peoples (1, 2). Increased oxygen extraction fraction (OEF) in patients with WMLs may represent the early stage of vascular dementia (3). Limited evidence exists on the relationships between severity of WMLs and cerebral vascular reserve capacity. Changes in cerebral vasoreactivity (CVR) associated with reduction of cerebral blood flow (CBF) during the development of WMLs have not been clarified. The aim of this study is to examine changes of CBF, oxygen metabolism, and CVR associated with severity of WMLs in patients with lacunar stroke by use of positron emission tomography (PET).

Methods: A total of 18 lacunar patients without large artery occlusive diseases were enrolled. Patients were divided into 2 groups according to the severity of WMLs, which were assessed by fluid-attenuates inversion recovery image of magnetic resonance images (MRI) using the Fazekas classification; grade 0-1 was defined as mild and grade 2-3 was as severe WMLs group. O-15 gas PET studies with a rapid dual autoradiography method (4) followed with water PET scans were performed to measure cerebral blood volume (CBV), cerebral metabolic rate of oxygen ($CMRO_2$), OEF, and CBF before and after acetazolamide (ACZ) administration. CVR was assessed as the ACZ reactivity, which was defined as percent change in CBF before and after the ACZ administration. A total of 30 circular regions of interest were placed in the frontal, parietal and occipital cortices, and the basal ganglia and central semiovale based on the automatic registration of MRI to PET.

Results: There were no significant differences in age, sex and vascular risk profiles between the two groups. In the central semiovale, lower CBF (20.6±4.4 vs. 29.9±8.2ml/100g/min, p=0.008), higher OEF (55.2±7.4 vs. 46.7±5.3%, p=0.013), and lower $CMRO_2$ (1.95±0.41 vs. 2.44±0.42ml/100g/min, p=0.025) were demonstrated in the severe WMLs group as compared with those in the mild WMLs group. There were no significant differences in the ACZ reactivity between the two groups (48.6±22.6% vs. 42.5±17.2%, p=0.524). The ACZ reactivity was not related with OEF as well as the severity of WMLs.

Conclusions: Reduced CBF, $CMRO_2$ and increased OEF were demonstrated in lacunar patients with severe WMLs. The CVR assessed as ACZ reactivity was preserved in both patients with severe and mild WMLs.

References:

1. Pantoni L, et al. *Stroke*. 1997;28:652-659.

2. Prins ND, et al. *Brain*. 2005;128:2034-2041.

3. Yao H, et al. *Stroke*. 1992;23:1673-1677.

4. Kudomi N, et al. *J Cereb Blood Flow Metab*. 2005;25:1209-1224.

464

IS TPA EXPRESSION INFLUENCED BY EPIGENETIC MECHANISMS?

P.Y. Obiang, A. Jullienne, C. Ali, V. Agin, D. Vivien

INSERM U919, Serine Proteases and Pathophysiology of the Neurovascular Unit (SP2U), UMR CNRS 6232 CI-NAPS, Centre for Imaging-Neuroscience and Applications to Pathologies, GIP CYCERON, University of Caen Basse-Normandie, Caen, France

Tissue type plasminogen activator is a pleiotropic serine protease of the central nervous system mainly described to promote fibrinolysis in the vascular compartment. More recently, tPA was also involved in brain functions such as learning and memory (Benchenane *et al*, 2007; Calabresi *et al*., 2000; Madani *et al*., 1999; Pawlak *et al*., 2002; Seeds *et al*., 2003).

Accordingly, we have reported that aging was associated with a selective lowering of brain tPA expression and proteolytic activity, notably in the hippocampus (Roussel *et al*., 2009), an observation related with an albumine D site-binding protein dependent transcriptional regulation (DBP, a member of the PAR bZIP transcription factors). On the other hand, the critical influence of environment on both tPA expression and cognitive performances during aging was recently evidenced (Obiang *et al*., In Revision). Indeed, enriched environment leads to a reversal of age-associated decrease in expression of hippocampal tPA and subsequent improvement in emotional and spatial memories. However, mechanisms by which age and environment modulate tPA expression and cognitive abilities remain unknown.

Our present *in vitro* studies evidenced that treatment of neurons with trichostatin A (TSA), an inhibitor of the histone deacetylases (HDA) improved the transcription rates of both DBP and tPA. Moreover, silencing of DBP in cultured neurons counteracted TSA-induced over-expression of tPA. These results suggest a HAD-dependent acetylation of DBP as an epigenetic process controlling the expression of brain tPA.

465

TEMPORAL STABILITY OF TSPO BINDING CLASS MEASURED WITH PBR28 IN HUMAN PLATELETS

D.R. Owen[1], G. Wadsworth[2], **I.A. Rabiner**[2], I. Bennacef[2], A. Lewis[1], P.M. Matthews[2], R.N. Gunn[2], C.A. Parker[2]

[1]Department of Medicine, Imperial College Faculty of Medicine, Hammersmith Hospital, [2]Clinical Imaging Centre, GSK, London, UK

Objectives: Microglial activation can be quantified with PET studies targeting the 18kDa Translocator Protein (TSPO). However, signal quantification with the TSPO radioligand [^{11}C]PK11195 is limited by poor signal to noise ratio (SNR). Novel radioligands (including [^{11}C]PBR28, [^{18}F]PBR06, [^{18}F]PBR111, [^{18}F]FEPPA, [^{11}C]DAA1106, [^{11}C]DPA713 and [^{11}C]AC-5216) have a more favorable SNR but, unlike [^{11}C]PK11195, they recognize two TSPO binding sites (1,2). In human brain, these tracers bind to a single class of high affinity sites in one group of subjects (high affinity binders, HABs), to a single class of low affinity sites in another group (low affinity binders, LABs), and in a third group (mixed affinity binders, MABs) both HAB and LAB sites appear to expressed in similar proportions (1).

The existence of these three binding classes represents a challenge for the quantitative interpretation of TSPO PET data, because differences in signal across subjects can only be interpreted as differences in target density if individuals are in the same binding class. However, binding class cannot be determined from an individual PET scan.

Knowledge of binding class in the brain, in addition to the specific signal, would allow valid comparisons between subjects. If binding class is stable over time and consistent across tissues within the same individual, it may be possible to determine it through assaying peripheral blood cells. The aim of this study was to investigate the temporal stability of TSPO binding class, in platelets derived from human blood samples collected at two time points.

Methods: Venous blood was drawn from 34 healthy volunteers on entry to the study and again 6 weeks later. Platelets were isolated as previously described (2) and the affinity constant (Ki) was determined by competition binding assays with [^{3}H]PK11195 and unlabelled PBR28. Data were analyzed using GraphPad Prism 5.0. Single site and two site competition models were fitted to the data using the least squares algorithm and model selection was performed with the F-test. MABs were defined as subjects that were best described with two binding sites. HABs and LABs were defined as subjects that were best described with a single binding site (HAB: Ki < 15nM, LAB: Ki > 100nM). No subject showed a best fit to a single binding site with Ki between 15 and 100 nM.

Results: 21/34 samples (62%) were HABs. 11/34 samples (32%) were MABs. 2/34 samples (6%) were LABs. These proportions are similar to ones reported in brain (1,2). There was no relationship between binding class and age or sex. Binding class did not change for any subject between the first and second time point.

Conclusion: This study suggests that TSPO binding class in human platelets does not change over a period of 6 weeks. These data are consistent with the notion that peripheral blood assays can be used to determine binding class, allowing valid comparisons to be made between subjects in TSPO PET studies. Ongoing work will elucidate whether, within the same subject, TSPO binding class in platelets matches that in the brain.

References:

1) Owen-et-al;JCBFM2010Sep;30(9):1608-18

2) Owen-et-al;JNM2010-in-press

467

REGIONAL BRAIN METABOLIC GLUCOSE CHANGES TO DIAZEPAM AND PROGRESSIVE MUSCLE RELAXATION ACCORDING TO JACOBSON: A FDG-PET STUDY

P. Pifarré[1], M. Simó[1], J.D. Gispert[2], P. Plaza[1], X. Jimenez[2], E. M.Miralles[3]

[1]Nuclear Medicine Department. CRC-Quiron Barcelona, [2]CRC-CIM, [3]CRC Corporation, Barcelona, Spain

Introduction: Orally administered Diazepam is commonly prescribed in standard PET-CT oncological studies to control patient anxiety. However, its usefulness and discretionary prescription is controversial. At present and according to Jacobson, drug-free methods have shown efficacy to induce relaxation and reduce anxiety in these patients, like progressive muscle relaxation (PR).

Aim: The aim of our study was to evaluate the changes in cerebral metabolic glucose rate induced after the administration of an anxiolytic medication and after PR as compared to a control group.

Material and methods: Seventy-seven oncological patients without neurodegenerative clinical disorders or metastatic brain lesions were included in this study; 30 patients were studied after sedative medication (Diazepam); 17 subjects were studied after PR. Another 30 patients scanned in resting conditions were also included as control group. All groups were age and gender matched.

Brain PET scans were acquired in a Siemens tomograph (Biograph) in 3D mode, 30 minutes after 18F-FDG administration. Regional cerebral glucose metabolism was compared among groups with SPM8, after intensity normalizing the global 18F-FDG PET uptake to that of white matter (WM). A WM mask was created by thresholding the a-priori WM image provided with SPM8. Voxels having a WM probability over 95% were selected and images were multiplicatively scaled to render identical WM uptake values. Two Student´s two-sample t-tests were conducted comparing the Diazepam and PR groups with respect the Control group. Statistical significance threshold was set to $p < 0.001$ uncorrected for multiple comparisons and no extent threshold was applied.

Results: Compared to the control group, both Diazepam and PR induced similar, although not identical, significant decreases in cortical metabolic activity. Statistical significance in hypometabolism was found. No statistically significant increases in 18F-FDG uptake were observed in either of the two groups.

Conclusion: The pattern of changes in cerebral glucose metabolic rate induced after diazepam administration was very similar than that observed after PR. In conclusion, the relaxation states achieved after PR and the pharmacological intervention were very similar, thus pointing at PR as an effective, drug-free and non-invasive alternative for the control of anxiety in patients undergoing oncological PET-CT scanning.

468

DEVELOPMENT AND EVALUATION OF STREPTOMYCIN SULPHATE LOADED SOLID LIPID NANOPARTICLES FOR THE TREATMENT OF CEREBRAL TUBERCULOSIS

M. Verma, I.P. Kaur

Department of Pharmaceutics, University Institute of Pharmaceutical Sciences, Chandigarh, India

Streptomycin the foremost of a class of drugs called aminoglycosides to be discovered is the only antibiotic remedy for tuberculosis. *Streptomycin cannot be given orally*, but must be administered by regular intramuscular injections as it is reported to degrade throughout the git. Further to this, its use in cerebral tuberculosis is minimal as *it does not cross the blood brain barrier* and *drug induced irreversible ototoxicity* (type B toxicity) additionally limits its use. Furthermore, streptomycin is majorly excreted unchanged in urine, as a result of which it is accumulated in kidneys, leading to *nephrotoxicity when given continuously for more than 2-3 months.* Hence the treatment with streptomycin cannot exceed beyond this period. **Envisaging the above it becomes imperative, to look upon the newer drug delivery concepts for effective delivery of streptomycin in a bioavailable form with minimal side effects.**

Aim of the present investigation was to prepare solid lipid nanoparticles (SLNs) of streptomycin so as to accomplish its rapid delivery to the brain and diminish the side effects associated with its use considering a controlled slow release from the developed system.

Streptomycin SLNs (S-SLNs) were prepared using microemulsification technique and characterized for particle size distribution (d_{50}=180 nm), TEM, drug content (89%), entrapment efficiency (60%), and zeta potential (-3mv). The results show minimal degradation of S-SLNs at pH1.2 and pH7.4, establishing its stability during transit through git. Biodistribution studies of S-SLNs and free streptomycin (F-S) in the brain and blood of mice following intranasal (IN) and intravenous (IV) administration, were examined using technetium labeled (99mTc-labeled) free drug solution or its developed SLNs. Brain/blood uptake ratios were calculated at 0.25h, 0.5h, 1h, 2h, 4h, 24h following IV and IN administration of S-SLNs vis-à-vis F-S. The results showed 4 times, higher brain/blood ratio in case of SLNs, in comparison to free drug administered similarly, suggesting effective transport of drug following S-SLNs administration. Results indicate 3.8 times higher C_{max}, in brain as compared to free drug when given as intranasal SLNs and t_{max} of drug incorporated in SLNs is 2 h, as compared to free drug in which t_{max} is 4 h. This investigation demonstrates a more rapid and larger extent of transport of streptomycin into the brain with intranasal S-SLNs, as compared to F-S. Further S-SLNs shows 6 times lower concentration in kidney as compared to the free drug indirectly indicating chances of fewer nephrotoxic side effects.

Conclusion: Enhancing bioavailability in brain and minimizing serious side effects of streptomycin would help alleviate systemic and cerebral tubercular infections with suggestion of noninvasive oral and nasal routes respectively.

470

CURCUMIN LOADED SOLID LIPID NANOPARTICLES: AN EFFICIENT FORMULATION APPROACH FOR CEREBRAL ISCHEMIC REPERFUSION INJURY IN RATS

I.P. Kaur[1], S. Muppu[2], K. Chopra[2], A.K. Mishra[3], K. Chuttani[3], V. Kakkar[1]

[1]Department of Pharmaceutics, [2]Department of Pharmacology, University Institute of Pharmaceutical Sciences, Chandigarh, [3]Radiology, DRDO, INMAS, Delhi, India

Background and purpose: To evaluate the efficacy of curcumin (a potent pluripharmacological molecule) and its solid lipid nanoparticles (C-SLNs) in the experimental paradigm of cerebral ischemic stroke in rats.

Method: Concentrated dispersion of C-SLNs (particle size: 134 nm; entrapment efficiency:82 %) were prepared and used for the study. Male Wistar rats were subjected to global cerebral ischemia (GCI) for 10 minutes by bilateral common carotid artery occlusion (BCCAO) followed by 72 h reperfusion. Rats were treated with free curcumin and C-SLNs (25 and 50 mg/kg) for 5 days prior and for another 3 days after BCCAO. Behavioral, biochemical (oxidative & nitrosative stress) including acetylcholinestrase, all four mitochondrial enzyme complexes and physiological parameters were evaluated. Biodistribution studies (oral/i.v) were performed with ^{99m}Tc labelled C-SLNs and solubilised curcumin (C-S) in mice. Brain sections of rats administered C-SLNs were evaluated by confocal laser scanning microscopy (CLSM).

Results: C-SLNs significantly improved neurobehavioral (Morris water maze-90.36 %, neurological scoring-79.32 %), biochemical (68-76 %) and cellular performance, while free curcumin showed no effect ($p < 0.05$). C-SLN showed 16.4 times higher bioavailability (AUC) and 10 times higher brain to blood ratio than C-S in γ- scintigraphic studies. CLSM gave a direct evidence of curcumin delivery to brain thereby establishing C-SLNs as a promising approach for cerebral pathologies.

Conclusion: Study establishes the potential of C-SLNs in alleviating pathologies associated with GCI.

471

LACTATE IS A DIRECT NEURONAL ENERGY SOURCE

M.T. Wyss[1,2], A. Buck[1], P.J. Magistretti[3], B. Weber[2]

[1]PET Center, Division of Nuclear Medicine, University Hospital of Zürich, [2]Institute of Pharmacology and Toxicology, University of Zürich, Zürich, [3]Brain Mind Institute, EPFL, Lausanne, Switzerland

Objectives: The perspective concerning the role of lactate in the brain has dramatically changed during the last decades. Initially regarded as a sign for bad prognosis in hypoxia and as a mere end product of energy metabolism it has been realized recently that lactate may play a variety of important roles in the brain. However, there is still a vigorous debate about the role of lactate as a neuronal energy source. Nevertheless, over the last two decades, a role of lactate released by astrocytes in fuelling the energetic needs of neurons has emerged. Most of the present evidence concerning lactate metabolism at the cellular level is based on *in vitro* data. Recent *in vivo* results have demonstrated that the brain uses lactate preferentially to glucose. Furthermore, a neuroprotective effect of lactate during hypoglycemia or cerebral ischemia has been reported. However, these studies do not directly address the issue of whether lactate is indeed consumed preferentially by neurons and if the neuroprotection is due to direct lactate use by the neurons.

Methods: In anesthetized Sprague Dawley rats we induced severe hypoglycemia (insulin i.p. 20 UI/kg) and continuously administered in three groups either saline, glucose or lactate. In a second and third set of experiments we used a dedicated beta scintillator to measure radiotracer kinetics. Using for the first time ^{11}C-L-lactate we measured the cerebral lactate oxidation at rest and during electrical infraorbital nerve stimulation. In a last set of experiments we quantified cerebral glucose utilization using ^{18}F-fluorodeoxyglucose during baseline conditions and during hyperlactemia and with changing activity levels.

Results: Glucose deprivation led to an arrest of the neuronal activity after about 150 minutes, whereas during glucose and lactate infusion the amplitude of the VSD signal remained high during the whole acquisition period (240 minutes). In the second set of experiments, we found an increase of radiolabel washout after ^{11}C-lactate injection during activation reflecting increased oxidation of lactate to CO_2. During baseline conditions, the cerebral glucose utilization decreased by on average 38% in a concentration-dependent manner. Upon activation the effect of lactate on the cerebral glucose utilization was further increased.

Conclusions: We provide for the first time *in vivo* evidence that lactate can sustain neuronal activity in the absence of glucose and thus has a direct neuroprotective role. It is furthermore shown that the brain readily oxidizes lactate at normoglycemic levels and that this lactate oxidation is an activity-dependent process presumably regulated at the level of the lactate dehydrogenase. Finally, it is confirmed that the brain prefers lactate over glucose as an energy substrate.

472

CEREBRAL BLOOD FLOW MEASUREMENT IN THE ASSESSMENT OF POST-TRAUMATIC CEREBRAL CONTUSIONS

P. Pifarré[1], G. Cuberas[1], B. Benejam[2], L. Frascherri[3], J. Sahuquillo[1], J. Castell-Conesa[1]

[1]Nuclear Medicine Department, [2]Neurosurgery Department, [3]Radiology Department, Hospital Universitari de la Vall d'Hebron, Barcelona, Spain

Brain trauma (BT) is the main cause of death and disability in the under-40 age group. The aim of this study was to establish a relationship between anatomical changes and deranged cerebral perfusion in patients with cerebral contusions, using CT scan in conjunction with SPECT.

Material: Twenty-two patients who had suffered BT were recruited. All patients underwent SPECT (20 mCi of 99mTcECD) and a CT head scan on the same day, within 24-48 hours following injury. Eighteen (81.8%) were men. Average age was 45.6 (range, 15-76). For each contusion, areas of bleeding, edema, and healthy perilesional tissue were distinguished.

Results: CT scan revealed a single lesion in 12 patients (54.54%), and more than one lesion in 10 patients (45.4%). Main lesions found on CT were located in the frontal region in 13 patients (59.04%). A total absence of perfusion was visible in the hemorrhagic area and in the edema in 18 patients (81.81%) and 14 patients (63.63%), respectively. In 7 cases SPECT showed hypoperfusion that did not correspond to any morphological changes on the CT scan. Quantitative assessment of fused lesions appearing on both CT scan and SPECT revealed severe perfusion defects in the hemorrhagic area (17.8% of maximum ±12) and in the edema (29.4% of maximum ±13.5).

Conclusion: For the main lesion the topographical findings of CT and SPECT coincided. SPECT revealed more secondary lesions, or dysafferentation lesions, as well as permitting cerebral flow assessment in regions directly involved in the contusion and areas adjacent to it.

474

RED BLOOD CELL INFLUENCE ON CORTICAL HEMODYNAMICS

J. Reichold[1], D. Obrist[1], A. Buck[2], B. Weber[3], P. Jenny[1]

[1]Institute of Fluid Dynamics, ETH Zurich, [2]Division of Nuclear Medicine, University Hospital Zurich, [3]Institute of Pharmacology and Toxicology, University of Zurich, Zurich, Switzerland

Introduction: Red blood cells (RBCs) are the primary means of oxygen transport to the brain. Their unique mechanical properties give rise to a number of interesting phenomena, which have been the topic of past and ongoing research [1-5]. Among them are the tank-treading motion of red cells in shear flow and their asymmetric deformation, leading to a movement across streamlines towards the blood-vessel midline.

However, not only the blood flow has an influence on the behavior of red blood cells, but also the opposite is true. This is especially prominent in capillary networks and has been discussed recently by Obrist and coworkers [6]. The model proposed by Obrist et al. is based on two central assumptions. First, the red cells increase the pressure drop across the vessel in which they reside, and second, at a bifurcation the red cells always follow the path of the steepest local pressure gradient. These two rules lead to a flow distribution that is dramatically different from a flow without red blood cells.

Methods: Here, we present an extension of the RBC transport model to realistic networks consisting of both capillaries and non-capillaries. As in the work of Obrist and coworkers, this is performed in a discrete form - in which all red cells are resolved -, as well as a continuum form where the hematocrit is assumed a continuous real number. The latter formulation has the advantage that it can be applied to large vascular networks, where the discrete representation would be computationally too expensive. The self-consistency of the model is shown by comparing the results of both formulations.

Results: The RBC transport model is applied to vascular networks of the rat somatosensory cortex. The influence of the red blood cells on the steady state blood flow, as well as on the hemodynamic response is demonstrated. Moreover, the implications of a loss in RBC elasticity (as in sickle-cell disease) are discussed.

1) Abkarian, M.; Faivre, M. & Viallat, A.

Swinging of red blood cells under shear flow. Phys Rev Lett, 2007, 98, 188302

2) Carr, R. T.

Estimation of hematocrit profile symmetry recovery length downstream from a bifurcation. Biorheology, 1989, 26, 907-20

3) Fischer, T. M.

Tank-tread frequency of the red cell membrane: dependence on the viscosity of the suspending medium. Biophys J, 2007, 93, 2553-61

4) Korin, N.; Bransky, A. & Dinnar, U.

Theoretical model and experimental study of red blood cell (RBC) deformation in microchannels. Journal of biomechanics, 2007, 40, 2088-95

4) Secomb, T. W.; Styp-Rekowska, B. & Pries, A. R.

Two-dimensional simulation of red blood cell deformation and lateral migration in microvessels. Annals of biomedical engineering, 2007, 35, 755-65

5) Skotheim, J. M. & Secomb, T. W.

Red blood cells and other nonspherical capsules in shear flow: oscillatory dynamics and the tank-treading-to-tumbling transition. Phys Rev Lett, 2007, 98, 078301

6) Obrist D, Weber B, Buck A, Jenny P.

Red blood cell distribution in simplified capillary networks. Philos Transact A Math Phys Eng Sci. 2010 Jun 28;368(1921):2897-918.

476

QUANTIFICATION OF [^{11}C]-(+)-PHNO BINDING IN THE HUMAN BRAIN: MASS EFFECTS AND SUITABILITY OF REFERENCE REGION

P. Shotbolt[1,2], A. Tziortzi[2,3], G.E. Searle[2], C. Plisson[2], M. Huiban[2], R.N. Gunn[1,2,4], E.A. Rabiner[1,2]

[1]Department of Neurosciences, Imperial College, [2]GSK Clinical Imaging Centre, GSK, London, [3]FMRIB Centre, Department of Clinical Neurology, [4]Department of Engineering Science, University of Oxford, Oxford, UK

Objectives: The comparability of a two-tissue-compartment model (2TCM) and a simplified reference tissue model (SRTM) in quantifying [^{11}C]-(+)-PHNO was demonstrated for baseline data[1], but test-retest and quantification of occupancy was only evaluated using SRTM quantification[2]. New evidence, suggesting that clinical [^{11}C]-(+)-PHNO studies are conducted under non-tracer conditions and that the cerebellar reference region may contain a measurable and displaceable specific binding component, complicate the interpretation of [^{11}C]-(+)-PHNO binding data. We examined both of these issues.

Methods: Six healthy male volunteers received four [^{11}C]-(+)-PHNO PET scans each. Two scans were performed on the same day within a 210 minute interval between injections of [^{11}C]-(+)-PHNO, in order to examine (+)-PHNO mass carry-over. One week later, two further [^{11}C]-(+)-PHNO scans were conducted, before and after a 15mg oral dose of aripiprazole, with a 300 min interval between them, to evaluate the magnitude of the specific [^{11}C]-(+)-PHNO binding component in the cerebellum. The range of injected mass of (+)-PHNO was 0.45-2.08 µg, but was tightly matched within each pair of scans. Regional volumes of distribution (V_T) for the Substantia Nigra (SN), Globus Pallidus (GP), Thalamus (TH), Ventral Striatum (VST), Dorsal Caudate (DCD), Dorsal Putamen (DPU) and the Cerebellum (CB), and binding potential relative to non-displaceable binding (BP_{ND}), were quantified using the 2TCM with a metabolite-corrected arterial input function and a cerebellar reference region. Regional occupancy values for aripiprazole were plotted against regional fractions of the [^{11}C]-(+)-PHNO signal attributable to D3 (f^{D3}PHNO), derived from previous studies[3], to estimate the D2 and D3 contributions to the total aripiprazole occupancy.

$$Occupancy_{Total} = f^{D3}PHNO\ (Occupancy_{D3} - Occupancy_{D2}) + Occupancy_{D2} \quad (Eq.1)$$

Results: Consecutive [^{11}C]-(+)-PHNO scans showed a significant reduction in BP_{ND} in regions with a high f^{D3}PHNO (SN; -19±12%, and GP; -27±14%), and a trend for reduction in the TH (11±12%). There was no change in the cerebellar V_T in consecutive [^{11}C]-(+)-PHNO scans (8±8%). A single oral dose of 15 mg of aripiprazole produced a significant reduction in the cerebellar V_T (-6±3%), consistent with a small specific binding component in the cerebellum. The plot of aripiprazole-induced occupancy against f^{D3}PHNO (Eq 1) indicated an occupancy of the D2 of ~55% with very little D3 occupancy (Figure 1).

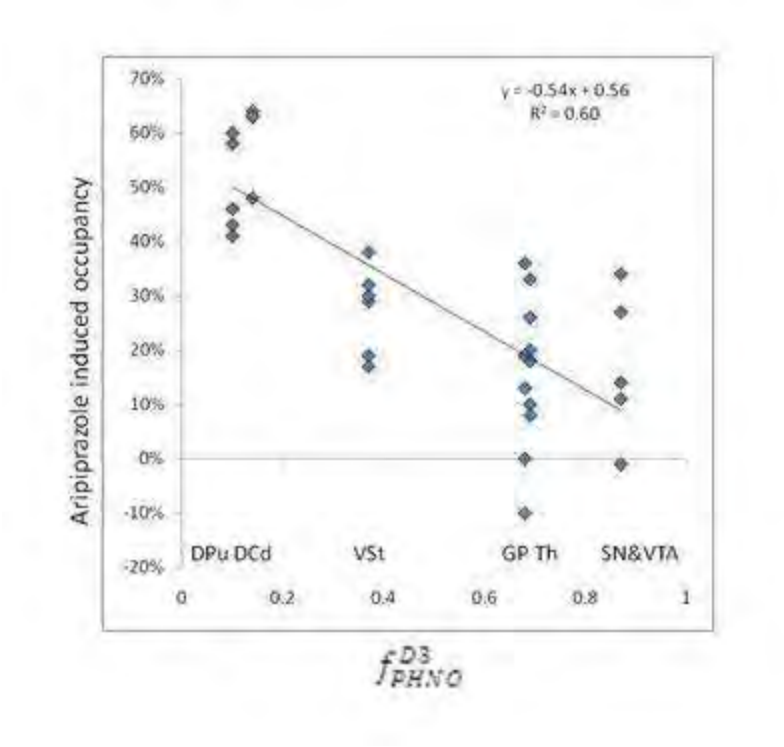

[Figure 1]

Conclusions: Mass carry-over is a significant confounder in the estimation of D3 occupancy with [^{11}C]-(+)-PHNO, particularly in the lower range. A small, but significant, specific binding component, attributable to D2 binding, was found in the cerebellum (but the presence of an additional D3 specific binding component is not excluded). The effect of this component may not be significant in the majority of studies. Estimation of the magnitude of the observed carry-over and specific binding in the reference region will help to plan and interpret future clinical studies with [^{11}C]-(+)-PHNO. Aripiprazole demonstrates significant selectivity for the D2 over the D3 in vivo.

1. Ginovart N et al. 2007. J Cereb Blood Flow Metab 27: 857-871

2. Willeit M et al. 2006. Biol Psychiatry 59: 389-394.

3. Searle GE et al. 2010. *NeuroImage* 52, S1: S20-S21

479

THERAPEUTIC EFFECT OF IL-12/23 AND THEIR SIGNALING PATHWAY BLOCKADE ON BRAIN ISCHEMIA MODEL

F. Konoeda[1,2], T. Shichita[2], H. Yoshida[2], N. Suzuki[1], A. Yoshimura[2]

[1]Neurology, [2]Microbiology and Immunology, Keio University School of Medicine, Tokyo, Japan

Objectives: It has been shown that the cytokine cascade, IL-23-IL-17 axis plays important role in the progression of brain injury by ischemia-reperfusion (I/R). In this study, we have tried to demonstrate therapeutic effects of blockade of IL-23 and its signaling by anti-IL-12/IL-23 (p40) antibody and CP-690550, a small molecule inhibitor of JAKs, on the onset of cerebral ischemia and neurological outcome after experimental stroke.

Methods: $CD3^+CD4^+CD44^-$ memory T cells or $CD3^+$TCRγδ+ cells purified by magnetic beads and FACS sorting were stimulated with anti-TCR mAb and anti-CD28 mAb in the presence or absence of IL-23 (25 ng/ml) with the indicated concentrations of CP-690550. After 24h, IL-17 production was determined through ELISA and quantitative RT-PCR. I/R injury of the brain was induced by standard suture methods using age- matched male C57/B6 mice. After 60 min of ischemia, we withdrew the filament to allow reperfusion of the right MCA territory. The treatment agents were administrated i.p. just before the filament evulsion. On days 3 and 7 after reperfusion, the mice were sacrificed by means of deep anesthesia and the infarct area was measured by TTC staining or MAP2 immunostaining. Neurological deficit was evaluated in a blinded fashion using a 4-point-scale neurological score by 7 days. Expression levels of inflammatory cytokines and other inflammatory factors were examined in the whole brain on day 3 after MCAO by quantitative RT-PCR. IL-17- and IFNγ-positive cells were estimated through intracellular cytokine staining and FACS.

Results: CP-690550 efficiently inhibited IL-17 production from memory T cells and γδT cells *in vitro*. CP-690550 (25 μg/g body weight) partly suppressed infarct volume and significantly improved the functional neurological deficit after I/R ($p< 0.05$). Anti-p40 antibody (25 μg/g body weight) also efficiently suppressed I/R injury. Infarct size on day 7 after MCAO was consistently and significantly ($n=9$, $p=0.002$) smaller in anti-p40 antibody-treated mice than in vehicle-treated controls. Recovery of neurological deficits were pronounced on day 1, 3, 5 and 6 by anti-p40 therapy ($p< 0.05$). IL-17-producing γδT cells were drastically reduced by anti-p40 antibody treatment ($p< 0.05$), although the expression of inflammatory factors including IL-1□, TNF□ and IL-6 produced and the numbers of CD4+ helper T cells and IFNγ-producing cells were not significantly altered.

Conclusions: Cytokine suppression by a JAK inhibitor or by anti-p40 antibody has a protective effect against brain damage induced by I/R injury. This finding will facilitate the development of new therapies for the treatment of stroke.

References:

1. F. Konoeda, T. Shichita, H. Yoshida, et al, Therapeutic effect of IL-12/23 and their signaling pathway blockade on brain ischemia model, Biochem Biophys Res Commun. 402 (2010) 500-506

2. T. Shichita, Y. Sugiyama, H. Ooboshi, et al, Pivotal role of cerebral interleukin-17-producing gammadeltaT cells in the delayed phase of ischemic brain injury, Nat Med. 15 (2009) 946-950

481

INFLUENCE OF A FREE RADICAL SCAVENGER ON CEREBRAL CIRCULATION EARLY AFTER RESUSCITATION IN A NEWBORN PIGLET HYPOXIC-ISCHEMIC MODEL

T. Kusaka[1], K. Koyano[1], S. Nakamura[2], M. Nakamura[2], S. Yasuda[1], K. Okubo[2], K. Isobe[2], S. Itoh[2], M. Ueno[3], T. Miki[4]

[1]Maternal Perinatal Center, [2]Department of Pediatrics, [3]Departments of Pathology and Host Defense, [4]Departments of Anatomy and Neurobiology, Kagawa University, Kitagun, Japan

Background: Hypoxic-ischemic encephalopathy remains a major cause of permanent neurodevelopmental disability and infant mortality. The origin of this secondary energy failure of asphyxiated infants is multi-factorial and related to a combination of excitatory amino acids, free radicals, immunocytotoxic reactions, impairment of protein synthesis, lack of growth factors, and decreased cerebral blood flow and oxygen delivery as a result of progressive cerebral edema. Several methods for preventing secondary brain damage have been proposed. Edaravone (Radicut, Tanabe Mitsubishi Pharmaceutical Co., Ltd.) is a neuroprotective agent (free radical scavenger) developed in Japan. In Japan, this agent is employed as a treatment for acute cerebral infarction in the adult field; it may be useful for treating hypoxic-ischemic (H.I.) encephalopathy.

Purpose: The purpose of this study was to examine the effects of edaravone on cerebral circulation early after resuscitation using a newborn piglet hypoxic-ischemic model.

Methods: Using newborn pigs within 24 hours after birth, we compared a H.I.-loaded, non-treated group (n=7) with a edaravone -treated group (n=6). Piglets were subjected to H.I. insult of 20-min low peak aEEG (LAEEG < 5μV). After 20min, the insult was maintained 10 min of low arterial blood pressure. But, the insult was stopped if CBV reached the rated value after 20 min LAEEG. The piglets were allowed to recover from anesthesia for 6 hr after the insult. At 5 days, the brains of the piglets were perfusion-fixed. Edaravone at 3 mg/kg was administered 6 times: immediately after resuscitation and at 12-hour intervals after loading until 60 hours after loading. We investigated the aEEG, and CBV and cerebral Hb oxygen saturation (ScO_2) using near-infrared time-resolved spectroscopy until 6 hr post-insult.

Results: There were no differences in the post-loading LAEEG duration or ScO_2 between the two groups. The CBV of 3 and 6 hours after loading was lower than the value immediately before resuscitation in the two groups. However, in the treated group, the rate of decrease was smaller than in the non-treated group.

Discussion: In this study, a decrease in the CBV following resuscitation in the treated group was less marked than in the non-treated group. This was possibly because active-oxygen scavenging reduced neurons and angiopathy, leading to improvement in brain edema or circulatory failure.

Conclusion: Edaravone reduced acute cerebral circulation failure related to H.I. loading.

483

AN ITERATIVE METHOD FOR THE ESTIMATION OF INPUT FUNCTIONS IN PET

C. Jouvie[1], S. de Gavriloff[1], M.-J. Santiago Ribeiro[2], V. Gaura[1], P. Rémy[1], P. Zanotti-Fregonara[1], R. Maroy[1]

[1]CEA,DSV,I2bm,SHFJ, Orsay, [2]Université François Rabelais, Tours, France

Introduction: Using Positon Emission Tomography for molecular imaging processes in vivo requires the knowledge of the arterial plasmatic activity concentration (PTAC). The reference method to obtain it is arterial sampling, not applicable in clinical studies since it is invasive and dangerous. Feng et al. [1] introduced the Simultaneous Estimation (SIME) method which deconvoluates the 18-FDG-three-compartments model. The present work proposes an improvement of the SIME through an iterative bootstrap approach taking as input up to 23 structures, instead of 3 or 4.

Methods and material: Feng's SIME is the minimization of a cost function ϕ representing the differences between the estimated input function and the real one, plus the distance (corrected for non stationary noise) of the estimated input function to input venous blood samples (BS), if any.

The Bootstrap-SIME method (B-SIME) consists in five steps. (A) From one set of n>3 kinetics, all possible sets of three different TTACs are built. (B) The best-ranked sets according to the three following criteria are chosen: noise and Partial Volume Effect (PVE) affection, TTACs differences. (C) For each of the selected sets, a SIME is performed. (D) The iteration final values of the analytical input function parameters are obtained by taking the weighted median of the values of the corresponding parameters in the results of C, the weights being equal to the inverse of ϕ at found minimum. They are used to set new constraints for the next iteration (initialization and parameters set values). Steps C and D are then repeated until an optimal input function is reached.

The method was validated on two datasets: simulated and real datasets of the human brain. The simulated dataset was composed of 100 sets of 16 TTACs each generated using the [18]FDG-three-compartments model and affected with realistic noise (1 to 20%). The real dataset included four healthy subjects with one T1-MRI image segmented into 16 structures and a PET image acquired on an Ecat HR+ PET system. Mean TTACs were extracted and corrected for PVE [2]. The figure of merit was the relative difference in area under curves (dAUC) between the estimated and reference curves.

Results: For simulated data, B-SIME (dAUC(1BS)=0.31xN+0.015, dAUC (noBS)=0.58xN+0.077, where N is the noise percentage) achieved better performances than SIME (dAUC(1BS)=0,32xN+0,045, while dAUC(noBS) varied randomly between 1% and 53%).

For real data (see fig.), dAUC(1BS) was lower than 5% for three subjects over four for B-SIME, while for SIME dAUC(1BS) was greater than 70% . The mean gain in dAUC using the bootstrap was 11.7. SIME failed to estimate the input function for two patients without bloodsamples.

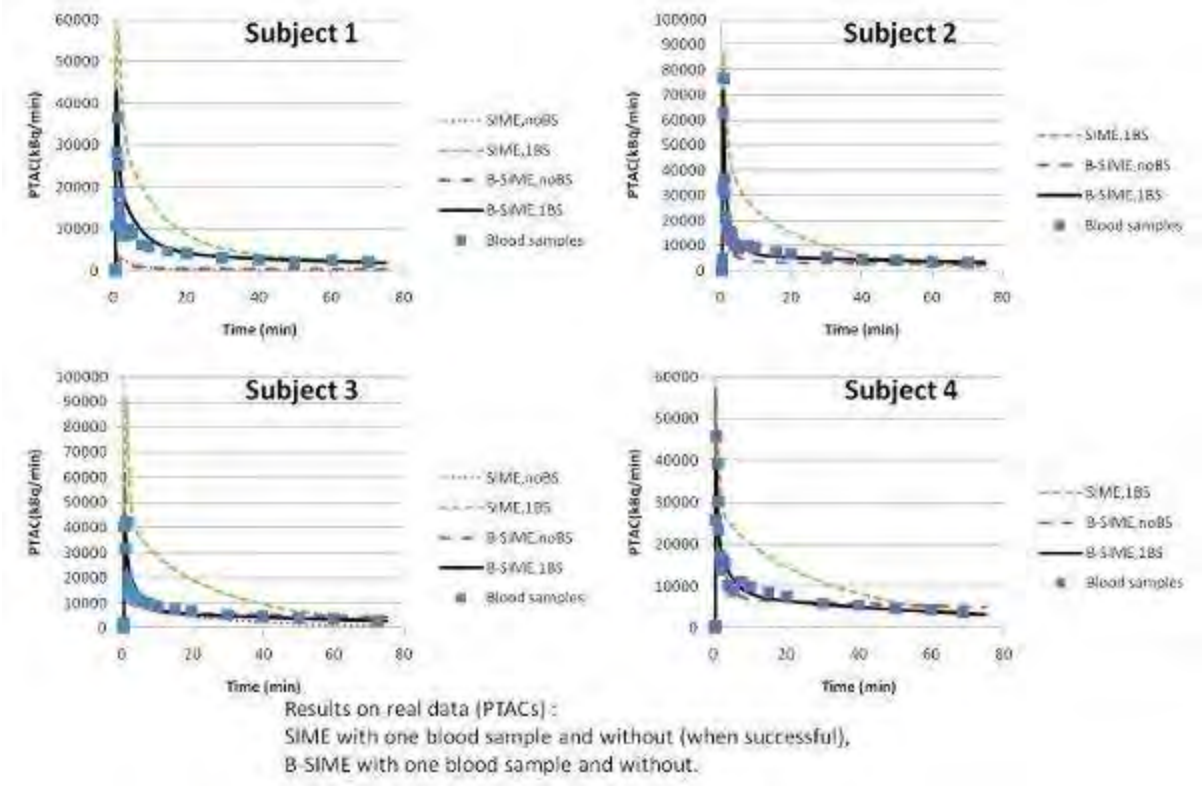

[Results on real data (PTACs)]

Conclusions: The B-SIME method, improvement of the SIME, obtained good results for the estimation of the PTAC, especially when using one late venous blood sample, for simulated and real data.

Acknowledgement: Thanks to the French National Research Agency for funding.

References:

[1] D. Feng et al., IEEE Trans. In Inform. Tech. in Biomed, December 1997.

[2] R. Maroy et al., Proc. AMSNM, 2009.

484

OCCUPANCY OF CEREBRAL A1 ADENOSINE RECEPTORS BY CAFFEINE: ASSESSMENT IN HUMANS WITH [18F]CPFPX AND PET

D. Elmenhorst[1], P.T. Meyer[1,2], A. Matusch[1], A. Bauer[1]

[1]*Institute for Neurosciences and Medicine INM-2, Research Center Juelich, Juelich,*
[2]*Department of Nuclear Medicine, University Hospital Freiburg, Freiburg, Germany*

Objectives: Caffeine is a non-selective antagonist at adenosine receptors and its stimulating effects at commonly consumed doses are supposed to be evoked through its action at adenosine receptors. [18F]CPFPX is a highly selective and affine ligand for the A1 adenosine receptors (A1AR) subtype and has been successfully implemented as PET ligand. A concentration of caffeine sufficient to inhibit 50% of binding (IC50, caffeine/[3H]CPFPX) in vitro is 150 µM. Here we present data on the in vivo occupancy of A1 adenosine receptors (A1AR) by caffeine in the human brain measured by [18F]CPFPX PET.

Methods: 18 subjects (24-68 years) underwent a 140 min bolus plus constant infusion [18F]CPFPX PET experiment after caffeine abstinence. Metabolite corrected blood samples were used to calculate steady-state distribution volumes (VT) at baseline (i.e., 70 to 90 min after start of [18F]CPFPX administration). Caffeine in increasing concentrations (0.5-4.3 mg/kg body weight) was given as a short infusion between 90 and 100 min. One subject received a placebo dose (saline only). Caffeine plasma levels were determined regularly. Occupancy VT values were then acquired using the time span 120-140 min (steady-state after displacement). Occupancy levels were calculated by applying the Lassen plot to 16 regions of interest including cortical and subcortical areas, cerebellum and pons. Based on these occupancies the IC50 value was estimated according to the equation: occupancy = dose / (dose + IC50).

Results: The applied doses of caffeine displaced [18F]CPFPX binding between 5 and 44% in a concentration dependent manner. No displacement (0.3%) was found after placebo administration. IC50 was estimated to be 65 ± 7.5 µM in plasma (± standard error of fit) which corresponds to 460 mg per 70 kg subject (approximately 4.5 cups of coffee).

Conclusions: Drug occupancy studies of A1AR can be performed with [18F]CPFPX bolus plus constant infusion protocols. Taking into consideration the biological half live of caffeine of about 5 h and the repeated consumption of caffeinated beverages during the day occupancies of 50% of cerebral A1ARs are probably a common phenomenon.

485

HYDROGEN-SUPPLEMENTED AIR DIMINISHES THE EFFECTS OF TRANSIENT GLOBAL ISCHEMIA ON EXPRESSION OF PRO-OXYDANT ENZYMES AND GAP JUNCTION PROTEINS

F. Bari[1,2], M. Hugyecz[2], E. Mracsko[2], P. Hertelendy[2], F. Domoki[2], E. Farkas[1]

[1]Department of Medical Physics and Informatics, [2]Department of Physiology, Faculty of Medicine, University of Szeged, Szeged, Hungary

Objectives: Inhalation of hydrogen (H_2) supplemented room air (RA+H_2) neutralizes reactive oxygen species (ROS). Various mechanisms, including oxidative stress and signals mediated by gap junctions appear to be involved in neuronal damage after global cerebral ischemia (GCI). We hypothesized that reduction of ROS affects the ischemia-induced changes in pro-oxidant and antioxidant enzyme expression in the brain, and that the modified expression of the gap junction element connexin (Cx) may also be an indicator of ischemic brain injury. Accordingly, we set out to characterize the changes induced by transient GCI in the expression of cyclooxygenase-2 (COX-2), endothelial, neuronal and inducible nitric oxide synthase (eNOS, nNOS and iNOS, respectively), manganese superoxide dismutase (MnSOD) and three characteristic Cxs (Cx43, Cx30 and Cx45) in rats.

Materials and methods: Adult male Wistar rats (n=70) were divided into 7 Groups:

1) naïve control,

2) GCI ventilated by RA during reperfusion,

3) GCI ventilated by RA+H_2,

4) sham-operated, ventilated by RA, and

5) sham-operated, ventilated by RA+H_2.

In Group 6, the peroxisome proliferator-activated receptor (PPAR) γ agonist rosigilitasone (RSG) was administered (6 mg/kg, i.p.) before the induction of GCI, while Group 7 served as vehicle treated control for the RSG group. In Groups 2, 3 and 6 10-min GCI was induced under halothane anesthesia by the combination of bilateral common carotid artery occlusion and hypovolemic hypotension (MABP ~ 40 mmHg). In Group 3, rats were ventilated with RA containing 2.1% H_2 during the first 30 min of reperfusion.

Tissue samples from the hippocampus and frontal cortex were taken 72 h following GCI. Protein levels were determined with Western blot analysis. For all investigated proteins, the concentration was normalized to β-actin, the level assessed in the naïve control group was taken as 100%, and changes were calculated with respect to this value for all other groups.

Results:

a) Hippocampus: GCI resulted in significant reduction of nNOS and Cx45 protein expression (56.0±17.5% and 54.8±6.4%, respectively) while RA+H_2- ventilation restored these levels to control value. After GCI, the expression of COX-2, Cx30 and Cx43 increased significantly with respect to the naïve control group (211.1±24.5%, 166.6±9.9% and 131.9±5.5%, respectively).

Inhalation of RA+H_2 reduced the GCI-induced elevation in COX-2 (136.8±7.8%) but remained uneffective in nNOS (101.9±11.4%), Cx45 (92.0±8.2%), Cx30 (101.1±7.3%) and Cx43 (88.2±7.0%) expression. We did not find any significant change due to GCI or either of the applied treatments in eNOS and MnSOD expression. RSG treatment counteracted the CGI-induced changes in nNOS, COX-2, Cx30, Cx43 and Cx45 expression.

b) Cortex: In the cortex, we did not observe apparent changes in the expression of COX-2, eNOS, nNOS, iNOS and MnSOD expression after GCI. However, Cx43 and Cx45 expression did change significantly (251.1±18.3% and 51.1±8.7%). Both levels were restored by RA+H_2 inhalation or RSG treatment.

Conclusion: Our study extends the sparse data indicating the beneficial effect of ventilation H_2-supplemented air in the post-ischemic period and confirms the advantageous consequences of RSG pre-treatment in GCI. Reduction of pro-oxidant enzymes would minimize the ROS production and reduce the cell injury.

Supported by OTKA (K81266).

487

CORTICAL μ-OPIOID RECEPTOR AVAILABILITY IS RELATED TO EATING BEHAVIOUR IN HEALTHY HUMAN MALES

A. Makwana[1], A. Colasanti[1,2], G. Searle[1], Z. Gerald[1], S. Hill[1], C. Long[1], R. Gunn[1,2], J. Beaver[1], E. Rabiner[1,2]

[1]GlaxoSmithKline Clinical Imaging Centre, [2]Division of Experimental Medicine, Imperial College, London, UK

Objectives: Pre-clinical and clinical studies implicate u-opioid receptor (μ-OR) neurotransmission in feeding behaviours[1]. A study of 8 female bulimia nervosa patients reported less μ-opioid binding in the insula than in healthy controls[2]. As part of an ongoing study, we examined the relationship between regional brain μ-OR availability and eating behaviours in healthy male volunteers.

Methods: Healthy male volunteers (n =37, Age =34 ± 8, BMI =25 ± 3) completed the three factor eating questionnaire (TFEQ-R18)[3] and were scanned post administration of the selective μ-OR radioligand [^{11}C]carfentanil, on two similar Siemens Biograph PET-CT scanners (Hi-Rez-6, n=24, and TruePoint-6, n=13). Simplified reference tissue model with the occipital lobe as the reference region was used to derive regional [^{11}C]carfentanil binding potential (BP_{ND}) for each of 10 *a priori* defined regions of interest (ROIs). Regional BP_{ND} were regressed against the three sub-scales of the TFEQ-R18 and the scanner type (multiple comparisons correction used the False Discovery Rate correction, p.adjust function in R).

Results:

ROI	*Regression ANOVA*	*Cognitive restraint*	*Uncontrolled eating*	*Emotional eating*	*Scanner type*
Frontal	**0.008**	**0.007**	0.082	0.585	0.058
Parietal	**0.008**	**0.026**	0.056	0.931	0.138
Insula	**0.010**	**0.008**	0.165	0.822	0.135
Temporal	**0.014**	**0.011**	0.065	0.600	0.199
Anterior cingulate	**0.034**	**0.014**	0.260	0.971	0.144
Nucleus accumbens	**0.015**	0.125	0.622	0.969	**0.002**

Thalamus	**0.033**	0.361	0.930	0.491	**0.006**
Caudate	**0.012**	0.840	0.185	0.761	**0.003**

[Table 1:]

Significance levels for ANOVA and regression coefficients for regional BP_{ND} regressions onto TFEQ-R18 scores and scanner typefor the 8 ROIs at FDR q* < 0.05.

In all ROIs, partial correlations of BP_{ND} were positive against Cognitive Restraint and negative against Uncontrolled Eating. Cortical ROIs demonstrated a significant relationship between μ-OR availability and Cognitive restraint. For the sub-cortical ROIs, any significant relationship seems to have been driven by differences between the two scanners.

Conclusions: Our data suggests that high cortical levels of μ-OR are related to the scale of Cognitive restraint in healthy males. Although μ-OR availability has been related in the past to the pathophysiology of bulimia, to our knowledge, this is the first direct demonstration of a link between opioid receptor density and eating behaviour in healthy humans.

References:

[1] C. Colantuoni et al., Excessive sugar intake alters binding to dopamine and mu-opioid receptors in the brain.. NEUROREPORT, 12, (2001), pp3549- 3552

[2] Bencherif, B. et al., μ-opioid receptor binding in insular cortex is decreased in bulimia nervosa and correlates inversely with fasting behaviour. Journal of Nuclear Medicine, 46, (2005), pp1349-1351,

[3] J Karlsson, et al., Psychometric properties and factor structure of the Three-Factor Eating Questionnaire (TFEQ) in obese men and women. Results from the Swedish Obese Subjects (SOS) study. International Journal of Obesity, 24, (2000), pp1715-1725

488

THE HIBERNATING BRAIN - CEREBRAL SUPPRESSION IN PATIENTS WITH CHRONIC HEMODYNAMIC ISCHEMIA

D. Jussen[1], A. Zdunczyk[1], L. Teichgräber[2], T. Picht[1], R. Buchert[2], P. Vajkoczy[1]

[1]Neurosurgery, [2]Nuclear Medicine, Charité - University Medicine Berlin, Berlin, Germany

Objective: Patients with chronic hemodynamic cerebral ischemia due to stenoocclusive cerebrovascular disease often suffer from reduced motor function and increased risk of stroke. This is associated with an impairment of cerebrovascular reserve capacity (CVRC). From clinical experience with patients improving after cerebral revascularization we hypothesize, in contrast to current doctrines, a reversible neuronal loss of function in these patients, similar to concept of hibernating myocardium in cardiology. In this study we prospectively determined the resting motor threshold (RMT) via navigated transcranial stimulation (nTMS) as a marker for reduced cortical excitability. We investigated the potential relationship between impaired RMT and cerebrovascular reserve capacity (CVRC) in chronically ischemic brain tissue and the course of cortical excitability after EC-IC bypass surgery.

Methods: Cortical excitability was determined by navigated TMS via identification of the RMT for both hemispheres. Brain perfusion SPECTs for measurement of CVRC had been acquired according to the EANM guidelines in 22 patients. Correlation analysis was used to test for a relationship betwen CVRC and RMT in these patients. Patients fulfilling criteria for EC-IC bypass surgery were operated via standard STA-MCA bypass. Electrophysiological, angiographic and clinical data were obtained preoperative as well as at follow-up one week and three months after surgery. In a first step a relationship between CVRC and RMT was tested in 22 patients by correlation analysis. To furthermore investigate a reversible neuronal loss of function we repetitively determined the RMT in 29 patients with unilateral symptomatic ICA or MCA-occlusion before and after revascularization.

Results: There was a statistically significant negative correlation between left-right difference of MCA CVRC and left-right difference of RMT (correlation coefficient = -0.446, p = 0.038). Concerning cortical excitability, RMT was higher in the symptomatic hemisphere compared to the contralateral asymptomatic side (50.9 ± 14.3 compared to 39.5 ± 8.4, p = < 0.001). Reduced cortical excitability normalized after revascularization (54.9 ± 14.1 → 45.9 ± 10.4, n=12, p < 0.05), while RMT in the asymptomatic hemisphere remained unchanged (42.5 ± 6.0 → 41.5 ± 5.7 p=0.7). RMTs of the harmed hemispheres assimilated to the unharmed hemispheres in terms of less asymmetry. In clinical examination there was an improvement in 80% of formerly thought fixed paresis and a 100% improvement of transitory ischemic attacks.

Conclusions: nTMS identifies patients with chronic hemodynamic cerebral ischemia and reduced cortical excitability. There is a significant relation between CVRC and RMT. Cerebral revascularization resulted in significant improvement of impaired cortical excitability. In contrast to current doctrines there was a parallel improvement of fixed neurological deficits and TIA after surgery. This supports the new concept of reversible neuronal loss of function: the Hibernating/Stunned Brain.

490

SELECT COMBINATION OF NEUROTROPHINS APPLIED OVER THE INJURED RAT SPINAL CORD ATTENUATES HEMEOXYGENASE-2 EXPRESSION, MICROVASCULAR PERMEABILITY AND CORD PATHOLOGY

H. Sharma[1], A. Sharma[1], H. Huang[2]

[1]Surgical Sciences, Uppsala University, Uppsala, Sweden, [2]Neuroscience Institute of Taishan Medical University, Chinese Academy of Neuroscience, Beijing, China

Previous reports from our laboratory show that neurotrophins when applied topically over the injured spinal cord in combination is able to reduce cord pathology and improves functional recovery. In this regard, a combination of BDNF and GDNF showed remarkable neuroprotection even when applied 90 min after spinal cord injury (SCI). However, a combination of BDNF or GDNF with NGF was not so effective. In present investigation, we wanted to know the role of CNTF in enhancing neuroprotection in SCI in combination with BDNF or GDNF treatment. Previously, we have shown that BDNF is able to attenuate nitric oxide (NO) production in the spinal cord after injury that correlates well with its neuroprotective ability. Since carbon monoxide (CO) is also a free radical gas and has many similarities with NO in inducing cell damage, in present investigation, we explored the role of neurotrophins in modulating CO production in the spinal cord in relation to neuroprotection. For this purpose, we used immunohistochemistry of the constitutive isoform of CO synthesizing enzyme, hemeoxygenase-2 (HO-2) to understand the functions of CO in SCI in relation to neurotrophins treatment.

A focal SCI on the right dorsal horn on the T10-11 segment markedly increased the HO-2 immunostaining in the T9 and T12 segments at 5 h. At this time, breakdown of the blood-spinal cord barrier (BSCB), edema formation and cell changes were seen in several spinal cord segments adjacent to the lesion site. Topical application of BDNF, CNTF and GDNF in combination (10 ng each in 10 µl, Total 30 µl from a solution of 1 µg/ml BDNF,GDNF or CNTF solution) 60, 90 and 120 min after injury over the exposed surface of the cord significantly reduced the BSCB breakdown, edema formation and cell injury. Functional recovery was also markedly improved by treatment with this combination of neurotrophins. Expression of HO-2 in the spinal cord was significantly reduced. However, co-application of CNTF with either BDNF or GDNF was not that effective in inducing neuroprotection or downregulation of HO-2 expression in SCI. These observations suggest that

(i) a combination of CNTF with BDNF and GDNF is necessary to induce effective neuroprotection even during the later phase of SCI (i.e., 120 min after primary insult), and

(ii) the neuroprotective effects of neurotrophins in SCI are some how interrelated with increased CO production. Taken together our novel observations suggest an active interaction of BDNF, CNTF and GDNF with CO system for inducing neuroprotection in the spinal cord after trauma.

491

UNVEILING AN EXCEPTIONAL ZYMOGEN: THE SINGLE-CHAIN FORM OF TPA IS A SELECTIVE ACTIVATOR OF NMDAR SIGNALING

J. Parcq[1], A.F. Baron[1], T. Bertrand[1], R. Macrez[1], J.-M. Billard[2], A. Briens[1], Y. Hommet[1], H.R. Lijnen[3], P. Dutar[2], E. Angles-Cano[1], D. Vivien[1]

[1]U919, INSERM, Caen, [2]U894, INSERM, Paris, France, [3]Center for Molecular and Vascular Biology, KU Leuven, Leuven, Belgium

Objectives: Tissue plasminogen activator (tPA) is an ubiquitous and exceptional serine protease in that it displays low zymogenicity. Indeed, the single-chain tPA (sc-tPA) and two-chain tPA (tc-tPA) display similar activity in the presence of blood templates such as fibrin. Interestingly, tPA was also highlighted in the brain to control neuronal migration, synaptic plasticity, learning and memory, through modulation of the N-methyl-D-aspartate receptor (NMDAR) signaling. Up to now, no difference has been underlined between the two forms of tPA regarding its neuromodulation. In the present study, we wonder whether sc-tPA and tc-tPA behave equally toward a non-fibrin substrate, the NMDAR, in the central nervous system.

Methods: tc-tPA was prepared by plasmin treatment from the commercial preparation of sc-tPA and conditioned in 0.5M bicarbonate ammonium buffer. Both forms were tested toward their modulation of NMDA-neurotoxicity and NMDAR signaling *in vitro* on cortical neurons and *in vivo* in the striatum and the hippocampus.

Results: Sc-tPA enhances NMDAR-mediated calcium influx (+34 % vs. tc-tPA), promotes NMDA Erk(½) activation (+19 % vs. tc-tPA) and NMDA neurotoxicity in cortical neurons (+51 % vs. tc-tPA) and in the striatum (+100 % vs. tc-tPA). We demonstrated that tPA mediates NMDA neurotoxicity through a plasminogen independent mechanism that requires its proteolytic activity. In the hippocampus only the sc-tPA is able to promote NMDAR-dependent long-term potentiation (LTP) in the CA1 network (+16 % vs. control), whereas tc-tPA does not. Moreover, only the sc-tPA can reverse a mild long-term depression (LTD) into LTP (excitatory post-synaptic potential slopes increased from 86 % of the baseline to 107 % in the presence of sc-tPA vs. 81 % in the presence of tc-tPA).

Conclusions: We have demonstrated, both *in vitro* and *in vivo*, the first differential function between sc- and tc-tPA, for that sc-tPA is the selective modulator of NMDAR signaling, via its proteolytic activity and through a plasminogen-independent mechanism. This finding opens a new area of investigations into plasminogen-independent functions of tPA in the brain, including mechanisms controlling its expression, its secretion and its proteolytic processing.

NEURORECEPTOR OCCUPANCY QUANTIFICATION WITH PET IN THE ABSENCE OF A REFERENCE REGION: AN ALTERNATIVE TO THE LASSEN PLOT

M. Koole[1,2], C. Casteels[1,2], J. Ceccarini[2], G. Bormans[1,3], K. Van Laere[2]

[1]IMIR, In Vivo Molecular Imaging Research Group, KU Leuven, [2]Division of Nuclear Medicine, UZ Gasthuisberg, [3]Laboratory for Radiopharmacy, KU Leuven, Leuven, Belgium

Objectives: Drug induced neuro-receptor occupancy O_{Drug} can be estimated with PET as the relative reduction of the non-displaceable binding potential $1-(BP_{ND}^{Drug}/BP_{ND}^{Base})$ with $BP_{ND}=V_s/V_{ND}$, V_{ND} being the non-displaceable distribution volume and V_s the distribution volume for specific binding. In case a reference region with negligible specific binding is unavailable, an graphical method has been proposed to estimate V_{ND} and occupancy while assuming differing target density in the brain, homogeneous nonspecific binding and uniform receptor occupancy [1, 2]. Using the same assumptions, we propose a straightforward method to estimate receptor occupancy without the need to estimate V_{ND}. We evaluate whether this new approach may lead to improved occupancy estimates.

Methods: Given V_T estimates for a range of brain regions for both a baseline and a post-drug scan, that is $V_{T\ Base} = V_s+V_{ND}$ and $V_{T\ Drug}=V_s x(1-O_{Drug})+V_{ND}$, the Lassen plot (LASSEN) gives an estimate for both receptor occupancy O_{Drug} and non-displaceable distribution volume V_{ND} by fitting $(V_{T\ Base}-V_{T\ Drug})=O_{Drug} x(V_{TBase}-V_{ND})$ (a) to the V_T estimates. We propose to estimate occupancy by fitting $(V_{T\ Drug}-V_T^{Avg}{}_{Drug})=(1-O_{Drug})x(V_{T\ Base}-V_T^{Avg}{}_{Base})$ (b) to the regional V_T estimates with V_T^{Avg} the average distribution volume of all regional estimates. Ordinary least squares fitting (OLS) of equation (b) gives the following estimate $(1-O_{Drug})=COVARIANCE(V_{T\ Base},V_{T\ Drug})/VARIANCE\ (V_{T\ Base})$. Using (a), this solution can be approximated by

$(1-O_{Drug})=STDEV(V_{T\ Drug})/STDEV\ (V_{T\ Base})$ (STDEV).

Synthetic kinetic data were generated using an up sampled measured input function and a two compartment model with V_{ND} = 1 and BP_{ND} ranging from 0 to 4 for the baseline scan. For the post-drug scans 20%, 50% and 80% occupancy levels were simulated. Gaussian noise was added to all time activity curves with a standard deviation of 5% of the mean activity value. V_T was determined using a 1 tissue compartment model, a constant weighted least squares cost function and Marquardt-Levenberg optimization. Using the covariance matrix of the Marquardt-Levenberg algorithm, estimates of the standard error for the fitted parameters could be calculated and used as weights for the weighted least squares fitting of both (a) and (b) [3]. Figure 1 gives an example of the graphical analysis as proposed by Lassen while Figure 2 demonstrates the new approach.

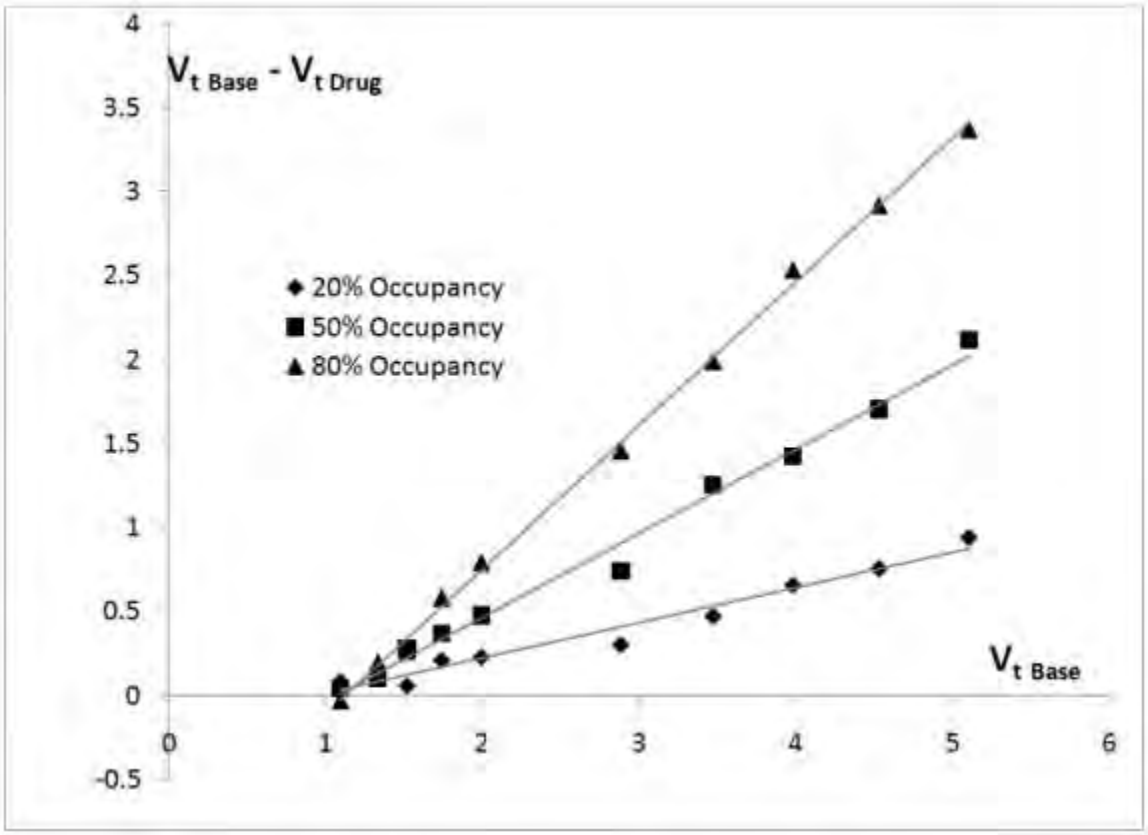
$V_{t\ Base} - V_{t\ Drug}$
20% Occupancy
50% Occupancy
80% Occupancy
$V_{t\ Base}$
4
3.5
3
2.5
2
1.5
1
0.5
0
-0.5
0
1
2
3
4
5
6

[Figure 1]

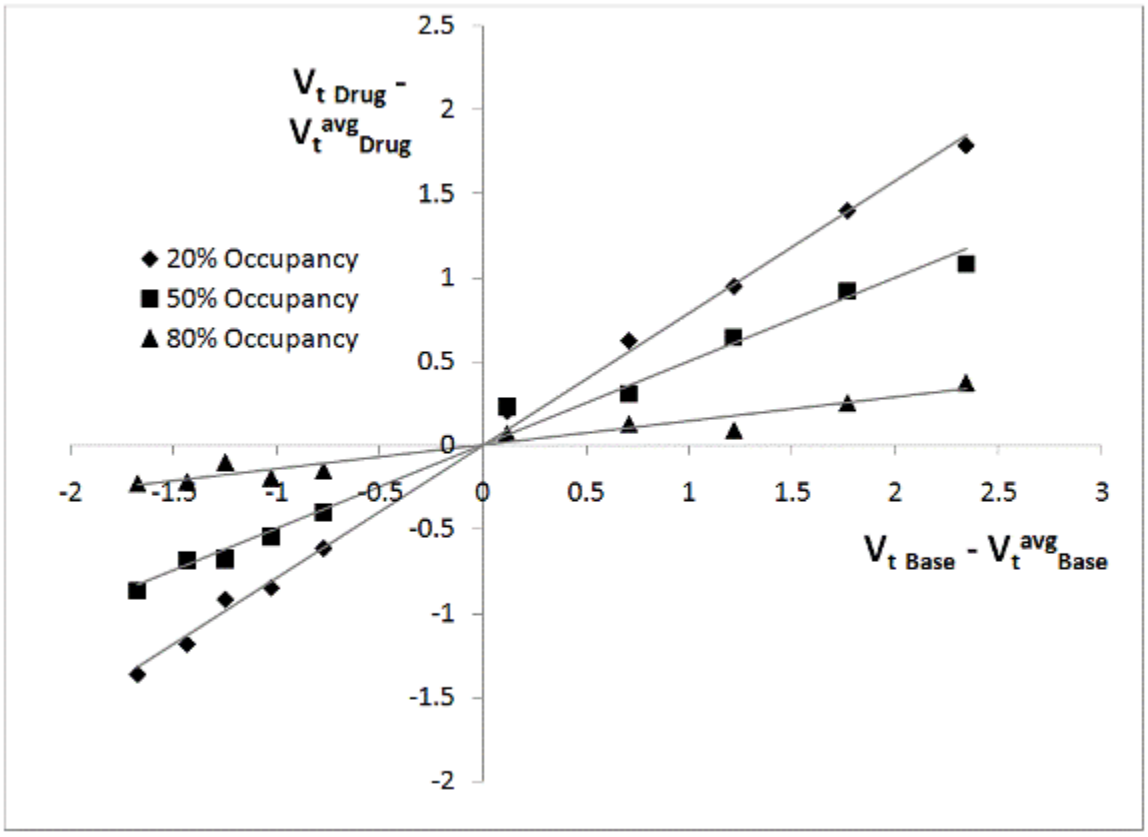

[Figure 2]

Results: Occupancy results of the simulations are summarized in Table 1 (avg ± stdev - min/max).

Occupancy	STDEV	OLS	WLS	LASSEN
20%	20.8±0.7% 19.8/22.3	20.6±0.8% 19.6/22.2	20.7±0.7% 19.5/22.0	20.9±1.2% 18.3/23.2
50%	52.5±1.8% 49.9/55.1	51.7±1.5% 49.8/54.9	52.4±2.3% 49.1/56.4	53.1±3.4% 48.4/60.1
80%	83.2±1.9% 80.1/85.9	82.4±1.8% 80.3/85.5	82.3±2.0% 80.4/85.7	82.3±2.7% 79.3/87.3

[Table 1]

Conclusions: Results show good agreement between theoretical and estimated occupancy levels for all methodologies. The proposed methodology proves to be as useful as the graphical analysis by Lassen and tends to reduce the positive bias that has been reported for the Lassen approach.

[1] Lassen et al, J Cereb Blood Flow Metab. 1995 Jan; 15(1):152-65.

[2] Cunningham et al, J Cereb Blood Flow Metab. 2010 Jan; 30(1):46-50.

[3] Numerical Recipes in C, second edition, Cambridge University Press 1992; p666-p670

496

CONSISTENT INJURY TO MEDIUM SPINY NEURONS AND WHITE MATTER IN THE MOUSE STRIATUM AFTER PROLONGED TRANSIENT GLOBAL CEREBRAL ISCHEMIA

H. Yoshioka[1], T. Yagi[1], T. Wakai[1], H. Sakata[2], T. Horikoshi[1], P.H. Chan[2], H. Kinouchi[1]

[1]Department of Neurosurgery, University of Yamanashi, Chuou, Japan, [2]Department of Neurosurgery, Stanford University, Stanford, CA, USA

Background and purpose: A reproducible transient global cerebral ischemia mouse model has not been fully established. Although striatal neurons and white matter of mouse brains are recognized to be vulnerable to ischemia[1), 2)], the mechanism of vulnerability after global ischemia has not been elucidated. The purpose of this study was to evaluate the damage of striatal neurons and white matter after ischemia in C57BL/6 mice and also to develop a reproducible global cerebral ischemia model. We also investigated the relationship between the ischemic vulnerability and the activation of NADPH oxidase, one of the major sources of superoxide.

Material and methods: Male C57BL6/J mice were subjected to transient global cerebral ischemia by bilateral common carotid artery occlusion. Mice whose cerebral blood flow after ischemia decreased to less than 13% of the pre-ischemic value were used. Histological changes in the striatum, hippocampal CA 1-4 subregions, thalamus, and cerebral cortex were evaluated 3 days after ischemia by cresyl violet and TUNEL staining. For the quantitative analysis of the ischemic injury, mitochondrial cytochrome *c* release and DNA fragmentation was analyzed. The difference in ischemic vulnerability among the striatal neuronal subpopulations and the activation of NADPH oxidase were evaluated by immunohistochemistry and Western blot analysis. Oxidative protein injury was detected by the carbonyl groups into proteins, and DNA oxidative damage was evaluated by 8-oxoG staining. Injury of axon and myelin was identified by SIM-32 and myelin basic protein (MBP) immunostaining, respectively.

Results: Histological analysis showed that striatal neurons 3 days after 22 minutes of ischemia were injured more consistently than those in other brain regions (n=15). In the striatum, cytochrome *c* in the cytosolic fraction significantly increased 24 hours after ischemia, and significant increment of DNA fragmentation 72 hours after ischemia was observed (n=6). Immunohistochemistry and Western blot analysis revealed that DARPP-32-positive medium spiny neurons (MSNs), the majority of striatal neurons, were the most vulnerable among the striatal neuronal subpopulations (n=4). NADPH oxidase was activated in the striatum 3-6 hours after ischemia, and MSNs were susceptible to ischemic oxidative stress (n=6). SMI-32 and MBP immunostaining showed that white matter in the striatum was also consistently injured 72 hours after 22 minutes of ischemia.

Conclusion: We propose a transient global cerebral ischemia model that consistently produces neuronal and white matter injury in the striatum by a simple technique. Since activation of NADPH oxidase and subsequent oxidative injury was observed in the striatum, especially in MSNs, NADPH oxidase activation might be a mechanism of the ischemic vulnerability of MSNs. This model can be highly applicable for elucidating molecular mechanisms in the brain after global ischemia.

Reference:

1. Pulsinelli WA, Brierley JB, Plum F. Temporal profile of neuronal damage in a model of transient forebrain ischemia. Ann. Neurol 11: 491-498, 1982

2. Pantoni L, Garcia JH, Gutierrez JA. Cerebral white matter is highly vulnerable to ischemia. Stroke 27: 1641-1647, 1996

498

MICRORNA AS THERAPEUTIC TARGETS FOLLOWING STROKE IN FEMALE RATS

F. Sohrabji, A. Selvamani, P. Sathyan, R. Miranda

Neuroscience and Experimental Therapeutics, Texas A&M Health Science Center, College Station, TX, USA

Objectives: Previous work from our lab shows that older females sustain a larger infarct as compared to younger females, and paradoxically, estrogen treatment to older females further increases cortical infarct volume (Selvamani and Sohrabji, 2008). In older animals, plasma and brain expression of the neuroprotective peptide hormone IGF-1 is significantly reduced and post-stroke infusions of IGF-1 (insulin-like growth factor-1) reverse estrogen-mediated toxicity (Selvamani and Sohrabji, 2010) in older females. Estrogen and IGF-1 interact to promote neuroprotection in several injury models and age-related loss of IGF-1 may promote greater ischemia-induced cell death in older animals. In order to promote neuroprotection in older animals, we focused on microRNA that regulate the expression of IGF-1. MicroRNAs (miRNAs) are small, non-coding RNA molecules of 18-25 nucleotides that control cellular function by inhibiting translation or by degrading mRNA. We hypothesized that inhibiting miRNA that bind to the 3' UTR of the IGF-1 gene would exert neuroprotection. Of the several miRNA that bind to the IGF-1 3' UTR, we selected mir1 because of its inverse correlation with IGF-1 and cardiac hypertrophy and Let7f, because of its role in angiogenesis.

Methods: Adult female Sprague-Dawley rats were subject to MCA occlusion via stereotaxic injections of endothelin-1 directed toward this vessel. Four hours after occlusion, animals were injected intracerebroventricularly with anti-mir1 or anti-Let7f or scrambled oligos. All animals were terminated 5 days post stroke and assessed for infarct volume. RNA from cortical and striatal tissue was subject to qPCR for genes known to be regulated by mir1 and Let7f target genes.

Results: ICV infusions of mir1 antagomirs significantly reduced cortical, but not striatal, infarct volume as compared to animals that received scrambled oligos. Animals that received ICV injections of Let 7f antagomirs given 4h post stroke robustly reduced both cortical and striatal infarct volume. Cortical infarct volume was reduced by 70% and striatal infarct volume was reduced by 83% as compared to animals that received scrambled oligo controls. Additionally animals treated with Let7f showed improved performance on the sensory motor tasks (rotarod and vibrissae evoked forelimb placement). Cortical tissue from anti-Let7f injected animals also showed elevated expression of 11 genes that contain Let7f binding sites in the 3'-UTR. These include BDNF, Aquaporin-4, synaptotagmin, glial glutamate transporter and other genes associated with neuroprotection.

Conclusions: Collectively these data support the hypothesis that miRNA that bind to the 3' UTR of the IGF-1 gene promote neuroprotection.

References: Selvamani and Sohrabji, Neurobiol Aging, 2008; Selvamani and Sohrabji, J. Neurosci, 2010.

499

NON-INVASIVE QUANTITATIVE MRI MEASUREMENTS OF CEREBRAL VASCULAR REACTIVITY USING A COMPUTER-CONTROLLED STIMULUS IN CHILDREN WITH SICKLE CELL DISEASE

A. Kassner[1,2], J. Leung[1], F. Nathoo[3], S. Dorner[4], J.A. Fisher[4,5], M. Shroff[1], G. deVeber[6], S. Williams[7]

[1]Diagnostic Imaging, Hospital for Sick Children, [2]Medical Imaging, University of Toronto, [3]Respiratory Therapy, Hospital for Sick Children, [4]Thornhill Research Inc., [5]Physiology, University of Toronto, [6]Neurology, [7]Hematology, Hospital for Sick Children, Toronto, ON, Canada

Objectives: Sickle cell disease (SCD) is the major cause of stroke in children leading to mortality or long-term disability[1]. A non-invasive means of measuring cerebral blood flow (CBF) reserve would facilitate assessment and clinical management of these patients[2]. Cerebrovascular reactivity (CVR), an indirect measure of CBF reserve, is defined as the CBF response to a vasodilatory stimulus. BOLD MRI has been used as a surrogate for CBF changes in response to a vasoactive stimulus such as partial pressure of CO_2 (PCO_2). The recent introduction of precise control of end-tidal PCO_2 ($PETCO_2$) and PO_2 ($PETO_2$) via a computer-controlled, model-driven prospective end-tidal targeting (MPET) system[3] has improved the reliability of BOLD based CVR measures in healthy and diseased adults. However, within the pediatric population, CVR studies are not common. Therefore, the aim of this study was to introduce this technique to a pediatric population with SCD and demonstrate the type of information that can be derived compared to existing CVR methods.

Methods: 11 SCD patients (7-18 years) were imaged on a 1.5T MRI system (GE Healthcare, Milwaukee, WI). PCO_2 and PO_2 targets were achieved using an MPET system (RespirAct™, Thornhill Research Inc., Toronto, ON). Imaging was performed in synchrony with the MPET using a standard BOLD sequence (TE=40ms, TR=2s, FOV=220mm, matrix=64×64, slices=25, slice thickness=4.5mm, volumes=240, scan time=8min). The data was assessed by correlating the BOLD signal change in time with the measured $PETCO_2$ values of each subject, and then normalizing over the mean signal to produce a voxel-wise map of CVR. Anatomical imaging and MR angiography (MRA) was also performed. Structural MRI, MRA and CVR maps were assessed visually by an experienced neuroradiologist (MS) as well as an imaging scientist (AK).

Results: There was a strong concordance between CVR and angiographic findings. Five patients had angiographic abnormalities and also had reduced overall CVR, three of which exhibited steal effect in the corresponding parenchymal territories. The six patients who had a normal angiogram also revealed lower CVR compared to healthy individuals, but was generally less severe than those with angiographic abnormalities. All patients in this study had ischemic changes in the brain parenchyma as identified with structural MR imaging. Nine patients demonstrated mapped reductions in CVR extending beyond the ischemic lesions (as identified with MR structural imaging) into normal appearing brain parenchyma.

Conclusions: The combined application of controlled reproducible changes in PCO_2

and BOLD MRI for generating whole brain CVR maps is a promising method for imaging the distribution of vasodilatory reserve in children with SCD. No complications of the procedure were encountered in this observational study. In our small cohort of 11 patients, CVR provided information on the severity and distribution of hemodynamic compromise that could not be

obtained from traditional clinical assessment and structural imaging. Further studies will be required to assess the reliability of this information for clinical management.

References:

[1] Ganesan V et al. *Ann Neurology* 2003, 53:167-73,

[2] Mandell D et al. *Stroke* 2008, 39:2221-8,

[3] Slessarev M et al. *J Physiology* 2007, 581:1207-19.

502

PRECLINICAL EVALUATION AND QUANTIFICATION OF [^{18}F]MK-9470 AS PET RADIOLIGAND FOR THE TYPE 1 CANNABINOID RECEPTOR IN RAT BRAIN

C. Casteels[1,2], M. Koole[1,2], S. Celen[2,3], G. Bormans[2,3], K. Van Laere[1,2]

[1]Division of Nuclear Medicine, [2]IMIR, In Vivo Molecular Imaging Research Group, [3]Laboratory for Radiopharmacy, KU Leuven, Leuven, Belgium

Objectives: We characterized the *in vivo* and *ex vivo* kinetics of the type 1 cannabinoid receptor (CB1-R) PET tracer [^{18}F]MK-9470 in rat brain.

Methods: Seven Wistar rats (female, 331±103 g) were scanned on a FOCUS-220 system for 5 half-lives (600 min), following a bolus injection of [^{18}F]MK-9470 (58±7 MBq; >95.2 GBq/μmol). Arterial blood samples were collected and parent intact fraction measured by HPLC to determine the metabolite-corrected plasma input function. Displacement and blocking experiments were performed using cold MK-9470 (n=1) and the CB1-R antagonist SR141716A (n=2). Time-activity curves were extracted for the caudate-putamen, cerebellum and cortex. The [^{18}F]MK-9470 distribution volume (V_T) was used as outcome measure. The use of standardized uptake value (SUV) in the 60-80 post-injection interval as simplified method of quantification was also evaluated. Additionally, *ex vivo* studies were performed in ten animals to determine the presence of radiometabolite(s) in perfused brain homogenates at 10, 30, 60, 120 and 240 min post-injection using HPLC.

Results: The percent fraction of intact [^{18}F]MK-9470 in arterial samples was 60±28% at 10 min, 38±30% at 40 min and 13±14% at 210 min. *Ex vivo* brain [^{18}F]MK-9470 concentration was consistent with the known CB1-R distribution [2]. In contrast, the radiometabolite concentration was uniform across the whole brain and remained relatively constant from 10 to 240 min, ~13% of the total activity concentration.

In vivo displacement studies demonstrated reversible binding of [^{18}F]MK-9470, and blocking studies showed that more than 60% of the brain activity was CB1-R specific.

Based on these findings, a model with two parallel compartments (2C), one for intact ligand and one for the metabolite, and corresponding input curves was used to describe brain kinetics. [^{18}F]MK-9470 V_T values were 40.3±18.7 in the cerebellum, 42.8±14.9 in the caudate-putamen and 49.3±22.8 in the cortex. The whole brain metabolite V_T was 0.95±0.81. A weak correlation between $SUV_{60\text{-}80}$ and [^{18}F]MK-9470 V_T was found (R^2=0.30, p=0.01; Fig.1A) but no correlation was seen between $SUV_{60\text{-}80}$ and the radiometabolite V_T.

The [^{18}F]MK-9470 V_T was also calculated using a single tissue compartment model (1T) ignoring the radiometabolite contribution. Although V_T(1T) overestimates the [^{18}F]MK-9470 V_T(2C), V_T(1T) and V_T(2C) values were correlated (R^2=0.51; p< 0.001; Fig.1B). No correlation was found between $SUV_{60\text{-}80}$ and 1T V_T values.

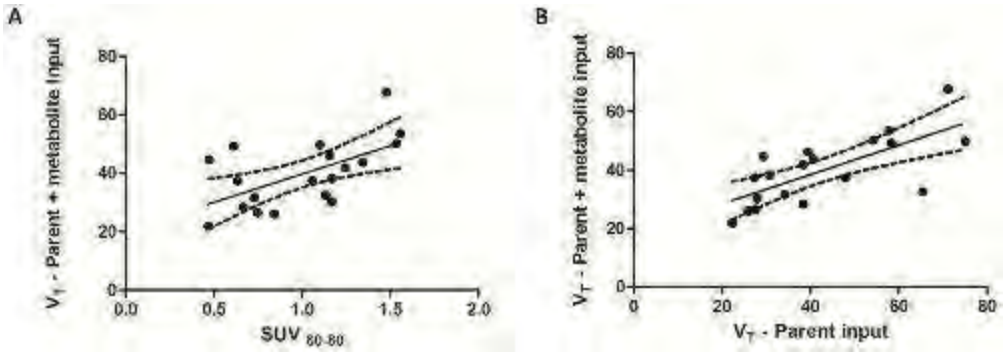

[VT 2C vs SUV and VT 1T]

Conclusions: A radiometabolite crossed the BBB, but displayed homogeneous distribution throughout the brain. The [^{18}F]MK-9470 signal accounts for 87% of the measured activity. Quantification of the tracer binding to CB1-R was possible using a model with the ligand and the radiometabolite input functions or the ligand input function alone. Additionally, a reasonable correlation between the [^{18}F]MK-9470 V_T

and SUV activity uptake was found.

References:

[1] Sanabria-Bohórquez SM. et al. Eur J Nucl Med Mol Imaging 2010.

[2] Herkenham M. et al. Proc Natl Acad Sci USA 1990.

503

COMPENSATORY INCREASE IN CEREBRAL PERFUSION PRECEDES ANGIOGENESIS AND LOSS OF ELASTICITY AFTER CEREBRAL ISCHEMIA USING PET/SPECT AND ULTRASONIC IMAGING

A. Martin[1,2,3], E. Macé[4], R. Boisgard[1,2], G. Montaldo[4], B. Thézé[1,2], M. Tanter[4], B. Tavitian[1,2]

[1]CEA,DSV,I2bm,SHFJ, [2]INSERM U1023 Université Paris Sud, Orsay, France, [3]Molecular Imaging Unit, CICbiomaGUNE, San Sebastian, Spain, [4]Institute Langevin,ESPCI ParisTech, Paris, France

Objectives: It is well known that after cerebral ischemia, brain suffers blood flow changes over time that have been correlated with functional recovery processes as compensatory growth of blood vessels to supply metabolic demand, inflammation and angiogenesis (Plate et al., 1999; Lin et al., 2008). Nevertheless, post-ischemic spatiotemporal changes of brain blood flow have not been fully investigated so far. Imaging methods may be helpful for a better characterization of the collateral circulation and angiogenesis providing angiographic information and perfusion data related to ischemic stroke evolution (Latchaw et al, 2003).

Methods: PET imaging with [^{15}O]H_2O, SPECT with [^{99m}Tc]HMPAO and Ultrafast Doppler imaging were performed to explore the changes in cerebral blood flow and Ultrasonic Shear imaging to detect viscoeslastic changes of ischemic brain during, and immediately (reperfusion) and 1, 2, 4 and 7 days after 2-hours transient middle cerebral artery occlusion (tMCAO) in rats. *In vivo* imaging studies were conducted in parallel with immunohistochemistry of rat brains.

Results: In the cerebral territory irrigated by the MCA, both PET and SPECT demonstrated a significant decrease of the signal during occlusion with respect to signals in the normal cerebral tissue. This was followed by a return to quasi-normal values during early reperfusion, after what signals dropped to 60% of control at day 1 and then rose steadily, reaching control values around day 2-4, and over shooting to twice the control values at day 7. This suggests a late compensatory increased perfusion in the ischemic area. Surprisingly, the same camel-shaped time course was observed in the contralateral, non-ischemic area. As a result, the ratio of PET and SPECT signals in the ischemic to contralateral areas varied from .5 at occlusion to 1.0 at day 4-7. Immunohistochemical analysis of CD31 positive vessels confirmed its results showing a steady increase of microvessel density on both brain hemispheres around 4-7 days after reperfusion. Cerebral blood flow increased in the ischemic area according with the loss of elasticity of the infarcted brain tissue measured by Shear Wave Imaging, appearing as a novel and relevant parameter for monitoring the evolution of cerebral ischemia over time. By contrast, Ultrafast Doppler intensity evidenced a significant increase at day 1, peaking at day 2 with respect to control values. This was followed by a reduction of the signals at day 4-7 to 50% of day 2, evidencing a high size increase of pre-existing vessel with a diameter greater than about 100 µm during first 48 hours after reperfusion.

Conclusions: Together, these findings evidenced size increase of pre-existing vessels during day 1 and day 2 after reperfusion followed by new vessel formation later on. Therefore, it suggests the existence of a preset pattern of brain vessel evolution in both ischemic territory and also in remote areas after cerebral ischemia which may support the removal of necrotic brain tissue and aid functional recovery.

References:

Plate, K. H (1999)*J. Neuropathol. Exp. Neurol*58; 313-320.

Lin, C., et al. (2008)*J Cereb Blood Flow Metab*28; 1491-1501.

Latchaw, R. E., et al. (2003)*Stroke*34; 1084-1104.

506

THE ROLE OF ASTROCYTES IN FUELING BRAIN DURING ACTIVATION

G.A. Dienel

Neurology, University of Arkansas for Medical Sciences, Little Rock, AR, USA

Brain activation increases energy demand and usually causes a disproportionate increase in consumption of glucose compared to oxygen, signifying enhanced flux of glucose into non-oxidative pathways. However, the fraction of glucose consumed by neurons and astrocytes in the activated tissue is not known, and the fate of blood-borne glucose is controversial. One model posits that astrocytes consume most of the glucose and release lactate for oxidation in nearby neurons, i.e., astrocyte-to-neuron lactate shuttle. An opposing model supports increased glucose utilization by neurons and a neuron-to-astrocyte lactate shuttle. In this system, glycogenolysis is predicted to raise glucose-6-phosphate concentration and feedback inhibit hexokinase while providing fuel for astrocytes; reduced astrocytic glucose use makes more blood glucose available for neurons. Experimental proof of cellular metabolism and cell-to-cell lactate trafficking within brain is technically difficult and remain to be established, but label trapping studies support the conclusion that lactate release rises during activation, and other studies support key roles for postsynaptic neurons in the energetics of metabolic activation.

In vivo studies in conscious rats have shown that glucose delivery to brain during rest and activation greatly exceeds demand and that blood flow quickly increases upon activation. Greater labeling of glutamate during activation indicates a rise in neuronal oxidative metabolism, but does not identify the labeling route. Increased glycogenolysis and acetate oxidation reveal that working astrocytes mobilize their fuel reserves and enhance fluxes in glycolytic and oxidative pathways. Also, glucose entry into the pentose-P shunt pathway rises during activation. Thus, flow of fuel into major pathways in both cell types is upregulated during brain activation. Due to the high yield of ATP from oxidative metabolism compared to glycolysis, it is difficult to simply assign ATP derived from either pathway to satisfy specific energy-requiring processes.

Evidence for rapid, substantial production and release of diffusible metabolites of glucose during brain activation has come from in vivo metabolic assays in several laboratories. Glucose utilization is underestimated by ~40-70% when assayed with [6-^{14}C]glucose compared to [^{14}C]deoxyglucose. Release of labeled and unlabeled lactate from brain to blood can account for 15-20% of the glucose entering brain. Focal registration of activation by trapping of metabolites of [^{14}C]glucose is enhanced by inhibition of gap junctions and lactate transporters, implicating metabolite spreading and lactate release from activated cells. Astrocytes are extensively coupled by gap junctions, and dye transfer within syncytial networks can involve 12,000 astrocytes and their perivascular endfeet. Lactate uptake into astrocytes from extracellular fluid is faster and greater than into neurons, and shuttling of lactate among gap junction-coupled astrocytes exceeds that to neurons; astrocyte-to-neuron glucose transfer can also occur. After microinfusion, ~30% of the [^{14}C]glucose-derived label recovered in brain is in the meninges, supporting the notion that perivascular routes are pathways for metabolite egress from brain. Thus, astrocytes can take up and disperse lactate within brain, discharge lactate into perivascular space, and serve as conduits for lactate release to blood. In vivo studies strongly support enhanced lactate production, trafficking, and release during activation compared to lactate use as fuel. (NS038230, DK081936)

507

EVOLUTION OF BLOOD BRAIN BARRIER PERMEABILITY IN PATIENTS WITH ACUTE ISCHEMIC STROKE: FROM ACUTE TO EARLY SUBACUTE PHASE

K. Huang[1], D. Mikulis[2], F. Silver[3], **A. Kassner**[1,4]

[1]Medical Imaging, University of Toronto, [2]Medical Imaging, [3]Neurology, Toronto Western Hospital, [4]Diagnostic Imaging, Hospital for Sick Children, Toronto, ON, Canada

Objectives: Blood-brain barrier (BBB) disruption following ischemia-reperfusion in stroke is associated with clinically important consequences including hemorrhagic transformation (HT). Previous data on BBB permeability changes after acute ischemic stroke (AIS) is limited to the first several hours and virtually non-existent in the subacute phase (days to weeks)[1,2]. We therefore reviewed our existing data that included data points from one hour to several days. Precise knowledge of BBB dynamics after ischemic stroke is of importance in considering future treatment possibilities including BBB leakage-blocking agents, and neuro-protective and neuro-restorative strategies[3]. The purpose of this study was to evaluate the time course of BBB disruption from acute to early subacute phase of AIS. We hypothesized that BBB permeability measured by DCE-MRI would continuously increase with time, a response caused initially by direct ischemic endothelial injury and subsequently by inflammatory reaction[4].

Methods: 39 patients (18 females, 21 males, 28-99 years) were included in the analysis. All patients received DCE-MRI as part of their acute stroke workup and were imaged on a 1.5T GE MR system (GE Healthcare, Milwaukee, USA) equipped with 8-channal head coil. 12/39 patients had follow-up DCE-MRI. 1/39 developed a new lesion at follow-up scan and was counted as 2 data points. Total data points were N=52. DCE-MRI parameters were as follows: dynamic 3D-GRE, FOV=240mm, 128×128 matrix, slice thickness=5mm, TR=5.9ms, TE=1.5ms, FA=35°, temporal resolution=9sec, volumes=31, acquisition time=4.48min. Data were analyzed on an independent workstation using in-house software (MR analyst) developed in MATLAB (MathWorks, Natick, MA). Regions of interest (ROIs) based on areas of ischemia were identified as regions of reduced diffusion on apparent diffusion coefficient maps. Coefficients of BBB permeability estimates (KPS) were calculated using a unidirectional, two-compartment kinetic model[1,5]. Mean KPS values (±SEM) were recorded for each ROI and each patient. KPS data were divided into three groups according to time between imaging and stroke onset and compared using a one-way ANOVA.

Results: MRIs in the first 16 hours showed mean KPS values in the lesion of 0.72 mL/100g/min. Scans taken between 16-50 hours showed mean KPS values in the lesion of 1.4 mL/100g/min, which was statistically significant when compared to MRIs taken in the first 16 hours (1.38±0.30 vs. 0.72±0.06 mL/100g/min, P=0.0007). After 50 hours, mean KPS values of the lesion decreased significantly (1.38±0.30 vs. 0.64±0.10 mL/100g/min, P=0.01).

Conclusions: Surprisingly, BBB permeability decreased after 50 hours. We believe that this represents transient stabilization of the initial ischemic endothelial BBB injury that stabilizes and reverses as a result of reperfusion[6]. The defect may again reappear due to the inflammatory phase in subsequent days to weeks after injury for which we currently do not yet have confirmatory data[6].

References:

1. Kassner A et al., AJNR, 2009. 30(10):p.1864-9;

2. Bang OY et al., Ann Neurol. 2007. 62(2):170-6;

3. Bauer AT et al., J Cereb Blood Flow Metab. 2010. 30(4):837-48;

4. Durukan A et al., Brain Res. 2009 Jul 14;1280:158-65;

5. Roberts, HC et al., Acad Radiol, 2001. 8(5):p. 384-91;

6. Huang et al 1999, Can J Neurol Sci. 1999. 26:298-304.

508

LONG-TERM ASSESSMENT OF MIGRATING NEURAL PROGENITOR CELLS IN MICE SUBJECTED TO CORTICAL ISCHEMIA

A. Osman[1,2], H.G. Kuhn[1]

[1]*Institute for Neuroscience and Physiology, University of Gothenburg, Gothenburg, Sweden,*
[2]*Faculty of Veterinary Medicine, University of Khartoum, Khartoum, Sudan*

Cortical ischemia has been reported to induce neural progenitor cells (NPC) migration toward the site of injury; however, whether these cells are capable to maintain the migratory response for longer period after the injury remains uncertain. Here, we analyzed the migratory response of neural progenitors at different time points after induction of a photothrombotic stroke lesion to the neocortex. Doublecortin (DCX), a microtubule-associated protein expressed in migrating progenitors, was assessed by immunohistochemistry and quantified stereologically. We detected elevated numbers of DCX positive cells (DCX^+) up to 3 months post-lesion in the striatum, whereas in the corpus callosum and the peri- infarct cortex DCX^+ cells were visible up to one year. The thymidine analogues chlorodeoxyuridine (CldU) and iododeoxyuridine (IdU) were utilized to birthdate the progenitor cells. CldU was applied to label cells generated during the first 10 days post-lesion, whereas IdU served to mark cells born within 2 weeks prior to perfusion. We only found DCX/ CldU co-labelling at 2 and 6 wks after injury, whereas DCX/ IdU co-expression was seen at all time points, indicating that the DCX^+ cells are recently generated progenitor cells rather than long- term DCX expressing cells. Finally, we determined the orientation of the leading processes of DCX^+ cells, and observed that the migrating cells are mostly aligned along the corpus callosum fibre tract at all time points; however, in the peri-infarct cortex they align parallel to the infarct border. From these results, we suggest that neural progenitors might have a role in replacing the dead cells and promote neural plasticity.

509

OSMOTIC AGENTS LOWER INTRACRANIAL PRESSURE INDEPENDENTLY OF REDUCING CEREBRAL BLOOD VOLUME

M. Scalfani[1], R. Dhar[1], A. Zazulia[1,2], T. Videen[1,2], W. Powers[3], M. Diringer[1,4]

[1]Neurology, [2]Radiology, Washington University in St. Louis School of Medicine, Saint Louis, MO, [3]Neurology, University of North Carolina at Chapel Hill School of Medicine, Chapel Hill, NC, [4]Neurological Surgery, Washington University in St. Louis School of Medicine, Saint Louis, MO, USA

Background: The mechanism by which osmotic agents such as mannitol and hypertonic saline reduce cerebral edema and intracranial pressure (ICP) has not been fully elucidated. We have previously demonstrated that brain volume is reduced when mannitol is administered to stroke patients with cerebral edema. There are two proposed mechanisms by which this reduction in intracranial volume (and ICP) occurs: (1) by reducing brain cellular and interstitial water content or (2) by reducing cerebral blood volume (CBV). This second theory is based on experimental models demonstrating that boluses of mannitol reduce blood viscosity and raise blood pressure, leading to increased cerebral blood flow (CBF). This rise in CBF induces reflex vasoconstriction, thereby reducing CBV and ICP. Hypertonic saline may also work in part through this rheological mechanism.

Objective: We used ^{15}O-PET to determine if mannitol or 23.4% saline (HS) acutely lowered CBV and how their response differed in a series of patients with severe brain injury.

Methods: We enrolled 21 patients with traumatic brain injury (n=8), ischemic (n=9) or hemorrhagic (n=4) stroke who were receiving osmotic therapy to treat intracranial hypertension or cerebral edema. Subjects were randomized to receive an equi-osmolar dose of either mannitol (1 g/kg, n=13) or HS (0.686 ml/kg, n=8). The study was timed so that the osmotic agent was administered at the same time they would normally have received their next dose of osmotic therapy. PET measurements of global CBV, CBF, oxygen extraction fraction (OEF) and cerebral metabolic rate for oxygen ($CMRO_2$) were obtained before and 1 hour after receiving osmotic therapy. At the time of each study, physiologic data were recorded (including ICP, when available). Intravascular volume was maintained by replacement of any net diuresis before the second PET study. Response to osmotic therapy was analyzed using 2-tailed paired t-tests while mannitol vs. HS groups were compared using repeated measures ANOVA.

Results: Baseline mean arterial pressure (MAP), cerebral perfusion pressure (CPP), ICP, CBF, CBV, OEF and $CMRO_2$ were similar in both treatment groups. Blood pressure did not change after osmotic therapy in either group. In the subset who had ICP monitoring, ICP fell (22.3±4.4 to 14.8±6.5 mm Hg, p=0.001) and CPP rose (83.4±16.6 to 89.7±17.9 mm Hg, p=0.01). CBF was increased in the mannitol group (34.0±11.3 to 37.2±16.6 ml/100g/min, p=0.04) but not in the HS group (32.8±14.6 to 33.9±13.4, p=0.61). However, CBV did not decrease, but was actually higher after osmotic therapy (3.4±0.8 to 3.7±1.0 ml/100g, p=0.03). This rise in CBV was evident in the mannitol group (3.6±0.7 to 4.0±1.0, p=0.04) but not in the HS group (3.1±0.8 to 3.2±0.8, p=0.537). However, the change in CBF and CBV with treatment did not differ significantly between mannitol and HS groups; this could be a result of small sample size. OEF and $CMRO_2$ did not change with either therapy.

Conclusion: Neither mannitol nor 23.4% saline lower CBV, arguing that their ability to reduce

ICP is not mediated through vasoconstriction but may occur due to other mechanisms such as a reduction in brain water.

511

NITRIC OXIDE DONORS IMPAIR ASTROCYTIC GAP JUNCTIONAL COMMUNICATION

N.F. Cruz, K.K. Ball, G.A. Dienel

Neurology, University of Arkansas for Medical Sciences, Little Rock, AR, USA

Objectives: Gap junctional communication in experimental diabetes is reduced by about 50% when astrocytes are grown in high (25 mmol/L) compared to low (5.5 mmol/L) glucose, and this decrement lags by several days the rise in reactive oxygen-nitrogen species (Gandhi et al., 2010). High glucose-induced inhibition of gap junctional dye transfer was prevented but not normalized by treatment with a superoxide dismutase mimetic or by inhibition of nitric oxide synthase, consistent with oxidative-nitrosative stress as a causative factor. Goals of the present study were to determine if dye transfer through gap junctions in astrocytes grown in high glucose could be restored by a reducing agent, if nitric oxide donors are sufficient to inhibit dye transfer in low glucose cultures, and if connexin protein levels are altered by growth in high glucose.

Methods: Astrocytes from cerebral cortex of one-day-old rats were grown on cover slips for 2-3 weeks in high or low glucose. A single astrocyte was impaled with a micropipette containing 4% Lucifer yellow, dye was allowed to diffuse for 2 min, and dye-labeled area determined (Gandhi et al., 2010). Immediately prior to dye transfer assay, high glucose cultures were treated with vehicle or dithiothreitol (10 mmol/L) for 10 min. Separate batches of low glucose cultures were treated for 1h prior to the dye transfer assay with vehicle and either sodium nitroprusside (200 µmol/L) or spermine-NO (250 µmol/L). Levels of immunoreactive connexin (Cx) proteins were evaluated by SDS-PAGE/Western blotting.

Results: Growth of astrocytes in high glucose medium reduced dye transfer by about 75%, from 20,110 ± 8,302 μm^2 (mean ± SD, n=11) to 5,303 ± 4,810 μm^2 (n=17) ($P< 0.001$). Brief treatment of high-glucose cultures with dithiothreitol normalized the dye-labeled area (21,103 ± 7,776 μm^2, n=21, $P< 0.001$, ANOVA and Bonferroni test). Treatment of a different batch of low glucose cultures with nitroprusside reduced the dye-labeled area by 65%, from 12,907 ± 6,718 μm^2 (n=22) to 4,573 ± 3,557 μm^2 (n=27) ($P< 0.001$, t-test). Treatment of a third low glucose culture batch with spermine-NO diminished the dye transfer area by 47%, from 5,581 ± 3,463 μm^2 (n=44) to 2,947 ± 1,380 μm^2 (n=28) ($P< 0.001$, t-test). Western blots showed no change in Cx26 level, a modest reduction of Cx30 level, and increased Cx43 level in high compared to low glucose cultures.

Conclusions: Gap junctional communication in cultured astrocytes is quite variable within and among culture batches. The hyperglycemia-induced decrement in dye transfer is rescued by dithiothreitol, consistent with oxidative-nitrosative modification of cellular proteins. Nitrosative stress is sufficient to reduce trafficking of material among coupled astrocytes in low glucose cultures. Gap junctional channels comprised of Cx30 are impermeant to Lucifer yellow (Manthey et al., 2001), whereas this dye goes through Cx26 and Cx43 channels (Elfgang et al., 1995). Thus, reduced Lucifer yellow transfer must be related to unidentified changes affecting Cx43 and/or Cx26 channels, not down-regulation of Cx30. (DK081936,NS038230)

References:

Gandhi et al.(2010) ASN Neuro 2(2):art:e00030.doi:10.1042/AN20090048

Elfgang et al.(1995) J Cell Biol 129:805-817.

Manthey et al.(2001) J Membr Biol 181:137-148.

512

IN VIVO IMAGING OF VASCULAR CELL ADHESION MOLECULE-1 IN A MOUSE MODEL OF CEREBRAL ISCHEMIA

M. Fréchou[1], **V. Beray-Berthat**[1], G. Louin[2], J.-S. Raynaud[2], S. Mériaux[3], M. Plotkine[1], C. Marchand-Leroux[1], E. Lancelot[2], I. Margaill[1]

[1]Pharmacologie de la Circulation Cérébrale EA4475, Université Paris Descartes, UFR des Sciences Pharmaceutiques et Biologiques, Paris, [2]Unité de Recherche Biologique, Division Recherche, Guerbet, Roissy, [3]Direction des Sciences du Vivant, CEA Neurospin, Saclay, France

Objective: Stroke is a multifactorial pathology for which nowadays there isn't any neuroprotective treatment. As inflammation plays a critical role in cerebral ischemia[1,2], the detection of inflammatory processes would therefore be of great interest, particularly in order to design individual therapeutic strategies after stroke. We have developed a specific contrast agent, an USPIO (ultrasmall particle of iron oxide) which targets a component of the neuroinflammatory response, namely VCAM-1 (vascular cell adhesion molecule-1). The aim of this study was to determine the relevance of this contrast agent to visualise VCAM-1 in MRI in a model of transient cerebral ischemia in mouse.

Methods: Ischemia was carried out in male Swiss mice by transient (1h) intraluminal occlusion of the left middle cerebral artery (MCA)[3]. In a first set of experiments, VCAM-1 expression was detected by immunohistochemistry at 6h, 24h and 72h post-ischemia (n=4-5). In a second set of experiments ischemic mice were intravenously injected with 100 µmol/kg of VCAM-1-USPIO or non-targeted USPIO 5h after the surgery. MRI (7T) was performed 6h (n=2-6) or 24h (n=2-5) after ischemia. Control ischemic animals without injection of USPIO were also included in our study (n=4-6). Just after MRI, mice were euthanized and their brains removed for *ex vivo* MRI (2.35T). Immunohistochemistry was performed on 20µm-thick cryostat-cut sections in order to search the presence of USPIO by Perls technique (revealing particles of iron) and the expression of VCAM-1 by immunohistochemistry.

Results: Time course of VCAM-1 on brain sections showed positive vessels 6h after ischemia and a significant up-regulation 24h after ischemia in the cortex and striatum of both hemispheres ($P < 0.05$). *In vivo* and *ex vivo* MRI showed at 6h and 24h hypointense foci corresponding to USPIO in the injured hemisphere of ischemic mice with VCAM-1-USPIO. Post-mortem analysis of these brains showed a co-localisation of the USPIO and its target VCAM-1. Ischemic animals without USPIO or with the non-targeted USPIO did not show hypointense foci on MRI. Further histological examination showed only the presence of VCAM-1.

Conclusion: Our USPIO seems able to detect VCAM-1 in our model of cerebral ischemia. However, the signal observed in MRI needs to be confirmed histologically by a more specific method than the Perls technique. This kind of contrast agent could be an interesting clinical tool for the design and the follow-up of specific therapeutic strategies targeting the inflammatory phenomenon.

References:

1. Frijns CJ, Kappelle LJ. (2002) Inflammatory cell adhesion molecules in ischemic cerebrovascular disease. *Stroke*. 33:2115-22.

2. Huang J, Upadhyay UM, Tamargo RJ. (2006) Inflammation in stroke and focal cerebral ischemia. *Surgical Neurology*. 66:232-245.

3. Haddad M, Rhinn H, Bloquel C, Coqueran B, Szabo C, Plotkine M, Margaill I. (2006) Anti-inflammatory effects of PJ34, a poly(ADP-ribose) polymerase inhibitor, in transient focal cerebral ischemia in mice. *Br J Pharmacol*. 149:23-30

514

BRAIN ENERGY METABOLISM IN MIGRAINE WITHOUT AURA INVESTIGATED BY ^{31}P- AND ^{1}H-MRS

H. Reyngoudt[1,2], E. Achten[1,2], B. Descamps[1,2], A. Dierickx[1,2], Y. De Deene[3], K. Paemeleire[4,5]

[1]Radiology and Nuclear Medicine, [2]Ghent Institute for Functional and Metabolic Imaging, [3]Laboratory for Quantitative Nuclear Magnetic Resonance in Medicine and Biology, [4]Basic Medical Sciences, Ghent University, [5]Neurology, Ghent University Hospital, Ghent, Belgium

Objectives: Magnetic resonance spectroscopy (MRS), a technique to obtain biochemical information non-invasively, has been performed in several migraine studies. Most of these studies were performed in migraine with aura (MA) [1-3]. Both proton MRS (^{1}H-MRS and functional ^{1}H-MRS) and phosphorus MRS (^{31}P-MRS) studies have been performed. The aim of our project was to perform absolute quantification of metabolites with ^{31}P-MRS and ^{1}H-MRS interictally in a homogeneous group of migraine without aura (MO) patients. We were interested in both resting state brain energy metabolism and the metabolic effects of prolonged photic stimulation (PS).

Methods:

Study 1: resting-state ^{31}P-MRS.

Study 2: resting-state ^{1}H-MRS.

Study 3: functional ^{1}H-MRS, i.e. PS study with black-and-white checkerboard stimulus at 8 reversals/second for 12 minutes.

Subjects: In each study we compared at least 20 MO patients with at least 20 controls. Patients experienced 2-8 attacks per month, were not on any prophylactic medication and were attack-free for at least 48 hours.

MRS: Spectra were acquired in the medial occipital lobe on a 3T Siemens TrioTim system with a double tuned ^{31}P/^{1}H birdcage head coil.

Quantification: Spectra were analyzed using jMRUI and Siemens software. Absolute quantification was performed using an external reference.

Statistics: A suitable statistical analysis was performed for all three studies (unpaired Student's *t*-tests for the resting state studies, repeated-measures ANOVA for the PS study).

Results: A significantly decreased phosphocreatine (PCr) was found as in previous studies. Whereas adenosine triphosphate (ATP) was considered to be constant in previously published work [2], we found a significant decrease in ATP in MO patients in study 1. No significant changes in inorganic phosphate, adenosine diphosphate, pH and magnesium were found between MO patients and controls. No significant differences in proton metabolites (N-acetyl aspartate, creatine, choline and myo-inositol) were observed between MO patients and controls in study 2. Resting state ^{1}H-MRS did also not show quantifiable lactate (Lac) in all subjects. Moreover we did not observe any significant differences in proton metabolites, including for Lac, between MO patients and controls, during and following PS in study 3.

Conclusions: Resting state ^{31}P-MRS demonstrated a significant decrease in the high-energy phosphates ATP and PCr, implying that brain energy metabolism in MO patients is impaired. The actual decrease in ATP adds further strength to the theory of the presence of a mitochondrial component in the pathophysiology of migraine. Since we did not observe Lac increases before, during and after PS, we can state these results argue against a significant switch to non-aerobic glucose metabolism in the resting state as well as during long-lasting PS of the visual cortex in MO patients. This observation is in contrast with studies in MA patients, where an increased Lac was found indeed [2,3], which implies that Lac increases are linked with aura symptoms rather than with migraine in general.

References:

[1] Neurology 1992;42:1209-1214

[2] Neurology 1996;47:1093-1095

[3] Cephalalgia 2005;30:552-559

515

ESTIMATION OF INTERSUBJECT VARIABILITY OF CEREBRAL BLOOD FLOW MEASUREMENTS USING MAGNETIC RESONANCE IMAGING AND POSITRON EMISSION TOMOGRAPHY

O. Henriksen[1], H.B.W. Larsson[1], A.E. Hansen[2], J.M. Grüner[3], I. Law[3], E. Rostrup[1]

[1]Functional Imaging Unit, Department of Clinical Physiology, Nuclear Medicine, [2]Dept. of Radiology, Glostrup Hospital, Glostrup, [3]Department of Clinical Physiology, Nuclear Medicine and PET, Rigshospitalet, Copenhagen, Denmark

Introduction: Quantitative cerebral blood flow (CBF) measurements can be performed by different methods, including positron emission tomography (PET) and various magnetic resonance imaging (MRI) techniques. Large variability in CBF measurements are often reported in studies of healthy subjects, irrespective of the method applied. Knowledge on the normal variability of CBF measurements is of key importance when designing studies involving CBF measurements.

Aims: To assess the within and between subject variability of repeated CBF measurements using three different MRI techniques: arterial spin labelling (ASL), dynamic contrast enhanced T1 weighted perfusion MRI (DCE) and intravascular velocity mapping (VM).

Methods: 18 healthy subjects (10 female and 8 male) aged 20-30 years (median age 23 years) were studied. In each subject repeated measurements using each of the three MRI techniques were performed within a single session. In 10 of the subjects repeated CBF measurements by ^{15}O labeled water PET had recently been performed and were also analyzed for comparison. Global CBF in mL/100g/min was calculated for each method. Between and within subject variability (s_{betw} and s_{with} respectively) was estimated using linear mixed model analysis. Coefficients of variation CV_{betw} and CV_{with} are calculated as s_{betw} and s_{with} respectively divided by the mean CBF value. All CBF values are reported as mL/100g/min.

Results: Results are presented in table 1. Good method agreement was observed with respect to mean values and between subject variability, whereas within subject variability varied substantially across modalities. VM and ASL yielded the lowest within subject variability indicating better reproducibility compared to PET and DCE. Only CBF measurements by VM and DCE was significantly positively correlated.

	Mean	Bias	p-value	s_{betw}	s_{with}	CV_{betw}	CV_{with}
VM	64.59§	0.74	0.671	10.91	4.68	16.9%	7.2%
ASL	37.27	-0.3	0.643	5.84	1.78	15.7%	4.8%
DCE	47.04	-3.77	0.115	8.37	6.65	17.8%	14.1%

PET	41.19	2.23	0.757	6.69	4.99	16.2%	12.1%

[Table 1. CBF measurements by different methods.]

Conclusions: These findings confirm a large between subject variability in CBF measurements that does not vary much across methods. In contrast, reproducibility is highly dependant on the method used. Limited method agreement despite significant between subjects variability may indicate that subject-method interaction contributes to variability of CBF measurements.

516

ROLE OF PERIPHERAL AND CENTRAL PAI-1 INHIBITION IN SECONDARY BRAIN DAMAGE AFTER EXPERIMENTAL BRAIN INJURY IN MICE

E.-V. Schaible, I. Petkovic, K. Engelhard, C. Werner, S.C. Thal

Department of Anesthesiology, University Medical Center of the Johannes Gutenberg University, Mainz, Germany

Objectives: The formation of microthrombi after experimental traumatic brain injury occurs about 1h after trauma[1] and can be observed by intra-vital microscopy in the pericontusional tissue[2]. This may lead to an aggravation of the secondary lesion volume via vascular occlusion and parenchymal ischemia. Plasminogen activator inhibitor (PAI)-1 inhibits the transformation of plasminogen to plasmin which leads to an enhanced clot formation. PAI-1 expression post injury is strongly upregulated with a 4fold increase after 3 hours and a 360fold peak after 12 hours[3]. The present study was planned to characterize the peripheral and central functional role of PAI-1 in secondary brain damage after traumatic brain injury.

Methods: Traumatic brain injury was induced in male C57Bl/6N mice anesthetized with isoflurane via pneumatic brain trauma (controlled cortical impact, CCI). The influence of peripheral PAI-1 inhibition on secondary brain damage was determined in animals randomized to vehicle solution (0.5 % DMSO) or to the PAI-1 inhibitor PAI-039 (1 mg/kg KG; sc injection 30 min and 6 h post CCI). The central effect of PAI-1 inhibition was investigated by intracerebroventricular injections in the ipsilateral cortex 15 min prior CCI of vehicle solution (0.5 % DMSO) or PAI-039 (0.1 mg/kg KG). The primary lesion was evaluated 15 min after CCI and the secondary contusion volume was defined after 24 h. Both were analyzed in Nissl stained sections. Statistics: ANOVA on ranks, $p < 0.05$

Results:

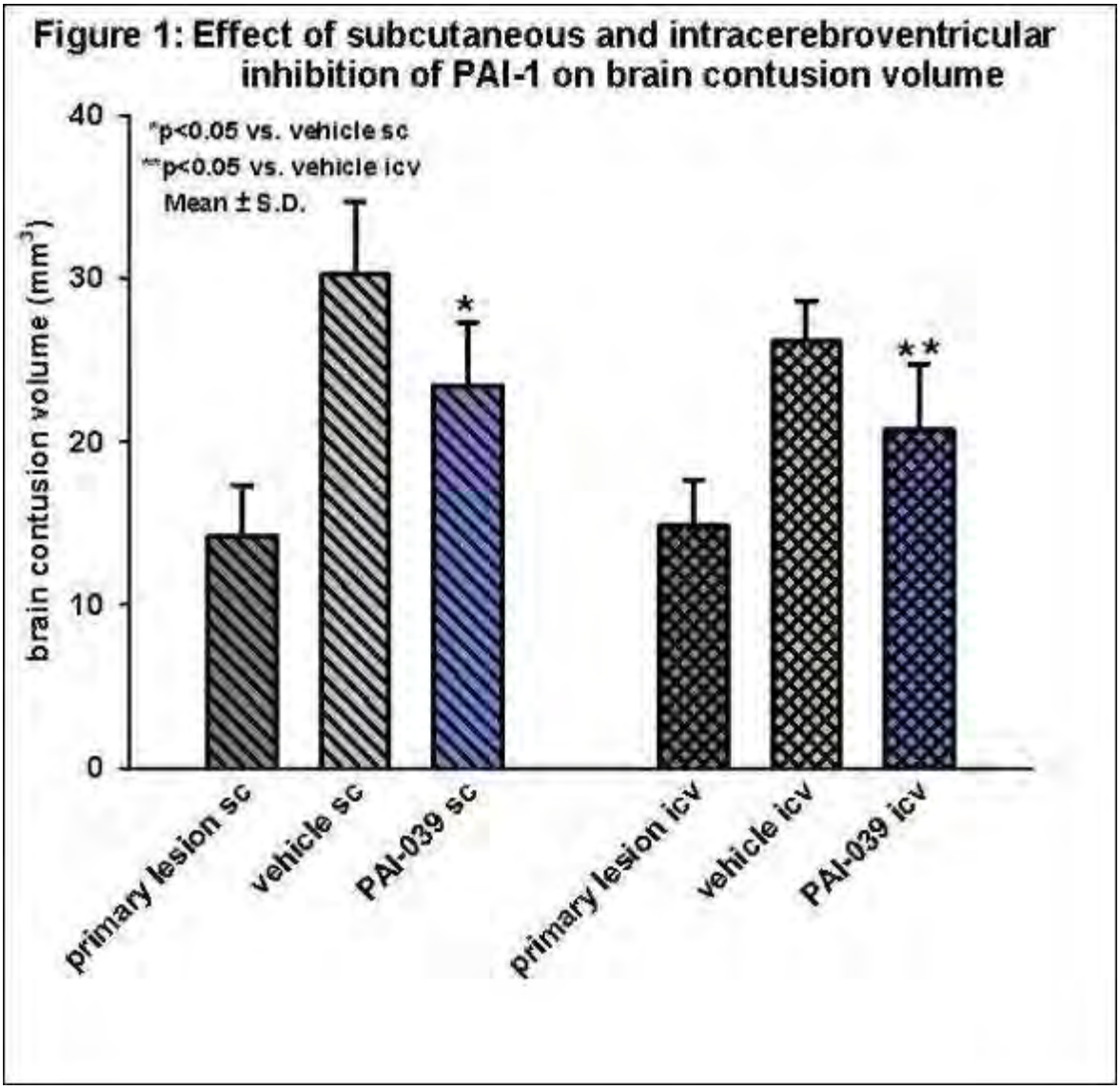

[Effect of sc and icv inhibition of PAI-1 on tbi]

Conclusions: PAI-1 as an inhibitor of tPA and uPA blocks the fibrinolysis and enhances clot formation which may interfere the balance between pro- and anticoagulation after traumatic brain injury. The inhibition of PAI-1 might deteriorate brain damage by increasing the propensity for bleeding or could reduce brain damage by prevention of clots which potentially obstruct the capillaries. In the present study the subcutaneous and central inhibition of PAI-1 decrease the secondary brain contusion volume possibly by restoring the fibrinolytic system. This might reduce the amount of thrombi which obstruct the vessels in the penumbra of the primary lesion. Furthermore, the risk for intracerebral bleeding was not increased by inhibition of PAI-1. The data demonstrate the importance to take care of the fibrinolytic system to limit the secondary brain lesion.

References:

1. W. D. Dietrich, O. Alonso, M. Halley, J Neurotrauma 11, 289-301 (1994).

2. S. M. Schwarzmaier, S. W. Kim, R. Trabold, N. Plesnila, J Neurotrauma 27, 121-130 (2010).

3. E.-V. Schaible, I. Petkovic, K. Engelhard, C. Werner, S. C. Thal, Annual Meeting of the American Society of Anesthesiologists, (2010), Abstract CD:A1246

520

QUANTIFICATION OF GLYT1 IN RHESUS MONKEY BRAIN USING [^{18}F]MK-6577 WITH VENOUS BLOOD SAMPLING AND AN IMAGE DERIVED INPUT FUNCTION

S.M. Sanabria-Bohórquez, A.D. Joshi, M.A. Holahan, L. Daneker, K. Riffel, M. Williams, T.G. Hamill

Imaging, Merck, West Point, PA, USA

Objective: [^{18}F]MK-6577 is a potent and selective inhibitor PET tracer for the glycine transporter 1 (GlyT1) which has been implicated in the pathophysiology of schizophrenia. Although differences in the ligand kinetics can be expected between non-human primates and humans, the tracer preclinical evaluation provides valuable information supporting protocol design and quantification in the clinical space. Here we propose a modeling approach to estimate the [^{18}F]MK-6577 input function required for the quantification of the tracer binding in the monkey brain without arterial blood sampling.

Methods: The proposed method takes advantage of the agreement between the [^{18}F]MK-6577 concentration in arterial and venous plasma from ~5 min following tracer IV bolus administration. Direct use of the tracer input curve measured in venous blood could result in significant bias in estimation of the tracer binding parameters (unpublished observations and Syvänen et al.). We model the early times of the tracer input curve by adding an exponential term $Ate^{-B(t-Tdelay)}$ to the measured venous curve (Sanabria-Bohórquez et al.). Assuming all brain regions share the same input, simultaneous fitting of several tissue time-activity curves to a compartment model was applied. The parameters of the exponential function A, B and T_{delay} were used as coupling variables. Regional tracer binding quantification was performed after estimation of the image derived [^{18}F]MK-6577. Although this method does not use information from the blood pool in the PET images, it uses the tracer kinetics throughout the brain and thus it can be considered an image-derived input function (IDIF) approach.

PET studies were conducted in three rhesus monkeys (10-16 kg) on an ECAT EXACT HR+ (CTI, Knoxville, TN). Catheters were placed for arterial and venous blood sampling and total activity and tracer fraction was measured in both sample sets. Dynamic emission scans (2h duration) were performed following injection of ~185 MBq of [^{18}F]MK-6577. Animals were studied under baseline conditions. Additionally, two occupancy studies with a GlyT1 inhibitor were performed in two of the animals.The IDIF parameters were estimated using the tracer kinetics in the cerebral cortex, striatum, thalamus, midbrain, pons, cerebellum nuclei and cerebral white matter. The regional [^{18}F]MK-6577 total volume of distribution V_T was calculated using Logan graphical analysis using the measured arterial and the image-derived input curves.

Results: Good agreement was found between the image derived and the measured arterial plasma curves. The figure shows an example of the measured tracer concentration in arterial and venous samples and the IDIF curve. Similar results were obtained in the other studies. V_T estimates using both curves were highly correlated (r^2~1.00). The slope and intercept values of the linear regression were in the interval [0.92, 1.06] and ±0.02, respectively.

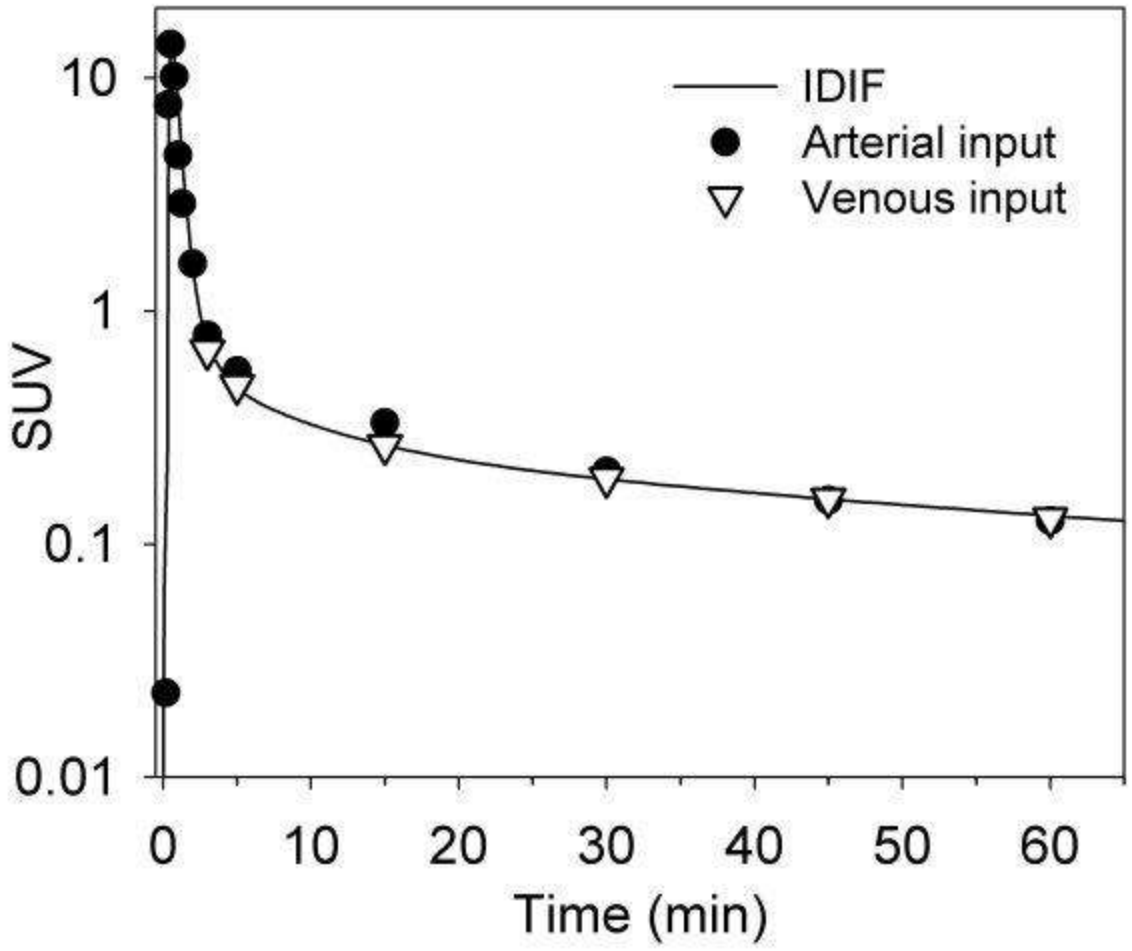

[Measured and image derived input curves]

Conclusion: The proposed method is suitable for [^{18}F]MK-6577 binding quantification in rhesus monkey brain requiring only a few venous samples to measure total activity and tracer metabolites.

References: Sanabria-Bohórquez SM, et al. 2003. Mol Imaging Biol 5:72-78.Syvänen et al. 2006. Eur J Clin Pharmacol 62:839-848.

521

AGED GARLIC EXTRACT AND S-ALLYLCISTEIN PREVENT CELL DEATH IN AN IN VITRO CHEMICAL HYPOXIA MODEL

M.E. Chanez-Cardenas[1], M. Orozco-Ibarra[2], B. Pineda[3], P.D. Maldonado-Jimenez[1], P. Aguilera[1], J. Pedraza-Chaverri[2,4]

[1]Patologia Vascular Cerebral, [2]Neurobiologia Molecular y Celular, [3]Neuroinmunologia, Instituto Nacional de Neurologia y Neurocirugia, Mexico, [4]Biologia, Universidad Nacional Autonoma de Mexico, Ciudad de Mexico, Mexico

Introduction: Using the middle cerebral artery occlusion model (MCAO) in rats, we have shown that aged garlic extract (AGE) delays the effects of ischemia/reperfusion- induced neuronal injury. AGE controls the free-radical burst induced by reperfusion and preserves antioxidant enzyme activity (1). Similar evidence was observed in a MCAO model using S-allylcistein (SAC) through the reduction of lipid peroxidation (2). In this work we evaluated the effect of AGE and SAC in an in vitro hypoxia model with $CoCl_2$ in PC12 cells. We observed that both compounds considerably reduced $CoCl_2$-induced cell death. The effect of AGE and SAC on mitochondrial activity, DNA fragmentation and apoptosis was evaluated.

Methods: PC12 cells were cultured and subjected to 24 or 48 h incubation with 0.5 and 1.0 mM $CoCl_2$ to generate chemical hypoxia. $CoCl_2$ and AGE (1%) or SAC (10 mM) co-incubation for 24 or 48 h were used for all determinations. Cell viability was determined by MTT assay. $SubG_o$ peak method and apoptosis were measured by PI and Annexin V assays by flow citometry (FC). For $SubG_o$ PI (50 ug/mL) cells were fixed in 70% ethanol. An Annexin V-PE and 7-AAD kit was used to early apoptosis determination. 10,000 total events were acquired with Facscalibur FL-4 (BD). Cell QuestPro and Flow Jo programs were used for data analysis.

Results: 10 mM SAC and 1% AGE were used based on toxicity assays (1-20 mM SAC and 0.25-1% AGE). 24 h: 0.5 and 1.0 mM $CoCl_2$ reduced cell viability to 60 and 50 % respectively, compared to control cells. $CoCl_2$-SAC 24 h co- incubation restored almost completely cell viability at 0.5 mM $CoCl_2$ but not at 1.0 mM $CoCl_2$. The same behavior was observed with AGE, 90% and 70% of MTT reduction was observed at 0.5 and 1.0 mM $CoCl_2$ respectively. 48 h: $CoCl_2$ reduced to 50 and 20% the MTT values at 0.5 and 1.0 mM $CoCl_2$, while SAC restores values to 90 and 50% respectively. $CoCl_2$-AGE incubation restored to 80 and 60% MTT reduction at 0.5 and 1 mM $CoCl_2$. FC: At 24 h 1.0 mM $CoCl_2$, $SubG_o$ cells increased from 2.53% (CT) to 23 %. This increase was reduced with AGE and SAC to control $SubG_o$ values. $CoCl_2$ 0.5 and 1.0 mM (48 h) rises $SubG_o$ values to 40 and 60 % respectively. SAC reduced to control values at both $CoCl_2$ concentrations. At 1.0 mM $CoCl_2$, AGE reduced from 60% to 34.5% $SubG_o$ values.

Conclusions: The reduction in cell viability observed with $CoCl_2$ at 24 and 48 h in PC12 cells where importantly prevented with 10 mM SAC or 1% AGE at both incubation times. The use of PI confirmed these results by the decrease of SubGo values when SAC or AGE were used. Cells with fragmented DNA are probably in apoptosis, and Annexin V assays are being performed to completely determine if the cells are undergoing apoptosis.

1. P. Aguilera et al (2010) Phytomedicine 17: 241-247
2. Numagami, Y. & Ohnishi, S.T. (2001). J Nutr 131:1100S-1105S

522

BEDSIDE DIFFUSE OPTICAL TOMOGRAPHY OF FUNCTIONAL CONNECTIVITY IN NEONATES

S.L. Ferradal[1], B.R. White[2], S.M. Liao[3], T.E. Inder[3], J.P. Culver[4]

[1]Biomedical Engineering, [2]Physics, [3]Pediatrics, [4]Radiology, Washington University in St. Louis, Saint Louis, MO, USA

Objectives: Characterizing the development of functional brain architecture in premature infants may provide valuable new insight and better define the functional lesions associated with prematurity that lead to neurodevelopmental impairments. Recent fcMRI studies have begun to establish the patterns of longitudinal functional network development in infants [1]. However, MRI techniques pose significant logistical barriers for use in preterm infants, largely related to challenges in transportation to the MRI scanner. Having previously developed functional connectivity diffuse optical tomography (fc-DOT) methods in adults [2], in this work, we apply these techniques to newborn infants at the bedside.

Methods: A high-density optode array consisting of 18 sources and 16 detectors was placed over the visual cortex (Fig. 1A). Resting-state data was collected from three term and four premature infants. One preterm infant had a unilateral occipital stroke (Fig. 1B). All other infants were healthy. DOT measurements were converted to 3D images of brain hemodynamics ([HbO_2] and [HbR]) using a sensitivity matrix derived from finite-element modeling. In this work a neonatal head atlas was used consisting of twelve T2-weighted MR images of healthy term-born infants (Fig. 1A). Resting-state brain function was analyzed using different approaches. First, two seeds (left and right visual cortex) based on anatomical landmarks were used to generate seed-to-voxel correlation maps. Second, we performed independent component analysis (ICA) using between 10 to 20 independent components. For each subject, a component corresponding to the visual resting-state network was chosen by visual inspection. Finally, we quantified the amplitude of low frequency fluctuations (ALFF) at each voxel. As it is hypothesized that hemodynamic oscillations below 0.1 Hz come from resting-state neural activity, we expect this calculation to give us a local measure of intrinsic brain activity.

Results: Correlation analysis on the healthy infants showed bilateral correlation patterns (Fig. 1C-D). In the infant with the stroke, the functional connectivity maps revealed that each seed only correlates with the ipsilateral hemisphere (Fig. 1E). ICA analysis also showed bilateral components in the healthy infants (Fig. 1F-G). Conversely, we could see only a component corresponding to the right hemisphere in the infant with the stroke (Fig. 1H). Analysis of low frequency fluctuations revealed similar bilateral patters in the healthy infants (Fig. I-J). In the infant with the brain injury, however, there is low frequency intensity only in the healthy hemisphere (Fig. 1K).

Conclusions: We have shown that imaging of functional connectivity of both term and preterm neonates is possible within the clinical environment. We expect that in the future fc-DOT can be used longitudinally to detect functional deficits before anatomical lesions are visible on conventional neuroimaging scans, allowing clinicians to assess brain function and track functional development at the bedside.

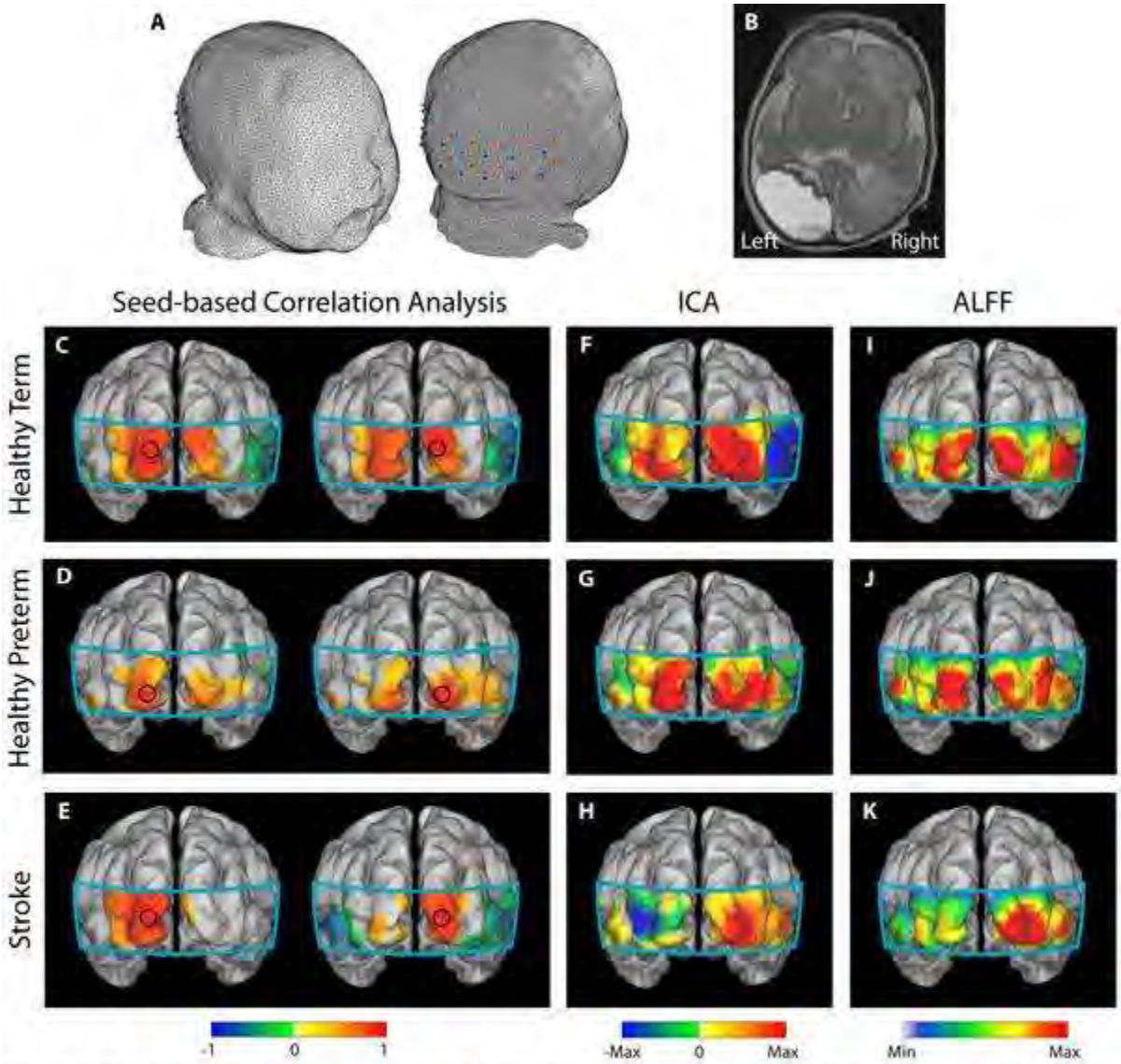

Figure 1: Neonatal fc-DOT. (The area covered by the imaging pad is shown in cyan. An average surface-based atlas of the neonatal cortex was used to perform the visualization of the functional connectivity maps.) **(A)** Infant head model and visual cortex imaging pad, with 18 sources (red) and 16 detectors (blue), placed over the occipital cortex. **(B)** An axial slice of a T2-weighted MRI of a preterm infant with an occipital stroke. **(C-D)** Correlation maps using a seed placed in the left and right visual cortices ([HbO_2]) of a healthy term infant (C), a healthy preterm infant (D) and a baby with an occipital stroke (E). (All correlation images are scaled from r=-1 to 1 and have a threshold at |r|>0.3). **(F-H)** ICA components corresponding to the resting-state visual network in both, a healthy term (F) and a healthy preterm infant (G). The ICA component in the infant with the unilateral stroke only shows activity in the healthy hemisphere (H). (All components are scaled to their maximum. Strong "correlations" are positive.) **(I-K)** Maps of amplitude of low frequency fluctuations (ALFF) at each voxel. ALFF in a healthy term (I) and a healthy preterm (J) infant show a bilateral pattern. The ALFF map in the infant with the stroke only shows high power in the healthy hemisphere (K).

[Figure1_small.jpg]

References:

1. Smyser, CD, et al. (2010) "Longitudinal analysis of neural network development in preterm infants." Cerebral Cortex 20:2852-62.

2. White, BR, et al. (2009) "Resting-state functional connectivity in the human brain revealed with diffuse optical tomography." NeuroImage 47:148-156.

523

ALTERED CEREBROVASCULAR REGULATION UPON RETURN FROM THE INTERNATIONAL SPACE STATION

R.L. Hughson[1], K.A. Zuj[2], D.K. Greaves[2], J.K. Shoemaker[3], A.P. Blaber[4], P. Arbeille[5]

[1]Schlegel Research Institute for Aging, [2]University of Waterloo, Waterloo, [3]University of Western Ontario, London, ON, [4]Simon Fraser University, Burnaby, BC, Canada, [5]University of Tours, Tours, France

Introduction: Prolonged space flight is associated with major alterations in cerebral perfusion pressure, elimination of the daily challenges of adaptation to changes in body position and a confined environment with elevated CO_2. On return from space astronauts experience greater incidence of orthostatic intolerance and the potential contribution of the cerebrovascular system to this is not completely understood.

Objective: To measure the dynamic cerebrovascular autoregulatory response to spontaneous changes in arterial blood pressure and the cerebrovascular responsiveness to changes in arterial PCO_2 after up to 199 days in space.

Methods: Five long-duration astronauts completed the 2-breath test (Am.J.Physiol. 283: R653-62, 2002) inhaling 2 breaths of 10% CO_2 once per minute for 5-minutes ~30 days before flight and less than 24-hours after return from space. Cerebral blood flow velocity (CBFV), mean arterial blood pressure (BP) and end-tidal PCO_2 were recorded. Beat-to-beat values were investigated by autoregressive moving average (ARMA) analysis to determine the independent influences of $PaCO_2$ and BP on CBFV and on the index of cerebrovascular resistance (CVRi).

Results: There were no significant differences in the BP-CBFV impulse and step responses computed from the ARMA; however, BP-CVRi responses showed a trend towards smaller CVRi changes post flight for both impulse and step responses (P=0.176, and P=0.141 respectively). The CO_2-CVRi showed significantly smaller step responses post flight (P=0.021). This result was also reflected in a trend towards a reduced CO_2-CBFV step response post flight (P=0.161).

Conclusions: The current data from five long-duration astronauts for the relationship between spontaneous fluctuations in BP and cerebrovascular resistance showed a trend to impaired autoregulation after spaceflight. The significant reduction in CO_2 responses after spaceflight might be related to chronic, slight increases in inspired PCO_2 on ISS. These changes could reflect an impaired ability of cerebral blood vessels to dilate with implications for cerebrovascular health as well as for the maintenance of cerebral blood flow on return to upright posture after long duration spaceflight.

Sponsored by the Canadian Space Agency.

524

D-CYCLOSERINE IMPROVES COGNITIVE DEFICITS IN A MOUSE MODEL OF NEUROINFLAMMATION

S. Liraz Zaltsman[1,2], A. Alexandrovich[1], R. Yaka[1], E. Shohami[1], A. Biegon[2,3]

[1]Pharmacology, Hebrew University, Jerusalem, [2]The Joseph Sagol Neuroscience Center, Sheba Medical Center, Ramat-Gan, Israel, [3]Brookhaven National Lab, Brookhaven, NY, USA

Background: Neuroinflammation can lead to significant and long lasting cognitive deficits in human subjects through an unknown mechanism. At present, there is no pharmacological intervention known to prevent or ameliorate cognitive deficits following a neuroinflammatory insult. In the present study, we examined the efficacy of D-cycloserine (DCS), a partial NMDA receptor agonist, on cognitive deficits induced in mice by intracisternal (ic) injection of endotoxin (LPS).

Methods: Male Sabra mice (N=10/treatment group) were given ic saline or LPS (10ug in 2ul) followed 24 h later by intraperitoneal saline or DCS (10ug/gr in 100ul/10gr). Memory function was assessed by the novel object recognition test (NORT) 2, 7, 16, and 30 days post LPS injections Electrophysiological recording of LTP was performed in hippocampal slices from animals killed after 8 days. The time course of LTP was evaluated in Saline (n = 11 slices, 5 mice), LPS (n = 12 slices, 7 mice), Saline+DCS (n = 9 slices, 7 mice) and LPS+DCS (n = 12 slices, 7 mice) treated mice. Initial fEPSPs slopes were measured, and the values were normalized in each experiment using the averaged slope value measured during the control period (time, 1 to 10 min). Tetanic stimulation (100Hz, 1 sec, 2 trains 10sec apart) was applied at time 10. Animals killed after 8 days and their brains processed for in vitro quantitative autoradiography with [3H]PK11195, an established marker of microgliosis, and [3H]MK801, a specific NMDA receptor antagonist. Statistical analysis was performed by one-way ANOVA (NORT) or 2 way ANOVA by treatment and region (Autoradiography), followed by Fisher's PLSD posthoc test.

Results: Intracisternal LPS induced a significant and long-lasting deficit in novel object recognition; which was reversed by DCS. Similarly, LPS impaired LTP and its magnitude was restored by DCS. Moreover, DCS treatment of LPS mice led to a significant reduction of regional neuroinflammation, and to up-regulation of NMDA receptor density as assessed by autoradiography ($p < 0.0001$ for region and treatment main effects).

Conclusion: These results suggest that neuroinflammation-induced cognitive deficits involve derangement of NMDAR function and can be prevented by DCS.

525

ARE SOMATOSENSORY EVOKED POTENTIALS (SEPS) RECORDINGS RELEVANT TO ASSESS THE EXTENT OF THROMBOEMBOLIC ISCHAEMIC STROKE IN THE ANAESTHETIZED MACACA MULATTA?

A. Balossier[1], E.M.L. Ribeiro[2], A.-S. Diependaele[2], M. Gauberti[1], C. Gakuba[1], P. Guedin[3], L. Chazalviel[1], V. Agin[1], E. Emery[1,4], D. Vivien[1], C. Orset[1], O. Etard[2]

[1]INSERM U919, Serine Proteases and Pathophysiology of the Neurovascular Unit (SP2U), UMR CNRS 6232 CI-NAPS, Centre for Imaging-Neuroscience and Applications to Pathologies, GIP CYCERON, University of Caen Basse-Normandie, [2]Laboratoire d'Explorations Fonctionnelles Neurologiques, Centre Hospitalier Universitaire de Caen, Caen, [3]Service de Neuroradiologie, Hôpital Lariboisière, Paris, [4]Service de Neurochirurgie, Centre Hospitalier Universitaire de Caen, Caen, France

Introduction: Validation of thromboembolic stroke models may benefit from electrophysiological recording to evaluate the extent of ischaemia. The N20, cortical wave reflecting the integrity of the somatosensory pathways, is related in human practice to the perfusion of areas surrounding the central sulcus. A reduction in amplitude of 50% or an increase of more than 1 ms in latency are critical signs of ischaemia. A cortical cartography similar to the human one was described in the primate model, the human N20 corresponding in this model to the N10.

Previous studies in anaesthetized monkeys showed that SEPs were reproducible, stable in latency and morphology but these studies measure SEPs variations only under stable conditions (anaesthetic, haemodynamic, stimulation) but not during surgery. Thus, not reflecting the impact of interactions between surgery and sedation.

Initially, we performed longitudinal SEPs recording in a primate model (*Macaca mulatta)* of cerebral ischaemia, induced by thrombin injection into the middle cerebral artery. During surgery, the anaesthetic and haemodynamic parameters remained constant. While we observed in the lesioned hemisphere a 50% decrease in amplitude after the occlusion correlated with cortical ischaemia, some variations happening before and after the occlusion in both hemispheres could not be explained.

In order to reproduce the different steps of the surgical procedure and the impact of low or high exteroceptive stimulations on SEPs variations, a second trial was performed on naïve monkeys during MRI recording, before surgery.

Objectives: To evaluate the validity of SEPs recordings in anaesthetized rhesus monkeys and to determine interaction between sedation and response to various exteroceptive supramaximal stimulation.

Materials and methods: Experiments were performed in 4 male macaques aged 5-6 years, body weights ranging from 7 to 11 kg.

The monkeys were either sedated with sevoflurane and N_2O or with sufentanil and propofol. Arterial pressure, temperature, heart rate, end-tidal CO_2 levels and SaO_2 concentration were measured continuously and maintained within normal physiological limits.

The median nerves were stimulated at each wrist alternatively, every 5 mn from sedation, using

a current square pulse of either 30 mA or 60 mA for 0.2 ms. All stimulations were supra-maximal. SEPs were recorded using subcutaneous needle electrodes according to the human 10-20 EEG system. Four channels were recorded: Erb´s point, C´3 or C´4 contralateral to the stimulated hand nerve and Fpz. Averaging runs of 100 stimuli at a repetition rate of 3.1 Hz were adequate to generate clear measurable responses.

Results: Whatever the anaesthetics used, exteroceptive stimulation at 60 mA induced a 30-50% increase in amplitude compared to 30 mA stimulation. This increase persisted in both hemispheres when stimulation returned to baseline (30 mA). Variations of cortical excitability were induced and spread all over the cortex, secondary to the doubling of stimulation intensity. This phenomenon probably resulted from modifications in sedation depth although no anaesthetic parameter was changed.

Conclusion: Fluctuations in sedation depth that cannot be controlled by physiological parameters engender great difficulties in the interpretation of SEPs monitoring, questioning the relevance of this technique for the development of a thromboembolic stroke model.

527

VASCULAR COGNITIVE IMPAIRMENT (VCI): CLINICAL CARDIOVASCULAR RISK FACTORS AND NEUROBEHAVIORAL PHENOTYPES ARE MIMICKED IN HYPERTENSIVE RAT VCI MODEL

F.C. Barone[1,2,3], J. Li[1], J. Zhou[1], M.G. Adamski[1,4], A.E. Baird[1,3], D.M. Rosenbaum[1,3], H. Crystal[1]

[1]Neurology, [2]Physiology & Pharmacology, [3]The Robert F. Furchgott Center for Neural & Behavioral Science, SUNY Downstate Medical Center, Brooklyn, NY, USA, [4]Neurology, Jagiellonian University Medical College, Krakow, Poland

Introduction: Cardiovascular disease and aging are major risk factors for dementia, including VCI. VCI symptoms include deficits in executive function, working memory, depression, and gait/balance that are associated with reduced forebrain perfusion (1, 2). Ischemic stress can mobilize progenitor CD34+ cells from bone marrow into peripheral blood (3). An animal model of VCI is needed to understand VCI pathology and intervention (1, 2). The ideal model should simulate the effects of specific, validated cardiovascular risk factors on cognition and capture ischemia-induced circulating cellular changes. Here we discover that identified cardiovascular risk factors for cognitive impairment from Clinical data can be manipulated to create a Preclinical rat model of VCI.

Methods:

Clinical Study: The relationship between independent predictors (carotid imaging measures, blood pressure, blood lipids, diabetes, previous MI) and dependent, cognitive outcome variables (Comalli-Kaplan Stroop and symbol-digit tests) were assessed in linear regression models (controlling for age, HIV-serostatus and AIDS, educational level, depression, and ethnicity). Participants were from the Women's Interagency HIV Study (WIHS).

Preclinical Study: Bilateral common carotid artery *Stenosis* surgery (i.e., guided by reduced forebrain microvascular perfusion) or *Sham* surgery was performed in spontaneously hypertensive rats (SHR). SHR were evaluated on a series of neurological (gait, balance, sensory-motor and activity) and cognitive (active place and passive avoidance) tests. The frequency of circulating CD34+ progenitor cells was measured using a fluorescence-activated cell analyzer. Two separate experiments (N=5-7/group) established model reliability.

Results:

Clinical Study: Carotid lesions and intimal-medial thickness ($p < 0.01$) and hypertension ($p < 0.05$) were significant and independent predictors of cognitive impairment.

Preclinical Study: *Stenosis* produced persistently decreased forebrain perfusion resulting in impaired active place avoidance (APA) learning and gait/balance deficits within 3 weeks and lasting for at least 3 months. An example of APA performance at 6 weeks (graph below; N=5/group) shows that *Stenosis* SHR do not learn to avoid entry into a shocked location in the test environment, while similar total path/movement is traveled by both groups. *Stenosis* deficits were not related to differences in general motor activity, severe sensory-motor deficits, blood pressure, heart rate or body weight. Simple passive avoidance performance was not affected by *Stenosis*. Circulating CD34+ progenitor cells were significantly increased by *Stenosis* compared to *Sham* surgery ($p< 0.02$).

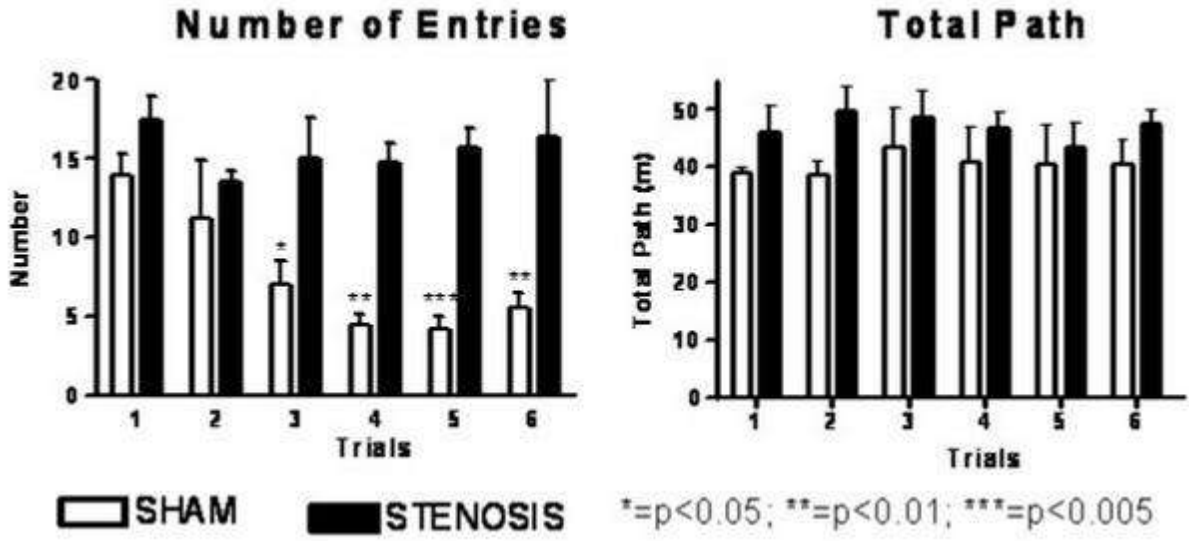

[SHR Stenosis vs Sham After 6 Weeks]

Conclusions: Carotid artery stenosis and hypertension are associated with cognitive impairment in middle-aged women (with or without HIV). Similar to the clinic, stenosis in the hypertensive rat results in cognitive and behavioral changes that mimic VCI. The APA paradigm requires complex cognitive control and is a sensitive detector of preclinical VCI (e.g., mimics executive function-like "decision making"). Increases in progenitor cells following stenosis suggests that a potential recovery from established VCI might be achieved in the future. This "carotid stenosis plus hypertension model" provides high throughput for in vivo work and is expected to be an important tool for well-controlled preclinical studies that probe VCI pathophysiology and intervention.

1. Curr Opin Investig Drugs. 10:624-637, 2009.
2. Stroke. 37:2220-2241, 2006.
3. Stroke. 40:1237-1244, 2009.

528

NEUROVASCULAR PRINCIPLES OF THE BLOOD-BRAIN BARRIER

N.J. Abbott

Institute of Pharmaceutical Science, King's College London, London, UK

The blood-brain barrier (BBB) is formed by the endothelial cells of the brain microvasculature, which also contribute to an anatomical and physiological association of cells termed the 'Neurovascular Unit' (NVU) (1). The NVU concept was originally developed in relation to control of cerebral blood flow, but it is also relevant to the control of molecular traffic between blood and brain and regulation of the neural microenvironment. This expanded concept of the BBB/NVU helps to explain embryonic development of the BBB, its normal adult function, and several neuropathologies involving disturbances of the brain vasculature. It also leads to re-evaluation of issues of drug discovery and delivery, whether for drugs required to reach targets within the CNS, or for those designed to act on peripheral targets and requiring restricted brain entry to reduce the risk of CNS side effects. Finally the NVU itself becomes a target for drug action, as a healthy BBB can help protect against neuronal damage mediated by dysfunction involving the NVU.

This new concept of the BBB/NVU involves new levels of complexity in investigation, understanding and modelling. The primary barrier site remains the brain endothelium, where the combination of tight junctions and tightly packed lipids in the plasma membrane contributes to the 'physical barrier'. A 'transport barrier' is created by the combination of apical and basolateral endothelial transport proteins (or carriers) regulating the entry and efflux of specific solutes, together with vesicular mechanisms for transcytosis (receptor-mediated and adsorptive mediated) of particular peptides and proteins. Finally several intracellular and extracellular enzymes contribute to the 'enzymatic barrier' function of the endothelium (1).

Associated with the adult brain endothelium within the NVU are pericytes, the end feet of perivascular astrocytes, smooth muscle cells in larger vessels, and microglia, the resident immune cells of the CNS; under normal conditions these cells support the function of the 'client' cells, the neurons. In inflammation found in several CNS pathologies, blood-derived leukocytes may accumulate around the vessels, invading further into the parenchyma in severe cases, and changing the organisation of the NVU. Recent studies show that the basic phenotype of endothelial tight junctions plus uptake transporters is induced during embryonic angiogenesis while subsequent down-regulation of the 'default' peripheral endothelial phenotype involves pericyte influences (2). Upregulation of further BBB features including efflux transporters requires later astrocytic influences. The complex basal laminae surrounding the endothelium also contribute to barrier function. In the adult BBB, pericytes and astrocytes continue to play critical roles in barrier induction and maintenance (2,3), but also act as a 'second line' of defence, able to supplement the physical, transport and enzymatic barrier functions of the endothelium, and to compensate to some degree if the endothelium is compromised in pathology (1).

The BBB/NVU is not a static structure, but is subject to change and modulation, both physiological and pathological. There are several important implications for drug discovery and delivery.

(1) Abbott et al. 2010 Neurobiol Dis. 37:13-25.

(2) Daneman et al. 2010 Nature 468:562-6.

(3) Bell et al. 2010 Neuron 68:409-27.

531

PHARMACOLOGICAL INDUCTION OF HEME OXYGENASE-1 PROTECTS AGAINST ISCHEMIC NEURONAL INJURY

F. Zhang[1,2], Z. Weng[1], S. Wang[1], M.B. Sporn[3], J. Chen[1,2,4]

[1]Neurology, Center of Cerebrovascular Disease Research, University of Pittsburgh, [2]Geriatric Research, Educational and Clinical Center, Veterans Affairs Pittsburgh Health Care System, Pittsburgh, PA, [3]Pharmacology and Medicine, Dartmouth Medical School, Hanover, NH, USA, [4]State Key Laboratory of Medical Neurobiology, Fudan University, Shanghai, China

Objectives: Heme oxygenase-1 (HO-1) is an inducible phase-2 enzyme that catalyzes the degradation of toxic heme, producing iron and the potentially cytoprotective biliverdin and carbon monoxide. While the role of HO-1 in cerebral ischemia is not fully understood, overexpression of HO-1 has been associated with enhanced resistance to oxidative stress in neurons. The current study was designed to test our hypothesis that chemical-induced upregulation of HO-1 expression protects neurons against ischemic injury.

Methods: Ischemic neuronal injury was induced in rat primary cortical neuronal cultures *in vitro* by means of oxygen-glucose deprivation (OGD) for 60 min followed by reperfusion. Transient global cerebral ischemia (12 min) was induced *in vivo* in male adult SD rats (300-350 *g* body weight) using the four-vessel occlusion method, with all physiological parameters controlled at normal ranges. Using both ischemic injury models, three sets of experiments were performed in parallel to determine: 1) whether CDDO-Im (2-cyano-3,12 dioxooleana-1,9 dien-28-oyl imidazolide), a robust inducer of phase 2 genes, can induce neuronal expression of HO-1, 2) whether administration of CDDO-Im protects against ischemic neuronal injury, and 3) whether inhibition of HO-1 activity disrupts the neuroprotective effect of CDDO-Im.

Results: In cultured neurons, HO-1 protein was barely detectable under resting conditions; however, CCDO-Im treatment (50-300 nM) resulted in robust upregulation of HO-1 expression within 6-24 hr, and protected against neuronal death at 24 hr after OGD (significantly reduced LDH release and increased cell viability, $p< 0.05$ *vs.* vehicle controls). Co-incubation with tin protoporphyrin IX (Sn-PPIX), a specific HO-1 inhibitor, abolished the neuroprotective effect of CCDO-Im against OGD. In rats, intracerebroventrical (*I.C.V.*) infusion of CCDO-Im (0.5-1.5 μg) augmented HO-1 expression in hippocampal CA1 neurons within 4 hr and lasting for 48-72 hr. At the optimal dose for HO-1 induction (1.5 μg), CCDO-Im treatment resulted in significant increases in CA1 neuronal survival at 3 days after global ischemia ($p< 0.05$ *vs.* vehicle group, n=8/group). Co-infusion of Sn-PPIX (30 μg/rat) significantly but partially ($p< 0.05$ *vs.* vehicle or CCDO-Im plus Sn-PPIX, n=8/group) reduced the neuroprotective effect of CCDO-Im against CA1 neuronal cell death after global ischemia

Conclusions: Our results demonstrate that administration of the phase-2 gene inducer CDDO-Im confers remarkable neuroprotection against ischemic neuronal injury in both *in vitro* and *in vivo* models by upregulating the expression of HO-1. Thus, enhancers for neuronal HO-1 expression may be a promising strategy for the therapeutic intervention of ischemic stroke.

(Supported by NIH grants NS45048, NS056118, NS036736, VA Merit Review grant, and AHA grant 10SDG2560122)

532

MOLECULAR AND CELLULAR MECHANISMS UNDERLYING CELL-BASED RESTORATIVE TREATMENT FOR NEUROLOGICAL DISEASE AND INJURY

M. Chopp

Neurology, Research, Henry Ford Hospital, Detroit, MI, USA

Cell-based therapies enhance recovery of function when employed to treat many neurological diseases. In injured brain, such as stroke, cell-based therapies act as catalysts to stimulate and amplify the endogenous restorative processes of angiogenesis, neurogenesis and synaptogenesis and white matter axonal outgrowth throughout the central nervous system. In this presentation, I will describe the coupling and interdependence among these restorative processes and how the astrocyte via the expression of vascular endothelial growth factor orchestrates brain plasticity and recovery of function after treatment with multipotent mesenchymal stromal cells (MSCs). I will also show that tissue plasminogen activator (rtPA) stimulated within parenchymal cells, primarily astrocytes, by MSCs, promotes recovery of neurological function after stroke. Cell-based therapies for neurological diseases and injury such as stroke, traumatic brain injury and multiple sclerosis in the adult remodel the injured brain indirectly via restorative action on parenchymal cells.

533

LOW-FREQUENCY REPETITIVE TMS IN EARLY PHASE OF STROKE ENHANCES ANGIOGENIC MECHANISMS IN RATS

T.R. Han, B.-M. Oh

Seoul National University, Seoul, Republic of Korea

Objectives: To investigate whether a unilateral application of repetitive transcranial magnetic stimulation (rTMS) changes angiogenesis-related gene expressions and thereby improves functional recovery after ischemic stroke in rats.

Materials and methods: Adult male Sprague-Dawley rats were subjected to middle cerebral artery occlusion (day 0) and subsequently treated with low- (1 Hz), high-frequency (20 Hz), or sham stimulation on their lesioned hemispheres for 2 weeks. Stimulation was applied using figure-of-8 coil with intensity set at 100% of motor threshold. Neurological function was evaluated performed on day 3, 10, and 17. Infarct volume, angiogenesis, angiogenic factor expression, and angiogenesis-related gene transcription were measured by histology, immunohistochemistry, Western blot, and real-time PCR, respectively.

Results: Neurological function and infarct volume were comparable between groups (P=0.636 and P=0.335). One-Hz rTMS significantly increased phosphorylation of Akt in ischemic border zones, and enhanced phosphorylation of endothelial nitric oxide synthase (eNOS) in infarct core, ischemic border zones, and contralesional cortex ($P< 0.05$ as compared to 20 Hz). Real-time PCR revealed that low-frequency stimulation significantly increased gene expression of Tie2 (tek), a receptor of angiogenic factors, in ischemic core region (1.22±0.39 and 0.49±0.07 in 1 Hz and Sham groups, mean fold change±SD of mRNA level relative to the GAPDH mRNA level, $P< 0.05$).

Conclusion: Low-frequency rTMS on lesioned hemisphere in acute phase after stroke promotes the expression of angiogenic factors and a related gene in the brain, especially in an ischemic core region. In addition to well-known effects of rTMS, regulation of Tie2, Akt, and eNOS seems to play vital roles in rTMS induced changes.

534

TUMORIGENESIS OF INDUCED PLURIPOTENT STEM CELLS IN ISCHEMIC MOUSE MODEL

T. Yamashita, **Y. Omote**, H. Kawai, F. Tian, Y. Ohta, K. Abe

Neurology, Okayama University Graduate School of Medicine, Dentistry and Pharmaceutical Sciences, Okayamashi, Japan

Objectives: Recent studies have indicated that induced pluripotent stem (iPS) cells may provide cures for various neurological diseases. However tumorigenesis of iPS cells is serious problem which should be overcome for clinical application. In this study, we evaluated the tumorigenesis of iPS cells in a mouse model of transient middle cerebral artery occlusion (MCAO).

Methods: Adult (20-25g, 8-10 week old) male C57BL/6N mice were used. The iPS cells (5×10^5) were injected into the ipsilateral striatum and cortex, which were considered as the ischemic boundary zone, at 24 hour after MCAO. We used the two different murine iPS cell lines. One was established with a retrovirus introducing four transcriptional factors, c-Myc, Sox2, Oct3/4 and Klf4 (classical iPS cells). The other was established with plasmid vectors expressing above four transcriptional factors (virus-free iPS cells). Histological analysis was performed 28 days after the cell transplantation.

Results: Classical iPS cells transplanted in brain after MCAO, formed teratoma with higher probability ($p < 0.05$) and larger volume ($p < 0.01$) compared with those in intact brain. Among of four transcriptional factors, c-Myc, Sox2 and Oct3/4 expression were significantly increased in iPS-derived tumors in ischemic brain ($p < 0.01$). On the other hand, virus-free iPS cells formed teratoma but there was no significant difference in tumor volume.

Conclusions: Our findings suggested that these four transcriptional factors which were integrated into the genome by retrovirus vectors, activated and promoted tumorigenesis in the ischemic brain condition. Virus-free iPS cells may be safer for transplantation therapy.

535

AMYLOID IMAGING IN ALZHEIMER DISEASE USING PET WITH [F-18]FACT: A NEURITIC PLAQUE IMAGING?

H. Ito[1], H. Shinotoh[1], H. Shimada[1], K. Yanai[2], N. Okamura[2], H. Takano[1], F. Kodaka[1], Y. Eguchi[1], M. Higuchi[1], T. Fukumura[1], T. Suhara[1]

[1]Molecular Imaging Center, National Institute of Radiological Sciences, Chiba, [2]Department of Pharmacology, Tohoku University School of Medicine, Sendai, Japan

Objectives: The characteristic neuropathologic changes in Alzheimer disease (AD) are deposition of amyloid senile plaques and neurofibrillary tangles. [C-11]BF227, a benxoxazole derivative, has been developed for in vivo imaging of amyloid senile plaques [1], which has been considered to bind more preferentially to dense-cored amyloid deposition than [C-11]PIB. The fluorine-18 labeled amyloid tracer, [F-18]2-[(2-{(E)-2-[2-(dimethylamino)-1,3-thiazol-5-yl]vinyl}-1,3-benzoxazol-6-yl)oxy]-3-fluoropropan-1-ol (Fluorinated Amyloid imaging Compound of Tohoku University; [F-18]FACT), which is one of benxoxazole derivatives and has similar structure with [C-11]BF227, has recently been developed. In the present study, deposition of amyloid senile plaques was measured by PET with both [C-11]PIB and [F-18]FACT in same subjects, and the regional uptake of both radiotracers were directly compared.

Methods: Two PET scans with [C-11]PIB and [F-18]FACT were performed sequentially on 6 normal control (NC) subjects, 2 mild cognitive impairment (MCI) patients, and 6 AD patients. The standardized uptake value (SUV) was calculated from time-integrated radioactivity with the integration intervals of 50 to 70 min and 40 to 60 min for [C-11]PIB and [F-18]FACT, respectively. Since SUV are affected by the non-specific accumulation of radiotracer in the white matter, the SUV per gray matter fraction in an ROI were calculated using MR images as follows:

SUV = SUVgray•TFgray + SUVwhite•TFwhite.

where SUVgray and SUVwhite are SUV in gray and white matter, respectively. TFgray and TFwhite are the tissue fraction of gray and matter, respectively, which are determined from MR images. The SUVgray were calculated by assuming SUVwhite to be equal to SUV in the centrum semiovale. The SUVgray ratio (SUVR) of brain regions to cerebellum was calculated.

Results: The SUVR of [C-11]PIB for cerebral cortical regions in NC subjects and AD patients were 1.15-1.40 and 3.10-4.91 in average, respectively. The SUVR of [F-18]FACT for cerebral cortical regions in NC subjects and AD patients were 1.22-1.33 and 1.58-1.70 in average, respectively. Significant positive correlations were observed between SUVR of [C-11]PIB and [F-18]FACT in all brain regions. Relatively lower uptake of [C-11]PIB in distribution were observed in the medial side of temporal cortex and occipital cortex as compared with [F-18]FACT. Relatively higher uptake of [C-11]PIB in distribution was observed in the frontal and parietal cortices.

Conclusions: Since [F-18]FACT has similar structure with [C-11]BF227, it might also bind more preferentially to dense-cored amyloid deposition. [C-11]PIB might bind to both diffuse and dense-cored amyloid plaques, and therefore such regional differences in cerebral cortical uptake between [C-11]PIB and [F-18]FACT might be due to differences in regional distribution between diffuse and dense-cored amyloid plaques. A histopathological study showed that diffuse amyloid plaque was not prominent in the occipital lobe as compared with the frontal and temporal lobe [2], corresponding to the present results. Because neuropathology in AD are

characterized by cortical neuritic plaque containing dense-cored amyloid deposition [3], selective radiotracer for neuritic amyloid plaque might be useful to distinguish normal aging process from AD.

References:

[1] Kudo Y, et al. J Nucl Med 2007; 48: 553-561.

[2] Yamaguchi H, et al. Acta Neuropathol 1988; 77: 113-119.

[3] Price JL. Neurobiol Aging 1997; 18: S67-70.

536

QUANTIFICATION OF [^{18}F]DPA714 BINDING IN THE HUMAN BRAIN: INITIAL STUDIES IN HEALTHY CONTROLS AND ALZHEIMER'S DISEASE PATIENTS

R. Boellaard[1], V. Oikonen[2], A. Hoffmann[3], B.N.M. van Berckel[1], A.D. Windhorst[1], J. Virta[2], M. Haaparanta-Solin[2], P. Luoto[2], N. Savisto[2], O. Solin[2], R. Valencia[3], A. Thiele[3], J. Eriksson[1], R.C. Schuit[1], A.A. Lammertsma[1], J.O. Rinne[2]

[1]Department of Nuclear Medicine & PET Research, VU University Medical Center, Amsterdam, The Netherlands, [2]Turku PET Centre, University of Turku and Turku University Hospital, Turku, Finland, [3]Bayer Schering Pharma AG, Berlin, Germany

Purpose: [^{18}F]DPA714 is a novel tracer of the 18-kDa translocator protein (TSPO). This protein is highly expressed in activated microglia. As microglia are known to be activated in conditions with chronic neuroinflammation, [^{18}F]DPA714 may be used to visualize and quantify neuroinflammatory processes. The purpose of this study was to identify the optimal kinetic model for quantification of [^{18}F]DPA714 binding in the brain of both healthy controls (HC) and patients with Alzheimer's disease (AD).

Methods: Following intravenous bolus injection of 250±10 MBq [^{18}F]DPA714, PET studies were performed in 16 subjects: 9 AD and 7 HC. The scanning protocol consisted of a dynamic emission PET scan with progressively increasing frame duration and a total duration of 150 min, including a short resting period, i.e. 0-90 min, rest, 120-150 min p.i.. Online arterial sampling was performed (n=14) and additional manual samples were taken for metabolite analysis. For each scan 56 volumes of interest in the brain were defined. All studies were analyzed using various plasma input and reference tissue kinetic models, the latter using cerebellum as reference region. The optimal pharmacokinetic model was selected using the Akaike Information Criterion (AIC). In addition, the impact of shorter overall scan durations (0-48, 0-60, 0-90 min) on model selection and parameter estimates was assessed. Finally, differences in tracer binding between subject groups were explored.

Results: The two tissue compartment model, including blood volume fraction was the preferred plasma input model in the majority of cases for scan durations of 60 min or longer. Average whole cerebrum grey matter V_T was 2.5±0.7 and 2.2±0.7 for HC and AD subjects, respectively. Corresponding BP was 1.00±0 and 0.86±0.50, respectively. In all cases the simplified reference tissue model (STRM) was preferred over the full reference tissue model. SRTM based BP_{ND} values equaled -0.05±0.15 and -0.09±0.04 for HC and AD subjects, respectively. Shortening scan duration from 150 to 60 min did not significantly affect V_T, BP and BP_{ND} values. In this exploratory study no significant differences in V_T, BP and BP_{ND} between subject groups in any of the studied regions were found so far.

Conclusions: The two tissue compartment model with blood volume fraction is the preferred plasma input model with minimum of 60 min scan duration for analyzing cerebral [^{18}F]DPA714 studies. SRTM with cerebellum as reference region provides reliable and accurate fits. So far, in this preliminary exploration no differences in binding between subject groups for any of the models and/or regions studied was observed.

537

EFFECTS OF IBUDILAST ON NO PRODUCTION, HYDROXYL RADICAL METABOLISM DURING CEREBRAL ISCHEMIA AND REPERFUSION IN MICE

N. Araki, Y. Asano, M. Yamazato, R. Nishioka, Y. Ito, K. Ishizwa

Department of Neurology, Saitama Medical University, Saitama, Japan

Introduction: Ibudilast is a relatively selective phosphodiesterase inhibitor (PDE3, PDE4, PDE10, PDE11), which showed vasodilator activity, antiinflammatory effects, and antithrombotic effects. Ibudilast improves subjective symptoms including dizziness of patients with cerebral infarction in chronic stage. The purpose of this study is to investigate the effects of ibudilast on NO production, hydroxyl radical metabolism.

Methods: (1) Male C57/BL6 mice [n=12] were used. Ibudilast 10 mg/kg/day was given in 6 mice 30 minutes prior to ishchemia (ibudilast group), and others were used as contol group. Both NO production and hydroxyl radical metabolism were continuously monitored by *in vivo* microdialysis. Microdialysis probes were inserted into the bilateral striatum. The *in vivo* salicylate trapping method was applied for monitoring hydroxyl radical formation via 2,3 dihydroxybenzoic acid (2,3-DHBA), and 2,5 dihydroxybenzoic acid (2,5-DHBA). A Laser Doppler probe was placed on the skull surface. Blood pressure, blood gases and temperature were monitored and maintained within normal ranges throughout the procedure. Forebrain cerebral ischemia was produced by occlusion of both common carotid arteries for 10 minutes. Levels of nitric oxide metabolites, nitrite (NO_2^-) and nitrate (NO_3^-), in the dialysate were determined using the Griess reaction.

Results:

(1) Blood Pressure: Ibudilast group (71.3 ± 6.8 mmHg; mean ± SD) showed significantly lower than that of the control group (84.2 ± 1.0), 20 minutes after the start of reperfusion ($p< 0.05$).

(2) Cerebral Blood Flow (CBF): There were no significant differences between the two groups.

(3) Nitric oxide metabolites:

1) NO_2^- ; Ibudilast group (81.4 ± 16.2 %) showed significantly higher than that of the control group (103.6 ± 14.3), 80-120 minutes after the start of reperfusion ($p< 0.05$).

2) NO_3^- ; There were no significant differences between the two groups.

(4) Hydroxyl radical metabolites:

1) 2,3-DHBA; ibudilast group (85.3 ± 5.9 %) showed significantly lower than that of the control group (95.2 ± 7.8 %), 20 minutes after the start of reperfusion ($p< 0.05$) (Figure 1).

2) 2,5-DHBA; There were no significant differences between the groups.

Conclusion: These *in vivo* data suggest that ibudilast, selective phosphodiesterase inhibitor, influences on the hydroxyl radical production in mice during reperfusion, and may protect against cerebral ischemic injury following ischemia and reperfusion.

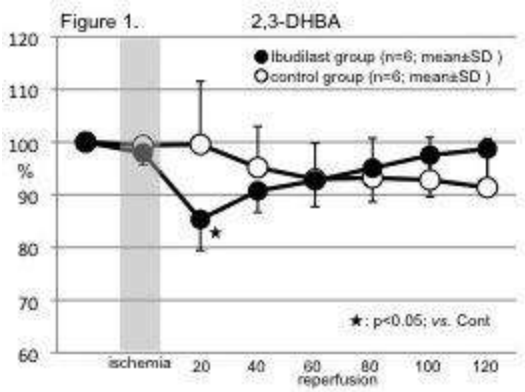
Figure 1.
2,3-DHBA
Ibudilast group (n=6; mean±SD)
control group (n=6; mean±SD)
120
110
100
%
90
80
70
60
★: p<0.05; vs. Cont
ischemia
20
40
60
80
100
120
reperfusion

[2.3 DHBA]

538

EVALUATION OF LASER SPECKLE CONTRAST IMAGE ANALYSIS TECHNIQUES IN THE CORTICAL MICROCIRCULATION OF PIGLETS

F. Domoki[1], D. Zölei[2], O. Oláh[1], V. Tóth-Szűki[1], B. Hopp[3], F. Bari[4], T. Smausz[2]

[1]Department of Physiology, [2]Department of Optics and Quantum Electronics, University of Szeged, [3]Research Group on Laser Physics, Hungarian Academy of Sciences and University of Szeged, [4]Department of Medical Physics and Informatics, University of Szeged, Szeged, Hungary

Background and aims: The closed cranial window has long been used to examine the vascular biology of pial arterioles in piglets. Despite the large number of such studies, we have little data on how diameter changes of pial resistance vessels affect cortical blood flow. Laser Speckle Imaging (LSI) yields vivid dynamic images of blood flow carrying information about the velocity of moving particles. Velocity is proportional to the reciprocal value of the autocorrelation decay time (1/τ) of local speckle contrast (K) by Laser Speckle Contrast Analysis (LASCA). However, K is affected by tissue static light scattering making the development of more sophisticated LASCA techniques necessary. We have recently shown *in vitro* (Ref1) and in skin that with multi-exposure LSI, 1/τ can be more precisely determined. A method based on a semi-empirical function obtained by introduction of two parameters (P_1 and P_2) was used to "rescale" the range of K according to the experimental data using the following equation:

$$K_2(T) = P_1\left\{\frac{\tau^2}{2T^2}\left[\exp\left(\frac{-2T}{\tau}\right)-1+\frac{2T}{\tau}\right]+P_2\right\}^{1/2}$$

[equation]

In the present study, we sought to determine how single or multiple exposure LSI followed by LASCA yields information on the contribution of pial arterioles to the cortical hyperemia in response to various vasodilator stimuli in newborn piglets.

Methods: Newborn pigs were anesthetized with Na-thiopental (40 mg/kg ip) followed by α-chloralose (40 mg/kg, iv), artificially ventilated and were fitted with a closed cranial window as described (Ref2). In Group1 (n=7), graded hypercapnia was elicited with inhalation of 5-10% CO_2 in room air followed by topical application of 1-10μM bradykinin. In Group 2 (n=6), the animals were ventilated first with 2.1% hydrogen in room air, followed by topical application of 100μM NMDA. A 200mW diode laser (λ=808nm) was used to illuminate the cranial window. Multiple exposure LSI series (0,5-100ms) were obtained under steady state conditions. Data are expressed as mean±SEM, and were analyzed with one-way or two-way repeated measures ANOVA, followed by the Student-Newman-Keuls test. $P< 0.05$, legend: * vs. baseline, ** vs. baseline+smaller dose, † vs. multiple exposure.

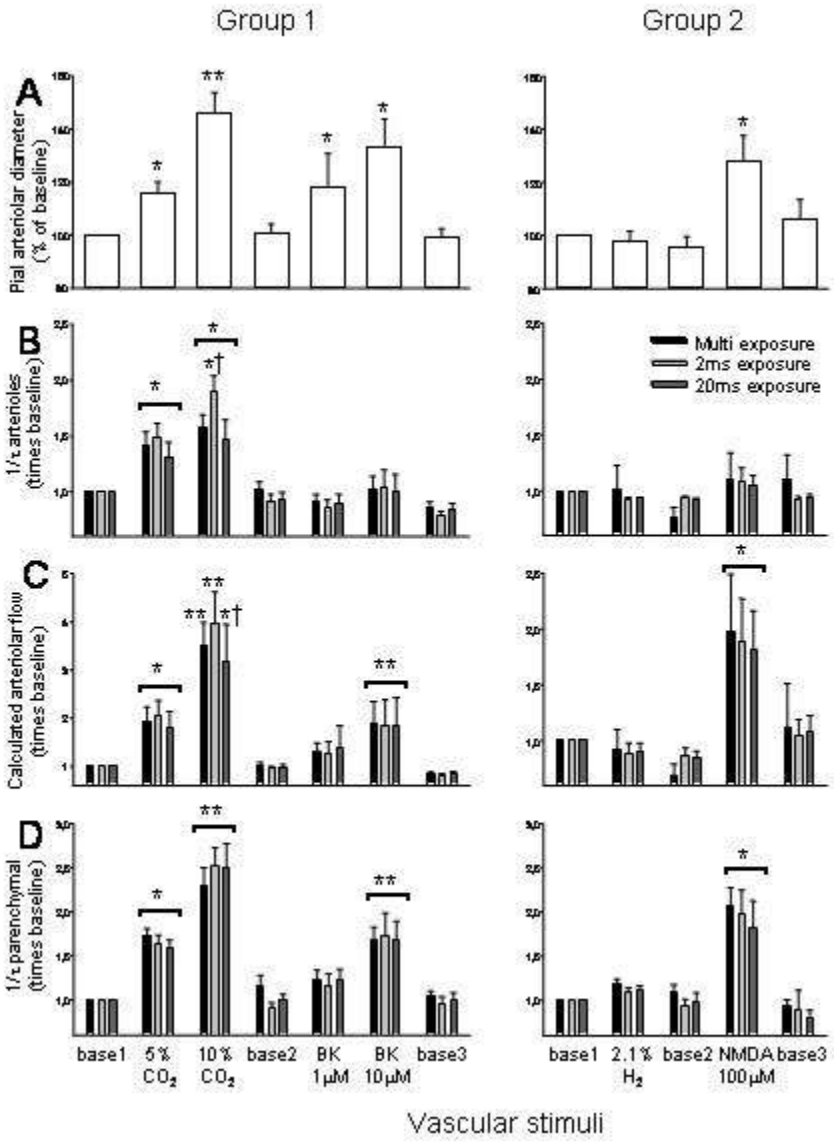

[figure]

Results: Hypercapnia, bradykinin (BK), and NMDA, but not hydrogen (H_2) resulted in dose-dependent, reversible pial arteriolar dilation (A). LASCA showed dose-dependent increases in 1/τ over the pial arterioles during hypercapnia only (B). Over parenchymal areas (D), 1/τ increased similar to the increases in pial arteriolar diameters. Interestingly, arteriolar flow changes (calculated by Δvelocity•Δcross sectional area, C) well matched the 1/τ increases measured over parenchymal areas. Typically, 1/τ values were similar when determined by different LASCA methods.

Conclusion: Unlike in skin, multi-exposure LASCA is probably not required to study the cortical

microcirculation. Our results indicate that pial arteriolar dilation results in cortical hyperemia at least in proportion with the increase in arteriolar cross sectional area in the piglet.

References:

(1) Smausz T. et al. *Applied Optics*, 48:1425-1429, 2009

(2) Domoki F. et al. *Am J Physiol Heart Circ Physiol* 289:H368-H373, 2005.

Support: OTKA K68976. F. Domoki is supported by the Bolyai János Research Scholarship.

539

THE NEUROPROTECTIVE EFFECT OF PTD-FNK PROTEIN AND HYPOTHERMIA COMBINED THERAPY ON RAT FOCAL BRAIN ISCHEMIA MODEL

M. Sakurazawa[1], K. Katsura[1], M. Saito[1], S. Asoh[2], S. Ohta[2], Y. Katayama[1]

[1]Department of Internal Medicine, Divisions of Neurology, Nephrology and Rheumatology, Nippon Medical School, Tokyo, [2]Department of Biochemistry and Cell Biology, Institute of Development and Aging Sciences, Graduate School of Medicine, Nippon Medical School, Kanagawa, Japan

Objective: We previously reported that PTD-FNK protein has a strong neuroprotective effect on rat focal brain ischemia models. FNK protein derived from anti-apoptotic protein Bcl-x_L by substituting three amino acids artificially and thereby gains a higher anti-cell death activity. FNK protein was fused with protein transduction domain(PTD) of the HIV/Tat protein to be able to pass through cell membranes and it was shown to be transduced to neuronal cells rapidly. The aim of this study is to investigate the effect of PTD-FNK protein and hypothermia combined therapy on cerebral infarction.

Methods: Eight-week-old SD rats were subjected to a 120min middle cerebral artery occlusion (MCAO) with an intraluminal thread. Rats were divided into 4 groups:

1) Normothermia(37°C) Vehicle administration,

2) Normothermia PTD-FNK administration,

3) Hypothermia(35°C) Vehicle administration, and

4) Hypothermia PTD-FNK administration.

PTD-FNK protein was intravenously administered 60min after the initiation of MCAO. Hypothermia was applied during 120min MCAO. Rats were sacrificed 24hours after ischemia and infarct volumes were measured.

Results: Infarct volumes were significantly reduced in groups of normothermic PTD-FNK group, hypothermic Vehicle group and hypothermic PTD-FNK group (176.9±40.7mm^3, 131.0±22.7mm^3 and 82.5±49.9mm^3, respectively) compared to normothermic vehicle group (246.9±22.0mm^3). Furthermore, hypothermia and PTD-FNK combination therapy significantly decreased total infarct volume than in hypothermia only group.

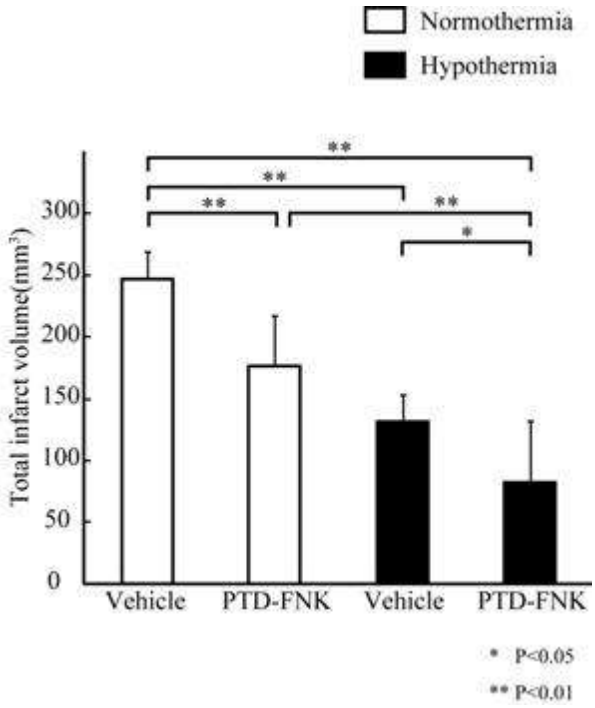
Normothermia
Hypothermia
Total infarct volume(mm³)
300
250
200
150
100
50
0
Vehicle
PTD-FNK
Vehicle
PTD-FNK
**
**
**
**
*
* P<0.05
** P<0.01

[Fig1]

540

COMBINATION THERAPY WITH BONE MARROW STROMAL CELLS AND FK506 ENHANCED AMELIORATION OF ISCHEMIC BRAIN DAMAGE IN RATS

S. Suda[1,2], K. Shimazaki[2], M. Ueda[1], T. Inaba[1], N. Kamiya[1], K. Katsura[1], Y. Katayama[1]

[1]Divisions of Neurology, Nephrology, and Rheumatology, Department of Internal Medicine, Nippon Medical School, Tokyo, [2]Department of Physiology, Jichi Medical University, Tochigi, Japan

Objectives: Transplantation of bone marrow stromal cells (MSCs) has been shown to ameliorate ischemic brain injury in animals. A strategy to enhance the abilities of MSCs may be desirable for its application in stroke therapy. FK506 (Tacrolimus), an agent widely used in clinical organ transplantation to prevent allograft rejection, in rheumatic arthritis, and atopic dermatitis, acts by inhibiting calcineurin-mediated T-cell activation via complex formation with FK506 binding protein 12. FK506 has also been found to confer neuroprotective effects against various types of ischemic injury models. In the present study, we investigated whether transplantation of MSCs combined with FK506, clinically used immunosuppressant, enhance neuroprotective effects in experimental stroke.

Methods: Male Sprague-Dawley rats underwent transient 90 min middle cerebral artery occlusion using an intraluminal suture technique. Two or 6 hours after ischemia onset, the rats were randomly assigned to receive intravenous administration of MSCs (1×10^6 cells) plus FK506 (0.3 mg/kg), MSCs alone, FK506 alone, or vehicle. Infarct volume, neurological and immunohistological assessments were performed to examine the effects of these therapies.

Results: In 2-hour post-ischemia treatment groups, significant improvement of infarct volume, edema index, and neurological scores were observed 1 day after combination therapy compared with monotherapies ($p< 0.05$), and this neuroprotection continued for 7 days. Combination therapy significantly reduced the number of TUNEL-positive apoptotic cells, increased Bcl-2 expression, decreased Bax expression, and suppressed neutrophil infiltration and microglia/macrophage activation compared to monotherapies ($p< 0.05$). In 6-hour post-ischemia treatment groups, only in combination therapy group, the significant reduction of infarct volume, edema index, and neurological score were observed ($p< 0.05$). Moreover, the number of engrafted MSCs on day 7 with combination therapy was significantly higher than with MSCs alone ($p< 0.05$).

Conclusions: Clinically relevant dose and a single injection of FK506 enhanced the anti-apoptotic and anti-inflammatory effects of MSC transplantation and increased the survival of transplanted cells, leading to an increase of the therapeutic time window for MSCs. Thus, a combination of cellular and clinically used pharmacological therapy may be feasible and valuable as a neuroprotective strategy for ischemic stroke.

541

EFFECTS OF INTRAVENOUS KETAMINE ON ISCHEMIC DEPOLARIZATION, NEURONAL DAMAGE AND PERIISCHEMIC EXTRACELLULAR GLUTAMATE CONCENTRATION IN GERBILS

H. Taninishi, Y. Takeda, T. Danura, K. Shiraishi, K. Morita

Anesthesiology and Resuscitology, Okayama University Graduate School of Medicine, Dentistry and Pharmaceutical Sciences, Okayama, Japan

Objectives: There are several reports that administration of ketamine during cerebral ischemia is neuroprotective. In the present study, the effects of intravenous ketamine on the duration of ischemic depolarization, histological outcome and dynamic change in extracellular glutamate concentration during cerebral ischemia were determined.

Methods: Thirty male Mongolian gerbils were randomly assigned to a group receiving 1 mg/kg/min of intravenous ketamine (Ketamine group, n = 15) and a group receiving 1% halothane as a control (Halothane group, n = 15). Forebrain ischemia was initiated by occlusion of bilateral common carotid arteries for 5 minutes in all animals. Duration of ischemic depolarization was recorded during cerebral ischemia, and histological outcome was evaluated 5 days after ischemia from the area reflecting bilateral hippocampal CA1 regions. In some animals, a microdialysis probe was inserted in the right hippocampal CA1 region and the dialysate (Ringer's solution at 3 µL /min) was collected every minute from 5 minutes before ischemia to 30 minutes after ischemia. Extracellular glutamate concentration was measured by the use of high-power liquid chromatography. During the experimental period, brain surface and rectal temperatures were maintained at 37.0 ± 0.5 °C from 30 minutes before ischemia to 90 minutes after ischemia. Statistical analysis was performed with Student's t-test (duration of ischemic depolarization and histological outcome) or multiple comparison followed by Tukey-Kramer`s test. A level of $p< 0.05$ was considered to be significant.

Results: Duration of ischemic depolarization in the Ketamine group (4.83 ± 0.99 minutes) was significantly shorter than that in the Halothane group (6.53 ± 1.24 minutes) ($p < 0.01$). The percentage of neuronal damage in the Ketamine group (21.2 ± 8.2 %) was significantly lower than that in the Halothane group (50.9 ± 22.8 %) ($p < 0.05$). Extracellular glutamate concentration in the Ketamine group was significantly lower than that in the Halothane group from the last two minutes during ischemia to the first minute after the reperfusion.

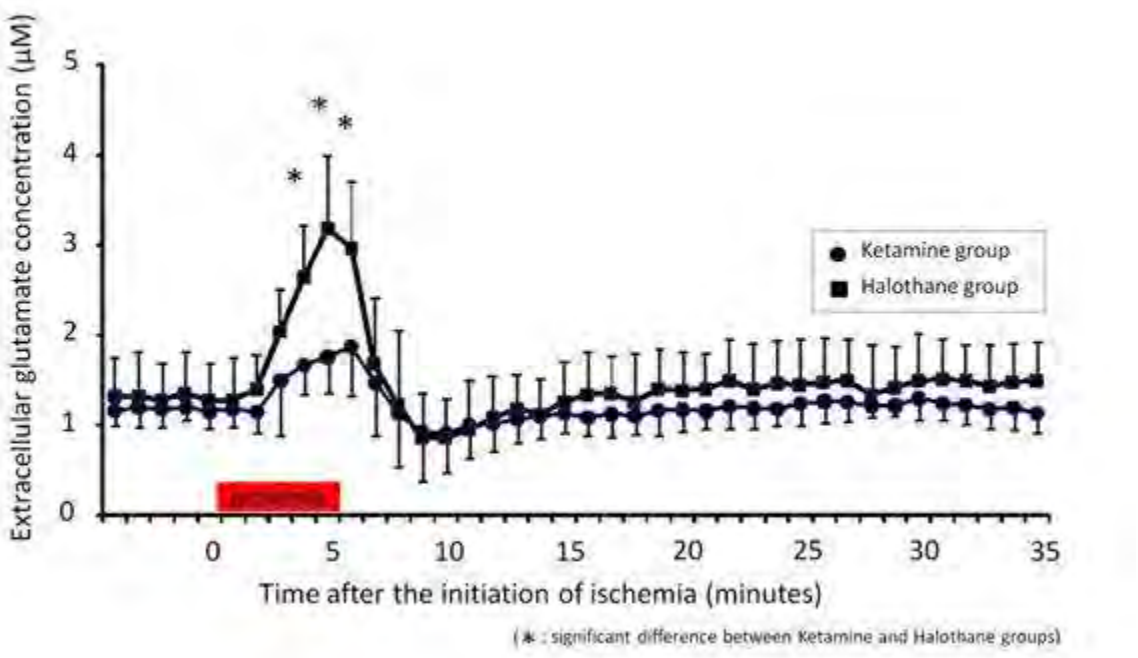

[Figure]

Mean maximum value of extracellular glutamate concentration in the Ketamine group (1.97 ± 0.52 μM) was significantly lower than that in the Halothane group (3.26 ± 0.79 μM) ($p < 0.01$). These values in the Ketamine group and Halothane group were 167% and 247% of pre-ischemic values, respectively.

Conclusion: Administration of intravenous ketamine reduced neuronal damage more than did halothane after 5 minutes of forebrain ischemia in gerbils. Reduction in the duration of ischemic depolarization and lower extracellular glutamate concentration during cerebral ischemia were the factors that contributed to the decrease in neuronal damage by ketamine.

543

IMPACT OF PRETREATMENT AND WITHDRAWAL INTERVALS ON NEUROPROTECTION BY ETHYL EICOSAPENTAENOIC ACID IN A RAT TRANSIENT FOCAL ISCHEMIA MODEL

M. Ueda, T. Inaba, C. Nito, S. Okubo, S. Suda, F. Kamiya, N. Kamiya, Y. Nishiyama, H. Nagayama, Y. Katayama

Neurology, Nippon Medical School, Tokyo, Japan

Objectives: Eicosapentaenoic acid (EPA) is one of the long-chain n-3 polyunsaturated fatty acids, which are derived from marine products. Recently, EPA has attracted considerable attention, because fish consumption is inversely related to stroke risk [1]. In addition, a clinical controlled trial has shown that ethyl EPA (EPA-E) reduces stroke recurrence in hypercholesterolemic patients [2]. We have previously shown that 7 days-pretreatment with ethyl EPA (EPA-E) reduces oxidative stress and ameliorated ischemic brain damage following transient focal ischemia in rats [3]. However pretreatment interval necessary for neuroprotection by EPA-E remains uncertain. The present study examined impact of pretreatment and withdrawal intervals on the neuroprotection by EPA-E using a rat transient focal ischemia model.

Methods: Male Sprague-Dawley rats, weighing 250-300g, were subjected to 90 min focal ischemia using an intraluminal suture technique following an overnight fast under halothane anesthesia. EPA-E (100mg/kg/day) or vehicle was orally administered once a day for 3, 5 or 7 days prior to ischemia induction (n=5, each). Another sets of animals were also subjected to focal ischemia with different withdrawal intervals of 3, 5, or 7 days following 7 days-pretreatment with EPA-E or vehicle in a same way (n = 5, each). Rectal temperature was maintained at 37˚C during ischemia and up to 2 hrs after reperfusion. Cerebral blood flow (CBF) and apparent diffusion coefficient (ADC) images at the level of the bregma were obtained just prior to reperfusion using a 7T MRI system. Neurological scores were assessed based on hemiparesis and abnormal posture using grading scale [4] at 24 hrs after reperfusion, and animals were decapitated to determine infarct volumes using 2,3,5-triphenyltetrazolium chloride (TTC) staining method. Statistical significance was set at $p < 0.05$.

Results: Pretreatment with EPA-E for 7 and 5 days, but not 3 days, showed significant reduction in infarct volumes, as well as significantly improved neurological scores, compared with the vehicle pretreatment. In addition, withdrawal of EPA-E administration for 3 days, but not 5 and 7 days, also demonstrated significant reduction in infarct volumes and significant improvement of neurological scores, compared with the vehicle treatment. Although reduced CBF areas (less than 60% of average in the non-ischemic hemisphere) were not different among the groups, decreased ADC areas (less than 80% of average in the non-ischemic hemisphere) were significantly smaller in EPA-E treated animals showing neuroprotection compared to vehicle-treated animals.

Conclusions: The present study showed that pretreatment with EPA-E for more than 5 days ameliorated brain damage without affecting CBF during ischemia in a rat transient focal ischemia model, and that withdrawal of EPA-E for more than 5 days abrogated the neuroprotective effects of EPA-E pretreatment in the model.

References:

[1] He K, et al. *Stroke* 2004; 35: 1538-1542.

[2] Tanaka K, et al. *Stroke* 2008; 39: 2052-2058.

[3] Ueda M, et al. *J Cereb Blood Flow Metabol* 2009; 29: S427-428.

[4] Amemiya S, et al. *Eur J Pharmacol* 2005; 516: 125-130.

545

IMPACT OF CO-MORBIDITY RISK FACTORS ON THE OUTCOME OF ISCHEMIC STROKE

H. Dhungana[1], T.M. Malm[1], T. Rolova[1], K. Savolainen[1], P.M. Sullivan[2], J. Koistinaho[1]

[1]University of Eastern Finland, Kuopio, Finland, [2]Duke University Medical Center, Durham, NC, USA

Objectives: Apolipoprotein E (ApoE) is a class of lipoproteins with an essential role in the catabolism of triglyceride rich lipid constituents. ApoE exists in three isoforms from which one variants, ApoE4 is associated with an increased risk of heart disease, stroke and Alzheimer's disease. Compared to ApoE3 allele ApoE4 has been demonstrated to be a risk factor also for cognitive impairment in the early phase after stroke. Even though most of the stroke patients suffer from co-morbidities, such as hypercholesterolemia and diabetes, a vast majority of the pre-clinical stroke studies are still carried out on healthy young male mice. Therefore, we investigated the impact of aging and high lipid diet on the severity of ischemic damage in the context of relevant human ApoE isoforms.

Methods: Focal cerebral ischemia was induced by permanent middle cerebral artery occlusion on 13-month-old ApoE3- and ApoE4 targeted replacement (tr) and wild type C57Bl mice fed with Western type diet for 15 weeks. The ischemic infarct was imaged with magnetic resonance imaging (MRI) 3 days post ischemia and the motor deficits were analyzed by using adhesive removal test. Total serum cholesterol was measure before and after the period the mice were onWestern type high fat diet.

Results: High fat diet alone induced deficits in adhesive removal test especially in ApoE4-tr mice. Importantly, also the un-operated ApoE4-tr mice on normal diet had deficits in adhesive removal test compared to ApoE3-tr mice. However, the deficits did not correlate with the size of the ischemic infarct. The total cholesterol levels in serum in ApoE3-tr mice were significantly higher compared to ApoE4-tr mice.

Conclusions: These results show that ApoE4-tr mice develop more severe deficits in motor functions upon high fat diet when compared to ApoE3-tr-mice, irrespective of infarct size and serum cholesterol level suggesting a human ApoE-isoform dependent effect in their overall motor performance.

546

VASCULAR REMODELING AND MICROSTRUCTURAL CHANGES IN A MODEL OF VASCULAR DEMENTIA: A LONGITUDINAL MRI STUDY IN RATS

G. Soria[1,2], R. Tudela[2,3], L. Camón[1], J. Puig[4], S. Pedraza[4], A. Prats-Galino[5], A.M. Planas[1,2]

[1]Dept. of Brain Ischemia and Neurodegeneration, Institut d´Investigacions Biomèdiques de Barcelona, IIBB-CSIC, IDIBAPS, [2]Experimental MRI 7T Unit, IDIBAPS, [3]CIBER de Bioingeniería, Biomateriales y Nanomedicina (CIBER-BBN), Group of Biomedical Imaging, University of Barcelona, Barcelona, [4]IDI Radiology Department, Hospital Universitario Dr. Josep Trueta. IDIBGI.Universitat de Girona, Gerona, [5]Laboratory of Surgical Neuroanatomy, University of Barcelona, Barcelona, Spain

Objectives: Cerebrovascular diseases are the second leading cause of cognitive decline. Damage of brain white matter induced by cerebral hypoperfusion is the main factor causing vascular dementia (1). These white matter lesions affect mainly the prefrontal subcortical circuit, which explains most of the cognitive impairments observed in patients (2). The aim of this work was to longitudinally study how vascular remodeling is developed in a chronic hypoperfusion model in rats, and how it correlates with grey and white matter tissue alterations.

Methods: Longitudinal MRI scans were performed under isofluorane anaesthesia in a BioSpec 70/30 horizontal animal scanner (Bruker BioSpin, Ettlingen, Germany), equipped with a 12 cm inner diameter actively shielded gradient system (400 mT/m) and a phased array surface coil for rat brain. A multimodal imaging study was performed before and 2h, 24h, 7 days, and 3, 7 and 12 weeks after bilateral carotid artery occlusion (BCCAO), or sham-operation, in male Wistar rats (weighting 280-300 gr). The MRI study comprised: T2 relaxometry for lesion evaluation, time of flight angiography to quantify the alterations of main cerebral arteries and Diffusion Tensor Imaging for assessing grey and white matter microstructural changes.

Results: As observed in figure 1, BCCAO significantly affected the vertebro-basilar artery system since it increased in length and tortuosity in comparison to pre-occlusion data ($p < 0.01$) already 10 days following BCCAO. Seven weeks later, these effects were enhanced and significant differences were also demonstrated in comparison to sham-operated animals ($p < 0.01$). In addition, the whole cerebral artery network was significantly increased 10 days after BCCAO compared to sham-operated animals ($p < 0.01$) and to pre-occlusion data ($p < 0.01$). As assessed by DTI, BCCAO significantly altered bilaterally grey and white matter microstructure in cingular and retrosplenial cortex, hippocampus, fornix and anteroventral thalamus. A significant decrease of DTI diffusivity indexes in comparison to sham operated animal ($p < 0.05$) could only be observed at the latest studied time point, i.e. 12 weeks after BCCAO.

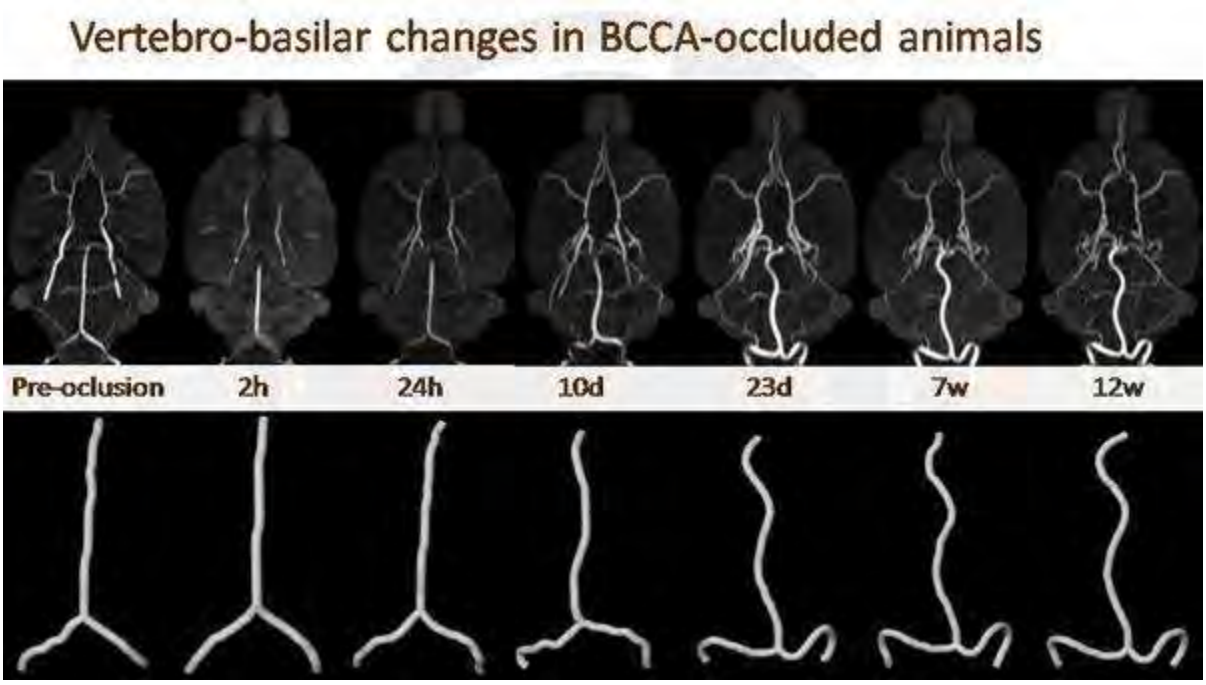

[Figure 1]

Figure 1. Time-course of vascular network increase (upper image) and vertebro-basilar artery increase in length and tortuosity (lower image) after bilateral common carotid artery occlusion in rats.

Conclusions: Under chronic hypoperfusion, the cerebral artery system compensates the decrease in blood flow by increasing the vascular network and by enlarging some of the main arteries, such as vertebro-basilar artery, in agreement with previous reports (3,4). This is the first study showing in living animals the temporal pattern of arteriogenesis induced by hypoperfusion. In addition, in vivo DTI evidenced alterations in grey and white matter microstructure within brain areas associated to cognitive deficits characteristic of vascular dementia.

Acknowledgements: This work was supported by Instituto de Salud Carlos III(FIS PS09/00527) and the European Union (FP7-ARISE 201024) and CIBER-BBN.

References:

1. O´Brien JT et al. 2003. The Lancet 2(2): 89-98.

2. Jokinen H, et al. 2006. J Neurol Neurosurg Psychiatry. 77(1):28-33.

3. Choy M, et al. 2006. J Cereb Blood Flow Metab. 26(8):1066-75.

4. Busch HJ,et al. 2003. J Cereb Blood Flow Metab. 23(5):621-8.

547

CORTICAL NEURONS LIKE GLUCOSE BUT THEY LOVE EATING LACTATE

A. Karagiannis[1], F. Plaisier[1], T. Gallopin[2], H. Geoffroy[2], C. David[3], F. Jarlier[1], S. Nomura[1], E. Guiot[1], B. l'Heureux[4], S. Burgess[4], B. Lambolez[1], J.F. Staiger[3], S. Seino[5], E.M.C. Hillman[4], J. Roeper[6], B. Cauli[1]

[1]Lab. Neurobiology of Adaptive Processes UMR7102, CNRS/UPMC, [2]Lab. Neurobiology UMR7637, CNRS/ESPCI, Paris, France, [3]Dept. of Neuroanatomy, Center of Anatomy, Georg August University, Göttingen, Germany, [4]Lab. Functional Optical Imaging, Dept. of Biomedical Engineering, Columbia University, New York, NJ, USA, [5]Dept. of Physiology and Cell Biology, Division of Cellular and Molecular Medicine, Kobe University, Kobe, Japan, [6]Institute of Neurophysiology, Neuroscience Center, Goethe-University, Frankfurt/Main, Germany

Introduction: Tight coupling between neuronal activity and energy supply is fundamental for functional imaging of the brain in health and disease. In the cerebral cortex, energy substrates fluxes evoked by neuronal activity lead to a transient increase in extracellular lactate while glucose levels remain fairly constant. However, the relative importance of these oxidative substrates to energy production is controversial and the functional consequence of an increased energy supply on neuronal activity is largely unexplored.

Objectives: We sought to evaluate the influence of energy substrates on neuronal activity with particular attention of ATP-sensitive K^+ (K-ATP) channels, which couple energy metabolism to membrane excitability. K-ATP channels are heteromers composed of the both different pore-forming subunits, Kir6.1 or Kir6.2, and distinct regulatory subunits, SUR1 or SUR2. The latter confer differential sensitivity to metabolic or pharmacological modulation. Monitoring the response of neuronal K-ATP channels to changes in extracellular glucose and lactate concentrations offers opportunities to decipher the impact of energy supply on neuronal excitability.

Methods: To evaluate the putative capacity of cortical neurons to sense changes in energetic states, we studied the functional modulation of K-ATP channels by combining patch-clamp recordings, single-cell RT-PCR and pharmacology in rodent acute cortical slices.

Results: Molecular characterization of glutamatergic and GABAergic cortical neurons revealed a promiscuous expression of Kir6.2 and SUR1 subunits and glucose (GluT3) and lactate (MCT1/2) transporters, suggesting that cortical neurons could indeed act as metabolic sensors. Consistently, in rats and wild-type mice, but not in Kir6.2 KO mice, intracellular ATP washout achieved by means of whole-cell recordings induced an outward current reversing near the expected K^+ equilibrium potential. Also, K-ATP channels were activated by the broad spectrum opener diazoxide but not by pinacidil, a SUR2-preferring opener, and closed by tolbutamide, a SUR1-preferring blocker. Using perforated-patch recordings in order to preserve intracellular energy metabolism, we found that decreasing glucose concentrations from 10 to 2.5 mM had no effect on the activity of individual neurons indicating that 2.5 mM glucose is a saturating concentration for ATP production. At 2.5 mM glucose in the extracellular solution, supplementation with lactate to reach an iso-energetic condition to 10 mM glucose enhanced the activity of cortical neurons from rats and wild-type mice, but not from Kir6.2 KO mice. Lactate also occluded the pharmacological blockade of K-ATP channels by tolbutamide. Conversely lactate-sensing in cortical neurons was blocked and reversed by lactate uptake inhibition or by activating K-ATP channels with diazoxide.

Conclusion: Our molecular, biophysical, pharmacological and genetic investigations revealed that cortical neurons express Kir6.2- and SUR1-containing K-ATP channels. We also found that cortical neurons preferentially act as lactate sensors but not as glucose sensors. These observations indicated that lactate, most likely supplied by neighboring astrocytes, is a major oxidative substrate for neurons and support the neuron-to-astrocyte lactate shuttle hypothesis. They also suggest that local lactate-sensing should be considered in the context of functional brain imaging.

548

EFFECT OF ANANDAMIDE ON EARLY INJURY DEVELOPMENT AND MICROGLIA RESPONSE FOLLOWING 4 HR CEREBRAL ISCHAEMIA IN RATS

J. Shearer, S. Coker, H. Carswell

University of Strathclyde, Glasgow, UK

Objectives: Cannabinoids are known to exert anti-inflammatory effects in vivo (Walter and Stella, 2004). As such, these compounds may affect inflammation which is involved in injury development in cerebral ischaemia. Indeed the endocannabinoid, anandamide, reduced infarct size at 24 hrs after transient cerebral ischaemia (Müller et al., 2008). On the other hand, exposure to anandamide in vitro increased microglia migration and enhanced production of the anti-inflammatory cytokine, IL-10 (Walter et al., 2003; Correa et al., 2010). The aim of this study was to investigate the effect of anandamide on injury development and the response of microglia after cerebral ischaemia.

Methods: Male Sprague Dawley rats (275-350 g) were anaesthetised with isoflurane and physiological measurements controlled within normal parameters. Middle cerebral artery occlusion (MCAO) was induced by insertion of a nylon intraluminal suture. Animals were randomly assigned into 3 groups: Group 1: FAAH inhibitor URB597 (0.3 mg/kg, s.c) administered immediately post-MCAO and the vehicle for anandamide administered at 30 min post-MCAO (n=6); Group 2: anandamide (10 mg/kg, s.c.) administered at 30 min post-MCAO and the vehicle for URB597 given immediately post-MCAO (n=5); and Group 3: vehicles for both URB597 and anandamide given at appropriate time-points (n=6). At 4 hrs post-MCAO, brains were snap frozen and injury volume determined. For immunofluorescence, microglia were stained with anti-Iba-1 and labeled with a FITC-conjugated secondary antibody. Positively stained cells were counted in 3 fields at the injury boundary (1 field in the cortex and 2 fields in the striatum) and corresponding areas in the contralateral hemisphere. Microglia numbers were expressed as cells per mm^3. The effect of treatment on microglia activation has yet to be elucidated. Injury volume and cell numbers were compared between groups using a one-way ANOVA.

Results: Physiological variables during the procedure did not vary between treatment groups. Treatment with anandamide and URB597 did not affect injury development at 4 hrs following occlusion (58.0±6.7mm^3 and 59.6±4.6mm^3, respectively) compared to vehicle (54.1±5.2mm^3). Numbers of microglial cells were similar in the ipsilateral and contralateral hemispheres in all of the treatment groups and did not vary among the groups (for ipsilateral versus contralateral striatum: anandamide: 0.32±0.04 vs 0.32±0.05; URB597: 0.34±0.03 vs 0.36±0.07; vehicle: 0.32±0.08 vs 0.36±0.09). A similar pattern was observed in the cortex.

Conclusions: These results demonstrate that anandamide, either administered exogenously or enhanced by metabolic inhibition, did not affect early injury development. There was no evidence of an effect on microglia migration.

References:

Correa F, Hernangómez M, Mestre L, Loría F, Spagnolo A, Docagne F et al. (2010). Anandamide enhances IL-10 production in activated microglia by targeting CB_2 receptors: roles of ERK1/2, JNK, and NF-kappaB. Glia 58(2), 135-147.

Müller H, Sommer C, Schwab S, Schäbitz W and Schomacher M (2008). Endocannabinoids mediate neuroprotection after transient focal cerebral ischemia. *Brain Res*. 1240:213-20.

Walter L, Franklin A, Witting A, Wade C, Xie Y, Kunos G et al. (2003). Non-psychotropic cannabinoid receptors regulate microglial cell migration. *J Neurosci.* 23: 1398-1405.

Walter L and Stella N (2004). Cannabinoids and neuroinflammation. *Br J Pharmacol* 141: 775-785.

549

POST-STROKE OF ADMINISTRATION OF ETHANOL PROTECTS AGAINST FOCAL ISCHEMIC BRAIN INJURY IN RATS

X. Ji[1,2], Y. Wang[1], F. Wang[1,3], Y. Luo[1], X. Liu[1], F. Ling[2], Y. Ding[1,4]

[1]Cerebral Vascular Disease Institute, [2]Department of Neurosurery, XuanWu Hospital, Capital Medical University, Beijing, [3]Ningxia Medical University, Yinchuan, China, [4]School of Medicine, Wayne State University, Detroit, MI, USA

Objective: Epidemiologic data suggest that although high level of alcohol consumption is linked to an increased risk for stroke, light or moderate alcohol consumption may render the brain more resistant to stroke. Several animal studies have shown that ethanol-induced preconditioning protects against ischemic injury in both heart and brain, and the underlying mechanism of neuroprotection may be attributable to the ability of ethanol to inhibit NMDA receptors or activate GABA neurotransmission. However, from the clinical point of view, it is unknown whether a post-stroke ethanol treatment is effective in reducing ischemic brain injury. Therefore, the present study was to test the neuroprotective efficacy of post-stroke administration of ethanol in a rat model of focal cerebral ischemia (FCI).

Methods: FCI was induced in adult male SD rats by intraluminal filament occlusion of the middle cerebral artery (MCAO) for 2 hr. In the first set of experiments, ethanol (0.5, 1.0, or 1.5 g/kg) or saline of the same volume (3 ml) was administrated intraperitoneally at the onset of reperfusion. Infarct volume was measured on TTC-stained sections 48 hr after MCAO. Sensorimotor functions of the animals were assessed 2-28 days after MCAO. In the second set of experiments, ethanol (1.5 g/kg) was administrated without or with induction of mild hypothermia (33^{o}C) in animals. Infarct volume was measured 48 hr after MCAO to determine whether combined ethanol and hypothermia offer additive neuroprotective effect compared to either treatment alone. The third set of experiments was to determine whether post-stroke administration of either ethanol or thrombolytic drug (t-PA, urokinase) or in conjunction increase hemorrhagic transformation (HT) during reperfusion. t-PA (2.5 mg/kg bolus followed by 30-minute infusion at 5 mg/kg/hr) or urokinase (170,000IU/kg infused at 4000IU/min) was administrated intravenously beginning at 15 min of reperfusion without or with preceding ethanol treatment (1.5 g/kg). Brain HT was quantitatively measured 48 hr after MCAO using the spectrophotometric hemoglobin assay.

Results: Compared to saline-treated group, post-stroke administration of ethanol at the dose of 1.5g/kg significantly reduced infarct volume (29.20±5.13% *vs.* 53.8±6.11% of contralateral hemisphere, $p< 0.05$, n=10/group) and improved sensorimotor functions ($p< 0.05$, n=10/group) after MCAO. Post-stroke administration of ethanol (1.5 g/kg) or transient induction of mild hypothermia during MCAO (starting 90 min after MCAO until the onset of reperfusion) offered comparable neuroprotective effect against infarction (29.20±6.10% for ethanol *vs.* 29.12±3.40% for hypothermia, $p>0.05$, n=6/group). However, the combination of ethanol and hypothermia treatment (26.55±8.09%, n=6) conferred no further neuroprotection compared with either treatment alone ($p>0.05$ *vs.* ethanol group or hypothermia group). Post-stroke administration of ethanol ((1.5 g/kg) followed by t-PA or urokinase infusion did not increase brain hemorrhagic transformation 48 hr after MCAO compared to either treatment alone.

Conclusions: Our results provide novel evidence that post-stroke administration of moderate dose of ethanol is neuroprotective against focal cerebral ischemia, resulting in reduced infarct volume and improved sensorimotor functions in stroked rats. We suggest that low to moderate

doses of ethanol may be safe either use alone or in conjunction use with a thrombolytic drug for the treatment of ischemic stroke.

550

PLASMA C3 AND C3A LEVELS IN CRYPTOGENIC AND LARGE VESSEL DISEASE STROKE: ASSOCIATIONS WITH OUTCOME

A. Stokowska[1], S. Olsson[2,3], L. Holmegaard[2,4], K. Jood[2,4], C. Blomstrand[2,4], C. Jern[2,3], M. Pekna[1]

[1]Medical Chemistry and Cell Biology, [2]Institute of Neuroscience and Physiology, Section for Clinical Neuroscience and Rehabilitation, [3]Department of Clinical Genetics, University of Gothenburg, [4]Department of Neurology, Sahlgrenska University Hospital, Gothenburg, Sweden

Background and aims: Inflammation seems to be a key player in the pathophysiology of stroke. There is, however, only a limited number of reports on systemic activation of the complement system in ischemic stroke. In this study, we intended to compare plasma C3 and C3a levels in two etiologically different ischemic stroke subtypes, namely among cryptogenic and large vessel disease (LVD) stroke survivors as well as control subjects, and to evaluate their association to functional outcome after three months and two years.

Methods: C3 and C3a in plasma of 79 cryptogenic and 73 LVD stroke patients, sampled within 10 days and at three months after stroke, and age- and sex-matched control subjects from the Sahlgrenska Academy Study on Ischemic Stroke was measured by ELISA. Functional outcome was assesed with the modified Rankin Scale.

Results: Plasma C3 was increased in both stroke groups at both time points. Systemic elevation of C3a was limited to the acute phase in the cryptogenic stroke group, wheras plasma C3a levels in the LVD group were also elevated at three-month follow-up. In the LVD group, three-month follow-up plasma C3 levels in the upper third were associated with unfavourable outcome after three months independently of age and sex (OR 5.56; 95% CI 1.03-29.93, *P*=0.045) as well as after two years (OR 4.75; 95% CI 1.11-20.30, *P*=0.036). In the cryptogenic stroke group, high plasma C3a levels in the acute phase were associated with unfavourable outcome after three months (OR 3.75; 95% CI 1.01-13.96, *P*=0.049) in the univariate analysis but not after adjustment for age and sex (*P*=0.050).

Conclusions: Plasma C3 and C3a levels are elevated in cryptogenic and LVD stroke and the predictive value of these markers may depend on stroke subtype.

551

NONINVASIVE TARGETING DELIVERY AND MRI DETECTION OF LIVE APOPTOTIC LESIONS IN RAT BRAINS AFTER CEREBRAL ISCHEMIA WITH MULTIFUNCTIONAL MAGNETIC NANOPARTICLE

A. Saito[1], M.M. Mekawy[2], A. Sumiyoshi[2], J. Riera[2], H. Shimizu[3], R. Kawashima[2], T. Tominaga[4]

[1]Neurosurgery, Kohnan Hospital, [2]Functional Brain Imaging, The Institute of Development, Aging and Cancer, Tohoku University, [3]Neuroendovascular Therapy, [4]Neurosurgery, Tohoku University Graduate School of Medicine, Sendai, Japan

Objectives: Apoptotic neuronal cell death is known to be programmed and delayed cell death after a variety of stimuli, such as cerebral ischemia, trauma, tumor expansion and metabolic abnormality. Apoptosis is facilitated by cell death signaling factors such as activated caspases. Precise evaluation and extrinsic control of these factors might protect lethal neuronal cells and have been focused as novel therapeutic strategy. In vivo detection of neuronal apoptosis is an expected methodology for regional assessment for the treatment of cerebral ischemia. However, high resolution image analysis of in vivo neuronal apoptosis has not been established. We developed novel magnetic resonance image (MRI) detection of in vivo neuronal apoptosis with nanomagnetic particle conjugated with caspase inhibitor.

Methods: Iron oxide magnetic nanoparticle (MNP) conjugated with FLIVO, pan-caspase inhibitor bound with fluorescent dye, sulphorhodamin B was newly fabricated as SR-FLIVO-MNP for MRI detection. As preliminary trial, cultured apoptotic cells induced by hydrogen peroxide were incubated with SR-FLIVO-MNP. SR-FLIVO expression and TUNEL immunopositivity was evaluated. Rat focal cerebral ischemia was induced by transient middle cerebral artery occlusion with intraluminal suture model. SR-FLIVO-MNP was intravenously administered to ischemic rat 1 hour before the scan and rat brains were scanned by 7T MRI.

Results: Intracellular accumulation of SR-FLIVO-MNP was specifically observed in vitro apoptotic cells. Accumulation of Iron oxide MNP was detected as hypointensty region of T2* mapping on MRI. Intracellular accumulation of SR-FLIVO-MNP was observed in apoptotic neuronal cells as colocalization of fluorescent SR-FLIVO with TUNEL immunopositivity in the T2* hypointensity region. Electromicroscope showed accumulation of Fe particles in morphological apoptotic cells. Immunopositivities of SR-FLIVO and TUNEL were significantly co-related to T2* signal reduction.

Conclusions: The newly developed MNP targeting activated caspases successfully detected apoptotic findings in live ischemic rat brains on MRI. The SR-FLIVO-MNP might be expected for a new moiety for noninvasive MRI detection of neuronal apoptosis and targeting delivery to live apoptotic cells.

552

UTILITY OF EARLY POSTTREATMENT SPECT IN EVALUATING THERAPEUTIC EFFICACY AND SAFETY OF INTRAVENOUS TISSUE PLASMINOGEN ACTIVATOR THERAPY

T. Abumiya, M. Kato, M. Yoshino, T. Aoki, H. Imamura, T. Aida

Hokkaido Neurosurgical Memorial Hospital, Sapporo, Japan

Background and purpose: Therapeutic efficacy and safety of intravenous tissue plasminogen activator (tPA) therapy is dependent on the timing and degree of cerebral reperfusion. In these days it becomes more necessary to know the therapeutic efficacy and safety early after intravenous tPA therapy because endovascular approach would be the next step when intravenous tPA therapy fails to get an early recovery. To evaluate the therapeutic efficacy and safety by the cerebral perfusion state we performed single photon emission computed tomography (SPECT) in patients treated with intravenous tPA therapy in the early posttreatment period.

Methods: We measured cerebral blood flow by 99mTc-HMPAO or 99mTc-ECD SPECT in 25 patients (mean age, 71.9 ± 8.7 years; 13 men) treated with tPA due to ischemia in the anterior circulation at one hour after tPA therapy. Asymmetry index depending on side-to-side (ipsilateral-to-contralateral) comparison was calculated on each SEPCT image by using Focus Image software. Hypoperfusion or hyperperfusion was defined as 25% lower or 25% higher CBF values in asymmetry index, respectively.

Results: Of 25 patients 16 had only hypoperfusion, 4 had both hypoperfusion and hyperperfusion, 2 had only hyperperfusion, and 3 had no significant hypo- and hyperperfusion. Volumes of hypoperfusion were significantly correlated with NIHSS scores at the end of tPA infusion ($r=0.820$, $p< 0.0001$) and modified Rankin scale (mRS) at 3months ($r=0.709$, $p=0.0001$). Six patients with hyperperfusion had relatively a good outcome compared to 16 patients with only hypoperfusion but the difference did not reach statistically significant level (mRS of patients with hyperperfusion; 1.67 ± 1.63 vs mRS of patients with hypoperfusion; 2.44 ± 2.03, $p=0.189$). Three of the 6 patients with hyperperfusion showed marked hyperperfusion area which went into reperfusion injury but not hemorrhagic transformation. Hemorrhagic transformation was observed in 6 patients (one symptomatic) and most of them occurred in the marked hypoperfusion area.

Conclusions: Early posttreatment SPECT after tPA therapy was useful in evaluating the therapeutic efficacy and safety. The results of this study demonstrated that volumes of hypoperfusion were associated with therapeutic outcome, marked hypoperfusion seemed to have a possibility of hemorrhagic transformations, and hyperperfusion seemed to be a sign of good outcome. These findings would be helpful in decision-making of the next therapeutic steps especially when we decide the option of endovascular approach.

553

CAVEOLIN-1 DELETION REDUCES EARLY BRAIN INJURY AFTER EXPERIMENTAL INTRACEREBRAL HEMORRHAGE

C.-F. Chang[1,2], S.-F. Chen[3,4], S.-K. Shyue[2]

[1]Graduate Institute of Life Sciences, National Defense Medical Center, [2]Institute of Biomedical Sciences, Academia Sinica, [3]Department of Physical Medicine & Rehabilitation, Cheng Hsin General Hospital, [4]Department of Physiology, National Defense Medical Center, Taipei, Taiwan R.O.C.

Purpose: Intracerebral hemorrhage (ICH) is a type of stroke with high mortality characterized by extravasation of blood into brain parenchyma and formation of hematoma. Despite its public importance, effective medical treatment has been unsatisfactory. Caveolin-1 (Cav-1) is the major component of caveolae, a membrane microdomain within lipid raft, known for its role in regulating cholesterol homeostasis and signal transduction. In central nerve system, the pathophysiological role of Cav-1 has been reported to maintain the nerve architecture and regulate neuronal plasticity. Overexpression of Cav-1 is associated with Alzheimer's disease; however, ablation of the Cav-1 gene increases the extent of cerebral ischemic injury. The role of Cav-1 in ICH remains unknown. In the present study, we investigated the role of Cav-1 and its underlying mechanisms in the pathogenesis of ICH.

Methods: ICH was induced by microinjecting collagenase VII-S into the striatum of both wild type (WT) and Cav-1 knockout (KO) mice. Primary cortical neuronal cultures were used to examine the contribution of Cav-1 to ICH-induced neuronal injury. Lentiviral vector transduction of shRNA and siRNA transfection were performed for validating the underlying mechanisms of Cav-1 inhibition in ICH.

Results: Cav-1 was up-regulated in the peri-hematomal area and the cellular distribution of Cav-1 was detected within neuron and endothelial cell in human and mouse brain. Cav-1 knockout (KO) mice had smaller injury volumes, milder neurological deficits, less brain edema and neuronal death 1 day after ICH than wild-type mice. The protective mechanism in Cav-1 KO mice was associated with marked reduction in leukocyte infiltration, decreased expression of inflammatory mediators, including macrophage inflammatory protein-2 and cyclooxygenase-2, and reduced matrix metalloproteinase-9 activity. Deletion of Cav-1 also suppressed heme oxygenase (HO)-1 expression and attenuated reactive oxygen species production after ICH. Moreover, deletion or knockdown of Cav-1 decreased neuronal vulnerability to hemin-induced toxicity and reduced HO-1 induction in vitro.

Conclusion: These data suggest that Cav-1 plays a deleterious role in early brain injury after ICH. Inhibition of Cav-1 may provide a novel therapeutic approach for the treatment of hemorrhagic stroke.

References:

1. Gaudreault SB, Dea D, Poirier J: Increased caveolin-1 expression in Alzheimer´s

disease brain. Neurobiol Aging 2004, 25:753-7592.

2. Razani B, Woodman SE, Lisanti MP: Caveolae: from cell biology to animal

physiology. Pharmacol Rev 2002, 54:431-4673.

3. Wang J, Dore S: Heme oxygenase-1 exacerbates early brain injury after intracerebral haemorrhage. Brain 2007, 130:1643-1652

4. Xi G, Keep RF, Hoff JT: Mechanisms of brain injury after intracerebral haemorrhage. Lancet Neurol 2006, 5:53-63

554

ACTIVATION OF SIGNAL TRANSDUCERS AND ACTIVATORS OF TRANSCRIPTION 3 IN THE HIPPOCAMPAL CA1 REGION OF RAT ISCHEMIC PRECONDITIONING MODEL

T. Yagi, H. Yoshioka, T. Wakai, T. Kato, T. Horikoshi, H. Kinouchi

Neurosurgery, Interdisciplinary Graduate School of Medicine and Engineering, University of Yamanashi, Chuo, Japan

Objectives: Ischemic tolerance is a well-known phenomenon in which ischemic preconditioning (PC) affords robust protection against subsequent lethal ischemia; however, its protective mechanisms are still obscure. The signal transducers and activators of transcription 3 (STAT3) are essential for the regulation of apoptosis and cell death initiated by a pro-survival signaling cascade. PC of the heart induces STAT3 tyrosine and serine phosphorylation, both of which seem to be necessary for full transcriptional activation of PC-associated genes. Also in cortical neurons, STAT3 serine phosphorylation was reported to play an important role in the protective effects of ischemic PC induced by oxygen-glucose deprivation. However, the precise role of STAT3 serine phosphorylation in ischemic tolerance of the brain remains unclear. In this study, we examined the phosphorylation status of ser727-STAT3 in the hippocampal CA1 region after nonlethal ischemia and lethal ischemia with or without PC.

Methods: Male Sprague-Dawley rats were subjected to transient forebrain ischemia by bilateral common artery occlusion with hypotension for 3 min as nonlethal ischemia or 5 min as lethal ischemia. For experiments of ischemic PC, the rats were first subjected to 3 min of ischemia, then 5 min of ischemia 2 days later. Ischemic neuronal injury was evaluated in the hippocampal CA1 region 5 days after ischemia by cresyl violet and Tunnel staining. Fresh brain tissue of each ischemic group was removed after 1, 4, 8 h and 1, 2 and 7 days (n=5) of reperfusion. Western blot analyses and immunohistochemistry of samples from the hippocampal CA1 region were used to investigate the expression of serine phosphorylation of STAT3. Localization of phosphorylated STAT3 was examined by double immunofluorescence. STAT3 inhibitor peptide was infused into the right intracerebral ventricle to investigate the role of STAT3 serine phosphorylation in PC.

Results: Western blot analysis showed that ser727-STAT3 phosphorylation was induced in the hippocampal CA1 region after transient forebrain ischemia. Phosphorylation of ser727-STAT3 transiently increased with maximal at 1 hour of reperfusion after lethal ischemia, in contrast, it gradually increased in a time-dependent manner and peaked at 2 day after nonlethal ischemia. In the preconditioned brains, phosphorylation of ser727-STAT3 increased at 1 h to 4h of reperfusion, and the decrease of its levels was delayed compared to the nonconditioned brains. A double immunofluorescent study revealed that phosphorylated-STAT3 positive cells colocalized with neuron-specific nuclear protein, suggesting phosphorylated-STAT3 expressed in CA1 neurons. Furthermore, inhibition of STAT3 phosphorylation abolished PC-induced neuroptotection.

Conclusions: These results suggest that phosphorylation of ser727-STAT3 after nonlethal ischemia is closely associated with neuroprotection and acquision of ischemic tolerance as one of the survival signals in hipoccampal CA1 neurons. Although further investigation is necessary to clarify the exact role of STAT3 serine phosphorylation in neuroprotection, STAT3 can be an important target for stroke therapy.

555

THE CLINICAL EFFICACY OF COMBINED THERAPY WITH OZAGREL AND EDARAVONE IN DIABETIC OR NON-DIABETIC PATIENTS WITH NONCARDIOEMBOLIC STROKE

T. Toyoda, I. Yonekura, S. Yoshida, T. Shiode

Neurosurgery, Tokyo Koseinenkin Hospital, Tokyo, Japan

Objectives: Ozagrel, a thromboxane A2 synthase inhibitor and antiplatelet agent, and edaravone, a free radical scavenger and neuroprotectant, were widely used for the treatment of acute ischemic stroke in Japan. The results of clinical trials that have investigated the effect of ozagrel or edaravone in acute ischemic stroke have been consistent. Theoretically, the combined use of both agents could be beneficial. We therefore conducted a retrospective study in which we compared the effect of combined therapy with each single agent therapy. Diabetes is a major risk factor for the stroke, and stroke patients with diabeted have poorer prognosis with higher morbidity. Little is known that beneficial effects of ozagrel and edaravone in stroke treatment for the patients with diabetes. We also investigated a retrospective study in which we compared the effects of these agents in the diabetic and nondiabetic patients.

Methods: The subjects consisted of 199 patients (141 male and 58 female, mean age of 68 years) with noncardioembolic cerebral infarction. All patients were divided into 4 treatment groups: Group Control: patients received without ozagrel or edaravone; Group Oz: patients administered with ozagrel; Group Ed: patients administered with edaravone; Group Oz-Ed: patients administered with ozagrel and edaravone. To evaluate the clinical efficacy of the combination of these drugs in patients with and without diabetes mellitus, each treatment groups were divided separately into diabetic and nondiabetic subjects. To evaluate neurological deficits, change in the Japan stroke scale (JSS) score and the National Institute of Health stroke scale (NIHSS) score were assessed from day 0 (before treatment initiation) to Week 4. To evaluate the functional outcome, the Modified Rankin scale (mRS) was assessed at 3 months after admission.

Results: The mean JSS score improvement was significantly higher in the Group Ed ($p=0.033$) and Group Oz-Ed ($p=0.0025$) than in the group Control. The mean NIHSS score improvement was also significantly higher in the Group Oz-Ed than in the Group Control ($p=0.024$). The mRS assessment results for each treatment group at 3-month after onset. Significant difference was observed for the Group Oz-Ed compared with the Group Control ($p=0.017$). We also demonstrate the mean improvement score in JSS and NIHSS in the patients with and without diabetes mellitus. Among diabetic patients, Group Ed achieved statistically significance in JSS score improvement compared with control ($p=0.0025$). Among diabetic patients, no significant intergroup differences were observed for the improvement of NIHSS score.

Conclusion: Our analysis suggests that combination therapy with ozagrel and edaravone is more effective for the treatment of acute ischemic stroke, while the efficacy of ozagrel is limited in diabetic patients.

References:

1.Shinohara Y. Saito Isamu, Kobayashi S, Uchiyama S. Edaravone (radical scavenger) versus sodium ozagrel (antiplatelet agent) in acute noncardioembolic ischemic stroke (EDO trial). Cerebrovasc Dis 2009; 27:485-492.

2.Van Swieten JC, Koudstaal PJ, Visser MC, Shouten HJA van Gijin J: Interobserver agreement for the assessment of handicap in stroke patients. Stroke 1998; 19:604-607.

556

SURGICAL TREATMENT OF CAROTID ARTERIAL STENOSIS WITH HIGH RISK PATIENTS

T. Tsukahara

Neurosurgery, NHO Kyoto Medical Center, Kyoto, Japan

Purpose: Choice of carotid endarterectomy (CEA) or carotid artery stenting (CAS) for cervical carotid stenosis has not been established. In this study we report our clinical results of CAS and CEA and suggest an appropriate treatment strategy.

Methods: From January 2001 to December 2009 we surgically treated carotid stenosis for 171 lesions by CEA and for 251 lesions by CAS. Symptomatic stenosis was 68% and average stenotic rate was 83% in CEA and symptomatic stenosis was 62% and average stenotic rate was 65% in CAS. Short-time surgical results and long-term results were also examined.

Results: Stenosis of carotid arteries was relieved in all cases after CEA or CAS. Surgical mortalities of CEA and CAS were 0.6% (1/167) and 0.4% (1/258), respectively. Surgical morbidities by ischemic stroke of CEA and CAS were 3.0% (5/167) and 1.1% (3/258), respectively. Surgical morbidity was not high in patients with medical risk factors or bilateral lesions. Long-term outcome after CAS is not inferior to it after CEA.

Conclusion: Carotid stenotic lesions can be treated with comparably low morbidity and mortality rates using CEA or/and CAS even with high risks, when choosing appropriate surgical methods considering each characteristic of carotid stenosis.

557

SHORT-TERM CLINICAL OUTCOME FOLLOWING MR-BASED TREATMENT IN STROKE PATIENTS WITHIN 3 HOURS OF ONSET DUE TO ACUTE CAROTID ARTERY OCCLUSION

T. Mori, H. Tajiri, T. Iwata, Y. Miyazaki, M. Nakazaki

Stroke Treatment, Shonan Kamakura General Hospital Stroke Center, Kamakura, Japan

Purpose: The purpose of our retrospective study is to investigate short-term clinical outcome following MR-based treatment in stroke patients admitted within 3 hours from sudden onset due to acute carotid artery occlusion.

Method: Criteria for retrospective analysis were acute stroke patients 1) who were admitted to our institution within 3 hours of stroke onset between Jan 2006 and March 2010, 2) who presented NIHSS score of 6 or more on admission, and 3) who underwent emergency MR imaging on admission, which suggested the affected carotid artery occlusion. Baseline features, mRS before admission (mRS-b), NIHSS on admission (NIHSS adm), DWI-ASPECT score, reperfusion therapy, NIHSS on the 7th day, hospitalization period, and in-hospital death were investigated. Variables to predict in-hospital death or reperfusion therapy were assessed with multivariate analysis and short-term clinical outcome was evaluated in patients with reperfusion therapy (group R) and without reperfusion therapy (group non-R).

Results: Sixty-three patients were analyzed. Age was 79.5±10.7 years (mean±SD), man was 33.3%(21/63), mRS-b (median) was 0, NIHSS adm (median) was 21, DWI-ASPECT score (median) was 6, twenty patients (31.7%: 20/63) underwent reperfusion therapy (intravenous rt-PA:2 pts, endovascular therapy: 18 pts), 7-day NIHSS (median) was 19, hospitalization period was 9 days (median), and in-hospital death rate was 36.5% (23/63). Multiple regression analysis showed that DWI-ASPECT score ($p < 0.01$) was an independent variable for in-hospital death and the ROC curve indicated that the cut-off value was 4 (sensitivity 73.9%, specificity 77.5%). The DWI-ASPECT score was an independent variable for reperfusion therapy and the cut-off value was 5.5 (sensitivity 61.9%, specificity 76.2%). In group R and non-R, in-hospital death was 5 (25%), NIHSS adm and 7-day NIHSS (median) were 19 and 13. In group non-R, 18 patients (41.9%) died within 3.5 days (median) after in-hospitalization. In the other survived 25 patients of group non-R, NIHSS adm and 7-day NIHSS (median) were 19 and 15, and thus their seven-day NIHSS score was improved.

Conclusion: MR imaging on admission was useful in providing acute stroke patients with appropriate treatment immediately, who were admitted within 3 hours of onset due to the carotid artery occlusion. The lower DWI-ASPECT score was the independent variable for in-hospital death and short-term clinical outcome was not unfavorable in patients of group R and non-R.

558

MAGNETIC RESONANCE IMAGING OF REDOX ACTIVITY IN THE BRAIN OF NORMAL AND CANCER-BEARING MAMMALIANS: A RADICAL DIAGNOSTIC APPROACH

Z. Zhelev[1], R. Bakalova[1], S. Shibata[1], L. Spasov[2], I. Aoki[1]

[1]Molecular Imaging Center, National Institute of Radiological Sciences, Chiba, Japan, [2]Medical Faculty, Sofia University 'St. Kl. Ohridski', Sofia, Bulgaria

Objectives: The present study shows that oxidation/reduction (redox) activity of the brain is a valuable diagnostic marker for carcinogenesis. This parameter could be evaluated in vivo (in the brain of intact mammalians), using magnetic resonance imaging (MRI) and redox-sensitive and blood-brain barrier (BBB) permeable nitroxide probes. The method allows a differentiation of cancer development from normal (healthy) condition.

Methods: The animals (Balb6 mice) were separated in two experimental groups - healthy mice (controls) and cancer-bearing mice (with experimental neuroblastoma or glioma). The mice were used 8-15 days after inoculation of cancer cells in the brain. They were subjected to anesthesia (1.5% isoflurane). The nitroxide probe (TEMPOL or SLENU; 1/2 of LD50 dose) was injected intravenously and T_1 weighted (gradient-echo) MRI of mouse brain was performed on 7 Tesla Magnet. Two regions of interests were selected - brain tissue (cortex) and soft tissues surrounding the brain. The nitroxide radical (which is characterized by T_1 contrast properties) participates in electron-transfer reactions (with cellular oxidants and reducers) with formation of non-contrast intermediate products. The rate constants of these reactions determine the MRI signal dynamics (enhancement, resp. decay) in the brain after injection of nitroxide, which could be used as a diagnostic marker for tissue redox activity.[1]

Results: In the brain of control mice, the MRI signal intensity increased slightly after injection of nitroxide probe, followed by rapid decay. The half-life ($t_{1/2}$) of MRI signal decay was about 1 min or 2 min 20 sec in the brain or surrounding tissues, respectively. These $t_{1/2}$ values could be considered as reference values for the redox activity of the respective tissues in norm. In the control group, the profile of the histograms and $t_{1/2}$ values are indicative of a high reducing activity of the brain and surrounding tissues to the nitroxide radical.In cancer-bearing mice, the profiles of MRI signal dynamics in the brain and surrounding tissues after injection of nitroxide probe were completely different from the reference profiles. The MRI signal intensity increased and remained high and stable over 14 min, without decay. The histograms were same in the cancer hemisphere of the brain, “normal” (non-cancer) hemisphere, and “normal” surrounding tissues. These profiles and $t_{1/2}$ values are indicative of a low reducing activity of the brain and surrounding tissues of cancer-bearing animals to the nitroxide probe. The “normal” tissues arround the tumor have a different metabolic activity from the pre-cancer state, making them more sensitive to damage.

Conclusions: There is a very clear difference between MRI signal dinamics of SLENU and TEMPOL in healthy and cancer-bearing brain, which is indicative of different metabolic (redox) activity of both tissues. The half-life of MRI signal decay is an appropriate diagnostic marker for carcinogenesis in the brain and a prognostic marker for efficiency of cancer therapy. The described methodology is also applicable in isolated tissue specimens (e.g., biopsy specimens).

References:

[1] Z. Zhelev, R. Bakalova, I. Aoki, V. Gadjeva and I. Kanno, Mol. BioSystems 2010, 6, 2386.

559

BRAIN ISCHEMIA PROMOTES FOCAL ANGIOGENESIS IN AGED RATS

Y.H. Tang[1], K.L. Jin[2], L.Q. Wang[3], Y. Wang[1], G.-Y. Yang[1,4]

[1]Neuroscience and Neuroengineering Center, Med-X Research Institute, Shanghai Jiao Tong University, Shanghai, China, [2]Buck Institute for Age Research, Novato, CA, USA, [3]Wenzhou Medical College, Wenzhou, [4]Department of Neurology, Shanghai Ruijin Hospital, School of Medicine, Shanghai Jiao Tong University, Shanghai, China

Introduction: Aging is a risk factor for cerebrovascular disease including ischemic stroke. Accumulating evidence suggests that aging slows down angiogenesis and vasculogenesis [1], which are both important processes for long term recovery after ischemic stroke [2]. However, it is unclear whether and how aging affects the outcomes of ischemia in aged rats. In this work we investigated angiogenesis and arteriogenesis in young and aged rat brain in response to focal ischemia.

Methods: Three-month young rats (n=4) and twelve-month aged rats (n=4) were conducted to distal middle cerebral artery occlusion (MCAO). Animals were sacrificed after two months of MCAO. The brains were removed and fixed in 4% paraformaldehyde. Paraffin coronal brain sections (4 μm in thickness) were acquired for immunohistochemistry. For infarction area analysis, brain sections were stained with cresyl violet and the infarct volume was calculated using NIH image J software. Lectin, CD-31, vWF, and alpha smooth muscle cell actin staining were used to quantify angiogenesis and arteriogenesis in both young and aged stroke rats.

Results: Under normal condition, aging did not affect the number of microvessel counts (aged sham 24±2 vs. young sham 26±1 microvessels per field, $p>0.05$, n=4). In contrast, decreased number of small arteries was observed in aged rats (aged sham 5±0.3 vs. young sham 6±0.2, $p< 0.05$, n=4). Our data showed that ischemia promoted angiogenesis and arteriogenesis in both aged and young rats compared to their corresponding shams ($p< 0.01$). Infarct volume in aged rats is larger than that in young rats ($p< 0.05$). Interestingly, similar number of microvessels was observed in young and aged rats following MCAO (young MCAO 62±1 vs. aged MCAO 58±1 microvessels per field, Figure 1A. $p>0.05$), while much more small arteries were observed in aged ischemic rats than in young ischemic rats (young MCAO 11±0.5 vs. aged MCAO 18±1.2 per field, Figure 1B. $p< 0.01$).

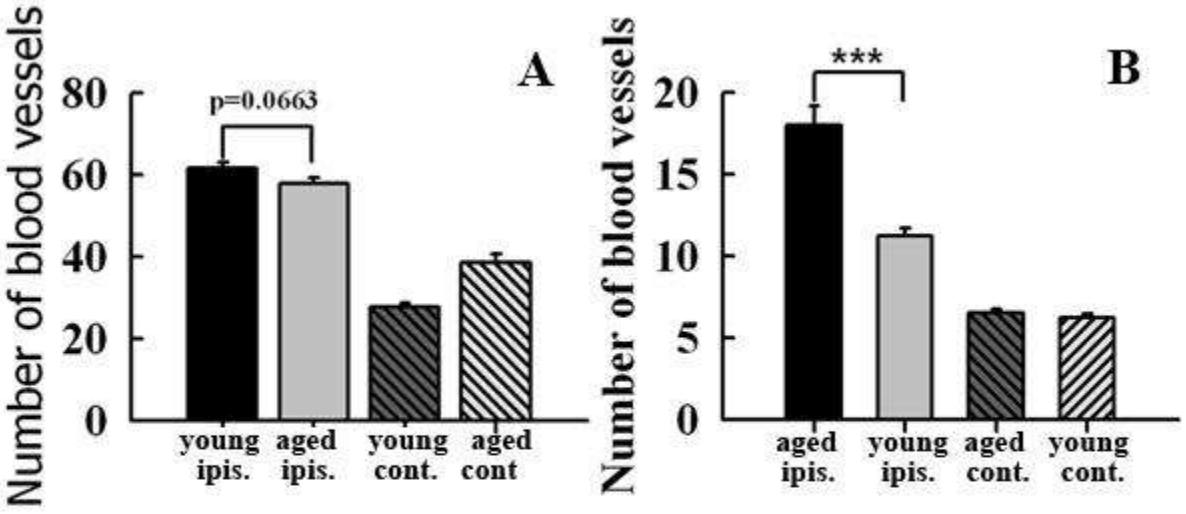

Figure 1. Lecin staining and number of microvessels were compared in both young and aged stroke rats (A). Immunohistochemistry of alpha smooth muscle cell actin and small arteries were compared in both young stroke rats and aged stroke rats (B).* p<0.01.**

[comparison microvessels and small arteries]

Conclusion: Our results indicated that the infarct volume was larger in aged stroke rats. Angiogenesis and arteriogenesis processes were induced in both young and aged rats after ischemic injury. Our study suggested that aging impeded recovery after ischemia may not due to the impaired angiogenesis and arteriogenesis processes, at least in rats. There is no significant difference in the microvessel counts between young and aged ischemic rats but much more small arteries in aged than in young ischemic rats.

Reference:

1. Rauscher, F., et al., Aging, progenitor cell exhaustion, and atherosclerosis. *Circulation*, 2003. 108(4): p. 457.

2. Slevin, M., et al., Serial measurement of vascular endothelial growth factor and transforming growth factor-beta1 in serum of patients with acute ischemic stroke. *Stroke*, 2000. 31(8): p. 1863-70.

561

ACETYL-L-CARNITINE AND -DL-A-LIPOIC ACID PROTECT AGAINST ACUTE GLUTAMATE-INDUCED NEUROTOXICITY IN RAT CEREBRAL CORTEX BY ALTERING MITOCHONDRIAL FUNCTION

N.B. Golla

REQUIMTE, Departamento de Química-Física, Faculdade de Farmácia, Universidade do Porto, Porto, Portugal

Objectives: Excessive activation of Glutamate (L-Glu) receptors by excitatory amino acids leads to a number of deleterious consequences, including generation of free radicals and activation of the mitochondrial permeability transition[1]. In L-Glu-induced neurotoxicity, L-Glu is implicated in two ways: excessive accumulation of L-Glu in the extracellular spaces during ischemia, and subsequent activation of L-Glu receptors in postsynaptic cells[2]. In addition, it is also reported that L-Glu causes neuronal death through p38 signaling pathway activated by TNF-α[3]. Whereas, acetyl-L-carnitine (ALCAR) and ± DL α- lipoic acid (LA) are known to be key players in the mitochondrial energy production. However, the protective mitochondrial functions involving ALCAR and LA have been mostly shown in aged rats and chronic neurological disorders. In the present study, we evaluated the possible protective role of chronic ALCAR and LA pre-treatment on acute L-Glu neurotoxicity.

Methods: To evaluate the effects of the above antioxidants, adult male rats were pretreated with ALCAR (100 mg/kg i.p for 21 days) and both ALCAR and LA (100 mg/kg i.p + 50 mg/kg i.p for 21 days), before stereotactically administering L-Glu bolus (1µmole/1 µl) in the cerebral cortex.

Results: Results showed that acute L-Glu increased ROS ($P < 0.001$), LPO ($P < 0.001$), Ca^{2+} ($P < 0.001$), TNF-α ($P < 0.001$), IFN-γ ($P < 0.001$), NO ($P < 0.001$) levels and mRNA expression of Caspase-3, Casapase-9, iNOS, and nNOS genes with respect to saline injected control group. Key antioxidant parameters such as SOD, CAT, GSH, GR along with mitochondrial transmembrane potential (Δψm) were decreased ($P < 0.05$), while ALCAR pretreatment prevented these effects by significantly inhibiting ROS ($P < 0.001$), LPO ($P < 0.001$), Ca^{2+} ($P < 0.05$), TNF-α ($P < 0.05$), IFN-γ ($P < 0.001$), NO ($P < 0.01$) levels and expression of the above genes. This chronic pretreatment of ALCAR also increased SOD, CAT, GSH, GR, and ($P < 0.0.01$, $P < 0.0.01$, $P < 0.05$, $P < 0.05$, and $P < 0.001$, respectively) with respect to L-Glu group. The addition of LA to ALCAR resulted in further increases in CAT ($P < 0.05$), GSH ($P < 0.01$), GR ($P < 0.05$), Δψm ($P < 0.05$) and additional decreases in ROS ($P < 0.001$), LPO ($P < 0.05$), Ca^{2+} ($P < 0.05$), TNF-α ($P < 0.05$) and mRNA expression of iNOS and nNOS genes with respect to ALCAR group. Hence, this "one-two punch" of ALCAR + LA may help in ameliorating the deleterious cellular events that occur after L-Glu.

Conclusions: This *in vivo* study has confirmed the neuroprotective role of ALCAR and also shown that the addition of LA to ALCAR provided a robust antioxidant and anti-inflammatory cover against acute L-Glu-induced neurotoxicity, thus, providing possible therapeutic implications for situations involving acute neuronal insult.

References:

1. Dong XX, Wang Y, Qin ZH (2009) Acta Pharmacol Sin 30:379-387.

2. Pellegrini-Giampietro DE (2003) Trends Pharmacol Sci 24: 461-470.

3. Chaparro-Huerta V, Flores-Soto ME, Gudino-Cabrera G, Rivera- Cervantes MC, Bitzer-Quintero OK, Beas-Zarate C (2008) Int J Dev Neurosci 26:487-495.

562

PHOSPHODIESTERASE III INHIBITOR IMPROVES AMYLOID B-INDUCED COGNITIVE DEFICITS IN MICE

S.H. Park[1], J.H. Kim[1], S.S. Bae[2], K.W. Hong[2], B.T. Choi[1], **H.K. Shin**[1]

[1]Division of Meridian and Structural Medicine, [2]Department of Pharmacology, School of Korean Medicine, Pusan National University, Yangsan-si, Republic of Korea

Objectives: Alzheimer's disease is characterized by amyloid β (Aβ) and tau deposition in the brain. Here, we investigated the preventive effect of a phosphodiesterase III inhibitor, cilostazol against cognitive decline in the C57BL/6J Alzheimer's disease mouse model.

Methods: For *in vitro* studies, we used N2a cells stably expressing human amyloid precursor protein Swedish mutation (N2aSwe). For *in vivo* studies, C57BL/6J mice underwent intracerebroventricular injection (ICV) of $A\beta_{25-35}$ and cognitive function was evaluated by the Morris water maze test.

Results: N2aSwe showed that cilostazol decreased the amyloid β (Aβ) levels in a concentration-dependent manner (1-30 μM) in the conditioned medium and cell lysates. Cilostazol attenuated the expression of ApoE, which is responsible for Aβ aggregation, in N2aSwe. ICV injection of $A\beta_{25-35}$ in C57BL/6J mice resulted in increased immunoreactivity of Aβ and p-tau, and microglia activation in the brain. Oral administration of cilostazol (20 mg/kg) for 2 weeks before $A\beta_{25-35}$ administration and once a day for 4 weeks post-surgery almost completely prevented the $A\beta_{25-35}$-induced increases of Aβ and p-tau immunoreactivity, as well as CD11b immunoreactivity. However, post-treatment with cilostazol 4 weeks after $A\beta_{25-35}$ administration, when Aβ was already accumulated, did not prevent the Aβ-induced neuropathological responses. Furthermore, cilostazol did not affect the neprilysin and insulin degrading enzymes involved in the degradation of the Aβ peptide, but decreased ApoE levels in $A\beta_{25-35}$ injected brain. In addition, cilostazol significantly improved spatial learning and memory in $A\beta_{25-35}$ injected mice.

Conclusions: The findings suggest that cilostazol significantly prevents memory impairment induced by $A\beta_{25-35}$. The beneficial effects of cilostazol might be explained by the reduction of Aβ accumulation and tau phosphorylation, not through an increase in Aβ degradation but via a significant decrease in ApoE-mediated Aβ aggregation. The phosphodiesterase III inhibitor, cilostazol may be the basis of a novel strategy for the therapy of Alzheimer's disease.

563

CRITICAL CLOSING PRESSURE AND RESISTANCE AREA PRODUCT OF THE CEREBRAL CIRCULATION IN PATIENTS WITH ALZHEIMER'S DISEASE AND VASCULAR DEMENTIA

J.-I. Cha, K.-M. Lee

Neurology, Seoul National University, Seoul, Republic of Korea

Introduction: Recording continuous blood flow velocity (FV) of middle cerebral artery and arterial blood pressure (ABP) simultaneously gives us information about the critical closing pressure (CrCP) and resistance area product (RAP). Cerebral CrCP is a sum of intracranial pressure (ICP) and vascular tone. If ICP is constant, CrCP is proportional to vascular tone, which increases in a situation of endothelial dysfunction due to atherosclerosis. The instantaneous FV-ABP relationship can be represented by a straight line and the slope of this linear regression means cerebrovascular compliance. The inverse of this value is called resistance area product (RAP), which reflects arterial stiffness and is associated with cerebrovascular resistance (CVR). Patients with vascular dementia may have multiple vascular risk factors, including diffuse atherosclerosis. We hypothesized that patients with vascular dementia have more atherosclerotic change than those with Alzheimer's disease, resulting increased vascular tone and decreased vascular compliance.

Patients and methods: Patients diagnosed as Alzheimer's disease and vascular dementia in Seoul National University Hospital were enrolled. Including normal controls, all subjects are of total 28. Non-invasive continuous BP monitoring via 2nd or 3rd digital artery of a non-dominant hand was performed with simultaneous measurement of both MCA flow velocity by transcranial Doppler ultrasound. CrCP is obtained from the first harmonics of the pulse waveforms of arterial blood pressure and MCA flow velocity. The slope of a line made by linear regression of FV-ABP relationship and its extrapolated point to reach the X-axis of ABP is considered as the RAP and CrCP, respectively. Each value of CrCP and RAP was obtained and compared patients with Alzheimer's dementia and vascular dementia.

Results: In all three groups, including the control group, there was no statistical difference in CrCP and RAP. No significant difference was also observed for vascular risk factors, body-mass index (BMI) except the age, which was significantly lower in the control group than those in dementia groups ($p < 0.001$). Although the difference of CrCP and RAP between the two dementia groups had no statistical significance, there was a consistent finding that in the vascular dementia group the mean CrCP was higher and the mean RAP was lower than those in Alzheimer's dementia group. There was also a tendency of increasing the number of vascular risk factors and scoring higher BMI in the vascular dementia group compared to Alzheimer's dementia group. These findings tell us the possible mechanism that the arteriosclerotic or arteriolosclerotic changes in vascular dementia made the vascular tone increased and the arterial compliance decreased. In Alzheimer's dementia, however, the capillary angiopathy is a predominant feature, resulting in no or less involvement of cerebral artery or arteriole, which made the CrCP less decreased and the RAP high.

Conclusions: CrCP and RAP are useful factors representing the cerebral hemodynamic states. Comparing Alzheimer's disease, diffuse atherosclerotic changes in cerebral artery or arterioles in vascular dementia are supposed to make a contribution to increased CrCP and a low RAP, although not supported by a statistical significance.

564

DIAGNOSTIC SIGNIFICANCE OF ^{123}I-METAIODOBENZYLGUANIDINE SPECT AND DIFFUSION MRI IN POSTERIOR FOSSA TUMORS

T. Sasajima[1], N. Shimada[1], T. Otani[2], K. Mizoi[1]

[1]Department of Neurosurgery, [2]Department of Radiology, Akita University School of Medicine, Akita, Japan

Introduction: ^{123}I-metaiodobenzylguanidine (MIBG) has been developed as a functional analog of the neurotransmitter norepinephrine. The success of MIBG as an imaging agent for the neural crest tumors is derived from its chemical similarities to norepinephrine. We have reported the feasibility of ^{123}I-MIBG in the diagnosis of intracranial embryonal tumors [1,2)]. The aim of this study is to explore whether delayed imaging of ^{123}I-MIBG, diffusion-weighted imaging (DWI) and apparent diffusion coefficients (ADC) maps are suitable for preoperative differential diagnosis of medulloblastomas from the other posterior fossa tumors.

Methods: Sixteen patients with histologically proven posterior fossa tumors (seven medulloblastomas, three ependymal tumors, six pilocytic astrocytomas) were examined with single-photon emission computerized tomography (SPECT) using ^{123}I-MIBG and ADC maps calculated from DWI. The uptake of the tracer for regions of tumors was calculated on SPECT images scanned 30 min (early images) and 6 hr (delayed images) after the intravenous injection of ^{123}I-MIBG at a dose of 111 MBq. The ratio of tumor (area of highest uptake) / nontumor (T/NT) was calculated as an indicator of selective uptake in the tumor. Furthermore, retention index (RI) was calculated as follows: RI = (delayed T/NT－early T/NT) / early T/NT. ADC value of each tumor was determined on ADC maps derived from isotrophic DWI. Absolute ADC values of solid portion of the tumors and ADC ratios (ADC of solid tumors to ADC of normal-appearing cerebellum) were compared with the histological diagnosis.

Results: The T/NT ratios on the early images for medulloblastomas, ependymal tumors, and pilocytic astrocytomas were 3.8 ± 2.1 (mean±SD), 1.4 ± 0.6, and 1.9 ± 0.4, respectively. On the delayed images, the T/NT ratios for medulloblastomas increased to 4.9 ± 3.4, while the delayed T/NT ratios for ependymal tumors and pilocytic astrocytomas remained low (1.2 to 1.6). The RI of medulloblastomas was 3.8 ± 2.1, significantly higher ($p < 0.01$) than that of ependymal tumors and pilocytic astrocytomas (-0.16 ± 0.08) with no overlapping of the range of RIs. The high RI of medulloblastomas indicated specific uptake of ^{123}I-MIBG in the tumors. In contrast, the RIs for the other tumors were negative value, suggesting early clearance of ^{123}I-MIBG. ^{123}I-MIBG was appropriated for a time-dependent strategy to reduce background radioactivity and increase the specificity of the resultant images with respect to intracellular localization of MIBG in tumor cells. Both of absolute ADC values and ADC ratios of medulloblastomas were significantly lower ($p < 0.01$) than those of the other posterior fossa tumors without overlap in the range of absolute ADC values and ratios.

Conclusion: ^{123}I-MIBG SPECT, especially 6-hr delayed imaging, provided important information on the differential diagnosis of medulloblastomas from ependymal tumors and pilocytic astrocytomas. Analysis of ADC values reflecting tumor cellularity, has also predictive value for medulloblastomas. Combination of ^{123}I-MIBG SPECT and ADC values analysis using DWI will yield a higher diagnostic accuracy in medulloblastomas by making full use of metabolic and morphological images preoperatively.

References:

1) Sasajima T, et al (2000) AJNR 21:717-720.

2) Sasajima T, et al (2006) J Nurooncol 77 :185-191.

565

THE EFFECT OF ELECTRO-ACUPUNCTURE ON THE EXPRESSION OF PLGF AND FLT-1 AFTER FOCAL CEREBRAL ISCHEMIA/REPERFUSION IN THE SD RATS

L. Wu, **Y. Luo**

The First Affiliated Hospital of Chongqing Medical University, Chongqing, China

Objective: To investigate the mechanism of electroacupuncture effects（EA）on promoting revascularization in the rat brain of focal cerebral ischemia/reperfusion by discussing the expression of PLGF/Flt-1 pathway after artery occlusion（MCAO）.

Methods: The SD rats received filament occlusion of the right middle cerebral artery for 2 hours. Rats were randomly divided into control group, model group, EA group. Accroding to accept reperfusion 1d, 3d, 7d after 2hischemia, the modle group and EA group were divided into three subgroups. After 1h of the reperfusion, EA was bilateral “Hegu”point（LI 4）in the EA group. Immunohistochemical method was used to detect the expression of PLGF and Flt-1 protein in the peripheral ischemic region.RT-PCR was used to detect the expressiom of PLGF mRNA and Flt-1 mRNA. Western blot was employed to detect the expression of PLGF protein.

Results: Compared with the control group,the expression of PLGF,Flt-1 protein and PLGF,Flt-1 mRNA in the peripheral ischemic region of the model group and EA group were significantly incressed ($P< 0.05$).Compared with the model group, EA group were significantly incressed($P< 0.01$) .

Conclusions: EA may up-regulate expression of PLGF, flt-1 protein and mRNA in the peripheral ischemic region, and PLGF/Flt-1 may promote revascularization in the rats brain of focal cerebral ischemia/reperfusion.

570

THE INFLUENCE OF CARBON DIOXIDE ON BRAIN ACTIVITY AND METABOLISM IN CONSCIOUS HUMAN

F. Xu[1], J. Uh[1], M.R. Brier[2], J. Hart[2], U.S. Yezhuvath[1], H. Gu[3], Y. Yang[3], H. Lu[1]

[1]Advanced Imaging Research Center, University of Texas Southwestern Medical Center, [2]Center of Brain Health, University of Texas at Dallas, Dallas, TX, [3]National Institute on Drug Abuse, National Institutes of Health, Baltimore, MD, USA

Objectives: A better understanding of the effect of carbon dioxide (CO2) on brain activity may have a profound impact on clinical studies using CO2 manipulation to assess cerebrovascular reserve and on the use of hypercapnia as a means to calibrate functional magnetic resonance imaging (fMRI) signal. A number of recent studies in brain slices and anesthetized animals provided evidence that higher CO2 partial pressure may reduce pH, decrease synaptic potentials, suppress seizure activities and increase sleep duration (1-4). But a systematic study on CO2 effect in the human brain is lacking. This present study used non-invasive MRI and electroencephalography (EEG) techniques to investigate how an increase in blood CO2 alters brain activity in awake humans.

Methods: Fifty young healthy subjects (27.9±6.5 yo, 32 M, 18 F) participated in the study. Hypercapnia was induced by breathing through an air bag filled with CO2 enriched gas (5% CO2, 21% O2 and 74% N2). Each parameter was measured twice under normocapnia and hypercapnia conditions, respectively.

Whole-brain CMRO2 (N=14) was measured using a recently developed MRI technique, which was based on arterial-venous oxygen differences (5, 6). To rule out the possibility that the CMRO2 change observed in hypercapnia was due to fatigue, mental stress, or anxiety, a sham control study (N=10) was performed following the same protocol as the hypercapnia study except that the gas valve was on room-air for the entire duration of the experiment.

Resting-state BOLD signal fluctuation (N=14) within the default mode network (DMN) was quantified by functional connectivity (fc) MRI. Three indices including cluster size, cross-correlation coefficient (cc) and amplitude of the fcMRI signal were quantified.

EEG was recorded using a 64-channel SynAmps II EEG system. Power spectra of the EEG time series were computed.

Results:

The CMRO2 study showed that mild hypercapnia resulted in a suppression of CMRO2 by 13.4%±2.3% ($p < 0.001$) and the CMRO2 change was proportional to the subject's end-tidal CO2 change ($p=0.014$), suggesting a dose dependent modulation of CO2 on CMRO2. No difference of CMRO2 was found in sham control experiment ($p=0.34$). In the fcMRI study, the cluster volume, cc and fcMRI signal amplitude were significantly ($p < 0.05$) reduced by 54.9%, 17.6% and 20.1% respectively. The reduced functional connectivity indicated that hypercapnia may suppress spontaneous activity of the brain. Hypercapnia altered the EEG power spectra such that delta band (1-3Hz) was increased ($p=0.049$), alpha band (8-13Hz) was decreased ($p=0.0003$) and theta band (4-7Hz) did not changed. The slower power spectra suggested that the brain enters a lower arousal state during hypercapnia.

Conclusions:

Our findings suggest that increased CO2 levels causes the brain reduce metabolism and spontaneous activity, and enter a lower arousal state.

References:

(1) Dulla et al. Neuron, 48:1011 2005. (2) Fraigne et al. Sleep 31:1025 2008. (3) Sicard and Duong Neuroimage 25:850 2005. (4) Zappe et al. Cereb Cortex 18:2666 2008. (5) Lu and Ge MRM, 60:357 (2008); (6) Xu et al. MRM 62:141 (2009).

571

TRANS CRANIAL DOPPLER STUDY OF CEREBRAL BLOOD FLOW IN PATIENTS TREATED BY INTRA-AORTIC BALLOON COUNTERPULSATION

M. Hachemi[1], C. Di Roio[1], E. Bonnefoy-Cudraz[2], O. Bastien[3], F. Dailler[1]

[1]Neuro Intensive Care Unit, [2]Cardiac Intensive Care Unit, [3]Cardiac Surgery Intensive Care Unit, Hospices Civils de Lyon, Lyon, France

Introduction: Intra-aortic Balloon Pump counterpulsation (IABP) therapy was proposed for optimizing cerebral blood flow during management of subarachnoid haemorrhage complicated by cerebral vasospasm or cardiac failure [1-3]. There is a few leak data concerning IABP and cerebral blood flow.

Patients and methods: Prospective monocentric study. Trans cranial Doppler of the middle cerebral arteries was performed through the temporal bone window (2 MHz EME Companion System, Nicolet Biomedical Inc. Madison, WI, USA) during five cardiac battments without and with IABP therapy (PCO2, SpO2, and hematocrit were stable). During procedure: medium arteriel pressure, cardiac frequency, systolic, diastolic and medium sylvian artery velocities, the pulsatility index (PI) and the resistivity index (RI) were recorded. Areas under curve of cerebral arteries velocimetries were determinated. Statistic anylasis of data by non parametric paired test of Wilcoxon ($p < 0.005$ was significant).

Results: 11 adult patients were included. The mean Pulsatility Index (PI) were 0.95 (± 0.2 SD) without IABP and 1.06 (± 0.18 Sd) with IABP therapy ($p = 0.026$). The mean Resistivity Index (RI) were 0.57 (± 0.07 SD) without IABP and 0.66 (± 0.2 SD) with IABP therapy ($p = 0.005$). The systolic middle cerebral artery velocity was 52 cm/s (± 18 SD) without and 59 cm/s (±19 SD) with IABP therapy($p = 0.89$). The diastolic middle cerebral artery velocity was 22 cm/s (± 10 SD) without and 16 cm/s (± 8 SD) with IABP therapy ($p = 0.082$).Area under curve of middle cerebral arteries velocimetries increases of 18% with IABP therapy.

Conclusion: In this study, Intra-aortic Balloon Pump Counterpulsation therapy increases over 18 % the Cerebral Blood Flow. IABP should be more studied in this setting.

Key words: Trans cranial Doppler - Subarachnoid Haemorrhage - Intra-aortic Balloon Pump Counterpulsation - Cerebral Blood Flow - Pulsatility Index - Resistivity Index

Reference:

[1] Solenski NJ, Haley EC Jr, Kassell NF, Kongable G, Germanson T, Truskowski L, et al. Medical complications of aneurysmal subarachnoid hemorrhage : a report of the multicenter, cooperative aneurysm study. Participants of the Multicenter Cooperative Aneurysm Study. Crit Care Med 1995; 23: 1007-17

[2] Hachemi M , Di Roio C, Tixier-Wulf S , Bonnefoy Cudraz E, Dailler F.

Optimization of Cerebral Blood Flow by Intra-aortic Balloon Pump Counterpulsation during Management of Neurogenic Pulmonary Oedema and Cardiac failure Associated with Subarachnoid Haemorrhage XXIV th International Symposium on Cerebral Blood Flow, Metabolism and Function and IX th International Conference on Quantification of Brain Function with PET, Chicago, IL USA, June 29-July 3rd, 2009. (Abstract)

[3] Taccone FS, Lubicz B, Piagnerelli M, Van Nuffelen M, Vincent JL, De Backer D.

Cardiogenic shock with stunned myocardium during triple-H therapy treated with intra-aortic balloon pump counterpulsation.Neurocrit Care. 2009; 10(1):76-82.

572

CORRELATION OF HYPOXIA-INDUCIBLE FACTOR-1 ALPHA AND ERYTHROPOIETIN PROTEIN AND MRNA TO CEREBRAL ISCHEMIC TOLERANCE IN A FOCAL ISCHEMIA/REPERFUSION MODEL

R. Zhao[1], C. Wang[2]

[1]*Department of Neurology, the Affiliated Hospital of Medical College, QingdaoUniversity,*
[2]*Qingdao Mental Health Center, Qingdao, China*

Background: Numerous studies have shown that transient ischemic preconditioning induces cerebral ischemic tolerance. However, the underlying mechanisms of endogenous protection following ischemic preconditioning remain unclear.

Objective: To dynamically measure erythropoietin and hypoxia-inducible factor-1α (HIF-1α) mRNA and protein expression at various times following preconditioning, and to investigate effects of erythropoietin and HIF-1α on cerebral ischemic tolerance in a model of focal ischemia/reperfusion established using the twice suture method.

DESIGN, TIME AND SETTING: The randomized, controlled study was performed at the Institute of Anatomy, Medical College, Qingdao University, China from March 2006 to March 2007.

Materials: Rabbit anti-rat HIF-1α monoclonal antibody and biotinylated goat anti-rabbit IgG (Boster, China), rabbit anti-rat erythropoietin monoclonal antibody (Santa Cruz Biotechnology, USA), and one-step RT-PCR kit (Qiagen, Germany) were used in this study.

Methods: A total of 99 healthy, male, Wistar rats were randomly assigned to three groups: sham surgery (n = 9), non-ischemic preconditioning (n = 45), and ischemic preconditioning (n = 45). In the ischemic preconditioning group, rat models of pre-ischemia-reperfusion-ischemia-reperfusion were established by occluding the left middle cerebral artery using the twice suture method. In the non-ischemic preconditioning group, pre-ischemia was replaced by sham surgery. Subsequently, the ischemic preconditioning and non-ischemic preconditioning groups were equally divided into five subgroups according to time of first reperfusion, including 1-, 3-, 7-, 14-, and 21-day subgroups. The sham surgery group received the sham surgery twice.

MAIN OUTCOME MEASURES: HIF-1α and erythropoietin protein expression was measured in the cerebral cortex, corpus striatum, and hippocampus of the ischemic hemisphere. HIF-1α and erythropoietin mRNA expression were determined in the frontal and parietal cortex of the ischemic hemisphere.

Results: (1) Intergroup comparison: compared with the non-ischemic preconditioning group, HIF-1α protein expression significantly increased in the rat cerebral cortex, corpus striatum, and hippocampus in the ischemic hemisphere at 1, 3, and 7 days following reperfusion in the ischemic preconditioning group ($P < 0.05$ or $P < 0.01$). Erythropoietin protein expression significantly increased in the cerebral cortex, corpus striatum, and hippocampus, as well as HIF-1α and erythropoietin mRNA expression in the frontal and parietal cortex in the ischemic hemisphere, at 3 and 7 days following reperfusion in the ischemic preconditioning group ($P < 0.05$). (2) Temporal expression: HIF-1α protein expression in the rat cerebral cortex, corpus striatum, and hippocampus, as well as HIF-1α mRNA expression in the frontal and parietal cortex, in the ischemic hemisphere increased at 3 days, and gradually decreased from 7 days

following reperfusion in the ischemic preconditioning group. Temporal erythropoietin protein and mRNA expression was consistent with HIF-1α protein expression. (3) Correlation: erythropoietin mRNA expression positively correlated with HIF-1α mRNA expression ($r = 0.737$, $P < 0.01$).

Conclusion: Ischemic preconditioning induced cerebral ischemic tolerance. Pre-ischemia-induced increase in endogenous HIF-1α expression, as well as its target gene erythropoietin, participated in the formation of cerebral ischemic tolerance.

573

IS ACETAZOLAMIDE-CHALLENGED SPECT NECESSARY BEFORE CEA/CAS?

H. Katano[1,2], M. Mase[1], K. Yamada[1]

[1]Neurosurgery, [2]Medical Informatics and Integrative Medicine, Nagoya City University Graduate School of Medical Sciences, Nagoya, Japan

Objectives: Though acetazolamide-challenged SPECT is recommended before carotid endarterectomy(CEA) and carotid stenting(CAS) due to the relationship between preoperative misery perfusion and postoperative hyperperfusion syndrome, it is controversy whether all cases should be checked or not in respect of the frequency of the event, invasiveness of the test and medical economics. We tried to predict the cases which need the examination by preoperative SPECT at rest and collateral vessels in MRA.

Methods: Pre- and postoperative ^{123}I-IMP-SPECT at rest were performed for the 46 consecutive operative cases of carotid stenoses (CEA:CAS=23:23, 70.6±6.0 y/o, M:F=38:8, mean degrees of stenosis 77.8±12.6%) and analyzed the regional quantitative CBF with the Fine-SRT, a technique using anatomical standardization and ROI template for the whole brain. We classified the cases with preoperative MRA into two groups; G: good collateral flow group with anterior communicating artery(AcoA), (CEA:CAS=11:13), P: poor collateral flow group without AcoA and/or ipsilateral posterior communicating artery (CEA:CAS=12:10).

Results: Postoperative regional CBF patterns were divided into two types; I: bilateral CBF increase (30 cases), II: unilateral (operative side) CBF increase (16 cases). Ten after CEA and 12 after CAS cases showed type I in group G and 9 after CEA and 5 after CAS cases showed type II in group P. Cases with high postoperative increase rate of rCBF were frequently found in group P and type II. Some patients showed high increase rate at the preoperative low rCBF site but 21 (45.7%, CEA:CAS=11:10) were not the case.

Conclusions: In the present study, the cases with poor collateral flow suspected from preoperative MRA and with unilateral postoperative rCBF increase in the operative side tended to demonstrate high increase rate of rCBF. These cases are recommended to have preoperative acetazolamide-challenge SPECT to check the vascular reserve and predict the possibility of postoperative hyperperfusion syndrome.

574

CHANGES IN SERUM CELLULAR ADHESION MOLECULE AND MATRIX METALLOPROTEINASE-9 LEVELS IN PATIENTS WITH CEREBRAL INFARCTION FOLLOWING HYPERBARIC OXYGEN THERAPY

R. Zhao[1], C. Wang[2]

[1]Department of Neurology, the Affiliated Hospital of Medical College, QingdaoUniversity,
[2]Qingdao Mental Health Center, Qingdao, China

Background: : Animal studies have confirmed that hyperbaric oxygen (HBO) therapy can reduce matrix metalloproteinase (MMP) activity and blood brain barrier (BBB) permeability, thereby exhibiting neuroprotective effects. However, at present, consensus does not exist in terms of its clinical efficacy.

Objective: To validate the significance of changes in serum cellular adhesion molecule and MMP-9 levels in patients with cerebral infarction following HBO therapy.

Design, time and setting: This randomized, controlled, neurobiochemical study was performed at the Department of Neurology, Affiliated Hospital of Qingdao University Medical College between December 2002 and March 2006.

Participants: A total of 112 patients with acute cerebral infarction of internal carotid artery, comprising 64 males and 48 females, averaging (67 ± 11) years, were recruited and randomized to a HBO group (n = 50) and a routine treatment group (n = 62). An additional 30 gender- and age-matched normal subjects, consisting of 17 males and 13 females, averaging (63 ± 9) years, were enrolled as control subjects.

Methods: The routine treatment group received routine drug treatment and rehabilitation exercise. HBO treatment was additionally performed in the HBO group, once a day, for a total of 10 days.

Main outcome measures: Serum levels of soluble intercellular adhesion molecule (sICAM), soluble vascular cell adhesion molecule (sVCAM), soluble E-selectin (sE-selectin), and MMP-9 were detected by enzyme linked immunosorbent assay.

Results: Upon admission, serum levels of sICAM, sVCAM, sE-selectin, and MMP-9 were significantly increased in patients with cerebral infarction, compared with control subjects ($P < 0.01$). Following HBO and routine treatments, serum levels of the above-mentioned indices were significantly reduced in the HBO and routine treatment groups ($P < 0.01$). Moreover, greater efficacy was observed in the HBO, compared with the routine treatment group ($P < 0.05$ or $P < 0.01$).

Conclusion: Intergroup comparison and case-control results indicated that HBO noticeably reduced serum levels of sICAM, sVCAM, sE-selectin, and MMP-9.

575

CHANGE OF BLOOD-BRAIN BARRIER PERMEABILITY AND MATRIX METALLOPROTEINASE-9 EXPRESSION IN RAT MODEL OF CEREBRAL ISCHEMIC TOLERANCE

R. Zhao[1], C. Wang[2]

[1]The Affiliated Hospital of Medical College ,Qingdao University, [2]Qingdao Mental Health Center, Qingdao, China

Background: Numerous studies have shown that transient ischemic preconditioning induces cerebral ischemic tolerance. However, the underlying mechanisms of endogenous protection following ischemic preconditioning remain unclear.

Objective: To investigate effects of change of blood-brain barrier(BBB) permeability and matrix metalloproteinase-9（MMP-9）expression on cerebral ischemic tolerance in a model of focal ischemia/reperfusion established using the twice suture method.

Methods: One hundred and fifty-four healthy Wistar rats were randomly assigned to three groups: sham surgery (n =14), non-ischemic preconditioning (NIP, n =70), and ischemic preconditioning (IP, n =70). For IP, the rats were given middle cerebral artery occlusion（MCAO） for 10 minutes. In the IP group, rat models of pre-ischemia-reperfusion-ischemia-reperfusion were established by MCAO using the twice suture method. In the NIP group, pre-ischemia was replaced by sham surgery. Subsequently, the IP and NIP groups were equally divided into five subgroups according to time of first reperfusion, including 1-, 3-, 7-, 14-, and 21-day subgroups. The sham surgery group received the sham surgery twice. The models were evaluated with examinating neurologic deficit scores and infarct volume. Change of BBB permeability were evaluated by measuring the content of Evan's blue (EB). MMP-9 protein and mRNA expression were determined by immunohistochemical staining and in situ hybridization respectively.

Results and conclusion:

(1) Intergroup comparison: compared with the NIP group, neurologic deficit scores, infarct volume, MMP-9 protein and mRNA expression significantly decreased in the 1, 3, 7d subgroups of IP group. Blood-brain barrier disruption and ischemic brain edema formation were significantly attenuated in 1, 3, 7d subgroups of IP（$p< 0.05$；$P < 0.01$).

(2) In the IP group, infarct volume and MMP-9 mRNA expression significantly decreased in the 1, 3, 7d subgroups. Blood-brain barrier disruption and ischemic brain edema formation were significantly attenuated in 3, 7d subgroups of IP compared with other subgroups（$p < 0.05$). These results indicated that attenuated disruption of BBB and decreased expression of MMP-9 induced by IP might contribute to brain ischemic tolerance.

576

THE EFFECTS OF NEUREGULIN ON EXPRESSIONS OF MMP-9 AND NSE IN BRAIN TISSUE FOLLOWING CEREBRAL ISCHEMIC REPERFUSION INJURY IN RATS

R. Zhao[1], C. Wang[2]

[1]Department of Neurology, the Affiliated Hospital of Medical College, Qingdao University,
[2]Qingdao Mental Health Center, Qingdao, China

Objective: To observe the expression alternation of matrix metalloproteinase-9 (MMP-9) and neuron-specific enolase (NSE) on brain tissue and the influence of neuregulin-1β (NRG-1β) in rats following cerebral ischemia/reperfusion.

Methods: The animal models of middle cerebral artery occlusion/reperfusion (MCAO/R) were established by a filament method from left external-internal carotid artery in adult healthy male Wister rats 100 cases. The rat models in the treatment group were injected 1.5％NRG-1β 5μL from internal carotid artery(ICA). The expressions of MMP-9 and NSE were determined by immunohistochemical and immumofluorescent double staining and western-blotting assay.

Results: Hypoxia and ischemia can cause the presence of MMP-9. With the ischemic time prolonging, the increased expression of MMP-9 can be detected in the control group. NRG-1β treatment could decrease the level of MMP-9 compared with that in the control group at the same timepoint and the corresponding region（$P< 0.01$）.The NSE immunoreaction could transiently elevate at the early stage of cerebral ischemia insuly, but accompanying with the extension of ischemic time its level gradually decreased. After the administration of NRG-1β, the level of NSE increased significantly and thus delayed the time course and the degree of neuronal damage. There were statistical differences in contrast to the control group($P< 0.01$). The expression of the two proteins lack of correlation according to the result of immumofluorescent double staining and western-blotting assay.

Conclusion: MMP-9 might aim at various target cells at different stages and contribute to the inflammatory reaction after ischemia-reperfusion cerebral insult by different methods. NRG-1β might regulate the activation of MMP-9 and NSE, disturb the development of inflammatory reaction, improve the microenvironment of neuron survival, delay the course and the degree of neuron by virious methods, and further play a neuroprotective role in ischemia cerebral insult .

577

RAPID EXPRESS-DIAGNOSIS OF ISCHEMIC STROKE: S-100B PROTEIN PLASMA MEASUREMENT

A. Vertkin, A. Skotnikov

Therapy, Clinical Pharmacology and Ambulance, Moscow State Medical Stomatological University, Moscow, Russia

Not least pressing urgent problem is the combination of cerebral and myocardial infarction. The aim of the study was to determine the dynamics of the concentration of serum protein S100β, depending on the severity of the clinical course of vascular pathology in patients with myocardial infarction and cerebral infarction.

Analyzed the 113 399 medical histories of patients admitted to a large multi-disciplinary hospital, out of which in 85 cases revealed a combination of cerebral infarction and myocardial infarction, leading to death.

The share of cardiovascular diseases in the structure of the overall mortality rate was 21,4%, and the combination of myocardial infarction and stroke - 2,1% of total mortality and 9,4% in the structure of the cardio- and cerebrovascular pathology.

The average age of deceased patients was 67±12 years. In 28,2% of cases they have been diabetes mellitus type 2, in 38,5% there were consequences stroke, 33,3% patients had myocardial infarction in the past, 30,7% and 10,4% persons had permanent and paroxysmal forms of atrial fibrillation, respectively, as well as other background diseases and comorbidities.

There was a lack of in vivo diagnosis of a combination of stroke and cerebral infarction (81% of cases). With the express determination of the content in the blood S-100β protein plasma has revealed that it corresponded to the maximum concentration of 24 hours from the development of cerebral infarction and was at 78,4% higher than after 12 hours of acute vascular accident. After 48 hours observed 297% decrease in the concentration of this biomarker and after 72 hours, its concentration reached the initial level. There was a direct correlation between the concentration of S-100β protein plasma in blood with clinical manifestations of stroke and the data computed tomography.

Thus, further study of clinical and laboratory parameters and the initiation of new clinical trials of biomarkers of brain tissue damage may be new and modern stage of stroke diagnosis.

578

HOW EVOLUTIONARY ANTHROPOLOGY INFORMS THE GROWTH, DEVELOPMENT, AND MATURATION OF THE VASCULAR DURA

A.R. Kunz[1], C. Iliadis[2]

[1]Harvard University (Extension), Boston, MA, USA, [2]Neurosursury, University of Patras Medical School, Patras, Greece

Introduction: The vascular dura mater, fibrous meningeal covering of the brain, is the principle source of integration between endocranial elements. Dural folds, falks cerebri/cerebelli and tentorium cerebelli (TC), compartmentalize vertically and horizontally, respectively, supporting the vascular brain.

Methods: This paper discusses current understandings of growth, development, and maturation, of the vascular dura. Dural growth, size changes, relate mainly to brain/skull expansion. Development, structural shape changes, are mostly associated with mechanical repositioning of dural connective tensors. Maturation changes encoporate a mathematical paradigm of inherited conserved regulatory genetic programs that allow changes in these ontological parameters in a relative short time.

Results/discussion: Growth of the vascular brain/dura is seen as multiphasic. What's important in evolution is not growth rates, but nonlinear growth phases, each with the allometric form $y=ax^b$ All descendants growth phases are extended by the same factor, **"proportional growth prolongation".** Data for chimpanzees show 4 phases + growth with post-embryonic breakpoints at 3.5, 7.75, 14.1, and 68 months conception. Likewise post-embryonic breakpoints for human + growth phases are 4.4, 9.3, 18.2, and 114 months conception. The human growth phase is prolonged 1.3 times at a similar growth rate.

Developmental repositioning of the vascular dura is due to tilting of the anterior cranial fossa where a mechanical structural link is exerted through the falx cerebri. Midline positioned TC rotates inferoposterior toward the foramen magnum, 30 degrees in humans, whose bipedal upright stance shifts the **"gravitational load"** onto the TC's surface, now almost parallel to a gravity vector. Non-human quadraped primates' TC's gravity vector is oblique. In a prenatal context, there is a tighter regulation of fetal development, human> non-human primates; anthropoid primates' cranial base (CB), with dura anchored, retroflexes 10 degrees after birth, whereas human's CB retroflexes 20 degrees 10-40 weeks prenatal and flexes 10 degree postnatal.

The evolutionary inheritance of our vertebrate lineage was expansion of homeobox regulatory gene networks, involved in embryonic pattern formation by cluster duplication. This was conserved in the mammalian lineage who evolutionary hallmark is neocortex expansion; Its superiority is implied from **"combinational power"** of epigenetic regulatory gene networks: prevertebral gene system of 1000 (2^{10}) states and 10^7 (50^{10}) epigenetic states; mammals 10^{12} (2^{40}) states and 10^{27} (5^{40}) epigenetic states. As primates, human/great apes are evolutionary hiers to this system, sharing a genome DNA 98.7% identical; again, positive selection of regulatory genes (promoters, operators, repressors) at embryonic stages in a minimum of 750 genes, $p< 0.05$, accounts for biological maturation differences translated into vascular cortical size/dura area, humans vs chimpanzees, respectively: age maximum brain size 15:7, neocortex surface area ratio 10:1; brain volume ratio 3.6:1; post-mitotic subventricular zone founder neurons ratio 15:1; ratio quantity protein (brain) secreted 4:3.

Conclusion: The importance of investigating the vascular dura's ontological parameters, growth, development and maturation, enlightens us to evolution's novel pathways of change and galvanizes us to possibilities for continued adaptive change.

579

PHARMACOLOGICAL MRI ASSESSMENT OF THE WHOLE BRAIN RESPONSE TO AN INTRAPERITONEAL GLUCOSE DOSE UNDER FASTING CONDITIONS

P.-W. So, K. O'Toole, D. Cash, S.C.R. Williams

Department of Neuroimaging, King's College London, Institute of Psychiatry, London, UK

Introduction: Neural glucose-sensing systems integrate glucose and energy homeostasis involving specialised 'glucosensing' neurones[1], receiving direct and indirect inputs from the periphery and brain areas involved in processing sensory, reward and blood nutrient levels information[1]. The neurons either increase activity (glucose-excited, GE) or decrease activity (glucose-inhibited, GI) as ambient glucose levels rise[1]. BOLD-MRI has been used to provide an indirect measure of neuronal activity in the hypothalamus following non-oral glucose administration in both rats[2] and humans[3]. In this study, we have adopted a pharmacological MRI (phMRI) approach to assess the effects of a single intraperitoneal (i.p.) glucose dose throughout the brain of a fasted rat model.

Methods:

Animals and Treatment: Sprague-Dawley rats (n=10, 252.7g ± 8.3g) were fasted overnight. Animals were anaesthesised (isoflurane in air/O_2) and an i.p. cannula implanted and MRI performed using a volume coil on a 7T MRI system. Following structural MRI, BOLD-MRI was performed using a multi-echo gradient echo sequence: TR, 125.18ms; TE, 5, 10 and 15ms (mean echo was analysed); 24 contiguous 1 mm slices; 32s per scan acquisition time. 40 scans were collected prior to, and 140 after, an i.p. injection of isotonic glucose (1g/kg, 20ml/kg water, n = 5) or 0.9% isotonic saline (n = 5). After MRI, animals were recovered for 40mins and then killed and terminal cardiac blood samples collected for glucose measurements.

Image Analysis: Data was analysed by SPM5 software. BOLD-MRI images were movement corrected, non-brain tissue masked and images normalised to a rat brain template, prior to Gaussian smoothing (2x in-plane resolution). The random effects general linear model (2^{nd} level analysis) was applied to test for changes in the BOLD signal between pre- and post-glucose images in the time-series. SPM{t}distribution was thresholded at $p< 0.001$ (uncorrected for multiple comparisons).

Results and discussions: Plasma glucose concentrations was significantly higher after injection of glucose compared to saline ($P< 0.05$). Significant widespread BOLD-MRI signal increases after glucose administration were observed in the cerebellum, brainstem, other hindbrain and midbrain regions, hippocampus, hypothalamus, thalamus and striatum. Only small increases in the posterior cortex and (unilateral) hippocampus were observed in the saline-treated animals. Both saline and glucose-treated animals showed significant BOLD-MRI decreases in the prefrontal cortex and olfactory regions, possibly related to i.p. volume administration. The significant hypothalamic and hippocampal activations are consistent with the presence of GE neurons in these brain areas[4,5]. We did not observe a transient decrease in hypothalamic activity previously reported[3,4] following i.p. glucose, possibly arising from methodological differences.

Conclusion: We have shown the ability to non-invasively assess regional brain changes following a glucose dose, suggesting the possibly use of phMRI to determine the functional role of various nutrients under different physiological states.

References:

[1] Levin (2002). Physiol Behav., 76:397-401.

[2] Mahankali et al., (2000). MRM, 43: 155-9.

[3] Smeets et al., (2007). Am. J. Physiol., 293: E754-8.

[4] Dunn-Meynell et al., (2002). Diabetes, 53: 549-598.

[5] Huang et al., (2007). J. Neurosci. Res., 85: 1468-77.

580

PROTEOMIC INVESTIGATION OF THE RESISTANCE OF CA3 NEURONS TO GLOBAL ISCHEMIA REVEALS HAMARTIN AS A NOVEL NEUROPROTECTIVE TARGET

M. Papadakis[1], L. Hoyte[1], S. Nagel[2], Z. Zhao[3], C. Wright[4], R. Chen[1], R. Deacon[5], S. Watt[6], K. Vekrellis[7], B. Kessler[4], B.M. Alastair[1]

[1]Acute Stoke Programme, Nuffield Department of Clinical Medicine, University of Oxford, Oxford, UK, [2]Department of Neurology, University of Heidelberg, Heidelberg, Germany, [3]Department of Clinical Neurosciences, University of Calgary, Calgary, AB, Canada, [4]Henry Wellcome Building for Molecular Physiology, Nuffield Depratment of Clinical Medicine, [5]Department of Experimental Psychology, University of Oxford, [6]Stem Cell Research Laboratory, NHS-Blood and Transpant, Oxford, UK, [7]Division of Basic Neurosciences, Biomedical Research Foundation of the Academy of Athens, Athens, Greece

Objectives: The molecular basis for the resistance of CA3 hippocampal cells to global cerebral ischemia has not been established and may provide novel neuroprotective targets. We carried out proteomic studies to investigate the events that are activated in the CA3 region. The gene product of Tuberous Sclerosis Complex 1 (TSC1), hamartin, which is a central regulator of protein synthesis[1] was identified as a neuroprotective target. Our objective was to demonstrate the importance of hamartin expression in ischemia, by performing preconditioning and protein knockdown experiments.

Methods: We performed label-free quantitative proteomic analysis of CA1 and CA3 membrane and cytoplasmic proteins from rats subjected to sham or 10min global ischemia, followed by 24h reperfusion. Ingenuity Pathway Analysis was used to analyze the proteomic dataset and identify proteins, pathways and protein networks selectively associated with events taking place in the CA3 area, following ischemia. The expression levels and distribution of proteins of interest were further studied by immunoblotting and immunofluorescence experiments. Their expression was also determined in CA1 and CA3 tissue homogenates from rats subjected to either 2min global ischemia (preconditioning stimulus) or sham preconditioning followed 7h later by 10min global ischemia and 24h reperfusion.

E-18 rat cortical neurons infected with either pLKO.1-puro control shRNA or pLKO.1-puro TSC1 shRNA lentiviral particles were subjected to 2h oxygen glucose deprivation (OGD) and cell death was assessed 24h later by Ethidium Homodimer III and Annexin V, fluorescence staining. TSC1 shRNA lentiviral particles were unilaterally injected in the CA3 area of the hippocampus, to rats subjected 2 weeks later to 10min global forebrain ischemia. Surviving pyramidal neurons were counted 7 days following reperfusion by hematoxylin and eosin staining on paraffin-embedded sections.

Results: Proteomic analysis of CA3 proteins revealed that the PI3k/Akt pathway and the downstream mediator hamartin were significantly associated with neuroprotection. Immunoblotting studies confirmed that hamartin was significantly upregulated selectively in the CA3 region by global ischemia and reperfusion. Immunofluorescence experiments demonstrated that hamartin expression was increased in the nuclear and perinuclear space. In the CA1 region, hamartin expression was unaffected by ischemia alone, but was upregulated by preconditioning preceding global ischemia, which protects the otherwise vulnerable CA1 cells.

Cortical cultures infected with TSC1 shRNA lentiviral particles, which inhibit the expression of hamartin, exhibited significantly higher cell death (83 ± 1%), following 2h OGD and 24h

reoxygenation compared to infection with control particles (56 ± 3%). Similarly, CA3 hippocampal neurons infected with TSC1 shRNA lentiviruses were significantly more susceptible to global ischemia and reperfusion.

Conclusions: Our multi-level proteomic analysis revealed that hamartin is selectively activated in the CA3 region by global cerebral ischemia and reperfusion. The upregulation of hamartin in the CA1 area of preconditioned rats supported its involvement in neuroprotection. The functional importance of hamartin expression levels to ischemic susceptibility was highlighted by knocking down its expression in vitro and in vivo. Neurons with suppressed hamartin levels were more susceptible to ischemia and reperfusion. Our results demonstrate hamartin as a novel target for neuroprotection.

References: 1. Tee et al. Curr Biol 2003; 13: 1259.

581

CAVEOLAE-ASSOCIATED SIGNALING IN HIV-1 AND AMYLOID BETA INTERACTIONS AT THE BLOOD-BRAIN BARRIER LEVEL

M. Toborek, I.E. András, L. Chen

Department of Neurosurgery, University of Kentucky Medical Center, Lexington, KY, USA

Objectives: HIV-1-infected brains are characterized by elevated depositions of amyloid beta; however, the interactions between amyloid beta and HIV-1 are poorly understood. In the present study, we hypothesize that exposure to HIV-1 may predispose brain endothelial cells to alterations of amyloid beta levels and contribute to brain amyloid pathology.

Methods: Te study was performed in an *in vitro* model of human brain microvascular endothelial cells exposed to HIV-1 in the presence or absence of amyloid beta. In addition, animal experiments were conduced in which HIV-1 specific protein Tat was administered into the cerebral vasculature of 50-52 week old double transgenic (B6C3-Tg) mice that express a chimeric mouse/human amyloid precursor protein (Mo/HuAPP695swe) and a mutant human presenilin 1 (PS1-dE9) and are characterized by increased amyloid beta depositions in the brain.

Results: Exposure to HIV-1 particles as well as to HIV-infected monocytes markedly increased endogenous amyloid beta levels and elevated accumulation of exogenous amyloid beta in brain endothelial cells. Importantly, caveolin-1 silencing or blocking of specific caveolae-associated signaling pathways protected against these effects. We next evaluated the effects of HIV-1 and/or simvastatin on expression of the receptor for lipoprotein related protein (LRP1) and the receptor for advanced glycation end products (RAGE) that are known to regulate amyloid beta transport across the BBB. LRP1 expression was not affected by HIV-1; however, HIV-1 significantly upregulated RAGE via caveolae-associated mechanisms in brain endothelial cells. In animal experiments, exposure to Tat increased permeability across cerebral capillaries, enhanced disruption of zonula occludens (ZO)-1 tight junction protein, and elevated brain expression of matrix metalloproteinase-9 (MMP-9) in B6C3-Tg mice as compared to age-matched littermate controls. These changes were associated with increased leukocyte attachment and their transcapillary migration. The majority of Tat-induced effects were attenuated inhibition of caveolae-associated Rho signaling.

Conclusions: The present data indicate that HIV-1 may directly contribute to amyloid beta accumulation at the BBB level via caveolae-associated mechanisms. Importantly, increased brain levels of amyloid beta can enhance vascular toxicity and proinflammatory responses associated with brain infection by HIV. Supported by MH63022, MH072567, and NS39254.

References:

András IE, Eum SY, Huang W, Zhong Y, Hennig B, Toborek M. HIV-1-induced amyloid beta accumulation in brain endothelial cells is attenuated by simvastatin. Mol. Cell. Neurosci. 43, 232-243, 2010.

András IE, Rha GB, Huang W, Eum SY, Couraud PO, Ignacio A. Romero, Hennig B, Toborek M. Simvastatin protects against amyloid beta and HIV-1 Tat-induced expression of inflammatory genes in brain endothelial cells. Mol. Pharmacol. 73, 1424-1433, 2008.

Zhong Y, Smart EJ, Weksler B, Couraud PO, Hennig B, Toborek M. Caveolin-1 regulates HIV-1 Tat-induced alterations of tight junction protein expression via modulation of the Ras signaling. J. Neurosci. 28, 7788-7796, 2008.

582

TEMPORAL PATTERN OF DTI CHANGES DURING THE FIRST 6H AFTER PERMANENT ISCHEMIA IN RATS

G. Soria[1,2], R. Tudela[2,3], J. Puig[4], S. Pedraza[4], A. Prats-Galino[5], D. Ros[3], J. Pavía[3], A.M. Planas[1,2]

[1]Dept. of Brain Ischemia and Neurodegenration, Institut d´Investigacions Biomèdiques de Barcelona, IIBB-CSIC,IDIBAPS, [2]Experimental MRI 7T Unit, IDIBAPS, [3]CIBER de Bioingeniería, Biomateriales y Nanomedicina (CIBER-BBN), Group of Biomedical Imaging, University of Barcelona, Barcelona, [4]IDI Radiology Department, Hospital Universitario Dr. Josep Trueta. IDIBGI.Universitat de Girona, Gerona, [5]Laboratory of Surgical Neuroanatomy, University of Barcelona, Barcelona, Spain

Objectives: About 20% of acute stroke patients wake up with stroke symptoms. The unknown time of infarct onset excludes these patients from thrombolysis. Diffusion Tensor Imaging (DTI) indexes such as fractional anisotropy (FA), mean diffusivity (MD), parallel (ParD) and perpendicular (PerD) diffusivities reveal information about the microstructural integrity of brain tissue and are very sensitive to ischemic episodes. We hypothesize that there is a time-dependent evolution of DTI indexes that could inform about the real duration of the infarction. The objective of this work was to investigate the hyperacute temporal pattern of changes in DTI indexes after permanent medial cerebral artery (MCA) occlusion in rats.

Methods: Longitudinal MRI scans were performed in rats under isofluorane anaesthesia in a BioSpec 70/30 horizontal animal scanner (Bruker BioSpin, Ettlingen, Germany), equipped with a 12 cm inner diameter actively shielded gradient system (400 mT/m) and a phased array surface coil for rat brain. Permanent MCA occlusion was performed in 8 male Wistar rats (weighting 280-300 gr). MRI scans consisting on apparent diffusion coefficient (ADC), T2 relaxometry, FA, MD, ParD and PerD were acquired before the surgery and for the next 6h, consecutively each 30 min, with a total of 12 time-points after MCA occlusion. All maps were generated with Paravision and processed with a custom-made Matlab program. Data were analyzed with two different approaches. First, regions of interest (ROI) were manually drawn for white and grey matter structures in both ipsi- and contralateral hemispheres. Secondly, a brain mask was applied to the images and whole-brain histograms of ADC, T2, FA, MD, Lpar and Lper were generated. Then, the mean, the skewness and kurtosis of each distribution was analyzed.

Results: Compared to pre-occlusion values, MD, PArD and PerD decreased progressively during the first 2h post-occlusion, and remained stable the following 4h in the ipsilateral cortex and striatum. No changes were observed in the corresponding contralateral structures. Ipsilateral FA increased during the first 60 min followed by a progressive decrease for the next 5 hours. MD and ParD progressively decreased in the ipsilateral Corpus Callosum and Internal Capsula. T2 relaxation time lineally increased with time after infarct onset in both white and grey matter, as previously described (1). Whole-brain volume analysis demonstrated that the skewness of ADC, T2, MD, ParD and PerD distributions progressively decreased with time after MCA occlusion. In addition, the kurtosis of FA distributions progressively increased after MCA occlusion.

Conclusions: In our conditions, DTI indexes were extremely sensitive to the microestructural hyperacute changes induced by MCA occlusion as assessed by both ROI and whole-brain volume analyses. ADC, MD, Lpar and Lper had a similar temporal pattern with a lineal phase,

while the FA pattern suggested a non-linear evolution after stroke. Our findings support that quantitative DTI studies are a promising tool to estimate the time of stroke onset.

Acknowledgements: This work was supported by Instituto de Salud Carlos III (FIS PS09/00527), the European Union (FP7-ARISE 201024) and CIBER-BBN.

References: Jokivarsi et al., 2010 Stroke. 41(10): 2335-40.

583

SCAVENGING OF MITOCHONDRIAL ROS IN THE BRAIN PREVENTS NEUROGENIC HYPERTENSION

J.Y. Jun, J. Zubcevic, Y. Qi, M.K. Raizada

Physiology and Functional Genomics, University of Florida, Gainesville, FL, USA

Introduction and objective: Increased oxidative stress in the brain has been implicated in chronic angiotensin II (AngII)-induced hypertension. However, the contribution of mitochondrial ROS generated in the cardiovascular (CV) relevant brain regions on this neurogenic model of hypertension remains to be studied. Thus, our objective in the present study was to test the hypothesis that mitochondrial ROS is critical to the development and establishment of neurogenic hypertension in this animal model. Antioxidant mitoTEMPO which targets mitochondria was used to scavenge ROS to test the hypothesis. Intracerebroventricular (ICV) infusion of mitoTEMPO for 4 weeks significantly reduced mean arterial pressure (MAP) in SD rats made hypertensive by subcutaneous infusion of Ang II (200ng/kg/min) [control: 98±2 mmHg (n=5), AngII: 177±6 mmHg (n=7), AngII+mitoTEMPO 150ug/kg/day: 146±12 mmHg (n=5)]. In addition, higher dose of mitoTEMPO ICV infusion (250ug/kg/day) completely blocked the increase of MAP induced by chronic AngII (n=5). Spectral analysis demonstrated an increase in sympathetic vasomotor activity [(ΔLF (SBP) control: +0.395±0.2 $ms^2/mmHg^2$, AngII: +2.201±0.3 $ms^2/mmHg^2$] and decrease in spontaneous baroreceptor reflex gain [(ΔsBRG(PI) control: +0.148±0.1 ms/mmHg, AngII: -0.247±0.06 ms/mmHg)] in AngII treated group at week 3 and week 4 compared to control group. However, these changes in sympathetic vasomotor activity and spontaneous baroreflex gain were attenuated by ICV infusion of mitoTEMPO [150ug/kg/day, 250ug/kg/day: (ΔLF (SBP) +0.997±0.7, +0.824±0.3 $ms^2/mmHg^2$, (ΔsBRG(PI): -0.07±0.04, -0.068±0.1 ms/mmHg]. In contrast to these profound ICV effects, subcutaneous infusion of mitoTEMPO at a same dose (150ug/kg/day) does not have any influence on MAP [176±5 mmHg (n=3)] in this hypertension animal model. Our data demonstrates that ROS produced from mitochondria in the brain is mainly responsible for the establishment of neurogenic hypertension by modulating sympathetic vasomotor drive and cardiac baroreflex gain. They suggest that mitochondria derived ROS in the cardiovascular relevant brain regions (i.e. PVN, NTS, RVLM) may be the principle driving factor in AngII-induced neurogenic hypertension

584

THE INFLUENCE OF HUMAN DEVELOPMENT IN THE QUALITY OF LIFE IN STROKE

F.J. Aidar[1], R.J.D. Oliveira[2], A.J. Silva[3], D.G.D. Matos[3], A.L. Carneiro[4], V.M. Reis[3]

[1]Minas Gerais State Military Fire and Rescue Dept, Uberlândia, [2]Brasilia University, Brasília, Brazil, [3]Tras-Os-Montes and Alto Douro University, Vila Real, Portugal, [4]Montes Claros University, Montes Claros, Brazil

Objective: The aim of this study was to analyze the effect of the Human Development Index (HDI) and of an active lifestyle on the quality of life of patients after stroke.

Methods: Two groups with subjects who had suffered a stroke over a year were studied, a group from Belo Horizonte (BHG) with 48 people (51.5 ± 8.7 years) and a group from Montes Claros (MCG) with 29 subjects (55, 4 ± 8.1 years). Subsequently, regardless of location, the groups were divided into Active and Insufficiently Active so their difference in terms of quality of life could be analyzed.

Results: There were no significant differences between BHG and MCG when it came to physical health (physical functioning 49.1 ± 6.0 / 47.5 ± 7.9; physical aspect 61.3 ± 6.7/ 59.4 ± 7.7; pain 48,2 ± 6,2 / 50.1 ± 6.0; health status 58.8 ± 7.9 / 59.3 ± 6.8) or mental health status (vitality 56,5 ± 7,6 / 55,2 ± 8,2, social aspect 55,2 ± 6,6 / 54,5 ± 8,4; emotional aspect 58,4 ± 5,4 / 59,3 ± 7,9; mental health 61,2 ± 4,5 / 59,1 ± 8,5), respectively. However, significant differences were found between groups Active and Insufficiently Active with respect to quality of life: physical health (physical functioning 56.2 ± 4.4 / 47.4 ± 6.9; physical aspect 66.5 ± 6.5 / 59.1 ± 6.7; pain 55,9 ± 6,2 / 47,7 ± 6,0; health status 67,2 ± 4,2 / 56,6 ± 7,8), and mental health (vitality 60,9 ± 6,8 / 54,1 ± 7,2; social aspect 60,4 ± 7,1 / 54,2 ± 7,4; emotional aspect 64,0 ± 5,5 / 58,1 ± 6,9; mental health status 66,2 ± 5,5 / 58,4 ± 7,5) respectively.

Conclusion: It was concluded that the location and the HDI did not affect quality of life, since no significant differences were found between a group from a city where the HDI is considered high and a group from another city where the HDI is considered low. However, with regard to physical activities, group Active showed significantly higher levels of quality of life, demonstrating that an active lifestyle can be essential to a better quality of life for individuals affected by stroke.

585

CHANGES IN CT PERFUSION-DERIVED CEREBRAL BLOOD VOLUME OUT TO 3 MONTHS WITHIN TISSUE THAT PROGRESSES TO INFARCTION IN ISCHEMIC STROKE

C. d'Esterre[1], E. Fainardi[2], A. Saletti[2], S. Ceruti[2], T.Y. Lee[1,3]

[1]Medical Biophysics, University of Western Ontario, London, ON, Canada, [2]Neurosciences and Rehabilitation, Azienda Ospedaliero-Universitaria, Ferrara, Italy, [3]Imaging, Lawson Health Research Institute, London, ON, Canada

Objective: CT perfusion (CTP)-derived cerebral blood volume (CBV) lesions (CBV ~ zero) are accepted as non-viable ischemic tissue[1,2]. However, extremely low CBV regions can remain prevalent up to 24 hours post stroke without an initial DWI abnormaility[3]. More recently, CBV defects larger than final infarct volumes from non-contrast CT (NCCT) or MR imaging have been reported, suggesting reversibility of such defects[4]. While controlling for technical and physiological factors that affect CBV, we examined a 3-month temporal profile of CTP-derived CBV to elucidate the possible reversibility of low CBV values within tissue that progressed to infarction.

Method: Twenty-five patients had a CTP/NCCT scan within 6-h and at 24-h, 7-d and 3-m post stroke. Final infarct regions of interest (IROIs) were traced on 3 month NCCT images. Each CTP study was examined for truncation of the tissue time-density curve (ITDC) obtained from the IROIs, defined as: the ratio of the increase in Hounsfield Unit (HU) value at the end of the CTP acquisition relative to that of the peak HU above baseline being greater than 0.5. Patients were excluded if ITDCs were truncated at any time point (n=7) or no IROIs were observed (n=8). For the remaining 10 patients, IROIs were superimposed onto registered CTP-derived perfusion weighted, cerebral blood flow and CBV functional maps, calculated using delay-insensitive deconvolution (CTP 4, GE Healthcare), at all time points. These regions were mirrored into the contralateral hemisphere. At all time points, average CBV ($ml \cdot 100g^{-1}$) within each infarct and contralateral ROI was determined with the exclusion of large vessel pixels[5]. For each patient, a weighted average CBV was calculated from all superimposed IROIs. To account for physiological fluctuations (arterial CO_2 tension and blood pressure) among time points, average CBV values from IROIs were divided by those from the contralateral ROIs to calculate relative CBV (CBV_r). The recanalization status was determined with computed tomography angiography at 24-h and 7-d post stroke.

Results: CBV_r (mean±stdev;$ml \cdot 100g^{-1}$) values at 6-h, 24-h, 7-d and 3-m were 0.75±0.23, 0.76±0.30, 0.84±0.13 and 0.51±0.13, respectively when averaged over all patients. There were no significant ($p>0.05$) CBV_r increases at any time point. Significant ($p< 0.05$) within-subject CBV_r increases occurred at one or more time points in 3 patients. Two of these patients recanalized within 24 hours and one within 7 days. The median (range) CBV (absolute value in $ml \cdot 100g^{-1}$ instead of CBV_r) from superimposed IROIs at 6-h, 24-h, 7-d and 3-m were 1.0(0.4-1.7), 1.1(0.6-1.4), 1.5(0.5-1.7), and 0.8(0.4-1.6) respectively.

Conclusion: Even with the use of delay-insensitive CTP software, exclusion of patients with ITDC truncation, and correction for physiological fluctuations among time points, we observed reversal of extremely low CBV out to one week in a limited number of patients irrespective of their recanalization status. Nevertheless, all CBV values obtained from IROIs remained below reported infarct thresholds[6] throughout the 3-m monitoring period.

References:

1. PW Schaefer.AJNR 2006

2. HM Silvennoinen. AJNR 2008

3. A McKinney. *AJNR* 2006

4. PW Schaefer. Stroke 2009

5. K Kudo. AJNR 2003

6. PW Schaefer. AJNR 2006

586

ON DELTA ACTIVITY AND CEREBRAL SINUS VEIN THROMBOSIS

S. Aharoni[1], H. Goldberg-Stern[1], L. Kornreich[2], A. Shuper[1]

[1]Pediatric Neurology, [2]Pediatric Imaging, Schneider Children's Medical Center of Israel, Petah Tikva, Israel

Introduction: Cerebral sinus vein thrombosis may be under-diagnosed. Although the introduction of advanced neuroimaging techniques has improved diagnostic capabilities, imaging studies may fail to reflect the true clinical picture. Despite the dominant clinical picture of seizures in CSVT, little attention has been paid to associated EEG changes in the English literature.

Case report: A 5-year-old boy, who presented with severe headache and focal seizures, had normal neurological examination and brain CT findings. The initial EEG showed focal delta activity. An emergent brain MRI disclosed a thrombosis of the left sigmoid sinus and jugular vein. The focal delta activity, which is presumed to represent the summation of effects of injured and viable neurons in the cortex and thalamus, was a significant diagnostic clue.

Conclusion: Cerebral sinus vein thrombosis should be considered in the differential diagnosis of focal delta activity. As EEG allows for the study of some aspects of the tissue damage in CSVT, it seems reasonable to include EEG in its routine diagnostic workup.

587

NIASPAN TREATMENT PROMOTES WHITE MATTER AND AXONAL REMODELING AND IMPROVES FUNCTIONAL OUTCOME AFTER STROKE IN TYPE 1 DIABETES RATS

J. Chen[1], X. Ye[1], A. Zacharek[1], Z. Liu[1], X. Cui[1], Y. Cui[1], T. Yan[1], C. Roberts[1], X. Liu[2], M. Chopp[1]

[1]Neurology, Henry Ford Hospital, Detroit, MI, USA, [2]Neurology, Jinling Hospital, Nanjing University School of Medicine, Nanjing, China

Diabetes mellitus (DM) patients are prone to develop more and earlier white matter lesions (WML) and DM leads to a higher risk of ischemic stroke. In this study, we investigated the changes and the molecular mechanisms of WM and axonal damage after stroke and tested the therapeutic effect of Niaspan in type-1 diabetic (T1DM) rats. T1DM was induced in male Wistar rats via injection of streptozotocin. These rats were subjected to middle cerebral artery occlusion (MCAo) and were treated with 40mg/kg Niaspan or saline starting 24h after MCAo daily for 14 days. WT-rats were also subjected to MCAo. All rats were sacrificed at 14 days after MCAo. A battery of functional tests were performed. Compared to WT-MCAo rats, the ischemic lesion volume was not increased in T1DM-MCAo rats, however, T1DM-MCAo rats exhibited worse functional outcome after stroke compared to WT-MCAo rats. T1DM-MCAo rats had significantly decreased high density lipoprotein (HDL) cholesterol levels. Using an ELISA assay, we found that Angiopoietin 1 (Ang1) was decreased in T1DM-MCAo in the iscehmci brain compared to WT-MCAo rats. To test whether T1DM-MCAo enhances WM impairment, SMI-31 (axonal neurofilament marker), Bielshowsky silver (axon marker), Luxol fast blue (LFB, myelin marker) and NG2 (oligodendrocyte progenitor cell marker) immunostaining were performed. SMI-31, Bielshowsky silver, LFB and NG2 expression were significantly decreased in T1DM-MCAo rats compared to WT-MCAo rats, indicating more severe WM damage. To investigate whether T1DM-MCAo affects axonal length, biotinylated dextran amine (BDA) was injected into the contralateral cortex at 14 days before sacrifice rats to retrogradely label pyramidal neurons. We found that the dendritic length of BDA positive neurons was significantly decreased in T1DM-MCAo rats compared with WT-MCAo rats. Niaspan treatment of stroke in T1DM-MCAo rats significantly increased HDL levels and improved functional outcome after stroke compared to saline treated T1DM-MCAo rats. Niaspan treatment significantly increased Ang1 expression in the ischemic brain as well as increased SMI-31, Bielshowsky silver, LFB and NG2 expression, and axonal length compared to saline treated T1DM-MCAo rats. In vitro data using a premature oligodendrocyte cell line (N20.1) and primary cortical neurons (PCN) show that high glucose (HG) significantly decreased OL proliferation and increased OL and PCN death as well as decreased Ang1 expression compared to normal conditions. Niacin and HDL treatment of OL and PCN significantly increased OL and PCN Ang1 expression. Niacin, Ang1 and HDL treatment significantly attenuated HG-induced cell death in cultured OL and PCN and increased neurite outgrowth in cultured PCN. Anti-Ang1 significantly decreased Niacin and HDL induced neurite outgrowth. These data indicate that T1DM decreases HDL levels and induces worse functional outcome after stroke. Increased WM and axonal damage in T1DM-MCAo rats may contribute to the reduced functional outcome after stroke. In addition, decreased Ang1 may be related to WM and axonal damage in T1DM-MCAo rats. Niaspan treatment increases serum HDL, and subsequent increased ischemic brain Ang1 expression may promote WM and axonal remodeling in the ischemic brain. WM and axonal remodeling may contribute to Niaspan induced improvement of functional outcome after stroke in T1DM rats.

588

ADVERSE EFFECTS OF BONE MARROW STROMAL CELL TREATMENT OF STROKE IN DIABETIC RATS

J. Chen[1], X. Ye[1], A. Zacharek[1], X. Cui[1], Y. Cui[1], T. Yan[1], X. Yang[2], C. Roberts[1], M. Chopp[1]

[1]Neurology, [2]Henry Ford Hospital, Detroit, MI, USA

Introduction: Diabetes mellitus (DM) is a major health problem associated with both microvascular and macrovascular disease and patients with DM have higher risk of atherosclerosis and ischemic stroke. Clinical studies have shown that hyperglycemia leads to poor recovery after ischemic stroke. Therefore, it is important to seek a therapeutic treatment for stroke in diabetes population. Previous studies have found that intravenous administration of bone marrow stromal cells (BMSCs) after stroke selectively targets the injury site, promotes angiogenesis and arteriogenesis, induces a neovascular response and improves functional outcome after stroke in wild-type (WT) animals. In this study, we investigated BMSC treatment of stroke in type 1 diabetic (T1DM) rats. The underlying mechanism of the effect of BMSCs on the ischemic brain tissue and macrovascular was investigated.

Methods: T1DM was induced in adult male Wistar rats via injection of streptozotocin (STZ) (65mg/kg, ip). At 14 days after induction of diabetes, rats were subjected to 2h transient middle cerebral artery occlusion (MCAO). BMSCs derived from normal WT rats were used for treatment. T1DM-MCAo rats were treated with BMSCs (3X10^6 and 5X10^6) or with saline intravenously via tail vein 24h after MCAo. Rats were sacrificed at 14 days after stroke (n=6-9/group). A battery functional tests, lesion volume, brain hemorrhage and immunostaining were performed. Another set of rats were sacrificed at 7 days after MCAo (n=5/group) for ELISA and Western blot assays.

Results: BMSC treatment in T1DM-MCAo rats increased early mortality rate, BBB leakage, and brain hemorrhage and decreased vascular stabilization and did not improve functional outcome after stroke compared to non-treatment T1DM-MCAo control. BMSC treatment also significantly increased neointimal formation and media thickness in the internal carotid artery and ischemic brain arterioles compared to non-treatment T1DM-MCAo control rats ($p< 0.05$). However, BMSC treatment also promoted angiogenesis and axonal regeneration in the ischemic brain measured by Bielshowsky silver (a marker for axons), Luxol fast blue (myelin marker) compared to non-treatment T1DM-MCAo rats ($p< 0.05$). To test the mechanism of BMSC induced BBB leakage and accelerated arteriosclerosis, Angiogenin, vascular endothelial growth factor (VEGF), and matrix metalloproteinases 9 (MMP9) ELISA assays and immunostaining were performed. BMSC treatment significantly increased Angiogenin, VEGF, and MMP9 levels in the ischemic brain and serum compared to T1DM-MCAo control group.

Summary: In summary, BMSC treatment of stroke in T1DM-MCAo rats does not improve functional outcome compared to control T1DM-MCAo rats. The increased Angiogenin, VEGF, and MMP9 levels by BMSC treatment after stroke in T1DM rats may contribute to BMSC treatment induced BBB leakage, brain hemorrhage and accelerated intracranial atherosclerosis in T1DM stroke rats. These data suggest that BMSC treatment of stroke has adverse effects in T1DM subjects.

589

PEROXISOMAL BIOGENESIS AFTER CEREBRAL ISCHEMIA

N.J. Alkayed

Oregon Health and Science University, Portland, OR, USA

Peroxisomes are small, single-membrane organelles found in almost every eukaryotic cell. They play an important role in the cellular response to oxidative and metabolic stress, and are the main site for hydrogen peroxide metabolism via catalase, fatty acid metabolism through β-oxidation and ether lipid synthesis, an essential component of myelin. They are highly adaptable and dynamic organelles, adjusting their number, size and enzyme composition to changing environment, metabolic demands and oxidative stress. Agents that proliferate peroxisomes, the so called peroxisome proliferator-associated receptor (PPAR) agonists, are used clinically for the treatment of diabetes and have been shown to exhibit neuroprotective properties in experimental models of neurodegeneration and cerebral ischemia. Finally, peroxisomes are required for normal brain development, and deficiencies in peroxisomal function in humans lead to severe and often fatal inherited disorders called peroxisomal biogenesis disorders (PBD, such as Zellweger syndrome), which are characterized by white mater damage and neurological abnormalities such as mental retardation and seizures. We have previously observed that the enzyme soluble epoxide hydrolase (sEH), a predominantly cytosolic protein, translocates to peroxisomes after ischemia, which is associated with peroxisomal proliferation and protection from ischemic injury. Accordingly, sEH-immunoreactivity increases in peroxisomes after ischemic injury, forcing sEH translocation enhances peroxisomal proliferation, and preventing its translocation and subsequent proliferation increases neuronal cell death. In this presentation, we will review peroxisomal biology and function, and mechanisms governing their proliferation and degradation in normal cells and in disease states, especially after cerebral ischemia. We will pay special attention to the unique role of sEH in triggering peroxisomal proliferation in response to ischemic stress and the potential therapeutic targeting of sEH to promote peroxisomal proliferation, neuroprotection and regeneration.

590

CHOLINERGIC MODULATION OF THE CORTICAL NEUROVASCULAR COUPLING AND NEURONAL RESPONSES TO WHISKER STIMULATION

C. Lecrux, C. Sandoe, X. Tong, S. Neupane, A. Shmuel, E. Hamel

Department of Neurology and Neurosurgery, Montreal Neurological Institute, McGill University, Montréal, QC, Canada

Background & objectives: Whereas neurovascular coupling appears to be driven by incoming afferent signals and their local processing in the activated region (1), the neuronal circuitry involved in this response is still poorly characterized. Acetylcholine (ACh) is a known modulator of sensory processing. Increased ACh levels, through basal forebrain (BF) stimulation, improve the cortical response gain by enhancing the action potential of pyramidal cells to afferent input, and reducing background activity within cortical circuits (2). However, little is known on the consequences of varying ACh levels on the neurovascular coupling response to sensory input. We investigated the cellular basis of the ACh modulation of neurovascular coupling to whisker stimulation, and assessed the mechanisms through which ACh modulates this response.

Methods: Sensory stimulation was induced in male Sprague-Dawley rats by mechanical stimulation of the whiskers. Activated neurons were identified by double immunohistochemistry for c-Fos and markers of pyramidal cells or GABA interneurons in perfused brain sections. CBF was measured by laser-Doppler flowmetry and extracellular local field potentials (LFP) were recorded with a multichannel electrode in the somatosensory cortex. Increase in ACh levels was achieved with linopirdine (10mg/kg, intraperitoneal) or physostigmine (0.1mg/kg, subcutaneous), whereas ACh levels were reduced by BF lesion with the selective cholinotoxin saporin (4mg/2mL, intracerebroventricular, icv). The role of ACh receptor subtypes was evaluated with antagonists at muscarinic (scopolamine, 0.1mg/kg, intravenous) and central nicotinic (chlorisondamine dichloride, 12mg/5mL, icv) receptors.

Results: ACh enhancement by linordipodine or physostigmine treatments potentiated the evoked CBF response to whisker stimulation (+31±4%, $p< 0.001$ and +40±8%, $p< 0.05$ relative to vehicle, respectively) without altering the activated cell populations or the extent of the c-Fos barrel. ACh decrease via selective cholinotoxic lesion diminished the evoked CBF response (-28±2%, $p< 0.001$) as well as the area of c-Fos activation in the barrel cortex whereas the activated cell types remained unchanged. In all conditions, ~21% of cyclooxygenase-2 (COX-2) pyramidal cells and ~13% of vasoactive intestinal polypeptide (VIP) interneurons, as compared to less than 8% of somatostatin interneurons, were recruited specifically in the activated barrel cortex. The enhanced CBF response induced by increased ACh transmission required activation of muscarinic but not nicotinic ACh receptors. Large CBF changes induced by enhanced ACh neurotransmission were associated with increased stimulus-evoked LFP power in the beta and gamma bands.

Conclusions: Our results indicate that increased ACh neurotransmission impacts the activity of selective populations of cortical neurons that drive the evoked CBF response, and that muscarinic receptors are required in this facilitation response to sensory input. The latter contrasts with the lack of involvement of these receptors in the neurovascular coupling response to sensory stimulation under baseline conditions. Investigations on how reduced ACh neurotransmission alters the CBF response to sensory stimulation are ongoing.

Supported by the Canadian Institutes of Health Research (CIHR, grants MOP-84209, EH and

MOP-102599, AS), the Human Frontier Science Program (HFSP RGY0080/2008, AS), a Heart and Stroke Foundation of Canada/Canadian Stroke Network Fellowship (CL) and a Jeanne Timmins studentship (CS).

References:

1. Lauritzen and Gold.J Neurosci.2003;23:3972-80.

2. Hasselmo and Giocomo.J Mol Neurosci.2006;30:133-5.

591

ACTIVATION OF ESTROGEN RECEPTOR A AND OF ACE2 SUPPRESSES ISCHEMIC BRAIN DAMAGE IN OOPHORECTOMIZED RATS

K. Shimada, K.T. Kitazato, T. Kinouchi, K. Yagi, Y. Tada, J. Satomi, T. Kageji, S. Nagahiro

Department of Neurosurgery Institute of Health Biosciences The University of Tokushima Graduate School, Tokushima, Japan

Background: The angiotensin II type 1 receptor blocker (ARB) is protective against cerebral ischemia in male rats. Estrogen is also neuroprotective and its effects are mediated by estrogen receptors (ERs). However, the detail actions of ERs and ARB on the brain renin-angiotensin system (RAS) after cerebral ischemia in estrogen deficient state remain obscure. We focused the relationship between ERs and the brain RAS in olmesartan-treated oophorectomized rats with ischemia

Methods: We performed oophorectomy (OVX^+) to 13-week-old female Wistar rats and compared OVX^+ rats with sham-oophorectomized rats (OVX^-) and OVX^+ rats treated with 0.3- or 3.0 mg/kg olmesartan for 2 weeks before middle cerebral artery occlusion. We accessed blood pressure, infarct volume, protein and mRNA expression of ERs and the brain RAS components in each group of rats. We used the ER inhibitor and agonist to further examine the role of ERs.

Results: Independent of blood pressure, the cortical infarct volume was larger in OVX^+- than OVX^- rats; it was smaller in olmesartan-treated OVX^+ rats. Activation of ERα but not ERβ in the cortical peri-infarct area was associated with a reduction in the infarct size. Interestingly, the activated ERα was correlated with the up-regulation of angiotensin-converting enzyme 2 (ACE2), Bcl-2 and Bcl-xL, and a reduction in angiotensin II and cleaved caspase-3. These effects were augmented in OVX^+ rats treated with olmesartan and abolished by the ER inhibitor. In OVX^+ rats treated with the ERα agonist alone, the infarct size was decreased and the neuroprotective genes were up-regulated. These findings suggest that the transactivation of neuroprotective genes and the reduction in brain angiotensin II are ERα dependent, and that this may augment neuroprotection together with an angiotensin II type 1 rectptor brockade.

Conclusion: Our study provides the new insight that the activation of ERα independent of estrogen contributes at least partly to limiting cerebral ischemic damage.

592

VERTEBRAL ARTERY OCCLUSION WITH VERTEBRAL ARTERY-TO-POSTERIOR INFERIOR CEREBELLAR ARTERY STENTING FOR PRESERVATION OF PICA IN TREATING RUPTURED VERTEBRAL ARTERY DISSECTION

Y.S. Shin

Seoul St Mary's Hospital, Catholic University of Korea, Seoul, Republic of Korea

We report two patients with ruptured vertebral artery (VA) dissecting aneurysms who were treated by placing an Enterprise stent (Cordis Neurovascular, Miami Lakes, FL) from the VA to the posterior inferior cerebellar artery (PICA) in order to save the patency of the PICA. First case: A 50-year-old man was admitted with a ruptured right VA dissecting aneurysm. The distal portion of the dissection involved the origin of the PICA. A 4.5×28-mm Enterprise stent was then placed through the contralateral VA and placed from PICA to distal VA. The dissected segment of the VA was completely occluded by coil embolization. The 2 weeks follow-up angiography showed that the dissected segment was completely occluded with patency of PICA. Second case: A 47-year-old man was admitted with a ruptured right VA dissecting aneurysm that involved the origin of the PICA. A 4.5×37-mm Enterprise stent was then placed through the proximal VA to the PICA. The dissected segment of the VA was completely occluded by coil embolization. The 1-year follow-up angiography showed that the dissected segment was completely occluded and the diameter of the PICA was slightly increased, and the PICA's patency was good.

Instead of the surgical revascularization of the PICA with VA occlusion, we report here on two patients who were treated by placing an Enterprise stent (Cordis Neurovascular, Miami Lakes, FL) from the proximal VA to the PICA in order to save the patency of the PICA, and we completely occluded the dissected segment by coiling. VA-to-PICA stenting with total occlusion of the VA by coil embolization might be a valuable treatment option to preserve the PICA's patency when treating a patient with VA dissection that involves the origin of the PICA.

594

BLOOD-BRAIN BARRIER INJURY IN ALCOHOL AND METHAMPHETAMINE ADDICTION

Y. Persidsky[1], S. Ramirez[1], H. Dykstra[1], N. Reichenbach[1], S. Fan[1], R. Potula[1], J. Haorah[2]

[1]Pathology and Laboratory Medicine, Temple University School of Medicine, Philadelphia, PA, [2]Pharmacology, University of Nebraska Medical Center, Omaha, NE, USA

Objectives: Alcohol and drug abuse result in multifaceted neurotoxic effects in central nervous system (CNS). Yet, their effects in brain endothelial cells, major part of blood brain barrier (BBB) controlling access of these substances to CNS remain undefined. Using primary human brain microvascular endothelial cells (BMVEC) we investigated functional changes in brain endothelium after exposure to ethanol (25-50 mM) and methamphetamine (50 mmol/L) in pathophysiologically relevant doses.

Methods: We assessed expression of EtOH metabolizing enzymes, tight junction (TJ) proteins, myosin light chain (MLC) kinase (MLCK), metalloproteases (MMP)-2 and 9 in primary human BMVEC by Western blot and immunostainung (TJ). Transendothelial electric resistance (TEER), permeability measured by FITC-labeled dextran, degradation of FITC-labeled collagen IV and transendothelial migration of monocytes served as functional assays of BBB impairment.

Results: *W*e demonstrated that exposure to ethanol (0.5-2 h) induced catalytic activity/expression of EtOH-metabolizing enzymes, which paralleled enhanced generation of reactive oxygen species (ROS), leading to Ca^{2+} release, activation of MLCK, phosphorylation of MLC and tight junction (TJ) proteins. These changes paralleled decrease in BBB integrity (in vitro and in vivo), and enhanced monocyte migration across BMVEC monolayers. We established that chronic exposure to EtOH (24-72 h) resulted in activation of MMP-2 and 9 via activation of protein tyrosine kinase, degradation of basement membrane components, increased barrier “leakiness” and monocyte migration across human brain endothelial monolayers. We found that all functional alterations and signal transduction events caused by EtOH exposure can be reproduced by application of acetaldehyde (major ethanol metabolite) or exogenous donors of ROS. Similarly, we found that methamphetamine increased BBB permeability *in vivo* (mice injected with escalating doses of methamphetamine, up to 10.0mg/kg for 9 days), and exposure of BMVEC to methamphetamine diminished tightness of BMVEC monolayers in a dose- and time-dependent manner by decreasing expression of cell membrane associated TJ proteins. These changes were accompanied by enhanced production of ROS, increased monocyte migration across methamphetamine-treated endothelial monolayers, and activation of MLCK in BMVEC. Anti-oxidant treatment attenuated or completely reversed all tested aspects of methamphetamine induced BBB dysfunction.

Conclusions: Our data suggest that BBB injury is caused by alcohol and methamphetamine - mediated oxidative stress, which activates MLCK and negatively affects the TJ complex. These observations provide a basis for antioxidant protection against brain endothelial injury in the setting of alcohol and/or methamphetamine abuse.

Supported by NIDA/DA025566 and NIAAA/AA017398, AA015913

595

BODY TEMPERATURE MIGHT BE A PROGNOSTIC FACTOR IN HYPOGLYCEMIC COM

T. Ikeda, M. Kanazawa, T. Takahashi, M. Nishizawa, T. Shimohata

Department of Neurology, Brain Research Institute, Niigata University, Niigata, Japan

Background: Hypoglycemic coma is a common and serious complication of insulin and/or oral hypoglycemia therapy, insulinoma, and malnutrition. The only treatment for hypoglycemia is blood glucose correction. Previous studies using rodent models have shown that a reduction in body temperature (BT) during hypoglycemia exerts protective effects against the development of hypoglycemia-induced neuronal injury. In addition, several studies on rodents have shown that post-treatment hyperglycemia should be avoided to prevent neuronal damage during glucose reperfusion. However, it remains unknown whether these findings are applicable to humans with hypoglycemic coma. The aim of our study was to test the following hypotheses: (1) low BT during hypoglycemic coma is a good prognostic factor in humans, and (2) hyperglycemia after glucose administration is a poor prognostic factor.

Objective: To investigate the effects of BT during hypoglycemic coma and hyperglycemia after blood glucose correction on the prognosis of patients with hypoglycemic coma.

Methods: A consecutive series of patients diagnosed as having hypoglycemic coma were studied. Medical records of the patients were used to identify the clinical features including blood glucose levels and body temperature during hypoglycemic coma and blood glucose levels after glucose administration. We also evaluated the therapeutic outcome of the patients on the day of discharge using the Glasgow outcome scale (GOS), and compared clinical features between the patients with poor outcome (GOS=1 to 4) and those with good outcome (GOS=5).

Results: During the observation period, we examined the clinical characteristics of 18 consecutive patients (11 men and 7 women) with hypoglycemic coma. The causes of hypoglycemic coma included drug-related (insulin and/or oral hypoglycemic agents) complication, insulinoma, and other factors such as inadequate diet and gastrointestinal diseases. The lowest blood glucose level during hypoglycemic coma was 26.9 ± 10.6 mg/dL. BT during hypoglycemic coma was 36.3 ± 1.2°C. Low BT during hypoglycemic coma was observed in 33% (BT < 36°C) and 12% (BT < 35°C) of the patients. The highest blood glucose level after treatment was 180.8 ± 92.9 mg/dL, and post-treatment hyperglycemia was observed in 22% of the patients.

There were no significant differences in the age, duration of hypoglycemic coma, and the blood glucose level during hypoglycemic coma between the good- and poor-outcome groups. The causes of hypoglycemic coma were not notably different between the 2 groups. BT during hypoglycemic coma in the good-outcome group was lower than that in the poor-outcome group (35.8 ± 1.2 vs. 37.2 ± 0.5; p = 0.026). Low BT (< 36°C) was observed only in the good-outcome group. Further, there were no significant differences in highest blood glucose level between the good- and poor-outcome groups (180.8 ± 100.8 vs. 180.6 ± 78.9, respectively). There was no statistically significant difference in the frequency of patients with post-treatment hyperglycemia between the 2 groups.

Conclusion: Low BT during hypoglycemic coma might be a good prognostic factor in patients with hypoglycemic coma.

596

TRANSPLANTED BONE MARROW STROMAL CELLS PROTECT NEUROVASCULAR UNITS AND AMELIORATE BRAIN DAMAGE IN STROKE-PRONE SPONTANEOUSLY HYPERTENSIVE RATS (SHR-SP)

M. Ito, S. Kuroda, T. Sugiyama, K. Maruichi, M. Kawabori, H. Shichinohe, K. Houkin

Neurosurgery, Hokkaido University Graduate School of Medicine, Sapporo, Japan

Background and purpose: Recently, there is increasing evidence that bone marrow stromal cells (BMSC) may protect and repair the damaged tissue through multiple mechanisms when transplanted into animal models of stroke. However, there is no study whether the BMSC can potentially prevent the occurrence of stroke in the high-risk patients. This study was aimed to test the hypothesis whether the BMSC can ameliorate brain damage when directly transplanted into the brain of stroke-prone spontaneously hypertensive rats (SHR-SP).

Methods: The BMSC or vehicle was stereotactically delivered into the right striatum of SHR-SP (male, 8 weeks old, n=3 and 4, respectively). Blood pressure was measured every week. 0.5% NaCl was loaded every day from 9 weeks of age to promote hypertension additionally. T2-weighted MR images were obtained at 11 weeks of age. They were sacrificed at 12 weeks of age for subsequent histological analysis. Wistar-Kyoto (WKY) rats were utilized as the control (n=3).

Results: Blood pressure gradually elevated up to higher than 200/150 mmHg in both the vehicle- and BMSC-transplanted SHR-SP at 12 weeks of age. T2-weighted MRI demonstrated neither cerebral infarct nor intracerebral hemorrhage, but identified abnormal dilatation of the lateral ventricles in the vehicle-transplanted SHR-SP. On HE staining, the lateral ventricle was significantly dilated in the vehicle-transplanted SHR-SP, compared with the WKY rats and the BMSC-transplanted SHR-SP. Double fluorescence immunohistochemistry revealed a decreased density of the collagen IV-positive microvasculature and a decreased number of the microvasculature that kept the integrity between basement membrane and astrocyte endfeet in the vehicle-transplanted SHR-SP. BMSC transplantation significantly inhibited these degenerative processes in the microvasculature.

Conclusion: These results strongly suggest that long-lasting hypertension may induce the damage of neurovascular units prior to the occurrence of stroke. The BMSC may ameliorate this damaging processes when transplanted into the CNS.

597

WNT/ BETA-CATENIN SIGNALING IS EVIDENT POST-STROKE AND ENHANCES ENDOGENOUS NEUROGENESIS WHEN UPREGULATED

I. Iordanova[1,2,3], M. Anderson[1], R. Nusse[4], T. Palmer[1], G.K. Steinberg[1,2,3]

[1]Neurosurgery, [2]Stanford Stroke Center, Stanford University School of Medicine, [3]Stanford Institute for Neuro-Innovation and Translational Neurosciences, Stanford University, [4]Developmental Biology, Stanford University School of Medicine, Stanford, CA, USA

Objectives: Wnt/ beta-catenin signaling is essential for maintaining endogenous neurogenesis in the adult brain[1]and enhancing post-stroke neurogenesis has been shown to be beneficial for recovery[2-4]. Having established that Wnt/ beta-catenin signaling is present within one of the two adult neurogenic niches: the subventricular zone, SVZ, we examined the dynamics of the signaling pathway following transient middle cerebral artery occlusion, MCAO. We also investigated the effect of upregulating the pathway on the endogenous post-stroke neurogenesis, by employing a novel Wnt-3a liposomal preparation.

Methods: - Young adult male Axin 2 reporter mice for Wnt/ beta-catenin signaling were subjected to 25 min MCAO and cohorts of 4 mice were sacrificed at 1 day, 3 days, 7 days and 14 days post-stroke. Immunohistochemistry was employed to visualize the cell types demonstrating Wnt/ beta-catenin signaling. Optical density values of images taken at each time point were compared using ImageJ in order to evaluate pathway activation levels.

- Wnt-3a liposomes were freshly made [5] and injected intra-parenchymally at 1, 3, 7 and 14 days post-stroke in two 1.5 ul boluses at 3mm and 1.5 mm depth (1.2 mm laterally, 0.6 mm anterior of bregma).

- DAB staining and stereology were employed to quantify the number of Doublecortin, DCX, positive newborn neurons at 1 month after MCAO.

Results: - Wnt/ beta catenin signaling was evident in GFAP, Nestin and Doublecortin cells present at the SVZ in both naïve and post-stroke animals, as well as in mature NeuN positive neurons within the cortex and striatum. In post-MCAO animals it was also present in GFAP positive astrocytes at the penumbra.

- We observed an oscillation in the upregulation pattern of Wnt/ beta-catenin signaling after stroke, which we are confirming with larger cohorts.

- Wnt-3a liposomes exhibited a potent ability to activate the Wnt/ beta-catenin pathway both *in vivo* (5 fold greater than baseline) and *in vitro* (comparable to recombinant Wnt-3a protein) and significantly increased the number of Doublecortin positive newborn neurons (up to 20 fold compared to PBS alone) when injected at 3 and 7 days post -stroke.

Conclusions: Here we show that the Wnt/ beta-catenin signaling pathway is active within the adult brain and upregulated following stroke. Activation of the pathway, in a novel liposome-mediated way, significantly enhances endogenous neurogenesis post-stroke.

References:

1. Lie, D.C.*, et al.* Wnt signalling regulates adult hippocampal neurogenesis. *Nature* 437, 1370-1375 (2005).

2. Greenberg, D.A. Neurogenesis and stroke. *CNS Neurol Disord Drug Targets* 6, 321-325 (2007).

3. Jin, K., Wang, X., Xie, L., Mao, X.O. & Greenberg, D.A. Transgenic ablation of doublecortin-expressing cells suppresses adult neurogenesis and worsens stroke outcome in mice. *Proc Natl Acad Sci U S A* 107, 7993-7998.

4. Jin, K.*, et al.* Evidence for stroke-induced neurogenesis in the human brain. *Proc Natl Acad Sci U S A* 103, 13198-13202 (2006).

5. Morrell, N.T.*, et al.* Liposomal packaging generates Wnt protein with in vivo biological activity. *PLoS One* 3, e2930 (2008).

599

ASSESSING THE ONTOGENY OF CB1 RECEPTORS IN ADOLESCENT AND ADULT RATS USING IN VIVO PET WITH [18F]MK9470

M. Verdurand[1,2], V. Nguyen[2], D. Stark[2], D. Zahra[2], M.-C. Gregoire[2], I. Greguric[2], K. Zavitsanou[1,2]

[1]Schizophrenia Research Institute, [2]ANSTO Life Sciences, Sydney, NSW, Australia

Objectives: Evidence suggests that cannabinoid CB1 receptors (CB1R) play a role in psychosis. In vivo studies of CB1R in both humans and animal models have been hampered by the lack of suitable radioligands. In the present animal study, we assessed the ontogeny of CB1R in adolescence and adulthood in vivo with Positron Emission Tomography (PET) and [^{18}F]MK9470, a selective high-affinity radioligand for CB1R[1].

Methods: [^{18}F]MK9470 was labeled with high specific activity (6000 Ci/mmol). Twelve male Wistar rats were imaged at adolescence (Post-Natal Day (PND) 35-37, n=6) and adulthood (PND70-72, n=6) with our Inveon PET/CT (Siemens). A 60-min PET scan was started at the same time of [^{18}F]MK9470 injection with a low mass (0.07 ± 0.001 nmol). Images were reconstructed, co-registered with CT and spatially normalized to a home-made atlas of rat brain with 8 Regions of Interest (ROI). Absolute and relative Standardized Uptake Values (SUV) were calculated for 8 ROI, based on the last 20 min of each scan, as a measure of CB1R binding[2].

Results: Levels of CB1R binding (SUV) were concordant with the literature with high to moderate CB1R density in cerebellum, cortical regions and hippocampus. Two-way ANOVA (age x region) looking at absolute [^{18}F]MK9470 SUV revealed a significant main effect of age ($F(1,80)=23.980$, $p< 0.001$) with adults having higher CB1R density than adolescents (+16.5% over 8 ROI). LSD's post-hoc tests revealed that CB1R density was significantly higher in adults compared to adolescents in the posterior cortex (+23.6%, p=0.017), the frontal cortex (+21.6%, p=0.035), and in the hippocampus (+21.3%, p=0.039). Percentage of change in relative SUV corroborated the absolute findings showing an increased CB1R expression in the adults compared to the adolescents in the cortical and hippocampal regions (posterior cortex (+9.2%, $p< 0.001$), the frontal cortex (+5.8%, p=0.003), the hippocampus (+5.8%, p=0.004)).

Conclusions: This study first confirms the feasibility of examining the ontogeny of CB1Rs in vivo with PET and [^{18}F]MK9470. The main finding of this study is that CB1R density is statistically increased from adolescence (PND35) to adulthood (PND70) in rats, in contrary to most other neuroreceptor systems undergoing pruning during this transitional period[3,4,5]. These in vivo results are in accordance with in vitro results obtained in rats[6] and humans[7]. This pilot study will provide the basis for future longitudinal in vivo studies looking at CB1R expression in animal models of psychosis.

References:

1. Burns et al., PNAS 104:9800-9805 (2007).

2. Casteels et al., Eur J Nucl Med Mol Imaging 37:1164-1173 (2010).

3. Andersen et al., Neurosci Biobehav Rev 27:3-18 (2003).

4. Verdurand et al., Brain Res 1351:238-245 (2010).

5. Zavitsanou et al., Neuroscience 169:315-324 (2010).

6. Belue et al., Neurotox Teratol 17:25-30 (1995).

7. Mato et al., Eur J Neurosci 17:1747-1754 (2003).

600

CEREBRAL BLOOD VESSEL MODEL SIMULATION FOR CEREBROVASCULAR CO_2 REACTIVITY AND AUTOREGULATION EXAMINED AFTER CHRONIC PRETREATMENT OF A CANDESARTAN

K. Nakamura, Y. Kondoh, S. Mizusawa, T. Kinoshita

Akita Research Institute of Brain and Blood Vessels, Akita, Japan

Introduction: Pretreatment of Angiotensin II type 1 (AT_1) antagonist, candesartan shows rather smaller value of CO_2 reactivity than normal rats[1]. The decreased response to CO_2 usually reflects vasodilatation of resistance vessels, and so smaller CO_2 reactivity should imply a shift in the autoregulation curve toward the higher blood pressures. However, previous results show that the autoregulation curve is shifted toward the lower blood pressure [2]. To interpret this discrepancy between CO_2 reactivity and autoregulation shift after candesartan, we prepare a mathematical model based on the mechanical and physiological aspects of cerebrovascular regulatory mechanisms.

Method: We used a mathematical model reported by Ursino for representing the autoregulation and CO_2 reactivity in human [3]. The model was based on the physiological aspects between mechanical tension of vessel wall and vessel radius[4]. Model parameters including a feedback parameter for expressing the autoregulation and CO_2 reactivity were fitted for normal rat and then applied to candesartan-treated model rat. For the candesartan-treated model rat, only a parameter of wall thickness was changed to thinner wall than normal condition [5].

Results: Figure1 shows simulation results of the autoregulation (left) and CO_2 reactivity (right) with same parameters. Open and closed sqares represent the normal and thinner wall conditions, respectively. According to the model simulation, autoregulation curve was shifted toward the lower blood pressure and CO_2 reactivity reduced simultaneously by only changing a parameter of wall thickness.

Discussion: Candesartan blocks AT_1 receptors that mediate vasoconstriction in large cerebral arteries, reducing blood pressure and increasing CBF. From a traditional viewpoint of autoregulation, small resistance vessels might be constricted in order to compensate for this large arteries extension [2]. It has not been revealed why candesartan effect is different for large and small arteries. As for vessel walls in candesartan treated rats, large arteriolar vessel wall is thinner than normal rats [5]. It is reasonable that all the vessels wall thickness changed to be thinner than normal condition. By using the mathematical model simulation, thinner vessel walls can be shifted autoregulation curve toward the lower blood pressure and can reduce CO_2 reactivity simultaneously. The experimental results of CO_2 reactivity and autoregulation shift in candesartan treated rats can be interpreted from the simulation results.

References: [1] Mizusawa et al., Proc Brain07 & BrainPET07, BP34-7M, 2007, [2] Vraamark et al., J Hypertension, 13, 1995, 755-761, [3] Ursino et al., Am J Physiol, 274, 1998, H1715 - 28, [4] Davis et al., Am J Physiol, 256, 1989, H630 - 40, [5] Ito et al., Stroke. 33, 2002, 2297-2303

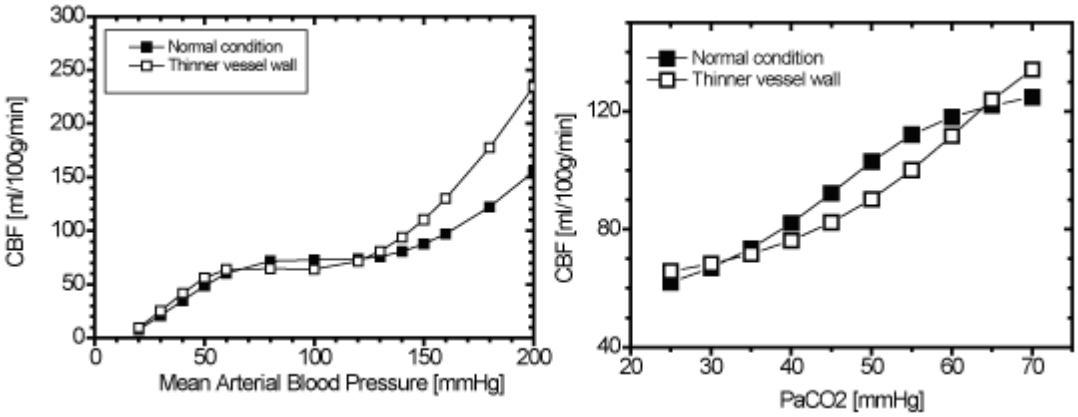

[Figure1 :]

Simulation results of the autoregulation (left) and CO2 reactivity (right) in different vessel wall thickness.

601

UNBIASED NON-INVASIVE QUANTIFICATION OF LIGAND-RECEPTOR DYNAMIC PET

Y. Zhou[1], J.R. Brasic[1], G.S. Smith[2], C.J. Endres[1], D.F. Wong[1]

[1]The Russell H. Morgan Department of Radiology and Radiological Science, [2]Department of Psychiatry and Behavioral Sciences, School of Medicine, Johns Hopkins University, Baltimore, MD, USA

Introduction: Tracer kinetic modeling using plasma input function (PIF) is regarded as the gold standard method for quantification of ligand-receptor dynamic PET study. The invasive arterial blood sampling for PIF is often a barrier to pursuing quantitative PET applications. Two strategies have been developed for PET kinetic modeling without blood sampling. The first strategy is to apply kinetic models that do not require PIF, and instead use a tissue-derived reference input. Unfortunately, reference tissue based quantitative methods are typically biased due to model simplification [1]. The second strategy is to estimate PIF from dynamic PET data. The existing methods for estimating an image-derived PIF have been studied mostly for [^{18}F]FDG [2-4].

Objective: The aim of this study is to evaluate a novel noninvasive tracer kinetic modeling technique for quantification of ligand receptor PET studies.

Methods: A non-parametric PIF based iterative estimation algorithm is proposed as below:

1) With given initial estimates of PIF_0 and ROI kinetics measured by dynamic PET (C(t)), the model parameter vector (K) was estimated by model fitting.

2) Based on the estimated parameter K from step 1, the PIF for each ROI was then estimated as $PIF = \Psi(PIF_0, C(t), K, t)$, where $\Psi(PIF_0, C(t), K, t)$ was determined by applying deconvolution to the tracer kinetic model. The mean of PIF (mPIF) over all ROIs was then computed.

3) The relative changes of mPIF compared to the PIF_0 was calculated. Steps 1 to 2 with the updated initial estimate of PIFnew = mPIF/AUC(PIF) were repeated if the relative change of PIF $\geq \varepsilon$, where ε is a given threshold value. The algorithm was evaluated by 55 [^{11}C]raclopride (D2 receptor) and 4 [^{11}C]DASB (serotonin transporter) human dynamic PET studies. Thirteen ROIs including reference tissue cerebellum were manually drawn on the co-registrated MRI images and then copied to dynamic PET images for ROI kinetics. Metabolite-corrected PIF were obtained in each PET study by arterial blood sampling. A 2-tissue compartmental model was used to fit the measured tracer kinetics. The binding potential (BP) was estimated via distribution volume (DV) as DV/DV(cerebllum)-1.

Results. The estimated PIFs were similar to the measured PIF in terms of curve shape. The BPs estimated by using a measured PIF were virtually identical to those obtained using an estimated PIF(see Fig), with no significant differences between BP estimates.

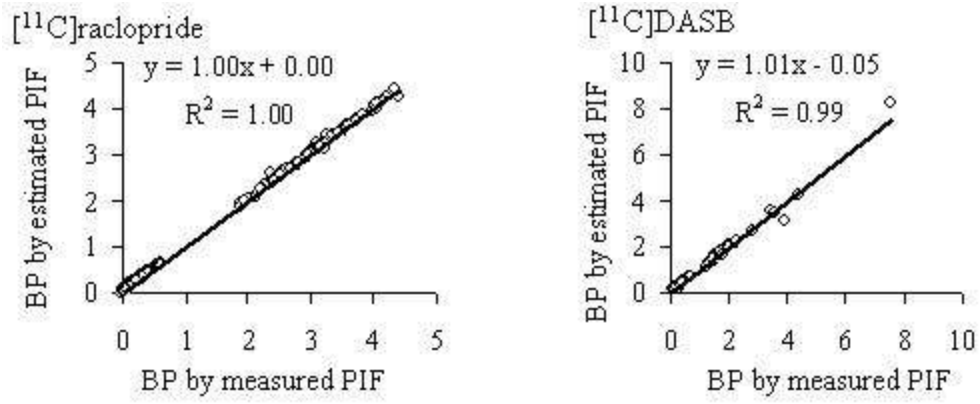

[Correlations of estimates]

Conclusions. The non-parametric PIF based iterative estimation algorithm was unbiased non-invasive approach for quantification of specific binding of [^{11}C]raclopride and [^{11}C]DASB as compared to the measured PIF. The applications of the proposed method to the dynamic PET studies without identified reference tissue such as [^{18}F]AZAN (nicotinic α4β2 receptor) and [^{11}C]DPA-713 (translocator protein) are under investigation.

References:

1. Zhou Y., et al. Neuroimage 18(4), 975-989.

2. Feng D, et al, 1997. IEEE Trans Inf Technol Biomed 1(4):243-254.

3. Wong KP, et al, 2001. IEEE Trans Inf Technol Biomed 5(1):67-76.

4. Ogden RT, et al. 2010. J Cereb Blood Flow Metab. 30(4):816-26.

603

SYNBIOTIC FLOATING BEADS OF GINGER-PROBIOTIC FOR EFFECTIVE TREATMENT OF CHRONIC FATIGUE SYNDROME (CFS)

P.K. Singh, **H. Singh**, I.P. Kaur

Department of Pharmaceutics, University Institute of Pharmaceutical Sciences, Panjab University, Chandigarh, India

Phenolic substances in ginger, possesse strong anti-inflammatory and antioxidative properties. Patients suffering from CFS show a disturbed intestinal microbial ecology and the host immune system. In the recent years the interface between neuropsychiatry and gastroenterology has converged into a new discipline 'enteric neuroscience'.

Ginger is reported to possess properties that make it beneficial for treating small intestinal bacterial overgrowth (SIBO) and associated problems. Of special benefit is the fact that ginger extract (GE) also acts as a prebiotic; however it shows a very slight solubility in water and a poor bioavailability. Prebiotics, non-digestible oligosaccharide are reported to promote and maintain the growth of probiotics. For probiotics to be effective, the bacteria must arrive in the intestine alive and in sufficient number such that a suitable packaging system which can maintain the viability and promote colonization of these probiotic organisms in gut is indicated. In view of this we entrapped *Lactobacillus acidophilus* and GE into sodium gel-polymeric beads. The developed beads possessed gastro-retentive property thus resulting in floating delivery system.

The study incorporates a novel concept of triforked therapy with a probiotic/ prebiotic/antioxidant agent as GE/suitable gel entrapment system resulting in an enhanced effect. Evaluation of the system in weight stress model of CFS in rats showed significant pharmacodynamic effect in terms of restoring the oxido-nitrosative stress, inflammatory cytokines and other behavioral and biochemical alternations associated with stress.

Conclusively, the system worked for curing CFS than providing a mere protective effect and is of great potential as therapeutics to treat CFS.

604

OPTIMIZING STATISTICAL PARAMETRIC MAPPING WITH A GENERAL LINEAR MODEL FOR DIFFUSE OPTICAL TOMOGRAPHY TO IMAGE RAPID BRAIN FUNCTION EVENTS

M. Hassanpour[1], B.R. White[1], A.T. Eggebrecht[2], J.P. Culver[2]

[1]Department of Physics, Washington University in St. Louis, [2]Department of Radiology, Washington University School of Medicine, St. Louis, MO, USA

Objectives: Recent advances in high-density diffuse optical tomography (HD-DOT) methods have demonstrated significant improvements in image quality which have potential utility in a wide variety of clinical and developmental studies. However, most HD-DOT studies have used slow (~20 sec) block-averaging behavioral paradigms. Both clinical studies and brain development studies in children would benefit from faster (~2-6 sec) event-related paradigms, and general linear model (GLM) analysis as used in fMRI and some Near Infrared Spectroscopy (NIRS) topography studies. In this work, we develop a GLM approach to generate statistical parametric maps (SPM) of visual activations. Several approaches to estimating the spatial and temporal parameters for DOT data sets are evaluated and optimized.

Methods: Using a high density imaging cap (Fig.1,a), visual cortex activations were recorded while subjects faced a LCD screen. Stimuli were flickering checkerboard wedge shapes (500s total run time) located at the lower left or right hand corner of the screen (Fig. 1,b). Data preprocessing included temporal filtering, global signal regression, image reconstruction and spectroscopy. In a three stage statistical analyses, first GLM was applied using a canonical hemodynamic response function (cGLM, Fig, 1,c), to oxy- deoxy- and total hemoglobin contrasts and three different combinations of contrasts. In the second stage subject-specific hemodynamic responses (HDRs) in two regions (left and right visual cortices) were estimated for each concentration. The third stage used the subject-derived HDRs to produce statistical parametric maps.

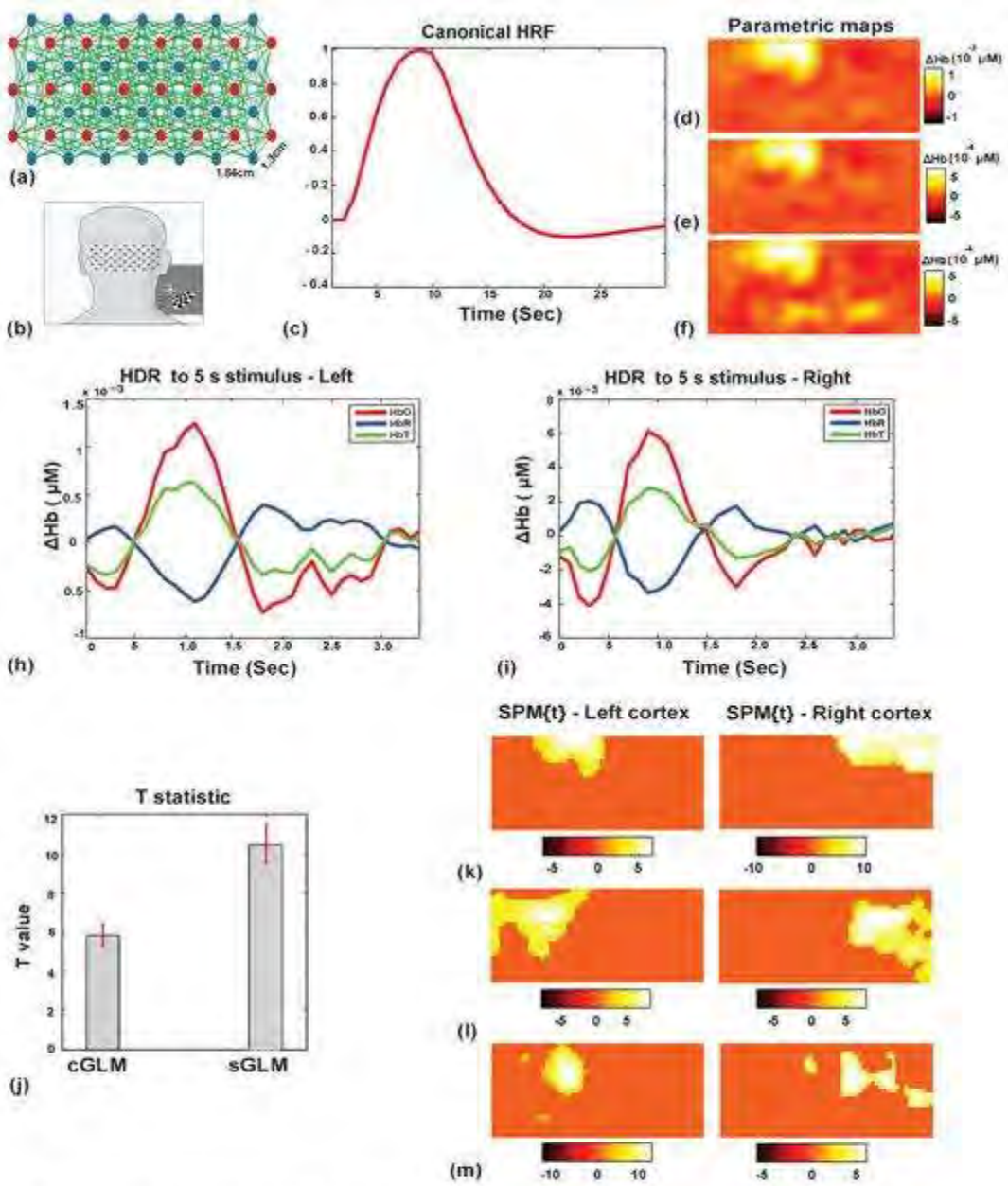

Figure1. (a) is schematic of HD-DOT imaging cap, (b) is schematic of cap position and subject viewing stimulus, (c) shows canonical hemodynamic response function. Parametric maps for HbO (d), HbR (e) and HbT (f) contrasts are qualitatively similar. (h) and (i) are measured hemodynamic responses to 5 s stimuli in left and right visual cortex respectively, (j) is comparison between cGLM and sGLM and (k,l,m) are statistical parametric maps in two regions for three subjects, p-value is 0.01.

[Figure 1]

Results: The first stage of analysis shows that for a 5s stimulus, parametric maps of activation for different contrasts are not significantly different (Fig. 1, d, e and f). The hemodynamic

response in regions of strong activation within the left and right cortex are estimated (Fig. 1, h and i) and used in the third stage of the GLM (sGLM). An improvement in the statistics is observed after the third stage (Fig. 1, j). Statistical parametric maps of three subjects are shown (Fig. 1, k-m) with the p-value set at 0.01. The analysis method evaluated the spatial and temporal properties of DOT data. A temporal correlation method was used to estimate the degrees of freedom. Both Gaussian field theory and Bonferroni correction were evaluated for solving the multiple comparison problem.

Conclusions: We have outlined a general statistical method for DOT. The three-stage procedure provides a more robust model with improved statistics in comparison to using only a canonical HDR. This approach provides us with an analytical tool to study more complex brain functions such as language development and learning processes in children.

References:

T.J. Huppert et al., “A temporal comparison of BOLD, ASL, and NIRS hemodynamic responses to motor stimuli in adult humans”, Neuroimage 29, 368-382 (2006)

F. M. Miezin et al., “Characterizing the Hemodynamic Response: Effects of Presentation Rate, Sampling Procedure, and the Possibility of Ordering Brain Activity Based on Relative Timing”, NeuroImage 11, 735-759 (2000).

605

ASSOCIATION BETWEEN RATING SCORES OF QUALITY OF LIFE AND REGIONAL BRAIN ACTIVITY IN ESOPHAGEAL CANCER PATIENTS UNDERGOING RADIOCHEMOTHERAPY

M. Tashiro[1], T. Yoshioka[2,3], M. Aikawa[1], G. Yamaura[3], S. Watanuki[1], K. Yanai[1,4]

[1]Cyclotron and Radioisotope Center, Tohoku University, Sendai, [2]Department of Clinical Oncology, Yamagata University School of Medicine, Yamagata, [3]Department of Clinical Oncology, Institute of Aging, Development and Cancer, Tohoku University, [4]Department of Pharmacology, Tohoku University Graduate School of Medicine, Sendai, Japan

Emotional responses such as depression and anxiety are often observed among patients with cancer. Though it is usually in a mild stage, depression is accompanied by reduction of regional cerebral glucose metabolism in the cancer patients. Such metabolic changes can be often observed in the prefrontal cortex by using PET with ^{18}F-fluorodeoxyglucose (FDG PET). However, invasive anticancer therapies such as radiotherapy and chemotherapy may also affect brain metabolism. The aim of the present study was to examine association between rating scores of quality of life and regional brain activity in esophageal cancer patients undergoing radiochemotherapy.

FDG PET was performed on 14 esophageal cancer patients (63.0 ± 9.4 y.o.) without brain metastases. They were scanned twice before and after the first cool of adjuvant radiochemotherapy using 5-FU and cisplatin. Their psychological aspect was evaluated using Hospital anxiety depression scale (HADS) and quality of life questionnaire developed by European Organization for Research and Treatment of Cancer (EORTC) QLQ-C30 (in Japanese translation).

In results, overall mean scores (global health status) were slightly deceased from 57.1 to 53.6 following treatment. Mean HADS scores showed decrease from 12.8 to 13.4, while depression component of HADS increased from 6.4 to 7.1. As for the symptom scales, dyspnea of QLQ-C30 showed considerable increase (2.4 to 9.5), that seemed to be associated with radiation pneumonitis. In brain PET image analysis, relatively-decreased regional brain activity was observed in the various neocortical regions including the posterior cingulate gyrus, temporo-parietal cortex, occipital and cerebellum, as well as in the prefrontal area. Relatively-increased metabolism was observed in the primary sensorimotor cortex, lentiform nucleus, thalamus, amygdala and posterior parietal cortex. Negative correlation to the scores of depression component was observed in the prefrontal cortex of patients both in the pre- and post-radiochemothearpy conditions. Negative correlation to the dyspnea component was observed in the parietal cortex etc., but such correlation was disappeared after therapy.

The difference in cognitive functioning component of QLQ-C30 ($D_{cognitive}$) between pre and post-treatment conditions was found to negatively correlate significantly to the change in the regional brain activity in the posterior cingulate cortex. In a similar manner, the difference in dyspnea ($D_{dyspnea}$) positively correlated well to the difference in the sensorimotor and premotor regions. In addition, the change in the scores of emotional functioning component correlated well to the metabolic change in the amygdala.

These results may suggest that the brain metabolic activity is associated with subjective feeling of quality of life and emotional responses and that the brain metabolic activity may be partly

affected by the central effects due to chemotherapy as well as by psychophysiological experiences induced by physical symptoms.

606

CAPILLARY PLUGGING CONTRIBUTES TO BLOOD FLOW REDUCTION IN MOUSE MODELS OF ALZHEIMER'S DISEASE

N. Nishimura[1], G. Otte[1], J. Zhou[1], J.D. Beverly[1], E. Slack[1], C. Iadecola[2], C.B. Schaffer[1]

[1]Biomedical Engineering, Cornell University, Ithaca, [2]Department of Neurology and Neuroscience, Weill Cornell Medical College, New York, NY, USA

Objectives: Alzheimer's disease is characterized by a loss of cognitive function that is likely linked to the toxic effects of aggregates of a small peptide, amyloid-beta, which eventually accumulates into dense plaques scattered throughout the brain. Clinical research in humans and experimental work in animals suggest that blood flow to the brain is impaired in Alzheimer's disease, implying that vascular dysfunction could be one result of this toxic environment [1]. In addition, chronically increased inflammation is observed in both patients and animal models [2]. We hypothesize that inflammation could contribute to the reductions in blood flow in Alzheimer's disease by leukocyte plugging of capillaries.

Methods: We used in vivo two-photon excited fluorescence microscopy to examine cortical blood flow in mouse models of Alzheimer's disease (B6.Cg-Tg(APPswe,PSEN1dE9)85Dbo/J) chronically implanted with sealed cortical windows (Figure). In this imaging method, we fluorescently label the blood vessels (red) by intravenous injection of Texas red-conjugated dextran, allowing us to image the location and structure of the capillaries in three dimensions in the brain. To determine whether individual brain microvessels are stalled or flowing, we monitor the movement of non-fluorescent blood cells that are visualized as dark patches within the dye-labeled blood plasma. Additionally, methoxy-X04 is used to fluorescently label the amyloid plaques (green) that are the pathological hallmark of Alzheimer's disease. Intravenous rhodamine-6G enables the discrimination of red blood cells from leukocytes (blue, white circle). Image and network analysis tools were developed to analyze the spatial and topological relationships between amyloid deposits, blood vessels and stalled blood vessels. Heart rate and saturation of peripheral oxygen were monitored during imaging using a pulse oximeter.

Results: In ~9 month old wild-type littermates of the Alzheimer mice, we found the fraction of capillaries stalled in the cortex to be 0.3%, while in same-aged transgenic mice this fraction rises to 1.8% (2475 capillaries across four wild-type and 2843 capillaries across six Alzheimer's mice, $p < 0.001$). A computational model, which is based on experimental measurement of blood flow decreases after single vessel clots [3], predicts that this six-fold increase in capillary stalls could reduce the overall blood flow to the brain by ~30%. We find approximately a third of the observed stalled vessels were plugged by rhodamine-6G positive occlusions, likely leukocytes.

Conclusions: This suggests that inflammation in Alzheimer's disease could cause significant, chronic leukocyte adhesion and capillary plugging. The resulting reductions in blood flow might contribute to the detrimental effects of AD.

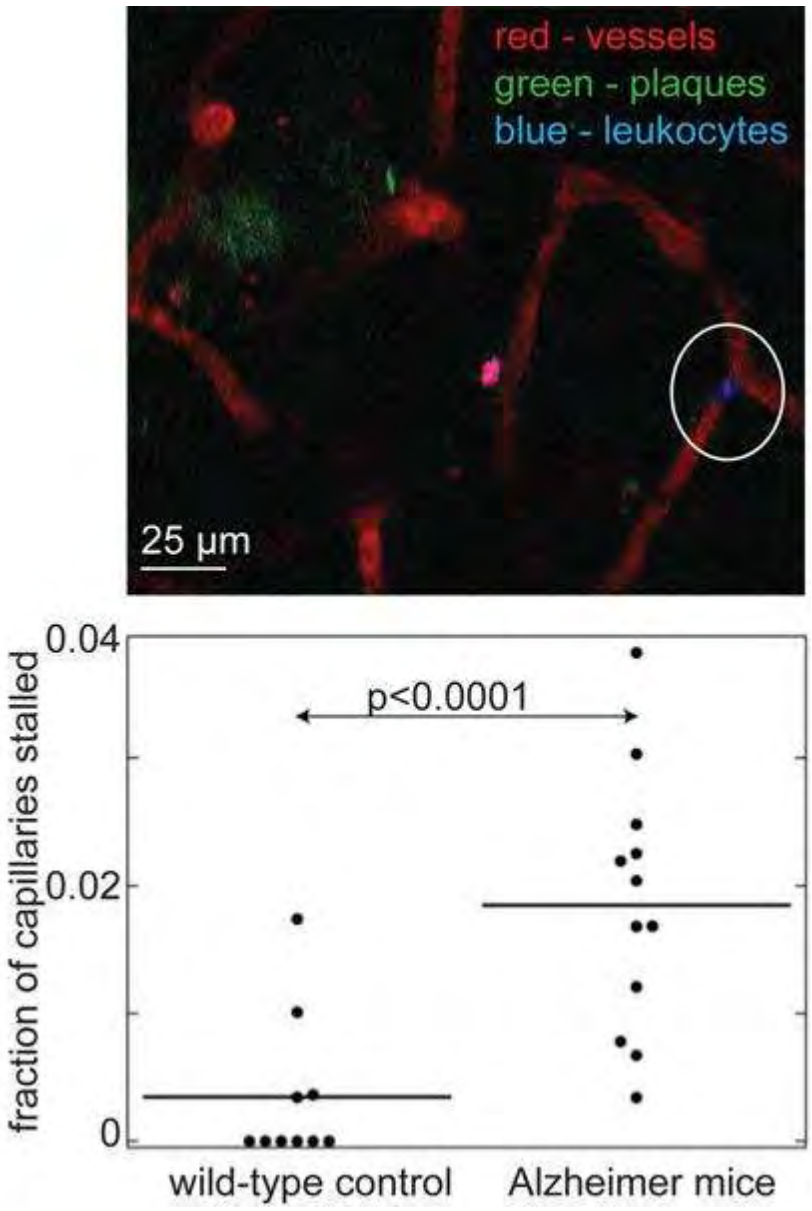

[Capillary stalls in AD mice]

References

[1] Girouard, J Appl Physiol, 2006.

[2] Wyss-Coray, Nat Med, 2006.

[3] Nishimura, Nat Meth, 2006.

607

EFFECT OF DOWN SYNDROME CANDIDATE REGION 1 (DSCR1) GENE OVER-EXPRESSION ON OUTCOME FOLLOWING CEREBRAL ISCHEMIA-REPERFUSION

V.H. Brait[1], K.R. Martin[2], T.V. Arumugam[3], M.A. Pritchard[2], C.G. Sobey[1]

[1]Department of Pharmacology, [2]Department of Biochemistry and Molecular Biology, Monash University, Clayton, VIC, [3]School of Biomedical Sciences, The University of Queensland, Brisbane, QLD, Australia

Objectives: The Down syndrome candidate region 1 (DSCR1) gene is thought to be important in Down syndrome and is a known inhibitor of calcineurin. DSCR1 protein is highly expressed in the brain and T lymphocytes, and following middle cerebral artery occlusion (MCAO) in mice, DSCR1 mRNA and protein was found to increase in the peri-infarct region. Using a DSCR1 transgenic (Tg) mouse that over-expresses isoform 1 of the human DSCR1 gene with the same temporal- and tissue-specific expression of the endogenous gene, we examined the effect of DSCR1 over-expression on outcome following MCAO, and investigated the possible mechanisms underlying this effect.

Methods: Flow cytometry was used to measure the number of circulating T lymphocytes in naïve DSCR1 Tg and matched Wt mice. Cerebral ischemia was produced by intraluminal filament-induced MCAO for 0.5 h followed by reperfusion for 23.5 h in male DSCR1 Tg (n=11) and Wt (n=11) mice. After 24 h, neurological impairment was assessed and brain infarct and edema volume were measured in thionin-stained coronal sections. In addition, the intrinsic resistance of neurons to ischemic stimuli was tested in primary neuronal cultures.

Results: There were fewer $CD4^+$ and $CD8^+$ circulating T lymphocytes in naïve DSCR1 Tg mice compared to Wt mice. 24 h after MCAO, Tg mice had significantly less neurological impairment than Wt mice, with a lower neurological score ($P< 0.05$) and a longer hanging wire time (Wt=17±5 s, Tg=40±5 s; $P< 0.05$). Tg mice also had a significantly smaller total (18±5 vs. 36±5 mm^3; $P< 0.05$) and subcortical infarct volume (12±2 vs. 33±5 mm^3; $P< 0.05$) than Wt mice, however, there was no difference in cortical infarct volume. Furthermore, edema volume was smaller in Tg than Wt mice (11±2 vs. 23±4 mm^3; $P< 0.05$), and Tg mice had a more rostral infarct distribution throughout the brain compared to Wt mice. Finally, in vitro studies revealed a significantly greater survival of DSCR1 Tg neurons after 24 h of glucose deprivation compared to neurons from Wt mice.

Conclusions: Thus, over-expression of DSCR1 in mice improves outcome following cerebral ischemia-reperfusion. We speculate that the mechanisms underlying this protection involve the inhibition of calcineurin by DSCR1 expressed primarily in neurons (but also potentially in T lymphocytes), thus reducing the transcription of some pro-inflammatory and pro-apoptotic cytokines, as well as reducing T lymphocyte infiltration through the lower numbers of circulating T lymphocytes.

608

PIVOTAL ROLES OF POSTERIOR COMMUNICATING ARTERIES IN THE MORTALITY OF MOUSE CEREBRAL ISCHEMIC MODEL

Y. Wang[1], F. Yuan[1], Y.H. Tang[1], Y. Guan[1], X. He[1], Y. Xi[2], G.-Y. Yang[1,3]

[1]Neuroscience and Neuroengineering Center, Med-X Research Institute, Shanghai Jiao Tong University, [2]Department of Biomedical Engineering, School of Life Sciences & Biotechnology, Shanghai Jiao Tong University, [3]Department of Neurology, Shanghai Ruijin Hospital, School of Medicine, Shanghai Jiao Tong University, Shanghai, China

Introduction: High mortality limits the application of mouse intraluminal suture middle cerebral artery occlusion (MCAO) models in stroke studies ADDIN EN.CITE ADDIN EN.CITE.DATA [1, 2]. Hypoplasia of posterior communicating arteries (PcomAs) may be the main cause of death after suture-induced MCAO. However, there is no direct evidence to prove this hypothesis. The aim of this study is to investigate the occurrence of the hypoplasia of PcomAs and the correlation between such hypoplasia and high mortality in a mouse intraluminal suture MCAO model.

Methods: In experiment 1: adult male CD-1 (n=15) and C57/BL6 (n=10) mice underwent 24 hours permanent MCAO (pMCAO). Bilateral common carotid arteries and thoracic aorta were ligated and right atrium was opened. Microfil (1 ml) was carefully perfused transcardially. The morphology of PcomAs was examined using a micro-CT and a microscope. In experiment 2: adult male CD-1 mice (n=17) and C57/BL6 (n=9) mice were subjected to synchrotron radiation angiography to detect the hypoplasia of PcomAs during MCAO using various sutures. We optimized suture with silicone coating to improve the blood flow of hindbrain which is supplied by PcomAs after the occlusion of posterior cerebral arteries. The length of silicone coating and the relationship between the patency of PcomAs and mortality was further analyzed.

Results: The occurrence of hypoplasia of PcomAs was higher in C57/BL6 mice (9 out of 10) than that in CD-1 mice(10 out of 15). Hypoplasia presents narrowness or absence of PcomA in one or both side. We found that the mortality following 7 days of MCAO was 82% in C57/BL6 and 43% in CD-1, respectively. Synchrotron radiation angiography showed that the PcomA was affected to different degree when using plain 6-0 suture. After modifying 8-0 suture with silicone coating, the mortality of MCAO was drastically decreased in both CD-1 and C57/BL6 mice compared with the plain 6-0 suture group ($P < 0.05$). The best coating length was 2 mm, which allows the perfusion of the posterior cerebral artery, regardless of the hypoplasia of PcomAs.

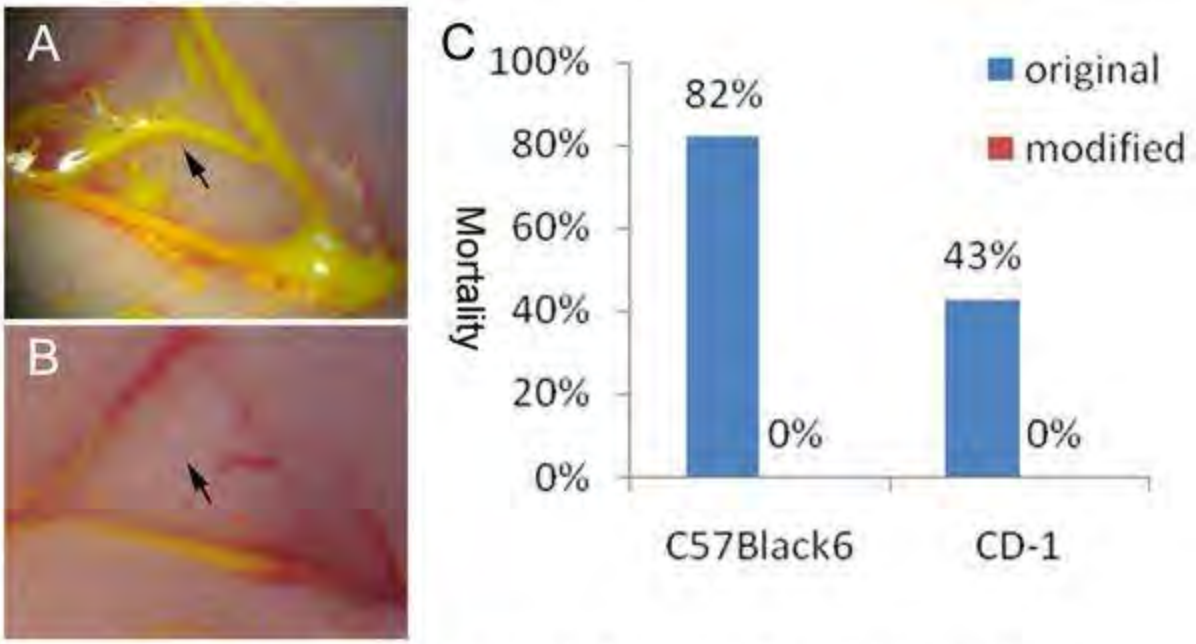

Figure (A): PcomAs were detected after microfil perfusion and arrow indicates one PcomA. (B) hypoplasia of missing PcomA . (C) Mortality comparison between original and modified models of C57/BL6 and CD-1 mice 7 days following pMCAO.

[PcomAs and mortality comparison]

Conclusion: Synchrotron radiation angiography provides a unique tool to directly detect cerebral vascular hemodynamic changes. High mortality is closely associated with the hypoplasia of PcomAs in both C57/BL6 and CD-1 mice. Modification of silicone coating length is critical for reducing mortality and generating stable infarction in mouse MCAO models.

Reference:

1. Kitagawa, K., et al., *Cerebral ischemia after bilateral carotid artery occlusion and intraluminal suture occlusion in mice: evaluation of the patency of the posterior communicating artery.* J Cereb Blood Flow Metab, 1998. 18(5): p. 570-9.

2. Chen, Y., et al., *Blocking pterygopalatine arterial blood flow decreases infarct volume variability in a mouse model of intraluminal suture middle cerebral artery occlusion.* J Neurosci Methods, 2008. 174(1): p. 18-24.

This study is supported by 973 Program of NBRP, China (2010CB834306 and 2011CB504405, GYY&YTW), NSFC 30973097 and the Shanghai STC Program 09140902400 (GYY).

609

RELATIONSHIP BETWEEN SLEEP SPINDLES AND CLINICAL OUTCOME IN PATIENTS WITH TRAUMATIC BRAIN INJURY: A SIMULTANEOUS EEG AND MEG STUDY

Y. Urakami

Psychiatry Section, Hospital, National Rehabilitation Center, Tokorozawa, Japan

Few methods can predict the prognosis and outcome of traumatic brain injury. Electroencephalographic(EEG) and magneto encephalographic(MEG) studies based assessments of consciousness provide valuable information for evaluation of residual function, formation of differential diagnosis, and estimation of prognosis. EEG examinations have a prognostic significance in the acute stage of post-traumatic coma, and some EEG variables have been correlated to outcome. Furthermore, spindle activity and reactivity in the acute stage have been associated with good recovery .This study investigated whether fast spindles could objectively evaluate recovery of the consciousness and cognitive function during the post-acute to chronic stages of diffuse axonal injuries. Sleep Stage 2 was examined in 7 healthy subjects and 8 patients with diffuse axonal injuries. Simultaneous EEG and MEG recordings were performed in the post-acute (mean 80 days) and chronic (mean 151 days) stages of recovery. MEGs enabled equivalent current dipole estimates of fast spindle sources. Clinical recovery was evaluated by consciousness, neuropsychological examination, and outcome. Six severe and two moderate injuries were studied in patients with favorable 1-year outcomes. In the sub-acute stage, significant decreases were detected in the frequency, amplitude, and cortical activation source strengths of spindle activities; these recovered in the chronic stage. In the chronic stage, the Wechsler adult intelligence factor scale and subset patterning revealed significant improvement in cognitive function. These results suggested that spindles may reflect recovery of consciousness and cognitive function following a diffuse axonal injury.

610

FUNCTIONAL LATERALIZATION OF SENSORIMOTOR CORTEX IN INFANTS MEASURED USING MULTI-CHANNEL NEAR-INFRARED SPECTROSCOPY

T. Kusaka[1], K. Isobe[2], T. Miki[3], M. Ueno[4], Y. Konishi[2], T. Kuboi[2], I. Kato[2], T. Nishida[5], S. Itoh[2]

[1]Maternal Perinatal Center, [2]Department of Pediatrics, [3]Departments of Anatomy and Neurobiology, [4]Departments of Pathology and Host Defense, Kagawa University, Kitagun, [5]Department of Education for Children with Special Needs, Kagawa University, Takamatsu, Japan

Introduction: During development, it is very important to investigate the process of specialization of the brain to functional areas in one hemisphere (lateralization) in order to understand reorganization after injury. We hypothesized that reliable and early cerebral functional assessments is useful for tailored early intervention and rehabilitation programs. In this study, we used multi-channel NIRS (MNIRS) to monitor the activities of the sensorimotor cortex as mirrored by hemodynamic responses in newborn infants subjected to passive unilateral knee and elbow joint movement.

Subjects and methods: The study was conducted involving two term infants and eight preterm infants (gestational age, 24 - 41 weeks; median age, 29.6 weeks) on days 3 - 99 after birth (median, days 6.0). We employed a 24 multi-channel NIRS (Hitachi Medico Co., Japan) and the probes were placed in the left or right parietotemporal region. Functional imaging tests were performed on infants who had been sedated. An examiner then flexed and extended the infant´s knee joint or elbow joint at a frequency of approximately 0.7 Hz.

Results: Contralateral knee and elbow movement caused a marked increase in the concentration of oxyhemoglobin ([oxyHb]) at site within the sensorimotor area. During ipsilateral knee and elbow movement, [oxyHb] showed smaller changes, equivalent to 64% and 66% of the changes that occurred with contralateral stimulation, respectively. The mean times corresponding to maximal changes in [oxyHb] were 16 sec for contralateral knee movement, and 18 sec for contralateral elbow movement. The mean time corresponding to maximal changes in [oxyHb] were not significant between during contralateral and ipsilateral knee or elbow movement. However, there is lateralization of the areas and degree of response during passive knee or elbow movement.

Discussion: In this study, there was no lateralization regarding the maximum response times of [oxyHb], but there was lateralization for areas and the degree of response during passive knee or elbow stimulation. An fMRI study of neonates reported that passive sensory motor stimulation of the hand resulted in a slight hemispheric dominance of the somatosensory area for the contralateral side (Erberich SG et al., NeuroImage 2006). However, a comparison of the area distribution of left and right hemisphere BOLD changes with hand stimulation revealed non-significant hemispheric specialization. The reasons for the difference in the distribution of results between MNIRS and fMRI may depend in the differences of method: 1) The time resolution of MNIRS is superior to that of fMRI, but the spatial resolution of MNIRS is inferior to that of fMRI. 2) The BOLD signal is derived from changes in [deoxyHb], but MNIRS can measure changes in [oxyHb] and [deoxyHb] separately.

Concliusion: The use of MNIRS is expected to facilitate investigation of the physiology of the developing brain and the brain's response to damage in premature infants, because MNIRS is a

noninvasive imaging tool that allows the identification of task-related activation changes not only in the term neonatal brain but also premature brain in the NICU.

611

G PROTEIN-COUPLED ESTROGEN RECEPTOR SIGNALING IN THE BRAIN WORSENS STROKE OUTCOME IN MALES BUT PROTECTS IN OVARIECTOMIZED FEMALES

B.R.S. Broughton[1], V.H. Brait[1], E. Guida[1], S. Lee[1], A.A. Miller[1], T.V. Arumugam[2], G.R. Drummond[1], C.G. Sobey[1]

[1]Department of Pharmacology, Monash University, Clayton, VIC, [2]School of Biomedical Sciences, University of Queensland, Brisbane, QLD, Australia

Background and aims: Experimental studies indicate that estrogen typically, but not universally, has a neuroprotective effect in stroke. Recent work from our laboratory and others has demonstrated that a novel membrane-bound estrogen receptor called G protein-coupled estrogen receptor (GPER), which is distinct from the classical estrogen nuclear receptors, is widely distributed throughout the male and female brain. We therefore hypothesized that GPER activity in the brain improves outcome after stroke in both genders.

Methods: To test this hypothesis, either vehicle (2% DMSO), the GPER agonist, G-1 (30µg/kg), or the GPER antagonist, G-15 (300µg/kg), was administered to male, intact female or ovariectomized female C57Bl/6J mice 1 h prior to 0.5 h cerebral ischemia by middle cerebral artery occlusion. We subsequently evaluated functional and histological endpoints of stroke outcome as well as apoptosis expression after 24 h ischemia-reperfusion. Furthermore, we used an *in vitro* glucose-deprived neuronal model to directly examine the effects of G-1 and G-15.

Results: Surprisingly, we found that in males, treatment with G-1 (n=10) vs vehicle (n=9) worsened both total infarct volume (G-1-treated: 53.2±6.9 mm^3 vs vehicle-treated: 22.6±7.6 mm^3; $P< 0.05$) and motor function (hanging wire time: 16.8±5.3 s vs 0.3±0.2 s; $P< 0.01$) after stroke. In addition, Western blot and immunohistochemical analysis showed that G-1 accelerated expression and distribution of the key apoptotic protein, caspase 3, in the brain following ischemia-reperfusion. Conversely, in a separate group of studies in males, G-15 reduced infarct volume by ~55% (G-15-treated: 14.7±3.9 mm^3 vs vehicle-treated: 32.5±11.1 mm^3; n=6/treatment) and improved motor function (23.8±6.7 s vs 13.8±2.5 s; $P=0.05$). Consistent with these *in vivo* observations in males, G-1 significantly augmented neuronal death and G-15 was neuroprotective following glucose deprivation *in vitro*. In contrast to males, however, G-1 improved infarct volume (G-1-treated: 11.6±2.1 s vs vehicle-treated: 32.9±7.3 s; $P< 0.05$, n=5-6) and neurological function (41.3±6.7 s vs 15.3±2.5 s; $P< 0.05$) in ovariectomized females after stroke, but had no significant affect in intact females (data not shown).

Conclusion: These data represent the first comprehensive pharmacological evaluation of GPER function in the brain after stroke and suggest that future therapies exploiting GPER modulation after stroke may need to be sex-specific.

612

VESSEL-BRANCH-BASED ANALYSIS FOR LOCAL AND GLOBAL BLOOD FLOW RESPONSE IN RAT SOMATOSENSORY CORTEX

H. Kawaguchi[1], K. Masamoto[1,2], T. Obata[1], I. Kanno[1]

[1]Molecular Imaging Center, National Institute of Radiological Sciences, Chiba, [2]The Education and Research Center for Frontier Science, University of Electro-Communications, Tokyo, Japan

Background and aims: The blood flow regulation system is of great interest for understanding energy demand and supply homeostasis in the brain. To investigate flow regulation system in vessels of various sizes, we developed a new method called vessel-branch-based analysis of spatiotemporal flow structures. The method was applied to characterize the hemodynamic response (plasma and RBC flow structure) under sodium nitroprusside (SNP) administration and electrical forepaw stimulation in individual vascular segments within the rat somatosensory cortex.

Material and methods: Sprague-Dawley rats (7-9w) were anesthetized with isoflurane (5% for induction and 1.3-1.5% for experiments), and area (3 x 3 mm^2) on the left parietal bone over the somatosensory cortex was thinned. The respiration rate was maintained at 0.87 Hz with mechanical ventilation. Time-lapse images of fluorescent signals were obtained in the rat somatosensory cortex, while a cocktail (0.02 ml) of plasma marker (Qdot-605, 1 μM) and FITC-labeled RBCs was injected at a rate of 2.23 ml/min from the internal carotid artery via external carotid artery. The image of RBC and plasma flow was simultaneously obtained through a band-pass filter (500-590nm and 595-615nm, respectively) with confocal microscopy at an excitation of 488 nm. The frame rate was 14.2 fps, the total measurement time was 18 s, and the field of view was 1.82x1.82 mm^2. In vessel-branch-based analysis, the artery and vein regions were extracted semi-automatically. Then, the vessel regions were separated to each vessel branch. All vessel-branches were classified into 6 types of segments with referencing diameter of plasma flow in control data: small artery (SA), medium artery (MA), large artery (LA), small vein (SV), medium vein (MV) and large vein (LV), where diameter range are as follows: LA, >50; MA, ≦50, >25; SA, ≦25; SV, ≦50; MV, ≦50, >100; LV, >100 μm. The diameter and transit time of both plasma and RBC flow-structures were determined for each segment. SNP administration and forepaw stimulation were induced and changes from the baseline were measured.

Results: Under SNP administration, RBC flow dilated more than plasma flow for all segment types (>5.1%). The venous transit time was longer than the arterial transit time for both plasma and RBC flow. The difference in diameter between RBC and plasma flow structure was maximum for the MA segment (MA, 26.4%; the others < 11.2%). During forepaw stimulation, plasma flow was unchanged in diameter (< 2.4 %) and slightly shortened in transit time (>0.26 sec) for most of the segments. The exception was the SA segment which unchanged in transit time (-0.08 sec) but increased in diameter (10.5%). The above results suggest that independent global and local flow regulation systems that depend on the vessel size may exist.

Conclusions: We developed a vessel-branch-based analysis method for spatiotemporal blood flow structures, which allows us independent evaluation of vessel-by-vessel flow regulation system. Our approach will be further applicable to the analysis of flow structures in various disease models.

614

THE IMPACT OF BLOOD TRANSFUSION ON CEREBRAL HEMODYNAMICS AND OXYGENATION IN ANEMIC PRETERM INFANTS

K. Koyano[1], S. Nakamura[2], K. Koyano[2], S. Yasuda[1], K. Okubo[2], M. Nakamura[2], T. Kusaka[1], K. Isobe[2], S. Itoh[2]

[1]Maternal and Perinatal Center Faculty of Medicine, Kagawa University, [2]Department of Pediatrics, Kagawa University Faculty of Medicine, Miki-cho Kita-gun, Japan

Background: Preterm infants with anemia receive multiple packed red blood cell transfusions to improve tissue oxygen levels. Transfusion is still an important therapy for preterm infants with anemia, and even recombinant human erythropoietin can be used. Anemia affects the clinical status of infants when the capacity to transport oxygen decreases under the demands of tissue oxygen consumption, especially in the brain. However, few studies have investigated the effect of blood transfusion on cerebral circulation and oxygen metabolism in anemic preterm infants.

Objective: The aim of this study was to investigate the influence of packed red blood cell transfusion on cerebral hemodynamics and oxygenation in anemic preterm infants.

Methods: The study was conducted involving ten preterm infants (gestational age, 23.5 - 30.4 weeks; median age, 27.1 weeks) on days 2 - 85 after birth (median, days 39). Informed consent in writing was obtained from the parents, and the protocol was approved by the ethical committee, Kagawa University. Transfusion therapy was provided according to the local guidelines. The mean blood Hb value (bHb) in infants before transfusion was 9.5g/dL, and the mean volume of packed red blood cells transfused in each period was 17.2mL/kg.

Using a portable three-wavelength near-infrared time-resolved spectroscopy (TRS) system (Hammamatsu Photonics K.K., Japan), the cerebral concentrations of oxyhemogobin ([oxy Hb]), deoxyhemoglobin ([deoxy Hb]), and total hemoglobin ([total Hb]) can be measured noninvasively in the NICU. The mean blood pressure, heart rate and anterior cerebral artery resistance index (were measured by echography) during this period. The cerebral blood volume (CBV) and cerebral oxygen saturation (ScO_2) were calculated using the following equations.

ScO_2 (%) = [oxy Hb] × 100 / [total Hb]

CBV (mL/100g) = [total Hb] × MW_{Hb} × 10^{-6} / bHb × 10^{-2} × D_t ×1 0

MW_{Hb}: 64,500 D_t: 1.05 g/mL (brain density).

Results: The measurements were conducted 15 times in 10 infants.

Before blood transfusion, the CBV and ScO_2 values were 2.54ml/100 g and 72.0%, respectively. After transfusion, the CBV and ScO_2 values were 2.10ml/100 g and 74.5%, respectively. CBV significantly decreased ($p = 0.007$) and ScO_2 increased ($p = 0.002$) after transfusion. The change in CBV values and bHb before transfusion showed a significant negative linear relationship ($P = 0.002$, $r = 0.814$).

Discussion: In this study, CBV significantly decreased and ScO_2 increased after transfusion in preterm infants. The reason for the decrease in CBV due to transfusion was improvement for a compensatory increase in cerebral blood flow in the anemic state. ScO_2 measured by TRS

represents the mixed vascular Hb oxygen saturation of capillaries, arteries, and veins in the brain. The reason for the decreased ScO_2 increasing after transfusion is that before transfusion, the capacity to transport oxygen decreases and this leads to a decrease in venous Hb oxygen saturation.

Conclusion: Measurements of CBV and ScO_2 in anemic premature infants and changes in CBV and ScO_2 during transfusion contribute supporting evidence for criteria for blood transfusion in infants to prevent brain damage.

615

OVEREXPRESSION OF NETRIN-1 REDUCES ISCHEMIC BRAIN INJURY FOLLOWING MIDDLE CEREBRAL ARTERY OCCLUSION

Y. Wang[1], H. Lu[1,2], F. Yuan[1], J. Liu[2], L. Zeng[1,2], G.-Y. Yang[1,2]

[1]Neuroscience and Neuroengineering Center, Med-X Research Institute, Shanghai Jiao Tong University, [2]Department of Neurology, Shanghai Ruijin Hospital, School of Medicine, Shanghai Jiao Tong University, Shanghai, China

Introduction: Netrin-1 (NT-1) is one of the axon-guiding molecules that are critical for neuronal development. Netrin-1 is able to stimulate proliferation and migration of human cerebral endothelial cells *in vitro* and also promotes focal neovascularization in the adult brain *in vivo*. In the present study, we investigate the role of overexpression of netrin-1 via adeno-associated virus (AAV) mediated gene transfer in a transient middle cerebral artery occlusion (tMCAO) model of mice.

Methods: We constructed adeno-associated virus-NT-1 (AAV-NT-1) and AAV-GFP vector (as a control). 2.5 µl of AAV-NT-1 suspension with 2×10^9 virus particles were injected stereotactically into the basal ganglia of male CD-1 mice at a rate of 0.2 ml/minute. Same amount of AAV-GFP or saline was injected as control (n=21 per group). Seven days after AAV-NT-1 injection, these mice underwent 60 minutes of tMCAO followed by 7 to 28 days of reperfusion. NT-1 expression was quantified by Western blot and NT-1 localization was determined by immunostaining. The infarct volume and animal behavioral outcomes (beam walk test and Rotor-Rod test) were examined until the end of the experiment. Lectin stained microvessels were counted to determine the effect of hyper-NT-1 on angiogenesis.

Results: NT-1 expression was induced in the ischemic penumbra of mouse brain following tMCAO. The expression of NT-1 in the ischemic hemisphere was further enhanced after AAV-NT-1 gene transfer. Both neurons and astrocytes but not endothelial cells could express NT-1 following AAV-NT-1 gene transfer. Overexpression of NT-1 improved focal cerebral blood flow recovery after MCAO in AAV-NT-1-transduced mice compared to control group of mice ($p< 0.05$). Long-term observation demonstrated that the infarct volume was decreased and neurobehavioral outcomes (beam walk test and Rotor-Rod test) were greatly improved in the AAV-NT-1-tranduced mice compared to the AAV-GFP or saline injected group of mice up to 28 days of tMCAO ($p< 0.05$). Further study demonstrated that the microvessel counts were significantly increased in the AAV-NT-1 transduced mice compared to the control group of mice ($p< 0.05$).

Conclusion: Our results demonstrate that NT-1 not only plays a key role in neuronal development as reported before, but also participates in neuroprotection and neovascularization and vessel remodeling in the ischemic brain.

References:

1. Shen F, Fan Y, Su H, Zhu YQ, Chen Y, Liu W, Young WL, and Yang GY. Adeno-associated viral vector-mediated hypoxia-regulated vascular endothelial growth factor gene transfer promotes angiogenesis following focal cerebral ischemia in mice. Gene Ther. 2008; 15:30-39.

2. Fan Y, Shen F, Chen Y, Hao Q, Liu W, Su H, Young WL, Yang GY. Overexpression of netrin-

1 induces neovascularization in the adult mouse brain. J Cereb Blood Flow Metab. 2008; 28:1543-1551.

616

CEREBRAL BLOOD VOLUME IS THE MOST EFFECTIVE GUIDE TO CONTROL FOR THE HYPOXIC/ISCHEMIC INSULT IN A NEWBORN PIGLET MODEL

T. Kusaka[1], S. Nakamura[2], K. Koyano[1], M. Nakamura[2], S. Yasuda[1], K. Okubo[2], K. Isobe[2], S. Itoh[2], M. Ueno[3], T. Miki[4]

[1]Maternal Perinatal Center, [2]Department of Pediatrics, [3]Departments of Pathology and Host Defense, [4]Departments of Anatomy and Neurobiology, Kagawa University, Kitagun, Japan

Background: A newborn hypoxic/ischemic piglet model with a consistent degree of survivable neuropathological damage can prove useful for examining potential neuroprotective therapies in the neonate brain. The variable degree of histopathological injury is caused by the variability in the response to hypoxia. A guide to control the degree of hypoxia is necessary to manipulate the response. Amplitude-EEG (aEEG) has been reported as a guide. Cerebral hemodynamic changes are as important as cerebral electrocortical activity. We developed the guide using changes in cerebral blood volume (CBV) with a near-infrared time-resolved spectroscopy system (TRS).

Objectives: The purpose of this study was to compare two hypoxic/ischemic insults using changes in cerebral electrocortical activity or changes in CBV as a guide to control hypoxia by aEEG and TRS, and to determine which protocol most effectively produces a consistent degree of survivable neuropathological damage in a newborn piglet.

Methods: All piglets were under general anesthesia and mechanically ventilated with an infant ventilator. Fourteen 1-day-old piglets were subjected to hypoxic/ischemic insult of 20-min low peak aEEG (LAEEG < 5μV). After 20 miniutes, the aEEG-guided insult (aEEG group: n=7) maintained 10 min of low mean arterial blood pressure (MABP < 70% of baseline). CBV-guided insult (CBV group: n=7) was stopped, if CBV reached the rated value after 20 min LAEEG. Control piglets (n=3) were in the normoxic group. The piglets were allowed to recover from anesthesia for 6 hr after the insult. We measured both the changes in CBV and cerebral electric activities until 6 hr post-insult. At 5 days, the brains of the piglets were perfusion-fixed and stained by hematoxylin/eosin.

Results: For both aEEG and CBV groups, the majority of neuronal loss occurred inthe cortex followed by the hippocampus, basal ganglia, and cerebellum. The CBV group had a greater number of piglets with neuropathological damage and survivors with a consistant degree of neuropathological damage than the aEEG group. LAEEG time during insult was not significantly different between aEEG and CBV groups, but changes in CBV were different between these groups.

Conclusion: We concluded that changes in CBV during insult using TRS can act as a guide to control the degree of insult and CBV-guided insult most effectively produces a consistent degree of survivable hypoxic/ischemic neuropathological damage in a newborn piglet.

618

EXPRESSION OF NEURAL STEM CELLS INDUCED BY TRANSIENT CORTICAL ISCHEMIA IN MICE

Y. Momota[1,2], T. Nakagomi[1], A. Nakano-Doi[1], O. Saino[1], Y. Kasahara[3], A. Taguchi[3], M. Takata[1], Y. Tsukamoto[4], M. Miyamae[5], J. Kotani[2], T. Matsuyama[1]

[1]Institute for Advanced Medical Sciences, Hyogo College of Medicine, Nishinomiya, [2]Anesthesiology, Osaka Dental University, Osaka, [3]Cerebrovascular Disease, National Cerebral and Cardiovascular Center Research Institute, Suita, [4]Surgical Pathology, Hyogo College of Medicine, Nishinomiya, [5]Internal Medicine, Osaka Dental University, Osaka, Japan

Introduction: We recently have reported generation of neural stem/progenitor cells (NSPCs) from the adult post-infarct cerebral cortex (Nakagomi, Eur J Neurosci, 2009). Others also have reported NSPCs activated by mild ischemic treatment in the cortex, suggesting that neurogenesis may be maintained in the adult cortex. However, the ischemic insult triggering neurogenesis has not been elucidated. In the present study, we investigated the expression of NSPCs following transient ischemia, which induces either lethal or non-lethal to cortical neurons, by using a highly reproducible murine model of cortical ischemia in the middle cerebral artery territory.

Materials and methods: The left middle cerebral artery (MCA) of 6- to 10-week-old male C.B-17/icr-+/+ (CB) mice was exposed, and various period of transient ischemia (10, 15 or 20 min) was produced using a 7.0 nylon monofilament to determine the lethal ischemic insult to cortical neurons. To detect the infarction, brain sections were made 3 or 5 days after the ischemia/reperfusion followed by staining with 2,3,5-triphenytetrazolium chloride (TTC). In another experiment, animals were perfusion-fixed 3 days after the ischemia, and frozen brain sections were subjected to immunohistochemistry for MAP2, GFAP, Iba-1, nestin and Sox2. Finally, RT-PCR was carried out to examine the expression of nestin and Sox2 within the ischemic regions 3 days after 15 or 20 min of ischemia.

Results: TTC staining revealed no infarcts in tissues collected 3 or 5 days after 10 or 15 min of ischemia. Clear cerebral infarction was observed in the cerebral cortex collected 3 or 5 days after 20 min of ischemia. No loss of MAP2-staining was observed after 10 or 15 min of ischemia, but expression of GFAP-positive and Iba-1-positive cells was up-regulated after 15 min of ischemia in ischemic regions. In the sections after 20 min of ischemia, loss of MAP2-staining was apparent in the core of infarction. A number of proliferating GFAP-positive and Iba-1-positive cells was observed in the boundary between infarct and peri-infarct regions, but in the core of ischemia no proliferation of GFAP-positive glia cells were detected. After 20 min of ischemia, proliferating nestin/Sox2 double-positive NSPCs were detected in association with the vessel wall within the core of infarct as well as in the ischemic boundary, as shown in the previous study (Saino, J Neuosci Res, 2010). The 10 min-ischemia did not induce the nestin/Sox2-positive cells in any layer of the cortex, but they are expressed both in the cortical layer 1 and in association with the vessel walls after 15 min of ischemia. RT-PCR showed expression of nestin and Sox2 mRNA in the ischemic tissue obtained from the animals undergoing 15 min or 20 min of ischemia but not from the 10 min-ischemic animals.

Conclusion: These results suggest that expression of NSPCs is up-regulated by the ischemic insult which is non-lethal to neurons but is activating glial reaction. Because NSPCs are expressed around the microvasculature in the ischemic core, the cell source of these two NSPCs may be different each other.

References:

Nakagomi, Eur J Neurosci, 2009

Saino, J Neuosci Res, 2010

620

CEREBRAL BLOOD VOLUME EVALUATION USING NEAR-INFRARED TIME-RESOLVED SPECTROSCOPY AFTER HYPOXIC-ISCHEMIC INSULT IN NEWBORN PIGLETS

T. Kusaka[1], M. Nakamura[2], S. Nakamura[2], K. Koyano[1], S. Yasuda[1], K. Okubo[2], K. Isobe[2], S. Itoh[2], T. Miki[3], M. Ueno[4]

[1]Maternal Perinatal Center, [2]Department of Pediatrics, [3]Departments of Anatomy and Neurobiology, [4]Departments of Pathology and Host Defense, Kagawa University, Kitagun, Japan

Background: Brain hypothermia (BHT) has been applied to severely asphyxiated infants to improve the neurological prognosis. Early induction of brain hypothermia, especially within 6 hours after birth, has been proposed to reduce neurological sequelae. Vital signs, blood gasses and EEG findings have been used as parameters for BHT indication; however, little has been reported about the non-invasive measurement of brain circulation in this period. As yet it is unclear which parameters are more useful to predict neurological outcomes.

Objective: To assess the relationship between cerebral blood volume (CBV) by near-infrared time-resolved spectroscopy (TRS) and neurological prognosis after hypoxic ischemic insult in newborn piglets.

Methods: Twenty anesthetized newborn piglets (within 24 hours of age) were studied. Hypoxic events were induced by low FiO_2 (0.02 to 0.04) for 30 to 40 minutes. FiO_2 was reduced to keep mean arterial blood pressure (MABP) under 70% of the baseline in the last 10 minutes. Then, piglets were resuscitated and vital signs and blood gasses recorded. CBV was measured with TRS (Hamamatsu TRS-10). MABP was recorded via an umbilical-arterial catheter and pressure transducer. Data were corrected until 6 hours after hypoxic events. Neurological outcomes were evaluated by the neurological score after 24 hours (Thorensen M, et al., Pediatr Res, 1996).

Results: Five piglets had increased CBV (increased group) and 15 had decreased CBV (decreased group) within 6 hours after resuscitation. Four piglets in the increased group and 1 piglet in the decreased group died within 5 days after resuscitation. All piglets in the increased group and 4 piglets in the decreased group had convulsions. MABP, HR, pH, and lactate showed no significant differences between the two groups.

Discussion and conclusion: The results suggested that the increased CBV group has a poor neurological prognosis. CBV values increased during the initial phase after resuscitation in the poor prognostic group (increased group) because of the dysfunction of cerebral autoregulation, which leads to arterial vasodilation after a hypoxic-ischemic insult. Marks et al. (Pediatr Res, 1996) reported delayed vasodilation and increased cerebral oxygen saturation by 12 h post-transient ischemia in late gestation fetal sheep. In the clinical setting, an increase in CBV was observed in asphyxiated infants within 48 hours of birth (Wyatt JS, et al., J Appl Physiol, 1990) and an increase in CBF was observed in asphyxiated infants within 24 hours of birth (Pryds O, et al., J Pediatr 1990). In conclusion, TRS is expected to measure CBV non-invasively and continuously at the beside side to predict the neurological outcome after hypoxic ischemic insult.

621

COMBINATION THERAPY WITH EDARAVONE AND MILD HYPOTHERMIA PREVENTS MMP-9 ACTIVIATION AND NEUROVASCULAR INJURY AFTER FOCAL CEREBRAL ISCHEMIA IN RATS

C. Nito[1], M. Ueda[1], T. Inaba[1], S. Okubo[1], K. Nomura[1], F. Kamiya[1], S. Ohta[2]

[1]Department of Internal Medicine, Divisions of Neurology, Nephrology, and Rheumatology, Nippon Medical School, Tokyo, [2]Department of Biochemistry and Cell Biology, Institute of Development and Aging Sciences, Graduate School of Medicine, Nippon Medical School, Kawasaki, Japan

Objectives: Edaravone, a potent scavenger of hydroxyl radicals has been widely used to treat acute ischemic stroke in Japan. It has been reported that edaravone protects not only neurons but the neurovascular unit, such as endothelial cells, astrocytes, microglia and neurons from ischemic damage. We previously shown the anti-edema effect of a combined therapy with edaravone and mild hypothermia following transient focal cerebral ischemia (tFCI). However, the detailed mechanisms of this combination therapy remain unknown.

Methods: SD rats were randomly devided into four groups. : (I) vehicle + normothermia (control) (II) vehicle + mild hypothemia (III) Edaravone + normothermia (IV) Edaravone + mild hypothermia. Temporal muscle and rectal temperatures were maintained during ischemia at 37 ± 0.2 °C in the normothermic groups or 35 ± 0.2 °C in the hypothermic groups using a thermal regulatory system. After 2h of MCAO, the rats were decapitated and the hemisphere of the affected side was removed at 24 h and 3 days. MMP-9 and MMP-2 activity by gelatin zymography and BBB permeability by Evans blue method were investigated. The size of the cerebral infarction or edema was evaluated by 2,3,5-triphenyltetrazolium chloride (TTC) stain.

Results: The combined treatment with edaravone and mild hypothermia significantly reduced Evans blue leakage ($p < 0.05$), MMP-9 activity ($p < 0.01$) 24h after reperfusion and diminished edema ($p < 0.01$) and infarct volume ($p < 0.05$) 3 days after reperfusion. The MMP-2 level was not significantly different between these four groups. Treatment with edaravone, or hypothermia alone reduced edema volume ($p < 0.05$, $p < 0.05$) but not infarct volume. We also found that the oxidized hydroethidine signals were markedly decreased in the combined therapy group compared with the control group.

Conclusions: These findings demonstrate that edaravone combined with mild hypothermia led to a reduction in BBB disruption and brain edema via blocking MMP-9 activity by suppressing free radical production on tFCI. We suggest that this combination therapy may have a potent effect of the neurovascular protection after acute ischemic stroke.

622

NEUROPROTECTIVE EFFECTS OF HYDROGEN GAS ON BRAIN IN THREE TYPES OF STRESS MODELS: A $^{1}H/^{31}P$-NMR AND ESR STUDY

C. Kuroki[1], O. Tokumaru[1], O. Kazue[1], T. Kitano[2], I. Yokoi[1]

[1]Department of Neurophysiology, [2]Medical Education Center, Oita University Faculty of Medicine, Yufushi, Japan

Introduction: It has recently been reported that hydrogen gas (H_2) acts as a radical scavenger by reducing hydroxyl radical and reduces acute oxidative stress on brain in ischemia-reperfusion stress (Ohsawa et al., Nat. Med. 2007). To clarify how the radical scavenging activity of H_2 contributes to its neuroprotective effect, we studied the capacity of H_2 as a radical scavenger using new spin traping reagent, 5-(2,2-dimethyl-1,3-propoxy cyclophosphoryl)-5-methyl-1-pyrroline N-oxide (CYPMPO). We compared the scavenging activity of H_2 with that of glucose and edaravone (3-methyl-1-phenyl-2-pyrazolin-5-one), which is widely used for the clinical treatment of acute cerebral ischemia-reperfusion stress as a radical scavenger. To elucidate the neuroprotective effect of H_2 on metabolites and energy metabolism, we measured cerebral metabolites and high-energy phosphates in rat brain slices by ^{1}H and ^{31}P nuclear magnetic resonance (NMR).

Methods: The capacity of H_2, edaravone and glucose to scavenge hydroxyl radicals was measured by ESR (JES-RE1X) by spin trapping method using CYPMPO. Hydroxyl radicals were produced using 5 s illumination of UV light to a dilute solution (0.5%) of hydrogen peroxide. We measured high-energy phosphates in rat brain slices by ^{31}P-NMR and evaluated neuroprotective effects of H_2 using a hypoxic stress model, an ischemia-reperfusion model and a high-K^+ stress model. Brain slices were superfused with well-oxygenated ($PO_2 \approx$ 500torr) artificial cerebrospinal fluid (ACSF) equilibrated with (H_2+ group) or without 4% H_2 (H_2- group) at 27.5°C. Following cerebral metabolites had been extracted from rat brain slices using perchloric acid before and after an ischemia-reperfusion stress, ^{1}H-NMR spectroscopy was also performed and the effect of H_2 in concentration of 28.2 and 56.4 μM was tested.

Result (ESR): The EC_{50} value of edaravone was 705 μM, while it is impossible to calculate that of H_2 since no significant decreases in relative ESR signal intensities after H_2 treatments were found using one-sample t tests. Furthermore, the scavenging activity of H_2 was obviously less potent than that of glucose.

Result (NMR): In the ischemia-reperfusion model, γ-ATP level of H_2+ group 1-2 hours after stress was significantly higher than that of H_2- group (H_2+: 60%, H_2-: 39%; $p < 0.05$). In the high-K^+ stress model, PCr level of H_2+ group at the early stage of the stress was significantly higher than that of H_2- group (H_2+: 71%, H_2-: 54%; $p < 0.05$). No significant effect of H_2 was found in N-acetylaspartate (NAA) on ^{1}H-NMR spectroscopy.

Conclusion: Our result in the ischemia-reperfusion model is consistent with Ohsawa et al. But we observed the significant difference of PCr level in the high-K^+ stress model and there was no significant effect of H_2 in NAA, both of which are not consistent. The scavenging activity of H_2 too weak to calculate EC_{50}, the scavenging activity of 1 mM glucose was, moreover, significantly higher than that of H_2 ($p < 0.05$). Our results might indicate that the radical scavenging activity of H_2 is so weak that the neuroprotective effect of H_2 cannot be attributed to its action as a radical scavenger.

623

MICRORNA-210：PREDICTION OF CLINICAL OUTCOME IN ACUTE ISCHEMIC STROKE

L. Zeng[1,2], Y. Wang[2], Y.H. Tang[2], C. Zheng[1], J. Liu[1], G.-Y. Yang[1,2]

[1]Department of Neurology, Shanghai Ruijin Hospital, School of Medicine, Shanghai Jiao Tong University, [2]Neuroscience and Neuroengineering Center, Med-X Research Institute, Shanghai Jiao Tong University, Shanghai, China

Introduction: Recent studies indicated that microRNAs may provide a useful blood biomarker in diagnosis and prognosis and a promising functional therapy of diseases including stroke. MicroRNA-210 (miR-210), a key and pleiotropic hypoxia-microRNA with antiapoptosis and angiogenesis feature, was expressed in both brain and blood in rat ischemia model. We hypothesize that blood miR-210 predicts clinical outcome in acute ischemic stroke.

Methods: Ischemic stroke patients were divided into good outcome group (mRS score >2, n=69) and poor outcome group (mRS score ≤2, n=43) by modified Rankin Score evaluation. Blood miR-210 was measured in patients with acute cerebral ischemia using a quantitative PCR technique. Plasma IL-6, an injury related cytokine, was examined in the same group by ELISA assay. Furthermore, we examined both blood and brain miR-210 in mice with middle cerebral artery occlusion, and the correlation between blood and brain miR-210 was investigated.

Results: MiR-210 level was higher in stroke patients with good outcome than in patients with poor outcome [Fig 1A 1.2 (0.56, 2.36) vs 0.44 (0.16, 1.57), P=0.012]. The receiver operator characteristic analysis showed that its prognostic cut off point is 0.46 [Fig 1B AUC 0.642 (0.539, 0.744), P=0.012]. Blood miR-210 of less than 0.46 suggested poor outcome after ischemic stroke (sensitivity 83.7% and specificity 50.7%). When miR-210 level is analyzed in combination with plasma IL-6 level, the prognostic specificity increased to 87.5%. Further study demonstrated that the correlation between blood miR-210 and brain miR-210 in ischemic mice was positive (R2=0.57, P=0.001).

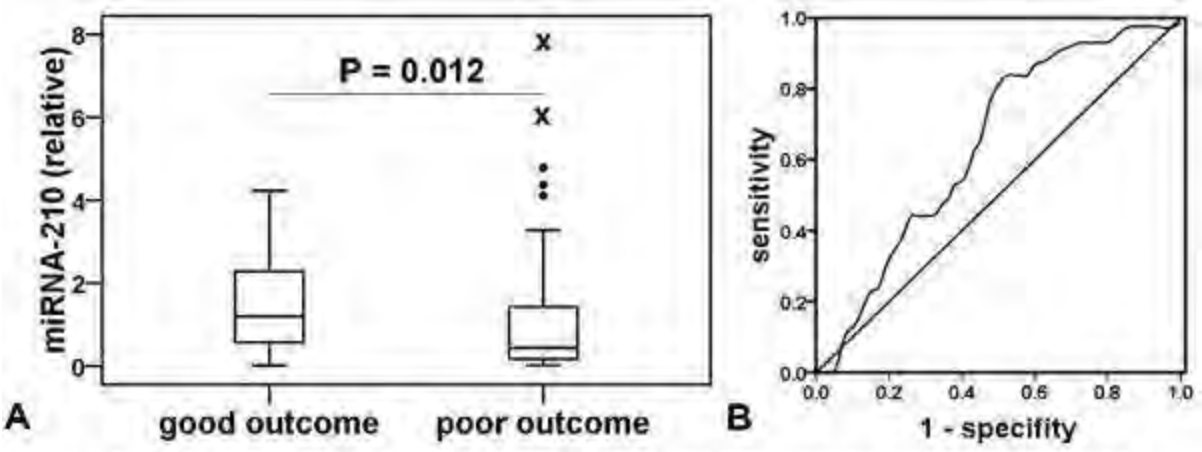

Figure 1 The relationship between blood miR-210 and the outcome of ischemic stroke.

[miR-210 and outcome of ischemic stroke]

Conclusion: As a repair related biomarker in nucleic level, blood miR-210 is useful to evaluate the potential overall recovery of ischemic tissue for predicting outcome after stoke.

Reference:

Liu DZ, Tian Y, Ander BP, et al. Brain and blood microRNA expression profiling of ischemic stroke, intracerebral hemorrhage, and kainate seizures. *J Cereb Blood Flow Metab* 2010;30:92-101.

This study is supported by 973 Program of NBRP, China (2011CB504405, GYY, YW), NSFC (30973097, GYY), the Science and Technology Commission of Shanghai Municipality (09140902400, GYY and 09ZR1415300, YW).

624

RAPIDLY RECURRING DEPOLARIZATIONS IN ADULT RAT BRAINSTEM - AN OWN ENTITY OR A SPECIAL CASE OF SPREADING DEPOLARIZATIONS (SD)?

F. Richter[1], R. Bauer[2], A. Lehmenkühler[3], H.-G. Schaible[1]

[1]Insitute of Physiology I/Neurophysiology, [2]Institute of Molecular Cell Biology, Jena University Hospital/Friedrich Schiller University Jena, Jena, [3]Pain Institute & Ctr. for Medical Education, Düsseldorf, Germany

Introduction: Previous studies revealed that the brain stem is rendered susceptible for KCl-evoked spreading depolarizations (SDs) by local superfusion with artificial cerebrospinal fluid (ACSF) in which 75% of the chloride ions were replaced by acetate and to which 10 mM KCl and 10 mM tetraethylammonium were added. KCl-elicited brainstem SDs are accompanied by transient increases in systemic blood pressure and in regional blood flow in the brainstem, but not in cerebral cortex [1]. Here we describe repetitive depolarizations in the adult brainstem that occur without KCl stimulation.

Methods: In 30 artificially ventilated anesthetized adult rats (sodium thiopentone, 100 mg/kg, i.p., paralyzed with pancuronium bromide, 1 ml/kg i.v.) we measured DC potentials in the brainstem (in trigeminal nucleus area and in nucleus tractus solitarii area, NTS) and in the cerebral cortex. In subsets of 6 rats we measured the release of calcitonin gene-related peptide (CGRP) from nociceptive dural nerve afferents and recorded action potentials from neurons in trigeminal nucleus or we monitored systemic blood pressure, heart rate and local blood flow at the surface of the brainstem or of the cerebral cortex.

Results: After at least 30 min of conditioning, episodes of recurring depolarizations were observed in more than 50 % of the rats. These occurred initially at intervals of several minutes and subsequently at intervals of 83.3±5.6 s with amplitudes of 9.8±0.6 mV (mean±SEM, n=597 depolarizations). Occasionally even DC amplitudes up to 35 mV were observed. Classical KCl-evoked SD with amplitudes up to 35 mV spread from the stimulation site to the ipsilateral NTS area, but did not propagate into the contralateral NTS area. In contrast, repetitive depolarizations were observed simultaneously in the whole brainstem including the contralateral NTS area (DC amplitudes of 10.8±0.3 mV, n=154 depolarizations). In some cases the onset of depolarizations in NTS and trigeminal nucleus was slightly different. As observed in classical SDs each recurring depolarization was accompanied by a burst of action potentials in trigeminal nucleus neurons and a subsequent transient cessation of neuronal firing. Similar to SD recurring depolarizations caused transient increases in systemic blood pressure and local blood flow. Neither classical KCl-evoked SDs nor recurring depolarizations caused any release of GGRP from nociceptive afferents in the dura mater. Concordantly to classical SD the blockade of NMDA receptors by 3 mg/kg MK-801 i.p. or the topical application of the P/Q-type VGCC blocker ω-agatoxin IVA 10^{-6} M to the surface of the brainstem abolished the recurring depolarizations.

Conclusions: Thus in these studies we discovered a previously unknown form of recurring depolarizations in adult rat brainstem that is closely linked to increased excitability. Typically these recurring depolarizations affected the whole brainstem simultaneously. At the mechanistic level, these depolarizations seem to involve the same receptors and ion channels as classical KCl-evoked SDs. We believe, therefore, that recurring depolarizations represent a spatially more extensive form of hyperexcitability than locally arising and spreading depolarizations.

Whether this form of depolarization might be of importance in brainstem pathophysiology has to be investigated in future experiments.

[1] Richter et al.,JCBFM 28,2008,984-994

625

A NOVEL APPROACH OF CEREBRAL VASCULAR SYSTEM CHARACTERIZATION IN MOUSE: SYNCHROTRON RADIATION PHASE-CONTRAST IMAGING

Y. Wang[1], B. Xie[1], F. Yuan[1], Y. Xi[2], Y.H. Tang[1], T. Xiao[3], G.-Y. Yang[1,4]

[1]Neuroscience and Neuroengineering Center, Med-X Research Institute, Shanghai Jiao Tong University, [2]Department of Biomedical Engineering, School of Life Sciences & Biotechnology, Shanghai Jiao Tong University, [3]Shanghai Institute of Applied Physics, Chinese Academy of Sciences, [4]Department of Neurology, Shanghai Ruijin Hospital, School of Medicine, Shanghai Jiao Tong University, Shanghai, China

Introduction: The visualization of cerebral vasculature in the entire brain of small animals is necessary to better understanding of morphological changes of cerebrovascular diseases. Despite massive efforts, changes of microvasculature in small animal brain remain to be completely elucidated. An imaging method providing both overall vascular morphology throughout the brain and detailed microvascular structures, will greatly facilitate the investigation of those aforementioned brain diseases. The aim of our study is to develop a high resolution phase-contrast imaging (PCI) technique using synchrotron radiation (SR) X-ray to study the entire cerebrovascular system in adult mice.

Methods: Adult male C57/Black6 mice were anaesthetized and heart perfused with normal saline and 4% PFA. Brains were removed immediately and then fixed in PFA buffer overnight at 4℃. The fixed brains were then dehydrated with 100% ethyl alcohol for 24 hours, and air dried at room temperature for another 24 hours. Phase-contrast imaging (PCI) was performed at the BL13W beam line of Shanghai Synchrotron Radiation Facility (SSRF). The beam was derived from a storage ring of electrons with storage energy of 3.5 GeV and average beam current of 200 mA. Phase-contrast and CT images were obtained by high resolution CCD with pixel sizes of 3.7 μm. The whole mouse brain vascular system in 1500 projections was re-constricted. 3-D mouse brain vascular system was rendered for studying brain structure in any angle. Acquired images were analyzed by image pro plus (IPP) and Adobe Photoshop software programs.

Results: We demonstrated that the optimal distance of high resolution phase-contrast imaging for mouse brain was 80 cm. We identified the cerebral vascular system, the ventricular system, and several nuclei in the entire mouse brain without contrast enhancement. After reconstructed the brain slices, we identified the vessel branches of cortex, the ventricle, and some of the deep structures of the brain. Compared to general pathology of brain, we demonstrated that reconstructed 3-D PCI images provided better brain morphological feature from different angles of view, suggesting that PCI images offer additional information to analyze mouse brain anatomy especially the vascular system.

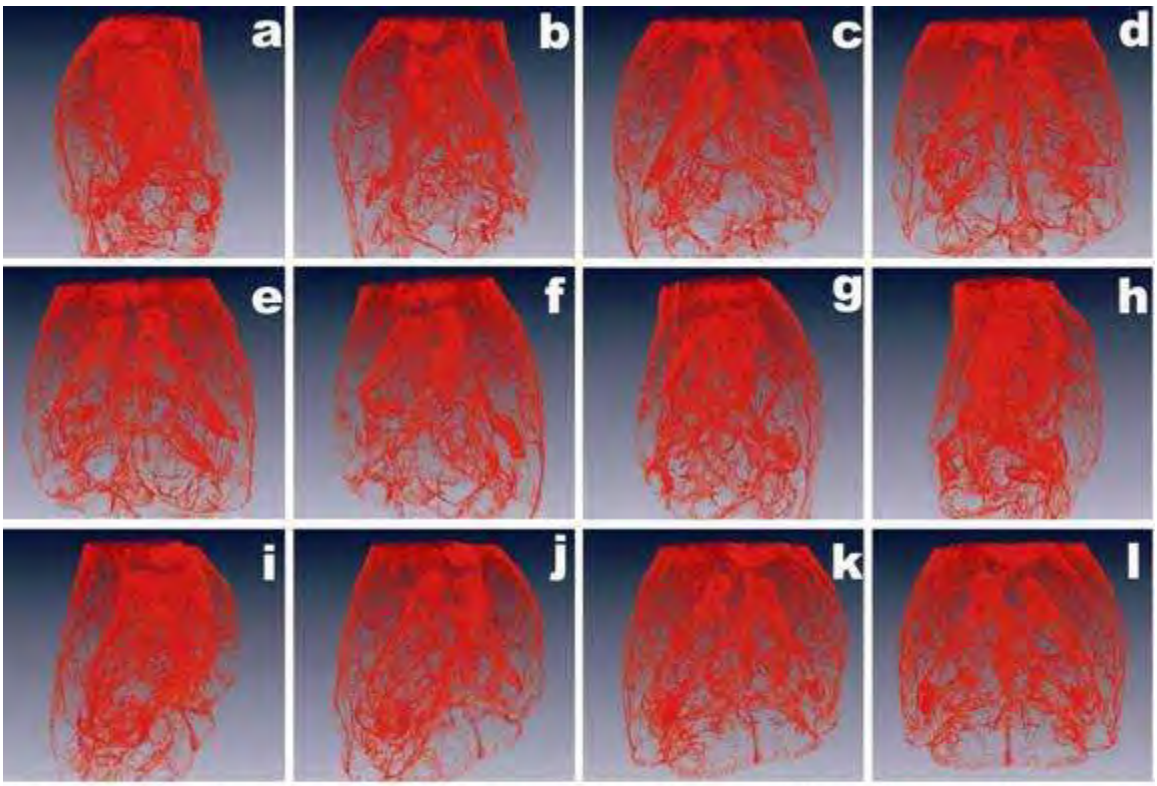

Figure 1. A series of 3-D PCI images show the structure of normal mouse brain. The reconstructed images are turned every 15°in each (a to i).

[3-D PCI images of normal mouse brain]

Conclusion: Our results demonstrated that phase-contrast synchrotron radiation imaging with high resolution CCD provides a unique technique to evaluate the changes of rodent brain vasculature.

Reference:

Pfeiffer F, Bunk O, David C, Bech M, Le Duc G, Bravin A, Cloetens P (2007) High-resolution brain tumor visualization using three-dimensional x-ray phase contrast tomography. *Phys Med Biol* 52:6923-30

Wu X, Liu H (2007) Clarification of aspects in in-line phase-sensitive x-ray imaging. *Medical physics* 34:737

This study is supported by 973 Program of NBRP, China (2010CB834306 and 2011CB504405, GYY&YTW), NSFC 30973097 and the Shanghai STC Program 09140902400 (GYY).

626

IN VIVO SYNCHROTRON RADIATION IMAGING FOR THE EVALUATION OF RAT INTRALUMINAL THREAD MODEL

Y. Guan[1,2], Y. Wang[2], F. Yuan[2], T. Xiao[3], K. Chen[1], G.-Y. Yang[2,4]

[1]Department of Radiology, Shanghai Ruijin Hospital, School of Medicine, Shanghai Jiao Tong University, [2]Neuroscience and Neuroengineering Center, Med-X Research Institute, Shanghai Jiao Tong University, [3]Shanghai Institute of Applied Physics, Chinese Academy of Sciences, [4]Department of Neurology, Shanghai Ruijin Hospital, School of Medicine, Shanghai Jiao Tong University, Shanghai, China

Introduction: Intraluminal filament model of middle cerebral artery occlusion (MCAO) is the most commonly used method for mimicking the focal cerebral ischemia in human. However, it remains a challenge to produce reproducible ischemia model with good consistency in outcome. Physiological property of suture has been proposed to be the key factor that causes variations in outcome. This issue was not adequately addressed due to the lack of a technique to monitor the occlusion of MCA in real-time. Here we developed a novel technique to dynamically monitor the cerebral blood flow after permanent MCAO in rat using synchrotron radiation angiography (SRA) with non-ionic iodine as contrast agent.

Methods: Twenty adult male SD rats underwent MCAO with 4-0 suture. Animals were divided into 5 groups corresponding to different suture preparations regarding silicone coating: 1) without silicone coating, 2) <2 mm, 3) 2 mm-3.3 mm, 4) >3.3 mm. *In vivo* imaging was performed at beamline BL13W1, Shanghai Synchrotron Radiation Facility in China. Imaging was carried out with 145 mA beam current, 33.7 keV x-ray energy. The CCD resolution is 13 mm and the field of view is 45 (H) ×5 mm (V). Non-ionic iodine contrast agent was injected during SRA through a PE-10 catheter at an injection rate of 100 μl/second by a microsyringe pump. The average exposure time of SRA is 20 ms. SRA images were jointed and processed by Adobe Photoshop CS4.

Results: SRA images could clearly display the hemodynamic changes following MCAO in rats. Contrast enhancement was detected in MCA when a suture without silicon coating was used. However, contrast enhancement was not detected in the MCA when a silicone-coated suture was used. Further study demonstrated that MCA was not or partially occluded when using nude suture or suture with silicone coating length less than 2 mm; MCA was successfully occluded when the silicone coating length was from 2 to 3.3 mm. However, when the coating length is longer than 3.3 mm, arteries including MCA, AChA, PCA and HTA were extensively occluded. Ischemia-induced infarct volume was closely related to the coating length and the optimal coating length is between 2 and 3.3 mm in order to completely occlude MCA with the lowest mortality compared with other groups ($p < 0.05$).

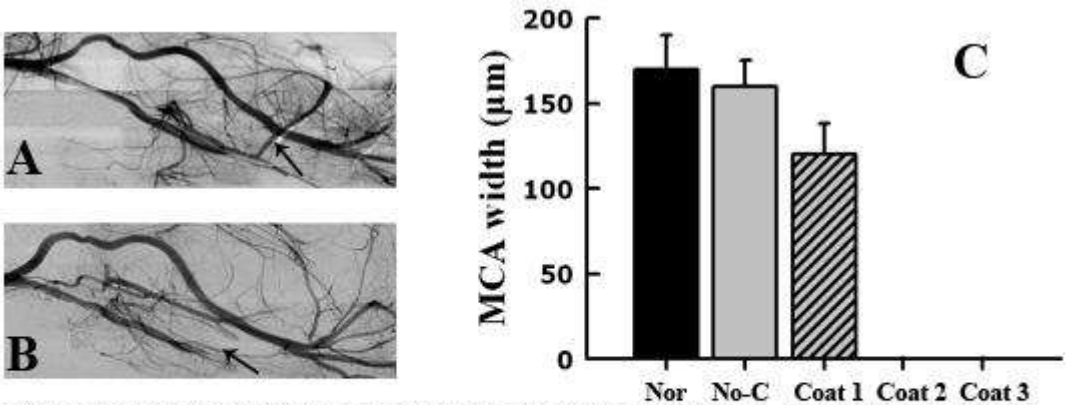

Figure 1 The effect of suture coating length during MCAO. A. suture head without sillicone coating. B. suture head with coating, arrows indicate MCA.C. bar graph shows the MCA width with different silicon coating of suture. No-C= no coating, Coat 1= <2mm, Coat 2= 2-3.3 mm, Coat 3= >3.3 mm.

[Effect of suture coating length during MCAO]

Conclusion: SRA provides a unique tool to study CBF changes and vascular morphology in real time in the rat brain. With SR imaging, the MCAO procedure can be monitored and adjusted when the suture was not in the right position. Well controlled infarct size could be induced by appropriate suture coating.

References:

Duverger, D. and E.T. MacKenzie; *J Cereb Blood Flow Metab*, 1988. 8(4): p. 449-61.

Shimamura, N., et al.; *J Neurosci Methods*, 2006. 156(1-2): p. 161-5.

Supported by The National Basic Research Program of China (*973 program 2010CB834306*) (GYY, YW), the Shanghai Science and Technology Commission Program *09140902400* (GYY, YW), and Shanghai Leading Academic Discipline Project *S30203* (GH, KMC).

627

"FASTFLOW" A SOFTWARE SUITE FOR WIDE-FIELD IMAGING OF BLOOD FLOW VELOCITY

T. Deneux[1,2], G.S. Masson[2], I. Vanzetta[2]

[1]Neurobiology, Weizmann Institute of Science, Rehovot, Israel, [2]INCM, Universitée de la Méditerranée, CNRS, Marseille, France

Introduction: Measuring the spatiotemporal properties of blood flow in vascular networks has important applications for biomedical and functional imaging, e.g. in the cortex or the retina. Wide-field optical imaging offers a simple and inexpensive way to do so, by quantifying the velocity of red blood cells (RBCs) inside optically accessible vessels. More precisely, it is possible to estimate RBC speed and its changes in comparatively large (several square mm) vascular networks at high temporal resolution (tens of ms), down to the individual vessel level and without the use of any exogenous contrast or fluorescent tracer. This estimation requires a number of processing steps, necessitates the handling of large size of data and requires the use of algorithms that are robust against noise.

Aim: A software suite is presented, which provides all the tools necessary to conduct such a blood flow velocity estimation in a vascular network of the kind encountered in functional imaging of the cortex (few square mm).

Methods: This suite consists of: 1) the coregistration of all the data to a reference frame, to correct for motions of the tissue; 2) the computation of a mask of the vasculature and a semi-automatic procedure to segment the shape of blood vessels; 3) pre-processing of the vessel data to produce spatio-temporal "trajectories images"; 4) two robust algorithms for velocity estimation that rely on complementary principles (one local based on the Radon transform, the second global based on the optical flow equation), and therefore serve as a control of one another; 5) post-processing of the estimation results, such as condition averaging, filtering, etc. The software is used through a graphic interface that enjoys the following features: 1) a unique window that displays all the important information at once 2) direct access to the tools and simplified parameter settings 3) intermediary results are accessible at any stage of the estimation and for any subpart of the data 4) smart data saving conventions allow the handling of large size data while being unnoticed by the user.

Results: We demonstrate the use of this software on physiological data obtained on an anesthetized rat during a spreading depression. We show that we can detect not only the strong response to the spreading depression in the flow velocity, but also the propagation in space of this response.

DEVELOPMENT OF A NEW STEADY-STATE METHOD USING INJECTABLE $^{15}O_2$ FOR MEASUREMENT OF OXYGEN METABOLISM IN THE RAT BRAIN

M. Kobayashi[1], T. Mori[2], Y. Kiyono[2], V.N. Tiwari[2], R. Maruyama[2], K. Kawai[1], H. Okazawa[2]

[1]School of Health Sciences, College of Medical, Pharmaceutical and Health Sciences, Kanazawa University, Kanazawa, [2]Biomedical Imaging Recearch Center, University of Fukui, Fukui, Japan

Objectives: A new injectable $^{15}O_2$ method using hemoglobin-containing vesicles ($^{15}O_2$-HbV) was developed to measure cerebral oxygen metabolism of rats [1]. However, the bolus injection method requires multipoint arterial blood sampling for quantitative measurement although the volume of sampling blood is limited in small animals. In this study, a less-stressful steady-state method was applied to $^{15}O_2$-HbV PET for measurement of cerebral metabolic rate for oxygen ($CMRO_2$).

Methods: Twenty rats including ten middle cerebral artery occlusion (MCAO) models were studied using a small animal PET scanner. Before emission scans, a transmission scan was performed for 60 min using $^{68}Ge/^{68}Ga$ source. A 3-min list mode PET scan was initiated at bolus intravenous administration of about 20 MBq $C^{15}O$ labeled HbV ($C^{15}O$-HbV) with injection volume and arterial blood was sampled every 1 min. After the decay of $C^{15}O$, 5-min list mode PET data was started at intravenous administration of $H_2{}^{15}O$ using the steady-state method [2]. In the program of the steady-state method, the injection speed was rapidly controlled for gradually increased administration rate to compensate for the decay of blood ^{15}O radioactivity. Arterial blood was sampled every 1 min during scan. After the $H_2{}^{15}O$ scan, 5-min list mode PET data acquisition was started with administration of $^{15}O_2$-HbV using the same injection program as $H_2{}^{15}O$ steady-state scans. About 200 uL arterial blood was sampled every 1 min during $^{15}O_2$-HbV scan, and whole blood and plasma radioactivity was counted. The cerebral blood flow (CBF), oxygen extraction fraction (OEF), $CMRO_2$ and cerebral blood volume (CBV) images were calculated using PET data and arterial blood radioactivity [3, 4].

	Normal	***MCAO***	
Hemodynamic parameters	Whole brain	Contralateral side	Ipsilateral side
CBF	54.3 ± 2.1	56.2 ± 1.8	23.8 ± 2.5
OEF	0.56 ± 0.04	0.53 ± 0.03	0.22 ± 0.05
CMRO2	5.9 ± 0.4	6.4 ± 0.5	1.2 ± 0.3
CBV	4.8 ± 0.6	5.2 ± 0.9	2.8 ± 0.5

[Hemodynamic parameters of normal and MCAO rats]

Results: In the steady-state method, radioactivity concentration of ^{15}O rapidly achieved equilibrium in blood and whole brain at about 2 min after $H_2{}^{15}O$ and $^{15}O_2$-HbV administration and stable PET counts were obtained. CBF, OEF, $CMRO_2$ and CBV in the whole brain of normal rats were 54.3±2.1 mL/100g/min, 0.56±0.04, 5.9±0.4 mL/100g/min and 4.8±0.6 mL/100g, respectively (Table). Average values of cerebral oxygen metabolism were not significantly different from the results reported previously in the normal rats. All hemodynamic parameters of the infarction areas showed a significant decrease compared with the corresponding region of contralateral side in the MCAO rats.

Conclusion: The $^{15}O_2$-HbV with the steady-state method is very useful in measurement of cerebral oxygen metabolism in small animal studies.

Reference:

[1] Tiwari VN, Kiyono Y, Kobayashi M, et al. *Nucl Med Biol.* 2010;37, 77-83.

[2] Kobayashi M, Kiyono Y, Maruyama R, et al. *J Cereb Blood Flow Metab*. In press.

[3] Frackowiak RS, Lenzi GL, Jones T, et al. *J Comput Assist Tomogr*. 1980;4, 727-736.

[4] Lammertsma AA, Wise RJ, Heather JD, et al. *J Cereb Blood Flow Metab*. 1983;3: 425-431.

629

THE PATHOPHYSIOLOGICAL ROLE OF NEUTROPHIL IN ISCHEMIC BRAIN

S.Y. Cheng, C.H. Wang, A.J. Chang, P.C. Hsu, C.M. Hsueh

Department of Life Sciences, National Chung Hsing University, Taichung, Taiwan R.O.C.

Objectives: Neutrophil possesses both phagocytic and pro-inflammatory activities in periphery its role in CNS however, is complex. The main purpose of the study was to evaluate the pathophysiological role(s) of infiltrating neutrophils in ischemic brain and the underneath mechanisms.

Methods: In the study, the capability of neutrophils entering ischemic brain and the underneath molecular mechanisms were investigated both in vivo and in vitro. Adhesive capability of 4´, 6-diamidino-2-phenylindole (DAPI)-labeled neutrophils to GOSD (glucose-, oxygen-, and serum-deprivation)-treated endothelial cells (EC) was first determined in vitro. DAPI-labeled neutrophils were also intravenously given into the ischemic animals (receiving 90 min bilateral common carotid artery occlusion plus unilateral middle cerebral artery occlusion also known as CCAO/MCAO, followed by 24 h reperfusion) to determine their migrating capabilities into ischemic brain using a fluorescence microscope with UV excitation. Neutrophil depletion by anti-polymorphonuclear leukocytes serum (anti-PMN) was further applied to evaluate the pathophysiological role of neutrophil in ischemic brain. In addition, GOSD-induced changes in tight-junction protein (occludin) and cell adhesion molecule (intercellular adhesion molecule or ICAM-1) on ECs and L-selectin on neutrophils were also analyzed by immunocytochemistry. In vitro production of interleukin1-β (IL-1β) and interferon-γ (IFN-γ), in response to GOSD was determined in neutrophils. The pathophysiological effect of IL-1β and IFN-γ on ischemic brain were also determined in vivo, using specific agonists and antagonists.

Results: The current results showed that GOSO significantly injured the ECs and decreased their expression of occludin. More DAPI-labeled neutrophils adhered to GOSD (6 h)-treated ECs than to the normal ECs in vitro. Neutrophil depletion in vivo significantly decreased the infarct volume of ischemic brain and slightly restored ischemia-decreased neurological function. Brain injection of low dose of IL-1β (5 ng/rat/intracisternal route) significantly reduced the infarct volume of ischemic brain, whereas at higher dose (10 ng/rat) IL-1β-mediated brain protection no longer existed. At present, entrance of DAPI-labeled neutrophils into the ishcemic brain; the expression of L-selectin on neutrophils and ICAM-1 on ECs in response to GOSD stress; and the pathophysiological roles of IL-1β and IFN-γ in ischemic brain and their possible correlations with neutrophil are still investigated in our laboratory.

Conclusions: Brain infiltrating neutrophils appeared to play a pro-inflammatory whereas IL-1β (at low dose) an anti-inflammatory role in ischemic brain. ECs may play a critical role in determining the entrance of neutrophils into ischemic brain. Would neutrophils rely on the release of high doses of IL-1β ad/or IFN-γ to exacerbate the infarction of ischemic brain are still unclear and currently under investigation. The adhesion molecules participate in the neutrophil/EC interaction are also evaluated and believed to be L-selectin and ICAM-1 related. Results from the study can further strengthen our knowledge about the immunological impact upon ischemic brain that might lead to a better therapeutic regimen in near future.

630

CEREBRAL BLOOD VOLUME IN ANEMIC PIGLETS USING NEAR-INFRARED TIME-RESOLVED SPECTROSCOPY

K. Koyano[1], S. Nakamura[2], K. Koyano[2], S. Yasuda[1], K. Okubo[2], M. Nakamura[2], K. Isobe[2], S. Itoh[2]

[1]Maternal and Perinatal Center Faculty of Medicine, Kagawa University, [2]Department of Pediatrics, Kagawa University Faculty of Medicine, Miki-cho Kita-gun, Japan

Background: Previously we have shown that Newborn Cerebral Blood Volume (CBV) becomes the important index in caring for NICU hospitalization infant. However, the effect of blood Hb concentrations on CBV is not found.

Purpose: The aim of this study is to determine the relationship between CBV and blood Hb concentrations in the anemic piglet model.

Methods: Seven newborn piglets, less than 24 h after birth, were used. To induce normovolemic anemia, 25 ml of arterial blood was drew from the arterial catheter while infusing a same volume of warmed 5% pig albumin solution via the peripheral vein. We used catecholamine for the maintenance of the blood pressure. This procedure was performed for each piglet at approximately 20 minutes until blood hemoglobin concentration became 6.0 g/dL or less. The reason is because the maintenance of the blood pressure becomes difficult if blood hemoglobin concentration becomes 6.0 g/dL or less. We used a portable three-wavelength Time-resolved Spectroscopy system for measurement of cerebral hemoglobin concentration.

Results: With the reduction in blood Hb concentrations, CBV increased. Blood hemoglobin concentration was 10.5 g/dL or more, the increase of CBV was slow. However, CBV increased rapidly when blood hemoglobin concentration was less than 10.5 g/dL.

Conclusion: It was confirmed the brain compensated it for an anemic progress, and to increase CBV. At first the increasing of CBV occurs gently and progresses it more rapidly than a certain hemoglobin blood level. It is thought that the same thing generates even the brain of the human. We may decide treatment strategy for the anemia as an index in CBV.

632

ISCHEMIA-INDUCED NEURAL STEM/PROGENITOR CELLS EXPRESS PYRAMIDAL CELLS-MARKERS IN VIVO AND IN VITRO

M. Clausen[1,2], A. Nakano-Doi[2], O. Saino[2], M. Takata[2], T. Nakagomi[2], P. Luiten[1], T. Matsuyama[2]

[1]University of Groningen, Groningen, The Netherlands, [2]Hyogo College of Medicine, Nishinomiya, Japan

Introduction: Adult brain-derived neural stem cells have acquired a lot of interest as an endurable neuronal cell source usable for CNS repair in a wide range of neurological pathologies, in particular as a therapeutic approach for neural regeneration in ischemic stroke. Recently, we identified injury induced neural stem/progenitor cells (iNSPC) in the post-stroke murine cerebral cortex, showing proliferating brain cells outside the conventional neurogenic regions. In this study we show that after differentiation the iNSPCs express the pyramidal cell markers, CaMKIIα and Emx1, as well as mature neuronal markers MAP2 and Tuj1 in vivo and in vitro. BrdU-positive neurons also express such pyramidal markers in the post-stroke cortex. The presence of newly regenerated pyramidal neurons in the post-stroke cortex might provide a non-invasive therapeutic strategy for stroke treatment with functional recovery.

Materials and methods: Male, 6-week-old SCID mice were subjected to cerebral ischemia through ligation of the middle cerebral artery (MCA). This causes a highly specific and reproducible infarction of the ipsilateral cerebral cortex. Bone marrow-derived mononuclear cells were obtained from 6-week-old normal male CB-17 and administered IV two days after stroke induction. BrdU was administered from day three post-stroke, three times per week until the animals were sacrificed on day 21 post-stroke. The animals were perfused, the brain was removed and subjected to immunohistochemistry for BrdU and the pyramidal marker Emx1.

7 Days after MCA, infarcted tissue was extracted from the post-stroke cerebral cortex of CB-17 mice. The ischemic tissue was cultured into neurospheres in vitro and differentiated. After 7 weeks of incubation and differentiation the cells were subjected to immunocytochemistry for the pyramidal cell markers Emx1 and CamKIIα and the mature neuron markers Tuj1 and MAP2. To confirm the immunocytochemistry, mRNA was isolated from the in vitro differentiated iNSPC and PCR was performed for the markers Emx1, CamkIIα, Otx1 and GAPDH.

Results: Similarly to our previous study in which neurosphere-like cell clusters were differentiated into neurons positive for the mature neuron markers MAP2 and Tuj1, the iNSPCs could differentiate into neurons which were double-positive for Tuj1 and Emx1 or MAP2 and CamKIIα. In addition, Emx1-positive cells displayed pyramidal-like morphology, while Emx1-negative but Tuj1-positive neurons were seen that showed non-pyramidal morphology. PCR revealed that the relative expression levels of Emx1 and CamKIIα in neurons differentiated from iNSPCs in vitro, were similar to those observed in the intact adult murine cortex. In contrast, expression levels of another pyramidal cell marker Otx1 were found to be significantly lower in iNSPC-derived cells than those in non-ischemic cortical brain tissue.

Discussion: In conclusion, the iNSPCs expressing pyramidal markers may indicate cortical neuron generation in the adult brain after ischemia. Stimulation of iNSPCs differentiation might provide a new non-invasive strategy in stroke treatment. Further studies are needed to confirm the regeneration of functional projecting neurons, such as their release of glutamate and NMDA-induced response as well as morphological connectivity to distant regions.

633

ROLE OF ENDOGENOUS NEUROMODULATOR IN ANGIOGENESIS

H.J. Jung[1], Y.H. Jeon[2], K.A. Park[1], J.E. Lee[2], W.T. Lee[1]

[1]Anatomy, [2]BK21 Project for Medical Science, College of Medicine, Yonsei University, Seoul, Republic of Korea

Objective: Angiogenesis results in the growth of new blood vessels which could be seen as a natural defense mechanisms involving endothelial cell proliferation, migration and tube formation. Several reports have demonstrated that increased adhesion molecule expression facilitates angiogenesis. Intercellular adhesion molecule-1 (ICAM-1) induced endothelial cell migration through organization of the actin cytoskeleton. Agmatine, is well known endogenous neuromodulator formed from L-arginine by the enzyme arginine decarboxylase (ADC), has the potential for new drug development based on animal studies. The aim of this study is to investigate the role of agmatine on angiogenesis and clarify the underlying molecular mechanism in brain endothelial cells (bEnd.3).

Methods: After 24 hours of starvation in 0.1% FBS media, agmatine (50, 100, 200 μM) was treated in bEnd.3 cells for 24 hours. Angiogenesis was assessed by measuring the proliferation and migration of bEnd.3 cells. Proliferation assay and migration assay were evaluated using 3-(4,5-dimethylthiazol-2-yl)-2,5-diphenyltetrazolium bromide (MTT) and Culture-insert which creates a cell-free gap of 500 μm. In order to investigate the molecular mechanism of migration regulated by agmatine, Vascular endothelial growth factor (VEGF), VEGFR-2 (KDR/Flk-1), PI3-kinase (PI3K), Akt, eNOS and Intercellular adhesion molecule-1 (ICAM-1) were detected and after treatment with wortmannin, known as potent PI3K inhibitor, ICAM-1 expression was confirmed by western blotting. Nitrite level was measured by griess reagent and actin cytoskeleton staining of endothelial cell monolayers was performed by immunocytochemistry.

Results: In bEnd.3 cells, agmatine treatment (50, 100, 200 μM) did not affect cell proliferation but the migration was significantly facilitated in a dose- and time-dependent manner. The treatment of agmatine markedly increased the level of vascular endothelial growth factor (VEGF) among angiogenic factors in a dose-dependent manner, and elevated VEGF level triggered PI3K/Akt/eNOS/ICAM-1 cascade. Agmatine led to a increase in cell migration, but these effects were significantly attenuated by wortmannin-induced inhibition of PI3K expression. These results suggest that agmatine may have the potential to regulate endothelial cell migration through controlled PI3K/Akt/eNOS and ICAM-1 expression. NO level was also found to be significantly increased by the treatment of agmatine. Further, induced migration by agmatine was associated with an elevated expression of actin cytoskeleton which may play a critical role in endothelial cell migration.

Conclusion: These data suggest that agmatine modulates endothelial cell migration through regulating PI3K/Akt/eNOS and ICAM-1 pathway.

This research was supported by Basic Science Research Program through the National Research Foundation of Korea (NRF) funded by the Ministry of Education, Science and Technology (2010-0012797)

635

THE CRUCIAL ROLE OF ENDOTHELIAL $G_{Q/11}$ IN REGULATION OF CEREBRAL BLOOD FLOW

S. Salinin[1], S. Muhammad[1], M. Rahman[1], D.A. Ridder[1], H. Schröck[2], S. Offermanns[1], M. Schwaninger[1]

[1]Department of Pharmacology, University of Heidelberg, Heidelberg, [2]Department of Neurophysiology, University of Heidelberg, Mannheim, Germany

Objectives: In many tissues the endothelium exerts a profound influence on blood flow. It regulates vascular tone by releasing nitric oxide (NO), prostacyclin (PGI_2), and other endothelium-derived relaxing factors in response to a range of chemical messengers. In most cases, the chemical message is transduced by G protein-coupled receptors (GPCRs), which are linked to the heterotrimeric G proteins $G_{q/11}$. However, the role of G proteins in brain endothelial cells was unclear.

Methods/Results: Using a genetic mouse model that allows for the conditional abrogation of Gq/11-mediated signaling pathways by inducible Cre/loxP-mediated mutagenesis in brain endothelial cells, we show that Gq/11-mediated signaling is essential for regulation of cerebral blood flow. Mice with Gq/11 deficiency exhibited a significantly reduced cerebral blood flow in the cerebral cortex, hippocampus, basal ganglia, and thalamus. Loss of $G_{q/11}$ lowered the production of NO and PGI_2 upon stimulation with vasodilating agents. Finally, mice lacking $G_{q/11}$ in brain endothelial cells had larger infarcts after middle cerebral artery occlusion.

Conclusions: Our findings suggest that impaired Gq/11 signaling in brain endothelial cells is crucial for regulation of the cerebral blood flow under physiological conditions and in cerebral ischemia.

638

THE EFFECT OF AGMATINE ON CEREBROVASCULAR DYSFUNCTION INDUCED BY PERMANENT BILATERAL COMMON CAROTID ARTERY IN RATS

H.J. Jung[1], B.E. Hur[2], K.A. Park[1], W.T. Lee[1], J.E. Lee[2]

[1]Anatomy, [2]BK21 Project for Medical Science, Yonsei University, College of Medicine, Seoul, Republic of Korea

Objective: The integrity of the vascular system is essential for the efficient functioning of the brain. Vascular dysfunction may be a key element in vascular dementia (VaD). The blood-brain barrier (BBB) comprises the microvascular endothelial cells, pericytes, and astrocytes, which are connected by the extracellular matrix (ECM). Previous studies have reported that agmatine possesses significant neuroprotective effects in brain ischemic injury and neuromodulatory functions in central nervous system (CNS). The aim of this study is to observe the effect of agmatine on the learning and memory abilities and vascular dysfunction of rats with VaD. This study was also intended to explore the mechanism of agmatine for the treatment of VaD.

Methods: SD rats were subjected to permanent ligatin of the both common carotid arteries (2VO) which leads to vascular dementia (VaD). Three groups, a sham operation group, a experimental control group and a agmatine treated group were set up. After 2VO, agmatine (100 mg/ kg) was administrated by i.p. for 5 weeks in treated group. We performed Morris water maze test and Laser Doppler to measure the learning and memory and cerebral blood flow (CBF) respectively. Levels of malondialdehyde (MDA) and glutathion (GSH) in brain tissue were detected by spectrophotometer. Furthermore, the activation of caspase-3 was detected by immunostaining and hematoxylin-eosin (H&E) to check neuronal cell death. CD31 (PECAM-1), vascular endothelial growth factor (VEGF), vascular endothelial growth factor receptor (VEGFR), matrix metalloproteinase-2 (MMP-2), MMP-9, glial fibrillary acidic protein (GFAP, astrocyte marker) and desmin (pericyte marker) were detected to confirm the effect of agmatine on disruption of cerebrovascular integrity.

Results: Agmatine improved learning and memory deficits in vascular dementia. A decrease of MDA and elevation of GSH level were seen in agmatine treated group after 2VO. Agmatine treatment group shortened the mean of escape latency time in Morris water maze, decreased neuronal cell death and restored the level of CBF compared to the experimental control group. Moreover, BBB integrity was strengthed by agmatine in VaD brain tissue as detected by immunohistochemistry and westernblot results for confirming vessel markers and angiogenic factors.

Conclusion: The results of the present observation suggest that agmatine has therapeutic potential for the treatment of vascular dementia, which is most likely related to its action to recover vascular dysfunction.

This research was supported by Basic Science Research Program through the National Research Foundation of Korea (NRF) funded by the Ministry of Education, Science and Technology (2010-0012797)

640

TRANSPLANTATION OF ADC GENE EXPRESSED NEURAL STEM CELLS (NSCS) IMPROVE CELL SURVIVAL AND BEHAVIORAL OUTCOME IN SPINAL CORD INJURY MODEL

Y.M. Park[1], S.K. Seo[1], Y.O. Lee[2], K.A. Park[2], W.T. Lee[2], J.E. Lee[1]

[1]BK21 Project for Medical Science, [2]Anatomy, College of Medicine, Yonsei University, Seoul, Republic of Korea

Objectives: Spinal cord injury results in loss of neurons, degeneration of axons, formation of glial scar, and severe functional impairments. Agmatine, a decarboxylated arginine catalysed by arginine decarboxylase (ADC) possesses to have neuroprotective effects. Recently, functional NSCs with transgenes proved to be a promising therapeutic strategy for targeting various stress models both in vitro and in vivo. Purpose of our present study was to observe the morphological and functional repair effects of the ADC-NSCs transplantation to the mice subjected to spinal cord injury.

Methods: Basing on our earlier reports describing the effects of exogenous agmatine treatment we investigated to develop new functional NSCs expressing ADC gene which can synthesize agmatine endogenously using retroviral vector expression system. PKH26 labeled ADC-NSCs were transplanted into spinal cord following compression injury at T10. Seven experimental groups were maintained: 1. normal control (NC); 2. experimental control (EC); 3. agmatine treatment (AGM); 4. NSCs transplantation (NSCs); 5. NSC transplantation combined with agmatine treatment (NSC+AGM); 6. Mock vector infected NSCs (LXSN-NSCs); 7. ADC-infected NSCs (ADC-NSCs). The Basso, Beattie, Bresnahan(BBB) functional scale was used to assess the locomotor capacity of rats after spinal cord injury. Animals were sacrified at 1, 2 and 5 weeks and then spinal cords were fixed, cryosectioned and analyzed. Stereologic methods were used to estimate the glial scar formation area. Immunostaining was also performed to determine the migration and differentiation of transplanted NSCs.

Results: (1) From 1 week to 5 weeks after injury, the BBB locomotion scores of ADC-NSCs transplanted groups were better than those of the agmatine treatment group and LXSN-NSCs transplanted group ($P < 0.05$). (2) ADC-NSCs integrated well into host tissue and appeared to migrate toward the lesion site. ADC-NSCs can be used as delivery vehicles for therapeutic proteins because they show an ability to migrate toward the lesion site. (3) ADC-NSCs might attribute partly to a reduction in tissue loss from secondary injury processes as well as diminished glial scarring. (4) Immunohistochemistry staining results showed the transplanted ADC-NSCs could survive and migrate until 5 weeks and they could differentiate into neurons, oligodendrocytes and astrocytes. (5) Histological and immunocytochemical staining results demonstrated that transplanted ADC-NSCs showed enhanced neurogenesis within the injury site and these neurons extended their processes and formed synaptic structures.

Conclusions: These results suggest that ADC gene delivery may promote grafted NSCs survival and differentiation after injury. Also ADC-NSCs transplantion could promote the functional recovery in the injured spinal cord. ADC-NSCs transplantation showed better results compared with NSCs transplantation alone, agmatine and NSCs co-treatment NSCs and mock vector transfected NSCs (LXSN-NSCs). Treatment with ADC-NSCs can facilitate functional recovery after traumatic spinal cord injury and may prove to be a useful therapeutic strategy to repair the injured spinal cord.

This research was supported by Basic Science Research Program through the National Research Foundation of Korea (NRF) funded by the Ministry of Education, Science and Technology (2010-0012797)

641

EXPERIMENTAL STROKE-INDUCED LEUKOCYTE RESPONSES IN THE BONE MARROW IN TWO DIFFERENT MODELS OF FOCAL CEREBRAL ISCHAEMIA

A. Denes[1], J. Pradillo[1], B.W. McColl[2], S.F. Leow-Dyke[1], K.Z. Chapman[3], S.M. Allan[1], N.J. Rothwell[1]

[1]Faculty of Life Sciences, University of Manchester, Manchester, [2]Neuropathogenesis Division, The Roslin Institute and R(D)SVS, University of Edinburgh, Roslin, UK, [3]Laboratory of Neurogenesis and Cell Therapy, Section of Restorative Neurology, Wallenberg Neuroscience Center, University Hospital, Lund, Sweden

Objectives: A large array of anti-inflammatory interventions has been tested in experimental stroke models as potential new therapies for stroke patients. However, we still lack an understanding of basic mechanisms that lead to and maintain the activation of peripheral inflammatory cells and cytokines, which contribute to brain damage after stroke. The effects of cerebral ischaemia on leukocyte responses in the bone marrow (BM), which is the primary source of circulating granulocytes and monocytes, have not been investigated in different experimental stroke models. Therefore in this study our aim was to establish key features of the BM response after experimental stroke in mice.

Methods: Transient middle cerebral artery occlusion (MCAo) was induced by two different (intraluminal filament and distal MCA ligation) approaches. Changes in BM and blood leukocyte populations, phosphorylation state and cytokine expression were analysed by flow cytometry, Western blotting, ELISA and cytometric bead array.

Results: MCAo induced by the intraluminal filament approach resulted in rapid (between 10min and 4h reperfusion) phosphorylation of NF-κB and P38 MAPK in BM myeloid cells and the release of CXCR2-positive granulocytes. Elevation of CXCL1 was seen in the plasma and circulating blood neutrophils. BM T cells and natural killer cells increased after MCAo at 24-72h reperfusion. BM leukocytes did not show a suppressed cytokine response to bacterial endotoxin stimulation *in vitro*. Both isoflurane anaesthesia and surgical stress had a profound effect on leukocyte responses in the BM. Release of granulocytes from the BM after distal MCA ligation (a model that involves craniotomy) was largely determined by the effect of surgery itself. We also show that both approaches result in a rapid increase of myeloid cells in the circulation, an effect also heavily influenced by surgical stress.

Conclusions: We present a detailed characterisation of BM responses in different MCAo models and identify targets for intervention. Our results also indicate that anaesthesia and surgical stress considerably affect multiple peripheral responses and therefore need to be accounted for in experimental stroke models.

The authors are grateful for funding provided by the Medical Research Council, the European Union's Seventh Framework Programme (FP7/2008-2013) under grant agreements no. 201024 and no. 202213 (European Stroke Network, NJR, AD).

642

CHARACTERIZATION OF RECOMBINANT NEURAL STEM CELLS AND PROSPECTS OF ITS DIFFERENTIATION

B.K. Kumar[1], Y.H. Jeon[2], S.U. Moon[1], K.A. Park[1], W.T. Lee[1], J.E. Lee[2]

[1]Anatomy, [2]BK21 Project for Medical Science, Yonsei University, College of Medicine, Seoul, Republic of Korea

Objectives: The use of Neural stem cells (NSCs), whether adult or embryonic for neuroprotective therapies require a homogenous population of mature and terminally differentiated cells. The neurosphere culture system is useful for expanding NSCs without affecting self-renewal potential and multipotency. Current area of intense interest is to characterize, maintenance, proliferation and subsequent differentiation of neural stem cells which are capable of replicating in the complex cellular environment existing *in vivo*. Agmatine is an amine and ionic cation synthesized following decarboxylation of L-arginine by arginine decarboxylase (ADC). Agmatine is considered a novel neuromodulator and possesses neuroprotective properties in the central nervous system. We already demonstrated that retrovirus-delivered human ADC genes (vhADC) in NSCs (ADC-NSCs) improve cell survival against oxidative insult *in vitro* but the characterization and cell fate of ADC-NSCs is not yet known. The specific aim of the present study is to characterize and explore the factors responsible for the differentiation of ADC-NSCs *in vitro*.

Methods: Cortical NSCs after 1-week culture were infected with empty retrovirus (vLXSN) and the vhADC genes. After 24 h of incubation with vLXSN and vhADC supernatants, the medium was replaced by NSC culture medium and were maintained for another week. The NSCs infected with vhADC (ADC-NSCs), NSCs infected with vLXSN (LXSN- NSCs), and retrovirus-noninfected control NSCs were used for the experiments. Stem ness was determined by checking the expression of SOX2 and OCT-4 by Western blot in control NSCs , LXSN-NSCs and ADC-NSCs. Immunocytochemial staining was done in all the experimental groups for determining the cell lineage (MAP2, GFAP, Oligo2). For exploring the cause for differentiation, the cell adhesion molecule integrin along with PI3K/AKT expressions was investigated in control NSCs, LXSN NSCs and ADC NSCs .

Results: The western blot results showed that the expression of stem cell markers: Nestin and Oct-4 appeared to be same in control NSCs, mock vector infected NSCs (LXSN-NSCs) and ADC-NSCs. Neural lineage was checked in all the experimental groups using MAP2 (mature neuron marker), GFAP (astrocyte marker) and Oligo-2 (oligodendrocyte marker) antibodies by using immunostaining. Results showed high number of MAP-2 positive cells in ADC-NSCs compared to control NSCs and LXSN NSCs depicting the ADC-NSCs lineage to neuron. Here, we also found that most of the ADC-NSCs were found attached and differentiated to the bottom surface of the culture plate. These outcomes were investigated by checking the expression profiles of PI3K /AKT and adhesion molecule, integrins.

Conclusions: The importance of PI3K /AKT and integrin expression in the differentiation of ADC-NSCs is highlighted as critical for neural lineage and consideration of the integrin expression profile should be made while differentiating neural stem cells for use in therapy

This research was supported by Basic Science Research Program through the National Research Foundation of Korea (NRF) funded by the Ministry of Education, Science and Technology (2010-0012797)

643

INFRINGEMENT OF PROCESSES CEREBROVASCULAR OF REGULATION AND COGNITIVE FUNCTION AT PATIENTS WITH HYPERTENSION, POSSIBILITIES OF CORRECTION

T. Ripp, V. Mordovin

Hypertension, Institut of Cardiology, Tomsk, Russia

Objectives: The aim of this study was evaluate state cerebrovascular reactions (CVR) in condition of hypercapnia- and hyperoxia- induced cerebrovascular reactivity up and after treatment of eprosartan (E) in hypertensive patients without complication.

Design and methods: Comparative research of 40 healthy volunteers and 66 patients with hypertension 2study, 1-2 degrees, without cerebral stroke during of the life history (age 40-56Y) have been made.We used ABPM, study and ultasonography of transcranial Doppler`s method in the study of middle cerebral arteries (MCA) from temporal window. We studied the changes of flow velocity mean (FVm) and diameter (D) starting, at the time of hypercapnia (4% CO_2) and hyperoxia (100%-O_2) and FmV in periods of recovery (rec) (air-inhalation 2min), We used coefficient and indexes of CVR and results of psychological testing. Patients had treatment of eprosartan 600mg/day during 24 weeks.

Results: Three types the damage of CVR it has been received at patients with a hypertensia: 1.decrease of hypercapnia reactions 19,2±2,8%, healthy 51,2±4,3% p=0,001, 2.decrease of hyperoxia reactions -10,4±2,6% p=0,04 or 3.distortion of hyperoxia reactions 4,9±2,3% p=0,00 in comparison with healthy -18,6±1,9% in MCA. Significant change of indicators of CVR was observed: at hypercapnia in a direction of normalisation of reaction (48,0±2,6% p=0,00), on hyperoxia - indicators have not reached normal values, but have got unidirectional natural character (-14,2±2,3 p=0,02) against therapy. The lowered initial factors and indexes of CVR aspired authentically to normal values after treatment. Improvement of indicators was observed: at an estimation of the test of G.Ajzenka at 75 %, function of memory at 86 %, degree of concentration and switching of attention at 62 % from total number of patients.

Conclusion: Patients with hypertension and *without cerebral stroke* had damage and decrease CVR and infringement cognitive functions, treatment with using eprosartan was effective and safe.

644

ELEVATION OF THE COMPARISON RESULTS OF THE CEREBRAL BLOOD FLOW CHANGES IN TEMPORARY CLIP APPLICATIONS USING DIFFERENT METHODS

S. Yavuz[1], M.E. Ustun[1], **M. Buyukmumcu**[2], M.T. Yılmaz[2], E.A. Cıcekcıbası[2]

[1]Neurosurgery, [2]Anatomy, Selcuk University, Meram Medical Faculty, Konya, Turkey

Objective: The major of this study is to define cerebral blood flow changes before, during and after temporary clip placement in aneursysm operation with QEEG and Bowman perfusion monitor and compare these methods with each other and also determine which QEEG parameter is valuable for following cerenral blood flow changes.

Material and methods: This study was achieved in Selcuk University Meram Faculty of Medicine Hospital Neurosurgery operating room between 2008 and 2009. The patients with single MCA or AcoA artery aneursysm which has no significant clinical or radiological vasospasm evidence and operated with in 3 days was included in this study. Temporary clip placement to main feding artery was performed before permanent aneursysm clipping in all of patients. Cerebral blood flow changes with Bowman perfusion monitor and also SEF 95, Median Frequence and Amplitude values obtained with QEEG determinated in the related arterial zone and these findings were compared which each other. Also QEEG changes were compared in three arterial zone.

Results: Cerebral blood flow decrease was started 10 minutes after temporary clip placement and this impairment became prominent 15 minutes after temporary clip placement. This cerebral blood flow impairment which was determinated with Bowman perfusion monitor had a high correlation with SEF 95 values of QEEG. 5 minutes after the withdrawal of temporary clip an increase in cerebral blood flow due to hyperperfusion was determinated with Bowman perfusion monitor had also a high correlation with SEF 95 values of QEEG. However median frequency and amplitude values have shown no correlation with perfusion changes observed with Bowman perfusion monitor.

Conclusion: The high correlation of SEF 95 values with the perfusion changes meassured with Bowman perfusion monitor led us to decide that SEF values can be used to monitor cerebral ischemia due to cerebral blood flow impairment alone or with Bowman perfusion monitor after temporary clip placement in intracranial aneursysm surgery.

645

ISCHEMIC PRECONDITIONING INCREASES THE LEVEL OF AGMATINE AND THE EXPRESSION OF ARGININE DECARBOXYLASE IN THE ISCHEMIC INJURED BRAIN

J.Y. Kim[1], H.S. Park[2], B.E. Hur[1], K.A. Park[2], J.E. Lee[1], W.T. Lee[2]

[1]BK21 Project for Medical Science, [2]Anatomy, Yonsei University, College of Medicine, Seoul, Republic of Korea

Objectives: Ischemic preconditioning (IP) is one of the most important endogenous mechanisms known for protecting cells against ischemic and reperfusion injury. Agmatine is an agonist for the α2-adrenergic and imidazoline receptors, an antagonist for NMDA receptors. Agmatine was shown to be neuroprotective in traumatic and ischemic CNS injuries. The purpose of this study is to establish the change between agmatine concentration and arginine decarboxylase (ADC) expression during ischemic preconditioning and its association with ischemic tolerance.

Methods: Male Sprague-Dawley rats (280±15g) were occluded at middle cerebral artery (MCA) for 10mins to establish IP 3days before 1hr occlusion. A 1hr occlusion was induced at 3days after a 10mins occlusion in IP group and parallel experimental control group without IP were also maintained throughout the experiment. Animals from the IP group were decapitated at 30min, 1day and 3days for measuring the agmatine concentration in brain, plasma and liver tissue using HPLC. Both EC and IP group animals were subjected to 1hr occlusion and were reperfused for 1hr, 3hr, 5hr and 23hr. Later animals both from EC and IP group were sacrificed and the brain edema, the infarct volume, the level of agmatine in brain, plasma and liver. The protein expression of ADC was checked by western blot analysis with or without ischemic preconditioning in ischemic injured brain of the rat.

Results: Ischemic preconditioning was found to be highly effective in inducing endogenous neuroprotection to the brain from ischemic injury. Infarct volume and the brain edema were markedly reduced in IP group. Concentration of agmatine in brain, plasma and liver tissue measured by HPLC shown ischemic preconditioning yielded higher agmatine levels and aided in protection against ischemic injury. The protein expression of ADC in preconditioning group was definite during the ischemic and reperfusion injury. The obtained data shows that the level of agmatine was increased during the IP and the increased level of agmatine facilitated the agmatine production by over expressed ADC gene during the ischemic and early reperfusion injury.

Conclusion: In this study, it has been concluded that ischemic preconditioning systemically increases the level of agmatine in the MCAO injured brain and this increased level of agmatine and ADC gene is maintained during ischemic period and found to be elevate a during early reperfusion period in the ischemic injured brain. These results demonstrate the possibility that agmatine and ADC gene may be one of the components of ischemic tolerance induced by ischemic preconditioning. It was suggested that agmatine concentration and ADC expression possess therapeutic potential to stroke.

This research was supported by Basic Science Research Program through the National Research Foundation of Korea (NRF) funded by the Ministry of Education, Science and Technology (2010-0012797)

646

O_2 CONSUMPTION DURING CHOLINERGIC GAMMA OSCILLATIONS IN HIPPOCAMPAL SLICE CULTURES AT AMBIENT ATMOSPHERE

C. Huchzermeyer[1], N. Berndt[2], H.-G. Holzhütter[2], O. Kann[1,3]

[1]Institute for Neurophysiology, [2]Institute of Biochemistry, Charité - Universitätsmedizin Berlin, Berlin, [3]Institute for Physiology and Pathophysiology, University of Heidelberg, Heidelberg, Germany

Gamma oscillations are fast network oscillations in the range of 30-80Hz. In hippocampal slice preparations they can be induced by bath application of acetylcholine (ACh), which mimics cholinergic input from the septum *in vivo*.

Using local field potential recordings, O_2 microsensor and theoretical modeling, we investigated the O_2 consumption of gamma oscillations in organotypic hippocampal slice cultures. We measured pO_2 depth profiles of slice cultures during gamma oscillations (GAM; 2µM ACh, 400nM physostigmine) as well as in the presence and absence (1µM tetrodotoxin, TTX) of spontaneous network activity (SPON). Experiments were made under optimized recording conditions in an interface chamber at ambient atmosphere (20% O_2, 5% CO_2), being closer to the situation *in vivo*.

Here, we show that gamma oscillations of high power were associated with lower pO_2 values in all layers (steps of ~16µm) of slice cultures compared to pO_2 values during spontaneous network activity (slice core: GAM, 25.45±4.9mmHg; SPON: 60.28±5.5 mmHg; slice bottom: GAM: 59.73±7.2mmHg; SPON: 73.66±5.4mmHg). Under the TTX condition, the pO_2 was much higher compared to SPON and GAM (slice core: 102.29±7.2mmHg; slice bottom: 105.12±7.9mmHg).

The observed pO_2 profiles were reproduced by a mathematical model taking into account oxygen diffusion and activity-dependent oxygen consumption. In this way, we are able to differentiate between the contributions of the oxygen diffusion and oxygen consumption to the depth profile and to quantify the O_2 consumption at different activity states.

Our data clearly show that gamma oscillations are highly O_2 consuming, even at lower experimental pO_2 levels.

647

SUICIDAL BEHAVIOR IS ASSOCIATED WITH REDUCED CORPUS CALLOSUM AREA

F. Cyprien[1,2,3], P. Courtet[1,2,3], A. Malafosse[1,4], J. Maller[5], C. Meslin[6], A. Bonafé[2,3], E. Le Bars[2,3], N. Menjot de Champfleur[2,3], K. Ritchie[1,2,7], S. Artero[1,2]

[1]Inserm U888, Montpellier CEDEX, [2]University of Montpellier I, [3]CHRU Montpellier, Montpellier, France, [4]Department of Psychiatry, University of Geneva, Geneva, Switzerland, [5]Monash Alfred Psychiatry Research Centre, The Alfred & Monash University School of Psychology and Psychiatry, Melbourne, [6]Centre for Mental Health Research, Australian National University, Canberra, ACT, Australia, [7]Faculty of Medicine, Imperial College, St Mary's Hospital, London, UK

Background: Corpus callosum (CC) size has been associated with cognitive and emotional deficits in a range of neuropsychiatric and mood disorders. As such deficits are also found in suicidal behavior, we investigated specifically the association between CC atrophy and suicidal behavior.

Methods: We studied 435 right-handed, non-demented individuals from a cohort of community-dwelling persons aged 65 years and over (the ESPRIT study). They were divided in three groups: suicide attempters (SA) (n=21), affective controls (AC) (n=180) without history of suicide attempt but with a history of depression, and healthy controls (HC) (n=234). T1-weighted magnetic resonance images were traced to measure the midsagittal areas of the anterior, mid and posterior CC. MANCOVA was used to compare CC areas in the three groups.

Results: Multivariate analyses adjusted for age, gender, childhood trauma, head trauma and total brain volume showed that the area of the posterior third of CC was significantly smaller in SA than in AC (p=0.02) and HC (p=0.01) individuals. No significant differences were found between AC and HC. No differences were found for the anterior and mid thirds of the CC.

Conclusions: Our findings emphasize a reduced size of the posterior third of the CC in subjects with a history of suicide, suggesting a diminished inter-hemispheric connectivity and a possible role of CC in the pathophysiology of suicidal behavior. Further studies are needed to strengthen these results and clarify the underlying cellular changes leading to these morphometric differences.

650

FUNCTIONAL NEURAL STEM/PROGENITOR CELLS EXPRESSING HUMAN ARGININE DECARBOXYLASE GENE TRANSPLANTATION PROMOTE NEUROLOGICAL FUNCTIONAL RECOVERY AND NEUROGENESIS AFTER EXPERIMENTAL STROKE

J.Y. Kim[1], B.E. Hur[1], Y.H. Jeon[1], K.A. Park[2], W.T. Lee[2], J.E. Lee*[1]

[1]BK21 Project for Medical Science, [2]Anatomy, Yonsei University, College of Medicine, Seoul, Republic of Korea

Objectives: The transplantation of neural stem/progenitor cells (NPCs) is a promising therapeutic strategy for Middle Cerebral Artery Occlusion (MCAO). However, transplanted NPCs have limited effect of transient recovery after CNS injury. Here, we suggested that transgenic neural stem cells, over-expressing human arginine decarboxylase gene exerts neuroprotective effects in CNS injury and regulated proliferation and differentiation of NPCs in vitro. In this study, we show the therapeutic efficacy of human arginine decarboxylase gene expressing adult mouse NPCs transplantation in rat brain after experimental stroke.

Methods: Male Sprague-Dawley rats (280±15g) were subjected to 60min MCAO by well established method. Animals were divided into 4 different groups; experimental control group, mNPCs transplantation alone group, vLXSN-mNPCs transplantation group and vhADC-mNPCs transplantation group. Animals were transplanted with vhADC-NPCs ($1*10^6$ cells/10$\mu\ell$) at 7days after MCAO injury. Behavior performance, rota-rod test was executed after MCAO. For confirmation of the cell lineage of transplanted vhADC-mNPCs in ischemic region, western blotting and immunohistochemistry was performed with anti-Ki67, BrdU, Sox2, Oct4, Neurog2, Doublecortin, Nestin, Tuj1, S100β and GFAP antibodies.

Results: Behavior tests supported that the therapeutic efficacy of vhADC-NPCs transplantation promotes neurological functional repair compared with NPCs transplantation alone and vLXSN-NPCs transplantation. Reflex response was regained to 70% in vhADC-NPCs transplantation group, but experimental control group recorded 50% reflex response for 4weeks after MCAO. Western blotting and immunohistochemistry results shown vhADC-mNPCs transplantation group increased stem cell maintenance and neuronal differentiation in ischemic region and promoted neurological functional recovery after ischemic injury.

Conclusions: The present investigation demonstrates that neural stem cells overexpressing arginine decarboxylase gene transplantation has a therapeutic clue for functional repair against CNS injury including experimental stroke.

This research was supported by Basic Science Research Program through the National Research Foundation of Korea (NRF) funded by the Ministry of Education, Science and Technology (2010-0012797)

652

MEMRI AS A TOOL TO OBSERVE CONNECTIVITY CHANGES IN RATS WITH MIDDLE CEREBRAL ARTERY OCCLUSION

C. Po[1], M. Gottschalk[1], T.D. Farr[1], A. Beyrau[1], M. Hoehn[1], G.A. Metz[2]

[1]*In-Vivo-NMR Laboratory, Max-Planck-Institute for Neurological Research, Köln, Germany,* [2]*Canadian Centre for Behavioural Neuroscience, University of Lethbridge, Lethbridge, AB, Canada*

Objectives: Manganese (Mn^{2+}) is taken up by voltage-gated calcium channels and actively axonally transported. Because Mn^{2+} is also a T_1 magnetic resonance imaging (MRI) contrast agent, it has been used to image brain circuitry (Soria, *et al*., 2008. Neuroimage. 41: 668-74) and to probe changes in brain connectivity after stroke. Significantly less Mn^{2+} was observed in the ipsilateral caudate and thalamic nuclei (ThN) after injection into the ipsilateral somatosensory cortex when compared to control rats (van der Zijden, *et al*., 2007. Neuroimage. 34: 1650-7). The aim of the present study was to observe potential ThN changes after stroke following injection into the non-ischemic ipsilateral primary motor cortex (M1), and to correlate this with behavior changes.

Methods: Wistar rats (n=21) were randomly divided into three groups: naïve controls (n=7), stroke via permanent distal occlusion of the middle cerebral artery (pdMCAO) (n=9), or the corresponding sham craniotomy procedure (n=6). MCAO and sham animals received a battery of sensorimotor behavioural tests before and weekly after surgery. Stroke damage was assessed immediately following surgery using diffusion-weighted imaging (DWI) at 7T: TR/TE= 5000/31ms, 7 b-values 0-1000s/mm^2, resolution= 156x156x500µm. Four weeks after surgery, in all animals, 0.3M $Mn^{2+}Cl_2$ solution was infused into the ipsilateral M1. Before and 24h after injection, all rats were scanned with a T_2-weighted sequence: TR/TE= 5000/13ms, 10 echoes, resolution= 234x234x500µm, and a T_1-weighted sequence: TR/TE/ = 2000/4.5ms, resolution= 117x117x500µm.

Results: Mn^{2+} was detected in the ipsilateral ThN of all rats (Figure1A). Signal intensity (S) was measured in the ipsilateral and contralateral ThN on the T_1 weighted images and normalized to S in muscle. The results were subsequently expressed as a ratio of S before and after Mn^{2+} injection (Safter/Sbefore). A significant difference in S was observed between groups ($F(2,19)=4.424$, $p=0.026$, two way mixed ANOVA), with the stroke group exhibiting the lowest values in the ipsilateral ThN. Furthermore, a significant difference was observed between ipsi and contralateral sides ($F(1,19)=47.7$, $p< 0.001$), with higher S in the ipsilateral ThN, though this did not achieve significance in the stroke group. Additionally, a significant negative linear correlation between S in the ipsilateral ThN and a bias towards turning in the ipsilateral direction in the open field was also observed.

Conclusions: In this study, Mn^{2+} was detected in the ipsilateral ThN of all rats but was only significantly higher than the contralateral ThN in sham and naïve animals. Combined with the correlation to the enhanced ipsilateral turn bias displayed in the open field, the MEMRI method could infer degeneration of ipsilateral M1 and ThN connectivity in stroke animals.

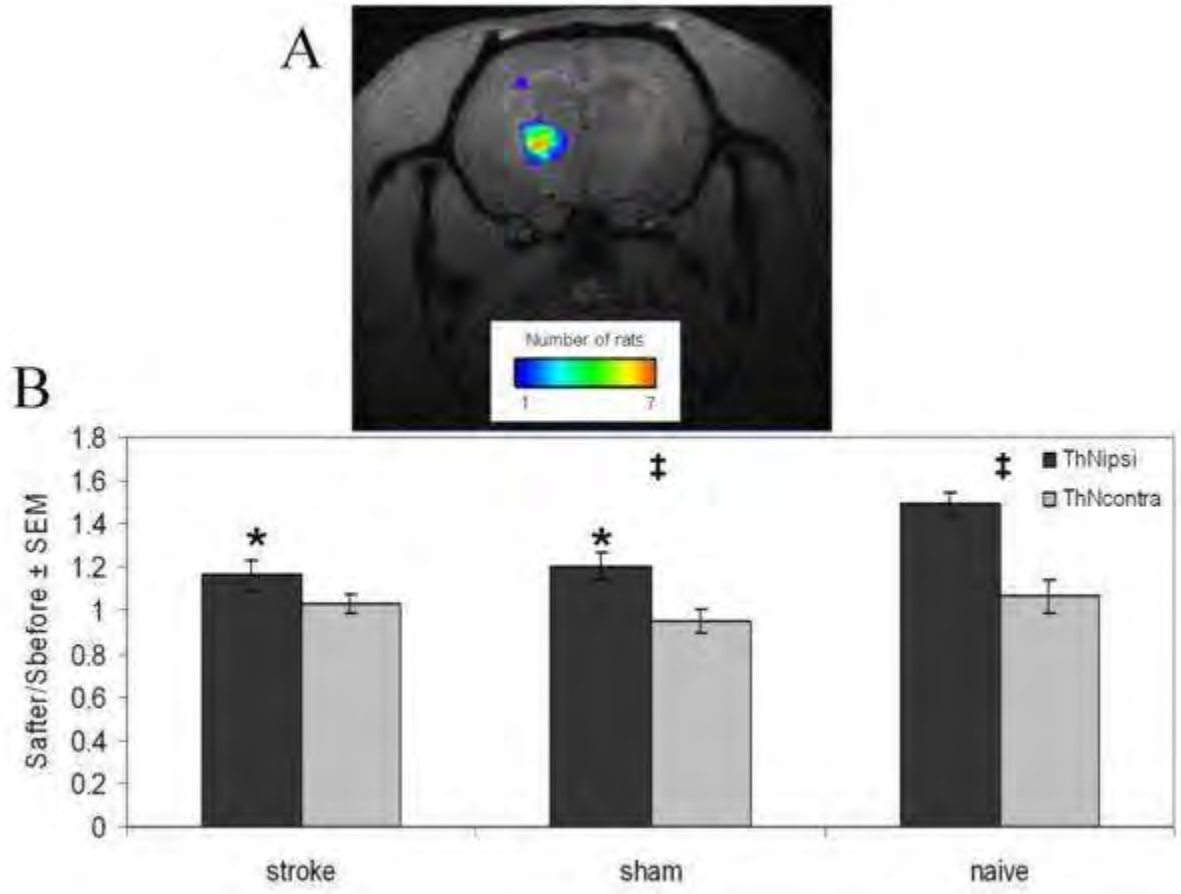

[Figure 1]

Figure1. A: Mn^{2+} incidence maps in the naive group. B: T_1 signal intensity as a ratio of the images before and after Mn^{2+} injection in the ipsilateral and contralateral ThN (⋆: $p < 0.05$ versus naive group, post-hoc Student Neuman Keuls; ‡: $p < 0.05$ ipsilateral versus contralateral, post-hoc pairwise comparison with Bonferonni correction).

654

REGULATION ON INFLAMMATION FOLLOWING TRANSIENT FOCAL CEREBRAL ISCHEMIA IN DIABETIC RATS

H.S. Choi[1], J.Y. Kim[2], C.H. Mun[2], B.N. Koo*[1], J.E. Lee*[2]

[1]Anesthesiology, Pain Medicine and Anesthesia, Pain Research Institute, [2]BK21 Project for Medical Science, Yonsei University College of Medicine, Seoul, Republic of Korea

Objectives: Diabetes mellitus is a metabolic disorder associated with structural and functional alteration of various organ systems including the central nervous system. The aim of this present study was to investigate the progresses and pathogenesis of cerebral ischemia in diabetes. It is also aimed to determine the neuroprotective effect of agmatine treatment during cerebral ischemic insult in diabetic rat. We established the streptozocine (STZ) induced diabetic model and middle cerebral artery occlusion (MCAO30) model in rat to demonstrate the difference in pathogenesis between simple cerebral ischemia and cerebral ischemia combined with diabetes.

Methods: Diabetes was induced with streptozotocin (60 mg/kg, i.p.) in male adult rats. Diabetes rats underwent 30min suture-occlusion of the middle cerebral artery (MCAO30), and was immediately injected with agmatine (100mg/kg, i.p.) followed by reperfusion for 1 and 3 days. Different neurobehavioral tests were performed. The brain infarct volume was assessed with 2 % solution of triphenyltetrazolium chloride (TTC). Western blot and immunohistochemical analysis were performed to determine nuclear factor kappa B (NF-kB)-dependent pro-inflammatory mediators interleukin-1β (IL-1β) and tumor necrosis factor-α (TNF-α) expression, neuronal nitric oxide synthase (nNOS) and inducible NOS (iNOS) expression in ischemic brain tissues. Moreover, microglial immunoreactivity was also determined. Caspase-3 activity and TUNEL staining were done to evaluate cellular apoptosis.

Results: Agmatine treatment decreased blood glucose level in STZ-induced rats mildly. Agmatine treatment significantly improved neurobehavioral activity, and reduced infarct size and edema volume in diabetic MCAO30 rats at 1 and 3 days reperfusion period compared with no treatment group ($P < 0.01$). Western blotting and immunohistochemistry results depicted that agmatine treatment significantly down-regulated NF-kB mediated inflammatory signaling, expression of nNOS and iNOS, and microglia immunoreactivity in diabetic MCAO30 rats at 1 and 3 days reperfusion period ($P < 0.05$). Moreover, Immunohistochemistry and TUNEL staining results showed that agmatine treatment significantly decreased number of caspase-3-positive and TUNEL-positive cells in diabetic MCAO30 rats at 1 and 3 days reperfusion period, respectively ($P < 0.01$).

Conclusion: The obtained results suggest that agmatine may protect brain from focal cerebral ischemic injury in diabetes partly due to its anti-inflammatory properties.

This research was supported by Basic Science Research Program through the National Research Foundation of Korea (NRF) funded by the Ministry of Education, Science and Technology (2010-0012797)

655

CAN EARLY MRI BE USED TO IMPROVE THE STATISTICAL QUALITY OF EXPERIMENTAL STROKE STUDIES?

C. Leithner, M. Füchtemeier, M. Foddis, U. Dirnagl, G. Royl

Experimental Neurology, Charite Universitaetsmedizin, Berlin, Germany

Objectives: Successful treatment of experimental stroke has not been translated to clinical use for a number of reasons, among them poor statistical quality of animal studies. Variability of infarct sizes induced by middle cerebral artery occlusion (MCAO) contributes to low power of statistical tests comparing placebo and treatment groups. Noninvasive early (pre-treatment) determination of ischemic lesion sizes could in principle be used to improve assessment of treatment effects. We therefore investigated whether combined information from early MRI and day two infarct size measurement can improve statistical parameters compared to infarct size measurement alone.

Methods: 103 C57/Bl6 mice were subjected to MCAO of 45 or 90 minutes duration. MRI measurements were performed either during, at 3h or 6h after MCAO and at day 2 for all animals. For early MRI ADC, DWI, CBF, T1 and T2 images were obtained. At day two, T2 was measured to determine infarct size. Timecourses of absolute hemispheric and regional ADC, T1 and CBF and lesion sizes for all MRI sequences were obtained. Correlation coefficients of early MRI parameters with day 2 T2 lesion sizes were calculated. The effect of early reperfusion (45 min. vs. 90 min.) was assessed statistically 1) by infarct size determination at day two alone and 2) by measurement of lesion size changes from early MRI to MRI at day two.

Results: During MCAO, CBF and ADC decreased in large parts of the affected hemisphere. At 3 hours after MCAO, CBF demonstrated reperfusion and ADC completely normalized in the 45 minutes MCAO group and partially in the 90 minutes MCAO group. At 6h after MCAO new ADC lesions could be detected in both groups compared to ADC lesions at 3h. Among the modalities investigated (CBF, ADC, DWI, T1, T2) ADC correlated best with day two lesion size. Correlation of early ADC with final lesion sizes was higher for ADC lesion during MCAO than at 3 hours after MCAO because of total (45 min MCAO) or partial (90 min MCAO) ADC normalization, but increased again substantially with decreasing ADC at 6h. The effect of early reperfusion on infarct sizes could be demonstrated with higher power and lower p-value when evaluating lesion size changes from early MRI to MRI at day two compared to assessment at day two alone.

Conclusions: Among routine MRI sequences, early ADC best predicted infarct sizes. Predicition accuracy temporarily decreased after reperfusion due to ADC normalization at 3 hours after MCAO and depended on brain region, duration of ischemia and timepoint of MRI measurement. A preliminary analysis evaluating the effect of early versus late reperfusion suggests that incorporating early ADC lesion measurement during MCAO in the statistical analysis may allow improvement of statistical parameters for experimental stroke studies compared to final lesion size measurement alone.

656

EFFECT OF A CXCR2 ANTAGONIST ON BRAIN INFLAMMATION AND INFARCT VOLUME AFTER STROKE IN MICE

C.G. Sobey, V.H. Brait, J. Rivera, B.R.S. Broughton, S. Lee, G.R. Drummond

Department of Pharmacology, Monash University, Clayton, VIC, Australia

Objectives: Stroke induces brain inflammation and the infiltration of leukocytes. Leukocyte chemotaxis is predominantly mediated by chemotactic cytokines, known as chemokines. CXCL1 and CXCL2 are chemokine ligands released by monocytes and neutrophils with strong neutrophil chemoattractant activity via the neutrophil CXCR2 receptor. This study aimed to identify chemokine-related targets in the brain after stroke, and to examine the efficacy of administering a CXCR2 antagonist as a potential therapeutic.

Methods: We examined the mRNA expression profiles of chemokines, chemokine receptors and chemokine-related genes, including CXCL1, CXCL2 and CXCR2, in the brain of male mice after 30 min intraluminal filament-induced middle cerebral artery occlusion (MCAO) using a SYBR green PCR array. We then confirmed these findings for CXCL1, CXCL2 and CXCR2 using specific Taqman gene expression assays. We next treated mice with vehicle (1% DMSO) or a CXCR2 antagonist, SB225002 (SB; 2 mg/kg per day, i.p.) commencing at reperfusion, and examined the effect on chemokine-related gene expression, neutrophil infiltration (myeloperoxidase immunohistochemistry) and stroke outcome.

Results: The mRNA expression of 49 chemokines, chemokine receptors and chemokine-related genes in the PCR array, including CXCL1, CXCL2 and CXCR2, increased by at least 2-fold at 4, 24 and/or 72 h after MCAO. When using specific Taqman gene expression assays, CXCL1 mRNA expression was increased 6-, 29- and 7-fold; CXCL2 was increased 17-, 101- and 77-fold; and CXCR2 was increased by 4-, 3- and 12-fold at 4, 24 and 72 h after MCAO, respectively. Expression levels of CXCL1, CXCL2 and CXCR2 after 24 h in SB-treated mice were reduced to 12%, 13% and 9%, respectively, of the levels in vehicle-treated mice. At 72 h, myeloperoxidase-positive cell infiltration was significantly reduced in SB-treated mice compared with vehicle-treated mice, and was similar to levels in sham-operated mice. However, while these findings indicate that SB effectively antagonized the interaction between CXCR2 and its chemokine ligands in the ischemic brain, we found that compared with vehicle treatment (n=7), mice treated with SB (n=9) had similar motor impairment as assessed by neurological deficit score or hanging wire latency (vehicle: 34±7 s; SB: 27±8 s; P=0.50) and a similar infarct volume (vehicle: 18±5mm^3; SB: 23±8mm^3; P=0.62) at 72 h.

Conclusions: The reduced neutrophil-related brain inflammation produced by SB administration does not improve outcome at 72 h after cerebral ischemia-reperfusion, and therefore CXCR2 is not likely to be a potential therapeutic target after ischemic stroke. However, this study also revealed that there is increased expression of many other chemokine-related genes in the brain after stroke and future studies will assess whether pharmacological targeting of some of their proteins might be beneficial post-stroke.

657

INTRAVENOUS PERFLUOROCARBONS WITH NORMOBARIC HYPEROXIA HAVE THE POTENTIAL TO SALVAGE ISCHAEMIC PENUMBRA IN ACUTE STROKE AND REDUCE FINAL INFARCT

G.A. Deuchar[1], C. Santosh[2], D. Brennan[2], W.M. Holmes[1], I.M. Macrae[1]

[1]Glasgow Experimental MRI Centre, Institute of Neuroscience and Psychology, College of Medical, Veterinary and Life Sciences, University of Glasgow, [2]Institute of Neurological Sciences, Southern General Hospital, Glasgow, UK

There is an urgent requirement for new safe & effective stroke therapeutics. Potentially salvageable penumbral tissue has a limited lifespan and, without intervention, becomes incorporated into irreversibly damaged ischaemic core in the first hours post-stroke. Although the use of hyperoxia has been proposed as a therapy in stroke, blood has a limited capacity to dissolve oxygen. Perfluorocarbons (PFCs, particle size ~0.2μm) are non-toxic oxygen carriers with an unrivalled capacity to dissolve gases including oxygen. Emulsified PFCs injected systemically can penetrate microcirculation normally only occupied by plasma and oxygenate ischaemic tissues where vasoconstriction or occluding emboli prevent perfusion of red blood cells.

Objectives: Using a rodent stroke model and magnetic resonance imaging (MRI) we tested the ability of PFC+hyperoxia to support penumbra survival and carried out a pilot neuroprotection study to investigate its potential as a novel stroke therapeutic.

Methods: Focal cerebral ischemia was generated in male Sprague Dawley rats (n=31) using the intraluminal filament model of permanent middle cerebral artery occlusion (MCAO).

Study 1: Following MCAO, serial scanning (Bruker 7T Biospec) produced maps of ischaemic injury (from apparent diffusion coefficient, ADC maps) and cerebral blood flow (arterial spin labelling) to define penumbra from perfusion diffusion mismatch.

Lactate data were generated in the following regions of interest: ischaemic core, corresponding contralateral striatum and penumbra, using localised ^{1}H MR spectroscopy. Initial baseline spectra were acquired for each region with the animal ventilated on air. Intravenous PFC (1.5ml, n=7) or saline (1.5ml, n=6) was followed by 30mins 100% O_2 during which 3 blocks of spectra were acquired. Ventilation was then switched back to normoxia for 30mins and a further 3 blocks of spectra acquired.

Study 2: For our pilot neuroprotection study (n=6 in each group) 60%O_2 was administered from 10mins post-MCAO for 6 hours along with either 1.5ml PFC or saline at 20min and 1ml at 3hrs post-MCAO. Normoxic controls were maintained on ~26%O_2 for 6 hours. Animals were recovered and infarct size determined 24hrs post-stroke. Data are presented as mean±SEM.

Results: Penumbra lactate increased by 7.1% during 30mins hyperoxia and by a further 33.7% following return to air (30mins) in the control saline group (Figure 1a). In the PFC group, penumbral lactate decreased by 20.8% during hyperoxia with a 15.2% increase on returning to air, thereby maintaining levels below the pre-hyperoxia baseline. ADC lesion expansion during 30mins O_2+30mins air, was 69±7mm^3 in the saline group and 37±10 mm^3 in the PFC group ($p< 0.05$). In Study 2, PFC+hyperoxia treatment significantly decreased infarct volume (149.9±22.9mm^3 vs 244.5±29.0mm^{33} in untreated MCAO rats, Figure 1b).

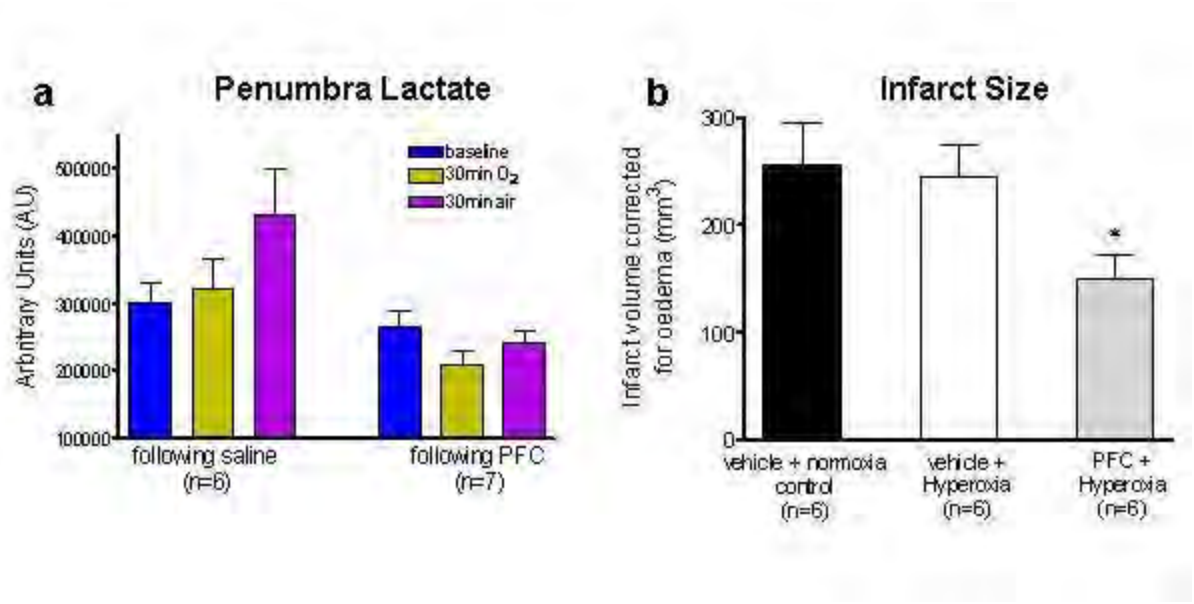

[Figure 1]

in saline+hyperoxia and 255.6±39.8mm**Conclusion:** PFC plus normobaric hyperoxia inhibited the temporal increase in lactate levels in the penumbra indicating maintenance of aerobic metabolism while preventing loss of penumbral tissue. This suggests the potential to prolong penumbra survival and extend the time window for intervention. Our neuroprotection study further substantiates the use of PFC with normobaric hyperoxia as a potential therapeutic strategy for acute ischaemic stroke.

658

IL-23 PRODUCTION FROM INFILTRATING MACROPHAGE IN THE ISCHEMIC BRAIN IS DEPENDENT ON TLR SIGNALING PATHWAY

T. Shichita[1,2], H. Ooboshi[3], I. Takada[1], T. Ishii[4], K. Kuroda[5], K. Miyake[6], A. Yoshimura[1]

[1]Department of Microbiology and Immunology, School of Medicine, Keio University, Tokyo, [2]Department of Medicine and Clinical Science, Graduate School of Medical Sciences, Kyushu University, [3]Department of Internal Medicine, Fukuoka Dental College Medical and Dental Hospital, Fukuoka, [4]Institute of Community Medicine, University of Tsukuba, Tsukuba, [5]Department of Immunology and Microbiology, Nihon University, School of Medicine, [6]Division of Infectious Genetics, Institute of Medical Science, University of Tokyo, Tokyo, Japan

Background: IL-23 plays an important role in the initiation of inflammatory response in the early phase of ischemic brain injury[1]. IL-17-producing γδT lymphocytes, which are induced by IL-23, exaggerate ischemic injury in the delayed phase. Recently, Toll like receptor (TLR) signaling is also implicated in the ischemic brain injury[2]. Therefore, we investigated the relationship between TLR signaling and IL-23/IL-17 pathway.

Method: Using MyD88 and TRIF knockout (KO) mice, the expression of inflammatory cytokines in the infiltrated cells which were collected by Percoll density centrifugation was investigated by real time PCR. The expression was also analyzed in bone marrow (BM) chimera using TLR2/4, TLR9 and IL-23 KO BM.

Results: Using gene depletion mice, we found that IL-23 production from infiltrated macrophage was completely dependent on MyD88, but not on TRIF, pathway. Using BM chimeric mice, it was clarified that TLR2 and TLR4 signaling pathway, but not on TLR9, induced IL-23 production from infiltrated macrophage. The expression of IL-1β and TNF-α was also mediated by TLR2/4 signals.

Conclusion: We found that IL-23 production from the infiltrated macrophage was MyD88 dependent and mediated by TLR signaling pathway in the ischemic brain. By targeting this specific inflammatory pathway, we may develop a new neuroprotective strategy.

Reference:

1 Shichita T, Sugiyama Y, Ooboshi H, Sugimori H, Nakagawa R, Takada I, Iwaki T, Okada Y, Iida M, Cua DJ, Iwakura Y, Yoshimura A. Pivotal role of cerebral interleukin-17-producing gammadelta T cells in the delayed phase of ischemic brain injury. Nat Med. 15(8):946-50 (2009)

2 Caso JR, Pradillo JM, Hurtado O, Lorenxo P, Moro MA, Lizasoain I. Toll-like receptor 4 is involved in brain damage and inflammation after experimental stroke. Circulation. 115(12):1599-1608 (2007)

659

MONITORING OF HEMODYNAMIC CHANGES USING A TELEMETRIC NIRS SYSTEM WITH HIGH TEMPORAL RESOLUTION DURING CAROTID ARTERY STENTING

T. Igarashi[1], K. Sakatani[1,2], N. Fujiwara[1], Y. Murata[1], T. Suma[1], T. Shibuya[3], T. Hirayama[1], Y. Katayama[1]

[1]Division of Neurosurgery, Department of Neurological Surgery, [2]Division of Optical Brain Engineering, Department of Neurological Surgery, Nihon University School of Medicine, Tokyo, [3]Department of Neuroendovascular Therapy, Sagamihara Kyodo Hospital, Sagamihara, Japan

Introduction: Carotid artery stenting (CAS) is a less invasive revascularization strategy than carotid endarterectomy (CEA) in patients with atherosclerotic carotid-artery stenosis. In order to avoid stroke and postprocedural embolic events, it is important to use embolic protection devices during CAS. It has been demonstrated that CAS with an emboli-protection device is not inferior to carotid endarterectomy among patients with severe carotid-artery stenosis. However, if blood flow in the internal carotid artery (ICA) is reduced by the device's filter, cerebral hyoperfusion occurs and this increases the probability of postprocedural ischemic stroke. Therefore, monitoring of hemodynamic changes is important to reduce surgical risk. In the present study, we employed a telemetric NIRS system with high time resolution to monitor hemodynamic changes during CAS with an emboli-protection device.

Materials and methods: We evaluated 16 patients with ICA stenosis who underwent CAS. CAS was performed by transfemoral intra-arterial catheterization under distal filter protection with an AngioguardXPR To verify filter patency, angiographic controls were obtained in all cases before and after stent replacement. We measured the concentration changes of oxy-Hb, deoxy-Hb and total-Hb in the bilateral frontal lobe using a NIRS equipped with a wireless communication device (Pocket NIRS, Hamamatsu Photonics K.K., Japan) during the whole CAS procedure. The sampling rate was 61.3 Hz (i.e., sampling time was about 16.3 msec). The NIRS probes were set symmetrically on the forehead with a flexible fixation pad. We analyzed the NIRS parameter changes using two kinds of analytical methods. First, we analyzed concentration changes of oxy-Hb, deoxy-Hb and, t-Hb. Second, we analyzed pulsatile fluctuations in oxy-Hb that synchronized with heart beats. We calculated mean values of five peak-to-peak amplitudes of oxy-Hb before and after dilation of the balloon.

Results: NIRS revealed decreases of oxy-Hb and t-Hb associated with an increase of deoxy-Hb immediately after ICA occlusion. We investigated whether the changes in Hb concentrations were influenced by the presence of anterior cross circulation. Total and oxy-Hb concentrations decreased during ICA occlusion in the cases with Cross Circulation (-), whereas Hb concentrations did not change or changed only a little in the cases with Cross Circulation (+). Analysis of fluctuations of oxy-Hb demonstrated decreases of the peak-to-peak amplitude of oxy-Hb not only in the cases with Cross Circulation (-), but also those with Cross Circulation (+). In addition, analysis of fluctuations of oxy-Hb could detect occurrence of filter obstruction (i.e., no/slow flow) which did not cause changes in Hb concentrations.

Conclusion: The fluctuation of oxy-Hb measured by the present NIRS system appears to reflect the oscillatory wave caused by heart beat. Analysis of the fluctuation was a more sensitive tool to detect hemodynamic changes during CAS compared with conventional analysis of Hb concentrations. We conclude that the present NIRS system is useful to monitor hemodynamic changes during CAS.Acknowledgement: This work was supported by Grants-in-

Aid from the Ministry of Education, Culture, Sports, Science and Technology of Japan (Strategic Research Program for Brain Sciences).

661

TARGETED MUTATION OF FAS LIGAND GENE ATTENUATES BRAIN INFLAMMATION IN EXPERIMENTAL STROKE

F.-N. Niu[1], X. Zhang[2,3,4], X.-M. Hu[5], J. Chen[5], Z. Liu[1,4,6], Z.-Y. Wang[2,3,4], L.-L. Chang[1], J.-W. Li[1,3,4], Y. Xu[1,2,3,4]

[1]Department of Neurology, Drum Tower Hospital of Nanjing Medical University, [2]Department of Neurology, Affiliated Drum Tower Hospital, Nanjing University Medical School, [3]The State Key Laboratory of Pharmaceutical Biotechnology, Nanjing University, [4]Jiangsu Key Laboratory for Molecular Medicine, Nanjing, China, [5]Department of Neurology, University of Pittsburgh School of Medicine, Pittsburgh, PA, USA, [6]The State Key Laboratory of Pharmaceutical Biotechnology,Nanjing University, Nanjing, China

Objective: Neuro-inflammation has a detrimental effect on the pathophysiology of ischemic stroke. Recent studies suggest that the Fas/FasL system, in addition to its importance in triggering apoptotic cell death, plays a central role in inflammation in central nervous system (CNS)[1, 2]. The purpose of this study was to investigate the inflammatory role of FasL in experimental stroke.

Methods: Focal cerebral ischemia was induced in the FasL mutant (gld) and wild type (B6) mice by transient middle cerebral artery occlusion (MCAO) for 2 h, followed by 24 h of reperfusion. Sensorimotor dysfunction was assessed by neurological severity score, infarct volume was measured by TTC staining and brain edema was determined by water content assessment. Real-time PCR was used to detect mRNA expression of several inflammatory cytokines and chemokines. Protein expression patterns of $GFAP^+$, $Iba1^+$, MPO^+ and $CD3^+$ and Annexin V were observed by immunostaining. T lymphocytes subpopulations were assayed by flow cytometry (FACS) and the activation of MAPK signal pathways (ERK, JNK and p38) was detected by western blot.

Results: FasL mutation profoundly decreased brain damage and improved neurological performance 24 h after ischemic stroke. The production of inflammatory cytokines and chemokines in the brain was attenuated in gld mice after ischemia in the absence of dramatic change in cell apoptosis. FasL mutation attenuated the recruitment of peripheral inflammatory cells (MPO^+ neutrophil) and the activation of residential glial cells ($Iba1^+$ microglia and $GFAP^+$ astrocyte). FasL mutation also resulted in T lymphocyte subset reprogramming, characterized by a reduction of $CD3^+CD8^+$ T cells and a skew of the Th1/Th2 balance towards Th2 in the brain and blood plasma. Moreover, our results suggest that the inflammatory role of FasL might be enacted through soluble FasL (sFasL). Finally, FasL mutation was found to block ischemia-induced JNK activation, but has no affect on p38 or ERK activation.

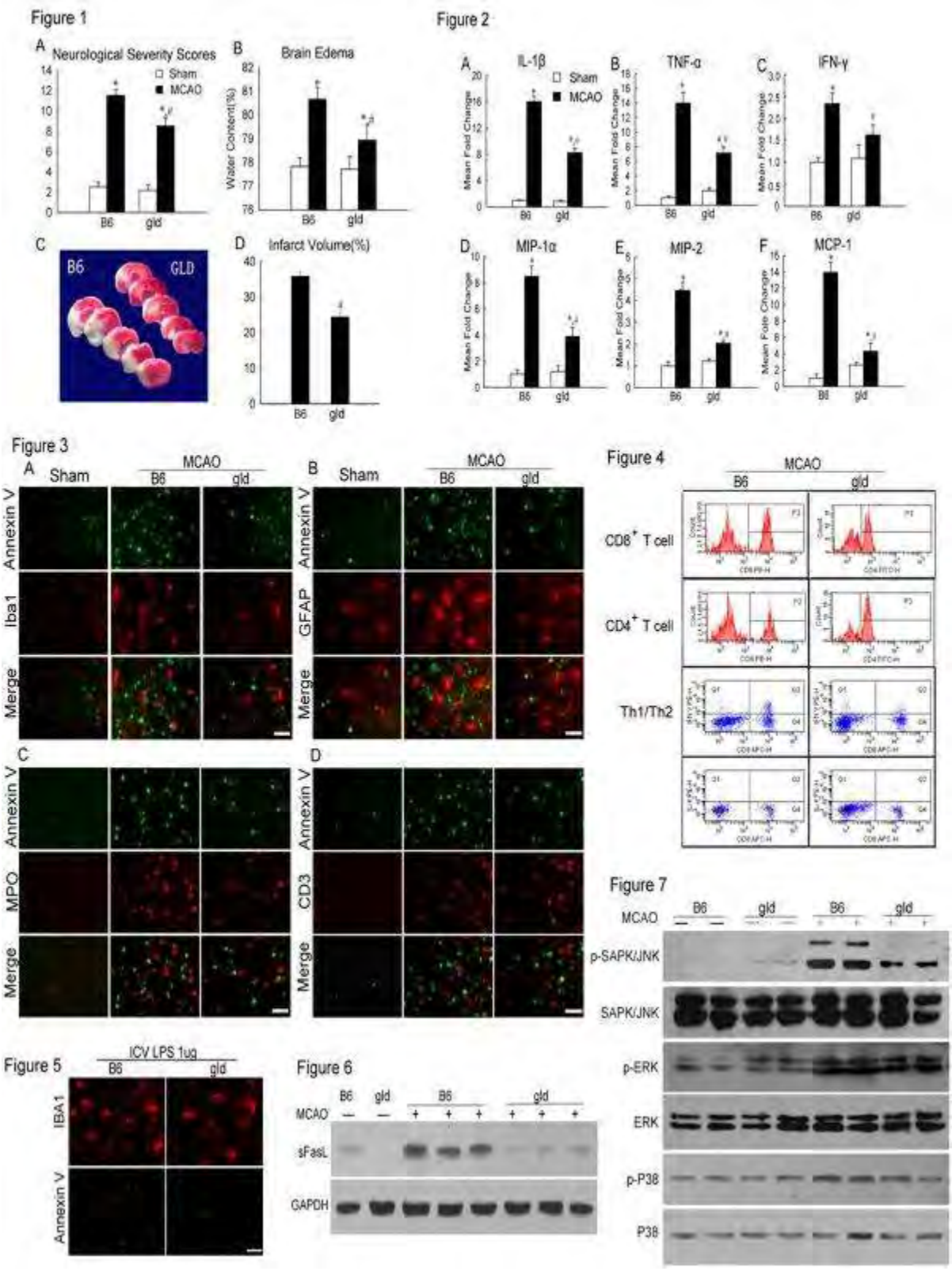

[Figure attachment]

Conclusion: Take together, these data support the hypotheses that: 1) FasL plays an inflammatory role in the pathophysiology of focal cerebral ischemia independent of the pro-apoptotic role of the Fas/FasL system, and 2) the recruitment of inflammatory cells through FasL and the activation of JNK pathway[3] might be an underlying mechanism of FasL-mediated inflammation. Immunotherapy targeting the FasL pathway may thus be promising avenue to prevent inflammatory reactions and improve the prognosis of patients with ischemic stroke.

Key Words: FasL, stroke, inflammation, T lymphocytes

Reference:

1. Askenasy N, Yolcu ES, Yaniv I, Shirwan H (2005) Induction of tolerance using Fas ligand: a double-edged immunomodulator. Blood. 105:1396-404

2. Lettau M, Paulsen M, Kabelitz D, Janssen O (2009) FasL expression and reverse signalling. Results Probl Cell Differ. 49:49-61

3. Sun M, Fink PJ (2007) A new class of reverse signaling costimulators belongs to the TNF family. J Immunol. 179:4307-12

662

INFLUENCE OF GESTATIONAL-AGE ON FIBRINOLYSIS FROM BIRTH TO POSTNATAL DAY 10

P. Leroux[1], L. Sentilhes[2], S. Radi[3], A. Ricbourg-Schneider[2], V. Laudenbach[1,3], L. Marpeau[1,2], J. Benichou[4], M. Vasse[5], S. Marret[1,3]

[1]EA4309- NeoVasc, University Rouen, [2]Obstetrics and Gynecology, [3]Neonate Pediatrics, [4]Biostatistics, [5]Dept. of Biological Resources, Rouen University Hospital, Rouen, France

Severe germinal matrix hemorrhage-intraventricular hemorrhage (GMH-IVH) with subsequent periventricular hemorrhagic infarction is a major source of adverse neurodevelopmental outcomes in preterm infants. Although GMH-IVH occurs in only about 5% of all preterm infants, PVHI rates of up to 20%-30% occur in infants weighing less than 750g at birth. The pathogenesis of GMH-IVH may involve immaturity of the germinal matrix vessels, whose endothelial cells proliferate actively. Differences between premature and full-term neonates in the levels of coagulation system components, most notably those involved in fibrinolysis, may facilitate the onset and progression of GMH-IVH in very preterm infants.

In this study, we compared the fibrinolytic status in neonates at different gestational age and in their mother. We measured the antigen levels of tissue-type plasminogen activator (t-PA), plasminogen activator inhibitors-1 (PAI-1) and -2 (PAI-2), and thrombin activated fibrinolysis inhibitor (TAFI), as well as PAI-1 activity at birth in cord blood, then in infants at day 3 and day 10 in extremely preterm (EP; < 30 gestation weeks (GW)), very preterm (VP; 30-33GW), moderately preterm (MP; 34-36GW) and full-term neonates (FT, 37 or more GW). The same components were also assessed for the mothers at delivery, as maternal fibrinolytic activity decreases during pregnancy, most notably in the third trimester, and as we could not exclude a relationship between maternal fibrinolytic status and fibrinolytic status in the infants. We studied 40 mother/child couples; 10 EP, 10 VP, 10 MP and 10 FT neonates.

Similar high PAI-2 levels were measured in mother's blood whatever the term of gestation end (1.03µg/mL (0.42-1.73); 1.13µg/mL (0.49-2.87); 1.03µg/mL (0.41-2.47) and 0.88µg/mL (0.21-1.35) in EP, VP, MP and FT groups, respectively). This observation is contradictory to the PAI-2 increase reported during the third gestation trimester. As PAI-2 levels were below detection limit in infants and as no correlation between mother and child concentration for any factor measured could be drawn, it appears that fibrinolytic status in infants does not depend on mother. t-PA levels did not significantly differ between groups at birth. While in VP, MP and FT infants the concentration decreased from birth to day 10, in EP group t-PA concentration undergoes significant increase to levels significantly higher than those in VP and MP ($p< 0.01$ and $p< 0.001$, respectively). Similar pattern is observed for PAI-1. On day 10, PAI-1 activity was higher in EP neonates than in the three other groups ($P< 0.001$). The fibrinolytic potential appreciated as t-PA/PAI-1 activity ratio was lower in the EP and VP neonates than in the full-term neonates ($P< 0.01$ and $P< 0.05$, respectively). No difference in TAFI concentrations was observed between groups or within groups.

Previous studies reported neonatal thrombosis associated with PAI-1 mutations. The present data show postnatal abnormal evolution of t-PA and PAI-1 levels in EP infants probably resulting in hypofibrinolytic (prothombotic) status. This observation is coherent with the hypothesis of postnatal increasing risk of deep vein obstruction/thrombosis and vascular ischemia in EP infants, resulting in PVHI in the early days postnatal actually observed in high proportions in these infants.

663

DICROTIC NOTCH DEEPENING AT TRANSCRANIAL DOPPLER PREDICTS THE DEVELOPMENT OF SYNCOPE DURING HEAD-UP TILT TEST

G. Rossato[1], D. Tonon[1], A.M. Corica[1], C. Bianconi[1], V.N. Thijs[2], **A. Adami**[3]

[1]Neurology Department, Ospedale Sacro Cuore, Negrar, Italy, [2]Neurology Department, Flanders Interuniversity Institute for Biotechnology, Leuven, Belgium, [3]Stroke Center, Ospedale Sacro Cuore, negrar, Italy

Introduction: Dicrotic Notch Deepening (DND) on Middle Cerebral Artery Blood Flow (MCA-BF) had been reported to precede the fall in systemic blood pressure and the onset of syncope symptoms. In this study we assessed sensitivity and specificity of this TransCranial Doppler (TCD) waveform pattern in the prediction of syncope during Head-Up Tilt test (HUT).

Methods: Patients with suspected neurocardiogenic syncope were consecutively enrolled and investigated with HUT and TCD. Systemic blood pressure and MCA-BF were continuously recorded by mean of non invasive devices (Portapres, FMS, the Netherlands; Multi-Dop T2, Sipplingen, Germany). HUT was concluded in the presence of syncope symptoms or after 30 minutes of tilting without symptoms. We measured at TCD the averaged dicrotic notch and diastolic velocities in the two minutes preceding the tilting (basal phase) and in the final two minutes of HUT (tilt phase). DND was quantified as the reduction in the difference between these two velocities between the basal and tilt phase. We finally compared DND values in patients who developed syncope and in asymptomatic patients.

Results: Twenty nine (52% females) patients were included. Mean age was 37±19 years. Twelve patients (51%) developed syncope symptoms. We observed DND in all patients. DND was however significantly greater in patients with syncope (12±5 Vs 5±3 cm/sec. $p< 0.001$). DND preceded the fall in blood pressure and syncope in all patients. A dicrotic notch deepening as higher as 7.5 cm/sec predicted syncope with 75% specificity and 88% specificity.

Conclusions: The use of TCD might improve the diagnosis of syncope during HUT.

665

INFARCT PREDICTION USING ADC MAPS DURING MCA OCCLUSION AND AFTER REPERFUSION IN RATS

R. Tudela[1,2], G. Soria[2,3], I. Pérez-De-Puig[3], D. Ros[1,4], J. Pavía[1,5], A.M. Planas[2,3]

[1]Research Networking Centre in Bioengineering, Biomaterials and Nanomedicine (CIBER-BBN), [2]Experimental MRI 7T Unit, IDIBAPS, Barcelona, Spain, [3]Department of Brain Ischemia and Neurodegeneration, Institut d'Investigacions Biomèdiques de Barcelona (IIBB)-Consejo Superior de Investigaciones Científicas (CSIC), [4]Biophysics and Bioengineering Laboratory, University of Barcelona, [5]Nuclear Medicine Department, Hospital Clinic, Barcelona, Spain

Objectives: Previous studies in animals have shown that magnetic resonance imaging (MRI) might be a useful tool for early prediction of tissue outcome after stroke (1). Studies of prediction of final infarction reveal the strong contribution of the apparent diffusion coefficient (ADC) (2). In this study we compared ADC maps at two different time points individually and combined in a voxel-by-voxel basis to estimate the infarct, which was determined by T2 mapping at 7 days.

Methods: Longitudinal MRI scans were performed in rats under isofluorane anesthesia in a BioSpec 70/30 horizontal animal scanner (Bruker BioSpin, Ettlingen, Germany), equipped with a 12 cm inner diameter actively shielded gradient system (400 mT/m) and a phased array surface coil for rat brain. MRI scans were performed with 9 male Wistar rats (weighting 250-300 gr), which underwent 90-min MCA occlusion. ADC maps were acquired before the occlusion, 60 min after the occlusion, and 60 min after reperfusion, and T2 maps were obtained 7 days later to assess final infarction. All the volumes were registered using Elastix (3) and relative differences in a voxel-by-voxel basis were computed using the pre-occlusion scans as reference values for each animal.

Results: Probability of infarct histograms were computed based on the relative ADC and T2 values obtained in 5 rats. Studies were carried out using the ADC data from occlusion and reperfusion, either separated or combined in a two-dimensional histogram. These histograms were then used to estimate the infarct in other rats using the ADC data obtained with the same experimental protocol. Predicted infarction in these animals was then compared to the actual lesion evaluated by T2 at 7 days. There were some differences between areas affected in the ADC maps obtained during occlusion and after reperfusion. While the ADC infarct values during occlusion had a relative decay from 20% to 60%, the change at reperfusion was from 40% to 80%. Topographically, the area affected during occlusion did not fully match the area affected at reperfusion. The information from the ADC during occlusion is more precise than that obtained at reperfusion to determine the location and extension of the infarct. Combining the ADC information from the two time points provided a more accurate estimation of the core of the infarct and of the areas differently affected during the occlusion and at reperfusion.

Conclusions: Hyperacute ADC data provide an estimation of the location and severity of infarction. By comparing data obtained during occlusion and after reperfusion, a better estimation of infarction was obtained when using the information acquired during the occlusion. Combining occlusion and reperfusion ADC maps, using a two-dimensional look-up table, provided a more accurate estimation of the affected areas and of the degree of alteration.

References:

1. O. Wu et al. 2007 J Cereb Blood Flow Metab 27:196-204
2. S. Huang et al. 2010 J Cereb Blood Flow Metab 30(9):1661-70.
3. S. Klein, et al., 2010 IEEE Transactions on Medical Imaging, 29(1):196-205.

667

SIGNIFICANCE OF DIASCHISIS IN FUNCTIONAL DEFICIT AND RECOVERY FOLLOWING FOCAL STROKE IN THE NON-HUMAN PRIMATE

E. Bihel, S. Valable, S. Roussel, J. Toutain, D. Divoux, M. Bernaudin, **O. Touzani**

University of Caen,UMR 6232 CI-NAPS, Caen, France

Objectives: Reduction in brain metabolism in remote regions following focal stroke has been reported both in patients and animal models. The significance of this phenomenon in functional deficits and their recovery is not well understood. In the present studies, we addressed this issue through the use of longitudinal positron emission tomography (PET) investigations and behavioural tests in a model of transient ischemia in the non-human primate.

Methods: Under anaesthesia with isoflurane, three marmosets were subjected to 3 hour intraluminal middle cerebral artery occlusion (MCAO) and two marmosets were sham-operated (Bihel et al., 2010). Each animal underwent 3 sessions of MRI (7T, Pharmascan; Bruker Biospin) at 60min, 7days and 42days following MCAO. Each MRI examination was followed by a PET scan (micro-PET INVEON Siemens) with [18F]-FDG. Glucose consumption (CMRglu) was quantified in the ischemic lesion and in remote areas known to display diaschisis: thalamus, substantia nigra (SN) and cerebellum. During 42days following the occlusion, a battery of behavioral tests were performed weekly to analyse the evolution of sensorimotor deficits.

Results: In sham-operated animals, no abnormality has been observed on MRI and PET images. In these animals CMRglu values were similar to those reported in human's brain (25-35 µmol/100g/min in the cortex). In animals subjected to ischemia, the MRI-defined lesion at the acute and subacute stages affected the striatum and in a lesser extent the cortex. At the chronic stage, no apparent lesion was visible on DWI and T2-MRI.

As early as 2 hours following the occlusion, a decrease in CMRglu was observed in the ipsilateral thalamus and substantia nigra (-13.9±4.3% and -17.4±3.8%, compared to the contralateral structures, respectively) and the contralateral cerebellum (-9.1±15.1%, compared to ipsilateral one). These data reveal the presence of diaschisis early following stroke. In the subacute stage (i.e. 7 days following MCAO), these remote alterations of CMRglu were more pronounced (-16.8±2.1; -22.1±5.6; -13.1±4.6, respectively in the ipsilateral thalamus, the ipsilateral SN and the contralateral cerebellum). At the chronic stage (i.e. 42 days post-MCAO), there was an increase of CMRGlu in the initially lesioned zone (+37.7±9.9% in the striatum) and the complete resolution of reduced GMRglu in the remote areas.

Transient ischemia in the marmoset induced several sensorimotor deficits that recovered progressively but only partially. To examine the relationships between diaschisis and the evolution of the functional deficits, the persistent contralateral sensorimotor impairments were correlated with the magnitude of the decrease in CMRglu in distant structures. Several significant correlations were found between the subacute diaschisis and the functional deficits assessed at 1 week following the occlusion (e.g. thalamic diaschisis and hemianesthesia R^2=0.73). Moreover, subacute diaschisis was also correlated with the chronic deficits assessed at 6 weeks following the occlusion (e.g. thalamic diaschisis and hemianesthesia R^2=0.96)

Conclusions: The data show for the first time that the values of brain glucose consumption in anaesthetized marmosets are similar to those measured in the human brain. The data also

suggest that the severity of functional deficits and the recovery after focal cerebral ischemia could be related to the magnitude of diaschisis.

670

SERIAL DIFFUSION TENSOR IMAGING SUGGESTS PROGRESSIVE PATHOPHYSIOLOGY FOR WEEKS FOLLOWING TRAUMATIC BRAIN INJURY, AND WHITE MATTER REPAIR MONTHS AFTER INJURY

V. Newcombe[1,2], G. Williams[2], J. Outtrim[1], D. Chatfield[1], M.G. Abate[1], T. Geeraerts[1], A. Manktelow[1], P. Hutchinson[1], J. Coles[1,2], D. Menon[1,2]

[1]Division of Anaesthesia, [2]Wolfson Brain Imaging Centre, University of Cambridge, Cambridge, UK

Introduction: It is becoming clear that many of the sequelae of Traumatic Brain Injury (TBI) are not just a direct consequence of the acute event, but represent a dynamic process, with changes occurring many years after the event. Such ongoing pathophysiology raises the hope for effective late treatments. However, a rational definition of the therapeutic window critically depends on being able to define the temporal pattern of such progression. Diffusion tensor imaging (DTI) is more sensitive than conventional CT or MR at showing the extent and distribution of injury following TBI, and so is a promising imaging marker for TBI. However, data on the temporal pattern of changes in diffusivity parameters remain incomplete.

Methods: Ten patients (six male) underwent MR imaging on a minimum of three occasions; within the first 48 hours of injury, at approximately six weeks post injury, and at least six months after injury. Of these, seven also had a scan at least one year post injury. Neuropsychometric testing including motor latency was undertaken with the six and one year scans, and correlated with imaging findings. 40 healthy volunteers were used as a control group. Ethical approval was obtained from the Local Research Ethics Committee and informed consent was obtained in all cases. MR imaging was performed using a 3 Tesla Siemens TIM Trio, and included DTI. Fractional anisotropy (FA) and apparent diffusion coefficient (ADC) maps were created using FDT. Mean FA and ADC for the anterior corpus callosum, the posterior corpus callous, frontal white matter and posterior white matter were calculated. Non-parametric statistics were used.

Results: In all ROIs at all time points the patients' FA was significantly lower than controls. FA continued to decrease from the first scan to a nadir at scan 3. FA in patient ROIs remained significantly lower than the control group at Scan 4, but was significantly higher than Scan 3 levels. ADC was significantly increased in the acute phase post injury in all ROIs except for the posterior corpus callous, and was significantly increased in all ROIs over the subsequent time points except for the posterior corpus callosal ADC in scan 4. The patterns of change in FA and ADC seen across the patient group were consistently reflected in individual data. All patients improved motor latency between Scans 3 and 4, and this change significantly correlated with the change in FA in the anterior and posterior corpus callosum ($r = 0.736$, $p = 0.036$ and $r = 0.607$, $p = 0.024$ respectively).

Conclusions: DTI measures of microstructural injury following TBI are consistent with ongoing subacute disease progression, and hint at the possibility of late repair. While further work is needed to correlate these structural data with neuropsychological parameters and functional outcome, and to examine longer time points, these results suggest that DTI may be a valuable tool to examine late neural injury and repair following TBI.

671

DIFFERENTIAL EFFECTS OF COLLAGEN-18 IN THE POST-ISCHEMIC BRAIN

K. Gertz, G. Kronenberg, M. Balkaya, J. Hellmann, J. Klohs, R. Heljasvaara, U. Dirnagl, M. Endres

Experimentelle Neurologie, Charité-Universitätsmedizin, Berlin, Germany

Collagen-18 is a proteoglycan component of vascular and epithelial basement membranes. Collagen-18 is involved in blood vessel development and Collagen-18 derived Endostatin functions as a potent inhibitor of angiogenesis.

Here, we investigated the differential effects over time of Collagen-18 in a model of mild ischemic stroke. Collagen-18 deficient mice and littermate controls were subjected to 30 minutes of filamentous left middle cerebral artery occlusion (MCAo) and reperfusion. Acute (48 hours) and chronic (28 days) ischemic lesion sizes were determined along with early and long-term functional outcome. Furthermore, we quantified absolute cerebral blood flow with the Iodo-C^{14}-antipyrine-technique and quantified perfused capillary density using Evans blue fluorescence within the ischemic lesion at 28 days after MCAo.

Collagen-18 deficient mice displayed increased acute lesion sizes and worse acute functional outcome. By contrast, lack of Collagen-18 conferred long-term histological and functional protection at four weeks. Collagen-18 deficient mice showed enhanced VEGF levels in serum and increased VEGF receptor mRNA expression in ischemic brain at 10 days after MCAo. In addition, we found enhanced numbers of von-Willebrand-factor/bromodeoxyuridine double-positive cells and higher densities of perfused vessels within the lesion at four weeks after MCAo, indicative of an enhanced angiogenic response in Collagen-18 deficient animals. Finally, increased vessel density was associated with higher absolute cerebral blood flow in Collagen-18 deficient mice.

In conclusion, lack of Collagen-18 aggravates acute stroke outcome, but mediates long-term protection at four weeks after the ischemic insult. These opposing effects are partially mediated by VEGF upregulation and accompanied by an enhanced angiogenic response. Interestingly, a single factor led to these widely differential outcomes after brain ischemia. Our finding underscores the need for researchers to explore complex endpoints in order to find effective new treatments for stroke.

674

ASSESSMENT OF CEREBRAL AUTOREGULATION WITH THE USE OF PSEUDORANDOM BINARY SEQUENCES

E. Katsogridakis[1], G. Bush[2], L. Fan[2], A.A. Birch[3], D. Simpson[4], R. Allen[4], R.B. Panerai[1]

[1]Department of Cardiovascular Sciences, University of Leicester, [2]Department of Medical Physics, Leicester Royal Infirmary, University Hospitals of Leicester NHS Trust, Leicester, [3]Neurological Physics Group, Department of Medical Physics and Bioengineering, Southampton University Hospitals NHS Trust, [4]Institute of Sound and Vibration Research, University of Southampton, Southampton, UK

Objectives: A wide range of methods have been proposed for the assessment of cerebral autoregulation (CA), but optimizing efficacy with clinical practicality remains a challenge. We propose a modification of the classical thigh cuff test[1], using pseudorandom binary sequences to drive the inflation and deflation of thigh cuffs, thus challenging the autoregulatory system with a broad spectrum of relatively small transients[2]. By increasing the variability of ABP in this way, we aim to improve robustness as well as the comfort of autoregulation tests. The objectives of the current report are to assess whether the intermittent inflation of thigh cuffs using random and non-random sequences[2] would result in increased ABP variability compared to baseline, and whether the increase in blood pressure variability would be dependent on the amplitude of the thigh cuff inflation pressure.

Methods: Arterial blood pressure (ABP)(Finapres, Ohmeda) and unilateral cerebral blood flow velocity (CBFV) (transcranial Doppler ultrasound, SciMed QVL 120, SciMed) were noninvasively monitored in 10 healthy adults at rest and during random and nonrandom inflation sequences with maximum thigh cuff pressures of 80 and 150mmHg. New hardware and software were developed to fill and empty bilateral thigh cuffs under strict safety controls. After obtaining the baseline recording, the sequence of four maneuvers was randomized. Power in ABP and CBFV were estimated for the frequency range of 0.05 to 0.15Hz. Mean heart rate as well as heart rate variability were calculated to assess effects on sympathetic outflow. To assess effects on CA estimates, CBFV step responses were also obtained for each maneuver. Repeated measures ANOVA was applied at $p< 0.05$.

Results: The use of pseudorandom sequences resulted in increased ABP ($p=0.001$) and CBFV ($p=0.001$) variability compared to baseline, with no significant effects on average heart rate variability ($p=0.108$) or mean heart rate ($p= 0.350$). Post hoc comparisons showed that the higher maximum pressure setting resulted in significantly higher ABP power ($p < 0.006$), whereas the lower thigh cuff pressure setting did not ($p > 0.22$) for both random and non-random sequences (Fig. 1).

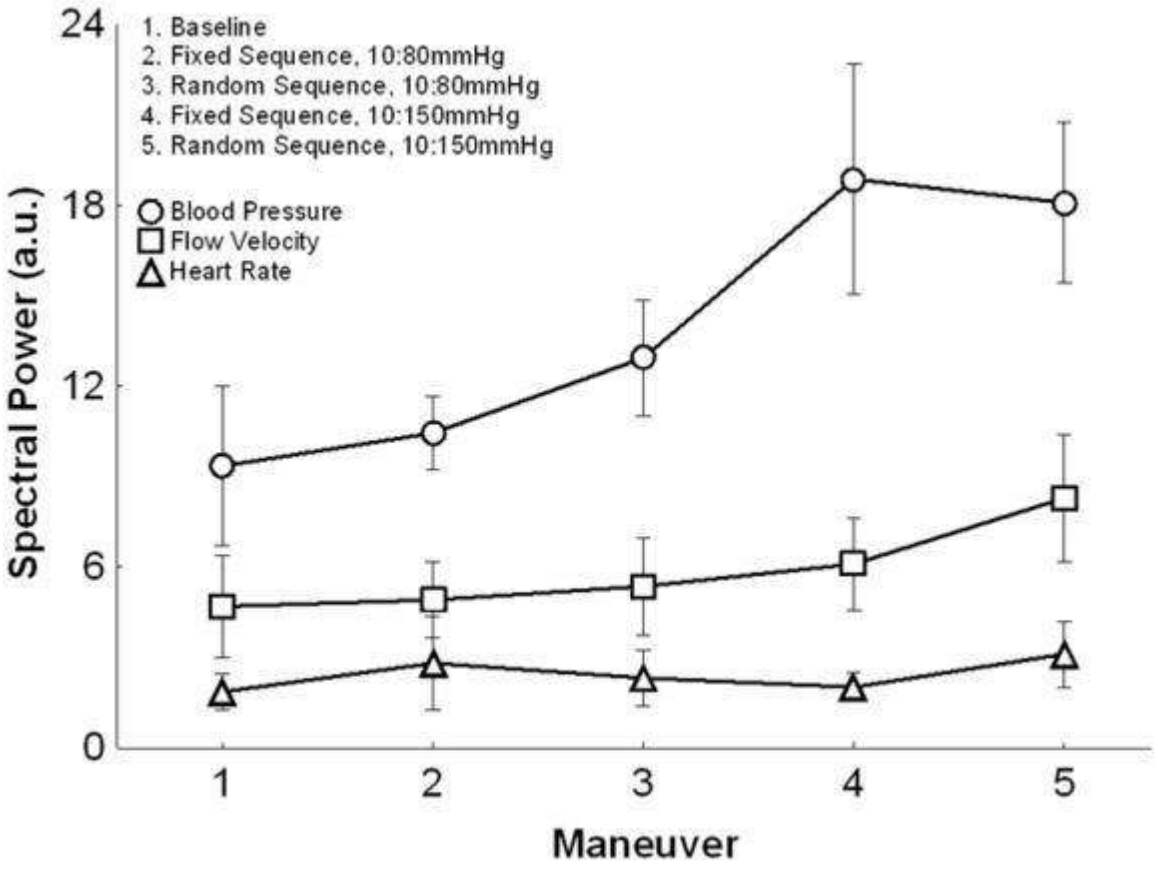

[Figure 1]

Conclusions: Pseudorandom binary sequences are an effective and safe alternative for increasing ABP variability. Significant sympathetic stimulation, or alterations in CA responses were not detected in comparison to baseline. Increased ABP variability is observed with the use of the higher thigh cuff pressure setting. This new approach shows great promise as a tool for the robust assessment of CA in different groups of patients.

675

HUMAN UMBILICAL CORD MESENCHYMAL STEM CELLS REDUCE INFLAMMATION AND PROMOTE REMYELINATION IN EXPERIMENTAL AUTOIMMUNE ENCEPHALOMYELITIS

Z. Zhang[1], R. Liu[1,2], J. Pan[1,2], L. Han[1], **Y. Xu**[1]

[1]Department of Neurology, The Affiliated Drum Tower Hospital of Nanjing University Medical School, [2]South East University Medical School, Nanjing, China

Objectives: Multiple sclerosis (MS) is a severe autoimmune disease characterized by perivascular inflammation, axonal damage and multifocal demyelination. Mesenchymal stem cell (MSC) transplantation has emerged as a promising therapeutic approach for the treatment of MS[1]. In particular, human umbilical MSCs (hUC-MSCs) exhibit a relatively high expansion capacity and low immunogenicity. The aim of this study is to examine the neuroprotective potential of transplanted hUC-MSCs on experimental autoimmune encephalomyelitis (EAE), and further explore the mechanism of immune suppression and remyelination.

Methods: Female C57BL/6 mice were inoculated with an emulsion containing 300μg of purified myelin oligodendrocyte glycoprotein (MOG) peptide in 100μl PBS and an equal volume of complete Freund's adjuvant on day 1 and day 8, respectively. In addition, 300ng of Bordetella pertusis toxin in 200μl PBS was administrated i.p.v. at both day 1 and day 3. Fifteen days following induction of EAE, hUC-MSCs (2×106 in 0.5mL, i.v.) were administered, and clinical scores were evaluated daily for 50 days. Mice were sacrificed for immunohistochemistry at 22 and 50 day post-EAE induction (acute and chronic phases, respectively) for inflammatory, axonal and myelin examination. Spleen cells were analyzed by flow cytometry for T cell populations, and the proliferation of spleen cells in vitro was assessed using the BrdU Flow kit. Cytokine levels were detected by ELISA using the supernatant of spleenocytes. The levels of the signaling pathway proteins SAPK/JNK and ERK-1/2 were measured by Western blot using phospho-specific antibodies. mRNA levels of lingo-1 were determined by quantitative Real-Time PCR assay. Statistical analyses were performed using ANOVA and Bonferroni's post-hoc comparisons, with $P< 0.05$ considered statistically significant.

Results: Treatment with hUC-MSCs decreased pathogenicity induced by MOG and improved clinical appearance. Treatment with hUC-MSCs induced a shift of T cells from Th1 toTh2 phenotype, significantly suppressed secretion of proinflammatory factors (IL-17) and increased the presence of anti-inflammatory cytokines (IL-4 and IL-10). Decreased JNK phosphorylation and increased ERK1/2 phosphorylation were evident in hUC-MSC treated mice compared to EAE-only mice. Additionally, lingo-1 mRNA was decreased by hUC-MSC treatment, suggesting the initiation of axonal regeneration following EAE when treated with MSCs.

Conclusions: These findings indicate that transplanted hUC-MSCs exert a profound beneficial effect on EAE. This effect is associated with the activation of ERK1/2 and suppression of SAPK/JNK signaling pathways. Additionally, the decreased levels of lingo-1 mRNA suggest a disinhibition of enhanced oligodendrocyte precursor cell differentiation and precocious myelination[2]. These results suggest that transplanted hUC-MSCs may serve as a potential therapeutic strategy for MS.

References:

1. Wiendl, H., Hohlfeld, R.. Multiple sclerosis therapeutics: unexpected outcomes clouding undisputed success. Neurology,2009;72(11): 1008-15.

2. Mi S, Hu B, Hahm K, Luo Y et al. LINGO-1 antagonist promotes spinal cord remyelination and axonal integrity in MOG-induced experimental autoimmune encephalomyelitis. Nat Med, 2007;13(10):1228-33.

676

LACK OF WALL TENSION IN RAT CEREBRAL ARTERIES CAUSE ENHANCED ENDOTHELIN B (ET_B) RECEPTOR CONTRATILE RESPONSES

M.N.P. Rasmussen[1], S.S. Larsen[1], L. Edvinsson[1,2]

[1]Department of Clinical Experimental Research, Research Institute Glostrup, Glostrup University Hospital, Glostrup, Denmark, [2]Division of Experimental Vascular Research, Institute of Clinical Sciences in Lund, University Hospital of Lund, Lund, Sweden

Objectives: Studies have demonstrated increased expression of ET_B receptors in cerebral vessels following a stroke or one day of organ culture. This upregulation of receptors is mediated via MAPK activation and is a transcriptional event; however, the initiating mechanism is elusive. We hypothesise that the upregulation of ET_B receptors in cerebral arteries is due to lack of tone in the vessel wall and therefore investigate the effect of isometric tension on ET_B receptor expression of cerebrovascular smooth muscle cells in middle cerebral arteries (MCA) of different size (main part and first branch segments) after myograph incubation for 4, 7 and 12 hours (h).

Methods: MCAs from adult male Wistar rats were used for the functional studies performed on wire-myographs. Concentration-response curves to S6c (10^{-13}M-3*10^{-9}M) were generated after 4, 7 and 12 h of incubation in the myograph with changes of buffer solution every 30 minutes and constant pH. The contractile response is given as % of max contraction to a 125 mM K^+ solution or in absolute milli Newton (mN). Isometric tension is defined as applying the vessel segments with a transmural pressure of 67.5 mmHg (9 kPa) independent of the internal circumference of the different segments.

Results: The first branch MCA segments, incubated without isometric tension, showed a significant increase in ET_B mediated contractility after 12 h (1.62mN/63.5% ± 0.24mN/4.9%) compared to first branch segments incubated with tension (0.37mN/24.5% ± 0.08mN/4.2%); $p < 0.05$ in all. In addition, a tendency to enhanced ET_B mediated contraction was seen in first branch segments without tension as compared to with tension after 7 h incubation (no tension: 29.1% ± 6.2%; tension: 14.6% ± 3.3%; $p = 0.05$). A significant increase in contractility via ET_B receptors was seen in MCA first branch segments with tension from 4 h (9.5% ± 2.5%) to 12 h (24.5% ± 4.2%), this was significantly less than that seen in vessel segments without tension after 12 h (1.62mN/64.1% ± 0.24mN/4.8%).

MCA main part segments showed after 12 h incubation without tension a somewhat stronger ET_B receptor activation than vessels with tension (no tension: 28.1% ± 6.8%; tension: 12.8% ± 6.5%; $p = 0.15$). Furthermore, there was a significant difference in the ET_B mediated contractility between the first branch (63.5% ± 4.9%) and the main part (28.1% ± 6.8%) of MCA following 12 h of incubation.

The ET_B upregulation in the first branch segments without tension is markedly reduced (from 59.8% ± 7.5% to 25.3% ± 4.9%) by adding the MEK-ERK1/2 inhibitor U0126 (10 µM).

Conclusions: In the absence of tone there is a time dependent increase in the ET_B mediated contraction of the MCA; this is more pronounced in the first branch as compared to the main trunk of the MCA. Thereby wall tension seems to have an inhibiting/stabilizing effect on the contractile response of ET_B. The ET_B mediated contractility is most likely due to increased ET_B

receptor transcription because the MEK1/2 inhibitor U0126 markedly reduced the ET_B mediated response.

677

CAMK INHIBITION ATTENUATES ENDOTHELIN RECEPTOR UP REGULATION AFTER SUBARACHNOID HEMORRHAGE

R. Waldsee, G. Povlsen, L. Edvinsson

Clinical Science, Experimental Vascular Research, Lund, Sweden

Objective: Delayed cerebral vasospasm has long been recognized as an important cause of poor outcome after a successful treatment of a ruptured intracranial aneurysm in subarachnoid hemorrhage (SAH) patients. It has been hypothesized that cerebrovascular upregulation of vasoconstrictor receptors has an important role in the development of late cerebral ischemia and vasospasm after SAH.

Increase in endothelin-1 (ET-1) and 5- carboxamidotryptamine (5-CT) induced contraction via elevated expression of ET_B and 5-hydraoxytryptamine ($5\text{-}HT_{1B}$) receptors have been shown after SAH and are related to late cerebral ischemia (Hansen-Schwartz, Hoel et al. 2003). This involves activation of mitogen activated protein kinase kinase (MEK) and extracellular signal regulated kinase 1/2 (ERK1/2) (Beg, Hansen-Schwartz et al. 2006).

We have shown that calcium calmodulin dependent protein kinase (CAMK) is involved in the endothelin receptor up regulation (Waldsee, Ahnstedt et al. 2009). Here we investigate if the intra-cellular pathways involving CAMK is activated in SAH and that receptor up regulation can be blocked by inhibition of CAMK.

Methods: Subarachnoid hemorrhage was induced by the injection of 250 µl of autologous blood into the basal cisterns. CAMK inhibitor (KN93) or saline (placebo) was administered first given at 1 h after SAH and then repeated at 12, 24, 36, 48, 60 h after the SAH. Gross sensorimotor function was assessed using a rotating pole test.

Results: Experimental SAH induced neurological symptoms associated with vasospasm after 3 days of observation. In vitro pharmacological examination of cerebral arteries showed significant increase in contraction induced by ET-1 and 5-CT in the SAH group as compared to sham. KN93 significantly attenuated contraction induced by ET-1 and 5-CT and somewhat improved functional outcome.

Conclusion. The study revealed an increase in ET_B and $5\text{-}HT_{1B}$ receptors in cerebral arteries after SAH associated with neurological deterioration. CAMK inhibition has a significant effect on receptor expression and a functional outcome.

References: Beg, S. A., J. A. Hansen-Schwartz, et al. (2006). "ERK1/2 inhibition attenuates cerebral blood flow reduction and abolishes ET(B) and 5-HT(1B) receptor upregulation after subarachnoid hemorrhage in rat." J Cereb Blood Flow Metab 26(6): 846-56.

Hansen-Schwartz, J., N. L. Hoel, et al. (2003). "Subarachnoid hemorrhage enhances endothelin receptor expression and function in rat cerebral arteries." Neurosurgery 52(5): 1188-94; 1194-5.

Waldsee, R., H. Ahnstedt, et al. (2009). "Involvement of calcium-calmodulin dependent protein kinase II in endothelin receptor expression in rat cerebral arteries." Am J Physiol Heart Circ Physiol.

678

NAD^+ TREATMENT PREVENTS MULTIPLE ROTENONE-INDUCED APOPTOTIC CHANGES OF PC12 CELLS

W. Ying, Y. Hong, W. Xia, S. Shi, Y. Ma, J. Shao

Med-X Research Institute, Shanghai Jiao Tong University, Shanghai, China

Introduction: NAD^+ plays critical roles in not only energy metabolism and mitochondrial functions, but also in calcium homeostasis and immunological functions. A number of studies have also indicated that NAD^+ treatment can prevent oxidative stress-induced necrosis of primary neurons and astrocytes, and NAD^+ administration can reduce ischemic brain damage. However, there has been little information regarding the effects of NAD^+ treatment on apoptotic changes, which are critical pathological changes in such neurological diseases as brain ischemia and Alzheimer's disease.

Objective: In this study we determined the effects of NAD^+ on multiple rotenone-induced apoptotic changes.

Material and methods: We conducted this study by applying flow cytometry-based Annexin V assay, TUNEL say, Hoechst staining and immunostaining of apoptosis-inducing factor (AIF).

Results: We found that treatment of NAD^+, but not nicotinamide, can markedly decrease all of these apoptotic changes, suggesting that NAD^+ can prevent cell apoptosis by mechanisms that are independent of its degradation product nicotinamide. Our study also showed that NAD^+ treatment can attenuate rotenone-induced cell necrosis. We further found that NAD^+ treatment can prevent rotenone-induced ATP depletion, which could in part underlie the protective effects of NAD^+.

Conclusions: Our study has provided first evidence that NAD^+ treatment can prevent multiple apoptotic changes, in addition to its reported preventive effects on cell necrosis. Because both apoptotic changes and necrosis are important pathological changes in brain ischemia, our study has suggested that NAD^+ may decrease ischemic brain damage by decreasing both apoptotic changes and necrosis.

684

VIGABATRIN INHIBITS MORPHINE-INDUCED DECREASES IN 18FDG UPTAKE IN ADULT ANIMALS

S.L. Dewey[1], A. Aarons[1], S. Agorastos[1], J. Carrion[1], K. Patel[1], S. Scherrer[1], A. Talan[1], C. Veith[1], J.D. Brodie[2], D. Eidelberg[3], W.K. Schiffer[1]

[1]Laboratory for Behavioral and Molecular Neuroimaging, Feinstein Institute for Medical Research, Manhasset, [2]Department of Psychiatry, NYU School of Medicine, New York, [3]Center for Neuroscience, Feinstein Institute for Medical Research, Manhasset, NY, USA

Objectives: Opiate abuse is on the rise worldwide and the United States alone has had a significant increase in first time users from 2008 (National Survey on Drug Use and Health, 2009). In an ongoing effort to develop vigabatrin (gamma vinyl-GABA, GVG) for the treatment of substance abuse, including opiates, we recently examined its effects on morphine-induced changes in ^{18}FDG uptake in adult animals using small animal positron emission tomography (PET). Previously, we demonstrated that acutely, vigabatrin blocked heroin-induced increases in extracellular dopamine, self-administration, and the acquisition and expression of conditioned place preference in freely moving animals. In the present study we examined vigabatrin's effects on ^{18}FDG uptake and behavior in adult animals prior to and following an escalating dose of morphine.

Methods: Two groups of adult male Sprague-Dawley rats (n=8/group) were studied. All animals received baseline scans (^{18}FDG uptake occurred for 45 mins in awake and freely moving animals) using a Siemens Inveon small animal tomograph. Group 1 animals then received morphine treatment for 14 days beginning at a dose of 10 mg/kg (ip) and ending at a dose of 42.5 mg/kg (doses were escalated by 2.5 mg/kg/day). 24 hours following their last dose, animals received another ^{18}FDG scan. These animals received subsequent ^{18}FDG scans at 7, 14, and 28 days post treatment. Group 2 animals received the identical morphine regimen as Group 1 animals except they also received daily injections of vigabatrin (100 mg/kg). 24 hours following their last dose, animals received another ^{18}FDG scan followed by subsequent ^{18}FDG scans at 7, 14, and 28 days post treatment. Behavioral measures of opiate-induced high followed by withdrawal were made throughout the study.

Results: In Group 1 animals, there was a significantly greater loss in weight than in Group 2 animals. Further, a significant decrease in ^{18}FDG uptake was noted in both cortical (frontal, parietal, and temporal cortices) and subcortical structures (deep cerebellar nuclei, striatum, and thalamus). These bilateral decreases returned to normal values by 28 days post treatment. Group 2 animals, however, failed to show significant decreases in ^{18}FDG uptake in either cortical or subcortical structures. In addition, their scans were identical to baseline values at all 4 time points (24 hours, 7, 14, and 28 days). These data suggest that subchronic morphine exposure produces profound cortical and subcortical decreases in ^{18}FDG uptake in adult animals, implying diminished brain activity in specific regions as a result of morphine exposure. Furthermore, these decreases are not readily reversible as they did not return to normal values until 28 days following cessation of treatment.

Conclusions: These studies demonstrated that vigabatrin inhibits morphine-induced decreases in ^{18}FDG uptake throughout the brain. Taken with our previous preclinical and clinical studies, these data further support the development of vigabatrin for the treatment of opiate dependence in adult populations. Perhaps most importantly, these data validate the use of functional imaging

with ^{18}FDG in behaving animals to understand the neural circuits that drive behavior, and provide a new platform to guide CNS drug development.

685

INVOLVEMENT OF CALCIUM CALMODULIN DEPENDENT PROTEIN KINASE ON CEREBROVASCULAR ENDOTHELIN RECEPTORS UP REGULATION

R. Waldsee, H. Ahnstedt, S. Eftekhari, L. Edvinsson

Clinical Science, Experimental Vascular Research, Lund, Sweden

Introduction: It is well known that calcium calmodulin dependent protein kinase (CAMK) is involved in contraction-excitation coupling but recent data suggest that CAMK has effects on gen regulation. Here we examine the influence of CAMK on endothelin receptors. The intracellular pathways and the relation between CAMK, calcium channels, and transcription factors in gene regulation of endothelin receptors have not been clarified.

Objective: We sought to investigate in detailed the CAMK intracellular pathway during organ culture of rat cerebral arteries using functional and molecular methods.

Methods: The time dependency of calcium channel expression during organ culture and the effect of inositol 1.4.5-triphosphate (IP3) receptor inhibitor xestospongin C (Xec), L-type Voltage operated calcium channel (VOCC) inhibitor nifedipine (Nif) and CAMK inhibitor (KN93) have been studied by incubation of arteries for 24 h with or without inhibitors. The mRNA level of inositol 1.4.5-triphosphate (IP3) receptors, ryanodine (Ryd) receptors, transient receptor potential canonical (TRPC) and VOCC have been evaluated by real time PCR. The effect of inhibitors on endothelin receptors were evaluated by myograph.Transcription factors as Downstream regulatory element antagonist modulator (DREAM),c-AMP-responsive element binding protein (CREB), and nuclear factor of activated T cells (NFAT) were evaluated by immunohistochemistry and real time PCR.

Results: Ring segments of middle cerebral artery (MCA) of rat were organ cultured for 24 hr; this results in transcription upregulation of endothelin ET_B receptor. Myograph results show that KN93 and Xec attenuate, and Nif promotes K^+, sarafotoxoin 6c (S6c) and endothelin-1 (ET-1)-induced contractions after organ culture. The mRNA level of IP3R, ryanodine receptors (RydR3), transient receptor potential canonical (TRPC1) but not VOCC decreased during organ culture as measured by real time PCR. Incubation of arteries with Xec and KN93, but not Nif increased the level of IP3R and TRPC1 channels and decreased the VOCC and RydR3. KN93 decreased the protein level of DREAM, Nif decreased the protein level of CREB, and Xec decreased the mRNA level of NFAT.

Conclusion: Taken together CAMK and IP3 channel activity and transcription factors DREAM and NFAT have significant roles in mechanism involved in endothelin receptor up regulation.

687

HUK ENHANCES CEREBRAL PERFUSION BY REGULATING ERK PATHWAY AND APELIN SYSTEM IN EXPERIMENTAL STROKE

Y. Xu[1], J. Li[1,2], G. Deng[1,2], J. LI[1,2]

[1]Department of Neurology, Drum Tower Hospital, Affiliated of Nanjing University Medical School, [2]Nanjing Medical University, Nanjing, China

Introduction: The kallikrein-kinin system (KKS) exerts beneficial effects on ischemic brain injury by enhancing neovascularization and restoring regional blood flow.[1] Human Urinary Kallidinogenase (HUK), a key member of KKS, has been used for more than 4 years in clinic for treating ischemic stroke patients in China; however, the mechanism of the angiogenic effects of the KKS is still unclear. In terms of angiogenesis, both ERK1/2 and the Apelin/APJ receptor signaling pathways have been implicated in the proliferation of vascular endothelial cells. Targeted blockade of ERK1/2 retards angiogenesis, and the APJ receptor and its endogenous ligand apelin are potent angiogenic agents in ischemia.[2] The present study was undertaken to investigate whether the HUK treatment can enhance cerebral perfusion by promoting blood flow and angiogenesis, and to determine if KKS angiogenic pathways are associated with activation of ERK1/2 and APJ signaling pathways.

Methods: Rats with or without HUK (20 PNAU/g per day, intravenous) were subjected to transient middle cerebral artery occlusion (MCAO) for 2h and followed by 1d, 3d, 7d and 14 d of reperfusion. Neurofunctional recovery was assessed using Longa scores. The cerebral blood flow of rats, including relative regional cerebral blood volume (rrCBV) and relative regional mean transit time (rrMTT) was detected by MRI and quantified by analysis software(BioMAP; Novartis, Basel, Switzerland). At various time post-reperfusion, brains were removed and stained with TTC staining for infarct size. RNA levels of VEGF, apelin, APJ, ACE2, CD31 in brain tissue was determined by Q-PCR, and serum concentration of VEGF, Apelin, ACE2 was verified by ELISA. Capillary density was detected by immunofluorescence. The activation of ERK1/2 were tested by western blotting. Statistical analyses were performed using ANOVA and Student's t-test (two-tailed), with $P< 0.05$ considered statistically significant.

Results: HUK treatment resulted in enchanced rrCBV and rrMTT in the regions of perfusion deficiency ($P< 0.05$, n=6/group). Total blood vessel and neovascular density significantly increased in rats exposed to HUK. CD31 and VEGF expression was increased at all time points tested in HUK-treated MCAO rats ($P< 0.05$, n=6/group). Increased activation of ERK1/2 pathway was detected 2d after reperfusion in HUK-treated animals, correlating with the early stage neovascularization($P< 0.05$, n=6/group). ACE2, apelin and APJ expression levels did not significantly increase until 14 d after reperfusion. HUK treatment significantly decreased infarct size following ischemia and lowered Longa mean scores at 3, 7, and 14 d ($P< 0.05$, n=6/group). No differences in blood pressure, SpO_2 and heart rate were observed between MCAO groups.

Conclusions: Neovascularization induced by HUK treatment is correlated with enhanced cerebral perfusion following experimental stroke. The underlying mechanism may involve the promotion of the ERK1/2 signaling in the early phase and the apelin/APJ pathway in the late phase.

References:

1. Xia CF, et al. Human Gene Therapy. 2006 ; 17:206-219.

2. Hiroyasu Kidoya, et al. Blood, 2010,115:3166-3174.

689

MKP-1 MRNA AND PROTEIN EXPRESSIONS ARE INDUCED IN NEURON AT ACUTE PHASE AFTER FOCAL CEREBRAL ISCHEMIA

H. Horikawa[1], H. Imai[1], Y. Chen[1], T. Ochi[1], A. Ito[1], H. Kanemitsu[2], H. Nakatomi[1], N. Saito[1]

[1]Department of Neurosurgery, The University of Tokyo, [2]Department of Radiological Technology, Faculty of Medical Technology, Teikyo University, Tokyo, Japan

Objectives: Ischemia-induced changes in gene and protein expression may provide important information relating to mechanisms of injury and potential recovery. Cells in the peri-infarct zone (penumbra) display a complex response including selectively increased mRNA levels of genes associated with stress, apoptosis, transcription, and inflammation. The study previously reported in our department by using the DNA microarray technique revealed the expression level of 246 transcripts were increased after ischemia (1) Of them, mitogen-activated protein kinase phosphatase (MKP-1) are known to show the 10-fold increase after ischemia. The MKP-1 gene encodes a dual specificity (Tyr/Thr) protein phosphatase that specifically inactivates mitogen-activated protein (MAP) kinase, and it seems to play an important role in controlling cellular proliferation, apoptosis and stress response (2). However, the function of MKP-1 in brain still remains to be unknown. We examined the expression pattern of MKP-1 mRNA and protein in the brain using *in situ* hybridization and immunohistochemistry at several time points after focal cerebral ischemia.

Methods: Permanent middle cerebral artery occlusion model was employed in Sprague Dawley rats (300-350g, n= 30). Rats were decapitated at 30minutes, 1hr(hour), 3hrs, 6hrs, 12hrs, 24hrs, 3days, and 7days after ischemia, and sham-operation without arterial occlusion. Sections of 20μm thickness were cut. For *in situ* hybridization, the sections were applied by Digoxigenin-labeled cRNA for MKP-1 probes. For immunohistochemical analysis, the specific antibody for MKP-1 was applied for the adjacent sections of *in situ* hybridization. The antibody against NeuN for neurons was applied for double immunohistochemistry.

Results: Histopathology showed ischemic damage was identified consistently in the ipsilateral MCA territory including the frontal cortex, dorsal parietal cortex, and the caudate. *In situ* hybridization showed the expression of MKP-1 mRNA emerged in the peri-infarct zone and remote cortex of ischemic side of cerebral hemisphere at 30 minutes after MCA occlusion, instead of the low expression in ischemic core. This expression of MKP-1 mRNA in these regions dramatically increased at 1 hour after MCA occlusion and was maintained until 3 hours after MCA occlusion. However, MKP-1 mRNA expression in the ischemic side of cerebral hemisphere was reduced markedly at 12 hours after MCA occlusion and almost lost at 24 hours. MKP-1 mRNA expressing cells were distributed predominantly in the ipsilateral cortex, with most cells displaying neuronal morphology. The double immunohistochemistry revealed the most MKP-1 positive cells in the peri-infarct cortex in the acute phase expressed NeuN and were thus identified as neurons.

Conclusions: The major observations were that MKP-1 mRNA was induced and strongly expressed in neurons of in the peri-infarct zone and remote cortex of ischemic side of cerebral hemisphere only at acute phase and that the expression pattern was very specific and sensitive to the ischemic insult after MCA occlusion

References:

1 Kawahara N et al. Genome-wide Gene Expression Analysis for Induced Ischemic Tolerance and Delayed Neuronal Death Following Transient Global Ischemia in Rats. J Cereb Blood Flow Metab. 2002 24:212-223

2 Keyse SM and Emslie EA Oxidative stress and heat shock induce a human gene encoding a protein-tyrosine phosphatase. Nature. 1992 359:644-7.

690

ASTROCYTIC AKAP12 REGULATE BLOOD-NEURAL BARRIER FORMATION THROUGH PROTEIN KINASECZ

J.H. Cha[1], Y.K. Choi[2], K.W. Kim[1]

[1]NVCRC College of Pharmacy, Seoul National University, Seoul, [2]Vascular System Research Center and Department of Molecular and Cellular Biochemistry, School of Medicine, Kangwon National University, Korea, Chun Chen, Republic of Korea

The Interaction of astrocytes and blood vessels has an important role in the formation and maintenance of the blood-neural barrier (BNB) including blood-brain barrier(BBB) and blood-retinal barrier(BRB). Astrocyte-derived A-kinase anchor protein 12 (AKAP12) influences BNB formation, but the mechanism of regulation of BNB functions by AKAP12 is not fully understood.

We have defined a novel pathway of barriergenesis in human retina microvascular endothelial cells (HRMECs) involving astrocytic AKAP12. The treatment of conditioned media from AKAP12-overexpressing astrocytes to vHRMECs reduced phosphorylation of protein kinase Cζ (PKCζ), decreased vascular endothelial growth factor (VEGF) and increased thrombospondin-1 (TSP-1) levels, which led to antiangiogenesis and barriergenesis. Transfection of a small interference RNA targeting PKCζ decreased VEGF levels and increased TSP-1 levels in HRMECs. Rho is a putative downstream signal of PKCζ, and inhibition of Rho kinase with a specific inhibitor, Y27632, decreased VEGF levels and increased TSP-1 levels.

These data suggest that AKAP12 in astrocytes differentially regulates the expression of VEGF and TSP-1 via the inhibition of PKCζ phosphorylation and Rho kinase activity in HRMECs.

691

INHIBITORY EFFECT OF SM6-SIM6-DG ON LPS-INDUCED COX-2 EXPRESSION AND THE UNDERLYING MECHANISM IN DIFFERENTIATED THP-1 MONOCYTES

L. Feng[1,2], X. Cai[1]

[1]Dept. of Neuropharmacology, [2]State Key Laboratory of Drug Research, Shanghai Institute of Materia Medica, Chinese Academy of Sciences, Shanghai, China

Cyclooxygenase (COX) is a rate-limiting enzyme in arachidonic acid (AA) metabolic pathways. COX has mainly two distinct isoforms, the constitutive COX-1 and inducible COX-2, both of which play an important role in many physiological and pathological processes. Nonsteroidal anti-inflammatory drugs (NSAIDs) are the most widely used anti-inflammatory drugs throughout the world, which act through inhibition of COX enzyme activity to reduce the generation of pro-inflammatory prostaglandins such as PGE_2. In view of the important physiological functions of COX, inhibition of either COX-1 or COX-2 may cause various side effects to some extent. We therefore aimed at specific suppression of COX-2 protein overexpression induced by proinflammatory agents to exert anti-inflammatory effect.

In this research, we used lipopolysaccharide (LPS)-stimulated human monocytic THP-1 cells as an in vitro inflammatory model to screen for COX-2 expression inhibitors with the combination of MTT assay to eliminate compounds with cytotoxicity and finally got the compound SM6-SIM6-DG with strong inhibitory effect and minimal cytotoxicity. Further investigation showed that SIM6-DG could suppress LPS-induced *COX-2* gene transcription in differentiated THP-1 cells, indicating that SIM6-DG downregulates COX-2 protein expression, at least partly, at transcription level. To clarify the underlying mechanism involved in the inhibitory effect of SIM6-DG, we examined the activation of two important signaling pathways, MAPK (mitogen-activated protein kinase) pathway and NF-κB (nuclear factor-κB) pathway, which have been demonstrated critical in COX-2 induction by LPS in macrophages. We found that SIM6-DG suppresses LPS-induced COX-2 expression through interfering with IKK (I-κB kinase)/I-κB (inhibitor κB)/NF-κB signaling pathway while it doesn't affect LPS-induced MAPK activation. Furthermore, we investigated the effect of SIM6-DG on COX metabolic pathways. The results showed that SIM6-DG suppresses LPS-induced generation of proinflammatory PGE_2 in a concentration-dependent manner, and this inhibitory action contributes to the downregulation of COX-2 protein expression rather than the inhibition of COX enzyme activity. In accordance with the *in vitro* data, SIM6-DG also shows a strong anti-inflammatory activity in carrageenan-induced paw edema in mice and neuroprotective effects on rat middle cerebral artery occlusion and reperfusion (MCAO) models.

Taken together, our results have showed that SIM6-DG exhibits strong anti-inflammatory effect both *in vitro* and *in vivo*. The different regulation mechanism of COX metabolic pathways from NSAIDs makes it theoretically reasonable for SIM6-DG to minimize the possible side effects resulting from inhibition of COX enzyme activity. SIM6-DG therefore has great potential as a candidate compound for anti-inflammatory drugs.

692

TIME-COURSE AND CORRELATION OF CEREBROVASCULAR VASOCONSTRICTOR RECEPTOR UPREGULATION, CEREBRAL BLOOD FLOW AND DELAYED CEREBRAL ISCHEMIA AFTER SUBARACHNOID HEMORRHAGE IN RATS

G.K. Povlsen[1], S.E. Johansson[1], C.C. Larsen[2], L. Edvinsson[1]

[1]Department of Clinical Experimental Research, [2]Department of Neurosurgery, Glostrup Research Institute, Glostrup University Hospital, Glostrup, Denmark

Background: Delayed cerebral ischemia is a major cause of death and disability after subarachnoid hemorrhage (SAH). Delayed cerebral ischemia occurs in the days following SAH when cerebral arteries constrict pathologically, a phenomenon termed cerebral vasospasm. Upregulation of vasoconstrictor endothelin-B (ET_B) and 5-hydroxytryptamine-1B ($5\text{-}HT_{1B}$) receptors have been demonstrated in smooth muscle cells of cerebral arteries after SAH, and it has been hypothesized that this contributes to cerebral vasospasm and delayed cerebral ischemia. However, the long-term time-course of cerebrovascular receptor changes and the correlation of these changes with reduced cerebral blood flow (CBF) and development of neurological deficits after SAH have not been studied.

Aim: The aim of the present study was to characterize, in a rat SAH model, the time-course and correlation of cerebrovascular vasoconstrictor receptor upregulation, changes in CBF and development of neurological deficits during the first 4 days after the SAH.

Methods: SAH was induced by intracisternal injection of 250 µl autologous blood at a pressure equal to the mean arterial blood pressure, thus mimicking bleeding from a ruptured artery. At 2, 3 and 4 days after SAH, smooth muscle endothelin-1 (ET-1) ET_B receptor and 5-hydroxytryptamine (5-HT) $5\text{-}HT_{1B}$ receptor expression and functionality were studied in isolated cerebral artery segments by immunohistochemistry and myograph contractility studies. Neurological deficits were assessed daily by a rotating pole sensorimotor test and observations of spontaneous behaviour. In a separate group of animals, CBF was determined at the same time-points after SAH by the [(14)C]-iodoantipyrine technique.

Results: We demonstrate that SAH induces upregulation of ET_B and $5\text{-}HT_{1B}$ receptors in cerebrovascular smooth muscle cells with the highest receptor expression and vasocontractile functionality at day 3 after the SAH. Thus, at day 3 after SAH, contractile responses to 10^{-8} M ET-1 and 5-carboxamidotryptamine (5-CT, a 5-HT1 receptor agonist) in basilar artery segments from SAH rats were increased to 191.1 ± 20.8 % and 199.6 ± 37.3 %, respectively, of the levels in sham-operated animals. In animals surviving until day 4 after the SAH, cerebrovascular ET_B and $5\text{-}HT_{1B}$ receptor expressions were normalized to levels observed in sham-operated animals. The time-course of CBF reduction and development of neurological deficits correlated with the time-course of cerebrovascular receptor upregulation. We also found that between day 3 and day 4 after SAH, around one third of the SAH animals die, with the group of dead animals displaying higher cerebrovascular vasoconstrictor receptor expression and stronger neurological deficits than the group of SAH-induced animals surviving beyond day 3.

Conclusion: Together, the correlation in time between cerebrovascular receptor upregulation, reduction in CBF and development of neurological deficits, and the association of mortality in the delayed ischemic phase with strong cerebrovascular vasoconstrictor receptor expression suggest a central role of cerebrovascular receptor upregulation in the pathophysiology of delayed cerebral ischemia after SAH.

693

THE NEUROVASCULAR RELATIONSHIPS OF THE OCULOMOTOR NERVE

E. Tuccar, A.F. Esmer, T. Sen, A. Comert, S.T. Karahan

Department of Anatomy, Ankara University, Ankara, Turkey

Introduction: In this study, the arterial supply of the cisternal (initial) and the subcavernous parts of the oculomotor nerve (ON) and the relation between the nerve and adjacent vascular structures like posterior cerebral artery (PCA) and superior cerebellar artery (SCA) were investigated.

Material and methods: A total of 140 formalin fixed hemispheres from 70 human cadaveric brains were examined. The nutrient branches reaching the cisternal and subcavernous parts of the ON were investigated, along with branches of adjacent vascular structures penetrating the nerve and passing through it.

Results: In the material examined, the ON, after arising from the midbrain, mostly continues laterally between PCA and SCA or between PCA and the rostral SCA trunk. However, in three hemispheres of our specimens, the ON run between the rostral and caudal SCA trunks. We observed that the branches of PCA-P1 segment supplied the cisternal part of the ON in all specimens. In one specimen, the cisternal part of the ON was supplied by a branch arising from the rostral SCA trunk which was also originating from PCA. Differently, in four hemispheres, branches arising from PCA or SCA perforated the cisternal part of the ON and passed through it. We also observed a tortuous caudal trunk of duplicated SCA in one of our specimens and considered it as a rare variation.

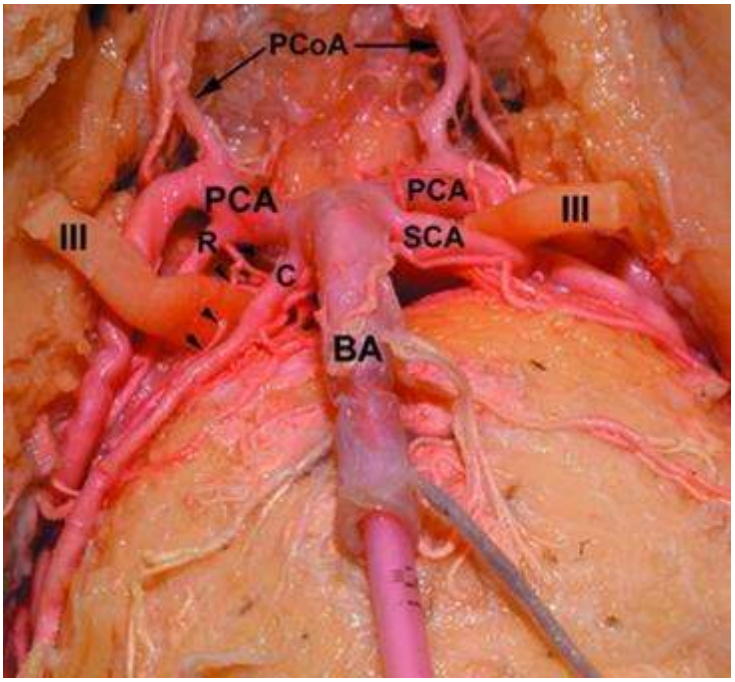

[oculomotor nerve]

Conclusion: The anatomy of the ON and its vascular relations is significant in terms of not only understanding the compression syndromes and its vascular dysfunctions, but the exact diagnosis and treatment as well.

Key words: oculomotor nerve, posterior cerebral artery, superior cerebellar artery

694

NMDA RECEPTOR MEDIATED CA^{2+} ELEVATIONS IN NEURONS ARE NOT NECESSARY FOR NEUROVASCULAR OR NEUROMETABOLIC COUPLING IN MOUSE SOMATOSENSORY CORTEX

B.L. Lind[1], A. Brazhe[2], S.B. Jessen[1], F.C.C. Tan[1], M. Lauritzen[1,3]

[1]Department of Neuroscience and Pharmacology, University of Copenhagen, Copenhagen N, Denmark, [2]Faculty of Biology, Moscow State University, Moscow, Russia, [3]Department of Clinical Neurophysiology, Glostrup Hospital, Glostrup, Denmark

The relationship between the cerebral blood flow (CBF) response seen in functional imaging studies and neuronal activity is not completely understood. The aim of this study was to investigate how the size of neuronal intracellular Ca^{2+} levels were related to the activity-dependent rises in CBF and O_2 consumption in the tissue.

Mouse sensory barrel cortex was activated *in vivo* by stimulation of contralateral whisker pad and studied through a craniotomy drilled over the right hemisphere. The frequency induced activity in layer 2/3 was studied by 2-photon based Ca^{2+} imaging, Laser-Doppler flowmetry of CBF, and measurements of oxygen tension in the tissue. Extracellular potentials were measured with a glass electrode. The tissue was stained by bulk-loading with Oregon green bapta in combination with sulphorhodamine that is selective for astrocytes. This allowed for the distinction between somas, while the neuronal dendrites and astrocytic processes were mixed in the neuropil. The blood-pressure, blood-gasses and CO_2 in the expired air was monitored during the experiment, to ensure that the animal was kept under physiological conditions.

Stimulation increased CBF and O_2 responses frequency-dependent with a max at between 2-3 Hz. This was in concordance with the size of the total Ca^{2+} signals in neuropil, neurons and astrocyte soma during stimulation. Blockade of NMDA receptors with MK801 reduced Ca^{2+} signals significantly in neuropil and neuronal somas, but not in astrocytes. We observed no reduction in the activity-dependent rises in cerebral metabolic rate of Oxygen ($CMRO_2$) and CBF or the size of the field potentials in response to MK801.

In conclusion, activity-dependent rises in CBF and $CMRO_2$ were accompanied by rises in astrocyte and neuronal Ca^{2+}. Reduction of the Ca^{2+} signals in neuronal soma and neuropil was possible with preserved CBF and $CMRO_2$ responses, which suggest that NMDA-related Ca^{2+} fluxes in neurons do not control oxygen consumption or neurovascular coupling.

695

EVALUATION OF CEREBRAL BLOOD FLOW IN PATIENTS WITH MISERY PERFUSION USING QUANTATIVE SPECT (QSPECT) AND PVELAB

K. Fukuda[1], H. Iida[2], C. Svarer[3], T. Zeniya[2], K. Iihara[1]

[1]National Cerebral and Cardiovascular Center-Hospital, [2]National Cerebral and Cardiovascular Center-Research Institute, Osaka, Japan, [3]Neurobiology Research Unit, University of Copenhagen, Copenhagen, Denmark

Objectives: Quantative SPECT (QSPECT) reconstruction program and a standardized protocol to assess rest and acetazolaminde CBF from single scanning has been validated by multicenter study that involved 12 clinical institutions. This study was aimed to develop the data processing pipeline suitable for evaluating effectiveness of new therapeutic trials based on multicenter clinical studies.

Methods: Clinical SPECT study using dual-table autoradiographic (DTARG) method and a dual administration of 123I-iodoamphetamine was carried out in five patients with symptomatic unilateral major cerebral arterial occlusion. Quantative regional CBF and cerebral vasoreactivity (CVR) in response to acetazolamide challenge were obtained, and misery perfusion was revealed. EC-IC bypass was performed in three patients because the degree of ischemia was severer. Two patients were medically treated. Follow up SPECT and MRI study were carried out at 6, 12 months. All images were registered to rest CBF at 0 month. To assess the CBF at rest and CVR, a standardized region of interests (ROI) we newly developed using PVElab was set automatically. SPECT study was analyzed using QSPECT reconstruction program. A systematic follow up evaluation was developed.

Results: The registration of all images could be completely achieved, and the data of CBF at rest and CVR could be correctly assessed . CBF at rest and CVR in patients with EC-IC bypass were significantly improved compared with medically treated patients (CBF at rest: +3.3±2.1 vs +0.5±0.8 mL/min/100g, CVR: +46.7±8.2 vs 4.2±21.8%). Reasonable reproducibility and timecourse in control area was confirmed (CBF at rest: -0.8±1.48mL/min/100g, CVR: 2.4±19.3%). No deterioration of symptom or ischemic change on MRI was confirmed in all patients.

Conclusion: Standardized protocol for data acquisition, image reconstruction and data-analysis pipeline appeared to be feasible to evaluate hemodynamic outcome in patients with misery perfusion. This system can be applicable to other study such as multicenter trial in patients with cerebrovascular occlusive disease. Limitation of this study is small number of subjects, from only single institution.

696

CORTICAL AND THALAMIC BRAIN TISSUE OXYGEN LEVELS DURING THE EARLY AND INTERMEDIATE PHASES OF POST-CARDIAC ARREST SYNDROME IN IMMATURE RATS

M.D. Manole[1], P.M. Kochanek[2], H. Alexander[2], M.J. Bell[2], E.L. Fink[2], H. Bayir[2], R.S.B. Clark[2]

[1]Pediatrics, [2]Critical Care Medicine, University of Pittsburgh School of Medicine, Pittsburgh, PA, USA

Introduction: Cerebrovascular disturbances after resuscitation from cardiac arrest (CA) may contribute to secondary neuronal injury and ultimate neurological outcome. As a first step in testing whether or not manipulating these cerebrovascular disturbances represents a therapeutic target, we measured brain tissue oxygen ($PbtO_2$) levels continuously during the early and intermediate phases of post-CA syndrome in immature rats.

Objectives: Determine cortical and thalamic $PbtO_2$ levels and the response to supplemental oxygen from 0-3 h (early phase) and 24 h (intermediate phase) after asphyxial CA in postnatal day (PND) 17 rats.

Methods: PND 17 Sprague-Dawley rats (n=48, 6/group) underwent tracheal intubation and vascular catheterization. Oxygen sensors were inserted in the parietal cortex (1-mm) and/or thalamus (6-mm) and $PbtO_2$ was measured continuously. Asphyxial CA of 9 min was induced by disconnecting the ventilator after neuromuscular blockade. Rats were resuscitated by resuming mechanical ventilation, chest compressions, epinephrine and bicarbonate. Cortical and thalamic $PbtO_2$ was measured at baseline and from 0-3 h after resuscitation (early phase), and then at 24 h after resuscitation (intermediate phase) in separate groups of rats. $PbtO_2$ was measured on a FiO_2 of 0.5, 0.21 and 1. $PbtO_2$ was also measured in shams on a FiO_2 of 0.5, 0.21 and 1. The response of cortical $PbtO_2$ to epinephrine infusion during the early post-CA phase was assessed.

Results: On a FiO_2 of 0.5 baseline cortical $PbtO_2$ was 39.3±8.7 mmHg decreasing progressively to 7.5±5.2 mmHg by 3h post-CA ($p< 0.05$ vs. baseline). On a FiO_2 of 0.5 baseline thalamic $PbtO_2$ was 66.9±16.3 mmHg, increasing to 281.8±25.4 mmHg at 5 min post-CA ($p< 0.05$ vs. baseline), then decreasing to baseline values by 3 h. Decreasing the FiO_2 from 1 to 0.21 resulted in a marked reduction in cortical $PbtO_2$ vs. sham on a FiO_2 of 0.21 (0.2±0.3 vs. 18.9±4.3). There was no response to a hyperoxic challenge (FiO_2 from 0.5 to 1) at 3h after CA in either the cortex or thalamus. Epinephrine infusion post-CA increased cortical $PbtO_2$ to baseline values in a dose-dependent manner. At 24 h after CA both cortical (2.5±1 mmHg) and thalamic (9±2 mmHg) $PbtO_2$ levels remained reduced compared to shams on a FiO_2 of 0.21. However, on a FiO_2 of 0.5 both cortical (47.8±15.1 mmHg) and thalamic (77.1±15.4 mmHg) $PbtO_2$ were similar to shams and pre-arrest baseline levels. There was no response to a hyperoxic challenge (FiO_2 from 0.5 to 1) at 24 h after CA in either cortex or thalamus.

Conclusions: Profound and sustained cortical hypoxia is seen during both the early and intermediate phases of the post-CA syndrome. In the thalamus, brief hyperoxia transitions to hypoxia between 3 and 24 h. $PbtO_2$ levels on room air are below generally regarded thresholds, particularly in cortex. Given that $PbtO_2$ is considered a realistic surrogate measure of cerebral blood flow, and that cerebrovascular disturbances measured by arterial spin labeling magnetic resonance imaging (JCBFM 2009;29:197-205) correspond to $PbtO_2$ measurements in this model, further study using a $PbtO_2$ goal-directed strategy to improve neurological outcome after CA appears warranted.Support: NIH HD058798 and HD045968

698

PROTECTIVE EFFECTS OF PRE-MEDICATED ANTI-PLATELET COMBINATION THERAPY IN FOCAL CEREBRAL ISCHEMIA RAT MODEL

Y. Toda, K.-I. Katsura, M. Sakurazawa, T. Kanemaru, S. Inaba, M. Saitou, Y. Katayama

Nippon Medical School, Tokyo, Japan

Objectives: Among several anti-platelet drugs using to prevent recurrent stroke, cilostazol has shown various effects including NO production, vascular smooth muscle relaxation, vascular endothelial protection, besides anti-platelet effect. We examined if cilostazol shows protection against acute cerebral ischemia and then the effect of combination therapy with aspirin was evaluated. We made rat transient middle cerebral artery (MCA) occlusion model which have pre-medicated anti-platelet drugs for seven days, and then examined the effect on infarct volume and neurological symptoms. We also explored the protective mechanisms immunohistochemically with Bcl-2, Bax, TUNEL, 8-OHDG, and 4-HNE staining.

Methods: We used 8 weeks male SD rats weighting 250 to 300g. After oral administration of anti-platelets for 7 days, we made transient MCA occlusion for 90 minutes, and examined infarct volume and neurological symptoms at 24 hours after ischemia. The dosage of drugs were as following: aspirin (30mg/kg/day), cilostazol (50mg/kg/day), and Vehicle, 0.5% CMC (carboxymethlcellulose).

Results: Compared with vehicle group, aspirin mono-therapy did not show significant decrease of infarct volume, however, cilostazol mono-therapy showed significant reduction of infarct volume. Aspirin plus cilostazol combination therapy showed significant decrease of infarct volume against cilostazole or aspirin mono-therapy. Similarly, neurological symptoms significantly improved in aspirin plus cilostazol combination group than the aspirin, or cilostazol mono-therapy group. In immunostaining result, Bcl-2 expression was significantly higher in combination therapy group. Bax, TUNEL, 8-OHDG, and 4-HNE expressions were significantly lower in combination therapy group than in aspirin or cilostazol mono-therapy group.

Conclusions: Using 2 to 3 anti-platelet drugs is a standard treatment to prevent re-attack of coronary artery events, however, in secondary stroke prevention therapy, single anti-platelet therapy is generally acceptable, because combination therapy increase hemorrhagic events without more efficacy in preventing recurrent stroke. However, there exist high risk patients to whom we want to treat with several anti-platelet drugs. From the results of CSPS2, cilostazol has fewer hemorrhagic complication than other anti-platelet. So it is clinically important to investigate hemorrhagic complication rate and the protective effects of aspirin plus cilostazol combination therapy. At first, we aimed to clarify the protective effect of the combination therapy in acute stroke model, which in turn may be interpreted that if taking aspirin plus cilostazol for secondary prevention, in case of unfortunate recurrence of stroke, the symptom may become less severe. We will further study the hemorrhagic complication rate and stroke recurrence rate in the aspirin plus cilostazol combination therapy in the rat experimental stroke model.

699

LOCAL ENHANCED CONTRACTILE FUNCTION OF ET_B, 5-HT_{1B} AND AT_1 RECEPTORS IN MIDDLE CEREBRAL ARTERY FOLLOWING DISTAL FOCAL PERMANENT OCCLUSION

M.N.P. Rasmussen[1], M. Hornbak[1], M. Sheykhzade[2], L. Edvinsson[1,3]

[1]Department of Clinical Experimental Research, Glostrup Research Institute, Glostrup University Hospital, Glostrup, [2]Department of Pharmacology and Pharmacotherapy, Faculty of Pharmaceutical Sciences, University of Copenhagen, Copenhagen, Denmark, [3]Division of Experimental Vascular Research, Institute of Clinical Sciences in Lund, University Hospital of Lund, Lund, Sweden

Objectives: Different experimental stroke models have been investigated regarding the pathophysiological mechanisms involved in upregulation of contractile receptors following cerebral ischemia. These models often result in either large infarcts or transient ischemia. However, no investigation has addressed the vascular changes proximal and distal to the occlusion site. Therefore we examined possible effects of minor stroke on the functionality and expression of the contractile endothelin-B (ET_B), 5-hydroxytryptamin-1B (5-HT_{1B}) and angiotensin-1 (AT_1) receptors in middle cerebral artery (MCA) segments proximal and distal to an occlusion.

Methods: Male Wistar rats underwent craniotomy where permanent occlusion of the distal part of the MCA was achieved by a suture and verified by laser Doppler flow analysis. Contractile responses were obtained by cumulative application of sarafotoxin 6c (S6c, selective ET_B receptor agonist), 5-carboxamidotryptamine (5CT, 5-HT_1 receptor specific agonist) and angiotensin II (Ang II, AT_{1+2} receptor agonist) at 24 and 48 hours after occlusion. Groups consisted of vessel segments proximal and distal to the occlusion, contralateral distal segments and distal segments from sham operated rats. Contractile response is given as % of 125 mM K^+ or in absolute milli Newton (mN). Protein localization and levels were examined by immunohistochemistry and ischemic damage by 2,3,5-Triphenyltetrazolium chloride (TTC) staining.

Results: TTC stainings showed no visible ischemic damage after 24 hours occlusion and only slight damage after 48 hours. After 24 hours of occlusion, ET_B and 5-HT_{1B} mediated contractile responses were significantly stronger in distal occluded MCA segments (113.0 %/1.4 mN ± 17.7 %/0.3 mN and 62.0 ± 9.7 % mean and s.e.m) compared to contralateral controls (16.8 ± 4.1 % and 28.2 ± 4.1%) and most interestingly to ipsilateral proximal segments (21.1 %/0.6 mN ± 5.7 %/0.2 mN and 31.9 % ± 6.2 %), respectively. These results were similar at 48 hours where also an AT_1 mediated contractile response was observed in the operated distal segments (41.2 ± 10.5 %) which was significantly higher compared to proximal segments, and distal segments from 24 hours occlusion (8.5 ± 1.7 % and 12.8 ± 3.7 %, respectively).

Immunohistochemistry revealed a tendency to up-regulation of ET_B and AT_1 receptors in the distal operated segments compared to control groups. In addition, it was disclosed that the receptors were localized in the smooth muscle cell layer.

Conclusions: A small focal vascular occlusion resulting in limited ischemic area leads to locally increased contractile function of ET_B and 5-HT_{1B} receptors after 24 hours, which persists after 48 hours, accompagnied by an additional increased contractile response from AT_1 receptors. The results suggest that the change in shear stress could be an initial trigger for the signaling pathways leading to increased contractility/elevated receptor expression of several receptors.

700

AKAP12 REGULATES VASCULAR AND BLOOD-BRAIN BARRIER STABILITY

K.W. Kim

College of Pharmacy and Department of Molecular Medicine and Biopharmaceutical Sciences, Seoul National University, Seoul, Republic of Korea

The initiation of brain vessel formation is the angiogenesis of primary vessel network and then brain vessel is processed the course of maturation known as barriergenesis in which Blood Brain-Barrier(BBB) is formed. Therefore, the strict regulation of angiogenesis and barriergenesis is necessary for the formation of complete brain vasculature.

We found that AKAP12, a scaffold protein that associates with protein kinase A (PKA) and protein kinase C (PKC) acting as a platform in various signal-transductions, is expressed in endothelial cells and astrocytes. Therefore, in the present study, we focus on the role of AKAP12 in the brain vascular stability and BBB integrity.

In zebrafish, loss of AKAP12 functions by morpholino knockdown resulted in severe cranial hemorrhage. We further revealed that AKAP12 morphants show impaired migrating behaviors of endothelial cells. These defects caused leaky vascular formation and abnormal patterning of vascular network. Furthermore *in vivo* time-lapse analysis revealed that the leakage is due to the contraction of the cells at the inter-endothelial cell-cell adhesions in AKAP12 morphants, suggesting the alteration of the actin cytoskeleton. These data imply that AKAP12 plays an important role in vascular stability.

We further studied that AKAP12 mediates anti-angiogenesis and BBB formation by down-regulating HIF-1α level, which leads to an increase in angiopoietin-1 and a decrease in VEGF expression in astrocytes. Conditioned media from AKAP12-overexpressing astrocytes induced BBB development by up-regulating the expression of tight junction proteins ZO-1, ZO-2 and claudin-5 in endothelial cells. These results indicate that AKAP12 regulates BBB formation by ceasing brain angiogenesis and by inducing barriergenesis.

Collectively, our data suggest that AKAP12 plays important roles in the vascular and BBB stability.

701

SINGLE CENTER SERIES AND SYSTEMATIC REVIEW OF DECOMPRESSIVE CRANIECTOMY IN PEDIATRIC PATIENTS

P. Schuss, E. Güresir, V. Seifert, H. Vatter

Department of Neurosurgery, Johann Wolfgang Goethe-University, Frankfurt am Main, Germany

Objective: Decompressive craniectomy (DC) is performed as a life-saving procedure in patients suffering from intractably elevated intracranial pressure following traumatic brain injury (TBI), bleeding, cerebral infarction or brain swelling of other etiologies. In the pediatric subgroup, DC is still controversially discussed. We therefore analyzed our institutional data and performed a review of literature.

Methods: Between April 2000 and December 2009 we performed 37 DCs in 34 pediatric patients (age 0-18 years). Patients were stratified according to the indication for DC: (1) traumatic brain injury (TBI), (2) cerebral infarction, (3) intracerebral hemorrhage (ICH), (4) subarachnoid hemorrhage (SAH) and (5) other non-traumatic reasons. Outcome was assessed according to the modified Rankin Scale (mRS) at 6 months (mRS 0-2 favorable vs. mRS 3-6 unfavorable). MEDLINE was searched for published studies or reports of DC in pediatric patients to gain a larger population. Two reviewers independently extracted data.

Results: Literature data, including the current series revealed a total of 172 pediatric patients. According to the underlying pathology, 136 procedures (79.1%) were performed due to TBI, 13 (7.5%) due to cerebral infarction, 5 (2.9%) due to ICH, 2 (1.2%) due to SAH, and 16 procedures (9.3%) due to other reasons. Overall 106 of 172 patients achieved a favorable outcome (62%). Favorable outcome was achieved in 25 of 36 patients without TBI vs. 81 of 136 patients with TBI (69% vs. 60%). Patients without signs of cerebral herniation achieved better outcome than patients with unilateral or bilateral dilated pupils (73% vs. 60% vs. 45%). The overall mortality rate was 13%.

Conclusion: The current data indicates that decompressive craniectomy in children with traumatic or non-traumatic brain swelling might be warranted, regardless of the underlying etiology. Despite mydriasis, favorable outcome might be achieved in a significant number of pediatric patients. Nevertheless, careful individual decision making is needed for each patient, especially when signs of cerebral herniation have persisted for a long time.

703

NEUROPROTECTIVE EFFECTS OF FRUCTOSE-1,6-DIPHOSPHATE ON BRAIN ENERGY METABOLISM AFTER ISCHEMIA-REPERFUSION INSULT: A ^{31}P-NMR STUDY

O. Tokumaru[1], C. Kuroki[1], K. Ogata[1], T. Kitano[2], I. Yokoi[1]

[1]Department of Neurophysiology, [2]Medical Education Center, Oita University Faculty of Medicine, Yufu, Japan

Objectives: Fructose-1,6-diphosphate (FDP) is an intermediate metabolite of glycolysis and functions as an energy substrate and a free radical scavenger. It is reported that FDP provides neuroprotection against ischemia-reperfusion insult. The neuroprotective effects of FDP on energy metabolism of rat brain slices exposed to ischemia-reperfusion insult were investigated by phosphorous nuclear magnetic resonance (^{31}P-NMR) spectroscopy.

Methods: Brain slices (400 μm-thick) prepared from a male Wistar rat (6 week-old) were superfused with standard artificial cerebrospinal fluid (ACSF) at a flow rate of 4 ml/min in an NMR sample tube at 27.5ºC. Ex-vivo ^{31}P-NMR spectra were obtained using an NMR spectrometer (DRX-300wb, Bruker Biospin). Free induction decays (FIDs) were acquired by 45° radio-frequency pulses repeated at intervals of 4 seconds. Accumulated data of 512 FIDs (32 min) or 1024 FIDs (64 min) were used for the analysis. Relative quantities of high-energy-phosphates, phosphocreatine (PCr) and ATP, and FDP were obtained from areas under curves fit to resonance peaks. Brain slices were exposed to ischemia by halting the perfusion for 64 min, followed by the recovery period for 128 min (the ischemia-reperfusion model). Neuron-rich slices superfused with 100 μM fluorocitrate, a selective glial poison, were also exposed to the ischemia-reperfusion insult. Capacity of FDP to scavenge reactive oxygen species (hydroxyl radical) was measured by electron spin resonance spectrometry (ESR) with the spin trapping method using CYPMPO.

Results: FDP signal decreased to 29% of pre-ischemic level during the ischemia and recovered gradually to 83% by 64 min after reperfusion, suggesting utilization of exogenous FDP as energy substrate. Recovery level of PCr 64 min after ischemia was significantly higher when superfused with ACSF with 1 mM FDP than when superfused with ACSF without FDP (67.9% vs. 53.8%, respectively; $p < 0.001$). But there was no significant difference in recovery of PCr between the two groups in neuron-rich slices pretreated with 100 μM fluorocitrate (FDP 60.9%, control 55.2%; $p = 0.483$). Although FDP was a potent radical scavenger with EC_{50} of 21.6 mM ($p < 0.001$), virtually no radical scavenging capacity was observed under the present experimental condition at 1 mM.

Conclusions: Our observation of decrease in FDP level indicated that FDP was utilized as energy substrate during the ischemic insult. The neuroprotective effects of FDP were observed in normal brain slices, but not in neuron-rich slices. The latter suggests that the neuroprotective effects of FDP depended on the presence of astrocytes. It might be suggested that the primary mechanisms of FDP as a potent neuroprotectant might be a metabolic substrate including one in glial aerobic glycolysis which provides neurons with lactate (astrocyte-neuron lactate shuttle), and secondary a radical scavenger, if any.

References:

Farias et al. (1990) *Stroke* 21:606-13

Hasegawa et al. (1997) *Brain Res* 750:1-10

Romsi et al. (2003) *J Thrac Cardiovasc Surg* 125:686-98

Sola et al. (1996) *Brain Res* 741:294-99

Tokumaru et al. (2009) *Neurochem Res* 34:775-785

Valério et al. (2009) *Br J Pharmacol* 158:558-568

Acknowledgments: The authors sincerely thank Dr. M. Kamibayashi who provided purified CYPMPO for ESR study.

704

ARTERIAL VASCULARIZATION OF THE ANTERIOR PERFORATED SUBSTANCE

E. Tuccar, T. Sen, A.F. Esmer, H.I. Acar, S.T. Karahan

Department of Anatomy, Ankara University, Ankara, Turkey

Introduction: Arteries of the anterior perforated substance (APS) are important because of their role in blood supply of the some important internal structures such as the internal capsule, putamen and caudate nucleus.

Objective: The purpose of this study was to investigate the arteries of the APS in detail.

Material and methods: The arteries of the APS were investigated in 60 cerebral hemispheres from 30 adult cadaveric brains. The internal carotid arteries were canulated and perfused with colored latex in fresh brains and then they were embalmed in 10% formaline solution for fixation. The branches of the middle cerebral artery (MCA) which penetrated the APS were investigated. These arteries are known as the lateral lenticulostriate arteries (LLAs).

Results: LLAs originated from the M1 segment of the MCA, early temporal and the early frontal branches of the MCA were recorded. And also, the LLAs arose from the superior trunk of the MCA were noted. The branches of the anterior choroidal artery which reached the APS were seen in all specimens. We found 1-3 branches which arose from A2 segment of anterior cerebral artery (ACA) to APS in all hemispheres. And also, 1-3 branches originated from A1 segment of ACA were seen in 48 hemispheres. In addition, two accessory MCAs originated from the A2 segment of the ACA were recorded as a variation and their perforating branches to APS were observed.

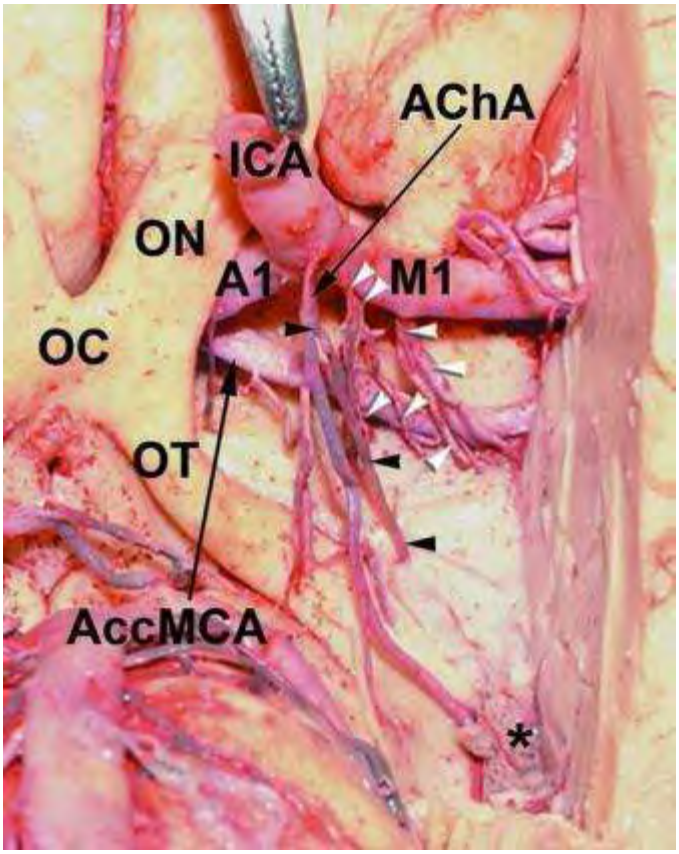

[Anterior Perforating Substance]

Conclusion: Serious complications like motor deficits can occur due to injuries of these arteries. Therefore the neurosurgeons must be aware during operations such as aneurysm or insular tumor surgeries.

Key Words: Anterior perforated substance, lateral lenticulostriate arteries, anterior perforating arteries, accessory middle cerebral artery

706

LYSOSOMAL TRAPPING OF A RADIOLABELED SUBSTRATE OF P-GLYCOPROTEIN AS A MECHANISM FOR POSITRON EMISSION TOMOGRAPHY SIGNAL AMPLIFICATION

P. Kannan[1,2], K.R. Brimacombe[3], W.C. Kreisl[2], J.-S. Liow[2], S.S. Zoghbi[2], S. Telu[2], Y. Zhang[2], V.W. Pike[2], C. Halldin[1], M.M. Gottesman[3], M.D. Hall[3], R.B. Innis[2]

[1]Clinical Neuroscience, Karolinska Institutet, Stockholm, Sweden, [2]Molecular Imaging Branch, National Institute of Mental Health, [3]Laboratory of Cell Biology, National Cancer Institute, Bethesda, MD, USA

Objectives: P-glycoprotein (P-gp) is a transporter that blocks the passage of substrates across the blood-brain barrier and has been shown to impede the delivery of many therapeutic compounds to the brain. P-gp function at the blood-brain barrier can be measured *in vivo* using positron emission tomography (PET) by co-administering the substrate radiotracer [^{11}C]*N-desmethyl*-loperamide ([^{11}C]dLop) and the P-gp inhibitor tariquidar. When P-gp is inhibited, [^{11}C]dLop, a potent opiate agonist, enters and becomes trapped in the brain[1]—a beneficial property for imaging because it amplifies the PET signal by accumulating radioactivity over time. Since we previously demonstrated that trapping was not due to binding to the opiate receptor[2], we hypothesized that [^{11}C]dLop, a weak base, is ionically trapped in acidic lysosomes.

Methods: We measured the accumulation of [^{3}H]dLop in human cells pretreated with increasing concentrations of four compounds that raise lysosomal pH and visualized lysosomal competition by a fluorescent marker using confocal microscopy. Because the *in vivo* trapping of dLop was seen after P-gp inhibition, we also measured the amount of [^{3}H]dLop in P-gp expressing cells pre-treated with increasing concentrations of tariquidar. Our *in vitro* results indicated that tariquidar may compete with dLop for lysosomes, so we used PET to investigate if lysosomal competition occurs *in vivo*. To examine the effects of tariquidar other than as a P-gp inhibitor, we measured the uptake of [^{11}C]dLop before and after injection of tariquidar (32 mg/kg, i.v.) in lysosome-rich organs (kidneys, spleen) and brains of P-gp knockout mice. Then, we performed a similar experiment in six healthy humans using [^{11}C]dLop and tariquidar (2 mg/kg, i.v.).

Results: *In vitro*, the cellular accumulation of [^{3}H]dLop was prevented ≥ 50% by compounds that raise lysosomal pH. Lysosomal competition of dLop was confirmed using confocal microscopy (Figure 1). In P-gp expressing cells, tariquidar had two effects on [^{3}H]dLop accumulation: at < 100 nM, it increased accumulation by 50%, but at > 100 nM, it decreased accumulation to baseline levels. *In vivo,* in both P-gp knockout mice and humans pre-treated with tariquidar, uptake of [^{11}C]dLop in the kidneys and spleen decreased by 35-40% ($P < 0.05$), but did not decrease in the brain.

Conclusion: Our results support our hypothesis that dLop is ionically trapped in lysosomes. We also showed that tariquidar, in addition to being a P-gp inhibitor, competes with dLop for lysosomal accumulation in human cells, *in vitro*, and in peripheral organs of mice and humans *in vivo*. However, tariquidar does not compete with dLop accumulation in the brain because tariquidar has negligible entry into the brain.[3] Thus, [^{11}C]dLop can still be used in combination with tariquidar to measure P-gp function at the blood-brain barrier.

References:

1. Kreisl WC, *et al.* (2010) *J Nucl Med* 51: 559-566.

2. Lazarova N, *et al.* (2008) *J Med Chem* 51: 6034-6043.
3. Kawamura, *et al.* (2010) *Ann Nucl Med* 24: 403-12.

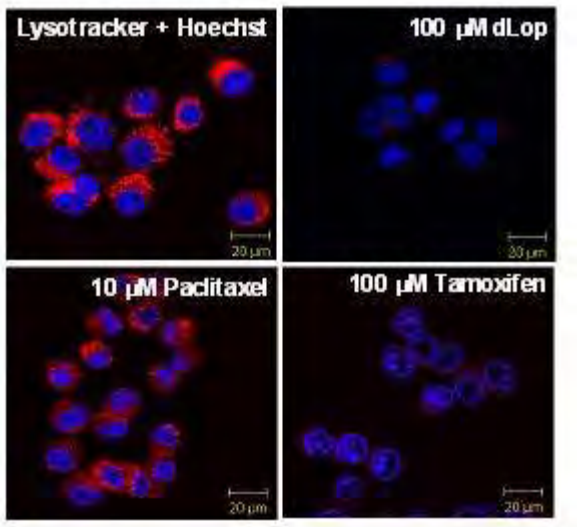

[Figure 1]

Displacement of fluorescent marker (Lysotracker) from lysosomes by dLop, tamoxifen (positive control), but not paclitaxel (negative control).

707

MULTI-SCALE HIERARCHICAL APPROACH FOR PARAMETRIC MAPPING: ASSESSMENT ON MULTI-COMPARTMENTAL MODELS

G. Rizzo[1], F.E. Turkheimer[2,3], S. Bose[3], A. Bertoldo[1]

[1]Department of Information Engineering, University of Padova, Padova, Italy, [2]Division of Experimental Medicine, [3]MRC Clinical Sciences Centre, Imperial College London, London, UK

Introduction: Following previous work [1], we developed a new hierarchical method to apply Basis Function Method (BFM) [2] to multi-compartmental models such as a 2 tissue compartment with 4 parameters (2T-4K) model and 1 tissue plus 1 blood compartment and three parameters (1T-3K) ones. The grids for the basis functions are generated automatically from the data, specifically for each Region of Interest (ROI), being consequently user-independent.

Material and methods: The local grids for voxel-by-voxel analysis were defined a priori, using the estimates obtained by application of the optimal model for the ROI Time Activity Curves (TACs) and solved with weighted non linear least squares (WLQ).

In order to investigate the impact of varying grid specifications, ROIs were obtained using both anatomical (atlas) and functional information (unsupervised clustering). Two datasets ([^{11}C]FLB457, high affinity dopamine D_2/D_3 receptor radioligand, and [^{11}C]SCH442416, highly selective adenosine A_{2A} antagonist), were used for the validation of the method applied to 2T-4K (2T-4K BFM) and 1T-3K model (1T-3K BFM) respectively. The parameter of interest was the Volume of Distribution (V_T). 6 and 18 subjects respectively underwent 90-min dynamic PET in a ECAT EXACT3D PET camera, following an injection with 280 to 380 MBq of [^{11}C]FLB and with 370 MBq of [^{11}C]SCH respectively. Arterial plasma input functions corrected for metabolites were created. An individualized maximum probability atlas was created for each subject and used to derive 83 ROIs for [^{11}C]FLB and 73 ROIs for [^{11}C]SCH.

The best model for each tracer was applied at voxel level and solved with WLQ and the estimates were compared to those obtained with 2T-4K BFM and 1T-3K BFM at voxel level.

Results: For both datasets, using grids defined on ROIs obtained by cluster analysis, V_T parametric maps were reliable, reproducing the known receptor distributions in the brain. There was strong agreement and excellent correlation among voxel BFM and voxel WLQ estimates ([^{11}C]FLB: $R^2 > 0.92$, Fig. 1A; [^{11}C]SCH: $R^2 > 0.93$, Fig 1B). V_T estimates out of physiological range were less than 3% using BFM, while around 20% using WLQ, being WLQ more sensitive to the noise in the data. Similar results held also when grids were defined on ROI obtained using the individualized maximum probability atlas.

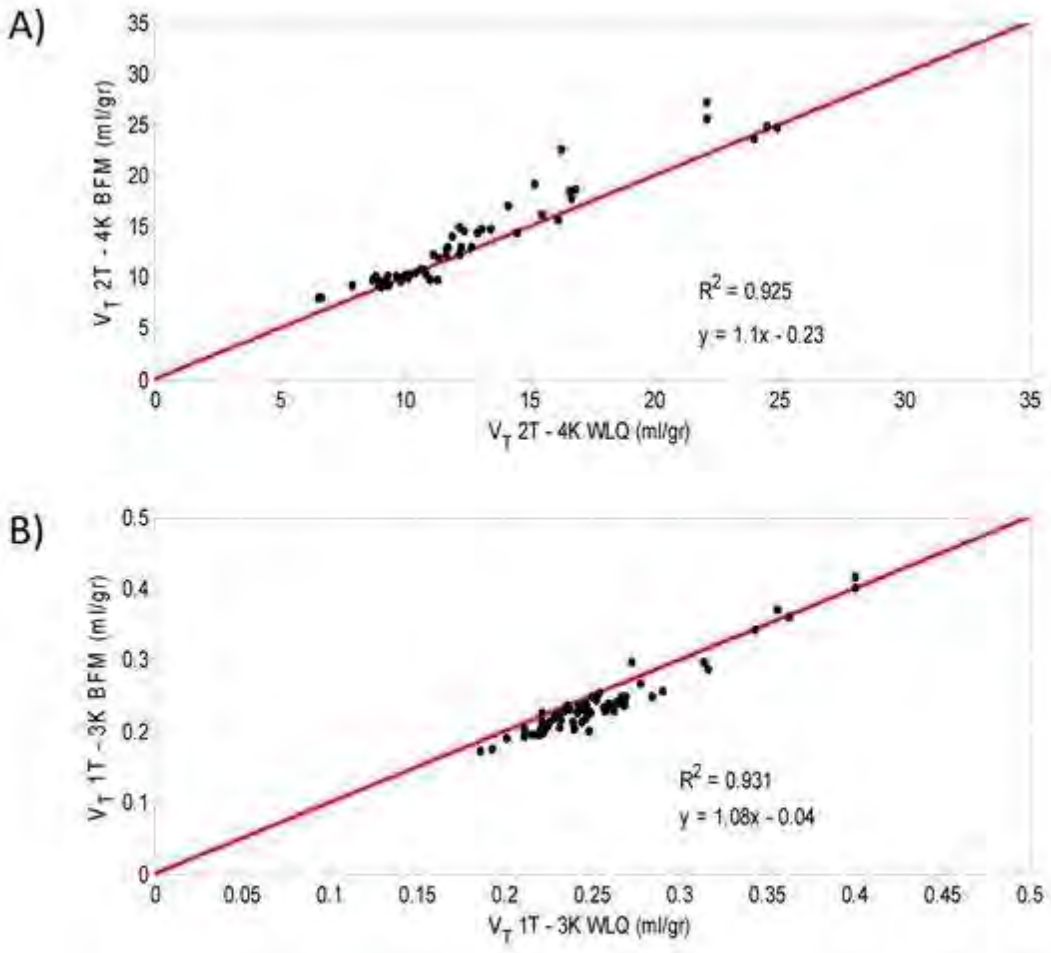

Fig 1. Scatterplot of average within the ROIs of V_T WLQ estimates (x axis) versus average of V_T 2T-4K BFM estimates for [^{11}C]FLB (A) and V_T 1T-3K BFM estimates for [^{11}C]SCH (B) (y axis). Pearson's correlation coefficient R^2, slope and intercept of the fitted regression line are presented.

[Fig1]

Conclusions: The new method is faster than WLQ (10-12 hrs vs 36-40 hrs) and robust. To the authors' knowledge there is only one previous work which developed the BFM for multi-compartmental models [3], but in that approach the grids were global and user-defined. Application of the novel methodology on both [^{11}C]FLB and [^{11}C]SCH allowed accurate quantification of V_T and good quality parametric maps. There is excellent agreement between the results obtained and the WLQ voxel level results. Moreover, we showed as functional clustering can be a good alternative for the ROIs' definition.

[1] Rizzo et al (2010) *Neuroimage* 52: S179 - S180

[2] Gunn et al (1997) *Neuroimage* 6: 279 - 287

[3] Hong and Fryer (2010) *Neuroimage* 51: 164 - 172

709

UNDERSTANDING THE EFFECT OF THE P-GP INHIBITOR CYCLOSPORIN ON ^{18}F-MPPF BRAIN UPTAKE IN NONHUMAN PRIMATE

N. Tournier[1], W. Saba[1], M. Bottlaender[1], F. Dollé[1], S. Cisternino[2], S. Goutal[1], M.A. Peyronneau[1], H. Valette[1]

[1]CEA,DSV,I2bm,SHFJ, Orsay, [2]INSERM U705; CNRS UMR8206, Paris, France

Introduction: The $5HT_{1A}$ radioligand ^{18}F-MPPF has been widely identified as a P-glycoprotein (P-gp) substrate in rodents as shown by a significant increase of its brain uptake in P-gp deficient mice or following P-gp pharmacological inhibition. However, our recent *in vitro* study using a reliable human P-gp specific model (transport assay using MDCKII-hMDR1 cells) failed to identify this compound as a human P-gp substrate. This result suggests a confounding interspecies variability. In the present work, the effects of the P-gp inhibitor cyclosporin a (CsA) on ^{18}F-MPPF peripheral blood clearance and brain uptake were studied in nonhuman primates.

Methods: Two *Papio Anubis* adult baboons were PET scanned twice (with and without P-gp inhibition) on a ECAT-EXACT-HR+ tomograph. P-gp inhibition was induced by infusion of CsA (15 mg/kg/h) starting 30 min prior to ^{18}F-MPPF injection (185-296 MBq) until the end of the PET scan (90 min). The percentage of unchanged ^{18}F-MPPF in arterial plasma was determined at selected times using radio-HPLC analysis. Plasma protein binding of ^{18}F-MPPF was measured on plasma samples collected from CsA-naïve and CsA-treated baboons using ultrafiltration. PET area under the curve ($AUC_{PET\ (0\text{-}90min)}$) were calculated in 3 regions of interest (ROI) defined manually: brain hemispheres, hippocampus and cerebellum (widely used as a region of reference for ^{18}F-MPPF PET analysis).

Results: ^{18}F-MPPF $AUC_{PET\ (0\text{-}90min)}$ were increased (~1.8 fold) in all the ROIs in CsA treated baboons compared to control. This effect could not be attributed to any increase in the arterial input function radioactivity or to any metabolic interaction between CsA and ^{18}F-MPPF (mean intact fraction of ^{18}F-MPPF at 60 min was ~13 % in both circumstances). However, CsA treatment seemed to lower ^{18}F-MPPF plasma protein binding, since the ^{18}F-MPPF free fraction was twice higher in CsA *vs* control baboons.

Conclusion: The increase of ^{18}F-MPPF brain uptake following CsA treatment in the absence of peripheral clearance change could suggest a role of P-gp efflux at the baboon blood-brain barrier. However, this effect could also be attributed to the release of ^{18}F-MPPF from plasma protein. Therefore, we cannot conclude that ^{18}F-MPPF is a P-gp substrate in baboons. Further investigations are required to evidence the interspecies variability in the P-gp substrate property of ^{18}F-MPPF and anticipate its impact in humans, with careful attention on plasma protein binding of ^{18}F-MPPF.

710

MODEL-BASED APPROACH APPLIED TO VISUAL SEARCH: SEPARATING INHIBITORY AND EXCITATORY TOP-DOWN PROCESSES

E. Mavritsaki, H. Allen, G.W. Humphreys

Department of Psychology, University of Birmingham, Birmingham, UK

This work focuses on understanding the neural processes underlying visual search. We use a model based approach that allows us to combine behavioural, modelling and fMRI data. In previous studies (Mavritsaki et al., 2010; in press), fMRI data on human search were assessed using activation functions predicted from the spiking search over time and space model (sSoTS; Mavritsaki et al., 2006).

We showed how a biologically plausible model can be used to decompose complex response patterns found in fMRI studies of human attention, separating circuits concerned with inhibition of attention function from those concerned with top-down enhancement.

This was possible because the sSoTS model incorporates different synaptic components (NMDA, AMPA, GABA) and a frequency adaptation mechanism based on [Ca2+] sensitive K+ current. This frequency adaptation current can act as a mechanism that suppresses previously attended items. When the passive process (frequency adaptation) is coupled with a process of active inhibition, new items can be successfully prioritised over older items and this occurs over time periods matching those found in psychological studies (Mavritsaki et al., 2006). We have also shown for the first time that activity in a central location map in the model, (which computes the saliency of a target relative to distracters) correlated with brain activation response in the right temporo-parietal junction (TPJ) - a key region

implicated in clinical studies of unilateral neglect.

These results indicate that excitatory and inhibitory circuits for visual selection can be separated, and that the right TPJ may be critical for responding to salient targets. Here, we take this a step further by applying the same to approach to a new fMRI study.

Participants were either told to ignore the old items and attend to the new items (as before), or told to attend to (or ignore) a particular category of search items. This allows us to clearly separate model and brain activity to inhibitory and excitatory processes.

References:

Mavritsaki E., Heinke D., Allen H., Deco G. and Humphreys G.W. (in press) “Bridging the gap between physiology and behavior: Evidence from the sSoTS model of human visual attention.” Psychological Review.

Mavritsaki E., Allen H.A., Humphreys G.W. (2010) “Decomposing the neural mechanisms of visual marking using an interconnected network of spiking neurons: The spiking search over time and space model (sSoTS).” NeuroImage, 52(3), 934-46.

Mavritsaki E., Heinke D., Deco G. and Humphreys G.W. (2006) “A computational model of visual marking using an interconnected network of spiking neurons: The spiking search over time & space model (sSoTS).” Journal of Physiology Paris, 100, 110-124.

711

ADAM17/TACE INHIBITS NEUROGENESIS AND PROMOTES GLIA GENERATION FROM NEURAL STEM CELLS: A MECHANISM THAT MAY IMPAIR RECOVERY IN CNS INJURY

M. Murillo-Carretero, C. Romero-Grimaldi, M.A. Lopez-Toledano, M. Carrasco-Viñuela, C. Castro, C. Estrada

Physiology, University of Cadiz, Cadiz, Spain

Introduction: Neural precursor cells (NPC) are activated in CNS lesions of different origin. However, in spite of being multipotential, they give rise to new glial cells, but not to new neurons, in the damaged area. This situation might be overcome by the induction of a neurogenic/non-gliogenic niche in the injured tissue.

Objective: The aim of this work was to investigate the role of the endogenously-activated epidermal growth factor receptor (EGFR) in the generation of gliogenic conditions, in search for a therapeutical target that could favour neuronal rather than glial differentiation.

Methods: NPC were isolated from postnatal mouse subventricular zone and maintained in neurosphere cultures for 3-10 passages. Then, cells were adhered and allowed to differentiate in the absence of added growth factors, and the generated cell phenotypes were analyzed by immunocytochemistry four days later. For *in vivo* experiments, discrete mechanical lesions were performed in the motor cortex of anesthetized adult mice. Animals were killed one week later and their brains were used for immunohistochemical studies or real time PCR. A group of mice was implanted with osmotic mini-pumps allowing continuous delivery of drug or vehicle in the lesioned area along the week of survival.

Results: Differentiating NPC in control cultures generated approximately 20% neuroblasts and 30% astrocytes four days after seeding, as detected by immunostaining for βIII-tubulin and GFAP, respectively. AG1478, a specific inhibitor of the EGFR, produced a significant increase in the number of neuroblasts and a significant decrease in the number of astrocytes. Similar results were obtained upon treatment with the broad spectrum metalloprotease inhibitor GM6001, thus revealing that some endogenous membrane-bound EGFR ligand was subjected to proteolytic cleavage, and activated the receptor. Differentiating NPC expressed the metalloproteases ADAM-10 and ADAM-17/TACE and the EGFR ligands TGF-α and HB-EGF. By using siRNA transfection, ADAM-17/TACE was identified as the specific metalloprotease which inhibited neurogenesis and promoted gliogenesis. TGF-α was detected by ELISA in control cultures, but not in those treated with GM6001.

In vivo experiments showed that ADAM-17/TACE, as well as TGF-α and EGFR, were upregulated in the NPC which appeared around the area of injury. Furthermore, local infusion with GM6001 produced the generation of new neuroblasts around the lesion, whereas these cells were only occasionally found in control mice or in mice infused with vehicle.

Conclusions: The results strongly suggest that the activation of ADAM-17/TACE in NPC initiates EGFR ligand shedding and EGFR activation in an autocrine manner, reducing neuroblast generation and leading to preferential glial differentiation. Inhibition of ADAM-17/TACE, the limiting step in this sequence, might be useful for the generation of neurogenic niches in areas of brain damage in patients.

712

INVOLVEMENT OF BOTH PLASMAMEMBRANE SODIUM CALCIUM EXCHANGER (NCX) AND SODIUM DEPENDENT GLUTAMATE TRANSPORTERS IN CELL ENERGY PRODUCTION

S. Amoroso, S. Magi, V. Lariccia, A.A. Nasti, S. Arcangeli, P. Castaldo

Neuroscience, University Politecnica of Marche, Ancona, Italy

Glutamatergic pathways seem to be involved in brain metabolism. In neuronal and glial cells Excitatory Amino Acid Transporters (EAATs) are responsible for glutamate transport coupled with Na^+. When glutamate enters the cell through EAATs, an increase in intracellular Na^+ occurs. In astrocytes it has been shown that Na^+ entry via EAATs may activate the reverse mode of the Na^+/Ca^{2+} exchanger (NCX), that couples the uphill extrusion of Ca^{2+} to the entrance of Na^+. Three different NCX1-3 isoforms have been identified and all are expressed in CNS. Both NCX and EAATs activities can be affected by the transmembrane Na^+ gradients to which these transporters are simultaneously exposed, so that their action may be co-modulated. In this study we characterized the expression and activity of EAATs and NCX and their possible involvement in energy production. We used two continuous cell lines, SH-SY5Y human neuroblastoma and rat C6 glioma. These cell lines express NCX1 and NCX3, and between the EAATs, they mainly express EAAC1. Exogenous glutamate promoted a significant increase in ATP production in both these systems. This effect was abolished when the cells were preincubated with DL-TBOA, an EAATs inhibitor. Moreover glutamate induced ATP synthesis was abrogated when EAAC1 was selectively knocked-out with antisense oligonucleotides. To establish the possible involvement of NCX in glutamate-induced ATP synthesis, we used KB-R7943, a selective NCX blocker. This compound reduced the glutamate-induced ATP production both in SH-SY5Y and C6. Moreover, by using specific antisense oligonucleotides against NCX1, we observed that, both in SH-SY5Y and C6, NCX1 knocking-out recapitulated the effect of KB-R7943; conversely, antisense oligonucleotides directed against either NCX2 or NCX3 were ineffective. Collectively, these results suggest that, in CNS, EAAC1 may be involved in the glutamate-induced ATP production and that glutamate may elicit ATP synthesis only if NCX1 activity is preserved.

713

NATURAL PROGRESSION OF CEREBRAL SMALL VESSEL DISEASE IN SH-SP RATS

C.Z. Büche[1,2], S. Schreiber[1,2], C. Garz[1,2], H.-J. Heinze[1,2], M.W. Goertler[1,2], K.G. Reymann[2,3], H. Braun[2,3]

[1]Department of Neurology, Otto-von-Guericke University, [2]German Center for Neurodegenerative Diseases, [3]Leibniz Institute for Neurobiology, Magdeburg, Germany

Objectives: Cerebral small vessel disease (CSVD) is one of the leading causes of lacunar strokes and vascular dementia, which is associated with vessel wall alterations, blood-brain barrier (BBB) disturbances, vasogenic edema and microbleeds. To assess occurrence and role of these pathological aspects we used spontaneous hypertensive stroke-prone (SHSP) rats as a model for CSVD.

Methods: Animals were divided into groups from 12 to 36 weeks of age. After transcardially perfusion brains were removed and frozen slices were stained with hematoxyline/eosine for detection of vessel wall changes, microbleeds and edema. Brain slices at different ages of the rats were immunohistochemically stained for IgG to describe a possible leakage of the BBB. Wistar rats from 12 to 36 weeks of age served as a control group. The number of stases and microbleeds was assessed in rats at different ages encompassing the brain regions corpus callosum, cortex, hippocampus and basal ganglia. Further, we determined the diameter of vessels containing stases. To describe a progression of BBB disturbance, the frequency of vessels positive for IgG was counted in the same brain regions.

Results: From the 12th week on, we found an accumulation of erythrocytes in the lumen of small vessels (stases) in all examined brain regions. SHSP rats were affected significantly more often than the controls. The number of vessels containing stases of erythrocytes significantly increased with age of SHSP group in all investigated brain regions. Furthermore, the diameter of affected vessels was significantly increased in the basal ganglia of SHSP animals older than 28 weeks. In addition to the occurrence of erythrocytes in small vessels, microbleeds were observed from the 32nd week on. Number of SHSP rats with microbleeds in the hippocampus and cortex significantly increased with age. Arteriolar wall thickening and occlusion accompanied by vasogenic edema and tissue infarctions were observed at the earliest in the 32nd week. Occurrence of IgG positive vessels, showing BBB disturbances, started in the 18th week and increased significantly with age of SHSP rats.

Conclusions: Accumulation of erythrocytes in small vessels without vessel wall changes represents the initial step in the pathologic cascade of CSVD. Secondly, BBB disturbances occuring some weeks after stases were detectable. Both phenomena are progressive and deteriorate with higher age. Microbleeds and finally, arteriolar wall thickening and occlusion leading to edema and tissue infarctions are the last steps of that pathological cascade.

715

SYSTEMIC STIMULATION OF TLR2 IMPAIRS NEONATAL MOUSE BRAIN DEVELOPMENT

X. Wang[1], X. Du[1], B. Fleiss[1], H. Li[1], C. Zhu[1], H. Hagberg[2,3], O. Levy[4], C. Mallard[1]

[1]Department of Neuroscience and Physiology, [2]Department of Obstetrics and Gynecology, The University of Gothenburg, Gothenburg, Sweden, [3]Imperial College, London, London, UK, [4]Harvard Medical School, Boston, MA, USA

Objectives: Perinatal brain injury is associated with inflammation but the underlying mechanisms are not completely characterized. Stimulation of Toll-like receptors (TLRs) through specific agonists induces inflammatory responses that trigger both antigen presenting cell and adaptive immune responses. The impact of engagement of TLR2 signaling pathways on the neonatal brain is still unclear. The aim of this study is to investigate the potential effect of TLR2 agonist on neonatal brain development.

Methods: Mice were injected intraperitoneally (i.p.) once a day with a TLR2 agonist, Pam_3CSK_4 (5mg/kg) from postnatal day (PND) 3 to PND11. Endotoxin-free saline injected mice were used as controls. Pups were sacrificed at PND12 or PND53. Brain, spleen and liver were collected and weighed. Brain sections were stained for brain injury markers. Long-term effects on memory function were assessed using the trace fear conditioning test at PND50.

Results: After 9 days of Pam3CSK4 administration, brain weight was decreased compared with endotoxin-free saline-treated animals at PND12. We also found a decreased volume of cerebral gray matter, white matter in the forebrain and cerebellar molecular layer that was accompanied by an increased spleen and liver weight at PND12. Forebrain gray matter volume: Pam3CSK4 139.4 ± 1.68 mm^3 *vs.* saline 145.1 ± 1.66 mm^3 (mean ± SEM, $p< 0.05$). Forebrain white matter volume: Pam3CSK4 9.4 ± 0.2 mm^3 *vs.* saline 10.1 ± 0.3 mm^3 (mean ± SEM, $p< 0.05$). Pam3CSK4-treated mice also displayed decreased neuronal density in the hippocampus (Pam3CSK4 360 000 ± 43 000 cell/μm^3 vs. saline: 400 000 ± 40 000 cell/μm^3, mean ± SEM, $p< 0.01$); and increased density of microglia (Pam3CSK4 145 9965 ± 23 387 cell/μm^3 vs. saline: 116 767 ± 13 451 cell/μm^3, mean ± SEM, $p< 0.01$), while there was no effect on caspase-3 or general cell proliferation. Pam_3CSK_4

administration did not have any effect on gray or white matter volume on PND53 or long-term memory function, as judged by the trace fear conditioning test conducted at PND50.

Conclusions: Repeated systemic exposure to the TLR2 agonist Pam_3CSK_4 can have a short-term negative impact on the neonatal mouse brain.

716

THE NCX3 ISOFORM OF THE NA^+/CA^{2+} EXCHANGER CONTRIBUTES TO NEUROPROTECTION ELICITED BY ISCHEMIC POSTCONDITIONING

G. Pignataro, E. Esposito, O. Cuomo, R. Sirabella, F. Boscia, A. Vinciguerra, G. Di Renzo, L. Annunziato

Neuroscience, Federico II University of Naples, Naples, Italy

It has been recently demonstrated that a short sub-lethal brain ischemia subsequent to a prolonged harmful ischemic episode may confer ischemic neuroprotection, a phenomenon termed ischemic postconditioning. Na^+/Ca^{2+} exchanger (NCX) isoforms, NCX1, NCX2, and NCX3, are plasmamembrane ionic transporters widely distributed in the brain and involved in the control of Na^+ and Ca^{2+} homeostasis and in the progression of stroke damage. Objective of this study was to evaluate the role of these three proteins in the postconditioning-induced neuroprotection.

NCX protein and mRNA expression was evaluated at different time points in the ischemic temporoparietal cortex of rats subjected to tMCAO alone or to tMCAO plus ischemic postconditioning.

Results of the present study showed that NCX3 protein and ncx3 mRNA were up-regulated in those brain regions protected by postconditioning treatment. These changes in NCX3 expression were p-AKT mediated, since the p-AKT inhibition prevented NCX3 up-regulation. The relevant role of NCX3 during postconditioning was further confirmed by results showing that NCX3 silencing, induced by icv infusion of siRNA, partially reverted the postconditioning-induced neuroprotection.

The results of the present study support the idea that the enhancement of NCX3 expression and activity might represent a reasonable strategy to reduce the infarct extension after stroke.

719

A NOVEL ROLE FOR THE GRANULOCYTE-MACROPHAGE COLONY STIMULATING FACTOR (GM-CSF) IN LEARNING AND MEMORY

M. Krieger[1], M. Klugmann[2], A. Schneider[1]

[1]Sygnis Bioscience, Heidelberg, Germany, [2]Department of Physiology & Translational Neuroscience Facility, School of Medical Sciences, UNSW Kensington Campus, Sydney, NSW, Australia

Objective: Previously, Granulocyte-Macrophage Colony Stimulating Factor (GM-CSF) has been shown to act as both a potent neuroprotective (1) and proneurogenic (2) factor in the rodent brain. This study was conducted to investigate a putative role of GM-CSF signaling in the mouse brain during cognitive processes of learning and memory.

Methods: GM-CSF knock-out (GMko) mice and wildtype controls were subjected to a cognitive test battery assessing both spatial and fear-related learning and memory. In a complementary approach, GM-CSF receptor alpha (GMRa) expression was specifically altered in the hippocampus of wildtype mice using adeno-associated virus (AAV) vectors. Here, the receptor was either overexpressed or knocked-down by a specific shRNA. The same cognitive test battery was then used on those mice.

Results: In GMko mice, cognitive deficits were observed in all paradigms tested. These animals showed impairments in i) fear memory to both context and conditioned cue in a fear conditioning experiment, ii) spatial learning in an active place avoidance paradigm, and iii) spatial memory in the Morris Water Maze (MWM). The inferior task performance observed in GMko animals were not due to confounding secondary factors related to motor function, inherent anxiety, or pain threshold levels, as judged by Rotarod, dark-light emergence, and plantar test analyses, respectively. Corroborating these data, AAV-mediated bidirectional modulation of GMRa expression in the hippocampus led to differential performance levels in hippocampus-specific tasks such as the MWM, meaning that spatial memory was enhanced or impaired dependent on GMRa overexpression or knock-down, respectively.

Conclusions: Collectively, these results suggest that GM-CSF signalling plays a hitherto unrecognized important role in hippocampus-dependent learning and memory in the mouse brain. This conclusion is supported by two fully different approaches to manipulating this system in the rodent. GM-CSF, which is in clinical use in indications such as neutropenia, could therefore present a novel therapeutic opportunity in neurodegenerative diseases with a cognitive component.

References:

(1) Schäbitz et al., A neuroprotective function for the hematopoietic protein granulocyte-macrophage colony stimulating factor (GM-CSF). *J Cereb Blood Flow Metab.* (2008) 28:29-43

(2) Krüger et al. (2007) The hematopoietic factor GM-CSF (granulocyte-

macrophage colony-stimulating factor) promotes neuronal differentiation of adult neural stem cells in vitro. *BMC Neurosci.*(2007); 8:88

722

ANALYSIS OF CEREBRAL BLOOD FLOW DURING CARDIOPULMONARY BYPASS DEPENDENT ON THE LEVEL OF CEREBRAL AUTOREGULATION USING COMPUTATIONAL FLUID DYNAMICS

T.A.S. Kaufmann[1], T. Schmitz-Rode[1], A. Moritz[2], U. Steinseifer[1]

[1]Cardiovascular Engineering, Institute of Applied Medical Engineering, Helmholtz Institute, RWTH Aachen University, [2]Thoracic and Cardiovascular Surgery, Johann Wolfgang Goethe-University Frankfurt am Main, Aachen, Germany

Objectives: Neurologic malfunction is a common problem during or after use of cardiopulmonary bypass (CPB). Headaches, mnemonic problems, loss of neural functions or coma can occur. These phenomena are related to decreased cerebral blood flow (CBF) and thus flow conditions in the cardiovascular (CV) system. As shown in recent studies [1,2], these conditions are affected by outflow cannula positioning.

Additionally, cerebral autoregulation (CA) plays an important role for CBF. It is defined as the body's intrinsic ability to provide sufficient CBF despite changes in cerebral perfusion pressure (CPP). Thus, it can be understood as a pressure-dependent change in cerebrovascular resistance.

In this study, a Computational Fluid Dynamics (CFD) model is presented to analyze CBF dependent on CA and cannula positioning during CPB.

Methods: A 3D-model of the human CV-system including aorta and greater vessels was generated from MRI records of healthy male volunteers. Numerical simulations of the flow in the CV-system were performed for physiological conditions and CPB. Flow rates were varied between 4.5-6 l/min, blood was modeled as a non-Newtonian fluid. The arterial outlets were set using a mathematical parameter model to represent CA by cerebrovascular resistance. Thus, CBF was calculated as a function of CPP.

In this function, CBF is kept constant for CPP of 80-120 mmHg. A deviation in CBF of up to 20% occurs for CPP between 55-80 mmHg and 120-145 mmHg, respectively. For CPP lower than 55 mmHg, CBF decreases drastically, so that the critical closing pressure is reached at approximately 20 mmHg.

Based on this model, the level of CA was varied between full and no regulation, to study the effect on CBF during CPB. The results from this study were compared to recent studies in which CA was neglected.

Results: CBF was not affected by the level of CA for physiological conditions. During CPB however, CBF is decreased to approximately 80% of baseline assuming full CA as mentioned above. Thus, CBF remains unchanged during a simulated native cardiac output of 5 l/min or CBP support of 6 l/min. Yet, by decreasing the level of CA, CBF can be regulated between 0 and 80% of baseline. Assuming slight or no CA, CBF is also highly dependent on cannula positioning.

Conclusions: The level of cerebral autoregulation has a strong impact on cerebral blood flow during cardiopulmonary bypass. It is therefore imperative to include this mechanism into CFD studies.

Furthermore, this study demonstrates that modeling of autoregulation by cerebrovascular resistance delivers feasible results. By varying parameters of the equation representing autoregulation, this model can be used to quantify the impact of different levels of regulation on cerebral blood flow. It can thus help to improve support conditions of extracorporeal circuits in general and cardiopulmonary bypass in particular.

References:

[1] Kaufmann et al. The impact of aortic/subclavian outflow cannulation for cardiopulmonary bypass and cardiac support: a computational fluid dynamics study. *Artif Organs*, 33(9):727-732, Sep 2009.

[2] Kaufmann et al. Flow distribution during cardiopulmonary bypass in dependency on the outflow cannula positioning. *Artif Organs*, 33(11):988-992, Nov 2009.

723

RECURRENT HYPOGLYCEMIA EXACERBATES CEREBRAL ISCHEMIC DAMAGE IN STREPTOZOTOCIN-INDUCED DIABETIC RATS VIA INCREASED FREE RADICAL GENERATION

K.R. Dave[1], F.J. Brand[1], A. Liu[1], S.K. Bhattacharya[2], A. Pileggi[3]

[1]Neurology, [2]Bascom Palmer Eye Institute, [3]Diabetes Research Institute, Department of Surgery, University of Miami, Miami, FL, USA

Objectives: Stroke and heart disease are the most serious complications of diabetes accounting for more than 65% of the mortality among diabetics (1). Intensive therapy to control blood glucose levels delays onset and retards the progression of secondary complications of diabetes. The major side effect of intensive therapy in both type 1 and type 2 diabetics is recurrent hypoglycemic (RH) episodes. Earlier we observed that RH exacerbates cerebral ischemic damage in insulin-treated streptozotocin diabetic (ITD) rats (2). Mitochondrial dysfunction is observed during hypoglycemia. We tested the hypothesis that RH-induced mitochondrial dysfunction is responsible for exacerbated cerebral ischemic damage in ITD rats.

Methods: Streptozotocin (Stz)-induced diabetic rats were used as an animal model. We included four experimental groups; namely, naïve (n=6), ITD (n=5), ITD+RH (n=6), and ITD+RH+Glucose (n=6) representing non-diabetics, diabetics on insulin therapy, diabetics on insulin therapy experiencing RH, and control for additional insulin that we injected to induce hypoglycemia. The RH model consisted of a total of ten hypoglycemic episodes per animal (~55-65 mg / dl blood glucose; two hypoglycemic episodes daily for 5 consecutive days). Hippocampal mitochondria were harvested overnight after the last hypoglycemia treatment and the relative quantities of mitochondrial proteins were measured using MudPIT / iTRAQ analysis.

Results: More than 1700 proteins were identified, of which 480 were identified with >95% confidence. Of these 480 proteins, the levels of NADH-ubiquinone oxidoreductase 24 kDa subunit (NDUFV2), translocase of outer mitochondrial membrane 22, and calretinin were increased more than 20% while levels of complex IV subunit Via (COXVIa) decreased more than 20% in the ITD+RH group (n = 3) as compared to three control groups (i.e. naïve, ITD, and ITD+RH+Glucose, n = 3 each). Since levels of NDUFV2 and COXVIa are altered in ITD+RH group, next we measured rate of substrate oxidation, and complex I and IV activity. We could not observe any significant differences in the rate of substrate oxidation or activity of either complexes among experimental groups. Because NDUFV2 is part of the FMN-containing NADH binding site of complex I and is one of the major sites of superoxide production in complex I, next we measured the rate of superoxide production. The rate of hydrogen peroxide production in the ITD+RH i.p. group was higher by 35% ($p< 0.05$), 29% ($p< 0.05$) and 33% ($p< 0.05$) as compared to the naïve, ITD, and ITD+RH+Glucose i.p. groups, respectively.

Conclusion: We are first to demonstrate that RH in diabetic animals exacerbates cerebral ischemic damage. Our results suggest that increased free radical release from mitochondria may be responsible for observed increased ischemic damage in ITD+RH rats.

References: 1) Biller and Love. Med Clin North Am, 77, 1993, 95

2) Dave et al. Stroke. 2008; 39:50.

Support: AHA (0735106N) and S.J. Glaser Research Grant.

724

ANTI-EDEMATOUS EFFECT BY SIMVASTATIN, AN HMG-COA REDUCTASE INHIBITOR, IN TRAUMATIC BRAIN INJURY: EVIDENCE AND PUTATIVE MECHANISMS

T. Béziaud, X.R. Chen, N. El Shafey, M. Frechou, F. Teng, B. Palmier, V. Beray Berthat, M. Soustrat, I. Margaill, **M. Plotkine**, C. Marchand-Leroux, V. Besson

Pharmacologie de la Circulation Cérébrale EA4475, Université Paris Descartes, UFR des Sciences Pharmaceutiques et Biologiques, Paris, France

Introduction: Traumatic brain injury (TBI) causes deleterious brain edema leading to high mortality and morbidity in affected individuals. Brain edema exacerbates neurological deficits and may be due to the breakdown of endothelial cell junction proteins, polymorphonuclear neutrophil (PMN) infiltration and matrix metalloproteases (MMP) activation. These all contribute to loss of blood brain barrier (BBB) integrity. As we previously showed that simvastatin, an HMG-CoA reductase inhibitor, reduced neurological deficit and brain edema in a rat model of TBI[1], we evaluated whether anti-edematous effect is associated with modulation of claudin-5, a tight junction protein, ICAM-1 expression, PMN infiltration, MMP2 and 9 activation and thus BBB permeability.

Methods: TBI was induced by lateral fluid percussion of the temporoparietal cortex on male Sprague-Dawley rats as previously described[1]. Simvastatin (37.5mg/kg) or its vehicle were given p.o. at 1h and 6h after brain injury. Brain edema was evaluated by measuring brain water content (BWC). Claudin-5 expression was determined by western blot. ICAM-1 expression was done by immunohistochemistry, PMN infiltration by measuring MPO activity and MMP2 and 9 activities by zymography. BBB permeability was assessed by extravasation of two fluorescent dyes, Evans blue (EB) and Fluorescein sodium salt (NaFl). The one of EB represents large MW molecule passage through BBB and the one of NaFl small MW molecule entry. PMN infiltration and BBB permeability were measured on temporoparietal cortex (contusion), frontal and occipital cortices (pericontusional areas) in order to evaluate more precisely areas affected. All other measures were done in the contusion.

Results: TBI induced brain edema (81.5±0.6 *versus* 79.5±0.1% for sham-operated rats, $P< 0.001$) that was reduced by simvastatin (79.9±0.1%, $P< 0.01$), showing the anti-edematous effect of this compound. Moreover, simvastatin suppressed post-TBI decrease in claudin-5 expression (20.2±2.1 *versus* 6.7±1.1 AU for TBI+vehicle rats, $P< 0.05$). TBI led to ICAM-1 staining (28.8±1.3 *versus* 14.4±0.7 for sham-operated rats, $P< 0.001$) and PMN infiltration in the contusion (0.049±0.017 *versus* 0.002±0.001 U MPO/g for sham-operated rats, $P< 0.05$) and pericontusional area (0.044±0.010 *versus* 0.003±0.002 U MPO/g for sham-operated rats, $P< 0.01$), which were decreased by simvastatin (for ICAM-1: 20.2±3.5, $P< 0.05$; for MPO activity in the contusion: 0.010±0.003 U MPO/g, $P< 0.05$ and in the occipital cortex: 0.013±0.005 U MPO/g, $P< 0.01$). At 24h post-TBI, BBB permeability was extended to the three cortical areas (for EB in frontal cortex: 447±89 *versus* 160±19% of control, $P< 0.01$, temporoparietal cortex: 868±94 *versus* 456±26% of control, $P< 0.001$ and occipital cortex: 592±62 *versus* 279±33% of control, $P< 0.001$). Even if simvastatin failed to reduce post-TBI MMP2 and 9 activities, it decreased EB extravasation in the pericontusional zones (frontal cortex: 236±27% of control; occipital cortex: 391±54% of control, $P< 0.05$).

Conclusion: Simvastatin is able to prevent post-TBI tight junction impairment, PMN parenchyma infiltration, and thus reduces BBB loss of integrity. These effects could contribute to

its anti-edematous effect. These results provide a solid basis for using simvastatin to reduce the edema resulting from TBI.

1- Chen *et al*, 2008. *J Pharmacol Exp Ther* 326(3): 996-74.

726

A DETAILED BEHAVIOURAL EXAMINATION OF THE TRANSIENT INTRALUMINAL MCAO MODEL OF STROKE

R.C. Trueman, D. Harrison, A. Fuller, S.B. Dunnett

Cardiff School of Biosciences, Cardiff University, Cardiff, UK

Objectives: In order to examine reconstruction of ischemic damaged brain tissue and functional recovery following neural transplantation, a focal model of stroke is required. Of particular use would be a model that produces predominantly striatal infarcts, as the benefits of neural transplantation into the striatum have already been proven in excitotoxic models of striatal damage. This work has led to clinical trials in neural transplantation of primary fetal tissue for Huntington's disease patients. One possibility for modelling such injury is the transient intraluminal filament middle cerebral artery occlusion model (MCAO), if short occlusion times of 30 - 60 minutes are performed. However, with such a mild model, spontaneous recovery is a common issue that prevents the use of a number of tests. We have evaluated a wide range of behavioural tests to identify key task(s) that reveal the most robust deficits in animals with small focal MCAO lesions.

Methods: Two cohorts of rats underwent 30 minutes of MCAO and were MRI scanned 24 hours later. Those that did not present signs of a developing lesion, or had indications of haemorrhage, were excluded from the study. The MCAO animals were tested, along with sham and naïve animals at 24 hours and 7 days following surgery on the adjusting steps task, cylinder test and assessed on a neurological score. At 1 month and 2 months following surgery the two cohorts were tested on a number of behavioural tasks. Tasks were chosen that are regularly used in models of stroke, and that are used to examine impairments in rodent models of basal ganglia disease (such as Huntington's and Parkinson's disease). Group 1 were tested on the following tasks: skilled reaching (in a cage), skilled reaching (in a “staircase” box), corridor task, grip strength analysis and rotarod. Group 2 were assessed on the following tasks: tapered balance beam, disengage, gait analysis, ladder rung test, adhesive removal, swim tank, and both amphetamine and apomorphine induced rotations. Following behavioural testing, brains were processed and stereological analysis of striatal neuronal counts were carried out, along with histological infract volumes.

Results: A number of tests were not sensitive to the mild dysfunction caused by the 30 min transient MCAO and deficits on some other tests recovered over the 2 month period. However, a small group of tests proved to be robust. The most reliable were those that assessed skilled motor function. The results were also correlated with MRI and histological measures.

Conclusions: Skilled paw reaching, forehand adjusting steps, disengage test and apomorphine induced rotations were the most reliable for analysing the 30 min transient MCAO model of stroke. These tasks may be of benefit for assessing striatal transplantation in the MCAO model.

727

EFFECT OF HYPEROXIA AND HYPERCAPNIA ON CEREBRAL AUTOREGULATION IN CORTICAL AND SUB-CORTICAL GREY MATTER (ARTERIAL SPIN LABELING MRI STUDY)

J. Cain, G. Thompson, L.M. Parkes, A. Jackson

Imaging Science and Biomedical Engineering, University of Manchester, Manchester, UK

Introduction: Cerebrovascular autoregulation maintains cerebral blood flow (CBF) in the presence of variations in cerebral perfusion pressure. This study was designed to identify potential imaging biomarkers of cerebral autoregulation in normal subjects. CBF is highly sensitive to changes in inhaled gas concentrations, in particular CO_2 and O_2. CBF decreases of 10-15% in subjects breathing 100% oxygen have been demonstrated using Phase contrast angiographic MRI, CBF increases of 20-30% when breathing 5% carbon dioxide. Previous groups using arterial spin labelling (ASL) have shown perfusion changes with CO_2 but have been unable to replicate the perfusion changes with oxygen. This study compares ASL perfusion results in cortical and sub-cortical areas under both hyperoxic and hypercarbic conditions building on previous work using PET imaging.

Methods: 10 health volunteers (19-32 year-old) underwent MRI imaging (3.0T Philips Achieva). The subjects were delivered gases via a mouthpiece using a Mapleson A anesthetic gas circuit during the MRI experiment. Subjects were given: 100% O_2, medical air and carbogen gas (95% O_2 5% CO_2) at a flow rate of 15 l/min. They received each gas for approximately 15 minutes in a random order. Imaging protocol consisted of a 3D structural acquisition followed by ASL acquisition under each gas. ASL imaging used STAR labeling collected at 4 inversion times: 800ms, 1200ms, 1600ms and 2000ms. ASL images were analysed using in-house code assuming a single blood compartment model. Control and labeled images were subtracted and a two-parameter fit for bolus arrival time (BAT) and perfusion was performed on a voxel by voxel basis, producing perfusion and BAT maps. Perfusion was calculated with units ml/100ml/min. Tissue segmentation masks were created for both cortical and sub-cortical grey matter structures including the thalamus, caudate nucleus, putamen, globus pallidus, hippocampus, amygdala and nucleus accumbens. To allow for the effect of 100% O_2 on the T1 of blood, measured vascular T1 values were used for perfusion calculations.

Results: In each subject CBF values were significantly higher ($P< 0.01$) during carbogen inhalation (76.01ml/100ml/min) than medical air (52.46ml/100ml/min) in all grey matter structures. However grey matter CBF (56.07ml/100ml/min) was not significantly different under hyperoxia in comparison with medical air. Cortical and sub-cortical BAT were increased ($p< 0.001$) during 100% oxygen inhalation(781.5ms) compared to medical air (675.4ms) and decreased ($p< 0.001$) during CO_2 inhalation (580ms).

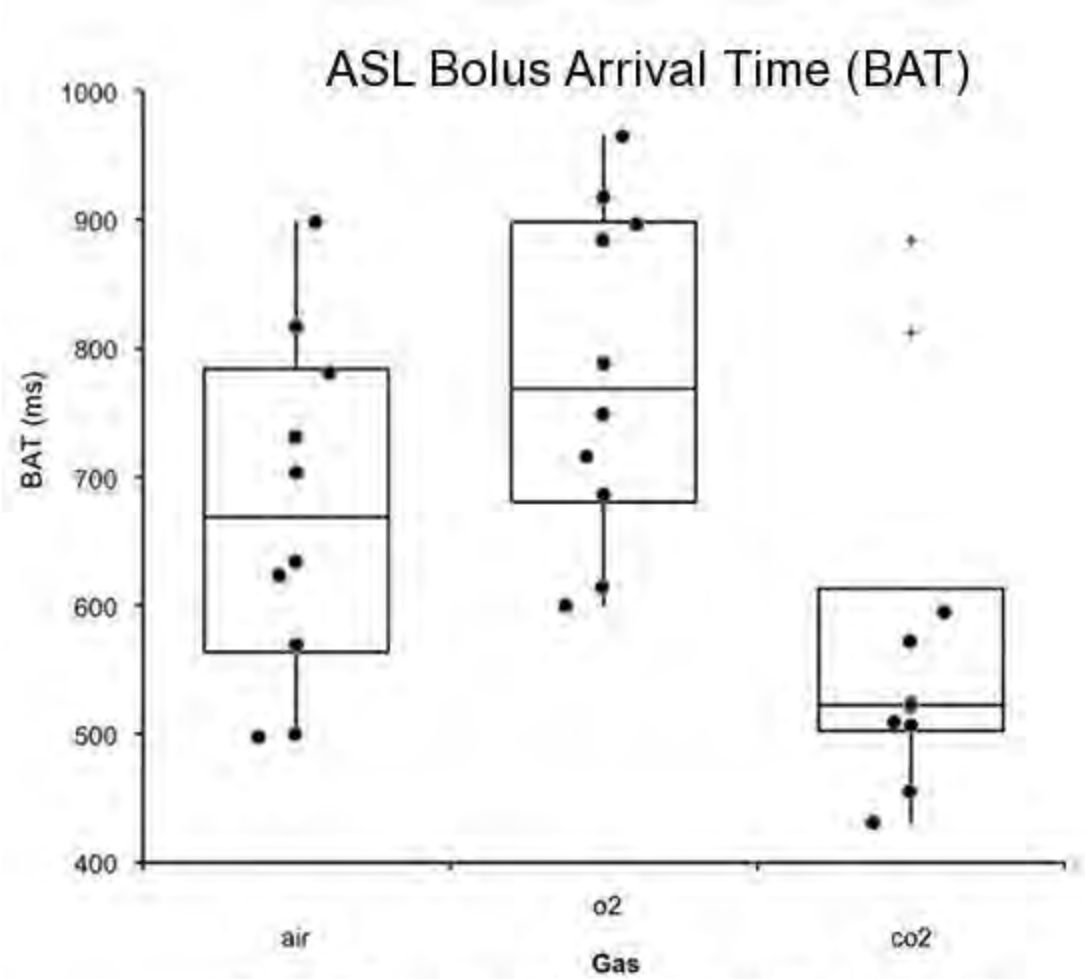

Figure 1: Box plot of ASL BAT under each gas stimulus

[ASL Bolus Arival Time (BAT)]

Conclusions: Variations in BAT induced by cerebral autoregulation secondary to gas inhalation are detectable with ASL MRI even when CBF is maintained. CO_2 causes marked vasodilatation and cerebral autoregulation is unable to compensate resulting in increased perfusion to grey matter structures. High concentrations of O_2 within the tissues may cause a degree of vasoconstriction leading to delay in arrival of blood but cerebral autoregulation is able to maintain grey matter perfusion. This study has shown STAR ASL is able to detect changes in CBF during CO_2. ASL imaging demonstrated increase in BAT during hyperoxia, although no change in CBF. ASL derived BAT provides a possible biomarker for autoregulatory studies.

728

A NON LINEAR MIXED EFFECT MODELING APPROACH FOR METABOLITE CORRECTION OF THE ARTERIAL INPUT FUNCTION IN PET STUDIES

M. Veronese[1], R.N. Gunn[2], S. Zamuner[3], A. Bertoldo[1]

[1]Department of Information Engineering, University of Padova, Padova, Italy, [2]Clinical Imaging Centre, GlaxoSmithKline, London, [3]Clinical Pharmacology and Biometrics, GlaxoSmithKline, Stockley Park, UK

Objective: Quantitative PET studies with the Arterial Input Function (AIF) normally require the correction of the measured total plasma activity for the presence of metabolites. This is achieved by fitting a Parent Plasma fraction (*PPf*) model to discrete HPLC measurements. More specifically, the commonly used method is based on an individual approach (IND): for each subject *PPf* model parameters are quantified from its own metabolite samples which are, in general, numerically limited and noisy. This fact can compromise the quality of the reconstructed AIF, and, therefore, affect the final estimates of tissue specific parameters.

In this study, we propose a Non Linear Mixed Effect Modelling (NLMEM) [1] approach to describe the metabolites kinetics. Since NLMEM has been developed to provide robust parameter estimates in case of sparse and/or noisy data, it has the potentialities to show a superior performance in comparison with IND approach.

Methods: We evaluated 3 different PET datasets: [^{11}C]-(+)-PHNO (54 scans), [^{11}C]-PIB (22 scans) and [^{11}C]-DASB (30 scans). For each tracer both simulated and measured data were considered. Residual Sum of Squares (RSS) and bias were used as performance indices. For each tracer the literature reference *PPf* model [2-4] was assumed.

When IND was used, *PPf* model parameters were estimated by non-linear weighted residual sum of squares. For NLMEM, the estimates were computed with NONMEM® by assuming log-normal distributions for the *PPf* parameters and a diagonal covariance matrix to model the inter-subject variability. The same model error description (additive, Gaussian with zero mean and SD defined by the metabolite measures uncertainty) was used in both IND and NLMEM.

Results: Simulations showed that NLMEM provides a more accurate metabolite description than IND (RSS_{pop}/RSS_{ind}=0.24), particularly in presence of outliers. NLMEM was shown to be superior to IND even when the simulated metabolite data are equal to the number of *PPf* model parameters, i.e. data poor scenario, (Figure) with a percent difference in the distribution volume (V_t) up to 10%.

In measured data analysis, the differences in *PPf* modeling between NLMEM and IND do not significantly affect neither the AIF reconstruction (Area Under Curve mean relative differences between 0.0% to 3.0%) nor V_t estimates (mean relative differences between 1% to 4%). However, even with real data, there are a few subjects (~5%) inside the evaluated populations for which high discrepancy between NLMEM and IND is found.

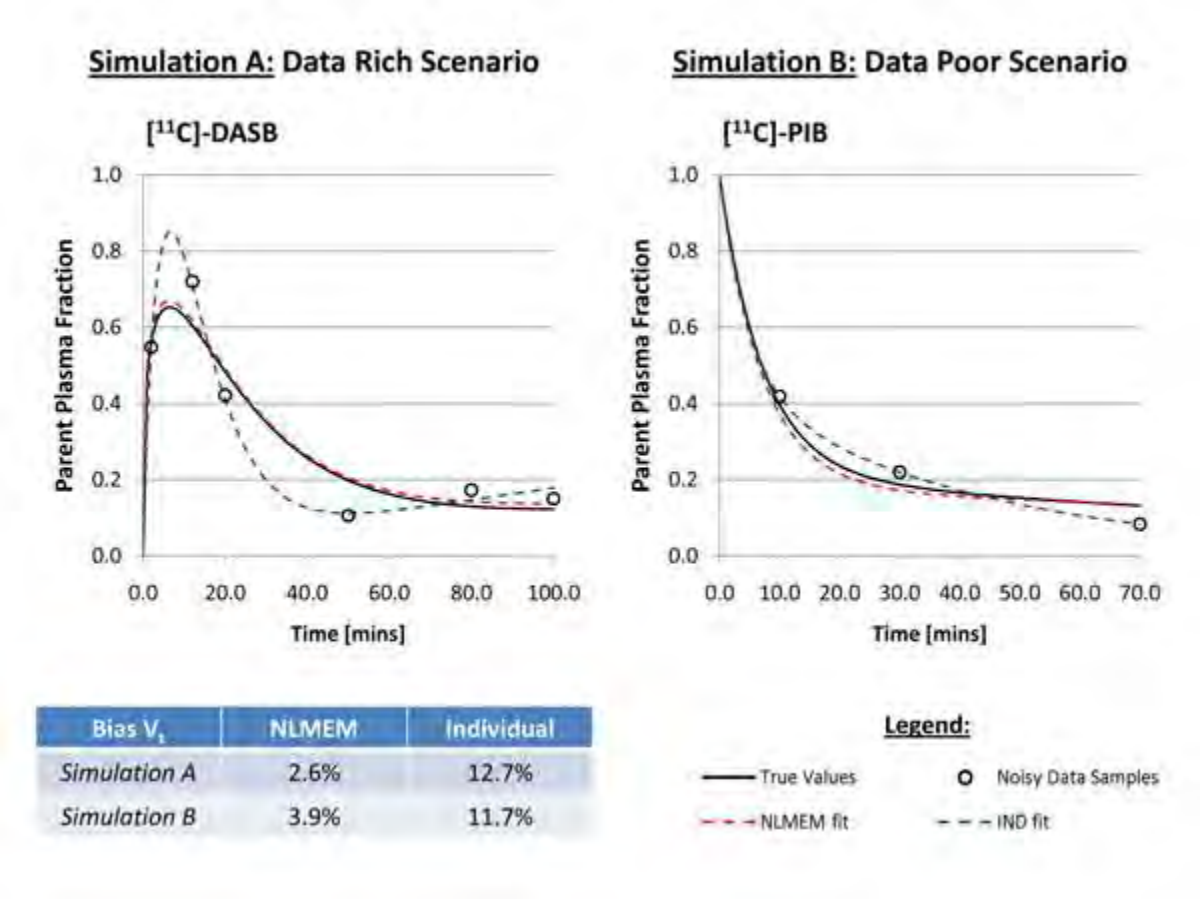

Bias V_t	NLMEM	Individual
Simulation A	2.6%	12.7%
Simulation B	3.9%	11.7%

[Impact of NLMEM vs IND for two simulated outliers]

Conclusions: NLMEM approach is shown to be superior to IND in the presence of outliers and/or when the number of the metabolites samples is very small (even equal to the number of *PPf* parameters). In the other cases, NLMEM has a similar performance to IND. However, NLMEM requires a population of at least 10 subjects to be viable.

References:

[1] Beal SL and Sheiner LB, *Crit Rev Biomed Eng.* 1982;8:195-222.

[2] Searle G *et al.*, *Biol Psychiatry* 2010;68:392-9.

[3] Lunk WE *et al.*, *Ann Neurol.* 2004;55:306-19.

[4] Parsey RV *et al.*, *J Nucl Med.* 2006; 47:1796-802.

729

RECURRENT HYPOGLYCEMIA EXACERBATES CEREBRAL ISCHEMIC DAMAGE IN GOTO-KAKIZAKI RATS

K.R. Dave[1], J. Tamariz[1], A.P. Raval[1], A. Pileggi[2]

[1]Neurology, [2]Diabetes Research Institute, Department of Surgery, University of Miami, Miami, FL, USA

Objectives: Stroke and heart disease are considered the most serious complications of diabetes, as they account for more than 65 % of mortality among diabetics (1). Clinical studies have demonstrated that intensive therapy targeted to control blood glucose and glycosylated hemoglobin was able to delay the onset and retard the progression of secondary complications of diabetes (2). The major side effect of intensive therapy in diabetics is hypoglycemia. Recurrent hypoglycemic (RH) episodes have been described in both patients with type 1 and type 2 diabetes receiving intensive therapy (3). We tested the hypothesis that RH may exacerbate cerebral ischemic damage in a rodent model of Type 2 Diabetes Mellitus (T2DM), the 16-week old Goto-Kakizaki (GK) rat. We chose this model, as the incidence of cerebral ischemia is greater in patients with T2DM than Type 1 Diabetes Mellitus (T1DM) (1).

Methods: Global cerebral ischemia was induced by tightening the carotid ligatures bilaterally following hypotension (50 mmHg) for eight minutes. We determined the extent of neuronal death at 7 days of reperfusion in CA1 hippocampus following global cerebral ischemia in control (age-matched Wistar rats), GK rats (diabetic), insulin-treated GK rats (insulin treatment was started at the age of 3.5 months using sustained release insulin implants; insulin treated diabetic: ITD) to represent the population taking glycemic control medication, and ITD rats exposed to 10 episodes of RH (ITD-RH; to represent RH in this population). Hypoglycemia (~55-65 mg / dl blood glucose) was induced twice daily for 5 consecutive days. Cerebral ischemia was induced overnight after the last hypoglycemia treatment. Number of normal neurons was counted in CA1 hippocampus to determine extent of neuronal death.

Results: At the time of ischemia induction, the mean blood glucose for control sham, control + ischemia, diabetic, ITD, and ITD-RH groups was 129±8, 147±20, 260±27, 193±10 and 189±17 mg / dl, respectively. The neuronal counts in all 4 groups were compared with sham-operated (without ischemia) control animals (100 % normal neurons). As expected, in the diabetic group only 17% (n = 3) neurons survived as compared to control ischemia group (55% neuronal survival, $p< 0.001$, n = 3). Insulin treatment was able to lower ischemic damage by 121 % ($p< 0.005$, n = 3, 59% normal neurons) as compared to the diabetic group. ITD-RH rats (28% normal neurons) had 52 % ($p< 0.05$, n = 3) and 51 % ($p< 0.05$, n = 3) more damage as compared to ITD or control ischemia groups, respectively.

Conclusion: This is the first report that RH episodes in T2DM animals exacerbate cerebral ischemic damage. RH thus may be an underappreciated but important factor responsible for increased ischemic damage in diabetes.

References: 1) Biller and Love. Med Clin North Am. 77,1993,952) TDCCTR group. N Engl J Med. 329, 1993, 977 3) Cryer Prog Brain Res. 153, 2006, 361

Support: AHA (0735106N) and S.J. Glaser Research Grant.

730

EXPRESSIONAL CHANGES IN CEREBROVASCULAR RECEPTORS AFTER EXPERIMENTAL GLOBAL CEREBRAL ISCHEMIA

S.E. Johansson, G. Klitgaard, Povlsen, L. Edvinsson

Department of Clinical Experimental Research, Research Institute Glostrup, Glostrup University Hospital, Copenhagen, Denmark

Background: Global cerebral ischemia occurs when the blood supply to the entire or a large part of the brain is disrupted or dramatically reduced, with the consequences of tissue deprivation of oxygen and glucose, which may result in permanent brain damage and stroke. It occurs commonly during cardiac arrest, which in Europe affects 1000 persons daily. We have previously demonstrated upregulation of vasoconstrictor receptors in cerebral arteries supplying ischemic tissue upon focal cerebral ischemia and subarachnoid hemorrhage, a phenomenon that contributes to reduced perfusion and worsened ischemic damage.

Aim: On this basis, we aimed to investigate whether vasoconstrictor receptor upregulation also occurs in cerebral arteries after global cerebral ischemia.

Materials and methods: Global cerebral ischemia most severely affecting the forebrain was induced in rats by 15 minutes two-vessel carotid artery occlusion combined with systemic hypotension, allowing minimal perfusion via the vertebral arteries. 48 hours later, cerebral arteries were isolated and the functional contractile responses to endothelin-1 (ET-1), 5-carboxamidotryptamine (5-CT, a 5-hydroxytryptamine (5-HT) agonist) and sarafatoxin 6c (S6c) were assessed by wire myography. Vasoconstrictor receptor expression in the smooth muscles of cerebral arteries was determined by immunohistochemical co-stainings with antibodies against β-actin and ET_A, ET_B, $5\text{-}HT_{1B}$ or $5\text{-}HT_{2A}$ receptors. Neurological deficits were evaluated daily by a grip strength test and a rotating pole sensorimotor test, showing significant deficits in ischemic rats.

Results: Contractile responses to ET-1 and 5-CT in middle cerebral arteries (MCA) and anterior cerebral arteries (ACA) were enhanced in ischemic rats compared to sham-operated rats resulting in leftwards shifted concentration-response curves. In ACA, the maximal responses to ET-1 and 5-CT were increased to 159±14% and 165±30%, respectively, of sham-operated rats. Furthermore, the contractile response to the specific ET_B receptor, S6c, in ischemic rats was enhanced to 279±48% of the responses in sham-operated rats. In contrast, contractile responses to all three agonists in basilar arteries (BA) were unchanged by the ischemia.

At the protein level, the expression of the ET_B receptor in ACA smooth muscle cells from ischemia-indcued rats was significantly increased compared to sham-operated rats. The $5\text{-}HT_{1B}$ receptor was also expressed in the smooth muscle cells in ACAs from ischemic rats with a non-significant tendency to an increased staining intensity compared to ACAs from sham-operated. In contrast, ET_A and $5\text{-}HT_{2A}$ receptor proteins showed no differences in staining intensity between ischemia-induced and sham-operated rats.

Conclusions: The ischemia-induced enhanced contractility and receptor expression observed in MCA and ACA but not BA suggest that contractile ET_B and $5\text{-}HT_{1B}$ receptors are upregulated selectively in the arteries supplying the forebrain, which is the most severely ischemic part of the brain in this model.

731

A CRITICAL RE-EXAMINATION OF THE INTRALUMINAL MCAO MODEL: IMPACT OF EXTERNAL CAROTID ARTERY TRANSECTION

R.C. Trueman[1], D. Harrison[1], D. Dwyer[2], M. Hoehn[3], S.B. Dunnett[1], T.D. Farr[3]

[1]Cardiff School of Biosciences, [2]School of Psychology, Cardiff University, Cardiff, UK, [3]In Vivo NMR Laboratory, Max-Planck-Institute for Neurological Research, Cologne, Germany

Objectives: In order to undertake behavioural testing of rodent models of stroke, it is important that there are no confounding effects of the surgical method employed. The most studied model of focal stroke is the intraluminal middle cerebral artery occlusion (MCAO). One common surgical technique used to produce this model requires permanent cauterisation or ligation of the external carotid artery (ECA) for insertion of the occluding filament. This artery has several branches and supplies the mastication and neck muscles, mandible, tongue, pharynx, scalp and ears. To date, no one has systematically examined how the unnecessary transection of the ECA affects behavioural outcome measures. We directly compared this method to other techniques that introduce the filament via the common carotid artery (CA), therefore maintaining perfusion through the ECA. The study was performed to establish if the ECA transection has detrimental effects on welfare and behaviour, which are secondary to the brain lesion, and therefore may confound outcome measures.

Methods: Three methods of the surgery were compared. The first was the traditional method, in which the filament was introduced via the transected ECA. The second inserted the filament via an incision in the CA, and following removal, sealed the incision in a way that maintained perfusion through the vessel. The third introduced the filament via the CA and then permanently tied off the CA. Corresponding sham groups were included in the study, in which each surgical method was performed only omitting the introduction of the filament. A group of naive animals were also included, to examine the effect of the sham surgeries. These 7 groups (n per group = 10 -12 rats) were compared over a period of 3 months on a number of measures including body weight, adhesive removal, paw reaching, adjusting steps, vibrissae evoked paw placing, apomorphine induced rotations and detailed analysis of drinking behaviour. Lesion volume was ascertained by both MRI and immunohistochemistry.

Results: No difference in lesion size was seen between the groups. However, transection of the ECA had a profound detrimental effect in both the corresponding MCAO and sham groups. The transection severely affected weight gain following surgery (fig. 1) and also compounded the effects of the brain infarct on a number of behavioural measures, included adhesive removal and drinking behaviour.

Conclusions: Transecting the ECA adds serious confounding factors to behavioural studies, and has additional detrimental effects on animal welfare. This study represents an important finding for all laboratories currently employing the intraluminal filament model.

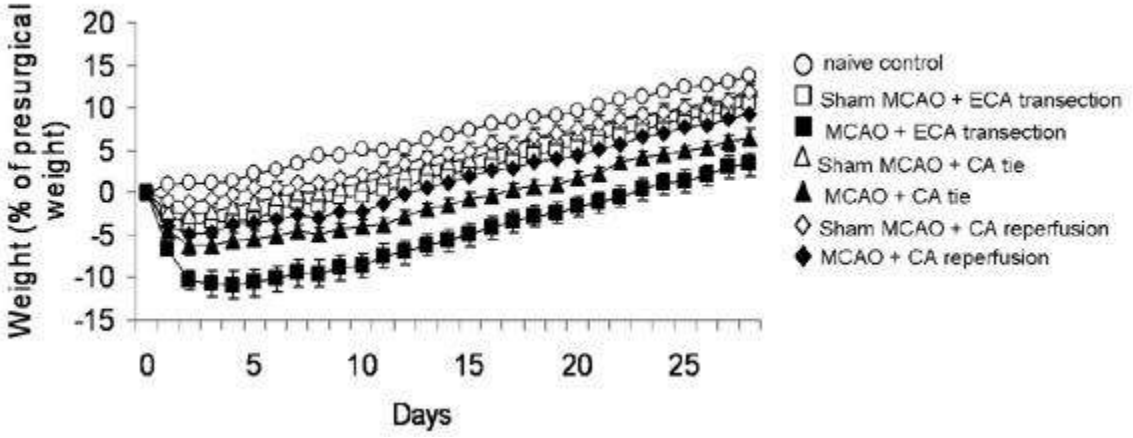

[Figure 1]

Fig 1. Change in body-weight over the first post-operative month

732

MECHANISMS UNDERLYING ENDOTHELIAL DYSFUNCTION BY ACUTE CIGARETTE SMOKING IN RATS

M. Iida[1], H. Iida[2], M. Takenaka[2]

[1]Internal Medicine, Gifu Prefectural General Medical Center, [2]Anesthesiology and Pain Medicine, Gifu University Graduate School of Medicine, Gifu-City, Japan

Objectives: We previously reported that acute single-cigarette smoking but not nicotine causes a dysfunction of endothelium-dependent vasodilation of cerebral vessels (1). Since cigarette smoking increases the production of free radicals, such as superoxide anions, it may induce endothelial dysfunction by inactivating NO, and the generation of angiotensin II (Ang II) which has been shown to promote the formation of superoxide anions, leading to reduced NO bioavailability. Other data have indicated that Rho-kinase may be substantially involved in Ang II-induced cardiovascular alterations and also enhance the oxidative stress associated with an upregulation of endothelial NADPH oxidase (2). Our aim is to clarify the mechanisms underlying the dysfunction of endothelium-dependent vasodilation in cerebral arterioles induced by acute cigarette smoking in vivo.

Material and methods: In pentobarbital-anesthetized, mechanically ventilated Sprague-Dawley rats (350g - 400g), we used a closed cranial window preparation to measure changes in pial vessel diameters. We initially examined the response of arterioles to an endothelium-dependent vasodilator [Ach (10^{-6}M and 10^{-5}M)] before smoking. Then, 1 hour after smoking (1 minute inhalation of 60 puffs per minute of mainstream cigarette smoke through tracheal canula) had been performed, we again examined the responses of arterioles to the larger doses of Ach for the control group (n=6). After intravenous valsartan (AT1-receptor blockade), fasudil (Rho-kinase inhibitor), apocynin (NADPH oxidase inhibitor), or varenicline (selective nicotine acetylcholine receptor partial agonist) pretreatment, we examined the pial vasodilator response to topical Ach (before and after cigarette smoking; n=6 each). Significance was set at $P < 0.05$. All values are presented as mean ± SD.

Results: Under control conditions, cerebral arterioles were dilated by 7.0 ± 4.5% and 13.8 ± 5.6% by topical Ach (10^{-6}M and 10^{-5}M, respectively). One hour after smoking, 10^{-5}M Ach constricted cerebral arterioles (-5.7 ± 2.7%). Vasodilator response to topical Ach was impaired after smoking. Valsartan, fasudil, apocynin, or varenicline pretreatment did not change the responses to topical Ach application obtained before smoking. One hour after smoking, 10^{-5}M ACh dilated cerebral pial arteries by 10.9 ± 3.7% in valsartan group, by 13.9 ± 1.4% in the fasudil group, by 15.5 ± 1.6% in the apocynin group, and by 15.0 ± 3.6% in the varenicline group, responses that were significantly different from those obtained without pretreatment. Thus, these four pretreatment completely prevented the smoking-induced impairment of Ach-induced vasodilation.

Conclusions: Acute single-cigarette smoking causes a dysfunction of endothelium-dependent cerebral vasodilation, and an inhibition of angiotensin II, Rho-kinase, or NADPH oxidase activity, prevents this impairment. Thus, the mechanism underlying such impairment would appear to involve mainly oxidative stress via acute smoking-induced increases in angiotensin II, Rho-kinase, and NADPH oxidase. However, it remains unclear why varenicline prevents such impairment, which nicotine itself does not induce.

References: (1) H. Iida, et al. Life Sci 2006, (2) M. Higashi, et al. Circ Res 2003

733

REMOTE POSTCONDITIONING INDUCED BY TRANSIENT FEMORAL ARTERY OCCLUSION PROTECTS THE BRAIN FROM STROKE INDUCED DAMAGE THROUGH NNOS ACTIVATION

G. Pignataro, E. Esposito, O. Cuomo, A. Vinciguerra, R. Sirabella, G. Di Renzo, L. Annunziato

Neuroscience, Federico II University of Naples, Naples, Italy

Introduction: It has been recently hypothesized that a sub-lethal ischemic insult induced in an organ is able to protect from a harmful ischemia occurring in a different and anatomically distant organ. In this paper, a new neuroprotective strategy termed remote ischemic postconditioning is described and characterized for the first time. This neuroprotective mechanism occurs in rats in which a harmful brain ischemia is followed by a sub-lethal ischemic insult applied at the femoral artery level.

Methods and results: Remote ischemic postconditioning was induced in adult male rats by subjecting them to 100 minutes of middle cerebral artery occlusion (MCAO) followed by several brief cycles of ipsilateral femoral artery occlusion-reperfusion. Within all the considered experimental protocols, the one in which 100 minutes of MCAO were followed by 10 minutes reperfusion and 20 minutes occlusion of the femoral artery was the most effective in reducing brain infarct, resulting in almost 50% reduction in the infarct volume if compared to animals subjected to 100' MCAO alone. Importantly, this protection was still present 7 days after remote postconditioning induction. Experiments carried out with specific inhibitors of each NO synthesizing enzyme, demonstrated that NO production through nNOS mediates part of the neuroprotective effect induced by remote ischemic postconditioning. In fact, the pharmacological blockade of nNOS was able to partially revert the neuroprotection induced by remote postconditioning. In addition, the neuroprotection induced by remote postconditioning was partially reverted when ganglion transmission was pharmacologically interrupted by hxamethonium, thus showing that neural factors are involved in this neuroprotective process.

Conclusion: Collectively, the results of the present study demonstrate that remote postconditioning induces a marked neuroprotection through nNOS activation and it may represent a new clinically feasible therapeutic approach to treat ischemic stroke.

734

USE OF SPECTRAL ANALYSIS WITH ITERATIVE FILTER FOR VOXELWISE DETERMINATION OF REGIONAL RATES OF CEREBRAL PROTEIN SYNTHESIS WITH L-[1-^{11}C]LEUCINE PET

M. Veronese[1], A. Bertoldo[1], G. Tomasi[2], C.B. Smith[3], K.C. Schmidt[3]

[1]Department of Information Engineering, University of Padova, Padova, Italy, [2]Comprehensive Cancer Imaging Center, Imperial College Faculty of Medicine, Hammersmith Hospital, London, UK, [3]Section of Neuroadaptation & Protein Metabolism, National Institute of Mental Health, National Institutes of Health, Bethesda, MD, USA

Objective: Regional rates of Cerebral Protein Synthesis (rCPS) in L-[1-^{11}C]leucine PET studies can be estimated voxelwise by a Basis Function Method (BFM) [1] that assumes kinetic homogeneity of the tissue within a voxel. By contrast, Spectral Analysis with Iterative Filter (SAIF) [2] can be applied to heterogeneous as well as homogeneous tissues. We have used SAIF to estimate rCPS at the region of interest (ROI) level. Because kinetic heterogeneity is not entirely eliminated by analyzing PET data at the voxel level [1], we explored the use of SAIF at the voxel level [3] for quantification of rCPS. In this study we compare BFM and SAIF voxelwise estimates of rCPS.

Methods: We analyzed a dataset of 6 healthy 18-24 year old male subjects. For each subject and both estimation methods, we computed the mean rCPS of all voxels within a ROI for 21 ROIs. We compared failure and outlier rates, computed respectively as the number of quantification failures and non-physiological estimates divided by the total number of voxels analyzed. We also examined the spatial distribution of the number of tissue components estimated with SAIF.

Results: Estimates of rCPS computed with SAIF and BFM were in good agreement. The relative rCPS difference across ROIs and subjects was 5±4% (mean±SD), and SAIF and BFM values were highly correlated (r^2, 0.96-0.99). The total rate of failures and outliers was low with both BFM (0.4±0.3%) and SAIF (1.7±1.0%). With BFM we found a higher incidence of rCPS estimates of zero (7.8±2.3%) compared with SAIF (0.5±0.3%) (Figure). With SAIF we found multiple tissue compartments in ~45% of voxels, suggesting the presence of heterogeneity; these voxels appeared to be concentrated at the borders between gray and white matter.

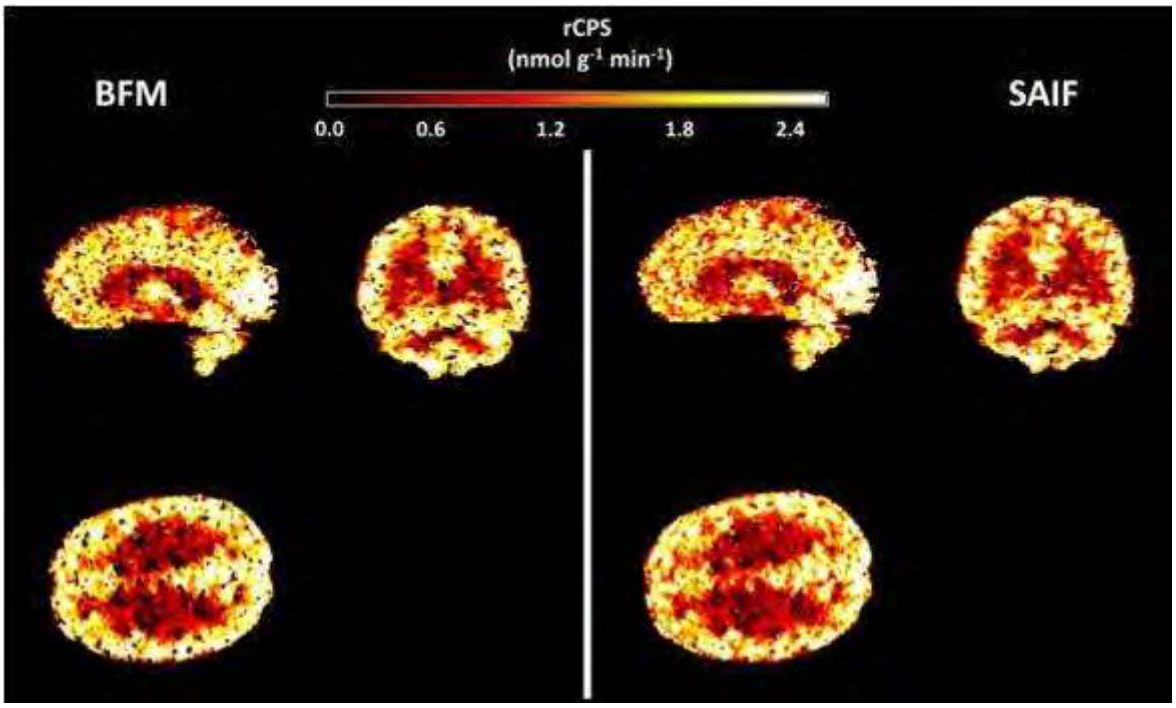

[Quantification of rCPS at voxel level]

Conclusions: SAIF and BFM provided comparable mean regional estimates of rCPS. Spatial maps of rCPS are more continuous with the SAIF method. SAIF may also provide useful information about voxel heterogeneity, although it appears that the presence of heterogeneity did not have a substantial impact on mean rCPS estimates. SAIF, however, requires more computation time than BFM. SAIF represents a robust alternative for determination of rCPS at the voxel level.

References:

[1] Tomasi G et al., *JCBFM* 2009, 29: 1317-1331;

[2] Veronese M et al., *JCBFM* 2010, 30:1460-76;

[3] Veronese M et al., *NeuroImage* 2010, 52(Supplement 1): S212.

Supported by IRP/NIMH/NIH

735

TARGETING NF-KAPPAB AND EPIGENETIC CHROMATIN REMODELLING IN THE THERAPY OF POST-ISCHEMIC BRAIN INJURY

M. Pizzi[1], G. Pignataro[2], A. Lanzillotta[1], I. Sarnico[1], M. Benarese[1], R. Ingrassia[1], C. Branca[1], G. Faraco[3], F. Blasi[3], O. Cuomo[2], A. Chiarugi[4], L. Annunziato[2], P.F. Spano[1]

[1]University of Brescia, [2]Federico II University of Naples, Brescia, [3]University of Florence, Florence, [4]University of Florence, Brescia, Italy

Diverse nuclear factor-kappaB (NF-kappaB) subunits can be responsible for opposite effects on neuronal survival and they are highly implicated in the pathophysiology of post-ischemic brain injury. NF-kappaB is a dimeric transcription factor that can be formed by the assembly of five diverse proteins, p50, p52, RelA (p65), RelB and c-Rel. We demonstrated that within the same neuronal cell the balance between activation of p50/RelA and c-Rel-containing complexes fine-tunes the threshold of neuron vulnerability to the ischemic insult. Both *in vivo* and *in vitro* experimental models of brain ischemia demonstrate that while p50/p65 dimer promotes the expression of proapoptotic genes Bim and Noxa and neuronal cell death, c-Rel-containing dimers can rescue neuronal cells by activating transcription of antiapoptotic Bcl-xL gene.

The neurotoxic effects of p50/RelA during ischemia is associated with epigenetic regulation of the NF-kappaB protein, i.e. site specific acetylation of RelA. RelA can be acetylated on five different lysines (Lys122, Lys123, Lys218, Lys221, and Lys310) and each lysine can differently regulate the activity of NF-kappaB. The acetylation status of RelA is modulated by a family of histone acetyl transferase (HAT) and by histone deacetylase (HDAC) belonging to class I and class II. A Class III HDAC, sirtuin 1 (SIRT1), activated by resveratrol, selectively deacetylates RelA at Lys310 residue. In neurons exposed to oxygen glucose deprivation, as well as in cortices of mice exposed to middle cerebral artery occlusion, the acetylation of RelA at the Lys310 residue increases, while the acetylation at the other lysine residues falls down. On the contrary, after a preconditioning ischemia able to limit the injury produced by lethal ischemia, total acetylation of RelA is predominant and acetylation at the Lys 310 is negligible. It can be inferred that during lethal ischemia the activation of p50/RelA is associated with unbalanced Lys310 RelA acetylation versus the total acetylation of RelA. Treatments able to restore the normal acetylation of RelA produce neuroprotection as well as treatment targeting RelA activation. Thus, administration of resveratrol, by deacetylating RelA on Lys310, can reproduce the protective effects of preconditioning. Likewise, treatment with the HDAC inhibitor MS-275 or SAHA, by increasing total acetylation of RelA, induce neuroprotection. These results suggest that acetylation status of p50/RelA has a key role in the epigenetic regulation of transcription and can represent a neuroprotective target in brain ischemia.

736

PIB RETENTION, WHITE MATTER LESIONS AND NEUROPSYCHOLOGICAL TEST PERFORMANCE AMONG COGNITIVELY NORMAL MEN

J. Becker[1], J. Price[2], L. Kingsley[3], D. Minhas[4], L. Teverovsky[5], C.R. Rinaldo[3]

[1]Psychiatry, Neurology and Psychology, [2]Radiology and Psychiatry, [3]Infectious Diseases and Microbiology, [4]Radiology, University of Pittsburgh, [5]Computer Science, Carnegie Mellon University, Pittsburgh, PA, USA

Introduction: Retention of the amyloid ligand, Pittsburgh Compound B (PiB) occurs in cognitively normal, elderly individuals. What is less clear is the extent to which there is a relationship between the extent of PiB retention and performance on neuropsychological tests among cognitively normal individuals who are, on average, younger than 65 years. In addition, the role of small vessel disease, as reflected by white matter lesions, may have a role in both increasing amyloid retention and in altering cognitive functions.

Objectives: We report here the results of the analysis of PiB data from a group of 22 young (age = 61.5 years) cognitively normal men (mean education = 15.9 years) who are participating in a study of amyloid deposition and cardiovascular risk factors.

Methods: Each of the subjects underwent a structural MRI scan, including FLAIR images, PET imaging using PiB, and a battery of neuropsychological tests.The MRI data were preprocessed with a bias field correction, inter- and intra-slice intensity normalization, spatial normalization to a custom template, and removal of non-brain tissue. The measurement of the total amount of white matter lesions was made using a semi-automated methodology, and the total lesion volume was expressed as a proportion of the total white matter volume (normal + abnormal).

PiB data were reconstructed and corrected for attenuation, scatter, and decay. Regions-of-Interest were applied to obtain regional time-activity data and analyzed to obtain measures of the standardized uptake value. The SUV measure was normalized to the cerebellum.

The scores from the neuropsychological test battery were reduced to T-scores adjusting for age, education, sex and race. The T-scores were then converted into Domain and Global Impairment scores using standard methods. 16/22 of the subjects (73%) had Global Impairment Ratings in the normal range; the remainder scored in the Borderline range.

The performance of the subjects on measures of cognitive speed were significantly associated with amyloid deposition in the Anterior Cingulate (rho=.45), Frontal Cortex (rho=.40) and Lateral Temporal Cortex (rho=.39). The highest level of PiB retention was found in the subjects classified as performing in the Borderline range. There was no association between performance in the Speed Domain and overall classification of PiB “positive”. There was also a significant association between the global performance rating, and the extent of white matter lesions (rho=.52). Further, there was a tendency for greater PiB retention to occur among the individuals with a higher proportion of abnormal white matter.

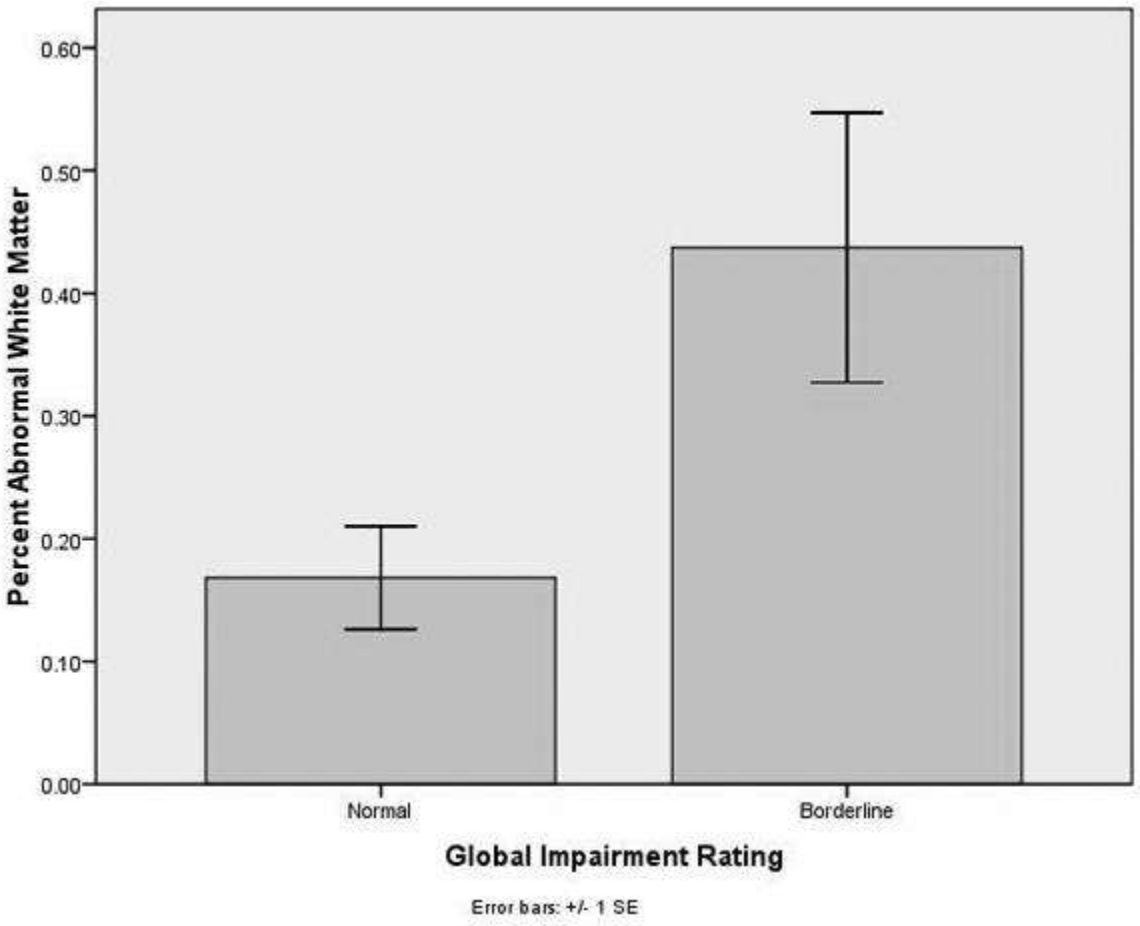

[White Matter Lesions and Cognition]

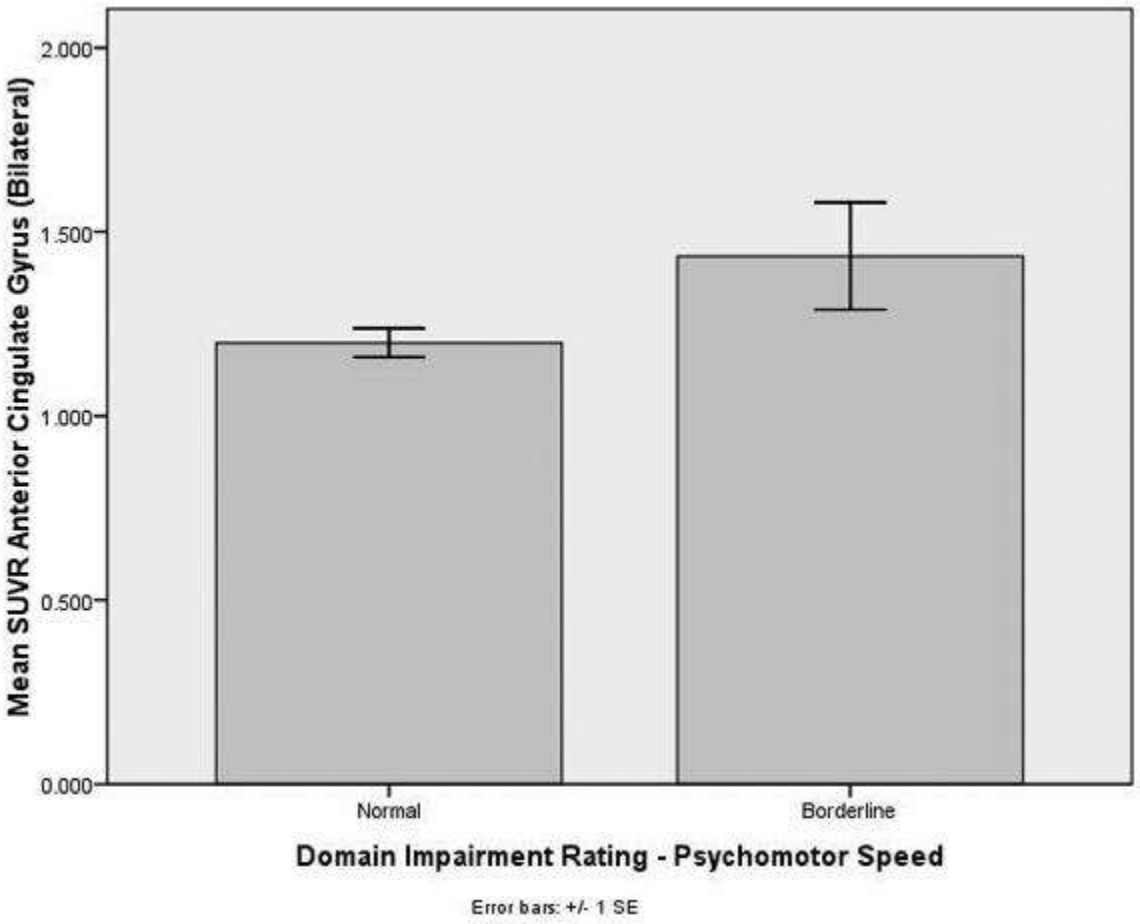

[PiB Retention and Psychomotor Speed]

Conclusions: The results of this initial analysis demonstrate that it is possible to find links between the amount of damage to brain white matter, the relative amount of PiB retention, and performance on measures of cognitive function. The findings are consistent with prior work that reported early amyloid deposition in anterior cortical regions in the absence of observed cognitive impairment.

737

ENERGETIC BASIS OF RESTING-STATE FLUCTUATIONS IN NEURAL AND NEUROIMAGING SIGNALS

P. Herman[1], B.G. Sanganahalli[1], D. Coman[1], H. Blumenfeld[2], F. Hyder[1,3]

[1]Department of Diagnostic Radiology, [2]Department of Neurology, [3]Department of Biomedical Engineering, Yale University, New Haven, CT, USA

Objectives: Task-evoked responses in functional studies show baseline dependence [1], i.e. in higher metabolic baseline state the functional response is smaller but delocalized, whereas lower metabolic baseline shows higher amplitude localized responses. Other human studies [2] showed that spontaneous fluctuations in BOLD signal seem to be important in local variability or trial-to-trial reproducibility of the functional response. In this study we examined activity energy differences between high and low energy baselines of light (Domitor) and deep (α-chloralose) anesthesia, and compared them with quantitative characterization of neural, cerebral blood flow (CBF) and BOLD signal fluctuations at rest.

Methods: Sprague-Dawley rats were tracheotomized and artificially ventilated (70% N_2O, 30% O_2). The anesthesia was switched to i.p. α-chloralose (40 mg/kg/hr) or s.c. Domitor (0.1mg/kg/h) from Isoflurane (1-2%) after the surgery. A femoral arterial line was used for monitoring blood pressure, acid-base balance and blood gases throughout the experiment. ***fMRI (n=10):*** All fMRI data were obtained on a modified 11.74T Bruker horizontal-bore spectrometer using a ^1H resonator/surface coil. All images were acquired with gradient-echo EPI (TR/TE=200/12.53 ms). Resting state BOLD data were obtained with NR of 4200. ***Neural and CBF (n=18):*** Rats were placed in a stereotaxic holder and tiny burr holes were made above left and right somatosensory regions. Tungsten microelectrodes were inserted together with laser Doppler probes for CBF recording. The multi-unit activity (MUA) and local field potential (LFP) were extracted from the raw signal with electronic filters. ***Analysis:*** Fluctuations of the BOLD signals were estimated using voxel by voxel standard deviation (SD), where the larger value means larger fluctuation. The SD of the voxel based time series were calculated, and then averaged by individual experiments and the two anesthetic groups were tested with Student's t-test. The temporal fluctuation of MUA signal (denser and rarer regions in the signal) was transformed into amplitude fluctuation with root mean square (RMS) method [3] with 1s binning. The fluctuations of LFP and CBF signals were also estimated by SD.

Results: The cortical activity measured by MUA in high baseline was characterized by high temporal frequency signaling, where the high density of neural firing converted into large amplitude RMS fluctuations. The fluctuation was significantly greater ($p=0.0015$) in high rather than low baseline state. Similarly, the SDs of fluctuations of LFP, LDF and BOLD signals were all much greater ($p< 0.005$) in the high instead of the low baseline state.

Conclusions: We characterized spontaneous fluctuations of multi-modal neuroimaging signals at two different baseline levels, where larger fluctuations (i.e., larger SD) were observed when baseline energy was high. The “power” of the baseline neural activity is correlated with the magnitude of the BOLD and LDF signal fluctuations. A plausible explanation of these results is that with light anesthesia and higher metabolic activity [1], the fluctuations in neural activity is larger due to high frequency signaling.

References:

[1] Maandag et al. (2007) PNAS, 104:20546-20551

[2] Fox et al. (2007) Neuron 56, 171-184,

[3] Stark and Abeles (2007) J Neurosci 27:8387-8394

Acknowlegements: Supported by NIH (R01 MH-067528, P30 NS-52519).

738

HIGH-RESOLUTION IMAGING OF RODENT CEREBRAL HEMODYNAMICS USING FUNCTIONAL MICRO-ULTRASOUND

M.E. van Raaij, L. Lindvere, A. Dorr, J. He, B. Sahota, F.S. Foster, B. Stefanovic

Imaging Research, Sunnybrook Research Institute, Sunnybrook Health Sciences Centre, Toronto, ON, Canada

Introduction: Quantitative mapping of the brain microvascular hemodynamics is important for understanding brain function in health and disease. Current imaging modalities lack either the spatial resolution or the penetration depth required to image blood volume changes in individual microvessels throughout the rodent cerebrum.

Objectives: We have developed a new high-frequency ultrasound imaging technique that enables functional imaging of the hemodynamics of the rat cerebral microvasculature at a spatial resolution of ~100 μm in-plane and 600 μm through-plane and a temporal resolution of 40 ms.

Methods: Adult male Sprague-Dawley rats (*m* = 120 - 250 g, *n* = 20) were anesthetized with isoflurane, tracheotomized, mechanically ventilated, and prepared with a 6 by 4 mm cranial window over S1FL. Anesthetic was switched to α-chloralose and an ultrasound contrast agent consisting of micrometer-sized bubbles of perfluorocarbon gas with a phospholipid shell was infused (IV). A near-sagittal plane of view (7 x 10 mm) encompassing both S1FL and VPL was imaged using a micro-ultrasound system with a 20 MHz transducer in a nonlinear contrast imaging mode. In this imaging mode, signal intensity is linearly related to the concentration of contrast agent in each voxel and thus to the local blood volume. The forelimb contralateral to the cranial window was electrically stimulated for either 2 or 10 second intervals while the physiological state of the animal was monitored. Detailed maps of vessel topography were obtained by averaging the nonlinear contrast ultrasound images, while color Doppler ultrasound images identified penetrating vessels as either venules or arterioles. Neuronal response to stimulation was confirmed independently by intracranial EEG measurements.

Results: Electrical stimulation of the contralateral forelimb reproducibly induced a hemodynamic response in S1FL with up to 22 % change in local blood volume in specific regions of the cortex (see figure). A general linear model analysis revealed the presence of regions ranging in size from 100 μm to 2 mm of stimulus-correlated increases as well as decreases in local blood volume. We also detect and quantify differences in the temporal evolution of the blood volume response in deep gray versus S1FL regions of the rat brain.

Conclusions: The significantly lower cost and higher spatial and temporal resolution of functional micro-ultrasound (fMUS) imaging compared to typical single-slice preclinical fMRI and the much deeper penetration depth compared to two-photon fluorescence microscopy should allow fMUS to become a valuable tool in the study of cerebral hemodynamics.

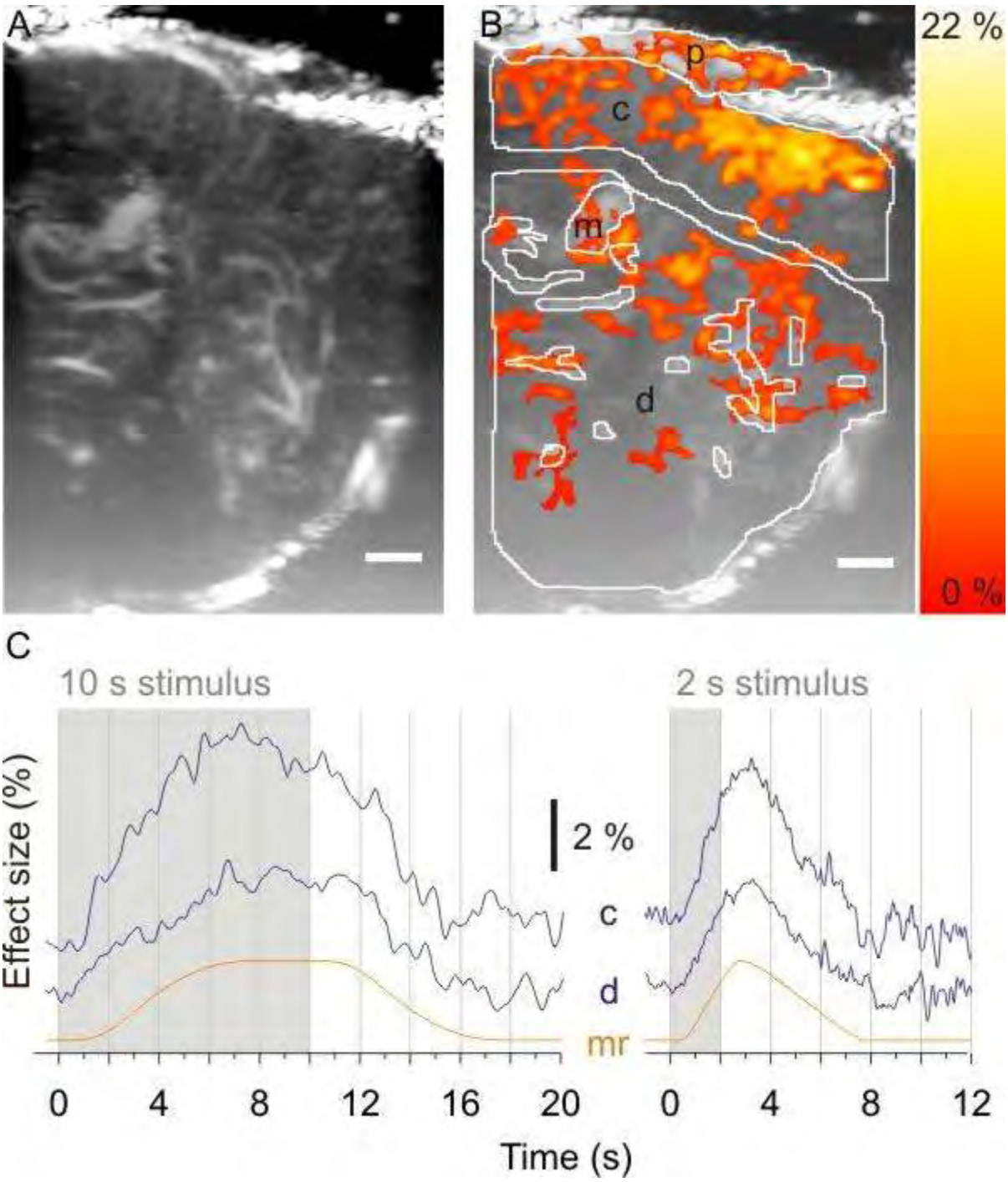

[Functional micro-ultrasound image of rat brain]

Figure caption: (A) Near-sagittal anatomical micro-ultrasound image of a rat brain encompassing S1FL (anterior = right side of image) showing vessel topography. (B)

Corresponding effect size map showing localized response to electrical somatosensory stimulus. p, pial vessels; c, cortex; m, major vessels in deep gray; d, deep gray.

Color scale in (B) corresponds to effect size in %. Scale bar in A and B is 1 mm.

(C) Blood volume responses averaged across 11 subjects in regions cortex (c) and deep gray (d) compared to the modeled reponse (mr).

739

NCX1 AND NCX3: TWO NEW EFFECTORS OF DELAYED PRECONDITIONING IN BRAIN ISCHEMIA

G. Pignataro[1], E. Esposito[1], A. Vinciguerra[1], O. Cuomo[1], P. Cerullo[1], F. Boscia[1], R. Sirabella[1,2], G. Di Renzo[1], L. Annunziato[1,2]

[1]Neuroscience, Federico II University of Naples, [2]SDN, Via Gianturco, Naples, Italy

Introduction and aim: It has been recently demonstrated that a short sub-lethal brain ischemia applied before a prolonged harmful ischemic episode may confer ischemic neuroprotection, a phenomenon named ischemic preconditioning. Na^+/Ca^{2+} exchanger (NCX) isoforms, NCX1, NCX2, and NCX3, are plasmamembrane ionic transporters widely distributed in the brain and involved in the control of Na^+ and Ca^{2+} homeostasis and in the progression of stroke damage. Objective of this study was to evaluate the role of these three proteins in the preconditioning-induced neuroprotection.

Methods: NCX protein expression was evaluated at different time points in the ischemic temporoparietal cortex of rats subjected to ischemia alone, to ischemic preconditioning alone or to ischemic preconditioning plus ischemia.

Results: Results of the present study showed that NCX1 and NCX3 were up-regulated in those brain regions protected by preconditioning treatment. These changes in NCX1 and NCX3 expression were p-AKT mediated, since the p-AKT inhibition prevented their up-regulation. The relevant role of NCX1 and NCX3 during preconditioning was further confirmed by results showing that NCX1 and NCX3 silencing, induced by icv infusion of siRNA, partially reverted the preconditioning-induced neuroprotection.

Conclusion: The results of the present study support the idea that the enhancement of NCX1 and NCX3 expression and activity might represent a reasonable strategy to reduce the infarct extension after stroke.

740

NCKX2 CONTRIBUTES TO NEUROPROTECTION ELICITED BY ISCHEMIC PRECONDITIONING AND POSTCONDITIONING

O. Cuomo, G. Pignataro, R. Sirabella, A. Vinciguerra, G. Di Renzo, L. Annunziato

Neuroscience, Federico II University of Naples, Naples, Italy

Introduction: Sodium/Calcium exchangers are neuronal plasmamembrane transporters which, by coupling Ca^{2+} and Na^{+} fluxes across neuronal membranes, may play a relevant role in brain ischemia. The exchanger gene superfamily comprises two arms: the K^{+}-independent (NCX) and K^{+}-dependent (NCKX) exchangers. In the brain, 3 different NCX and NCKX family members have been described (Annunziato et al., 2004; Cai and Lytton, 2004). Previous studies showed that more than 60% of calcium extrusion was mediated by sodium calcium exchangers and that 90% of this exchange was NCKX-mediated (Lee et al., 2002). Recently, it has been shown NCKX2 is involved in the progression of the ischemic lesion, since both its knocking down and its knocking out induced a worsening in ischemic damage (Cuomo et al., 2008)

Objectives: To further confirm the role played by NCKX2 in cerebral ischemia, here we examined its involvement in two endogenous recently characterized neuroprotective strategies: brain ischemic preconditioning and postconditioning. The main aim of this study was to elucidate whether NCKX2 might take part as effector in the neuroprotection evoked by preconditioning and postconditioning. For this purpose, we investigated the effect of ischemic preconditioning and postconditioning on (1) NCKX2 protein expression in the temporoparietal cortex and striatum of rats at different time intervals after pre- or postconditioning induction; (2) the effect of p-AKT and calpain inhibition on NCKX2 expression during preconditioning and postconditioning and (3) the effect of nckx2 silencing on the protection exerted by pre- and postconditioning in nckx2+/+ and nckx2-/- mice.

Methods: Ischemic preconditioning and postconditioning were experimentally induced in adult male rats and mice by subjecting them to different protocols of middle cerebral artery occlusion and reperfusion.

Results: The results of the present study showed that NCKX2 expression increased in both the neuroprotective processes and its knocking-out significantly reverted the protection exerted by both preconditioning and postconditioning.

Conclusions: Overall, our results suggest that NCKX2 plays a fundamental role in the neuroprotective effect mediated by preconditioning and postconditioning and support the idea that the enhancement of its expression and activity might represent a reasonable strategy to reduce the infarct extension after stroke.

References:

- Annunziato L, Pignataro G, Di Renzo GF. Pharmacology of brain Na+/Ca2+ exchanger: from molecular biology to therapeutic perspectives. Pharmacol Rev. 2004; 56(4):633-54.
- Cai X, Lytton J. The cation/Ca(2+) exchanger superfamily: phylogenetic analysis and structural implications. Mol Biol Evol. 2004 Sep;21(9):1692-703
- Cuomo O, Gala R, Pignataro G, Boscia F, Secondo A, Scorziello A, Pannaccione A, Viggiano D, Adornetto A, Molinaro P, Li XF, Lytton J, Di Renzo GF, Annunziato L. A

Critical Role for the Potassium-Dependent Sodium/Calcium Exchanger NCKX2 in Protection Against Focal Ischemic Brain Damage J Neurosci 2008; 28:2053-63.
- Lee SH, Kim MH, Park KH, Earm YE, Ho WK. K+-dependent Na+/Ca2+ exchange is a major Ca2+ clearance mechanism in axon terminals of rat neurohypophysis. J Neurosci. 2002; 22:6891-9.

741

ACUTE CO_2-INDEPENDENT VASODILATATION OF PENETRATING AND PRECAPILLARY ARTERIOLES IN MOUSE CEREBRAL PARENCHYMA UPON HYPOXIA REVEALED BY A THINNED-SKULL WINDOW METHOD

T. Nakamura[1,2], M. Kajimura[1], T. Morikawa[1], K. Hattori[1], M. Ishikawa[3], Y. Yukutake[1], S. Uchiyama[2], M. Suematsu[1]

[1]Biochemistry, School of Medicine, Keio University, [2]Neurology, Tokyo Women's Medical University, Tokyo, [3]Neurosurgery, Saitama Medical Center, Jichi Medical University, Saitama, Japan

Purpose: Investigating spatio-temporal relationship between regional metabolic changes and microvascular responses in hypoxic brain is critical for unraveling local O_2-sensing mechanisms. However, no reliable method to examine the relationship has been available *in vivo* because of inherent disadvantages associated with use of a conventional cranial-window preparation. With a conventional cranial-window preparation, brain might be exposed to unwanted atmospheric gases, and protrude from cranial window by hypoxia-induced brain swelling. We aimed to devise a method to solve the problem and visualized O_2-dependent regional metabolic changes and regional microvascular responses *in vivo* in subsurface cerebral parenchyma and arterioles composing neurovascular unit with surrounding astrocytes and neurons.

Methods: Anesthetized C57BL/6J mice (male, 22 to 28 g, 8-9 weeks old) were equipped with either a conventional cranial-window with craniotomy or a thinned-skull preparation. In some set of experiments, an arterial catheter connected to a pressure transducer was placed in the left femoral artery to continuously monitor mean arterial pressure. Mice were mechanically ventilated to avoid hypercapnia and exposed to systemic isobaric hypoxia which was induced by the inhalation of 10% O_2 balanced with N_2 for 30 min. A small aliquot of arterial blood (~70 μL) was sampled before and after the 30 min of hypoxia, and analyzed with a blood gas analyzer. Using two-photon laser scanning microscopy (TPLSM), NADH autofluorescence and diameter changes in penetrating and precapillary arterioles within the parenchyma were visualized to examine their temporal alterations.

Results: With the conventional cranial-window preparation, marked vertical displacement of the tissue occurred through edema within 30 seconds after inducing hypoxia and made it difficult to obtain optical images seamlessly from the same axial plane. With a thinned-skull preparation, however, such hypoxia-induced displacement was diminished, enabling us to examine acute spatio-temporal changes in diameters of penetrating and precapillary arterioles and NADH autofluorescence. Vasodilatation of these microvessels was evoked within 1 min after hypoxia, and sustained during the entire observation period despite the absence of hypercapnia. This event coincided with parenchymal NADH elevation, but the onset and peak dilatory responses of the penetrating arterioles preceded the local metabolic response of the parenchyma.

Conclusion: Our results demonstrate that: (i) the cerebral cortex herniates rapidly through a craniotomy hole upon hypoxic insults with a closed cranial window preparation; (ii) the use of a thinned-skull preparation for atmospherically gas-tight conditions helps to alleviate such herniation; and (iii) the combination of TPLSM and the thinned-skull preparation makes it possible to detect acute changes in tissue metabolism indicated by NADH autofluorescence and small arteriolar diameters. Observation of hypoxia-exposed brain by the thinned-skull preparation combined with two-photon intravital microscopy revealed rapid vasodilatory responses in penetrating arterioles preceding parenchymal NADH elevation, suggesting the

presence of acute hypoxia-sensing mechanisms involving a specific hierarchy of cortical arterioles within the neurovascular unit.

742

ELEVATED STRIATAL DOPAMINE SYNTHESIS CAPACITY IN SUBJECTS WITH PRODROMAL SIGNS OF PSYCHOSIS: CONFIRMATION IN A SECOND COHORT

A. Egerton[1,2], C.A. Chaddock[1,2], T.T. Winton-Brown[1,2], S. Bhattacharyya[1,2], M.A. Bloomfield[2], P.K. McGuire[1], O.D. Howes[1,2]

[1]Psychosis Studies, Institute of Psychiatry, King's College London, [2]Psychiatric Imaging, MRC Clinical Sciences Centre, Imperial College London, London, UK

Introduction: Elevated striatal dopaminergic activity is the major neurochemical abnormality which has been associated with schizophrenic illness. Using 18F-DOPA positron emission tomography (PET), we recently demonstrated that presynaptic dopamine synthesis capacity is increased in individuals with prodromal symptoms of psychosis, indicating that dopamine over-activity predates the onset of a frank psychotic disorder (Howes et al., 2009). This raises the possibility that presynaptic dopamine synthesis capacity, as determined using 18F-DOPA PET, may form an imaging biomarker for psychosis risk.

Aim: To determine the reproducibility of our previous finding in a second, independent cohort of subjects.

Methods: 24 individuals with prodromal symptoms of psychosis (At Risk Mental State, ARMS) were matched with 17 controls from the same geographical area. This represents an entirely new sample from our previous study. The ARMS is characterised by attenuated psychotic symptoms and a marked decline in socio-occupational functioning, with a high (~20-30%) risk of transition to psychosis over the next 1-2 years (Yung et al., 2005). All subjects received carbidopa (150 mg) and entacapone (400 mg) orally 1 hour before ^{18}F-DOPA imaging. Presynaptic dopaminergic activity (^{18}F-DOPA uptake, k_i) was estimated using graphical analysis in striatal regions of interest relative to a cerebellar reference region.

Results: Relative to controls, individuals with prodromal symptoms of psychosis showed elevated 18F-DOPA k_i in the whole striatum (t_{39} = -2.13; P = 0.04) and the associative striatum (t_{39}=-2.18; P = 0.03). In contrast, no group differences were apparent in the limbic (t_{39} = 0.92; P = 0.36) or sensorimotor (t_{39}=-1.20; P = 0.24) striatum.

Conclusions: These findings confirm, in a second, independent cohort, that presynaptic dopaminergic activity is elevated in subjects with prodromal symptoms of psychosis. As in our previous study (Howes et al., 2009), these increases were particularly apparent in the associative striatum, suggestive of a link to frontal or executive dysfunction. Together with the initial cohort, these ARMS individuals are currently being followed up clinically. This will allow future investigation of the relationship between striatal ^{18}F-DOPA uptake and subsequent transition to psychosis.

References:

Howes OD, Montgomery AJ, Asselin MC, Murray RM, Valli I, Tabraham P, Bramon-Bosch E, Valmaggia L, Johns L, Broome M, McGuire PK, Grasby PM. Elevated striatal dopamine function linked to prodromal signs of schizophrenia. Arch. Gen. Psychiatry. 2009; 66(1):13-20.

Yung AR, Yuen HP, McGorry PD, Phillips LJ, Kelly D, Dell'Olio M, Francey SM, Cosgrave EM, Killackey E, Stanford C, Godfrey K, Buckby J. Mapping the onset of psychosis: the

Comprehensive Assessment of At-Risk Mental States. Aust N Z J Psychiatry. 2005;39(11-12):964-971.

743

EFFECT OF SPONTANEOUS RESTING-STATE FLUCTUATIONS ON TRIAL-TO-TRIAL VARIABILITY OF BOLD TASK-EVOKED RESPONSES

P. Herman[1], B.G. Sanganahalli[1], R.S.N. Sachdev[2,3], F. Hyder[1,4]

[1]Department of Diagnostic Radiology, [2]Department of Neurobiology, [3]Kavli Institute of Neuroscience, [4]Department of Biomedical Engineering, Yale University, New Haven, CT, USA

Objectives: Resting state fluctuations in BOLD signal are used for functional connectivity studies [1]. It has been suggested that these baseline fluctuations may influence trial-to-trial variability of the evoked BOLD response [2]: The *amplitude* of the spontaneous fluctuation has significance for the strength of the functional connectivity and the *phase* of the BOLD signal fluctuation just preceding the stimulus can affect the trial-to-trial variability of the evoked BOLD response. We measured the BOLD signal spontaneous fluctuations and whisker functional responses in rat cortex with two slightly different baseline states (lightly anesthetized and awakened animals) to investigate these suggestions.

Methods:

Pre-experimental procedure: Long Evans rats (n=5) were habituated to restraint and scanner noise, and then surgically prepared for head post implantation. After recovery from surgery, they were re-acclimated to restraint.

Experimental procedure: On the experimental day, animals were anesthetized with domitor (0.1 mg/kg/hr) and fixed to the holder via the implanted head post. Whisker stimulus (8Hz, 30s) evoked functional responses, and baseline BOLD signals were acquired. The anesthetic was stopped and functional responses with baseline fluctuations were acquired at several time points after the anesthetic wore off.

fMRI: All fMRI data were obtained on a modified 11.7T Varian horizontal-bore spectrometer using a ^{1}H surface coil. The functional images were acquired with gradient echo EPI sequence (TR/TE=1000/15 ms).

Analysis: The power spectra of the BOLD fluctuations in the low frequencies (to 1Hz) were computed for both domitor anesthetized and awakened animal. The Student's t-score of the BOLD responses were compared voxel by voxel to the last baseline value of the signal. The variability of the evoked BOLD responses as function of the baseline amplitude was calculated.

Results: Spontaneous fluctuations in the BOLD signal have the same frequency distributions in the domitor anesthetized and awakened state. The frequency analysis of the awakened and anesthetized animals shows high power in the range of 0.05-1Hz fluctuation and this power does not show significant difference across states (p=0.19), but the difference is much smaller in the lower (0.1-0.5Hz) frequency range (p=0.89). The time series of evoked BOLD responses were collected according to activated voxels, and the variability of the BOLD responses were estimated from their standard deviation. The variability of the awakened BOLD responses was ~3 times higher than in the anesthetized state, although the magnitudes of evoked BOLD responses were similar. We also found that the pre-stimulus BOLD values did not predict the BOLD response amplitude or the rate of rise of the evoked BOLD response.

Conclusion: Our results show that while there is a significant difference in the variability of the

functional responses during whisker stimulation between anesthetized and awakened animals, the spontaneous fluctuations do not show significant differences in their frequency power. Thus the trial-to-trial variability of task-evoked functional responses could not be explained by the phase of the spontaneous fluctuations in the resting-state BOLD signal.

References:

[1] Biswal et al. (1995) *Magn Reson Med* 34:537-541

[2] Fox et al. (2007) *Neuron* 56:171-184

Acknowledgements: Supported by NIH (R01 MH-067528, P30 NS-52519).

744

HETEROGENEOUS HIPPOCAMPAL CHOLINERGIC CHANGES IN ALZHEIMER'S DISEASE SUBJECTS SHOWN BY AUTORADIOGRAPHY WITH [^{18}F]FEOBV, AN ACETYLCHOLINE VESICULAR TRANSPORTER PET TRACER

J.-P. Soucy[1], L. Minuzzi[2], A. Alliaga[2], R. Quirion[2], S. Gauthier[2], M.-A. Bédard[3], P. Rosa-Neto[2]

[1]McConnell Brain Imaging Centre, Montreal Neurological Institute, [2]Douglas Hospital, [3]Université du Québec à Montréal, Montreal, QC, Canada

Objectives: In prior studies performed in rats and in cynomolgus monkeys, we have established that [^{18}F]FEOBV is a highly promising tracer for evaluation of the *in vivo* distribution of cholinergic terminals with PET in humans. This agent could be useful in the field of Alzheimer's disease, where it might have diagnostic applications, as well as in assessing disease progression and efficacy of therapeutic interventions. In order to further evaluate that potential, we have measured its autoradiographic distribution in the hippocampal formation from both Alzheimer's Disease subjects and age-matched controls, using tissue from the Douglas Hospital Brain Bank (Montreal).

Methods: Hippocampi from AD patients (N=4, age 72 ± 4.39 y.) and healthy controls (N=4, age 69.67 ± 5.61 y.) were used. Tissue was cryosectioned to 20 mm, and binding was carried out at a single concentration of [^{18}F]FEOBV, with pre-incubation for 30 min. in buffer (50 mM Tris, 120 mM NaCl, 5 mM KCl, 2 mM CaCl2, 1 mM MgCl2; pH 7.4) and incubation for 60 min with [^{18}F]FEOBV (S.A. > 1250 Ci/mmol) at room T°. Non-specific binding was determined by addition of 10 mM FEOBV in adjacent slices. Slides were washed in cold buffer, dried, and exposed for 10 min. to phosphor imaging plates. Binding of the radioligand in both groups was normalized to the slice area with the highest binding.

Results: [^{18}F]FEOBV showed markedly heterogeneous hippocampal distribution. In both groups, the highest density was found in the hilus, dentate gyrus, CA3 and CA4 as compared to other hippocampal regions (ANOVA, $F=7.3$, $p< 0.001$), and the lowest in CA2 ($p< 0.05$). Uptake was higher in controls than in AD patients in the hilus, parasubiculum and subiculum sub-fields ($p < 0.05$), but higher in AD subjects in the dentate gyrus (superior & inferior granular cells; specific binding increased by 45%, post-hoc multiple comparison analysis, $p< 0.05$).

Conclusions: The heterogeneity shown here by [^{18}F]FEOBV autoradiography generally agrees with results in a mice and rats study (Aznavour et al.), although the exact pattern was slightly different. Compensatory responses in the cholinergic system already have been shown in humans with Alzheimer's disease (DeKosky et al). In fact, increased acetylcholinergic innervation of the dentate gyrus after entorhinal lesioning in the rat, abolished after septal lesioning, has been reported (Cotman et al) and could be of relevance to the present findings. Overall, whether the changes seen here are the result of cholinergic sub-systems with different susceptibility to the disease process projecting to different fields of the hippocampus, or of different local molecular parameters conferring “resistance” to cholinergic terminals in those areas, remains to be established, but our results indicate a complex response of the cholinergic system to changes associated with Alzheimer's.

References: Aznavour et al: Hippocampus 12: 206-217 (2002); DeKosky et al: Ann Neurol 51: 145-155 (2002); Cotman et al : Proc. Nat. Acad. Sci. USA 70: 3473-3477 (1973).

745

TEXTURE ANALYSIS OF POLY-ADENYLATED MRNA STAINING FOLLOWING GLOBAL BRAIN ISCHEMIA AND REPERFUSION

J. Szymanski, J. Jamison, D. Degracia

Physiology, Wayne State University, Detroit, MI, USA

Objectives: We previously showed that cytoplasmic polyadenylated mRNAs form mRNA granules in post-ischemic neurons which correlate with translation arrest and hence cell death [1]. The cytoplasmic mRNA granules are ostensibly particulate structures showing variations in area and intensity from animal to animal. We therefore sought to quantify mRNA granules variations amongst animals. Here we apply the methods of texture analysis (TA) to quantify mRNA granules in photomicrographs of CA3 in the rat hippocampus around 1 hour of reperfusion after 10 min of global cerebral ischemia. Additionally, we use TA methods to quantify the effect of pre- and post-ischemic treatment of animals with the translation inhibitor cycloheximide (CHX).

Methods: Normothermic global forebrain ischemia was induced adult male Long Evans rats by bilateral carotid artery occlusion as we have described previously [1]. Treatment groups (n = 5 animals/group) were: 10 min ischemia and (1) 45 min reperfusion, (2) 60 min reperfusion, (3) 75 min reperfusion, (4) CHX pre-treatment + 60 min reperfusion, and (5) CHX treatment at 15 min reperfusion and a total of 60 min reperfusion. Vehicle-treated controls were also run for groups 4 and 5. mRNA granules were visualized by fluorescent in situ hybridization for polyadenylated mRNA and co-stained for the mRNA-binding protein HuR. TA was performed using MaZda ver 4.6. TA workflow involved: (1) image segmentation into regions of interest (ROI), (2) computing a 155-texture feature vector for each ROI, (3) feature reduction to 10 most discriminate features by Fisher analysis, and (4) principle component analysis of the 10-vector obtained by Fisher analysis. PCA results were compared by ANOVA with $p < 0.05$.

Results: The TA workflow allowed statistically significant discrimination between the 45, 60 and 75 min reperfused groups that could be correlated to the time course of mRNA granule formation. CHX pretreatment prevented formation of mRNA granules, but CHX treatment at 15 min reperfusion did not prevent mRNA granules at 60 min reperfusion.

Conclusions: The TA procedure described here provided an effective means for quantifying the complex morphology of mRNA granulation induced in post-ischemic neurons. The differential effect of CHX via pre- and post-ischemic treatment supports the conclusion that mRNA granule formation is dependent upon polysome dissociation. The methods described here provide a novel means for quantifying the dynamics of cellular processes in photomicrographs of post-ischemic neurons.

References:

[1] Jamison JT, Kayali F, Rudolph J, Marshall M, Kimball SR, DeGracia DJ. Persistent redistribution of poly-adenylated mRNAs correlates with translation arrest and cell death following global brain ischemia and reperfusion. Neuroscience. 2008;154(2):504-20.

746

MAST CELL MEDIATED MICROVASCULAR GELATINASE ACTIVATION AFTER TRANSIENT CEREBRAL ISCHEMIA IN RAT

O.S. Mattila[1], D. Strbian[1,2], J. Saksi[1], T.O. Pikkarainen[1], V. Rantanen[3], T. Tatlisumak[2], P.J. Lindsberg[1,2]

[1]Research Program of Molecular Neurology, University of Helsinki, [2]Department of Neurology, Helsinki University Central Hospital, [3]Genome-Scale Biology Program, University of Helsinki, Helsinki, Finland

Background and aims: Ischemic blood-brain barrier (BBB) damage causes hazardous expansive brain edema and hemorrhages. Recent evidence suggests that perivascularly positioned immunocompetent granulous mast cells (MCs) compromise the integrity of BBB following sudden ischemia. We studied whether MCs regulate the enzymatic gelatinase activity produced by matrix metalloproteinases (MMPs) -2 and -9 known to degrade the main constituents of basal membrane following ischemia.

Methods: Genotypically altered rats ($WsRc^{Ws/Ws}$) born with no MCs (n=7) and their wild-type (WT) littermates (n=7) were subjected to 60-min middle cerebral artery occlusion (MCAO) followed by 3-h reperfusion. In the pharmacological groups rats were treated with an inhibitor of MC degranulation (sodium cromoglycate, n=8), MC-activating secretagogue (compound 48/80, n=6) and saline (n=7). The activity of gelatinase enzymes (mainly MMP-2 and -9) was visualized by *in situ* zymography (ISZ) in coronal brain sections. Gelatinase-positive areas were quantified as percentage of the total infarcted area from montage images. Microvascular gelatinase activity was quantified with automated image analysis from ISZ and endothelial marker double-stained sections. The cellular localization of gelatinase activity was demonstrated by double stainings: ISZ plus markers of vascular endothelium (vWF), neurons (NeuN), astrocytes (GFAP) and mast cells (TRITC-conjugated Avidin). Microvascular basal membrane disruption was evaluated with collagen IV immunostaining. Data are presented as mean±SD.

Results: MC-deficiency significantly reduced the *mean gelatinase activity* of microvessels ($p=0.002$) and the *percentage of microvessels with high gelatinase activity* in the ischemic hemisphere ($p=0.003$) compared to WT animals. The pharmacological interventions showed a significant effect on the *percentage of microvessels with high gelatinase activity* ($p=0.02$, Kruskal-Wallis ANOVA), and a trend towards a difference between *mean microvascular gelatinase activity* ($p=0.054$, Kruskal-Wallis ANOVA) in the ischemic hemisphere. Total area of gelatinase activity within the ischemic lesion was reduced in MC-deficient rats (7.3±2.7%) compared to WT (23.5±8.8%, $p< 0.001$). In the pharmacological interventions the MC-activating compound 48/80 was associated with increased area of gelatinase activity (34.4±9.9%), but cromoglycate (21.2±10.2%) failed to influence it compared to the control group (22.2±12.0% $p=0.07$, 1-way ANOVA). Gelatinase activity localized in microvessels but also in neuronal somas within the infarcted area. A halo of gelatinase positive granules was seen around activated mast cells in the ipsilateral hemisphere. Furthermore, visualization of the gelatinase substrate collagen IV showed loss of immunoreactivity and fragmentation of vessel profiles in the ischemic hemisphere, which was mitigated by MC inhibition.

Conclusions: These results demonstrate that MCs are involved in the regulation of microvascular gelatinase activity and subsequent basal membrane disruption in early ischemia-reperfusion injury in the rat brain. These observations further support the involvement of MCs in

disrupting the integrity of BBB and suggest novel therapeutic avenues in stroke based on regulation of MCs.

747

NCX3 AS A NEW MOLECULAR TARGET FOR SUMOYLATION AFTER FOCAL CEREBRAL ISCHEMIA

O. Cuomo, G. Pignataro, R. Sirabella, A. Scorziello, C. Savoia, M.J. Sisalli, G. Di Renzo, L. Annunziato

Neuroscience, Federico II University of Naples, Naples, Italy

Introduction: The small ubiquitin-like modifier (SUMO) is a post-translational protein modification mechanism activated by several stresses that has been investigated in experimental models of cerebral ischemia only in the last years (Yang et al., 2008). Convincing evidences showed that sumoylation can confer neuroprotection against stressful stimuli by regulating the function and the fate of proteins involved in stress signalling pathways (Lee et al., 2007). Recently, it has been shown that sumoylation enzymes and substrates are expressed not only in the cytoplasmic and nuclear compartments, but also at the plasma membrane level (Rajan et al., 2005). Within the numerous plasmamembrane proteins involved in the pathophysiology of cerebral ischemia and able to control ionic homeostasis, we have recently demonstrated that the sodium calcium exchanger, NCX, plays a relevant role. In particular, we demonstrated that NCX3, one of the three NCX brain isoforms, is tightly related to the pathophysiology of the ischemic event. In fact, NCX3 knock-out or knock-down significantly worsen ischemic damage (Molinaro et al., 2008).

Objectives: In the light of these premises, the aims of this study were: (1) to analyze the activation of sumoylation after focal cerebral ischemia, ischemic pre- and postconditioning (2) to analyze whether NCX3 is a target for sumoylation (3) to evaluate, if it occurs, the biological meaning of the interaction between NCX3 and SUMO.

Methods: Focal ischemia and ischemic preconditioning and postconditioning were experimentally induced in adult male rats by subjecting them to different protocols of middle cerebral artery occlusion and reperfusion. SUMOylation was evaluated by Western Blot analysis. SUMO and NCX interaction was analyzed by confocal microscopy and immunoprecipitation assay.

Results: The results of the present study showed that sumoylation is significantly activated after both cerebral ischemia, preconditioning and postconditioning and that NCX3 may be a target for sumoylation.

Conclusions: Overall, these results indicate that NCX3 may represent a new potential target to be investigated in the study of the SUMO-mediated molecular pathways involved in cerebral ischemia.

References:

- Annunziato L, Pignataro G, Di Renzo GF. Pharmacology of brain Na+/Ca2+ exchanger: from molecular biology to therapeutic perspectives. Pharmacol Rev. 2004; 56(4):633-54.
- Molinaro P, Cuomo O, Pignataro G, Boscia F, Sirabella R, Pannaccione A, Secondo A, Scorziello A, Adornetto A, Gala R, Viggiano D, Sokolow S, Herchuelz A, Schurmans S, Di Renzo GF, Annunziato L. “Targeted Disruption of NCX3 Gene Leads to a Worsening of Ischemic Brain Damage” J Neurosci 2008; 30;28(5):1179-84.

- Yang W, Sheng H, Homi HM, Warner DS, Paschen W.Cerebral Ischemia/Stroke and Small Ubiquitin-Like Modifier (SUMO) Conjugation - A New Target for Therapeutic Intervention? J Neurochem. 2008;106(3):989-99.
- Lee YJ, Miyake S, Wakita H, McMullen DC, Azuma Y, Auh S, Hallenbeck JM Protein SUMOylation is massively increased in hibernation torpor and is critical for the cytoprotection provided by ischemic preconditioning and hypothermia in SHSY5Y cells. J Cereb Blood Flow Metab. 2007;27(5):950-62.
- Rajan S, Plant LD, Rabin ML, Butler MH, Goldstein SA. Sumoylation silences the plasma membrane leak K+ channel K2P1. Cell 2005;121(1):37-47.

748

CELL-SELECTIVE GENE ABLATION AS A TOOL TO RESOLVE SITE-SPECIFIC ROLES OF CCL2 AT THE BLOOD-BRAIN BARRIER DURING NEUROINFLAMMATION

D. Paul, S. Ge, J.S. Pachter

Cell Biology, Blood-Brain Barrier Laboratory, University of Connecticut Health Center, Farmington, CT, USA

Introduction: Alterations in blood-brain barrier (BBB) permeability accompany neuroinflammatory disorders such as multiple sclerosis (MS). It nonetheless remains unclear whether such permeability changes are a “cause” or “effect” of the neuroinflammatory process, and the mediators responsible await clarification. Despite this, chemokine CCL2 has emerged as a critical mediator in experimental autoimmune encephalomyelitis (EAE), well-accepted animal model for MS, and thought to be a pathological feature in MS. Specifically, CCL2 is linked to leukocyte-extravasation at the sites of BBB-breakdown in the central nervous system (CNS), implying an intricate functional correlation between CCL2 expression, paracellular leukocyte influx into CNS parenchyma, and BBB-leakage. To begin resolving CCL2's role in neuroinflammatory disease, we recently created the first cell-conditional chemokine knockout-mice, separately eliminating CCL2 gene from two cell types considered crucial in neuroinflammation: *astrocytes* (Astro-KO) or *endothelial* cells (Endo-KO).

Aim:

1. To characterize, *qualitatively* and *quantitatively,* the heightened BBB-permeability and leukocyte-influx in CNS during various stages of EAE progression in wild-type (WT) animals, and correlating these observations with CCL2 expression in various segments of the spinal cord and brain.
2. To employ Astro-KO and Endo-KO mice to determine the relative contributions of astrocyte- and endothelial cell-derived CCL2, respectively, to the histopathological changes in BBB-permeability and leukocyte invasion that accompany different stages of EAE.

Methods:

- EAE induction was carried-out by active-immunization with myelin oligodendrocyte glycoprotein (MOG) peptide$_{35\text{-}55}$.
- Epifluorescence microscopy was employed to identify leukocytes, TJs, basement membranes (BMs), IgG and CCL2 in WT, Astro-KO & Endo-KO mice.
- Three-dimensional (3-D) projections of Z-stacked confocal images were volume rendered by IMARIS, uniquely allowing qualitative and quantitative assessment of *holistic* pathological-changes around the entire surface of CNS microvessels during EAE progression (e.g., expression/localization of tight-junction [TJ] proteins, IgG leakage, step-wise penetration of leukocytes through endothelium and successive endothelial and parenchymal BMs, and sites of CCL2 expression).

- ELISA was performed to detail the time-course of changes in CCL2 expression in the lumbar, thoracic and cervical spinal cord, as well as brain, with ascending progression of EAE.

Results:

- BBB-permeability and leukocyte infiltration into the CNS parenchyma progressively increased from day 9 - day 19 during EAE in WT mice, with an associated decrease in Claudin-5 expression at TJs of inflamed vessels in white matter.
- BBB-permeability correlated with CCL2 expression, which peaks at day 12 post-injection, in the cervical spinal cord of WT mice.
- WT showed high CCL2 expression in astrocytes during EAE; this was absent from Astro-KO mice, which, along with Endo-KO mice, showed diminished neuroinflammatory activity at the BBB.

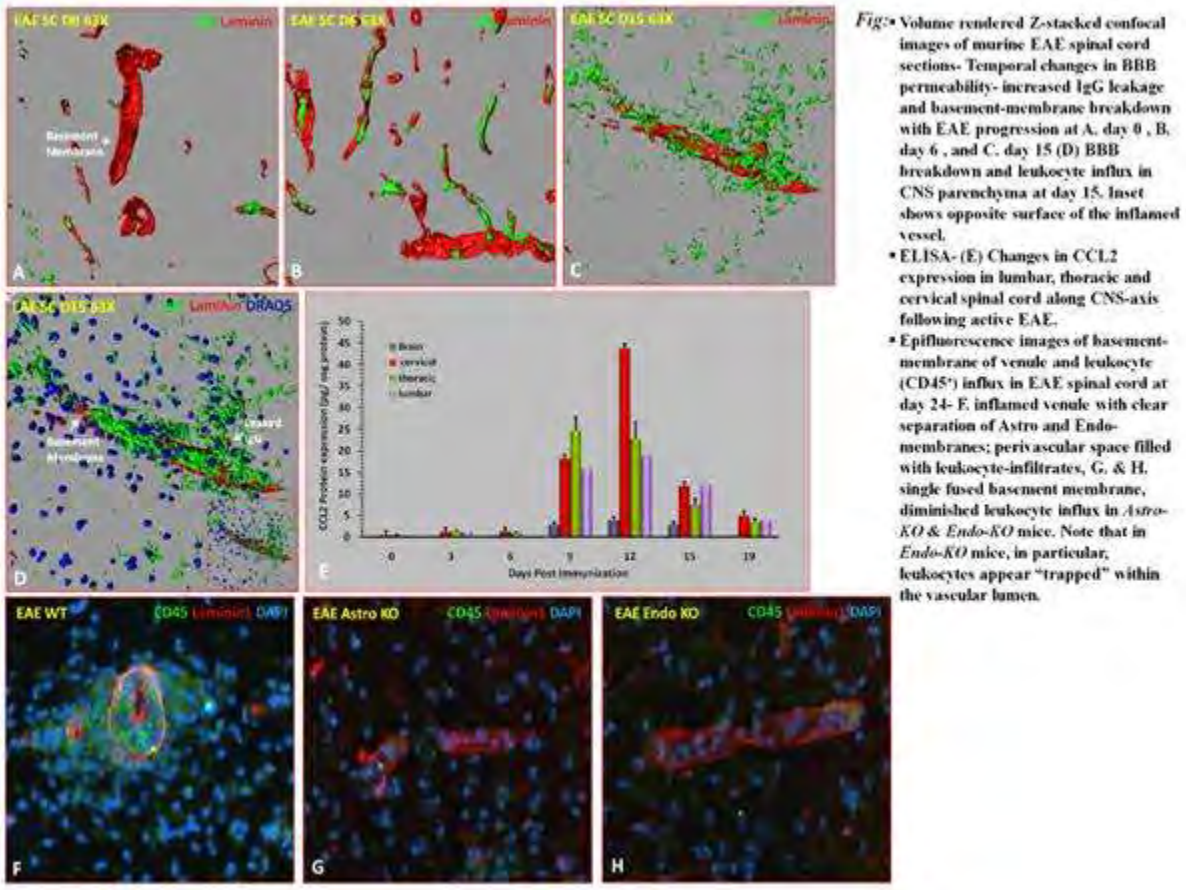

Fig: • Volume rendered Z-stacked confocal images of murine EAE spinal cord sections- Temporal changes in BBB permeability- increased IgG leakage and basement-membrane breakdown with EAE progression at A. day 0 , B. day 6 , and C. day 15 (D) BBB breakdown and leukocyte influx in CNS parenchyma at day 15. Inset shows opposite surface of the inflamed vessel.
• ELISA- (E) Changes in CCL2 expression in lumbar, thoracic and cervical spinal cord along CNS-axis following active EAE.
• Epifluorescence images of basement-membrane of venule and leukocyte ($CD45^+$) influx in EAE spinal cord at day 24- F. inflamed venule with clear separation of Astro and Endo-membranes; perivascular space filled with leukocyte-infiltrates, G. & H. single fused basement membrane, diminished leukocyte influx in *Astro-KO & Endo-KO* mice. Note that in *Endo-KO* mice, in particular, leukocytes appear "trapped" within the vascular lumen.

[Figure]

Conclusion: Our study unveiled a close association between increased CCL2 production by reactive astrocytes and progressive reduction in TJs, increased leukocyte extravasation and elevated BBB-permeability at the BBB during EAE. Cell specific knockout of CCL2 alleviated the neuroinflammation observed in WT EAE mice. These results highlight CCL2 as a potential therapeutic target **f**or neuroinflammatory disease.

749

LASER-INDUCED THROMBUS FORMATION IN BRAIN MICROVASCULATURE OF ANGIOTENSIN II TYPE 2 RECEPTOR-KNOCKOUT MICE

H. Maruyama, H. Takeda, T. Fukuoka, N. Tanahashi

Neurology, International Medical Center, Saitama Medical University, Hidaka, Japan

Objectives: There are two known major angiotensin II receptor subtypes, type 1 (AT1) and type 2 (AT2), both of which are present in the brain. The major cardiovascular actions of angiotensin II have been reported to be mediated by the subtypes of angiotensin II receptor. However, the functions of two angiotensin II receptors have been still unclear in thrombus formation of the brain. Using a laser, we developed a technique to induce thrombus formation in murine brain microvasculature instantaneously. The purpose of this study was to observe the effect of AT2 receptor deficient on the process of laser-induced thrombus formation and platelet behavior in the brain microvasculature of mice using intravital fluorescence microscopy.

Methods: Adult male C57BL/6J mice (control group, N=7) and AT2 receptor-knockout mice (AT2 knockout group, N=10) were used in this study. The mice were anesthetized with chloral hydrate and inserted a catheter in their cervical vein. Their head was fixed with a head holder, and a cranial window was prepared in the parietal region. Platelets were labeled in vivo by intravenous administration of carboxylfluorescein succinimidylester (CFSE). Laser irradiation (1000 mA, DPSS laser 532 nm, TS-KL/S2; Sankei) was spotted for 4 seconds on pial arteries to induce thrombus formation. Labeled platelets and thrombus were observed continuously with a fluorescence microscope.

Results: After laser irradiation to the pial artery, thrombus formation started in the irradiated area in gradually. The complete occlusion rate was not significantly different between in the control group (60%, 12/20 vessels, vessel diameter 26.9±3.3μm) and in the AT2 knockout group (48%, 12/25 vessels, vessel diameter 26.2±3.4μm). The area of platelet thrombus on 30 minutes after laser irradiation was significantly larger in the AT2 knockout group (555±488 μm^2) than in the control group (358±256 μm^2; P=0.028) .

Conclusion: The present study suggests that the AT2 receptor is related to the inhibition of the laser-induced thrombus formation in murine pial arteries.

750

NEUROLOGICAL DEFICIT, NAD LOSS AND NUCLEAR SIRT1 UPREGULATION AFTER AN ACUTE *IN VIVO* CEREBRAL OXIDATIVE STRESS

C. Gueguen, C. Guiziou, A. Paucard, B. Palmier, **M. Plotkine**, I. Margaill, C. Marchand-Leroux, V. Besson

Pharmacologie de la Circulation Cérébrale EA4475, Université Paris Descartes, UFR des Sciences Pharmaceutiques et Biologiques, Paris, France

Introduction: Acute central nervous system injuries, such as cerebral ischemia and traumatic brain injury, induce a deleterious oxidative stress. *In vitro* studies showed that oxidative stress, which leads to cell death, decreases NAD level and Sirtuin 1 (SIRT1) activity[1]. SIRT1 is a NAD-dependent deacetylase involved in various biological functions such as development, metabolism and cell death[2]. Increasing NAD could restore SIRT1 activity and decrease oxidative stress-induced cell death[1]. This led us to study whether an *in vivo* cerebral oxidative stress modulates SIRT1 and level of NAD, its substrate.

Methods: *In vivo* cerebral oxidative stress was induced by the infusion of malonate, a mitochondrial toxin that promotes free radicals production, into the left striatum of anaesthetized male Sprague-Dawley rats[3]. The neurological evaluation was performed using a global motor and behavioral score (ranging from 0=worst to 15=best) at 24, 48, 72h and 7d after malonate. Striatum levels of glutathione (GSx) and NAD were evaluated 1, 2, 4, 24, 48, 72h and 7d after malonate. GSx is a major antioxidant whose decrease reflects an oxidative stress. SIRT1 expression was evaluated 1, 2, 4, 6 and 24h after malonate by western-blot in 2 subcellular fractions, cytoplasm and nucleus, as SIRT1 is present in these both cellular compartments.

Results: Malonate reduced the neurological score from 24h (5.7±0.9 vs 13.2±0.5 for sham operated rats, $P< 0.001$) until at least 7d post-injury (9.0±1.0, $P< 0.01$) demonstrating a long lasting neurological deficit. GSx level was decreased as early as 1h after malonate (75±2 vs 89±3% of control for sham operated rats, $P< 0.001$) until at least 7d (60±7 vs 92±3% of control for sham operated rats, $P< 0.01$) showing a long-lasting oxidative stress. In addition GSx loss was correlated with neurological deficit ($P< 0.001$). Malonate decreased NAD level as early as 4h (0.17±0.02 vs 0.27±0.02 nmol/g for sham operated rats, $P< 0.05$) that persisted until 48h (0.16±0.02 nmol/g, $P< 0.01$). Whereas cytoplasmic SIRT1 expression was not modified between 1 and 24h after malonate, nuclear SIRT1 expression was upregulated at 6h (234±30 vs 155±15 AU for sham operated rats, $P< 0.05$).

Conclusion: *In vivo* cerebral oxidative stress induces a long-lasting neurological deficit correlated with important long-lasting GSx loss. Oxidative stress upregulates SIRT1 expression at 6h in the nucleus. As NAD, its substrate, is decreased by oxidative stress at this time, SIRT1 activity could be modified. Further studies are necessary to measure SIRT1 activity in nuclear and cytoplasmic compartments after *in vivo* cerebral oxidative stress.

1. Furukawa et al., 2007, *Cell Physiol Biochem*, 20: 45-54.

2. Michan & Sinclair, 2007, *Biochem J*, 404: 1-13.

3. Besson et al., 2003, *Free Radic Res*, 37: 1201-1208.

753

QUANTITATIVE INHIBITION OF P-GLYCOPROTEIN AT THE HUMAN BLOOD-BRAIN BARRIER AFTER TARIQUIDAR ADMINISTRATION: AN (R)-[11C]VERAPAMIL PET STUDY

M. Bauer[1], M. Zeitlinger[1], R. Karch[2], P. Matzneller[1], J. Stanek[1], E. Lackner[1], W. Wadsak[3], M. Müller[1], O. Langer[1,4]

[1]Department of Clinical Pharmacology, [2]Computer Sciences, [3]Nuclear Medicine, Medical University of Vienna, Vienna, [4]Health and Environment Department, Molecular Medicine, AIT Austrian Institute of Technology GmbH, Seibersdorf, Austria

Introduction: Positron emission tomography (PET) with (R)-[11C]verapamil (VPM), a substrate of the multidrug efflux transporter P-glycoprotein (Pgp), can be used to assess Pgp function at the blood-brain barrier (BBB). We have shown in rats that performing VPM PET scans after half-maximum inhibition of Pgp with the third-generation P-gp inhibitor tariquidar (TQD) has higher sensitivity for detection of regional differences in cerebral Pgp function than VPM baseline scans [1].

Objective: For translating this study approach to humans a knowledge of the dose-response relationship of TQD for enhancing VPM brain activity uptake is required, which was investigated in the present work.

Methods: Healthy male subjects (n=3 per dose group) underwent VPM PET scans and arterial blood sampling at 1 h after i.v. infusion of TQD at doses of 3, 4, 6 and 8 mg per kg body weight. Radiolabelled metabolites of VPM in plasma were assessed with a previously described solid-phase extraction protocol [2]. Brain activity uptake was quantified in terms of the volume of distribution (VT) derived from Logan analysis. Data were pooled with data from a previous pilot study in 5 healthy male subjects who underwent VPM PET scans before and after administration of 2 mg/kg TQD [2] and sigmoidal dose-response curves were fitted to the data using the Hill-equation.

Results: Administration of TQD dose-dependently increased VPM brain activity uptake with an estimated half-maximum effect dose (ED50) of 3.09±0.30 mg/kg. The maximum increase in brain activity uptake as compared to baseline scans (without TQD administration) was 2.4-fold (Fig. 1). Administration of TQD exerted no effect on the fraction of polar radiolabelled metabolites of VPM in plasma. For comparison, in rats the ED50 of TQD was 2.95±0.19 mg/kg and the maximum increase in brain activity uptake compared to baseline 10.7-fold [1].

Conclusions: This is to our knowledge the first study where quantitative inhibition of Pgp at the human BBB is reported. Our data suggest that the ED50 of TQD to enhance VPM brain activity uptake in humans is similar to the value previously determined in rats using an identical study protocol [1]. The maximum increase in brain activity uptake was several-fold lower in humans as compared to rats. The exact reasons for these differences are unknown but might be related to differences in TQD pharmacokinetics, binding of VPM in brain tissue or the relative contribution of other efflux transporters to VPM brain distribution, such as multidrug resistance proteins (MRP1).

References:

1. Kuntner C et al. Dose-response assessment of tariquidar and elacridar and regional

quantification of Pglycoprotein inhibition at the rat blood-brain barrier using (R)-[11C]verapamil PET. Eur J Nucl Med Mol Imaging 2010, 37:942-53.

2. Wagner CC et al. A pilot study to assess the efficacy of tariquidar to inhibit P-glycoprotein at the human blood-brain barrier with (R)-[11C]verapamil and PET. J Nucl Med 2009, 50:1954-61.

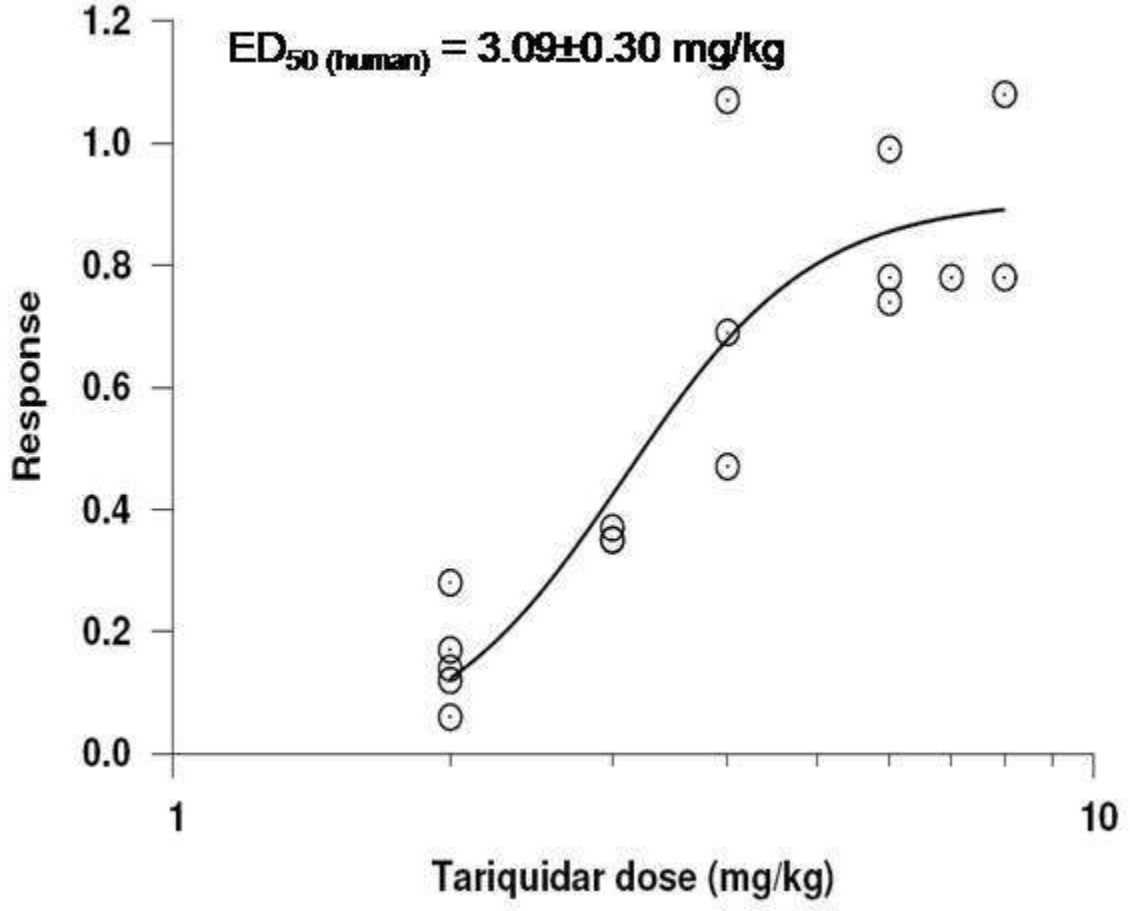

[Dose-response curve of TQD]

Fig. 1.: Dose-response curve of TQD for increasing brain activity uptake of VPM in humans. Response is VT increase of VPM in whole brain relative to baseline scan without TQD administration.

755

A SMALL MOLECULE BRAIN-DERIVED NEUROTROPHIC FACTOR MIMETIC, ADMINISTERED BEGINNING THREE DAYS AFTER STROKE, IMPROVES FUNCTIONAL RECOVERY IN MICE

J. Han, J. Pollak, T. Yang, K.P. Doyle, K. Taravosh-Lahn, E. Cekanaviciute, J.Z. Goodman, A. Han, M.R. Siddiqui, F.M. Longo, **M.S. Buckwalter**

Neurology and Neurological Sciences, Stanford School of Medicine, Stanford, CA, USA

Objectives: Stroke is a leading cause of long-term disability. Although acute revascularization therapies can be used to abort or reduce stroke burden, there are currently no FDA-approved drugs that improve functional recovery after stroke. We hypothesized that brain-derived neurotrophic factor (BDNF) might promote functional recovery because it is a key stimulator of neurogenesis and brain rewiring after stroke. Also, relative BDNF deficiency occurs with aging in association with decreased functional recovery. But BDNF is not a good drug candidate - it is a protein that has a short plasma half-life and only poorly penetrates the blood brain barrier and brain parenchyma. Tropomyosin-related kinase B (TrkB) is one of two BDNF receptors, and mediates its effects on neurogenesis, axonal sprouting, and synapse formation. We therefore tested the small molecule BDNF mimetic LM22A-4, which specifically activates the TrkB pathway, to determine if it improves functional recovery after hypoxic-ischemic stroke.

Methods: Five month old mice were trained on three tasks (ladder, Noldus Catwalk and rotarod) prior to stroke or sham surgery. After stroke, rotarod and ladder test results were used to randomize mice into two equally impaired groups. Mice received either 0.22 mg/kg LM22A-4 or saline vehicle, given intranasally, beginning 3 days after stroke, and were treated daily until ten weeks after stroke. Fifty mg/kg BrdU was also administered on days 3-8.

Results: After stroke, LM22A-4 treatment improved limb swing speed on Catwalk, and gait accuracy on ladder testing ($P = 0.0032$ and 0.0289, respectively, repeated measures ANOVA). There was no recovery in rotarod testing in either group. Stereological analysis of BrdU+/NeuN+ cells revealed that LM22A-4 treatment increased neurogenesis in areas adjacent to the stroke core. We found a 1.8-fold increase in BrdU+ mature neurons in penumbral cortex and a 2.7-fold increase in dorsolateral striatum ($P = 0.004$ and < 0.0001, respectively, Student's t test), but no significant increase in the unaffected ventral striatum. Immunostaining for the immature neuronal marker doublecortin also demonstrated a two-fold increase in LM22A-4-treated animals. Golgi staining revealed no drug-induced differences in dendritic complexity in contralateral motor cortex and dorsal lateral striatum.

Conclusions: Increased TrkB pathway activation improves recovery from stroke and increases neurogenesis. LM22A-4 or its derivatives might therefore serve as “pro-recovery” therapeutic agents for people with stroke.

References: None.

756

SPATIALLY-RESOLVED REFLECTANCE MEASUREMENTS AT THE CORTEX SURFACE DURING SUSTAINED STIMULATION DEMONSTRATE MARKED VARIATIONS OF ABSORPTION AND SCATTERING COEFFICIENT

S.R. Chamot[1,2], E. Migacheva[2], N. Calcinaghi[3], M.T. Wyss[3], B. Weber[3], M. Rudin[4], C. Depeursinge[2], P.J. Magistretti[1,2], P. Marquet[1,2]

[1]Centre de Neurosciences Psychiatriques (CHUV), [2]Swiss Federal Institute of Technology Lausanne, Lausanne, [3]University of Zurich, [4]Swiss Federal Institute of Technology Zurich, Zurich, Switzerland

Introduction: The study of neurovascular coupling examines the relationship between oxidative metabolism and cerebral blood flow in brain cortex during neural activation. Investigations of the transient variations in tissue and blood oxygenation occurring within the early times of neuronal activation carried with functional magnetic resonance imaging (fMRI) or optical intrinsic signals (OIS), in some case, reported a rapid decrease called 'initial dip' in tissue oxygenation. This dip would have important implications for the interpretation of the physiological mechanisms at stake and its existence is today still debated. Regarding the interpretation of OIS, the discrepancy of results obtained by different groups may be due to the lack of accurate information regarding the changes of cortex optical properties induced by neuronal activity, thus justifying the need for quantitative.

Material and methods: We report here in vivo spatially-spectrally-resolved reflectance (SSRR) measurements carried with a custom small optical probe through thinned skull bone on rat brain somatosensory cortex regions activated during forepaw stimulations. With the animal anesthetized, ventilated and fully monitored, and the optical probe placed directly at the tissue surface, SSRR measurements were repeatedly performed at 1.5 seconds intervals during a 3-min. protocol (1st min.: baseline, 2nd min.: sustained stimulation, 3rd min.: recovery). Forepaw stimulation were obtained with two electrodes inserted subcutaneously (0.8 mA pulses @ 4Hz).

Results: The SSR measurements show that the light intensity detected in the 9 fibers of the optical probe can vary significantly and with a good reproducibility up to 20% over an extended wavelength range (500-900 nm) during stimulation. The post-processing of these experimental data indicates that both absorption and reduced scattering coefficients vary significantly and independently during sustained cortex activity, with amplitudes depending on the wavelength. A fit of the absorption spectrum with a linear combination of the spectral extinction coefficient of Hb and HbO2 allows computing blood oxygen saturation, which, in some case, markedly increases up to 40% during stimulation.

Conclusions: Intrinsic optical signals due to sustained cortical activity are locally measurable with SSRR. As a great advantage, this technique allows a distinct evaluation of the absorption and reduced scattering coefficients of the tissue. For the correct interpretation of OIS acquired with different optical imaging techniques dedicated to explore neurovascular and neurometabolic coupling mechanisms, this information is of ample interest.

757

VOXEL-WISE QUANTIFICATION OF 5HT$_{2A}$ RECEPTOR WITH [^{11}C]MDL100907

G. Rizzo[1], R.M. Moresco[2], F.E. Turkheimer[3], I. Florea[2], M. Matarrese[2], A. Panzacchi[2], A. Bertoldo[1]

[1]Department of Information Engineering, University of Padova, Padova, [2]IBFM-CNR, University of Milan Bicocca, Nuclear Medicine Department, San Raffaele Scientific Institute, Milan, Italy, [3]Division of Experimental Medicine, Imperial College London, London, UK

Introduction: [^{11}C]MDL100907 is a high affinity PET ligand for 5-HT$_{2A}$ receptor quantification in vivo. On the basis of ROI analysis, the tracer is usually assumed to be reversible as its kinetics are well described by a two-tissue four-rate constant model [1]. In literature [^{11}C]MDL data have been previously evaluated only with plasma input reversible compartmental models [1] and with reference input models (graphical and compartmental models) [2]. Our study aimed to define the best quantitative model for [^{11}C]MDL100907 considering its kinetics at voxel level and using Spectral Analysis (SA) in order to avoid the problem of tissue heterogeneity implied by the ROI approach.

Materials and methods: We analyzed two [^{11}C]MDL datasets, made available by Imperial College (London, UK) and San Raffaele Scientific Institute (HSR, Italy). The Imperial dataset consisted in 5 healthy subjects undergone twice a 90-min PET scan following injection of 361 MBq of [^{11}C]MDL (baseline condition and after administration of mirtazapine, a 5HT$_{2A}$ blocking), complete with plasma input functions. HRS dataset consisted in 6 healthy subjects, scanned twice in baseline condition, complete with plasma input functions and 12 Obsessive Compulsive Disorder (OCD) patients, scanned twice (baseline condition and after administration of a SSRI). All HSR subjects underwent a 90-min PET after injection of 190-370 MBq of [^{11}C]MDL.

SA both linear [3] and nonlinear [4] was used to quantify the data. A reference region was automatically extracted from the cerebellum area by using cluster analysis. The impact of the different drug treatments on the reference region was evaluated.

Results: SA results clearly showed at voxel level the presence of an irreversible component, especially in cortical regions (more than in 70% of the voxels both in Imperial and HRS dataset) (Fig1) likely associated with the tracer's specific binding. Only in cerebellar voxels it was possible to properly identify two reversible components, probably due to the lack or reduced density of 5-HT$_{2A}$.

The reference region extracted by cluster analysis for both datasets for baseline condition showed no changes in the kinetics, neither between patients and control subjects nor between the two datasets. Instead after administration of SSRI, there was an alteration in the reference kinetic; this change didn't occur after administration of mirtazapine.

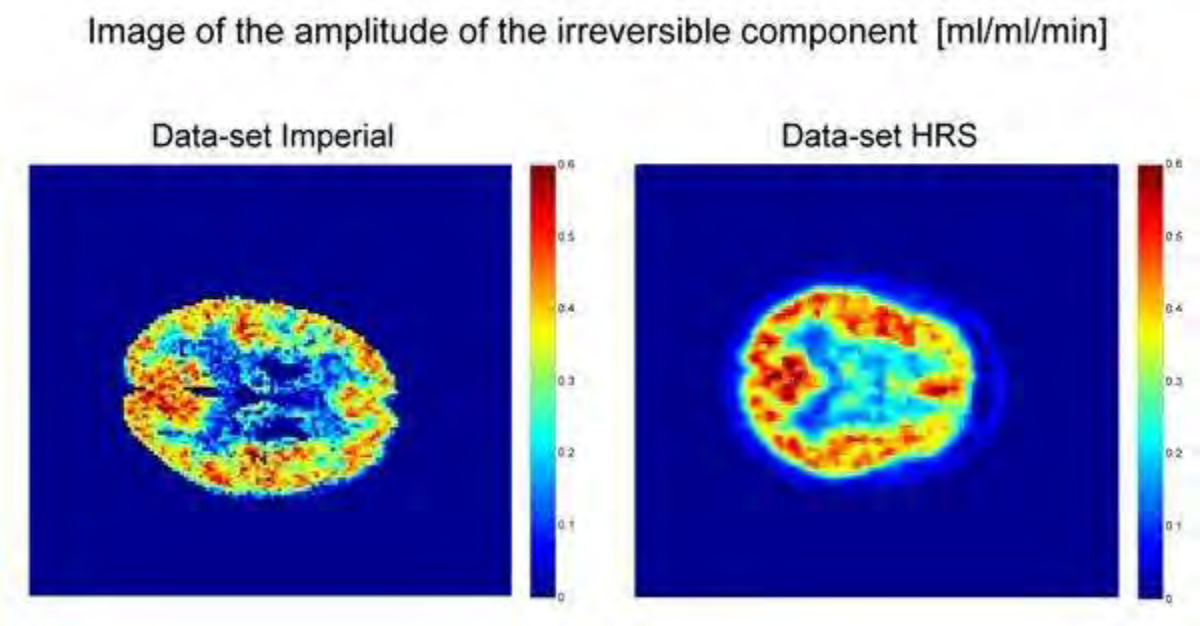

[Fig1]

Conclusions: Using SA we identify an irreversible component in the two different datasets, while in the cerebellum it was possible to identify mainly two reversible components. Moreover we analyzed the validity of the use of the cerebellum as reference region and we found out that when subjects are administered with SSRI the kinetic of cerebellum changes probably for drug induced modifications of tracer metabolism. This finding strongly indicates that cerebellum cannot be used as true reference region in presence of pharmacological treatment that potentially modifies metabolic enzymes like SSRI [5].

References:

[1] Hinz et al (2007) *JCBFM* 27: 161-172

[2] Meyer et al (2010) *Neuroimage* 50: 984-993

[3] Cunningham and Jones (1993) *JCBFM* 13: 15-23

[4] Bertoldo et al (1998) *IEEE Trans Biomed Eng* 45:1429-1448

[5] Brosen et al (1993) *Clin Investig* 71: 1002-1009

758

BRAIN REGIONAL ANGIOGENIC POTENTIAL OF THE AGING CEREBRAL MICROVASULATURE

N. Murugesan, J.S. Pachter

Cell Biology, University of Connecticut Health Center, Farmington, CT, USA

Introduction: Mounting evidence indicates that during normal aging, angiogenesis - the sprouting of new blood vessels from pre-existing vasculature - is significantly impaired in peripheral organ beds. However, little is known of how normal aging impacts angiogenesis in the brain, where increased susceptibility to stroke and age-associated cerebrovascular disorders could partly derive from a similar impairment. As angiogenesis is the product of an intricate balance between proangiogenic

and anti-angiogenic genes, it is critical to understand how this delicate balance may

be altered in the healthy aging brain. Furthermore, since certain brain regions appear particularly vulnerable to age-related cerebrovascular complications and display reduced vascular density with aging, the prospect that cerebral angiogenic potential is affected by the aging process in a regional manner warrants critical attention.

Our hypothesis: **Expression of the complement of genes governing angiogenesis is dysregulated in the brain, in a regional manner during**

normal aging, is tested here in two specific aims.

Aim:

1. Focuses on assessing regional, cerebral angiogenic potential in situ during normal aging.

   Specifically, expression of a set of recognized angiogenesis-associated genes was analyzed along the neurovascular unit (NVU) using Immuno-LCM/qRT-PCR, in distinct brain regions (cerebral cortex, corpus callosum and hippocampus) of young vs. aged mice.

2. Examines how physical exercise (treadmill training) influences brain regional expression of these angiogenesis-associated genes across age.

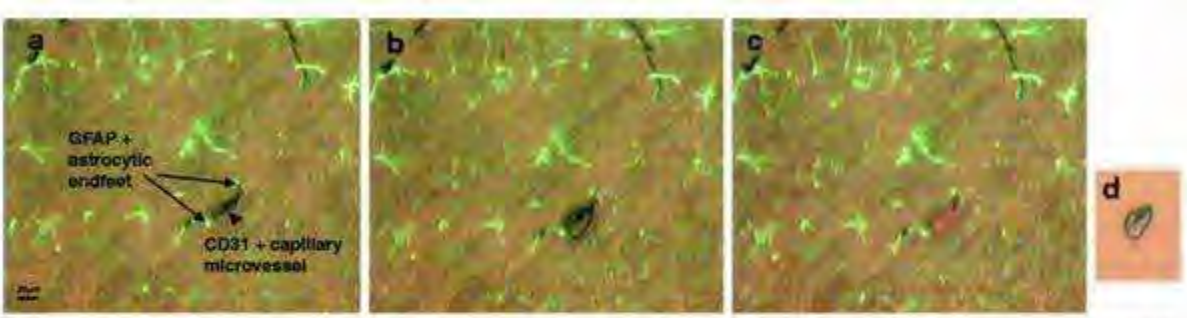

Selective retrieval of brain microvascular endothelial cells using Immuno-LCM. A 7 µm thick frozen coronal section of mouse brain double-immunostained with antibodies against CD31 and GFAP is shown. CD31 immunoreactivity was visualized by alkaline phosphatase and NBT-BCIP substrate, and GFAP was detected by immunofluorescence. (**a**) *Prelift:* Tissue stained with anti-CD31 (*dark purple*) and anti-GFAP (*green*), viewed under bright-field and epifluorescence optics simultaneously, prior to LCM. *Arrows* indicate the CD31+ stained endothelial cells of the microvessel (*dark purple*) and the perivascular distribution of astrocytic endfeet (*green fluorescence*). (**b**) *Tissue during-lift:* Tissue section is shown during the laser-melting, with the LCM cap placed over the CD31+ capillary microvessel. (**c**) *Tissue postlift:* Tissue after LCM shows that the entire endothelial layer was removed and the fluorescent distribution of astrocytic end-feet was not disturbed. (**d**) *Cap:* Tissue transferred to cap after LCM, showing intact endothelium, was retrieved, with no detection of astrocytic end-feet. (Ref: *Analysis of mouse brain microvascular endothelium using laser capture microdissection coupled with proteomics. Murugesan N, Macdonald JA, Lu Q, Wu SL, Hancock WS, Pachter JS. Methods Mol Biol. 2011;686:297-311.)*

[Immuno-LCM]

Results:

- The impact of aging on the relative expression of angiogenesis-associated genes is not constant across brain regions - implying region-specific adaptation to the aging process. Different ´cassettes´ of angiogenic genes were altered in expression in the three brain regions studied across age. While all three areas also showed capillary loss in aged subjects, the white matter appeared to change most drastically.
- The response to physical exercise training also exhibited regional differences as well. Moreover, the effect of exercise on the expression patterns of angiogenesis-associated genes differed in the aged exercised mice in comparison to that observed in the corresponding brain region in young exercised mice. In the cortex, physical exercise increased expression of MMP2 and decreased expression of Flk1 - thus reversing the trend observed in this region during normal aging. In the hippocampus, exercise similarly reduced Flk1, also reversing the aging trend in this region. Preliminary studies have also shown that, in addition to reversing some age-associated gene trends, physical exercise positively impacted cerebral capillary density and branching - in a region-dependent way.

Conclusions: Profiling the entire ´angiome´ in this manner will help identify the key repertoire of angiogenic genes that regulate angiogenesis in distinct brain regions as a function of age and highlight prospective targets for therapeutic angiogenesis. Moreover, physical exercise could potentially be used as a therapeutic intervention to correct/reverse age-associated changes in cerebral angiogenesis.

759

ELEVATED BLOOD CONTENT OF FIBRINOGEN INCREASES MOUSE PIAL VENULAR PERMEABILITY IN VIVO, IMPLICATION OF MATRIX METALLOPROTEINASE-9

N. Muradashvili[1], **D. Lominadze**[2]

[1]Physiology and Biophysics, University of Louisville School of Medicine, [2]Physiology and Biophysics, University of Louisville, Louisville, KY, USA

Objectives: An increase in blood content of fibrinogen (Fg) accompanies many inflammatory cardiovascular and cerebrovascular diseases commonly associated with vascular dysfunction. Previously we showed that pathologically high (4 mg/ml) content of Fg disrupts integrity of endothelial cell (EC) layer (1) affecting endothelial tight junction proteins (2). We tested the hypothesis that at high levels Fg increases cerebrovascular permeability activating matrix metalloproteinases (MMPs) and affecting vascular endothelial cadherin (VE-cadherin).

Methods: Undegraded Fg (a total blood content of 4 mg/ml) or similar volume of phosphate buffered saline (PBS) was infused to wild-type (WT) or MMP-9 gene knockout (MMP9-/-) mice. Leakage of fluorescein isothiocyanate -labeled bovine serum albumin to Fg or PBS and to topically applied histamine (10^{-5} M) were assessed in mice pial circulation. Intravital fluorescence microscopy and off-line image analysis were used for observation and assessment of pial venular permeability (3). The effect of Fg on mouse brain EC (MBEC) layer integrity was assessed by measuring transendothelial electrical resistance (TEER). Confocal imaging, Western blotting, and RT-PCR analyses and immunohistochemistry were used to define effects of Fg on expression of VE-cadherin in MBECs and brain samples, respectively.

Results: Pial venular leakage was increased in response to Fg infusion (150±3 percent of baseline, %) compared to PBS infusion (128±2%) in WT mice. Although still higher (135±4%) than after PBS infusion (110±1%), Fg-induced cerebrovascular leakage was less in MMP9-/- than in WT mice. Macromolecular leakage from pial venules induced by histamine was greater in Fg-infused (172±4%) than in PBS-infused (140±1%) WT mice. Again, although histamine-induced cerebrovascular leakage was greater in MMP9-/- mice infused with Fg (149±1%) than in those infused with PBS (123±2%), it was still less than in respective groups of WT mice. Presence of MMP-9 activity inhibitor decreased destructive effect of Fg on EC layer integrity. High content of Fg decreased expression of VE-cadherin in brain vessels and in MBECs. This effect was ameliorated in MMP9-/- mice and in the presence of MMP-9 activity inhibitor in MBECs.

Conclusions: Thus that an increase in blood content of Fg compromises cerebrovascular integrity by activating MMP-9 and affecting VE-cadherin. Fg may directly affect VE-cadherin function through activation of an extracellular signal-regulated kinase-1/2 (4) and formation of filamentous actin (1). In addition, Fg-activated MMP-9 may digest VE-cadherin leading to disruption of cell-to-cell interaction and cell to subendothelial matrix attachment. The present study suggests that at high levels Fg increases cerebrovascular permeability confirming findings that it may act as an inflammatory agent.

Supported in part by NIH grants HL080394 and HL080394S2 to DL.

References:

1. Tyagi N, Roberts AM, Dean WL, Tyagi SC, Lominadze D. Fibrinogen induces endothelial cell permeability. Mol.Cell.Biochem. 2008;307(1-2):13-22.

2. Patibandla PK, Tyagi N, Dean WL, Tyagi SC, Roberts AM, Lominadze D. Fibrinogen induces alteration of endothelial cell tight junction proteins. J.Cell.Physiol. 2009;221(1):195-203.

3. Lominadze D, Roberts AM, Tyagi N, Tyagi SC. Homocysteine causes cerebrovascular leakage in mice. AJP. 2006;290:H1206-H1213.

4. Sen U, Tyagi N, Patibandla PK, Dean WL, Tyagi SC, Roberts AM, Lominadze D. Fibrinogen-induced production of endothelin-1 from endothelial cells. AJP. 2009;296(4):C840-C847.

760

RESTING STATE AND TASK EVOKED NEURAL ACTIVITY WITH HYPOTENSION

P. Herman[1], S.S. Kannurpatti[2], B.G. Sanganahalli[1], F. Hyder[1,3]

[1]Department of Diagnostic Radiology, Yale University, New Haven, CT, [2]Department of Radiology, UMDNJ-New Jersey Medical School, Newark, NJ, [3]Department of Biomedical Engineering, Yale University, New Haven, CT, USA

Objectives: Blood oxygen level dependent (BOLD)-fMRI signals is believed to represent the output of a filter system through which input is modulated by neural and vascular sources in both task-induced (T-fMRI) and resting-state (R-fMRI) responses. R-fMRI studies have used physiological modulation such as hypotension (through exsanguination) that significantly enhanced the amplitude of the low frequency BOLD fluctuations (LFFs) and spatial spread of the temporal coherence of the LFFs in cortical structures of anesthetized rats [1]. Since these changes may originate from neural and/or vascular sources, we studied the effect of hypotension on neural signal activity to distinguish the underlying neural and vascular (non-neural) components of the hypotension-induced T-fMRI and R-fMRI responses.

Methods: Sprague-Dawley rats (n=5, 280-310g) were anesthetized with 2% isoflurane (surgical phase) and i.p. 40 mg/kg/h α-chloralose (recording phase). The animal was artificially ventilated, temperature was monitored and maintained at physiological range. The left femoral artery was cannulated for blood pressure measurements. The lower body of the animal was fixed into a plastic tube which was connected to a vacuum source through a controlled pressure regulator [2]. Suction of the lower half of the body, i.e. lower body negative pressure (LBNP), decreased venous return inducing hypotension. We measured neural activity using extracellular tungsten electrodes (2-4 MOhm) inserted into the S1FL region of the cortex. We stimulated the forepaw on the contralateral side with electric current (2mA, 3Hz, 0.3ms pulses with 60s duration). 10 minutes hypotensive steps of 80, 60, 40 mmHg were applied, and the animal was stimulated 3 minutes prior to hypotension and during hypotension. Multi Unit Activity (MUA) and Local Field Potential (LFP) were collected at 20kHz and separated by band pass filtering [3].

Results: Hypotension induced by LBNP from the control value of 100mmHg to 80, 60 and 40 mmHg had no significant effect on the neural activity in the cerebral cortex in the resting state. The resting state fluctuation of electrical amplitude (RSFEA) values for LFP and MUA, respectively, changed from 0.064±0.021 and 0.003±0.001 at control blood pressure (100mmHg) to 0.056±0.015 and 0.003±0.001 at the lowest blood pressure (40mmHg). Forepaw stimulation-induced responses showed a tendentious but non-significant decrease in MUA 274±204 to 116±93 from 100mmHg to 40mmHg and remained constant in LFP (14.4±7.2 vs. 17.8±13.6).

Conclusion: High inter-hemispheric symmetry in fMRI-BOLD fluctuations with similar phase characteristics across cortical regions in anesthetized rats is believed to represent distinct functional neural networks [1]. However, the functional networks were modulated during hypotension, speculated to be neural or myogenic in origin [1]. The present studies measuring neural activity during normal and hypotensive states indicate that the neural activity remains mostly undisturbed during hypotension. above, near and below flow autoregulatory limits. Thus, resting-state fMRI network modifications in perturbed physiological states such as exsanguination and LBNP, in anesthetized rats, predominantly occur through a non-neural mechanism.

References:

[1] Biswal & Kannurpatti (2009) Methods Mol Biol 489:255-274.

[2] Herman & Eke (2006) JCBFM 26:1189-1197.

[3] Maandag et al. (2007) PNAS, 104:20546-20551

Acknowledgements: Supported by NIH (R01 MH-067528, P30 NS-52519).

761

T2'- AND PASL-BASED PERFUSION MAPPING AT 3 TESLA: INFLUENCE OF OXYGEN-VENTILATION ON CEREBRAL AUTOREGULATION

M. Wagner[1], J. Magerkurth[1], S. Volz[2], A. Jurcoane[1], T. Neumann-Haefelin[3], F.E. Zanella[1], O.C. Singer[4], R. Deichmann[2], E. Hattingen[1]

[1]Institute of Neuroradiology, [2]Brain Imaging Center, Goethe University, Frankfurt am Main, [3]Klinik für Neurologie, Klinikum Fulda, Fulda, [4]Klinik für Neurologie, Goethe University, Frankfurt am Main, Germany

Introduction: There is a close relationship between the CBF and the cerebral O_2-metabolism. In addition to covering the basic O_2-demand of the brain, the elevated O_2-demand during dynamically elevated neuronal activation has to be met. It is known that oxygen ventilation leads (1) to cerebral vasoconstriction and (2) to an increase of the oxygen saturation of haemoglobin in the arterial blood. The aim of this study was to obtain simultaneous information about the cerebral oxygen metabolism and the resulting cerebral vasoreactivity under normoxic and hyperoxic conditions using noninvasive MRI techniques. In particular, the goals were (1) to test the hypothesis that hyperoxic ventilation causes vasoconstriction with a subsequent rCBF decrease, and (2) to investigate to what extent the resulting rCBF decrease influences the oxygen content of cerebral grey matter in the cortex and thalamus.

Materials and methods: To quantify the oxygen content of the brain parenchyma, we used T2' mapping. As was demonstrated on the basis of the blood oxygen level dependent (BOLD) effect, paramagnetic DeoxyHb causes accelerated spin dephasing due to magnetic susceptibility differences between deoxygenised blood and the surrounding diamagnetic tissue, resulting in reduced values of the effective transverse relaxation time T2* and thus reduced signal in T2* weighted images. However, T2* is also affected by changes of the transverse relaxation time T2. To account for this effect, the relaxation time T2' may be calculated from 1/T2* - 1/T2 = 1/T2'. T2' provides mainly information about local field inhomogeneities and thus about local concentrations of DeoxyHb. Due to the requirement of performing gradient echo imaging with relatively long TE, T2*-mapping is very sensitive to motion artifacts, resulting in erroneous T2* values. To avoid this effect, a newly developed motion correction was performed.

To evaluate the regional CBF (rCBF) without the use of intravenously administered contrast agents, we used perfusion mapping based on pulsed arterial spin labelling (PASL).

Twelve healthy volunteers aged between 20 and 34 years were investigated. All experiments were performed on a 3T MR scanner (Magnetom Trio; Siemens Medical Solutions, Erlangen, Germany) using an eight-channel phased-array head coil for signal reception and a whole body coil for RF transmission. First, each subject underwent MRI while breathing room air. Subsequently, each subject was ventilated with 10l/min 100% O_2, and the second scan was performed.

Results: Both cortical CBF and T2' values decreased significantly under hyperoxic ventilation as compared to room air ventilation. In particular: T2' (room air): 199.6±72.6ms; T2' (hyperoxia): 156.0±29.1ms; p=0.04; CBF (room air): 61.2±9.6ml/100g/min; CBF (hyperoxia): 56.2±8.5ml/100g/min; p=0.01.

Conclusion: Motion corrected and highly resolved quantitative evaluation of T2' determinating the deoxygenation level of the cerebral blood can be used together with the PASL- based

quantification of the CBF to detect the correlation between oxygen content and cerebral vasoreactivity. In this study, we could show that hyperoxic ventilation in young, healthy volunteers does not cause an increase but a decrease of the saturation level of Hb in the cerebral cortex, which is most likely caused by the reactive hyperoxic-induced vasoconstriction.

762

CHANGES IN NEUROVASCULAR COUPLING DURING BRAIN ISCHAEMIA AND REPERFUSION USING REMOTE MIDDLE CEREBRAL ARTERY OCCLUSION

B.A. Sutherland[1], B.M. Witgen[2], C. Martin[3], J.C. Fordsmann[2], N.R. Sibson[3], M. Lauritzen[2,4], A.M. Buchan[1]

[1]Acute Stroke Programme, Nuffield Department of Clinical Medicine, University of Oxford, Oxford, UK, [2]Department of Pharmacology and Neuroscience and Center for Healthy Aging, The Panum Institute, University of Copenhagen, Copenhagen, Denmark, [3]Experimental Neuroimaging Group, CR-UK/MRC Gray Institute for Radiation Oncology and Biology, University of Oxford, Oxford, UK, [4]Department of Clinical Neurophysiology, Glostrup Hospital, Glostrup, Denmark

Objectives: The intraluminal filament model of middle cerebral artery occlusion (MCAO) is commonly used for experimental stroke. However, technical challenges preclude monitoring neurovascular coupling (NVC) during ischaemia and reperfusion. We aimed to develop a model of remote MCAO with a stimulation paradigm that assessed NVC during acute ischaemia and reperfusion.

Methods: Male Wistar and Sprague-Dawley rats (240-340g) were used. Transient MCAO was based on Longa *et al*. (1989). To occlude remotely, a long filament (10cm for stereotaxic frame (SF) experiments, 100cm for magnetic resonance imaging (MRI) experiments, (Doccol, USA)) was placed in the right internal carotid artery through some guide tubing (ID 0.4mm) in the right common carotid artery, ready to advance. For SF experiments, stimulation electrodes were positioned in the left barrel cortex and cerebral blood flow (CBF) and tissue oxygen (tO_2) were monitored in the right hemisphere. Transcallosal stimulation (TC; 10Hz, 15sec, 1.5mA, 120sec interstimulation interval) was used to evoke hemodynamic responses in the right barrel cortex, which forms part of the penumbra following acute MCAO. For MRI experiments, stimulation electrodes were placed in the left barrel cortex or whisker pad, and a Laser Doppler probe attached over the right barrel cortex. TC or whisker pad stimulation (10Hz, 16sec, 1.6mA, 60sec interstimulation interval) evoked hemodynamic responses, which were monitored concurrently with Laser Doppler and T2* gradient echo imaging for the BOLD response.

Results: Prior to MCAO in the SF, TC evoked a large increase in CBF and tO_2 in the right hemisphere. Remote advancement of the filament produced MCAO (confirmed by a decrease in CBF). Evoked CBF and tO_2 increases by TC were consistently diminished during MCAO. Remote retraction of the filament reperfused the right hemisphere (confirmed by an increase in CBF) and TC evoked an increase in CBF and tO_2, but was not as large as pre-MCAO levels. MRI experiments produced similar results. Left whisker pad stimulation evoked CBF and T2* BOLD increases in the right barrel cortex. A drop in CBF and T2* signal indicated remote MCAO, and whisker stimulation then evoked minimal BOLD and CBF responses in the right barrel cortex. Retraction of the filament increased CBF and T2* signal denoting reperfusion. Evoked BOLD and CBF responses during reperfusion were restored in the right hemisphere but not to pre-MCAO levels. In both setups, various lengths of ischaemia were used (range 6mins to 90mins). It was noted that evoked responses during the later stages of ischaemia were larger than the start of ischaemia. However, evoked responses during reperfusion were attenuated following longer ischaemia compared to shorter periods.

Conclusions: The remote MCAO and stimulation technique allows novel assessment of acute NVC changes immediately upon ischaemia and reperfusion. NVC was significantly impaired

during remote MCAO, which could be partially restored during reperfusion. With this model, brain function can be assessed during acute stages of stroke and reperfusion, but could also be used to investigate functional effects of pharmacological agents being tested for stroke, particularly during reperfusion.

References: Longa EZ et al. 1989. *Stroke* 20(1):84-91

763

MEASURING THE CEREBRAL METABOLIC RATE OF OXYGEN USING TWO-PHOTON LASER SCANNING MICROSCOPY IMAGING OF OXYGEN GRADIENTS IN TISSUE

S. Sakadzic[1], A. Devor[1,2], M.A. Yaseen[1], P. Saisan[2], E. Roussakis[3], E.T. Mandeville[4], V.J. Srinivasan[1], E.H. Lo[4], S.A. Vinogradov[3], D.A. Boas[1]

[1]Department of Radiology, Massachusetts General Hospital / Harvard Medical School, Charlestown, MA, [2]Departments of Neurosciences and Radiology, University of California, San Diego, La Jolla, CA, [3]Department of Biochemistry and Biophysics, University of Pennsylvania, Philadelphia, PA, [4]Departments of Radiology and Neurology, Massachusetts General Hospital / Harvard Medical School, Charlestown, MA, USA

Objectives: The ability to measure oxygen tension (pO_2) with high spatio-temporal resolution is crucial for understanding oxygen delivery and consumption in brain. Until now, the lack of technologies for direct 3D mapping of brain oxygen availability has been a limiting factor in investigations of oxygen metabolism. This was overcome by recent development of the two-photon-enhanced phosphorescent nanoprobe, which allowed us to obtain for the first time extensive pO_2 maps in rat's cortical microvasculature and tissue.[1] Most importantly, high density tissue pO_2 maps allow for the first time calculation of the cerebral metabolic rate of oxygen ($CMRO_2$) based on tissue pO_2 gradients with unprecedented spatial resolution.

Methods: Imaging of pO_2 is based on two-photon laser scanning microscopy (TPLSM) measurement of oxygen-dependent phosphorescence lifetime of a specially designed oxygen-sensitive dye (PtP-C343) with enhanced two-photon excitation cross-section. Sprague Dawley rats (90-120 g) were ventilated with a mixture of air, oxygen, and isoflurane, and controlled for temperature, blood gases, and blood pressure. We created a sealed cranial window over fore-paw area of SI with the dura removed. Before sealing the window, we pressure-injected ~0.1 µl of PtP-C343 (1.4×10^{-4} M) with a micropipette ~300 µm below the surface of the brain. We imaged a few hundred micrometers from the injection site.

Results: Dense baseline tissue pO_2 maps reveal steep pO_2 gradients around both pial and descending arterioles. In contrast, pO_2 maps around ascending venules and capillaries indicate significant heterogeneity of the tissue oxygen concentration in venous and capillary compartments. We take the advantage of unique configuration of the cortical vasculature, where the space around arterioles that descend from the pial surface is largely devoid of capillaries.[2] This geometry allows for direct calculation of $CMRO_2$ from measured tissue pO_2 gradients by fitting the simple equation that describes O_2 diffusion from a cylinder (Krogh's model). In alpha-chloralose anesthetized rats we have measured baseline $CMRO_2$ between 1.92±0.13 and 2.21±0.17 µmol $O_2/(cm^3$ min), in a good agreement with the previously measured 2.6 µmol $O_2/(cm^3$ min) under similar experimental conditions[3]. By increasing the anesthesia level, a clear ~15% decrease in $CMRO_2$ was observed. We also present the measurements of $CMRO_2$ changes during fore-paw stimulation.

Conclusions: The developed methodology enables high-resolution depth resolved mapping of cortical tissue pO_2 and assessment of $CMRO_2$. In comparison with other $CMRO_2$ measurement modalities, novel $CMRO_2$ detection based on tissue pO_2 gradients is very unique in requiring a single imaging parameter, and poses unprecedented spatial resolution. This technology will provide critical insight into the metabolism and function of the normal brain as well as into various neurological conditions and stroke.

References:

1. Sakadzic, S. et al., “Two-photon high-resolution measurement of partial pressure of oxygen in cerebral vasculature and tissue,” Nat. Methods 7, 755-761 (2010).

2. Kasischke K.A. et al., “Two-photon NADH imaging exposes boundaries of oxygen diffusion in cortical vascular supply regions,” J. Cereb. Blood Flow Metab. (2010).

3. Herman et al., “A multiparametric assessment of oxygen efflux from the brain,” J Cereb Blood Flow Metab 26, 79 (2006).

764

PHOSPHORYLATION OF SYNAPSIN I FOLLOWING SUBARACHNOID HEMORRHAGE IN RATS

H. Yuan[1], L.L. Mao[2], M.F. Yang[2], M. Zhao[1], B.L. Sun[2]

[1]The Affiliated Hospital of Taishan Medical College, [2]Taishan Medical College, Taian, China

Aim: This study aimed to investigate the possible role of phosphorylation of synapsin I in the process of cerebral injury following subarachnoid hemorrhage (SAH).

Methods: Wistar rats were divided into non-SAH, sham-operated group, SAH90min, SAH24h, SAH3d, SAH5d and SAH 14d groups. Autologous arterial hemolysate was injected into rats´ cisterna magna to induce SAH.synapsin I protein and phosphosynapsin-I protein were measured from brain tissues by westernblot and immunohistochemistry.

Results: Synapsin I and phosphosynapsin-I positive cells were found in frontal penum-bral cortex and hippocampus in every groups. The expression of synapsin I was mildly decreased after the establishment of SAH. However, expression of phosphorylation of synapsin-I was significantly decreased. A considerable reduction of phosphosynapsin-I was observed in SAH3d group, suggesting a selective defect in synapsin-I phosphorylation.

Conclusions: It was concluded that phosphorylation of presynaptic proteins was probably impaired before cerebral vasospasm following SAH .The synaptic transmission may be blocked in cerebral injury following SAH.

765

FOCAL CEREBRAL ISCHEMIA IN THE TNFA-TRANSGENIC RAT: EFFECT ON LONG-TERM POTENTIATION AND COGNITIVE PERFORMANCE

L.C. Pettigrew[1,2,3], C.M. Norris[2,4], R.J. Kryscio[2,5]

[1]Department of Veterans Affairs Medical Center, [2]Sanders-Brown Center on Aging, [3]Department of Neurology, [4]Department of Molecular and Biochemical Pharmacology, [5]Department of Statistics/School of Public Health, University of Kentucky, Lexington, KY, USA

Objectives: Tumor necrosis factor-alpha (TNFα) is an inflammatory mediator that is elevated in ischemic brain. To complement its role as a determinant of cell survival after physiological stress, TNFα is also recognized as an important contributor to neurotransmission and synaptic plasticity. Using a transgenic (TNFα-Tg) rat selectively overexpressing the murine TNFα gene in its brain, we tested the following dual hypotheses: 1) that constitutive upregulation of TNFα protein synthesis will alter long-term potentiation (LTP) and 2) will affect cognitive performance after focal cerebral ischemia.

Methods: Construction of the TNFα-Tg rat has been described (Pettigrew et al., 2008). To evaluate the effect of constitutive upregulation of TNFα protein synthesis on synaptic function, LTP was measured 60 min after 100-Hz stimulation of hippocampal slices taken from TNFα-Tg and wild type (WT) rat brain. In separate experiments, TNFα-Tg and WT rats underwent middle cerebral artery occlusion (MCAO) for 1 hr. Parallel groups of animals were examined for cognitive performance in a Morris water maze, before and 7 days after MCAO, or in serial Rotarod tasks performed up to 28 days after MCAO.

Results: In naïve rat hippocampus, LTP was increased in TNFα-Tg animals compared to WT littermates ($p \leq 0.05$). During probe testing of reference memory retention 7 days after MCAO, WT animals selectively targeted one of 4 water maze pool quadrants from which an escape platform had been removed (39.3 ± 14 sec; $p \leq 0.03$ compared to random [25% targeted search]). TNFα-Tg rats did not follow differential search strategy (36.5 ± 13.2 sec; p=NS). In the Rotarod task performed after sham-MCAO, there was no difference between TNFα-Tg and WT rats (p=NS). After MCAO, TNFα-Tg rats performed inferiorly to sham-ischemic animals on 6 of 10 serial test dates up to 28 days ($p \leq 0.05$ per comparison). Ischemic WT rats performed inferiorly on only 3 dates ($p \leq 0.05$).

Conclusions: We found that TNFα-Tg rats had increased LTP compared to WT littermates, perhaps due to greater activation of voltage-dependent calcium channels on hippocampal neurons. Our LTP data imply that TNFα-Tg animals may harbor an underlying alteration in synaptic integrity that could affect cognitive phenotype. In water maze testing of reference memory, TNFα-Tg rats displayed weakened retention of reference memory 7 days after MCAO. In the Rotarod task, ischemic TNFα-Tg animals performed inferiorly to sham-ischemic TNFα-Tg rats with two-fold greater frequency than by the same comparison among WT littermates. We conclude that upregulated synthesis of TNFα protein alters synaptic integrity and will amplify cognitive impairment after focal cerebral ischemia.

Reference: Pettigrew LC, Kindy MS, Scheff S, et al. Focal cerebral ischemia in the TNFalpha-transgenic rat. *J Neuroinflammation* 2008:5; 47

Grant Support: United States Department of Veteran Affairs Merit Review Award (LCP)

766

EARLY METABOLIC CHANGES IN THE AMYOTROPHIC LATERAL SCLEROSIS SOD1 MOUSE BRAIN ARE REVEALED USING ^{1}H MRS

H. Lei[1,2], E. Dirren[3], C. Poitry-Yamate[2], B.L. Schneider[3], P. Aebischer[3], R. Gruetter[1,2,4]

[1]Radiology, University of Lausanne, [2]LIFMET, École Polytechnique Fédérale de Lausanne, [3]Brain Mind Institute, Ecole Polytechnique Fédérale de Lausanne, Lausanne, [4]Radiology, University of Geneva, Geneva, Switzerland

Introduction: Mice overexpressing the human mutant G93A superoxide dismutase 1 (SOD1) develop a progressive limb paralysis that closely mimics the familial ALS, so is a model of choice for elucidating the biochemical/metabolic changes in motor-neuron rich areas previously reported in patients. The progressive nature of this disease highlights the need for longitudinal and non-invasive measurements of brain function, structure and metabolism. The aim of study was to explore regional biochemical variations in brain and brain stem during the pre- and post-symptomatic defined phases using ^{1}H MRS.

Methods: G93A-SOD1 mice were bred and genotypied. Based on preliminary electromyographical measurements and swimming abilities, we designated post-natal day 60 (P60) as pre-symptomatic, and P100 as minor post-symptomatic phases. The mean lifespan of our animals was ~125 days. During the entire experimental period, animals were maintained under isoflurane anesthesia (0.8-1.5%) and physiological parameters were continuously monitored. At 9.4T, localized ^{1}H MRS was applied on motor cortex, striatum and brainstem using SPECIAL as previously. Water signals with no water suppression (NT=8) were acquired for further absolute quantification. MR spectra were processed and quantified using the LCModel and water content was 80% for motor cortex and striatum and 75% for brainstem.

Results: At 9.4T, quality anatomical imaging data allowed precise localization of the volume of interests (VOIs) in SOD1 mouse brain, striatum, motor cortex and brainstem (Figure 1A). With improved field homogeneities, and satisfactory water suppression performance and sufficient scan number, localized MR spectra of striatum, motor cortex and brainstem were obtained with satisfactory quality (Figure 1B). The resulting linewidths and SNRs were 7±1Hz and 14±3 in striatum; 10±1Hz and 14±3 in motor cortex; and 13±2Hz and 16±2 in brainstem. The resulting neurochemical profile of 20 metabolites per region was quantified using the LCModel (Figure 1C). Regional metabolic profiles were quantitatively distinguishable from MR spectra (Figure 1, $p < 0.0001$, two-way ANOVA). metabolic changes were observed in motor cortex, striatum and brainstem of SOD1 mice as early as P60 (Table 1). At P100, the level of lactate was decreased in all 3 regions (Table 1) although plasma lactate levels were comparable to that in controls. This finding is contrary to previously reported increases of lactate levels in SOD1 mice obtained *in vitro*, which could be explained by postmortem effects. Overall, our results indicated that the progression of over-expressing superoxide dismutase in mice (Table 1) may be linked to excitotoxicity, i.e. increased glutamate levels at P60 and followed by increased glutamine levels at P100.

AGE	TISSUE	Relative increase (%, p-value)	Relative decrease (%, p-value)

P60	brainstem	Glu (+8, 0.017)	Lac (-19, 0.04)
	motor cortex	Asc (+51, 0.017)	GABA (-30, 0.003); NAA (-5, 0.04)
	striatum	Glu (+13, 0.02)	
P100	brainstem	Gln (+33, 0.0005); Asp (+49, 0.03); PCr (+20, 0.006)	Lac (-21, 0.04)
	motor cortex	Gln (+22, 0.02)	Glu (-12, 0.0004); Lac (-61, 0.002); Ins (-14, 0.03)
	striatum	PCr (+22, 0.006)	Lac (-44, 0.03); Cr (-11, 0.004)

[Summary of significant metabolic changes observed]

Conclusion: This was first time to report *in vivo* ^{1}H MRS of brainstem in mouse brain. Whatever the underlying pathogenic mechanisms, studying such animal models longitudinally using ^{1}H MRS is an effective and powerful strategy towards identifying potential biomarkers of ALS during the early post-symptomatic phase.

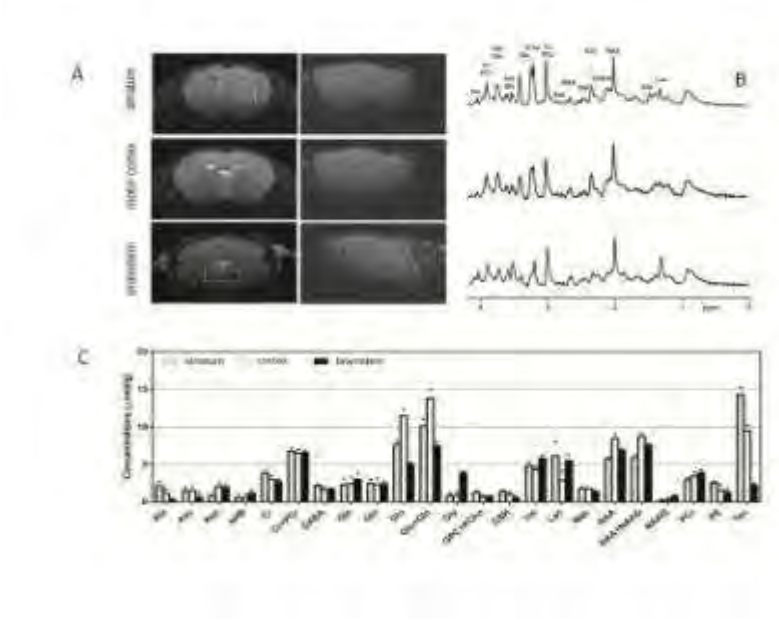

[Figure 1 Typical MRI (A), localized 1H MR spectra]

768

PRENATAL ALCOHOL EXPOSURE AFFECTS THE ASSOCIATION BETWEEN STRESS RESPONSE AND SEROTONIN 5-HT1A BINDING IN NONHUMAN PRIMATES

B.T. Christian[1], D.W. Wooten[1], D. Tudorascu[1], A.T. Hillmer[1], J. Moirano[1], R.J. Nickles[1], J. Mukherjee[2], M.L. Schneider[1]

[1]University of Wisconsin-Madison, Madison, WI, [2]University of California-Irvine, Irvine, CA, USA

Introduction: There is compelling data from animal models that the development of the serotonergic system is adversely affected by fetal alcohol exposure (FAE). The involvement of serotonin regulation on the HPA-axis is believed to be mediated in part by the 5-HT_{1A} and is implicated in the neurobehavioral pathology associated with prenatal alcohol exposure. The goal of this work is to use in vivo PET imaging to examine the relation between serotonin 5-HT_{1A} binding and stress response in a group of rhesus monkeys that received prenatal alcohol exposure.

Methods: The macaca mulatta (rhesus) monkeys for this work are part of a cohort used to examine the effects of prenatal alcohol exposure. This cohort consists of monkeys that received moderate FA-exposure (n=8) along with control monkeys (n=8) treated identically from birth with the exception of alcohol exposure. The measure of cortisol response (CR) at 6 months of age following maternal separation was used to represent the trait-like quality of these subjects for stress responsivity carried into adulthood. The FAE group (n=9, 6 f, 20.1±0.9 yr) and the non-alcohol group consists of (n=9, 6 f , 20.4±0.1 yr). PET imaging on a high resolution primate scanner (microPET P4) was performed using the 5-HT_{1A} antagonist, [F-18]mefway, to obtain a measure of 5-HT_{1A} binding. Parametric images of specific binding (DVR) were generated for each subject using the cerebellum as a reference region and spatially normalized into a common space. Regions of interest were extracted from the mesial temporal cortex (MTC), raphe nuclei (RN) and anterior cingulate gyrus (aCG). The relationship between 5-HT_{1A} binding, FAE and CR was examined using regression methods. Voxelwise analysis was also performed to examine mid- to low-level 5-HT_{1A} binding regions using a threshold of $p < 0.005$.

Results: Statistically significant interaction was found between CR and alcohol exposure in the RN and aCG. The slope of the linear relationship between [F-18]mefway DVR values and CR was found to be varying with the alcohol exposed and non-exposed group in the RN ($p = 0.024$) and the aCG ($p = .0348$). In addition to these regions, voxelwise regression analysis of this interaction also found significant group differences in the posterior CG (max $t = 6.06$). There were no main effect group differences in the high 5-HT_{1A} binding regions of the brain, but in the mid- to low-receptor areas reduced binding was found in the FAE group in the region of the globus pallidus (max $t = 4.32$).

Conclusion: The significant group differences between the cortisol response and 5-HT_{1A} receptor binding suggests that FA-exposure may have enduring effects in altering this interaction.

769

LEPTIN AUGMENTS CEREBRAL HEMODYNAMIC RESERVE IN A NON-LETHAL MODEL OF RAT BRAIN OLIGEMIA

H.-J. Busch[1], S.H. Schirmer[2,3], M. Jost[1], S. van Stijn[4], S.L. Peters[4], J.J. Piek[2], C. Bode[1], I.R. Buschmann[5], **G. Mies**[6]

[1]Department of Cardiology and Angiology, Albert Ludwigs University, Freiburg im Breisgau, Germany, [2]Department of Cardiology, Academic Medical Center, Amsterdam, The Netherlands, [3]Department of Cardiology, Angiology and Intensive Care Medicine, Homburg/Saar, Germany, [4]Department of Pharmacology & Pharmacotherapy, Academic Medical Center, Amsterdam, The Netherlands, [5]Research Group for Experimental and Clinical Arteriogenesis, Charité, Berlin, [6]Max Planck Institute for Neurological Research, Cologne, Germany

Introduction: The adipocytokine leptin has distinct pro-inflammatory properties acting via the Ob-receptor in regulating vascular tone, inflammation and collateral artery growth. Arteriogenesis is an inflammatory process and provides a mechanism to overcome the effects of vascular obstruction. Leptin has been described to stimulate endothelial cell proliferation and angiogenesis. We, therefore, tested the arteriogenetic and hemodynamic effects of leptin treatment for one week in the chronically hypoperfused rat brain.

Materials and methods: A 3-vessel occlusion (3-VO) rat model was applied to induce cerebral oligemia by interruption of arterial blood supply via vertebral arteries and one common carotid artery (n=53) in adult male Wistar rats under halothane anesthesia and physiological control of body temperature. After one week, changes in the cerebral angioarchitecture following 3-VO were examined using the cerebrovascular latex perfusion method. The CO_2 challenge was achieved by delivery of 6% CO_2 in the breathing air while taking an arterial blood sample for blood gas analysis. The effect of leptin and granulocyte macrophage colony stimulating factor (GM-CSF) on cerebral CO_2 reactivity and arteriogenesis were compared to vehicle treatment. Furthermore, the underlying mechanisms of vasoreactive responses were investigated in an isolated rat carotid artery ring assay in rats following 3-VO.

Results: Leptin treatment significantly reduced total body weight compared to baseline values (control: 317 ± 6 g; leptin: 275 ± 6 g*; GM-CSF: 307 ± 10 g; *p< 0.001). A one week application of GM-CSF significantly increased the external diameter of the ipsilateral posterior communicating artery (PCA) whereas leptin was not effective (vehicle: 250 ± 11µm; leptin: 281 ± 11µm; GM-CSF: 317 ± 13 µm*; *p < 0.05). Systemic leptin administration for one week after 3-VO increased the cerebral hemodynamic reserve similar to that of GM-CSF as indicated by improved CO_2 reactivity (vehicle 0.53 ± 0.26 %; GM-CSF 1.13 ± 0.25 %; leptin 1.05 ± 0.6 % per mmHg apCO_2, $p < 0.05$). Pre-incubation of isolated rat carotid artery rings with different concentrations of leptin did not have an effect on the methylcholine-induced vasodilation. However, pre-incubation of carotid artery segments with leptin for 24 h significantly damped cumulative concentration response curves for phenylephrine, demonstrating a weakened contractile capacity of the carotid artery. The vasoconstrictive response of carotid artery rings after phenylephrine was attenuated after 24 h pre-incubation with leptin, which was unaffected by endothelium removal. However, it was abrogated by co-culture with L-NAME, pointing towards an iNOS-mediated mechanism.

Conclusion: The present study shows that the adipocytokine leptin improves cerebrovascular reactivity in a non-lethal model of hypoperfused rat brain. Leptin treatment improved cerebrovascular reactivity upon three-vessel occlusion *in vivo,* attenuated carotid artery

contractility *in vitro* but failed to induce a significant improvement of arteriogenesis. Our results, for the first time, reveal a protective role of leptin on vascular function in hemodynamically compromised brain tissue. Further studies are necessary to clarify involved pathogenetic mechanisms in more detail.

770

THE NEGATIVE BOLD SIGNAL IN THE SOMATOSENSORY SYSTEM IS ASSOCIATED WITH PERFUSION DECREASES

K. Schaefer[1], F. Blankenburg[2], R. Kupers[3,4], I. Law[5], M. Lauritzen[6,7], H.B.W. Larsson[1]

[1]Department of Clinical Physiology and Nuclear Medicine, Glostrup Hospital, Copenhagen, Denmark, [2]Department of Neurology and Bernstein Center for Computational Neuroscience, Charité, Berlin, Germany, [3]PET Unit, Rigshospitalet, University of Copenhagen, [4]Institute for Neuroscience & Pharmacology, University of Copenhagen, [5]Department of Clinical Physiology, Nuclear Medicine and PET, Rigshospitalet, University of Copenhagen, [6]Department of Clinical Neurophysiology, Glostrup Hospital, [7]Department of Medical Physiology, Panum Institute, University of Copenhagen, Copenhagen, Denmark

Objectives: There is still an ongoing dispute about the neurophysiological basis of the negative Blood Oxygenation Level Dependent (BOLD) signal in functional Magnetic Resonance Imaging (fMRI). In recent years, it has been shown that a negative BOLD signal can be reliably induced by electrical hand stimulation in the ipsilateral primary somatosensory cortex (SI). Here, we used this paradigm during fMRI and Positron Emission Tomography (PET) recording in order to directly study the relationship between the negative BOLD signal and regional blood flow changes. In addition, we performed a psychophysical experiment to investigate possible extenuating effects of the negative BOLD signal on sensory function.

Methods: 11 subjects (7 male, age 28 ± 7) were scanned with a high-resolution research tomography (HRRT) PET camera (Siemens Medical Solutions) following intravenous bolus injection of 400 MBq of [^{15}O] labeled water as well as a 3T fMRI scanner (Phillips Intera Achieva) during an identical stimulus protocol. Monophasic square wave pulses (6.8 mA ± 2.16 mA; duration 200 μs; frequency 7 Hz) were applied in a block design (60 s stimulation, 39 s rest) to the right median nerve. Both data sets were analyzed with SPM8. To assess effects that are common in both data sets we performed inclusive masking and Volume of Interest (VOI) analyses. Uncorrected p values were chosen due to a strong anatomical a priori hypothesis. In a separate psychophysical experiment (9 subjects of the original 11, 6 male, age 28 ± 9) detection thresholds of the left index finger with and without concurrent right median nerve stimulation were recorded and analyzed in Matlab with a two -sided Wilcoxon signed-rank test.

Results: We found the expected negative BOLD signal in ipsilateral SI ($p< 0.001$ and $p< 0.005$). Interestingly the PET-data showed a decrease in regional blood flow in the same anatomical location ($p < 0.001$). Furthermore, positive BOLD signaling in contralateral SI and secondary somatosensory cortex (SII) was accompanied by perfusion increase ($p< 0.001$) with high spatial congruence. The psychophysical experiment returned detection thresholds that were significantly higher during concurrent median nerve stimulation than without (1.04 mA and 0.90 mA; $p = 0.004$).

Conclusions: The negative BOLD signal in ipsilateral SI during median nerve stimulation is caused by perfusion decreases, or increased oxygen use without concomitant perfusion changes. The positive BOLD signal in contralataral SI and SII is shown to be caused by a perfusion increase. Elevated detection thresholds of the left index finger during concurrent stimulation of the right median nerve indicate synaptic inhibition that may relate to the ipsilateral negative BOLD signal.

References:

1. Ramsey et al., *J Cereb Blood Flow Metab* 1996*;* 16, 755-764

2. Logothethis et al., *Nature* 2001; 412, 150-157

771

DILATION OF THE MIDDLE CEREBRAL ARTERY IN RESPONSE TO ACIDOSIS IS LOST DURING EXPERIMENTAL HYPONATREMIA

M. Aleksandrowicz[1], K. Klapczyńska[1], **E. Koźniewska**[1,2]

[1]Laboratory of Experimental Neurosurgery, Department of Neurosurgery, Mossakowski Medical Research Centre PAS, [2]Department of Experimental and Clinical Physiology, Medical University of Warsaw, Warsaw, Poland

Objectives: Hyponatremia is diagnosed in approximately 30% of neurosurgical patients after head trauma, subarachnoid or intracerebral haemorrhage. It deteriorates the general state of the patients, aggravates brain damage and increases mortality. The symptoms of hyponatremia correlate with the severity and duration of sodium ions imbalance. Despite the importance of blood vessels for the adequate brain supply of nutrients, surprisingly little is known about the influence of hyponatremia on vascular function. The present study was undertaken to investigate the effect of acute and prolonged hyponatremia on the response of the middle cerebral artery (MCA) of the rat to changes in perfusion pressure, to acidosis and to the increase in extravascular concentration of potassium ions.

Material and Methods: The experiments were performed on seventy five vessels. For acute hyponatremia (AH) studies, MCAs isolated from normonatremic rats and placed in normonatremic buffer in the organ chamber were subjected to hyponatremia (120mM Na^+) one hour prior to the reactivity tests. Prolonged hyponatremia (PH) was induced *in vivo* with a help of vasopressin and rodent liquid diet (AIN-76). Vasopressin was delivered continuously by subcutaneously implanted ALZET osmotic minipumps. After 3.5 days, plasma Na^+ concentration in these rats ranged from 116 to 122 mM. MCAs were isolated and mounted in the organ chamber containing 120 mM Na^+ buffer. MCAs placed in normonatremic buffer (Na^+=144 mM) served as a reference group.

Results: In normonatremia MCA dilated on average by 18±2% ($p< 0.05$) when pH of the extravascular buffer was lowered from 7.4 to 7.0 and by 41±7% ($p< 0.05$) during increase of the extravascular K^+ concentration from 3.5 to 20 mM. In AH group acidosis constricted MCA by 4±2% ($p< 0.01$) and hyperkalemia did not affect its diameter. In PH group MCA did not respond to acidosis but dilated by 38±5% ($p< 0.005$) in response to hyperkalemia which was not different from the response of normonatremic MCA. .

Conclusion: Our results demonstrate for the first time that hyponatremia selectively disturbs the regulatory mechanisms of cerebral blood vessels. They also show that acute hyponatremia impairs regulation of the MCA more than the prolonged one. In conclusion, vascular impairment may be an important component of intracranial pathology during hyponatremia.

Acknowledgements: This study was financially supported by the grant N401 19032/3924 from the Ministry of Science and Higher Education.

772

TIME-RESOLVED NEAR-INFRARED AND DIFFUSE CORRELATION SPECTROSCOPY FOR CONTINUOUS MEASUREMENT OF ABSOLUTE CEREBRAL BLOOD FLOW

M. Diop[1,2], T.-Y. Lee[1,2,3], K. St. Lawrence[1,2]

[1]Imaging Division, The Lawson Health Research Institute, St. Joseph's Health Care, London, [2]Department of Medical Biophysics, [3]Robarts Research Institute, University of Western Ontario, London, ON, Canada

Objective: A central focus of neurointensive care practice is detecting and treating secondary events that can exacerbate brain injury. A common cause of secondary brain injury is cerebral ischemia, which has led to the recognition that bedside monitoring of absolute cerebral blood flow (CBF) could improve the clinical management of patients. The focus of this research was to develop a hybrid optical system combining a time-resolved near-infrared (TR-NIR) technique, capable of single time-point measurements of absolute CBF, with diffuse correlation spectroscopy (DCS), which can continuously monitor relative CBF [1,2]. A portable instrument combining these two technologies was assembled. Measured perfusion changes obtained from both TR-NIR and DCS in an animal model were compared for validation.

Methods: Experiments were conducted on five newborn piglets (age < 4 days). Animals were anaesthetized with 1.75% isoflurane and mechanically ventilated. Cerebral blood flow was altered by changing the arterial pressure of CO_2 and by temporarily occluding both carotid arteries. Piglets were placed in a prone position and two sets of emission and detection optodes (one for each technique) positioned 20 mm apart on the head.

Absolute CBF was measured using a dynamic contrast-enhanced technique. A bolus of contrast agent (indocyanine green, ICG) was injected intravenously, and brain and arterial blood ICG concentration curves obtained with TR-NIR and dye densitometry, respectively. A stable deconvolution algorithm was used to extract CBF from the brain and arterial blood ICG data [3]. Changes in the intensity autocorrelation functions measured with the DCS technique were converted into CBF changes and compared to the TR-NIR results [4].

Results: Figure 1 demonstrates a strong correlation between perfusion changes measured by TR-NIR and DCS techniques (slope of 0.98 and R^2 of 0.96). Since these results show that the same perfusion changes are measured by the two techniques over a wide range of CBF values, one single time-point CBF measurement by TR-NIR could be used to convert continuous DCS data into units of absolute CBF (ml of blood/ g of tissue /min). Furthermore, the DCS technique can sample at a rate of 38 Hz [5], which suggests this hybrid instrument could be used to study dynamic autoregulatory mechanisms controlling CBF.

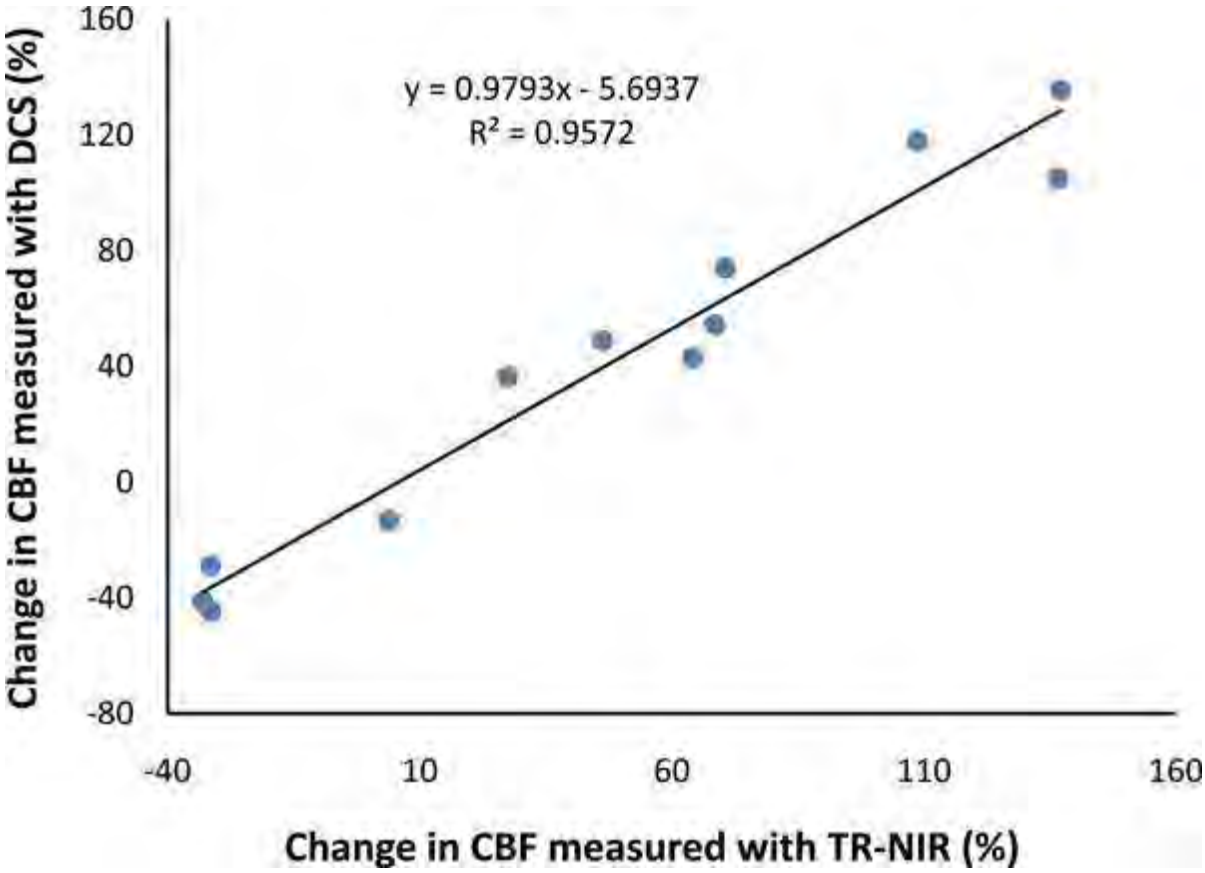

[Figure 1]

Figure 1 - Absolute cerebral blood flows measured with the TR-NIR technique, converted into perfusion changes, and compared with changes in CBF measured with the DCS technique.

Conclusion: Cerebral perfusion changes derived from the absolute CBF measurements obtained by the TR-NIR technique were in excellent agreement with relative perfusion changes measured with DCS. Since the TR-NIR part of the apparatus can continuously measure tissue optical properties simultaneously at three wavelengths (760, 800, and 830 nm) to yield cerebral blood oxygenation, the hybrid instrument has the potential to continuously monitor both absolute CBF and cerebral metabolic rate of oxygen.

References:

1) Diop *J Biomed Opt.*, 15; 057004

2) Cheung Phys. Med. Biol., 46; 2053

3) Brown *Pediatr Res*, 51;564

4) Zhou *J Biomed Opt.*, 14; 034015

5) Dietsche *Appl Opt.*, 46; 8506

774

ENRICHED ENVIRONMENT IMPROVES FUNCTIONAL RECOVERY BY ATTENUATION OF INFLAMMATION AND INHIBITION OF THE STROMAL-DERIVED-FACTOR 1/CXC RECEPTOR 4 PATHWAY AFTER STROKE

K. Ruscher[1], E. Kuric[1], Y. Liu[2], A.R. Inácio[1], S. Issazadeh-Navikas[2], T. Wieloch[1]

[1]Laboratory for Experimental Brain Research, University of Lund, Lund, Sweden, [2]BRIC, Copenhagen University, Copenhagen, Denmark

Objectives: After stroke, inflammation hampers beneficial mechanisms important for tissue reorganization in the ischemic hemisphere. The aim of the present study was to investigate if enriched environment (EE) effects improved functional recovery specifically by attenuation of inflammation in the ischemic hemisphere (Ruscher et al., 2009). We also aimed at evaluating if we can mimick by pharmacological means mechanisms of inflammation affected by enriched environment to improve recovery after experimental stroke.

Methods: Spontaneous hypertensive rats were subjected to permanent occlusion of the middle cerebral artery (pMCAO). Two days after stroke, rats with a significant neurological deficit were randomly allocated and kept in standard or enriched housing cages for 3 consecutive days. To study the effect of SDF-1/CXCR4 inhibition on functional recovery after transient MCAO (tMCAO), the specific CXCR4 antagonist 1,1′-[1,4-Phenylenebis(methylene)]bis [1,4,8,11-tetraazacyclotetradecane] octohydrobromide dihydrate (AMD3100) was injected for 3 consecutive days (ip, 0.5mg/kg every 12h) starting 2 days after tMCAO. FACS analysis was performed to study immune cells in the injured and noninjured hemisphere and peripheral secondary immune organs.

Results: Analysis of the ischemic core and the peri-infarct area revealed that EE profoundly attenuated the level of the pro-inflammatory cytokines interferon-gamma, TNFalpha, IL-1beta, IL-4, and IL-5. Importantly, cytokine levels in the cerebro-spinal fluid and serum were not altered in respective animals. Along with changes of pro-inflammatory cytokines we found a significant reduction of the otherwise upregulated chemokine receptor CXCR4 and its natural ligand stromal-derived-factor 1 (SDF-1) in rats housed in EE after pMCAO. We also found that AMD3100 treated rats (n=8) showed an improved recovery compared with saline treated rats (n=8) at day 5 after tMCAO. Accompanied we found a reduction of infiltrating immune cells, in particular CD4(+) T-cells were inhibited to invade in the ischemic hemisphere. Moreover, AMD3100 treatment prevented spleen atrophy which however was observed in saline treated animals (n=8) after tMCAO. Preliminary results also suggest antibacterial properties of AMD3100 by suppression of poststroke bacteriemia. Importantly, Infarct size was unaffected by the treatment.

Conclusions: We conclude that attenuation of poststroke inflammation obtained by housing rats in an enriched environment together with specific inhibition of the SDF-1/CXCR4 pathway significantly improves functional recovery and prevents detrimental secondary systemic effects in rats subjected to experimental stroke.

References: Ruscher K, Johannesson E, Brugiere E, Erickson A, Rickhag M, Wieloch T. 2009. Enriched environment reduces apolipoprotein E (ApoE) in reactive astrocytes and attenuates inflammation of the peri-infarct tissue after experimental stroke. J Cereb Blood Flow Metab 29:1796-1805.

775

DIFFERENTIAL EFFECTS OF ACUTE HYPERGLYCAEMIA ON FOCAL ISCHAEMIC DAMAGE IN RATS WITH AND WITHOUT METABOLIC SYNDROME

D.J. Tarr[1], D. Graham[2], J. Mullin[3], C. McCabe[3], W.M. Holmes[3], I.M. Macrae[1], D. Dewar[1], K.W. Muir[1]

[1]Institute of Neuroscience and Psychology, [2]Institute of Cardiovascular and Medical Sciences, [3]Glasgow Experimental MRI Centre, University of Glasgow, Glasgow, UK

Objectives: In stroke patients with acute hyperglycaemia, >50% are subsequently diagnosed with an insulin resistant state including impaired glucose tolerance, diabetes mellitus or impaired fasting glucose, features associated with metabolic syndrome[1]. The effects of acute hyperglycaemia in subjects with and without metabolic syndrome have not been studied in preclinical models of experimental stroke and the majority of preclinical studies of acute hyperglycaemia have not assessed clinically relevant blood glucose levels. The aim of this study was to determine if clinically relevant levels of acute hyperglycaemia exert differential effects on normal healthy rats and in those displaying features of metabolic syndrome[2], following permanent focal cerebral ischaemia.

Methods: Adult male Wistar-Kyoto (WKY) rats were randomly allocated to normoglycaemic (N; n=5) or hyperglycaemic (HN; n=4) groups. Adult male fructose-fed spontaneously hypertensive stroke-prone (SHRSP) rats[1] were randomly allocated to metabolic syndrome (MS; n=6) or hyperglycaemic plus metabolic syndrome (HMS; n=6) groups. HN and HMS groups received 15% glucose (i.p., 10ml/kg) while N and MS groups received saline (i.p., 10ml/kg), 10min prior to permanent distal diathermy occlusion of the middle cerebral artery (MCAO). Diffusion weighted imaging (DWI) was carried out from 1-4h post stroke (8 coronal slices of 1.5mm thickness). Apparent diffusion coefficient (ADC) maps generated from DWI displayed ischaemic injury and lesion volume was calculated using in-house strain specific thresholds of abnormality. Arterial blood glucose was measured hourly using a blood glucose monitor. Infarct volume was measured by histology 24h after MCAO. Data are expressed as mean±SD.

Results: Blood glucose in N and MS groups 30min following saline injection were not significantly different (5.6±0.3 vs 5.7±0.2mmol/l)). Blood glucose 30min post glucose administration in HN and HMS groups was not significantly different (11.7±1.3 vs 11.5±1.2). At 1h post-MCAO the HN group had a significantly larger ADC lesion than the N group (94±26 vs 42±22 mm^3, $P< 0.01$, Fig.1A). The HMS group had a significantly greater ADC lesion than the MS group at 1h after MCAO (152±23 vs 111±23 mm^3, $P< 0.05$, Fig.1B). The % difference between HN and N groups was substantially greater than the % difference between MS and HMS groups (121% vs 37%). The HN group had a significantly larger infarct volume than the N group (158±32 vs 93±15 mm^3, $P< 0.001$, Fig.1A). The HMS group had a significantly larger infarct than MS group (191±25 vs 153±9 mm^3, $P< 0.05$, Fig.1B). The % difference between HN and N groups was 69% while the difference between MS and HMS groups was 24%.

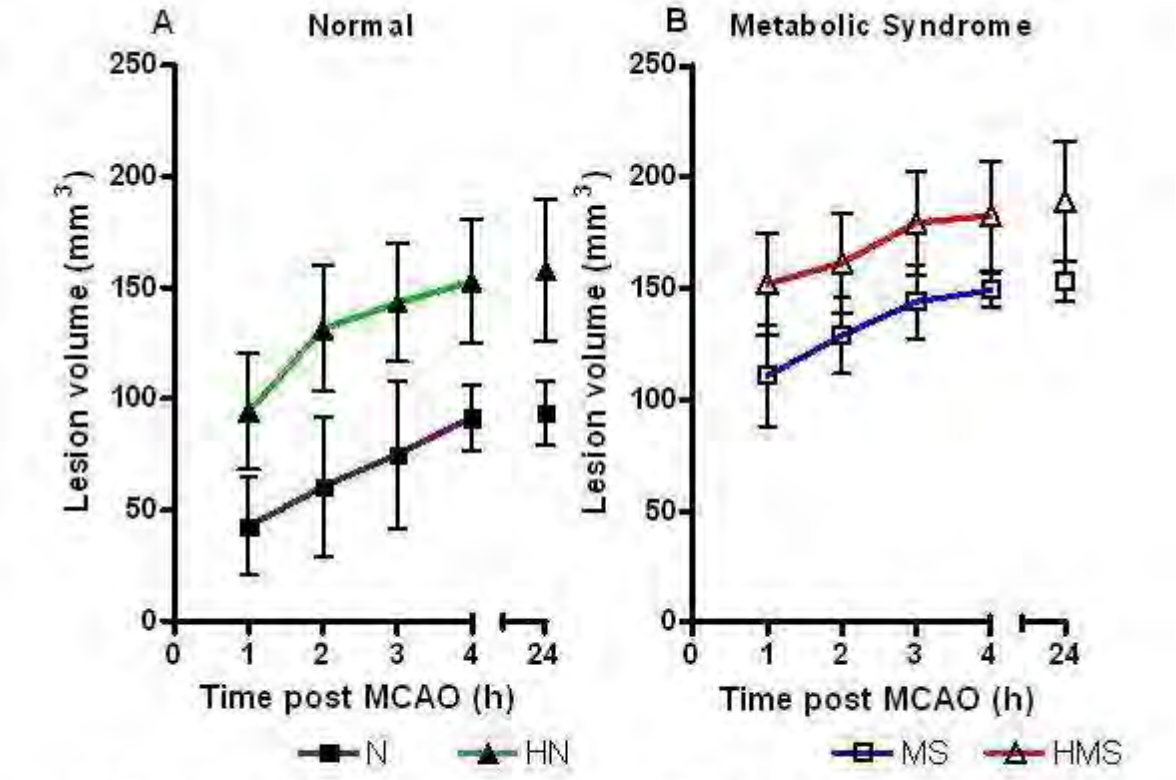

Figure 1: N and MS groups, normoglycaemic. HN and HMS groups, hyperglycaemic. Lesion volume obtained 1-4h from ADC maps and at 24h from histology. Data analysed using 2-way repeated measures ANOVA

[Lesion volumes for Normal and Metabolic Syndrome]

Conclusions: Acute hyperglycaemia, at clinically relevant levels, exacerbates early ischaemic damage and final infarct volume in both normal and metabolic syndrome rats. The effect of acute hyperglycaemia in the rat metabolic syndrome model was less pronounced than in normals. This suggests that management of hyperglycaemia may be most beneficial in the absence of an underlying dysglycaemia.

Acknowledgement: Funded by CSO, Scotland and a MRC Studentship (DT).

References:

[1] McCormick MT, Muir KW. Cerebrovascular Diseases 2006,21:62

[2]Strahorn. P et al. J.Hypertens. 2005,23:2179-86

777

COMPARATION BETWEEN BONE MARROW AND ADIPOSSE TISSUE MESENCHYMAL STEM CELLS IN THE TREATMENT OF ACUTE CEREBRAL INFARCT IN RATS

B. Rodríguez-Frutos, M. Gutiérrez-Fernández, J. Álvarez-Grech, M. Expósito-Alcaide, M.T. Vallejo Cremaddes, E. Díez-Tejedor

La Paz University Hospital, IdiPAZ, UAM, Madrid, Spain

Introduction: Several cell lines have been used in experimental stroke models, such as embryonic, haematopoietic and mesenchymal stem cells and between those, the more used are: bone marrow stem cells (BMSCs) and adipose tissue (ASCs).

Aims: To analyze the beneficial effect of intravenous (i.v) injection of both MSC allogenic cellular lineages on repair and neurological recovery in acute cerebral infarct.

Material and methods: Model of medium cerebral artery occlusion in Sprague Dawley male rats in 4 groups (n=7): a) Sham: surgery without infarct; b) control: surgery + infarct; c) i.v BMSCs: surgery + infarct + i.v injection of BMSCs ($2X10^6$ cells); d) i.v ASCs: surgery + infarct + i.v injection of ASCs ($2X10^6$ cells). We analyzed: Neurological evaluation and lesion volume by Magnetic Resonance Imaging (MRI) and Hematoxilin- Eosin (H-E), neuronal death by TUNEL, migration of MSC by inmmunohistochemistry and MRI, plasmatic levels of pro-inflammatory cytokines (IL-6 and TNF alpha) by ELISA. Rats were sacrificed at 14 days.

Results: Treated animals with BMSCs and ASCs showed better neurological evaluation score in comparison with control group at 24h and 14 days ($p< 0,05$), without differences between them. Neither treatment reduced infarction volume but decreased the TUNEL+ cells ($p< 0,05$). Treated groups increase inflammatory response respect to control group ($p< 0,05$).

Conclusion: Both therapies with mesenchymal stem cells, BMSCs and ASCs, have demonstrated equal effectiveness on neurological recovery and decrease brain damage (reduction neuronal death). The advantage of ASCs could be their easy obtained to be used in translational applications.

Supported by grants from RENEVAS (RD07/0026/2003) (Spanish Research Neurovascular Network), Research Institute Carlos III, Ministry Science and Innovation.

779

EFFECTS OF CITICOLINE AND MESENCHYMAL STEM CELLS IN ACUTE CEREBRAL INFARCT. EXPERIMENTAL STUDY IN RATS

M. Gutiérrez-Fernández, J. Álvarez-Grech, B. Rodríguez-Frutos, M. Expósito-Alcaide, M.T. Vallejo-Cremades, E. Díez-Tejedor

La Paz University Hospital, IdiPAZ, UAM, Madrid, Spain

Introduction: The stimulation of endogenous trophic factors or exogenous administration of mesenchymal stem cells (MSC) can enhanced neurological repair and recovery.

Aims: To analyze citicoline, MSC and combination therapeutic effects on repair and functional recovery in a model of brain infarct in rats.

Materials and methods: 35 Sprague Dawley male rats distribuited in 5 groups: 1 - Sham (surgery without infarct); 2 - control (surgery + infarct); 3 - Citicoline (surgery + infarct + citicoline ip (500 mg/kg); 4 - MSC (surgery + infarct + MSC i.v. (2×10^6 cells); 5 - Combination (surgery + infarct + MSC i.v. (2×10^6 cells) + citicoline ip (500 mg/kg)). We analyzed: Neurological evaluation and lesion volumen by Magnetic Resonance Imaging (MRI) and Hematoxilin-Eosin (H-E), Neuronal death by TUNEL, Proliferation cellular (BdrU) by immunohistochemistry and VEGF by immunofluorescence, Migration of MSC by inmmunohistochemistry and MRI, Plasmatic levels of IL-6 and TNFalpha by ELISA.Rats were sacrificed at 14 days.

Results: All treatment groups at 24h and 14 days showed better neurological score than control groups with significant differences ($p< 0,05$), but there were not differences between them. Neither treatment reduced infarction volume but decreased the TUNEL+ cells respect to control group ($p< 0,05$), increased of BrdU + cells and VEGF in peri-infarct zone (increasing neurogenesis and angiogenesis).Citicoline reduced inflammatory response.

Conclusions: Citicoline and MSC administration show equal efficacy in the neurological recovery, decrease neuronal death and increase repair, but the combination not increase the benefit. Moreover, citicoline decrease inflammatory response.

Supported by grants from Center of Innovation and business development (CIDEM), Ferrer Group, RENEVAS (RD07/0026/2003) (Spanish Research Neurovascular Network), Research Institute Carlos III, Ministry Science and Innovation.

780

PARENTERAL OR ENTERAL SUPPLEMENTATION IN ALPHA-LINOLENIC ACID PROTECTS FROM STROKE IN MICE

C. Nguemeni[1,2], C. Rovere[1,2], E. Gouix[1], N. Simon-Rousseau[3], C. Heurteaux[1,2], N. Blondeau[1,2]

[1]CNRS, Institut de Pharmacologie Moléculaire et Cellulaire/ UMR 6097, Valbonne, [2]University of Nice, Nice, [3]Onidol, Paris, France

Objectives: Stroke is a major cause of mortality and morbidity associated with a significant socioeconomic cost and a marked patient/families burden. Treatment for stroke is almost reduced to fibrinolysis, a therapy that unfortunately can be only delivered to around 5% of patients. Neuroprotective post-treatments have failed in clinical trials drawing attention to the importance of prevention. It has also promoted further interest in dietary functional foods/nutraceuticals as an important tool in preventing stroke damage. Beneficial effects of diets rich in seafood, which contain high levels of long chain omega-3 fatty acids, have been demonstrated in cardiovascular diseases, with increasing attention devoted to neurological diseases. Little is known on the role of the precursor, alpha-linolenic acid (ALA). Our work aimed to design and compare preventive strategies by ALA supplementation either by injections (parenteral) or by diets (enteral) in a stroke mice model.

Methods: Focal ischemic stroke was induced by introducing a siliconated filament into the proximal middle cerebral artery (MCA) of anesthetized mice. Parenteral ALA supplementation consisted in 3 injections of 500 nmole/kg of ALA on days 1, 3 and 7. Enteral supplementation was achieved feeding mice an experimental diet in which ALA represented 0, 0.4, 0.8 or 1.6% of the total weight. Infarct size was measured 24h post-MCA occlusion. Oxidative stress and polyunsaturated fatty acid peroxides were assessed by measuring the generate malondialdehyde (MDA) levels. Since, neuroplasticity stimulation and reduction of post-stroke depression improve stroke recovery, their pre-existing level may modify the impact of stroke. The potential effects of ALA on neuroplasticity were evaluated through the expression of proteins involved in synaptic functions and glutamatergic neurotransmission. For the sensibility to depression, Porsolt Forced Swim Test and Tail Suspension Test that are commonly accepted to predict antidepressant efficiency were used. To analyze whether ALA action was direct or not, neuroprotection against oxygen glucose deprivation (OGD) and neuroplasticity were also tested *in vitro*.

Results: Three repeated ALA injections reduced by approximately 30% the post-ischemic infarct volume 24 hours post-surgery. Diet containing 0.8 or 1.6% of ALA reduced MCAO-induced cortical infarct volume. A significant reduced mortality rate, infarct size and increased probability of spontaneous reperfusion in the post-ischemic period were also observed with these ALA supplemented diets. ALA enteral supplementation did not alter the basal lipid peroxidation levels but drastically decreased the lipid peroxidation in the ischemic cortex 24 hours post-MCAO. Supplementation by injection induced neuroplasticity and antidepressant-like effects. These effects were only seen comparing diet-lacking ALA with the richest in ALA content. ALA also promoted protection against OGD and neuroplasticity *in vitro*.

Conclusion: A direct role of ALA in stroke protection and neuroplasticity was established *in vitro* and *in vivo*. While the brain protection was also obtained with ALA supplementation through experimental diet, the effect on neuroplasticity and depression were slightly different of those observed with ALA injections. Taken together our findings provide new insights into the potential of ALA as nutraceutical aiding in stroke prevention and protection.

781

CEREBROVASCULAR CAPILLARY TO THOROUGHFARE CHANNEL SHUNT FLOW TRANSTION AT HIGH INTRACRANIAL PRESSURES IN RATS

E.M. Nemoto, D.E. Bragin, R.C. Bush

Neurosurgery, University of New Mexico, Albuquerque, NM, USA

Objectives: The critical cerebral perfusion pressure (CPP) for maintenance of cerebral blood flow (CBF) is reduced by approximately 50% from 60 mmHg to 30 mmHg when CPP is reduced by decreasing mean arterial pressure (MAP) as opposed to increasing intracranial pressure (ICP). We hypothesized that this is due to a pathological shift from capillary (CAP) to thoroughfare channel (TFC) shunt flow resulting in a pathologically elevated CBF at a lower CPP. The aim of this study was to show by two photon laser scanning microscopy (2PLSM), that a transition from CAP to TFC shunt flow occurs when CPP is decreased by raising ICP but not by reducing MAP which is associated with tissue hypoxia and brain edema.

Methods: Anesthetized male Sprague-Dawley rats were intubated and mechanically ventilated. Arterial blood pressure and rectal temperature were continuously monitored. ICP was monitored and manipulated by a catheter in the cisterna magna connected to a reservoir of mock cerebrospinal fluid. A cranial window sealed with a glass plate was used for *in vivo* 2-photon laser scanning microscopy to record microvascular RBC flow velocity (by fluorescein dye) and NADH fluorescence. CAP flow = flow velocities < 1.0 mm/sec and TFC shunt flow = flow velocities >1.0 mm/sec. Brain tissue water was measured by wet/dry weight. The relationship between CAP and TFC shunt flow at CPP of 70 (normal) 50 and 30 mmHg was determined by manipulating CPP by decreasing MAP or increasing ICP. Rats were studied in three groups (ten rats/group): Group I (control)- CPP maintained at 70 mmHg; Group II - CPP reduced by increasing ICP; and Group III -CPP reduced by decreasing mean arterial pressure (MAP).

Results: Reduction of CPP from 70 to 50 and 30 mmHg by increasing ICP progressively increased TFC shunt flow (Table). Reduction of CPP from 70 to 50 and 30 mmHg by increasing ICP shifted the CAP/TFC ratio from 70/30 to 60/40 and 50/50, respectively. Decreasing CPP from 70 to 50 and 30 mmHg by reducing MAP changed the CAP/TFC distribution from 65/35 to 70/30 and 86/14, respectively, reflecting a reduction in TFC shunt flow and maintenance of CAP flow.

Increasing ICP markedly increased NADH fluorescence from baseline by 20.3 ± 6.8% and 58.1 ± 8.2% at CPP of 50 and 30 mmHg, respectively. Decreasing CPP by lowering MAP resulted much smaller increases in NADH by 11.7 ± 5.9 and 17.3 ± 7.5% 8 above baseline at CPP of 50 and 30 mmHg, respectively.

Brain tissue water content at a CPP of 70 mmHg was 69.3 ± 1.51%. A decrease in CPP from 70 to 50 and 30 mmHg by increasing ICP resulted in a significant increase in water content to 74.4 ± 3.21% and 77.8 ± 2.42%,, respectively. In contrast, water content was not affected by MAP reduction of CPP.

CPP (mmHg)	ICP Group (%)	ICP Group (%)	MAP Group (%)	MAP Group (%)	P<

	< 1.0 mm/s	> 1.0 mm/s	< 1.0 mm/s	>1.0 mm/s	
	CAP	TFC	CAP	TFC	
70	69.6±5.4	30.4±2.3	64.8±6.1	35.2±4.3	0.145
50	58.4±4.6	41.6±3.4	70.7±6.4	29.3±4.5	0.001
30	48.8±4.7	51.2±5.1	86.1±6.9	13.9±2.6	0.001

[Percent CAP and TFC Flow]

Conclusions: The lower critical CPP at high ICP is attributable to a transition from CAP to TFC shunt flow resulting in brain tissue hypoxia and edema.

783

CORRELATION BETWEEN [^{18}F]FDG PET AND [^{11}C]FLUMAZENIL PARAMETRIC RELATIVE DELIVERY (R_1) OR EARLY UPTAKE IMAGES IN EPILEPSY PATIENTS

M. Lubberink[1,2], T. Danfors[1,3], E. Kumlien[3], J. Sörensen[1]

[1]PET Centre, [2]Medical Physics, [3]Neurology, Uppsala University Hospital, Uppsala, Sweden

Objective: Both [^{18}F]fluorodeoxyglucose (FDG) and [^{11}C]flumazenil (FMZ) PET are of use in pre-surgical evaluation of epilepsy, revealing areas with glucose hypometabolism and reduced GABA-A receptor density. Apart from receptor density, a dynamic [^{11}C]FMZ scan can be used to calculate the relative delivery (R_1) of [^{11}C]FMZ, reflecting relative cerebral blood flow (CBF). Early images of [^{11}C]FMZ uptake may reflect relative CBF as well. Since glucose metabolism has been shown to be closely coupled to cerebral blood flow, it is of interest to compare early [^{11}C]FMZ uptake or R_1 and [^{18}F]FDG images. A high agreement between [^{11}C]FMZ relative delivery and [^{18}F]FDG images may allow for assessment of both GABA-A receptor density and hypometabolism in a single dynamic [^{11}C]FMZ scan.

Methods: Data from 5 consecutive epilepsy patients was used. All patients underwent 40 min dynamic scans after injection of 4 MBq/kg [^{11}C]FMZ and 20 min scans starting 30 min after injection of 3 MBq/kg [^{18}F]FDG. Data were acquired using an ECAT Exact HR+ scanner (Siemens/CTI, Knoxville) and images were reconstructed using filtered back projection applying all appropriate corrections. Volumes of interest were drawn over pons on a co-registered T2-weighted MRI scan. [^{11}C]FMZ R_1 images were constructed using reference parametric mapping (RPM) which is a basis function implementation of the simplified reference tissue model (1,2), using pons as reference tissue (3). [^{18}F]FDG and [^{11}C]FMZ images were co-registered using a mutual information algorithm, brain voxels were extracted using SPM and images were normalised relative to their mean total grey matter values. [^{11}C]FMZ R_1 and [^{11}C]FMZ early uptake (1-2 min p.i.) images were post-smoothed with a 5 mm Gaussian filter. Correlations between [^{18}F]FDG, early [^{11}C]FMZ uptake, and [^{11}C]FMZ R_1 images without and with post-smoothing were assessed using linear regression of individual brain voxels.

Results: Figure 1 shows typical [^{18}F]FDG , [^{11}C]FMZ early uptake and [^{11}C]FMZ R_1 images, as well as a correlation plot between [^{18}F]FDG and [^{11}C]FMZ R_1 for individual voxels. Similar correlation between [^{18}F]FDG and [^{11}C]FMZ R_1 or [^{11}C]FMZ 1-2 min images was found (Pearson correlation coefficient r = 0.83 and 0.86, respectively, for all brain voxels, and r = 0.75 and 0.79 for grey matter voxels only). Slope between [^{18}F]FDG and [^{11}C]FMZ R_1 or early [^{11}C]FMZ uptake voxel values did not differ significantly from 1. Visual assessment revealed a better image quality of [^{11}C]FMZ R_1 images than early uptake images. Post-smoothing of [^{11}C]FMZ delivery images did not improve correlation with [^{18}F]FDG images.

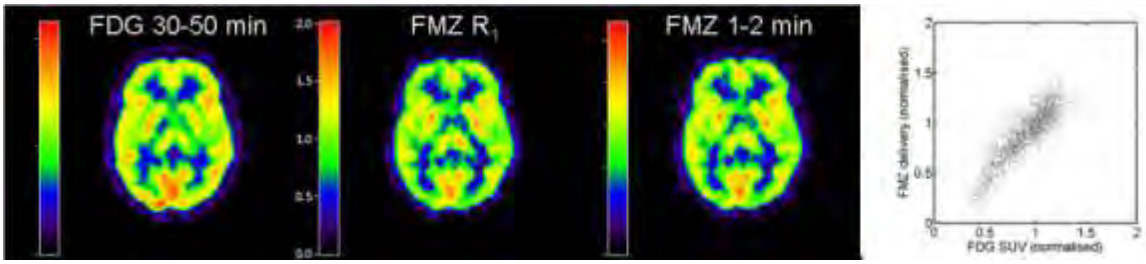

[Figure 1]

Conclusion: A good correlation between [^{18}F]FDG, early [^{11}C]FMZ uptake and [^{11}C]FMZ R_1 images was found. Further investigations are needed to assess the accuracy of [^{11}C]FMZ R_1 images in revealing hypometabolic areas in comparison to [^{18}F]FDG.

References:

1. Gunn et al, Neuroimage 1997
2. Lammertsma & Hume, Neuroimage 1996
3. Klumpers et al, J Cereb Blood Flow Metab 2008

784

TAK1 IN BRAIN ENDOTHELIAL CELLS MEDIATES FEVER AND SICKNESS BEHAVIOR

D.A. Ridder, M.-F. Lang, S. Salinin, M. Schwaninger

Institute of Pharmacology, University of Heidelberg, Heidelberg, Germany

Objectives: Infections, tissue injury, and autoimmune disorders trigger a systemic inflammatory response, which comprises immune, autonomic, and behavioral changes. Upon immune challenge, endogenous or exogenous pyrogens that are present in the periphery are capable of altering brain functions, resulting in fever, anorexia, lethargy, and activation of the hypothalamus-pituitary-adrenal axis. This sickness response has been shown to involve different brain structures especially the anterior hypothalamus and to depend on the induction of cyclooxygenase-2 (Cox-2) and increased prostaglandin E2 (PGE2) production (Pecchi et al., 2009). The route, how peripheral inflammatory signals reach the brain is still a matter of debate. The prevailing view is that upon immune stimuli, brain endothelial cells in proximity to the thermoregulatory centers are producing Cox-2 and are consequently releasing PGE2 into the brain tissue. PGE2 in turn is thought to act on neuronal EP3 receptors leading to fever and sickness behavior.

Cox-2 induction has been shown to depend on p38 MAPK and on the transcription factors NF-κB and c-jun (Singer et al., 2003; Yamaguchi et al., 2005) and all of these pathways are downstream of transforming growth factor-β-activated kinase 1 (Tak1) (Shim et al., 2005). We therefore wanted to investigate the role of Tak1 in brain endothelial cells in the sickness response.

Methods: In this study we have generated a Cre-mouse line to delete Tak1 specifically in the blood-brain barrier and challenged these mice with the endogenous pyrogen interleukin-1β (IL-1β).

Results: Mice lacking Tak1 in brain endothelial cells showed a blunted fever response and reduced lethargy upon intravenous stimulation with the endogenous pyrogen IL-1β, whereas anorexia and corticosterone release were not affected by deletion of Tak1. We could also show that Cox-2 induction upon stimulation with IL-1β in brain endothelial cells *in vitro* depends on Tak1, although Tak1 inhibition does not affect the activation of NF-κB upon stimulation with IL-1β.

Conclusion: We could show that Tak1 in brain endothelial cells is necessary for the induction of fever and sickness behavior and that this effect is most likely mediated by activation of p38 MAPK and c-jun.

References:

Pecchi, E., M. Dallaporta, A. Jean, S. Thirion, and J.D. Troadec. 2009. Prostaglandins and sickness behavior: old story, new insights. *Physiol Behav* 97:279-292.

Shim, J.H., C. Xiao, A.E. Paschal, S.T. Bailey, P. Rao, M.S. Hayden, K.Y. Lee, C. Bussey, M. Steckel, N. Tanaka, G. Yamada, S. Akira, K. Matsumoto, and S. Ghosh. 2005. TAK1, but not TAB1 or TAB2, plays an essential role in multiple signaling pathways in vivo. *Genes Dev* 19:2668-2681.

Singer, C.A., K.J. Baker, A. McCaffrey, D.P. AuCoin, M.A. Dechert, and W.T. Gerthoffer. 2003. p38 MAPK and NF-kappaB mediate COX-2 expression in human airway myocytes. *Am J Physiol Lung Cell Mol Physiol* 285:L1087-1098.

Yamaguchi, K., A. Lantowski, A.J. Dannenberg, and K. Subbaramaiah. 2005. Histone deacetylase inhibitors suppress the induction of c-Jun and its target genes including COX-2. *J Biol Chem* 280:32569-32577.

785

EFFECTS OF INTRANASAL DELIVERY OF CALCITONIN GENE-RELATED PEPTIDE ON CEREBRAL VASOSPASM AND NO-CGMP PATHWAY IN ARTERY WALLS IN RATS

B.-L. Sun[1], Y. Wang[2], M.-F. Yang[3], H. Yuan[3], X. Liang[4]

[1]Department of Neurology, Affiliated Hospital of Taishan Medical University, Taian, [2]Shandong Provincial Hospital, Jinan, [3]Key Laboratory of Cerebral Microcirculation in Universities of Shandong, Affiliated Hospital of Taishan Medical University, [4]Department of Neurology, First Hospital of Taian, Taian, China

Objectives: Cerebral vasospasm is the primary cause of sequelae and poor clinical conditions of subarachnoid hemorrhage (SAH) and it is imperative to relieve vasospasm and improve cerebral blood supply. Calcitonin gene-related peptide (CGRP) is a potent vasodilator that is normally released by trigeminal sensory fibers but depleted following SAH. The aims of this study were to investigate the effects of intranasally CGRP on SAH-related cerebral vasospasm and NO-cGMP pathway in artery walls.

Methods: Wistar rats were divided into normal control, SAH, SAH and intranasal normal saline (IN NS+SAH), SAH and intranasal CGRP (IN CGRP+SAH) groups. SAH was induced by double-injection of autologous blood into the cisterna magna. After second cisternal injection of blood, rats received 30μl normal saline and 30μl(30μl/μg) CGRP intranasally in IN NS+SAH and IN CGRP+SAH groups, respectively. The brain was removed and the arteries of Willi's Circle were harvest. Levels of nitric oxide (NO) were detected by nitrate reductase technique. eNOS and iNOS mRNA were determined by Reverse transcriptive PCR. cGMP content was measured by a radioimmunoassay. Diameters of basilar arteries were observed in brain sections.

Results: NO levels in arterial walls reduced significantly in SAH and IN NS+SAH groups. NO levels in IN CGRP+SAH group were higher than those in SAH and IN NS+SAH groups. Decreased expression of eNOS mRNA and increased expression of iNOS mRNA were found in SAH, IN NS+SAH and IN CGRP+SAH groups. Intranasal delivery of CGRP antagonized the alteration of eNOS mRNA and iNOS mRNA expression. cGMP levels in arterial walls in SAH and IN NS+SAH groups decreased markedly as compared with normal controls. cGMP levels were higher in IN CGRP+SAH group compared with those in SAH and IN NS+SAH groups. Diameters of basilar artery decreased significantly in rats of SAH and IN NS+SAH groups as compared with normal controls. Intranasal delivery of CGRP partly reversed the decrease of diameters of basilar artery caused by SAH.

Conclusions: The impairment of NO-cGMP pathway are involved in the development of cerebral vasospasm following SAH in rats. Intranasal delivery of CGRP up-regulate the expressions of eNOS mRNA and iNOS mRNA and increase cGMP and NO levels in cerebral aterial walls, and thus reverse cerebral vasospasm after SAH.

787

QUANTITATIVE MEASUREMENT OF CEREBRAL BLOOD FLOW IN AN ADULT PORCINE MODEL OF ISCHEMIA USING A TIME-RESOLVED NEAR-INFRARED TECHNIQUE

J.T. Elliott[1,2], M. Diop[1,2], L.B. Morrison[1,3], J.A. Hadway[1,3], T.-Y. Lee[1,2,3], K.S. St. Lawrence[1,2]

[1]Imaging Division, Lawson Health Research Institute, [2]Department of Medical Biophysics, University of Western Ontario, [3]Imaging Research Laboratories, Robarts Research Institute, London, ON, Canada

Introduction: Following traumatic brain injury (TBI), patient outcome is reliant on maintaining adequate oxygenation of brain tissue. Complications can occur during recovery, resulting in reduced cerebral blood flow (CBF) and worsening outcome, and include systemic hypotension, increased intracranial pressure and spontaneous cerebral vessel constriction. For this reason, bedside monitoring of CBF could significantly improve patient management. While optical dye-dilution techniques have been used successfully to measure cerebral blood flow (CBF) in infants, the presence of a more substantial scalp and skull has prevented accurate measurements of CBF in adult patients. And while much effort has been made in improving depth-sensitivity through advances in instrumentation and modeling [1], the extraction of uncontaminated dye dilution curves suitable for quantitative CBF measurements relies heavily on *a priori* knowledge of patient-specific anatomy and accurate Monte Carlo modeling.

Here we demonstrate the use of a spatially and time-resolved near-infrared (TR-NIR) technique that can independently and accurately measure CBF under normal and ischemic conditions. We also present computed tomography (CT) perfusion data as an independent measure of CBF during ischemia.

Methods: In three adult pigs, TR-NIR measurements of cerebral blood flow were made at baseline and immediately following infusion of endothelin-1 (ET-1), a potent ischemia-producing vasoconstrictor. Following a bolus injection of indocyanine green (ICG), temporal point-spread functions (TPSFs) were obtained every 0.4 seconds at 1, 2 and 3-cm source-detector (SD) distances, simultaneously. Total differential pathlength and the time-dependent changes in attenuation at each probe were determined from TPSFs. The scalp contamination was removed from each channel using a two-step process. First, TPSFs collected from the 1-cm SD pair at each time-point were fit to the diffusion approximation to retrieve the time-varying change in attenuation coefficient. The attenuation coefficient function was then fit with a tracer kinetic model (tissue-homogeneity model) to extract the flow and impulse residue function of the scalp [2]. The modeled scalp function was subtracted from the change in attenuation measured at each detector, and the resulting brain curves deconvolved to retrieve CBF [3].

Results: Mean CBF measured by TR-NIR was 59.2 ± 1.1 during baseline. Following ET-1 injection, TR-NIR revealed that CBF decreased to 37.2 ± 1.1 $mL \cdot min^{-1} \cdot 100g^{-1}$, which was in good agreement with a mean CBF of 34.5 ± 1.0 $mL \cdot min^{-1} \cdot 100g^{-1}$ determined by CT perfusion.

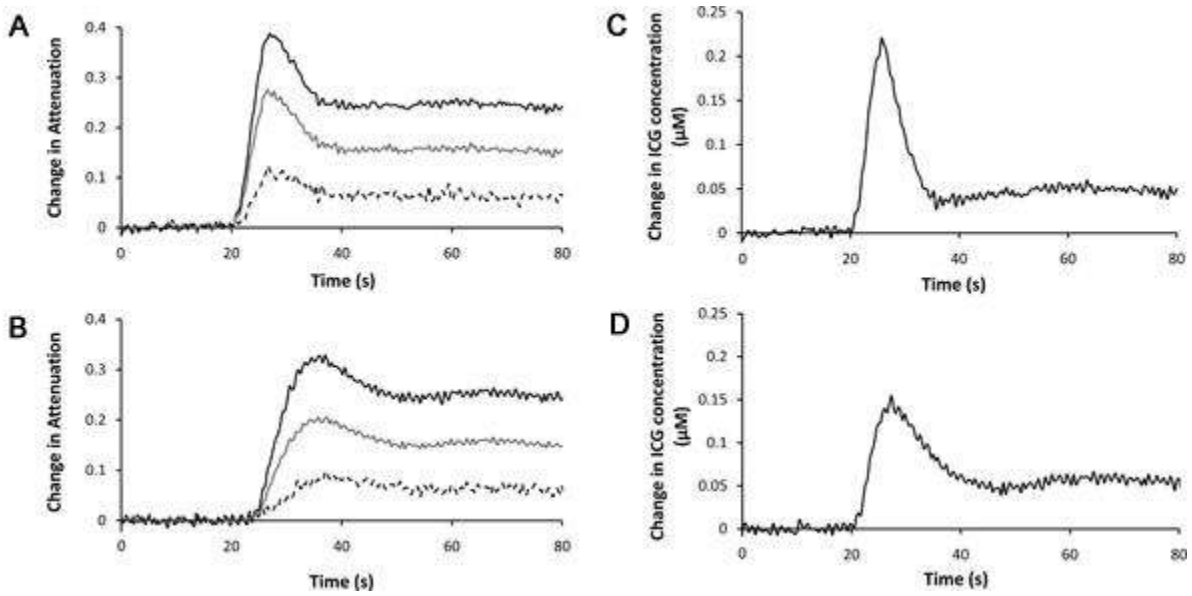

[figure]

Fig. Change in attenuation following ICG injection at baseline (A) and post endothelin-1 infusion (B), measured at source-detector distances of 3 cm (black line), 2 cm (grey line) and 1 cm (dashed line); and the recovered brain tissue ICG curves (C, D) at the two conditions, respectively.

Conclusions: These preliminary results suggest that spatially resolved TR-NIR can be used to accurately quantify cerebral blood flow in adults. Furthermore, fitting the time-varying scalp attenuation coefficient function with the tissue homogeneity model eliminates the need for accurate *a priori* knowledge of mean partial pathlengths.

1. Liebert *Appl Opt* **43**(15):3037-3047

2. St.Lawrence. *J Cereb Blood Flow Metab* **18**:1365-77

3. Brown *Pediatr Res* **51**(5):564-570

789

TBI INDUCED ALTERATIONS IN ENDOTHEIN RECEPTOR EXPRESSION: A TEMPORAL CORRELATE TO HEMODYNAMIC DYSFUNCTION

C. Reynolds[1], J. Rafols[1], A. Kropinski[1], J. Graves[1], C. Kreipke[1,2]

[1]Anatomy and Cell Biology, Wayne State University School of Medicine, [2]John D Dingell Veterans Administration Hospital, Detroit, MI, USA

Introduction: Traumatic brain injury (TBI) results in multiple pathologies, including cerebrovasospasm resulting in impaired cerebral autoregulation and significant reductions in cerebral blood flow (CBF). Recently, it has been suggested that endothelin-1 (ET-1) acting through two receptors, A and B (ETrA and ETrB), plays a major role in the induction of cerebral vasospasm following head trauma, thus diminishing the autoregulatory capacity of reacting blood vessels and, in turn, promoting secondary tissue damage. In the current study we sought to determine the relative contributions of ETrA and B to the pathotrajectory of TBI-induced changes in vascular reactivity and whether manipulation of receptors can mitigate hypoperfusion.

Methods: A rodent model of diffuse TBI was used to determine regional and temporal changes in cerebral blood flow (CBF) as measured by arterial spin labeling MRI. Additionally, at 4, 24, and 48 hours following TBI animals were sacrificed for semiquantitative measurement of regional endothelin receptor expression by western analysis. The observed temporal course of TBI-induced modulation of receptor expression was compared with changes in CBF. Furthermore, injured animals were given several doses of ETrA or B antagonists and CBF was measured.

Results: TBI resulted in a significant ($*p < 0.05$) decrease in CBF which persisted for 24 hours in sensorimotor cortex and through 48 hours in hippocampus. The observed decrease in regional blood flow correlates temporally with a significant increase in endothelin receptor expression following TBI. Antagonist studies revealed that ETrA, but not ETrB, antagonism improves blood flow.

Conclusion: These data suggest that endothelin receptor expression following head trauma plays an important role in the altered vascular reactivity, causing vasospasm and decreased CBF. Furthermore, manipulation of ET-1 receptors may prove effective as clinical treatments for TBI victims. (supported by NIH-NINDS NS064976 and VA RR&D Merit Award RX000224)

790

LIVER X RECEPTOR BETA ACTIVATION PROMOTES LIPID MICRODOMAIN FORMATION AFTER EXPERIMENTAL STROKE

E. Kuric, T. Wieloch, K. Ruscher

Laboratory for Experimental Brain Research, University of Lund, Lund, Sweden

Objectives: Mechanisms are required to scavange the massive release of cellular lipids which otherwise exacerbates neuronal death and infarct expansion after stroke. Liver X receptors (LXRs) are transcription factors regulating the expression of lipid transport proteins and are up-regulated following experimental stroke. The present study was conducted to investigate if LXRs are involved in lipid transport mechanisms in models of experimental stroke.

Methods: Male spontaneous hypertensive rats were subjected to permanent occlusion of the middle cerebral artery (MCAO). After selective sorting, animals were assigned into standard cages or enriched environment cages for 3 days. Complementary, primary cultures of cortical astrocytes were exposed to combined oxygen glucose deprivation (OGD). DNA binding activity and levels of LXRs were analyzed from the infarct core/ peri-infarct border zone and posthypoxic astrocytes by gel shift assay and Western blotting, respectively. LXR regulated proteins were analyzed in lipid microdomains prepared differential ultracentrifugation (Ruscher et al., 2010).

Results: Activation of the transcription factor liver X receptor beta (LXRβ) promotes the formation of caveolin-1 positive lipid microdomains in astrocytes after combined oxygen glucose deprivation. Accompanied, we observed the integration of the LXRβ regulated proteins ATP-binding cassette transporter 1 *(ABCA1)* and apolipoprotein E (ApoE) into lipid microdomains. In rats housed in an enriched environment which significantly improves functional recovery after experimental stroke, elevated LXRβ activation were evident at the peri-infarct area/infarct core border zone compared to rats housed in standard cages after MCAO. Similar to astrocytes *in vitro*, the accumulation of ABCA1, ApoE, and ApoA into lipoprotein particles strongly corroborate an optimized clearance of free lipids in the ischemic hemisphere.

Conclusion: Our data support the notion that lipid clearance mechanisms involving LXRb and LXRb regulated proteins are activated in the peri-infarct area/ infarct core border zone and associated with an improved recovery after experimental stroke with implication for the development of regeneration enhancing medicines after stroke.

Reference: Ruscher K, Shamloo M, Rickhag M, Ladunga S, Gisselsson L, Toresson T, Urfer R, Johansson BB, Nikolich K, and Wieloch T. Sigma-1 receptor regulates mechanisms of functional recovery after experimental stroke. *Brain, 2010. In press.*

791

5-LIPOXYGENASE IS INVOLVED IN INFLAMMATION RESOLUTION AFTER PPARGAMMA ACTIVATION BY POLARIZATION OF MACROPHAGE/MICROGLIA TOWARDS A M2 PHENOTYPE AFTER EXPERIMENTAL STROKE

I. Ballesteros[1], M.I. Cuartero[1], M. Sobrado[2], J.G. Zarruk[1], T. Atanes[1], O. Hurtado[1], J. Vivancos[2], F. Nombela[2], A.L. Corbí[3], I. Lizasoain[1], M.A. Moro[1]

[1]Universidad Complutense, [2]Hospital Universitario La Princesa, [3]CIB, CSIC, Madrid, Spain

Objectives: Regulation of microglial activation to promote conditions that support repair and return to tissue homeostasis has been proved to be beneficial in the treatment of several animal models of CNS pathologies with an inflammatory background. In this context, M2 polarized macrophages play a role in resolution of inflammation through high endocytic clearance capacities and trophic factor synthesis, accompanied by reduced pro-inflammatory cytokine secretion (1). Peroxisome Proliferator-Activated Receptor gamma (PPARgamma) has emerged as a crucial regulator of M1/M2 macrophage polarization which actively promotes resolution and tissue repair (2,3). We have recently showed that PPARgamma-induced neuroprotection and inhibition of inflammation is a 5-lipoxygenase (5-LO)-dependent process in the injured brain after cerebral ischemia in rodents (4). Now, we report new evidence on the mechanisms recruited by 5-LO induction after PPARgamma activation in experimental stroke.

Methods: WT and 5 LO-deficient mice were subjected to permanent focal cerebral ischemia prior to an intraperitoneal administration of vehicle (saline) or 3 mg/kg of the PPARgamma agonist rosiglitazone (RSG). Infarct volume was evaluated by magnetic resonance imaging (MRI) 24 hours after ischemia. Protein extracts were collected from periinfarct and infarct areas to measure the expression of the M2 markers arginase I and CD36. Neutrophil infiltration and microglial reactivity were studied by inmunofluorescence staining of NIMPR14 and Iba1.

Results: RSG administration conferred neuroprotection on wild type mice but not in 5-LO KO mice as determined by MRI. RSG was able to up-regulate the expression of arginase I and CD36 24 hours after ischemia on wild-type mice but this effect was absent in 5-LO KO mice. Finally, RSG failed to reduce neutrophil infiltration and microglial reactivity on 5-LO KO animals.

Conclusions: Our results demonstrate the implication of 5-LO in PPARgamma-induced M2 polarization and reduction of neutrophil infiltration and of microglial activation after stroke. These effects, together with our previous work on 5-LO implication in PPARgamma anti-inflamatory properties, highlight the importance of 5-LO metabolites on PPARgamma signaling pathways implicated on resolution of inflammation and repair. A better characterization of these 5-LO derived compounds and the study of the downstream pathways could contribute to the development of new drugs to promote resolution of inflammation and neurorepair after stroke.

References:

1. Martinez FO et al. (2008). Front Biosci. 13:453-461

2. Odegaard JI et al. (2007). Nature 447:1116-1120

3. Ricote M et al. (1998). Nature 391:79-82

4. Sobrado M et al. (2009). J.Neurosci. 29:3875-3884

Supported by RETICS-RENEVAS RD06/0026/0005 and SAF2009-08145

792

DIFFUSE AXONAL INJURY AND ENDOTHELIN: A COUPLING OF CONCURRENT PATHOLOGIES?

J. Rafols[1], C. Reynolds[1], A. Kropinski[1], J. Graves[1], C. Kreipke[1,2]

[1]Anatomy and Cell Biology, Wayne State University School of Medicine, [2]John D Dingell Veterans Administration Hospital, Detroit, MI, USA

Introduction: Two common pathologies associated with traumatic brain injury (TBI) are diffuse axonal injury (DAI) and hypoperfusion of the microcirculation from enhanced contractility of reacting microvessels (Rafols et al, 2007). Over the past decade our laboratory has focused its attention on strategies to mitigate the TBI-induced hypoperfusion through the use of endothelin receptor antagonism (Kreipke and Rafols, 2010). Selective antagonism of the endothelin receptor A (ETrA), was previously shown to decrease both the hypoperfusion and the extent of cell injury (assessed by FluoroJade, FJ), as well as ameliorate cognitive behavioral (radial arm maze) deficits following TBI. However, recently we have uncovered a potentially novel consequence of selective ETrA blockade—decrease in the extent of DAI.

Methods: In order to confirm this observation, TBI was induced in adult (400-450 g) male Sprague Dawley rats using a modified (after Marmarou's weight impact/acceleration, 1994) model of diffuse TBI. Shortly after impact animals were given a 1.0 mg/kg IV injection of BQ123, a selective ETrA antagonist. At 24 and 48 hours post TBI, coronal brain sections through the rostro-caudal extent of the corpus callosum were collected and morphometric analyses of beta amyloid peptide (b-APP) stained retraction bulbs resulting from DAI were conducted.

Results: Compared to control (non-TBI and sham operated), ETrA antagonism significantly reduced (>30%) the number of retraction bulbs in corpus callosum, this reduction temporally coinciding with both improved histopathologic (Fluorojade staining in layers II-II of sensorimotor cortex) and behavioral (radial arm maze) outcomes.

Conclusions: While the precise mechanism is currently unknown, the results suggest that improving CBF via ETrA blockade can ameliorate TBI-induced DAI. Alternatively endothelin (known to be upregulated after TBI) via the ETrA, could directly impact on the pathotrajectory of DAI. Future studies will be performed to determine whether dysregulation of ETrA signaling may be part of the molecular cascade leading to DAI (supported by NIH-NINDS NS064976 and VA RR&D Merit Award RX000224)

793

ETRA ANTAGONISM AND TRAUMATIC BRAIN INJURY: TOWARDS A CLINICAL TRIAL

C. Kreipke[1,2], C. Reynolds[1], J. Graves[1], A. Kropinski[1], D. Kuhn[2,3], W. Armstead[4], J. Rafols[1]

[1]Anatomy and Cell Biology, Wayne State University School of Medicine, [2]John D Dingell Veterans Administration Hospital, [3]Psychiatry and Behavioral Neurosciences, Wayne State University School of Medicine, Detroit, MI, [4]Anesthesiology, University of Pennsylvania, Philadelphia, PA, USA

Introduction: Traumatic brain injury results in multiple pathologies, including a significant reduction in cerebral blood flow. Our combined laboratories have shown that endothelin-1 plays a major role in the induction of hypoperfusion.

Methods: Therefore, using a rodent model of diffuse traumatic brain injury, we sought to test the effects of IV administration of various selective and non-selective endothelin receptor antagonists on CBF (as measured using arterial spin labeling MRI), cellular injury (as measured using Fluoro-Jade labeling), and behavioral outcome (as measured using a radial arm maze-spatial learning task) following TBI.

Results: Our results indicate that ETrA antagonism causes a decrease both in hypoperfusion and cellular injury, and improves behavioral outcome. Conversely, ETrB antagonism did not improve any measure of outcome at any dose given. Furthermore, mixed ETrA/B antagonism did not improve outcome.

Conclusion: These data suggest that specific ETrA antagonists may be effective in ameliorating the deleterious effects of TBI. (supported by NIH-NINDS NS064976 and VA RR&D Merit Award RX000224)

794

MICRODIALYSIS STUDY OF METRONIDAZOLE CEREBRAL DISTRIBUTION IN PATIENTS WITH ACUTE BRAIN INJURY

C. Dahyot-Fizelier[1,2], D. Frasca[1,2], O. Mimoz[2,3], W. Couet[2,4], S. Marchand[2,4]

[1]Neuro Critical Care Unit, University Hospital of Poitiers, [2]INSERM ERI-23, University of Poitiers, [3]Intensive Care Unit, [4]Pharmacokinetic Laboratory, University Hospital of Poitiers, Poitiers, France

Objectives: Metronidazole is part of the standard therapy of bacterial brain abscess and considered to penetrate well blood-brain barrier (BBB) [1]. However dosing regimens are based on plasma and few cerebral spinal fluid (CSF) pharmacokinetic (PK) studies [2,3]. As infections mainly occur in tissue extracellular fluid (ECF), corresponding unbound ECF antibiotic concentrations are responsible for the antimicrobial effect. This study aims to explore metronidazole distribution in patients with acute brain injury, by comparing their unbound concentrations in brain and plasma.

Methods: After local ethic approval and written informed consent, four brain injured patients, sedated, mechanically ventilated, monitored by cerebral microdialysis (CMA 71, membrane lenght 10 mm, membrane diameter 0.6 mm, molecular cut-off 100 kDa; CMA, Stockholm, Sweden) and receiving metronidazole for an infection or prophylaxis, were enrolled. PK study succeeded to 500 mg of metronidazole over 30 minutes and brain dialysates and blood samples were collected over 400 minutes. *In vivo* probes recoveries were evaluated individually by retrodialysis. Metronidazole was assayed by HPLC.

Results: Mean metronidazole brain to plasma AUC ratio was 0.86 ± 0.14 (range from 0.74 to 1.06). All patients had metronidazole concentrations versus time curves in brain delayed (mean time-to-peak = 69 ± 30 min) and peaks were smoother than corresponding curves in plasma with mean C_{max} in brain and plasma of 14.5 ± 1.2 and 19.1 ± 2.4 µg/mL, respectively (figure). Mean half-lives was 379 ± 131 min in plasma; C_{min} were 7.2 ± 4.0 µg/mL in plasma and 5.5 ± 1.3 µg/mL in brain. Mean probe recovery was 78.8 ± 1.3%.

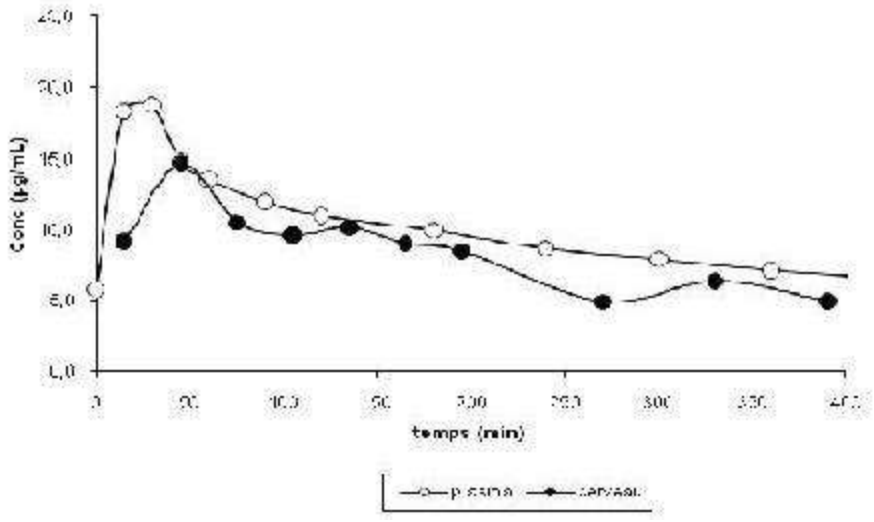

[Figure: 1 representative patient]

Conclusion: Our findings confirm previous studies in CSF, metronidazole penetrates well BBB. Indeed, in acute brain injury patients, unbound metronidazole AUCs in brain and plasma are close. So, unbound metronidazole concentrations in plasma could be a good surrogate of metronidazole active concentrations in brain for PK monitoring in routine.

References:

1-Nau R. Clin Microbiol Rev 2010;23:858-883.

2-Hoffmann HG. Arzneimittelforschung 1984;34:830-831.

3-Warner JF. Arch Intern Med 1979. 139;167-169.

795

EXPERIMENTAL VALIDATION OF THE GENERAL 1/f^{β} MODEL IN PRODUCING RESTING-STATE BOLD SIGNAL TOPOLOGY IN THE RAT BRAIN

P. Herman[1], B.G. Sanganahalli[1], F. Hyder[1,2], A. Eke[3]

[1]Department of Diagnostic Radiology, [2]Department of Biomedical Engineering, Yale University, New Haven, CT, USA, [3]Institute of Human Physiology and Clinical Experimental Research, Semmelweis University, Budapest, Hungary

Objectives: The cross-correlation analysis of spontaneous low frequency fluctuations (LFF) of resting-state BOLD signal in rodents have proven instrumental in localizing coupled brain networks as resting-state connectivity maps [1,2]. In human studies the autocorrelation structuring of the BOLD signal, mainly BOLD-LFF, was reported to follow a 1/f^{β} model with β as a physiologically responsive variable [3]. Fractal analysis is used to detect the presence of power-law scaling frequency distribution according to the formalism of the 1/f^{β} model, which is related to autocorrelation in the signal and characterizes its temporal complexity [4]. We investigated BOLD-LFF in anesthetized rat brain to validate the general 1/f^{β} model and associated fractal autocorrelation structure by comparing its spectral index β obtained *in vivo*, *post mortem*, and *in vitro* (phantom) to assess the extent to which LFF is related to underlying physiology and to demonstrate if instrument noise could influence the fractal nature of *in vivo* BOLD-LFF.

Methods: All fMRI data (n=10) were obtained by a modified 11.7T Bruker horizontal-bore spectrometer using a ^{1}H surface coil (1.4 cm diameter). All fMRI data were collected with sequential sampling gradient echo planar imaging (EPI) sequence (TR/TE=200/13ms). In every series of EPI sequence we acquired 4200 images creating BOLD time series in adequate length for fractal analysis. The *in vivo* EPI data were recorded in steady state after the animals were stabilized in the MRI scanner. The *post mortem* data were collected after one hour following the sacrifice of the animal. We modeled the BOLD-LFF in the frequency domain by using β as its scaling exponent characterizing the autocorrelation structure of the signal as β=0 for random, β>0 for correlated, and β< 0 for anticorrelated signal.

Results: Cortical β values dropped from 0.62±0.1 (strongly correlated) at *in vivo* to 0.17±0.07 (weakly correlated) at *post mortem*. Similar trends were observed for subcortex: β dropped from weakly correlated (0.2±0.11) at *in vivo* to near random (0.06±0.03) at *post mortem*. Cortical and subcortical β values were significantly different (P=0.0002 and 0.002 at *in vivo* and *post mortem*, respectively), whereas β values *post mortem* and *in vitro* were similar.

Conclusions: These results demonstrate that i) β is a variable with topology accentuating grey matter areas, ii) near-zero powers across *in vitro* BOLD-LFF spectra indicates that LFF of *in vivo* and *post mortem* signals are not influenced by instrument noise, iii) and - although at low power - BOLD-LFF is still present *post mortem* when the brain has ceased functioning. Our *post mortem* and *in vitro* data suggest that the LFF captured in the resting-state BOLD signal at high magnetic fields is dominated by underlying physiology and thus may reliably capture the correlation structure of underlying neurovascular and neurometabolic processes with the caveat of some “residual” power seen in BOLD-LFF *post mortem*.

References:

[1] Pawela et al (2008) MagnResonMed 59:1021-1029.

[2] Zhao et al (2008) Neuroimage. 39:248-260

[3] Bullmore et al (2009) Neuroimage 47:1125-1134

[4] Eke et al (2002) PhysiolMeas 23:R1-38

Acknowledgements: Supported by NIH (R01 MH-067528, P30 NS-52519).

796

GENISTEIN AND DAIDZEIN HAVE NEUROPROTECTIVE EFFECTS THROUGH LIGAND-BINDING-INDEPENDENT PPARΓ ACTIVATION

O. Hurtado[1], I. Ballesteros[1], M.I. Cuartero[1], M. Torres[2], J. Sánchez-Prieto[2], M. Castelló-Ruiz[3,4], M.C. Burguete[4], E. Alborch[3,4], I. Lizasoain[1], M.A. Moro[1]

[1]Universidad Complutense, [2]Veterinary School, Universidad Complutense, Madrid, [3]Hospital Universitario La Fe, [4]Universidad de Valencia, Valencia, Spain

Objectives: Phytoestrogens are a group of plant-derived compounds that include mainly isoflavones (genistein, daidzein, glycitein and equol), lignans, coumestans, flavonoids, stilbenes and mycotoxins. Phytoestrogens prevent neuronal damage (1) and improve outcome in experimental stroke (2); however, the mechanism of this neuroprotective action has not been fully elucidated. In this context, it has been postulated that phytoestrogens might act through the peroxisome proliferator-activated receptor-γ (PPARγ), which exerts anti-inflammatory effects in several settings, including cerebral ischemia (3). The aim of this study was to determine whether phytoestrogen-induced neuroprotection in experimental stroke is brought about by activation of PPARγ.

Methods: Primary cultures of rat cortical neurons and oxygen and glucose deprivation (OGD) were performed as described (4). In some experiments, genistein and daidzein 0.05, 0.5 and 5 μM was included 24 hours before, during and after OGD, in the absence or presence of the specific PPARγ antagonist T0070907 (Cayman, Ann Arbor, USA). As a marker of necrotic tissue damage, LDH (lactate dehydrogenase) activity was determined 24 h after OGD. Nuclear extracts were prepared as described (5) and PPARγ activity was assessed using PPARγ Transcription Factor Assay kit (Cayman, Ann Arbor, USA). LanthaScreen™ TR-FRET PPARγ Coactivator Assay (Invitrogen) was used for screening of phytoestrogens as ligands for PPARγ (6).

Results: Treatment with genistein or daidzein decreased lethal OGD-induced LDH release in neuronal cultures (LDH: 92, 88 and 72 % vs 100% OGD with 0.05, 0.5 and 5 μM genistein and 92, 46, 45 % vs 100% OGD with 0.05, 0.5 and 5 μM daidzein). The PPARγ antagonist T0070907 (1μM) inhibited the protective effect caused by the administration of 5 μM genistein or daidzein. Both phytoestrogens induced an increase in PPARγ transcriptional activity: 129 and 125% vs control (100%) with 0.5 and 5 μM genistein and 122 and 117% vs control (100 %) with 0.5 and 5 μM daidzein. Rosiglitazone induced FRET in a concentration-dependent manner with an intensity at 1 nM (EC_{50} values). However, neither genistein nor daidzein showed any response in the same assay.

Conclusions: These results demonstrate that 1) genistein and daidzein are neuroprotective in an in vitro stroke model using rat cortical neurons and 2) that both phytoestrogens induce an increase in PPARγ transcriptional activity in pure neuronal cultures, although this effect is not mediated by direct binding to the receptor ligand-binding domain.

References:

1. Kajta et al. 2007. Neuroscience. 145:592-604.

2. Burguete et al. 2006. Eur J Neurosci. 23:703-10.

3. Jiang et al. 2008. CNS Drugs. 22:1-14.

4. Hurtado et al. 2002. J Cereb Blood Flow Metab. 22:576-85.

5. Cárdenas et al. 2000. J. Neurochem. 74:2041-48.

6. Stafslien et al. 2007. Mol Cell Endocrinol. 29:82-9.

Supported by RETICS-RENEVAS RD06/0026/0005, RD06/0026/0006 and SAF2009-08145.

797

PROTEOMICS DIFFERENCES IN BRAIN VESSELS FROM ALZHEIMER'S DISEASE MICE AND WILDTYPE CONTROLS: NORMALIZATION BY THE PPAR-Γ AGONIST PIOGLITAZONE

A. Badhwar[1], R. Brown[2], C.E. Delaney[2], D.B. Stanimirovic[2], A.S. Haqqani[2], E. Hamel[1]

[1]Montréal Neurological Institute, McGill University, Montréal, QC, [2]National Research Council of Canada, Institute for Biological Sciences, Ottawa, ON, Canada

Introduction: Cerebrovascular dysfunction appears prior to Aβ-plaque deposition and memory deficits in Alzheimer's disease (AD) patients and amyloid precursor protein (APP) transgenic mice. Current evidence points to the soluble, highly toxic Aβ fragment generated from the amyloidogenic processing of APP as the primary instigator of cerebrovascular deficits. In aged (1) and young (2) APP mice, we found that the PPAR-Y agonist pioglitazone normalized cerebrovascular reactivity and the neurovascular coupling response to whisker stimulation.

Objectives: The cerebrovascular proteome of APP mice compared to that of wildtype (WT) mice is unknown, and its alteration related to the therapeutic benefit of pioglitazone remains uncharacterized. We address this gap in knowledge by performing mass spectroscopy (MS)-based quantitative proteomics in isolated cerebral arteries of WT and APP-transgenic mice, treated and untreated with pioglitazone. We aim to identify proteins and networks that orchestrate pioglitazone-mediated recovery of cerebrovascular function.

Methods: Three-month-old APP (line J20) and WT mice were treated (16 weeks) with pioglitazone (20 mg/kg/day) or control diet. Thereafter, mice were transcardially perfused and the main cerebral arteries and their primary branches removed under a dissecting microscope and cleaned of any attached tissue. Proteins were extracted, trypsin-digested, fractionated by strong cation exchange (gel-free method) and 1D SDS-PAGE (gel-based method), and analyzed by nanoLC-MS/MS using nanoAcquity UPLC (Waters) and ESI-LTQ Orbitrap (Thermo). MatchRx software (3) version QnD-2.0 was used to define peptide peaks, quantify and normalize intensities, and align LC-MS runs among fractions. Differentially-expressed proteins were compared at >1.5 and 2 fold changes, and at $p < 0.05$ and $p < 0.01$.

Results: We identified 6,566 proteins in murine cerebral arteries. Compared to WT mice, 975 proteins (15%) showed differential expression (>1.5-fold up- or down-regulated, $p < 0.05$) in the arteries of APP mice. A more stringent analysis (>2-fold up- or down-regulation, $p < 0.01$) narrowed down these to 90 proteins (1.4%) differentially expressed between the two groups. The altered proteins were associated with pathways related to oxidative stress, inflammation, apoptosis, protein signaling, and amyloidosis. Pioglitazone treatment partly or totally normalized the majority (~60% of 975, and ~80% of 90 proteins) of the differentially expressed proteins to levels comparable to those of WT mice. Pioglitazone exerted beneficial effects in all pathways that were altered between APP and WT mice.

Conclusions: We characterized the effects of soluble Aβ peptide on the cerebrovascular proteome of APP mice. Further, we showed that functional recovery with pioglitazone (1, 2) is associated with normalization of the majority of altered proteins in the vessel wall and, particularly, those related to oxidative stress and inflammation known to impair cerebrovascular function. The identified proteins could represent potential biomarkers for diagnostic and therapeutic efficacy. The results demonstrate, at the proteome level, that pioglitazone counters the deleterious cerebrovascular effects of soluble Aβ.

References:

1. Nicolakakis N, et al, 2008. J Neurosci. 2008;28(37):9287-96

2. Badhwar A, et al., 2010. Alzheimer´s & Dementia. 2010;6(4):S5-6

3. Haqqani AS, et al., 2008. Methods Mol Biol. 2008;439:241-56

Supported by grants (EH) from the Canadian Institutes of Health Research (CIHR grant MOP-84275) and Takeda Pharmaceuticals Inc, and a CIHR studentship (AB).

798

EXAMINING THE RATE OF CONTRAST EXTRAVASATION FOR INTRACEREBRAL HEMORRHAGE: A CT PERFUSION STUDY

C. d'Esterre[1], T.Y. Lee[2], R.I. Aviv[3]

[1]Medical Biophysics, University of Western Ontario, [2]Imaging, Lawson Health Research Institute, [3]Neuroradiology, Sunnybrook Health Sciences Center, London, ON, Canada

Objective: CT perfusion (CTP)-derived permeability surface area product (PS) is a novel method of measuring the rate of contrast extravasation from the intra- to extra-vascular compartment. Knowing the rate of contrast extravasation may provide insight into the pathophysiology of hematoma expansion by identifying the target abnormality most likely to contribute to hematoma growth. This study assessed whether CTP-PS measures can distinguish between different rates of contrast extravasation for patients with and without CT angiography (CTA) Spot Sign or post contrast CT contrast leakage (PCL). We hypothesize that the rate of contrast extravasation will be higher in CTA Spot Sign regions compared to PCL and hematoma regions in patients without extravasation.

Methods: Spot sign and PCL extravasation were identified by the presence of contrast extravasation on the CTA or PCCT, respectively. Of 16 screened patients, 7 demonstrated contrast extravasation. Nine foci of contrast extravasation were present on each of the CTA and PCCT for a total of 18 regions.

We report CT perfusion (CTP)-derived blood brain barrier (BBB) permeability findings of 16 consecutively screened ICH patients with and without confirmed contrast extravasation within 3 hours of symptom onset. CTP-derived parametric maps of permeability surface area product (PS) were analyzed using custom software (IDL v6.1, RSI Inc, Boulder, Colo. USA). Four regions of interest were placed on perfusion-weighted average images: 1) Extravasation positive regions (CT angiographic Spot Sign and post contrast leakage (PCL)), 2) mirrored contralateral hematoma volumes, 3) background hematoma excluding extravasation and 4) region within hematoma volume for patients without extravasation. Baseline and follow up hemorrhage volumes were measured.

Results: Mean PS was 3.8 ± 2.9 $ml^{-1}\times min^{-1}(100g)^{-1}$, 0.12 ± 0.39 $ml^{-1}\times min^{-1}\times (100g)^{-1}$, 0.10± 0.26 $ml^{-1}\times min^{-1}\times (100g)^{-1}$ and 0.38 ± 0.26 $ml^{-1}\times min^{-1}\times (100g)^{-1}$ in the extravasation positive, hematoma excluding extravasation, contralateral mirror regions, and extravasation negative patients, respectively. Extravasation positive group was significantly different *($p < 0.05$)*. Within the extravasation group, Spot Sign and PCL regions had a mean PS of 6.5 ± 1.6 $ml^{-1}\times min^{-1}\times (100g)^{-1}$ and 0.95 ± 0.39 $ml^{-1}\times min^{-1}\times (100g)^{-1}$ respectively. These values were significantly different from each other and all other regions of interest *($p < 0.05$)*. Average absolute or percent hematoma volume increased from 34.1 ± 41.0 ml to 40.2 ± 46.1 ml or 27.8% in contrast extravasation positive patients. In extravasation negative patients absolute and percent volume decreased from 19.8 ± 31.8 ml to 17.4 ± 27.3 ml, or -1.5% *($p < 0.05$).*

Conclusion: A clinical technique that quantifies the rate of extravasation provides objective assessment of hematoma expansion risk rather than the qualitative approach currently used. Such information may become increasingly important as novel ICH treatments are developed that will target specific lesions. The gradation of contrast leakage reported in this study supports our assertion that CTA Spot Sign and PCL are entities associated with different rates of extravasation.

799

FRACTAL DYNAMICS IN NEUROVASCULAR COUPLING IN THE SOMATOSENSORY CORTEX OF THE RAT

P. Herman[1], F. Hyder[1,2], A. Eke[3]

[1]Department of Diagnostic Radiology, [2]Department of Biomedical Engineering, Yale University, New Haven, CT, USA, [3]Institute of Human Physiology and Clinical Experimental Research, Semmelweis University, Budapest, Hungary

Objectives: Recent observations that the spontaneous fluctuation in neural signals, especially in gamma range, is well correlated with that in cerebral blood flow or fMRI temporal records [1,2] may well bring attention to a novel aspect of neurovascular coupling that could underlie the dynamics in the hemodynamic response elicited by functional activation. The question here is how and to what extent the neural and vascular modalities are coupled as assessed by their autocorrelation structures. We studied the fractal dynamics [3] of concurrently recorded hemodynamic (i.e. CBF) and neural (i.e. local filed potentials, LFP) signals prior to and during forepaw stimulation in deeply anesthetized animals.

Methods: Sprague-Dawley rats (n=13, 280±35 g) were tracheotomized and artificially ventilated (70% N_2O, 30% O_2). The anesthesia was switched to i.p. α-chloralose (40 mg/kg/hr) from Halothane (1-2%) after the surgery. A femoral arterial line was used for monitoring blood pressure, acid-base balance and blood gases throughout the experiment. Rats were placed in a stereotaxic holder and tiny burr holes were made above the left and right S1FL somatosensory regions. Tungsten microelectrodes were inserted together with laser Doppler probes for simultaneous neural and CBF recording. LFP signal was extracted from the raw signal with a low-pass electronic filter (0-150Hz), then down sampled to 2000Hz. LDF signal was recorded at 100Hz. Electrical forepaw stimulation was applied for 30s duration (2mA, 3Hz, 0.3 ms). All signals demonstrated significant stimulus-induced increases in their respective baseline means. The extent of scale-free (i.e. fractal) autocorrelation in each signal was characterized by the extended Hurst exponent ($0< {}^{e}H< 2$) for all experimental conditions (i.e., 30s baseline and 30s stimulus), by our Signal Summation Conversion (SSC) [4] method based on the scaled window variance (SWV) method.

Results: The LDF signal revealed a two-tiered pattern yielding a split dynamics separated by a breakpoint at ~1Hz (i.e. separating low and high frequency dynamics, LF and HF, respectively). The autocorrelation of LF CBF fluctuations was strongly anti-persistent (${}^{e}H$=1.29±0.08) and didn't change during stimulation while the HF CBF fluctuations were strongly correlated (${}^{e}H$=0.78±0.29) at rest which correlation increased during stimulation (${}^{e}H$=0.94±0.23 at a significance of p=0.02). The LFP signals showed weak correlation at rest (${}^{e}H$=0.62±0.18), that became random during stimulation (${}^{e}H$=0.48±0.21 at a very high significance of p< 0.001).

Conclusions: These results demonstrate that apparently stochastic fluctuations in neurophysiologic signals are, in fact, driven by complex processes of robust correlation. The LF dynamics in the LDF signal is not even influenced by the stimulation. While at rest, the dynamics in the HF LDF and LFP signals are similar to each other - both being a correlated signal -, during stimulation, their scale-free structuring turn the opposite. Therefore the dynamics of neurovascular coupling seen at rest probably undergo significant changes during stimulation

References:

[1] Liu et al (2010) Cereb Cortex. Jun 7. [Epub]

[2] Schölvinck et al (2010) PNAS 107:10238-10243

[3] Eke et al (2002) Physiol Meas 23:R1-38

[4] Eke et al (2000) Pflugers Arch 439:403-415

Acknowledgments: Supported by NIH R01 DC-003710, R01 MH-067528, P30 NS-52519.

800

QUANTIFYING MICROVASCULAR PROPERTIES IN HEALTHY AGING: A PILOT 7T DCE-MRI STUDY

V.C. Anderson[1], D.P. Lenar[1], J.F. Quinn[2], J.A. Kaye[2], X. Li[3], W.D. Rooney[3]

[1]Neurological Surgery, [2]Neurology, [3]Advanced Imaging Research Center, Oregon Health & Science University, Portland, OR, USA

Introduction and objectives: The blood brain barrier (BBB) regulates capillary blood volume and plays a key role in water homeostasis throughout the brain. Although increasingly recognized, age-related changes in BBB permeability have been poorly characterized.(1) Dynamic contrast enhanced magnetic resonance imaging (DCE-MRI) provides a sensitive *in vivo* measure of BBB permeability. In this pilot study, we used ultra-high field DCE-MRI to quantify the effects of healthy aging on capillary blood volume and BBB water permeability of normal-appearing white matter (WM).

Patients and methods: Eighteen elderly subjects (55-73 yrs, 13/18 female) were enrolled. Individuals were excluded with BP> 160/95, diabetes, history of stroke, TIA or cardiac disease. All MR data were acquired at 7T (Siemens Magnetom). Axial 2D T_1-weighted images (IR-tFLASH; TI/TE/FA 300/1.4 ms/5°) centered on a slice just superior to the lateral ventricles were collected every 2.5 sec during and for 3 min post bolus contrast reagent (CR) injection (gadoteridol, 0.11 mmol/kg). ^1H_2O R_1 ($\equiv 1/T_1$) maps were prepared at each time point by voxelwise evaluation of the Bloch equation for the IR-tFLASH sequence, accounting for all RF pulses and delays.(2) After rigid-body registration and WM masking of serial R_1 maps (3), mean R_1 values were determined in each of 4 quadrants (frontal/parietal and right/left). Blood R_1 values were calculated from a voxel contained entirely in the sagittal sinus. Capillary blood volume (v_b), the rate constant for water extravasation (τ_b^{-1}), and P_wS (the BBB water permeability surface area product; $\equiv v_{b^*} \tau_b^{-1}$) were determined using a two compartment (intravascular/extravascular) tissue model that accounts for equilibrium intercompartmental exchange of water and CR (4).

Results: Among all individuals, WM v_b was 0.50 ± 0.19 mL/100 g and showed a strong tendency to decrease with age (r= -0.36, P= 0.07). Regional (frontal> parietal) and hemispheric (left> right) effects on v_b were significant (P< 0.05). Mixed effect linear models showed that after controlling for region and hemisphere, v_b decreased by approximately 0.01 mL/100 g for every 1 year of age increase. τ_b^{-1} was not associated with age or hemisphere, but was increased in parietal compared to frontal WM (6.6 ± 4.5 s^{-1} and 5.1 ± 3.8 s^{-1}, respectively). P_wS was 4.7 ± 2.1 mL/100 g/s among all individuals and showed no statistical association with age, region, or hemisphere.

Conclusions: After controlling for region and hemisphere, there was a strong trend towards reduced WM blood volume with age. However, the rate of water extravasation and water permeability surface area product (intrinsic markers of BBB integrity) were unaffected. If confirmed in a larger sample, these results would suggest that age-related changes in microvascular properties are less likely to involve compromised BBB water permeability than decreased density of WM microvessels.

References:

(1) Farrall AJ, Wardlaw JM. Neurobiol Aging 30: 337-352 (2009).

(2) Fritz-Hansen T, Rostrup E, Larsson HB, Sondergaard L, Ring P, Henriksen O. Magn Reson Med 36: 225-231 (1996).

(3) www.fmrib.ox.ac.uk/fsl.

(4) Yankeelov TE, Rooney WD, Li X, Springer CS. Magn Reson Med 50: 1151-1169 (2003).

801

GLIOBLASTOMA TREATMENT: COMPARATIVE STUDIES OF THREE ROUTES OF ADMINISTRATION, PLATINUM FORMULATIONS AND COMBINATION OR NOT WITH RADIATION. -IN VIVO EXPERIMENTS

G. Charest[1], D. Fortin[2], D. Mathieu[2], L. Sanche[1], B. Paquette[1]

[1]Radiobiologie, Université de Sherbrooke, Sherbrooke, [2]Neurochirurgie, Neuro-Oncologie, Université de Sherbrooke, Sherbooke, QC, Canada

Objectives: Despite recent advances, the radiotherapy and chemotherapy protocols only marginally improve the overall survival of patients bearing glioblastoma (GBM). In our study, the anticancer efficiency with and without radiation combination of five platinum compounds was tested: cisplatin, oxaliplatin, their liposomal formulation Lipoplatin™ (cisplatin), Lipoxal™ (oxaliplatin) and carboplatin. The liposomal formulations were included since they can potentially reduce the toxicity of cisplatin and oxaliplatin[1]. We also investigated the tumor drug uptake according to three different routes of administration that are intra venous (i.v.), intaarterial (i.a.) by the carotid artery and i.a. with prior brain blood barrier disruption (BBBD). The aim of this study is to find a better route of administration, a better chemotherapy formulation and a better post-administration time to combine ionizing radiation in clinical GBM therapy.

Methods: The tumor F98 glioma implanted in the brain of Fischer rats was used as model to mimic the human glioblastoma[2, 3]. Although intra venous i.v. injection is the usual way to administrate the chemotherapeutic agents, the blood brain barrier (BBB) largely limits drug uptake to brain tumor. To improve the efficiency of chemotherapeutic agents, the drugs were injected via carotid artery and the BBB was temporary disrupted BBBD prior to i.a. administration[4]. The post-administration time corresponding to the maximal tumor drug uptake was determined to optimize the concomitant treatment with radiotherapy delivered by Gamma Knife.

Results: Experiments using the i.v. and i.a. route of drug administration treatment were completed. The i.a. route allows preferential uptake (up to 140X) into the tumor DNA compared to the i.v. administration. Our study confirms that the liposomal formulations allow to bypass the toxicity and considerably improving the life span of the animals. The anticancer efficiency of oxaliplatin was increased when incorporated in Lipoxal™ resulting in a considerable improvement of the life span of animals implanted with a GBM. The efficiency of Lipoxal™, Lipoplatin™ and carboplatin were similar with a median survival times of 29-32 days (i.a.) and 23-25 days (i.v.), compared to 22 days for untreated rats. Concomitant i.a. treatment with radiotherapy further extend the median survival times with the highest efficiency obtained with of Lipoxal™ (37 days) and carboplatin (47 days), compared to 34 days with radiation only. The same drugs given by i.v. don't show significant difference compare to the radiation alone.

Conclusions: Our study confirms that the liposomal formulations allow to bypass the toxicity and considerably improving the life span of the animals. Intraarterial drug administration improves considerably the tumor uptake and the life span compare to i.v. injection. We expect that i.a. plus BBBD should increase the tumor uptake and the tumor control.

References:

1. Boulikas. *Oncol Rep.* 2004;12: 3-12.

2. Mathieu et al. *Can J Neurol Sci.* 2007;34: 296-306.

3. Blanchard et al. *Can J Neurol Sci.* 2006;33: 86-91.

4. Blanchette et al. *Methods Mol Biol.* 2011;686: 447-463.

802

EFFECTS OF DIPYRIDAMOLE IN BRAIN ENDOTHELIAL CELLS: MODULATION OF INFLAMMATORY AND TROPHIC FACTOR MECHANISMS

S. Guo[1], A.T. Som[1], M. Stins[2], M. Ning[1,3], E.H. Lo[1,3]

[1]Neuroprotection Research Laboratory, Dept. of Radiology and Neurology, Massachusetts General Hospital & Harvard Medical School, Charlestown, MA, [2]Neurology, Johns Hopkins Medical Center, Baltimore, MD, [3]Clinical Proteomics Research Center, Deptartment of Neurology, Massachusetts General Hospital & Harvard Medical School, Boston, MA, USA

Objectives: Emerging evidences suggest that beyond its antiplatelet properties, dipyridamole may have pleiotropic effects on other cells within the neurovascular elements of brain. Here, we tested the effects of dipyridamole on endothelial cells in terms of inflammation and trophic factor pathways.

Methods: Human brain endothelial cells were grown in culture, and exposed to TNFa (continuously for 24 h) or subjected to oxygen-glucose deprivation (OGD, 6 h of insult followed by 18 h recovery). Expression of ICAM-1, VCAM-1 and PECAM-1 were measured by immunoblotting. Matrix metalloproteinase-2 (MMP-2) and MMP-9 in the conditioned media were quantified via zymography. MTT mitochondrial activity and LDH release were measured to assess endothelial cell viability. For trophic factors, endothelial cells were exposed to dipyridamole for 2 h, then mRNA levels of BDNF and VEGF were measured by qPCR; after 20 h protein levels of these two factors in the conditioned media were measured by ELISA.

Results: Exposure of human brain endothelial cells to TNFa (12.5-50 ng/ml) induced a clear increase in protein levels of ICAM-1, VCAM-1 and MMP-9, but no increase in PECAM-1. Dipyridamole (1-5 mM) significantly attenuated ICAM-1 and MMP-9 levels after this inflammatory insult. No significant effects of dipyridamole were noted for VCAM-1. Six-hour OGD induced moderate endothelial cell death with a release of MMP-9. Dipyridamole significantly decreased MMP-9 levels and cell death after this metabolic insult. Also, exposure of endothelial cells to dipyridamole induced slight but significant increase of mRNA level and protein level in conditioned media of BDNF.

Conclusions: These results suggest that dipyridamole may ameliorate brain endothelial injury after metabolic insults. These beneficial effects of dipyridamole may involve a modulation of inflammatory mechanisms and trophic factor(s) expression. How these putative cellular mechanisms may relate to clinical outcomes and conditions in stroke patients warrants further investigation.

803

ANALYSIS OF OGD-INDUCED CHANGES IN SUMO CONJUGATION USING A SILAC BASED QUANTITATIVE PROTEOMIC APPROACH

W. Yang, L. Wang, Z. Wang, J.W. Thompson, M.W. Foster, M.A. Moseley, W. Paschen

Duke University Medical Center, Durham, NC, USA

Objectives: Small ubiquitin-like modifier (SUMO1-3) is a group of small proteins binding to lysine residues of target proteins and thereby modifying their activity, stability and subcellular localization. SUMO2/3 conjugation has been shown to be dramatically activated after ischemia (1,2). We have also found that SUMO2/3 conjugation protects neurons from ischemia-like conditions (Daetwyler et al., Brain '11), suggesting that this is a protective stress response shielding neurons from damage induced by ischemia. In a first attempt to identify the main players in this process, we subjected neuroblastoma B35 cells to transient oxygen and glucose deprivation (OGD) and analyzed OGD-induced changes in the pattern of SUMO conjugated proteins using a SILAC (stable isotope labeling with amino acids in cell culture) based quantitative proteomic approach.

Methods: B35 cells were stably transfected with HA-SUMO3 and grown in normal medium (control), or heavy medium (OGD, lysine and arginine replaced by $^{13}C_6$ L-lysine and $^{13}C_6/^{15}N_4$ L-arginine). Cells were subjected to 6h OGD followed by various reoxygenation times. OGD-induced changes in SUMO conjugation were evaluated by Western blotting. For proteomic analysis, proteins were extracted from control and 30 min re-oxygenated cells when SUMO2/3 conjugation was maximally activated, and the same amount of proteins was mixed from both extracts. Proteins conjugated with HA-SUMO3 were pulled down, precipitated with aceton, and loaded onto NuPAGE 4-12% gels. After electrophoresis, the gel was cut into 5 slices for LC-MS/MS analysis (nanoAcquity and Synapt HDMS). Data analysis was performed in both Rosetta Elucidator and Scaffold. For verification of identified proteins, western blots were performed using the respective antibodies.

Results: Transient OGD induced a pattern of SUMO2/3 conjugation similar to that induced by transient ischemia *in vivo* (Figure 1). Using Scaffold and Elucidator Identification Metrics, we found 90 and 158 proteins respectively, identified by 2 or more unique peptides. Since we sliced gels into 5 samples, we could quantify changes in levels of individual SUMO3 conjugated proteins and shifts in the extent of SUMO conjugation. We found only very few proteins where SUMO3 conjugation was decreased after OGD. Several proteins were SUMO3 conjugated after OGD but not in control cells, including HNRPM and PIAS2, while some proteins showed a shift towards higher molecular weight, suggesting increased length of poly-SUMO chains or conjugation at multiple sites in post-OGD cells.

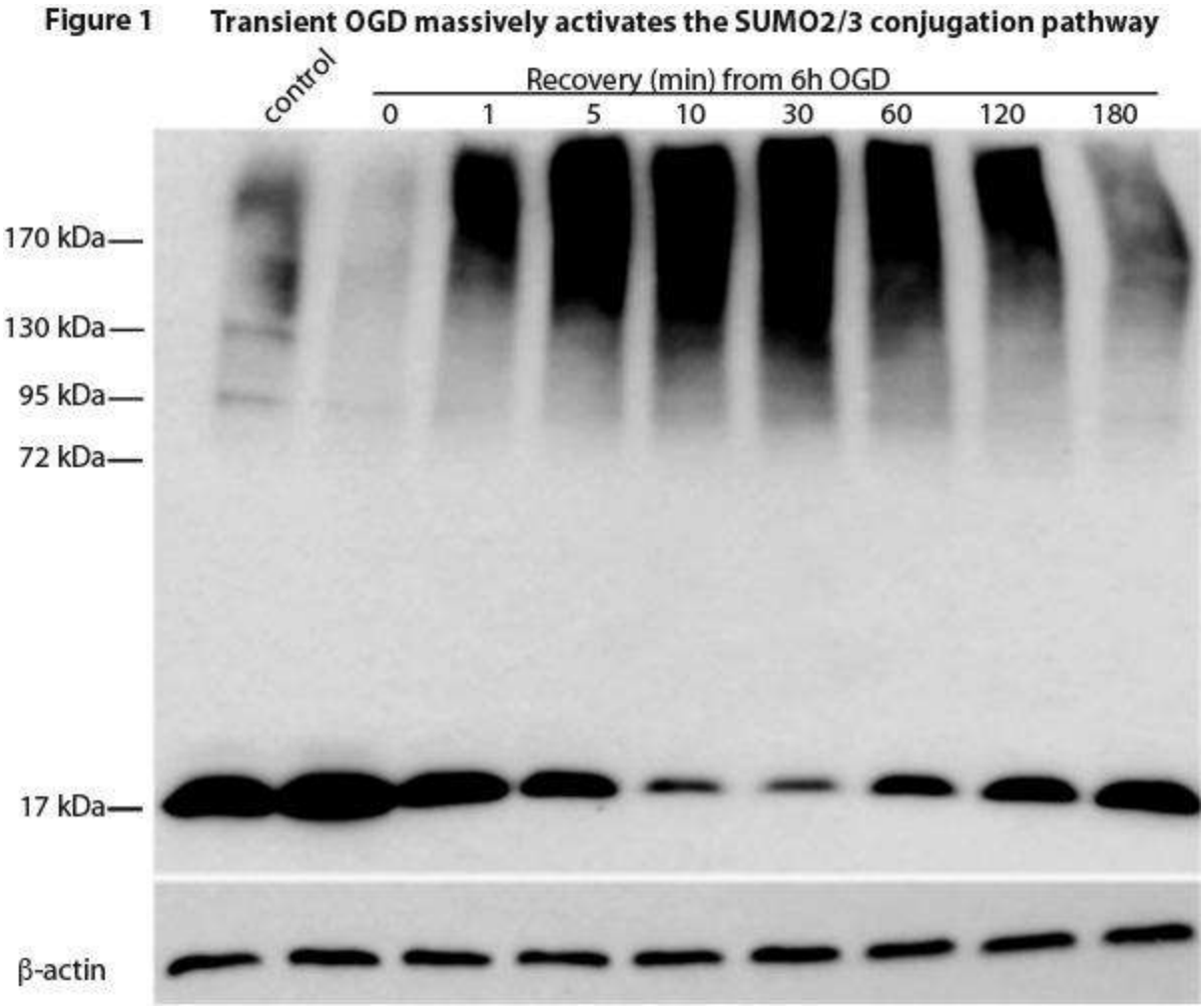

[Figure 1]

Conclusion: The SILAC based quantitative proteomic approach is an accurate means to identify differentially regulated proteins. Using this approach, we have identified some target proteins where SUMO conjugation was regulated by OGD treatment. Since a duration of OGD that produced only minor cell damage was used, we therefore expect identified targets to play a role in shielding cells from damage caused by a transient metabolic stress.

804

USE OF PRECISE CO2 MANIPULATION AND TRANSCRANIAL DOPPLER IN THE ASSESSMENT OF CEREBRAL AUTOREGULATION AFTER ANEURYSMAL SUBARACHNOID HEMORRHAGE

L. da Costa[1], D. Houlden[1], J. Fierstra[1], M. Schwartz[1], J. Fisher[2]

[1]Department of Surgery - Division of Neurosurgery, [2]Department of Anesthesia - Division of Neurosurgery, University of Toronto, Toronto, ON, Canada

Objectives: Transcranial Doppler is frequently used in the management of subarachnoid hemorrhage (SAH) patients. The most common use is as a tool to aid in the diagnosis of intracranial vasospasm. Cerebral autoregulation can be affected by SAH, and its state may be an important factor in many clinical decisions. The objective of this study was to access the utility of transcranial Doppler (TCD) coupled with precise CO_2 manipulation using a new re-breathing device, the Respiract®, in the evaluation of cerebral autoregulation after aneurysmal subarachnoid hemorrhage.

Methods: 25 healthy controls and 10 patients with SAH were screened. Bilateral TCD was used to record middle cerebral artery (MCA) blood flow velocity (BFV) coupled with precise CO_2 manipulation using the Respiract® re-breathing system. CO_2 was changed according to study protocol: CO_2 levels were normalized from baseline to 40 mmHg, kept stable for2 minutes, increased to 45 mmHg for 2 minutes and then decreased to 40 mmHg for another 2 minutes. Continuous bilateral TCD recording of middle cerebral artery blood flow velocity was done. Autoregulation was define as unit Δ MCA BFV / Δ PCO_2. Changes in MCA BFV and autoregulation were compared for each brain hemisphere between controls and patients. All aneurysms were secured either with microsurgical clipping or endovascular coiling before the test.

Results: Tests were performed between days 2 and 6 after SAH. The male:female ratio was higher in the SAH group than in the control (2, 1.67). SAH patients were also older (mean age = 54.5, controls - mean age = 38.6). Overall increase in MCA blood flow velocity occurred in both groups with increase in CO_2 levels. However, in controls MCA BFV showed a constant pattern of increased velocity with increased CO_2 levels with similar changes in both hemispheres. Autoregulation was intact, with quick and predictable response to CO_2. In SAH patients, blood flow velocity does not have an establish pattern, with different responses between SAH patients and even between hemispheres in the same patient. Autoregulation was found to be disturbed in most patients and differences between hemispheres in the same subject were frequent. This difference in response was not related to clinical condition at the time of the test.

Conclusion: TCD coupled with precise control of CO_2 levels is useful in accessing changes in autoregulation in patients with SAH. The MCA BFV response to CO_2 challenge was significantly reduced in SAH patients in both hemispheres (right $p=0.03$, left $p=0.05$). Our study confirms that autoregulation is affected by SAH and suggests that the change may not be symmetrical in the whole brain. Further investigation is required to access the relationship of this finding with delayed ischemic neurological deficits.

805

PET IMAGING OF CEREBRAL NICOTINIC ACETYLCHOLINE RECEPTORS (NACHRS) IN EARLY ALZHEIMER'S DISEASE (AD) ASSESSED WITH THE NEW RADIOLIGAND (-)-[18F]-NORCHLORO-FLUORO-HOMOEPIBATIDINE (NCFHEB)

O. Sabri[1], S. Wilke[1], S. Graef[2], P. Schoenknecht[2], B. Habermann[1], G. Becker[1], J. Luthardt[1], M. Patt[1], K. Kendziorra[1], P. Meyer[1], S. Hesse[1], G. Wagenknecht[3], A. Hoepping[4], U. Hegerl[2], P. Brust[5]

[1]Department of Nuclear Medicine, [2]Department of Psychiatry, University of Leipzig, Leipzig, [3]Central Institute for Electronics (ZEL), Research Center Juelich, Juelich, [4]Advanced Biochemical Compounds (ABX), Radeberg, [5]Research Site Leipzig, Helmholtz-Zentrum Dresden-Rossendorf, Leipzig, Germany

Objectives: Post mortem studies have shown a degeneration of cholinergic neurons in the brain of AD-patients. Further evidence suggests that the loss of nAChRs is a major contributor to the cognitive deterioration in AD, whereby the alpha4beta2-nAChR subtype is thought to be the most severely reduced in the onset of AD. Using 2-[18F]F-A85380 PET we showed a significant decline in alpha4beta2-nAChRs in early AD-patients which correlated significantly with the loss of cognitive function (1, 2). However, this tracer was not well suited as a biomarker in a routine clinical set-up for early AD-diagnosis because of unfavourable properties (slow kinetics, long acquisition times up to 7 hours, limited alpha4beta2-receptor selectivity). We, therefore, developed the new radiotracer [18F]NCFHEB (epibatidine derivative without toxicity in humans) with significantly improved brain uptake, nAChR affinity and selectivity (3). Here, we present the results of the worldwide first ongoing NCFHEB-PET study in humans.

Methods: 6 mild AD-patients (NINCDS-ADRDA, age 76.7±5.9, MMSE 23.8±3.0) and 5 age-matched healthy controls (HC, age 71.1±5.3, MMSE 28.4±1.1) underwent NCFHEB-PET (370 MBq, 3D-acquisition, ECAT Exact HR+). All were nonsmokers and naïve for central acting medication. In each subject, 4 scans (41 frames) were acquired from 0-270 min post injection and motion correction was performed with SPM2. Kinetic modeling was applied to the VOI-based tissue-activity curves generated for 29 brain regions (irregularly anatomically defined via MRI co-registration) using a one tissue compartment model with measured arterial input-function. Total distribution volume (DV) and binding potential (BP, reference region: corpus callosum) were used to characterize specific binding. Additionally, parametric images of DV were computed (Logan plot).

Results: Image quality of NCFHEB scans was clearly superior to 2-[18F]F-A85380, and a 20 minutes scan already adequate for visual analysis. All 29 regions were well described with one tissue compartment. PET data acquired over only 90 minutes were sufficient to estimate all kinetic parameters precisely indicating a fast receptor binding kinetic (much faster than for 2-[18F]F-A85380). DVs in HCs increase as expected with receptor density: Corpus callosum (DV: 4.81±0.32), posterior cingulate (8.92±0.66), temporal (9.03±0.44), pons (11.00±1.19), thalamus (24.32±2.96). The AD-patients showed extensive BP reductions in frontal, parietal, temporal, anterior and posterior cingulate cortices, caudate, and hippocampus (all $p < 0.05$) compared to HCs.

Conclusions: Due to the significant shorter acquisition time and superior image quality NCFHEB appears to be a much more valuable tracer than 2-[18F]F-A85380 to image alpha4beta2-nAChRs in humans. Early AD-patients show significant declines of alpha4beta2-

nAChRs in brain regions typically affected by AD-pathology. These results indicate that NCFHEB-PET has a great potential to be tested as a biomarker for early AD-diagnosis.

References:

1. O. Sabri, ..P. Brust: Acetylcholine receptors in dementia and mild cognitive impairment. Eur J Nucl Med Mol Imaging 2008; 35 (Suppl. 1): 30-45.

2. K. Kendziorra, ..O. Sabri: Decreased cerebral a4ß2 nicotinic acetylcholine receptors in living patients with mild cognitive impairment and Alzheimer disease with positron emission tomography. Eur J Nucl Med Mol Imaging 2010; DOI 10.1007/s00259-010-1644-5.

3. P. Brust, ..O. Sabri: In-vivo measurement of nicotinic acetylcholine receptors with [18F]norchloro-fluoro-homoepibatidine (NCFHEB). Synapse 2008; 62: 205-218.

808

AWAKE ANIMAL SPECT/CT TO STUDY THE EFFECTS OF ANESTHESIA ON THE UPTAKE OF ^{123}I-DATSCAN™

H. Jung[1], J. Baba[2], C. Endres[1], J. Goddard[2], S.J. Lee[3], J. McKisson[3], S. Nimmagadda[1], M. Pomper[1], M. Smith[4], A. Stolin[5], A. Weisenberger[3]

[1]Radiology, Johns Hopkins University, Baltimore, MD, [2]Measurement Science & Systems Engineering Division, Oak Ridge National Laboratory, Oak Ridge, TN, [3]Radiation Detector and Imaging Group, Thomas Jefferson National Accelerator Facility, Newport News, VA, [4]Radiology, University of Maryland, Baltimore, MD, [5]Radiology, West Virginia University, Morgantown, VA, USA

Objective: Apply awake animal SPECT/CT to investigate the effect of anesthesia on the uptake of ^{123}I-DaTSCAN™ in mouse striatum.

Method: A SPECT / X-ray CT system capable of imaging unrestrained, un-anesthetized mice was used in this study. The system was built by Thomas Jefferson National Accelerator Facility and Oak Ridge National Laboratory[1]. The SPECT-CT system is built around a modified MicroCAT II Small Animal Imaging system equipped with 80 kV (max), 40W x-ray source and CCD based x-ray detector. SPECT imaging was accomplished using a pin hole equipped custom gamma camera 10 cm x 20 cm in size composed of a 2 x 4 array of Hamamatsu H8500 flat panel position sensitive photomultiplier tubes. A real-time optical tracking system utilizing three infrared cameras provides time stamped pose data of an awake mouse's head during a SPECT scan[2]. The six degrees of freedom (three translational and three rotational) pose data are used for motion correction during tomographic list-mode iterative image reconstruction[3].

Twelve mice were used in this study including five awake and seven anesthetized with 2% isoflurane. For each mouse, small regions on the head had the fur thinned to allow gluing attachment of three hemispherical IR reflective markers. Mice were injected via tail vain with the dopamine transporter ligand ^{123}I DaTSCAN™ (4.52±0.23 mCi), then placed ina a transparent cylindrical burrow and positioned for brain imaging. Two 25 minute scans were acquired at 15 minutes and 45 minutes post injection.

Results: On average 10% of pose data in awake animals were unavailable because of loss of tracking, and the corresponding SPECT list-mode data were discarded. The remaining SPECT data were reconstructed using 3D-MLEM. SPECT and CT images were co-registered manually. Regions of interest were drawn, and tracer activity computed, in left and right striata (STR), and cerebellum (CER). Tracer binding potential (BP) was calculated as STR/CER-1. For the first scan (15-40 minutes post-injection), there was roughly a 20% decrease in striatal BP in awake mice relative to anesthetized, but the difference was not statistically significant. For the 2nd scan (45-70 minutes post-injection), there was over a 30% statistically significant decrease seen in the awake mice (Table 1).

	1st scan Left BP	1st scan Right BP	2nd scan Left BP	2nd scan Right BP

Anesthetized	1.52±0.50	1.49±0.56	2.00±0.38	1.95±0.33
Awake	1.11±0.09	1.23±0.17	1.31±0.26	1.36±0.19
TTESTS	0.107	0.35	0.005	0.005

[Table 1]

Conclusions: This study demonstrated significantly higher uptake of DaTSCAN™ in striata of anesthetized mice as compared to awake mice, indicating that anesthesia can have a substantial effect on tracer studies. The awake animal SPECT system is useful for investigating distinct tracer pharmacokinetics in awake animals.

References:

[1] Weisenberger, A.G., et al, IEEE Transactions on Nuclear Science, vol., 52, no. 3, June 2005.

[2] Goddard, J.S., et al., Conference Record of the 2008 IEEE Nuclear Science Symposium and Medical Imaging Conference, Dresden, 2008

[3] Weisenberger, A.G., et al, Conference Record of the 2008 IEEE Nuclear Science Symposium and Medical Imaging Conference, Dresden, 2008.

810

CELLULAR RESPONSE OF CEREBRAL WHITE MATTER TO CARDIOPULMONARY BYPASS IN A PORCINE BYPASS SURVIVAL MODEL

N. Ishibashi[1], J. Scafidi[2], A. Murata[1], L. Korotcova[1], D. Zurakowski[3], V. Gallo[2], R.A. Jonas[1]

[1]Children's National Heart Institute, [2]Center for Neuroscience Research, Children's National Medical Center, Washington, DC, [3]Department of Surgery, Children's Hospital Boston, Boston, MA, USA

Objectives: Clinical MRI studies have demonstrated a high incidence of white matter (WM) injury after neonatal cardiac surgery leading some to suggest that surgery should be avoided in this population. The purpose of this study is to investigate the WM cellular response to cardiopulmonary bypass (CPB) using neonatal piglets. This study will elucidate the risk of surgery in neonates and young infants.

Methods: We evaluated normal WM development in three age-group piglets (1week, 3week, and 7week). Thirty animals were assigned to one of 3 different CPB induced brain insults: i) no surgery (Control); ii) 34^{o}C full-flow bypass for 60min (Mild-CPB insult; Systemic Inflammatory Response Syndrome (SIRS)); and iii) 25^{o}C circulatory arrest for 60min (Severe-CPB insult; SIRS and I/R-injury). Cerebral tissue-oxygenation index (TOI) was measured by NIRS and systemic inflammation was assessed by plasma IL-6 concentration. Cellular response in 5 WM regions [Corpus Callosum (CC), Medial- and Lateral-Periventricular WM (M- and L-PVWM), Internal Capsule (IC), Subcortical WM (SCWM)] was assessed on postoperative day 3 and week 4 using established markers of oligodendrocyte (OL) lineage cells.

Results: Myelin basic protein (MBP) expression in CC and M-PVWM significantly increased with age, while the expression in other areas did not change. Transcription factor Olig2+ OL lineage cells and CC1+ mature OLs numbers in CC and M-PVWM also significantly increased with age; however, the numbers in IC decreased. There were no significant differences in L-PVWM and SCWM, indicating that WM development in IC preceded L-PVWM and SCWM followed by CC and M-PVWM. In CPB groups, Severe-CPB insult significantly increased caspase3+ numbers in all WM area, whereas Mild-CPB insult did not cause injury. The number of O4+/caspase3+ immature OLs was significantly greater than the number of CC1+/caspase3+ OLs. This suggests that O4+ OLs are more vulnerable to CPB induced brain insults compared with CC1+ OLs. The caspase3+ numbers differed significantly according to WM area, and the numbers were inversely correlated with advancing maturation stage. At 4weeks after surgery, Olig2+ OL lineage cell numbers were not different among groups; while CC1+ OLs after Severe-CPB insult, but not Mild-CPB insult, were significantly reduced. Similarly, MBP expression after Severe-CPB insult was significantly reduced. Furthermore, the percentage of Olig2+/CC1- immature OLs after Severe-CPB insult was significantly increased compared with Control and Mild-CPB insult, suggesting that Severe-CPB insult causes arrested OL maturation and/or delayed myelination. When the logistic regression model was applied, there were significant inverse relationships between damage probability and TOI as well as maturation stages. The model also indicated that maintaining high TOI minimizes the risk of WM damage independent of maturation stage. Similarly, a high level of inflammation had a significant effect on caspase3+ numbers; however, this effect is observed only for immature areas. On the other hand, when IL-6 was less than 250pg/ml, there were no significant differences in caspase-3+ numbers between maturation stages.

Conclusions: Severe-CPB insult causes significant WM injury, while mild insult carries minimal

risk. Cardiac surgery in neonates and young infants should therefore avoid I/R injury and efforts should be made to reduce inflammation.

811

IMAGING OF INHIBITORY NEUROTRANSMISSION IN CHRONIC PAIN

B.R. Foerster[1], M. Petrou[1], N.L. Hoefling[1], T.L. Chenevert[1], P.C. Sundgren[1], D.J. Clauw[2], R.E. Harris[2]

[1]Radiology, [2]Anesthesiology, University of Michigan, Ann Arbor, MI, USA

Objective: Widespread pain sensitivity in fibromyalgia subjects suggests a central nervous system (CNS) processing problem. Several neuroimaging studies have reported increased in 'Glx' (combined measure of glutamate and glutamine) in pain processing regions in the brain suggesting an elevation in exicitatory neurotransmitters [1,2]. However, there is a paucity of data evaluating the neuroinhibitory pathway in chronic pain. The purpose of this study was to assess for decreases in of gamma-aminobutyric acid (GABA), the major inhibitory neurotransmitter in the CNS, (as measured by magnetic resonance spectroscopy imaging) in a number of brain regions implicated in pain processing in fibromyalgia subjects compared to healthy controls.

Methods: The subjects in this study were eleven female subjects (aged 22-52 years, mean age 33.7 years) who met the 1990 American College of Rheumatology (ACR) criteria for fibromyalgia as well as 9 female healthy controls (aged 22-52 years, mean age 31.4 years). MRI examinations were performed on a Philips Achieva 3T MRI (Best, Netherlands). Subjects underwent conventional MR point resolved spectroscopy (PRESS); the MR spectral editing technique, MEGA-PRESS [3], was used to measure GABA relative to NAA. Voxels were placed in brain regions which have been implicated in pain processing in other neuroimaging studies including the anterior insula, posterior insula and the anterior cingulate cortex. LCModel was used to calculate creatine, choline, N-acetylaspartate (NAA), myo-inositol and Glx concentrations. Determination of GABA/NAA ratio as well as GABA concentrations were carried out in Matlab (The Mathworks, Natick, MA) using in-house software. GABA concentrations were quantified in institutional units (i.u.) as the ratio between the GABA integral and the NAA integral multiplied by the NAA concentration calculated in LCModel. Differences in GABA measurements between the different brain regions were analyzed using unpaired t-tests ($p< 0.05$).

Results: There was a significantly lower GABA/NAA ratio in the posterior insula in fibromyalgia subjects (0.219 ± 0.013) compared to healthy controls (0.244 ± 0.032; $p = 0.03$). There was also a significantly lower GABA concentration in the posterior insula in fibromyalgia subjects (1.443 i.u. ± 0.164)) compared to healthy controls (1.645 i.u. ± 0.262; $p = 0.05$). There were no significant differences in the GABA/NAA ratios or GABA concentration in the anterior insula or the anterior cingulate cortex.

Conclusion: Diminished inhibitory neurotransmission resulting from lower concentrations of GABA within the posterior insula may play a role in the pathophysiology of FM and other central pain augmentation syndromes.

References:

1. Harris RE, Sundgren PC, Craig AD, et al. Elevated insular glutamate in fibromyalgia is associated with experimental pain. *Arthritis Rheum* 2009;60:3146-3152.

2. Harris RE, Sundgren PC, Pang Y, et al. Dynamic levels of glutamate within the insula are

associated with improvements in multiple pain domains in fibromyalgia. *Arthritis Rheum* 2008;58:903-907.

3. Mescher M, Merkle H, Kirsch J, et al. Simultaneous in vivo spectral editing and water suppression. *NMR Biomed* 1998;11:266-272.

813

TRACER KINETIC RESPONSES TO PROPOFOL-INDUCED REDUCTION OF BRAIN PERFUSION: COMPARISON OF [11C]YOHIMBINE AND [11C]SCH23390

J.E. Holden[1], S. Jakobsen[2], A.K. Olsen Alstrup[2], D.J. Doudet[3,4], A. Landau[3]

[1]Medical Physics, University of Wisconsin-Madison, Madison, WI, USA, [2]PET Center, [3]PET Center and Center of Functionally Integrative Neuroscience, Aarhus University Hospital, Aarhus, Denmark, [4]Department of Medicine/Neurology, University of British Columbia, Vancouver, BC, Canada

Objective: The baseline scans from two studies, performed in Göttingen minipig with the tracers [11C]yohimbine and [11C]SCH23390 respectively, but with different anesthetics, have provided the opportunity to study the variety of kinetic responses to the known reductions in brain perfusion caused by the anesthetic propofol [1].

Methods: Ninety-minute dynamic PET studies were performed in 10 animals with yohimbine and in 12 animals with SCH23390; in both cases half with isoflurane (2%) and half with intravenous propofol (3.8 mg/kg/h). Time-activity curves (TACs) were generated from cortical and sub-cortical regions and analyzed using both Logan analysis [2,3] and UGA [4] (yohimbine: plasma-input; SCH23390: cerebellum tissue-input) UGA is an extension of modified Patlak analysis [5] that estimates uptake rate constant (Ki) and distribution volume (DV) for plasma-input, or normalized uptake rate constant (Ki*) and distribution volume ratio (DVR) for tissue-input. The first-order rate constant for the loss of tracer from the most slowly clearing kinetic component (kloss) is also estimated.

Results: There were no effects due to anesthetic in the yohimbine results (Table 1:average of five regions). In contrast, for SCH23390 (Table 2) Ki* values with propofol were about 2/3 those with isofluorane in all regions. Striatal kloss was very similar for the two anesthetics, and thus the DVR values were reduced by the same 2/3 factor. However, non-striatal kloss values fell by the same factor as the Ki* values, resulting in similar values of the DVR for the two anesthetics. The Logan plots showed positive curvature throughout the studies for SCH23390.

Anesthetic	Ki (mL/g min)	kloss (1/min)	UGA DV (mL/g)	Logan DV (mL/g)
isoflurane	0.189(0.03)	0.040(0.007)	4.73(0.67)	4.59(0.66)
propofol	0.187(0.03)	0.039(0.008)	4.94(1.23)	4.81(1.20)

[Table 1. Yohimbine (mean(std)n=5)]

Region	Anesthetic	Ki* (1/min)	kloss (1/min)	UGA DVR	Logan DVR
Striatum	isoflurane	0.0465(0.018)	0.009(0.004)	6.22(1.71)	5.13(1.17)
	propofol	0.0298(0.008)	0.010(0.003)	4.02(1.06)	3.00(0.64)
Extra-striatal	isoflurane	0.0268(0.008)	0.032(0.011)	1.63(0.28)	1.58(0.25)
	propofol	0.0166(0.007)	0.023(0.010)	1.65(0.47)	1.44(0.25)

[Table 2. SCH23390(mean(std)n=6)]

Discussion: The absence of any anesthetic effects on uptake or loss for yohimbine remains unexplained. For SCH23390 both Ki* and kloss were sensitive to propofol-induced changes in regions of low specific binding, and cancellation of the two effects led to preservation of the DVR. The large DVR in striatum is due to both increased uptake and diminished loss rate. Propofol reduced the uptake rate, but failed to further diminish the loss rate, resulting in a significant ($p < 0.02$) reduction of the DVR relative to that measured under isoflurane.

References:

[1] Moss and Price Br J Anaesth. (1990) 65:823-5.

[2] Logan et al JCBFM (1990) 10:740-747.

[3] Logan et al JCBFM (1996) 16:834-840.

[4] Graner et al Neuroimage (2008) 41: (supp 2) T24

[5]] Patlak and Blasberg JCBFM (1985) 5: 545-553

814

TIME COURSE FOR EXPRESSION OF VASCULAR ENDOTHELIN ET_B RECEPTORS AFTER EXPERIMENTAL STROKE IN THE RAT

L. Edvinsson[1], K.A. Kristiansen[2], G.K. Povlsen[2], J. Hansen-Schwartz[3], F.F. Johansen[3]

[1]Lund University, Lund, Sweden, [2]Glostrup Research Institute, Glostrup University Hospital, [3]University of Copenhagen, Copenhagen, Denmark

Objectives: Several experimental stroke models have been used to investigate pathophysiological mechanisms involved in upregulation of contractile receptors that follow a cerebral ischemic attack. Thrombo-embolic stroke gives rise to an immediately infarcted volume of tissue surrounded by a critically perfused penumbra, which is potentially salvageable. The fate of this penumbral tissue and in consequence the neurological outcome is dependent on restoration of perfusion. Since changes in the expression of vasoconstrictor receptors in cerebral arteries may disturb the perfusion of ischemic regions after a stroke, we have examined the time-dependent upregulation of the contractile endothelin-B (ET_B) receptors in cerebral arteries following occlusion and reperfusion.

Methods: Male Wistar rats underwent craniotomy and the right middle cerebral artery (MCA) was occluded for 120 minutes with a microsurgical hook, followed by reperfusion. Using confocal microscopy for analysis of receptor protein and myographs for assessment of ET_B receptor-mediated contractile responses, we studied the time course over a 48 hour period of ET_B receptor expression in the MCA. For comparison, isolated MCA segments subjected to organ culture were used as a model of ET_B receptor upregulation. Contractile responses were obtained by cumulative application of sarafotoxin 6c (S6c, a selective ET_B receptor agonist) at 1, 24 and 48 hours after occlusion. Contractile response is given as % of responses induced by 125 mM K^+ or in milli Newton (mN). Protein localization and levels were examined by immunohistochemistry.

Results: The occluded and reperfused MCA became significantly more sensitive to the contractile ET_B agonist S6c at 24 hrs, with responses declining at 48 hrs. In MCA from fresh rats there was no contractile effect of S6c. After one hour of reperfusion, a contractile response with an E_{max} of 17±11% with a pD_2 of 9.5±0.2 was observed. After 24 hours of reperfusion, E_{max} had increased to 94±3% ($p< 0.05$), dropping to 45±11% after 48 hours of reperfusion. The pD_2 values at 24 and 48 were not significantly different compared to the pD_2 at 1 hour after reperfusion.

Concomitantly, the immunohistochemical staining showed a significant increase in ET_B receptor protein at 24 hours subsiding at 48 hours. In MCA segments subjected to organ culture, the protein levels rose significantly over the entire period of activation, in parallel with elevated contractile responses to S6c.

Conclusions: Functional ET_B receptor upregulation has been established as an observed phenomenon both after whole vessel culture as well as in rat models of focal cerebral ischemia and subarachnoid haemorrhage. The present data clearly shows that the increased functional response of the ET_B receptor corresponds to an increase in ET_B receptor protein in the smooth muscle cells within the cerebral vessel walls during reperfusion after experimental stroke. Thus, the increased contractile ET_B receptor response was associated with an increase in receptor protein in this stroke model with an optimum ET_B receptor upregulation after 24 hours of reperfusion.

815

TITLE: PPARA AGONISTS DILATE THE MOUSE MIDDLE CEREBRAL ARTERY AND DELETION OF PPARA CAUSES ENDOTHELIAL DYSFUNCTION

J. Andresen[1], N.K. Parelkar[2]

[1]University of Missouri-Kansas City, Kansas City, MO, [2]University of Arkansas for Medical Sciences, Little Rock, AR, USA

Introduction: Peroxisome proliferator activated receptors (PPARs) are nuclear hormone receptors that are divided into three subtypes PPARα, PPARβ, and PPARγ. PPAR agonists are clinically important and have cardioprotective and lipid lowering effects and deletion of PPARγ causes cerebrovascular dysfunction and hypertension.

Objective: The purpose of this study was to investigate the cerebrovascular role of PPARα by examining vasomotor function in mice deficient for PPARα (Pparα-/-) and by determining if PPARα agonists could acutely alter vascular diameter.

Background: PPARα is important for fatty acid metabolism, glucose homeostasis, and the inflammatory response. PPARα is widely expressed in the vasculature including in the middle cerebral artery (MCA). Chronic treatment with PPARα agonists promoted endothelium-dependent dilation of the MCA and increased endothelial nitric oxide synthase expression in cultured endothelial cells. Potent and selective PPARα agonists are also known to have acute effects although this has not been examined in the vasculature.

Materials and methods: Pharmacological PPARα agonists included gemfibrozil, WY14643, and GW7647. Vascular function of wild-type (WT) and Pparα-/- mice was assessed using isobaric myography for the MCA and isometric tension myography for the aorta. Fura-2 ratiometric calcium imaging studies were performed in vitro using mouse aortic smooth muscle cells (MOVAS).

Results: PPARα protein was detected throughout the wall of the MCA by immunofluorescence. Acute application of PPARα agonists concentration-dependently dilated pressurized MCAs of WT mice in an endothelium-independent manner where the more selective the PPARα agonist, the more potent was the vasodilation. The maximum dilation to gemfibrozil at 10-4 M was only 28±6% whereas WY14643 and GW7647 both elicited greater than 90% dilation. GW7647 with a log EC50 of -5.86±0.14 was, however, nearly 50-fold more potent than WY14643. Dilation to GW7647 was resistant to inhibition of nitric oxide synthase, cyclooxygenase, potassium channels, and occurred even in MCAs from Pparα-/- mice. GW7647 maximally dilated MCAs preconstricted with the L-type calcium channel activator Bay K8644. Likewise, in MOVAS cells GW7647 prevented depolarization- (with 100 mM KCl) or agonist-induced (with Bay K8644) elevations of intracellular calcium. Endothelium-dependent responses were selectively impaired in both the MCA and aorta of Pparα-/- mice. Dilation of the MCA to acetylcholine (ACh) and Bradykinin was reduced by 11% and 16% respectively in Pparα-/- mice vs. WT mice. Likewise, relaxation of the aorta to ACh was reduced by 30% in Pparα-/- mice. Agonist and depolarization-induced contractions were unimpaired in either the MCA or aorta of Pparα-/- mice. Similarly, endothelium-independent dilations were also indistinguishable from WT in Pparα-/- mice.

Conclusions: Pharmacological PPARα agonists are excellent endothelium-and PPARα-independent vasodilators that appear to act by inhibiting L-type calcium channels. Genetic

deletion of PPARα impairs endothelial function of the aorta and of the MCA. Thus, chronic treatment with PPARα agonists may have both direct and indirect benefits for the cerebrovasculature.

816

GLOBAL CEREBRAL EDEMA AND BRAIN METABOLISM AFTER SUBARACHNOID HEMORRHAGE

R. Helbok[1,2], S.-B. Ko[2], M. Schmidt[2], S.E. Connolly[2], K. Lee[2], N. Badjatia[2], S.A. Mayer[2], J. Claassen[2]

[1]Clinical Department of Neurology, Neurocritical Care Unit, Medical University Innsbruck, Innsbruck, Austria, [2]Columbia University Medical Center, Department of Neurology, Division of Neurocritical Care, NY, NY, USA

Introduction: Global cerebral edema (GCE) is common amongst poor-grade subarachnoid hemorrhage (SAH) patients and associated with poor outcome. Currently no targeted therapy exists largely due to an incomplete understanding of the underlying mechanisms.

Methods: This is a prospective observational study including 39 consecutive poor-grade SAH patients with multimodal neuromonitoring. Levels of microdialysate lactate/pyruvate ratio (LPR), episodes of cerebral metabolic crisis (MC; LPR >40 and brain-glucose < 0.7 mmol/L), brain tissue oxygen tension (PbtO2), cerebral perfusion pressure (CPP), and transcranial Doppler sonography flow velocities were analyzed.

Results: Median age was 54 years (45-61) and 62% were female. Patients with GCE on admission (n=24, 62%) had a higher incidence of MC in the first 12 hours of monitoring than those without GCE (n=15; 15% v.s. 2%, $P< 0.05$) and during total time of neuromonitoring (20% v.s. 3%, $P< 0.001$). There was no difference in PbtO2 and CPP between the groups, however, in patients with GCE a higher CPP was associated with lower LPR ($P< 0.05$). Episodes of crisis were associated with poor outcome (modified Rankin Score 5 or 6, $P< 0.05$).

Conclusions: In poor-grade SAH patients, GCE is associated with early brain metabolic distress. Optimizing cerebral blood flow and homeostasis early after SAH may prove beneficial for patients with GCE.

817

ACUTE ETHANOL ADMINISTRATION REDUCES METABOLIC DISORDER AND APOPTOSIS IN ISCHEMIC STROKE

Y. Ding, R. Kochanski, T. Higashida, C. Peng, M. Guthikonda

Wayne State University School of Medicine, Detroit, MI, USA

An elevated blood ethanol level is associated with increased survival in patients with moderate to severe traumatic brain injury (TBI), suggesting that an acute exposure to a relatively high dose of alcohol is neuroprotective. In the present study, the potential neuroprotective benefits of acute alcohol intoxication in ischemic stroke were determined. Hypoxia inducible factor (HIF)-1a is a master regulator of the cellular response to hypoxic stress. HIF-1a expression likely mediates both adaptive and pathological functions by regulating multiple genes, including glycolytic enzymes and apoptotic proteins. In the present study, we determined whether post-stroke ethanol administration induced neuroprotection by regulating glycolysis in association with HIF-1a up-regulation.

Adult male Sprague Dawley rats were subjected to a 2-hour middle cerebral artery (MCA) occlusion using an intraluminal filament, followed by 3 or 24 hour reperfusion. Ischemic animals were administered with ethanol at doses of 0.5, 1.0 and 1.5g/kg prior to reperfusion. Pro-apoptotic protein expression (caspase-3 and Apoptosis-inducing factor, AIF) was determined by Western blot. Cerebral metabolism was determined by ADP/ATP ratio and brain glycolysis was determined by glycolytic enzyme expression [Lactate dehydrogenase (LDH), phosphoryated 5'AMP-activated protein kinase (pAMPK) and Phosphofructokinase-1 (PFK-1) protein levels]. Protein levels of HIF-1a were analyzed using Western blot in ischemic rats.

Our preliminary data reveals that acute administration of ethanol at a moderate dose of 1.5 g/kg, which translates to a blood alcohol content barely above the legal limit for driving (80mg/dL), most effectively reduced protein expression of caspase-3 and AIF at 3 and 24 hours after reperfusion in association with enhanced expression of HIF-1a at these two time points. Ethanol also reduced the ADP/ATP ratio in the ischemic brain in association with normalized glycolytic enzyme expression after reperfusion at 3 and 24 hours.

The data from this study assesses the feasibility of a novel investigation of administration of ethanol in stroke therapy. The work presented here suggests that acute moderate ethanol administration induces neuroprotection by regulating brain metabolism and glycolysis through the HIF-1a signaling pathway. This data could lead to a preclinical therapy development for stroke patients.

818

ARTERIAL CONTRIBUTION TO THE BOLD AND CBF FMRI RESPONSE TO SOMATOSENSORY STIMULATION IN RATS

Y. Hirano, A.C. Silva

CMU, LFMI, NINDS, NIH, Bethesda, MD, USA

Introduction: Biophysical models of BOLD have assumed full oxygen saturation of the arterial vasculature (Ogawa et al., Biophys J. 1993; Davis et al., PNAS 1998), so that BOLD originates in the capillaries and the venous vasculature. Recently, optical imaging experiments coupled with direct PO_2 measurements showed a significant oxygen loss from large arteries to arterioles in the cerebral cortex, with the largest fractional increases in oxygenation upon functional activation occurring in the arterial vasculature (Vazquez AL et al., JCBFM 2010), implying that a measurable fraction of the BOLD response may be of arterial origin. Here, we measured the BOLD and CBF fMRI responses to somatosensory stimulation in α-chloralose anesthetized rats under different levels of arterial oxygenation to examine the arterial contribution to BOLD.

Methods: Adult Sprague-Dawley rats (n=6, 298±40g) were orally intubated and anesthetized with α-chloralose. Simultaneous BOLD and CBF-fMRI was performed at 7T using the dynamic ASL (DASL) sequence (Barbier EL et al., MRM 2001) with parameters: TE/TR=25/250ms, spatial resolution=400×400×2000μm^2, acquisition bandwidth=170kHz. A pair of needle electrodes was inserted into each forelimb and bilateral forepaw stimulation was accomplished by paired electrical stimulation (333μs-pulses, 2mA-amplitude, 3Hz) for 4s in each 30s epoch. The fraction of inspired oxygen (FiO2) was varied between 21% and 40% in different fMRI sessions. Arterial blood gasses were sampled periodically during experiments. Moderate hypoxia, normoxia and hyperoxia states were defined for each animal based on PaO2. Region-of-interest analysis of the BOLD and CBF responses to somatosensory stimulation was performed.

Results: PaO2 were 71.3±11.3, 98.6±8.8 and 144.3±21.4mmHg in hypoxia, normoxia and hyperoxia, respectively. Robust BOLD and CBF responses were obtained in all conditions. The BOLD response obtained in normoxia had the highest peak amplitude, while responses obtained during normoxia and hyperoxia were smaller. The amplitudes of the CBF responses in normoxia or hypoxia were similar, slightly higher than the response in hyperoxia. Hypoxia caused a significant delay in the onset-time (OT) and time-to-half-maximum (THM) of the BOLD response compared to normoxia, but the times-to-peak (TTP) under all conditions were similar. The different levels of arterial oxygenation had no effect on the CBF OT, THM and TTP, which were all significantly shorter than their respective BOLD counterparts. Relative to normoxia and hyperoxia, hypoxia significantly increased the OT difference between CBF and BOLD, indicating a significant delay in onset of BOLD.

Conclusion: Moderate hypoxia affected neither the amplitude nor the OT of the CBF response to somatosensory stimulation, suggesting that the CBF response is not critically dependent on the level of arterial oxygenation. Interestingly, under normoxia and hyperoxia, the OT difference between CBF and BOLD (~150ms) is significantly shorter than the arteriole-venule transit-time (~0.5s) (Hutchinson EB et al., Neuroimage 2006), suggesting that at least some small fraction of the BOLD response comes from the arterial side of the vasculature. Hypoxia significantly extended the BOLD OT, elongating the transit of oxygen across the vasculature. Based on the BOLD amplitude at 0.5s following stimulus onset, we estimate that the relative arterial contribution to the overall BOLD response is ~5%.

819

NICOTINE AND ESTROGEN SYNERGISTICALLY EXACERBATE CEREBRAL ISCHEMIC INJURY

A.P. Raval[1], N. Hirsch[1], K.R. Dave[1], H. Bramlett[2], I. Saul[1]

[1]Neurology, [2]Neurological Surgery, University of Miami, Miami, FL, USA

Objectives: Nicotine addiction elevates risk of cardiac arrest, which is magnified in women smokers using oral contraception (OC). Cardiac arrest typically results in global cerebral ischemia (GCI) causing delayed neuronal death in the hippocampal CA1 region. Here we examined the hypotheses that a nicotine plus OC (NOC) exacerbates post-ischemic hippocampal damage in female rats, and nicotine directly inhibits estrogen-mediated intracellular signaling in the hippocampus.

Methods: Female Sprague-Dawley rats (290±20g) were implanted with osmotic pumps containing nicotine (in saline) for 16 days. To mimic OC use in women, nicotine/saline-exposed rats were administered OC (3 days) + placebo (1 day) orally. At end of these treatments (day 16) rats were exposed to an episode of GCI (10 min of bilateral carotid occlusion and systemic hypotension (50mmHg)) and brains were examined for histopathology at 7 days of reperfusion. Further, to identify direct inhibitory effects of nicotine on estrogen signaling in hippocampus we used an organotypic slice culture model of GCI. Slices were exposed to nicotine (100ng/ml in saline) for 15 days. In a second set of experiments, slices were transiently exposed to 17beta-estradiol (1nM; 4h) on day 13 of nicotine/saline exposure. On day 15 slices were exposed to oxygen-glucose deprivation for 40 min or collected for western blot analysis of phosphorylated cyclic-AMP response element binding (CREB) protein. Results are expressed as mean ± SEM. Statistical significance was determined with an ANOVA test followed by a Bonferroni's post-hoc test.

Results: The data are expressed as a percentage of surviving neurons of the sham (saline-treated rats without GCI). The number of normal neurons in the CA1 hippocampal region in sham rats was 1204 ± 105 (n=6), and administered GCI to saline-treated rats decreased the normal neuronal count to 44% (525 ± 22, n=6; $p < 0.001$). Nicotine exposure followed by GCI decreased the neuron count to 368 ± 56 (n=6), which amounted to 32% of normal neurons. OC treatment alone did not significantly affect the post-ischemic number of normal neurons (567±21; n=6) as compared to saline group. GCI insult to NOC rats resulted in only 16% (197±13; n=6) normal neurons as compared to sham. Interestingly, we observed a significant ($p < 0.001$) difference in the post-ischemic number of normal neurons between nicotine alone and the NOC group. These results demonstrate that NOC did indeed exacerbate post-ischemic CA1 damage as compared to nicotine alone in naive female rats. In slice cultures, we found that nicotine alone or with 17beta-estradiol directly inhibits phosphorylation of CREB, a process required for neuronal survival and also exacerbates ischemic damage.

Conclusions: Nicotine can affect the outcome of cerebral ischemia by influencing brain endocrine function directly rather than through indirect systemic effects.

Grant support: AHA-SDG-#0730089N and James and Esther King Biomedical Research Program# 07KN-10 (APR)

821

REAL-TIME MONITORING OF BRAIN MITOCHONDRIAL FUNCTION AND CEREBRAL BLOOD FLOW BEFORE, DURING AND FOLLOWING FOCAL ISCHEMIA

A. Mayevsky, E. Barbiro-Michaely, A. Livnat

The Mina & Everard Goodman Faculty of Life-Sciences, Bar-Ilan University, Ramat-Gan, Israel

Objectives: Focal ischemia leads to a gradual injury, ranging from severe injury in the core of the lesion towards moderate damage in penumbral regions. The difference in blood supply to these 2 areas affects the metabolic balance in the tissue, leading to lower ATP levels and a massive mitochondrial injury in the core, while the penumbra suffers from limited mitochondrial damage. The present study introduces a novel method, which combines the evaluation of cerebral blood flow (CBF) and mitochondrial function in the core and the penumbra, before, during and following focal cerebral ischemia in various degrees of severity.

Methods: Wistar rats underwent focal cerebral ischemia by MCAO for 10, 30 and 60 minutes, followed by reperfusion. Animals were monitored using a unique Multi-Site - Multi-Parametric (MSMP) system, which measures mitochondrial NADH redox state using surfaceflourometry and CBF using Laser Doppler Flowmetry (LDF).

Results: At the onset of the occlusion, CBF decreased and NADH increased significantly. In the 3 ischemic durations, CBF levels were significantly lower and NADH levels were significantly higher in the core compared to the penumbra. Three minutes following the occlusion, reflectance levels increased in the core, but not in the penumbra, remaining in higher than baseline levels throughout the ischemic period. At reperfusion, CBF increased and NADH decreased in both core and penumbra. As the ischemic period was shorter, the hyperemic response seen in CBF was higher. Ischemia for 60 minutes led to the disappearance of the hyperemic response in CBF following reperfusion. Mitochondrial activity following reperfusion was higher than baseline following 10 and 30 minutes, but not following 60 minutes of ischemia.

Conclusions: Our show that ischemic damage increase according to duration and location in the brain. These results demonstrate the importance of the MSMP system in stroke monitoring, by adding information regarding cerebral metabolic state under ischemic conditions, with emphasis on mitochondrial function.

References:

1. Livnat A, Tolmasov M, Barbiro-Michaely E and Mayevsky A. Real-Time Monitoring of Mitochondrial Function and Cerebral Blood Flow following Focal Ischemia in Rats. JIOHS 1: 63-69, 2008.

2. Mayevsky A and Rogatsky G. Mitochondrial function in vivo evaluated by NADH fluorescence: from animal models to human studies. Am J Physiol Cell Physiol 292: C615-C640, 2007.

3. Sims NR and Muyderman H. Mitochondria, oxidative metabolism and cell death in stroke. Biochimica et Biophysica Acta (BBA) - Molecular Basis of Disease 1802: 80-91, 2010.

822

VARIABILITY OF CEREBRAL BLOOD FLOW MEASUREMENTS BY ^{133} XENON SPECT

O. Henriksen[1], C. Kruuse[2], J. Olsesen[3], L.T. Jensen[4], E. Rostrup[1]

[1]Functional Imaging Unit, Dept. Clin. Physiology / Nuclear Medicine, [2]Dept. Neurology, [3]Danish Headache Center, Dept. Neurology, [4]Dept. Clin. Physiology / Nuclear Medicine, Glostrup Hospital, Glostrup, Denmark

Introduction: Measurement of cerebral blood flow (CBF) is of great importance both for clinical use and for neuroscience. In healthy subjects large between subject variability is often reported. To which extent this is caused by methodological imprecision or true between subjects differences has not been investigated in large studies.

Aims: The aims of the present study were to establish between and within subject variability of CBF measurements using ^{133} Xenon single photon emission tomography (SPECT) in healthy subjects and to assess the effects of physiological variables on CBF measurements..

Methods: Retrospective analysis of ^{133} Xenon SPECT studies performed in healthy subjects from 1998 to 2007. Only baseline studies and placebo measurements were include for analysis. Within and between subejct variability was estimated using a mixed liniar model. Sex, age, end expiratory pCO_2, mean arterial blood pressure (MAP), hematocrit (Hct in %) and body mass index (BMI) were included in the analysis as covariates .

All CBF values are reported as mL/100g/min. CO_2 reactivity is reported as mL/100g/min per kPa.

Results: A total of 439 measurements from 154 subjects (100 males and 54 females) were included in the analysis. Mean age was 25.1 ± 4.1 years.

Mean CBF was 61.05 ± 12.56 (range 34.44 to 103.44). CBF was positively correlated to female gender (β=8.46, 95% 5.35 to 11.57), but not to age, MAP or BMI.

Between subject CO_2 reactivity (β 5.68, 95%CI 3.22 to 8.13) was not different from within subject CO_2 reactivity (β 3.92, 95%CI 1.95 to 5.89). Males tended to have higher CO_2 reactivity than females did (β 2.82, 95%CI 0.15 to 5.62).

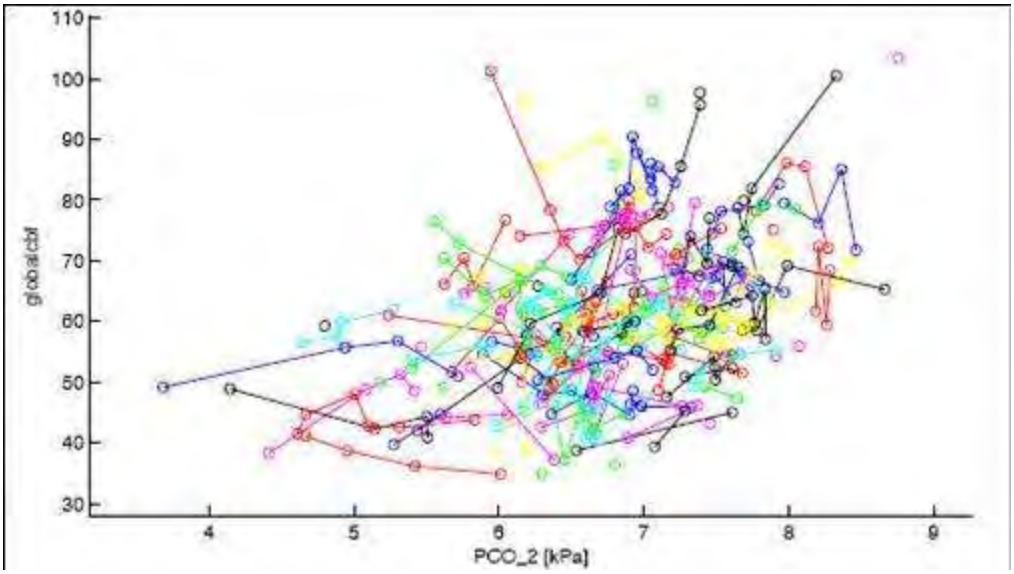

[133 Xe SPECT CBF measurements vs pCO2]

Hct was negatively correlated to CBF (β -0.785, 95%CI -1.302 to -0.267) When Hct was included in the model gender differences were no longer apparent, both in respect to CBF and to CO_2 reactivity.

Adjusting for pCO_2 and Hct decreased between and with subject variability from 8.81 and 5.27 mL/100g/min respectively to 6.98 and 4.75 mL/100g/min respectively, corresponding to 32% decrease in the total variance.

Conclusions: This analysis confirms a significant between subject variability in CBF measurements that cannot only be attributed to differences in Hct and pCO_2. Also the analysis shows that CO_2 reactivity is preserved across different pCO_2 values suggesting that individuals are not habituated to different pCO_2 levels. The CO_2 reactivity estiamted from spontaneous variations in pCO_2 is lower than previously reported when arterial CO_2 is actively manipulated [1]. Apparent gender differences seem to be related to different Hct levels in males and females.

[1] Rostrup, Neuroimage (2005)

823

OPTICAL IMAGING OF NEUROVASCULAR COUPLING DURING NEONATAL DEVELOPMENT

M. Kozberg, S.E. De Leo, M. Bouchard, E.M.C. Hillman

Departments of Biomedical Engineering and Radiology, Columbia University, New York, NY, USA

Objectives: Upon applying an external stimulus, particular regions of the adult brain will experience an increase in both oxy- and total hemoglobin (HbO_2 and HbT), with a corresponding decrease in the local concentration of deoxy-hemoglobin (HbR). This classic hemodynamic response has been observed in adult mammals using both fMRI and optical imaging techniques. However, there are numerous reports that hemodynamic responses to stimuli in the early stages of postnatal brain development differ from those of the developed brain. How and why neonatal responses differ has been highly disputed. Past studies have identified three different responses in neonates: an increase in the level of HbR throughout the stimulus (as opposed to the decrease observed in adults), a phase shift in HbR relative to HbO_2, and a classical adult hemodynamic response. Many of these studies were performed in human infants, were unable to follow the subjects over the course of various developmental stages, and often focused on premature infants, whose clinical condition may have been a confounding factor. Therefore, the evolution of changes in the hemodynamic response in early development has yet to be systematically characterized.

While these changes in hemodynamics may ultimately prove to be important markers of developmental progress, such changes in the hemodynamic response may also hold information about how neurovascular coupling develops at a mechanistic level. Hypotheses to explain the various findings to date include that the vasculature is still maturing postnatally and may not be able to respond to a call for oxygen and other nutrients with the same efficiency as that of an adult. Additionally, the presence of fetal hemoglobin may alter the measurement, manifestation, or demands of the hemodynamic response. Also, during the first weeks of life, substantial cellular migration, neurogenesis and synaptic pruning occur, and these changes in cytoarchitecture may affect neurovascular coupling processes.

In this study, we used high-resolution, high-speed optical imaging of the exposed cortex in a neonatal rat model to seek a better understanding of the changes in neurovascular coupling that occur throughout development. Our goal is to gain a clearer picture of how neurovascular coupling in the adult brain is assembled and actuated.

Methods: Our ongoing study utilizes sets of Sprague-Dawley littermates. From a given litter, the pups are imaged in five distinct age groups: P9-P11 (equivalent to premature human infants), P12-P20 (equivalent to newborn), P21-33 (the age at which the rats are weaned), P34-P48 (adolescence), and adult rats (7 weeks or older, based on sexual maturity). Each rat underwent surgery to expose and thin the skull bilaterally, and then received forepaw and hindpaw stimuli while both somatosensory cortices were imaged simultaneously using high-speed 3-color optical intrinsic signal imaging.

Results and conclusions: While further data is being acquired to control for effects of anesthesia and stimulus amplitudes across the age groups, our initial analysis has revealed a range of 'abnormal' responses in pups up to at least age P21 that are suggestive of an immature neurovascular response. We will present the results of our continued analysis.

824

IN-VIVO OPTICAL IMAGING OF GLIOMA PATHOGENESIS

S.E. De Leo[1], B.R. Chen[1], M.G. Kozberg[1], O.D. Gil[2], P.D. Canoll[3], E.M.C. Hillman[1]

[1]Biomedical Engineering and Radiology, Columbia University, [2]Pathology and Cell Biology, [3]Department of Neurological Surgery, Columbia University Medical Center, New York, NY, USA

Objectives: Glioma is the most aggressive and common form of brain cancer, with a 2-year survival rate of only 25%. Yet little is understood about how glioma develops and proliferates within the brain, how it affects brain function and perfusion, and how different treatments affect disease evolution. Most studies of glioma rely on ex-vivo histology and immunohistochemistry, with a few studies using in-vitro brain slice models.

We have developed a retrovirus-mediated rodent model of glioma that induces adult glial progenitors to form tumors that closely resemble human glioblastomas, while also expressing green fluorescent protein (GFP)[1]. Time-lapse microscopy of slice cultures generated from these model brain tumors show that glioma cells migrate along blood vessels as they invade the surrounding brain tissue[2]. This may lead to disruption of the blood brain barrier and peritumoral edema. However, these results have not yet been confirmed in-vivo.

In this work, we are applying advanced in-vivo optical imaging methods to study the pathogenesis of glioma in the intact rodent brain. Using high-resolution, high-speed optical imaging and two-photon microscopy of the exposed cortex, we can image the migration and behavior of GFP-labeled glioma cells three-dimensionally in-vivo, without disrupting neural and vascular networks as in the earlier brain-slice model. In turn, this allows us to study real-time interactions between glioma cells and the intact vasculature as well as their effects on both baseline and evoked neuronal and hemodynamic responses.

Methods: In this study, each rat underwent surgery to remove the skull overlying the somatosensory cortices bilaterally. Gliomas had been previously induced in each animal on one side of the brain, just rostral to bregma, 10-15 days prior to imaging. Functional imaging data was acquired using high-speed 3-color optical intrinsic signal imaging [3] to resolve bilateral oxy- deoxy- and total hemoglobin responses to forepaw and hindpaw stimuli, as well as fluctuations in hemodynamics during baseline. The same animals were then transferred to our custom-built in-vivo two-photon microscope system to investigate the morphology of glioma-astrocyte-vasculature interactions at the tumor perimeter. To explore the effects of glioma on blood brain barrier integrity, we acquired dynamic in-vivo two-photon microscopy images during a bolus injection of fluorescent dextran conjugated dyes into the blood stream. Following imaging, the animals were sacrificed and their brains were examined using conventional histology to confirm the location and size of the tumor.

Results and conclusions: Our preliminary studies have demonstrated that we can readily observe GFP-positive cells in this rodent glioma model using in-vivo two-photon microscopy. We have observed increased blood vessel density and tortuosity at tumor sites, consistent with known glioma pathology. We have also been able to acquire hemodynamic responses to bilateral functional stimulus. We are continuing to acquire data in larger numbers of animals to characterize the migration dynamics of glioma cells over discrete 3-6 hour epochs, as well as to investigate the effects of glioma on functional reactivity.

References:

[1] Assanah M.et al, JNeurosci, 2006, 26(25):6781-6790

[2] Farin A. et al, Glia, 2006, 53(8), 799-808

[3] Bouchard M.B. et al, OptExpress, 2009, 17 (18), 15670-15678

826

EFFECT OF EARLY MEK1/2 INHIBITION ON VASOCONSTRICTOR RECEPTOR UPREGULATION AND DELAYED CEREBRAL ISCHEMIA AFTER EXPERIMENTAL SUBARACHNOID HEMORRHAGE IN RATS

G.K. Povlsen, L. Edvinsson

Department of Clinical Experimental Research, Glostrup Research Institttute, Glostrup University Hospital, Glostrup, Denmark

Background: Delayed cerebral ischemia is a major cause of death and disability after subarachnoid hemorrhage (SAH). Upregulation of vasoconstrictor endothelin-B (ET_B) and 5-hydroxytryptamine-1B ($5\text{-}HT_{1B}$) receptors have been demonstrated in smooth muscles of cerebral arteries after SAH, and it has been hypothesized that this contributes to delayed cerebral ischemia. It has also been shown earlier that the Ras-Raf-MEK-ERK1/2 signalling pathway is involved in mediating the cerebrovascular upregulation of vasoconstrictor receptors. The aim of this study was to investigate the effect of early treatment with the MEK1/2 inhibitor U0126 on the longer-term cerebrovascular receptor upregulation and development of delayed cerebral ischemia in a rat model of SAH.

Methods: SAH was induced by intracisternal injection of autologous blood. U0126 or vehicle treatment was administered intracisternally at 6, 12, and 24 after SAH. Rats were terminated at day 2, 3 or 4 after SAH induction, and smooth muscle ET_B and $5\text{-}HT_{1B}$ receptor expression and functionality were studied in isolated cerebral artery segments by immunohistochemistry and myograph contractility studies. Gross sensorimotor function of the rats was assessed daily by a rotating pole test.

Results: We demonstrate that SAH induces upregulation of ET_B and $5\text{-}HT_{1B}$ receptors in cerebrovascular smooth muscles with the highest receptor expression and functionality levels observed at day 3 after SAH. Thus, at day 3 after SAH, contractile responses to 10^{-8} M ET-1 and 5-carboxamidotryptamine (5-CT, a 5-HT1 receptor agonist) in basilar artery segments from SAH rats were increased to 191.1 ± 20.8 % and 199.6 ± 37.3 %, respectively, of the levels in sham-operated animals. Treatment with U0126 completely abolishes this receptor upregulation, rendering the levels of ET_B and $5\text{-}HT_{1B}$ receptor contractile responses in U0126 treated animals similar to the responses in sham-operated animals. Furthermore, SAH resulted in sensorimotor deficits on day 2 and 3 after the SAH that were strongly alleviated by the early U0126 treatment.

Conclusion: These findings suggest that MEK-ERK1/2-mediated cerebrovascular vasoconstrictor receptor upregulation is critically involved in delayed cerebral ischemia after SAH, and MEK1/2 inhibition may be a promising novel SAH treatment strategy. Specifically, we here demonstrate that inhibition of MEK1/2 activity during the first 24h after the SAH is enough to abolish vasoconstrictor receptor upregulation throughout the delayed ischemic phase.

827

ISCHEMIA-INDUCED STIMULATION OF CEREBRAL MICROVASCULAR ENDOTHELIAL CELL NA-K-CL COTRANSPORTER ACTIVITY INVOLVES JNK AND ERK1/2 MAP KINASES

B.K. Wallace, M.E. O'Donnell

Physiology and Membrane Biology, University of California-Davis, Davis, CA, USA

Objectives: In the early hours of ischemic stroke, edema forms in the presence of an intact blood-brain barrier (BBB) by mechanisms involving increased secretion of Na, Cl and water from blood into brain. Our previous studies have provided evidence that a luminal BBB membrane Na-K-Cl cotransporter (NKCC) participates in ischemia-induced cerebral edema formation. NKCC activity of cerebral microvascular endothelial cells (CMEC) is stimulated by hypoxia, aglycemia and arginine vasopressin (AVP), three prominent factors present in ischemia. In addition, inhibition of BBB NKCC activity by intravenous bumetanide significantly reduces edema and infarct in the rat permanent middle cerebral artery occlusion model of stroke. Previous studies have shown that ischemic conditions activate AMP kinase (AMPK) and also p38, JNK and ERK1/2 MAP kinases (MAPK) in the brain. We recently found that hypoxia, aglycemia and AVP activate p38 MAPK and AMPK in CMEC as early as 5 min after exposure and that stimulation of CMEC NKCC activity by these ischemic factors is reduced by inhibition of p38 MAPK and/or AMPK activity. We have also confirmed that p38 MAPK and AMPK are present in rat BBB *in situ*. Here, we extend these studies to evaluate the possibility that JNK and/or ERK1/2 MAPK also participate in ischemia-induced stimulation of BBB NKCC activity. Our aims were to: 1) test whether ischemic factors activate CMEC JNK and/or ERK1/2; 2) determine whether SP600125 and FR180204, specific inhibitors of JNK and ERK1/2 respectively, attenuate hypoxia- and/or aglycemia-induced stimulation of CMEC NKCC activity; and 3) determine whether JNK and ERK1/2 are present in rat BBB endothelial cells *in situ.*

Methods: CMEC were exposed to hypoxia (7% or 2% O_2), aglycemia, or AVP for 5-120 min. Cell lysates were subjected to Western blot analysis to determine the abundance JNK and ERK1/2 as well as the level of phosphorylated JNK (p-JNK) and ERK1/2 (p-ERK1/2), using antibodies that specifically recognize JNK and ERK1/2 (both non-phosphorylated and phosphorylated) or only the phosphorylated (activated) kinase proteins. NKCC activity of CMEC exposed to ischemic factors with or without SP600125 and FR180204 was determined as bumetanide-sensitive K influx. *In situ* experiments were conducted using perfusion fixed rat brain and immunofluorescence confocal microscopy.

Results: Both JNK and ERK1/2 are activated following exposure to the ischemic factors, although with different time courses. We found that CMEC p-JNK is increased by hypoxia after 5 min, and by aglycemia and AVP after 30-120 min exposures. CMEC p-ERK1/2 is increased by hypoxia after 5 and 30 min, by aglycemia after 5-120 min and by AVP only after 5 min exposure. We also found that both SP600125 and FR180204 significantly reduce hypoxia- and aglycemia-induced stimulation of NKCC activity. Further our immunofluorescence studies revealed the presence of both total and activated JNK and ERK1/2 in rat cortex BBB endothelial cells *in situ*.

Conclusions: These findings support the hypothesis that ischemic factor activation of BBB endothelial cell NKCC activity involves activation of JNK and ERK1/2, and suggests that these kinases may provide additional targets for stroke therapy.

Supported by NINDS (MEO) and HHMI (BKW)

828

NON-ANEURYSMAL SUBARACHNOID HEMORRHAGE: PATIENTS CHARACTERISTICS, CLINICAL OUTCOME AND PROGNOSTIC FACTORS

J. Konczalla, E. Güresir, H. Vatter, V. Seifert

Department of Neurosurgery, Johann Wolfgang Goethe University Frankfurt, Frankfurt am Main, Germany

Objective: Subarachnoid hemorrhage (SAH) is mainly caused by ruptured cerebral aneurysms. In some patients cerebral angiography is negative for an aneurysm. Our objective was to analyze patient characteristics, clinical outcome and prognostic factors in these patients.

Methods: From 1999 to 2009, 125 patients had a non-aneurysmal SAH. Patient and specific characteristics were entered into our prospectively conducted database. Outcome was assessed according to the modified Rankin Scale (mRS) at 6 months (mRS Score 0-2 favourable vs. 3-6 unfavourable). All patients underwent digital subtraction angiography (DSA).

Results: 106 of 125 patients were in good WFNS grade (I-III) at admission (84.8%). Overall, favourable outcome was achieved in 104 of 125 patients (83.2%). Favourable outcome was associated with younger age (54 ± 13 vs. 66 ± 11, $p < 0.001$), good admission status ($p < 0.0001$), and no signs of hydrocephalus ($p=0.001$).

52 of the 125 patients had a non perimesencephalic and non-aneurysmal SAH. 40 of 52 patients were in good grade at admission (76.9%) and favourable outcome was achieved in 40 patients (76.9%).

73 of the 125 patients had a perimesencephalic SAH and 66 patients of them were in good condition at admission (90.4%) and 64 patients had a favourable outcome (87.7%).

In the ISAT-study, 2018 of 2143 patients were in a good grade at admission (94.2%) and a favourable outcome after 1 year was achieved in 1161 of 1594 patients (72.8%).

Our group with 125 patients has a better outcome compared to the ISAT-group (odds ratio 1.85, $p=0.011$ for Fisher's exact test).

Conclusions: Non-aneurysmal SAH has a better prognosis compared to aneurysm related SAH. The present data suggest that age, poor admission status, and hydrocephalus are prognostic factors for poor outcome.

830

BRAIN TUMOR INFILTRATION IN A NOVEL HUMAN GLIOBLASTOMA STEM CELL MODEL AS DETECTED BY DIFFUSION TENSOR IMAGING

F. Mauconduit[1], F. Tiar[2], T.-A. Perles-Barbacaru[1], D. Wion[2], F. Berger[2], H. Lahrech[1]

[1]Functional and Metabolic Neuroimaging, [2]Brain Nanomedicine Group, INSERM U836, Grenoble Institute of Neurosciences, University Joseph Fourier, Grenoble, France

Introduction: Recently, a new slowly growing glioblastoma mouse model was developed in our laboratory [1]. The hypothesis of an infiltrating growth pattern is put forward, and assessed using diffusion tensor imaging (DTI) in this study.

Methods: Two months after tumor implantation (5×10^5 human glioblastoma stem cells) in the caudate nucleus (Bregma level, 2 mm right, 2.5 mm depth), nude mice (n = 6) were imaged in a 47/40 Bruker Biospec USR AV III scanner (FOV = 15 ´ 15 mm^2, matrix 128 ´ 128, 7 slices of 0.7 mm). Diffusion maps were acquired using a spin echo sequence (TR/TE = 2000/30 ms, NA = 1, duration 30 min) with two identical diffusion gradients of 5 ms duration and 10 ms separation time. Six different gradient diffusion directions ([1 1 0],[1 -1 0],[0 1 1],[0 1 -1],[1 0 1],[-1 0 1]) with a b-value of 1000 s/mm^2 were used. Symmetrical ROIs in the tumors and in contralateral striatal tissue were drawn on the T_2-weighted images (TR/TE = 3500/33 ms, NA = 6, duration = 5 min 36 s) and copied to the diffusion maps.

Mean diffusivity (MD), maximum, median and minimum apparent diffusion coefficients (ADC) and fractional anisotropy (FA) were computed from the diffusion weighted images according to [2].

Results and discussion: Tumor occurrence was detectable on T_2-weighted acquisitions as a slight hyperintensity with respect to the normal brain tissue. As shown in the figure, all diffusion parameters were increased in the tumor tissue compared to the contralateral brain tissue, except the FA with an average of 0.35 ± 0.08 in both regions. As reported in [3,4] this is compatible with a predominantly infiltrative growth pattern of this slowly growing tumor model. Although the FA does not change and the MD does not reach the value of free water, necrosis or edema might be present in subparts of the tumors, since tumors are generally heterogeneous. However, a spatially resolved analysis was not possible due to the small tumor size.

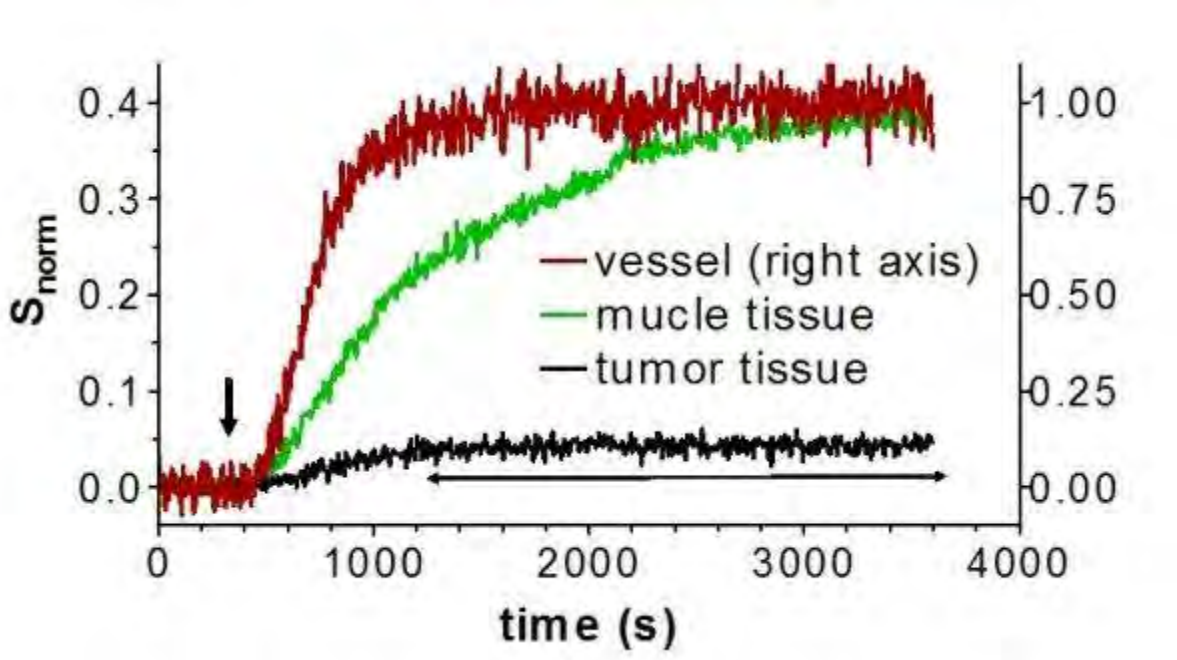

[dia]

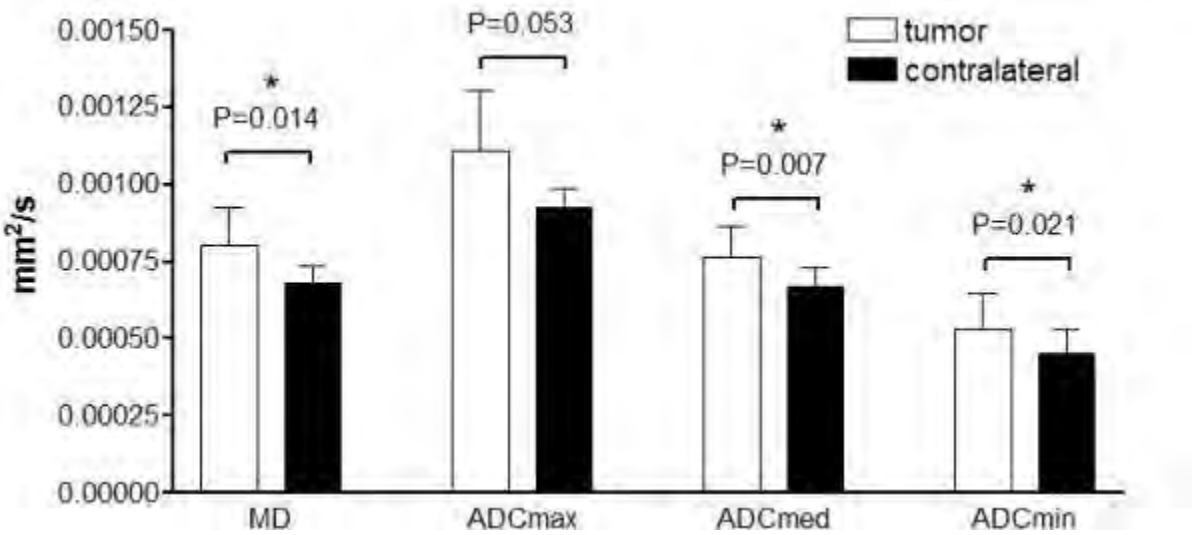

[figure]

Conclusion: The findings of this study suggest that the mouse tumor model has an infiltrative growth pattern. Histologic validation using fluorescently labeled glioblastoma cells is under way. Spectroscopy will be used as a complementary noninvasive technique to DTI to confirm the presence of proliferating tumor cells from the metabolic profiles.

References:

[1] Platet et al, Cancer Lett. 2007;

[2] Pierpaoli, MRM 1996;

[3] Wright, MRM 2009;

[4] Price, Eur Radiol 2007

831

ISCHEMIC POST-CONDITIONING MAINTAINS TISSUE VITALITY FOLLOWING FOCAL CEREBRAL ISCHEMIA IN RATS

A. Livnat, E. Barbiro-Michaely, A. Mayevsky

The Mina & Everard Goodman Faculty of Life-Sciences, Bar-Ilan University, Ramat-Gan, Israel

Objectives: Ischemic post-conditioning is a phenomenon in which interruptions to cerebral blood flow (CBF) during the post ischemic reperfusion phase protect the brain from reperfusion injury and reduced infarct size (1). The present study investigated the effects of transient bilateral carotid occlusion (BCO) prior to reperfusion of focal ischemia on mitochondrial metabolism and CBF.

Methods: Male Wistar rats underwent middle cerebral artery occlusion (MCAO) for 60 minutes, with or without BCO, which was induced 15 minutes before reperfusion. Monitoring in the core and the penumbra of the ischemic brain was performed using a unique Multi-Site - Multi-Parametric (MSMP) system, which measures mitochondrial NADH using surface fluorometry, and CBF using laser Doppler flowmetry (2). Short anoxia and cortical spreading depression (CSD) waves were induced in order to test the ability of the tissue to cope with oxygen deficiency and metabolic challenges following reperfusion.

Results: MCAO led to a decrease in CBF to 15% (of the control values) in the core and to 40% in the penumbra. Simultaneously, fluorescence increased to 129% in the core and 121% in the penumbra. NADH levels increased to 110% in both core and penumbra, followed by a decrease in the core, due to an artifact caused by an increase in reflectance levels (3). BCO 45 minutes later lead to a further decrease in CBF to 5% in the core and 15% in the penumbra. Reflectance and fluorescence levels further increased in both core and penumbra, leading to levels of 115% in the penumbra. In the core, NADH levels remained low due to the further increase in reflectance. Removal of the occluding filament lead to an increase in CBF in both areas toward levels of 50%, as the rest of the parameters showed no significant change. Restoration of carotid blood perfusion led to an increase in CBF to 180% in both areas, while reflectance, fluorescence and NADH levels decreased toward baseline. CBF levels returned to baseline as well 60 minutes later. Short anoxia and CSD waves, which were induced 60 minutes following carotid reperfusion, showed no significant changes in parameters compared to control.

Conclusions: These results imply that ischemic post-conditioning by BCO assists in maintaining tissue vitality following cerebral focal ischemia and may serve as a protective mechanism to ischemic and reperfusion damage.

References:

1. Pignataro G, Scorziello A, Di Renzo G and Annunziato L. Post-ischemic brain damage: effect of ischemic preconditioning and postconditioning and identification of potential candidates for stroke therapy. FEBS J 276: 46-57, 2009.

2. Livnat A, Barbiro-Michaely E and Mayevsky A. Variability in Mitochondria function and Cerebral Blood Flow following Middle Cerebral Artery Occlusion in Rats. Journal of Neuroscience Methods 188(1): 76-82, 2010.

3. Mayevsky A and Rogatsky G. Mitochondrial function in vivo evaluated by NADH

fluorescence: from animal models to human studies. Am J Physiol Cell Physiol 292: C615-C640, 2007.

833

METABOLIC AND HEMODYNAMIC RESPONSES TO HEMORRHAGIC HYPOTENSION UNDER BRAIN PARTIAL ISCHEMIA MEASURED IN THE BRAIN AND SMALL INTESTINE

M. Mandelbaum-Livnat, E. Barbiro-Michaely, A. Mayevsky

The Mina & Everard Goodman Faculty of Life-Sciences, Bar-Ilan University, Ramat-Gan, Israel

Objectives: During hemorrhage, blood is redistributed in favor of the vital organs and on the expense of the less vital organs. Bilateral carotid occlusion (BCO) is an animal model of arteriosclerosis, which is considered to be the leading cause of mortality in industrialized countries due to reduced blood supply to the brain.

The purpose of the present study was to investigate how BCO influences the responses of the brain (vital organ) and small intestine (less vital organ) to hemorrhagic hypotension.

Methods: Rats were bled until reaching mean arterial pressure (MAP) of 40mmHg, with or without BCO 24 hours prior to the bleeding session. MAP level was maintained for 15 minutes, after which the animals were resuscitated with the withdrawn blood. Metabolic and hemodynamic monitoring from both organs were carried out using the Multi-Site Multi-Parametric system, which simultaneously monitors tissue blood flow using Laser Doppler Flowmeter and mitochondrial NADH redox state using surface fluorometry.

Results: While hemorrhage under normoxic conditions caused a decrease in blood supply (30±7%, $p< 0.01$) and mitochondrial dysfunction (132±10% ($p< 0.01$) to the intestine, the brain preserved its normal function. However, under ischemic conditions hemorrhage caused deterioration in both organs. Blood supply to both brain and intestine rapidly decreased and remained low for the entire hemorrhage period (79.5±8% ($p< 0.001$) and 56±10% ($p< 0.001$), respectively). In addition, mitochondrial dysfunction was observed in both brain (137±9%, $p< 0.01$) and intestine (145±12%, $p< 0.01$). Furthermore, the responses of the cerebral parameters to hypotension, exhibited Ischemic-Depolarization (ID) and Secondary Reflectance Increase (SRI) - biphasic changes, where the immediate response was followed by a further response.

Conclusions: The Impaired blood supply to the brain decreases cerebral autoregulation abilities and therefore decreases its protection during hemorrhage. The ID demonstrates the severity of the ischemic damage to normal mitochondrial function under combination of partial ischemia and hemorrhagic hypotension, while the SRI implicates the severity of the damage to normal hemodynamic. These highlight the importance of adequate cerebral perfusion for the maintenance of body homeostasis.

References:

Mandelbaum MM, Barbiro-Michaely E, Tolmasov M and Mayevsky A. Effects of Severe Hemorrhage on *In Vivo* Brain and Small Intestine Mitochondrial NADH and Microcirculatory Blood Flow. *Journal of Innovation in Optical Health Sciences* 1: 177-183, 2008

Mayevsky A and Rogatsky GG. Mitochondrial function in vivo evaluated by NADH fluorescence: from animal models to human studies. *Am J Physiol Cell Physiol* 292: C615-C640, 2007.

834

SYNERGISTIC INHIBITORY EFFECT OF NICOTINE PLUS ORAL CONTRACEPTIVE COMBINATION ON MITOCHONDRIAL COMPLEX-IV IS MEDIATED BY ESTROGEN RECEPTOR-BETA IN FEMALE RATS

A.P. Raval, K.R. Dave, I. Saul

Neurology, University of Miami, Miami, FL, USA

Objectives: The rise in the number of female smokers is a global public health concern. The primary reason that people continue to consume tobacco products is nicotine addiction. The results of our research indicate that chronic nicotine exposure makes female rats more susceptible to ischemic brain damage. The severity of ischemic brain damage is far greater in female rats simultaneously exposed to oral contraceptives (OC) than to nicotine only. One of the well-known consequences responsible for post-ischemic hippocampal neuronal death is mitochondrial dysfunction. Thus, in the current study we investigated effects of nicotine alone or in combination of oral contraceptives on hippocampal mitochondrial functions.

Methods: Female Sprague-Dawley rats (290±20g) were implanted with osmotic pumps containing nicotine (in saline) for 16 days. To mimic the use of OC in women, nicotine /saline exposed rats were administered OC (3 days) + placebo (1 day) orally for 16 days. On the last day of these treatments rats were sacrificed and hippocampus was isolated. We measured mitochondrial oxygen consumption and individual complex I to IV activities using a spectrophotometer assay in mitochondria isolated from rat hippocampus.

Results: The mean rate of mitochondrial respiration in the presence of pyruvate plus malate as substrates (providing electrons to complex I), and oxygen consumption in the nicotine and nicotine plus OC (NOC) groups were lowered by 45% (79 ± 19; n =3; $p< 0.05$) and 43% (83 ± 6; n = 10; $p< 0.001$), respectively, when compared to saline group (144 ± 22; n = 10). No significant differences were found between the saline- and OC- treated groups. The rate of respiration was comparable among all groups when succinate plus glycerol-3-phosphate were used as substrates for complex II. Oxygen consumption in the nicotine, OC and NOC groups was reduced by 28 % (620 ± 83; n = 5; $P < 0.05$), 17% (715 ± 64; n = 5; $P < 0.05$) and 34% (571 ± 70; n = 4; $P < 0.05$) as compared to the saline-treated group (859 ± 103; n = 10) in presence of ascorbate plus tetramethyl-p-phenylenediamine (complex IV substrates), respectively. Results of individual mitochondrial complex activities demonstrated that neither nicotine nor NOC treatment to rats altered complex I, II or III activities as compared to the saline group. Interestingly, we observed significant decrease in the activity of complex IV in NOC-exposed groups as compared to rest of the experimental groups.

Conclusion: Overall our study presents evidence that NOC reduces mitochondrial respiration by reducing complex IV activity in hippocampal mitochondria, which might be manifested after ischemic stress, exacerbating CA1 neuronal death in female rats.

Grant support: AHA-SDG-#0730089N and James and Esther King Biomedical Research Program# 07KN-10 (APR)

835

IN VIVO EFFECTS OF SIMVASTATIN ON MEMORY AND CEREBROVASCULAR DEFICITS IN APP/TGF BITRANSGENIC MICE

P. Papadopoulos, X.-K. Tong, E. Hamel

McGill University, Montreal, QC, Canada

Background: Cognitive and cerebrovascular deficits are two manifestations of Alzheimer's disease (AD) to consider when aiming for effective therapy. Animal models have been invaluable in dissecting the pathogenic mechanisms and identifying drug targets, primarily for memory deficits. However, very few of these drugs have ameliorated the human condition. Here, we use bitransgenic APP/TGF mice that recapitulate the cerebrovascular and cognitive AD landmarks (1) to evaluate the efficacy of simvastatin on these clinical markers.

Objectives: APP/TGF mice, which overexpress a mutated form of the human amyloid precursor protein (hAPPSwe,Ind) and a constitutively active form of transforming growth factor-b1 (TGF), display the salient cerebrovascular and cognitive impairments of AD as early as six months of age. Using these mice, we aim to test the therapeutic potential of simvastatin, a 3-hydroxy-3-methylglutaryl coenzyme A reductase inhibitor with proven efficacy against these two deficits in singly APP mice (2,3).

Methods: Three-month-old APP/TGF and wildtype (WT) mice were treated with simvastatin (40 mg/kg/day in water). At age 6 and 9 months, mice were tested for learning in the hippocampal-based spatial Morris Water Maze (MWM), as described by DeIpolyi and colleagues (4) with visible and hidden platform; and for memory in the probe trial test. Post-training, the evoked cerebral blood flow (CBF) response to whisker stimulation was measured as an index of functional hyperemia. Mice were then sacrificed and the posterior cerebral artery (PCA) was used for assessment of cerebrovascular reactivity.

Results: Simvastatin treatment failed to improve spatial learning and memory deficits of APP/TGF mice tested at 6 and 9 months in the MWM. The decreased CBF response evoked by whisker stimulation in APP/TGF mice (-59%, $p< 0.001$) was also not normalized by simvastatin. Similarly, the 46% and 58% respective loss of dilatory ability to acetylcholine and calcitonin gene-related peptide of isolated PCA were not restored, but rather reversed to weak constrictions in treated APP/TGF mice. In contrast, the decreased synthesis of nitric oxide (-45%) in the vessel wall was totally normalized by treatment. Simvastatin had no deleterious effects on any parameters in WT animals.

Conclusion: In contrast to the beneficial cerebrovascular and mnemonic effects exerted by simvastatin in singly APP mice (2,3), our data show that the underlying mechanisms that allowed these improvements have been altered by the TGF transgene, making the bitransgenic APP/TGF mice more resistant to simvastatin. Together, these results suggest that therapeutic benefits in APP/TGF mice, which display a more complete array of AD salient features, are not as readily obtained as in APP mice. Further, as these mice better reflect the complexity that one faces when attempting to rescue function in AD patients, they may represent an improved model to test new therapeutic strategies.

References:

1. Ongali et al. 2010, Am J Pathol. 177: 3071- 3080.

2. Li et al. 2006, Ann Neurol 60:729-739.

3. Tong et al. 2009, Neurobiol Dis. 35:406-414.

4. DeIpolyi et al. 2008, Neurobiol. Aging. 29: 253-266.

Support: Supported by the Canadian Institutes of Health Research (CIHR grant MOP-84275 to EH), and Jeanne Timmins Costello Fellowship (PP).

836

MODEL CHOICE REDUCES ANIMAL REQUIREMENTS TO PROVE SUCCESSFUL MICROBUBBLE STROKE SONOTHROMBOLYSIS WITHOUT TPA IN RABBITS

W.C. Culp[1], A.T. Brown[1], J.D. Lowery[2], S.D. Woods[1], E. Erdem[1], P.K. Roberson[3]

[1]Radiology, [2]Laboratory Animal Medicine, [3]Biostatistics, University of Arkansas for Medical Sciences, Little Rock, AR, USA

Objectives: Microbubbles (MB) combined with ultrasound (US) have demonstrated effective clot lysis without exogenous tissue plasminogen activator (tPA) *in vitro* and *in vivo*. We compare two variations of an angiographic rabbit model of ischemic stroke and evaluate sonothrombolysis with MB compared with standard tPA therapy.

Methods: For large strokes New Zealand White rabbits (n=57) received angiography, and a single 4.0-mm clot was injected into the internal carotid artery, occluding its branches. Emboli were prepared from fresh rabbit blood in 1.5-mm glass tubes. Clotting proceeded for 6 hours at 37ºC, then at 4ºC for 72 hours total before cutting to precise length. Large stroke rabbits were randomly assigned groups: 1) control (n=11) rabbits embolized without therapy; 2) tPA without US (n=20); 3) tPA+US (n=10); 4) MB+US (n=16). Treatment began one hour following occlusion. Rabbits with US received transcutaneous pulsed US (1 MHz; 0.8 W/cm^2) for 1 hour (Sonicator 716, Mettler Electronics). Rabbits with tPA received intravenous tPA (0.9 mg/kg) over 1 hour. MB dose was high dose intravenous lipid MB (0.16 mg/kg) (Definity; Lantheus Medical Imaging) over 30 minutes. In the small stoke model (n=145) the same technique was followed except the clots were smaller, 1-mm long, and were clotted in 1-mm tubes for only 3 to 6 hours at 37ºC. All clots in both sizes were about 0.6-mm in diameter after shrinkage. Small stroke rabbits were assigned to 5 groups: 1) Control (n=44); 2) US alone (n=26); 3) tPA (n=26); 4) tPA+US (n=22); 5) MB+US (n=27). Rabbits were sacrificed at 24 hours and infarct volume was determined using vital stains on brain sections.

Results: In large strokes mean infarct volume was significantly lower (p=0.01) for rabbits treated with MB+US (0.8%±0.8%) compared with control rabbits (3.5%±0.8%). Infarct volume averaged 2.2%±0.6% and 1.7%±0.8% for rabbits treated with tPA alone and tPA+US, respectively, and did not differ significantly from control and MB groups with this sample size. In small strokes infarct volumes were smaller and larger numbers of animals were required in all groups to prove significance: Control 1.2%; US alone 1.4% (vs control p=NS); tPA alone 0.3% (p=0.05); tPA+US 0.2% (p=0.05); MB+US 0.3% (p=0.05).

Conclusions: 1) Using an appropriate model fewer animals are required to reach statistical significance. Future studies can be designed with this consideration. 2) MB+US sonothrombolysis without exogenous tPA administration is effective in reducing infarct volumes in treatment of both small and large ischemic strokes. Human trials are now justified and urgently needed.

References:

1. Culp, BC, Brown, AT, Erdem, E, Lowery, JD, Culp, WC. Selective Intracranial Magnification Angiography of the Rabbit: Basic Techniques and Anatomy. *Journal of Vascular Interventional Radiology*, 2007, 18:187-192.

2. Brown AT, Flores R, Hamilton E, Roberson PK, Borrelli MJ, Culp WC. Microbubbles improve

sonothrombolysis in vitro and decrease hemorrhage in vivo in a rabbit stroke model. *Investigative Radiology* 2011;46(3)*In Press*

3. Culp, WC, Porter, TR, Lowery, J, Xie, F, Roberson, PK, Marky L. Intracranial Clot Lysis with Intravenous Microbubbles and Transcranial Ultrasound in Swine. *Stroke* 2004; 35: 2407-2411

837

CYCLIC PATTERN OF 17BETA-ESTRADIOL PRETREATMENT PROTECTS THE HIPPOCAMPAL CA1 REGION AGAINST CEREBRAL ISCHEMIA VIA ESTROGEN RECEPTOR BETA

A.P. Raval, N. Hirsch, I. Saul

Neurology, University of Miami, Miami, FL, USA

Objective: The failure of the Women's Estrogen for Stroke Trial raised concern regarding the safety of chronic estrogen treatment in women. In contrast to chronic 17β-estradiol treatment, our recent study demonstrated that a single 17beta-estradiol bolus 48h prior to ischemia induces neuroprotection in the hippocampal CA1 region in slice culture and rat models of global cerebral ischemia. We hypothesized that cyclical 17β-estradiol treatment provides neuroprotection against cerebral ischemia in the rat model, and that estrogen receptor(s) (ER) were required for induction of estrogen-mediated neuroprotection.

Method: Female rats were ovariectomized (OvX) and 7 days later injection of 17beta-estradiol (5 µg/Kg; i.p.) or vehicle (oil) was started at intervals of every 48 or 72h for 4 cycles over the period of one month. 48 or 72h following the last hormone treatment rats were exposed to cerebral ischemia produced by 10 min of bilateral carotid occlusion and systemic hypotension (50 mmHg). Seven days later, rat brains were fixed for histopathological assessment.

The role of ERs was determined by exposing slices to the medium containing an ER subtype alpha (PPT) or beta (DPN) selective agonist for 4h. In parallel, slices were incubated in a medium containing estradiol-17beta (1 nM) for 4h followed by ERs inhibitor (ICI 182780; 1 µM; DMSO; for 24h). Forty eight hours after the slices were exposed to 40min of oxygen-glucose deprivation. Propidium Iodide (PI) fluorescence images were obtained using a SPOT CCD camera and were digitized using SPOT advanced software. The percentage of relative optical intensity was used as an index of cell death. Results are expressed as mean ± SEM. Statistical significance was determined with an ANOVA test followed by a Bonferroni's post-hoc test.

Results: The number of normal neurons per slice in the CA1 hippocampal region in naïve rats was 1100±45 (n=4). Ischemia in OvX rats decreased the number of normal neurons by 82% (192±10, n= 6, $p< 0.05$). Intermittent estradiol-17beta treatment of OvX rats prior to cerebral ischemia increased the number of normal neurons 51% (556±13, n=8, every 48h) and 41% (446±14, n=7, every 72h) compared to the OvX group ($p< 0.05$). Neither vehicle treatment nor sham-OvX showed any significant difference in the number of normal neurons versus OvX groups. In slice model, quantification of cell death using PI technique demonstrated that the activation of ER-beta was neuroprotective while ER-alpha activation did not. Inhibition of ERs significantly increased CA1 neuronal loss as compared to vehicle group. The PI fluorescence values of vehicle and ERs inhibitor were 55±6 (n=3) and 76±4 (n=5; $p< 0.05$).

Conclusion: Cyclic 17beta-estradiol treatment conferred protection against ischemia in OvX rats. Furthermore, ERs activation after estrogen pretreatment was required to rescue CA1 neurons after ischemia.

Grant support: AHA-SDG-#0730089N and James and Esther King Biomedical Research Program# 07KN-10 (APR)

838

EFFECT OF CHRONIC HYPERGLYCEMIA ON GLUCOSE TRANSPORT KINETICS AND CEREBRAL METABOLISM IN THE RAT BRAIN IN VIVO USING ^{1}H MRS

P. Lee[1,2], W.-T. Wang[1], H. Yeh[3], I.V. Smirnova[4], I.-Y. Choi[1,5]

[1]Hoglund Brain Imaging Center, [2]Molecular and Integrative Physiology, [3]Biostatistics, [4]Physical Therapy and Rehabilitation Sciences, [5]Neurology, University of Kansas Medical Center, Kansas City, KS, USA

Introduction: The chronic hyperglycemia and diabetes may cause neuropathologic conditions via altered cerebral glucose metabolism and/or transport. The effect of long-term uncontrolled hyperglycemia on cerebral metabolite levels and glucose transport has not been well characterized. In this study, we used streptozotocin (STZ)-induced diabetic rats as an experimental model of uncontrolled type-1 diabetes to characterize metabolic alterations in the brain. We have measured the neurochemical profile in chronic uncontrolled hyperglycemic conditions and normalized glycemic conditions via insulin as well as the glucose transport kinetics using in vivo ultra-short echo time ^{1}H MRS.

Materials and methods: Total thirteen Sprague-Dawley rats (8 weeks old) were injected with STZ i.p. to induce type-1diabetes and were maintained for 10 weeks. MR experiments were performed before STZ injection (CTL) and after 10 weeks (DM70). After completing DM70 scans, five rats were further studied for glucose transport kinetics by concurrent infusion of insulin and glucose to achieve various stready-state target glycemic levels. All MR experiments were performed on a 9.4 T MR system (Varian Inc.). Neurochemical levels were measured using ultra short echo-time STEAM (TE/TM=2/20 ms, TR=5s)[1] and quantified using LCModel. Glucose transport kinetic constants at the blood brain barrier (BBB) were calculated from the relationship between glucose levels in the brain and plasma using both reversible and standard Michaelis-Menten (MM) kinetic equations. Confidence intervals of the kinetic constants were estimated using a non-parametric bootstrapping method written in R software.

Results and discussions: Uncontrolled hyperglycemia resulted in elevation of several neurochemical levels such as beta-hydroxybutyrate (bHB), glycerophosphoryl-choline (GPC), myo-inositol (Ins), and taurine (Tau), consistent with previous findings. Prolonged uncontrolled hyperglycemia 10 weeks (DM70) caused decreases of the levels of alanine (Ala), aspartate (Asp), glutathione (GSH), and N-acetylaspartate (NAA). When glycemic levels were normalized with insulin infusion, the levels of most metabolites (bHB, GPC, Tau, Asp, GSH) were normalized to the levels of CTL, while NAA, Ala and Ins remained altered. Persistent reduction of NAA after the glycemic normalization suggests potential alterations of neuronal integrity caused by prolonged hyperglycemia.

Brain and plasma glucose levels showed an apparent linear relationship over a wide range of plasma glucose concentration, which is consistent with the reversible MM model for glucose transport across the BBB. The best fit to the data resulted in an apparent MM constant K_t of 0.51 (0.00 - 2.44, 95% confidence interval) mM and the ratio of the maximal transport rate relative to cerebral metabolic rate of glucose, T_{max}/CMR_{glc}, was 1.65 (1.55 - 1.76) with the reversible MM model, and Kt of 10.93 (7.07 - 14.98) and T_{max}/CMR_{glc} of 3.86 (3.48 - 4.35) with the standard MM model. Current values of K_t and T_{max}/CMR_{glc} were within the error range compared to those reported previously in both control and STZ-treated rats[2]. Our data support the notion that glucose transport capacity across BBB was not altered by prolonged uncontrolled hyperglycemia.

References:

[1] Tkac et al., MRM 41:649 (1999).

[2] Duarte et al., J Neurochem 111:368 (2009).

This work is partly supported by NIH (R21DK081079).

841

PERLECAN DOMAIN V IS NEUROPROTECTIVE, ENHANCES BRAIN REPAIR AND LIMITS CHRONIC GLIAL SCAR FORMATION IN EXPERIMENTAL BRAIN ISCHEMIC STROKE

B. Lee[1], A. Al Ahmad[1], D.N. Clarke[1], M. Kahle[1], C. Parham[1], **G.J. Bix**[1,2]

[1]Molecular & Cellular Medicine, [2]Neuroscience & Experimental Therapeutics, Texas A&M Health Science Center, College Station, TX, USA

Introduction: Stroke is the leading cause of long-term disability and third leading cause of death. While most research has focused on acute stroke treatment and neuroprotection, the additional exploitation of brain self-repair and the inflammatory response may provide better therapies. Unfortunately, many factors that prevent cell death also inhibit repair, or vice versa, depending upon when they are administered post-stroke. Furthermore, the glial driven inflammatory response is critical to acutely stabilizing post-stroke brain injury, but ultimately detrimental to reparative responses inasmuch as they are physically limited by glial scar formation. Thus, there is a need for a stroke therapy that is neuroprotective, a promoter of brain repair, and a suppressor of scar formation regardless of when administered. Here we describe the naturally occurring extracellular matrix fragment of perlecan, domain V (DV), as such a triple functioning stroke treatment.

Methods: Adult C57/Bl6 mice were transiently (2 h) stroked by the tandem ipsilateral CCA/MCA occlusion technique. The mice then received i.p. injections of human recombinant DV (1mg/kg) on post-stroke days 1, 3, 5 and 7, the first dose given 24 h after stroke. Animal motor function was assessed throughout by the cylinder test. Brain tissue was also harvested for immunohistochemical and western blot analysis. Finally, DV effects on primary mouse brain endothelial cells, neurons, and astrocytes were assessed.

Results: Post-stroke DV treatment resulted in smaller infarct sizes with fewer peri-infarct apoptotic neurons, increased post-stroke neurogenesis and angiogenesis (reparative processes), and acute glial activation followed by chronic (i.e. by post-stroke day 14) suppression of glial scar formation. Furthermore, DV appeared to work via two distinct mechanisms of action: DV interacted with brain endothelial cell a5b1 integrin resulting in the release of vascular endothelial growth factor, and astrocyte a2b1 integrin resulting in the release of nerve growth factor. Finally, DV was well-tolerated, specifically targeted peri-infarct brain tissue, was effective when initially administered 24 hours after stroke (an important consideration given the limited 3-4.5 hour therapeutic window of tPA), and restored stroke-affected motor function to baseline pre-stroke levels.

Conclusion: These results highlight DV as a versatile stroke treatment capable of positively affecting multiple components of the neurovascular unit. Specifically, by protecting neurons, enhancing post-stroke angiogenesis and neurogenesis, and suppressing chronic glial scar formation, DV may represent a novel triple threat in the battle against stroke.

842

ENDOCRANIAL HEAT DISSIPATION AND THE INFLUENCE OF THE CEREBRAL CIRCULATORY SYSTEM IN BRAIN THERMOREGULATION AND HUMAN EVOLUTION

J.M. de la Cuétara[1], F. Musso[2], E. Bruner[1]

[1]Centro Nacional de Investigación sobre la Evolución Humana (CENIEH), [2]Universidad de Burgos, Burgos, Spain

Objectives: Compared with non-human primates, the human brain is characterized by a clear increment in its size, and by a considerable increment of its metabolic costs (Leonard and Robertson, 1992). Considering that brain function is highly influenced by changes in temperature, in the way that slight temperature variations may produce irreversible brain damage or even cause death, the removal of heat produced by neural metabolic activity is a relevant issue for understanding the development and evolution of the human brain (Caputa, 2004). In this context, the cerebrovascular system has been proposed to play a relevant role in brain thermoregulation. Interestingly, it has also been proposed that a more developed cerebrovascular network may have evolved in modern humans (Bruner and Sherkat, 2008). In order to look for morphological correlates of brain metabolism, this study introduces a novel approach to investigate the heat production/dissipation patterns associated to the brain gross morphology, and how these patterns are affected by the presence of the main endocranial vessels. Some comments about the heat dissipation patterns in modern humans, fossil hominids and non-human primates are provided.

Methods: Three-dimensional digital reconstructions of the endocranial anatomy (endocasts) and the cerebral vessels are obtained through the segmentation of standard tomographic and angiotomographic data. Then, numerical modeling is used to provide quantitative and qualitative evaluations of the heat distribution patterns within the endocranial cavity (Bruner et al., 2011). The quantitative evaluation of the results is performed through the analysis of the distribution of the temperature values, while a qualitative description is provided by the generation of endocranial thermic maps, in living and extinct species.

Results: Despite some minor differences, all modern humans show similar heat dissipation patterns along their endocranial cavity. Such models allow to quantify the contribution of the vascular system in cooling the endocranial volume according to its geometry. On the other hand, interspecific comparisons show that modern humans display quantitatively and qualitatively different heat dissipation patterns to those of fossil hominid and non-human primates.

Conclusions: The preliminary results of this study evidences the utility of this new methodology to quantify and evaluate the heat production/dissipation differences between different human (modern and non-modern) and non-human species, as well as the potentiality to generate numerical models that integrate information of different anatomical components such as the brain and the cerebrovascular system in order to investigate physiology, development and evolution of the modern human brain.

References:

Bruner E, Sherkat S. 2008. The middle meningeal artery: from clinics to fossils. Child´s Nerv Syst 24: 1289-1298.

Bruner E, Mantini S, Musso F, de la Cuétara JM, Ripani M, Sherkat S. 2011. The evolution of the meningeal vascular system in the human genus: From brain shape to thermoregulation. Am J Hum Biol 23: 35-43.

Caputa M. 2004. Selective brain cooling: a multiple regulatory mechanism. J Therm Biol 29: 691-702.

Leonard WR, Robertson ML. 1992. Nutritional requirements and human evolution: A bioenergetics model. Am J Hum Biol 4:179-195.

843

DIFFERENTIAL VASOACTIVE EFFECTS OF SILDENAFIL AND TADALAFIL ON CEREBRAL ARTERIES -RELEVANT TO MIGRAINE?

C. Kruuse[1], S. Gupta[2], E. Nillson[3], L.S. Kruse[4], L. Edvinsson[3,5]

[1]Dept. Neurology, Glostrup Hospital, University of Copenhagen, [2]Dept. Neurology, Glostrup Research Institute, Glostrup University Hospital, Glostrup, Denmark, [3]Division of Experimental Vascular Research 4, Department of Internal Medicine, University Hospital of Lund, Lund, Sweden, [4]Neurology, Glostrup Research Institute, Glostrup University Hospital, [5]Departments of Clinical Experimental Research, Glostrup Research Park, Glostrup Hospital, Glostrup, Denmark

Background: Phosphodiesterase 5 (PDE5) is associated with migraine pathophysiology, stroke recovery and vasospasm treatment (1, 2). We have shown previously that vasodilatation was not a prerequisite for migraine induction; sildenafil elicited migraine-like attacks in migraine patients without measurable changes in intra- or extra-cerebral artery diameter. Further, sildenafil was found to not affect neurovascular response or excitability (3). However, dural artery responses were not accounted for in the human studies and minor vascular changes of functional importance may not have been detected.The potential vascular interplay of PDE5 inhibitors sildenafil, tadalafil and UK-114,542 were studied by intra- versus extra-luminal administration in rat middle cerebral arteries (MCA) in vitro and on middle meningeal arteries (MMA) in vivo.

Aim: To examine 1) the effects of PDE5 inhibitors in vitro dilatation of the middle cerebral artery (MCA) with controlled luminal or extra-luminal application of the drugs and 2) the in vivo effects of intravenous PDE5 inhibitors on the middle meningeal artery (MMA) dilatation in a closed cranial window model in rats.

Methods: Rat MCA diameter was investigated using pressurised arteriography, applying UK-114,542, sildenafil, and tadalafil intra- or extra-luminally. Effects on MMA were studied in the in vivo closed cranial window model.

Results: At high concentrations, abluminal sildenafil and UK-114,542, but not tadalafil, induced dilatation. Luminal application elicited a contraction of 4 % (sildenafil, $p = 0.03$) and 10 % (tadalafil, $p = 0.02$). In vivo, sildenafil, but not tadalafil, dose-dependently dilated MMA concomitant to blood pressure reduction (1-3 mg/kg);1 mg/kg sildenafil inducing 60 ± 14 % ($p = 0.04$) and vehicle (DMSO) 13 ± 6 % dilatation.

Conclusion: PDE5 inhibitors applied luminally had contractile effect on MCA. Abluminal sildenafil induced MCA dilatation above therapeutic levels. In vivo, sildenafil dilated MMA. Tadalafil had no dilatory effects. PDE5 inhibitors show differential vascular activity in arteries, although clinically the potential for headache induction appears similar. Therefore these findings support non-vasodilatory origin of headache by PDE5 inhibition.

References:

1. Kruuse C, Thomsen LL, Birk S, Olesen J. Migraine can be induced by sildenafil without changes in middle cerebral artery diameter. Brain 2003;126(Pt 1):241-247.

2. Zhang R, Wang Y, Zhang L, Zhang Z, Tsang W, Lu M, et al. Sildenafil (Viagra) induces

neurogenesis and promotes functional recovery after stroke in rats. Stroke 2002;33(11):2675-80.

3. Kruuse C, Hansen AE, Larsson HB, Lauritzen M, Rostrup E. Cerebral haemodynamic response or excitability is not affected by sildenafil. J Cereb Blood Flow Metab 2009;29(4):830-9.

844

LONGITUDINAL IMAGING OF GLIO-VASCULAR REMODELING INDUCED BY CHRONIC HYPOXIA IN MOUSE SOMATOSENSORY CORTEX

K. Masamoto[1,2], Y. Tomita[3], H. Takuwa[2], M. Unekawa[3], H. Toriumi[3], Y. Itoh[3], N. Suzuki[3], I. Kanno[2]

[1]University of Electro-Communications, Chofu, [2]Molecular Imaging Center, National Institute of Radiological Sciences, Chiba, [3]School of Medicine Keio University, Tokyo, Japan

Objectives: To better understand the morphological association of gliovascular units, *in vivo* two-photon imaging of gliovascular remodeling elicited by chronic systemic hypoxia was performed in mouse cerebral cortex.

Methods: C57BL/6J mice (20-23 g, N = 4) and Tie2-GFP transgenic mice (20-26 g, N = 5) anesthetized with isoflurane were used for the experiments. Animal use and experimental protocols were approved by the Institutional Animal Care and Use Committee. A custom-made attachment device was fixed on the skull, and 3-mm diameter of closed cranial window (Tomita et al., 2005) was made over the somatosensory area. The animals were housed into hypoxic chamber (8-9% oxygen in nitrogen balance gas). One day before putting the animal into the chamber, two-photon volume imaging of cerebral microvessels and astroglia preliminarily labeled with sulforhodamine 101 (SR101) were performed in the somatosensory barrel cortex. An excitation light was 900 nm and image signals of green fluorescent protein and SR101 were simultaneously acquired with a bandpass filter of 525/50 nm and 610/75 nm, respectively. A single image plane consists of 1024 by 1024 pixels, and a volume image was acquired up to a depth of 0.5 mm from the cortical surface with a z-step size of 5 μm and 4 μm for microvessels and astroglia, respectively. After the experiment was completed, the animal was allowed to wake up from anesthesia and back to the chamber provided with enough food and water. The imaging experiment was repeatedly performed every 3 to 7 days until one month after hypoxic exposure. On a separate date, hemodynamic responses to whisker stimulation and behavior performances were concurrently measured with laser-Doppler flowmetry and optical motion sensor, respectively (Takuwa et al., 2010).

Results and discussion: We observed that chronic hypoxia preferentially induced dilation of parenchyma microvessels (43% increases in a lumen space) within 7 days after the onset of hypoxic induction, but smaller changes in a diameter of surface arterioles (19%) and venules (37%). The morphological changes in astroglia was not significantly observed during this early period (until 7 days), but a distinct increase in cell volume was developed after 2 weeks of hypoxic induction. These results indicate that the vascular remodeling elicited by chronic hypoxia is independently regulated apart from the morphological changes in astroglia. Supporting this notion, a new vessel appeared at capillary regions where the astroglial wrapping was normally preserved in 1 to 2 weeks from hypoxic induction. And then, a new vessel in which blood flow was opened was covered by astroglia as has been seen in normal structures. On the other hand, if newly-appeared vessels fail to meet the partner vessels, those immature vessels disappeared within one week. These observations may indicate that the both opening of blood flow and astroglial remodeling are required for stabilizing newly-appeared vessels.

References:

Tomita Y, Kubis N, Calando Y, Dinh AT, Méric P, Seylaz J, Pinard E, JCBFM (2005) 25, 858-867

Takuwa H, Autio J, Nakayama H, Matsuura T, Obata T, Okada E, Masamoto K, Kanno I, Brain Res (2010) online published

847

THE M.3243A>G MTDNA MUTATION IS ASSOCIATED WITH ALTERATIONS IN PERMEABILITY OF THE BBB

M. Davidson[1], W. Walker[1], E. Young[2], H. Huang[3]

[1]Radiation Oncology, [2]Center for Radiation Research, [3]Neurology, Columbia University, New York, NY, USA

Introduction: Mitochondrial Encephalopathy, Lactic Acidosis and Stroke-like episodes (MELAS)), is a common mitochondrial disease most frequently associated with the m.3243A>G point mutation in the $tRNA^{Leu(UUR}$ of mitochondrial DNA and characterized by stroke-like episodes with vasogenic edema and lactic acidosis. The pathogenic mechanism of recurrent strokes and brain edema is not known. Alterations in the blood brain barrier, (BBB), perhaps caused by respiratory chain defects in the cortical microvasculature, could explain the pathogenesis of stroke-like episodes.

Aim: The goal is to generate an in vitro model of the normal BBB and the MELAS BBB to test this hypothesis.

Materials and methods: Immortalized normal human brain capillary endothelial cells (hMEC/D3) and human fetal astrocytes (IHFA) were used. The cell lines harboring homoplasmic levels of the mtDNA mutation were generated. The mutation levels were checked by RFLP analysis.

Biochemical and cytochemical analyses of the complexes of the respiratory chain were performed on the wild type and MELAS constituent cell types of the BBB.

Results: Severe defects of complex I and complex IV activities, and and a moderate deficiency of complex II activity were demonstrated in astrocytes and endothelial cells (EC) with the mutation. The respiratory chain defects in the mutant EC segregated with lower transendothelial electrical resistance (TEER), in contrast to wild type EC, indicating that the integrity of the BBB was compromised. Furthermore, when the resistance measurements were recorded in the presence of BBB stabilizers, the TEER values returned to almost wild type levels. Currently, studies of the expression of tight junction proteins, transporters and paracellular permeability measurements in co-cultures of EC and astrocytes on transwell inserts are in progress.

Conclusion: These data support our hypothesis that respiratory chain defects in the constituent cells of the BBB may cause changes in permeability of the blood brain barrier. This *in vitro* model of the BBB has the potential to unravel the complex pathogenic mechanism beyond molecular characterization of a devastating disease and to allow testing interventional strategies.

848

BRAIN ENDOTHELIUM PROTECT NEURONS FROM CASPASE-DEPENDENT CELL DEATH THROUGH PI3K/AKT SIGNALING

S. Guo[1], M.F. Stins[2], E.H. Lo[1]

[1]Neuroprotection Research Laboratory, Deptartment of Radiology and Neurology, Massachusetts General Hospital & Harvard Medical School, Charlestown, MA, [2]Neurology, Johns Hopkins Medical Center, Baltimore, MD, USA

Objectives: The concept of neurovascular unit emphasizes that cell-cell signaling between neuronal, glial and vascular compartments underlies the homeostasis of normal brain function. Correspondingly, disruptions in cell-cell signaling in the neurovascular unit may also explain dysfunction during pathology and CNS disease. Previously, we reported that conditoned media from cerebral endothelial cells can protect neurons against a wide range of insults including hypoxia, metabolic injury, and oxidative stress. Here, we tested the mechanism(s) that may underlie the ability of cerebral endothelium to protect neurons against hypoxic injury.

Methods: Primary rat cortical neurons were cultured and objected to hypoxia on DIV7. Human brain endothelial cells were grown in culture and endothelial-conditioned media were collected after 24 h incubation with NBM-RPMI (1:1). Endothelial-conditioned media was transferred to neurons before the beginning of hypoxia. After hypoxia, MTT mitochondrial activity was measured to assess neuronal cell viability. Cell lysates were collected to measure caspase activation by immunoblotting. Cell lysates from neurons treated with endothelial-conditoned media for short time (within 30min) were also collected to measure the activation of Akt signaling. To confirm the role of PI3K/Akt on the protective effect of cerebral endothelial cells, the PI3K inhibitor LY294002 was used to block this signaling pathway.

Results: Hypoxia activated caspases and induced cell death in neurons. Addition of endothelial-conditioned media significantly reduced hypoxic neuronal death. Neuroprotection was accompanied with a decrease in the amount of cleaved Caspase-3 (19 kDa) and cleaved Caspase-9 (38 kDa and 17 kDa) Incubation with endothelial-conditioned media also promptly increased the phosphorylation levels of Akt (Ser 473) and GSK-3beta (Ser 9). Blocking this PI3-K/Akt pro-survival pathway with the potent PI3-K inhibitor LY294002, eliminated the ability of endothelium to protect neurons against hypoxia.

Conclusions: Brain endothelial cells enhanced the pro-survival PI3-K/Akt pathway in neurons and reduced the activation of the caspase-dependent apoptosis pathway. These effects appeared to be required for the ability of endothelium to protect the neurons from hypoxic stress. These results again emphasize the importance of cell-cell interactions within neurovascular unit and non-cell autonomous mechanisms of neuron death. How these putative cellular mechanisms may relate to the damage and/or recovery in stroke or other neurodegenerative diseases in vivo, remains to be elucidated.

849

BRAIN GLUCOSE AND KETONE METABOLISM IN AGED RATS: A DOUBLE TRACER PET STUDY

M. Roy[1], J. Tremblay-Mercier[1], S. Tremblay[2], M. Fortier[1], M. Bentourkia[2], S.C. Cunnane[1]

[1]Physiology and Biophysics, [2]Nuclear Medicine and Radiobiology, Université de Sherbrooke, Sherbrooke, QC, Canada

Introduction: Brain ^{18}F-fluorodeoxyglucose (^{18}F-FDG) uptake is significantly reduced in Alzheimer´s disease (AD). This abnormality correlates well with cognitive impairment in AD. Brain glucose uptake has also been reported to be lower during healthy aging[1] but there is no clear consensus on this[2]. Ketones (b-hydroxybutyrate [b-HB] and acetoacetate [AcAc]) are the brain's main alternative fuel to glucose and mild, experimental ketosis appears to have a beneficial effect on cognitive function in AD[3]. Rats fed on a ketogenic diet for 5 wk presented an increase of b-HB brain uptake of 40 fold[4] while ^{18}F-FDG brain uptake linearly decreased with increasing blood ketone concentration[5].

Objectives: Using PET imaging, to assess: (1) whether brain glucose and ketone metabolism are reduced in healthy aged rats; (2) the effect of a short term ketogenic diet on brain glucose and ketone metabolism in aged rats.

Methods: Brain uptake of ^{11}C-AcAc and ^{18}F-FDG were measured by PET imaging (Triumph; Gamma Medica) in Sprague-Dawley rats at 4, 18, 21 and 24 mo of age (n=6/group). A second group of 24 mo old rats were scanned before and after consuming a ketogenic diet (Dyets, Bethlehem) for 14 d. The double tracer PET protocol consisted of a first injection of ^{11}C-AcAc (50MBq) with a 20 min dynamic scan, 10 min wash-out, and a second injection of ^{18}F-FDG (50MBq) with a 40 min dynamic scan. Each group also underwent a magnetic resonance imaging scan for brain volume assessment. PET data were expressed as a percentage of radiotracer uptake relative to the injected dose/brain volume and as cerebral metabolic rates of ^{18}F-FDG and ^{11}C-AcAc. Brains were removed after the PET scans and used to assess brain glucose and ketone transporter density.

Results: Brain ^{11}C-AcAc and ^{18}F-FDG uptake were not statistically different in the 18, 21 and 24 mo old groups compared to the 4 mo old group. ^{18}F-FDG uptake was 5.7 times higher than ^{11}C-AcAc uptake ($p < 0.0001$). In the 24 mo old rats, plasma ketone level was 0.1 mM before the ketogenic diet and 0.38 mM after 2 wk on the ketogenic diet. ^{11}C-AcAc uptake was 26% higher after 2 wk on the ketogenic diet ($p = 0.04$). ^{18}F-FDG uptake was not different after the ketogenic diet. Whole brain volumes were not statistically different in the 4, 18 and 21 mo old groups. Brain biochemical studies are ongoing.

Conclusions: Energy substrate uptake by the healthy aging rat brain appears to be maintained at levels similar to that of young rats, an observation commonly but not universally reported in humans[2]. Providing a ketogenic diet for a short term facilitates brain uptake of ^{11}C-AcAc but not ^{18}F-FDG in aged rats. The difference between our results and those of LaManna et al[5] may be due to the fact that their rats had much higher ketonemia (plasma b-HB = 4.8 mM).

References: [1]Kalpouzos et al Neurobiol Aging 2009 [2]Cunnane et al Nutrition 2010 [3]Henderson et al Nutr Metab 2009 [4]Puchowicz et al Am J Physiol Endocrinol Metab 2007 [5]LaManna et al Adv Exp Med Biol 2009

850

A STUDY OF PERIPHERAL RESPONSE DURING CEREBRAL ISCHEMIC INFARCT PROGRESSION USING TEMPORAL QUANTITATIVE PROTEOMIC SCREENING

M. Ning[1], M. Lopez[2], D. Sarracino[2], M. Athanas[3], D. McMullin[1], F.S. Buonanno[1], E.H. Lo[1]

[1]Clinical Proteomics Research Ctr, Dept of Neurology, Mass General Hospital/Harvard Medical School, Boston, [2]ThermoFisher Scientific, [3]VAST Scientific, Cambridge, MA, USA

Introduction: While previous studies of clinical biomarkers have been limited to known individual measurable factors, new proteomic techniques may help to simultaneously identify both known and unknown factors directly at the bedside, to improve our understanding of complex disease entities such as stroke, which most probably involves multiple gene interactions. New isotope labeling technology now allows for more accurate quantitative comparison of multiple samples to discover unknown molecular triggers. Coupled with rigorous study design to avoid confounders, we present preliminary data of quantitative proteomic screening in patients with ischemic infarct progression over time.

Patients and methods: Plasma obtained from acute ischemic stroke patients in accordance with IRB approval was labeled with a six-plex isotope tag and data obtained from Orbitrap XL MS. Patients were age, gender, and co-morbidity matched and blood sampled at 2 time-points (6h & 72h) post stroke onset. All patients had worsened clinical outcome with increased infarct size and NIHSS over this time period.

Results: Pathway analysis of quantitative proteomic profiles with respect to cellular compartment suggests novel interaction of circulatory candidates. Both established (S100) and novel (TSP-4) markers are found to increase over time (Figure A). TSP-4, secreted by endothelial cells, interacting with circulating proteins such as SPARC (secreted protein, acidic and rich in cysteine), is important in cell differentiation and response to injury. In the setting of clinical worsening, we found a statistically significant decease of matrix proteases such as ADAMTS-13 - potentially interactive with significantly elevated vWF (Von Willebrand factor), as infarct size increased over 72 hours (Figure B). ADAMTS-13 inactivates vWF by cleaving the bond between tyrosine-842 and methionine-843 in the A2 domain of vWF multimers. This coagulation pathway is important in acute stroke: a deficiency of ADAMTS-13 has been reported to correlate to increased vWF and more clotting events.

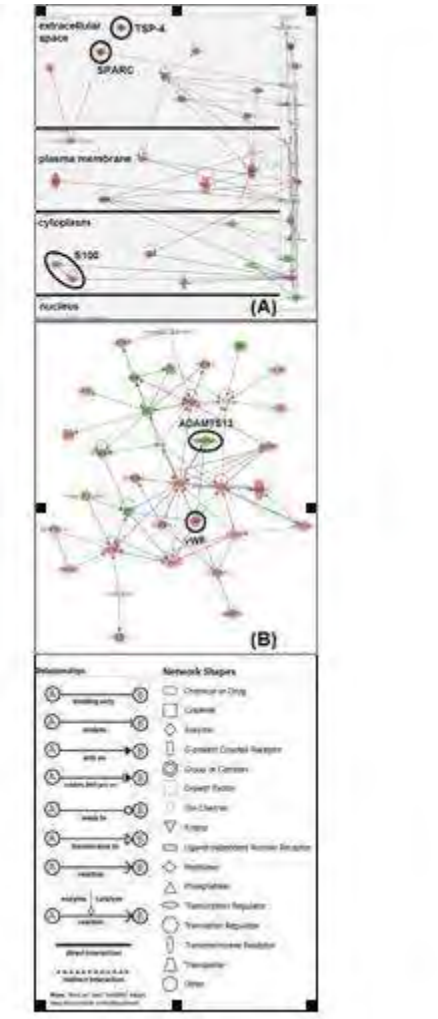

[Figure A and B]

Conclusion: Our proof-of-concept study illustrates the feasibility and potential of direct bedside proteomics as an initial step in understanding ischemic injury progression from the circulation. Quantitative analysis of protein-protein interactions with respect to clinical outcome revealed both an increased expression of relevant injurious markers, and a decrease of novel “protective” factors in disease-relevant pathways. However, further validation is underway to better understand the role of these novel biomarkers for ischemic infarct progression.

851

GENOME-WIDE EXPRESSION PROFILES OF CORTICAL MICROVESSELS AFTER TRAUMATIC BRAIN INJURY

J. Lok[1,2], S. Zhao[1], W. Leung[1], A.T. Som[1], K. Hayakawa[1], X. Wang[1], E.H. Lo[1], **S. Guo**[1]

[1]Neuroprotection Research Laboratory, Deptartment of Radiology and Neurology, Massachusetts General Hospital & Harvard Medical School, Charlestown, [2]Department of Pediatrics, Pediatric Critical Care Medicine, Massachusetts General Hospital, Boston, MA, USA

Objectives: It is increasingly suspected that perturbations in the functioning of blood vessels play a critical role in the pathophysiology of stroke, traumatic brain injury and neurodegeneration. Here, we use a systematic genome-wide transcriptome screening approach to investigate the responses of brain microvessels after brain trauma in mice.

Methods: Male C57Bl/6 mice with 10-12 weeks of age were subjected to controlled cortical impact (CCI) model following standard methods.

Twenty four hrs after CCI, brains were removed and directly damaged tissues in the core of the traumatic lesions were dissected away. Remaining cortex was extracted from non-damaged ipsilateral hemisphere as well as the contralateral hemisphere. Cortical microvascular fragments were isolated by gradient centrifugation in 18% Dextran solutions. Samples from four mice were pooled for each preparation and RNA extraction. A parallel preparation of microvascular was used for immunostaining.

Total RNA samples were used for labeling with Affymetrix 3' IVT Express kit and hybridization with Mouse Genome 430 2.0 Array. Raw expression data for each chip was summarized and normalized using RMA algorithm after quality checking. Differentially expressed genes were identified with SAM algorithm. Quantitative real-time PCR (qPCR) was used to validate differentially expressed genes. Pathways associated with the trauma response were determined using Gene Set Enrichment Analysis (GSEA) algorithm, based on terms from Gene Ontology (GO).

Results: The specificity of purified mouse brain microvascular fragments was confirmed with staining of endothelial markers. In this preparation, CD31 and lectin signals were high compared with low signals for GFAP (astrocyte marker) and SM-actin (smooth muscle cell/pericyte marker).

Applying a criteria of p value < 0.01 and fold change > 2 or < 0.5, we identified 141 genes that were upregulated, and 331 genes that were downregulated in microvessels derived from non-damaged ipsilateral cortex after CCI. The differentially expressed genes came from categories comprising a wide range of functions, including extracellular matrix (fibromodulin and Tenascin C), ECM proteinase (MMP-3, TSP-1 and Adamts 1/4/9), cytokines (IL-6, IL-11 and LIF), growth factors and receptors (VEGF-C, PDGF-D and IGF1-R) and transcription factors (Fos b, Id4 and ATF4). Some of these genes, e.g. BDNF, c-fos, CD-44, IL-6, STAT-3, TIMP-1 have previously been reported to change in the brain after trauma. The expressions of randomly selected 6 genes were all confirmed with q-PCR.

Based on GO analysis, statistically enriched pathways that were upregulated in the microvessels of ipsilateral cortex include inflammatory response and cytokine activity, and

extracellular matrix. Enriched pathways that were downregulated include those related to mitochondrial functions, oxidation reduction and several transport pathways.

Conclusions: This study explored the responses of microvessels to brain trauma with genome-wide gene expression profiles. The results indicate that traumatic brain injury induces a wide spectrum of responses in the cerebral endothelium. Importantly, these gene responses come from areas of non-directly-damaged cortex, indictaing that microvascular perturbations can be widespread and not necessarily localized to focal areas of trauma per se. Further investigations of these microvascular phenomenons may reveal new mechanisms and/or therapeutic targets relevant for the acute treatment of traumatic brain injury.

852

CD36 EXPRESSED IN THE PERIPHERY AND BRAIN SYNERGIZE IN ISCHEMIA-REPERFUSION INJURY

E. Kim[1], M. Febbraio[2], Y. Bao[1], A.T. Tolhurst[1], **S. Cho**[3]

[1]Research, W M Burke Medical Research Institute, White Plains, NY, [2]Molecular Cardiology, Cleveland Clinic, Cleveland, OH, [3]Neurology/Neuroscience, Weill Cornell Medical College at Burke Med Res Inst, White Plains, NY, USA

Background: CD36, an inflammatory mediator, has been implicated in ischemic brain injury (*Cho et al.,* 2005). It expresses in several types of cells in the CNS (microvascular endothelial cells, astrocytes, and microglia) and in the periphery (monocytes, macrophages, and platelets). Our previous study showed that elevating plasma cholesterol levels at the time of stroke increased infarct size and this exacerbation was associated with enhanced expression of CD36 in ischemic brain as well as in peripheral monocytes/macrophages (*Kim et al.*, 2008). The current study investigates the extent to which peripheral CD36 influences ischemic inflammation/injury and defines a role of brain CD36 in attaining the peripheral effect in hyperlipidemic conditions.

Methods: Eight week-old male CD36-expressing ApoE knock-out (**AKO**) and CD36-deficient ApoE knock-out (**DKO**) mice were subjected to whole body irradiation and received $1x10^7$ stem cells from AKO bone marrow (AKO^{bm}) or DKO bone marrow (DKO^{bm}). After 11 weeks of a high fat diet, the mice were subjected to 20 min MCAO by an intraluminal thread method. Mice were sacrificed at 72 h after ischemia. Infarct volume and CD36, MCP-1 and CCR2 mRNA levels were determined in the brain.

Results: Eleven weeks of a high fat diet significantly elevated plasma cholesterol levels ~900 mg/dl in both AKO and DKO mice regardless of the source of bone marrow (n=12-14/group, *ns*). CD36 gene expression in the ischemic brain was absent in mice transplanted with CD36-deficient DKO^{bm} but present in mice transplanted with CD36-expressing AKO^{bm}, suggesting that CD36 expression in the ischemic brain originates from the periphery. Compared to AKO mice that received AKO^{bm} (control transplant), the AKO mice transplanted with DKO^{bm} resulted in 30% reduction in infarct volume (n=12-14, $p< 0.05$, Fig. 1) and MCP-1 and CCR2 mRNA levels were reduced by 27% and 35% respectively ($p< 0.05$). In contrast, infarct volume (Fig. 1), MCP-1 or CCR2 mRNA levels were not different between DKO mice received either AKO^{bm} or DKO^{bm} (n=11-15, *ns*), suggesting that peripheral CD36 effect did not occur in the absence of brain CD36. Correlation analyses of MCP-1 or CCR2 against infarct volume revealed blunted MCP-1/CCR2 responses in DKO compared to AKO host mice (Fig 2).

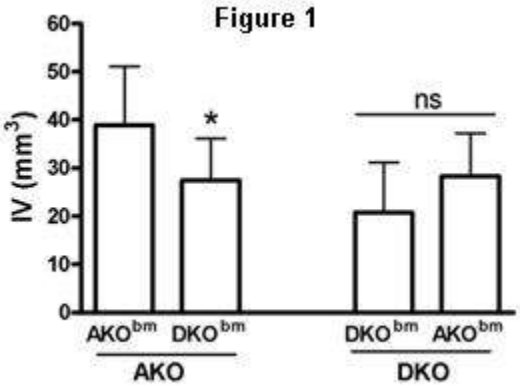

[Figure 1]

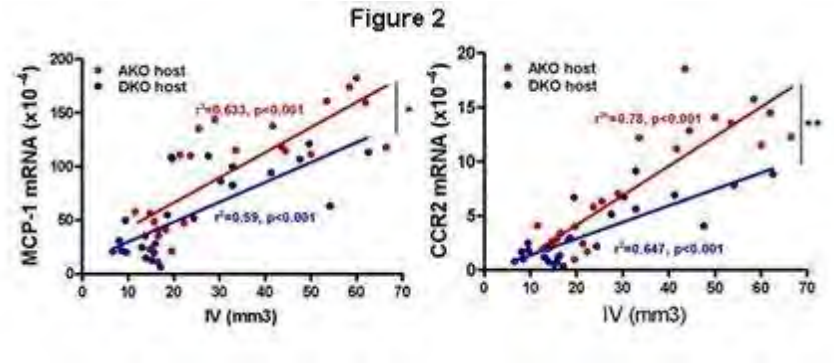

[Figure 2]

Conclusion: The data unequivocally demonstrate that peripheral CD36 is the major source of stroke-induced CD36 expression in the brain and that it contributes to stroke-induced brain injury. The peripheral effect on stroke injury is dependent upon the modulation of MCP-1 and CCR2 expression, and additionally requires the expression of CD36 in the host brain. The synergy implies that targeting peripheral CD36, in addition to brain CD36, provides added protection from stroke-induced brain injury. (Supported by NIH grants HL82511 to SC)

References:

1. Cho et al., J Neurosci. 2005 Mar 9;25(10):2504-12.

2. Kim et al., J Neurosci. 2008 Apr 30;28(18):4661-70.

853

ESSENTIAL ROLE OF 14-3-3Γ AND ITS MECHANISM IN PROTECTING ASTROCYTES FROM APOPTOSIS DURING ISCHEMIA AND PRECONDITIONING

Y. Pang, Y. Dong, R. Zhao, A.C.-H. Yu

Neuroscience Research Institute, Department of Neurobiology, Peking University, Beijing, China

The 14-3-3 family, a group of multifunctional acidic proteins, exists predominantly in the brain. Our group has demonstrated that 14-3-3γ expresses in cultured astrocytes and specifically up-regulated under ischemia. Furthermore, up-regulation of 14-3-3γ is neuro-protective and crucial in protecting astrocytes from ischemic induced apoptosis with the mechanism through binding to phosphorylated Bad to prevent Bad from getting into mitochondria. Then we examined the signaling pathways and found JNK/c-Jun/AP-1 pathway to be responsible for the up-regulation of 14-3-3γ in astrocytes under ischemia. Preconditioning, happening under non-lethal ischemia stress, can induce endogenous self-protection to enhance tolerance to the subsequent ischemic insult and promoting survival. 14-3-3γ may be an indicative endogenous protective protein in astrocytes preconditioning. We established a preconditioning model in vitro using cultured astrocytes. We investigated the expression of 14-3-3γ after ischemia for 0.5h, 1h and 2h and detected that it remains in high level after reverting back to normal culture condition in 72h. Furthermore, we found out that preconditioning for 0.5h and then reverting to 6h's normal culturing condition could produce significant protective role facing ischemia again. Once JNK signaling pathway was inhibited, up-regulation of 14-3-3γ induced by preconditioning abolished. Our studies infer that 14-3-3γ could be one of the protective proteins induced during preconditioning. This provides a foundation for the future development of pharmacotherapy to manipulate its intrinsic levels, thus might provide an important means to lengthen therapeutic window for ischemia treatment.

Acknowledgement: Supported by the National Natural Science Foundation of China (Grant No.: 30870818); and the Beijing National Natural Science Foundation of China (Grant No.: 7051004).

Key Words: 14-3-3γ, Astrocytes, Apoptosis, Ischemia, Preconditioning

854

DYNAMICS OF OXYGEN TRANSPORT IN A CAPILLARY NETWORK

C.S. Park, P. Orlowski, M.A. Chappell, V. Grau, **S.J. Payne**

Department of Engineering Science, University of Oxford, Oxford, UK

Objectives: The dynamics of oxygen transport within the microvasculature are complex, due to the high degree of interconnectedness of the capillary network. However, a better understanding of how these dynamics vary with the local network properties would be valuable in helping to interpret how oxygen supply is affected under different pathological conditions. The mass transport equation is solved here for a general capillary network to quantify how the concentration changes locally in response to altered arteriolar oxygenation. This could also be used to help to interpret results obtained using dynamic susceptibility MRI and ASL, for example, which are dependent upon an arterial input function, which is not currently directly related to the underlying physiology.

Methods: A capillary network matching both length and radial distribution obtained experimentally [1] is created using a specific algorithm, described elsewhere. The one-dimensional mass transport equation is solved for the created capillary network assuming Poiseuille flow and that the concentration is solely driven by convection. Two different cases, with and without diffusion through the capillary membranes to the surrounding tissue, are considered to investigate the importance of this diffusion on the dynamics.

Results: A specific signal is considered at the inlet of our capillary network in order to observe the signal produced at the outlet. Figure 1 shows the concentration at the outlet along time with a sinusoidal inlet signal with a mean concentration of 1mol and amplitude of 1mol. For the case without diffusion through the capillary membranes a general exponential recovery in the concentration is observed modulated with oscillations due to the oscillatory nature of the signal at the inlet. A similar trend is observed for the case with diffusion through the capillary membranes. There is however a difference in the amplitude of the oscillations at the outlet, this being primarily dependent on the magnitude of the diffusion coefficient across the capillary membranes. The concentration in the tissues will determine the magnitude of the exponential recovery. Mathematical analysis shows that the time constant is unaffected by the presence of diffusion, whereas the amplitude is affected.

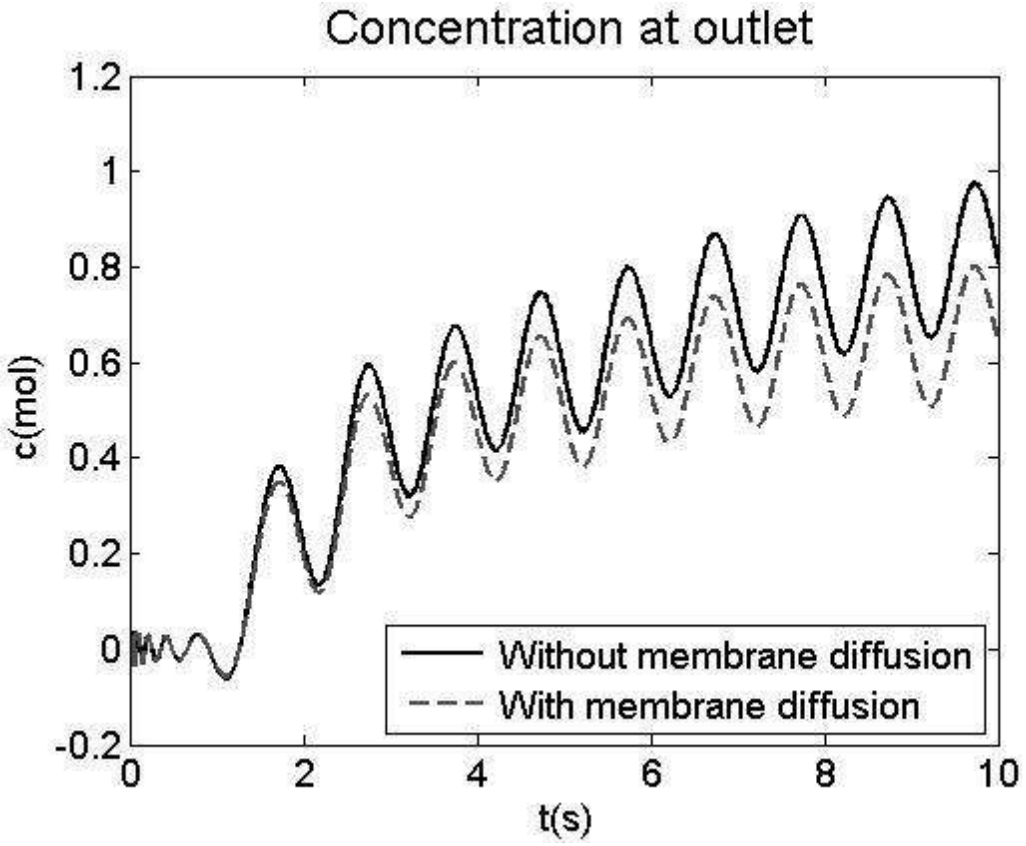

[Figure 1]

Conclusions: We have presented a model to quantify the concentration within the vessels in a simple capillary network. The difference in the concentration at the inlet and outlet at a given time determines the rate of supply from the capillary network. Preliminary results confirm that the model responds in a first order way. We plan to investigate how different networks responds and thus to characterize the response in terms of the network connectivity and vessel length distribution. This will be very helpful in developing accurate models of the microvasculature that can be used within more lumped models of the cerebral circulation, both in the context of oxygen supply and in interpreting results from imaging techniques such as ASL and dynamic susceptibility MRI.

[1] F. Cassot et al. Microcirculation, 13:1-18, 2006.

855

IMPAIRED CBF REGULATION CONTRIBUTES TO LARGER ISCHEMIC VOLUME IN SPONTANEOUSLY HYPERTENSIVE RATS

B.T. Kang, R. Leoni, A. Silva

Cerebral Microcirulation Unit, Laboratory of Functional and Molecular Imaging, National Institute of Neurological Disorders and Stroke/National Institutes of Health, Bethesda, MD, USA

Objectives: Spontaneously hypertensive rats (SHR) have increased susceptibility to ischemic stroke compared with the normotensive rats. Reduced collateral blood flow has been considered as a major contributing factor. The purpose of this study was to investigate the correlation between temporal changes of cerebral blood flow (CBF) and the severity of ischemic stroke in SHR and Wistar-Kyoto rats (WKY).

Methods: Focal cerebral ischemic stroke was induced during 1 hour by transient middle cerebral artery occlusion (MCAO). T2-, diffusion- and perfusion-weighted magnetic resonance imaging were performed serially with a 7-tesla MR system at six different time points; before and during MCAO, 1 hour after reperfusion, and 1 day, 4 days and 7 days after MCAO. Lesion volumes were estimated on apparent diffusion coefficient (ADC) maps and T2-weighted images. Regional CBF values were measured within and outside the perfusion deficient lesion and normalized by the CBF in the corresponding region of the contralateral hemisphere.

Results: Ischemic lesion volumes were significantly larger in SHR than in WKY at all time points ($p< 0.05$). The difference in lesion volumes between the two species increased up to 7 days after MCAO (during MCAO, 8.82%; 7 days after MCAO, 18.81%). Even though perfusion lesion volumes were not different between two species (WKY, 32.52%±4.3; SHR, 34.86%±3.01, $p>0.05$), the CBF ratio within the perfusion lesion was significantly lower in SHR than in WKY during MCAO (WKY, 0.32±0.04; SHR, 0.25±0.07, $p< 0.05$). On the other hand, hyperperfusion was observed in the perfusion lesion of SHR at 4 days (CBF ratio: WKY, 1.04±0.26; SHR, 1.53±0.34, $p< 0.05$) and 7 days (WKY, 1.14±0.34; SHR, 1.57±0.34, $p=0.05$) after MCAO.

Conclusions: SHR has more severe ischemic damage than WKY during ischemic period and post-ischemic periods. The impaired CBF regulation in the hyper-acute and acute post-ischemia period is closely related to the increased sensitivity to ischemic stroke in SHR. These results suggest that restoring normal CBF values is a potential therapeutic target in hypertensive patients following an ischemic attack.

857

NITROXYL SUPPRESSES CEREBROVASCULAR REACTIVE OXYGEN SPECIES GENERATION AND CONSTRICTOR RESPONSES TO ANGIOTENSIN II VIA INHIBITION OF NOX2-NADPH OXIDASE

A.A. Miller, K.F. Maxwell, S. Chrissobolis, S. Selemidis, G.R. Drummond, C.G. Sobey, B.K. Kemp-Harper

Vascular Biology & Immunopharmacology Group, Department of Pharmacology, Monash University, Melbourne, VIC, Australia

Objectives: Accumulating evidence suggests that elevated production of reactive oxygen species (ROS) by Nox2-NADPH-oxidase is an important underlying cause of cerebrovascular dysfunction in a number of vascular diseases. For example, Nox2-NADPH oxidase-derived ROS has been implicated in mediating angiotensin II-induced constrictions and endothelial dysfunction in the cerebral circulation. Nitroxyl (HNO), the reduced and protonated congener of nitric oxide ($NO^{\cdot}$), is emerging as a novel entity with distinct pharmacology and therapeutic advantages over $NO^{\cdot}$. Nitric oxide (NO.) has been reported to suppress NADPH oxidase superoxide ($\cdot O_2^-$) generation. The aims of this study were to test the hypothesis that HNO limits ROS levels and constrictor responses to angiotensin II in the cerebral circulation via inhibition of Nox2-NADPH oxidase.

Methods: Basilar and middle cerebral arteries (MCA) were isolated from male C57Bl6/J wild-type (WT) and Nox2-deficient ($Nox2_{-/-}$) mice. The effect of the HNO donor, isopropylamine NONOate (IPA/NO; 0.1-1μmol/L) on angiotensin II (0.1μmol/L)-stimulated $\cdot O_2^-$ production, and angiotensin II (0.1μmol/L)- and phorbol 12,13-dibutyrate (PDB, Nox2-activator; 10μmol/L)-stimulated hydrogen peroxide (H_2O_2) production were assessed using lucigenin (5μmol/L)-enhanced chemiluminescence and Amplex red fluorescence, respectively. The effect of IPA/NO (1μmol/L) on constrictor responses to angiotensin II (1nmol/L-1μmol/L) was assessed in isolated cannulated MCA using a perfusion myograph.

Results: Angiotensin II-stimulated $\cdot O^{2-}$ levels in cerebral arteries from WT mice (150±25 10^3 counts/s/mg; n=21) were suppressed in a concentration-dependent manner by IPA/NO such that at 1μmol/L, IPA/NO decreased levels by ~60% (n=8; 63±18 10^3 counts/s/mg; P< 0.05). IPA/NO (1μmol/L) also suppressed angiotensin II- and PDB-stimulated H_2O_2 levels in cerebral arteries from WT mice by ~40% (n=11-13; P< 0.05). The ability of IPA/NO (1μmol/L) to decrease $\cdot O_2^-$ levels was reversed by the HNO scavenger L-cysteine (3mmol/L; vehicle + L-cysteine, 98±21; IPA/NO + L-cysteine, 100±8; 10^3 counts/s/mg; n=8; P< 0.05), yet sustained in the presence of the $NO^{\cdot}$ scavenger hydroxycobalamin (100μmol/L; n=7), the soluble guanylate cyclase inhibitor ODQ (10μmol/L; n=6), and the protein kinase G inhibitor Rp-8-pCPT-cGMPs (10μmol/L; n=6). Angiotensin II-stimulated $\cdot O_2^-$ levels were lower in cerebral arteries from $Nox2^{-/-}$ versus WT mice (WT, 191±26; $Nox2^{-/-}$, 103±10; 10^3 counts/s/mg; n=5; P< 0.05). Moreover, IPA/NO (1μmol/L) had no effect on angiotensin II-stimulated $\cdot O_2^-$ levels in cerebral arteries from $Nox2^{-/-}$ mice (IPA/NO, 102±9 10^3 counts/s/mg; n=5). Finally, IPA/NO (1μmol/L) abolished angiotensin II (1nmol/L-1μmol/L)-induced constrictions of MCA from WT mice (Δ diameter for 1μmol/L angiotensin II: Control, -13±3%; IPA/NO, 1±0.6%; n=5; P< 0.05) without affecting constrictor responses to high K^+ (124 mM; n=5).

Conclusions: In summary, we report for the first time that HNO acutely suppresses angiotensin II-stimulated ROS generation in mouse cerebral arteries via cGMP-independent inhibition of Nox2-NADPH-oxidase. Furthermore, HNO attenuates Nox2-dependent angiotensin II-induced

constrictions of MCA i*n vitro.* Thus, an ability of HNO to suppress ROS generation by Nox2-NADPH oxidase may facilitate the use of HNO donors in the treatment of cerebrovascular dysfunction associated with hypertension and other vascular diseases.

858

DELETION OF NOX2 PREVENTS EXCESSIVE SUPEROXIDE PRODUCTION AND REDUCED NITRIC OXIDE BIOAVAILABILITY IN CEREBRAL ARTERIES FOLLOWING TRANSIENT ISCHEMIA

A.A. Miller, T.M. De Silva, V.H. Brait, G.R. Drummond, C.G. Sobey

Vascular Biology and Immunopharmacology Group, Department of Pharmacology, Monash University, Melbourne, VIC, Australia

Objectives: Following cerebral ischemia and reperfusion the function and integrity of cerebral arteries are critical for maintaining cerebral blood flow and thus minimizing further neuronal injury. Experimental studies have reported that reperfusion after partial or complete cerebral ischemia results in cerebral endothelial dysfunction. Although such changes are proposed to result from oxidative stress, the contributing molecular mechanisms are unclear. Here, we tested the hypothesis that enhanced superoxide ($\cdot O_2$-) production by Nox2-containing NADPH oxidase leads to impaired cerebral endothelial function following transient ischemia.

Methods: Cerebral ischemia was induced in male C57Bl6/J wild-type (WT; n=42) and Nox2-deficient ($Nox2^{-/-}$; n=14) mice by middle cerebral artery occlusion (MCAO) for 0.5 h followed by reperfusion (23.5 h). Control mice (WT; n=7) were subjected to sham surgery. MCA were isolated from the ischemic and non-ischemic cerebral hemispheres of mice following MCAO, and from corresponding left and right hemispheres of sham mice. Basal and phorbol 12,13-dibutyrate (PDB, Nox2-activator; 10µmol/L)-stimulated $\cdot O_2^-$ production by MCA were measured by L-012 (100 µmol/L)-enhanced chemiluminescence. Endothelial function was assessed in isolated cannulated MCA using a perfusion myograph via the vasoconstrictor response to the nitric oxide synthase inhibitor, *N*-nitro-L-arginine methyl ester (L-NAME; 100 µmol/L).

Results: At 24 h after MCAO, $Nox2^{-/-}$ mice had smaller infarct volumes than WT mice ($Nox2^{-/-}$: 14.7±3.8 mm^3, n=7; WT: 36±3.4 mm^3, n=15, P< 0.05). In WT mice, both basal and PDB-stimulated ·O2- production by ischemic MCA (basal, 71±24; PDB, 3077±834, 10^3 counts/mg; P< 0.05, n=8-9) were elevated compared with the non-ischemic MCA (basal, 21±4; PDB, 536±66, 10^3 counts/mg; n=8-9) or MCA from sham mice (basal, 33±11; PDB, 641±32, 10^3 counts/mg; n=7). However, in $Nox2^{-/-}$ mice, $\cdot O_2^-$ production by ischemic MCA was not elevated (basal, 21±2; PDB, 14±4, 10^3 counts/mg, n=6; versus non-ischemic MCA: basal, 20±3; PDB, 18±7, 10^3 counts/mg, n=5). In WT mice, the magnitude of L-NAME-induced constriction of ischemic MCA (Δ diameter = -14±3 %; P< 0.05, n=8) was < 40% of that in non-ischemic MCA (-27±5 %; n=6), whereas similar constrictor responses to the thromboxane A2 mimetic U46619 (1nM-1µmol/L) were observed in ischemic and non-ischemic MCA. In Nox2-/- mice L-NAME-induced constriction of ischemic MCA was unchanged (-24±4 %, n=6; non-ischemic: -22±5 %, n=6).

Conclusions: Excessive $\cdot O_2^-$ production and endothelial dysfunction occur in ischemic MCA at 24 h following transient ischemia. These changes appear to be exclusively due to increased activity of Nox2-NADPH oxidase. Thus, limiting Nox2-derived O_2^- production may be a potential therapeutic strategy for improving cerebral vascular function following cerebral ischemia and reperfusion.

859

THE EXTRACELLULAR CALCIUM-SENSING RECEPTOR (CASR) IS INVOLVED HIPPOCAMPAL NEURONAL DEATH IN TRANSIENT GLOBAL ISCHEMIA MOUSE MODEL: SUPPRESSION BY HYPOTHERMIA

J.Y. Kim[1], Z. Cheng[2], N. Kim[3], M.A. Yenari[3], W. Chang[2]

[1]Neurology & Endocirne Research Unit, [2]Endorine Research Unit, [3]Neurology, UCSF, VAMC, San Francisco, CA, USA

Cerebral ischemia induces neuronal hyperactivity that leads to intracellular calcium overload and cell death. The extracellular calcium-sensing receptor (CaSR), which is a member of family C G-protein-coupled receptors was originally described in parathyroid tissues, but is now recognized to be broadly expressed in the brain, including all subpopulations of hippocampal neurons. The CaSR senses minute changes in extracellular [Ca^{2+}] and couples to multiple signaling responses and secretory function in the cells. Activation of CaSR promotes Ca^{2+} release from intracellular stores and Ca^{2+} influx through membrane ion channels in many cell systems. To test the hypothesis that changes in the expression and activity of neuronal CaSRs are involved in promoting neuronal injury after cerebral ischemia, we generated $^{CamK2a}CaSR^{-/-}$ mice with CaSR knockout (KO) targeted to hippocampal neurons by breeding a floxed-CaSR mouse with a transgenic CamK2a-Cre mouse line. Global cerebral ischemia was performed on 3-months-old male KO and control littermates by occlusion of both common carotid arteries (2-VO) for 10 min, followed by 3-days of reperfusion. Brain sections from KO and controlled mice were prepared for immunohistochemistry for CaSR expression and TUNEL staining. In uninjured WT mice, CaSR expression was localized to the CA1, CA3, and dentate gyrus (DG) of the hippocampal formation. CaSR expression in these regions was absent in the KO mice, confirmed by immunohistochemistry. In WT mice, ischemia profoundly increased CaSR expression in the CA1, CA3 and DG when compared to sham controls. TUNEL-positive neurons were also increased in the hippocampus of injured mice. In contrast, the number of TUNEL-positive neurons was significantly ($p< 0.05$) decreased in CA1 (by ~25%), CA3 (by ~70%), and DG (by ~85%) of ischemic $^{CamK2a}CaSR^{-/-}$ mice compared to ischemic WT ($P< 0.05$). Hypothermia has been shown to be effective in improving neurological outcome from cardiac arrest. To test whether changes in CaSR expression contribute to the neuroprotective effects of hypothermia, we compared CaSR expression in hippocampus of mice subjected to 2-VO at 33 ^{o}C and 37^{o}C. Cooling was initiated at the onset of reperfusion and maintained for 3 h. Brains were assessed by immunohistochemistry and TUNEL staining 3 days later. Immunistaining indicated that hypothermia prevented ischemia-induced CaSR overexpression and neuronal death in all sub-regions of hippocampus ($P< 0.05$). Our data support a new role for the CaSR in potentiating ischemic neuronal death. We conclude that the CaSR may be a new therapeutic target for treatment of ischemic brain injury.

Study supported by DOD W81XWH-05-2-0094 and NIH AG-21353 (WHC) and DOD DAMD17-03-1-0532 and NIH NS-40516 (MAY)

860

VASCULAR NITRIC OXIDE AS PART OF A MOLECULAR MOSAIC IN THE DEVELOPMENT OF ALZHEIMER´S DISEASE

J.C. de la Torre

Alzheimer Research Unit, Banner Research Institute, Sun City, AZ, USA

Vascular nitric oxide (vNO) has been reported to be involved in Alzheimer´s disease (AD) but its role in the development of this disorder is unclear. Based on post-mortem data, endothelial dysfunction involving vNO in the cerebral microvasculature of AD patients has been reported, adding fuel to the mystery. Because mounting evidence indicates that AD is a vascular disorder with neurodegenerative consequences and is preclinically accompanied by chronic brain hypoperfusion (CBH), the role of vascular NO in the pathology of this dementia takes on special meaning. We report that CBH in aging rats appears to ´upregulate´ vNO in the hippocampus prior to spatial memory impairment and to Abeta 1-40 accumulation in the hippocampus. Experimental upregulation of vNO may be a ´futile´ compensatory reaction that attempts to diminish the damage posed by the persistent CBH and the shear stress it creates on the endothelial surface of the microvasculature. However, the neuronal energy hypometabolic changes promoted by CBH that precede AD onset as measured by FDG-PET studies, may explain in part, the subcellular cascade that include not only vNO release but also the participation of epoxyeicosatrienoic acids (EETs) and hypoxia-inducible factor-1 in endothelial cells. These interrelated endothelial cell molecules largely participate in the convoluted mosaic that characterizes AD. Vascular-related factors and their attending endothelial cell vasoactive agents that form the preclinical AD mosaic present a realistic therapeutic target to how and why AD onset can be prevented in asymptomatic individuals .

861

MAPPING THE BOLD RESPONSE DYNAMICS USING RESPIRATORY CHALLENGES IN HEALTHY AND CLINICAL POPULATIONS

M.G. Bright[1,2], D.P. Bulte[2], P. Jezzard[2], J.H. Duyn[1]

[1]Advanced MRI Section, Laboratory for Functional and Molecular Imaging, National Institute of Neurological Disorders and Stroke, Bethesda, MD, USA, [2]FMRIB Centre, University of Oxford, Oxford, UK

Objectives: Recently, a novel hypocapnic respiratory challenge of Cued Deep Breathing (CDB) was proposed and the dynamics of the resulting BOLD response were characterized [1]. In this study, we better measure the healthy variation in the BOLD response to respiratory challenges, and apply challenges in patients to compare the response timing maps of the non-invasive CDB method with more traditional bolus-tracking results.

Methods: Healthy Volunteers: Six volunteers were scanned using a 3 Tesla Siemens scanner equipped with a 12-channel receive head coil. A 460-volume BOLD EPI scan was acquired (TR/TE=1250/40ms, FOV=240mm, resolution=3.0x3.0x5mm^3, 17 slices). Six CDB trials were performed, interleaved with 60 seconds of normal breathing. CDB task instructions were presented using visual cues (Figure, top-left panel): four breathing instructions were prompted at two-second intervals. A structural MP-RAGE image was acquired for registration purposes. The BOLD data were motion corrected (MCFLIRT), and the timecourse of each voxel was interpolated to a temporal resolution of 0.2s and smoothed with a 3.0s Gaussian kernel. The average response to the six trials was determined, and the time-to-peak of the BOLD signal dip was identified. For every subject, the EPI data were aligned to the structural image (FLIRT, FSL), which was aligned to a template brain (Montreal Neurological Institute). The MNI brain was segmented to create a gray matter mask (FAST, FSL) and the mean TTP within gray matter voxels was calculated. After normalizing every voxel to the mean subject response time, the six datasets were combined to create a mean group map of relative CDB response timing.

Patient Study: In chronic stroke patients exhibiting significant uni- or bilateral stenosis of the carotid arteries but negligible neurological symptoms (not receiving a carotid endarterectomy), DSC bolus tracking data were acquired as part of a separate clinical study. In five of these patients, a BOLD EPI scan during five CDB challenges was executed. Four subjects did not complete the scan or did not exhibit robust BOLD signal changes that could be characterized. In one subject, BOLD data enabled whole-brain mapping of CDB TTP using the analysis method discussed above. Voxelwise TTP of the bolus passage was also mapped. These results were aligned to a structural image and masked to display only gray matter voxels.

Results: Good consistency in the regional heterogeneity of the BOLD response timing following CDB challenges was observed in healthy subjects (top-right panel). The delayed response in posterior cortical areas agrees with bolus arrival time maps in the literature [2]. In the TTP maps of the stenosis patient (bottom panel), similarities are visible between bolus- and respiration-derived results. Most strikingly, asymmetry in the TTP in the posterior cortex can be observed in both maps.

Conclusions: Non-invasive respiratory challenges such as the CDB task may provide similar information as traditional, but invasive, contrast agent methods, opening possibilities for application in a broader range of environments.

References:

[1] Bright MG, et al. (2009) Neuroimage 48(1):166-75.

[2] van Gelderen P, et al. (2000) Radiology 216(2):603-8.

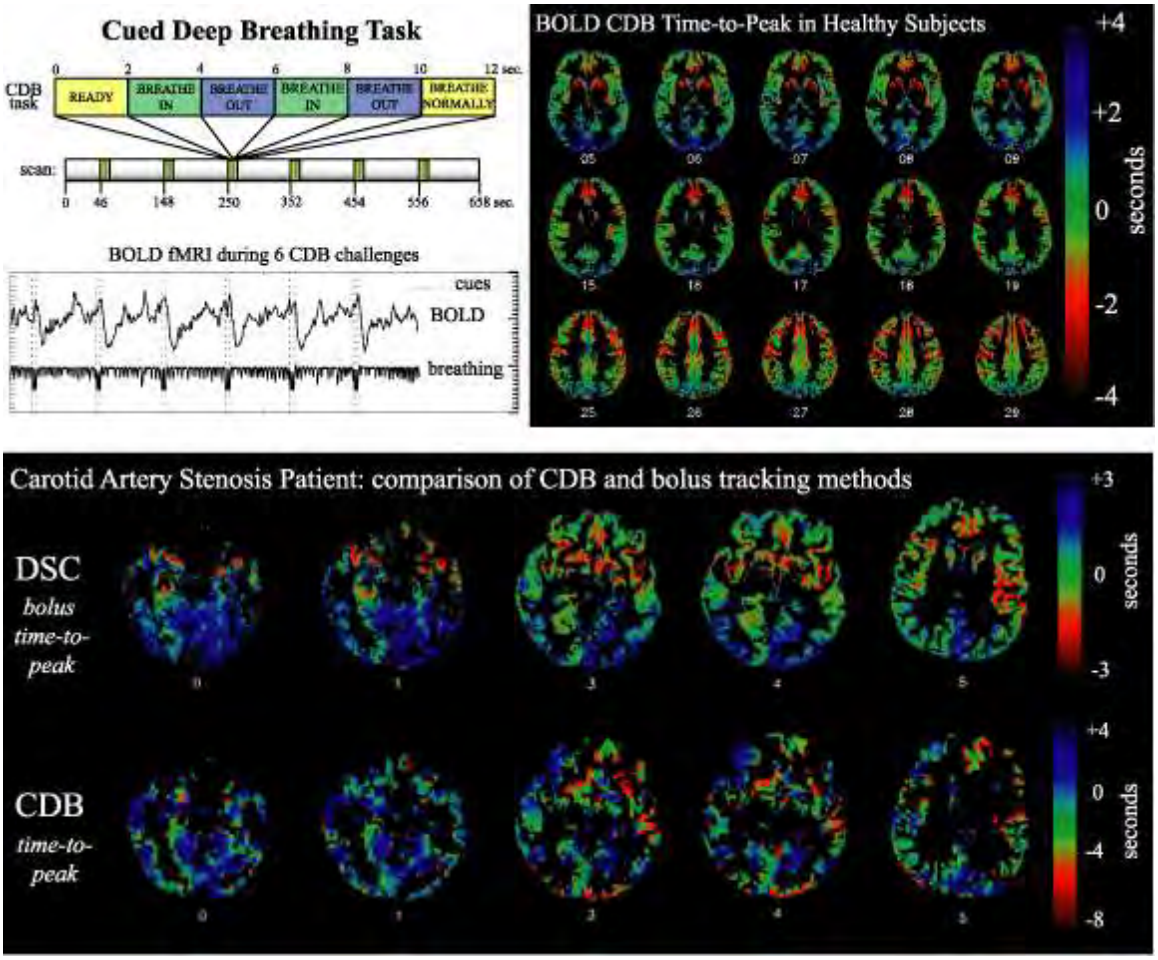

[Figure]

862

HSP70 OVEREXPRESSION DECREASES MMP ACTIVITY AND IMPROVES HEMORRHAGE AND MOTOR RECOVERY AFTER TRAUMATIC BRAIN INJURY

J.Y. Kim[1], N. Kim[1], L.J. Noble-Haeusslein[2], M.A. Yenari[1]

[1]Neurology, UCSF, VAMC, [2]Neurological Surgery & Physical Therapy & Rehabilitation Science, UCSF, San Francisco, CA, USA

Disruption of the blood brain barrier (BBB) leads to complication of brain trauma including brain edema and hemorrhage. Recent work has implicated matrix metalloproteinases (MMPs) in the breakdown of the extracellular matrix and BBB. MMP-2 and MMP-9 are both increased in the brain and spinal cord following cerebral ischemia and brain trauma, and mice lacking MMP-9 are protected from damage, in part, by preventing BBB disruption. We and others have shown that the 70kD heat shock protein (HSP70) protects against various cerebral insults including ischemia, excitotoxicity, oxidative stress and apoptosis. Whether it also protects against traumatic brain injury (TBI) has surprisingly not yet been demonstrated. HSP70 is increased within brain including vascular structures following various brain insults. While thought to protect by preventing protein aggregation, more recent work has shown that it can directly inhibit other brain injury pathways such as suppression of immune responses and expression and processing of the MMPs. In this study, HSP70 transgenic or wildtype mice were subjected to TBI using controlled cortical impact (CCI). After drilling a burr hole at: AP: -2.5 mm, ML: 2.0mm, an impactor was applied at a depth of 1 mm and dwell time of 8. This model leads to impairment of corresponding motor functions as well as consistent BBB disruption and hemorrhage. 3d following CCI, mice were assessed for BBB disruption and MMP activity. Mice were also assessed for lesion size and neurological behavior 14 d post CCI. We found that HSP70 overexpression protected the brain following TBI as evidenced by decreased cell loss ($n=6$/group, $P< 0.05$) and improved behavior indices using the elevated body swing and corner tests, and improved walking on an inclined beam ($P< 0.05$). Brain hemorrhage and MMP activity were also decreased among the HSP70 transgenic brains. To our knowledge, this is the first direct demonstration of brain protection due to HSP70 overexpression in a model of TBI. This would support the development of strategies to increase HSP70 in the brain for prophylaxis or direct treatment of TBI.

Study supported by DOD grant DAMD17-03-1-0532

863

THE STUDY OF DISTURBANCE OF CEREBRAL BLOOD FLOW FOR PATIENTS WITH SUBARACHNOID HEMORRHAGE IN EARLY PHASE

M. Honda[1], K. Yokota[1], H. Masuda[2], H. Uekusa[2], R. Ichibayashi[1], K. Yosihara[1], S. Sase[3], T. Kishi[4]

[1]Department of Critical Care Center, [2]Department of Neurosurgery, Toho University School of Medicine, [3]Anzai Medical Co., Ltd., [4]Department of Education Planning and Development, Toho University School of Medicine, Tokyo, Japan

Introduction: Subarachnoid hemorrhage (SAH) is widely known to cause a dynamic change in cerebral blood flow (CBF). Especially, a decrease in CBF due to secondary brain insult has been reported. There is not only delayed ischemia due to vasospasm, but also early perfusion deficits before vasospasm phase. The purpose of this study was to clarify the disturbance of CBF in this early phase and the possibility of assessing outcome.

Methods: In 109 patients with SAH we performed Xe-CT and perfusion CT to evaluate cerebral circulation at the same time during Day 1 - Day 4. We measured CBF using Xe-CT and mean transit time (MTT) using perfusion CT and calculated cerebral blood volume (CBV) by AZ-7000W98 computer system.

Results: Analysis of variance in grading on admission and outcome was done (Table 1 & Table 2). We tried to predict the outcome by discriminate analysis using these parameters. The probability was 71.3%.

Conclusion: We could evaluate the condition of cerebral circulation for patients with SAH by these parameters. These parameters can be helpful for the evaluation of circulation disturbance and prediction of outcome for the patients with SAH.

Hunt and Kosnik grading	CBF(ml/100g/min)	MTT(sec)	CBV(ml/100g)
II	34.7±11.3	6.2±1.0	3.4±1.0
III	29.9±9.3	6.8±1.4	3.3±1.2
IV	25.4±8.3	7.4±2.4	3.0±1.2
V	18.6±6.8	7.2±1.0	2.1±0.8
	P<0.001	P< 0.05	P < 0.05

[Table 1. Grading on admission and parameters]

Outcome	CBF(ml/100g/min)	MTT(sec)	CBV(ml/100g)
GR	34.5±11.5	6.2±0.8	3.4±1.4
MD	29.2±8.6	6.2±0.8	2.9±0.7
SD	26.3±5.9	7.2±1.6	3.0±0.7
VS	23.1±12.8	7.4±0.8	2.7±1.5
D	21.9±6.8	8.3±2.9	3.0±1.4
	P＜0.001	P＜0.001	P＝0.253

[Table 2. Outcome and parameters]

864

COMPUTATIONAL ANALYSIS OF CEREBRAL BLOOD FLOW

N. Vaicaitis, B. Sweetman, A. Linninger

Bioengineering, University of Illinois at Chicago, Chicago, IL, USA

The dynamics of cerebral blood flow and its role in maintaining homeostasis of the central nervous system (CNS) is of high clinical relevance. A mechanistic understanding of intracranial dynamics may lead to greater insight of cerebrovascular disorders and cerebral blood flow autoregulation. Computational models of the cerebral vasculature can assist neurosurgeons in diagnosis and rational design of patient-specific treatments. To this end, computer models of cerebral vasculature which capture hemodynamic properties of human vasculature are constructed using modern medical imaging combined with automatic vessel generation techniques. The novel synthesis method seamlessly fuses large arterial and venous vessels obtained from patient-specific images with automatic space-filling algorithms to emulate the microvasculature into a realistic model of the entire cerebral blood flow network. The artificially generated networks enable the simulation of blood flow and pressure distribution throughout the cerebral vasculature bed. These studies permit a quantitative investigation of cerebral hemodynamics and demonstrate the feasibility of complete patient-specific models of cerebral vasculature based on modern medical imaging combined with advanced scientific computing methods.

865

SEX-SPECIFIC ENDOTHELIAL DYSFUNCTION AFTER FOCAL CEREBRAL ISCHEMIA

M. Liu[1], W. Zhang[1], S. Jouihan[1], X.J. Nie[1], M. Grafe[2], C.E. Roselli[3], M.L. Edin[4], D.C. Zeldin[4], P.D. Hurn[1], N.J. Alkayed[1]

[1]Department of Anesthesiology & Perioperative Medicine, [2]Department of Pathology, [3]Department of Physiology and Pharmacology, Oregon Health & Science University, Portland, OR, [4]National Institute of Environmental Health Sciences, NIH, Research Triangle Park, NC, USA

Introduction: Sex differences in endothelial function and sensitivity to ischemia are in part due to the vasoprotective effects of estrogen in females. Estrogen is produced by P450 aromatase, which in addition to ovaries is expressed in multiple tissues, including vascular endothelium. We tested the hypothesis that sex differences in endothelial function and protection from ischemic dysfunction in brain are linked to endothelial aromatase.

Methods: Aromatase immunoreactivity was localized in brain after MCA occlusion by immunohistochemistry. Aromatase activity and expression were measured in isolated cerebral vessels and cultured endothelial cells from male and female mice. Endothelial function was assessed *in vivo* in male and female wild-type (WT) and aromatase knockout (ArKO) mice. Endothelial cells injury was assessed *in vitro* by lactate dehydrogenase (LDH) release after oxygen-glucose deprivation (OGD).

Results: Aromatase immunoreactivity was localized in cerebrovascular endothelium. Mouse cerebral vessels express a functionally active aromatase, which is upregulated after ischemia in a sex-specific manner, with higher post-ischemic levels in female vs. male vessels. Aromatase gene deletion attenuates acetylcholine (ACh) dose-response curve in female, but not male cerebral vessels. Female endothelial cells express higher levels of aromatase mRNA and protein, and produce higher levels of NO in response to ACh stimulation than male endothelial cells. Female endothelial cells were more resistant to OGD than male endothelial cells. Aromatase gene deletion exacerbates ischemic injury in female, but not male endothelial cells, and the sex difference in response to OGD was not present in ArKO endothelial cells.

Conclusions: We conclude that endothelial cell function and response to ischemia are sexually dimorphic, in part due to higher aromatase expression in female vs. male endothelial cells. The findings suggest that P450 aromatase plays a critical role in sex-specific endothelial cell function after cerebral ischemia.

References:

1. Liu M, Hurn PD, Roselli CE and Alkayed NJ. Role of P450 aromatase in sex-specific astrocytic cell death. Journal of Cerebral Blood Flow & Metabolism. 2007;27:135-41.

2. Liu M, Oyarzabal EA, Yang R, Murphy MJ, Hurn PD. A novel method for assessing sex specific and genotype specific response to injury in astrocyte culture. Journal of Neuroscience Methods. 2008; 171:214-217.

867

LABEL-FREE LONGITUDINAL OPTICAL-RESOLUTION PHOTOACOUSTIC MICROSCOPY OF ISCHEMIC STROKE THROUGH INTACT MOUSE SKULLS

S. Hu[1], E. Gonzales[2], E. Gong[1], B. Soetikno[1], K. Maslov[1], **J.-M. Lee**[2], L.V. Wang[1]

[1]Department of Biomedical Engineering, Washington University in St. Louis, [2]Department of Neurology and the Hope Center for Neurological Disorders, Washington University School of Medicine, St. Louis, MO, USA

Objectives: Studying cerebrovascular responses to brain ischemia has been limited by a variety of imaging modalities that have either good tissue penetration but low resolution, or high resolution but requiring invasive preparations (open-skull windows). Here, we report a study of cerebrovascular hemodynamics in a mouse model of focal ischemia using a novel minimally invasive, high-resolution technique known as optical-resolution photoacoustic microscopy (OR-PAM).

Methods: Using OR-PAM[1, 2] we serially imaged cerebral blood vessels through the intact skull before, during, and after 1-hr transient middle cerebral artery occlusion (MCAO) in Swiss Webster mice up to 24 days following ischemia. Vessels were imaged using two different wavelengths to quantify the relative concentrations of oxy- and deoxy-hemoglobin, from which the hemoglobin oxygen saturation (sO_2) and the oxygen extraction fraction (OEF) were calculated. In addition, vessel diameter was measured by calculating the full-width-at-half-maximum value of the vessel cross section.

Results: Arteries could be easily distinguished from veins based on the baseline image (average arterial sO_2: 0.86; average venous sO_2: 0.73). During MCAO, the average sO_2 values of arteries/arterioles and veins/venules within the stroke core region dropped ~10% and ~34%, respectively. After reperfusion, arterial sO_2 recovered back to baseline; however, the venous sO_2 increased above the baseline value by ~7%. Thereafter, venous sO_2 values were close to the arterial sO_2 values. OEF increased from 0.15 at the baseline to 0.48 during the MCAO, and then progressively dropped to near-zero levels after reperfusion. Vasodilation of both arteries and veins was observed during and after MCAO.

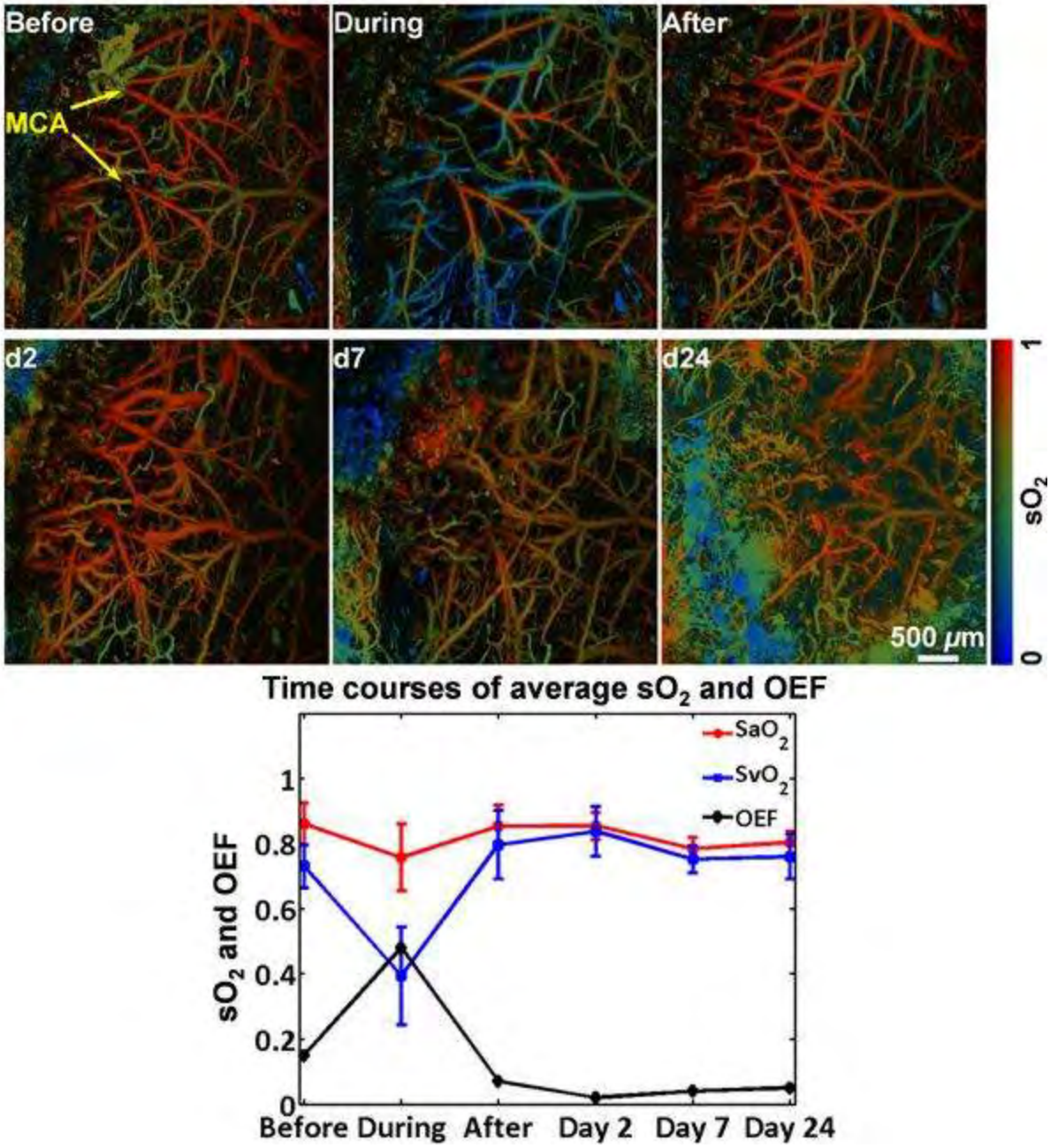

[Transcranial OR-PAM monitoring of ischemic stroke]

Conclusions: We demonstrate, for the first time, longitudinal transcranial OR-PAM monitoring of morphological (i.e., vessel diameter) and functional (i.e., HbT and sO_2) hemodynamic alterations during transient focal ischemia in mice. Consistent with previous PET studies in human stroke, we found OEF increased during acute ischemia, but progressively decreased after reperfusion, suggesting eventual brain tissue infarction. OR-PAM can be a valuable tool to longitudinally study cerebrovascular hemodynamics in intact mouse models of ischemic stroke.

References:

1. S. Hu, K. Maslov, V. Tsytsarev and L. V. Wang, "Functional transcranial brain imaging by optical-resolution photoacoustic microscopy," J. Biomed. Opt. 14(4), 040503 (2009).

2. K. Maslov, H. F. Zhang, S. Hu and L. V. Wang, "Optical-resolution photoacoustic microscopy for in vivo imaging of single capillaries," Opt. Lett. 33(9), 929-931 (2008).

868

CHARACTERIZING GLYCOLYTIC AND OXIDATIVE METABOLISM IN BRAIN SLICES USING 2-PHOTON LIFETIME IMAGING OF NADH AND PO_2

M.A. Yaseen[1], S. Sakadžic[1], J. Lee[1], V.J. Srinivasan[1], M.A. Yucel[1], S.A. Vinogradov[2], D.A. Boas[1]

[1]Martinos Center for Biomedical Imaging, Massachusetts General Hospital & Harvard Medical School, Charlestown, MA, [2]Department of Biochemistry and Biophysics, University of Pennsylvania, Philadelphia, PA, USA

Objectives: Over the past several years, a number of hypotheses have arisen to explain intricacies of cerebral metabolism, postulating the cooperative shuttling of metabolites between astrocytes and neurons. These ideas remain the subject of longstanding debate, as conventional techniques lack the necessary resolution for definite validation. Here, building on observations reported previously [1-3], we propose to use 2-photon lifetime microscopy to identify different enzyme-bound formulations, or ´species´, of reduced nicotinamide adenine dinucleotide (NADH) and classify them as indicators of glycolysis or oxidative metabolism. These species will be measured in astrocytes and neurons in organotypic brain slices and correlated with measurements of extracellular oxygen pressure (pO_2).

Methods: Organotypic brain slices will be prepared from male neonatal Sprague Dawley rats. By modifying our custom-designed imaging system, we will combine 2-Photon microscopy with time-correlated single photon counting (TCSPC) to measure the phosphorescence lifetime and fluorescence lifetimes of pO_2- sensitive PtP-C343 and various species of NADH, respectively. Brain slices will be exposed to reagents used to modulate glycolysis, the Kreb´s cycle, or the electron transport chain. Lifetime measurements will be performed in cytosolic and mitochondrial compartments of astrocytes and neurons and correlated with metabolic state and local pO_2. Multiple, disparate lifetimes of NADH are indicative of variations in enzyme bound state. Specific enzymes will be identified by comparing the in vitro lifetime measurements with those of solutions containing NADH and several enzymes known to bind to NADH[4, 5].

Results: Similar to published results[1-3], multiple NADH species will be identified with fluorescence lifetimes ranging from picoseconds to nanoseconds, corresponding to free, unbound NADH or NADH bound to various metabolic enzymes. Different species have been reportedly segregated in distinct cellular compartments, either the cytosol or the mitochondria, of astrocytes and neurons.

Conclusions: 2-photon fluorescence lifetime imaging allows for resolution between different enzyme-bound states of NADH, extending its utility to indicate metabolic activity with greater specificity. Future in vivo experiments to monitor NADH species representing glycolysis or oxidative metabolism in astrocytes and neurons will help to resolve the dispute surrounding metabolic shuttling hypotheses.

References:

1. H. D. Vishwasrao, A. A. Heikal, K. A. Kasischke and W. W. Webb, "Conformational Dependence of Intracellular NADH on Metabolic State Revealed by Associated Fluorescence Anisotropy," *J. Biol. Chem.* 280, 25119-25126 (2005)

2. T. H. Chia, A. Williamson, D. D. Spencer and M. J. Levene, "Multiphoton fluorescence lifetime

imaging of intrinsic fluorescence in human and rat brain tissue reveals spatially distinct NADH biding," *Optics Express* 16, 4237-4249 (2008)

3. Q. Yu and A. A. Heikal, "Two-photon autofluorescence dynamics imaging reveals sensitivity of intracellular NADH concentration and conformation to cell physiology at the single-cell level.," *J. Photochem. Photobiol. B Biol.* 95, 46-57 (2009)

4. D. H. Williamson, P. Lund and H. A. Krebs, "The Redox State of Free Nicotinamide-Adenine Dinucleotide in the Cytoplasm and Mitochondria of Rat Liver," *The Biochemical Journal* 103, 514-527 (1967)

5. B. Chance and H. Baltscheffsky, "Respiratory Enzymes in Oxidative Phosphorylation VII: Binding of Intramitochondrial Reduced Pyridine Nucleotide," *J. Biol. Chem.* 233, 736-739 (1958)

869

CHARACTERISATION OF A NEW MODEL OF MIDDLE CEREBRAL ARTERY OCCLUSION IN THE SHEEP

R.J. Turner, A.J. Wells, S.C. Helps, R. Vink

Anatomy and Pathology, The University of Adelaide, Adelaide, SA, Australia

Objective: More than 60 000 Australians suffer a stroke each year, with devastating consequences. However, many animal models of cerebral ischaemia, such as those in rodents, fail to accurately translate to the human condition. Rodents have a small lissencephalic brain with a small amount of white matter. In contrast, sheep have a large human-like gyrencephalic brain with a large proportion of white matter. Accordingly, we have developed a novel model of large animal ischaemic stroke in the sheep.

Methods: After mapping the anatomy on post mortem tissue we then developed a novel surgical approach to the middle cerebral artery (MCA). Merino sheep (n=16) were subject to either sham surgery or MCA occlusion achieved by either diathermy (permanent), ligature (2h occlusion) or the application of an aneurysm clip (2h occlusion). Brain tissue oxygenation (licox), intracranial pressure (ICP), blood pressure and blood gases were recorded. Animals were monitored for 4h after the induction of stroke and killed by perfusion fixation. Brains were subsequently processed for histological examination with H&E, weil stain and albumin immunohistochemistry.

Results: MCA occlusion by diathermy or ligature was commonly associated with complications, such as bleeding. Accordingly, the aneurysm clip approach was found to be the superior method. Aneurysm clip application produced a 52% reduction in brain tissue oxygenation, which recovered upon reperfusion. Cerebral perfusion pressure and blood gases remained stable. Marked ischaemic cell damage was evident within the MCA territory on the H&E, with tissue pallor also observed on the weil stain. Albumin immunohistochemistry revealed a loss of blood brain barrier integrity within the MCA territory.

Conclusions: The sheep model of MCAO, in particular, the aneurysm clip approach, may represent a new method for investigation of the pathophysiology associated with ischemic stroke and provide an appropriate vehicle for pre-clinical testing of therapeutic agents.

870

LONG LASTING PROTECTION IN BRAIN TRAUMA BY LIPOPOLYSACCHARIDE PRECONDITIONING

L. Longhi[1], R. Gesuete[2], C. Perego[2], F. Ortolano[1], N. Sacchi[1], P. Villa[2,3], N. Stocchetti[1], M.G. De Simoni[2]

[1]Anesthesia and Critical Care Medicine, University of Milano. Fondazione IRCCS Ospedale Policlinico, [2]Neuroscience, Mario Negri Institute, [3]CNR, Institute of Neuroscience, Milano, Italy

Objectives: We tested the hypothesis that a low dose of lipopolysaccharide (LPS) could act as a preconditioning stimulus and attenuate the neurobehavioral and histological sequelae induced by a subsequent traumatic brain injury (TBI). We investigated the time window of LPS effects, its persistence and the associated molecular mechanisms.

Methods: C57/Bl6 mice received 0.1 mg/Kg LPS or saline intraperitoneally and subsequently TBI at various time intervals. Outcome measures included motor (Neuroscore and Beam walk test) and cognitive (Morris water maze) function, contusion volume and mRNA expression of genes known to be modulated by preconditioning and/or acute brain injury.

Results: Mice receiving LPS 3, 5 or 7 days prior to TBI showed a significant attenuation of motor deficits at 1 week postinjury compared to mice receiving saline. Those receiving LPS 5 days before injury had also a significant reduction in contusion volume (7.9±1.3 vs. 12±2.3 mm^3). One month after TBI, the protective effect of LPS on contusion volume was still present (14.5±1.2 vs. 18.2±1.2 mm^3) together with an improvement in neurological function. Traumatic brain injury significantly increased GFAP, CD11b, CD68, TNF-α, IL-10 and IL-6 mRNA expression 24 hours postinjury. Lipopolysaccharide induced a persistent increase in the expression of CD11b (233%) and IFNβ (500%) in uninjured mice. In preconditioned injured mice, the expression of CD68 was dampened (by 46%) while that of IL-6 was increased (by 52%) compared to non preconditioned mice.

Conclusions: Lipopolysaccharide preconditioning conferred a long lasting neuroprotection following TBI, which was associated with an early modulation of microglia/macrophages activity and cytokine production.

871

SUBSTANCE P ALTERS THE PROFILE OF ENDOGENOUS NEUROGENESIS AFTER DIFFUSE AXONAL INJURY

J.M. Ziebell, H.L. Carthew, L. Giorgio, E. Thornton, R. Vink

Anatomy and Pathology, The University of Adelaide, Adelaide, SA, Australia

Objectives: Over the past 30 years many studies have focused on improving outcome following traumatic brain injury (TBI). With the discovery of endogenous neurogenesis, recent research has been directed at encouraging newly generated cells to effectively integrate and survive. We have previously reported that the substance P antagonist, n-acetyl- tryptophan (NAT), improves outcome in rats following TBI. However, whether such improvement correlates with increased new cell integration is unknown. This question is addressed in the current study.

Methods: Male Sprague-Dawley rats (360-420 g) were anaesthetized with 3% isoflurane and subjected to acceleration-induced TBI. Rats were treated 30 minutes post-injury with either 2.5 mg/kg NAT or vehicle. Twice daily pulses of 100 mg/kg BrdU were injected on days 1-4. Brains were collected at 1, 2, 4 or 7 weeks post-TBI (n=4-7/treatment/timepoint). Sham animals were anaesthetized but did not receive injury or treatment (n=5 at 1, 4 and 7 weeks). Additional rats were treated as above but received ICV infusion of substance P from 48-96 hours post-injury and then killed at 1 week post-injury. Motor function of all rats was tested from 1 to 7 days post-injury via the rotarod.

Results: Injury significantly increased the number of BrdU positive cells 7 days post-TBI ($p< 0.001$), with a further increase observed in animals treated with Substance P ± NAT ($p< 0.001$). Double-labeling of BrdU with cell markers for immature neurons (double-cortin (Dcx)) or microglia/macrophages (Iba1) revealed relatively small numbers of neurons following injury. Interestingly, treatment with substance P ± NAT did not alter the number of neurons 7 days following injury. At this time point, SP treatment did increase the number of BrdU positive microglia in the subventricular zone (SVZ), hippocampus and the corpus callosum ($p< 0.05$ compared to vehicle). Futhermore, treatment of animals with NAT alone decreased the number of BrdU positive microglia observed as well as significantly improving motor performance from day 2-7 ($p< 0.05$ compared to vehicle).

Conclusion: Current data indicate that substance P infusion ameliorates the NAT-induced improvement in functional outcome despite increasing the number of BrdU positive cells. NAT treatment alone decreases microglia proliferation post-injury and is associated with improved functional outcome.

872

CART IMPROVES COGNITIVE IMPAIRMENT BY REGULATING SYNAPTIC EFFICIENCY IN APP/PS1MICE

J.L. Jin[1], L. Qian[1], X.L. Zhu[2], R. Liu[3], Y. Xu[1]

[1]Department of Neurology, The Affiliated Drum Tower Hospital of Nanjing University Medical School, [2]Department of Neurology, Nanjing Drum Tower Hospital Clinical College of Traditional Chinese and Western Medicine, Nanjing University of Chinese Medicine, [3]Department of Neurology, South East University Medical School, Nanjing, China

Objectives: The key pathological feature of Alzheimer´s disease (AD) is described as the accumulation and deposition of amyloid β protein (Aβ) (neuritic plaques) in the brain. These plaques are present in the APP/PS1 double transgenic mouse model, and are associated with reduced mRNA expression of several immediate early genes (IEGs), including Arc, Zif268, NR2B, Homer-1a and Nur77/TR3, which are required for synaptic plasticity and memory formation. Our previous work indicated that the cocaine- and amphetamine-regulated transcript (CART) peptide had neuroprotective effects following stroke. The aims of this study are: 1) to determine whether CART has the ability to inhibit neurotoxicity induced by Aβ; 2) to investigate the effects of CART on synaptic impairment induced by Aβ; 3) to explore the impact of CART on the expression of IEGs.

Methods: APP/PS1 transgenic mice (10 months old, n=9/group) were injected with CART or vehicle (2.5ug/kg, intra-vena caudalis). Learning and memory impairment was tested by Morris water maze, and the induction of synaptic plasticity was assessed electrophysiologically. For in vitro studies, primary cortical neurons were treated with Aβ42, and cell viability or death was assayed by MTT and Fluorescence Activated Cell Sorter (FACS) analysis, respectively. The structure and function of synapses were determined by immunohistochemistry and transmission electron microscope (TEM) both in vivo and in vitro. The expression of synaptic-related proteins was measured by real time PCR or western blot, and the expression of IEGs was determined by a reporter gene assay. Statistical analyses were performed using ANOVA and *post hoc* Fisher's PLSD tests, with $P< 0.05$ considered statistically significant.

Results: CART administration significantly protected against learning and memory impairments in APP/PS1 mice ($P< 0.05$, n=9/group), and partially improved LTP induction and synaptic efficiency. The expression of synaptic related proteins, number of synaptic vesicles (SV) and the thickness of the postsynaptic density (PSD) in APP/PS1 mice brains were all significantly increased following CART administration. Cholinergic neurons and synaptic activity were significantly improved in CART-treated animals compared to vehicle treatment. ACh release was enhanced by 62.72% and 35.89% in cortex and hippocampus, respectively, in CART-treated mice compared to vehicle treatment. CART treatment in cortical neurons induced several IEGs, including Homer1a, Nur77 and Arc (1.27, 1.87 and 1.54-fold over $A\beta_{42}$ treated only, respectively), and regulated the expression of Homer1a by increasing promoter activity. Furthermore, CART significantly decreased neuronal death induced by $A\beta_{42}$

($P< 0.05$, n=3/condition).

Conclusion: Our findings suggest that CART significantly improves synaptic plasticity and cholinergic neuronal function in AD models, correlated with neuroprotection. The improvement in synaptic plasticity was also associated with the upregulation of critical IEG gene expression.

Thus, CART and its downstream mechanism of action may serve as novel therapeutic targets for AD.

873

CEREBROVASCULAR RESPONSES TO BRIEF HYPOXIA IN FETAL SHEEP: CONTRIBUTION TO SELECTIVE VULNERABILITY OF WHITE MATTER IN THE DEVELOPING BRAIN?

A.A. Baburamani, D.W. Walker, M. Castillo-Melendez

The Ritchie Centre for Baby Health, Monash Institute of Medical Research, Monash University, Melbourne, VIC, Australia

Objective: Transient hypoxia can injure the fetal brain, causing oedema formation, vascular leakage, haemorrhage, and oxidative damage, with white matter regions being the most susceptible. In the adult brain, angiogenic responses to cerebral hypoxia-ischemia include up-regulation of vascular endothelial growth factor (VEGF), promoting endothelial cell proliferation and formation of new blood vessels. VEGF actions are modulated by other factors (e.g., angiopoietin-1 [Angpt-1]) that influence endothelial cell survival and attachment to surrounding structures. Whether or not a similar response occurs in the developing cerebrovasculature following an *in utero* global hypoxic insult has not been widely investigated.

Aim: The aim of this study was to determine the effects of an *in utero* hypoxic insult (umbilical cord occlusion; UCO) on the cerebral vasculature in late gestation fetal sheep.

Methods: At 124-127 days gestation (term = 145 days), singleton fetal sheep underwent surgery for catheterization and placing of an inflatable cuff around the umbilical cord. At 132 days gestation, UCO was produced for 10 mins causing transient fetal hypoxia, hypercapnia and acidemia. Control fetuses underwent a sham UCO. All fetuses were then allowed to recover *in utero*, and brains were collected once labor had started from control (n=5) and UCO (n=5) fetuses and immersion fixed with 4% paraformaldehyde for 48 h. Immunohistochemistry was carried out on 10 µm sections using mouse monoclonal anti-VEGF, rabbit polyclonal anti-VEGFR-2 and rabbit polyclonal anti-Angpt-1 primary antibody; the antigen-antibody reaction was visualized with metal-enhanced diaminobenzydine. Expression of VEGF, VEGFR-2 and Angpt-1 specifically associated with blood vessels in white matter (periventricular and subcortical) and gray matter (cortex) was quantified using Image J. Data is expressed as mean ± SEM.

Results: The UCO fetuses went into labor significantly earlier (140.2 ± 1.3 days) than controls (144.0 ± 1.0 days, $p < 0.05$). No change of parenchymal expression of VEGF occurred in the cortex or white matter, however the proportion of blood vessels containing VEGFR-2 expression was significantly increased in subcortical (64.9 ± 2.0%) and periventricular (58.5 ± 2.2%) white matter compared to controls (53.2 ± 3.4%, 46.2 ± 4.4% respectively, $p < 0.05$). Parenchymal cellular expression of VEGFR-2 was also significantly increased in periventricular white matter in UCO brains (1959.2 ± 238.4 cells/mm^2 vs. 1300.3 ± 117.9 cells/mm^2, $p = 0.05$). A significant decrease in Angpt-1 expression associated with blood vessels was seen only in periventricular white matter of UCO fetuses (39.8 ± 3.5% vs. 61.0 ± 4.5%, $p < 0.05$).

Conclusions: The increased vascular expression of VEGFR-2, but not VEGF is consistent with adult brain focal ischemia studies. Angpt-1, a key angiogenic protein important for vascular development and maturation, was *decreased* in periventricular white matter only, a region known to be susceptible to haemorrhage. The predilection of the perinatal brain to white matter lesions may be explained, in part, by these regionally-selective vascular responses to transient global hypoxia.

875

NO PRODUCTION, CBF DURING CEREBRAL ISCHEMIA AND REPERFUSION IN ATII TYPE 1A KO AND ATII TYPE 2 KO MICE

Y. Masamizu[1], Y. Ito[2], R. Nishioka[2], Y. Asano[2], K. Ishizawa[2], M. Iwai[3], M. Horiuti[3], N. Araki[2]

[1]Neurology, Saitama Medical Center, Saitama Medical School, Kawagoe, [2]Department of Neurology, Saitama Medical University, Moroyama, [3]Ehime University, Touon, Japan

Introduction: Nitric oxide (NO) and angiotensin II play an important role in the regulation of cerebral blood vessels. Angiotensin II stimulates the production of NO and peroxynitrite in endothelial cells. Pretreatment with angiotensin II AT1 receptor antagonists protects against cerebral ischemia (1). Moreover, a significant correlation was found between brain NO synthase and AT1 receptor mRNAs (2). Therefore, we examined the generation of NO metabolites and hydroxyl radicals during global ischemia and reperfusion in angiotensin II type 1a receptor knockout mice and type 2 receptor knockout mice.

Methods: (1) Male ATII type 1a receptor KO mice [n=8], male ATII type 2 receptor KO mice [n=5], and control C57/BL6 mice [n=8] were used. Both NO production and hydroxyl radical metabolism were continuously monitored by *in vivo* microdialysis. Microdialysis probes were inserted into the bilateral striatum. A Laser Doppler probe was placed on the skull surface. Blood pressure, blood gases and temperature were monitored and maintained within normal ranges throughout the procedure. Forebrain cerebral ischemia was produced by occlusion of both common carotid arteries for 10 minutes. Levels of nitric oxide metabolites, nitrite (NO_2^-) and nitrate (NO_3^-), in the dialysate were determined using the Griess reaction.

Results: (1) Blood Pressure (Figure 1): AT1a KO (50.3 ± 2.6 mmHg; mean ± SE) showed significantly lower than that of AT2 KO (80.8 ± 4.1), and the control group (63.3 ± 4.5) before ischemia, during ischemia and 10-110 minutes after the start of reperfusion ($p< 0.05$).

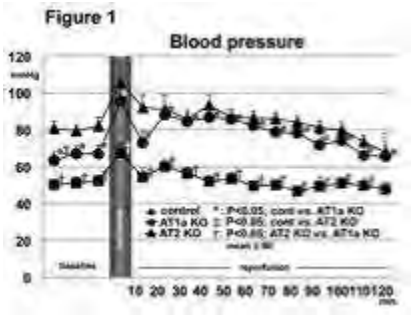

[Blood pressure]

(2) Cerebral Blood Flow (CBF): AT1a KO (97.6 ± 15.8) showed significantly lower than that of the control group (115.3 ± 15),20-30 minutes after the start of reperfusion ($p< 0.05$). AT1a KO showed significantly lower than that of the AT2 KO group (97.6 ± 15.8),10-20 minutes after the start of reperfusion ($p< 0.05$). (3) Nitric oxide metabolites: 1) NO_2^- ; There were no significant differences between the groups. 2) NO_3^- (Figure 2); AT1a KO (1.07 ± 0.5 mol/L) showed significantly lower than that of the AT2 KO group (27 ± 0.3) before ischemia, and 30-110 minutes after the start of reperfusion ($p< 0.05$).

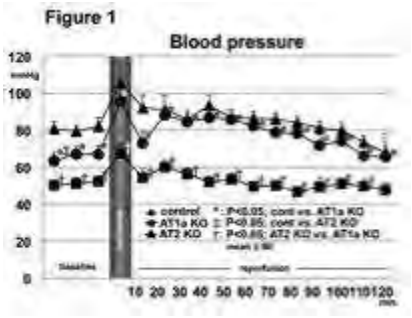

[NO3-]

Conclusion: These *in vivo* data suggest that AT1a and AT2 influences on the blood pressure, CBF and NO production in mice, and especially AT1a is more closely related to .the cerebral blood flow and nitric oxide production in brain during ischemia and reperfusion.

References:

[1] Ito T, Yamakawa H, Bregonzio C, Terron JA, Falcon-Neri, Saavedra JM ; *Stroke* 33 2297-2303 (2002)

[2] Krizanova O, Kiss A, Zacikova, Jezova,D; Physiol Res 50 473-480 (2001)

876

THE EFFECT OF DIMENSIONALITY ON GROWTH AND DIFFERENTIATION OF NEURAL PROGENITORS FROM DIFFERENT REGIONS OF FETAL RAT BRAIN IN VITRO

H. Lu[1], K. Searle[2], Y. Liu[1], T. Parker[2]

[1]Institute of Neurobiology, Environment and Genes Related to Diseases Key Laboratory of Education Ministry, Xi'an Jiaotong University College of Medicine, Xi'an, China, [2]Institute of Neuroscience, Department of Human Anatomy and Cell Biology, School of Biomedical Sciences, University of Nottingham, Nottingham, UK

Introduction: Cell culture is an essential tool in biological sciences, clinical sciences and biomedical sciences. It is generally recognized that cells growing on flat and hard glass or plastic substrates results in the bio-behaviour change due to the loss of tissue specific architecture, mechanical and biochemical cues and cell-cell communication. The striking similarity of in vivo morphologies and behaviors of cell grown in three dimension culture environments has also been well accepted. However, the effect of dimensionality on bio-behaviour of neuroprogenitors remains an unmet need.

Objective: To address the differences of growth and differentiation of neuroprogenitors in different dimensional culture environment.

Material and methods: Neuroprogenitor cells were isolated from cerebral cortex, cerebella and brainstem of fetal rat brain, then cultured in serum free DMEM/F12 medium and DMEM with 10% FBS. The character of neuroprogenitor cells was identified by morphological and immunocytochemical criteria. The growth and differentiation of neuroprogenitors in 3 dimensional spheroids was compared with that in 2 dimensional monolayer cultures.

Results: These cells keep dividing and forming neurospheres on 5-7 days in vitro (DIV). There is no significant difference among the different brain regions regarding the growth of neurospheres, which shown by the 12-17 % increases of neuroshperes' diameter over 10 days. Most of the cells were immature undifferentiated nestin positive neural progenitor cells which were mononuclear and lined the edge of spheroids. Some of them differentiated spontaneously into NF positive neurons and GFAP positive astrocytes as shown by the formation of immature synaptic contacts and abundant extracellular collagen production, respectively. More neuroprogenitors undertook neuronal differentiation in spheroids than that in 2 dimensional monolayer cultures. Approximately 74%, 74.5% and 74.5% of cells in neural spheroids from cerebral cortex, cerebelum and brain stem, respectively, were NF positive neurons. They are significantly higher than that in the monolayer culture (8%, 6.5% and 3.5%, repsectively) at 3 DIV. On the contrary, the population of astrocytes in spheroids from cerebral cortex (37.5%), cerebellum (15.7%) as well as brainstem (29.4) were significantly lower than that in monolayer cultures from same regions (45%, 45% and 48%, respectively). In comparison with the undissociated brain tissue, the neuron/astrocyte ratio in spheroids from cerebral cortex and cerebella is similar to that found in adult rat tissue, while the ration in spheroids from brainstem is more close to fetal brain tissue.

Conclusion: Our results suggested that three-dimensional spheroid culture system mimics the in vivo cytoarchitecture to a greater extent that more closely reflects adult brain tissue cellular composition. The niche in spheroids is more favorable for neuronal precusors' survival and differentiation while the cue in artificial 2 dimensional monolayer cultures could be favoring glial

cells survival. The differences between brainstem and other two brain regions could be due to the specific spatio-temporal cues that are essential for neuronal development.

877

OMEGA-3 POLYUNSATURATED FATTY ACIDS IMPROVE LONG-TERM NEUROLOGICAL OUTCOMES AFTER ISCHEMIC STROKE VIA ENHANCING ANGIOGENESIS AND NEUROGENESIS

X. Hu[1], F. Zhang[1], Y. Gao[2], J. Chen[1,2]

[1]Center of Cerebrovascular Disease Research, University of Pittsburgh, Pittsburgh, PA, USA, [2]State Key Laboratory for Medical Neurobiology and Institute of Brain Sciences, Fudan University School of Medicine, Shanghai, China

Backgound: Stroke is a devastating disease as currently no therapy is available to prevent stroke-induced neurological deficits. The current study was conducted to assess whether omega-3 polyunsaturated fatty acids (n-3 PUFAs) could improve long-term neurological outcomes after experimental stroke and to investigate the effect of n-3 PUFAs on post-stroke neurovascular remodeling including angiogenesis and neurogenesis.

Methods: Transgenic mice over-expressing the *C. elegans fat-1* gene, which encodes an enzyme that converts endogenous n-6 to n-3 PUFAs, was created to study the effect of n-3 PUFAs on cerebral ischemia. Focal cerebral ischemia was induced for 60 min by right MCAO. Brains were assessed for cerebral tissue loss at 2 and 14 days of reperfusion. Neurological performance was analyzed up to 14 days after ischemia. Neovasculation was identified by transcardial perfusion of FITC-conjugated tomato lectin. Immunohistochemistry staining and immunoblot assay for specific markers were used to evaluate angiogenesis and neurogenesis after stroke.

Results: *fat-1* mice with elevated brain levels of n-3 PUFAs were remarkably resistant to focal cerebral ischemia compared to their wildtype (WT) littermates, showing reduced infarct size at not only acute (2 days post-ischemia, n=6/group, $p< 0.01$) but also delayed (14 days post-ischemia, n=7/group, $p< 0.001$) phase after MCAO. Acute sensorimotor dysfunction (1-7 days after ischemia) was significantly improved in *fat-1* mice as assessed by rotarod performance (n=7/group, $p< 0.01$), foot fault (n=7/group, $p< 0.05$), and corner test (n=7/group, $p< 0.01$). The *fat-1* mice also showed improved long-term sensorimotor performance as assessed by corner test 14 days post-ischemia (n=7/group, $p< 0.01$). The post-stroke neovasculation, as measured by three vascular density parameters (vascular surface area, branch points, and vascular length per mm^3 tissue volume), in the peri-infarct regions were significantly decreased compared to the contralateral counterparts in WT mice 7 days after MCAO (n=6/group, $p< 0.05$). In contrast, neovascularization in the peri-infarct regions of *fat-1* mice was robustly increased compared to WT mice (n=6/group, $p< 0.05$), suggesting that n-3 PUFAs enhanced the post-stroke neovascularization. As an index of active angiogenesis, double-labeling of BrdU and intravascular tomato lectin was significantly higher in *fat-1* mice compared to WT mice 7 days after MCAO (n=6/group, $p< 0.01$). The expression levels of three angiogenesis-promoting proteins (angiopoietin1, angiopoietin2 and meteorin) were also significantly increased in *fat-1* mice compared to their WT littermates (n=4/group, $p< 0.05$). Both BrdU and DCX staining demonstrated robustly enlarged ipsilateral subventricular zone (SVZ) 14 days post-ischemia in WT mice, suggesting an increased progenitor cell proliferation and early neuronal differentiation. The *fat-1* mice showed even more enlarged ipsilateral SVZ compared to their WT littermates. The number of DCX+ cells and the percentage of DCX+Brdu+ cells, which represents newly generated neuronal progenitor cells, also increased significantly in the peri-infarct striatum in *fat-1* mice compared to their WT littermates (n=5/group, $p< 0.05$).

Conclusion: This study suggests that n-3 PUFAs supplementation is a promising strategy to improves long-term neurological outcomes after stroke. Angiogenesis and neurogenesis were robustly enhanced in *fat-1* mice compared to WT littermates, suggesting that n-3 PUFAs promote post-ischemic brain repair and neurovascular remodeling.

878

GABAPENTIN REDUCES INFARCT VOLUME BUT DOES NOT SUPPRESS PERI-INFARCT DEPOLARIZATIONS IN MICE

U. Hoffmann[1], J.-H. Lee[1], T. Qin[1], K. Eikermann-Haerter[1], C. Ayata[1,2]

[1]Radiology, Stroke and Neurovascular Regulation Lab, [2]Neurology, Stroke Service and Neuroscience Intensive Care Unit, Massachusetts General Hospital, Harvard Medical School, Charlestown, MA, USA

Introduction: Cortical spreading depression (CSD) is an intense depolarization wave implicated in the pathophysiology of brain injury states and migraine aura. In focal cerebral ischemia, recurrent peri-infarct depolarization (PID) waves akin to CSD worsen ischemic injury by exacerbating the blood flow-metabolism mismatch. We recently showed that gabapentin elevates the electrical threshold for CSD induction and suppresses recurrent CSDs evoked by topical KCl in rats (Hoffmann et al.2010). We therefore sought to assess its potential to modulate injury depolarizations and infarct volume in acute stroke.

Methods: Mice (C57BL/6, male, 25-30 g) were pretreated with a single dose of Gabapentin 200 mg/kg (intravenous) or vehicle (saline) 60 min before the onset of stroke. Under isoflurane anesthesia (2.5% induction, 1.5% maintenance, in 70% nitrous oxide and 30% oxygen), middle cerebral artery was occluded (MCAO) for 1 hour using an intraluminal filament. Successful occlusion and reperfusion were monitored using a laser Doppler flow probe over the ischemic core. Infarct volume (TTC staining) and neurological deficits (6 point scale) were assessed 24 hours after stroke onset. To detect PIDs, a separate group of mice were placed in a stereotaxic frame for extracellular steady (DC) potential recordings using two capillary microelectrodes placed outside the ischemic cortex (mm from bregma: 3.5 posterior, 1.5 lateral; 1.0 anterior, 1.5 lateral [300 µm deep]) for 2 hours starting 25-30 min after MCAO.

Results: Gabapentin significantly reduced the infarct volume after 1 hour transient MCAO in mice. In contrast, the frequency and cumulative duration of PIDs were not suppressed by gabapentin. Cerebral blood flow reduction in ischemic core as well as the systemic physiological parameters did not differ between groups.

		Infarct	Neuro deficit		CBF (%)			PID	
Group	N	(indirect, mm3)	(score 0-5)	CCAO	MCAO	Reperfusion	N	Frequency (total)	Cumulative duration (sec)
Saline	12	55.7 ± 9.2	2 [2-5]	57 ± 7	10 ± 4	90 ± 18	10	5.1 ± 2.3	291 ± 132
Gabapentin 200 mg/kg	9	72.8 ± 12.1	2 [1-5]	67 ± 13	11 ± 5	91 ± 14	9	5.9 ± 2.3	306 ± 158

P value		<0.05	n.s.	n.s.	n.s.	n.s.		n.s.	n.s.

[Gabapentin Table]

Conclusion: Gabapentin reduces infarct volume after acute stroke in mice, as previously reported (Williams et al.2006). However, despite its inhibitory efficacy on CSD, the mechanism of neuroprotective action of gabapentin in focal cerebral ischemia does not appear to involve suppression of PIDs.

References: Hoffmann U, Dilekoz E, Kudo C, Ayata C. (2010). Gabapentin suppresses cortical spreading depression susceptibility. J Cereb Blood Flow Metab 30(9):1588-92

Williams AJ, Bautista CC, Chen RW, Dave JR, Lu XC, Tortella FC, Hartings JA. (2006) Evaluation of gabapentin and ethosuximide for treatment of acute nonconvulsive seizures following ischemic brain injury in rats. J Pharmacol Exp Ther 318:947-955

879

QUANTITATIVE ANALYSIS OF AMYLOID BETA DEPOSITION IN ALZHEIMER'S DISEASE PATIENTS USING PET AND [^{11}C]BF-227 AND [^{18}F]FACT

M. Tashiro[1], N. Okamura[2], S. Watanuki[1], S. Furumoto[1,2], K. Furukawa[3], Y. Funaki[1], R. Iwata[1], Y. Kudo[4], H. Arai[3], K. Yanai[1,2]

[1]Cyclotron and Radioisotope Center, Tohoku University, [2]Department of Pharmacology, Tohoku University Graduate School of Medicine, [3]Department of Geriatrics and Gerontology, Institute of Development, Aging and Cancer Tohoku University, [4]Innovation of New Biomedical Engineering Center, Tohoku University Hospital, Sendai, Japan

In vivo detection of amyloid deposits is useful for early diagnosis of Alzheimer´s disease (AD) and for prediction of potential converters from the mild cognitive impairment (MCI) to AD. Our original imaging probe, [^{11}C]BF-227, has been shown to be useful for clinical evaluation of AD, MCI and various neurodegenerative disorders using positron emission tomography (PET). Afterward, we have also developed [^{18}F]-labeled probe, [^{18}F]FACT for better throughput. Purpose of the present study is to examine multiple methods for quantitative analysis of amyloid deposition in human brain using PET and [^{11}C]BF-227 and [^{18}F]FACT.

Six AD patients (mean age: 73.0 y.o.) and six healthy aged controls (mean age: 61.3 y.o.) were studied using PET and [^{11}C]BF-227. In addition, ten AD patients (mean age: 74.5 y.o.) and nine healthy aged controls (mean age: 68.3 y.o.) were studied using PET and [^{18}F]FACT. Regions of interest (ROIs) were placed on various cortical and subcortical regions in dynamic PET images of 60-min- and 90-min-long duration, based on the coregistered MRI T1 images. Results of quantification using arterial inputs were compared to those calculated by Logan graphical analysis with arterial data (LGA) and with the reference data (LGAR), and to those calculated by full kinetic analysis based on 1- and 2-tissue compartmental models (1TM and 2TM). These results were compared to the standardized uptake values (SUV) in the cortex and their ratios to that in the cerebellum (SUVR), as well.

The results of [^{11}C]BF-227 displayed significantly higher distribution volume ratio (DVR) values in AD patients than in controls in various cortical regions such as the cingulate, temporal and occipital regions, especially in the temporo-occipital regions. 2TM demonstrated better fitting result compared to 1TM. The correlation of distribution volume ratio (DVR) values calculated by LGA and LGAR to those by 2TM was very good. In addition, these values correlated well to the SUV values.

The results of [^{18}F]FACT also displayed significantly higher DVR values in AD patients than in controls in various cortical regions such as the cingulate, temporal and occipital regions, especially in the temporo-occipital regions. 2TM demonstrated better fitting result compared to 1TM. The correlation of DVR values calculated by LGA and LGAR to those by 2TM was very good. In addition, these values correlated well to the SUV values.

These findings have demonstrated that [^{11}C]BF-227 and [^{18}F]FACT are promising PET probes and that DVR values based on LGA, LGAR and SUVR can be good indices of amyloid deposition in AD patients and MCI.

880

DOWN-REGULATION OF CD133 IN CANCER STEM CELLS SUPPRESSES GLIOMA GROWTH

C.-C. Wu[1], Y.-H. Chiang[1], K.-Y. Chen[1], J.-W. Lin[2], W.-T. Chiu[3]

[1]Department of Neurosurgery, Taipei Medical University Hospital, [2]Department of Neurosurgery, Taipei Medical University-Shuang Ho Hospital, [3]Taipei Medical University, Taipei, Taiwan R.O.C.

Malignant gliomas are common primary brain tumors which have poor prognosis. Even though recent advances in chemotherapy proves to be effective in controlling the disease progression, the duration of disease control is still limited. Limitation of chemotherapy effect is frequently observed in cancer stem cells, which in many aspects are similar to normal stem cells. Despite the rarity of cancer stem cells, they have very different characteristics such as their resistance to chemotherapy and radiotherapy. Because neither chemotherapy nor radiotherapy are capable of eradicating all cancer stem cells, these residual stem cells repopulate the tumor and allow cancer relapse. Malignant gliomas frequently rapidly recur even after gross total surgical removal followed by chemotherapy and radiotherapy. A possible cause is the presence of residual stem cells of gliomas. Methods in removing or disabling glioma stem cells (GSC) may lead to the control and limitations of the malignancy of the gliomas.

CD133 was recently identified as an important cancer stem cell marker, with increased expression in various human malignancies, including gliomas. Here, we successfully isolated CD133 positive glioma stem cells (GSC-CD133+) from brain tumor specimen and demonstrated that GSC-CD133 + are capable of self-renewal and express high levels of embryonic stem cell markers (Oct-4, Nanog, Sox-2, Klf-4, and c-Myc). To investigate the changes of GSC cell biology by different CD133 expression in vitro and in vivo, we used a lentiviral vector expressing shRNA to knock down CD133 expression (shCD133) in GSC-CD133+. MTT assay showed that silencing of CD133 in GSC-CD133+ significantly reduced proliferation about 40-50% within 3days. We further examined whether the growth suppression is through apoptosis or autophagy. By western blot analysis, we found that down-regulated CD133 decreased the expression of XIAP, Bcl-2, and increased the expression of autophagy-related gene ATG5, Beclin, and LC3. Importantly, GSCs with decreased CD133 levels have lower tumorigenicity when xenotransplanted into the brains of nude mice. These results support an important role of CD133 in regulating proliferation and survival of GSCs. Targeting CD133 may offer improved therapeutic approached for gliomas.

882

INHIBITION OF HISTONE DEACETYLASES REDUCES ISCHEMIC INJURY BY REGULATION OF THE 3'UTR STABLIZATION OF PRO-INFLAMMATORY CYTOKINE MRNAS

Y. Chen[1], X. Zhu[2], X. Wu[2], S. Huang[1], X. Zang[3], Y. Xu[3]

[1]Department of Neurology, The Affiliated Drum Tower Hospital of Nanjing University Medical School, [2]Department of Neurology, Nanjing Drum Tower Hospital Clinical College of Traditional Chinese and Western Medicine, Nanjing University of Chinese Medicine, [3]Department of Neurology, the Affiliated Drum Tower Hospital of Nanjing University Medical School, Nanjing, China

Objectives: Inflammation is an important pathophysiological mechanism involved in ischemic brain injury. In experimental stroke, inhibition of histone deacetylases (HDACs) exerts anti-inflammatory effects and reduces postischemic brain damage. However, it is unknown whether HDAC inhibition can influence poststroke inflammation by a post-transcriptional control mechanism involving mRNA stabilization.

Methods: Middle cerebral artery occlusion (MCAO) was induced in adult male mice for 2 h followed by 2 h of reperfusion. For in vitro studies, cortical neurons were subjected to oxygen glucose deprivation (OGD) for 2 h and returned to normal culture conditions. Specific isoforms of HDACs were inhibited by lentivirus-mediated short hairpin RNA (shRNA) interference or HDAC inhibitors (HDACi). Ischemic infarct volume and neurological function were evaluated through 2,3,5-triphenyltetrazolium chloride (TTC) staining and Neurological Severity Scores (NSS), respectively. Expression of HDAC isoforms, proinflammatory inflammatory cytokines, AU-rich element RNA binding proteins (AUBPs) and p38 were quantified by real-time polymerase chain reaction (PCR) and western blotting. The half-lives of proinflammatory cytokine mRNAs in OGD neurons treated with actinomycin D were determined using northern blot. Expression of luciferase reporter constructs containing the 3´-untranslated regions (3´UTR) of pro-inflammatory cytokines were measured by fluorospectrophotometer.

Results: Inhibition of HDACs decreased levels of pro-inflammatory TNF-α and iNOS cytokines and reduced infarct volume and neurological deficit following MCAO. HDAC inhibition also decreased the half-life of proinflammatory cytokine mRNAs in OGD neurons. Northern blot and promoter analyses showed that HDACi reduced mRNA stability of proinflammatory cytokines by targeting the AU-rich element (ARE) of the 3´UTR. HDAC inhibition also induced upregulation of Tristetraprolin (TTP), an AUBP that mediates destabilization of mRNAs, and was accompanied by lower phosphorylation of p38. Inhibition of p38 with SB253080 blocked induction of TTP by HDACi in OGD neurons.

Conclusions: Inhibition of HDACs attenuates poststroke inflammation and protects against ischemic brain damage. These protective effects are associated with mRNA destabilization of pro-inflammatory cytokines. The post-transcriptional regulation of HDAC inhibition involves TTP-dependent p38 MAPK pathway. Therefore, this pathway may be a promising therapeutic target in the treatment of ischemic stroke by modulating post stroke inflammation.

883

PERICYTES, ASTROCYTES AND MMPS PLAY KEY ROLES IN CEREBROVASCULAR REMODELING AFTER ISCHEMIC STROKE IN RAT BRAIN

Y. Yang, J.F. Thompson, T. Mcavoy, J.W. Hill, V.M. Salayandia, E.Y. Estrada, G.A. Rosenberg

Neurology, University of New Mexico, Albuquerque, NM, USA

Introduction: Angiogenesis and blood-brain barrier (BBB) remodeling is important in stroke recovery, but the molecular and cellular mechanisms underlying neurovascular unit remodeling are uncertain.

Background and aims: Matrix metalloproteinases (MMPs), which increase the permeability of BBB by degrading tight junction proteins (TJPs) after stroke, are beneficial during angiogenesis. We observed MMP-expressing populations of astrocytes around the border of the infarct in ischemic hemispheres at 3-5 days of reperfusion after stroke. We hypothesized that astrocytes surrounding the lesion areas play an important role in the remodeling of TJPs. This study focused on: 1) investigation of the roles of astrocytes and other neurovascular cells in the remodeling of TJPs and the restoration of BBB integrity, and 2) determination of involvement of MMPs in the neurovasculature unit during recovery after ischemia-reperfusion injury.

Material and methods: A 90-minute transient middle cerebral artery occlusion (MCAO) was induced in adult rats with 24 and 48 hours, 7 days and 3 weeks reperfusion. Immunohistochemistry, Western blot, confocal microscopy and other methods were employed.

Results: From 24 hours to 7 days, we observed a significant loss of vessels in the ischemic hemispheres. We found a loss of expression of TJPs, claudin-5, occludin and ZO-1, in vessels in lesioned hemispheres at 24 or 48 hours. By 3 weeks, there was a remarkable increase of vessels in the core and penumbral areas compared to 7 days. Double immunohistochemical staining with RECA-1, an endothelial cell marker, and NG2, a marker of immature pericytes, showed that these vessels are newly formed. Ki67 expression in pericytes and endothelial cells confirmed the proliferation of cerebral vessels in lesioned hemispheres. Protein levels of TGF-β receptors, ALK1 and ALK5, were evaluated at 3 weeks. There was an increase in ALK1 and a decrease in ALK5 in lesion hemispheres. In addition, increased vascular endothelial growth factor (VEGF) was seen in NG2-positive pericytes and astrocytes at 3 weeks. These results suggested cellular proliferation and angiogenesis.

By 3 weeks, TJPs reappeared in the newly formed vessels. Occludin and ZO-1 were expressed by astrocytes around the lesion area, which sent processes to the new vessels. ZO-1 was also seen in NG2-positive pericytes around endothelial cells that expressed claudin-5. Increased pro and active MMP-2 and -3 were detected in the ischemic hemisphere at 3 weeks. MMP-2 co-localized with astrocytes that expressed ZO-1 and occludin. Unexpectedly, NG2-positive pericytes around endothelial cells of the newly formed vessels appeared to be the main source of MMP-3.

Conclusion: Pericytes and astrocytes play critical roles in formation of neurovasculature, including the remodeling of TJPs in BBB and migration of new vessels during angiogenesis after stroke. MMP-2 and -3 are involved in the remodeling of TJPs in BBB and migration of new vessels. Our results suggest that although MMPs are known to be detrimental early after stroke, they improve new vessel formation and remodeling of injured tissues at later stages of the

ischemic insult. Each cell type plays a unique role, and works with other types to respond to angiogenesis and BBB remodeling.

886

NON-INVASIVE OPTICAL MEASUREMENT OF CEREBRAL BLOOD VOLUME, CEREBRAL BLOOD FLOW, AND OXYGEN METABOLISM IN INFANTS

M.A. Franceschini[1], N. Roche-Labarbe[1], A. Fenoglio[2], A. Surova[1], A. Aggarwal[3,4], P.E. Grant[2,3]

[1]Radiology, Athinoula A. Martinos Center for Biomedical Imaging, Massachusetts General Hospital, Harvard Medical School, Charlestown, [2]Fetal-Neonatal Neuroimaging and Developmental Science Center, [3]Division of Newborn Medicine, Children's Hospital Boston, [4]Department of Newborn Medicine, Brigham and Women's Hospital, Boston, MA, USA

Newborn brain injury occurs in more than 6 of every 1000 live term births and is a major cause of neurodevelopmental disability. Global effects on cognition and memory deficits with or without motor and visual impairment are increasingly recognized. Although MRI is the current gold standard for brain injury detection, it is impractical as a screening tool and cannot provide bedside monitoring to optimize individual responses to therapies.

Since its introduction 30 years ago, researchers have been exploring the potential role of near-infrared spectroscopy (NIRS) as a bedside monitor for newborn brain health. The results have not generated much enthusiasm, however, due to the insensitivity of oxygen saturation. Recently, thanks to the development of more sophisticated and more quantitative systems such as frequency domain (FD) NIRS and diffuse correlation spectroscopy (DCS), we are developing the ability to characterize normal brains and detect changes with injury [1-3]. These new approaches do not focus on oxygen saturation (SO_2) alone but use quantitative cerebral blood volume (CBV) and independent measures of blood flow (CBF) to estimate cerebral oxygen consumption ($CMRO_2$).

In the past four years we have used a custom-modified ISS FDNIRS system to quantify CBV and SO_2 in > 250 babies and shown the high sensitivity and specificity of CBV and $rCMRO_2$ in detecting brain injury [2]. In the past two years we have also used a DCS system in sequence with the FDNIRS, and measured an index proportional to blood flow (BF_i) in ~150 babies, demonstrating the feasibility of sequential measures. When DCS BF_i is used to calculate $rCMRO_2$ instead of an estimate of CBF based on CBV, variance decreases significantly [3]. This improvement enables us to detect changes in $rCMRO_2$ with cGA or region.

We have now started measurements in subjects undergoing therapeutic hypothermia (33.5^oC for 72 hrs). To date we have measured 7 infants and all but 2 showed marked decreases in $rCMRO_2$ during hypothermia compared to healthy neonates. BF_i, CBV and SO_2 do not distinguish at-risk neonates on hypothermia from normal as well as $rCMRO_2$, and the combination of $rCMRO_2$ and BF_i shows potential for an increased ability to discriminate between them. Abnormalities were more pronounced in parietal regions, suggesting regional vulnerability. One of 5 measured after cooling had a rebound $rCMRO_2$ elevation, suggesting the need for individualized care. Further studies are needed to determine whether $CMRO_2$ response correlates with outcomes.

1. Franceschini et al. Pediatr Res 61, 546-551.

2. Grant et al. J Cereb Blood Flow Metab 29, 1704-1713.

3. Roche-Labarbe et al. Hum Brain Mapp 31, 341-352.

887

A STUDY OF D2/D3 DOPAMINE RECEPTOR DISTRIBUTION IN A RARE FORM OF TOURETTE SYNDROME WITH [^{11}C]PHNO AND POSITRON EMISSION TOMOGRAPHY

J.-D. Gallezot[1], W.A. Williams[1,2], K. Lim[1], M.-Q. Zheng[1], E.C. Loring[3], R.E. Carson[1], J.H. Krystal[2], M.W. State[3], Y.-S. Ding[1]

[1]Department of Diagnostic Radiology, [2]Department of Psychiatry, [3]Department of Genetics, Yale University, New Haven, CT, USA

Objective: The goal of the study was to evaluate the distribution of D2/D3 dopamine receptors using [^{11}C]PHNO in members of a family with a Tourette Syndrome (TS) that carries a rare mutation in the L-histidine decarboxylase (HDC) gene, and compare them with gender, age and weight matched healthy controls.

Methods: Three members of a family with TS and a mutated HDC gene and 9 healthy controls (HC) were included in the study: 2 males and 1 female (age=29±15; BMI=30±5) were part of the TS group; 6 males and 3 females (age=29±11; BMI=28±7) were included in the HC group. Each subject underwent one [^{11}C]PHNO scan on a HRRT scanner. Injected activities were 292±129 MBq with a total injected mass of 0.028±0.004 µg/kg (max=0.032 µg/kg). Specific radioactivity was 58±27 MBq/nmol at the end of synthesis and 32±15 MBq/nmol at injection time. Head motion was tracked during the scan using a Vicra polaris optical tool. Images were reconstructed using the MOLAR algorithm (with 2 iteration and 30 subsets) with all corrections. Regions of interest (ROI) were delineated in the caudate, putamen and pallidum using the AAL template and nonlinear wrapping between the template MRI and each subject MRI. A region corresponding to the substantia nigra was also added to the template. Binding potentials were quantified using cerebellum as the reference region and SRTM (Ginovart et al., 2007, J Cereb Blood Flow Metab, 27:857-71) for ROI-based kinetic modeling and SRTM2 for computation of parametric images.

Results: [^{11}C]PHNO binding potentials (BP_{ND}) estimated with SRTM were higher in the caudate (+11%), putamen (+19%) and pallidum (+48%), but not significantly, and more markedly in the substantia nigra (+139%, p≤0.01, Mann-Whitney rank-sum test) for members of the TS family as compared to HCs (see figure). Results were similar when SRTM2 was used to compute parametric images: increases were +8%, +17%, +30% and +93% (p≤0.01, Mann-Whitney rank-sum test), respectively.

Conclusion: [^{11}C]PHNO is a dopamine receptor radioligand that binds to both D2 and D3 subtypes with a higher affinity for the D3 subtype (approx. 30-50 fold). Due to the relative distribution of these two subtypes, [^{11}C]PHNO BP_{ND} in caudate and putamen is mostly due to the contribution of D2 subtype, and the BP_{ND} in the pallidum and substantia nigra is mostly due to the contribution of the D3 subtype. The fact that the highest increases of [^{11}C]PHNO BP_{ND} seen in this study were in the pallidum and substantia nigra may indicate that the observed effect is due to changes in D3 receptors. Further studies would be useful to investigate whether the observed effect is linked to the rare mutation, or if it can also be found in patients with idiopathic Tourette Syndrome.

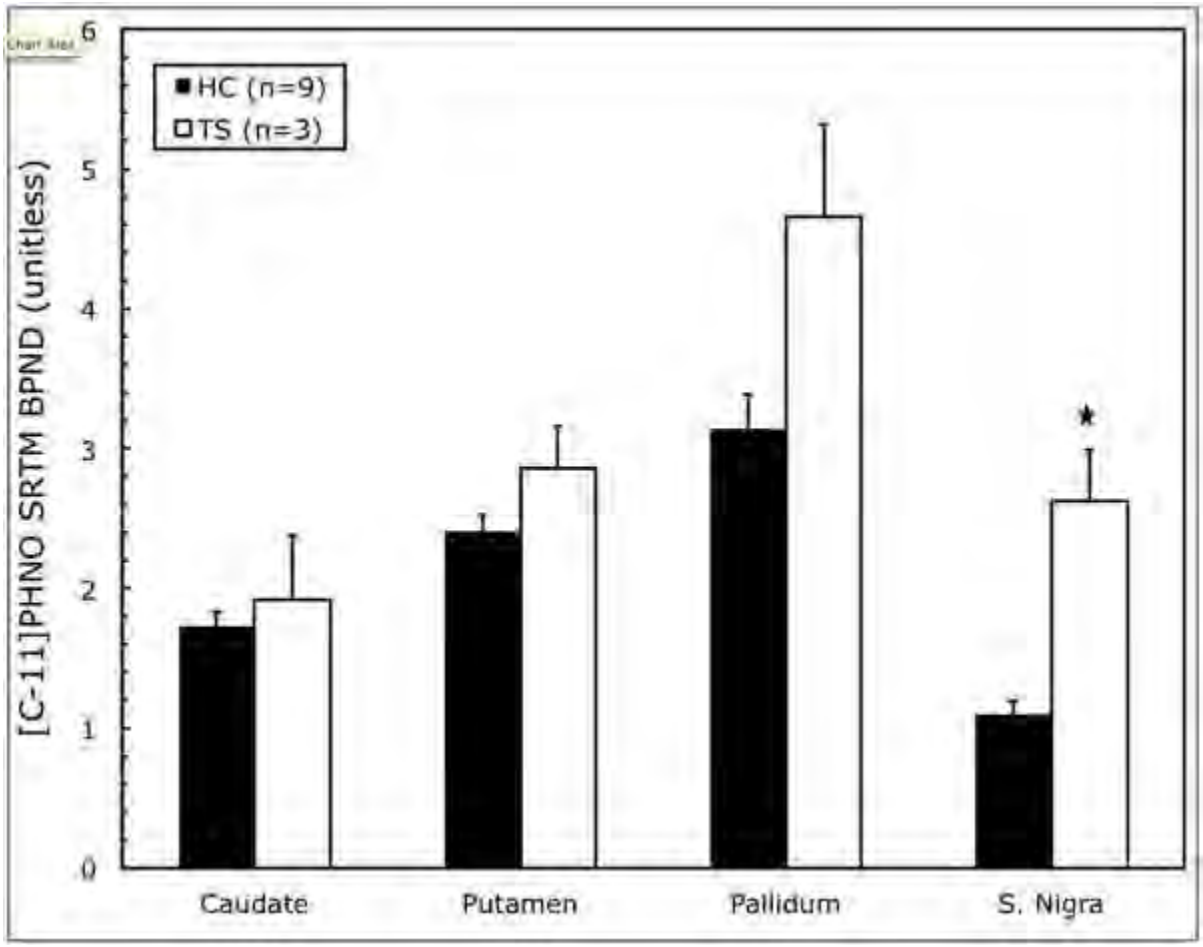

[Regional Distribution in TS vs HC]

888

CYCLOOXYGENASE-2 ACTIVITY CONTRIBUTES TO BLOOD-BRAIN BARRIER DISRUPTION IN ISCHEMIC STROKE BY INCREASING MATRIX METALLOPROTEINASE EXPRESSION

E. Candelario-Jalil[1], Y. Yang[1], F. Bosetti[2], G.A. Rosenberg[1]

[1]Department of Neurology, University of New Mexico, Albuquerque, NM, [2]National Institute on Aging, National Institutes of Health (NIH), Bethesda, MD, USA

Introduction: Cyclooxygenase-2 (COX-2) activity exacerbates ischemic brain injury. We showed that COX-2 inhibition reduced blood-brain barrier (BBB) breakdown, edema, and neutrophil infiltration following focal cerebral ischemia. However, the mechanisms through which COX-2 activity enhances BBB permeability are unknown.

Hypothesis: Since matrix metalloproteinases (MMPs) contribute to BBB opening and neuronal death during ischemia, we hypothesized that COX-2 increases BBB opening and tissue damage by increasing MMP expression or activity in the ischemic brain.

Methods: The contribution of COX-2 to stroke-induced MMP-9 and MMP-3 protein expression was investigated using COX-2 knockout mice or their wild-type controls subjected to 90 min of middle cerebral artery occlusion (MCAO). Brain IgG levels were utilized to quantify increased BBB permeability 24 h following ischemia. MMP-3 and MMP-9 protein levels were measured by immunoblotting. MMP-9 activity was determined using a newly developed immunocapture assay coupled to a fluorescence resonance energy transfer peptide.

Results: COX-2 deficient mice showed a significant reduction in BBB breakdown in the cerebral cortex compared to their wild-type controls after ischemia and 24 h of reperfusion. COX-2 knockout mice had a significant reduction in MMP-3 and MMP-9 protein expression compared to wild-type controls. COX-2 gene deletion prevented the loss of type IV collagen and degradation of the tight junction proteins, occludin and zona occludens-1 (ZO-1), following ischemia.

Conclusions: These data indicate that COX-2 is actively involved in BBB damage in ischemic stroke through modulation of MMP expression and activity.

890

ISOFLURANE INDUCES ENHANCED NEUROAPOPTOSIS AND PRONOUNCED REDUCTION OF BRAIN OXIDATIVE METABOLISM IN INTRAUTERINE GROWTH RESTRICTED NEWBORN PIGLETS

R. Bauer[1], H. Schubert[2], B. Walter[1,3], H. Fritz[4], M. Brodhun[5]

[1]Institute of Molecular Cell Biology, [2]Insitute of Laboratory Animal Science and Conservation, University Hospital Jena, Friedrich Schiller University, Jena, [3]Department of Neurosurgery, Zentralklinik, Bad Berka, [4]Department. of Anesthesiology and Intensive Care, Martha-Maria Hospital, Halle/Saale, [5]Institute of Pathology, HELIOS Klinikum Wuppertal, Erfurt, Germany

Background and aims: Neurodegeneration following exposure to anesthetics and sedatives has been clearly established in developing animals. However, while some of the biochemical pathways have been revealed, the impact of pre-existing disturbances in brain development on extent of resulting brain injury remains unclear. Intrauterine growth restriction (IUGR) is a leading cause of perinatal neurodevelopmental morbidity. Causal mechanisms of poor neurological outcome in IUGR are less well understood, but may likely include abnormal maturation patterns of neurotransmitter networks and increased vulnerability to extrinsic factors. Therefore, we asked if exposure of the frequently used inhalational anesthetic isoflurane may provoke an altered response on acute brain functioning and enhanced propensity to neurodegenerative effects.

Methods: We used 1-day old piglets (n=25). Animals were divided into normal-weight piglets (NW, n=13; BW:1557 ± 105g) and IUGR piglets (n = 12, BW:823 ± 55g) according to their birth weight. Correct allocation was confirmed afterwards by estimation of the brain to liver ratio. Surgical preparation was performed under a minimal alveolar concentration (MAC, respiratory gas monitor controlled) of 1.0 for isoflurane in 70% nitrous oxide and 30% oxygen (duration ~2h). After completion, anesthesia was reduced to 0.25 MAC for isoflurane and the piglets were allowed to stabilize for two hours (baseline conditions). Neuro- and cardiorespiratory monitoring was performed during baseline conditions and subsequent 1-h periods of 0.5 MAC, 1.0 MAC and recovery (0.25 MAC). Cardiac output and regional blood flows were measured by colored microspheres. Brain $AVDO_2$ was determined using arterial and sagittal sinus blood samples ($CMRO_2$= $CBF \cdot AVDO_2$).Total time of gradual isoflurane exposure was seven hours. Experiments were finished by intravital perfusion fixation of the brain for immunohistochemistry (IHC).

Results: At baseline conditions, systemic cardiovascular and other physiological values including organ blood flows, brain electrical activity and brain oxidative metabolism were similar in NW and IUGR piglets. Gradually increased isoflurane administration caused a more pronounced restriction of myocardial contractility and cardiac output in NW piglets resulting in a pronounced reduction in heart, forebrain and kidney blood flows ($P < 0.05$). In contrast, the expected gradual restriction in brain oxidative metabolism by stepwise elevated isoflurane MACs was markedly more pronounced in IUGR animals ($P < 0.05$). However, the extent of depressed brain electric activity (burst suppression index) was similar in both groups. Importantly, a manifold increase of TUNEL-positive cells appeared in IUGR piglets exposed to different levels isoflurane inhalation compared to NW animals of similar conditions ($P < 0.05$). NW piglet brains did not show any differences in histology and IHC compared to isoflurane non-exposed siblings.

Conclusions: An enhanced number of TUNEL-positive cells in brain slices indicate an

increased vulnerability of IUGR piglets to isoflurane exposure under conditions, which are comparable with ongoing clinical practice. The increased brain oxygen delivery to uptake ratio at MAC 1.0 in IUGR piglet brains suggest that the more pronounced suppression of brain oxidative metabolism may not induce a hypoxia-induced neuronal injury.

891

EXTRACELLULAR SIGNAL-REGULATED KINASE 1/2 DEPENDENT NEUROPROTECTION OF ISCHEMIC PRECONDITIONING AGAINST ISCHEMIC STROKE OF MICE

J.A. Shin[1], H.-S. Kim[2,3,4], E.-M. Park[1,4]

[1]Department of Pharmacology, [2]Department of Molecular Medicine, School of Medicine, Ewha Womans University, [3]Tissue Injury Defense Research Center, [4]Department of Brain & Cognitive Sciences, Ewha Womans University, Seoul, Republic of Korea

Objectives: Experimental stroke studies have suggested several signaling pathways that play important roles in the tolerance induced by preconditioning stimuli. Extracelluar signal-regulated kinase 1 and 2 (ERK 1/2) is one of major signaling pathways regulating tight junction (TJ) of blood-brain barrier (BBB) and affecting neuronal survival after ischemic stroke. However, the activity of ERK1/2 and its role in the ischemic preconditioned brain has not been clearly defined. This study was aim to examine whether the protective effect of ischemic preconditioning (IP) was associated with modulation of TJ proteins via ERK1/2 activity.

Methods: IP of brief bilateral common carotid artery occlusion (BCCAO) was induced in male C57BL/6 mice 24 h before transient middle cerebral artery occlusion (MCAO). A specific ERK1/2 inhibitor U0126 (30ug/kg, i.v.) was given to some of mice 1 h before MCAO to examine the role of ERK1/2 in the preconditioned brain. Behavior tests (neurological score and hanging wire test) were performed and infarct volume was measured 3 days after reperfusion. To asses BBB break down, 2% Evans blue (5 ml/kg) was injected to tail vein right after BCCAO, and then the amount of Evans blue in the brain was measured at 24 h later. The expression changes of tight-junction proteins (occludin and claudin5), total and phosphorylated ERK1/2 were analyzed by Western blot. Microglial activation during the tolerance period was evaluated by immunofluorescence staining of Iba1.

Results: Phosphorylated form of ERK1/2 was increased while tight junction proteins were down-regulated in the preconditioned brain. Microglial activation was slightly increased by IP during the tolerance period. Evans blue extravasation was observed in the preconditioned brain although there was no statistical significance between IP and sham groups. When mice were pretreated with U0126 after IP, improvements of infarct volumes and behavior tests were disappeared. Also, down-regulated tight junction proteins and mild activated microglia were reversed by inhibition of increased ERK 1/2 phosphorylation.

Conclusions: The findings suggest that increased activity of ERK1/2 in the preconditioned brain affects the tightness of via regulation of endothelial tight junction proteins to induce brain tolerance against ischemic stroke.

Acknowledgements: This research was supported by the National Research Foundation of Korea (NRF) grant funded by the Korea government (MEST) (2010-0029354).

892

MODIFIED SHAPE (NON-INPUT) ANALYSIS FOR MEASUREMENT OF METABOLIC RATE WITH PET USING INCOMPLETE TRAPPING IRREVERSIBLE TRACER

T. Ohya, T. Kikuchi, T. Irie, M.-R. Zhang, T. Fukumura

Molecular Imaging Center, National Institute of Radiological Sciences, Chiba, Japan

Introduction: 'Shape analysis' proposed by Frey et al. (1997) is one of non-input analyses for irreversible tracer. The method enables direct estimation of metabolic rate (k_3) without a reference site nor an input function. However, the mismatched setting of final scan frame and the extent of measurement error in the final frame cause large bias. Thus, we modified Shape analysis and assessed the reliability of parameter estimation by a simulation using the experimental monkey PET data with metabolic complete ([^{11}C]MP4A) and incomplete ([^{18}F]FEP4MA) trapping irreversible tracers.

Methods: Theory: Brain-TAC in the first period (~ 2000 sec) is fitted by the function f_1 and f_2 (Figure Eq.1) for interpolation of data points. The C_1 and C_2 curves are calculated by Eq.2 assuming $C_2(t=0)=0$ and $dt \approx \Delta t \approx 1$ sec, where C_1 and C_2 represent the concentration of authentic and metabolite of tracer in the brain. When the metabolite is eliminated with k_{el}, the Brain-TAC in the middle to latest period (1400 sec ~) is described by Eq.3. The parameters k_3 and k_{el} in Eq.2 are determined to minimize the residual sum of squares for two C_2 curves based on Eq.2 and Eq.3 in the overlapping region (1500 - 1800 sec).

Simulation: Monte Caro simulation was performed to examine the effect of measurement noise on the parameter estimation using the monkey PET data estimated by non-linear least square method (NLS); each input function, K_1=.47, k_2=.13, k_3=.10, k_{el}=.0036 (/min) in [^{11}C]MP4A, K_1=.65, k_2=.14, k_3=.10, k_{el}=.012 (/min) in [^{18}F]FEP-4MA, where K_1 represents the tracer influx rate from blood pool to brain, k_2 the efflux rate from brain to blood pool. On the basis of the experimental data, we also examined the effect of the fluctuation of the rate parameters (K_1±10%, k_2±20%, k_3±15%, k_{el}±10%) on the reliability of parameter estimation: Only k_3 parameter was changed (30% decrease) under various rate parameter conditions, and the relative k_3 change was measured by the relative bias ($RB = (rk_3 - rk_{3\text{-true}})/rk_{3\text{-true}} \times 100$, $rk_{3\text{-true}}$=0.7). In shape analysis, we adopted the condition reported by Tanaka et al. (2001).

Results: The negative bias and positive bias were increased in Shape and the modified method as the measurement noise was increased. The precision of k_3 parameter in Shape is higher than that in the modified method with only FEP-4MA. However, RB of k_3 in Shape (18-26%) was also larger than that in the modified method (2-7%) for both tracer conditions. The effect of analytical conditions in the modified method on the precision and bias of k_3 parameter was lower than those in Shape; especially the effect of the noise added in final frame on the data reliability was lowed in the modified method. From the PET study with [^{18}F]FEP-4MA, we also found that relative k_3 estimated by Shape was large different from that by NLS.

Conclusion: E-method can be considered as an alternative analysis to Shape especially for an incomplete trapping irreversible tracer.

References: Frey et al. (1997) JCBFM 17:S328, Tanaka et al. (2001) JCBFM 21:295-306

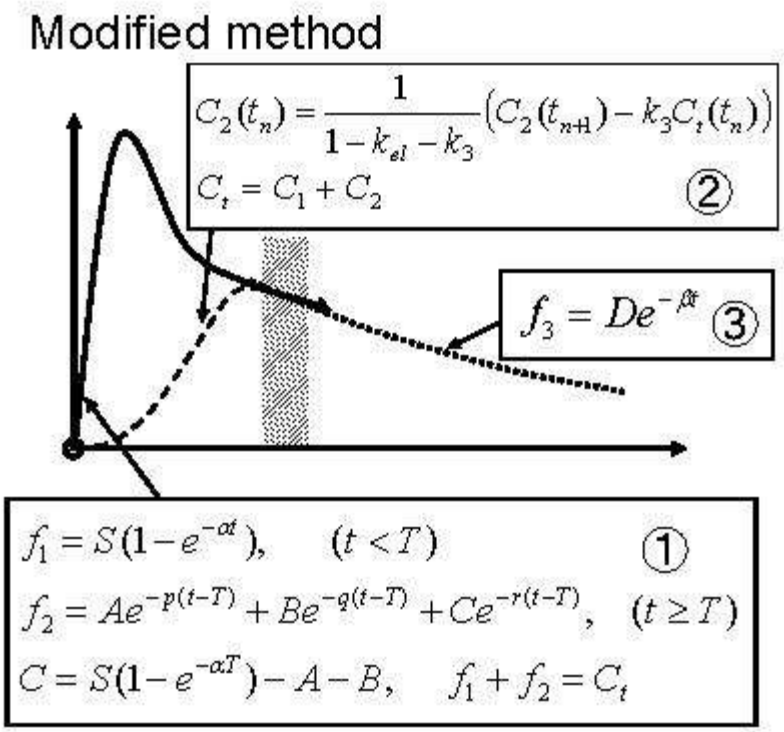

[modified method]

893

ACUTE TREATMENT WITH A CB2R SELECTIVE AGONIST DECREASES PARENCHYMAL PRO-INFLAMATORY AND ANTIINFLAMATORY CYTOKINES AFTER BRAIN ISCHEMIA IN MICE

J.G. Zarruk[1], D. Fernández-López[1], M.I. Cuartero[1], I. Ballesteros[1], I. García-Yébenes[1], F. Nombela[2], J. Vivancos[2], J. Manzanares[3], I. Lizasoain[1], **M.A. Moro**[1]

[1]Pharmacology, Universidad Complutense, [2]Hospital Universitario La Princesa, Madrid, [3]Instituto de Neurociencias, CSIC, Alicante, Spain

Background and purpose: Ischemic stroke continues to be one of the main causes of death worldwide (1). Inflammation accounts for a large part of damage in this pathology (2). Interestingly, the cannabinoid type 2 receptor (CB2R) has been proposed to have neuroprotective properties in neurological diseases (3, 4). Therefore, our aim was to determine the effects of the activation of CB2R on infarct outcome and on the expression of ischemia-induced pro- and anti-inflammatory markers.

Methods: Swiss wild type and CB2R knock-out male mice were subjected to a permanent middle cerebral artery oclussion (pMCAO). Mice were treated with either a CB2R agonist (JWH133; 1.5mg/kg), a CB2R antagonist (SR144528; 3-5mg/kg) or vehicle 10 min after the pMCAO. Neurological symptoms were evaluated using the modified Neurological Stroke Scale (mNSS) 24 and 48 hours after MCAO. To determine infarct volume, brains were removed 48 hours after MCAO and stained with 2% TTC (2,3,5-triphenyltetrazolium chloride). An additional group of animals was used to assess mRNA and protein expression of CB2, IL-1β, IL-6, TNF-α, MCP-1, MIP-1α, RANTES, iNOS, COX-2, IL-4, IL-10, TGF-β, arginase I and Ym1.

Results: Administration of the CB2R agonist JWH-133 significantly improved infarct outcome, as shown by a reduction in brain infarction and neurological impairment. This effect was reversed in mice treated with the CB2R antagonist and absent in CB2R knock-out mice. Additionally, ischemia-induced expression of IL-6, TNF-α, MCP-1, MIP-1α, RANTES, iNOS, IL-10, TGF-β, and Ym1 was significantly decreased in mice treated with JWH133 compared with vehicle-treated mice.

Conclusions: Our data demonstrate that the acute administration of CB2 activation induces neuroprotection in experimental permanent ischemia in mice, as shown by a reduction in neurological symptoms and infarct volume. In addition, inhibition of MCAO-induced expression of pro-inflammatory cytokines and chemokines may account for the neuroprotective effect of this CB2 selective activation, as well as a diminished expression of anti-inflammatory cytokines would be suggesting not only reduced infiltration but also a central inhibition of microglia/macrophages activation.

References:

1. D. Lloyd-Jones *et al.*, *Circulation*, (2008).

2. A. Denes, P. Thornton, N. J. Rothwell, S. M. Allan, *Brain Behav.Immun.*, (2009).

3. R. I. Grundy, M. Rabuffetti, M. Beltramo, *Mol.Neurobiol.* **24**, 29 (2001).

4. R. Mechoulam, D. Panikashvili, E. Shohami, *Trends Mol.Med.* **8**, 58 (2002).

Acknowledgments: Supported by RETICS-RENEVAS RD06/0026/0005 and SAF2009-08145. Zarruk JG is supported by the Programme Alban, scholarship No. E07D400805CO.

894

SUBDIVISIONAL DISTRIBUTION OF STRIATAL DOPAMINE D_1 RECEPTORS AND THEIR ASSOCIATION WITH THOSE OF EXTRA-STRIATAL REGIONS USING [^{11}C]SCH23390: A PET STUDY

H. Fujiwara, H. Ito, F. Kodaka, Y. Kimura, H. Takano, T. Suhara

National Institute of Radiological Sciences, Chiba, Japan

Objectives: Mesencephalic dopamine (DA) system is the main DA system which relates to affective and cognitive functions such as reward processing. The system is divided into three cell groups A8, A9 and A10, whose cells are located in different regions of the midbrain. The striatum is the main input structure of the basal ganglia from the mesencephalon. In human, the striatum is functionally organized into sensorimotor, associative and limbic subdivisions [1)], which process information related to motor, cognitive and emotional functions, respectively. DA projections ascending from the midbrain provide regulatory input to these subdivisions. However, the associations between DA functions of each subdivision and those of extra-striatal regions remain unknown. The aim of the study was to investigate the relation in DA D_1 function using PET.

Methods: A PET study was performed on 30 healthy male subjects using [^{11}C]SCH23390 to measure striatal and extra-striatal D1 receptor (D_1R) binding[2)]. The binding potentials (BP_{ND}) of D1R was quantified using the simplified reference tissue model using the cerebellum as a reference region. Regions of interest were manually defined for each striatal subdivision. A multiple regression analyses was undertaken to find extra-striatal regions which are associated with each striatal functional subdivision in terms of their D_1R BP_{ND} using statistical parametric mapping 5. The regions in which BP_{ND} were correlated with those of striatal subdivisions were visualized in the form of statistical parametric maps.

Results: The BP_{ND} values of D1R were 0.61±0.11, 1.46±0.27, and 0.33±0.05 in the sensorimotor, associative, and limbic subdivisions, respectively (mean±SD). BP_{ND} values in the sensorimotor and associative subdivisions were significantly correlated with those in various brain regions, i.e., fronto-temporal and parieto-occipital cortices including cingulate cortices. No correlations was found between BP_{ND} values in the limbic subdivision and extra-striatal regions. With regard to the interrelationships among BP_{ND} of three striatal subdivions, mutual correlations were found between the sensorimotor and associative ones, whereas not between the limbic and the other subdivisional ones.

Conclusion: Although the DA projections to the sensorimotor and associative subdivisions of striatum and extra-striatal regions would originate from different cell groups (A9 and A10) in the midbrain, the relation in BP_{ND} between the striatal subdivisions and extra-striatal regions suggests that the sensorimotor and associative striatum might have similar backgrounds to those of cortical regions in terms of D_1R expression. For the projections to the limbic subdivision and cortical regions, they are considered to originate from the same cell group (A10). However, the background of D_1R expression in the limbic subdivision might be different from that in the cortical regions. The BP_{ND} of the sensorimotor and associative subdivisions were mutually correlated, but not with limbic ones, indicating the similarity between the sensorimotor and associative subdivisions, and the difference of limbic one from the other subdivisions in terms of D1R expression.

References:

1. Martinez D et al. J Cereb Blood Flow& Metabolism 23: 285-300, 2003.

2. Okubo Y at al. Nature 385: 634-6, 1997.

895

PREDICTIVE VALUE OF BRAIN CT FOR FUNCTIONAL OUTCOME AND MOTOR RECOVERY IN DEEP SEATED INTRACEREBRAL HEMORRHAGE

H. Hwang, T. Lee, J.H. Jeong, I.Y. Shin, S.-M. Moon

Neurosurgery, Hangang Sacred Heart Hospital, College of Medicine, Hallym University, Seoul, Republic of Korea

Background: In deep seated intracerebral hemorrhage, functional outcome and motor recovery are very important as well as variable. We would like to predict functional outcome and motor recovery through only initial brain CT image.

Methods: In a retrospective review, 80 patients with spontaneous ICH (S-ICH) around internal capsule were identified among 136 cases of S-ICH between January 2006 and December 2007. We investigated age, sex, past medical history, Glasgow coma scale, Glasgow outcome scale, ICH volume, ICH location and the degree of motor recovery. We divided cases into 4 groups according to the location of hematoma. In addition, all types were subcategorized into two groups depending on the involvement of corona radiate. The difference of functional outcome and motor recovery according to type was statistical analyzed.

Results: The mean age was 59 years old and the mean volume of hematoma was 23cc. Some hemtomas were operated by stereotaxic and navigation guides but small hematomas were treated conservatively. The mean follow-up period was 35.7 months. Among 80 cases, type A was 13 (16.3%), type B 24(30%), type C 16, (20%) and type D 27(33.8%). On univariate analysis to Glasgow Outcome Scale (GOS), there were significant differences for ICH volume, ICH type, corona radiata involvement and Glasgow Coma Scale (GCS). To initial motor grade, there were significant differences for ICH type and corona radiata involvement. But, there was not statistically significant factor to motor recovery. The average motor grade improvement of lower extremity was better (1.3) than the upper extremity (1).

Conclusion: On S-ICH, initial motor grade should be related with the amount of damage of pyramidal tract from corona radiate to internal capsule but initial brain CT could not show the difference of functional outcome and motor recovery precisely.

896

MEASUREMENT OF CEREBRAL METABOLIC RATE OF OXYGEN (CMRO2) USING QBOLD TECHNIQUE IN RESTING STATE

X. He[1], D.A. Yablonskiy[2], K.T. Bae[1]

[1]Department of Radiology, University of Pittsburgh School of Medicine, Pittsburgh, PA, [2]Mallinckrodt Institute of Radiology, Washington University in St. Louis School of Medicine, St Louis, MO, USA

Introduction: Quantitative brain hemodynamic parameters, such as oxygen extraction fraction (OEF), cerebral blood flow (CBF), and cerebral metabolic rate of oxygen (CMRO2) in a baseline resting state or during functional activation, are essential for both understanding the biophysical processes underlying blood oxygenation level depend (BOLD) phenomenon (1), as well as for determining the consequences of neurological impairments associated with common brain diseases. Previous studies developed (2) and validated (3) MRI-based quantitative BOLD (qBOLD) methods that allow for non-invasive regional measurement of OEF. In this study, we propose a new MR approach, ASL-qBOLD (arterial spin labeling qBOLD), to simultaneously measure both CBF and OEF, thereby providing quantitative CMRO2 mapping.

Methods: All experiments were performed on a 3.0 T Siemens Trio scanner. FAIR perfusion sensitive preparation pulses (4) were used to generate perfusion weighted GESSE (gradient echo sampling of spin echo) qBOLD images. QUIPSS II technique (5) was incorporated for a robust CBF quantification. Three studies were conducted on healthy volunteer subjects. The MR imaging parameters were: TR = 3000 ms; total labeling time (TI) of 2000 ms; 90 gradient echoes with spin echo at 15th echo; echo spacing of 1.5 ms; sampling matrix of 64 x 48 with voxel size of 4x4x8 mm^3. After the correction for motion and Bo field, the averaged GESSE data between the labeling and control conditions was fitted by the qBOLD signal model (2) to estimate the absolute OEF maps. ASL signal was the averaged MR signal difference between labeling and control GESSE images. CBF was subsequently quantified by assuming typical T1 of GM, WM and blood. The CMRO2 was determined by the product of OEF and CBF.

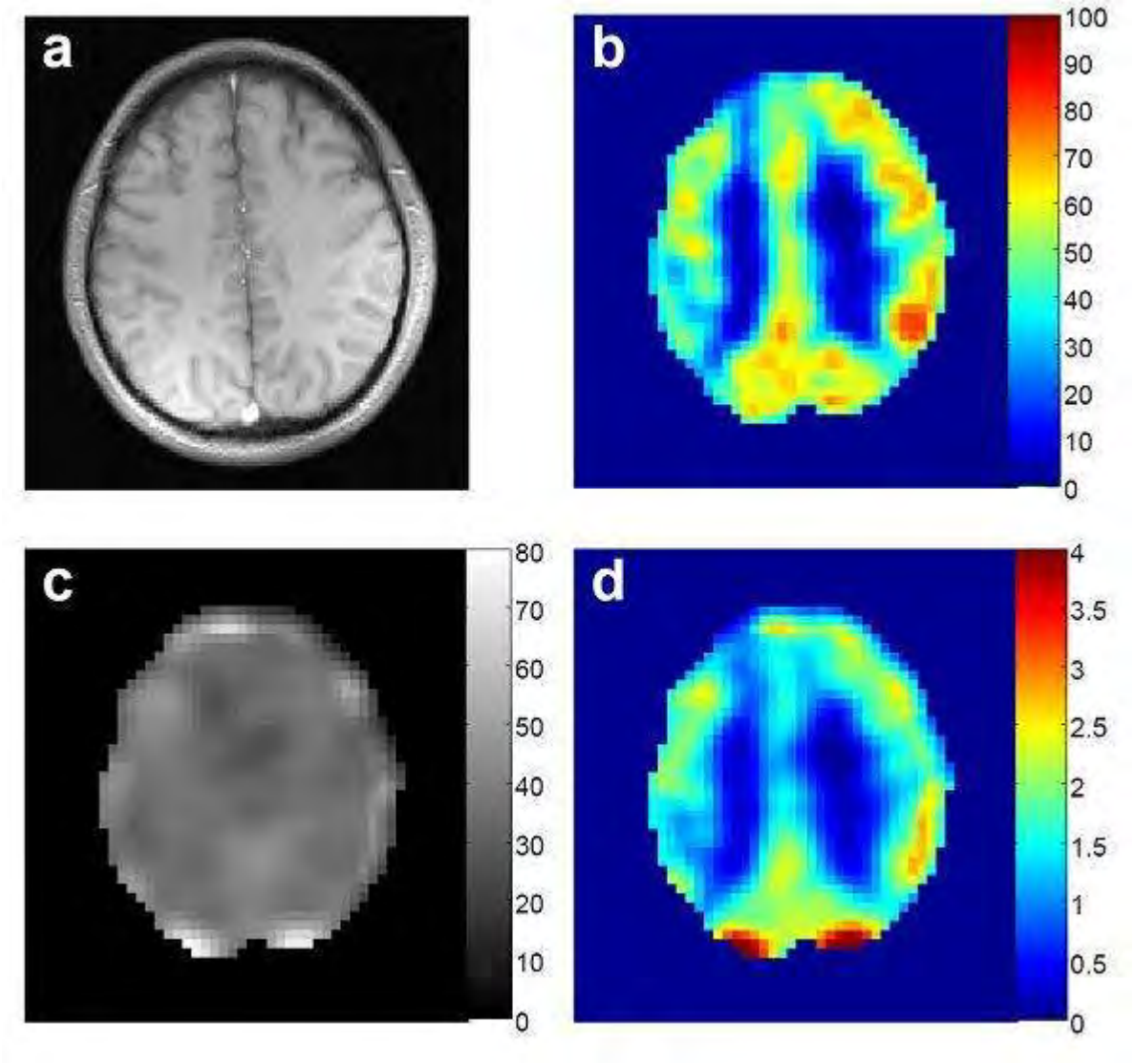

[Figure 1]

Results: Figure “a” depicts a typical case in point of a high resolution T1-weighted anatomy image from a healthy subject. The brain area was manually segmented. Areas close to the brain surface were masked out to avoid a possible contamination from large veins at the surface, reflected by the higher qBOLD fitting residue. Figure “b” is the estimated CBF map (in ml/100g/min), delineating the contrast between GM and WM. The mean CBF was 52±10 ml/100g/min in GM. Figure “c” illustrates the estimated OEF map, which is relatively uniform across the brain parenchyma with mean values of 38±9 %. Figure “d” shows the CMRO2 map (in μmol/g/min). Note that the CMRO2 was much higher in the cortical GM than the WM. The mean CMRO2 in GM area was 1.77±0.56 μmol/g/min, which is consistent with that measured by PET imaging.

Conclusion: We have developed and implemented an ASL-qBOLD technique to determine

quantitative MR-based in vivo absolute CMRO2 maps of the brain. The estimated CMRO2 was within a physiological range of those reported by PET imaging (the current in vivo gold standard).

References: 1. Ogawa, et al, PNAS 1990; 87:9868-72; 2. He and Yablonskiy., MRM 2007; 57:115-126; 3. He, *et al.*, MRM 2008; 60:882-888; 4. Kim, *et al*., MRM 1995; 34:293-301; 5. Wong, *et al.*, MRM 1998; 39:702-708.

897

HOPEAHAINOL A TARGETS OXIDATIVE STRESS INDUCED BY AMYLOID-B PEPTIDES (AB) AND AMYLOID-B ALCOHOL DEHYDROGENASE (ABAD) INTERACTION IN APP/PS1MICE

Z.X. lei[1], Y. lan[2], L. Rong[2], G.H. min[3], T.R. xiang[3], Y. Xu[1]

[1]Nanjing Drum Tower Hospital Clinical College of Traditional Chinese and Western Medicine, Nanjing University of Chinese Medicine, [2]Medical School of Southeast University, [3]Institute of Functional Biomolecules State Key Laboratory of Pharmaceutical Biotechnology School of Medicine, Nanjing University, Nanjing, China

Objectives: Oxidative stress caused by the formation of the Aβ-ABAD complex is regarded as one of the most important molecular mechanisms of Alzheimer's disease (AD). A polyphenol isolated from *Hopea exalata* (Hopeahainol A, $C_{28}H_{16}O_8$) has demonstrated antioxidant capacities beyond its ability to inhibit acetylcholinesterase. In this study, we aim determine if Hopeahainol A improves cognitive impairment by an antioxidative capacity in APP/PS1 mice, focusing on the potential inhibition of the interaction between Aβ and ABAD.

Methods: APP/PS1 mice were treated with Hopeahainol A (2 mg/kg/2d, 30 days). For in vitro studies, primary cortical neurons were treated with Aβ with or without 2μM Hopeahainol A for 24 hours. ROS and indicators of oxidative damage (4-HNE, 3-NT and 8-OHdG) were measured by immunofluorescence and ELISA, respectively. Aβ-ABAD complex formation was assessed by confocal microscope and co-immunoprecipitation. High performance liquid chromatography (HPLC) was performed to quantify levels of free (unbound) Hopeahainol A. Behavioral performance was evaluated by the Morris Water Maze test, field EPSPs were measured, and immunohistochemical staining of cholinergic neurons was performed to determine protective outcomes of Hopeahainol A against neural impairment in APP/PS1 mice. Statistical analyses were performed using ANOVA and *post hoc* Fisher's PLSD tests, with $P< 0.05$ considered statistically significant.

Results: Hopeahainol A significantly decreased ROS and oxidative damage both in vivo and in vitro ($p< 0.05$). In addition, the presence of the Aβ-ABAD complex was attenuated by Hopeahainol A ($p< 0.05$). The presence of free Hopeahainol A was depleted by addition of $Aβ_{1-42}$ but not $Aβ_{42-1}$, suggesting that Hopeahainol A binds directly with $Aβ_{1-42}$. Finally, performance on the Morris Water Maze, field-excitatory postsynaptic potential (fEPSP) in the CA1 stratum and immunohistochemistrical staining for cholinergic neurons were all significantly improved with Hopeahainol A treatment, suggesting that Hopeahainol A protects APP/PS1 mice at both the functional and pathological levels.

Conclusions: Hopeahainol A protected APP/PS1 mice from both cellular and functional neural damage. These protective effects were associated with inhibition of oxidative stress and reduced formation of the $Aβ_{1-42}$-ABAD complex. Furthermore, our results indicate that Hopeahainol A appears to bind directly with $Aβ_{1-42}$. Thus, Hopeahainol A may be a promising drug therapy for the treatment of AD.

898

INFLAMMATION-INDUCED TLR4 EXPRESSION AND REACTIVE OXYGEN SPECIES ARE ATTENUATED BY DIHYDROTESTOSTERONE IN HUMAN PRIMARY VASCULAR SMOOTH MUSCLE CELLS

R. Gonzales[1], R. Techapinywat[1], D. O'Connor[1], K. Osterlund[1,2]

[1]Basic Medical Sciences, University of Arizona COM Phoenix, Phoenix, AZ, [2]Biomedical Sciences, Colorado State University, Fort Collins, CO, USA

Experimental studies have demonstrated that androgens modulate vascular inflammation, a critical regulator in the development and progression of cerebrovascular disease, particularly stroke[1]. In rats, low doses of androgens have been shown to be protective during cerebral ischemia[2]. Our most recent data has demonstrated that the potent endogenous androgen, dihydrotestosterone (DHT), attenuated endotoxin-induced[3] and oxygen glucose deprivation (OGD; in vitro model for ischemia)-induced cyclooxygenase-2 (COX-2) in human vascular smooth muscle (VSM) cells. It has been implicated that COX-2 plays a role in vascular inflammation and may serve as a source of reactive oxygen species (ROS)[4]. Expression of COX-2 as with many other proinflammatory mediators such as cytokines, chemokines and iNOS can be regulated by the activation toll-like receptor 4 (TLR4) following exposure to endotoxin or injury[5]. TLR4 expression significantly increases after middle cerebral artery occlusion in rodents and these increases in TLR4 correlate with increased damage[6,7].

Objective: Because TLR4 is implicated in pathogenic endotoxin-induced inflammation and, more recently, implicated in injury-induced inflammation in the absence of endotoxin the goal of this proposal is to determine if DHT's ability to attenuate COX-2 following endotoxin, hypoxia, or OGD involves in part alterations in TLR4 levels and ROS production.

Methods: TLR4 localization was detected via immunocytochemistry and visualized using confocal microscopy in rat pial arteries and primary human brain VSM cells. TLR4 protein levels were measured in whole lysate from primary human brain VSM or human coronary artery VSM cells via western blot following a pre-treatment with vehicle or DHT (10nM, 18h) and 6h exposure to the endotoxin LPS (100 ng/ml), hypoxia (1% O_2), or OGD (1% O_2 in glucose-free media) in the continued presence of hormone. OGD studies were repeated in the presence of the androgen-receptor antagonist bicalutamide (1μM). ROS generation was measured using the indicator dye carboxy-H2DCFDA (30μM) in human brain VSM cells pre-treated with vehicle or DHT (10nM, 18h) followed by the cytokine IL1-beta (5ng/ml, 30min) in the continued presence of hormone.

Results: TLR4 was detected in both the cytosol and nucleus of human brain VSM cells, as well as both the endothelium and VSM of rat pial arteries. Endotoxin, hypoxia, and OGD all increased TLR4 levels in VSM cells compared to controls. In contrast, endotoxin and OGD-induced TLR4 levels were attenuated in the presence of DHT (10nM). In the OGD studies, DHT's effect on TLR4 was androgen receptor independent. Similar to the TLR4 studies, cytokine-induced ROS production was blunted by DHT.

Conclusion: In conditions of oxidative stress, androgens may confer protection from vascular injury in part by attenuating both TLR4 protein levels and ROS production.

References: [1] del Zoppo and Mabuchi 2003 *Journal of Cerebral Blood Flow & Metabolism*. [2]Uchida et al 2009 *J Cerebral Blood Flow & Metabolism*. [3]Osterlund et al 2010 *AJP*

Endocrinology & Metabolism. [4]Masferrer et al 1995 *American Journal of Therapeutics*. [5]Dauphinee and Karsan 2006 *Laboratory Investigation*. [6]Hyakkoku et al 2010 *Neuroscience*. [7]Arumugam et al 2009 *Shock*.

Support: AHA SDG (RJG), UA Sarver Heart Center Grants: (KLO, RAT).

899

TWO-PHOTON IN VIVO IMAGING REVEALS CEREBRAL CIRCULATION DISRUPTIONS IN MOUSE MODELS OF MYELOPROLIFERATIVE NEOPLASMS

T.P. Santisakultarm[1], C. Paduano[1], N. Nishimura[1], T. Stokol[2], R.C. Skoda[3], W.L. Olbricht[4], A.I. Schafer[5], R.T. Silver[5], C.B. Schaffer[1]

[1]Biomedical Engineering, [2]Population Medicine and Diagnostic Services, Cornell University, Ithaca, NY, USA, [3]Biomedicine, University Hospital Basel, Basel, Switzerland, [4]Chemical and Biomolecular Engineering, Cornell University, Ithaca, [5]Medicine, Weill Cornell Medical College, New York, NY, USA

Objectives: Myeloproliferative neoplasms (MPNs) are caused by hyperactive bone marrow, leading to overproduction of platelets in essential thrombocythemia (ET), or red blood cells (RBCs), white blood cells, and platelets in polycythemia vera (PV). Vascular obstructions and other rheological complications due to the high blood viscosity lead to abnormal flow in many organs including the brain, where decreased blood flow potentially contributes to cognitive decline(1). An activating mutation in a cytoplasmic tyrosine kinase, JAK2V617F, is associated with MPNs in humans, and transgenic mice carrying this mutation develop ET and PV phenotypes(2). Here, we quantify the alterations in cerebral circulation in PV and ET mice and determine the mechanisms that disrupt blood flow in microvessels, with the goal of identifying potential therapeutic targets.

Methods: We used JAK2V617F transgenic mice as donors for bone marrow transplantation into wild type mice. The recipient mice were classified as PV or ET based on blood composition. In order to understand the contribution of elevated RBCs, another group of wild type mice received erythropoietin (EPO, 10-100 IU daily subcutaneous injections for 5 days) to increase hematocrit. All animals were anesthetized and imaged, through a craniotomy, using in vivo two-photon excited fluorescence microscopy(3). Texas-red dextran (0.05 mL of 2.5% w/v) and rhodamine 6G (0.05 mL of 0.1% w/v) were intravenously injected to reveal vascular topology and label leukocytes and platelets, respectively. Cortical capillaries were determined to be flowing or stalled by recording the position of blood cells in individual vessels over time. For flowing arterioles, capillaries, and venules, flow speed was measured.

Results: The average hematocrits of control, ET, EPO-injected, and PV groups were 48%, 44%, 60%, and 63%, respectively. The fraction of microvessels stalled in the top 350 μm of the cortex increased from 3% in controls (2431 vessels, 13 mice) to 14%, 20%, and 22% in ET (6060 vessels, 11 mice, $p < 0.01$), EPO-injected (6594 vessels, 12 mice, $p < 0.01$), and PV (6605 vessels, 8 mice, $p < 0.01$) mice, respectively (Figure). These stall were frequently associated with leukocytes that were firmly adhered to the endothelium in both models with elevated leukocytes (ET and PV) and models with elevated RBCs (EPO-injected and PV) (Figure). Flow speeds decreased in brain capillaries by 38%, 25%, and 46%, relative to controls (92 vessels, 23 mice), in ET (143 vessels, 9 mice, $p < 0.05$), EPO-injected (105 vessels, 11 mice, $p < 0.05$), and PV (91 vessels, 6 mice, $p < 0.05$) groups, respectively. Slowed flow was also observed in surface arterioles and venules in the MPN models..

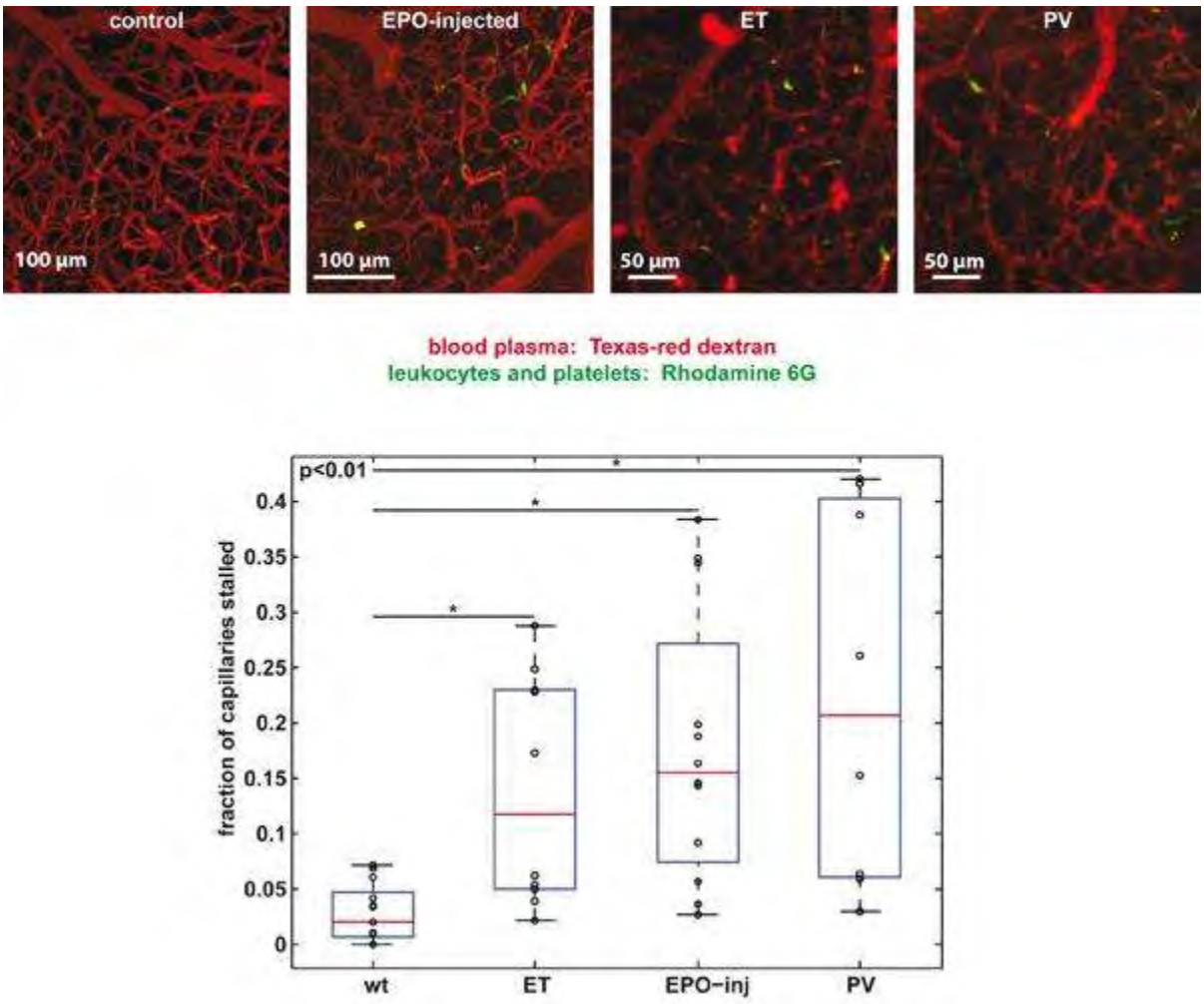

[Figure 1]

Conclusions: Our findings suggest that leukocyte adherence plays a crucial role in obstructing cortical perfusion in MPNs where abnormal rheology results from altered blood composition. Targeting leukocyte adhesion and activation may be clinically important in patients to restore normal cerebral microcirculation.

References:

1. Heinicke, K., et al., *Excessive erythrocytosis in adult mice overexpressing erythropoietin leads to hepatic, renal, neuronal, and muscular degeneration*. Am J Physiol Regul Integr Comp Physiol, 2006. 291: p. R947-956.
2. Tiedt, R., et al., *Ratio of mutant JAK2-V617F to wild-type Jak2 determines the MPD phenotypes in transgenic mice.* Blood, 2008. 111(8): p. 3931-40.
3. Schaffer, C.B., et al., *Two-photon imaging of cortical surface microvessels reveals a robust redistribution in blood flow after vascular occlusion.* PLoS Biol, 2006. 4(2): p. e22.

900

PSD-93 POTENTIATES SREBP-1 ACTIVATION BY IMPACTING THE PHOSPHORYLATION OF FYN AND NR2B FOLLOWING FOCAL CEREBRAL ISCHEMIA

M. Zhang, J. Sun, Y. Xu

Department of Neurology, Affiliated Drum Tower Hospital, Nanjing University Medical School, Nan Jing, China

Introduction: Under ischemic settings, the Postsynaptic Density Protein-93 (PSD-93) and the Src-family kinase Fyn appear to regulate NDMA receptor (NMDAR) function. Targeted disruption of the PSD-93 gene attenuates the excitotoxicity triggered by NMDAR,and Fyn physically binds to and phosphorylates a critical tyrosine residue on the NR2B subunit of NMDAR following cerebral ischemia. However, the crosstalk between these two regulators has not been investigated following cerebral ischemia. A key downstream element in NMDAR-induced excitotoxic signaling pathways is the activation of the sterol regulatory element binding protein-1 (SREBP-1). Therefore, in this study, we explored the role of PSD-93 in neuroprotection and activation of Fyn and SREBP-1 following experimental stroke.

Methods: PSD-93 knockout(KO) and wild type (WT) mice were subjected to 2-hour MCAO and sacrificed at 6, 24 and 72 hours after reperfusion. Brains were removed and assessed for infarct size using 2,3,5-triphenyltetrazolium chloride(TTC). The ischemic condition of longterm potentiation like (i-LTP) phenomenom was measured in fresh hippocampal slices submerged in artificial CSF with or without MK-801 or PP2. Tyrosine phosphorylation of NR2B was detected by western blot using phospho-tyrosine specific NR2B antibodies. Interaction between the NDMAR subunit NR2B and Fyn was detected using coIP. Tyrosine phosphorylation of Fyn was detected using coIP. The presence of SREBP-1 in nuclear extracts was detected by western blot, and mRNA expression of malic enzyme was determined by Q-PCR as an indicator of SREBP-1-induced transcriptional activity. Statistical analyses were performed using ANOVA and *post hoc* Fisher's PLSD tests, with $P< 0.05$ considered statistically significant.

Results: PSD-93 knockout mice had significant reduction in infarct size following MCAO ($P< 0.05$, n=10/group; 6h: 0.06±0.021 in KO vs 0.27±0.04 in WT; 24h:0.16±0.05 in KO vs 0.35±0.05 in WT; 72h:0.12±0.03 in KO vs 0.40±0.09 in WT) and improvement in behavioral outcomes ($P< 0.05$, n=10/group: 24h: 9.78±0.68 in KO vs 12±0.40 in WT; 72h: 9.6±0.27 in KO vs 10.5±0.58 in WT). i-LTP was impaired in the PSD-93 KO group and WT groups pretreated with either MK-801 (an NMDAR antagonist) or PP2 (a Src family antagonist). PSD-93 gene deletion decreased the phosphorylation of the NR2B subunit at Tyr1472 following MCAO and decreased the interaction between NR2B and Fyn. Furthermore, a marked reduction in the presence of the active form of Fyn(phosphorylation at Tyr416) and promotion of the inactive form (phosphorylation at Tyr518) was observed in PSD-93 mice compared to WT.Knockout of PSD-93 reduced the activation of SREBP-1, as evidenced by decreased presence of the N-terminal active form of SREBP-1 in nuclear extracts and the decreased expression of malic enzyme.

Conclusions: The findings suggest that cerebral ischemic activation of the NMDA NR2B subunit and Fyn signaling is potentiated by PSD-93. Deletion of PSD-93 abrogates SREBP-1 activation and leads to significant neuroprotection and functional recovery. Therefore, targeting of PSD-93 and the Fyn signaling pathway may represent a therapeutic target against ischemic insult.

903

P2Y12 DEFICIENCY OR INHIBITION BY CLOPIDOGREL AMELIORATES DELAYED NEURONAL DEATH IN EXPERIMENTAL BRAIN ISCHEMIA

M. Hokari, C.M. Webster, X.N. Tang, A. McManus, M.A. Yenari

UCSF, VAMC, San Francisco, CA, USA

Microglial activation, migration, and proliferation have critical roles in brain injuries and diseases. How microglia are activated by ischemic insults is not precisely known, but may involve extracellular release of nucleotides from necrotic cells. Nucleotides can bind any number of purinergic receptors, and can thus directly participate in cell signaling. The P2Y12 receptor is one such purinergic receptor expressed on platelets and exclusively on microglia. Clopidogrel, a commonly used antiplatelet drug used to prevent stroke in patients, also acts by inhibiting the P2Y12 receptor. However, there have been few studies about the role of P2Y12 in the microglia activation in brain ischemia ischemia. Here, we employed models of ischemia-like insults in vitro and global cerebral ischemia in vivo. To determine the significance of microglia in ischemia-like insults, we prepared enriched neuron cultures with or without added microglia. These cultures were subjected to oxygen glucose deprivation (OGD) and the extent of neuron cell death was estimated from a MAP-2 viability assay. The addition of microglia to enriched-neuron cultures doubled the extent of neuron cell death ($P < 0.05$, 3 replicates). Further, OGD appeared to induce clustering of microglia around neurons. The P2Y12 receptor was then knocked down in microglia using siRNA. P2Y12 knockdown led to the prevention of OGD-induced neuron cell death and prevented microglial clustering. We then studied mice deficient in the P2Y12 receptor (C57/BL6 background), after confirming that their cerebrovascular anatomy was no different from wildtype littermates.We compared P2Y12-heterozygous mice (P2Y12(+/-), lacking one copy of P2Y12)with wild type (WT) littermates, and wildtype mice treated with clopidogrel (25 mg/kg po) to block P2Y12 (CL). Mice were subjected to 12-min bilateral common carotid artery occlusion (BCCAO). Carbon black perfusion was performed to assess the plasticity of the posterior communicating artery (PComm). Homozygote P2Y12 knockout mice were not studied because in pilot studies, these mice suffered higher mortality than the heterozygote mice, and the extent of neuron damage was highly variable. This could be due to indirect effects of changes in hemostasis resulting from complete P2Y12 deficiency in platelets among the homozygote knockouts. There were no significant differences in the caliber of PComm's between groups. In most cases, PComm's were atretic or absent. Histological analysis was performed to evaluate the effect of the P2Y12 receptor on delayed neuronal death at 72 h after 12-min BCCAO. The percentage of viable neurons in the hippocampus CA1 sector was significantly higher in P2Y12(+/-) than in WT mice (P2Y12 knockout 40.2% vs. WT92.3% cell death, $P < 0.05$). Clopidogrel treatment also increased the percentage of viable neurons in the hippocampus CA1 sector (CL35.8 % cell death, $P < 0.01$). Moreover, the knockout and CL groups exhibited decreased in microglial activation as evidenced by decreased lectin staining.

These data indicate that P2Y12 deficiency can reduce activity of microglia and ameliorate delayed neuronal death in the hippocampus after transient global ischemia. These observations also suggested an additional benefit of clopidogrel.

905

HIF-1 PROLYL HYDROXYLASE (PHD) INHIBITORS ARE NEUROPROTECTIVE IN A NEONATAL RAT MODEL OF HYPOXIC-ISCHEMIC BRAIN INJURY

N. Jones, A. Galle

Pharmacology / School of Medical Sciences, University of New South Wales, Sydney, NSW, Australia

Objectives: Hypoxia-inducible factor-1 (HIF-1) is the key transcription factor regulating the expression of many hypoxia-responsive genes (Sharp & Bernaudin, 2004). Under normoxic conditions HIF-1α protein is constantly being degraded due to HIF-1 prolyl hydroxylase enzymes (PHDs) which hydroxylate proline residues on HIF-1α causing ubiquitination and proteosomal degradation of HIF-1α and consequently, constitutive levels of HIF-1α protein are almost undetectable. Hypoxia and drugs that can inhibit PHD activity can cause accumulation of HIF-1 and subsequently increase target gene expression. Previously, we have shown that preconditioning with hypoxia and PHD Inhibitors (cobalt chloride ($CoCl_2$) and desferrioxamine (DFX)) can protect the brain against hypoxic-ischemic (HI) brain injury and this protective effect is largely due to expression of HIF-1 and its target genes (Jones & Bergeron 2001; Jones et al, 2008). In the present study, we have examined whether PHD Inhibitors administered after injury can be neuroprotective.

Methods: Sprague-Dawley rat pups (postnatal day 7) were anaesthetised with isofluorane (2-5% in oxygen) and underwent a unilateral common carotid artery ligation and were then exposed to 3 hours of 8% oxygen. A single injection of drug treatment (DFX (200mg/kg, s.c.), $CoCl_2$ (60 mg/kg, s.c.), ethyl-3,4-dihydrobenzoate (EDHB, 200mg/kg, s.c.) or saline vehicle control (s.c.) was performed immediately after the HI procedure. At 5 days after hypoxic-ischemic insult, pups were sacrificed and brains removed foe sectioning, histological staining and lesion volume analysis. **Results:** This combined HI procedure results in a significant reduction in volume of the ipsilateral hemisphere. Treatments with DFX (n=12), CoCl2 (n=12) and EDHB (n=10) reduced the degree of damage in the ipsilateral hemisphere by 38%, 42% and 37%, respectively, when compared with vehicle treated littermate controls (n=18) ($p< 0.05$, ANOVA).

Conclusions: Overall, our findings indicate that modulation of HIF-1 and its target gene expression using PHD inhibitors after HI brain injury is an effective neuroprotective strategy. We believe that stimulating the body's endogenous protective mechanisms (i.e. HIF-1 and downstream mediators) is a valid strategy for saving brain cells in the injured brain.

References:

Sharp, F.R. & Bernaudin, M. (2004) HIF1 and oxygen sensing in the brain. *Nature Rev Neuroscience* **5**: 437-448.

Jones, N.M., Kardashyan, L., Callaway, J.K., Farso, M., Lee, E.M., Jarrott, B. and Beart, P.M. (2008) Long term functional and protective actions of preconditioning with hypoxia, cobalt chloride and desferrioxamine in neonatal rats exposed to hypoxic-ischemic injury. *Pediatric Research* **63:** 620-624.

Jones, N.M. & Bergeron, M. (2001) Hypoxic preconditioning in rat brain induces changes in HIF-

1 target genes in neonatal rat brain. *Journal of Cerebral Blood Flow and Metabolism,* **21:** 1105-1114.

906

DEFEROXAMINE REDUCES NEURON DEATH AND HEMATOMA LYSIS AFTER INTRACEREBRAL HEMORRHAGE IN AGED RATS

T. Hatakeyama, Cerebral Hemorrhage

Neurological Surgery, Kagawa University, Kita-gun, Japan

Introduction: Deferoxamine (DFX), an iron chelator, reduces brain edema, neurological deficits, and brain atrophy after intracerebral hemorrhage (ICH) in aged rats. In the present study, we investigated whether DFX can reduce ICH-induced neuron death and hematoma lysis in aged rats.

Material and methods: Male Fisher 344 rats (18 months old) had an intracaudate injectin of 100 µL autologous whole blood into the right basal ganglia and were treated with DFX (100mg/kg) or vehicle 2 hours post-ICH and then every 12 hours up to 7 days. Rats were killed 1, 3, or 7 days later for neuron death, ferritin and hematoma lysis measurement. Plasma ferritin levels and behavioral outcome following ICH were also examined.

Results: We found that DFX treatment significantly reduced ICH-induced neuron death, neurological deficits and suppressed hematoma lysis (13.20±1.17 vs. 3.78±1.17 mm^3 in vehicle-treated group, $p < 0.01$) in aged rats. DFX also reduced the ferritin levels in the ipsilateral basal ganglia. However, DFX had not significantly effect on plasma ferritin levels after ICH.

Conclusion: In conclusion, DFX reduces neuron death, neurological deficits, and suppressed hematoma lysis after ICH in aged rats supporting the suggestion that DFX may reduce brain injury in ICH patients.

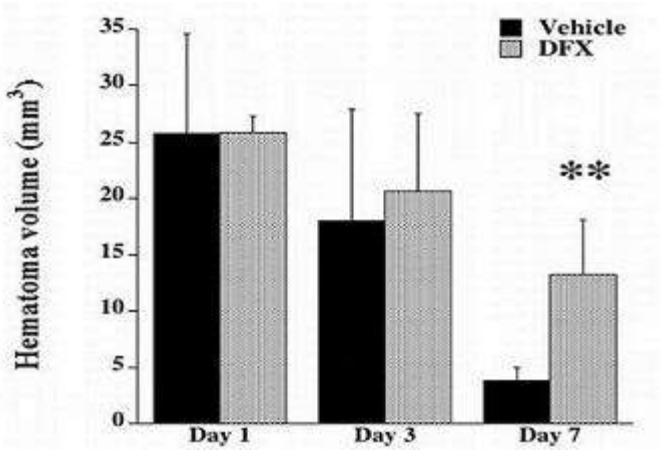

[hematoma volume]

907

ROLE OF NADPH OXIDASE 1 IN ISCHEMIA/REPERFUSION- INDUCED BRAIN INJURY AFTER STROKE

D.-H. Choi[1], K.-H. Lee[1], M.Y. Kim[1], S.-H. Han[1], J. Lee[1,2]

[1]Center for Geriatric Neuroscience Research, Institute of Biomedical Science & Technology, Konkuk University, [2]Department of Rehabilitation Medicine, Konkuk University Medical Center, Seoul, Republic of Korea

Background and purpose: While oxidative stress has been implicated in the pathogenesis of neuronal injury after stroke, molecular mechanism underlying selective vulnerability of the ischemia-reperfusion (I/R) injury to oxidative damage remains unknown. We investigated to determine the role of NADPH oxidase 1(Nox1) in cerebral I/R-induced brain injury.

Materials and methods: Primary rat cortical neuron cultures were exposed to oxygen-glucose deprivation (OGD) and reoxygenation. Nox1 expression, ROS generation and cell death were evaluated. Male SD rats (8 weeks, n = 5~6 each group) were subjected to 90 min middle cerebral artery occlusion (MCAo) followed by reperfusion. At 24hr of reperfusion, infarction size, level of superoxide and 8-hydroxy-2'-deoxyguanosine (8-oxo2dG) immunoreactivity were determined. Either RNAi-mediated knock down of Nox1 or inhibition of Rac1 by overexpressing dominant negative Rac1 (T17N Rac1) were used to investigate the role of NOX1 in I/R-induced oxidative damage and neuronal death.

Results: In primary cortical neurons treated with OGD and reoxygenation, Nox1 expression and peri-nuclear 8-oxo2dG immunoreactivity was increased. Either RNAi-mediated knock down of Nox1 or inhibition of Rac1 by T17N Rac1 led to reduction of ROS generation and neuronal cell death. After MCAo and reperfusion, Nox1 expression and 8-oxo-2dG immunoreactivity was increased in cortical neurons of ischemic penumbra. Both infarction size and neuronal death in I/R injury were significantly reduced by adeno-associated virus-mediated transduction of Nox1 shRNA or T17N Rac1.

Conclusion: Our data suggest that Nox-1 may be responsible for oxidative damage to DNA and subsequent cortical neuronal degeneration in ischemic penumbra after stroke.

908

NEUROVASCULAR COUPLING IN PHARMACOLOGICAL MRI: INVESTIGATING ELECTROPHYSIOLOGICAL AND NEUROIMAGING SIGNAL RELATIONSHIPS DURING A SEROTONERGIC CHALLENGE AND UNDER DIFFERENT ANESTHETIC REGIMES

C. Martin, N.R. Sibson

Gray Institute for Radiation Oncology and Biology, University of Oxford, Oxford, UK

Introduction: Functional brain imaging methods are increasingly applied to study the effects of neuropharmacological agents on brain function in both human and animal subjects. A problem is that neuroimaging signals such as the blood oxygen level dependent (BOLD) functional magnetic resonance imaging (fMRI) signal, commonly used in pharmacological MRI, are indirectly related to neuronal activity. Additionally, little is known about neuronal-phMRI signal coupling under drug-related experimental manipulations. To investigate this, we acquired phMRI and electrophysiological data from animals undergoing a pharmacological challenge of the serotonergic (5-HT) system, using the 5-HT releasing agent fenfluramine. We further investigated the effects of choice of anesthetic agent on the signal measurements and neuronal-phMRI signal coupling.

Methods: Animals were anesthetized with isoflurane, halothane, alpha-chloralose or urethane. Animals were tracheotomized for artificial ventilation and cannulated for administration of drugs and monitoring of physiological parameters. Recording electrodes were constructed from carbon fibre bundles (diameter ~50μm) and inserted into the somatosensory cortex. Imaging was performed on a 7-Tesla horizontal bore magnet. Anatomical scans covering the whole brain were acquired using a T2-weighted fast spin-echo sequence (field of view 30X30mm, matrix size 128X128, slice thickness 0.5mm). Functional data spanning the entire brain were acquired using a T2*-weighted multi-echo gradient-echo sequence (effective TE 12ms, field of view 30 X 30 mm, matrix size 128 X 64, slice thickness 0.5mm). Fenfluramine (10mg/Kg) was injected intravenously after a period of baseline data acquisition. Data were analyzed using FSL tools including FEAT from the Oxford Centre for Functional Magnetic Resonance Imaging of the Brain (FMRIB). Imaging-related and stimulation artifacts were removed from electrophysiological data prior to band-pass filtering.

Results & conclusions: We demonstrate that electrophysiological measures of both baseline and stimulation-evoked neuronal activity can be obtained concurrently with phMRI data acquisition in order to interrogate neuronal-phMRI coupling relationships during neuropharmacological manipulations. Fenfluramine administration produced simultaneous decreases in the BOLD signals (**A**) and in EEG power fluctuations (**B**) in cortical regions. Neuronal responses to stimulation could be extracted from the data following processing to remove MR gradient artifacts (**C**: red - before processing, blue - after processing). Neuronal responses were transiently attenuated by fenfluramine administration (**D**).

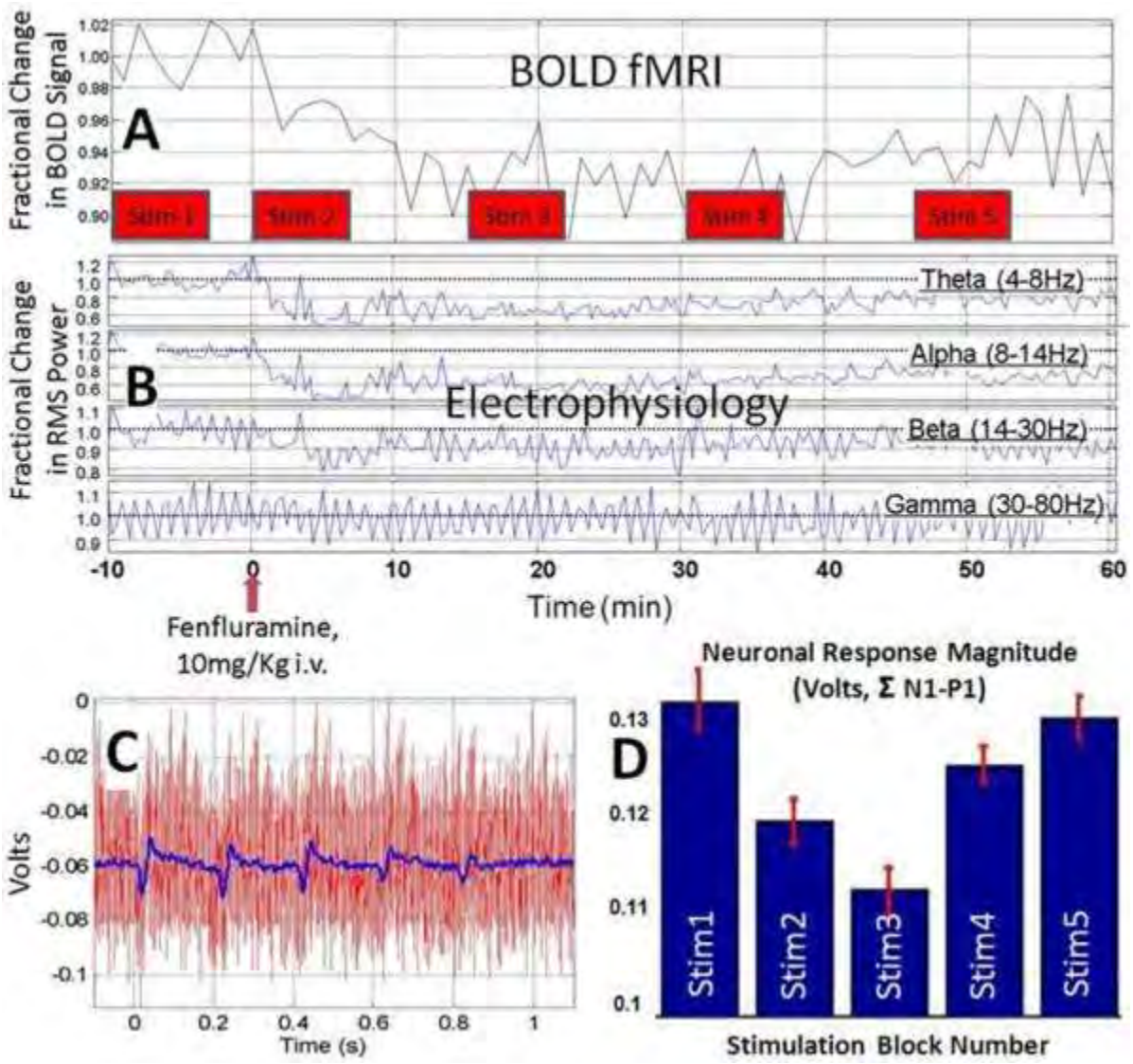
BOLD fMRI
A
Fractional Change in BOLD Signal
Stim 1
Stim 2
Stim 3
Stim 4
Stim 5
B
Electrophysiology
Fractional Change in RMS Power
Theta (4-8Hz)
Alpha (8-14Hz)
Beta (14-30Hz)
Gamma (30-80Hz)
Time (min)
Fenfluramine, 10mg/Kg i.v.
C
Volts
Time (s)
D
Neuronal Response Magnitude
(Volts, Σ N1-P1)
Stim1
Stim2
Stim3
Stim4
Stim5
Stimulation Block Number

[FIG A-D]

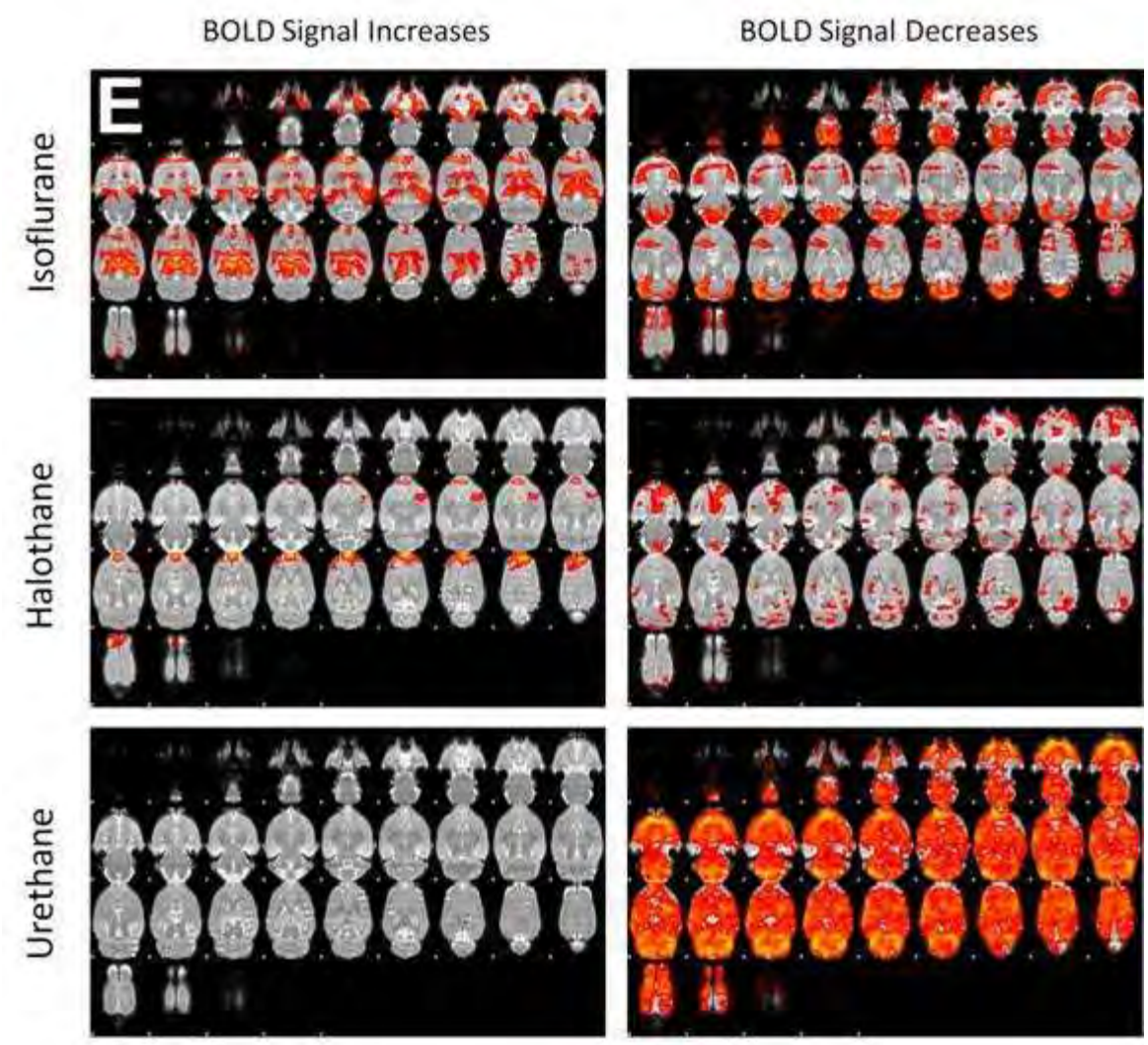

[FIG E]

This study also demonstrated that the choice of anesthetic regime can profoundly affect the pattern of phMRI responses observed across the brain **(E)**. Where phMRI signals are being used as a marker of neuronal function, any interaction of anesthetic regime and pharmacological stimulus may confound interpretation of results. Experiments are ongoing to determine other characteristics of neuronal-phMRI coupling and how this is affected by drug-anesthetic interactions.

909

NADPH OXIDASE-DERIVED SUPEROXIDE MEDIATE CARDIOVASCULAR EFFECTS OF UROTENSIN II IN SPONTANEOUSLY HYPERTENSIVE RATS

N. Lu, Y.C. Zhu

Fudan University, Shanghai, China

Central Urotensin II (U-II) may participate in the regulation of cardiovascular functions by stimulating sympathy pathway. However, their central mechanism remained unknown. Recent studies have shown that brain reactive oxygen species (ROS) mediates the sympatho-excitaory effects. In present study, we tested the hypothesis that ROS mediate central cardiocvascular effects of U-II. Experiments were completed in Wistar-Kyoto (WKY) rats and spontaneously hypertensive rats (SHR). The following observations were made: 1) Expressions of U-II receptors of rostral ventrl medulla (RVLM) and Nucleus tractus solitarii (NTS) were increased in SHR rats compared with WKY rats. 2) Doubling Immunoflurescence analysis showed that U-II receptor and NADPH oxidase subunit $gp91^{phox}$ were co-localization in the RVLM and NTS. 3) Intracerbroventricular U-II or microinjection U-II in RVLM significantly increased mean arterial pressure (MAP) and heart rate (HR). Tempol (a superoxide dismutase mimetic) or Apocinin (NADPH oxidase inhibitor) pretreatments eliminated these effects of U-II . 4) Brain superoxide levels were enhanced in U-II-treated rats compared with CSF-treated rats. 5）Intracerbroventricular UⅡ significantly increased gp91phox or p47phox mRNA level in the RVLM. More importantly, a significant elevation in phosporylated P47phox was detected 5 min after microinjection of UⅡ into the RVLM. These results indicate that superoxide mediates central cardiovascular effects of U-II and provide evidence for a novel relationship between U-II and ROS.

910

ETHYL PYRUVATE TREATMENT ATTENUATES WHITE MATTER INJURY AND IMPROVES NEUROLOGICAL RECOVERY AFTER TRAUMATIC BRAIN INJURY IN RATS

H. Shi[1], H. Pu[2], M. Chu[2], Y.L. Guo[2], J. Zhang[2], P.Y. Zhang[2], W.M. Liang[1], J. Chen[2,3], Y.Q. Gao[2]

[1]Department of Anesthesiology of Huashan Hospital, [2]State Key Laboratory of Medical Neurobiology, Fudan University, Shanghai, China, [3]Center of Cerebrovascular Disease Research, University of Pittsburgh School of Medicine, Pittsburgh, PA, USA

Objective: Traumatic brain injury (TBI) is a leading cause of death and neurological disability in young adults, for which a clinically effective neuroprotective strategy is currently unavailable. TBI triggers a cascade of events such as oxidative stress and inflammation, leading to secondary brain injury and long-term neurological deficits. Recent studies suggest that ethyl pyruvate (EP), a stable lipophilic ester derivative of pyruvate, is remarkably effective in protecting organs (brain, heart, and kidney) against ischemia/reperfusion injury. Since the neuroprotective effects of EP involve ROS scavenging and inflammation suppression, the present study was performed to test the potential beneficial effect of EP treatment in a rat model of TBI.

Methods: Male adult SD rats were subjected to unilateral cortical contusion injury (CCI) and then randomly assigned to either vehicle (n =10) or EP treatment (10, 30 or 50 mg/kg, n=10/dose). EP was injected intraperitoneally immediately after CCI and again at 12, 24, 36, 48, and 60 h post-CCI. For the first set of experiments, neurobehavioral assessments (beam balance, adhesive removal, and foot fault tests) were performed 1-3 days after CCI and brain lesion volume was determined 3 days after CCI. In the second set of experiments, rats (n=8/group) were subjected to sham operation or CCI followed by either vehicle or EP (the optimal dose). Sensorimotor function (foot fault tests) was examined at 3, 5, 7, 14, 21, and 28 days after CCI, and spatial learning and memory was assessed using Morris water maze at 21-28 days after CCI. In the third set of experiments, rats were subjected to CCI and then treated with either vehicle or EP. Brains were assessed for white matter injury at 3, 7, 14, and 28 days after CCI using immunohistochemical staining for myelin basic protein (MBP), oligodendrocyte transcription factor 2 (Olig2), and glial fibrillary acidic protein (GFAP).

Results: Compared to vehicle-treated group, none of the EP-treated groups showed significantly reduced cortical lesion volume 3 days after CCI (all $p>0.05$ vs. vehicle treatment). However, EP treatment at 30 mg/kg significantly improved the foot fault scores on day 3, 5, 7, 14 and 28 after CCI, and significantly enhanced the cognitive performance in Morris water maze (latency to find the hidden platform and the working memory; $p< 0.05$ vs. vehicle group). Moreover, at the same dose that showed neurobehavioral improvement (30 mg/kg), EP treatment also significantly attenuated the remarkable loss of MBP+- and Olig2+-immunoreactive cells in both corpus callosum and striatum at 3-28 days after CCI compared to vehicle-treated groups ($p< 0.05$ vs. vehicle group, n=5/group). In contrast, CCI-induced astrogliosis (the numbers and intensity of GFAP-immunoreactive cells) in the cortical lesion border, corpus callosum and striatum was markedly decreased in EP-treated rats at 7-28 days.

Conclusion: Our results demonstrate that post-injury administration of EP was effective in improving sensorimotor and cognitive functions in a rat model of TBI. The neuroprotection afforded by EP is likely achieved through its salvaging effect on white matter injury, an important secondary injury event thought to contribute to long term neurological deficits after TBI.

911

LARGE-SCALE VECTORIZATION AND ANALYSIS OF THE NEUROVASCULAR UNIT IN MOUSE CORTEX

P. Blinder[1], P.T. Tsai[1], J.P. Kaufhold[2], D. Kleinfeld[1,3,4]

[1]Physics, University of California, San Diego, La Jolla, CA, [2]Intelligent Systems Division, SAIC, Arlington, VA, [3]Center for Neural Circuits and Behavior, [4]Graduate Program in Neurosciences, University of California-San Diego, La Jolla, CA, USA

Background and aims: We study the complete three-dimensional organization of the vasculature and associated neurons and non-neuronal cells in the vibrissa area of mouse parietal cortex. We use an all optical histology block-face imaging technique (Tsai *et al.* Neuron 2003) to acquire volumetric data and analytical tools to segment the data (Tsai *et al.* J Neurosci 2009) across several cubic millimeters (Fig 1). Ongoing vectorization and post-processing of these datasets result in a fully-connected digital representation of the vascular topology as well as the positions of all surrounding nuclei. Auxiliary data sets are used to colocalize contractile elements and other cellular components.

Results: We focus on the neural units of the vibrissa cortical columns, or “barrels”. The vasculature shows at least one geometrical feature that relate to the columnar stricture: penetrating vessels, which either source blood from the surface to the subsurface microvasculature or return blood to the surface, tend to cluster along the edges of the individual columns. Yet our work shows that the density an connectivity of the underlying microvasculature is independent of both the columnar and the laminar cortical structure.

Our recent work shows that penetrating arterioles uniquely source a given, cylindrical region of cortex (Nishimura *et al.* PNAS 2007; Blinder *et al.* PNAS 2010). This could result form a lack of collateral flow in a fully connected microvascular network or from a modular form of arteriole sources and venous sinks. We find support for the first scenario. The microvasculature forms a lattice of interconnected loops that typically contain eight capillary segments; this corresponds to a path length of 460 ± 190 μm (mean ± SD). A small fraction of each loop passes through one or more neighboring barrels to form a fully interconnected microvascular network, in which the lateral resistance is too high to promote widespread collateral flow. Further, features such as the well known increased neuronal density in layer IV are not accompanied by a concomitant increase in the density of microvessels.

Conclusion: The location of the contractile elements, and the source of their afferent inputs, are key to modeling and understanding the partitioning of blood flow in the highly interconnected microvasculature network. Anatomical and analytical work toward this goal will be presented.

Funded by the NIH (EB003832, MH085499, NS059832, and OD006831).

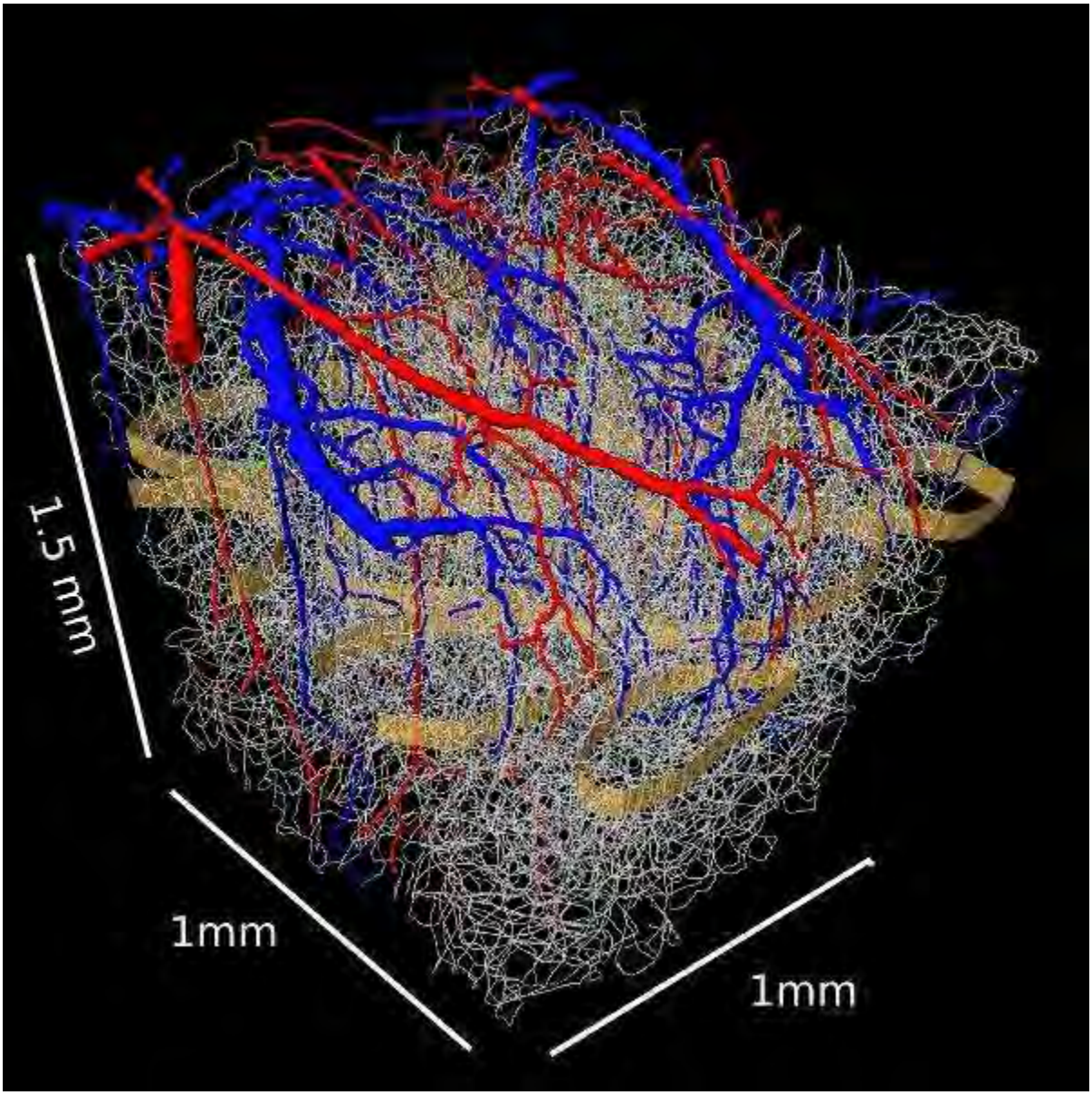

[PB_fig1]

Figure 1. Fully vectorized AOH data over 1.5 mm^3 of mouse S1 cortex. Arteries (red) and veins (blue) are labeled based on tracing to their origin. Layer IV barrels (golden) are labeled based on neuronal nuclei location (not shown).

912

EPAC2-DEFICIENCY LEADS TO MORE SEVERE NEUROLOGICAL DEFICIT AND LARGER INFARCT WITH HIGHER GLIAL REACTIVITY AFTER TRANSIENT MIDDLE CEREBRAL OCCLUSION

L. Cheng[1], P. Yeung[1], S.S.M. Chung[2], S.K. Chung[1,3]

[1]Department of Anatomy, Li Ka Shing Faculty of Medicine, The University of Hong Kong, Hong Kong, Hong Kong S.A.R., [2]Division of Science and Technology, United International College, Zhuhai, China, [3]Research Center of Heart, Brain, Hormone and Healthy Aging, Li Ka Shing Faculty of Medicine, The University of Hong Kong, Hong Kong, Hong Kong S.A.R.

Introduction: Exchange proteins activated by cAMP (Epac1 and Epac2) belong to a family of cAMP-regulated guanine nucleotide exchange factors (cAMPGEFs) for the small GTPases, Rap1 and Rap2[1]. Epac1 was thought to be important in maintenance of tight and adhesion junctions between endothelial cells[2] , suggesting that Epac may play an important role in blood brain barrier (BBB) function.

Objective: Previously, it was shown that Epac2 mRNA is expressed in the brain[3]. Here, the protein expression of Epac2 was determined and compared to that of Epac1. In addition, the role of Epac2 was determined in the BBB and brain function after ischemia/reperfusion injury.

Method: Six regions of brain from Epac2 wild type ($Epac2^{+/+}$) mice was dissected, and proteins were extracted in order to determine the expression of Epac1 and Epac2 under normal and ischemic condition by Western blot analysis. $Epac2^{+/+}$ and homozygous Epac2 knockout ($Epac2^{-/-}$) [4] mice were exposed to 2 hrs of middle cerebral artery occlusion followed by 22 hrs of reperfusion (tMCAO). Then, the neurological score was determined. The infarct and edema in ipsilateral side was determined by TTC stained brain section. After tMCAO, contralateral and ipsilateral hemispheres of brains were collected for histological and biochemical analyses, including Western blot analysis, RT-PCR, and immunocytochemistry.

Results: Under normal condition, Epac1 and Epac2 are widely expressed in the various regions of brain of $Epac2^{+/+}$ mice, including olfactory bulb, cerebellum, brainstem, cortex, midbrain and hippocampus. We have confirmed that Epac2 is absent in the brain of $Epac2^{-/-}$ mice. Interestingly, there was no compensation by Epac1 in brain of $Epac2^{-/-}$ mice, which showed no obvious abnormality in brain. However, $Epac2^{-/-}$ knockout mice showed significantly more severe neurological deficits, larger infarct volume and edema compared to those of $Epac2^{+/+}$ mice after tMCAO. The ipsilateral hemisphere of $Epac2^{-/-}$ brain also showed higher GFAP expression.

Conclusion: Taken together, Epac2 may not contribute to brain function under normal condition. However, Epac2 may protect the brain from ischemia/reperfusion injury. Currently, the detailed mechanisms of protective role of Epac2 in I/R brain injury is being further investigated.

References:

[1] Bos JL. Epac proteins: multi-purpose cAMP targets. TRENDS in Biochemical Sciences. 2006, 31: 680-686.

[2] Gloerich M and Bos JL. Epac: Defining a New Mechanism for cAMP Action. Annu. Rev. Pharmacol. Toxicol, 2010, 50: 355-375.

[3] Kawasaki H et al. A family ofcAMP-binding proteins that directly activate Rap1. Science, 1998, 282: 2275-2279

[4] Seino S et al. Essential role of Epac2/Rap1 signaling in regulation of insulin granule dynamics by cAMP. PNAS, 2007, 104: 19333-19338.

913

TORTUOSITY OF CORTICAL PENETRATING VESSELS IN THE TGCRND8 ALZHEIMER'S DISEASE MOUSE MODEL

A. Dorr[1], B. Sahota[1], J. He[1], M. Hill[2], J. McLaurin[2], B. Stefanovic[1]

[1]Sunnybrook Research Institute, Sunnybrook Health Sciences Centre, [2]Centre for Research in Neurodegenerative Diseases/ University of Toronto, Toronto, ON, Canada

Objectives: Alzheimer´s disease (AD) involves a strong cerebrovascular component,

evidenced by amyloid deposition on arterial walls, hypoperfusion, and reduced hemodynamic

responses to stimulation (1). Human postmortem AD histology has shown morphological changes in blood vessels, decreased vascular density and increased curvature (2), endothelial degeneration of smooth muscle, and vascular endothelium alterations (3,4). Many transgenic AD mouse models present cerebrovascular abnormalities, such as cortical microvascular basement membrane thickening (5) and significant amyloid deposition on penetrating cortical arterioles (6) which are critical for amyloid drainage from the brain, as well as cortical blood flow control. The present work investigates the effect of AD progression on in-vivo morphology of penetrating cerebral blood vessels in the TgCRND8 mouse AD model which presents early CAA and parenchymal plaque onset. We compare TgCRND8 mice with age matched wildtype (WT) littermates from 2 to 11 months of age.

Methods: Two-photon fluorescence microscopy following closed cranial window implantation and intravenous administration of fluorescent dextran (Texas Red, 70kDa, 33mg/kg) was employed to acquire ~ 300 slices, parallel to cortical surface in the forelimb representation in isoflurane anesthetized mice, every 1.5um (in-plane resolution of 1µmx1µm). Mice were divided into three age groups: early stage with little to no plaques (2-3 months), middle stage with moderate plaque load (4-6 months), late stage AD with heavy plaque load (7-11 months). The microvascular network was segmented using semi-automatic intensity-based segmentation algorithm (Imaris, Bitplane).

The degree of curvature (tortuosity) of the penetrating vessel was compared between groups, defined as the length along the vessel between the beginning and endpoints divided by the 3D Euclidian distance between beginning and endpoints (higher values indicate a more tortuous vessel).

Results: A mixed effects linear model was employed, with subject as random effect, time and state as fixed effects. Individual vessel curvature (tortuosity) values for all subjects ranged from 1.0-1.14. The WT cohort did not vary over time ($p>0.05$). The curvature in TgCRND8, in contrast, increased so that vessels in late stage TgCRND8s were more tortuous than the ones in early or middle stage ($p< 0.05$). The tortuosity of the TgCRND8 was found to be larger by 3 +/-1% than that of WT littermates ($p< 0.05$). Figure 1 shows a 3D rendering of penetrating vessel segmentation in a sample 8 month AD versus 7 month WT.

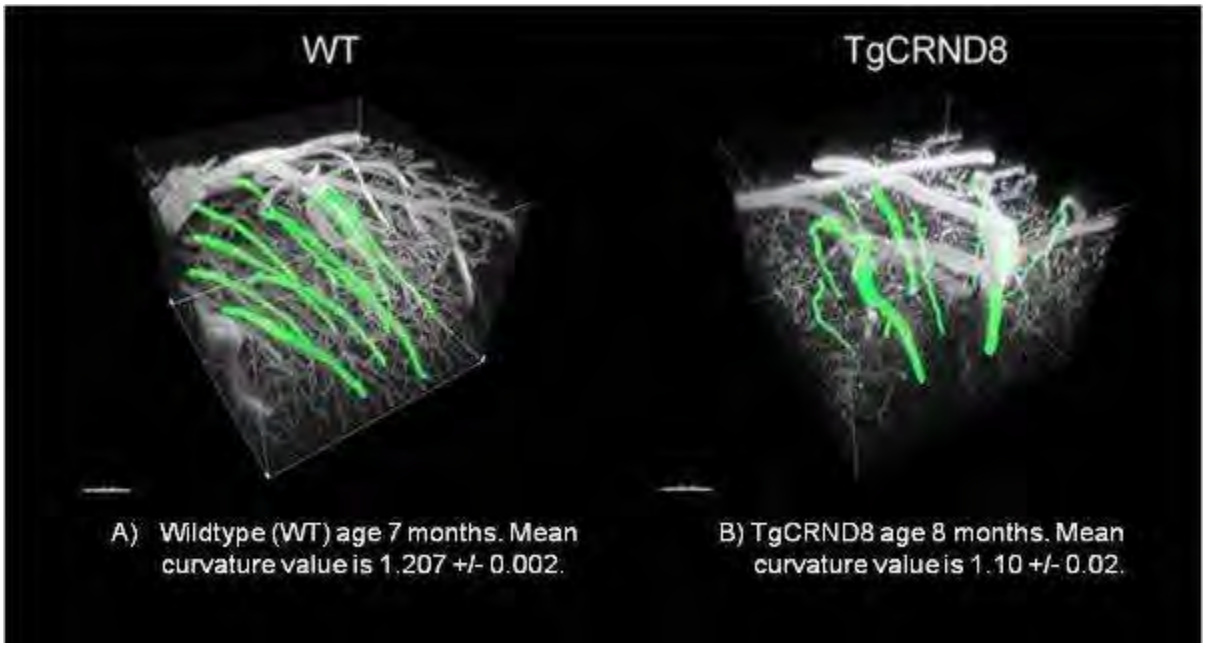

[dorr-abstract-figure]

Conclusions: We observe a time-dependent divergence in the tortuosity of the penetrating vessels in the AD group compared to WT group. CAA deposition on penetrating vessel walls, soluble amyloid cellular toxicity leading to degradation/hypertrophy of vascular layers, and/or side effects due to interstitial fluid drainage insufficiency may all contribute to observed topographical changes. Studies are currently underway exploring the mechanism underlying this phenomenon.

References:

1) Girouard, J Appl Physiol. 2006;100(1):328-35.

2) Fischer., Acta Neuropathol. 1990;79(6):672-9.

3) Kalaria, Cerebrovasc Dis. 2002;13(Suppl2):48-52.

4) Kalaria, Pharmacol Ther. 1996;72(3):193-214.

5) Bourasset, Neuropharmacology. 2009;56(4):808-13.

6) Weller, Alzheimers Res Ther. 2009;1(2):6.

915

NANOPARTICLES LOADED WITH A CASPASE-3 INHIBITOR AND BASIC FIBROBLAST GROWTH FACTOR (BFGF) CONCURRENTLY PROVIDES BETTER NEUROPROTECTION

M. Yemisci[1], S. Caban[2], S. Lule[1], Y. Gursoy-Ozdemir[1], E. Fernandez-Megia[3], R. Novoa-Carballal[3], R. Riguera[3], K. Andrieux[4], P. Couvreur[4], Y. Capan[2], T. Dalkara[5]

[1]Institute of Neurological Sciences and Psychiatry, Department of Neurology, Faculty of Medicine, [2]Department of Pharmaceutical Technology, Faculty of Pharmacy, Hacettepe University, Ankara, Turkey, [3]Departamento de Química Orgánica, Facultad de Química and Unidad de RMN de Biomoléculas Asociada al CSIC, Universidade de Santiago de Compostela, Santiago de Compostela, Spain, [4]Physico-Chimie, Pharmacotechnie, Biopharmacie, Faculté de Pharmacie, Université Paris-Sud, Châtenay-Malabry, France, [5]Institute of Neurological Sciences and Psychiatry and Department of Neurology, Faculty of Medicine, Hacettepe University, Ankara, Turkey

Objectives: Caspase inhibitors such as N-benzyloxycarbonil-Asp(OMe)-Glu(OMe)-Val-Asp(OMe)-flouromethyl ketone (Z-DEVD-FMK) and neurotrophins such as basic fibroblast growth factor (bFGF) inhibit ischemic cell death and are thought to be promising neuroprotective agents. However, these peptides cannot pass through the blood brain barrier (BBB) when they are applied systemically. Therefore, an effective drug carrier system is needed to achieve sufficient brain drug concentration that provides neuroprotection on systemic administration.

Methods: Polyethylene glycol-coated nanospheres were conjugated to the anti-mouse transferrin receptor monoclonal antibody (TfRMAb) that selectively recognizes the TfR type 1, which is highly expressed on the cerebral vasculature. The nanospheres were loaded with either Z-DEVD-FMK or bFGF and administered systemically alone or in combination. To evaluate the neuroprotective effect of the nanospheres, four groups of mice were subjected to 2 h of proximal middle cerebral artery (MCA) occlusion and 24 h of reperfusion. In all groups, nanospheres were administrated intraperitoneally (ip) just before inducing ischemia. The first group received drug-loaded nanoparticles lacking TfRMAb (control) and the test groups received nanospheres functionalized with TfRMAb. The second group received nanoparticles loaded with bFGF; the third group, with Z-DEVD-FMK and the fourth group both with bFGF and Z-DEVD-FMK. Corrected infarct volumes and neurological deficit scores were measured and the nanosphere penetrance to the brain was examined by immunofluoresence microscopy.

Results: After 2 hours of ischemia and 24 hours of reperfusion, the infarct volume of the control group was 50.7±1mm^3 (mean±SEM). The infarct volumes decreased significantly to 37.3±3mm^3 in mice receiving Z-DEVD-FMK, to 33.2±1 mm^3 in mice receiving bFGF, and to 26.5±3mm^3 in mice receiving a mixture of bFGF and Z-DEVD-FMK. The neurological deficit scores parallely improved. The infarct volumes did not significantly differ in mice receiving bFGF ip or intravenously (33.2±1mm^3 versus 37.1±3mm^3, respectively).

Conclusions: This study shows that the nanospheres loaded with large as well as small peptides can be efficiently transported across the BBB when administred systemically and could provide neuroprotection. Moreover, they show synergistic neuroprotective action when concomitantly administered. Thus, these new nanomedicine open exciting opportunities for the delivery of biologically active peptides to brain that are useful for the treatment of ischemic stroke as well as other central nervous system disorders.

References:

1) Aktaş Y, Yemisci M, Andrieux K, Gürsoy RN, Alonso MJ, Fernandez-Megia E, Novoa-Carballal R, Quinoa E, Riguera R, Sargon MF, Çelik HH, Demir AS, Hincal AA, Dalkara T, Çapan Y, Couvreur P,´´Development and brain delivery of chitosan-PEG nanoparticles functionalized with the monoclonal antibody OX26´´, Bioconjugate Chem, 16, 1503-1115 (2005).

2) Fisher, M., Meadows, M.E., Do, T., Weise, J., Trubetskoy, V., Charette, M. ve diğerleri. Delayed treatment with intravenous basic fibroblast growth factor reduces infarct size following permanent focal cerebral ischemia in rats. J Cereb Blood Flow Metab, 15, 953-959 (1995).

3) Karatas H, Aktas Y, Gursoy-Ozdemir Y, Bodur E, Yemisci M, Caban S, Vural A, Pinarbasli O, Capan Y, Fernandez-Megia E, Novoa-Carballal R, Riguera R, Andrieux K, Couvreur P, Dalkara T. ´´A nanomedicine transports a peptide caspase-3 inhibitor across the blood-brain barrier and provides neuroprotection´´, J Neurosci, 44, 13761-9 (2009).

916

IN-VIVO DETECTION OF AGE-RELATED CEREBRAL GLUCOSE UPTAKE EVOLUTION BY PET IN MICROCEBUS MURINUS PRIMATES

O. Dorieux[1,2,3], N. Joseph-Mathurin[1,2], M. Chaigneau[1,2], D. Houitte[1,2], M. Guillermier[1,2], C. Josephine[1,2], N. Van-Camp[1,2], P. Hantraye[1,2], F. Metzger[4], M. Perret[3], M. Dhenain[1,2]

[1]URA 2210, CEA/CNRS, [2]MIRCen, CEA,DSV,I2bm, Fontenay-aux-Roses, [3]UMR 7179, CNRS/MNHN, Brunoy, France, [4]CNS Preclinical Research, F. Hoffmann-La Roche Ltd., Basel, Switzerland

Objectives: Aging and associated pathologies are a major public health challenge. Implementation of new animal models and associated biomarkers monitoring aging processes are critical to better evaluate future therapies. In humans, [18]-fluoro-deoxyglucose-Positron Emission Tomography (FDG-PET) is widely used to characterize metabolic changes associated to aging in many organs including the brain. It reveals a glucose uptake reduction in some brain regions such as the frontal lobe[1]. In pathologies such as Alzheimer´s disease, early functional alterations are detected[2].

Microcebus murinus (M.m) are small lemurian primates. During aging some M.m develop cognitive impairments[3], brain amyloid plaque deposition and altered Tau protein accumulation[4], as well as macroscopic alterations such as brain atrophy that can be detected by MRI[4]. As cognitive alterations are associated to cerebral atrophy[5], the aim of this study was to evaluate age-associated evolution of glucose uptake in lemurs by using non-invasive 18F-FDG PET.

Methods: Twenty female M.m (1.5 to 9 years) were evaluated by PET and MRI. For PET and MRI scans, M.m were anesthetized (Isoflurane 5% induction, 1-2% maintenance, respiratory rate and temperature monitoring). PET scans were recorded with a MicroPET® Focus 220 system after FDG intravenous injection (900µCurie/100g). Animals´ heart were within the field of view and heart´s time activity curve allowed to control for correct FDG injection. Glycaemia was evaluated in all animals. Two animals with extra-scale glycaemia were excluded from the analysis. 3D-MR images were recorded (7-Tesla PharmaScan Bruker, T2-weighted-sequence, IR-RARE; TR/TE=2500/69, resolution=234*234*234µm^3). MR images were registered on TEP images by rigid transformations to define volumes of interest (VOI). Activities were extracted from PET images in whole brain, frontal cortex, hippocampus, caudate nucleus, and cerebellum. Standard Uptake Values (SUV=Activity/(activity injected/animal weight)) as well as relative values as compared to whole brain activity were evaluated for each VOI.

Results: The PET study revealed a strong relationship between age and SUVs in frontal cortex and cerebellum ($p < 0.01$) and an age-associated decrease of SUV in the whole brain and in hippocampus ($p < 0.05$), but not in caudate nucleus. However, relative values normalized by whole brain activity were not correlated with age.

Conclusion: An age-associated evolution of glucose uptake as measured by SUVs could be detected in healthy lemur primates and resembles evolution of the regional cerebral metabolic rates for glucose (rCMRGlc) observed in humans[1]. This study is a first step toward the characterization of age-associated changes of brain glucose uptake in M.m. and will be useful as a first reference to understand the effects of aging in mouse lemur brains. Further studies based on the evaluation of rCMRGlc will provide more information on cerebral metabolism changes in lemurs.

Work supported by: Hoffmann-La Roche Ltd, France-Alzheimer association, CNRS longevity program, National Foundation for Alzheimer's Disease and Related Disorders, National Institute on Aging.

1. Kalpouzos, G. et al. *Neurobiology of aging* (2009).

2. Mosconi, L. et al. *E.j. nuclear medicine and molecular imaging* (2006).

3. Picq, J.-L. *Experimental gerontology* (2007).

4. Kraska, A. et al. *Neurobiology of aging* (2009).

5. Picq, J.-L. et al. *Neurobiology of aging*. (2010).

917

RELATIONSHIP OF DISTURBANCES OF CEREBRAL VENOUS BLOOD FLOOW AND WHITE MATTER INJURIES IN HYPERTENSIVE PATIENTS

N. Afanasyeva, V. Mordovin, P. Lukyanenok

Research Institute of Cardiology, Tomsk, Russia

Objective: In phatogenesis of chronic forms of disturbances of cerebral blood floow important role play as insufficiency of inflow of blood to brain, and difficulty of cerebral venous outflow. Working out of diagnostic criteria of cerebral venous blood floow at hypertensive angioencephalopathy is necessary for more effective treatment of this numerous group of patients.The aim of the present study was to investigate relationship of disturbances of cerebral venous blood floow and structural attributes of hypertensive angioencephalopathy in hypertensive patients.

Methods: We examined 72 asymptomatic, non complicated essential hypertensives, aged between 28-60 years. All patients underwent clinical exam, magnetic resonance (MRI) a brain and MR venography a brain.

Results: According to MR-venography at 60% attributes of disturbances of cerebral venous blood floow are revealed. At 35 % asymmetry of venous sine less than 30 %, at 65 %- more than 30% has been revealed. At 82 % of patients with the expressed asymmetry of cerebral venous sine expansion of the linear sizes of lateral ventricles a brain was marked, at 59 % of patients expansion of subarachnoidal spaces was marked (c^2=14.73, p=0.0001). In hypertensive patients with asymmetry more than 30 % leucoaraiosis (LA) met significantly more often (c^2=7.97, p= 0.0048). In hypertensive patients with asymmetry more than 30 % significantly met LA 2 degree (c^2=5.34, p=0.020) and LA 3 degree (c^2= 10.2, p=0.0014), than LA 0 degree is more often. At asymmetry more than 30 % significantly met the focal white matter lesions (FWML) (c^2=7.36, p= 0.0067) and lacunae (c^2=4.3, p=0.0382) is more often.

Conclusions: At asymmetry of cerebral venous sine more than 30 % define the expressed hypertensive angioencephalopathy, including expansion of subarachnoidal spaces and lateral ventricles a brain, leucoaraiosis high degree and presence of the focal white matter lesions and lacunae.

918

TEMPERAMENT TRAIT HARM AVOIDANCE ASSOCIATES WITH μ-OPIOID RECEPTOR AVAILABILITY IN LIMBIC CORTEX: A PET STUDY USING [^{11}C]CARFENTANIL

L. Tuominen[1,2], J. Salo[3], J. Hirvonen[1], K. Någren[4], P. Laine[2], T. Melartin[5], E. Isometsä[5], J. Viikari[6], O. Raitakari[7], L. Keltikangas-Järvinen[3], J. Hietala[1,2]

[1]Turku PET-Centre, [2]Department of Psychiatry, University of Turku, Turku, [3]Department of Behavioural Sciences, University of Helsinki, Helsinki, Finland, [4]Department of Nuclear Medicine, PET and Cyclotron Unit, Odense University Hospital, Odense, Denmark, [5]Department of Psychiatry, University of Helsinki, Helsinki, [6]Department of Internal Medicine, [7]Department of Clinical Physiology, University of Turku, Turku, Finland

Introduction: Harm Avoidance is a temperament trait that regulates one's sensitivity to stress and fear-provoking stimuli and predisposes to anxiety and affective disorders. Opioid and particularly the μ-opioid system is related to emotions such as fear, anxiety and sadness as well as stress reactivity. We hypothesized that variability in μ-opioid receptor availability would explain interindividual differences in Harm Avoidance.

Methods: 22 Healthy subjects (10 male, 12 female) with pre-existing TCI scores (Temperament and Character Inventory) consistently in either upper or lower quartiles for the Harm Avoidance trait were selected from a population-based cohort in Finland (N=2075). We measured brain μ-opioid receptor availability in vivo using [^{11}C]carfentanil, a selective μ-opioid receptor agonist, and positron emission tomography (PET).

Results: In a priori defined regions of interest significant positive correlations between Harm Avoidance and μ-opioid receptor availability were found in medial frontal cortex, lateral orbital frontal cortex and in anterior cingulate cortex. Voxel-wise analysis of the whole brain revealed a statistically significant cluster comprising parts of prefrontal, temporal and anterior cingulate cortices ($p=0.009$). These associations were driven by two subscales of Harm Avoidance; Shyness with strangers and Fatigability & Astenia.

Conclusion: Higher Harm Avoidance score is associated with higher limbic μ-opioid receptor availability. As [^{11}C]carfentanil binding in the brain is sensitive to activation and deactivation of the endogenous opiate system, we assume that high μ-opioid receptor availability predicts low endogenous μ-opioidergic neurotransmission. Thus, subjects with high Harm Avoidance score may have lower endogenous opioid drive in a stressful situation (i.e. PET scan) which could partly explain why these people feel easily distressed and anxious. This finding has implications in etiological considerations of anxiety and affective disorders.

919

TOLL-LIKE RECEPTOR 3: A PROMISING NEW TARGET TO PROTECT THE BRAIN FROM ISCHEMIC DAMAGE

A.E.B. Packard, P.Y. Leung, T. Yang, R. Bahjat, M.P. Stenzel-Poore

Molecular Microbiology and Immunology, Oregon Health and Science University, Portland, OR, USA

Objectives: Ischemic tolerance is a phenomenon whereby preconditioning with a small dose of an otherwise harmful stimulus can protect against damage caused by a subsequent ischemic challenge. Among the known preconditioning stimuli, small doses of Toll-like receptor (TLR) ligands can induce significant neuroprotection and reprogram the brain's response to ischemia. To shed light on this molecular process, we have begun to test TLR3, unique among the TLR family for its distinctive signaling cascade via the adaptor TRIF while all other TLRs signal through MyD88. Our objective is to evaluate the efficacy of the TLR3 ligand Poly I:C to induce neuroprotection.

Methods: *Oxygen Glucose Deprivation (OGD):* Primary mouse mixed cortical cultures were prepared from E15-E17 mouse fetuses. Cultures were treated with either Poly I:C or media for 24 hours prior to 3 hours of OGD. Cell death was determined 24 hours following OGD by propidium iodide staining.

Middle cerebral artery occlusion (MCAO): C57 Bl6 or TLR3 knockout male mice 8 to 14 weeks old were used for all MCAO experiments. Mice were treated with either vehicle or Poly I:C 72 hours prior to MCAO. The right carotid artery was exposed and a 7-0 silicone-coated nylon filament was used to block blood flow to the MCA for 45 minutes. A laser doppler probe was used insure occlusion reduced flow to less than 20% of baseline. Infarct was determined by removing the brain promptly following perfusion, then slicing it into 1mm coronal sections and stained in 1.5% 2,3,5 triphenyltetrazolium chloride (TTC) in saline. The indirect infarcted area was calculated over 6 slices and averaged to determine an overall infarct volume.

Results: We have discovered that preconditioning with the TLR3 ligand Poly I:C confers robust neuroprotection from ischemic injury (MCAO) in mice. Poly I:C preconditioning significantly reduced infarct size and decreased neurological deficit following ischemia. Furthermore, primary mouse cortical cells treated with Poly I:C prior to exposure to OGD significantly protects against cell death. Finally we investigated TLR3's role in the endogenous response to ischemia and found that TLR3 exacerbates ischemic damage as TLR3 knockout mice had decreased infarct size following MCAO.

Conclusion: Poly I:C preconditioning induces robust ischemic tolerance illustrating that TLR3 is a new target for neuroprotection. TLR3 promises to be a valuable tool for elucidating the mechanisms of TLR-mediated neuroprotection.

920

DECREASE IN DYSTROPIN EXPRESSION PRIOR TO DISRUPTION OF BRAIN-BLOOD BARRIER WITHIN THE RAT PIRIFORM CORTEX FOLLOWING STATUS EPILEPTICUS-INDUCED VASOGENIC EDEMA

T.C. Kang[1], S.Q. Kang[2]

[1]Anatomy & Neurobiology, College of Medicine, Hallym University, Chuncheon, [2]Neurosurgery, Soonchunhyang University Hospital, Seoul, Republic of Korea

Backgrounds: Status epilepticus (SE) is a potential life-threatening neuroloical condition that affects both adult and children. The BBB disruption has been reported in experimental and human epilepsy. A leakage of serum-derived components into the extracellular space is associated with hyperexcitability and seizure onset. Furthermore, dysfunction of the BBB leads to epileptogenesis and contributes to progression of epilepsy. However, the changes in structural components mediating BBB disruption still remain unclear.

Objectives: Since **BBB disruption** induced by epileptogenic insults is not fully clarified, we identified **wheather changes in BBB-related molecules are associated with vasogenic edema in the PC** after pilocarpine-induced status epilepticus model in the rats.

Materials and methods: Status epilepticus induction was followed by LiCI 9127/mg/kg, i.o.) 20hrs before pilocarpine injection. Pilocarpine (25mg/kg) was injected intraperitonealy 30 minute after scopolamine butylbromide (2mg/kg,i.p.) Animals was perfused transcranially with phosphate-buffered saline (PBS) followed by 4 % paraformaldehyde in 0.1 M PB (phosphate buffer, pH 7.4) under urethane anesthesia (1.5 g/kg, i.p.). Brain was removed, postfixed in the same fixative for 4 hrs. and rinsed in PB containg 30 % sucrose at 4'C for 2 days. Tissue were frozened and sectioned with a cryostat at 30 microm and consecutive sections were collected in six-well plates containg phosphate buffered saline (PBS). For a stereological study, every sixth section throught the entire hippocampus and PC was used in the series.

Results: One day after status epilepticus (SE), PC neurons and astrocytes showed a pyknotic nucleus and shrunken cytoplasm accompanied by vasogenic edema. At this point, SMI-71 (an endothelial barrier antigen) immunoreactivity had decreased in the PC. Prior to vasogenic edema formation (12 h after SE), dystropin immunoreactivity disappeared within astrocytes, while the change in glial fibrillary acidic protein immunoreactivity was negligible. However, glucose transporter-1 (an endothelial cell marker) had increased at 12 h after SE.

Conclusions: These findings indicate that dysfunction of dystropin induced by SE may result in endothelial and astroglial damage with BBB breakdown and increase vascular permeability, leading to vasogenic edema that is involved in pathogenesis of epileptogenesis. Therefore, these findings suggest that disruption of astroglio-interaction may be one of the important factors to maintain BBB permeability rather than endothelial cells themselves.

921

THE ROLE OF PARVALBUMIN IN THE CEREBRAL BLOOD FLOW RESPONSE TO SOMATOSENSORY STIMULATION

A. Kocharyan, A.C. Silva

Cerebral Microcirculation Unit, Laboratory of Functional and Molecular Imaging, National Institute of Neurological Disorders and Stroke, National Institutes of Health, Bethesda, MD, USA

Introduction: The role of individual thalamic nuclei in the local vascular response to functional stimulation remains uncertain. The ventroposterolateral (VPL) and reticular (RT) thalamic nuclei are important processors of proprioceptive information from the forelimbs (FL) to their representation in primary somatosensory cortex (S1FL). Recently, we reported that electrical stimulation of rat FP activates specific subset of contralateral cortical neurons. In the present study, we investigated the cerebral blood flow (CBF) response, evoked neuronal activity and identity of involved cells to VPL stimulation in chloralose-anesthetized rats.

Methods: Laser-Doppler flowmetry and somatosensory-evoked potentials (SEPs) were recorded during electrical stimulation of the contralateral FP (2mA, 333μs, 3Hz, 5s) or ipsilateral VPL (50μA, 200μs, 3-100 Hz, 3s). Individual cortical and thalamic cell types expressing c-fos in response to stimulation were identified and quantified using double-immunohistochemistry. The influence of local superfusion of Parvalbumin (PV, 10^{-12} - 10^{-7}M) on the CBF response to FL stimulation was also investigated.

Results and discussion: We found that direct electrical stimulation of the ipsilateral VPL produced robust CBF responses in S1FL that increased with the stimulus frequency (Fig. 1A). At the maximum tested frequency of 100Hz, VPL stimulation increased cortical CBF by 36.6 ± 7.1%. In comparison, electrical FL stimulation increased CBF by 25.4 ± 5.4%.

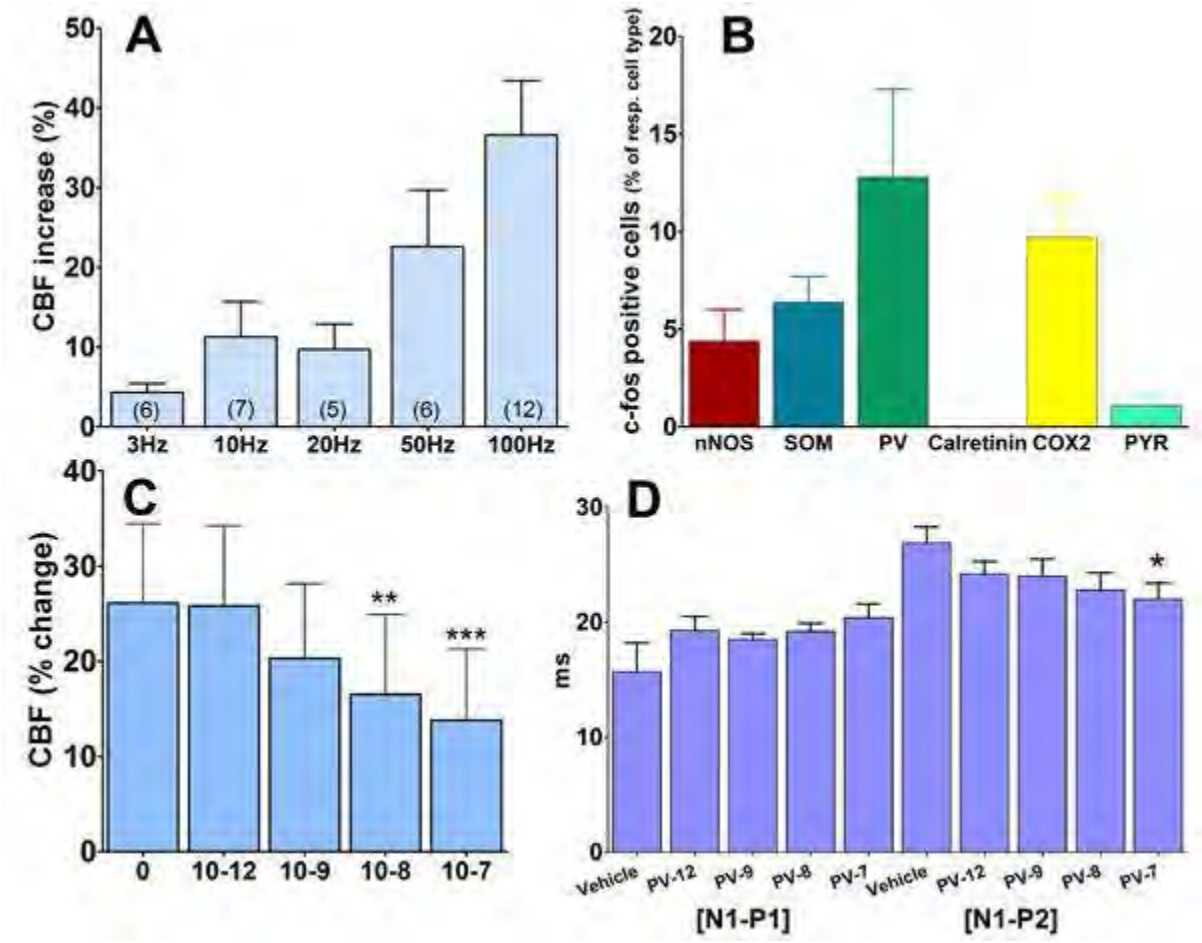

[fig.1]

Localized ipsilateral c-fos activation in RT and in S1FL was observed after VPL stimulation. In RT, 39.0 ± 12.8% of PV-positive cells also expressed c-fos. In contrast, FL stimulation did not induce c-fos expression in RT. In S1FL, 43.3 ± 5.6% of all c-fos-positive nuclei co-expressed the rat pyramidal cell marker (PYR). As well, 4.4 ± 1.6%, 6.4 ± 1.3%, 12.8 ± 4.5% and 9.7 ± 2.1% of neuronal nitric oxide (nNOS), somatostatin (SOM), PV and cyclooxygenase-2 (COX-2) interneurons, respectively, co-expressed c-fos on a layer-specific basis. None of the numerous investigated calretinin-positive interneurons co-expressed c-fos (Fig. 1B).Local superfusion of S1FL with PV for 20 minutes decreased the CBF response by up to 47% (Fig. 1C) and shortened the N1-P2 latency by up to 18% (Fig. 1D), on a concentration dependent basis, without changing SEP amplitudes.

These results demonstrate that i. the cortical CBF increase elicited by VPL stimulation is accompanied by activation of specific subpopulation of both excitatory and inhibitory neurons; and that ii. cortical and RT originated PV-neurons and PV itself (as a local calcium “buffer”) are important participants of the somatosensory pathway and neurovascular unit. This research was supported by the Intramural Research Program of the NIH, NINDS.

922

PRE-TREATMENT WITH RESVERATROL REDUCES ISCHEMIC INJURY FOLLOWING RECURRENT STROKE AND PROTECTS ENDOTHELIAL CELLS FOLLOWING OXYGEN-GLUCOSE DEPRIVATION

D.L. Clark[1,2], R. Thompson[1], Á. Institóris[2,3], A. Kulynych[1], D. Busija[3], U. Tuor[1,4]

[1]University of Calgary, Calgary, AB, Canada, [2]University of Szeged, Szeged, Hungary, [3]Wake Forest University School of Medicine, Winston-Salem, NC, USA, [4]National Research Council of Canada, Institute for Biodiagnostics West, Calgary, AB, Canada

Background: There is a high risk of recurrent stroke following a transient ischemic attack (TIA) or minor stroke. Accordingly, there is an opportunity for treatment with neuroprotective agents after the initial insult. We employed a novel in vivo model of recurrent stroke to investigate whether resveratrol, a dietary polyphenol, might be an effective treatment after a mild stroke and prior to a second stroke. We hypothesized that resveratrol would have beneficial actions on brain parenchyma, microvessels or both. In addition to our rat model of recurrent stroke, we used rat primary cultures to determine the effectiveness of resveratrol to protect both cortical neurons and brain microvessel endothelial cells against ischemic injury.

Methods: A total of 42 rats received either a single mild stroke consisting of a 30 min transient middle cerebral artery occlusion or a combination of two mild strokes (2x30 min). Rats in the single mild group received resveratrol (25 mg/kg/day) or vehicle orally for 4 days including surgery day. Those undergoing a double stroke were treated upon recovery after the first stroke and with 3 additional doses thereafter. The second stroke was produced on day three. To study 'in vitro' models of stroke, cultures of brain microvessel endothelial cells or cortical neurons were pretreated with resveratrol (10nM-100μM) for 3 days before undergoing oxygen and glucose deprivation.

Results: There were no differences in blood gases, blood pressure, temperature or ischemic levels of Doppler blood flow between treatment groups. Brain damage 7 days following recurrent stroke was greater than a single mild stroke. Resveratrol administered prior to a single mild stroke or following a mild stroke but prior to a second stroke reduced cell death. In addition, resveratrol treatment reduced immunohistochemical markers of astrocyte activation, nitrosative stress and macrophage infiltration in the affected hemisphere, following recurrent stroke. In vitro, pretreatment with lower doses (< = 1μM) protected brain microvessel endothelial cells 24 h following oxygen and glucose deprivation but did not improve viability of cortical neurons. Resveratrol did reduce reactive oxygen species production in neurons following oxygen and glucose deprivation. Larger doses (>=10μM) reduced viability in both cell types. Co-application of the non-selective nitric oxide synthase inhibitor, L-NAME, did not block the protection of pre-treated brain microvessel endothelial cells that underwent oxygen and glucose deprivation but blockade of SIRT1 with sirtinol significantly reduced benefit.

Conclusions: Nutritional supplements of resveratrol may be an effective and low risk strategy to protect the brain from recurrent stroke damage occurring after a TIA or a mild stroke. Low concentrations are sufficient to provide protection in brain microvessel endothelial cells and reduce oxygen free radical production in neurons.

Acknowledgements: This work was supported by CIHR (grant MOP 84407). DC is supported by a Heart and Stroke Fellowship.

923

THE EFFECT OF IRBESARTAN AND LOSARTAN ON BLOOD PRESSURE AND COGNITIVE FUNCTION IN HYPERTENSIVE PATIENTS

N. Afanasyeva, V. Mordovin, G. Semke

Research Institute of Cardiology, Tomsk, Russia

Background and purpose: Hypertension is important predictor of dementia. Cognitive impairment also arises already at early stages of hypertension. Angiotensin receptor blocker (ARB) suppress activity of sympathetic nervous system and are capable to eliminate factors which raise vascular risk in hypertensive patients. The aim of the present study was to study hypotensive and cerebroprotective efficacy of ARB irbesartan and losartan in hypertensive patients.

Methods: Forty five hypertensive patients (21 women and 24 men), aged between 28-56 years, were randomized to treatment with either blockers irbesartan (Sanofi-aventis) 150-300 mg or losartan (Zentiva) 50-100 mg during 6 month. 24-hours ambulatory blood pressure monitoring and neurocognitive assessment by Wechsler Memory Scale (WMS) were performed in all patients at baseline and in course of the treatment.

Results: Irbesartan reduced significantly 24-h SBP (with 156.8 mm Hg up to 134.0 mm Hg; P=0.009), 24-h DBP (with 96 mm Hg up to 88 mm Hg; P=0.012), time-index 24-h SBP (with 72% up to 44%; P=0.014) and time-index 24-h DBP (with 64% up to 42%; P=0.018). Losartan reduced significantly 24-h SBP (with 148.8 mm Hg up to 132.0 mm Hg; P=0.008), 24-h DBP (with 98 mm Hg up to 89 mm Hg; P=0.024), time-index 24-h SBP (with 58% up to 42%; P=0.028) and time-index 24-h DBP (with 46% up to 38%; P=0.034). Later 6 months hypotensive therapies by results of proof test were marked statistically significant reduction the quantity of errors (irbesartan with 6 up to 1.8; P=0.003, losartan with 5 up to 4.2; P=0.062). By results of tables of Shulte psychomotor speed has increased (irbesartan with 48 sec up to 36 sec; P=0.026, losartan with 48 sec up to 44 sec; P=0.242), indicators of long-term memory have increased (irbesartan with 68.5 word up to 52.6 word; P=0.005, losartan with 60.4 word up to 56.2 word; P=0.084).

Conclusions: Our study demonstrates, that long controllable treatment of hypertension with irbesartan and losartan reduces blood pressure and improves cognitive function. The most expressed positive effect on cognition rendered irbesartan.

925

NITRIC OXIDE IS IMPLICATED IN PATHOGENESIS OF ISCHEMIC CEREBRAL DAMAGE VIA INDUCTION OF INDOLEAMINE 2,3-DIOXYGENASE

S.J. Kim, C.H. Woo, S.A. Hwang, J.S. Joo, C.D. Kim, **W.S. Lee**

Department of Pharmacology, and MRCITR, Pusan National University School of Medicine, Yangsan, Republic of Korea

Nitric oxide (NO) is being recognized as an important mediator of cellular and molecular events which impacts the pathophysiology of cerebral ischemia. Indoleamine 2,3-dioxygenase (IDO), which catalyzes the initial and rate-limiting step of L-tryptophan metabolism and leads to rapid depletion of intracellular tryptophan, has been reported to be highly expressed in the ischemic brain. In the ischemic brain injury, the precise role of IDO and its mechanism of induction are not yet clearly identified. Thus, this study aimed to investigate whether IDO is induced in the ischemic cerebral cortex by NO and vice versa using an animal model of photothrombotic focal cerebral ischemia. Male C57BL/6 mice were subjected to cortical photothrombosis and sacrificed 24 h after ischemic insult. Pretreatments with NO synthase (NOS) inhibitors and IDO inhibitor markedly decreased the cerebral infract size as well as the expression of IDO in the ischemic cortex. Pretreatment with IDO inhibitor was without effect on the expression of iNOS. Treatment with peroxynitrite markedly increased the expression of IDO and 3-nitrotyrosine, both of which were significantly reduced by FeTPPs, a peroxynitrite decomposition catalyst. Furthermore, transfection of siRNAs for iNOS and nNOS markedly reduced the expression of IDO, TNF-α and 3-nitrotyrosine, whereas significantly increased the expression of p-Akt and p-GSK-3β. These results indicate that NO is implicated in the pathogenesis of ischemic cerebral damage via induction of IDO in ischemic cerebral cortex

927

METABOLIC MISMATCH BETWEEN GLUCOSE-UPTAKE AND BLOOD-FLOW THROUGH SPM ANALYSIS WITH NEUROIMAGING STUDIES IN A CASE WITH SEVERE HYPOGLYCEMIC ENCEPHALOPATHY

S. Park[1], M.-K. Sunwoo[1], H.-J. Kim[1], J.-Y. Hong[1], M.-K. Lee[1], H.-J. Park[2], E.-Y. Kim[3]

[1]Neurology, [2]Neuclear Medicine, [3]Neuroradiology, Yonsei University College of Medicine, Seoul, Republic of Korea

Background: In case of pure hypoglycemia-induced encephalopathy, theoretically the blood flow was maintained in spite of poor supply of glucose on the brain if hypoxia and hypotensive shock were not combined. The functional neuroimages seemed to be thought to show a mismatch between the blood flow and glucose uptake in cortex. We tried to study the possibility of a mismatch through SPM (statistical parametric mapping) analysis with Tc-99m EDC SPECT and 18F-FDG PET in a diabetic patient with severe hypoglycemic encephalopathy.

Case Report: A-76-year-old man was admitted due to coma underlying hypoglycemia. He took oral antidiabetic medication regulary on that day in spite of poor oral intake. He was found unconscious with seizure at morning. Blood glucose level was 27 mg/dl on admission. Blood pressure was 135/108 and arterial blood gas was as followings: pH 7.361, pCO2 29.9 mmHg, pO2 71.9 mmHg. He was immediately infused 40 ml of 50% glucose to reach 120 mg/dl without mental recovery. Brain MRI which was taken at emergency room showed diffusion restriction at bilateral hippocampus. Follow up Brain MRI on 3rd day showed extensively diffuse cortical involvement in addition to hippocampus with decrease in apparent diffusion coefficient (ADC) map. Blood flow with Tc-99m EDC SPECT, taken on 2nd day, seemed to be maintained grossly but FDG PET on next day showed markedly decreased FDG uptake in entire cerebral cortex including bilateral basal ganglia. SPM analysis showed marked decreased glucose uptake in entire cortex compared to normal control group except bilateral occipital cortex. In contrast, blood flow was higher in occipital area, and lower in inferolateral frontal areas including bilateral insular and cingular than normal control group. Patient expired due to sepsis without recovery of consciousness.

Conclusions: These results showed there was clear metabolic mismatch of brain in severe hypoglycemic condition, which showed different patterns depending on the area of cortex. The increased blood flow with no change of glucose uptake was noted on the occipital areas. In contrary, decrease or no change of blood flow with decrease of glucose uptake in the remaining cortex inevitably gave rise to functional decline. This metabolic mismatch could explain the regional difference for the hypoglycemic brain insult.

928

HEMISPHERIC PECULIARITIES OF BASIC BRAIN METABOLITES' CHANGES IN MALES AFTER ISCHEMIC STROKE

V. Kuznietsov, S. Kuznietsova, D. Shulzenko

Institute of Gerontology, Kiev, Ukraine

Aim: to research metabolic state (N-acetilaspartat (NAA), creatin (Cr), cholin (Cho) content) in brain and peculiarities of metabolic and cerebral hemodynamics interrelations in males after ischemic stroke.

Materials and methods: 128 aged males after ischemic (atherothrombotic) stroke in recovering period and 58 males of control group; metabolites' content was essessed in white substance of frontal region and grey substance of occipital region on scanner 1,5 T Magnetom Vision Plus (Siemens). Cerebral hemodynamics rates were analyzed by ultrasound duplex scanning method on Sonoline Elegra (SIEMENS).

Results: In males with ischemic focus localization in right hemisphere in comparison with control group was more marked decreasing of NAA in frontal (21,74±0,52*, CG 23,87±0,44) and occipital areas of injured hemisphere (21,13±0,62, CG 24,75±0,59) than in ones with left hemispheric stroke localization. In patients with localization of ischemic focus in left hemisphere in injured hemisphere in frontal area was significantly higher NAA content (23,73±0,5), Cr (13,47±0,66), Cho (13,12±0,46) than in patients with right-sided stroke in left frontal area (21,74±0,52, 8,9±0,31 and 9,22±0,48 accordingly). In patients with ischemic focus localization in left and right hemisphere in intact hemisphere wasn't adjusted significant changes in content of basic metabolites.

The influence of cerebral hemodynamics on brain metabolic processes and changes of NAA, Cr, Cho in males with ischemic stroke determined reasonability of study of metabolism and cerebral hemodynamics interrelations. We establish that in males with ischemic stroke there occurs qualitive and quantitive structural reorganization of correlation relations content of basic metabolites in grey and white brain substances and cerebral hemodynamics rates in vessels of carotid and vertebral-basilar basins and type of these interrelations had hemispheric peculiarities. In males with left-sided stroke metabolism and hemodynamics interrelation strengthen (24 relations), with right-sided ischemic stroke - the range of these interrelations decreases (6 relations) in comparison with control group (15 relations).

Thus, hemispheric peculiarities of interrelations metabolism reorganization of basic metabolites in grey and white brain substances and cerebral hemodynamics describe more active metabolism recovering in males with ischemic stroke in left hemisphere.

929

THERAPEUTIC ADMINISTRATION OF ALPHAB-CRYSTALLIN IN CEREBRAL ISCHEMIA

A. Arac[1,2,3], S.E. Brownell[4,5], J.B. Rothbard[6], C. Chen[2,3,4], R.M. Ko[6], M.P. Pereira[1,2,3], G.W. Albers[2,3,4], L. Steinman[3,4], G.K. Steinberg[1,2,3]

[1]Neurosurgery, Stanford University, [2]Stanford Stroke Center, [3]Stanford Institute for Neuro-Innovation and Translational Neurosciences, [4]Neurology and Neurological Sciences, [5]Biology, [6]Medicine, Stanford University, Stanford, CA, USA

Introduction: AlphaB-crystallin (cryab), a member of the small heat shock protein superfamily of molecular chaperones. It functions as a potent negative regulator, acting as a brake on several inflammatory pathways in both the immune system and central nervous system and has anti-apoptotic and neuroprotective functions. Stroke is the leading cause of disability and the third most common cause of death in adults. Each year almost 800,000 individuals are affected in the US. Here, we investigated the role of cryab in cerebral ischemia.

Methods: We exposed wild-type (WT) and cryab-knockout (KO) mice to 30min of middle cerebral artery occlusion. We assessed lesion size at 2days(2d) by TTC and at 7days(7d) by silver stain. We administered 50ug/100ul of recombinant human cryab, intraperitoneally. After the stimulation of splenocytes, the cytokines were assessed by ELISA, and other cellular inflammatory responses were measured in spleen, blood and brain by flow cytometry.

Results: Cryab-KO mice had significantly larger lesions than WT mice at both 2d and 7d and had worse neurologic deficits at both time points. Flow cytometry showed increased neutrophils and macrophages in KO mice brains 2d after stroke. At 7d after stroke, there were more T cells in the brains of KO mice. This difference was only in gamma-delta T cell population, not in CD4 or CD8 T cell populations. The gamma-delta T cells in the blood were also increased in KO group at 7d after stroke. Bone marrow chimera experiments showed that deficiency of cryab both in the immune system and the brain separately contributed to larger lesions. Futhermore, the plasma level of cryab was significantly increased at 12h after stroke with a gradual decrease over the ensuing 7d in WT mice. The cryab plasma levels were also high in stroke patients. This led us to investigate whether restoration of the cryab in the plasma of KO mice would decrease the lesion size. Recombinant cryab administration daily for a week decreased the lesion size in KO group to the level of WT group, suggesting that the increased lesion size in KO mice was due to deficiency of cryab rather than other potential causes. Moreover, upon stimulation, the KO splenocytes from mice 7d after stroke produced more pro-inflammatory (interferon-gamma, IL2, IL12, TNF, IL17) and less anti-inflammatory (IL10) cytokines as compared to splenocytes from both WT and cryab treated KO mice. These results prompted us to try cryab as a therapeutic in WT mice. Starting the treatment 1h before stroke, we were able to decrease the lesion size at 7d, compared to subjects with saline. Furthermore, starting the treatment even 12h after stroke conferred significantly smaller lesion size compared to treatment with saline.

Conclusion: In conclusion, our data indicate that cryab is an endogenous neuroprotectant against cerebral ischemia and that it can be administered as an exogenous therapeutic even 12 hours after stroke.

930

AGE-RELATED CHANGES IN THE AVAILABILITY OF GABAA RECEPTORS IN HEALTHY SUBJECT: IMAGING STUDY WITH F-18 FLUMAZENIL PET

Y.K. Kim, Y.-I. Kim, B.C. Lee, J.S. Lee, J.M. Jeong, S.E. Kim, D.S. Lee

Department of Nuclear Medicine, Seoul National University College of Medicine, Seoul, Republic of Korea

Background and aims: GABA(gamma-aminobutyric acids)ergic neurotransmission, as the most important inhibitory neuromodulation in the brain, has been issued in neuronal plasticity related with brain damage or neurodegenerative disorder, and the changes in GABAergic regulation with age has been also suggested. To evaluate the effect of aging on cortical GABAergic system, we applied the PET imaging with [18F]-flumazenil ([18F]-FMZ) which showing a high affinity to the GABA/BZ receptors in the brain.

Material and methods: Thirteen healthy volunteers (age range: 29-65 years) were participated in this study. All subjects performed 3D T1 MRI, FDG PET and [^{18}F]-FMZ PET. Parameterized images of GABA/BZ receptor availability were generated. Correlation of age with gray matter volume, relative glucose metabolism and GABA receptor availability were evaluated using optimized VBM and SPM.

Results: As usual, age-related metabolic decline with volume loss was observed in the bilateral frontal cortex and peri-insular areas on FDG PET and MRI. Whereas, higher receptor availability of GABA/BZ receptors was found in the cerebral cortex (mainly frontal and temporal cortices) and the cerebellum on [^{18}F]-FMZ PET as the subjects' age was increased.

Conclusion: Through our study, we can provide normal human database of GABAa receptor mediated inhibitory neuronal system in aging. By ensuring the association with metabolic decline in aging, we can understand the role and change of inhibitory neuromodulatory system in normal aging.

931

EFFECTS OF IRBESARTAN ON NO PRODUCTION, HYDROXYL RADICAL METABOLISM DURING CEREBRAL ISCHEMIA AND REPERFUSION IN MICE

R. Nishioka, Y. Asano, M. Yamazato, Y. Ito, K. Ishizawa, N. Araki

Neurology, Saitama Medical University, Saitama, Japan

Introduction: Irbesartan is an ARB (angiotensin Ⅱ receptor blocker), which is designed for the long acting type ARB strongly bound with AT1 type receptors, and expected for the saving effect not only for heart and kidney but also for brain. The purpose of this study is to investigate the effects of irbesartan on NO production, hydroxyl radical metabolism and ischemic change of hippocampal CA1 during cerebral ischemia and reperfusion in mice.

Methods: (1) Male C57BL/6 mice [n=21] were used in the study. Irbesartan(10 mg/kg/day) was administered once a day per os for 7 days before cerebral ischemia in 7 mice (Irbesartan group), and the drug was not given in the remaining 14 mice (control group and sham group). Both NO production and hydroxyl radical metabolism were continuously monitored by *in vivo* microdialysis. Microdialysis probes were inserted into the bilateral striatum. The *in vivo* salicylate trapping method was applied for monitoring hydroxyl radical formation via 2,3-dihydroxybenzoic acid (2,3-DHBA), and 2,5-dihydroxybenzoic acid (2,5-DHBA). A laser Doppler probe was placed on the skull surface. Blood pressure and temperature were monitored and maintained within normal ranges throughout the procedure. Transient forebrain cerebral ischemia was produced by clipping both common carotid arteries for 10 minutes. Levels of nitric oxide metabolites, nitrite (NO_2^-) and nitrate (NO_3^-), in the dialysate were determined using the Griess reaction.

(2) CA1 neurons: Hippocampal CA1 neurons were analyzed into three phases (severe ischemia, moderate ischemia, survive), and the ratio of the number of surviving neurons was calculated (survival rate).

Results:

(1) Blood Pressure: Irbesartan group (44.6±15.3 mmHg; mean ± SD) showed significantly lower than that of the control group (65.6±10.1 mmHg), 30 minutes before ischemia, and 30-70 minutes after the start of reperfusion ($p< 0.05$).

(2) Cerebral Blood Flow (CBF): There were no significant differences between irbesartan group and control group.

(3) Nitric oxide metabolites: 1) NO_2^- ; There were no significant differences between the groups. 2) NO_3^- ; Irbesartan group (210.7 ± 65.4 %; mean ± SD) showed significantly higher than that of the control group (171.2 ± 36.5), 30 and 80 minutes after the start of reperfusion ($p< 0.05$).

(4) Hydroxyl radical metabolites:

1) 2,3-DHBA; irbesartan group (99.3 ± 4.8%; mean ± SD) showed significantly lower than that of the control group (108.7 ± 7.2), 20 minutes after the start of reperfusion ($p< 0.05$) (Figure 1).

2) 2,5-DHBA; There were no significant differences between the groups.

(5) Survival rate in CA1 area: There were no significant differences between the groups (Figure 2).

Conclusion: These *in vivo* data suggest that irbesartan influences on the CBF and hydroxyl radical production during cerebral ischemia and reperfusion in mice, and may protect against cerebral ischemic injury following ischemia and reperfusion.

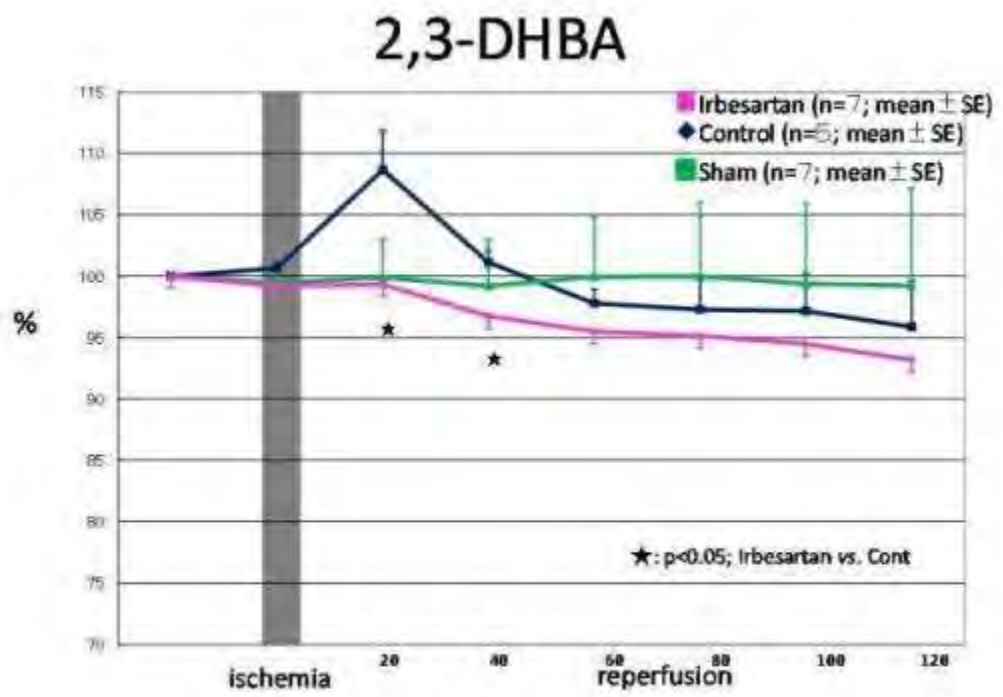

[Figure 1]

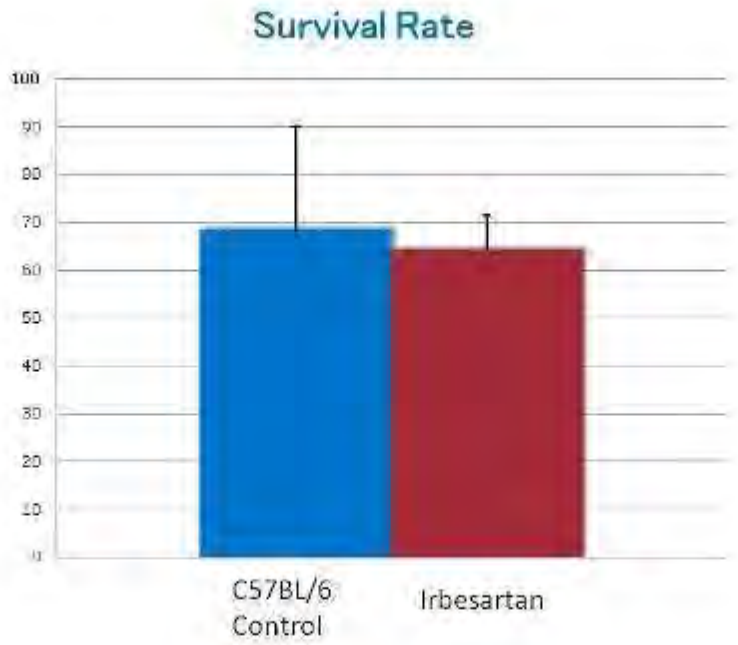
Survival Rate
100
90
80
70
60
50
40
30
20
10
0
C57BL/6
Control
Irbesartan

[Figure 2]

932

PRECLINICAL SAFETY ASSESSMENT OF THE 5-HT_{2A} AGONIST PET TRACER [^{11}C]CIMBI-36

A. Ettrup[1], M. Wasim[1], S. Holm[2], M.A. Santini[1], M. Hansen[3], J. Paine[3], M.M. Herth[2,3], M. Palner[1], J. Madsen[2], G.M. Knudsen[1]

[1]Neurobiology Research Unit and Center for Integrated Molecular Brain Imaging (Cimbi), [2]PET and Cyclotron Unit, Copenhagen University Hospital, Rigshospitalet, [3]Department of Medicinal Chemistry, Faculty of Pharmaceutical Sciences, University of Copenhagen, Copenhagen, Denmark

Objectives: We have recently validated [^{11}C]Cimbi-36 as a PET tracer for mapping and quantification of serotonin (5-HT) 2A receptor (5-HT_{2A}) agonist binding in the living brain[1]. Such a PET tracer may also be more displaceable by elevated levels of endogenous 5-HT as compared with 5-HT_{2A} antagonist tracers. However, the radiation dose absorbed in conjunction with [^{11}C]Cimbi-36 PET scanning is not known, and since most 5-HT_{2A} receptor agonists have potent hallucinogenic effects in humans[2], the possibility of adverse effect from Cimbi-36 administration needs to be evaluated. Here we assess safety issues for the clinical use of [^{11}C]Cimbi-36, including dosimetry and in vivo pharmacology in rodents.

Methods: [^{11}C]Cimbi-36 dosimetry was examined in 16 adult male Sprague-Dawley rats. The animals were injected with 20.6 ± 2.4 MBq [^{11}C]Cimbi-36 i.v. in the tail vein and decapitated after 5, 15, 30, and 60 minutes. After decapitation, 15 distinct tissues, including liver, stomach wall, spleen, kidney, adrenal, lung, heart wall, bone, adipose tissue, testis, muscle, blood, frontal cortex, cerebellum, and rest of brain were taken out. Tissue radioactivity was measured in a gamma-counter, and residence times were calculated as the area under the time-activity curve. The extrapolated human dosimetry for [^{11}C]Cimbi-36 was calculated using the OLINDA software applying similar assumptions regarding hepatobiliary and renal excretion as previous studies[3]. To assess the pharmacological effects of 5-HT_{2A} receptor stimulation, the head-twitch response (HTR) was assessed in mice by giving increasing doses of Cimbi-36. Forty NMRI mice were injected i.p. with saline, 2,5-dimethoxy-4-iodoamphetamine (DOI), or increasing doses of Cimbi-36, and their HTR was scored for 20 min starting 5 min after injection using video recordings.

Results: [^{11}C]Cimbi-36 accumulation measured as standardized uptake values (SUV) was highest in rat lungs, where SUV = 30 was found 5 minutes after injection. The human target organ with highest absorbed dose was the urinary bladder wall receiving 0.04 mGy/MBq. The total effective dose as extrapolated from the rat data was also low (5 μSv/MBq). After administration of 0.5 mg/kg Cimbi-36, the mice displayed HRT comparable to 2.5 mg/kg DOI and significantly higher than with saline (Fig. 1). 0.05 mg/kg Cimbi-36 did not elicit a significant HTR relative to saline, while Cimbi-36 doses at and above 2.5 mg/kg had prominent sedative effects. Thus, significant pharmacological effects of Cimbi-36 were not observed by doses ~350 times greater than that given in conjunction with a PET scanning (with 10 μg as maximal injected mass in a 70 kg subject).

Conclusions: The extrapolated effective radioactive dose of [^{11}C]Cimbi-36 was 5 μSv/MBq which is a similar to that of most other carbon-11 labelled neuroreceptor PET radioligands. [^{11}C]Cimbi-36 can be safely administered in relation to PET scanning since tracer dose administration is given at doses ~350 times lower than those associated with pharmacological effects in rodents.

[1] Ettrup et al., *Eur J Nucl Med Mol Imaging*, in press.

[2] Gonzalez-Measo et al., *Neuron*, 2007. 53(3):439-52.

[3] Wilson et al., *Nucl Med Biol*, 2002. 29(5):509-15.

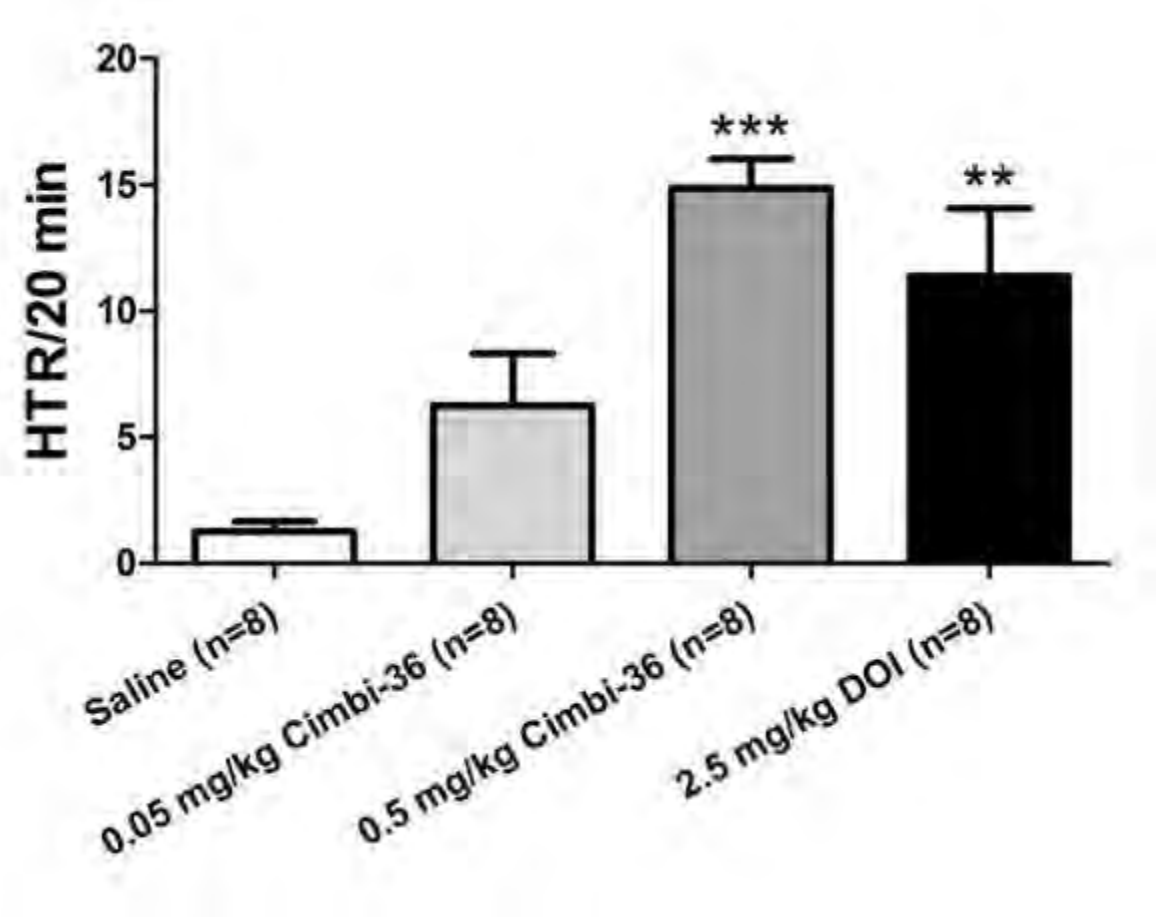

[Fig.1]

934

MODELS OF CREATINE DEFICIENCY SYNDROMES BY RNAI IN 3D REAGGREGATED BRAIN CELL ORGANOTYPIC CULTURES

O. Braissant, E. Béard, J. Uldry

Clinical Chemistry Laboratory, University Hospital of Lausanne, Lausanne, Switzerland

Creatine deficiency syndromes, either due to deficiencies in AGAT and GAMT, the two enzymes of the creatine synthesis pathway, or in the creatine transporter SLC6A8, lead to a complete absence, or a very strong decrease, of creatine within the brain, as measured by magnetic resonance spectroscopy. CNS appears as the main organ affected in patients suffering from creatine deficiency syndromes, who show severe neurodevelopmental delay and present neurological symptoms in early infancy, in particular mental retardation, disturbance of active and comprehensible speech, autism, automutilating behavior, hypotonia, and, in GAMT- and sometimes SLC6A8-deficient patients, intractable epilepsy. The creatine / phosphocreatine / creatine kinase system plays essential roles in the brain to maintain the high energy levels necessary for its development and functions, through regeneration and buffering of ATP levels. Moreover, recent works also suggest new roles for creatine in CNS, where it may act as neuromodulator or even true neurotransmitter. In these last years, we have brought evidence that blood brain barrier has a limited permeability for creatine, and that CNS has to synthesize an important proportion of its own creatine. We have further shown that AGAT, GAMT and SLC6A8 are differentially expressed by brain cells, in most cases under a dissociated pattern.

To better understand the effects of creatine deficiencies on developing brain cells, we have developed new experimental models by gene knock-down through RNAi of AGAT, GAMT and SLC6A8 in 3D organotypic rat brain cell cultures in aggregates, which were transduced by 2 different adeno-associated virus (AAV) serotypes, AAV2 and AAV5, driving the expression of specific shRNAs for AGAT, GAMT and SLC6A8.

We show that both AAV2- and AAV5-transduced shRNAs were able to efficiently knock down the genes for creatine synthesis and transport. Moreover, AGAT, GAMT and SLC6A8 knock-down by RNAi strongly affected brain cell development, as shown by the use of specific brain cell (NF-M for neurons; GFAP for astrocytes; MBP for oligodendrocytes) as well as apoptotic (activated caspase 3) markers in immunohistochemistry and western blots experiments.

AAV2 or AAV5 viruses appear as powerful tools for knocking down AGAT, GAMT and SLC6A8 expression by RNAi in developing brain cells, allowing the analysis of specific alterations of CNS development in creatine deficiency syndromes.

935

COGNITIVE DYSFUNCTION AND CEREBRAL BLOOD FLOW IN 5 CASES OF BILATERAL MEDIAL THALAMIC INFARCTION

H. Maruyama[1], A. Osawa[2], S. Maeshima[2], H. Takeda[1], T. Dembo[1], H. Nagoya[1], Y. Kato[1], Y. Oe[1], I. Deguchi[1], T. Fukuoka[1], Y. Horiuchi[1], N. Tanahashi[1]

[1]Neurology, [2]Rehabilitation Medicine, International Medical Center, Saitama Medical University, Hidaka, Japan

Objectives: There are various fiber communications between thalamus and cerebral cortexes. Therefore, various symptoms appear in patients of thalamic infarction. Since Segarra and Castaigne reported the clinical and anatomical examination of bilateral median thalamic and midbrain infarctions, some similar cases have been reported. However, there are only a few reports of cognitive dysfunction and cerebral blood flow (CBF) in patients with bilateral median thalamic infarction. The aim of this study was to investigate cognitive dysfunction and cerebral blood flow in patients with bilateral medial thalamic infarction.

Methods: Subjects were 5 patients (3 men and 2 woman, aged 72.6±7.7 years) who were diagnosed as bilateral median thalamic infarction by MRI-DWI (diffusion weighted image) and were admitted in our hospital from April, 2007 to November, 2010. One of 5 patients had not only thalami but also midbrain infarction. As the clinical type of brain infarction, 4 patients were cardioembolic stroke, another one patient was atherothrombotic infarction. They were taken neuropsychological assessment and measurement of CBF using ^{99m}Tc-ECD single photon emission computed tomography (SPECT). SPECT was done within two weeks from admission (acute phase) in all cases, 2 of 5 patients in one month later after admission (chronic phase).

Results: All 5 patients had a serious disturbance of consciousness at the time of the hospitalization. In 3 patients, consciousness was almost recovered within a few days after hospitalization. In other 2 patients, disturbance of consciousness was prolonged after hospitalization. In patients who were examined neuropsychological assessment, each patient had inattention, amnesia, mental deterioration and executive dysfunction. In all patients, SPECT on acute phase showed a marked hypoperfusion in the bilateral thalamic lesion, and an associated hypoperfusion of the overlying cortex, mainly in the frontal lobes. In chronic phase, CBF in the frontal lobes was still decreased.

Conclusions: It was suggested that the cognitive dysfunction and hypoperfusion of the wide cerebral cortex were caused by the thalamic damage and remote effect of fiber communication from thalamus to cerebral cortex.

936

ASSOCIATION BETWEEN CHRONIC PSYCHOSOCIAL STRESS AND REGIONAL BRAIN GLUCOSE METABOLISM IN NORMAL ELDERLY FEMALES

H. Park[1], S.S. Cho[2], S.E. Kim[2], J. Chey[1]

[1]Psychology, Seoul National University, [2]Nuclear Medicine, Seoul National University College of Medicine, Seoul, Republic of Korea

Neuroimaging studies in human have shown that basal cortisol level is related to hippocamal volume; however, little have been known about the association between chronic psychosocial stress and regional glucose metabolism. In attempt to investigate the cortical and subcortical metabolic correlates of chronic psychosocial stress in human brain, we conducted the correlation analysis between regional brain glucose metabolism and chronic psychosocial stress in normal older females. Thirty nine healthy right-handed volunteers (age 67-85 [mean 72.72±4.467]) participated in the study. After neuropsychological evaluation for cognitive decline, chronic psychosocial stress were assessed with the Traumatic Stress Inventory (TSI) that inquired into individual's severe stress experiences after 60 years old. FDG-PET images were taken at resting state and correlation between regional glucose metabolism and stress was tested using SPM2. A significant negative correlation between TSI score and glucose metabolism was observed in the putamen, inferior and dorolateral prefrontal regions. These data demonstrate metabolic correlates of chronic psychosocial stress in normal older females. These results suggest that chronic psychosocial stress decreases frontostriatal metabolism in normal older adults and that frontostriatal circuit is involved in stress processes.

937

LITHIUM STIMULATES CELL PROLIFERATION AND INHIBITS INFLAMMATION AFTER NEONATAL HYPOXIA-ISCHEMIA

C. Zhu[1], H. Li[2], Q. Li[2], X. Du[2], X. Wang[1], K. Blomgren[1]

[1]University of Gothenburg, Gothenburg, Sweden, [2]Zhengzhou University, Zhengzhou, China

Objective: To evaluate long-term effects of lithium on neonatal hypoxic-ischemic brain injury as well as cell proliferation and inflammation.

Methods: Nine-day-old male rats were subjected to unilateral hypoxia-ischemia (HI) and 2 mmol/kg lithium chloride was injected i.p. immediately after the insult. Additional lithium injections, 1 mmol/kg, were administered at 24 h intervals. Pups were sacrificed 24 h, 72 h or 7 weeks after HI.

Results: Lithium reduced total tissue loss from 89.4 ± 14.6 mm^3 to 27.6 ± 6.2 mm^3 (69.1 %) (n=15) compared with vehicle (n=14) at 7 weeks after HI ($P< 0.001$). Injury was reduced in the cortex, hippocampus, thalamus and striatum at the histopathological level. Lithium promoted both cell proliferation and the survival of newborn cells in the dentate gyrus of hippocampus, but had no effect on neuronal differentiation. Microglia activation after HI was inhibited by lithium treatment, as judged by reduced levels of IL-1β and MCP-1 .

Conclusion: Lithium could mitigate the brain injury after neonatal hypoxia ischemia by inhibiting inflammation and promoting cell proliferation and survival in the neurogenic area of the hippocampus

938

COMPLEX PATHOLOGY IN THE THALAMUS FOLLOWING CEREBRAL ISCHEMIA

J. Jolkkonen, M. Hiltunen

Institute of Clinical Medicine - Neurology, University of Eastern Finland, Kuopio, Finland

Focal cerebral ischemia in the cortex leads to the secondary pathology in areas distant from but connected to the infarct. The thalamus is spared from acute ischemic damage, but because of its synaptic connections delayed retrograde degeneration of thalamocortical neurons occurs. In addition to degenerative process, thalamic pathology includes parallel inflammatory reaction, impaired calcium homeostasis, complex alterations in beta-secretase-mediated amyloid precursor protein processing and increased angiogenesis. Together these result in the unique pathology remote from the initial insult that has intriguingly similar features as to that in Alzheimer's disease. The causal relationships between different pathologies and their functional meaning are poorly understood. Given the integral role of the thalamus in the sensorimotor information flow and processing, however, the damage to the thalamus or its projections is likely to have detrimental consequences. Further understanding the secondary pathology in the thalamus is expected to aid in drug discovery aiming at neurorestoration following various neuronal insults.

940

COMBINED THERAPY OF MILD HYPOTHERMIA AND EDARAVONE ENHANCES THE EFFECT OF THROMBOLYSIS ON EMBOLIC ISCHEMIC MODEL IN RATS

S. Okubo, T. Inaba, C. Nito, M. Ueda, Y. Katayama

Divisions of Neurology, Nephrology, and Rheumatology, Department of Internal Medicine, Nippon Medical School, Tokyo, Japan

Objectives: There are clinical demands for neuroprotective therapy that can extend the therapeutic time window of thrombolysis for cerebral ischemia. Edaravone, a free radical scavenger, has the neuroprotective effects and mild hypothermia enhances the effect of neuroprotective drugs following transient focal ischemia in rat. The aim of this study is to determine whether combined therapy of Edaravone and mild hypothermia enhances effect of thrombolysis on embolic ischemic model in rats.

Methods: 18 pieces of 1mm length from the fibrin rich portion in clots were gently infused via ICA of Sprague-Dawley rats (n=30). Intravenously, 3 mg/kg of Edaravone or vehicle was administered after 90 minutes from embolization. 10% of total 10 mg/kg of Alteplase or vehicle was injected as a bolus and remainder was infused continuously for 30 minutes at 90 minutes after embolization. Until 3 hours from embolization, temporal muscle and rectal temperatures were maintained 37degrees C in the normothermic animals and 35 degrees C in the hypothermic animals. Five groups (n=6 respectively); (a) vehicle, vehicle, normothermia, (b) vehicle, Alteplase, normothermia, (c) Edaravone, Alteplase, normothermia, (d) vehicle, Alteplase, hypothermia, (e) Edaravone, Alteplase, hypothermia, were compared by neurological symptom and infarct and edema volume from TTC stain at 24 hours after treatment.

Results: There were no significance in infarct volume between the group (a) and (b), or (c) and (d). Edaravone or mild hypothermia with Alteplase significantly reduced neurological dysfunction (p=0.01, 0.05) and infarct volume (p=0.03, 0.03), but not edema volume (p=0.2, 0.2) compared with the group (a). Combined therapy of Edaravone and mild hypothermia with Alteplase more significantly reduced neurological dysfunction, infarct volume and edema volume (p=0.05, 0.01, 0.05) compared with the group (a).

Conclusions: Combined therapy of Edaravone and mild hypothermia may enhance the effect and extend the therapeutic time window of thrombolysis on embolic ischemic model in rats.

941

AN EARLY OCCIPITAL SPECIALIZATION FOR DETECTION AND CATEGORIZATION ABILITIES IN HEALTHY INDIVIDUALS

S. Chokron[1,2], C.D. Cavézian[1,2], C. Peyrin[2], G. Doucet[3], O. Coubard[2], J. Savatovsky[4], F. Héran[4], O. Gout[5], C. Perez[1,2]

[1]Unité Fonctionnelle Vision & Cognition, Fondation Ophtalmologique Rothschild, Paris, [2]Laboratoire de Psychologie & NeuroCognition - UMR5105, Grenoble, [3]Centre d'Imagerie-Neurosciences et Applications aux Pathologies - UMR 6232, Caen, [4]Service d'Imagerie, [5]Service de Neurologie, Fondation Ophtalmologique Rothschild, Paris, France

To assess if visual processing for detection and categorization abilities can be distinguished as early as the occipital lobe, 14 healthy male volunteers (55 years ± 11.4) completed an fMRI paradigm including a detection and a categorization task differing only by the task demand. Filtered (in high [HSF] or low [LSF] spatial frequencies) and non-filtered [NF] images were briefly presented centrally on a computer screen. Participants were required to respond when a natural scene was presented (detection task) or to indicate if the stimulus was a city or a highway (categorization task). Accuracy (error rate) and response times (RT) were recorded. Behaviourally, compared to LSF or NF -images, ER was greater and RT was longer when HSF-images were presented in the detection task. However, the type of images did not modulate performance in the categorization task. Imaging data revealed that the two tasks differentially recruited the occipital lobe although they differed only regarding the cognitive demand. Although the left inferior occipital gyrus was activated in both tasks, the detection task recruited the right inferior occipital gyrus whereas the categorization task recruited the left medium occipital gyrus. Besides, increased signal was observed in the left middle occipital gyrus when HSF-images had to be categorized as compare to LSF-images. Altogether, data confirm the coarse-to-fine time course for spatial frequency processing as well as the specific implication of the left middle occipital gyrus for HSF processing. Interestingly, imaging result suggest an early hemispheric specialization for detection and categorization abilities (even when only the instruction changes).

942

IMPORTANCE OF NADPH OXIDASES AND ENDOTHELIAL NITRIC OXIDE SYNTHASE IN ANGIOTENSIN II-INDUCED OXIDATIVE STRESS AND ENDOTHELIAL DYSFUNCTION

S. Chrissobolis[1,2], B. Banfi[3], C.G. Sobey[1], F.M. Faraci[2,4]

[1]Pharmacology, Monash University, Melbourne, VIC, Australia, [2]Internal Medicine, [3]Anatomy and Cell Biology, [4]Pharmacology, University of Iowa, Iowa City, IA, USA

Objective: Angiotensin II (Ang II) contributes to cerebrovascular disease during hypertension by producing oxidative stress and endothelial dysfunction. NADPH oxidases and uncoupled endothelial nitric oxide synthase (eNOS) are potential mediators of oxidative stress in the vasculature. The objective of this study was to examine the involvement of Nox1 and Nox2-containing NADPH oxidases and eNOS in Ang II-induced oxidative stress and endothelial dysfunction in cerebral arteries.

Methods: Nox1-deficient ($Nox1^{-/Y}$), Nox2-deficient ($Nox2^{-/-}$), and eNOS deficient ($eNOS^{-/-}$) mice and appropriate controls (wild-type littermates or C57Bl/6 mice) were treated for 7 days with vehicle (saline) or Ang II (1.4 mg/kg/day) using an osmotic minipump. Blood pressure was measured using tail-cuff plethysmography, superoxide levels were measured using L-012 chemiluminesence, and vasodilation was measured using isolated, pressurized basilar arteries.

Results: Ang II treatment increased blood pressure to a similar degree in all groups of mice. In C57Bl/6 mice, Ang II reduced vasodilation of pressurized arteries to acetylcholine (ACh, an endothelium-dependent agonist) compared to vehicle (eg. %Δ diameter caused by 10^{-4} M ACh in vehicle-treated mice: 46±2%; Ang II-treated: 31±3%, $P< 0.05$), confirming that Ang II causes endothelial dysfunction. Ang II treatment also reduced vasodilation to ACh in $eNOS^{-/-}$ mice (eg. %Δ diameter caused by 10^{-4} M ACh in vehicle-treated mice: 57±6%; Ang II-treated: 30±3%, $P< 0.05$), suggesting that uncoupled eNOS is not involved in Ang II-induced endothelial dysfunction. In contrast, Ang II had no effect on responses to ACh in $Nox2^{-/-}$ mice (eg. %Δ diameter caused by 10^{-4} M ACh in vehicle-treated mice: 46±3%; Ang II-treated: 49±10%, $P>0.05$), suggesting that Nox2 mediates cerebral endothelial dysfunction in response to Ang II. Ang II treatment also had a small but significant inhibitory effect on dilation to ACh in $Nox1^{-/Y}$ mice, suggesting Nox1 may contribute to Ang II-induced cerebral endothelial dysfunction. Ang II treatment did not impair responses to papaverine in any group. Superoxide levels tended to increase (ie. were ~1.6 fold greater) in cerebral arteries of Ang II vs vehicle-treated mice, although this effect was not statistically significant. Interestingly, superoxide production in response to phorbol-12,13-dibutyrate (a Nox2-dependent stimulus) was ~2-fold greater in cerebral arteries from Ang II vs vehicle-treated mice ($P< 0.05$), and this effect was abolished in Nox2-deficient mice.

Conclusions: These data suggest a major role for Nox2-containing NADPH oxidase in Ang II-induced oxidative stress and endothelial dysfunction, with a potential minor role for Nox1. Uncoupling of eNOS may not contribute to Ang II-induced impairment of endothelial function in cerebral arteries.

943

THE PARAMETERS OF BIOELECTRICAL ACTIVITY AS MARKERS SOME STRUCTURAL CHANGES OF THE BRAIN IN HYPERTENSIVE PATIENTS

G. Semke, V. Mordovin, N. Afanaseva

Tomsk Research Institute of Cardiology, Tomsk, Russia

Objective: To study relationship between bioelectrical activity and structural changes of the brain in order to find possible early markers of hypertensive encephalopathy

Material and methods: 16-channel EEG was recorded using “Orion” (Hungary) and brain MRI were performed using 0.2 T Magnetom-OPEN (Germany) in 162 patients aged between 28-56 years (mean age 12.4±2.4), 94 men and 68 woman (mean duration of hypertension 12.4±6.7). Selective mapping of power of EEG d, t, a rhythms across the brain (in microV/Hz/0.5) was performed using Fourier spectral analysis of digital EEG records. Cluster analysis was applied to the maps for identification of distinctive types. Correlation and variation statistical analysis were used to find relationships between spectral characteristics of bioelectrical activity and structural changes of the brain

Results: Four distinctive types of the EEG maps were identified with statistically significant difference in spectral power of EEG rhythms in all regions of brain (F=26,79-93,05, p=0,0000) reflecting progressive impairment of functional activity of the brain: going from a type 1 to type 4 power of slow rhythms increases while power of a-rhythm decreases. Type 1 (13,5%) was defined as normal, types 2-4 were defined as consecutive stage of progressive impairment of bioelectrical activity of the brain - from mild (type 2 - 29.5%) to severe (type 4 - 24.5%). Brain MRI detected liquorodynamic disturbance in 67.1%, leucoaraiosis - in 40.8%, focal damage of white matter - in 65.8%, lacunar infarcts - in 19.1% of patients. Going from type 1 to type 4 decrease of power of a-rhythm and increase of power of slow rhythms was related to increase in severity of liquorodynamic disturbance (F=4,1, p=0,019 and F=3,4, p=0,038 respectively) and leucoaraiosis (F=2,7; p=0,048 and F=3,9, p=0,01 respectively). Greatest impairments of bioelectrical activity of the brain were observed in the regions with most severe structural changes. There was no relation between impairments of bioelectrical activity and presence focal damage of white matter and lacunar infarcts. The deterioration of functional activity of the brain (increase of spectral power of slow rhythms and decrease - of α-rhythm) in hypertensive patients correlated with index of time for daytime systolic BP (r = 0.42; p=0.001) and for 24-h systolic BP (r=0.46; p=0.009).

Conclusion: Identified types of the brain EEG maps (spatial distribution of power of EEG rhythms) characterize severity of impairment of rhythmic structure of cortical bioelectrical activity. They are determined by the presence of structural changes of the brain and reflects stages of morphological manifestations of hypertensive encephalopathy. The increase of the index of slow activity and decrease (reduction) of the index of a-rhythm in the hypertensive patients can be considered as markers of increase of subarachnoidal spaces and presence of leucoaraiosis.

944

IMAGING THE IN VIVO EFFECT OF HYPERAMMONEMIA IN THE RAT BRAIN: A SPECTROSCOPIC IMAGING AND DIFFUSION TENSOR IMAGING STUDY

C. Cudalbu[1], N. Kunz[1], B. Lanz[1], Y. Van de Looij[1], V. Mlynárik[1], R. Gruetter[1,2]

[1]Laboratory for Functional and Metabolic Imaging (LIFMET), Ecole Polytechnique Fédérale de Lausanne (EPFL), Lausanne, [2]Departments of Radiology, Universities of Lausanne and Geneva, Lausanne and Geneva, Switzerland

Objectives: Ammonia is a neurotoxin that is implicated in the pathogenesis of hepatic encephalophaty (HE). Brain edema represents a major complication. In hyperammonemic (HA) conditions, glutamine is generated in astrocytes from ammonia and glutamate in a reaction catalyzed by glutamine synthetase (GS). In vitro observations suggested that during HA, alterations in brain metabolites other than glutamine can occur (1,2). Diffusion tensor imaging (DTI) measures the relative translational motion of water proton across cell membrane, which is expressed as the ADC value. Changes in ADC reflect the presence of edema. The in vivo spatial distribution of brain metabolites can be measured using proton spectroscopic imaging (SI). The aim of the study was: 1) to assess the effects of HA per se in the rat brain by DTI; 2) to image for the first time the in vivo effect of hyperammonemia per se on 12 brain metabolites (i.e. Gln, Glu, tCr, tCho, Ins, Tau, Lac, NAA+NAAG, Lac, etc) in different brain regions and the net glutamine synthesis rates.

Methods: Experiments were performed on a 9.4T MRI system using SD rats. NH_4Cl was infused (4.5mmol/h/kg) for 6h. Diffusion tensor acquisitions were performed (3) and diffusivity values (ADC, FA) were derived from the tensor. ADC was measured in ROIs positioned in: Cortex (Cx), Striatum (St), Hippocampus (Hip) and Ventricles (Ven). Ventricles sizes were also calculated on the ADC maps with a threshold set to 10mm2/s. Metabolic maps were obtained using short-echo-time proton-spectroscopic-imaging (4).

Results: The results are presented in Fig 1. ADC measurements showed a decrease along the infusion (6%), significant only 6 hours after infusion. In addition, an increase of the ventricles size was visible (V_{before}=18 ± 6ml, V_{+6h}=31±13ml, $p< 0.05$). The increase in the Gln pool at different time points during infusion was apparent from the maps. The Gln concentration increased more in cortex than in hippocampus (5.5hh of infusion 16.2± 2.7mmol/kg_{ww} Cx and 11.5±1.2mmol/kg_{ww} Hip, p=0.03). The maps of the other brain metabolites did not show any visible difference before and after ammonia infusion. From the linear fit of the time-evolution of Gln we obtained a net glutamine synthesis rate of 0.039±0.007µmol/min/g Cx and 0.024±0.007µmol/min/g Hip (p=0.05).

Discussion: We propose that HA per se induces late in time a mild brain edema, as indicated by the decrease in ADC at 6h. Nevertheless, the origin of the ventricles increase and the presence of mild brain edema remain unclear and will need further investigations. High resolution metabolic maps enabled to observe the in vivo spatial distribution of 12 metabolites in various brain structures under HA. Contrary to other models of HA associated with experimental acute liver failures (1,2), no changes in spatial distribution of metabolites were observed except for Gln. The net glutamine synthesis rates were significantly higher in the cortex than in the hippocampus.

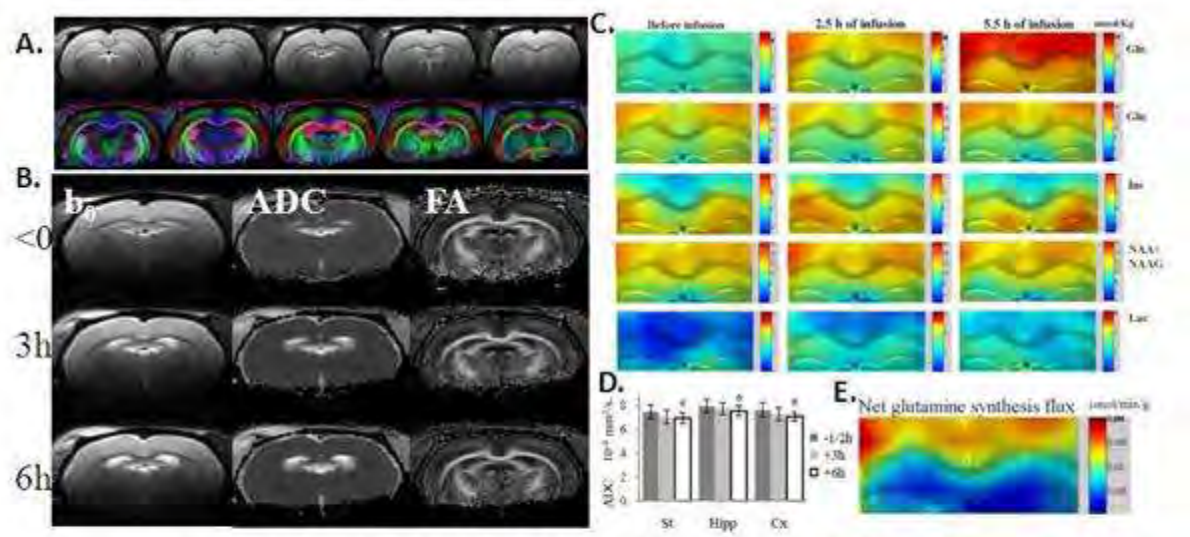

A) Images acquired with the semi-adiabtic SE-EPI before infusion, with the diffusion coefficient maps. $\mathbf{b_0}$ image (b = 0 mm²/s) and color encoded map (**Cmap**). B) $\mathbf{b_0}$ image (b = 0 mm²/s), diffusion tensor trace (**ADC**) and fractional anistropy (**FA**) maps acquired before infusion (<0), +3h after infusion, +6h after infusion. C) Metabolic maps of Gln, Glu, Ins, NAA+NAAG, Lac superimposed on the anatomical T_{2w} images and acquired at different time points during ammonia infusion. D) Mean ADC values before infusion, 3h and 6h after infusion in the striatum (**St**), hippocampus (**Hipp**) and cortex (**Cx**). *: $p < 0.05$ compared to control. E) Net glutamine synthesis rates imaged over the VOI and superimposed on the anatomical T_{2w} images.

[Fig 1]

References:

[1]Zwingmann C, J Neurosc Res. 85:3429,2007. [2]Rao KV et al, Metab Brain Dis. 16:67,2001. [3]Kunz N, Proceedings ISMRM2008. [4]Mlynárik V *et al.* Magn Reson Med. 59:52,2008.

945

METABOLITE CONCENTRATION CHANGES DURING VISUAL STIMULATION USING FUNCTIONAL MAGNETIC RESONANCE SPECTROSCOPY (FMRS) ON A CLINICAL 7T SCANNER

B.M. Schaller[1], R. Mekle[2], L. Xin[3], R. Gruetter[1,3,4]

[1]Laboratory of Functional and Metabolic Imaging, Ecole Polytechnique Fédérale de Lausanne, Lausanne, Switzerland, [2]Physikalisch, Technische Bundesanstalt, Berlin, Germany, [3]Department of Radiology, University of Lausanne, [4]Department of Radiology, University of Geneva, Lausanne, Switzerland

Objectives: FMRS allows direct measurement of metabolic changes during neuronal activation (within 0.2µmol/g) and provides insight into brain metabolism. The aim of the study was to use the spin echo based sequence SPECIAL (SPin ECho full Intensity Acquired Localized Sequence) combined with the advantages of increased sensitivity and spectral resolution at 7T [2], to investigate the temporal concentration changes of metabolites during neuronal activation in humans.

Methods: Six healthy subjects gave informed consent according to the procedure approved by the local ethics committee. Experiments were performed on a 7T Siemens scanner using quadrature transmit/receive surface RF coil. A brief checkerboard fMRI experiment (frequency 9Hz, 10s ON, 20s OFF, TA=2.5min) was used to place the acquisition voxel for the subsequent fMRS scans in an area of high visual activation. Shimming was performed using FASTMAP. For fMRS, subjects were exposed to the same visual stimulation consisting of five alternate periods of 5min of rest and visual stimulation (25min total) and ^{1}H MRS spectra were continuously acquired using the SPECIAL sequence (TR/TE=5000/6ms, BW=4000Hz, vector size=2048pts, VOI=20*22*20mm^3, 300scans) [2]. The unsuppressed water signal was measured at the end of the experiment (nt=8scans) for absolute quantification using LC Model [4]. For the inter-subject analysis, spectra were summed across the 6 subjects in blocks of 24 spectra (4scans per subject) yielding a time resolution of 20s.

Results: Spectra displayed typical water linewidths of ~13Hz and SNR of 30-40 for a single spectrum of 2 scans. The SPECIAL sequence with a carefully selected set of OVS bands, to minimize lipid contamination, ensured reliable quantification of the concentration of Lactate. Averaging 24 spectra allowed quantification of 18 metabolites with CRLB less than 30%, in particular, Lactate and Aspartate with CRLB below 25%, and Glutamate below 5%. The BOLD effect increases T_2^* and thus induced line-narrowing of the activated spectra [3] which could be observed in the time course of the Creatine peak height. The time courses from six subjects are plotted (fig. 1) with a moving average (sliding offset=4scans). Inter-subject analysis revealed an increase of [Lac] of 25±9% ($p< 0.05$) and [Glu] of 4±1% ($p< 0.02$) in the visual cortex during the second part of the activation. A decrease of [Asp] of 9%±3.5% ($p< 0.05$) has also been measured. A trend for [Glc] decreasing during activation was further observed.

Conclusion: The use of SPECIAL sequence at 7T yielded increased SNR compared to STEAM providing twofold increased resolution for the time courses of different metabolites concentration compared to a previous study performed on twelve subjects [1] and further support the notion of predominant oxidative metabolism during activation. By increasing the number of subjects a detailed study on the dynamics of amino acid changes should be feasible. The metabolites changes agree with previous studies [1] though at a reduced subject number.

References: [1] S. Mangia, JCBFM, 27:1055-1063, 2007 [2] R. Mekle et al, MRM, 61(6):1279-85, 2009 [3] Zhu X-H et al, MRM, 2001:46 [4] S. Provencher, MRM, 30, 1993.

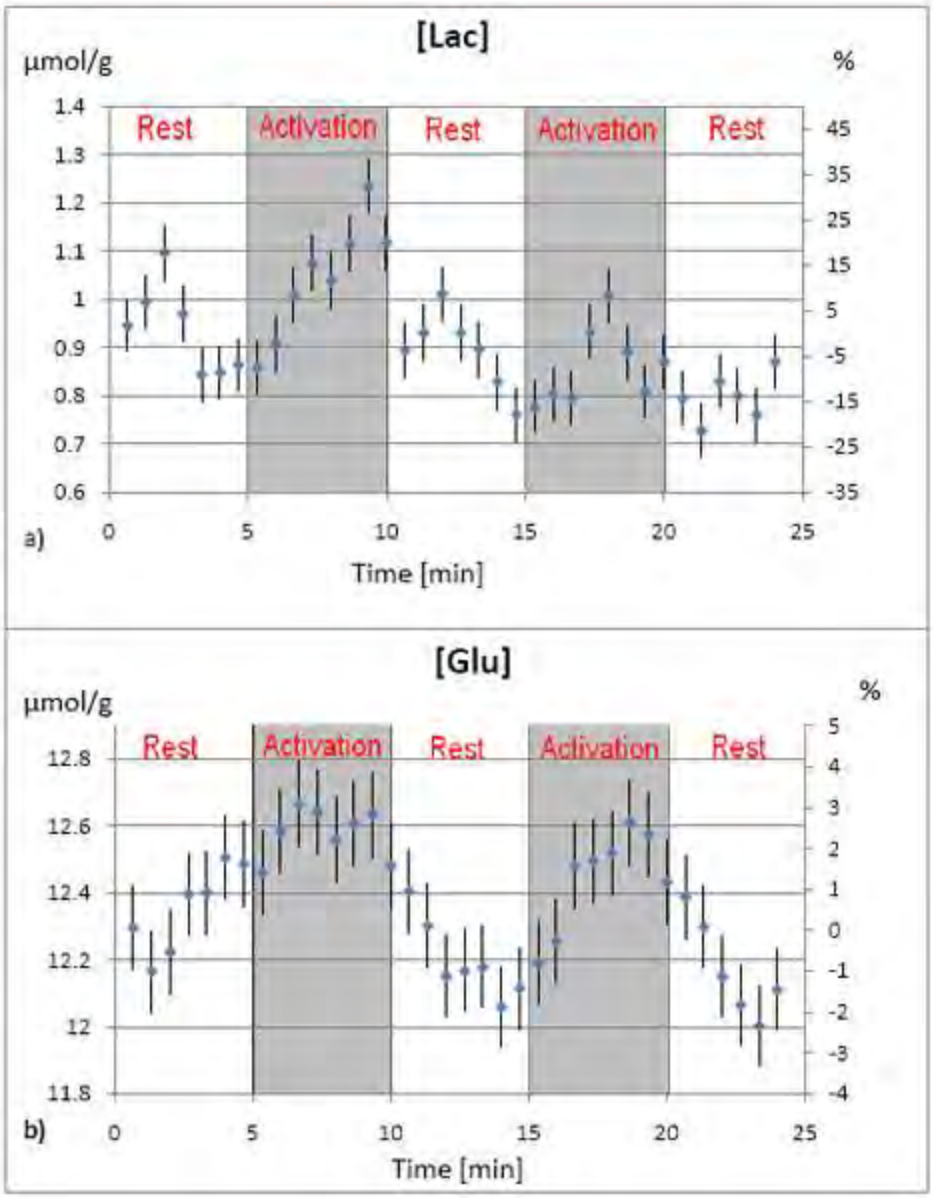

Figure 1.a) and b): *Time courses for Lactate and Glutamate during the functional paradigm plotted with moving average (sliding offset=4scans). Each time point corresponds to 24 averaged spectra.*

[Time courses for Lactate and Glutamate]

947

NEUROTOXIC TRANSFERRIN EXTRAVASATES AND ACCUMULATES IN THE POSTISCHEMIC BRAIN AREAS IN EXPERIMENTAL STROKE

T. GASULL[1], M.C. Burguete[2], S. Guardia[1], N. Degregorio-Rocasolano[1], O. Martí-Sistac[3], J.B. Salom[2,4], E. Alborch[4,5], A. Dávalos[1,6]

[1]Department of Neurosciences, Fundació d'Investigació en Ciències de la Salut Germans Trias i Pujol, Badalona, [2]Departamento de Fisiología, Universidad de Valencia, Valencia, [3]NON, Universitat Autònoma de Barcelona, Bellaterra, [4]Centro de Investigación, Hospital Universitario 'La Fe, [5]Hospital Universitario La Fe, Valencia, [6]Department of Neurosciences, Hospital Universitario Germans Trias i Pujol, Badalona, Spain

Background and Objectives: Impairment of blood brain barrier function by stroke disturbs the otherwise exquisitely regulated blood-to-brain transport of molecules, producing accumulation in ischemic brain areas of water and of some other molecules whose abundance in serum is much higher than in cerebrospinal fluid (1-2). Peripheral iron overload has been associated with neurological worsening in stroke patients after thrombolytic treatment (3). We have recently demonstrated that the iron-transporting protein transferrin is harmful to postischemic neurons exposed to an in vitro model of stroke (4). Transferrin is highly abundant in serum (5), and no studies are available so far about its extravasation after stroke. The objective of the present work was to investigate the efflux of serum transferrin towards the extravascular space and its accumulation in ischemic areas at risk of infarction in two experimental rat stroke models.

Methods: Transient middle cerebral artery occlusion (tMCAO) was performed by using either ligature or intraluminal filament in rats. To evaluate transferrin extravasation, labelled transferrin was injected intravenously 15 min after reperfusion following 90 min of tMCAO using intraluminal filament. Rats were sacrificed after 2 hours of reperfusion, brains were extracted, and the label present in the ipsilateral and contralateral hemispheres was quantified. In addition, we studied the accumulation of endogenous transferrin in the brain areas of interest after 60 min of tMCAO by ligature and 2 hours of reperfusion by Western blot.

Results: After tMCAO by intraluminal filament we found a 30-fold increase in the levels of labelled transferrin in the ipsilateral as compared to the contralateral hemisphere (fig below). Western blot after tMCA by ligature showed a 11-fold increase of endogenous transferrin levels in the brain postischemic areas as compared with contralateral areas. The concentration of transferrin estimated in the postischemic area was in the range that we previously found to exacerbate neuronal death in vitro.

Conclusions: These findings confirm that both early extravasation and accumulation of serum transferrin in the postischemic areas occur in experimental stoke models in vivo; the concentration of transferrin reached in the postischemic areas was in the range we previously found to be neurotoxic to postischemic neurons. Therapeutic interventions preventing blood transferrin to reach postischemic areas or preventing the uptake of transferrin by neurons might, thus, protect from reperfusion damage in stroke patients.

References:

1. Chi OZ et al. Neurochem Res 34:1249-1254, 2009

2. Abulrob A et al. Mol. Imaging 7:248-262, 2008

3. Millán A et al. Stroke 38:90-95, 2007

3. Gasull T et al. ESC 2010

4. Gaasch JA et al. Neurochem Res 32:1196-1208, 2007

948

HIGH SALT INTAKE UNDER HYPOESTROGENECITY DETERIORATES ISCHEMIC BRAIN DAMAGE WITHOUT AFFECTING BLOOD PRESSURE

M. Sumiyoshi, T. Kinouchi, T. Tsutsumi, K. Kitazato, K. Shimada, N. Matsushita, Y. Kanematsu, J. Satomi, S. Nagahiro

Neurosurgery, Institute of Health Biosciences, The University of Tokushima Graduate School, Tokushima, Japan

Objectives: Hypertension is one of risk factors of cerebral infarction. Overintake of salt is thought to be a causal factor of hypertension. The incidence of cerebral stroke is typically higher in middle-aged men than women, which is considered to be attributable to estrogen deficiency. To verify the effects of hypoestrogenesity and over-salt intake on cerebral ischemic damage, we performed this study.

Methods: 5 weeks-old female rats were subjected to oophrectomy(OVX) and given normal- or high salt diet (OVX/ND, OVX/HSD) for 2 weeks since 2 weeks after OVX. At 4 weeks post OVX, middle cerebral artery was transiently occluded (MCAO) by 4-0 nylon suture for 90 min. The ischemic brain damage were assessed at 24h after MCAO-reperfusion and compared with age-matched male rats (M/ND,M/HSD).

Results: In both male and female rats, infarct size was significantly larger in HSD- than ND rats ($p < 0.05$). Interestingly , in OVX/HSD rats, the infarct seize was larger than M/HSD rats($p < 0.05$). However, the blood pressure level in OVX/HSD rats was normal and similar to M/ND and OVX/ND. Notably, the blood pressure level in M/HSD rats was significantly higher than in M/ND($p < 0.05$). These results indicated that the expansion of infarct size in male rats was correlated with the elevated blood pressure, while in OVX rats the severity after ischemic insult was not necessarily reflected by blood pressure, suggesting the gender difference of pathophysiology on cerebral ischemic damage.

Conclusion: OVX rats may be more susceptible to sodium-induced deterioration of ischemic damage than male rats. To establish an optimal therapeutic strategy in male and female patient, further studies are required.

949

THE INFLUENCE OF GENDER ON PENUMBRA IN EXPERIMENTAL STROKE: AN MRI PWI/DWI MISMATCH STUDY

T.A. Baskerville, C. McCabe, W.M. Holmes, I.M. Macrae

Glasgow Experimental MRI Centre, University of Glasgow, Glasgow, UK

In rodent experimental stroke models, females exhibit less ischaemic injury than males, however, the reason for this it is not fully understood. Preservation of cerebral blood flow (CBF) and/or the ischaemic penumbra (potentially salvageable tissue) are two proposed mechanisms that may underlie the neuroprotection afforded to females.

Objectives: CBF and penumbra have been investigated in both male and female Sprague-Dawley rats up to 4hrs from stroke onset.

Methods: Male (n=7, 300-350g) and female (n=8, 220-260g) rats were anaesthetised (isoflurane: 5% induction, 2-3% maintenance, 30%:70% O_2:N_2O), artificially ventilated and the middle cerebral artery (MCA) permanently occluded by intraluminal filament. Rats were immediately transferred for MRI scanning (Bruker Biospec 7T/30cm with 4 channel phased-array surface coil). Physiological variables (blood pressure and blood gases) were monitored throughout. Diffusion-weighted imaging (DWI) and perfusion-weighted imaging (PWI) were performed (on 6x1.5mm coronal slices throughout MCA territory) from 1-4hrs post-stroke. A RARE T_2 scan was performed at 24hrs post-stroke to determine final infarct size (corrected for oedema) and to derive gender-specific diffusion and perfusion thresholds. Histogram analysis was used to asses CBF profiles in both hemispheres. Thresholded apparent diffusion coefficient (ADC) maps were used to define ischaemic injury and PWI/DWI mismatch to define penumbra. Diffusion and perfusion abnormality thresholds were derived by spatially matching the 4hr ADC and CBF lesion size with T_2-defined infarct at 24hrs. All data are presented as mean±S.D.

Results: Diffusion and perfusion thresholds derived for males and females were 0.60±0.05 and 0.55±0.09x$10^{-3}$$mm^2$/s, 35±15.2 and 35±20ml/100g/min, respectively. ADC lesion volume was significantly larger in males at all time points post-stroke (e.g. 143±32mm^3 and 72±29mm^3 at 1hr post-MCAO, respectively, Figure 1). However, the PWI-derived perfusion deficit was similar between the sexes (e.g. 212±27mm^3 versus 188±20mm^3 in males and females, respectively at 1hr post-MCAO). Histogram analysis of CBF profiles in ischaemic hemispheres showed no sex differences and no change throughout the experimental time course. Females displayed comparatively more penumbral tissue than males at all timepoints post-stroke (e.g. 70±26mm^3 in males versus 116±40mm^3 in females at 1hr post-MCAO, $P< 0.05$, Figure 1B) with less penumbra loss over the first 4 hrs. As predicted, females exhibited smaller infarcts than males at 24hrs post-stroke (146±67mm^3 versus 218±33mm^3, $P< 0.05$).

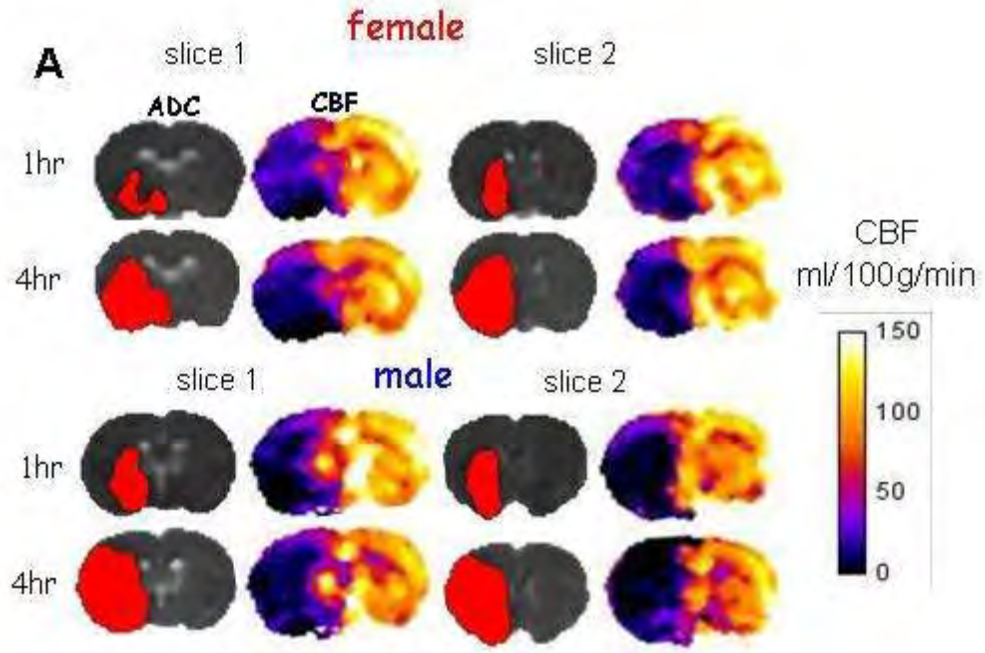
A
female
slice 1
slice 2
ADC
CBF
1hr
4hr
male
slice 1
slice 2
1hr
4hr
CBF
ml/100g/min
150
100
50
0

[Figure 1A]

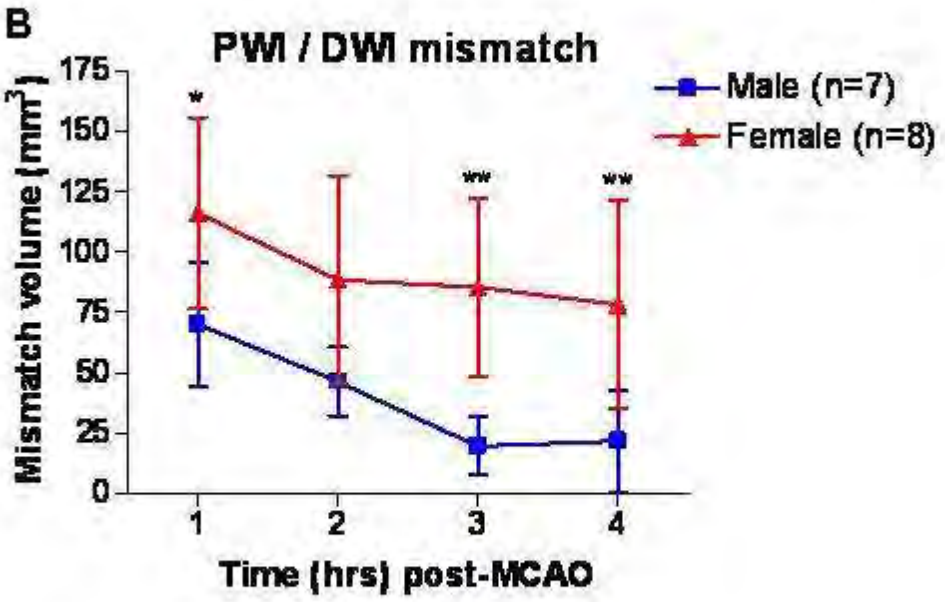

[Figure 1B]

Figure 1: A. Representative CBF maps and thresholded ADC maps, tracking changes in perfusion deficit and ADC lesion growth (red shading) in a representative female (top) and male (bottom) rat. B. Penumbra volume (PWI/DWI mismatch) in males and females 1-4hrs post-stroke (*P< 0.05, **P< 0.01, Two-way ANOVA with Bonferroni post-tests).

Conclusions: Following stroke, despite similarities in perfusion deficit between the sexes, females have more penumbra tissue which is also better preserved than in males. Differences in tissue response to ischaemia rather than vascular mechanisms appear to account for the sex-specific responses during ischaemic stroke.

This work was supported by a TMRC award from the consortium of 4 Scottish Universities and NHS Health Boards, Scottish Enterprise and Wyeth Pharmaceuticals.

950

THE ROLE OF TUMOR NECROSIS FACTOR-A AND TNF-A RECEPTORS IN CEREBRAL ARTERIS FOLLOWING CEREBRAL ISCHEMIA IN RAT

A. Maddahi, L. Edvinsson

Department of Clinical Sciences, Division of Experimental Vascular Research, Lund University, Lund, Sweden

Objective: Tumour necrosis factor-α (TNF-α) is a pleiotropic pro-inflammatory cytokine, which is rapidly upregulated in the brain after injury. TNF-α is involved in mediating the harmful processes that are initiated following stroke and is responsible for some of the signalling events within cells that lead to necrosis or apoptosis.

The aims of this study was (i) to investigate the expression of TNF-α and its receptors

(TNF-R1 and TNF-R2) in cerebral arteries following global or focal ischemia, and (ii) to determine if the enhanced expression is regulated via activation of the Raf-MEK-ERK1/2 pathway

Methods: The hypothesis was tested by two in experimental subarachnoid haemorrhage (SAH) and transient middle cerebral artery occlusion (TMCAO), and by in vitro organ culture of isolated cerebral arteries. The localization and amount of TNF-α, TNF-R1 and -R2, phosphorylated ERK1/2 and ELK-1 proteins expression were analyzed with immunohistochemistry using confocal microscopy and western blot after 48 h in both SAH and MCAO models and after 24 h and 48h in organ culture.

Results: Immunohistochemistry revealed enhanced expression of TNF-α, TNF-R1 and TNF-R2 in the cerebral arteries wall after MCAO and SAH at 48 h when compared with their control groups. Co-localization study showed that TNF-α, TNF-R1 and TNF-R2 were mostly localized in the cell membrane and cytoplasm of the smooth muscle cells (SMC). There is a fair expression of TNF-R2 in the endothelial cells. Both immunohistochemistry and western blot analysis showed that these proteins were upregulated in culture after 24 h and 48 h, and this upregulation was time-depended, reaching a maximum at 48 h of organ culture. In addition, treatment with U0126 (a specific MEK1/2 inhibitor) given intraperitoneal at zero or 6 hours after the ischemic event normalized the enhanced vascular expression of TNF-α, pERK1/2 and pELK-1.

Conclusion: The present study shows that both cerebral ischemia and organ culture induce expression of TNF-α, and its receptors (TNF-R1 and TNF-R2) in the walls of cerebral arteries. This is transcriptional regulated via the MEK/ERK pathway.

References:

Cerebral ischemia induces microvascular pro-inflammatory cytokine expression

via the MEK/ERK pathway. Maddahi and Edvinsson, Journal of Neuroinflammation 2010, 7:14

Tumor necrosis factor and its receptors in the neuroretina and retinal vasculature after ischemia-reperfusion injury in the pig retina. Gesslein, Håkansson, Gustafsson, Ekström and Malmsjö, Journal of Molecular vision 2010; 16:2317-2327

951

OPTIC NEURITIS AND HOMONYMOUS HEMIANOPIA DIFFERENTIALLY ALTER SPATIAL FREQUENCY PROCESSING FOR DETECTION AND CATEGORIZATION

C. Cavézian[1,2], A.-C. Viret[3], I. Gaudry[1,2], O. Coubard[2], C. Peyrin[2], C. Vignal[4], O. Gout[3], S. Chokron[1,2]

[1]Unité Fonctionnelle Vision & Cognition, Fondation Ophtalmologique Rothschild, Paris, [2]Laboratoire de Psychologie & NeuroCognition - UMR5105, Grenoble, [3]Service de Neurologie, [4]Service d'Ophtalmologie, Fondation Ophtalmologique Rothschild, Paris, France

Cortical reorganization seems to occur following peripheral as well as cerebral damage of the visual system. Although the central visual field of such types of patients remains often (partly) preserved, few studies assessed visual processing quality following either peripheral or central visual impairment. To assess if spatial frequency processing in the central visual field differs between peripheral and central damage of the visual system, 8 patients with recovered right (n=4) or left (n=4) optic neuritis (for one month) and 8 patients with right (n=4) or left (n=4) homonymous hemianopia (following a contralateral occipital lobe damage) completed a detection and a categorization task of natural scene images. Stimuli were filtered (in high or low spatial frequencies) or not and were briefly presented centrally on a computer screen. In the detection task, participants were had to press one button when an image was presented and another one when no stimulus was present. In the categorization task, they had to press one button when a city was presented and another button when it was a highway. Error rate (ER) and response time (RT) were recorded in both tasks. Compared to 16 young healthy controls, optic neuritis patients showed degraded performance when they completed the task with their (previously) pathologic eye (either right or left), and especially for low spatial frequency (ER) and in the categorization task (RT). Compared to 16 aged healthy participants, left hemianopes showed longer RT in both tasks (regardless the spatial frequency) whereas right hemianopes only tended to show longer RT for high spatial frequency images presented in the categorization task. Altogether, our data suggest that a peripheral or a cerebral visual impairment as well as the lateralization of the brain damage differentially alters visual processing: i) a peripheral disorder such as optic neuritis specifically alters low spatial frequency processing; ii) a brain damage of the left occipital lobe alters high spatial frequency processing; iii) a brain damage of the right occipital lobe alters both low and high spatial frequencies processing.

954

ROLE OF NUCLEAR RECEPTORS ON NEUROPROTECTION AFTER EXPERIMENTAL CEREBRAL ISCHEMIA IN FEMALE RATS

K.T. Kitazato, T. Kinouchi, K. Shimada, N. Matsushita, M. Sumiyoshi, Y. Kanematsu, J. Satomi, T. Kageji, S. Nagahiro

Department of Neurosurgery, Institute of Health Biosciences, The University of Tokushima Graduate School, Tokushima, Japan

Objectives: The protective role of estrogen in brain function has been confirmed experimentally. The binding of estrogen to estrogen receptor alpha (ERa) or beta (ERb) can alter the expression of many genes involved in neuro- and cardioprotection. However, there are few studies regarding the effects of nuclear receptors ERa, ERb and PPARg against ischemic brain damage in female patients and animals. The goal of this study is to verify the role of these receptors on neuroprotection by estrogen against ischemic brain damage.

Methods: Ten week-old female Wistar rats were subjected to bilateral oophorectomy (OVX^+) and sham-oophorectomy (OVX^-) 4 weeks before the induction of middle cerebral artery occlusion for 90 minutes and reperfusion (MCAO-R) .

Results: At 24 hr post-MCAOR, the cortical- but not basal ganglia infarct volume was larger in OVX^+- than OVX^- rats ($p< 0.01$), while there is no significant difference on their blood pressure. The increased infarct size was inversely correlated with the expression of ERa and PPARg but not ERb in the peri-infarct area ($p< 0.05$). Each inhibitor of ERa and PPARg eliminated the neuroprotective effects in the presence of estrogen. Interestingly, activation of PPARγ but not ERa was attributable to STAT3 phosphorylation in the peri-infarct area. The increase of p-STAT3 was associated with the transactivation of anti-apoptotic- and survival genes and the reduction of caspase-3 in the peri-infarct area. The phosphorylation of ERa was also associated with the transactivation of neuroprotective genes. These effects suggest that activation of each nucleus receptor by estrogen contributes synergistically to the neuroprotection after ischemic insult.

Conclusion: Our study first demonstrated that estrogen may exert the diverse neuroprotective effects mediated by nucleus receptors to prevent cerebral ischemic damage.

955

FIRST EVALUATION OF THE 5-HT_{2A} RECEPTOR AGONIST RADIOLIGAND [^{11}C]CIMBI-36 IN PRIMATE BRAIN

S.J. Finnema[1], A. Ettrup[2], V. Stepanov[1], A. Varrone[1], G.M. Knudsen[2], C. Halldin[1]

[1]Department of Clinical Neuroscience, Karolinska Institutet, Stockholm, Sweden, [2]Neurobiology Research Unit, Copenhagen University Hospital, Rigshospitalet, Copenhagen, Denmark

Introduction: Antagonist radioligands for the serotonin 2A (5-HT_{2A}) receptor have been used in clinical PET studies investigating the 5-HT system in several neuropsychiatric disorders. Development of an agonist radioligand has been pursued to allow for study of the high affinity state of 5-HT_{2A} receptors *in vivo*. Very recently the first agonist PET radioligand, [^{11}C]CIMBI-5, was found suitable for 5-HT_{2A} receptor imaging in pig [1]. Further development of a series of substituted ^{11}C-phenetylamines has identified [^{11}C]CIMBI-36 to provide higher BP_{ND} values, than for [^{11}C]CIMBI-5 [2]. In this study, we for the first time evaluated the binding characteristics of [^{11}C]CIMBI-36 in the primate brain.

Methods: [^{11}C]CIMBI-36 was prepared by ^{11}C-methylation in a two-step synthesis, starting from the *N*-Boc-*O*-desmethyl precursor, similarly as previously described [2]. A total of four PET measurements were performed in two female cynomolgus monkeys (3.3 and 6.6 kg). On two experimental days, a baseline measurement was followed by a pretreatment measurement with the 5-HT_{2A} receptor selective antagonist ketanserin (1.5 mg/kg). After intravenous administration of [^{11}C]CIMBI-36, PET measurements were performed for two hours in the HRRT PET system. Blood samples were collected for measurement of radioactivity and for analysis of radiometabolism, as measured by HPLC. Time activity curves of brain regions were obtained after co-registration with individual monkey MRI-templates. Specific binding and binding ratios were calculated with the cerebellum as reference region.

Results: Baseline PET measurements in two monkeys showed a peak in brain activity, of 2.4 and 2.6 %ID, between 10 and 20 minutes after [^{11}C]CIMBI-36 injection. In both monkeys, binding ratios of the cortical regions over cerebellum approximated 2.8 at the end of the PET measurement, and specific binding in cortical regions reached a plateau ~80 minutes after [^{11}C]CIMBI-36 injection. Administration of ketanserin significantly reduced the radioactivity in 5-HT_{2A} receptor-rich cortical regions and decreased cortical binding ratios to ~1.5. Radiometabolism of [^{11}C]CIMBI-36 was found relatively fast with 50% remaining after 4 minutes, and 10-15% remaining after 30 minutes until the end of the PET measurements. A total of six different radiometabolites were distinguished with HPLC, and three of them had retention times near to that of [^{11}C]CIMBI-36. However, the quantity of these three relative lipophilic radiometabolites was for each of them less than 1%, already 15 minutes after [^{11}C]CIMBI-36 injection.

Conclusions: This preliminary work indicates that [^{11}C]CIMBI-36 sufficiently enters the primate brain. Regional radioactivity after [^{11}C]CIMBI-36 injection distributed similarly as reported in the pig, and binding was found specific to 5-HT_{2A} receptors. The regional distribution and binding ratios in the primate brain were found similar as previously reported for the 5-HT_{2A} receptor antagonist [^{11}C]MDL 100907 [3,4]. No significant amount of lipophilic radiometabolites was observed. In conclusion, [^{11}C]CIMBI-36 is a promising radioligand for evaluation of the high affinity state of 5-HT_{2A} receptors *in vivo*.

References:

1. Ettrup, JNM, 2010. **51**: p. 1763-1770.

2. Ettrup, EJNM&MI, in press.

3. Lundkvist, Life Sciences, 1996. **58**(10): p. PI187-PI192.

4. Hall, Synapse, 2000. **38**(4): p. 421-431.

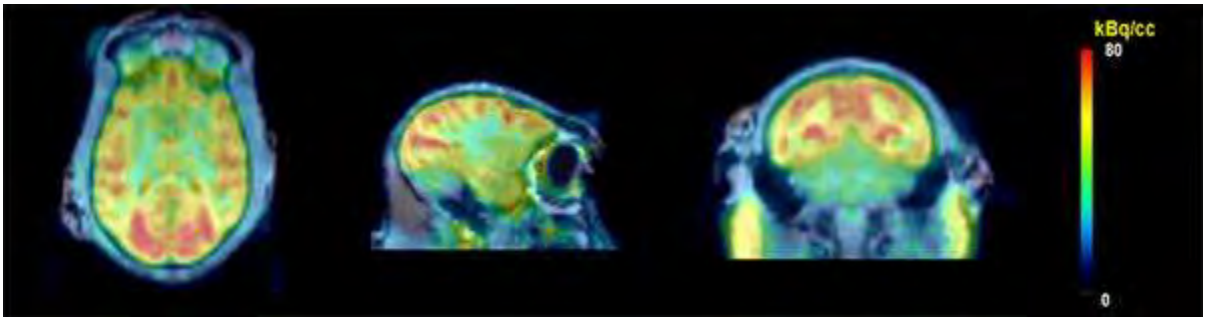

[Co-registered PET images (9-123') of [11C]CIMBI-36]

956

EFFECTS OF ACETAZOLAMIDE CHALLENGE ON CEREBRAL HEMODYNAMICS IN PATIENTS WITH SEVERE CAROTID ARTERY STENOSIS AND HEALTHY CONTROLS

P. Zirak[1], R. Delgado-Mederos[2], J. Martí-Fàbregas[2], L. Dinia[2], T. Durduran[1]

[1]ICFO - The Institute of Photonic Sciences, Castelldefels Barcelona, [2]Neurology, Hospital de la Santa Creu i Sant Pau, Barcelona, Spain

Objectives: We have previously[1] demonstrated and validated the use of combined diffuse optics/Doppler-ultrasonography(TCD) to assess cerebral-vasomotor-reactivity (CVR) in healthy controls in both micro- and macro-vasculature where Acetazolamide (ACZ) was the stimulus. Here we extend the study to patients with severe carotid artery steno-occlusive lesions whose CVR assessment is of prognostic significance due to a higher stroke risk in those who suffer impaired CVR[2]. Although several groups reported the use of near-infrared-spectroscopy (NIRS) together with TCD to assess CVR, we use diffuse-correlation-spectroscopy(DCS) to directly assess relative-cerebral-blood-flow (rCBF) which is superior to the use of NIRS alone[3].

Methods: Intravenous administration of ACZ (1g/10ml Saline) is used as a stimulus to determine CVR. A hybrid diffuse optical ,DCS/NIRS, device followed rCBF (with DCS), oxy-hemoglobin(HbO2) and deoxy-hemoglobin(Hb) concentration changes (with NIRS), in real-time and at the bed-side. Simultaneously, the relative-cerebral-blood-flow-velocity (rCBFV) in the right and left middle-cerebral-artery (MCA) was measured with clinical TCD. The methods are described previously[1]. Ten healthy controls (8 male, 2 female, age (27.5, IQR-26-34) years (median- Interquartile range

(IQR)) and 12 patients (10 male, 2 female, age (65.5, IQR-60-74), 50% symptomatic) with hemodynamically significant carotid artery steno-occlusions (>70%) in right or left internal-carotid-artery (ICA) were recruited. The exclusion criteria was stenosis >50% contralateral to the side with ICA steno-occlusive lesion.

Results: In healthy subjects, there was no significant difference between right and left hemispheres. Therefore, the right and left hemispheres were averaged. In patients, the affected side is compared to the normal side. Table shows the results. Overall[4], a significant increase in HbO2, rCBF and rCBFV for healthy subjects and affected and normal sides of the patients was observed. The DCS and TCD measures are in agreement for all three groups.

Conclusions: We have demonstrated that the combined NIRS, DCS and TCD technique could assess CVR both in micro- and macro-vascular levels upon ACZ administration. Our observations showed that the micro-vascular CVR measures are in agreement with the macrovascular CVR values in healthy controls and in patients with carotid artery steno-occlusive complications. While we did not find a significant difference for affected and normal sides of the patients, the rCBFV and HbO2 data for the affected sides show a tendency to decrease. Based on these data, power calculation shows that a minimum of 30 patients is needed to get enough statistical power. In the coming 3 months we expect to have >30 patients. Based on these results and other reports[5], we believe that diffuse optical techniques are promising technologies for continuous, real-time and bed-side monitoring

of the CBF changes and provide complimentary information for individualized treatment of the patients with severe cerebrovascular diseases like stroke.

Grant support:Fundació Cellex Barcelona, EC-FP7 and Inst. Salud Carlos III.

parameter	Patient						Healthy		
	affected side			normal side					
	median	IQR	p-value	median	IQR	p-value	median	IQR	p-value
$\Delta HbO_2\ (\mu M)^*$	6	3.7:10.8	<0.001	9.8	5.75:14.1	<0.001	9.5	5:15.9	0.0039
$\Delta Hb\ (\mu M)$	-1	-1.48:0.18	0.1475	-1.25	-2.3:-0.1	0.137	-0.8	-2:0.4	0.131
Δ rCBF$^*_{DCS}$ (%)	27.8	13.1:17.6	<0.001	25.1	12:39.7	0.0029	27	12.9:42.9	0.0019
Δ rCBFV$^*_{TCD}$ (%)	10.3	-2.6:29.3	0.04	23.5	11:27.6	0.0068	34.7	31.3:45.3	0.0078

Median (IQR) and p-values. Superscript, *, implies statistically significant change ($p<0.05$).

[Table]

References:

1. P.Zirak et al Biomedical Optics Express, 1(5):1443-1459,2010.

2. B. Kleiser et al Stroke, 23(2):171,1992.

3. H.W.Schytz et al European Journal of Neurology, 16(4):461-467,2009.

4. G.Settakis et al European Journal of Neurology, 10(6):609-620,2003.

5. T.Durduran et al Reports on Progress in Physics, 73:076701,2010.

957

THE EFFECT OF PHENYLEPHRINE VERSUS EPHEDRINE ON FRONTAL LOBE CEREBRAL OXYGENATION AND MCA FLOW VELOCITY DURING CAROTID ENDARTERECTOMY

C.W.A. Pennekamp[1], R.V. Immink[2], F.L. Moll[1], W.F. Buhre[2], G.J. de Borst[1]

[1]Vacular Surgery, [2]Anaesthesia, University Medical Centre Utrecht, Utrecht, The Netherlands

Objectives: Carotid endarterectomy (CEA) is the recommended treatment for symptomatic high degree stenosis of the internal carotid artery (ICA). ICA obstruction may affect cerebral autoregulation (CA), i.e. the ability to keep cerebral blood flow constant during changes in blood pressure (BP). Therefore, to preserve cerebral perfusion, one of the main objectives is to prohibit intraoperative BP decrease. Different short-acting agents such as phenylephrine, an α-agonist, or ephedrine, a combined α- and β-agonist, can be used to correct hypotension. In healthy subjects with intact CA, cerebral tissue oxygenation is decreased during phenylephrine administration and is preserved with ephedrine use.[1,2] In our centre, we monitor frontal lobe cerebral tissue oxygenation (rSO_2) and middle cerebral artery blood flow velocity (V_{MCA}) in patients undergoing CEA. In this study we describe the effect of phenylephrine- and ephedrine induced changes in BP on rSO_2 and V_{MCA} during CEA.

Methods: In 19 patients undergoing CEA: continuous radial mean arterial BP (MAP), Transcranial Doppler (TCD) derived V_{MCA} and frontal lobe oxygenation (rSO_2,) measured using Near Infra Red Spectroscopy (NIRS) were monitored .To correct hypotension, in 10 patients ephedrine was used and in 9 phenylephrine. For statistical analysis linear regression analysis was performed.

Results: Ephedrine increased MAP 41±13 mmHg and phenylephrine 18±9 mmHg (mean±SD). rSO_2 Increased 5±2% when ephedrine was used but declined 3±2% during phenylephrine administration. The V_{MCA} increase was larger during ephedrine than during phenylephrine; 11±10 versus 2±3 $cm \cdot s^{-1}$.

Compared to baseline, the absolute change in rSO_2 were positively related to the change in MAP ephedrine (0.046% per mmHg, 95% CI 0.034-0.059). However, for a phenylephrine induced increase in MAP an inversely related change in rSO_2 compared to MAP was seen (-0.045% per mmHg (95% CI 0.079- 0.11). Changes in V_{MCA} were positively related to changes in MAP for both the ephedrine and phenylephrine group (0.035 $cm \cdot s^{-1}$ per mmHg, 95% C.I. 0.130-0.270 and 0.080 $cm \cdot s^{-1}$ per mmHg, 95% C.I. 0.043- 0.117, respectively).

Conclusions: Phenylephrine and ephedrine both increase blood pressure in patients undergoing carotid endarterectomy. Phenylephrine and ephedrine both lead to increase in V_{MCA}. However, phenylephrine results in frontal lobe rSO_2 decrease, while ephedrine leads to rSO_2 increase.

References:

(1) Nissen P, Brassard P, Jorgensen TB, Secher NH. Phenylephrine but not ephedrine reduces frontal lobe oxygenation following anesthesia-induced hypotension. Neurocrit Care 2010 Feb;12(1):17-23.

(2) Lucas SJ, Tzeng YC, Galvin SD, Thomas KN, Ogoh S, Ainslie PN. Influence of changes in blood pressure on cerebral perfusion and oxygenation. Hypertension 2010 Mar;55(3):698-705.

958

WHAT IS A NORMAL PET 18-FDG BRAIN IMAGE? A CORRELATIVE STUDY WITH AGE AND SEX

A. Anjum[1], P. Bertrand[1], P. Payoux[2], P. Celsis[2], K. Boulanouar[2]

[1]Unit 825, INSERM U825; UPS, [2]INSERM U825, INSERM; UPS; CHU Purpan, Toulouse, France

Objectives: When clinicians are presented with PET-FDG images to decide either these images are normal or not, they need normal reference images to compare with. There is no single answer to that need, since we know that cerebral metabolism depends on age and sex. To better answer the question we thus investigated age and sex related cerebral metabolic changes in healthy subjects using (F-18 FDG).

Materials and methods: 1 156 healthy subjects (86 males, 70 females), aged 59 to 81 years, were included in the present study. Cerebral metabolic images were obtained from ADNI database (http://adni.loni.ucla.edu/). Age and sex related effects and their interaction were assessed through group analysis using SPM8. (http://www.fil.ion.ucl.ac.uk/spm/software/spm8/).

Results: Age-associated changes of FDG uptake in females were found in right temporal lobe, right precuneus and right inferior parietal lobe. In males , significant chages were observed in right Lingual Gyrus, right middle frontal Gyrus, left posterior cingulate, right parietal lobe, left precuneus and right insula. Males show higher age associated metabolic changes than females. Gender-related changes with normal aging in females were observed in the left supramarginal gyrus , the right lingual gyrus ,right superior temporal gyrus, and left Precentral gyrus , whereas in males changes were restricted to the right frontal lobe and right Precentral gyrus.

The figure below shows the mean images obtained in male subjects from two different age groups, showing noticeable changes in cerebral metabolism.

Conclusion: When interpreting PET-FDG images, the clinician should be aware that brain metabolism is age and sex dependent. Our study evidenced the localization of the main differences. For some regions, our results are consistent with previous studies (Kim IJ et al, 2009 and Fujimoto T, 2008) but we also observed significant changes in other regions than those previously reportedThe images showed in fig 1 are an example of images which can be used as a reference for normal subjects and give an idea for the cerebral metabolic changes in two different age groups.

Bibliography:

1. Kim IJ et al, Acta Radiol : 50 (2009)1169-1174

2. Fujimoto T et al, Psychiatry Research: Neuroimaging 164 (2008) 58- 72

3. Kawachi T et al, Journal of the Neurological sciences: 199 (2002) 79-83 **Acknowledgments:** We are really thankful to Dr Michel Weiner and all ADNI (Alzheimer's disease Neuroimaging Initiative) team for providing us the access to their data collection and making this research work possible.

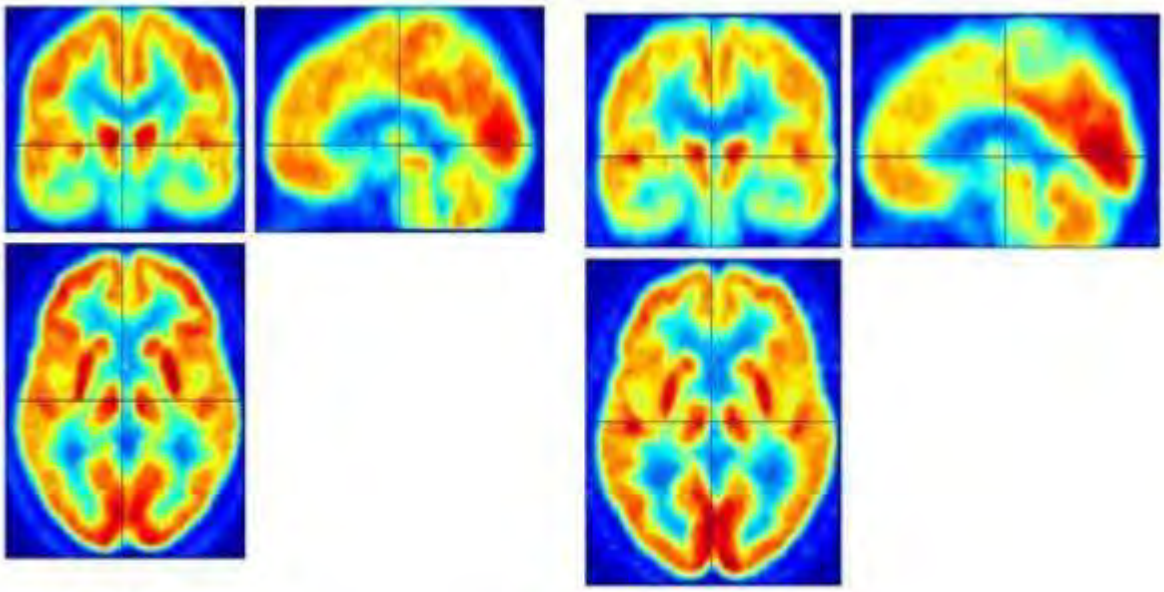

Fig "a "

Fig "b"

Fig.a Mean image of male subjects in the group aged 59 to 70
Fig.b Mean image of male subjects in the group aged 75 to 81.

[example of reference images]

959

BRAIN PERFUSION (ASL-MRI) AND GLUCOSE METABOLISM (FDG-PET): PATTERNS IN PARKINSON'S DISEASE

L.K. Teune[1], M.F. Masman[1], R.J. Renken[2], B.M. de Jong[1], A.T.M. Willemsen[3], M.J.P. van Osch[4], R.A. Dierckx[3], K.L. Leenders[1]

[1]Neurology, University Medical Center Groningen, [2]BCN Neuro Imaging Center, University of Groningen, [3]Nuclear Medicine and Molecular Imaging, University Medical Center Groningen, [4]Department of Radiology, Leiden University Medical Centre, Groningen, The Netherlands

Objectives: Specific regional changes in brain metabolism has been demonstrated previously using FDG-PET imaging in Parkinson's Disease (PD).(1)

In a normal brain the spatial distribution of resting cerebral blood flow and cerebral metabolic rate of glucose are closely related. A relatively new MR technique, Arterial Spin Labeling (ASL), is used to measure brain perfusion. It produces perfusion weighted images in a noninvasive way by using the signal of magnetically labeled blood.(2) In this study we wanted to investigate whether ASL MR imaging is able to detect areas of changed perfusion in PD compared to healthy controls and if these patterns are similar to changes in brain metabolism.

Methods: 14 PD patients and 17 age-matched healthy controls underwent pseudo-continuous arterial spin labeling (pCASL) on a 3T MRI scanner (8 channel head coil, Philips Intera) and FDG-PET imaging on a high resolution PET camera (Biograph, mCT, Siemens). These sequences were scanned as part of a larger study. FDG-PET images were spatially normalized onto the dimensions of a PET template in MNI space and smoothed with an 8 mm FWHM kernel. The 30 ASL time frames of labeled and control images were realigned separately (motion correction), and subsequently coregistered for each subject. Next, frames were smoothed (FWHM = 8mm) and filtered against a time course selected for WM and CSF. Thereafter, control images were subtracted from labeled images and a mean ASL image was calculated and normalized to MNI space using an EPI template. The FDG-PET and mean ASL images were proportionally scaled to the cerebral global mean and compared using Matlab 7.10 and Statistical Parametric Mapping (SPM8).

Results: Decreased metabolic activity in PD patients, compared to controls, was found in postparietal, premotor and prefrontal cortices and primary visual and visual association areas. Hypoperfusion was seen in the same areas although less widespread. Relatively increased metabolic activity was found in pallidothalamic, cerebellar and pontine areas. Relatively increased perfusion was seen predominantly in the cerebellum.

Conclusions: Arterial spin labeling MR imaging was able to detect regional differences of brain perfusion in PD patients in a generally similar pattern to that found with FDG-PET imaging. Our findings support the data on spatial covariance patterns expressed in CASL and FDG-PET in PD patients reported by Ma et al.(3) Therefore, ASL MR imaging is a promising technique, which can be used to detect regional differences of brain perfusion in PD and may thus be helpful to assist in the differential diagnosis of PD.

References:

(1) Teune LK, Bartels AL, de Jong BM, Willemsen AT, Eshuis SA, de Vries JJ, et al. Typical

cerebral metabolic patterns in neurodegenerative brain diseases. Mov Disord 2010 Oct 30;25(14):2395-404.

(2) van Osch MJ, Teeuwisse WM, van Walderveen MA, Hendrikse J, Kies DA, van Buchem MA. Can arterial spin labeling detect white matter perfusion signal? Magn Reson Med 2009 Jul;62(1):165-73.

(3) Ma Y, Huang C, Dyke JP, Pan H, Alsop D, Feigin A, et al. Parkinson´s disease spatial covariance pattern: noninvasive quantification with perfusion MRI. J Cereb Blood Flow Metab 2010 Mar;30(3):505-9.

960

BEHAVIOURAL DEFICIT AFTER MIDDLE CEREBRAL ARTERY OCCLUSION IN THE RAT - A LONGITUDINAL STUDY

S.S.J. Rewell[1,2], T.K. Sidon[1,2], M.J. Porritt[1,2], D.W. Howells[2]

[1]Department of Medicine, University of Medicine, [2]Florey Neuroscience Institutes, Heidelberg, VIC, Australia

Objective: Neuroprotection for stroke patients has to date failed to translate from promising animal studies into a positive clinical trial. One explanation for this may be the discrepancy between the endpoints in animal studies (early after stroke onset - most commonly 24 hours) and clinical studies (3-6 months). Additionally, the outcomes measured differ, in that infarct volume has been the focus of many experimental studies whilst the primary assessment in clinical trials is neurological deficit. Behavioural outcome measures at later timepoints after experimental stroke may provide a key to translating neuroprotection from animals to the clinic. The purpose of this study was to examine the evolution of ischemic damage over time with both behavioural and histological outcomes. We propose that behavioural tests that are simple and quantitative will show long term deficits in stroke rats. This will provide a tool to investigate recovery in animals post stroke.

Methods: Using our optimised model of rat Middle Cerebral Artery thread occlusion (MCAo), we aimed to evaluate the usefulness of behavioural tests in detecting long term deficits out to 24 weeks post stroke. 105 male Spontaneously Hypertensive Rats were randomly allocated to one of nine groups. Stroke animals underwent 90 minute transient MCAo while the sham group underwent identical surgery without thread insertion. The surgery was followed by a range of recovery times: 24 hours, 3, 7, 14, 21, 28 days, 12 and 24 weeks (n³11 per group). Neurological deficit was assessed at each time point (and additionally at 8, 16 and 20 weeks) using three behavioural tests: basic behavioural deficit (assessment of reflex and mobility); a modified sunflower seed task (fine motor skill) and an adhesive sticky tape removal test (sensory neglect and motor skill).

Results: Stroke animals showed an average laser Doppler drop of 70.6±14.6% at MCAo. Macroscopic cortical infarct (or cavity formation) was observed in 91% of stroke animals. Basic behavioural deficit resolved within 14 days in most animals. Of its components, forelimb flexion was affected for the longest duration. A simplified analysis of the sunflower seed task, which involved counting untouched seeds and the number of broken seed pieces, did not show differences between stroke and sham animals beyond 14 days. The sticky tape test highlighted continual neglect of the contralateral forepaw both in the acute period and for the 24 weeks following stroke. There was also a delay in time to remove both left and right tape in the acute stroke period. This implies that there may be contralateral consequences of the ischemic event.

Conclusion: Initial examination of behaviour over time identified the sticky tape test as the most sensitive in demonstrating sustained differences between stroke and sham animals. The Basic Behavioural Test is useful for identifying animals that have ischemic damage in the early time period after MCAo. Alone it is not sensitive enough to show long term deficits. Further analysis of behavioural change over time, together with histological examination will provide insights into the development of damage and process of behavioural recovery.

961

STROKE PENUMBRA DEFINED BY AN MRI-BASED OXYGEN CHALLENGE TECHNIQUE: VALIDATION USING A FOCAL ISCHAEMIA MODEL WITH REPERFUSION

C. Robertson[1], C. Mccabe[1], L. Gallagher[1], M.R. Lopez-Gonzalez[2], W.M. Holmes[1], B. Condon[3], K.W. Muir[1,3], C. Santosh[3], I.M. Macrae[1]

[1]Glasgow Experimental MRI Centre (GEMRIC), Institute of Neuroscience and Psychology, [2]Department of Clinical Physics, SINAPSE Collaboration, University of Glasgow, [3]Institute of Neurological Sciences, Southern General Hospital, Glasgow, UK

Diffusion- and perfusion-weighted MRI (DWI/PWI mismatch) is used to identify the ischaemic penumbra (potentially salvageable tissue) following stroke. However this indirect technique has not been fully validated and provides no information on metabolic status or oxygen-extraction capacity of the tissue. We have developed a novel MRI technique combining T_2*-weighted imaging with normobaric hyperoxia (Oxygen Challenge (OC)) as a metabolic biotracer, allowing alternative penumbral identification based on oxygen-extraction fraction and $CMRO_2$. Penumbra displays a greater T_2* signal change during OC than surrounding tissue. Since timely CBF restoration should salvage penumbra, T_2*OC was tested by examining the consequences of reperfusion on T_2*OC-defined penumbra.

Male Sprague Dawley rats (n=8) were anaesthetised, ventilated (air) and the middle cerebral artery (MCA) occluded by an intraluminal filament. Multi-slice MR imaging of MCA territory was performed pre- and post-reperfusion, induced by filament withdrawal 109±20min after filament insertion. T_2*-weighted MRI was run during OC (4min air then 6min 100% oxygen inhalation), with maps of T_2*% signal change generated. These T_2* maps were thresholded (set at mean plus 2 standard deviations) to define penumbral region (Figure). Apparent diffusion coefficient (ADC) maps (from diffusion-weighted images) displayed ischaemic injury and CBF maps (from continuous arterial-spin labelling) revealed perfusion deficit. Final infarct was assessed at day 7 (T_2). MRI parameters were analysed in regions of interest (ROIs): ischaemic core, caudate nucleus and penumbra (from thresholded ADC and T_2*OC maps, respectively), diffusion-perfusion (DWI/PWI) mismatch and control contralateral cortex and caudate nucleus.

Mean time to commence OC was 78±15min post-MCAO for ischaemia scans and 180±31min for the reperfusion scans. OC resulted in a 3.4% increase in T_2* signal in contralateral ROIs which was unaffected by reperfusion. In OC-defined penumbra, a T_2* signal increase of 8.9±3.6% during ischaemia normalised to 3.45±1.1% ($p< 0.01$) following reperfusion. In ischaemic core, the negligible T_2* signal change during OC was unchanged following reperfusion. There were no significant T_2*% signal changes from ischaemia to reperfusion in any other ROI. Penumbral blood flow increased significantly from 41.94±26 to 116.5±44mL/100g/min ($p< 0.001$) on reperfusion, whereas equivalent contralateral cortex CBF did not change significantly (162±39 to 134±37mL/100g/min). Upon reperfusion, mean CBF in ischaemic core increased from 4.3±6.7 to 32±42 mL/100g/min, but remained significantly reduced compared to the equivalent contralateral ROI ($p< 0.001$). During ischaemia, ADC values in OC-defined penumbra, ischaemic core and DWI/PWI mismatch were significantly reduced compared to the equivalent contralateral ROIs ($p< 0.001$), remaining significantly reduced following reperfusion ($p< 0.05$, $p< 0.01$ and $p< 0.001$, respectively). At day 7, T_2*% signal change in OC-defined penumbra (1.69±0.6%) was not significantly different from equivalent contralateral cortex (1.72±0.6%). Co-registration of the OC-defined penumbra (derived from the acute ischaemia scans) onto day 7 T_2 scans revealed that penumbra was not

incorporated into the final infarct in any animal, providing evidence of penumbral salvage by reperfusion.

Therefore, tissue identified as penumbra using the T_2*OC technique was capable of recovery following blood flow restoration, providing validation of the utility of the technique in acute stroke management.

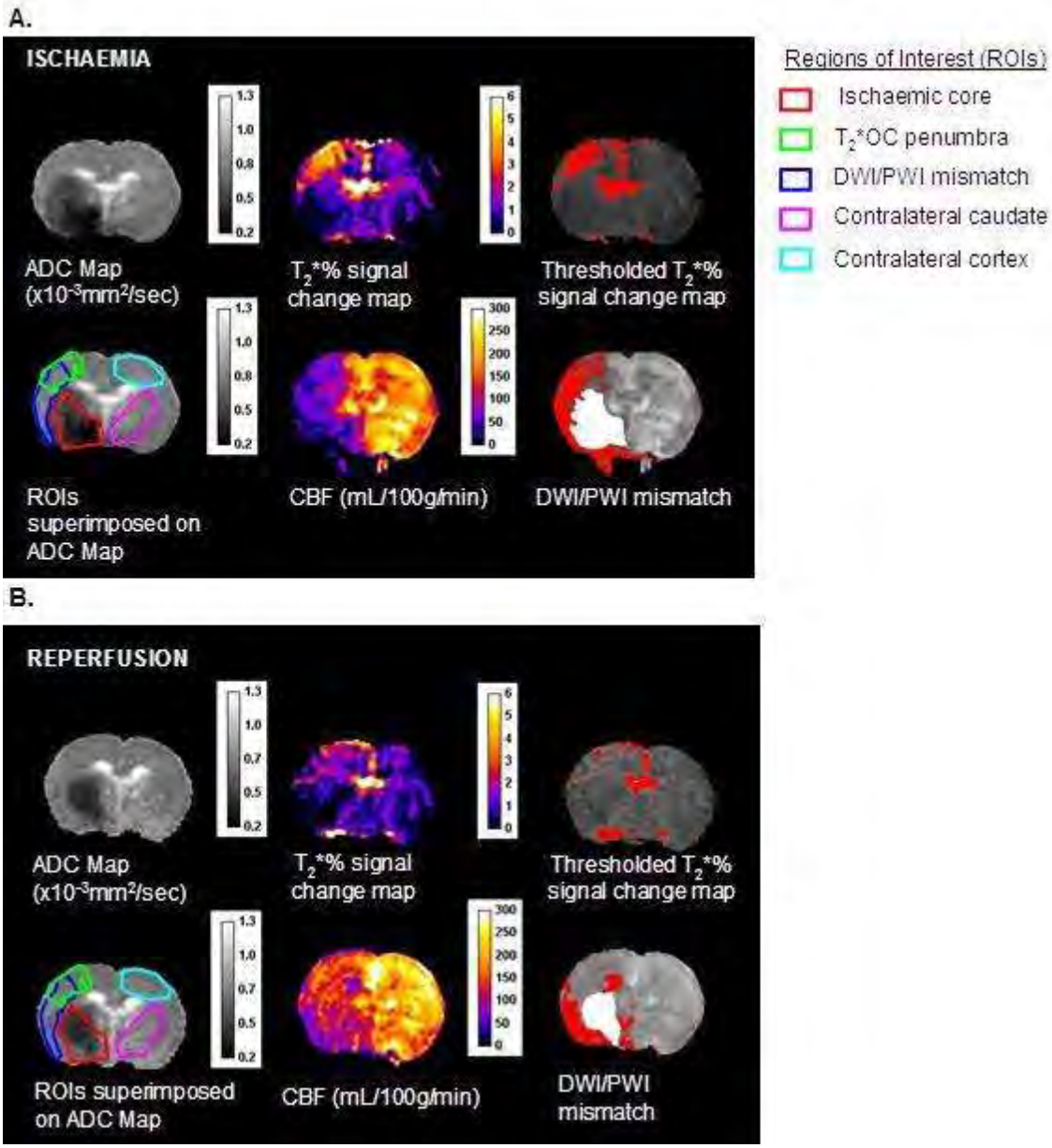

[Ischaemia (A) & Post-Reperfusion (B) Scans]

962

QUANTITATIVE EVALUATION OF NEUROPROTECTIVE EFFECTS ON BRAIN ISCHEMIA AFFORDED BY VOLATILE ANESTHETICS; ISOFLURANE, SEVOFLURANE AND HALOTHANE

M. Kobayashi, Y. Takeda, H. Taninishi, K. Shiraishi, T. Danura, K. Morita

Okayama University Hospital, Okayama, Japan

Introduction: We evaluated the effects of three volatile anesthetics on ischemic neuronal injury and ischemic depolarization in same anesthetic strength standardized with minimum alveolar concentration (MAC). With the use of probit curves, we determined the ischemic time necessary for causing 50% neuronal damage (P_{50} of ischemic time) and the duration of ischemic depolarization necessary for causing 50% neuronal damage (P_{50} of duration of ischemic depolarization). And we quantitatively compared the neuroprotective effects of halothane, isoflurane and sevoflurane on brain ischemia by P_{50}.

Methods: Forty-five male gerbils were used. Animals were randomly assigned to one of three groups. In the halothane group (Halo: n=15), halothane was maintained at 1% (1.33MAC). In the isoflurane group (Iso: n=15), isoflurane was maintained at 1.5% (1.33MAC). In the sevoflurane group (Sevo: n=15), sevoflurane was maintained at 2.3% (1.33MAC). Brain ischemia was initiated by occlusion of bilateral common carotid arteries for a pre-determined duration (3, 5 or 7 min) and DC-potentials in bilateral CA1 regions were measured. Histological evaluation of the CA1 region was performed 5 days after the brain ischemia.

Results: Percentage of damaged neurons in the hippocampus CA1 region after 7 min ischemia are 94±7%, 65±21% ($p< 0.01$ vs. Halo) and 79±30% in Halo, Iso and Sevo, respectively. (Figure 1) Onset time of ischemic depolarization was significantly prolonged both in Iso (2.0±0.6 min; $p< 0.05$) and Sevo (1.9±0.4 min; $p< 0.05$) compared with that in Halo (1.4±0.3 min). But there is no significant difference between the three groups in the duration of ischemic depolarization. P_{50} of ischemic time in Halo, Iso and Sevo was estimated to be 5.2 min, 6.3 min and 5.7 min, respectively. P_{50} of duration of ischemic depolarization in Halo, Iso and Sevo was estimated to be 7.0 min, 9.2 min and 7.5 min, respectively.

Conclusion: Isoflurane is the most neuroprotective volatile anesthetic agent in same anesthetic strength standardized with MAC.

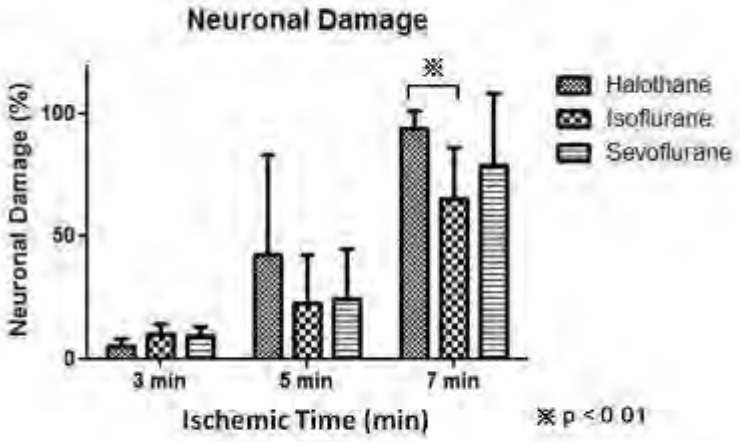

Figure 1

[Figure 1]

963

CEREBRAL BLOOD CIRCULATION IN EXPERIMENTAL CAROTID-JUGULAR FISTULA

V. Musienko

Department of Pathophysiology, Lugansk State Medical University, Lugansk, Ukraine

Objectives: The disturbances of the cerebral blood circulation, which complicate the clinical course of the extracranial arteriovenous fistulas and aneurysms, require the detailed study because they are the etio-pathogenic base of the brain damage at this pathology.

Methods: The aim of the research was to study the cerebral circulatory disorders in experimental carotid-jugular fistula that was modelled on 40 dogs. Physiological and morphological methods were used. The experiments were conform to internationally accepted ethical standards in the care and use of animals.

Results: The study shows the complex character of the cerebral circulatory disorders at carotid-jugular fistula. They were stipulated by relative hypovolemia due arteriovenous blood shunting, decreased blood inflow to the brain by affected arteria and impaired venous outflow from the skull cavity by affected vein and the veins engaged in drainage of the shunting blood. Morphological changes of the brain venous system within acute period of the arteriovenous fistula were characteristic for venous plethora. Reconstruction of the arterial system was directed on improvement of the blood supply of the brain hemisphere on the side of defeat. Total expansion of the cerebral microcirculatory bed, a thickening of the capillary basal membrane and its damage by the swollen pericyte sprout, and the ultrastructural changes of the capillary endotheliocytes were found. The hydropsic transformation of neurocytes accompanied by fragmentation of the cytoplasm organelles, especially mitochondrion, a widening of endoplasmatic cisterns, an increasing of vacuoles number and reduction of ribosome quantity, the peripheral translocation of both diffuse and condensed nuclear chromatin, an enlargement of nuclear pores and perinuclear space were discovered. Increase of both the intracranial pressure and intracranial venous pressure was defined. The level of common water of the cerebral tissue was increased that supports development of the brain oedema-swelling. Morphological rebuilding of the vessels resulted in forming vascular system of the arteriovenous fistula and arterial and venous collateral ways of the blood circulation. Development of the vascular system of the arteriovenous fistula was expansive in dynamics because the system involved new and new vessels including the cerebral ones in the arteriovenous blood shunting that was the morphologic base of “robbery” syndrome. Heart overload by volume was accompanied by disorder of the heart electrical activity and development of cardiovascular insufficiency. Increased disproportion of the arterial inflow to the brain and drain possibilities of the ways of collateral venous outflow formed predispositions for relative arterial stenosis syndrome. Transformation of the cerebral microcirculatory bed formed the ways for intracerebral arteriovenous blood shunting, pathological acceleration ("centralizations") of cerebral blood flow and hypoxic damage of the brain.

Conclusion: Complex and progressive character of the disturbances of the cerebral blood circulation requires radical surgical treatment of the extracranial arteriovenous fistulas and aneurysms.

964

EVALUATION OF HYPOXIC TISSUE DYNAMICS WITH ^{18}F-FMISO PET IN A RAT MODEL OF PERMANENT CEREBRAL ISCHEMIA

S. Rojas Codina[1], J.R. Herance[1], S. Abad[1], X. Jiménez[1], D. Pareto[1,2], A. Ruíz[1], È. Torrent[1], F.P. Figueiras[1], F. Popota[1], F.J. Fernández-Soriano[1], A.M. Planas[3], J.D. Gispert[1,2]

[1]Institut d´Alta Tecnologia-PRBB, CRC Corporació Sanitaria, Barcelona, [2]CIBER en Bioingeniería, Biomateriales y Nanomedicina (CIBER-BBN)., Zaragoza, [3]Department of Brain Ischemia and Neurodegeneration, Institut d'Investigacions Biomèdiques de Barcelona (IIBB)-Consejo Superior de Investigaciones Científicas (CSIC), Institut d'Investigacions Biomèdiques August Pi i Sunyer (IDIBAPS), Barcelona, Spain

Objectives: 18F-FMISO is a nitrimidazole derivate that has been proposed as a PET radiotracer to detect the hypoxic tissue in vivo. This compound accumulates in hypoxic but viable tissue and may be a good candidate for evaluating the ischemic penumbra.Our objective in this work was to characterize in vivo the uptake pattern of ^{18}F-FMISO in rats subjected to permanent cerebral ischemia and to determine the time course of radiotracer accumulation. We also evaluated the correlation between histological alterations and ^{18}F-FMISO. To our knowledge, this is the first PET study in rats with permanent cerebral ischemia using ^{18}F-FMISO to characterize the binding of the radiotracer up to 24 hours after ischemia.

Methods: Rats (n=14) were subjected to permanent ischemia by intraluminal occlusion of the middle cerebral artery in order to asses by PET the kinetics of ^{18}F-FMISO uptake. Each rat received an intravenous bolus injection of ^{18}F-FMISO 999±146 µCi (mean±SD), and then was returned to their cages for 120 min. PET data was collected for 30 minutes in an animal dedicated camera (microPET R4; Concorde, Siemens, Knoxville, TN, USA). Radiotracer was administered immediately after the surgery (n=6), after 4 (n=4) or 8 hours (n=4) and animals PET scans were performed at 2, 6 and 10 hours post occlusion. To follow up the evolution of ^{18}F-FMISO uptake a second PET study was performed after 24 hours from the surgery in four animals. After the scan, animals were sacrificed, their brains removed and processed for histological evaluation with 2,3,5-triphenyltetrazolium chloride (TTC) and Nissl staining.

Results: The uptake of ^{18}F-FMISO was quite evident in the area of the occluded middle cerebral artery. Animals injected immediately after occlusion or 4 hours after the surgery present extensive and similar uptake, which was detected in the infarcted area up to 8 hours after occlusion but was no longer detected at 24 hours. This time point was coincidental with the pan necrosis of the tissue. The comparison of these histological findings with the uptake of ^{18}F-FMISO strongly suggests that radiotracer uptake occurs in viable neurons.

Conclusions: Our study suggests that survival of some hypoxic tissue in this animal model of stroke may be extended through a relatively long period (up to 8h). This result supports the view that a therapeutic window longer that 3-4 hours may exist under certain conditions of brain ischemia. We therefore propose PET with ^{18}F-FMISO as a useful tool to explore the penumbra in ischemic stroke.

References:

Varghese et al. Cancer Res. 1980;40:2165-2169

Markus et al.. Neuroimage. 2002;16:425-433

Markus et al. Stroke. 2003;34:2646-2652

Markus et al. Brain. 2004;127:1427-1436

Read et al. Ann Neurol. 2000;48:228-235

Read et al. Neurology. 1998;51:1617-1621

Saita et al. Stroke. 2004;35:975-980

Spratt et al. Stroke. 2006;37:1862-1867

Spratt et al. Brain Res. 2009;1288:135-142

Takasawa et al. J Cereb Blood Flow Metab. 2007;27:679-689

967

STUDYING POTENTIALLY SALVAGEABLE PENUMBRA AND ITS LIFESPAN IN THE STROKE-PRONE SPONTANEOUSLY HYPERTENSIVE RAT (SHRSP): A MRI PERFUSION-DIFFUSION MISMATCH STUDY

E. Reid[1], L. Gallagher[1], J.M. Mullin[1], W.M. Holmes[1], M.R. Lopez-Gonzalez[2], D. Graham[3], A.F. Dominiczak[3], I.M. Macrae[1], C. McCabe[1]

[1]Glasgow Experimental MRI Centre (GEMRIC), Institute of Neuroscience & Psychology, [2]Department of Clinical Physics, SINAPSE Collaboration, [3]BHF Glasgow Cardiovascular Research Centre, Institute of Cardiovascular & Medical Sciences, University of Glasgow, Glasgow, UK

Objectives: SHRSPs represent a clinically relevant model of cerebrovascular disease characterised by progressive development of severe hypertension, a major stroke risk factor. SHRSP were exposed to experimental stroke to investigate the influence of hypertension on potentially salvageable penumbra and its lifespan. Serial perfusion-diffusion (PWI/DWI) mismatch MRI scans were undertaken to assess penumbra. Diffusion-weighted imaging reveals injured tissue and perfusion-weighted imaging identifies the perfusion deficit, the mismatch between the two providing an approximation of penumbra. In addition, since there is no consensus on diffusion or perfusion threshold values used to define the diffusion abnormality and perfusion deficit, these were calculated for each strain.Our aims were to apply these threshold values to assess and compare penumbra size and lifespan in SHRSP compared to the normotensive control strain, Wistar-Kyoto (WKY). We postulated that penumbra size and lifespan would be compromised in SHRSP.

Methods: Permanent middle cerebral artery occlusion (MCAO) was induced in age-matched WKY (n=8) and SHRSP (n=7) by intraluminal filament. MR diffusion- (DWI) and perfusion-weighted (PWI) images were obtained hourly for 4hrs post-stroke. Final infarct was determined at 24hrs by T_2-weighted imaging. Strain-specific cerebral blood flow (CBF) and apparent diffusion coefficient (ADC) thresholds were calculated from final infarct and applied to quantitative ADC and CBF maps to assess the evolution of ischaemic injury, perfusion deficit and mismatch volume (from spatial assessment of ADC lesions superimposed onto perfusion deficits on each coronal slice). Data are presented as mean±SD in text and figure.

Results: Infarct volume was significantly larger in SHRSP (405±50mm^3) than WKY (322±43mm^3, P=0.004). ADC and CBF thresholds were 0.59±0.03 x 10^{-3} mm^2/sec and 39±10 mL/100g/min respectively, for SHRSP and 0.62±0.03 x 10^{-3} mm^2/sec and 26±6 mL/100g/min for WKY. ADC-derived injury increased over time and was greater in SHRSP from 30min (353±83mm^3, WKY; 213±80mm^3, P< 0.01) out to 4hrs post-stroke. SHRSP perfusion deficit was significantly larger than in WKY at all time points. Perfusion deficit significantly increased between 1-4hrs in both strains (SHRSP; 34±24mm^3, WKY; 56±22mm^3, P< 0.01). Mismatch volume was larger in WKY at 1hr (28±17mm^3 vs 13±12mm^3 in SHRSP, P=0.07) and comparable between strains thereafter (Figure, P>0.05). In WKY, mismatch volume decreased from 28±17mm^3 at 1hr post-MCAO to 20±11mm^3 at 4hrs, (P>0.05) and in SHRSP, mismatch volume decreased from 13±12mm^3 at 1hr to 11±11mm^3 at 4hrs, (P>0.05).

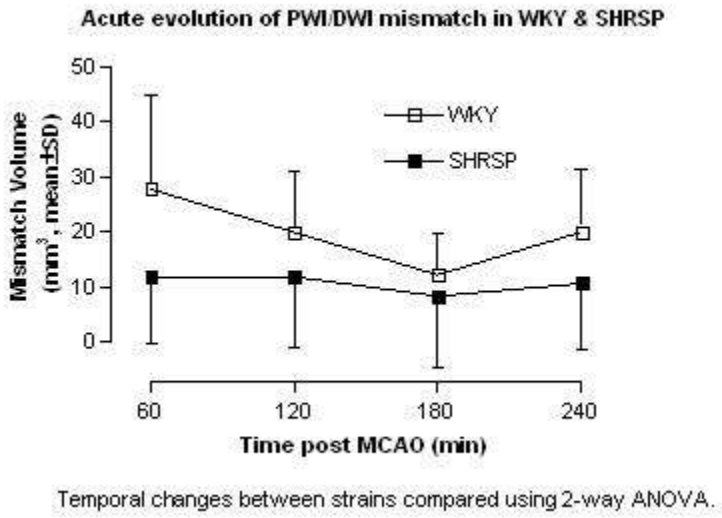

Temporal changes between strains compared using 2-way ANOVA.

[Acute evolution of PWI/DWI Mismatch in WKY & SHRSP]

Conclusions: Penumbra volumes, assessed by PWI/DWI mismatch, were small in both strains by 1hr post-stroke with a trend towards less penumbra and significantly more ADC-defined injury in SHRSP. The apparent persistence of penumbra beyond 1hr in both strains can be attributed to the temporal increase in perfusion deficit alongside ADC-defined injury, which suggests a failure of collateral flow.

968

PLASMINOGEN ACTIVATOR INHIBITOR-1 PROTECTS AGAINST INFECTION-SENSITIED AND PURE HYPOXIC-ISCHEMIC BRAIN INJURY IN NEWBRONS BY DISTINCT MECHANISMS

C.-Y. Kuan[1], D. Yang[2], N. Nemkul[2], D. Lindquist[2]

[1]Pediatrics, Division of Neurology, [2]Cincinnati Children;s Hospital Medical Center, Cincinnati, OH, USA

Objectives: Intrauterine infection and fetal inflammatory responses either directly trigger or greatly increase brain vulnerability to secondary insults such as hypoxia-ischemia (HI). Evidence also indicates that infection may alter the pathogenic mechanisms of neonatal HI brain injury, but details of this process are unclear. We recently reported that therapeutic administration of plasminogen activator inhibitor-1 (PAI-1) markedly protects against HI brain injury in rodent pups (Yang et al., 2009). The objectives of the present study are to clarify (a) the efficacy of PAI-1 treatment in infection-sensitized HI brain injury; (b) different mechanisms between infection/HI versus pure-HI brain injury in neonates.

Methods: P7 Wistar rat pups were injected with lipopolysaccharide (LPS) at 4 h before the Rice-Vannucci model of neonatal cerebral HI (unilateral carotid-ligation and 90-min hypoxia). After LPS/HI, animals received intracerebroventricle (ICV) injection of PAI-1 or saline as controls. The brain samples were prepared at 4 and 24 hrs post-injury for mechanistic analysis, including NFkB gel-shift assay, tPA and MMP activity, cytokines, and BBB permeability. The extent of brain tissue loss was quantified at 7 d recovery. Some of the animals were housed until 2 months of age for behavioral and diffusion tensor imaging (DTI)-based analysis of WM functions.

Results: We found that the addition of LPS to HI dampened non-vascular tPA activity, but greatly increased the NF-kB signaling activity (Fig. 1A). PAI-1 treatment mitigated LPS/HI-induced NFkB activity and BBB damage (Fig. 1B). PAI-1 significantly reduced brain tissue loss, and the therapeutic window is at least 4 h post-LPS/HI. PAI-1 treated animals showed near-normal motor functions and WM development at 2 months (Fig. 1C).

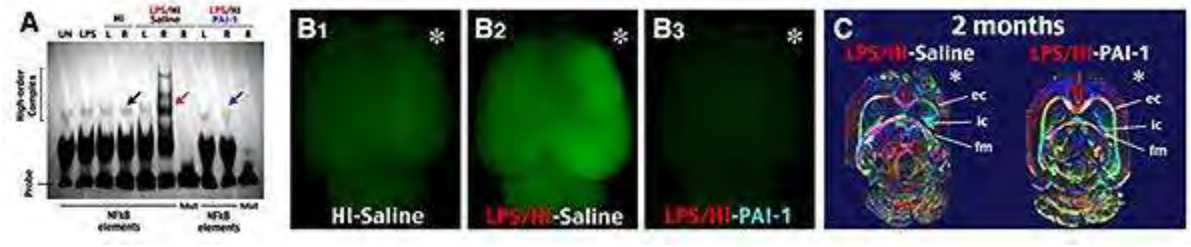

[Figure 1: Efficacy of PAI-1 in LPS/HI injury]

Conclusion: Inflammatory responses modify HI brain injury by up-regulation of NFkB signaling at the expense of non-vascular tPA activity. Yet, PAI-1 treatment markedly opposes both neonatal injuries, suggesting a strong therapeutic potential. Because the anti-infection/HI ability

of PAI-1 is unique among serine protease inhibitors, further study is warranted to determine the domains in PAI-1 for these distinct protective functions.

References:

Yang D, Nemkul N, Shereen A, Jone A, Dunn RS, Lawrence DA, Lindquist D, Kuan CY (2009) Therapeutic administration of plasminogen activator inhibitor-1 prevents hypoxic-ischemic brain injury in newborns. J Neurosci 29:8669-8674.

969

DYNAMIC CHANGES OF CROSS SECTION IN ATHEROSCLEROTIC STENOSIS IN MIDDLE CEREBRAL ARTERY DETECTED BY 3.0T MRI

A. Mizuma[1], T. Ishikawa[1], S. Takizawa[1], Y. Okumura[2], A. Horie[2], T. Yanagimachi[2], S. Takagi[1]

[1]Neurology, [2]Radiology, Tokai University School of Medicine, Isehara, Japan

Purpose: Atherosclerotic stenosis in middle cerebral artery (MCA) is one of the cause of ischemic stroke, but the studies evaluating its stenosis are rare except using MRA. The purpose of this study is to assess dynamic changes of cross section in MCA between systolic and diastolic phases in patients with cerebral infarction using 3.0 Tesla MRI.

Subjects and methods: Twelve patients with M1 stenosis in MCA and twelve healthy volunteers were investigated. We measured the cross sections in MCA (proximal and distal parts to stenosis, and just on stenosis) in both systolic and diastolic phases by synchronizing with heart beats, as well as the maximum flow velocity, using cine mode MRI. We also underwent the conventional MRA in them.

Results: Difference in cross sections between systolic and diastolic phases just on M1 stenosis was significantly smaller than in distal part of stenosis in the patients ($P < 0.01$) and in non-stenotic M1 portion in the control group ($P < 0.01$). Difference in blood maximal velocity between systolic and diastolic phases just on M1 stenosis was significantly larger than in the proximal part of MCA stenosis ($P < 0.05$).

Conclusion: We clearly demonstrated dynamic changes of cross section just on stenosis by 3.0 Tesla MRI, suggesting the induction of hemodynamic shear stress. This phenomenon may enhance further atherosclerosis in MCA.

970

MORPHOLOGICAL CHANGES IN BRAIN TISSUE AFTER LOCAL HYPERTHERMIA

M.I. Nebieridze

Cerebral Blood Flow and Metabolism, Life Science Research Centre (former Beritashvili Institute of Physiology), Tbilisi, Georgia

The clinical use of hyperthermia for cancer treatment become actually nowadays. The goal of present study was to obtain some specific data pertaining to sensitivity of cerebral tissue to hyperthermic exposure, because still there is not consensus regarding the tolerance of CNS to the hyperthermic influence.

Methods: Experiments were performed on adult mail Wistar rats weighing 250-300g., anesthetized by Chloral Hydrate. Through the cranial window a local area of cerebral surface was during 60 minutes irrigated by Saline Solution heated up to the temperature 41, 43 or 45^0C. Serial brain frontal sections stained with Azur-Eozin were analyzed under light microscope.

Results: At 41^0C just superficial lesions of the cerebral cortex and a few cases of thrombosed cerebral arterioles have been observed. 43^0C resulted in very severe lesions of cerebral tissue. The layered structure of the cerebral cortex was impaired. 45^0C caused complete destruction of the cortex layered structure.

Conclusion: Our results confirmed very high sensitivity of brain tissue to hyperthermic exposure even at temperature of 41^0C and this finding suggests the need for very quick preventive actions if core body temperature for some reasons is rising above 41^0C. Most significant reasons for extensive damage of nervous tissue under hyperthermic exposure are the formation of micro thrombi and occlusion of cerebral vessels. The role of free radicals also has to be taken into account.

Key words: Hyperthermia, brain tissue, thrombosis.

971

EVIDENCE FOR THE EFFICACY OF STATINS IN THE ANIMAL STROKE MODELS: A META-ANALYSIS

M. Campos[1], L. Garcia-Bonilla[1], D. Giralt[1], D. Salat[2], J. Álvarez-Sabín[2], A. Rosell[1], J. Montaner[1]

[1]Neurovascular Research Laboratory, Research Institute Vall d'Hebron, [2]Neurology Department, Vall d'Hebron Hospital, Barcelona, Spain

Objectives: Statins have been well documented for their protective effects in ischemic stroke(1), independent of their lowering cholesterol properties, and are suggested to be candidate drugs for acute stroke therapy. Here, we used a systematic review and meta-analysis to assess evidence of their beneficial effects in animal models of stroke. In addition, using a rat embolic stroke model, we confirmed the effects of simvastatin on post-stroke outcome in our laboratory.

Methods: One hundred thirteen studies describing statin treatment in animal models of cerebral ischemia were identified from PubMed and manual searching of abstracts of scientific meetings (1998 to 2008) using the search terms of [statin, brain and ischemia]. [statin and stroke] and [statin and cerebral infarction] limited to 'animal species'. A total of 39 works describing procedures of middle cerebral artery occlusion and reporting the effect of statins on infarct size (involving 1118 animals) or neurological outcome (330), were included in the analysis. Data on 10 points study quality (2), both type and dose of statins, time of administration and outcome, measured as infarct volume or functional deficit, were extracted. The number of animals used, mean and SEM (standard error of mean) or SD (standard deviation) of each comparison (statin vs control) were calculated and meta-analysis was performed using weighted mean difference with random effects model. The effect of simvastatin found in the stratified meta-analysis was then compared to our data using a clot embolism model in rat.

Results: The quality of the studies (range scale 0-10) was modest (4, interquartile range, 3-5). Overall, statins reduced infarct volume by 25.5 % [95% confidence interval (CI), 21%-30%, $p< 0.001$] and the reduction was higher when statin administrating was given as pre-treatment (33.8%; 95% CI, 27.7-39.8%, $p< 0.001$) compared with post-treatment (16.2%; 95% CI, 10.8-21.6%, $p< 0.001$). Consistent with this, a considerable improvement in neurological outcome was observed (19%; 95% CI, 9.1%-29%, $p< 0.001$). Moreover, when stratifying the meta-analysis by type of statin, the effect size was significantly higher in animals treated with Simvastatin (38%; 95% CI, 33.2%-43.3%, $p< 0.001$) as compared to those treated with artovastatin (28%; 95% CI, 20.6%-35.4%, $p< 0.03$). Our results using the clot embolism model showed a significant improvement in neurological outcome in rats receiving a single dose of simvastatin administered as post-treatment by 48% (95% CI, 28.6%-64.59%) as compared with vehicle group.

In conclusion, this meta-analysis provides further evidence of the efficacy of statins in stroke treatment, supporting their use as potential neuroprotective drugs for human stroke therapy.

References:

1- Salat D, Ribosa R, Garcia-Bonilla L, Montaner J. Statin use before and after acute ischemic stroke onset improves neurological outcome. Expert Rev Cardiovasc Ther. 2009 Oct; 7 (10):1319-30

2- Macleod MR, O´Collins T, Howells DW, Donnan GA. Pooling of animal experimental data reveals influence of study design and publication bias. Stroke. 2004 May;35(5):1203-1208.

972

EFFECT OF ANESTHESIA ON DEEP BRAIN STIMULATION IN RATS

M.L. Soto-Montenegro[1,2], J. Klein[3], J. Pascau[1,2], L. Günther[4], A. Kupsch[5], C. Winter[3,4], M. Desco[1,6]

[1]Laboratorio de Imagen. Medicina y Cirugía Experimental, [2]CIBER de Salud Mental (CIBERSAM), Hospital General Universitario Gregorio Marañón, Madrid, Spain, [3]Department of Psychiatry and Psychotherapy, Charité Campus Mitte, [4]Department of Psychiatry and Psychotherapy, Technical University Dresden, [5]Department of Neurology, Charité Campus Virchow Klinikum, University Medicine, Berlin, Germany, [6]Departamento de Bioingeniería e Ingeniería Aeroespacial, Universidad Carlos III, Madrid, Spain

Objectives: Deep brain stimulation (DBS) is an approved treatment for neurological or psychiatric disorders (Kuhn et al 2009). In the preclinical use, DBS also serves as a tool to selectively affect neuronal function of brain regions and associated networks in order to depict (patho-)physiological circuitries (Winter et al 2008). FDG-PET functional imaging provides an *in vivo* technique for analyzing consequences of DBS on brain activity-patterns and as such has clinically been applied in various diseases. The aim of this study is to analyze the effect of different type of anesthesia on brain glucose metabolism in rats that have been performed a DBS study.

Methods: A concentric bipolar electrode with connector (platinum-iridium, Nano-biosensors Nazareth, Israel) was implanted unilaterally into the left STN under anesthesia in twelve adult male Wistar rats. PET and CT scans were performed in the 7 and 9 days after surgery. Two groups of animals were studied according to the type of anesthesia while performing the study of DBS: A) isoflurane (N=6) and B) medetomidine and atracurium. 2-deoxy-2-[18F]fluoro-D-glucose (FDG) was intravenously injected and DBS started: day 7 (without stimulacion) and day 9 (with stimulation) during 45 minutes. Stimulation time matches tracer uptake period. DBS was performed in a constant current mode at 130 Hz and 300 μA using an isolated stimulator. Imaging was performed on a small-animal PET-scanner. PET-scans were reconstructed using 2D-OSEM algorithm. All images were spatially registered, smoothed with a 2 mm isotropic Gaussian kernel and masked to remove extracerebral tissues. Voxel values were normalized to the overall brain average, analyzed with Statistical Parametric Mapping software (SPM5).

Results: SPM analysis in group A revealed increased metabolic activity in the brainstem, the hipothalamus, the globus pallidus ipsi- and contralateral as well as in the mediodorsal thalamus and the caudate ipsilateral to the stimulation site. Furthermore, we found decreased FDG-uptake in the entorhinal cortex, visual cortex and inferior colliculus ipsi- and contralateral as well as in the amygdala, and somatosensory cortex and hippocampus contralateral and the ventral pallidum ipsilateral to the stimulation site. In group B, the analysis showed increased and decreased metabolic activity in those regions than group A but with less intensity (lower T value). We did not found decreased FDG-uptake in the visual cortex and inferior colliculus.

Conclusions: The FDG-PET study revealed distinct changes in the naïve rat brain metabolic activity following unilateral STN-DBS affecting to the motor, cognitive and emotional system. The choice of a type of anesthesia may be crucial for the interpretation of results after DBS since the depth of anesthesia could affect to the brain glucose metabolism.

References:

Kuhn J, Gaebel W, Klosterkoetter J, Woopen C. Deep brain stimulation as a new therapeutic approach in therapy-resistant mental disorders: ethical aspects of investigational treatment. Eur Arch Psychiatry Clin Neurosci 2009; 259 (Suppl. 2): 135-141.

Winter C, Mundt A, Jalali R, Joel D, Harnack D, Morgenstern R, et al. High frequency stimulation and temporary inactivation of the subthalamic nucleus reduce quinpirole-induced compulsive checking behavior in rats.. Exp Neurol 2008; 210: 217-228.

973

GENDER-LINKED DIFFERENCES IN RAT HIPPOCAMPUS AFTER TRANSIENT GLOBAL CEREBRAL ISCHEMIA

M. Hugyecz[1], D. Drakulic[1,2], E. Farkas[3], P. Hertelendy[1], J. Toth[1], F. Bari[3]

[1]Department of Physiology, Faculty of Medicine, University of Szeged, Szeged, Hungary, [2]Laboratory of Molecular Biology and Endocrinology, "Vinča" Institute of Nuclear Sciences, University of Belgrade, Belgrade, Serbia, [3]Department of Medical Physics and Informatics, Faculty of Medicine, University of Szeged, Szeged, Hungary

Objectives: Transient global ischemia (TGI) may occur in serious cardiovascular disorders that deprive the brain of oxygen and glucose for a short period of time. Reperfusion injury plays a critical role in the pathophysiology of brain damage most likely mediated by reactive oxygen species (ROS). Impairment of physiological pro- and antioxidant enzyme levels by ROS leads to delayed neuronal death through apoptotic pathways in the hippocampus, the most vulnerable part of the brain to oxidative damage. Although, some fundamental mechanisms have already been elucidated, the obvious sex-specific differences are still unexplored.

Methods: Adult male and female Wistar rats were divided into 3 groups: naive, sham-operated and a group subjected to TGI. TGI was induced by occluding the common carotid arteries and hypovolemic hypotension (~40 mmHg) for 5 or 10 min. One month before this procedures females were bilaterally ovariectomised, while males underwent sham operation. Three days after TGI, all animals were sacrificed and by immunoblotting pro- and antioxidant enzymes, pro- and antiapoptotic molecules as well as connexin protein expression in whole cell extracts were detected.

Results: TGI lasting 5 min in males caused decrease of nNOS and Cx30 enzyme levels, while the expression of MnSOD, Bax, and Bcl-2 were less affected. All males subjected to 10-min TGI died within a day, probably due to body overweight, age and hormone status. In female rats, 5 min TGI did not significantly change the expression of the investigated proteins, but after 10 min, enhanced Bcl-2/Bax protein ratio was obtained.

Conclusions: TGI in male and female hippocampus differently alters protein expression and results in cascade of events leading to a number of vital cellular changes. In this model system in male hippocampus, 5 min TGI evoked alterations in protein expressions whereas 10-min TGI was already a lethal insult. Decreased nNOS level in male hippocampal area may be the result of high degree of cell damage caused by TGI. Lower Cx30 protein level could lead to modulation of intercellular diffusion of necrotic or apoptotic signals and may allow diffusion of ions and substances from healthy to injured cells. In females, 5-min TGI was insufficient to induce changes in expression of investigated molecules, whereas 10-min TGI, due to increase of Bcl-2/Bax protein ratio, most likely triggers intracellular signaling pathways involved in cell survival and regenerative processes. In both gender, TGI did not influence MnSOD expression, indicating that ischemic stress is not directly involved in regulation of expression of this enzyme. Basically, understanding gender differences in ischemic brain injury, as well as revealing critical cell and molecular mechanisms of brain cell death may contribute to the development of more effective therapies for ischemic stroke.

This study was supported by OTKA K81266 & ETT 375-04 to FB

974

OPTOGENETIC APPROACH TO STROKE CELL THERAPY

M. Daadi[1], I. Goshen[2], J. Klausner[1], C. Lee-Messer[2], G. Sun[1], K. Deisseroth[2], G. Steinberg[1]

[1]Neurosurgery, Stanford University, [2]Bioengineering and Psychiatry, Stanford University School of Medicine, Stanford, CA, USA

Objectives: Stroke is one of the leading causes of death and long-term disability in the world. There are no effective treatments targeting the residual anatomical and behavioral deficits resulting from stroke. It is known that after stroke the brain undergoes limited self-repair to compensate for the lost structures. Changes in reorganization or neuroplasticity are thought to underlie the partial spontaneous functional recovery that often occurs over time following stroke. To understand this innate functional repair process, it is necessary to improve our comprehension of the mechanisms mediating stem cell functional recovery in stroke damaged brain tissues. This understanding will help move forward the field of cell transplantation, a promising therapeutic strategy for brain repair. It has been shown that the transplantation of stem cell progeny from multiple sources ameliorates motor deficits after stroke. However, it is currently unknown to what extent the electrical activity of grafted neural stem cell progeny participates in the improvement of motor deficits and whether excitatory phenotypes of the grafted cells are beneficial or deleterious to motor performances.

Methods: We first derived multipotent neural stem cells (NSCs) from human embryonic stem cells. The NSCs were then transduced with lentiviral vectors carrying the channelrodopsin-2 (ChR2) gene fused with enhanced yellow fluorescent protein (ChR2-EYFP) under the EF1alpha promoter. ChR2 is a transmembrane conductance regulator that when expressed by a cell, can generate action potentials in response to blue light stimulation. The ChR2 expression was confirmed in vitro. To test the function of these cells in stroke model, Sprague Dawley rats were subjected to 65 min middle cerebral artery occlusion. One week later, immunosuppressed rats were transplanted with NSCs (2 x 105) into the ischemic boundary zone in the striatum. Animals were biweekly tested for the use of their forelimbs in the cylinder test and for locomotor activity.

Results: After 12 weeks survival time, the animals were perfused and brains processed for histo-pathology and immunocytochemistry. Grafted NSCs, identified with a human-specific nuclear marker survived in the stroke-damaged peri-infarct tissue, expressed the ChR2 transgene and extended neurites into the host parenchyma. Our behavioral analysis demonstrated that light stimulation of animals grafted with the ChR2 optogenetically engineered NSCs increased their forelimb use in comparison to vehicle animals. In addition, animals that received the ChR2 expressing NSCs increased their motor activity and total distance covered during light stimulation relative to vehicle-treated animals subjected to light stimulation.

Conclusions: Our data suggested that excitatory influences of grafted neural stem cells may offer benefit in experimental stroke.

981

[^{11}C]-METHIONINE POSITRON EMISSION TOMOGRAPHY IN PATIENTS WITH MALIGNANT GLIOMAS DEMONSTRATING NON OR VERY SUBTLE CONTRAST-ENHANCMENT

N. Galldiks[1], V. Dunkl[1], **L. Kracht**[2]

[1]Department of Neurology, University Hospital of Cologne, [2]Max-Planck-Institut for Neurological Research, Cologne, Germany

Purpose: Neurooncologists are in practice commonly confronted with ill-defined and ambiguous MRI findings in WHO grade III glioma, especially with noncontrast-enhancing lesions or lesions with minimal abnormalities (e.g., nodular enhancement less than 1 cm^3).

To further investigate this issue we identified a subgroup of patients with histologically proven glioma WHO grade III in which MRI displayed a minimal or even lack of contrast-enhancement. We employed [^{11}C]-methionine Positron-Emission-Tomography (MET) in these patients to assess the metabolically active tumour volume. We hypothesized that a volumetric assessment of MET-PET can be used to detect additional subareas of active tumour volumes, complementary to the information provided by Gd-DTPA enhancement or T2-weighted images alone.

Procedures: Eleven patients with gliomas WHO grade III underwent MET-PET- and MR-imaging (contrast-enhanced T1- and T2-images). To calculate the volumes in cm^3, threshold-based volume-of-interest analyses of the metabolically active tumour (MET-uptake index ≥1.3), contrast-enhancement, and the T2-lesion, respectively, were performed after coregistration of all images.

Results: As defined by study design, MRI showed minimal volumes of Gd-DTPA enhancement less than one cm^3 (in 9 of 12 MRI-/MET-PET-scans), or even complete absence thereof (3/12). In contrast, in all patients metabolically active tumour tissue was depicted by MET-PET with an increased MET uptake index ≥ 1.3. The mean MET-uptake index of tumour-to-contralateral activity was 1.96 ± 0.51. When assessing the volume of active tumour tissue, defined by the increased MET-uptake index ≥ 1.3, the metabolically active tumour volume was larger than the volume of Gd-DTPA enhancement in all patients (20.8 ± 18.8 vs. 0.29 ± 0.25 cm^3; $p < 0.001$, Rank Sum Test). With the exception of one patient, in all patients the volumes of Gd-DTPA enhancement were located within the metabolically active tumour volume .

The mean volume of the T2-lesion on MRI was 30.9 ± 27.7 cm^3 . MET-PET identified smaller tumour volumes than T2-MRI in six patients, with MET positive volumes with an average of 39.6 ± 35.6 % of the T2 volume. In a minority of patients (in 2 of 12 MRI-/MET-PET-scans), the active tumour volume on MET-PET fell entirely within the localization of the T2-lesion volume. In contrast, in the majority of patients MET uptake overlapped with the T2-lesion and, furthermore, reached beyond it (in 10 of 12 MRI-/MET-PET-scans). In these imaging studies, the active tumour volume on MET-PET was often eccentric and partially located outside the volume of the T2-lesion. Up to an extent of 10 % in eight MRI-/MET-PET-scans, parts of the metabolically active tumour were located outside the area of the T2-lesion. In two further MRI-/MET-PET-scans, the extent ranged between 20 - 50 %).

Conclusions: The present data suggest that in patients with glioma WHO grade III with minimal or lack of contrast-enhancement MET-PET delineates metabolically active tumour tissue. These findings support the use of combined PET / MR imaging with radiolabeled amino acids (e.g.,

MET) for the delineating of the true extent of active tumour in the diagnosis and treatment planning of patients with gliomas.

982

DISTRIBUTION OF CD200 AND CD200R IN THE DEVELOPING C57BL/6 MICE BRAIN BEFORE AND AFTER HYPOXIA/ISCHEMIA INJURY

K. Shrivastava, G. Llovera, P. Gonzalez, L. Acarin

Medical Histology, Faculty of Medicine, Department of Cell Biology, Physiology and Immunology, Neuroscience Institute, Universitat Autonoma Barcelona, Bellaterra, Spain

Introduction: CD200, a membrane glycoprotein has been identified as the ligand of a myeloid cell receptor designated as CD200R. There are reports on the significance of CD200/CD200R in inducing immune tolerance and had recently been highlighted to contribute to immune privileged status of the central nervous system. The developing brain exhibits distinct morphological as well as physiological characteristics determining a peculiar response to injury showing an aggravated susceptibility to excitotoxicity and pro-inflammatory cytokines, along with an exacerbated inflammatory response.

Objectives: Hence, the aim of this study is to characterize the expression pattern of CD200-CD200R in the developing mice brain before and after Hypoxia/Ischemia injury by immunofluorescence and western blotting.

Methods: Wild-type C57BL/6 mice postnatal day- 1,3,5,7,10,14,21 and adult were used for developmental studies; while P7 mice were used for H/I injury and samples were collected 3h, 12h, 24h, 48h, 72h & 7 days after hypoxia following unilateral carotid artery occlusion.

Results: CD200 is highly expressed in gray matter regions including cerebral cortex, hippocampus and striatum where immunoreactivity appeared surrounding $NeuN^+$ neurons and along the blood vessels (Tomato $lectin^+$) at all the age groups displaying decrease in intensity with increasing age. CD200 labelling was also observed in the hippocampal fissure along with the meninges at all ages with decreasing intensity from P1 to adult. At P21 and adult, hippocampal CD200 was found as a stronger labelling in the inner commissural-associational zone of the molecular layer of DG. The western blot showed a gradual decrease in CD200 expression with increasing age. $CD200R^+$ labelled microglia/macrophages ($Iba1^+$) were observed in ventricle linings and meninges; and also in cingulum from P1-P7. The expression decreased with increasing age. After H/I injury, activated microglia were observed as early as 3h even in parenchyma. $CD200R^+$ & $CD200^+$ cell numbers increased with lesion size and were nearly back to basal level by 7 days. $CD200R^+$ cells were also observed in hippocampus and lesioned white matter.

Conclusions: These data indicate that CD200-CD200R expression mediates immune regulation in neonates. Further studies with characterization of these cell types expressing the ligand and receptor will shed light on the neuron-glial interactions and their role in the exacerbated inflammatory response in neonatal brain.

References:

Chitnis T, Imitola J, Wang Y, Elyaman W, Chawla P, Sharuk M, Raddassi K, Bronson RT, Khoury SJ (2007) Elevated neuronal expression of CD200 protects Wlds mice from inflammation-mediated neurodegeneration. Am J Pathol 170:1695-1712.

Gorczynski R, Chen Z, Kai Y, Lee L, Wong S, Marsden PA (2004). CD200 is a ligand for all members of the CD200R family of immunoregulatory molecules. J Immunol 172:7744 -7749.

Koning N, Swaab DF, Hoek RM, Huitinga I (2009) Distribution of the immune inhibitory molecules CD200 and CD200R in the normal central nervous system and multiple sclerosis lesions suggests neuron-glia and glia-glia interactions. J Neuropathol Exp Neurol 68:159 -167.

Minas K, Liversidge J (2006). Is the CD200/CD200 receptor interaction more than just a myeloid cell inhibitory signal? Crit Rev Immunol 26(3):213-30.

983

VERY-LOW-FREQUENCY OSCILLATIONS OF CEREBRAL HEMODYNAMICS AND BLOOD PRESSURE ARE INFLUENCED BY AGING AND COGNITIVE ACTIVATION

A. Vermeij[1,2], A.S.S. van den Abeelen[1], R.P.C. Kessels[2,3], A.H.E.A. van Beek[1], J.A.H.R. Claassen[1]

[1]Department of Geriatric Medicine, Medical Centre, [2]Donders Institute for Brain, Cognition and Behaviour, [3]Department of Medical Psychology, Medical Centre, Radboud University Nijmegen, Nijmegen, The Netherlands

Objectives: The origin of spontaneous slow oscillations in cerebral hemodynamics and metabolism is controversial. Very-low-frequency oscillations (VLFOs, 0.02-0.07 Hz) are hypothesized to result from neurogenic activity, whereas low-frequency oscillations (LFOs, 0.07-0.20 Hz) are possibly caused by activity in microvascular smooth muscle cells. High-frequency oscillations (HFOs, 0.20-0.35 Hz) are due to respiratory activity. The influence of blood pressure oscillations is however frequently neglected. Evidence exists that aging is accompanied by a degeneration of the vascular system and changes in neurovascular coupling, which may have consequences for regional cerebral blood flow and cognitive performance. Therefore, we aimed to establish interactions between oscillations in pressure and the effect of age and cognitive activation by using functional Near-Infrared Spectroscopy (fNIRS), a noninvasive neuroimaging technique.

Methods: In this study, 15 healthy young (21-32 years) and 16 older adults (64-78 years, MMSE=29.1±1.0) performed a verbal n-back working-memory task. Oxygenated ([O_2Hb]) and deoxygenated hemoglobin ([HHb]) concentration changes, as indices of brain activation, were registered by two fNIRS channels located over left and right dorsolateral prefrontal cortex. Concentration changes in total hemoglobin ([tHb]), defined as the sum of changes in [O_2Hb] and [HHb], are used as an indicator of alterations in total blood volume. Blood pressure (BP) was measured in the finger by photoplethysmography (Finapres).

Results: [O_2Hb] increased in both groups under influence of cognitive activation. Mean BP was higher in older adults than in young adults during all conditions. In comparison to baseline measurements, BP increased slightly under high working-memory load (2-back) in young (4.2 mmHg, $p=.002$) and older adults (6.0 mmHg, $p< .001$), but the increase did not differ between groups. Power spectral density analysis showed that VLFOs of BP, [O_2Hb], [HHb], and [tHb] are influenced by both age and working-memory load. In the control condition (0-back), VLFOs of BP were equal in power for young and older adults. However, high working-memory load resulted in declined VLFOs of BP in young adults ($p=.007$), while in older adults the VLFOs increased ($p=.06$). VLFOs of [O_2Hb] ($p=.005$) and [tHb] ($p=.020$) were stronger in young adults in comparison to older adults during the control condition. However, under high working-memory load, in young adults the VLFOs of [O_2Hb] ($p=.006$), [HHb] ($p=.033$), and [tHb] ($p=.008$) were reduced and became similar to those in older adults. LFOs were not influenced by working-memory load, but declined with age (BP, [O_2Hb], [tHb] $p\leq.005$, [HHb] $p< .05$). HFOs were not dependent on either age or working-memory load.

Conclusions: Our study shows that VLFOs and LFOs in cerebral hemodynamics decline with age. VLFOs are influenced by intensity of cognitive activation, but only in young adults. This age-dependency may indicate age-related changes in neurovascular coupling. Moreover, our results on BP oscillations show that not only local vasoregulatory processes, but also systemic processes influence the cerebral hemodynamic signals. To conclude, the effects of age and BP

should be taken into account in the interpretation of neuroimaging studies that rely on blood oxygen levels.

984

EXTRASYNAPTIC $GABA_A$ RECEPTORS REGULATE CEREBRAL BLOOD FLOW AND OXYGEN METABOLISM IN MOUSE NEOCORTEX IN VIVO

S.B. Jessen[1], B.L. Lind[1], C. Mathiesen[1], K. Jensen[2], M. Lauritzen[1,3]

[1]Department for Neuroscience and Pharmacology, University of Copenhagen, Copenhagen, [2]Department of Physiology and Biophysics, Aarhus University, Aarhus, [3]Deparment of Clinical Neurophysiology, Glostrup Hospital, Glostrup, Denmark

Introduction: The GABA receptors are the most important inhibitory receptors in the nervous system and postsynaptic $GABA_A$ receptors ($GABA_AR$) are indispensible for normal neuronal activity.

The spillover of synaptically released GABA activates extrasynaptic $GABA_AR$, and tonic inhibition contributes to the modulation of network dynamics, and emerging evidence suggest that neurons respond to tonic inhibition mediated by extrasynaptic $GABA_A$ receptors in a differentiated way in brain slices. We also previously showed that increases in cerebellar GABA activity decreased activity-dependent rises in cerebral blood flow (CBF) and oxygen metabolism ($CMRO_2$) in vivo, but it is unknown whether this effect was mediated via synaptic or extrasynaptic $GABA_AR$, and the extent to which this observation may be generalized to other brain regions.

Purpose: To investigate how activation of extrasynaptic and synaptic $GABA_A$ receptors regulate neurovascular coupling and brain metabolism in mouse cerebral cortex

Methods: 8 weeks old male NMRI mice were anesthetized with xylazine/ketamine during surgery and alfa-chloralose during experiments. End-respiratory CO_2 and blood pressure were monitored continuously. A cranial window was drilled above the right cortex and dura was removed. A laser-Doppler probe was placed just above and a recording electrode and an oxygen electrode were inserted 150 µm (layer 2/3) into the right hemisphere. The left whisker pad was activated using stimulation frequencies of 0.5, 1.0, 2.0, 3.0 and 5.0 Hz for 15 s. The $GABA_A$ agonist, THIP (4,5,6,7-tetrahydroisoxazolo[5,4-c]pyridin-3-ol) was used to activate extrasynaptic $GABA_AR$.

Ongoing experiments are conducted using Zolpidem, a synaptic $GABA_AR$ agonist, to elucidate the effect of synaptic $GABA_AR$ on neurovascular coupling.

Results: Activation of extrasynaptic $GABA_A$ receptors by THIP caused profound effects on both cerebral oxygen metabolism, calculated as $CMRO_2$, and evoked cerebral blood flow responses.

In low concentrations THIP increased CBF and $CMRO_2$ responses, whereas at higher concentrations, activation of extrasynaptic $GABA_AR$ caused a reduction in oxygen use and CBF responses.

Conclusion: Extrasynaptic $GABA_A$ receptors are important regulators of cerebral blood flow and metabolism, and ongoing experiments are conducted to further elucidate the effects of activation of synaptic $GABA_A$ receptors. This will provide information that will help disentangle the mechanisms by which GABA exerts its control on neurovascular coupling in cerebral cortex.

We postulate that a decline in extrasynaptic GABA-receptor activity may lead to insufficient

substrate supply (blood flow) during activity, which is known to be accompanied by impairment of cognitive function.

985

PROGRAMMED INFUSION SCHEME FOR [^{11}C] FLUMAZENIL PET - IS TRACER STEADY-STATE ATTAINED FASTER THAN BOLUS INFUSION?

L. Feng[1], C. Svarer[1], M. Ziebell[1], A. Ettrup[1], H.D. Hansen[1], K. Madsen[1], H.M. Arfan[2], S. Yndgaard[3], G.M. Knudsen[1], L.H. Pinborg[1,4]

[1]Neurobiology Research Unit, Rigshospitalet, Copenhagen University Hospital, Copenhagen, [2]Epilepsihospitalet, Dianalund, [3]Department of Anaesthesia, [4]Epilepsy Clinic, Department of Neurology, Rigshospitalet, Copenhagen University Hospital, Copenhagen, Denmark

Objective: Full quantification with an image-independent input should ideally be used in the evaluation of [^{11}C] Flumazenil ([^{11}C]FMZ) PET (1). However, the need for an arterial line reduces the feasibility in a clinical setting. An alternative approach is to use the bolus infusion (BI) approach to hasten the time to attain tracer steady-state in brain and blood (2). At steady-state the venous concentration of [^{11}C]FMZ is used as a representation of the input to the brain. However, it is a challenge to attain steady-state with C-11 labeled tracers, due to the short half-life. A programmed infusion (PI) system governed by a feed-back controller has been developed, which potentially attains steady-state faster than a BI approach.

Methods: To accommodate the kinetics of [^{11}C]FMZ to the system, we conducted 3 bolus dynamic PET studies on healthy volunteers, lasting 1.5 h each. Arterial blood sampling was performed for measuring tracer concentrations and metabolites. The PI scheme was designed based on kinetic modeling of the bolus studies, using a model that simulates brain tissue time activity courses (TACs) directly from tracer injection. The model consists of two parts: a) a 3-compartment model of the tracer activity in the arterial plasma from tracer injection; and b) a one-tissue compartment model of the TACs from the plasma activity (3). By applying methods from automatic control systems and a P-controller the injection scheme was obtained, and the simulation showed that steady-state could be attained rapidly. Two young healthy volunteers were double scanned using the BI paradigm (B/I ratio=35 min) and the PI method.

Results:

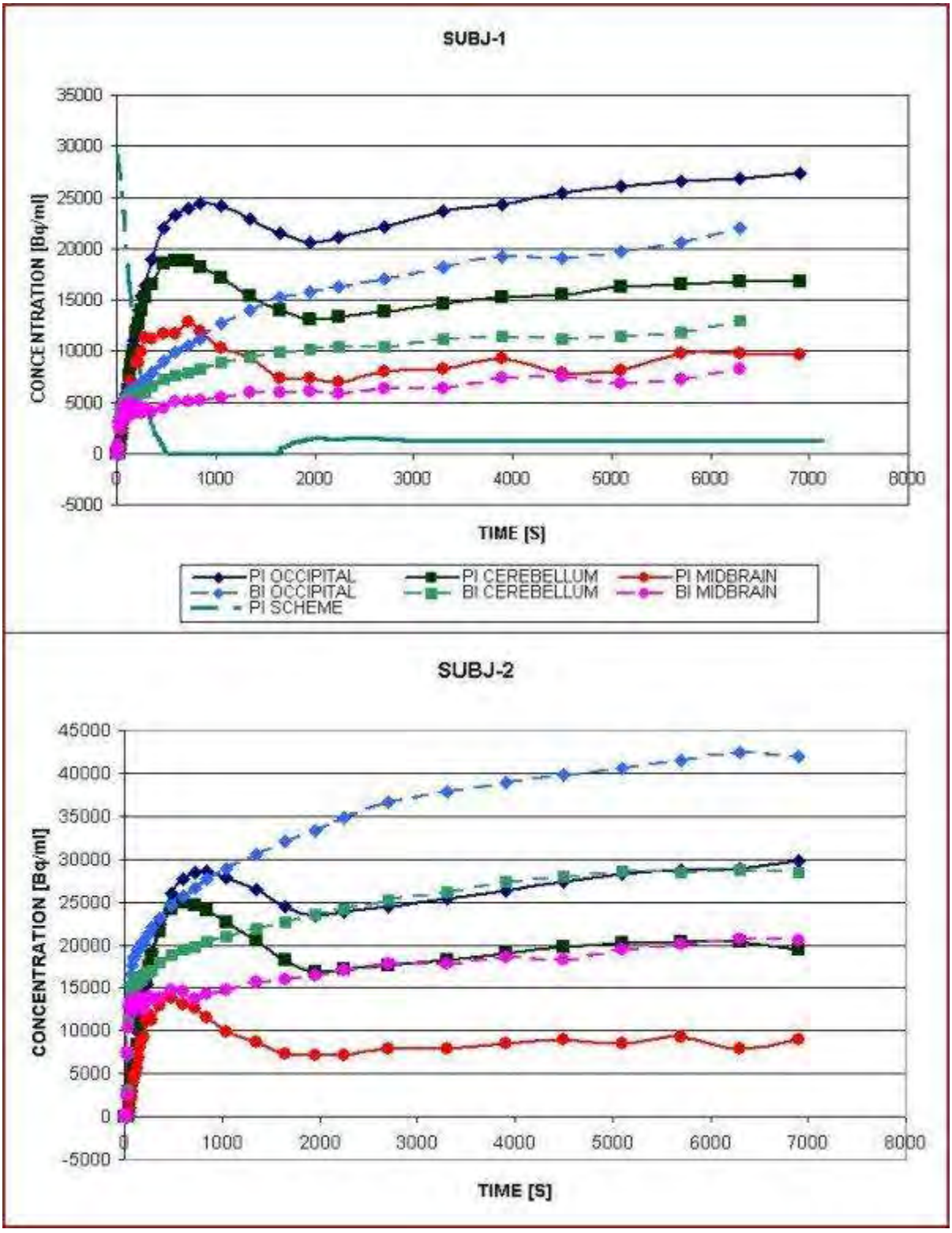

[Programmed Infusion vs. Bolus Infusion]

Measured TACs from PI and BI were compared. Three brain regions are shown: occipital cortex

(occ), cerebellum (cb) and midbrain (mb). Regions were defined by aligning PET images with MRI. The low binding region (mb) reached steady-state. However the binding in the other regions: occ and cb for subj-1; and occ for subj-2, did show an increasing tendency for both BI and PI. In comparison to BI, PI has a tendency to reach steady-state faster, but it is still slower than expected.

Conclusions: For the BI studies the results suggest a higher B/I ratio for attaining faster steady-state especially in receptor rich cortical regions. However, earlier experiments conducted with a B/I ratio up to 60 min, did not result in a faster steady-state. The occ TACs in both PIs showed a drop after the initial peak, which is contrary to the simulation. This may indicate that the system, built upon these bolus experiments, was not able to fully capture the dynamic and physiological characteristics of [^{11}C]FMZ. Furthermore, inter-individual differences may introduce discrepancy between the model and experiments. More optimizations of the system are needed, and further experiments will be conducted.

References:

1. Hammers, A., Panagoda, P., et. al, *J Cereb Blood Flow Metab* 28, 207-216 (2008)

2. Carson R.E., Channing M.A., et. al. *J Cereb Blood Flow Metab* 13(1):24-42 (1993)

3. Koeppe R.A., Holthoff V.A., et. al. *J Cereb Blood Flow Metab* 11(5):735-44 (1991)

986

LATERALITY OF SILENT ISCHEMIC LESIONS IN PATIENTS WITH ASYMPTOMATIC INTERNAL CAROTID ARTERY STENOSIS IS ASSOCIATED WITH REDUCED CEREBRAL VASOREACTIVITY

M. Isozaki[1], K. Fukuda[1], K. Fukushima[2], Y. Kaku[1], H. Kataoka[1], N. Nakajima[1], H. Iida[3], K. Iihara[1]

[1]Neurosurgery, [2]Radiology, [3]Center Research Institute, National Cerebral and Cardiovascular Center, Osaka, Japan

Objectives: This study aimed to investigate the relationship between silent ischemic lesions (SILs) and cerebral hemodynamics. SILs were defined as hyperintense lesions on fluid-attenuated inversion recovery (FLAIR) magnetic resonance imaging (MRI) scans of the white matter of the brain, and cerebral hemodynamics was defined in terms of baseline cerebral blood flow (CBF) and cerebral vasoreactivity (CVR). CVR was reported to be useful for predicting the risk of cerebral hemodynamic impairment and was assessed using the acetazolamide (ACZ) challenge test. Cerebral hemodynamic impairment was measured in patients with asymptomatic internal carotid artery (ICA) stenosis by using N-isopropyl-p-[^{123}I]iodoamphetamine (^{123}I-IMP) single- photon emission computed tomography (SPECT).

Methods: Between January 2007 and April 2010, 168 patients with ICA stenosis (>50%) had been admitted to our hospital for consideration of carotid endarterectomy. Of these patients, 72 patients (men, 62; age, 70 ± 5.7 y) with asymptomatic ICA stenosis were included in this study. These patients underwent FLAIR MRI, diffusion-weighted (DWI) MRI, and ^{123}I-IMP SPECT for evaluation of asymptomatic SILs, acute infarction, and cerebral hemodynamics, respectively.

Results: DWI revealed that 2 patients (2.8%) had spotty asymptomatic acute infarction in the ipsilateral hemisphere. 72 patients studied were divided into 2 groups on the basis of distribution of the SILs: the Asymmetry group (n = 33), which had a greater number of SILs in the ipsilateral hemisphere than in the contralateral hemisphere, and the Symmetry group (n = 39), which had symmetrical distribution of SILs or did not have any SILs. The CVR values for the ipsilateral hemisphere for the Symmetry group (41.7% ± 22.8%) were significantly higher than those for the Asymmetry group (29.2% ± 23.1%) ($P < 0.05$, paired t test). The SILs of the patients in the Asymmetry group were further divided into 2 subtypes: the Internal subtype, where the patients had only subcortical SILs, and the External subtype, where the patients had SILs involving the cortex. The ipsilateral CVR values for the Internal subtype and the External subtype were 10.4% ± 14.6% and 40.2% ± 13.6%, respectively, and this difference was statistically significant ($P < 0.001$, paired t test).

Conclusions: The increase in ipsilateral asymmetrical SILs was related to CVR reduction, which was assessed by the ACZ challenge test. Therefore, this finding may help in predicting the risk of cerebral infarction in patients with asymptomatic ICA stenosis.

References:

[1] Kristina S, et al. Stroke 2001; 32: 1323-1329.

[2] Kuroda S, et al. Stroke 2001; 32: 2110-2116.

[3] Ogasawara K, et al. J Cerebral Blood Flow Metab 2002; 22: 1142-1148

987

DIFFUSION TENSOR IMAGING-NEUROPATHOLOGY CORRELATION IN A MURINE MODEL OF THROMBOTIC STROKE: ACUTE AXONAL, OLIGODENDROCYTIC, AND DENDRTITC INJURY

C.-Y. Kuan[1], A. Shereen[2], D. Yang[2], D. Lindquist[2]

[1]Pediatrics, Division of Neurology, [2]Cincinnati Children;s Hospital Medical Center, Cincinnati, OH, USA

Objectives: White-matter (WM) injury is an important cause of functional disabilities in stroke and a desired target of acute therapy, but this goal is hindered by inability to monitor WM damage with imaging methods. Diffusion tensor image (DTI) is a powerful technology to visualize WM and quantify its functions. Yet the utility of DTI in acute stroke remains uncertain due to the lack of corresponding neuropathologic data. The objective of the present study is to determine neuropathological correlates of DTI changes within 24 hours of stroke-onset in a mouse model of thrombotic stroke.

Methods: Ten-to-twelve week-old male CD-1 mice were subjected to unilateral carotid-artery ligation followed by hypoxia to induce thrombosis. At 6, 15, and 24 h post-injury, mice were divided into 3 groups for (1) in-vivo T2- and diffusion-weighted magnetic resonance imaging (MRI) on a 7T system followed by histochemistry, (2) ex-vivo DTI and electron microscopy (EM) correlation, and (3) additional staining and biochemical analysis of the reactive oxidative stress responses. In DTI, regions-of-interest were drawn in external capsule, internal capsule, and the fimbria/fornix to compare temporal progression and spatial differences in fractional anisotropy, axial diffusivity, and radial diffusivity among the three axonal bundles.

Results: We found that hypoxia-ischemia caused rapid reductions of axial and radial diffusivities in all three axonal bundles. A large decrease in fractional anisotropy is associated with structural breakdown of the axons (Fig. 1A). The reduction of radial diffusivity correlates with swelling of myelin sheaths and compression of the axoplasma (Fig. 1B). The damage to oligodendrocytes is associated with oxidative stress. Finally, the gray matter of the hippocampus exhibits a high level of diffusion anisotropy, and its reduction signifies dendritic degeneration (Fig. 1C).

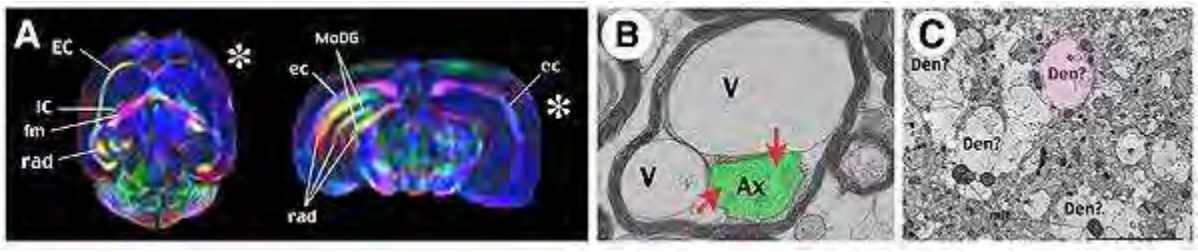

[Figure 1: DTI-neuropathology correlations.]

Conclusion: DTI has a far greater resolution of WM than T2- or conventional diffusion-weighted MRI. Cross-evaluation of multiple DTI parameters provides a fuller picture of axonal,

oligodendrocytic, and dendritic injury in acute ischemic stroke. If these DTI-neuropathological correlates are confirmed in patients, DTI could become a powerful tool for monitoring WM injury in acute stroke.

988

COMPARATIVE EFFECTS OF ANESTHETICS ON CORTICAL SPREADING DEPRESSION

C. Kudo, M. Tsunokawa, H. Niwa

Department of Dental Anesthesiology, Osaka University Graduate School of Dentistry, Suita, Japan

Cortical spreading depression (CSD) is a transient neuronal and glial depolarization and disruption of membrane ionic gradients that propagates slowly across the cerebral cortex. It is now widely recognized to be involved to pathophysiology of migraine. CSD susceptibility can be experimentally assessed by recording the frequency of CSDs evoked upon continuous topical application of KCl (1M). We systematically studied the influence of different anesthetic types, isoflurane, propofol and dexmedetomidine which are widely used in the current clinical situations, on CSD susceptibility in this model. Male Sprague-Dawley rats were intubated and mechanically ventilated. Femoral arteries were cannulated for arterial blood pressure and blood gas analysis, and femoral veins were cannulated for drug continuous administrations. CSD occurrence and propagation speed were recorded using two intracortical glass micropipettes (350 micron depth). One of 3 different anesthetics was tested in each rat: isoflurane (1%, 0.7MAC), propofol (14 mg/kg loading, followed by 28 mg/kg/hr, 0.7MAC) and dexmedetomidine (1 microg/kg/min). We found that highest CSD frequency was observed under propofol anesthesia (42±5, $P< 0.05$ vs isoflurane). Isoflurane reduced the frequency of CSDs compared to other two groups (25±5). Dexmedetomidine tended to reduce the CSD frequency (32±8, $P=0.1$ vs propofol). The propagation speed and amplitude of CSD did not differ among groups. In summary, CSD susceptibility is modulated by the choice of anesthetic, as previously reported using other drugs (Kudo et al. 2008). The mechanism of CSD suppression by isoflurane may involve the blockade of gap junctions, whereas it has been reported that CSD is not inhibited by drugs that augment GABAergic transmission and it is consistent with the result of propofol ($GABA_A$ receptor agonist) seen in this study. Dexmedetomidine is an $alpha_2$-adrenergic full agonist and more potent than clonidine which has been reported to inhibit SD initiation and propagation by topical application to the cortical surface (Richter et al, 2005). In this study, dexmedetomidine was administered systemically that is more relevant to the clinical situation, and tended to reduce CSD frequency. Our experiments tested anesthetics widely used clinically, and may help to elucidate the mechanism of CSD and establish the new therapy for migraine.

Acknowledgement: This study was supported by Grants-in-aid for Young Scientist (B) (21791992, CK)

989

EARLY PREDICTIVE BIOMARKERS FOR LESION DEVELOPMENT AFTER TRANSIENT CEREBRAL ISCHEMIA

C. Berthet[1], **H. Lei**[2,3], R. Gruetter[2,3], L. Hirt[1]

[1]Clinical Neurosciences, CHUV, [2]LIFMET, EPFL, [3]Radiology, UNIL, Lausanne, Switzerland

The course of ischemic episodes is very variable and it is difficult to predict the outcome of an individual patient early after ischemia. A better prediction of the outcome at early time points would greatly facilitate clinical decisions. Several cerebral imaging techniques are available for the diagnosis and management of stroke patients, including computed tomography and magnetic resonance imaging. However, none of them is able to reliably estimate the severity of ischemia or identify transient ischemic attacks (TIAs). Therefore, the aim of the present study was to use magnetic resonance spectroscopy to identify neurochemical markers for outcome prediction at very early time points after transient and permanent ischemia.

ICR-CD1 mice were subjected to 10-minute (n=11), 30-minute (n=9) or permanent (n=18) endoluminal filament middle cerebral artery occlusion (MCAO). The regional cerebral blood flow (CBF) was monitored in all animals by laser-Doppler flowmetry with a flexible probe fixed on the skull with < 20% of baseline CBF during ischemia and >70% during reperfusion. All MR studies were carried out in a horizontal 14.1T magnet. Fast spin echo images with T_2-weighted parameters were acquired to localize the volume of interest and evaluate the lesion size. Immediately after adjustment of field inhomogeneities, localized ^{1}H MRS was applied to obtain the neurochemical profile from the striatum (6-8µl) or the cortex (2.2-2.5µl). Six animals (sham group) underwent nearly identical procedures without MCAO.

By comparing the evolution of several metabolites in ischemias of varying severity, we observed an increase in glutamine in all ischemic mice after reperfusion, but not in permanent ischemia. We also observed a decrease in the sum of N-acetyl aspartate + glutamate + taurine in all irreversibly damaged tissues, independently of reperfusion, severity and tissue type. Finally, we observed a GABA increase after permanent ischemia only. We have thus identified two metabolites which can be used to determine if reperfusion has occurred (glutamine increase) or not (GABA increase). We have also identified a biomarker, N-acetyl aspartate+glutamate+taurine, which can be used to determine if a tissue is already irreversibly damaged or not. In permanent ischemia, we have also identified an exponential decrease of specific metabolites which could be used to determine the time of ischemia onset.

In conclusion, magnetic resonance spectroscopy can be used as a diagnostic tool to monitor reperfusion, identify reversibly and irreversibly damaged tissue and evaluate the time of ischemia onset. If these results can be translated to stroke patients, this technique would greatly improve the diagnosis and help with clinical decisions.

990

IDENTIFICATION AND CHARACTERIZATION OF PARENCHYMAL PROSTAGLANDINERGIC CELLS IN THE RAT CEREBRAL CORTEX

F. Plaisier[1], A. Karagiannis[1], P. Chausson[1], F. Jarlier[1], A.F.H. McCaslin[2], X. Toussay[3], E. Hamel[3], E.M.C. Hillman[2], **B. Cauli**[1]

[1]Lab. Neurobiology of Adaptive Processes UMR7102, CNRS/UPMC, Paris, France, [2]Lab. Functional Optical Imaging, Dept. of Biomedical Engineering, Columbia University, New York, NJ, USA, [3]Lab. Cerebrovascular Research, Montreal Neurological Institute, McGill University, Montréal, QC, Canada

Introduction: The spatiotemporal coupling between neuronal activity and increased cerebral blood flow, termed functional hyperemia, is a highly regulated physiological phenomenon at the basis of functional brain imaging. In the cerebral cortex this hyperemic response which initiates in diving arterioles and propagates upstream at the pial level, is achieved by a delicate interplay between neurons, astrocytes and arterioles. Among the various messengers involved in cortical functional hyperemia the vasodilatory prostaglandin E2 (PGE_2) was shown to play a major role, but the cellular origins of this arachidonic acid derivative are still under debate.

Objectives: We sought to determine the expression profile of the synthesizing enzymes of PGE_2 in astrocytes and identified neurons of supragranular layers of the rat somatosensory cortex.

Methods: Astrocytes and cortical neurons were characterized in acute rat cortical slices by means of whole-cell patch-clamp recordings and single-cell RT-PCR. The amplification protocol was designed to probe for the expression of the two rate-limiting enzymes cyclooxygenases type 1 and 2 (COX-1 and -2) as well as of the three different downstream synthesizing enzymes, cytosolic and microsomal type 1 and type 2 PGE_2 synthases (cPGES, mPGES-1 and mPGES-2). Astrocytes, were recorded after vital staining with the fluorescent astrocytic markers Sulforhodamine 101 (SR101) or Texas Red Hydrazide (TexRed), and were further identified according to their electrophysiological properties and expression of GFAP and/or S100 beta. Similarly, neurons were identified according to their intrinsic firing properties and to the expression of well established molecular markers of neuronal types.

Results: Cells labeled with SR101 or TexRed exhibited the typical passive membrane properties of mature astrocytes and expressed S100 beta and/or GFAP. These astrocytes were subdivided according to the location of their endfeet as parenchymal (n=19) if their perivascular processes enwrapped diving arterioles and superficial (n=24) if their processes targeted the pial membrane. Superficial astrocytes expressed more frequently COX-1 (29%) than parenchymal astrocytes (11%) and COX-2 was only observed in a small proportion of superficial astrocytes (13%). cPGES was detected in 38 and 26% of superficial and parenchymal astrocytes, respectively. In contrast, of the two microsomal isoforms, only mPGES2 was detected in parenchymal astrocytes (11%). In neurons COX-1 and COX-2 were respectively detected in 43% and 33% of glutamatergic neurons (n=21), and in 25% and 10% of GABAergic interneurons (n=48). Interestingly, VIP interneurons were the only GABAergic neurons expressing COX-2 (18%, n=28). Finally, the terminal PGE_2

synthase most frequently observed in neurons was cPGES, which was detected in 86 and 46% of pyramidal neurons and VIP-expressing interneurones, respectively.

Conclusion: Our study indicates that glutamatergic neurons, over interneurons and perivascular astrocytes, are the major parenchymal source of the COX-2 derived PGE_2. Together with the reported spatiotemporal dynamics of dilations evoked by sensory stimulations, our observations suggest that the PGE_2-mediated hyperemic response would initially involve pyramidal neurons and, possibly, VIP interneurons, superficial astrocytes being only recruited in a secondary phase.

991

PET WITH ^{11}C-FLUMAZENIL IN THE RAT SHOWS PRESERVATION OF BINDING SITES DURING THE ACUTE PHASE AFTER 2H-TRANSIENT FOCAL ISCHEMIA

S. Rojas Codina[1], A. Martin[2], D. Pareto[1,3], J.R. Herance[1], S. Abad[1], A. Ruíz[1], N. Flotats[1], J.D. Gispert[1,3], J. Llop[2], V. Gómez-Vallejo[2], A.M. Planas[4]

[1]Institut d´Alta Tecnologia-PRBB, CRC Corporació Sanitaria, [2]Molecular Imaging Unit, Asociación Centro de Investigación Cooperativa en Biomateriales - CIC BiomaGUNE, Barcelona, [3]CIBER en Bioingeniería, Biomateriales y Nanomedicina (CIBER-BBN)., Zaragoza, [4]Department of Brain Ischemia and Neurodegeneration, Institut d'Investigacions Biomèdiques de Barcelona (IIBB)-Consejo Superior de Investigaciones Científicas (CSIC), Institut d'Investigacions Biomèdiques August Pi i Sunyer (IDIBAPS), Barcelona, Spain

Objective: Precise in vivo evaluation of the ischemic penumbra might help to advance in stroke management, since it is assumed that penumbral tissue is salvageable by therapeutic intervention. The benzodiazepine receptor antagonist Flumazenil (FMZ) binds to the benzodiazepine binding site of GABA-A receptors that are mainly located on neurons and are widely expressed in brain tissue. ^{11}C-FMZ and its single-photon gamma emitter counterpart 123I-iomazenil have been proposed as PET and SPECT markers of neuronal viability, respectively. PET studies in humans have used ^{11}C-Flumazenil (FMZ) to assess neuronal viability after stroke. Here we aimed to study whether ^{11}C-FMZ binding was sensitive to neuronal damage in the acute phase following ischemia/reperfusion in the rat brain.

Method: Transient (2h followed by reperfusion) and permanent intraluminal middle cerebral artery occlusion was carried out in male Sprague-Dawley rats. ^{11}C-FMZ binding was studied by PET up to 24 hours after the onset of ischemia. Tissue infarction was evaluated post-mortem at 24h with 2,3,5-triphenyltetrazolium chloride (TTC) staining. Immunohistochemistry against a neuronal marker (NeuN) was also performed to assess neuronal injury.

Results: No decrease in ^{11}C-FMZ binding was detected in the ipsilateral cortex up to 24 h post-ischemia in the model of transient occlusion despite the fact that rats developed cortical and striatal infarction. Moreover, at 24h, a slight but significant increase in the binding of ^{11}C-FMZ was observed at the level of the ipsilateral cortex. In contrast to transient ischemia, animals subjected to permanent ischemia showed a marked reduction of ^{11}C-FMZ uptake in the ipsilateral hemisphere at 24 hours. Transient ischemia and permanently occluded animals presented TTC alterations irrespective of the differences in binding of ^{11}C-Flumazenil observed between these models. Similar results of the TTC and Neu-N immunostaining staining were found in the brains obtained from the animals sacrificed at 24 hours. In fact a similar pattern of panecrosis with extense loss of Neu-N immunoreactivity was observed in both types of ischemia at the level of ipsilateral hemisphere. The similarities in the gross histopathological findings in both animal models strongly contrasts with the completely different images obtained in the ^{11}C-FMZ PET scans performed 24 hours after surgery.

Conclusions: This finding evidences that ^{11}C-FMZ binding is not sensitive to neuronal damage on the acute phase of ischemia/reperfusion in the rat brain.

References:

Abe K et al, (2004) Synapse 53:234-239.

Debruyne D et al, (1991) Eur J Drug Metab Pharmacokinet 16:141-152.

Dohmen C et al, (2003) Stroke 34:2152-2158.

Heiss WD et al, (1997). Stroke 28:2045-2051.

Heiss WD et al, (1998). Stroke 29:454-461.

Heiss WD et al, (2000). Stroke 31:366-369.

Matsuda H et al, (1995). Nucl Med Commun 16:581-590.

Sette G et al, (1993). Stroke 24:2046-2057.

Watanabe Y et al, (2000). Eur J Nucl Med 27:308-313

992

TLR4 INCREASES BRAIN CELL PROLIFERATION AFTER EXPERIMENTAL STROKE

A. Moraga, R. Cañadas, J.G. Zarruk, V.G. Romera, J.M. Pradillo, D. Fernández-López, O. Hurtado, M.A. Moro, I. Lizasoain

Pharmacology, Universidad Complutense, Madrid, Spain

Background: Stroke is the second-third leading cause of death, the first of disability and the second of dementia in Western countries. A specific innate immunologic response starts after stroke that is mediated through toll-like receptors (TLR). TLR4 has been implicated in the brain damage caused by stroke (1). In addition, TLR4 has been also involved in adult hippocampal neurogenesis under normal conditions (2). However, it is unknown the role that TLR4 plays on cell proliferation after stroke. The objective of this study is therefore to determine the role of TLR4 in this process.

Methods: Focal cerebral ischemia was induced by permanent occlusion of the middle cerebral artery in mice of 10 months of age. It was performed on TLR4-deficient mice (C57BL/10ScNJ) and animals that express TLR4 normally (C57BL/10ScSn). 5-bromo-2′-deoxyuridine (BrDu, 50 mg/kg) was injected intraperitoneally twice daily from days 5 to 6 after ischemia. Cerebral infarct size was measured by magnetic resonance imaging (MRI) at 48h and by Nissl staining at 7 and 14 days. Cell proliferation and differentiation were quantified 7 and 14 days after ischemia by immunohistochemical studies. Dorsolateral striatal projection of the subventricular zone and peri-infarct zone in parietal cortex were dissected as previously described (3).

Results: We did not find any difference in the infarct volume measured at 2, 7 and 14 days after stroke between both groups. Different reasons (model used, infarct size and age of the animals) might explain this result. Our findings reveal that after stroke TLR4 promotes cell proliferation, increasing the number of BrdU+ cells and the number of microglial cells (Iba1+ cells) in the ipsilateral parietal cortex and SVZ at 7 and 14 days after ischemic insult.

Conclusions: Our results suggest that after stroke the presence of TLR4 promotes cell proliferation, suggesting that although TLR4 mediates brain damage in the acute phase, it might be necessary for neurorepair mechanisms during the chronic phase of stroke.

References:

(1) Caso et al., Circulation. 2007.

(2) Rolls et al., Nature Cell Biol. 2007.

(3) Fernández-López et al., Stroke 2010.

Supported by Spanish Ministry of Education (SAF2008-03122) and Health (RENEVAS RD06/0026/0005)

993

DETECTION OF PENUMBRAL FLOW WITH QUANTITATIVE PERFUSION WEIGHTED-MRI IN ACUTE STROKE: MAPS, OPTIMAL FLOW THRESHOLDS AND CALIBRATION OF PW MAPS

O. Zaro-Weber[1,2], W.D. Heiss[1], J. Sobesky[2]

[1]Max Planck Institute for Neurological Research, Cologne, [2]Department of Neurology and Center for Stroke Research Berlin, Charité-Universitätsmedizin, Berlin, Germany

Background and purpose: Perfusion weighted (PW) magnet resonance imaging (MRI) is used to identify the tissue at risk. However, the accuracy of perfusion weighted magnet resonance imaging (PW-MRI) based quantitative maps remains a matter of debate. Obstacles are the choice of the best PW map and the adequate threshold. By comparative positron emission tomography (PET), we evaluated a simple MR based and PET validated calibration of PW maps.

Methods: PW-MRI and quantitative 15O-water-PET was performed in acute stroke patients. In a regions of interest (ROI) based approach, maps of time to peak (TTP), time to maximum (Tmax), mean transit time (MTT) and cerebral blood flow (CBF) were analyzed in order to identify the most predictive PW-map and the best threshold for each PW map with the sensitivity and specificity to define penumbral flow (< 20 ml/100g/min). We also calibrated the PW-maps to improve quantification.

Results: 22 acute stroke patients were included (median time from stroke: 8.9 hours; median time MRI to PET: 60 min). The averaged thresholds (median/IQR) were; rTTP 4.2 seconds (s) (2.8-5.8); Tmax 5.5 (3.9-6.6) s, MTT 5.2 s (3.9-6.9); CBF 21.7 ml/100g/min (19.9-32). The corresponding ratios for sensitivity/specificity (%) were: 91/82, 88/89, 88/78 and 89/87. The large individual variability was well explained by the mean value of the hemispheric reference (HR) (R^2: TTP 0.95, Tmax 0.9, MTT 0.83, CBF 0.76 Thus look-up tables were calculated that identified the individual best thresholds according to the individual HR value on PW images.

Conclusion: The individual variation of PW values remains a major problem in quantitative PWI and can be significantly improved by a simple MR based calibration. Easily applicable lookup-tables identify the individual best threshold for each PW map to optimize mismatch detection.

994

CEREBRAL BLOOD FLOW MEASURED BY PSEUDO-CONTINUOUS ARTERIAL SPIN LABELLING MRI: A POTENTIAL MARKER FOR OUTCOME IN SUBARACHNOID HAEMORRHAGE

M. Kelly[1,2], M. Rowland[1,2], T. Okell[1], J. Xie[1], M. Chappell[1], J. Westbrook[2], P. Jezzard[1], K. Pattinson[1,2]

[1]Oxford Centre for Functional Magnetic Resonance Imaging of the Brain, [2]Nuffield Department of Anaesthetics, University of Oxford, Oxford, UK

Objectives: Delayed ischaemic neurological deficit (DIND) is the major cause of morbidity and mortality following subarachnoid haemorrhage (SAH). Following either surgical clipping or endovascular coiling to secure the initial bleed, ~30% of survivors go on to develop DIND. Vasoconstrictive processes have been considered fundamental in the genesis of DIND. Recently other mechanisms have been proposed[1]. Early brain injury (EBI) describes global brain changes in the first 72 hours post SAH. A component of EBI, transitory ischaemia (global reduction in cerebral blood flow (CBF)), is thought to play a role in the development of DIND post SAH. In this study, we investigate the feasibility of using the non-invasive perfusion MRI technique, arterial spin labelling (ASL), to track CBF changes following SAH.

Methods: 5 SAH patients (4 x Grade I and 1 x Grade II) were scanned on a 3 Tesla Siemens Trio MRI scanner (12 channel head coil), using a pseudo-Continuous ASL (pCASL) sequence[2]. Patients were scanned on varying days post endovascular coiling (patient one: days 2 and 4, patient two: day 1, patient 3: days 1, 5 and 7, patient 4 days 1, 3 and 10, patient 5, day 1). The pseudo-CASL sequence consisted of a 1.4s labelling duration, followed by five post labelling delays and a gradient-echo EPI readout (TR=3.75s, TE=13ms). Total ASL scanning time was 9.5 mins (15 averages). Additional scans acquired included time-of-flight angio for optimal placement of the labelling plane (1.5 min duration) and two ASL calibration scans (2 x 11sec) for quantification of CBF in absolute units (ml/100g/min). CBF and arterial arrival time (AAT) maps were generated by fitting the pCASL data to the ASL kinetic model[3], using a Bayesian inference approach[4].

Results: The average grey matter CBF and AAT values obtained across all subjects were 34.42 ± 6.29 ml/100g/min and 0.59 ± 0.06 sec (mean ± s.d.) respectively. Sample CBF and AAT maps are shown in figure 1(a) and (b). Figure 1(c) shows the trend in CBF in the two patients that were scanned on three occasions. Both patients demonstrated a global CBF reduction on the second scan day and a subsequent return towards baseline CBF on the third scan day.

Conclusions: The findings of this study demonstrate the feasibility of using ASL to reproducibly track changes in CBF in SAH patients. The CBF values obtained were lower than pulsed ASL (PASL) CBF values in the literature[5] . Further investigation of the method (specifically an assessment of the inversion efficiency of the pseudo-CASL sequence[6]) is required. However, the CBF trend displayed in figure 1 (c), although preliminary, demonstrates the potential of the ASL technique as a predictor of outcome in SAH patients and holds much potential for future work.

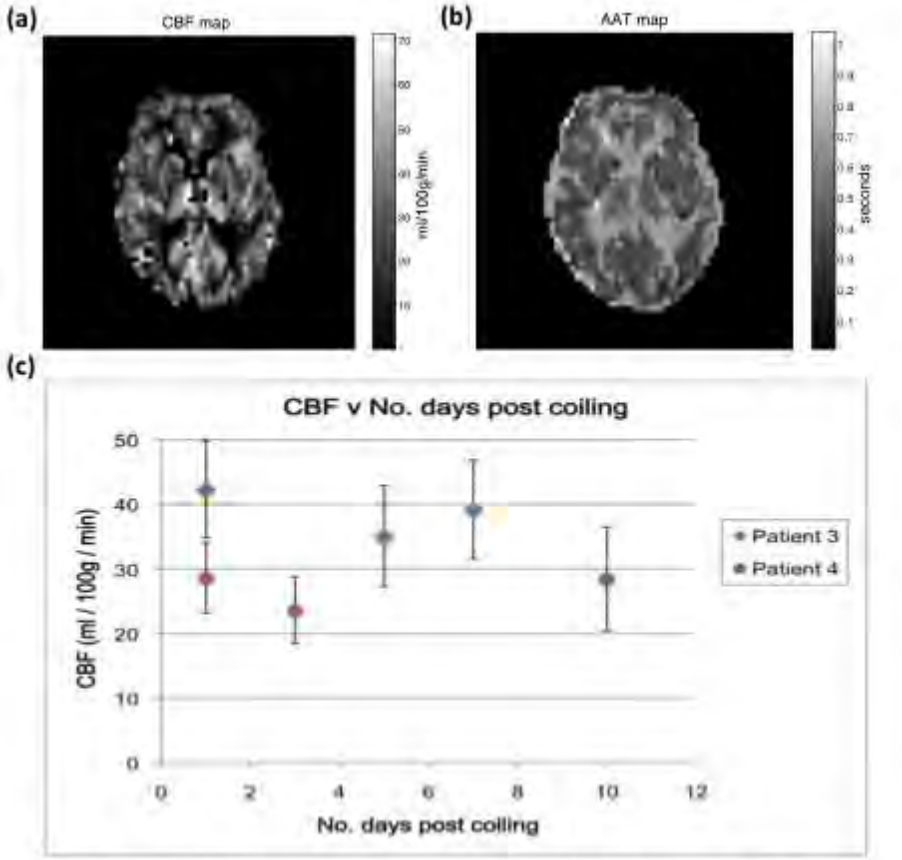

Fig.1 (a) sample CBF map **(b)** sample AAT map **(c)** CBF versus number days post endovascular coiling, patient 3 and 4

[figure 1]

References:

1. Cahill J, *et al*. Stroke 2009:(40):S86-7.

2. Dai W, *et al.* Magn.Reson.Med 2008:(6):1488-97.

3. Buxton RB, *et al.* Magn.Reson.Med 1998:(3):383-96.

4. Chappell M, *et al.* IEEE.Trans.Sig.Proc 2009:(45):795-809.

5. MacIntosh BJ, *et al.* J.Cereb.Blood.Flow.Metab 2008:(28):1514-22.

6. Aslan S, *et al*. Magn.Reson.Med 2010:(63):765-71

995

SIMULTANEOUS ACQUISITION OF FMRI AND EEG IN THE PICROTOXIN MODEL OF EPILEPSY

C. Simmons, D. Cash, S. Williams, M.B. Mesquita

Neuroimaging, King's College London, London, UK

Objectives: One of the greatest challenges in epileptology is the identification and localisation of those brain areas responsible for eliciting and maintaining epileptiform activity. Furthermore, it is also important to ascertain whether there is any dynamic interaction between those different brain areas. Research has, to date, focused primarily on EEG. Although EEG has high temporal resolution, it lacks spatial resolution due to the inverse problem of dipole source localization. On the other hand, fMRI has great spatial resolution but a relatively poor temporal resolution due to the delayed haemodynamic response. In the present study, we take advantage of the temporal resolution of EEG and spatial resolution of BOLD-fMRI to evaluate the changes in brain activity following ip injection of Picrotoxin.

Methods: Male adult Wistar rats (330g) were anaesthetized with urethane (140mg/kg,i.p.) and carbon fibre EEG surface electrodes were placed over the skin of both cerebral hemispheres. The signals from the electrodes were amplified inside the bore of the fMRI scanner by a x2000 pre-amplifier, placed 25cm away from the head of the rat to decrease “magnetic gradient interference”. The signals were then taken out of the magnet via optical fibre cables, reconverted into electrical signals, conditioned (CyberAmp380-Axon Instruments; amplification=200; high-pass filter=0.1Hz; low-pass filter=60Hz; Notch filter 50Hz) and then converted to digital data (MP100-Biopac Systems; sampling rate=500spl/s). Two raw signal channels were recorded and two digitally filtered channels were calculated in real time (low-pass filter at 60Hz with Q=1 + band-stop filters in 38, 76 and 114Hz). Physiological monitoring (respiration and temperature) was performed throughout the experiment. Dynamic MR images were acquired using a 7T imaging system (Varian; Gradient-echo; TR=500; TE=5/10/15ms; 24 slices per volume affording one whole brain scan each 30sec for a total scan duration of 60mins.). Picrotoxin injection (8mg/kg,i.p.) was remotely performed after acquisition of the first 30 volumes, without interruption of imaging or EEG recording. EEG data was used to determine presence of electrodecremental response and time of seizures onset, in order to select the 30 volumes immediately before seizure. MRI data was analyzed using a random effects approach with SPM8.

Results: we were able to acquire good quality EEG and fMRI data from all subjects. During the experiments all animals presented a typical evolution of the EEG morphology: electrodecremental response followed by isolated spikes, poli-spikes and spike-and-waves, culminating in *status epilepticus*. The MR images acquired showed a robust negative BOLD response (global minimum) in the caudate and nucleus accumbens and a positive response (global maxima) in the amygdale, during the electrodecremental period.

Conclusion:

(1) The methodology described above is suitable for simultaneous acquisition of EEG and fMRI in anaesthetized animals.

(2) The analysis of the images acquired during the electrodecremental response showed robust negative BOLD in the caudate and nucleus accumbens.

(3) The negative BOLD signal change observed during the electrodecremental response suggests a correlation between amplitude variation of the EEG and the BOLD contrast.

998

CHARACTERIZATION OF GLOBAL CEREBRAL ISCHEMIA-INDUCED PERI-INFARCT DEPOLARIZATION (PID) WITH MULTIMODAL IMAGING IN THE RAT BRAIN

Z. Bere[1,2], A. Kulmany[1,2], T.P. Obrenovitch[1,3], F. Bari[1], E. Farkas[1,2]

[1]Department of Medical Physics and Informatics, [2]Department of Physiology, Faculty of Medicine University of Szeged, Szeged, Hungary, [3]Division of Pharmacology, School of Life Sciences, University of Bradford, Bradford, UK

Objectives: Propagating electrical inactivation called peri-infarct depolarization (PID) spontaneously occurs during cerebral ischemia in the cerebral cortex. PIDs are speculated to be initiated near the ischemic core or in the penumbra. The pathophysiological significance of PID lies in that the associated changes in cerebral blood flow (CBF) may contribute to the extension of brain infarcts. The purpose of this study was to identify and characterize PID-related changes in membrane potential and hemodynamic variables by multi-modal imaging of the rat cerebral cortex through a closed cranial window.

Methods: A closed cranial window was mounted over the parietal bone in halothane anesthetized, adult, male Sprague-Dawley rats (n=13). The left femoral artery and vein were cannulated for the monitoring of mean arterial pressure (MAP) and latter blood withdrawal. The cranial window was loaded with a voltage sensitive (VS) dye (RH-1838). Global cerebral ischemia was induced by bilateral common carotid artery occlusion combined with subsequent hypovolemic hypotension (MAP< 40 mmHg). Each experiment was terminated by cardiac arrest, achieved by the injection of 1 ml 1% KCl through the venous line. Using two cameras and carefully selected illuminations, multiple image sequences of the cortex were captured. This multi-modal strategy, allowed the study of synchronous changes in the following variables: membrane potential (VS dye method); cerebral blood volume (CBV) with green (540-550 nm) illumination; hemoglobin (Hb) deoxygenation with red (620-640 nm) illumination, and CBF by laser speckle contrast imaging.

Results: The experiments fell into 3 categories based on whether depolarization evolved, and if so, during which phase of the experimental procedures: in group 1 (n=4) no PID could be detected, in group 2 (n=6) PID appeared during the induction of hypovolemic hypotension, in group 3 (n=3) PID emerged after cerebral ischemia had been completed by hypovolemic hypotension. PID typically occurred at a MAP value of 41.2±3.7 mmHg and at CBF value of 43.4±4.9%. The depolarizations displayed a clear wave front, invaded the window from the frontolateral corner, and propagated at a rate of 2.9±0.3 mm/min to caudomedial direction. In 7 cases, the depolarization was not followed by the recovery of membrane potential, and these events were associated with CBF reduction (19±3.6%) decreasing the already low ischemic value further. In 2 cases, repolarization was seen, and the PID coincided with mild CBF elevation (7.1±2.6%) with respect to the ischemic flow.

Conclusions: In global cerebral ischemia, PID appears to be generated at the lower limit of the autoregulatory range of CBF. PID originates at a focus probably located in an area with high vulnerability to ischemia, and propagates similar to that known for cortical spreading depression, whether or not the PID involves the recovery of membrane potential. CBF responses associated with PID most often display inverse neurovascular coupling.

Acknowledgements: This work was supported by grants from the EGT Norwegian

Financial Mechanisms (NFM, NNF 78902), and Hungarian Scientific Research Fund (OTKA, K81266).

999

SELECTIVE INHIBITION OF NR2B-CONTAINING N-METHYL D-ASPARTATE RECEPTORS ATTENUATES NEURONAL INJURY *IN VITRO* AND *IN VIVO* VIA SUPPRESSION OF CALPAIN ACTIVITY

Y. Terasaki, T. Sasaki, M. Kawamura, Y. Sugiyama, N. Oyama, E. Omura-Matsuoka, Y. Yagita, K. Kitagawa

Department of Neurology, Osaka University Graduate School of Medicine, Suita, Japan

Introduction: Glutamate is a key excitatory neurotransmitter in the central nervous system and plays an essential role in brain insults such as stroke. The global N-methyl D-aspartate (NMDA) glutamate receptor antagonists have neuroprotective effect in experimental stroke model, however, the agents failed to show efficacy in clinical trials. The NMDA receptors are heterometic assemblies composed of an NR1 subunit combined with one or more NR2 or NR3 subunits. Among four subtypes of NR2, NR2A and NR2B subunits are considered as the main subtypes of functional NMDA receptor. While activation of NR2A receptors is involved in synaptic plasticity and cell survival, activation of NR2B is shown to promote neuronal death. The present study is aimed to investigate whether the selective inhibition of NR2B is neuroprotective in *in vitro* oxygen glucose deprivation (OGD) model and *in vivo*

permanent middle cerebral artery occlusion (MCAO) model.

Methods: Primary cortical neuronal cultures were prepared from 16-day-old Wistar rat embryos. As *in vitro* ischemia, neurons were exposed to 210-minute OGD or 15-minute 100 μM glutamate-containing bathing medium. Cells were treated after OGD with one of the following chemicals: global NMDA receptor antagonist MK-801 (10 μM), non NMDA receptor antagonist CNQX (10 μM), L-type calcium channel blocker nifedipine (5 mM), NR2A-specific antagonist NVP-AAM077 (200 nM), and NR2B-specific antagonist Ro25-6981 (500 nM). Neuronal death was quantified 24 hours later by measurement of lactate dehydrogenase released by dead neurons into the bathing medium. The level of fodrin proteolysis was analyzed by Western blotting. For *in vivo* ischemia, male 8-week-old Wistar rats were anesthetized with halothane, and right MCA was occluded permanently by introducing a 4-0 nylon monofilament suture. Animals were divided into Ro and Vehicle group. Ro group rats were given Ro25-6981 (6mg/kg) intraperitoneally 3 hours after MCAO and vehicle group rats were given vehicle in a same way. Those rats were sacrificed 12 hours after MCAO, and cerebral cortex was dissected into the core of MCA, the peripheral area of MCA, and the ACA area. The level of fodrin proteolysis was analyzed by Western blotting. The other rats were sacrificed 24 hours later, and infarct size was measured with 2,3,5-triphenyltetrazolium chloride staining.

Results: Treatment with Ro25-6981 was protective *in vitro* as well as MK-801 compared with vehicle treatment in both lethal OGD ($p=0.004$) and glutamate toxicities ($p< 0.001$). In contrast, other agents such as CNQX, nifedipine, and NVP-AAM077 did not affect the cell injury after lethal injuries. Cells treated with Ro25-6981 were shown to attenuate the level of fodrin proteolysis after both OGD and glutamate exposure. Ro25-6981 treatment resulted in a significant reduction in infarct volume compared with vehicle treatment in permanent MCAO model (250 ± 101 vs. 354 ± 50 mm^3, mean±s.d, $p=0.008$). In Ro group rats, the proteolysis of fodrin was significantly attenuated compared with vehicle group in the penumbra area 12 hours after MCAO.

Conclusions: In conclusion, NR2B inhibition shows a marked reduction of neuronal injury via

suppression of calpain activity both *in vitro* OGD and glutamate exposure and *in vivo* MCAO model.

1000

NITRIC OXIDE PRODUCTS (NO_X) IN HUMAN BRAIN MICRODIALYSATES AND THEIR RELATIONSHIP WITH CEREBROVASCULAR PRESSURE REACTIVITY IN ACUTE BRAIN INJURY

K.L.H. Carpenter[1,2], I. Timofeev[3], P.G. Al-Rawi[3], M. Czosnyka[3], P. Smielewski[3], D.K. Menon[2,4], J.D. Pickard[2,3], P.J. Hutchinson[2,3]

[1]Division of Neurosurgery, Dept. of Clinical Neurosciences, University of Cambridge Nuffield, [2]Wolfson Brain Imaging Centre, Dept. of Clinical Neurosciences, [3]Division of Neurosurgery, Dept. of Clinical Neurosciences, [4]Division of Anaesthesia, Dept. of Medicine, University of Cambridge, Cambridge, UK

Objective: This pilot study's objective was to apply microdialysis, in patients with acute brain injury, to assess the relationship between nitric oxide products (total nitrite plus nitrate, termed NO_x) and pressure parameters: intracranial pressure (ICP), cerebral perfusion pressure (CPP), arterial blood pressure (ABP) and cerebrovascular pressure reactivity index (PRx). Microdialysis continuously samples the chemistry of a small focal volume of the cerebral extracellular space. Nitric oxide (endothelial-derived relaxing factor) is a short-lived reactive species, but its products nitrate and nitrite are readily measurable retrospectively. The PRx is a moving correlation coefficient between 30 mean values (10s window) of ICP and mean ABP (mABP), and reflects status of cerebral vascular autoregulation. Positive PRx values imply that increases in mABP are positively associated with increases in ICP, suggesting autoregulatory impairment, whereas negative PRx values indicate preserved vascular reactivity, with vasoconstriction and decrease in intracranial pressure in relation to surges in mABP. The PRx was previously validated against other indices of cerebral autoregulation [1], and is related to outcome [2].

Methods: Microdialysis catheters (CMA70 or CMA71) were inserted into the cerebral cortex of 12 patients (11 head injury; 1 subarachnoid haemorrhage) together with an intracranial pressure sensor (Codman), via a cranial access device (Technicam). Catheters were perfused at 0.3 microlitres/minute with CNS perfusion fluid (CMA); microdialysate collection vials were changed hourly. Pressure monitoring data were recorded on a bedside computer, using ICM+ software. Microdialysates were analysed for energy-related molecules (on a CMA600 or ISCUS analyser), and analysed for NO_x using a purge vessel (vanadium (III) chloride plus hydrochloric acid at 95^{o}C, purged with nitrogen gas) connected to a Sievers NOA 280i nitric oxide analyser [3]. Data were analysed by Spearman's rank correlation. The level of significance was $p< 0.05$.

Results: The mean of mean NO_x concentration (±SD) for the 12 patients was 32.5±16.7 micromol/litre, ICP 27.3±17.4 mmHg, CPP 73.2±3.8 mmHg, ABP 100.5±16.4 mmHg and PRx 0.07±0.23. Increasing NO_x concentrations correlated significantly with decreasing PRx values ($r = -0.66$, $p=0.028$) (Fig. 1).

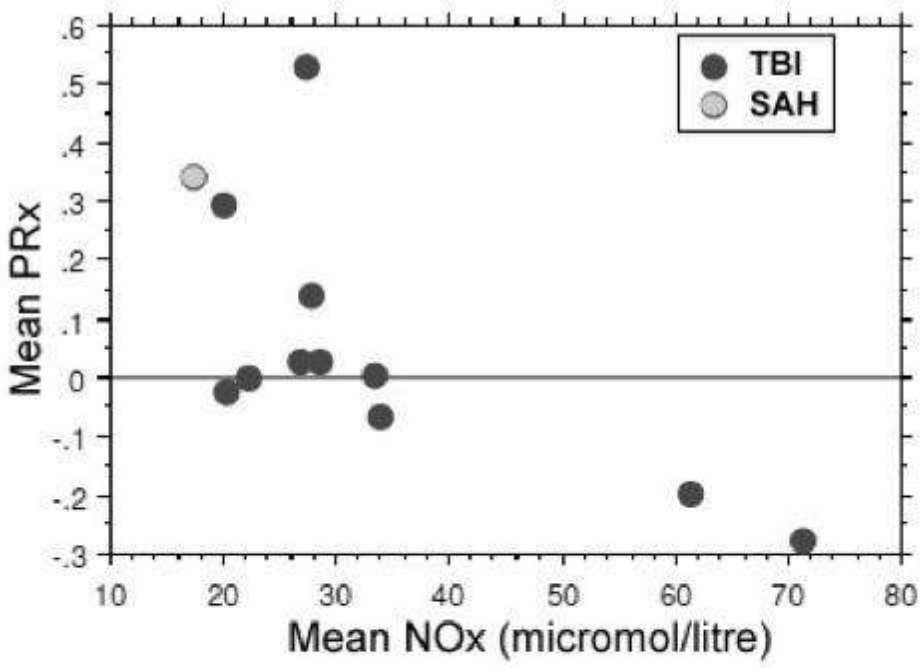

Figure 1. Relationship between the cerebrovascular pressure reactivity index (PRx) and NO_x concentration (micromol/litre) in human brain microdialysates (acute brain injury, 12 patients). Each data-point represents the mean value for each patient. The relationship was significant by Spearman's rank correlation (r = -0.66, p=0.028, n=12).

[Figure 1.]

There were no significant relationships between NO_x and ICP, CPP or ABP. Increasing NO_x

concentrations correlated significantly with decreasing lactate/pyruvate ratio (r = -0.73, p=0.015), with decreasing lactate concentration (r = -0.63, p=0.037), with decreasing glycerol concentration (r = -0.69, p=0.040) and with increasing glucose concentration (r = 0.69, p=0.029).

Conclusions: These pilot data suggest that in injured brains, higher concentrations of nitric oxide are associated with better autoregulation, evidenced by more negative PRx values, and with better metabolism. Nitric oxide may act beneficially by increasing responsiveness in the cerebral vasculature, enabling more favourable metabolism. Further patients' samples will be analysed.

References:

[1] Czosnyka M et al. Neurosurgery 1997;41:11-7 [2] Czosnyka M et al. J Neurosurgery 2005;102:450-4 [3] Carpenter KLH et al. Acta Neurochir Suppl 2008;102: 207-13.

1001

INVESTIGATION OF BLOOD-BRAIN BARRIER DYSFUNCTION IN SUBARACHNOID HAEMORRHAGE AND TRAUMATIC BRAIN INJURY PATIENTS USING MRI, SPECT AND PLASMA S-100B LEVELS

C. Winter[1,2], J. Cardinal[3], A. Coulthard[4], D. Mcfarlane[5], S. Rose[6]

[1]Neurosurgery, Royal Brisbane and Women's Hospital, [2]Neurosurgery, University of Queensland, [3]Chemical Pathology, [4]Radiology, [5]Nuclear Medicine, Royal Brisbane and Women's Hospital, [6]Centre for Advanced Imaging, University of Queensland, Brisbane, QLD, Australia

Objectives: Disruption of the blood-brain barrier (BBB) is one of the secondary mechanisms of brain injury that occurs following aneurysmal subarachnoid haemorrhage (SAH) and traumatic brain injury (TBI). We aim to demonstrate BBB dysfunction in patients with SAH and TBI using DCE-MRI (Dynamic Contrast Enhanced Magnetic Resonance Imaging) and SPECT (Single Photon Emission Computed Tomography) brain scans, to quantify the extent of BBB disruption using these imaging techniques and to correlate with plasma S-100B levels. A positive correlation may provide support for the hypothesis that plasma S-100B could be used as a bedside test for assessment of BBB damage, which may in turn alter management. Within the cohort of aneurysmal SAH patients we aim to investigate changes in BBB dysfunction secondary to global poor grade haemorrhage and regional damage related to the onset of cerebral vasospasm and delayed ischaemic neurological deficit (DIND).

Methods: A prospective study of 15 patients presenting with aneurysmal SAH and 15 patients with TBI were enrolled. The patients included World Federation of Neurosurgical Societies (WFNS) SAH grades 1-3 and mild to moderate head injuries with a Glasgow Coma Score (GCS) of 9 - 15. Severe TBI and poor grade SAH (WFNS grades 4 and 5) patients were included once they no longer required artificial ventilation. Serial blood samples were collected during the patients' admission and the plasma stored at - 80 degrees for analysis for S-100B levels.

Results: The DCE-MRI used $K^{trans,}$, a volume transfer constant of contrast agent between blood plasma and the extravascular extracellular space, to determine vascular permeability. The integrity of the BBB was evaluated using (99m)Tc-DTPA brain SPECT. The MRI and SPECT images clearly demonstrate different patterns of BBB disruption secondary to specific brain injuries such as focal cortical contusion, diffuse axonal injury, poor grade aneurysmal subarachnoid haemorrhage and delayed cerebral vasospasm. Quantification of BBB dysfunction using the two imaging modalities was performed and a correlation with plasma S-100B levels sought. Plasma S-100B levels were elevated in the majority of the participants compared to known baseline values. In general, the more severe the acquired brain injury (SAH or TBI) the higher the S-100B level.

Conclusion: DCE-MRI and SPECT brain scans can be used to assess the extent of BBB dysfunction following aneurysmal SAH or TBI brain injured patients. For both SAH and TBI patients the heterogeneity of the primary brain injury, the small number of participants in each group, coupled with variable patient factors, ensures that any correlations between BBB damage and plasma S-100B levels are unlikely to reach statistical significance.

References:

1. Barzo P et al. Contribution of vasogenic and cellular oedema to traumatic brain swelling measured by diffusion-weighted imaging. J Neurosurg. 1997; 87(6):900-907.

2. Blyth BJ, Farhavar A, Gee C, Hawthorn B, He H, Nayak A, Stocklein V, Bazarian JJ. Validation of Serum Markers for Blood-Brain Barrier Disruption in Traumatic Brain Injury. J Neurotrauma. 2009 Sep;26(9):1497-1507.

3. Korn A et al. Focal cortical dysfunction and blood-brain disruption in patients with post-concussion syndrome. J Clin Neurophysiol. 2005; 22(1):1-9.

1002

THE EFFECT OF HYPOCAPNIA AND HYPERCAPNIA ON CEREBRAL HAEMODYNAMICS, OXYGENATION AND METABOLISM: COMBINING MODELLING AND EXPERIMENTAL APPROACHES

J. Panovska-Griffiths[1], M. Banaji[2], I. Tachtsidis[1], T. Moroz[1], C.E. Cooper[3], C.E. Elwell[1]

[1]Medical Physics and Bioengineering, University College London, London, [2]Department of Mathematics, University of Portsmouth, Portsmouth, [3]Biological Sciences, University of Essex, Colchester, UK

Background and aims: Following the blossoming of systems biology in the last decade, experimental research on the brain circulation is being complemented by mathematical modelling. Such interdisciplinary approaches attempt to combine the predictive or explanatory power of model simulations with more traditional approaches to the analysis of experimental data. One long-term goal is the development of patient-specific models to help interpret the outputs of medical monitoring, and shed light on the behaviour of quantities which are important but hard to measure experimentally.

Methods: We explore the ability of a previously developed physiological model of brain circulation and metabolism [1] to explain the responses of five measured signals to hypocapnia and hypercapnia in ten healthy volunteers [2]. Hypercapnia was induced by increasing the levels of CO_2 in the inspired gases. During the challenge, end tidal CO_2 concentration, mean arterial blood pressure, and arterial oxygen saturation were measured, and these three signals served as inputs to the model. Near infrared spectroscopy (NIRS) [3] was used to measure cerebral tissue oxygen saturation (TOI) and changes in the oxidation level of oxidised cytochrome c oxidase (CCO). Finally, cerebral blood flow velocity (Vmca) was measured using transcranial Doppler. The last three signals provided measures of model performance: model-predicted and experimentally measured TOI, CCO and Vmca were compared.

Results: Our model simulations suggest that there should be respective decrease and increase in all three output signals (namely TOS, Vmca and CCO) during the hypocapnia and hypercapnia challenges. The temporal evolution of the monitored variables obtained experimentally (red) and from the model simulations (green) from a single subject are shown in Figure 1. We observe good qualitative and quantitative agreement between the two sets of profiles. Preliminary work suggests that different physiological mechanisms may be needed to improve the fits between modelled and measured data. We are currently exploring the effects on the model-to-data fit of changing sensitivity of blood flow to CO_2 levels, and are also exploring possible effects of hypocapnia and hypercapnia on metabolic demand.

Conclusions: This preliminary work shows that there is qualitative agreement between the predictions of a published model and measured data. It demonstrates that an interdisciplinary approach has the potential to inform on the effects of hypocapnia and hypercapnia on brain metabolism and circulation, with the possibility of application to the monitoring of brain injury. Qualitative agreement between model predictions and data, and systematic discrepancies, may highlight gaps in our understanding of physiological mechanism which remain to be explored.

References:

[1.] Banaji M. et al., PLoS Comp.Biol., 4(11), 2008

[2.] Tachtsidis I. et al. , Adv. Exp. Med. Biol., 645, p315, (2009)

[3.] Highton D. et al., Curr Opin Anaesthesiol., 23, p576, (2010)

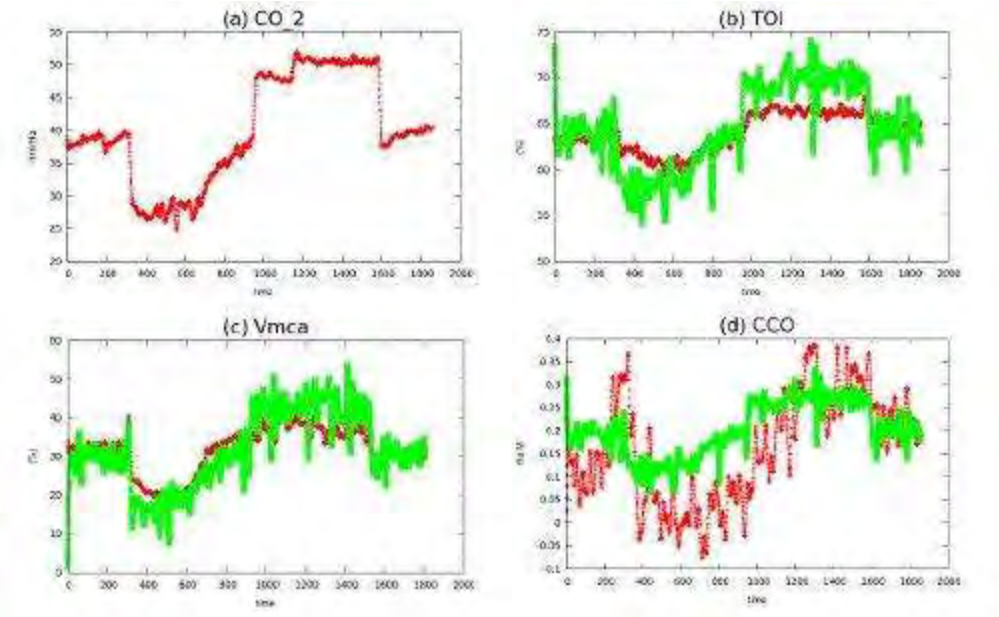

[Figure 1]

Figure 1: Comparison between the experimental (red) and the model derived (green) profiles

1003

STACHYBOTRYS MICROSPORA TRIPRENYL PHENOL-7 (SMTP-7), A NOVEL THROMBOLYTIC AGENT, ATTENUATES REPERFUSION INJURY AFTER TRANSIENT FOCAL CEREBRAL ISCHEMIA IN RATS

Y. Akamatsu[1], A. Saito[2], H. Shimizu[3], M. Mekawy[4], H. Sawada[5], H. Kasuya[5], K. Hasumi[6], T. Tominaga[1]

[1]Neurosurgery, Tohoku University Graduate School of Medicine, [2]Neurosurgery, Kohnan Hospital, [3]Neuroendovascular Therapy, [4]Tohoku University Graduate School of Medicine, Sendai, [5]TMS. Ltd, [6]Tokyo University Agriculture and Technology, Tokyo, Japan

Background and purpose: Fibrinolytic therapy is one of the most effective treatment for acute ischemic stroke, however, the indication is limitted due toa risk of hemorrhagic transformation. The purpose of the present study was to investigate the effect of a new fibrinolytic agent, Stachybotrys microspora triprenyl phenol-7 (SMTP-7) on transient focal cerebral ischemia in rats

Method: A total of 84 rats underwent 2 hr of transient focal cerebral ischemia using intraluminal suture to occlude the origin of the middle cerebral artery (MCA). 10mg/kg of SMTP-7 or vehicle was intravenously administered; bolus injection of 10% of the total amount followed by continuous infusion for 30-min. Regional cerebral blood flow (rCBF) was measured using a laser speckle blood flow imaging system during and after ischemia. Volume of ischemic lesion was evaluated at 24 hr after reperfusion, and several factors related to reperfusion injury, such as superoxide, nitrotyrosine, endothelin-1 (ET-1), matrix metalloproteinase-9 (MMP9), and aquaporine-4 (AQP4), were compared between the groups.

Results: The lesion volume was significantly smaller (17.4±13.0% vs. 26.5±6.98 % of bilateral hemispheric volume,*P*=0.03). rCBF at 60 minutes after reperfusion improved better in the SMTP-7 than in the vehicle group. Expressions of superoxide, nitrotyrosine, ET-1, MMP-9, and AQP4 were decreased significantly in the SMTP group compared with the vehicle group.

Conclusion: SMTP-7 reduced the ischemic lesion volume and the factors related to reperfusion injuries. Further investigation will be expected to clarify a clinical relevance of SMTP-7 .

1004

MEASURING CEREBRAL BLOOD FLOW, OXYGEN, TEMPERATURE AND INTRACRANIAL PRESSURE IN A SINGLE MULTI-PARAMETER CATHETER: FIRST DATA FROM A PORCINE STUDY

G. Wöbker[1], A. Heimann[2], P.S.M. Mayr[3], A.N. Obeid[3], R.L. Pauly[4], O. Kempski[2], B. Alessandri[5], Multi-Parametric Brain Sensor

[1]Intensive Care Medicine, HELIOS Klinikum Wuppertal, Wuppertal, [2]Insitute for Neurosurgical Pathophysiology, University Medical Center of the Johannes Gutenberg-University Mainz, Mainz, Germany, [3]Oxford Optronix Ltd., Oxford, UK, [4]Millar Instruments Inc., Houston, TX, USA, [5]Institute for Neurosurgical Pathophysiology, University Medical Center of the Johannes Gutenberg-University Mainz, Mainz, Germany

Introduction: Treatment of pathophysiological processes after traumatic brain injury on the basis of continuous monitoring of tissue oxygen tension (ptiO2) as single modality or in combination with intracranial pressure (ICP) or microdialysis is a major concern for decades. It became obvious that continuous multi-parametric monitoring of brain injured patients should include cerebral blood flow (CBF). Therefore, we combined sensors for $ptiO_2$, ICP, temperature and CBF in a single catheter (multi-parameter brain sensor = MPBS) and validated its functionality in 5 pigs against standard sensors such as Licox® CCI.SB, Raumedic PTO® and Hemedex QFlow 500® probe. The study is supported by the 'Else Kröner-Fresenius Stiftung' (Homburg, Germany, study A33/2008).

Method: The experimental protocol consisted of a oxygen challenge (paO_2 >400 mmHg), hypercapnia ($paCO_2$ >75 mmHg) and hypoxia (paO2 < 40 mmHg) for 5 to 15 min. Each period was preceeded by a normalization period. Due to the different location of catheters in the brain and different measuring principles baseline levels varied between sensors. Therefore, results were described as percent changes from baseline. A total of 20 MPBS, 10 Licox, 5 Raumedics and 5 Hemedex sensors were used and allowed to equilibrate for 2 hours after insertion. Values are given as mean ± SD.

Results: Equilibration time to tissue oxygen following insertion was longer for MPBS compared to Licox. Increased inspired oxygen fraction elevated $ptiO_2$ by 161.5% (±116) for MPBS, 107.1% (±49) for Licox and 221.6% (±218) for Raumedic sensors,. A few sensors from each manufacturer showed a drop of $ptiO_2$ during oxygen challenge that could only partially be explained by simultaneous CBF changes. A slight CBF decrease was observed with several MPBS sensors at the time of increasing inspired oxygen.

Hypercapnia increased CBF measured by MBPS by 29.3% (±27) in 4 animals. In parallel ICP assessed by MPBS and Raumedics sensors rose by 64.2% (±36) and by 139.6% (±143), respectively. CBF showed an inverse reaction in one animal with a decrease in all 4 implanted sensors (-34±22%) and a subsequent $ptiO_2$ reduction. ICP was elevated as expected.

A short hypoxic period (5 min) produced an immediate increase of perfusion which was picked up by MPBS and Hemedex sensors. As soon as mean arterial blood pressure fell below autoregulation this process was inversed and a simultaneous decrease of ptiO2 and CBF could be detected. CBF measured by MPBS dropped by 32,3% (±23). Simultaneously $ptiO_2$ fell by 60.8% (±16). Licox and Raumedics sensors showed a decrease of tissue oxygen by 64.5% (±21) and 66.2% (±20), respectively. The expected ICP increase during hypoxia was 87% for MBPS and 147% for Raumedic sensors. Unfortunately, quick and steep changes of perfusion

following hypercapnia and hypoxia initiated a re-calibration of Hemedex sensors. Thus, perfusion values could often not be recorded and compared to values from MPBS.

Conclusion: Evoked physiological and pathophysiological changes of ICP, CBF and ptiO2 were detected reliably by our new multi-parameter MPBS sensor and by Licox and Raumedic catheters. Additional monitoring of CBF can provide valueable information in respect to treatment (e.g. hyperoxygenation).

1005

A ROLE FOR TORC1-CREB SIGNALING IN NEURONAL SURVIVAL AFTER ISCHEMIA

T. Sasaki[1], H. Takemori[2], Y. Terasaki[1], N. Oyama[1], Y. Sugiyama[1], M. Kawamura[1], Y. Yagita[1], K. Kitagawa[1]

[1]Department of Neurology, Osaka University Graduate School of Medicine, [2]Laboratory of Cell Signaling and Metabolism, National Institute of Biomedical Innovation, Osaka, Japan

Background: The transcription factor cAMP responsive element-binding protein (CREB) mediates diverse responses in the nervous system. The phosphorylation of CREB at Ser133 has been proposed to be a trigger for CREB-dependent gene expression. Recently, the discovery of a family of coactivators named transducer of regulated CREB activity (TORC, also known as CREB Regulated Transcriptional Co-activator (CRTC), with TORC1-3 isoforms), provided new insights on CREB activation (Conkright et al.,Mol Cell, 2003). However, it remains to be clarified whether the intracellular signaling of TORC coactivator is crucial for CREB-dependent neuronal survival.

Methods: Neuronal cultures were prepared from the cortex of embryonic day 16 (E16) rat embryos. To directly detect the CREB-TORC1 activity after OGD, we have transfected adeno-CRE-luciferase reporter, GAL4-CREB, GAL4-bZIP less CREB, or GAL4-TORC1 and rTK-luciferase to cortical neurons and measured these activities using luciferase assays. Immunohistochemistry and Western blot analysis were performed to examine phosphor-CREB (Ser133), TORC1, and phospho-TORC1 (Ser167) after OGD. To elucidate the role of TORC1 in neuronal survival, we have transfected TORC1, TORC1 S167A mutant, or dominant negative TORC1 (DN-TORC1, N-terminal 56 amino acids). Also, CREB-dependent gene expression, such as *Ppargc-1a* (PGC-1a) and *BDNF,* have been examined.

Results: A significant enhancement of CRE activity was detected after 3 hr and continued after 12 h. The activity of the full-length CREB, but not bZIP-less CREB, was enhanced after OGD. TORC1 translocated from the cytoplasm into the nucleus after OGD-reoxygenation, accompanied by the dephosphorylation of TORC1 at Ser 167 followed by the enhancement of its coactivator activity. We found that CRE activity in cortical neurons was enhanced by the overexpression of TORC1, and a constitutively active TORC1 (S167A) further up-regulated CRE activity. The overexpression of TORC1 or the TORC1S167A mutant resulted in a significant decrease of ischemic neuronal death. The overexpression of TORC1 in cortical neurons induced the mRNA expression of PGC-1a and *BDNF* .

Conclusion: The present study demonstrated that TORC1-CREB plays a crucial role in neuronal survival after OGD.

1007

THE ROLE OF FCΓ-RECEPTORS IN CEREBRAL INFLAMMATION AND SECONDARY BRAIN DAMAGE AFTER EXPERIMENTAL TRAUMATIC BRAIN INJURY IN MICE

C. Luh, R. Timaru-Kast, C. Werner, K. Engelhard, S. Thal

Anesthesiology, University Medical Center of the Johannes Gutenberg University Mainz, Mainz, Germany

Objectives: Traumatic brain injury (TBI) results in the development of a marked inflammatory response, including activation of microglia and increased C-reactive protein (CRP) plasma levels during the early post-traumatic period[1]. Evidence from in-vitro BBB (blood-brain barrier) model indicates that e.g. CRP mediates BBB opening via Fcγ-receptors (FcγR)[2]. After neuronal trauma the FcγR may, therefore, not only play an important role for the humoral defense system, but possibly also contribute to brain edema formation. The present study was designed to assess the role of FcγR on histological brain damage, cerebral inflammation, and edema formation following experimental TBI in mice.

Methods: FcγR-/- mice (deficient for FcγRI, FcγRII and FcγRIII) and wild-type mice with the same genetic background (C57Bl6, WT) were randomized to: (1) WT + sham surgery; (2) WT + CCI; (3) FcγR-/- + sham surgery; (4) FcγR-/- + CCI (n=7 per group) and subjected to controlled cortical impact brain injury (CCI). 24h post CCI brain contusion volume was determined in Nissl stained sections and microglia activation (Iba-1 positive cells) in the pericontusional tissue and CRP plasma levels were quantified as markers for inflammatory response. In a separate set of animals hemispheric brain water content were determined 24h after CCI in animals randomized to: (1) WT + sham surgery; (2) WT + CCI; (3) FcγR-/- + sham surgery; (4) FcγR-/- + CCI (n=4 per group); Statistics: Wilcoxon Mann Whitney rank sum test, $p< 0.05$.

Results: The brain damage was significantly smaller in $FcγR^{-/-}$ mice (31.31 ± 4.87 mm^3) compared to the WT mice (41.11 ± 6.84 mm^3). In line with the histological damage microglia activation was markedly reduced in $FcγR^{-/-}$ animals (261.9 ± 31.5 Iba-1 pos. cells / mm^2) vs. WT (356.7 ± 80.5 Iba-1 pos. cells / mm^2). After experimental TBI CRP plasma levels increased only in WT (12.0 ± 3.1 µg/ml), but not in $FcγR^{-/-}$ mice (7.3 ± 1.4 µg/ml) mice compared to sham operated animals (FcγR-/-: 5.1 ± 1.4 µg/ml, WT: 5.7 ± 0.8 µg/ml). 24 hours after CCI brain water content increased significantly in comparison to sham operated animals (WT + sham surgery: 78.89 ± 0.8 %; FcγR-/- + sham surgery: 78.80 ± 0.5 %) without difference between WT (81.16 ± 0.6 %) and FcγR-/- (81.02 ± 0.6 %) mice.

Conclusion: FcγR seems to play a crucial role in the posttraumatic inflammatory response. Prevention of action at the FcγR significantly limited microglia activation, CRP plasma levels and resulted in a reduced secondary brain damage. Accordingly, infarct volume and inflammatory response after focal cerebral ischemia was reduced in FcγR deficient mice in comparison to wild-type litter mates[3]. In contrast to in-vitro data suggesting a FcγR-induced BBB disruption[2], brain water content was not reduced in FcγR deficient mice. Therefore, posttraumatic brain edema formation is not mediated by Fcγ receptors.The present data suggest that post CCI FcγR activate cerebral microglial and, thereby, contribute to secondary brain damage by enhancing cerebral inflammation.

Litrature: 1.) Meisner. Crit Care 2006; Feb;10(1):R1; 2.) Kuhlmann, Stroke 2009;40:1458-1466; 3.) Komine-Kobayashi, Stroke 2004;35:958-963

1008

SERUM FERRITIN IS NOT AN ACUTE PHASE PROTEIN AFTER EXPERIMENTAL STROKE

I. García-Yébenes[1], V.G. Romera[1], A. Moraga[1], M. Sobrado[1], J.M. Pradillo[1], T. Sobrino[2], T. Gasull[3], A. Dávalos[3], M. Castellanos[4], J. Serena[4], M.A. Moro[1], I. Lizasoain[1]

[1]Pharmacology, Universidad Complutense, Madrid, [2]Neurología, Hospital Santiago de Compostela, Santiago de Compostela, [3]Neurociencias, Hiospital Germans Trias i Pujol, Barcelona, [4]Neurología, Hospital Dr Josep Trueta. IdiBGi., Girona, Spain

Background and objectives: Ischemic stroke is one of the leading causes of death and disability in developed countries. Some clinical studies pointed out that high levels of iron measured as serum ferritin, were associated to a worse outcome after stroke (1) and even to a higher risk of hemorrhagic transformation after t-PA treatment (2). However, it is not known whether ischemic damage might increase ferritin levels as an acute phase protein or rather if iron overload shown as high serum ferritin affects stroke outcome (3). The objective of this work is to study the effect of stroke on serum ferritin.

Methods: Mice weighing 15 g were fed for 8 weeks with a standard diet or with a diet supplemented with 2.5% carbonyl iron to simulate iron overload. Mice were submitted to permanent and transient focal ischemic models and an additional sham group was made as a control. Focal permanent ischemia was carried out by using an in situ thromboembolic model whereas transient model was induced by a ligature model with further reperfusion. In situ thromboembolic model was carried out as previously described (4) injecting thrombin in the bifurcation of the middle cerebral artery (MCA) and excluding animals with spontaneous reperfusion (n=5). In the ligature model the ipsilateral common carotid and the MCA were tied for 1 or 3 hours (transient model)(n=6). 100 µl of blood was collected through the tail before, 3 and 24 hours after the ischemia. Finally, serum ferritin was measured.

Results: Treatment with iron diet produced a significant increase on the basal levels of serum ferritin in all the groups studied (100±30% in control group, 380±119% in iron overload group; basal level in control group was 170±59 ng/ml). However, serum ferritin did not change after permanent or transient ischemia in any group (control groups: 137±48% and 97±23% at 3 and 24 hours respectively after ischemia; and iron overload groups: 394±115% and 372±129% at 3 and 24 hours respectively after ischemia).

Conclusions: Serum ferritin levels do not change after cerebral ischemia. Ferritin is a good indicator of iron levels but it is not an acute phase reactive protein after experimental ischemia.

References:

(1) Davalos et al. Neurology, 2000

(2) Millan et al. Stroke, 2007

(3) Millerot et al. J Cereb Blood Flow Metabol. 2005

(4) Orset et al. Stroke, 2007

Supported by Spanish Ministry of Education (SAF2008-03122) and Health (RENEVAS RD06/0026/0005)

1010

RESVERATROL-MEDIATED NEUROPROTECTION IN GLOBAL CEREBRAL ISCHEMIA CORRELATES WITH CREB AND GSK-3B ACTIVATION-DEPENDENT OF PI3-K/AKT

F. Simao, A. Matte, C.A. Netto, C.G. Salbego

Biochemistry, Federal University of Rio Grande do Sul, Porto Alegre, Brazil

Objectives: Accumulating evidence indicates that the polyphenol resveratrol (RSV) potently protects against cerebral ischemia damage due to its oxygen free radicals scavenging and antioxidant properties. However, the role and contribution of PI3-K/Akt/GSK-3b and cyclic-AMP response element binding protein (CREB) is unclear and was the subject of the current study. The purpose of this study was determine whether resveratrol protects against delayed neuronal cell death in hippocampal CA1 following transient global cerebral ischemia in rats and investigate the signaling mechanism responsible for the neuroprotective effects of RSV.

Methods and results: Experimental model of transient global cerebral ischemia was induced in Wistar rats by the four vessel occlusion method for 10 min and followed by different periods of reperfusion. Nissl stained indicated extensive neuronal death at 7 days after I/R. Administration of resveratrol by i.p. injections (30 mg/kg) for 7 days before ischemia significantly attenuated neuronal death. Akt/GSK-3b and CREB signaling pathways appear to play a critical role in RSV neuroprotection, as RSV pre-treatment increased the phosphorylation of Akt/GSK-3b and CREB in 1h and 4h in CA1 hippocampus after global cerebral ischemia. Furthermore, administration of LY294002, an inhibitor of PI3-K, compromised the neuroprotective effects of RSV and decreased the level of p-Akt, p-Gsk-3b and p-CREB after injury.

Conclusions: Taken together, the results suggest that RSV protects against delayed ischemic neuronal death in the hippocampal CA1 by maintaining the pro-survival states of GSK-3b and CREB signaling pathways dependent of PI3-K/Akt.

1011

IRON OVERLOAD INCREASES BRAIN DAMAGE INDUCED BY EXPERIMENTAL ISCHEMIA

I. García-Yébenes[1], V.G. Romera[1], A. Moraga[1], M. Sobrado[1], T. Gasull[2], A. Dávalos[2], M. Castellanos[3], J. Serena[3], M.A. Moro[1], I. Lizasoain[1]

[1]Pharmacology, Universidad Complutense, Madrid, [2]Neurociencias, Hiospital Germans Trias i Pujol, Barcelona, [3]Neurología, Hospital Dr Josep Trueta, IdiBGi, Girona, Spain

Background and objectives: Ischemic stroke is one of the leading causes of death and disability in developed countries. Clinical and experimental studies (1,2) showed that higher levels of iron were associated to a worse outcome after stroke. In addition, it has been demonstrated that treatment with iron chelating agents after stroke might reduce ischemic injury (3,4). However, other authors did not observe this deleterious effect of iron in experimental ischemia (5). The objective of this study was to evaluate the contribution of iron overload to ischemic damage using different models.

Methods: Mice weighing 15 g were fed for 8 weeks with a standard diet or with a diet supplemented with 2.5% carbonyl iron to simulate iron overload. Mice were submitted to permanent and transient focal ischemic models. Focal permanent ischemia was carried out by using an in situ thromboembolic model or by using a distal ligature model, whereas transient model was induced by the ligature model with further reperfusion. In situ thromboembolic model was carried out as previously described (6) injecting thrombin in the bifurcation of the middle cerebral artery (MCA) and excluding animals with spontaneous reperfusion (n=5). In the ligature model, the ipsilateral common carotid and the MCA were tied permanently (permanent model), or for 1 or 3 hours (transient model)(n=7). 24 hours after surgery, animals were sacrificed, the brain was removed and the infarct volume was measured by TTC staining.

Results: Animals submitted to permanent ischemia had the same infarct volume, either in the in situ thromboembolic model (17.5±3.8% vs 16.5±4.1%) or in the ligature model (11.7±2.9% vs 13.4±3.8%), with or without iron overload respectively. However, in mice submitted to transient ischemia, early (1 hour; 9±6.1% vs 3.4±1.9% in control group) but not late reperfusion (3 hours; 11.2±4.7 vs 13.5±2.9 in control group) increased ischemic damaged in the iron overload group.

Conclusions: Iron worsens ischemic damaged induced by early reperfusion in the transient model. These results strongly suggest that iron plays an important role in penumbra evolution to infarct and subsequent worsening in the outcome after stroke.

References:

(1) Davalos et al. Neurology, 2000

(2) Castellanos et al. Brain Res. 2002

(3) Patt et al. J Pediatric Surg. 1990

(4) Millerot-Serrurot et al. Neurochem Int. 2008

(5) Millerot et al. J Cereb Blood Flow Metabol. 2005

(6) Orset et al. Stroke, 2007

Supported by Spanish Ministry of Education (SAF2008-03122) and Health (RENEVAS RD06/0026/0005)

1012

A DECREASE OF INHIBITORY INFLUENCE OF HORMONES ON ADENYLYL CYCLASE SYSTEM IN THE BRAIN OF RATS WITH DIABETES AND HYPERGLYCEMIA

A.O. Shpakov, K.V. Derkach, O.V. Chistyakova, V.M. Bondareva

Biochemistry, Sechenov Institute of Evolutionary Physiology and Biochemistry, St. Petersburg, Russia

A wide spectrum of the disturbances of the functions of the nervous system is occurred in the patients with the diabetes mellitus of the types 1 and 2 (DM1 and DM2). It is supposed that one of the main causes of these disturbances is the alteration of sensitivity of the tissues of nervous system to regulatory action of the hormones realized via hormone-sensitive G protein-coupled signaling systems. We studied the functional activity of AC inhibiting and stimulating signaling pathways in the brain of rats with 5-days streptozotocin DM1, 180-days neonatal DM2, as well as acute one-hour hyperglycemia induced by using of the high doses of glucose. It was found that in the brain of control animals the hormones activating Gi proteins-coupled receptors decrease forskolin-stimulated AC activity in a dose-dependent manner and selectively increase GTP binding activity of Gi proteins. The most effective inhibitors of AC were somatostatin, selective D2-agonist bromocryptine, as well as 5-methoxy-N,N-dimethyltryptamine and 5-nonyloxytryptamine, the selective agonists of 5-hydroxytryptamine receptor of the type 1. In the condition of DM1 which is characterized by insulin deficiency and strongly expressed hyperglycemia the significant weakening of both AC inhibiting effects of these hormones and a decrease of their stimulating effects on GTP binding was observed. In the brain of rats with EDM2 and acute hyperglycemia these changes in the sensitivity of AC system to hormones inhibiting AC have been expressed more poorly, and the regulatory effects of bromocryptine are not changed. At the same time, the stimulating effects of relaxin, pituitary AC-activating polypeptide and β-agonist isoproterenol on AC activity and Gs proteins in the condition of DM and hyperglycemia did not change or slightly decreased. Thus, we found the decrease of the response of AC signaling system to the hormones, inhibitors of AC activity, in the brain of rats in the conditions of DM and acute short-term hyperglycemia, the most expressed in the case of DM1. The main disturbances are localized at the level of Gi proteins that be connected both with decrease in their expression and with disturbances of interaction between Gi proteins and other signaling proteins in the condition of high level of glucose.

1013

REPERFUSION AFTER RECANALIZATION OF THE MCA STARTS FROM THE PERIPHERY OF THE ISCHEMIC AREA

Y. Gursoy-Ozdemir, H. Karatas, S.E. Erdener, T. Dalkara

Dept. of Neurology and Institute of Neurological Sciences, Hacettepe University, Ankara, Turkey

Objective: Recent clincal trials indicate that reperfusion and recanalization are independent factors to predict a good neurological outcome after tPA treatment (1, 2). These observations suggest that no-reflow may be one of the mechanisms responsible for this discrepancy between recanalization and reperfusion and that reperfusion may partly be obtained in the penumbra area. In this study, we aimed to investigate the kinetics of microcirculatory recovery in the ischemic penumbra and core after tPA induced recanalization.

Methods: Distal middle cerebral artery occlusion in mice was performed with application of 10% $FeCl_3$-soaked filter paper strip over the trunk of the artery. FITC-Dextran-70S (Sigma, 0.5 mg in 0.1 ml saline) was injected to visualize vessels and monitor the clot formation in the distal MCA through a cranial window. Intravenous tPA (Actilyse; INN alteplase, Boehringer Ingelheim) was started 10 minutes after FeCl3 application. Live imaging of clot formation and recanalization were monitored with intravital fluorescent microscopy. The tissue reperfusion was monitored with laser-speckle imaging.

Results: 10% $FeCl_3$ application triggered clot formation at multiple foci within the distal MCA 3 minutes after application and, the lumen was completely obliterated in 10-20 minutes. Flow recordings showed a rapid rCBF drop in 10 minutes after $FeCl_3$ in the ischemic hemisphere. Reperfusion was obtained with early (10 minutes after $FeCl_3$) tPA administration in half of the mice, whereas recanalization was fully achieved in 2/3rd and partially in 1/3rd of the mice. Two hours after tPA, the rCBF reached twice the ischemic values in the periphery of ischemic area, whereas there was no significant rCBF change in the core during the 2-hour follow-up period as previously reported in rats subjected to clot embolism and treated with tPA (3).

Discussion: Our results suggest that although recanalization is achieved via tPA administration, it may not lead to reperfusion of deeply ischemic tissue. Microvascular stasis and no-reflow may be the mechanism of failed reperfusion. To elucidate the mechanisms of reperfusion failure, further studies are warranted to increase the success of reperfusion therapies.

References:

1) De Silva DA, Fink JN, Christensen S, Ebinger M, Bladin C, Levi CR, Parsons M, Butcher K, Barber PA, Donnan GA, Davis SM; Echoplanar Imaging Thrombolytic Evaluation Trial (EPITHET) Investigators. Assessing reperfusion and recanalization as markers of clinical outcomes after intravenous thrombolysis in the echoplanar imaging thrombolytic evaluation trial (EPITHET). Stroke. 2009 Aug;40(8):2872-4.

2) Recanalization and reperfusion therapies for acute ischemic stroke. Molina CA, Alvarez-Sabín J. Cerebrovasc Dis. 2009;27 Suppl 1:162-7.

3) Niessen F, Hilger T, Hoehn M, Hossmann KA (2002) Thrombolytic treatment of clot embolism

in rat: comparison of intra-arterial and intravenous application of recombinant tissue plasminogen activator. *Stroke* 33:2999-3005.

1014

BRAIN METABOLISM BY HIGH RESOLUTION *IN VIVO* ^{13}C NMR SPECTROSCOPY

J.M.N. Duarte[1,2], B. Lanz[1], R. Gruetter[1,3]

[1]Laboratory for Functional and Metabolic Imaging, Center for Biomedical Imaging, Ecole Polytechnique Federale de Lausanne, [2]Faculty of Biology and Medicine, University of Lausanne, [3]Department of Radiology, Universities of Lausanne and Geneva, Lausanne, Switzerland

Objectives: The combination of dynamic ^{13}C nuclear magnetic resonance (NMR) spectroscopy with the infusion of ^{13}C-enriched substrates is a powerful method to probe metabolic fluxes in vivo. With this work we aimed to study brain metabolism with higher sensitivity and spectral resolution provided by the increased magnetic field at 14.1T.

Methods: Male Sprague-Dawley rats (n=5, 276±11 g) were prepared and maintained during the NMR experiment as previously described [1]. Under α-chloralose anaesthesia, [1,6-^{13}C]glucose was infused to induce a step function in plasma fractional enrichment (FE) [2], while ^{13}C spectra were measured. Localized ^{1}H and ^{13}C NMR spectroscopy was performed on a 14.1 T, 26 cm VNMRS spectrometer (Varian, Magnex) with a coil consisting of a ^{1}H quadrature surface coil and a ^{13}C linearly polarized surface coil. ^{13}C NMR spectra were acquired using semi-adiabatic distortionless enhancement by polarization transfer (DEPT) combined with ^{1}H localization [2], and quantified with LCModel [5]. Metabolic modelling was performed as in previous studies [6].

Results: Excellent sensitivity was evident from the measured ^{13}C spectra. High spectral resolution allowed complete separation of C2 and C3 resonances of glutamate and glutamine, which was not possible at lower fields, as well as good observation of their multiplets resulting from homonuclear coupling in multiply labelled metabolites. FE in aliphatic carbons of glutamate and glutamine were determined in 5 animals with high reproducibility, thus increasing accuracy in determination of cerebral metabolic fluxes with appropriate mathematical models. Multiplets were clearly observed and isotopomer analysis can be performed in vivo for different metabolites, including glutamate, glutamine, aspartate and GABA. FE of glutamate and glutamine carbons was accurately determined with 3 minutes of time resolution. At lower temporal resolution there was reliable determination of labelling incorporation into carbons of metabolites with slow synthesis rate or occurring at lower concentration, like aspartate and GABA (12 minutes) or glutathione and N-acetylaspartate (30 minutes). Preliminary modelling of the observed data resulted in V_{TCA} of 0.37±0.01mmol/kg/min in neurons and 0.12±0.01mmol/kg/min in glia and V_x=0.57±0.05mmol/kg/min.

Conclusions: Direct detection of ^{13}C enrichment of cerebral metabolites with DEPT was improved at 14.1 T with gain in sensitivity and especially in spectral resolution. Upon infusion of [1,6-^{13}C]glucose, numerous ^{13}C-enriched metabolites could be quantified over the entire time course. In addition, LCModel allowed maximizing the amount of information that can be extracted from ^{13}C spectra. All this together may increment the reliability of complex mathematical models describing cerebral energy metabolism.

References: [1] Duarte et al. (2009) J Neurochem 111:368. [2] Henry et al. (2003) MRM 50:684. [3] Gruetter (1993) MRM 29:804. [4] Mlynárik et al. (2008) J Mag Reson 194:163. [5] Henry et al. (2003) NMR Biomed 16:400. [6] Gruetter et al. (2001) AJP 281:E112.

This work was supported by Centre d'Imagerie BioMédicale (CIBM) of the UNIL, UNIGE, HUG, CHUV, EPFL and the Leenaards and Jeantet Foundations; and by SNF grant 131087.

1015

SUB-CHRONIC TREATMENT WITH MERCURIC CHLORIDE ELICITS BEHAVIORAL DEFICITS AND INCREASES BRAIN SEROTONIN AND DOPAMINE METABOLISM IN RATS

H. Naz, Neurochemistry and Biochemical Neuropharmacology Research Unit

Biochemistry, University of Karachi, Karachi, Pakistan

Introduction: The function of the brain can be modulated by a number of environmental factors such as stress, toxins, exercise, diet, physical and mental abuse, organic solvents, pesticides and other innumerable sources. Unlike other environmental factors, Mercuric Chloride is not an atmospheric pollutant. Its pollution and hazards are related to its extensive use in antiseptics, photographic operations, skin ointments, PVC boots, dental amalgam and also to occupational exposure. These subsequently lead to autoimmune side effects, neurasthenia, epilepsy, hematemesis and neurotoxic side effects. Role of serotonin and dopamine has been well documented in various psychological and neuropsychiatric disorders.

Objective: In view of the neurotoxic effects of Mercuric Chloride the study was designed to explore the behavioral and neurochemical effects in terms of brain Serotonin and Dopamine metabolism in experimental animals.

Material and methods: Mercuric Chloride was injected at a dose of 1mg/ml/kg on alternate days to locally bred female Albino Wistar Rats. The controls received injection of saline. The experiment continued for ten days. Food intakes and body weights were monitored on alternate days. Open field activity was monitored five minutes after the injection on the tenth day. Animals were decapitated on the eleventh day and brain was dissected for neurochemical analysis using HPLC-EC (High Perfomance Liquid Chromatography using ElectroChemical Detector) method. The experimental procedure was carried out keeping in view the ethical conditions approved by Local Animal Care Committee.

Results: Mercuric Chloride increased locomotor activity, decreased latency to move, corner sittings and food intake. Neurochemical analysis revealed that brain tryptophan concentration, 5-Hydroxy indole acetic acid (5-HIAA) and Dihydroxy phenyl acetic acid (DOPAC) were increased, while 5-hydroxy tryptamine (5-HT) and Dopoamine (DA) were decreased in the Mercuric Chloride injected rats. The results also showed an increase in brain 5-HT and DA turnover ratio in Mercuric Chloride injected rats.

Conclusion: To conclude we can suggest that along with tissue necrosis and other adverse effects; administration of mercuric chloride induced increases of brain 5-HT and DA metabolism may tend to contribute to Anorexia and Hyperactivity seen in Mercuric Chloride exposed rats. Thus Mercuric Chloride could be a risk factor in the development of neurological disorder.

The full length paper is published in: Pak.J.Pharm.Sci., 21(1), January 2008. pg 7-11.

1017

MODEL SELECTION IN MRI DCE-T_1 STUDIES IN GLIOBLASTOMAS

J.R. Ewing[1], H. Bagher-Ebadian[2], S. Nejad-Davarani[2], A.S. Arbab[3], L. Scarpace[4], Q. Jiang[1], T. Mikkelsen[4], R. Jain[3]

[1]Neurology, [2]Henry Ford Hospital, [3]Radiology, [4]Neurosurgery, Henry Ford Hospital, Detroit, MI, USA

Objectives: To determine the appropriate model for analyzing Magnetic Resonance Imaging (MRI) Dynamic Contrast Enhanced T_1-weighted (DCE-T_1) studies.

Methods: In a 3T GE Excite HD MR system, DCE-T_1 studies were conducted in eight treatment-naïve patients with Glioblastoma (GBM). Before contrast agent (CA) administration, T_1 mapping was performed using DESPOT1 [1] TR ~ 5.8 ms, flip angles 2, 5, 10, 15, 20 and 25º , 256X128, FOV 240mm, sixteen 5mm slices, no gap.Twenty seconds after the start of the DCE-T_1 sequence CA (Magnevist, 0.1 mmol/kg) was injected. Seventy image sets - 20º flip angle and other parameters as above - were acquired in 6.8 min. The change in R_1 ($R_1=1/T_1$) with time was used as a measure of CA concentration.

The full model is shown in Equation 1 [2 , 3] (see Figure). Ct(t) and Cp(t) are the tissue and plasma concentration-time traces of CA, v_D is the vascular distribution volume fraction, K^{trans} is the forward vascular transfer constant, and k_b is the reverse vascular transfer constant.

A set of nested models was fitted [4], each identified by its number of model parameters: Model 1 - no leakage, v_D only; Model 2 - leakage with no vascular reabsorption, v_D and K^{trans}; Model 3 - the full model, v_D , K^{trans}, and k_b. Two F statistics (2 vs 1 and 3 vs 2) were computed to assess the contribution of the higher-order model, with the p=0.05 level used as a mask in the formation of parameter maps. This yielded three maps of parameters: a full brain map of v_D; inside that was a map of K^{trans}, and inside that, a map of k_b. Additionally, using Patlak's extended model, the final fit in the area defined by the full model was fitted in a linear regression, and R^2 calculated.

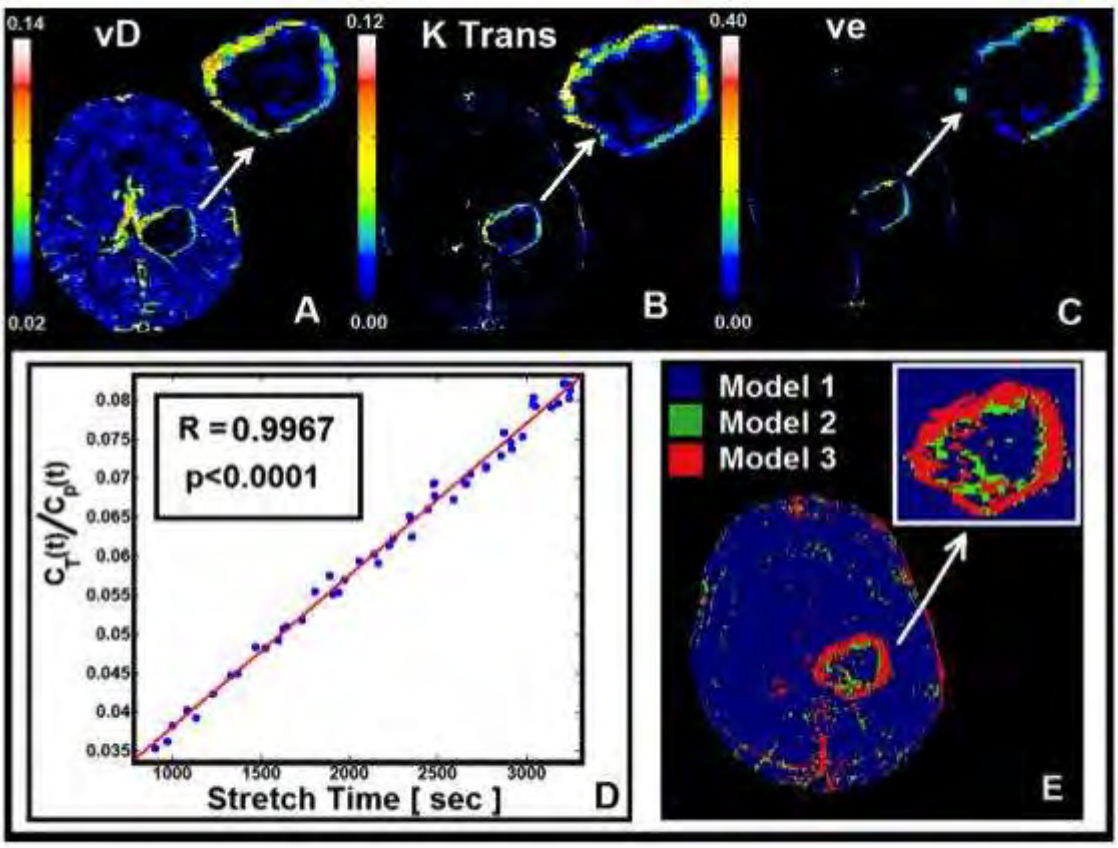

$$C_t(t) = K^{trans} \int_0^t e^{-k_b(t-\tau)} C_p(\tau) d\tau + v_D C_p(t) \qquad [1]$$

[Model Parameters in GBM]

Results and conclusion: The Figure shows maps of v_D, K^{trans}, and v_e in a typical patient, along with the regions where the 3 models hold. It shows that in a typical GBM the proportion of the lesion fitted with the full model is mostly confined to the rim of the lesion. In this region R^2 was 0.99, making any additional model parameters unnecessary. Forty-seven slices in eight patients contained tumor. Mean values: Model 1 (normal tissue), white matter v_D = 0.7%, grey matter v_D = 2.2%. Model 2, v_D = 2.8%, K^{trans} = 5.8x10^{-3} [min^{-1}]. Model 3, v_D = 6.6%, K^{trans} = 4.2x10-2 [min^{-1}], k_b = 0.31 [min^{-1}], yielding an interstitial volume fraction, v_e ~ 13%. Group mean R^2 = 0.97. This lends a note of caution to wholesale fitting of DCE-T_1 data in GBMs without attention to the validity of the model.

References: [1] S. C. Deoni , et al., Magn Reson Med, 53, 237-41, 2005. [2] C. Patlak and R. Blasberg, J CBF Met, 5, 584-590, 1985.[3] P. S. Tofts, et al., J MRI, 10, 223-32, 1999.[4] J. R. Ewing, et al., J CBF Met, 26, 310-320, 2006.

1018

INFLUENCE OF INTRANASAL ADMINISTRATION OF INSULIN AND SEROTONIN ON COGNITIVE FUNCTIONS IN FEMALE RATS WITH TYPE 2 NEONATAL DIABETES MELLITUS

O.V. Chistyakova, I.B. Sukhov, V.N. Shipilov, V.M. Bondareva, A.O. Shpakov

Biochemistry, Sechenov Institute of Evolutionary Physiology and Biochemistry, St. Petersburg, Russia

Insulin- and serotonin-regulated signaling systems play a key role in development and differentiation of the nervous system, memory formation and regulation of cognitive functions. The numerous data obtained show that the disturbances in these systems in the condition of diabetes mellitus (DM) led to nervous system dysfunctions and neurodegenerative diseases. Using the Morris Water-Maze task we studied spatial memory formation in the rats with the type 2 DM compared and the influence of intranasal insulin and serotonin treatment on the formation of cognitive functions after intranasal administration of the hormones (25 mkg/kg of body weight). Hormone treatment spent daily, beginning for a week prior to the experiments and continuing in the course of testing (for 30 min prior to the beginning of the test). It was showed that in control rats the formation of long-term memory were active than in diabetic animals. The control animals did not expose a reliable effect of insulin on spatial learning, while in the case of diabetic rats insulin exerted a positive influence on the processes of learning and memory, the efficiency of learning, as well as on decreasing the time of spatial memory formation. Intranasal application of serotonin induced the improvement of the spatial memory, whereas on the case of animals with DM2 serotonin treatment led to positive influence on the long-term memory, but not essentially changed the spatial memory. The conclusion was made that intranasal insulin and serotonin delivery can be considered as successful approach for treatment of cognitive dysfunctions in DM2.

1019

PRIMITIVE REFLEXES IN PREMATURE AND HIGH RISK INFANTS

M. Sohn, Y. Ahn, S. Lee

Department of Nursing, Inha University, Incheon, Republic of Korea

Objectives: Despite the advances in medical technology and improved neonatal care, premature infants still have higher mortality and morbidity rates and higher rates of neurological and developmental disorders compared to full-term matured infants. Careful neurological assessments provide important information for their early diagnoses and treatments. However, neurological assessment for premature infants is often difficult to perform due to their small body sizes and lack of vocal and motor responses. Primitive reflexes have been used as one of the earliest, simplest, and most frequently used assessment tools among health care providers for neonatal and young children,[1] but the lack of evidence in the following areas still exist: First, the responses of primitive reflexes have been categorized mostly as dichotomous responses, but primitive reflexes often present various degrees of neurological response to stimulus, and clinicians are missing those responses which might be clinically meaningful. Second, few data exists about primitive reflexes in premature and high-risk infants and it is not clear how their incomplete reflexes are related to clinical conditions. This study is a cross-sectional descriptive study to 1) evaluate three primitive reflexes in Korean high risk infants to describe the various levels of their responses, and 2) examine relationships between primitive reflexes and clinical variables to explore the meaning of primitive reflexes in clinical context.

Methods: A neonatal intensive care unit nurse assessed the Moro, Babinski and sucking reflexes and summarized clinical variables from medical records. Clinical variables included birth-related variables, brain sonogram results, the Clinical Risk Index for Babies, Anderson Behavioral State Scale and Infant Coma Scale.[2]

Results: Data of total 67 infants were analyzed. Among them, 52% were male, 75% were preterm births, and 67% had pathologic abnormalities. The mean gestation age was 33.60 (±3.58) weeks and the mean birth weight was 2048.12 (±741.73) grams. The sucking reflex presented normal response most frequently (61.2%), followed by the Babinski reflex (58.2%) and the Moro reflex (41.8%). Abnormal responses were most frequently presented in the Moro reflex (38.1%), followed by the Babinski reflex (33.3) and the sucking reflex (11.1%). Infants who presented normal responses of the Babinski and sucking reflexes were more likely to have older gestational ages, heavier birth weights, heavier current weights, and higher Apgar scores. They also presented a statistically significant negative correlation with length of hospitalization and worse respiratory conditions. Abnormal brain sonogram results presented a statistically significant negative correlation with only the Babinski reflex.

Conclusion: Primitive reflexes in high-risk infants are an important part of clinical assessment. Primitive reflexes were highly associated with healthier birth and neurological conditions, but may reflect birth outcomes more than pathologic problems.

References:

1. Zafeiriou, D. I. (2004) Primitive reflexes and postural reactions in the neurodevelopmental examination. *Pediatr Neurol. 31*(1):1-8.

2. Ahn, Y. M., Sohn, M., & Lee, S. M. (2010) Evaluation of mental status in high-risk neonates using infants coma scale. *J Korean Acad Nurs, 40*(4), 561-570.

1023

HESC-DERIVED NEURAL PROGENITORS ENHANCE FUNCTIONAL RECOVERY ASSOCIATED WITH THE REGULATION OF INFLAMMATION AND NEUROGENESIS IN MICE WITH STROKE

K. Puttonen[1], K. Savolainen[1], M. Ruponen[1,2], T. Malm[1], S. Paulo[1], J. Koponen[3], S. Ylä-Herttuala[3], J. Koistinaho[1,2], O. Hovatta[3], A. Muona[1,4]

[1]Neurobiology, A.I. Virtanen Institute, University of Eastern Finland, [2]School of Pharmacy, University of Eastern Finland, [3]Biotechnology and Molecular Medicine, A.I. Virtanen Institute, University of Eastern Finland, [4]Medeia Therapeutics Ltd, Kuopio, Finland

Objectives: Treatment of cerebral stroke, the 3rd leading cause of death worldwide, is restricted to the tPA-therapy in a 3-hour window and rehabilitation afterwards. Since the late degenerative processes, i.e. inflammation and apoptosis, contribute to the infarction, therapeutic approaches targeted to subacute or late phases of the injury may be beneficial. Cell replacement is among the most promising neurorestorative therapies. Human embryonic stem cells (hESCs) divide indefinitely and differentiate into any kind of cells. Studies have shown that transplanted ESC-derived neural progenitor cells (NPCs) survive and enhance functional recovery in rodents with cerebral stroke(1), but the mechanism is still obscure. While direct neuronal replacement may not play a prominent role in the recovery, it has been proposed that modulation of inflammation would be behind the beneficial outcome. Here we studied both short- and long-term integration, migration, survival and maturation of hESC-derived NPCs in the brains of mice with cerebral stroke. An *in vitro* co-culture study was used to dissect cell-mediated response to hypoxia.

Methods: 200 000 hESC-derived neural progenitors(2,3) were labeled with either ultra small superparamagnetic iron-oxide (USPIO) nanoparticles or green fluorescent protein (lenti-GFP) and then transplanted into the ipsilateral striatum of aged middle cerebral artery occluded Balb/c mice. MRI was proceeded every 1-2 weeks to visualize lesion and transplanted cells. Sensomotoric function was evaluated weekly by the adhesive removal tape test and by CatWalk automated gait analysis (Noldus). Immunohistochemical (IHC) staining with various neuronal (DCX, Tuj1) and astrocytic (GFAP) markers was used to phenotype the grafted cells. To detect the involvement of mouse cells, CD45 (detecting all leucocytes), Iba-1 (microglia), COX-2 (inflammation marker expressed in neurons in the CNS), and CD3 (early T-cell lineages) stainings were done. To determine the role of cytokines and growth factors in the cell-mediated recovery, hNPCs were co-cultured with hypoxic mouse cortical cells, medium was collected, and analysed by ELISA.

Results: MRI showed that USPIO-labeled hNPCs migrated towards the ischemic site already 3 days post-transplantation and in *in vitro* co-cultures hNPCs matured into neurons within a week. CatWalk revealed a long-term and significant ($p < 0.001$) functional recovery already two weeks after transplantation. With tape test, significant recovery ($p < 0.05$) was achieved at 12 week time point. Preliminary IHC suggests that transplanted cells in ischemic brain may enhance endogenous neurogenesis and regulate inflammation by attenuation of neuronal COX-2 and by recruiting protective microglia.

Conclusions: Human ESC-derived NPCs injected into the striatum of mice with cortical ischemia migrate towards the adjacent cortical infarct. They improve long-term sensomotoric recovery most likely by attenuation of harmful inflammation and by up-regulation of endogenous neurogenesis.

References:

(1) Bliss et al., Stroke. 38(2 Suppl):817-26, 2007.

(2) Nat et al., Glia. 55(4):385-99, 2007.

(3) Hicks et al., Eur J Neurosci. 29(3):562-74, 2009.

1024

THE SIMON EFFECT IN RATS: BEHAVIORAL ANALYSIS COMBINED WITH FUNCTIONAL µPET IMAGING USING [^{18}F]FLUORODEOXYGLUCOSE

H. Endepols[1], C. Marx[1], B. Lex[2], C. Calaminus[2,3], W. Hauber[2], B. Neumaier[1], H. Backes[1], G. Mies[1], R. Graf[1]

[1]Max Planck Institute for Neurological Research, Cologne, [2]Institute of Biology, University of Stuttgart, Stuttgart, [3]Laboratory for Preclinical Imaging and Imaging Technology, University of Tübingen, Tübingen, Germany

Objectives: In stimulus-response tasks, reaction times and error rates are increased if stimulus and response sides are incongruent, a phenomenon termed “Simon effect”. Such a response conflict arises for example, if the tone pitch of an auditory stimulus presented on the subject´s right side indicates that a response to the left is required. It is thought that stimulus dimensions (tone pitch, speaker location) are processed via different channels ("dual-route model" [1]), and response conflicts may occur during binding of feature codes ("event file model" [2]) and/or during sensorimotor integration, if stimulus-response associations of the two routes are not compatible. Little is known about the neural bases of dual-route and event file processing, but anterior cingulate cortex and dorsomedial prefrontal cortex seem to be involved in conflict monitoring and resolution in humans [3]. Using behavioral positron emission tomography (PET) in rats, our aim was to assess brain areas, which are metabolically active during the occurrence of response conflicts, and whether we can identify mechanisms of post-conflict adjustments.

Methods: An auditory Simon task for rats was established in an operant chamber, and was combined with metabolic PET to identify brain regions involved in conflict monitoring and resolution as well as regions of the “automatic route” audiomotor pathway for processing of stimulus location. Eight male Lister hooded rats were subject to behavioral testing, and four of them underwent behavioral PET using the tracer 2[^{18}F]fluoro-2-deoxy-D-glucose (FDG, 2 mCi, i.p.). During four separate PET sessions, each rat performed the Simon task (50 % conflict probability) and three control tasks (1. conflict trials only, 2. non-conflict trials only, 3. trials without spatial information), starting 5 min after FDG injection. After 50 min, rats were anesthetized with 2 % isoflurane and submitted to a 30 min static PET scan starting 60 min after FDG injection. Regional metabolic activity during the Simon task was compared to control tasks using VOI analysis.

Results: Rats revealed a robust Simon effect, which was reduced if incongruent trials preceded ("sequential modulation"). Conflict-related decreases of metabolic activity occurred in the anterior premotor cortex (M2), motor cortex (M1) and dorsocentral striatum. Enhanced metabolic activity during response conflicts was found in the prelimbic and anterior cingulate cortex. Furthermore, metabolic activity of M2 was related to reaction times and error rates.

Conclusions: Sequential modulation of the Simon effect in rats indicates post-conflict adjustments. The decrease of metabolic activity found in M1, M2, and the dorsocentral striatum during conflicting trials may reflect automatic route suppression as one mechanism of sequential modulation. The correlation of metabolic activity with reaction times and error rates during response conflicts provides further evidence that M2 plays a role in conflict processing. Similar to the situation in humans, activation of prelimbic and anterior cingulate cortex may be associated with conflict monitoring.

References:

[1] Hommel B. et al. (2004) Psychol Res 68: 1-17.

[2] Zhang H.H. et al. (1999) Cogn Psychol 38: 386-432.

[3] Wittfoth M. et al. (2009) Neuroimage 44: 1201-1209.

1025

IMPROVEMENT OF NEUROLOGICAL OUTCOME AND REDUCTION OF SECONDARY BRAIN DAMAGE BY AT1-INHIBITION AFTER EXPERIMENTAL TBI IN YOUNG AND OLD ANIMALS

S.C. Thal, R. Timaru-Kast, P. Gotthardt, C. Werner, K. Engelhard

Department of Anesthesiology, Johannes Gutenberg-Universität, Mainz, Germany

Objectives: In a previous study we demonstrated a reduced neurofunctional impairment and decreased secondary brain damage by Angiotensin II receptor type 1 (AT1) inhibition 24 hours after experimental traumatic brain injury (TBI) in young adult mice (1). In contrast to young, the ability of old animals to recover from TBI is reduced (2;3). The aim of the present study was to investigate the age dependent effect of AT1 inhibition.

Methods: Young (2 months) and old (21 months) male C57Bl6 mice were anesthetized with fentanyl, midazolam and medetomidine and were subjected to a pneumatic brain trauma on the right parietal cortex (controlled cortical impact, CCI). Animals of both ages were randomly assigned to vehicle or to the AT1 inhibitor candesartan (0.1 mg/kg, s.c.) 30 min after trauma and then daily until day 4. Neurological outcome was assessed at day 1, 3 and 5 after CCI using a modified Neurological Severity Score (no impairment = 0, highest deficit = 15 points). Contusion volume was measured at day 5 in Nissl stained sections. In a separate set of non-treated animals of both age groups mRNA expression of AT1 and AT2 was determined before and 15 min, 24h and 72h after CCI. Statistics: Wilcoxon Mann Whitney rank sum test.

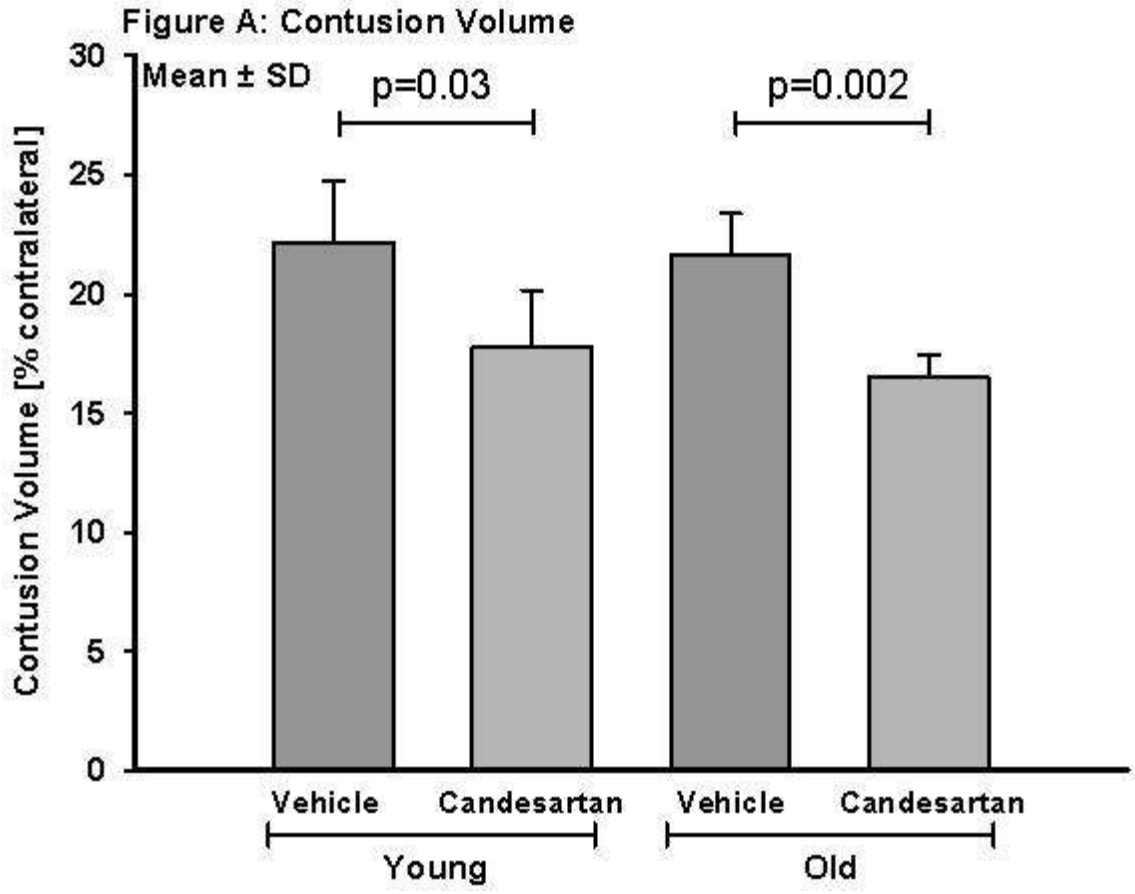

[Figure A]

Results: Without treatment expression of AT1 was not influenced by CCI in young animals, while AT1 expression in old was significantly reduced 72h post TBI. AT2 expression increased 24 h post insult in young, but not in old animals. Candesartan treated old mice showed a lower mortality than vehicle treated old mice (12.5 % vs. 30 %), whereas all young animals survived the 5 days period. Neurological deficit was higher in vehicle treated animals in both age groups on day 3 and 5. Histological brain damage was reduced in candesartan treated mice compared to vehicle treated mice in both age groups (see figure A).

Conclusions: The present study demonstrates an improved neurological function and a reduced secondary brain damage by post-treatment with low dose candesartan after TBI in young mice and in old mice, while in the latter the results were even more pronounced. This suggests that AT1-inhibition after TBI might be more effective in aged animals. Possible mechanisms of AT1-inhibition are the shift of angiotenin II action from the proinflammatory AT1 that is reduced in aged animals after TBI to the protective AT2 with reduction of cerebral inflammation (4) and increased liberation of neurotrophic effects (5). Old animals are known to demonstrate an earlier and more pronounced inflammatory response (2), which is possibly limited by AT1-inhibition. The present study suggests that AT1-inhibition is a promising therapeutic strategy to prevent secondary brain damage after TBI in both aged and young.

References: 1. Timaru-Kast R, et al. Brain 2009, Abstract No. 507; 2. Onyszchuk G, et al. J Neurotrauma 2008; 3. Timaru-Kast R, et al. ASA Meeting Abstracts 2009; 4. Takemori K, et al. Am J Hypertens 2000; 5. Mogi M, et al. Hypertension 2006

1027

TRANSCRIPTOMIC ALTERATIONS IN THE CHOROID PLEXUS OF THE EXPERIMENTAL AUTOIMMUNE ENCEPHALOMYELITIS MICE MODEL

F. Marques[1], S. Mesquita[1], J. Sousa[1], D. Geschwind[2], S. Columba-Cabezas[3], F. Aloisi[3], G. Coppola[2], J. Cerqueira[1], M. Correia-Neves[1], J. Palha[1]

[1]Life and Health Sciences Research Institute (ICVS), School of Health Sciences, University of Minho, Braga, Portugal, [2]Program in Neurogenetics, Department of Neurology, David Geffen School of Medicine-UCLA, Los Angeles, CA, USA, [3]Department of Cell Biology and Neuroscience, Istituto Superiore di Sanità, Rome, Italy

The choroid plexus (CP) is clearly on the interface between the central nervous system (CNS) and the periphery, and thus in a privileged position to mediate interactions between the periphery and the CNS. In addition to it's principal function that is the CSF production our lab several laboratories have showed that the CP is mediating immune signals from the periphery into the brain during acute and sustained peripheral inflammation. The CP transcriptome promptly responds in both conditions and this leads to an alteration in the CSF composition that, consequently, might influence several regions of the brain parenchyma. Despite of such observations, little attention has been paid to the CP in neurodegenerative disorders like Multiple Sclerosis (MS). By using the experimental autoimmune encephalomyelitis (EAE) animal model of MS we characterized the CP response in the course of the different clinical phases of the disease. The data obtained show that the CP displays a sustained response to the EAE mice model by altering the expression profile of several genes. From a total of 24,000 genes, at the onset of the disease 633 are up-regulated and 290 are down-regulated, while at the remission phase of the disease the number decreases to 484 and 180 respectively and in the relapse phase it come back diminish to 309 and 96 respectively. When genes with altered expression are clustered into classes, a strong CP immune response becomes evident in all phases of the disease, being the chemokine, the JAK-STAT and the T cell receptor signalling pathways the most affected.

1029

CHARACTERISING THE PERFORMANCE OF SIMPLIFIED AND PSEUDO REFERENCE TISSUE MODELS FOR A RANGE OF COMPARTMENTAL TOPOLOGIES

C. Salinas[1], G. Searle[1], R. Gunn[1,2,3]

[1]Clinical Imaging Centre, GSK, London, [2]Department of Engineering Science, University of Oxford, Oxford, [3]Division of Neuroscience, Imperial College, London, UK

Introduction: Quantitative analysis of PET data using reference tissue models is appealing because it obviates the need for invasive blood sampling. Of the reference tissue models in use, the simplified reference tissue model (SRTM) is the simplest and most commonly applied. The main assumptions of SRTM are that there is one tissue compartment in both the target and reference tissues and that there is negligible specific binding in the reference region. Recently, a pseudo reference tissue model (PRTM) was introduced to extend SRTM so that it can accommodate specific binding in the reference region. Computer simulations were used to characterise the performance of SRTM and PRTM for a range of situations where assumptions about the number of tissue compartments and validity of the reference region were violated.

Methods: A measured arterial input function and compartmental models were used to simulate dynamic reference and target tissue data. Different compartmental topologies were explored for target and reference tissues (Fig 1.). BP_{ND} values from 0-10 were considered for the target tissue and reference tissue. SRTM and PRTM were applied to the noiseless simulated data and the % bias in the BP_{ND} outcome measure of interest was calculated. For PRTM, the specific binding in the reference tissue was assumed to be known. Additional simulations were performed in the presence of noise (100 realisations for each combination) and the reference tissue models were applied again. The performance was then assessed in terms of % bias and %COV of BP_{ND}.

Results: Figure 1 presents the results from the noise free simulations. As expected, SRTM was unbiased when there was one tissue compartment in each region, whilst with the addition of more than one compartment in either or both regions a bias was introduced. With the introduction of increasing specific binding in the reference tissue BP_{ND} became increasingly underestimated. When PRTM was applied to the simulations involving one tissue compartment in each region, the true BP_{ND} value was recovered in all cases. However, when there was more than one compartment in either or both of the regions, biases were introduced into the estimate of BP_{ND}. When noise was added to the simulations the underlying bias was similar, demonstrating that the methods are fairly unbiased in the presence of noise.

Conclusion: SRTM can underestimate the true BP_{ND} when there is more than one compartment in either of the tissue regions or when there is specific binding in the reference tissue. Application of PRTM can correct for the presence of specific binding in the reference tissue but may still be biased when there is more than one compartment in either of the tissue regions. Characterisation of these reference tissue models through simulations allows for informed decisions to be made about the application of them to PET studies.

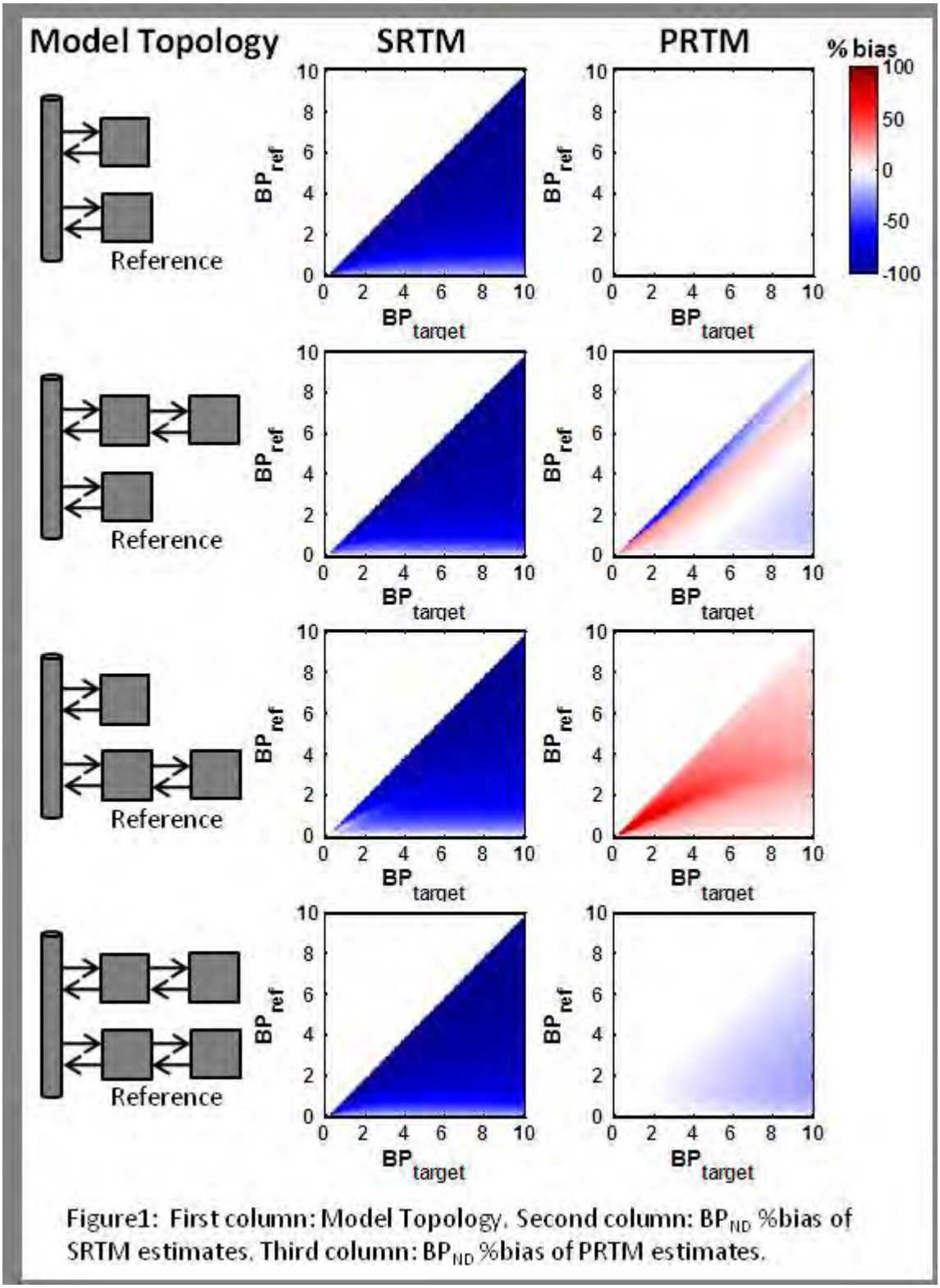

Figure1: First column: Model Topology. Second column: BP_{ND} %bias of SRTM estimates. Third column: BP_{ND} %bias of PRTM estimates.

[Figure 1]

1030

FUNCTIONAL STIMULATION INDUCED CHANGE IN CEREBRAL BLOOD VOLUME: A TWO PHOTON FLUORESCENCE MICROSCOPY MAP OF THE 3D VASCULAR NETWORK RESPONSE

L. Lindvere[1,2], A. Dorr[2], D. Chartash[2], J.G. Sled[1,3], B. Stefanovic[1,2]

[1]Medical Biophysics, University of Toronto, [2]Imaging Research, Sunnybrook Research Institute, Sunnybrook Health Sciences Centre, [3]Toronto Centre for Phenogenomics, Toronto, ON, Canada

Objective: The goal of this work is to characterize the spatial pattern of the cerebral microvascular network response to stimulation under physiological conditions. To date, there is limited data on the *in vivo* reactivity of deep cerebral microvessels to functional stimulation and the behavior of individual microvessels has been reported to be highly heterogeneous. The current work uses a model based tracking algorithm to detect temporal changes in the 3D morpholology of the vascular network as seen on high-resolution two-photon fluorescence microscopy (2PFM) volumetric images.

Methods: Adult male Sprague-Dawley rats were anesthetized with isoflurane, tracheotomized and mechanically ventilated. To enable 2PFM imaging of the brain, stereotaxic surgery was done to prepare a small (~5 mm in diameter) closed (1% agarose) cranial window, over the forelimb representation in the primary somatosensory cortex. Imaging was performed following intravenous administration of fluorescent dye during rest and electrical stimulation of the contralateral forepaw. The stimulation was presented in an off/on/off paradigm with each on period lasting approximately 2.5 seconds and consisting of 7 pulses, each 0.3 ms in duration, 2 mA in amplitude, and repeated at a frequency of 3Hz.

200 slices were collected parallel to the cortical surface, every 3 μm, with the nominal in-plane resolution of 1 x 1 μm. The microvascular network was segmented from these high resolution stacks using 3D anisotropic diffusion filtering followed by user defined signal intensity thresholding (Imaris, Bitplane). Coarser resolution functional stacks acquired at each time point (100 slices of 1.6 x 1.6 x 3 μm) were subjected to motion correction, median filtering, intensity normalization across cortical depths, and were segmented using a semi-automated multi-scale tracking algorithm (Fridman et al., Med Image Anal 2004;8(3),169-176). The algorithm follows the centreline of a vessel and all of its branches using the high resolution data based network segmentation as the initial guess. Circular vessel cross sections, but anisotropic point spread function of 2PFM, were assumed when estimating vessel diameters and centreline positions at each time point. General linear model analysis (AFNI, 3Ddeconvolve) was applied to identify regions of statistically significant stimulus correlation at the omnibus significance level of 0.05 after correction for multiple comparisons. Pronounced volume changes relative to baseline are thus observed at discrete segments of the microvascular network in response to electrical stimulation.

Results: The map shows the 3D microvascular response to the stimulus presentation (figure). As expected, dilation was the predominant response of the microvasculature, though many focal instances of stimulation-induced constriction were also observed.

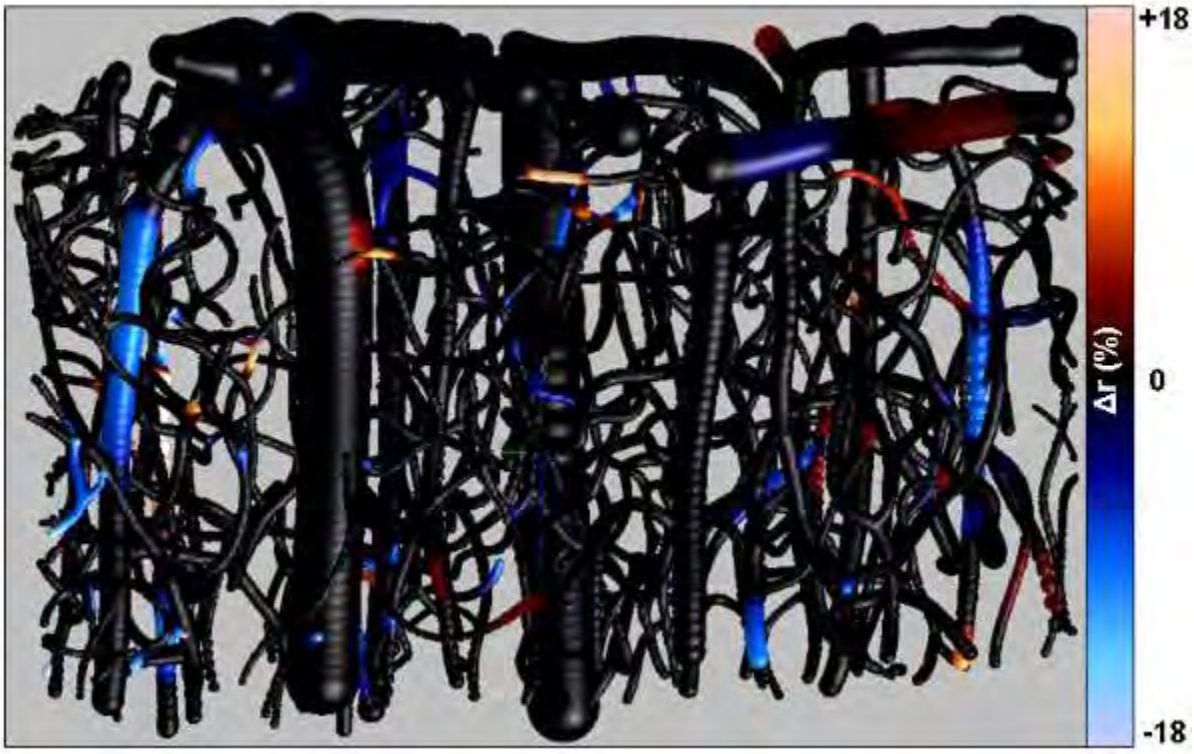

[Stimulus induced change in radii (%)]

Figure: Map of stimulus induced changes in radii (%) estimated through general linear model following 3D clustering and masking by thresholded t-map.

Conclusions: The presented detailed account of the microvascular network reactivity will further our understanding of the *in vivo* microvascular reactivity and the hemodynamically weighted responses measured in neuroimaging, most notably blood oxygenation level dependent (BOLD) fMRI. The current methodological developments also provide a platform for future investigations of the perturbations in neurovascular coupling at the microscopic scale.

1031

METABOLIC CYTOPROTECTORS AS A TREATMENT OF CARDIOEMBOLIC STROKE

V. Kuznetsov[1], S. Kuznetsova[2], M. Iegorova[2]

[1]Neurology, [2]Institute of Gerontology AMS Ukraine, Kiev, Ukraine

Atrial fibrillation (AF) is a supraventricular tachyarrhythmia characterized by disorganized atrial electrical activity and progressive deterioration of atrial electromechanical function. AF is the most common arrhythmia encountered in clinical practice and is a significant public health problem in every country. AF is a major risk factor for ischemic stroke, congestive heart failure and mortality. The prevalence of AF is influenced by age, gender, cardiovascular disease (CVD) such as valvular heart disease, and CV risk factors such as hypertension, diabetes, obesity, and insulin resistance. The prevalence of AF increases dramatically with age. For example, the prevalence of AF in the general population is estimated to increase from 2.3 million in 2001 to 5.6 million in 2050 in the United States. However, the the interrelations between cerebral hemodynamics and bioelectrical activity in patients after ischemic stroke is still unknown.

Aim: to conduct a complex analysis of Mexicor's influence on cerebral hemodynamics in elderly patient with cardioembolic stroke (CES).

Materials and methods: The study groups were composed of the 60-80-years old patients (30 subjects, 14 females, 16 males): 15 patients with AF had CES in left hemisphere and 15 patients with AF had CES in right hemisphere.Duplex scanning of brain and neck vessels were performed on an ultrasound device Sonoline Elegra, Siemens. Magnetic resonance tomography was done on a tomograph 1.5 T Magnetom Vision Plus (Siemens).

Results and discussion: In patients with CES after Mexicor's treatment cerebral hemodynamics improved in vertebral - basilar basin (in PCA before treatment linear systolic blood flow (LSBF) - 43,74±2,05, after treatment - 47,15±1,12, $p < 0,05$). This fact told us about Mexicor's compensatory influence on cerebral blood flow.In patients with left-sided CES Mexicor decreases peripheral resistance (Pi) (Pi before treatment 0,84±0,06, Pi after treatment 0,73±0,03, $p < 0,05$) and increases flexibility (before treatment 0,63±0,01, after treatment 0,67±0,02, $p < 0,05$)only in vessels of vertebral - basilar basin of intact hemisphere.In patients with right-sided CES Mexicor decreases peripheral resistance and increases flexibility in cerebral vessels of both hemispheres.

1032

CONFIRMATION OF AMPHETAMINE EFFECT ON A_{2C}-ADRENOCEPTOR BINDING OF [^{11}C]ORM-13070 USING AN EQUILIBRIUM APPROACH

S.J. Finnema[1], V. Stepanov[1], A. Varrone[1], R. Nakao[1], M. Haaparanta-Solin[2], O. Solin[2], K. Ingman[3], J. Sallinen[3], M. Scheinin[4], L. Farde[1], C. Halldin[1]

[1]Department of Clinical Neuroscience, Karolinska Institutet, Stockholm, Sweden, [2]Turku PET Centre, University of Turku, Turku University Hospital and Åbo Akademi University, [3]Orion Pharma R&D, Orion Corp., [4]Department of Pharmacology, Drug Development and Therapeutics, University of Turku, Turku, Finland

Introduction: [^{11}C]ORM-13070 has recently been reported as the first promising antagonist radioligand for imaging of α_{2C}-adrenoceptors in the brain [1]. Initial characterization of [^{11}C]ORM-13070 in the rat demonstrated *ex vivo* striatum to cerebellum ratios of 2.6 and confirmed specific binding to α_{2C}-adrenoceptors [1]. The first human PET study with [^{11}C]ORM-13070 yielded striatal binding potential (BP_{ND}) values of ~0.6, but kinetic modeling indicated the presence of a radioactive metabolite in brain [2]. We previously demonstrated that an amphetamine-induced increase in neurotransmitter release dose-dependently decreased [^{11}C]ORM-13070 receptor binding in monkey brain [3]. In the current study, we developed a bolus infusion protocol (BI-protocol) suitable for quantification of BP_P. This approach was expected to permit quantitative determination of *BP* in the presence of a brain-penetrant radioactive metabolite with homogenous brain distribution. The BI-methodology was applied to evaluate the effect of amphetamine, initially in one monkey.

Methods: Five preparative PET measurements were performed to evaluate the optimal K_{bol} to achieve rapid steady state conditions. [^{11}C]ORM-13070 was administered with the BI-protocol to two rhesus monkeys, using K_{bol} values ranging from 30 to 90 min. The subjects were anaesthetized with sevoflurane (2-8 %) and emission data were acquired for 123 min using the HRRT PET system. During each PET experiment, seven venous blood samples were obtained for measurement of total radioactivity in blood and plasma, and for determination of [^{11}C]ORM-13070 and possible metabolites with HPLC. Next, two PET measurements were performed using the optimized BI-protocol in one cynomolgus monkey. The effect of pretreatment with *D*-amphetamine (1.0 mg/kg given i.v. 25 min before tracer injection) was estimated as relative change (%) in BP_P. BP_P ((C_T-C_{ND})/C_P) was calculated for the striatum (C_T) using the cerebellum for determination of the non-displaceable concentration (C_{ND}). An improved metabolite system allowed for determination of [^{11}C]ORM-13070 plasma concentrations at every six minutes in the amphetamine challenge study.

Results: Administration of [^{11}C]ORM-13070 with the BI-protocol resulted in a rapid equilibrium in receptor binding. Equilibrium for specific binding (C_S = C_T-C_{ND}) was achieved for all evaluated K_{bol} values, while C_{ND} values, in contrast, increased continuously over time, until the end of the PET measurement. A K_{bol} value of 30 min was found optimal for the amphetamine challenge. Amphetamine decreased the radioactivity in striatum, and to a smaller extent in cerebellum. The striatal BP_P decreased from 1.7 to 1.3 (-20 %) after 1.0 mg/kg amphetamine.

Conclusions: This preliminary work confirms that [^{11}C]ORM-13070 may be a sensitive tool to investigate alterations in synaptic norepinephrine concentrations *in vivo* with PET. Future studies are, however, required to further understand a potential contribution of dopamine to the amphetamine-induced effect.

Acknowledgement: NEWMEDS - the work leading to these results has received funding from the Innovative Medicines Initiative Joint Undertaking (IMI), within NEWMEDS, under Grant Agreement N° 115008.

References:

1. Arponen, E., et al., Neuroimage, 2010. **52**: p. S125.

2. Data on file, Orion Corp., Orion Pharma.

3. Finnema, S.J., et al., Neuroimage, 2010. **52**: p. S61-S62.

1033

A NOVEL METHOD FOR GLOBAL CEREBRAL METABOLIC VOLUME MEASUREMENT USING FDG-PET: APPLICATION IN ALZHEIMER'S DISEASE

E.S. Musiek[1], B. Saboury[2], Y. Chen[3], S. Mishra[2], J.S. Reddin[2], A.B. Newberg[4], J.K. Udupa[2], F. Hofheinz[5], J.A. Detre[1,3], D.A. Torigian[2], **A. Alavi**[2]

[1]Neurology, [2]Radiology, [3]Center for Functional Neuroimaging, University of Pennsylvania, [4]Myrna Brind Center for Integrative Medicine, Thomas Jefferson Medical College, Philadelphia, PA, USA, [5]ABX GmBH, Radeberg, Germany

Imaging of cerebral metabolism using FDG PET is widely used in the diagnosis of neurologic diseases, including Alzheimer's Disease (AD), though few quantitative analysis methods for brain FDG PET data are available for clinical use. Herein, we describe the application of a novel quantitative image analysis package, termed ROVER (Region of interest Visualization, Evaluation, and Image Registration), to the examination of brain FDG PET images, and apply this method in 14 patients with AD and 16 age-matched controls. ROVER provides automated partial volume corrected measures of brain volume (whole brain and cortex-only), average glucose uptake (mean SUV), and whole brain glucose metabolism (metabolic volumetric product, MVP) without the need for concurrent MRI data, and is facile enough for clinical use. We compared ROVER-derived cortex-only volumes to MRI grey matter volumetric measurements in a subset of subjects, and found that mean brain volume of controls was very similar between methods (avg. volume 747 ± 98 cm^2 for MRI vs. 720 ± 106 cm^2 for ROVER, difference of 4.8%, non-significant), and correlated very closely (R^2=0.93, slope=0.88). However, ROVER-derived cortical volumes in a subset of 5 AD patients were on average 59.4% lower than MRI-derived grey matter volumes (840 ± 123 for MRI vs. 547 ± 106 for ROVER, $p< 0.01$), as ROVER provides a unique measure of metabolically active brain volume. ROVER-derived brain volumes were 22.3% lower in AD patients ($P< 0.001$), and very accurately distinguished between AD patients and controls (AUC of ROC curve 0.89, $p< 0.001$). MVP was also significantly lower in AD patients (21.1% for whole brain, 31.6% for cortex-only measurements, $p< 0.01$ for both), and provided good diagnostic accuracy (AUC of ROC curve 0.86, $p< 0.001$). Thus, ROVER analysis of FDG-PET images provides a unique index of metabolically-active brain volume, and can accurately distinguish between AD patients and controls. Our findings suggest that ROVER may serve as a useful clinical tool for quantitative analysis of whole-brain metabolism in AD and other neurologic and psychiatric diseases.

1035

STRIATAL AND EXTRASTRIATAL DISTRIBUTION OF THE RATIO OF DOPAMINE D_1 AND D_2 RECEPTOR DENSITIES IN HEALTHY MALE SUBJECTS

Y. Kimura, H. Ito, H. Fujiwara, F. Kodaka, H. Takano, T. Suhara

Molecular Imaging Center, National Institute of Radiological Sciences, Chiba, Japan

Objectives: Although no alteration in dopamine D_1 and D_2 receptors was observed in striatal regions in schizophrenia using a positron emission tomography (PET)[1,2], a postmortem studies showed imbalance between dopamine D_1 and D_2 receptors in schizophrenia[3]. Building a database of the ratio of D_1 and D_2 receptor densities in striatal and extrastriatal regions in the living human brain could be useful to understand the pathophysiology of neuropsychiatric disorders. The purpose of the study was to investigate *in vivo* striatal and extrastriatal distribution of the ratio of D_1-like and D_2-like receptor densities using PET.

Methods: Three PET scans were performed on each of nine healthy men after intravenous injection of ^{11}C-SCH23390, ^{11}C-raclopride, or ^{11}C-FLB457. Binding potential (BP_{ND}) for each radioligand were calculated by the simplified reference tissue model using cerebellum as a reference region. BP_{ND} images were normalized by the value of putamen. Maps of the ratio of D_1/D_2 were created dividing the normalized BP_{ND} images of ^{11}C-SCH23390 by those of ^{11}C-raclopride and ^{11}C-FLB457 for the striatal regions and the extrastriatal regions, respectively.

Results: In the striatum, the D_1/D_2 ratio was almost uniform, but the D_1/D_2 ratio in the sensorimotor striatum was significantly lower than that in the associative striatum. The limbic striatum showed a slightly higher ratio than the sensorimotor striatum with a trend level difference.

In the extrastriatam, the D_1/D_2 ratios were ~6 times higher than those of the striatum and were the lowest in the medial temporal cortex. The lateral and medial temporal cortex showed a significantly lower ratio than the frontal cortex. The medial temporal cortex showed a significantly lower ratio than the lateral temporal cortex. The occipital cortex showed a higher ratio with a trend level difference as compared to the parietal cortex and medial temporal cortex.

Conclusions: *In vivo* distribution of the ratio of D_1-like and D_2-like receptor densities in the striatal and extrastriatal regions were investigated in the living human brain. In the striatum, the relative predominance of D_2-like receptors in the sensorimotor striatum is in accordance with the finding that the D_2-receptor-rich extrastriosomal matrix is related to sensorimotor processing. In the extrastriatam, the relative predominance of D_2-like receptors in the medial temporal cortex is in accordance with previous studies with autoradiography.

References:

1. Farde et al. Arch Gen Psychiatry (1990)

2. Okubo et al. Nature (1997)

3. Hess et al. Life Sci (1987)

		D_1/D_2 ratio (the ratio in the putamen as 1.00)
Striatal regions	Associative striatum	1.07 ± 0.03
	Sensorimotor striatum	0.97 ± 0.03*
	Limbic striatum	1.10 ± 0.11
Extrastriatal regions	Frontal cortex	5.90 ± 1.62
	Lateral temporal cortex	4.36 ± 1.37§
	Medial temporal cortex	3.67 ± 0.70†
	Parietal cortex	5.59 ± 2.63
	Occipital cortex	7.44 ± 5.02
* $p < 0.05$ v.s. the associative striatum, † $p < 0.01$ v.s. the frontal cortex and $p < 0.05$ v.s. the lateral temporal cortex, § $p < 0.05$ v.s. the fromtal cortex		

[The D1/D2 ratio in the striatum and extrastriatum]

1036

ROLE OF NEUROINFLAMMATION IN MICROEMBOLISM-INDUCED CHANGES IN AFFECTIVE BEHAVIOR

G.N. Neigh[1,2], C.L. Nemeth[1,2]

[1]Physiology, [2]Psychiatry & Behavioral Sciences, Emory University, Atlanta, GA, USA

Introduction: In the aged human brain alterations to vasculature, including the development of small cerebral infarcts, precipitate larger ischemic events and changes of affective behavior. Nearly 94% of people who develop depression after age 65 exhibit diffuse cerebral lesions, but a causative relationship has not been determined. These vascular-associated depressive behaviors appear to be clinically distinct from classic depression and are resistant to anti-depressant treatments. Pro-inflammatory cytokines have pleiotropic effects immediately following ischemic events and their upregulation is linked to the development of depressive behaviors and anti-depressant resistance in humans suggesting a possible role of neuroinflammation in vascular-associated depression. Recent work has shown that elevations of pro-inflammatory cytokines (IL-6, IL-1β, and TNF-α) in the hypothalamus trigger activation of both the hypothalamic-pituitary-adrenal axis and the sympathetic nervous system which are both linked to behavioral disruption.

Objectives: The current experiment was designed to use a rat model of diffuse cerebral microembolism infarcts to determine if induction of small cerebral infarcts was sufficient to induce depressive-like behaviors. The second objective of the study was to examine the potential role of increased activity of pro-inflammatory cytokines in altered affective behavior following microembolism infarcts.

Methods: Rats were anesthetized and the left carotid artery was isolated and ligated inferior to the external carotid artery and at the junction between the internal and external carotid arteries. Microemboli (ME) were induced by injection of microspheres into the left internal carotid artery. SHAM animals underwent the same procedure without injection of microspheres. After a two week recovery, affective behavior was assessed in one cohort of rats. Tests included the open field, elevated plus maze, sucrose preference test, and forced swim test. Microembolism load and location was assessed in this cohort of rats. A second cohort of rats was used for tissue collection at the two week post-operative time point and these tissues were assessed for neuroinflammatory markers using quantitative RT-PCR.

Results: Rats with microembolism infarcts demonstrated the depressive-like behavior of anhedonia as evidenced by a reduced preference for sucrose in the sucrose preference test, compared to the SHAM group ($p < 0.05$). In addition, although motor behavior was normal in rats with microemboli ($p > 0.05$ compared to SHAM), rats with microemboli exhibited decreased exploratory behavior in the open field ($p < 0.05$) suggesting an increase in anxiety-like behavior. Stereological assessments of microembolism load and location established that the microembolism procedure induced cerebral damage but neither the location nor magnitude of the damage correlated with the assessed behavioral endpoints. Expression of neuroinflammatory markers in rats with microemboli diverged from expression in the SHAM group.

Conclusions: The current study demonstrates that induction of microemboli is sufficient to induce behaviors in the rat which are similar to depression and anxiety in the human. These data are congruent with human studies which have correlated small cerebral infarcts and

depression. In addition, the data demonstrate that neuroinflammation may play a role in altered affective behavior following small cerebral infarcts and provide an avenue for assessment of alternative therapies for vascular-associated depression.

1038

PREDICTING INFARCT CORE AND PENUMBRA WITH CT PERFUSION (CTP) FOLLOWING ISCHAEMIC STROKE IN RAT

D. McLeod[1,2], M. Parsons[2,3], C. Levi[2,3], D. Buxton[4], S. McCann[1,2], B. Hiles[1,2], N. Spratt[1,2,3]

[1]School of Biomedical Sciences & Pharmacy, University of Newcastle, Callaghan, [2]Hunter Medical Research Institute (HMRI), [3]Neurology, [4]Hunter Health Imaging, John Hunter Hospital, New Lambton, NSW, Australia

Objectives: It is not known whether CT perfusion thresholds defining infarct core and penumbra change over time following ischaemic stroke, because serial scanning is not feasible in humans due to cumulative radiation and intravenous iodinated contrast dosage. Better definition and validation of the best perfusion thresholds for infarct core and penumbra would strengthen the use of CTP, which is already being used in patient selection for thrombolysis. Our aim was to determine infarct core and penumbra thresholds at serial timepoints following middle cerebral artery occlusion (MCAo) by coregistration of serial CTP scans with histological maps of infarction at 24 hours in our established rat CTP stroke model.

Methods: Adult male outbred Wistar rats underwent CTP scanning prior to, immediately after, and every 30 min for 2 hours following either permanent or temporary intraluminal MCAo. CTP maps of cerebral blood flow (CBF, ml.100g.min^{-1}), cerebral blood volume (CBV, ml.100g^{-1}) and mean transit time (MTT, sec) were generated at each scan time-point. Animals were sacrificed at 24 hours for standard histology and areas of infarction and normal tissue were outlined. These traces were coregistered with coronal plane CTP maps at each time point. 'Penumbra + core' was defined as the tissue region that progressed to infarction at 24 hours in the absence of vessel reperfusion (permanent MCAo (pMCAo), N= 5). 'Infarct core' was defined as tissue that progressed to infarction despite vessel reperfusion at 1 or 2 hours post MCAo (N= 7). Pixel-by-pixel analyses were performed on the coregistered CTP maps to determine the best (most accurate) perfusion thresholds for 'penumbra + core' and 'infarct core' for each individual perfusion variable (CBF, CBV, MTT), testing both absolute thresholds and relative (relative to contralateral) thresholds. A modification of previously established receiver operator curve analysis was performed, with validation by volumetric analysis of the defined regions.

Results: In the pMCAo group, the best relative 'penumbra + core' thresholds for CBF, CBV and MTT did not change over time up to 2 hours following MCAo. The best thresholds were (in descending order of accuracy) 65% (CBF), 75% (CBV) and 115% (MTT). Relative thresholds had greater predictive accuracy than absolute thresholds. In the 1 and 2 hour reperfusion groups, the best relative thresholds for predicting 'infarct core' at 1 or 2 hours following MCAo were 50% (CBF), 60% (CBV) and 145% (MTT). The best thresholds were no different in groups reperfused at either 1 or 2 hours.

Conclusions: This preliminary data indicates that the CTP thresholds for predicting 'penumbra + core' and 'infarct core' change little over time within the first 2 hours after stroke onset. This provides reassurance that when imaging patients at varying times after onset of acute stroke, the duration of symptoms is unlikely to alter the reliability of the infarct core and penumbra maps. Ongoing studies will expand on this dataset and determine which CTP variable or combination of variables most accurately predicts infarct core and penumbra following ischaemic stroke.

1041

PLASMA INSULIN AND TRIGLYCERIDE LEVELS CORRELATE INVERSELY WITH THE CEREBRAL METABOLIC RATE OF GLUCOSE IN HEALTHY HUMANS

S. Nugent[1], E. Croteau[2], F. Pifferi[1,3], M. Fortier[1], E. Turcotte[2], S.C. Cunnane[1,3]

[1]Research Center on Aging, [2]Nuclear Medicine and Radiobiology, CIMS, [3]Medicine, Université de Sherbrooke, Sherbrooke, QC, Canada

Cerebral metabolic rate of glucose (CMRg) is lower in individuals affected by cognitive decline and dementia, especially in Alzheimer's disease. However, as yet there is no consensus as to whether CMRg decreases during normal, healthy aging. Epidemiological studies show that weekly consumption of fish abundant in ω3 fatty acids has a protective effect on cognition during aging. Animal studies suggest the ω3 fatty acid, docosahexaenoic acid (DHA) is a key modulator of GLUT transporter activity and hence glucose transport across the blood brain barrier.

The primary objective of this human study was therefore to evaluate whether supplementation with a fish oil rich in ω3 fatty acids (680 mg of DHA and 323 mg EPA/day) increases CMRg in healthy young or elderly adults.

CMRg was determined using positron emission tomography analysis with the tracer ^{18}F-fluorodeoxyglucose and was expressed as a ratio over the cerebellum in order to minimize inter-individual variation. CMRg, oral glucose tolerance and fasting plasma glucose, triglycerides, cholesterol, and free fatty acids were measured in healthy young (23±5 y old; n = 5) and elderly (76±3 y old; n = 6) women and men.

Oral glucose tolerance was worse in the elderly but was not affected by ω3 supplementation. With or without correction for the cerebellum, neither age nor ω3 supplementation altered CMRg (μmol/100 g/min) in any of the brain regions measured. However, CMRg corrected for the cerebellum were significantly negatively correlated with plasma insulin in the frontal (r = -0.679, p = 0.022), occipital (r = -0.727, p = 0.011), parietal (r = -0.775, p = 0.005), and temporal lobes (r = -0.614, p = 0.044), as well as in the whole brain (r = -0.762, p = 0.006). CMRg corrected for the cerebellum were also negatively correlated with fasting plasma triglycerides in the frontal (r = -0.619, p = 0.042), parietal lobes (r = -0.602, p = 0.050), and in the posterior cingulate cortex (r = -0.738, p = 0.009).

Hence, there was no significant effect of age or ω3 supplementation on CMRg in any of the brains regions studied. However, higher fasting plasma triglyceride and insulin levels were associated with lower CMRg in several brain regions, suggesting that a trend towards the metabolic syndrome may also be associated with cerebral hypometabolism, irrespective of age. The metabolic syndrome in turn is associated with a higher risk of adult-onset diabetes, which is a major non-genetic risk for cognitive decline in the elderly. Screening for normal fasting plasma triglycerides, and insulin is recommended when evaluating CMRg, especially when selecting criteria to define a group of healthy elderly. Future studies in this area should address whether glucose intolerance or other conditions linked to the metabolic syndrome impact negatively on brain glucose metabolism and cognition.

Funding for this project was provided by the Natural Science and Engineering Research Council of Canada, Canadian Institutes of Health Research, Canadian Foundation for Innovation,

Canada Research Chairs Secretariat (S.C.C.). Excellent technical assistance was provided by Jennifer Tremblay-Mercier, Julie Desgagné and Conrad Filteau.

1042

OBSERVING ACTIVE CEREBROVASCULAR AUTOREGULATION IN CORTICAL AND SUB-CORTICAL GREY MATTER USING LOWER BODY NEGATIVE PRESSURE AND ARTERIAL SPIN LABELING MRI

J.R. Cain, G. Thompson, L.M. Parkes, A. Jackson

Imaging Science and Biomedical Engineering, University of Manchester, Manchester, UK

Introduction: The maintenance of constant cerebral blood flow throughout a wide range of cardiac outputs is controlled by a complex homeostatic mechanism known as cerebral autoregulation. We present MRI perfusion data demonstrating active cerebral autoregulation in healthy volunteers. Traditional orthostatic challenges that elicit cerebral autoregulation such as tilt-table tests are incompatible with MRI experiments. A stimulus equivalent to 70^0 tilt-table test can be reproduced by lower body negative pressure (LBNP) of -20mmHg, created by applying an external vacuum to the lower limbs and torso. We have constructed a MRI compatible LBNP chamber and investigated the effects of LBNP on cerebral perfusion and bolus arrival time (BAT) with particular reference to the cortical and sub-cortical gray matter using arterial spin labeling (ASL) and phase contrast angiography (PCA).

Materials & methods: Ten healthy volunteers (24-31years 7-male 3-female) underwent imaging with a 3T Phillips Achieva MR scanner with their legs and lower torso within the Manchester MRI compatible LBNP chamber. Imaging consisted of high-resolution 3D T1 sequence, ASL and PCA acquisition both at rest (control) and under -20mmHg LBNP. ASL imaging used STAR labeling collected at 4 inversion times: 800ms, 1200ms, 1600ms and 2000ms. PCA acquisition was collected using 2D cine phase-contrast images. Throughout scanning the subjects pulse and blood pressure were monitored. Cardiac output was calculated from PCA flow volumes in ascending and descending aorta. ASL images were analysed using in-house code assuming a single blood compartment model. Control and labeled images were subtracted and a two-parameter fit for BAT and perfusion was performed on a voxel by voxel basis, producing perfusion and BAT maps. Perfusion was calculated with units ml/100ml/min. Automated tissue segmentation masks were created from aligned T1 images applied to co-registered perfusion and BAT maps for both cortical and sub-cortical grey matter structures, including the thalamus, caudate nucleus, putamen, globus pallidus, hippocampus and amygdala.

Results: During -20mmHg LBNP cardiac output was reduced on average by 0.5 l/min, blood pressure remained constant and pulse was raised by 7bmp. This represents a normotensive hypovolemic stimulus. There was no difference between ASL grey matter perfusion values (mean 39.2ml/100ml/min and 42.3ml/100ml/min respectively) or sub-cortical grey matter perfusion values (31.3ml/100ml/min and 33.1ml/100ml/mim) between control and -20mmHg. The BAT was significantly delayed ($p< 0.05$) during -20mmHg LBNP compared to control in both the cortical (782ms and 831ms) and sub-cortical grey matter (896ms and 1033ms). Comparing the sub-cortical structures, the hippocampus (19.5%) caudate (21%) and putamen (28%) showed the greatest % increase in BAT during -20mmHg LBNP.

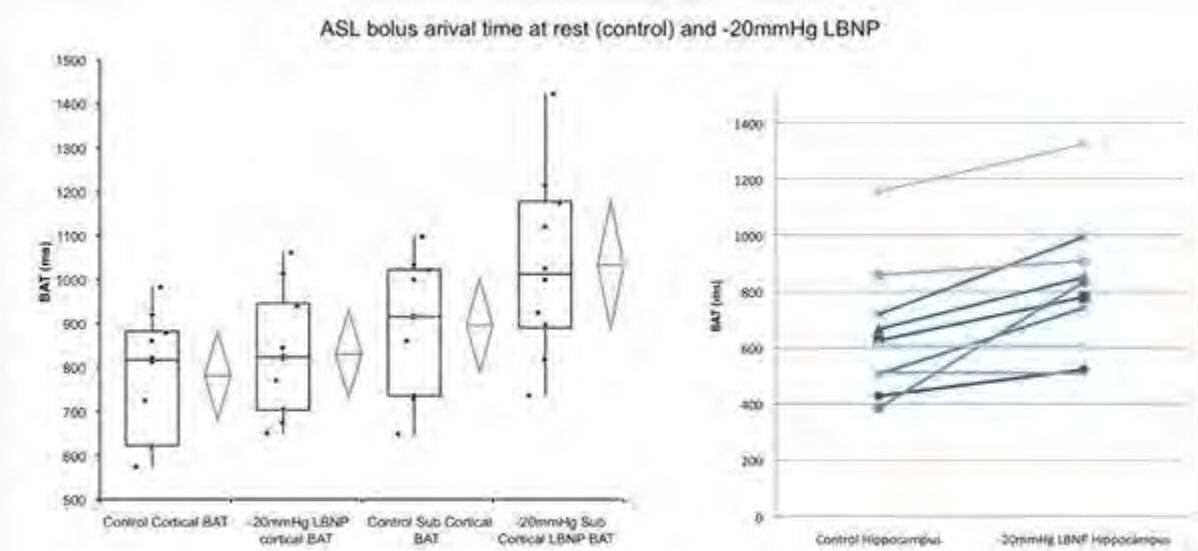

Figure 1: Box plot of cortical and sub-cortical areas BAT at rest (control) and during -20mmHg LBNP (diamond = mean and 95% confidence interval). Plot of individual subjects BAT in hippocampus.

[ASL Bolus Arrival Time LBNP]

Conclusion: LBNP produces a normotensive hypovolemic challenge in the MRI environment. In young healthy individuals cerebral autoregulation is able to compensate for -20mmHg LBNP and maintain constant perfusion. Sub-cortical grey matter perfusion was lower than cortical perfusion. BAT was delayed more in sub-cortical areas in keeping with the longer arteriolar inflow paths for these structures. BAT may prove to be an important biomarker in detecting cerebral autoregulation. This experiment demonstrates that normal cerebral autoregulation is observable using MRI.

1043

ESTROGEN SUPPLEMENTATION WORSENS STROKE OUTCOME FOLLOWING MIDDLE CEREBRAL ARTERY OCCLUSION IN AGED RATS

J.D. Huber[1], R.L. Leon[2], X. Li[2], C.L. Rosen[2]

[1]Basic Pharmaceutical Sciences, [2]Neurosurgery, West Virginia University, Morgantown, WV, USA

Introduction: Estrogen has been shown to be neuroprotectant in animal models of ischemic stroke; however, data from the Women´s Health Initiative indicates that hormone replacement therapy is a causative factor for increase incidence and severity of ischemic stroke. We contend that age is a primary risk factor accounting for the contrast between animal studies and clinical trial findings. Despite statistics from the Centers for Disease Control and Prevention indicating that 72% of people who suffer a stroke are over the age of 65, the vast majority of research in stroke, including studies on hormone replacement therapy, utilize young animal models. The mechanism of estrogenic actions on the aged post-ischemic brain are unknown. Studies have confirmed that neuropoietic cytokines and their target receptor, glycoprotein 130 (gp130) play a primary role in the complex relationship between aging and pathology. In the present study, we hypothesized that post-ischemic gp130 signaling would be attenuated following experimental stroke in aged rats supplemented with estrogen.

Materials & methods: To test this hypothesis, female Sprague-Dawley rats (3 & 9 months old) were randomly divided into three treatment groups: Group 1 (Estrogen) received bilateral ovariectomy and implanted with 17-β estradiol pellet. Group 2 (OVX) received bilateral ovariectomy and implanted with placebo. Group 3 (Control) received a sham ovariectomy and implanted with placebo. Estrogen was administered to the 3 month old rats for 30 d, and pellets e aged rats were changed every 90 d, until the rats reached 18 months of age. At 4 and 18 months of age, rats underwent occlusion of the middle cerebral artery (MCAO) and tPA reperfusion under isolfurane anesthesia (4% induction, 2% maintenance), as previously described. At 24 h following MCAO, functional assessments were measured on all of the rats using a modified Neurological Severity Score (mNSS) and then one or more of the following assays were peformed: staining with 2 , 3, 5-triphenyltetrazolium (TTC) to quantify infarct volume and edema formation, immunostaining for degenerating neurons (FluoroJade B) and activated astrocytes (glial fibriallry acidic protein) and microglia (ionic calcium binding protein), extraction of RNA and protein for real-PCR, gene expression assay, or immunoblot for gp130 associated targets.

Results: The results showed that aged female rats supplemented with estrogen had increased cortical and total infarct size and higher mortality compared to aged control and young rats supplemented with estrogen following MCAO and tPA reperfusion. Estrogen supplementation also changed post-ischemic expression of neuropoietic cytokines and gp130 signaling modulators in aged rats following ischemic brain injury. Among the changes, we observed a several fold decrease in erythropoietin receptor and an increase in prolactin and prolactin recpetor.

Conclusion: Aged rats chronically treated with estrogen suffer worsened stroke outcomes, which parallel the findings of the large-scale clinical trials. The study also found changes in the gp130 associated targets: prolactin and erythropoietin that may allow us to identify novel targets to explain the increased prevalence and severity of ischemic stroke in women taking estrogen supplementation.

1044

[^{18}F]ALTANSERIN-PET IN PRE- AND POSTMENOPAUSAL WOMEN IS NOT INFLUENCED BY PHYSIOLOGICAL ESTRADIOL, PROGESTERONE, AND PROLACTIN LEVELS

T. Kroll, A. Matusch, D. Elmenhorst, A. Bauer

Institute of Neurosciences and Medicine, Jülich Research Center, Jülich, Germany

Objective: Gonadal hormones like estradiol and progesterone influence key elements of serotonergic neurotransmission including transcriptional regulation of 5-HT_{2A} receptor gene expression in rats. But, up to now, little is known about potential changes in serotonergic receptor expression throughout the human menstrual cycle. Here we correlate cerebral 5-HT_{2A} receptor densities, as measured with [^{18}F]altanserin PET in pre- and postmenopausal women, with gonadal hormone levels in order to evaluate the hormonal influence on cerebral 5-HT_{2A} receptor availability in women.

We also investigate the peptide hormone prolactin which regulates milk production during lactation and is known to be influenced by antidepressants acting via serotonergic and dopaminergic receptors. Physiological concentrations of prolactin are varying e.g. by daytime and might therefore also influence cortical 5-HT_{2A} receptor availability.

Methods: [^{18}F]Altanserin-PET was performed using a bolus plus continuous infusion protocol on 19 healthy women (mean age: 51.5 y, range 30-70 y) without any known neuropsychological disorders or medication affecting the hormonal status. Dynamic emission scans were acquired 120-180 min after initial administration of [^{18}F]altanserin under equilibrium conditions. As outcome parameter the binding potential relative to the plasma concentration corrected for metabolites (BP_P) was chosen, which is directly proportional to 5-HT_{2A} receptor availability. Cerebellum was used as a reference region. Regions of interest were delineated on individual anatomical MRI planes.

Levels of 17β-estradiol, progesterone, and prolactin were analyzed for each subject.

Since 5-HT_{2A}-BP_P decreases with age, individual binding potentials were detrended linearly based on previous published findings to control for ageing effects. Subjects were divided into three groups (proliferative, luteal, and postmenopausal phase) in order to investigate differences in 5-HT_{2A} receptor availability during the menstrual cycle. Furthermore, levels of each hormone were correlated with the 5-HT_{2A}-BP_P.

Results: Comparison of cerebral [^{18}F]altanserin binding potentials between pre- and postmenopausal women did not reveal significant differences (mean cortical BP_P, one-way ANOVA p=0.18). Average parametric BP_P images of premenopausal subjects (n=11) show a trend of increase in cortical 5-HT_{2A} receptor densities during the luteal phase of the menstrual cycle without reaching the level of significance (two tailed t-test p=0.07). There was neither a correlation between physiological prolactin levels and cortical 5-HT_{2A} receptor expression (R^2=0.006; n=19) nor a relationship between gonadal hormone levels and cortical 5-HT_{2A} receptor densities in premenopausal women (estradiol: R^2=< 0.01; progesterone: R^2=0.1; n=11).

Conclusions: We found no evidence that [^{18}F]altanserin PET imaging in women is affected by varying gonadal hormone levels throughout the menstrual cycle. Moreover individual prolactin levels did not influence cortical 5-HT_{2A} receptor expression.

1045

PET-CT IMAGING TO MEASURE TRANSPORTER MEDIATED DRUG-DRUG INTERACTIONS AT THE BLOOD-BRAIN BARRIER

M.L. Vlaming[1], T. Läppchen[2], H.T. Jansen[1], S. Kivits[3], A. van Driel[3], D. Grossouw[1], J.W. van der Hoorn[4], C.F. Sio[2], H.M. Wortelboer[1], M. Verwei[1], O.C. Steinbach[2], J. De Groot[1]

[1]Pharmacokinetics, TNO, Zeist, [2]Biomolecular Engineering, [3]Life Science Facilities, Philips Research Europe, Eindhoven, [4]Vascular and Metabolic Disease, TNO, Leiden, The Netherlands

Reaching sufficiently high therapeutic concentrations of drugs acting in the brain is often hampered by the activity of the efflux transporters P-glycoprotein (P-gp, ABCB1) and Breast Cancer Resistance Protein (BCRP, ABCG2) at the blood-brain barrier (BBB). The broad substrate specificity of P-gp and BCRP can also cause transporter-mediated drug-drug interactions (DDIs), for example when co-medicated drugs compete for efflux by these transporters. This can lead to increased brain concentrations of a drug in patients, potentially resulting in unexpected brain toxicity. It is therefore highly important to determine whether a drug may be involved in transporter-mediated drug-drug interactions at the BBB.

To detect possible P-gp and/or BCRP mediated DDIs at the murine BBB, we synthesized the PET tracer [^{18}F]-gefitinib. By imaging the pharmacokinetics of [^{18}F]-gefitinib in wild-type, Bcrp1$^{-/-}$, P-gp$^{-/-}$ and Bcrp1;P-gp$^{-/-}$ mice we showed that P-gp and Bcrp1 together limit the brain penetration of [^{18}F]-gefitinib, when administered at a dose of 1 mg/kg. Furthermore, the DDI between the Bcrp1 and P-gp inhibitor elacridar (10 mg/kg) and [^{18}F]-gefitinib (1 mg/kg) at the BBB could be quantified using PET-CT imaging. We conclude that [^{18}F]-gefitinib is a useful tool to non-invasively analyze potential P-gp and Bcrp1 mediated DDIs in vivo. Combining such quantitative PET-CT animal imaging data with in vitro human drug transporter assays and PBPK-modeling, could provide a powerfull approach to predict drug pharmacokinetics in humans.

1046

A ROLE FOR METALLOTHIONEINS AS MOLECULAR SENSORS OF OXIDATIVE STRESS IN ANESTHETIC PRECONDITIONING

S.D. Edmands, A. Ziemba, A.C. Hall

Biological Sciences, Smith College, Northampton, MA, USA

Objectives: Delayed preconditioning is a conserved biological response to oxidative stress in which pre-exposure to sublethal stimuli induces cellular and molecular adaptations that can protect against subsequent ischemic insults. The zinc binding proteins metallothioneins I + II (MT-I + II) have recently been shown to play an important role in modulating isoflurane-mediated delayed preconditioning against oxygen-glucose deprivation (OGD) in mouse mixed neuronal cultures*(1).* Recent work on oxidative signaling pathways suggests that metallothioneins may act as cellular sensors of oxidative stress by reacting with reactive oxygen and nitrogen species to release MT-bound zinc*(2).* Released zinc, in turn, can complex with the metal-responsive transcription factor-1 (MTF-1) enabling it to translocate to the nucleus and regulate gene expression*(3)*. In the current study we investigated this pathway looking specifically at whether isoflurane induces increases in cellular free zinc and whether MT-I + II participate in delayed anesthetic preconditioning via modulation of MTF-1 localization.

Methods: Isoflurane induced zinc release: Murine neuroblastoma cells (NIE-115) were cultured and loaded with the zinc-binding fluorophore Fluozin-3. Dye loaded cells were treated with 1.0, 2.5, and 5.0 minimum alveolar concentration (MAC) isoflurane for periods of 1-5 hours and zinc-mediated changes to fluozin-3 fluorescence were measured by spectrofluorimeter. MTF-1 Translocation: Primary dissociated cultures of neurons and glia were derived from mouse (P2) cortex. Changes to nuclear MTF-1 levels were assessed by Western blot analysis following exposure to either the nitric oxide donor *S*-nitroso-*N*-acetyl-l,l-penicillamine (SNAP),the superoxide generator paraquat, or isoflurane in wild-type (WT) and MT-I + II knockout derived cultures. MTF-1 localization was also assessed following isoflurane-preconditioning in cells treated with AG or the superoxide dismutase mimetic manganese (III) tetrakis (4-benzoic acid) porphyrin chloride (MnTBAP). In parallel with the MTF-1 localization studies, protection studies were performed for each preconditioning regimen using lactate dehydrogenase (LDH) release assays to assess survival following OGD.

Results: Isoflurane-induced zinc release: Isoflurane treatment resulted in statistically significant increases in cellular free zinc at 2.5 and 5.0, but not at 1.0 MAC isoflurane after 3 and 5 hrs of treatment. MTF-1 Translocation: Preconditioning with SNAP, paraquat, and isoflurane produced significant levels of protection against OGD with concomitant nuclear translocation of MTF-1 in WT cultures. Treatment of isoflurane preconditioned cultures with AG or MnTBAP significantly reduced the level of protection and decreased levels of nuclear MTF-1. Knockout of MT-I + II abrogated preconditioning and decreased levels of nuclear MTF-1 levels for all agents tested.

Conclusions: We conclude that isoflurane treatment leads to increased intracellular free zinc through a mechanism that relies on nitric oxide production. Furthermore, we conclude that MT-I + II are important for anesthetic mediated preconditioning, via activation of MTF-1and may play roles as sensors of oxidative stress and as end effectors of protection.

References:

ADDIN BB1. S. D. Edmands, A. C. Hall, *Anesthesiology* (2009).

2. C. M. St Croix *et al.*, *Am J Physiol Lung Cell Mol Physiol* 282, L185 (2002).

3. M. S. Stitt *et al.*, *Vascul Pharmacol* 44, 149 (2006).

1048

MRI DETECTION OF BRAIN GLUCOSE UPTAKE USING GLUCO-CEST

X. Golay[1], C.X. Yong[2], Y.M. Wang[2], G.K. Radda[2], K.-H. Chuang[2]

[1]Institute of Neurology, University College London, London, UK, [2]Singapore Bioimaging Consortium, Agency for Science, Technology and Research, Singapore, Singapore

Introduction: Measurement of glucose uptake and metabolism is usually performed using ^{18}F labelled fluorodeoxyglucose (FDG) (1), a radio-labelled compound accumulating in cells after phosphorylation. Chemical exchange saturation transfer (CEST) based MRI has recently been used to show amplification factors of detection by up to 500,000 (2). A recent study demonstrated that glycogen production could be detected by CEST (3). Here we propose to measure the uptake of unlabelled 2-deoxy-glucose (2DG) using CEST in the rat brain.

Methods: Animal experiments were approved by the institutional animal care and use committees (BMSI, Singapore). Male Lister Hooded rats (240-350g; n = 4) were fasted for 24 h before imaging. The rats were anesthetized with isoflurane, orally intubated and mechanically ventilated. End-tidal CO_2 was monitored and rectal temperature was maintained at 37°C by a feedback-controlled air-heater. 0.5-1g/kg of 2DG was injected i.v. in a bolus, followed by repeated scanning for a least 1.5 h to assess uptake curves. MRI was conducted on a Varian 9.4 T magnet (Agilent, Inc, USA). Single-shot SE-EPI imaging was used to acquire a slice crossing the somatosensory area with thickness = 2 mm, 64x32 matrix and FOV= 32 x 32 mm2. A train of saturation pulses of 1.5uT amplitude and 58 ms duration was applied at 33 different frequency offsets spanning ±4ppm to produce the desired CEST spectra in 10.2 min. To calibrate for B0 shifting, the WASSR method (4) was used with 0.1uT pulse amplitude and offset frequencies within ± 1ppm in 1.2 min.The data at each pixel was corrected for the B0 offset using polynomial fitting in phantom or WASSR in vivo. The z-spectra were processed according to (5). The CEST image was created by integration of the spectra intensity within [0.75ppm-1.25ppm].

Results: The calculated CEST maps are very similar to published FDG PET in rat brains. The benefit of this method compared to ^{13}C NMR is that it provides an intrinsic molecular amplification factor, allowing for a much larger signal to be detected. This technique therefore opens up new possibilities to map the glucose uptake in vivo for diagnosis and prognosis of diseases like neurodegeneration.

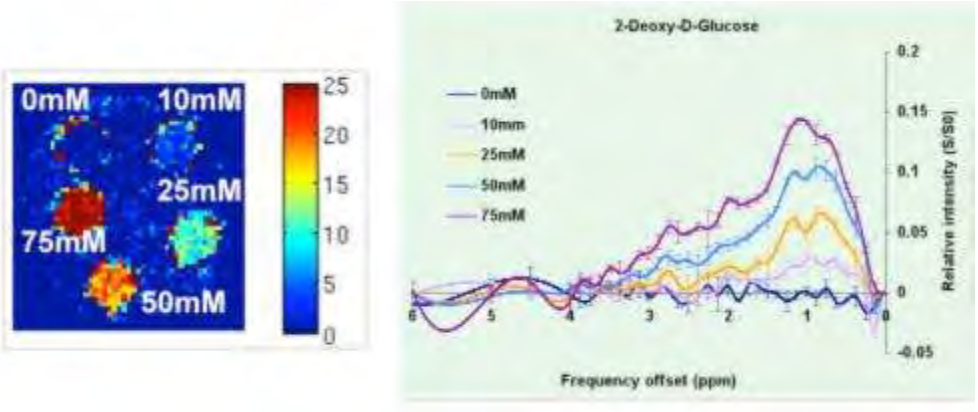

[Fig.1: CEST signal of 2DG at 1ppm]

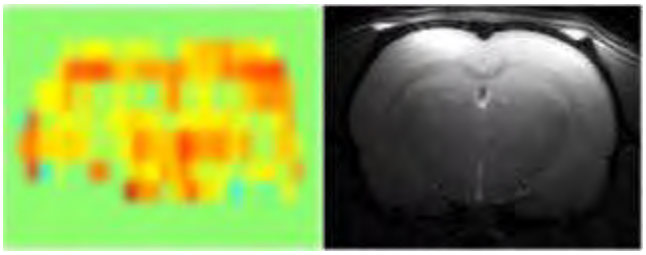

[Fig. 2: 2DG-CEST rat brain image]

Conclusion: We demonstrated in this abstract that 2DG uptake can be detected by CEST MRI.

References:

1. Alavi, A., Dann, R., Chawluk, J., Alavi, J., Kushner, M. & Reivich, M. (1986) Semin Nucl Med 16, 2-34.

2. Goffeney, N., Bulte, J. W. M., Duyn, J., Bryant, L. H. & van Zijl, P. C. M. (2001) J Am Chem Soc 123, 8628-8629.

3. van Zijl, P. C., Jones, C. K., Ren, J., Malloy, C. R. & Sherry, A. D. (2007) Proc Natl Acad Sci U S A 104, 4359-64.

4. Kim, M., Gillen, J., Landman, B. A., Zhou, J. & van Zijl, P. C. (2009) Magn Reson Med 61, 1441-50

5. Zhou, J., Payen, J. F., Wilson, D. A., Traystman, R. J. & van Zijl, P. C. (2003) Nat Med 9, 1085-90.

1049

ANGIOTENSIN(1-7) HAS THERAPEUTIC POTENTIAL IN HEMORRHAGIC STROKE

R.W. Regenhardt, P. Ritucci-Chinni, F. Desland, J.P. Joseph, A.P. Mecca, C. Sumners

Physiology, University of Florida, Gainesville, FL, USA

Stroke is a major cause of death and disability worldwide. There are two types of stroke: ischemic and hemorrhagic. Few treatments exist for this devastating condition; therapeutic options for the hemorrhagic type are particularly lacking. Its pathophysiology is multifactorial, yet growing evidence supports a major role of the angiotensin system. We have previously shown that angiotensin(1-7) [Ang(1-7)], a breakdown product of angiotensin II, has cerebroprotective actions in ischemic stroke, mediated by a blunting of increased iNOS expression. Because iNOS and inflammation are also responsible for much of the damage in hemorrhagic stroke, we examined the potential cerebroprotective role of Ang(1-7) using stroke-prone spontaneously hypertensive rats (spSHR) and also a model of collagenase-induced intrastriatal hemorrhage. Male spSHR received a 4% salt diet at 5 weeks of age to exacerbate their spontaneous hypertension and hemorrhagic stroke occurrence. Two weeks later rats received osmotic pumps to infuse Ang(1-7) or control artificial cerebrospinal fluid intracerebroventricularly (ICV). The rats treated with Ang(1-7) showed a significant increase in survival (median 175 d vs 110 d, $p< 0.05$ Chi Square, 95% CI of ratio 1.268 to 1.913) and a trend toward improvement on a sunflower seed eating task, where they were able to more efficiently shell seeds. Further, we show that during Ang(1-7) treatment, systemic arterial pressure is not different from controls. Ang(1-7), when administered ICV 7 d before collagenase-induced hemorrhagic stroke in 8 week old SD rats also shows some therapeutic potential. Rats treated with Ang(1-7) performed significantly better on the sunflower seed eating task, both in terms of time to eat the seeds ($p< 0.05$) and efficiency to shell seeds ($p< 0.05$). These data are the first demonstration that Ang(1-7) exerts beneficial actions in hemorrhagic stroke, and may ultimately provide a novel therapeutic target.

1052

DIFFERENT UNITS FOR EXPRESSING PET DATA HAVE A SIGNIFICANT IMPACT ON INTERPRETING POSSIBLE AGING-RELATED DIFFERENCES IN BRAIN GLUCOSE UPTAKE

S. Nugent[1], E. Croteau[2], F. Pifferi[1], M. Fortier[1], E. Turcotte[2], S.C. Cunnane[1,3]

[1]Research Center on Aging, [2]Nuclear Medicine and Radiobiology, CIMS, [3]Medicine, Université de Sherbrooke, Sherbrooke, QC, Canada

Despite more than 25 years of study involving nearly 1000 subjects, presently, there is no consensus as to whether the cerebral metabolic rate of glucose (CMRg) decreases during normal, healthy aging. A number of confounding biological and methodological factors contribute to the difficulties in interpreting CMRg in healthy aging and may contribute to this lack of consensus. Various techniques can be used to determine metabolic activity including the Standardized Uptake Value (SUV), Patlak analysis, non-linear regression models, 3 compartment model, or more recently, voxel-based analysis.

The primary objective of this study was to compare methods of expressing CMRg in different human brain regions in order to evaluate how the method used to express CMRg affects the interpretation of results obtained during healthy aging.

Cerebral glucose metabolism was determined using positron emission tomography analysis with the tracer ^{18}F-fluorodeoxyglucose (^{18}F-FDG) and was expressed as a ratio over the cerebellum in order to minimize inter-individual variation. CMRg and SUVs were determined in fasted healthy young (23±5 y old; n = 5) and elderly (76±3 y old; n = 6) women and men. Exclusion criteria included a MMSE score < 25/30, smoking, diabetes, evidence of overt hepatic or renal disease, untreated hypertension, dyslipidemia or thyroid disease and any medication other than that prescribed for elevated blood pressure, hyperlipidemia or inflammatory joint pain. For CMRg, the input function was derived from MRI-guided ROIs of the carotid arteries.

SUVs showed the elderly had significantly lower glucose uptake compared with young adults (5.7±0.6 vs. 7.1±1.1; mean decrease of 18-24% across several brain regions), including the anterior and posterior cingulate gyrus, frontal, parietal, and temporal lobes as well as the whole brain (all $p \leq 0.05$). However, CMRg for the elderly was not significantly different from CMRg for the young participants (48.0±8.2 vs. 48.4±10.0 µmol/100 g/min). Hence, with or without correction for the cerebellum, age did not have an effect on CMRg in any of the brain regions measured.

Expressing these data as SUV or CMRg clearly affects the interpretation of whether the brain glucose metabolism changes with age. The age-related differences observed for SUVs could be due to a number of factors. First, subject weight and body composition could be an issue, since fat has a much lower uptake of ^{18}F-FDG than other tissues. Therefore, lean body mass may be a better denominator than body mass for the calculation of the SUV. Secondly, the SUV does not take into account plasma glucose, thus brain ^{18}F-FDG uptake would be decreased if plasma glucose is high due to competitive inhibition of ^{18}F-FDG uptake by glucose. Future studies will aim to apply a correction from MRI scans for atrophy associated with aging.

Funding for this project was provided by the Natural Science and Engineering Research Council of Canada, Canadian Institutes of Health Research, Canadian Foundation for Innovation,

Canada Research Chairs Secretariat (S.C.C.). Excellent technical assistance was provided by Jennifer Tremblay-Mercier, Julie Desgagné and Conrad Filteau.

1054

IMAGING OF THE 5-HT$_{1B}$ RECEPTORS IN PARKINSON´S DISEASE WITH [^{11}C]AZ10419369

A. Varrone[1,2], P. Svenningsson[3], A. Forsberg[1], M. Tiger[1], P. Marklund[2,4], H. Fatouros-Bergman[1], K. Varnäs[1], C. Halldin[1,2], L.-G. Nilsson[2,4], L. Farde[1,2]

[1]Department of Clinical Neuroscience, Karolinska Institutet, [2]Stockholm Brain Institute, [3]Department of Physiology and Pharmacology, Karolinska Institutet, [4]Department of Psychology, Stockholm University, Stockholm, Sweden

Introduction: In Parkinson´s disease (PD) depression or cognitive impairment are common problems potentially related to changes of non-dopaminergic neurotransmitters such as serotonin (5-HT). Pre-clinical and post-mortem studies have shown that the serotonin system is implicated in PD [1,2]. Moreover, pre-clinical studies suggest that the 5-HT$_{1B}$ receptor and the associated p11 protein are implicated in depression-like states [3] and in L-dopa induced dyskinesias [4]. The 5-HT$_{1B}$ receptor might be a potential candidate target for the investigation of the serotonin function in PD and its relation to mood or cognitive function.

Aim: The aim of this study was to investigate the availability of 5-HT$_{1B}$ receptors in PD using positron emission tomography.

Methods: Ten PD patients (6M, 4F, age 57-75 y, mean 67, Hoehn and Yahr stage: 1-2.5, UPDRS-motor: 10-25, mean 14) and nine healthy controls (7M, 2F, age 53-69 y, mean 63) were included. Subjects were not depressed according to psychiatry assessment, including Beck Depression Inventory and the Montgomery & Åsberg Depression Rating Scale. Cognitive function was evaluated with the assessment of episodic, semantic, working memory, verbal/spatial span, and visual attention. PET measurements were performed with the 5-HT$_{1B}$-radioligand [^{11}C]AZ10419369 [5] using the HRRT system. 5-HT$_{1B}$ receptor availability was evaluated in cortical regions (occipital, visual, prefrontal, orbitofrontal, anterior and posterior cingulate, temporal), limbic regions (amygdala and hippocampus), and subcortical regions (caudate, putamen, ventral striatum, globus pallidus, thalamus, substantia nigra). The outcome measure was the binding potential (BP_{ND}) estimated using the simplified reference tissue model and the cerebellum as reference region. Differences between groups were assessed with unpaired *t*-test ($p < 0.05$) without Bonferroni correction.

Results: PD patients showed a significantly lower BP_{ND} as compared with healthy controls in orbitofrontal cortex (0.77±0.16 vs. 0.95±0.20), posterior cingulate (0.61±0.20 vs. 0.81±0.19), temporal cortex (0.65±0.12 vs. 0.81±0.18) and hippocampus (0.27±0.17 vs. 0.42±0.09). A significant decrease in episodic memory, creative ability, and spatial span (working memory capacity) was also observed in PD patients. A positive correlation was found between episodic memory and BP_{ND} in posterior cingulate (r^2=0.418, $p < 0.01$) and between creative ability and BP_{ND} in orbitofrontal, prefrontal, cingulate cortex, temporal cortex and thalamus (r^2=0.349-0.546, p=0.001-0.016) when PD and healthy controls were analysed together.

Conclusions: These preliminary data indicate a mild (~20%) decrease of 5-HT$_{1B}$ receptor availability in PD. Decreased 5-HT transporter availability in orbito-frontal cortex, cingulate cortex, and hippocampus has already been found in previous PET studies in PD patients [6,7], suggesting that impairment of serotonin innervation in those regions might be present in PD. Preliminary correlation analysis suggest that 5-HT$_{1B}$ receptor availability might be associated with episodic memory and creative ability, cognitive domains that were found to be affected in PD.

Acknowledgements: This study was supported by Stockholm Brain Institute and by the Swedish Foundation for Strategic Research.

References:

1. Carta M. Brain 2007;130:1819-1833.
2. Kish SJ. Brain 2008;131:120-131.
3. Svenningsson P. Science 2006;311(5757):77-80.
4. Zhang X. Proc Natl Acad Sci U S A 2008;105(6):2163-2168.
5. Pierson, ME. Neuroimage 2008;41(3):1075-85
6. Guttman M. Eur J Neurol 2007;14(5):523-528.
7. Albin RL. J Cereb Blood Flow Metab 2008;28(3):441-444.

1055

ATLAS-BASED ANALYSIS OF A FUNCTIONAL NEAR INFRARED SPECTROSCOPY MOTOR STUDY

D. Contini[1], M. Caffini[1], L. Zucchelli[1], L. Spinelli[2], R. Cubeddu[1], D.A. Boas[3], A. Torricelli[1]

[1]Dept. of Physics, Politecnico di Milano, [2]Istituto di Fotonica e Nanotecnologie (IFN) - CNR, Milan, Italy, [3]Martinos Center for Biomedical Imaging, Massachusetts General Hospital, Charlestown, MA, USA

Aim: Implementation of a tool for the spatial fNIRS data visualization on the basis of an atlas-based reconstruction method.

Introduction: Functional Near Infrared Spectroscopy (fNIRS) systems have been developed with a relatively large number of sources and detectors that use tomographic methods to reconstruct 3D images of brain activation [Zeff B. et al., Proc. Natl. Acad. Sci. U.S.A. 104, 12169 (2007)]. To further improve images of brain activity, subject-specific spatial priors of the head anatomy can be exploited to inform the optical tomography problem [Boas D. et al., Appl.Opt. 44, 1957 (2005)]. We apply a method to image the hemodynamic response to brain activation using an atlas head model to guide the optical tomography problem [Custo, A. et al., NeuroImage 49, 561 (2009); Caffini M. et al., OSA Technical Digest, JMA87 (2010)]. This MRI-free approach to obtaining optical images is based on registering a selected head template (atlas) to the subject head surface and solving the photon migration forward problem on the registered atlas [Fang Q. et al., Optics Express 17, 20178 (2009)]. From the map of the cortical absorption at two different wavelengths (690 nm and 820 nm) a map of the oxygenated and deoxygenated hemoglobin concentration changes can be obtained.

Material and methods:

Protocol: We have collected data from 10 subjects during a hand grasping motor task. The protocol we adopted has been a 40 s long task (10 s baseline, 20 s task and 10 s recovery), 10 repetitions.

Probe: We designed a probe that covered surface of the scalp above the motor areas. 8 sources and 15 detectors have been arranged in a squared pattern with 3 cm source-detector distance accordingly to the 10/20 EEG positions.

Instrumentation: fNIRS data have been acquired with the 16 channels time domain medical device developed at Politecnico di Milano [Contini D. et al., Optics Express, 14, 5418 (2006)].

Data analysis: From each source and detector position a Monte Carlo photon migration simulation has been run in the segmented atlas volume and then the forward matrix operator have been computed. Image reconstruction has been performed solving the inverse model.

Results:

Standard visualization: the classical fNIRS time series analysis features the visualization of the oxygenated and deoxygenated hemoglobin signals vs. time and spatial information is limited to source-detector relative positions. Spatial arrangement of fNIRS time series using the 10/20 EEG reference could help the spatial interpretation of data.

Atlas visualization: Conversely, the atlas approach gives an immediate visualization of the activation spatial profile and of its time course. A movie could also be created to better visualize the time evolution of the cortical activation.

Conclusion: The use of an atlas-based reconstruction method for the analysis of fNIRS data can be useful for the spatial visualization and interpretation of optical measurements even without an MRI subject-specific anatomy. Further work is in progress to apply this method to time resolved fNIRS data in order to exploit time information and increase the accuracy in the discrimination between superficial and brain hemodynamic changes.

1058

ACUTE HYPOGLYCEMIA INDUCES INCREASED BRAIN LACTATE UPTAKE AND METABOLISM IN RATS

H.M. De Feyter[1], K.L. Behar[2], L.R. Drewes[3], R.A. de Graaf[1], D.L. Rothman[1,4]

[1]Department of Diagnostic Radiology, [2]Department of Psychiatry, Yale University, New Haven, CT, [3]Department of Biochemistry and Molecular Biology, University of Minnesota, Duluth, MN, [4]Department of Biomedical Engineering, Yale University, New Haven, CT, USA

Objectives: To investigate the blood-brain lactate transport and cortical lactate metabolism during hypoglycemia.

Methods: *In vivo* ^{1}H-[^{13}C] magnetic resonance spectroscopy (MRS) in combination with [3-^{13}C]-lactate infusion during hyperinsulinemic euglycemic and hypoglycemic conditions was performed in Long Evans rats using a 9.4T horizontal bore magnet interfaced to a Varian spectrometer. A combined quadrature ^{13}C and single loop ^{1}H surface coil set-up was placed on top of the skull to acquire ^{1}H-[^{13}C] MR spectra from a 180 mL voxel positioned in the middle of the cortex. ^{1}H-[^{13}C] MR spectra were acquired at steady state plasma glucose levels of ~6 mM (euglycemia) or ~2.3 mM (hypoglycemia). Data are presented as mean ± standard deviation.

Results: Mean plasma glucose levels were 5.8 ± 0.7 and 2.3 ± 0.3 mM in euglycemic and hypoglycemic rats, respectively (n=5, 5). Steady state plasma lactate concentrations were 3.3 ± 0.5 mM during euglycemia and 3.6 ± 0.9 mM for hypoglycemia, whereas fractional enrichments of plasma lactate where 19.8 ± 1.8 and 25.1 ± 3.7 % in euglycemic and hypoglycemic rats, respectively. Figure 1a depicts the ^{13}C signal of glutamate C4 (Glu4) expressed in arbitrary units, determined after scaling total (^{12}C+^{13}C) spectra to the creatine peak at 3.02 ppm. The ^{13}C signal of glutamate C4 (Glu4) in hypoglycemic rats was ~ twice the level of euglycemic rats. Mean ^{13}C fractional enrichment calculated for Glu4 from spectra acquired after 75 min of lactate infusion was 6.3 ± 0.7 % for euglycemic animals and 13.0 ± 1.8 % for hypoglycemic animals. To confirm the apparently fast change in brain lactate transport and metabolism two-stage glycemic clamps were performed within the same animals resulting in euglycemic levels followed by acute hypoglycemia, while keeping the [3-^{13}C]-lactate infusion constant (Figure 2). Glu4 ^{13}C fractional enrichments were 7.4 ± 0.7 % at average glucose concentration of 6.4 ± 0.2 mM (45 min) and increased to 11.9 ± 0.2 % when glucose was dropped to 2.3 ± 0.7 mM (120 min).

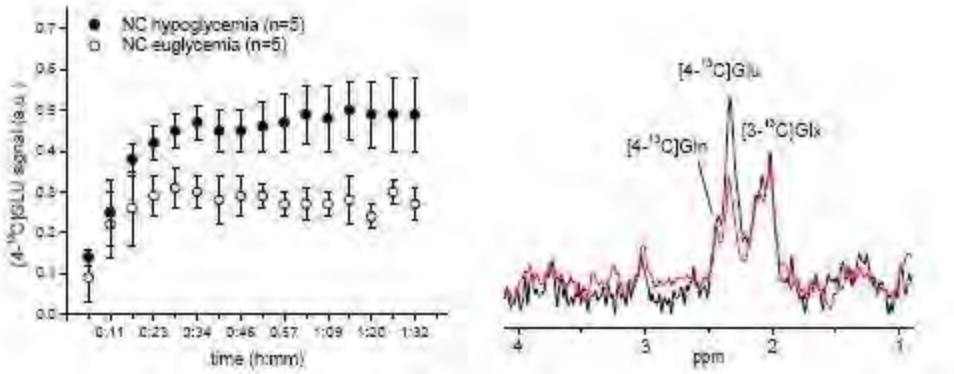

Figure 1 a) ^{13}C signal amplitude of brain Glu4 of fitted POCE difference spectra during the infusion of [3-^{13}C]-lactate under euglycemic (open symbols) and hypoglycemic (filled symbols) conditions (n=5). **b)** POCE difference spectra acquired after 75 min of [3-^{13}C]-lactate infusion during euglycemia (red) and acute hypoglycemia (black). Peak annotations: Glu: glutamate; Gln: glutamine; Glx: glutamate+glutamine. The peak at 3.02 ppm is natural abundance ^{13}C signal of total creatine (tCr). Total (^{12}C+^{13}C) spectra were scaled to the 3.02 ppm tCr peak before subtraction.

[Figure 1]

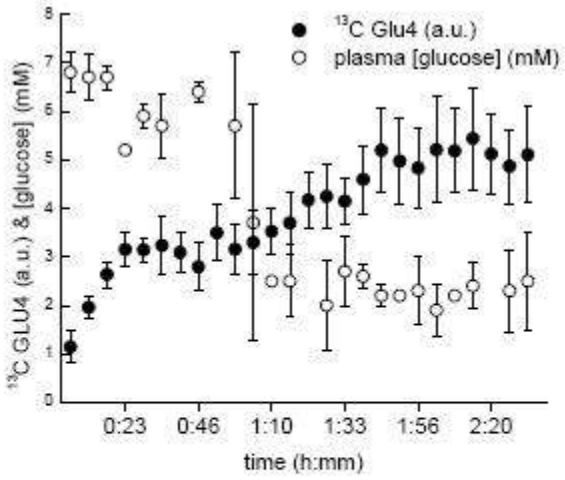

Figure 2 ^{13}C signal amplitude of brain Glu4 of fitted POCE difference spectra during the infusion of [3-^{13}C]-lactate during euglycemia and subsequent hypoglycemia (n=3).

[Figure 2]

Conclusions: Levels of ^{13}C fractional enrichment of Glu4 during infusion of [3-^{13}C]-lactate were increased following acutely induced hypoglycemia compared to euglycemic rats, suggesting rapid upregulation of lactate transport upon lowering plasma glucose levels. Indeed, rats studied under euglycemia immediatley followed by hypoglycemia displayed a rapid increase in lactate transport and/or oxidation, as Glu4 enrichment increased to a new steady state level when glucose levels were lowered. The higher level of Glu4 ^{13}C enrichment induced by hypoglycemia can be the result of increased brain metabolism of lactate, a higher transport capacity of lactate at the blood-brain barrier or a combination of both. The ability of the brain to rapidly upregulate monocarboxylixc acid transport and metabolism during hypoglycemia may be an important mechanism for adapting to hypoglycemia and could play an important role in the pathogenesis of hypoglycemia unawareness.

1059

NITRIC OXIDE DYNAMICS COUPLES NEURONAL ACTIVITY WITH HIPPOCAMPUS MICROCIRCULATION: A MECHANISM IMPAIRED IN A TRIPLE-TRANSGENIC MOUSE MODEL OF ALZHEIMER DISEASE

C.F. Lourenço[1], R.M. Santos[1], R.M. Barbosa[1], E. Cadenas[2], R. Radi[3], J. Laranjinha[1]

[1]University of Coimbra - Center for Neurosciences and Cell Biology, Coimbra, Portugal, [2]University of Southern California, Los Angeles, CA, USA, [3]Universidad de la Republica, Montevideo, Uruguay

Introduction: The neurovascular coupling (NVC) is the process of local increase in cerebral blood flow (CBF) in response to rising metabolic neuronal demands, being essential for the brain to maintain its functional and structural integrity. Disturbing the mechanisms that couple neuronal activity to CBF will lead to brain dysfunction and disease. The concept that nitric oxide ($^{\cdot}$NO) formed upon ionotropic glutamate receptor activation, may play a critical role in NVC has been a tempting suggestion but difficult to substantiate *in vivo*. That is, the sequence of events encompassing $^{\cdot}$NO signals, CBF and O_2 changes need to be simultaneously and quantitatively measured *in vivo* and in a way that the dynamics of all the processes is clear visible.

By simultaneously measuring $^{\cdot}$NO dynamics and CBF in hippocampus *in vivo* we aimed at establishing the role of neuronal NMDA receptor-dependent $^{\cdot}$NO dynamics in the regulation of local blood flow. Moreover, we addressed how NVC developed during Alzheimer disease (AD) progression.

Methods: The simultaneous measurements of $^{\bullet}$NO production and cerebral blood flow were achieved by using an array formed by a $^{\bullet}$NO-selective microelectrode (or to O_2), an ejection glass micropipette and a laser Doppler probe assembled in a pre-defined geometry. Two animal models were used: male Wistar rats and a triple-transgenic mouse model of AD (3×Tg-AD). The array was sterotaxically positioned in the hippocampus of the urethane-anesthetized animals. $^{\bullet}$NO production was induced by a localized stimulation with L-glutamate (0.5 nmol, 25 nL). The recorded signals were modulated with several pharmacological tools.

Results and discussion: The *proof of concept* of the $^{\bullet}$NO-mediated wireless connection between neurons and arterioles requires the demonstration of a spatial, temporal, and amplitude association between vascular changes, O_2 tension and neural functioning. Glutamatergic activation showed to promote a time, spatial and amplitude coupled increase in $^{\cdot}$NO concentration and local CBF, both dependent on the activation of NMDA receptor and nNOS activation, identifying the pathway that paves the NVC process and recognizing nNOS-derived $^{\cdot}$NO as the coupler molecule in hippocampus.

In the triple transgenic model of AD, neuronal derived $^{\cdot}$NO was unaffected during disease progression, a significant impairment in the corresponding CBF change was found in the later stages of the disease (12 months-old). Data supports that the impairment in NVC in AD likely results from a dysfunction at the transducer site (vasculature), rather than at the signal producer site ($^{\cdot}$NO-producing neurons). Furthermore, it is suggested that oxidative stress may be critically contribute to the NVC impairment.

Conclusions: In hippocampus, nNOS-derived nitric oxide mediates neurovascular coupling via a diffusional wireless connection between active glutamatergic neurons and blood vessels. The neurovascular coupling is impaired in the later stages of AD at the transducer level

(vasculature). Overall, these findings (1) *establish causality*, for specific and quantitative approaches *in vivo* link nitric oxide-driven signaling pathways to cerebral blood flow changes, (2) *provide a conceptual advance* of how the brain maintains its integrity by controlling its own blood supply, and (3) may be conducive to the development of therapeutic interventions in Alzheimer´s disease.

1060

IDENTIFICATION AND VALIDATION OF NOVEL TARGETS FOR STROKE TREATMENT BY AN INNOVATIVE IN VITRO SYSTEM

B. Wielsch, **M. Mueller**

Fraunhofer Institute for for Cell Therapy and Immunology, Leipzig, Germany

Objective: The leading cause of chronic disability in humans is stroke, due to the lack of an effective treatment beyond a 4.5 hour time window.- currently leaving more then 90% of patients untreated. Aim of the project is the establishment of a novel and highly innovative *in vitro* system of interacting primary neural cells, in particular neurons, astro- and microglia, as a test system for novel stroke therapies. The system will be used for the analysis of new endogenous key factors which are regulated or activated after oxygen-glucose-deprivation in order to find new therapeutically relevant molecules which play an important role in the regulation of the (patho-) physiological processes after stroke beyond a 4.5 hour time window and may therefore be addressed in new regenerative approaches.

Material and methods: Neurons and Glia were harvested from fetal mouse brain at embryonic day 18.5. The cells are cultured under normoxic (21% O_2,4,5% Glucose) or ischemic (1% O_2, no glucose) conditions for a defined period of time and analysed after 0h, 6h, 24h, 48h and 72h reoxygenation.

Results and conclusion: Our recently developed in vitro system allows the analysis of new endogenous key factors which are regulated or activated after oxygen-glucose-deprivation. Among others, two protein families seem to be extremely promising and interesting candidates in our analysis. SUMOs and SENPs (small ubiquitin like modifiers/ SUMO proteases) are implicated in the regulation of a broad range of cellular processes and have been shown to be up regulated during cerebral ischemia. These proteins can have an important function in stroke regeneration and/or decrease the inflammatory processes - a major reason for cell loss following cerebral ischemia.

Expression patterns show that the candidate proteins are expressed in neural tissue under normoxic and ischemic conditions. Loss of function as well as overexpression experiments shall demonstrate their protective function during the regeneration process after oxygen glucose deprivation.

Overall, our findings and further studies will help to elucidate the molecular signalling pathways activated after oxygen-glucose-deprivation, in order to enhance the therapeutic intervention during cerebral ischemia.

1061

DISTRIBUTION OF TEMPERATURE CHANGES AND DYNAMICS IN RAT BRAIN INDUCED BY MDMA

D. Coman[1], B.G. Sanganahalli[1], L. Jiang[1], F. Hyder[1,2], K. Behar[3]

[1]Diagnostic Radiology, [2]Biomedical Engineering, [3]Psychiatry, Yale University, New Haven, CT, USA

Objectives: 3,4-Methylenedioxymethamphetamine (MDMA, ecstasy) is a heavily abused psychostimulant which has seen explosive growth in its use during the last decade [1]. The most severe and potentially fatal acute effects of MDMA involve extreme hyperthermia and its consequences on multiple organ systems [2,3]. The magnitude, distribution, and dynamics of MDMA induced temperature changes are thus of critical importance in neurotoxicity, where core body temperature is most frequently reported. Recently, we showed that biosensor imaging of redundant deviation of shifts (BIRDS) in conjunction with a new exogenous temperature-sensitive probe based on the complex between thulium ion (Tm^{3+}) and macrocyclic chelate 1,4,7,10-tetraazacyclododecane-1,4,7,10-tetramethyl-1,4,7,10-tetraacetate ($DOTMA^{4-}$) can be used to obtain temperature distributions in rat brain within minutes [4]. In the present study we use the $TmDOTMA^-$ agent to measure time-dependent temperature distributions, and from these we calculate the maps of temperature changes and of MDMA-induced warming rates in rat brain.

Methods: Sprague-Dawley rats (250-300g) were tracheotomized and artificially ventilated. The animals were anesthetized with an intraperitonial injection of urethane (1.3g/Kg). The anesthetized rats were prepared with renal ligation as previously described [4]. $TmDOTMA^-$ was continuously infused for ~2 hours, followed by the MDMA injection (20mg/kg,i.p.). A gaussian pulse of 200 ms was used for excitation of a 6mm slice with FOV of 2.56cmx2.56cm. The following parameters were used: 16x16 encode steps, TR=11ms, 100 averages and 4min 40s acquisition time. The temperature maps were calculated from the chemical shifts of $TmDOTMA^-$ methyl group according to the equation: $\boldsymbol{T=(34.45\pm0.01)+(1.460\pm0.003)\cdot(\delta_{CH3}+103)+(0.0152\pm0.0009)\cdot(\delta_{CH3}+103)^2}$**.** For each animal, the MDMA-induced warming rates were calculated by fitting the temperature variation over time to a linear function as a first-order approximation to represent the initial speed of heating.

Results: The results indicate a relatively homogenous distribution across the whole cortex for both warming rates and temperature changes, with standard deviations of less than 0.2 ^{0}C/h and 0.3 ^{0}C, respectively. The average warming rates were very similar for all animals investigated (~2.0 ^{0}C/h), while the average cortical temperature change was different for each animal investigated, spanning a relatively large range of values, from 1.0 to 2.4 ^{0}C. A strong linear correlation (R=0.9987) was observed between changes in the average cortical temperature, ΔT_{brain}, and the body temperature, ΔT_{body}: $\boldsymbol{\Delta T_{brain}=(0.53\pm0.03)\times\Delta T_{body}+(0.45\pm0.07)}$. These results were further confirmed by thermocouple based temperature measurements. Cortical brain temperature increased from 34.3±0.4 ^{0}C to 35.9±0.8 ^{0}C after the MDMA injection, with a similar warming rate.

Conclusions: The current results indicate that a single bolus injection of MDMA (20mg/kg,i.p.) led to a rapid initial rate of heating of ~2^{0}C/h with a maximum temperature change of 2.4 ^{0}C observed at 2 hours post injection. Future studies should investigate the consequences of repetitive MDMA injections as well as other brain regions where MDMA neurotoxicity is known to manifest.

References:

[1] http://www.drugabuse.gov/PDF/RRmdma.pdf, (2006);

[2] Hall AP and Henry JA. *Br J Anaesth.*, **96**(6):678-685, (2006).

[3] Green AR et al., *Pharmacol Rev.,* **55(3)**:463-508**, (**2003);

[4] Coman D et al. (2009) *NMR Biomed.*23(3):277-285.

Acknowledgements: Supported in part by a pilot grant from P30 NS052519 of the QNMR Program.

1063

OCCUPANCY AT BRAIN 5-HT$_{1B}$ RECEPTORS WITH AZD3783 IN NON-HUMAN PRIMATES AND HUMAN SUBJECTS: A PET STUDY WITH [^{11}C]AZ10419369

K. Varnäs[1], S. Nyberg[2], P. Karlsson[1], E. Pierson[3], M. Kågedal[2], Z. Cselényi[1,2], D. Mc Carthy[4], A. Xiao[4], M. Zhang[4], C. Halldin[1], L. Farde[1,2]

[1]Clinical Neuroscience, Karolinska Institutet, Stockholm, [2]Clinical Neuroscience, AstraZeneca Pharmaceuticals, Södertälje, Sweden, [3]CNS Discovery, [4]Clinical Pharmacology, AstraZeneca Pharmaceuticals, Wilmington, DE, USA

Introduction: The serotonin 1B (5-HT$_{1B}$) receptor has attracted interest for its potential involvement in the pathophysiology and treatment of depression. Positron emission tomography (PET) determination of 5-HT$_{1B}$ receptor occupancy with drug candidates targeting this receptor in non-human primate and human subjects may facilitate translation of research from animal models and guide dose-selection for clinical studies. AZD3783 is an orally bioavailable 5-HT$_{1B}$ receptor antagonist recently developed by AstraZeneca.

Objectives: To determine the relationship between plasma concentration of AZD3783 and occupancy at non-human primate and human brain 5-HT$_{1B}$ receptors using PET and the radioligand [^{11}C]AZ10419369.

Methods: PET studies with [^{11}C]AZ10419369 were performed in three non-human primates at baseline and after intravenous injection of AZD3783. Subsequently, PET measurements were undertaken in six human subjects at baseline and after administration of different single oral doses of AZD3783 (1-40 mg). Receptor occupancy was calculated from binding potential (BP_{ND}) values for the occipital cortex and striatum estimated with the simplified reference tissue model and the cerebellum as reference region. The relationship between AZD3783 plasma exposure and receptor occupancy was modeled to estimate the AZD3783 plasma concentration required for 50% receptor occupancy ($K_{i,\ plasma}$).

Results: After administration in non-human primates and human subjects AZD3783 reduced regional [^{11}C]AZ10419369 binding in a dose-dependent and saturable manner. The AZD3783 $K_{i,\ plasma}$ value for non-human primates was 25 and 27 nmol/L in occipital cortex and striatum, respectively (Figure 1). Corresponding estimates for human occipital cortex and ventral striatum were 24 and 18 nmol/L, respectively (Figure 2).

Conclusions: The correspondence between $K_{i,\ plasma}$ values for AZD3783 obtained in non-human primate and human subjects *in vivo* provides support for the validity of PET studies using [^{11}C]AZ10419369 in non-human primates for prediction of 5-HT$_{1B}$ receptor pharmacology in humans. [^{11}C]AZ10419369 can be successfully used to determine 5-HT$_{1B}$ receptor occupancy and constitutes a useful tool for dose-selection in clinical studies with 5-HT$_{1B}$ receptor compounds.

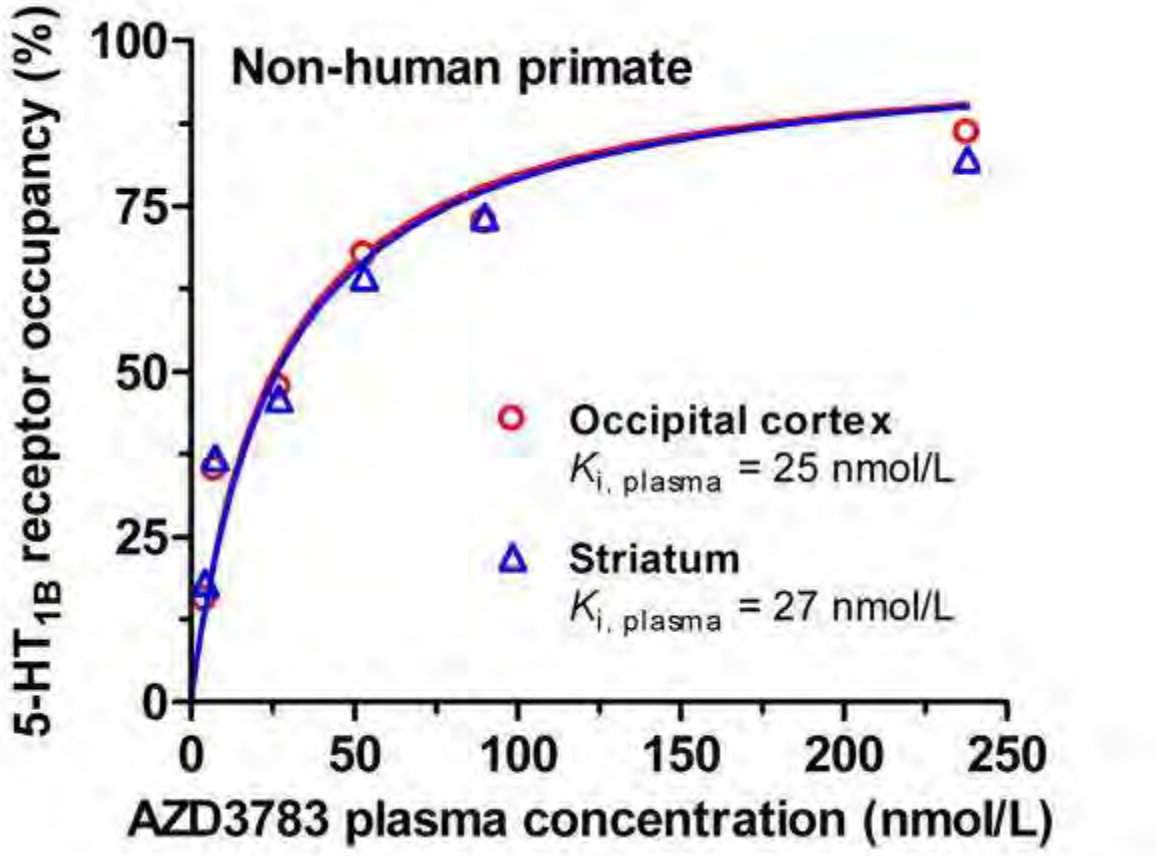
Non-human primate
5-HT1B receptor occupancy (%)
100
75
50
25
0
0
50
100
150
200
250
AZD3783 plasma concentration (nmol/L)
Occipital cortex
Ki, plasma = 25 nmol/L
Striatum
Ki, plasma = 27 nmol/L

[Figure 1]

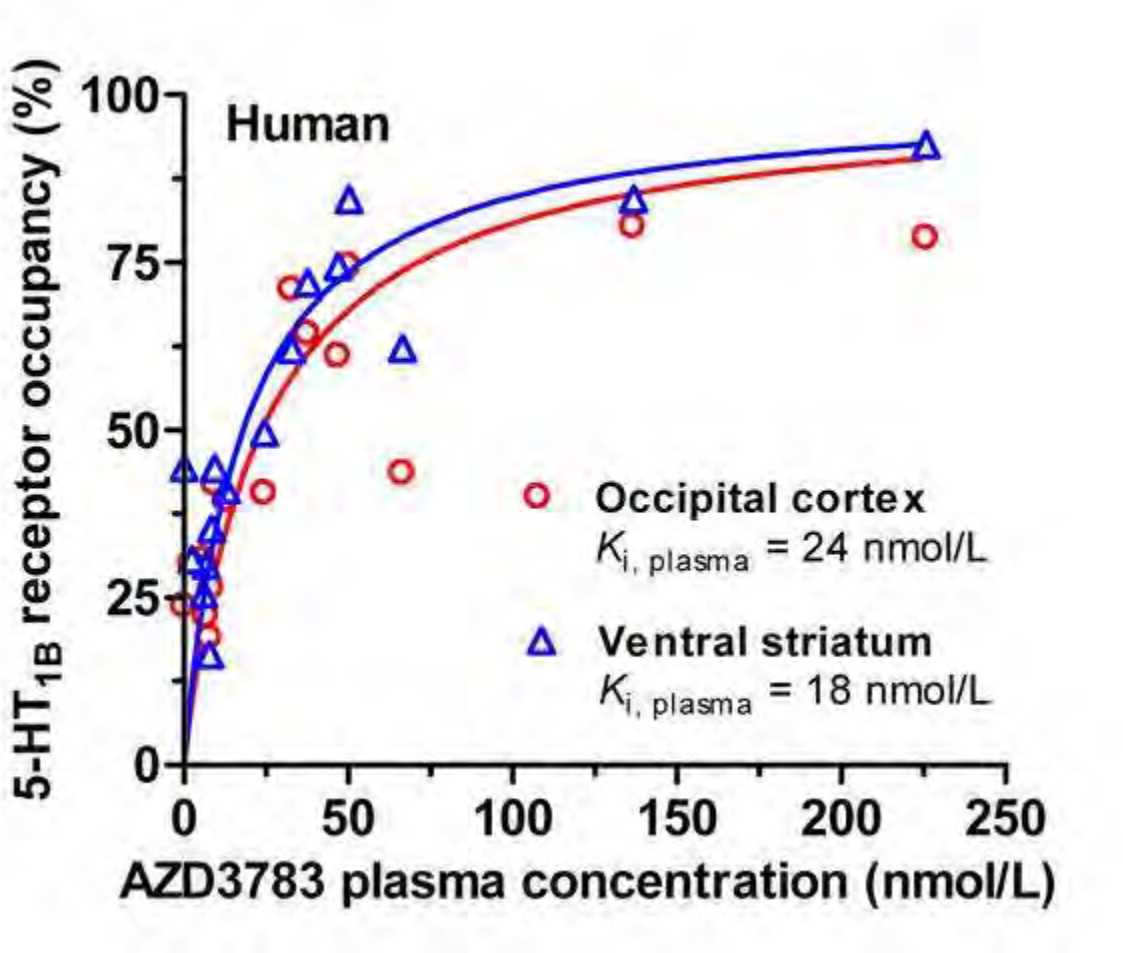
Human
5-HT1B receptor occupancy (%)
100
75
50
25
0
0
50
100
150
200
250
AZD3783 plasma concentration (nmol/L)
Occipital cortex
Ki, plasma = 24 nmol/L
Ventral striatum
Ki, plasma = 18 nmol/L

[Figure 2]

1065

LONGITUDINAL MRI EVALUATION OF PROTECTION AGAINST BRAIN DAMAGE AFTER TRANSIENT ISCHEMIA IN MICE DEFICIENT IN MANNOSE-BINDING LECTIN

X. de la Rosa[1,2], Á. Cervera[2,3], G. Soria[1,2,4], C. Justicia[1,2], Á. Chamorro[2,3,5], A.M. Planas[1,2,4]

[1]Department of Brain Ischemia and Neurodegeneration, Institut d'Investigacions Biomèdiques de Barcelona (IIBB)-Consejo Superior de Investigaciones Científicas (CSIC), [2]Institut d'Investigacions Biomèdiques August Pi i Sunyer (IDIBAPS), [3]Comprehensive Stroke Unit, Hospital Clinic, [4]Experimental MRI 7T Unit, IDIBAPS, [5]Medical School, University of Barcelona, Barcelona, Spain

Objectives: The complement system has been shown to participate in brain damage after stroke. The complement can be activated through the lectin pathway, which involves mannose-binding lectin (MBL). We recently showed that experimental animals and patients with deficient production of MBL are protected after stroke (1). Up to two days after brain ischemia, MBL-deficient (MBL-null) mice showed smaller infarct volume and better neurological outcome than the wild type (wt) (1). Here we carried a longitudinal MRI study in wild type and MBL-null mice by examining the progression of the brain lesion up to day 7. We also evaluated the acquired neurological deficit at 1 and 7 days after transient ischemia.

Methods: Intraluminal middle cerebral artery (MCA) occlusion was induced for 90 min in adult male MBL-null mice of the C57/Bl6 background (n=8) and corresponding wt mice (n=6) under isofluorane anesthesia. Cortical cerebral blood flow (CBF) was recorded with laser Doppler flowmetry (Perimed). Longitudinal MRI scans were performed under isofluorane anaesthesia in a BioSpec 70/30 horizontal animal scanner (Bruker BioSpin, Ettlingen, Germany), equipped with a 12 cm inner diameter actively shielded gradient system (400 mT/m) and a phased array surface coil for mouse brain. MRI studies (Apparent Diffusion Coeficient, ADC, and T2 relaxometry) were performed during MCA occlusion, and at 1 and 7 days post-ischemia. The volume of infarction was measured from the T2 map images. The neurological deficit was assessed with the tape-removal behavioral test that required training the animals before induction of ischemia.

Results: The mean cortical perfusion during ischemia (expressed as percent of basal pre-occlusion levels) was similar in the MBL-null group (27±7%) than in the wt group (22±7%). By measuring the volume of infarction at 1 and 7 days in the same animals we showed a significant reduction from day 1 to 7 in both groups. The percentage of infarct volume reduction from day 1 to 7 was 41% ($p< 0.01$) and 46% ($p< 0.05$) in wt and MBL-null groups, respectively. MBL-null mice showed significantly smaller infarct volumes that the wt at day 1 ($p< 0.05$) with a 32% reduction in infarct volume. Likewise, at day 7, infarct volume in MBL-null mice was 38% smaller ($p< 0.05$) than in the wt, demonstrating that the protection reported before was maintained at day 7. Also, the neurological deficit was significantly attenuated in MBL-null mice versus the wt at day 1 ($p< 0.01$) and at day 7 ($p< 0.05$).

Conclusions: This study shows that protection from transient brain ischemia/reperfusion in MBL-null mice is maintained for 7 days. The results support that MBL negatively contributes to stroke outcome.

Reference: Cervera A et al., 2010. Plos One;5(2):e8433.

Acknowledgements: XR was supported by a grant from the Spanish Ministry of Science and

Innovation (MICINN). Financed in part by the European Community (FP7/2007-2013; grant agreement number 201024), the MICINN (SAF2008-04515-CO2-01) and the Spanish Ministry of Health: *Fondo de Investigaciones Sanitarias* (FIS).

1066

IMPACT OF MICROVASCULAR ENDOTHELIAL CELLS ON GLUTAMATE-INDUCED EXCITOTOXICITY IS AGE- AND T-PA-DEPENDENT

V.J. Henry[1], M. Lecointre[1], P. Leroux[1], D. Vivien[2], B.J. Gonzalez[1], V. Laudenbach[1,3]

[1]EA 4309 'Neo Vasc', University of Rouen, Rouen, [2]'Sérines Protéases et Physiopathologie de l'Unité Neurovasculaire', INSERM U919, Serine Proteases and Pathophysiology of the Neurovascular Unit (SP2U), UMR CNRS 6232 CI-NAPS, Centre for Imaging-Neuroscience and Applications to Pathologies, GIP CYCERON, University of Caen Basse-Normandie, Caen, [3]'Pédiatrie Néonatale et Réanimation, Centre d'Education Fonctionnelle', CHU Rouen, Rouen, France

Despite the improvement in obstetrics and newborn intensive care, neurological disabilities of perinatal origin do not decrease. Pathophysiology of neonatal lesions is multifactorial, but excitotoxicity has been pointed out as a common pathway of most deleterious processes in brain injuries. High brain vascularisation and detection of functional NMDA-receptor on endothelial cells support a contribution of brain microvascular endothelial cells (BMEC) on neuronal death during an excitotoxic process. Recently, we demonstrated phenotypic and functional differences between newborn (n) and adult (a)-derived BMECs[1]. In particular, these data suggested different responses of nBEMC versus aBEMC to excitotoxic concentrations of glutamate (Glu).

In order to compare the impact of BMEC released factors on cortical neurons in excitotoxic conditions, we performed mice nBMEC and aBMEC cultures. BMECs were exposed during 6h to low (50 µM) and high (1 mM) concentrations of Glu. Afterwards, culture media from treated BMECs were applied on mature cortical neurons at 11 days *in vivo* (DIV11). Neuronal death was quantified by lactate deshydrogenase activity released in media.

At low concentration of Glu (50 µM), neuronal death was significantly increased by the culture medium from nBMEC, whereas aBMEC did not induced any variation of neuronal mortality. At high concentration of glutamate (1 mM), both nBMEC and aBMEC culture media increased neuronal death. However, the neurotoxicity of nBMEC was higher than that of aBMEC. Neuronal death induced by nBMEC and aBMEC culture media was significantly blocked by the NMDA-receptor antagonist MK-801 (10 µM) and by the tissue-Plaminogen Activator (t-PA) inhibitor: PAI-1 (1 µg/ml). The contribution of t-PA on BMEC neurotoxicity was confirmed using nBMEC from t-PA$^{-/-}$ knock-out mice which didn't increased the excitotoxic effect of Glu. Consistent with these results, treatment of mature cultured neurones with t-PA (20µg/ml) mimicked the effect of nBMEC on glutamate-induced toxicity. Interestingly, when t-PA (20µg/ml) was added to immature cortical neurons (DIV 4), it exerted a neurotrophic effect, suggesting a dual action of t-PA depending on neuronal maturity. In order to confirm this hypothesis, acute cortical slices of 10 days-old mice were treated by t-PA and/or Glu. Compared to Glu alone, t-Pa + Glu significantly increased necrosis in the cortical layers V and VI (containing high proportion of mature neurones at this stage), whereas, it decreased Caspase-3 activity in cortical layer II-IV (containing mostly immature neurones at this stage).

Taking together these results suggest a differential contribution of nBMEC and aBMEC on glutamate-induced neuronal death. In mature neurons, nBMEC are more potent than aBMEC to promote glutamate-induced toxicity. This effect is mediated, at least in part, by t-PA. In contrast, in immature neurons, nBMEC seems to exert neurotrophic activities. This dual action of BMEC

depending on neuronal maturity reinforces a vascular contribution on glutamate-mediated excitotoxicity, especially in neonate pathophysiology.

Reference:

[1]Legros *et al.* (2009) *J. Cereb. Blood. flow. Metab. 29, 1146-1158*

Acknowledgements: *foundation « les gueules cassées », université de Rouen, région Haute-Normandie, ANR, ELA*

1067

PROTEIN CCM3 REGULATES TIGHT JUNCTION COMPLEX STABILITY AT BLOOD BRAIN BARRIER

A.V. Andjelkovic[1], S.M. Stamatovic[1], R.F. Keep[2]

[1]Pathology, [2]Neurosurgery, University of Michigan, Ann Arbor, MI, USA

Objectives: Accumulating evidence suggests that impairment in intercellular barrier function and tight junction (TJ) complex defects at the endothelium are the major cause for cerebrovascular malformation type-3 (CCM-3) lesions. However, only few studies were analyzed alterations in the Tj complex in CCMs and particularly it was very limited data regarding the alteration of TJ complex in CCM3 lesion. This study is focused to elucidate the alteration of Tj complex in condition of absent CCM3 protein in vitro.

Methods: To study effect of CCM3 on Tj complex it was generated CCM3 knockdown human brain microvascular endothelial cells, by stable transfection with CCM3-shRNA. The morphological (immunocytochemistry), biochemical (cell fractional analysis, Western blot and immunoprecipitation) as well as functional analysis were performed in order to detect the CCM3 effect on Tj complex stability.

Results: CCM3-KO cells showed selective increase permeability for small molecular weight tracer FITC-inulin evaluated by in vitro permeability assay. Morphological and biochemical analysis of the pattern of Tj complex in CCM3-KO cells indicated that the transmembrane TJ proteins claudin-5, occludin and JAM-A were “correct” localized on the membrane of brain endothelial cells. On the other hand the scaffolding Tj protein ZO-1 and ZO-2, physiologically localized in cytosol and actin cytoskelatel cell fractions, showed complete shifting from actin cytoskeleton to cytosol fraction. This was result of absence of ZO-1 interaction with actin cytoskeleton, one of pivotal interaction for stability of tight junction. Analyzing the potential link of CCM3 with Tj proteins ZO-1 and actin cytoskeleton, we found that CCM3 was generated complex with cortical actin ring protein cortactin with support of cortactin binding protein -2 (CNTTP2). Furthermore by binding CCM3 to cortactin was regulated the phosphorylation status of cortactin (increase phosphorylation of Ser residues) directly and cortactin-ZO-1 interactions which in turn lead to ZO-1 association with F-actin. Rescuing the CCM3-KO cells by adding CCM3 cDNA showed de novo establishment of CCM3-Corcatin and ZO-1-cortactine complex increasing the stability of brain endothelial barrier and preventing further leaking.

Conclusions Collectively, this study provides new information related to CCM3 regulation of tight junctional complex and highlighted the presence of new complex with CCM3 (CNTTP2-cortcatine-CCM3), which could play important role in regulation of brain endothelial barrier permeability.

1068

COMPARISON OF BOLUS VS. BOLUS PLUS CONSTANT INFUSION OF THE MGLUR5 TRACER [^{18}F]FPEB IN HUMANS

J.M. Sullivan[1], K. Lim[1], D. Labaree[1], S.-F. Lin[1], T.J. McCarthy[2], J. Seibyl[3], G. Tamagnan[3], R.E. Carson[1], E.D. Morris[1], Y.-S. Ding[1]

[1]Yale PET Center, Yale University, New Haven, [2]Pfizer Global R&D, Groton, [3]Institute for Neurodegenerative Disorders, New Haven, CT, USA

Objectives: [^{18}F]FPEB is a PET tracer that has shown high specificity and selectivity toward the metabotropic glutamate receptor 5 (mGluR5)[1]. It possesses the potential to be used in human studies to evaluate mGluR5 functions in a range of neuropsychiatric disorders, such as anxiety and Fragile X syndrome[2-4]. The goal of the present study is to compare bolus (B) and bolus plus constant infusion (B/I) [^{18}F]FPEB administration methods and to determine which approach is best suited for future studies.

Methods: Healthy human subjects were scanned on the HRRT for up to 6hrs (with two 30min breaks) following a B injection (n=5) or B/I (n=5) of [^{18}F]FPEB. Arterial blood samples were collected and parent fraction measured by HPLC to determine the metabolite-corrected plasma input function. Specific activity at the end of synthesis was 5.62±1.90mCi/nmol (mean±SD), injected mass was 0.35±0.16μg, and the injected activity was 4.62±0.42mCi. Time activity curves (TACs) were extracted from 13 regions of interest (ROIs): caudate, cerebellum, cerebellum white matter, anterior cingulate, posterior cingulate, frontal cortex, hippocampus, occipital cortex, pallidum, parietal cortex, putamen, temporal cortex, and thalamus. Regional TACs were fitted with the 2T model to estimate distribution volume (V_T). For B/I scans, regional V_T was also estimated by the equilibrium method. Additionally, for both B and B/I data, reduced scan time TACs (i.e. 240, 180, 120mins) were fitted by the 2T model to determine if scan time could be shortened.

Results: Highest V_T values were observed in the anterior cingulate, putamen, temporal cortex, and caudate. Lowest V_T values were observed in the thalamus, posterior cingulate, pallidum, and cerebellum. In B/I studies (K_{bol}=190 minutes), equilibrium was generally reached within 90-120mins but time to equilibrium varied across regions and subjects. Decreasing scan time from 360 to 120mins had little effect on V_T estimation or variability in both B and B/I tracer administrations. Average V_T values across all subjects and regions for B studies of 360 and 120mins were 20.4±4.14 and 20.4±3.65mL/cm^3. For B/I studies, V_T values across all subjects and regions for 360 and 120min studies were 19.4±2.50 and 18.7±2.40mL/cm^3. Similar V_T values were estimated by the equilibrium method from 90-120min data, however equilibrium V_T values were significantly ($p < 0.001$, *) higher than 2T V_T values (Table 1). Both V_T values derived from B/I scans were less variable as than those derived from the B scans.

Table 1. Group mean V_T and standard deviations (SD) for selected ROIs for different [^{18}F]FPEB administrations (B or B/I) and analysis methods (2T or Equilibrium Method). ‡ Means in last row include all 13 regions (data from all regions not shown).

	Group Mean V_T (mL/cm^3)			Group Mean SD		
ROIs	**B (2T)**	**B/I (2T)**	**B/I (Equilibrium)**	**B (2T)**	**B/I (2T)**	**B/I (Equilibrium)**
caudate	25.7	22.9	25.3	17%	13%	10%
cerebellum	9.3	9.5	11.2	22%	11%	9%
cerebellum white matter	5.3	5.2	6.1	15%	12%	14%
anterior cingulate	30.1	27.2	29.9	15%	13%	13%
frontal	23.7	21.8	25.0	23%	10%	7%
hippocampus	23.4	20.7	21.9	15%	15%	17%
putamen	26.5	24.4	27.7	17%	11%	10%
thalamus	16.8	15.7	18.6	16%	11%	12%
‡ Mean	**20.4**	**18.7**	***21.2**	**18%**	**13%**	**12%**

[.]

Conclusions: Initial imaging of [^{18}F]FPEB in humans shows high uptake and specific binding in regions known to be rich in mGluR5 receptors. It displays high contrast (binding potentials of 3-6) and appears to be a suitable radiotracer for comparative mGluR5 studies in various disease populations. It is possible to shorten the scan time of [^{18}F]FPEB from 360 to 120mins without effecting V_T estimation. B/I of [^{18}F]FPEB is recommended for future studies as there is less variability in V_T across subjects with this method.

References:

[1]Wang JQ. 2007. *Synapse*. 61(12):951-961.

[2]Porter RH. 2005. *JPharmacolExpTher.* 315(2):711-721.

[3]Montana MC. 2009. *JPharmacolExpTher.* 330(3):834-843.

[4]Berry-Kravis E. 2009. *JMedGenet.* 46(4):266-271.

1069

IN-VIVO MOLECULAR IMAGING OF THE GABA-A/BENZODIAZEPINE COMPLEX IN AGING: A PET-STUDY OF [11C]-FLUMAZENIL BINDING IN THE RAT BRAIN

E.A. Hoekzema[1], S. Rojas[2], R. Herance[2], D. Pareto[2,3], S. Abad[4], X. Jiménez[4], F.P. Figueiras[2], F. Popota[4], A. Ruiz[4], N. Flotats[4], F.J. Fernández-Soriano[4], M. Rocha[5], M. Rovira[4], V.M. Víctor[6], J. Gispert[2,3,4]

[1]Dept. de Psiquiatria i Medicina Legal, Universitat Autònoma de Barcelona, [2]Institut d'Alta Tecnologia - PRBB, Barcelona, [3]Centro de Investigación Biomédica en Red en Bioingeniería, Biomateriales y Nanomedicina (CIBER BBN), Zaragoza, [4]CRC Centre d'Imatge Molecular, Barcelona, [5]University Hospital Doctor Peset Foundation and CIBERehd, [6]Department of Physiology, University of Valencia, Valencia, Spain

Introduction: Gamma-amino butyric acid (GABA) signal transmission plays a crucial role in cortical development, and the GABAergic system has been postulated to mediate neurodegenerative processes in aging as well. Reports of altered benzodiazepine (BDZ) pharmacology and age-related neuroprotective effect of BDZ agents in aged subjects suggest a role for BDZ modulation in cerebral aging.

Aims: We applied positron emission tomography (PET) and voxel-wise kinetic modeling to quantify the in-vivo the in-vivo binding to the GABA-*BDZ-ionophore*

receptor complex in the aged rat brain.

Methods: PET acquisitions were performed in a microPET system in young adult (14.8±2.64 weeks) and aged (85.16±1.72 weeks) rats. To visualize BDZ recognition site availability, we injected the radioligand [^{11}C]-flumazenil, a high-affinity competitive antagonist of the central $GABA_A$/BDZ receptor complex. Flumazenil has been associated with age-related cognitive and cellular neuroprotective effects, and has not previously applied in aging research. We applied parametric modeling to allow detection of localized effects in heterogeneous neuroanatomical regions and control for variance relating to the criteria for neuroanatomical delineation.

Results: Comparing the young and old rats, we observed localized clusters of reduced cerebral flumazenil uptake in the aged rats in the bilateral hippocampus, cerebellum, and frontal and parietal lobes of the cerebral cortex ($p < 0.001$). The contrast 'Old>Young' rendered no significant results. Region of interest analyses replicated these findings, and a comparison between the ROI-based and voxel-wise [^{11}C]-flumazenil binding indicated a high consistency between the quantification methods.

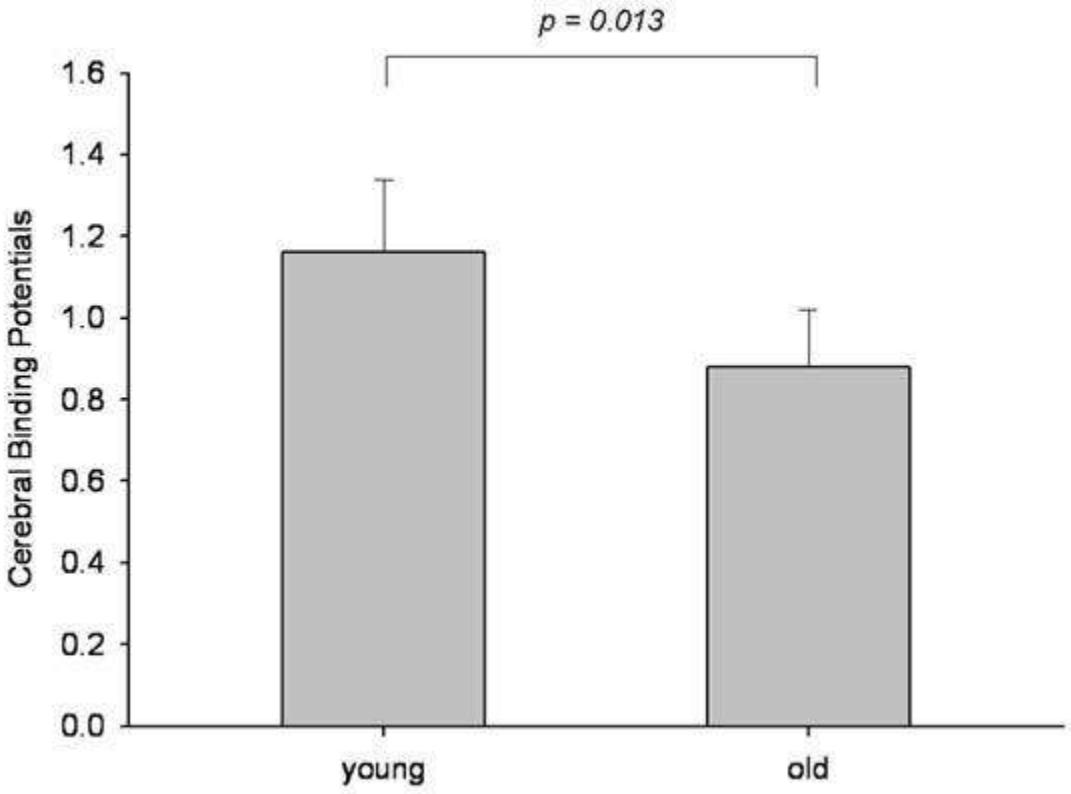

[Global [11C]-FMZ uptake]

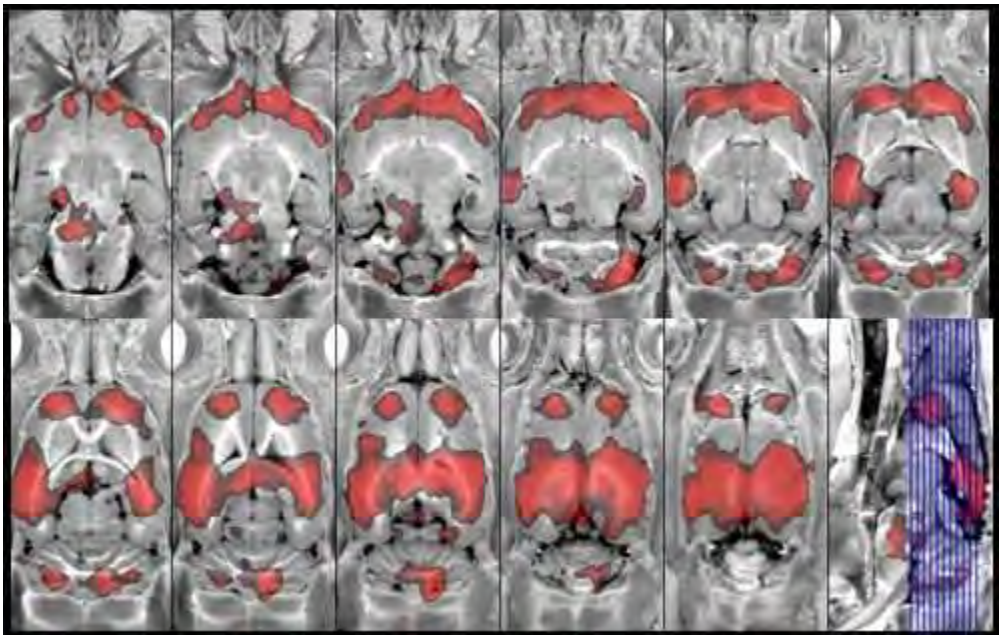

[Reduced regional 11C-FMZ uptake in old rats]

Conclusions: These results support the pertinence of voxel-wise kinetic modeling in dynamic microPET data. Moreover, our findings indicate that the GABA system is susceptible to age-related neurodegeneration, and cerebral aging is characterized by localized reductions of GABA-A/BDZ availability in the hippocampal formation, fronto-parietal cortex and cerebellum. The observed decreases in $GABA_A$/BDZ receptor binding may reflect a compensatory down-regulation of the number of neocortical BDZ recognition sites, manifested by changes in polypeptide subunit expression that alter the molecular composition and pharmacological properties of the central $GABA_A$ receptor.

1071

FLOW TRANSIENTS PREDICT OUTCOME IN RAT FOCAL BRAIN ISCHEMIA

J. Lückl[1,2], J.P. Dreier[1], T. Szabados[2], F. Bari[3], J.H. Greenberg[2]

[1]Experimental Neurology, Charite Universitatsmedizin, Berlin, Germany, [2]Department of Neurology, University of Pennsylvania, Philadelphia, PA, USA, [3]Department of Medical Physics and Informatics, University of Szeged, Szeged, Hungary

Purpose: Spreading depolarisations are accompanied by transient changes in cerebral blood flow (CBF) in experimental ischemia. In our practice with filament occlusion we noticed that CBF data collected by a single laser Doppler probe may predict outcome. We found also that the cortical infarct size shows a bimodal distribution (75% of the animals show decent cortical infarct while the rest don't). In a post-hoc analysis of the controls of prospective studies we tested whether intra-ischemic flow, reperfusion, and the different parameters of flow transients (amplitude, duration etc) can predict this bimodal outcome. Our secondary aim was to put all of the collected data into a matrix and find correlations between them in this large animal population.

Methods: Sprague-Dawley rats (n=56) undergoing 90-minute filament occlusion and surviving for 72 hours, were enrolled in the post-hoc analysis. The infarct size was determined by 2,3,5-triphenyltetrazolium chloride, relative blood flow changes were monitored by laser Doppler at the same locus (4-5 mm lateral and 1-2 mm posterior to Bregma), and physiological variables were recorded. The lack of cortical infarct or high (>50% of baseline) intra-ischemic flow was not an exclusion criterion. The animals underwent either halothane (n=23) or isoflurane (n=33) anesthesia. Another filament occlusion study in rat (n=12) was performed prospectively to validate that the flow transients were coupled to typical direct current (DC) shifts of spreading depolarization.

Results: The prospective study showed that every flow transient was associated with a negative DC shift typical of spreading depolarization. The post-hoc analysis revealed that the parameters of the outcome and the flow transients did not show significant differences between the halothane and isoflurane anesthetized animals. We found that the onset latency of the first flow transient, the magnitude of the mean reperfusion (0-10. min) and the total duration of flow transients combined with the intra-ischemic flow can best predict the bimodal outcome whereas intra-ischemic flow is not correlated with the outcome parameters. Spearman's analysis of the matrix revealed further significant correlations between the data collected (table).

Conclusions: We demonstrated in a large animal pool that intra-ischemic flow is not an independent predictor of outcome, but instead the measurement of flow transients does serve as a biomarker for predicting outcome and can be useful in the quality control of experimental ischemia.

Table - The table summarizes the results of Spearman's analysis of the combined isoflurane and halothane anesthetized animals. The “matrix” contains the parameters of cerebral blood flow (mean intra-ischemic flow, mean reperfusion (0-10 min.)), flow transients (total duration, average duration, positive amplitude, onset latency of the first transient) and outcome (striatal infarct, cortical infarct, edema).

	Intra-ischemic flow							
Total duration	◆	*Total duration*						
Pos. amp.	◆◆◆	n.s.	*Pos.amp*					
Avg. duration	◆	n.s.	n.s.	*Avg. duration*				
Onset latency	n.s.	◆◆	n.s.	n.s.	*Onset latency*			
Striatal Infact	n.s.	◆◆◆	n.s.	n.s.	n.s.	**Striatal Infarct**		
Cortical Infarct	n.s.	◆◆◆	n.s.	◆◆	n.s.	◆◆	**Cortical Infarct**	
Edema	n.s.	◆◆	n.s.	◆◆	◆	◆	◆◆◆	**Edema**
Reper-fusion	n.s.	◆◆◆	n.s.	◆◆◆	n.s.	n.s.	◆◆◆	◆◆◆

◆◆◆ $p<0.0001$, ◆◆ $p< 0.01$, ◆ $p< 0.05$, n.s. non significant

[Table]

1072

GLYCINE N-METHYLTRANSFERASE EXPRESSION IN THE MOUSE HIPPOCAMPUS AND ITS ROLE IN NEUROGENESIS AND COGNITIVE PERFORMANCE

M. Carrasco[1], L.G. Rabaneda[1], S. Ortega-Martínez[1], M. Murillo-Carretero[1], A.J. Macías-Sánchez[1], E. Miguel[1], M.L. Martínez-Chantar[2], A. Woodhoo[2], Z. Luka[3], C. Wagner[3], S.C. Lu[4], J.M. Mato[2], J.A. Micó[1], **C. Castro**[1]

[1]University of Cadiz, Cadiz, [2]CIC BioGune, Bizkaia, Spain, [3]Vanderbilt University, Nashville, TN, [4]University of Southern California, Los Angeles, CA, USA

Alterations in one carbon metabolism have long been linked to the development of neurological disorders, such as neurodegenerative and vascular dementia, Alzheimer´s disease, depression or schizophrenia. Since one carbon reactions determine the availability of the methyl donor S-adenosylmethionine (SAMe), and of its demethylated form S-adenosylhomocysteine thus modulating the cellular methylation potential, it is reasonable to hypothesize that alterations in the cellular methylation potential might play a key role in the etiopathology of neurological disorders associated to cognitive decline. It has been shown that hyperhomocysteinemia, elevated plasma level of homocysteine, induces cognitive impairment in animal models and reduces the neurogenic capacity of the adult brain. Several reports indicate that adult brain neurogenesis might be modulated by epigenetic mechanisms involving methylation reactions.

In order to understand whether other alterations in one carbon metabolism might affect neurogenesis and cognitive impairment, we have analyzed herein hippocampal neurogenesis, cognitive performance, and brain SAMe levels in two mice models with elevated levels of plasma methionine: methionine adenosyltransferase (MAT) and glycine N-methyltransferase (GNMT) knockout mice (Mat1a-/- and Gnmt-/- respectively). GNMT deficiency in mice, impaired spatial memory and reduced neurogenic capacity, whereas no effect was exerted by MAT1A deficiency. The enzyme GNMT was found in hippocampal homogenates and its deficiency resulted in increased levels of SAMe in this area. Finally, incubation of neural progenitor cells (NPC) *in vitro* with SAMe exerted an antiproliferative effect on NPC cultures, leading to the downregulation of cyclin E expression. Our findings indicate that elevated SAMe impairs neurogenesis and cognitive performance in adult mice, and show some of the molecular and cellular mechanisms involved in this SAMe-induced antiproliferative effect. Identical mechanisms might contribute to facilitate the development of cognitive decline in neurological disorders.

1073

NEUROANATOMICAL DIFFERENCES IN A MOUSE MODEL OF EARLY LIFE NEGLECT REAVELED BY HIGH RESOLUTION DTI

D. Coman[1], A. Duque[2], E.D. George[3], X. Papademetris[1,4], F. Hyder[1,4], A.A. Simen[3]

[1]Diagnostic Radiology, [2]Neurobiology, [3]Psychiatry, [4]Biomedical Engineering, Yale University, New Haven, CT, USA

Objectives: Early life neglect and abuse is a common problem in the USA with little discrimination for race, gender or socio-economical status. Changes in white matter (WM) are associated with a variety of psychiatric conditions. Diffusion tensor imaging (DTI) has shown reduced fractional anisotropy in the medial and posterior corpus callosum of maltreated children with post-traumatic stress disorder (PTSD) **[1]** and in the anterior limb of the internal capsule, a fiber tract with important projections to the PFC, of macaques with disrupted mother-infant attachment, but not the posterior limb or occipital white matter **[2]**. Recently, a novel mouse model of early life neglect based on maternal separation with early weaning (MSEW) was developed **[3]**. In the present work we used DTI to examine the consequences of MSEW with regard to neuroanatomical structure.

Methods: The animals were anesthetized with chloral hydrate (1500mg/kg IP), followed by intracardiac perfusion with phosphate buffered saline (PBS) was followed by ice cold 4% paraformaldehyde (PFA) in 0.01 M PBS. After perfusion, the brains were harvested and stored in 4%PFA in PBS at 4°C for 2 weeks. One hour before the DTI scans, the brains were washed with PBS and placed into an MRI compatible tube, filled with Fluorinert, an MRI susceptibility-matching fluid. The DTI datasets were obtained on a 9.4T horizontal bore magnet using a custom-made ^{1}H radio frequency coil. The six elements of the diffusion tensor were calculated from the intensities of 16 diffusion-weighted images. The tensor eigenvalues and the corresponding eigenvectors were obtained by matrix diagonalization. First smoothed versions of the fractional anisotropy (FA) images were non-rigidly registered to a single smoothed FA map using a non-linear intensity-based warping parameterized in terms of a tensor b-spline grid with uniform control point spacing of 3mm using BioImage Suite (http://www.bioimagesuite.org). Next the unsmoothed FA maps were warped to this common coordinate space following which average FA maps for each group were computed**.**

Results: Coronal slices spaced 100μm and representing mean averages for each condition show reduced FA in different brain areas of the MSEW animals as compared to controls. MSEW animals showed decreased FA in several WM fiber tracks including the cingulum, corpus callosum, anterior commissure and septofimbria. We also observed decreased FA in multiple gray matter regions including the cingulate gyrus, basolateral amygdala, thalamus, and middle and deeper cortical layers.

Conclusions: DTI imaging clearly demonstrated that both hemispheres of MSEW mice are abnormal. Although both hemispheres were affected, asymmetric involvement of the WM, for example in the corpus callosum and WM near the basolateral amygdala, were evident. In addition, histological studies reveal slight left-right asymmetry in MSEW vs control. Future DTI analysis should co-register each hemisphere of each group independently to highlight such asymmetry.

References:

[1]Jackowski AP et al. (2008) Psychiatry Res 162:256-261.

[2]Coplan JD et al. (2010). Neurosci Lett 480:93-96.

[3]George ED et al. (2010). BMC Neurosci *11*, 123.

Acknowledgements: Supported in part by P30 NS052519 of the QNMR Program.

1074

STRIATO-CORTICAL RELATIONSHIP OF DOPAMINE $D_{2/3}$ RECEPTOR BINDING IN HEALTHY HUMANS: A POSITRON EMISSION TOMOGRAPHY STUDY WITH [^{11}C]RACLOPRIDE AND [^{11}C]FLB457

F. Kodaka, H. Ito, H. Fujiwara, Y. Kimura, H. Takano, T. Suhara

Clinical Neuroimaging Team, Molecular Neuroimaging Group, Molecular Imaging Center, National Institute of Radiological Sciences, Chiba, Japan

Introduction: Dopaminergic neurotransmission system is of a main interest of pathophysiology of schizophrenia. The system has three distinct cell groups, referred to as A8, A9 and A10. As for each cell group, the striatum plays important roles, for it receives various inputs from brain regions within the system. The striatum could be divided into the tripartite functional organization, i.e, associative, limbic, and sensorimotor subdivisions, from the viewpoint of their anatomical connections with other brain regions. These subdivisions have connections with the dorsolateral prefrontal cortex (DLPFC), medial prefrontal cortex (MPFC), and motor/premotor cortex, respectively. Although functional anatomy of such striatal subdivisions has been studied, little is known about the role of dopaminergic neurotransmission for them. In the present study, we examined the relationship of dopamine $D_{2/3}$ receptor bindings between each functional striatal subdivision and corresponding brain regions by using [^{11}C]raclopride and [^{11}C]FLB457.

Methods: Twenty-two healthy male volunteers underwent a series of positron emission tomography (PET) studies with [^{11}C]raclopride and [^{11}C]FLB457 on the same day. This study protocol was approved by the Ethics and Radiation Safety Committees of the National Institute of Radiological Science, Chiba, Japan. For each anatomically standardized PET image, parametric binding potential (BP_{ND}) images were calculated using simplified reference tissue model. VOIs were defined according to tripartite striatal organization [i.e., the associative striatum (AST), limbic striatum (LST), and sensorimotor striatum (SMST)], and corresponding cortical regions (i.e., DLPFC, MPFC). BP_{ND} values in each striatal subdivision and corresponding cortical region were obtained from parametric PET images of [^{11}C]raclopride and [^{11}C]FLB457. To estimate the statistical significance of striato-cortical correlation coefficients of dopamine $D_{2/3}$ receptor binding, a voxel-wise regression analysis with [^{11}C]FLB457 was performed for each striatal subdivision. Subsequently, for cortical regions that showed significant correlations, VOI-based correlation analysis between each striatal subdivision and each cortical region was performed, and obtained correlation coefficients were compared for each striatal subdivision.

Results: BP_{ND} values in the AST, LST and SMST from [^{11}C]raclopride were 3.0±0.38, 2.7±0.38, and 3.7±0.45, respectively (mean±SD). BP_{ND} values in the DLPFC and MPFC from [^{11}C]FLB457 were 1.2±0.26, 1.4±0.25. The voxel-wise regression analysis showed that all subdivisions had significant correlation in the DLPFC, MPFC, and motor/premotor cortex. VOI-based correlation analysis showed the highest correlation coefficients between the DLPFC and SMST ($r = 0.68$). On the other hand, the LST and SMST showed higher correlation coefficients with the MPFC ($r = 0.76$) than the AST($r = 0.61$).

Conclusion: We did not find identical striato-cortical relationship with past functional anatomical studies. However, all the assumed cortical regions have significant correlations with each functional striatal subdivision, raising the possibility that the tripartite striatal organization has correlation with corresponding cortical regions as a whole. Moreover, VOI-based correlation analysis showed the difference of correlation coefficients by each subdivision, suggesting that

the degree of correlation could have relationship with similarity of given striato-cortical dopamine $D_{2/3}$ receptor expression

References:

1. Martinez D et al. J Cereb Blood Flow& Metabolism 23: 285-300, 2003.

1075

COMPARISON OF ARTERIAL SPIN LABELED MRI AND FDG-PET IN ALZHEIMER'S DISEASE

Y. Chen[1], J.S. Reddin[2], A.B. Newberg[3], P. Julin[4], S. Arnold[1,5], J. Greenberg[1], J.A. Detre[1]

[1]Neurology, [2]Radiology, University of Pennsylvania, [3]Myrna Brind Center of Integrative Medicine, Thomas Jefferson University and Hospital, Philadelphia, PA, USA, [4]Research and Development, Astra Zeneca, Södertälje, Sweden, [5]Psychiatry, University of Pennsylvania, Philadelphia, PA, USA

Introduction: FDG-PET is an established diagnostic modality in Alzheimer's Disease (AD), and has consistently demonstrated a pattern of hypometabolism in parieto-temporal and posterior cingulate/precuneus areas of AD patients. However, PET is costly and requires injection of a radioactive tracer. Arterial spin labeled (ASL) MRI uses blood as an intrinsic tracer to measure cerebral blood flow (CBF). In this study, we compared ASL and FDG-PET acquired concurrently in Alzheimer's patients and controls.

Methods: Fifteen clinically diagnosed AD patients and 19 age-matched controls were included in this study. High-resolution anatomical MRI and pseudo-continuous ASL[1] scans were collected on a 3T Siemens MR scanner, All subjects were injected with FDG during the ASL MRI scan, and PET images were acquired according to ADNI PET imaging protocol on a Philips Allegro scanner 40 minutes later.

Imaging data were processed using SPM5 (Wellcome Institute, UK) and Matlab (Mathworks, Natick MA). ASL images were converted to quantitative CBF images in units of ml/100g/min using a single compartment model and spatially normalized to an age-specific template. PET images were first co-registered to the high-resolution MR images and then spatially normalized to the same template. Both ASL and PET images were first corrected for atrophy by the method proposed by Du et al.[2], then normalized by each subject´s mean global value to remove global effects. A 2x2 factorial design with condition and modality as factors, age and years of education as nuisance covariates was used to generate voxel-wise statistical maps. All statistical maps were masked at $p < 0.05$ (FDR multiple comparison correction) and cluster threshold of 200 voxels. A lower threshold of $p < 0.01$ (uncorrected) was used to detect areas of significant conditionxmodality interaction.

Results: Thresholded statistical maps overlaid on high resolution MR images are shown in the figure. Row a) shows the FDG-PET areas of hypometabolism in patients relative to controls. Row b) shows the corresponding ASL detected hypoperfusion pattern. Locations of the slices are indicated by blue lines on the rightmost image. Both ASL and FDG-PET show very similar patterns of decreased CBF and metabolism, especially in the parieto-temporal and precuneus areas. The main discrepancy is in the ventromedial temporal lobe, where only FDG-PET hypometabolism was observed, likely due to reduced sensitivity of ASL in this area of high field inhomogeneity. No significant AD-related hypermetabolism or hyperperfusion was detected. While no interaction survived the multiple comparison threshold, a lower statistical threshold revealed an interaction in precuneus, anterior cingulate, left hippocampus, lingual gyrus and right inferior temporal lobe (row c).

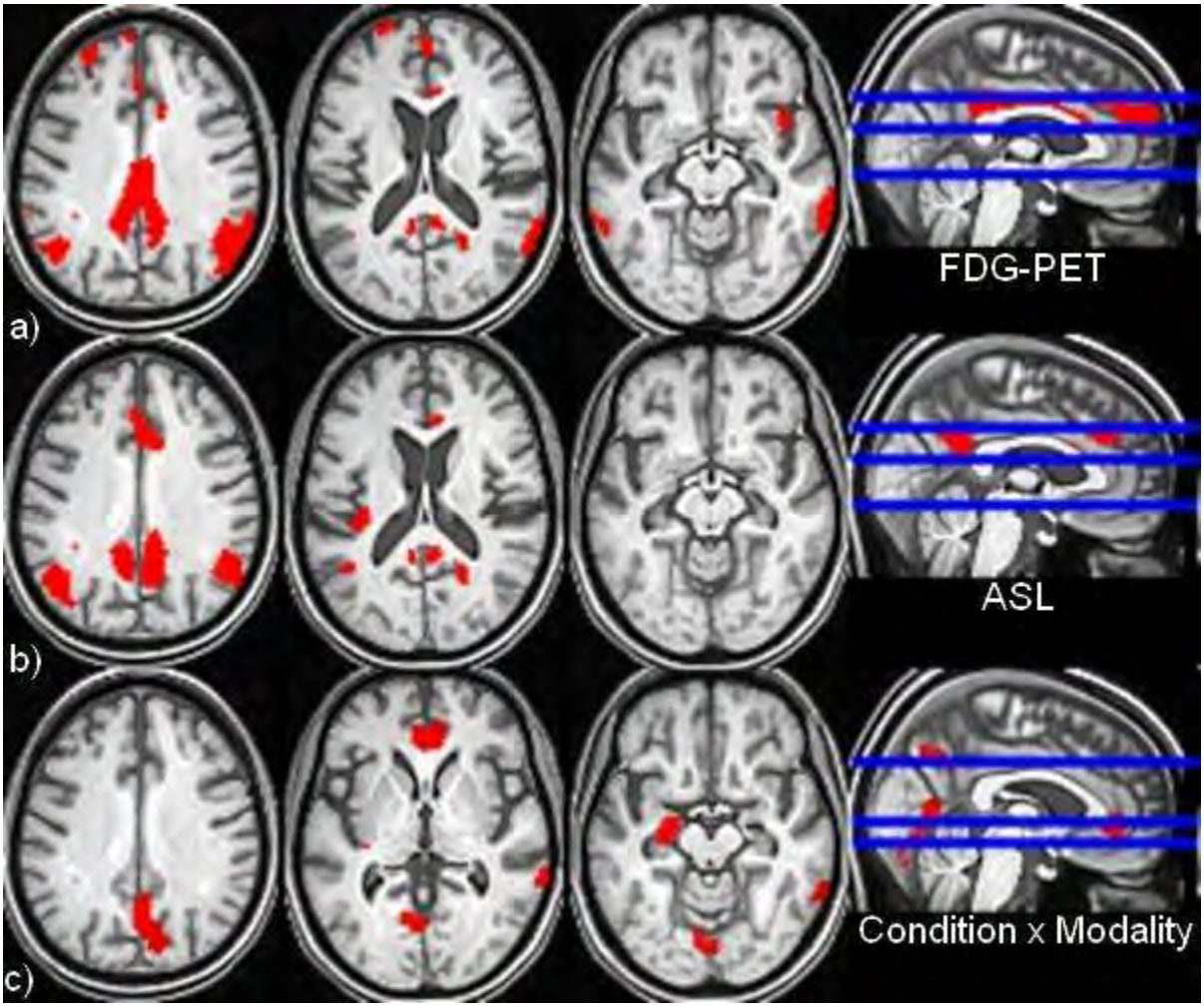

[Figure]

Conclusions: Our data demonstrates excellent agreement between FDG-PET and ASL in detecting AD-related hypometabolism and hypoperfusion, and confirms ASL can be an alternative noninvasive imaging biomarker for AD. Our data also suggest a dissociation between perfusion and metabolism in brain regions most severely affected by AD. Further studies are necessary to better understand the mechanism underlying this perfusion-metabolism mismatch.

References:

1. Dai, W.*, et al.*, MRM, 2008. 60(6):1488-97.

2. Du, A.T.*, et al.*, Neurology, 2006. 67(7):1215-20.

1076

NEUROGLOBIN ASSOCIATED WITH MITOCHONDRIA FUNCTIONS AND ISCHEMIA PROTECTION IN ASTROCYTES AND NEURONS

R. Zhao, L.T. Yang, **A.C.-H. Yu**

Neuroscience Research Institute, Peking University, Beijing, China

Neuroglobin (Ngb) was discovered as a member of the mammalian globin family ten years ago. It was identified as an oxygen transport protein in nervous system and suggested to be able to protect against brain hypoxic/ischemic injury. At first, Ngb was thought to present only in neurons. We have reported that Ngb could also be expressed in primary culture of astrocytes and using antisense oligo to reduce Ngb protein level would induce apoptosis in astrocytes under ischemic treatment. Now, by over-expressing Ngb into both neurons and astrocytes, we observed that Ngb specifically could co-localize with mitochondria in both cell types, while Western blot showed that ischemia treatment could elevate the level of Ngb in mitochondria isolated from neuronal and astrocytic cultures. Based on these result, we speculate that Ngb may exert its protective effects by facilitating oxygen delivery to the mitochondria of astrocytes or neurons subjected to ischemic exposure. We also curiously found that some specific mutation in exons of mouse may facilate Ngb co-localization with mitochondria. All these evidences showed that Ngb might play an active role in oxygen transport in astrocytes and neurons under physiological and pathological conditions.

1077

OMEGA-3 FATTY ACIDS AND BRAIN GLUCOSE UTILIZATION: AN ^{18}F-FLUORODEOXYGLUCOSE POSITRON EMISSION TOMOGRAPHY (FDG-PET) STUDY IN THE RAT

E. Harbeby[1], S. Tremblay[2], J. Mercier-Tremblay[2], M. Archambault[2], M. Roy[2], J.-F. Beaudoin[2], J. Rousseau[2], P. Guesnet[1], A. Huertas[3], R. Lecomte[2], S. Cunnane[4]

[1]INRA, Jouy-en-Josas, France, [2]2 Department of Nuclear Medicine and Radiobiology, Université de Sherbrooke, Sherbrooke, QC, Canada, [3]Lesieur, Asnières-sur-Seine, France, [4]The Research Center on Aging, Sherbrooke, QC, Canada

Background: Several *in vivo* and *in vitro* studies suggest that docosahexaenoic acid (DHA, 22:6w3), the main omega-3 fatty acids of brain membranes, may be a regulator of brain energy metabolism by affecting glucose metabolism and its transporter GLUT1.

Objective: The purpose of this study was to evaluate whether cerebral glucose metabolism measured by FDG-PET would reflect decreased GLUT1 expression in the brain of omega-3 deficient rats.

Methods: We measured the cerebral metabolic rate for glucose with FDG-PET for small animal (microPET) in adult rats (10 wk-old) receiving an omega-3 fatty acid-adequate (control, n = 6) or an omega-3 fatty acid-deficient (omega-3 def, n = 6) diet. Dynamic PET scans were performed during 45 min after injection of ^{18}F-FDG (60 MBq). Data were reconstructed and superposed with MRI slices of the rat brain to calculate radioactivity in regions of interest (ROIs). Fatty acid content in brain phospholipid classes was determined by gas chromatography and the mRNA and protein expression of GLUT1 using real-time PCR (TaqMan low-density array, TLDA) and western blotting, respectively.

Results: Omega-3 PUFA-deficient rats had 60-70% lower DHA in their brain membrane phospholipids. Significantly decreased ^{18}F-FDG uptake was observed in the brain of omega-3 deficient rats, corresponding to both a lower rate of FDG uptake during the early phase (0-15 min) and a lower plateau level of ^{18}F-FDG incorporation during the later plateau phase (15-45 min). The gene and protein expression of GLUT1 was also lower in the omega-3 def group.

Conclusion: In rats deficient in omega-3 PUFA, lower expression of GLUT1 in the brain is consistent with in vivo results using FDG-PET that show glucose hypometabolism in the brain. Dietary intake of omega-3 fatty acids therefore clearly appears to modulate brain glucose uptake, a mechanism by which omega-3 fatty acid status may influence cognitive function known to be at risk during aging.

Acknowledgements: Financial support was provided by the Canada Research Chaires (SCC), CIHR, INRA and E. Harbeby was supported by grants from Lesieur and INRA.

1078

FUNCTIONAL CONNECTIVITY OPTICAL IMAGING OF THE MOUSE BRAIN

A.Q. Bauer[1], B.R. White[1], A.Z. Snyder[1,2], B.L. Schlaggar[1,2,3,4], J.-M. Lee[2], J.P. Culver[1,5,6]

[1]Radiology, [2]Neurology, [3]Anatomy and Neurobiology, [4]Pediatrics, [5]Biomedial Engineering, Washington University in St. Louis School of Medicine, [6]Physics, Washington University in St. Louis, Saint Louis, MO, USA

Objectives: Translation between human functional neuroimaging (e.g., with fMRI) and mouse models of disease is hampered by the difficulty in determining molecular correlates of cognitive neuroscience findings and vice versa. A method to easily perform large-scale functional neuroimaging in mice, where molecular studies are common, would provide a bridge between the two fields. To satisfy this need, we propose a new technique combining resting-state functional connectivity mapping and optical intrinsic signal (OIS) imaging.

Methods: We aimed to map functional connectivity using a custom-built high-speed (30 Hz) OIS system. This set-up captures a large field of view of the mouse brain visible through the intact skull, from which the brain was manually segmented. Data from multiple wavelengths were synthesized using a tissue spectroscopy model to yield time traces of changes in oxy- and deoxyhemoglobin at all visible brain locations. Imaging was performed on five mice (all male ND4 Swiss Webster anesthetized with Ketamine/Xyalzine); resting-state data were acquired for at least 15 minutes on each mouse.

Results: Resting-state functional connectivity methods evaluate spatio-temporal correlation patterns in spontaneous brain activity (here viewed indirectly through the neurovascular response). After filtering the data to the band 0.009-0.08 Hz, functional connectivity patterns were measured by performing a simple Pearson´s correlation analysis between anatomically determined seed regions and all other cortical locations[1]. Using a histological atlas [2], seed locations were chosen at coordinates expected to correspond to the left and right visual, motor, somatosensory, frontal, cingulate, and retrosplenial cortices, as well as the right and left superior colliculi and olfactory bulbs (16 total seeds, Fig. 1A). To generate atlas divisions in a data-driven manner, the brain was parcellated into functional regions by evaluating the resting-state brain signals with an iterative strategy. Each pixel was assigned to a parcel with which it correlated most highly (Fig. 1B), organizing the cerebral surface into functional zones in a pattern similar to that found in histology. Individual parcels were combined into larger functional regions using a clustering algorithm (Fig. 1C). The parcel-to-parcel correlation matrix (Fig. 1D) illustrates how the clustering of Fig. 1C arranged the parcels into networks.

Conclusions: These results demonstrate that functional connectivity OIS (fcOIS) is able to map both functional regions and their connections. This methodology has the potential to be a powerful tool for detecting when functional connectivity networks are disrupted (either in the distribution of the neuroarchitecture or in the pattern of connections). Thus, fcOIS could be used to examine functional consequences in disease models including genetic and surgical disruptions. We expect that future fcOIS studies will connect fcMRI neuroimaging results of human disease with advances in mouse models.

References:

1. Fox MD, Snyder AZ, Vincent JL, Corbetta M, Van Essen DC, et al. (2005) The human brain is intrinsically organized into dynamic, anticorrelated functional networks. PNAS 102: 9673-9678.

2. Franklin KBJ, Paxinos G (2008) The Mouse Brain in Stereotactic Coordinates. New York: Academic Press.

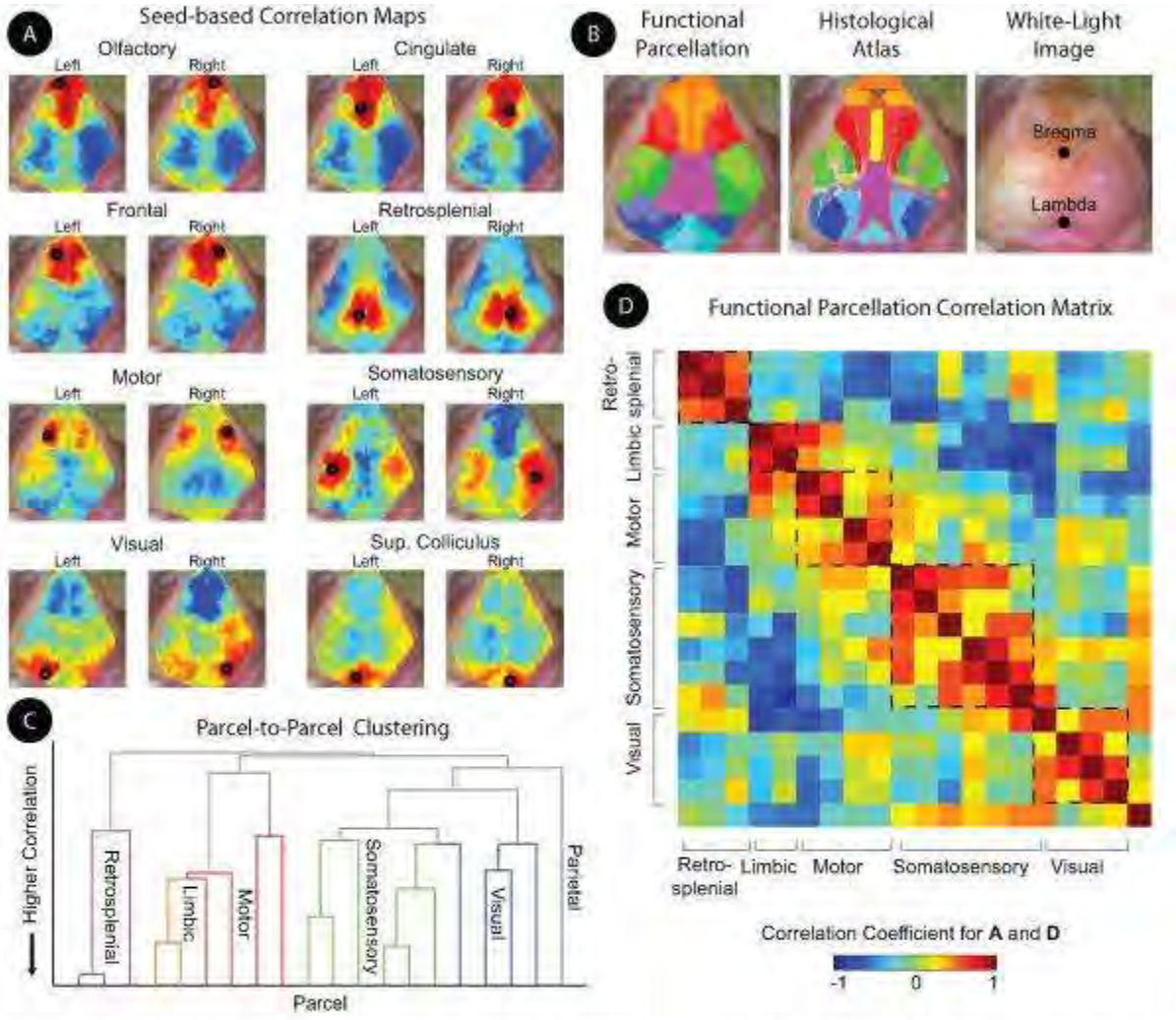

Functional connectivity optical intrinsic signal (fcOIS) imaging in the mouse brain. A. Overhead view of the mouse brain with retracted scalp showing correlation maps for seeds chosen using the expected cortical positions of various functional areas. Seed positions and sizes are shown with black circles. The scale for all correlation maps is from r = -1 to 1. Maps are shown overlaid on a white light image of the brain viewed through the intact skull. Field of view approximately 1 cm x 1 cm. Note the bilateral patterns for all seed locations. **B.** The results of iterative parcellation using the first twenty singular vectors from the full brain correlation matrix (not shown) as an initial condition. We see clear delineation of a frontal/olfactory/cingulate (limbic) network (oranges), a motor network (reds), a somatosensory network (greens), a visual network (blue), the retrosplenial cortex (magenta), and the superior colliculus (light blues). To the right are a histological atlas applied to this mouse brain and a white-light image for comparison **C.** Dendrogram showing clustering of the parcels based on their correlations. Each terminal branch is a parcel (color-coded for visualization); parcels that share similar correlation maps have branches that meet lower on the tree. Note the tight correlations within the frontal network, in turn connecting to first medial and then lateral motor areas. In total, there are main branches for all of the main networks we expect. **D.** Correlation matrix between parcels. Each row and column corresponds to a parcel with a functional assignment. We see a block-diagonal pattern showing how the clustering has arranged the parcels into networks (dashed boxes shown for visualization). Off-diagonal elements show the relationships between networks; in particular, note the anticorrelations between frontal and somatosensory and between retrosplenial and motor.

[fcOISinMice]

1079

COMBINATION OF INTRACORTICAL ANGIOGLIONEURIN ADMINISTRATION AND ENVIRONMENTAL ENRICHMENT ENHANCES BRAIN PROTECTION IN DEVELOPING RATS

E.G. Argandoña[1], H. Bengoetxea[2], S. Bulnes[2], N. Ortuzar[2], A. Garcia-Blanco[2], I. Rico-Barrio[2], J.V. Lafuente[2]

[1]Unit of Anatomy, Department of Medicine, University of Fribourg, Fribourg, Switzerland,
[2]Department of Neuroscience, University of the Basque Country UPV/EHU, Leioa, Spain

Introduction: Postnatal development of the visual cortex is modulated by experience, especially during the critical period. In rats, a stable neuronal population is only acquired after this relatively prolonged period. The term angioneurins have recently been proposed to name molecules with neuroprotective,neurogenic, neurotrophic and angiogenic effects. They induce a variety of cellular responses, not only neuronal and vascular, but also glial. These molecules play a pivotal role in the development of CNS and in maintenance of the optimal condition for survival of nervous cells in adult. Among the main angioneurins are: the proangiogenic factor VEGF, the neurotrophin BDNF, the IGF-1 and the glycoprotein EPO. A decrease of angioneurins expression was found in aging and in pathological conditions like neurodegenerative diseases, stroke, TBIs or ischemia. As they actions include all the elements of the neurogliovascular unit as well as the unit as a whole, here we propose the term angioglioneurins to define molecules acting to the three elements of the neurogliovascular unit.

Environmental enrichment improves brain function in health and disease, including morphological, physiological and behavioural changes at all levels of the neurogliovascular unit. These changes include the increase of neuronal activity and plasticity, the glial population, structure and function and the angioarchitecture and the maturation of the microvascular network. In disease, beneficial effects of environmental enrichment include functional recovery and prevention of neurodegenerative, traumatic, ischemic and even tumoral diseases. These effects are attributed in part to an increase of angioglioneurin production and release.

Aim: Our aim is to investigate the vascular and neuronal effects of combining VEGF infusion and environmental enrichment on the visual cortex during the initial days of the critical period.

Material and methods: VEGF was administered for one week using intracerebral osmotic minipumps placed in middle cortical layers of P18 Long Evans rats. Different visual stimulation conditions were studied in each experimental group (VEGF infused, PBS infused and non infused controls). Vascular, neuronal and Caspase-3 positive cell densities were measured by the optical dissector method. To assess if Caspase-3 positive cells correspond to neurons or astrocytes, double-label immunofluorescence by confocal microscopy was used.

Results: Results showed that a small percentage of Caspase-3 positive cells colocalized with neuronal markers. The lesion produced by the cannula implantation resulted in decreased vascular, neuronal and Caspase-3 positive cell densities. Rearing under enriched environment was unable to reverse these effects in any group, whereas VEGF infusion alone partially corrected those effects. A higher effectiveness was reached by combining both the procedures, the most effective combination being when enriched-environment rearing was introduced only after minipump implantation. In addition to the angiogenic effect of VEGF, applied strategies also had synergic neuroprotective effects, and the combination of the two strategies had more remarkable effects than those achieved by each strategy applied individually.

Conclusion: Exposure to enriched environment implies an enhancement of angioglioneurins expression which could improve the evolution of most brain diseases. The combination of angioglioneurins administration and environmental enrichment may be a promising therapeutical strategy for brain restoration.

1081

EXPRESSION OF ESTROGEN RECEPTOR A AND B IN RAT ASTROCYTES IN PRIMARY CULTURE: EFFECTS OF HYPOXIA AND GLUCOSE DEPRIVATION

M. Al-Bader, S. Malatiali, **Z. Redzic**

Department of Physiology, Faculty of Medicine, Kuwait University, Kuwait, Kuwait

Objectives: Neuroprotective role of estrogen in cerebral ischemia could be partially associated to increased expression of glutamate transporter in astrocytes, an effect that could be protective against deleterious effects of increased glutamate concentration. Estrogen regulates gene expression through estrogen receptors alpha (ERα) and beta (ERβ). The aim of this study was to explore effects of hypoxia and glucose deprivation (HGD), alone or followed by 1h recovery, on estrogen receptor alpha (ERα) and beta (ERβ) expression in rat astrocytes in primary culture.

Methods: Rat cortical astrocytes were cultured as explained earlier [1, 2] and exposed to the following conditions: a) 5%CO_2 in air for 1h (control group-CG); b) 2%O_2 / 5%CO_2 in N_2 with glucose deprivation (HGD group-HGDG) for 1h; or c) the HGDG protocol followed by 1h CG protocol (recovery group-RG). ERα and ERβ mRNA expression was assessed by real time PCR using the gene expression assays that had intron-spanning primers and hydrolysis probes labeled with 6-carboxyfluorescein (FAM) as a reporter dye and 6-carboxy-tetramethyl-rhodamine (TAMRA) as a quencher dye; the relative gene expression was calculated using the efficiency corrected calculation model for multiple samples and based on one reference gene [3]. ERα and ERβ protein expression was assessed by immunoblotting and expressed as relative to expression of beta-actin [4].

Results: ERα mRNA expression decreased in HGDG and increased in RG, when compared to CG. ERβ mRNA expression did not change. At the protein level, full-length ERα (67 kDa) and three ERα-immunoreactive protein bands (63, 60 and 52 kDa) were detected in rat astrocytes. A significant decrease in the 52 kDa band was seen in HGDG, while a significant decrease in expression of the full length ERα was seen in the RG. ERβ protein was detected as full length, 54 kDa, single band and its expression did not change in HGDG or RG.

Conclusion: This study revealed that 1h HGD and 1h HGD followed by recovery caused a decrease and an increase in ERα mRNA, respectively, while 1h HGD followed by recovery caused a decrease in ERα protein expression. The decrease in ERα protein may change the cell ERα/ERβ ratio and alter estrogen signaling in astrocytes.

References:

1. Dolman D, Drndarski S, Abbott NJ, Rattray M. (2005) Induction of aquaporin 1 but not aquaporin 4 messenger RNA in rat primary brain microvessel endothelial cells in culture. J Neurochem. 93:825-833.

2. Redzic ZB, Malatiali SA, Al-Bader M, Al-Sarraf H. (2010) Effects of hypoxia, glucose deprivation and recovery on the expression of nucleoside transporters and adenosine uptake in primary culture of rat cortical astrocytes. Neurochem Res. 35:1434-1344.

3. Pfaffl MW (2001) A new mathematical model for relative quantification in real-time RT-PCR. Nucleic Acids Res. 29:2002-2007.

4. Al-Bader MD, Abdallah AA, Redzic ZB. (2008) Ontogenic profile of estrogen receptor alpha and beta mRNA and protein expression in fetal rat brain. Neurosci. Lett. 440:222-226.

1082

DETERMINATION OF CBF-RELATED TISSUE COMPARTMENTS IN A NEW SHEEP STROKE MODEL BY MEANS OF [^{15}O]H_2O-PET

V. Zeisig[1,2], G.-A. Becker[1], U. Grossmann[1], T. von Geymueller[2,3], B. Nitzsche[2], A. Dreyer[2], M. Kluge[1], N. Plesnila[4], O. Sabri[1], J. Boltze[2,5], H. Barthel[1]

[1]Department of Nuclear Medicine, University of Leipzig, [2]Department of Cell Therapy, Fraunhofer Institute for Cell Therapy and Immunology, [3]Institute of Pathology, Faculty of Veterinary Medicine, University of Leipzig, Leipzig, Germany, [4]Royal College of Surgeons in Ireland, Dublin, Ireland, [5]Translational Centre for Regenerative Medicine, University of Leipzig, Leipzig, Germany

Objectives: Our group recently managed to establish a new large animal model of ischemic stroke in sheep (Boltze et. al., J Cereb Blood F Metab 2008). One of the advantages of this model is the possibility to employ clinical imaging systems and protocols, allowing for a quick translation of the imaging knowledge achieved into the clinic. As most experimental stroke treatment approaches currently under investigation target the ischemic penumbra, the aim of this present study was to establish a method to determine this “tissue at risk” together with the infarction core by using [^{15}O]H_2O-PET and to test whether this can be achieved without arterial blood sampling.

Material and methods: Adult merino sheep were 2 to 3 hours after permanent occlusion of the left medial cerebral artery (pMCAO) i.v. injected with ~1GBq [^{15}O]H_2O and were dynamically imaged over 5 min (ECAT EXACT HR+ scanner). PET acquisition run parallel to continuous arterial blood sampling using an automated device (ALLOG AB blood sampler). Individual arterial input functions (I-AIF) from 32 PET scans were used to create a normalized (injected activity, bodyweight) population-based arterial input function (PB-AIF). For both AIFs, kinetic modeling of the cerebral blood flow (CBF) was performed on a voxel-wise base using a 1-tissue-compartment model (Alpert et al. J Cereb Blood F Metab 1984) implemented in PMOD. In the two resulting CBF maps per PET scan (I-AIF and PB-AIF), three stroke-related tissue regions were defined applying established CBF thresholds: the infarction core (< 8ml x $100g^{-1}$ x min^{-1}), the ischemic penumbra (8-22ml x$100g^{-1}$ x min^{-1}), and normal brain tissue (>22ml x $100g^{-1}$ x min^{-1}).

Results: Using the I-AIF for CBF modeling, 6.8± 3.6ml (7.4% of total brain volume) and 12.5±5.5ml (13.6%) were determined as ischemic penumbra and infarction core per sheep brain. The volumes of the infarction core, ischemic penumbra, and normal brain as obtained using the PB-AIF were linearly correlated to those obtained using the I-AIF ($r = 0.97$, 0.62, and 0.84, each $p=0.01$). The volumes of the tissue regions obtained using PB-AIFs deviated from the ones obtained using I-AIFs by 0.01%, 0.5%, and 0.5% for infarction core, ischemic penumbra, and normal brain.

Conclusion: These results demonstrate that in the sheep stroke model recently implemented by our group, 2 to 3 hours after pMCAO a relevant portion of ischemic penumbra is present, making this model interesting for testing new ischemia-targeting stroke therapies. Further, it was shown that it is in this model possible to apply a population-based arterial input function for kinetic modeling of the CBF without losing accuracy in penumbra volume definition. The further imaging work on this sheep stroke model will, amongst other projects, involve the implementation of simultaneous PET-MRI imaging.

1083

INCREASED IN VIVO EXPRESSION OF AN INFLAMMATORY MARKER IN TEMPORAL LOBE EPILEPSY

J. Hirvonen[1], W.C. Kreisl[1], M. Fujita[1], I. Dustin[2], O. Khan[2], S. Appel[2], Y. Zhang[1], C. Morse[1], V.W. Pike[1], R.B. Innis[1], W.H. Theodore[2]

[1]Molecular Imaging Branch, National Institute of Mental Health, National Institutes of Health, [2]Clinical Epilepsy Section, National Institute of Neurological Disorders and Stroke, National Institutes of Health, Bethesda, MD, USA

Background and aims: Animal studies and clinical observations suggest that epilepsy is associated with inflammation. Translocator protein 18 kDa (TSPO), a marker of inflammation, is increased *in vitro* in surgical samples from patients with temporal lobe epilepsy. TSPO can be measured in the living human brain with positron emission tomography (PET) and the novel radioligand [^{11}C]PBR28. In this study, we sought to determine if *in vivo* expression of TSPO is increased ipsilateral to the seizure focus in patients with temporal lobe epilepsy.

Methods: Sixteen patients with unilateral temporal lobe epilepsy and 30 healthy subjects were studied with [^{11}C]PBR28 PET and magnetic resonance imaging (MRI). Low-affinity binders were excluded. Uptake of radioactivity after injection of [^{11}C]PBR28 was measured from regions of interest drawn bilaterally onto MR images. Brain uptake from ipsilateral and contralateral hemispheres was compared using a paired samples t-test.

Results: Brain uptake was higher in the ipsilateral than in the contralateral hemisphere in hippocampus (10%), parahippocampal gyrus (8%), amygdala (8%), fusiform gyrus (4%), and choroid plexus (16%), but not in other brain regions. This asymmetry was more pronounced in patients with hippocampal sclerosis than in those without. Repeated measures analysis of variance confirmed that asymmetry in normal brain was significantly smaller than the difference between ipsilateral and contralateral hemispheres in patients with epilepsy.

Conclusions: We found increased hippocampal expression of TSPO, as evidenced by increased uptake of radioactivity after injection of [^{11}C]PBR28, suggesting a neuroinflammatory response on the side of the epileptogenic focus, associated with increased density of reactive astrocytes and/or activated microglia. Fully quantitative analysis of [^{11}C]PBR28 binding requires arterial catheterization and will be done in the future to determine whether patients with epilepsy have increased TSPO binding only in the hemisphere containing the epileptogenic focus or in both hemispheres.

1084

IDENTIFICATION OF NEURONAL POPULATIONS INVOLVED IN THE NEUROVASCULAR COUPLING RESPONSE TO LOCUS COERULEUS STIMULATION

X. Toussay, K. Basu, E. Hamel

Laboratory of Cerebrovascular Research, Montréal Neurological Institute, McGill University, Montreal, QC, Canada

Background and objectives: The mechanisms that govern the tight control between increased neuronal activity and cerebral blood flow (CBF) remain largely unknown, but the afferent input and its local processing by the activated neurons have been implicated (1, 2). The locus coeruleus (LC) is the major source of noradrenalin (NA) in brain and it provides a widespread innervation to the cerebral cortex. NA has been associated with decreases in CBF, and with brain homeostasis, metabolism, and blood-brain barrier permeability (2, 4). Using a multidisciplinary approach, we aimed at identifying the neuronal targets of NA afferents in the cerebral cortex, the CBF response induced by LC stimulation, and the mediators involved in this neurovascular coupling response.

Methods: Paraformaldehyde-fixed brains of male Sprague-Dawley rats were used in double-immunohistochemistry for NA and specific populations of pyramidal cells and GABA interneurons (parvalbumin, PV; somatostatin, SOM and vasoactive intestinal polypeptide,VIP), and innervation density quantified in semithin sections. In functional studies, rats were chronically implanted with electrodes in the LC, and CBF evoked by electrical stimulation of LC (100Hz, 80μA, 1sec on/1sec off, 20secs) measured by Laser-Doppler Flowmetry. The messengers involved in the CBF response were investigated in rats injected intracisternally (3μL of 10^{-4}M solution) with antagonists of α-adrenergic (phentolamine), β-adrenergic (propranolol), and NMDA (MK-801) receptors, and inhibitors of epoxyeicosatrienoic acids (EETS) synthesis (MS-PPOH) or their vehicles. Some rats were treated with the selective NA toxin DSP-4.

Results: Double-immunostaining indicated that NA fibers targeted cortical neurons to similar extent, with comparable proportions of PV (25%), SOM (20%) and VIP (18%) interneurons contacted by NA terminals on their cell soma or proximal dendrites. Cortical CBF increased bilaterally during LC stimulation, the ipsilateral increase was about twice as large as that in the contralateral (40 vs 22%) side. DSP-4 treated rats exhibited a dramatic reduction in the density of cortical NA nerve fibers, and in the evoked CBF response (-75%) compared to saline injected rats. Phentolamine and propranolol significantly decreased the evoked CBF (-48% and -30%, respectively). Blockade of NMDA receptors or EETs synthesis also significantly reduced the evoked CBF response (-60% and -58%, respectively). Blood gases, pH, and arterial blood pressure were not altered by treatments, and the small changes in blood pressure induced by LC stimulation did not account for the CBF increase.

Conclusions: The data demonstrate comparable NA innervation density for most cortical neuronal populations. The results indicate that stimulation of NA LC afferents increases CBF through α- and β-adrenergic receptors, and that excitatory transmission is involved. Further, the results indicate that vasoactive EETs, presumably released from astrocytes, contribute to this response. Additional studies are ongoing to identify the role of inhibitory interneurons and the cortical neuronal circuitry activated by NA afferent pathways.

References:

1. Logothetis et al., (2001) Nature 12;412: 150-7.

2. Lauritzen and Gold (2003) J Neurosci 23: 3972-3980.

3. Goadsby et al., (1985) Brain Res 326: 213-7.

4. Adachi et al., (1991) Biogenic Amines 8: 19-31.

Supported by the Canadian Institutes of Health Research (CIHR, grant MOP-84209, EH).

1086

MOLECULAR ANALYSIS OF GLYCOCALYX AND ITS SHED COMPONENTS IN HUMAN BRAIN ENDOTHELIAL CELLS AFTER IN VITRO ISCHEMIA-REPERFUSION

A.S. Haqqani[1], C.E. Delaney[1], P.O. Couraud[2], **D.B. Stanimirovic**[1]

[1]National Research Council of Canada, Institute for Biological Sciences, Ottawa, ON, Canada, [2]Université Paris Descartes, Paris, France

Background: The lumen of brain vasculature is decorated with a thick coating of glycocalyx that is made up of proteins, glycoproteins and proteoglycans. The glycocalyx is involved in various vascular functions including endothelial permeability, leukocyte adhesion/emigration and vascular blood flow. In response to ischemia-reperfusion or inflammatory insults, the endothelial glycocalyx undergoes significant alterations, such as changes in expression of cell adhesion glycoproteins for anticipated interactions with leukocytes, as well as shedding of proteolytically cleaved components into the circulation. In addition to affecting physiological functions of brain vessels, these molecular changes are attractive sources of biomarkers useful in diagnosis or therapeutic targeting since they are blood-accessible. However, due to the complex nature of brain endothelial glycocalyx, detailed analyses of protein and glycoprotein changes in response to pathological conditions have been lacking.

Objectives: To perform quantitative molecular profiling of human cerebral microvascular endothelial glycocalyx and its shed components (secretome) in response to *in vitro* ischemia-reperfusion using mass spectrometry (MS) based proteomics and glycoproteomics.

Methods: Human brain endothelial cell line, hCMEC/D3 (1), was exposed to 4-h oxygen and glucose deprivation (OGD) followed by a 24-h recovery as previously described (2). Proteins from luminal/apical membranes (containing glycocalyx) and secreted fractions (containing secreted proteins and shed components of the glycocalyx) were isolated using recently described methods (3), enriched for glycoproteins using hydrazide capture (4) and analyzed using gel-free, nanoLC-MS-based quantitative proteomics to identify differentially expressed molecules (5).

Results: More than 650 proteins and glycoproteins were identified in the glycocalyx of the brain endothelial cells, mostly consisting of signal transduction proteins, adhesion molecules and transporters. About 15% of the proteins responded significantly to the ischemia-reperfusion treatment, showing >2.5-fold up- or down-regulation (Table 1). The secreted fraction consisted of more than a hundred extracellular signalling molecules and >200 membrane-derived proteins and glycoproteins, likely resulting from the cleavage from the membrane by specific proteases (Table 1). The majority has not been previously reported as ischemia/reperfusion-responsive.

Table 1. Molecular changes in luminal glycocalyx and secreted fractions of hCMEC/D3 in response to OGD/reoxygenation as identified by nanoLC-MS/MS-based proteomics

Cell fraction	Total identified	OGD-responsive	Examples of proteins over-expressed after OGD
Glycocalyx (luminal membranes)	663 proteins and glycoproteins	15%	Cell adhesion molecules (e.g., ICAM1, ALCAM), Tight junction proteins (e.g., ZO1) and extracellular/membrane proteases (e.g., MMPs, ADAMs)
Secreted molecules	>100 cytokines, chemokines and growth factors	45%	MCP1, RANTES, CCL19
Glycocalyx-shed molecules	>200 proteins, glycoproteins and glycans	>65%	ICAM1, ALCAM, Syndecan-4, LRPs, fractalkine

[Table 1]

Conclusions: This study is the most comprehensive profiling of human brain endothelial glycocalyx, demonstrating molecular complexity of the endothelial luminal layer and identifying a subset of modified proteins that are shed from this layer in response to in vitro ischemia. OGD-responsive 'shed' glycoproteins can be exploited as peripheral biomarkers of ischemic brain disease.

References:

1. B.B. Weksler et al, FASEB J, 19, 1872-1874, 2005.
2. A. S. Haqqani *et al*, J Proteome Res, 6, 226-239, 2007.
3. A. S. Haqqani *et al*, Methods Mol Biol, 686, 337-53, 2011.
4. J. J. Hill *et al*, Proteomics, 9, 535-549, 2009.
5. A. S. Haqqani *et al*, Methods Mol Biol, 439, 241-256, 2008.

1087

INVOLVEMENT OF THE CAMP SPECIFIC PDE4B2 SPLICE VARIANT IN EXPERIMENTAL AUTOIMMUNE ENCEPHALOMYELITIS

C. Sanabra[1], E. Johansson[1], M. Conti[2], G. Mengod[1]

[1]*Institut d´Investigacions Biomèdiques de Barcelona, IIBB-CSIC, IDIBAPS, Barcelona, Spain,*
[2]*Center for Reproductive Sciences, University of California, San Francisco, CA, USA*

Inflammatory responses involve cAMP and pharmacological manipulation of cAMP levels by using specific phosphodiesterase (PDE) inhibitors provokes an anti-inflammatory response. Experimental autoimmune encephalomyelitis (EAE) is an animal model of the chronic inflammatory, neurodegenerative demyelinating disease multiple sclerosis (MS). Previously we demonstrated that in the brain and spinal cord of EAE rats there was a dramatic increase in the mRNA expression levels of the PDE4B isoenzyme, solely due to the splicing mRNA variant PDE4B2. This expression was found in the infiltrating T-cells and macrophage/microglia in microvessels and brain parenchima. We present here the study on the alterations in the expression of the cAMP-specific PDE4 and of several inflammatory cytokine mRNAs in the brain and spinal cord of C57BL6 EAE mice model by neuroanatomical techniques (double *in situ* hybridization histochemistry and immunohistochemistry), and quantitative real time RT-PCR. We observed a PDE4B2 mRNA upregulation after the onset of the EAE model, being significant 30 days post-immunization. No changes on PDE4B3 mRNA splice variant could be detected. Double *in situ* hybridization and immunohistochemistry studies showed that cellular infiltrates in brain and spinal cord tissues of EAE mice are overexpressing PDE4B isoform. Studies performed on PDE4A and PDE4B knockout (KO) mice showed an early onset of EAE in PDE4B KO mice, suggesting a “protective/retarding” role of PDE4B in this disease. RT-PCR experiments also detected a downregulation of some pro-inflammatory cytokines, like interferon-g (IFNγ), in PDE4A KO mice and a trend to upregulation of interleukin 1b (IL1β) and IL6 in PDE4B KO mice. This differential response to EAE of PDE4A and PDE4B KO mice contrast with results obtained for EAE wt mice treated with a PDE4 inhibitor, rolipram. These findings support an important and distinctive role of different PDE4 isoforms during the neuroinflammatory response produced in a EAE model and their importance as a therapeutic target for the treatment of some neuroinflammatory diseases using subtype-selective PDE4 inhibitors.

Financed by CICYT-MICINN and FEDER (SAF2006-10243, SAF2009-11052) and by a grant from the Sandler Foundation to MC. C.S. and E.J. are respectively recipients of fellowships from IDIBAPS and MICINN.

1088

OPTOGENETICS-GUIDED CORTICAL PLASTICITY FOLLOWING NERVE INJURY

N. Li[1,2], J. Downey[1], A. Bar-Shir[3,4], A.A. Gilad[3,4], P. Walczak[3,4], H. Kim[3,4], S.E. Joel[1,3], J.J. Pekar[1,3], N.V. Thakor[2], **G. Pelled**[1,3]

[1]F. M. Kirby Research Center for Functional Brain Imaging, Kennedy Krieger Institute, [2]The Department of Biomedical Engineering, [3]The Russell H. Morgan Department of Radiology and Radiological Sciences, [4]Cellular Imaging Section, Vascular Biology Program,Institute for Cell Engineering, Johns Hopkins University School of Medicine, Baltimore, MD, USA

Introduction: Peripheral nerve injury causes sensory dysfunctions that are thought to be attributable to changes in neuronal activity occurring in the somatosensory cortices contralateral and ipsilateral to injury. Recent studies suggest that the distorted functional responses observed in the deprived rat's primary somatosensory cortex (S1) originate in increases in inhibitory interneurons activity and are mediated via the transcallosal pathway. In order to decrease the cortical inhibition mediated by the transcallosal pathway, the excitatory neurons in rat S1 were engineered to express a light sensitive pump which triggers neuronal hyperpolarization (halorhodopsin: eNpHR). The neuronal activity of the healthy cortex was optogeneticly manipulated and multimodal *in vivo* techniques were applied to evaluate functional responses in the deprived S1. The results demonstrate that decreases in the inhibitory activity of the deprived cortex can be achieved by optogenticly manipulating the transcallosal activity and propose a novel therapeutic strategy to facilitate rehabilitation.

Materials and methods: The halorhodopsin plasmid (Lenti-CaMKIIa-eNpHR-EYFP-WPRE) was injected into the pups' right lateral ventricle. Denervation of the right forepaw was performed after 7 weeks. (denervated n=16, control n=16). Forepaw stimulation: 2 mA pulses were repeated at 3 and 9Hz. Light activation of eNpHR: An optic fiber coupled to a 594nm wavelength laser was placed directly over the right exposed S1. Functional MRI: Images were acquired using a Bruker 9.4 T. A GE EPI sequence with a 128 × 128 matrix, TE=21 ms, TR=1000 ms, and 3, 1-mm thick slices was used. Electrophysiology: Single unit and local field potentials were collected simultaneously. Optical imaging: Cerebral blood flow (CBF) responses were measured by laser speckle imaging (LSI). Laser with 632nm wavelength was used to provide coherent illumination.

Results: Single unit responses: In denervated rats, eNpHR activation of the healthy, contralateral S1 resulted in increased firing rate of neurons located within the deprived, ipsilateral S1 during stimulation of the left, intact forepaw ($P< 0.05$). CBF responses: In denervated rats, eNpHR activation of the healthy, contralateral S1 resulted in increased CBF responses of the deprived, ipsilateral S1 during stimulation of the left, intact forepaw ($P< 0.05$) BOLD fMRI responses: Stimulation of the left, intact forepaw in denervated rats resulted in increased BOLD responses both in healthy, contralateral and deprived ipsilateral S1 cortices ($P< 0.05$). Consistent with electrophysiology and optical imaging measurements, in denervated rats, eNpHR activation of the healthy, contralateral S1 resulted in increases in BOLD responses of the deprived, ipsilateral S1 during stimulation of the left, intact forepaw ($P< 0.05$).

Discussion: Electrophysiology, optical imaging and fMRI results show that the increased inhibitory activity usually observed in the denervated rats' deprived cortex, can be reversed by optogeneticaly manipulating the neuronal activity of the healthy cortex. Human and animal studies suggest the involvement of the transcallosal projection in shaping neuroplasticity with increased cortical inhibition following injury may be crucial in dictating the rehabilitation

probability. Thus, our findings demonstrate that in the denervated rat, the transcallosal communication can be manipulated in a manner that could potentially promote recovery. This offers a novel therapeutic strategy to facilitate rehabilitation.

1091

OCT FOR IN VIVO, LONGITUINDAL IMAGING OF NEUROVASCULAR REMODELING DURING ISCHEMIC STROKE RECOVERY

V.J. Srinivasan[1], E.T. Mandeville[2], H. Radhakrishnan[1], S. Sakadzic[1], J.Y. Jiang[3], S. Barry[3], A.E. Cable[3], E.H. Lo[2]

[1]Martinos Center for Biomedical Imaging, [2]Neuroprotection Research Laboratory, Departments of Radiology and Neurology, MGH/HMS, Charlestown, MA, [3]Thorlabs, Inc., Newton, NJ, USA

Objectives: Neurovascular responses underlie a transition from acute injury to delayed repair over time scales of days to weeks as the brain begins to initiate endogenous angiogenesis that facilitates neuronal plasticity and remodeling. Volumetric, in vivo imaging may provide additional insight into the spatiotemporal evolution of these endogenous responses that cannot be obtained from sectioning and histology. While two-photon microscopy achieves subcellular spatial resolution, the imaging speed, penetration depth, and field-of-view are limited. Conversely, while diffusion- and perfusion-weighted MRI can assess flow and tissue viability concurrently, much higher resolution imaging is desirable for mouse models. The goal of our study was to investigate the novel technique of Optical Coherence Tomography (OCT) for longitudinal imaging of neurovascular remodeling during ischemic stroke recovery in the mouse cortex.

Methods: A thinned-skull, glass coverslip-reinforced cranial window over the cerebral cortex was created in C57BL6/6 mice (n=3) from Charles River Lab, enabling imaging of the boundary between middle cerebral artery (MCA) and anterior cerebral artery (ACA) territories. OCT imaging was performed under isoflurane anesthesia just prior to permanent distal middle cerebral artery occlusion (dMCAO) and one week after occlusion. Imaging was performed using a 1300 nm spectral / Fourier domain OCT system operating at 47,000 axial scans per second. Including time required for instrument alignment, OCT imaging could be performed in less than 30 minutes.

Results: Figure 1A shows an OCT angiogram obtained before occlusion, revealing the pial vessels (orange) as well as a dense capillary network (green). Concentric rings of 1 mm, 2 mm and 3 mm radius centered on a large MCA branch are shown as white dotted lines. Figure 1B shows the absolute CBF values measured by Doppler OCT in concentric annuli. A clear gradient in flow is seen from the MCA supplied territory to the ACA supplied territory. Locations at which the flow difference (pre-MCAO vs. post-MCAO) is statistically significant are shown (two-tailed, $p < 0.05$). Since imaging was performed in the same mice at two different time points, a paired t-test could be used. A recovery of flow to pre-ischemic levels is seen near the boundary of the MCA and ACA territories. High-resolution imaging of the penumbra (Figure 1C-D) revealed dramatic diameter increases in surface collaterals (white arrows), and possible capillary network changes (capillaries colored green), both of which may account for the flow recovery in the border zone. Diameter increases in dural vessels (which could be distinguished from pial and parenchymal vessels in the volumetric data) were evident as well.

Conclusions: We have demonstrated longitudinal imaging of vascular remodeling in the ischemic stroke penumbra using OCT. Imaging can be performed chronically, through the thinned skull, without the application of exogenous dyes or contrast agents, and over time scales of weeks. This novel imaging platform can be used in the future to assess cell-based or pharmacological therapies that promote endogenous repair.

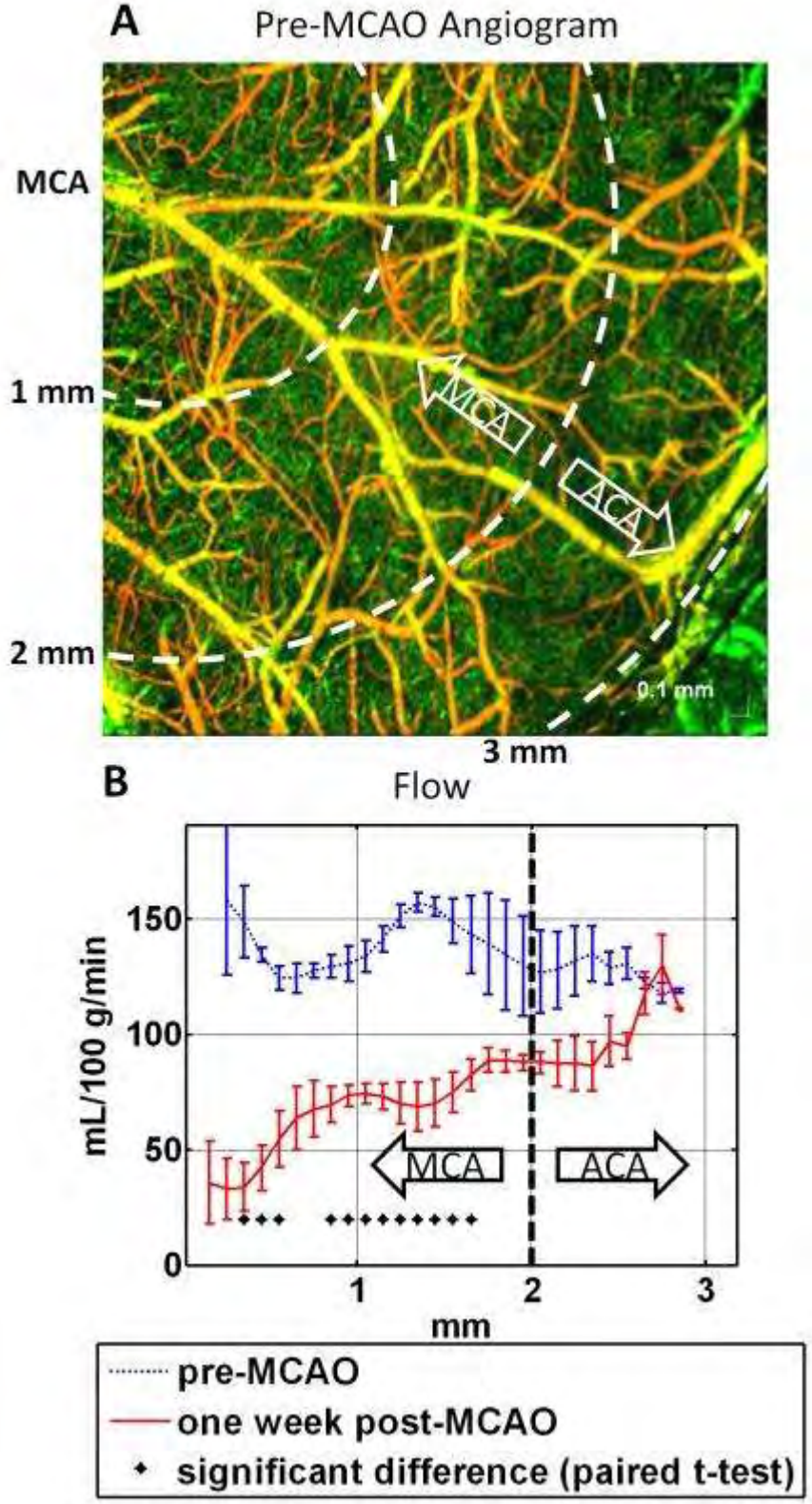
A
Pre-MCAO Angiogram
MCA
1 mm
2 mm
3 mm
MCA
ACA
0.1 mm
B
Flow
mL/100 g/min
150
100
50
0
1
2
3
mm
MCA
ACA
pre-MCAO
one week post-MCAO
significant difference (paired t-test)

[Figure 1AB]

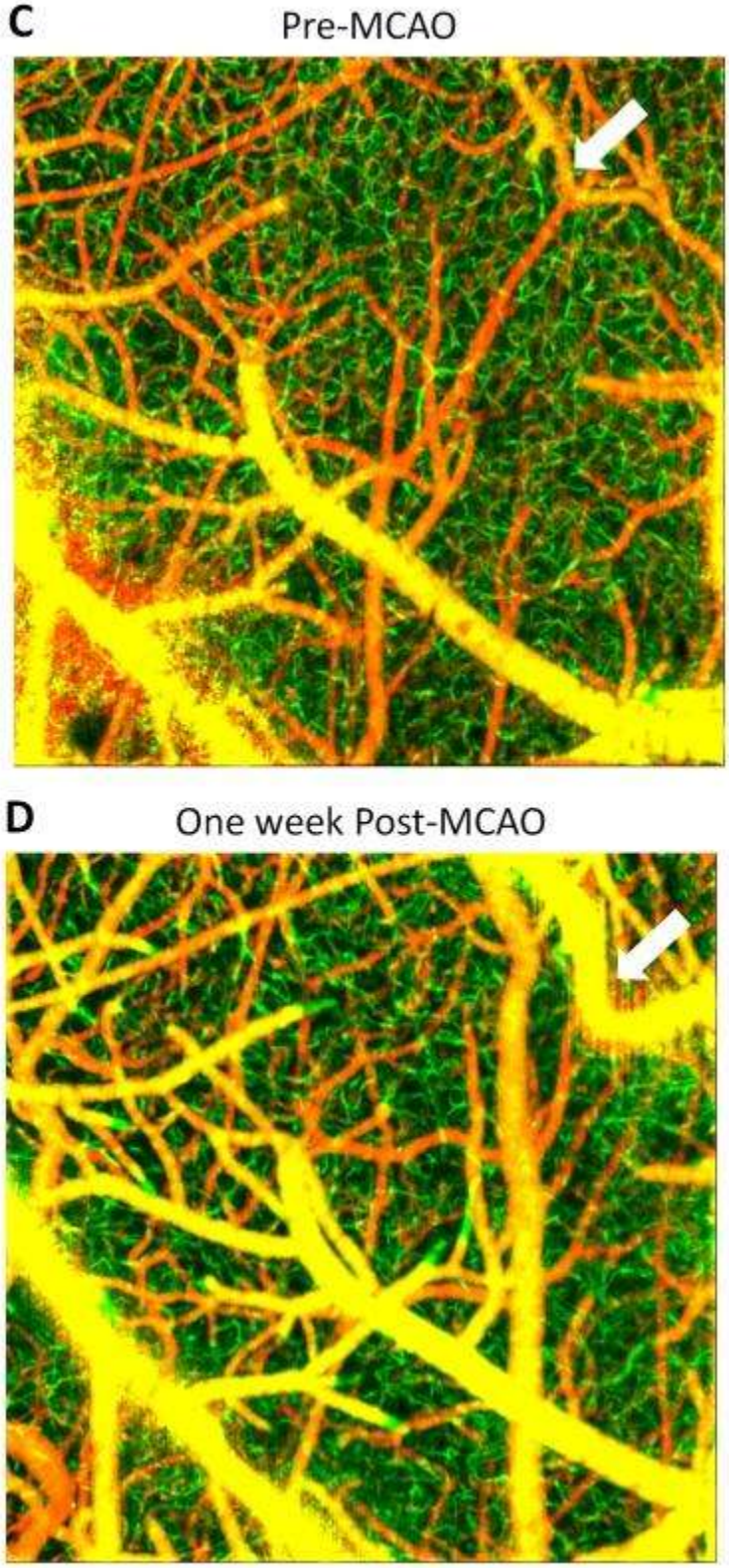

[Figure 1CD]

1092

PEROXISOME PROLIFERATOR-ACTIVATED RECEPTOR Γ ACTIVATION REDUCES NEURONAL DAMAGE IN THE SUBSTANTIA NIGRA AFTER FOCAL CEREBRAL ISCHAEMIA IN RATS

Y. Zhao[1], M. Zuhayra[1], E. Henze[1], U. Lützen[1], T. Herdegen[2], J. Culman[2]

[1]Department of Nuclear Medicine, [2]Institute of Experimental and Clinical Pharmacology, University Hospital of Schleswig-Holstein, Campus Kiel, University of Kiel, Kiel, Germany

Objectives: Activation of peroxisome-proliferator-activated receptor(s) γ (PPARγ) in the brain exerts beneficial effects after ischaemic stroke. We studied in rats the function of brain (neuronal) PPARγ in the delayed degeneration and loss of neurones in the substantia nigra (SN) occurring after occlusion of the middle cerebral artery (MCAO) followed by reperfusion.

Methods: The PPARγ agonist, pioglitazone, or vehicle was infused intracerebroventricularly over a 5-day period before, during and 5 days after MCAO (90 min). The neuronal degeneration in the SN pars reticularis (SNr) and pars compacta (SNc), the analysis of the number of tyrosine hydroxylase - immunoreactive (TH-IR) neurones and the expression of the PPARγ in these neurones was studied by immunohistochemistry and immunofluorescence staining. The effects of PPARγ activation on excitotoxic and oxidative neuronal damage induced by 6-hydroxydopamine (6-OH DA) or glutamate were investigated in primary cortical neurones expressing the PPARγ. The cell viability and cytotoxic effects were assessed by the WST - and lactate-dehydrogenase assay in neurones treated with vehicle (control) or pioglitazone with or without the selective PPARγ antagonist, GW 9662, prior to the exposure to 6-OH DA or glutamate.

Results: Pioglitazone reduced the total and striatal infarct size by 36 % and 48 %, respectively. Rats treated with pioglitazone displayed less sensory impairments than vehicle-treated rats on days 3, 4 and 5 after MCAO. MCAO initiated a delayed neurodegeneration of neurones in the SN, no apoptotic neurones were detected. In vehicle treated rats, the number of TH - IR neurones in the ipsilateral SNc was reduced (- 40 %) in relation to the corresponding contralateral side. Pioglitazone prevented the loss of TH - IR neurones in the SNc and reduced the number of neurones displaying signs of degeneration in both parts of the ipsilateral SN. Activation of PPARγ decreased the accumulation of activated microglia/macrophages and increased the number of PPARγ - positive TH-IR neurones. In primary cortical neurones, pioglitazone reduced the glutamate - and 6-OH DA - induced LDH release and increased the viability of neurones as revealed by the enhanced reduction of the WTS reagent. Both effects were completely reversed by the selective PPARγ antagonist, GW 9662, implying a PPARγ - dependent mechanism.

Conclusions: The present data demonstrate that activation of neuronal PPARγ prevents the delayed loss of neurones in the SN after transient focal cerebral ischaemia and provide evidence that PPARγ agonists confer neuroprotection after ischaemic stroke by reducing neuronal damage within the peri-infarct zone and delayed degeneration of neurones and neuronal death in areas remote from the site of ischaemic injury. Pioglitazone and other PPARγ agonists may be useful therapeutic agents for preventing the progression of brain damage after cerebral ischaemia.

1093

PARAMETERS OF FLOW AND OXY HEMOGLOBIN TRANSIENTS SHOW SPATIAL HETEROGENEITY IN RAT FOCAL BRAIN ISCHEMIA

J. Lückl[1,2], W. Baker[3], Z.-H. Sun[2], T. Durduran[3,4], A.G. Yodh[3], J.H. Greenberg[2]

[1]Experimental Neurology, Charite Universitatsmedizin, Berlin, Germany, [2]Department of Neurology, [3]Department of Physics and Astronomy, University of Pennsylvania, Philadelphia, PA, USA, [4]ICFO-Institut de Ciències Fotòniques, Mediterranean Technology Park, Barcelona, Spain

Objectives: It is well known that spreading depolarisations are accompanied by transient changes in cerebral blood flow in experimental ischemia. In a previous study we demonstrated that the morphology of flow transients show regional heterogeneity (Luckl et al. 2009). In the present study we investigated if the parameters (amplitude, duration, morphology) of different hemoglobin (oxy, deoxy) transients show similar spatial heterogeneity.

Methods: Sprague-Dawley rats were prepared using 1.2% isoflurane anesthesia. The middle cerebral artery was occluded by photothrombosis (4mW) and the ipsilateral common carotid artery was ligated permanently. Physiological variables were constantly monitored during the experiment. A 6x6 mm area centered 3 mm posterior and 4 mm lateral to Bregma was thinned for laser speckle and optical spectroscopic imaging. Nine circular regions-of-interests (0.3 mm in diameter) (figure) were evenly spaced on the images for the analysis of blood flow, oxy- and deoxy-hemoglobin transients and metabolic changes. The amplitudes (peak to peak, both positive and negative components), duration, and the five different types of morphology (type) of the transients were determined as described previously (Luckl et al. 2009).The animals underwent neurological examinations 24 h after ischemia at which point all animals were sacrificed and the infarct size was determined by triphenyltetrazolium chloride staining.

Results: The physiological variables were in a normal range. The mean intraischemic flow (29-35% of baseline), the neurological score (3.8±1.9) and the infarct volume (126±38 mm^3) indicated succesful occlusions in the animals. The transients (flow and hemoglobin) did not propagate over ROI 1,2,3 which is the core of the MCA territory and so only the transients between ROI 4,5,6 (penumbra) and ROI 7,8,9 (peri-ischemic area) were compared. The peak-to-peak amplitudes of the flow transients, and the positive component of these transients were significantly higher over the peri-ischemic area. The type 1 morphology (monophasic increase) of the flow transients showed a a greater occurence over the peri-ischemic area. Similarly, the peak-to-peak amplitudes and the positive components of the oxy-hemoglobin transients were higher over the peri-ischemic area, and the type 1 (monophasic increase), type 2 (biphasic) and type 4-5 (monophasic decrease) transients showed significant spatial heterogeneity. The parameters of the deoxyhemoglobin transients did not show any difference between penumbra and peri-ischemic area.

Conclusions: In the present study we demonstrated that not only the parameters of the flow transients but also the oxy hemoglobin transients show spatial heterogeneity and therefore might serve as biomarkers in the distinction between penumbra and peri-ischemic area.

References:

Luckl J, Zhou C, Durduran T, Yodh AG, Greenberg JH (2009) Characterization of periinfarct

flow transients with laser speckle and Doppler after middle cerebral artery occlusion in the rat. *J Neurosci Res* 87:1219-1229

Figure Legend

Schematic figure of the thinned skull with the positions of the nine regions of interests (ROI). The shadowing shows the peri-ischemic area in animals after mapping the infarct area with the map of ROIs

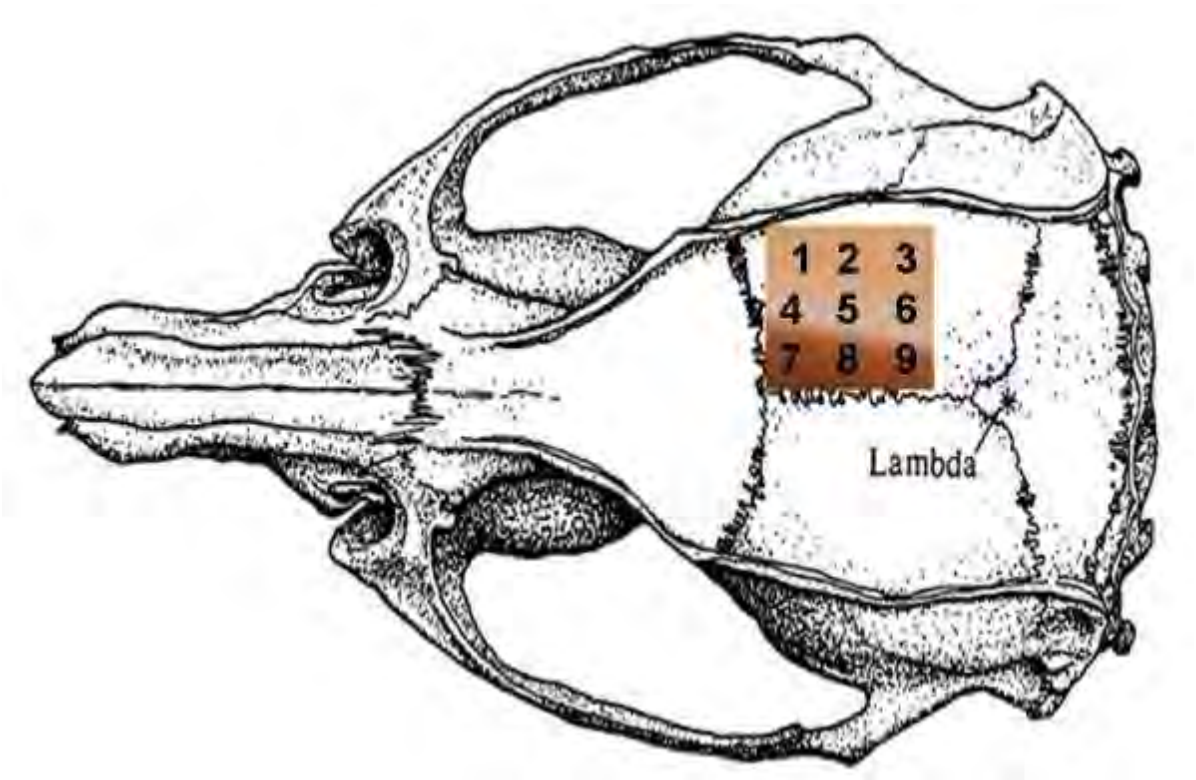

[Figure]

1094

SEX DIFFERENCES IN PROTECTION PROVIDED BY PHARMACOLOGICAL AND GENETIC INHIBITION OF TRPM2 CHANNELS AGAINST EXPERIMENTAL STROKE IN MICE

P.S. Herson[1], J. Jia[1,2], S.L. Mader[1], S. Nakayama[1], M.R. Grafe[1,2], P.D. Hurn[1]

[1]Department of Anesthesiology & Perioperative Medicine, [2]Department of Pathology, Oregon Health Sciences University, Portland, OR, USA

Objectives: Stroke is a sexually dimorphic disease that affects men more severely than women. Transient receptor potential (TRP) channels have been implicated in ischemia-induced neuronal damage. Our previous data demonstrated that TRPM2, a member of the TRP channel superfamily, contributed to oxygen-glucose deprivation (OGD) induced cell death in vitro only in male neurons, failing to benefit female neurons. In this study, we examined the effect of pharmacological and genetic inhibition of TRPM2 channels on tissue infarction after focal cerebral ischemia in male and female mice.

Methods: Intact and castrated male and female C57BL/6 mice were subjected to 90 min middle cerebral artery occlusion (MCAO) under isoflurane anesthesia. Mice were acutely injected with the TRPM2 inhibitor clotrimazole 30 mg/kg), or vehicle (Veh), via subcutaneous injections, at the time of occlusion and reperfusion. Infarct volumes (% contralateral structure) were determined 24 hr after reperfusion by analysis of coronal sections stained with TTC. A separate cohort of male and female C57BL/6 mice received intrastriatal injection of lentivirus expressing shRNA against TRPM2, or control virus, 2 weeks before MCAO. Infarct volume was determined by analysis of cresyl violet stained sections. Cerebrocortical laser-Doppler perfusion (LDP) was continuously monitored during occlusion.

Results: Male mice treated with clotrimazole had significantly smaller cortical and hemisphere infarcts compared to vehicle treated animals (Hem: 42.0 ± 2.7% (n=10) in Veh vs. 27.0 ± 4.5% (n=10; $P < 0.05$) in clotrimazole.; cortex: 45.1 ± 3.8% in Veh vs. 28.5 ± 5.9% ($P < 0.05$) in clotrimazole; striatum 91.2 ± 2.7% in Veh vs. 71.6 ± 8.5% ($P < 0.1$) in clotrimazole. In contrast, in female mice, clotrimazole had no effect on infarct volume; 31.4 ± 5.6% (n=10) in Veh vs. 28.1 ± 3.8% (n=10; $P > 0.7$) in clotrimazole. Consistent with involvement of TRPM2 in ischemic outcome in male brain, male mice receiving intrastriatal injection of lentivirus expressing TRPM2 targeted shRNA had significantly smaller striatal infarcts compared to male mice injected with control virus; striatum: 94.0 ± 1.6% (n=9) in control vs. 84.1 ± 3.2% (n=12; $P < 0.05$) in shRNA. In contrast, shRNA expressing lentivirus had no effect on infarct volumes in female mice, striatal infarct volumes of 90.7 ± 2.2% (n=8) in control vs. 82.7 ± 7.5% (n=9; $P > 0.3$) in shRNA. Finally, the role of androgens was assessed by tested the ability of clotrimazole to protect castrated male mice. Surprisingly, castrated mice treated with clotrimazole had larger infarcts compared to vehicle treated castrated mice; 24.5 ± 6.2% (n=6) in Veh vs. 38.4 ± 10.4% (n=5) in clotrimazole.

Conclusion: Pharmacological and genetic inhibition of TRPM2 channels protect against cerebral ischemia in male mice, while having no effect in females. Thus, inhibition of TRPM2 channels represents a potential therapeutic strategy to improve outcome following stroke in men.

1095

QUANTITATIVE PET IMAGING AT SIMULTANEOUS 3T MR-PET HYBRID MEASUREMENTS

C. Weirich[1], J. Scheins[1], L. Tellmann[1], D. Brenner[1], E. Rota Kops[1], H. Herzog[1], N.J. Shah[1,2]

[1]Institute of Neuroscience and Medicine - 4, Forschungszentrum Jülich, Jülich, [2]Department of Neurology, Faculty of Medicine, RWTH Aachen University, Aachen, Germany

Objectives: A 3T MR-PET hybrid scanner for brain investigation has been installed in our institute. The MR component is a 3T MAGNETOM Trio scanner, whereas the PET component is constructed as an insert and located within the bore of the MR scanner to allow simultaneous MR and PET scans. Here we report our results on quantification of PET images acquired during simultaneously performed MRI sequences.

Methods: The high quality of the PET images is related to a high spatial resolution (3 mm in the transaxial centre), a high detection efficiency (6% point-source sensitivity) and minimal artefacts. Recently, methods were developed and implemented to quantify the PET images that are acquired simultaneously with the MR measurements. Effects of the simultaneously performed MRI sequences on the PET sensitivity are corrected. These methods have been evaluated with phantom studies, covering a wide range of countrates. Furthermore, phantoms with different shapes were measured to study the influences of shape and countrate on the quantification and to determine the quantification error. Finally, a phantom consisting of two compartments, filled with ^{11}C and ^{18}F, respectively, was studied.

The PET data were acquired in listmode and corrected for deadtime and radioactive decay of the isotope. The influences of the MR hardware on the PET measurement have been analysed for different MR sequences (no imaging). A correction procedure based on the weighing of the listmode is suggested

The prompt coincidences are filled directly into a sinogram, whereas the estimated random sinogram is computed from the measured delayed coincidences. The final image reconstruction is performed with an ordinary Poisson (OP) OSEM algorithm, taking into account the measured data, the normalisation for the crystal efficiencies and the attenuation and the scatter properties of the measured subject. Finally, the image is calibrated with a separately determined calibration factor, leading to quantitative images with the unit of kBq/ml.

Results: The calibration factor was found to be stable, determined with 23 measurements during 8 weeks. Counting rates with a dynamic range from 20 to 400 kcps true coincidences were measured during the phantom studies. The error of quantification in the reconstructed images, in references measured with a gamma counter, were found to be between -2.4% and 4.7%. MRI sequences such as MP-RAGE have a negligible influence on the PET sensitivity, whereas sequences with fast switching gradients and a high gradient duty cycle (e.g. EPI) show an instantaneous, correctable countrate drop of 3 %. In the combined ^{11}C-^{18}F experiment, the maximum error in the compartment of ^{18}F was 1.6%, whereas the error in the ^{11}C compartment was found to vary between -2.4% for high and 4.7% for low countrates.

Conclusions: Quantitative PET imaging acquired simultaneously with MRI is possible for objects with different shapes and sizes and a wide range of countrates.

1096

BEHAVIORAL AND HISTOLOGICAL CHARACTERIZATION OF BRAIN INJURY AFTER EXPERIMENTAL CARDIAC ARREST

C. Dezfulian[1,2,3], A. Alekseyenko[1], H.M. Bramlett[4], M.A. Perez-Pinzon[2], C.M. Atkins[4]

[1]Medicine, [2]Neurology, University of Miami, Miami, FL, [3]Critical Care Medicine, University of Pittsburgh School of Medicine, Pittsburgh, PA, [4]Neurological Surgery, University of Miami, Miami, FL, USA

Introduction: Long-term human survivors of cardiac arrest are known to suffer from short-term memory loss, executive frontal lobe dysfunction, anxiety, mild depression, fatigue, sleep rhythm disturbances and loss of psychomotor speed and coordination. Although numerous neurological scales and individual behavioral tasks have been applied to animal models of cardiac arrest, systematic evaluation using established neurobehavioral testing is lacking. In addition, most histological evaluation of brain injury after cardiac arrest focuses only on the highly sensitive hippocampal CA1 neurons.

Aims of study: To characterize behavioral deficits in rat survivors of asphyxial cardiac arrest (ACA) utilizing a battery of neurobehavioral tasks selected based on human clinical outcomes and to correlate these deficits with histological changes.

Methods: Male Sprague-Dawley (250-300g) rats underwent 8 min ACA and were resuscitated with CPR and epinephrine and survived 2 weeks (n=3). This cohort was compared to sham (surgery but no ACA, n=4), and naïve (no surgery, n=6) rats using a series of neurobehavioral tests administered 7-16 days after ACA (Table). Sixteen days post-ACA rats were perfused with formaldehyde under anesthesia and brains removed for histological evaluation.

Neurobehavioral test	Domain or behavior tested	Anatomical localization	Days post-ACA when tested
Morris Water Maze (MWM)	Spatial learning and memory; working memory; coordination	Hippocampus; Pre-frontal and motor cortex; Cerebellum	7 to 11
Fear Conditioning	Emotional memory	Amygdala; Hippocampus	9 to 11
Sucrose preference	Depression (anhedonia)	Limbic system (includes amygdala and hippocampus)	11 to 14
Rotarod	Motor and coordination	Motor cortex and cerebellum	14 to 15

[Neurobehavioral testing]

Results: This model of ACA is associated with 50-70% neuronal loss in CA1 of hippocampus. Sham and naïve rats were nearly indistinguishable except in the sucrose preference test where both surgical groups (sham, ACA) lost preference to a similar extent. Animals surviving ACA had increased latency in the hidden platform version of the water maze task which diminished by day 3 suggesting motor/coordination deficits (Figure 1). No deficits were noted in a working memory. The motor/coordination deficits were also seen using the rotarod where ACA survivors remained on the beam significantly less than shams (* in figure denotes p< 0.001; Figure 2). ACA animals exhibited less freezing behavior during fear conditioning training and had significant deficits in both contextual and cue fear conditioning when tested at 24 hr post-training in contrast to sham animals (*, p< 0.001; $, p< 0.05; Figure 3).

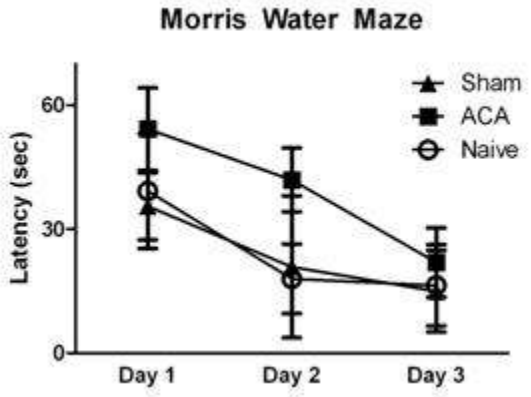

[Figure 1: Morris Water Maze]

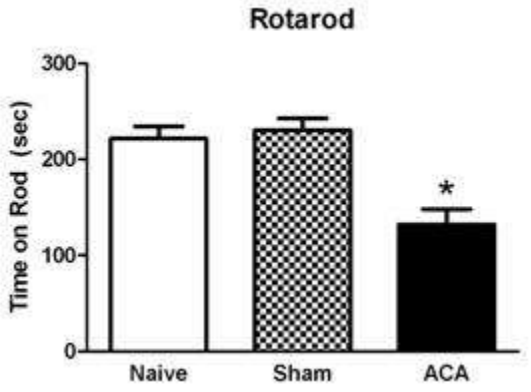

[Figure 2: Rotarod]

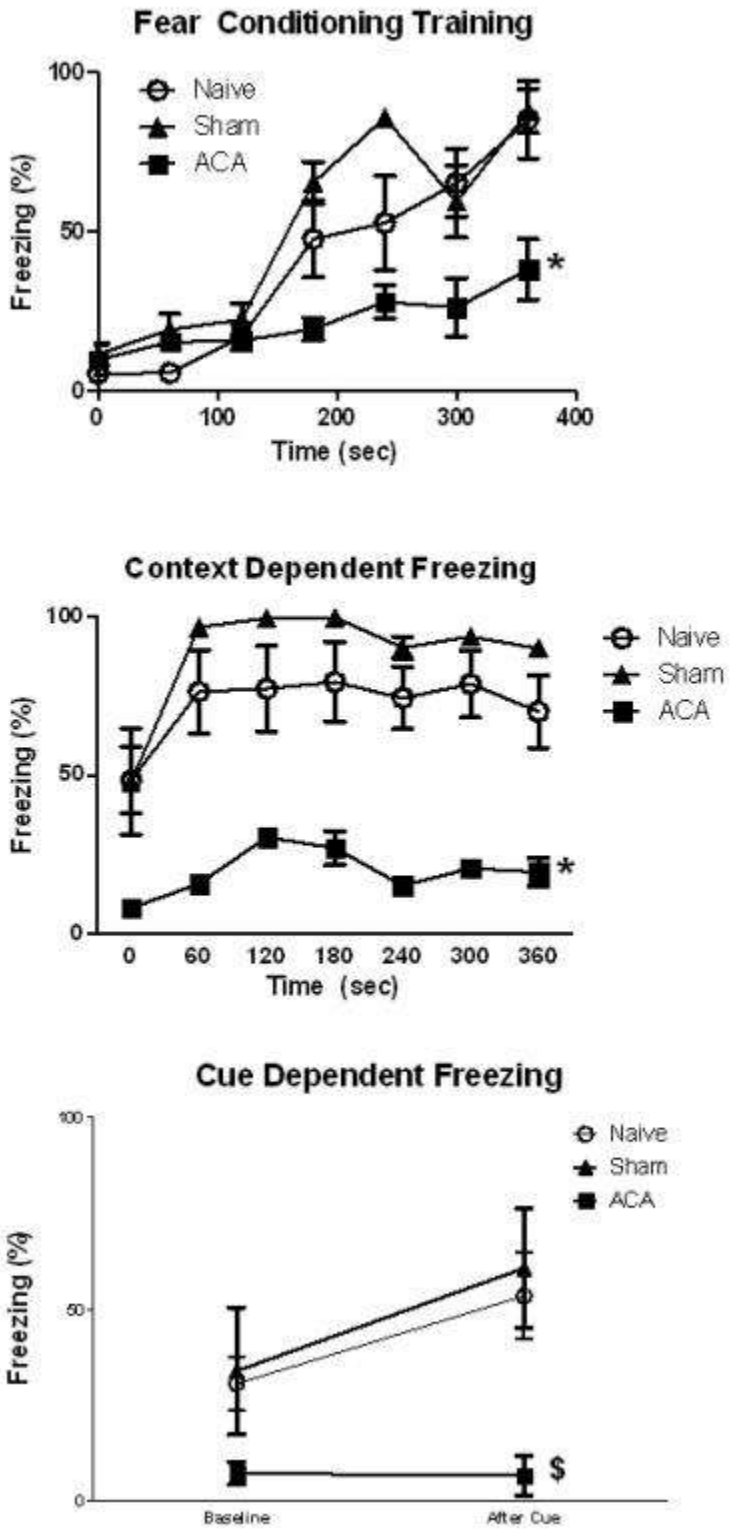

[Figure 3: Fear Conditioning]

Conclusion: ACA results in acquired neurobehavioral deficits similar to humans which are normally associated with injury to the hippocampus, amygdala and cerebellum. Histological evaluation of these regions is ongoing.

1097

ASTROCYTE ACTIVATION IN RESPONSE TO BRAIN METASTASIS

E. O'Brien[1], S. Serres[1], C. Bristow[1], D. Anthony[2], N. Sibson[1]

[1]Gray Institute of Radiation Oncology Biology, [2]Neuroinflammation, Department of Pharmacology, Oxford University, Oxford, UK

Introduction and Aim: A diverse range of CNS insults induce morphological and transcriptional changes in astrocytes, known collectively as astrogliosis. This reactive phenotype has varied consequences in a range of pathologies, and recent studies in vitro and in vivo studies suggest astrocyte activation occurs during the development of secondary cancer (metastasis) in the brain [1,2,3]. Brain metastasis is predicted to affect 20-40% of all cancer patients, yet the factors governing tumour development remain largely unknown [4]. The aim of this study, therefore, was to quantify astrocyte activation during metastasis induction and pathogenesis in a mouse model of metastatic breast cancer, with a view to determining the role of astrocytes in tumour pathogenesis.

Methods: Astrocyte activation in response to brain metastasis was quantified over a 28 day period. Brain metastases were induced via intra-cardiac injection of a Green Fluorescent Protein (GFP) transfected murine breast cancer cell line, 4T1, into female BALB/c mice, at 6-7 weeks of age. Brains perfused-fixed at days 10, 14 and 28 post-injection (n=3 at each time point). Tumours were detected using immunohistochemical detection of GFP, whilst astrocyte activation was detected via immunohistochemical staining of Glial Fibrillary Acidic Protein (GFAP).

Results: Brain metastases were found to be surrounded by a ring of activated astrocytes throughout the time course studied (Figure 1), and a positive correlation was found between the extent of astrogliosis and tumour size (r^2= 0.2, P value = 0.01). The area of astrocyte activation increased significantly with time (P value= 0.01, Figure 1), and interestingly to a greater extent than tumour area.

Figure1: Brain metastasis is associated with astrocyte activation. In a day 28 brain, asterix denotes activated astrocytes, stained with anti-Glial Fibrilary Acidic Protein, arrow depicts brain metastasis, counter-stained with Cresyl Violet. As shown in the graph, the area of astrocyte activation surrounding the tumours increases with time. P value < 0.01.

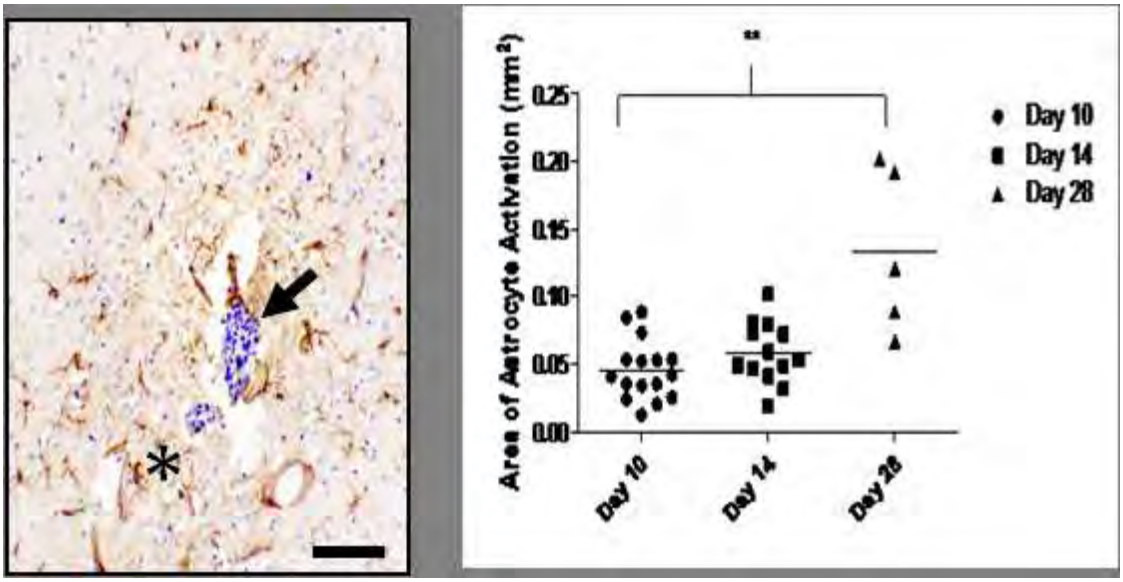

[Astrocyte activation]

Conclusion: This study demonstrates robust activation of astrocytes in response to brain metastases, suggesting that astrocytes may play an important role in tumour pathogenesis. These findings provide the basis for further investigations aimed at ascertaining the positive and negative components of this interaction, and to determine the molecular pathways that drive the relationship.

References:

1. He BP et al., (2006) Differential reactions of microglia to brain metastasis of lung cancer, *Molecular Medicine*, 12(7-8), 161-70

2. Fitzgerald, D.P. et al., (2008). Reactive glia are recruited by highly proliferative brain metastases of breast cancer and promote tumor cell colonization. *Clinical & experimental metastasis*, 25(7), 799-810.

3. Seike, T. et al., 2011. Interaction between lung cancer cells and astrocytes via specific inflammatory cytokines in the microenvironment of brain metastasis. *Clinical & Experimental Metastasis*, 28(1), 13-25.

4. Soffietti, R., Rudā, R. & Mutani, R., (2002). Management of brain metastases. *Journal of Neurology*, 249(10), 1357-1369.

1098

OPTICAL COHERENCE MICROSCOPY FOR IN VIVO, DEEP TISSUE BRAIN IMAGING

V.J. Srinivasan[1], H. Radhakrishnan[1], J.Y. Jiang[2], S. Barry[2], A.E. Cable[2]

[1]Martinos Center for Biomedical Imaging, Charlestown, MA, [2]Thorlabs, Inc., Newton, NJ, USA

Objectives: In vivo optical imaging techniques have recently emerged as important tools for studying neurobiological development and pathophysiology. In particular, two-photon microscopy has proved to be a robust and highly flexible method for in vivo imaging in highly scattering tissue. However, two-photon microscopy typically requires extrinsic dyes or contrast agents, and imaging depths are limited to a few hundred microns. Here, we introduce Optical Coherence Microscopy (OCM) for in vivo imaging of neuronal cell nuclei and cortical myelination up to depths of ~1.3 mm in the rat cortex.

Methods: Male Harlan Sprague-Dawley rats (weight 200-350 g) were prepared with closed cranial windows. A gas mixture of 80% air and 20% O2 was used for ventilation and 1-2.5% isoflurane was administered via face mask during surgery. A tracheotomy for mechanical ventilation and cannulations of the femoral artery and vein were performed. A heating blanket maintained a core temperature of 37°C. Imaging was performed under alpha-chloralose anesthesia, and blood pressure and blood gases were frequently monitored. A 1300 nm spectral / Fourier domain OCM system operating at 47,000 axial scans per second was used for imaging.

Results: Figure 1 shows "virtual," coronal sections of the rat somatosensory cortex, obtained from volumetric OCM data. Since imaging is non-destructive, these histology-like sections can be obtained in vivo, without directly cutting tissue. OCM imaging does not require addition of dyes or contrast agents, and is achieved through intrinsic scattering contrast and image processing alone. Furthermore, OCM enables in vivo, quantitative measurements of optical properties (index of refraction, scattering coefficient) in the cortex. OCM imaging techniques enable direct visualization of morphological changes during depolarization and repolarization and may provide novel optical markers of cell viability.

Conclusions: Staining methods used by Golgi, Cajal, and Nissl led to seminal observations about the microscopic organization of the brain. Even today, staining either bulk tissues, specific cell populations, or organelles in histological specimens and light microscopy are widely used for studies of cyto-architecture in the brain. More recently, advances in light microscopy and cell-labeling techniques have enabled in vivo imaging of neuro-anatomy and function. Two-photon microscopy, in particular, has become the method of choice for in vivo imaging of cortex at depths of up to a few hundred microns. However, two-photon microscopy suffers from limited penetration depths, typically requires either exogenous dyes or genetic labeling, and requires the use of costly, bulky femtosecond lasers. We present an alternative in vivo cellular brain imaging strategy based on Optical Coherence Microscopy (OCM) that uses intrinsic contrast, e.g. contrast arising from endogenous tissue properties. Furthermore, we use this novel imaging platform to quantify the refractive index and scattering of brain tissue. We also show data that suggests OCM may provide novel optical markers of cell viability.

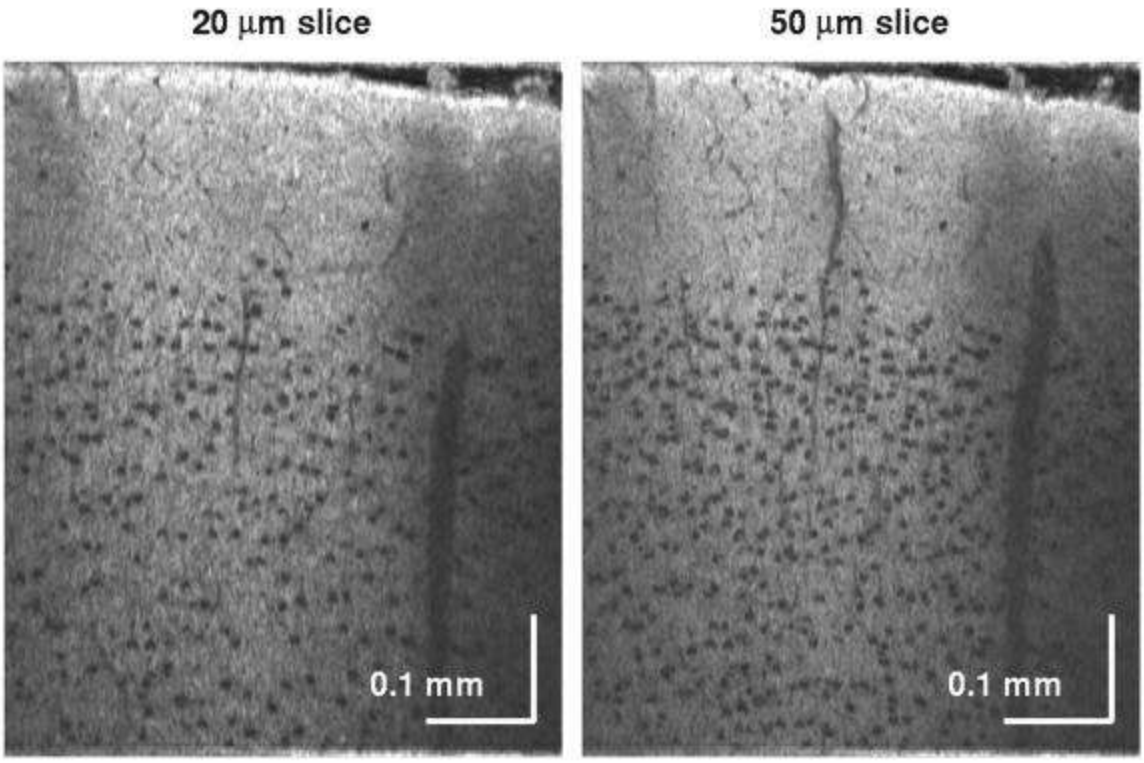

[Figure 1]

1101

HUMAN UMBILICAL CORD BLOOD MESENCHYMAL STEM CELLS PROTECT MICE BRAIN AFTER TRAUMA

E.R. Zanier[1], F. Pischiutta[1], M. Viganò[2], M. Montinaro[1], P. Villa[1,3], S. Fumagalli[1], L. Longhi[1,4], M. Leoni[1,4], P. Rebulla[2], N. Stocchetti[4], L. Lazzari[2], M.G. De Simoni[1]

[1]Mario Negri Institute, [2]Cell Factory, Center of Transfusion Medicine, Cellular Therapy and Cryobiology, Department of Regenerative Medicine, [3]CNR, Intitute of Neuroscience, [4]University of Milan, Department of Anesthesia and Critical Care Medicine, Fondazione IRCCS Ca' Granda Ospedale Maggiore Policlinico, Milan, Italy

Objectives: human umbilical cord blood mesenchymal stem cells (CB-MSC) are emerging as a novel source of progenitors with multilineage potential[1,2] . Here we investigated if CB-MSC: 1) decrease traumatic brain injury sequelae and restore brain function; 2) are able to survive and migrate in the injured brain; 3) induce relevant changes in the environment in which they are infused.

Methods: CB-MSC were isolated from cord blood through a negative depletion of the erythroid component. C57Bl/6 male mice were subjected to controlled cortical impact (CCI)/sham brain injury followed by an intracerebroventricular injection of CB-MSC (150,000/5ul) or PBS (control group) contralateral to the injured side, 24h postinjury. Immunosuppression was achieved by cyclosporine A (10 mg/kg ip). Neurological motor function was evaluated by Neuroscore (NS) and Beam-Walk (BW) tasks. Cognitive function was assessed by Morris Water Maze (MWM). The expression of brain derived neurotrophic factor (BDNF) was determined by western blot analysis. The activation of microglia/macrophage and the effect on gliotic scar was determined by immunohistochemistry. For BW, NS, MWM, contusion volume and BDNF concentrations, the comparison between groups was performed by 2-way ANOVA and Tukey post hoc test. Unpaired t-test was used for CD11b, CD68 and GFAP quantification.

Results: CB-MSC transplantation induced an early improvement of motor dysfunctions that was already present 1 week postinjury and persisted for the whole study [4 weeks postinjury, median NS: 7(range:6-9) and 5(3-9); BW: 24(8-37) and 38(24-51) in CB-MSC transplanted and control mice respectively, n=16]. Moreover, 1 month postinjury CB-MSC mice also showed attenuated learning dysfunction at MWM ($p< 0.05$) and reduced contusion volume compared to control mice (13.7±1.7 mm^3 and 17.3±1.3 mm^3, respectively $p< 0.01$). Assessment of cell distribution revealed that Hoechst positive CB-MSC survived in the injured brain up to 5 weeks and homed to lesioned tissue as early as 1 week postinjury in 67% of mice. By 3 days postinjury cell infusion significantly increased BDNF concentration in cortical contusion core and bordering region, restoring BDNF expression close to the levels observed in sham operated mice (n=8). By 7 days postinjury, we observed a selective rise (260%) in CD11b-positive cells of CCI CB-MSC compared to control mice. Conversely we observed a significant decrease (58%) in CD68 (a marker of active phagocytosis) positive cells in CCI CB-MSC compared to control mice indicating a non phagocytic activation of microglia/macrophage population. Five weeks after injury, in the scar region, CCI CB-MSC mice showed a selective decrease of GFAP positive cells compared to control mice (n=8, $p< 0.01$).

Conclusions: these findings suggest that CB-MSC stimulate the injured brain and evoke protective events through trophic and immunomodulatory mechanisms that remodel the brain and lead to significant improvement of neurological outcome. Based on these results we

propose that CB-MSC may be regarded as a novel therapeutic strategy for traumatic brain injury.

References:

1. Salem HK, Stem Cells. 2010; 28:585-96

2. Malgieri A, Int J Clin Exp Med. 2010; 3:248-69

1102

MICRORNA-320A AS A POTENTIAL THERAPEUTIC TARGET IN CEREBRAL ISCHEMIA

K. Jeyaseelan[1], S. Sepramaniam[1], K.Y. Lim[1], D.S. Karolina[1], A. Armugam[1], J.R. Tan[1], Y.X. Koo[1], P. Kaur[1], F.J. Liu[1], K.S. Tan[2], C.W. Wang[2], P.T.H. Wong[3], The Stroke Program

[1]Biochemistry, National University of Singapore, Singapore, Singapore, [2]Molecular Medicine, University Malaya, Kuala Lumpur, Malaysia, [3]Pharmacology, National University of Singapore, Singapore, Singapore

Objective: Stroke forms one of the leading causes of death and disability worldwide. Our previous studies using animal models[1-2] and young stroke patients[3] have shown that microRNAs (miRNAs) present in peripheral blood are temporally regulated during cerebral ischemic conditions. The objective of this study is to find specific microRNAs that could be developed as novel therapeutic targets for treating cerebral ischemia.

Methodology:

miRNA profiling was performed using miRCURY LNA technology on blood samples from stroke patients and animal models (including brain tissue). The profiling results were further confirmed using quantitative stem-loop PCR. Target genes of the selected miRNAs were analyzed using mRNA arrays and quantitative real-time PCR. The positive interaction between the miRNA and its targets were shown using reporter binding studies. Modulation of miRNA expression in embolic animal models was carried out to understand the effect of the selected LNA based miRNAs. These studies were also conducted with rtPA treatment.

Results: Based on our profiling studies, several miRNAs and their target genes that are involved in endothelial dysfunction, dysregulation of neurovascular integrity, anti-angiogenesis, pro-apoptosis, inflammation and cytoskeletal remodeling have been identified. From these we have found that miR-320a, which regulates the expression of Aquaporins 1 and 4, serves as an excellent target to reduce ischemic infarct volume in animal models of stroke created by suture method. These observations were extended in this study for embolic stroke models. Modulation of miR-320a in such embolic stroke models also showed positive outcome. Moreover our studies show that combination therapy, using miR-320a and rtPA in embolic stroke models, results in better neurological outcomes compared to that of rtPA treatment alone.

Conclusion: miR-320a presents itself as a useful therapeutic target in cerebral edema. Our findings implicate a role for miR-320a as an universal therapeutic target for different forms of ischemia. More studies are needed to further evaluate and establish its importance in the treatment of cerebral ischemia.

References:

1. Jeyaseelan K, Lim KY, Armugam A. MicroRNA expression in the blood and brain of rats subjected to transient focal ischemia by middle cerebral artery occlusion. *Stroke.* (2008) **39**: 959-966.

2. Lim KY, Chua JH, Tan JR, Swaminathan P, Sepramaniam S, Armugam A, Wong PT, Jeyaseelan K. MicroRNAs in cerebral ischemia. *Transl. Stroke Res.* (2010) **1**: 287-303.

3. Tan KS, Armugam A, Sepramaniam S, Lim KY, Setyowati KD, Wang CW, Jeyaseelan K. Expression profile of microRNAs in young stroke patients. *PLoS ONE* (2009) **4**: E7689.

4. Sepramaniam S, Armugam A, Lim KY, Karolina D S, Swaminathan P, Tan JR, Jeyaseelan K. MicroRNA 320a functions as a novel endogenous modulator of aquaporins 1 and 4 as well as a potential therapeutic target in cerebral ischemia. *J. Biol. Chem.* (2010) **285:** 29223-29230.

1103

THE IMMEDIATE HEMODYNAMIC EFFECTS OF TDCS ON BRAIN ACTIVATION

C. Paquette, M. Sidel, B. Radlinska, A. Thiel

Neurology, McGill University at SMBD Jewish General Hospital & Lady Davis Institute for Medical Research, Montreal, QC, Canada

Introduction: Transcranial direct current stimulation (tDCS) is a non-invasive method used to modulate neuronal excitability in humans. This technique uses small direct currents applied through surface electrodes on the scalp affecting neuronal resting membrane potential(1). Anodal currents increase excitability while cathodal currents decrease excitability, resulting in increased or decreased amplitude of motor evoked potentials (MEP; 1, 2). These electrophysiological aftereffects are observed up to one hour following stimulation. Imaging studies using surrogate markers to measure this aftereffect of tDCS on rCBF over the motor cortex showed rCBF changes in widespread networks of motor-associated brain regions and not at the stimulation site(3-5). These widespread aftereffects observed at a network level might be secondary adaptations of the network to the previous stimulation rather than the direct effects of stimulation. The objective of this study was to determine the immediate effects of tDCS on resting- and activation-induced rCBF during stimulation rather than tDCS aftereffects, using a bilateral electrode mount in young healthy subjects.

Methods: tDCS electrodes were affixed on 9 healthy subjects (3 males; mean age: 28 years) with the cathode over the non-dominant M1 and anode over the dominant M1. Twelve scans of positron emission tomography (PET) were collected for each subject during a motor task (finger opposition task at 70bpm) with either hand, or no motor task. tDCS was turned on for 4 minutes (2mA) in half of the trials and sham tDCS was used in the remaining trials. 370 MBq of O-15 water radioactive tracer was injected 2.5 minutes after the start of real or sham tDCS. PET images were acquired in the last minute of tDCS. Activation images were calculated as difference images of rCBF change for contrast with the no finger task during sham. A 5cm diameter disk (1cm deep) was used as volume-of-interest at the center of each M1(6).

Results: *tDCS during movement:* Activation from finger movements was significantly decreased relative to sham stimulation during bilateral tDCS under the cathode (↓1.84 in Z-score, p=0.02). tDCS under the anode however, did not significantly differ from sham tDCS during finger movement (↑0.67 in Z-score, p=0.31). *tDCS only:* There was no significant effect of tDCS under the cathode or anode on rCBF (mean increase in Z-score< 2.0). Also, no change was observed in rCBF when contrasting tDCS stimulation versus sham tDCS with finger movements.

Conclusions: Activation-induced rCBF changes measured during tDCS differ from more wide-spread brain activity-related changes measured 5 to 60minutes after tDCS. It seems to be the interaction of tDCS with motor-induced change in activity that modulates rCBF change. Stimulation alone seems to have little effect if neuronal activity does not change between two activation states. This finding has implications for the use of tDCS as supportive treatment in post-stroke rehabilitation, since it suggests that therapy might be more effective during tDCS then with post-tDCS aftereffects.

References: (1)Nitsche *et al.*(2000)*JPhysiol* 527Pt 3:633-9. (2)Furubayashi *et al.*(2008)*ExpBrainRes* 185:279-86. (3)Baudewig *et al.*(2001)*MagnResonMed* 45:196-201. (4)Jang *et al.*(2009)*NeurosciLett* 460:117-20. (5)Lang *et al.*(2005)*EurJNeurosci* 22:495-504. (6)Thiel *et al.*(2006)*JCerebBloodFlowMetab* 26:1122-7.

1107

CRITICAL IMPORTANCE OF EARLY PERFUSION VARIATIONS ON TISSUE FATE DURING ACUTE CEREBRAL ISCHEMIA

H. An[1], A.L. Ford[2], C. Eldeniz[1], Y. Yang[1], Y. Chen[1], K.D. Vo[3], W.J. Powers[4], J.-M. Lee[2], W. Lin[1]

[1]Radiology, University of North Carolina at Chapel Hill, Chapel Hill, NC, [2]Neurology, [3]Radiology, Washington University in St. Louis, St. Louis, MO, [4]Neurology, University of North Carolina at Chapel Hill, Chapel Hill, NC, USA

Background: While the importance of early reperfusion on tissue salvage and neurological improvement in stroke patients is well-established. The impact of early worsening perfusion has not been systematically studied. In this study, we directly quantified the effect of both types of tissue perfusion changes within the first 6 hours of stroke onset on ultimate tissue outcome.

Methods: Sixteen tPA treated patients underwent three consecutive MR scans at 2.7 ± 0.7 hours (tp1), 6.4± 0.4 hours (tp2) and 1 month (tp3) after stroke onset. Dynamic susceptibility contrast (DSC) was performed to obtain mean transit time (MTT) maps at both tp1 and tp2. Final tissue infarction was defined using tp3 FLAIR and all scans were co-registered within individuals. MTT prolongation for each voxel was calculated as MTT - median MTT of the contralateral hemisphere. Tp1 and tp2 MTT prolongations ranging from 0 to 25 seconds were used to construct 26*26 bins with each bin representing a specific tp1 and tp2 MTT prolongation using 1-sec intervals. All voxels were combined from all patients for this analysis. The % of total voxels falling within each bin was calculated and plotted in Fig A. In addition, tissue survival rate was also calculated (# of surviving voxels/total # of all voxels within a specific bin) and plotted in Fig B.

Results:

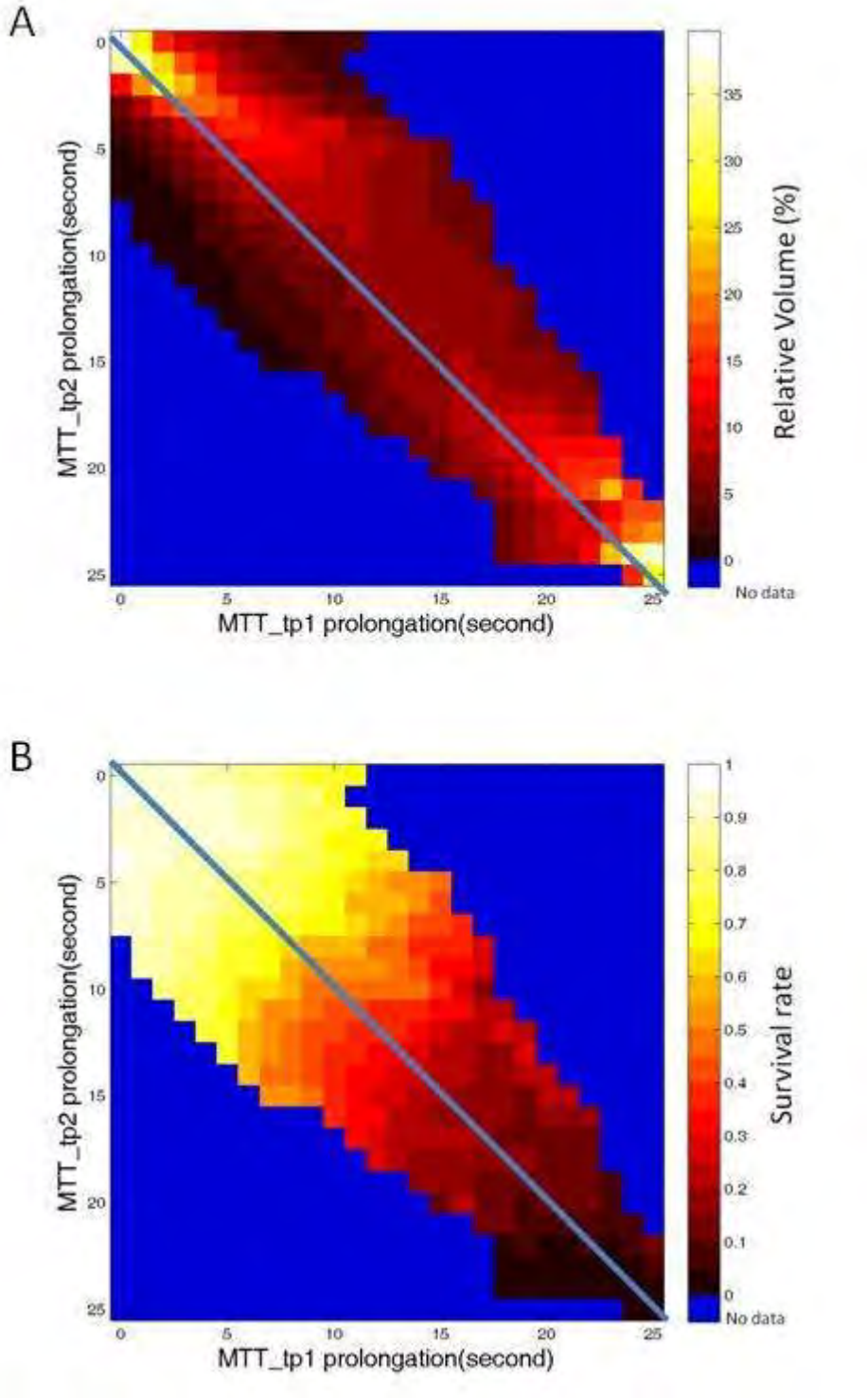

[Fig]

Fig. A shows the relative amount of tissue with a tp1 MTT which evolved to a corresponding tp2 MTT value (blue bins indicate no tissue with these values). The diagonal line indicates regions

in which MTT did not change. All bins above this line represent tissue with increased perfusion, while those below the line represent decreased perfusion. The figure demonstrates that perfusion changes in both directions are quite common during early ischemia despite that all patient received tPA treatment. Fig, B shows the tissue survival rate for each bin. At extremes of tp1 MTT values (< =4 sec or >20 sec) survival rates had little change regardless of the tp2 MTT values, suggesting that tissue outcome was already determined at tp1. On the other hand, voxels with intermediate values of tp1 MTT (5 to 20 sec) had highly variable tissue. Worsening perfusion was just as important as improved perfusion for determining tissue. For example, voxels with tp1 MTT=12 sec could either have a survival rate >80% if tp2 MTT improved to 3 sec, or have a survival rate < 30% if tp2 MTT worsened to 18 sec.

Conclusions: Within the first hours after ischemia, perfusion is highly dynamic. While perfusion changes do not affect outcome in tissue with extremely low or high initial perfusion, the ultimate fate of tissue with moderate perfusion deficits (MTT prolongation ranges from 5-20 sec) is highly dependent on both subsequent perfusion improvement or deterioration. These findings demonstrate for the first time the critical importance of worsening perfusion in determining tissue outcome in acute stroke patients treated with intravenous thrombolysis.

1108

PREDICTING THE IN VIVO UTILITY OF TSPO PET RADIOLGIANDS WITH BIOMATHEMATICAL MODELS THAT ACCOUNT FOR TSPO BINDING CLASSES

Q. Guo[1,2], D.R.J. Owen[1,2], I. Bennacef[2], C.A. Parker[2], E.A. Rabiner[1,2], F. Turkheimer[1], R.N. Gunn[1,2]

[1]Centre for Neuroscience, Imperial College London, [2]Clinical Imaging Centre, GlaxoSmithKline, London, UK

Objectives: ^{11}C-PK11195, the most widely used TSPO imaging probe, suffers from high non-specific binding and low signal to noise ratio. New radioligands have been developed with higher affinity and/or lower nonspecific binding, however unlike ^{11}C-PK11195, they have been shown to bind in vitro to two sites with differing affinity. Individuals fall into one of three binding classes, namely high (HABs), low (LABs) or mixed (MABs) affinity binders [1,2]. Here, we simulated the binding of 4 radioligands (^{18}F-PBR111, ^{11}C-PBR28, ^{11}C-DPA713 and ^{11}C-PK11195) in humans using biomathematical models, in order to evaluate their performance in within-subject (e.g. longitudinal studies) and between-subject (e.g. disease characterisation) studies in the presence and absence of TSPO binding class information.

Methods: The within-subject variability for each ligand was assessed in terms of their reproducibility of the in vivo binding potential (%COV[BP_{ND}]). Biomathematical modelling predictions [3] of %COV[BP_{ND}] derived from in silico/in vitro data were obtained for each TSPO binding class at normal and diseased states (50% density increase). To evaluate the between-subject variability, the minimum sample sizes (90% power) required for each ligand to distinguish healthy controls and patients were determined. When the subjects' binding class information is unavailable, we estimated the sample sizes by simulating the binding potential of a large population of controls and patients, with a mixture of binding classes (HAB:MAB:LAB=62:32:6). We also simulated the population for each binding class separately and estimated the corresponding sample sizes required when prior knowledge of the binding class exists.

Results: The within-subject variability for ^{18}F-PBR111, ^{11}C-PBR28 and ^{11}C-DPA713 (2.4% to 7.8%) was significantly lower than ^{11}C-PK11195 (20% to 45%) for HABs and MABs at both normal and diseased states. The %COV[BP_{ND}] values of all the ligands for LABs are above 10%.

Sample sizes required to detect 50% differences in TSPO density between two groups are presented in Table 1. When binding class information is available, the novel ligands allow sample sizes 3-fold lower than ^{11}C-PK11195, but without it, the sample sizes required for all the ligands are similar.

Conclusions: Biomathematical models predict that ^{18}F-PBR111, ^{11}C-PBR28 and ^{11}C-DPA713 will be better ligands than ^{11}C-PK11195 for both longitudinal studies and disease characterisation if binding class information is known a priori, due to their lower within-subject variability. Ongoing studies are investigating whether TSPO binding class can be identified through a peripheral blood assay.

References:

1. Owen et al. NeuroImage 2010; 52:S30

2. Owen et al. JCBFM 2010;,30:1608-1618

3. Guo et al. JNM 2009; 50:1715-1723

Radioligands	TSPO binding class info is unknown	TSPO binding class info is known		
	ALL	HAB	MAB	LAB
^{18}F-PBR111	23	10	10	18
^{11}C-PBR28	32	10	10	16
^{11}C-DPA713	29	10	10	23
^{11}C-PK11195	29	30	29	26

[Sample sizes required to detect 50% increase]

1109

IN-VIVO ABETA CONCENTRATIONS LINKED TO DECREASE IN ENERGY SUPPLY IN ALZHEIMER´S DISEASE

A. Rodell[1], J. Aanerud[1], A. Gjedde[2]

[1]PET-Centret, Aarhus Sygehus, Aarhus, [2]Department of Neuroscience and Pharmacology, Copenhagen University, Copenhagen, Denmark

β-amyloid (Abeta) products are of intense interest as implicated in Alzheimer´s disease (AD), both in relation to Abeta plaque deposits and in upstream products such as Abeta oligomers.

The dye [^{11}C]Pittsburg Compound B (PIB) is an emerging radiotracer for imaging of Abeta plaque load. However, as a considerable number of healthy human volunteers have buildup of Abeta plaques without apparent disease or cognitive decline, we suggest that Abeta plaque formation is one only of multiple factors influencing the development of AD. The plethora of risk factors predisposing to AD is broad but includes a wide variety of mechanisms also implicated in vascular diseases. We therefore investigated the possible links between the formation of Abeta products in the human brain and factors governing the cerebral blood flow (CBF) and metabolism by means of Positron Emission Tomography (PET). The tracers used were [^{11}C]PIB, [^{15}O]H_2O, and [^{15}O]O_2. Healthy aged controls (HC, n=8) and patients suffering from AD (n=6) underwent PET and we derived parametric images from the tomography to obtain quantitative measures of binding potential or rate constants for the radiotracer uptake. The effect of CBF on the PIB quantification is apparent as is the intrasubject variability stemming from variations of pCO_2.

We use a novel method for extracting semiquantitative CBF measures directly from the [^{11}C]PIB dynamic uptake curves alongside the binding potential, eliminating future needs for both CBF and PIB tomography for this analysis.

The results reveal highly significant ($p=0.0018$) reduction of cortical CBF in AD compared to healthy aged subjects, while the K1 of oxygen transfer into the tissue remained relatively constant. These relations gave a significant ($p=0.013$) increase of oxygen extraction fraction in cerebral cortex in AD compared to HC. This finding is in concordance with the theory that AD is linked to aberrations in brain energy metabolism and vascularisation. It also raises the possibility that at high concentrations Abeta acts as a neurotrophic factor, which, in conjunction with high extraction of oxygen, could lead to apoptosis imposed by excessive mitochondrial ROS signalling.

1110

DELTA PROTEIN KINASE C MODULATES PRESYNAPTIC TARGETS OF CORTICAL MICROVESSELS IN VIVO

H.W. Lin, R.A. DeFazio, K.C. Morris, S.V. Narayanan, V.L. Gresia, K.R. Dave, J.W. Thompson, M.A. Perez-Pinzon

Neurology, University of Miami, Miami, FL, USA

Protein kinase isozymes mediate signal transduction pathways, including the fate of neuronal cell survival. Our previous studies suggest that protein kinase C delta (deltaPKC) enhanced apoptosis in hippocampal neurons by activation of caspase-3 activity following cerebral ischemia. In addition, rats pretreated with the selective deltaPKC inhibitor (deltaV1-1) induced attenuation of latent hypoperfusion 24 hrs after asphyxial cardiac arrest (ACA) and afforded neuroprotection in the rat hippocampus and cortex regions 7 days after ACA. In order to define the vascular target(s) of deltaPKC modulation of cerebral blood flow (CBF), the rat skull was thinned to visualize red blood cell speed (an indicative measure of CBF) in microvessels of the neocortex via 2-photon microscopy. We tested the hypothesis that deltaPKC inhibited nitric oxide (NO)-mediated vasodilation modulating CBF. L-arginine (L-arg, 100 mg/kg) infusion (IV) enhanced CBF by serving as a substrate for NO synthesis in presynaptic terminals to cerebral vessels. As expected, infusion of L-arg increased flow by 46 ± 25 %. Since sodium nitroprusside (SNP, 0.75 mg/kg, a nitric oxide donor) bypasses NO synthesis in the presynaptic terminal and directly elevates NO levels within vascular targets, infusion with SNP also increased CBF (90 ± 32 %). To evaluate the role of deltaPKC, we pretreated the rat with deltaV1-1. After deltaV1-1 treatment, L-arg infusion significantly increased CBF compared to L-arg alone (312 ± 70.3 %), while the response to SNP was minimal (4.75 ± 37.2 %). The enhanced CBF response to L-arg after deltaV1-1 treatment suggests that deltaPKC may be a tonic modulator of NO-mediated vasodilation during delayed hypoperfusion after cerebral ischemia. The presence of L-arg plus deltaV1-1 but not SNP plus deltaV1-1 treated rats enhanced cortical CBF suggesting that deltaPKC is acting on presynaptic targets by enhancing presynaptic NO production via the L-arg to L-citrulline NO synthase pathway, while inhibiting postsynaptic targets of NO in cortical microvessels. Since NO signaling is also largely derived from sympathetic outflows to the brain, we examined the superior cervical ganglion (SCG), the origin of sympathetic innervation of cerebral arteries. Western blots were performed suggesting the presence of deltaPKC in the SCG, further defining a possible role in cerebral vascular (sympathetic) innervation in the brain. These results suggest the therapeutic potential of deltaV1-1 in providing neuroprotection by regulating CBF through NO modulation during cerebral ischemia.

1111

SERUM SDF1-A LEVELS SIGNIFICANTLY INCREASE FOLLOWING STROKE AND ARE ASSOCIATED WITH INCREASED HEMATOPOETIC STEM CELL MOBILIZATION

A. Afzal[1], S. Ansari[1], C.P. Kellner[2], S.A. Sosunov[2], B.L. Hoh[1], E.W. Scott[3], E. Connolly[1], J. Mocco[1]

[1]Neurosurgery, University of Florida, Gainesville, FL, [2]Neurosurgery, Columbia University, New York, NY, [3]Molecular Genetics and Microbiology, University of Florida, Gainesville, FL, USA

Background: Hematopoietic Stem Cells (HSC)/ Hematopoietic Progenitor Cells (HPC) have recently been demonstrated to correlate with improved neurological function following stroke, suggesting a potentially critical role for HSC/HPC's in limiting stroke injury and/or facilitating stroke recovery. HSC/HPC's are known to mobilize to the peripheral circulation from bone marrow in response to stroke. Stromal Derived Growth Factor 1-Alpha (SDF1-A) along with its receptor CXCR4 is a potent chemo attractant released by areas of injury. SDF1-A has been shown to mobilize HSC/HPC from the bone marrow to the blood and lead to 'homing' of the cells to an area of injury.

Methods: Animals underwent a murine intraluminal filament model of focal cerebral ischemia. Animals were divided into 4 groups (n=5 each): 4hrs sham surgery, 4hrs post reperfusion, 24hrs sham surgery, and 24hrs post reperfusion. Neurological deficit score was recorded prior to euthanasia and serum SDF1-A was assessed in all groups. HSC/HPC were enriched using nanoparticles tagged with LIN negative and SCA1 positive markers and counted on a hemacytometer.

Results: Serum SDF1-A levels were elevated at 4hrs and 24 hours compared to sham controls (107±3.8% and 137±11% versus 100±0.04% and 100±0.06%, respectively; 4hrs vs sham: P=NS, 24hrs vs sham: $p< 0.05$). Bone marrow showed an increased production of HSC/HPC at 4 hrs (106±26%) and significantly higher at 24 hrs (272±35%). Mobilization of the HSC/HPC was slightly higher at 4 hrs (167±26%) and significantly higher at 24 hrs (606±91%; $P< 0.05$). Neurological deficit score at 4hrs and 24hrs post reperfusion were 1.846±0.21 and 2.04±0.178, respectively.

Conclusions: Serum SDF1-A levels significantly increased following cerebral ischemia, leading to increased mobilization of HSC/HPC from the bone marrow to the blood. These data suggests that SDF1-A mobilization of HSC/HPC in response to cerebral ischemia may be a relevant pathway for cerebral injury repair following stroke.

1114

COMBINED EFFICACY OF ANTI-OXIDANT AND ANTI-APOPTOTIC INTERVENTIONS FOLLOWING HYPOXIA/REOXYGENATION IN B50 NEURONAL CELLS

E.N.J. Ord[1], R. Shirley[1], C. McCabe[2], I.M. Macrae[2], A.H. Baker[1], L.M. Work[1]

[1]Institute of Cardiovascular and Medical Sciences, [2]Institute of Neuroscience and Psychology, University of Glasgow, Glasgow, UK

Objectives: We propose that a combined intervention strategy, involving neuroglobin (Ngb) overexpression and JNK inhibition using a novel gene- and drug-based system, will have a greater beneficial effect following cerebral ischaemia than either agent alone. Efficacy has been determined in vitro using a hypoxia/reoxygenation model.

Methods: A lentivirus was generated to overexpress neuroglobin under the control of the spleen focus-forming virus (SFFV) promoter. B50 neuronal cells were placed in a hypoxic chamber (1% O_2, 5% CO_2, balance N_2) with serum starvation for 9 h before 24 h reoxygenation in complete media. Cells were either left untreated, pre-treated with lenti-Ngb or a control reporter gene (green fluorescent protein, GFP) expressing virus, lenti-GFP (MOI 5 virus particles/cell for 4h, 48h prior to hypoxia), the JNK inhibitor, SP600125, alone (20μM, 30 mins prior and immediately after hypoxia) or with combined treatments. Cell viability and oxidative stress assays were then performed. Experiments were performed on three independent occasions and results are shown as mean ± s.e.m. Electron paramagnetic resonance (EPR) was used to measure extracellular superoxide production for 60 mins at the end of the 24 h reoxygenation period. EPR utilises a CPH spin probe, that when oxidised forms the nitroxide CP radical, this CPH to CP radical conversion is measured by the spectrometer giving a reading in counts/minute normalised to protein. A malondialdehyde (MDA) assay was used as a surrogate marker of oxidative stress through lipid peroxidation.

Results: Hypoxia resulted in a 1.5 fold increase in superoxide generation compared to normoxic cells (Fig 1A). Lenti-GFP, DMSO (vehicle) and SP600125 had no effect on superoxide production it was significantly lowered by lenti-Ngb (Fig 1A). The combined treatment with lenti-Ngb and SP600125 further lowered superoxide to the levels of the time-matched normoxic control cells (Fig 1A). In contrast to EPR data each therapy alone and in combination lowered MDA levels maximally from hypoxic cells with treatments restoring levels to that of the time-matched normoxic cells (Fig 1B).

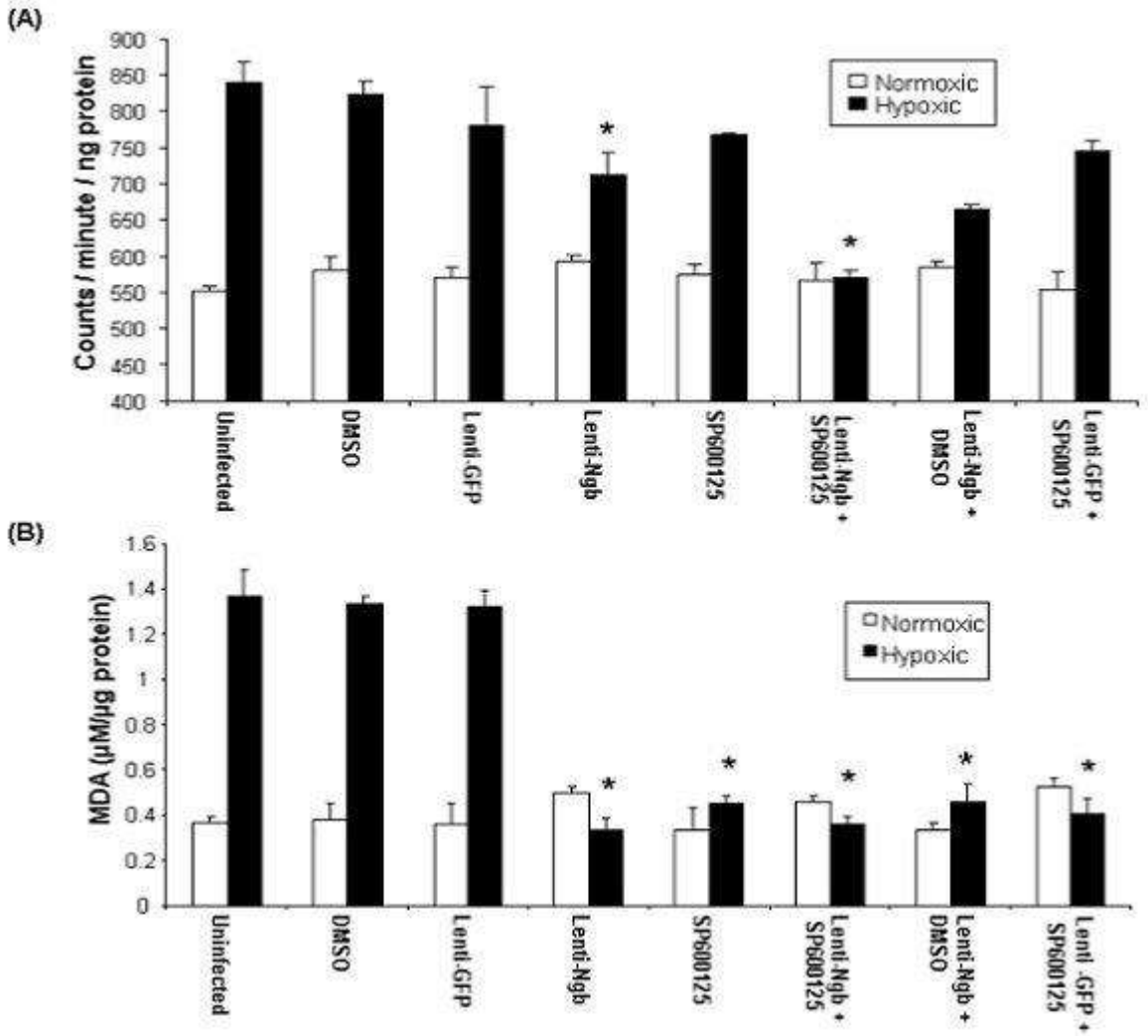

[EPR & MDA]

Figure 1: The effect of Ngb overexpression, JNK inhibition or their combination was assessed using (A) EPR to determine effects on superoxide generation or (B) MDA assay for assessment of lipid peroxidation. *p< 0.05 vs. uninfected hypoxic control.

Apoptosis was determined by caspase 3 immunocytochemistry, where following hypoxia the caspase 3 localises to the nucleus. Singular treatments with SP600125 or lenti-Ngb lowered levels of caspase 3 nuclear expression but in concordance with the other assays, the combination therapy reduced levels of caspase 3 to that of normoxic cells.

Conclusions: These in vitro data demonstrate that combined therapy results in a significant reduction in the effects of hypoxia/reoxygenation injury on neuronal cells across a variety of assays. In conclusion, we have completed a comprehensive in vitro study showing a more than additive effect of our combination therapy across a variety of assays. In vivo studies are ongoing

to assess the single and combined efficacy of Ngb overexpression or JNK inhibition in male SHRsp rats following transient MCAo.

1115

INCLUDING THE EFFECTS OF HYPOXIA IN SIMULATIONS OF NEURAL NETWORKS

B.-J. Zandt[1,2], S. Visser[2,3], M. Cloostermans[2,4], B. ten Haken[1,2], M.J.A.M. van Putten[2,4]

[1]LT-Biomagnetism, University of Twente, [2]MIRA-Institute for Biomedical Technology and Technical Medicine, [3]Applied Analysis & Mathematical Physics, [4]Clinical Neurophysiology, University of Twente, Enschede, The Netherlands

Objectives: The network properties of neurons are essential for the proper functioning of the brain. The energy needed for the signalling processes of the neurons is provided by the oxygen and sugar in the blood. An insufficient supply of energy (ischemia) to the brain will hamper the workings of the synapses and the molecular ion-pumps [1], which in turn will alter the signaling properties of the neurons. In that case, we expect the network to show changes in activity, both in amplitude and frequency, which can be visible in EEG or MEG. In this project, which is part of the PID-ON project "ViP-Brain Network", we want to investigate the possibilities for new diagnostic methods for pathologies related to ischemia. On this poster, we will present our approach and work in progress.

Methods: We build a model of network activity during hypoxia, by calculating the oxygen distribution in a volume of tissue, and modify an existing neural simulation by altering neuron behavior depending on the oxygen concentration.

The oxygen distribution in the cortex is calculated by modeling the supply from the blood vessels and the diffusion through the tissue. Oxygen distributions will be different in each layer of the cortex, because the layers have different microvascular densities. [2] This may be important to take into account, because the layers contain different types of neurons (e.g. inhibiting/exciting). A realistic microvascular structure is constructed from optical measurements on slices of human cortex.

In a simulation of a neural network [3] in the human cortex, the ionic concentrations [4] and synaptic potentials [1] will be changed to alter the electrophysiological behavior of the neurons that are supplied with insufficient oxygen. With this, the activity of a neural network located in hypoxic tissue, and the resulting EEG, can be simulated.

Results: A model is obtained with which the effects of insufficient blood supply on neural activity can be calculated.

Conclusions: A start was made in building a computational model of a neural network suffering from hypoxia. This model will be used to find markers for hypoxia in EEG or MEG. Preliminary conclusions will be presented on the poster.

References:

[1] Krnjevic, 1999, Early Effects of Hypoxia on Brain Cell Function, CMJ 40(3):375-380

[2] Cassot, 2006, A Novel Three-Dimensional Computer-Assisted Method for a Quantitative Study of Microvascular Networks of the Human Cerebral Cortex, Microcirculation, 13: 1-18

[3]Visser, 2010, Comparing Epileptiform Behavior of Mesoscale Detailed Models and Population Models of Neocortex, J.of Clinical Neurophysiology: Volume 27 - Issue 6 - pp 471-478

[4] Dronne, 2003, A Mathematical Study of Volume Shifts and Ionic Concentration Changes during Ischemia and Hypoxia, J. theor. Biol. (2003) 220, 83-106

1116

EFFECT OF HYPOXIA ON MICRORNA EXPRESSION IN RAT CORTICAL PERICYTES

P. Dore-Duffy[1], J. Treuttner[2], W.D. Dietrich[2], V. Katyshev[3]

[1]Neurology, Wayne State University, Detroit, MI, [2]Neurological Surgery, Miller School of Medicine, University of Miami USA, Miami, FL, [3]Neurology, Wayne State University School of Medicine, Detroit, MI, USA

kMicrovascular adaptation to environmental stress is important in the maintenance of tissue homeostasis. Nowhere is this more important than in the central nervous system (CNS). Recently the role of microRNAs (miRNAs) in modulating gene expression post-transcriptionally has been shown to be of major importance in cellular responses to injury. MiRNAs are small 19-25 nt noncoding RNAs that regulate gene expression post-transcriptionally by targeting mRNA for degradation and/or translational repression. MiRNAs have been found to play an important regulatory role in cell differentiation, growth and proliferation, cell cycle, lineage determination, and metabolism. We have questioned the role of miRNAs in the CNS capillary pericyte response to hypoxic stress. Micro array analysis (LC Sciences, Houston, Tx) was used to examine the expression of 444 rat miRNAs in primary rat cortical pericytes with and without exposure to low oxygen (1%) for 3 hr, 24 hr, or 48 hr. Changes in levels of miRNAs after hypoxia were compared to control, normoxic cultures. Pericytes subjected to hypoxia for 24 hr showed 19 miRNAs that were higher than control and 31 that were lower. After 48 hr of hypoxia, 27 miRNAs were increased and 31 were decreased. Further validation and quantification was performed by Real Time RT-PCR on several of the miRNAs of interest from the arrays. MiR-145, expressed in pericytes, was the most highly enriched (up to 346% of control). miR-140* was the most decreased (26% of control at 3 hr). miR-140 on the opposite strand, targets Smad3 and suppresses the TGF-β pathway. miR-24, which is known to be associated with the microvasculature, was reduced at both the 24 hr and 48 hr times. miR-345-5p was increased and targets genes involved in the cell cycle and protein localization. Systematic and integrative analysis of possible gene targets analyzed by DAVID (the database for annotation, visualization and integrated discovery) bioinformatics resource (http://david.abcc.ncifcrf.gov) for some of these miRNAs will help determine possible gene targets and pathways that may be affected by the post-transcriptional changes after hypoxic insult.

1118

AQUAPORIN-4 SINGLE NUCLEOTIDE GENOMIC VARIANT AS A PREDICTOR OF WORSE FUNCTIONAL OUTCOME AFTER INTRACEREBRAL HEMORRHAGE

G. Appelboom[1], M. Piazza[1], A. Bratt[1], A. Duren[1], S. Smith[1], A. Carpenter[1], R. Hwang[1], S.A. Mayer[2], E.S. Connolly[1]

[1]Neurosurgery, [2]Neurocritical Care, Columbia University, New York, NY, USA

Introduction: Intracerebral hemorrhage (ICH) remains the deadliest form of stroke, and effective treatments that improve clinical outcome are currently lacking. The identification of common genomic variants may serve as predictors of poor outcome after ICH that would facilitate appropriate risk stratification for clinical trials as well as potential therapeutic targets. Aquaporin-4 (AQP-4) is the most common permeable water channel of the central nervous system. Studies have demonstrated the importance of AQP-4 in edema formation post-ICH. Recent studies have demonstrated a link between single nucleotide polymorphisms (SNP) rs9951307 and edema formation in ischemic stroke. We hypothesize rs9951307 may be associated with worse clinical outcome post-ICH.

Methods: Patients admitted to the Columbia University Medical Center Neurological Intensive Care Unit with spontaneous, hypertensive ICH and enrolled in the Intracerebal Hemorrhage Outcomes Project (ICHOP) during February 2009 and May 2010 were included in this study. DNA was extracted and purified from buccal swabs using standard techniques; PCR amplification and sequencing of rs9951307 was performed using previously published primers. Demographic, clinical, radiographic, and outcome data were prospectively collected. Functional outcome at discharge was assessed using modified Rankin Scale (mRS) dichotomized as 1-2 vs. 3-6. Chi-square, Fisher's Exact, and independent t-Test were used for comparison of clinical variables with outcome.

Results: Sixty-four consecutive patients with spontaneous, hypertensive ICH were prospectively enrolled in ICHOP. Genetic samples were obtained from fifty-one patients. Median age was 61; 35% of patients were female. Mean admission Glasgow Coma Scale (GCS) score was 10.5±4.2. 11.8% of a patients were homozygous for the GG genotype, 49.0% were heterozygotes, and 39.2% were homozygous for the AA genotype. 84.3% of patients had poor outcome at discharge. The presence of the G allele was associated with poor outcome ($p=0.045$) at discharge with an OR of 6.21 (95% CI 1.24-30.2). Furthermore, admission GCS (15.0±0.0 vs. 9.65±4.0, $p=0.001$) and hematoma size (4.10cc±4.15cc vs. 25.1cc±26.3cc, $p=0.03$) differed among patients with mRS 1-2 vs. 3-6, respectively, while age ($p=0.105$), admission intraventricular hemorrhage ($p=0.24$), and admission hydrocephalus ($p=0.053$) were not associated with poor outcome.

Conclusion: The precise mechanism by which AQP-4 influences the pathophysiology of ICH is not well understood. AQP-4 is largely expressed at the glial membrane in astrocytic processes adjacent to cerebral capillaries and pial membranes lining the subarachnoid space. Following ICH, expression of AQP-4 is upregulated in astrocytic foot processes and is believed to facilitate water movement into and out of the cerebral tissue, thus critically defining brain edema volume. Moreover it has been implicated in cerebral response to brain injury through astrocyte migration, neuronal activity, and increased neurogenesis. An alteration in its function would also lead to increased excitotoxicity in the setting of massive K+ release following erythrocyte lysis. Further studies are needed to capture the exact alteration in AQP-4's function, but this study underscores its importance in the secondary injury following ICH. Moreover, the presence of this

genotype may allow identification of individuals at high risk for poor functional outcome after ICH and could be a potential therapeutic target if confirmed in larger studies.

1119

THE EFFECT OF CAFFEIC ACID PHENETHYL ESTER ON PERACUT ISCHEMIA-REPERFUSION INJURY IN RAT BRAIN

M.E. Altuğ[1], I.M. Melek[2], S. Erdoğan[3], V. Düzgüner[3], A. Öztürk[1], A. Küçükgül[3]

[1]Dept. of Surgery, Faculty of Veterinary Medicine, [2]Dept. of Neurology, Tayfur Ata Sökmen Medical School, [3]Dept. of Biochemistry, Faculty of Veterinary Medicine, Mustafa Kemal University, Hatay, Turkey

Objectives: The aim of the present study was to investigate the effects of caffeic acid phenethyl ester (CAPE) on cyclic AMP (cAMP) levels and cAMP-phosphodiesterase 4 (PDE4) transcripts, oxidative and antioxidative events in ischemia-reperfusion (I/R) injured rat brains.

Methods: Cerebral ischemia was produced in ischemia (n=7) and ischemia + CAPE groups (n=7) by bilateral occlusion of common carotid arteries (BCCA) for 30 min followed by reperfusion. Rats in control group (n=7) were underwent only surgical intervention. The rats were sacrificed 24 h after I/R. CAPE was administered intraperitoneally to the treatment group at the dose of 15 μmol kg^{-1} twice, 1 h before occlusion and at 12^{th} h of reperfusion. Glutathione peroxidase (GSH-Px), catalase (CAT) and superoxide dismutase (SOD) and xanthine oxidase (XO) activities, nitric oxide (NO) and malondialdehyde (MDA) levels were analyzed in the cerebral cortex homogenates. The cAMP concentrations were analyzed by ELISA and PDE4 isozyme mRNA transcriptions were evaluated by RT-PCR methodology. Neurological evaluations were performed 24 h after the onset of ischemia-reperfusion, or sham operation using a neurologic deficit score (NDS) as described previously (Geocadin *et al*., 2000; Brambrink *et al*., 2006; Zhou et *al*., 2010).

Results: The neurological evaluations showed that CAPE non-significantly reduced the neurological deficit scores compared with the ischemia group. Ischemia-induced nitric oxide (NO) production was significantly attenuated by CAPE administration in the cerebral cortex ($p< 0.05$). There was a decrease in brain homogenate's CAT ($p>0.05$) and GSH-Px activities ($p< 0.05$) along with increase in SOD ($p< 0.01$) and XO ($p< 0.005$) activities in the ischemia group compared to control after 24 h of reperfusion. CAPE treatment significantly enhanced GSH-Px activity ($p< 0.05$), while SOD, XO and CAT activities remained unaffected compared to ischemia group. CAPE treatment unchanged cerebral intracellular cAMP levels but it decreased PDE4A and PDE4B transcripts by 1.2 and 2.3-folds, respectively, and PDE4D was not changed in the brain cortex.

Conclusions: These results suggest that CAPE administrations slightly modulate the antioxidant defense system and NO release of rat brain during peracute transient global cerebral ischemia-reperfusion injury, without changing second messenger cAMP levels.

Key words: global cerebral ischemia-reperfusion, caffeic acid phenethyl ester, antioxidant activity, cAMP-phosphodiesterase 4 (PDE4)

References:

Zhou Q, Cao B, Niu L, Cui X, Yu H, Liu J, Li H, Li W. Effects of permissive hypercapnia on transient global cerebral ischemia-reperfusion injury in rats. Anesthesiology 2010; 112:288 -97

Brambrink AM, Koerner IP, Diehl K, Strobel G, Noppens R, Kempski O: The antibiotic

erythromycin induces tolerance against transient global cerebral ischemia in rats (pharmacologic preconditioning). Anesthesiology 2006; 104:1208 -15

Geocadin RG, Ghodadra R, Kimura T, Lei H, Sherman DL, Hanley DF, Thakor NV: A novel quantitative EEG injury measure of global cerebral ischemia. Clin Neurophysiol 2000; 111:1779 - 87

1120

ISSUES FOR CBF QUANTIFICATION IN CAROTID ARTERY DISEASE

K. Jann[1], M. Hauf[2], F. Kellner-Weldon[2], M. El-Koussy[2], R. Wiest[2], A. Federspiel[1], G. Schroth[2]

[1]Department of Psychiatric Neurophysiology, University Hospital of Psychiatry / University of Bern, [2]University Institute of Diagnostic and Interventional Neuroradiology, Inselspital / University of Bern, Bern, Switzerland

Arterial spin labeling (ASL), a non-invasive MR method to quantify cerebral perfusion (cerebral blood flow; CBF), is of increasing interest not only in basic research but also in diagnostic applications. In carotid artery disease (CAD) the application of ASL provides similar information about altered perfusion in vascular territories like PET (Bokkers et al. 2010). Furthermore, the assessment of ASL during the administration of a vasodilatory agent allows the calculation of the cerebro-vascular reserve (CVR). However, during our ongoing work investigating perfusion and CVR in patients with CAD we encountered several critical issues for quantification as well as interpretation of results. Conventionally, in CAD CBF is calculated for flow territories of main feeding arteries but often the watershed areas are ignored although they frequently show the first effects related to diminished CBF and CVR. Furthermore, calculation of CBF is rarely corrected for white matter voxels although white matter is known to have higher transit times and the validity of ASL signal in white matter is debatable (van Gelderen et al. 2008; van Osch et al. 2009).

To account for these issues we adapted out analysis routine to provide WM corrected CBF and CVR values. To this end we segmented the T1 weighted images into gray and white matter using the segmentation batch implemented in SPM8 that then served as masks for CBF quantification in the flow territories. This step also excluded non brain tissue voxels at the boarders form analysis. Analysis was performed in the main vascular territories according to Tatu et al. (1998) and additionally in watershed territories of the middle cerebral arteries (MCA).

WM and non-brain voxel correction increased the CBF value in all analysed flow territories in hemisphere without upstream stenosis. In the hemisphere with highgrade carotid stenosis CBF showed a reduction of 4 ml/100g/min in the MCA territories. At first this seems contradictory since WM voxels usually have lower CBF values. However, CBF values in WM often are focally extremely high most likely resulting from labeled blood in arteries that has not yet perfused the parenchyma due to prolonged transit times (Kluytmans et al. 2008), which leads to an overestimation of perfusion. Furthermore, CVR values were more pronounced after WM correction. Correction for CBF and CVR values originating only from GM voxels removes artificial signals and thus increases validity of the quantification.

With respect to flow territories the watershed areas seem to be a better indicator of pathological alterations than conventional vascular territories (compare Abstract by Hauf et al.) and CBF in watershed areas might be the most promising marker for cognitive impairments (Abstract by Kellner-Weldon et al.).

References:

Bokkers et al. (2010) J Cereb Blood Flow Metab. 30(1):222-9

Tatu et al. (1998) Neurology 50:1699-1708

Kluytmans et al. (1998) J Magn Reson Imaging 8(4):767-74

van Gelderen et al. (2008) Magn Reson Med 59(4):788-95

van Osch et al. (2009) Magn Reson Med 62(1):165-73

This study was partially financed by the Swiss National Science Foundation: SPUM Consortium (33CM30-124114).

1122

DIAGNOSTIC ULTRASOUND AND SONOVUE OPEN THE BLOOD-BRAIN BARRIER AND ITS EFFECT ON COGNITIVE FUNCTION IN RATS

L. Zhang[1], Q. Wang[1], X. Zhou[2], H. Su[2], S. Wang[1], Z. Zhang[2], B. Wang[1], L. Xiong[1]

[1]Department of Anesthesiology, [2]Department of Ultrasound, Xijing Hospital of the Forth Military University, Xi'an, China

Objectives: The objective of this work was to investigate the recovery time of the change of the blood-brain barrier's permeability by diagnostic ultrasound and contrast agent in rat, and determine whether the opening could affect the cognitive ability.

Materials and methods: All animals were anesthesed by Phenobarbital, the hair of the right eye to ipsilateral ear to the top of skull was removed before treatment. The SonoVue was administrated intravenously at the dosage of 7 ml/ kg, and the ultrasound was delivered to rat brain at 1. 3 mechanical indexes (MI) for 10 minutes, then the permeability of the BBB was investigated at different times after the contrast imaging by evans blue dye exudation . Morris water maze was used for assessing the spatial learning and memory 24 hours after the treatment. Arterial blood gas samples were obtained at three time points: before the SonoVue injection, right at 5mins of the ultrasound exposure, after the treatment. The cerebral blood flow was measured before ultrasound exposure with SonoVue and after the treatment.

Results: Evens blue could be detected in the local brain after the contrast imaging and the permeability' change recovered in 6 hours ($P< 0.05$). The escape latency and pathlength to the platform decreased compared to the control groups ($P< 0.05$). Ph, PaO_2, $PaCO_2$ were no different among the three time points ($P>0.05$).Cerebral blood flow increased after contrast imaging ($P< 0.05$).

Conclusions: Blood-brain barrier could open after diagnostic ultrasound and contrast agent in rat. The cognitive function was improved after ultrasound with SonoVue. Arterial blood gas is not affected. Cerebral infusion improves after the treatment.

1123

TISSUE PLASMINOGEN ACTIVATOR IMPAIRS STEM CELL FUNCTION, THUS LIMITING RECOVERY FOLLOWING STROKE

A. Afzal[1], S. Ansari[1], C.P. Kellner[2], S.A. Sosunov[2], B. Hoh[1], E.W. Scott[3], E.S. Connolly[2], J. Mocco[1]

[1]Neurosurgery, University of Florida, Gainesville, FL, [2]Neurosurgery, Columbia University, New York, NY, [3]Molecular Genetics and Microbiology, University of Florida, Gainesville, FL, USA

Background: Intravenous Tissue Plasminogen Activator (tPA) is the only FDA approved pharmacological recanalization therapy for stroke, however tPA has been associated with deleterious effects on the blood brain barrier in experimental models. A potential contributor to vascular integrity and/or repair following stroke are Hematopoietic Stem Cells (HSCs)/ Hematopoietic Progenitor Cells (HPCs), circulating bone marrow derived mononuclear cells that promote repair in areas of injury. HSC/HPC's have recently been shown to mobilize to the peripheral circulation from bone marrow in response to stroke. Furthermore, increasing levels of circulating HSC/HPCs have been demonstrated to correlate with improved neurological function following stroke, suggesting a potentially critical role for HSC/HPC's in limiting stroke injury and/or facilitating stroke recovery. Stromal Derived Growth Factor 1-Alpha (SDF1-A) along with its receptor CXCR4 is a potent chemo attractant released by areas of injury. SDF1-A has been shown to mobilize HSC/HPC from the bone marrow to the blood and lead to 'homing' of the cells to an area of injury. We hypothesized that tPA inhibits HSC/HPC's function, potentially limiting tPA's beneficial effects in acute stroke therapy.

Methods: Animals (n=10) were euthanized 24 hours post ischemia/reperfusion following a murine intraluminal filament model. Infarction was confirmed using TTC staining of 2 mm sections of the brain. HSC/HPC were harvested from bone marrow and blood using LIN negative and SCA1 Positive labeled nanoparticles. The harvested cells were counted using a hemacytometer; the HSC/HPC were then either left untreated or treated with 10nM TPA and migrated towards SDF1-A in a Boyden Chamber. The level of the SDF1-A receptor (CXCR4) was also assessed by real time PCR of the untreated and tPA treated HSC/HPC. Experiments, and their analysis, were performed in a blinded manner.

Results: Mean infarct volume was 43±10%. Pre-treatment with 10nM tPA reduced HSC/HPC migratory capability towards SDF1-A (100±1.3% versus 173±1.0%, $p< 0.05$). Pre-treatment with 10nM tPA also reduced expression of CXCR4 from 100±7.9% to 35.8±7.1%, $p< 0.05$).

Conclusion: These data indicate that exposure of HSC/HPC's to tPA abrogates their migratory response to SDF1-A. mRNA analysis of HSC/HPC cells following treatment with tPA demonstrates a down regulation of the CXCR4 receptor. These results suggest that tPA may reduce the ability of the HSC/HPC to home to ischemic brain following stroke and possibly interferes with repair mechanisms associated with HSC/HPC.

1124

P-GLYCOPROTEIN OVEREXPRESSION IN PATIENTS WITH PHARMACO-RESISTANT TEMPORAL LOBE EPILEPSY MEASURED WITH PET AND (R)-[^{11} C]VERAPAMIL

M. Feldmann[1,2], M.-C. Asselin[2], S. Wang[2], A. Mcmahon[2], M. Walker[1,2], R. Hinz[2], J. Duncan[1], S. Sisodiya[1], M. Koepp[1]

[1]Department of Clinical and Experimental Epilepsy, University College London, London, [2]School of Cancer and Enabling Sciences, Wolfson Molecular Imaging Centre, The University of Manchester, Manchester, UK

Objectives: Overexpression of the multidrug efflux transporter P-glycoprotein (P-gp) at the blood-brain-barrier (BBB) is thought to be involved in pharmacoresistance in epilepsy by extruding antiepileptic drugs (AEDs) from their target site [1]. To evaluate P-gp function in pharmaco-resistant mesial temporal lobe epilepsy (mTLE), we performed positron emission tomography (PET) scans with the P-gp substrate (R)-[^{11}C]verapamil (VPM) in pharmaco-resistant and -sensitive mTLE patients and healthy controls. We hypothesize that VPM uptake is reduced in pharmaco-resistant patients compared to pharmaco-sensitive patients and healthy controls.

Methods: We studied 8 pharmaco-resistant (3 females, 30-56yrs) and 5 pharmaco-sensitive (3 females, 39-50yrs) mTLE patients with unilateral hippocampal sclerosis, and 4 healthy controls (3 females, 37-55yrs). All subjects underwent a VPM PET scan to assess P-gp function. The pharmaco-sensitive patients underwent a second VPM PET scan on the same day to assess test-retest variability. The rate constant of transfer from plasma to brain, K_1, was estimated using a single-tissue compartment model with a VPM-in-plasma arterial input function. Analysis was performed on the first 10min of dynamic data containing limited radiolabeled metabolites [2]. Regions were defined automatically using an anatomical template, and ratios of K_1 values were calculated between a reference region (parietal cortex) and target regions. Additionally, asymmetry indices (AI) were calculated using K_1 values as AI(%)=(ipsi-contra)/((contra+ipsi)/2)x100. Differences were tested by one-way analysis of variance (ANOVA) and the level of significance was set at $p < 0.05$.

Results: K_1 values were significantly higher globally in patients compared to controls ($p< 0.001$) and in pharmaco-sensitive compared to pharmaco-resistant patients ($p< 0.01$). Ratios of K_1 values between reference and target regions were significantly lower globally in pharmaco-resistant patients compared to both pharmaco-sensitive patients and controls ($p< 0.03$), but not significantly different between controls and pharmaco-sensitive patients ($p=0.56$) (Fig). There was also a significant regional effect ($p< 0.001$), but no group by region effect ($p=0.96$). Test-retest reproducibility for pharmaco-sensitive patients of K_1 in whole brain is 7.8% (n=5) and without an order effect of the time of day when scans are performed ($p=0.73$). Asymmetry indices did not show significant side differences in temporal nor extratemporal brain regions ($p=0.34$).

Conclusions: Lower K_1 values and ratios in pharmaco-resistant compared to pharmaco-sensitive patients support the hypothesis of P-gp overexpression in pharmaco-resistant mTLE. The global rather than regional differences in K_1 could point to subtle BBB leakage in patients [3] or be attributed to differences in radiotracer peripheral metabolism between controls and patients. Using a P-gp inhibitor, such as Tariquidar, to increase VPM signal may elicit regional differences.

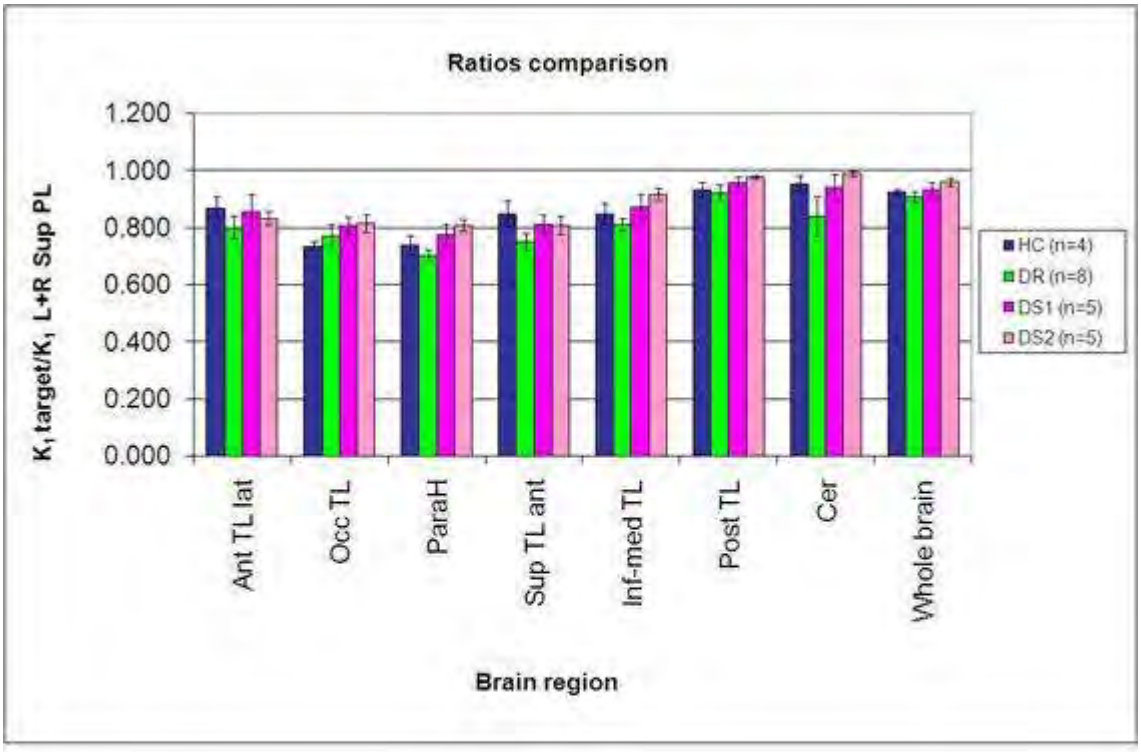

[Fig]

Fig: VPM K_1 ratios between reference region (parietal cortex) and target regions for 4 healthy controls (HC), 8 pharmaco-resistant (DR) and 5 pharmaco-sensitive (DS1=test, DS2=retest) mTLE patients in 6 different temporal lobe regions of interests (ROI) as well as cerebellum and whole brain.

References:

[1] Löscher and Potschka (2002) JPharmacolExpTher.301:7-14.

[2] Muzi et al (2009) JNuclMed.50:1267-75.

[3] Van Vliet et al. (2007) Brain.130:521-534.

1126

MOLECULAR NEUROIMAGING OF THE GABAERGIC AND SEROTONINERGIC SYSTEMS IN ESSENTIAL TREMOR: CORRELATION WITH SYMPTOM SEVERITY

A. Gironell[1], F.P. Figueiras[2], J. Pagonabarraga[1], R. Herance[2], B. Pascual[1], C. Trampal[3], **J.D. Gispert**[2,3,4]

[1]Servei de Neurologia, Hospital de la Santa Creu i Sant Pau, [2]Institut d'Alta Tecnologia - PRBB, [3]CRC Centre d'Imatge Molecular, Barcelona, [4]Centro de Investigación Biomédica en Red en Bioingeniería, Biomateriales y Nanomedicina (CIBER BBN), Zaragoza, Spain

Introduction: Essential tremor (ET) is the most common movement disorder. However, the underlying pathophysiological mechanisms are still poorly understood. Primary overactivity of cerebello-thalamo-cortical pathways is the most conspicuous finding in ET, as indicated both by positron emission tomography (PET) studies in ET patients and tremor models in animals.

Aims: The goal of this study was to investigate two important neurotransmitter systems in patients with ET, compared to healthy controls and to correlate ligand uptake with clinical symptom severity scales. We studied the serotonin transporter activity using [^{11}C]DASB PET and the gamma-aminobutyric acid ($GABA_A$) receptor binding with ^{11}C-flumazenil ([^{11}C]FMZ) PET scan. We also sought for correlations between ligand binding and the clinical symptom severity as measured by the Tremor Clinical Rating Scale (TCRS) and the Glass Scale.

Methods: FMZ and DASB bindings were measured in 8 patients with the diagnosis of ET (5 male, 3 female; range 50 - 78 ys), and in 2 healthy controls (1 male, 1 female; range 69 - 78 ys). Each subject underwent two 90 min high resolution [^{11}C]DASB and [^{11}C]FMZ PET scan, with approximately one week in between sessions. An MRI scan of the brain was obtained within one month of the PET scans.

Images were analyzed with pixel-wise modeling. Parametric images were estimated using the simplified reference tissue method (SRTM). In [^{11}C]DASB analysis, the cerebellum was used as reference region to measure nondisplaceable uptake (free plus nonspecifically bound). In [^{11}C]FMZ analysis the reference region was the pons. The WFU Pickatlas template was used to define the regions of interest.

Results: Analysis of [^{11}C]DASB BP_{ND} parametric images showed significant reductions in serotonin receptor binding in the thalamus and striatum in patients with ET compared to controls. Mean thalamus values were 2.287 ± 1.62 (controls) and 1.049 ± 0.86 (patients), mean striatum values were 1.301 ± 0.43 (controls) and 0.807 ± 0.47 (patients).

In the [^{11}C]FMZ BP_{ND} parametric images there were also differences between patients and controls. In cerebellum and parietal cortex, patients with ET had significant increases in FMZ BP_{ND} compared to controls. Mean cerebellum values were 1.497 ± 0.164 (controls) and 1.933 ± 0.47 (patients), mean parietal cortex were 1.584 ± 0.09 (controls) and 2.089 ± 0.49 (patients). There were slight increases in FMZ BP_{ND} values in the frontal, occipital and temporal cortex and thalamus. Moreover, a statistically significant ($p < 0.001$) correlation was observed in cerebellar FMZ BP_{ND} values and TCRS.

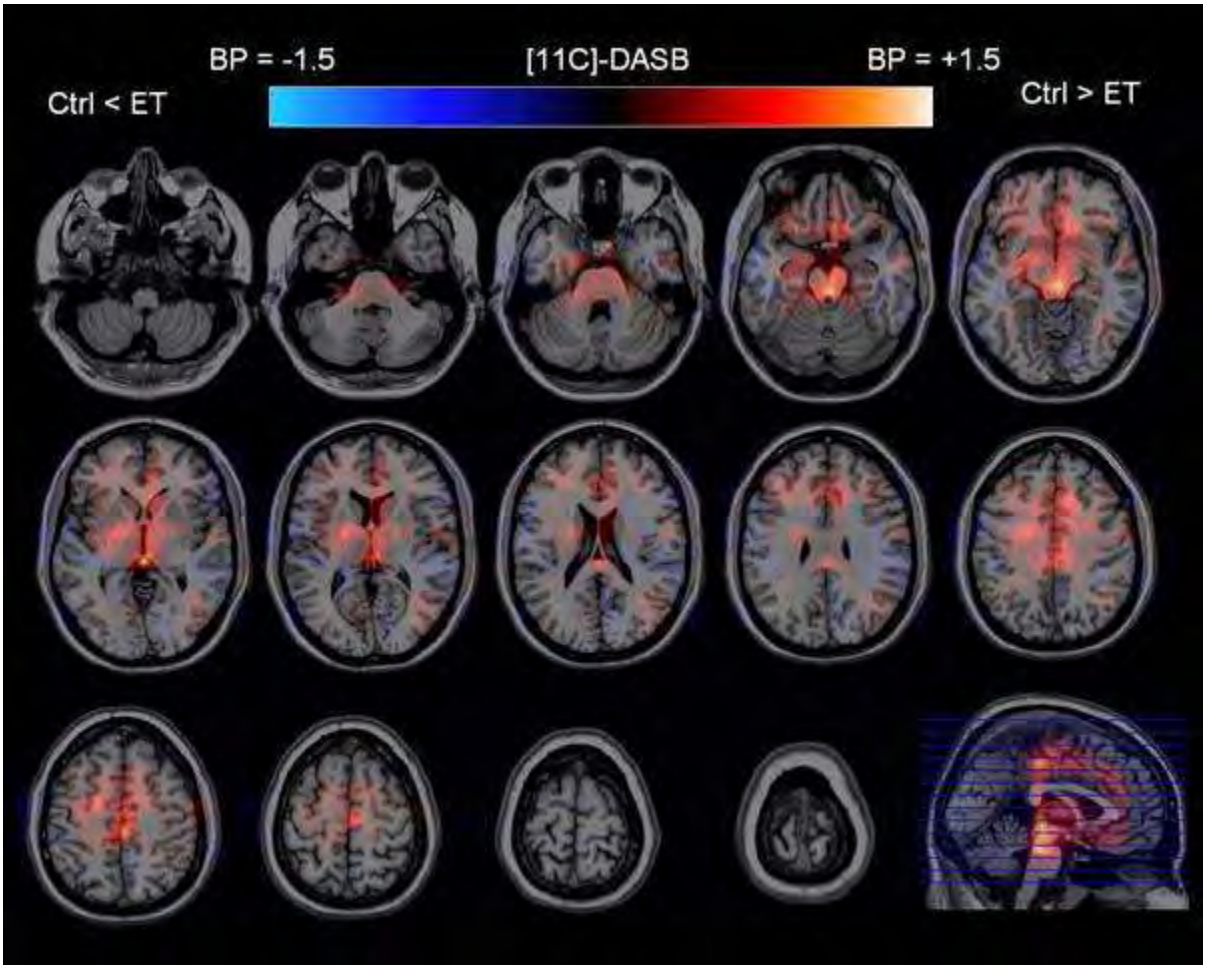

[[11C]DASB: ET vs Ctrl]

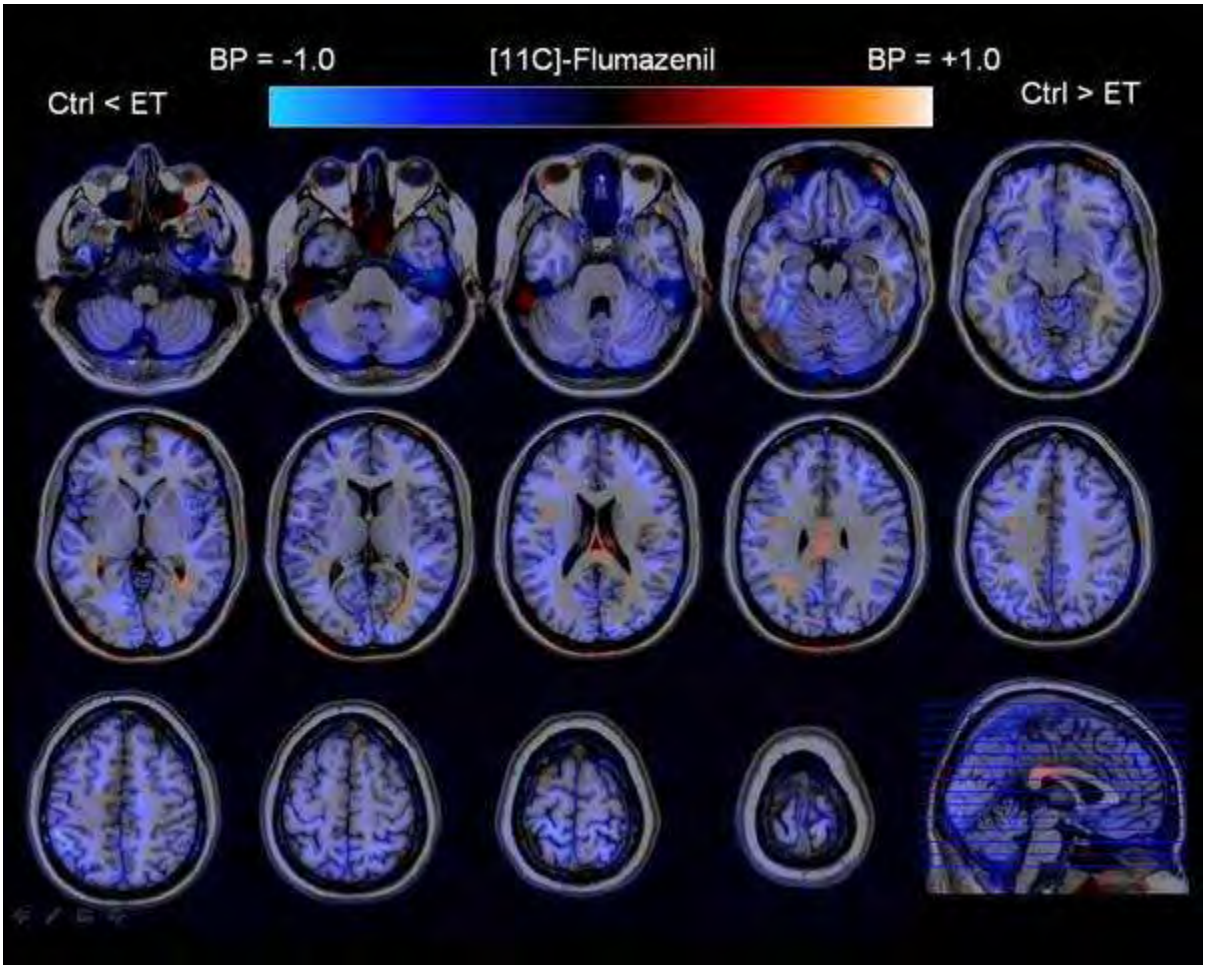

[[11C]FMZ: ET vs Ctrl]

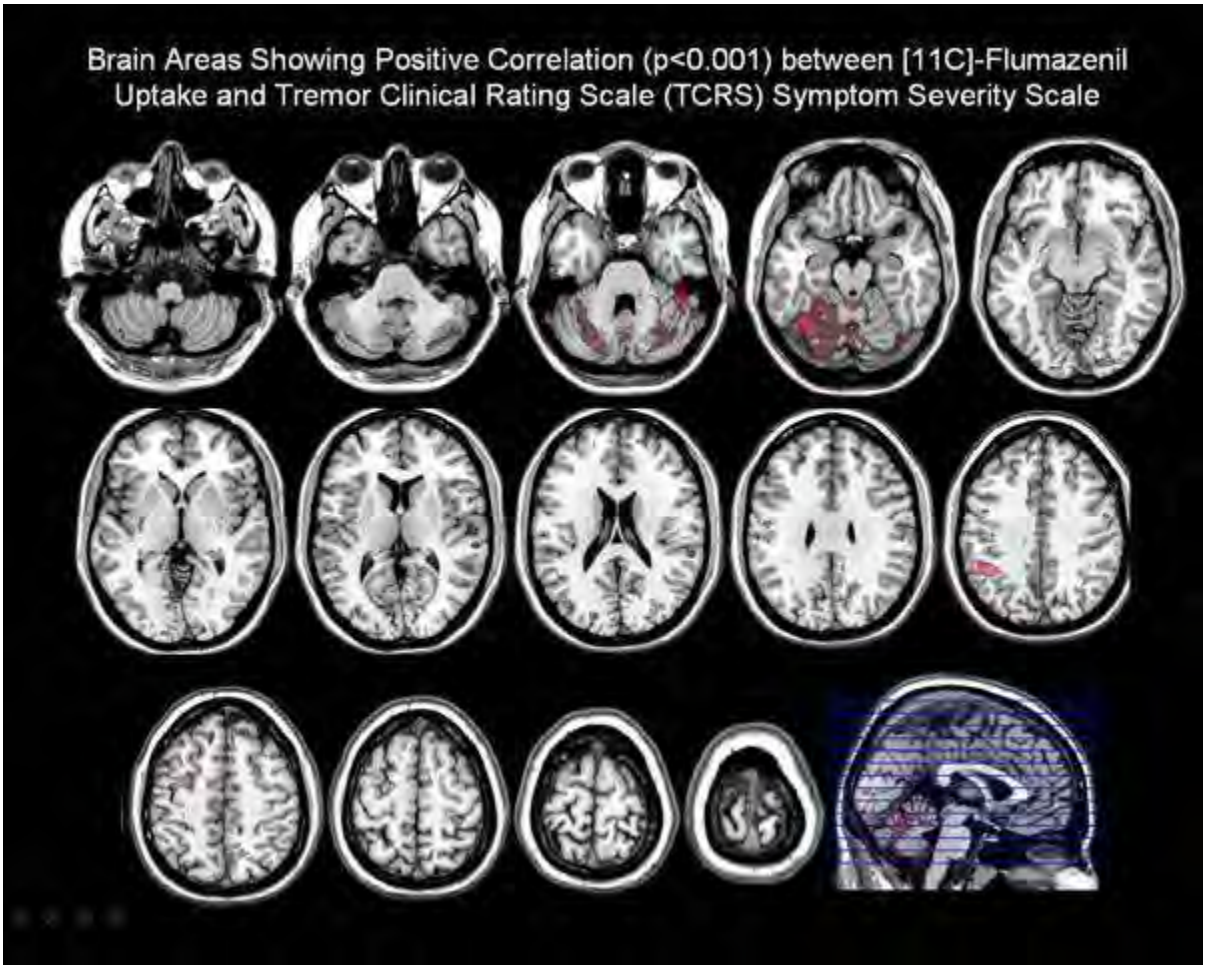

[[11C]FMZ vs. FTMS]

Conclusions: This finding suggests that both serotonin and GABAergic systems are critically involved in the neurophysiologic changes in ET patients. Furthermore, [^{11}C]FMZ binding in the cerebellum was found to closely correlate with the TCRS clinical symtom scale. PET may be an important and useful tool to understand the underlying pathophysiological mechanisms of ET.

1127

EFFECT OF A NEUROPROTECTIVE AGENT ON THE INFLAMMATORY RESPONSE DURING CEREBRAL ISCHEMIA

C. Benakis[1], A. Vaslin[2], C. Pasquali[2], C. Bonny[2], L. Hirt[1]

[1]Department of Clinical Neurosciences, CHUV, [2]Xigen Pharmaceuticals, Lausanne, Switzerland

Objectives: After an ischemic event affecting the brain, glial cells become activated and numerous inflammatory cells infiltrate the site of the lesion secreting a large variety of cytokines and chemokines. It is less known whether this brain inflammation is detrimental or beneficial for tissue recovery. Here, we evaluated whether the strongly neuroprotective peptide XG-102 (formely D-JNKI1), an inhibitor of the pro-apoptotic Jun Kinase pathway (Borsello et al., 2003), modulates post-ischemic inflammation in animal models of stroke.

Methods: XG-102 (0.1mg/kg) or vehicle (saline) was administered intravenously 3 h after transient middle cerebral artery occlusion (MCAO) in mice. Lesion size and microglial cell activation were assessed using histology. The secretion of the inflammatory mediators interleukin-6 (IL-6) and keratinocyte chemokine (KC/CXCL1) in the brain and systemic circulation was analysed by ELISA at 4 h, 7 h, 48 h and 5 days after ischemia in sham-operated, MCAO+vehicle and MCAO+XG-102 mice.

Results: Lesion size at 48 h was significantly reduced in the treated group. Quantification of the average intensity of CD11b positive microglia within the ischemic tissue showed no significant difference between groups (Benakis et al., 2010). In the plasma samples of vehicle mice, IL-6 and KC were secreted early after ischemia and returned to basal level at late time points. XG-102 showed a trend towards reducing plasma levels of IL-6 but not KC. Interestingly, we found a significant release of IL-6 and KC at 48 h in the brain of XG-102-treated mice, compared with vehicle-treated mice.

Conclusions: These results demonstrate that the neuroprotectant peptide XG-102 does not modify the activation and accumulation of microglial cells in the brain lesion. Interestingly, its neuroprotective effect may be linked, at least partly, to the secretion of inflammatory mediators after stroke.

References:

Benakis C, et al. JNK inhibition and inflammation after cerebral ischemia. Brain Behav Immun. 2010;24:800-11.

Borsello T, et al. A peptide inhibitor of c-Jun N-terminal kinase protects against excitotoxicity and cerebral ischemia. Nat Med. 2003;9:1180-6.

1128

STEM CELLS ENHANCE MOTOR RECOVERY FOLLOWING STROKE IN LONG-EVANS RATS

J. Mocco[1], A. Afzal[1], N. Thomas[2], Z. Warraich[2], B. Hoh[1], E.W. Scott[3], J.A. Kleim[2]

[1]Neurosurgery, [2]Neuroscience, [3]Molecular Genetics and Microbiology, University of Florida, Gainesville, FL, USA

Background: Stroke is the leading cause of disability in the Unites States resulting in upper extremity motor impairments.

Methods: Male Long-Evans hooded rats (350-420g) underwent stroke surgery using Endothelin-1 induced MCAO. Animals were housed in standard laboratory cages on a 12hour light/dark cycle. Animals were pretrained to familiarize them with the reaching accuracy task. Trained animals were then divided into 3 groups (controls, n=7; stroke, n=3; stroke with post-reperfusion administered endothelial progenitor cells (EPC's), n=6); The EPC's were enriched from the bone marrow of a separate group of donor rats using nanoparticles tagged with LIN negative and CD90 markers. Ten million EPC's were injected into the tail vein immediately following reperfusion. Animals were assessed at 3 and 5 weeks following the surgery for reaching task performance. All assessments were performed in a blinded manner.

Results: Reaching accuracy: Control animals scored a reaching accuracy of 41±8.1% and 46±11% at 3 and 5 weeks, respectively. Stroke decreased this task to 12±21% and 18±28%, respectively ($p < 0.05$, compared to controls at both time points). Injection of EPC's following reperfusion led to an increase in reaching accuracy to 27±26% and 32±24%, at 3 and 5 weeks, respectively ($p < 0.05$, compared to stroked non-EPC cohort at 5 weeks).

Conclusions: These data suggest that Hematopoietic EPC's play a significant role in the amelioration of stroke injury following cerebral ischemia.

1131

BRAIN PERFUSION STUDIES BY ARTERIAL SPIN LABELING (ASL) IN INTRACRANIAL ARTERIAL STENOSIS - DIAGNOSTIC ISSUES AND TREATMENT EFFECTS

M. Hauf[1], F. Kellner-Weldon[2], K. Jann[3], M. El-Koussy[2], M. Wapp[2], R. Wiest[2], A. Federspiel[3], G. Schroth[2]

[1]Neuroradiology, University of Bern, [2]Neuroradiology, University of Bern, Inselspital, [3]University Hospital of Psychiatry, University of Bern, Bern, Switzerland

Objectives: Treatment guidelines for intracranial arterial stenosis are not well established. Assessment of the hemodynamic compromise may aid in the diagnostic workup.

Methods: 8 patients (5 males, mean age 41 years, range 36-62 years) with symptomatic intracranial arterial stenosis were assessed in the diagnostic workup of a revascularisation therapy. Brain perfusion measurements using pseudocontinuous ASL (TR 4000 ms, label time 1.72 s, post labeling delay 1.5 s) at rest and under a vasodilatory stimulus of inhalative CO2 7% were performed before and after revascularisation therapy. CBF values were calculated using a self written Matlab script. CBF values were extracted from the cortical territory of the middle cerebral arteries (MCA) and of the anterior and posterior MCA watershed areas. Digital subtraction angiography (DSA; Siemens Axiom Artis zee, Siemens, Erlangen, Germany) of each patient was analyzed for the grade of stenosis according to NASCET criteria and evidence of collaterals (visual grading 1-4). SPSS 17.0 (SPSS, Chicago, USA) was used for statistical analyses.

Results: Five patients had proximal MCA, 3 intracranial internal carotid artery stenosis. Mean stenosis grade was 70.2%. All patients underwent successful revascularisation therapy, 7 by PTA/stent, 1 by extra-intracranial bypass. Before treatment CBF values (in ml/100g/min) were lower in the MCA territory with upstream stenosis (44.6 (SD 11.6)) compared to the non stenotic side (51.9 (SD 12.2)) at rest (p=0.03, t-test) and under vasodilatatory stimulus (stenotic 53.0 vs non-stenotic 59.0 (n.s)). In the MCA watershed regions the difference in resting CBF was accentuated (stenotic 39.2 vs non-stenotic 50.2; p=0.01, t-test). After revasularisation therapy no CBF differences were observed at rest and under vasodilatation (stenotic 52.2/58.6 vs non-stenotic 54.6/60.4). No correlation with the grade of stenosis and the collateral flow grading reached significance.

Conclusion: Brain perfusion measurements using ASL show reduced CBF values in territories with upstream high grade intracranial stenosis. Hemodynamic compromise is predominantly present in the affected watershed areas. A successful revascularisation therapy resulted in a normalisation of the CBF values. Future work on prognostic and diagnostic predictors may integrate analysis of watershed areas.

This projet is granted by the Swiss National Foundation: Impact of quantitative MR perfusion imaging on the management of patients with carotid artery disease, 33CM30-124114

1133

THE NOVEL TRKB AGONIST, 7,8-DIHYDROXYFLAVONE ENHANCES STEM CELL MOBILIZATION AFTER STROKE

J.A. Kleim[1], A. Afzal[2], N. Thomas[1], Z. Warraich[1], B.L. Hoh[2], E.W. Scott[3], **J. Mocco**[2]

[1]Neuroscience, [2]Neurosurgery, [3]Molecular Genetics and Micorbiology, University of Florida, Gainesville, FL, USA

Background: Increasing levels of circulating Hematopoietic Stem Cells (HSC)/Hematopoietic Progenitor Cells (HPC), bone marrow derived mononuclear cells that promote repair in areas of injury, have been demonstrated to correlate with improved neurological function following stroke, suggesting a potentially critical role for HSC/HPC's in limiting stroke injury and/or facilitating stroke recovery. Flavonoids, found in plants and fruit, exert anti-oxidative effects. Recent studies have demonstrated that 7,8 Dihydroxyflavone (DHF) is a potent TrkB agonist mimicking Brain Derived Neurotropic Factor, thus making it a powerful potential tool for treating neurological disorders. Stromal Derived Growth Factor 1-Alpha (SDF1-A) along with its receptor CXCR4 is a potent chemo attractant released by areas of injury. SDF1-A has been shown to mobilize HSC/HPC from the bone marrow to the blood and lead to 'homing' of the cells to an area of injury. We investigated the effect of DHF on HSC/HPC function following cerebral ischemia.

Methods: Ischemic damage was induced in adult male Long Evans hooded rats (350-400g) with a peri-MCA injection of the vasoconstriction peptide ET-1. The rats were sacrificed at 24 hours post surgery and their bone marrow and blood HSC/HPC enriched using nanoparticles tagged with LIN negative and CD90 markers.

Results: Stroked animals showed an increase in bone marrow production of HSC/HPC versus control animals (31.9±7 versus 2±0.5, $p< 0.05$). The mobilization of the HSC/HPC from the bone marrow to the blood was also significantly higher in the stroked animals versus control animals (43±19 versus 3.6±0.3, $p< 0.05$). Following stroke, DHF pre-treated HSC/HPC's demonstrated significantly improved migration along an SDF-1 gradient compared to controls (129±1.0 versus 108±1.15, $p< 0.05$), despite the fact that DHF alone provided no independent migratory stimulus.

Conclusions: The results suggest that DHF may be a viable compound to facilitate HSC/HPC migration post-stroke.

1134

ASSESSMENT OF THE INCREASED ANAPLEROSIS IN THE HYPERAMMONEMIC RAT BRAIN USING IN VIVO ^{13}C MRS

B. Lanz[1], C. Cudalbu[1], J.M. Duarte[1], R. Gruetter[1,2,3]

[1]Laboratory of Functional and Metabolic Imaging, Ecole Polytechnique Fédérale de Lausanne, [2]Department of Radiology, University of Lausanne, Lausanne, [3]Department of Radiology, University of Geneva, Geneva, Switzerland

Objectives: Past ^{13}C-glucose NMR studies in hyperammonemic rats used [1-^{13}C] glucose to analyze the GluC4 turnover or [2-^{13}C] glucose, which labels GluC3 and GluC2 to assess pyruvate carboxylase (PC) [1,2]. In this study, we combine ammonium chloride and [1,6-$^{13}C_2$] glucose infusions, in order to investigate the effect of hyperammonemia and anaplerosis on the time courses of the C4 and C3 positions of glutamate and glutamine simultaneously. PC beeing a dilution flux only for the labeling position C3, can be assessed directly from the different labeling dynamics of the C4 and C3 positions, in a single experiment.

Methods: Localized ^{13}C spectra were measured on 3 control and 3 hyperammonemic rats (Sprague-Dawley, 275±25g, VOI=5x8x8mm^3) artificially ventilated. An exponentially decaying bolus of 99%-enriched [1,6-$^{13}C_2$] glucose was administrated over 5min, followed by a continuous infusion of 70%-enriched glucose for 6h, adapted to maintain a constant glycemia level (around 350 mg/dl). To create hyperammonemic conditions, ammonium chloride was infused continuously at a stable rate (4.5mmmol/h/kg) after a 1 min bolus [3], starting 3 hours before the glucose injection. All data were acquired on a 9.4T system with a surface coil as RF transceiver and the semi-adiabatic DEPT polarization transfer sequence [4]. ^{1}H spectra were acquired before the glucose injection using the SPECIAL spectroscopy sequence in the same VOI. For the hyperammonemic rats, the evolution of glutamate and glutamine concentrations was followed over the ammonia infusion period preceding the glucose injection.

Results: The total glutamate concentration [Glu] remained constant in hyperammonemic rats, while glutamine [Gln] was linearly increasing. Using both the preinfusion ^{1}H MRS data and the measurement of [Gln] derived from the GlnC4 multiplets at steady-state, a net glutamine synthesis rate of 0.04±0.02 µmol/g/min (mean±SEM) was calculated.

Fig.1 shows that under hyperammonemia, the isotopic enrichment FE of GlnC4 and GlnC3 are reaching a dynamic steady-state level, which is different from the control, especially for GlnC3 (FE=20±1% vs 32±5% in controls (mean±SEM))(table 1). This suggests a significant increase in PC, responsible for the net glutamine synthesis. Since most of the glutamine is located in the glial cells while glutamate is mainly neuronal, this explains why the glutamine steady-state enrichments are significantly affected by hyperammonemia but not the GluC4 and GluC3 FE.

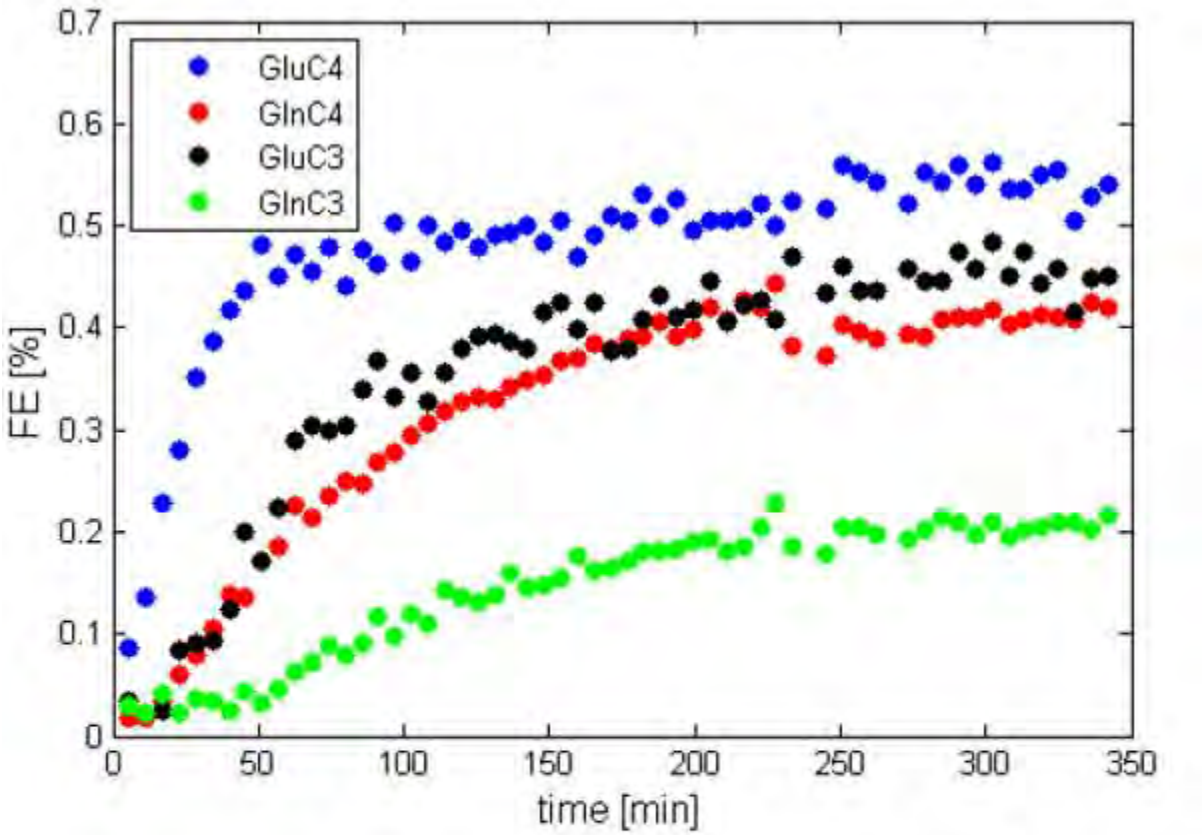

Fig.1: *time course of the FE of the metabolites in hyperammonemic rats (n=3)*

FE	*GluC4*	*GlnC4*	*GluC3*	*GlnC3*
Control	*0.54±0.03*	*0.35±0.06*	*0.46±0.01*	*0.32±0.05*
Hyper-ammonemia	*0.52±0.05*	*0.43±0.02*	*0.43±0.04*	*0.20±0.01*

Table 1: *fractional enrichment levels at steady-state*

[Figures]

Conclusion: From the glutamine enrichment curves, anaplerosis appears to be the major ammonia detoxification pathway, while neuronal metabolism is less affected, as indicated by GluC4 and GluC3 FE. The linearly increasing glutamine concentration over several hours leads to a dynamic steady-state of the FE in the glutamine C4 and C3 positions, reflecting constant metabolic fluxes during the infusion. The obtained PC flux is in good agreement with the values estimated in our previous ^{15}N MRS study [5].

References:

1.N. Sibson et al., *J.Neurochem.* 76:975 (2001) 2.N. Sibson et al., *Proc. Natl. Acad. Sci. U S A.*94(6):2699 (1997) 3.K. Kanamori et al., *NMR Biomed.* 6:21(1993) 4.P.G. Henry et al., *Magn. Reson. Med.* 50(4):684(2003) 5.C. Cudalbu et al., *Proc. Intl. Soc. Mag. Reson. Med.* 18:314 (2010)

1135

ANTIOXIDANT CARBON-BASED NANOTUBES: *IN-VITRO* CHARACTERIZATION AND *IN-VIVO* EFFECTS ON CEREBROVASCULAR REGULATION FOLLOWING MILD TRAUMATIC BRAIN INJURY

T.A. Kent[1,2], B.R. Bitner[3], J.M. Berlin[4], C.R. Robertson[5], D.C. Marcano[4], R.H. Fabian[1,2], R.G. Pautler[3], J.M. Tour[4]

[1]Department of Neurology, Baylor College of Medicine, [2]Michael E. DeBakey VA Medical Center, [3]Department of Molecular Physiology and Biophysics, Baylor College of Medicine, [4]Department of Chemistry and the Smalley Institute for Nanoscale Science and Technology, Rice University, [5]Department of Neurosurgery, Baylor College of Medicine, Houston, TX, USA

Introduction: Dysfunction of the cerebrovasculature, manifested acutely by loss of autoregulation, is a feature of TBI and impedes recovery. Oxidative stress is implicated in this injury. To date, small molecule antioxidants and enzymes have not proven clinically effective in TBI, suggesting a need for novel antioxidants. Nanomaterials are an emerging class of antioxidants with several potential advantages, including quenching of oxidative radicals without need for enzymatic transformation as well as favorable biodistribution *in-vivo*.

Objectives: We tested whether the carbon nanomaterials, poly(ethylene gylcol)-functionalized hydrophilic carbon clusters (PEG-HCCs) are antioxidants in biological settings and performed a preliminary experiment to determine their effect on cerebral blood flow following mild experimental TBI and hypotension.

Methods: HCCs were generated by treating single wall carbon nanotubes with oleum and nitric acid. Following purification, the HCCs were functionalized with PEG via coupling to the carboxcylic acids present on the HCCs. The ability to quench superoxide anion reduction of cytochrome c generated by xanthine/xanthine oxidase was determined spectrophotometrically in solution. Ability to reduce superoxide anion production and protect cells from injury following treatment with the electron chain transport inhibitor Antimycin A (AntA), was tested in b.End3 cultured brain endothelial cell line using dihydroethidium (DHE) fluorescence flow cytometry and trypan blue exclusion. *In-vivo* studies were performed in Long Evans rats following mild TBI (3m/s; 2.5 mm deformation; 80 ms duration) or sham along with hemorrhagic hypotension for 50 minutes, followed by resuscitation first with Lactated Ringers then by shed blood. Treatment with PEG-HCCs (2 mg/kg PEG-HCCs in 1 mL) or PBS was initiated prior to restoration of the shed blood. Hemispheric laser Doppler relative perfusion (LDF) was measured from baseline to 6 hours post-TBI.

Results: PEG-HCCs were effective antioxidants *in-vitro*. The IC50 for prevention of reduction of cyctochrome c for the PEG-HCCs was 200mg/L relative to the carbon core. At that concentration, there was no innate toxicity following incubation determined by a clonogenic and trypan blue assay. DHE fluorescence induced by AntA was eliminated by post-treatment with PEG-HCCs (2-4 mg/L; 15 mins post-AntA). Interestingly only pre-treatment with an excess of superoxide dismutase (SOD; 14 hours prior) achieved comparable level of DHE fluorescence reduction. PEG-HCC post-treatment also improved cell survival following a higher dose of AntA, to 65% of baseline compared to 23% for SOD. *In-vivo* following TBI, hypotension reduced relative LDF to approximately 50% compared to sham TBI (Figure). At 2 hours following resuscitation, nanotubes restored LDF to 86% of sham, while the vehicle group remained significantly lower at 56% of sham. LDF declined in all groups over time.

Conclusions: PEG-HCCs are biocompatible with b.End3 cells and the PEG-HCCs rapidly protected these cells from oxidative stress. Preliminary results, administering PEG-HCCs at a clinically realistic time point, improved post-TBI/hypotension LDF. Experiments are underway to establish that oxidative stress was reduced by treatment and longer term survival studies are planned to establish whether outcome is improved. Because PEG-HCCs are able to sequester proteins, it is conceivable that specific targeting is possible.

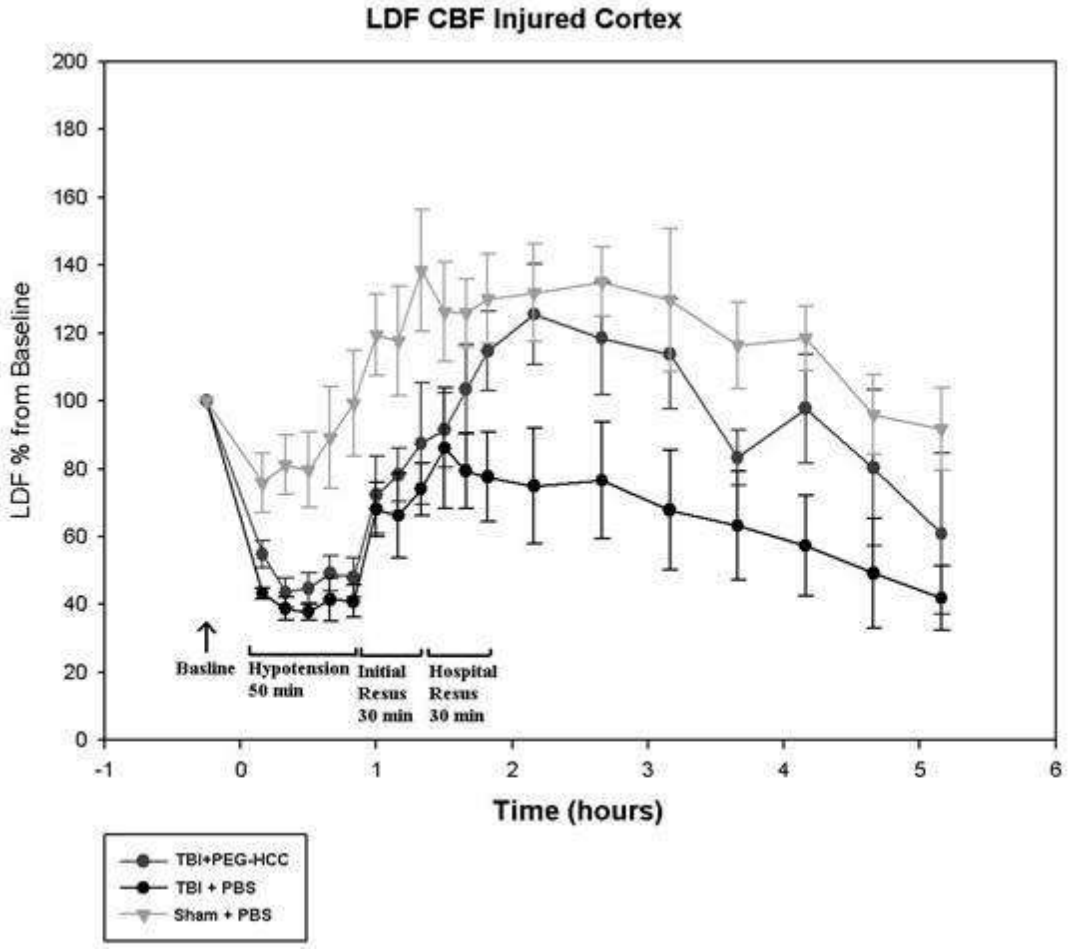

[Laser Doppler Flow Following TBI and Hypotension]

1136

EFFECTS OF NEUROPROTECTIVE INTERVENTIONS ON GENOMIC RESPONSE TO REPERFUSION INJURY AFTER CARDIAC ARREST AND CARDIOPULMONARY RESUSCITATION IN PORCINE BRAIN

C. Martijn, L. Wiklund

Surgical Sciences/Anesthesiology and Intensive Care, Uppsala University, Uppsala, Sweden

Objectives: Cerebral ischemia/reperfusion injury is a common secondary effect of cardiac arrest which is largely responsible for postresuscitative mortality. Therefore development of therapies which restore and protect the brain function after cardiac arrest is essential. The present study analyzed whole-genome cerebral transcriptional profiles in a porcine model of cardiac arrest in order to elucidate the mechanisms of action of therapeutical 34-32°C hypothermia and a few drugs having been experimentally proven to possess neuroprotective effects.

Methods: Pigs were subjected to 12 min of cardiac arrest, 8 min of cardiopulmonary resuscitation (CPR) and spontaneous reperfusion during 3 hours. Hypothermia, Methylene Blue (MB) or S-PBN (sodium 4-[(tert-butylimino) methyl]benzene-3-sulfonate *N*-oxide) was induced or administered during CPR and reperfusion. Genome-wide transcriptional profiling using the Affymetrix porcine microarray was performed to 1) gain understanding of delayed neuronal death initiation in porcine brain during ischemia and after 30, 60 and 180 min following reperfusion and 2) identify the mechanisms behind the neuroprotective effect after ischemic injury of MB (at 30, 60 and 180 min), hypothermia (at 60 and 180 min) and S-PBN (at 180 min) respectively.

Results: Our results confirmed that restoration of spontaneous circulation (ROSC) induces major transcriptional changes related to stress response, inflammation, apoptosis and even cytoprotection. Furthermore, our data showed that the neuroprotective role of MB is fulfilled by regulation of the expression of soluble guanylate cyclase and diverse biological processes as early as 30 min after ROSC. Finally comparison of transcript profiles from hypothermia, MB and S-PBN allowed us to identify a group of genes commonly induced by all three therapies as well as sets of genes specifically regulated after each intervention.

Conclusions: Our results support that MB could be a valuable intervention and should be investigated as a therapeutic agent against neural damage associated with ischemia/reperfusion injury induced by cardiac arrest. Moreover, our data show that combining MB with hypothermia could potentially enhance overall protection. Therefore a combinatorial approach is at present being tested in our porcine model.

1139

FEASIBILITY AND SAFETY OF COMBINED INTERMITTENT HYPOXIA AND INTENSIVE MOTOR REHABILITATION FOR CHRONIC STROKE PATIENTS

S. Pundik[1], W.D. Lust[2], E. Fredrickson[3], K. Strohl[4], J.J. Daly[1]

[1]Neurology, Cleveland VA Medical Center and Case Western Reserve University School of Medicine, [2]Neurosurgery, Case Western Reserve University School of Medicine, [3]Neurology, Cleveland VA Medical Center, [4]Medicine, Cleveland VA Medical Center and Case Western Reserve University School of Medicine, Cleveland, OH, USA

Introduction: Some brain repair and return of function can be achieved with intensive rehabilitation even years after stroke; however, function does not return to normal. It is increasingly evident that improved therapies are needed to further improve outcomes. Intermittent Hypoxia (IH) is a promising therapy. Specific cellular processes in the brain are required in order for brain plasticity to occur which drives motor function recovery. IH induced these same cellular processes, specifically neurogenesis, neuronal dendrite outgrowth, and synthesis of neuronal and vascular growth factors. There is potential that IH could work in concert with intensive neurorehabilitation, inducing an additive effect in motor recovery.

Objective: The study objective was to test the feasibility and safety of IH therapy in combination with upper extremity motor rehabilitation in chronic stroke. We tested tolerability of an escalating IH protocol.

Methods. Eight subjects (>6mos post-stroke) with upper extremity motor deficits were treated with combination intensive motor learning (12wks, 5 days/wk, 5hrs/day) and IH (5wks; total, 25 sessions). Twenty nine historical controls, age and gender matched stroke subjects had intensive motor therapy alone. Functional measures were Arm Mobility Assessment Test (AMAT) and Fugl-Myer (FM), acquired before and after the combined therapies. Safety and tolerability of IH treatments were monitored with cognitive measures of attention (Stroop, Digit span and Trail Making tests) and vital signs (blood pressure, heart rate, respiratory rate, blood oxygen saturation (SpO_2)). Serum erythropoietin and hematocrit were measured at baseline, midway and final evaluation.

Results. The average ages were 58.5±8.8yrs and 57±13.7yrs in control and IH groups, respectively. There was a trend toward greater functional gains based on AMAT and FM scores (trend did not reach significance). AMAT score gains were 1465±1374secs vs. 1927±1644secs ($p>0.05$) in motor learning alone and motor learning plus IH groups, respectively. Median FM gains were 9(IQ range7.8) vs. 10(IQ range 7.8) for motor therapy and motor therapy plus IH groups, respectively. The average minimum SpO_2 during IH sessions for all the subjects was 81.5±1.42% where the average baseline SpO_2 was 96.4±1.3%. IH treatments were well tolerated by the cohort of chronic stroke survivors. The score for measures of attention before and after each IH session were either unchanged or improved. Mean arterial pressure (MAP) before and after each session was 88.4±7.5mmHg and 86.5±7.4mmHg ($p< 0.05$), respectively. Heart rate before and after each IH session was 71±4 and 68.8±7.2 ($p< 0.05$). There was a small increase in MAP while inhaling the hypoxic air versus while breathing room air, 89.18±7.7mmHg vs. 87.1±8.5mmHg($p=0.01$), respectively. For the IH therapy group, serum erythropoietin levels were 10.9±4.26MIU/ml, 13.2±5.1MIU/ml and 11.9±3.6MIU/ml at baseline, midway and at the final evaluation, respectively.

Conclusions. According to measures of cognitive function, vital signs and erythropoietin levels,

IH therapy was safe and well tolerated by chronic stroke survivors. The trend toward an additive advantage for combined IH and motor therapy versus motor therapy alone supports the conduct of a larger study to determine the efficacy of this promising combined therapy for motor recovery in chronic stroke survivors.

1140

ESTIMATION OF IN VIVO SELECTIVITY OF A TRIPLE MONOAMINE REUPTAKE INHIBITOR IN NON-HUMAN PRIMATE AND HUMAN

J. Van der Aart[1], R.A. Comley[1], C.A. Salinas[1], M. Slifstein[2], M. Petrone[3], M. Neve[3], R.O. Gomeni[4], F.A. Gray[5], R.N. Gunn[1], E.A. Rabiner[1]

[1]Clinical Imaging Centre, GlaxoSmithKline, London, UK, [2]Columbia University, New York, NY, USA, [3]Clinical Pharmacology Modelling and Simulation, GlaxoSmithKline, Verona, Italy, [4]GlaxoSmithKline, Pharmacometrics, Upper Marion, PA, USA, [5]GlaxoSmithKline, Clinical Pharmacology and Discovery Medicine, Stevenage, UK

Introduction: Early examination of therapeutic doses of a novel compound can lead to a significant reduction in risks associated with drug development. Determination of the in vivo affinity of a compound in pre-clinical species and humans can be used to refine the dose range tested in phase I and II of clinical development. The affinity of GSK1360707, a triple monoamine re-uptake inhibitor, was evaluated at the serotonin, dopamine and noradrenaline transporters (SERT, DAT and NAT) in the non-human primate and SERT and DAT in human, to provide information for go/no-go decisions in clinical development.

Methods: The occupancy at the SERT, DAT and NAT by GSK1360707 was assessed in *Papio Anubis* by using the radioligands [^{11}C]DASB, [^{11}C]PE2I and [^{11}C]MeNER (i.e. MRB). In each scanning session, a baseline PET scan was conducted, followed by 30 minute intravenous infusion of GSK1360707. The post-drug scan commenced 15 minutes after the end of the infusion. Several venous blood samples were obtained over the course of the post-drug scan to estimate the plasma concentration time-course of GSK1360707. PET emission data were obtained for 120 minutes, and regional V_T values for each ligand were derived from an appropriate compartmental model with metabolite corrected arterial plasma input function. [^{11}C]MeNER V_{ND} values were obtained with a modified occupancy plot [1].

Subsequently, SERT and DAT occupancy was assessed in 12 healthy male human volunteers with [^{11}C]DASB and [^{11}C]PE2I. Each subject received one baseline and two post dose scans of 100 minutes each in a sequential adaptive design [2] which maximises information by adjusting drug doses (between 15 and 150 mg) and scan times (between 2.2 and 27.5 hours post dose). BP_{ND} for each ligand was derived from a simplified reference tissue model with the cerebellum as a reference region, and target occupancy was estimated. For all studies, estimated occupancy for each target was fitted to the measured plasma concentration using a direct and indirect Emax model to derive a measure of in vivo affinity (IC_{50}).

Results: In *Papio Anubis,* IC_{50} were estimated at 19 ng/mL at the SERT and DAT, and 2 ng/mL at the NAT. In humans, SERT and DAT IC_{50} were 6.3 ng/mL and 18.5 ng/mL respectively (Figure 1)

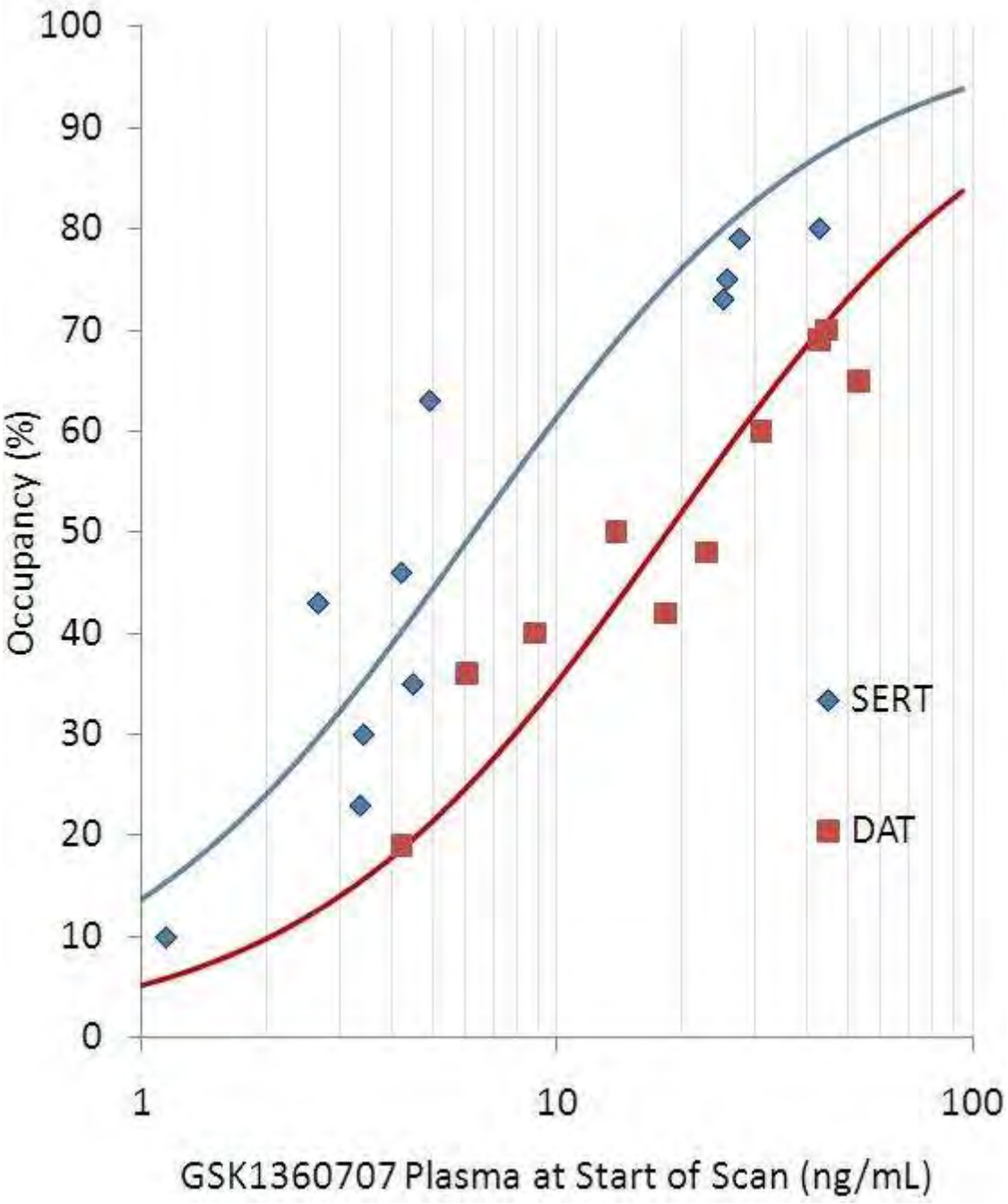

[Figure 1]

Conclusion: In vitro, the affinity ratio of GSK1360707 for human SERT, DAT and NAT is 16 : 1 : 1.3 respectively. In vivo, GSK1360707 exhibited an affinity ratio of 1 : 1 : 9.5 in *Papio Anubis* (SERT:DAT:NAT), and 3 : 1 in humans (SERT:DAT). Our data suggest that in vitro binding assays may deviate from in vivo data. The acquisition of human in vivo affinity estimates can reduce the risks associated with early drug development and improve clinical trial designs.

References:

1 - V. J. Cunningham, et al. JCBFM (2010) 30, 46-50.

2 - S. Abanades, et al. JCBFM (2010)*DOI*:10.1038/jcbfm.2010.175.

1141

VALUE OF LASER DOPPLER FLOWMETRY FOR FILAMENT MCAO IN EXPERIENCED AND INEXPERIENCED EXPERIMENTAL SURGERY

J.J. Jung[1], H. Sheng[1], Z. Wang[1], **D.S. Warner**[2]

[1]Duke University Medical Center, [2]Anesthesiology, Duke University Medical Center, Durham, NC, USA

Objective: The rodent filament MCA occlusion (fMCAO) model is employed widely. It offers the advantage of decreased surgical invasiveness (vs. craniotomy). This allows decreased morbidity in long-term recovery protocols and also may be performed by individuals with limited surgical expertise. One problem, though, is that the quality of MCAO cannot be directly observed leading to potential major variability in outcome from a standardized ischemic insult. Laser Doppler flowmetry (LDF) has been advocated to standardize MCAO and reperfusion. LDF correlates with CBF, but the instrumentation is expensive and the procedure requires additional scalp and skull surgery in recovery animals. We explored the utility of the LDF as a function of surgical experience.

Methods: Two animal surgeons, 1 having >10 years MCAO experience and the other having 1 month experience, each subjected 19-20 rats to 90 min fMCAO. In all cases, LDF values were recorded at baseline, during occlusion, and early reperfusion by another experimenter. In ½ of the animals (randomized), both surgeons were allowed to observe the LDF values. In the remaining animals, both surgeons were blinded to the LDF values. Neurologic function was scored at 1 hr (simple scoring scale 0-3, 3 = circling) and 7 days (complex functional scale 0-48, 0 = no deficit) post-MCAO. Infarct size was then measured using subtraction analysis to control for edema. Each surgeon was considered as an independent experiment for statistical analysis.

Results: For the experienced surgeon there was no effect of LDF use on immediate neurologic score. All rats had a score of 3 ($P>0.99$). For the inexperienced surgeon, immediate neuroscores were 3 for all rats with LDF use, but scattered between 0-3 without LDF ($P=0.01$). At 7 days post-ischemia, there was no effect of LDF on neuroscore for either surgeon. Cortical ($P=.81$), subcortical ($P=.73$), and total ($P=.95$) infarct volumes were not affected by access to LDF values for the experienced surgeon. For the inexperienced surgeon, infarct volumes were smaller without LDF assistance (cortical $P=0.05$, subcortical $P=.11$, and total $P=.03$). When LDF was used infarct sizes were similar to those obtained by the experienced surgeon (e.g., experienced surgeon total infarct volume =147±50 mm^3, inexperienced surgeon total infact volume = 148±31 mm^3). LDF values were corrected to % pre-ischemic baseline. Mean ± sd intra-ischemic CBF (% of baseline) was decreased with LDF for both surgeons (Experienced No LDF = 39 ± 19, LDF = 31 ± 15, $P< 0.01$; Inexperienced No LDF = 42±14, LDF = 56± 29, $P< 0.01$). There was no effect of LDF on reperfusion CBF for either surgeon.

Conclusions: LDF use had no effect on neurologic score or cerebral infarct size when used by an experienced surgeon. LDF use served to standardize severity of acute ischemic deficit and infarct size when used by an inexperienced surgeon. This study failed to demonstrate value of LDF in experienced surgical hands performing fMCAO, but showed benefit for the novice.

1142

NONINVASIVE IMAGING OF POLYMERIC DRUG DELIVERY WITH POSITRON EMISSION TOMOGRAPHY

R. Sirianni[1], M.-Q. Zheng[1], T. Patel[2], J. Zhou[3], T. Schafbauer[1], W.M. Saltzman[3], Y. Huang[1], R.E. Carson[1]

[1]Diagnostic Radiology, [2]Neurosurgery, Yale School of Medicine, [3]Biomedical Engineering, Yale University, New Haven, CT, USA

Objectives: One strategy to deliver drugs to the brain is to encapsulate the drug within a solid polymer nanoparticle. Polymeric drug delivery methods have shown promise in their ability to treat central nervous system disease, however, imaging their distribution in brain tissue is a challenge. Most currently available methods are invasive, which prevents the comparison of drug distribution with therapeutic outcome in a single subject and does not allow for imaging in humans. In this work, we use Positron Emission Tomography (PET) to quantify the distribution of radiolabeled nanoparticles that were infused directly into the rat striatum via convective enhanced delivery.

Methods: Nanoparticles composed of poly(lactic-co-glycolic acid) (PLGA) and containing the fluorescent compound coumarin-6 (C6) were prepared by single emulsion and surface modified with avidin-palmitate, a conjugate that will bind up to four biotins per molecule. For radiolabeling, avidin-palmitiate modified nanoparticles were incubated with ([^{18}F]fluorobenzylamine-poly(ethylene glycol)4-biotin, NPB4) in saline and sonicated for up to 30 minutes. Nanoparticles were infused into the striatum of rats (20µg/20µl , 0.67µl/min). Emission data were acquired during the infusion and for 30 minutes after on a microPET Focus 220. Rat brains were frozen immediately after the PET scan and later sectioned for fluorescent microscopy. The spatial volume of distribution ($V_{d\text{-}sp}$) was obtained by cropping images to exclude the injection tubing and thresholding to a fraction of the maximum value at the injection point.

Results: When nanoparticles were incubated with [^{18}F]NPB4 (0.6mCi/7mg) and centrifuged to pellet the nanoparticles, no radioactivity was detected in the wash. We estimate that < 1% of the avidin sites present on the nanoparticle are occupied by [^{18}F]NPB4, suggesting that nanoparticles can easily be labeled with a high quantity of [^{18}F]NPB4 while leaving abundant avidin sites for targeting or protective ligands. Features of the reconstructed PET images matched well with fluorescent microscope images of sectioned tissue. Nanoparticles were observed to distribute in brain tissue with a $V_{d\text{-}sp}$ that increased over time and depended on the size of the nanoparticle (figure 1). Small nanoparticles (diameter=70nm) were observed to travel significantly further than large nanoparticles (diameter=150nm), with an average $V_{d\text{-}sp}$ of 16±1mm^3 versus 57±8mm^3 (p=0.0088), presumably because small nanoparticles are better able to navigate the small extracellular space in the brain. $V_{d\text{-}sp}$ values obtained by PET are greater than values obtained by fluorescence, which reflects both the high sensitivity and inherent loss of spatial resolution encountered with PET imaging.

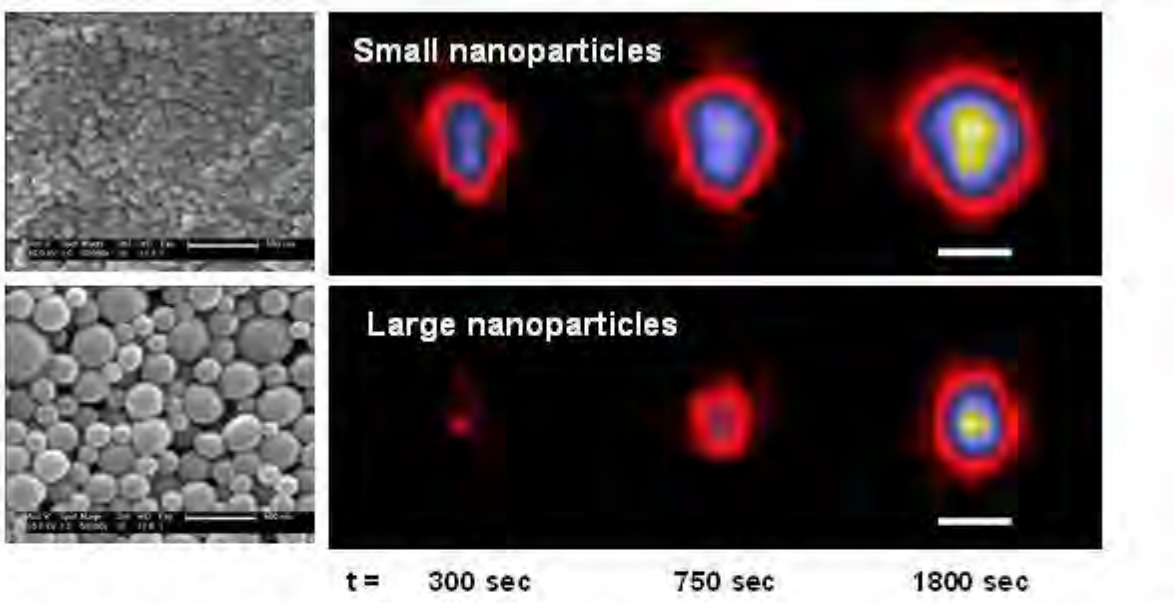

Figure 1: (Left panel) Scanning electron microscope images of small and large nanoparticles (scale bar = 500nm). (Right panel) Coronal sections of OSEM-reconstructed PET images show the distribution of small and large nanoparticles at the beginning, middle, and end of the infusion. Small nanoparticles infiltrated brain tissue at a faster rate and achieved a wider volume of spatial distribution than large nanoparticles (scale bar = 5mm).

[Figure 1]

Conclusion: One advantage of PET over other imaging methods is that it is directly quantitative. We have previously developed methods to measure the distribution of locally delivered compounds with PET, and work is ongoing to apply these methods to local and systemic delivery of radiolabeled nanoparticles. In other experiments, we are surface-modifying PLGA nanoparticles to pass through the BBB for treatment of glioblastoma multiforme in rats. The new imaging methods presented here are an exciting advancement in the ability to measure, noninvasively, the distribution of polymeric drug delivery vehicles in the body.

1144

CEREBRAL HEMODYNAMIC EFFECTS OF BLOOD TRANSFUSIONS IN NEONATES MEASURED WITH DIFFUSE OPTICS

E. Buckley[1], D.A. Goff[2], D. Hance[1], T. Durduran[1], M.N. Kim[1], R. Mesquita[1], J. Greenberg[3], M.A. Putt[4], D.J. Licht[5], A.G. Yodh[1]

[1]Physics and Astronomy, University of Pennsylvania, [2]Cardiology, Children's Hospital of Philadelphia, [3]Neurology, [4]Biostatistics, University of Pennsylvania, [5]Neurology, Children's Hospital of Philadelphia, Philadelphia, PA, USA

Objectives: Approximately 6-8 in 1,000 infants born each year are diagnosed with congenital heart defects (CHD), a third of whom require major surgical repair in the first month of life. These neonates have a high incidence (>50% (Galli, Zimmerman et al. 2004)) of hypoxic-ischemic white matter injury after heart surgery. There is emerging evidence that the greatest risk for this injury is during post-operative care when transfusions (Mahle, Tavani et al. 2002), aimed at maintaining tissue oxygenation, are common. Thus, the goal of this work is to investigate the cerebral hemodynamic effects of blood transfusions in post-operative CHD neonates.

Methods: A hybrid diffuse optical spectroscopy and diffuse correlation spectroscopy (Boas, Campbell et al. 1995; Boas and Yodh 1997) (DOS/DCS) optical device constructed in our laboratory (described previously (Durduran, Zhou et al. 2010)) acquired cerebral oxygenation and cerebral blood flow data at a rate of 0.13 Hz. All patients were monitored for 10 to 12 hours after returning from cardiopulmonary bypass surgery. The optical probe consisted of two source-detector pairs, both separated 2.5 cm apart, one designated for DOS measures of oxy-, deoxy- and total hemoglobin concentrations (ΔHbO_2, ΔHb, ΔTHC respectively), the other designated for DCS measures of rCBF. The optical probe was repositioned on the forehead routinely every two hours, or as needed in the case of poor signal quality or movement of the child. Anatomical MRI scans reveal a combined skull, scalp, and cerebral spinal fluid thickness of 0.74±0.10 cm, thus the optical techniques were probing the a few millimeters into the surface of the frontal cortex. To quantify the effects of transfusion, changes were computed from a 5-minute mean of each parameter (ΔHbO_2, ΔHb, ΔTHC, and rCBF) immediately before and after transfusion.

Results: We have captured a total of 16 blood transfusions of varying duration and amount from the 12 CHD patients we have recruited. The median (range) duration of transfusion was 24.1 (34.5) minutes and median amount of transfusion was 25.3 (10.7) mL. DTHC showed a significant median (range) increase of 9.5 (10.9) uM after transfusion ($p=0.002$, Wilcoxon signed rank test (Wilcoxon 1945)). Transfusions had mixed effects on rCBF, leading to a non-significant ($p=0.21$) population averaged change in CBF of 4.5 (24.5)%. Additionally, after dividing results into palliative and corrective CHDs (N=9 and 7, respectively), we observe a significant difference in $DHbO_2$ response to transfusion. Patients with corrected CHD show a significantly greater increase in $DHbO_2$ than those with a palliative repair of their CHD.

Conclusions: Blood transfusions are common in post-operative CHD patients. We have observed significant increases in total hemoglobin concentrations with transfusions, with varying effects on cerebral blood flow. Currently we are investigating a piglet model of transfusion in order to have normative data to compare our CHD population results and to validate the optical modalities during transfusion using well-established CBF methods.

1145

THE STABILITY OF RELATIVE CEREBRAL BLOOD FLOW (CBF) IN THE WHITE AND GRAY MATTER WITH MULTI-SLICE ARTERIAL SPIN LABELING MEASUREMENTS

B. Piotrowska[1,2], H.O. Karnath[1], U. Klose[2]

[1]Neuropsychology Section, Centre of Neurology, [2]MR-Research Group, Diagnostic and Interventional Neuroradiology, University Hospital Tuebingen, Tuebingen, Germany

Introduction: Arterial spin labeling (ASL) is a noninvasive MRI technique to measure perfusion. This method involves the measurement of pairs of tag/control images to produce the magnetization difference (ΔM) maps. ΔM is proportional to the volume of labeled arterial blood that has entered the tissue at imaging slab during the inversion time (TI2), and depends on T1 relaxation time of blood. In typical multislice ASL, after a delay TI1 a saturation pulse is applied to define the arterial bolus, and after another delay (w) the image of a slice is collected (TI2=TI1+w). If several slices are acquired within a time ta for each slice, then TI2 for the n-th slice is given by TI2(n) = TI1+w+(n-1)*ta. In this study, the influence of different TI2s on the CBF values in the gray (GM) and white matter (WM) was analyzed.

Materials and methods: Four healthy subjects were examined on a 3T Siemens MR scanner. The PASL sequence with FAIR QUIPSSII tagging scheme [1] was used to collect 8 slices, 5 mm thick with 20% gap, 30 pairs of control/tag images with following parameters: FoV = 220, matrix = 64x64, TE/TR = 19ms/3000ms, TI1 = 800ms. TI2 for the first slice was 1800ms, and respectively longer for further slices (60ms per slice). After ASL measurement, high resolution T1 MPRAGE images were collected for coregistration, normalization and segmentation. Data sets were preprocessed using SPM8 and home-written routines in Matlab 9.10. The pair-wise subtractions were generated from realigned pairs of control/tag images, and the CBF was calculated using General Kinetic Model [2]. From segmented anatomical scans, the white (WM) and grey matter (GM) masks were extracted for the further data evaluation. The mean CBF values in dependence on the number of slice were investigated.

Results: The calculated CBF maps were in good quality for all subjects examined. Fig.1 shows the mean CBF values for GM and WM versus slice position, averaged across all subjects. There was no dependence of the CBF values on the slice position, however the calculated CBF in the WM showed higher values in the first four slices. Averaged over all subjects and slices, the CBF was 50.8 ± 5.6 for the GM, and 18.7 ± 4.0 ml/100g/min for the WM.

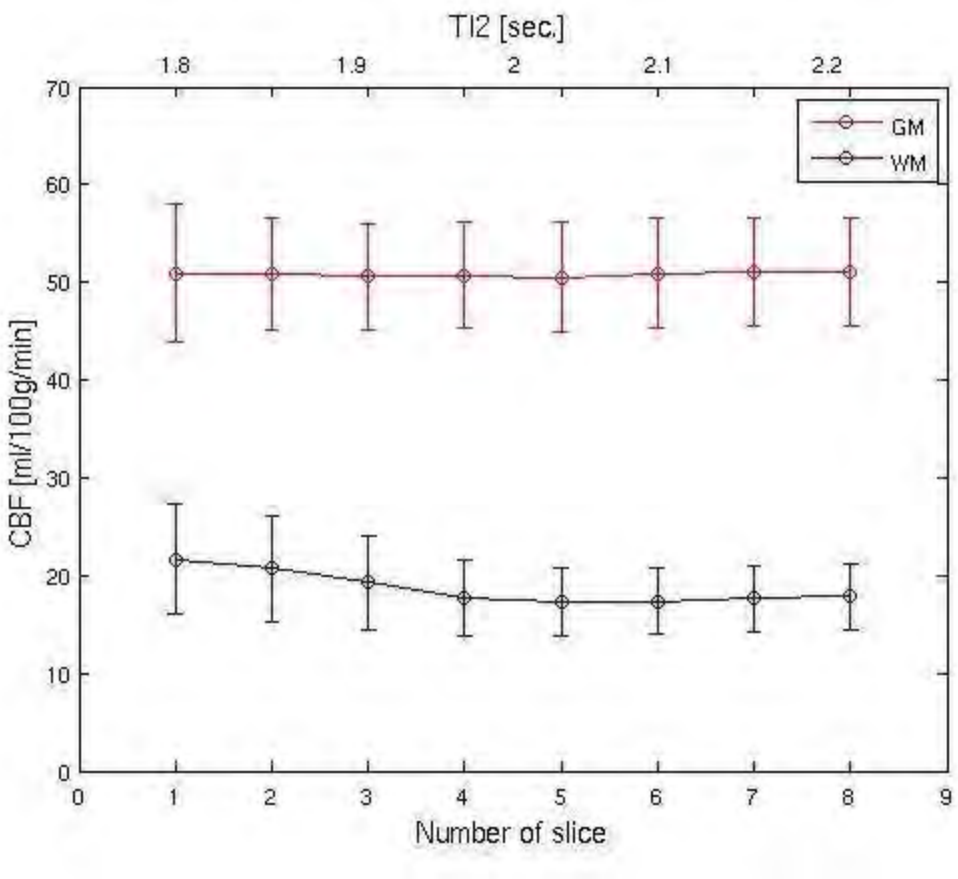

[The mean CBF values in the GM (red) and WM (blue)]

Discussion: The results are consistent with previous studies [3,4]. Small differences between CBF values can be due to the saturation by neighboring slices, but they are too small to affect the pathological findings in the relative CBF values.

Acknowledgements: This study was supported by a research stipend of the Werner Reichardt Centre for Integrative Neuroscience in Tübingen, Pool project 2008/13.

References:

[1] Wong E.C. et al, Magn Reson Med., 39:702-708, 1998.

[2] Buxton R.B. et al, Magn Reson Med., 40:383-396, 1998.

[3] Campbell A.M., Beaulieu Ch., Magn Reson Imaging, 24:869-876, 2006.

[4] Calamante F. et al, J Cereb Blood Flow Metab., 19:701-35, 1999.

1147

NEUROVASCULAR COUPLING INVESTIGATED USING COMBINED OPTICAL COHERENCE TOMOGRAPHY AND ELECTROPHYSIOLOGY MEASUREMENTS IN RATS

H. Radhakrishnan, V.J. Srinivasan, M.A. Yaseen, W. Wu, **M.A. Franceschini**

Athinoula A. Martinos Center for Biomedical Imaging, Massachusetts General Hospital, Charlestown, MA, USA

Objective: Neurovascular coupling has been investigated predominantly using simultaneous measures of electrophysiological data with measurements of hemodynamic changes using intrinsic optical imaging and spectroscopy laser Doppler flowmetry. In this study, we present a novel method of combining Optical Coherence Tomography (OCT) with electrophysiology measurements to investigate neurovascular coupling. Frequency-Domain OCT (FD-OCT) offers sufficient penetration depth to image most of the brain cortical layers, and good spatial resolution to detect relatively small vessel diameter changes. This enables quantification of depth-resolved blood flow changes using the Doppler effect in response to stimulation (Srinivasan et al. 2009; 2010). The goals of this study were (i) to test whether there are differences in the neural and vascular responses in different cortical layers and (ii) to establish whether a surface measure (electrical and/or vascular) is sufficient to describe the neurovascular relationship.

Methods: Eighteen Sprague-Dawley rats were used, divided into 3 groups based on the maintaining anesthetic (Alpha-Chloralose, Ketamine/Xylazine, and Isoflurane). Hemodynamic changes in a 1-mm line scan by 1-mm depth were obtained from a commercial frequency-domain OCT system (FD-OCT) simultaneously with electrophysiology data obtained using a standard profile tungsten electrode inserted to ~600 microns in the rat cortex and a ball electrode positioned in contact with the thinned skull from a region of maximal activation previously determined. A total of 6 runs, each lasting 6 minutes and consisting of varying frequency (1-5 Hz, mean ISI = 12 sec) event-related parametric forepaw stimuli, were conducted on each animal. Relative blood flow changes and neuronal responses (LFP, MUA, and surface potentials) were calculated for each stimulus condition and anesthetic group. Flow responses were resolved by depth and correlated with the electrophysiology data using a linear convolution model.

Results: Neuronal responses showed varying habituation effects for the three anesthetics - alpha-chloralose exhibited strong habituation at frequencies higher than 2 Hz while ketamine/xylazine did not habituate. Depth-resolved flow changes showed habituation patterns similar to the neuronal responses, but were not significantly different across depths. To determine the best predictor of flow, area under the neuronal response curves were used as inputs to a linear convolution model. Results show that the N1

surface potential component and LFP from layers III-IV are better predictors of blood flow responses than P1 surface potential component while MUA is the worst predictor of blood flow.

Conclusion: We have, for the first time, successfully integrated electrophysiology measurement with OCT to investigate neurovascular coupling in an animal model. The finding of N1 being a better predictor of hemodynamic changes than P1 agrees with results from our previous macroscopic NIRS-EEG experiments (Franceschini et al. 2008; 2010). This is further proof of the predominant role of secondary synaptic activity in driving hemodynamic responses.

Moreover, our results suggest that surface measures of electrical and flow responses could be sufficient to determine neurovascular coupling.

References:

Franceschini, M.A., et al. 2008. Neuroimage 41, 189-203.

Franceschini, M.A., et al. 2010. Neuroimage 51, 1367-1377.

Srinivasan, V.J., et al. 2009. Optics Letters 34, 3086-3088.

Srinivasan, V.J., et al. 2010. Optics Express 18, 2477-2494

1148

INHIBITION OF THE ENDOTHELIAL NOS AFTER CONTROLLED CORTICAL IMPACT IN MICE

S. Schwarzmaier[1], N. Terpolilli[2], N. Plesnila[1]

[1]Neurodegeneration, Royal College of Surgeons in Ireland, Dublin, Ireland, [2]Neurosurgery, Ludwig-Maximilians University Munich, Munich, Germany

Objective: Traumatic brain injury (TBI) is associated with a multitude of microvascular alterations resulting in secondary brain damage. Among others NO synthases (NOS) are suspected to be involved in these mechanisms. In a previous study we showed that administration of the NOS inhibitor VAS203 has beneficial effects after CCI (Terpolilli et al. 2009). The mechanisms underlying this effect could not be fully explained by inhibition of the inducible NOS (iNOS) which is up-regulated only after injury. Therefore we investigated the effect of VAS203 on cerebral vessel diameter in order to determine whether also the upregulation of one of the constitutive NOS, in this study the endothelial NOS (eNOS), is involved in secondary brain damage.

Method: C57/Bl6 mice (n=12) were intubated and ventilated under continuous control of end tidal CO_2. After preparation of a cranial window and baseline recordings, animals were subjected to controlled cortical impact (CCI; 6m/s, 0.5mm). 30 min after CCI either VAS203 or control NaBP were administered. Arteriolar and venular lumen was visualized in vivo by FITC-dextrane and vessel diameters were monitored by intravital microscopy (IVM) both before and up to 2.5h after CCI.

Results: Animals had normal end tidal CO_2 and MABP values during IVM. The arteriolar diameter was stable during baseline monitoring, after CCI, however, it increased to 108.2+/-2.7% or 109.8+/-6.5% of baseline before any treatment. Administration of NaPB had a small but not significant constrictive effect on cerebral arterioles. By contrast, administration of VAS203 resulted in a significant vasoconstriction, i.e. 92.2+/-2.1% of baseline or to 85.3 % of posttraumatic diameter in arterioles. No significant effect of both VAS206 and NaBP was seen in sham operated animals.

Conclusion: The arteriolar dilatation that occurs after CCI could be completely inhibited by VAS203. Hence this vasodilatation is very likely to be induced by an upregulation of eNOS after TBI. The vasoconstrictive effect did not induce a reduction of CBF but resulted in a reduction of posttraumatic ICP. This might be due to a restoration of cerebral compliance. Thus the acute effect of VAS203 on ICP can be explained by the inhibition of post-traumatically increased eNOS activation.

Reference List:

Terpolilli NA, Zweckberger K, Trabold R, Schilling L, Schinzel R, Tegtmeier F, Plesnila N (2009) The novel nitric oxide synthase inhibitor 4-amino-tetrahydro-L-biopterine prevents brain edema formation and intracranial hypertension following traumatic brain injury in mice. J Neurotrauma 26:1963-1975

1151

SURROGATE MRI SIGNATURERS FOR GD-DTPA CONTRAST-ENHANCED IMAGING THAT MAY PREDICT ACUTE BLOOD-BRAIN BARRIER DAMAGE AFTER REPERFUSION FOLLOWING CEREBRAL ISCHEMIA

R.A. Knight[1], T.N. Nagaraja[2], J.R. Ewing[1], K. Karki[1], V. Nagesh[1], J.D. Fenstermacher[2]

[1]Neurology, [2]Anesthesiology, Henry Ford Hospital, Detroit, MI, USA

Background and aims: Gadolinium-diethylenetriaminepentaacetic acid (Gd-DTPA) contrast-enhanced MRI is widely used to measure blood-brain barrier (BBB) damage after stroke. However, Gd-DTPA MRI is contra-indicated in cases with compromised kidney function. There is a need, therefore, for alternative MRI techniques that can portend the likelihood of BBB damage. This study examined the temporal and quantitative relationships between some non-contrast MRI measures and Gd-DTPA contrast-enhanced data to test whether the former serve as surrogate markers of BBB damage in acute stroke.

Methods: Male Wistar rats (~300 g; N=22) were subjected to cerebral ischemia via suture occlusion of the right middle cerebral artery (MCA). The suture was then withdrawn to initiate reperfusion 3 hours after occlusion. During occlusion and after reperfusion, the rats were studied using multiparametric MRI in a 7 Tesla magnet. The MRI parameters measured were: cerebral blood flow (CBF), T_2, MT-related parameters such as T_1 and T_1 under off resonance saturation (T_{1sat}). Quantitative maps of these data were constructed. All the data except CBF were expressed as contralateral-to-ipsilateral ratios (C-I). About 2.5 hours after reperfusion, Gd-DTPA contrast-enhanced imaging was performed using quantitative Look-Locker (LL) technique. The LL data were used to construct Patlak plot maps of blood-to-brain influx rate constant (K_i). The multiparametric MRI maps were compared to the K_i map from the same region of interest (ROI). Scatter plots with Pearson correlation coefficients (r) were used to compare separately CBF from the two sets of flow maps to K_i. Significance was inferred at $P< 0.05$.

Results: All the rats were affected by MCA occlusion, albeit to slightly varying degrees. Brain regions of preoptic area (PoA) and striatum (Str) were found ischemic in nearly all, whereas the neocortical areas were less affected. During occlusion, CBF (mean±SD) was 42±18 and 26±15 ml/100g/min (20-25% of contralateral side) in the preoptic area (PoA) and striatum (Str), respectively. After reperfusion, CBF was 78±27 and 99±50 ml/100g/min (45-55% of the contralateral side) in the PoA and Str, respectively. Contrast enhancement or BBB damage was observed in the PoA in all the 22 rats and in Str too in 17 out of 22. The C-I values of T_2, T_1 and T_{1sat} were elevated between occlusion and reperfusion periods and such elevations were associated with increased K_i values suggesting they were indicative of impending BBB damage. Comparison of CBF in such regions showed that the extent of reductions during occlusion were significantly, but negatively, correlated with increased K_i ($r= -0.5$; $P=0.03$) and that this relationship was lost after reperfusion ($r=0.3$; $P=0.3$).

Conclusions: These data suggest that changes in parameters such as T_2, T_1, T_{1sat} are predictive of impending acute BBB damage in this experimental model of stroke. Reduction in CBF during stroke also turned out to be a good predictor of BBB damage. The utility of these potential surrogate MRI signatures needs to be tested using clinically relevant embolic stroke models with a thrombolytic drug. If confirmed, it may lead to a non-contrast based MRI evaluation of the BBB in stroke in cases where Gd-DTPA is contra-indicated.

1152

MODELLING DRUG CONCENTRATION-TIME PROFILE IN BRAIN: PHYSIOLOGICALLY-BASED PHARMACOKINETICS (PBPK) WITH AND WITHOUT DIFFUSION LIMITED PERMEABILITY

L. Gaohua[1], C. Rosenbaum[2], S. Neuhoff[1], T.N. Johnson[1,3], M. Jamei[1], A. Rostami-Hodjegan[1,4]

[1]Simcyp Limited, Sheffield, UK, [2]Faculty of Pharmacy, Uppsala University, Uppsala, Sweden, [3]Department of Pharmacy, Sheffield Children's Hospital, Sheffield, [4]Centre of Applied Pharmacokinetic Research, The School of Pharmacy and Pharmaceutical Sciences, The University of Manchester, Manchester, UK

Objectives: The drug concentration-time profile in brain may differ from that in plasma. Perfusion limitation in the absence of any diffusion barrier must be considered in any dynamic (non-steady state) investigation to obtain an expected profile prior to reaching conclusions on the impact any active influx or efflux transporters may have. The purposes of this study were two fold:

1- To provide an example through modelling and using known physiological parameters on potential disparity between drug concentration-time profile in brain in two group of subjects in the absence of any transporter involvement in despite drug concentration-time profile in plasma being the same (paediatrics *vs* adults),

2- To outline a modelling approach for incorporation of a multiple compartmental brain representation within an existing and commonly used PBPK model (Simcyp Population-Based Simulator) which is feasible and of practical value.

Methods:

Part I - A perfusion limited PBPK model (Simcyp Population-Based Simulator V9) was used to evaluate kinetics of 4 compounds with varying tissue-to-blood equilibrium ratios (K_P): diclofenac, theophylline, sildenafil and dextromethorphan. Both oral and intravenous administrations were investigated in different age groups (fixed mg/kg dose; three different rates). The ratios of the maximum drug concentration in brain ($C_{max,br}$) and plasma ($C_{max,p}$) were calculated and compared with those in adults.

Part II - Literature were reviewed to obtain the physiological and anatomical attributes for the three barriers that primarily limit drug transport from blood to the brain and cerebrospinal fluid (CSF) (i.e. the blood-brain barrier (BBB), the blood-CSF barrier, the ependyma (CSF-brain barrier)) and to evaluate various compartmental models representing lumped or fully separated segments (1 to 5 compartments) taken from previous reports. Using the Simulink (Matlab), various simulations were carried out to explore “what-if” scenarios.

Results:

Part I - Major disparities in C_{max} ratios (brain/plasma) were observed, particularly for the compounds with high K_P. The discrepancies were related to age, rate of administration, and type of drug.

Part II - Drug concentration in the 4 compartments could be simulated based on existing data. These showed a difference in drug concentration-time profile in spinal CSF in comparison to

that in cranial CSF (consistent with differences in the spinal CSF concentration obtained from the lumbar puncture and the concentrations in the ventral CSF or brain mass).

Conclusions: The differences in drug brain/plasma ratio between paediatric and adults are possible in the absence of any transporter related effects in the BBB; simply due to physiological changes occurring during the first few years of life particularly those related to brain blood perfusion. Hence, any investigation into the effect of transporter expression in various groups should consider the hemodynamic variations.

Our simulation of compartmental brain model suggested feasibility of dividing CSF into 2 compartments (cranial and spinal parts) for exploring the distribution of drugs to brain and CSF and the utilization of lumber puncture in monitoring drug disposition in the CNS.

1153

AXONAL OUTGROWTH AND MYELINATION IN THE CORTICAL PERI-INFARCT AREA AFTER HUMAN AND EXPERIMENTAL STROKE

Y. Ueno[1], M. Chopp[1,2], L. Zhang[1], B. Buller[1,2], N.L. Lehman[3], X.S. Liu[1], C. Roberts[1], Z.G. Zhang[1]

[1]Neurology, Henry Ford Hospital, Detroit, [2]Physics, Oakland University, Rochester, [3]Pathology, Henry Ford Hospital, Detroit, MI, USA

Aims: Axonal and dendritic remodeling are critical to brain repair after stroke. Neurofilaments are the most abundant cytoskeletal element in axons and dendrites. The phosphorylated high molecular weight neurofilament (pNFH) participates in axonal and dendritic growth. We analyzed the temporal and spatial profiles of pNFH levels and axonal myelination in ischemic rat and human brains after stroke and investigated the signaling pathways that mediate pNFH expression and axonal growth.

Methods: Adult rats subjected to permanent middle cerebral artery occlusion were sacrificed at 7, 28, and 56 days after stroke (n=6/group). Sham operated rats (n=6) were used as a control group. Human brain samples with acute ischemia (n=3) and infarction (n=2) were also studied. The pNFH and myelin basic protein (MBP, an oligodendrocytic marker) expression were measured immunohistologically. Golgi-Cox staining was performed to measure morphological changes of dendrites and spines. In vitro, cortical neurons isolated from E17 rat embryos were challenged by oxygen-glucose deprivation (OGD) and cultured in a Standard Neuron Device which separated axons from neuronal cell bodies. Co-culture of neurons with differentiated N20.1 cells, an oligodendrocyte progenitor cell line, was employed for analysis of axonal myelination. OGD challenged axons were treated with pharmacological inhibitors of PI-3K/Akt and GSK-3β.

Results: Sham-operated rats exhibited abundant $pNFH^+$ neuronal fibers in the cortex and the majority of pNFH fibers were myelinated as measured by co-localization with MBP. At 7 days after stroke, $pNFH^+$ fibers substantially decreased in the ipsilateral cortex (25±11%) compared to the homologous areas of sham-operated rats (33±14%, $p< 0.01$). However, the percentage of $pNFH^+$ fibers in the peri-infarct cortical areas significantly increased to 19% and 52% at 28 and 56 days after ischemia, respectively, compared to the percentage of $pNFH^+$ fibers at 7 days of ischemia ($P< 0.05$). A majority of $pNFH^+$ fibers were myelinated at 56 days from the levels at 7 days after ischemia (72% vs 42%, $P< 0.01$). Golgi-Cox staining revealed that cortical neurons in the peri-infarct areas had significant increases in the numbers of dendritic spines at 56 days after ischemia (16±5% vs 6±2% at 7 days of ischemia, $P< 0.01$). Furthermore, in human brains, $pNFH^+$ axons substantially increased in peri-infarct areas compared to that in ischemic boundary regions of acute ischemia (42±10% vs 23±6%, $P< 0.01$). Many of pNFH axons in peri-infarct area were co-localized to MBP. In vitro, neurons challenged by OGD exhibited reduction of axons at 24h, whereas axonal elongation and increase in pNFH protein levels were detected at 96h after OGD ($P< 0.05$). These axons were myelinated by oligodendrocytes. Concurrently, reduction of phosphorylated PTEN and increases of phosphorylated Akt and GSK-3β protein levels were detected at 96h after OGD ($P< 0.05$), suggesting that downregulation of PTEN activates Akt that inhibits GSK-3β activity. Blockage of PI3K/Akt suppressed the elevated pNFH, whereas GSK-3β inhibitors augmented the pNFH ($P< 0.05$).

Conclusions: Stroke induced axonal outgrowth occurs in rodent and human ischemic brains

during stroke recovery. Newly generated axons are myelinated. The PTEN/Akt/GSK-3β signaling pathway may mediate pNFH expression and axonal outgrowth after ischemia.

1154

INCREASED NEUROINFLAMMATION IN THE BRAIN OF AGEING CORPULENT (JCR:LA-CP) RATS: A POSITRON EMISSION TOMOGRAPHY STUDY

H. Boutin[1], K. Burnett[1], C. Drake[1], A. Denes[1], A. Smigova[2], P. Julyan[3], R. Maroy[4], M. Kassiou[5], G. Brown[2], K. Herholz[2], S. Allan[1], N. Rothwell[1]

[1]Faculty of Life Sciences, [2]Wolfson Molecular Imaging Centre, University of Manchester, [3]North Western Medical Physics, Christie Hospital, Manchester, UK, [4]SHFJ, CEA, Orsay, France, [5]School of Chemistry, University of Sydney, Sydney, NSW, Australia

Introduction: Despite intense research and development of several animal models, drugs efficient in preclinical model of cerebral ischaemia have failed so far when reaching clinical trial[1]. One striking feature of the animal models is the lack of co-morbidities and risk factors when compared to clinical set-up, in which patients have atherosclerosis, high blood pressure, chronic and/or acute inflammation due to chronic inflammatory diseases and infections. Inflammation and neuroinflammation in particular are known aggravating factors of stroke outcome[2]. Here we investigate the impact of known risk factors of stroke such as obesity and atherosclerosis in JCR:LA-cp (corpulent) rats on neuroinflammation as measured by TSPO expression in activated microglia.

Methods: Neuroinflammation was assessed with [18F]DPA-714 by PET in Lean (control: Cp/?) and JCR:LA-cp (corpulent: Cp/Cp) rats PET imaging. 2 groups of rats were scanned at 9 months or 12 and 15 months of age (n=3~4 per group). PET images were co-registered with a MRI template[3] for analysis and automatic segmentation performed for user-independent ROI determination[4,5], a simplified digital Paxinos atlas was also used for anatomical ROI quantification. Euthanasia was performed at 9 months and 15 months of age 3 to 7 days after PET imaging to assess various neuroinflammation biomarkers (GFAP, IBA1, VCAM) by immunohistochemistry (IHC).

Results: Neuroinflammation, as quantified by [18F]DPA-714 PET imaging, was significantly increased in corpulent rats when compared to lean rats in peri-ventricular and subcortical brain structures (+53%, Figure 1) and in less extent in the rest of the brain (+37%) at 15 months of age. Similar trend were also observed at 12 months of age, but only reached significance (+35%) in cortical areas of corpulent rats. IHC for microglial activation confirmed the PET data in 15 months old animals (Figure 1).

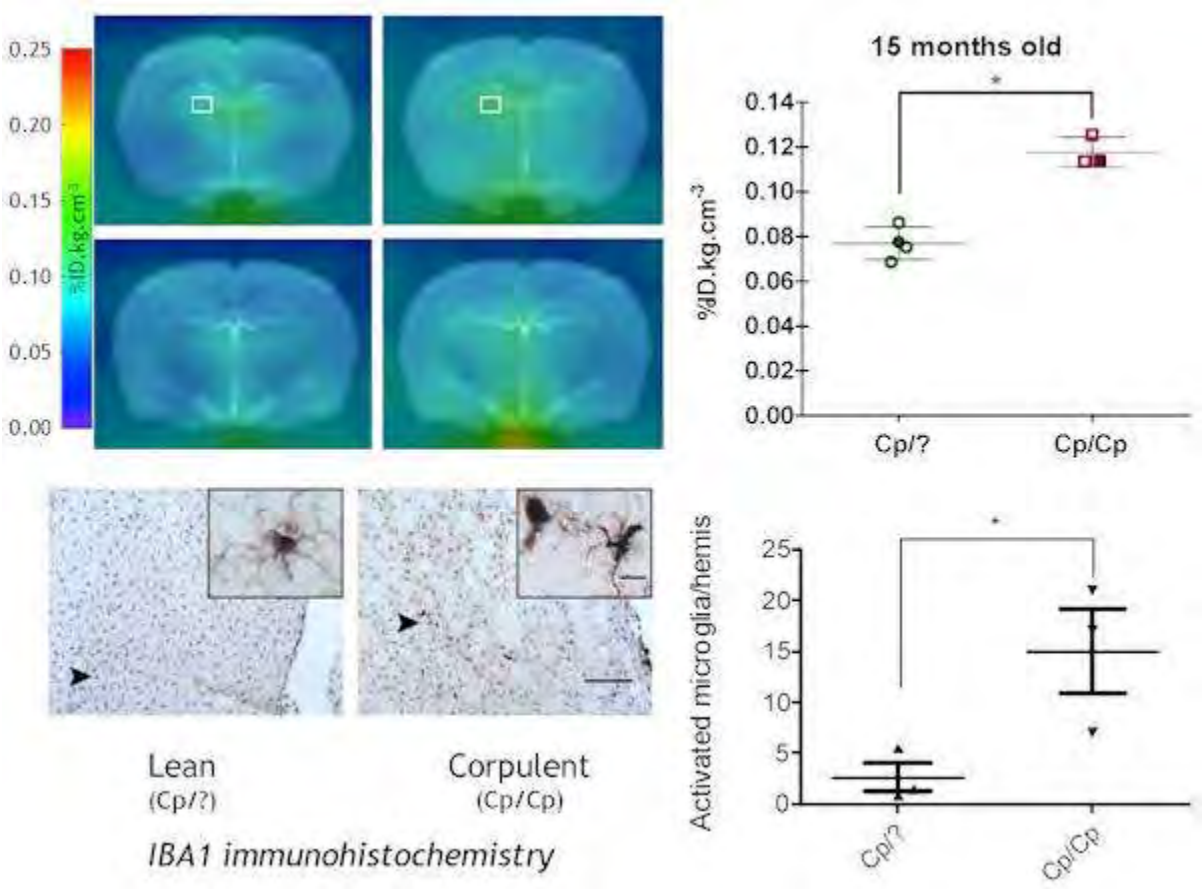

[Figure 1]

Conclusions: Our data show here the importance of taking into account risk and co-morbidity factors in preclinical models of stroke as they have a significant impact on neuroinflammation. This study shows the crucial role of molecular imaging with the high translational value of PET imaging to investigate such paradigms. The effect of stroke in these animals and potential neuroprotection by interleukin-1 receptor antagonist are presented by Pradillo et al. at this meeting.

References: [1]. Dirnagl U. (2006) J Cereb Blood Flow Metab. 26:1465-1478; [2]. McColl B.W. et al. (2009) Neuroscience. 158:1049-1061;[3]. Schwarz A.J. et al. (2006) Neuroimage. 32:538-550; [4]. Maroy R. et al. (2008) IEEE Trans.Med.Imaging. 27:342-354; [5]. Maroy R.et al. (2010) The Journal of Nuclear Medicine (Submitted).

Acknowledgement: Prof. N. Rothwell and Dr H. Boutin are funded by MRC. We are grateful for funding provided by the European Union´s Seventh Framework Programme (FP7/2008-2013) under grant agreements n° 201024 and n° 202213 (European Stroke Network, NR, AD). This study was carried out within the EC-FP6 project DiMI (LSHB-CT-2005-512146) framework.

1155

EARLY BRAIN TISSUE OXYGENATION IS RELATED TO SELECTIVE NEURONAL LOSS FOLLOWING CLINICAL HEAD INJURY

V. Newcombe[1,2], I. Timofeev[3], C. Williams[1], D. Chatfield[1], P. Hutchinson[3], J. Coles[1,2], J. Pickard[2,3], G. Williams[2], A. Gupta[1], D. Menon[2,3]

[1]Division of Anaesthesia, [2]Wolfson Brain Imaging Centre, [3]Academic Department of Neurosurgery, University of Cambridge, Cambridge, UK

Introduction: We have previously used ^{11}C-flumazenil positron emission tomography to show that selective neuronal loss in the thalamus is pervasive after traumatic brain injury (TBI) and correlates with functional outcome,[1] findings that are concordant with previous post-mortem data.[2] The mechanisms responsible are unclear, but may involved global hypoxia/ischaemia as well as retrograde degeneration.

Objectives: We hypothesised that early brain tissue oxygenation would correlate with late diffusion tensor imaging (DTI) abnormalities in the thalamus, and therefore, help to provide an explanation for late neuronal loss.

Methods: Nine patients underwent brain tissue oximetry (PbO_2) following acute TBI, using a Licox PbO_2 probe, sited in structurally normal frontal white matter. Mean PbO_2 was calculated for the duration of their intensive care admission. At a median of 11.6 months (range 237 to 702 days) they underwent magnetic resonance imaging, including DTI. Apparent diffusion coefficient ADC (maps) were created, ADC calculated in regions of interest in the frontal lobes, splenium of the corpus callosum and thalami, and correlated with mean PbO_2 using Spearman's Rho. Ethical approval was obtained from the Local Research Ethics Committee, and assent from next-of-kin was obtained in all cases. **Results:** Mean PbO_2 was inversely related to ADC in both frontal lobes ($r = -0.73$ & -0.72; $p = 0.025$ & 0.031), and with the ADC in the thalamus bilaterally ($r = -0.87$ & -0.80; $p = 0.002$ & $p = 0.010$). In contrast, no correlation was seen between mean PbO_2 and ADC in the splenium of the corpus callosum, a common site of traumatic axonal injury (TAI; $p = 0.265$).

Discussion: The inverse correlation of mean PbO2 associated with ADCs in the monitored brain region is unsurprising, but the correlations observed with contralateral regions and deep grey matter suggest that the burden of tissue hypoxia has a significant impact on secondary neuronal loss across the brain. In contrast, the lack of correlation with ADC changes in an area at risk of traumatic axonal injury (TAI) suggests a less significant impact of hypoxia on the progression or maturation of TAI. The correlations with measures of thalamic microstructural injury are particularly significant, since they establish a clear link between acute physiology, tissue fate in key brain regions, and clinical outcome.

References:

1.Coles J, et al. Evidence for selective neuronal loss following clinical head injury (abstract) J Neurotrauma 2009 26:A2-A101

2. Maxwell WL, et al. Differential responses in three thalamic nuclei in moderately disabled, severely disabled and vegetative patients after blunt head injury. Brain 2004;127:2470-8

1157

PROTECTION OF OGD-CHALLENGED ASTROCYTE DYSFUNCTION IS PREDOMINANT OVER PREVENTION OF THEIR DEATH IN NEURONAL SURVIVAL

E. GOUIX[1,2], N. Blondeau[1,3], A. Buisson[4], L. Had-Aissouni[2]

[1]Institut de Pharmacologie Moléculaire et Cellulaire, CNRS UMR 6097- Université of Nice, Valbonne, [2]Institut de Biologie du Développement de Marseille Luminy, CNRS UMR 6216 - Université de la Méditerranée, Marseille, [3]Université de Nice-Sophia Antipolis, Nice, [4]Centre CYCERON, CNRS UMR 6232 CiNAPS- Université de Caen Basse Normandie, Caen, France

Objectives: During decades, astrocytes were thought being only “supportive” brain cells. Nowadays it is acknowledged that they are potent regulators of neuronal plasticity and activity in physiological conditions. Although astrocyte dysfunction and/or death are suspected to be detrimental for neurons, their contribution in pathological conditions like stroke is poorly understood. Our study aimed at determining whether the prevention of astrocyte dysfunction and/or death may be important for neuronal survival.

Methods: To reproduce stroke in vitro, we used the oxygen glucose deprivation model (OGD). Differentiated astrocytes were obtained adding Dibutyryl-AMPc to the culture medium. The viability of astrocytes was estimated by LDH release and MTT assay. The phenotype of astrocytic death was determined by microscopy and cleaved caspase-3 western blot analysis. The viability of neurons that were co-cultured with OGD-challenged astrocytes was assessed by LDH and MTT assay. Anti-inflammatory or antioxidant strategy with AA861, a 5-lipoxygenase inhibitor, or N-acetylcysteine (NAC promotes glutathione synthesis) was respectively used to protect astrocytes against OGD. The impact of astrocyte death inhibition was then evaluated on neuronal survival. Alteration of glial Excitatory Amino Acid Transporters (EAAT) pathways was investigated by immunocytochemistry of EAAT1 and 2 (GLAST and GLT1), HPLC measurements of extracellular glutamate and detection of intracellular glutathione (GSH) with a nonenzymatic fluorescent reagent.

Results: OGD shorter than 3 hours didn't elicit cell death in undifferentiated and differentiated astrocytes cultures. 3h-OGD induced a massive death in differentiated astrocytes, while it triggered a less pronounced death and a transformation into Alzheimer type II-like astrocytes of the undifferentiated astrocytes.

3h-OGD decreased GSH intracellular content of both types of astrocyte cultures. GSH depletion and abolition of glutamate re-uptake were more pronounced in differentiated astrocytes, which also displayed an impaired expression of EAAT 1 and 2.

In differentiated astrocytes, 3h-OGD induced oxidative/inflammatory mechanisms leading to caspase-3 mediated apoptosis. Application of AA861, NAC or DEVD-CHO, a caspase-3 selective inhibitor, reduced differentiated astrocytes death induced by 3h-OGD.

Fifty percent of the naïve neurons that were placed and co-cultured in the well of 3h-OGD challenged astrocytes (differentiated or undifferentiated) died the first day of co-culture. Interestingly, neuronal death was not exacerbated by differentiated astrocyte death, suggesting that astrocyte loss is not the neuronal death driving mechanism. Indeed, single application of AA861 or NAC that inhibited astrocytes death throughout 3 days post-OGD didn't protect neurons from death induced by OGD-challenged astrocytes.

Conclusions: Our results suggest that:

1/ the vulnerability of differentiated astrocytes to 3h-OGD could be related to impaired expression/distribution of EAAT resulting in an inactivation rather than an inversion of EAAT function.

2/ Impaired distribution and function of EAAT trigger oxidative and inflammatory pathways and apoptosis.

3/ Astrocyte EAAT dysfunction is highly detrimental for neurons while differentiated astrocyte death does not exacerbate neuronal death.

Our results suggest that targeting the astrocyte dysfunction may constitute an interesting strategy to indirectly protect neurons from stroke. Therefore the understanding of the mechanism leading to EAAT inactivation is crucial especially if the inactivation is due to an enzymatic activity that could be the target of new therapeutic.

1158

LONG-TERM ASSESSMENT OF FUNCTIONAL IMPAIRMENT IN ISCHEMIC MICE

M. Montinaro[1], P. Villa[1,2], E.R. Zanier[1], M. Leoni[1,3], F. Pischiutta[1], E. Micotti[1], A. Paladini[1], M.G. De Simoni[1]

[1]Neuroscience, Mario Negri Institute, [2]CNR, Institute of Neuroscience, [3]University of Milan, Department of Anesthesia and Critical Care Medicine, Fondazione IRCCS Ca' Granda Ospedale Maggiore Policlinico, Milan, Italy

Objectives: There is an urgent need to develop predictive preclinical long term functional outcome tests that can be used, along with neural pathological markers, to help in translational research. Whereas behavioural impairments after stroke are increasingly studied in the rat, little is known about the long-term functional consequences of focal ischemia in mice. This study was designed to identify an array of complementary tests to reveal both short and long-term sensorimotor, behavioural and cognitive consequences of transient cerebral artery occlusion (tMCAo) in mice.

Methods: Adult C57Bl/6 male mice (26-28g) were anesthetized with isofluorane and subjected to right tMCAo (30 min) or sham surgery. Sensorimotor performance was assessed at 1, 3, 6, 9 and 12 weeks postinjury by performing rotarod, negative geotaxic (NG), composite neuroscore (NS), beam-walk time (BWt) and footfaults (BWf), grip and corner tests (n=12). Exploratory behaviour was assessed at 3 and 9 weeks by means of the open field test (n=9). Cognitive function was assessed at 5 and 11 weeks postinjury using the Morris water maze (MWM) and passive avoidance (PA), n=12. All investigators who performed behavioural assessments were blinded to the surgery.

Results: tMCAo mice showed a significant reduction in time spent on the rotarod from 1 up to 12 weeks postinjury (47% reduction at 12 weeks). Similarly, the NG test revealed a significant increase in right turns from 1 up to 12 weeks in tMCAo compared to sham mice (% of right turns at 12 weeks postinjury: tMCAo 89%, sham 46%). A smaller although significant difference between tMCAo and sham mice at all time points considered was also evident both at NS and BWt tests (12 weeks postinjury NS: median 10(range:8-11) and 12(11-12); BW: mean±SD 115.8±128.4 and 48.7±18.5 in tMCAo and sham mice respectively). No significant impairments could be detected by delivering BWf and grip tests. tMCAo mice also showed a significant impairment in exploratory behaviour at both time points assessed (time in contact with objects 9 weeks postinjury: tMCAo 12.8±9.1, sham 47.9±29.5 seconds, $p< 0.05$) as well as in spatial learning abilities at MWM both at 5 and 11 weeks post-injury (11 weeks postinjury latency to platform: tMCAo 42.7±12.8, sham 23.3±4.9 seconds, $p< 0.0001$). No significant cognitive impairment could be detected by PA.

Conclusions: Our findings demonstrate that rotarod, NG, open field and MWM tests are reliable tools to assess sensorimotor and cognitive function impairment up to 12 weeks after ischemia. The weak impairment detected by NS and BWt questions their usefulness to detect a protective effect. These results provide an array of tests that can help to reveal the long term effectiveness of protective or regenerative therapies in stroke murine models.

References:

1. Bouet V, Exp Neurol 2007; 203: 555-67
2. Hicks A, Cell Stem Cell 2009; 5:139-40

1159

ASSESSMENT OF TREATMENT RESPONSE IN PATIENTS WITH GLIOBLASTOMA MULTIFORME USING [^{18}F]FLUOROETHYL-L-TYROSINE PET

N. Galldiks[1,2], M.D. Piroth[3,4], R. Holy[3,4], M. Pinkawa[3,4], G. Stoffels[4,5], H.J. Kaiser[4,6], G.R. Fink[1,2], H.H. Coenen[4,7], M.J. Eble[3,4], K.J. Langen[4,5]

[1]Institute of Neuroscience and Medicine 3, Cognitive Neurology, Forschungszentrum Jülich, Jülich, [2]Dpt. of Neurology, University of Cologne, Cologne, [3]Dpt. of Radiation Oncology, RWTH Aachen University Hospital, Aachen, [4]Jülich-Aachen Research Alliance (JARA) - Section JARA-Brain, Jülich-Aachen, [5]Institute of Neuroscience and Medicine 4, Medical Imaging Physics, Forschungszentrum Jülich, Jülich, [6]Dpt. of Nuclear Medicine, RWTH Aachen University Hospital, Aachen, [7]Institute of Neuroscience and Medicine 5, Nuclear Chemistry, Forschungszentrum Jülich, Jülich, Germany

Objectives: The assessment of treatment response in patients with glioblastoma multiforme (GBM) is difficult since treatment-related contrast-enhancement in MRI can mimick tumor progression or pseudoresponse, especially during and after radiochemotherapy. The aim of this prospective study was to evaluate the prognostic impact of PET using O-(2-[^{18}F]fluoroethyl)-L-tyrosine (^{18}F-FET) during treatment of patients with GBM.

Methods: In a prospective study 25 patients with GBM were investigated by MRI and ^{18}F-FET PET after cytoreductive surgery (MRI-1 and FET-1), 7-10 days (MRI-2 and FET-2) and 6-8 weeks after completion of radiochemotherapy with temozolomide (RCX) (MRI-3 and FET-3). Volumes of the metabolically active tumor in ^{18}F-FET PET with a tumor/brain ratio (TBR) >1.6 ($T_{vol\ 1.6}$), maximum TBR, and the volume of Gd-DTPA contrast enhancement on MRI (Gd-Volume) were determined. For $T_{vol\ 1.6}$ and Gd-Volume stable values or reduction in comparison to baseline were defined as treatment response. For TBR_{max} a reduction of ≥10% was considered as treatment response. The median follow-up time of the patients was 13.8 (3-29) months. The prognostic impact of changes of the different parameters in MRI and ^{18}F-FET PET was evaluated using Kaplan-Maier estimates for disease-free survival (DFS) and overall survival (OS).

Results: Changes of $T_{vol\ 1.6}$ and TBR_{max} between FET-1 and FET-2 or FET-3, respectively, were significant predictors of DFS and OS (Table 1).

Table 1: Summary of results		MRI/FET-2 versus MRI/FET-1				MRI/FET 3 versus MRI/FET 1			
		DFS [months]	p-value	OS [months]	p-value	DFS [months]	p-value	OS [months]	p-value
$T_{vol\ 1.6}$	Responder	10.3	0.016*	15.4	0.19	10.3	0.001*	16.1	0.04*
	Non-Responder	5.8		9.8		5.1		9.9	
TBR_{max}	Responder	9.3	0.002*	15.4	<0.001*	8.3	0.07	15.4	0.021*
	Non-Responder	4.7		8.5		5.1		9.3	
Gd-Volume	Responder	9.4	0.93	14.8	0.75	10.3	0.16	14.8	0.31
	Non-Responder	7.8		9.9		5.8		9.9	

*significant difference

[Table 1]

A decrease of TBR_{max} ≥10% after completion of RCX was highly predictive for DFS and OS. At 6-8 weeks after completion of RCX, measurement of $T_{vol\ 1.6}$ appeared to be a more reliable parameter to estimate prognosis. In contrast, changes of the Gd-Volume between MRI-1 and MRI-2, and MRI-1 and MRI-3, respectively, revealed no significant differences of DFS and OS.

Conclusions: In comparison to Gd-Volumes on MRI, our data indicate that changes of metabolically active ^{18}F-FET tumor volumes and TBR_{max} are better parameters to assess treatment response and to predict survival time.

1160

MAPPING CEREBRAL BLOOD FLOW TERRITORIES IN EXPERIMENTAL ISCHEMIC STROKE WITH ARTERIAL SPIN LABELING

R.F. Leoni[1,2], B.T. Kang[1], F.F. Paiva[1], D.B. de Araujo[2], A.C. Silva[1]

[1]Cerebral Microcirculation Unit, National Institute of Neurological Disorders and Stroke - NIH, Bethesda, MD, USA, [2]Department of Physics and Mathematics, University of Sao Paulo, Ribeirao Preto, Brazil

Introduction: The investigation of the perfusion territories of major cerebral arteries may contribute to a better understanding of the functional role of collateral circulation in patients with cerebrovascular diseases [1, 2]. Amongst the different MRI techniques to measure cerebral blood flow (CBF), arterial spin labeling (ASL) can be used to selectively label blood flowing through specific cerebral arteries [3]. Here, we aim to investigate the feasibility of ASL to obtain quantitative CBF territory maps in a rodent model of ischemic stroke.

Methods: Twenty-six male adult rats (295±34g) were anesthetized under isoflurane, orally intubated and mechanically ventilated. A small surface coil was positioned under the neck of the animal (Fig. 1a) to allow selective labeling of blood flowing through the right (θ=+60°), the left (θ=-60°), or both (θ=0°) common carotid and vertebral arteries [3]. CBF maps were acquired at 7T MRI using a spin-echo EPI sequence (TR/TE=10000/30ms, FOV=2.56x2.56cm^2, matrix=64x64, labeling time=8849ms, and post-labeling delay=500ms). In twelve rats, whole brain magnetic resonance angiography was also obtained. The remaining rats were subjected to temporary (1 hour) occlusion of the middle cerebral artery (MCAO) using intraluminal filaments. Perfusion territories were obtained before and during the MCAO, and 45 minutes after reperfusion, or one and seven days after the procedure.

Results: Whole brain CBF maps showed equal sensitivity to perfusion in both hemispheres. Right and left perfusion territories were complementary, but not symmetric with respect to midline. Asymmetries varied among rats, including encroachment of the left territory into the right hemisphere, and vice-versa. Most asymmetries were explained by anatomical variations of the Circle of Willis. Moreover, these asymmetries changed after MCAO (Fig.1b). In this particular example, prior to brain ischemia, there was encroachment of the right territory (green) into the left hemisphere (red). During occlusion of the right MCA, blood flow redistribution caused the left circulation to supply regions of the right hemisphere. Immediately following reperfusion, the right circulation was restored. However, it occupied a smaller territory due to a residual presence of collateral blood flow, which persisted even seven days after MCAO. Similar results were observed in all other rats.

Conclusions: We successfully used ASL to observe the changes in perfusion territories in an animal model of experimental stroke. Future studies will compare perfusion territory maps with both diffusion- and T2-weighted MRI to investigate the relationship between collateral circulation and stroke outcome.

References:

[1] van Laar et al., *Radiology* 246(2008)354-364. [2] Hendrikse et al., *Stroke* 40(2009)1617-22. [3] Paiva et al., *JMRI* 27(2008)970-977.

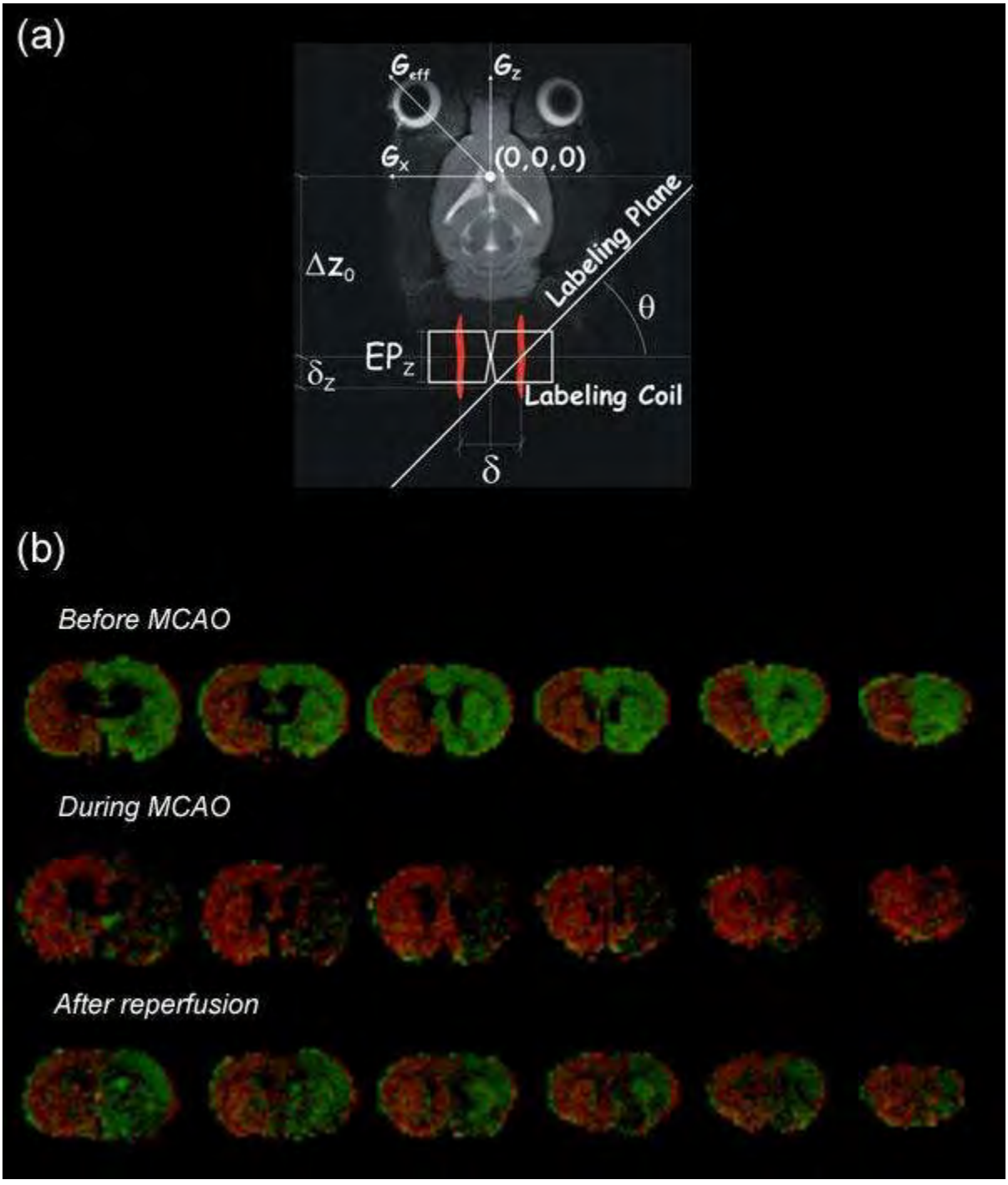

[Figure 1]

Figure 1: (a) Schematic diagram of perfusion territory mapping with ASL. (b) CBF territory maps of the left (red) and right (green) common carotid arteries in a representative rat before (top row) and during MCAO (middle row), and 45 minutes after reperfusion (bottom row).

1161

MRI BRAIN PERFUSION MEASUREMENTS IN THE FOLLOW-UP OF CUTTING-EDGE RADIATION THERAPY TECHNIQUES

P. Deman[1,2], M. Vautrin[1,2,3], M. Edouard[1,2], V. Stupar[1,2], L. Bobyk[1,2], R. Farion[1,2], H. Elleaume[1,2], C. Remy[1,2], E. Barbier[1,2], F. Estève[1,2,4], J.-F. Adam[1,2]

[1]u836, INSERM U836, Grenoble Institute of Neurosciences, University Joseph Fourier, [2]Institut des Neurosciences, Université Joseph Fourier, Grenoble, [3]DOSIsoft, Cachan, [4]CHU, Grenoble University Hospital, Grenoble, France

Objectives: The significant benefits of perfusion imaging in brain tumor radiotherapy treatment follow-up and survival prognosis has been reported in the past decade by various authors (1-3). This is of particular interest if the radiation therapy targets the blood vessels, which is the case with microplanar irradiations (MRT) using intense x-rays from a synchrotron source (4). The aim of this study was to evaluate the potential of MRI brain perfusion measurements in the follow-up of a new radiation therapy technique derived from MRT: monochromatic x-rays minibeams radiotherapy (5). The objective was to use high resolution MRI morphological (T2w and diffusion mapping) and functional (perfusion) imaging to study healthy tissue and brain glioma response to this cutting edge radiation therapy technique.

Methods: Two groups of five healthy rats were irradiated with a single anteroposterior minibeams incidence in the right hemisphere (four minibeams, 130 Gy prescribed dose at 1 cm depth in the brain) and with two interleaved incidences (57 Gy prescribed dose in a 5x5x4.8 mm^3 volume centered in the right hemisphere), respectively (Figure 1). MRI follow-up was performed over one year post-irradiation. T2 weighted images (T2w), apparent diffusion coefficient (ADC) and blood vessel permeability maps were acquired on a 4.7 or 7 T MRI preclinical magnet. Twenty three F98 tumor bearing rats were also irradiated with interleaved minibeams (57 Gy in a 8x8x7.8 mm^3 volume centered on the tumor). Anatomic and functional MRI follow-up was performed about every 10 days after irradiation. T2w images, ADC and perfusion maps were acquired on a 7 T MRI. Perfusion maps were computed on using a gamma variate model.

Results: All healthy rats didn't present any clinical alteration visible by simple examination during the whole follow-up period. T2w and ADC measurements remain stable for the single incidence irradiation group. Localized Gd-DOTA permeability was however observed 9 months after irradiation for the interleaved incidences group.

The irradiated glioma bearing rats had a mean survival time significantly different from the untreated animals (200% increased). A trend to decrease has been observed in the tumoral cerebral blood flow and blood volume values, after irradiation. These values increase when the tumors start to grow again.

Conclusions: This preclinical study demonstrates the potential of MR brain perfusion measurements for the follow-up of cutting edge radiotherapy techniques.

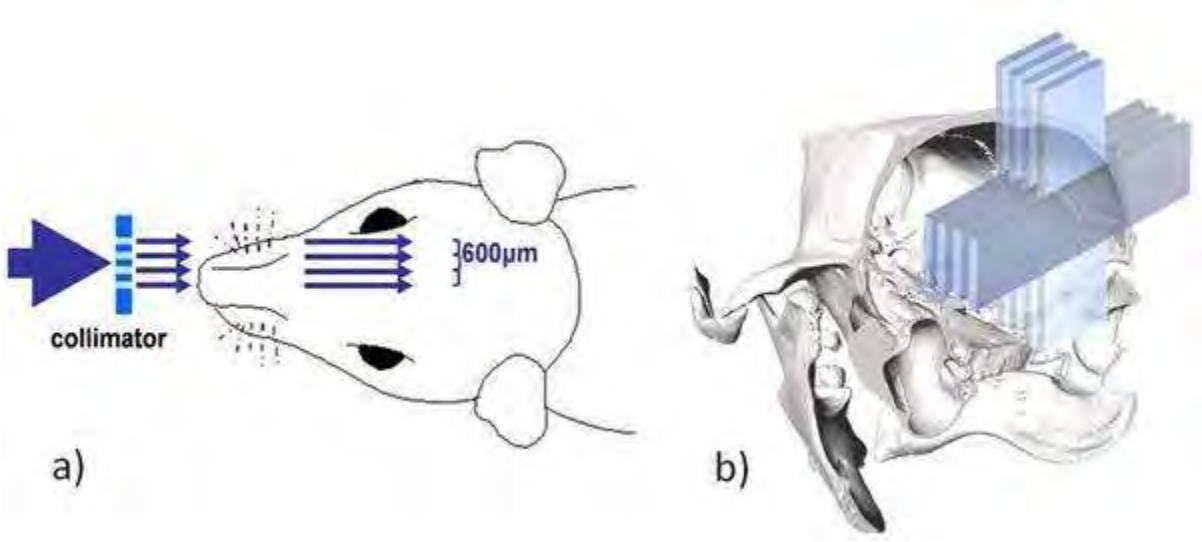

[Figure 1]

Figure 1: Minibeam radiation therapy irradiation geometries for rodents preclinical studies: a) one incidence protocol: 4 beams of 600 µm width, 5 mm height, separated by 600µm width non-irradiated zones. b) two interleaved incidences protocol: 4 beams in each incidence, 600 µm high, 5 mm width; interleaved in the rat right striatum

References:

1 Cao, Y et al, IJROBP, 64, 876-885 (2006)

2 Fuss, M et al, IJROBP, 51, 478-482 (2001)

3 Marcus, C.D et al, Critical Reviews in Oncology Hematology, 72, 217-238 (2009)

4 Van der Sanden, B et al, IJROB, 77, 1545-1552 (2010)

5 Dilmanian, F.A et al, PNAS USA, 103, 9709-9714 (2006)

1162

AMYLOID DEPOSITION AND MICROGLIA ACTIVATION IN PATIENTS AFTER ISCHEMIC STROKE

A. Thiel[1], B. Radlinska[1], R. Schirrmacher[2], J.-P. Soucy[3], **W.-D. Heiss**[4], V. Hachinski[5]

[1]Neurology & Neurosurgery, McGill University at SMBD Jewish General Hospital & Lady Davis Institute for Medical Research, Montreal, QC, [2]Montreal Neurological Institute, McGill University, Montreal, PE, [3]Montreal Neurological Institute, McGill University, Montreal, QC, Canada, [4]Max Planck Institute for Neurological Research, Cologne, Germany, [5]London Health Science Centre, University of Western Ontario, London, ON, Canada

Introduction: The risk to develop relevant cognitive impairment after a stroke is 3.5 to 5.8 times larger than in age-matched controls (Leys et al., 2005). Even patients who are cognitively intact 3 months after a stroke still have a 4 to 9 fold greater risk of developing dementia in the following year. This manifestation of clinically relevant cognitive impairment after a stroke might be related to the interaction of vascular pathology and metabolic changes typical for Alzheimer diseases (Snowdon et al., 1997). Animal experiments (Cechetto et al., 2008) also indicated the importance of inflammation for the progression of these metabolic changes. We thus studied the burden of amyloid deposition and inflammatory reaction in the brain after the stroke uisng positron emission tomography.

Methods: 5 Patients with a confirmed first supratentorial ischemic stroke underwent 2 MRI-scans within 2 weeks and 5-7 months and two PET-scans between 5 and 7 months after the event. MRI was performed on a clinical 1.5T MRI scanner (Siemens Magnetom, 1mm resolution, T1-weighted, T2-weighted, and FLAIR), PET-scanning was performed on two separate days, on an ECAR HR+ scanner (Siemens) after a transmission scan of 10 minutes duration. Patients receive 370MBq of ^{11}C-PIB and 370MBq of ^{11}C-[R]-PK11195 PIB in separate scanning session 1-2 days apart. For the PIB-scans dynamic data acquisition started 30 minutes after injection (7 frames 600 sec each), for the ^{11}C-[R]-PK11195-PET a series of 21 dynamic scans was acquired. Images were reconstructed using filtered back-projection (Hanning filter: kernel FWHM=3 mm) after correction for attenuation, scatter and decay. Standardizes uptake value ratios (SUVR) were calculated for cerebellar reference regions.

Results: Preliminary results indicate a significant increase in global PIB uptake (SUVR > 1.5) in the entire cortex compared to cerebellum. The increased amyloid deposition often was asymmetric and peak uptake was found in pre-frontal (SUVR = 2.29 +/- 0.325) or parieto-temporal areas (SUVR = 2.02 +/- 0.202). Increased PK-uptake as a marker of microglia activation was mainly found in connecting fiber tracts, especially in the pyramidal tracts, and could be observed also distant from the ischemic lesion, e.g. in the brain stem.

Conclusion: These preliminary demonstrate amyloid deposition, in patients suffering from stroke. These changes are in the range of PIB-binding described in Alzheimer patient's and may reduce the reserve capacity of the brain. Together with increased vascular lesion load, they may contribute to impair cognitive performance post-stroke. The relationship between amount of amyloid deposit before the stroke and the importance of microglia activation for the progression of cognitive impairment will be investigated in larger follow-up studies.

Cechetto DF et al, Expert Rev Neurother 8:743-750.

Leys D et al. Lancet Neurol 4:752-759.

Snowdon DA et al.JAMA 277:813-817.

1164

IMPAIRMENT OF EXECUTIVE FUNCTION IN PATIENTS WITH CAROTID ARTERY STENOSIS CORRELATES WITH DECREASED PERFUSION IN FRONTAL LOBE WITH UPSTREAM STENOSIS

F. Kellner-Weldon[1], K. Jann[2], Y. Burren[1], R. Wiest[1], C. Kiefer[1], M. El-Koussy[1], R. Everts[1], P. Michel[3], M. Wapp[1], A. Federspiel[2], G. Schroth[1], M. Hauf[1]

[1]Institute of Diagnostic and Interventional Imaging, Support Center for Advanced Neuroimaging, [2]Department of Psychiatric Neurophysiology, University of Berne, Bern, [3]Departement of Neurology, University of Lausanne, Lausanne, Switzerland

Objectives: Cognitive function is likely to decline in patients with Carotid Artery Disease (CAD) in about 1/3 of patients with asymptomatic carotid stenosis.[1] To determine the correlation between neuropsychological deficits and brain perfusion deficits in CAD, resting state CBF and CVR was measured with arterial spin labeling (ASL) in patients with carotid artery stenosis without prior stroke.

Methods: Eighteen patients (15 males, mean age 68.8 y Range: 53-83y) with internal carotid stenosis of ≥70% without prior stroke underwent brain perfusion measurement with ASL before and after intravenous administration of acetazolamide (1 g). Pseudocontinous ASL with TR 4000ms, label time 1.72s, post labeling delay 1.5 s[2] was used. Calculation of CBF values was performed using a self written Matlab script. CBF and CVR were measured in the gray matter of the anterior cerebral artery- and the frontal middle cerebral artery territory (frontal lobe hereafter). The asymmetry index (AI) was calculated for the frontal lobes and for the territory of the posterior cerebral artery as reference region. Executive function was assessed by stroop-interference- and trail-making-B-test [3,4]. SPSS 17.0 (SPSS, Chicago, USA) was used for statistical analyses.

Results: Seven of 18 patients showed executive deficits (pathological group). In the pathological group CBF AI of the frontal lobe of the stenotic side was -8.7% (Range: -18.4 to 0.9%) compared to -3.3% (Range: -7.7 to 1.1%) in the normal group ($p< 0.19$). No significant correlation to the stenosis grade and age was found. The average increase of CBF under vasodilatatory stimulus was 35.6 % for both frontal territories. Under vasodilatory stimulus the AI for CBF of the frontal lobe on the stenotic side was -9.2% and -2.9% and for the pathological and normal group respectively (not significant).

Conclusion: 38 % of otherwise asymptomatic patients with CAD showed impaired executive function.

CBF measurements at rest and under vasodilatatory stimulus showed a decreased brain perfusion in the frontal lobe with upstream stenosis. No correlation to the degree of stenosis was present suggesting the importance of collateral flow on CBF measurements and neuropsychological performance in patients with CAD. The ongoing study envisages further assessment of the neuropsychological performance and CBF and CVR in CAD.

References:

1. S. Claiborne Johnston et al 2004 Ann Intern Med February 17, 2004 140:237-247

2. Dai W. et al. (2008) Magn Reson Med 60: 1488-1497;

3. Bench CJ et al. (1993) Neuropsychologia Sep;31(9):907-22; Investigations of the functional anatomy of attention using the Stroop test.

4. Oosterman JM et al. (2010) Clin Neuropsychol. Feb;24(2):203-19;

This project is granted by the Swiss National Foundation: Impact of quantitative MR perfusion imaging on the management of patients with carotid artery disease SPUM 33CM30-124114

1165

MULTIPLE PRECONDITIONING PARADIGMS CONVERGE ON IRF-DEPENDENT SIGNALING TO PROMOTE ISCHEMIC TOLERANCE

S.L. Stevens[1], K.B. Vartanian[1], P.Y. Leung[1], B. Gopalan[2], R.P. Simon[3], M.P. Stenzel-Poore[1]

[1]Molecular Microbiology & Immunology, Oregon Health & Science University, Portland, OR, [2]Genomic Medicine Institute, Cleveland Clinic, Cleveland, OH, [3]The Neuroscience Institute, Morehouse School of Medicine, Atlanta, GA, USA

Objectives: To determine whether ischemic tolerance through preconditioning with the Toll-like receptor (TLR) ligands lipopolysaccharide (LPS) or unmethylated CpG ODNs share a common mechanism of protection with preconditioning via brief ischemia. Through this comparison, our goal is to identify key features of the neuroprotective program elicited by brain ischemia in the setting of prior preconditioning.

Methods: C57BL/6 mice (n=4) were treated with either the TLR4 ligand LPS (0.2mg/kg; s.c.), the TLR9 ligand CpG (0.8mg/kg; s.c.) or brief transient ischemia (12 min middle cerebral artery occlusion (MCAO)). RNA was isolated from the brain cortex at 3, 24 and 72 h following treatment with additional groups undergoing a subsequent 45 min MCAO and cortical tissue collected at 3 and 24 h post injury. Gene chip arrays (Affymetrix MOE430 2.0) were performed to identify genes differentially regulated in each group. Pathway and promoter region analysis of the regulated genes identified key elements associated with neuroprotection. Knockout mice were selected (interferon regulatory factor (IRF) 3 and IRF7 knockouts) for additional studies using MCAO.

Results: We found that preconditioning with each stimulus induced genomic changes in the brain that indicated activation of a TLR pathway. Following MCAO, all three preconditioning stimuli caused the genomic response to ischemic injury to be reprogrammed leading to expression of a subset of 13 genes which were not expressed in the brains of mice not so preconditioned. Promoter analysis of these 13 genes revealed a shared IRF regulatory element, which suggests that IRFs may play a role in ischemic tolerance. To determine whether IRF3 or IRF7 are important neuroprotective mediators, we tested mice deficient in either IRF3 or IRF7 for their ability to be preconditioned by LPS, CpG or brief ischemia. We found that preconditioning induced protection was significantly attenuated in mice lacking IRF3 or IRF7—a finding that suggests a seminal role for these IRFs in neuroprotection.

Conclusions: These studies suggest that the neuroprotective pathways induced by multiple, distinct preconditioning stimuli converge on a common mechanism that involves IRF mediated transcription. There appears to be an initial TLR signaling event in the brain that results in a reprogrammed response to injury. The reprogrammed response directs signals down an IRF dependent cascade as evinced by induction of a subset of 13 IRF-regulated genes in response to ischemia in preconditioned mice only. The protective nature of this IRF signaling is underscored by our findings that mice deficient in IRF3 or IRF7 failed to be protected or showed reduced protection with the preconditioning stimuli. These results highlight a shared mechanism of ischemic tolerance, which depends on the transcription factors IRF3 and IRF7 and culminates in the reprogramming of the brains response to stroke injury.

1166

PPARA ACTIVATION IMPROVES CEREBRAL BLOOD FLOW AFTER ISCHEMIC STROKE AND ATTENUATES BRAIN INFLAMMATION

S. Namura, G. Wang, Q. Guo

Neurobiology and Neuroscience Institute, Morehouse School of Medicine, Atlanta, GA, USA

Objectives: Fibrates, originally developed as drugs for dyslipidemia, are peroxisome proliferator-activated receptor alpha (PPARα) agonists. Fibrates have been shown to attenuate infarct size after ischemic stroke in mice [1,2]. We investigated how PPARα activation protects the brain against ischemic stroke. Two animal models were used to demonstrate potential two mechanisms: (1) middle cerebral artery occlusion (MCAO) model for blood flow mechanism; and (2) lipopolysaccharide (LPS) intra-cerebral injection model for inflammation mechanism. To seek the molecular mechanism, we measured the influences of fibrates on superoxide dismutase (SOD) in the brain.

Methods: Male C57BL6 or PPARα deficient mice were used. Wy-14643 or fenofibrate was given trans-orally for 7 days. MCAO was induced by intraluminal filament insertion under isoflurane anesthesia. Cerebral blood flow (CBF) was measured by laser speckle imaging. LPS was injected into the somatosensory cortex using a stereotaxic apparatus under isoflurane anesthesia. Activation of PPARα protein was measured by electrophoretic mobility shift assay. Gene expression levels of PPARα, pro-inflammatory molecules, and SODs were measured by quantitative real-time PCR. Microglia/macrophage activation and leukocyte infiltration were analyzed by immunostaining for Iba and neutrophil elastase. Neuronal injury was evaluated by Fluoro-Jade B or Nissl staining. Brain microvessels were separated by multi-step fractionations using a mesh technique. SOD activity was determined by measuring the inhibition rate of diformazan production after adding xanthine and xanthine oxidase. Oxidative stress level in the brain tissue was measured by two different methods: superoxide production determined by hydroethidium fluorescence and protein oxidation by derivitized protein carbonyls detection. Plasma homocysteine was measured by a commercial ELISA kit.

Results: Wy-14643 and fenofibrate (30 mg/kg) increased the amount of active PPARα protein and SOD activity in the brain, improving CBF during MCAO and early reperfusion. Such improvements by fenofibrate were not seen in PPARα deficient mice. In addition, Wy-14643 and fenofibrate significantly attenuated the signal levels of the two oxidative stress indicators. These treatment protocols profoundly attenuated the elevations of many cytokines and cellular adhesion molecules, microglia/macrophage activation, neutrophil recruitment, and neuronal injury at 3 days after LPS. These beneficial effects were not seen at 100 mg/kg of fenofibrate under which plasma homocysteine level was significantly elevated.

Conclusions: Our findings suggest that fibrates protect the brain after ischemic stroke by improving ischemic CBF and by attenuating brain inflammation, at least in part. SOD may be a potential downstream effector for the cerebrovascular protection by PPARα activation. Since homocysteine is pro-oxidant, the observed homocysteine elevation by the higher dose of fenofibrate might counteract the beneficial effects by fenofibrate. Further studies are required for minimizing the worsening side effect by homocysteine so that the cerebrovascular protection by fibrates could be maximized.

References:

1. Inoue H et al. “Resveratrol and fenofibrate require PPARalpha expression to limit brain infarct resulting from permanent focal ischemia in mice.” Neurosci. Lett 352:203-206, 2003.

2. Guo Q et al. “Effects of gemfibrozil on outcome after permanent middle cerebral artery occlusion in mice.” Brain Res. 1279:121-130, 2009.

1167

TOWARDS PERSONALIZED TREATMENT PLANNING FOR ISCHEMIC STROKE PATIENTS

P. Orlowski, M. Chappell, C. Sub Park, V. Grau, S. Payne

Department of Engineering Science, University of Oxford, Oxford, UK

Objectives: The identification of salvageable brain tissue is a major challenge at stroke presentation. Standard techniques used in this context, as the *perfusion-diffusion mismatch*, have limitations. There is a need for new methods that would help guide treatment. Our hypothesis is that perfusion and diffusion imaging could be complemented with pH imaging. Indeed, a pH threshold of 6.3-6.4 exists, below which cellular pH related damage is triggered [1]. Furthermore, for values of pH ~6.5 apoptosis is likely to begin [2]. Therefore, we have developed a physiologically-based model to simulate cellular pH dynamics under conditions of ischemia.

Methods: Excessive production of H^+ ions in the cell after stroke is due to two factors: consumption of cell energy stores, and a high concentration of CO_2. To describe the change of pH an existing model of the brain metabolism was adapted [3]. The model is composed of four compartments: astrocytes, neurons, extracellular volume and capillary vessels. ATP, glucose, glycogen, lactate, phosphocreatine, O_2 and CO_2 dynamics are all included. Four adjustments were made to the model to account for H^+ production : 1) baseline intracellular pH was set to 7.2; 2) the decrease of ATP concentration by a mole increases H^+ concentration by a mole; 3) further H^+ is produced at the same rate as lactate; 4) additional H^+ is produced at the same rate as phosphocreatine concentration increase in the cell. The regulation of pH was modelled by introducing a buffer solution composed of HCO_3^-, CO_3^{2-} and H_2CO_3 inside the cell and modelling the extrusion of H^+ ions outside of the cell with two channels: MCT (the lactate-H^+ co-transporter) and NHE (Na^+/H^+ antiporter). The function of the channels was coupled with ATP.

Results: Cerebral blood flow (CBF) was reduced to 80% of its baseline value. According to [4] the expected fall of pH under total ischemia is to a values of 6.4. Here pH drops to a value of 6.7. Furthermore, Fig. 1 shows the evolution of the neuron energy stores and the concentration of sodium ions in the cell. The regulation of sodium concentration is effective for as long as energy stores are available in the cell.

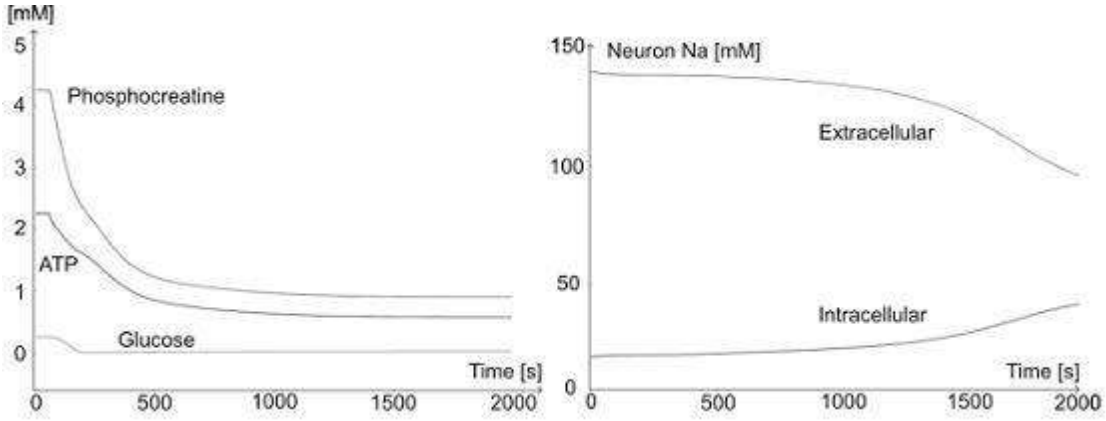

[Fig.1 Phosphocreatine, ATP, glucose and sodium dyn]

Fig.1 Phosphocreatine, ATP, glucose and sodium dynamics in neurons after a 80% CBF fall.

Conclusions: There is a good qualitative agreement between predicted and physiological variation of pH and cell metabolites under ischemia conditions. Refinement of the model requires further incorporation of CO_2 kinetics, metabolites diffusion in the brain tissue, buffering with carbon anhydrase, metabolism under total ischemia, cell volume regulation, and inclusion of less important pH regulation mechanisms

References:

[1] Kaila K, Ransom BR. pH and brain function. *Wiley & Sons*, 1998.

[2] Barry MA, Eastman A. Endonuclease activation during apoptosis: the role of cytosolic Ca^{2+} and pH. Biochem Biophys Res Commun 186:782-789, 1992.

[3] Cloutier M et al. *J Comput Neurosci*, 27:391-414, 2009.

[4] Ljunggren B, et al. Brain Res 73:291:307, 1974.

1168

CONTRAST-ENHANCED MRI OF DISCRETE VASCULAR CHANGES IN THE THALAMUS AFTER FOCAL CEREBRAL ISCHEMIA IN RATS

P. Yanev, P.R. Seevinck, M.J. Bouts, I.A. Tiebosch, A. van der Toorn, R.M. Dijkhuizen

Biomedical MR Imaging and Spectroscopy Group, Image Sciences Institute, University Medical Center Utrecht, Utrecht, The Netherlands

Objectives: Secondary neuronal damage in the thalamus may occur following focal cerebral ischemia in cortical tissue as a result of retrograde degeneration of the thalamocortical pathway.[1] Recent studies suggest that these pathological changes may be followed by neurogenesis and angiogenesis at chronic stages,[2,3] which may be associated with post-stroke tissue plasticity.

The goal of the present study was to noninvasively characterize the temporal pattern of vascular remodeling in relation to macroscopic tissue status in the thalamus from subacute to chronic time-points after focal cerebral ischemia in rats.

Material and methods: Male Wistar rats were mechanically ventilated with air and 2% isoflurane. Focal cerebral ischemia was induced by 60-min middle cerebral artery occlusion (MCAO) with an intraluminal filament.[2] Only rats with cortical and subcortical lesions were included in the study. Animals were scanned at 1 (n = 4), 7 (n = 6), 20 (n = 6) and 70 days (n = 8) after stroke.

MRI was conducted on a 4.7 T animal MR system. For steady state susceptibility contrast-enhanced (ssCE-)MRI, we performed multiple spin-echo ($TR/TE_1/\Delta TE$ = 3500/13/13 ms) and multiple gradient echo ($TR/TE_1/\Delta TE$ =1800/4/4 ms) pulse sequences, respectively, before and after injection of ultrasmall particles of iron oxide USPIO (P904, Guerbet, France) (16.5 mg/kg). Multislice MR images were obtained with a field-of-view of $32 \times 32\,mm^2$, 128 × 256 matrix size, and 1 mm slice thickness. Subsequently, ΔR_2^* and ΔR_2 were calculated as measures of total and microvascular cerebral blood volume (CBV), respectively.[4] The region of interest was the ventroposterior nucleus (VPN) of the thalamus and a homologous contra-lateral area, in which ΔR_2 and ΔR_2^* values were estimated.

Results: Animals developed ischemic lesions, characterized by prolonged T_2, in the ipsilateral somatosensory cortex and caudate putamen. The thalamus was invariably outside the lesion territory and revealed no significant alterations in tissue T_2. Nevertheless, significant changes in vascular contrast-induced ΔR_2^* and ΔR_2 were observed in the ipsilateral VPN. ΔR_2^* was significantly increased at all time-points as compared to contralateral values. Significant elevations of ΔR_2 were detected after day 7, with a significant further increase at days 20 and 70 as compared to day 1.

Conclusions: We demonstrate that steady state USPIO-enhanced MRI can serve as a sensitive method for assessment of (changes in) vascularity in the thalamus by probing total and microvascular CBV.

At early time points following cerebral ischemia, increased total CBV in the VPN may reflect vasodilation or recruitment of previously nonperfused vessels. Gradual increase in microvascular CBV between 1 week and 10 weeks post-ischemia may be associated with ongoing angiogenesis, which might contribute to restoration of neuronal networks.

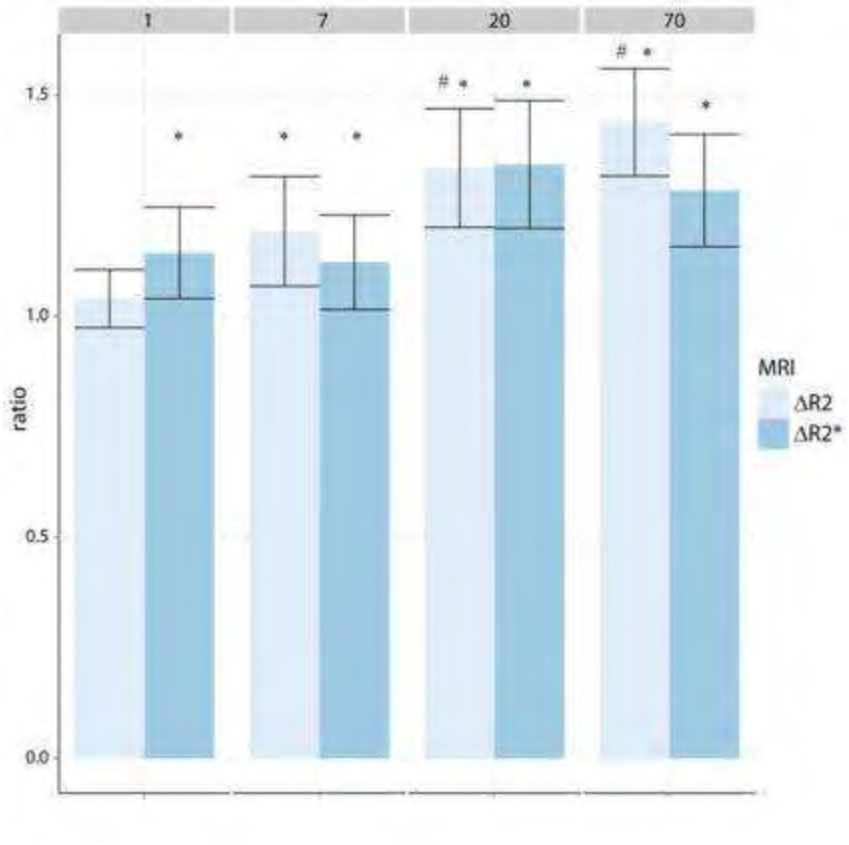

[Figure 1]

Figure 1. ΔR_2 and ΔR_2^* ratios in ipsilateral VPN (relative to contralateral) at different post-stroke time-points. *P< 0.05 vs. contralateral. #P< 0.05 vs. day 1.

References:

1. Iizuka et al. Stroke. 1990; 21:790-4.

2. Hayward et al. J Cereb Blood Flow Metab. 2010; in press.

3. Ling et al. J Cereb Blood Flow Metab. 2009; 29:1538-46.

4. Seevinck et al. Angiogenesis. 2010;13:101-11.

1169

EXTRA-CEREBRAL REFERENCE TISSUE FOR FDG-PET IN RATS - APPLICATION TO TISSUE WITH NON-PRESERVED LUMPED CONSTANT

H. Backes[1], M. Walberer[2], H. Endepols[1], B. Neumaier[1], G. Mies[1], R. Graf[1], K. Wienhard[1]

[1]Max Planck Institute for Neurological Research, [2]Neurology, University of Cologne, Cologne, Germany

Objectives: Diseases and dysfunction of the central nervous system are often associated with regional changes in cerebral glucose metabolism, which can be measured in vivo by positron emission tomography (PET) using [18F]-fluoro-2-deoxyglucose (FDG) as tracer. For quantification, the arterial tracer input function must be determined. For rodents in particular, direct measurement of blood radioactivity is scarcely feasible for follow-up of individual animals due to the invasiveness of blood sampling. We show that the whiskers area of the rat's muzzle serves as an extra-cerebral reference region. The derived model also takes into account local variations of the lumped constant, which is crucial in pathological tissue as we demonstrate by application of the method to rats subjected to acute focal cerebral ischemia.

Methods: To validate the whiskers area in the rat´s muzzle as an appropriate extra-cerebral reference region, arterial blood activity was continuously determined in a blood sampler for the first 2 minutes after injection of FDG. Thereafter, activity was measured in discrete blood samples taken during the PET acquisition time of 60 min (wistar rats; n=11). FDG kinetic parameters were calculated using a two-tissue compartment model with either the directly measured or the whiskers area derived input function.

The reference tissue model was applied to five rats subjected to acute focal cerebral ischemia. The middle cerebral artery was occluded using macrospheres. After 45 minutes, cerebral blood flow was determined with [15O]H2O-PET followed by a 60 minutes FDG-PET measurement. FDG net influx rate constant and unidirectional transport rate constant were calculated. Local cerebral glucose metabolic rates were calculated taking into account local variations of the lumped constant.

Results: A) Input functions derived from the whiskers reference region using an average set of kinetic parameters agreed well with the directly measured input functions. The resulting cerebral kinetic parameters were not significantly different and showed a high correlation (K1: r=0.93, p=0.82; k2: r=0.96, p=0.128; k3: r=0.88, p=0.72; k4: r=0.85, p=0.19; Ki: r=0.89, p=0.96; p values from paired t-test). B) In rats subjected to focal cerebral ischemia, FDG kinetic parameters in healthy tissue were not significantly different from whole brain kinetic parameters in naïve rats. The ischemic region was characterized by preserved glucose metabolism although FDG uptake was elevated significantly, i.e. the lumped constant in the ischemic tissue was significantly different from that in healthy brain tissue (Fig 1). C) In the ischemic region, the unidirectional FDG transport rate constant correlated significantly with cerebral blood flow measured with [15O]H2O-PET.

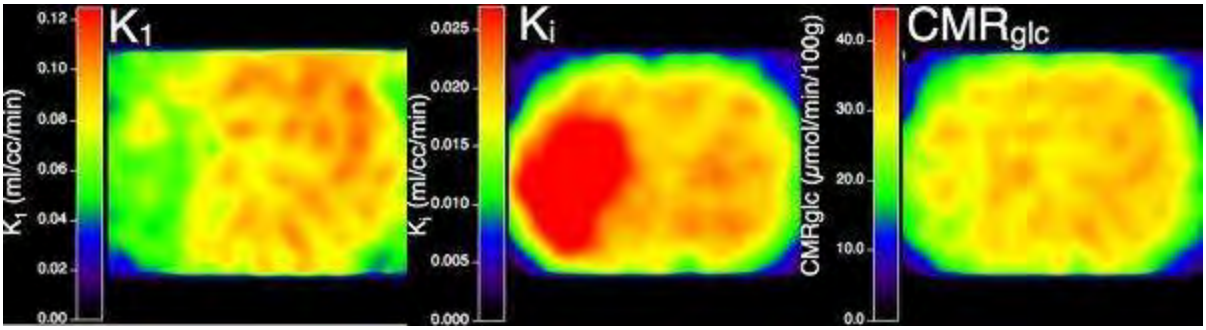

[Fig 1]

Conclusions: The method presented here allows for the quantitative non-invasive determination of cerebral glucose consumption in rats, takes into account local variations of the lumped constant, and is suitable for follow-up measurements of individuals. In hypo-perfused tissue the unidirectional flow constant of FDG is a good surrogate marker for cerebral blood flow.

1171

RELEVANCE OF COMPLEMENT LECTIN PATHWAY IN CEREBRAL ISCHEMIA

F. Orsini[1], E.R. Zanier[1], R. Gesuete[1], M. Stravalaci[2], D. De Blasio[1], R. Ottria[3], J. Reina[3], A. Bernardi[3], M. Gobbi[2], M.G. De Simoni[1]

[1]Neuroscience, [2]Molecular Biochemistry and Pharmacology, Mario Negri Institute, [3]Department of Organic and Industrial Chemistry, University of Milan, Milan, Italy

Objectives: We have recently demonstrated that the powerful protective effect of recombinant human complement C1-inhibitor (rhC1-INH) in cerebral ischemia is due to its ability to inhibit the activation of complement lectin pathway by binding to mannose binding lectin (MBL)(1), likely through its mannose-enriched N-terminal domain. To explore the relevance of the lectin pathway in cerebral ischemia we have: 1) assessed whether the lectin pathway was activated following ischemia; 2) determined the presence and localization of MBL-A and MBL-C in ischemic tissue; 3) studied the susceptibility of MBL-A and MBL-C double knock-out ($MBL^{-/-}$) mice to transient and permanent ischemia; 4) determined if newly synthesized mannosilated molecules, characterized and selected for their binding to MBL, are able to prevent ischemic injury in mice.

Methods: The activation of lectin pathway after ischemia was analyzed by measuring circulating functional MBL/MASP-2 complexes by ELISA. MBL-A/MBL-C presence on cerebral vessels was assessed by immunostaining and confocal microscopy. Transient or permanent focal cerebral ischemia was induced in C57Bl/6 (WT) or $MBL^{-/-}$ mice and neurological deficits and infarct volumes were evaluated 48h later. The affinity of mannosilated molecules to MBL were measured by surface plasmon resonance (SPR). The molecule showing the highest affinity to MBL was administered intravenously to ischemic mice and neurological deficits and infarct volume were evaluated 48h later.

Results: Cerebral ischemia led to a significant increase in the number of functional MBL/MASP-2 complexes and induced the deposition of both MBL-A and MBL-C on cerebral endothelial wall. $MBL^{-/-}$ mice showed a significantly lower susceptibility to transient and permanent ischemia (reduction of ischemic volume 28% and 41%, respectively compared to WT). Polyman002, a dendrimeric molecule exposing multiple copies of synthetic mannoside and binding MBL with a KD=2.3±0.7μM, induced a significant reduction of neurological deficits and ischemic volume *in vivo.*

Conclusions: The lectin pathway is activated by ischemic injury. Our results obtained in $MBL^{-/-}$ mice and in WT mice treated with a MBL-binding molecule indicate that the inhibition of this protein leads to neuroprotection. Our findings, together with those recently published by Cervera et al. (2), indicate that MBL inhibition may represent a novel therapeutic target for stroke.

References:

1) Gesuete R, Storini C, Fantin A, Stravalaci M, Zanier ER, Orsini F, Vietsch H, Mannesse ML, Ziere B, Gobbi M, De Simoni MG. RECOMBINANT C1-INHIBITOR IN BRAIN ISCHEMIC INJURY. Ann Neurol. 2009 Sep;66(3):332-42.

2) Cervera A, Planas AM, Justicia C, Urra X, Jensenius JC, Torres F, Lozano F, Chamorro A. GENETICALLY-DEFINED DEFICIENCY OF MANNOSE-BINDING LECTIN IS ASSOCIATED

WITH PROTECTION AFTER EXPERIMENTAL STROKE IN MICE AND OUTCOME IN HUMAN STROKE. PLoS One. 2010 Feb 3;5(2):e8433.

1172

AUDITORY MISMATCH NEGATIVITY IN ISOFLURANE-ANAESTHETIZED RATS: FESEABILTY STUDY AND INHIBITION WITH NMDA ANTAGONIST MK801

C. Simmons[1], D. Cash[1], D. Virley[2], S. Williams[1], M.B. Mesquita[1]

[1]Neuroimaging Reseach Group, Institute of Psychiatry / King's College London, London, UK,
[2]Porsolt and Partners Pharmacology, Paris, France

Objectives: Mismatch negativity (MMN) is an EEG method used in both humans and animals to assess cognitive functions[4,6]. The processes involved in the evoked response measured in MMN studies are preattentive and therefore can be measured in both the conscious and unconscious state, although there is still controversy over whether it is detectable under anaesthesia. Under urethane and pentobarbital anaesthesias a few groups have shown that MMN-like responses can be detected and inhibited with an NMDA antagonist[1,7,8], whereas others have shown no MMN-like response under urethane/xylazine or ketamine/zylazine anaesthesia[3,9]. The aim of the present study was to determine if a mismatch negativity-like response could be detected in isoflurane-anaesthetised rats and inhibited with an NMDA antagonist.

Methods. Male Sprague Dawley rats were anaesthetized with isoflurane (1.5% in 20/80% air/oxygen mixture @1L/min) and a monopolar EEG electrode was inserted into the skull above the auditory cortex. MMN protocol consisted in alternate presentation of two vowel tones (e125 and e275@95dB-SPL) one being presented more frequently than the other at a ratio of 1:10 (deviant:familiar). Animals were recorded before and five minutes after being given MK801 (0.1mg/kg or 0.3mg/kg ip) or saline. Mean evoked response was calculated with a customised MatLab function and amplitude and latency of P1 and N1 peaks were measured for statistical analysis.

Results: Typical MMN response was observed in saline-treated animals, with significantly higher amplitude for deviant (in both P1 and N1 peaks) when compared to frequent tone, but no difference in latency. MK801 was able to block this MMN-like response in amplitude in both doses tested. In addition, within deviant tone, 0.1mg/kg MK801 caused a significant decrease in latency for the N1 peak and a significant decrease in amplitude compared to the other groups (fig01).

Conclusions: Auditory MMN can be detected under isoflurane anaesthesia as has been seen under urethane/pentobarbital anaesthesia and in conscious animals. This is shown as an increase in amplitude of the early peaks of the evoked response to the deviant tone, which is in line with previously published studies. NMDA antagonists like MK801, as demonstrated by other groups[2,5], can inhibit this effect.

References:

1-ASTIKAINEN, P. et.al.(2006) *Neuroreport,* 17**,**1561-4.

2-EHRLICHMAN, R. S. et.al.(2008) *J Cogn Neurosci,* 20**,**1403-14.

3-ERIKSSON, J. & VILLA, A. E.(2005) *Biosystems,* 79**,**207-12.

4-JAVITT, D. C. et.al.(1998) *Electroencephalogr Clin Neurophysiol,* 108**,**143-53.

5-JAVITT, D. C. et.al.(1996) *Proc Natl Acad Sci U S A,* 93**,**11962-7.

6-PEKKONEN, E.(2000) *Audiol Neurootol,* 5,216-24.

7-RUUSUVIRTA, T. et.al.(1998) *Neurosci Lett,* 248**,** 45-8.

8-TIKHONRAVOV, D. et.al.(2008) *Brain Res,* 1203**,**97-102.

9-LAZAR, R. & METHERATE, R.(2003) *Hear Res,* 181,51-6.

1173

THE INITIATION OF ESTROGEN REPLACEMENT THERAPY AFTER OVARIECTOMY IS CRITICAL ON IN VIVO GLUCOSE UPTAKE

R. Lopez-Grueso[1], C. Borras[2], J. Gambini[2], D. Monleon[3], K.M. Abdelaziz[2], M. Ahmed El-Alami[2], V. Bonet[2], J. Vina[2]

[1]Physiology, INCLIVA-FIHCUV University of Valencia, [2]Physiology, University of Valencia, [3]INCLIVA-FIHCUV University of Valencia, Valencia, Spain

Objectives: Females live longer than males and these differences may be explained by estrogens. Our aim was to study the effect of the initiation of the estrogen replacement therapy (ERT) after the ovariectomy on *in vivo* glucose uptake.

Methods: Female Wistar rats were ovariectomized and treated for 0, 3, 6 or 9 weeks with 17b-estradiol (1 ug/kg/day) or vehicle subcutaneously. After 18F-fluordeoxyglucose (FDG) intravenous administration in vivo, brain glucose uptake was measured by positron emission tomography (PET).

Results: We found that the brain glucose uptake was lower in ovariectomized compared with control rats. Immediate administration of ERT after ovariectomy prevented the loss of glucose uptake. Implementation of ERT after 3, 6 or 9 weeks after ovariectomy did not recover the glucose uptake.

Conclusion: Immediate administration of estradiol after ovariectomy recovers brain glucose uptake. However, ERT, 3, 6 or 9 weeks after ovariectomy is not efficient to prevent detrimental ovariectomy effects. Therefore, we suggest that ERT is only effective if administered immediately after menopause.

References:

· Maki PM (2006) Potential importance of early initiation of hormone therapy for cognitive benefit. *Menopause*, 13, 6-7.

· Resnick SM, Henderson VW (2002) Hormone therapy and risk of Alzheimer disease: a critical time. *JAMA*, 288, 2170-2

· Resnick SM, Maki PM, Golski S, Kraut MA, Zonderman AB (1998) Effects of estrogen replacement therapy on PET cerebral blood flow and neuropsychological performance. *Horm Behav*, 34, 171-82.

1175

MONITORING RESPONSE TO DISEASE-MODIFYING DRUGS IN MS WITH MRI AND DEFORMATION-BASED MORPHOMETRY

W.R. Riddle[1], S.C. DonLevy[2], S. Shokouhi[3]

[1]Radiology and Radiological Sciences, Vanderbilt University, [2]Pediatric Nurse Practitioner, [3]Radiology and Radiological Sciences, Vanderbiilt University, Nashville, TN, USA

Introduction: The current paradigm to diagnose and monitor the progression of multiple sclerosis (MS) includes evaluating the number and volume of cerebral white matter lesions identified with T2-weighted MRI, the number and frequency of patient reported relapses, and progression of physical disability. While these metrics provide global indicators of disease progression, they do not identify brain specific responses to the treatment.

Objective: To evaluate if volume changes on serial MR scans measured with deformation-based morphometry can be used to monitor response to treatment in MS.

Methods: Serial brain MRI scans were acquired on a single MS patient from 2001 to 2003 during treatments with mitoxantrone and from 2007 to 2010 during treatments with mycophenolate mofetil. There were nine scans with mitoxantrone and fourteen scans with mycophenolate mofetil. Scans included 3-D T1-weighted images, T2-weighted FLAIR images, and diffusion tensor images. Volume changes relative to the scan obtained before treatment were quantified with deformation-based morphometry. These volume changes were mapped into fifteen bins and displayed as color overlays over the second MRI volume. The brains were divided into ten regions (frontal lobe, parietal lobe, occipital lobe, temporal lobe, cingulate cortex, sublobar region, cerebellum, midbrain, pons, and medulla). Plots of the fraction of voxels in each region that expanded or contracted over the treatment times were created. Fiber tracts associated with white matter changes were identified with diffusion tensor images.

Results: Deformation-based morphometry demonstrated different changes in brain white matter during the treatments with mitoxantrone and mycophenolate mofetil. With mitoxantrone, the number of expansion in the sublobar region, which included the internal capsule, increased for the first year, then declined over the next 1½ years. There was a smaller response with mycophenolate mofetil. In the frontal lobe, there were expansions with both therapies that corresponded to the superior longitudinal fasciculus. With mitoxantrone, the number of expansions in the cerebellum increased for the first year, then declined over the next 1½ years. With mycophenolate mofetil, the number of expansions increased over the three years of treatment.

Conclusions: Deformation-based morphometry may be a useful technique for evaluating the response to disease-modifying therapies in multiple sclerosis.

1177

ENDOTHELIAL TRPC1 AND TRPC3 CHANNELS CONTRIBUTE TO ATP-MEDIATED CALCIUM REGULATION AND VASODILATION IN MOUSE CEREBRAL ARTERY

S.P. Marrelli[1,2], R.C. Noel[1], J. Abramowitz[3], L. Birnbaumer[3], M.Y. Kochukov[1]

[1]Anesthesiology, [2]Molecular Physiology and Biophysics, Baylor College of Medicine, Houston, TX, [3]National Institute of Environmental Health Sciences, NIH, Research Triangle Park, NC, USA

Objectives: Canonical transient receptor potential (TRPC) channels are expressed in vascular endothelial cells (EC) and may play a role in intracellular calcium ($[Ca^{2+}]_i$) regulation and subsequent vasodilation. The goal of this study was to determine the role of TRPC1 and TRPC3 channels in endothelial-mediated vasodilation in mouse cerebral artery. We specifically tested the hypothesis that *TRPC1 and/or TRPC3 contribute to ATP-mediated vasodilation of posterior cerebral artery (PCA) by regulating endothelial $[Ca^{2+}]_i$ signaling*.

Methods: TRPC1 and TRPC3 KO and littermate WT mice on a C57BL/6 background were used for all studies. Mouse PCA were mounted in a pressurized artery chamber with a Krebs/bicarbonate buffer. Luminal pressure was increased to 80 mm Hg and flow was established through the lumen of the artery. Endothelin-1 (Et-1, 10 μM) was administered abluminally to constrict the artery before luminal delivery of ATP at 10 and 100 μM. Aorta EC (AoEC) and cerebral artery EC (CAEC) were cultured using a Matrigel explant technique and used for studies at passage 1. EC $[Ca^{2+}]_i$ was measured by fura-2 fluorescent dye.

Results: Baseline diameter in response to Et-1 was not different between groups. Diameter for WT, TRPC1 KO, and TRPC3 KO was 124±3 μm (n=8), 122±4 μm (n=6), and 122±7 μm (n=5), respectively. Maximal diameter (dilation to Ca^{2+}-free solution) was greater in the TRPC3 KO group compared to WT (P=0.007) and averaged 172±4 μm, 180±2 μm, and 190±4 μm, respectively.

Luminally-delivered ATP (10 and 100 μM) produced dose-dependent dilation in all groups. However, the dilations were significantly reduced in the KO arteries compared with WT control. Dilations (% of maximal) to 10 & 100 μM ATP were 78±7 & 96±1% (WT), 30±12* & 76±10% (C1 KO), and 33±10* & 51±11* % (C3 KO) (2 way RM-ANOVA with Holm-Sidak test*).

Application of ATP (1 to 100 μM) to CAEC and AoEC produced a dose-dependent increase in EC $[Ca^{2+}]_i$ that was entirely blocked by PLC inhibition (U73122, 2-4 μM) and a non-specific TRPC channel blocker (1 mM La^{3+}). Additional studies in AoEC demonstrated that the ATP-stimulated Ca^{2+} response was significantly reduced in TRPC1 and TRPC3 KO with 10 μM ATP. The response to 100 μM ATP was still significantly reduced in the TRPC1 KO, however, the TRPC3 KO response was comparable to WT. Application of a newly described TRPC3 selective blocker (Pyr3, 10 μM), significantly attenuated the 100 μM ATP-stimulated Ca^{2+} response in WT and TRPC1 KO but not TRPC3 KO. Continuing studies are being performed with CAEC from KO mice to confirm these latter results in cerebral arteries.

Conclusions: TRPC1 and TRPC3 channels contribute significantly to endothelial-mediated dilation to ATP but not vasoconstriction to Et-1. The attenuated ATP-mediated vasodilation is likely due to impaired endothelial $[Ca^{2+}]_i$ signaling.

Supported by NIH R01 HL088435 (SPM) and NIEHS Z01-ES-101684 (LB)

1178

CAROTID OCCLUSION SURGERY STUDY (COSS): FAILURE OF CONCEPT OR METHODOLOGY?

H. Yonas, A. Carlson, E.M. Nemoto

Neurosurgery, University of New Mexico, Albuquerque, NM, USA

Objectives: The Carotid Occlusion Surgery Study (COSS) (1) represented a significant methodological advance over the failed Extracranial-Intracranial (EC-IC) Bypass Study (2) but does the recent termination of the COSS trial mean that there is no clinical benefit of EC-IC bypass surgery or was it due to failure of the methodology used to identify patients at high risk for stroke? Careful examination of the PET methodology used in COSS could provide insight into understanding the possible reasons for failure of COSS and more importantly, guidance on how to proceed to define the role of EC-IC bypass surgery.

Methods: Increased oxygen extraction fraction (OEF) measured by PET is the accepted gold standard of ischemic stress. Less certain is whether qualitative OEF ratios used in the COSS study and quantitative OEF values are equivalent in identifying ischemic stress. Also at issue are the threshold values used for both qualitative OEF ratios and quantitative OEF as indicators of ischemic stress and hemodynamic compromise.

Results: Studies using absolute, quantitative OEF measurements with appropriate reference 95% confidence intervals to define the absolute OEF thresholds of >50% showed that *increased OEF is an independent predictor of increased stroke risk*. Yamauchi et al (3) reported 57% stroke risk in patients with high OEF and 15% strokes in patients with OEF below the threshold. Others have also shown that an ischemic OEF threshold of 50% is an independent predictor of increased stroke risk. .

COSS was based on the study by Grubb et al (4) in a prospective study in patients with carotid occlusion where *qualitative* OEF was measured by the count rate ratio method. The upper limit of the OEF ratio obtained in normal volunteers (1.082) was used as the threshold which identified a stroke risk of 30% in patients with increased OEF ratio and 7% in patients with normal OEF ratio. Derdeyn et al (5) compared quantitative OEF and qualitative and quantitative OEF ratios in predicting stroke risk from the data of Grubb et al (4) and concluded that all were equivalent. However, the threshold was based on the mean ± 2 SEM and a threshold of 44% which predicted 8/9 strokes (6). Had the correct threshold of 56% been used only 3/9 strokes would have been predicted. An independent NIH funded study comparing quantitative and qualitative PET OEF as done in COSS did not identify the same patients as being at increased stroke risk.

Conclusions: Based on our analysis, we believe that the statistical methods used in studies on which COSS was based were flawed. Therefore the failure of COSS we believe is due to a failure of the OEF methodology.

References:

1. Derdeyn, CP, PI. *Carotid Occlusion Surgery Study [SPOTRIAS].http://www.strokecenter.org/trials/TrialDetail.aspx?tid=91*
2. N Engl J Med 1985; 313:1191-1200

3. J Nucl Med 1999; 40:1992-1998. .
4. JAMA 1998; 280: 1055-1060.
5. J Nucl Med 2001; 42: 1195-1197
6. Brain 2002; 125: 595-607.

1179

JUVENILE TRAUMATIC BRAIN INJURY IS ASSOCIATED WITH LATE CHANGES IN MYELIN BASIC PROTEIN AND BEHAVIORAL DYSFUNCTIONS

D. Ajao[1], J.E. Kamper[2], V. Pop[3], A. Adami[4], E. Rudobeck[4], L. Huang[4], R.E. Hartman[2], R. Vlkolinsky[4], S. Ashwal[3], A. Obenaus[3,4,5,6], J. Badaut[1,3]

[1]Physiology, [2]Psychology, [3]Pediatrics, [4]Radiation Medicine, [5]Biophysics & Bioengineering, [6]Radiology, Loma Linda University, Loma Linda, CA, USA

Objectives: Traumatic brain injury (TBI) within the juvenile population results in high mortality and in short- and long-term motor and cognitive impairments. Only a few experimental studies in rodents, however, have investigated these functional impairments in the long-term or attempted to match observed changes in the white matter tract with these behavioral changes.

Methods: Moderate right frontal cortical injury was induced using controlled cortical impact (CCI, 3mm diameter, 1.5mm depth) in 17-day-old rats. Lesion volumes at 3, 30, and 60 days post-injury were quantified using T2-weighted MRI. Motor function and behavioral outcomes were assessed at 1, 3, 7, 30, and 60 days after jTBI using: i) beam balance and foot-fault (sensorimotor, coordination, and proprioception), ii) rotarod (sensorimotor coordination and balance), iii) open field (activity levels), iv) turn bias, and v) zero maze (anxiety) tests. Electrophysiological recordings were acquired along the ipsi-(stimulating electrode) and contralateral (glass electrode) corpus callosum fiber tracks. Myelin Basic Protein (MBP) immunostaining was performed to investigate the consequences of jTBI on neuronal networks both at the level of and remotely from the site of injury.

Results: Lesion volumes remained constant at ~3% of brain volume over 60 days post-injury. Increased sensorimotor deficits in the foot-fault test were observed in TBI compared to sham-operated control rats from 3 to 60 days ($p < 0.05$). Rotarod tests confirmed motor deficits in TBI rats at 30 and 60 days ($p < 0.05$). The TBI rats also travelled significantly less distance on the balance beam up to 60 days ($p < 0.05$). A left turn bias (contralateral to the injured hemisphere) was observed in the TBI rats at 30 and 60 days related to the right brain cortical lesion. Anxiety-like behaviors were detected in TBI rats using the zero maze at 60 days post-injury with increased time spent in the dark ($p < 0.05$). Quantitative infrared-MBP demonstrated a significant global increase throughout all white matter structures in TBI animals (25%±4.39 increase in MBP-IR between P20 and P50 in the corpus callosum, $p < 0.005$), suggesting altered myelination. Electrophysiological measurements revealed reduced compound action potential (CAP) measured in the corpus callosum ($p < 0.005$) consistent with altered myelinated axons.

Conclusions: We have shown that moderate CCI in juvenile rats induced long-term sensorimotor deficits that continued into adulthood. Interestingly in our jTBI model, cognitive deficits appeared 60 days after injury with motor disabilities and an increase in anxiety-like behavior. These lasting deficits are associated with globally-altered myelin basic protein and reduced compound action potentials despite the fact that the initial injury was localized. These results suggest that increased MBP expression does not necessarily improve behavior. The molecular mechanisms have not yet been identified but they could be related to cerebrovascular dysfunctions.

Funded By NIH 1RO1HD061946-01

1180

PET IMAGING OF CANNABINOID CB1-RECEPTOR SYSTEM WITH [^{11}C]JHU75528. IMPROVEMENTS IN IMAGE QUANTIFICATION USING WILD-TYPE AND KNOCKOUT MICE

J.R. Herance[1], S. Rojas Codina[1], S. Abad[1], X. Jiménez[1], J.D. Gispert[1,2], E. Martín[3], A. Burokas[3], M.-À. Serra[3], R. Maldonado[3], D. Pareto[1,2]

[1]Institut d´Alta Tecnologia-PRBB, CRC Corporació Sanitaria, Barcelona, [2]CIBER en Bioingeniería, Biomateriales y Nanomedicina (CIBER-BBN)., Zaragoza, [3]Laboratory of Neuropharmacology, Department of Experimental and Health Sciences, Universitat Pompeu Fabra (UPF) - PRBB, Barcelona, Spain

Objective: The endocannabinoid system is integrated by the cannabinoid receptors, the endogenous cannabinoid ligands and the enzymes involved in their synthesis and degradation. At least two types of cannabinoid (CB) receptors have been identified: CB1 mainly expressed in the central nervous system that is the most abundant G protein-coupled receptor in the brain; and the CB2 receptor mostly found in the immune system. In this study we assessed the feasibility of using PET and the tracer [^{11}C]JHU75528, an analog of rimonabant, to study, in vivo, the brain cannabinoid type 1 (CB1) receptor system in genetically modified mice.

Methods: Wild-type (WT, n=8) and CB1 knock-out (KO, n=8) animals were imaged with [^{11}C]JHU75528 in baseline and after pretreatment with blocking doses of Rimonabant (2mg/kg) using a animal dedicated camera (microPET R4; Concorde, Siemens, Knoxville, TN, USA) Concoorde R4. Autoradiagraphic studies with the same radiotracer were performed in an additional set of WT mice to evaluate the binding of the radiotracer in the different brain regions

Results: The CB1 cannabinoid receptor radiotracer [^{11}C]JHU75528 showed a clear brain uptake in WT animals that was 50% higher than in KO mice. Pretreatment with Rimonabant reduced the binding of the radiotracer to the levels of the KO mice. No brain specific uptake was seen in CB1 KO mice. These sets of experiments demonstrate that [^{11}C]JHU75528 binds specifically to the CB1 receptor at the level of mice central nervous system. Brain distribution of [^{11}C]JHU75528 was rather homogeneous in PET images indicating a similar uptake in the different brain regions. Autoradiographic studies verified this behaviour.

Conclusions: Taken together, the results of this study support the feasibility of using PET technology to study the CB1 receptor in vivo, in the brain of genetically modified mice. Interestingly, [^{11}C]JHU75528 can be used to investigate the cannabinoid receptor system, and assess the effect of new drugs and treatments in preclinical studies. In fact the present work presented the kinetics of the radiotracer in mice brain and this binding pattern, which is quite homogeneous between the different brain regions. Finally we demonstrate that in mice the specific binding observed for [^{11}C]JHU75528 corresponds completely to CB1 receptor.

References:

Horti AG et al, 2006 Oct;47(10):1689-96.

Burns HD et al, Proc Natl Acad Sci U S A. 2007 Jun 5;104(23):9800-5.

Terry GE et al, Neuroimage. 2009 Nov 1;48(2):362-70.

Wong DF et al, Neuroimage. 2010 Apr 18.

Fan H et al, J Label Compd Radiopharm 2006; 49: 1021-1036.

Fan H et al, Eur J Med Chem. 2009 Feb;44(2):593-608.

Thanos PK et al, J Nucl Med. 2002 Nov;43(11):1570-7.

1182

METABOLITE ANALYSIS OF (-)-[^{18}F]FLUOROBENZOYL BENZOVESAMICOL, A PROMISING PET TRACER FOR IMAGING VACHT

Z. Tu[1], J. Cui[1], J. Fan[1], L. Shihong[1], L.A. Jones[1], P.K. Padakanti[1], A. Li[1], R. Wang[1], S.M. Parsons[2], J.S. Perlmutter[1], R.H. Mach[1]

[1]Washington University in St. Louis School of Medicine, St. Louis, [2]University of California at Santa Barbara, Santa Barbara, MO, USA

Objective: The vesicular acetylcholine transporter (VAChT) is a unique biomarker for studying cholinergic neurons in neurodegenerative diseases such as Alzheimer´s disease, Parkinson disease and other brain disorders. A PET radiotracer that can image VAChT will be useful for assessing cholinergic neurons in neurodegenerative diseases. MicroPET studies of (-)-*trans*-2-hydroxy-3-(4-(4-[^{18}F]fluorobenzoyl)piperidino)tetralin, (-)-[^{18}F]FBBV, one of a new class of carbonyl-containing benzovesamicol VAChT inhibitors,[1] displayed promising results in monkey brains.[2] To determine if (-)-[^{18}F]FBBV could be a clinical tracer for quantifying VAChT, the *ex vivo* metabolite analysis of (-)-[^{18}F]FBBV was performed on rhesus monkey plasma samples during a PET imaging session and on rat brain and plasma samples.

Methods: (-)-[^{18}F]FBBV was synthesized according reported procedure[2] with slightly modification. The specific activity at end of synthesis was >2000 mCi/μmol. After injection of (-)-[^{18}F]FBBV (~ 7.5 mCi) into a male rhesus, blood was collected at 5, 15, 30, 60 and 90 min during a 120 min dynamic scan with the microPET Focus 220. Images were reconstructed; regions-of-interest (ROI) were drawn on the summed image and time-activity curves were generated. Rats were euthanized and blood and brain harvested at 15, 30, 60 min post-injection of 1.67, 2.92 and 2.91 mCi of (-)-[^{18}F]FBBV. Rat brain was homogenized on ice with 2 mL of ice cold acetonitrile and centrifuged; the same solvent extraction process was used for plasma samples. For each solvent extract, 200 μL was injected onto a pre-conditioned reverse phase HPLC system and eluted with acetonitrile: 0.1 M Ammonium formate buffer. HPLC fractions were collected at 1 min intervals for 16 min; the radioactivity was counted and decay corrected to the time of injection and then generated the HPLC chromatograph.

Results: for the monkey plasma samples, at 5, 15, 30, 60 and 90 min post-injection, the parent compound, (-)-[^{18}F]FBBV retained 95%, 75%, 57% and 40% and 32% respectively. (-)-[^{18}F]FBBV was eluted from 9-12 min, in addition, two addition radioactive metabolites were collected; a major metabolite that was eluted 2-4 min and a minor metabolite that was eluted at 4 - 5 min. The same two metabolite peaks were observed in rat blood plasma. However, only parental compound, (-)-[^{18}F]FBBV was observed in the rat brain, which suggested major radioactive metabolite from the plasma samples of both species does not appear to cross the blood brain barrier. The microPET studies demonstrated (-)-[^{18}F]FBBV specifically bound to VAChT in the striatum of the monkey brain.

Conclusions: MicroPET Studies and radiolabeled metabolism studies indicate that (-)-[^{18}F]FBBV is a promsing radioligand for PET imaging of VAChT in the brain. The majority of activity in rhesus blood for the first 30 min was parent compound. *Ex vivo*

metabolite analysis of rat blood and brain showed a similar profile of radiolabeled metabolites in blood which suggested only parent compound entered into the brain of animal. Acknowledgments:

This work was supported by NIH/NINDS-R21NS061025-01A2.

Reference:

1. *Journal of Medicinal Chemistry* 2010, *53*, 2825.

2. *J Med Chem* 2009, *52*, 1359.

1184

MATERNAL FOOD RESTRICTION INCREASES THE VULNERABILITY OF FETAL CEREBRAL ARTERIES TO ISCHEMIC DAMAGE

S.M. Butler[1], S.M. Charles[1], J.M. Abrassart[1], O. Khorram[2], W.J. Pearce[1]

[1]Center for Perinatal Biology, Loma Linda University, Loma Linda, [2]Obstetrics and Gynecology, Harbor UCLA, Torrance, CA, USA

Objectives: Maternal food restriction (MFR) during gestation produces a broad variety of changes in fetal cardiovascular structure and function that persist through adulthood. Numerous studies suggest that these changes increase risk for metabolic syndrome, hypertension, and myocardial infarction in adult offspring (1). The present study examines that hypothesis that maternal food restriction also alters cerebrovascular structure and function in the developing fetus, and thereby enhances cerebrovascular vulnerability to ischemic injury during the perinatal period.

Methods: Pairs of female Sprague-Dawley littermates were bred at the same time, and the Control dam was given free access to food whereas the MFR dam was given 50% of the calories consumed by the Control dam. Pups were cross-fostered at birth, and on the 10^{th} postnatal day (P10) underwent either sham treatment or ischemic treatment consisting of unilateral carotid ligation followed by 105 min at 8% O2 with 24 hrs reperfusion. Middle cerebral arteries (MCA) from Sham and Ischemic groups of Control and MFR rats were studied using myography of pressurized segments and confocal colocalization of smooth muscle alpha-actin and myosin heavy chain isoforms, which are markers for smooth muscle phenotype.

Results: Confocal colocalization measurements revealed that MCA from MFR offspring exhibited a significantly greater fraction of smooth muscle cells in the non-contractile phenotype compared to Control offspring. Relative to Controls, MFR dramatically increased arterial stiffness in non-ischemic arteries. Ischemia depressed stiffness in MFR offspring, but enhanced it in Control offspring. Ischemia also depressed myogenic reactivity to a significantly greater extent in MFR than in Control offspring, and this differential effect was attributable to selective depression of pressure-induced increases in cytosolic Ca++ and myofilament Ca++ sensitivity in the MFR offspring.

Conclusion: These results demonstrate that maternal food restriction produces phenotypic changes in fetal arterial smooth muscle that increase arterial stiffness, attenuate the coupling between increased transmural pressure and increased cytosolic calcium, and depress myofilament calcium sensitivity in P10 rat middle cerebral arteries. Together, these structural and functional changes enhance the vulnerability to ischemic damage in fetal cerebral arteries. These results support the hypothesis that ischemic damage to immature cerebral arteries causes phenotypic transformation in cerebrovascular smooth muscle, which in turn, contributes to the depressed vasoreactivity that is characteristic of the post-ischemic fetal cerebral circulation.

References:

1. Le Clair C, Abbi T, Sandhu H, Tappia PS. Impact of maternal undernutrition on diabetes and cardiovascular disease risk in adult offspring. Can J Physiol Pharmacol 87: 161-79, 2009.

1185

COUPLING OF CEREBRAL BLOOD FLOW AND GLUCOSE METABOLISM DURING SPREADING DEPOLARISATIONS - A MULTIMODAL STUDY

D. Feuerstein, M. Gramer, T. Kumagai, M. Takagaki, S. Vollmar, M. Sué, H. Backes, R. Graf

Max Planck Institute for Neurological Research, Cologne, Germany

Objectives: Several clinical studies have recently suggested that multiple spreading depolarisations (SDs) in the human injured brain lead to a failure of cerebrovascular coupling [Dreier 2009] and glucose metabolism [Feuerstein 2010]. To decipher the mechanisms underlying this metabolic “uncoupling”, we have characterized SDs in intact brain using a multimodal approach. SDs and their cerebral blood flow correlates were observed with laser speckle flowmetry (LSF) and, simultaneously, glucose metabolism was assessed by positron emission tomography (PET) of [18F]-2-fluoro-2-deoxy-D-glucose (FDG) and rapid-sampling microdialysis (rsMD) of glucose and lactate every minute.

Methods: Male Wistar rats were positioned in a custom-built LSF/PET holder for simultaneous laser speckle contrast imaging and FDG-PET measurement. The temporo-parietal cortex of the animals was exposed to laser illumination through thinned skull and dura mater. A microdialysis probe was slowly inserted through a small craniectomy/durectomy and perfused at 1.6 µL/min with artificial cerebro-spinal fluid. The dialysate was assayed for glucose and lactate at 1-minute intervals using rsMD [Hashemi 2009]. After baseline measurements of rsMD and LSF, FDG was injected and PET images were acquired for 90 min. SDs were induced 20 min after FDG injection by either a needle prick or by continuous epidural application of potassium chloride (3M at 10 µL /hour).

Results: The LSF maps and PET images were co-registered using a specially made fudiciary marker. SD waves were detected by LSF as hyperemic waves propagating over the surface of the brain at a rate of 2 to 5 mm/min. Using a region of interest analysis, the number and the duration of the SD-associated hemodynamic waves were correlated to the PET and rsMD data.

The passage of one single SD wave (needle prick group, n=5) caused a moderate and transient fall in microdialysis glucose concentrations (by 15% of baseline values) and increase in FDG uptake compared to the contra-lateral hemisphere. By twenty minutes post-SD, FDG uptake was no different from the contra-lateral hemisphere and glucose concentrations had recovered their initial levels.

Following multiple SDs (potassium group, n=5), FDG preferentially accumulated in regions with a high frequency of SDs. Locally, the duration and amplitude of FDG increased uptake correlated with the frequency of propagating SDs (Pearson's correlation coefficient, r=0.729, p=0.002). Similarly, dialysate glucose concentrations gradually decreased with the occurrence of SD waves past the MD probe. Both responses were sustained and showed no apparent sign of recovery.

Conclusions: These data indicate that the passage of an SD wave causes a local transient increase in energy utilization. To account for the normalization of FDG uptake and glucose levels post-SD, this hypermetabolism seems to be followed by reduced energy consumption during a resting phase. However, as the SDs repeat frequently, the energy demand increases again during the resting phase, leading to sustained changes in FDG uptake and depletion of

glucose. This energy “crisis” during multiple SDs would be amplified in already compromised tissue following brain injury.

References:

Dreier et al., Brain, 2009,**132**(7):1866-1881

Feuerstein et al. JCBFM, 2010, **30**(7):1343-55

Hashemi et al. JCBFM, 2009, **29**(1):166-75

1186

JUVENILE TRAUMATIC BRAIN INJURY-INDUCED LESION VOLUME AND NEUROBEHAVIORAL DEFICITS ARE AMELIORATED BY D-JNKI1 THERAPY

D. Ajao[1], J.E. Kamper[2], A. Fukuda[1], V. Pop[3], D. Sorensen[1], R.E. Hartman[2], A. Obenaus[3,4,5,6], S. Ashwal[3], J. Badaut[1,3]

[1]Physiology, [2]Psychology, [3]Pediatrics, [4]Radiation Medicine, [5]Biophysics & Bioengineering, [6]Radiology, Loma Linda University, Loma Linda, CA, USA

Objectives: Traumatic brain injury in juvenile population (jTBI) is associated with a high risk of mortality and long-term disability. The neuropathological sequelae that result from TBI are a complex matrix of events including edema, excitotoxicity and apoptosis. The juvenile brain is particularly vulnerable to these events due to their unique developmental features. The c-Jun N terminal kinase (JNK) pathway has been recognized as playing a critical role in mediating post-traumatic cascade of events related to glial and neuronal survival. Our objective was to determine the therapeutic effectiveness of D-JNKI1, a protease-resistant, global JNK-inhibiting peptide, in improving neuroimaging and behavioral outcomes post-jTBI.

Methods: We carried out a moderate controlled cortical impact (CCI) injury to the right parietal cortex (CCI, 2.7mm-diameter impactor tip, 1.5mm depth; impact coordinates: 3mm AP, 4mm ML) in 17-day-old rats. D-JNKI (11mg/kg) or saline was intraperitoneally administered at 3 hours post-injury. Lesion volumes at 1, 3, 7, 30, and 60 days post-injury were quantified using T2-weighted MRI. Edema formation and brain water mobility were evaluated using T2-weighted (T2WI) and diffusion-weighted imaging (DWI). Motor function and behavioral outcomes were measured at 1, 3, 7, 30, and 60 days post-injury (dpi) using: (i) beam balance and foot-fault (sensorimotor, coordination, and proprioception), (ii) rotarod (sensorimotor coordination and balance), (iii) open field (activity levels), (iv) turn bias, (v) Morris water maze (MWM, learning and memory), and (vi) zero maze (anxiety) tests.

Results: D-JNKI1-treated animals showed significant improvement in neurological tests over the first 30 dpi (Foot-fault: p = 0.007, 0.009, and 0.021 for 3, 7 and 30dpi respectively; rotarod test [10rpm]: p = 0.007 at 7dpi). Behavioral tests at 30 and 60dpi also revealed improvements in D-JNKI1-treated animals compared to the saline group. MWM probe (measuring percent time spent in target quadrant for second day) showed significant interaction for day vs. group (p < 0.01) with DJNKI1-treated rats spending more time in target quadrant (p = 0.04), suggesting improvement in spatial memory for DJNKI treated rats at 30dpi. This result was confirmed at 60 dpi when D-JNKI1-treated animals performed better on cued MWM (p = 0.01). Saline-treated rats displayed turn bias showing asymmetry of motor function (p = 0.05). This functional improvement correlated with MRI-derived lesion volume results showing a 50 percent reduction in lesion volume in the DJNKI1-treated animals over the first 7dpi. There were no significant differences in raw T2 values between the two groups.

Conclusions: These results show that a single dose of D-JNKI1 administered at 3 hours post-injury in juvenile rats results in a reduction in lesion volume and improvements in several motor and cognitive functions, similar to that reported in adult stroke models. This lends credence to the idea that D-JNKI1 might be a potential clinical therapeutic agent for jTBI.

Funded By NIH 1RO1HD061946-01

1187

ARTERIAL RETE MIRABILE IN BLOOD SUPPLY SYSTEM OF MAMMALIAN BRAIN IN SOME TAXONS

H. Frąckowiak

Animals Anatomy, Poznan University of Life Sciences, Poznan, Poland

Aim and Objectives: The internal carotid artery and its input to blood supply to the arterial circle of the brain in 56 species of *Artiodactyla* order, representing families of *Suidae, Tayassuidae, Hippopotamidae, Camelidae, Giraffidae, Moschidae, Cervidae* and *Bovinae* and in 11 species of *Felidae* family (*Carnivora* order) as well as in cattle foetuses and newborns (n= 21) was analysed.

Methods: The cast preparations were made filling the arteries with stained solutions of plastics, introduced under pressure to bilateral common carotid arteries. Following solidification of the plastics the investigated material was subjected to maceration, which yielded arterial casts on the osseous framework of the skull.

Results: In multiple species of *Artiodactyla* order and in studied *Felidae* the original or extracranial fragment of internal carotid artery was found to undergo obliteration in ontogenesis. The complete internal carotid artery in these species of animals was present only in cattle foetuses and newborns.

Obliteration of the extracranial segment of internal carotid artery in the studied animals resulted in a principal modification of blood supply system to the arterial circle of the brain. The function of the obliterated extracranial segment in internal carotid artery was taken over by maxillary artery. In *Artiodactyla*, in species of *Ruminantia* suborder the maxillary artery yielded rostral branches and a caudal branch to rostral epidural rete mirabile, in which intraretis fragment of internal carotid artery ran, but only the supraretis fragment of the artery joined arterial circle of the brain. In *Felidae* rete mirabile of maxillary artery was noted, which through rami retis joined the intracranial segment of internal carotid artery, and through it, arterial circle of the brain.

In the examined *Artiodactyla* belonging to *Ruminantia* suborder a rostral epidural rete mirabile was detected, with branches forming anastomoses with maxillary artery. In *Suiformes* the rostral epidural rete mirabile was joined by a branch originating from the original, obliterated segment of internal carotid artery. In species of *Tylopoda* suborder a thin extracranial segment of internal carotid artery was preserved, which joined the rostral epidural rete mirabile.

In the arterial system of mammalian head rete mirabile are thought to provide morphological grounds for the so called „selective cooling of the brain" (Johnsen and Folkowa 1988). Dieguez et al. (1987, 1988) demonstrated that arteries forming epidural rete mirabile in *Artiodactyla* cannot participate in active control of blood supply to the brain.

Conclusions:

1. In the *Artiodactyla* order blood supply system to the brain contains an epidural adrostral rete mirabile.

2. Rete mirabile of maxillary artery can be demonstrated in species of *Felidae* family.

3. The studied animals manifest obliteration of extracranial segment in innernal carotid artery.

References:

Diaguez G., Garcia-Villalon A.L., Gomez B., Lluch S. (1988): Hemodynamic significance of the carotid rete during changes in arterial blood pressure. Am. J. Physiol. 254:770-775.

Lluch S., Dieguez G., Garcia A.L, Gomez B. (1985): Rete mirabile of goat: its flow-damping effect on cerebral circulation. Am. J. Physiol. 18:482-489.

1188

A STEP TOWARDS PERFUSION BENCHMARK MEASUREMENTS IN CLINICAL IMAGING DEVICES

P. Deman[1,2], M. Vincent[1,2], H. Elleaume[1,2], J.-F. Le Bas[1,2,3], A. Krainik[1,2,3], F. Estève[1,2,3], J.-F. Adam[1,2]

[1]u836, INSERM U836, Grenoble Institute of Neurosciences, University Joseph Fourier, [2]Institut des Neurosciences, Université Joseph Fourier, [3]CHU, Grenoble University Hospital, Grenoble, France

Objective: In recent decades, new methods aiming to assess quantitative brain perfusion have been developed [1] and tentatively applied to clinics in cerebrovascular diseases, oncology and trauma. However, all available methods require the use of tracer kinetics models for the extraction of absolute perfusion values [2].The results vary with the imaging technique and protocols, the algorithms and the operator [2]. In particular, it is not known to what extent blood brain barrier leakage affect the results [2]. Of the parameters blood volume, flow and permeability surface area product (PS, one of the capillaries permeability coefficients), only blood flow has been experimentally validated [3]. As a necessary step towards validating absolute perfusion measurements procedures used in clinics, we propose a novel method usable with both CT and MRI based on a phantom that mimics perfused tissue under defined conditions.

Methods: So far, only CT-perfusion measurements procedures were evaluated. The phantom is a bundle of porous capillaries each about 215 µm in diameter. Theoretical fluid volume and flow were derived from the phantom physical characterization for a given input flow. Theoretical PS was derived from two photons microscopy experiments on one capillary. Values have been compared with those derived from different models implemented in clinical analysis workstations. We have also tested the robustness of these models under various input flow rates and sizes of contrast agent to mimic various perfusion rates and capillary permeabilities.

Results: The adiabatic approximation of the Johnson and Wilson model [4] gave the best results in presence of permeable capillaries whereas the models based on gamma-variate fitting gave reliable results only for non-leaking capillaries conditions and large errors (> 300%) in case of contrast extravasation. For example, with theoretical flow and volume values set at 19.8 ml/100g/min and 22.9 ml/100g, respectively; the Johnson and Wilson model returned 17.4 ± 4.5 ml/100g/min and 21.2 ± 1.5 ml/100g, respectively, whereas the gamma variate model returned 73.3 ml/100g/min and 124 ml/100g, respectively. PS values were found almost equal to zero (7 ± 13 ml/100g/min) for the Johnson and Wilson model when using a micrometric size contrast agent (barium, Micropaque®). These values raised to 44 ± 10 ml/100g/min when using a small iodinated contrast agent (Iomeron®), which is coherent with the theory.

Conclusion: To our knowledge, this is the first report of a robust experimental method for validating CT perfusion measurement procedures and shedding the light on controversial absolute perfusion measurements methods recently developed. Further investigations are underway to use this methodology in MR perfusion measurements, for calibration purposes and absolute perfusion values retrieval, when the relationship between the signal and the contrast agent concentration is controversial.

References:

1. M. Wintermark, et al. *Stroke* 36 (9), 2032 (2005).

2. *Multi-Detector Computed Tomography in Oncology: CT Perfusion Imaging*, Miles K.A., Charnsangavej C., Cuenod C.A. ed. (Informa Healthcare, U.K., 2007).

3. A. Cenic, et al. *Am J Neuroradiol* 20 (1), 63 (1999)

4. K. S. St Lawrence and T. Y. Lee*. J Cerebr Blood F Met* 18 (12), 1365 (1998).

1190

AMYLOID IMAGING AND CORRELATION WITH CLINICAL SYMPTOMS IN A COHORT OF PARKINSON´S DISEASE PATIENTS

M. Petrou, N. Bohnen, M. Muller, R. Koeppe, K. Frey

University of Michigan, Ann Arbor, MI, USA

Objectives: Amyloid deposition is one of the earliest findings in patients with Alzheimer disease (AD); there have been variable reports regarding abnormal amyloid deposition in patients with Parkinson disease (PD)[1,2]. Our investigation aimed at quantifying cortical and striatum amyloid deposition in a cohort of Parkinson's disease patients with mild cognitive impairment using PET imaging with Pittsburgh compound B (PIB). We also examined the association between corticostriatal amyloid deposition and cognitive function in this patient group.

Methods: 22 patients with Parkinson's disease and mild cognitive impairment (mean age 69.7±6.7, range 60-82, 18 males, 4 females; mean Montreal Cognitive Assessment Test score of 25.4±2.1, range 21-29) underwent dynamic amyloid brain PET imaging with Pittsburgh compound B (18 mCi [C-11]PIB), MRI and neuropsychological assessment. PET studies were performed on a Siemens ECAT HR+ tomograph in 3D. Brain MRI was also performed on all subjects on a 3 Tesla Philips Achieva MR unit. Dynamic PET image frames were spatially coregistered within subjects with a rigid-body transformation and registered to the MRI using Neurostat software (U Washington, Seattle, WA). IDL image analysis software (Research systems, Inc., Boulder, CO) was used to manually trace volumes of interest (VOIs) on the MRI. Cortical VOI were defined using semi-automated thresholding delineation of cortical gray matter signal on the MRI. PIB PET data were analyzed using the Logan graphical method and the cerebellum as reference region to determine global cortical PIB distribution volume ratio (DVR). Composite z-scores were calculated for intelligence and different cognitive domains (memory, visuospatial attention, working memory/attention, and executive functions) based on normative data.

Results: Mean cortical PIB DVR in this cohort was 1.13±0.0.05, range 0.98-1.41. Mean striatal PIB DVR was 1.35±0.01, range 1.19-1.68. There was significant correlation of corticostriatal PIB binding and various cognitive parameters. For example, significant correlations were noted between cortical PIB binding and attention measures ($r=0.55$, $p=0.009$) as well as the Weschler Adult Intelligence Score ($r=-0.55$, $p=0.007$). Significant correlations were also found between striatum PIB binding and attention scores ($r=0.48$, $p=0.02$) as well as the Weschler Adult Intelligence Score ($r=-0.61$, $p=0.002$).

Conclusion: Although average cortical PIB binding in PD is in the range below than those commonly used to classify a PIB PET scan as “positive”, these apparent low binding values have significant correlation with cognitive functions. Furthermore, similar findings were seen with striatal PIB activity. These findings suggest that subcortical and cortical amyloid binding in PD and mild cognitive impairment, even at mildly elevated levels, are of pathophysiological significance.

References:

1. Foster ER, Campbell MC, Burack MA et al. Amyloid Imaging of Lewy Body- Associated disorders. Movement Disorders 2010; 25: 2516-2523.

2. Edison P, Rowe CC, Rinne JO, et al. Amyloid load in Parkinson´s disease

dementia and Lewy body dementia measured with [^{11} C]PIB positron emission tomography. J Neurol Neurosurg Psychiatry 2008; 79: 1331-8.

3. Logan J, Fowler AH, Volkow ND, Wang G-J, Ding Y-S, Alexoff DL. Distribution volume ratios without blood sampling from graphical analysis of PET data. J Cereb Blood Flow Metab 1996; 16: 834-40.

1191

THE IMPACT OF SOFTWARE MOTION CORRECTION ON PET DRUG OCCUPANCY STUDIES

M. Savli[1], A. Hahn[1], D. Häusler[2], C. Philippe[2], P. Baldinger[1], A. Höflich[1], C. Kraus[1], G.S. Kranz[1], S. Zgud[1], E. Akimova[1], W. Wadsak[2], M. Mitterhauser[2], R. Lanzenberger[1], R. Dudczak[2], S. Kasper[1]

[1]Psychiatry and Psychotherapy, [2]Department of Nuclear Medicine, Medical University of Vienna, Vienna, Austria

Introduction: Positron emission tomography (PET) has become a powerful instrument in imaging of receptor and transporter molecules in the living human brain. One of its major drawbacks is the mostly long acquisition time of about 90 minutes up to sometimes 240 minutes depending on the tracer radionuclide and the metabolism. Neat data quantification requires a stable head position throughout the entire scan, which can become a burdensome procedure for the patient. Usually face mask systems help to keep the head in position, however such equipments cannot totally prevent movements. This results in blurred images or artifacts and thus might lead to data misinterpretation, particularly in small brain regions. The objective of our study was to demonstrate the impact and relevance of software motion correction in PET studies exemplified on drug occupancy data investigating the serotonin transporter (SERT).

Methods: 18 MDD outpatients (mean age=42.06 years, SD=8.0) participated in this study and received an equivalent amount of the enantiomer S-citalopram for at least three weeks. Total PET acquisition time was 90min. (15x1min. and 15x5min. frames). Dynamic scans were inspected visually and motion correction using SPM8 was carried out by coregistration of each frame to the mean of the patient's motionfree frames. Subsequently, dynamic PET scans were normalized onto a tracer-specific template in Montreal Neurological Institute (MNI) space. Regions of interest (ROIs) were defined using a template (AAL, [1]), which involved eight a priori defined brain areas: Dorsal Raphe Nucleus (DRN), Median Raphe Nucleus (MRN), Midbrain, Thalamus, Putamen, Nucleus Caudatus, Nucleus Accumbens, and Amygdala. SERT occupancy was derived by quantification of [^{11}C]DASB binding using the MRTM2 reference region approach and the following equation: $\text{Occupancy}(\%)=(1-BP_{treatment}/BP_{baseline})x100$.

Results: Head motion was observed in 12 out of 18 subjects. On average, first movements were registered after 30±14 minutes. Repeated measures ANOVA revealed a significant influence of motion correction on occupancy values ($F=5.16$, $df=1,17$, $p=0.036$) as well as a ROI by motion correction interaction ($F=4.17$, $df=7,119$, $p=0.007$). Whereas motion corrected values were significantly lower in the amygdala, nucleus caudatus, putamen, thalamus, and MRN; midbrain and DRN showed no significant differences, and nucleus accumbens were even significantly higher (all p-values < 0.05).

Conclusion: This study demonstrated the influence of head motion during data acquisition on drug occupancy, one of the most relevant outcome variables in PET studies. Interestingly, in 67% of our sample head movements were already identified upon visual inspection. Although six patients showed no perceivable head motion, small movements cannot be completely ruled out. Hence software motion correction might be an essential benefit in the data processing cascade, especially when reference region methods are applied for quantification. Even though motion correction on our scans yielded significantly lower drug occupancy values in almost all ROIs investigated, modifications in both directions can be expected. The accuracy of such

outcomes is of particular interest in PET studies investigating the optimal dosage of psychotropic drugs.

References:

[1] Tzourio-Mazoyer et al. Neuroimage 2002

1192

DEFICIENCY OF NA,K-ATPASE ALPHA ISOFORMS DIFFERENTIALLY MODULATE THE THRESHOLD FOR SPREADING DEPOLARIZATIONS IN MICE

C. Reiffurth[1,2], M. Alam[3], M. Zahedi-Khorasani[4], J.P. Dreier[1,2,5]

[1]Center for Stroke Research, [2]Experimental Neurology, Charité - University Medicine Berlin, Berlin, [3]Department of Neurosurgery, Hannover Medical School, Hannover, Germany, [4]Laboratory of Cerebrovascular Research, Physiological Research Center, University of Medical Sciences, Semnan, Iran, [5]Department of Neurology, Charité University Medicine Berlin, Berlin, Germany

Objectives: Mutations in ATP1A2, the gene encoding the Na,K-ATPase alpha2 subunit, have been identified in patients suffering from a severe form of migraine with aura: familial hemiplegic migraine type 2 (FHM2)[1]. It has been hypothesized that spreading depolarization (SD, spreading depression), the neurophysiological process underlying migraine aura, might be facilitated by a loss of function of a single allele of the gene encoding the alpha2 subunit[2]. To address the question whether a specific reduction of the alpha2 isoform affects the threshold for SD ignition we employed heterozygous knockout mice lacking one copy of the α2 subunit encoding allele (alpha2+/-) and provoked SD by various stimuli.

Methods: In acute brain slices, SD was triggered focally by droplet application of 1 M KCl solution, by electrical stimulation or by stepwise increasing the K+ concentration in the bathing solution. We recorded changes in extracellular K+ concentration, the accompanying slow extracellular potential shift, as well as changes in intrinsic optical signals to assess spatiotemporal patterns. To further investigate whether the observed effects were specific for a reduced amount of the alpha2 isoform, alpha1 and alpha3 heterozygous (alpha1+/- and alpha3+/-) mice were included in this study.

Results: We found a slightly but significantly lowered ($P < 0.001$) threshold concentration of K+ to trigger SD in alpha2+/- mice (13,03 ± 1,24 mmol/l, n = 18) compared to their wild-type littermates (14,92 ± 1,59 mmol/l, n = 23). This fact was reflected by a shortening of the wash-in time needed to induce SD. No significant reduction in threshold concentration was found in alpha1+/- or alpha3+/- mice compared to their wild-type littermates indicating that the observed effect in the alpha2 group is specific for this isoform.

Conclusions: The present results bolster the notion that different catalytic Na,K-ATPase alpha isoforms have distinct functional properties and substantiates the hypothesis that functional haploinsuffiency may underlie the increased susceptibility to SD in FHM2.

References:

1. De Fusco M, Marconi R, Silvestri L, Atorino L, Rampoldi L, Morgante L, Ballabio A, Aridon P, Casari G (2003) Haploinsufficiency of ATP1A2 encoding the Na+/K+ pump alpha2 subunit associated with familial hemiplegic migraine type 2. Nature Genetics 33:192-6.

2. Pietrobon D, Striessnig J (2003) Neurobiology of migraine. NatRevNeurosci 4:386-98.

1193

BLOOD-BRAIN BARRIER (BBB) PROTECTION IN SPHINGOSINE KINASE 2-MEDIATED ISCHEMIC TOLERANCE

B.K. Wacker, A.B. Freie, J.L. Perfater, J.M. Gidday

Neurosurgery, Washington University School of Medicine, Saint Louis, MO, USA

Objectives: Hypoxic preconditioning (HPC) protects against neurovascular dysfunction caused by cerebral ischemia, providing a platform to study endogenous pathways of ischemic protection. Previously, we demonstrated that pharmacological inhibition of sphingosine kinase (SphK) activity abrogates HPC-induced ischemic tolerance, blocking the increase in the activity of the SphK2 isoform we measured 2-4 hours after HPC.[1] Since SphK2 catalyzes the production of sphingosine-1-phosphate (S1P), a bioactive lipid known to enhance vascular barrier integrity via junctional protein regulation,[2] we hypothesized that a vasculoprotective phenotype, secondary to the hypoxia-mediated production of S1P by SphK2, contributes to HPC-induced neurovascular ischemic tolerance. The present studies were designed to document a role for SphK2 signaling induced by HPC in reducing infarct volume and preventing postischemic blood-brain barrier (BBB) disruption. In addition, we sought to identify the mechanistic basis of this BBB protection by evaluating junctional protein regulation in response to HPC and ischemia.

Methods: Adult SphK2 knockout mice and matched wild-types (C57BL/6) were subjected to HPC (4 h of 8% oxygen, systemic) two days prior to undergoing 45-min middle cerebral artery occlusion by intraluminal suture. After 24 h of reperfusion, infarct volume was determined, and IgG permeability was quantified to measure vasogenic edema. In separate cohorts, changes in cortical expression of several BBB junctional proteins were measured by immunoblotting of brain lysates 48 h after HPC (coinciding with the time of onset of ischemia). In addition, triton-insoluble fractions were analyzed to determine expression changes specific to cytoskeletally-linked cell junctions.

Results: While HPC significantly reduced infarct volumes in wild-type mice subjected to focal stroke ($p < 0.05$), HPC-induced tolerance was completely lost ($p < 0.05$) in SphK2 knockout mice. Significant ($p < 0.05$), HPC-mediated reductions in postischemic IgG permeability were also lost ($p < 0.05$) in SphK2 knockout mice. Additionally, protection against BBB disruption was more evident as a reduction in the intensity, rather than the area, of extravascular IgG, suggesting that this improvement in BBB integrity was not the result of a smaller infarct area. Examination of BBB junctional proteins revealed a significantly decreased expression of occludin and VE-cadherin in the triton-insoluble fraction of SphK2-null mice relative to wild-types following HPC. The significant increase in triton-insoluble claudin-5 expression following HPC was reduced ($p < 0.05$) in SphK2 knockout mice.

Conclusions: These findings confirm that HPC-induced ischemic tolerance and protection of the BBB depend on SphK2 signaling. Moreover, SphK2 signaling participates in both the maintenance of VE-cadherin and occludin at cell junctions, as well as the mediation of HPC-induced localization of claudin-5 to cytoskeletally-linked cell junctions, which may be compulsory for induction of a vasculoprotective phenotype by HPC. Analysis of changes in post-ischemic junctional protein expression, currently in progress, may further illuminate SphK2-regulated mechanisms of BBB protection induced by HPC. Elucidation of the mediators of this endogenous, HPC-activated lipid signaling pathway, and its role in BBB protection after stroke, may provide new therapeutic targets that can be modulated for cerebrovascular protection in stroke patients.

References:

1. Wacker BK, Park TS, Gidday JM. *Stroke* 2009; 40(10):3342-3348

2. Wang L, Dudek S. *Microvasc Res*. 2009; 77(1):39-45

1194

DEPLETION AND DYSFUNCTION OF BONE MARROW ENDOTHELIAL PROGENITOR CELLS IN NEUROGENIC HYPERTENSION

V. Shenoy[1], J. Zubcevic[1], J.Y. Jun[1], Y. Qi[1], A. Afzal[2], J. Mocco[2], M.K. Raizada[1]

[1]Physiology and Functional Genomics, [2]Neurological Surgery, University of Florida, Gainesville, FL, USA

Introduction: Neurogenic hypertension is a complex polygenic trait characterized by a dysfunctional autonomic nervous system and endothelium, resulting in part from increased oxidative stress and inflammation. Bone marrow (BM)-derived endothelial progenitor cells (EPCs) contribute to the repair and maintenance of endothelial damage to maintain the vascular homeostasis. Dysfunctional EPCs and elevated pro-inflammatory mediators may exaggerate vascular dysfunction and contribute to the pathophysiology of neurogenic hypertension. Thus, we propose that there is an imbalance between the BM EPCs and pro-inflammatory cells (PICs) in the spontaneously hypertensive rat (SHR), an established rodent model of human neurogenic hypertension.

Methods: Femur and tibia from nine weeks old SHR (MAP=152) and its aged matched normotensive control, the Wistar-Kyoto (WKY) rat (MAP=94) were used to study the function of BM cells. CD90+ and CD34+ cells were used as representative of EPCs, and their function was assessed by their ability to migrate and proliferate upon stimulation with growth factors (*STEMCELL Technologies*). BM-derived CD4+ and CD8+ cells (T lymphocytes) and CD68+ cells (macrophages) were used as representatives of the PICs, and were fluoro-labeled (*AbD Serotec*) and analysed by FACS.

Results: We observed a 2 fold increase in the BM PICs, and a 19 fold decrease in the BM EPCs in the SHR compared to the WKY. As a result, the SHR BM showed a 40 fold increase in the PIC/EPC ratio. The decrease in the EPC numbers in the SHR was associated with a 3 fold decrease in their ability to migrate to the site of endothelial damage, and a 2 fold decrease in their proliferative capacity. Furthermore, there was a ~20% increase in the levels of reactive oxygen species (ROS) in the BM EPCs of the SHR compared to the WKY.

Conclusion: These data demonstrate that the BM PIC/EPC ratio is increased, which is associated with EPC dysfunction in the SHR. These alterations in EPC numbers and function could be a consequence of the altered sympathetic/parasympathetic regulation of the BM, and key in a decreased vasoreparative mechanisms leading to pathophysiology of hypertension.

1195

ANALYZING BRAIN CHANGES IN ALZHEIMER'S DISEASE WITH DEFORMATION-BASED MORPHOMETRY FROM SERIAL MRIS AND CORRELATIONS WITH PET FDG AND PIB

W.R. Riddle[1], S. Shokouhi[1], S.C. DonLevy[2]

[1]Radiology and Radiological Sciences, Vanderbilt University, Nashville, TN, [2]Pediatric Nurse Practitioner, Nashville, TX, USA

Introduction: The distinguishing factor between Alzheimer´s disease and other dementias is the presence of beta-amyloid plaques that are thought to cause the death of brain cells. Previously, a definitive diagnosis of the disease could only be made post-mortem at autopsy. Studies have demonstrated that C-11 labeled Pittsburg Imaging Compound B (PIB) can detect the accumulation of these plaques in vivo.

Objective: To evaluate volume changes on serial MR scans measured with deformation-based morphometry and to correlate these changes with C-11 PIB retention and F-18 uptake.

Patients and methods: Serial T1-weighted MRI volumes, FDG uptake volumes, PIB retention volumes, and accompanying Mini-Mental Status Exam scores were obtained from the Alzheimer's Disease Neuroimaging Initiative. Using the serial MRI volumes, volume changes relative to the first scan were quantified with deformation-based morphometry. These expansions/contractions were mapped into fifteen bins and displayed as color overlays over the second MRI volume. The MRI volumes were divided into ten regions (frontal lobe, parietal lobe, occipital lobe, temporal lobe, cingulate cortex, sublobar region, cerebellum, midbrain, pons, and medulla). For each subject, plots of the fraction of voxels in each region that expanded or contracted were created. The FDG uptakes and PIB retention images were co-registered to the MRI volumes and overlaid over the MRI images.

Results: The expansions/contractions of the MRI volumes were different for each patient. For some patients, areas of contractions in the superior longitudinal fasciculus corresponded to initial decreases in Mini-Mental Status Exam scores. In the temporal lobe, areas of contraction corresponded to PIB retention, which occurred after the Mini-Mental Status Exam scores had declined.

Conclusion: Deformation-based morphometry of serial MRI volumes may provide useful information for early detection and understanding the pathogenesis of Alzheimer's disease.

1196

EARLY HEMISPHERIC SWELLING IN FOCAL BRAIN ISCHEMIA: COMPARING THE ROLES OF BRADYKININ AND VASCULAR ENDOTHELIAL GROWTH FACTOR

N.E. Lapina, J.D. Seiffge, **L. Schilling**

Neurosurg. Res., Med. Fac. Mannheim, Univ. Heidelberg, Mannheim, Germany

Following an ischemic or traumatic brain insult hemispheric edema followed by subsequent swelling of the affected hemisphere is considered an important pathophysiological mechanism in the early phase of tissue reaction. The development of edema appears to be a multifactorial process with thev release of bradykinin (Bk) following activation of the kallikrein-kinin system (KKS) and of the vascular endothelial growth factor (VEGF)-flt1 system due to tissue hypoxia potentially involved. We have, therefore, compared activation of these two systems in a rat model of transient focal brain ischemia.

Male Sprague Dawley rats anesthetized with Isoflurane (2.5- 3.0%) were used throughout. In the right skull bone a laser Doppler fibre (LDF) probe was inserted in the supply territory of the middle cerebral artery (MCA) for continuous recording of cerebral perfusion. In the right side of the neck the external carotid artery (ECA) was visualized and a 4-0 filament with the tip covered with silicone was introduced. The filament was pushed into the internal carotid artery until MCA occlusion (MCAO) was achieved as indicated by a sharp drop of >50% of the LDF signal. The animals were allowed to recover before removal of the filament after 2 h. Part of the animals received an anti-hypoxic treatment for 8 h including normobaric hyperoxygenation. The experiments were terminated 8 or 24 h after MCA occlusion and the brain removed. Serial coronal sections were taken at a distance of 1 mm for subsequent silver nitrate staining to planimetrically determine ischemic damage and hemispheric swelling. The tissue between the sections was sampled for subsequent extraction of total RNA from the ischemic and the contralateral hemisphere and subjected to reverse transcription followed by real time quantitative PCR. Results were analysed using ΔCt methodology and elongation factor-1 as house keeping gene.

The target genes studied included the B1 und B2 receptor, kallikrein, VEGF and the VEGF-receptor, flt1 with elongation factor-1 (EF-1) serving as house keeping gene. The results (mean±SEM of n= 4-8 measurements per group) are shown in the table below (with * p< 0.05 vs. control).

		Δ Ct				
	Swelling (%)	B1	B2	Kininogen	VEGF	flt1
Control no MCAO	-	not expressed	12.8±2.0	12.7±1.3	8.5±0.9	7.4±0.5
MCAO 8h	20.6±4.1	13.7±1.4	9.3±0.5	7.2±0.9	7.7±0.7	6.8±0.6

no treatment						
MCAO 8h NBH treatment	7.7±0.9	14.2±0.6	9.2±0.4	6.9±1.0	7.6±0.9	6.9±0.6
MCAO 24h no treatment	38.4±4.7	11.4±2.4	8.6±2.3*	1.4±0.3*	7.3±1.1	6.0±1.6*
MCAO 24h NBH treatment	18.6±2.4	14.6±1.3	8.9±0.6*	4.8±0.9*	6.8±0.5*	5.8±0.5*

[Results]

Correlation analysis revealed a significant relationship of hemispheric swelling with the level of gene expression only for the B1 receptor ($r=0.817$, $p< 0.001$) and for kininogen ($r=0.814$, $p< 0.001$).

The results indicate a time-related activation of the KKS and the VEGF-flt1 system in a rat model of transient focal brain ischemia. However, only the B1 and the kininogen expression appear to significantly contribute to hemispheric swelling within the first 24 h. The role of the activation of the VEGF/flt1 system may become important at a later time, e.g. when tissue remodelling occurs.

1199

THE ROLE OF NF -KB IN AUTOPHAGIC CELL DEATH AFTER BARRAL CORTEX ISCHEMIA

L. Wei[1], W.-L. Li[2], T.C. Carter[2], Q.L. Kern[2], S.P. Yu[2]

[1]Anesthesiology and Neurology, [2]Emory University School of Medicine, Atlanta, GA, USA

Objective: Autophagy is a required process for cellular homeostasis under physiological condition. Recent data suggest that autophagy may contribute to cell death in the mammalian brain after ischemic stroke (Rami et al., 2008; Cherra and Chu, 2008). The exact role of autophagy after acute ischemic stroke is obscure. Moreover, the mechanism that controls the post-stroke autophagy is not well defined. The transcription factor, nuclear factor kappa B (NF-κB), is an important regulator of apoptosis in cerebral ischemia. The present investigation explored the role of NF-κB p50 gene in ischemia-induced autophagic cell death.

Methods: Adult wild type (WT) and NF-κB p50 knockout (p50-/-) mice were subjected to permanent occlusion of branches of middle cerebral artery supplying to the barrel cortex (Wei et al. 1995; Li et al., 2006; Whitaker et al., 2007). The activity of autophagy was detected by immunofluorescence staining and/or Western blotting of Beclin-1 and LC-3. Neuronal and vascular damage was determined by TUNEL co-stained with NeuN and Collagen IV (a vessel marker). Immunostaining of endothelial cell tight junction marker occludin was used to detect blood brain barrier (BBB) integrity.

Results: The activity of autophagy was significantly enhanced in p50-/- mice compared with WT mice 12 and 24 hrs after ischemic stroke. This increased autophagic activity contributed to cell injury, evidenced by co-labeled TUNEL staining. The number of Beclin-1/TUNEL positive cells in the stroke border was significantly increased in p50-/- mice than in WT mice. The autophagy associated cell death was seen in neurons as well as in endothelial cells. Compared with WT, TUNEL-positive cells co-stained with either NeuN or Collagen IV increased in $p50^{-/-}$ mice. Reduced immunostaining of endothelial cell tight junction marker occludin revealed an increase in damage to the BBB in $p50^{-/-}$ mice. Western blotting of the penumbra tissue showed a reduction of Akt-mTOR signaling in $p50^{-/-}$ mice after ischemia.

Conclusion: These findings demonstrate that ischemic insult activates autophagy, this form of cell death may contribute to ischemic injury, and NF-kB activation plays a protective, anti-autophagic role, likely by regulating mTOR signaling.

Reference:

Rami A, Langhagen A, Steiger S. Focal cerebral ischemia induces upregulation of Beclin 1 and autophagy-like cell death. Neurobiol Dis. 29:132-141, 2008.

Cherra SJ, Chu CT. Autophagy in neuroprotection and neurodegeneration: A question of balance. Future Neurol. 3:309-323, 2008.

Wei L, Rovainen CM, Woolsey TA. Ministroke in rat barrel cortex. Stroke. 26:1459-1462, 1995.

Whitaker VR, Cui L, Miller S, Yu SP, Wei L., Whisker stimulation enhances angiogenesis in the barrel cortex following focal ischemia in mice. J Cereb Blood Flow Metab. 27:57-68, 2007.

Li Y, Lu Z, Keogh CL, Yu SP, Wei L. Erythropoietin-induced neurovascular protection, angiogenesis, and cerebral blood flow restoration after focal ischemia in mice.

J Cereb Blood Flow Metab. 27:1043-1054, 2006.

1200

AMYLOID AND ACETYLCHOLINESTERASE IMAGING AND OLFACTION IN PARKINSON´S DISEASE

M. Petrou, N. Bohnen, M. Muller, R. Koeppe, K. Frey

University of Michigan, Ann Arbor, MI, USA

Objectives: Hyposmia is an early, often prodromal symptom, that can occur both in Alzheimer's (AD) and Parkinson's disease(PD). We recently reported that severity of PD hyposmia correlated with the degree of cholinergic denervation and cognitive impairment. Amyloid deposition is one of the earliest findings in AD and has been considered to underlie olfactory changes in AD. There are variable reports regarding abnormal amyloid deposition in PD. Our investigation examined the association of amyloid deposition, cholinergic denervation and hyposmia in a cohort ofPD patients.

Methods: 22 patients with PD and mild cognitive impairment (mean age 69.7±6.7, range 60-82, 18 males, 4 females; mean Montreal Cognitive Assessment Test score of 25.4±2.1, range 21-29) underwent dynamic amyloid brain PET imaging with Pittsburgh compound B (18 mCi [C-11]PIB), MRI and olfactory assessment. Subset of 16 of these patients also underwent acetylcholinesterase imaging using the [C-11]PMP ligand (18 mCi). PET studies were performed on a Siemens ECAT HR+ tomograph in 3D. Brain MRI was also performed on all subjects on a 3 Tesla Philips Achieva MR unit. Dynamic PET image frames were spatially coregistered within subjects with a rigid-body transformation and registered to the MRI using Neurostat software (U Washington, Seattle, WA). IDL image analysis software (Research systems, Inc., Boulder, CO) was used to manually trace volumes of interest (VOIs) on the MRI. PIB PET data were analyzed using the Logan graphical method with cerebellum as reference region to determine global cortical PIB distribution volume ratios (DVR). PMP hydrolysis rates were estimated using the Nagatsuka method with the striatum as input function. Odor identification was assessed using the University of Pennsylvania Smell Identification Test (UPSIT).

Results: Mean cortical PIB binding in this cohort was 1.13±0.05, range 0.98-1.41. Mean striatal PIB binding was 1.35±0.01, range 1.19-1.68. Mean cortical PMP hydrolysis rates was 0.0268 ± 0.0033^{-1}, range $0.0219\text{-}0.0343^{-1}$. There was robust correlation between UPSIT scores and cortical PMP ($r=0.74$, $p< 0.001$) but not PIB activity ($r=0.006$, $P=0.98$). Cortical PIB binding showed no significant correlation with cortical PMP activity ($r=0.085$, $P=0.75$) in the subset of 16 patients that underwent both scans.

Conclusion: Hyposmia is robustly correlated with cholinergic denervation but not with abnormal amyloid binding in PD. Lack of correlation between cortical acetylcholinesterase and amyloid activity suggests that amyloid deposition and cholinergic denervation are concurrent but relatively independent pathophysiologic processes.

Support: NIH P01 NS015655 & R01 NS070856

References:

1. Bohnen NI, Muller MLTM, Kotagal V, Koeppe RA, Kilbourn MA, Albin RL, et al. Olfactory dysfunction, central cholinergic integrity and cognitive impairment in Parkinson disease. Brain 2010; 133: 1747-54.

2. Logan J, Fowler AH, Volkow ND, Wang G-J, Ding Y-S, Alexoff DL. Distribution volume ratios without blood sampling from graphical analysis of PET data. J Cereb Blood Flow Metab 1996; 16: 834-40.

3. Nagatsuka S, Fukushi K, Shinotoh H, Namba H, Iyo M, Tanaka N, et al. Kinetic analysis of [(^11)C]MP4A using a high-radioactivity brain region that represents an integrated input function for measurement of cerebral acetylcholinesterase activity without arterial blood sampling. J Cereb Blood Flow Metab 2001; 21: 1354-66.

1201

THE EFFECT OF VAGUS NERVE STIMULATION DURING FOCAL CEREBRAL ISCHEMIA: CHRONIC OUTCOME IN RATS

T. Hiraki[1], W. Baker[2], Z. Sun[1,3], J.H. Greenberg[1]

[1]Neurology, [2]Physics and Astronomy, University of Pennsylvania, Philadelphia, PA, USA, [3]Neurosurgery, General Hospital of Chinese PLA, Beijing, China

Objectives: Vagus nerve stimulation (VNS) is known as a safe and effective treatment for epilepsy and treatment resistant depression (Beekwilder and Beems, 2010) and is likely to serve as an effective treatment for protection against ischemic brain injury. We have previously shown that VNS is neuroprotective in models of both transient (filament occlusion of the middle cerebral artery) and permanent (photothrombosis of the middle cerebral artery) focal ischemia (Sun et al., 2010). These studies examined infarct volume, neurobehavioral indices and cerebral blood flow only one day after occlusion. Because acute studies may not correctly demonstrate neuroprotection, it is important to assess long-term outcome. The current study was designed to investigate the effect of VNS on infarct volume and neurological recovery up to three weeks following transient focal cerebral ischemia.

Methods: Transient ischemia was produced by filament occlusion of the proximal middle cerebral artery in Sprague-Dawley rats. The right vagus nerve was stimulated starting 30 minutes after MCA occlusion and consisted of 30 second pulse trains (20 Hz) delivered to the animal's right vagus nerve every 5 minutes for a total period of 60 minutes (n=10). All the procedures were duplicated but no stimulus was delivered in a control group (n=10). Cerebral blood flow in the MCA territory was continuously monitored with laser Doppler flowmetry and neurological evaluations were performed in all animals at 24 hours, 48 hours, 1 week, 2 weeks and 3 weeks after MCAO and animals were euthanized and neuronal damage evaluated in H&E stained sections.

Results: The ischemic lesion volume was smaller in the VNS-treated animals in comparison to the non-stimulated group ($p < 0.01$). Although the functional score in both treated and non-treated groups improved over the three week observation period, there was still a statistically significant improvement due to VNS treatment at all time points compared with control animals ($p < 0.05$). CBF changes in the MCA territory during ischemia did not differ between the VNS-treated animals (31.9±10.4 % of baseline) and control (29.9±9.1 %) animals ($p=0.6$). Similarly there were no differences between the groups during the early reperfusion period.

Conclusions: Stimulation of the vagus nerve for only a brief period early in ischemia provides neuroprotection in both transient and permanent ischemia. This neuroprotection persists for at least three weeks following the ischemia. Although the precise mechanism of this effect remains to be determined, it is not mediated through any changes in cerebral blood flow in the cortex.

References:

Beekwilder JP and Beems T: Overview of the clinical applications of vagus nerve stimulation. J Clin Neurophysiol. 2010;27:130-8.

Sun Z, Hiraki T, Baker W, Greenberg JH: Neuroprotection from ischemia with vagal nerve stimulation may be model dependent. Program 466.19. 2010 Neuroscience Meeting Planner. San Diego, CA; Society for Neuroscience, 2010

1202

THE NEW METHOD OF RECOVERY OF THE CBF REGULATION AFTER STROKE

N.V. Kazantseva

Neurology, Medical State Academy of Tver, Russia, Tver, Russia

Objectives: Linear dependence of atmospheric pressure and CO2 content in the expired air was discovered in the 19-th century (Firord). However, it was only due to the works of M.V.Fok (1919-2008) that the mechanisms of the effects of a surplus outer pressure became cleare. He formed the basis of the regulation of O2 transport in the organism through the non-specific pores of cellular membranes appearing when the double lipid layer of the membrane turns to a two-dimensional crystal from two-dimensional liquid.

On the basis of the research carried out a method of effective impact on the tissue respiration and microcirculation in stroke has been developed. It was named the normoxic curative compression (NCC).

Methods: Comparative studies of the clinical efficacy of various regimens of hyperbaric treatment (HBT) in stroke were carried out in previous studies. In this investigation the main groups included 100 patients with stroke received sessions of NCC (less than 1.1 ATA at less than 30% O2 content in chamber) with or without antioxidants (Q10 and picnogenol). The control groups included patients with stroke who received sessions at atmospheric pressure with 100% or 30% content of O2 in the chamber. The complex of investigations included: the score estimation of neurological symptoms, acid-base state, capnography, rapid oxymetry, lipid peroxidation, blood viscosity and rheology, EEG, transcranial Dopplerography.

Results: PCO2 was observed to decrease in all previously used hyperbaric treatment (HBT) regimens and in control groups after sessions in a chamber. When the pressure in the chamber was more than 1.1 ATA unpredictable impairments of acid - base balance were noted and undesirable hyperoxic after-effect such as increased blood viscosity and activation of lipid peroxidation were observed to become more pronounced after each subsequent treatment session. Normalization of PCO2 and an increase in CO2 content in the expired air was only observed in the main groups receiving curative compression (NCC). The maximum clinical effect was observed when NCC was used in combination with antioxidants. An increased number of NCC sessions resulted in the increased clinical effect accompanied by the normalization of acid-base balance, of microcirculation and of lipid peroxidation.

Conclusions: Increased outer pressure within a very narrow range of values (at NCC) allows one to activate tissue respiration in the hypoperfusion zone in the brain and thus to restore microcirculation and the CBF regulation in stroke. An increase in surplus pressure in the chamber or the use of 100% O2 at atmospheric pressure is accompanied by blood plasma hyperoxigenation and leads to advers effect.

References: The phenomenon discovered is due to the impact of outer pressure on the rare of oxidative and reducing reactions with molecular gases (O2 and CO2) dissolved in liquids. However, the linear relationship of outer pressure and the rate of the oxidative phosphorylation are only observed within the narrow range of surplus pressure values before blood plasma hyper oxygenation develops.

1203

IN VIVO IMAGING AFTER STROKE INVESTIGATED BY INTRACRANIAL 2-PHOTON MICROSCOPY

M. Riek-Burchardt[1], **K.G. Reymann**[1,2], J. Neumann[3], H. Heinze[3], M. Görtler[3], M. Gunzer[4]

[1]Leibniz Institute for Neurobiology, [2]Pathophysiology of Dementia, DZNE, [3]Neurology, [4]Institute for Immunology, University Magdeburg, Magdeburg, Germany

Cerebral ischemia is accompanied by an acute immunological reaction and consists activation of resident brain microglia and recruitment of leucocytes, mainly neutrophils and monocytes from the blood circulation. How these different immune cell types contribute to the neuronal outcome after cerebral ischemia is still under discussion. Various significant actions of immune cells are just to reveal by imaging them either in vitro / ex vivo or in vivo. We developed a postischemic ex vivo model of immune cell (fluorescently labeled) application on hippocampal slices (eYFP expression in neurons). We observed two significant neuroprotective properties of microglia. On the one hand microglia was found in close proximity or in physical cell-cell contact to the neurons after ischemia; on the other hand microglia eliminated infiltrating neutrophil granulocytes very fast and effective. Blocking both properties pharmacologically yields in an exacerbation of neuronal damage.

Methods: For induction of cerebral ischemia we use a model of permanent middle cerebral artery occlusion combined with an occlusion of the common carotid arteries for 20 min. To test our hypothesis in vivo we generated a mouse transgenic for neutrophils (Lys-EGFP) and microglia (CX3CR1-EGFP). These mice allow the visualization of both cell types in the same animal, using large differences in morphology and migration characteristics as a marker for the identification despite similar colour.

Results: To date we observed a rapid infiltration of neutrophils and a very fast response of microglia to damaged vessels after ischemia. In the first 24 h local microglia changed their morphology dramatically. We are presenting the first post-ischemic intravital microscopy study from different microglial activation phases after ischemia within the ischemic injured parenchyma.

Conclusion: Intracranial in vivo 2-photon microscopy is a suitable method to investigate immune cell interactions directly within vital tissue. This implies a new quality and new possibility to examine the immunological reaction in the brain after cerebral ischemia.

1204

CYCLOSPORIN-A REDUCES GREY MATTER ATROPHY AND STABILIZES AXONAL INTEGRITY, BUT FAILS TO REINSTATE BRAIN ACTIVATION AFTER EXPERIMENTAL TRAUMATIC BRAIN INJURY

N.G. Harris, D.R. Verley, M.S. Nogueira, D.A. Hovda, R.L. Sutton

Department of Neurosurgery & UCLA Brain Injury Research Center, UCLA, Los Angeles, CA, USA

Objectives: Cyclosporin-A (CsA) has shown promise as a neuroprotectant after traumatic brain injury (TBI). Acute intervention with CsA after experimental TBI results in a significant reduction in axonal disconnection and grey matter atrophy, and a preservation of callosal compound axon potentials. Successful completion of safety trials in TBI patients also indicates the potential use of CsA as a therapeutic modality. However, much of the data indicating efficacy has been collected in the first 1-7 days after experimental TBI, and the available behavioral data at more chronic time-points show inconsistent improvements. No structural-functional data exists beyond the first week, and no data exists on the ability of CsA to prevent the acute deficits in interhemispheric connectivity that occurs after TBI. To investigate this we acquired diffusion-tensor and functional-MRI (DTI/ fMRI) data at acute and chronic time points after experimental TBI to look specifically at grey/white matter integrity and brain activation.

Methods: T2-weighted, anatomical and DTI data were acquired before, and at 7, 14, 21 and 28 days after unilateral SM-cortex, controlled cortical impact in adult rats (n=3/group). FMRI data were acquired during electrical forelimb stimulation at 28-days (n=4/group). CsA or saline-vehicle (n=3-4/group) was given after injury (20mg/kg,I.P., followed by 10mg/kg/day pump infusion for 7-days).

Results: CsA significantly reduced the volume of contused tissue compared to vehicle-treated at 7-days (35±4.7 & 21±1.3mm^3; $P< 0.05$) and this effect was still present at 28-days, albeit non-significantly when assessed by manual lesion tracing on anatomical data. Voxel-based morphometry analysis of grey matter between pre-injury and 28-day data confirmed that there were significant changes in brain voxels in both groups compared to pre-injury, but the number of significant voxels was lower for CsA treated. Axonal integrity was assessed by tract-based-spatial-statistics of fractional anisotrophy data at 28-days. In injured+vehicle rats there were significant regions of reduced FA compared to baseline ($P< 0.01$, uncorrected) - chiefly within ipsilateral corpus callosum and internal capsule. There were far fewer, and smaller, significant clusters of low FA in injured-CsA rats. The volume of total white matter with low FA (< 0.25) was reduced by CsA compared to vehicle treatment (19.4±1.6 vs 12.6±2.0mm^3, respectively; $P=0.056$). Within the white matter regions of low FA in injured+vehicle rats, mean FA was significantly higher in the same regions in injured+CsA rats (0.34 ±0.007 vs 0.37 ±0.005, respectively; $P=0.011$). DTI Tractography analysis at 28-days revealed CsA did not attenuate the >50% reduction in inter-hemispheric tracts. However, there was some amelioration of the deficits in ipsilateral corticospinal projections after CSA treatment. Compared to unaffected limb, brain activation resulting from affected limb stimulation was absent in injured S1/M1 forelimb cortex at 28-days after injury+vehicle. In contrast to the structural data however, CsA treatment did not reinstate S1/M1 functional activation at 28-days. In both injured groups, a novel region of activation was present in ipsilateral S2 cortex.

Conclusions: These preliminary data suggest a structural-functional dissociation after CsA

treatment. More chronic time-point data is required to determine whether functional deficits ultimately resolve after CsA.

Support: NINDS NS055910 & UCLA Brain Injury Research Center.

1205

INFLUENCE OF ERYTHROPOIETIN ON LESION DEVELOPMENT AND INFLAMMATORY RESPONSE FOLLOWING CLOSED HEAD INJURY IN NEWBORN RATS

A. Heimann[1], A. Grings[1], G. Di Vincenzo[1], F. Dehghani[2], O. Kempski[1], B. Alessandri[1], H. Bächli[3]

[1]Institute for Neurosurgical Pathophysiology, University Medical Center of the Johannes Gutenberg-University Mainz, Mainz, [2]Institute for Anatomy, University of Leipzig, Leipzig, [3]Neurosurgery, University of Heidelberg, Heidelberg, Germany

Introduction: Erythropoietin (EPO) is an endogenous hormone that plays a key role in hematopoiesis. Production of and receptors for EPO have been discovered in brain tissue. Since EPO has anti-apoptotic and anti-inflammatory properties it has been tested as neuroprotective compound in stroke and head-injury. It could be shown that anti-apoptotic defense response to traumatic brain injury (TBI) is suppressed and that inflammation is stronger in neonatal rat pups in comparison to adult rats. Furthermore, endogenous production of EPO after TBI is delayed. Therefore we hypothesized that a neuroprotective effect of EPO is rather based on an anti-inflammatory action.

Method: 7-day old Sprague-Dawley rats were traumatized using a 'weight-drop injury' (WDI) device. A weight of 50 g was dropped from a height of 14 cm onto the exposed skull over the left hemisphere. After WDI rat pups were returned to their litter. At the end of each assigned survival period (1, 3, 7 or 14 days) rats were euthanized, brains removed, fixed for 48h in paraformaldehyde followed by dehydration in 30% sucrose. Cryo-sections were taken throughout the brain and stained for histology (cresyl-violet) and for immunohistochemistry.

Activated astrocytes and microglia were stained with GFAP (Glial fibrillary acidic protein) and with Iba (calcium binding adaptor molecule), respectively. IL-1β (interleukin-1β) has been chosen as inflammatory marker. Animals were treated with either 0.9% NaCl or EPO 5000 IU/kg body weight. Half of the sham-operated group received EPO but no injury. All animals were injected i.p. 60 min

after sham operation or WDI (n>5/group).

Results: Histological analysis revealed a significant reduction of number of surviving cortical cells and cortex thickness at day 14 post-injury when compared to sham group (cell counts: 659±316 vs. 1176±118; thickness: 1.0±0.4 vs 2.1±0.2 mm; $p < 0.001$). WDI induced an expansion of the ipsilateral ventricle. A single injection of EPO tended to increase number of surviving cortical cells (843±252) and cortex thickness (1.2±0.3 mm).

Activation of astrocytes was increased in both injury groups already at post-injury day 1. Whereas GFAP immunoreactive area remained at an unchanged, elevated level in EPO group, it increased in trauma controls and was significantly larger at day 14 compared to the EPO group (8.4±1.5 vs. 5.4±0.5; $p < 0.05$). Similarly, Iba immunoreactive area was significantly increased in both injury groups when compared to sham. In comparison to trauma controls, however, EPO reduced Iba-positive area throughout the experiment significantly (7.9±1.2 vs. 6.3±0.6; $p=0.027$). In more lateral cortical areas EPO produced weaker effects on GFAP and Iba. Double-staining of IL-1β with GFAP and Iba showed that this cytokine is mainly released by activated astrocytes. EPO reduced this reaction.

Conclusion: A single injection of EPO 5000 IU/kg was not sufficient to reduce histological damage following WDI in newborn rats. The same dose was, however, able to reduce activation of astrocytes and microglia concomitant with a weaker IL-1β production. We suggest that anti-apoptotic pathways could not be stimulated strongly enough to prevent cell death, but that the anti-inflammatory effect may provides a basis for better recovery of brain functions.

1206

CEREBRAL UPTAKE OF KETONE BODIES FOR A KETOGENIC DIET IN RATS BY PET STUDIES WITH [^{11}C]ACETOACETATE TRACER

S. Tremblay[1,2], F. Pifferi[3], M. Fortier[1], J. Tremblay-Mercier[1], E. Croteau[2], R. Lecomte[2], S. Cunnane[1,4]

[1]Research Center on Aging, Sherbrooke University Geriatric Institute, [2]Radiobiology and Nuclear Medicine, Molecular Imaging Center of Sherbrooke, Faculty of Medicine and Health Sciences, Université de Sherbrooke, Sherbrooke, QC, Canada, [3]Adaptative Mechanisms and Evolution, CNRS/MNHN, Brunoy, France, [4]Medicine, Faculty of Medicine and Health Sciences, Université de Sherbrooke, Sherbrooke, QC, Canada

Objectives: Cerebral energy requirements are supplied mainly by glucose. When glucose is missing, as in prolonged fasting or in low carbohydrate diet (ketogenic diet), the brain energy requirements can be satisfied by alternative energy substrates, such as the ketone bodies acetoacetate and β-hydroxybutryrate[1]. In Alzheimer's disease (AD), glucose hypometabolism is observed in specific brain regions using ^{18}F-FDG positron emission tomography (PET). Raising blood ketones is known to induce short-term improvement in cognitive function both in AD[2-3] and in hypoglycemic type 1 diabetics[4]. A better understanding of the mechanisms underlying the brain's ability to utilize alternative energy sources would potentially enhance the benefits of ketones on neurodegenerative diseases or aging. In this study, ketone bodies cerebral metabolic rate (CMR) and expression of the glucose transporter 1 (GLUT1) and monocarboxilic transporter type 1 (MCT1) were measured in Fisher rats subjected to mild experimental ketonemia induced by a ketogenic diet or by 48 h fasting to investigate brain energy metabolism.

Methods: The PET tracer ^{11}C-acetoacetate (^{11}C-AcAc) was used as a bolus injected intravenously to determine ketone bodies CMR. Each animal was used as its own control, starting first on a normal diet, then undergoing 48 h fasting (FS), followed by 2 wk ketogenic diet (KD). In each diet group, expression GLUT1 and MCT1 were measured in brain microvessel preparations, and relevant metabolites were measured in blood. Dynamic PET images were acquired for brain and heart in list mode for 20.5 min. The arterial input function was derived from the left ventricle blood pool in the heart image. The AcAc CMRs were obtained by Patlak analysis.

Results: Compared to the controls, a significant two-fold increase of MCT1 expression was measured in the KD group, but did not change in FS and no difference was observed for GLUT1. In plasma, significant differences across the three groups were observed for β-hydroxybutyrate, AcAc, glucose, triglycerides, glycerol and cholesterol. A linear correlation was observed between AcAc plasma level and AcAc CMR measured by PET, with an approximate rate of 25 nmole·mL^{-1}·min^{-1} for each mM of plasma AcAc. No correlation was observed between MCT1 expression and ^{11}C-AcAc uptake.

Conclusions: The cerebral metabolic rate of AcAc per mM of AcAc plasma obtained by the non-invasive PET tracer ^{11}C-AcAc (25 nmole·mL^{-1}·min^{-1}) is in good agreement with the invasive ^{14}C-AcAc experiment of Daniel et al[5] (19 nmole·gr^{-1}·min^{-1}), Bates et al[6] (25 nmole·gr^{-1}·min^{-1}) and Hawkins et al[7] (22.9 nmole·gr^{-1}·min^{-1}). Furthermore, these studies also evidenced a linear correlation between AcAc CMR and the plasma AcAc concentration. The proposed method is being implemented in clinical trials to evaluate the balance between ketone and glucose metabolic rates in healthy aging subjects.

References:

1. Owen OE et al. 1967
2. Reger MA et al. 2004
3. Henderson ST et al. 2008
4. Page KA et al. 2009
5. Daniel PM et al. 1971
6. Bates MW et al. 1968;110
7. Hawkins RA et al. 1986.

1207

AMPK SIGNALING MODUALATES RESVERATROL-MEDIATED SIRT3 EXPRESSION AND PROTECTION AGAINST ISCHEMIC DEATH

K.C. Morris, J.W. Thompson, K.R. Dave, A.P. Raval, M.A. Perez-Pinzon

Neurology, University of Miami Miller School of Medicine, Miami, FL, USA

Objectives: We have previously shown that the antioxidant resveratrol protects against ischemic injury by activating the transcription coregulator SIRT1 and by regulating mitochondrial dynamics in a protective manner (Della-Morte et al. 2009). Resveratrol has been shown to increase activity of AMP-activated protein kinase (AMPK) (Dasgupta & Milbrandt, 2007), an enzyme that enhances mitochondrial functioning. The goals of this study were to:

o Determine whether AMPK plays a role in resveratrol-mediated ischemic protection

o Assess whether resveratrol regulates expression of mitochondrial sirtuins in AMPK-dependent manner

Methods: Preconditioning was induced by exposing primary cortical cultures to resveratrol (25uM or 50uM), AMPK inhibitor Compound C (CC) (15uM), or AMPK activator AICAR (0.5mM or 1.0mM) for 1 hour, then subjecting cultures to manipulations 48hr later. For western blotting, mitochondrial fraction was collected by centrifugation and analyzed for SIRT3, SIRT4, and SIRT5. For oxygen-glucose deprivation (OGD), cultures were bathed in glucose-free medium and incubated in an oxygen free environment ($5\%H_2$--$5\%CO_2$--$90\%N_2$) for 3 hours, then returned to normoxic conditions. Cell death was measured 48hr after OGD using a lactate dehydrogenase (LDH) assay. Results analyzed using one-way ANOVA followed by multiple comparisons procedure, the null hypothesis was rejected at $p< 0.05$.

Results:

· Preconditioning with resveratrol (RPC) or AICAR (APC) led to significant protection against OGD. At low RPC concentrations, cell death was decreased by more than 40% and the addition of CC had no effect. High RPC concentrations decreased cell death by about 10% and more robust decreases in cell death were observed with the addition of CC. APC at low and high concentrations both significantly decreased cell death by about 30%.

· RPC led to significant increases in SIRT3 expression which could be blocked with the application of CC. Conversely, APC led to significant decreases in SIRT3 expression. RPC had no effect on SIRT4 or SIRT5 expression, but the addition of CC during RPC increased SIRT5 protein levels.

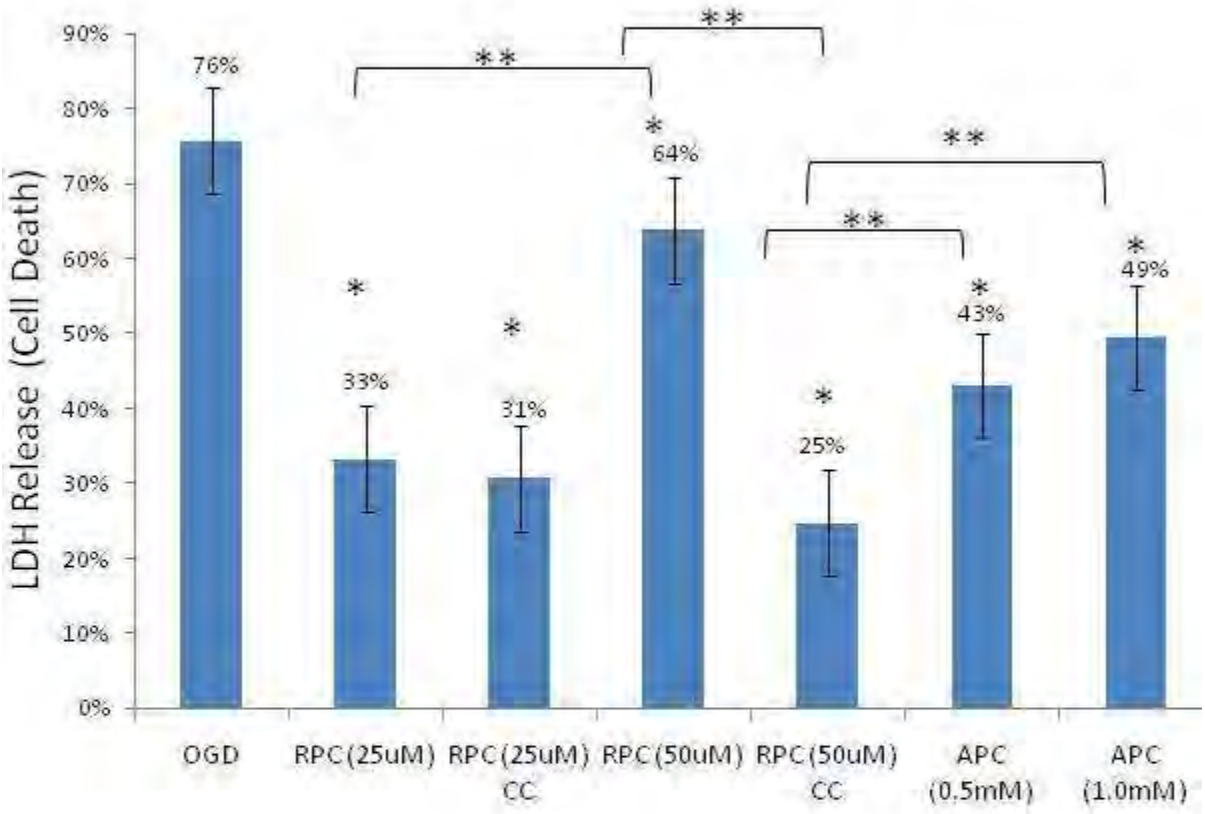

[RPC and APC Protect Against OGD-Induced Death]

Conclusion: We show that APC led to decreased cell death after OGD which suggests AMPK can play a protective role in resveratrol-mediated signaling. However, at high RPC blockade of AMPK actually led to more robust neuroprotection against OGD which means resveratrol-mediated AMPK activation at this concentration may overstress neurons. Indeed, high RPC alone only mildly protected against cell death, while low RPC more drastically protected neurons. The fact that AMPK inhibition at low RPC had no effect could mean that AMPK activation after RPC may not be a major contributor to resveratrol-mediated protection against ischemic death. However, AMPK may play a role in other aspects of resveratrol-mediated protection as blockade of AMPK, inhibited RPC-mediated increases in SIRT3, an enzyme known to enhance oxidative capacity (Ahn et al. 2008) and decrease oxidative stress (Sundaresan et al. 2009). We plan to further investigate the exact relationship between AMPK and resveratrol-mediated mitochondrial protection.

References:

Ahn et al. (2008). *PNAS*

Dasgupta & Milbrandt (2007) *PNAS*

Della-Morte et al. (2009) *Neuroscience*

Sundaresan et al. (2009) *J Clin Invest*

1208

BLOOD-BRAIN TRANSPORT OF LACTATE BY MCT-1: REGULATORY MECHANISMS

Z. Liu, M. Sneve, L.R. Drewes

Biochemistry and Molecular Biology, University of Minnesota Medical School, Duluth, MN, USA

Background and aims: The cellular interface between the blood and brain functions as a dynamic, responsive multicellular complex referred to as the neurovascular unit (NVU)[1]. The NVU consists of vascular endothelial cells, pericytes, astrocytes and their endfoot processes that link neuronal activity to the blood, the source of nutrients and oxygen for metabolism. Recent evidence strongly implicates signaling pathways that rapidly modulate the influx (or efflux) of blood-borne nutrients and other substances by the NVU[1,2,3]. Specifically, the transport of lactate by the monocarboxylic acid transporter, MCT1, is rapidly altered by a cAMP/protein kinase A-dependent mechanism in cultured rat brain endothelial cells[1]. MCT1 is highly expressed in brain endothelial cells and transports short chain carboxylates such as lactate, pyruvate and ketone bodies. It also transports valproate, anti-cancer drugs and a number of other pharmaceutical agents. Basigin (EMMPRIN/CD147) is an accessory protein capable of associating with MCT1 to form a heterodimer and traffic to the plasma membrane, a process that is essential for transporter function. MCT1 transport activity is thus dependent on its membrane localization and prior association with basigin. The aims of this study were 1) to evaluate specific signaling pathways and phosphorylation mechanisms for MCT1 localization and regulation and 2) to examine MCT1-protein interactions in the NVU.

Methods: Immortalized rat brain endothelial cells (RBE4), a gift from F. Roux were cultured as described previously [1]. MCT1 protein on the plasma membrane exterior surface of treated and untreated RBE4 cells was isolated by biotinylation and quantified by immunoblot detection. Phosphorylated proteins were separated using phosphoprotein purification columns (Qiagen) and MCT1 in fractions was quantified by immunoblot and spot densitometry (FluorChem, Alpha Innotech). The preparation of a MCT1-antibody immobilized column, co-immunoprecipitation (Co-IP) and subsequent immunoblot detection were according to the vendor instructions (Pierce Co-IP Kit). Following Co-IP and SDS-PAGE electrophoresis, mass spectrometry (MS) was used to identify protein bands.

Results: Both phosphorylated and unphosphorylated forms of MCT1 were detected in RBE4 cells. Brief treatment with cAMP caused rapid dephosphorylation (-29%) of MCT1. The same treatment caused an 18% decrease in the exterior cell surface localization of MCT1. Basigin was shown by Co-IP to be associated with MCT1 in RBE4 cells, although to a lesser extent than in cultured rat liver cells. MS analysis suggested several other proteins possibly associated with MCT1.

Conclusion: These results indicate that MCT1 in the NVU is associated with basigin and possibly other proteins involved in intracellular trafficking and linkages to the cytoskeleton. The results also suggest that MCT1 transporter activity may be regulated by its plasma membrane location and exposure to the surrounding medium. Furthermore, the outer surface exposure may be dependent on its state of phosphorylation and cAMP/protein kinase A signaling. Regulation of MCT1 activity may be relevant to stroke, changes in glycemic status (diabetes) or brain drug delivery.

References:

1. Abbott et al, Nat Rev Neurosci (2006) 7:41.

2. Smith and Drewes, J Biol Chem (2006) 281:2053.

3. Hartz, et al, Mol Pharmacol (2006) 69:462

(Funded by American Heart Association)

1209

NEUROINFLAMMATION IN HEALTHY AGING: AN IN VIVO POSITRON EMISSION TOMOGRAPHY STUDY WITH [^{18}F]-FEPPA

R. Mizrahi, P. Rusjan, T. Selvanathan, A.A. Wilson, S. Houle

PET Centre, Centre for Addiction and Mental Health, Toronto, ON, Canada

Background and objectives: Microglia modulate cytokines in the central nervous system (CNS) and are important in regulating neuronal plasticity and neurotransmitter synthesis. Although older patients appear to have low levels of circulating cytokines, and postmortem studies show increased interleukin IL1 and histocompatibility complex HLA-DR in the hippocampus and cortex, little is known about the role of activated microglia in the human brain in normal aging (Griffin, Sheng, & Mrak, 1998; Sheng, Mrak, & Griffin, 1998). Translocator protein 18K (TSPO) is upregulated in activated microglia and has been evaluated as a potential biomarker for neuroinflammation in a variety of imaging studies. Positron emission tomography (PET) imaging of TSPO binding thus becomes a marker for activated microglia and neuroinflammation processes in-vivo.

Studies of TSPO in aging are limited (Cagnin et al., 2001). However, the few studies available suggest increased TSPO binding with aging in mouse models or human platelets with aging (Marazziti et al., 1994; Nomura et al., 1996; Venneti et al., 2009). There are only two PET studies in humans that showed that in normal individuals, regional [^{11}C](R)-PK11195 or [^{11}C]DPA-713 binding did not significantly change with age, except in the thalamus, where an age-dependent increase was found[107]

We recently completed the feasibility and modeling studies of [^{18}F]-FEPPA, a novel TSPO PET ligand (Wilson et al., 2008) (Rusjan, Wilson, Bloomfield, Houle, & Mizrahi). [^{18}F]-FEPPA has high affinity for TPSO, an appropriate metabolic profile, with high brain penetration and good pharmacokinetics (Bennacef I et al., 2008). High levels of specific and reversible binding to TPSO have been found in both pig and rats(Kudo G, 2008). Finally [^{18}F]-FEPPA is demonstrably sensitive to neuroinflammation in a rat model (Hatano et al.).

Aim: Our specific aim is to determine whether normal aging is accompanied by increased neuroinflammation as measured with [^{18}F]-FEPPA.

Methods: Subjects: 19 healthy controls (ages 24 to 78) were given a bolus injection of [^{18}F]-FEPPA and PET scanned for 120 mins in a CPS-HRRT head only scanner. Arterial blood samples were taken throughout the scanning period to measure plasma radioactivity and generate a metabolite corrected arterial input function used for quantitative analysis. An MRI was obtained for each subject for Region of Interest (ROI) delineation. Distributions volume of specific binding (V_S) were quantified using a two tissue compartmental model(Rusjan, Wilson, Bloomfield, Houle, & Mizrahi).

Results: We found no relationship between age and [^{18}F]-FEPPA binding in any ROI (frontal, temporal, occipital, cingulate, thalamus, caudate, putamen, hyppotalamus, middle brain). A large variability was observed within subjects with may explain the lack of association with age in this study.

Conclusions: These preliminary data suggest no evidence of increased [^{18}F]-FEPPA binding in normal aging.

1210

AN ANGIO-TOMOGRAPHIC APPROACH TO THE STUDY OF THE VARIATION OF THE MIDDLE MENINGEAL ARTERY IN HUMANS

S. Mantini[1], M. Ripani[1], B. Colaiacomo[1], F. Spano[2], F. Marziali[2], E. Bruner[3]

[1]Università degli Studi di Roma Foro Italico, [2]Policlinico Umberto I, Roma, Italy, [3]Centro Nacional de Investigacion de la Evolucion Humana, Burgos, Spain

Objectives: The middle meningeal artery usually enters the endocranial cavity through the foramen spinosum, running within the dura mater and developing a vascular network on the frontal, parietal, and occipital surfaces of the brain. Little information is available on its morphogenesis and variation in human populations or within primates (Falk 1993). Its imprints on the endocranial walls can be recognised on fossil specimens, allowing inferences on the evolution of this vascular system. While extinct human species display a limited reticulation of this vessels, *Homo sapiens* shows a definite increase of its complexity (Bruner et al., 2005). Current hypotheses on the evolution of a complex meningeal vascularization in our species include biomechanical protection and thermoregulation of the brain surface (Bruner et al., 2011). Taking into account the limited knowledge on the variation of this arterial network, this study is aimed at quantifying individual differences in the branching patterns, as well as at investigating the spatial relationships between middle meningeal arteries, cerebral arteries, and neurocranial bones.

Methods: Angiotomography and digital anatomy are used to reconstruct in vivo the meningeal vascular system in 46 individuals.. Three-dimensional reconstructions of the cerebral and meningeal vascular systems have been computed by using Osirix. Variations in basic branching patterns have been described by standard anatomical approaches, as well as by using standard morphometrics. Complexity of the branching pattern has been quantified also by using fractal approaches (Zamir; 1999).

Results: Anatomical descriptions and metrics are reported for different age classes, sexes, and hemispheres, providing mean values and ranges of distribution accounting for the vascular patterns.

Conclusions: Although the middle meningeal network shows a variable and complex geometry, its spatial organization can be quantified in terms of branching patterns and topological relationships with the neurocranial elements. This information allows to test evolutionary hypothesis by quantifying individual or between-groups differences. At the same time this information is helpful in biomedical and neurosurgical context, providing statistical values for the position and distribution of the vessels.

1211

CORRELATION BETWEEN CORTICAL TISSUE DAMAGE AND HYPERPERFUSION AFTER EXPERIMENTAL SUBARACHNOID HEMORRHAGE

A. Hamming[1,2], I.A.C.W. Tiebosch[1], M.J.R.J. Bouts[1], M.J.H. Wermer[2], W.M. van den Bergh[3], R.M. Dijkhuizen[1]

[1]InvivoNMR Group, Imaging Scienses Institute, Utrecht University, Utrecht, [2]Department of Neurology, Leiden University Medical Center, Leiden, [3]Department of Intensive Care, Academic Medical Center, University of Amsterdam, Amsterdam, The Netherlands

Objectives: Survivors of a subarachnoid hemorrhage (SAH) carry a poor prognosis, which has been attributed to vasospasm-related delayed cerebral ischemia (Dankbaar et al. 2009). Little is known about the development of perfusion and tissue changes towards chronic time points. More insight into the progression of these secondary complications could provide targets for therapeutic intervention. Goal of the current study was to relate brain tissue status to perfusion changes from subacute to chronic stages after experimental SAH.

Methods: SAH was induced in isoflurane-anesthetized adult male Wistar rats (n=30) by puncturing the right middle cerebral artery or the internal carotid artery at the level of their bifurcation, with a sharpened 4-0 polypropylene suture (Dankbaar et al. 2009). MRI was conducted on a 4.7 T animal MR system after 2 and 7 days, and included, T2-weighted MRI, diffusion-weighted MRI for lesion detection and dynamic susceptibility contrast-enhanced MRI for assessment of tissue and perfusion status (Dijkhuizen et al 2001). A lesion incidence map, based on manual outlines of tissue with prolonged T2, was calculated to select tissue that was most susceptible to SAH-induced damage.

Results: 13 animals survived up to the final MRI session at 7 days, of which two were excluded for not having relevant ischemic lesions. Highest lesion incidence was observed in the ipsilateral somatosensory cortex. At day 2, the cerebral blood flow index (CBF_i) was notably increased (210 ± 56%, relative to unaffected tissue), while the apparent diffusion coefficient (ADC) and T2 were reduced and elevated, respectively, reflective of cytotoxic and vasogenic edema formation. Increased CBF_i correlated significantly with elevated T2 at both time-points ($r = 0.78$ and 0.84, $P < 0.05$). Significant negative and positive correlations were found between CBF_i and ADC at das 2, but positive correlations at day 7. Furthermore, subacute CBF_i at day 2 was positively related to elevated T2 at day 7 ($r = 0.66$, $P < 0.05$).

Conclusions: Although vasospasm occurs after SAH, we found hyperperfusion in the area of secondary brain damage at day 2 in this rat SAH model. This does not seem to support the idea that vasospasm is the cause of reduced cortical perfusion and delayed lesion development. Up until day 7 the ipsilateral cortical regions displayed hyperperfusion together with tissue damage. Furthermore, subacutely increased CBF_i was predictive of chronic tissue edema. This indicates that these affected regions do not recover as a result of improved blood flow. This post-SAH hyperperfusion may be caused by dysfunctional regulation of blood flow. We conclude that SAH-induced brain injury may not necessarily be caused by delayed vasospasms and can be associated with progressive changes in tissue perfusion.

References: Dankbaar JW et al. Relationship between vasospasm, cerebral perfusion, and delayed cerebral ischemia after aneurysmal SAH. Neuroradiology. 2009;51(12):813-9.

Bederson JB et al. Cortical blood flow and cerebral perfusion pressure in a new noncraniotomy model of SAH in the rat. Stroke. 1995;26(6):1086-91.

Dijkhuizen RM et al. Delayed rt-PA treatment in a rat embolic stroke model: diagnosis and prognosis of ischemic injury with MRI. JCBFM 2001;21(8):964-71.

1213

IS VIP INVOLVED IN NEUROVASCULAR COUPLING IN THE RAT IN VIVO?

F. Vetri, H.-L. Xu, D.A. Pelligrino

Neuroanesthesia Research Laboratory, University of Illinois at Chicago, Chicago, IL, USA

Objectives: Electrical stimulation of GABAergic interneurons co-expressing VIP has been shown to induce vasodilation in vitro (1). Moreover, anatomical pathways connecting those interneurons to pial arterioles have been demonstrated (2). VIP has a dilatory effect on cerebral vessels of different mammals, however, the role of VIP in the regulation of pial arteriole diameter in vivo in the rat has not yet been studied. In the present study, we tested the following hypotheses: a) exogenous VIP elicits vasodilation of pial arterioles in rats in vivo; b) VIPergic pathways contribute to sciatic nerve stimulation (SNS)-induced pial arteriolar dilation.

Methods: In rats equipped with closed cranial windows (n=7), we monitored pial arteriolar dilations evoked by SNS and topically-applied VIP, in the absence and presence of the VIP receptor ($VPAC_{1-2}$) blocker, VIP6-28 fragment.

Results: VIP induced a non-linear dose-dependent dilation of pial arterioles within a broad concentration range (from 10^{-10} to 10^{-6} M), with the dilation peaking at 10^{-8} M and decreasing at higher concentrations. Those dilations were suppressed in the presence of VIP6-28 (1 μM). Moreover, SNS elicited a robust dilation of pial arterioles overlying the contralateral somatosensory cortex. In the presence of VIP receptor blockade, an 18% decrease in the arteriolar response to SNS was found, but, due to the high variability in the effect of the drug (Fig.1), statistical significance was not achieved.

Discussion: In the present study, we show that VIP acts to dilate pial arterioles in vivo in the rat through $VPAC_{1-2}$ receptors, since that dilation could be blocked by VIP6-28. Results also revealed a tendency toward VIPergic influence on SNS-induced vasodilation, as suggested by a 40-50% reduction in that response in 5 of the 7 rats studied. However, in 2 instances the opposite phenomenon was seen. This discrepancy may reflect complex interactions existing between VIPergic pathways and pial arterioles, especially during somatosensory activation.

Conclusions.: These data indicate that VIP is able to dilate pial arter

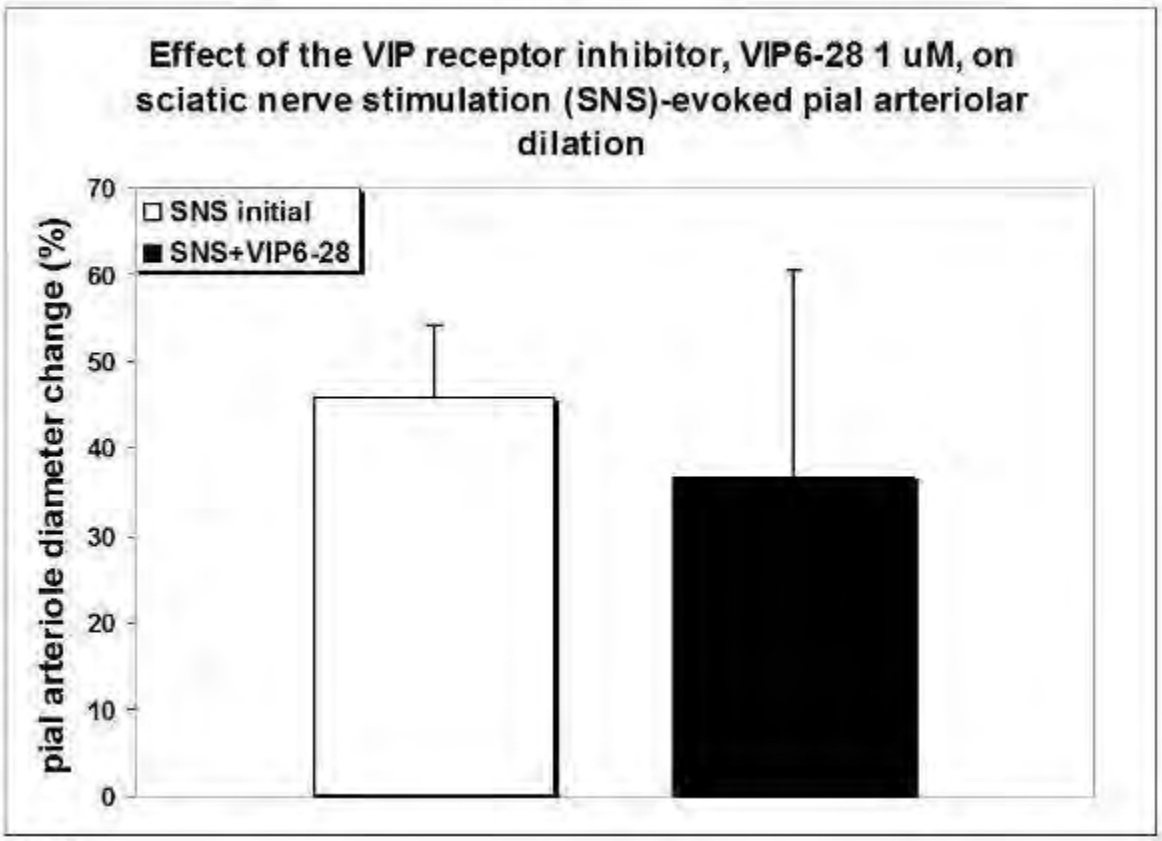

Fig.1

[Fig.1]

ioles in vivo via a VPAC-receptor-dependent process. It remains unclear whether SNS-induced pial dilations in rats have an important VIPergic component. Further studies are certainly necessary to better understand the role of VIP in neurovascular coupling.

References:

(1) Cauli B, Tong XK, Rancillac A, Serluca N, Lambolez B, Rossier J, Hamel E. Cortical GABA interneurons in neurovascular coupling: relays for subcortical vasoactive pathways. J Neurosci. 2004 Oct 13;24(41):8940-9.

(2) Fahrenkrug J, Hannibal J, Tams J, Georg B. Immunohistochemical localization of the VIP1 receptor (VPAC1R) in rat cerebral blood vessels: relation to PACAP and VIP containing nerves. J Cereb Blood Flow Metab. 2000 Aug;20(8):1205-14.

1214

SUMOYLATION IN NEURONS - STRATEGIES TO COPE WITH STRESS

A.L. Datwyler[1], G. Lättig[1], W. Yang[2], W. Paschen[2], U. Dirnagl[1], M. Endres[1], C. Harms[1]

[1]Center for Stroke Research and Clinic for Neurology, Berlin, Germany, [2]Duke University Medical Center, Durham, NC, USA

Objectives: The SUMO2/3 (small ubiquitin-like modifier) conjugation pathway is activated in various pathological states of high clinical relevance like deep hypothermia (1) and transient global or focal cerebral ischemia (2,3). The post-ischemic pattern of SUMO2/3 conjugation suggests that activation of this pathway could be an endogenous protective stress response shielding neurons from damage induced by ischemia. To test the hypothesis that SUMO2/3 is indeed neuroprotective, we reduced induction of endogenous SUMO2/3 conjugation by RNA interference. Survival of mouse primary cortical neurons was analyzed after different durations of transient Oxygen-Glucose deprivation (OGD) and compared to control conditions *in vitro*.

Methods: Transient global cerebral ischemia was carried out *in vivo* and primary cortical neurons as well as mixed glial cultures were separately subjected to OGD with different reoxygenation times *in vitro*. Specific patterns of SUMO1 versus SUMO2/3 conjugation were evaluated by Western blotting. Primary cortical neurons were lentivirally transduced (>95% efficiency) with SUMO2/3 miRNA driven by the neuron specific Synapsin promoter to inhibit endogenous induction of SUMO2/3 conjugation. After subjection to different durations of OGD (15min/45min/75min) neuronal survival was evaluated compared to baseline values through analysis of prospectively selected positions on DIV 6, 9, 12 and 13 (Two Way Repeated measures ANOVA with $p < 0.001$ for interaction, Tukey posthoc test, power ($a=0.05$) is 1).

Results: Transient global cerebral ischemia markedly activated SUMO2/3 but not SUMO1 conjugation *in vivo*. Furthermore, SUMO2/3 but not SUMO1 conjugation was induced in neurons after OGD, but not in mixed glial cultures. Interference with endogenous SUMO2/3 induction through lentivirally delivered miRNA did not modify viability of neurons unless stressed by transient OGD. Efficacy and neuronal specificity of SUMO2/3 miRNA versus neg miRNA was proven through immunohistochemistry and Western blotting. We titrated OGD damage (15min/45min/75min) which correlated to a gradual decrease in ATP levels to approximately 75%, 50% and 25%, respectively. Shorter OGD durations (15min and 45min) did not result in significant neuronal cell loss which was reflected through recovery of ATP to approximately 80% (subthreshold OGD). In contrast, longer OGD duration (75min) lead to a gradual decrease in neuronal survival due to the lack of recovery in ATP levels (only to approximately 50% after 180min, severe OGD). SUMO2/3 miRNA increased susceptibility of neurons to OGD. Subthreshold OGDs (15min and 45min) damaged more than 70% of SUMO2/3 miRNA expressing cells, whereas severe OGD (75min) lead to almost 100% loss of SUMO2/3 miRNA expressing neurons.

Conclusions: We show that blocking SUMO2/3 conjugation dramatically increases vulnerability of neurons to ischemia-like stress. This implies that post-ischemic activation of SUMO2/3 conjugation is an endogenous neuroprotective stress response. Considering the SUMO2/3 conjugation pathway for establishing new therapeutic strategies could thus be of considerable clinical interest for all pathological states associated with an insufficient blood supply to the brain and for surgical procedures requiring a period of circulatory arrest.

References:

1) Yang et al., J Cereb Blood Flow Metabol. 2009; 29:886-890. 2,3) Yang et al., J Cereb Blood Flow Metabol 2008; 28:269-279 + 892-896.

1215

CONTINUOUS MEASUREMENT OF RELATIVE CHANGES IN $CMRO_2$ USING SIMULTANEOUS MRI AND DIFFUSE OPTICAL METHODS DURING HYPERCAPNIA & HYPEROXIA

D.L. Minkoff[1], T. Durduran[1,2,3], M.N. Kim[1], D. Hance[1], E.M. Buckley[1], M. Tobita[4], J. Wang[3], J.H. Greenberg[4], J.A. Detre[3,4], A.G. Yodh[1]

[1]Department of Physics & Astronomy, University of Pennsylvania, Philadelphia, PA, USA, [2]ICFO- The Institute of Photonic Sciences, Barcelona, Spain, [3]Department of Radiology, [4]Department of Neurology, University of Pennsylvania, Philadelphia, PA, USA

Objectives: Diffuse correlation spectroscopy (DCS) is an optical technique for the bed-side, non-invasive, continuous measurement of microvascular cerebral blood flow (CBF). We compare estimates of relative changes in the cerebral metabolic rate of oxygen ($CMRO_2$) during hypercapnia and hyperoxia using concurrent arterial spin labeling MRI (ASL), DCS, and diffuse optical spectroscopy (DOS/NIRS). Since $CMRO_2$ should remain approximately constant during hypercapnia, we examined deviations from the idealized behavior to examine the influence of partial volume effects on DOS/DCS estimates of $CMRO_2$ and to help elucidate discrepancies between ASL and DCS measurements of CBF.

Methods: DCS/DOS data were acquired continuously throughout the experiment. Details of the optical instrumentation and analysis have been reported previously [1]. MRI scans were performed using a 3T Tim-Trio whole-body scanner (Siemens, Germany) with an eight channel array coil. Perfusion images were obtained using a dual-echo pseudo-continuous arterial spin labeling (pCASL) sequence. ASL estimates of CBF were extracted from ROIs drawn over the left and right frontal poles on high resolution anatomical images for comparison with DCS. The protocol consisted of five minutes breathing room air, followed by five minutes breathing either a 5% CO_2 gas mixture (for hypercapnia) or 100% oxygen (for hyperoxia), followed by ten minutes breathing room air to recover. We estimate relative changes in $CMRO_2$ using a model derived from Fick´s Law: $rCMRO_2$=rOEF*rCBF, where rOEF is the relative oxygen extraction fraction (estimated using DOS), and rCBF is the relative, local CBF (by ASL/DCS).

Results: Although DCS and ASL CBF time series show excellent correlation (R^2=0.81, p=5.2e-9), the magnitude of relative CBF changes estimated by DCS is approximately one-third that of ASL. This underestimation of the relative CBF change estimated by ASL is similar to an ASL/DCS study in rats [2], but contrasts with previous studies comparing DCS to xenon-CT in adults [3] and to ASL in neonates [4]; the latter two studies both showed excellent correlation in the time series and agreement in the magnitude of the CBF changes. Taken together, the results thus far [5] suggest that the underlying mechanism for this discrepancy likely extends beyond partial volume effects. Therefore, we have explored $CMRO_2$ variation during hypercapnia/hyperoxia which we expect to remain unchanged (or slightly altered). These results indicate that our assumption that ASL and DCS measure the same compartment may be incorrect. Preliminary $rCMRO_2$ results for hypercapnia using ASL show an increase of 73+/-40%, while results using DCS show an increase of 18+/-11% (mean+/-std). We are currently developing a correction algorithm that takes both the partial volume effects and the assumption that $CMRO_2$ should be unchanged into account to modify DCS estimates.

Conclusions: DCS/DOS and ASL were utilized simultaneously to study the microvascular, cerebral hemodynamics in adults during hypercapnia and hyperoxia. $CMRO_2$ is estimated by two methods and then used to calibrate the DCS measures.

References:

[1]Durduran et al., Opt. Express 17,3884(2009).

[2]Carp et al., Biomed. Opt. Express 1,125(2010).

[3]Kim et al., Neurocrit. Care 12,173(2010).

[4]Durduran et al., J. Biomed. Opt. 15,037004(2010).

[5]Durduran et al., Rep. Prog. Phys. 73,076701(2010).

1216

CHRONIC ANGIOTENSIN II TREATMENT INDUCES CEREBRAL INFLAMMATION AND ALTERS COGNTIVE FUNCTION IN MICE

S. Duchemin[1], M. Beauvillier[1], M. Boily[1], J. Viard[1], R. Wu[1], E. Belanger[2], G. Ferland[2], H. Girouard[1]

[1]Pharmacology, [2]Nutrition, Université de Montréal, Montréal, QC, Canada

Hypertension is a major risk factor for cerebrovascular diseases and cognitive impairment. Recent studies have shown that hypertension is associated with several inflammatory markers and mediators. In turn, chronic inflammation appears to affect brain functions. We sought to investigate the effect of angiotensin II, an hormone involved in the onset of hypertension, on cognitive functions and cerebral inflammation. Mini-pumps containing angiotensin II (2,74 $mg \cdot kg^{-1} \cdot day^{-1}$) or a saline solution as a vehicle, were placed subcutaneously in C56BL6 mice for a duration of 7 to 28 days. Blood pressure was carefully monitored by the non-invasive tail-cuff method and significantly rose ($p < 0.001$) during the traitment. To evaluate the influence of angiotensin II on cognitive functions, spatial memory was assessed using the water maze test after two (n=10) and three (n=13) weeks of treatment. The results indicated a significant ($p < 0.05$) memory deficit in the angiotensin II group, in comparison to the vehicle group, starting at the 3rd week of treatment. The swimming speed and visual acuity were equivalent in both groups. The memory deficit was accompanied by a decreased resting cerebral blood flow in the hippocampus. Cerebral inflammation was determined by immunofluorescence of the Glial fibrillary acidic protein (GFAP) and the ionized calcium binding adaptor molecule 1 (Iba-1), markers of astrogliosis and activated microglia respectively. Seven days of angiotensin II infusion significantly induced astrogliosis ($p < 0.01$) and activated microglia ($p < 0.05$). Our results show for the first time that angiotensin II causes brain inflammation preceding cognitive dysfunctions. These results suggest that inflammation may have additive or synergistic effects to cerebrovascular alterations in the development of cognitive deficit associated to hypertension.

1217

CONTRIBUTION OF EPOXYEICOSATRIENOIC ACIDS TO THE CEREBRAL BLOOD FLOW RESPONSE TO HYPOXIC HYPOXIA

R.C. Koehler[1], X. Liu[1], D. Gebremedhin[2], D.R. Harder[2]

[1]Department of Anesthesiology and Critical Care Medicine, Johns Hopkins University, Baltimore, MD, [2]Department of Physiology and the Cardiovascular Research Center, Medical College of Wisconsin, Milwaukee, WI, USA

Objectives: Cerebral vasodilation during hypoxia is a fundamental physiological response but the mechanisms are incompletely understood. Some studies have shown that the response to hypoxia can be attenuated by theophylline, a non-specific adenosine receptor antagonist, and glibenclamide, an inhibitor of ATP-sensitive K+ (KATP) channels. We have shown that epoxyeicosatrienoic acids (EETs) are released from astrocytes exposed to hypoxia [1]. EETs can open Ca-activated K+ channels in astrocytes and vascular smooth muscle and produce vasodilation. Stimulation of astrocyte metabotropic glutamate receptors (mGluR) can produce vasodilation by an EETs-dependent mechanism. Here, we tested the hypothesis that EETs and mGluR activation contribute to hypoxic vasodilation. With the use of specific antagonists, we also tested whether adenosine A2A and A2B receptors are involved.

Methods: Mechanically ventilated male rats anesthetized with chloralose were subjected to 10-min periods of stepwise reductions of inspired O2 while hypocapnia was prevented with supplemental CO2 as needed. Cortical blood flow was measured by laser-Doppler flow (LDF). In 5 groups of rats, the cortical surface was superfused for 1 h before hypoxia and during hypoxia with CSF containing vehicle (n=18), the EETs antagonist 14,15-EEZE (30 μM; n=13), the EETs synthesis inhibitor MS-PPOH (20 μM; n=13), glibenclamide (10 μM; n=13), the A2A antagonist SCH58261 (1 μM; n=14), or the A2B antagonist MRS1754 (1 μM; n=13). A sixth group (n=15) received a combined mGluR subtype 1 antagonist MPEP (0.5 mg/kg, iv) and a mGluR subtype 5 antagonist LY367385 (0.5 mg/kg, iv) 20 min before hypoxia. Doses were based on those that inhibit the LDF response to whisker stimulation [2, 3]. In each rat, hypoxic reactivity was calculated as the slope of LDF (fraction of baseline) vs the reciprocal of arterial oxygen content (ml O2/dL) over the arterial O2 saturation range of 50-100%. Data were excluded if arterial pressure decreased by >20%. Slopes were calculated from 3-5 values per rat. Comparisons of reactivity were made to the vehicle group by ANOVA and Dunnett's test.

Results: Hypoxic reactivity significantly decreased from 9.1±4.1 in the vehicle group to 2.6±2.4 in the 14,15-EEZE group, to 3.0±2.5 in the MS-PPOH group, and to 5.6±2.0 in the glibenclamide group. Reactivity was also markedly suppressed to 1.9±4.1 by the combined mGluR antagonists. However, reactivity was not significantly changed by SCH58261 (7.0±4.6) or MRS1754 (6.7±2.9), although SCH58261 significantly reduced the LDF response with severe hypoxia (50-70% arterial O2 saturation) by 62%.

Conclusions: These data indicate that EETs and mGluRs make a major contribution to the increase in cerebral blood flow during acute hypoxic hypoxia, possibly by mGluR stimulation of EETs release in astrocytes. EETs are known to promote opening of KATP channels in mesenteric arteries [4], and a similar mechanism may be operative in the neurovascular unit. Adenosine A2A receptors appear to contribute to vasodilation during severe hypoxia.

References: 1. Yamauro et al. Neuroscience 2006;143:703-16. 2. Shi et al. J Cereb Blood Flow

Metab 2008;28:111-25. 3. Zonta et al. Nat Neurosci 2003;6:43-50. 4. Lu et al. J Physiol 2006;575.2:627-44.

1218

QUANTITATION OF GLUTAMATE MGLUR5 RECEPTOR WITH 18F-FPEB PET IN HEALTHY CONTROLS AND NEURODEGENERATIVE DISEASE

J. Seibyl, O. Barret, G. Tamagnan, J. Batis, D. Alagille, D. Jennings, G. Zubal, D. Russell, K. Marek

Institute for Neurodegenerative Disorders, New Haven, CT, USA

Background: Altered glutaminergic function is implicated in a number of neurodegenerative diseases including Huntington disease and Parkinson disease. Medications with potency at the mGluR5 receptor are now in clinical trials to help manage dyskinetic symptoms. The purpose of this study is to further characterize 18F-FPEB [1], a novel mGluR5 tracer, in humans using non-invasive kinetic modeling with the cerebellum as the reference region (where the mGluR5 levels are known to be very low) and a simple tissue ratio in subjects with neurodegenerative conditions.

Methods: 7 healthy control (HC), 8 Parkinson disease (PD), 3 Parkinson disease with dyskinesia (PD-dys) and 2 Huntington Disease (HD) subjects were injected with 4.1±1.1 mCi of 18F-FPEB and were imaged on the ECAT EXACT HR+ for up to 4.5 hours. PD-dys subjects were only able to tolerate 2 hours of imaging due to their dyskinetic movements. Images were corrected for motion and spatially normalized using an internally developed FPEB template. 11 VOI templates were overlaid to obtain regional brain time activity curves (TAC). Metabolite analysis by HPLC, invasive and non-invasive modeling of the 18F-FPEB data as well as estimates stability as a function of scan duration have been previously reported [2, 3]. In this analysis, we estimated the binding potential (BPnd) with the multilinear reference tissue model (MRTM2) using 2 hours of data, as well as the tissue ratio at 2h post injection of the radiotracer (apparent BPnd under quasi-equilibrium conditions).

Results: MRTM2, with t* set to 30 min, satisfactorily described the TACs in all regions. Strong correlation was found between the MRTM2 BPnd estimate and the tissue ratio at 2h post injection (R^2=086, 0.75, 0.72, 0.52, 0.93 in putamen, caudate, anterior cingulate, temporal and thalamus, respectively). Both MRTM2 BPnd and the tissue ratio demonstrate reduced 18F-FPEB binding in HD subjects and increased 18F-FPEB binding in PD-dys subjects consistent with the current understanding of glutaminergic dysregulation in these conditions (Figure1).

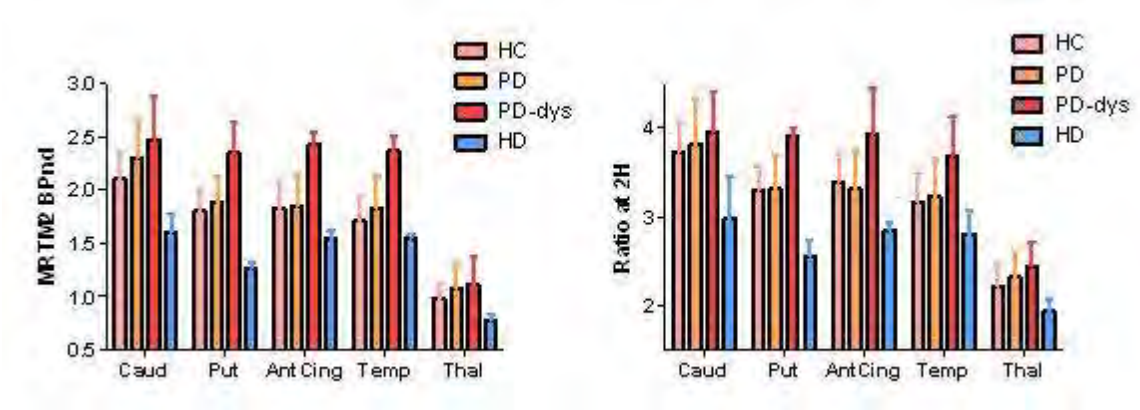

[MRTM2 BPnd and ratio to cerebellum at 2h post inje]

Conclusions: These data suggest that quantitation of glutamate mGluR5 receptor with 18F-FPEB with non-invasive modeling using the cerebellum as the reference region is feasible. The strong correlation of the simple tissue ratio apparent BPnd with the estimate from non-invasive modeling makes it an interesting outcome measure. The results obtained across the neurodegenerative diseases are in agreement with the mGluR5 pathophysiology for these conditions.

Reference:

[1] Hamill TG, Krause S, Ryan C, Bonnefous C, Govek S *et al*., "Synthesis, characterization, and first successful monkey imaging studies of metabotropic glutamate receptor subtype 5 (mGluR5) PET radiotracers", Synapse 2005; 56(4):205-216

[2] Barret O, Tamagnan G, Batis J, Jennings D, Zubal G, Russell D, Marek K and Seibyl J, "Quantitation of glutamate mGluR5 receptor with 18F-FPEB PET in humans", J. Nucl. Med. 2010; 51(Supplement 2): 215.

[3] O.Barret, G.Tamagnan, J.Batis, D. Alagille, A. Koren, D.Jennings, G.Zubal, D.Russell, K.Marek, J.Seibyl, "Quantitation of glutamate mGluR5 receptor with [18F]-FPEB PET in humans", Poster 123, Neuroreceptor Mapping 2010, Glasgow, UK.

1219

CEREBROVASCULAR ENDOTHELIAL CELLS ARE PROTECTED FROM ISCHEMIC INJURY BY STAT3

C.M. Davis, N.J. Alkayed

Anesthesiology and Perioperative Medicine, Oregon Health & Science University, Portland, OR, USA

Signal Transducer and Activator of Transcription 3 (STAT3) plays a protective role in the brain following ischemia/ reperfusion injury. The function of STAT3 in cerebral endothelial cells in response to ischemic injury has not been investigated. Since neuronal- specific ablation of STAT3 does not alter infarct size, endothelial STAT3 may be responsible for the STAT3-mediated protection in the brain. We therefore hypothesized that STAT3 protects endothelial cells from ischemic injury. We used primary adult mouse cerebrovascular endothelial cells and subjected them to oxygen and glucose deprivation (OGD), an in vitro model of ischemia. Using Western blot analysis, we found that STAT3 protein levels and its phosphorylation on tyrosine residue 705 are regulated by OGD; they are decreased immediately following OGD but increase to exceed pre-OGD levels by 24 hours of reoxygenation. Using a pharmacological inhibitor of STAT3 activation, we show that attenuation of STAT3 signaling induces endothelial cell death. STAT3 is therefore a survival factor for endothelial cells, and plays an important role in determining susceptibility to ischemic damage. We demonstrate that STAT3 is essential for correcting endothelial dysfunction after ischemic injury. Since endothelial dysfunction is a contributing factor, as well as an outcome of pathological states, regulation of endothelial STAT3 may have important consequences in cerebrovascular disease.

This work was supported by a Pacific Mountain Affiliate Postdoctoral Fellowship from the American Heart Association to C. M. Davis.

1220

NEGATIVE BOLD EFFECT IN THE STRIATUM CORRELATES WITH A DECREASE IN CBV IN FMRI OF THE RAT BRAIN

M. Selt, D. Kalthoff, M. Hoehn

Max-Planck-Institute for Neurological Research, Cologne, Germany

Objectives: Functional magnetic resonance imaging (fMRI) based on blood-oxygenation level-dependent (BOLD) contrast is a widely used technique to study brain function [1]. Mediated by neurovascular coupling, neuronal activity triggers hemodynamic responses of increased cerebral blood volume (CBV) and flow (CBF), leading to a net increase of the BOLD fMRI signal. Lately reported negative BOLD responses [2] may point towards complex interaction of neuronal systems, though origin and interpretation are to be further investigated. Here we describe negative BOLD responses in striatum alongside positive BOLD in thalamus and somatosensory cortex upon electrical forepaw stimulation and their behaviour after CBV weighting.

Materials and Methods: Four male Wistar rats were anesthetized with Isoflurane. Needle electrodes were inserted in both forepaws for electrical stimulation and a tailvein-catheter was placed for contrast agent administration. Isoflurane was discontinued after subcutaneous administration and subsequent continuous infusion of Medetomidine solution [3].

Functional MRI was performed on an 11.7 T BioSpec-system using gradient-echo EPI (TR=3s). The stimulation paradigm consisted of 5 repetitions of 45 seconds off-period followed by 15 seconds on-period. After contrast agent injection (Endorem, 30mg Fe/kg) fMRI scans were repeated.

fMRI data were motion corrected, co-registered and normalized to 100% baseline signal. Datasets were averaged across animals, activation-maps were calculated and signal timecourses of somatosensory cortex (S1) and striatum (CPu) were extracted.

Results: BOLD activation-maps (Fig 1B) show increased BOLD signal in thalamus and S1 of the right hemisphere upon stimulation of the left forepaw. Simultaneously we observe bilateral signal decreases in the striatum. These results are reflected by the signal changes over time (Fig 1A). With stimulus onset the signal in S1 increases rapidly and reaches its peak after the first third of the stimulation period. At the same time the striatum shows decreases in signal intensity in both hemispheres. Interestingly, the time courses of the striatal areas reach the lowest signal intensity at the same time the S1 signal peaks.

In contrast, signal intensity in contralateral S1 of the CBV-weighted images decreases while the striatal signals increase (Fig 1C and D).

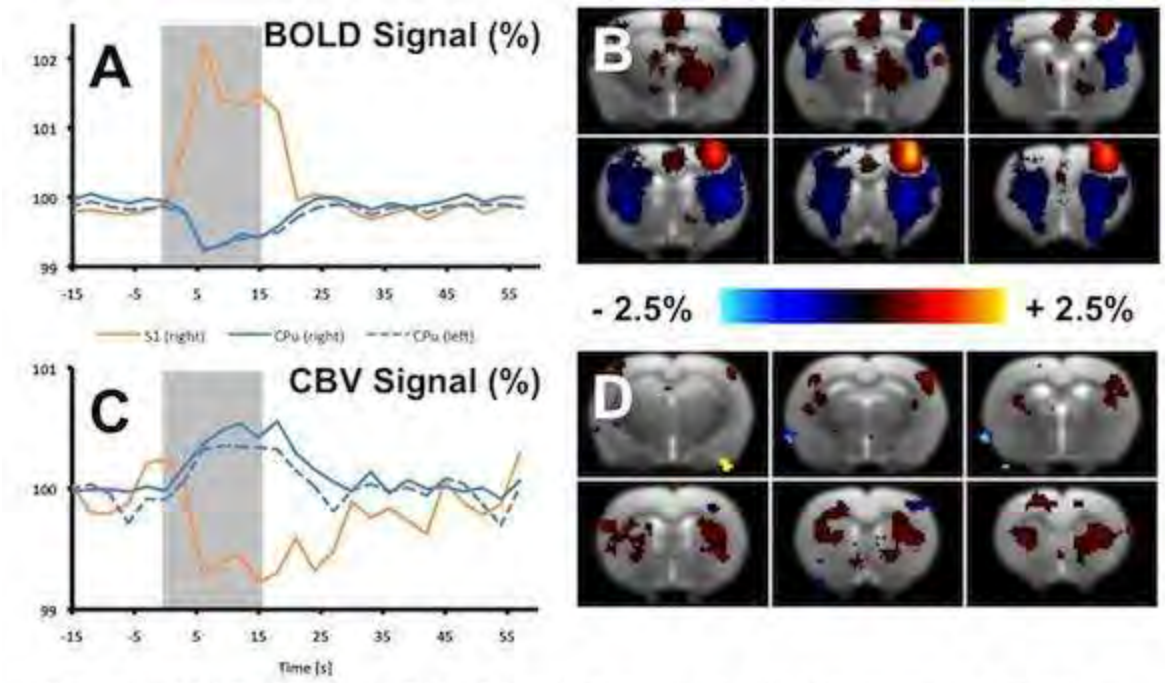

Figure 1: BOLD (1B) and CBV (1D) activation-maps with corresponding signal timecourses for S1 and caudate putamen (Cpu) of the right hemisphere as well as Cpu of the left hemisphere. The grey bars indicate the duration of stimulation.

[Figure 1]

Conclusions: Observed positive BOLD responses in S1 turn into negative signal changes after contrast-agent administration, indicating a substantial CBV weighting and expected vasodilatation upon neuronal activity. Opposed signal behaviour in the striatum and a clear anti-correlation of S1 and CPu BOLD signals indicate direct coupling between these structures. CBV-weighted MRI signal increase in the striatum suggests a stimulus-related vasoconstriction and rules out an instantaneous “vascular-steal” phenomenon in favor of cortical regions. In fact, the observed signal characteristics could point to stimulus-related inhibition of striatal activity with tightly coupled hemodynamics, potentially promoted through the α_2-receptor agonist Medetomidine [4]. Further imaging experiments, electrophysiological and metabolic assessment will be necessary to elicit the origin of the observed negative BOLD responses.

References:

[1] Ogawa et al. (1990); Magn Reson Med 14(1):68-78

[2] Boorman et al. (2010); Neurosci 30(12):4285-4294

[3] Weber et al. (2006); Neuroimage 29(4):1303-1310

[4] Trendelenburg et al. (1994); Naunyn Schmiedebergs Arch Pharmacol 350(5):473-481

1221

MITOCHONDRIAL BIOGENESIS CONTRIBUTES TO THE NEUROPROTECTIVE EFFECT OF LPS PRECONDITIONING AGAINST NEURONAL ISCHEMIA VIA AKT AND JNK PATHWAYS

R.A. Stetler[1,2,3], W. Yin[1], S. Wang[1,3], J. Chen[1,2,3]

[1]Neurology, University of Pittsburgh School of Medicine, Pittsburgh, PA, USA, [2]State Key Laboratory of Medical Neurobiology, Fudan University, Shanghai, China, [3]Geriatric Research, Educational and Clinical Center, Veterans Affairs Pittsburgh Health Care System, Pittsburgh, PA, USA

Objectives: The exposure of neurons to a sublethal stimulus (preconditioning) such as lipopolysacchride (LPS) prior to a subsequent ischemic challenge has been extensively demonstrated to decrease infarct and afford lasting neuroprotection. However, the mechanisms are not well understood. Bolstering energetic reserves to face subsequent ischemic conditions has been postulated to underlie the preconditioning phenomenon, and implicitly suggests the involvement of mitochondrial biogenesis. Using an in vitro neuronal ischemic model, we explored the contribution of mitochondrial biogenesis to the neuroprotection afforded by LPS preconditioning.

Methods: Primary neuronal cultures were derived from E15 rat embryos. On 11DIV, cultures were treated with LPS (0.1-4μg/mL) or vehicle for 3, 6 or 24 h. For ischemic conditions, cultures were subjected to 60 min of oxygen/glucose deprivation (OGD) following 24 h of LPS preconditioning (1μg/mL), and assessed for cell survival at 24 h following OGD. Induction of mitochondrial biogenesis was assessed by FACS analysis of mitochondrial DNA (mtDNA) and RT-PCR quantification of key transcription factor gene expression (PGC-1, NRF-1 and TFAM). Critical components of the electron chain transport (COXI-IV and VDAC) were measured by 2D and western blotting, and energetic stores were assessed by quantification of ATP levels and citrate synthase activity. Mitochondrial flux and length were measured using image analyses from cultures transiently transfected with DsRed2. Contribution of mitochondrial biogenesis in LPS-mediated neuroprotection against OGD was ascertained by transfection of TFAM siRNA. The effect of kinase family inhibitors on TFAM mRNA expression was determined by RT-PCR. Statistical analyses were performed using ANOVA and *post hoc* Fisher's PLSD tests, with $P < 0.05$ considered statistically significant.

Results: LPS preconditioning (1μg/mL, 24 h prior to OGD) led to significant neuroprotection against OGD in cultured neurons. The conditioning event alone significantly increased mtDNA content and upregulated NRF-1 and TFAM within 3 h of LPS exposure, and PGC-1 at 24 h, following addition of LPS to the cultures. Furthermore, expression of electron transport chain protein complexes and VDAC, ATP content and citrate synthase activity were significantly increased following LPS preconditioning. The increased biochemical content of mitochondria induced by sublethal LPS exposure was correlated with increased mitochondrial flux but without changes in mitochondrial length, suggesting that newly formed mitochondrial are functional and healthy. Knockdown of TFAM abrogated the capacity of LPS to increase mtDNA levels, but had no effect on control cells. Neuroprotection against OGD induced by LPS preconditioning was significantly decreased in the presence of TFAM siRNA. The induction of TFAM was decreased by inhibitors of Akt and JNK signaling pathways.

Conclusions: Our findings indicate that the LPS preconditioning event induces functional mitochondrial biogenesis, involving both the Akt and JNK signaling pathways. Importantly, the

mitochondrial biogenetic response significantly contributes to LPS-mediated neuroprotection against a subsequent ischemic event. These results support a functional role for mitochondrial biogenesis in the preconditioning effect against neuronal ischemia.

1223

VASCULAR MITOCHONDRIAL DYSFUNCTION ASSOCIATED WITH INSULIN RESISTANCE IMPAIRS ACTIVATION OF CA^{2+} SPARKS AND MITOCHONDRIAL CA^{2+} UPTAKE

D.W. Busija, P.V.G. Katakam

Pharmacology, Tulane University School of Medicine, New Orleans, LA, USA

Introduction: Mitochondrial depolarization and subsequent generation of reactive oxygen species (ROS) have been shown to trigger vasodilation via activation of 'Ca^{2+} sparks' and Ca^{2+}-activated K^+ (K_{Ca}) channels (Xi Q, Cheranov SY, Jaggar JH, Circ. Res. 97:354-62, 2005). Previously, we reported reduced mitochondrial depolarization and ROS generation resulting in impaired mitochondria-mediated cerebral vasodilation in insulin resistant (IR) Zucker obese (ZO) rats compared to lean (ZL) rats (Katakam PV, Domoki F, Snipes JA, Busija AR, Jarajapu YP, Busija DW, Am. J. Physiol. 296:R289-98, 2009). However, the role of calcium dynamics in impaired mitochondrial-induced dilation in Zucker obese rats is unclear.

Objective: We evaluated the impact of mitochondrial dysfunction with insulin resistance on 'Ca^{2+} sparks' -activation and mitochondrial Ca^{2+} (mitoCa^{2+}) in cerebral artery smooth muscle cells (SMC).

Methods: Middle and posterior cerebral arteries (140 to 180 μm) were isolated from ZO and ZL rats, transferred into a vessel bath (Living Systems, Burlington, VT, USA) filled with PSS, secured between glass pipettes, and superfused with oxygenated (20%O_2/5% CO_2/75% N_2 at 37°C) physiologic saline solution (PSS). Intraluminal diameter was measured using a video dimension analyzer (Living Systems, Burlington, VT, USA). Arteries were slowly pressurized to 70 mmHg with PSS under no flow conditions until a stable myogenic tone (30% to 45% of passive diameter) developed. 'Ca^{2+} sparks' activation and changes in mitoCa^{2+} were evaluated utilizing fluoroprobes Fluo-4 AM and Rhod-2AM, respectively, and a Zeiss Live-7 confocal microscope. Mitochondrial depolarization with or without accompanying ROS generation was achieved by applying the putative mitochondrial K_{ATP} channel activators 100 μM diazoxide (DZ) or 50 μM BMS-191095 (BMS), respectively.

Results: Baseline calcium spark activity (sparks/min) was reduced in ZO compared to ZL (156±21 versus 231±26, $p< 0.05$). BMS and DZ responses were diminished in ZO (207±48 and 257±32, $p< 0.05$) versus ZL (318±54 and 366±63). BMS and DZ promoted a greater increase in mitoCa^{2+} in SMCs of ZL compared to ZO. The protonophore carbonyl cyanide m-chlorophenylhydrazone (10 mM) abolished calcium sparks and diminished mitoCa^{2+} in all arteries.

Conclusion: Mitochondrial dysfunction associated with IR leads to impaired calcium spark activity and mitoCa^{2+} uptake and thus appears to be a major cause of reduced mitochondrial-mediated vasodilation. Thus, restoring mitochondrial function appears to be a novel therapeutic target for protecting the cerebral vasculature in IR in order to maintain normal hemodynamics and lessen the incidence of strokes.Acknowledgements:

Supported by NIH grants (HL-093554, HL-030260, HL-065380).

1224

ACTIVITY MEASURED BY ACCELEROMETER CORRELATES WITH INFARCT VOLUME AND NEUROLOGICAL BEHAVIOR IN A RHESUS MACAQUE ISCHEMIC STROKE MODEL

F.R. Bahjat[1], R.L. Williams-Karnesky[1], G.A. West[2], S.G. Kohama[3], H.F. Urbanski[3], M.P. Stenzel-Poore[1]

[1]Molecular Microbiology and Immunology, Oregon Health & Science University, Portland, OR, [2]Neurotrauma Research Laboratory, Colorado Brain & Spine Institute, Swedish Medical Center, Englewood, CO, [3]Division of Neuroscience, Oregon National Primate Research Center, Beaverton, OR, USA

Objectives: Hemiparesis is commonly observed following stroke and a wide-range of motor deficits exist in both humans and experimental animals. Quantification of the extent of motor deficit has been historically limited to the use of subjective neurological scales that have great value but require significant expertise to implement. Stroke studies in humans have used wrist-worn miniaturized accelerometers to compare activity of affected versus unaffected limbs [1]. Similarly, behavior studies in rhesus macaques have validated the use of accelerometers worn on collars that instead detect total movement [2]. The purpose of this study was to determine whether activity monitoring could quantify changes in spontaneous activity resulting from ischemic stroke in the rhesus macaque. We determined whether accelerometer-derived activity data correlated with infarct volume and/or neurological score.

Methods: Ten adult male rhesus macaques (Macaca mulatta; 6-12 years of age and 6-12kg) were housed individually in 12-hr light/dark cycle and fed twice daily with water ad libitum. Animals fitted with Actiwatch Mini devices (Respironics) attached to aluminum collars (Primate Products) were continually monitored over ~30 days. Devices recorded the integration of intensity, amount, and duration of movement in all directions with force sensitivity of 0.05g and 32Hz maximum sampling frequency [3]. Cerebral ischemia was induced and infarct volume using T2-weighted magnetic resonance imaging (MRI) at 48 hours post-stroke and cumulative neurological score (days 3-8 post-stroke) were determined, as previously described [4]. Three neurological scales were scored each day (Modified-Spetzler, Lessov, and Simon scales). Activity data were analyzed using Actiware Sleep version 3.4 (Cambridge Neurotechnology Ltd). Percent change in activity was calculated using mean pre-stroke and mean post-stroke average daily values. The percent changes in total daily, mean daytime (between 0700 to 1900 hr), mean nocturnal (between 1900 to 0700 hr) and mean ratio daytime:nocturnal activities were tabulated for each animal and Spearman correlation analysis performed using Prism 5.0 (GraphPad).

Results: Percent infarcts ranged from 1 to 26 percent of total hemispheric volume in this study and the extent of infarct correlated well with cumulative neurological score ($p < 0.007$ for all three neurological scales). Significant correlations also existed between the three different neurological scales ($p < 0.0001$). The mean percent change (pre- versus post-stroke) in the ratio of daytime:nocturnal activity compared to infarct volume or cumulative neurological score also revealed significant correlations ($p < 0.0007$).

Conclusions: Stroke in the rhesus macaque results in a consistent reduction in daytime activity with relatively unchanged nocturnal activity compared to pre-stroke values and these changes are related to the extent of infarct present. A resultant decrease in the ratio of daytime:nocturnal activity is observed following stroke which significantly correlates with infarct and neurological

outcomes. Thus, activity monitoring in this experimental stroke model could improve the quality of motor function assessment with a non-invasive and less subjective approach.

References:

1. Gebruers et al. Arch Phys Med Rehabil, 2010. 91(2):288-97.

2. Papailiou et al. Am J Primatol, 2008. 70(2):185-90.

3. Mann et al., Lab Anim, 2005. 39(2): p.169-77.

4. West et al. J Cereb Blood Flow Metab, 2009. 29(6):1175-86.

1226

NOVEL TLC-TECHNIQUES FOR 6-[^{18}F]FLUORODOPA AND [^{18}F]FP-CIT RADIOMETABOLITE ANALYSIS IN HUMAN PLASMA

A. Matusch[1], O.H. Winz[2], J. Schmaljohann[2], S. Prinz[3], I. Vernaleken[3], A. Bauer[1,4]

[1]Institute of Neuroscience and Medicine (INM-2), Research Center Jülich, Jülich, [2]Dept. of Nuclear Medicine, [3]Dept. of Psychiatry, University Hospital Aachen, Aachen, [4]Dept. of Neurology, University Düsseldorf, Düsseldorf, Germany

Objectives: HPLC is a current standard for metabolite analysis of diverse radiotracers. The self-evident advantage of an excellent separation performance is outweighed by some shortcomings inherent to the general design of online detection and sequential runs. Here we report on novel thin layer chromatography (TLC) protocols for 6-[^{18}F]fluorodopa and [^{18}F]FP-CIT.

Methods: [^{18}F]FP-CIT was selectively liquid-liquid (L-L) extracted from 700µl plasma by adding 1/5 volume of 0.8 M Na-carbonate pH9.7, a defined volume of dichloromethane containing 10 µg ml^{-1} cold FP-CIT. 100 µl of the organic under-phase were sprayed onto a 60Å normal phase M&N Sil G25 TLC-plate. Elution used tert-butylmethylether / n-hexane / triethylamine 3/7/1 (v/v/v) under gas phase saturation.

200 µl plasma samples from [^{18}F]FDOPA studies (under carbidopa) underwent protein precipitation (PP) by adding 800 µl of methanol spiked with 5µg ml^{-1} cold 6-FDOPA re-extraction of co-precipitated FDOPA by adding 200µl H_2O and shaking prior to centrifugation. 2 × 20µl of the supernatant were sprayed onto an aluminium oxide plate (M&N ALOX25). The eluent was acetonitrile / (0.25 M Na-carbonate, pH 10.5, containing 0.1% Na-metabisulfit and 10 mM EDTA) 30/70 under gas phase saturation.

Spraying was performed with the CAMAG ATS4 automated TLC sprayer. Developed plates were imaged for 2h using a Packard InstantImager.

Results: TLC after L-L extraction or PP and ß/γ-imaging of developed TLC plates allowed parallel measurements of large numbers of plasma samples which required only small volumes and achieved high count rates for hours after the PET scan. A complete balance of every step and every device was possible. In contrast, HPLC requires large sample volumes and each run is different, as specific activity and consequently the signal to background ratio are decreasing. Furthermore, baseline drifts are likely to occur and radioactivity remaining in the column is not accounted for in the measurement.

[^{18}F]FDOPA metabolites were analysed in 22 and [^{18}F]FP-CIT metabolites in 3 PET studies, respectively. The relative standard deviation of residuals describing the scatter of data points from the fitted course of plasma parent, as a measure of precision, was 2.3% for [^{18}F]FDOPA and 2.7% for [^{18}F]FP-CIT. The fractions of [^{18}F]FDOPA after 30 and 90 min were 48% and 26% (literature 39% and 22%) that of [^{18}F]OMFD 36% and 52% (literature 39% and 56%), respectively. The analogue values for [^{18}F]FP-CIT were 44% and 14% (measured) and 27% and 13% (literature).

Conclusions: TLC is an attractive alternative to HPLC especially when a large number of samples is analysed.

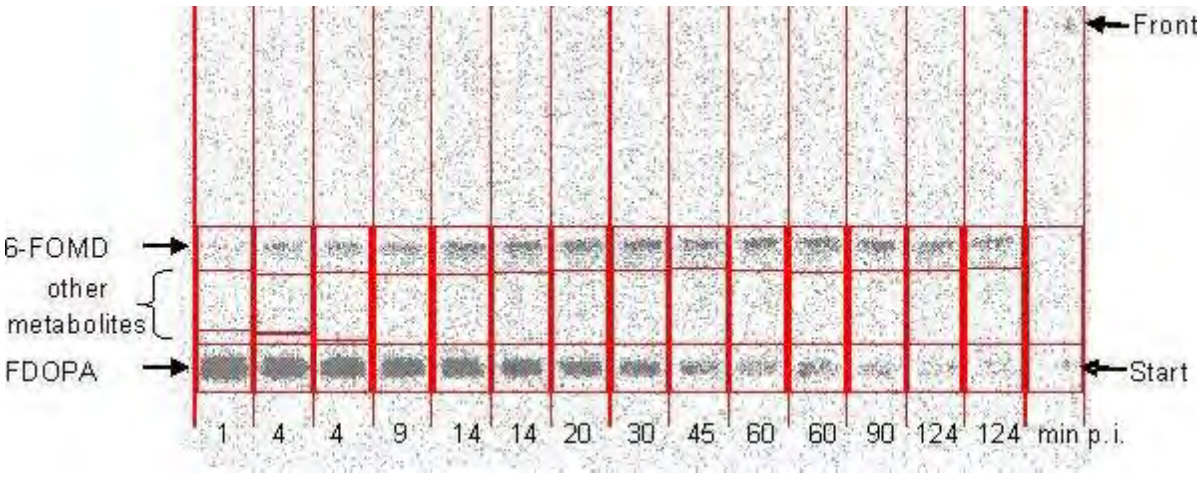

[Figure 1]

Caption of Figure 1

Representative thin layer plate after separating [^{18}F]FDOPA radiometabolites of 14 plasma samples from a kinetic study.

1228

ACTIVATION OF THE S100B/RAGE PATHWAY CONTRIBUTES TO SUBARACHNOID HEMORRHAGE (SAH)-ASSOCIATED CEREBROVASCULAR DYSFUNCTION

C. Paisansathan, H. Xu, L. Mao, F. Vetri, D. Pelligrino

Anesthesiology, University of Illinois at Chicago, Chicago, IL, USA

Objective: Vasospasm is a complication of SAH, which usually occurs several days after the initial bleed and can be associated with a sustained vasoconstriction. Although the underlying pathologic mechanism remains unresolved, findings suggest inflammation as a critical contributor to the pathogenesis of cerebral vasospasm. Evidence points to release of the astrocyte-derived inflammatory protein, S100B, following SAH. In this study, we addressed the hypothesis that, S100B, as a RAGE (receptor for advanced glycation end-products) ligand, may trigger a S100B/RAGE -related pro-inflammatory pathway, which ultimately results in the impairment of cerebral vasodilating function even at sites remote from the initial bleed (e.g., neocortex). To that end, we examined: (1) whether SAH is accompanied by loss of pial arteriolar dilating function; (2) whether the above changes are associated with increased presence of S100B and its receptor, RAGE; and (3) whether blocking RAGE-S100B interactions, via sRAGE (soluble RAGE) application, restores SAH-impaired cerebrovascular function.

Methods: SAH was established using a rat anterior cerebral artery perforation model. Rats were divided into three groups: (1) sham operation control, (2) vehicle-treated SAH, and (3) sRAGE-treated SAH. In the last two groups, the vehicle and sRAGE solution were delivered intracerebroventricularly (starting at 30 min following SAH) via an osmotic pump. Vascular function was evaluated, up to 3 days post-SAH, by measuring pial arteriolar responses to vasodilating stimuli using intravital microscopy/videometry. In groups 1 and 2, brain samples were collected at the end of each experiment (6, 24, 48, or 72 h post-SAH) for western blot analysis of cortical expression of S100B and RAGE.

Results: Western blot analysis revealed increased RAGE expression in samples obtained at 6-72 h post-SAH; whereas S100B expression was increased at 6-24 h, and fell back to normal levels over 24-72 h. In a separate study, using ELISA analysis, we found a steep increase of S100B in cisternal CSF that appeared by 6 hrs following SAH, and persisted up to 7 days. Compared to sham controls, substantially attenuated pial arteriolar responses to hypercapnia and cortical activation (sciatic nerve stimulation [SNS]) were observed, with maximum effects seen at 48 h post SAH. Additionally, the vasodilatory response to the topically-applied endothelium-dependent vasodilator, acetylcholine (ACh), was completely eliminated by SAH at 24, 48, and 72 h. Normal pial arteriolar responses to adenosine and S-nitroso-N-acetyl penicillamine (NO donor) were observed at 24 and 72 h post-SAH, with substantial repression seen only at 48 h post-SAH. Application of sRAGE was associated with partial or complete restorations of vascular reactivity, except SNS-induced vasodilation, which was not affected.

Conclusion: Enhanced activity of the S100B/RAGE pro-inflammatory pathway appears to contribute to cerebrovascular dysfunction following SAH. This impaired vasodilating function can be restored, in part, by interruption of S100B-RAGE interactions.

1229

INFRARED OPTICAL IMAGING OF MATRIX METALLOPROTEINASES (MMP) UP REGULATION FOLLOWING ISCHEMIA REPERFUSION IS AMELIORATED BY HYPOTHERMIA

U.I. Tuor[1], D. Rushforth[1], P. Barber[2]

[1]Experimental Imaging Centre, National Research Council of Canada, Institute for Biodiagnostics West, [2]Department of Clinical Neuroscience, University of Calgary, Calgary, AB, Canada

Introduction: The activity of matrix metalloproteinases (MMPs) are considered to be key factors in blood brain barrier (BBB) permeability through the direct degradation of constituents of the neurovascular matrix. Non-invasive imaging of MMP activity may provide important insight into the spatial and temporal proteinase activity following ischemia reperfusion.

Objective: To investigate whether an MMP activated optical probe (MMP 750 FAST, Visen) could be used to visualize early MMP activity in cerebral cortex following focal ischemia.

Methods: Experimental stroke was induced by 30 minutes of middle cerebral artery occlusion (MCAO) in the mouse (C57 bl). Following MCAO optical imaging was performed using an Olympus BX 51 microscope fitted with a back-thin CCD camera linked to image-capture software. Excitation and emission filters were in the near infra-red (NIR) range of 749 and 755 nm, respectively. The animal groups consisted of sham MCAO, MCAO with early reperfusion imaging, MCAO with early hypothermic (33oC) ischemic reperfusion imaging and MCAO with reperfusion and imaging at 24 hr. A pial window was created by thinning the bone with a high speed micro drill over the ischemic injured cortex. A control window was made on the contralateral side. Baseline images were acquired starting at 120 min or 24 hours after reperfusion over the ipsilateral and contralateral cortex, after which 150 micro litres of MMP 750 FAST was slowly infused over 60 seconds. Optical imaging was repeated every 5 to 10 min for 3 hours. Brain tissue was collected for MMP enzyme ELISA quantification. Ipsilateral - contralateral differences in gray levels were converted to a percentage of contralateral values. Data were analyzed using a 2 way-repeated ANOVA for comparison between groups and a paired t-test for within groups.

Results: Following optical probe injection in sham animals there were no significant ipsilateral-contralateral differences in intensity over the 3 hour observation period. In contrast, in ischemic reperfused brain there were left-right intensity differences that increased with time. Differences in gray levels between ipsilateral and contralateral cortex were significant by 2-3 hours post MMP 750 FAST administration ($P < 0.001$ for 4-5 hr reperfusion and 24 hr reperfusion). Such increases were not observed in the MCAO group with hypothermia, resulting in significant differences in this group compared to the MCAO group with acute reperfusion. ELISA measures demonstrated that this corresponded with a significant ipsilateral increase in total MMP9 5 hrs following ischemia reperfusion ($P < 0.05$) and a trend at 24 hours ($P < 0.09$). There were no significant increases in MMP2 at any of the time points. Increases in MMP9 were not observed in the hypothermic reperfusion group.

Conclusions: The results indicate that early MMP 9 upregulation in ischemia reperfusion can be imaged early and non-invasively with NIRF using an MMP activatable optical probe. Hypothermia attenuates both MMP9 protein expression and the increase in optical gray scale

intensity after MMP 750 FAST administration supporting the proof of concept that NIRF can be used to assess potential therapeutic strategies for stroke treatment.

1232

NOVEL SPATIAL AND TEMPORAL PATTERNS OF CYTOKINE EXPRESSION IN BRAIN AND PLASMA AFTER EXPERIMENTAL STROKE

M.P. Pereira[1,2,3], A. Arac[1,2,3], H. Keren-Gill[1,2,3], T.M. Bliss[1,2,3], G.K. Steinberg[1,2,3]

[1]Neurosurgery, Stanford University School of Medicine, [2]Stanford Stroke Center, [3]Stanford Institute for Neuro-Innovation and Translational Neurosciences, Stanford, CA, USA

Background and purpose: Inflammation plays a major role in the pathophysiology of brain ischemia with inflammatory cytokines implicated in tissue injury in the acute stage of stroke. Anti-inflammatory strategies have shown beneficial effects in experimental stroke; however, their clinical translation has been unsuccessful due in part to lack of detailed knowledge of post-stroke neuroinflammatory processes. A major issue is that cytokines form a complex network of molecules and can have pleiotropic effects that are either detrimental or beneficial depending on their microenvironment, which is influenced by the timing and location of cytokine release, and other cytokines in their vicinity. This study profiles the spatial and temporal response of 20 cytokines in the brain and plasma after ischemia, and offers new insight to an immune-modulatory approach for stroke.

Methods: 6 hours to 1 month after experimental stroke in rats, cytokine profiles were determined in infarct and peri-infarct regions of the brain, and in plasma, by multiplexed immunoassay.

Results: Novel patterns of cytokine expression were observed in the peri-infarct compared to the infarct region, with some cytokines (i.e.KC and RANTES) being uniquely expressed in the infarct. The temporal profile revealed a biphasic expression pattern for some cytokines (e.g. IL-1a, IFNg), with a known peak in the acute phase of stroke and a second novel peak at 1 week. Cytokine changes in plasma, in general, did not mirror those observed in the brain; bi-phasic immunodepression was observed, with many plasma cytokines decreasing below baseline at 6h and again at 1 week post-stroke, interspersed with a peak of expression at 1 day. IL-6 peaked a second time at 1 month. Common to brain and plasma, cytokine profiles had not returned to baseline by 1 month.

Conclusions: A critical temporal and spatial profile exists regarding cytokine expression in the brain and plasma after stroke, with the inflammatory response remaining perturbed to at least one month post-stroke. These data imply that a more targeted approach to modulating the inflammatory response is required with emphasis on the timing and location of therapeutic intervention.

1233

CEREBRAL GLUCOSE METABOLISM IS INCREASED WITH INSULIN DETEMIR COMPARED TO NPH INSULIN IN HUMAN TYPE 1 DIABETES

L.W. van Golen[1], M.C. Huisman[2], R.G. Ijzerman[1], N.J. Hoetjes[2], L.A. Schwarte[3], P. Schober[3], R.P. Hoogma[4], M.L. Drent[1], A.A. Lammertsma[2], M. Diamant[1]

[1]Endocrinology, [2]Nuclear Medicine and PET Research, [3]Anaesthesiology, VU University Medical Center, Amsterdam, [4]Endocrinology, 'Groene Hart' Hospital, Gouda, The Netherlands

Objective: The purpose of this study was to test the hypothesis that subcutaneous administration of insulin detemir, a basal insulin analogue that has been shown to result in less weight gain[1], leads to a more pronounced effect on brain glucose metabolism, particularly in regions associated with appetite regulation, than NPH insulin in men with type 1 diabetes (T1DM).

Methods: In a randomised cross-over study, male T1DM patients were treated with a basal-bolus regimen for two periods of 12 weeks, starting with either insulin detemir or NPH insulin, in combination with insulin aspart. After each period of treatment, patients were scanned in the fasted state early in the morning. All patients had injected their last basal insulin the previous night. Dynamic [^{18}F]-fluoro-2-deoxy-D-glucose (FDG) brain scans were acquired over 60 minutes using a High Resolution Research Tomograph PET scanner (Siemens/CTI). The input function was obtained using continuous arterial sampling. Various brain regions were defined by automatic delineation on an MRI scan, which was acquired within one week of the first PET scan. Cerebral metabolic rate of glucose uptake (CMRGlu) was obtained by non-linear regression of the regional time activity curves using an irreversible 2-tissue compartment model with blood volume parameter together with the arterial plasma input function. Differences between treatments were tested by paired 2-tailed t-tests.

Results: Seventeen male T1DM patients (mean ± SD; age 38 ± 9 years, body weight 83.4 ± 13.9 kg, BMI 24.7 ± 2.7 kg×m^{-2}, diabetes duration 14.8 ± 7.0 years , HbA1c 7.5 ± 0.6%) were included. After 12 weeks, daily insulin doses and HbA1c were similar between treatments. Insulin detemir decreased body weight by 0.3 kg, whereas patients on NPH insulin gained 0.4 kg (between-group difference p=0.27). CMRGlu in total brain was 7.1% higher after treatment with insulin detemir versus NPH insulin (p=0.02). Arterial glucose levels during scanning were not significantly different between treatments (p=0.7).

Conclusion: Treatment with insulin detemir versus NPH insulin resulted in an increase in total brain glucose metabolism in men with T1DM. In parallel, compared with NPH insulin, insulin detemir showed a trend towards weight loss. These findings support the hypothesis that a differential effect on cerebral glucose metabolism may contribute to the observed weight sparing effect of insulin detemir. **References:**

1. De Leeuw I, Vague P, Selam JL, Skeie S, Lang H, Draeger E, Elte JW. Insulin detemir used in basal-bolus therapy in people with type1 diabetes is associated with a lower risk of nocturnal hypoglycemia and less weight gain over 12 months in comparison to NPH insulin. Diabetes Obes Metab. 2005 Jan;7(1):73-82.

1234

CHANGES IN APPARENT DIFFUSION COEFFICIENT (ADC) AND T2 RELAXATION TIME IN A RAT MODEL OF SUBARACHNOID HAEMORRHAGE (SAH)

S.M. Fredriksson[1], N. Singh[1,2], J. Galea[1,2], A. Greenhalgh[1], A. Parry-Jones[2], C. Smith[2], S. Hulme[2], S. Hopkins[2], A. Vail[2], H. Patel[2], N.J. Rothwell[1], A.T. King[2], P.J. Tyrrell[2], S.M. Allan[1]

[1]Faculty of Life Sciences, University of Manchester, [2]Brain Injury Research Group, Manchester Academic Health Sciences Centre, Salford Royal NHS Foundation Trust, Manchester, UK

Background: In subarachnoid haemorrhage (SAH) 20-30 % of patients that survive the acute phase caused by the bleeding are affected by secondary delayed cerebral ischaemia (DCI) 3-14 days after the bleed (Eddleman *et al*., 2009). DCI is a potentially fatal complication and underlying mechanisms may involve a combination of constriction of the brain microcirculation and microthrombosis (Vergouwen *et al*., 2008). However, more evidence is needed to establish the mechanism of DCI, and it is currently not established whether DCI occurs in animal models of SAH. Therefore our objective was to investigate the evolution of ischaemic brain injury in a rat model of SAH, to determine whether it correlates with the appearance of DCI in SAH patients.

Methods: Male Sprague-Dawley rats weighing 330-500 g were used. Animals were injected after withdrawal of 100 µl CSF with 300 µl blood followed by 200 µl blood after 24h. Injections were made into cisterna magna through a catheter and heads were tilted 30° to introduce blood under base of the brain. One group of rats were imaged 1, 2, 3, 4, 5, 14 and 28 days (n=3 per time point and treatment), one group was only assessed histologically after 28 days (n=6) and another group 1, 3 and 6 days (n=3) after the second injection. Control groups received saline injections or catheter implantation without injection.

T1-, T2- and diffusion-weighted sequences were run on a 7T Bruker scanner using ParaVision software to run the magnet and acquire and analyse the images. Parametric maps were calculated and average ADC and T2 measured for cortex and striatum.

After the last scanning session, brains were perfuse-fixed with saline/paraformaldehyde, removed and sectioned for subsequent assessment of neuronal damage using cresyl violet.

Results: Preliminary results show that the group of animals imaged at 1, 2, 3, 4, 5, 14 and 28 days displayed changes in T2 and ADC coefficients corresponding to histological change in the form of unilateral or bilateral cortical areas of pyknotic nuclei and areas of decreased cell density. Increased ADC values may signify vasogenic oedema (Cernak *et al*., 2010), and increased T2 values possibly indicate vasogenic oedema and chronic ischaemic lesions (Wegener *et al*., 2006). The animals that were only assessed histologically did not display any signs of ischemic lesions. The occurence of what appeared to be ischemic lesions in the imaged group but not the other, may be due to small n numbers or an effect of repeated anaesthesia and injection of contrast agent in the scanned animals.

Conclusions: Diffusion-weighted and T2-weighted MRI can be used as a non-invasive method to follow ischemic processes in the rat brain after subarachnoid blood injection. This may be useful for investigating possible development of DCI after SAH.

1236

NOVEL SETUP FOR COMBINED MEASUREMENT OF LASER SPECKLE FLOWMETRY, RGB REFLECTOMETRY AND POSITRON EMISSION TOMOGRAPHY:VALIDATION AND IN VIVO APPLICATION

M.M. Gramer[1], A. Steimers[2], M. Takagaki[1], T. Kumagai[1], D. Feuerstein[1], H. Backes[1], M. Kohl-Bareis[2], R. Graf[1]

[1]Max Planck Institute for Neurological Research, Cologne, [2]RheinAhrCampus Remagen, University of Applied Science Koblenz, Remagen, Germany

Objectives: Spreading depolarizations (SDs) are transient waves of local depolarization that propagating slowly over the cortex with a speed of 3-5 mm/min [1]. There is increasing evidence that these waves play a major role in the secondary deterioration of cortical tissue in the immediate vicinity of initial lesions. However, the underlying mechanisms of the neurometabolic coupling during the passage of SDs are still unclear. Therefore, we developed a setup to combine a) Laser Speckle Flowmetry (LSF) to track the SD waves and their hemodynamic responses with b) Positron Emission Tomography (PET) of [18F]-fluoro-2-deoxyglucose (FDG) to measure glucose consumption and c) RGB Reflectometry (RGBR) to measure tissue concentrations of oxy-haemoglobin (HbO2) and deoxy-haemoglobin (HHb).

Methods: For simultaneous acquisition of optical and positron emission data, a commercially available animal bed (MACU, MEDRES, Germany) was modified to allow not only regulation of basic systemic parameters (anesthesia, body temperature, breathing rate) but also minimum attenuation of gamma rays by the optical equipment. For this purpose, optical signals were redirected onto the CCD camera outside the PET gantry using a mirror.

To co-register the 2d optical images and the 3d FDG-PET maps, we developed a spatially well-defined fiduciary marker visible in all modalities. It included small light reflecting spheres detectable in the optical images and a ring-shaped radiotracer tubing visible in the PET data.

We used double illumination consisting of a laser diode in the near-infrared range and high power white light LEDs in the visible spectrum for LSF and RGBR respectively. Reflected signals were spectrally separated by a prisma and directed to two CCD chips within a single camera [2].

Sensitivity and intermodal interference of each modality were determined using phantoms. Furthermore, the setup was tested in vivo. In male Wistar rats the temporoparietal cortex was exposed through thinned skull. The medial cerebral artery was occluded by injection of macrospheres in the carotid artery (MCAO) [3] causing SDs.

Results: In a set of validation experiments we showed that there is minimal interference between the modalities with no visible artefacts and preserved sensitivities.

The combined LSF and RGB reflectometry showed that the spatiotemporal patterns of tissue oxygenation matched the haemodynamic response (Fig. 1, arrows indicate direction of wave propagation). During the first SD event following MCAO we observed an oligemic wave that was time-locked with a congruent wave of decreased HbO2 and increased HHb.

The local FDG-uptake on the PET images could be correlated with the propagation of the SD waves after co-registration.

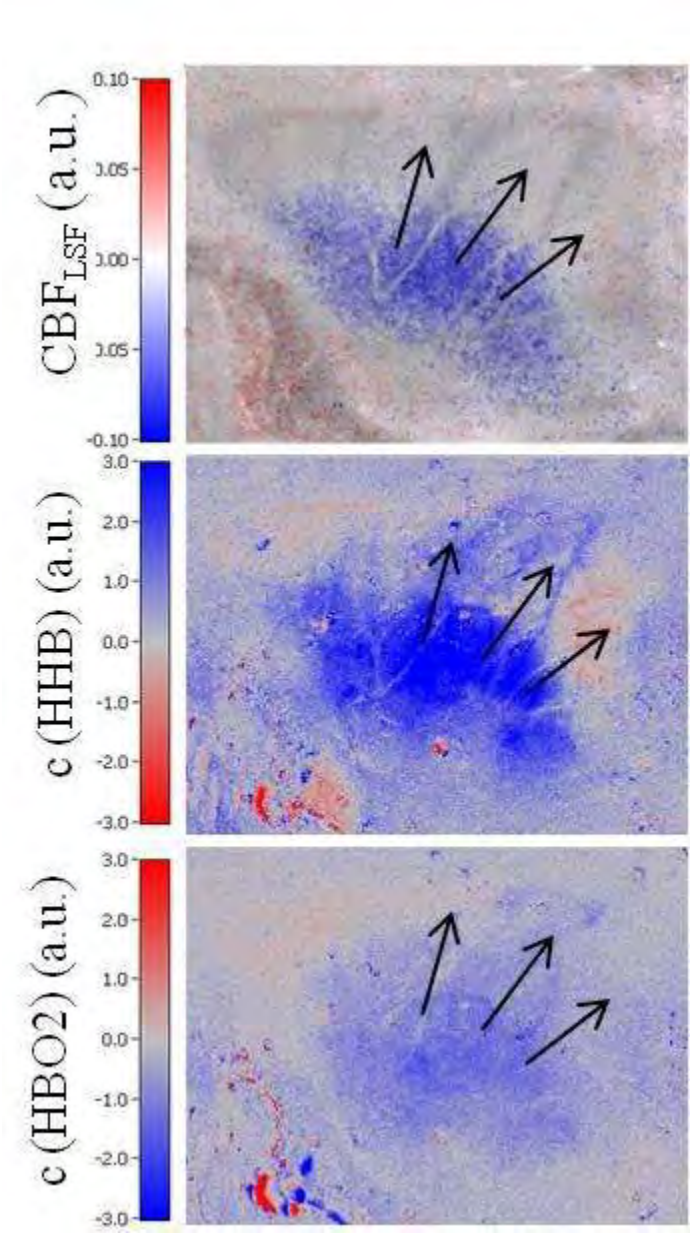

[Response to a hypoemic SD in CBF, HHb and HbO2]

Conclusions: This setup allows for the examination of dynamic vascular and metabolic disturbances in the rodent brain with high spatiotemporal accuracy.

References:

[1] Kumagai et al., JCBFM 2010, doi:10.1038/jcbfm.2010.128

[2] Steimers et al., Proc. SPIE 2009;7368-30

[3] Gerrits et al., Brain Res 2004;12(3):137-43

1239

FUNCTIONAL NETWORKS IN THE RAT BRAIN: DEPENDENCE ON ANESTHETIC REGIMES REVEALED VIA INDEPENDENT COMPONENT ANALYSIS

D. Kalthoff, C. Po, D. Wiedermann, M. Hoehn

In-Vivo NMR Laboratory, Max Planck Institute for Neurological Research, Cologne, Germany

Objectives: Functional Magnetic Resonance Imaging of the brain's "resting state" (rsfMRI) has evolved into an important tool to investigate intrinsic functional networks of the brain [1]. Applied in animal models, rsfMRI has an enormous potential to study progression, recovery or therapy of various diseases. Animal MRI, however, generally requires anesthesia, which potentially confounds functional connectivity results. The aim of this study was thus to compare functional connectivity networks in an established protocol of Medetomidine (MED) sedation vs. Isoflurane (ISO) anesthesia.

Methods: Male Wistar rats (n=17) were anesthetized with ISO kept at ~1.5% with O_2 and N_2 (30/70). MRI was performed on a 11.7 T Bruker BioSpec system. After adjustments, a 5 min rsfMRI scan was acquired using gradient-echo-planar-imaging (TE=17.5ms/TR=2.84s). Subsequently, a bolus and continuous infusion of MED solution were administered subcutaneously while ISO was discontinued [2]. After settlement of ~30 min, rsfMRI acquisition was repeated under MED.

Functional datasets were motion corrected, co-registered structural template and analyzed via probabilistic independent component analysis (ICA) with FSL MELODIC software. Spatial maps and frequency spectra of all components were inspected, and those exhibiting patterns of physiological noise [3] were excluded. Remaining components were automatically grouped based on their spatial similarity using a hierarchical clustering algorithm: In brief, pairwise correlation coefficients were calculated from probability maps, compiled in a weighting-matrix and clustered using MultiDendrograms software. For the identified clusters, incidence maps were calculated across animals using thresholded probability maps.

Results: ICA identified 10-19 independent components (ICs) in each dataset (Median/SD: 15/3 ISO, 13/3 MED). In ISO data, more than 90% of all ICs had to be removed as artifacts of physiological or non-physiological origin; only 7% of ISO ICs were retained as meaningful with respect to functional connectivity analysis. In MED data, 32% of all ICs were considered for further analysis. Clustering of ICs via their spatial features revealed a bilateral cortical and bilateral striatal group. While those components were only present in < 30% of ISO datasets, incidence was > 75% in the MED regime. Moreover, ICs in the MED regime could be segregated into consistent subgroups that were often found in parallel within the subjects (Figure for illustration of IC networks incidence).

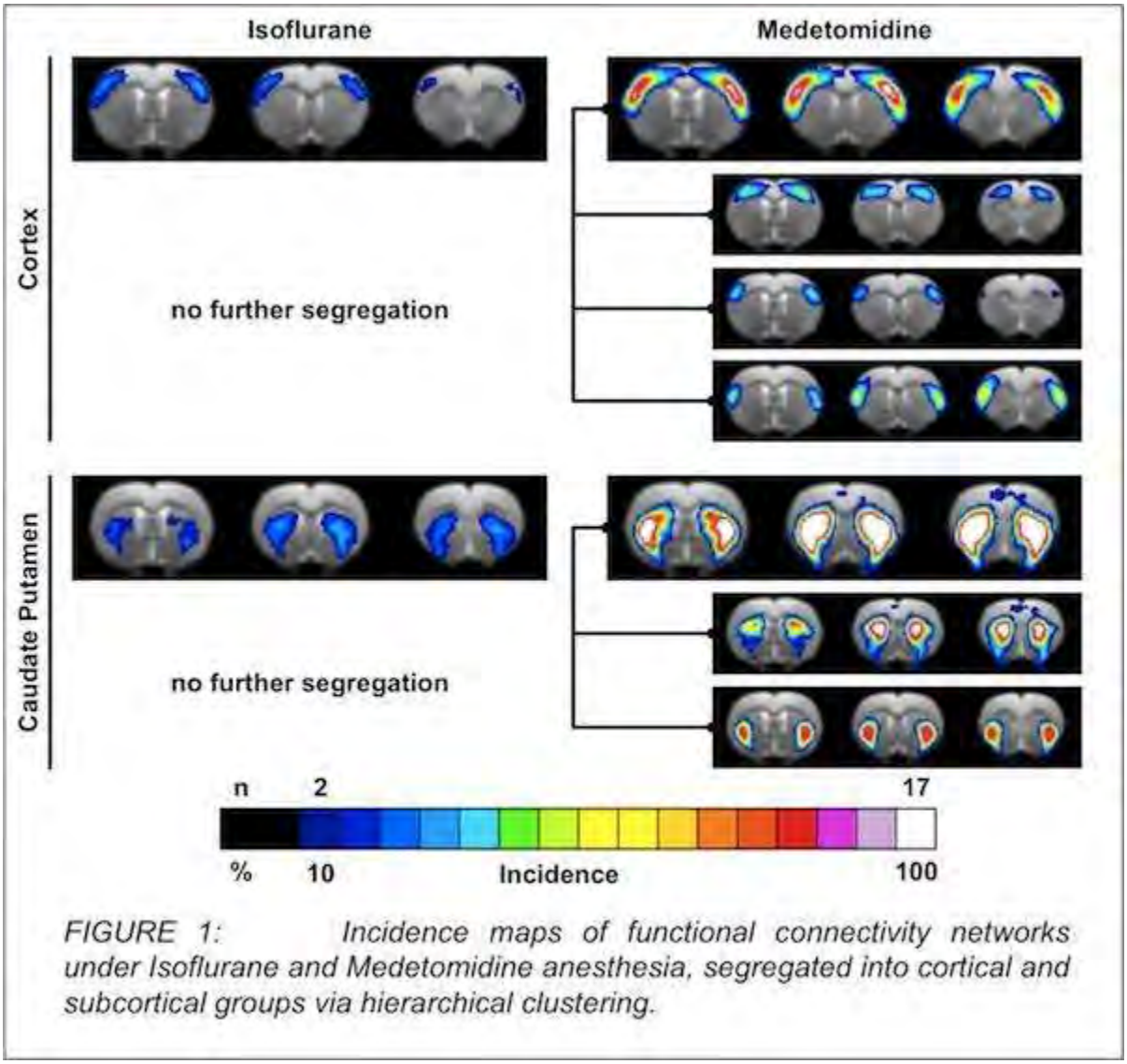

FIGURE 1: Incidence maps of functional connectivity networks under Isoflurane and Medetomidine anesthesia, segregated into cortical and subcortical groups via hierarchical clustering.

[Functional Networks - Incidence Maps]

Conclusions: Our results show that connectivity networks in the rat brain revealed via ICA differ significantly in MED sedation vs. ISO anesthesia. Connectivity networks identified in the MED regime are stronger, more reproducible and spatially more coherent, which is supported by a recent report using a seed-based analysis approach [4] and comparison to other studies [5,6]. We conclude that MED sedation of the rat is to favor over ISO anesthesia whenever functional connectivity networks are to be studied in their complexity and greater level of detail.

References:

[1] Biswal et al., MagnResonMed 34, 537(1995)

[2] Weber et al., Neuroimage 29, 1303(2006)

[3] Kalthoff et al., Neuroimage(2010)

[4] Williams et al., Magn Reson Imaging(2010)

[5] Hutchison et al., J Neurophysiol 103, 3398(2010)

[6] Kannurpatti, Neuroimage 40, 1738(2008)

1241

MITOCHONDRIAL DEPOLARIZATION ALONE ENHANCES CA^{2+}-SPARKS GENERATION INDEPENDENT OF REACTIVE OXYGEN SPECIES

D.W. Busija, P.V.G. Katakam

Pharmacology, Tulane University School of Medicine, New Orleans, LA, USA

Introduction: Mitochondrial depolarization and subsequent generation of reactive oxygen species (ROS) in response to diazoxide application have been shown to trigger cerebral vasodilation via activation of calcium-sparks and calcium-activated K^+ (K_{Ca}) channels (Xi Q, Cheranov SY, Jaggar JH, Circ. Res. 97:354-62, 2005). However, it is unclear if mitochondrial depolarization alone, independent of ROS generation, is capable of promoting calcium sparks. Although it is generally believed that depolarization of mitochondria is always associated with enhanced release of ROS, we have shown that these two events can be uncoupled (Busija DW, Gaspar T, Domoki F, Katakam PV, Bari F. Adv. Drug Deliv. Rev. 60:1471-7, 2008; Gáspár T, Snipes JA, Busija AR, Kis B, Domoki F, Bari F, Busija DW. J. Cereb. Blood Flow Metab. 28:1090-103, 2008).

Objective: To determine whether BMS-191095 (BMS), a putative mitochondrial K_{ATP} channel opener that depolarizes mitochondrial without increasing mitochondrial ROS release, could induce calcium sparks in vascular smooth muscle cells of rat cerebral arteries. We tested the hypothesis that mitochondrial depolarization independently of ROS production could increase the generation of calcium sparks.

Methods: Middle and posterior cerebral arteries (140 to 180 μm) were isolated from Sprague Dawley rats, transferred into a vessel bath (Living Systems, Burlington,VT, USA) filled with physiologic saline solution (PSS), secured between glass pipettes, and superfused with oxygenated (20%O_2/5% CO_2/75% N_2 at 37°C) PSS. Intraluminal diameter was measured using a video dimension analyzer (Living Systems, VT, USA). Arteries were slowly pressurized to 70 mmHg with PSS under no flow conditions until a stable myogenic tone (30% to 45% of passive diameter) developed. Fluorescence microscopy and a Zeiss Live-7 confocal microscope were used to measure the calcium sparks (Fluo-4 AM). In addition, the affect of BMS on mitochondrial membrane potential (TMRE), ROS (mitoSOX) and calcium (Rhod-2AM) were determined. Mitochondrial depolarization without accompanying ROS generation was achieved by applying the putative mitochondrial K_{ATP} channel activator BMS (50 µM).

Results: Compared to the vehicle treated arteries, BMS depolarized mitochondria without producing ROS. BMS also enhanced generation of calcium sparks (54±9 versus 117±18 sparks/min in response to vehicle and BMS respectively, $p< 0.05$) and promoted calcium uptake by mitochondria. BMS also dilated cerebral arteries and this effect was reduced by iberiotoxin.

Conclusions: Our study has shown for the first time that mitochondrial depolarization induces calcium sparks via a ROS-independent mechanism and that subsequent activation of K_{Ca} channels results in cerebral vascular dilation. Thus, both mitochondrial ROS and mitochondrial depolarization independently induce increased calcium spark activity by cerebral vascular smooth muscle cells. These results show that a previously unknown signaling pathway originating in the mitochondria can alter cerebral vascular tone.

Acknowledgement: Supported by NIH grants HL-093554, HL-077731, and HL-030260.

1242

USE OF BOLD-MRI TO EVALUATE CEREBROVASCULAR REACTIVITY AFTER SAH: AN EARLY DIAGNOSTIC TOOL FOR VASOSPASM?

L. da Costa[1,2], J. Fierstra[1], J. Fisher[3], D. Mikulis[2], M. Tymianski[1]

[1]Department of Surgery - Division of Neurosurgery, [2]Department of Medical Imaging, [3]Department of Anesthesia, University of Toronto, Toronto, ON, Canada

Objective: Delayed ischemic neurological deficit (DIND) is still a major problem in neurosurgical centers. Despite massive research, no new predictive factor was identified in many years, and patients require prolonged intensive care (ICU) stay for monitoring. We developed a pilot project to evaluate cerebral autoregulation (CVR) after subarachnoid hemorrhage (SAH) and its relationship with radiographic vasospasm and DIND using BOLD-MRI images and precise control of CO_2 using a newly developed re-breathing circuit, the Respiract™.

Methods: Five patients with aneurysmal SAH were enrolled. After securing the aneurysm, patients were submitted to an MRI/MRA with functional imaging protocol (BOLD) and continuous CO_2 manipulation during image acquisition. MRIs were performed between day 2 and 6 after the SAH. All patients were in good clinical grade. BOLD MRI signal was then analyzed, color coded and superimposed on anatomical images to generate the maps. Treatment followed standard institutional SAH protocol after, with follow up imaging based on clinical needs.

Results: There were 3 males and 2 females. Hunt-Hess scale was II for all patients. In two patients the maps suggested disturbed CVR: one patient had paradoxical decrease of flow with increasing CO_2 levels (blue zones in the map, figure 01) and another disturbed CVR without paradoxical flow. The correlation between the areas of disturbed CVR and future ischemic symptoms appears to be good: a stroke occurred in the patient with “blue” areas who also had angiographic vasospasm in the same regions. The patient with mild CVR disturbance evolved with contralateral motor deficits responsive to increase in volume and blood pressure (Figure 02). None of the patients with normal CVR according to MRI had ischemic symptoms, despite the presence of angiographic vasospasm in 2.

Conclusion: Early assessment of the state of cerebral autoregulation after aneurysmal subarachnoid hemorrhage using BOLD-MRI and precise CO_2 manipulation with the Respiract™ may be useful to identify patients at risk for DIND. MRI has the advantage of very good anatomical detail what may help to guide future interventions. More cases are needed to confirm the relationship between disturbed CVR and DIND.

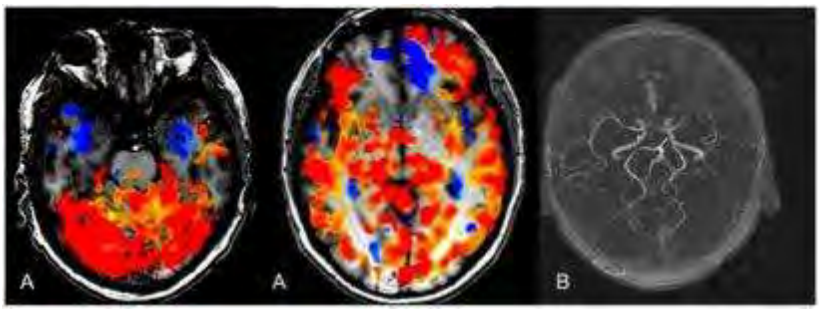

[Figure 01]

Figure 01: CVR maps with “blue” (paradoxical flow decrease with increasing CO_2 levels) obtained 36 h after SAH (A) and late MRA (9 days) showing severe vasospasm in the corresponding territories (B).

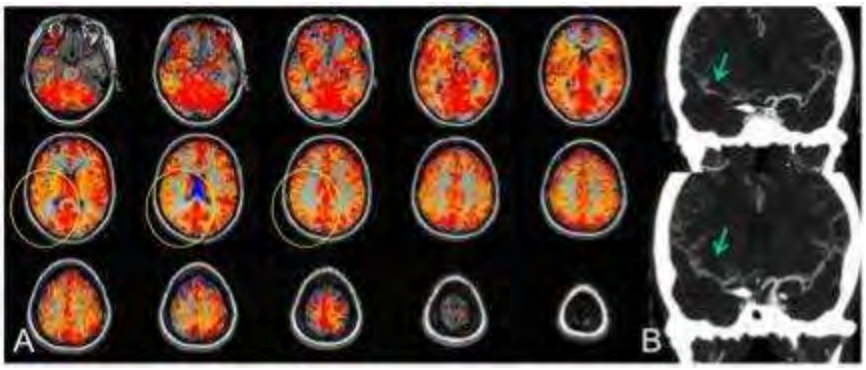

[Figure 02]

Figure 02: Decreased CVR (A - yellow circles) on the right hemisphere on day 3 post-SAH corresponding well with DNID a week later (left arm weakness) and angiographic vasospasm (B - arrows).

1243

ANGIOTENSIN AT_2 RECEPTOR STIMULATION SIX HOURS AFTER STROKE CAUSES POTENT NEUROPROTECTION IN CONSCIOUS RATS

J. Callaway[1], C.A. Mc Carthy[2], B. Broughton[2], A. Vinh[2], R.E. Widdop[2]

[1]Pharmacology, The University of Melbourne, Parkville, [2]Pharmacology, Monash University, Clayton, VIC, Australia

Objectives: Neuroprotection in stroke induced by AT_1 receptor antagonists such as candesartan, may be due to unmasking the effects of AT_2 receptor stimulation[1]. To this end we have previously demonstrated that pre-treatment with an AT_2 receptor agonist is neuroprotective independent of any changes in blood pressure[2]. Therefore, in the current study, we have examined the potential neuroprotective effect of AT_2 receptor stimulation following intracerebroventricular (icv) administration of the AT_2 receptor agonist CGP42112, initiated 6 hours after stroke in conscious spontaneously hypertensive rats (SHR).

Methods: Male SHR rats (250-350g) were stereotaxically implanted with a guide cannula above the middle cerebral artery (MCA) under ketamine/xylazine (75/10 mg/kg) anaesthesia for later administration of endothelin-1. A second cannula was implanted into the left lateral ventricle for icv drug administration. After 5 days recovery, stroke was induced in conscious rats by titrating infusion of endothelin-1 via the cannula above the MCA until stereotypical stroke behaviours were observed[3]. Experimenter was blinded to treatment. Rats were randomly allocated to one of several treatment groups prior to stroke: CGP42112 (3µg/kg/dose); CGP42112 (3µg/kg/dose) + PD123319 (104µg/kg/dose): PD123319 alone (104µg/kg/dose) or vehicle (saline) only control. Drugs were administered at 4 time points after stroke, 6, 24, 48 and 72h post stroke. Motor coordination and limb function were assessed at 24, 48 and 72h using the ledged beam test[3]. After the last behavior test, rats were transcardially perfused with PBS and brains removed and frozen. 16 µm coronal sections throughout the infarct were used for determination of infarct volume[5], neuronal survival (NeuN), microglial activation (OX42) and apoptosis (cleaved caspase-3 immunohistochemistry).

Results: Administration of CGP42112 (3µg/kg/dose centrally) at 6, 24, 48 and 72 hours after stroke induction reduced both cortical and striatal infarct volume and improved motor function. We confirmed that CGP42112 was acting via the AT_2 receptor by reversing the protection with the coadministration of an AT_2 receptor antagonist, PD123319. Furthermore, we have demonstrated that AT_2 receptor stimulation after stroke increases neuronal survival and the number of activated microglia in the core region of damage. Increased neuronal survival is likely due to a reduction in cell death. CGP42112 inhibited the number of cleaved caspase-3 positive cells in the core and peri-infarct regions.

Conclusions: Thus, the current study has shown for the first time that delayed central AT2 receptor stimulation following a cerebral incident is neuroprotective in a conscious rat model of stroke. The mechanism of neuroprotection is likely to involve improved neuronal survival.

References:

1. Lou M, Blume A, Zhao Y *et al*. *J. Cereb.Blood Flow. Metab.* 2004;24:536-547.

2. McCarthy C, Vinh A, Callaway J, Widdop R. *Stroke.* 2009;40:1482-1489.

3. Schallert T, Woodlee M, Fleming S. In: J Krieglstein (Ed.) Pharmacology of Cerebral Ischemia 2002, Medpharm Scientific Publishers Stuttgart, pp. 201-216.

4. Roulston C, Callaway J, Jarrott B *et al*. *Eur. J. Pharmacol.* 2008;584:100-110.

5. Callaway J, Knight M, Watkins D *et al*. *Stroke.* 1999. 30;2704-2712.

1244

HIPPOCAMPAL METABOLISM AS A KEY EFFECTOR MECHANISM FOR COGNITIVE EFFECTS OF BOTH INSULIN AND BETA-AMYLOID

E. McNay

Neuroscience, University at Albany, Albany, NY, USA

Background: The exact mechanism underlying cognitive deficits associated with Alzheimer´s disease (AD) remains unknown; however, both elevated levels of amyloid-derived diffusible ligands (ADDLs) and impaired brain insulin signalling are associated with AD, and ADDLs have been shown *in vitro* to impair hippocampal insulin signalling. We recently demonstrated that intact hippocampal insulin signalling is required for both optimal cognitive functioning and regulation of hippocapal glucose metabolism. Hence, we hypothesized that ADDLs may directly impair memory by attenuating hippocampal insulin signalling and, thus, metabolism. In addition, we investigated the effects of both insulin and amyloid on hippocampal blood flow *in vivo* using laser doppler flowmetry (LDF).

Methods: Rats were given either insulin, ADDLs or vehicle to the left hippocampus 10 min prior to testing in a four-arm maze using a spatial memory (spontaneous alternation) task. *In vivo* microdialysis was used to examine the impact of ADDL adminstration on local hippocampal metabolism, LDF measurements of blood flow were taken, and post mortem analyses of insulin signalling were performed.

Results: ADDL administration produced a significant impairment in memory performance, translocation of glucose transporter 4 (GluT4), and insulin signalling. Conversely, as expected, insulin administration enhanced both cognitive performance and local hippocampal metablism, as well as GluT4 translocation.

Conclusions: ADDLs act rapidly to downregulate hippocampal insulin signalling, leading directly to impaired cognitive performance. We have previously shown that impaired central insulin signalling, such as that characterising type 2 diabetes (T2DM), is associated with elevations in amyloid accumulation. Hence, mutually-opposing regulation of hippocampal metabolism by insulin and beta-amyloid may be a central component of not only normal physiological function, but the impairments seen in both AD and T2DM.

1245

SYMPTOMATIC POSTPRANDIAL CEREBRAL HYPOPERFUSION

M. Mohapl, D. Netuka, F. Kramar, V. Benes

Neurosurgery Department Central Military Hospital, Prague, Czech Republic

Background: The majority of ischemic strokes are of tromboembolic origin. However, in certain cases even minor flow redistribution may cause symptomatic cerebral hypoperfusion in some patients.

Case report: A 68-year-old right-handed Caucasian male suffered repeated ischemic attacks causing right upper extremity paresis and aphasia with incomplete restoration. Ischemic attacks occurred regularly shortly after meal consumption. Neither change of blood pressure nor heart rate changes were recorded. Clinical presentation upon admission indicated moderate weakness of the right arm and mild speech disturbance. Single photon emission computerized tomography (SPECT) with ^{99m} Tc-HM-PAO was performed. Hypoperfusion of the whole left hemisphere was found. Another SPECT examination was done during ischemic attack that occurred after meal ingestion. This investigation demonstrated further reduction of cerebral blood flow (CBF) after digestion with minimal perfusion in the territory of the middle cerebral artery (MCA). Severe stenosis of the left internal carotid artery was disclosed. The patient underwent carotid endarterectomy.

Result:

Mild improvements of motor functions and speech disturbance were observed immediately after surgery. The patient was found to be free of any ischemic attacks.. The SPECT scan, performed 3 months post-surgery, showed only slight asymmetry in cerebral perfusion. Psychological examination revealed improved cognitive functions. The patient also gained 4 kg after surgery.

Conclusion: This case report provides evidence suggesting a hemodynamic origin of ischemic attacks. Carotid endarterectomy relieved the patient's symptoms. Hemodynamics should be considered in differential diagnostics in patients with ischemic attacks.

1246

AUGMENTATION OF RESPIRATORY CAPACITY BY PYRUVATE IN NEURONS, SYNAPTOSOMES, AND ORGANOTYPIC HIPPOCAMPAL SLICES

B.M. Polster[1], P. Clerc[1], H. Hwang[1], Z. Mehrabian[1], R.A. Schuh[2,3]

[1]Anesthesiology and Center for Shock Trauma and Anesthesiology Research, [2]Department of Neurology, University of Maryland School of Medicine, [3]Research Service, Maryland VA Healthcare System, Baltimore, MD, USA

Introduction: Spare respiratory capacity, defined as the difference between basal respiration and maximal respiration in the presence of mitochondrial uncoupler, was shown to influence the ability of neurons to survive excitotoxic glutamate exposure [1,2]. Pyruvate is neuroprotective in brain injury models that involve glutamate excitotoxicity [3,4]. Furthermore, pyruvate supplementation is known to enhance uncoupler-stimulated mitochondrial O_2 consumption in synaptosomes [5] and cultured neurons [4].

Objectives: Our objectives were to 1) adapt microplate-based cell respirometry for organotypic hippocampal slices, 2) compare the spare respiratory capacity of slices to that of cultured neurons or synaptosomes, and 3) determine whether acute pyruvate addition enhances respiratory capacity in the slice model with preserved neural architecture.

Methods: The Seahorse Extracellular Flux Analyzer (XF24) was used to measure glucose-supported O_2 consumption rates from cultured forebrain neurons, plate-attached forebrain synaptosomes, or organotypic hippocampal slices cultured on nylon mesh inserts. Pyruvate (10 mM) was injected after respiration was stimulated by the uncoupler FCCP and O_2 consumption rates were monitored in real-time.

Results: Mouse organotypic hippocampal slices oxidizing glucose displayed significantly less spare respiratory capacity compared to forebrain neurons or synaptosomes. Pyruvate enhanced uncoupler-stimulated respiration in all three model systems. Pyruvate also augmented the O_2 consumption rate of forebrain neurons exposed to excitotoxic glutamate.

Conclusions: We were able to successfully adapt microplate-based respirometry for hippocampal slices, enabling improved throughput and maintained neural circuitry compared to traditional O_2 electrode-based methods. The reduced spare respiratory capacity measured in slices compared to cultured neurons or synaptosomes suggests a greater basal utilization of mitochondrial respiratory capacity. This may be due to the energy demands of spontaneous neuronal activity. However, it is also possible that the difference is due to the added presence of glia within slices. Pyruvate stimulated uncoupled respiration in all three model systems, including slices with preserved neural architecture. This finding suggests that substrate supply may limit the maximal respiration of neural cells in vivo. Finally, the ability of pyruvate to augment the respiration of forebrain neurons after excitotoxic glutamate exposure suggests that an improvement of mitochondrial substrate supply may be related to its neuroprotective potential.

References:

1. Yadava N, Nicholls DG: Spare respiratory capacity rather than oxidative stress regulates glutamate excitotoxicity after partial respiratory inhibition of mitochondrial complex I with rotenone. *J Neurosci* 2007, 27: 7310-7317.

2. Johnson-Cadwell LI, Jekabsons MB, Wang A, Polster BM, Nicholls DG: ´Mild Uncoupling´ does not decrease mitochondrial superoxide levels in cultured cerebellar granule neurons but decreases spare respiratory capacity and increases toxicity to glutamate and oxidative stress. *J Neurochem* 2007, 101: 1619-1631.

3. Izumi Y, Zorumski CF: Neuroprotective effects of pyruvate following NMDA-mediated excitotoxic insults in hippocampal slices. *Neurosci Lett* 2010, 478: 131-135.

4. Jekabsons MB, Nicholls DG: In situ respiration and bioenergetic status of mitochondria in primary cerebellar granule neuronal cultures exposed continuously to glutamate. *J Biol Chem* 2004, 279: 32989-33000.

5. Choi SW, Gerencser AA, Nicholls DG: Bioenergetic analysis of isolated cerebrocortical nerve terminals on a microgram scale: spare respiratory capacity and stochastic mitochondrial failure. *J Neurochem* 2009, 109: 1179-1191.

Supported by NIH grant NS064978 (to B.M.P.) and Rehabilitation R & D REAP (to R.A.S.) and CDA-02 Biomedical R & D grant (to R.A.S.) from the VA Research Service

1247

DAY-TIME ELEVATION OF 1.5% PER HOUR OF OXYGEN CONSUMPTION OF HUMAN BRAIN

J. Aanerud[1,2], A. Gjedde[1,3]

[1]PET Center, [2]Department of Nuclear Medicine, Aarhus University Hospitals, Aarhus, [3]Department of Neuroscience and Pharmacology, University of Copenhagen, Copenhagen, Denmark

Introduction. The reasons for the mammalian brain's need to sleep are not clear. Recent experiments suggest that the build-up of spines during the day and the scaling-down of these spines at night are the main mechanisms subserving the induction of sleep (1). From these results arise the prediction that brain energy metabolism and hence brain oxygen consumption would rise during the day and decline during the night when the need to support spine functions would abate as spines were scaled down (2-5). Measures of cerebral blood flow further show that blood flow as indicative of brain activity rises about 20% during a 20-hour wake (6), implying that brain energy metabolism could rise about 1% for every hour of wakefulness.

Methods. To test this hypothesis, we analyzed repeated PET measurements of brain oxygen consumption made with $[^{15}O]O_2$ inhalation with an interval of 2 hours in the morning in 23 healthy young volunteers of both genders.

Results. Average gray matter $CMRO_2$ rose from 162$\pm$6 mmol/hg/min to 172$\pm$6 mmol/hg/min (SEM, n=23) during the 2 hours. For 14 regions and 23 subjects, two-way ANOVA revealed significant effects of order ($P< 0.05$) and region ($P< 0.0001$) with no interaction. The average increase during the 2 hours was 2.9+0.33% (SEM) in the 14 regions.

Conclusion. The increase of brain energy metabolism averaged approximately 1.5%/hour. The reason for the increase remains unclear but the increase may be related to the support of spines constructed or reconstructed in the course of functional brain activity during the two hours. Previous evidence of glucose consumption also implies that some of the increase may be related to the actual use of carbon skeletons from glucose engaged in the physical build-up of the spines.

References.

1: Olcese U, Esser SK, Tononi G. J Neurophysiol. 2010 Oct 6. [Epub ahead of print].

2: Picchioni D, Killgore WD, Balkin TJ, Braun AR. Int J Neurosci. 2009;119(11):2074-99.

3: Horovitz SG, Braun AR, Carr WS, Picchioni D, Balkin TJ, Fukunaga M, Duyn JH. Proc Natl Acad Sci U S A. 2009 Jul 7;106(27):11376-81.

4: Picchioni D, Fukunaga M, Carr WS, Braun AR, Balkin TJ, Duyn JH, Horovitz SG. Neurosci Lett. 2008 Aug 15;441(1):81-5.

5: Fukunaga M, Horovitz SG, de Zwart JA, van Gelderen P, Balkin TJ, Braun AR, Duyn JH. J Cereb Blood Flow Metab. 2008 Jul;28(7):1377-87.

6: Balkin TJ, Braun AR, Wesensten NJ, Jeffries K, Varga M, Baldwin P, Belenky G, Herscovitch P. Brain. 2002 Oct;125(Pt 10):2308-19.

1248

INFLUENCE OF GEOMETRY OF HUMAN BRAIN CORTEX ON THE PROPAGATION OF SURFACE WAVES: RELATION TO THE CORTICAL SPREADING DEPRESSION

D. Milakara[1,2], M. Dahlem[3], G. Bohner[1], J. Dreier[2]

[1]Radiology, [2]Neurology, Charité - Universitätsmedizin Berlin, [3]Theoretical Physics Dept., Technische Universität Berlin, Berlin, Germany

Objectives: It has been suggested (Dahlem, Hadjikhani, PLoS ONE 2009, Vol 4, Issue 4) that cortical spreading depression (CSD) effect is based on reaction-diffusion of regional ion concentrations. Since the CSD has been observed in the gray matter, we conducted numerical simulation of the surface waves spreading across the cortical surface to compare clinically recorded data and the data generated in the simulation, respectively. This is attempt to localize the region(s) generating CSDs in patients suffering from aneurismal subarachnoid hemorrhage (aSAH).

Methods: During the period of 15 days, 68 CSDs were recorded in a single patient suffering from aSAH using subdural electrocorticography (ECoG). ECoG recordings were acquired continuously in 5 active channels from the 6-electrode (linear array) subdural strips. Electrode 1 served as ground while electrodes 2-6 (interelectrode distance 10 mm) were connected in sequential unipolar fashion to an amplifier, each referenced to an ipsilateral subgaleal platinum electrode. CSD was defined by the sequential onset in adjacent channels of a propagating slow potential change (SPC). A CT scan was performed during ECoG monitoring to visualize the platinum electrodes which are invisible in MRI scans. The single electrodes were then superimposed from the CT scan onto the 3D rendered brain surface of the MRI. The simulation has been conducted on the rendered cortical surface using cellular automaton, where the wave propagates on the discrete surface in form of 2-manifold mesh. The form of circular wave has been chosen for simulation. Since the spatial position of electrodes was known, this information was used for picking-up the activation signal generated in the simulation. Five points at the rim of the alleged CSD generator region have been selected as initial wave sources. Best fit was calculated by summing absolute time differences between recorded and simulated channel.

Results: The table shows best fits calculated for three different velocities 3,4 and 5 mm/sec. Since the velocity is always expressed in mm/min, the time differences is expressed in minutes.

	3 mm/min			4 mm/min			5 mm/min		
SOURCE	**#CSD best fit**	**Time difference for best fit**	**All CSDs time difference mean / std**	**#CSD best fit**	**Time difference for best fit**	**All CSDs time difference mean / std**	**#CSD best fit**	**Time difference for best fit**	**All CSDs time difference mean / std**

1	13	3.403	15.523 / 7.763	62	4.144	15.322 / 7.626	62	3.962	14.999 / 7.399
2	13	3.137	15.657 / 7.692	13	4.388	15.489 / 7.551	62	4.234	15.209 / 7.342
3	13	4.4047	15.569 / 7.564	13	5.071	15.379 / 7.430	62	4.964	15.062 / 7.273
4	13	4.199	15.411 / 7.505	13	5.184	15.182 / 7.383	62	5.601	14.800 / 7.277
5	10	3.433	15.606 / 7.575	10	4.912	15.406 / 7.540	10	5.799	15.087 / 7.605

[Table]

Conclusion: The results show certain conservatism, since only 3 of 68 CSDs are calculated best fits. The question of remaining temporal aberations might be explained with co-registration error or rounding error during simulation. Future investigation should provide the answer to that question.

1249

TISSUE-TYPE PLASMINOGEN ACTIVATOR IS AN ENDOGENOUS NEUROPROTECTANT IN THE ISCHEMIC HIPPOCAMPUS

M. Yepes[1], R. Echeverry[1], W. Haile[1], J. Wu[1,2]

[1]Neurology, Emory University, Atlanta, GA, USA, [2]Neurology, Tianjin Huanhu Hospital and Graduate School of Tianjin Medical University, Tianjin, China

Objectives: Tissue-type plasminogen activator (tPA) is a serine proteinase that activates the zymogen plasminogen into plasmin. The hippocampus is not only a brain structure critical for learning, memory and the development of navigational strategies crucial for survival, but also one of the areas of the brain with the highest levels of tPA activity. Paradoxically, the presence of tPA has been linked to neurotoxicity and cell death in the hippocampus. Thus, the goal of this study is to investigate the association between tPA and neuronal survival in the ischemic hippocampus.

Methods: To test the effect of tPA on neuronal death we used four different methods: MTT, LDH release and TUNEL assays, and trypan blue exclusion test. To study the effect of tPA on cell survival we used an *in vitro* model of hypoxic preconditioning and an *in vivo* model of ischemic preconditioning in neurons and mice deficient in either tPA or plasminogen. Akt phosphorylation and cleavage of the NMDA receptor were studied by Western blot analysis. Delayed neuronal death was studied in vivo with Cresyl violet, fluoro Jade and TUNEL staining.

Results: We found that incubation with tPA does not induce hippocampal neuronal death *in vitro* and that hippocampal areas lacking tPA activity are more vulnerable to delayed neuronal death *in vivo*. Exposure to hypoxia induces the rapid release of tPA from hippocampal neurons and incubation with tPA induces tolerance against a lethal hypoxic insult applied either immediately after (early hypoxic preconditioning) or 24 hours later (delayed preconditioning). However, whereas tPA-induced early preconditioning is independent of tPA's proteolytic activity and instead requires the engagement of a member of the low density lipopoprotein (LDL) receptor family, tPA-induced delayed preconditioning requires tPA's proteolytic activity, and is mediated by plasmin, the N-methyl-D-aspartate receptor and protein kinase B phosphorylation. Our results also indicate that treatment with tPA cleaves the NR2A sub-unit of the NMDA receptor and abrogates kainic acid-induced cell death. We also observed that endogenous tPA induces tolerance against a subsequent lethal hypoxic insult. Accordingly hypoxic preconditioning induces tolerance in wild-type but not in tPA deficient ($tPA^{-/-}$) neurons. Our results also indicate that sub-lethal ischemia *in vivo* increases tPA activity and Akt phosphorylation in the hippocampal CA1 layer, as well as ischemic tolerance in wild-type but not tPA- or plasminogen-deficient mice. Finally, inhibition of either NMDAR or Akt phosphorylation abrogates the protective effect of tPA.

Conclusions: Our work indicates that tPA is devoid of neurotoxic effects and instead it suggests that tPA is an endogenous neuroprotectant in the ischemic brain.

1250

HISTOLOGICAL CHANGES AFTER EXPERIMENTAL SAH AND CAROTID ARTERY OCCLUSION IN RATS: PERFUSION WEIGHTED IMAGING, VASOSPASM AND CLINICAL ASSESSMENT

E. Güresir[1], N. Vasiliadis[1], S. Dias[1], P. Raab[2], V. Seifert[1], H. Vatter[1]

[1]Department of Neurosurgery, [2]Department of Neuroradiology, Goethe-University, Frankfurt/Main, Germany

Objective: The time course of cerebral vasospasm and clinical changes in the rat double-SAH model are well understood. However, data of histological changes are still missing. Our objective was to determine histological changes in correlation to clinical and perfusion weighted imaging (PWI) changes in the double-SAH model of the rat.

Methods: Cerebral vasospasm (CVS) was induced by injection of 0.25ml autologous blood twice in the cisterna magna of 8 Sprague-Dawley rats with common carotid artery ligation on the left side. The animals were examined on days 2, 3, 4 and 5 and compared to the sham-operated control group without SAH (n=8). The functional deficits were graded between 0 and 3. PWI at 3 tesla magnetic resonance (MR) tomography was performed on day 5 to assess CBF. The brains were fixed, stained and evaluated for histological changes.

Results: Neurological state was significantly worsened on days 2 and 5 in rats with SAH (medians grade 2 and 3). Sham-operated animals were grade 0 at any time. The relative CBF/muscle blood ratio in rats with SAH was 3.5 ± 0.6 versus 7.9 ± 1.5 (sham, $p< 0.001$). Basilar artery (BA) diameter was 79 ± 5 µm (SAH) vs. 147 ± 4 µm (sham, $p< 0.001$). Neuronal cell count in the hippocampal areas CA1-CA4 was significantly reduced by SAH on day 5 ($p< 0.001$). In CA1 cell count was reduced from 77 ± 7 to 45 ± 4, in CA2 from 69 ± 5 to 43 ± 7, in CA3 from 54 ± 7 to 27 ± 5, in CA4 from 51 ± 6 to 31 ± 8.

Conclusions: SAH in the modified rat double-SAH model with additional carotid artery occlusion leads to vasospasm proven by PWI, neurological worsening and reduced BA diameter. Correlated to these findings, reduction of neuronal cell count in all hippocampal areas is pronounced compared to the conventional double-SAH model. Therefore, the double-SAH model of the rat seems to be an ideal model to investigate cerebral vasospasm and the resulting cerebral lesions.

1251

CHARACTERIZATION OF A MOUSE MODEL OF THROMBOEMBOLIC STROKE

S. Ansar[1], P. Heiler[2], S. Grudzenski[1], M. Fatar[1], L. Schad[2], S. Meairs[1]

[1]Department of Neurology, [2]Computer Assisted Clinical Medicine, Heidelberg University, Mannheim, Germany

Objectives: Substantial efforts have been made to understand the pathophysiologic mechanisms involved in ischemia-induced cerebral damage and to develop drugs that protect the brain from damage once a stroke has occurred. Although several treatment strategies have shown a beneficial effect in animal models of experimental ischemia, translation to major clinical trials has been poor. Apart from a multitude of factors related to poor experimental study design, the animal model itself may contribute to this lack of translation through its inability to adequately represent the pathophysiology of naturally occurring cerebral ischemia. Thus, new models may be warranted, which more closely reproduce crucial criteria of the clinical situation. The aim of the present study was to characterize a novel reproducible mouse model of thromboembolic stroke that may provide new insights into the mechanisms of ischemic stroke.

Methods: Thromboembolic stroke was induced by local injection of purified thrombin directly into the right MCA of C5 black/6J mice. Cerebral blood flow (CBF) velocity was measured continuously throughout the duration of the study by laser Doppler flowmetry. The stability of the clot was determined by investigating the time point when the clot was spontaneously dissolved. In addition, the efficiency of recombinant tissue-type plasminogen activator (rtPA) to induce thrombolysis was examined at different time points after clot formation. The effect of different concentration of thrombin (1,5 and 3 UI) and rtPA (5 and 10 mg/kg) was examined in the study. The efficiency of rtPA to induce thrombolysis and its subsequent effect on infarct volume were measured by laser Doppler flowmetry, histology and magnetic resonance imaging (MRI). MRI was performed on a 9,4 T Biospec 94/20 USR with 740 mT/m.

Results: Thrombin injection resulted in clot formation and cortical brain injury. The clot is stable up to 2 hours after the formation, subsequently 20% of the animals recanalize spontaneously. There is a significant variability in the response to rtPA at different time-points after clot formation. At 20 minutes after the clot formation, rtPA treatment results in 100% recanalization. However, rtPA-induced thrombolysis only dissolves the clot in 30% of the animals when administrated 40 minutes after the clot formation.

In addition, the infarct size depends on the concentration and manufacturer of thrombin.

Conclusion: We characterize a novel and reproducible mouse model of in situ clot formation and reperfusion, which could be used to investigate new treatment strategies to improve cerebral ischemia. We have demonstrated how important it is to carefully analyse the experimental settings in animal studies before new treatment strategies are started. The outcome of the study will depend on the selected criteria.

1252

[^{11}C]PHNO PARAMETRIC IMAGING AND TEST-RETEST STUDY IN HUMANS USING THE HRRT SCANNER

J.-D. Gallezot[1], D. Matuskey[1,2], K. Lim[1], M.-Q. Zheng[1], S.-F. Lin[1], Y.-S. Ding[1], R.E. Carson[1], R.T. Malison[2]

[1]Department of Diagnostic Radiology, [2]Department of Psychiatry, Yale University, New Haven, CT, USA

Objective: [^{11}C]PHNO is a D2/D3 dopamine receptor radioligand with preferential affinity for the D3 subtype. The goal of the study was to the evaluate the variability of [^{11}C]PHNO binding parameter estimates, as well as potential carry-over effects, using a within-day test-retest design.

Methods: Eight subjects were studied. Each subject was scanned twice for two hours using the HRRT scanner, with injections separated by at least 4 hours. 328±107 MBq of [^{11}C]PHNO were injected (mass=0.025±0.005 µg/kg). Specific activities were 83±36 MBq/nmol at the end of synthesis and 45±18 MBq/nmol at the time of injection. The metabolite-corrected arterial input function was measured. Head motion was tracked during the scan using the Vicra system. Images were reconstructed using the MOLAR algorithm with all corrections. Regions of interest (ROI) were delineated in the caudate, putamen and pallidum using the AAL template and nonlinear methods used to 'warp' subject and template MRIs. A region corresponding to the substantia nigra was also added to the template. The two-tissue compartment model (2T), MA1, SRTM and SRTM2 were tested to estimate distribution volumes (V_T) and/or binding potentials (BP_{ND}). Test-Retest variability was estimated by computing the mean and standard deviation of $\Delta V_T = 2*(V_T^{retest} - V_T^{test})/(V_T^{retest} + V_T^{test})$ and/or $\Delta BP_{ND} = 2*(BP_{ND}^{retest} - BP_{ND}^{test})/(BP_{ND}^{retest} + BP_{ND}^{test})$.

Results: The 2T model did not provide stable V_T or BP_{ND} estimates. MA1, with a t* of 30 min, was chosen to estimate distribution volumes. V_T estimates ranged from 4.6±0.8 mL/cm^3 in the cerebellum to 18.7±4.1 mL/cm^3 in the pallidum, and BP_{ND} estimates ranged from 0.4±0.1 in the thalamus to 3.1±1.0 in the pallidum (n=5). There were no systematic changes in the test and retest measures, with absolute mean ΔV_T and ΔBP_{ND} values less than 4% in all regions, while the standard deviation of ΔV_T and ΔBP_{ND} ranged form 11% to 20% (n=8) (see table for details). SRTM and SRTM2 BP_{ND} estimates were all well correlated with the gold standard MA1 BP_{ND} estimates. Both SRTM and SRTM2 BP_{ND} parametric images had low noise (see figure of representative images from a single scan). Test-retest variability of SRTM and SRTM2 BP_{ND} estimates was comparable or slightly less than that of MA1 BP_{ND} estimates.

Conclusion: Low noise parametric images of [^{11}C]PHNO binding potential can be estimated with SRTM or SRTM2. No reduction in binding in the retest scan (i.e., no carry-over effect) was observed in any brain region when scans were separated by at least 4 hours and injected mass is kept below 0.03 µg/kg. With a high-resolution scanner such as the HRRT, small structures, such as the substantia nigra, can be clearly visualized and reproducibly assessed.

	MA1	MA1	Parametric SRTM	Parametric SRTM2

Region	V_T	ΔV_T	BP_{ND}	ΔBP_{ND}	BP_{ND}	ΔBP_{ND}	BP_{ND}	ΔBP_{ND}
Cerebellum	4.6±0.8	3±20%						
Caudate	13.1±1.3	1±11%	1.9±0.5	-1±16%	2.1±0.5	-3±13%	2.0±0.5	-3±13%
Putamen	15.7±1.7	0±12%	2.5±0.4	-3±13%	2.6±0.5	-4±11%	2.6±0.5	-3±11%
Pallidum	18.7±4.1	3±14%	3.1±1.0	2±18%	3.1±1.0	2±14%	3.0±1.0	0±14%
S. Nigra	10.1±1.8	4±20%	1.2±0.6	3±20%	1.4±0.5	-1±15%	1.2±0.5	-3±16%

[Test-Retest *Table]*

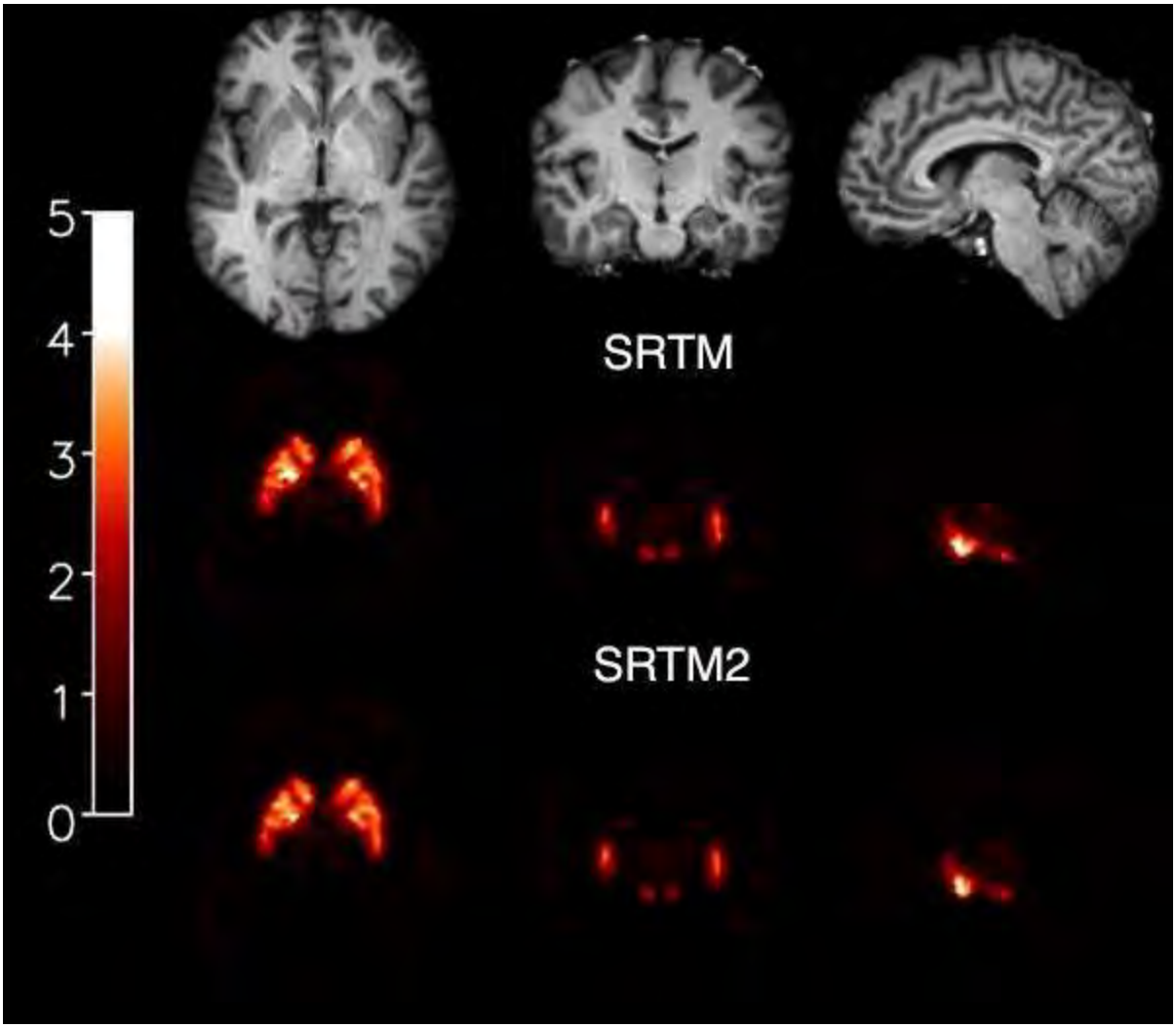

[Parametric images]

1254

SODIUM IMAGING IN ANIMAL MODELS OF CEREBRAL ISCHEMIA BY QUANTITATIVE ^{23}NA MRI

S. Ansar[1], P. Heiler[2], F. Wetterling[2], L. Tritschler[1], M. Fatar[1], L. Schad[2], S. Meairs[1]

[1]Department of Neurology, [2]Computer Assisted Clinical Medicine, Heidelberg University, Mannheim, Germany

Objectives: The use of ^{23}Na imaging in animal models of stroke is of growing interest because of its possible use as an intrinsic marker for brain integrity. The ability to accurately quantify TSC (tissue sodium concentration) in vivo could allow development of a direct bio-marker for tissue viability in stroke. The apparent diffusion coefficient (ADC) of tissue water is an established marker for initial ischemic damage to the brain. However, it is inadequate for describing stroke severity. Recently ^{23}Na MRI has been explored as a complementary MRI technique for ischemic stroke characterization and suggested as a means to determine precisely the stroke onset time for establishing patient eligibility for thrombolytic therapy. The aim of this study was to establish the ^{23}Na MRI as a diagnostic tool for stroke in experimental models of cerebral ischemia.

Methods: Two experimental animal models of stroke were used in this study; a mouse model of thromboembolic stroke and the middle cerebral artery occlusion (MCAO) in the rat. Thromboembolic stroke was induced by local injection of purified thrombin directly into the right MCA of C5 black/6J mice. The MCAO in rats was induced by the intraluminal filament occlusion technique. Magnetic resonance imaging (MRI) experiments were performed on a 9,4 T Biospec 94/20 (Bruker, Germany) USR small animal system equipped with 740 mT/m gradients. The center slice of each scan was used for further data analysis to calculate SO and $T2^*$

parameter maps.

Results: Both animal models of cerebral ischemia resulted in a significant increase of sodium concentration in the stroke regions compared to healthy tissue. The hyperintense sodium image in the infracted area correspond to the T2 weighted images and the infracted area investigated by histology.

We have demonstrated that ^{23}Na-CSI is feasible for sodium imaging at adequate resolution for the small anatomical size of the murine brain. The combination of the high field of 9.4 Tesla, the inductive coupled surface coil and the weighted ^{23}Na-CSI sequence enable a spatial resolution of 0.6 x 0.6 x 1.2 mm3. To the best of our knowledge, this is the highest reported resolution in sodium magnetic resonance imaging measured below 21 Tesla. Furthermore, the acquired data allows the calculation of S0 and T2* parameter maps and therefore a quantitative evaluation of the sodium signal change in stroke.

Conclusion: Sodium MRI is a promising diagnostic tool in stroke, since pathological processes can alter this ion gradient. It can be used as a marker for tissue death and for determining the duration of ischemia. Combined MRI data may provide a tool for preclinical testing of new treatments and may also have the potential to facilitate decision-making in the management of acute stroke patients.

1257

DISTRIBUTION AND THERAPEUTIC BENEFITS OF INTRANASALLY ADMINISTRATED HYPOXIA-PRECONDITIONED BONE MARROW STEM CELLS AFTER BARREL CORTEX STROKE

S.P. Yu, N. Wei, M. Chau, T.C. Deveau, L. Wei

Anesthesiology, Emory University School of Medicine, Atlanta, GA, USA

Objectives: Stem cell-based cell therapy has provided encouraging hope to repair damaged brain structures and stimulate regenerative mechanism in the post-ischemic brain. Most methods of cell-based therapy involve invasive administration of cells into the brain while the intravenous infusion of cells results in insufficient delivery to the brain. Moreover, the homing of transplanted cells to the injured brain region depends on migration of these cells. The present investigation explored a non-invasive intranasal route for introducing hypoxia-preconditioned bone marrow mesenchymal stem cells (HP-BMSCs) into the brain and ischemic region after the barrel cortex stroke in mice. Based on our recent investigations we predicted that hypoxic-preconditioning will promote cell survival as well as homing to the ischemic cortex (Theus et al., 2008; Francis and Wei, 2010)

Methods: BMSCs were isolated from Wistar baby rats (21 days) and preconditioned with sublethal hypoxia (0.5% oxygen) for 24 hours. Barrel cortex stroke was induced by selective ligations of branches of middle cerebral artery based upon the optical imaging of the whisker barrel cortex activities (Whitaker et al., 2007). One day post barrel cortex ischemia, adult male C57BL/6 mice were intranasally administered with Hoechst labeled BMSCs ($5x10^5$ cells/animal). Infarct size was assessed 4 days after stroke with TTC staining. Before, during and 14 days after stroke, local blood flow was measured with the Periscan system. Behavioral tests were performed before and 1 to 14 days after stroke. Expression of neurotrophic/migration factors was examined by Western blotting.

Results: Our data demonstrated hypoxia-preconditioned BMSCs significantly increased VEGF, SDF-1, CXCR4 and MMP2 expression compare to the normal oxygen cultured cells. Intranasally administrated HP-BMSCs can migrate to the ischemic region as early as 1 hour post delivery; Hoechst prelabeled BMSCs were seen in the contralateral and ipsilateral cortex and also in olfactory bulb, in and around ischemic region, primary somatosensory cortex. Delayed (24 hours after stroke) intranasal BMSCs reduces infarct volume measured 4 day after stroke, it also attenuates neurological functional deficits 4 days after stroke. Western blot analysis shows increased VEGF, BDNF, SDF-1, CXCR4 expression in ischemic brain. Two weeks after stroke the intranasal BMSCs treatment significantly improves blood flow recovery at ischemic region.

Conclusions: Intranasal administration of cells offers a non-invasive alternative method for cell-based therapy in ischemic stroke treatment. BMSCs subjected to hypoxia-precondition showed ability to migrate to the stroke area and provide neuroprotective effects and increase functional recovery after stroke.

References:

Theus MH, Wei L, Cui L, Francis K, Hu X, Keogh C, Yu SP. In vitro hypoxic preconditioning of embryonic stem cells as a strategy of promoting cell survival and functional benefits after transplantation into the ischemic rat brain. Exp Neurol. 210:656-670, 2008.

Francis, K.R. and Wei, L., Human embryonic stem cell neural differentiation and enhanced cell survival promoted by hypoxic preconditioning, Cell Death & Diseases, In press. e22; doi:10.1038/cddis.2010

Whitaker VR, Cui L, Miller S, Yu SP, Wei L., Whisker stimulation enhances angiogenesis in the barrel cortex following focal ischemia in mice. J Cereb Blood Flow Metab. 27:57-68, 2007.

1258

NEUROPROTECTIVE EFFECT OF FLUVOXAMINE IN AN MCAO RAT MODEL OF STROKE

K. Galley O'Toole[1], D. Cash[1], J. Beech[2], M. Bernanos[1], M. Lima[3], S. Williams[1]

[1]Neuroimaging, King's College London, London, [2]Radiation Oncology and Biology, University of Oxford, Oxford, UK, [3]Nucleo de Neurosciencias, Instituto de Ciencias Biologicas, Universidade Federal de Minas Gerais, Belo Horizonte, Brazil

Objectives: SSRI's, including fluvoxamine, are effective antidepressants acting via increasing serotonergic transmission in the CNS. Recently SSRI's have been shown to promote neurogenesis and neuronal cell survival, increase concentration of growth factors and even suppress inflammation - the effects that might be effective in ameliorating acute and chronic brain trauma including ischemia[1,2]. However some controversy exists over whether SSRI's are beneficial or even harmful in various types of stroke. Here we set out to test if fluvoxamine is neuroprotective in a rat model of transient focal ischemia, middle cerebral artery occlusion (MCAO).

Methods: Using stratified randomization (by weight), 28 male SD rats (380.1g ± 11.10 g) were randomly assigned to either the control (saline) or the treatment group. The middle cerebral artery (MCA) was occluded by a 5.0 intraluminal thread (Doccol Corporation, USA) under isoflurane anaesthesia (in O2/air 10:90) as previously described[3]. The reperfusion was achieved by withdrawing the thread after 60 minutes. The treatment was 25mg/kg fluvoxamine administered by 2 intraperitoneal injections: the first at 30min before occlusion and the second at reperfusion. T2W MRI images were acquired at 24 hours and 9 weeks after MCAO on a 7T MRI system. Lesions were quantified by semi-automatically countering the hyperintense lesion in the T2W images by Jim software (Xinapse systems).

Results: Lesion sizes in the control group were (mean±sd) 121±74mm^3 at 24h, and reduced to 70±64 mm3 at 9 weeks after MCA occlusion - of these 47% of animals had lesions encompassing cortical and subcortical tissue and 53% were subcortical-only (caudate-putamen), following a pattern previously described[4]. In the fluvoxamine group, the lesions were 85±56 (24h) and 32±44 (9wk), and 44% animals had full lesions. Measurement of the lesions' change over time from acute to chronic revealed a significant effect of fluvoxamine treatment in the subcortical lesion cohort (p=0.04 Man Whitney two tailed t-test, 77% reduction in fluvoxamine group vs. 57% reduction in control group).

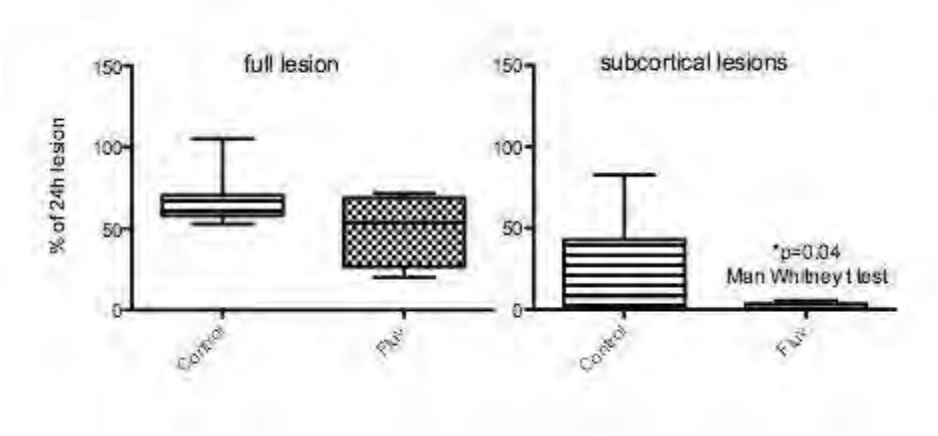

[graph]

Conclusion: Fluvoxamine showed a small but significant neuroprotective effect on reducing the size of the subcortical stroke lesions in MCAO rats. This result corroborates and substantiates the findings of improved function in experimental stroke in rodents by SSRI's.

References:

[1] Jin et al. (2009) Brain Res. 1281:108.

[2] Li et al. (2009) J Neurosci Res. 87:112.

[3] Virley et al. (2000). J Cereb Blood Flow Metab. 20(3): 563.

[4] Wegener et al. (2005) J Mag Res Imaging 21:340.

1259

EXTRACRANIAL - INTRACRANIAL BYPASS IN CEREBRAL ISCHEMIA TREATMENT

M. Mohapl, V. Benes

Neurosurgery Department, Central Military Hospital, Prague, Czech Republic

Extracranial-intracranial bypass was almost abandoned after publication of the results of ECIC bypas study in 1985 and new data from ongoing studies ith PET are awaited. Authors present long term results of series where indication for revascularisation was based on SPECT evaluation.

Material and Methods: In patients after transient ischemic attack or after non-disabling stroke and proved carotid artery ^{99}TcHMPAO SPECT in rest and after stimulation either by hypercapnia or acetazolamid was performed and patients with impaired cerebrovascular reserve capacity occlusion were considered for revascularization - 20 patients underwent extracranial - intracranial bypass. The presentig symptoms were repeated TIAs orRIND in 5 pts, minor non-disabling stroke in 15 pts, in al patients the embolic origin of their symptoms were ruled out. There was no operative mortality or morbidity, in al patients the function of bypass was proved by angiography. In all the patients the improvement of CVRC was proved by SPECT. In follow-up of 72-103 months recurrency of ischameic stroke in 2 pts was observed, in 8 pts with minor stroke presentation clinical improvement was recorded.

Conclusion: ECIC bypass is a valuable method in the treatment of strictly selected subgroup of patients with cerebrovascular occlusive disease.

1260

DYNAMICS OF MITOCHONDRIAL FISSION AND FUSION IN NEURONAL CELL CULTURE FOLLOWING OXYGEN-GLUCOSE DEPRIVATION (OGD)

E.A. Wappler, J.A. Snipes, P.V.G. Katakam, D.W. Busija

Wake Forest University School of Medicine, Winston Salem, NC, USA

Introduction: Mitochondria, containing small number of mitochondrial genes and lacking efficient DNA repair mechanisms, constantly undergo fission and fusion to optimize mitochondrial functions including ATP synthesis. However, the effects of pathophysiological stimuli and pharmacological agents on fission and fusion are not fully understood.

Objectives: To investigate the effect of oxygen-glucose deprivation (OGD) on mitochondrial (mito) fission and fusion processes in primary cultures of rat cortical neurons together with its modulation with several relevant drugs.

Methods: Primary rat cortical neurons were isolated from E18 Sprague Dawley fetuses and were plated at a density of approximately 10^6 cells/cm^2 onto poly-d-lysine coated plates or dishes. Experiments were carried out on 7-9-day old cultures, during which period the neurons expressed NMDA, α-amino-3-hydroxy-5-methylisoxazole-4-propionate, and kainate receptors and were vulnerable to OGD. Neurons were exposed to OGD for 180 min followed by up to 24 hrs of recovery. Mito dynamics were characterized by analyzing levels of mito fission [dynamin related protein-1 (Drp1)] or fusion [mitofusin-2 (Mfn2); optic atrophy-1 (OPA-1)] proteins, electron transport chain proteins, mito DNA, and mito morphology. The effects of application of the fission blocker 15d-Prostaglandin J_2 (5-20 μM) (15-d-PGJ_2) and the mito ATP-sensitive K^+ channel opener diazoxide (125-750 μM) were also investigated.

Results: 3h OGD followed by 24 hr recovery resulted in an increase in mito DNA and complex II, IV, and V proteins, and the mitochondria became enlarged in size. Fission protein Drp1 was significantly lower by the end of OGD, and was totally degraded by 6 hr of reoxygenation. The amount of fusion proteins Mfn-2 and OPA-1 also decreased significantly after OGD. 15d-PGJ_2 pretreatment dose-dependently decreased viability in control neurons, which was further decreased following OGD. Furthermore, 15-PGJ_2 treatment decreased Drp1 in controls, but increased it after OGD while changing the shape and the number of mitochondria in the neurons. Diazoxide, which was previously proved to be neuroprotective against OGD, increased the expression of protein II and Drp1, but did not change the Mfn2 expression at the 250-750 μM concentration.

Conclusions: Thus, OGD increased respiratory complex proteins and mito DNA in neurons, while levels of fission protein Drp1, fusion protein Mfn2 and OPA1 decreased. Additionally, PGJ2 treatment may promote neuronal cell death by inhibiting Drp1 in untreated and OGD conditions. Lastly, the neuroprotective effects of diazoxide may involve increased mito fission as well as previously described mechanisms (Gáspár T, Snipes JA, Busija AR, Kis B, Domoki F, Bari F, Busija DW. J. Cereb. Blood Flow Metab. 28:1090-103, 2008.

Acknowledgement: Supported by NIH grants HL-07731 and HL093554.

1261

LONG-TERM ALTERATIONS IN THE BLOOD-BRAIN BARRIER, COGNITIVE IMPAIRMENT, AND DEVELOPMENT OF ALZHEIMER-TYPE NEUROPATHOLOGY AFTER JUVENILE TRAUMATIC BRAIN INJURY

V. Pop[1], D. Sorensen[1,2], J. Kamper[3], D. Ajao[2], A.M. Fukuda[2], A. Obenaus[1,2,4], R.E. Hartman[3], J. Badaut[1,2]

[1]Pediatrics, [2]Basic Science, [3]Psychology, [4]Radiation Medicine, Radiology, Biophysics and Bioengineering, Loma Linda University, Loma Linda, CA, USA

Objectives: Clinical and animal studies suggest that traumatic brain injury (TBI) hastens the development of cognitive decline and neuropathology associated with brain aging and Alzheimer disease (AD), but the mechanisms remain unknown. In parallel, recent studies in both human AD patients and transgenic AD models have shown that a blood-brain barrier (BBB) characterized by low levels of vascular P-glycoprotein (P-gp) correlates with a high quantity of beta-amyloid (Aβ) deposition in the brain, suggesting a deficit of Aβ clearance. We evaluated how juvenile TBI alters the BBB to predispose the brain to accelerated aging and AD pathogenesis in rats.

Methods: A single TBI at post-natal day 17 in male Sprague-Dawley rats was delivered via a moderate controlled cortical impact (CCI) to the right parietal cortex overlying the hippocampus (2.7mm-diameter impactor tip, 1.5mm depth, impact coordinates: 3mm posterior, 4mm lateral to Bregma). Sham control animals were treated identically but without TBI. Morris water maze (MWM) testing (cued and spatial) was administered 30 and 60 days after injury, and brain samples for histology were collected at the final 60 day timepoint. The protein expression of P-gp, IgG, endothelial brain antigen 1 (EBA1), and Aβ neuropathology were investigated using immunohistochemistry and quantified with semi-automatic histology software.

Results: MWM testing at 30 and 60 days detected no significant differences in cued or spatial performance, or swim speed. However, an categorical analysis of the strategies used by the animals to find the platform at 60 days post-injury revealed that TBI animals used systematic, but inefficient, maze searches as opposed to relying on spatial memory like the sham controls ($p < 0.05$). At 60 days, TBI animals had globally decreased levels of P-gp and decreased levels of EBA1 (both $p < 0.05$), suggesting BBB alteration despite the absence of BBB leakage measured by IgG staining intensity. Interestingly, TBI animals exhibited diffuse extracellular Aβ plaques in multiple regions. Notably, we detected higher levels of Aβ in the temporal cortex, a region highly sensitive to age-associated Aβ accumulation in humans with AD.

Conclusions: Our research suggests that juvenile brain injury affects P-gp expression at the BBB and may impair effective clearance of toxic proteins, as suggested by increased intracerebral Aβ plaque formation. The initial injury, along with dysregulation of BBB proteins and accumulation of neuropathology may contribute to the strategy impairment in MWM. Thus, early life brain injury can permanently alter and interfere with the composition of the BBB, which may accelerate brain aging and contribute to cognitive decline.

Funded by: NIH 1R01HD061946-01 (Badaut)

1262

CILOSTAZOL ATTENUATES ISCHEMIC BRAIN INJURY AND ENHANCES NEUROGENESIS IN THE SUBVENTRICULAR ZONE OF ADULT MICE AFTER TRANSIENT FOCAL CEREBRAL ISCHEMIA

Y. Tanaka[1], R. Tanaka[2], L. Meigi[1], H. Nobutaka[1], T. Urabe[1]

[1]Juntendo University School of Medicine, Tokyo, [2]Juntendo University Urayasu Hospital, Chiba, Japan

Evidence suggests that neurogenesis occurs in the adult mammalian brain, and that various stimuli, for example, ischemia/hypoxia, enhance the generation of neural progenitor cells in the subventricular zone (SVZ) and their migration into the olfactory bulb. In a mouse stroke model, focal ischemia results in activation of neural progenitor cells followed by their migration into the ischemic lesion. The present study assessed the in vivo effects of cilostazol, a type 3 phosphodiesterase inhibitor known to activate the cAMP-responsive element binding protein (CREB) signaling, on neurogenesis in the ipsilateral SVZ and peri-infarct area in a mouse model of transient middle cerebral artery occlusion. Mice were divided into sham operated (n=12), vehicle- (n=18) and cilostazol-treated (n=18) groups. Sections stained for 5-bromodeoxyuridine (BrdU) and several neuronal and a glial markers were analyzed at post-ischemia days 1, 3 and 7. Cilostazol reduced brain ischemic volume ($P < 0.05$) and induced earlier recovery of neurologic deficit ($P < 0.05$). Cilostazol significantly increased the density of BrdU-positive newly-formed cells in the SVZ compared with the vehicle group without ischemia. Increased density of doublecortin (DCX)-positive and BrdU/DCX-double positive neural progenitor cells was noted in the ipsilateral SVZ and peri-infarct area at 3 and 7 days after focal ischemia compared with the vehicle group ($P < 0.05$). Cilostazol increased DCX-positive phosphorylated CREB (pCREB)-expressing neural progenitor cells, and increased brain derived neurotrophic factor (BDNF)-expressing astrocytes in the ipsilateral SVZ and peri-infarct area. The results indicated that cilostazol enhanced neural progenitor cell generation in both ipsilateral SVZ and peri-infarct area through CREB-mediated signaling pathway after focal ischemia.

1263

VERY EARLY-INITIATED PHYSICAL REHABILITATION PROTECTS AGAINST FOCAL ISCHEMIC BRAIN INJURY AND IMPROVED NEUROLOGICAL OUTCOME IN RATS

Z. Pengye[1], P. Hongjian[2], G. Yanqin[2], C. Jun[2,3], H. Yongshan[1]

[1]Department of Rehabilitation of Huashan Hospital, State Key Laboratory of Medical Neurobiology, Department of Sports Medicine and Rehabilitation and Institute of Brain Sciences, [2]State Key Laboratory of Medical Neurobiology and Institute of Brain Sciences, Fudan University, Shanghai, China, [3]Department of Neurology, University of Pittsburgh School of Medicine, Pittsburgh, PA, USA

Objectives: Physical rehabilitation is a clinically promising strategy for promoting neurological recovery in ischemic stroke patients. In animal studies, enforced excises initiated 5-7 days after stroke appear to be able to enhance functional recovery without affecting ischemic brain lesions. However, recent clinical data suggest that very early initiated physical rehabilitation (VEIPR) within 48 hr after stroke may offer beneficial effects in patients; whereas the evidence for a neuroprotective effect of VEIPR in experimental stroke is scant and the underlying mechanism for EIPR-afforded neuroprotection is unknown. In the present study, we have investigated the effect of EIPR on brain damage, inflammation, and neurobehavioral outcomes in a rat model of transient focal cerebral ischemia (tFCI).

Methods: tFCI was induced in adult male Sprague-Dawley rats by middle cerebral artery occlusion for 60 min, and the animals were then randomly assigned to VEIPR or non-excise groups. Beginning at 24 hr after tFCI, VEIPR was induced by enforced treadmill training on a daily basis for a maximum of 14 days. The daily excises gradually reached the full amount (12 meters/min for 30 min) at the 3rd day of VEIPR. For outcome assessments, neurological scores and sensorimotor deficits (foot fault test and adhesive remove test) were determined at 1-7 days after tFCI, while spatial learning and memory were measured by Morris water maze at 21-28 days after tFCI. In additional rats, infarct volume, brain edema (wet and dry weight), and blood brain barrier integrity (Evans blue extravasation) were assessed at 7 days after tFCI. The expression of pro-inflammatory cytokines (mRNAs) and cell adhesion proteins (ICAM and VCAM) were measured at 3 and 7 days after tFCI using real-time PCR and Western blots, respectively.

Results: Compared to non-excise stroke animals (n=8), animals received VEIPR exhibited significantly improved neurological scores and performed significantly better in the foot fault tests ($p < 0.05$ *vs.* non-excise controls, n=8), but not in the adhesive removal tests, at 4-7 days after tFCI. Animals under VEIPR also showed significantly improved working memory in Morris water maze compared to non-excise animals ($p < 0.05$, n=6/group). In consistent with the early improvement of functional outcomes, animals under VEIPR had significantly reduced infarct volume, brain water content, and blood brain barrier damage at 7 days after tFCI compared to non-excise animals ($p < 0.05$, n=6/group). Moreover, the neuroprotection afforded by VEIPR was associated with significantly reduced expression of proinflammatory cytokines (IL-1α, IL1-β, IL-6, iNOS, COX2, and TNFα) and cell adhesion molecules at 3 and 7 days after tFCI ($p < 0.05$ vs. non-excise controls, n=5/group), respectively.

Conclusion: Our results provide novel evidence that very early initiated physical rehabilitation confers marked neuroprotection against focal ischemic brain injury in rats. This neuroprotection by VEIPR is associated with the attenuation of pro-inflammatory reactions, brain edema, and

blood brain barrier damage after ischemia and reperfusion. Further work is required to elucidate the precise underlying mechanisms.

1264

TEMPORAL AND SPATIAL QUANTIFICATION OF FDG UPTAKE IN CEREBRAL ISCHEMIC LESIONS IN RELATION TO ADC LESIONS ON RAT MODEL

H. Yuan, B. Yoder, J. Nie, H. An, D. Shen, W. Lin

Radiology, University of North Carolina at Chapel Hill, Chapel Hill, NC, USA

Cerebral glucose metabolism is disturbed in ischemic stroke due to reduced glucose delivery and cascading tissue response. However, the spatial and temporal distribution of disturbed glucose metabolism under ischemic insults remains largely elusive particularly during the acute phase. While MR imaging has been employed as a means to potentially predict tissue outcomes subsequent to ischemic insults, FDG PET imaging may offer additional information to delineate tissue viability. This study aimed to quantify temporal and spatial distribution of glucose metabolism using PET in conjunction with MRI on cerebral ischemia stroke rat model.

Methods: Permanent middle cerebral artery occlusion (MCAO) was induced in rats. Animals were divided into three groups including control, 90min, and 180 min of MCAO groups. Dynamic PET imaging was acquired with F18-FDG immediately followed by MR imaging including anatomical and diffusion weighted imaging. CT imaging was also taken to facilitate registration between MRI and PET images. Ischemic lesion was first identified from the DWI/ADC MR images. ROI of ischemic core was then manually drawn on PET images in low signal regions. Ratios of FDG uptake between the ischemic core and the homologous regions in the contralateral hemisphere were measured. Compartmental model was developed to calculate the time constants k1 (indicating perfusion level), K2 (back flux) and K3 (phosphorylation) in ischemic core and normal tissue. Patlak graphical analysis was used to produce a map of K-trans constant. The k-trans map and apparent diffusion coefficient (ADC) map were compared after registering PET/MRI images.

Results: In all three groups, significant reduction of FDG uptake was observed in ischemic core in both 90min and 180min MCAO animals with the reduction ratio of 35.5+/-10.5% and 49.0+/-12.2%, respectively. The dynamic curves showed that FDG uptake reached plateau 5min post injection in the control group as well as the contralateral hemisphere in the ischemic groups. However, FDG uptake continued to increase in the ischemic tissue in both ischemic groups throughout the 45min imaging time, although the overall uptake level was lower than that of the normal brain tissue. Results from the compartmental model further showed almost two times decrease in K1 in ischemic core of 90min and 180min group, indicating reduced perfusion in MCAO animals. On the contrary, K3 was much higher in the core of the 90min and 180min MCAO rats when compared to the contralateral tissue. Interestingly, both PET images and Patlak k-trans map showed a hyper-uptake band surrounding ischemic core in 90min MCAO rats with a large ischemic lesion. However this hyper-uptake band was not observed in 180min MCAO animals or 90min MCAO animals with smaller subcortical lesions. Although results showed no significant correlation between PET and ADC map, the hyper-uptake band was clearly within the ADC lesion and on the edge of the ADC lesion.

Conclusion: Spatially heterogeneous and temporally progressed FDG uptakes were observed in ischemic rats. In particular, a hyper-uptake band surrounding ischemic core but within the ADC lesion suggests that a combination of both FDG PET and MRI may offer additional insight into ischemic lesion.

1265

PRO-ANGIOGENIC EFFECTS OF RESVERATROL IN BRAIN ENDOTHELIAL CELLS: NITRIC OXIDE-MEDIATED REGULATION OF VASCULAR ENDOTHELIAL GROWTH FACTOR AND METALLOPROTEINASES

F. Simao[1], C.G. Salbego[2], E.H. Lo[1]

[1]Neurology and Radiology, Harvard Medical School, Charlestown, MA, USA, [2]Biochemistry, Federal University of Rio Grande do Sul, Porto Alegre, Brazil

Objectives: Modulating the sirtuin signaling pathway with resveratrol (RSV) is a powerful way of protecting the brain against a wide variety of stress and injury. Recently, it has been proposed that RSV not only reduces brain injury but also promotes recovery after stroke. Resveratrol has been shown to function as a nodal point of converging signaling pathway in endothelial cells to regulate vessel growth, but the signaling mechanisms determinant for angiogenesis is unknown. In the present study, we test the hypothesis that RSV promotes angiogenesis in brain endothelial cells by activating the NO/VEGF/MMPs signaling axis.

Methods: A human brain endothelial cell line was stimulated with resveratrol (0.1-10 uM) and cell proliferation, migration and tube formation were measured as in vitro assays of angiogenesis. Conditioned medium was used to measure responses in NO, VEGF and MMPs. Akt, ERK, eNOS, VEGF and VEGFR2 expression was measured with western blots.

Results: Treatment of cerebral endothelial cells with RSV promoted proliferation, migration and tube formation in Matrigel assays. Consistent with these pro-angiogenic responses, RSV altered endothelial morphology resulting in cytoskeletal rearrangements of beta-catenin and VE-cadherin. These effects of RSV were accompanied by activation of PI3-kinase/Akt and ERK MAP kinase signaling pathways that led to eNOS upregulation and increased NO levels. Subsequently, elevated NO signaling increased VEGF and MMP levels. Sequential blockade of these signaling steps prevented RSV-induced angiogenesis in cerebral endothelial cells.

Conclusions: Our findings suggest that RSV activates PI3-kinase/Akt and ERK MAP kinase signaling pathways that upregulate eNOS and increases extracellular levels of VEGF and MMPs. These findings provide a mechanistic basis for the potential use of RSV as a candidate therapy to promote angiogenesis and neurovascular recovery after stroke.

1267

RNA INTERFERENCE AGAINST AQUAPORIN-4 PREVENTS EDEMA FORMATION AFTER JUVENILE TRAUMATIC BRAIN INJURY

J. Badaut[1,2], A. Adami[3], D. Sorensen[1,2], V. Pop[1], L. Huang[4], S. Ashwal[1], A. Obenaus[1,3,4]

[1]Dpt. of Pediatrics, [2]Dpt. of Physiology, [3]Dpts. of Radiology and Radiation Medicine, [4]Dpt. of Biophysics, Loma Linda University, Loma Linda, CA, USA

Aim: Traumatic brain injury (TBI) is a leading cause of death and a permanent disability in infancy and childhood. The brains of young animals have more water content than adult animals and as a result the juvenile brain typically swells more than the adult brain after TBI. We recently developed a method using siRNA against the aquaporin 4 (AQP4), a water channel, to decrease its expression *in vivo*. The aim of this study was to determine if injection of the siRNA against AQP4 could prevent the edema formation and improve behavioural outcomes after juvenile-TBI.

Methods: We carried out a moderate controlled cortical impact (CCI) injury to the right parietal cortex (CCI, 2.7mm-diameter impactor tip, 1.5mm depth; impact coordinates: 3mm AP, 4mm ML) in 17-day-old rats. RNAi was performed using specific small interference RNA against AQP4 (400ng/4ul) and a non-targeted-siRNA (siGLO, 400ng/4ul) as a control. Silencing RNA was injected into the cortical tissue adjacent to the TBI-induced lesion. Lesion volumes at 1, 3, and 7 days post-injury were quantified using T2-weighted MRI. Edema formation and alterations in water diffusion in the rats were studied via T2-weighted and diffusion-weighted imaging (T2WI, DWI). Motor function and behavioral outcomes were measured at 1, 3 and 7 days post-injury (dpi) using: (i) beam balance and foot-fault (sensorimotor, coordination, and proprioception) and (ii) rotarod (sensorimotor coordination and balance) tests.

Results: *In vivo*, control injections of non-targeted siRNA (siGLO) tagged with CY3 revealed positive staining in GFAP-labelled astrocytes, showing an efficient transfection. MRI derived lesion volumes, with 2.5% of average, were not significantly changed between the siGLO and siAQP4 treated juvenile-TBI rats at 1, 3 or 7 days. The siAQP4 treatment injected at 10 min after CCI reduced edema levels by 28% (T2-MRI) and decreased water mobility by 47% in the injured cortex. The effects of siRNA on T2 values in the injured cortex were maintained at 3days after CCI, with 64% decrease in siAQP4 compared to siGLO animals. At distance from the impact site, the T2 and ADC values were not significantly altered. In addition, the decreased edema within the tissue at 1 and 3 days correlated with improved motor functions. The number of foot-faults were significantly decreased in siAQP4 vs siGLO rats ($p< 0.05$) at 1d and 3d after CCI. Similarly, the time spent on the rotarod was increased in siAQP4 compared to siGLO treated rats ($p< 0.05$). Overall, motor functions were improved by inhibition of the AQP4 expression.

Conclusions: Our findings demonstrate for the first time that *in vivo* injection of siAQP4 prevented edema formation after juvenile TBI which correlated with behavioral improvements.

Supported by the Swiss Science Foundation (FN 31003A-122166), NIH 1R01HD061946-01, NMTB 2000-180

1268

INTRANASAL ADMINISTRATION OF CRGP ALLEVIATES CEREBRAL VASOSPASM AND PROMOTES VEGF EXPRESSION FOLLOWING EXPERIMENTAL SUBARACHNOID HEMORRHAGE

B.-L. Sun[1], F.-P. Shen[2], M.-F. Yang[3], H. Yuan[4], F.-M. Xie[4]

[1]Key Laboratory of Cerebral Microcirculation at the Universities of Shandong, Department of Neurology, Affiliated Hospital of Taishan Medical University, Tanan, [2]Department of Neurology, Longnan Hospital of Daqing Oil Field General Hospital Group, Daqing, [3]Key Laboratory of Cerebral Microcirculation at the Universities of Shandong, Taishan Medical University, [4]Affiliated Hospital of Taishan Medical University, Taian, China

Objectives: The purpose of this study is to investigate intranasal administration of extrinsic calcitonin gene-related peptide (CGRP) whether or not to reverse cerebral vasospasm (CVS) following subarachnoid hemorrhage (SAH).

Methods: Using wistar rats as experimental animal, subarachnoid hemorrhage (SAH) models of Wistar rats were established by double injection of autologus arterial blood into cistema magna. Animals were divided into normal control group, SAH group and intranasal administration of CGRP plus SAH group. Dynamic changes of regional cerebral blood flow (rCBF) within 12 hours were detected. Diameters of basilar artery were measured and immunohistochemical staining and RT-PCR for VEGF protein and VEGF mRNA expression were used 72 hours after second cisternal injection of blood.

Results: Above parameters did not altered significantly in rats of normal control group during the experiment. However, in SAH group, rCBF reduced immediately after induction of SAH, reached nadir at 1 hour, persisting at low levels within 12 hours. Diameters of basilar artery significantly decreased, VEGF protein and VEGF mRNA expression increased 72 hours after induction of SAH in rats of SAH group. The decrease of rCBF and decrease of diameters of basilar artery in rats of intranasal administration of CGRP plus SAH group were not so obvious as in rats of SAH group. VEGF protein and VEGF mRNA expression increased more significantly increased in rats of intranasal administration of CGRP plus SAH group were not so obvious as in rats of SAH group.

Conclusions: Intranasal administration of CGRP reverses CVS and secondary ischemic cerebral injury following SAH in rats by improving cerebral blood perfusion and angiogenesis.

1270

EXERCISE STRENGTHENS THE BLOOD-BRAIN BARRIER PRIOR TO TRAUMATIC BRAIN INJURY

V. Pop[1], D. Sorensen[1,2], K. Castellanos[1], J.S. Coats[3], R.E. Hartman[4], T. Garland, Jr.[5], A. Obenaus[1,2,3], J. Badaut[1,2]

[1]Pediatrics, [2]Basic Science, [3]Radiation Medicine, Radiology, Biophysics and Bioengineering, [4]Psychology, Loma Linda University, Loma Linda, [5]Biology, University of California-Riverside, Riverside, CA, USA

Objectives: Exercise following traumatic brain injury (TBI) has been reported to provide cognitive benefits in humans and improve behavioral outcomes in rodents. Forced exercise pre-conditioning studies in rat models of stroke have shown beneficial effects, such as reduced stroke volume and strengthening of the blood-brain barrier (BBB) through thickening of the basal lamina. However, pre-injury exercise has not been studied in TBI. We evaluated whether exercise prior to TBI in mice may be protective at a behavioral and cellular level.

Methods: We used High Runner (HR) mice genetically selected for high levels of voluntary wheel-running for 57 generations and compared them to non-genetically selected control (C) mice. Sedentary C groups were kept in standard cages, while HR mice received two weeks of pre-injury exercise in cages with attached wheels for voluntary running (thus minimizing potential stress effects of forced exercise paradigms). A single TBI was induced using a moderate controlled cortical impact (CCI) injury at the level of the hippocampal formation (5 mm craniotomy, 3 mm impact diameter, 1.5 mm depth, 5 m/sec speed, 100 msec dwell time). In the first week post-TBI, the injury was evaluated using T2-weighted magnetic resonance imaging (MRI) and animals were tested for general activity and sensorimotor function on balance beam and open field. Brain samples for histology were collected at two weeks post-injury and protein expression for IgG and glial fibrillary acidic protein (GFAP) were investigated using immunohistochemistry and quantified with semi-automatic histology software.

Results: At 3 days post-injury, MRI revealed that exercised mice had a significant 34% reduction in lesion volume compared to sedentary mice ($p=0.003$). MRI-derived T2 maps showed a significant reduction in edema at regions distant from the impact site, namely at the temporal cortex and hippocampus ($p< 0.05$), with no changes in edema detected in the lesional or perilesional areas. Behaviorally, exercised animals exhibited increased activity during open field testing ($p=0.02$), as well as improved motor function on balance beam that correlated inversely with reduced lesion volume ($p=0.011$). For histology at two weeks after TBI, exercised animals had significantly lower IgG staining indicative of a less permeable BBB ($p< 0.05$), as well as decreased GFAP staining suggesting fewer reactive astrocytes.

Conclusions: Our results indicate that pre-injury exercise can be neuro-protective by being vaso-protective, as suggested by lower lesion volume and edema, improved motor function, and a stronger BBB with decreased IgG leakage and reduced glial scar formation. While the genetic selection of HR animals may play a role, our data indicate that exercise maintains the normal integrity of the brain's vascular network to provide a more resistant interface in response to TBI, thus maintaining adequate nourishment of neurons in the surrounding environment.

Funded in part by: NIH 1R01HD061946-01 (Badaut), NSF IOB-0543429 (Garland), DCMRP # DR080470 (Obenaus)

1271

NEURONAL DELETION OF CASPASE 8 PROTECTS AGAINST BRAIN INJURY IN MOUSE MODELS OF CONTROLLED CORTICAL IMPACT AND KAINIC ACID-INDUCED EXCITOTOXICITY

S. Krajewski[1], Z. You[2,3], J. Rong[1], C. Kress[1], X. Huang[1], J. Yang[2,4], T. Kyoda[1], R. Leyva[1], S. Banares[1], Y. Hu[5,6], M.J. Whalen[2], L. Salemena[7,8], R. Hakem[7], B.P. Head[5], J.C. Reed[1], M. Krajewska[1]

[1]Program on Apoptosis & Cell Death, Sanford-Burnham Medical Research Institute, La Jolla, CA, [2]Neuroscience Center, Harvard Medical School, Charlestown, [3]Tufts University Sackler School of Graduate Biomedical Sciences, Boston, [4]Department of Radiology, Massachusetts General Hospital & Harvard Medical School, Charlestown, MA, [5]Department of Anesthesiology, University of California, San Diego, [6]VA San Diego Healthcare System, La Jolla, CA, USA, [7]Department of Medical Biophysics, Ontario Cancer Institute, Toronto, ON, Canada, [8]Beth Israel Deaconess Medical Center, Boston, MA, USA

Acute brain injury is an important public health problem worldwide. Multiple lines of evidence demonstrate a critical role for caspases in neuronal cell death. Given the critical position of caspase 8 at the crossroads of cell death pathways, we generated a new viable mouse line (Ncasp8$^{-/-}$), in which the gene encoding caspase 8 was selectively deleted in neurons by *cre-lox* system. For deletion of the *caspase 8 (casp8)* gene specifically in neurons, homozygous *casp8*-floxed mice (*casp8*$^{fl/fl}$) were bred with pan-neuronal CRE3 (Banares et al., 2005), the homozygous transgenic mice line of FVB/N background. Deletion of caspase 8 reduced rates of neuronal cell death in primary cortical cultures and in whole brain organotypic coronal slice cultures (BOCSC) prepared from young adults and cultivated up to 72 h *in vitro*. Representative slices at bregma levels from -1.22 to 3.08 were maintained in culture for 72 hours, and then treated with TRAIL (Calbiochem, La Jolla, CA, USA) at 250 ng/mL for 4 h. Following treatment, the slices were fixed in Z-fix solution and processed into paraffin blocks, sectioned and immunostained. A protective role of caspase 8 deletion in vivo was also demonstrated using a controlled cortical impact (CCI) model of traumatic brain injury (TBI) and seizure-induced brain injury caused by kainic acid (KA). In the TBI model, homozygous deletion of caspase 8 resulted in reduced lesion volumes, improved post-injury motor performance (wire grip, beam walk), decreased apoptosis, diminished proteolytic processing of caspases and caspase substrates, and less neuronal cell loss and degeneration. In the KA model, Ncasp8$^{-/-}$ mice demonstrated superior survival, reduced seizure severity, less apoptosis, and reduced caspase 3 processing. Thus, neuron-specific deletion of caspase 8 reduces brain damage and improves post-traumatic functional outcomes, suggesting an important role for this apical caspase in the pathophysiology of brain trauma.)

All morphometric analyses in this study were done using scanning system and image analysis algorithms; the cutting edge technology of image analysis. By employing virtual images of hundreds of brain coronal sections, we were able to perform morphometry of histo- and immunostainings on entire brain sections or selected regions in an unbiased manner.

1272

HYPERGLYCEMIA AFTER TRAUMATIC BRAIN INJURY CAN BE NEUROPROTECTIVE

R. Sutton, N. Moro, S. Ghavim, N.G. Harris, D.A. Hovda

Department of Neurosurgery, David Geffen SOM at UCLA, Los Angeles, CA, USA

Objectives: The impact of hyperglycemia (HG) after traumatic brain injury (TBI), and even the administration of glucose to head injured patients, remains controversial [1,2]. This study determined effects of single or multiple bouts of mild HG on neuronal injury and regional cerebral metabolic rates of glucose (rCMRG) after experimental TBI.

Methods: Adult male Sprague-Dawley rats (n>8 /group) underwent surgery to induce sham injury or left cortical contusion injury (CCI), followed by injection (i.p.) with either 8% saline (Sal) or 50% glucose (Glc, 2g/kg) immediately (1X) or at 0, 1, 3 and 6 h (4X) post-surgery. At 24 h rCMRG (µmol/100g/min) were assessed in 8 cortical and 10 subcortical regions of interest (ROI) using ^{14}C-2DG procedures and alternating tissue sections were stained for Fluoro-Jade B (FJB) to quantify neuronal damage in cortex and hippocampus.

Results: Dead/dying neurons (Mean ± SEM) in the ipsilateral midline peri-contusional cortex and the ipsilateral hippocampus (hilus and CA3) were significantly reduced (p's< 0.05) in the CCI-Glc 1X and CCI-Glc 4X groups compared to Sal-treated groups (see Table). In all CCI groups rCMRG was reduced significantly compared to sham operates in ipsilateral cortex remote from the impact site (11-20% in prefrontal, entorhinal cortex) and in cortex proximal to the injury site (30-50% in peri-contusional, auditory and occipital cortex) and in ipsilateral hippocampus and thalamic regions. Statistical analyses are ongoing, but for all ipsilateral ROI analyzed to date, there has been a significant effect of Injury (Sham vs. CCI, p's< 0.05), but no effect of Treatment and no Injury X Treatment interaction.

Table. FJB-positive cell density counts (neurons/mm^2) 24 h post-injury.

CCI-Sal 1X CCI-Glc 1X CCI-Sal 4X CCI-Glc 4X

48.1 ± 6.9; 26.0 ± 7.6*; 50.6 ± 13.3; 28.0 ± 9.2* Cortex

59.6 ± 5.8; 30.6 ± 5.2**; 66.6 ± 6.6; 44.5 ± 4.4* Hilus

105.9 ± 11.8; 52.2 ± 9.2**; 15.4 ± 13.1; 54.8 ± 4.9** CA3

*p< 0.05, **p< 0.01 versus CCI-Sal counterparts

Conclusions: Single or multiple episodes of HG acutely (0-6 h) after TBI confers neuroprotection, but exogenous glucose does not appear to affect rCMRG 24 h after injury. These neuroprotective effects suggest that the increased availability of glucose may satisfy increased energy demands acutely after TBI [3], but it does not prevent the metabolic depression induced by TBI. Further research is needed in this area given the recent trend towards tight glycemic control in TBI patients [4].

References: [1] Hill J. et al., 2010, J. Neurotrauma. [2] Meierhans R. et al., 2010, Crit. Care. [3] Lee S.M. et al, 1999, Ann. N.Y. Acad. Sci. [4] Vespa P.M. 2008, Crit. Care.

Support: NINDS P01NS058489 and UCLA Brain Injury Research Center.

1273

APPLICATION OF 18F-FDG, 18F-FLT AND 18F-FET PET IN PATIENTS WITH GLIOMA

S.Q. Park[1], S.H. Sheen[2], H.S. Hwang[2], C.H. Rhee[3], B.I. Kim[4]

[1]Neurosurgery, Soonchunhyang University, College of Medicine, Seoul, [2]Neurosurgery, Hallym University, College of Medicine, Chuncheon, [3]Neurosurgery, [4]Nuclear Medicine, Korea Cancer Center Hospital, Seoul, Republic of Korea

Purpose: 18F-FDG is the most widely used tracer for oncologic PET imaging. However, because of the high glucose metabolism in normal brain tissue FDG is not the ideal tracer for the detection of glioma. The aim of this study was to compare with the differences of 18F-FDG, fluoroethyl tyrosine(18F-FET) and fluorothymidine(18F-FLT) PET for detection of glioma.

Material and methods: Twenty nine patients(high grade: low grade=22: 7) who were newly diagnosed(n=5) or suspicious of recurrence(n=24) were included in this retrospective study. Brain MRI with Gd enhancement was performed and then FLT, FET and FDG brain PET were succeeded within 1 week for all patients. ROIs corresponding to Gd enhancement in MR were manually drawn on each PET scan. Then, maximal SUV(SUVmax) and the respective ratio to the background(BG) were measured. Sensitivity for each modality were evaluated. Abnormal Gd enhancement in MR and abnormal tracer uptake greater than BG on PET scan were regarded as viable tumor.

Results: Histological confirmation was performed in 7(newly diagnosed in 5) of 29 patients, and 22 of 29 patients were clinically follow up. Among 24 patients who were suspicious of recurrence, 18 patients were recurred. In all patients, each sensitivity of FDG, FLT, FET PET and MRI were 55%, 85%, 100% and 100%, and each specificity were 100%, 100%, 50% and 67%. In recurred patients with FDG positive, sensitivity of FLT, FET and MRI was 100%. In recurred patients with FDG negative, sensitivity of FLT was decreased to 77%. Mean SUVmax of FLT, FET and FDG were 1.26, 2.20 and 6.08. Mean tumor to BG ratio of FLT, FET and FDG were 4.00, 1.90 and 1.17, In recurred patients, mean tumor to BG ratio of FET had statistically significant differences between high grade and low grade(tumor to BG ratio, 2.15 vs. 1.71; p=0.049) but mean tumor to BG ratio of FDG and FLT had no significant differences.

Conclusion: Tumor to BG ratio of FET could be useful in grading of glioma. When the decision of recurrence with MRI is difficult, combination of FLT and FET PET could be useful, considering sensitivity, specificity and image contrast.

1274

AUTOMATED FUZZY C-MEANS CLUSTER ANALYSIS RELIABLY IDENTIFIES ISCHEMIC BRAIN IN DYNAMIC CONTRAST ENHANCED CT IMAGING

D. Lelli[1], C. Gomez-Laberge[2], M. Bussiere[1], S. Chakraborty[3], M. Sharma[1], M.J. Hogan[1]

[1]Medicine (Neurology), University of Ottawa, [2]Neuroscience Program, Ottawa Hospital Research Institute, [3]Diagnostic Imaging, University of Ottawa, Ottawa, ON, Canada

Objectives: CT perfusion (CTP) is an important aspect of acute stroke imaging that allows model based calculation of cerebral blood flow (CBF), cerebral blood volume (CBV) and time-to-peak (TTP) maps that represent brain tissue perfusion. Acute clinical decisions are often based on the inferred perfusion status of brain tissue. Current technologies require manual identification of arterial regions of interest to extract the contrast input curves that generate the CTP maps. We seek to develop a method that requires no a priori model of tissue perfusion and automatically extracts segments of brain tissue that have significantly different perfusion states. Fuzzy c-means clustering, a method of analyzing data for groups (clusters) that behave similarly with respect to a measure of similarity (distance metric), is our chosen method.

Methods: Our CTP data is generated from subjects with acute onset of stroke before treatment with thombolysis or revascularization. Contrast material is injected and two 512 by 512 pixel axial slices of the head are scanned every 0.5 seconds for 45-50 seconds, generating a 4D dataset. The raw data is pre-processed to realign the skull over time and isolate brain parenchyma. We then analyze this 4D CTP data with a fuzzy c-means clustering algorithm using the Pearson correlation as a distance metric (EvIdent, National Research Council of Canada, Winnipeg, MB, Canada). This segments the data into clusters that meaningfully differ from one another in how they respond to intravenous contrast over time. We then analyze each cluster´s aggregate perfusion curve to determine TTP and relative CBV and attempt to identify normal, ischemic and infarcted tissue. Final infarcts are confirmed with follow up plain CT scans.

Results: In scans of 13 subjects with acute stroke, the automated analysis identified the ischemic hemisphere in 13 scans (100%). Aggregation of the data points not belonging to other clusters revealed a region of tissue in the ischemic hemisphere that had little response to contrast. This was identified in 12 scans (92%), and was felt to represent infarcted tissue. The volume of the identified infarcted tissue correlated well with the final infarct seen on follow up CT scans ($r = 0.99$). The only scan on which an infarct was not apparent on follow up CT also did not have an infarct identified with our analysis. In 4 scans (31%), a cluster of uncertain significance was identified.

Conclusions: Model free clustering with fuzzy c-means can identify normal, ischemic, and infarcted tissues in acute stroke. The multiple clusters identified may represent tissue with varying risk of infarction and may help clinical decision making in acute stroke. Future research directions include integrating other metrics into the clustering distance measure, such as contiguity and Euclidean distance, and using entirely different clustering algorithms. In addition, the inclusion of larger numbers of concurrent axial slices may improve the detection of clusters. These strategies may allow the discovery of other clusters of tissue that could be of significance in clinical decision making.

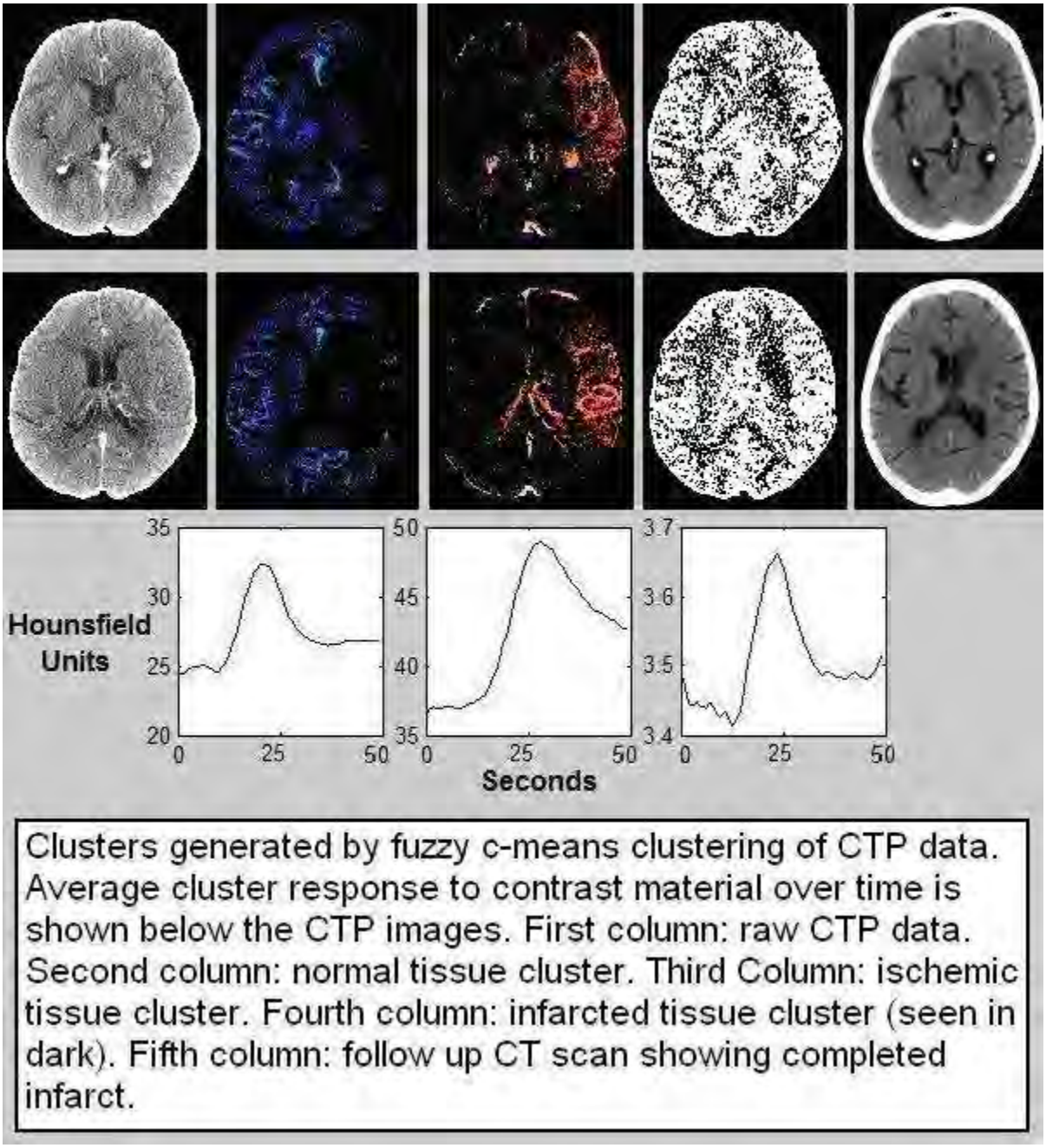

Clusters generated by fuzzy c-means clustering of CTP data. Average cluster response to contrast material over time is shown below the CTP images. First column: raw CTP data. Second column: normal tissue cluster. Third Column: ischemic tissue cluster. Fourth column: infarcted tissue cluster (seen in dark). Fifth column: follow up CT scan showing completed infarct.

[Clusters identified in a subject with acute stroke]

1275

POST-ISCHEMIC XENON NEUROPROTECTION IN A PHYSIOLOGICALLY CONTROLLED LONG-TERM TEMPORARY MCAO OUTCOME RAT MODEL: POTENTIAL MILD HYPOTHERMIA ADJUNCT

H. Sheng[1], P. Sheng[2], M. Maze[3], N.P. Franks[4], R. Pearlstein[5], **D. Warner**[1]

[1]Anesthesiology, Duke University Medical Center, Durham, [2]University of North Carolina at Chapel Hiill, Chapel Hill, NC, [3]Anesthesiology, University of California, San Francisco, CA, USA, [4]Biophysics, Imperial College London, London, UK, [5]Surgery, Duke University Medical Center, Chapel Hill, NC, USA

Objective: Xenon is a nobel gas proven to provide neuroprotection through antagonism of the NMDA receptor glycine-recognition site. Xe efficacy has not been evaluated in the context of post-MCAO treatment. Xe offers advantages including rapid BBB penetration, absence of effects on blood and intracranial pressure and negligible metabolism. Xe is not psychotomimetic and does not promote apoptosis. At high concentrations Xe is an anesthetic, but at lower concentrations sedation is minimal. We performed a series of studies to define Xe efficacy in a temporary MCAO post-treatment paradigm.

Methods: Rats were subjected to 70 min awake MCAO with pericranial temperature held at 37.5°C. At 90 min post-MCAO, rats were restrained by harness in a closed gas system with servoregulation of pericranial temperature and Xe, O_2, and N_2 concentrations. Saline was infused at 1 ml/hr IV. Rats were randomly assigned to experimental groups. **Dose-Response** (n=12-13): Rats breathed 0, 15%, 30% or 45% Xe in 30% O_2/balance N_2 for 20 hrs. **Treatment Duration** (n=15-17): Rats breathed 30% O_2 in N_2 or 30% Xe for 0 8, 20 or 44 hrs. Neurological function (scores = 0-48, 0=no deficit, Kruskal-Wallis) and infarct volumes (1-way ANOVA) were evaluated, with investigator blinded to group, at 7 days post-ischemia. **Hypothermia Adjunct** (n=19-20): Rats breathed 30% Xe in 30%O_2/40%N_2 or 30%O_2/70%N_2 for 20 hrs while normothermic (37.5^{o}C) or mildly hypothermic (36^{o}C). Outcome was assessed at 4 weeks.

Dose-Response Results. There were no differences for peri-ischemic glucose, MAP, blood gases or Hct. A U-shaped dose-response was observed. A main effect was present (P=0.023). Total cerebral infarct sizes for 0, 15, 30, and 45% Xe were 212±27, 176±55, 160±32, and 198±54 mm^3, respectively. Between group differences were present (P< 0.05) for 0% vs. 15%, 0% vs. 30% and 30% vs. 45% Xe. Reduced infarct size was present in both cortex and subcortex. Neurologic scores followed a similar pattern: 0, 15, 30, and 45% Xe = 18±2, 14±5, 12.5±5.5, and 14±6.5 (P=0.002), respectively. Moderate sedation was observed at 45%Xe, but not lower doses. **Treatment Duration Results:** A main effect was absent for infarct size (0, 8, 20, and 44 hrs Xe=209±46, 169±36, 168±54, and 170±35 mm^3, respectively, P=0.09), but neurologic score improved (P=0.002) at all Xe exposure durations (0, 8, 20, and 44 hrs Xe exposure = 17±4, 12.5±5, 14±5.5, and 14±6.5, respectively). With Xe treatment duration collapsed, cerebral infarct size was decreased versus 30% O_2/70% N_2 (209±46 vs. 169±54 mm^3, P=0.009).

Hypothermia Adjunct Results: A main effect was present for group (P=0.01). Hypothermia alone decreased infarct size. This was enhanced (P=.04) by Xe (37.5/No Xe = 224±51, 36.0/No Xe = 177±72, 37.5+Xe = 212±76, 36.0+Xe = 157±82 mm^3). Neurologic scores had a similar pattern (P=0.003).

Conclusions: Delayed Xe neuroresuscitation onset reduced infarct volume and improved

neurological function. 30% Xe offered optimal efficacy without observable sedation. Xenon exposure >8hrs did not impact efficacy. Xe served as a therapuetic adjuvant to mild hypothemia with long-term efficacy. Post-ischemic Xe therapy may have clinical potential and should be explored as a bridge to thrombolysis.

1276

INFLAMMATORY RESPONSE AFTER INJURY IN THE RAT CNS - MACROPHAGES AT THE INJURY SITE EXHIBIT DIFFERENT PHENOTYPES

C. Loy[1,2], J. Favaloro[1,2], V. Perreau[3], M. Porritt[1], S. Dieni[1], M. Katz[1], P.E. Batchelor[1,2], D.W. Howells[1,2]

[1]Medicine, University of Melbourne, [2]Florey Neuroscience Institutes, [3]Neurogenomics and Neuroproteomics Platform, University of Melbourne, Melbourne, VIC, Australia

Introduction: Macrophages, the first cells to respond to injury, have been studied extensively, and are recognized as highly dynamic and heterogeneous cells. They exhibit different phenotypes, changing and responding to environmental fluctuations. Macrophage behaviour has a dual role in the aftermath of injury. In the injured mammalian CNS, macrophages have been implicated in both exacerbating, and ameliorating damage to tissue at the injury site. They produce both pro-inflammatory and neurotrophic factors, and appear to support axonal sprouting.

Previous work in the injured mouse striatum showed axons sprouting in the periphery of the macrophage-filled wound. The fibres course towards the wound edge, forming varicosities with microglia along the way. These sprouting fibres terminate in dense plexuses, within which lie macrophages. The fibres do not extend into the wound cavity, where macrophages of apparently identical morphology and immunoreactivity are found less than 100µm away**.** This suggests the presence of at least two macrophage phenotypes: one that supports regenerating fibres and one that does not.

Aims: The aims of this study are to (1) verify that different macrophage phenotypes exist after injury to the CNS in the rat, and (2) develop immunohistochemical markers of the different macrophage phenotypes.

Hypotheses: We hypothesize that : (1) at least two different macrophage phenotypes exist within the injured CNS - macrophages located at the wound edge exhibit a neurosupportive phenotype, while macrophages found in the wound core exhibit a non-supportive, possibly cytotoxic phenotype. (2) These different phenotypes can be identified using immunohistochemical biomarkers and by their location in the wound.

Methods: Adult male rats were given bilateral brain axonal injury using a Scouten wire-knife. These rats were perfused two weeks after injury with 4% paraformaldehyde. Tissue was processed for immunohistochemistry and laser microdissection. OX42-positive macrophages located at the wound core or edge were laser-catapulted into Trizol. RNA was prepared from the two populations of cells and purified with a Qiagen RNeasy kit. cDNA was prepared using the Invitrogen Superscript III Amplification Kit and the gene expression profiles compared on Affymetrix Rat Genome 230 2.0 Array.

Results: 30000 genes were analyzed and many genes characteristic of macrophages were expressed as anticipated. 928 genes had a minimum 2-fold change in expression, and at least 90 genes exhibited a 30-fold change - between macrophages from the two locations. We identified potentially targetable families of genes. These included transcription factors and regulators of axonal growth. We have shortlisted possible immunohistochemical markers that may identify, and differentiate between the supportive and non-supportive macrophages.

Conclusion: The macrophages from two different locations at the wound exhibited considerable differential gene expression, even though they were isolated from locations less than 100μm apart.

Limiting the development of cytotoxic or non-supportive macrophages, or directing macrophage activation towards a growth-supportive phenotype immediately after trauma, may contribute towards creating a cellular environment that encourages repair. This study leads towards identifying potential therapeutic targets, as well as identifying genes whose expression might allow development of more specific markers of macrophage function than currently available.

1277

EFFECTS OF LONG-TERM ADMINISTRATION OF HMG-COA REDUCTASE INHIBITOR, ATORVASTATIN, ON MICROVESSELS IN THE BRAIN OF STROKE-PRONE SPONTANEOUSLY HYPERTENSIVE RATS

K. Nomura, K. Muraga, T. Katsumata, M. Ueda, C. Nito, K. Katsura, Y. Katayama

Neurology, Nippon Medical School, Tokyo, Japan

Background: It is reported that long-term administration of atorvastatin suppressed the incidence of stroke and delayed stroke death in stroke-prone spontaneously hypertensive rats (SHR-SPs). It is also indicated that long-term administration of atorvastatin prevented vasodilatory remodeling in anterior cerebral artery (ACA) in SHR-SPs.

Objective: The objective of this study was to determine whether the long-term administration of an HMG-CoA reductase inhibitor, atorvastatin, confers anti oxidative and anti inflammatory effect in microvessels in the brain of SHR-SPs. Atorvastatin (20 mg/kg) or vehicle was orally administered to 8-week-old SHR-SPs for 5 weeks. As normal controls, vehicle was orally administered to 8-week-old WKYs over the same period.

Methods: The animals were decapitated and the brains were removed. The brains were then quickly frozen, and were sliced into horizontal sections of 6-mm-thickness using a cryostat. The markers for oxidative stresses on lipids (4-HNE) and DNA (8-OHdG) were immunohistochemically detected. LOX-1 was used as the maker for inflammation. The numbers of positive vessels in the 12 randomized 0.25 mm^2 areas in a horizontal section were counted. The ratio of positive vessels for each maker to all vessels (positive for von Wille brand factor) was calculated.

Results: The positive ratios of oxidative stress markers and inflammatory maker were significantly higher in the vehicle group than in the normal controls. Then the positive ratios were significantly lower in the atorvastatin group than in the vehicle group. Atorvastatin significantly reduced immunoreactivities for oxidative stress markers and inflammatory makers in microvessels. Lipids such as total cholesterol (T-cho), HDL-cholesterol (HDL-cho), LDL-cholesterol (LDL-cho), and triglyceride (TG) did not differ among in the same species (SHR-SPs or WKYs). **Conclusion:** The results suggest that statins may confer the anti oxidative and anti inflammatory properties and have the protective effects in the endothelial cells, even in the brain microvessels.

1278

QUANTITATED T1 AND T2 MR IMAGING OF ACUTE ISCHEMIC STROKE IN HUMANS

S. Bal[1], R.K. Kosior[2,3], M.L. Lauzon[3], R. Frayne[1,3], U. Tuor[1], P.A. Barber[1]

[1]Department of Clinical Neurosciences, Foothills Medical Centre, [2]Biomedical Engineering, [3]Seaman Family MR Centre, Foothills Medical Centre, University of Calgary, Calgary, AB, Canada

Introduction: Thrombolytic therapy for acute ischemic stroke remains the only available treatment for acute disabling stroke but despite significant benefit its overall effect is limited by concerns regarding increased risk of fatal outcome and symptomatic intracranial hemorrhage (SICH). However, it remains difficult to identify patients at greater risk for hemorrhagic transformation and increased morbidity and mortality before administration of tissue plasminogen activator (tPA). Preclinical studies have shown the potential of quantitated MR imaging (qMR) to determine the tissue properties of the ischemic brain.(1,2)

Objectives: We hypothesize that *the use of qMR T1 and T2 measurements might provide an index of stroke severity and therefore, reliably predict both response to tPA and risk of hemorrhagic transformation, allowing treatment decisions to be stratified according to the "tissue properties" of cerebral ischemia rather than by arbitrary time windows.*

Methods: Patients with acute ischemic stroke presenting were prospectively enrolled in the study. All patients had hemispheric syndromes with NIHSS >8 indicating moderate to severe stroke. All patients underwent MR imaging at 3T within 6 hours of onset of symptoms. For T1 mapping, a nonlinear fit was performed to data from a 3D-GRE-LL sequence that acquires images over 22 phases with a flip angle of 3.5 degrees, an inversion time of 13 ms and a repetition time of 3 ms. For T2 mapping, a nonlinear fit was performed to data from a CPMG sequence that acquires images at eight echo times (30 to 240 ms).

Results: Four patients fulfilled the criteria for this study and their images were analyzed. The mean time from onset of stroke symptoms to MR imaging was 203 minutes (SD 21 min). Preliminary analysis revealed all patients had ADC changes in the middle cerebral artery territory. There were early quantifiable T1 and T2 increase in three patients. Lesion extent detected on T1 maps in two patients exceeded the area outlined on T2 maps indicating difference in pathophysiology (Figure 1). T1 values of symptomatic side (ROI 2: 2913 ms, ROI 4: 2317) showed 41% increase as compared to contralateral side (ROI 1:1875, ROI 3: 1825). One patient with MR done at 240 minutes of onset of stroke had T2 weighted changes exceeding the T1 lesion size.

Conclusion: We conclude that there is a quantifiable increase in T1 and T2 in acute ischemic stroke. The precise interpretation of these quantifiable MR imaging changes remains to be established, but the presence of qT2 concomitant to reduced ADC suggests the existence of both cytotoxic and vasogenic edema. These preliminary observations suggest qMR can define "tissue properties" during acute ischemic stroke, which may help in determing stroke severity and risk of hemorrhagic transformation.

References

1. Barber PA, et al. *Neurosci Lett* 2005;388:54.

2. Kaur J, et al. *Int J Stroke* 2009;4:159.

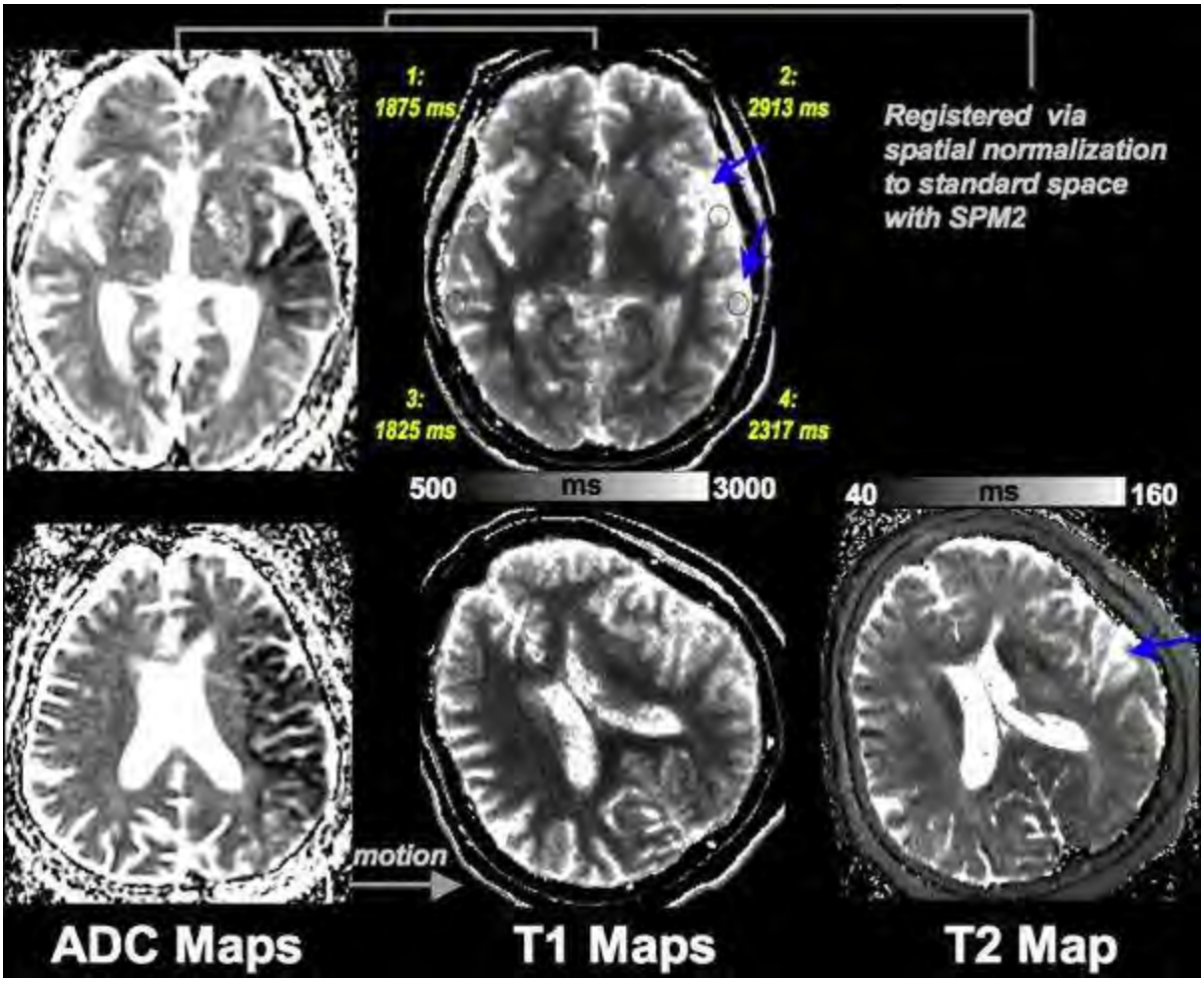

[Figure 1]

Figure 1: Patient with ADC lesion within 3 hours of symptom onset with concurrent qT1 and qT2 changes. The T1 and T2 maps show a hyperintense lesion corresponding to the ADC lesion (arrow).

1279

EFFECTS OF INTRANASAL ADMINISTRATION OF RHG-CSF ON EXPRESSION OF FAS L AND HO-1 AFTER CEREBRAL ISCHEMIA IN RATS

B.-L. Sun[1], M.-Q. He[2], M.-F. Yang[1], Y.-B. Zhang[1], H. Yuan[1], X.-Y. Han[3]

[1]Key Laboratory of Cerebral Microcirculation at the Universities of Shandong, Department of Neurology, Affiliated Hospital of Taishan Medical University, [2]Department of Internal Medicine, Taishan Chronic Disease Hospital, Taian, [3]Jining First Hospital, JIning, China

Objectives: The Study was carried out toobserve the effects of rhG-CSF given intranasally on expression of FasL and HO-1 in rats after cerebral ischemia.

Methods: Sixty adult male Sprague-Dawley rats were randomly assigned into normal, sham-operated, middle cerebral artery occlusion group (MCAO), MCAO+NS, MCAO+rhG-CSF subcutaneously, and MCAO + rhG-CSF intranasally groups. Rats were sacrificed at the first and third day after MCAO. The brain of rats were taken out and made into the coronal frozen sections. Immunohistochemical staining was used to detect the expression of Fas ligand (FasL) and hemeoxygenase-1 (HO-1) in peri-infarct and collateral hippocampus respectively.

Results: There were little FasL and HO-1 positive cells expressed in rats'brain of the nomal and sham groups. The expressions of FasL and HO-1 were up-regulated in MCAO group, 1d>3d. FasL and HO-1 positive cells mainly distributed in ischemic penumbra and collateral hippocampus. There was no obvious difference between the two group-MCAO and NS ($P>0.05$). rhG-CSF treatment significantly decreased the expression of FasL while increased that of HO-1. The average number of FasL positive cells of the intranasal group was lower than that of the subcutaneous group. On the contrary, the average number of HO-1 positive cells in the intranasal group was higher than that in the subcutaneous group obviously. ($P< 0.05$).

Conclusions: It suggested that rhG-CSF given intranasally exterts neurological protection by inhibiting the expression of FasL and upregulating the expression of HO-1 in. rats with cerebral ischemic.

* This work was supported by the National Natural Science Foundation of China (No. 30570651, No. 30670724)

1280

PSTAT3 IS A COMPONENT OF ASTROGLIAL CELL ACTIVATION AFTER NEONATAL HYPOXIA/ISCHEMIA IN MICE

G. Llovera, K. Shrivastava, L. Acarin

Institute of Neuroscience, Universitat Autònoma de Barcelona, Bellaterra, Spain

Introduction: Neonatal hypoxia/ischemia (H/I) is the major cause of morbidity and mortality as a result of the complications during birth, causing a wide range of neurological dysfunctions. H/I induces both white and gray matter abnormalities and activation of the inflammation cascade in the damaged areas, which is responsible for the release of different cytokines which further increase inflammation-induced damage. These cytokines activate the JAK/STAT pathway activating the STAT3 protein by phosphorylation into pSTAT3, which dimerizes and translocates into the nucleus, where it binds to the DNA triggering the expression of more pro-inflammatory molecules.

Objectives: In this sense, we hypothesized that pSTAT3 is an important component of the activation of glial cells after neonatal injury, and the aim of this project was to explore the pattern of pSTAT3 activation at several survival times following H/I in the newborn mouse brain.

Methods: For this study we used 7-day old postnatal wild-type C57BL6 mice, which were subjected to unilateral carotid ligation followed by 55 minutes of hypoxia. To evaluate lesion progression we used histological techniques, and for the evaluation of spatiotemporal and cellular pattern of pSTAT3 triple immunohistochemistry and confocal analysis were used.

Results: Alltogether, data indicates that the most damaged region of the neonatal brain after H/I was the ipsilateral hippocampus, more concretely the CA region, although the corpus callosum was also affected. The main cell type showing nuclear pSTAT3 were the astrocytes. However, not all of injury-activated astrocytes were pSTAT3+, only a subpopulation located in the hippocampus and in the corpus callosum. pSTAT3+ cells were observed as early as 3 hours post-injury, although the peak of pSTAT3+ cells was not observed until 48 hours after hypoxia-ischemia.

Acknowledgement: Supported by BFU2009-08805 from the Ministry of Science and Innovation, Government of Spain.

1281

ASSOCIATION OF D3/D2 RECEPTORS IN COCAINE DEPENDENCE IN HUMAN SUBJECTS WITH PHNO

D. Matuskey[1,2], J.-D. Gallezot[2], K. Lim[2], M.-Q. Zheng[2], S.-F. Lin[2], R.E. Carson[2], R. Malison[1], Y.-S. Ding[2]

[1]Psychiatry, [2]Diagnostic Radiology, Yale University, New Haven, CT, USA

Objectives: The role of Dopamine-D2 has been well established in the importance of cocaine dependence (CD). Dopamine-D3, however, has gained more interest recently for a possible role in CD. This project aims to elucidate the role of D3 in CD as compared to healthy control (HC) subjects with the new D3 preferring radioligand PHNO.

Methods: 10 medically healthy, non-treatment seeking CD subjects (mean age 42±7) were compared to 17 HC subjects (mean age 30±10) with no past or current history of cocaine/illicit substance abuse. CD subjects were admitted to a research-dedicated psychiatric inpatient unit where they resided for the duration of the study. After an acclimatization period, participants received a MRI and then underwent PHNO acquisition using a High Resolution Research Tomograph (HRRT) for purposes of quantifying brain D3/D2 binding potential (BP_{ND}), a measure of available receptors. Subjects received a bolus injection of 316±140 MBq of [^{11}C] PHNO with a total injected mass of 0.028±0.004 µg/kg. The specific radioactivity was 63±29 MBq/nmol at the end of synthesis and 35±17 MBq/nmol at injection time. Parametric images were computed using the simplified reference tissue model (SRTM2) with the cerebellum as the reference region.

Results: Subcortical regions rich in D2 and D3 were chosen for region-of-interest (ROI) analyses. The results are shown in the table below. No statistically significant changes were seen between HC and CD subjects in the caudate (-9%,), pallidum (-7%) putamen (-7%), substantia nigra (22%, P=.13) and the thalamus (1%). Statistical significance differences were seen when the ratio of D3 to D2 areas (SN/Striatum) were compared (30%, P=.02).

ROI (BPND)	Caudate	Putamen	Pallidum	Substantia Nigra (SN)	Thalamus	SN/Striatum Ratio
HC Mean (SD)	1.95 (.34)	2.54 (.41)	3.48 (.61)	1.14 (.30)	0.41 (.08)	.50 (.10)
CD Mean (SD)	1.78 (.56)	2.37 (.36)	3.23 (.78)	1.38 (.52)	0.42 (.09)	.68 (.26)

[Subcortical Regions (BPnd)]

Conclusions: The results suggest that that D2 rich regions (caudate, putamen and pallidum) are down-regulated and D3 rich areas (substantia nigra) are up-regulated in cocaine subjects. These differences did not reach statistical significance, unlike the SN/Striatum (D3 to D2) ratio, which was statistically significant. 2 CD subjects who were 1 SD outside of the mean likely

altered the later result. These preliminary results are continuing to be actively studied to more fully understand the relationship of D3 receptor availability in cocaine dependence.

1282

ALTERATIONS OF RCBF AND EXPRESSION OF FAS L BY CEREBRAL LYMPHATIC BLOCKADE, AND INFLUENCE OF PYRIDOXOL IN RATS WITH SAH

B.-L. Sun[1], Z.-C. Cheng[2], M.-F. Yang[1], H. Yuan[3], Y.-B. Zhang[3]

[1]Key Laboratory of Cerebral Microcirculation at the Universities of Shandong, Department of Neurology, Affiliated Hospital of Taishan Medical University, [2]Taian Traditional Chinese Medical Hospital, [3]Affiliated Hospital of Taishan Medical University, Taian, China

Objectives: The study was designed to observe the effects of cerebral lympatic pathway on cerebral blood flow and the expression of Fas L and the influence of pyridoxol following experimental subarachnoid hemorrhage(SAH).

Methods: Healthy adult male Wistar rats were divided into normal control, SAH, SAH+cerebral lymphatic blockade(CLB), SAH+CLB+vehicle, and SAH+CLB+pyridoxol groups. SAH models were replicated by double iscternal injection of autologus arterial blood. CLB was accomplished 1 day prior to the insuction of SAH by ligating the cevical lymphatic input and output tubes and removal of bilateral shallow and deep lymphatic nodes. Pyridoxol (25mg/kg bw) was injected intraperitoneally 30 minutes after the first cisternal injection, and was repeated twice a day with the half dose. On the third day after SAH, regional cerebral blood flow (rCBF) of candate nucleus was recorded by a laser Doppler flow-meter probe. Expressions of fasL mRNA of cortex and hippocampus were detected by RT-PCR. Expressions of fasL protein was determined by a immunohistochemistry assay.

Results: It was found that rCBF of candate nucleus decreased after SAH, which was deteriorated by CLB and was partially reversed by pyridoxol. The expressions of fasL mRNA and its protein weres induced after SAH, and were further enhanced by CLB. Alterations of the expressions were antagonized by the use of pyridoxol.

Conclusions: It was concluded that cerebral lympatic pathway exerts intrinsic protective effects against the decrease of cerebral blood flow and the up-regulated expression of fasL mRNA and its protein. Pyridoxol may have beneficial effects against secondary cerebral ischemic injury following experimental SAH.

* This work was supported by the National Natural Science Foundation of China (No. 30570651, No. 30670724)

1283

NEUROPROTECTIVE EFFECTS OF EMODIN IN TRAUMATIC BRAIN INJURY MODEL

K.-Y. Chen[1], Y.-H. Chiang[1], C.-C. Wu[1], Y.-W. Yu[1], J.-W. Lin[2], W.-T. Chiu[3]

[1]Department of Neurosurgery, Taipei Medical University Hospital, [2]Department of Neurosurgery, Taipei Medical University -Shuang Ho Hospital, [3]Department of Neurosurgery, Taipei Medical University, Taipei, Taiwan R.O.C.

Background and aims: Emodin has previously reported to exhibit neuroprotective effects in cerebral ischemia-reperfused injury and glutamate induced neuronal damage. It is extracted from Polygonum cuspidatum Sieb. et Zucc, a traditional Chinese medicinal herb widely used to treat acute hepatitis. This study investigates neuroprotective effects of Emodin in traumatic brain injury (TBI) model both in vitro and in vivo.

Methods: Primary cortical neurons and PC12 cells were exposed to hypoxic conditions to similate neural injury, and involved signaling pathways and results of Emodin treatment was evaluated by western blot and MTT assay. In addition, cortical impact was induced in Male SD rats to establish TBI model. Results of the Emodin treatment 30 minutes after cortical impact were evaluated with behavioral examinations with water maze. Mechanisms of Emodin treatment in animal model were also analyzed with Western blot.

Results: Neuroprotective effect in in vitro study as decreased cell death was observed in cultures treated with Emodin. In addition, neuroprotective effect was observed as animals show a more rapid recovery of memory in group treated with Emodin. Furthermore, Western blot analysis shows p38-mitogen-activated protein kinases (MAPK) pathway is involved in neuroprotective effect of Emodin.

Conclusion: Emodin demonstrates neuroprotective effects in TBI model both in vitro and in vivo via p38-MAPK pathway.

1284

NEURAL NETWORK PLASTICITY DURING TASK ACQUISITION AFTER TRAUMATIC BRAIN INJURY

F.G. Hillary[1], J. Medaglia[1], K. Gates[2], P. Molenaar[2], D. Good[3], Brain Injury

[1]Psychology, Pennsylvania State University, [2]HDFS, Pennsylvania State University, [3]Neurology, Hershey Medical Center, University Park, PA, USA

There is a growing literature using functional brain imaging methods to examine working memory (WM) deficits in individuals with neurological disorders such as traumatic brain injury (TBI). These studies represent the foundation for understanding the basic brain changes occurring after moderate and severe TBI, but the focus on topographical brain "activation" differences ignores potential alterations in how nodes communicate within a distributed neural network. The current study makes use of the most recently developed connectivity modeling (extended unified structural equation model; eu-SEM) (Gates et al. 2010a; Gates et al. 2010b) to examine performance during a well-established WM task (the n-back) in individuals sustaining moderate and severe TBI. The goal is to use the findings observed in topographical activation analysis as the basis for second-level effective connectivity modeling. Findings here reveal important between-group differences in within-hemisphere connectivity, with the control sample demonstrating rapid within-left hemisphere connectivity increases and the TBI sample demonstrating consistently elevated within-right hemisphere connectivity. These findings also point to important maturational effects from "early" to "late" during task performance, including diminished right PFC involvement and an anterior to posterior shift in connectivity with increased task exposure. We anticipate that this approach to functional imaging data analysis represents a important future direction in the understanding how neural plasticity is expressed in brain disorders.

1285

ROLE OF LYMPHATIC DRAINAGE PATHWAY IN PROLIFERATION AND DIFFERENTIATION OF NEURAL STEM CELLS DURING SUBARACHNIOD HEMORRHAGE IN RATS

B.-L. Sun[1], X.-C. Liu[2], M.-F. Yang[3], H. Yuan[3]

[1]Key Laboratory of Cerebral Microcirculation at the Universities of Shandong, Department of Neurology, Affiliated Hospital of Taishan Medical University, Taian, [2]Penglai People's Hospital, Penglai, [3]Affiliated Hospital of Taishan Medical University, Taian, China

Objectives: This experiment was to determine effect of cerebral lymphatic drainage pathway on neural stem cells (NSCs) proliferation and differentiated after experimental subarachnoid hemorrhage (SAH).

Methods: Adult male Wistar rat were used as experimental animals and were divided into normal control, SAH, and SAH+ cerebral lymphatic blockade(CLB) groups. SAH models were replicated by double iscternal injection of autologus arterial blood. CLB was accomplished 1 day prior to the insuction of SAH by ligating the cevical lymphatic input and output tubes and removal of bilateral shallow and deep lymphatic nodes. At dfferent time after SAH, NSCs were labelled by Brdu. Immunofluorescence double staining was used to detect the co-expression of Brdu+,GFAP+ and Neurod+. A Laser Confocal Microscopy was applied to count the numbers of the positive cells.

Results: It was found that Brdu+ cells in SAH group were more than that in control group.The positive cells in CLB+SAH group were more than that in SAH group. The number of GFAP+ and Brdu+ cells in SAH group were more than that in control group. The positive cells in CLB+SAH group were more than that in SAH group.

Conclusions: It was concluded that blockage of cerebral lymphatic drainage after SAH facilitate proliferation of NSCs, but it is a disadvantage to NSCs' differentiation to neurons.

* This work was supported by the National Natural Science Foundation of China (No. 30570651, No. 30670724)

1286

CHANGES IN RESTING STATE FUNCTIONAL CONNECTIVITY DURING RECOVERY FROM TRAUMATIC BRAIN INJURY

F. Hillary[1], G. Wylie[2], J. Slocomb[3], J. Medaglia[1], D. Good[3], Brain Injury

[1]Psychology, Pennsylvania State University, University Park, PA, [2]Kessler Foundation Research Center, West Orange, NJ, [3]Neurology, Hershey Medical Center, Hershey, PA, USA

In the present study we investigate changes in resting state functional connectivity (RSFC) at separate time points during the first 6 months following moderate and severe traumatic brain injury (TBI). The goal of this study was to examine how regional off-task connectivity is altered during a critical period of recovery from moderate and severe TBI. This was achieved by examining regional changes in the BOLD fMRI signal in separate resting networks: 1) regions linked to goal-directed (or external-state) networks and 2) default mode (or internal-state) networks. Findings here demonstrate significant increased resting connectivity in both external-state and goal-directed networks in the TBI sample during the first six months following recovery. These findings were dissociable from repeat measurements in a matched healthy control sample. The current findings are interpreted in the context of on-task activation findings in this literature and offer some insight into how neural systems adapt to severe disruption during the first six months following injury.

1288

ACTIVATION OF 5-HT3 RECEPTOR DISRUPTS DEVELOPMENT OF GAMMA OSCILLATIONS IN HIPPOCAMPAL CA1

Y. Huang[1,2], K. Yoon[2], H. Ko[3], A. Morozov[2]

[1]Physiology and Pathophysiology, Fudan University, Shanghai, China, [2]NIMH, NIH, Bethesda, MD, USA, [3]Department of Neuroscience, Physiology and Pharmacology, University College London, London, UK

5-HT3 receptor has been implicated in learning and memory processes. Activation of this receptor has been suggested to impair cognition whereas its inhibition is thought to facilitate memory. Gamma oscillations are proposed to play an important role in cognition and memory; however, the role of 5-HT3 receptor in gamma oscillations remains unclear. Hippocampal gamma oscillations are driven by interplay between fast-spiking parvalbumin (PV)-positive interneurons and pyramidal cells, the roles of other interneurons are poorly understood. A subpopulation of PV-negative but cholecystokinin (CCK)-positive hippocampal interneurons expresses 5-HT3 receptor. Here we investigated how 5-HT3 receptors modulate carbachol-induced gamma oscillations through these interneurons in hippocampal area CA1. 5-HT3 receptor agonist *m*-CPBG attenuated development of gamma oscillations. It increased afterhyperpolarization (AHP) and reduced firing frequency in 5-HT3 cells in a Ca^{2+}- and small conductance potassium (SK)-channel-dependent manner, reduced inhibitory input to PV cells and increased but desynchronized PV cells' firing, which interfered with the development of gamma oscillations. Our findings provide a novel mechanism whereby 5-HT3 interneurons modulate gamma oscillations by changing inhibition of PV interneurons, which might be involved in the modulation of cognitive functions by 5-HT3 receptors.

1289

ANTIBODY MEDIATED INHIBITION OF MADCAM-1 AGGRAVATES ISCHEMIC STROKE PATHOLOGY

C.V. Ganta[1], A. Minagar[2], J.S. Alexander[1]

[1]*Molecular & Cellular Physiology, Louisiana State University School of Graduate Studies,*
[2]*Neurology, Louisiana State University School of Medicine, Shreveport, LA, USA*

Ischemic stroke induces the expression of several adhesion molecules that facilitate the adhesion and penetration of immune cells into the post-ischemia reperfused (I/R) brain. Several reports have shown that while T-cell infiltration into the brain aggravates post-ischemic injury, specific populations of T-cells e.g. regulatory T- cells (T-Regs) can attenuate ischemic damage. 'MAdCAM-1' (mucosal addressin cell adhesion molecule) a receptor for the a4b7 integrin expressed on T-cells plays an important role in the endothelial cell-T-cell binding interaction and can regulate homing of T-cells into the postischemic brain. Unlike intercellular cell adhesion molecule-1 (ICAM1), vascular cell adhesion molecule-1 (VCAM1), P- and E-Selectin, the role of MAdCAM-1 in the pathology of stroke is not well known. We found that ischemic stroke (by occluding MCAo for 2h and reperfused for 24h in a mouse model of focal cerebral ischemia) induced the expression of MAdCAM-1 in the I/R brain. Interestingly, not only was MAdCAM-1 induced in the brain vasculature but also on the neurons of the the ipsilateral hemisphere compared to contralateral hemisphere. Further, serum levels of MAdCAM-1 were observed to be significantly increased in the post-stroke mice compared to the sham operated mice. More importantly, western blots of human stroke patients' CSF samples also showed higher levels of MAdCAM-1 compared to controls' CSF. *In vitro* studies using human neurons and human brain endothelium subjected to oxygen and glucose deprivation (OGD) for 3h and reperfused for 24h (to mimic ischemic conditions) showed that neurons and brain endothelial cell MAdCAM-1 is induced by I/R. In order to understand the role of MAdCAM-1 in the pathophysiology of stroke, monoclonal MAdCAM-1 antibody (MECA-367, 200ug/mouse) was administered (intra-peritoneally) to mice 30min before the occlusion of the MCAo; (controls received PBS). After 24h reperfusion, control stroke mice and MAdCAM-1 treated stroke mice were sacrificed and their brains were sliced (2mm thickness), and TTC stained, scanned and infarct sizes were measured (using NIH image J software). MAdCAM-1 antibody treated mice had significantly higher infarct sizes (compared to control stroke animals) and also exhibited significantly higher behavior deficit compared to controls. Whether the observed increased infarct size was due to the initiation of MAdCAM-1 signaling ('agonist' mode of MAdCAM-1 ab mediated signaling on post-ischemic neuro-vasculature) or due to defective recruitment of beneficial T-Regs into the brain or due to MAdCAM-1 ab interference with circulating MAdCAM-1 in I/R stroke mice is currently under investigation.

1290

EFFECTS OF CEREBRAL LYMPHATIC DRAINAGE PATHWAY ON CEREBRAL VASOSPASM AND CEREBRAL ISCHEMIC INJURY AFTER SAH IN RATS

B.-L. Sun[1], X. Wang[2], L.-L. Jia[2], M.-F. Yang[3], H. Yuan[4]

[1]Key Laboratory of Cerebral Microcirculation at the Universities of Shandong, Department of Neurology, Affiliated Hospital of Taishan Medical University, Taian, [2]Zhangqiu People's Hospital, Jinan, [3]Key Laboratory of Cerebral Microcirculation at the Universities of Shandong, Taishan Medical University, [4]Affiliated Hospital of Taishan Medical University, Taian, China

Objectives: Cerebral lymphatic drainage pathway may play an important role in the removal of substances in the brain and cerebrospinal fluid (CSF) in normal conditions. After the onset of subarachnoid hemorrhage (SAH), large amount of macromolecular substances were accumulated in the brain tissure and CSF, which contribute to cerebral vasospasm (CVS) and related cerebral ischemic injury. The experiment was carried out to investigate the possible role of cerebral lymphatic drainage pathway in the development of CVS and related cerebral ischemic injury.

Methods: Wistar rats were divided into normal control, SAH, SAH+ cervical lymphatic blockade (CLB). SAH models were replicated by double iscternal injection of autologus arterial blood. CLB was accomplished 1 day prior to the insuction of SAH by ligating the cevical lymphatic input and output tubes and removal of bilateral shallow and deep lymphatic nodes. 48 hours after SAH, diameter of basilar artery (BA) was detected via a transclivus approach. The pathological alterations of BA were examed under light microscope. Immunofluorescent technique was used to detecte caspase-3 expression in brain section. DAPI staining was used to observe the morphological alterations of cellular nuclei.

Results: It was found that diameters of BA decreased remarkably after SAH. The increased thickness of BA wall and decread cavity were also observed SAH induction. There were a lot of caspase-3 positive cells in SAH group. The number of aspase-3 positive cells increased in SAH+CLB group. By DAPI staining, apoptotic changes of some cells in SAH goup were found. More apoptotic cells were seen in SAH+CLB group. Above resultes indicated that CLB deteriorates SAH-induced CVS and related cerebral ischemic injury.

Conclusions: It was concluded that cerebral lymphatic drainage pathway exerts intrinsic protective effects against CVS and related cerebral ischemic injury by removal of macromolecular substances in the brain and subarachnoid spaces.

* This work was supported by the National Natural Science Foundation of China (No. 30570651, No. 30670724)

1291

EPHRIN/EPH RECEPTOR EXPRESSION ON BRAIN MICROVASCULAR ENDOTHELIAL CELLS AND MICROPARTICLES: REGULATION BY INFLAMMATORY CYTOKINES

J.S. Alexander[1], C.V. Ganta[2], A.W. Orr[3], S. Funk[3], A. Yurdagul[3], W. Cromer[4], J.M. Mathis[4], A. Erdreich-Epstein[5], R.M. Nagra[6], A. Minagar[7], I. Tsunoda[8], F. Sato[8], N. Martinez[8], S. Omura[8]

[1]Molecuar & Cellular Physiology, Louisiana State University Health Sciences Center - Shreveport, [2]Molecular & Cellular Physiology, Louisiana State University School of Graduate Studies, [3]Pathology, Louisiana State University School of Medicine, [4]Cell Biology & Anatomy, Louisiana State University School of Graduate Studies, Shreveport, LA, [5]Hematology/Oncology, Children's Hospital Los Angeles, CA, [6]UCLA Multiple Sclerosis (MS) Human Neurospecimen Bank, UCLA, Los Angeles, CA, [7]Neurology, Louisiana State University School of Medicine, [8]Microbiology & Immunology, Louisiana State University School of Graduate Studies, Shreveport, LA, USA

Endothelial cells which are exposed to stressful or pro-apoptotic stimuli shed small (< 1um) Annexin V+ plasma membrane derived particles, termed 'microparticles' (MPs) that often bear cell surface markers derived from the cell membrane. Brain endothelial MPs represent an important new marker of disease activity and may contribute to pathophysiology in cerebrovascular and neurodegenerative diseases. Ephrin receptors (Ephs) and ephrins expressed on endothelial cells are increased by TNF-a, IL-1b and oxidized LDL and may regulate vascular pathology / dysfunction in atherosclerosis, stroke and multiple sclerosis by inducing adhesive determinants e.g. VCAM1 and E-selectin. Whether brain endothelial cells express ephrins and Eph receptors, or transfer these ligand/receptors to MPs is unclear but could represent a novel mechanism underlying neurovascular inflammation. Using the stable brain capillary endothelial cell line (HBMEC-2) we found that the formation of of annexin V+ brain endothelial microparticles was induced by exposure to TNF-a, IL-1b or IFN-g (48h). Some markers e.g. vascular cell adhesion molecule (VCAM1) appears to be transferred to MPs, while occludin, a tight junctional adhesive determinant, and pan-reactive cadherins, were excluded from MPs, suggesting that MPs are derived from the apical (rather than lateral or basolateral) cell surfaces. Interestingly, Ephrin receptor A2 and ephrinA1 were both persistently expressed by cultured brain endothelial cells. Treatment of brain endothelial cells with inflammatory cytokines induced the transfer of these markers into brain endothelial derived MPs. Samples of control and multiple sclerosis (MS) serum showed increased ephrin A1; EphA2 expression was elevated in vessel structures in MS brain tissue (compared to control). These data show that brain microvascular endothelial express ephrinA1 and EphA2 and following exposure to inflammatory stimuli, transfer these markers to MPs. Elevated levels of circulating ephrinA1 in MS and increased vascular EphA2 staining in MS. This is the first report of brain endothelial MP expression of ephrins and Eph receptors which represent novel biomarkers (and possibly mediators) of neurovascular inflammation.

1292

SYMPATHETIC PERIVASCULAR NERVES MEDIATE VASOTROPHIC EFFECTS OF CHRONIC HYPOXIA IN FETAL SHEEP CEREBRAL ARTERIES

O.O. Adeoye, S.M. Butler, J.M. Abrassart, J.M. Williams, W.J. Pearce

Center for Perinatal Biology, Loma Linda University, Loma Linda, CA, USA

Objectives: Multiple pathologies alter cerebral artery structure and function through mechanisms that remain largely unidentified. A common feature among many of these pathologies is cerebral hypoxia. In turn, recent evidence suggests that hypoxia increases production of Vascular Endothelial Growth Factor, which stimulates the growth and differentiation of the perivascular sympathetic innervation. Other studies have clearly indicated that the perivascular sympathetic innervation can exert potent trophic effects on cerebral arteries, and thereby influence their structure and function. In light of these findings, the present study explores the hypothesis that the perivascular sympathetic innervation of cerebral arteries mediates hypoxic changes in the smooth muscle phenotype, structure, and function of fetal lamb middle cerebral arteries.

Methods: Time-dated pregnant sheep were maintained either at sea level or at the White Mountain Research Station (altitude 3280m) for the final 110 days of gestation. In both normoxic and hypoxic animals, a right superior cervical ganglionectomy was performed on the exteriorized sheep fetuses at 124 days of gestation, after which the fetus was returned to the uterus, the defect was surgically repaired, and the fetus was allowed to mature another 14 days after which the fetal middle cerebral arteries were harvested and subjected to a series of structural, functional and compositional analyses.

Results: Chronic hypoxia decreased NE content (ng NE/mg protein) from 35.3 (normoxic) to 25.5. Similarly, chronic hypoxia decreased NE uptake capacity (pmol/mg protein/min) from 1.11 (normoxic) to 0.90. In contrast, chronic hypoxia increased the contractile response to transmural nerve stimulation at 8 Hz by approximately 10-fold. Chronic hypoxia significantly increased arterial wall thicknesses in hypoxic relative to normoxic cerebral arteries by 36%. Sympathetic denervation significantly decreased arterial wall thicknesses in hypoxic fetuses by up to 12%, but had no effect in normoxic fetuses. Efficacy values for norepinephrine (%Kmax) averaged 106% in normoxic fetal MCA but only 16% in hypoxic fetal arteries. Denervation restored NE efficacy to 42% of Kmax. Similarly, NE potency (-log EC50) was decreased from 6.11 in normoxic arteries to 5.61 in hypoxic arteries, and this effect was reversed by denervation; NE potency averaged 6.18 in denervated hypoxic arteries. Confocal colocalization of smooth muscle alpha actin with myosin heavy chain isoforms revealed that chronic hypoxia induced a phenotypic transformation of cerebrovascular smooth muscle cells resulting in an intramural cell population with a greater proportion of synthetic and a smaller proportion of contractile phenotypes. Confocal colocalization of Myosin Light Chain Kinase and its substrate 20 kD Regulatory Light Chain was tightly coupled to changes in contractility.

Conclusions: These results demonstrate that chronic hypoxia significantly alters the density and enhances the function of the perivascular sympathetic innervation in fetal cerebral arteries. These changes, in turn, appear to mediate major changes in artery structure (increased wall thickness) and function (depressed NE efficacy) that can be reversed, at least in part, by sympathetic denervation. Together, these data strongly support the hypothesis that the perivascular sympathetic innervation of cerebral arteries mediates hypoxic changes in the smooth muscle phenotype, structure, and function of fetal lamb middle cerebral arteries.

1293

ESTROGEN REDUCES CEREBROVASCULAR TONE THROUGH BOTH ENDOTHELIAL-DEPENDENT AND -INDEPENDENT MECHANISMS

D.N. Krause[1], Y. Zhao[1], I. Jansen-Olesen[2], S.P. Duckles[1]

[1]Pharmacology, University of California-Irvine, Irvine, CA, USA, [2]Neurology, Glostrup Hospital, University of Copenhagen, Copenhagen, Denmark

Estrogen has well-known vasoprotective effects. In cerebral arteries, we have demonstrated that estrogen affects contractility by enhancing release of endothelial vasodilators nitric oxide (NO) and prostacyclin. These effects involve both genomic and non-genomic mechanisms. For example, activation of estrogen receptor (ER) alpha increases expression of endothelial NO synthase mRNA and protein as well as phosphorylation of this enzyme by Akt. We recently discovered an additional mechanism by which estrogen acutely alters cerebrovascular tone independent of endothelial mechanisms. Isolated, precontracted segments of female mouse basilar artery relaxed upon exposure to either estrogen (EC50 = 1 x 10-6 M) or the ERalpha agonist, PPT (EC50 = 7 x 10-7 M); these effects were inhibited by the ER antagonist, fulvestrant. In contrast, DPN, an ER beta agonist, was relatively ineffective. Surprisingly the effects of estrogen and PPT were not blocked by inhibitors of NO synthase or cyclooxygenase, nor did they require the presence of functional endothelium. These findings indicate that ER alpha on the vascular smooth muscle mediates direct relaxation of cerebral arteries. This effect would complement the endothelial effects of estrogen to release vasodilators NO and PGI2. It is hypothesized that the smooth muscle may respond to local estrogen synthesized by aromatase found in cerebrovascular endothelium as well as to circulating estrogen. Moreover, through direct stimulation of smooth muscle relaxation, protective effects of estrogen may persist under conditions of endothelial dysfunction. [NIH Grant HL50775; Lundbeck Fdn; Candice Fdn]

1294

NEUROVASCULAR INTERACTIONS REGULATE ANTI-ANGIOGENIC VEGF164B MEDIATED ISCHEMIC BRAIN PATHOPHYSIOLOGY

C.V. Ganta[1], W. Cromer[2], J.M. Mathis[3], P.J. Mccarthy[4], L.S. Keith[5], A. Minagar[6], J.S. Alexander[7]

[1]Molecuar & Cellular Physiology, [2]Cell Biology & Anatomy, Louisiana State University Health Sciences Center - Shreveport, [3]Cell Biology & Anatomy, Louisiana State University School of Graduate Studies, [4]Medicine & Neurosurgery, [5]Medicine & Pediatrics, [6]Neurology, Louisiana State University School of Medicine, [7]Molecular & Cellular Physiology, Louisiana State University School of Graduate Studies, Shreveport, LA, USA

Introduction: Despite many advances in stroke research, therapeutic options are still limited. Restitution of brain tissue in the post-ischemic cerebrum is facilitated by *de novo* angiogenesis and induction of neurogenesis by exogenous administration of stem cells which is proving to be invaluable for stroke therapy. Angiogenic molecules like VEGF which actively regulate angiogenesis are highly pleiotropic in the brain. Two of the most important mechanisms in ischemic brain pathology are blood brain barrier damage and neuronal death. Although VEGF-A is neuroprotective, it is also well known to promote hyper-permeability of the blood brain barrier making it difficult to consider as a stroke therapy. However, it is still unclear which is more detrimental during the etiology of stroke: BBB dysfunction or neuronal damage.

Objectives: We hypothesized that the anti-angiogenic VEGF isoform, VEGF164b might efficiently block the hyper-permeability effect of VEGF on BBB protect from stroke.

Design: To understand the influence of VEGF165b on the components of neurovascular unit (neurons, astrocytes and endothelium) during stroke, *in vitro* simulated stroke model (oxygen and glucose deprivation, reperfusion) using 3D co-cultures of: 1) human neurons / human brain endothelium, 2) human astrocytes / human brain endothelium and 3) human brain endothelium alone were used. We found that neurons and astrocytes differentially regulate BBB permeability in the presence of VEGF165b.

Results: We observed that in a mouse model of focal cerebral ischemia (middle cerebral artery occlusion (MCAo) for 2h and reperfusion for 24h) serum and the brain levels of VEGF164 are upregulated. In vitro, following I/R, brain endothelium co-cultured with astrocytes progressively lost barrier, while brain endothelium co-cultured with neurons retained the barrier till 5d. Importantly, co-cultures as well as brain endothelium alone treated with VEGF165b showed a net higher barrier compared to all other conditions indicating a protective effect of VEGF165b on the BBB. However, interestingly, I/R treated human neurons treated with VEGF165b showed statistically lower survival at 24h than untreated cells. Moreover, immunoblot analysis showed that CSF samples of sub-arachnoid hemorrhage patients (collected with patients' approval) had higher levels of VEGF 165b compared to VEGF165. These results indicate that even though VEGF promotes BBB permeability, its function may be more important in protection neuronal survival and compromise in its function through inhibitory isoforms e.g. VEGF164b may contribute to aggravation of ischemic pathology.

Conclusions: These results indicate that even though VEGF165b protects barrier, it can also antagonize the beneficial effect of VEGF165 in neuronal survival thereby contributing to neuronal degeneration during stroke.

1296

NOVEL INSIGHTS INTO ADOLESCENT OPIATE ABUSE REVEALED WITH PRECLINICAL BEHAVIORAL IMAGING

W.K. Schiffer[1,2], J. Carrion[1,3], S. Agorastos[1], A. Talan[1], C. Veith[1], A. Aarons[1], S. Dewey[1], S. Scherrer[1]

[1]Feinstein Institute for Medical Research, North Shore University Hospital, Manhasset, [2]Department of Psychiatry, NYU School of Medicine, [3]The City College of New York, New York, NY, USA

Objectives: A recent surge in the misuse of prescription pain medications by adolescents and teens has led to an even more alarming rise in heroin abuse, which is often easier to find in schools and much less expensive than the popular pain medication, Oxycontin. Opiate abuse is well known to cause lasting changes in cognition in the developing brain. However there also exists a considerable literature demonstrating that classic withdrawal symptoms following opiate cessation are milder in adolescents compared to adults; adolescent rodents exhibit only moderate signs of withdrawal-associated anxiety, and reduced negative affect during abstinence has been observed in adolescent humans as compared to adults. The diminished negative consequences of opiate abuse in adolescents is thought to be a key factor in the development of opiate addiction in this vulnerable population (reviewed in O'Dell 2006). Our premise is that functional imaging in freely moving rodents can be used to establish a metabolic 'signature' of brain activity that, when combined with simultaneous behavioral measures, provides a comprehensive animal model with significant clinical relevance. Here we used serial imaging with FDG PET together with behavioral measures to capture the metabolic signature of opiate use and withdrawal in adolescents. Identical measures from adult animals revealed a unique time course and magnitude of functional impairment in the adolescent group.

Methods: Two groups of male Sprague-Dawley rats (n=8/group) were studied; adolescents (PN day 40) and adults (PN day 100) underwent identical morphine treatment, scanning and behavioral regimens. After a baseline scan, both groups received escalating doses of morphine from 10mg/kg to 42.5mg/kg over 14 days. 24 hours following their last dose, both groups received a second FDG scan followed by serial PET measurements at 7, 14, and 28 days post treatment. For all scans, FDG uptake occurred in awake, freely moving animals, followed by anesthesia and a 10 min image acquisition. An observational time-sampling procedure was used to capture previously identified behavioral characteristics of opiate withdrawal in predetermined time bins. Composite behavioral scores established individual withdrawal severity and group differences (adolescent versus adult). Images were spatially normalized to stereotaxic space using PMOD software. An ROI template determined regional changes FDG uptake. Voxel-based image analysis using Statistical Parametric Mapping (SPM) identified regions where individual differences in FDG uptake correlated with the severity of opiate withdrawal.

Results: In adults, marked reductions in FDG uptake were evident in both cortical (frontal, parietal, temporal cortices) and subcortical structures (deep cerebellar nuclei, striatum, thalamus). However adolescent animals showed only a moderate decline in FDG uptake in cortical regions that recovered after 7 days of cessation, with commensurate behavioral withdrawal signs.

Conclusions: Functional imaging in behaving animals allows us to map laboratory models to clinical studies by examining opiate use in paradigms that produce similar activation patterns in

animals and humans. These functional assays of physiological withdrawal can be repeated longitudinally to follow the evolution of changes that are known to occur temporally in the brain, and now we have shown to distinguish adolescent from adult opiate abuse.

1297

BAYESIAN MIXTURE MODELS AND SOURCE SEPARATION IN MEG

E. Somersalo, L. Homa, D. Calvetti

Department of Mathematics, Case Western Reserve University, Cleveland, OH, USA

Objectives: Magnetoencephalography (MEG) is a totally non-invasive research tool with excellent temporal resolution and, combined with EEG, it may provide valuable information, e.g., about the foci of the onset of epileptic seizures. Despite of the magnetic shielding, a major challenge for clinical MEG is its sensitivity to electromagnetic noise, which in a hospital environment may be a significant nuisance. Therefore, it is important to develop efficient computational methods that make it possible to extract the signal induced by a focal source from the biological noise and the signal due to outside magnetic sources. Moreover, different sources within the brain may elicit similar or equal magnetic fields, and distinguishing between such sources must be based on complementary information. The design of algorithms that meet these challenges is the objective of the research in [2].

Methods: Magnetic noise, due to outside sources or to biological processes, is difficult to filter out by traditional techniques that rely solely on the properties of data. As an alternative to using the spatio-temporal properties of the signals themselves, we propose a source separation method that is based on the differences in spatial statistical properties of sources of different nature. A focal source has significantly different spatial characteristics from a virtual source explaining a disturbance from an outside source, as well as from a spatially distributed source that gives rise to the biological noise. The methodology is based on Bayesian mixture models and hierarchical prior models.

Results: We demonstrate with simulated examples that the methodology is capable to distinguish between a signal coming from inside the brain and one due to outside sources. Moreover, the methodology, augmented with variable source surface model leads to a new `` onion peeling'' algorithm that helps identify deep sources, that are of significant interest in using MEG for guiding epilepsy surgery. Previously, it was demonstrated [1] that Bayesian hierarchical models with Markov Chain Monte Carlo methods are able to identify deeps sources, indicating a great promise of the new mixture models.

Conclusions: Bayesian methods, augmented with the inclusion of complementary information to guide the MEG inverse problem have been extensively studied previously. The novel feature in this work is the use the Bayesian methods to discriminate between useful signal and noise, based on the different spatial statistics exhibited by the sources, real or virtual, that explain the data. Results obtained with simulated data are very promising, and we are now in the process of validating the methodology with real data.

References:

1. Calvetti D, Hakula H, Pursiainen S and Somersalo E (2009) Conditionally Gaussian hypermodels for cerebral source localization. SIAM J. Imaging Sci. 2:879-909

2. Calvetti D, Homa L and Somersalo E (2011) Bayesian mixture models and source separation in MEG. Manuscript.

1299

FUNCTIONAL ANGIOGENESIS IN THE EARLY STAGE OF THE ACUTE ISCHEMIC STROKE: A PRELIMINARY MICROPET/CT STUDY

J. Huang[1], Y. Wang[1], Q. Huang[1], S. Liang[2], B. Li[2], K. Chen[1,3], **G. Yang**[1]

[1]Med-X Institute, Shanghai Jiao Tong University, [2]Shanghai JiaoTong University Affiliated Ruijin Hospital, Shanghai, China, [3]Banner Alzheimer's Institute, Phoenix, AZ, USA

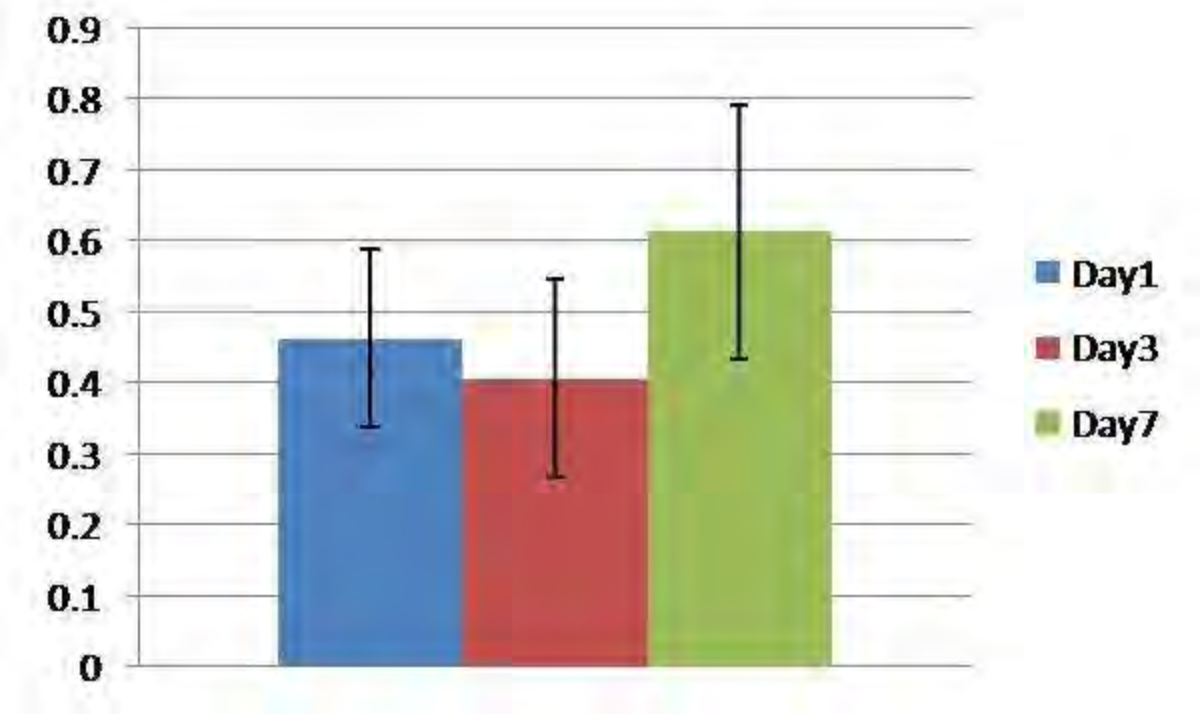

[SUVr for data acquired at Day 1, Day 3 and Day 7.]

[SUVr for data acquired at Day 1, Day 3 and Day 7.]

Objective: To investigate the feasibility of utilizing microPET/CT system and fluorodeoxyglucose (FDG) measured cerebral metabolic rate for glucose to image mouse model for cerebral ischemic stroke for the future potential use as treatment evaluation biomarker.

Methods: To mimic acute focal ischemia in humans, middle cerebral artery occlusion (MCAo) in mice were performed to build the focal cerebral ischemia model. The cerebral blood flow (CBF) was then measured after the MCAo using the Laser Doppler Flowmetry. FDG-PET and CT data were acquired 1 day (n=8), 3 days (n=7) and 7 days (n=11) afterwards.

After brain images were extracted from the whole body PET data with the assistance of CT scans, re-sliced and positioned approximately in the coordinate space of the MRI template in the SPM mouse toolbox (http://www.wbic.cam.ac.uk/~sjs80/spmmouse.html), a region of interest (ROI) on the ischemia core and on the a normal reference region were defined for each mouse. The normal reference region was generated by symmetrically mapping the ischemia ROI to the other side of the brain where normal metabolism was observed. The ratio of the ischemia ROI standard uptake value relative to the normal reference region (SUVr) was calculated. For data acquired at Day 1 after MCAo, linear correlation between SUVr and the ischemic CBF ratio over the normal half brain (CBFr) was studied.

Results: The correlation coefficient between SUVr and CBFr is 0.52777(n=8). After the MCAo, the SUVr decreases to its extremum at Day 3 followed by a recovery, as shown in Figure 1. The figure shows the mean value of SUVr with the error bar indicating the standard deviation. The SUVr values for Day 1, Day 3 and Day 7 are (mean±std) 0.46385±0.12, 0.40649±.0.14 and 0.61398±0.18 (ANOVA p=0.0238.) respectively.

Conclusion: The cerebral blood flow measured by Doppler flowmetry and the glucose uptake in the brain is correlated. After the ischemic stroke happens, there is a natural angiogenesis as demonstrated by the FDG-PET findings

This study confirms that animal FDG-PET imaging can *non-invasively* detect the MCAo induced ischemia functional changes over time. It provides a potentially more sensitive and non-invasive functional imaging tool to investigate different treatment strategies (for instance, the EPC transplantation (Zhang, et al., Circ Res, 2002. Ohta, et al., Neurosurgery, 2006. Fan, et al., Ann Neurol. 2010)) in promoting functional angiogenesis in the early stage of the acute ischemic stroke. With additional validation and possible combination of FDG-PET and other imaging modalities (such as CT or MRI), we believe neuroimaging techniques will provide biomarkers with high sensitivity and specificity in cerebral ischemic stroke studies.

1300

MÉNAGE À TROIS AND THE BALANCE OF CARBONS AND AMINO GROUPS DURING EXCITATION AND INHIBITION

D. Calvetti, E. Somersalo

Mathematics, Case Western Reserve University, Cleveland, OH, USA

Objectives: Predictive models of brain cellular metabolism are important when trying to determine which biochemical processes are directly or indirectly affected by the type and intensity of neuronal activity. The complexity of cerebral metabolism is further complicated by the presence of glutamatergic and GABAergic neurons, which interact with each other and with astrocytes at tripartite synapses, which are where the interplay between excitation and inhibition occurs. Brain energy metabolism has received a lot of attention in the past decade, fueling a debate on the primacy of glucose or lactate as a substrate to meet the energetic needs of neuronal (excitatory) activity, with only a few studies addressing the balance of amino groups, essential for the synthesis and recycling of neurotransmitters and their precursors. The integration of carbon and amino group balances in connection with the metabolic and neurovascular changes brought on by neuronal activities may offer some explanations for changes in the blood flow and metabolic rate which are yet to be explained. Our objective is to follow the shifts in metabolic activation with a detailed multi-compartment mathematical model of brain cellular metabolism comprising glutamatergic and GABAergic neurons, astrocyte, extracellular space and capillary blood compartment, tracking the balancing of both carbon skeletons and amino groups. For this purpose a new stoichiometric model of brain cellular metabolism will be assembled, and its configurations during high and low inhibitory and excitatory neuronal activity will be analyzed.

Methods: Bayesian Flux Balance Analysis (BFBA) will be performed with a new model of much higher metabolic complexity than what can be found in the literature. BFBA is based on the assumption that different ensembles of flux values and reaction rates can support a given steady state, hence these quantities, of primary interest for flux balance analyses, are regarded as random variables and described by their distributions rather than by given values. The new methodology, applied to analyze the energetic of inhibition and excitation separately, is particularly attractive for complex metabolic networks where classical flux balance analysis may fail due to inconsistencies between input, steady state assumptions, stoichiometry and other constraints.

Conclusions: Different levels of neuronal inhibition and excitation activate different portions of the metabolic pathway of the cerebrovascular unit which up- or down-regulate the shuttling of reducing equivalents across the mitochondrial membrane. Likewise, the malate-aspartate shuttle seems to be responsive to the transfer of amino groups between the different cell types accompanying the recycling of neurotransmitters. An elevated oxidative phosphorhylation activity to maintain redox balance may explain in part the brain's consumption of oxygen in excess of what needed for ATP production.

References:

1. Calvetti D, Somersalo E: Ménage à trois: the role of astrocyte during excitation and inhibition (submitted)

2. Occhipinti R, Somersalo E, Calvetti D (2009) Astrocytes as the glucose shunt for glutamatergic neurons at high activity: an in silico study. J Neurophysiol 101:2528-2538.

3. Occhipinti R, Somersalo E, Calvetti D (2010) Energetics of inhibition: insights with a computational model of the human GABAergic neuron-astrocyte cellular complex. Cereb. Blood Flow Metabolism 30:1834-1846.

1301

COALESCENCE OF SMALL-SCALE STROKES AS A PATHOLOGICAL MECHANISM IN CEREBROVASCULAR DEMENTIA

A.Y. Shih[1], J.D. Driscoll[1], P. Blinder[1], P. Tsai[1], B. Friedman[1], P.D. Lyden[2], D. Kleinfeld[1]

[1]Physics, University of California, San Diego, [2]Cedars-Sinai Medal Center, Los Angeles, CA, USA

Silent strokes are rarely investigated experimentally as clinical symptoms tend to be mild or inconspicuous due to their small size. However, small strokes have the potential to accumulate and lead to long lasting deficits in function and cognition. We use targeted laser thrombosis of single vessels in rodents to study the cumulative effect of single vessel strokes on cortical function and viability. Occlusion of only a single penetrating vessel, either arteriolar or venular in origin, could generate a columnar-shaped micro-infarction ~ 500 μm in diameter and 1000 μm deep after 7 days. This was due to the bottleneck-like architecture of penetrating vessels, as occlusion of highly interconnected surface and subsurface vascular networks were incapable of generating overt infarction. Penetrating vessel occlusions placed greater than 1 mm apart within the same imaging window led to distinct infarctions. However, occlusions placed less than 1 mm apart led to coalescence of the two infarcts into a single entity over the course of 7 days. The infarctions grew non-linearly in size as the number of occluded penetrating vessels increased to 5-9 placed sparsely throughout the imaging window. Longitudinal studies showed that infarct expansion involved rapid subsurface clotting and disruption of flow in penetrating vessel in regions bordering the stroke core. Further hallmarks of ischemic injury were observed acutely in the stroke border, including cortical spreading depression, seizure activity, vascular leakage, and leukocyte infiltration, and may contribute to infarct expansion. The coalescence of small infarcts was completely blocked by the NMDA receptor blockade using MK-801. Ongoing experiments will test the effectiveness of mild NMDA receptor antagonism and various immunomodulators. The non-linear expansion of small cortical strokes may be an unappreciated mechanism of tissue damage that accelerates cognitive deficit in vascular dementia and multi-infarct dementia.

1303

TRANSPLANTATION OF AUTOLOGOUS BONE MARROW STROMAL CELLS FOR ISCHEMIC STROKE - STRATEGY AND TACTICS FOR CLINICAL APPLICATION

S. Kuroda, H. Shichinohe, T. Sugiyama, M. Ito, M. Kawabori, K. Houkin

Department of Neurosurgery, Hokkaido University Hospital, Sapporo, Japan

Background: There is increasing evidence that the transplanted bone marrow stromal cells (BMSC) significantly promote functional recovery after central nervous system (CNS) damage in the animal models of various kinds of CNS disorders, including cerebral infarct, brain contusion and spinal cord injury. However, there are several shortages of information when considering clinical application of BMSC transplantation for patients with neurological disorders. In this paper, therefore, we discuss what we should clarify to establish cell transplantation therapy in clinical situation and describe our recent works for this purpose.

Methods and Results: The BMSC have the ability to alter their gene expression profile and phenotype in response to the surrounding circumstances and to protect the neurons by producing some neurotrophic factors. They also promote neurite extension and rebuild the neural circuits in the injured CNS. Using optical imaging and MRI techniques, the transplanted BMSC can non-invasively be tracked in the living animals for at least 8 weeks after transplantation. Functional imaging such as PET scan may have the potential to assess the beneficial effects of BMSC transplantation. The BMSC can be expanded using the animal protein-free culture medium, which would maintain their potential of proliferation, migration, and neural differentiation. The BMSC significantly promote functional recovery when stereotactically injected into the brain, but not when intravenously infused, at 7 days after the onset of cerebral infarct. In vivo optical imaging and histological analysis support the findings. G-CSF can enhance the in vitro proliferation of BMSC isolated from the aged animals, promising clinical application for donor cell expansion.

Conclusion: It is urgent issues to develop clinical imaging technique to track the transplanted cells in the CNS and evaluate the therapeutic significance of BMSC transplantation in order to establish it as a definite therapeutic strategy in clinical situation in the future.

1304

MERGING MOLECULAR IMAGING AND BEHAVIORAL NEUROSCIENCE: SEEING ANIMAL MODELS IN A NEW LIGHT

W.K. Schiffer[1], J. Carrion[2], D.L. Alexoff[3], S.L. Dewey[4], J.D. Brodie[1]

[1]Department of Psychiatry, NYU School of Medicine, [2]The City College of New York, New York, [3]Department of Environmental and Atmospheric Sciences, Brookhaven National Laboratory, Upton, [4]Feinstein Institute for Medical Research, North Shore University Hospital, Manhasset, NY, USA

Objectives: Behavioral neuroimaging in animals allows us to map preclinical models to clinical studies by examining both behavior and molecular imaging endpoints simultaneously. We will describe the development and validation of a new paradigm in which PET and many receptor specific radiotracers can capture dynamic molecular events in behaving animals. Present imaging approaches rely mostly on non-specific changes that relate regional brain activity to associated behavioral changes. While powerful, we are now using specific molecular probes in behaving animals. This change in emphasis from imaging nonspecific brain targets to specific molecular events represents a significant paradigm shift and offers a new tool for understanding brain/behavior relationships.

Methods: Key to our paradigm, radiotracer uptake occurs while animals move freely in a range of test environments, followed by anesthesia and scan. Using ^{11}C-raclopride (^{11}C-rac) as a prototypical probe whose displacement reflects changing dopamine, we validated this paradigm with drug challenges designed to directly perturb ^{11}C-rac (loading doses of cold rac) or indirectly change ^{11}C-rac by changing dopamine (METH to increase and AMPT to decrease dopamine). Systematic variations in uptake duration, type and presence of anesthetic, route of ^{11}C-rac administration and image acquisition methods were used to optimize the protocol. For these validations, paired scans were performed where uptake occurred in the awake state, followed by anesthesia and scanning. While still in the gantry, a second scan gave full time activity data from the same animal. Comparing these data allowed us to validate derivations of binding potential used to quantitate awake uptake. All awake studies were videoed and analyzed with behavioral phenotyping software. With this information, individual behaviors were directly related changes in ^{11}C-rac binding.

Results: Behavioral challenges revealed striking parallels analagous to human PET studies. First, stress decreased ^{11}C-rac binding, an effect that significantly correlated with behavior and was similar in magnitude to that following METH. Second, cue exposure in cocaine-addicted animals significantly decreased ^{11}C-rac, and this decrease correlated with individual measures of craving using the CPP model. The magnitude was similar to the decrease in ^{11}C-rac from an acute dose of cocaine. Microdialysis data revealed that cue exposure produces lower but sustained increases in dopamine, while cocaine produces large, rapid increases that quickly return to baseline. This is one explanation for why a behavioral challenge (ie drug cues) produces the same magnitude of 11C-rac displacement as the drug itself, yet the reward is very different.

Conclusions: Perhaps the most important message, individual changes in ^{11}C-rac binding were closely linked to individual differences in behavior in each model tested. Animals with little genetic variation and no difference in rearing will, for example, respond uniquely to stress and this response closely reflects ^{11}C-rac. This reflects inherent variability common to clinical PET studies, but in animals it is obscured by examining group responses in single-focus behavioral

or biological experiments. Finally, these data address a burgeoning problem in clinical behavioral PET experiments by demonstrating that the shape of the dopamine pulse plays an important role in the magnitude of radiotracer displacement.

1305

INTRACEREBRAL VERSUS INTRAVENOUS BONE MARROW STROMAL CELL ADMINISTRATION IN A RODENT MODEL OF STROKE

M. Kawabori[1], S. Kuroda[1], M. Ito[1], T. Sugiyama[1], H. Shichinohe[1], K. Houkin[1], Y. Kuge[2], N. Tamaki[3]

[1]Department of Neurosurgery, [2]Department of Tracer Kinetics and Bioanalysis, [3]Department of Nuclear Medicine, Hokkaido University Graduate School of Medicine, Sapporo, Japan

Objectives: Recent studies have indicated that bone marrow stromal cells (BMSC) have the potential to improve neurological function when transplanted into animal model of central nervous system (CNS). However, there still exist a several questions that has not been solved, such as the route of cell delivery and timing of the transplantation. In the present study, we compared the effect of systemic and local administration of BMSC in adult rodent model of stroke at the subacute stage.

Methods: The rats were subjected to permanent middle cerebral artery occlusion. 7 days after the insult, 1×10^7 or 3×10^7 quantum dots labeled BMSC were transplanted directly into the ipsilateral striatum (intracerebral group)or systematically into the tail vein (intravenous group) consecutively. Motor function and non-invasive cell tracking using near infrared fluorescence was performed to assess the efficacy. The fate of the transplanted BMSC was examined at 5 weeks after transplantation, using immunohistochemistry.

Results: BMSC transplantation significantly enhanced functional recovery in intracerebral group, while intravenous group showed no significant functional recovery compared with the vehicle. NIR fluorescence imaging can also detect cell migration only with direct injection group. Histological analysis revealed that some of the transplanted BMSC showed neural and glial differentiation in the infarct brain.

Conclusions: Intracerebral transplantation of BMSC may provide better functional recovery when compared with intravenous transplantation at the subacute stage of rodent stroke model. Therapeutic time window must be call into account when considering the route of BMSC transplantation.

1307

SUFFICIENT SURGICAL REVASCULARIZATION IMPROVES CEREBRAL HEMODYNASMICS AND ATTENUATE HEADACHE IN PEDIATRIC MOYAMOYA DISEASE

M. Kawabori[1], S. Kuroda[1], N. Nakayama[1], T. Ishikawa[2], K. Houkin[1]

[1]Department of Neurosurgery, Hokkaido University Graduate School of Medicine, Sapporo,
[2]Department of Surgical Neurology, Research Institute for Brain and Blood Vessels-Akita, Akita, Japan

Objectives: Headache is one of the major clinical presentations of moyamoya disease especially in pediatric patients. Because not a few Patients who complained preoperative headache recognize attenuation of headache after surgery, hemodynamic stress is thought to play an important role in the development of headache. However, the precise mechanism is still unknown. To clarify the pathophysiological feature of headache in pediatric moyamoya disease, the authors have conducted a questionnaire and reviewed the data of pre- and postoperative hemodynamics using PET or SPECT in relation with headache.

Methods: The authors surveyed 29 children with moyamoya disease younger than 17 years of age who underwent bypass surgery consecutively between 1997 and 2010 in our institute. The headache was regarded as significant if they disturbed their daily activity, required rest and/or medication. Surgery was performed to the hemodynamically compromised hemisphere, using direct and indirect bypass as a general rule. MRI/A, CT, angiography, and SPECT and/or PET were performed preoperatively and postoperative 3 months or later.

Results: Preoperative headache was documented in 38% (11 of 29 patients), and postoperative headache was observed in 9% (1 of 11) of the patient with preoperative headache and in 6% (1 of 18) of those without preoperative headache. In the patient with preoperative headache, 81% (9 of 11) of them developed headache at the awakening or in the morning. The location of the headache and the local impaired hemodynamics were well correlated in the preoperative headache.

Conclusions: Preoperative headache in the pediatric moyamoya disease is strongly correlated with local impaired hemodynamics and migraine may play an important role in the development of preoperative headache. Most of the preoperative headache can be attenuated with sufficient surgical revascularization.

1309

MODULATION OF STRESS INDUCED ANXIOGENESIS AND BRAIN OXIDATIVE INJURY BY NEUROSTEROIDS: POSSIBLE ROLE OF NITRIC OXIDE

K. Gulati, A. Chakraborti, A. Ray

Vallabhbhai Patel Chest Institute, University of Delhi, Delhi, India

A variety of emotional and environmental stressors are known to influence brain functions thus resulting in precipitation of several neuropsychiatric illnesses. Since the inception of concept of stress in medicine and biology, stress has considerably evolved into a highly interactive system and complex neurochemical mechanisms in the brain have been proposed. Oxidative injury results from imbalance between prooxidant and antioxidant forces and the brain is highly susceptible to such damage. Neurosteroids are important endogenous modulators of CNS activity and behavioral processes and alterations of their concentrations may contribute to neurobehavioral disorders. Nitric oxide (NO), a versatile, neuromodulatory molecule with multidimensional effects, is localized in brain regions (eg. hypothalamus, amygdala and hippocampus) involved with anxiety. Thus, the present study evaluated the effects of the neurosteroid, dehydroepiandrosterone sulphate (DHEAS) on stress induced anxiogenesis and brain oxidative injury in rats and the possible involvement of nitric oxide (NO) during such modulatory effects. Restraint stress (RS for 1h at room temperature) was used as the experimental stressor and the elevated plus maze (EPM) test was used to assess the anxiogenc/anxiolyitc profile. Following behavioral studies, the animals were sacrificed and the brains were dissected out, homogenized and assayed for oxidative/nitrosative stress markers. Exposure to RS induced significant reductions in percent open arm entries (OAE) and time spent in open arms (OAT) in the EPM test - suggestive of an anxiogenic response. Pretreatment with DHEAS (20 and 40 mg/kg), prior to RS significantly increased both OAE and OAT values. Prior treatment with the NO synthase inhibitor, L-NAME (50 mg/kg) blocked the stress-attenuating effects of DHEAS and this was evident for both OAE and OAT values. On the other hand, the NO precursor, L-Arginine (100 mg/kg) potentiated the action of DHEAS (5 mg/kg) and there was significant reversal of both OAE and OAT towards normalcy. Biochemical assay of brain homogenates showed that RS suppressed NOx (stable NO metabolites) and GSH (reduced glutathione, endogenous antioxidants) while enhancing MDA (melondialdehyde, index of lipid peroxidation) levels. Pretreatment with DHEAS (20 and 40 mg/kg) significantly attenuated the RS induced suppression of NOx and GSH levels while decreasing MDA levels. Further, L-Arginine (100 mg/kg) pretreatment potentiated the action of DHEAS (5 mg/kg) and there was significant reversal of both NOx and MDA. On the other hand L-NAME (50 mg/kg) blocked the attenuating effect of DHEAS (40 mg/kg) and this was evident for NOx, GSH as well as MDA values. Neurosteroids like DHEAS are known to stimulate NO synthesis due to enhanced expression and stabilization of NOS enzyme and may also rapidly activate NOS through a non-transcriptional mechanism. It is thus possible that DHEAS may have increased NO generation which might have prevented the RS induced anxiogenic response. It can also be inferred from the present results that neurosteroids like DHEAS exert protective effects on stress induced anxiogenesis and brain oxidative injury in rats and NO-dependent mechanisms may be involved.

1310

BRAIN TARGETING OF PLGA NANOPARTICLES OF DONEPEZIL FOR TREATMENT OF NEUROLOGICAL DISORDERS

J. Ali[1], M. Bhavna[1], M. Ali[1], S. Babootа[1], A. Bhatnagar[2]

[1]Department of Pharmaceutics, Jamia Hamdard, [2]Institute of Nuclear Medicine and Allied Sciences, New Delhi, India

Objective: To formulate poly(lactide-co-glycolide) (PLGA) nanoparticles of donepezil coated with Tween-80 to deliver donepezil by intravenous route for neurodegenerative disorders.

Methods: Donepezil loaded PLGA nanoparticles were prepared by emulsion solvent diffusion evaporation method using Tween 80 as a stabilizer. Donepezil was encapsulated in these nanoparticles and evaluated by Transmission electron microscopy (TEM), Scanning electron microscopy (SEM) and zetesizer. A method for radiolabeling the optimized formulation of radiolabeled donepezil loaded PLGA nanoparticles with ^{99m}Tc was standardized using stannous chloride as reducing agent. The biodistribution studies were performed in animal model of Sprague Dawley rats and the prepared nanoparticles were injected i.v. The levels of donepezil was determined in various organs in comparison to drug solution as a positive control. The gamma scintigraphic images were also captured to show the localization effect of released drug from the PLGA nanoparticulate formulation in the brain of animal model of Sprague Dawley rats.

Results: The prepared nanoparticles were in the range of 20 - 100 nm having a spherical shape and smooth surface and the coating of tween-80 on the nanoparticles was clearly observed. It is anticipated that this coating of tween-80 could inhibit the efflux system, especially P-glycoprotein (Soppimath et al., 2001) contributing towards enhanced drug delivery to brain via BBB. Radiolabeling of optimized nanoformulation with ^{99m}Tc consistently gave a radiolabeling efficiency of >95% using stannous chloride as reducing agent. The radiolabeled preparation was found to be fairly stable up to 24 h. The biodistribution data of drug loaded nanoparticulate system and drug solution via intravenous route revealed higher % of radioactivity/g in the brain for the nanoparticulate formulation as compared with the drug solution ($p < 0.05$). When the nanoparticulate suspension was given intravenously, there was an increased concentration of drug in brain due to the small particle size of nanoparticles (< 200 nm) which crosses the BBB faster. The gamma scintigraphic images showed localization of released drug from the PLGA nanoparticulate suspension and drug solution. As the drug comes into the circulation within seconds the images were captured for initial 5 min. The region of interest (ROI) of brain showed increased radiation intensity from the radiolabeled drug in the brain region for PLGA nanosuspension as compared with that for drug solution.

Conclusions: This study proves that the coating of nanoparticles with tween-80 resulted in greater transport of nanoparticles across the BBB, allowing brain targeting following an intravenous injection. The donepezil loaded PLGA NPs, due to the receptor mediated transport at the BBB and prolonged circulation of NPs in blood as a result of surface coating with tween-80 exhibited improved uptake and significantly longer presence in brain. It may reduce dose and/or frequency of the drug presently administered by parenteral route. Hence, i.v. administration of donepezil loaded nanoparticles could be an alternative approach to deliver drug to brain.

1312

CNS-IMMUNE INTERACTIONS DURING STRESS AND ITS REGULATION BY NITRIC OXIDE (NO) IN RATS

A. Ray, K. Gulati

Vallabhbhai Patel Chest Institute, University of Delhi, Delhi, India

Psychoneuroimmunology expresses the interactions betweenbrain, behavior and immunity. A bi-directional link exists between the central nervous system (CNS) and immune systems and such CNS-immune interactions play a crucial role on maintaining the homeostasis. Stress in any external and internal stimulus capable of disrupting such homeostatic mechanisms and is capable of influencing both neurobehavioral and immune functions. Complex petrochemical mechanisms regulate stress responses and nitric oxide (NO) is widely documented as a unique, multidimensional messenger molecule with neuromodulatory properties. The present study thus evaluated the role nitric oxide (NO) and its signaling pathways in CNS-Immune interactions during stress. Acute restraint stress (RSx1) suppressed neurobehavioral activity in the elevated plus maze test suggestive of anxiogenic response, and this was associated with suppressions in brain NO metabolite (NOx) and elevations in brain ADMA activity. Pretreatment with the NO mimetic, L-arginine attenuated both behavioral responses and brain biochemical markers, whereas, the NO synthase inhibitor, L-NAME, aggravated them. Acute RS, however, had no appreciable effects on adaptive immune markers, viz. humoral and cell mediated immune responses. Antibody responses were suppressed, delayed type hypersensitivity reactions were inhibited and differential modulations of cytokines (TNF-α, IL-1β , IL-6, IL-4) were observed. On the other hand, chronic RS (RSx15) resulted in greater degree of behavioral suppression and brain NOx, and in addition, both humoral and cell mediated immune responses were markedly suppressed. These changes were accompanied by enhancements in lipid peroxidation (MDA levels) in both brain homogenates and plasma . The chronic Rs induced neurobehavioral, biochemical and immunological changes were attenuated by melatonin and alpha-tocopherol pretreatments and α-tocopherol by L-NAME. Sex differences also influences RS induced behavioral and immune responses and male rats showed greater anxiogenic and immunosppressive responses, and these were associated with lower NOx and brain MDA levels, as compared to females. Similarly. `high emotional` rats showed greater stress susceptibility in behavioral and immune responses as also lower levels of brain and plasma NOx as compared to `low emotional` rats. It is proposed that stress may be an integrated output of several physiological responses and behavioral stressors like restraint may be effectively used as a unique model for studying neural-immune reactions. Further, the data are strongly suggestive of the involvement of NO and its interactions with reactive oxygen species in the regulation of such CNS-Immune interactions.

1314

NICOTINE AMELIORATES BEHAVIORAL DEFICITS AND OXIDATIVE STRESS IN A 6-HYDROXYDOPAMINE RAT MODEL OF PARKINSON'S DISEASE

A.S. Ciobica[1], L. Hritcu[1], M. Padurariu[2], C. Joacabine[2]

[1]Alexandru Ioan Cuza University, [2]Gr. T. Popa University, Iasi, Romania

Background: Parkinson's disease (PD) is a human neurodegenerative disorder which is mainly characterized by a massive and progressive degeneration of the dopaminergic neurons in the substantia nigra (SN). As a result, one of the most widely used animal models of PD involve injecting of 6-OHDA directly into the SN, in order to induce selective neurodegeneration of dopamine nerve terminals. We previously demonstrated that 6-OHDA-induced lesion of SN results in memory deficits and increase brain oxidative stress.

Some authors suggested that tobacco smoking may represent a form of self-medication in some brain disorders. Experimental studies showed contradictory results regarding the influence of nicotine on memory formation. In addition, the effects of nicotine on oxidative stress are controversial.

The aim of the present study was to examine the effects of nicotine, on behavioral deficits and brain oxidative stress induced by 6-OHDA in a rat model of PD.

Material and methods: 30 male Wistar rats weighing 200-250 g at the start of the experiment were used. Specific right-unilateral lesions of the dopaminergic neurons located in the SN were produced with 6-OHDA. 8 µg 6-OHDA, dissolved in 4 µl physiological saline containing 0.1% ascorbic acid were administrated through Hamilton syringe. The following coordinates were used: 5.5 mm posterior to bregma; 2.0 mm lateral to the midline; 7.4 mm ventral to the surface of the cortex.

Two weeks after operation, all surviving animals showing no evident neurological abnormalities were admitted to drug treatment. Nicotine was dissolved in saline and injected intraperitoneally at the dose of 0,3mg/kg/day for consecutive 7 days. Control animals received an injection of saline alone with the same procedure.

Two-way active avoidance and Y maze tasks were used for memory assessment. We also assessed the levels of some enzymatic antioxidant defences like superoxide dismutase (SOD) and glutathione peroxidase (GPX), as well as lipid oxidation makers like malondialdehyde (MDA), from the temporal lobe, using chemiluminometric and spectrophotometric methods.

Results: Administration of nicotine resulted in a significant facilitation of spatial short-term memory, explored by Y-maze task, as indicated by an increase of spontaneous alternation percentage ($F(1,28)=53$, $P< 0.006$), compared to control rats. This effect could not be attributed to increased motor activity, since the number of arm entries was not significantly changed.

Also, nicotine induced a decrease ($F(1,28)=94.21$, $p< 0.00001$) of the latency time in the two-way active avoidance, suggesting positive effects on long-term memory.

At the biochemical level, we observed an increase in the specific activity of SOD and GPX, in the temporal lobe of nicotine-treated rats, compared to control group. Moreover, Pearson's

correlation coefficient and regression analysis revealed a significant positive correlation between latency time in two-way active avoidance and antioxidant enzymes specific activities.

Conclusions: Taken together, our data suggest that nicotine (0,3mg/kg/day) may counteract both behavioral and biochemical changes induced by 6-OHDA in a rat model of PD. Our study also suggests that these positive behavioral responses could be correlated with some antioxidant actions of nicotine. This could be useful for future investigations and clinical applications of nicotine.

1315

THE IMPLICATION OF PERIPHERAL OXIDATIVE STRESS IN MILD COGNITIVE IMPAIRMENT AND ALZHEIMER´S DISEASE

M. Padurariu[1], A.S. Ciobica[2], V. Bild[1], C. Joacabine[1]

[1]Gr. T. Popa University, [2]Alexandru Ioan Cuza University, Iasi, Romania

Background: Alzheimer's disease (AD) is the most common cause of dementia in the elderly, affecting several million of people worldwide. The diagnosis of AD may be preceded by a long stage of neuropathological changes and cognitive decline, known as Mild Cognitive Impairment (MCI), without significant impact on the activities of daily life. The progression of MCI into AD is estimated with a probability of 50% within 4 years, approximately 12% per year, supporting the concept that MCI represents a prodromal stage of AD. In this context, it is fundamental to identify and biochemically characterize these patients during the predementia phase, where pharmacological intervention would have the greatest potential to inhibit or delay disease progression.

A large body of evidence suggests that oxidative stress plays an important role in the pathogenesis of AD, and that it occurs early in the course of the disease, preceding the development of the pathological hallmarks, like neurofibrillary tangles and senile plaques.

In this way, the aim of this study was to determine the peripheral oxidative stress status in MCI and AD patients.

Methods: The patients were selected using Petersen criteria for Mild Cognitive Impairment and NINCDS ADRDA criteria for Alzheimer's disease. The cognitive performance was assessed using MMSE (Mini Mental State Examination), ADAS-cog (Alzheimer´s Disease Assessment Scale- cognitive subscale), Clock Drawing Test and Verbal Fluency Test. We assessed the levels of some enzymatic antioxidant defences like superoxid dismutase (SOD) and glutathione peroxidase (GPX), as well as lipid oxidation makers like MDA (malondialdehyde), using chemiluminometric and spectrophotometric methods. The results were compared to an aged-matched control group.

Results: Biochemical analyses showed a similar decrease of the main enzymatic antioxidant defences (SOD and GPX) and increased production of lipid peroxidation marker (MDA) in the serum of the MCI and AD patients, compared to age-matched control group.

We also looked for correlations between antioxidant levels and clinical variables in the different diagnostic groups. We found that in MCI patients the cognitive function positively correlates with antioxidant levels.

Conclusions: These results support the hypothesis that oxidative damage is an important event in the pathogenesis of neurodegenerative diseases. Also, it seems that some peripheral markers of oxidative stress appear in MCI with a similar pattern to that observed in AD, which suggest that oxidative stress might represent an early event of the AD pathology.

In this context, new antioxidant strategies appear to be an encouraging focus of therapeutic interventions and should be proposed as primary prevention measures, maybe years before the dementia age risk.

Further studies of antioxidants as therapeutic intervention for AD, therefore, appear to be warranted. Also, the ability to identify oxidative damage at early stages such as MCI will have a potentially great importance.

1316

THE ROLE OF THE SYSTEMIC INFLAMMATORY RESPONSE IN THE DEVELOPMENT OF BRAIN METASTASES

A.M. Hamilton, S. Serres, A. Khrapichev, S. Ferjancic, R.P. Choudhury, D.C. Anthony, N.R. Sibson

University of Oxford, Oxford, UK

Objectives: The mechanism of tumour metastasis to the brain is poorly understood. Mechanisms that govern tumour cell arrest in blood vessels are likely to be similar to those of the leukocyte adhesion cascade[1], which relies on expression of adhesion molecules such as vascular cell adhesion molecule-1 (VCAM-1)[2]. We hypothesized that up-regulation of these molecules via a systemic inflammatory response would lead to an increase in the number of tumour cells that arrest in cerebral blood vessels and the number of metastases. VCAM-1 expression can be monitored in vivo using a novel VCAM-1-targeted contrast agent (VCAM-MPIO)[3]. The aim of this study was to quantify both VCAM-1 expression and tumour burden in a mouse model of brain metastasis with or without systemic inflammatory challenge.

Methods: 8-10-week-old female balb/c mice were injected with 10^5 4T1-GFP tumour cells intracardially. In some animals IL-1β-producing replication-deficient adenovirus (AdIL-1) was injected intravenously either one day PRE- or five days POST-tumour cell injection. At day 10 post-4T1 cell injection, all animals underwent T2*-weighted MRI using VCAM-MPIO to detect VCAM-1 expression. Brains were taken for immunohistochemistry to assess tumour burden and to co-localize tumour location with MRI-based detection of VCAM-1. Control mice injected with AdIL-1 only were imaged either 5 or 11 days after Ad-injection to determine the level of hypo-intense MRI signal, and the level of VCAM-1 expression on blood vessels in the brain immunohistochemically.

Results: Injection with AdIL-1 led to a significant increase in both the number and size of tumours in the brain (Fig 1(b)). An eight-fold increase in the volume of VCAM-MPIO-induced hypo-intensity on T2*-weighted images was observed in 4T1-injected animals compared to naive. Similar increases in signal volume were seen both in 4T1-injected animals pre-treated with AdIL-1, and animals imaged 11 days after AdIL-1 alone. A fifteen-fold signal increase was observed in animals injected with AdIL-1 five days post-tumour cell injection compared to naive. However, the same level of signal change was seen in control animals injected with AdIL-1 alone (5 days post-virus). Ca. 60% of all blood vessels in the brain were VCAM-1 positive 1, 5 and 11 days post-adenovirus injection. Surprisingly, the majority of VCAM-1 expression was located on arterioles rather than venules.

Conclusions: Injection of an AdIL-1 in animals pre- and post-tumour injection induces an increase in VCAM-1 expression on blood vessels in the brain and an increase in size and number of tumours in the brain. These changes are associated with T2*-weighted VCAM-MPIO-contrast changes using MRI. Tumours above a threshold of ca. 1/1000 µl can be reliably detected from hypo-intense signals with VCAM-MPIO-contrasted T2*-weighted imaging.

References:

1) Yilmaz et al. Trends Mol. Med. 13:535-541 (2007)

2) Ley et al. Nat. Rev. Immunol. 7:678-689 (2007)

3) McAteer et al. Nat. Med. 13:1253-1258 (2007)

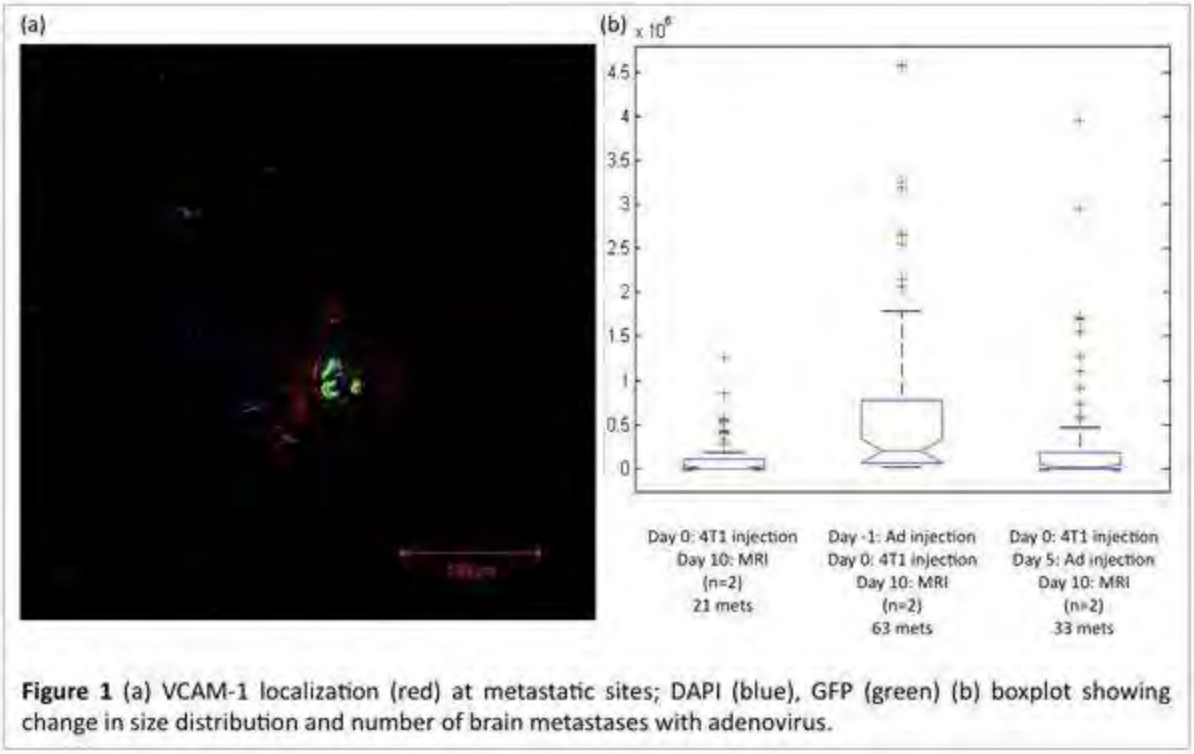

Figure 1 (a) VCAM-1 localization (red) at metastatic sites; DAPI (blue), GFP (green) (b) boxplot showing change in size distribution and number of brain metastases with adenovirus.

[Figure 1]

1317

DEVELOPMENT OF AN HSP70-REGULATED FAR-RED FLUORESCENT REPORTER MOUSE FOR IMAGING THE ISCHEMIC PENUMBRA

X. de la Rosa[1,2], T. Santalucía[1,2], J. Purroy[1,2,3], M. Calvo[4], A. Salas[1,2], C. Justicia[1,2], A.M. Planas[1,2]

[1]Department of Brain Ischemia and Neurodegeneration, Institut d'Investigacions Biomèdiques de Barcelona (IIBB)-Consejo Superior de Investigaciones Científicas (CSIC), [2]Institut d'Investigacions Biomèdiques August Pi i Sunyer (IDIBAPS), [3]Parc Científic de Barcelona, Universitat de Barcelona, [4]Servei de Microscopia, Serveis Cientifico-Tècnics, Universitat de Barcelona (UB), Barcelona, Spain

Objectives: Neurons surrounding the ischemic area express Hsp-70 and this is regarded as a marker of the ischemic penumbra (1,2). Hsp-70 is also strongly induced in blood vessels within the ischemic territory. Our aim was to obtain transgenic mice expressing a fluorescent reporter to image the induction of Hsp70. For such applications, the use of a far-red fluorescent protein reporter is desirable so that fluorescence absorption and scattering by the cerebral parenchyma are reduced (3).

Methods: An Hsp70 promoter-driven reporter vector for the far-red fluorescent protein mPlum (4) was constructed with Invitrogen's Multisite Gateway Vector Construction kit. NIH3T3 cells were transfected with this vector and stimulated with sodium arsenite (50 uM) to induce Hsp-70 expression (5) mPlum and Hsp70 protein expression was detected with specific antibodies by Western blotting and immunocytochemistry. mPlum fluorescence was detected with a fluorescence inverted-microscope. Transgenic mice were generated at the “Norsk Transgen Senter” (Norway). Transient middle cerebral artery occlusion (MCAO) was performed on adult transgenic or wt mice as previously described (6). A cranial window sealed with a cover slip was opened on ketamine/xylacine-anesthetised mice over the ipsilateral hemisphere for live observation under high speed confocal microscope (590nm ex, 649nm em) 24h after ischemia. Mice were killed thereafter and the brain was processed for immunohistochemistry. In another set of animals, brain samples were obtained 24h after MCAO and were processed for either quantitative real time RT-PCR or Western blotting.

Results: Cells transfected with the Hsp-70 reporter vector showed induction of mPlum when Hsp-70 expression was stimulated, showing the usefulness of our construct to track Hsp-70 induction. In transgenic mice, MCAO induced expression of mPlum and hsp70 mRNAs and proteins in the ipsilateral hemisphere. Intravital confocal microscopy showed mPlum fluorescence in superficial blood vessels of the ipsilateral hemisphere. Immunohistochemistry on post-mortem brain sections revealed expression of mPlum in the infarct area, which co-localised with endogenous Hsp70 expression in blood vessels and neurons. Despite mPlum's limited intensity of fluorescence signal, our studies reveal that mPlum fluorescence can be detected in live animals after brain ischemia, mainly in cortical blood vessels that show the strongest induction of Hsp-70 and mPlum.

Conclusions: Our results show that our Hsp70-mPlum reporter vector in the transgenic mice responds to ischemia in a parallel way to endogenous Hsp70, and that it is possible to track Hsp-70 expression *in vivo* through mPlum fluorescence.

References:

1. Planas et al. (1997) Prog Neurobiol; 51: 607-36.

2. Zhang et al. (2010) Brain Res; 1343:143-52.

3. Deliolanis et al. (2010) J Biomed Opt; 13:044008.

4. Wang et al. (2004) PNAS; 101 : 16745-9

5. Fauconneau et al. (2002). J Neurochem ; 83:1338-48.

6. Cervera et al (2010) PloS One; 5: e8433.

Acknowledgements: We thank Roger Tsien (UCSD) for providing the mPlum cDNA. X. R. has a fellowship from the Spanish Ministry of Science and Innovation (MICINN). T.S. participates in the Program for Stabilization of Investigators from the “Generalitat de Catalunya”, Spain. Financed in part by the EC (FP6 Diagnostic Molecular Imaging) and MICINN (SAF2008-04515).

1318

VALIDITY OF ^{18}F-FLUORODEOXYGLUCOSE PET IN IDENTIFYING INFLAMED AND VULNERABLE CAROTID PLAQUE - A RADIOLOGICAL AND PATHOLOGICAL STUDY

S. Kuroda[1], N. Nakayama[1], K. Hirata[2], T. Shiga[2], K. Houkin[1], N. Tamaki[2]

[1]Department of Neurosurgery, [2]Department of Nuclear Medicine, Hokkaido University Hospital, Sapporo, Japan

Objective: In this report, we assessed whether ^{18}F-fluorodeoxyglucose (FDG) PET can identify inflamed and vulnerable plaque at higher risk for subsequent ischemic stroke in patients with internal carotid artery (ICA) stenosis.

Methods: This prospective study included 23 patients with ICA stenosis of more than 70%, including 18 males and 5 females. Their age ranged from 48 to 85 years. All 23 patients underwent ^{18}F-FDG PET, CT, MRI, and ultrasound to evaluate the plaque morphology and composition prior to carotid endarterectomy (CEA). Following surgery, the specimens were examined, using HE staining and immunohistochemistry.

Results: Carotid plaque had a high uptake of ^{18}F-FDG in 9 (39%) of 23 patients. Intraoperative observations revealed that their carotid plaques were lipid-rich and vulnerable. Histological analysis detected a dense accumulation of lipid and activated macrophages in these plaques. On the other hands, such high uptake of ^{18}F-FDG was not observed in other 14 patients (61%). Of these, 12 were fibrous and were considered as “stable” plaques. Other two lesions had large subintimal hemorrhage associated with ulcer formation.

Conclusion: The present results suggest that ^{18}F-FDG PET would be valuable to identify the inflamed, vulnerable plaque and predict the risk for subsequent ischemic stroke in patients with severe ICA stenosis.

1319

BRAIN PLASTICITY AND REGENERATION

B.B. Johansson

Clinical Neuroscience, Wallenberg Neuroscience Center, Lund University, Lund, Sweden

The value of aim-directed training-induced plasticity in a stimulating environment is well established after brain lesions. Current knowledge on the organization and connection of networks from the level of individual cells and synapses to sensory-motor and cognitive systems, and how unilateral lesions can disrupt networks on both sides of the brain, suggests that we should pay more attention to networks and multisensory interaction in stroke rehabilitation. Methods based on multisensory integration of motor, cognitive and perceptual processes such as action observation, motor imagery, mental training, and training in virtual reality, are currently being tested with promising preliminary results. Rhythmic music activates motor and premotor cortices and can enhance gait and arm motor training. Listening to music also activates many brain structures related to sensory processing, attention, and memory, and various music therapies are tried in cognitive rehabilitation. Repetitive trans-cranial magnetic stimulation, rTMS, and transient direct cortical stimulation, tDCS are neurophysiological methods that are increasingly being used both in diagnosis and in treatment after brain damage. To avoid the confounding effect of spontaneous improvement, most trials with new techniques have so far been performed ≥ 3 months post stroke. Randomized trials earlier after stroke and longer follow-ups are needed. More attention should be given to stroke heterogeneity, cognitive rehabilitation, social adjustment and quality of life.

Regeneration is the optimal goal for treatment of acute and chronic brain disorders. To understand to what extent that is possible needs much further research. Main research lines concern regeneration by stimulation of endogenous neuronal cell proliferation and differentiation, and transplantation of various stem cells or progenitor cells. Other research lines include neutralizing myelin inhibitory factors in the brain and spinal cord, and methods aimed to optimize the extracellular environment and vascularization. In addition to neurogenesis, regeneration requires astrocytes, oligodendrocytes and other brain cells, vascularization and a submissive extracellular environment for cell survival and myelin production. It is an extensive research area that includes most acute and chronic neurological disorders from stroke and trauma to multiple sclerosis, amyotrophic lateral sclerosis, Parkinson disease (PD), Alzheimer disease and Huntington Dementia. A wide variation of animal models of brain disorders are currently used, and it has been shown that housing in cages allowing various activities and stimulation can have epigenetic effects and influence survival and functional outcome.

Environment and genes interact throughout life and genetic polymorphism can influence the response of the human brain to injury and disease. In healthy individuals, a common single nucleotide polymorphism (BDNFval66met) reduces the activity-related cortical plasticity in human motor cortex, and is associated with greater error and poorer retention in short-term motor learning, and with reduced cognitive performance. It has been reported to predict poor outcome among survivors of aneurismal subarachnoid hemorrhage. Furthermore, it can interact with dopamine and increase early and severe hyperkinesias in patients with PD treated with L-DOPA. Genetic studies in humans are likely to play an important role for finding the optimal treatment for individual patients in the future.

1321

IMAGING DOPAMINE D3 RECEPTORS IN ALCOHOLISM WITH [^{11}C]-(+)-PHNO

D. Erritzoe[1], A. Tziortzi[2,3], D. Bargiela[1], G. Searle[2], R.N. Gunn[2], J.D. Beaver[2], D. Nutt[1], A. Waldman[4], M. Bani[5], E. Merlo-Pich[5], E.A. Rabiner[2], A. Lingford-Hughes[1]

[1]Neuropsychopharmacology Unit, Imperial College London, [2]Clinical Imaging Centre, GSK, London, [3]FMRIB Centre, Department of Clinical Neurology, University of Oxford, Oxford, [4]Department of Imaging, Charing Cross Hospital, London, UK, [5]CEDD for Neurosciences, GlaxoSmithKline, Verona, Italy

Background: Several lines of evidence support a role for dopamine-D3 receptors (DRD3) in alcohol reinforcement or liking[1]. The lack of PET ligands suitably selective for the DRD3 over the DRD2 has so far hindered the direct evaluation of DRD3 status in alcoholic patients. The introduction of the DRD3 preferring PET radioligand [^{11}C]-(+)-PHNO, when used in combination with a selective DRD3 antagonist, has allowed the examination of DRD3 in the human brain in vivo [2-4]. We are using this method to compare regional DRD3 density in alcohol dependent patients to that of healthy controls.

Methods: Male alcohol dependent patients and age, sex and smoking status matched healthy controls are scanned with [^{11}C]-(+)-PHNO PET before and after a single oral dose of GSK598809. Previous data indicates that 60mg of GSK598809 blocks a substantial proportion of the DRD3, without affecting the DRD2 signal. The alcohol dependent patients are >4 weeks alcohol abstinent. To date 3 healthy controls and 1 patient have been examined.

Results: Three healthy controls (age 38±5 years) and one alcohol dependent patient (age 55 years, 8 weeks abstinent) have received two [11C]PHNO-PET scans each (Injected dose and injected mass, 224±64 MBq and 1.9±0.3 µg respectively). Consistent with previously published data [5], 60mg dose of GSK598809 produced occupancy of 40-60% in DRD3 predominant regions (substantia nigra and hypothalamus). The DRD3 occupancy seen in the patient with alcohol dependence is similar to that seen in healthy controls.

Conclusion: Quantification of DRD3 expression in patients with alcohol dependence will provide important information on the role of DRD3 in the pathophysiology of alcohol abuse.

References:

1. Heidbreder C. Selective antagonism at dopamine D3 receptors as a target for drug addiction pharmacotherapy: a review of preclinical evidence. *CNS Neurol Disord Drug Targets.* Nov 2008;7(5):410-421.

2. Wilson AA, McCormick P, Kapur S, et al. Radiosynthesis and evaluation of [11C]-(+)-4-propyl-3,4,4a,5,6,10b-hexahydro-2H-naphtho[1,2-b][1,4]oxazin-9 -ol as a potential radiotracer for in vivo imaging of the dopamine D2 high-affinity state with positron emission tomography. *J Med Chem.* Jun 16 2005;48(12):4153-4160.

3. Graff-Guerrero A, Redden L, Abi-Saab W, et al. Blockade of [11C](+)-PHNO binding in human subjects by the dopamine D3 receptor antagonist ABT-925. *Int J Neuropsychopharmacol.* Sep 15 2009:1-15.

4. Rabiner EA, Slifstein M, Nobrega J, et al. In vivo quantification of regional dopamine-D3

receptor binding potential of (+)-PHNO: Studies in non-human primates and transgenic mice. *Synapse.* Sep 2009;63(9):782-793.

5. Searle G, Beaver JD, Comley RA, et al. Imaging dopamine D3 receptors in the human brain with positron emission tomography, [11C]PHNO, and a selective D3 receptor antagonist. *Biol Psychiatry.* Aug 15 2010;68(4):392-399.

1323

CALCIUM SIGNALLING IN BRAIN MITOCHONDRIA: THE ROLE OF THE CALCIUM-DEPENDENT MITOCHONDRIAL METABOLITE CARRIERS

J. Satrustegui[1], J. Traba[2], I. Amigo[2], I. Llorente-Folch[2], P. Marmol[2], S. Cavero[2], C. Rueda[2], B. Pardo[2], A. del Arco[3]

[1]Department of Molecular Biology and Centre for Molecular Biology Severo Ochoa CSIC-UAM, [2]Autonomous University of Madrid, [3]Area of Biochemistry and Centre for Biomedical Research, University of Castilla-La Mancha, Madrid, Spain

The calcium-binding mitochondrial carriers of glutamate/aspartate (AGCs) and ATP-Mg/Pi (SCaMCs) provide a mechanism to transmit Ca^{2+} signals to mitochondria independent of the entry of calcium to the organelle. The AGCs Aralar/AGC1 and citrin/AGC2 are components of the malate aspartate NADH shuttle and citrin is also a component of the urea cycle. The presence of calcium binding motifs facing the intermembrane space in both AGCs results in the activation by extramitochondrial calcium of these shuttles at calcium levels below those required by the calcium uniporter. The $S_{0.5}$ for Ca^{2+} activation of the shuttle in tissues where aralar is the predominant isoform (brain, skeletal muscle, insulin-secreting beta cells) is about 300 nM, and Aralar mutants blocking calcium binding fin aralar fully prevent this activation. In neurons utilizing glucose, small calcium signals activating the malate aspartate shuttle appear to “push” pyruvate into mitochondria and thus greatly stimulate mitochondrial NAD(P)H production independently of Ca^{2+} entry in mitochondria. However, this mechanism is blunted with large Ca^{2+} signals. Mammalian SCaMCs have a lower affinity for Ca^{2+} than the AGCs but, unlike AGCs, are strictly Ca^{2+} dependent. SCaMC-3 is the ATP-Mg/Pi mitochondria carrier present in brain. The role of this carrier in the control of mitochondrial adenine nucleotide levels and Ca^{2+} concentrations will be discussed.

1324

IMAGE GUIDED HEMICRANIECTOMY OR STROKECTOMY FOR MALIGNANT INFARCTION OF THE MIDDLE CEREBRAL ARTERY

B.T. Jankowitz, D.B. Kostov, **P.V. Parry**

Department of Neurological Surgery, University of Pittsburgh Medical Center, Pittsburgh, PA, USA

Objectives: To assess the feasibility of intra-operative image guidance for the determination of ischemic versus viable brain and to guide the extent of resection for the surgical treatment of malignant infarction of the middle cerebral artery.

Methods: Patients with acute onset hemispheric stroke involving >50% of the MCA distribution causing depressed mental status and midline shift were chosen for an operative intervention. Intraoperative image guidance was used to decide between performing a standard hemicraniectomy or a radical strokectomy with replacement of the bone flap. Image guidance was also used to guide the extent of brain resection. A pre-operative fine cut CT (1.25 mm slices) was used in conjunction with the Stryker Navigation System to allow intraoperative localization of the stroke. The noncontrast CT could be fused with the preoperative MRI. Indocyanine green (ICG) videoangiography was also used to evaluate brain perfusion and the extent of stroke.

Results: Four patients were assessed intraoperatively. The use of a hand held wand (Stryker Navigation) allowed localization of ischemic brain using both the noncontrast CT and DWI from MRI. These imaging modalities were also fused to show that the ischemic burden was uniform between the noncontrast CT and MRI. ICG videoangiography showed no evidence of blood flow to the ischemic territory as deduced by visual inspection of blanched brain and using the wand, although it depicted a more accurate delineation of the presumably ischemic border allowing us to more accurately distinguish between dead and potentially salvageable brain. Based on persistent perfusion to a significant portion of the temporal lobe, two of the four patients underwent a hemicraniectomy only. The remaining two patients underwent radical strokectomies with replacement of the bone flap facilitated with navigation and repeat ICG videoangiography showing continued absence of perfusion to deeper structures as the cortex was removed. All patients showed amelioration of their midline shift with improvement in their neurological status postoperatively. No patient required repeat surgery.

Conclusions: The use of image guidance during the surgical treatment of malignant infarction of the middle cerebral artery facilitates distinguishing ischemic brain from potentially viable brain. This may enable surgeons to perform more aggressive strokectomies allowing replacement of the bone flap and avoidance of further surgery.

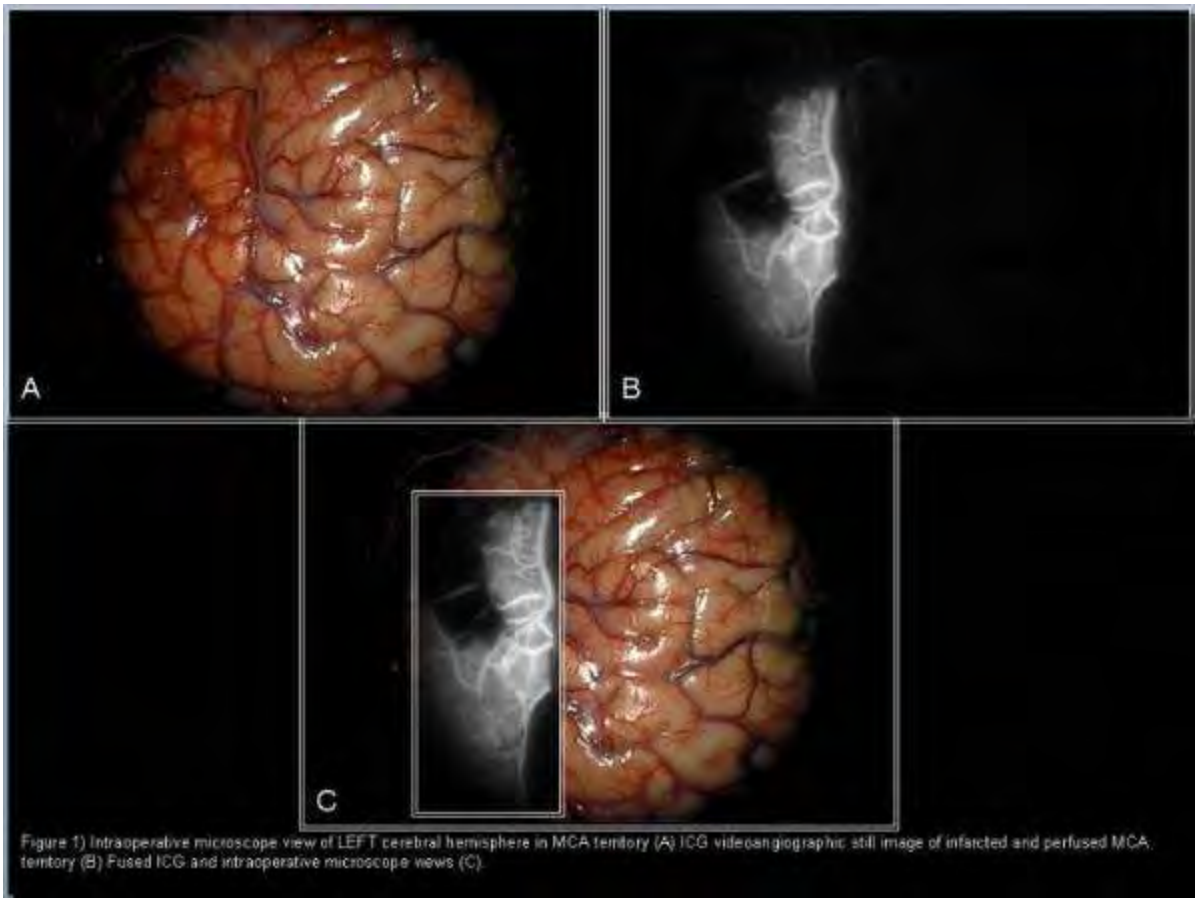

Figure 1) Intraoperative microscope view of LEFT cerebral hemisphere in MCA territory (A) ICG videoangiographic still image of infarcted and perfused MCA territory (B) Fused ICG and intraoperative microscope views (C).

[Figure 1]

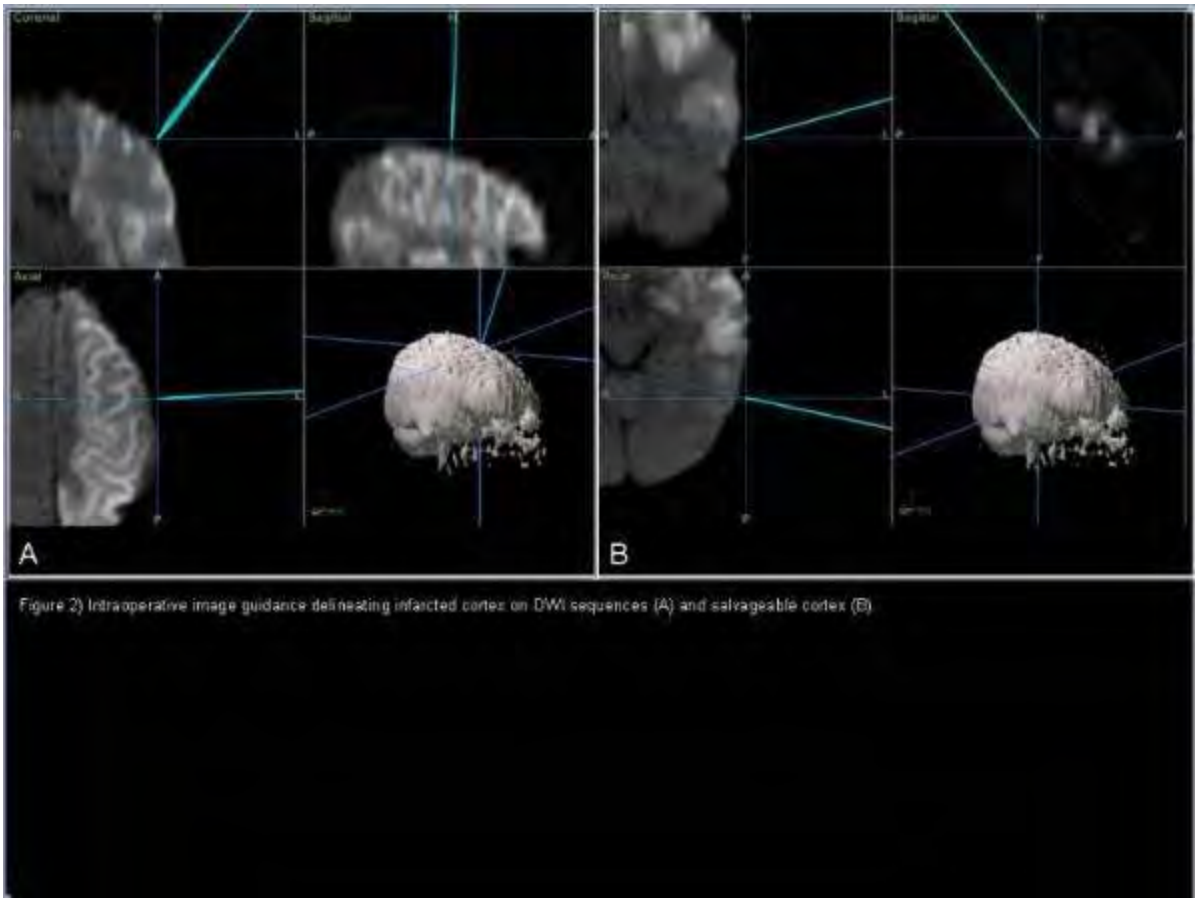

Figure 2) Intraoperative image guidance delineating infarcted cortex on DWI sequences (A) and salvageable cortex (B)

[Figure 2]

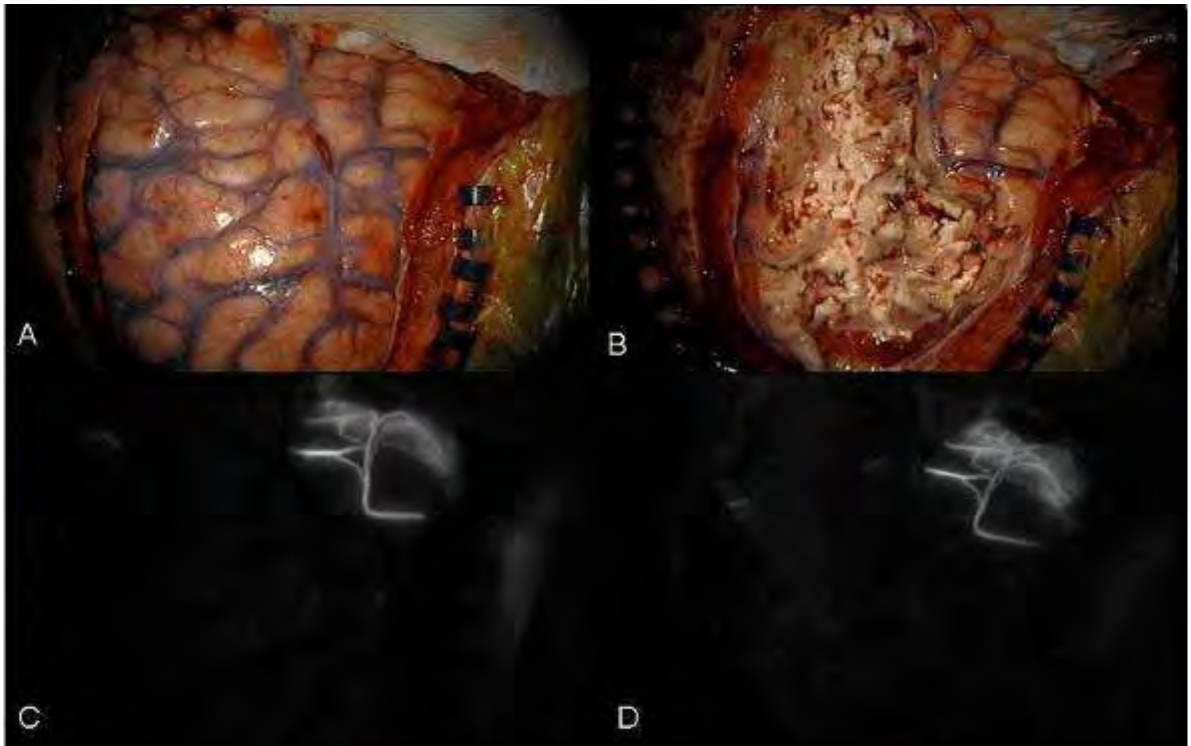

Figure 3) Preoperative microscope view of infarcted right MCA territory (A). Postoperative microscopic view of strokectomy resection cavity (B). Corresponding ICG videoangiographic still images of the pre (C) and postoperative (D) infarcted cortex demonstrating preserved perfusion in the right anterior temporal lobe.

[Figure 3]

Disclosure: We have no disclosures to submit.

1325

MULTIMODAL IMAGING OF GL261 GLIOMA IN MICE *IN VIVO* USING PET/MRI/CT

M. Balcerzyk[1], A. Parrado[1], I. Fernandez[1], S.F. Garcia[1], J. Cobos[1], A. Guisado[2], A. Villaran[2], J.J. Minguez[2], K. Gabrusiewicz[3], B. Kaminska[3]

[1]Centro Nacional de Aceleradores, Universidad de Sevilla, Sevilla, [2]Guadiamar Servicios Veterinarios de Referencia, Sanlucar la Mayor, Spain, [3]Nencki Institute of Experimental Biology, Warszawa, Poland

Objectives: Our objective was to determine the size of the tumor *in vivo* for subsequent therapy monitoring of intracranial murine glioma. The previous method of slicing of the removed and fixed brain and following fluorescent microscope examination of GFP transfected glioma cells was not allowing the therapy monitoring in the same animal *in vivo*, although was giving very high precision of the measurement.

Methods: C57 wild type adult 4 month male mice were injected with 50000 EGFP-GL261 glioma cells in stereotactic apparatus at the location (AP +1.5 mm; L -1.5 mm; DV -3 mm). Control mouse was injected with saline. Starting 16th day after implantation, the animals were tomographically scanned in PET (Mosaic, Philips) with FDG (for cell glucose consumption) and immediately after in CT (nanoCT, Bioscan) for anatomical information and vascularization with iodine contrast Iomeron 350 mg iodine per ml (Iomeprol). The second full body scan of animal injected with contrast was taken followed by scanning in MRI (Vet-MR, ESAOTE) and with PET (FMISO for possible hypoxia in the tumor) and immediately after in CT. CT resolution was 0.2 mm.Tumors were localized in PET-FDG scan in the region of cell injection, and then in MRI image. For detailed localization of the tumor and its volume measurement, CT images before the injection of the contrast and after were analyzed using percentage difference image algebra ([contrasted]-[before])/([contrasted]+[before])/2*100 (BIA units) and smoothed with Gaussian 0.4 mm FWHM filter.

Results:

[Figure 1]

Figure 1. MRI T2 image of the tumor on 22th day after implantation in dorsal view. Light white on the right side is tumor-affected area.

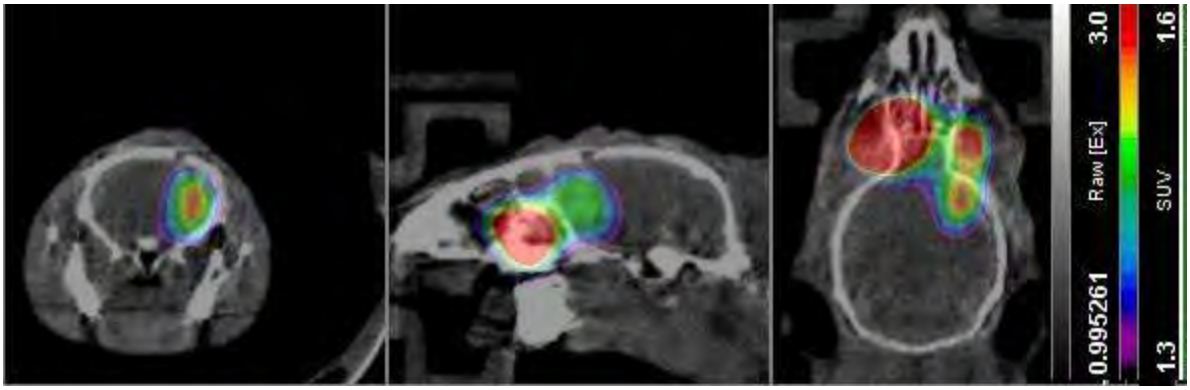

[Figure 2]

Figure 2. PET FDG image (color UCLA scale) overlaid on CT image (grayscale) taken on 17th day after tumor implantation. On CT image in transversal and sagittal views cut through the skull is seen. Ventral from this point tumor can be seen. More anterior on dorsal and sagittal view Harderian glands can be seen. Volume of interest drawn at 1.49 SUV level gave 9.9 microl volume, definitely influenced by partial volume effect. Tumor is not hypoxic as indicated by FMISO scan (not shown).

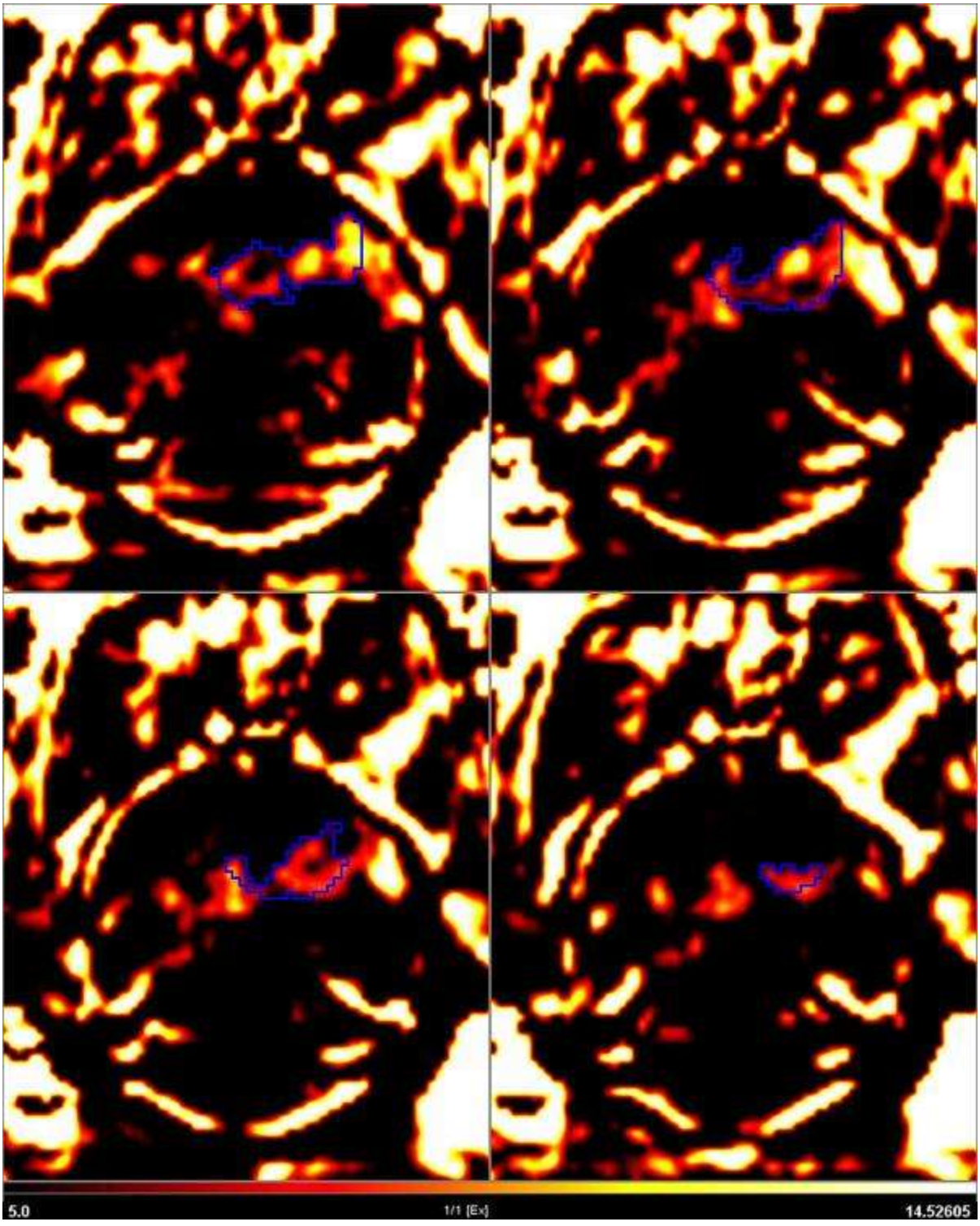

[Figure 3]

Figure 3. Image derived from the percentage difference (see above text) between image with iodine contrast and base CT scans. In blue, VOI drawn at 2.4 BIA. The volume of the VOI is 6.4 microl.

Conclusions: Contrast enhanced CT shows vascularization of the tumor with high resolution and is suitable for determination of tumor volume *in vivo*. FDG-PET in isoflurane anesthetized animal´s brain gives relatively low non specific signal due to suppressed neuronal activity. Such study may be indicative of tumor volume, measuring the metabolic activity of the cells, and quite reliable in longitudinal study of tumor progression and treatment. Veterinarian MRI can give high resolution in plane, but low interplane resolution and may serve to indicate linear dimensions of the tumor.

1326

EMBOLUS EXTRAVASATION: A MECHANISM OF MICROVASCULAR RECANALIZATION WITH IMPLICATIONS IN STROKE AND NEURODEGENERATION

J. Grutzendler

Neurology, Northwestern University, Chicago, IL, USA

Microvascular occlusion by emboli occurs spontaneously throughout life and is common in a variety of disease processes. Although these small vessel occlusions may produce little acute symptomatology, their cumulative effect is likely to lead to organ dysfunction. This is especially relevant in the brain where micro-occlusions may eventually lead to cognitive impairment. The current view is that microvascular emboli are normally cleared by hemodynamic forces and the fibrinolytic system. However, we recently discovered an alternative cellular mechanism that effectively removes from the cerebral microvasculature emboli composed of virtually any substance including those not susceptible to fibrinolysis such as atheromatous cholesterol fragments. Clearance occurs by a previously unknown process of microvascular plasticity involving the engulfment of entire emboli by endothelial membrane projections and their subsequent translocation into the perivascular parenchyma leading to rapid reestablishment of blood flow and vessel sparing. Matrix metalloproteases 2/9 were found to be involved in the extravasation process. The extravasation mechanism was found to be severely impaired in aging leading to synaptic loss and perivascualr cell death. Our results could have important implications in vascular biology, systemic embolic disorders, stroke and dementia

1329

IMMUNOMODULATORY EFFECT OF ACUTE INJECTION OF MORPHINE IN LPS-INDUCED NEUROINFLAMMATION

F. Rostami[1,2], L. Dargahi[2], A. Ahmadiani[2]

[1]Tarbiat Moalem Tehran, [2]Brain Research Institute, Shahid Beheshti University, Tehran, Iran

Introduction: Morphine possesses immunomodulatory effects but its intrinsic mechanisms are only partially understood.

Aim: In this study, We investigated how morphine preconditioning may alter lipopolysaccharide (LPS)-induced neuroinflammatory responses in the rat brains.

we evaluated the effects of three doses of morphine(4,7,1o mg/kg) on TNFα, IL-1 beta and cox-2 expression rat hippocampus and identified the involvement of MOR and TLR4 of different opioid receptors

Material and method: male wistar rats used in all exprements. Animals received LPS(1mg/kg ip) and 4 hour later they were sacrificed and their hippocampus rapidly removed and frozen in liquid nitrogen and stored at -80 ˚C until the time of protein extraction for western blot analysis. three another groups were injected by morphine (4,7,10 mg/kg ip) 30 min before LPS and in another group naloxone was injected(4 mg/kg ip) 5 min befor morphine and 2 hour later for inhibition of opioid receptor .Hippocampus lysates were used for assessment of proinflammatory cytokines (IL-1 beta, TNF-α) , COX-2 measurment and caspase3 activation.

Results: Morphine inhibited the production of proinflammatory cytokines in hippocamps of LPS-treated rats in a dose dependent manner and it seems that therapeutic and subtherapeutic doses of single dose of morphine may exert a protective role in neuroinflammatory conditions.

Conclusion: Inhibition of morphine anti inflammatory effect by naloxone demonstrates the involvement of MOR in this pathway .However TLR4 is also scored as opioid receptor and antagonized by Naloxone , so antagonization of TLR4 by a specific antagonist is necessary to clarify the exact role of each receptors , which will be done in continue.

1330

SPLENECTOMY MODULATES EXPERIMENTAL SEIZURES; A ROLE FOR T CELLS IN EPILEPSY?

V. Puvenna, N. Marchi, W. Tierney, D. Janigro

Cleveland Clinic, Cleveland, OH, USA

Background and aims: A neurocentric approach has characterized the study of epilepsy. However, the research field has recently considered the fact that the cerebral vasculature could be involved in the maintenance of proper neuronal activity and pathogenesis of seizures. While a role for the blood-brain barrier (BBB) in seizures has been accepted, only recently an unexpected contribution of circulating immune cells to the development of acute seizures has been demonstrated in animal models. Endothelial-leukocyte interactions have been shown to contribute to pilocarpine-induced epileptogenesis, and anti-inflammatory regimens aimed at reducing adhesion of white blood cells to the vascular wall prevented *status epilepticus* (SE; *Nat.Med.* 14, 1377-1383 (2008); *Neurobiol.Dis. 33*, 171-271 (2009)). In particular, $CD8^+$ natural killer T cells appear to be involved ; however, the molecular players involved in this cascade of events are unknown. Since the spleen is a chief regulator of leukocyte activation, and in particular $CD8^+$ mobilization, we wished to test whether immunosupression by splenectomy or lack of perforin, a downstream factor of natural killer and cytotoxic T-cells, could reduce seizure onset. Since both cholinergic and glutamatergic receptors are expressed on B- and T-cells (*J.Immunol.* 170, 4362-4372 (2003); *J.Neuroimmunol.* 194, 83-88 (2008)), kainic acid and pilocarpine were used as SE inducers.

Methods: Rats or mice were monitored for EEG and behavioral changes throughout the experiments. Splenectomy was performed either before (>4 hrs.) or after (3 hrs.) exposure to pilocarpine (350 mg/kg) or kainate acid (10 or 15 mg/kg). Immunocytochemical analysis was used to measure $CD3^+$ cells in spleen. Seizures were quantified by joint time frequency analysis. FACS analysis was performed on spleen and brain tissue of wild type and perforin-deficient deficient mice treated, or not, with pilocarpine.

Results: After SE, the spleen displayed a great increase of $CD3^+$ cells regardless of the trigger used to induce seizures. Splenectomy prevented seizure development in all pilocarpine-treated rats (n=9 per group). Low dose kainate caused behavioral modifications that were entirely prevented by splenectomy (n=3). At the convulsive dosage, KA seizures were decreased but not entirely abolished in splenectomized rats (n=4). Splenectomy also prevented SE-induced mortality. Pilocarpine increased spleen NK 1.1 and CD8+ cells; in contrast, brain inflammatory cells remained unchanged at time of pilocarpine SE. Seizure onset and mortality were decreased in perforin deficient mice (n=12 per group, $p< 0.05$). BBB damage was also negligible in the perforin deficient pilocarpine-treated mice, while increased cerebrovascular permeability was the hallmark of seizure activity in wild type animals.

Conclusions: Our results show for the first time that splenectomy prevents SE (pilocarpine) or decreases seizure burden (kainate) in animal models of acute seizures based on chemical activation of glutamatergic or muscarinic receptors. A study conducted on temporal lobe epileptic patients demonstrated an increase in circulating natural killer (NK) and cytotoxic T lymphocytes (*Exp. Neurol.* **211**, 370-377 (2008)). We hypothesize that white blood cell activation by kainate or pilocarpine may mimic BBB disruption that precedes seizures.

1332

THE STUDY ON THE BRAIN TARGETING OF INTRANANSAL ADMINISTRATION XIONGBING MICROEMULSION BY MICRODIALYSIS TECHNIQUE

W. Lisheng, L. Baolin, C. Xiaodan

College of Chinese Traditional Medicine, Guangzhou University of Chinese Medicine, Guangzhou, China

Objective: To evaluate the brain targeting of intranansal administration Xiongbing microemulsion and investigate its feasibility by the representative constituent of tetramethylpyrazine(TMP).

Method: Blood and striatum dialysate samples were continuously collected by blood and brain microdialysis technique in rats after intragastric (i.g.),intravenous (i.v.) and intranansal(i.n.) administration. The concentration of TMP in dialysate samples were measured by HPLC,the pharmacokinetic parameters were calculated by pharmacokinetic software DAS2.1,and evaluated the brain targeting by the value of drug targeting index (DTI).

Results: The measured pharmacokinetics of free TMP concentration in blood and brain all fited single compartment model after i.g. administration,and two-compartment model after i.n. ,i.v. administration.The absolute bioavailability(F) of i.g. administration was 41.89±5.16%, the $T_{1/2}$ and $MRT_{0-\infty}$ of TMP in brain was approximate compared with i.n. administration,but the C_{max} and $AUC_{0-\infty}$ was significantly lesser than its.The F of i.n. administration was 86.60±2.02%, and its $AUC_{0-\infty}$ in brain was approximate to i.v. administration,but the $T_{1/2}$ and $MRT_{0-\infty}$ was significantly prolonged,and increased by nearly 1.16,1.24 respectively.Its DTI value was 1.07.

Conclusion: The $AUC_{0-\infty}$ values of TMP in brain were approximate between intravenous and intranansal, part of TMP could be straight transported into brain by the intranasal administration, which could improve the brain targeting of Xiongbing Microemulsion,and showed a prolonged duration of TMP concentration in the brain. Therefor,intranasal administration of Xiongbing Microemulsion could be a promising alternative to traditional administration routes.

Key words: Xiongbing microemulsion; Intranansal administration;Brain targeting ; Microdialysis technique

1333

AGING AND MASTICATORY DEPRIVATION ALTER LAMINAR DISTRIBUTION OF CA1 ASTROCYTES AND SPATIAL MEMORY IN MURINE MODEL

M. Almeida[1], F. Mendes[1], A. Felício[1], M. Andrade[1], M. Falsoni[1], J. Bento-Torres[1], C.W. Picanço Diniz[2], **M. Sosthenes**[2]

[1]*Instituto de Ciências Biológicas, Lab de Investigações em Neurodegeneração e Infecção,*
[2]*Instituto de Ciências Biológicas, Universidade Federal do Pará, Belém, Brazil*

It has been suggested that longer periods and higher numbers of dental elements may protect against aging cognitive decline. However there is not a single quantitative report based on unbiased stereological method to investigate the cellular basis of that hypothesis. We investigated the impact of the reduced mastication on spatial memory of adult female albino Swiss mice in correlation with stereological analysis of the laminar distribution of CA1 astrocytes. All assays were done at 3, 6 and 18 months of age and reduced mastication was imposed to the experimental group with soft diet (SD) whereas the control group was fed with hard diet (HD). The results demonstrated that SD had differential effects on the number of astrocytes in the CA1 hippocampal field and on the performances in water maze memory tests. After 3 months all mice, no matter the diet regime (HD or SD) find and remember the position of a hidden platform. After 6 months, SD but not HD mice exhibited significant spatial memory dysfunction whereas after 18 months, both SD and HD presented spatial memory decline. SD as compared to age matched HD presented astrocytic hypoplasia at 3 and 6M and hyperplasia at 18M in the molecular, radiatum and pyramidal layers. In the stratum oriens hypoplasia was detected at 3M but not at 6M age and hyperplasia was found at 18M of age. Taken together the results suggest that the abnormal cognitive development and aging induced by masticatory deprivation may be connected with altered laminar gliogenesis in CA1.

1336

COMBINED INTERVENTION STRATEGIES IN AN *IN VITRO* MODEL OF HYPOXIA/REOXYGENATION

R. Shirley[1], E.N.J. Ord[1], C. McCabe[2], I.M. Macrae[2], A.F. Dominczak[1], A.H. Baker[1], L.M. Work[1]

[1]Institute of Cardiovascular and Medical Sciences, [2]Institute of Neuroscience and Psychology, University of Glasgow, Glasgow, UK

Objectives: To silence neuronal-specific pro-apoptotic enzyme c-jun N-terminal kinase 3 (jnk3) and assess the effects of this either alone or in combination with anti-oxidant protection afforded by tempol in an in vitro model of hypoxia/reoxygenation.

Methods: B50 rat neuronal cells were exposed to 9 hrs hypoxia (1% O_2, 5% CO_2, balance N_2) and serum deprivation followed by 24 hrs reoxygenation in complete media. Short hairpin RNA (shRNA) directed against the jnk3 gene was incorporated into lentivirus. Cells were left untreated or pre-treated 48 hrs prior to hypoxia with lenti-shRNA or control virus lenti-NC (50 virus particles/cell). Selective knockdown of jnk3 was assessed at the mRNA and protein level by Taqman^{TM} qRT-PCR and western blot, respectively. Effects of jnk3 knockdown on levels of oxidative stress were assessed by electron paramagnetic resonance (EPR); lipid peroxidation levels were quantified by malondialdehyde (MDA) assay and caspase 3 levels assessed by immunocytochemistry (ICC). For all experiments, n=3, values are mean±SEM and statistical analysis was performed using ANOVA with Bonferroni post-test.

Results: Following in vitro hypoxia/reoxygenation, mRNA expression levels showed a time-dependent up-regulation in jnk3 levels, whilst jnk1 and jnk2 expression remained unchanged (ΔCt vs GAPDH jnk1 11.7, jnk2 8.3, jnk3 16.3 after 9 hrs hypoxia vs jnk1 12.0, jnk2 8.9, jnk3 18.0 in normoxia). Levels of activated JNK3 protein also reflected these changes. Selective and significant knockdown of hypoxia/reoxygenation-stimulated jnk3 expression was achieved with lenti-shRNA at the level of both mRNA expression and protein, with both showing levels of jnk3 being reduced to levels equivalent to that of normoxic control cells (ΔCt vs GAPDH 17.1 compared to 15.7, respectively). EPR analysis showed a 2.5 fold increase in oxidative stress levels in hypoxic cells compared to normoxic cells. Levels of oxidative stress were significantly reduced in hypoxic cells pre-treated with lenti-shRNA, but not lenti-NC (Figure 1A). Furthermore, knockdown of jnk3 resulted in significantly reduced levels of MDA in hypoxic cells pre-treated with lenti-shRNA but not lenti-NC (Figure 1B). The addition of the anti-oxidant tempol also reduced MDA levels, both alone and in combination with lenti-NC and lenti-shRNA. Caspase 3 ICC was carried out as a measure of apoptosis and showed that levels of nuclear-localised caspase 3 were reduced after treatment with lenti-shRNA but not lenti-NC.

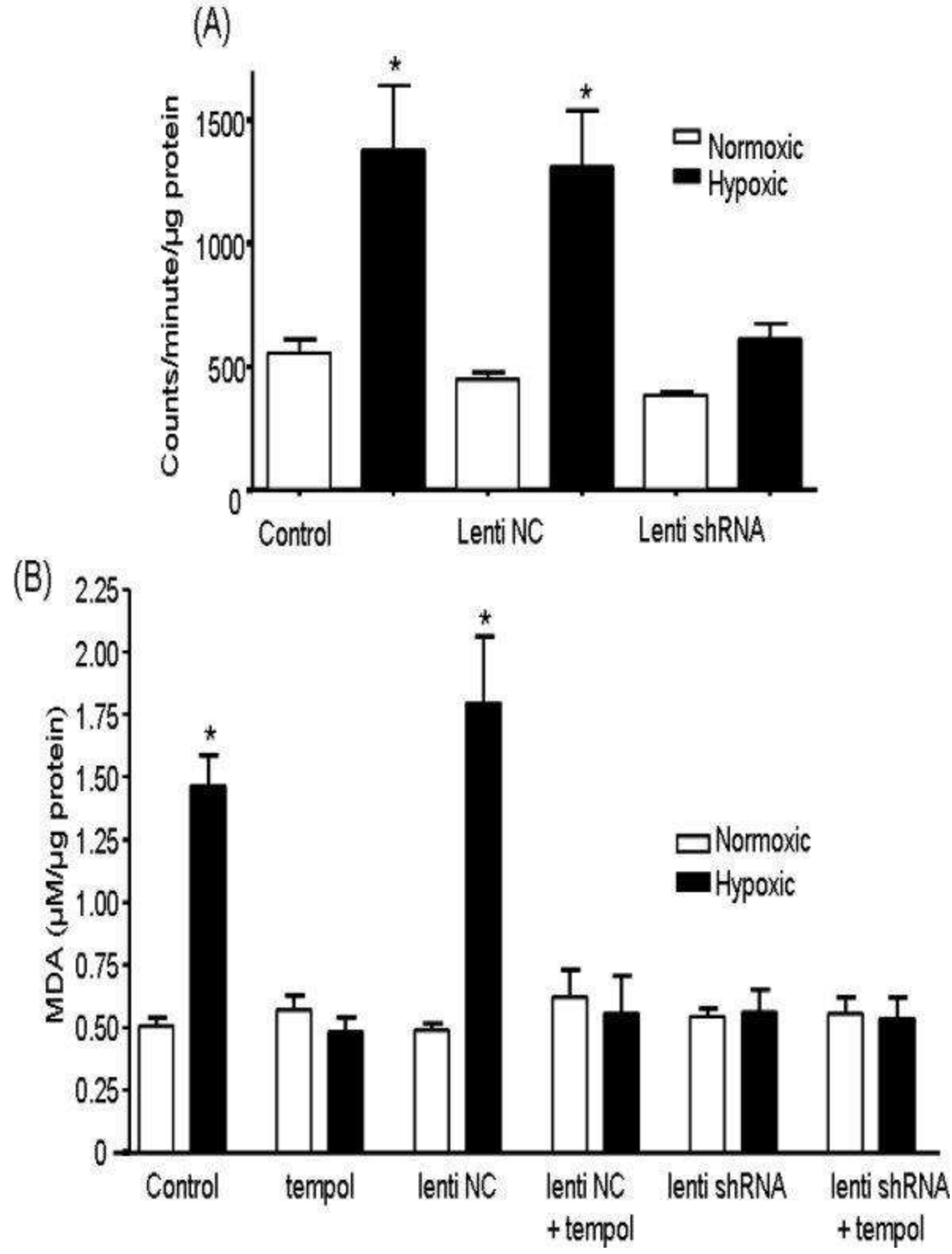
(A)
Counts/minute/µg protein
1500
1000
500
0
*
*
Normoxic
Hypoxic
Control
Lenti NC
Lenti shRNA
(B)
MDA (µM/µg protein)
2.25
2.00
1.75
1.50
1.25
1.00
0.75
0.50
0.25
0
*
*
Normoxic
Hypoxic
Control
tempol
lenti NC
lenti NC + tempol
lenti shRNA
lenti shRNA + tempol

[Figure 1]

Figure 1: The effects of jnk3 knockdown on (A) superoxide production as assessed by EPR (a measure of spin-probe CPH to CP radical conversion) and (B) lipid peroxidation assessed by MDA assay. *p< 0.05 vs normoxic control by one way ANOVA and Bonferroni post-test.

Conclusions: Lentiviral-shRNA mediated selective jnk3 knockdown significantly decreases oxidative stress, lipid peroxidation levels and inhibits apoptosis in vitro. Studies to assess the effect of jnk3 knockdown on cerebral damage and neurological outcome in SHRSP rats following transient MCAO will help further elucidate the role of jnk3 in stroke-induced ischaemia/reperfusion injury.

These studies were supported by BHF PG/07/126/24223 and a capacity building award in Integrative Mammalian Biology funded by the BBSRC, BPS, KTN, MRC, SFC.

1337

CAMP SPECIFIC PDE4B SPLICE VARIANTS EXPRESSION IN MALE AND FEMALE MOUSE BRAIN DURING ACUTE SYSTEMIC INFLAMMATION

E. Johansson, C. Sanabra, G. Mengod

IIBB, CSIC, Barcelona, Spain

PDE4 represents a family of cAMP-specific PDEs consisting of four paralog genes (PDE4A-D) each distinguishable by its unique N-terminal sequence. Publications indicate that the PDE4B gene is the predominant subtype involved in inflammatory induction by lipopolysaccaride (LPS) in mouse monocytes and macrophages. Together with previous reports of expression of the three PDE4 isoforms PDE4A, PDE4B and PDE4D in oligodendrocytes (Olgs), we show that the PDE4B3 mRNA is readily present in Olgs and neurons which imply a role for this PDE4B splice variant in the central nervous system (CNS).

cAMP has been shown to play an important role in protecting myelin from excitotoxic cell death and considering the sexual dimorphism in Olgs functional properties and in disease susceptibility observed for e.g. multiple sclerosis (MS) together with the alterations in the two PDE4B splice-variants (PDE4B2 and PDE4B3) mRNA expression observed after LPS administration, we focused on possible gender differences for these enzymes during the acute immediate neuroinflammatory process observed during septic shock. Furthermore, sex-related differences have been observed in the incidence and severity of sepsis in humans and also in the response towards LPS administration in rodents for several cytokines.

We have analyzed the influence of an intra peritoneal LPS injection on the distribution pattern and expression levels of the PDE4B3 mRNA splicing variant in both male and female mice brain. Characterization of the cell populations involved in the PDE alterations was established by double *in situ* hybridization histochemistry and immunohistochemistry. By semi-quantitative analyses of the autoradiograms we observed that PDE4B3 mRNA levels showed clear changes in females 24h post-injection, whereas, in male the altered expression was less evident and peaked 8h after treatment. Furthermore, we discovered that this downregulation was reflected in a lower percentage of oligodendrocytes positive for the PDE4B3 mRNA.

Knowledge about PDE4B mRNAs expression in mouse brain in both sexes and the alterations provoked by LPS administration might help us to clarify sex-related differences in the susceptibility to autoimmune diseases.

Financed by 2006-10243 & SAF2009-11052. EJ is a recipient of a fellowship from Ministerio de Educación y Ciencia (BES-2007-16588).

1338

LONG TERM DECREASE IN ALPHA 2 RECEPTOR DISTRIBUTION VOLUME AFTER ACUTE STIMULATION OF NA RELEASE

D. Doudet[1,2], A.M. Landau[2], S. Dyve[3], S. Jakobsen[4], A.K. Alstrup[4], A. Gjedde[4,5]

[1]Neurology, University of British Columbia, Vancouver, BC, Canada, [2]PET Center and CFIN, [3]Neurosurgery, [4]PET Center, Aarhus University Hospital, Aarhus, [5]Neurosciences and Pharmacology, University of Copenhagen, Copenhagen, Denmark

Objective: To evaluate the binding of yohimbine to alpha2 receptors after acute, short-term stimulation of noradrenaline (NA) release. Microdialysis studies in rodents showed that vagal nerve stimulation (VNS) at 1mA induces NA release, rapidly returning to baseline following interruption of the stimulus. We have previously demonstrated that 11C-yohimbine, a tracer of the alpha2 receptors, was displaceable by its endogenous ligand. We used Gottingen minipigs to investigate the changes in yohimbine binding to the alpha2 receptors in response to changes in NA release induced by VNS stimulation.

Methods: Three minipigs were implanted with VNS stimulators. Four to six weeks following surgical recovery with the stimulator off, three 11C-yohimbine PET scans were performed within one day in each of the propofol anesthetized minipigs. A 90 min yohimbine scan was obtained at baseline. After the end of the scan, the VNS stimulator was turned ON at a current intensity of 1mA and a second yohimbine scan was obtained within 30 min of initiation. The VNS stimulator was turned OFF at the end of this acute scan and a third injection of yohimbine was performed 2 hrs later with the stimulator remaining in the OFF position. The images were co-registered to an atlas of the minipig brain and time activity curves were obtained for thalamus, frontal and temporal cortices, striatum and cerebellum. Kinetic analysis was performed using the Logan multilinear graphical analysis method using a standard plasma time activity curve as the input function and yielded the distribution volume (DV).

Results: Acute VNS stimulation resulted in a significant decrease in yohimbine DV ranging from 11-15 % in regions of known high alpha2 receptor density (thalamus and cortex) to 8 -9% in regions of mid to low binding (striatum and cerebellum). After turning off of the VNS stimulator and presumably, interruption of the NA release, the yohimbine DV continued to decrease by another 9-10% across all regions considered. The total mass of yohimbine injected across all 3 studies (i.e. over 7-8 hrs) was below the demonstrated dose necessary for inducing a pharmacological mass effect of yohimbine.

Discussion: In the absence of combined microdialysis data, it is impossible to confirm the interruption of NA release in parallel with the interruption of VNS stimulation in the minipig, as was previously reported in the rat. We are currently initiating combined PET/dialysis studies in this model. However, the observation of a prolonged decrease in DV after acute stimulation of NA release is reminiscent of a similar behavior of another monoaminergic system, the dopamine D2 receptors. Using raclopride as the surrogate marker of DA release and microdialysis, the prolonged decrease in raclopride binding potential after acute amphetamine challenge, which persists long after return to baseline of the extracellular concentrations of dopamine, is well known, and the mechanism(s) responsible have been the subject of animated debate for many years. The current observation raises the possibility of similar processes in the two receptors systems. The similitude in these observations in the behavior of alpha2 and D2 receptors is being further investigated.

1339

IMPAIRED HEMODYNAMIC RESPONSE IN MIGRAINEURS: EVIDENCE FOR 0.4-0.5 HZ OSCILLATIONS

A. Akin[1], A. Ozdemir[2], H. Bolay[3]

[1]Institute of Biomedical Engineering, [2]Department of Electronics, Bogazici University, Istanbul, [3]Department of Neurology, Gazi University Medical Faculty, Ankara, Turkey

We exploited the capability of the functional near infrared spectroscopy system (fNIRS) in quantifying the cerebrovascular regulation of migraineurs during a cognitive task. A computerized version of the color-word matching Stroop task was employed to stimulate the hemodynamic oscillations that are generated as a result of sustained neuronal activation. The spectral analysis yielded significant differences in the energies computed between the 0.4-0.5 Hz frequency interval in favor of the controls (Power of Controls (13 subjects): 2.14±1.68, Power of Migraineurs (20 subjects): 0.59±0.67 mM^2Hz, $p< 0.05$). This finding strengthens the argument that there is an impairment in neurovascular coupling and cerebrovascular autoregulation in migraineurs with auora.

1340

ANGIOGRAPHY AND VENOGRAPHY OF BAT INTRACRANIAL VESSELS: ADAPTATION TO PROLONGED INVERSION

J.O. Ashaolu

Depatment of Anatomy, Bowen University, Iwo, Nigeria

Bats contend with prolonged inversion in their roosting colonies, and both inversion and valsalva maneuver in Man has been reported to increase intracranial pressure (Flanagan, 2001).The aim of this study is to verify if bats possess accessory drainage system(s) or arterial shunt(s) for regulating intra-cranial circulation. 4 bats captured irrespective of sex weighing between 250-260g were divided into 2 groups of 2 each (A and B). The group A and B bats were anaesthetized with chloroform and administered with 3mls Urografin (a radiographic contrast) through the left and right ventricles to study angiography and venography respectively. X-ray images were taken and placed on a viewing box, and photographic records obtained for analysis showed that; the posterior vena cava was highly enlarged, the superior sagittal sinus communicated with the facial veins, the vertebral arteries have a midline origin that appears to emanate from the arch of aorta other than the origin from the subclavian artery, the vertebral arteries communicated by shunts with each other and, the common carotid arteries appear visually narrower compared to the vertebral arteries. All these arterial and venous modifications suggest reasons for bat protection against increased intracranial pressure or increased hemodynamics when inverted in their roosting colonies.

Key Words: Bats, Eidolon Helvum, Angiography, Venography, Vertebral artery, Common carotid artery, Posterior vena cava, Facial veins

1343

QUANTIFYING THE EFFECTS OF ARTERIAL BLOOD GAS LEVELS ON CEREBRAL BLOOD FLOW AND REGULATION USING NIRS

S.J. Payne[1], J. Mohammad[1], M.M. Tisdall[2], I. Tachtsidis[3]

[1]Institute of Biomedical Engineering, Department of Engineering Science, University of Oxford, Oxford, [2]Department of Neurosurgery, National Hospital for Neurology and Neurosurgery, Queen's Square, London, [3]Department of Medical Physics and Bioengineering, UCL, London, UK

Introduction: Autoregulation is a term used to characterise many complex processes that act together to maintain cerebral blood flow within tight limits. However, it is known that these are strongly influenced by changes in blood gas levels. The high temporal resolution of NIRS allows it to be potentially a valuable tool to provide additional information about cerebral blood flow regulation, in addition to that gained from traditional MBP/CBFV analysis.

Objective: We investigated how measures of oxyhaemoglobin and deoxyhaemoglobin are affected by changes in arterial blood gas levels, using a variety of experimental data from previously published studies. In particular, we quantified the phase angle between MBP/CBFV, MBP/O2Hb and MBP/Hbdiff (where Hbdiff is equal to O2Hb-HHb and all signals were sampled at 1 Hz) at 0.1 Hz, since this provides a robust metric of cerebral autoregulation, at different arterial blood gas levels.

Methods: Using wavelet analysis, we measured the time-varying phase angles, using a synchronisation threshold of 0.5. We also adapted an existing mathematical model of the cerebral vasculature to predict these phase angles and their response to arterial blood gas levels, assuming that autoregulation was unaffected by these levels.

Results: We found that the phase angle for MBP/O2Hb and MBP/Hbdiff shows negligible change with baseline SaO2, although the MBP/CBFV phase angle increases by approximately 0.75 deg/%. This indicates that there is some influence of SaO2 on cerebral autoregulation strength or speed, which has not previously been considered. Using the mathematical model to predict the response to changes in autoregulation, it can be estimated that autoregulation is reduced by approximately 2 % per % decrease in SaO2. Although this effect is relatively small, it should be considered when quantifying cerebral autoregulation in patients with variable SaO2.

The response to changes in CO2 is more complicated, since there are associated alterations to vascular reactivity and baseline flow, which affect the phase angle, as do changes in autoregulation strength with CO2. We used the mathematical model to compensate for the changes in vascular reactivity for MBP/CBFV phase angle and hence to estimate the influence of CO2 on autoregulation. We then did the same analysis on the MBP/O2Hb and MBP/Hbdiff phase angles and found that all three phase angle sensitivities to changes in CO2 were in good agreement with each other, yielding an estimate of -4.6 % change in autoregulation strength per mmHg changes in CO2 partial pressure.

Conclusions: We were able to quantify the effects of both SaO2 and CO2 partial pressure on cerebral autoregulation through analysis of the phase angles measured for both MBP/CBFV and MBP/O2Hb and MBP./Hbdiff, recorded using NIRS. The good agreement shown indicates how NIRS can be used to interrogate cerebral autoregulation, when measurements are analysed

correctly. This opens up very interesting possibilities for looking at spatial variations in cerebral autoregulation, in particular in subjects with brain disease or injury.

1344

EVALUATION OF SEROTONERGIC RADIOLIGANDS AS SUITABLE SPECT TRACERS IN RODENTS

N. Dumas[1], M. Moulin[1,2], B. Tournier[1], N. Ginovart[1], Y. Charnay[3], P. Millet[1]

[1]Unité de Neurophysiologie Clinique et Neuroimagerie, Hôpitaux Universitaires de Genève, Service de Neuropsychiatrie, Geneva, Switzerland, [2]U877, INSERM, Grenoble, France, [3]Unité de Morphologie, Hôpitaux Universitaires de Genève, Service de Neuropsychiatrie, Geneva, Switzerland

Objectives: Our point was to evaluate SB207710[1], p-MPPI[2] and ADAM[3] radioligands, respectively 5HTR4, 5HTR1A and SERT ligands, as suitable SPECT tracers for *in vivo*

imaging and receptor quantification in mice and rats using small animal SPECT scanner.

Methods: Radioligands were obtained by iododestannylation. Purification and apparent specific activity measurement were performed by HPLC. Radiotracers were tested by *ex vivo* or *in vitro* binding on brain sections and autoradiography. Preliminary *ex vivo* autoradiographic studies were performed for SB207710 and p-MPPI to determine the best delay after injection for static SPECT image recording. Alternatively, for ADAM, a dynamic SPECT acquisition was performed. Static SPECT images were recorded at the previously determined times to investigate the potential of the tracers for SPECT imaging in rodents.

Results: Radiochemistry : Radioiodinated ligands were successfully obtained with ^{125}I and ^{123}I. Specific activities observed were constantly above 50% of the carrier-free specific activity for either ligand.

Ex vivo and *in vitro* binding autoradiographies : amongst other structures, p-MPPI intensely labeled the hippocampus. SB207710 showed strong binding to the nucleus accumbens and olfactive tubercle. ADAM labelled numerous SERT rich structures like substantia nigra, dorsal raphe nucleus or olfactory tubercles.

Ex vivo autoradiographic time course studies: the maximum specific to unspecific binding ratio was reached around 1 hour time post injection for SB207710 and around 30 minutes after injection for p-MPPI.

Dynamic SPECT experiment : ADAM SPECT images were considered most specific after 2 hours post injection.

SPECT experiments in mice were performed by recording static images at the previously determined times. [^{123}I]-SB207710 gave no detectable specific signal in brain, however *ex vivo* autoradiographies of the same animal after the SPECT experiment showed identical labelling to that seen in *in vitro* experiments. With [^{125}I]-p-MPPI, labelling of the hippocampus was detectable although the quality of the data was hampered by strong binding in the harderian glands. [^{123}I]-ADAM allowed for higher quality SPECT acquisitions due to its longer residence time (lower K_{off}) in target structures, which allowed late acquisitions, thus limiting the impact of the blood flow.

Conclusions: In our hands, SB207710 gave poor results for SPECT imaging in mouse but it remains a very powerful tool for autoradiographic *ex vivo* or *in vitro* experiments. p-MPPI could

be a promising tool for the study of the serotoninergic system by *in vivo* SPECT imaging, although its quick washout from the brain will require adaptations in the SPECT acquisition protocol. The SERT ligand ADAM, already used in humans, appears suitable for in vivo imaging in rodents due to its convenient pharmacokinetics.

References:

1. Pike, V.W.*, et al.* Radioiodinated SB 207710 as a radioligand in vivo: imaging of brain 5-HT4 receptors with SPET. *Eur J Nucl Med Mol Imaging* 30, 1520-1528 (2003).

2. Kung, H.F.*, et al.* In vivo SPECT imaging of 5-HT1A receptors with [123I]p-MPPI in nonhuman primates. *Synapse* 24, 273-281 (1996).

3. Oya, S.*, et al.* 2-((2-((dimethylamino)methyl)phenyl)thio)-5-iodophenylamine (ADAM): an improved serotonin transporter ligand. *Nucl Med Biol* 27, 249-254 (2000).

1345

ENVIRONMENTAL AND AGING INFLUENCES ON SECONDARY DENV INFECTION OUTCOMES IN IMMUNOCOMPETENT MURINE MODEL: CLINICAL SIGNS AND PATHOLOGICAL CHANGES

M.C.P. Turiel[1], D.G. Diniz[1], C.A.R. Foro[1], M.C.K. Sosthenes[1], S. Demacki[1], G.F. Gomes[1], C.M.D. Rego[1], M.C. Magalhães[1], B.G. Pinto[2], J.P. Ramos[3], S.M.M. Casseb[4], J.A.P. Diniz[4], P.F.C. Vasconcelos[4], C.W.P. Diniz[1]

[1]Universidade Federal do Pará, [2]Centro Universitário do Pará, [3]Universidade Estadual do Pará, [4]Instituto Evandro Chagas, Belém, Brazil

Recent studies demonstrated that memory DENV-specific T cells from a prior infection respond with altered cytokine production to heterologous DENV serotypes and that the level of activation and expansion of these memory cells during acute DENV infection correlates with disease severity. Since recent studies demonstrate that enriched environment enhances T cell activity during viral infections (Sousa et al. 2010) and aging may reduce immunocompetence (Castle, 2000) we tested the hypothesis that severe disease progression would affect a higher number of subjects from enriched environment (EE) as compared to the ones from impoverished environment (IE) and that aging will reduce this impact. Nine and 19 months old female albino Swiss mice were housed from weaning either in impoverished or in enriched conditions. To mimic serial and multiple infections as it may occur in human disease we have done serial i.p. weekly injections following one of two experiments. In the 1st experiment multiple infections with infected brain homogenate with a single serotype DENV3 (genotype III) or with anti-DENV3 hyperimmune serum containing high titers of anti-DENV3 antibodies followed 24 h later by DENV3 genotype III infected brain homogenate. In the 2nd experiment to simulate antibody-enhanced DENV replication and infection with two serotypes, animals were serially inoculated with anti-DENV2 hyperimmune serum containing high titers of anti-DENV2 antibodies followed 24hours later by DENV3 infected brain homogenate. Control subjects received uninfected brain homogenate. After inoculations all EE subjects from experiment 2 revealed significant decrease in the surviving probability earlier than IE subjects. Both groups presented at 39 days post-infection (dpi) a significant decrease in the probability of surviving but the decay was much higher in EE as compared to IE Kaplan-Meier survival plots. EE aged subjects present higher surviving probability than the EE young ones. At this time point both groups presented after inoculation acute disease signs including dyspnea, tremor, hunched posture, ruffled fur, immobility and eventual death. These symptoms were more intense in EE as compared to IE. To assess hippocampal function we measured burrowing and open field activities before and after DENV secondary infection and found significant changes in burrowing activity of EE subjects but no changes in IE subjects and earlier changes in EE as compared with IE subjects in open field (two-tail t-test, $p < 0.05$). Animals from the first experiment not only survived for longer periods post-challenge but also exhibited distinct and less intense clinical signs. Liver and lungs of EE subjects, died after acute symptoms in the experiment 2, presented mononuclear infiltrates, intense and disseminated vascular congestion and dilated blood vessels. Focal necrotic hepatocytes with lymphocytes and macrophages infiltrates, tumefaction, steatosis and regeneration signs were detected in various liver lobules with focal mononuclear infiltrates around efferent veins and Kupffer cell hypertrophy. Low viral titers were detected at this time point by RT-PCR using specific primers but the higher values were found in the liver as compared with spleen, lungs or brain. Apart from behavioral changes no remarkable neuropathological changes were observed in the brain.

1346

QUANTIFICATION OF RECEPTOR-LIGAND BINDING POTENTIAL IN SUB-STRIATAL DOMAINS USING PROBABILISTIC AND TEMPLATE REGIONS OF INTEREST

N. del Campo[1], R.J. Tait[2], J. Acosta-Cabronero[3], Y.T. Hong[4], D. Izquierdo-Garcia[4], R. Smith[4], F.I. Aigbirhio[4], B.J. Sahakian[1], U. Muller[1], T.W. Robbins[2], T.D. Fryer[4]

[1]Department of Psychiatry, University of Cambridge, [2]Behavioural and Clinical Neuroscience Institute, University of Cambridge, [3]Department of Clinical Neurosciences, University of Cambridge, [4]Wolfson Brain Imaging Centre, University of Cambridge, Cambridge, UK

Objectives: Sub-striatal regions of interest (ROIs) are widely used in PET studies to investigate the role of dopamine in the modulation of neural networks implicated in emotion, cognition and motor function. One common approach is that of Mawlawi et al. (2001) and Martinez et al. (2003), where each striatum is divided into five sub-regions. This study focuses on the use of two spatial normalization-based alternatives to manual sub-striatal ROI delineation per subject: manual ROI delineation on a template brain and the production of probabilistic ROIs from a set of subject-specific manually delineated ROIs.

Methods: Two spatial normalization algorithms were compared: SPM5 unified segmentation (Ashburner and Friston, 2005) and ART (Ardekani et al., 2005). The ability of these methods to quantify sub-striatal regional non-displaceable binding potential (BP_{ND}) and BP_{ND} % change (following methylphenidate) was tested on 32 subjects (16 controls and 16 ADHD patients) scanned with the dopamine D_2/D_3 ligand [^{18}F]fallypride. The T1-weighted ICBM152-2009a template was used (Fonov et al., 2009).

Results: Probabilistic ROIs produced by ART provided the best results, with similarity index values against subject-specific manual ROIs of 0.75 - 0.89 (mean 0.84) compared to 0.70 - 0.85 (mean 0.79) for template ROIs. Correlations (r) for BP_{ND} and BP_{ND} % change between subject-specific manual ROIs and these probabilistic ROIs of 0.90 - 0.98 (mean 0.95) and 0.98 - 1.00 (mean 0.99) respectively were superior overall to those obtained with template ROIs, although only marginally so for BP_{ND} % change. The significance of relationships between BP_{ND} measures and both behavioural tasks and methylphenidate plasma levels was preserved with ART combined with both probabilistic and template ROIs. SPM5 virtually matched the performance of ART for BP_{ND} % change estimation but was inferior for BP_{ND} estimation in caudate sub-regions.

Conclusions: ART spatial normalization combined with probabilistic ROIs and to a lesser extent template ROIs provides an efficient and accurate alternative to time-consuming manual sub-striatal ROI delineation per subject, especially when the parameter of interest is BP_{ND} % change.

References:

Ardekani, B.A., Guckemus, S., Bachman, A., Hoptman, M.J., Wojtaszek, M., Nierenberg, J., 2005. Quantitative comparison of algorithms for inter-subject registration of 3D volumetric brain MRI scans. J Neurosci Methods 142, 67-76.

Ashburner, J., Friston, K.J., 2005. Unified segmentation. Neuroimage 26, 839-851.

Fonov, V.S., Evans, A.C., McKinstry, R.C., Almli, C.R., Collins, D.L., 2009. Unbiased nonlinear average age-appropriate brain templates from birth to adulthood. Neuroimage 47, S102.

Martinez, D., Slifstein, M., Broft, A., Mawlawi, O., Hwang, D.R., Huang, Y., Cooper, T., Kegeles, L., Zarahn, E., Abi-Dargham, A., Haber, S.N., Laruelle, M., 2003. Imaging human mesolimbic dopamine transmission with positron emission tomography. Part II: amphetamine-induced dopamine release in the functional subdivisions of the striatum. J Cereb Blood Flow Metab 23, 285-300.

Mawlawi, O., Martinez, D., Slifstein, M., Broft, A., Chatterjee, R., Hwang, D.R., Huang, Y., Simpson, N., Ngo, K., Van Heertum, R., Laruelle, M., 2001. Imaging human mesolimbic dopamine transmission with positron emission tomography: I. Accuracy and precision of D(2) receptor parameter measurements in ventral striatum. J Cereb Blood Flow Metab 21, 1034-1057.

1348

PKCB INHIBITION PREVENTS INCREASED BLOOD-BRAIN BARRIER PERMEABILITY AND EDEMA FORMATION DURING HYPERGLYCEMIC STROKE

Q. Huang, J. Sweet, **M. Cipolla**

Neurology, University of Vermont, Burlington, VT, USA

Introduction: Hyperglycemia is common in stroke patients and worsens outcome after middle cerebral artery occlusion (MCAO). PKCβ activity is increased in the vasculature during hyperglycemia, an effect that is known to phosphorylate tight junction proteins and increase blood-brain barrier (BBB) permeability. Thus, we hypothesized that increased PKCβ activation during hyperglycemia is an underlying mechanism by which BBB permeability and edema formation are increased during hyperglycemic (HG) stroke.

Methods: Male Wistar rats that were HG for 6 days by STZ (50mg/kg) underwent MCAO for 2 hours of ischemia with 2 hours reperfusion or sham surgery. BBB permeability was assessed in isolated and pressurized MCA from the ischemic (ipsilateral) side of the brain by measuring the flux of water in response to hydrostatic pressure. BBB permeability was compared between sham vessels (n=8), MCAO vessels (n=6) and MCAO vessels perfused with a PKCβ inhibitor (CG53353;0.5μM; n=6). Separate sets of HG animals were treated with a PKCβ inhibitor (CG53353;10μg/mL; n=6) or vehicle (n=6) intraveneously 15 minutes prior to reperfusion after 1.75 hours of ischemia and the brain removed for measurement of edema by wet:dry weights. Percent water content in the ipsilateral and contralateral sides of the brain were then compared.

Results: BBB permeability was significantly increased in MCAO vessels compared to sham (flux = 184 ± 17 vs. 106 ± 22 μm^3; $p < 0.05$). Perfusion of the PKCβ inhibitor prevented the increase in permeability in the MCAO vessels (flux = 96 ± 31 μm^3; $p < 0.05$ vs. MCAO). HG vehicle-treated animals had significantly increased edema formation in the ipsilateral vs. contralateral brain after transient MCAO (% water = 78.64± 0.09 vs. 81.26 ± 0.24; $p < 0.01$). Normoglycemic vehicle-treated animals (n=6) that underwent the same duration of MCAO did not have an increase in water content (78.84± 0.11 vs. 79.13 ± 0.19; $p > 0.05$). Inhibition of PKCβ during postischemic reperfusion prevented the increase in edema in the ipsilateral brain of HG animals (78.39 ± 0.12 vs. 79.54 ± 0.56; $p > 0.05$).

Summary and conclusions: The presence of acute hyperglycemia significantly increased BBB permeability and edema formation in response to transient focal ischemia, an effect that was prevented by inhibition of PKCβ. Thus, PKCβ may be an important therapeutic target to protect the BBB and prevent edema formation during HG stroke.

1349

SUPERSELECTIVE ENDOVASCULAR CANINE MODEL OF ISCHEMIC STROKE

N.R. Gonzalez[1], J.R. Dusick[2], A. Laiwalla[3], B. Evans[2], F. Vinuela[4]

[1]Departments of Neurosurgery and Radiology, [2]Department of Neurosurgery, [3]UCLA David Geffen School of Medicine, [4]Department of Radiology, UCLA David Geffen School of Medicine, Los Angeles, CA, USA

Introduction: Large-animal models of ischemic stroke offer several advantages: anatomic similarities to humans, larger brain tissue volume, larger cerebral arteries for endovascular techniques and thus avoidance of open surgery, and easy use of diagnostic and therapeutic techniques used for human clinical stroke. Most existing canine models use carotid injection of autologous clots, producing inconsistent embolic patterns and not permitting reperfusion. We aimed to develop a highly reproducible canine model of ischemic stroke for translational stroke research.

Materials & Methods: Ten mongrel dogs were used for endovascular induction of ischemic stroke. A first group of 6 dogs underwent MCA occlusion via ICA route with a GDC coil. A second group of 4 animals underwent MCA(M1) or MCA(M1)-ACA(A1) occlusion via vertebral artery route. All animals had MRI studies at 3-hours after occlusion. Four animals were reperfused by removing the coils.

Results: In 4 of 6 dogs with the ICA route the MCA was successfully catheterized and MCA strokes resulted. In two animals navigation was not possible given the marked ICA tortuosity. There was severe vasospasm and one ICA perforation. In the second group superselective navigation into the MCA was successful in all animals. When isolated M1 occlusion was performed, MRI revealed small infarctions in diverse locations of the MCA territory. In animals with A1 and M1 occlusions, MRI and gross histology revealed large, consistent MCA infarctions.

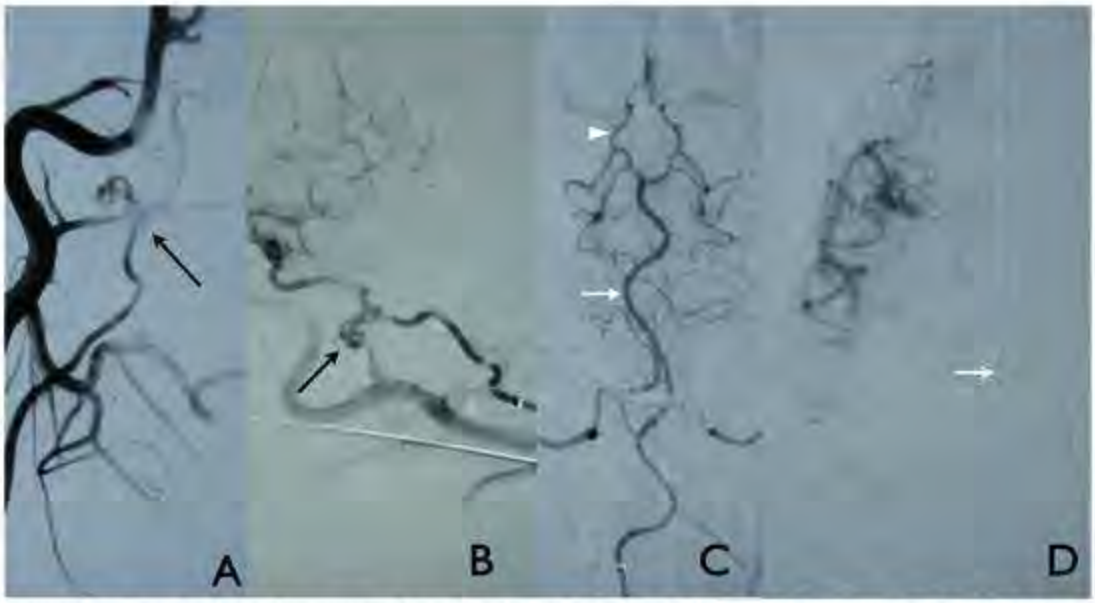

Figure 1: Cerebral angiograms. A and B: AP and lateral of R ICA injection. C: Vertebral angiogram. D: Superselective R MCA angio via vertegral route. Notice the highly tortuous course of the high cervical ICA (black arrows), compared with the less sinuous course of the vertebral route (white arrows). The large P-comm (arrowhead) allows for each intracranial ICA and MCA catheterization. Catheter course is shown in picture with the white arrow.

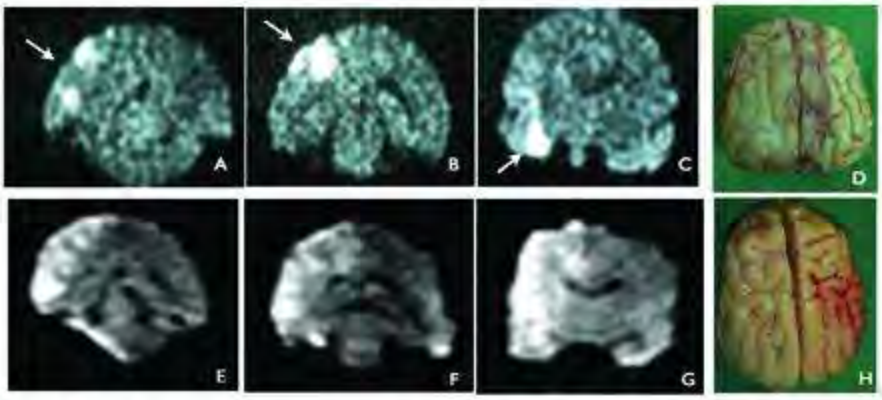

Figure 2: MRI and Gross Pathology. A-C: Coronal DWI MRI views of dogs with only M1 occlusion. Note the small size and inconsistent location of infarctions. D: Brain of dog with only M1 occlusion. No obvious areas of infarction visible. E-G: Coronal DWI MRI of dogs with both A1 and M1 occlusion. Note the large infarction of the entire MCA. H: Brain of dog with A1 and M1 occlusion after intra-arterial formalin fixation demonstrating complete MCA infarction consistent with MRI findings.

[Figures]

Conclusions: We have developed a superselective endovascular canine model of ischemic stroke. The vertebral route provided easier access than the torturous ICA. Occlusion of the A1

and M1 decreases collateral circulation and greatly increases reproducibility and infarct volume. The use of removable-coils allows for ischemic territory reperfusion. This model allowed for use of standard human MRI equipment and provided large amounts of tissue for histological and immunohistochemical analysis. This model is suitable for use in translational stroke research.

1350

A MINIMALLY-INVASIVE RAT MODEL OF SUBARACHNOID HEMORRHAGE AND VASOSPASM

N.R. Gonzalez[1], J.R. Dusick[2], A. Laiwalla[3], B. Evans[2], S. Krahl[4], N.A. Martin[2]

[1]Department of Neurosurgery, UCLA, [2]Department of Neurosurgery, [3]UCLA David Geffen School of Medicine, [4]West Los Angeles VA Medical Center, Los Angeles, CA, USA

Introduction: Double-injection models of subarachnoid hemorrhage in rats are the most effective in producing vasospasm, delayed neurological deficits and infarctions. However, models previously described in the literature require two large surgeries to expose the femoral artery, to obtain arterial blood, and the atlanto-occipital membrane, to access the cisterna magna. We have developed a minimally-invasive modification that prevents possible confounding effects of surgical procedures, leakage of blood from the subarachnoid space and minimizes risk of wound infection.

Materials & Methods: Adult Sprague-Dawley rats are anesthetized. The ventral tail artery is exposed through a small (5mm), midline incision, 0.2mL of arterial blood is taken from the artery and gentle pressure is applied for hemostasis. The incision is closed. The rat is flipped prone and, with the head flexed to 90 degrees in a stereotactic frame, a 27G angiocath is advanced in a vertical trajectory, level with the external auditory canals. Upon puncturing the atlanto-occipital membrane, the needle is removed and the catheter is advanced and observed for cerebrospinal fluid. A syringe withdraws 0.1mL of CSF and the blood is injected into the subarachnoid space.

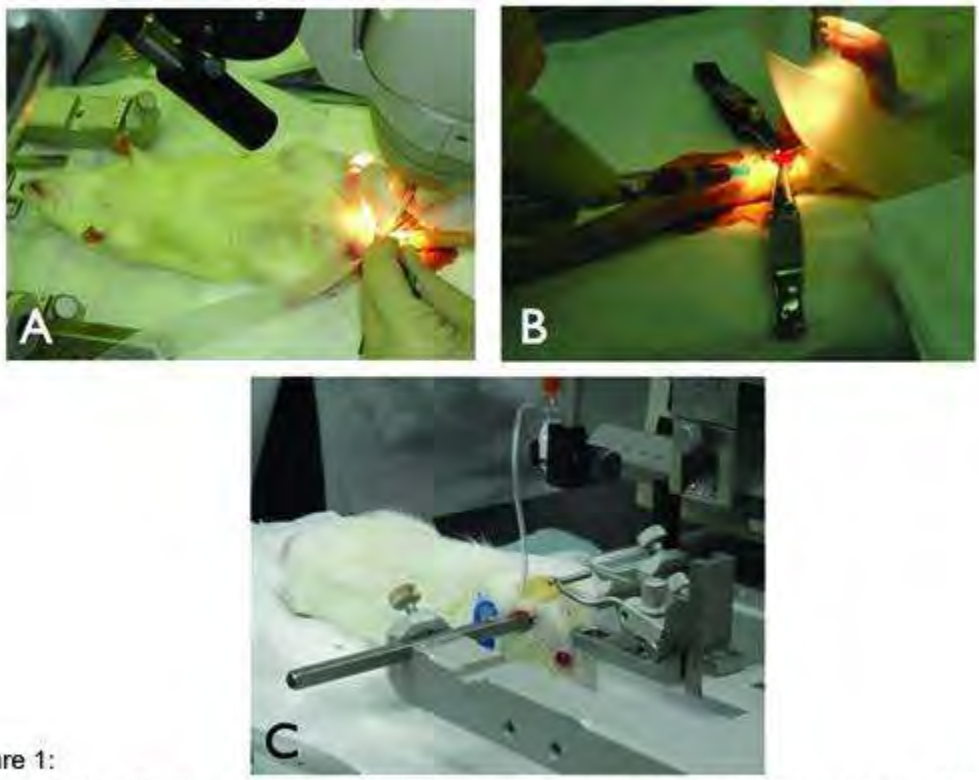

Figure 1:
Arterial blood collection and cisternal injection procedure: A) Under the microscope, a 5mm incision is opened to expose the ventral tail artery. The small amount of soft tissue facilitates exposure and reduces surgical trauma. B) 0.2mL of arterial blood is obtained. C) Once the rat is in the stereotactic frame with head positioned at 90 degrees, the cisterna magna is aligned with the intermeatal line.

[Figure 1]

The rat is kept in a head-down position while awakening from anesthesia. The procedure is repeated 24 hours later by re-opening the tail incision. If need be, the artery can be exposed more proximally to obtain this blood sample. At 8 days, the rats are euthanized and their brains harvested, sectioned and incubated with triphenyltetrazolium chloride (TTC).

Results: Neurological deficits consistent with vasospasm and infarction were observed as previously described in double-injection models. Cortical and deep nuclei infarctions were demonstrated by the TTC staining technique.

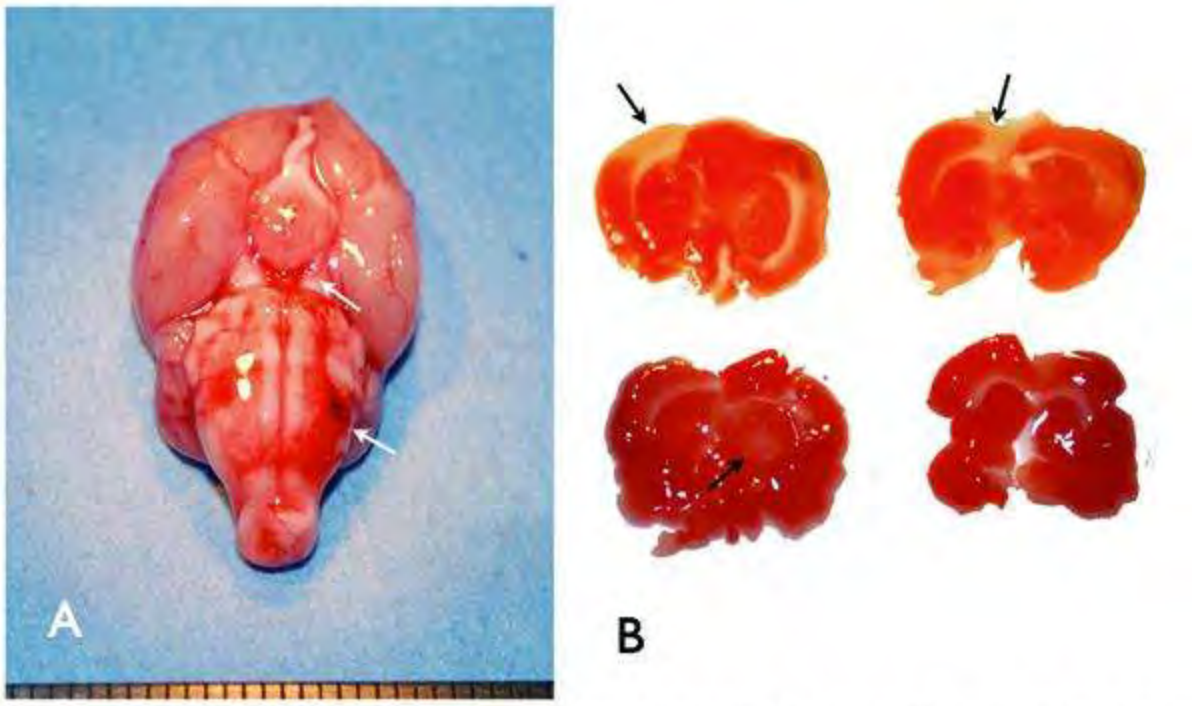

Figure 2: (A) Gross pathology and (B) coronal brain slices after TTC stain. The cisternal injection produced accumulation of blood in the prepontine and interpeduncular cisterns (white arrows). The neurological deficits developed by the rat correlated with cortical and thalamic strokes.

[Figure 2]

Conclusions: A minimally-invasive, double-injection rat model of SAH and vasospasm is feasible and produces neurological deficits and infarction. This model can be used to study neuroprotective treatments for vasospasm and delayed neurological deficits following SAH, reducing the confounding effects of surgical interventions.

1351

INVESTIGATING THE REPRODUCIBILITY OF THE NOVEL CANNABINOID TYPE 1 (CB_1) RECEPTOR PET LIGAND [^{11}C]MEPPEP

D.A. Riaño Barros[1], C.J. McGinnity[1], P. Su[1], L. Rosso[1], R.A. Heckemann[1,2], D.J. Brooks[1], J.S. Duncan[3], F.E. Turkheimer[1], M.J. Koepp[3], A. Hammers[1,2]

[1]MRC Clinical Sciences Centre, Imperial College London, London, UK, [2]The Neurodis Foundation, CERMEP Imagerie du Vivant, Lyon, France, [3]Department of Clinical and Experimental Epilepsy, Institute of Neurology, University College London, London, UK

Introduction: The cannabinoid type 1 (CB_1) receptor is one of the most abundant G protein-coupled receptors in the brain[1]. MePPEP is a novel CB_1 inverse-agonist that has been labelled with ^{11}C for use in positron emission tomography (PET). The reliability of [^{11}C]MePPEP PET has so far only been investigated for standard uptake values (SUVs) and two-compartment modelling[7].

Objective: To optimise the quantification of [^{11}C]MePPEP test-retest data using additional analytical strategies.

Design: Fourteen healthy controls were studied twice with 95-minute dynamic PET scans on a Siemens/ECAT 962 scanner, after intravenous injection of approximately 370MBq (mean: 365.9MBq, range 347-389MBq) of [^{11}C]MePPEP. Data were motion-corrected with a frame-to-frame co-registration method and T1-weighted structural 3D MRI images were spatially aligned to PET data[2]. Arterial plasma input function (IFs) were obtained by continuous blood withdrawal for 15 minutes in combination with discrete plasma samples over the entire duration of the scan, to allow correction for radio-labelled metabolites and incorporation of plasma-over-blood ratio within Clickfit Software[3]. Regions-of-interest (ROIs) were defined using an automated multi-atlas region-of-interest (ROI) definition method[4]. We selected six ROIs with high/moderate CB_1 receptor density (hippocampus, anterior cingulate gyrus, inferior frontal gyrus, caudate nucleus, globus pallidus, and nucleus accumbens) and two with low CB_1 receptor density (thalamus and brainstem) and masked the cortical regions with 50% grey matter contribution derived from SPM5 (www.fil.ion.ucl.ac.uk). We calculated total volumes of distribution (V_Ts) using 1) Spectral analysis (SA) on parametric maps generated within RPM6[5] using a low frequency boundary of 0.00063 s^{-1} [$\log_{10}$ = -3.2]; 2) the rank shaping (RS) regularisation of SA[6] (using Clickfit[3]), 3) calculated SUVs in the same regions. Outcome measures were intraclass correlation coefficient (ICCs), the between-subject coefficient of variation (CV), and within-subject percent variability

Results: Seven women and seven men with an average age of 41.4 years (25-65 years) were studied. Mean V_Ts in high/moderate ROIs ranged from 12.94 to 18.24; while the lowest mean V_T was in brainstem (6.22). Overall, ICCs for SA were high in all regions ranging from 0.83 to 0.92. For RS, ICCs ranged between 0.84 to 0.92, except in the nucleus accumbens and globus pallidum, where ICCs were 0.73 and 0.74 respectively. For SUV, ICCs ranged between 0.84 to 0.92 (Table 1).

	Intraclass Correlation Coefficients (ICC)			Between-subject Coefficients of Variation (CV)			Within-subject Percent Variability		
	Spectral Analysis	Rank Shaping	SUV	Spectral Analysis	Rank Shaping	SUV	Spectral Analysis	Rank Shaping	SUV
Hippocampus	0.92	0.87	0.91	32.8%	36.9%	31.3%	11% (1 - 30)	17% (1 - 39)	13% (1 - 34)
Anterior Cingulate Gyrus	0.91	0.93	0.92	33.3%	35.4%	33.1%	13% (0 - 35)	13% (0 - 25)	13% (3 - 25)
Inferior Frontal Gyrus	0.92	0.92	0.92	35.1%	36.3%	33.8%	13% (0 - 32)	15% (3 - 33)	13% (1 - 29)
Caudate Nucleus	0.86	0.84	0.84	37.9%	42.6%	34.7%	15% (0 - 55)	17% (1 - 61)	15% (2 - 46)
Brainstem	0.83	0.90	0.86	25.0%	30.7%	27.7%	14% (4 - 26)	14% (0 - 51)	14% (3 - 30)
Globus Pallidus	0.86	0.74	0.87	33.9%	39.1%	33.2%	13% (1 - 42)	23% (2 - 54)	16% (2 - 27)
Thalamus	0.88	0.80	0.89	34.3%	36.1%	31.4%	15% (1 - 37)	15% (0 - 37)	15% (6 - 38)
Nucleus Accumbens	0.86	0.73	0.88	35.6%	38.9%	33.8%	17% (2 - 57)	27% (0 - 83)	13% (0 - 46)

Table 1. Comparison between intraclass correlation coefficients (ICC), coefficients of variation (CV; expressed as percentages) and the average percentage test–retest differences in VD (expressed as percentages with range) between-subjects coefficients by bilateral regions of interest, for spectral analysis (SA), rank shaping (RS) and standard uptake value (SUV).

[Table 1.]

Conclusions: [^{11}C]MePPEP V_Ts obtained with spectral analysis and rank shaping provide a highly reproducible measure of CB_1 receptor availability; SUVs are similarly consistent. Superior quantification of CB_1 receptor availability was achieved with a mean injection of less than 60% of the radioactivity used in previous studies[7]. Scanning beyond 90 minutes post-injection and arterial blood sampling are not prerequisites for studies with this radiotracer. Our findings open opportunities for a range of applications for [^{11}C]MePPEP PET in neurological and psychiatric research.

References:

[1]Yasuno F et al. *Neuropsychopharmacology* 2008;33:259-69.

[2]Hammers A et al. *NeuroImage* 2007;38:82-94.

[3]MRC Cyclotron Unit, Hammersmith, London, UK).

[4]Heckemann RA et al. *NeuroImage* 2006;33:115-26.

[5]Gunn RN et al. *NeuroImage* 1997; 6:279-287.

[6] Turkheimer et al. *Phys Med Biol* 2003; 48:3819-3841.

[7]Terry GE et al. *NeuroImage* 2009;48: 362-370.

1352

THE AT2R AGONIST COMPOUND 21 IS CEREBROPROTECTIVE IN A RAT MODEL OF ISCHEMIC STROKE

J.P. Joseph[1], A.P. Mecca[1], R.W. Regenhardt[1], N.A. Patel[1], U.M. Steckelings[2], T. Unger[2], M.J. Katovich[3], C. Sumners[1]

[1]Department of Physiology and Functional Genomics, McKnight Brain Institute, University of Florida, Gainesville, FL, USA, [2]Center for Cardiovascular Research, Charité-Universitätsmedizin Berlin, Berlin, Germany, [3]Department of Pharmacodynamics, McKnight Brain Institute, University of Florida, Gainesville, FL, USA

An increasing number of studies indicate that the angiotensin type 2 receptor (AT2R) in the CNS exerts beneficial actions in ischemic stroke. Furthermore, evidence indicates that AT2R expression is increased in the penumbra region that surrounds the cerebral infarct following ischemic insult. Here we tested the effects of a specific AT2R agonist, Compound 21 (Cp21), on the cerebral deficits produced by endothelin-1 (ET-1) induced middle cerebral artery occlusion (MCAO). Adult male Sprague Dawley rats were pre-treated with Cp21 (0.0075 or 0.075 µg/h) or artificial cerebrospinal fluid (aCSF) via intracerebroventricular (ICV) infusion for 7 days prior to ET-1 induced MCAO. Cp21 treatment (0.0075 µg/h) reduced neurological deficits and infarct size measured 72 h after MCAO induction. Infarct size was reduced to 28.17 ± 3.99% of ipsilateral gray matter in Cp21 treated rats (n=16) compared with 54.05 ± 4.73% in aCSF controls (n=21; p=0.0006). Additionally, neurological deficits were reduced by Cp21 treatment as indicated by a lower Bederson Exam Score of 0.3 ± 0.1 compared to 1.6 ± 0.2 in control rats ($p < 0.0001$) and a higher Garcia Exam Score of 16.9 ± 0.28 compared to 14.3 ± 0.75 in control rats (p=0.0011). Similar results were obtained with ICV infusion of 0.075 µg/h Cp21. This data is the first demonstration of a non-peptide AT2R agonist exerting cerebroprotective actions following ET-1 induced MCAO.

1353

DODECAFLUOROPENTANE EMULSION DECREASES INFARCT VOLUME IN A RABBIT ISCHEMIC STROKE MODEL USING PERMANENT ARTERIAL OCCLUSION

W.C. Culp[1], S.D. Woods[1], A.T. Brown[1], J.D. Lowery[2], R.D. Skinner[3], M.J. Borrelli[1], P.K. Roberson[4]

[1]Radiology, [2]Laboratory Animal Medicine, [3]Neurology, [4]Biostatistics, University of Arkansas for Medical Sciences, Little Rock, AR, USA

Objectives: Excellent absorption and transportation of oxygen *in vitro* and *in vivo* have been demonstrated using dodecafluoropentane emulsion (DDFPe). Additionally, DDFPe enhanced resuscitation and survival in severely anemic rats and improved oxygenation and nitrogen washout in pigs. DDFPe may protect tissues during hypoxic episodes such as stroke, heart attack, trauma, or surgical procedures. In acute stroke, tissue plasminogen activator must be given within 4.5 hours of onset. Few patients meet this requirement. Agents that can extend this time by preventing or delaying cellular damage during ischemic periods promise more time for successful intervention and return of blood flow. Using a rabbit model of acute insoluble ischemic stroke, we assessed DDFPe efficacy in decreasing infarct volume without lysis of arterial obstructions.

Methods: New Zealand White rabbits (n=40) received selective angiography. Three embolic spheres (diameter=700-900 μm) were injected into the internal carotid artery typically occluding the middle cerebral and anterior cerebral arteries. Rabbits were randomly assigned to a time-course of therapy: control, no treatment (n=8), immediate DDFPe (n=8), DDFPe at 30 minutes (n=6), 1 hour (n=7), 2 hours (n=5), and 3 hours (n=6). DDFPe dose was two 2% w/v DDFPe intravenous injections, 0.6 mL/kg, the first at the designated time and the second 90 minutes later. Following euthanasia at 4 hours infarct volume was determined using vital stains on brain sections.

Results: Mean percent infarct volume was decreased for each treatment group (Immediate DDFPe=0.75%±0.69%, p=0.01; DDFPe at 30 minutes=0.65%±0.79%, p=0.02; 1 hour=1.1%±0.74%, p=0.04; 2 hours=0.72%±0.87%, p=0.03; 3 hours=0.48%+0.79%, p=0.01) compared to control (3.31%±0.69%).

Conclusions: Intravenous DDFPe protects ischemic brain from hypoxia and decreases infarct volumes. An undefined mechanism allows the beneficial effect of this potential neuroprotective agent to be observed even at 3 hours. Further development and investigation are justified.

References:

1. Culp BC, Brown AT, Erdem E, Lowery JD, Culp WC. Selective Intracranial Magnification Angiography of the Rabbit: Basic Techniques and Anatomy. *Journal of Vascular Interventional Radiology*, 2007; 18:187-192.

2. Brown AT, Skinner RD, Flores R, Hennings L, Borrelli M, Lowery J, Culp WC. Stroke Location and Brain Function in an Embolic Rabbit Stroke Model. *Journal of Vascular Interventional Radiology,* 2010; 21:903-9.

3. Johnson JLC, Dolezal MC, Kerschen A, Matsunaga TO, Unger EC. In vitro comparison of dodecafluoropentane (DDFP), perfluorodecalin (PFD), and perfluoroctylbromide (PFOB) in the

facilitation of oxygen exchange. *Artificial Cells, Blood Substitutes, and Biotechnology*, 2009; 37:156-162

4. Donnan GA. The 2007 Feinberg Lecture: a new road map for neuroprotection. *Stroke,* 2008; 39:242-248.

5. Lundgren CEG, Bergoe GW, Tyssebotn IM. Intravascular fluorocarbon-stabilized microbubbles protect against fatal anemia in rats. *Artificial Cells, Blood Substitutes, and Biotechnology*, 2006; 34:473-486.

1354

IMAGING PARKINSON'S DISEASE: FROM PATHOGENESIS TO PLACEBO RESPONSES

R. de la Fuente-Fernandez

Neurology, Hospital A. Marcide, Ferrol, Spain

Functional neuroimaging studies have provided most valuable insight into the mechanisms involved in Parkinson's disease (PD) neurodegeneration and related compensatory mechanisms.

Recent in vivo evidence suggests that PD pathology leads to an exponential decline in nigrostriatal dopamine function with a compensatory increase in dopamine turnover. While increased dopamine turnover may initially be beneficial by helping delay the onset of PD symptoms, it most likely contributes to the development of treatment-related motor complications during the symptomatic phase of the disease.

PET studies with raclopride led to the puzzling discovery of the biochemical basis of the placebo effect in PD. Converging evidence indicates that placebo-induced release of dopamine is a key mechanism underlying clinical placebo responses, not only in PD but also in other medical conditions. Placebo responses often complicate the interpretation of results of trials of neuroprotective therapies for PD.

While functional neuroimaging is a most powerful research tool, its role in clinical practice is not yet clear. Histopathological confirmation of neuroimaging patterns assumed to be specific for PD is still lacking. Until this information is available, PD remains a clinical diagnosis in the vast majority of cases.

1355

DEFINITION OF A STEREOTACTIC 3D MODEL OF THE HUMAN INSULAFOR NEUROSURGICAL APPROACH (EPILEPSY AND STEREOTAXIC SURGERY)

A. Afif, P. Mertens

Department of Neurosurgery, University Lyon 1, Lyon, France

Purpose: Design a method for 3D reconstruction of the insula, including its gyri and sulci , in AC-PC reference usable individually for imaging or for epilepsy and stereotactic surgery.

Material and methods: Morphometric study using 56 MRI of normal insular region. 26 male/30 female, 28 left/28 right hemispheres.

Stage 1 : Reconstruction in AC-PC reference of the insula from 3D-T1-MRI slices 1 mm thick.

Stage 2 : Digitalization and superposition of data in 3D using PhotoStudio software (Photo Editing Software) system with PC as the center of coordinates.

Stage 3 : MATLAB software (Mathworks Inc.) was used to transform in color values each pixel to obtain a color scale corresponding to the probability of insula sulci localization between 0% and 100%.

Results: Demonstration of very significant correlations between the coordinates of the main insular structures (angles, sulci ..) and the length of AC-PC (Spearman r = 0.5; two-tailed P = 0.0001).

This close correlation allows to describe a method for 3D reconstruction of the insula on MRI slices that requires only the positions of Ac and PC and then the inter-commissural (AC-PC) length. This procedure defines an area containing insula with 100% probability.

Conclusion: 3D reconstruction of insula will be potentially useful for:

1 - To improve localization of cortical areas, allowing to differentiate insular cortex from opercular cortex during stereoelectroencephalographic exploration of patients with epilepsy (SEEG) or in morphological and functional imaging.

2 - For microsurgical approach of Insula using Neuronavigation techniques.

3 - Identification of Insula during stereotactic surgery (SEEG, biopsy).

1359

FTY720 REDUCES POST-ISCHEMIC BRAIN LYMPHOCYTE INFLUX BUT DOES NOT IMPROVE OUTCOME IN PERMANENT MURINE CEREBRAL ISCHEMIA

A. Liesz[1], L. Sun[1], S. Schwarting[1], E. Mracsko[1], H. Bauer[2], C. Sommer[2], R. Veltkamp[1]

[1]Department of Neurology, University Heidelberg, Heidelberg, [2]Department of Neuropathology, University Mainz, Mainz, Germany

Objectives: The contribution of neuroinflammation and specifically brain lymphocyte invasion is increasingly recognised as a substantial pathophysiological mechanism after stroke. FTY720 is a potent treatment for primary neuroinflammatory diseases by inhibiting lymphocyte circulation and brain immigration. Previous studies using transient focal ischemia models showed a protective effect of FTY720 but did only partially characterize the involved pathways. We tested the neuroprotective properties of FTY720 in permanent cortical ischemia and analyzed the underlying neuroimmunological mechanisms.

Methods: Focal cerebral ischemia was induced by permanent transtemporal middle cerebral artery occlusion (MCAO) or reversible filament-induced MCAO for 60min. Mice received 1mg/kg body weight FTY720 per oral gavage as a single dose or daily treatment, control animals were administered PBS. Infarct volume and behavioural deficits ("Corner Test", "Cylinder Test") were determined at several time points after MCAO. Brain edema was analyzed 3d after MCAO by measuring brain water content with the dry/wet weight method. The treatment impact on lymphocyte subsets was characterized by flow cytometry. Brain invasion of leukocyte subsets was analyzed by immunohistology, cerebral cytokine expression was measured by RT-PCR and serum cytokine levels were detected by ELISA.

Results: FTY720 treatment resulted in substantial reduction of circulating lymphocytes while blood monocyte counts were significantly increased. The number of brain invading T- and B lymphocytes was significantly reduced in FTY720 treated mice. However, despite testing a variety of treatment protocols, infarct volume and behavioural deficits were not reduced 7d after permanent occlusion of the distal middle cerebral artery (MCAO). Additionally, we did not measure a significant reduction in infarct volume at 24h after 60min filament-induced MCAO, and did not see differences in brain edema between PBS and FTY720 treatment. Analysis of brain cytokine expression revealed complex effects of FTY720 on postischemic neuroinflammation comprising a substantial reduction of delayed proinflammatory cytokine expression at 3d but an early increase of IL-1β and IFN-γ at 24h after MCAO. Also, serum cytokine levels of IL-6 and TNF-α were increased in FTY720 treated animals compared to controls.

Conclusions: In the present study we were able to detect a reduction of lymphocyte brain invasion by FTY720 but could not achieve a significant reduction of infarct volumes and behavioural deficit. This lack of neuroprotection despite effective lymphopenia might be attributed to a divergent impact of FTY720 on cytokine expression and possible activation of innate immune cells after brain ischemia.

1360

ABSOLUTE CBF QUANTIFICATION WITH ARTERIAL SPIN LABELING MRI DURING HYPEROXIA

D.T. Pilkinton[1,2], J.A. Detre[1,3], R. Reddy[1,2]

[1]Center for Magnetic Resonance and Optical Imaging, Department of Radiology, [2]Biochemistry & Molecular Biophysics, [3]Center for Functional Neuroimaging, Department of Neurology, University of Pennsylvania, Philadelphia, PA, USA

Introduction: A number of studies have used arterial spin labeling (ASL) approaches to investigate the regional cerebral blood flow (CBF) changes with hyperoxia. Although it is well-known that inhaled oxygen creates a significant reduction in the T_1 of arterial blood (T_{1a}), and that T_{1a} has a substantial effect on CBF measurements using ASL, none of these studies have measured T_{1a} changes and CBF simultaneously during hyperoxia.

Aim: In this study, our aim was to simultaneously measure CBF and T_{1a} *in vivo* during normoxia and hyperoxia. These data will allow for an accurate correction of CBF data due to reduction in T_{1a} on a per subject basis to quantify the degree to which the reduction in CBF measured with ASL is due to the reduction in T_{1a}.

Material and Methods: All images were collected on a clinical 3T MRI scanner with a body coil transmitter and 35mm receive-only surface coil. Adult male Sprague-Dawley rats (n=5; 430-470 g) were maintained on 1.5% isoflurane in 30% oxygen delivered at 1.5 L/min through a nose cone. Gases were manually switched from 30% O2 to 100% O2 for ten minutes of hyperoxia, and then were switched back to 30% for a five minute baseline. This paradigm was repeated three times for each measurement of T_{1a} and CBF. A pulsed ASL (PASL) approach was used in this study for regional quantification of CBF. Control minus tag images were calculated according to the equation, $\mathbf{\Delta M = 2\ a\ M_{0a}\ f\ TI_1\ exp(-TI_2/T_{1a})}$, where a is the inversion efficiency, M_{0a} is the fully relaxed longitudinal magnetization of arterial blood, f is cerebral blood flow in ml blood/g tissue/min, and T_{1a} is the longitudinal relaxation time of arterial blood. Measurements of T_{1a} were performed using a technique employing a similar pulsed arterial spin labeling approach that was inversion prepared at multiple inversion times allowing for a monoexponential fit for T_{1a}.

Results: The measured values of T_{1a} during hyperoxia were found to decrease significantly compared to normoxia ($p < 0.01$). Mean T_{1a} decreased from 1.62 ± 0.06 s during normoxia to 1.50 ± 0.04 s during hyperoxia. Average whole-brain CBF was calculated to be 109.8 ± 13.4 and 92.0 ± 9.1 mL/100g/min during normoxia and hyperoxia, respectively. CBF calculated in the hyperoxic condition corrected for T_{1a} exhibited a reduced (100.4 ± 10.0 mL/100g/min) , but still statistically significant change from the normoxic condition. The correction for the change in T_{1a} during hyperoxia accounted for approximately 47.5% of the overall decrease in the calculated CBF.

Discussion and Conclusions: Simultaneous *in vivo* measurements of T_{1a} and CBF were performed using PASL approaches during normoxia and hyperoxia in rat brains. Baseline values of T_{1a} and CBF measured during normoxia show very close agreement with previous studies. Significant reductions in T_{1a} and CBF were measured during hyperoxia, also in agreement with previous studies. Although the effect of the correction of T_{1a} of the CBF data due to hyperoxia was substantial, it represented a smaller correction factor compared with previous studies.

1363

SUPPRESSION OF TRPC6 DEGRADATION PREVENTED ISCHEMIC BRAIN DAMAGE

Y. Wang

Institute of Neuroscience, SIBS, CAS, Shanghai, China

Brain injury after focal cerebral ischemia develops from a series of pathological processes. However, the results of clinical trials to prevent ischemic brain damage by blocking the detrimental effects are disappointing. We report that suppression of proteolytic degradation of transient receptor potential canonical (TRPC) 6 prevented ischemic neuronal cell death. The TRPC6 protein level in neurons was reduced in ischemia via N-methyl-D-aspartate (NMDA) receptor-dependent calpain proteolysis of N-terminal domain of TRPC6 at Lys^{16}. A fusion peptide derived from the calpain cleavage site in TRPC6 inhibited its degradation, reduced infarct size and improved behavior outcome of ischemic rats. Thus, suppression of TRPC6 degradation prevented ischemic brain damage.

1364

ANTI-APOPTOTIC EFFECT OF ACTIVATED PROTEIN C IN HIPPOCAMPAL NEURONAL CULTURE DURING GLUTAMATE TOXICITY

L. Gorbacheva[1], S. Strukova[1], G. Reiser[2]

[1]The Lomonosov Moscow State University, Moscow, Russia, [2]Institute for Neurobiochemistry, Otto-von-Guericke University, Medical Faculty, Magdeburg, Germany

Introduction: Brain injury is associated with hyperstimulation of glutamate receptors by glutamate (Glu) and led to induction of neuronal death during apoptosis or necrosis. We have previously shown that activated protein C (APC), a serine protease of hemostasis has protective effects in hippocampal and cortical neurons at glutamate-induced excitoxicity through protease activated receptor-1 (PAR-1) or endothelial receptor of protein C (EPCR)/PAR-1. The molecular cascade responsible for neuronal apoptosis at Glu-induced toxicity includes many transcription factors and molecular regulators.

Aim of our study is to detect possible molecular mechanism of neuroprotective action of APC.

Methods: Studies were performed using primary culture of neurons from cortex or hippocampus of brain of Wistar rat pups. Cell death was determined by biochemical (LDH) and morphological methods (Hoechst33342, Ethidium bromide and Syto-3). By immunostaining and Western blot the nucleus and cytoplasm levels of pro-apoptotic proteins (p53, AIF, Bax and caspase-3) were assessed during Glu-toxicity and incubation with APC or (and) with NF-κBp65 inhibitor, helenalin.

Results: We observed that exposure neurons to Glu led to the increase of apoptotic cells (to 33%) at 24 h. The pretreatment of culture with APC (Sigma) (0,05-10 nM) significantly (on average in two times) reduced the Glu-induced neuronal death. We show that APC inhibits translocation of NF-κBp65 into the nucleus of cultured rat hippocampal neurons, induced by 100 μM glutamate. The blocking effect of APC on NF-kB translocation was observed at 1 and 4 h after treatment of neurons with glutamate, when the NF-kBp65 level in the nucleus was significantly above the basal level. Then we investigated whether the binding of APC to EPCR/PAR-1 is required to control NF-κB activation. Using antibodies blocking PAR-1 or EPCR abolished the APC-induced decrease of nuclear level NF-κBp65 at glutamate-induced toxicity. More over incubation neurons with helenalin, a special inhibitor of NF-κBp65, blocks neuronal death during Glu-toxicity similarly to APC. Thus, we demonstrate that the activation of NF-κB in hippocampal neurons mediates the glutamate-activated cell death program, which is reduced by exposure of cells to APC. Both PAR-1 and EPCR mediate the APC-induced reduction of the nuclear level of NF-κBp65 on hippocampal neurons at glutamate-induced.

It is known, NF-κB, as transcription factor, can regulate level of some pro-apoptotic proteins. But it is not clear how APC influences on these key signalling molecular during Glu-induced toxicity. Our studies showed that in hippocampal neurons APC inhibits Glu-induced caspase-3 activity with maximum effect 24h after treatment. APC inhibits AIF translocation into nucleus. Incubation of neurons with APC blocks the increase of nuclear level of p53 as well as 4 h and 24 h after exposure cells to Glu. APC protects neurons from Glu-toxicity due to blockage of both caspase-dependent and -independent apoptosis. APC reduces of the nuclear level of NF-κBp65 at Glu-toxicity.

Conclusion: Thus APC can suppress the molecular cascade responsible for neuronal

apoptosis at Glu-induced toxicity via inhibition of p53 or blockage the activation of caspases and NF-kB. (RFBR grant 08-04-01123a).

1365

SYNERGISTIC EFFECTS OF MCI-186 ON TRANSPLANTATION OF BONE MARROW STROMAL CELLS IN RAT ISCHEMIC STROKE MODEL

L.H. Shen[1], X.S. Ding[2], M. Ye[3], Q. Han[4], C. Zhang[4], H. Huang[4], E.B. Wu[4], H.F. Huang[4]

[1]Neurology, The Affiliated Hospital of Nantong University, Nantong, [2]Neurology, The First Affiliated Hospital of Nanjing Medical University, [3]The BenQ Neurological Institute of Nanjing Medical University, Nanjing, [4]The Affiliated Hospital of Nantong University, Nantong, China

Aims: Transplantation of bone marrow stromal cells (BMSCs) is a potential therapy for ischemic stroke due to their inherent characteristics of self renewal, proliferation and ability to differentiate into multiple cell phenotypes. But the poor environment such as insufficient nutrition supply and oxygen free radical toxicity in brain leision limits the efficacy. Here, we hypothesized and verified the synergistic effects of MCI-186, a free radical scavenging, on BMSC transplantation in rat ischemic model.

Methods: In vitro, cultured BMSCs (passage4) were divided into 3 groups, including the normal group, ischemia-reperfusion (I/R) group and MCI-186 treated I/R group, cell apoptotic rate of each group was measured by flow cytometer respectively. In vivo, rat transient middle cerebral artery occlusion (MCAO) model was established. Two separate groups of rats were administered with MCI-186 (3 mg/kg) or phosphate buffered solution (PBS) immediately after artery occlusion and then killed 1, 3, 7and 14 days respectively following MCAO to monitor the expressions of brain-derived neurotrophic factor (BDNF) and vascular endothelial growth factor (VEGF), superoxide dismutase(SOD) activity/ malondialdehyde (MDA) level in ischemic brain chronologically, and compared with sham operation group. Furthermore, another three separate groups of MCAO rats were administered with either PBS or BMSCs (2×106, marked with BrdU) or combination of MCI-186 and BMSCs. At 14d after MCAO, immunohistochemistry was used to observe the engrafted-BMSCs and caspase-3 protein in ischemic brain, infarct volume and neurological function were also evaluated.

Results: In vitro, apoptotic rate of BMSCs was significantly decreased following MCI-186 treatment after I/R. In vivo, the expressions of BDNF and VEGF were both up-regulated in ischemic brain after MCAO, probably MCI-186 could enhance and prolong the secretions. MDA level in brain lesion was significantly reduced in MCI-186 treated group while SOD activity rose. When compared with BMSC monotherapy, combination therapy obviously enhanced BrdU positive cell number and decreased caspase-3 expression in ipsilateral brain , and NSE/ BrdU, GLUT-1/ BrdU double staining cells also increased. Infarct volumes were notablely reduced in two BMSC treated groups, especially in combination treated group, functional restoration was accordingly improved.

Conclusions: The present study suggests MCI-186 can protect BMSCs from I/R injury and produce synergistic effects on BMSC transplantion in ischemic stroke by ameliorating the poor environment of brain lesion.

Keywords: Bone marrow stromal cells (BMSCs), ischemic stroke, MCI-186, Nutrition factor, Oxygen free radical

1366

MEASUREMENT OF DOPAMINE D_2 RECEPTORS IN LIVING HUMAN BRAIN USING [^{11}C]RACLOPRIDE WITH ULTRA-HIGH SPECIFIC RADIOACTIVITY

Y. Fujimura[1,2], H. Ito[1], H. Takahashi[1], F. Yasuno[1], Y. Ikoma[1], M.-R. Zhang[3], S. Nanko[2], K. Suzuki[3], T. Suhara[1]

[1]Molecular Neuroimaging Group, Molecular Imaging Center, National Institutes of Radiological Sciences, Chiba, [2]Department of Psychiatry, Teikyo University School of Medicine, Tokyo, [3]Molecular Probe Group, Molecular Imaging Center, National Institutes of Radiological Sciences, Chiba, Japan

Objectives: High specific radioactivity is preferable in the measurement of neuroreceptor bindings with positron emission tomography (PET) because receptor occupancy by the mixed cold ligand hamper an accurate estimation of receptor binding. Recently, we succeeded in synthesizing [^{11}C]raclopride, a dopamine D_2 receptor ligand, with ultra-high specific radioactivity, i.e., several thousand GBq/mmol. In the present study, we compared the [^{11}C]raclopride bindings to dopamine D_2 receptors between radioligands with ultra-high specific radioactivity and ordinary high specific radioactivity in healthy human subjects.

Methods: Two PET studies using [^{11}C]raclopride with ultra-high specific radioactivity (4302-7222 GBq/mmol) or ordinary high specific radioactivity (133-280 GBq/mmol) were performed on different days in 14 healthy men. Binding potential (BP) was calculated by the simplified reference tissue method, peak equilibrium method, and area-under-the-curve method for each region-of-interest using time-activity data in the cerebellum as a reference brain region.

Results: BP values for radioligands with ultra-high specific radioactivity and ordinary high specific radioactivity calculated by the simplified reference tissue method were 4.06 ± 0.29 and 4.10 ± 0.25 in the putamen, 0.44 ± 0.07 and 0.47 ± 0.07 in the thalamus, and 0.37 ± 0.06 and 0.38 ± 0.06 in the temporal cortex, respectively (mean ± SD). No significant difference in BP was observed between ultra-high specific radioactivity and ordinary high specific radioactivity in any of the brain regions.

Conclusion: The correlations for BP values between ultra-high SA and ordinary high SA by each quantification method were very well (r^2 >0.99). No significant differences were observed in BP values between both SA. Although, use of [^{11}C]raclopride with ultra-high SA does not have merit over ordinary high SA in human study, it must be desirable in small animal study like mouse since injected dose per body is usually much higher than that in human.

References:

1) Noguchi J, Zhang MR, Yamamoto K, Nakao R, and Suzuki K. In vitro binding of [^{11}C]raclopride with ultrahigh specific activity in rat brain determined by homogenate assay and autoradiography. Nucl Med Biol. 2008;35:19-27.

2) Noguchi J, Suzuki K. Automated synthesis of the ultra high specific activity of [^{11}C]Ro15-4513 and its application in an extremely low concentration region to an ARG study. Nucl Med Biol. 2003;30:335-43.

1367

ASSESSMENT OF THE EFFICIENCY OF NEUROMEDIATORY THERAPY OF VEGETATIVE STATE PATIENTS USING PET

E. Kondratyeva[1], V. Panuntsev[2], S. Kondratyev[2], L. Zenciper[2], M. Chachkhaliya[2]

[1]Intensive Care, [2]Polenov Neurosurgical Institute, Saint Petersburg, Russia

The aim: To evaluate the influence of super selective neuromediatory metabolic therapy at patients in a vegetative state using PET.

Materials and methods: In our investigation we enrolled 26 patients in vegetative state, aged from 2.4 to 57 years. Duration of a vegetative state in all patients had been longer than 4 months by the time of hospitalization. For clinical examination we used Spiral Computer Tomography («Brilliance 6-S - Phillips»), MRI-tomography («Signa Excite Medical System»), Positron Emission Tomography («SCANDY-TRONIX»), angiographic complex «Phillips-integris», transcranial dopplerography.

For super selective arterial catheterization we used microcateters MAGIC STD (BALT), PROWLER plus (CORDIS). All 26 patients had undergone PET with glucose twice (before intra-arterial infusion and 10 days after infusion).

The arterial catheter was installed into internal carotid artery (left - in 12 patients, right - in 8 patients) or into left vertebral artery (6 patient). Continuous intra-arterial infusion of Nimodipime 0,15 mg /kg/ day, Phosphocreatine -30 mg/ kg /day, Citicoline 100 mg /kg /day and together with heparin was carried on for 7 days.

Before the infusion in all patients we observed significant decrease in brain glucose metabolism on PET. After realization of intra-arterial infusion, the metabolism of glucose according to PET remained at former level in 12 patients, in 14 patients we observed positive dynamic on EEG and increase of glucose metabolism (from 5 to 20%) in different brain fields (mainly near the catheter) by PET.At all patients with positive dynamics according to PET the increase in an index of fast waves according to EEG was marked also. Only in 7 cases from those 14 with gained positive dynamics based on PET results, we have observed transition to the minimal consciousness state.

The resume: This results shows that it is necessary to be careful with the conclusions about interrelation of structure, a metabolism of a brain and a consciousness phenomenon.

Thus, provisional data allowed assuming significant efficiency of an offered technique of super selective intra-arterial infusion in treatment of patients in vegetative state and that is why this method needs following investigation.

1368

GCEE PROTECTS CEREBRAL MICROVASCULAR ENDOTHELIAL CELLS AND DECREASES BLOOD-BRAIN-BARRIER PERMEABILITY AFTER EXPERIMENTAL BRAIN TRAUMA

L. Josephine[1,2], W. Leung[1,2], S. Zhao[2,3], A. Yalcin[4,5], S. Pallast[2], X. Wang[2], S.-Z. Guo[2], K. van Leyen[2], E.H. Lo[2,6,7]

[1]Pediatric Critical Care Medicine, Massachusetts General Hospital / Harvard Medical School, Boston, [2]Neuroprotection Research Laboratory, Massachusetts General Hospital / Harvard Medical School, Charlestown, MA, USA, [3]Department of Orthopedics - Spine Division, The First Hospital of Jilin University, Changchun, China, [4]Department of Biochemistry, [5]Faculty of Pharmacy, Ege University, Izmir, Turkey, [6]Department of Neurology, [7]Department of Radiology, Massachusetts General Hospital / Harvard Medical School, Boston, MA, USA

Objectives: Oxidative stress has been implicated in the pathogenesis of many acute and chronic neurological pathologies. The endothelial cells of the blood-brain-barrier are an important target of oxidative stress because they are rich in polyunsaturated fatty acids, which are prone to lipid peroxidation in the presence of free radicals generated during oxidative processes. Glutathione (GSH), the major intracellular antioxidant molecule, limits oxidative stress-induced cell injury, but GSH depletion is an important consequence of oxidative stress. Efforts to administer GSH as a therapeutic agent has been limited by the fact that it does not readily cross cell membranes. γ-glutamyl cysteine ethyl ester (GCEE), a precursor of GSH synthesis, crosses lipid membranes easily. Intraperitoneal administration of GCEE has been shown to increase brain GSH levels. In this study, we ask whether GCEE protects the endothelium during brain injury. Our objectives are to investigate the effect of GCEE on cultured human brain microvascular endothelial cells (HMBECs) in two *in-vitro*

models of injury, and to determine its effect on acute blood-brain-barrier permeability in an in-vivo model of brain trauma.

Methods: *In vitro* studies examined the effects of GCEE on human brain endothelial cells which were subjected to two injury paradigms: incubation with hydrogen peroxide (H2O2) to simulate oxidative stress, and oxygen-glucose deprivation (OGD) to simulate hypoxia and ischemia. Measured outcomes include intracellular ROS levels and GSH levels, mitochondrial membrane potential, and cell survival. In vivo studies were performed using a standard controlled cortical impact model of traumatic brain injury. GCEE or vehicle was administered by intraperitoneal injection 10 minutes after trauma. Evans blue dye was injected intravenously 30 minutes after trauma, and leakage of Evans blue dye from the ipsilateral and contralateral hemispheres were quantified at 2 hrs.

Results: GCEE was significantly protective in human brain endothelial cell cultures. GCEE increased intracellular GSH levels during baseline conditions. GCEE decreased ROS formation and restored GSH levels during H2O2-induced injury. GCEE preserved mitochondrial membrane potential during OGD. These biochemical effects of GCEE were consistent with its ability to decrease endothelial cell death after H2O2-induced injury and OGD. In the *in vivo* brain trauma studies, GCEE-treated mice showed a significant reduction in acute blood-brain-barrier permeability.

Conclusions: These data suggest that the beneficial effects of GCEE on brain endothelial cells

and microvessels may contribute to its potential efficacy as a neuroprotective agent in traumatic brain injury.

References:

Lai, Y., Hickey, R. W., Chen, Y. et al. (2008) Autophagy is increased after traumatic brain injury in mice and is partially inhibited by the antioxidant gamma-glutamylcysteinyl ethyl ester. J Cereb Blood Flow Metab, 28, 540-550.

Drake, J., Kanski, J., Varadarajan, S., Tsoras, M. and Butterfield, D. A. (2002) Elevation of brain glutathione by gamma-glutamylcysteine ethyl ester protects against peroxynitrite-induced oxidative stress. J Neurosci Res, 68, 776-784.

Pun, P. B., Lu, J. and Moochhala, S. (2009) Involvement of ROS in BBB dysfunction. Free Radic Res, 43, 348-364.

1370

BINDING POTENTIAL ESTIMATES OF Γ-AMINOBUTYRIC ACID A BENZODIAZEPINE RECEPTOR BINDING: A TEST-RETEST STUDY IN NONHUMAN PRIMATES

D.E. Lee[1], T. Kloczynski[1], C. Sandiego[1], D. Weinzimmer[1], D. Labaree[1], E.D. Morris[1], R.E. Carson[1], K.P. Cosgrove[1,2]

[1]Diagnostic Radiology, Yale University, New Haven, [2]Psychiatry SPECT Brain Imaging, VA Connecticut Healthcare System, West Haven, CT, USA

Changes in numbers of γ-Aminobutyric Acid type A benzodiazepine receptors ($GABA_A$-BZRs) during the recovery from alcohol dependence likely play an important role in alcohol withdrawal symptoms and craving associated with early withdrawal [1]. However, it is difficult to distinguish between preexisting differences in patients compared to controls versus differences due to the chronic effects of alcohol on $GABA_A$-BZR availability. A nonhuman primate model is critical to examine these changes within subjects. As a prelim to the establishment of a useful animal model, we examined the test-retest reliability of [^{11}C]flumazenil, a radiotracer for PET, in drug-naïve animals. Ten adolescent male, rhesus macaques (4-6 kg) were injected with 6.19 ± 0.75 mCi of [^{11}C]flumazenil (injected mass of 0.74 ± 0.33 μg) and scanned for 90 min using the bolus plus constant infusion (B/I) paradigm (K_{bol}=90 min). To measure the variability and reliability of [^{11}C]flumazenil binding, we computed the binding potential (BP_{ND}) using the equilibrium approach, and the simplified reference tissue model (SRTM) [2] using the pons as a reference region. The reproducibility of BP_{ND} in all regions between days 1 and 2 were examined by percent change in BP_{ND} (Δ BP_{ND}), test-retest variability (TRV: $|BP_{day1} - Bp_{day2}|/[(BP_{day1} + BP_{day2})/2]$), and intraclass correlation coefficient (ICC) comparisons. Highest BP_{ND} values were observed in the occipital (3.13 ± 0.37), frontal (2.53 ± 0.21), temporal (2.19 ± 0.18), insula (2.59 ± 0.23) cortices followed by caudate (0.93 ± 0.19), putamen (1.04 ± 0.19), and cerebellar regions (1.16 ± 0.10) where lower BP_{ND} values were observed (Figure 1). Further, the cortical regions with the highest BP_{ND} values also had lower ΔBP_{ND} (1.48 ± 1.38 %) than non-cortical regions (3.21 ± 3.78 %). Consistently, % TRV was lower in the cortical regions compared to non-cortical regions (6.47 ± 1.43 vs. 11.84 ± 4.98, respectively). SRTM yielded reliable BP_{ND} estimates with higher ICC (0.94) than estimates using the equilibrium approach (ICC = 0.88). These studies provide support for the use of SRTM with pons as an input function as a robust and reproducible method for studying GABA-A BZR availability using [^{11}C]flumazenil. Future imaging studies in the same group of animals will be conducted during the recovery from chronic alcohol exposure to determine changes in GABA-A BZR availability underlying alcohol addiction. [1]Staley J. et al., 2005 Arch Gen Psychiatry. 62:877-88 [2]Lammertsma, A.A. and Hume, S.P., 1996 NeuroImage. 4:153-58

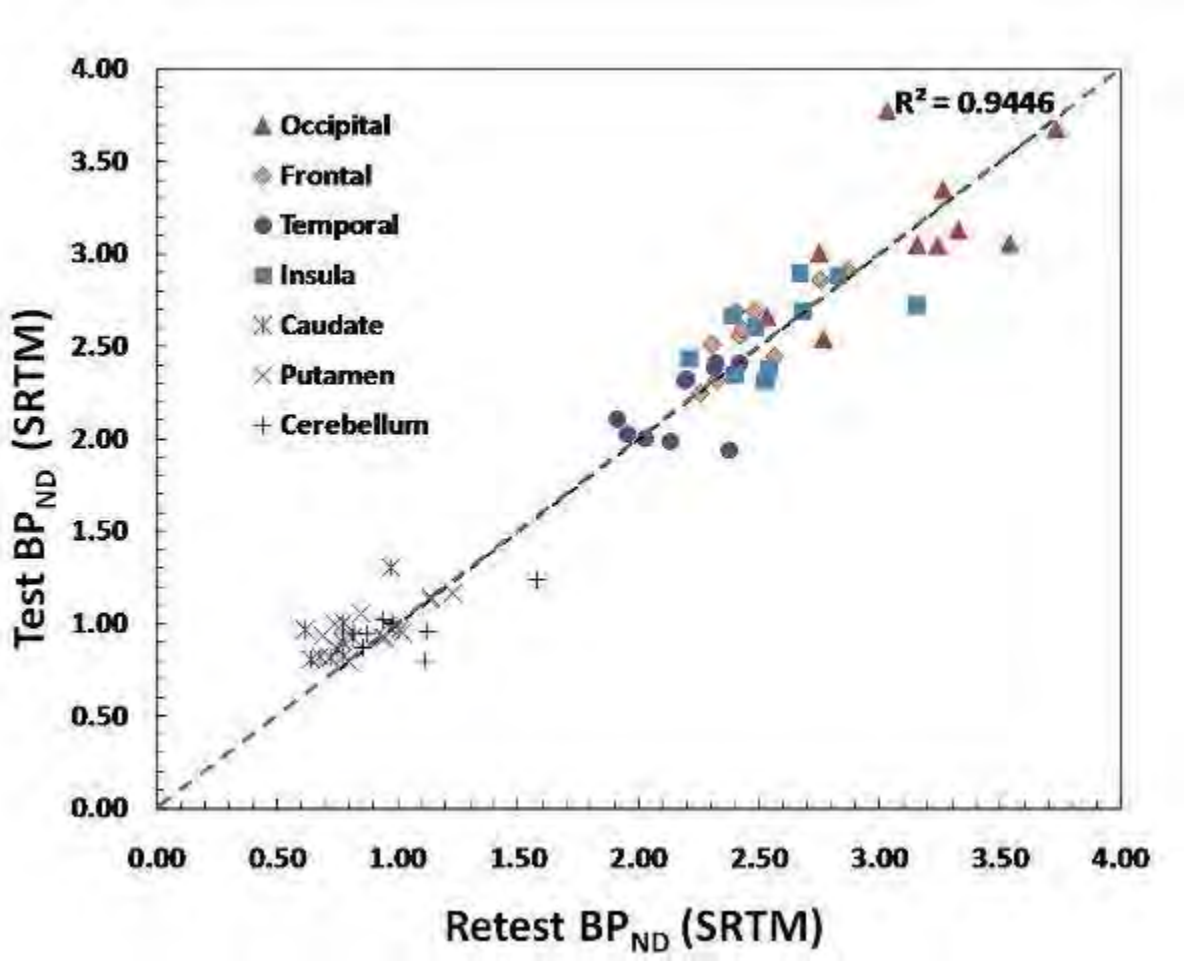

[Test-retest BPND of 11C-flumazenil in 10 NHP-brain]

1371

DETECTION OF ENDOGENOUS OPIOID RELEASE *IN VIVO* IN THE HUMAN BRAIN WITH [^{11}C]CARFENTANIL PET

A. Colasanti[1,2], G. Searle[1], S. Hill[1], R. Reiley[1], A. Tziortzi[1], D. Quelch[1,2], R. Gunn[1], A. Waldman[3], K. Schruers[4], D. Nutt[2], E.A. Rabiner[1,2]

[1]GlaxoSmithKline Clinical Imaging Centre, Hammersmith Hospital, [2]Division of Experimental Medicine, [3]Department of Imaging Sciences, Imperial College London, London, UK, [4]Department of Psychiatry and Neuropsychology, Maastricht University, Maastricht, The Netherlands

Objectives: Changes in the binding of the PET ligand [^{11}C]carfentanil to the μ-opioid receptor, following physiological and psychological interventions, have been interpreted as evidence of its sensitivity to endogenous opioid (EO) fluctuations. However, direct pharmacological confirmation has not been performed. We evaluated, in humans, the effect of pharmacological intervention designed to increase [amphetamine [1]] and decrease [hydrocortisone [2]] synaptic EO concentration, on [^{11}C]carfentanil binding.

Methods: Twelve healthy male volunteers were examined with [^{11}C]carfentanil PET, before, and 3 hours after, an oral administration of d-amphetamine (either a "high" dose, 0.5 mg/kg, n=6, or an inactive "ultra-low" dose [3], 1.25 mg total dose, n=6). One week later, nine of the subjects underwent a third scan 16 hours after an oral administration of 100 mg hydrocortisone. Regional binding potential (BP_{ND}) values were derived using a simplified reference tissue model with the occipital cortex as the reference region. Changes from Baseline to Post-Amphetamine scans (Δ_{amp} BP_{ND}), at "high" and "ultra-low" amphetamine dose and from Baseline to Post-Hydrocortisone scans (Δ_{hc} BP_{ND}) were assessed in predefined automatically-delineated regions of interest (ROI) (Putamen, Caudate, Thalamus, Frontal Lobe, Anterior Cingulate, Insula) and manually-delineated ROI (Ventral Striatum, Amygdala, and Hypothalamus).

Results: Δ_{amp} BP_{ND} was significantly different from 0 in the "high" but not the "ultra-low" group, in Putamen, Caudate, Thalamus, Anterior Cingulate, Insula ($p < 0.005$, corrected for multiple comparisons) and was significantly higher in the "high" than in the "ultra-low" group in the Putamen and Thalamus ($p \leq 0.05$, corrected for multiple comparison). We saw no main effect on Δ_{hc} BP_{ND} in any of the ROI examined, though $\Delta_{hc}BP_{ND}$ was higher in those who had previously received the "high" amphetamine dose (n=4) relative to those who previously received the "ultra-low" amphetamine dose (n=5) in the Ventral Striatum and Thalamus ($p \leq 0.05$, corrected for multiple comparisons).

Conclusions: This is the first direct demonstration of a dose-dependent, pharmacologically induced release of endogenous opioids in the human brain *in vivo*. The reason for the lack of effect in the hydrocortisone group is not clear, but may be related to inadequate dose of hydrocortisone, low baseline levels of EO, small sample size or persistent effects of amphetamine administration in the previous 7 days. Amphetamine challenge in combination with [^{11}C]carfentanil PET promises to be a useful tool to investigate opioid neurotransmission in neuropsychiatric disorders.

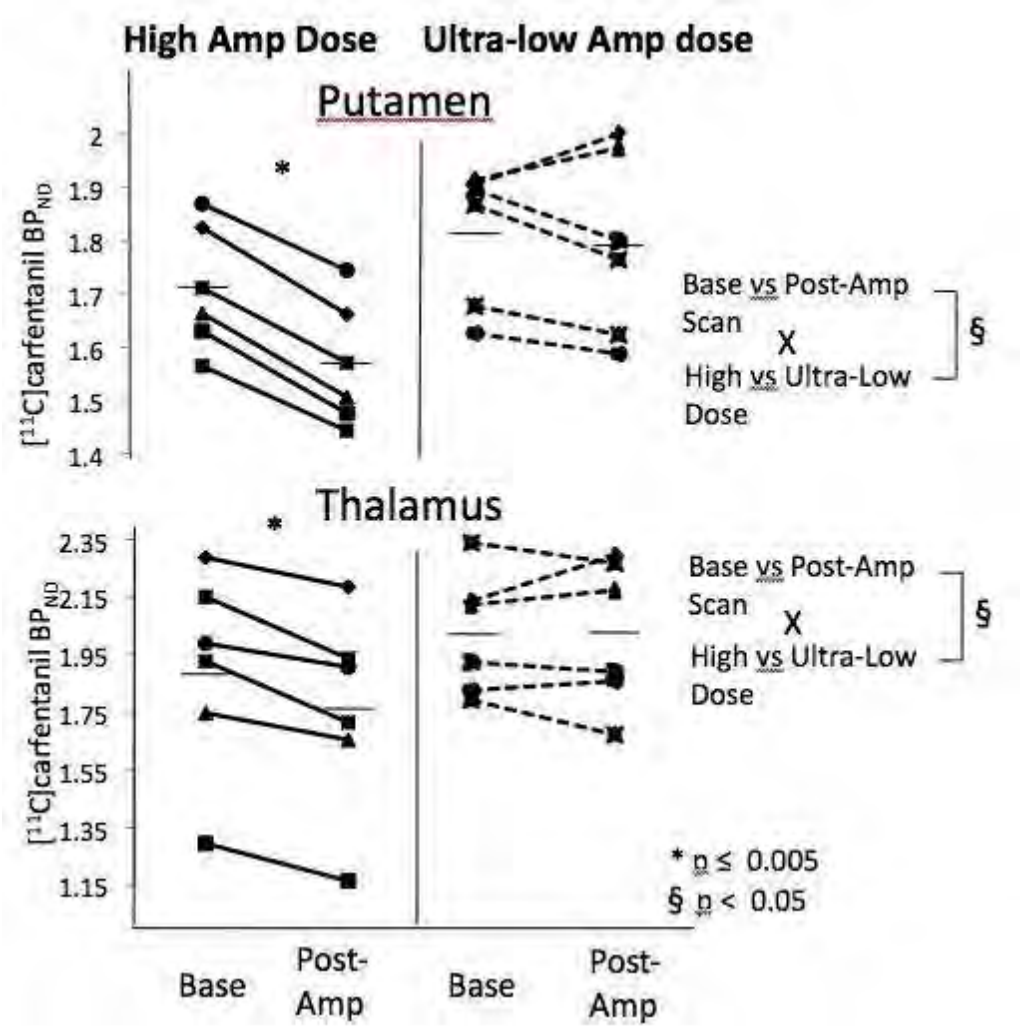

[Fig.1]

References:

[1]. Olive MF et al. *J Neurosci*. 2001 21: RC184.

[2]. Krantz DE & Brown WA. *Psychoneuroendocrinology*. 1985 10: 211-214.

[3]. Grilly DM & Loveland A. *Psychopharmacology (Berl)*. 2001 153: 155-169.

1372

SIMULTANEOUS TRACKING OF BLOOD BRAIN BARRIER DISRUPTION AND DRUG DELIVERY BY OPTICAL PHARMACOKINETICS

S. Joshi[1], M. Wang[1], A. Ergin[2], I.J. Bigio[2]

[1]Anesthesiology, Columbia University, New York, NY, [2]Biomedical Engineering, Boston University, Boston, MA, USA

Objectives: By observing changes in spectrum of back-scattered visual-near infrared light, it is possible to measure *in-vivo* the tissue concentrations of certain drugs and tracers that have an absorption spectrum that is distinct from hemoglobin and deoxy-hemoglobin. The technique has been called as optical pharmacokinetics (OP). OP measurements are tissue non-invasive and can track concentrations of drugs/tracers in virtual real-time. Rapid drug/tracer concentration measurements are particularly useful in tracking drugs/tracers when injected by the intraarterial route that are beyond the temporal resolution of tissue biopsy or microdialysis. Osmotic disruption of the blood brain barrier (BBBD) by intraarterial mannitol injection is often the key step in the delivery of chemotherapeutic drugs to brain tissue. BBBD with mannitol can be highly variable. Objective of this study is to investigate the possiblility of simultaneous quantification of BBBD and tissue drug concentrations using the OP method, which could generate novel insights into pharmacokinetics of CNS drugs.

Methods: After IACUC approval the study was conducted on New-Zealand white rabbits. Surgical preparation included: tracheotomy for mechanical ventilation, femoral and selective internal carotid artery (ICA) catheterizations, skull screws for monitoring electrocerebral activity, bilateral placement of laser Doppler probes and skull shaving to the inner table for the placement of fiber OP probe. For this experiment we measured brain tissue concentrations of indocyanine green (ICG, a marker of BBBD) and mitoxantrone (a chemotherapeutic drugs effective in experimental glioma models) using the OP method. Animals were randomized into two groups with (mannitol, intracarotid mannitol injection) or without (control, intravenous saline injection) BBBD. Immediately after mannitol injection intracarotid 1 mg of ICG was injected followed the injection of intracarotid mitoxantrone (3mg).

Results: The study involved 8 control and mannitol treated animals, each. Preliminary analysis of the data reveals that intracarotid ICG was rapidly cleared from the brain tissue, however, there was a small but significant retention of ICG concentrations after BBBD 0.005± 0.003 (control) vs. 0.041± 0.03 µg/ml (mannitol, $P< 0.005$) at the end of 5 minutes. The concentration MTO concentrations was also significantly higher after BBBD (0.02±0.03 (control) vs. 0.583±0.51 (µg/ml, mannitol, $P< 0.008$). There was a linear correlation between the tissue concentrations of mitoxantrone and the area under the mitoxantrone concentration time curve and the end ICG concentrations, Figure.

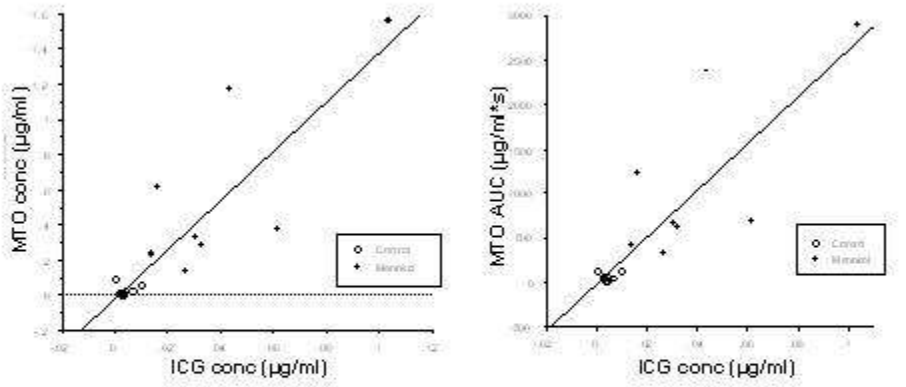

Figure: A linear relationship was observed between the ICG concentrations (µg/ml) and mitoxantrone (MTO, µg/ml) concentrations at the end of 30 minutes (N=16, R=0.85 and P<0.0001) A similar relationship was observed with the area under the concentration time curve (AUC) for mitoxantrone and the ICG concentrations (N=16, R=0.84, P<0.0001)

[sj1]

Conclusion: This study shows the feasibility of optical monitoring of blood brain barrier disruption with intraarterial ICG injections. That tissue concentration of mitoxantrone was linearly related to the degree of BBB disruption as assessed by the ICG. While most of the ICG dose was rapidly cleared from the brain tissue trace concentrations remained detectable in the brain tissue after BBB disruption. If such concentrations of ICG could be detected in human brain tissue by NIRS spectroscopy then, optical monitoring of the barrier could help improve intraarterial delivery of drugs. Inadequate disruption might require additional dose of mannitol while excessive disruption might result in reducing the dose of chemotherapeutic drugs.

Funded: NIH (NCI) R01 127500 (SJ)

1373

HISTONE DEACETYLASE-5 (HDAC-5) MRNA QUANTIFICATION BY NANOTECHNOLOGY USING *IN VIVO* GENE TRANSCRIPT TARGETING MRI AND *EX VIVO* RT-QPCR

P.K. Liu, J. Yang, C. Liu, J. Ren, H. Wang, K. Rasakham, C.-M. Liu

Radiology/A.A. Martinos Center for Biomedical Imaging, Mass General Hospital/Harvard Medical School, Charlestown, MA, USA

Epigenetic modulation of histon deacetylase (HDAC) activities is controlled, in part by a class of post-transcriptional gene-regulating micro RNAs (miR). However, currently, methods to detect epigenetic processes can only be performed in post mortem samples. We have developed a targeted magnetic resonance imaging (MRI) technique. This technology is based on fast exclusion of unbound, non-targeted MR probe by normal active brains, while bound and targeted MR-visible probe having an extended window for MRI. Here, we investigated the expression of HDAC-5 mRNA in mice exposed to amphetamine, a common neuropsychostimulant.

We aimed to compare in vivo MRI and ex vivo RT-qPCR. An oligodeoxynucleotide (ODN) with sequence antisense to the HDAC5 mRNA was made with phosphorothioate-modification (sODN) and this sODN-hdac5 was linked to an MR-visible contrast agent containing superparamagnetic iron oxide nanoparticles (SPION). SPION was chemically modified to contain NeutrAvidin (NA) and the overall hydrodynamic diameter was 30 nanometers (nm) (SPION-NA, core size of 10 nm); SPION-NA has a capacity to bind 2 $x10^{-15}$ mol of target mRNA per signal reduction frequency ($\Delta R2^*$, sec^{-1}). Our preliminary studies show that SPION-hdac5 targeted HDAC5 transcript from the total cDNA of the hippocampus and striatum of C57black6 mice in vitro. We delivered SPION-hdac5 via intraperitoneal (i.p.) injection to mice with a bypass to the blood-brain barrier (BBB). SPION-hdac5 was distributed globally. Using quantitative RT-PCR, we examined the mRNA levels of Actin, GFAP and HDAC5 in striatal and hippocampal samples of mice that received saline, acute amphetamine or chronic amphetamine treatment. We found agreement between in vivo MRI data and ex vivo RT-qPCR for all three mRNA transcripts.

Supported by grants from NIH (AT004974 [JQR], DA024235, DA026108; DA029889 [PKL] and RR14075 [AA Martinos Center]), from American Heart Association (09GRNT2060416); the Stanley Center for Mental Health Research at the Broad Institute [PKL].

1376

LOSS OF DOPAMINE SYNTHESIS CAPACITY DURING HEALTHY AGING PREDICTS COGNITIVE SPEED AND IS NOT CAUSED BY ATROPHY

J. Kalbitzer[1], L. Deserno[1], F. Schlagenhauf[1], A. Beck[1], T. Mell[1], H.-G. Buchholz[2], M. Plotkin[3], R. Buchert[3], Y. Kumakura[4], P. Cumming[5], A. Heinz[1], M.A. Rapp[1]

[1]Department of Psychiatry, Charite Berlin, Berlin, [2]Department of Nuclear Medicine, University Hospital Mainz, Mainz, [3]Department of Nuclear Medicine, Charité Berlin, Berlin, Germany, [4]Research Center for Advanced Science and Technology, Tokyo, Japan, [5]Department of Nuclear Medicine, Ludwig-Maximilians University Munich, Munich, Germany

Cortical dopamine synthesis capacity declines during the process of healthy aging. It has been argued that this decline is responsible for the age-related decrease of cognitive speed. But it is still unclear whether this loss as measured with positron emission tomography (PET) is caused by a general atrophy.

The aim of this study was to (1) show the correlation between cognitive speed and dopamine synthesis capacity, (2) test for an age-related loss of dopamine synthesis capacity, and (3) test if this age-related loss is caused by general atrophy.

In a first and second step, we used SPM analysis to estimate the correlation between (1) cognitive speed and (2) age with dopamine synthesis capacity as measured with 6-[18F]fluoro-L-DOPA (FDOPA) and PET in 16 healthy, right-handed men with an age ranging from 22 to 61 years. As expected, cognitive speed was associated with the unidirectional net blood brain clearance of FDOPA (kinapp, ml g-1 min-1) and, described by other groups, kinapp decreased in cortical but not subcortical regions relative to age. Statistical significance of both these results survived correction for all voxels of the brain. In a third step (3), we used the biological parametric mapping (BPM) toolbox which allows multimodal imaging analysis to estimate to which degree the age-related decrease of kinapp is related to gray matter density as measured with magnetic resonance (MR) imaging. No significant association was observed.

Our data indicate that age-related decline of dopamine synthesis capacity in cortical regions is responsible for the decrease of cognitive speed. Our data also indicate that this process is not related to general atrophy but most likely to changes in dopamine metabolism.

1378

IMPROVEMENT IN CEREBRAL GLUCOSE METABOLISM IN PATIENTS WITH SYMPTOMATIC CAROTID ARTERY OCCLUSION OR SEVERE STENOSIS AFTER STENTING: A PET STUDY

Y.-W. Wu[1], M.-S. Lin[2], W.-C. Wu[3], H.-L. Kao[2]

[1]Nuclear Medicine, [2]Internal Medicine, [3]Radiology, National Taiwan University Hospital, Taipei, Taiwan R.O.C.

Background and Aim: Chronic cerebral hypoperfusion may lead to impairment in neurocognitive performance in patients with chronic internal carotid artery stenosis or occlusion, and the long-term effects of carotid artery stenting on neurocognitive function remained unclear. The purpose of the study was to investigate cerebral glucose metabolism by using ^{18}F-FDG PET after carotid stenting.

Methods: We prospectively enrolled 19 patients (69±13y, 15 male) with cerebral ischemia detected on brain perfusion CT or MRI. Fifteen subjects had prior ischemic stroke before enrollments. Brain ^{18}F-FDG PET before and one year after endovascular intervention were performed.

Results: The overall technical success rate was 70% (16 of 23 procedures). Two patients were excluded from analysis due to dissection/ embolization and intracranial hemorrhage during procedure with neurologic sequelae. There was no new cerebral ischemic event or neurologic death for a mean follow-up of 29±5 (15-36) months except one died for gallbladder cancer 15 months after the index procedure. Brain PET scans before and 18±8 (12-31) months after endovascular intervention were compared by using a voxel-based Statistical Parametric Mapping (SPM) analysis. In 13 patients with unilateral disease, 6 (66%) of 9 patients showed improvement of cerebral glucose metabolism after successful stenting (ipsilateral in 2, controlateral in 2 and bilateral in 2 cases). Of 4 patients with recanalization failure, 2 exhibited decline in ipsilateral glucose metabolism, and another 2 showed mild improvement in bilateral cerebral glucose metabolism. In 4 patients with bilateral diseases, all showed improvement of cerebral glucose metabolism (unilateral in 2 and bilateral in 2 cases) after successful stenting.

Conclusion: Successful carotid artery stenting improves cerebral glucose metabolism in patients with chronic carotid severe stenosis or occlusion which could be associated with long-term benefits of neurocognitive function.

1380

TRANSHEMISPHERIC EFFECT OF CORTICAL SPREADING DEPRESSION: ELECTROENCEPHALOGRAM WAS SUPPRESSED BUT ERYTHROCYTE VELOCITY IN INTRAPARENCHYMAL CAPILLARIES WAS NOT AFFECTED IN RAT

M. Unekawa[1], **Y. Tomita**[1], H. Toriumi[1], K. Masamoto[2], I. Kanno[3], N. Suzuki[1]

[1]Neurology, Keio University, School of Medicine, [2]Center for Frontier Science and Engineering, University of Electro-Communications, Tokyo, [3]Molecular Imaging Center, National Institute of Radiological Sciences, Chiba, Japan

Objectives: We have reported propagating profile of DC potential and cerebral blood flow (CBF) by potassium-induced cortical spreading depression (CSD) and its suppressive effect on red blood cell (RBC) velocities in intraparenchymal capillaries of the rat cerebral cortex in spite of CBF elevation. This study is intended to examine the neuronal activity may directly affect on RBC velocities in single capillaries. We found sustained suppression of electroencepharogram (EEG) on contralateral hemispheric in response to CSD induction by potassium and examined RBC velocities in intraparenchymal capillaries.

Methods: In isoflurane-anesthetized rats, DC potential, EEG, partial pressure of oxygen (PO_2) and CBF were simultaneously recorded at the cranial window made in the both side of temporo-parietal region (n=7). EEG was obtained by digital filtering of DC potential recording and CBF was measured with laser Doppler flowmetry. Velocity of FITC-labeled RBCs flowing at the layer I was calculated with high-speed camera (500fps) laser-scanning confocal fluorescence microscopy and MatLab-domain original software KEIO-IS2 (n=10). CSD was elicited by topical application of KCl (1 M) on the posterior brain surface.

Results: Transient deflection of DC potential and PO_2 and increase of CBF were repeatedly detected on only ipsilateral hemisphere by KCl application, whereas these parameters of contralateral hemisphere were not affected at all. On the contrary, relative power of EEG was bilaterally reduced (ipsilateral; -70.7±14.0 %, contralateral; -57.6±22.8 %). The minimum value was obtained 5 min after KCl application which is much longer than DC potential deflection (1.5 min after KCl application). Mean RBC velocity in capillaries was slightly but significantly reduced from 1.49±1.05 to 1.18±0.66 during CSD and 1.18±0.53 mm/s 5 min after KCl application in the ipsilateral hemisphere, whereas it was changed from 1.69±0.97 to 1.60±0.98 and 1.71±0.96 mm/s at the same timing in the contralateral hemisphere in the same rats. Frequency distribution of RBC velocity in capillaries slightly shifted to slower on the ipsilateral hemisphere during and after passage of CSD, namely during EEG suppression. On the other hand, RBC velocity in capillaries of the contralateral hemisphere was not affected during EEG suppression.

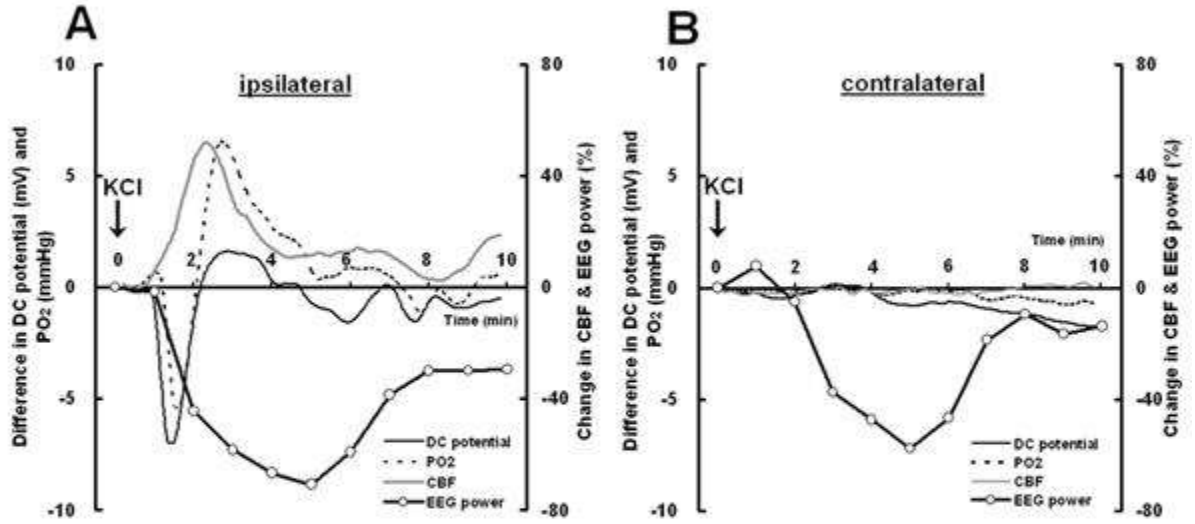

Figure: Change of physiological parameters (DC potential, PO_2 and CBF) and EEG power in response to KCl-induced CSD in the ipsilateral (A) and contralateral (B) hemisphere.

[Figure]

Conclusion: CSD-induced neuronal depression represented as EEG suppression may not affect on RBC velocity in intraparenchymal capillaries.

References: Tomita M, et al., JCBFM. 2005;25:742-7. Unekawa M, et al., JCBFM. 2009;29:S298.

1381

EFFECT OF INJECTION OF ARTIFICIAL RBCS ON HEMORRHAGIC HYPOTENSION IN MICE

Y. Tomita[1,2], M. Unekawa[1], H. Toriumi[1], K. Masamoto[3], H. Sakai[4], E. Tsuchida[4], H. Horinouchi[5], K. Kobayashi[5], I. Kanno[3], N. Suzuki[1]

[1]Department of Neurology, Keio University, School of Medicine, Tokyo, [2]Department of Neurology, Tomita Hospital, Okazaki, [3]Biophysics Group, Molecular Imaging Center, National Institute of Radiological Sciences, Chiba, [4]Research Institute for Science and Engineering, Waseda University, [5]Division of General Thoracic Surgery, Department of Surgery, Keio University, School of Medicine, Tokyo, Japan

Background: Availability of suitable blood for emergency transfusion is sometimes insufficient, so substitutes are needed. Recently, artificial RBCs (aRBCs: 0.25 μm in diameter) that can be stored for more than 2 years at room temperature have been developed (Artif Cells, Blood Substitutes, Biotechnol. 35: 81, 2007). In the present study, we examined the effect of injection of rhodamine-labeled aRBCs on systemic blood pressure, partial pressure of oxygen in brain tissue (PO_2), cerebral blood flow, blood gases, and survival of mice with hemorrhagic hypotension.

Methods: Under isoflurane anesthesia, a cranial window was opened above the left parieto-temporal cortex of C57BL/6J mice (n=18). A femoral artery and tail vein were catheterized. An oxygen electrode (Bio Research Center) was placed near the branch of the left MCA with a reference Ag-AgCl electrode inserted into the space between scalp and skull bone. Changes in brain microvasculature, blood pressure, PO_2 , and CBF measured by laser Doppler flowmetry were continuously recorded. Blood gases were regularly measured. FITC-labeled RBCs were injected into the circulating blood in all cases, and their movement through single capillaries in the ROI of brain parenchyma (50 μm depth) was monitored and recorded continuously with a video camera (30 frames/s) at 488 or 533 nm (J. Cereb. Blood Flow Metab. 25: 858-867, 2005). Hemorrhagic hypotension was induced by blood withdrawal (0.6 ml, 20 min) (n=18), then the same amount of saline (n=6) or aRBCs (n=6) or whole blood (n=6) was systemically injected and parameter values in the three groups were compared.

Results: Hemorrhagic hypotension to 31.8±3.6% of the baseline blood pressure produced severe microvascular derangement with sluggish flow, disappearance of most FITC-labeled RBCs from capillaries, and development of RBC sludge and aggregates in arterioles and venules. Tissue PO_2 decreased to 70.0±5.2% ($P< 0.05$) of the control value after hypotension.

- Saline injection group: BP, CBF, and tissue PO_2 showed slight but temporary improvement. These parameters then decreased gradually and all mice died within 5 hours after injection.

- aRBCs injection group: Penetration of red 0.25 μm aRBCs through capillaries and transient resumption of capillary flow were observed. BP, CBF, and tissue PO_2 improved gradually. One hour after injection, tissue PO_2 had recovered almost to the baseline level. The survival rate was increased compared with the saline injection group.

- Whole blood injection group: High cerebral circulation and high tissue PO_2 (above baseline) were maintained. The survival rate was increased further, compared with the aRBCs group.

Discussion: Administration of aRBCs to emergent ischemic tissue transiently improved the

microcirculation. Supply of oxygen via improved capillary flow might temporarily rescue anoxic neurons.

Conclusion: Use of aRBCs transiently improved the brain microcirculation in hemorrhagic hypotension, and might be therapeutically effective when immediate blood transfusion is not possible.

1383

CHANGES IN CEREBRAL BLOOD FLOW IN DEMENTIA PATIENT WITH HYPER SEXUALITY AFTER ANTI-ANDROGEN THERAPY

M. Inoue[1], K. Kiuchi[2], J. Kosaka[3], S. Kitamura[2], T. Nagashima[4], T. Shinkai[2], T. Kishimoto[2]

[1]Shouraiso Hospital, [2]Nara Medical University, Nara, [3]Sakai Mental Health Center, Osaka, [4]National Institute of Radiological Sciences, Chiba, Japan

Objective: To investigate the changes in cerebral blood flow in dementia patient with hyper sexuality after anti-androgen therapy.

Methods: We performed 99mTc-ECD SPECT studies before and after anti androgen therapy in a senile dementia patient with hyper sexuality using statistical parametric mapping analysis.

Results: Statistical parametric mapping analysis showed that increased cerebral blood flow occurred in both frontal gyri especially. Although there are not significant changes, both temporal gyri and both precneus gyri showed increased cerebral blood flow compared with baseline study. Patient improved the sexual problem after therapy, but cognitive function did not change throughout the study.

Conclusions: Our findings indicate that the frontal and temporal cortices may be the structures for the response to anti-androgen therapy in patient with hyper sexuality.

1384

AGE-DEPENDENT IMPAIRMENT OF FUNCTIONAL HYPEREMIA IS ASSOCIATED WITH B-AMYLOID ACCUMULATION IN SMALL ARTERIES IN APP TRANSGENIC MOUSE SOMATOSENSORY CORTEX

H. Takuwa[1], K. Masamoto[2], C. Seki[1], M. Maruyama[1], T. Obata[1], M. Higuchi[1], I. Kanno[1]

[1]Molecular Imaging Center, National Institute of Radiological Sciences, Chiba, [2]University of Electro-Communications, Tokyo, Japan

Objectives: In order to explore the causal relationship between cerebrovascular dysfunction and pathogenesis of Alzheimer's disease, we performed a repeated longitudinal evaluation of CBF response to whisker stimulation and accumulation of β-amyloid in APP transgenic mouse somatosensory cortex.

Methods: Long-term evaluation of CBF response and behavior activity was performed (Takuwa et al., 2010), every 2 to 4 weeks with laser-Doppler flowmetry (LDF) and an optical motion sensor, respectively in awake APP transgenic mice (3-27 months). Whisker stimulation was performed to provoke CBF response. On a separate date, amyloid and microvessels were fluorescently labeled with a compound X (newly-developed by our group) and sulforhodamine 101, respectively, and two-photon imaging (1024 by 1024 pixels) was performed with a z-step size of 4 μm (Fig. 1). Accumulation of vascular amyloid and tissue amyloid were evaluated separately. The thickness of the vascular amyloid was evaluated at several point along a particular vessel as the difference between the outer diameter of the vessel wall and the outer diameter of the amyloid. The fraction of the vessel covered by vascular amyloid was evaluated by measuring the length of non-amyloid spaces. The tissue amyloid was evaluated by calculating the area covered by labeled amyloid in the parechymal tissue.

Results: We observed that evoked CBF age-dependently declined with age from 3 months (23%) to 27 months (5.5%), while animal locomotion and heart rate were preserved. Further detailed analysis suggested that the age-dependent decline of cerebrovascular functions increased dramatically after about 17 months (6.8% at minimum). On the other hand, the accumulation of amyloid was found to be detectable in the parenchyma tissue and the vessel wall of small arteries at 14 months. The accumulation of the tissue amyloid gradually increased and the vascular amyloid expanded from the arteries to arterioles between the ages from 14 to 19 months. The thickness of the vascular amyloid at 19 months was 60% higher than that at 14 months. The length of non-vascular-amyloid spaces at 19 months decreased to 82% of that at 14 months. The size of the tissue amyloid at 19 months increased by 70% relative to that at 14 months.

Discussion: The results indicate that the impairment of CBF response is caused by i) age-dependent decline of the proteolytic activity and/or clearance of the parenchymal β-amyloid, and/or ii) direct toxic effects of the cerebral amyloid angiopathy at small arteries and arterioles on the cerebrovascular function.

Reference:

Takuwa H, Autio J, Nakayama H, Matsuura T, Obata T, Okada E, Masamoto K, Kanno I. (2010) Reproducibility and Variance of a Stimulation-Induced Hemodynamic Response in Barrel Cortex of Awake Behaving Mice. Brain Res. In press

1386

CEREBRAL BLOOD FLOW RESTORATION MECHANISMS AFTER UNILATERAL COMMON CAROTID ARTERY OCCLUSION IN MICE

S. Yamada[1], H. Guo[1,2], Y. Itoh[1], H. Toriumi[1], Y. Tomita[1], H. Hoshino[1], N. Suzuki[1]

[1]Department of Neurology, School of Medicine, Keio University, Tokyo, Japan, [2]Department of Neurology, People's Hospital, Peking University, Beijing, China

Objective: With major artery stenosis, collateral blood flow may gradually develop to prevent cerebral infarction. To clarify the mechanisms of cerebral blood flow restoration after major artery occlusion, we presented first dynamic changes in cortical vessel morphology observed through a cranial window in mice after unilateral common carotid artery (CCA) occlusion.

Methods: Ten male C57BL/6J mice (8-12 weeks old) weighing 20 to 25 g were used for the measurement of cerebral blood flow (CBF) before and after ischemia (n=5) or sham operation (n=5). Tie2-GFP transgenic mice (8-12 weeks old) weighing 17 to 24 g (purchased from Jackson Lab were used for the measurement of capillary density, 7 in ischemia group and 6 in sham group. CBF measured by Matlab software (The MathWorks, Inc.) and an original Program(KEIO IS-1). The density and diameter of capillaries as well as diameters of pial arteries were measured by confocal laser-scanning microscopy and fluorescent microscopy, respectively. The diameter of the branches of anterior cerebral artery (ACA) and middle cerebral artery (MCA), and anastomosis artery connecting ACA and MCA (ConA) was measured with the software of LuminaVision. Possible angiogenesis was evaluated by detecting any outgrowth of endothelial cells from preexisting vessels or intussusception in Tie2-GFP mice.

Results: The cerebral blood flow index, the reciprocal of mean transit time, before CCA occlusion was 0.88 ± 0.09 (1/sec)(mean ± SD). It decreased to 0.70 ± 0.03 (1/sec) after left CCA occlusion and returned to 0.85 ± 0.09 (1/sec) at Day15 in ischemia group, whereas it remained constant in sham group (0.87 ± 0.15, 0.91 ± 0.09 and 0.91 ± 0.08 (1/sec), respectively)(Fig 1). The decrease in cerebral blood flow index was significant when compared with that before occlusion ($p < 0.05$) and with that at Day15 ($p< 0.05$) in ischemia group. Repeated observation of the cortical vessels did not reveal any angiogenesis. Whereas, the mean capillary daiameter was 4.8±0.9 and 8.3± 1.9 μm at Day1 and Day15 in ischemia group, and 5.2± 0.6 and 6.7± 1.6μm at Day1 and Day15 in sham group(Fig 2A). The capillaries dilated by 74% and became as large as arterioles. The diameter of ACA and ConA increased significantly 14 days after induction of ischemia ($P< 0.05$), whereas the differences was not significant in sham group(Fig 2B). ACA and ConA also dilated significantly. The capillary dilatation to the size of arteriole in the settings of collateral growth and CBF restoration suggested capillary arterialization.

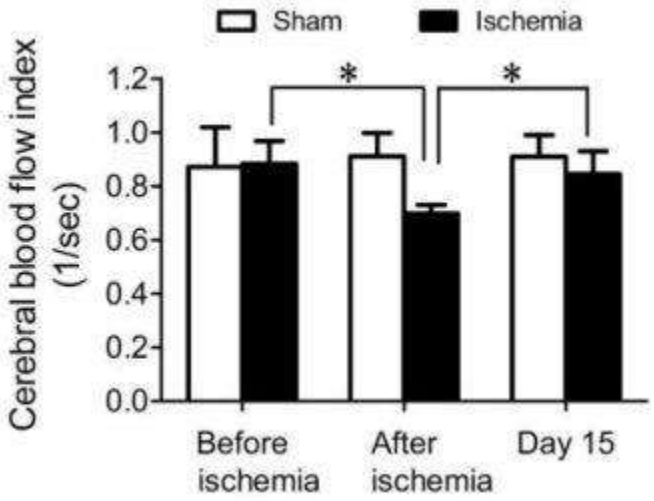

[Fig 1]

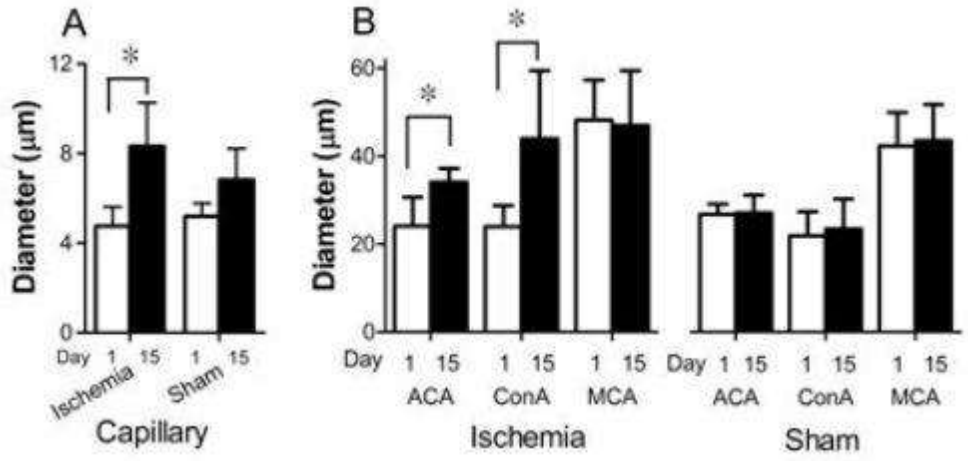

[Fig 2]

Conclusions: Our results indicate that capillary remodeling, pial artery dilatation and collateral growth without angiogenesis are sufficient mechanisms to restore normal cerebral blood flow after unilateral CCA occlusion.

1387

NEUROPROTECTIVE EFFECTS OF OLEIC ACID ON FOCAL ISCHEMIA RATS BY PEROXISOME PROLIFERATOR-ACTIVATED RECEPTOR Γ ACTIVATION

J. Kim[1], J.-G. Kim[2], D. Lee[2], S.-H. Lee[2], B.-J. Kim[1], D.W. Lim[1], M. Song[1], M.-Y. Kim[1], **H. Kim**[1,2]

[1]Herbal Pharmacology, College of Oriental Medicine, Kyunghee University, [2]Korea Institute of Science and Technology for Eastern Medicine (KISTEM), NeuMed Inc, Seoul, Republic of Korea

Backgroud and aims: Oleic acid (OA), a monounsaturated ω-9 fatty acid, is most abundant in all dietary fats and oils, and is normally present in small amounts in the brain but accumulate under ischemia. The role of OA has not been paid attention or known for exacerbating neuronal cell death in ischemic conditions. Since free fatty acids including OA is an endogenous ligand and activator with high affinity for the three isoforms of peroxisome proliferator-activated receptors, in the present study, we hypothesized that OA may exert important role on the neuroprotective effect in ischemic rat brain and this effect exert through PPARγ activation.

Methods: We used transient middle cerebral artery occlusion (MCAo) for 1.5 h followed by 24 h reperfusion in rats. After reperfusion, infarction volume was measured by TTC staining. Metabolic profiling of oleic acid level was in brain from Normal rats, OA treated rats, MCAo rats, OA treated MCAo rats by GC/MS. In order to determine whether PPARγ activation is critical for this effect, pretreatment of PPARγ antagonist, GW9662 was also performed. For mechanism study, expressions of mRNAs and proteins related inflammation were assessed by western blotting, RT-PCR and immunohistochemistry.

Results: OA decreased infarct size induced by MCAo as late as 3 h after injury, and the effect of OA was inhibited by GW9662. OA content of brain increased OA treated MCAo rats compared to in the other rats. OA also inhibited COX-2 and MMP-9 expression and induced HO-1 gene in MCAo rats.

Conclusions: Neuroprotective effect of OA is through the mechanism of PPARγ activation, contributing anti-inflammatory effect by inhibition of COX-2 and MMP-9 expression, and anti-oxidative effect by induction of HO-1.

1390

GENE EXPRESSION PROFILING IN THE CORTEX OF SPONTANEOUSLY HYPERTENSIVE RATS SHOWS ABNORMAL METABOLISMS AND REDUCED HYPOXIC/OXIDATIVE STRESS TOLERANCE CAPACITIES

M.-F. Ritz[1], S. Engelter[2], P. Lyrer[2]

[1]Neurobiology Laboratory, Department of Biomedicine, [2]Neurology Clinic, Stroke Unit, University Hospital Basel, Basel, Switzerland

Objectives: Cerebral small vessel disease (SVD) is an important cause of stroke, cognitive decline and vascular dementia (VaD). The molecular mechanisms involved in the development and progression of SVD are not yet completely understood. As hypertension is one of the major risk factors for developing the disease, Spontaneously Hypertensive Rats (SHR) are considered a good experimental model for the study of neuropathological changes appearing in the brain, as they share several similarities with essential hypertension in human. We previously described cellular differences in the brain of this rat strain such as imbalance between the number of blood microvessels and astrocytes at the level of the neurovascular unit in young, pre-hypertensive SHR, leading to signs of neuronal hypoxia in the brain of older animals (1).

Methods: To identify genes and pathways involved in the development of small vessel disease, we performed comparison of gene expression in the cortex of 2 and 9-month-old SHR with age-matched normotensive Wistar Kyoto (WKY) rats using oligonucleotide-based microarray technology. Quantitative qPCR was used to confirm the differences in expression for selected genes.

Results: This analysis revealed significant downregulations in the expression of genes involved in the energy and lipid metabolisms, in mitochondrial function, in oxidative stress, and in hypoxia preconditioning in 2 as well as 9-month old SHR. Moreover, genes involved in endothelial proliferation were overexpressed in both SHR groups, confirming our histological observations.

Conclusions: These results indicate that the brains of SHR suffer form mitochondrial dysfunction, energy failure and increased oxidative stress. These observations suggest that SHR may be unable to tolerate hypoxia-like conditions, and may be more vulnerable than WKY to high-energy consumption conditions. This genetic analysis gives new insights about pathways accounting for the development of deep ischemic infarcts observed in small vessel disease which will ultimately lead to the establishment of preventive therapeutic options for patients at risk.

References: (1) Ritz MF, Fluri F, Engelter ST, Schaeren-Wiemers N, Lyrer PA. Cortical and putamen age-related changes in the microvessel density and astrocyte deficiency in spontaneously hypertensive and stroke-prone spontaneously hypertensive rats. Curr Neurovasc Res. 2009 Nov;6(4):279-87.

1391

PATHOPHYSIOLOGICAL ROLE FOR B1 KININ RECEPTORS IN TWO MOUSE MODELS OF TRAUMATIC BRAIN INJURY

C. Albert-Weissenberger[1], F. Raslan[2], T. Schwarz[1], C. Várallyay[3], A.-L. Sirén[2], C. Kleinschnitz[1]

[1]Department of Neurology, [2]Department of Neurosurgery, [3]Department of Neuroradiology, University of Würzburg, Würzburg, Germany

Objectives: Traumatic brain injury (TBI), a leading cause of death and disability, is a result of an outside force causing mechanical disruption of brain tissue and delayed pathogenic events which collectively exacerbate the injury [1]. Kinins are released during tissue damage after TBI and trigger proinflammatory events by activation of specific kinin B1 and B2 receptors [2]. In order to study the role of kinin receptors in the expansion of secondary brain damage following TBI and the potential of kinin antagonists as a novel treatment strategy for acute brain injury, we investigated the influence of the B1 and B2 receptor deletion on functional and morphological recovery in two mouse models of TBI.

Methods: To assess the discrete impact of the B1 and B2 receptors on TBI, we used mice deficient for either the B1 or B2 receptor, and wild type mice treated with selective pharmacological antagonists of the B1 and B2 receptors. Considering the broad range of pathomechanisms associated with TBI [1], the cryogenic lesion model was used to produce a focal lesion and a marked brain edema, and the weight-drop model with the gravitational forces of a free falling weight to induce an injury incorporating focal and diffuse brain damage [1]. In the cryogenic model, the lesion size and blood-brain barrier integrity was determined by using 2,3,5-triphenyltetrazolium chloride and Evan´s Blue tracer, respectively. In the weight-drop model, the initial trauma severity and progression of brain injury was assessed by neurological scoring immediately after injury and on day 1, 3, and 7 post-injury and by magnetic resonance imaging. In both models, histological analyses and real-time PCR analyses were used to assess the expansion of secondary brain damage and inflammatory processes.

Results: Genetic B1 receptor deficiency or an acute pharmacological antagonism of B1 receptors with the selective inhibitor, R-715 (Ac-Lys-[D-ß Nal7, Ile8]-des-Arg9-BK; 0.5-1 mg/kg, i.v.) attenuated secondary lesion size, inflammation, and the development of vasogenic edema after focal brain injury. B1 receptor deficient mice showed also a better neurological outcome after weight-drop injury than the wild type mice demonstrating protection by B1 receptor depletion also in a brain injury model that reflects the heterogeneity of human TBI. In contrast, deficiency or blockade of B2 receptors with the selective inhibitor, Hoe-140 (D-Arg0-Hyp3-Thi5-D-Tic7-Oci8-BK, 0.2-0.4 mg/kg, i.v.) had no significant protective effect.

Conclusion: Our results demonstrate a role for the B1 kinin receptors in the pathophysiology of TBI and suggest that pharmacological inhibition of the B1 receptor may offer a novel therapeutic strategy in acute traumatic brain injuries.

References:

[1] Albert-Weissenberger C. and Sirén A.-L., Exp. & Transl. Stroke Med. (2010), 2:16.

[2] Raslan F. et al., J. Cereb. Blood Flow Metab. (2010), 30:1477-1486.

1392

REGIONAL CEREBRAL METABOLIC CHANGES IN RESPONSE TO ALTERNATIVE TREATMENTS: CHIROPRACTIC AND ANIMAL ASSISTED THERAPY: [^{18}F]FDG PET STUDIES

M. Tashiro[1], T. Ogura[1], A. Sugawara[1], M.M. Masud[1], S. Watanuki[1], K. Shibuya[1,2], K. Yamaguchi[1,3], M. Itoh[1], K. Yanai[1,2]

[1]Cyclotron and Radioisotope Center, Tohoku University, [2]Department of Pharmacology, Tohoku University Graduate School of Medicine, [3]Advanced Image Medical Center, Sendai Welfare Hospital, Sendai, Japan

Alternative therapies, recently, are getting more and more popular. While the alternative therapies are used very often among patients and ordinary people, the brain responses to these interventions have not been elucidated in terms of functional neuroanatomy. In the present study, regional brain metabolic changes in response to alternative therapies, chiropractic spinal manipulation (CSM) and animal-assisted therapy (AAT), were studied using positron emission tomography (PET) and [^{18}F]fluorodeoxyglucose ([^{18}F]FDG).

Fourteen participants with neck/shoulder pain were enrolled for the study on CSM, and another 12 participants were recruited for the study on AAT. Brain PET scanning was performed twice on each subject in a resting control condition and in an intervention condition under certain therapeutic effects (following CSM intervention or being accompanied by a familiar dog). Questionnaires such as stress response scale (SRS-18) were used for evaluation of subjective perception of stress. In addition, an electrocardiograph was recorded to assess heart rate variability (HRV). Using the HRV data, autonomic nervous activity was examined. Brain PET images were processed for voxel-by-voxel analysis using statistical parametric mapping (SPM) program. Regional metabolic changes were examined between the resting control and the intervention conditions.

In results, SRS-18 scores were significantly higher ($p< 0.05$) in the resting control conditions than in the intervention condition, suggesting the presence of relaxing effects of the therapeutic interventions in both studies. In results of heart rate variability, increased parasympathetic nerve activity was observed in the both studies on CSM (significantly increased) and on AAT (threshold level). As for the results of SPM analysis in the study on CSM, increased glucose metabolism was observed in the prefrontal cortex, anterior cingulated gyrus and in the temporal cortex, whereas decreased glucose metabolism was found in the cerebellar vermis and visual association cortex ($P< 0.001$). On the other hand, in the results of SPM analysis in the study on AAT, decreased glucose metabolism was observed in the frontal cortex, the right fusiform gyrus, the left putamen and the thalamus in the presence of the familiar dog, while no regions manifested increased metabolism.

Based on the whole results, it seems that different therapeutic intervention might induce regional brain responses in different ways while the resultant clinical effects are looking similar. It may be worthwhile to examine the regional brain responses to different alternative therapies. Functional neuroimaging technique is a very effective tool for that.

1395

MODIFICATIONS IN LOCAL HEMODYNAMIC PRECEEDS EPILEPTIC SPIKE: SIMULTANEOUS ECOG AND NEAR INFRARED SPECTROSCOPY ANALYSIS IN RATS AND CHILDREN

E. Bourel-Ponchel, V. Osharina, A. Aarabi, R. Grebe, F. Wallois

GRAMFC EA 4293, University of Picardie Jules Verne, CHU Amiens, Amiens, France

Objective: Whatever may be the complex pre-spike mechanism that propels these neurones from physiological dynamic synchronization to a freezing of synchronization resulting in tight coupling, it can induce neurovascular coupling or not. NIRS is a recently developed technique for haemodynamic studies suitable for dynamic recordings. It has the advantage to have an excellent temporal resolution and to measure changes in the concentrations of both oxy-, deoxy- hemoglobin in tissues. We evaluate combined EEG-NIRS recordings in rats, and in some children to get further insight in the relationship between spikes and the hemodynamism.

Method: Acute experiments were performed on urethane anaesthetized rats.ECoG electrodes, light sources and detectors were inserted bilaterally. The epileptic spikes were induced by local application of bicuculline methiodide to the left SI cortex. The ECoG and NIRS data were recorded simultaneously. The time of the spike peak was used for averaging ECoG and NIRS Data.A grand average was performed between the different rats. In epileptic children with partial epilepsy and spontaneous focal discharges the procedure of analysis was similar.

Results: The hemodynamic changes precede the epileptic spike in all rats. The hemodynamic changes are characterized by a biphasic pattern. The "initial dip" in oxygenated (HbO) and total (HbT) haemoglobin occurred before the spike onset and was followed by postspike increasing in the HbO/HbT. In children, a focal increase in HbO and a small increase in Hbr were observed in the area of the spikes.

Conclusion: In rats, we demonstrate hemodynamic changes which precedes the onset of spike activity. Such hemodynamic modulation has other than highly synchronized pyramidal cells origin. Glial cells, non synchronized activities or low level synchronized activities are likely to participate in this early hemodynamic modulation tightly associated with the mechanism of spike onset. In children changes in HbO and HbR are focal and predominate after the spikes.

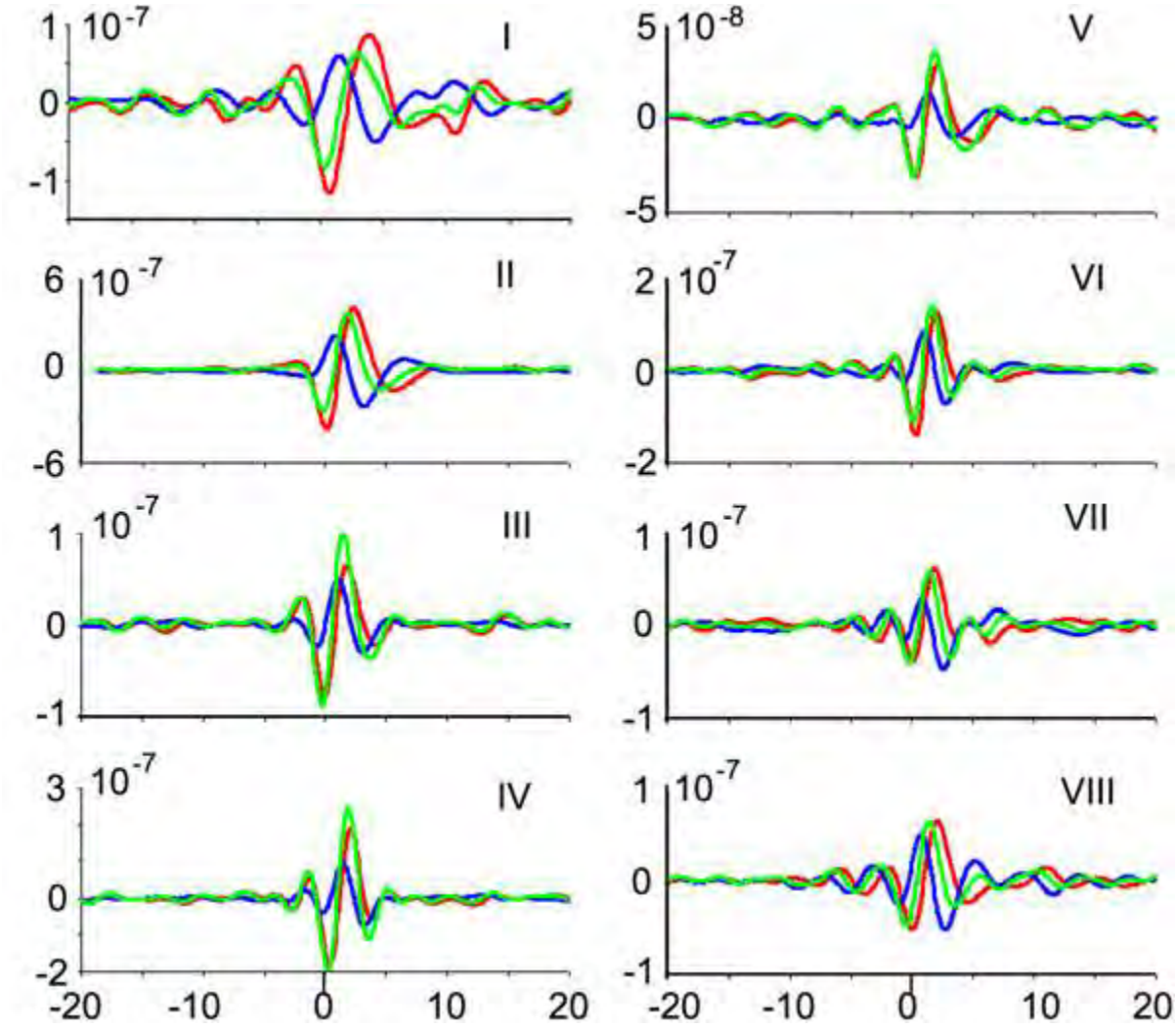

[Figure]

Figure:

Averaged HbO(red)/HbR(blue)/HbT(green) epochs from each rat (from I to VIII; only ipsilateral data are shown). The scale of the y axis is different for each rat (molar concentration). The x axis is the same for all experiments. The epochs are chosen from -20 s before the EcoG P1 appearance (0s) up to +20 s after

1396

EVALUATION OF RE-GP GRAPHICAL ANALYSIS METHODS FOR V_T ESTIMATES OF A NOVEL KAPPA OPIOID RECEPTOR AGONIST TRACER IN HUMANS

S.J. Kim[1], G. Tomasi[1], M. Zheng[1], N. Nabulsi[1], Y. Huang[1], R. Carson[1], L. Jacobsen[2], E.D. Morris[1]

[1]PET Center, Yale University School of Medicine, New Haven, [2]Pfizer Global R&D, Groton, CT, USA

Objective: (1) To assess the utility of the relative equilibrium-based graphical analysis method with the Gjedde-Patlak correction (Zhou et al, [1]) (RE-GP) for estimation of total distribution volume (V_T) for a novel kappa-opioid receptor agonist tracer with slow kinetics, [^{11}C]GR103545 [2, 3]. (2) To investigate an alternative implementation of RE-GP which uses smoothed emission images in a two-step construction of V_T images from [^{11}C]GR103545 data.

Methods: Ten dynamic [^{11}C]GR103545 PET scans on the Siemens HRRT were acquired for 120-150 min in 5 healthy human subjects (two scans each). Arterial blood samples were obtained and plasma input functions were constructed based on metabolite-corrected parent fraction. Brain regional time-activity curves were fitted using the two-tissue compartment model (2TCM). ROI based and pixel-by-pixel graphical analyses were used for calculation of V_T according to Zhou et al [1]. We initially implemented the method as proposed by Zhou for making V_T images that smooths the K_p (slope of the GP plot) and β (intercept of the GP plot) images from the GP step of a two-step process.

Results: For the ROI analysis, results of the RE-GP plot were well correlated with those from 2TCM (y=1.10x-0.69, r^2=0.65; see Fig.1). The agreement between methods was insensitive to choice of relative equilibrium time (t*). However, the V_T images that were produced were very noisy (see Fig. 2A) despite smoothing the K_p and b images according to [1]. To improve the performance of RE-GP, we smoothed the dynamic emission data used for the GP step *instead* of the parametric images produced by RE-GP. Our modified RE-GP plot was much more stable, but there appeared to be a critical dependence on the size of the smoothing kernel. A 9x9 pixel kernel (pixel size=1.2 x 1.2 mm^2) produced V_T images that were in good agreement with ROI values (Fig. 2B).

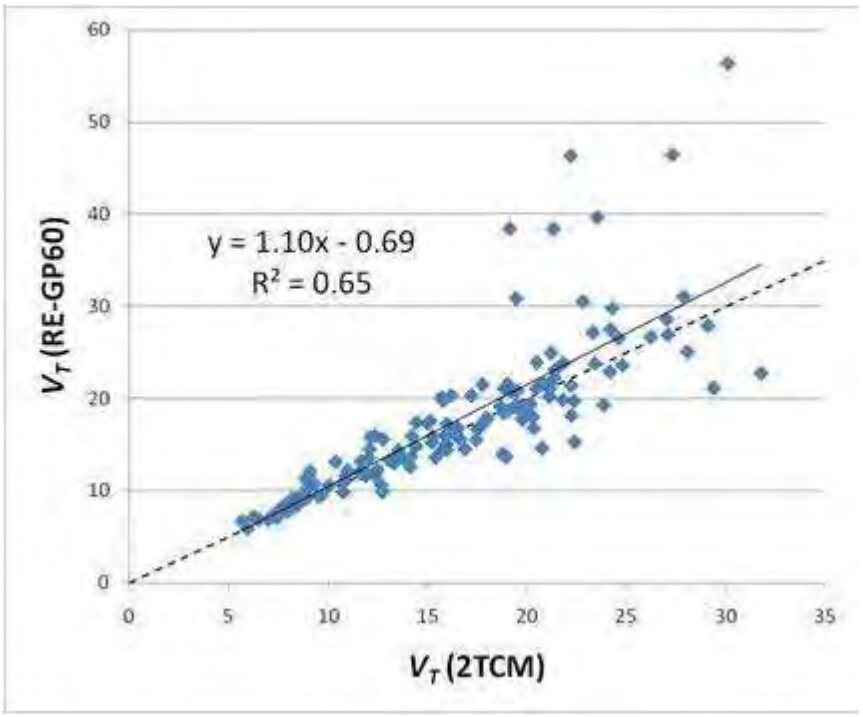

[Figure 1.]

Figure 1. Correlation between RE-GP and 2TCM for ROI data. 10 scans x 13 regions are displayed.

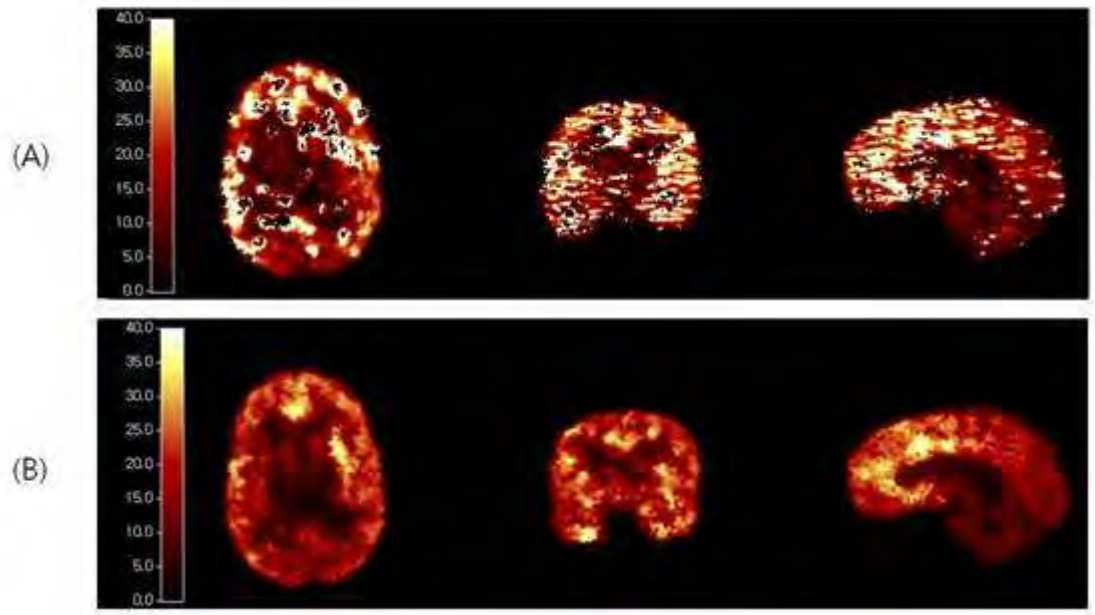

[Figure 2.]

Figure 2. (A) V_T image (3 orientations) for [^{11}C]MKAP data - note instability of result spatially. (B) V_T image using modified RE-GP graphical method as described in text.

Conclusion: The modified RE-GP plot appears to be an appropriate method for making regional estimates of V_T for the new kappa-opioid agonist ligand, [^{11}C]GR103545. Smoothing of emission images instead of the intermediate parametric images may extend the applicability of the method for creation of V_T

images with slow kinetics.

References:

[1] Zhou Y., Ye W., Brasic J.R., Wong D.F. (2010) Multi-graphical analysis of dynamic PET *Neuroimage* 49:2947-2957

[2] Talbot, P. S.; Narendran, R.; Butelman, E. R.; Huang, Y.; Ngo, K.; Slifstein, M.; Martinez, D.; Laruelle, M.; Hwang, D. R., 11C-GR103545, a radiotracer for imaging kappa-opioid receptors in vivo with PET: synthesis and evaluation in baboons. *J Nucl Med* 2005, 46, (3), 484-94.

[3] Tomasi, G.; Zheng, M.-Q.; Weinzimmer, D.; Lin, S.-F.; Nabulsi, N.; Williams, W.; Ding, Y.-S.; Jacobsen, L.; Huang, Y.; Carson, R. E., Kinetic modeling of the kappa agonist tracer [^{11}C]GR103545 in humans. *J Nucl Med* 2010, 51, (S2), 1293.

1397

CUMULATIVE ASSOCIATION OF SIX VARIANTS IN THE *KCNK17*, *LRP, NOS3, SCNN1A* AND *MMP12* GENES WITH ISCHEMIC STROKE

S. Domingues-Montanari, I. Fernández-Cadenas, A. del Rio-Espinola, A. Penalba, M. Rubiera, M. Ribó, A. Rosell, J. Alvarez-Sabin, J. Montaner

Neurovascular Research Laboratory and Neurovascular Unit, Department of Neurology, Institut de Recerca, Vall d'Hebron Hospital, Barcelona, Spain

Objectives: We previously reported the association of single nucleotide polymorphisms (SNPs) in five chromosomal regions with ischemic stroke (IS). Each SNP alone showed a moderate association, with odds ratios (OR) ranging from 1.35 to 3.05, so we hypothesized that their combination could reveal a stronger association with IS.

Methods: We evaluated the combined association with IS of 6 SNPs around the KCNK17 (rs10947803), LRP1 (rs7956957), MMP12 (rs2276109), NOS3 (rs10275136 and rs310585) and SCNN1A (rs5742912) genes in a Spanish population comprising 540 IS subjects and 540 control subjects. IS subjects were divided in cardioembolic (44.8%), atherothrombotic (20.9%) and undetermined (34.3%) etiologies. Statistical analysis and logistic regression were performed under an additive model. Predicted probabilities were calculated with receiver operating characteristic (ROC) curves and compared using the MedCalc software.

Results: Each SNP was significantly associated with IS after adjustment for the other SNPs and established risk factors, including male gender, age over 55, diabetes mellitus, dislipidemia, hypertension and cigarette smoking. IS risk increased depending on the number of risk alleles carried. Additionally, the combination of 6 SNPs showed clear contribution to risk in comparison with conventional clinical stroke risk factors only, with predictive probabilities of 69.1% vs. 63.4% ($p< 0.001$). In subjects who had any five or more of these SNPs, the predictive probability for IS was significantly higher compared with subjects carrying none or only one SNP (OR=26.06, $p< 0.001$). Moreover the risk increased with the number of genetic plus clinical risk variable carried, although no subject in our population carried more than 9 markers. Finally, a risk score was assigned to each variable depending on the b value from the logistic regression and a risk scale from 1 to 45 was then used to classify subjects into three categories. 51.0% of IS cases were in the low risk category (score ≤ 18) compared to 72.4% in the moderate (19 < score ≤ 26, $p< 0.001$ vs. low) and 92.3% in the high risk (35 < score, $p< 0.001$ vs. low). This model permitted to reclassify 10% of the subjects with a moderate risk determined by classical risk factors into the high risk category considering both genetic and clinical data.

Conclusions: Six SNPs plus classical stroke risk factors showed a cumulative and significant association with IS. These results open diagnostic and therapeutic expectations in stroke.

1398

MULTIMODAL CT IMAGING FOR ACUTE STROKE PATIENTS COULD DIFFERENTIATE ISCHEMIC PENUMBRA AND ACUTE MISERY PERFUSION

J. Nakagawara, Y. Yamaguti, H. Endou, K. Kamiyama, H. Takada, T. Osato, H. Nakamura

Neurosurgery, Nakamura Memorial Hospital, Sapporo, Japan

Objectives: In the management of acute stroke patients, multimodal CT imaging could be useful for selecting adequate treatments based on the assessment of stroke subtypes and pathophysiological mechanisms from diagnostic information consisted of cerebral tissue damages, cerebral hemodynamics and occlusive vascular lesions[1)]. In this clinical study, we evaluated cerebral hemodynamic parameters such as cerebral blood flow (CBF), cerebral blood volume (CBV) and mean transit time (MTT) obtained from whole brain CT perfusion (CTP) by multi-detector row CT (MDCT) for acute stroke patients with ischemic penumbra or acute misery perfusion.

Methods: Twenty acute stroke patients who suffered from the occlusion of major cerebral arteries were involved in this clinical study. Whole brain CTP and CT angiography (CTA) was obtained by 64 x 2-row MDCT (SOMATOM Definition AS+) which scan patients' brain with spiral mode and shuttle motion of patient's table with 96mm width per 1.5 sec. For the safety from X-ray radiation to patients head during CTP, radiation dose was limited to less than 100 mGy around the orbit and less than 250 mGy in the center of scalp. For the image reconstruction of hemodynamic parameters, vascular components which could interrupt accurate evaluation were completely removed from raw data. Tomographic images and 3-dimentional surface projection images (3D-CTP) on each parameter were obtained promptly for assessing the ischemic core and penumbra or acute misery perfusion in the territory of the occlusion of major cerebral arteries.

Results: In 10 patients with cardioembolic stroke, decrease of CBF and increase of MTT were observed in the territory of affected arteries, CBV was decreased in the ischemic core, and not increased in peripheral area around the ischemic core. These data suggested that CBV was not increased in the area of ischemic penumbra, and time window for thrombolytic therapy using t-PA was limited within several hours. In other 10 patients with atherothrombotic stroke, decrease of CBF and increase of MTT were observed in the territory of affected arteries, CBV was decreased in the ischemic core, but increased in peripheral area around the ischemic core. These data suggested that CBV was increased in the area of acute misery perfusion, and time window for acute revascularization using EC-IC Bypass or Stenting which prevents progression of cerebral infarction was preserved within several days.

Conclusions: Multimodal CT imaging by MDCT could be useful for selecting thrombolytic therapy or revascularization therapy for acute stroke patients. Especially, CBV in whole brain CTP could be key findings for assessment of indication of therapeutic intervention. Increase of CBV was a compensatory response based on vasodilation for reduced cerebral perfusion pressure (CPP) in hemodynamic cerebral ischemia, such compensatory response could not functioned in the area of ischemic penumbra, but well functioned in the area of acute misery perfusion. Increase of CBV could preserve longer therapeutic time window for acute misery perfusion. Multimodal CT imaging for acute stroke patients could be diagnostic tool for differentiating ischemic penumbra from acute misery perfusion, and estimating therapeutic time window.

References:

1. Carlos A et al: Stroke 2005;36:2311-2320

1399

IMPACT OF NEONATAL INTRAVENTRICULAR HEMORRHAGE ON AUDITORY HEMODYNAMIC RESPONSE

M. Mahmoudzadeh[1], G. Dehaene-Lambertz[2], G. Kongolo[1], S. Goudjil[1], R. Grebe[1], F. Wallois[1]

[1]GRAMFC EA 4293, University of Picardie Jules Verne, CHU Amiens, Amiens, [2]Unité INSERM 592 'Neuroimagerie Cognitive', CEA/SAC/DSV/DRM/NeuroSpin, Gif-sur-Yvette, France

Objective: Learning more about the neural basis of developmental disorders after prematurity is essential. Such information may explain the developmental disorders that follow prematurity. Functional imaging contributs to our understanding of brain function in the aftermath of prematurity. Children with delays in language and speech development are at high risk for later disorders in reading, spelling, and writing, academic skills which are highly dependent on language abilities. Brain injuries have been found to be associated with language and speech outcomes among children born prematurely. Severe grades of intraventricular hemorrhage (IVH) are risk factors for adverse neurodevelopmental outcomes, including cognitive impairment and cerebral palsy [1, 2, 3, 4].

Method: Eight healthy and five ill preterm neonates (IVH grade III and IV) (GA:28-34 weeks) participated in an optical topography study designed to assess the specific characteristic of neurovascular coupling to auditory syllabic stimuli in healthy and ill neonate brains. Tests consisted of 108 blocks; each block contained 20s of auditory stimulation followed by 40s of silence. Auditory stimuli consist of two digitized syllables /ba/ and /ga/, naturally produced by a male and a female speaker. Neonates were tested while they slept. We used 16-channel Near-Infra Red Spectroscopy (NIRS) device to assess changes in the concentration of deoxyhemoglobin (HBR) and oxyhemoglobin (HBO) in response to auditory syllabic stimuli in the right and left hemispheres.

Result: We found that temporal areas of healthy neonates showed significantly more activation (increase in [HBO], decrease in [HBR] than ill neonates when were exposed to auditory stimuli.

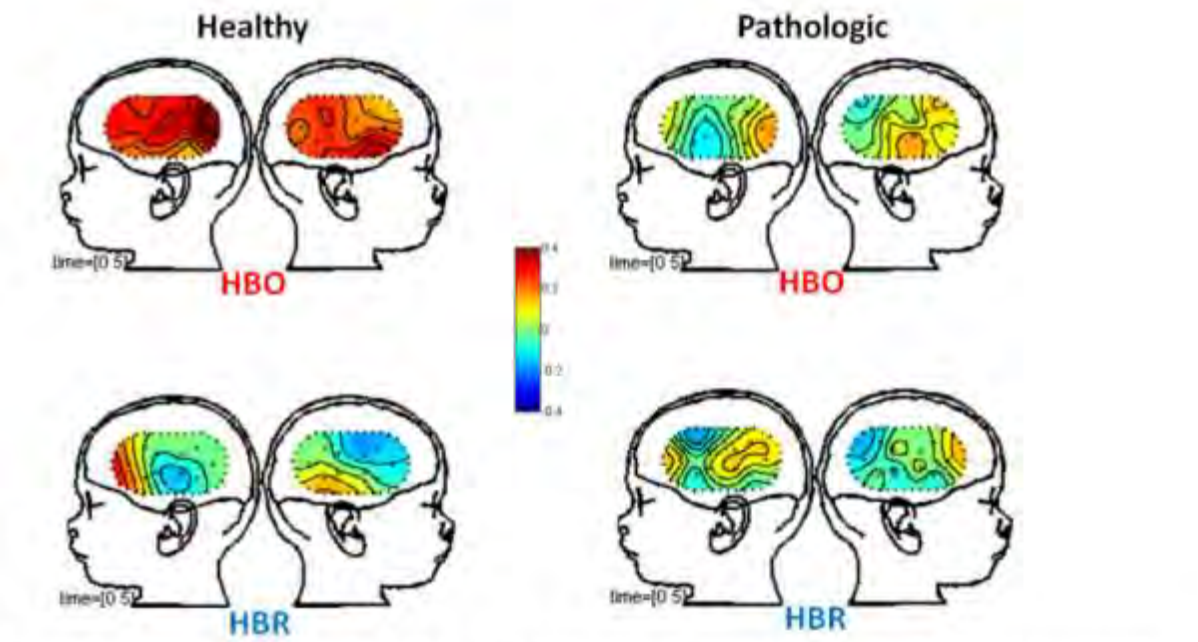

Figure: Grandaverage topographies of raw hemodynamic responses (changes in HBO/HBR concentration) after onset of auditory stimulation.

[Figure]

Conclusion: The present data confirm the existence of neurovascular coupling in healthy premature brain. It also shows that ill premature neonates are unable to process syllabic stimuli, a step for language acquisition ability. The results are in accordance with what we previously described concerning abnormalities of spontaneous neurovascular coupling in pathological EEG discontinuity in ill premature neonates [5]. This inability of pathological brain to adapt to either endogenous or exogenous stimuli by an increase in blood flow can represent a mechanism by which the pathological brain enters in a deleterious pathological loop. This might explain cerebral disabilities observed latter in acquisitions throughout the neurodevelopment.

References:

[1] Vohr B, Allan WC, Scott DT, et al. Early-onset intraventricular hemorrhage in preterm neonates: incidence of neurodevelopmental handicap. Semin Perinatol 1999; 23: 212-17.

[2] Hemphill L, Feldman HM, Camp L, et al. Developmental changes in narrative and non-narrative discourse in children with and without brain injury. J Commun Disord 1994; 27: 107-33.

[3] Feldman HM, Evans JL, Brown RE, et al. Early language and communicative abilities of children with periventricular leukomalacia. Am J Ment Retard 1992; 97: 222-34.

[4] Ment LR, Vohr BR, Makuch RW, et al. Prevention of intraventricular hemorrhage by indomethacin in male preterm infants. J Pediatr 2004; 145: 832-4.

[5] Roche-Labarbe, N., Ponchel, E., Kongolo, G., Grebe, R., and Wallois, F. Coupled oxygenation oscillations measured by NIRS and intermittent cerebral activation on EEG in premature infants. Neuroimage, 36, 718-727, 2007.

1400

HAEMODYNAMIC CHANGES DURING SEIZURE-LIKE ACTIVITY IN A NEONATE: A SIMULTANEOUS AC EEG-NIRS AND HIGH-RESOLUTION DC EEG RECORDING

F. Wallois, A. Patil, G. Kongolo, S. Goudjil, R. Grebe

GRAMFC EA 4293, University of Picardie Jules Verne, CHU Amiens, Amiens, France

Objective: We sought to define the interaction between neonatal epileptic discharges and the haemodynamic activities in a control situation (i.e. in the absence of cardiorespiratory perturbation or any interaction with normal, ongoing, synchronized neuronal activity).

Method: Alternating-current electroencephalography (AC EEG), near-infrared spectroscopy (NIRS), and high-resolution direct-current (HR DC) EEG were performed in a curarized, ventilated neonate with a flat interictal EEG. The seizure-like discharges (SLD) first spike was used as a trigger for further averaging of NIRS, AC and DC EEG. Source localization was performed on the averaged spike and the averaged, negative DC shift.

Results: SLD were of maximal amplitude in centroparietal areas and induced a change in local haemodynamic parameters characterized by a first increase in [HHb] followed by an increase in [HbO2] and [HbT]. [HHb] returned to baseline at the end of the seizure and decreased thereafter. The negative DC shift started before the first spike and the increase in haemodynamic parameters. It then became positive and returned to baseline at the end of the seizure. Source localization revealed different positions for the first spike and the negative DC shift.

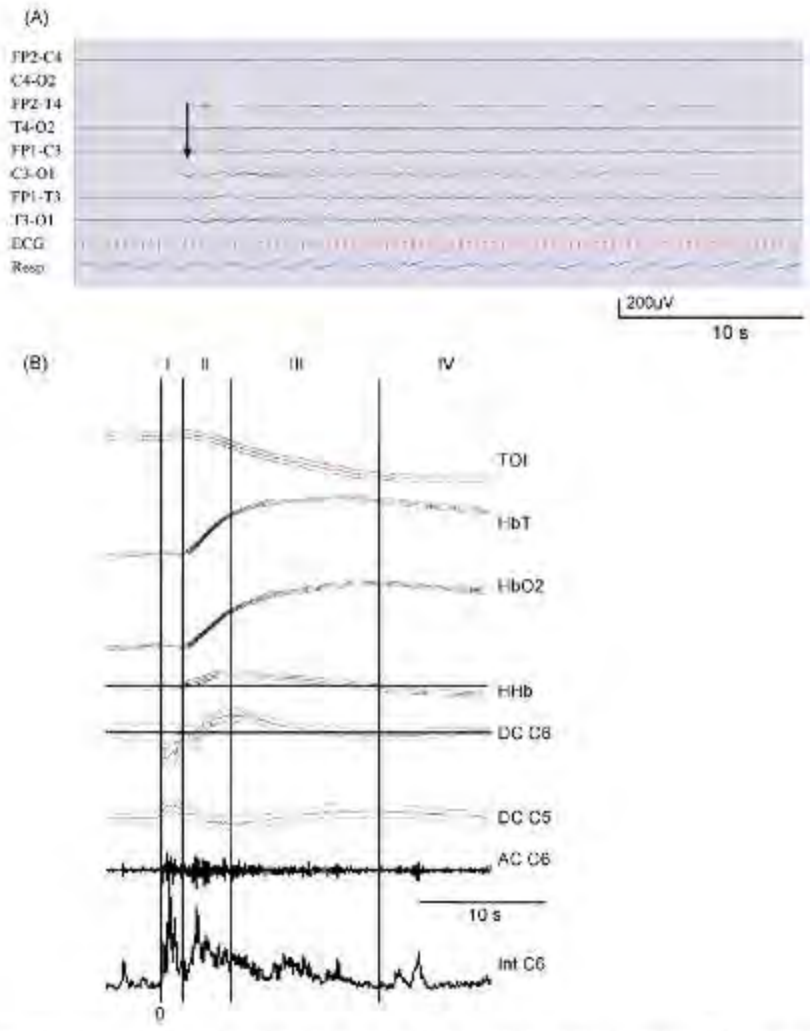

Figure 1 A. Seizure-like activity recorded in a bipolar montage. The arrow indicates the onset of the seizure, concomitant with the first spike. Calibration 1 s and 200 µV. B. Average change in haemodynamics (TOI, [HbT], [HbO_2], [HHb]), DC EEG (DC C6, DC C5), AC EEG (C6), integrated EEG (Int C6).
The first vertical line at 0 marks the seizure onset. The second vertical line is the onset of an averaged increase in HbO_2. The third vertical line is the peak increase in the AC EEG. It corresponds to the peak of [HHb] and to the inflexion of the [HbO_2] increase. The fourth vertical line corresponds to the zero intercept for [HHb], the normal value of AC C6 and the inflexion of HbO_2 towards a control value. I corresponds to an activation in the absence of haemodynamic changes. II corresponds to an increase in haemodynamics, the occurrence of rapid rhythms on EEG and a progressive increase in DC EEG. III corresponds to a plateau in haemodynamics, together with the inversion of HHb and DC EEG. IV corresponds to the end of the seizure and recovery.

[Figure]

Discussion: Pure SLD in neonates might induce a negative blood oxygen level-dependent (BOLD) effect on the cortex, which occurs after the negative DC shift and which has a closer temporal relationship with the neuronal discharge than a positive BOLD effect.

1401

AUTOMATIC EXTRACTION OF REFERENCE REGION USING SUPERVISED CLUSTERING FOR PET STUDY WITH [^{11}C]PIB

Y. Ikoma[1,2], F.E. Turkheimer[1], P. Edison[3], A. Ramlackhansingh[3], D.J. Brooks[3]

[1]MRC Clinical Sciences Centre and Division of Experimental Medicine, Hammersmith Hospital, Imperial College, London, UK, [2]Biophysics Group, Molecular Imaging Center, National Institute of Radiological Sciences, Chiba, Japan, [3]MRC Clinical Sciences Centre and Division of Neuroscience, Hammersmith Hospital, Imperial College, London, UK

Objectives: Positron emission tomography with [^{11}C]PIB has been utilized for imaging amyloid plaque deposition in patients with Alzheimer's disease (AD). The specific binding of [^{11}C]PIB is usually quantified by an accumulated radioactivity ratio of target and reference regions or a graphical analysis method using the cerebellum as a reference region where the specific binding is negligible. Recently, however, the retention of [^{11}C]PIB in the cerebellum was reported to increase in familial AD compared with normal volunteers (1), suggesting that this region may not be suitable as a reference region. In this study, we devised a supervised clustering procedure for extracting the reference region automatically in [^{11}C]PIB PET studies, and validated this method in the [^{11}C]PIB studies of control and AD subjects.

Methods: First, the supervised clustering approach of automatic reference extraction for [^{11}C]PIB PET study was established by applying the procedure developed for [^{11}C]PK11195 study (2). A set of kinetic classes that represent the typical kinetic pattern of normalized radioactivity in the gray matter with and without specific binding and in the blood pool was defined from the time-activity curves (TACs) of control and AD subjects. In PET dynamic image, the combination of each kinetic class was calculated by the linear-least squares for each voxel in the gray matter. The TAC of reference region was derived from voxels in which the ratio of normal gray matter class was high. Next, this extraction method was applied to [^{11}C]PIB PET studies of normal volunteers and AD patients. For the validation of proposed method, the TACs of extracted reference region were compared with those of the cerebellum for each subject, and distribution volume ratio (DVR) estimated by the Logan Plot using the input function of extracted reference TAC was compared with DVR using the cerebellum TAC and with DVR calculated by the Logan Plot using an arterial input function.

Results: The TACs of extracted reference region agreed well with those of the cerebellum region in both control and AD patients. There was little difference between DVR of the Logan Plot with the extracted reference region and with the cerebellum, and they were correlated with the DVR estimated with the arterial input function.

Conclusions: Reference tissue extraction with supervised clustering could detect the voxels of reference region without specific binding in [^{11}C]PIB PET study, and it would be a useful tool for the quantification of amyloid plaque deposition, especially for studies in which the retention in cerebellum becomes higher.

References:

1. Knight WD et al. Carbon-11-Pittsburgh compound B positron emission tomography imaging of amyloid deposition in presenilin 1 mutation carriers. *Brain*, in press

2. Turkheimer FE et al. Reference and Target Region Modeling of [^{11}C]-(R)-PK11195 Brain Studies. *J Nucl Med* 48:158-167, 2007

1402

HYPERCAPNIA CAUSES A SLIGHT BUT SIGNIFICANT DECREASE OF BRAIN ELECTRICAL ACTIVITY UNDER THIOPENTAL ANAESTHESIA

E.J. Kang, D. Jorks, S. Major, J.P. Dreier

Center for Stroke Research Berlin (CSB), Charité University Medicine, Berlin, Germany

Objectives: Hypercapnia is employed to calibrate the Blood Oxygen Level Dependent (BOLD) signal. It is assumed that hypercapnia isolates the cerebral blood flow (CBF) component of the BOLD signal since it does not lead to changes in neuronal activity/oxygen metabolism. Here, we studied the response of brain electrical activity, DC potential, interstitial pH and K^+ concentration ($[K^+]_o$) as well as regional CBF to hypercapnia in a rat cranial window preparation to test whether hypercapnia is not associated with changes in neuronal activity.

Methods: Male Wistar rats (n = 51; 250-350 g) were anaesthetized with thiopental-sodium (100mg/kg, i.p.), tracheotomised, and artificially ventilated. Systemic arterial pressure was monitored via the left femoral artery. K^+- and pH-sensitive microelectrodes as well as a laser-Doppler flow (LDF) probe were placed at an open parietal cranial window. The epidural DC potential was measured by an Ag/AgCl electrode at a frontal window. Two hypercapnic episodes were produced by ventilation with a gas mixture containing 10% CO_2 for 5 min at an interval of 30 min. Blood gas analysis was performed before, during and after hypercapnia.

Results: During hypercapnia, arterial pCO_2 increased significantly from 44.1 (40.4, 49.3) to 79.1 (75.5, 83.5) mmHg. Arterial pO_2 remained within physiological limits but decreased significantly from 110.0 (97.3, 116.8) to 73.8 (68.2, 80.3) mmHg similar to the arterial blood pressure that decreased from 124.8 (111.5, 133.6) to 91.0 (83.4, 102.0) mmHg. The interstitial pH decreased from 7.39 (7.34, 7.40) to 7.26 (7.20, 7.36). This pH reduction was significantly less pronounced than the arterial pH reduction from 7.36 (7.34, 7.39) to 7.17 (7.16, 7.19). The intracortical DC potential showed a significant positive shift of 3.1 (2.4, 3.5) mV that reached a plateau after 136 (107, 153) s similar to the epidural DC potential that shifted by 0.6 (0.3, 0.9) mV (n = 35). The power of the brain electrical activity (bandpass: 0.5 - 45 Hz) decreased significantly from 5.2 (3.6, 7.1) to 4.8 (2.4, 7.7) mV^2s during the plateau phase followed by a significant increase to 6.5 (4.2, 11.2) mV^2s during the early recovery phase. $[K^+]_o$ increased first insignificantly from 2.86 (2.70, 3.08) to 2.88 (2.64, 3.20) mM during the plateau phase but the early recovery phase showed a significant increase to 2.93 (2.74, 3.20) mM (n = 37). CBF increased from 100 to 191 (169.61, 208.80) % and returned to the baseline after 612 (559, 673) s. CO_2 reactivity was found to be 4.20 (3.59, 5.23) %/0.1kPa (n=47). The power of low-frequency vascular fluctuations (LF-VF) (bandpass: 0.05-0.1 Hz) showed a significant increase from 1.12 (0.73, 1.80) to 4.31 (1.72, 8.98) during the plateau phase, which promptly diminished to 1.93 (1.27, 3.21) PU^2. The power of high-frequency vascular fluctuations (HF-VF) (bandpass: 0.5-5 Hz) increased from 0.20 (0.10, 0.76) to 0.55 (0.20, 2.83) during the plateau phase followed by a slight decrease to 0.52 (0.18, 2.09) PU^2 and finally returned to the baseline.

Conclusions: Our present data show that hypercapnia affects not only CBF but also brain electrical activity which decreases slightly but significantly.

1404

HIPPOCAMPAL HEAD VOLUME CORRELATES WITH IN VITRO [^{3}H]ABP688 BINDING POTENTIAL IN MESIAL TEMPORAL LOBE EPILEPSY

L. Minuzzi[1], E. Kobayashi[2], J. Hall[2], A. Aliaga[1], M.C. Guiot[2], P. Rosa-Neto[1,2]

[1]Translational Neuroimaging Laboratory, Douglas Hospital, [2]Department of Neurology and Neurosurgery, McGill University, Montreal, QC, Canada

Introduction: Hippocampal sclerosis (HS) is the main pathological substrate in refractory mesial temporal lobe epilepsy (MTLE) patients, with abnormalities predominating in the anterior hippocampal segment. HS can be identified in vivo through MRI, with reduced dimensions and increased T2 signal characterizing hippocampal atrophy (HA). We have previously demonstrated using in vitro quantitative autoradiography that epileptogenic MTLE hippocampi presented nearly 50% reduction in metabotropic glutamate receptor type 5 (mGluR5) allosteric binding sites as compared to necropsy controls without history of seizures.

Objective: The objective of this study is to evaluate whether pre-operative MRI hippocampal head volumes (HHV) correlate with in vitro [^{3}H]ABP688 binding in resected hippocampal tissue.

Methods: All patients signed REB approved informed consent for research. We analyzed pre-operative MRIs and in vitro hippocampal [^{3}H]ABP688 binding data from 17 MTLE patients. Eleven patients had MRI diagnosis of HA based on visual analysis. HHV were determined by manual segmentation on T1 images. Patients were divided in two groups: “atrophic” group (N=11) comprising patients with HA on MRI and confirmed HS, and “non-atrophic” group including patients without HA but neuronal loss/gliosis (N=3) or normal pathology (N=3). Hippocampal surgical specimens were immediately frozen after selective amygdalohippocampetomy or anterior temporal resection including the anterior portion of the hippocampus. Tissue was cryosected at 20 um, and mGluR5 saturation binding was carried out using increasing concentrations of [^{3}H]ABP688 (specific activity 74 Ci/mmol). Non-specific binding was defined by addition of 10 μM MPEP into adjacent sections. Saturation binding parameters (Bmax and KD) were calculated using one-binding site model. Regions of interest (containing at least a section of dentate gyrus, hilus and Ammon horn) were manually drawn onto the autoradiograms. In vitro binding potential (BP_{iv}) was defined as BP_{iv}=Bmax/KD.

Results: Non-atrophic group presented higher HHV (1850 ± 111.6 vs 975.7 ± 57.35 mm^3, $p< 0.001$, Figure 1A). There was a positive linear correlation between Bmax and KD (R^2=0.5, p=0.002), as well as between BP_{iv} and HHV for all patients (R^2=0.26, p=0.04, Figure 1B), but none between HHV and Bmax or KD. Lower KD (0.6 ± 0.11 nM) and Bmax (0.23 ± 0.01 pmol/mg) were found in the non-atrophic group, but only KD was significantly different (p=0.04, Figure 1C and 1D). BP_{iv} was lower in the atrophic group (0.63 ± 0.08 mmol/mgxM) as compared to non-atrophic group (0.90 ± 0.07, p=0.04).

Conclusions: The positive correlation between degree of atrophy in the resected tissue measured by HHV and [^{3}H]ABP688 BPiv suggests pathology-specific adaptations in mGluR5 allosteric binding sites. These adaptations should be considered for interpretation of in vivo binding studies in MTLE patients.

References:

Minuzzi et al (2009). “Reduction of mGluR5 binding sites in hippocampi from patients with

pharmaco-resistant temporal lobe epilepsy: an autoradiographic study." J Cereb Blood Flow Metab 29, S581-S599

Kobayashi et al (2009). "In vivo/in vitro evidence for altered metabotropic Glutamate Receptor Type 5 (mGluR5): a biomarker for epileptogenicity in Mesial Temporal Lobe Epilepsy (MTLE)?" Epilepsia, 2009:50(Suppl. 11):83-84.

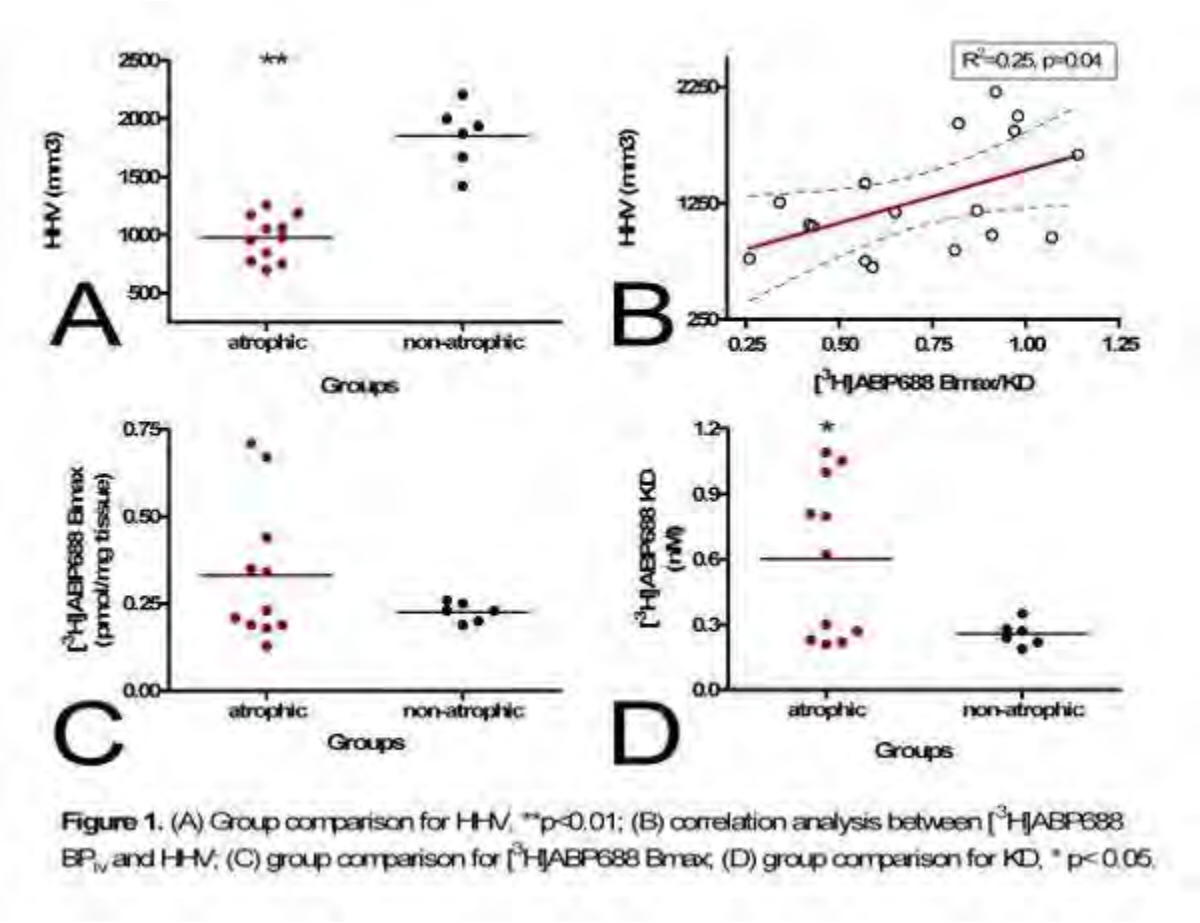

Figure 1. (A) Group comparison for HHV, **p<0.01; (B) correlation analysis between [^{3}H]ABP688 BP_{ND} and HHV; (C) group comparison for [^{3}H]ABP688 Bmax; (D) group comparison for KD, * p< 0.05.

[Figure 1]

1407

THE RELATIONSHIP BETWEEN RADIOACTIVE DOSE AND PRECISION OF OUTCOME PARAMETERS IN QUANTITATIVE PET IMAGING OF THE HUMAN BRAIN

Y.H. Nai, M.L. Cunneen, R.S. Dimber, W.A. Hallett, G.E. Searle

Clinical Imaging Centre, GlaxoSmithKline, London, UK

Objectives: The amount of radioactivity injected in a Positron Emission Tomography (PET) experiment is a significant factor in the quality of the resulting images and data. However, the amount that can be injected is limited by safety considerations as well as practical issues relating to radiochemical production and delivery. Sometimes, when a lower-than-ideal dose is produced, investigators must use subjective judgement to decide whether to go ahead with the injection or to cancel the experiment. The aim of this work is to determine recommended minimum doses that could be expected to result in adequate quantification for a selection of [^{11}C]-labelled PET radiotracers.

Methods: Dynamic data from fifteen human PET scans with [^{11}C]-PHNO, [^{11}C]-DASB, [^{11}C]-carfentanil and [^{11}C]-raclopride were used to simulate the effects of injecting less than the actual 158 - 300 MBq doses used. Each list mode data set was repeatedly halved to produce 30 additional data sets, which were reconstructed into simulated images corresponding to two dynamic images with half the full dose, four images with ¼ of the dose, and so on to 16 images with 1/16 of the dose. The images were processed using an image analysis pipeline and the simplified reference tissue model to produce estimates of binding potential (BP_{ND}) in various regions of interest (ROIs). Thus, for each activity level, multiple estimates of BP_{ND} value were produced. Relationships between the precision and bias of these estimates and the simulated doses were explored. For each ROI and radiotracer, the maximum relative BP_{ND} error was calculated at each activity level. These values were then interpolated to estimate the minimum injection dose required to ensure that estimated BP_{ND} values should be within 5% of the original (full activity image).

Results: The variability in BP_{ND} estimates increased with decreasing injected activity. For most datasets, no significant bias was observed. However for some scans and ROIs, there was an apparent decrease in median BP_{ND} with decreasing activity. This was found to result primarily from poorer correction of subject motion at low activities. Table 1 shows the recommended minimum injection doses for each radiotracer in selected regions (empty cells correspond to ROIs not considered for that tracer). As expected, regions with high target density and / or large volumes tended to produce lower minimum doses.

	Amygdala	Caudate	Putamen	Thalamus	Midbrain	Striatum	Substantia Nigra	Globus Pallidus	Ventral Striatum
Carfentanil (MBq)	100	56	37	58					

DASB (MBq)				120	155	67			
Raclopride (MBq)		65	21	147			204	153	133
PHNO (MBq)		92	28	124			151	136	125

[Table 1: Recommended minimum injection doses]

Conclusions: The results presented here can be used to make rapid, informed decisions about whether to proceed with injection of a radiotracer. This could minimise unnecessary scan cancellations whilst ensuring that any procedures which do go ahead are likely to produce useful data. Also, given the low thresholds established for some tracer and ROI combinations, new experimental designs might now be considered using lower doses and a greater number of scans per subject.

1409

THE PERMEABILITY TRANSITION IN MITOCHONDRIA, REGULATED BY BRAIN-SPECIFIC PROTEINS - A BROAD TARGET FOR NEUROPROTECTION IN ISCHEMIC DAMAGE

T. Azarashvili[1,2], **G. Reiser**[1]

[1]Institut fuer Neurobiochemie, Otto-von-Guericke University, Magdeburg, Germany, [2]Russian Academy of Science, Pushchino, Russia

In all neurodegenerative disease states, the sudden increase of the permeability of the inner mitochondrial membrane in response to threshold calcium concentration or oxidative stress leads to the formation of an unselective permeability transition pore (PTP) complex. Intense studies of the PTP phenomenon did not yet allow unravel the biochemical mystery and the structure of this pore complex. Gene knockout experiments ruled out the earlier accepted involvement of voltage-dependent anion channel and adenine nucleotide translocase as structural elements of PTP. Interestingly, the peripheral benzodiazepine receptor (PBR), now designated the 18-kDa translocator protein (TSPO) of the outer membrane, seems to take part in PTP regulation. We present data on evidence how ligands of TSPO or PBR (PK11195, Ro5-4864, protoporphyrin and diazepam binding inhibitor) are able to modulate the induction of Ca^{2+}-induced PTP in rat brain mitochondria. Furthermore, we summarize the recently revealed contribution of two novel proteins, 2',3'-cyclic nucleotide 3´-phosphodiesterase and $p42^{IP4}$ (centaurin α1; ADAP 1), to Ca^{2+} efflux from rat brain mitochondria loaded by threshold [Ca^{2+}] and thus to induction of PTP. In conclusion, the mitochondria permeability transition pore complex in brain with its interacting proteins and the small molecule ligands presents a promising target for protection in many neurodegenerative diseases, especially in brain damage after ischemic injury.

1410

MECHANISMS OF STROKE RECOVERY MEDIATED BY REGULATION OF GABA-MEDIATED TONIC NEURONAL INHIBITION

B.S. Huang, S.T. Carmichael, I. Mody

Neurology, UCLA, Los Angeles, CA, USA

Objectives: Stroke is the leading cause of adult disability; yet no pharmacological therapy is currently available for promoting recovery. Most patients, however, show partial recovery over time and after physical rehabilitation, revealing the brain's capacity for self-repair. We aimed to examine what constrains this endogenous repair from occurring sooner and how such constraint could be overcome pharmacologically to enhance stroke recovery.

Methods: Using patch-clamp electrophysiology, in cortical slices obtained from a photo-thrombotic mouse model of focal ischemia, we previously discovered that GABA-mediated tonic inhibition is significantly increased after stroke in the peri-infarct cortex (1). Using type-specific GABA transporter (GAT) inhibitors (NO-711 and SNAP-5114), we found that the post-stroke increase in tonic inhibition is caused by an impairment in glial GABA transporters (GAT-3), suggesting that a diminished GABA clearance after stroke leads to excessive extracellular transmitter accumulation, which in turn over-activates extra-synaptic GABA(A) receptors to elevate tonic inhibitory currents (1). We tested the effect of dampening tonic inhibition on motor recovery by chronic treatment with an α5-GABA(A)R-selective inverse agonist (L655,708) starting at 3-days after stroke, and we found a significant (~50%) reduction in motor deficits in treated animals (1). These findings indicate that excessive tonic inhibition critically constrains the plasticity necessary for functional recovery, and thus, the regulation of tonic inhibition is a promising new therapeutic approach.

Results: Here, we sought to understand the mechanisms underlying the treatment-induced functional recovery and compare it with the endogenous repair process without treatment. We found that both endogenous and treatment-induced repairs are mediated by regulation of tonic inhibition. To study endogenous recovery, we measured the level of tonic inhibition and GAT function at 3, 7, 14, and 42-day-post-stroke (corresponding to previous behaviorally studied time-points). We found that peri-infarct tonic inhibition has returned to control level by 42-day-post-stroke and is associated with an up-regulation of neuronal GAT-1 function, while glial GAT-3 remains impaired, suggesting a neuronal homeostatic mechanism is activated to regulate proper level of GABA clearance. To determine the mechanism underlying the enhanced plasticity following the reduction of tonic inhibition, we studied peri-infarct neurons at 14-day-post-stroke from mice chronically-treated with L655,708 and found a significant increase in their spontaneous EPSC amplitudes. Notably, this increased synaptic excitation is found only in treated animals and not in non-treated controls even at 42-day-post-stroke (when tonic inhibition has re-normalized endogenously), suggesting that treatment-induced repair differs from endogenous recovery in its activation of enhanced excitatory plasticity, which likely leads to the cortical reorganization necessary for functional restoration.

Conclusions: Together, these findings constitute a new conceptual model for functional recovery after stroke and possibly other brain injuries. The long-term time course of recovery also provides a rational basis for designing optimal clinical treatment strategies.

Reference:

(1) Clarkson, A.N.*, Huang, B.S.*, MacIsaac, S.E., Mody, I., Carmichael, S.T. (2010) Reducing excessive GABA-mediated tonic inhibition promotes functional recovery after stroke. *Nature*, 468: 305-309. (*co-first-authors)

1411

THE ROLES OF MELATONIN RECEPTOR 1 AND 2 IN THE TREATMENT OF STROKE

E. Kilic[1], B. Yilmaz[1], M. Ugur[1], B. Cevreli[1], B. Yulug[1], D.M. Hermann[2], U. Kilic[1,3]

[1]Physiology, Yeditepe University, Istanbul, Turkey, [2]Neurology, University of Essen, Essen, Germany, [3]Medical Biology, Bezmialem Vakif University, Istanbul, Turkey

Objectives: Melatonin is a potent antioxidant with neuroprotective activity in animal models of ischemic stroke (Kilic et al., 1999; 2008). Based on melatonin's lack of serious toxicity, it has raised hopes that this indolamine might be used for human stroke treatment in the future. However, the roles of melatonin receptors (MT1 and MT2) in the neuroprotective effects of melatonin are not known after brain injury. In this study, we have investigated the roles of MT1 and MT2 in the neuroprotective effects of melatonin in melatonin receptors 1-2 knockout mice (*mt1/2*$^{-/-}$).

Materials and Methods: In this study, adult male melatonin receptors 1-2 knockout mice (*mt1/2*$^{-/-}$), with a C3H/HeN strain background and their *wt* littermates were used. In the first series of experiments, the animals were divided into four groups and submitted to focal cerebral ischemia, as induced by 90 minutes of intraluminal middle cerebral artery (MCA) occlusion, followed by 24 hours of reperfusion (Kilic et al, 2010). The animals were treated with melatonin (4 mg/ kg; i.p. day) or vehicle just after 90 mins of ischemia. In these animals, infarct volume and brain swelling were analyzed.

In the second series of experiment, the animals were divided into four groups and submitted to focal cerebral ischemia, as induced by 30 minutes of intraluminal middle cerebral artery (MCA) occlusion, followed by 25 days of reperfusion. Melatonin (4 mg/ kg; i.p. day) or vehicle was administrated daily, beginning on the 5th day after induction of ischemia and continuing for 25 days. Thirty days after induction of ischemia, neuronal survival and lesion areas were analyzed.

Results: Laser Doppler measurements showed no difference after 90 or 30 minutes of ischemia between *mt1/2*$^{-/-}$, or *wt* animals. Ninety min episodes of MCA occlusion resulted in focal infarcts of the cerebral cortex and underlying striatum. The infarct volume and brain swelling did not significantly differ between vehicle-treated *mt1/2*$^{-/-}$, or *wt*. Melatonin treatment significantly decreased infarct size and brain swelling in both groups of animals as compared with their vehicle-treated control animals. Interestingly, melatonin was found to be significantly more effective in mt1/2$^{-/-}$ animals as compared with melatonin-treated with wt animals.

Thirty minutes of ischemia caused disseminated cell death in striatum. The number of surviving neurons was higher and lesion areas lower in *mt1/2*$^{-/-}$ animals, as compared with vehicle-treated wt animals. Although, the treatment was started five days after ischemia, significantly higher number of surviving neurons and lower lesion areas were observed in melatonin-treated *mt1/2*$^{-/-}$ animals, compared with the control groups. Melatonin treatment was not effective in wt animals as compared with vehicle-treated control animals.

Conclusion: We provide evidence that absence of melatonin receptors 1-2 has no deleterious effect on brain injury induced by MCAo and reperfusion. Melatonin protection of the brain from ischemic injury in wt and MT1-2 knockout animals indicates that the neuroprotective efficacy of melatonin is independent from its receptors membrane receptors.

References:

Kilic et al (1999) 19: 511-516; (2010) 30:969-84. J Cereb Blood Flow Metab.

Kilic et al (2008) 45: 142-148 J of Pineal Research

1412

ELECTROPHYSIOLGICAL MAPPING OF HORIZONTAL MERIDIAN IN THE PRIMARY VISUAL AREA OF THE DIURNAL SOUTH AMERICAN RODENT DASYPROCTA AGOUTI

C.W. Picanço-Diniz[1], E.G. Rocha[1], L.C.D.L. Silveira[1], G. Elston[2], E. Oswaldo-Cruz[3]

[1]Institute of Biologic Sciences, Federal University of Pará, Belém, Brazil, [2]Centre for Cognitive Neuroscience, Sunshine Coast, Sunshine Coast, QLD, Australia, [3]Instituto de Biofísica Carlos Chagas Filho, Rio de Janeiro, Brazil

Objectives: In the present investigation we mapped the primary visual area of the South American diurnal rodent, *Dasyprocta aguti*, by standardized electrophysiological mapping techniques.

Methods: We used six adult male agoutis (*Dasyprocta aguti*), obtained from the Museu Paraense Emílio Göeldi animal colony in the present study. In particular, we performed a series of mapping experiments of the visual streak in the primary visual cortex. Electrophysiological mapping techniques have been described in detail elsewhere (Picanço-Diniz et al. 1991).

Results: We found that the representation of the visual streak in V1 is greatly expanded: the nasal 10 degrees of the visual streak representation occupies ten times more cortical area than equivalent areas in the central or temporal representation of the visual streak. Comparison of these data with those on the density of ganglion cells in the retina at corresponding locations in the visual field reveal an interesting mismatch between these two variables. The nasal representation is greatly expanded along the horizontal meridian in V1 as compared to the central and temporal regions whereas the density of ganglion cells decreases with progression along the visual streak from central region towards the nasal or temporal visual field.

Conclusions: A review of the available data reveals that all lateral-eyed mammals exhibit a similar mismatch between the retinal and cortical representation of the visual field, and this mismatches is greater in those species with well defined visual streaks such as rabbit and agouti.

References:

Picanço-Diniz CW, Silveira L, Oswaldo-Cruz E. 1992. A Comparative Survey of Magnification Factor in V1 and Retinal Ganglion Cell Topography of Lateral-Eyed MammalsEnglish. In: Lent R, editor. The visual system from genesis to maturity. Rio de Janeiro: ed. Boston, U.S.A. Birkhäuser. p 187-198.

Silveira LC, Picanco-Diniz CW, Oswaldo-Cruz E. 1989a. Distribution and size of ganglion cells in the retinae of large Amazon rodents. Visual Neuroscience 2(3):221-235.

Hughes A. 1977. The topography of vision in mammals of contrasting life styles: Comparative optics and retinal organization. In: Cresctelli F, editor. Handbook of Sensory Physiology. Berlin: Springer-Verlag. p 813.

1413

NEUROPROTECTİVE EFFECT OF MELATONİN COMBİNED WİTH MEMANTİNE İN ISCHEMİC-BRAİN İNJURY

U. Kilic[1,2], M. Ugur[1], S. Eyuboglu[1], B. Cevreli[1], A. Cumbul[3], B. Seker[1], B. Yilmaz[1], E. Kilic[1]

[1]Physiology, Yeditepe University, [2]Medical Biology, Bezmialem Vakif University, [3]Histology and Embryology, Yeditepe University, Istanbul, Turkey

Objectives: Brain injury following transient or permanent focal cerebral ischaemia (stroke) develops from a complex series of pathophysiological events, including excitotoxicity, peri-infarct depolarizations, inflammation and apoptosis. Melatonin is a potent antioxidant with neuroprotective activity in animal models of ischemic stroke (Kilic et al, 2008). Memantine is a non-competitive NMDA receptor blocker characterized by its low affinity and fast unblocking kinetics (Liu et al, 2009). Based on their lack of serious toxicity has raised hopes that they might be used for human stroke treatment in the future. We hypothesized that co-administration of melatonin and memantine would be highly effective to attenuate brain injury after focal cerebral ischemia in mice.

Materials and methods: In this study, adult male C57/BL6 mice were used. In the first series of experiments, the animals were divided into four groups and submitted to focal cerebral ischemia, as induced by 90 minutes of intraluminal middle cerebral artery (MCA) occlusion, followed by 24 hours of reperfusion (Kilic et al, 2010). The animals were treated with (1) vehicle, (2) melatonin (4 mg/kg, i.p.), (3) memantine (20 mg/kg, i.p.) and (4) melatonin add on to memantine after stroke onset. Twenty-four hours later neurological scores, infarct volume, brain swelling, Serum Igg extravasation, the number of apoptotic and nNOS positive cells were analyzed.

Results: Laser Doppler measurements showed no difference between animal groups. Ninety min episodes of MCA thread occlusion resulted in focal infarcts of the cerebral cortex and underlying striatum. The infarct volume was significantly reduced in melatonin, memantine and melatonin/memantine treated animals. Infarct volume was also significantly lower in melatonin/memantine treated animals compared to memantine treated animals. Brain swelling was significantly lower in melatonin and melatonin/memantine injected animals. Serum Igg extravasation the number of TUNEL positive cells were significantly reduced in cortex in melatonin and melatonin/memantine treated animals. nNOS positive cells were observed in ischemic and non-ischemic hemispheres. In the control animals, number of nNOS positive cells was significantly reduced compared to melatonin and melatonin/memantine treated animals.

Conclusion: Melatonin and memantine have been shown to be safe and beneficial in human and are approved for the treatment of Alzheimer disease and sleep disorders, respectively. In the present study, we provide evidence that melatonin, memantine and their combination reduce ischemic injury. Their combination appears to be more effective especially in ischemic injury and serum Igg extravasation.

References:

Kilic et al (2008), 45: 142-148 Journal of Pineal Research

Liu et al (2009), 1282: 173-182 Brain Research

Kilic et al (2010) 30:969-84. J Cereb Blood Flow Metab.

1414

EXPLORATORY ANALYSIS OF RELATIONSHIP BETWEEN MR BASED CONVENTIONAL PERFUSION PARAMETERS AND THE PERFUSED BLOOD VOLUME (PBV) MEASURED USING C-ARM SYSTEMS

M. Kamran[1], P. Schweder[1], Y. Deuerling-Zheng[2], B. Mueller-Allissat[2], J.V. Byrne[1]

[1]University of Oxford, Oxford, UK, [2]Siemens AG, Forchheim, Germany

Purpose: Developments in the flat detector technology and high frame rate rotational imaging with C-arm systems have, made it possible to measure one of the perfusion parameters (perfused blood volume, PBV) in the neuro-interventional suite[1]. For its measurement, an optimized contrast injection protocol is used to account for the longer scan-times characteristic of C-arm systems. PBV, therefore, carries unknown weightings of the parameters traditionally used to describe cerebral perfusion. We aim to explore the relationship of conventional MRI perfusion parameters to PBV measured using a C-arm systems.

Materials and methods: Patients (n=17) with suspected vasospasm scanned using a biplane angiography system (Axiom Artis dBA; Siemens Healthcare, Germany). For PBV measurement two 8-seconds rotational acquisitions were obtained, each comprising approximately 400 projection images at 0.5 degree steps. 80ml of Iopamidol 300mg/ml was injected at 4ml/sec using a mechanical injector before the second rotational acquisition. PBV maps were constructed using a dedicated prototype software (Siemens AG, Healthcare). Contemporaneous perfusion weighted MR scan (MR-PWI) was performed (dynamic susceptibility contrast, TR 2018ms; TE 44ms). Perfusion maps (cerebral blood volume CBV, cerebral blood flow CBF, mean transit time MTT) were calculated using block circulant deconvolution based analysis. MR-CBV, CBF, and MTT maps were co-registered with C-arm PBV maps. A region of interest analysis of voxel intensities was carried out. Multiple regression analysis was used to characterize the relationship between MR and C-arm based perfusion parameters.

Results: Voxel intensities of C-arm PBV maps showed consistent relationships with MR based perfusion measurements maps of various regions of interest (figure 1). Multiple regression demonstrated MR-CBF was the strongest individual predictor in the model (b 0.2194, $P < 0.0001$) while MR-CBV had the highest correlation with C-arm PBV, followed by MR-CBF.

Conclusion: PBV measured using a C-arm system represents a measurement related to conventional perfusion parameters (CBV, CBF, and MTT). PBV maps likely represent components of both CBV and CBF to differing degrees. PBV likely reflects not solely the ischemic penumbra or the infarct core, but a measure which is a component of the two, which may be influenced by contrast injection and image acquisition protocols.

References:

1. Struffert T, Deuerling-Zheng Y, Kloska S, et al. Flat Detector CT in the Evaluation of Brain Parenchyma, Intracranial Vasculature, and Cerebral Blood Volume: A Pilot Study in Patients with Acute Symptoms of Cerebral Ischemia. *AJNR Am J Neuroradiol* 2010;31:1462-1469

1416

EFFECTS OF INTRAVENOUS AUTOLOGOUS TRANSPLANTATION OF MESENCHYMAL STEM CELLS AFTER PHOTOTHROMBOTIC RING STROKE IN ADULT RATS

L. Larsson, M. Brohlin, W. Gu, X. Hu, L. Novikov, M. Wiberg, P. Wester

Umeå University, Umeå, Sweden

Introduction: The photothrombotic ring stroke model in adult rats features late spontaneous reperfusion and morphological tissue recovery within the cortical region at risk. Mesenchymal stem cell (MSC) transplantation has suggested therapeutic benefits in mechanical cerebral artery occlusion models of stroke. Since clinical ischemic stroke is mostly thromboembolic, the photothrombotic ring stroke model may be of greater clinical relevance.

Objective: The aim of this study was to assess the therapeutic effects of intravenous delivery of autologous MSC in a modified photothrombotic ring stroke model targeting the primary motor and sensory cortex of inbred Fischer rats.

Methods: The exposed crania of adult male Fischer rats (250-320 g) were subjected to a ring-shaped (5.0 mm outer diameter; 0.35 mm thick) laser-irradiation beam (514.5 nm; 1.25 W/cm^2) for 2 min simultaneously with intravenous infusion of the photosensitizing dye erythrosin B (17 mg/kg) during the first 30 s. After stroke induction, the rats received repeated injections of the cell proliferation specific marker 5-bromodeoxyuridine (BrdU). MSC were isolated from the bone marrow of naïve Fischer rats, cultured for 4 passages, and labeled with the fluorescent dye PKH26. 3×10^6 cells were injected intravenously at seven days after stroke, and the rats were sacrificed at 14 days after stroke by transcardial paraformaldehyde perfusion. Current experiments are exploring whether the endogenous and/or exogenous neurogenesis, gliogenesis, and angiogenesis in the ischemic penumbra are increased in rats treated with MSC compared with control animals. The frequency and phenotypes of BrdU positive cells (endogenous proliferation) and PKH26 positive cells (exogenous proliferation) are determined by double immunofluorescence staining for neuron- (NeuN), endothelial- (vWF), and glial- (GFAP) specific markers, and stereological cell counting.

Results: The photothrombotic ring stroke model was successfully modified to target the primary motor and sensory cortex of inbred Fischer rats. An accumulation of transplanted PKH26 positive MSC could be observed in the ischemic core and the penumbra at 14 days after photothrombotic ring stroke. Preliminary results demonstrated some cells in the cortical ischemic penumbra that were double-positive for PKH26 and GFAP whereas a few other cells were double-labeled with PKH26 and NeuN.

Conclusions: Mesenchymal stem cells, systemically administrated, preferentially migrate to the ischemic penumbra after photothrombotic ring-stroke. Intravenous autologous mesenchymal stem cell transplantation may enhance the endogenous angiogenesis, gliogenesis and neurogenesis.

1418

EXPRESSION OF THE ANGIOTENSIN II AT1 RECEPTOR AFTER TRAUMATIC BRAIN INJURY IN MICE

S. Villapol[1,2], A. Yaszemski[1], E. Sanchez-Lemus[2], J.M. Saavedra[2], A.J. Symes[1]

[1]Centre for Neuroscience and Regenerative Medicine, and Departament of Pharmacology, Uniformed Services University of the Health Sciences, [2]Pharmacology, National Institute of Mental Health, National Institutes of Health, Bethesda, MD, USA

Objectives: Traumatic brain injury (TBI) results in complex pathological reactions. Damage from the initial lesion is worsened by secondary inflammation and edema. Angiotensin II is produced in the brain and is known to have anti-inflammatory reactions. However, little is known about the response of the Renin Angiotensin ystem (RAS) after TBI. Angiotensin II receptor (ATR) expression is indicative of RAS activation, and is upregulated by inflammation and stress. In the present study, we characterize the expression of components of the Angiotensin II pathway in the brain at specific time points after controlled cortical impact (CCI) injury to mice.

Methods: We performed moderate CCI injury on 8-week-old male C57BL/6 mice. CCI, sham and naïve animals were sacrificed at 1, 3, 7, and 28 days post lesion. We analyzed temporal and spatial expression of AT1R via autoradiography and immunohistochemistry using several antibodies together with neuronal and glial markers. The amount of cell death was also examined. To test neurological function in mice that had undergone CCI, three different behavioral tests were performed: rotarod, open field, and Morris water maze.

Results: We found strong nuclear staining of AT1R in apoptotic cells in the injured cortical areas at 1 and 3 days after injury. This aberrant nuclear AT1R expression was found mainly in the lesion core and apoptotic hippocampal neurons. Strong cytoplasmic AT1R expression was also observed in some reactive astrocytes and brain microvessels in the border of the lesion. In the penumbra of the lesion neuronal AT1R expression was cytoplasmic, in contrast to that in the lesion core. Cytoplasmic neuronal AT1R expression was also observed in the contralateral cortex and in the cortex of sham and naïve mice. Autoradiography and immunohistochemistry also indicated AT1R binding in the paraventricular nucleus, lateral septum, and subfornical organ in the brain in all experimental groups. Behavioral assays indicated that CCI injured mice had deficits in motor function up to 7 days after injury, and deficits in memory three weeks after injury.

Conclusions: AT1R expression is upregulated in the damaged cortex and hippocampus after CCI injury. We therefore hypothesize that pharmacological antagonism of AT1Rs may reduce neuronal cell death in the cortex and hippocampus after CCI, and thereby improve functional recovery. Our data suggest that angiotensin II receptor blockers may have efficacy in treating TBI.

1419

HOLD THE DEEP BRAIN STIMULATION: THE ROLE OF IMAGING IN CHALLENGING PSYCHOGENIC PARKINSONISM

M.H. Pourfar[1], **V. Dhawan**[2], C.C. Tang[2], A.Y. Mogilner[3], D. Eidelberg[2]

[1]Departments of Neurology and Medicine, North Shore University Hospital, [2]Feinstein Institute for Medical Research, [3]Department of Neurosurgery, North Shore University Hospital, Manhasset, NY, USA

Objectives: As many as 15% of subjects enrolled in recent early Parkinson's disease (PD) trials have been found to lack evidence of a dopaminergic deficit following PET or SPECT imaging. The frequency with which non-PD patients with advanced parkinsonian symptoms undergo deep brain stimulation (DBS) procedures is unknown. However, the potential exposure of these patients to unnecessary surgical risks makes their identification critical. In this study, we examined two female patients (Patient 1: age = 54 y; Patient 2: age = 40 y) with probable psychogenic parkinsonism who were referred for DBS surgery.

Methods: We quantified dopaminergic and metabolic function in both patients by concurrent PET studies with [^{18}F]-fluorodopa and [^{18}F]-FDG. [^{18}F]-fluorodopa uptake was measured in the striatal subregions with a volume of interest (VOI) approach. Metabolic profiles in individual patients were assessed on a voxel basis by using single-case statistical parametric mapping analysis and by quantifying network expressions of spatial covariance patterns associated with PD and multiple system atrophy (MSA).

Results: [^{18}F]-fluorodopa uptake in both patients was normal in caudate and putamen relative to 15 healthy control subjects (mean/SD = 2.27±0.27). The uptake values in the patients were symmetric in the caudate nucleus, anterior putamen and posterior putamen.

Patient	L Caudate nucleus	R Caudate nucleus	L Anterior putamen	R Anterior putamen	L Posterior putamen	R Posterior putamen
1	2.26	2.27	2.35	2.29	2.21	2.17
2	2.29	2.28	2.26	2.27	2.15	1.99

[Table 1. Caudate and putamen FDOPA uptake values.]

In Patient 1, increased regional metabolic activity was evident ($p < 0.05$, uncorrected) in the cerebellum and motor cortex, without changes in the basal ganglia. In Patient 2, regional metabolic increases were present in the cerebellum, without changes in the motor cortex or basal ganglia. These findings contrasted with those observed in PD patients, who typically display metabolic increases in the putamen/GP, thalamus, cerebellum, and motor cortex, and those in MSA patients with characteristic metabolic decreases in the basal ganglia and the cerebellum.

Subject scores quantifying the expression of the PD-related metabolic spatial covariance pattern (PDRP) were normal in both cases. By contrast, PDRP scores were abnormally elevated in the PD reference subjects (>2.0, corresponding to 2 SD above the normal mean) and were normal

(< 2.0) in the MSA reference group. Additionally, subject scores for MSA-related spatial covariance pattern (MSARP) were also found to be normal in the two patients. By comparison, MSARP scores were abnormally elevated (>2.0) in 21 of 23 MSA reference patients and were normal (< 2.0) in 24 of the 25 PD reference subjects.

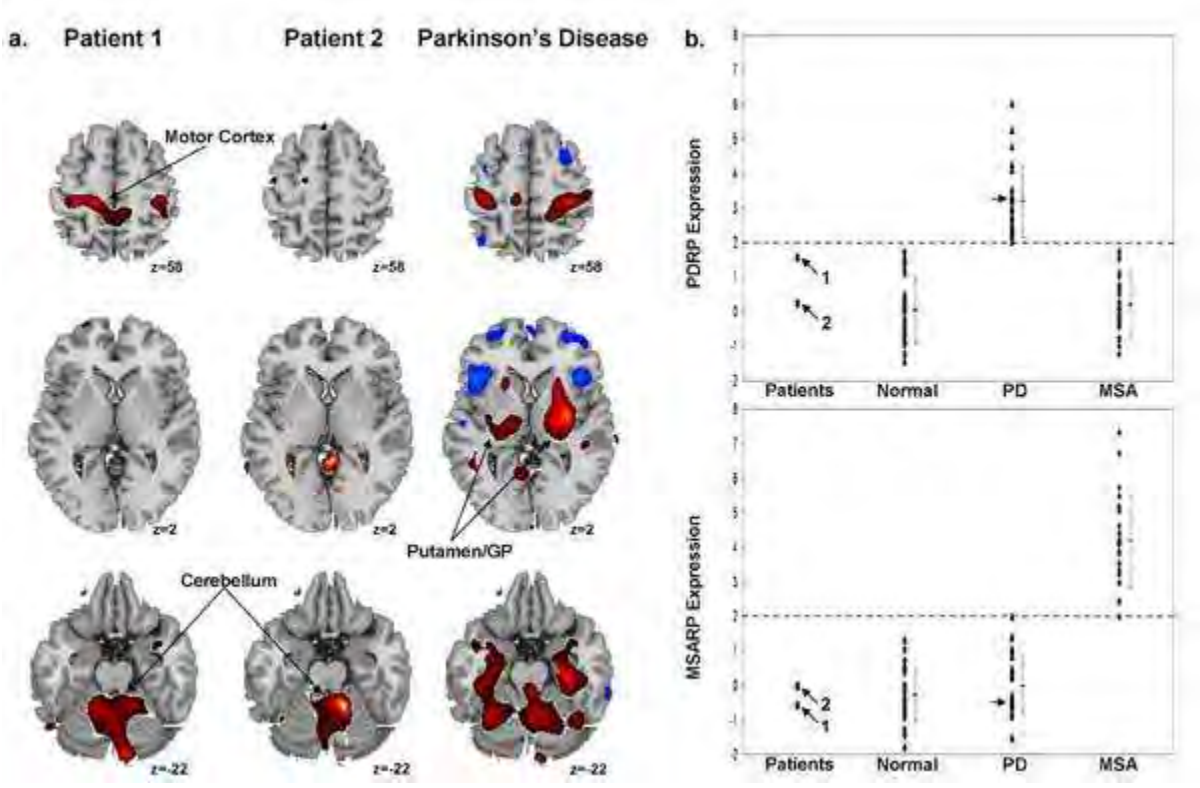

[Fig 1. Single-case diagnosis and network analysis.]

Conclusions: We found that both patients had normal caudate and putamen [^{18}F]-fluorodopa uptake, along with normal expression of disease-related regional metabolic covariance patterns for PD and MSA. Their clinical features and PET findings highlight the role of functional imaging in assisting clinical decision-making when the diagnosis remains unclear.

1420

THEORETICAL TIME-RESOLVED NEAR-INFRARED MEASUREMENTS OF INDICATOR-DILUTION IN THE ADULT HEAD USING TRACER KINETIC MODELING AND SERIAL MONTE CARLO SIMULATIONS

J.T. Elliott[1,2], M. Diop[1,2], T.-Y. Lee[1,2,3], K.S. St. Lawrence[1,2]

[1]Imaging Division, Lawson Health Research Institute, [2]Department of Medical Biophysics, University of Western Ontario, [3]Imaging Research Laboratories, Robarts Research Institute, London, ON, Canada

Introduction: Indicator-dilution based optical techniques have emerged as a promising tool for bedside monitoring of cerebral hemodynamics in critical care settings [1]. To increase the sensitivity of these techniques to brain tissue, a combination of instrumentation and modeling approaches have been proposed [2,3]. However, these solutions need to be validated by numerical and animal experiments prior to clinical application. To this end, we have developed a model that generates time-resolved data for a variety of instrumental configurations applied to arbitrary three-dimensional media such as CT imaging datasets. Although this model is flexible enough to investigate a wide variety of clinical and technical issues, we present the clinical case of subdural hematoma and numerical experiment results as a proof-of-principle.

Methods: A segmented CT volume of a patient with a subdural hematoma (Figure A, inset) was divided into five tissue-types-scalp, skull, CSF, brain and hematoma-and optical properties were assigned to each [4]. Scalp and hematoma were given a flow value of 8 $mL \cdot min^{-1} \cdot 100g^{-1}$, and CBF set to 70 $mL \cdot min^{-1} \cdot 100g^{-1}$.

To simulate time-resolved data during indicator-dilution, first, tissue-specific indicator-dilution curves were determined by convolving modeled tissue-specific impulse residue functions [5,6] with experimental arterial input functions. These indicator-dilution curves were then used to determine the time-varying attenuation coefficient, inputted into the Monte Carlo simulations [7] to generate temporal point spread functions (TPSFs) at 1-, 2-, and 3-cm source-detector distances. Thereafter, the TPSFs were convolved with an experimental instrument response function to yield “experimental” TPSFs comparable to that typically measured with a time-resolved system.

Data were simulated for two conditions-presence or absence of hematoma. The homogeneous and partial pathlength (PPL) approaches were applied to the data to extract brain concentration curves, which were used to determine CBF as previously described [3].

Results: With respect to the simulated TPSFs, in the absence of hematoma the total intensity was $8.98x10^5$, $3.18x10^5$, and $3.11x10^4$ photons for 1-, 2-, and 3-cm source-detector distances respectively. With the hematoma present, the total intensity was reduced to $6.25x10^5$, $1.66x10^5$, and $1.28x10^4$ photons at the three distances, respectively. Presence of the hematoma reduced the signal-to-noise ratio by 75.5%, 71.1%, and 50.3% for 1-, 2-, and 3-cm source-detector distances, respectively. CBF was calculated using both the homogenous [9] and PPL approaches [3]. In the absence of hematoma, recovered CBF values were 50.42 and 64.07 $mL \cdot min^{-1} \cdot 100g^{-1}$ with the homogenous and PPL approaches, respectively. In the presence of the hematoma, the two approaches recovered the same value of CBF (14.7 $mL \cdot min^{-1} \cdot 100g^{-1}$).

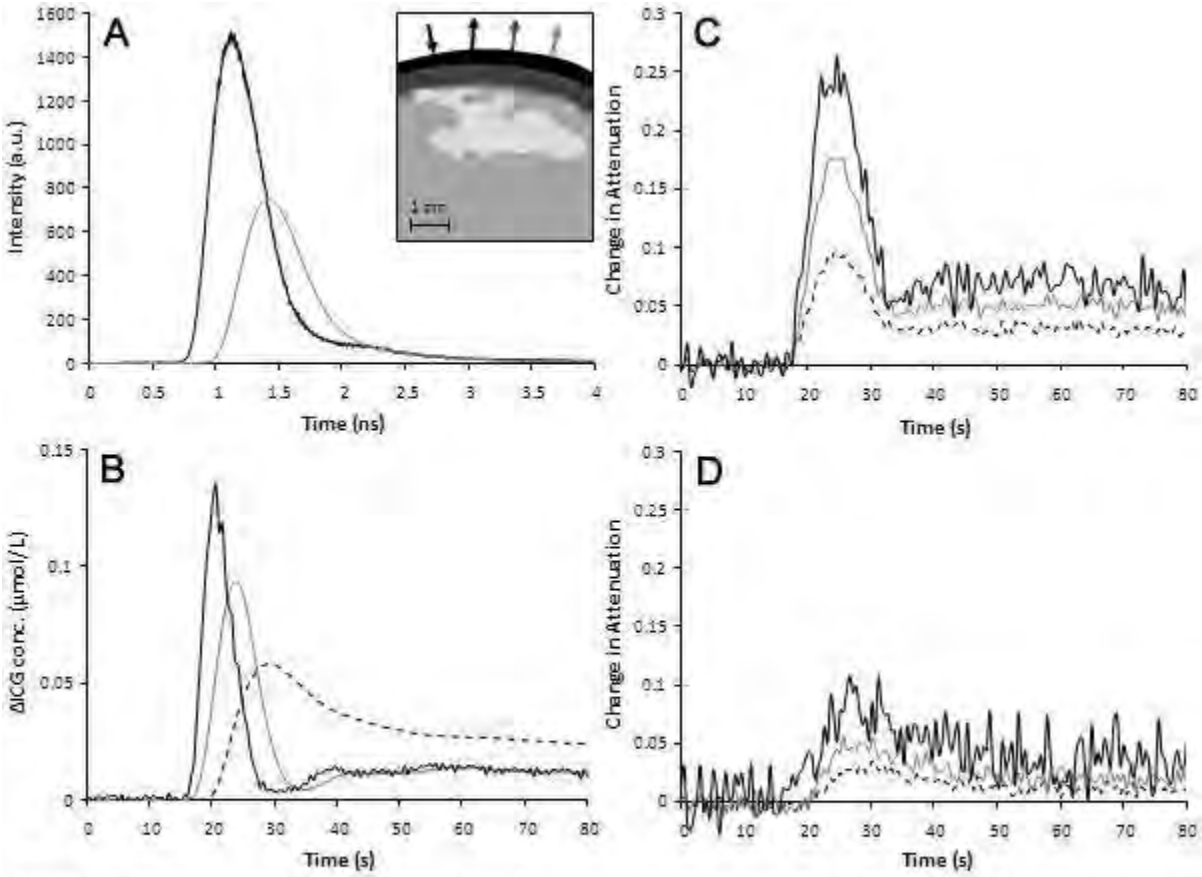

Figure. (A) IRF (black line) and simulated TPSF for 3-cm distance (gray line). (B) Arterial input (black), modeled brain (gray) and scalp (dashed) dye-dilution curves. (Arterial and scalp curves have been scaled by factors of 0.01 and 5, respectively.) (C) Change in attenuation at 3-cm (black), 2-cm (gray) and 1-cm (dashed) distances without hematoma and (D) the same measurements with hematoma present.

[fig_cap]

Conclusion: As a proof-of-principle, we demonstrate the ability of the presented model to describe the influence of a subdural hematoma on time-resolved measurements of CBF. Using this model, it is possible to investigate a wide variety of clinical and technical challenges and to evaluate novel fitting approaches—a necessary step before these techniques can be implemented clinically.

References:

1.Steinkellner *JBO* 15(6):061708

2.Liebert *ApplOpt* 43:3037-3047

3.Elliott *JBO* 15(3):037013

4.Strangman *JNeuroimage* 18(4):865-879

5.Thompson *Circ Res* 14:502-14.

6.St.Lawrence *JCBFM* **18**:1365-77

7.Fang *OptExp.* **17**(22):20178

8.Gora *J Neurosurg Anesthesiol* 14(3):218-222

1421

AGING AND ENVIRONMENTAL ENRICHMENT ALTER OBJECT RECOGNITION, SPATIAL LEARNING, AND LAMINAR DISTRIBUTION OF CA1-CA2 AND CA3 ASTROCYTES

C.M. de Lima, D.G. Diniz, J. Bento Torres, M. Sosthenes, C. Picanço Diniz

Universidade Federal do Pará, Belem, Brazil

Studies of environmental effects on brain plasticity have focused on altered neuronal morphology; however, substantial morphological changes have also been shown to occur in glial cells. An enriched environment has been defined as that which offers social interactions with conspecifics and stimulation of exploratory and motor behavior with periodic changes in the variety of toys, ladders, tunnels, ropes, bridges, and running wheels for voluntary physical exercise. In contrast, an impoverished environment offers standard cages with reduced sensorial, motor and cognitive stimulation. In the present report, we assessed the integrated memories of young adult (6 months) and aged (20 months) mice raised in either enriched or impoverished environments, and we investigated whether affected memories were correlated with changes in the number of astrocytes in the CA1-CA2 and CA3. After these behavioral tests, mice were sacrificed. Aldehyde-fixed brain sections were immunolabeled for glial fibrillary acid protein. We used unbiased, stereological methods to estimate the laminar distribution of astrocytes in CA1-CA2 and CA3. Episodic-like memory was absent in mice raised in impoverished conditions, but was preserved in both young and aged mice raised in enriched conditions. Morris water-maze performances were affected by both aging and environmental conditions. Learning rates were highest in young mice raised in enriched conditions, and lowest in aged mice raised in impoverished conditions. Thus, the effects of environmental enrichment on episodic-like memory were not dependent on age and may protect water maze spatial learning and memory from declines induced by aging or impoverished environment. In the hippocampus the number of astrocytes changed with both aging and enriched environment suggesting that impoverished conditions may be associated with abnormal cognitive development and an altered laminar distribution of astrocytes in the CA1-CA2 and CA3. We concluded that long-term experience-induced glial plasticity by enriched environment may represent at least part of the circuitry groundwork for improvements in behavioral performance in the aged mice brain.

1422

DYNAMIC SUSCEPTIBILITY CONTRAST MRI CEREBRAL BLOOD FLOW IMAGING WITH POSITRON EMISSION TOMOGRAPHY CORRELATION IN TRAUMATIC BRAIN INJURY AND STROKE

J.R. Alger[1], T.J. Schaewe[1], D.L. Mc Arthur[2], D.S. Liebeskind[1], H.S.C. Huang[3], P.M. Vespa[2]

[1]Neurology, [2]Neurosurgery, [3]Pharmacology, University of California, Los Angeles, CA, USA

Introduction: At our center, dynamic H2O PET is used to study cerebral blood flow (CBF) after traumatic brain injury (TBI). We sought to explore the question of whether Dynamic Susceptibility Contrast Magnetic Resonance Imaging (DSC-MRI) could provide equivalent CBF information in small cohorts of normal subjects, TBI patients and patients with cerebrovascular abnormalities. Proof of equivalence would be valuable because MRI is somewhat easier to perform.

Methods: Seven normal subjects, 7 patients who had experienced recent severe TBI (< 5 days) and 6 cerebrovascular patients underwent DSC-MRI and dynamic PET studies within 24 hrs of each other. Dynamic MRI scanning was performed for 120 sec using 1.5 T gradient echo EPI (TR/TE 2000/55) and a single dose of Omniscan. CBF images were derived from the PET data in the customary fashion. For DSC-MRI, the arterial input function (AIF) was automatically sampled. An automatically sampled venous outflow function (VOF) was used to correct the AIF for partial volume effect. A conventional non-parametric truncated singular values decomposition approach was employed together with a correction for AIF shape, SVD truncation and sampling rate. Absolute MRI-CBF images were then calculated from the measured absolute cerebral blood volume and the initial value of the deconvoluted residue function. A capillary to artery R2* relaxivity ratio of 2.4 was used in the calculation for all subjects. The PET-CBF images were then aligned to the DSC-CBF image space using an automated image registration routine. Images were compared visually and a Bland-Altman (BA) analysis (regression of the difference between the PET and DSC CBF readings versus their average) was performed for the whole brain mean CBF values derived from each technique.

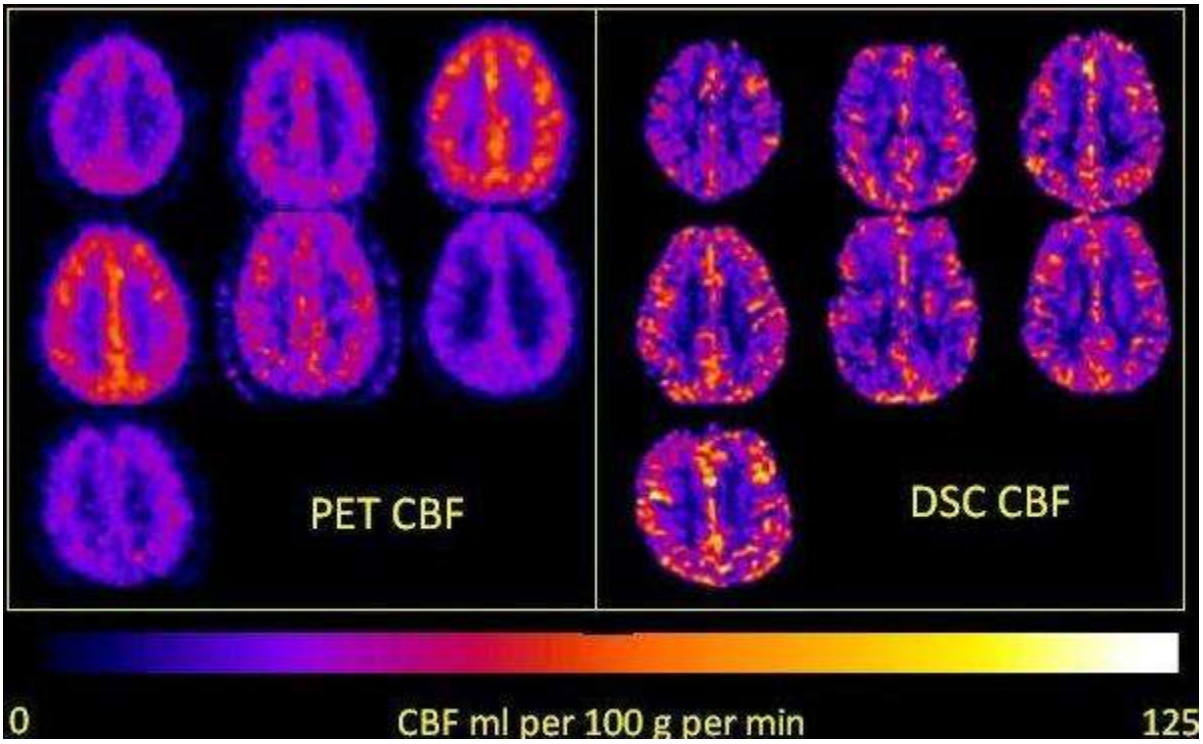

[PETMRICBF]

Results: The figure shows selected aligned slice images from the normal subjects. DSC-CBF images showed substantially more vascular and gray matter “shine-through” in comparison with PET-CBF images. Agreement in white matter regions was better. The mean BA PET-DSC difference was -30 ml/100g/min and was marginally different from zero ($p = 0.49$). The BA slope was 0.37 and was not significantly different from zero. Regression of mean total brain CBF readings produced by the two techniques showed insignificant correlation ($p = 0.67$).

Conclusions: CBF images produced by DSC do not match well with those produced by H_2O PET. Some correctable bias in the DSC CBF readings was detected. The pronounced differences in how the two techniques report CBF in gray matter and vascular regions may be due to the insensitivity of PET to high flow and/or to some unknown bias of the DSC methodology in regions of high flow and volume. The observed agreement in lower flow white matter areas suggests that DSC-CBF might be useful for problems related to detection of ischemia.

1424

DIFFUSION TENSOR IMAGING OF THE SUBSTANTIA NIGRA DOES NOT CORELATE WITH STRIATAL DOPAMINERGIC ACTIVITY OR MOTOR SYMPTOMS IN PARKINSON'S DISEASE

T. Marentis, M. Petrou, M. Muller, R. Koeppe, K. Frey, N. Bohnen

Radiology, University of Michigan, Ann Arbor, MI, USA

Introduction: Diffusion tensor imaging (DTI) is a novel MR technique to characterize microstructural abnormalities in the brain. Recently, DTI measurements in the substantia nigra (SN) showed differences in fractional anisotropy (FA) between Parkinson's disease (PD) patients and healthy control subjects [1]. It is however unknown if DTI based microstructural abnormalities reflect dopaminergic loss in PD patients.

Objective: The objective of our study was to assess the relationship between SN DTI measurements and degree of nigrostriatal dopaminergic denervation as quantified by [^{11}C]dihydrotetrabenazine (DTBZ) PET imaging as well as clinical symptoms in PD.

Methods: 76 PD subjects (mean age 64.6±7.1 years; Hoehn and Yahr stages 1-4) underwent brain MRI with DTI. Imaging protocol included T1 and FLAIR images as well as DTI. For DTI, a single shot spin-echo multislice EPI technique was used with 2 b-values (0 and 800 s/mm2) for each of 32 diffusion encoding directions, plus one B0 image set, TR/TE=7075/62 ms, matrix 112x112 pixels, 2 mm slice thickness with no gap, number of slices 60. DTI images were analyzed as previously described [1]; in brief, 3 circular VOIs (area= 4 voxels)were placed in the rostral, middle and caudal aspects of the SN bilaterally, one slice below the level of maximum visualization of the red nucleus. VOI placement was performed on the B0 set of images. FA values were computed using DTI studio software. Mean values for the different regions were estimated for each patient using the right and left sided computed parameters.

To estimate nigrostriatal terminal integrity participants underwent vesicular monoaminergic type 2 (VMAT2) (+)-μ-[^{11}C]DTBZ PET imaging. Logan analysis method was used to estimate striatal Distribution Volume Ratio (DVR). Striatal VOIs (putamen and caudate) were placed on the T1 weighted images of the MRI for PET analysis purposes.

Unified Parkinson's Disease Rating Scale (UPDRS) was used to score motor impairments. Subjects on dopaminergic drugs were examined and underwent PET imaging in the clinically-defined ”off” state.

Results: Mean FA values were 0.55 ± 0.02 for the rostral, 0.518 ±0.02 for the middle and 0.52 ± 0.02 for the caudal SN; overall mean SN FA value was 0.529 ± 0.016.

Mean striatal [^{11}C]DTBZ DVR in this group was 1.94 ± 0.06 . Mean UPDRS scores were 27.0 ± 2.6. Overall mean SN FA did not correlate with striatal [^{11}C]DTBZ DVR (r=-0.04, P=0.74)) or total UPDRS motor score (r=-0.04, P=0.73).

Conclusion: Although fractional anisotropy measurements of the substantia nigra have been proposed as a novel diagnostic biomarker of PD they do not appear to have a significant correlation to striatal dopaminergic activity and clinical function to serve as a disease progression or outcome biomarker.

Support: NIH P01 NS015655

1425

NEUROINFLAMMATORY SIGNALING AND P-GLYCOPROTEIN

D. Miller

Laboratory of Toxicology and Pharmacology, NIH/NIEHS, Research Triangle Park, NC, USA

P-Glycoprotein is an ATP-driven drug efflux pump that is highly expressed in the luminal plasma membrane of the brain capillary endothelium. Because of its wide specificity limits and ability to drive active drug efflux, p-glycoprotein is a major obstacle to the delivery of small therapeutic drugs to the CNS. It may also have a neuroprotective function, but that possibility is only just beginning to be explored. Experiments with animal models show that in vivo inflammation causes tissue-specific, time-dependent and signal-specific changes in P-glycoprotein activity and expression. Our in vitro studies with isolated rat brain capillaries have disclosed complex signaling following exposure to the proinflammatory cytokine, TNF-alpha, with short-term exposures (minutes) reducing transport activity without affecting protein expression and long-term exposures (hours to days) increasing both transport activity and expression. In both cases, TNF-alpha signals through TNFR1, endothelin receptors, iNOS and protein kinase C (PKC). Signaling bifurcates at PKC. TNF exposure activates both PKCbeta1 and PKCbeta2, with the former signaling rapid loss of transporter activity and the latter signaling increased expression. Our recent work has focused on the PKCbeta1 pathway. When PKCbeta1 is activated in brain capillaries it rapidly signals to P-glycoprotein through a sphingosine-1-phosphate pathway coupled to a protein phosphorylation cascade. The latter involves activation of pathways containing PI3-kinase, Akt and p38 MAPK. Using in situ brain perfusion in rats we have validated key elements of the PKCbeta1 pathway in vivo. Detailed mapping of the PKCbeta1 pathway has the potential to provide pharmacological tools to transiently reduce P-glycoprotein activity and thus improve CNS pharmacotherapy without compromising neuroprotection.

1427

ISCHEMIC BRAIN DAMAGE, TISSUE SODIUM CONCENTRATION AND PERFUSION DEFICIT

F. Boada[1], E. Nemoto[2], Y. Qian[1], C. Tanase[1], C. Jungreis[3], J. Weimer[1], V. Lee[1]

[1]Radiology, University of Pittsburgh, Pittsburgh, PA, [2]Neurosurgery, University of New Mexico, Albuquerque, NM, [3]Radiology, Temple University School of Medicine, Philadelphia, PA, USA

Introduction: The outcome of reperfusion and/or recannalization therapies is dependent on the physiologic status of the ischemic tissue. It has been demonstrated previously that reperfusion of non-viable ischemic tissue can lead to hemorrhage or the development of edema. Unfortunately, we currently lack tools for the prospective determining which patients could benefit from reperfusion/recannalization therapies because the viability of the tissue at risk cannot be determined using the standard neuroimaging tools. Tissue sodium concentration (TSC) has been shown to increase in a linear fashion as the duration of ischemia increases. Moreover, reports suggest that once the TSC exceeds a threshold of about 65mM irreversible tissue damage (ITD) is likely to have taken place. Because of the coupling between energy metabolism and sodium-potassium-ATPase, however, the time at which this threshold is reached is likely to depend on the underlying perfusion deficit. In this paper, we explore the relationship between TSC increase and perfusion deficit in a non-human primate (NHP) model of reversible focal ischemia. Our results support the belief that the threshold for ITD is perfusion dependent.

Methods: Reversible focal ischemia was induced on pigtail monkeys (N=5) using an endovascular approach to block the middle cerebral artery. After ischemia was established, and verified by fluoroscopic means, the animals were quickly transported to the MRI suite where serial angiographic (MRA), sodium (TSC), diffusion (ADC) and perfusion (PWI) MRI was performed continuously for 6hrs. All images were collected on a clinical 3 Tesla scanner (Siemens Medical Systems, Erlangen, Germany) using commercial-grade pediatric imaging coils that were modified for this purpose (Advanced Imaging Research, Inc, Cleveland, Ohio). The balloon was removed at 3 hours post ischemia and imaging continued until the animal was sacrificed under general anesthesia. Harvested brains were perfused, stained for infarction using inmunohistochemistry (MAP2) and digitized for pixel-by-pixel image analysis.

Results: The MAP2 images were used to delineate the area of infarction. The contours from the infracted area were then used to identify the volume of non-viable tissue prior to reperfusion on the TSC, PWI and ADC images. Pixel-wise correlations on the volume of non-viable tissue for the TSC and PWI images were performed to study the relationship between the rate of TSC increase and the perfusion deficit. In addition, a histogram analysis of this volume was performed on the TSC images to determine the mean TSC of the non-viable tissue. These data demonstrated that the non-viable tissue had a median of 60mM and that within this tissue the TSC slope correlated with the perfusion deficit.

Conclusions: Our data support the hypothesis that ischemic tissue with elevated TSC (>65mM) carries an increased risk of infarction after tissue reperfusion. Additionally, the rate of TSC increase appears to depend on the perfusion deficit of the tissue and, therefore, the time at which ITD is reached could vary from individual to individual. As a consequence, TSC might be a useful parameter to predict low-risk reperfusion treatment windows on a subject-by-subject basis.

1428

EFFECTS OF OXYGEN-GLUCOSE DEPRIVATION (OGD) AND REOXYGENATION (REOX) ON NA^+/H^+ EXCHANGER ISOFORM 1 (NHE-1) ACTIVITY IN HIPPOCAMPAL REACTIVE ASTROCYTES

P. Cengiz[1], P. Kendigelen[1], D. Kintner[2,3], G. Begum[3], E. Akture[1], P. Ferrazzano[1,3], D. Sun[2,3]

[1]Pediatrics, [2]Neurological Surgery, University of Wisconsin-Madison, [3]Waisman Center, Madison, WI, USA

Background: Hypoxia ischemia (HI) is a common cause of brain injury in neonates. One hallmark characteristic of HI in neonates is selective hippocampal injury. Mechanisms underlying ischemic hippocampal neuronal injury and subsequent long term deficits in learning and memory are not exactly understood. Hippocampal astrocytes respond to HI by developing reactive astrogliosis. During this process, up-regulation of glial fibrillary acid protein (GFAP) expression, astrocyte hypertrophy, and astrocyte proliferation are seen. NHE-1 was dramatically increased in the hippocampal $GFAP^+$ reactive astrocytes at 3 days after neonatal HI[1]. Moreover, inhibition of NHE-1 with its selective and potent inhibitor HOE 642 decreased CA1 pyramidal neurodegeneration and improved motor and spatial learning. Inhibition of NHE-1 may offer neuroprotection in part via blocking NHE-1 activity in reactive astrocytes. We hypothesize that up-regulation of NHE-1 in hippocampal reactive astrocytes contributes to hippocampal pyramidal neurodegeneration after HI via changing the intracellular pH.

Methods: Hippocampal astrocyte cultures are prepared from postnatal day 4 Black6/C57 mouse hippocampus (>99% astrocytes). OGD is induced by incubating cells with a bicarbonate-buffered OGD solution (pH_o 7.4) at 37°C in a hypoxic incubator for 2 hours, maintained at 94% N_2, 1 % O_2, plus 5% CO_2. In REOX studies, the OGD solution is replaced with the normoxic control solution and the cells placed in a normoxic incubator under atmospheric conditions plus 5% CO_2 at 37°C. Cells grown on cover slips are incubated with 1.0 mM BCECF-AM, a H^+-sensitive dye. Live cell imaging is performed using the Nikon TiE inverted epifluorescence microscope as described previously. After 2 hours (h) of OGD and 1-5 h of REOX, hippocampal astrocytes are undergone immunohistochemical staining to identify GFAP and NHE-1 expressions. Intracellular pH is measured in $GFAP^+$ astrocytes after 2 h of OGD, 1-5 h of REOX. In HOE studies, 1 μM HOE 642 is added to the media during OGD and REOX in order to establish the effect of NHE-1 inhibition pharmacologically.

Results: Stimulation of NHE-1 resulted in H^+ efflux from hippocampal astrocytes, which coincided with a sustained intracellular alkalosis between 0-1 h REOX following 2 h OGD. Addition of HOE 642, resulted in less intracellular alkalosis. Moreover, we observed that exposure of hippocampal astrocytes to OGD led to a significant transient elevation of NHE-1 protein expression with a peak level at 5 h of REOX after 2 h OGD.

Conclusions: We concluded that HI causes overstimulation and up-regulation of NHE-1 increasing its function in hippocampal reactive astrocytes after OGD and REOX. This may result in intracellular alkalosis and disruption of ionic homeostasis contributing to the damage of pyramidal neurons in the hippocampus by activation of Na^+-Ca^{+2} exchanger, subsequent increase in intracellular Ca^{+2} and release of gliotransmitters.

References: 1. Cengiz P, et al. Antioxid Redox Signal. 2010 Dec 4. [Epub ahead of print].

Acknowledgement: This work was supported University of Wisconsin Department of Pediatrics

Research & Development Grant (Cengiz P), 1UL1RR025011 from the ICTR Award program of NCRR and NIH (Ferrazzano P), NIH grants RO1NS38118 and RO1NS48216 (Sun D), NIH grants RO1NS42803 and NIH P30 HD03352 (Waisman Center).

1429

VIRAL INFECTION AND CHRONIC NEURODEGENERATION IN MURINE MODEL OF PRION DISEASE: INFLUENCES OF THE ENVIRONMENTAL ENRICHMENT AND INFLAMMATORY RESPONSE

M.C.P. Turiel[1], L.L. Sobral[1], A.K.G. Martins[1], R.R. Reis[1], L.F. Jesus[1], P.S. Barros[1], J.B. Torres[1], P.F. Da Costa Vasconcelos[2], C.W.P. Diniz[1]

[1]Universidade Federal do Pará, [2]Instituto Evandro Chagas, Belém, Brazil

Prion diseases have been used as a model for chronic neurodegeneration studies and peripheral infections to aggravate disease progression. We previously tested the hypothesis that environmental enrichment leads to less CNS neuroinvasion and/or more rapid viral clearance in association with T cells without neuronal damage. The results suggested that an enriched environment has a profound effect of the rate of clearance of virus and or neuroinvasion in a non-lethal encephalitis and promotes a more effective immune response not at the cost of CNS damage. In the present report we tested the hypothesis that environmental enrichment may reduce behavioral changes and inflammatory response induced by prion agent ME7 intracerebral infection aggravated by arbovirus inoculation in murine model. Stereology-based estimates of activated microglia in the septal region were correlated with behavioral changes in 6 different experimental groups infected or not infected by prion agent and arbovirus Piry and maintained in either impoverished or enriched environments. Two-month-old female mice maintained in impoverished (IE) or enriched environments (EE) for 3 months were behaviorally tested for open field and burrrowing. After these tests, an equal volume of either normal (NBH) or infected brain (ME7) homogenates were inoculated in the striatum. 17 weeks after inoculation two experimental groups (ME7PiryEE and ME7PiryIE) received into nostrils an equal volume of 10^{-6} suspension of arbovirus Piry infected brain homogenate whereas the other experimental groups (ME7EE and ME7IE, NBHEE and NBHIE) received an equal volume of uninfected brain homogenate. Eight days post-instillation (dpi) all animals were behavioral tested again and sacrificed. Brains were fixed and processed to detect activated microglia, viral antigens, astrocytes and PrPsc by histochemistry or immunohistochemical reactions. Stereological estimations of microglia revealed a higher number of cells in ME7PyIE (59056±7322) followed by ME7IE (37746±8523) as compared to the other groups (OneWay ANOVA $p< 0.05$). The level of microglial activation in the ME7PyEE (20039±5768) was very much similar to the NBHEE (20053±6302), $p>0.05$. Open field and burrowing were significantly altered. As compared to the baseline ME7PyIE and ME7IE presented significant reduction in distance travelled at 18wpi whereas ME7PyEE and ME7EE did not present open field changes (One-Way ANOVA $P< 0.05$). Taken together the results confirmed as hypothesized that prion agent induced significant microglial activation with typical behavioral changes mostly in IE as compared to EE groups. Central arbovirus infection aggravated the inflammatory response and environmental enrichment seems to reduce it. The molecular mechanism associated to the neuroprotection induced by environmental enrichment remains to be investigated.

1433

EFFECT OF ENRICHED ENVIRONMENT ON PROTEOMIC PROFILING OF CONTRALATERAL CORTEX AFTER FOCAL CEREBRAL ISCHEMIA

X.-L. Hu, P. Dahlqvist, M. Brink, S.-A. Bergström, I. Söderström, T. Olsson

Department of Public Health and Clinical Medicine, Medicine, Umeå University Hospital, Umeå, Sweden

Introduction: Enriched environment (EE), a combination of enhanced social interaction, physical exercise and stimulation of novelty, can strongly influence the structure and function of the adult mammalian brain. Earlier studies have demonstrated that exposing laboratory rats to an enriched environment increase brain weight, cortical thickness, neuron size, number of glial cells, dendritic spines, synapses, neurogenesis and long term potentiation [1]. We and others have shown that housing rats in an enriched environment result in better performance in several behavioral tests, including improved sensorimotor and cognitive function in naive rats [2] and after brain lesions including ischemic stroke [3,4]. The molecular mechanisms behind the EE-induced functional and structural brain plasticity are largely unknown.

Aims of study: The current study aims to investigate the effect of EE on changes in protein expression in the contralateral motor cortex two weeks after experimental stroke in rats.

Material and methods: Sven-eight weeks old male Sprague-Dawley rats were subjected to middle cerebral artery occlusion (MCAo) by using modified suture model. Two days after MCAo, rats with sustained hemiparesis were randomized to either EE (n=10) or deprived environment (DE) (n=10). Protein isolation was performed at 14 days after ischemia. Protein samples were labeled with Cy 3 and Cy5 and analyzed with two-dimensional differential in-gel analysis (2D-DIGE). The interesting protein-spots were identified by MALDI-ToF mass spectrometry and further confirmed by western blots.

Results:

Analysis with 2D-DIGE revealed 9 protein-spots differentially expressed in the contralateral motor cortex between rats housed in enriched environment or deprived environment. Among these nine proteins, six showed increased expression (22-56%) and three showed decreased expression (21-125%) in enriched environment rats compared with deprived environment rats ($p < 0.05$). Protein Enriched in Astrocytes of

15 kDa (PEA-15) was the protein with most significant change (fold change -2,25, $p = 0.00033$). The ongoing experiment is to confirm the proteomics findings by western blot.

Conclusion:

The present study revealed new insights into the molecular changes taking place in the brain of rats, which successfully recovered after focal cerebral ischemia in an enriched environment. We suggested a putative role for PEA-15 in brain plasticity. The roles for these proteins in brain plasticity need further characterization and may lead to possible future applications in clinical stroke rehabilitation.

References:

1. M.C. Diamond, Response

of the brain to enrichment, An Acad Bras Cienc, 73 (2001) 211-20.

2. H. van Praag, G. Kempermann and F.H. Gage, Neural consequences of environmental enrichment, Nat Rev Neurosci, 1 (2000) 191-8.

3. B.B. Johansson and P.V. Belichenko, Neuronal plasticity and dendritic spines:

effect of environmental enrichment on intact and postischemic rat brain, J

Cereb Blood Flow Metab, 22 (2002) 89-96

4. P. Dahlqvist, A. Ronnback, S.A. Bergstrom, I. Soderstrom and T. Olsson, Environmental enrichment reverses learning impairment in the Morris water maze after focal cerebral ischemia in rats, Eur J Neurosci, 19 (2004) 2288-98.

1434

INTRAVENOUS GRAFTS OF AMNIOTIC FLUID-DERIVED NEURAL PROGENITOR CELLS INDUCE ENDOGENOUS CELL PROLIFERATION AND AMELIORATE BEHAVIORAL DEFICITS IN ISCHEMIC STROKE RATS

N. Tajiri[1], S. Acosta[1], S. Yu[1], P.C. Bickford[1], A. Solomita[2], I. Antonucci[2], L. Stuppia[2], Y. Kaneko[1], C.V. Borlongan[1]

[1]University of South Florida, Tampa, FL, USA, [2]Department of Biomedical Sciences, G. d'Annunzio University, Chieti-Pescara, Italy

Introduction: We recently reported isolation of viable neural progenitor cells from rat amniotic fluid (Antonucci et al., Cell Transplant., 2010).

Objective: Here, we tested the therapeutic benefits of amniotic fluid-derived neural progenitor cells in a rodent of model of ischemic stroke.

Methods: Adult, male Sprague-Dawley rats (about 8 weeks old at study initiation and weighing ~250g) were initially trained in the cognitive task, Morris water maze. Only those animals (n=16 from original 20 rats) reaching the learning criteria (e.g., ability to reach the hidden platform in less than 30 sec) were subsequently tested in motor tasks (elevated body swing test, rotorod test) and neurologic test, which further confirmed that these animal subjects were exhibiting normal behaviors (i.e., 50% swing activity to both left and right directions, ability to stay on rotating rod for at least 60 sec, and a neurologic mean score of close to zero based on a battery of somatosensory tests). These animals then received a one-hour occlusion of the middle cerebral artery followed by reperfusion, which was verified by laser Doppler and with routine physiologic parameters (e.g., blood gases) validating a homogenous stroke subject population. At 5 weeks post-stroke, animals that showed significant cognitive, motor, and neurologic deficits (n=14) subsequently received intravenous transplants of rat amniotic fluid-derived neural progenitor cells (1 million viable cells in 1 ml of sterile saline; n=7) or vehicle (equivalent volume of saline; n=7) delivered over a period of 1 minute. At about one month after transplantation, animals were subjected again to the same behavioral tests then euthanized for immunohistochemical evaluation of brain pathology.

Results: Statistical analyses revealed significant recovery of cognitive, motor and neurologic function in stroke animals that received the amniotic fluid-derived neural progenitor cells compared to vehicle-infused stroke animals ($p's < 0.05$). Although the hematoxylin and eosin staining revealed no significant differences in the infarcted core areas between the two stroke groups, the cell proliferation marker, Ki67, demonstrated at least a two-fold increase in Ki67-positive cells along the subventricular zone of the stroke animals that received the amniotic fluid-derived neural progenitor cells compared to those that received the vehicle infusion. Moreover, there was also a corresponding increase in cells immunostained with Ki67 and doubled labeled with the migratory neural immature marker doublecortin. This increased cell proliferation along a neural fate occurred despite very few surviving grafts of amniotic fluid-derived neural progenitor cells. Parallel ELISA and gene microarray analyses revealed significant upregulation of the chemokine receptor for stromal cell-derived factor-1, CXCR4, and the vascular endothelial growth factor (VEGF), implicated in cell migration and cell proliferation, respectively.

Conclusion: This study reports the therapeutic potential of amniotic fluid-derived neural progenitor cells in stroke animals, characterized by attenuation of stroke-induced behavioral

deficits, possibly via enhancement of endogenous repair mechanisms. Such allogeneic transplantation and minimally invasive intravenous route of cell administration have direct clinical applications.

Disclaimer: CVB has patent applications relating to the use of amnion tissue and fluid for cell therapy.

1435

COMPARISON OF MAGNETIC RESONANCE IMAGING (MRI) AND HISTOPATHOLOGY IN A RABBIT STROKE MODEL

A. Brown[1], J. Meek[1], L. Hennings[2], J. Lowery[3], M.D. Amerson[1], J. Hatton[1], S. Woods[1], W.C. Culp[1]

[1]Radiology, [2]Pathology, [3]Laboratory Animal Medicine, University of Arkansas for Medical Sciences, Little Rock, AR, USA

Objectives: A method for evaluating infarct areas in an animal model of embolic stroke is needed for progressive non-invasive evaluation of infarct areas. We describe techniques for comparing progressive magnetic resonance imaging (MRI) in the rabbit model of embolic stroke and comparing infarct incidence, location and size to histology.

Methods: Infarct was induced by direct delivery of insoluble embolic spheres in three mature New Zealand White rabbits by angiographical deposition of spheres in the middle cerebral artery (MCA). Animals first received baseline 3T MRI scan series (Day 0) then were followed longitudinally and scanned at four additional times (Days 1, 20, 50 and 79) and were analyzed for change in infarct location and size. Animals were sacrificed at Day 80 followed by a 7T MRI T1 Flash and T2 weighted scans post mortem.

Results: Results from two non-operative shams were used to establish normal rabbit brain MRI series in both 3T and 7T MRI. Scans were followed longitudinally and analyzed for change in infarct location and size. For detecting infarcts diffusion the 7T MRI T2 weighted series best approximated infarct incidence, location and size compared to 2,3,5-triphenyltetrazolium chloride (TTC) staining. Neurological assessments remained constant throughout the later time points.

Conclusions: Rabbit MCA embolic occlusive models can be documented by real-time MRI scanning and can be used to reliably demonstrate changes in infarct size prior to sacrifice. This provides a useful means of evaluating induced ischemic stroke similar to clinical stroke.

References:

Brown AT, Flores R, Hamilton E, Roberson PK, Borrelli MJ, Culp WC. Microbubbles improve sonothrombolysis in vitro and decrease hemorrhage in vivo in a rabbit stroke model. Investigative Radiology 2011;46(3):In Press.

Brown AT, Skinner RD, Flores R, Hennings L, Borrelli M, Lowery J, Culp WC. Stroke Location and Brain Function in an Embolic Rabbit Stroke Model. Journal of Vascular Interventional Radiology 2010;21:903-9.

1436

KINETIC MODELING OF [^{11}C]4DST PET IMAGING DNA SYNTHESIS RATE: INITIAL CLINICAL TRIALS IN BRAIN TUMORS

M. Sakata[1], J. Toyohara[1], T. Nariai[2], K. Oda[1], K. Ishii[1], T. Kawabe[3], K. Kubota[4], K. Ishiwata[1]

[1]Positron Medical Center, Tokyo Metropolitan Institute of Gerontology, [2]Department of Neurosurgery, Tokyo Medical and Dental University, Tokyo, [3]Department of Neurosurgery, Katsuta Hospital Mito Gamma House, Ibaraki, [4]Department of Radiology, National Center for Global Health and Medicine, Tokyo, Japan

Objectives: It is well known uncontrolled cell proliferation is one of the hallmarks to characterize tumor phenotypes and measuring DNA synthesis rate with [^{3}H]thymidine was used as a gold standard for characterizing cell proliferation. Therefore, measuring the DNA synthesis rate of tumor tissues is considered to be an ultimate goal of tumor diagnosis, and in line with this theory, much efforts have been paid to develop the radiotracers for *in vivo* imaging of DNA synthesis rate. Recently, we developed [methyl-^{11}C]4'-thiothymidine ([^{11}C]4DST) as an ideal DNA synthesis marker.[1] This compound certainly has a potential to visualize *in vivo* DNA synthesis status in rodent.[2] This study shows the initial clinical trial of the [^{11}C]4DST PET in the brain tumors and the kinetic analysis.

Methods: Dynamic [^{11}C]4DST PET scans with arterial blood samplings and the metabolite analyses were performed in five patients with brain tumors (48 ± 5 years old; two astrocytoma grade 3, one oligodendroglioma grade3, one *metastatic brain tumor from lung cancer*, and one malignant lymphoma). The injected dose was 710 ± 108 MBq and the specific activity was 273 ± 121 MBq/nmol. [^{11}C]methionine ([^{11}C]MET) PET scan was also performed within 3 weeks prior to [^{11}C]4DST scan. Gadolinium-enhanced MRI was used for confirmation of breakdown of the blood-brain barrier. ROI-averaged time-activity curves (TACs) of tumor and normal brain regions were analyzed using Patlak plot graphical analysis (t* = 10 min) and the two-tissue compartmental model (2T model) analysis. Parametric images of the uptake rate (K_i) were also calculated using the Patlak plot.

Results: [^{11}C]4DST showed little uptake in the normal brain regions, resulting in low background for imaging of brain tumors. TACs in tumor regions were rapidly increased, and they were reaching plateau according to the decrease of the input function (Fig. 1). Patlak plots showed a linear increase, and the K_is of clinically aggressive tumor regions (0.02-0.05) were higher than those of normal regions (~ 0.01) and clinically stable tumor regions (~ 0.01). The distribution pattern of [^{11}C]4DST was not always identical to that of [^{11}C]MET. Particularly, the [^{11}C]4DST image of the patient whose tumor was successfully controlled by chemotherapy did not show obvious uptake at the region where the high accumulation of [^{11}C]MET was observed (as shown in Fig. 2, right). Although we have not determined the kinetic model because of the limited sample size, the estimated k_4 (≤ 0.01) in 2T model was much lower than the k_3 (> 0.07) in tumor regions.

Conclusions: [^{11}C]4DST was suggested to be a feasible and irreversible tracer for imaging brain tumors.

References :

1. Toyohara J, et al. *J Nucl Med* 2006;47:1717-22.

2. Toyohara J, et al. *Nucl Med Biol* 2008;36:67-74.

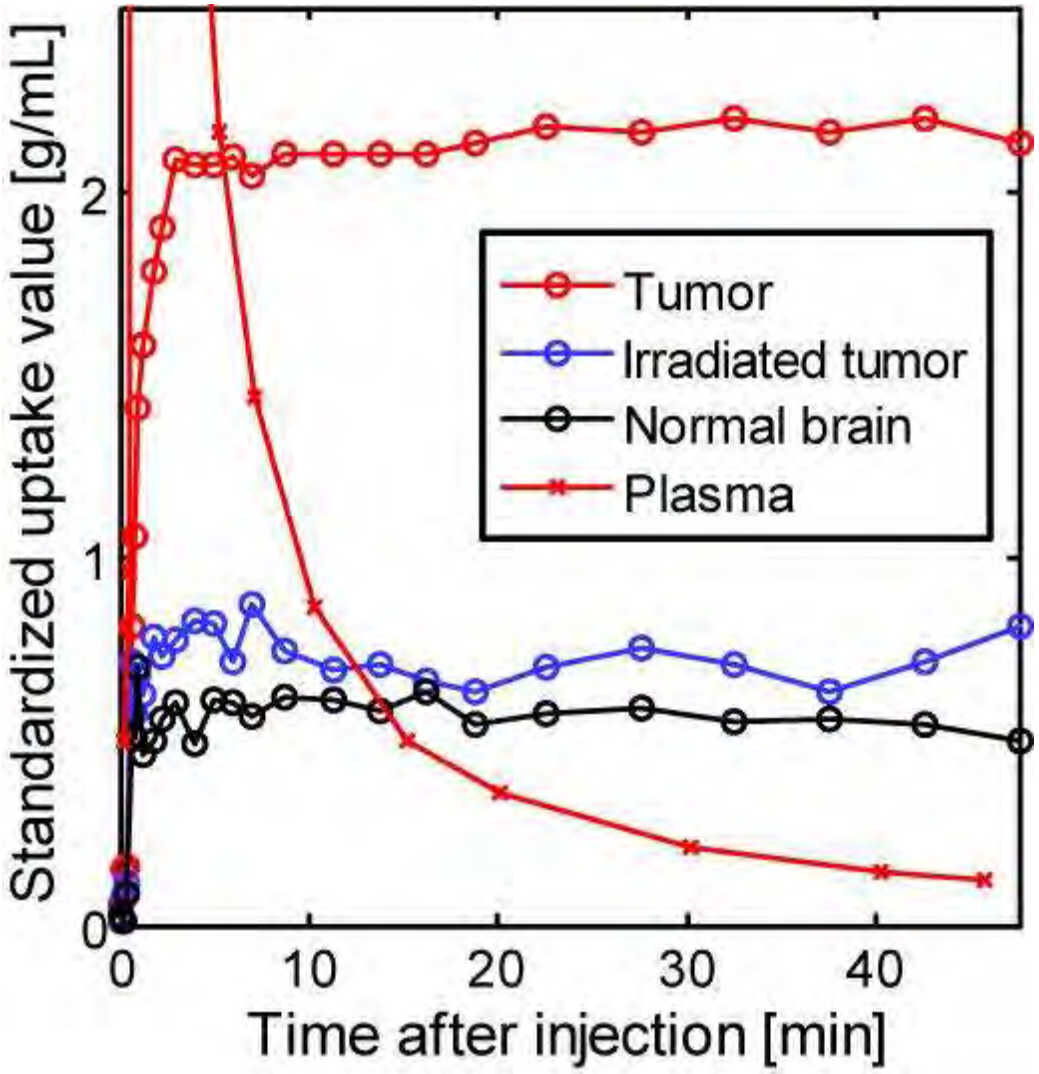

[[11C]4DST TACs]

Figure 1: Typical time activity curves of [^{11}C]4DST.

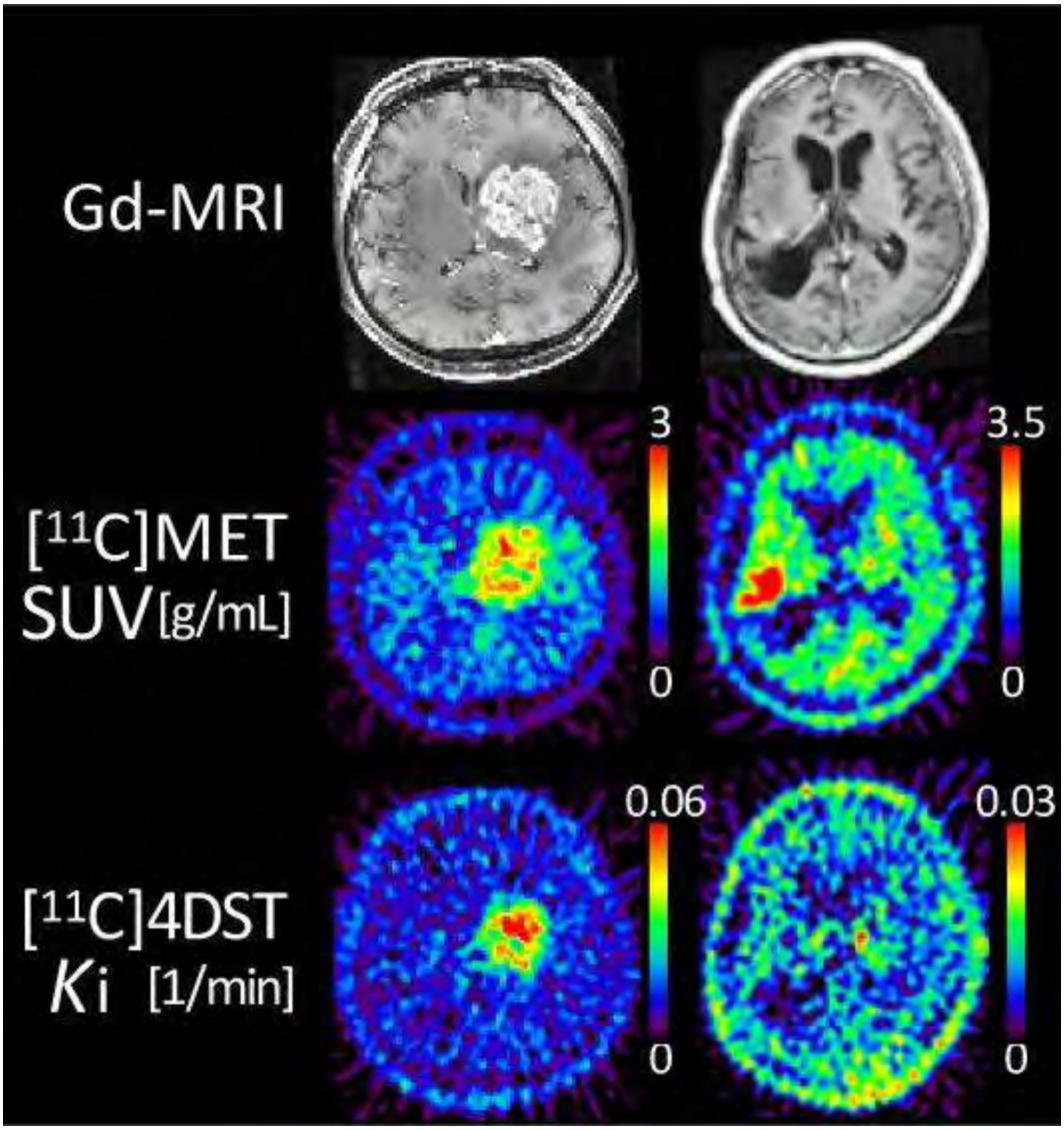

[Images]

Figure 2: Sample images of two patients with oligodendroglioma (left) and astrocytoma (right).

1437

EXPRESSION OF V_{1A} RECEPTORS IN CEREBRAL BLOOD VESSELS INCREASES AFTER SUBARACHNOID HAEMORRHAGE AND CORRELATES WITH THE SEVERITY OF ACUTE VASOSPASM

K. Rosmanowska[1], A. Oniszczuk[1], R. Michalik[1], R. Gadamski[2], P. Piotrowski[2], R. Wojda[2], J. Rafałowska[2], **E. Koźniewska**[1]

[1]Laboratory of Experimental Neurosurgery, Department of Neurosurgery, [2]Department of Experimental and Clinical Neuropathology, Mossakowski Medical Research Centre PAS, Warsaw, Poland

Objectives: Concentration of vasopressin has been reported to increase in the blood and in the cerebrospinal fluid during intracranial hypertension in acute phase after subarachnoid haemorrhage (SAH). The main recognized targets of vasopressin are vascular V_{1a} and renal V_2 receptors. Acting on V_{1a} receptor, vasopressin constricts blood vessels and stimulates vascular smooth muscle cells proliferation. The participation of this peptide in cerebral blood vessels constriction observed after SAH is not fully elucidated. Our study aimed to investigate the correlation of dynamics of the expression of V_{1a} receptors mRNA and the degree of constriction of the middle cerebral (MCA) and basilar (BA) artery of the rat subjected to subarachnoid hemorrhage (SAH).

Methods: The experiments were performed on 60 adult, male Sprague-Dawley rats according to the protocol approved by the Local Ethical Committee. SAH was induced by the puncture of the bifurcation of the intracranial portion of the right internal carotid artery. The severity of SAH was assessed by monitoring cerebral cortical microcirculation with laser Doppler flowmeter. Right MCA and BA were harvested from 36 animals 24, 48 and 72 hours after SAH, immediately frozen and stored at -80°C. At the same time points brains of the remaining 24 rats were isolated and fixed in 10% formaldehyde solution. The frozen arteries served as material for V_{1a} receptors mRNA studies using rtPCR. The formaldehyde fixed brains were cut to obtain the sections containing right MCA and BA, stained with orcein and studied with the light microscope The degree of vasospasm was assessed based on the corrugation of the internal elastic lamina (IEL). It was expressed as a ratio of the total length of IEL to its internal circumference.

Results: The increased expression of V_{1a} receptor gene was observed in both MCA and BA already 24 hours following SAH but only in animals which had smaller bleeding (more efficient acute vasospasm) after SAH (decrease of microflow in cerebral cortex by 70% for about 15 min). In the case of the ruptured vessel (right MCA) the increase of V_{1a} receptor mRNA amounted to 98% ($p< 0.05$ vs. sham) at 24 hours and was maintained at about that level during 48 and 72 hours after SAH. The increase of V_{1a} receptor mRNA in the BA was smaller than in the MCA at 24 and 46 hours after SAH (60% and 33%, respectively) but did not differ at 72 hours. The index of corrugation of IEL was larger in the MCA and BA after the small than the large bleeding . This index was increasing with time after SAH but the decrease of the diameter of the MCA and BA at 72 hours did not exceed 30% of control.

Conclusion: Our results strongly suggest that vasopressin and V_{1a} receptors participate in the acute vasospasm after SAH. They also suggest that vasopressin may potentially play a role in the development of the late vasospasm.

1438

IMPROVED ESTIMATES OF AUTOREGULATION FROM SPONTANEOUS VARIATIONS IN BLOOD FLOW AND PRESSURE

D. Simpson, N. Angarita-Jaimes, H. Kouchakpour, R. Allen

ISVR, University of Southampton, Southampton, UK

Objectives: The relatively small spontaneous variations in arterial blood pressure excite the autoregulatory system, and this has been extensively exploited to quantify autoregulation, with minimal interference with the patient. In the current work, we test different parameters to quantify autoregulation from such data, and recommend methods that provide improved distinction between functioning and impaired cerebral haemodynamic control.

Methods: In 13 healthy adult subjects at rest and supine, arterial blood pressure (ABP - from Finapres), blood flow velocity (BFV - from Trancranial Doppler in the middle cerebral artery) and respiratory pCO2 were simultaneously acquired for approximately five minutes. Recordings were repeated with subjects inhaling 5% CO2 in air, to provoke hypercapnia and hence impairment of autoregulation. Signal quality was visually checked, and beat-averaged values of ABP and BFV calculated. End-tidal values of pCO2 (et-CO2) were calculated for each breathing cycle. Different mathematical models with ABP as input and BFV as output were estimated, and in some cases etCO2 was used as a second input. Both linear (FIR filter) and quadratic models (Wiener Laguerre) were tested. Autoregulation parameters were extracted from the models according to methods previously used (phase, ARI, Mx, coherence, step-response), as well as the response to a smoothed pulse in ABP (centred at 0.1 Hz). The autoregulation parameters were compared based on the standard deviation (across the 13 subjects) relative to the mean difference between normocapnia and hypercapnia, the average intra-subject variability (estimation errors calculated from theory and Monte Carlo simulation), and the fraction of subjects where degraded autoregulation was evident during hypercapnia.

Results: Many conventional parameters used extensively in previous work were clearly not optimal in terms of distinguishing between normal and impaired autoregulation, in these relatively short recordings. Large differences in intra-subject variability of parameters between individual recordings were evident. As expected, higher-order, non-linear and bivariate models fitted the training data well, but generalized poorly to the validation data. In spite of this, they provided a good measure of autoregulation, when assessed using the band-limited pulse. The simplest (1^{st} order FIR filter) gave a poor fit to both training and test data, but was among the best in distinguishing between normal and impaired autoregulation.

Conclusions: Considering both simplicity and performance, this latter method is recommended, overall. The results show clearly that in choosing an autoregulation parameter based on a mathematical model of the pressure-flow relationship during spontaneous variations in the signals, model fit to the data should not be the overriding concern; adding etCO2 also gave only minor improvements. Furthermore, large differences in standard deviation of autoregulation parameter estimates from different recordings were observed, confirming the need to provide confidence limits in the estimates, as used here. The methods recommended provide clear improvements in distinguishing between normal and impaired autoregulation compared to the most established parameters, but still, robustly inferring autoregulation from individual recordings with only spontaneous variability remains an on-going challenge.

Acknowledgements: to Drs. Stephanie Foster and Lingke Fan, and Prof. David Evans (Leicester Royal Infirmary) for anonymized data, and Innovation China UK for funding.

1439

MATRIX METALLOPROTEINASE-2/9 MEDIATE BLOOD BRAIN BARRIER DAMAGE IN THE HYPERACUTE PHASE OF CEREBRAL ISCHEMIA IN RATS

X. Jin, K.J. Liu, J. Liu, **W. Liu**

College of Pharmacy, University of New Mexico, Albuquerque, NM, USA

Disruption of the blood brain barrier (BBB) is an antecedent event to intracerebral hemorrhage (ICH) in ischemic stroke. Interestingly, our previous studies showed that tPA-induced ICH invariably occurred in subcortical areas and in the piroform cortex, where we also observed BBB disruption as a much earlier stroke stage. In the present study, we sought to determine whether severe BBB damage occurs in the hyperacute stroke stage relevant to acute thrombolytic therapy and whether matrix metalloproteinase (MMP)-2 and 9 contribute to this BBB damage. Rats were subjected to 1, 2 or 3 hrs filament occlusion of the middle cerebral artery (MCAO), followed by 10 min reperfusion. Successful MCAO was confirmed by 2,3,5-triphenyltetrazolium chloride (TTC) staining. Fluorescent tracer fluorescein isothiocyanate-dextran (FITC-dextran) was injected to observe severe BBB damage, and MMP-2/9 were measured by in situ and gelatin gel zymography. Extravsation of FITC-dextran was seen in brain sections after 2 hrs MCAO, with the tracer leakage limited to subcortical regions and the piroform cortex, indicating hyperacute BBB damage in these brain regions. Interestingly, TTC stain showed that this hyperacute BBB damage was not necessarily occurred in brain regions with neuronal cell death, reflected by positive staining for Fluoro-Jade B. With the prolongation of ischemia duration to 3 hrs, FITC-dextran leakage was spread to the other MCAO territories including ischemic cortex. Rats subjected to 1-hr MCAO did not show any FITC-dextran leakage. Paralleling to BBB damage, MMP-2/9 were significantly increased in the ischemic brain after 2 and 3 hrs, but not 1 hr, of MCAO. Moreover, in situ zymography demonstrated the colocalization of increased MMP-2/9 activities with FITC-dextran extravasation. Pretreatment of rats with MMP inhibitor GM6001 (30 mg/kg body weight, ia, 10 min before MCAO) drastically reduced FITC-dextran leakage, but did not reduce tissue infarction. Taken together, BBB damage occurs in the hyperacute stroke stage relevant to acute thrombolytic therapy, and MMP-2/9 critically contributes to this early ischemia-induced BBB disruption. MMP inhibition may be an important strategy to preserve BBB integrity in the hyperacute phase of stroke, though it alone may not interrupt the evolution of tissue infarction.

1442

ABSOLUTE REGIONAL PERFUSION MEASURED WITH ARTERIAL SPIN LABELING CALIBRATED USING PHASE CONTRAST MRI

N. Alperin[1], C. Wright[2], A. Bagci[2]

[1]University of Miami, [2]School of Medicine, University of Miami, Miami, FL, USA

Objectives: Arterial spin labeling (ASL) uses water in the blood as an endogenous contrast to assess cerebral blood perfusion (CBF). However, absolute values of CBF obtained using ASL depend on the type of ASL technique, the imaging parameters, and influenced by the subject's hemodynamics. We have developed a method to calibrate CBF measurements using an independent measurement of the total cerebral blood flow (tCBF) with velocity encoding MRI. The method performance was assessed by comparing CBF values in deep gray matter and cerebral cortex regions obtained with calibrated and with non-calibrated ASL in healthy subjects and subjects with cognitive impairment.

Methods: MRI scans of 5 healthy subjects (2M:3F, age 24-44) and 5 patients with cognitive impairment (3M:2F, age 56-82) were acquired with a 3T Siemens scanner. Scans included whole brain 2D-ASL, cine phase contrast (PC), T1-weighted MPRAGE, and 2D TOF MRA. The correspondence between the ASL images and the T1-weighted images was obtained by registration of T1- weighted to the reference EPI through a rigid body transformation. The T1-weighted image was parcellated using the subcortical segmentation routine in FreeSurfer. The CBF values for seven gray matter regions produced by this parcellation were obtained by integrating the perfusion values provided by ASL over all voxels that fall within each region. Total cerebral blood flow was obtained by summation of the arterial inflow through the two internal carotids and vertebral arteries. A calibration factor was then calculated using the tCBF and whole brain ASL based CBF. A mask containing the major arteries was created using the MRA data and was used to exclude labeled blood that has not perfused into the brain for the calculation of the absolute CBF in deep gray matter regions.

Results: The mean CBF values obtained for each deep gray matter structure and cerebral cortex is provided for healthy and patient groups, along with the calibrated mean CBF values with PCMRI in Fig. 1. Calibrated CBF values were significantly higher than uncalibrated CBF values for all investigated structures for both groups ($p < 0.05$). It was also observed that the mean CBF in most regions including the cerebral cortex is lower in the elderly patients than the younger healthy subjects, consistent with previous literature reports]. The mean (SD) CBF value in hippocampus for healthy subjects before and after calibration was 40.3 (7.5) and 66.2 (8.2) mL/min/100g, respectively where the calibrated value is in agreement with recently reported values. Similarly, the mean (SD) CBF value averaged over the thalamus, putamen, and caudate for healthy controls before and after calibration was 33.8 (10.5) and 55.1 (13.3) mL/min/100g respectively where the calibrated value is closer to the reported values.

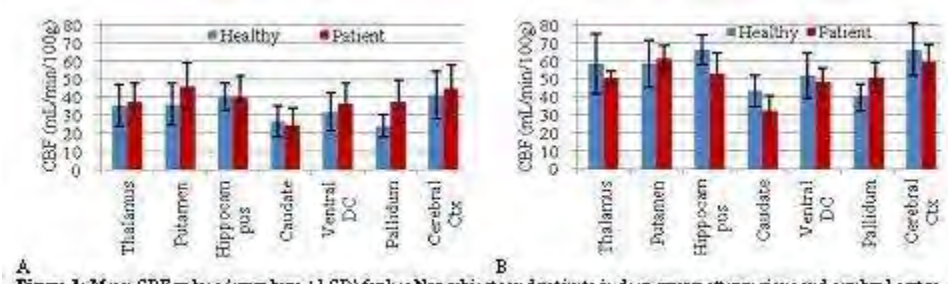

Figure 1: Mean CBF values (error bars ±1 SD) for healthy subjects and patients in deep gray matter regions and cerebral cortex before (A) and after calibration (B).

[CBF values using non-calibrated vs. calibrated ASL]

Conclusions: PCMRI calibrated regional CBF values are more consistent with previously reported values compared with CBF values derived by ASL alone. CBF measurements using ASL in combination with PCMRI may help overcome the limitations of ASL in providing reliable absolute CBF values.

1443

INFLUENCE OF EXERCISE ON RECEPTIVE FIELDS AND ASTROCYTE NUMBERS IN THE HINDPAW CORTICAL REPRESENTATION OF SENILE RATS: AN ELECTROPHYSIOLOGICAL AND STEREOLOGICAL STUDY

R.P. Borges[1], L.C. Viana[1], M.A. Oliveira[1], T.T. Cardoso[1], I.N.F. Almeida[1], D.G. Diniz[1], J.B.T. Neto[1], C.W.P. Diniz[1], A. Pereira[1], M. Batista-de-Oliveira[2], R. Abadie-Guedes[2], A. Amancio dos Santos[2], D.S. Lima[2], R.C.A. Guedes[2]

[1]Lab of Neurodegeneration and Infection, Universidade Federal do Pará, Belém, [2]Department of Nutrition, Universidade Federal de Pernambuco, Recife, Brazil

The aim of the present work was to investigate the influence of treadmill exercise on the number of astrocytes on the cortical hindpaw representation on the somatosensory S1 area of senescent rats, as well as its influence on multiunit receptive fields size and hindpaw footprints. Eight Wistar senescent rats, 16-22 months old and housed in standard conditions were submitted to 3 months of 20 min daily exercise in the treadmill (n=4), or left sedentary (n=4). Before and after training sessions all subjects had their footprints collected by placing them to explore an arena, walking on a white paper with black ink on the hindpaws. The footprints were scanned and had their areas measured by using Adobe Photoshop and Image J software. After that, both exercised and sedentary subjects were submitted to electrophysiological recordings in the primary somatosensory cortex, where microelectrodes were placed into the hindpaw representative area. Somatosensory cortical mapping was performed with tactile stimuli consisting of light touches with fine probes and brushes or hair displacement. The correlation between the multiunit receptive field and the recording site allowed the construction of detailed maps of the somatotopic representation of hindpaw on the cortex. After electrophysiological recording subjects were perfused with aldehyde fixatives and had their brains processed for Glial Fibrilary Acidic Protein (GFAP) immunohistochemistry. Serial anatomical reconstructions of the responsive recording sites to hindpaw tactile stimulation were done for each subject in order to place the optical fractionator probes inside the area of interest. Cell counts and total cell numbers were estimated for cortical hindpaw representation area in the supragranular layers of somatosensory cortex by optical fractionator stereological procedure. Parametric statistical analysis was performed and two-tail t-test was used to determine the significance of statistical differences. The number of astrocytes estimated by optical fractionator in the hindpaw representation area of somatosensory cortex was significantly increased in exercised (62652.71±3915.79 S.E.) as compared to sedentary (33414.94 ± 823.35 s.e.m.) group (two tail t-test $p< 0.05$). Significant differences were also found between exercised and sedentary subjects in the multiunit receptive field areas (5513.3±1556.6 vs 7242.3±2578.5 arbitrary units), with smaller receptive fields observed in the exercised group. Measurements of footprint areas also revealed significant difference between exercised (1.97cm^2 ± 0.17) and sedentary groups (2.23cm^2 ± 0.05, two-tailed T-test $p< 0.01$), with smaller footprints on the exercised subjects. Taken together the results suggested a reduction in the age-induced changes in hindpaw somatosensory S1 cortex of exercised senile rats that may be associated to the increase of astrocytes number and neuroprotection.

1444

SENSORIMOTOR MAPPING OF CORTICAL PERFUSION PATTERNS IN NON-ISCHAEMIC BRAINS: AN MR AND CT PERFUSION ANALYSIS

M. Kamran, P. Schweder, J. Byrne

University of Oxford, Oxford, UK

Purpose: The cortical homunculus represents the anatomical organization of the primary motor and sensory cortices. Degrees of topographic representation of cerebral organization reflect complexity of innervation of certain body parts. The sensorimotor cortex is often studied with functional magnetic resonance (fMRI) modalities to locate task specific activation for pre-surgical planning. We analyzed the normal perfusion patterns of primary motor and sensory cortices in 15 non-ischaemic brains using MR and C-arm CT perfusion imaging modalities.

Methods: C-arm CT based perfusion data was acquired using a biplane angiography system (Axiom Artis dBA; Siemens Healthcare, Germany). The imaging protocol included two 8-seconds rotational acquisitions: mask and contrast enhanced runs, each comprising of 400 projection images at 0.5 degree steps. CBV maps were constructed after registration of the two volumes, voxel-by-voxel subtraction, and normalization with an automatically estimated input function. Perfusion weighted imaging data (PWI), T1, T2 and diffusion weighted data was acquired on a 1.5 T Philips Achieva Magnet. PWI data was acquired using T2* weighted gradient echo planar imaging (TR: 2018 ms; TE 44 ms; FOV 248×248 mm; reconstruction matrix 256×256; bandwidth 806 Hz/pixel; SENSE factor 2.1; 15 slices with 4mm slice thickness at 50 time points were acquired following administration of 0.2 mmol/kg at 5 ml/s in the antecubital vein using a power injector) Time-of-flight MR angiograms were obtained to exclude significant abnormalities of arterial patency. Initial processing of PWI data was performed using a deconvolution based software package (NordicNeuroLab, Bergen, Norway). C-arm based CBV maps as well as MR based CBV and CBF maps were aligned onto a stereotactic brain using affine registration. Mean perfusion was calculated across each modality.

Results: Perfusion topography reflected homuncular innervation. Significantly higher CBV and CBF were demonstrated in the face and tongue areas of the motor and sensory cortices. ($p < 0.05$), however not evident with C-arm CT. Variability in perfusion topography was evident in both motor and sensory cortices between subjects.

Conclusions: Perfusion of primary motor and somatosensory cortices demonstrated topographic organization of perfusion patterns with highest perfusion measured in the inferior lateral divisions. This reference atlas can aid in the understanding of motor and sensory neurophysiology as well as aid in the interpretation of functional MRI studies measuring haemodynamic response of these areas.

1445

ANALYSIS OF SIGNAL TO NOISE RATIO USING DYNA-CT AND MR PERFUSION IMAGING: EVIDENCE OF INTER-MODALITY AND CEREBRAL REGIONAL VARIANCE

M. Kamran, P. Schweder, J. Byrne

University of Oxford, Oxford, UK

Purpose: Developments in flat detector technology and high frame rate rotational imaging with C-arm systems allows rapid acquisition of three-dimensional (3D) volumes with contrast resolution comparable to conventional computed tomography (CT). Acquired volumes allow whole brain coverage with a spatial resolution comparable to current CT and MR imaging protocols. Consequently C-arm imaging can be applied to generate soft tissue images of brain parenchyma as well as 3D cerebral angiography, to allow perfusion imaging of the brain. We implemented a novel protocol to estimate cerebral blood volume (CBV) with the C-arm technique. We compared the signal to noise ratios (SNR) of C-arm CBV maps with MR perfusion weighted imaging based calculation of CBV, and cerebral blood flow (CBF).

Methods: C-arm based perfusion data was acquired for 12 patients using a biplane angiography system (Axiom Artis dBA; Siemens Healthcare, Germany). The imaging protocol included two 8-second rotational acquisitions: mask and contrast enhanced runs, each comprising of 400 projection images at 0.5^0 steps. CBV maps were constructed after registration of the two volumes, voxel-by-voxel subtraction, and normalisation with an automatically estimated input function. The reconstruction was performed on a dedicated prototype software (Siemens AG, Healthcare). Perfusion weighted imaging data (PWI), T1, T2 and diffusion weighted data was acquired for the same 12 patients on a 1.5 T Philips Achieva Magnet. PWI data was acquired using T2* weighted gradient echo planar imaging (TR: 2018 ms; TE 44 ms; FOV 248×248 mm; reconstruction matrix 256×256; bandwidth 806 Hz/pixel; SENSE factor 2.1; 15 slices with 4mm slice thickness at 50 time points were acquired following administration of 0.2 mmol/kg at 5 ml/s in the antecubital vein using a power injector) Time-of-flight MR angiograms were obtained to exclude significant abnormalities of arterial patency. Initial processing of PWI data was performed using a deconvolution based software package (NordicNeuroLab, Bergen, Norway). C-arm based CBV maps as well as MR based CBV, CBF and MTT maps were then aligned into stereotactic space using 12 degrees of freedom affine registration. A signal to noise analysis was then performed across all subjects with regions of interest specified using atlas mapping techniques.

Results: Mean MR CBF CBV maps of all subjects demonstrated highest SNR in white matter and thalamus. C-arm CBV analysis demonstrated superior SNR of the basal ganglia compared with MR based methods ($p< 0.05$) (figure1). Regions of interest analyses of specific structures allowed quantification of SNR and determination of the optimal modality for each region.

Conclusions: Clinical diagnosis of perfusion abnormalities directly influence patient therapy, thus accurate diagnostic tools and algorithms are essential in management of ischaemic patients. Each perfusion imaging modality demonstrates specific advantages and disadvantages. C-arm perfusion acquisition demonstrated an optimal SNR profile, especially for deep subcortical grey matter areas, vulnerable to ischaemia. SNR of perfusion modalities demonstrates significant potential for improvement with noise reduction algorithms.

1446

METABOLIC ALTERATIONS IN THE AMYGDALA DURING CONSOLIDATION AND RECONSOLIDATION OF AN INHIBITORY AVOIDANCE TASK

L. Sandusky[1], A. Byrne[1], R. Flint[2], E. McNay[1]

[1]Neuroscience, University at Albany, [2]Neuroscience, College of Saint Rose, Albany, NY, USA

Objective: There is a long-standing debate as to whether the memory process of consolidation (he physical and psychological changes that take place as the brain organizes and structures information to make a permanent memory trace) is neurochemically the same as reconsolidation (which occurs after a memory is activated and made apparently labile for re-storing, triggered by cued recall). Furthermore, although we have previously shown that initial memory processes in the hippocampus are metabolically taxing, causing a drainage of hippocampal glucose, it is unknown what metabolic changes occur elsewhere in the brain or during reconsolidation.

Method: We used in vivo microdialysis (mD) of amygdala extracellular fluid (ECF) before, during and following initial learning and cued recall of an avoidance task. Male rats (3 months old) received mD cannulae into the left basolateral amygdala. Animals were placed in a novel, brightly-lit white chamber for 30 seconds after which a door opened, allowing entry to a dark chamber. Upon entry on day one, animals immediately received a mild foot shock; they returned to the lit chamber and were then returned to their home cages for 24h. On day two, the animals were re-exposed to the white box, where the memory from day one was recalled, and increased latency to cross was used as a measure of memory, with cued recall assumed to be a period of reconsolidation.

Results: ECF samples were analysed for glucose, lactate, and pyruvate (to assess local glucose metabolism) and while neurotransmitter release (glutamate and norepinephrine), using either a CMA 600 Metabolic Analyzer or standard HPLC methods. On both day one and day two, there was a marked dip in ECF glucose whose start coincided with task performance but which persisted beyond task completion. Concurrent with this decrease in ECF glucose, there was a marked rise in ECF lactate. The magnitude and duration of both changes was very similar across days, and suggests a similar elevation in local metabolism on each day. Further, on both day one and day two there was a similar marked rise in glutamate during the Inhibitory Avoidance task.

Interestingly, on day one there was a marked rise in pyruvate during and following the test period, while on day two there was a marked dip. This difference across days suggests that although both initial learning and reconsolidation are metabolically demanding, there may perhaps be a difference in oxidative phosphorylation between the two processes, and that despite many similarities suggested by the glucose, lactate, and glutamate data, consolidation may be neurochemically different from reconsolidation.

Conclusions: Consistent with our previous hippocampal data, avoidance training and testing caused an acute elevation of local metabolism within the basolateral amygdala, causing a drainage of ECF glucose and increased ECF lactate and glutamate. To our knowledge, these are the first microdialysis measurements of local metabolism in the amygdala during affective processing, and also the first attempt to compare neurochemical processes in the amygdala during both consolidation and reconsolidation.

1447

NEW STRIATAL NEURONS FORM PROJECTION TO SUBSTANTIA NIGRA IN ADULT RAT BRAIN AFTER STROKE

X. Sun[1], Q.-W. Zhang[1], M. Xu[1], J.-J. Guo[1], F.-Y. Sun[1,2]

[1]Department of Neurobiology and State Key Laboratory of Medical Neurobiology, Shanghai Medical College, Fudan University, [2]Institute of Biomedical Sciences, Fudan University, Shanghai, China

Introduction: Neurogenesis is reported to exist in the adult mammalian brain in both neurogenic and non-neurogenic areas. In recent years, lots of evidence revealed that newborn neurons were observed in the injured brain in many pathology conditions, such as stroke, AD and transient brain injury. Our previous studies demonstrate functional neurogenesis in the striatum of rat brain. In this study, we determined whether ischemia-induced newborn striatal neurons can anatomically integrate into the preexisted neural circuits in adult brains.

Methods: Cerebral ischemic injury was induced by a transient middle cerebral artery occlusion (MCAO) in adult rats. 5'-bromodeoxyuridine (BrdU) and retrovirus containing GFP report gene was used to label proliferated newborn cells. Fluorogold, a retrograde tracer, was injected into the substantia nigra to trace projection neurons from the striatum. Multiple immunostating combined with confocal microscopy was used to identify whether newborn striatal neurons can be develop projection to the substantia nigra.

Results: We further detected that $BrdU^+$ cells could express mature neuronal markers neuron-specific enolase（NSE）or NeuN in ipsilateral striatum of ischemic rat brain after reperfusion of 12 weeks. To exclude possibility that these $BrdU^+$-$NeuN^+$ cells may be caused by DNA repair or apoptosis, we further used retroviral vectors targeted with GFP to label striatal newborn neurons. We found that GFP expressed cells also can be labeled with NSE or NeuN in the ipsilateral striatum to MCAO. The results suggest that newborn striatal mature neurons are still survivor even 3 month after their birth.

Then, we used this model to investigate if these newborn striatal neurons can form projection to the substantia nigra. We found that florescent signals fluorogold, injected into substantia nigra one week before sacrificed, can be detected in the striatum ipsilateral to injection in the control and MCAO-operated rats. Most interestingly, these newly generated striatal neurons ($BrdU^+$-$NeuN^+$ cells / GFP^+-NeuN) contained strong fluorogold signals, demonstrating that newborn striatal neurons could form a long projection to the substantia nigra in adult rat brain.

Conclusion: These data indicate that new generated striatal neurons can differentiate into mature neurons and form axon to project into the ipsilateral substantia nigra. The result revealed that newly generated striatal neuron could integrated into the striatal-nigra neural networks, an important pathway to modulate movement.

1449

THE BBB IN LYSOSOMAL STORAGE DISEASES

D.J. Begley

Institute of Pharmaceutical Science, Kings College London, London, UK

Approximately 50 lysosomal storage disorders (LSDs) have been described. These diseases are inherited metabolic disorders which arise from mutations affecting the activity of either lysosomal hydrolases or transferases involved in transport across the lysosomal membrane, or in ancillary proteins which affect post-translational processing of enzyme or trafficking of enzyme into and out of the lysosome. The lysosomal storage disorders are classified as rare diseases with an overall occurrence of 1:7000 live births. However, they represent globally a very significant health and economic burden. In some geographical regions and societies the occurrence of specific lysosomal storage disorders can be relatively much higher. A defect in a lysosomal hydrolase or another protein affecting lysosomal function usually results in the accumulation of specific storage products in cells or tissues.

The storage product that accumulates is usually the substrate for the affected enzyme. However, other storage products may also accumulate. In fact, a single degradation pathway is rarely involved and a bottle-neck in one degradation pathway may then overload other parallel pathways, or cause accumulation of substrate further down the degradation pathway as some catalysed steps may be more rate limited than others. The precise genetic defect and the resulting change in amino acid sequence, structure and activity of the affected and damaged protein is now well documented for most of these diseases. Up to 70% of the lysosomal storage disorders involve substrate accumulation in brain tissue with resulting neuropathology and CNS cell death. Again neuronopathic progression may be rapid and severe with death in early years or more prolonged and attenuated with a number of decades of survival.

A number of therapies exist for treating the lysosomal storage disorders ranging from (i) enzyme replacement therapy (ERT), where the defective enzyme is replaced by the regular intravenous infusion of working copies of the enzyme which are then scavenged by affected cells, endocytosed and incorporated into their lysosomes, where they restore functional activity. Unfortunately these large enzymes do not cross the BBB and the neurological decline is not halted or reversed; (ii) Substrate reduction therapies (SRT) where a drug inhibiting an early stage in the degradation pathway is administered with a view to reducing the metabolic load on the severely rate-limited pathway produced by the defective enzyme; or (iii) Small molecules, termed chaperones, which resemble the natural substrate of the defective lysosomal enzyme.

There is also evidence that in some of the lysosomal storage disorders the function of the blood-brain barrier itself is compromised perhaps leading directly to further cascade processes within the brain resulting in neuropathology.

References:

Begley DJ, Pontikis CC, Scarpa M. 2008. Lysosomal Storage Diseases and the Blood-Brain Barrier. Curr Pharm Des 14: 1566-1580

Pontikis C C, Zaccariotto E, Begley DJ. (2009) In situ brain perfusion reveals functional changes in the blood-brain barrier on mouse models of Sanfilippo syndrome Types A and B. International J Clin Pharm and Thera 47: 147

1450

PET ACQUISITION AND RECONSTRUCTION: CORRECTIONS AND FBP VERSUS ITERATIVE RECONSTRUCTION METHODS

R. Boellaard

Nuclear Medicine & PET Research, VU University Medical Centre, Amsterdam, The Netherlands

Introduction: Brain neuroreceptor PET studies often require dynamic studies in order to explore the kinetic behaviour of a (new) radiotracer *in vivo*. During these studies multiple acquisition frames are collected sequentially across a wide range of count rates and activity distributions. From these dynamic studies various pharmacokinetic parameters can be derived provided that the PET studies are performed and reconstructed using quantitatively robust methods. In order to obtain quantitative accurate results various corrections during acquisition and reconstructions must be applied, such as e.g. randoms, scatter, attenuation, normalisation and dead time corrections. Moreover, image reconstruction methods can have a large impact on image quality and quantification.

Filtered back projection (FBP) is an analytical and still frequently used reconstruction method for dynamic PET studies. The method is relatively fast, linear and quantitatively robust. A disadvantage of FBP is the potentially poor image quality, especially for low count acquisition frames, showing severe streak artefacts. Consequently, iterative reconstructions algorithms were developed and are nowadays more frequently used. During iterative reconstruction an image, that represents the tracer distribution in the patient, is iteratively estimated such that the corresponding estimated projection data (sinogram) shows the least discrepancy with the measured one. However, certain implementations of iterative reconstructions methods may suffer from bias (quantitative inaccuracies) under conditions that may specifically occur during dynamic acquisitions. Yet, by applying randoms, scatter and attenuations correction in a more sophisticated way, e.g. by including these during the iterative reconstruction process rather than as a precorrection to the measured sinograms, much of the bias can be avoided. Moreover, the PET systems resolution properties can also be incorporated in the system matrix, thereby enhancing the image spatial resolution and/or its uniformity. Several other strategies may be applied to enhance image quality, for example, by including priors during the reconstruction process.

Aim of this presentation: In this presentation an overview of data acquisition, corrections and image reconstruction methods will be provided. Mechanism of various image reconstruction methods will be discussed and illustrated. Finally impact of data collection and image reconstruction methods on image quality and quantitation will be explained and demonstrated.

1451

NONCODING RNAS AND THERAPEUTIC PLASTICITY OF NEURAL STEM CELLS

S. Pluchino

Cambridge Centre for Brain Repair and Cambridge Stem Cell Initiative, University of Cambridge, Cambridge, UK

Compelling evidence exists that somatic stem cell-based therapies protect the central nervous system (CNS) from chronic inflammation-driven degeneration, such as that occurring in experimental autoimmune encephalomyelitis (EAE), multiple sclerosis (MS) and cerebral ischemic/hemorrhagic stroke. However, while it was first assumed that stem cells may act trough direct replacement of lost/damaged cells, it has now become clear that they are able to protect the damaged nervous system through a number of '*bystander'* mechanisms other than cell replacement. In immune-mediated experimental demyelination and stroke - both in rodents and non-human primates - others and we have shown that transplanted neural stem/precursor cells (NPCs) possess a constitutive and inducible ability to mediate efficient '*bystander'* myelin repair and axonal rescue. Yet, a comprehensive understanding of the multiple mechanisms by which NPCs exert their therapeutic impact is lacking. We envisage that the remarkable therapeutic plasticity of NPCs results from their capacity to engage highly sophisticated programmes of horizontal cell-to-cell communication at the level of the (micro)environment and we attribute a key role to the transfer of secreted membrane vesicles (MVs) from (*donor*) NPCs to (*recipient*) neighbouring cells. We are starting to define whether this form of communication is biologically relevant for NPCs, and look forward to establishing whether it is associated to cell-to-cell trafficking of non-coding RNAs (ncRNAs), and indeed on elucidating its molecular signature and therapeutic significance.

We believe that the true innovation of this approach relies in its unique peculiarity to *look into an innate cellular mechanism* with the visionary focus of *translating the knowledge of basal stem cell functions into innovative high-impact clinical therapeutics for invalidating neurological diseases*.

1452

THE EVOLVING ROLE OF IMAGING IN TRANSLATIONAL RESEARCH FOR PARKINSON'S DISEASE

M. Emborg

Medical Physics, Wisconsin National Primate Research Center, University of WIsconsin, Madison, WI, USA

Preclinical and clinical research in Parkinson's disease (PD) has been at the forefront on the application of PET imaging. In the case of PD, investigating dopamine function *in vivo* using neuroimaging allows for the evaluation of an endpoint in animals that is exactly the same as in the clinic. Neuroimaging functional methods can be used to estimate dopaminergic cell degeneration, adaptive responses to injury and, importantly, the effect of therapeutic interventions. Different tracers labeled with positron emission positrons, such as ^{18}F or ^{11}C, [e.g.: Fluoro-L-3,4-dihydroxyphenylalanine (F-DOPA), that targets the enzyme aminoacid decarboxylase] provide insight at different levels of the integrity of the dopaminergic system. An alternative to the use of radio-labeled markers of the dopaminergic pathway (that maybe influenced by dopamine replacement therapies), is the study of the pattern of resting glucose metabolism as measured by [^{18}F]2-fluoro-2-deoxy-D-gluocose (FDG). Rather than focus on the neurochemical aspects of the specific lesioned areas, the FDG method can evaluate the metabolic responses to these lesions in the entire brain. The evaluation of therapies based on the resolution of the abnormal pattern back to the normal one has been performed for levodopa and ablation of the subthalamic nucleus, among others. As our understanding of PD evolves, so does the animal models and the tools needed to evaluate them. An example is the development of PD models with non-nigrostriatal neurodegeneration such as heart dysautonomia. Our lab has developed such a monkey model and used ^{11}C meta-hydroxyephedrine PET scans to evaluate and map regional changes in catecholaminergic innervation. The role of PET is evolving from an interesting method to observe the state of the system to a true tool to affect diagnoses, treatment selection and assess if a therapy is effective. The increased level of sophistication in the applied methods of analysis, matches the increasing need of noninvasive biomarkers of diagnoses, monitoring of disease progression and treatment monitoring. Perhaps the factor that may influence the most the application of PET imaging is the creation of interdisciplinary teams to help discover new applications for imaging, such as the identification of possible targets for cell-replacement strategies. The main challenge for PET today is the application of rigorous experimental designs to demonstrate the correlations between PET results, clinical and anatomical changes. A continuous communication between preclinical and clinical researchers is needed to bridge and validate the data and facilitate the interpretation of the results for clinical application

1453

LIVE IMAGING AND FUNCTION OF MICROGLIAL ACTIVATION IN BRAIN ISCHEMIA

J. Kriz

Dept. Psychiatry and Neuroscience, Faculty of Medicine, Laval University, Quebec City, QC, Canada

Introduction: Microglial cells are the main effectors of the innate response following CNS injuries, including ischemia. However, whether microglial activation has beneficial or detrimental effects on adjacent ischemic neurons remains controversial. Moreover, the spatial and temporal dynamics of microglial activation following ischemic injury is not yet well understood.

Aim: To investigate microglial activation/innate immune response in real time, we generated transgenic mouse model bearing the dual reporter system luciferase/green fluorescent protein under transcriptional control of a murine Toll like receptor 2 (TLR2) gene promoter. In this transgenic reporter model, transcriptional activation of TLR2/ microglial activation can be visualized from the brains of live animals using biophotonic/bioluminescence molecular imaging and high resolution/high sensitivity charged coupled device (CCD) camera.

Results: The analysis of our *in vivo* imaging results revealed some intriguing primary findings. First, the TLR2 induction/microglial activation after ischemic injury was associated with marked chronic component which may last several months after the initial attack. Secondly, the pro-inflammatory response was not restricted to the site of ischemic injury being also evident in the olfactory bulb. Interestingly, a significant TLR2 response was seen first in OB (6hrs after stroke), several hours before the increase in photon emission over the site of infarction thus suggesting that OB microglia may serve as modulators of brain inflammation. However, although development of model systems for live imaging of microglial activation provided novel and intriguing information on spatial and temporal dynamics of the whole process, the molecular mechanisms underlying potential neuroprotection by microglial cells remain elusive. We investigated several molecules and pathways linked to microglial activation and, in particular, microglial proliferation following ischemic injury. Using a mouse model for selective ablation of proliferating microglia, we demonstrated that selective ablation of resident microglia markedly alters the pro-inflammatory brain response and exacerbates ischemic injury. Moreover, our results revealed an important neuroprotective potential of proliferating microglial cells serving as an endogenous pool of neurotrophic and antiapoptotic molecules such as IGF-1. Recently, we studied involvement of other molecules including galectin-3 in the modulation of microglial proliferation that yielded similar results.

Conclusions: Altogether our results suggest that microglial activation following ischemic injury in adult mice is associated with marked chronic component. Furthermore, a well synchronized and functional microglial proliferative response following ischemic injury is instrumental in limiting early as well as later stages of ischemia-induced brain damage.

1454

THE ROLE OF PPARΓ IN NEUROPROTECTION

J. Aronowski, X. Zhao

Neurology, University of Texas - HSC Houston, Houston, TX, USA

Recently transcription factor PPARγ emerged as a new promising target for the treatment of cerebrovascular diseases including ischemic and hemorrhagic stroke. It is now recognized that besides its established role in metabolic processes in adipose tissue. PPARγ appears to be abundant in the brain where it plays a role in cell signaling in neurons and glia. PPARγ also acts as an auspicious pleiotropic regulator of lipid and glucose metabolism, mitochondrial function, inflammation, oxidative stress, differentiation, phagocytosis, cell cycle and cell death. Such amalgam of multimodal biological effect of PPARγ offers a unique suitability for PPARγ-activating agents to help combat manifold pathogenic pathways underlying brain damage caused by stroke.

To study the mechanisms of how PPARγ may help brain after stroke, we employed pharmacologic agents that alter this transcription factor, as well as neuron- and microglia-specific PPARγ knockout mice. Animal models of ischemic (modeled by the middle cerebral artery occlusion) and hemorrhagic (modeled by intracerebral injection of autologous blood) stroke, as well as tissue culture systems simulating stroke events were employed.

Our *in vitro* studies indicate that PPARγ acts as an endogenous cytoprotective modulator for most brain cells and protect them from various types of injury. Stroke itself induces expression of PPARγ while activation of PPARγ with pharmacological agents protects brain from damage caused by both ischemic and hemorrhagic stroke. In agreement with the notion of these pharmacological studies, mice lacking PPARγ in neurons as compared to control developed more brain damage after ischemic stroke, corroborating an important role of PPARγ in protecting neurons. This increased vulnerability of neurons was associated with impaired expression of PPARγ -targeted anti-oxidative enzymes and selected mitochondrial protein and coincided with increased oxidative stress in neurons. Increased ischemic injury was also evident in mice lacking PPARγ in microglia. This neuroprotective effect however is likely due to a secondary damage since mice deficient in PPARγ showed increased dysfunction, as compared to wild type mice, only after more than 24h following the stroke. Finally, after hemorrhagic stroke, PPARγ in microglia appeared to help in the cleanup of hematoma from the hemorrhagic brain by improving the efficiency of microglia/macrophage-mediated phagocytosis of erythrocytes and other cellular debris. This PPARγ effect is likely mediated via increased expression of scavenger receptor, CD36 (PPARγ target gene), improved anti-oxidative capacity and reduced pro-inflammatory response.

1456

PATHOPHYSIOLOGY OF THE NEUROVASCULAR UNIT: INTERCELLULAR COMMUNICATION AND SIGNALLING

D. Stanimirovic

Institute for Biological Sciences, National Research Council of Canada, Ottawa, ON, Canada

The neurovascular unit (NVU) is composed of functionally integrated cells (brain endothelial cells, astrocytes, pericytes, and smooth muscle cells) and acellular (i.e., collagens, fibronectin, tenascin, and proteoglycans) elements that form the vascular basement membrane. The blood-brain barrier (BBB), neurovascular coupling and neuroimmune interface are three principal functions of the NVU. All three functions are profoundly changed in pathophysiological conditions affecting the brain, including cerebrovascular pathologies (e.g., stroke), neurodegenerative (e.g., Alzheimer's disease) and autoimmune diseases (e.g., multiple sclerosis). Although each neurological disease affecting NVU exhibits unique characteristics, among common denominators across the disease spectrum that trigger NVU dysfunction are hypoxia and inflammation. To examine global molecular changes that occur in the NVU in response to hypoxia and inflammation, we used a spectrum of targeted 'systems biology' approaches. One of these approaches examines cellular components of the NVU (endothelial cells, astrocytes, inflammatory cells) subjected to hypoxia or inflammatory stimuli using proteomics and glycoproteomics on subcellular compartments (luminal/abluminal membranes, secreted and shed proteins, lipid rafts, and exosomes) [1, 2]. Inter-cellular molecular interactions (e.g., cell-cell contacts, paracrine communication, etc.) important for NVU pathology (e.g., T-cell transmigration, BBB permeability) were then identified using in silico interactomics. The second approach analyses NVU protein changes in animal models of disease (e.g., stroke, Alzheimer's disease) using laser capture microdissection (LCM) technique to extract brain microvessels in situ, coupled to genomic/proteomic analyses. Dynamic protein changes in the NVU are then correlated with the aberrant function of the NVU during the course of disease. For example, differentially expressed NVU proteins between control and ischemic brain vessels in global forebrain ischemia model in rat were categorized in four groups that correlate closely with temporal patterns of the BBB disruption, inflammation, cell cycle initiation/angiogenesis and extracellular matrix remodeling in this disease model [3]. Based on these global scale analyses of molecular changes in the NVU in response to ischemic and inflammatory triggers, the complex dynamic picture of NVU remodeling processes has emerged. At the microanatomy level, alterations include the increased interaction (adhesion, transmigration) of peripheral inflammatory cells with brain endothelial cells, disruption of inter-endothelial tight junctions, retraction of pericytes from the abluminal surface of the capillary, release of proteases from the activated endothelial cells, breakdown of the basal lamina with transudation of plasma, degradation of the ECM surrounding vessels, endothelial cell proliferation and migration toward chemotactic stimuli, maturation of the newly formed vessels and initiation of blood flow. At the molecular level, this remodeling is accompanied by increased expression of endothelial cell-leukocyte adhesion receptors, loss of endothelial cell and astrocyte integrin receptors, loss of their matrix ligands, expression of members of several matrix-degrading protease families, and the appearance of receptors associated with angiogenesis and neovascularization. Several of these mediator families are also involved in neuronal remodeling, thus providing for integration of vascular and neuronal responses to the pathologic state.

References:

1. Haqqani AS et al. (2008) *Methods Mol Biol* 439:241-56.

2. Haqqani AS et al. (2011) *Methods Mol Biol*. 686:337-53.

3. Haqqani AS et al. (2005) *FASEB J*. 19:1809-21

1457

VASCULAR-MEDIATED NEURODEGENERATION - THE ROLE OF PERFUSION STRESS AND BLOOD-BRAIN BARRIER BREAKDOWN

B.V. Zlokovic

CNVBD, University of Rochester, Rochester, NY, USA

The neurovascular unit is comprised of vascular cells (i.e., endothelial cells pericytes, vascular smooth muscle cells), glial cells (i.e., astrocytes, microglia, oliogodendroglia) and neurons. The blood-brain barrier (BBB) is a highly specialized brain endothelial structure within the neurovascular unit. In concert with pericytes, astrocytes, and microglia, the BBB separates components of the circulating blood from neurons. Moreover, the BBB maintains the chemical composition of the neuronal "milieu" which is required for proper functioning of neuronal circuits, synaptic transmission, synaptic remodeling, angiogenesis and neurogenesis in the adult brain. Recent findings indicate that brain perfusion stress, from one hand, and the BBB breakdown with accumulation in brain of different proteinacious cytotoxic and neurotoxic macromolecules, from the other, may initiate and/or contribute to a loss of synapto-dendritic connections, neuronal dysfunction and neuronal loss in neurodegenerative diseases such as Alzheimer's disease and amyotrophic lateral sclerosis. A recent evidence suggests that pericytes control key functions within the neurovascular unit and are necessary for maintaining key neurovascuar functions and neuronal structure and function in the adult brain and during aging process. Pericytes degeneration can initiate vascular-mediated secondary neurodegenerative changes through either a chronic brain hypoperfusion and/or the BBB breakdown with a leakage of blood-derived endogenous neurotoxins, and/or both. The double-hit vascular hypothesis for Alzheimer's disease suggests that an initial vascular damage precedes the cerebrovascular and brain accumulation of Alzheimer's toxin amyloid b-peptide (Aβ) (hit 1) which in turn amplifies the neurovascular dysfunction preceding neurodegenerative changes (hit 2). The role of brain vascular-specific genes relevant to AD discovered through genomic screening (e.g., MEOX2, MYOCARDIN) and cerebrovascular receptors at the BBB (i.e., LRP1, RAGE) in controlling the reductions in brain microcirculation, cerebral blood flow and a faulty amyloid b-peptide clearance at the BBB preceding neuronal loss will be discussed. Potential therapeutic approaches that could be developed for chronic neurodegenerative disorders based on the vascular concept of neurodegeneration will be presented with examples of cellular and molecular targets within the neurovascular unit and at the BBB.

1458

FOCAL CEREBRAL ISCHEMIA MODELS OF BOTH LISSENCEPHALIC AND GYRENCEPHALIC SPECIES

H. Imai, N. Saito

Department of Neurosurgery, The University of Tokyo, Tokyo, Japan

Animal stroke models are indispensable for both the investigation of the pathophysiology of cerebral ischemia and the evaluation of preclinical pharmacological intervention. It is crucial to choose the most suitable experimental stroke models depending on the scientific question being investigated. In this paper we focus on the focal cerebral ischemia models of both lissencephalic and gyrencephalic species.

Of lissencephalic species, the occlusion of the middle cerebral artery (MCAO) in the rat using either an intraluminal approach (Koizumi et al., 1986) or by exposure and direct surgical occlusion of the blood vessel (Tamura et al., 1981) has been widely used since the 1980s and is one of the most relevant animal stroke models. Briefly, we refer to the inherent advantages and disadvantages of each model focusing on the reproducibility of the infarction volume. Indeed the latter, Tamura model has a robust advantage in terms of the reliability and reproducibility of the production of ischemic lesions in the ipsilateral MCA territory including the frontal cortex, dorsal parietal cortex, and the lateral part of the caudate- putamen. However, the use of this model has become less prevalent than the intraluminal model presumably due to the substantial requirement for microsurgical expertise. Then, in this course we explain the tips of the neurosurgical procedures for direct exposure and MCA occlusion in the rat including anesthesia, physiological monitoring, positioning and neuro-vascular anatomy. In addition, this paper describes a method for quantitation of white matter (axonal) injury after MCA occlusion in rats and its application to the study of the pharmacological intervention (Imai et al., 2002).

In gyrencephalic species, we have recently introduced the new model of the focal cerebral ischemia of miniature pig (Imai et al., 2006) which provides a reproducible amount of ischemic damage in both gray and white matter with significant utility for studying the pathophysiology of ischemia. Moreover, advancing this model, lacunar infarction model was introduced by selective obstruction of the anterior choroidal artery which causes selective white matter ischemia in internal capsulae (Tanaka et al., 2008). We review the miniature pig stroke model focusing on the methodology, pathophysiology, new findings and applicability for the future investigation.

References:

Tamura A et al. Focal ischemia in the rat. Part I: description of technique and early neuropathological consequences following middle cerebral artery occlusion. J Cereb Blood Flow Metab 1981 1:53-60

Koizumi J et al. Experimental studies of ischemic brain edema, I: a new experimental model of cerebral embolism in rats in which recirculation can be introduced in the ischemic area. Jpn J Stroke. 1986;8:1- 8.

Imai H et al. New method for the quantitative assessment of axonal damage in focal cerebral ischemia. J Cereb Blood Flow and Metab (2002) 22: 1080-1089.

Imai H et al. A new model of focal cerebral ischemia in the miniature pig. J Neurosurg 2006 104: 123-132.

Tanaka Y et al. Experimental model of lacunar infarction in the gyrencephalic brain of the miniature pig: neurological assessment and histological, immunohistochemical, and physiological evaluation of dynamic corticospinal tract deformation. Stroke 2008 39:205-212.

1459

IS BRAIN AFTER NEONATAL STROKE BETTER OFF WITHOUT MICROGLIA?

Z. Vexler

Neurology, University of California, San Francisco, CA, USA

The inflammatory and oxidative responses are the major contributors to ischemic injury in both immature and adult brain, but there are several areas where these responses diverge. In contrast to adult, the early post-stroke macrophage population is predominantly comprised of resident microglia, not invading monocytes and deletion of microglial cells prior to stroke induction in neonatal rodents is protective. We will discuss relationships between the state of microglial activation, removal of apoptotic neurons, which are in abundance after focal ischemia-reperfusion in neonatal rats, and injury. In particular, we will focus on the effects of modulation of intracellular glutathione metabolism in microglia on ischemic injury in neonatal rodents and discuss emerging data on both the supportive and adverse roles of these cells.

1460

TRANSLATIONAL PERSPECTIVES OF MOLECULAR IMAGING IN ALZHEIMERS DISEASE

T. Suhara

Molecular Imaging Center, National Institute of Radiological Sciences, Chiba, Japan

Amyloid β peptide (Aβ) and tau protein are well known as the pathological features Alzheimer's disease (AD) and mechanistically implicated in the illness as initiators of molecular and cellular cascades underlying the pathogenesis. Radiolabeled amyloid ligands are used for positron emission tomography (PET) like Pittsburgh Compound-B labeled with ^{11}C ([^{11}C]PIB), which has promising binding properties with affinities for amyloid in a nanomolar range and has been shown to be of great utility for detection of amyloid at early symptomatic stages of AD. Despite clinical data, PET experiments using animal models did not provide unequivocal evidence in PET analyses of APP transgenic (Tg) mouse brains. However, with high specific radioactivity, we have successfully performed PET visualization of progressively depositing Aβ aggregates in brains of APP Tg mice. In addition, our in vitro assays revealed preferential binding of PIB to N-terminally modified Aβ, Aβ-N3-pyroglutamate. The notion, N- and C-terminal heterogeneities of Ab were analyzed by immunostaining of human and mouse brain sections, Ab40 and Ab42, major constituents of C-terminal heterogeneity, were abundantly observed in all APP transgenic strains relative to AD brains, and thus showed no overt correlation with binding of [^{11}C]PIB. N-terminally unmodified Ab, Ab_{N1D}, intensely accumulated in mouse brains but Ab_{N3pE}, which lacked 2 N-terminal amino acid residues and was pyroglutamylated, was detected only at low levels in mice, and its amount and localization were intimately correlated with those of [^{11}C]PIB radiolabeling consistently across human and mouse brains. Multi-tracer, multi-scan PET study is also of pivotal importance in the mechanistic evaluation of Aβ immunization and other related anti-amyloid treatments, as a PET ligand for peripheral benzodiazepine receptor, termed [^{18}F]fluoroethyl-DAA1106 (FE-DAA1106), which we developed for capturing glial activation can be used in combination with amyloid probes to longitudinally assess the contribution of neuroinflammation to both therapeutic and adverse effects. Injection of monoclonal antibody against N-terminal portion of Ab into the unilateral hippocampus strongly induced neuroinflammation putatively by activated microglia, and gave rise to elimination of nearby amyloid. We also examined detectability of microgliosis in living tau transgenic mice. The mice exhibited noticeable hippocampal atrophy as determined by MRI, accompanied with increased binding of the [^{18}F]FE-DAA1106. The utility of imaging agents for microglial activation, altered neurotransmission and other key processes downstream of amyloid formation should also be taken into account in order to therapeutically regulate the entire pathological cascade of AD. Neuroimaging biomarkers would also promote bidirectional translational research between clinical and preclinical levels, since they serve as common indices shared by humans and animal models and thus ease extrapolation of pathobiological information in a reciprocal manner.

1462

PPARΓ AS A THERAPEUTIC TARGET IN ALZHEIMER'S DISEASE

E. Hamel

Montreal Neurological Institute, McGill University, Montréal, QC, Canada

Introduction: Alzheimer's disease (AD) is clinically characterized by gradual impairment of cognitive function, decreased cerebral glucose uptake and chronic cerebral hypoperfusion. At the neuropathological exam, AD brains display amyloid-beta (Aβ) peptide aggregated in parenchymal plaques and in blood vessels, neurofibrillary tangles, and signs of oxidative stress and neuroinflammation. In addition to Aβ deposition, cerebral blood vessels exhibit structural alterations reminiscent of vascular fribrosis, such as accumulation of extracellular matrix (ECM) proteins collagen, laminin and fibronectin. Here, the role of PPARγ activation in counteracting several of these pathogenic processes will be presented, and discussed in view of the apparent benefit in both AD animal models and patients.

PPARγ positive effects in AD pathology: Drugs with PPARγ activity relevant to AD therapy correspond primarily to NSAIDs such as ibuprofen, and a class of oral anti-diabetics, the thiazolidinediones (TZDs) that include rosiglitazone and pioglitazone, which have been associated with decreased AD risk or pathology. Consistently, PPARγ agonists have been associated with brain anti-inflammatory effects with reduced levels of cytokines, and astroglial or microglial inflammatory markers in various AD mouse models that overexpress mutated forms of the human amyloid precursor protein (APP). Additionally, reduced astroglial activation was apparent in a model of AD cerebrovascular pathology, the transforming growth factor-β1 overexpressing mice (TGF mice). In contrast, contradictory findings have been obtained on the ability of PPARγ to counter the Aβ pathology, whether related to soluble forms of Aβ or to Aβ plaques. At the level of the cerebral circulation, the PPARγ agonist pioglitazone fully normalized cerebrovascular reactivity, the hemodynamic response to increased neuronal activity, the Aβ-induced cerebrovascular oxidative stress, as well as the dysfunctions, but not the structural alterations, related to cerebrovascular fibrosis in TGF mice. These effects were corroborated by the capacity of pioglitazone to directly act upon proteins involved in vascular oxidative stress and fibrosis. Similar to data on amyloidosis, there is currently no agreement on the ability of PPARγ agonists to rescue learning and memory in AD animal models or AD patients, despite beneficial effects on neuronal function, such as neurometabolic coupling.

Conclusions: Evidence suggests that PPARγ ligands exert beneficial effects, primarily related to inflammation, oxidative stress, glucose metabolism and signaling processes, in the neuronal, glial and cerebrovascular compartments affected by AD pathology. However, these have not translated into unequivocal improvement in learning and memory in AD animal models or AD patients. Further studies are needed to establish if this is due to a too advanced age or a too severe pathology at treatment onset, or to a clear failure of these drugs to rescue memory in AD.

Supported by research grants (to EH) from the Canadian Institute of Health research (CIHR), the Society Alzheimer Canada and Takeda Pharmaceuticals North America, Inc.

1463

OUTCOME MEASURES - BEHAVIOURAL TESTING AND BRAIN DAMAGE

D. Corbett

Dept Cellular & Molecular Medicine, University of Ottawa, Ottawa, ON, Canada

While animal models of stroke will never perfectly capture all of the elements of the human condition it is essential that key clinical features be incorporated into preclinical models. For example, animal models should reflect the injury patterns (e.g. location, extent) and behavioural sequelae (e.g. specific functional domain, chronicity) of human stroke as much as possible, language being an obvious exception! For these reasons, I will emphasize a “bedside to bench” approach in my workshop instead of the universal “bench to bedside” line of thinking that currently characterizes much of preclinical stroke research.

The first question to be addressed is: What are you trying to model? When using rodent stroke models it seems obvious that the model should be relevant to the clinical problem being investigated but this is often not the case. Accordingly, a brief but critical review of commonly used rat and mouse models of global and focal ischemia will be presented highlighting the key advantages and disadvantages of each model and their similarity to stroke in humans.

While histological outcome measures (e.g. infarct volumes and cell counts) provide valuable information behaviour is the most important clinical outcome measure. Consequently, investigators need to select a battery of tests that are appropriate for the specific type of injury being modeled (e.g. global versus focal ischemia). The choice of behavioural tests is critical since it can ultimately determine the “apparent” level of neuroprotection or functional recovery. A number of widely used sensory-motor and cognitive tests will be discussed and critically evaluated with regard to their sensitivity and relevance to human stroke. Differences in the timing and repetition of behavioural testing can also markedly affect outcome and illustrative examples will be provided. Special consideration will be given to behavioural tests in mice since they are increasingly being employed in stroke studies and in a number of cases tests developed in rats do not always transfer to the mouse. An issue of considerable importance is the extent to which the stroke-damaged brain is able to recover or whether the reestablished behaviour is largely or entirely the result of compensation.

At the conclusion of the workshop attendees will have acquired new knowledge that will help them approach and design more thoughtful and valid experiments that better mimic the clinical condition of interest. In so doing, there is a greater likelihood that results from the laboratory will be successfully translated to the clinic.

1464

SUPPRESSING MICROGLIAL FUNCTIONS IN ACUTE NEUROLOGICAL INSULTS IN THE ADULT BRAIN

M.A. Yenari[1,2], T.M. Kauppinen[1,2], R.A. Swanson[1,2]

[1]Neurology, University of California, San Francisco, [2]Neurology, San Francisco Veterans Affairs Medical Center, San Francisco, CA, USA

Recent work in the area of stroke and related acute neurological insults suggests that microglia may contribute to its worsening. Thus, an understanding of how microglia participate in the process may lead to the identification of appropriate therapeutic targets.Microglial activation is an early brain response to stroke and related insults. Microglia normally monitor changes in brain homeostasis including specific signaling molecules expressed or released by neighboring cells. These signaling molecules, including ATP,glutamate, cytokines, prostaglandins, zinc, reactive oxygen species, and HSP60, may induce microglial proliferation and migration to the sites of injury. They also induce a non-specific innate immune response that may exacerbate acute ischemic injury. This innate immune response includes release of reactive oxygen species (ROS), cytokines, and proteases. Microglial activation requires hours to days to fully develop, and thus presents a target for therapeutic intervention with a much longer window of opportunity than acute neuroprotection. Effective agents are now available for blocking both microglial receptor activation and the microglia effector responses that drive the inflammatory response after stroke. Effective agents are also available for targeting the signal transduction mechanisms linking these events. Evidence in experimental models of stroke and ischemia-like injury indicate that microglia most certainly exacerbate neuron cell death and increase stroke lesion size. Inhibition of microglia through its ability to activate or generate damaging substances such as ROS and damaging proteases can reduce the extent of ischemic injury and improve behavioral outcomes. Novel anti-inflammatory targets and treatments have been identified recently, including pyruvate, HSP70 and sphingolipid agonists/antagonists. However, the innate immune response can have salutary as well deleterious effects on outcome after stoke, and a challenge will be to find ways to selectively suppress the deleterious effects of microglial activation after stroke without compromising neurovascular repair and remodeling.

1468

BLOOD-BRAIN BARRIER NA TRANSPORTERS IN ISCHEMIA-INDUCED CEREBRAL EDEMA

M.E. O'Donnell

Physiology and Membrane Biology, University of California, Davis, CA, USA

Cerebral edema is a major cause of morbidity and mortality in ischemic stroke yet much is unknown about the processes involved. Blood-brain barrier (BBB) endothelial cell ion transporters play an important role in regulating the volume and composition of brain interstitial fluid (ISF). In this regard, BBB ion transporters are responsible for secreting up 30% of brain ISF, comprised largely of Na, Cl and water, and also maintaining appropriate K concentrations in brain ISF. Evidence suggests that BBB ion transporters also participate in ischemia-induced edema formation. During the early hours of ischemic stroke, edema forms by mechanisms involving increased secretion of Na, Cl and water across the intact BBB from blood into brain. Previous studies have provided evidence that luminal BBB membrane Na transport is rate limiting in this process. We have identified two Na transporters, a Na-K-Cl cotransporter and Na/H exchanger, that reside in the luminal BBB membrane and are stimulated by hypoxia, aglycemia and arginine vasopressin (AVP), three prominent factors present during cerebral ischemia. We have hypothesized that ischemic factor stimulation of the BBB Na-K-Cl cotransporter and/or Na/H exchanger causes increased secretion of Na and water from blood into brain through functional coupling of the luminal Na transporters with abluminal Na/K pump and Cl efflux pathway. In support of this, we have found that administering intravenous bumetanide and/or HOE642 to inhibit BBB Na-K-Cl cotransporter and/or Na/H exchanger activity, respectively, significantly attenuates cerebral edema formation and brain Na uptake, assessed by magnetic resonance imaging and Na spectroscopy, in the rat permanent middle cerebral artery occlusion (MCAO) model of ischemic stroke. Bumetanide and HOE642 also significantly reduce TTC-defined brain lesion volume and improve neurologic outcome. These Na transport inhibitors are effective whether given immediately before, or 2-3 hours after, induction of ischemia. While reducing activity of these BBB Na transporters appears to be promising for acute treatment of ischemic stroke, identifying the signaling pathways whereby ischemic factors stimulate BBB Na-K-Cl cotransporter and Na/H exchanger activities offers the possibility of developing preventative therapies for patients at risk for stroke. AMP kinase as well as p38 and JNK MAP kinase signaling pathways are activated by hypoxic/ischemic stress in a variety of cells, suggesting the possibility that one or more of these kinases is involved in ischemic factor stimulation of BBB Na transporter activity. Recently, we have found that all three of these kinases are rapidly activated by hypoxia, aglycemia and/or AVP in cerebral microvascular endothelial cells (CMEC) and further, that Compound C, SB239063 and SP600125, inhibitors of AMPK, p38 and JNK, respectively, greatly reduce or abolish ischemic factor stimulation of CMEC Na-K-Cl cotransporter activity. These findings, together with evidence from other studies that these kinase inhibitors provide neuroprotection in ischemic stroke, suggest therapeutic promise in targeting AMPK, p38 and/or JNK to attenuate ischemia stimulation of BBB Na transporter activity and edema formation in at-risk patients prior to onset of ischemia.

1469

COMBINING MOLECULAR IMAGING WITH PET AND FMRI (PART I)

J.C. Price

Department of Radiology, University of Pittsburgh School of Medicine, Pittsburgh, PA, USA

Molecular imaging is a multi-faceted science that encompasses the in vivo study of normal and pathological events at the cellular and molecular levels, as well as the development and application of molecular imaging probes/paradigms that utilize methods from molecular biology and genetics. The Molecular Imaging framework includes methods for in vivo visualization, evaluation and assessment. Positron emission tomography (PET) is an established molecular imaging tool that has been used to sensitively trace physiological processes and to identify and assess function of desired targets or pathways (e.g., enzyme activity, ligand-binding interactions, reporter gene assays). Magnetic Resonance imaging (MRI) provides visualization of structural anatomy for molecular imaging applications, and additionally offers the capacity to assess brain function through Blood Oxygenation Level Dependent (BOLD) fMRI (e.g., task-induced activation, resting state connectivity) and metabolic brain activity through spectroscopy.

Part 1 of Combining Molecular Imaging with PET and MRI will focus on the methodology involved in a combined PET/MR imaging study. Basic technical aspects of PET and MR imaging will be reviewed to highlight the relative strengths, weaknesses, similarities and differences between these modalities and between the methods utilized within the modalities. This will include discussion of study design issues and the presentation of example results from multi-modal investigations of PET ligand-binding interactions and BOLD fMRI. Recent advancements in combined PET/MR imaging technology will also be discussed in the context of future directions. The overall goal is to provide a basic understanding of: 1) important methodological considerations for PET/fMRI molecular imaging investigations and; 2) how a combined PET/fMRI molecular imaging data set could be used to enhance understanding of disease processes, improve early disease detection, and inform drug discovery.

1470

THE REGULATION OF NEURONAL CELL DEATH BY GLYCOLYTIC ENZYMES

P. Mergenthaler

Department of Experimental Neurology, Charité University Medicine Berlin, Berlin, Germany

Regulation of energy metabolism and programmed cell death is tightly connected and critical for homeostasis. All organisms have evolved strategies to promote survival when challenged by deprivation of metabolic substrates. The transcription factor hypoxia-inducible factor-1 (HIF-1) is a master regulator of the cellular response to these evolutionary pressures and emerging evidence suggests that key pathways leading to hypoxia tolerance as well as tumorigenesis share HIF-1-dependent regulation. In particular, HIF-1 plays a critical role in mediating endogenous protection in the brain. However, the underlying molecular mechanisms leading to 'endogenous tolerance' against substrate deprivation are largely unknown.

Glycolytic enzymes are of vital importance for all cells. However, in addition to their role in cellular metabolism, additional functions of these enzymes have emerged. Specifically, it has recently been described that different enzymes in the glycolytic cascade play important roles in the regulation of cell death. We found that the glycolytic enzyme Hexokinase II is activated after HIF-1 induction in primary neurons. When bound to mitochondria, Hexokinase II potently inhibits cell death under hypoxia. Furthermore, Hexokinase II relies on its binding partner Pea-15, a protein known to be involved in the regulation of cell death and multiple aspects of cellular homeostasis, to mediate protection from hypoxic cell death. In the absence of glucose or Pea-15, Hexokinase II induces neuronal cell death. Therefore, Hexokinase II acts as a molecular sensor of the metabolic state of the cell, determining its fate depending on substrate availability. Thus, Hexokinase II functionally links the regulation of cell death and glucose metabolism and provides novel insight for understanding the regulation of neuronal cell death under various physiological and pathophysiological conditions.

1471

MONITORING THE EFFECT OF INHALATIVE NO ON CBF IN THE LEIPZIG SHEEP STROKE MODEL BY [^{15}O]H_2O PET

H. Barthel[1], V. Zeisig[1], B. Nitzsche[2], U. Großmann[1], A. Dreyer[2], G. Becker[1], M. Kluge[1], T. von Geymüller[2], N. Terpolilli[3], O. Sabri[1], N. Plesnila[3], J. Boltze[2]

[1]University of Leipzig, [2]Fraunhofer Institute for Cell Therapy and Immunology, Leipzig, Germany, [3]Royal College of Surgeons in Ireland, Dublin, Ireland

Based on the successful evaluation of inhalative NO (iNO) in small animal stroke models we thought to determine a possible therapeutic benefit by iNO on the cerebral blood flow (CBF) in the ischemic penumbra of a sheep stroke model recently implemented by our group. This new large animal stroke model allows to employ human imaging techniques and protocols and by that to quickly translate preclinical into clinical research. Using positron emission tomography (PET) in this model, the ischemic penumbra can be accurately described both for its localization as well as for the CBF.

In 6 female Merino sheep, the medial cerebral artery was permanently occluded (pMCAO). Two hours after pMCAO, 50ppm iNO was given for 60min in the randomly selected treatment group. The control group comprised of pMCAO sheep without iNO. In all sheep, CBF was visualized and absolutely quantified using [^{15}O]H_2O PET (1GBq, ECAT EXACT HR+ scanner, 3D mode, 5min acquisition). CBF-PET was carried out each before (PET1), 30min (PET2), and 60min after start of iNO (PET3), as well as 30min after end of iNO (PET4). The PET imaging was paralleled by arterial blood sampling for absolute quantification of CBF in a voxel-wise manner. Kinetic modeling of the PET and blood data was performed using PMOD software employing the Alpert method. The following established CBF thresholds were used to separate the pMCAO-related brain tissue compartments: < 8 ml x $100g^{-1}$ x min^{-1} for infarction core, 8-22ml x $100g^{-1}$ x min^{-1} for ischemic penumbra, and >22 ml x $100g^{-1}$ x min^{-1} for normally perfused brain tissue. 3D volumetry of these three tissue compartments was carried out using PMOD. Further, stroke-specific magnet resonance imaging was performed 1h after the last PET scan (i) to confirm the MCA occlusion, (ii) to confirm the presence of a territorial infarction, and (iii) to provide a reference for anatomical co-registration with the PET data.

The baseline CBF PET data showed in the brain hemisphere ipsilateral to the pMCAO an infarction core of 11.7 ± 5.2ml which was surrounded by an ischemic penumbra of 8.8 ± 3.4ml. In the control sheep, the penumbra volume did not change within the time span investigated (PET2: 8.9 ± 2.2ml, PET3: 8.6 ± 2.4ml, PET4: 9.4 ± 3.6ml). This was in contrast to the sheep treated with iNO, in which the penumbra volume significantly decreased by ~50% ($p < 0.05$ for PET2 and PET3 vs. PET1 and vs. control group) in favor of the normally perfused tissue compartment.

In this small pilot trial using CBF PET to perform individual volumetry of the ischemic penumbra over time in the new sheep stroke model we were able to demonstrate a therapeutic effect of iNO. These data support the encouraging small-animal data and call for a clinical trial testing iNO in the human stroke situation. It is also planned to expand these sheep PET experiments to test for the optimal iNO dose and duration to achieve a maximal penumbra CBF improvement as well as to perform long-time clinical outcome experiments.

1473

MULTI-SET DATA ANALYSIS

S. Strother

Rotman Research Institute, Baycrest & University of Toronto, Toronto, ON, Canada

The aim of this presentation is to introduce the audience to multi-set analysis approaches and their possibilities with simple diagrams and examples from the literature using a minimum of mathematics. I will start by briefly summarize the primary options for merging multi-modal data and the pros and cons of the different approaches as outlined by Horwitz and Poeppel [1]. These include the traditional univariate approach for combining molecular (e.g., modality 1 = serotonin receptor measures) and functional brain imaging data (e.g., modality 2 = fMRI BOLD), using correlations between predefined volumes of interest, as exemplified by Rhodes et al. [2].

To obtain a 2-way multi-set analysis the univariate correlations between multiple modalities can be generalized using partial least squares (PLS), or its close relative, canonical correlation analysis (CCA). The modern use of these approaches with multiple modalities in neuroimaging is exemplified by the work of Chen et al with PLS [3], and paired with independent components analysis (ICA) by Calhoun´s group as reviewed by Correa, et al. [4]. However, to my knowledge these approaches have yet to be applied to the fusion of molecular and functional data sets, and it is unclear if ICA is important in this context. These and an alternative approach called "data stacking" rely on extracting a single summary or feature image per subject as an initial step. This is unnecessary for typical molecular and functional PET images since only a single image is available per subject, but an fMRI study must first be compressed to a single statistical parametric map per subject, for example using GLM. Data stacking then proceeds by concatenating the 2 multimodal images per subject to create a matrix with dimensions (# subjects) x (# spatial locations in [modality 1 + modality 2]). This extended data matrix may now be analyzed using any of a range of multivariate analysis techniques such as principal components analysis, ICA, PLS, linear discriminants, SVM, etc. Finally, I will briefly comment on further extensions to > 2-way multi-set analyses involving more than 2 modalities (e.g., receptors, fMRI and MRI), and indicate where software implementing multi-set approaches is available.

In general this area of multi-modal data analysis using multi-set approaches involving molecular imaging seems ripe for further research and development as the vast majority of the literature focuses on single modality studies or simple correlation analyses between two modalities.

1. Horwitz and Poeppel. How can EEG/MEG and fMRI/PET data be combined? Hum Brain Mapp. 17:1-3, 2002.

2. Rhodes, RA; Murthy, NV; Dresner, MA, et al., Human 5-HT transporter availability predicts amygdala reactivity in vivo. J. Neuroscience, 27(34):9233, 2007.

3. Chen, K., Reiman, E.M., Huan, Z., Caselli, R.J., Bandy, D., Ayutyanont, N., and Alexander, G.E. Linking functional and structural brain images with multivariate network analyses: a novel application of the partial least square method. Neuroimage *47*, 602-610, 2009.

4. Correa, N.M., Adali, T., Li, Y.O., and Calhoun, V.D. (2010). Canonical Correlation Analysis for Data Fusion and Group Inferences. IEEE Signal Process. Mag. *27*, 39-50, 2010.

1474

AN OVINE LARGE ANIMAL STROKE MODEL IN SHEEP - A NEW TOOL FOR TRANSLATIONAL BRAIN ISCHEMIA RESEARCH

J. Boltze[1], A. Förschler[2,3], B. Nitzsche[1], D. Waldmin[1], A. Hoffmann[4], C. Boltze[1], A. Dreyer[1], W. Härtig[5], H. Barthel[6], U. Gille[4]

[1]Department of Cell Therapies, Fraunhofer Institute for Cell Therapy and Immunology, [2]Department for Neuroradiology, University of Leipzig, Leipzig, [3]Department for Neuroradiology, University Clinic rechts der Isar, Munich, [4]Institute of Veterinary Anatomy, Faculty of Veterinary Medicine, [5]Paul-Flechsig-Institute for Brain Research, [6]University Clinic of Nuclear Medicine, University of Leipzig, Leipzig, Germany

Despite thorough research activities during the past decades, numerous neuroprotective drugs that have been successfully evaluated in rodent models have not been beneficial in clinical trials. This can partly be attributed to species differences between rodent and humans and emphasizes the demand for close-to-practice models, in particular large animal models of focal cerebral ischemia. To overcome common limitations of existing large animal models (high mortality, ethical concerns) we developed a novel ovine model of middle cerebral artery occlusion (MCAO), which allows control of induced lesion size and subsequent neurological dysfunctions and implementation of sophisticated imaging procedures.

Twenty five adult Merino rams were randomly assigned to transcranial 1-branch-, 2-branch- or total cortical MCAO, sham operation (craniotomy without MCAO) and control group (no operation, n=5 each). The left cortical MCA or branches of the vessel were permanently occluded using high frequency bipolar forceps. Neurological investigation was performed using an especially designed score point system before surgery and at days 1, 4, 7, 10, 16, 25, 32 and 42 following MCAO. Impact of focal cerebral ischemia MCAO were evaluated by magnetic resonance imaging (MRI) including T1-, T2-, T2*-sequences, diffusion weighted (DW) and diffusion tensor (DT) imaging and magnetic resonance angiography (MRA) using a Philips 1.5T or a Siemens 3.0T clinical scanner at days 1, 14 and 42. Moreover, positron emission tomography (PET) was performed to assess cerebral blood flow by $[^{15}O]H_2O$ or glucose metabolization ($[^{18}F]$FDG, day 42 only). Animals were then for neuropathological investigation.

Total MCAO induced the large cortical lesion ($p< 0.05$) and most severe and most severe ($p< 0.05$) neurological dysfunctions including absent/delayed motoric reflexes, ataxic movement, circling and torticollis lasting until the end of the observation period. 1- and 2-branch MCAO caused smaller cortical lesions ($p< 0.05$) as well as more limited, transient functional deficits ($p< 0.05$). MCAO was confirmed by MRA on day 14 in all cases. Sham operated subjects showed very mild dysfunctions lasting for no longer than 2 days and and small cortical contusion damage at the day 1. Control animals did not show any pathology, while ischemic lesions were neither observed in controls nor sham operated subjects by MRI and PET. DTI at 3.0T is feasible in sheep. No animal died during the surgical intervention or the post-MCAO observation period.

The sheep MCAO model represents a translational stroke model to study the mechanisms of focal cerebral ischemia and potential impact of novel therapies in a large animal model. The model further allows control of lesion size and functional deficits for different experimental paradigms. The ovine brain can easily be imaged using clinical scanners. Since MCAO causes a severe, but not total loss of motor functions in sheep, animals can easily be housed in a

species-appropriate environment. Method-related mortality is very low. The model also allows to perform stereotaxic interventions and can be modified for hemorrhage induction.

1475

HOW NO GIVEN TO THE LUNG AFFECTS THE HEALTHY AND ISCHEMIC BRAIN - INTRODUCTION OF THE CONCEPT

N. Plesnila

Royal College of Surgeons in Ireland (RCSI), Dublin, Ireland

Nitric oxide (NO) is a gaseous signalling molecule produced by nitric oxide synthases (NOS). NO produced by endothelial NOS (eNOS) diffuses from endothelial cells into smooth muscle cells, where it initiates a cascade resulting in smooth muscle relaxation and dilation of vessels. Due to its short half life (only a few seconds in tissue) the activity of NO is believed to be confined to the immediate vicinity of its production. For instance, in the treatment of pulmonary hypertension NO given by inhalation (iNO) specifically dilates the vessels in the lung; due to its short half life (and scavenging by haemoglobin) it is inactivated before it reaches other organs.

However, indirect evidence from the literature suggests that NO may, in certain instances, leave the pulmonary vascular bed and have extrapulmonary effects. In order to investigate possible cerebral effects of iNO we ventilated mice with 5-50 ppm NO and directly visualized the arterioles and venules of the cerebral microcirculation by intravital fluorescence microscopy. Our results show that iNO results in the formation of NO carriers in blood and in dilation of cerebral venules thereby proving that iNO can have an effect on the cerebral circulation.

1476

CLINICAL APPLICATION OF INO - WHERE DO WE STAND?

M.A. Moskowitz[1,2]

[1]Neurology and Neurosurgery, Massachusetts General Hospital & Harvard Medical School, Charlestown, [2]Health Sciences and Technology, Massachusetts Institute of Technology, Boston, MA, USA

The potential therapeutic role for nitric oxide in cerebral ischemia is multifaceted. When generated within neurons in large amounts nitric oxide forms peroxynitrite after combination with superoxide anion, and peroynitrite kills cells. When generated within endothelial cells, NO exhibits antiplatelet, anti-inflammatory effects and is also a recognized vasodilator. There is accumulating data indicating that the upregulation of NO by the endothelium protects tissue under ischemic conditions, including for example, following the administration of L-arginine and NO donors, statins, steroid hormones, nutrients, rho kinase inhibitors and physical activity. The mechanism in part appears to involve improved tissue perfusion and enhanced blood flow. Inhaled nitric oxide plays a role as a therapeutic agent such as in myocardial ischemia-reperfusion injury. Nagasaka and colleagues found that breathing of NO diminishes myocardial ischemia in a model of reperfusion injury. In one experimental paradigm, breathing NO for 5 min or 5 or 60 min prior to reperfusion reduced the size of myocardial infarction size by approximately 32%. This presentation will review the experimental evidence and the potential clinical importance of NO in cerebral ischemia.

1478

BIOMARKERS FOR VASCULAR COGNITIVE IMPAIRMENT

G. Rosenberg

Neurology, University of New Mexico, Albuquerque, NM, USA

Introduction: Vascular cognitive impairment (VCI) is a major form of dementia in the elderly. The heterogeneous nature of the illness makes separation of VCI from neurodegenerative diseases difficult, particularly in the early stages. Biomarkers that aid diagnosis and treatment are needed.

Background and aims: There are two major forms of VCI: multiple strokes most commonly due to large vessel and embolic disease, and small vessel disease, which leads to lacunar strokes and damage to the white matter. When the white matter is extensively involved, the patients have a progressive illness that has hallmarks of an inflammatory process. Potential biomarkers based on the underlying pathophysiology include proton magnetic resonance spectroscopy (^{1}H-MRS), albumin elevation in the CSF, blood-brain barrier (BBB) disruption in the white matter, and the presence of matrix metalloproteinases (MMPs) in the CSF.

Material and methods: Patients with suspected VCI were entered into a longitudinal study to identify biomarkers. They underwent yearly neurological and neuropsychological testing, MRI with ^{1}H-MRS to measure N-acetylaspartate (NAA), dynamic contrast-enhanced MRI (DCEMRI) to quantify the BBB permeability, and measurements of MMPs and albumin index in the CSF.

Results: We separated patients into groups based on the clinical, neuropsychological testing and MRI findings. Patients with extensive white matter hyperintensities on MRI, focal findings and poor balance were classified as subcortical ischemic vascular disease (SIVD), and they were separated from those with multiple strokes (MI). Several patients with white matter lesions could not be classified and were called leukoaraiosis (LA). We found that white matter NAA correlated negatively with size of the lesions and with albumin index. DCEMRI showed BBB disruption in the white matter in both SIVD and MI patients. MMP-2 index was reduced in the CSF particularly in the SIVD group.

Conclusion: We have identified a series of multimodal biomarkers that are present in patients with the small vessel form of VCI. Long-term follow-up will be needed to determine the natural history of the illness and the optimal set of biomarkers to use in determining progressive disease.

1480

DESIGNING A CLINICAL PET STUDY

A.M. Catafau

Barcelona Imaging Group, S.L., Barcelona, Spain

PET is a highly valuable, cutting-edge technology for research. However, it is also complex in its procedure, requiring both sophisticated equipment and a very well coordinated team of people with niche expertise in different disciplines. A PET tracer is always needed and in most cases is not registered. This implies that PET studies for research need to comply with similar regulatory requirements as in typical clinical trials with investigational drugs. Given the particularity of the short half life of the positron emitters, these requirements add difficulty to the procedure. The above reasons make the PET study cost is high. A careful protocol writing and study set up are crucial to maximize the chances of success for every single PET scan and therefore to obtain useful, reliable data out of the study.

Aspects to be considered for clinical PET studies protocol writing include: a) ensure feasibility, i.e. that appropriate tools (tracer, equipment) and specific population (healthy volunteers or patients) with required characteristics (inclusion-exclusion criteria) are available at the selected or targeted site(s) to achieve the objective of the study; b) consider potential contingencies (e.g. tracer synthesis failures, delays in arterial cannulation, etc) and allow for flexibility using time windows or giving suitable alternatives in the text.

The PET study set up should include: a) ensuring that all investigators and participants understand the protocol and the reason for particular procedures (e.g. tracer administration, arterial cannulation, blood sampling times); b)PET staff training for the particular procedure requirements in each protocol, such as coordination between radiochemistry lab and PET camera staff, times for blood sampling and analysis, drug administration if required, etc; c) coordination between clinicians and PET staff (e.g. agreements on how to communicate, calendar slots and contingency plans); d) preparation of study documents (clinical histories at PET center, meaningful CRFs, working sheets).

In summary, detailed, careful planning and preparation are key to get the most from a clinical PET study, by minimizing scan failures and enhancing efficiency in terms of study costs and length.

1481

SUB-(HALF)-MM SPECT AND SIMULTANEOUS SPECT/PET OF MOLECULES AND TISSUE IN ACTION

F.J. Beekman[1,2]

[1]Radiation Detection and Medical Imaging, Delft University of Technology, Delft, [2]MILabs BV, Utrecht, The Netherlands

Pivotal questions in pharmacology and biology concern how function of localized cells relates to disease. In experimental neuroscience we have dreamt about a magnifying glass that would allow us to see neurotransmitters in action, in cardiovascular research about a system that would provide us simultaneously with myocardial anatomy, mechanical function and cell function, and in cancer research for simultaneous detailed dynamic distributions of pharmaceuticals and tumor response, in small animals serving as models for human disease. Such studies have been limited by the availability of methods to study such molecular dynamics. Recently focussing SPECT systems (U-SPECT) have been developed that can quantify tracer dynamics in < 0.35mm structures by applying clever focusing pinhole geometries together with unique 3D focusing technology, list mode data acquisition and accelerated iterative reconstruction. Recently, a new way to perform sub-mm SPECT and PET simultaneously has been developed named VECTor: Versatile Emission Computed Tomography, based on a proprietary clustered multi-pinhole technology. U-SPECT/CT and VECTor/CT images will be shown as well as movies with sub-minute resolution. Examples include imaging density and occupancy of dopamine transporters in (sub)compartments of the brain, sub-half-mm resolution imaging of tumor markers and anti-cancer agents (e.g. antibodies) in micrometastasis, during a range of points in time. Applied to different models of disease this will aid our understanding of dynamic processes that underlie tissue functions and human pathology.

1482

TRACER DISCOVERY & DEVELOPMENT: FROM FIRST IN HUMAN TO QUALIFIED TRACER

M. Schmidt

Experimental Medicine, Janssen Research & Development, Beerse, Belgium

One of the more rewarding aspects of the discovery of tracers for in vivo imaging in human subjects is that preclinical studies can be highly predictive of the clinical results. As complicated as PET imaging can be; ultimately, the performance of tracers is heavily dependent on basic pharmacology and pharmacokinetic properties. These characteristics translate far more readily across mammalian species than behaviour, disease, and long term tolerability: the major hurdles for clinical CNS drug development. Once a ligand can be identified as having suitable properties for in vivo imaging in preclinical species, the probability of technical success for use in humans is high. Nonetheless, clinical testing and qualification involves a series of studies necessary to determine the safety of new tracers that require judgement, inclusion of a number of technical specialties, and serious advance planning. Necessary preclinical studies from pharmaceutical sponsors include receptor profiling and functional assays, physical chemistry relevant to formulation and bioanalytics, and in vivo pharmacology such as plasma protein binding. The standard toxicology approach is 'extended I.V.' studies in rat including 100 x to 1000 x the anticipated carrier mass, while additional safety studies (cardiovascular) or gentox studies may be added depending on sponsor practices, target distribution, or structural 'alerts'. A critical consideration for most pharmaceutical sponsors is meeting Good Manufacturing Practice (GMP) guidelines. This typically involves audits of the PET center by sponsor Quality Assurance representatives. Audits and requirements focus on the reliability and integrity of synthesis and dose preparation, sterility, and staff training and practices. Many aspects of GMP can be product specific and can require significant time and resource commitments from PET centers. Once all the approvals are in place, initial testing and characterization can be quite rapid. As one example, the introduction of PET/CT has significantly improved the reliability and speed with which dosimetry can be measured. Consideration should be given early to including blood flow studies to evaluate blood flow dependence of tracer delivery. Analysis concerns beyond the appropriate compartmental, graphical, or reference region approach include adequacy of acquisition, image QC, determination of human specific metabolism of the tracer, and careful post-processing. Points to consider for occupancy studies include acute versus steady state studies and the potential for 'dynamic' effects on the tracer target such as displacement by endogenous tracer, and up and down regulation of the target as a consequence of previous treatment with pharmacological doses of drugs of interest. Methods of data acquisition and analysis are of critical concern if the tracer is evaluated beyond a single PET center, especially if the tracer is to be employed in patient and treatment studies.

1483

IMAGING IN VIVO PHARMACOLOGY

A. Abi-Dargham

Columbia University, New York, NY, USA

PET has been used to image acute fluctuations in neurotransmitters. This technique relies on measuring change in the binding potential of a radiotracer induced by a pharmacological challenge administered between two scans. The most reliable paradigms have involved imaging aspects of the dopaminergic system, and have been restricted to the striatal structures where D2 receptors are most abundant, leading to very consistent findings in schizophrenia and addiction, and emerging observations in depression. Here we will review some of the validation work that supports the concept of imaging transmitter release, the findings that have emerged, and describe two novel paradigms that may lead to an expansion of our capability to image transmitters across different systems and different areas of the brain.

The first development relates to the evidence for measuring dopamine release in the cortex using [11C]FLB 457, a high affinity D2/3 radiotracer, combined with the amphetamine challenge. This method, if used within certain mass limits and full quantification, leads to measurable dopamine release capacity in areas of the brain involved in working memory and implicated in the cognitive deficits and negative symptoms observed in schizophrenia. This can lead to the examination of the role of cortical dopamine dysfunction in schizophrenia and addictive disorders.

The second new development is the suggestion that imaging fluctuations in glutamate levels may be feasible, using [11C]ABP688, a PET radiotracer that binds to an allosteric site on the mGluR5 receptor, combined with N-acetylcysteine (NAC), a drug shown to increase extracellular glutamate through stimulation of the cystine-glutamate antiporter. In this pilot study, PET in anesthetized baboons showed a significant decrease in [11C]ABP688 binding potential following NAC. There were no significant differences between test and retest, indicating the observed difference following NAC was not likely due to mass-carryover or some other effect of scan order. Although consistent with an allosteric interaction in which the affinity of [11C]ABP688 for mGluR5 is reduced compared to baseline due to increased glutamate levels following NAC, more studies are needed to replicate the finding and validate the method. If confirmed, [11C]ABP688 PET imaging will be a potential tool for detecting changes in glutamate levels in vivo.

Ultimately understanding the alterations in vivo allow us to develop animal models in a translational effort to study the corresponding cellular mechanisms of the disorders. Thus in vivo pharmacological studies with PET imaging play an important role in unraveling the cellular and molecular basis of psychiatric disorders.

1485

PRECLINICAL IMAGING IN BRAIN PET

R. Carson

Diagnostic Radiology, Yale University, New Haven, CT, USA

Preclinical imaging plays a key role in use of PET imaging for studies in the brain. Such studies are important, first in tracer development, and subsequently, to study brain mechanisms with appropriate animal models of neuropsychiatric diseases. In the tracer development phase, the goals of the studies are to assess whether there is appropriate levels of brain penetration, target specificity (assessed by pharmacological competition), dosimetry, and appropriate imaging characteristics (i.e., distribution, contrast, and kinetics). In addition, tracer kinetic modeling is used to assess whether binding measures can be obtained quantitatively. Mechanistic studies, on the other hand, tend to occur after a tracer has been validated and human studies have begun. Often their goal is to develop a hypothesis or validate a model to explain imaging alterations found in human disease. For example, measures of neurotransmitter release are inferred from changes in PET binding potential values. However, validation and proper interpretation of such findings can require preclinical studies, especially if they are linked with more invasive approaches such as microdialysis.

There are a number of important experimental design choices that must be addressed in designing a proper preclinical PET study. Rodent studies are quite common, and the resolution of current state-of-the-art small animal systems permits brain imaging, at least in the rat. However, not all tracers or target systems are well suited to proper quantification of brain signals in the rodent, at resolutions of 1-2 mm. In some ways, rodent brain imaging today is comparable to human PET brain imaging in the 1980's, where image resolution was measured in tens of mm. If rodent imaging is appropriate, quantification becomes a challenge, especially if arterial input functions are required, given limits in blood volume and the technical expertise required. For reversible receptor systems, constant infusion is one approach to simplify the quantification, and avoid misinterpretation of imaging data caused by tracer clearance.

For preclinical brain studies, nonhuman primates (NHP) are highly suitable. Their brain size is appropriate for imaging with clinical systems, and there is sufficient blood availability for input function measurements. Further, the imaging results in NHPs are typically more similar to those found in humans. In the tracer development phase, anesthetized animal studies are usually the rule. However, when mechanistic studies are performed, anesthesia can become a substantive confound. For example, Tsukada and others have shown that anesthesia affects the interpretability of binding measures, either by increasing endogenous neurotransmitter or altering receptor availability. Thus, the development of awake NHP imaging, while technically demanding, offers the possibility of a groundbreaking improvement in the interpretation and utility of translational neuroimaging studies.

1486

TRACER KINETIC MODELING AND ANALYSIS: THEORETICAL CONSIDERATIONS, COMPREHENSIVE METHODS AND PRACTICAL ADAPTATIONS

M. Slifstein[1,2]

[1]Psychiatry, Columbia University, [2]Division of Translational Imaging, New York State Psychiatric Institute, New York, NY, USA

PET imaging is a powerful and unique tool for obtaining quantitative information about brain neurochemistry, non-invasively in the in vivo setting. A critical step in this process is the development of parsimonious pharmacokinetic models; these are mathematical representations that are comprehensive enough to enable characterization of the essential elements of the biological processes being studied, but simple enough to allow robust statistical parameter estimation to be performed with real data. The balance between detail and practicality depends on the interplay between tracer properties (isotope used for radiolabeling, speed of peripheral kinetics, target specificity, affinity, signal to noise ratio), the target molecule or process being studied (abundant or sparse, homogeneous or heterogeneous distribution, existence or absence of suitable reference tissues), and the subjects being imaged (preclinical species, healthy humans, patients). The result is a range of data-fitting techniques, which are based on similar models of the underlying pharmacokinetics but are different in implementation.

Broadly, models fall into two classes: irreversible (typically used to image metabolic processes in which the radiolabel becomes “trapped” at some stage) and reversible (bimolecular association with, and unimolecular dissociation from, receptors or other target molecules). The mathematical starting points for both of these are compartment models, systems of differential equations which characterize the rates at which the tracer passes between different states (parent compound and metabolite for irreversible tracers, bound and unbound for reversible tracers).

In this presentation, we will discuss the underlying theory of the compartment models and the information that can be derived from them, in the context of reversible and irreversible models. We will review the methods used for actual analysis, including the most comprehensive approaches that compare tracer concentration in brain to concentration in arterial plasma, reference tissue models which are less invasive and less technically challenging than the comprehensive models but provide more limited information and are only feasible in some circumstances, and equilibrium analysis (tissue ratios) which also requires special conditions. We will also briefly touch on other issues that relate to making analysis simpler, such as direct implementation of the compartment models vs. graphical or basis function approaches, and other procedures for making studies more tolerable for subjects, such as determination of minimal scan durations necessary to obtain quantitatively reliable data.

1487

DEVELOPMENT OF RADIOTRACERS FOR PET IMAGING OF ENZYMES IN THE CNS

A. Wilson

PET Centre, CAMH and University of Toronto, Toronto, ON, Canada

As targets for CNS PET imaging it could be argued that enzymes have taken a backseat to other targets, most notably receptor proteins. However, because enzymes effect chemical transformations on their substrates, a variety of mechanisms exist for their imaging over and above simple recognition/binding of a radiotracer. This provides both opportunities and challenges in enzyme radiotracer design. For example, the position of the radiolabel within the radiotracer can be crucial for success. Consideration must also be paid to the rate determining step of the enzymatic mechanism, and the curious problems of high levels of target protein.

Several innovations in PET radiochemistry have been driven by the desire to image enzymes including incorporation of nucleophilic [^{18}F]-fluoride into unactivated aromatic rings, advances in [^{11}C]-phosgene radiochemistry, [*carbonyl*-^{11}C]carbamate/urea radiosynthesis, and the use of deuterium isotope effects to fine tune pharmacokinetics.

An overview of the types of mechanisms involved in PET radiotracers for enzymes in the CNS will be presented along with historical and recent examples of the synthesis and use of said radiotracers.

1488

GLOBAL ISCHEMIA AND ALTERNATE ANIMAL MODELS

U.I. Tuor[1,2,3]

[1]Institute for Biodiagnostics West, National Research Council of Canada, [2]Physiology and Pharmacology and Hotchkiss Brain Institute, University of Calgary, [3]Experimental Imaging Centre, Faculty of Medicine, Univerity of Calgary, Calgary, AB, Canada

This presentation will review briefly several models of global ischemia and alternate stroke models such as those for transient ischemic attack or recurrent stroke.

Global cerebral ischemia is fundamental to the morbidity and mortality occurring following resuscitation from cardiac arrest. Models of global ischemia commonly used to investigate the brain damage produced and its treatment include 4-vessel occlusion and 2-vessel occlusion in the rat and bilateral carotid occlusion in the gerbil. Cerebral injury following global ischemia includes neuronal death in hippocampal pyramidal cells and selective neuronal necrosis in cortex and striatum. Hypothermia is a treatment shown to be effective in reducing neuronal brain damage in global ischemia models; and, clinically, cooling has also been shown to be effective for reducing mortality and increasing favourable outcomes following circulatory arrest.

An alternate model of stroke to be presented is a recent model of recurrent stroke in the rat. Recurrent stroke consisting of a transient ischemic attack or minor stroke followed by a second stroke occurs frequently and provides an opportunity for treatment after the first attack. This rat model involves producing a minor stroke using a short transient middle cerebral artery occlusion followed days later by a second mild or moderate stroke. In contrast to pre-conditioning studies, if the first mild stroke is sufficient to produce selective neuronal necrosis then damage produced by the second stroke is enhanced. There is evidence for resveratrol administration to be protective in this recurrent stroke model.

1489

FUTURE DIRECTIONS AND CHALLENGES FOR REALISING THE FULL POTENTIAL OF BRAIN PET

T. Jones

The PET Research Advisory Company, Wilmslow, UK

Given the unique sensitivity and specificity of PET based molecular imaging, many of us who have seen the field develop feel it has under achieved with respect to its impact in clinical neuroscience, translation and healthcare. Few centres world-wide practice state-of-the-art PET. This is due in part to the modest outcomes to date but also because of the high buy-in, the cost of sustaining a PET research centre and extensive regulatory requirements. Added to this is the complex logistics of exploiting the application of imaging bio-markers labelled with short lived positron emitting radioisotopes such as carbon-11. However, there are promising developments with significant investments currently being made in PET bio-markers of amyloid and microglial activation which will provide appreciable boosts for the field on a number of fronts.

Future directions: Extend the biological entities quantified by PET such as the function of glial cells and astrocytes, processes down-stream to the neuro receptor, the neurochemistry of memory, blood brain barrier transport including strategies to enhance drug transport into the brain. Such developments, which are not exhaustive, would attract broader appreciation of being able to non-invasively research the human brain in health and disease.

The challenges:

· To realise the full potential of Brain PET in clinical neuroscience and healthcare

· Engage many more chemists and biologists

· Engage many more clinical neuroscientists

· Discover and develop specific PET based imaging biomarkers

· Continue to maximise the signal-to-noise within the PET data

· Maintain and enhance quantitative Brain PET through image derived input functions · Heighten the impact of PET by expanding its use across internal medicine.

Meeting the Challenges:

· Make PET research much more affordable, accessible and less logistically complex by exploiting the new generation of easy to install, simple to operate, low cost and low radiation emitting micro-cyclotrons

· Develop innovative chemistry to overcome the low radiochemical yields and specific activities associated with the micro-cyclotrons; especially through cyclotron target research, along with overcoming the inherent difficulties of labelling certain chemical structures

· Developing to GMP standards, reliable, low cost, small scale, micro-fluidics based disposable integrated radio labelling and analytical equipment

· Exploit the strengths of antibody technology for expanding PET based imaging bio-markers

· Make quantitative PET more easily accessible which is becoming ever important in healthcare with respect to removing the subjectivity of radiological reporting.

Strategies:

· Build on the investments and expertise developed to date

· Engage in tracer studies that are less stringent on high specific activity

· Place the modern technology for generating positron emitting radioisotopes (the reagents), namely micro-cyclotrons to where developments are foremost needed namely into premier chemistry and biology departments world-wide

· Encourage the commercial development of the next generation of low cost, high spatial resolution dedicated brain PET cameras

· Reinforce the progress that has been made in enhancing the signal to noise in reconstructed PET data and de-noising techniques

· Encourage the establishment of commercial photo-shops for standardising protocols for the recording and processing of kinetic PET data.

1490

A RAT MODEL FOR EMBOLIC ENCEPHALITIS

L.B. Astrup[1], T. Iburg[2], B. Aalbæk[2], R. Rasmussen[3], F. Johansen[3], J. Agerholm[2]

[1]Institut for Veterinær, Frederiksberg, [2]Faculty of Life Sciences, Copenhagen University Hospital, [3]Copenhagen Stroke Unit, Copenhagen University, Copenhagen, Denmark

Methods: 63 Male Sprague-Dawley rats were randomly assigned to three groups: control, sterile and septic. The right external carotid artery (ECA) was catheterized after anesthesia and 300µl blood was aspired. The blood was mixed with 30µl thrombin (2.5 IU/ml) in a catheter until coagulated. A sterile fibrin-clot of 5 mm was selected for embolization and injected via the ECA catheter. The common carotid artery was clamped during injection thereby directing the embolus via the internal carotid artery to the brain. The clot-diameter ensures occlusion at the origin of the middle cerebral artery. Occlusion was verified by angiography. In the septic group *Staphylococcus aureus* was added to the clot-mixture resulting in 600 CFU/5 mm fibrin clot. The control-group received no embolus. The body temperature was kept at 37.0 ±0.5°C during anesthesia. Animals were killed after 48 hours. Within each group animals were randomly assigned into two sub-groups, one formalin-perfused and one snap-frozen. Formalin fixed brains were cut into coronal sections and stained by haematoxylin & eosin and by immunohistochemistry.

Results: 11 animals in each group completed the survival period. Premature death occurred more than 2.5 times as often in the septic group than in the sterile group. Bacteriological cultivation showed rapid growth of bacteria in the brain during the survival time. Histology of the formalin-fixed brains showed uni-or bi-focal abscesses in the right hemisphere in the septic group. The abscesses stained positively for *Staphylococcus aureus* antigen in the center of the abscesses. Histology showed sterile infarction in the right hemisphere in the sterile group. No brain lesions were detected in the control animals.

Conclusions: We hereby present a novel animal model of haematogenous brain infection. A model of cerebral ischemia was modified to haematogenously introduce bacteria to an area of brain necrosis and damage to the blood-brain-barrier. Our model has several advantages: the surgical intervention is minimized, the bacteria gain access to the brain by the circulation and, no foreign materials other than bacteria are implated in the brain. This ensures high face-validity and high construct-validity of the model for three reasons: 1) Cerebral infarction by thrombosis or disseminated intravascular coagulation is a key mechanism involved in neurologic complications to human bacteriaemia. 2) *Staphylococcus aureus* is a leading cause of human brain abscesses. 3) Human brain abscesses are primarily confined to one anatomical site in the frontal lobe. This model therefore offers a tool for several scientific areas within research of brain infection and inflammation.

References:

Sharma, R. *et al.* (2009): *Infection*

Kielian, T. *et al*. (2004): *Journal of Neuropathology and Experimental Neurology.*

Rasmussen, RS. *et al.* (2003): *Acta Neurol Scand*

Syrjänen, J. (1989): *Scand J Infect Dis*

1491

THE STRUCTURAL BASIS OF POST-TRAUMATIC DISABILITY?

W. Maxwell

University of Glasgow, Glasgow, UK

Magnetic Resonance Imaging (MRI) provides evidence for loss of both white and grey matter, in terms of tissue volume, from the cerebral hemispheres in the chronic phase of traumatic brain injury (TBI). However, quantitative histopathological data is lacking.

The cortex and subcortical white matter in Brodmann Areas BA 11, BA 10, BA 24a and BA4 in 48 patients (Control n = 9, Moderately disabled [MD] n = 13, Severely Disabled [SD]n = 12 and Vegetative state [VS] (n = 12) that survived TBI for at least 3 months were examined using routine stereological techniques. Some patients from the archive were diagnosed with Diffuse Axonal Injury (DAI) post-mortem. The hypotheses tested were that thinning of the cerebral cortex occurred after TBI and different changes occurred for glial and neuronal number within cortex and underlying frontal white matter across GOS groups.

There was a greater loss of large pyramidal and large non-pyramidal neurons with more severe GOS from all four cortical regions with the greatest loss from the prefrontal cortex of DAI patients. Changes of number of medium and small pyramidal and non-pyramidal neurons differed between cortical regions and between DAI and non-DAI patients. Neurons did not follow a Poisson distribution but pyramidal neurons were usually scattered while medium and small non-pyramidal neurons were clustered. Nearest neighbour spacing increased in MD and SD but fell in VS patients. Reactive GFAP positive astrocytes occurred in all cortical layers in VS patients but only in cortical layers 1 and 2 in MD and SD patients. Numerous reactive microglia CR3/43 positive microglia occurred in lower layer 6 and subcortical white matter in SD and VS patients.

It is concluded that loss of neurons and increased numbers of reactive microglia in subcortical white matter reflect ongoing post-traumatic degeneration of gray and white matter in the chronic phase after TBI and contribute to the reduced executive and integrative capability reported in patients after traumatic brain injury. Although there is an initial loss of neurons and nerve fibres in the acute and post-acute phases after TBI, there is a continued lower level of loss in the chronic phase. There is more widespread loss in DAI patients ($p < 0.01$).

1492

ACTIVATION OF G-PROTEIN COUPLED K^+ CHANNEL (GIRK) SUPPRESSES NEURONAL REGENERATION IN THE DORSAL ROOT GANGLION

A. Cooper, E. Reuveny

Department of Biological Chemistry, Weizmann Institute of Science, Rehovot, Israel

G-protein coupled inwardly rectifying K+ (GIRK) channels generate slow inhibitory postsynaptic potentials in the central nerves system (CNS), and were implicated in various functions including pain, memory, reward and motor coordination. The GIRK channels are activated by various $G_{i/o}$-protein-coupled receptors ($G_{i/o}$ PCRs) such as a_2 adrenergic, g-aminobutyric acid type B ($GABA_B$), d, m and k opioids. Dorsal root ganglion (DRG) neurons are the primary neurons for somatic and visceral afferentation. The DRG cells are subclassified into two major groups: mechanosensors and nociceptors divided by size, while the aforementioned are smaller. All 4 types of GIRK subunits (GIRK1-4) are expressed in the nociception neurons.

The current study assessed the manifestation of GIRK current to regeneration of adult mouse DRG neurons *in-vitro*.

We found a significant reduction in neurite sprouting of small DRG neurons with GIRK2 trisomy. These neurons were dissected from a mouse line that harbors three copies of the *kcnj6* gene, the human gene encoding for GIRK2, one of GIRK subunits (Smith et al., 1995). In addition, treatment of tertiapin, a GIRK blocker, results in significant elevation in the amount of neurite sprouting of DRG neurons.

Electrophysiological measurements indicate that GIRK channels are expressed and functionally coupled with both $GABA_B$ and opioids receptors in the adult mouse DRG. Moreover, basal but not $GABA_B$ induced GIRK current is larger in triploid neurons, in primary hippocampal culture. The increase in GIRK current in these cells might explain the suppressed neurite sprouting, it is remained to be seen whether the activation of $GABA_B$ receptors are involved in this process.

To summarize, we suggest a novel role of GIRK channels in neuronal regeneration in the adult mouse DRG.

Reference:

Smith DJ, Zhu Y, Zhang J, Cheng JF, Rubin EM (1995) Construction of a panel of transgenic mice containing a contiguous 2-Mb set of YAC/P1 clones from human chromosome 21q22.2. Genomics 27:425-434.

1493

POST STROKE FUNCTIONALITY OF T CELLS

A. Vogelgesang[1], V.E. May[1], U. Grunwald[2], M. Bakkeboe[1], C. Kessler[1], B.M. Bröker[2], A. Dressel[1]

[1]Department for Neurology, [2]Institute for Immunology and Transfusion Medicine, University of Greifswald, Greifswald, Germany

Objectives: The close and complex relationship between the immune system and the brain in ischemic cerebral stroke has been in the focus of clinicians and immunologist for some time. More recently it has become apparent that stroke induces rapid and extensive alteration in the cellular compartment of the peripheral immune system including a dramatic loss of peripheral blood T-cells leading with subsequent infections. This study therefore addressed the functional consequences of immunological changes induced by stroke in humans. Of special interest were the kinetics of serum cytokine concentrations and differences in T cell function between stroke patients and healthy controls and between stroke patients with and without subsequent infection additionally.

Methods/ Results: For this purpose peripheral blood T-cells were isolated from 93 stroke patients. The expression of activation makers was determined. In addition ex vivo stimulation assays were applied to asses the functionality of T cells derived from blood of stroke patients.

Compared to healthy controls, stroke patients demonstrated an enhanced surface expression of HLA-DR ($p < 0.0001$) and CD25 ($p = 0.02$) on T cells, revealing that stroke leads to T cell activation, while CTLA-4 remained undetectable by immunfluorescent staining. In vitro studies revealed that catecholamines inhibit CTLA-4 upregulation in activated T cells. Ex vivo, T cells of stroke patients proliferated unimpaired and released increased amounts of the proinflammatory cytokine TNF-alpha ($p < 0.01$) and IL-6 ($p < 0.05$). Also, in sera of stroke patients HMGB1 concentrations were increased ($p = 0.0002$).

Besides T cell loss Treg have been extensively discussed as mediators of immune suppression in stroke. The relative resistance of Treg to steroid-mediated apoptosis could lead to the selective survival of this T cell subset. In this study the percentage of CD4+T-cells expressing high levels of CD25 was increased in stroke patients suggesting a survival advantage of this cell population. The total number of CD4+ CD25high cells was lower in the infected group, also the relative percentage of CD4+CD25high T-cells was not altered compared to the infected cohort either.

Conclusion: In summary, here we provide a detailed analysis of T cell functionality in stroke patients. We demonstrate a rapid activation of T cells that are primed towards a Th1 response. This was true for both patient subgroups; those with and those without subsequent infection.

Our data point towards two mechanisms which may mediate the activation of T cells in stroke patients: while increased HMGB1serum levels may activate surviving lymphocytes in stroke patients a downregulatory mechanism, the expression of CTLA-4 remains suppressed.

Further studies are needed to characterize the immunosuppressive cascades triggered by cerebral ischemia.

1494

MICRORNAS CONTROL BRAIN ENDOTHELIAL CELL BARRIER FUNCTION

A. Reijerkerk[1], B. van het Hof[1], K.A.M. Lakeman[1], J. Drexhage[1], J.B. Vos[1], M. Blommaart[1], D. Geerts[2], R. Agami[3], A. Prat[4], A.J. van Zonneveld[5], A. Horrevoets[1], **H.E. de Vries**[1]

[1]Blood-Brain Barrier Research Group, Molecular Cell Biology and Immunology, VU Medical Center Amsterdam, [2]Department of Human Genetics, Academic Medical Center, University of Amsterdam, [3]Division of Gene Regulation, The Netherlands Cancer Institute, Amsterdam, The Netherlands, [4]Neuroimmunology Research Laboratory, Center of Excellence in Neuromics, CHUM-Notre-Dame Hospital, Faculty of Medicine, Université de Montréal, Montréal, QC, Canada, [5]Department of Nephrology and Einthoven Laboratory for Experimental Vascular Research, Leiden University Medical Center, Leiden, The Netherlands

Endothelial cells in the body display a remarkable diversity and are perfectly adapted to the needs of the underlying tissue. One of the best examples of specific endothelial cell function is found in the blood-brain barrier (BBB) which is required for optimal brain homeostasis and neuronal performance. Brain capillaries are surrounded by and closely associated with several other cell types, including the perivascular endfeet of astrocytes, pericytes, microglia and neuronal processes that have been shown to contribute to barrier function.

Perturbations of BBB function are hallmarks of a variety of brain diseases. On the other hand, multiple efforts are focused on developing strategies to overcome the BBB and to effectively deliver active drugs to the brain. Understanding the mechanisms involved in the regulation of the blood-brain barrier may therefore open novel therapeutic avenues for treatment of neurological diseases. Yet, little is known regarding the molecular mechanisms that support the function of the BBB.

Using a combined genetic and bioinformatics approach, we uncovered a novel mechanism by which astrocytes mediate BBB function, i.e. through the activity of a new class of gene regulators called microRNAs. microRNAs regulate gene expression by binding to partially complementary sites in the 3' untranslated regions (UTR) of target genes, thereby causing degradation or translational repression.

We believe that detailed knowledge about these genes will allow us to design novel therapeutic approaches for several neurological diseases in which blood-brain barrier repair is required or controlled opening is needed for effective treatment. Our latest findings will be presented.

1495

A MINIMAL TWO-STAGE MODEL OF ENERGY METABOLISM AND ENERGY EFFICIENCY IN THE BRAIN

F.A. Dehmelt, C. Machens

Ecole Normale Sup´erieure, Paris, France

Objectives: most prominent of which are electrical activity (as measured by electrodes, EEG, etc.) and haemodynamic activity (as measured by fMRI). While much work has focused on how these two are linked [1][2], little quantitative or computational work has addressed the question of why there is haemodynamic activity in the first place. Given that blood flow is tightly linked to the regulation of cellular metabolism [3], the haemodynamic response is likely to balance two needs of the organism. One is to supply cells with necessary resources in a timely manner, thus avoiding starvation. The other is to avoid constant oversupply, as this would be an inefficient drain on the overall resources available. To quantify how these needs are balanced in practice, we construct a minimal metabolic model, linking the supply of metabolites from blood to the production of ATP. Our aim is to obtain as concise a model as possible while retaining key features of cerebral metabolism, to quantify the efficiency of ATP replenishment following brain activation. Identifying an optimally efficient policy could then reveal the constraints shaping the haemodynamic response. Local brain activity produces a wide range of experimentally accessible signals, the **Methods:** an aerobic pathway (TCA cycle, oxidative phosphorylation) consuming glucose and oxygen. At first, we assume constant concentrations of these metabolites. These interdependent pathways are linked by the intermediate product pyruvate. We assume Michaelis-Menten kinetics and product inhibition by ATP. We then specify a loss function reflecting the energetic cost of this policy, including both maintenance cost and operating cost. The former results from providing steady state metabolite concentrations. The latter arises from deviations from this state, such as temporary drops in the ATP/ADP ratio. Given the ATP consumption evoked by neural activity, this loss function can be applied to any policy regulating the uptake of metabolites, and the assumption of constant concentrations can be relaxed. We investigate the dynamics of ATP production via an anaerobic pathway (glycolysis) and **Results:** Furthermore, the time needed to approach this state is mostly determined by glucose, not oxygen concentration - except if the latter falls to an order of magnitude below its common resting value. These results may hint at glucose playing an important role in shaping the haemodynamic response. However, oxygen supply is likely to be a crucial factor with respect to efficiency, and whenever large quantities of pyruvate are exported or imported in the form of lactate. Our results indicate that steady-state ATP concentration should not depend on oxygen concentration. **Conclusions:** quantifying the efficiency of potential control mechanisms regulating metabolite uptake during ATP consumption. Incorporating available models of neurovascular coupling, it can be extended to quantify the efficiency of vascular control. This model further allows for **References:** Med. 39(6), 1998, 855-864; [2] Friston et al., NeuroImage 12(4), 2000, 466-477; [3] Mangia et al., J. Cereb. Blood Flow Metab. 29(3), 2009, 441-463. [1] Buxton et al., Magn. Reson.

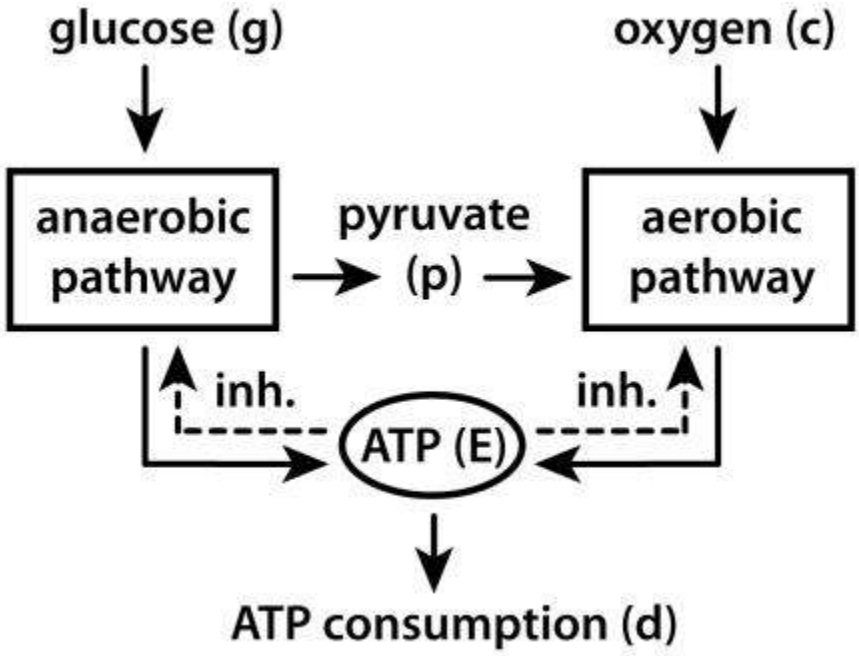
glucose (g)
oxygen (c)
anaerobic pathway
pyruvate (p)
aerobic pathway
inh.
inh.
ATP (E)
ATP consumption (d)

[GRAPH1]

1496

IMAGING IN CNS DRUG DEVELOPMENT

E.A. Rabiner

Clinical Imaging Centre, GlaxoSmithKline, London, UK

Rising costs necessitate the search for greater efficiency in the drug development process. Imaging technologies have the potential to reduce the time and resources necessary to progress a down the development pipeline. However, imaging technologies are expensive and complicated both in their use and in the interpretation of the data they generate. Optimal integration of imaging methods into drug development requires the understanding of the critical decision-making points in the drug development process. For imaging techniques to justify the resource required for their effective implementation, they have to be deployed at critical points to provide information that will lead to go/no-go decision making. I will propose that the use of molecular imaging methods can provide critical information refining the dose of novel medication, through the quantification of drug occupancy of its molecular target.

Such knowledge can be used to; make the choice of a candidate molecule, determine the range of doses to be examined in Phase I studies, and define the dose range to be used in proof-of-concept studies in Phase II. Target occupancy studies utilizing well characterized radioligands are ideally suited to provide these data. The optimal design of PET occupancy studies designed to meet these objectives will be explored. In the absence of a well characterized PET radioligand, quantification of the bio-distribution and tissue kinetics of a radiolabelled drug may be used to provide useful information. Optimal design and expected outcomes of biodistribution studies will be examined. Lastly, I will explore the integration of molecular imaging methods that characterize tissue pharmacokinetics, with functional imaging studies that provide information about cellular, tissue and system responses to pharmacological challenge. Examples of the integration of target occupancy studies with functional MRI studies will be presented and the role of such studies in aiding decision making will be discussed.

1497

INTRINSIC NEUROGENESIS IN CEREBRAL ISCHEMIA

N. Kawahara

Neurosurgery, Graduate School of Medical Sciences, Yokohama City University, Yokohama, Japan

In 1990's, several studies demonstrated that endogenous neural stem cells/progenitors (neural progenitors, NP) exist in the adult mammalian brain. One of them is located in the anterior subventricular zone (aSVZ), where these stem cells continuously divide and proliferated, and migrate towards the olfactory bulb to replace olfactory neurons (neurogenic regions). The other population resides under the dentate gyrus (subgranular zone, SGZ), where they similarly proliferate, migrate, and differentiate into mature granule cells. Following these findings, many studies have been carried out to see whether these endogenous NP can be utilized to replace lost neurons after brain insult, such as ischemia.

To utilize endogenous NP for the treatment of brain ischemia, several issues have to be addressed. To achieve replacement of lost neurons, NP should first change the pathway towards the ischemic lesion, where constitutive neurogenesis does mot normally occur (non-neurogenic regions). An epoch-making finding was then reported which demonstrated that NP in the aSVZ actually proliferate, migrate, and differentiate to mature neurons in the striatum after MCA occlusion. This study clearly demonstrated that adult mammalian brain still retains the intrinsic mechanism for neuronal regeneration in the non-neurogenic region. At the same time, several issues were found.

The first is that few neurons actually maturate in the lesion, which would account for the difficulty of functional recovery after ischemic injury. To overcome such low efficiency of endogenous neuronal regeneration, several studies tried to increase the number of proliferating NP by employing growth factors. Indeed these growth factors increased the number of NP and increased the final mature neurons. For example, in the striatum, up to 10-15% of the lost neuron were replaced by these treatments following ischemic lesion.

Another issue is whether such neuronal regeneration can be achieved at other non-neurogenic regions such as hippocampal CA1 and cortex. In the hippocampal CA1, quiescent neural NPs were found in the subventricular zone over the hippocampus, that could be potently activated by growth factors after ischemia and lead to successful regeneration of lost CA1 neurons. Similarly in the cortex, quiescent NPs were found to proliferate after ischemia leading to mature neurons. These studies demonstrated that quiescent NPs remain in the non-neurogenic region, implying that endogenous approach would be applicable to relatively broader regions.

It has also been questioned that such new neurons become functionally active. Recent studies revealed that such regenerated neurons mature electrophysiologically and become integrated in the pre-existing neuronal circuit in the striatum and hippocampus(dentate gyrus and CA1), leading to improvement of lost functions.

Though these studies have provided evidence for remarkable regenerative capacity of adult mammalian brain after ischemia, many other issues should be further addressed, such as low survival, inflammation response, migratory cue, and regulation of differentiation. Future studies are expected to clarify these issues to provide endogenous approach as a future clinical therapeutic option.

1498

ROLE OF IONIC CHANGES IN ER STRESS RESPONSES UNDER ISCHEMIC CONDITIONS

D. Sun

Neurological Surgery, University of Wisconsin-Madison, Madison, WI, USA

Dysregulation of endoplasmic reticulum Ca^{2+} (Ca^{2+}_{ER}) can disrupt proper peptide folding and trigger the unfolded protein response and ER stress. Maturation and folding of membrane and secretory proteins rely on the activity of Ca^{2+}-regulated ER chaperones and enzymes. Depletion of Ca^{2+}_{ER} will perturb the function of these proteins and result in formation of misfolded proteins which are subsequently degraded by the ubiquitin-proteasomal system. Therefore, maintenance of Ca^{2+}_{ER} homeostasis is important for appropriate protein folding. Moreover, release of Ca^{2+} from intracellular Ca^{2+} stores is a key component in astrocyte function under physiological conditions. This includes ATP-mediated Ca^{2+} release, which leads to a spatial expansion of astrocyte activation and plays an important role in coordination and synchronization of astrocyte responses to synaptic transmission. On the other hand, ER Ca^{2+} stores sequester Ca^{2+} to prevent intracellular Ca^{2+} overload in astrocytes. This event is accompanied with changes in mitochondrial function including increase of mitochondrial Ca^{2+} and depolarization of mitochondrial membrane potential. However, the temporal changes in Ca^{2+} homeostasis of ER and mitochondria, as well as in mitochondrial Cyt c release are not well studied. Our recent studies elucidate relationships between ER Ca^{2+} dysregulation and organelle damage (ER and mitochondria) under ischemic conditions. Supported by NIH R01NS38118 and R01NS048216.

1499

DESIGN OF NEUROPROTECTION STUDIES

K.-A. Hossmann

Max Planck Institute for Neurological Research, Cologne, Germany

Objectives: Alleviation of ischemic brain damage succeeds under various experimental conditions but suffers from poor translation to clinical trials. The Stroke Therapy Academic Industry Roundtables attributed this failure to various methodological and conceptual deficits and provided recommendations for improvement of preclinical research, notably the definition of time windows of neuroprotection, the use of different animal species and the study of permanent and transient vascular occlusion[1]. However, even strict adherence to these recommendations did not improve clinical outcome, which raises concerns about the appropriate design of experimental stroke studies.

Background and aims: Under experimental conditions, 3 basically different stroke models can be distinguished.

Permanent vascular occlusion as induced by mechanical clipping, coagulation or intraluminal filament insertion produces a gradient of flow with a central core which suffers energy failure, and a peripheral penumbra in which energy state is preserved. With ongoing ischemia time the infarct core expands into the penumbra, progressing to near maximal infarct volume within 3 hours. Neuroprotection may alleviate infarct growth but only as long as penumbral tissue is preserved, i.e. within a time window of similar to 3 hours.

Transient vascular occlusion with protracted recanalisation as induced by clot embolism followed by spontaneous or pharmacologically enhanced thrombolysis does not reverse core injury but prevents infarct growth due to improvement of penumbral blood flow. However, as infarct growth is not affected prior to the initiation of thrombolysis, time windows do not differ from those of permanent ischemia, i.e. also similar to 3 hours.

Transient vascular occlusion with sudden recanalisation: If ischemia is promptly reversed within 1-2 hours, core metabolism transiently recovers but suffers secondary energy failure after a free interval of up to 12 hours. The window of neuroprotection is much longer but the mechanisms of injury differ from those of permanent or clot lysis models. Moreover, prompt reperfusion within 1-2 hours can only be achieved under experimental conditions, notably the release of vascular clips or intraluminal filament withdrawal. Data are, therefore, not readily translatable to naturally occurring stroke.

This incompatibility is widely ignored in preclinical stroke research[2]. A PubMed search revealed that 62% of experimental treatments have been carried out using transient mechanical occlusion models. The review of preclinical data preceding the NX-059 (SAINT) trials[3] disclosed that the clinical time window of 6 hours was matched to experimental neuroprotection achieved after transient mechanical occlusion (up to 8 hours) but not to the clinically more relevant permanent ischemia models (mean treatment delay 45 min). This explains that SAINT and probably all other phase 3 neuroprotection trials (time windows 4-12 hours, median 6 hours) failed, whereas tPA thrombolysis trials with time windows of 3-4.5 hours (but not those with windows of 6-9 hours) were positive.

Conclusions:

These results strongly suggest that clinical relevance is a major reqirement for the design of experimental neuroprotection studies and that transient mechanical occlusion models should be abandoned in the future.

[1] Fisher et al, Stroke 40: 2244-2250, 2009

[2] Hossmann, Neuropharm. 55: 257-270, 2008

[3] Bath et al, Br.J.Pharmacol. 157: 1157-1171, 2009

1500

MR PERFUSION PARAMETERS: TESTING OF MODELS AND THRESHOLDS

L. Østergaard

Center of Functionally Integrative Neuroscience & MINDLab, NeuroCampus Aarhus, Aarhus University, Aarhus, Denmark

Background: Perfusion weighted MRI is sensitive to hemodynamic disturbances in acute ischemic stroke. Based on the temporal characteristics of passages of intravenously injected contrast media, perfusion maps may display indices relating to relative cerebral blood flow (rCBF), relative blood volume (rCBV), mean transit time (MTT) and vascular dispersion (Tmax). There is, however, a general lack of consensus regarding the physiological significance of these parameters, as well as their utility as predictors of tissue outcome, given the wealth of other relevant imaging and clinical data available to the physician.

There is hence an urgent need to better understand the physiological significance of perfusion parameters, and to develop more comprehensive models of infarct progression in acute stroke.

Objectives: The talk will discuss two avenues towards a better understanding of the ischemic penumbra based on multimodal MRI.

First, predictive models may compare multimodal imaging information in single voxels with the final outcome (infarcted, non-infarcted) of the voxel, to detect patterns associated with poor outcome. The talk will discuss how such ´multidimensional thresholds´ may allow not only better prediction of outcome - put also serve as research tools by allowing identification of strong predictors of infarct growth (inference), and comparison of infarct progression across groups subdivided according to the patients clinical, epidemiological or treatment characteristics.

Secondly, experimental findings and recent reanalysis of oxygen transport in tissue suggest that perfusion parameters may not reflect the metabolic impairment of ischemic tissue. The talk will briefly outline a crucial difference between tissue *ischemia* and tissue *hypoxia*, and discuss how an incomplete understanding of the flow-metabolism coupling in the ischemic penumbra may challenge the use of perfusion imaging in acute stroke.

Conclusion: Predictive models may better reflect the complexity of stroke pathophysiology than single perfusion thresholds, and serve to disentangle the roles of multiple factors in the progression of tissue damage.

A clearer distinction between tissue ischemia and tissue hypoxia may be crucial for our understanding of the pathophysiology of tissue damage in ischemia-reperfusion. **References:**

1. Wu O, Koroshetz WJ, Østergaard L, Buonanno FS, Copen WA, Gonzalez RG, Rordorf G, Rosen BR, Schwamm LH, Weisskoff RM, Sorensen AG (2001) Predicting tissue outcome in acute human cerebral ischemia using combined diffusion- and perfusion-weighted MR imaging. *Stroke* 32:933-942

2. Calamante F, Christensen S, Desmond PM, Østergaard L, Davis SM, Connelly A (2010) The physiological significance of the time-to-maximum (Tmax) parameter in perfusion MRI. *Stroke* 41:1169-1174.

3. Østergaard L, Jonsdottir KY, Mouridsen K (2009) Predicting tissue outcome in stroke: new approaches. *Curr Opin Neurol* 22:54-59.

1501

TWO-PHOTON PHOSPHORESCENCE LIFETIME MICROSCOPY (2PLM) FOR HIGH RESOLUTION OXYGEN IMAGING IN THE BRAIN

S. Vinogradov

Biochemistry and Biophysics, University of Pennsylvania, Philadelphia, PA, USA

Imaging brain oxygenation is a challenging problem in modern neuroscience. We present a method for imaging of oxygen in biological tissues with micron-scale resolution and three-dimensional capability. The technique is based on the combination of *phosphorescence quenching* with *two-photon laser scanning microscopy*. The key to the method are special two-photon-enhanced oxygen probes whose phosphorescence upon two-photon excitation is enhanced *via* intramolecular Förster-type energy transfer from covalently attached two-photon antennae. The probe´s oxygen sensitivity is tuned by way of encapsulation of phosphorescent chromophores inside dendrimers, while peripheral functionalization prevents interactions of the probes with biological macromolecules and ensures their high selectivity for oxygen. We also address design of a two-photon microscope required for 2PLM and discuss the interplay between the probe photophysics, spatial and temporal imaging resolution. 2PLM was applied to obtain the first depth-resolved intravascular and interstitial high-resolution oxygen maps *in vivo* in the brain. The unique properties of the probe allowed simultaneous 3D mapping of oxygen in vasculature and tissue as well as measurements of the rate of blood flow in individual capillaries.

1502

OPTICAL COHERENCE TOMOGRAPHY OF MICROVASCULAR CEREBRAL BLOOD FLOW

R.K. Wang

Department of Bioengineering, University of washington School of Medicine, Seattle, WA, USA

Advances in optical technologies have spurred many new applications of light in biology and medicine. The expanding fields of optical diagnostics and therapeutics include such diverse topics as photodynamic therapy for cancers and other diseases, fluorescence endoscopy for early tumor detection, photoacoustic imaging for deep tissue vascular visualization, and optical coherence tomography (OCT) for superficial tissue assessment. OCT is a new medical imaging modality in which the coherent interference of a wide spectrum light source is used to create a high resolution (micron-scale) subsurface image of tissue microstructure. Recently, we have supplemented the microstructural OCT images with additional contrast mechanisms such as blood flow imaging using the static and dynamic (Doppler) speckle effects, which provide us the ability to perform label-free optical microangiography (OMAG) of microcirculatory tissue beds. The ability to visualize tissue blood flow at the microcirculation level is important in a variety of biomedical applications, some of which (along with the OCT basics and the enabling technologies) will be highlighted in this talk. Examples using OMAG to delineate the dynamic blood perfusion, down to capillary level resolution, within living tissues will be given, including cerebral blood flow in small animals and retinal blood flow in humans.

1503

CELL DEATH MECHANISMS IN OLIGODENDROCYTES

C. Matute[1,2]

[1]Departamento de Neurociencias, Universidad del País Vasco, [2]CIBERNED, Leioa, Spain

White matter (WM) cells and axons possess the molecular machinery to signal by means of neurotransmitters, a property whose functional significance remains elusive. Yet, it is now well established that excessive neurotransmitter signalling is deleterious to WM and that it can trigger disease and/or contribute to its progression. In my presentation, I will summarize progress in the understanding of the mechanisms by which neurotransmitters cause structural and functional damage to WM, and their relevance to multiple sclerosis and stroke, and emphasize the case of glutamate and ATP, two major excitatory transmitters that can act as potent neurotoxins.

Sustained activation of ionotropic glutamate receptors of the AMPA, kainate and NMDA subclasses damages oligodendrocytes, a feature which depends entirely on Ca^{2+} overload of the cytoplasm and which can be initiated by disruption of glutamate homeostasis. Thus, inhibition of glutamate uptake by activated microglia can compromise glutamate homeostasis and induce oligodendrocyte excitotoxicity. Moreover, non-lethal, brief activation of kainate receptors in oligodendrocytes rapidly sensitizes these cells to complement attack as a consequence of oxidative stress.

In addition to glutamate, ATP signalling can directly trigger oligodendrocyte excitotoxicity via activation of Ca^{2+}-permeable P2X7 purinergic receptors which mediates ischemic damage to WM and causes lesions that are reminiscent of multiple sclerosis plaques. Conversely, blockade of P2X7 receptors attenuates post-ischemic injury to WM and ameliorates chronic experimental autoimmune encephalomyelitis, a model of multiple sclerosis. Importantly, P2X7 expression is elevated in normal-appearing WM in multiple sclerosis patients, suggesting that signalling through this receptor in oligodendrocytes may be enhanced in this disease.

Altogether, these observations reveal novel mechanisms by which altered glutamate and ATP homeostasis can trigger oligodendrocyte death. This knowledge will generate new therapeutic avenues to treat more efficiently acute and chronic WM pathology.

Funded by CIBERNED, Universidad del País Vasco, MICINN and European Leukodystrophy Association.

Selected references:

Matute C, Cavaliere F. Neuroglial interactions mediated by purinergic signalling in the pathophysiology of CNS disorders. Semin Cell Dev Biol. 2011 Feb[Epub ahead of print] .

Domercq M, Alberdi E, Sanchez-Gomez MV, Ariz U, Perez-Samartin A, Matute C.

DUSP-6 phosphatase and ERK mediate AMPA receptor-induced oligodendrocyte death. J Biol Chem. 2011 Feb 7. [Epub ahead of print]

Matute C. Glutamate and ATP signalling in white matter pathology. J Anat. 2011

Jan 20. doi: 10.1111/j.1469-7580.2010.01339.x. [Epub ahead of print]

Domercq M, Perez-Samartin A, Aparicio D, Alberdi E, Pampliega O, Matute C.

P2X7 receptors mediate ischemic damage to oligodendrocytes. Glia. 2010 Apr 15;58(6):730-40.

1504

IMAGING EPIGENETIC FACTORS BY PET

J.G. Gelovani

Experimental Diagnostic Imaging, UT M.D. Anderson Cancer Center, Houston, TX, USA

With the recent advances in epigenetic research and improvement in our understanding of various epigenetic mechanisms, chromatin and DNA modifying enzymes, such as histone deacetylases (HDACs), histone methylases (HMs), and DNA methylating enzymes have emerged as important regulators of gene expression, development, physiology and life span. This presentation will cover a series of comprehensive imaging studies in rodents and non-human primates to assess the efficacy of novel radiolabeled agents non-invasive PET imaging of Class-II and Class-III histone deacetylase enzymes in the brain and other organs and tissues. The availability of novel HDAC class- and isoform-specific PET radiotracers will have a significant positive impact on the pace or research in the field of epigenetics.

Our group was the first to develop a radiotracer for PET imaging of HDAC expression and activity, the 6-([^{18}F]fluoroacetamido)-1-hexanoicanilide, termed ^{18}F-FAHA [1]. We have demonstrated, that after i.v. injection ^{18}F-FAHA rapidly accumulates in the brain in rats and in rhesus macaques, and that the rate of ^{18}F-FAHA accumulation in the brain is inhibited in a dose-dependent manner by HDAC inhibitor SAHA (vorinostat) [2, 3]. The most recently, the NIDA researchers confirmed our in vivo imaging results in non-human primates [4]. Using quantitative PET/CT/MRI imaging and pharmacokinetic modeling, a dose-dependent nature of SAHA-induced reduction in ^{18}F-FAHA accumulation in the baboon brain was demonstrated. Based on these initial studies, we developed a novel SIRTs-specific radiotracer 6-(4-[^{18}F]**F**luoro-**Ph**enyl-**A**cetamido)-**H**exanoic-**A**nilide (^{18}F-PhAHA), established it's substrate specificity to SIRTs in a panel of human recombinant enzymes from all classes of HDACs, and performed initial evaluation of this novel radiotracer *in vitro* in tumor cell lines and *in vivo* in mice using PET/CT.

These PET imaging agents will enable non-invasive and repetitive *in vivo* imaging of expression and activity of HDACs in the brain and different organs and tissues (including cancer) and help to understand the mechanisms of HDACs involvement in normal physiology and in the mechanisms of different diseases. The utilization of invasive biopsies of normal tissues (i.e., brain, heart, etc.) is prohibitive in humans due to obvious reasons of traumatism and morbidity. Therefore, PET/CT(MR) imaging using HDACs-specific substrate-type radiotracers should enable non-invasive monitoring of pharmacodynamics and therapeutic efficacy of novel HDACs-specific inhibitors (or activators) in experimental animals and in humans, and facilitate their translation into clinic.

References:

1. Mukhopadhyay U, T.W., Gelovani J, Alauddin M. J Label Comp Radiopharm., 2006. **49**: p. 997-1006.

2. Nishii R, et al. J Nucl Med, 2007. **48**(Suppl.2): p. 336.

3. Sanabria S, et al. NeuroImage, 2008. **41**(Suppl.2): p. T15.

4. Reid, A.E., et al. Nucl Med Biol, 2009. 36(3): p. 247-58.

1505

LOSS-OF-FUNCTION OF NSF LEADS TO DELAYED NEURONAL DEATH AFTER BRAIN ISCHEMIA

B. Hu, C. Liu

University of Maryland School of Medicine, Baltimore, MD, USA

Neurons are particularly susceptible to the toxic effect of misfolded proteins, which is underscored by the fact that protein misfolding occurs in virtually all neurodegenerative disorders. Recent studies provide strong evidence that protein misfolding/aggregation also occurs in postischemic neurons, where it induces multiple organelle damage and plays a prominent role in neuronal death after brain ischemia.

Emerging evidence suggests that many established ischemia-induced damage mechanisms converge to generate protein damage including: mitochondrial dysfunction, acidosis, increased intracellular Ca^{2+}, reactive oxygen species (ROS), and dysfunction of protein quality control systems. Collectively these lead to dramatic deposition of misfolded proteins on subcellular organelle membranes in postischemic neurons. Postischemic neurons respond to overload of misfolded proteins by: (i) shutting off protein synthesis to reduce the load of the major cellular unfolded nascent polypeptides, (ii) expression of molecular chaperones/stress proteins to prevent misfolded protein-induced toxicity; i.e., proteotoxicity, and (iii) upregulating the ubiquitin-proteasomal and autophagy protein degradation pathways for eliminating misfolded proteins. The importance of protein misfolding is further supported by: (i) studies showing that overexpression of molecular chaperones protects neurons from ischemic injury; and (ii) ischemic preconditioning is able to create a state that can cope with accumulation of neuronal misfolded proteins, thus offering neuroprotection. Therefore, proteotoxicity appears to be a key nodal point in the constellation of events underlying post-ischemic delayed neuronal death. It is therefore timely to bring together information pertinent to post-ischemic proteotoxicity to disseminate findings and foster further interest and research in this area.

One of the key mechanisms of proteotoxicity is that unfolded/misfolded proteins trap critical active cellular proteins, thereby converting them into inactive protein aggregates. Loss-of-function of critical cellular proteins that are necessary for cell survival will eventually lead to cell death after brain ischemia. N-ethylmaleimide-sensitive fusion ATPase (NSF) is one such critical protein trapped into inactive protein aggregates after brain ischemia. NSF is a homohexameric ATPase, and a central component of the cellular machinery in the transfer of intracellular membrane vesicles/organelles from one membrane compartment to another. We recently discovered that functional NSF is severely and irreversibly depleted by protein aggregation in neurons after brain ischemia. We therefore generated both NSF loss-of-function mutation and gain-of-function overexpression transgenic mouse lines. Our studies show that NSF deficiency by dominant negative mutation in transgenic mice can replicate neuronal pathology seen after brain ischemia, while the gain-of-function type offers cell protection. Damage to two prominent organelles, the Golgi apparatus and the autophagosome-lysosome, were clearly seen in both postischemic neurons and NSF-deficient transgenic mice. The organelle damage develops over time and eventually results in delayed neuronal death after brain ischemia.

1506

CELL-BASED STRATEGIES FOR FUNCTIONAL REGENERATION FOLLOWING SPINAL CORD INJURY

X.-M. Xu

Indiana University School of Medicine, Indianapolis, IN, USA

Injury to the spinal cord is devastating because of the inability of injured spinal descending and ascending axons to regenerate and to rebuild their functional connections. The consequences of injury are not just a break in communication between neurons, but also a cascade of events leading to neuronal degeneration and cell death. Thus, regeneration in the adult spinal cord requires a multi-step processes. First, the injured neurons must survive, and then the damaged axons must extend to innervate their original targets. Once the contact is made, the axons need to be remyelinated and functional synapses need to form on the surface of the targeted neurons. Several strategies could be considered to achieve these objectives, such as cell replacement, neurotrophic factor delivery, removal of the inhibitory molecules at the site of injury, bridging the lesion gap with artificial substrates, and modulation of the immune responses. In our laboratory, a spinal cord hemisection and Schwann cell (SC)-seeded guidance channel transplantation model in adult rats was developed. We demonstrated that grafted SCs formed an effective bridge promoting robust regeneration of damaged axons. When glial cell line-derived neurotrophic factor (GDNF) was co-administered with SCs, it enhanced axonal regeneration and myelination. To promote axon growth beyond the bridge transplant, three strategies showed promise which include (1) infusion of brain-derived neurotrophic factor (BDNF) and/or neurotrophin-3 (NT-3) into the distal spinal cord, (2) infusion of chondroitinase ABC (ChABC) into the distal spinal cord, and (2) delayed transplantation of SC-seeded guidance channels at 2-4 wks post-SCI. Synaptic bouton-like structures were found between regenerated axons and target neurons. We propose that a complete regeneration strategy may include the following steps (1) prevention of axonal die-back from the lesion site, (2) promotion of axonal regeneration through permissive bridge transplants, (3) removal of inhibitory gliotic environment at graft-host interfaces, (4) provision of growth-promoting pathways for extension of regenerating axons, and (5) target innervation of regenerated axons. Combination of these strategies may lead to meaningful recovery of function following CNS injuries.

1508

THE ROLE OF PPARΓ IN PROTECTING THE FEMALE BRAIN DURING HYPERTENSION

M. Cipolla

Neurology, University of Vermont, Burlington, VT, USA

Cardiovascular disease (CVD) and stroke are leading causes of death for women as well as men. Since 1984, the number of deaths from CVD for females exceeded those for males. Hypertension is also common in women, a leading risk factor for CVD and stroke. Hypertension has profound effects on the cerebral circulation in males, causing inward remodeling and capillary rarefaction that can limit vasodilator reserve and worsen stroke outcome. In contrast, little is known regarding how hypertension affects the cerebral circulation in females, where the hormonal milieu is significantly different. In relation to mechanisms that may underlie these changes, peroxisome proliferator-activated receptor-γ (PPARγ) is a ligand-activated transcription factor expressed in vascular cells that has been shown to be involved in cerebral vascular remodeling and hypertension. Here, we have begun to explore how hypertension affects the cerebral circulation in female rats and the role of PPARγ in mediating those changes. We found that just three weeks of hypertension induced by inhibition of NO synthase (NOS) caused significant inward remodeling and capillary rarefaction of cerebral arteries that was reversed by treatment with rosiglitazone, a PPARγ agonist. In addition, hypertension by NOS inhibition caused increased hydraulic conductivity of the blood-brain barrier that was also reversed by treatment with rosiglitazone. Lastly, we show that treatment of normotensive female rats with rosiglitazone caused selective outward remodeling of penetrating brain arterioles, but not upstream arteries, that was associated with decreased vascular resistance and hyperperfusion during acute hypertension, a model of severe preeclamsia/eclampsia. Together these results suggest that the cerebral circulation of females undergo similar changes during hypertension, including inward remodeling and increased permeability that can be reversed by PPARγ activation. Thus, PPARγ-dependent signaling may be an important regulator of cerebrovascular structure and function in both males and females.

1509

TRANSCRANIAL, NON-INVASIVE MEASUREMENTS OF MICROVASCULAR CEREBRAL BLOOD FLOW, BLOOD OXYGENATION, BLOOD VOLUME AND CMRO2 IN HUMANS WITH HYBRID DIFFUSE OPTICS

T. Durduran

ICFO- The Institute of Photonic Sciences, Castelldefels/Barcelona, Spain

Two related but fundamentally different diffuse optical methods — near-infrared spectroscopy (NIRS) and diffuse correlation spectroscopy (DCS) — were developed in hybrid probes towards translational studies at the bed-side in the neuro-intensive care units (NICU). Together, these methods allow for transcranial, non-invasive measurement of microvascular, cerebral blood flow (CBF), blood oxygenation, blood volume and cerebral metabolic rate of oxygen extraction (CMRO2).

I will briefly describe the fundamentals of both methods, their technological implementation, hybrid probes and the developments (mainly at University of Pennsylvania) that led from in-vivo studies on experimental rodent models (“bench-top”) to pilot clinical studies (“bed-side”). I will discuss potential applications with examples in ischemic stroke management, traumatic brain injury monitoring and neonatal intensive care management.

1510

CNS DRUG DELIVERY

T.P. Davis, P.T. Ronaldson

Medical Pharmacology, University of Arizona College of Medicine, Tucson, AZ, USA

The blood-brain barrier (BBB) constitutes a physical and biochemical barrier between the brain and the systemic circulation. This dynamic structure regulates critical processes of nutrient uptake and waste removal, thus enabling the BBB to maintain brain homeostasis. However, BBB characteristics involved in homeostatic control (i.e., tight junction (TJ) protein complexes, expression/activity of endogenous drug transport proteins) are also significant obstacles to CNS drug delivery. As paracellular permeability is limited by TJs between adjacent endothelial cells, transcellular permeability is governed by a discrete balance between uptake and efflux transporters. Furthermore, complexity of mechanisms involved in CNS drug delivery is underscored by the fact that BBB integrity may be compromised in response to pathophysiological stressors. In this “teaching session” on CNS drug delivery, data from our laboratory has shown that hypoxia/reoxygenation, oxidative stress, and peripheral inflammatory pain can dramatically alter both TJ protein complexes and endogenous drug transport mechanisms using both in vitro and in vivo models. In order to characterize BBB mechanisms involved in brain drug delivery, our laboratory has utilized multiple in vitro and in vivo methodologies. Using bovine brain microvessel endothelial cells, we demonstrated that hypoxic stress increased paracellular flux of sucrose, a vascular marker that does not typically cross the BBB. Hypoxic stress also decreased transendothelial resistance in this same model system, which further implies reduced barrier properties. However, use of in vitro cell culture systems to study CNS drug delivery is not without limitations. In fact, an effective in vitro model of the mammalian BBB has yet to be developed, primarily because vascular endothelial cells lose their barrier properties when subjected to cell culture conditions. Therefore, our laboratory continues studying CNS drug delivery in vivo using the in situ brain perfusion technique. This method enables us to directly examine mechanisms of permeability and/or transport at the BBB in healthy animals and in animals subjected to pathophysiological stress under more representative physiological conditions than can be obtained in vitro. Such studies have shown that paracellular permeability to vascular markers (i.e., sucrose) and drugs (i.e., morphine, codeine) were increased in response to hypoxia/reoxygenation stress and/or peripheral inflammatory pain. These increases in xenobiotic permeability were directly related to changes in constituent proteins of BBB TJ complexes. We also demonstrated that peripheral pain/inflammation can significantly alter functional expression of CNS drug transporters that are endogenously expressed at the BBB endothelium (i.e., P-glycoprotein, Organic Anion Transporting Polypeptide 1a4 (Oatp1a4)). Although CNS efflux, mediated by P-glycoprotein, is increased during pain/inflammation, we identified Oatp1a4 as a transporter target that may be exploited to optimize delivery of therapeutic agents to the brain. Overall, results from our studies can profoundly impact drug development and/or design as well as treatment of CNS disease. This teaching session will highlight techniques utilized by our laboratory for the study of CNS drug delivery and how data obtained from such experiments can translate to optimization of pharmacotherapy to the patient.

Studies described in this abstract were supported by National Institutes of Health Grants R01-NS39592, R01-NS42652, and R01-11271 to TPD.

1511

PHYSIOLOGICAL MONITORING AND EFFECTS OF TEMPERATURE

T. Nowak

Department of Neurology, University of Tennessee Health Science Center, Memphis, TN, USA

Unrecognized variations in physiological parameters are major contributors to variability in brain ischemia models, and continue to confound many studies of experimental interventions. Ischemia models differ markedly in their sensitivity to particular variables, and different monitoring standards therefore apply.

Global ischemia models, by design, produce profound and homogeneous reductions in CBF. Other than cardiac arrest, all such models rely on the efficacy of vascular occlusions to reduce perfusion, which is influenced by blood pressure. In models that employ systemic hypotension this is specifically measured and controlled. In other cases it remains a potential source of systematic variability, dependent on animal strain and choice of anesthetic. Blood glucose can also influence the acute time course of ischemic depolarization, but has a minor impact unless there is substantial residual CBF. With additional effort, direct monitoring of ischemic depolarization as an index of insult severity can essentially eliminate variability arising from these two sources.

Temperature is the most critical parameter in global ischemia. Independent monitoring and control of head/brain temperature is essential to avoid heat loss during occlusion. Spontaneous hyperthermia is a recognized complication during early recirculation in some models, exacerbating injury and increasing sensitivity to artifactual cooling in the context of intervention studies. Due to the prolonged time course of days to weeks during which selective neuron injury evolves after global ischemia, and its sensitivity to even slight cooling, long term temperature monitoring is essential. This is best done by telemetry.

Focal ischemia models require comprehensive assessment of all physiological variables, especially in the context of transient occlusions. Insult severity is determined by the graded CBF deficit in the territory of the occluded artery, which depends on collateral perfusion, and therefore blood pressure. For a given distribution of perfusion deficit, blood oxygenation establishes the position in the gradient at which normal metabolism can be maintained, and blood glucose levels in turn determine the extent of tissue in which ATP production can be sustained by anaerobic glycolysis. All of these parameters are affected by anesthesia, which is often maintained for the duration of transient occlusions. Monitoring is less critical for permanent occlusion models, in which anesthesia duration is brief and the insult is sustained in the awake state.

Focal models are somewhat less sensitive to incidental cooling, but routine temperature control during surgical anesthesia is essential. The greatest risk of artifact arises due to hyperthermia, secondary to the hypothalamic ischemia often produced by intraluminal filament occlusions. As noted above for global ischemia, this worsens the impact of the insult and therefore amplifies the protective effect of artifactual cooling that might result following administration of a test agent. Since infarcts evolve more slowly after transient occlusions, the interval of potential susceptibility to temperature effects is more prolonged. Furthermore, transient filament insertions that produce vascular damage can induce a prothrombotic state, further prolonging the time course of flow deficit and infarct progression. Long term telemetry is also the definitive method for identifying temperature artifacts in focal ischemia.

1512

ENERGY METABOLISM AND REGULATION OF CEREBRAL BLOOD FLOW

U. Lindauer

Dept. of Neurosurgery, Experimental Neurosurgery, Klinikum rechts der Isar, Technical University Munich, Munich, Germany

Although neurovascular coupling has been investigated for almost 120 years, the cellular and molecular mechanisms that couple neuronal activity to metabolism and blood supply are still incompletely understood, and concepts are currently changing (Attwell et al., 2010). The traditional 'metabolic' hypothesis implicates that neurons or astrocytes, triggered by a fall in oxygen or glucose or by a rise in carbon dioxide concentration, release vasoactive metabolic products, such as H+ or adenosine. However data from the literature show that neither hyperoxia or mild hypoxia nor hyperglycemia or mild hypoglycemia significantly changes the blood flow responses to functional activation (Lindauer et al, 2010; Mintun et al., 2001; Wolf et al., 1997; Powers et al., 1996), pointing against a direct sensing mechanism of oxygen or glucose concentration involved in activity induced CBF regulation. The 'neuronal' hypothesis, on the other hand, postulates that neuronal energy demand is communicated to the vasculature (either directly or through astrocytes) in an anticipatory, feedforward manner by vasoactive neurotransmitters or products of synaptic signaling.

Neurons can tolerate only small changes in energy supply. Beside a change in blood flow, adaptation to nutrient supply may also occur by changing the balance between aerobic glycolysis and oxidative phosphorylation. During aerobic glycolysis, glucose is utilized in excess of that used for oxidative phosphorylation despite availability of sufficient oxygen for completely metabolism of glucose to carbon dioxide and water. Aerobic glycolysis is present in the normal human brain at rest, showing high regional variation (Vaishnavi et al., 2010), and has been observed to increase locally in the brain during task-induced increases in cellular activity (Fox and Raichle 1988). In addition to glucose supplied by the blood, it has recently been shown that glycogen reservoir in astrocytes not only provide energy substrate during short lasting hypoglycemia, but glycogen turnover also occurs in the presence of glucose (glycogen shunt activity) (Dienel et al., 2007; Walls et al., 2009). It can be hypothesized that transient increases of glucose metabolism and / or transient changes in astrocytic glycogen content may also transiently alter the relation between aerobic glycolysis and oxidative phosphorylation.

In this presentation, preliminary and indirect evidence for a variability of the balance between aerobic glycolysis and oxidative phosphorylation will be provided from studies in anesthetized rats using optical methods to measure blood flow and blood oxygenation changes during physiological activation.

Reference:

Attwell et al., Nature 468: 232-243, 2010

Dienel et al., J Neurochem 102: 466-478, 2007

Fox et al., Science 241:462-464, 1988

Lindauer et al., J Cereb Blood Flow Metab 30: 757-768, 2010

Mintun et al., Proc Natl Acad Sci 98:6859-6864, 2001

Powers et al., Am J Physiol Heart Circ Physiol 270: H554-559, 1996

Vaishnavi et al., Proc Natl Acad Sci 107: 17757-17762, 2010

Walls et al., Neuroscience 158: 284-292, 2009

Wolf et al., Brain Res 761:290-299, 1997

1514

IN-VIVO OPTICAL IMAGING AND MICROSCOPY OF NEUROVASCULAR COUPLING

E.M.C. Hillman

Biomedical Engineering and Radiology, Columbia University, New York, NY, USA

Neurovascular coupling is the tight relationship between neuronal activity and blood flow modulations in the brain. An increase in blood flow accompanies almost all neuronal activity that occurs in the cortex. The resulting local decrease in deoxy-hemoglobin concentration is the basis of functional Magnetic Resonance Imaging (fMRI).

However, very little is understood about how and why blood flow is modulated in the brain. The 'hemodynamic response' to a stimulus generally starts several hundred milliseconds after stimulus onset, peaking 2-5 seconds later, irrespective of when the stimulus ends. Furthermore, the response corresponds to an *increase* in local oxygenation, suggesting that the additional oxygen supplied by an increase in blood flow far exceeds any increase in oxygen consumption.

Nevertheless, this hemodynamic response is a vital part of normal brain function, and it is thought that impaired neurovascular coupling may underlie a range of disorders including age-related neurodegeneration and even Alzheimer's. A proper understanding of how the hemodynamic response is controlled, and what it represents in terms of brain energetics would both provide potential therapeutic targets for disease, while also improving interpretation of fMRI data.

Our approach to studying neurovascular coupling is to utilize high-speed, high-resolution optical imaging and microscopy of the intact, in-vivo exposed rodent cortex. Imaging in-vivo maintains the natural timing of the response to stimulus, while also ensuring that blood flow and central nervous system innervation are in place. Imaging contrast is provided by the differing absorption properties of oxy- and deoxy-hemogloin, intrinsically fluorescent metabolites NADH and FAD, intravascular tracer dyes, cell-specific dyes such as astrocyte-specific sulforhodamine 101, active dyes such as calcium sensitive dyes, and transgenic animals expressing fluorescent proteins.

To date, we have carefully characterized the evolution of the hemodynamic response in terms of its vascular manifestations within arterioles, capillaries and veins. We have combined these studies with in-vivo two-photon microscopy to explore astrocyte-vascular interactions, and their potential role as mediators of vascular control. Our work has led to an exciting 3-phase model of neurovascular coupling that accommodates many previous observations that were seemingly contradictory.

In addition to characterizing neurovascular coupling in the normal brain, in response to stimulus, we are also using our imaging tools to explore brain development and the effects of pathologies such as glioma on neurovascular coupling. Further work is focused on characterizing the nature of baseline fluctuations in cortical hemodynamics as captured during 'resting state' fMRI, to determine the underlying basis of functional connectivity mapping fMRI.

1515

GENETIC APPROACHES DEFINE CELL-SPECIFIC ROLES FOR PPAR GAMMA IN THE VASCULATURE

F. Faraci

University of Iowa, Iowa City, IA, USA

Peroxisome proliferator-activated receptor-gamma (PPARg) is a ligand-activated transcription factor expressed in many cell types including the vasculature. Thiazolidinediones (TZDs) are synthetic activators of PPARg used to treat type II diabetes. When administered systemically, TZDs reduce blood pressure and have beneficial vascular effects in many experimental models. While this pharmacological strategy has provided examples of potentially new therapeutic uses for activators of PPARg, the approach does not provide insight into cell-specific effects of PPARg. In addition, such studies do not unmask the functional importance of PPARg in the absence of TZD treatment. Patients with mutations in the ligand-binding domain of PPARg (eg, P467L) exhibit early-onset hypertension and diabetes. These mutations act in a dominant negative fashion to inhibit transcriptional activity of wild-type PPARg. To gain insight into cell specific roles for PPARg, we initiated studies using mice in which human dominant negative mutations in PPARg are expressed in all cells or selectively in vascular cells. The approach mimics the reductions in activity of PPARg seen in some diseases (or with other genetic polymorphisms) and provides insight into the functional importance of PPARg when driven by endogenous ligands. Using heterozygous knock-in mice with the P467L mutation in all cells, we found that PPARg protects against oxidative stress, endothelial dysfunction, and inward vascular remodeling under normal conditions. These effects were much greater in the cerebral circulation than in carotid artery or aorta. In transgenic mice expressing P467L under control of the smooth muscle myosin heavy chain promoter (S-P467L), there was no change in body weight, adipose tissue, plasma glucose, insulin, or leptin. Using this model in which interference with PPARg was targeted to smooth muscle, there was marked impairment of dilator responses to nitric oxide (NO) in cerebral arteries. In contrast, responses to NO were modestly impaired in carotid artery and unaffected in small mesenteric arteries. In vivo, dilation of cerebral microvessels to endogenously produced or exogenously applied NO was reduced by more than 50%. In relation to mechanisms, dilation of the basilar artery to NO in S-P467L mice was restored to normal following treatment with an inhibitor of rho kinase (Y-27632). Interference with PPARg in vascular muscle also produced hypertrophy and inward remodeling in cerebral arterioles as well as increased constrictor responses of cerebral arteries to endothelin-1 (ET-1). ET-1 is thought to be a key mediator of vasospasm. In S-P467L mice, vascular sensitivity to ET-1 was increased ~10-fold and maximal responses were more than doubled. These findings support the concept that PPARg in smooth muscle plays a major role in regulating structure and function in both large and small cerebral blood vessels. The impact of PPARg appears to be particularly prominent the cerebral circulation in the absence of exogenous ligand.

1517

ROLE OF INFLAMMATION AND IMMUNITY IN ACUTE STROKE

U. Dirnagl

Center for Stroke Research Berlin, Charite Universitaetsmedizin Berlin, Berlin, Germany

Stroke affects the normally well balanced interplay of the two supersystems - the nervous and the immune system. Recent research elucidated some of the involved signals and mechanisms, and importantly, was able to demonstrate that brain-immune interactions are highly relevant for functional outcome after stroke. Stroke induces immunodepression and increases the succeptiblity to infection, the most relevant complication in stroke patients. However, immunodepression after stroke may also have beneficial effects, for example by suppressing autoaggressive responses during lesion-induced exposure of CNS specific antigens to the immune system. It is important to note that immune responses generated on antigen encounter are determined by the microenvironment of the tissue. Co-stimulatory molecules are necessary for the priming of immune responses. In the brain, such molecules are only expressed at low levels in the normal brain, but become upregulated upon brain damage, such as stroke. In addition, systemic infection, which may accompany stroke, induces the upregulation of co-stimulatory as well as MHC class I and II molecules in the periphery and the brain, thus sensitizing T- and B-cells to brain antigens. Stroke induces activation of microglia and astrocytes, which result in the production of pro-inflammatory cytokines. As a result of systemic inflammation, for example during infection, additional cytokines are produced outside and within the brain and mediate aspects of sickness behaviour. In the context of stroke, systemic inflammation may thus lead to an exaggerated pro-inflammatory phenotype. At present it is clear that the interaction of brain and adaptive as well as innate immunity after stroke is highly relevant for tissue damage, regeneration, as well as systemic infection. However, the exact mechanisms and consequences of the interplay between circulating cells of the immune system and brain immune cells (e.g. microglia) remain to be elucidated. It is likely that a deeper understanding of brain immune interaction after stroke will supply us with a host of targets for protecting the brain, fostering its regeneration, and preventing systemic complications such as infection.

1518

ROLE OF MICROGLIA IN NEURODEGENERATIVE DISEASE (AD)

H. Boutin, S. Allan

Faculty of Life Sciences, University of Manchester, Manchester, UK

Alzheimer's disease (AD) and other forms of dementia represent a massive and growing global social and economic burden, estimated at between 66-150 billion €/year in Europe (Ferri C.P. *et al.* (2005) *Lancet* 366:2112-17 and World Alzheimer Report 2010).

It is well established that AD is a multi-factorial, complex disease. Several abnormalities, such as elevated levels of Ab(40-42) leading to b-amyloid plaque formation, neurofibrillary tangles (NFT), alteration of the cholinergic system, brain atrophy, decreased brain metabolism, have all been extensively documented as characteristic features of the disease. However, Ab plaques and NFT alone do not seem sufficient to explain the full features of AD, as the presence of abnormally high levels of Ab plaques are also observed in control subjects. Furthermore, recent clinical trials found no improvement in cognitive function in patients immunised against Aβ, despite evidence of plaque clearance on the brains post-mortem. In parallel, animal models of AD do not show significant neurodegenerative changes/atrophy despite high levels of expression of Aβ and/or tau and behavioural deficits. These findings suggest that factors additional to Aβ plaques and NFT are required for AD to develop fully and there is now a wealth of evidence that neuroinflammation is an active contributor to AD pathophysiology. Neuroinflammation relates mainly to the activation of astrocytes and microglial cells, and cytokines and chemokines production. Neuroinflammation also involves the response of the brain vasculature to the brain inflammation (e.g. expression of adhesion molecules) which leads to infiltration of neutrophils and macrophages. Microglial activation and elevated cytokine expression have been demonstrated *in vivo* and in post-mortem human tissues in AD, whilst it has been demonstrated *in vitro* that Ab induces cytokine release from brain cells. However, the temporal cytokine expression profile and the precise contribution of neuroinflammation to AD pathology remain unknown. Whether neuroinflammation is purely an epiphenomenon of the disease or is contributing to AD pathogenesis has not been resolved; although increasing evidence suggests that inflammation is an active contributor to the disease process in AD. For instance, AD patients deteriorate faster following systemic/peripheral infections which are known to induce neuroinflammation. In addition, retrospective studies of individuals on long-term treatment with non-steroidal anti-inflammatory drugs (NSAIDs) have demonstrated delayed onset and reduced severity of AD symptoms, although recent prospective trials have failed to confirm this. Recent genome-wide association studies have also identified some inflammatory genes as having a role in AD. However, during the slow progression of AD, some neuroinflammatory processes may actually be beneficial whereas others are clearly detrimental. Overall, there is some consensus that moderate activation of glia might be beneficial, through an increase in Ab clearance. Whereas strong activation of microglial cells may lead to a phagocytic profile which might slow down Ab clearance, increase production of detrimental pro-inflammatory cytokines and speed-up neuronal damage and cognitive decline. Consequently, understanding the role of the different components of the neuroinflammatory response *in vivo* in animal models and in patients is therefore essential to establish the contribution of neuroinflammation in AD and for development of new therapeutic strategies.

1524

SIGNALING FOR NEUROGENESIS

D.A. Greenberg

Buck Institute for Research on Aging, Novato, CA, USA

Neurogenesis—the process through which new neurons are produced from proliferating neural precursor cells—is regulated by a variety of physiological, pharmacological, and pathological factors. One such factor is cerebral ischemia, which stimulates the production of new neurons in the hippocampal dentate gyrus (DG) and rostral subventricular zone (SVZ) and their migration from SVZ to the site of ischemic injury. Diverse signaling molecules, including growth factors, neurotransmitters, and intracellular mediators, can influence neurogenesis, but which are critical for signaling from ischemic brain to neuroproliferative sites and for directing the migration of new neurons is uncertain. In this review, representative signaling mechanisms that may be involved in these events will be discussed.

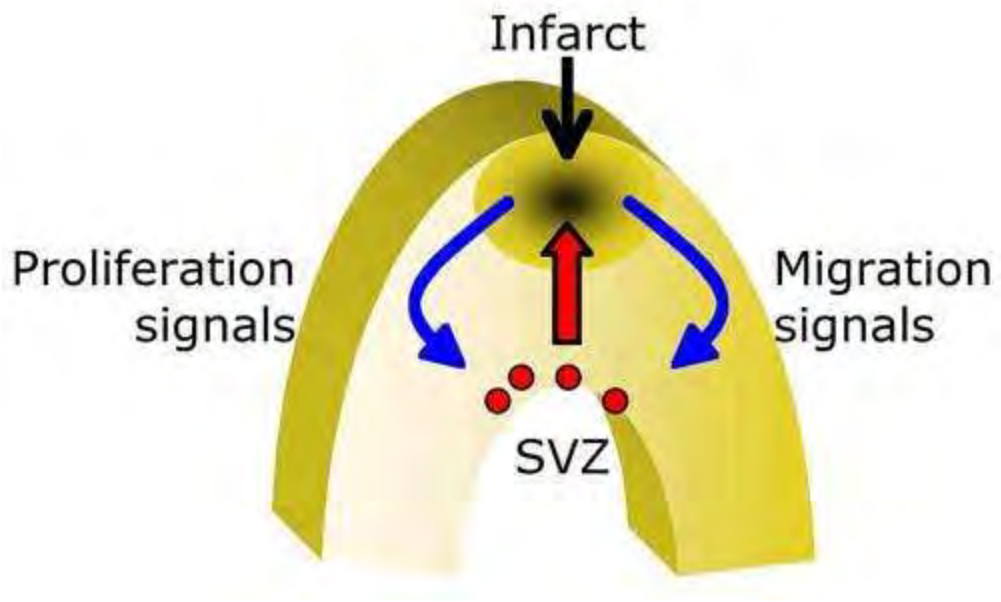

[Figure 1]

1525

TWO-PHOTON NADH IMAGING EXPOSES BOUNDARIES OF OXYGEN DIFFUSION IN CORTICAL VASCULAR SUPPLY REGIONS

K. Kasischke

Dept. of Neurology, Center for Neural Development and Disease, University of Rochester Medical Center, Rochester, NY, USA

Oxygen transport imposes a possible constraint on the brain´s ability to sustain variable metabolic demands, but oxygen diffusion in the cerebral cortex has not yet been observed directly. We show that concurrent two-photon fluorescence imaging of endogenous nicotinamide adenine dinucleotide (NADH) and the cortical microcirculation exposes well defined boundaries of tissue oxygen diffusion in the mouse cortex. NADH fluorescence increases rapidly over a narrow, very low pO_2 range with a p_{50} of 3.4 ± 0.6 mmHg, thereby establishing a nearly binary reporter of significant, metabolically limiting hypoxia. The transient cortical tissue boundaries of NADH fluorescence exhibit remarkably delineated geometrical patterns, which define the limits of tissue oxygen diffusion from the cortical microcirculation and bear a striking resemblance to the ideal Krogh tissue cylinder. The visualization of microvessels and their regional contribution to oxygen delivery establishes penetrating arterioles as major oxygen sources in addition to the capillary network and confirms the existence of cortical oxygen fields with steep microregional oxygen gradients. Thus, two-photon NADH imaging can be applied to expose vascular supply regions and to localize functionally relevant micro-regional cortical hypoxia with micrometer spatial resolution.

1526

OLIGODENDROGENESIS AND WHITE MATTER RESCUE AFTER CNS INJURY AND NEURODEGENERATION

M. Chopp[1,2]

[1]Neurology, Research Division, Henry Ford Hospital, Detroit, [2]Department of Physics, Oakland University, Rochester, MI, USA

White matter damage and degeneration, which leads to neurological deficits, is a hallmark of stroke, traumatic brain injury and multiple sclerosis; therefore reducing white matter damage, by promoting oligodendrogenesis, remyelination and enhanced neurite outgrowth in response to neural injury may yield beneficial therapeutics effects. In this presentation, data on white matter-axonal remodeling post neural injury in stroke patient's and in animal models of neural injury and degenerative disease will be presented. We will show that white matter remodeling is present in the periphery of human brain after stroke. In the experimental animal, we will demonstrate that the cell and pharmacological restorative therapies can stimulate oligodendrogenesis and white matter remodeling in the ipsilateral as well as the contralateral hemispheres to injury. The molecular bases for the induction of oligodendrogenesis and white matter restorative events will be discussed and will include identification of novel miRNA families that regulate white matter remodeling and oligodendrogenesis.

1527

IMAGING THE HUMAN PENUMBRA, HISTORICAL PERSPECTIVES, CHALLENGES AND OPPORTUNITIES

G.A. Donnan

Florey Neuroscience Institutes, Carlton South, VIC, Australia

The concept of the ischaemic penumbra, first developed by Astrup and Symon in the 1970's has matured over the years with the introduction of imaging modalities to assess its quantitative and topographical extent. However, the original concept of tissue which is functionally impaired but anatomically intact and which is salvageable has been maintained. The introduction of Positron Emission Tomography (PET) allowed an in vivo topographical and quantitative image of the ischaemic penumbra to be achieved for the first time. The concept of “misery perfusion” with a reduced cerebral blood flow in the face of preserved metabolism and elevated oxygen and extraction fraction (OEF) was the first definition of the penumbra in vivo in humans. Other PET techniques such as PET 18F MISO, PET 11C flumazinal also provided alternative means of imaging potentially salvageable tissue. The introduction of MR with DWI/PWI mismatch revolutionized penumbral studies because of its broad availability and repeatability. Latterly, CT perfusion has provided similar opportunities.

When using MR to generate mismatch images, the most challenging issues relate to the definition of thresholds. For example for DWI, while originally thought to accurately reflect infarct core, was subsequently found to have components which were reversible. However, it has been subsequently shown that the extent of this is quite modest, so that DWI does remain a good index of infarct core volume. For PWI, the upper threshold between benign oligaemic tissue and true penumbra has been difficult to establish. Recent developments suggest that the T-max haemodynamic parameter may be the most reliable and that T-max + 2 seconds may be a reasonable estimate of penumbral tissue. More recent studies modelling predictable infarct expansion or correlations with PET haemodynamic gold standards suggest that T-max + 6 seconds is the most appropriate penumbral measure.

For CT perfusion, the challenge has been to provide similar perfusion thresholds, particularly for infarct core and upper penumbral levels. The latter may be determined in a similar way to that of MR perfusion indices, while the infarct core has more recently been defined more precisely with cerebral blood flow rather than the original cerebral blood volume parameters.

The real opportunities that now exist for penumbral imaging is to be incorporated into mainstream clinical usage. For this to occur, it must be clearly demonstrated that penumbral identification is a useful way to maximise clinical responsiveness to therapy. A number of studies are underway endeavouring to prove this very point.

1528

STEM CELL THERAPY IN CHRONIC STROKE PATIENTS-PHASE II TRIAL

S.-Z. Lin[1,2,3], D. Liu[1], W.-C. Shyu[1,3]

[1]Center for Neuropsychiatry, China Medical University Hospital, Taichung, [2]Department of Neurosurgery, China Medical University Beigang Hospital, Yunlin, [3]Graduate Institute of Immunology, China Medical University, Taichung, Taiwan R.O.C.

Our pilot clinical trial was performed in 6 chronic stroke patients (stroke duration more than 6 months) by implanting autologous hematopoietic stem cells into the infarct brain. The results show that the damaged corticospinal tract might be regenerated within 3 to 6 months after the transplantation. However, the corticospinal tract regeneration and motor improvement were much better in young stroke patients (age less than 60 years old) than the elder (age more than 61 years old). We hypothesized that the age dependent regeneration of the corticospinal tract may be related to the molecular systems of the chemoattractants and stress proteins.

The most common and strongest chemoattractant protein is the stromal-cell-derived factor-1 alpha (SDF-1 alpha) and its receptor CXCR4. These two proteins together with cellular prion protein (PrPsc) are upregulated in the acute injured brain and stem cells. Stress induced protein such as secretoneurin is also upregulated during acute brain injury. In animal studies, overexpression of these proteins not only protects the injured brain from neural apoptosis, but also attracts bone marrow as well as neural stem cell to the injured site. Stem cells secrete various nurotrophic factors, angiogenic factors, stress proteins, and chemoattractants to enhance neuroprotection, tractogenesis and neuroplasticity. In addition, stem cells may also rejuvenate the surrounding cells.

We are currently conducting a randomized, double blind control trial for chronic stroke patients by implanting CD34 stem cells into the infarct brain. Our preliminary results show that there were a significant increment of corticospinal tract fiber density ratio (CTFDR) assessed by diffusion tensor image (DTI) in treatment group than control. The neurological improvements were better in the treatment group as compared to control patients in regarding to NIHSS, ESS, EMS, and Barthel Index. Details will be presented in the meeting.

This randomized control study demonstrates that a therapeutic strategy using G-CSF combined with autologous implantation of PBSCs mobilized by G-CSF transplantation for old stroke patients is safe, feasible, and shows preliminary evidence of improved neurological outcomes.

1529

NEUROPROTECTIVE TARGETS OF OXIDATIVE STRESS

P. Chan

Neurosurgery, Stanford University, Stanford, CA, USA

Brain mitochondria are known to be the powerhouses of the cell. These subcellular organelles are also the determinants for cellular survival and death after neurological injury, cerebral ischemia, and reperfusion, in particular. Superoxide and other reactive oxygen species (ROS) are produced in mitochondria during ischemia/reperfusion and are known to generate oxidative stress and cellular damage. We have demonstrated that manganese-superoxide dismutase (MnSOD, SOD2; a highly inducible antioxidant enzyme), its transcriptional activity and expression are highly regulated by STAT3 (signal transducer and activator of transcription 3). Ischemic reperfusion causes STAT3 inactivation, decreases SOD2 expression, and enhances brain damage. We now present data that demonstrates that the inflammatory cytokine IL-6, in particular, activates the IL-6 receptor (IL-6R), which leads to increased expression of STAT3 phosphorylation (Y705), dimerization, and nuclear translocation, resulting in activation of the SOD2 promoter for transcriptional activation of SOD2 and subsequent neuroprotection. We propose IL-6R as a molecular target for neuroprotection against reperfusion-induced oxidative stress and cell injury by up-regulation of mitochondrial SOD2.

1531

STIMULATION-INDUCED INCREASES OF ASTROCYTIC OXIDATIVE METABOLISM IN RATS AND HUMANS INVESTIGATED WITH 1-^{11}C-ACETATE

M.T. Wyss[1,2], B. Weber[2], T. Valerie[1], S. Heer[1], L. Pellerin[3], P.J. Magistretti[4], A. Buck[1]

[1]PET Center, Division of Nuclear Medicine, University Hospital of Zürich, [2]Institute of Pharmacology and Toxicology, University of Zürich, Zürich, [3]Physiology Department, University of Lausanne, [4]Brain Mind Institute, EPFL, Lausanne, Switzerland

Brain metabolism is a highly compartmentalized process in which astrocytes have been shown to play substantial roles rather than being passive elements. In order to elucidate aspects of their metabolism, we investigated oxidative astrocytic metabolism with the use of the radiolabeled astrocyte-specific substrate acetate (1-^{11}C-acetate). Using a β-scintillator we evaluated 1-^{11}C-acetate kinetics in the somatosensory cortex of anesthetized rats during several conditions 1. Baseline, 2. Peripheral sensory stimulation, 3. Increased cerebral blood flow by acetazolamide and 4. Pharmacological inhibition of the pyruvate dehydrogenase complex. In addition, we report the straightforward translation of the methodology into human studies where tracer kinetics were measured in human visual cortex with positron emission tomography. Based on a classical one-tissue compartment model rate constants for delivery (K_1) and for radiolabel washout from tissue (k_2) were determined from our data by kinetic modeling. Beside the fact that k_2 demonstrates a significant increase during stimulation in rats (from 0.014 ± 0.007 to 0.027 ± 0.006 min^{-1}) and in humans (from 0.016 ± 0.01 to 0.026 ± 0.006 min^{-1}) further support for the notion that k_2 is tightly linked to astrocytic oxygen consumption is provided. 1-^{11}C-acetate is a promising tracer to investigate astrocytic oxidative metabolism *in vivo* and our results point to a substantial increase of astrocytic oxidative metabolism during brain activation. Finally, we will report more recent work of our lab that has focused on the use of 1-^{11}C-lactate for the study of cerebral lactate oxidation.

1532

QUANTIFICATION OF MICROGLIA AND AMYLOID-ß BY PET

A. Lammertsma

Nuclear Medicine & PET Research, VU University Medical Center, Amsterdam, The Netherlands

There is growing evidence that activation of microglia cells is an early and ongoing event in neurodegeneration. Activated microglia are characterized by increased expression of the 18 kDa translocator protein (TSPO), formerly known as the peripheral type benzodiazepine receptor. In recent years, several new TSPO ligands have been proposed, but none has been fully characterized for human use yet. Moreover, at least for some of the newer ligands, there appear to be two affinity states, making *in vivo* quantification essentially impossible. This problem does not exist for *(R)*-[^{11}C]PK11195, the only ligand that has been validated quantitatively. Nevertheless, even quantification of this ligand is not trivial, as it suffers from noise, partly due to the relatively high level of non-specific binding. Using a range of both plasma input and reference tissue models, it has been shown that the method of choice for quantifying *(R)*-[^{11}C]PK11195 is the simplified reference tissue model (SRTM). This method allows for quantitative assessment of microglia activation without the need for arterial sampling. A problem associated with neurodegenerative diseases is that no anatomical region can be assumed to be (completely) free of microglia activation. Therefore, it is recommended to use a (modified) supervised cluster analysis algorithm as an objective means of defining the reference tissue curve of *(R)*-[^{11}C]PK11195. Finally, it is possible to generate parametric binding potential (BP_{ND}) images using RPM2, a basis function implementation of SRTM with fixed k_2'.

Senile plaques, caused by accumulation of amyloid-beta (Aβ), are one of the main neuropathological features of Alzheimer's disease. With the development of new drugs, aimed at either preventing Aβ deposition or increasing its clearance, quantification of Aβ burden *in vivo* becomes essential in order to follow disease progression and its (early) modification by therapy. Although several promising tracers of amyloid-ß are available, most quantitative studies have been performed using [^{11}C]PIB. In fact, in most clinical trials, static scans acquired some time after [^{11}C]PIB injection are used and data are quantified using standardised uptake value ratios with cerebellum (SUVr). This approach inherently assumes that the ratio of specific to non-specific binding remains constant, an assumption that might be violated especially in the case of novel amyloid modifying therapies. A better approach is to use full kinetic modelling. Again, using a range of both plasma input and reference tissue models, it has been shown that the method of choice for quantifying [^{11}C]PIB is SRTM. As for *(R)*-[^{11}C]PK11195, parametric BP_{ND} images can again be obtained with RPM2.

1534

PET IMAGING OF NEUROINFLAMMATION

B. Tavitian

Laboratoire d'Imagerie Moléculaire Expérimentale, Inserm-CEA U1023, Orsay, France

Imaging of neuroinflammation is assigned with several objectives: (i) follow the time course of neuroinflammation during acute insults of the CNS such as ischemic stroke, traumatic brain injury, or during flares of multiple sclerosis (MS); (ii) reveal the presence of persistent neuroinflammation found in chronic disorders such as Alzheimer's disease (AD), schizophrenia, and others; (iii) document the anti-inflammatory activity of drugs.

Microglia are CNS-resident patrolling cells that depict a dramatic change in their morphology and pattern of gene expression in the first hours following tissue an injury of the cerebral tissue. This “activated” phenotype resembles that of macrophages in the periphery and persists as long as the insult to the cerebral tissue has not been resolved. A protein called TSPO that is part of an outer mitochondrial complex is expressed in activated microglia, while it is absent or barely detectable in resident microglia from intact cerebral tissue. Therefore, imaging of TSPO expression using PET radioligands for this protein is considered a surrogate for the imaging of acute and chronic neuroinflammation. TSPO is a transporter of cholesterol that may participate in the production of neurosteroids known to act on various CNS cells types including neurons. The discovery that AD senile plaques are surrounded by activated microglia, that long-term anti-inflammatory treatments may reduce the prevalence of AD, that microglia respond to TNF alpha and interferon, and that some compounds binding to TSPO have anti-apoptotic activity, has brought further support to PET imaging of TSPO. Many questions remain concerning the exact role of TSPO and of its associated proteins, the time course of its expression during neuroinflammation in microglia as well as in other cell types, the expression of TSPO in the intact CNS and the existence of different binding sites. In recent years, over 50 new PET radiotracers binding to TSPO have been described and several clinical trials have been initiated with the most promising ones. Here I will review the data obtained in our laboratory with new TSPO PET radiotracers imaging animal models of neuroinflammation.

Supported by the EU-FP6 networks EMIL (LSHC-CT-2004-503569) and DiMI (LSHB-CT-2005-5121146)

1535

NOVEL ADHESION MOLECULES OF THE BBB

A. Prat

Université de Montréal, Neuroimmunology Unit, CHUM-Notre-Dame Hospital, Montreal, QC, Canada

The Blood Brain Barrier (BBB) protects the central nervous system by regulating molecular and cellular exchanges between the brain and the blood. The BBB is made of a network of tightly adherent endothelial cells (ECs) surrounded by astrocytic processes which provide factors that contribute to BBB maintenance. Several proteomic based-profiling of human and animal BBB endothelial cells have revealed the presence of unique regulatory proteins involved in BBB physiology and trans-endothelial leukocyte migration, including proteins involved in cellular adhesion, cell structure, BBB development, immunity and defense, transport and trafficking and signal transduction. Recent work, using animal models of MS and spinal cord contusion, as well as human in vitro, in situ and ex vivo analysis revealed that these new BBB candidate proteins, including ALCAM, MCAM, Ninjurin-1 and VAP-1 are involved in the regulation of immune cell trafficking across vascular structures of the CNS. This presentation will provide a short overview of the progresses that were made over the last 5 years to identify novel pathways that are involved in the selective recruitment of specific immune cells to the CNS. These molecules are currently seen as the basis for the development of future therapies in MS.

1536

IN VIVO IMAGING OF IMMUNE CELL ENTRY INTO THE CNS

A. Flugel, *Institute for Multiple Sclerosis Research, Department of Neuroimmunology, University of Göttingen, Germany*.

The healthy CNS tissues are shielded from the periphery by the blood brain barrier (BBB) preventing the unrestricted access of immune cells and macromolecules. However, during experimental autoimmune encephalomyelitis (EAE), an animal model of multiple sclerosis T cells reactive against myelin components readily overcome this barrier and locally evoke a massive inflammatory process resulting in severe neurological deficits. Using intravital 2-photon imaging of green fluorescent protein-expressing T cells in a Lewis rat model of EAE, we follow the transgression of the BBB and the locomotion behavior of pathogenic effector T cells in real time. We found that encephalitogenic effector T cells arriving at the BBB enter the tissue in at least three distinct stages: (i) The movement of the effector T cells is initially arrested but then they start to crawl within the lumen of pial vessels, preferentially against the blood stream. (ii) They then transgress the vascular walls and migrate on their outer surface. (iii) Upon contact with perivascular phagocytes, the T cells become re-activated and spread throughout the meningeal surface before they enter deep into the CNS parenchyma. Within the parenchyma, the T cells move seemingly at random (references Bartholomäus et al. 2009 and Kawakami et al. JEM 2005). Our current work is focused on finding out which factors and mechanisms underlie the locomotion behavior of autoaggressive effector T cells at the blood brain interface and how these cells can be prevented from penetrating into nervous tissue. These studies aim at defining new therapeutic targets and understanding how established therapies influence T cell migration *in vivo*.